ACTA CHEMICA SCANDINAVICA 10 (1956) 1—8

On the Structure of the Crystal Form A of Lauric Acid

ERIK von SYDOW

Institute of Chemistry, University of Uppsala, Uppsala, Sweden

The A-form of lauric acid, $C_{11}H_{23}COOH$, is triclinic with space group $P\bar{1}$. For structural reasons the centered cell $A\bar{1}$ has been used. It has the dimensions $a = 5.41$ Å, $b = 26.27$ Å, $c = 35.42$ Å, $\alpha = 69° 36'$, $\beta = 113° 9'$, and $\gamma = 121° 21'$. The centered cell contains 12 molecules. The hydrocarbon chains are arranged in a triclinic packing and from this point of view the structure can be regarded as a sixfold superstructure. There are no layers in the crystals with only carboxyl groups or methyl groups, respectively. They appear together in the same layers in groups of six.

Like all the other crystal forms of normal fatty acids the crystalline A-form of acids with an even number of carbon atoms was first detected in a "long spacing" investigation [1]. Trillat and v. Hirsch [2] determined the smallest axis-plane of stearic acid with electron-diffraction. Lomer [3] has recently determined the unit cell dimensions of the A-forms (γ-form) of lauric acid and myristic acid from powder data. He suggests that the cells are monoclinic, which however seems to be wrong. For the A-form of lauric acid he gives a volume which is about 6 % less than the volume of the one described here. Lomers observed density data are also inconsistent with these results.

PREPARATION OF CRYSTALS

The very pure lauric acid used was prepared by Professor E. Stenhagen and his collaborators. It melts at 44.5—44.8° C.

According to Stenhagen and the author [4,5] lauric acid may crystallize exclusively in the form A from light petroleum, pentane, acetone, ethyl alcohol, and carbon disulfide. The best single crystals for the X-ray investigation were obtained from carbon disulfide.

Crystals of normal fatty acids are usually in form of thin plates, but the A-form of lauric acid crystallizes in elongated parallelepipeds with irregular shortsides. The crystals are biaxial positive. No twinning could be observed under the polarizing microscope.

X-RAY DATA

Rotation and Weissenberg photographs were taken with Cu-K radiation using a calibrated camera. The following data were obtained:

Molecular formula: $C_{12}H_{24}O_2$.
Molecular weight: 200.31.
Density calculated: 1.027 ± 0.013 g cm^{-3}.
Density observed: 1.033 g cm^{-3}.
Unit cell: triclinic (primitive).
Six molecules per unit cell.
Number of electrons: 672.
Space group: C_i^1—$P\ \bar{1}$.

For structural reasons the following cell will be used in the text:

Unit cell: triclinic (A-centered).
$a = 5.41 \pm 0.01$, $b = 26.27 \pm 0.07$, $c = 35.42 \pm 0.13$ Å.
$\alpha = 69°\ 36' \pm 30'$, $\beta = 113°\ 9' \pm 26'$, $\gamma = 121°\ 21' \pm 34'$.
d(001) $= 32.02 \pm 0.06$ Å.
Twelve molecules per unit cell.
Number of electrons: 1 344.
Absent reflexions: (hkl) when $(k+l)$ odd.
Space group: C_i^1—$A\ \bar{1}$.

The absence of the piezo-electric effect (I am indebted to Mr. J. Baecklund for help with the measurements) is consistent with a center of symmetry.

No twinning was observed.

The intensities were estimated by eye from two different sets of multiple films exposed for different times. They were corrected with the normal polarization and Lorentz factors, but no absorption corrections were applied. The relative, observed structure factors obtained were later brought to an absolute scale by comparison with the calculated structure factors. The intensities of the low angle reflexions (002), (011) and (01$\bar{1}$) were estimated from a powder photograph.

Subcell

In the triclinic reciprocal lattice strong reflexions appear periodically along (hkl) when $k = 6n$. They give rise to a larger reciprocal cell, which also is triclinic. Its dimensions agree very well with those of the cell having triclinic packing of hydrocarbon chains, described by Müller and Lonsdale [6] and Vand and Bell [7]. The triclinic subcell coincides approximately with the A-centered cell of the A-form of lauric acid having two axes equal to a and a value close to $b/6$. Considering the chainpacking the main crystal structure can be regarded as a sixfold superstructure.

Patterson projections

If the carbon atoms lie strictly according to the triclinic subcell, they contribute only to structure factors $F(hkl)$ with $k = 6n$. The oxygen atoms in the carboxylic groups, however, contribute to all structure factors and are the only cause of $F(hkl)$ with $k \neq 6n$.

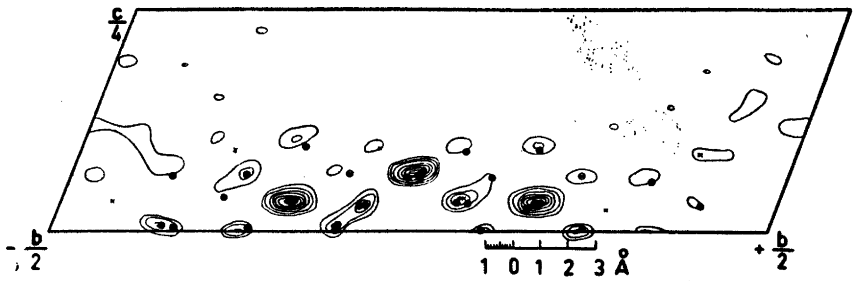


Fig. 1. Patterson projection with $F^2(0kl)$ *values for* $k \neq 6n$. *Origo: 15 contours.* × *single,* ⊗ *double oxygen-oxygen vectors calculated with the final oxygen coordinates.*

A Patterson synthesis with $F^2(hkl)$ for which $k = 6n$ should thus give interatomic distances in the hydrocarbon chains and a synthesis with $F^2(hkl)$ for which $k \neq 6n$ should give peaks which either represent at least approximate oxygen-oxygen vectors or have no significance at all. The latter is due to the fact that the contribution from the oxygen atoms to $F(hkl)$ with $k = 6n$ is not taken into consideration. This contribution may be comparatively large as there are two oxygen atoms bonded to each of the twelve hydrocarbon chains in the centered cell.

Two Patterson projections were carried out, one with $F^2(0kl)$ where $k = 6n$ and the other with $F^2(0kl)$ where $k \neq 6n$. Both were sharpened by multiplication by the function

$$M(S) = \left(\frac{1}{\hat{f}}\right)^2 \exp\left(-\frac{\pi^2}{p} S^2\right) \text{ with } p = 7.25$$

as suggested by Lipson and Cochran [9, p. 172].

The first gave carbon-carbon distances which fitted well with the subcell data given by Vand and Bell [7]. The second projection (Fig. 1) consisted of many peaks concentrated round (0, 0, 0) and (0, ½, ½) in agreement with the centering. It was treated by Buergers vector set method [10] and a set of relative positions was obtained. The carboxylic group and the hydrogen bonding between two acid molecules was supposed to be very similar to those in the other crystal forms of normal fatty acids, *e. g.* the C-form of lauric acid investigated by Vand, Morley and Lomer [8]. With this assumption it could be seen that some of the positions obtained by the vector set method were impossible and thus caused by the fact that the oxygen contribution to $F(0kl)$ with $k = 6n$ had not been accounted for. The remaining positions were supposed to be relative oxygen positions and agreed well with the assumptions above. From the knowledge of other crystal forms (*e. g.* Refs.[8, 13, 14]) they were placed relative to the carbon atoms.

Structure factors and electron-density projections

If all carbon atoms are assumed to be situated strictly according to the triclinic subcell, the structure factors can be calculated using the coordinates

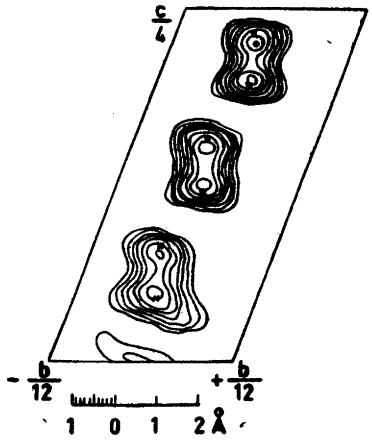


Fig. 2. Fourier projection along the shortest axis with 27 F(0kl) *where* k = 6n. *Arbitrary contour scale. The correct positions of the carbon atoms are marked with crosses.*

of only six carbon atoms (later with two hydrogen atoms each) and six oxygen atoms. This will cause small errors in the structure factors due to the non-existence of hydrogen atoms at the carbon atom in the carboxylic group, the existence of a hydrogen atom in the hydroxyl group and of a third hydrogen atom in the methyl group. This effect is, however, insignificant and has been ignored.

With the information obtained from the Patterson projections, structure factors were calculated without the hydrogens. Atomic scattering factors were taken from McWeeny [11] using for oxygen $f = \frac{1}{3}(f^{\perp} + 2f^{\parallel})$ and for carbon the values for "valence states".

A Fourier synthesis was carried out with relative, observed $F(0kl)$ values for $k = 6n$ using 27 signs from the first structure factor calculation. The projection obtained is given in Fig. 2 and shows clearly the six carbon atoms.

In order to obtain the oxygen positions another synthesis with relative, observed $F(0kl)$ values for $k \neq 6n$ was performed using 105 calculated signs (none of these was later found to be wrong). This projection can be seen in Fig. 3. For comparison the final coordinates of the atoms are marked with crosses in both figures.

Structure factors were now calculated again and a total electron-density projection along the shortest axis was prepared. The coordinates were refined using several $(F_o - F_c)$-syntheses and the hydrogen atoms were included in the

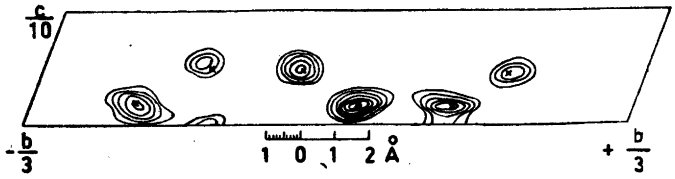


Fig. 3. Fourier projection along the shortest axis with 105 F(0kl) *where* k ≠ 6n. *Arbitrary contour scale. The correct positions of the oxygen atoms are marked with crosses.*

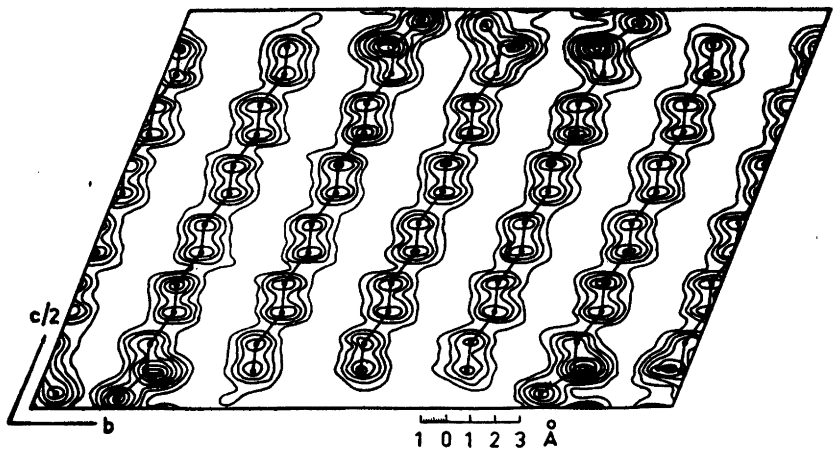


Fig. 4. The A-form of lauric acid. Electron-density projection along the shortest axis. Contour scale: 1 e Å^{-2}.

structure factor calculations as was mentioned above. Their positions relative to the carbon atoms were calculated from data given by Vainshtein and Pinsker [12]. A temperature factor, $\exp\left(-B\frac{\sin^2\Theta}{\lambda^2}\right)$ with $B = 4.2$, was applied.

The final coordinates are collected in Table 1, and observed and calculated structure factors in Table 2. The electron-density projection prepared with the values from Table 2 is shown in Fig. 4. The reliability index $R_1 = 0.15$

Table 1. Coordinates of the atoms.

Atom	y/b	z/c	Atom	y/b	z/c
O_1^1	0.0323	0.0180	C_1	$0.9922 + n \cdot \frac{1}{6}$	0.0445
O_2^1	0.9555	0.0475	C_2	$0.9795 + n \cdot \frac{1}{6}$	0.0803
O_1^2	0.1337	0.0128	C_3	$0.9979 + n \cdot \frac{1}{6}$	0.1196
O_2^2	0.1820	0.0435	C_4	$0.9850 + n \cdot \frac{1}{6}$	0.1553
O_1^3	0.3663	0.4872	C_5	$0.0035 + n \cdot \frac{1}{6}$	0.1947
O_2^3	0.3180	0.4565	C_6	$0.9908 + n \cdot \frac{1}{6}$	0.2302
O_1^4	0.4677	0.4820	C_7	$0.0092 + n \cdot \frac{1}{6}$	0.2698
O_2^4	0.5445	0.4525	C_8	$0.9965 + n \cdot \frac{1}{6}$	0.3053
O_1^5	0.7142	0.4834	C_9	$0.0150 + n \cdot \frac{1}{6}$	0.3447
O_2^5	0.6449	0.4530	C_{10}	$0.0021 + n \cdot \frac{1}{6}$	0.3804
O_1^6	0.7858	0.0166	C_{11}	$0.0205 + n \cdot \frac{1}{6}$	0.4197
O_2^6	0.8551	0.0470	C_{12}	$0.0078 + n \cdot \frac{1}{6}$	0.4555

Table 2. Observed and calculated structure factors.

hkl	$\frac{1}{2}F_o$	$\frac{1}{2}F_c$	hkl	$\frac{1}{2}F_o$	$\frac{1}{2}F_c$	hkl	$\frac{1}{2}F_o$	$\frac{1}{2}F_c$
0, 0, 0	336		0, 3, 15	12	−12	0, 6, 10	21	−23
0, 0, 2	12	12	0, 3, 17	12	−12	0, 6, 12	59	−55
0, 0, 4	< 2	1	0, 3, 19	10	−10	0, 6, 14	35	26
0, 0, 6	11	−12	0, 3, 21	8	− 7	0, 6, 16	15	7
0, 0, 8	20	−22	0, 3, 23	< 3	− 3	0, 6, 18	8	5
0, 0, 10	24	−27				0, 6, 20	7	4
0, 0, 12	27	−31	0, 3, $\bar{1}$	14	−15	0, 6, 22	< 3	4
0, 0, 14	5	3	0, 3, $\bar{3}$	12	−14	0, 6, 24	< 3	3
0, 0, 16	< 3	− 4	0, 3, $\bar{5}$	7	− 9	0, 6, 26	33	28
0, 0, 18	< 3	2	0, 3, $\bar{7}$	3	− 1	0, 6, 28	9	− 6
0, 0, 20	5	3	0, 3, $\bar{9}$	8	7	0, 6, 30	8	− 5
0, 0, 22	< 3	4	0, 3, $\bar{11}$	13	12	0, 6, 32	7	− 4
0, 0, 24	6	6	0, 3, $\bar{13}$	16	14	0, 6, 34	< 4	− 4
0, 0, 26	28	27	0, 3, $\bar{15}$	11	12	0, 6, 36	< 4	− 3
0, 0, 28	20	−17	0, 3, $\bar{17}$	8	8	0, 6, 38	4	− 4
0, 0, 30	10	−10	0, 3, $\bar{19}$	< 3	3	0, 6, 40	6	5
0, 0, 32	5	− 7				0, 6, 42	< 4	0
0, 0, 34	< 4	− 5	0, 4, 10	< 3	− 1			
			0, 4, 12	5	− 6	0, 6, $\bar{2}$	43	−41
0, 1, 1	30	30	0, 4, 14	11	−10	0, 6, $\bar{4}$	19	−16
0, 1, 3	24	25	0, 4, 16	12	−11	0, 6, $\bar{6}$	14	−12
0, 1, 5	15	15	0, 4, 18	10	−10	0, 6, $\bar{8}$	13	−11
0, 1, 7	6	5	0, 4, 20	7	− 8	0, 6, $\bar{10}$	9	− 9
0, 1, 9	< 3	− 3	0, 4, 22	< 3	− 5	0, 6, $\bar{12}$	6	− 6
						0, 6, $\bar{14}$	17	−23
0, 1, $\bar{1}$	29	29	0, 4, $\bar{8}$	< 3	2	0, 6, $\bar{16}$	< 4	− 4
0, 1, $\bar{3}$	21	21	0, 4, $\bar{10}$	6	6			
0, 1, $\bar{5}$	11	12	0, 4, $\bar{12}$	7	8	0, 6, $\bar{22}$	< 4	4
0, 1, $\bar{7}$	4	2	0, 4, $\bar{14}$	7	8	0, 6, $\bar{24}$	5	6
0, 1, $\bar{9}$	< 3	− 4	0, 4, $\bar{16}$	7	7	0, 6, $\bar{26}$	13	15
			0, 4, $\bar{18}$	4	4	0, 6, $\bar{28}$	16	−16
0, 2, 8	< 3	− 2	0, 4, $\bar{20}$	< 3	1	0, 6, $\bar{30}$	< 4	− 4
0, 2, 10	6	− 5						
0, 2, 12	9	− 7	0, 5, 1	12	13	0, 7, 1	4	3
0, 2, 14	9	− 7	0, 5, 3	12	13	0, 7, 3	< 3	1
0, 2, 16	6	− 6	0, 5, 5	9	10			
0, 2, 18	4	− 4	0, 5, 7	< 3	6	0, 7, 17	< 4	0
0, 2, 20	< 3	− 1				0, 7, 19	5	2
			0, 5, $\bar{1}$	11	11	0, 7, 21	4	2
0, 2, $\bar{8}$	< 3	0	0, 5, $\bar{3}$	4	6	0, 7, 23	< 4	2
0, 2, $\bar{10}$	6	3	0, 5, $\bar{5}$	< 3	2			
0, 2, $\bar{12}$	9	7	0, 5, $\bar{7}$	4	− 2	0, 7, $\bar{1}$	4	3
0, 2, $\bar{14}$	9	7	0, 5, $\bar{9}$	6	− 4	0, 7, $\bar{3}$	5	3
0, 2, $\bar{16}$	6	6	0, 5, $\bar{11}$	6	− 4	0, 7, $\bar{5}$	4	2
0, 2, $\bar{18}$	< 3	4	0, 5, $\bar{13}$	3	− 3	0, 7, $\bar{7}$	4	2
			0, 5, $\bar{15}$	3	− 2	0, 7, $\bar{9}$	3	2
0, 3, 1	11	−12	0, 5, $\bar{17}$	< 3	− 1	0, 7, $\bar{11}$	4	2
0, 3, 3	6	− 7				0, 7, $\bar{13}$	5	3
0, 3, 5	4	− 2	0, 6, 0	157	157	0, 7, $\bar{15}$	5	3
0, 3, 7	< 3	− 1	0, 6, 2	28	27	0, 7, $\bar{17}$	< 4	2
0, 3, 9	4	− 2	0, 6, 4	9	7			
0, 3, 11	6	− 6	0, 6, 6	3	− 5	0, 8, 10	< 3	− 2
0, 3, 13	13	−10	0, 6, 8	11	−14	0, 8, 12	3	− 5

Table 2. Continued

h k l	½ F_o	½ F_c	*h k l*	½ F_o	½ F_c	*h k l*	½ F_o	½ F_c
0, 8, 14	6	− 8	0, 10, 20	5	− 6	0, 12, $\bar{2}$	32	−37
0, 8, 16	7	− 9	0, 10, 22	4	− 4	0, 12, $\bar{4}$	8	− 9
0, 8, 18	8	− 9	0, 10, 24	< 4	− 1	0, 12, $\bar{6}$	4	− 2
0, 8, 20	7	− 7				0, 12, $\bar{8}$	< 4	1
0, 8, 22	< 4	− 4	0, 10, $\bar{8}$	< 4	1	0, 12, $\bar{10}$	< 4	2
			0, 10, $\bar{10}$	5	4	0, 12, $\bar{12}$	< 4	− 1
0, 8, $\bar{6}$	< 3	3	0, 10, $\bar{12}$	6	6	0, 12, $\bar{14}$	13	−17
0, 8, $\bar{8}$	6	8	0, 10, $\bar{14}$	< 4	5	0, 12, $\bar{16}$	< 4	2
0, 8, $\bar{10}$	10	11						
0, 8, $\bar{12}$	12	14	0, 11, 1	10	−12	0, 12, $\bar{26}$	< 5	8
0, 8, $\bar{14}$	12	12	0, 11, 3	11	−11	0, 12, $\bar{28}$	6	−11
0, 8, $\bar{16}$	7	9	0, 11, 5	10	− 9	0, 12, $\bar{30}$	< 5	1
0, 8, $\bar{18}$	< 4	6	0, 11, 7	5	− 6			
			0, 11, 9	< 4	− 3	0, 13, 1	5	− 6
0, 9, 1	3	− 2				0, 13, 3	5	− 8
0, 9, 3	< 3	4	0, 11, $\bar{1}$	9	−10	0, 13, 5	5	− 8
0, 9, 5	6	8	0, 11, $\bar{3}$	6	− 6	0, 13, 7	4	− 1
0, 9, 7	9	9	0, 11, $\bar{5}$	< 4	− 3	0, 13, 9	< 4	2
0, 9, 9	6	6						
0, 9, 11	5	0	0, 12, 0	27	35	0, 13, $\bar{1}$	4	− 3
0, 9, 13	3	− 6	0, 12, 2	< 4	0	0, 13, $\bar{3}$	< 4	1
0, 9, 15	8	−11	0, 12, 4	5	− 8			
0, 9, 17	13	−13	0, 12, 6	7	−10	0, 18, 0	10	10
0, 9, 19	10	−12	0, 12, 8	8	−10	0, 18, 2	< 5	3
0, 9, 21	8	− 9	0, 12, 10	8	− 9			
0, 9, 23	< 4	− 5	0, 12, 12	36	−35	0, 18, 10	< 6	2
			0, 12, 14	12	11	0, 18, 12	20	−24
0, 9, $\bar{5}$	< 3	− 2	0, 12, 16	8	5	0, 18, 14	< 6	4
0, 9, $\bar{7}$	3	3	0, 12, 18	4	3			
0, 9, $\bar{9}$	8	9	0, 12, 20	< 4	1	0, 18, $\bar{2}$	13	−17
0, 9, $\bar{11}$	13	13	0, 12, 22	< 4	− 1	0, 18, $\bar{4}$	< 5	− 1
0, 9, $\bar{13}$	11	13	0, 12, 24	< 4	− 4			
0, 9, $\bar{15}$	7	11	0, 12, 26	15	18	0, 18, $\bar{12}$	< 6	− 1
0, 9, $\bar{17}$	< 4	7	0, 12, 28	< 5	1	0, 18, $\bar{14}$	10	−12
						0, 18, $\bar{16}$	< 6	5
0, 10, 14	< 4	− 4	0, 12, 36	< 5	− 1			
0, 10, 16	5	− 7	0, 12, 38	5	− 5			
0, 10, 18	4	− 7	0, 12, 40	< 5	5			

for all observed (0*kl*) reflexions and $R_1 = 0.16$ for observed (0*kl*) reflexions with $k \neq 6n$.

The 66 vectors between the oxygen atoms in six adjacent carboxylic groups calculated from the final coordinates are marked in the Patterson projection with $F^2(0kl)$ and $k \neq 6n$ in Fig. 1.

DISCUSSION OF THE RESULTS

The hydrocarbon chains of the A-form of lauric acid are arranged in the triclinic packing first found by Müller and Lonsdale [6] in a low-temperature form of a paraffin. In this packing all chain-planes are parallel. Form A′ of

acids with an odd number of carbon atoms [13,14] has the same hydrocarbon chain packing.

The dimers of the A-form of lauric acid are, however, entirely differently arranged, as compared with the A'-form. From the chain-packing point of view the structure of the A-form of lauric acid is a sixfold superstructure (Fig. 4). The carboxylic groups and the methyl groups are situated together in the same layers in the crystal in groups of six units (Fig. 4) giving rise to equal binding forces in every such layer (hydrogen bonds and van der Waals bonds). This is not the case with the other crystal forms of normal fatty acids where the carboxylic groups and the methyl groups, respectively, are situated in alternate layers. The binding forces are then much weaker in the methyl group layers (van der Waals bonds) than in the carboxylic group layers (hydrogen bonds). These different molecular arrangements affect the macrocrystalline shape as well as the cleavage properties. As was stated earlier normal fatty acids usually crystallize in thin plates, which can easily be split up into thinner plates, but the A-form of lauric acid grows in parallelepiped-shaped crystals, which do not split up in the same regular way as the crystals of the other polymorphic forms. The absence of twinning is also in accordance with the molecular arrangement.

The carboxylic groups fit so well into the chain-packing that none of the carbon atoms need be moved from its position in the subcell to allow hydrogen bonding between two carboxylic groups.

The increment of long spacing for this crystal form of acids with an even number of carbon atoms is 2.36 Å according to Stenhagen and the author [4]. Thus the angle of tilt will be between 69° and 65° if the distance between alternate carbon atoms is between 2.521 Å, given by Vand, Morley and Lomer [8], and 2.610 Å, given by Morley and Vand [15].

I am indebted to Professor Gunnar Hägg, Professor Einar Stenhagen and Dr. Ingvar Lindqvist for their interest in this work. I am also grateful to Mr. C. O. Jansson for help with the X-ray work and computations. The expenses involved have been defrayed by grants from the *Swedish Natural Science Research Council.*

REFERENCES

1. Piper, S. H., Malkin, T. and Austin, H. E. *J. Chem. Soc.* **1926** 2310.
2. Trillat, J. J. and v. Hirsch, Th. *Compt. rend.* **195** (1932) 215.
3. Lomer, T. R. *Nature* **176** (1955) 653.
4. Stenhagen, E. and von Sydow, E. *Arkiv Kemi* **6** (1953) 309.
5. von Sydow, E. *Acta Chem. Scand.* **9** (1955) 1685.
6. Müller, A. and Lonsdale, K. *Acta Cryst.* **1** (1948) 129.
7. Vand, V. and Bell, I. P. *Ibid.* **4** (1951) 465.
8. Vand, V., Morley, W. M. and Lomer, T. R. *Ibid.* **4** (1951) 324.
9. Lipson, H. and Cochran, W. *The Determination of Crystal Structures*, Bell and Sons Ltd. London 1953.
10. Buerger, M. J. *Acta Cryst.* **4** (1951) 531.
11. Mc Weeny, R. *Ibid.* **4** (1951) 513.
12. Vainshtein, B. K. and Pinsker, Z. G. *Doklady Akad. Nauk SSSR* **72** (1950) 53.
13. von Sydow, E. *Acta Cryst.* **7** (1954) 529.
14. von Sydow, E. *Ibid.* **8** (1955) 845.
15. Morley, W. M. and Vand, V. *Nature* **163** (1949) 285.

Received November 4, 1955.

ACTA CHEMICA SCANDINAVICA 10 (1956) 9—14

Studies on Pyrazolones

IX. Reactions between Pyrazole Blue and Ethyl Cyanoacetate

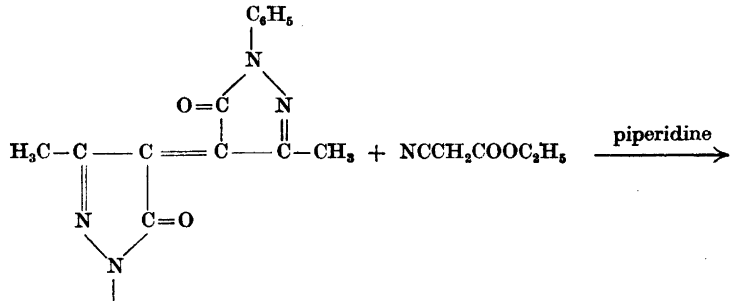
GUNNEL WESTÖÖ

Institute of Organic Chemistry, University of Lund, Lund, Sweden

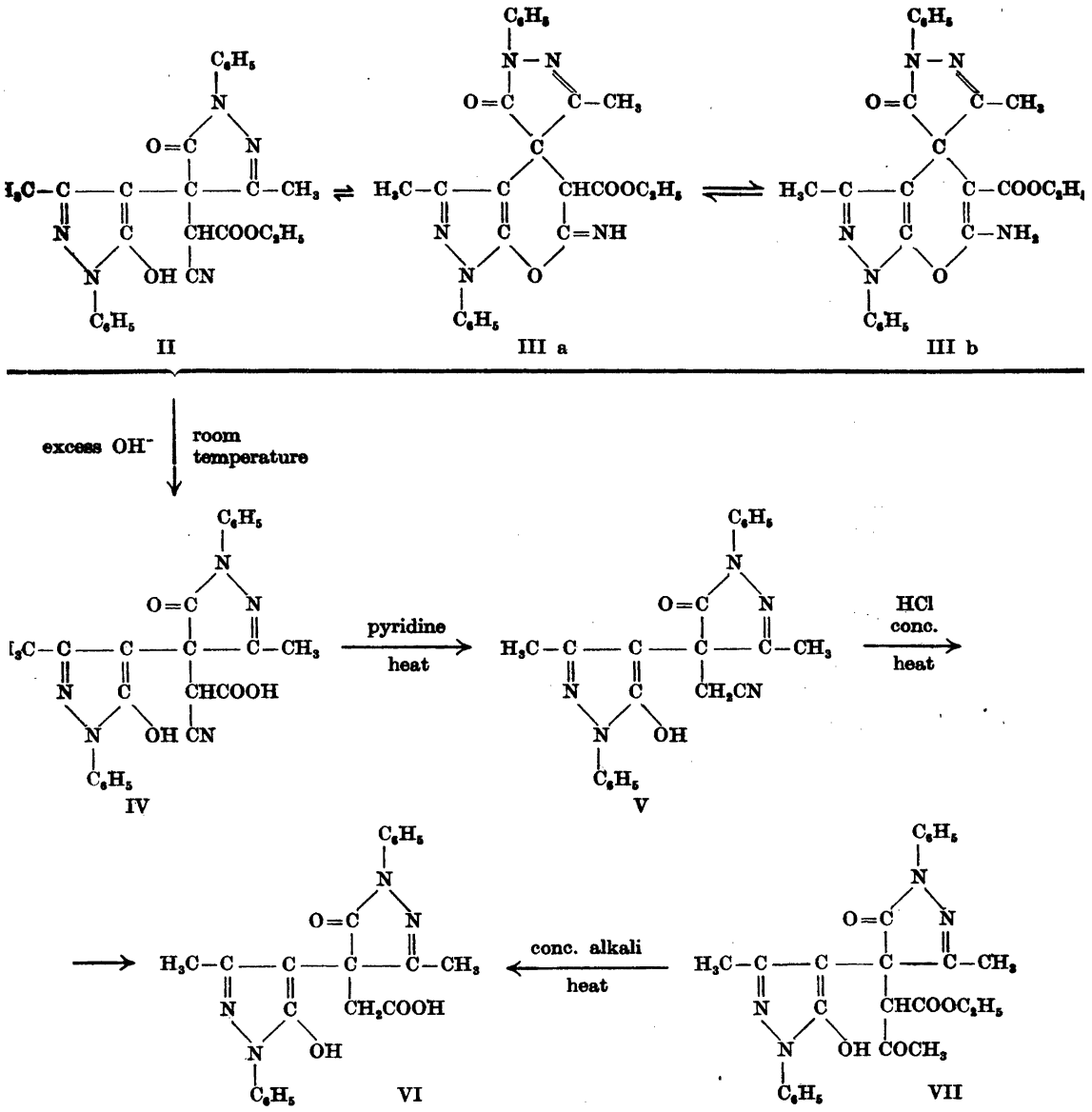
The addition compounds II and III have been prepared from pyrazole blue (I) and ethyl cyanoacetate. By degradation of the adducts some 4-substituted 1,1′-diphenyl-3,3′-dimethyl-[4,4′-bi-2-pyrazoline]-5,5′-diones have been synthesized, *viz.* bispyrazolonyl-cyanoacetic acid (IV), 4-cyanomethylbispyrazolone (V) and bispyrazolonylacetic acid (VI).

In the presence of a small amount of piperidine, a chloroform solution of pyrazole blue (I) was rapidly decolorized when boiled with an equimolar amount of cyanoacetic ester. The reaction product obtained was a neutral addition compound, $C_{25}H_{23}N_5O_4$. On treatment with excess of alkali at room temperature it yielded an acid, $C_{23}H_{19}N_5O_4$, for which structure IV is suggested on the basis of the following facts. It is a dibasic acid. On decarboxylation it gave a cyanomethylated bispyrazolone (V), which could be hydrolysed to the acid VI, identical with the product obtained by acid cleavage of the adduct, VII, from pyrazole blue and ethyl acetoacetate.

These degradation reactions show that both the bispyrazolonyl group and the cyanoacetic acid skeleton are present in $C_{25}H_{23}N_5O_4$. These facts together with the neutral reaction of the compound indicate that III (a, b or — presumably — an equilibrium of both) is the correct structure for this adduct.



I



The first step in the formation of III is considered to be a normal Michael addition of ethyl cyanoacetate to pyrazole blue giving the bispyrazolonylcyanoacetate, II. It is a well-known fact that both Michael condensations [1] and the reversible addition of alcohols to nitriles with formation of iminoethers are catalysed by basic compounds (Nef [2], Marshall and Acree [3]). In spite of the fact that the hydroxyl group of II has acidic properties, it is reasonable to

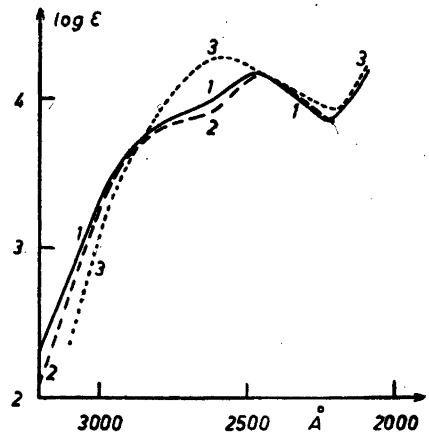


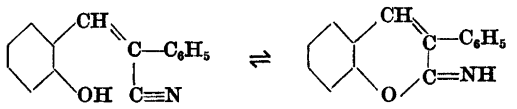
Fig. 1. UV absorption curves of the compounds II (1), III (3) and IV (2) in ethanol solution.

suppose that it adds to the cyano group of II in a way analogous to an alcoholic hydroxyl, *i. e.* that II is isomerized to III a (III a ⇌ III b). The ring closure ought to be facilitated since a six-membered ring is formed and since the structure III b is stabilized by resonance.

In order to check the proposed mechanism it was of interest to prepare and examine compound II. By performing the addition of ethyl cyanoacetate to pyrazole blue at room temperature, a mixture of the neutral compound, III, and the isomeric, acidic product, II, could be obtained. The components were separated by virtue of their different solubilities. The UV absorption curves of the two products were distinctly different. The curve of the acidic compound was very similar to the corresponding curve of IV (Fig. 1). Excess of dilute alkali at room temperature hydrolysed both products with formation of IV.

An ethanol solution of II was slowly isomerized to III even at room temperature. This isomerization was catalysed by a small amount of piperidine. In boiling chloroform containing a trace of piperidine (the same conditions as prevailed when III was prepared directly from pyrazole blue and ethyl cyanoacetate), the ring closure of II to form III was rapid. Dry hydrogen chloride (*cf.* Pinner [4]) in ethanol solution or heating of the solid compound also caused isomerization of II. All these facts are in favour of the proposed reaction sequence I→II→III. — The easy ring closure observed with II did not take place with the acids IV or V.

o-Hydroxy-*α*-phenylcinnamic nitrile [5] (VIII) has been found to isomerize in a similar manner to compound II but with greater ease. In ethanol solution it was completely transformed into the iminolactone, 2-imino-3-phenylcoumarine (IX) in a few hours. The solid nitrile slowly changed into the coumarine derivative even at room temperature.



VIII IX

The isomerization of II to form III is reversible, for brief treatment of III with an equivalent amount of alkali yielded compound II, in addition to compound IV. Long treatment with excess of alkali gave only IV.

Houben and Pfankuch [6] made the similar observation that the iminolactone ring of 2-imino-3-phenylcoumarine is split by alkali to form *o*-hydroxy-α-phenylcinnamic nitrile (*cf.* Schlesinger [7]).

The acidic properties of compound II are of interest. The introduction of the electron attracting bispyrazolonyl group into the ethyl cyanoacetate molecule increases the acidity of the active hydrogen atom in the α-position of the cyano group with the result that, though ethyl cyanoacetate is only slightly acidic towards alizarine yellow in ethanol-water solution, its bispyrazolonyl derivative could be titrated as a dibasic acid using the same indicator, though with a poor end point. In IV (and of course in III and V) the cyanoacetate hydrogen is not acidic towards alizarine yellow.

The IR spectra[9] of the two addition compounds of pyrazole blue and ethyl cyanoacetate have been studied. The acid II had a distinct, though not very strong nitrile band at 2 240 ± 15 cm^{-1}, whereas the neutral compound exhibited no C≡N absorption. This provides further support for III as the structure of the neutral adduct. However, great caution is necessary when drawing conclusions from the IR spectra of the nitriles. Thus a study of the absorption of IV, which compound certainly contains a cyano group, showed that the existence of a C≡N band in the spectrum of the free acid was doubtful, whereas the potassium salt of IV had a strong C≡N absorption band at 2 240 ± 15 cm^{-1}. Compound V (prepared from IV by decarboxylation) had a distinct but not very intense nitrile band at 2 240 ± 15 cm^{-1} (*cf.* Kitson and Griffith [8]).

EXPERIMENTAL

Preparation of compound III from pyrazole blue and ethyl cyanoacetate. Pyrazole blue (13.5 g), ethyl cyanoacetate (7 ml), chloroform (50 ml) and a few drops of piperidine were boiled until decolorization was complete (about 5 minutes). On standing a colourless product separated from the cooled solution. It was collected by filtration and washed with ethanol and ether. Impurities were removed by extraction with boiling ethanol. The product was dried *in vacuo* at 100°. Yield 17.4 g (97 %); m. p. about 245° with decomposition. The compound was only slightly soluble in most solvents. (Found: C 65.1; H 5.1; N 15.2. $C_{25}H_{23}N_5O_4$ requires C 65.6; H 5.1; N 15.3.) For UV absorption curve see Fig. 1.

Alkaline hydrolysis of compound III with the formation of IV. A suspension of III (7.6 g) in a solution of potassium hydroxide (8 g) in methanol (75 ml) and water (5 ml) was shaken for half an hour and then left overnight. The hydrolysate was precipitated with water and dilute sulphuric acid and the precipitate filtered, washed with water and air-dried. The crude product was dissolved in ethyl acetate at room temperature. From the solution the pure acid soon separated as colourless crystals. Yield 5.9 g of purified product, m. p. about 160° (decomp.) (Found: C 64.1; H 4.5; N 16.2; equiv. wt. 215. $C_{23}H_{19}N_5O_4$ requires C 64.3; H 4.5; N 16.3; equiv. wt. 215.) UV absorption see Fig. 1.

Decarboxylation of IV with formation of 1,1′-diphenyl-3,3′-dimethyl-4-cyanomethyl-[4,4′-bi-2-pyrazoline]-5,5′-dione (V). The bispyrazolonylcyanoacetic acid (IV) (5.8 g), ethyl alcohol (50 ml) and pyridine (0.75 ml) were boiled on a water bath for ten minutes. The decarboxylated product was precipitated with water and dilute hydrochloric acid. The precipitate was collected by filtration, washed with water and air-dried. After crystallization from ethyl acetate and ethanol, 2.9 g (56 %) of the colourless 1,1′-diphenyl-3,3′-dimethyl-4-cyanomethyl-[4,4′-bi-2-pyrazoline]-5,5′-dione (V) was obtained. It was

dried at 0.1 mm Hg, 100°. M. p. 160°. (Found: C 68.6; H 5.1; N 18.1; equiv. wt. 385 on titration using thymolphthalein indicator, 391 determined by means of the cyano group. $C_{22}H_{18}N_5O_2$ requires C 68.6; H 5.0; N 18.2; equiv. wt. 385.) The product was soluble in ethanol, chloroform and acetone, but only slightly soluble in ether and benzene.

Hydrolysis of 1,1'-diphenyl-3,3'-dimethyl-4-cyanomethyl-[4,4'-bi-2-pyrazoline]-5,5'-dione. The decarboxylated product (V) (0.2494 g) was boiled with a few ml of concentrated hydrochloric acid for one hour. The hydrolysate was precipitated with water, filtered, washed with water and air-dried. Impurities were removed by boiling the product once with ethyl acetate. The substance was then dissolved in ethyl alcohol and the solution evaporated to dryness, when an unstable modification was obtained, which was soluble in ethyl acetate. On scratching colourless crystals separated from the solution, m. p. 213° (decomp.) (Found: C 65.4; H 5.2; N 13.7; equiv. wt. 202. $C_{22}H_{20}N_4O_4$ requires C 65.3; H 5.0; N 13.9; equiv. wt. 202.)

To the mother liquor from the hydrolysis a large excess of sodium hydroxide was added, and the ammonia formed was distilled into 0.1050 N hydrochloric acid (10.00 ml). After distillation, 4.26 ml of 0.0966 N barium hydroxide solution was needed for neutralization. Hence the equiv. wt. of the cyano compound was 391 (calc. for the cyanomethylated bispyrazolone (V) 385).

Addition of ethyl acetoacetate to pyrazole blue with the formation of VII. Pyrazole blue (5.0 g), ethyl acetoacetate (2.4 g), ethyl alcohol (25 ml) and piperidine (0.5 ml) were mixed together. A rapid decolorization took place at room temperature. The colourless addition product separated immediately, but was dissolved by boiling the mixture briefly to ensure complete reaction. After cooling, the precipitation was completed by addition of water and dilute hydrochloric acid. The product was filtered off and washed with water and ethanol. Yield 6.7 g. Impurities were removed by extraction with ether and by crystallization from ethanol. The product was dried *in vacuo* (0.1 mm Hg) at 80°. It was difficult to obtain a solvent free product without decomposition taking place. M. p. 106°. (Found: C 64.8; H 6.0; N 11.6; equiv. wt. 475. $C_{26}H_{26}N_4O_5$ requires C 65.8; H 5.5; N 11.8; equiv. wt. 475.)

Acid cleavage of compound VII. The preceding product (VII) was heated on a boiling-water bath with ethanol and excess of concentrated potassium hydroxide solution for 5 minutes. On acidification the cleavage product separated. It was filtered off, washed with water and air-dried. Impurities were removed as previously described. M. p. 214° (decomp.) (Found: C 65.1; H 4.9; N 13.9; equiv. wt. 203. Calc. for $C_{22}H_{20}N_4O_4$: C 65.3; H 5.0; N 13.9; equiv. wt. 202.) The light absorption of this compound was identical with the absorption of the product obtained by hydrolysis of V.

Preparation of compound II from pyrazole blue and ethyl cyanoacetate. A mixture of pyrazole blue (1.35 g), ethyl cyanoacetate (0.7 ml), chloroform (5 ml) and a trace of piperidine was shaken at room temperature until decolorization took place. On addition of ethanol and scratching, crystals of III (0.25 g) separated.

The chloroform was rapidly removed from the filtrate *in vacuo* at room temperature, and the ethanol solution was immediately poured into N hydrochloric acid. The acid II, which precipitated, was collected by filtration, washed with water and dried *in vacuo*. The product could be purified by solution in cold benzene and precipitation with light petroleum. Benzene insoluble crystals (1.7 g) were obtained. The last trace of benzene was removed *in vacuo*. The product, which was hygroscopic, melted at 116—120°. When the heating was continued, the melt solidified, owing to ring closure with formation of III. At 240—245° it melted again with decomposition. (Found: C 65.2; H 5.0; N 15.3; equiv. wts 454 (potentiometric titration) and 230 (titration with sodium methoxide [10]). Calc. for $C_{25}H_{23}N_5O_4$: C 65.6; H 5.1; N 15.3; equiv. wts 457 and 229.) For UV absorption curve see Fig. 1.

The acid was isomerized to the neutral compound III, a) when heated in solid form or in solution, b) when kept in ethanol solution for several days (with piperidine as catalyst one day was sufficient), c) when its ethanol solution was treated with dry hydrogen chloride. The isomer III formed was in all cases identified by its melting point, neutral reaction, slight solubility in most solvents and UV absorption curve.

At room temperature alkali hydrolysed the ester but not the cyano group of II, compound IV being formed.

Partial hydrolysis of III. Product III (1.45 g) was shaken with 5 ml of 1.3 N methanolic potassium hydroxide solution for ten minutes. Undissolved material was removed by

filtration, and the filtrate was poured into N hydrochloric acid. The precipitate formed was washed with water and air-dried. The colourless product melted partly at 120°, solidified again and was decomposed at 160°. These facts as well as the equivalent weights of the product and the UV absorption (maximum at 250 mμ) indicate that a mixture of II and IV was formed.

o-Hydroxy-α-phenylcinnamic nitrile (VIII) and 2-imino-3-phenylcoumarine (IX). *o*-Hydroxy-α-phenylcinnamic nitrile (VIII) was prepared according to Borsche and Streitberger [5] and treated with alkali to transform any 2-imino-3-phenylcoumarine present into the hydroxynitrile. (Found: C 80.3; H 5.0; N 6.1. Calc. for $C_{15}H_{11}NO$: C 81.4; H 5.0; N 6.3.) 2-Imino-3-phenylcoumarine (IX) was prepared according to Houben and Pfankuch [6].

Treatment of an ethanolic solution of VIII with a small amount of piperidine for three hours and subsequent acidification with acetic acid yielded product IX. When a solution of VIII in ethanol was kept overnight without any catalyst, the same isomerization took place. The products were identified by their light absorption and different solubilities in concentrated hydrochloric acid (*cf.* Houben and Pfankuch [6]).

The analyses were performed by Mr. A. Grossman, Department of Organic Chemistry, University of Copenhagen, or by Miss M. Westerdahl, Department of Analytical Chemistry, University of Lund. I am indebted to Dr. Andreas Rosenberg, University of Uppsala, for carrying out the IR measurements.

The author wishes to thank *Statens naturvetenskapliga forskningsråd* for financial support and Prof. S. Bergström for permission to carry out this investigation at his Institute.

REFERENCES

1. Michael, A. *J. prakt. Chem.* **35** (1887) 349.
2. Nef, J. U. *Ann.* **287** (1895) 265.
3. Marshall, Jr. E. K. and Acree, S. F. *Am. Chem. J.* **49** (1913) 127.
4. Pinner, A. *Die Iminoäther und ihre Derivate*, Verlag R. Oppenheim, Berlin 1892.
5. Borsche, W. and Streitberger, F. *Ber.* **37** (1904) 3163.
6. Houben, J. and Pfankuch, E. *Ber.* **59** (1926) 1594.
7. Schlesinger, H. *Am. Chem. J.* **39** (1908) 738.
8. Kitson, R. E. and Griffith, N. E. *Anal. Chem.* **24** (1952) 334.
9. Schiedt, U. and Reinwein, H. *Z. Naturforsch.* **7 b** (1952) 270.
10. Fritz, J. S. *Anal. Chem.* **24** (1952) 674.

Received September 10, 1955.

ACTA CHEMICA SCANDINAVICA 10 (1956) 15—19

Bifunctional Amines and Ammonium Compounds

V*. Bis-trialkylammoniumethyl Disulfides, Sulfoxides, and Sulfones

JØRGEN FAKSTORP

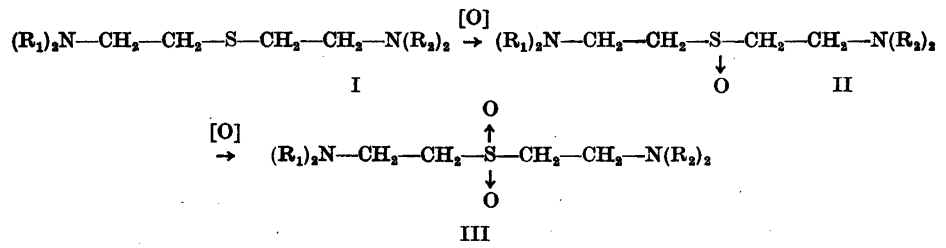
Aktieselskabet Pharmacia, Copenhagen V., Denmark

Oxidized derivatives of bis-alkylammonium sulfides were obtained by oxydation of the *tert.* thiols and sulfides with iodine and bromine water, followed by alkylation. The oxidation with acid or alkaline permanganate gave the expected *tert.* sulfones. However, the quaternization gave products which, most probably, were *1,1-dioxy-4,4-dialkylthiazanium salts.*

In continuation of work concerning the relation between structure and neuropharmacological activity within a series of simple "bolaform" [1] bis-onium salts containing a hetero atom in the alkylene chain, several substances containing an oxidized sulfur function have been prepared for pharmacological evaluation.

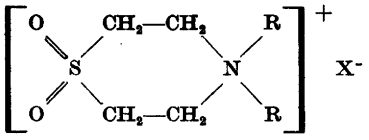
Bis-quaternary ammoniumalkyl sulfoxides and sulfones were available through the corresponding bis-chloro derivatives as described by Lawson and Reid [2] (*cf.*, however, Alexander and McCombie [3]) but in the work described here these types of substances were obtained starting from the corresponding bis-*tert.* aminoalkyl sulfides [4], by oxidation in acid solution with hydrogen peroxide, potassium permanganate or bromine water by conventional procedures[5].

Three sulfoxides were prepared and transformed to the six bis-quaternary salts containing only methyl and ethyl substituents at the nitrogen.



* Part IV. *Acta Chem. Scand.* 8 (1954) 350.

The alkylation of the sulfones to the quaternary ammonium salts met with unexpected difficulties. The products obtained could only in a single instance be purified to correct analysis. The main product of the reaction gave analytical values which were much better in accord with a ring closed product, 1,1-dioxy-4,4-dialkylthiazanium halide (IV).



IV

The appearance of this product is explained in terms of an intramolecular alkylation by a carbonium ion resulting from a cleavage of trialkylamine from normally formed monoquaternary sulfone,

$$(R_1)_2N—CH_2—CH_2—SO_2—CH_2—CH_2—N^+(R_2)_2R_3 \rightarrow$$

$$(R_1)_2N—CH_2—CH_2—SO_2—CH_2—CH_2\oplus + (R_2)_2NR_3 \rightarrow \text{IV}$$

The product obtained might also have been a trialkylammonium vinyl sulfone (V).

$$R_3(R_1)_2N^+—CH_2—CH_2—SO_2—CH=CH_2$$

None of the addition reactions expected are shown by the product obtained. It is also difficult to account for the appearance of the same salt from different starting products in terms of a vinyl sulfone. This appearance necessitates a retention of the N-alkyl substituents present in the original sulfone, while the vinyl sulfone salt should contain N-alkyl substituents of which at least one originated from the alkylating agent.

A dioxy-thiazanium salt (IV) should also result if a dioxy-thiazane was quaternized. The formation of dioxy-thiazane directly from the bis-*tertiary* sulfone is less easy to explain, although some earlier observations support it (see Lawson and Reid [2]). However, this route would also require thiazanium salts (IV) containing both ethyl and methyl at nitrogen. Such products have not been observed.

The four disulfide salts were obtained by the quaternization of bis-2-dimethylaminoethyl disulfide (*cf.* Andrews, Bergel and Morrison [9]) and bis-2-diethylaminoethyl disulfide which in turn resulted either from the corresponding sodium mercaptides by oxidation with iodine (*cf.* Gilman *et al.*[6]) or from iodine oxidation of the sodium aminoalkyl thiosulfates (Bunte salts) according to Bretschneider [7] (*cf.* Westlake and Dougherty [8], and also Peak and Watkins [5]).

Unfortunately no method is available for the preparation of "asymmetric" disulfides, a type of compound which would be of considerable pharmacological interest.

A report on the pharmacology of the compounds reported in this paper will appear elsewhere.

EXPERIMENTAL *

Bis-2-dimethylaminoethyl sulfoxide (II, $R_1 = R_2 = CH_3$)

The bis-hydrobromide was obtained according to Peak and Watkins [5] by oxidation of 17.6 g (0.1 mole) of bis-2-dimethylaminoethyl sulfide dissolved in 75 ml of water with 20 (approx. 0.2 mole) of bromine dissolved in 1 000 ml of water and 1 500 ml of 99 % ethanol. The evaporation residue was dissolved in 1 500 ml of 99 % ethanol containing 75 ml of water. Upon cooling the *bis-hydrobromide* separated. Yield 29 g (85 %), m. p. 215° C. (Found: Br 44.75. Calc. for $C_8H_{22}N_2SOBr_2$ (354.1): Br 45.13). It was not possible to isolate the free sulfoxide in a pure form neither from the bis-hydrobromide nor by oxidation of sulfide with hydrogen peroxide (v. s.) owing to decomposition of the free base during distillation.

The *bis-methoiodide* (As-7366) was obtained from 14.5 g (0.042 mole) of the bis-hydrobromide dissolved in 50 ml of anhydrous ethanol in which 1.94 g of sodium (0.084 mole) were previously dissolved. After removal of sodium bromide, 8 g of methyl iodide was added to the solution and this mixture kept overnight. There was obtained 12.5 g (64 %) of bis-methoiodide, m. p. 230–233° C (decomp.) (from methanol-water 5:1). (Found: I 53.19. Calc for $C_{10}H_{26}N_2SOI_2$ (476.2): I 53.30).

Bis-ethobromide (As-7367) obtained in like fashion from 14.5 g of the bis-hydrobromide and 11 g of ethyl bromide. Yield 11 %, m. p. 205–208° C (diss. methanol, reprecipitd. ether). (Found: Br 38.81. Calc. for $C_{12}H_{30}N_2SO\ Br_2$ (410.3): Br 38.96).

Bis-2-diethylaminoethyl sulfoxide (II, $R_1 = R_2 = C_2H_5$)

Bis-2-diethylaminoethyl sulfide, 11.6 g (0.05 mole) was mixed with 50 ml of water and then added to a cooled mixture of 8.4 g of 30 % hydrogen peroxide and 12 ml of concentrated hydrochloric acid in 70 ml of methanol. The volume was made up to 200 ml with water and the mixture allowed to stand at room temperature for two days. The contents were made strongly alkaline with sodium hydroxide solution, extracted with ether after supersaturation with sodium chloride, the ether extract dried over potassium carbonate, the ether removed through a 30 cm Vigreux column. The residue distils under evolution of a gas. There was obtained 9.5 g (78 %) of a deeply yellow oil, b. p. 148–149° C at 1 mm Hg. (Found: C 57.14; H 11.30; N 11.20. Calc. for $C_{12}H_{28}N_2SO$ (248.4): C 58.01; H 11.36; N 11.30).

Bis-methoiodide (As-7432) obtained at room temperature as previously described from base and an excess of methyl iodide in acetone containing ethanol. Yield 38 %, m. p. 235–238° C (decomp.) (from ethanol-water 5:1). (Found: N 5.31; I 46.48. Calc. for $C_{14}H_{34}N_2SOI_2$ (532.3): N 5.46; I 47.71).

Bis-ethobromide (As-7490). From 2.48 g (0.01 mole) of sulfoxide and 2.78 g of ethyl bromide in 25 ml of acetone containing 5 ml of ethanol. Yield 3.5 g (75 %), m. p. 211° C (acetone-methanol 2:1). (Found: Br 35.17. Calc. for $C_{16}H_{38}N_2SOBr_2$ (466.3): Br 34.29).

Bis-(2-dimethyl-2′-diethyl)-aminoethyl sulfoxide (II, $R_1 = CH_3$; $R_2 = C_2H_5$)

A bis-hydrobromide was prepared from 20.4 g of the corresponding sulfide. Yield 31 g (81 %), m. p. 210–212° C. (Found: Br 41.92. Calc. for $C_{10}H_{26}N_2SO\ Br_2$ (382.2): Br 41.81). The free base decomposed upon treatment of the hydrobromide with alkali and was not obtained pure.

Bis-methoiodide (As-7588). From the bis-hydrobromide in ethanol-sodium ethylate. Yield 59 %, m. p. 223–224° C (ethanol-water 5:1). (Found: I 50.55. Calc. for $C_{12}H_{30}N_2SOI_2$ (504.4): I 50.32).

* All melting points and boiling points are uncorrected. The nitrogen and halogen values are semi-micro determinations by Mrs. G. Speggers of this laboratory. Carbon and hydrogen values are micro determinations by Messrs. W. Egger and A. Grossmann, University of Copenhagen.

Bis-ethobromide (As-7589). The reaction was carried out in a sealed glass tube at 100° C for 3 hours. Yield 36 %, m. p. 163–170° C (methanol). (Found: Br 38.34. Calc. for $C_{14}H_{32}N_2SOBr_2$ (438.3): Br 36.46).

Bis-2-dimethylaminoethyl sulfone (III, $R_1 = R_2 = CH_3$)

The bis-hydrochloride prepared according to Peak and Watkins [5] by permanganate oxidation in acetic acid solution *. Yield 41 % m. p. 245–247° C (from ethanol-methanol-water 10:5:3). (Found: Cl 25.27. Calc. for $C_8H_{22}N_2SO_2Cl_2$ (281.3): Cl 25.21).

Bis-methoiodide (As-7696) directly from the bis-hydrochloride. Yield 30 %, m. p. 268–272° C (decomp.) (from dilute ethanol). (Found: I 49.37. Calc. for $C_{10}H_{26}N_2SO_2I_2$ (492.2): I 51.56). Another product is isolated by the fractional crystallization, m. p. 294° C, apparently a ring-closed product, *1,1-dioxy-4,4-dimethylthiazanium iodide* (IV, R = CH_3). (Found: I 44.13. Calc. for $C_6H_{14}NSO_2I$ (291.2): I 43.58).

1,1-dioxy-4,4-dimethylthiazanium bromide (IV, R = CH_3). Directly from the bis-hydrochloride. Yield approx. 10 %; m. p. 320° C (decomp.). (Found: C 29.35; H 5.77; Br 32.50. Calc. for $C_6H_{14}NSO_2Br$ (244.1): C 29.53; H 5.78; Br 32.73). It was not possible to secure any of the desired bis-ethobromide.

Bis-2-diethylaminoethyl sulfone (III, $R_1 = R_2 = C_2H_5$)

2-Diethylaminoethyl sulfide (23.8 g) dissolved in a stirred solution of 11.8 g of concentrated sulfuric acid in 150 ml of water was cooled to room temperature and a solution of 21.1 g of potassium permanganate was added at a rate sufficient to keep the mixture at a temperature of approximately 60° C. After one night the mixture is made strongly alkaline, the precipitate removed by suction on a layer of Theorit, the mixture extracted continuously with 400 ml of ether for 12 hours in a *Kutscher-Steudel* extractor, the ether extract dried over potassium carbonate and the bis-hydrochloride precipitated by addition of dry HCl gas. Yield 16.7 g (50 %), m. p. 204° C (Ref.[5] reports 202° C). (Found: Cl 21.10. Calc. for $C_{12}H_{30}N_2SO_2Cl_2$ (337.4): Cl 21.11). The free base decomposes when distilled or even by being kept in alkaline solution.

1,1-dioxy-4,4-diethylthiazanium iodide (IV, R = C_2H_5). Directly from an aliquot part of the ether extract by dilution with acetone and addition of a 50 % excess of methyl iodide. Yield 35 %, m. p. 225–227° C (dilute ethanol). (Found: I 39.83. Eq. w. (perchloric acid titration) 312. Calc. for $C_8H_{18}NSO_2J$ (319.2): I 39.76). None of the desired open chain methoiodide was ever isolated in numerous experiments.

1,1-dioxy-4,4-diethylthiazanium bromide (IV, R = C_2H_5). Prepared in similar fashion. Yield 11 %, m. p. 234° C (from dilute ethanol). (Found: Br 28.85. Calc. for $C_8H_{18}NSO_2Br$ (272.2): Br. 29.32).

Bis-(2-dimethyl-2'-diethyl)-aminoethyl sulfone (III, $R_1 = CH_3$, $R_2 = C_2H_5$).

A *bis-hydrochloride* prepared from 20.4 g of bis-(2-dimethyl-2'-diethyl)-aminoethyl sulfide was obtained by alkaline permanganate oxidation in a yield of 12 g (40 %), m. p. 250° C (from dilute ethanol). (Found: Cl 22.96. Calc. for $C_{10}H_{26}N_2SO_2Cl_2$ (309.4): Cl 22.96.)

Attempts to prepare the bis-methoiodide and the bis-ethobromide resulted in the above mentioned 1,1-dioxy-4,4-diethylthiazanium halides.

* There is an error in Peak's and Watkins' [5] experimental description. The amount of permanganate used should be three times higher.

Bis-2-dimethylaminoethyl disulfide

a) From 18.0 g (0.171 mole) of 2-dimethylaminoethane thiol according to the procedure of Gilman *et al.*[6]. Yield 11.3 g (32 %) of faintly yellow, pungent smelling liquid, b. p. 136—138° C at 18—20 mm Hg. (Found: C 45.88; H 9.47; N 13.00. Calc. for $C_8H_{20}N_2S_2$ (208.4): C 46.10; H 9.65; N 13.44).

b) From 36 g of the hydrochloride of 2-dimethylaminoethyl chloride was obtained 9.0 g (17 %) of sodium 2-dimethylaminoethyl thiosulfate, m. p. 152° C (from ethanol), following the procedure of Peak and Watkins[5]. (Found: N 6.73. Calc. for $C_4H_{10}O_3S_2NNa$ (207.3): N 6.77). The thiosulfate decomposes when exposed to moist air, presumably under formation of disulfide.

This product, 5.2 g (0.025 mole), dissolved in 90 ml of 1 % hydrochloric acid and treated with excess iodine according to Bretschneider [7] gave 2.7 g (42 %) of the disulfide, b. p. 134° C at 12 mm Hg. (Found: N 13.36. Calc. N 13.44). It was not possible to obtain the disulfide from the thiosulfate *in situ*.

Bis-methoiodide (As-11032). Yield 85.2 %, m. p. 238—240° C (washed with acetone). (Found: I 51.32. Calc. for $C_{10}H_{26}N_2S_2I_2$ (492.3): I 51.55).

Bis-ethobromide (As-11031). Yield 86.6 %, m. p. 237° C (from ethanol). (Found: Br 36.16. Calc. for $C_{10}H_{26}N_2S_2Br_2$ (426.4): Br 37.48).

Bis-2-diethylaminoethyl disulfide

Obtained in 37 % yield by the mercaptide-iodine procedure, b. p. 172° C at 12 mm Hg (Gilman *et al.* [6] report 155—160° C at 20 mm Hg). From the original alcoholic oxidation mixture a precipitate is secured which upon crystallization from dilute ethanol melts at 197° C and has been shown to be a *bis-hydroiodide*. (Found: N 5.34; I 47.36. Calc. for $C_{12}H_{30}S_2N_2I_2$ (530.3): N 5.38; I 48.78). This is obtained in amounts corresponding to 18 % free sulfide.

The total yield obtained *via* the thiosulfate route (*cf.* Bretschneider [7]) was 68 %. The disulfide could not be obtained directly from the thiosulfate reaction mixture.

Bis-methoiodide (As-8872). Yield 83 %, m. p. 208—210° C (from acetone-methanol 2:1). (Found: I 47.26. Calc. for $C_{14}H_{34}S_2N_2I_2$ (548.4): I 46.31).

Bis-ethobromide (As-8802). Yield 37 %, m. p. 215° C (from acetone-methanol 2:1). (Found: Br 33.76.) Calc. for $C_{12}H_{30}S_2N_2I_2$ (520.5): Br 33.16).

Acknowledgement: The technical assistance of Miss Jytte Christiansen is gratefully acknowledged.

REFERENCES

1. Fuoss, R. M. and Edelson, D. *J. Am. Chem. Soc.* **73** (1951) 269.
2. Lawson, W. E. and Reid, E. E. *Ibid.* **47** (1925) 2821.
3. Alexander, J. R. and McCombie, H. *J. Chem. Soc.* **1931** 1913.
4. Fakstorp, J. and Christiansen, J. *Acta Chem. Scand.* **8** (1954) 346.
5. Peak, D. A. and Watkins, T. I. *J. Chem. Soc.* **1951** 3292.
6. Gilman, H., Plunkett, M. A., Tolman, L., Fulhart, L. and Broadbent, H. S. *J. Am. Chem. Soc.* **67** (1945) 1846.
7. Bretschneider, H. *Österr. Akad. Wiss. Math. naturw. Klasse Sitzber. Abt. II b* **159** (1950) 385.
8. Westlake, H. E. Jr. and Dougherty, G. *J. Am. Chem. Soc.* **64** (1942) 149.
9. Andrews, K. J. M., Bergel, F. and Morrison, A. L. *J. Chem. Soc.* **1953** 2998.

Received September 13, 1955.

ACTA CHEMICA SCANDINAVICA 10 (1956) 20—25

Enzymatic Formation of Nitrous Oxide from Nitrite

T. YAMADA* and ARTTURI I. VIRTANEN

Laboratory of the Foundation for Chemical Research, Biochemical Institute, Helsinki, Finland

A halotolerant *Micrococcus* strain evolved gas from nitrite (and nitrate) by reduction. Both dried cell preparations and a cell-free enzyme solution prepared from the organism was used in the experiments. The predominant product of the reduction was nitrous oxide. Nitrogen could not be established with certainty in the gas evolved. Practically no reduction of nitrite to hydroxylamine could be detected.

Several authors have observed the formation of nitrous oxide in experiments with denitrifying bacteria. Beijerinck and Minkman [1] and Kluyver and Verhoeven [2] succeeded to accumulate nitrous oxide in the gaseous products by using a higher concentration of nitrate and "vacuum experiments", respectively. The main product of the gas evolved by denitrifying bacteria under ordinary conditions was, however, nitrogen. Sacks and Barker [3] and Allen and van Niel [4] rejected the possibility that nitrous oxide might be a normal intermediate in denitrification. In their remarkable work Kluyver and Verhoeven are, on the other hand, of the opinion that molecular nitrogen is formed through reduction of nitrous oxide even if it is very probable that a part of the nitrogen can be formed also directly from the precursor of nitrous oxide.

The stepwise assimilatory reduction of nitrate to ammonia differs from denitrification on the stage between nitrite and hydroxylamine (*cf.* below). The original aim of the present investigation was to obtain further knowledge about the hitherto obscure reduction of nitrite to hydroxylamine, *i. e.* a reaction stage belonging to the assimilatory nitrate reduction. For this purpose we used both a dry cell preparation and a cell-free enzyme solution from the same halotolerant *Micrococcus* which Egami *et al.*[5] had used when establishing that specific nitrate reductase, nitrite reductase and hydroxylamine reductase act successively in assimilatory nitrate reduction which leads to ammonia. In our experiments even living cells of *Micrococcus* did not reduce nitrate and nitrite to ammonia but formed practically only gaseous products. This was also the case both with our dry cell preparations and cell-free enzyme

* Fellowship from the Travelling Fund of the Ministry of Education of Japan.

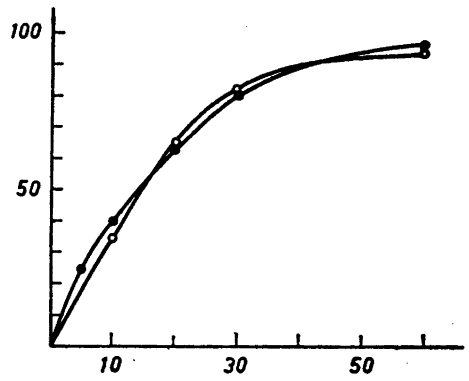


Fig. 1. Gas evolution in experiments with dried cells. Main chamber: 1 ml bacterial suspension (20 mg/ml), 0.5 ml 1/2 M phosphate buffer (pH 6.8), 0.1 ml methylene blue solution 0.01 M. Side arm: 0.5 ml 0.02 M NO_3^- or NO_2^- solution added into the main chamber after 30 min. preincubation. Temp. 35° C. O—O NO_2^-, ●—● NO_3^-.

solutions. Our investigations came thus to be directed on the formation of nitrous oxide from nitrite.

Robinson *et al.*[6] using *Micrococcus halodenitrificans* and Najjar and Allen [7] using *Pseudomonas stutzeri* and *Bacillus subtilis* obtained cell-free enzyme systems which evolved gas from nitrite. In the former case the gas was suggested to be nitrogen and also in the latter case the predominant product was nitrogen (with smaller amounts of nitric oxide and nitrous oxide).

EXPERIMENTAL

Cultivation of Micrococcus *and preparation of dried cells.* The test organism was a strain of *Micrococcus*, isolated in the laboratory of Japan Marine Product Co., named tentatively halotolerant bacteria No. 203. The cultural medium was peptone broth containing 10 % of NaCl and 3 % of KNO_3. The cells harvested from 36—48 hours liquid cultures were washed several times with 10 % NaCl solution and lyophilized.

Preparation of enzyme solution. The dried cell suspension (2 g/80 ml) which had been dialysed overnight against diluted phosphate buffer, pH 6.8, was centrifuged at 0° C

Table 1. Gas evolution from nitrite by dried cells.

Total volume of reaction mixture	Volume of gas evolved if calculated as			
	N_2		N_2O	
ml	μl	10^{-5} M	μl	10^{-5} M
3.0	92	0.81	102	0.91
6.0	80	0.71	105	0.93
9.0	61	0.54	104	0.93

Main chamber: 1 ml bacterial suspension (20 mg/ml), 0.5 ml 1/2 M phosphate buffer (pH 6.8), 0.1 ml 0.01 M methylene blue solution, appropriate amount of water.

Side arm: 0.5 ml 0.02 M $NaNO_2$ solution added into the main chamber after 30 min. preincubation.

Table 2. The mass spectrometrical data of the gas evolved.

	Voltage observed on each peak			
	without NO_2^-		with NO_2^-	
Mass	Expt. 1	Expt. 2	Expt. 1	Expt. 2
28 (N_2)	1.13	2.33	1.43	1.42
30 (NO)	0.06	0.03	0.320	0.240 *
40 (Ar)	0.032	0.060	0.039	0.038
44 (N_2O)	0.127	0.076	1.17	0.950

for 30 min. at 15 000 × g. From the supernatant thus obtained the active protein was precipitated by potassium citrate between half and full saturation. The precipitate was resolved into 20 ml of distilled water and used as enzyme solution.

Measurement of gas evolution. The conventional Warburg apparatus was used. The gas phase was nitrogen unless otherwise mentioned. The *dried cells* maintained a rather strong activity of formic dehydrogenase, and formate was therefore used as hydrogen donor in the following experiments with dried cells. Methylene blue was added as intermediate hydrogen carrier to make the reaction rapid enough. The dehydrogenase activity of the *cell-free enzyme solution* was not strong enough and therefore leuco-methylene blue produced from methylene blue by hydrogen in the presence of palladium black carried on $BaSO_4$ was used as hydrogen donor in experiments with enzyme solution. Hydroxylamine was estimated according to the method of Csàky [8], ammonia to that of Conway [9].

RESULTS

In the present experiments with the halotolerant *Micrococcus* No. 203 the dried cells reduced nitrate to nitrite, and hydroxylamine to ammonia almost quantitatively, while on the other hand practically no, or possibly only a very weak, reduction of nitrite to hydroxylamine and ammonia could be detected. The principal end products of nitrite reduction were gaseous (Fig. 1).

The gas evolved was identified as follows. Because it was reasonable to suppose that the gaseous reduction product of nitrite would be nitrogen or/and nitrous oxide the solubility of the gas evolved was estimated. Table 1 shows the volumes of gas when the volume of the liquid phase in Warburg flasks was varied by addition of water. The values calculated as pure nitrogen or nitrous oxide suggest that the gas should be practically exclusively nitrous oxide.

By a mass spectrometric method Dr. Burris in the laboratory of the Department of Biochemistry, University of Wisconsin, kindly analysed the gas samples which were collected from Warburg flasks and sent to him. The gas phase was in these experiments hydrogen. The analytical data are presented in Table 2. The great differences between experiments with and without nitrite were observed at mass 30 and 44. The former peak corresponded de-

* Because a peak of about 1/5 the height of the N_2O peak is obtained as a NO peak arising from the cleavage of N_2O in the instrument the gas mixture contained practically no NO.

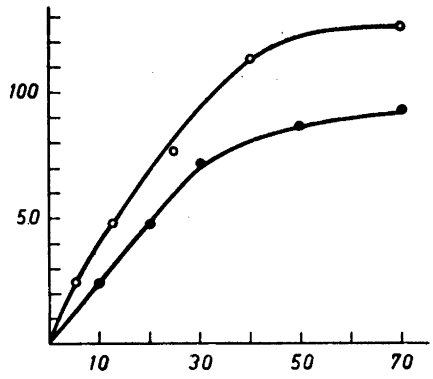


Fig. 2. Gas evolution in experiments with cell-free enzyme solution. Main chamber: 1 ml enzyme solution, 2 ml 1/2 M phosphate buffer (pH 6.8), 3 ml leuco-methylene blue solution. Side arm: 0.5 ml 0.02 M NO_2^- or NO_3^- solution added into the main chamber after 30 min. preincubation. Temp. 35° C. O—O NO_2^-, ●—● NO_3^-

finitely to nitric oxide. Although the latter could correspond both to carbon dioxide and nitrous oxide the possibility of carbon dioxide was excluded because the flasks contained KOH in the center wells. There was another peak at mass 28 corresponding to nitrogen but this probably was due to air contamination because a mass 40 peak for argon also was evident. There is, moreover, a considerable cleavage of nitrous oxide to nitric oxide in the mass spectrometer. A peak of about 1/5 the height of the parent nitrous oxide peak is obtained as a nitric oxide peak arising from the cleavage of nitrous oxide in the instrument. Thus a good share of the mass 30 peak could have arisen from nitrous oxide. Therefore, it may be concluded that the predominant product in the present experiments also on the basis of the mass spectrometric analysis was nitrous oxide.

The gas evolution from nitrite and nitrate even in experiments with cell-free enzyme preparation was strong, and no noticeable amounts of hydroxyl-

Table 3. Reduction of nitrite and hydroxylamine by cell-free enzyme solution and formation of hydroxylamine and ammonia.

Substrate	Substrate reduced	Reduction products (gaseous not estimated)	
	10^{-6} mole	NH_2OH 10^{-6} mole	NH_3 10^{-6} mole
$NaNO_2$	7.5	0.5 ? *	0.2
NH_2OH	6.9	—	4.9

Thunberg tubes were used. The contents were as follows: 1 ml enzyme solution, 2 ml 0.5 M phosphate buffer (pH 6.8), leuco-methylene blue solution 3 ml for NO_2^- and 2 ml for NH_2OH. Reaction time 1 h.

* After treatment with urea no hydroxylamine could be found. The presence of hydroxylamine is therefore not probable.

amine or ammonia were detected as shown in Fig. 2 and Table 3. In the experiment presented in Fig. 2 no nitrite could be found in the solution at the end of the experiment and also no hydroxylamine.

DISCUSSION

In our experiments the predominant product of nitrite reduction with halotolerant *Micrococcus* has been nitrous oxide, not only with dried cells but also in a system which consisted of cell-free enzyme solution, nitrite and leucomethylene blue. The results suggest that the reaction might proceed according to the following scheme:

$$2\ HNO_3 \rightarrow 2\ HNO_2 \rightarrow 2\ (=NOH) \rightarrow N_2O$$

In the same halotolerant micro-organism, used in the present work, Egami *et al.* have established the specific nitrate, nitrite and hydroxylamine reductases. They have thus corroborated the conception that assimilatory nitrate reduction proceeds *via* the following reaction stages:

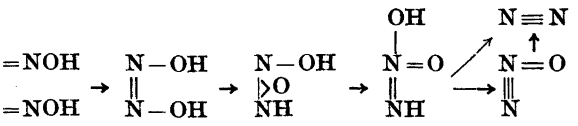
$$\underset{}{HNO_3} \xrightarrow[a]{} \underset{}{HNO_2} \xrightarrow[b]{} \underset{}{(?)} \xrightarrow[c]{} \underset{}{NH_2OH} \xrightarrow[d]{} \underset{}{NH_3}$$

In our experiments with dried cells as well as with cell-free enzyme solution the reactions *a* and *d* could be realized almost quantitatively. On the other hand nitrite was not reduced to hydroxylamine (and of course not to ammonia either) at least not in amounts which could be established with certainty. As the reduction product of nitrite practically only nitrous oxide was formed. Nitrogen could not be established in the gas mixture, not with certainty anyhow. Reaction stage *c* was accordingly inhibited under our reaction conditions and the reduction of nitrite was on account of this dissimilatory, nitrous acid being the only reaction product which could be established with certainty. It is difficult to understand why reaction *c* was lacking in our experiments although Egami *et al.* succeeded in reducing nitrite to hydroxylamine with the same bacteria. The only explanation is that the bacteria in our experiments for some unknown reason were lacking in the enzyme which catalyses reaction *c*.

The radical =NOH is the logical first reduction product of nitrite. It can be assumed that one molecule of water is split off under formation of one molecule of nitrous oxide when two radicals combine with each other: $2(=NOH) \rightarrow N_2O+H_2O$. When discussing possible precursors of nitrous oxide or molecular nitrogen, respectively, formed in denitrification Kluyver and Verhoeven have fixed their attention on imido-nitric acid, $HN=N=O$, for

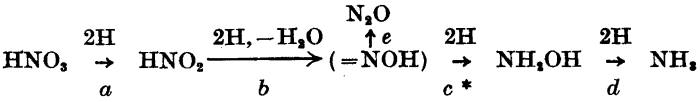
$$\begin{array}{l} \\ | \\ OH \end{array}$$

which the wrong name "nitramide" has generally been used. They found that this compound rapidly and spontaneously decomposes into nitrous oxide and water at pH ranges where denitrification takes place. There is accordingly an experimental basis for the concept that this compound could be formed in denitrification and should thus be the long sought precursor of nitrous oxide. As Kluyver points out its formation is, however, obscure. He proposes tentatively the following mechanism



The concept about the formation of nitrous oxide from the radical = NOH *via* a simpler mechanism (*cf.* above) is tempting.

When taking into consideration the observations made by Egami *et al.* about the reduction of nitrite to hydroxylamine and our results concerning the formation of nitrous oxide as the only with certainty established reduction product of nitrite the following pathway can be proposed for assimilatory and dissimilatory nitrate reduction with the *Micrococcus* in question



Reaction stages *a*, *b*, *c*, and *d* are enzymatic, *e* at least partly spontaneous.

According to this idea the assimilatory nitrate reduction differs from denitrification because of lack of the enzyme which reduces the intermediate between nitrite and hydroxylamine. Thus bacteria causing denitrification could be formed *via* mutation from bacteria which reduce nitrate to ammonia and use it as their nitrogen source.

The authors are greatly indebted to Dr. R. H. Burris for his advice and his kindness in performing the mass spectrometric analyses.

REFERENCES

1. Beijerinck, M. W. and Minkman, D. C. *Centr. Bakteriol. Parasitenk. II* **25** (1910) 30.
2. Kluyver, A. J. and Verhoeven, W. *Antonie van Leeuwenhoek J. Microbiol. Serol.* **20** (1954) 241; Verhoeven, W. *Aerobic sporeforming nitrate reducing bacteria* (Diss.) Delft 1952.
3. Sacks, L. E. and Barker, H. A. *J. Bacteriol.* **64** (1952) 247.
4. Allen, M. B. and van Niel, C. B. *J. Bacteriol.* **64** (1952) 397.
5. Egami, F., Yamada, T. and Taniguchi, S. *II^e Congrès international de biochimie, Paris, 21–27 Juillet 1952*, M. Declume, Lons-le-Saunier, 1952; Taniguchi, S., Mitsui, H., Nakamura, K. and Egami, F. *Ann. Acad. Sci. Fennicæ II Chem.* **60** (1955) 200, ("Biochemistry of Nitrogen").
6. Robinson, J., Gibbons, N. E. and Thatcher, F. S. *J. Bacteriol.* **64** (1952) 69.
7. Najjar, V. A. and Allen, M. B. *J. Biol. Chem.* **206** (1954) 209.
8. Csàky, T. Z. *Acta Chem. Scand.* **2** (1948) 450.
9. Conway, E. J. *Microdiffusion analysis and volumetric error*, Crosby Lockwood & Son Ltd., London 1947.

Received October 1, 1955.

* Enzyme lacking in our experiments

ACTA CHEMICA SCANDINAVICA 10 (1956) 26—31

*iso*Thiocyanates XV. *p*-Methoxybenzyl *iso*Thiocyanate, a New Natural Mustard Oil Occurring as Glucoside (Glucoaubrietin) in *Aubrietia* Species

ANDERS KJÆR, ROLF GMELIN and ROALD BOE JENSEN

Chemical Laboratory of the University of Copenhagen, Denmark

Fresh plants and seeds of various species of the crucifer genus *Aubrietia* have been demonstrated to contain a new glucoside, *glucoaubrietin*, enzymically hydrolysed to sulphuric acid, glucose and *p*-methoxybenzyl *iso*thiocyanate. This mustard oil, which has not been previously recognised in nature, has been identified by comparison of the crystalline derivatives, formed upon reaction with ammonia and benzylamine, with authentic specimens of *p*-methoxybenzylthiourea (I) and *N*-(*p*-methoxybenzyl)-*N'*-benzylthiourea (II).

In the course of studies of *iso*thiocyanates in plants it was incidentally noticed that fresh parts of the crucifer *Aubrietia hybrida* hort. possessed a sharp, anis-like taste which made a closer investigation desirable. Paper chromatography [1] revealed the presence of a single glucoside in fresh parts of various species of the genus *Aubrietia*, a hitherto unrecognised source of mustard oils. With *n*-butanol:acetic acid:water (4:1:3) as a solvent system, the *Aubrietia*-glucoside appeared as a spot possessing an R_F-value slightly above that of glucotropaeolin, the well-known glucoside containing benzyl *iso*thiocyanate. This location, in conjunction with the spectroscopical characteristics discussed below, precluded the identity of the *Aubrietia*-compound with any of the previously recognised glucosides. In accordance with common usage, the name *glucoaubrietin* has been adopted for the new glucoside.

Ultra-violet absorption spectra of various mustard oil glucosides in aqueous solutions have been determined here. Provided strongly absorbing groups are absent from the aglucone side chains the glucosides display a single maximum at 228 mμ (ε *ca.* 8 000) as seen from the examples in Fig. 1. A partly purified specimen of glucoaubrietin exhibited maximum absorption at about the same wave-length but had in addition a broad band of medium intensity at about 270 mμ (Fig. 2). This pattern was retained after enzymic hydrolysis (Fig. 2), indicating unusual absorption properties of the corresponding *iso*thiocyanate.

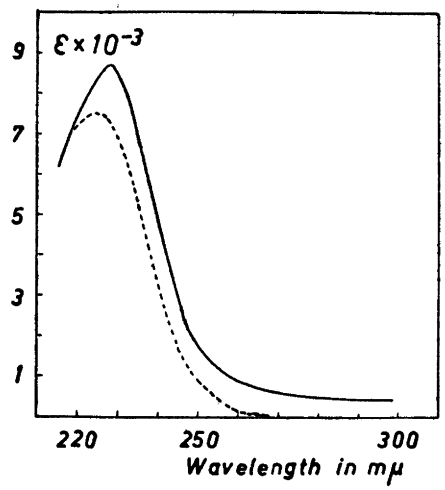


Fig. 1. Ultra-violet absorption spectra of aqueous solutions of : ———— *sinigrin;* — — — — *glucoiberin*[1].

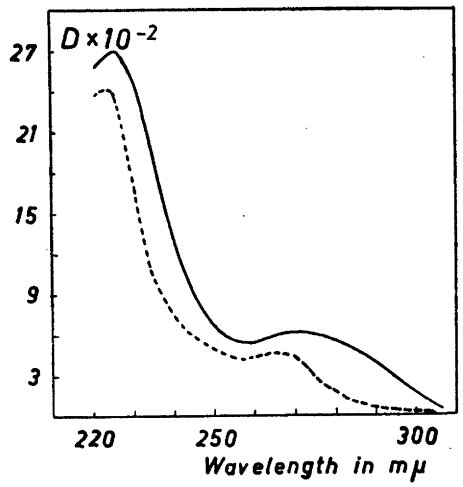


Fig. 2. Ultra-violet absorption spectra of: ———— *a partly purified extract of the glucoside of fresh parts of* Aubrietia columnae *Guss.;* — — — — *the corresponding crude* iso*thiocyanate. Solvent: water.*

The absorption curve suggested that the latter was of aromatic character, most likely substituted by one or more auxochromic groups. The spectral similarity with compounds such as *p*-hydroxy- and *p*-methoxy-benzylpenicillin [2], tyrosine [3], the cresols [4] *etc.* was striking. No colour appeared on spraying the chromatograms with diazotised sulphanilic acid [1], a fact precluding the presence of free aromatic hydroxy- and amino-groups in the glucoside. During the enzymic action, the concomitant formation of sulphate and glucose was established, the latter by paper chromatography in two solvent systems. Hence, glucoaubrietin appears to be a glucoside of the usual type. No attempts were made to crystallise or further characterise the genuine glucoside.

Whole, fresh plants of *Aubrietia deltoidea* DC. served as the starting material for the provision of further quantities of the glucoside. A methanolic extract was partly purified by percolation through aluminium oxide and then submitted to enzymic hydrolysis. The liberated *iso*thiocyanate was isolated by ether extraction and without further purification transformed into well-crystallising thioureas by reaction with ammonia and benzylamine. Analyses of both derivatives proved the presence of one methoxy-group and established the composition C_9H_9ONS for the parent *iso*thiocyanate. The ultra-violet absorption spectrum of the simple thiourea in 96 % ethanol exhibited a maximum at 245 mμ (ε 14 000), displaced in water to 237 mμ (ε 15 900), and an auxiliary band at 275 mμ (ε 1 900), practically unchanged in aqueous solution. In the present case, the high-extinction band could be regarded as diagnostic of an aralkyl-substituted thiourea, because the only alternative, a substituted arylthiourea, should possess quite different absorption data. For example,

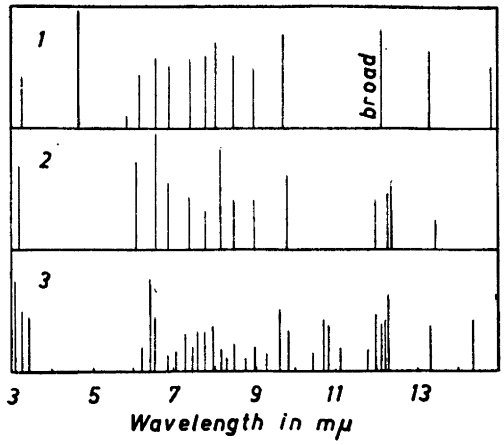
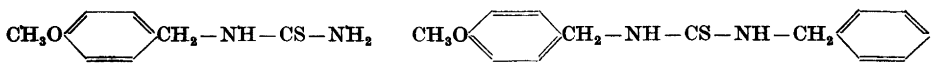


Fig. 3. Schematic presentation of the infra-red absorption spectra of: 1. p-*methoxybenzyl* isothiocyanate *(neat liquid, 0.1 mm layer); 2.* p-*methoxybenzylthiourea (I) (KBr pellet); 3.* N-(p-*methoxybenzyl*)-N'-*benzylthiourea (II) (KBr pellet).*

phenylthiourea in 96 % ethanol exhibits a maximum at 266 mμ (ε 15 400) with an inflection at 245 mμ (ε 10 000) and minimum at 227 mμ (ε 8 000), changed in water to a split peak at 248 and 240 mμ (ε 14 700 and 15 700). Hence, the mustard oil of glucoaubrietin must be one of the isomeric methoxybenzyl *iso*thiocyanates. In the literature [5,6] *p*-methoxybenzylthiourea is recorded with the m. p. 133—135°, sufficiently close to the m. p. 137° of the *Aubrietia*-thiourea to warrant a synthesis of an authentic specimen for comparison purposes.

p-Methoxybenzylamine was prepared in 34 % yield by reduction of anisaldoxime with zinc and acetic acid, according to Sunagawa *et al.*[7], or, more conveniently, from anisaldehyde by a Leuckart-reaction in 23 % yield as described by Lewis [8]. The amine was transformed into *p*-methoxybenzyl *iso*thiocyanate in 75 % yield by the Kaluza-Hodgkins synthesis, successfully employed recently by Ettlinger and Lundeen [9] for the preparation of the corresponding *m*-isomeride. The *iso*thiocyanate was formerly described by v. Braun and Deutsch [10] as a colourless liquid boiling over a rather wide range and suffering extensive decomposition on distillation at 16 mm. Here, the mustard oil appeared as a colourless, constant-boiling oil of agreeable odour and a burning taste, resembling that of fresh *Aubrietia* plants.



I II

By reaction with ammonia and benzylamine the synthetic mustard oil afforded the corresponding thioureas, (I) and (II). Analyses, melting points, mixed melting points and infra-red spectra served to establish the identity of the two *Aubrietia*-thioureas with the authentic specimens. The infra-red

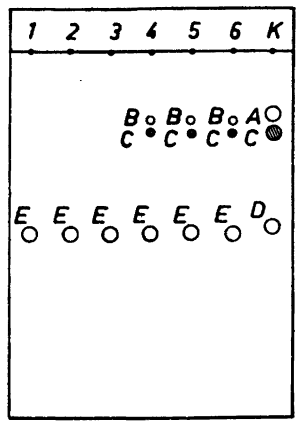


Fig. 4. *Schematic presentment of descending paperchromatographic analyses of the glucosides in various* Aubrietia *species. Solvent system:* n-*butanol:acetic acid:water (4:1:3).*

1. A. deltoidea *DC.*
2. A. hybrida *hort.*
3. A. columnae *Guss.*
4. A. deltoidea *DC (seed).*
5. A. erubescens *Griseb. (seed).*
6. A. intermedia *Heldr.* et *Orph. (seed).*
K. a control solution.
A. sinigrin; B. unknown glucoside; C. sinalbin;
D. glucotropaeolin; E. glucoaubrietin.

spectra are schematically reproduced in Fig. 3. It has thus been proved that *p*-methoxybenzyl *iso*thiocyanate represents an addition to the rather extensive series of naturally occurring *iso*thiocyanates.

Besides its occurrence in fresh plants of *Aubrietia deltoidea* DC., *A. hybrida* hort. and *A. columnae* Guss., glucoaubrietin has been demonstrated to be present in seeds of *A. deltoidea* DC., *A. erubescens* Griseb. and *A. intermedia* Heldr. *et* Orph. In the seed samples, however, the glucoside is accompanied by the *p*-hydroxybenzyl *iso*thiocyanate glucoside and an unidentified glucoside, the latter two being present in minor amounts only (Fig. 4). Glucoaubrietin therefore appears to be a rather constant and characteristic constituent of the genus *Aubrietia*. Its possible occurrence in other genera is being investigated at present. The detection of *p*-methoxybenzyl *iso*thiocyanate in nature is not altogether surprising in view of the long recognised existence of *p*-hydroxybenzyl *iso*thiocyanate (*cf.* ref. 11) as the aglucone of the glucoside sinalbin which occurs in white mustard and a few other plants. Biological methylation of aromatic hydroxy-groups is a reaction too well-known in phytochemistry to need further comments.

At the conclusion of the present work, the authors were informed that Ettlinger and Lundeen [9] have recently established the occurrence of the isomeric *m*-methoxybenzyl *iso*thiocyanate in seed of the American plant *Limnanthes douglasii* R.Br., belonging to the family *Limnanthaceae*. The latter finding is remarkable because of the rare occurrence of *m*-disubstituted aromatic compounds in nature.

EXPERIMENTAL

All melting points are uncorrected and determined in capillary tubes in a glycerol bath.

Paper chromatography of Aubrietia *species.* Methanolic extracts of whole, fresh plants and seeds of various *Aubrietia* species were applied to Whatman paper No. 1 and chromatographed in *n*-butanol:acetic acid : water (4:1:3) by the descending technique. The chromatograms were developed as previously described [1] and the results are schematically presented in Fig. 4. Whereas extracts of the fresh plants gave only one glucoside-spot, the seed samples contained minor amounts of two additional glucosides. One of these (C in Fig. 4), appeared to be identical with the glucoside containing *p*-hydroxybenzyl *iso*thiocyanate. Like an authentic specimen of the latter, the *Aubrietia*-compound C developed a red colour on spraying the chromatogram with diazotised sulphanilic acid [1]. The nature of the other minor glucoside, (B), is unknown.

Properties of glucoaubrietin. A specimen of fresh parts of *Aubrietia columnae* Guss. (1 g) was extracted three times with boiling methanol. The solvent was removed *in vacuo* and the residue taken up in water (20 ml). Insoluble material was removed by filtration and the filtrate passed through a column of acid-washed aluminium oxide (2 g). After the column had been washed with water the glucoside was eluted with 1 % K_2SO_4-solution[1].

A small fraction of the eluate was used, after appropriate dilution, for the determination of the ultra-violet spectrum, while the remaining part was subjected to enzymic hydrolysis by adding a drop of a cell-free myrosinase preparation. After some hours, the reaction mixture was extracted with ether, the solvent removed and the residue dissolved in water. Again, the ultra-violet absorption spectrum of this solution was determined. The original aqueous phase was chromatographed in 1) *n*-butanol:acetic acid:water (4:1:3) and 2) pyridine:amyl alcohol:water (30:35:30), in both solvent systems accompanied by glucose as a reference substance. The R_F-values were 0.24 and 0.42, respectively, the same as of glucose in the two systems.

A separate plant extract, which was not further purified, served to establish the presence of sulphate after enzymic hydrolysis of the glucoside.

Crystalline derivatives of the Aubrietia *isothiocyanate.* It was established in preliminary experiments that the *iso*thiocyanate, corresponding to glucoaubrietin, was volatile with steam. The steam distillation, however, was accompanied by a considerable loss of material for reasons which are not quite clear. Therefore, it was preferred to extract the free mustard oil by ether after enzymic hydrolysis.

Fresh, whole plants of *Aubrietia deltoidea* DC. (1.2 kg) were repeatedly extracted with a total of 5 l of methanol. After removal of the latter, the residue was taken up in water (1 l) and filtered. The filtrate was divided into four parts and each was allowed to flow slowly through a column of acid-washed aluminium oxide (35 g). The percolates were pooled, a few ml of a myrosinase solution was added and the mixture set aside overnight. Next day, the *iso*thiocyanate was collected by ether extraction (3 × 100 ml) and the ether solution was divided into two parts.

Thiourea. To one of these was added a solution of ammonia in ethanol. After 12 hours, the solvents were removed and the partly oily residue was treated with charcoal in hot water and filtered. On cooling, the solution deposited colourless needles (49 mg). The product was recrystallised from water (3.5 ml) for analysis (43 mg), m. p. 137.5—138.5°. Paper chromatography of the thiourea in chloroform gave a spot with an R_{Ph}-value [12] of 1.03. The ultra-violet and infra-red spectra were determined. (Found: C 55.10; H 6.02; N 13.93; S 15.90; OCH_3 15.90. Calc. for $C_9H_{12}ON_2S$: C 55.05; H 6.17; N 14.27; S 16.33; OCH_3 15.83).

Benzylthiourea. To the other half of the ether solution was added an excess of benzylamine. Next day, the solvent was removed and the residue treated with water, containing a drop of hydrochloric acid. The partly crystalline product was recrystallised three times from 50 % ethanol to give colourless, nacreous platelets (66 mg), m. p. 105°. (Found: C 67.25; H 6.24; N 9.87; S 11.04; OCH_3 10.94. Calc. for $C_{16}H_{18}ON_2S$: C 67.10; H 6.34; N 9.78; S 11.20; OCH_3 10.83). The ultra-violet and infra-red spectra of the disubstituted thiourea were determined.

Synthesis of p-*methoxybenzyl* iso*thiocyanate.* *p*-Methoxybenzylamine was prepared by reduction of anisaldoxime with zinc and acetic acid, according to Sunagawa *et al.*[7], who

reported a yield of 75 %. Our yields were considerably smaller (30—40 %) and it was therefore preferred to prepare the amine by the Leuckart-reaction proposed by Lewis [8]. The stated yield (23 %) was obtained. The amine was distilled *in vacuo*, b. p. 115° at 12 mm.

The synthesis of the *iso*thiocyanate was performed exactly as described by Ettlinger and Lundeen [9] for the corresponding *m*-isomeride and proceeded in 75 % yield. The mustard oil appeared as a colourless liquid of a faint odour, but possessing a sharp and aromatic taste, b. p. 133° at 0.7 mm; n_D^{25} 1.5935. (Found: C 60.30; H 5.21; N 7.98; S 17.86. Calc. for C_9H_9ONS: C 60.31; H 5.06; N 7.82; S 17.89).

p-*Methoxybenzylthiourea* (I). The synthetic mustard oil was allowed to react with ammonia in dilute ethanol overnight. The resulting thiourea was obtained as clusters of colourless needles after recrystallisation from water, m. p. 138° alone or when mixed with the *Aubrietia*-thiourea above. (Found: C 55.20; H 6.15; N 14.24. Calc. for $C_9H_{12}ON_2S$: C 55.05; H 6.17; N 14.27.) The infra-red spectrum was found identical with that of the *Aubrietia*-thiourea.

N-*(p-Methoxybenzyl)*-N'-*benzylthiourea* (II). An ether solution of the mustard oil and benzylamine was left standing at room temperature overnight. Next day, the crystals were collected and recrystallised from 50 % ethanol. The benzylthiourea separated as colourless plates, m. p. 105°, alone or in admixture with the *Aubrietia*-derivative. (Found: C 67.00; H 6.33; N 9.82. Calc. for $C_{16}H_{18}ON_2S$: C 67.10; H 6.34; N 9.78). Again, the infra-red spectrum served to establish the identity of the compound with the benzylthiourea, derived from the *Aubrietia* mustard oil.

The authors wish to thank the *Botanical Garden of the University of Copenhagen* for placing at our disposal all the plant materials employed in the present investigation. Microanalyses were made in this laboratory by Mr. P. Hansen. The work is part of investigations supported by *Statens Almindelige Videnskabsfond (The Danish State Research Foundation)* and *Carlsbergfondet (The Carlsberg Foundation)*.

REFERENCES

1. Gmelin, R. *Präparative und analytische Versuche über Senfölglucoside* (Diss.), University, Tübingen 1954.
2. *The Chemistry of Penicillin*, Princeton University Press, Princeton, N. J. 1949, p. 423, 670.
3. Kretchmer, N. and Taylor, R. *J. Am. Chem. Soc.* **72** (1950) 3291.
4. Hunter, R. F., Morton, R. A. and Carpenter, A. T. *J. Chem. Soc.* **1950** 441.
5. Hüter, F. *Chem. Ber.* **80** (1947) 273.
6. Saijo, S. *J. Pharm. Soc. Japan* **72** (1952) 1009; *cf. Chem. Abstracts* **47** (1953) 3298.
7. Sunagawa, G., Kushima, T. and Ichii, T. *J. Pharm. Soc. Japan* **72** (1952) 1570; *cf. Chem. Abstracts* **47** (1953) 9285.
8. Lewis, K. G. *J. Chem. Soc.* **1950** 2249.
9. Ettlinger, M. G. and Lundeen, A. J. *J. Am. Chem. Soc.* **78** (1956). *In press.*
10. v. Braun, J. and Deutsch, H. *Ber.* **45** (1912) 2188.
11. Kjær, A. and Rubinstein, K. *Acta Chem. Scand.* **8** (1954) 598.
12. Kjær, A. and Rubinstein, K. *Acta Chem. Scand.* **7** (1953) 528.

Received October 25, 1955.

ACTA CHEMICA SCANDINAVICA 10 (1956) 32—36

Diels-Alder Reaction of α-Phellandrene and Cinnamaldehyde

INGVALD AUGESTAD

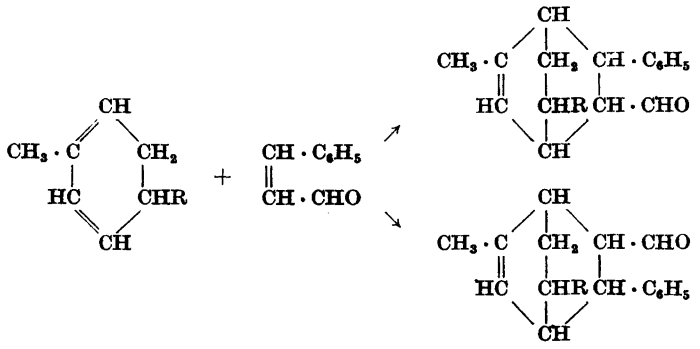
Universitetets kjemiske institutt, Blindern-Oslo, Norway

An adduct of laevorotatory α-phellandrene and cinnamaldehyde has been prepared. The adduct, which is liquid and dextrorotatory seems to consist of one predominating form with at least one other isomeride present. On regenerating the adduct from its phenylhydrazone in methanolic solution the crystalline methyl acetal of the adduct was formed. The adduct of maleic anhydride and α-phellandrene is transformed into a lactonic acid by boiling with water.

Diels-Alder reactions of α-phellandrene have previously been carried out with symmetrical dienophiles such as maleic anhydride and naphthoquinone and with the unsymmetrical dienophiles acrolein and crotonaldehyde; for summary see Northon [1]. In the present paper the reaction with cinnamaldehyde is described. The α-phellandrene used was a commercial laevorotatory sample (Eastman) with a specific rotation of —124°. In order to check its reactivity it was treated with maleic anhydride when it readily gave a crystalline adduct as described by Diels and Alder [2]. It was found that this adduct by boiling with water was isomerized to the lactonic acid previously prepared by West [3].

The reaction of α-phellandrene with cinnamaldehyde was carried out by heating to 150°. On fractionating the reaction product in a vacuum a crude adduct was obtained which was purified by treatment with sodium hydrogen sulphite. After redistillation the adduct was obtained as an oil with the expected composition $C_{19}H_{24}O$ and with a specific rotation of +17.8°.

Theoretically the addition of an unsymmetrical dienophile to one of the optical components of α-phellandrene could give 8 isomeric adducts of two structurally different types as seen from the scheme (R = *iso*propyl)



In accordance with what has been found by Alder and Stein [4] the diene synthesis seems also in this case to lead mainly to one product with one other adduct present in small amount. If the adduct was treated with 2,4-dinitrophenylhydrazine two crystalline hydrazones could be isolated, the one being strongly dextrorotatory and the other strongly laevorotatory. With phenylhydrazine one crystalline hydrazone only was isolated and in good yield. It was dextrorotatory and is evidently a derivative of the predominating isomeride. An attempt to regenerate the aldehydic adduct from the phenylhydrazone by boiling with a methanolic solution of pyruvic acid led to a new crystalline compound $C_{21}H_{30}O_2$, m. p. 71°, $[\alpha]_D^{20} = +68°$ which was found to be the methyl acetal of the adduct. The acetal on catalytic hydrogenation took up one mole of hydrogen.

From the acetal the adduct itself could only partially be regenerated. Hydrolysis led to a mixture of crystalline acetal and oily adduct, the methoxyl content and rotation of which permitted the calculation of an approximate specific rotation of + 27° for the adduct. The oily part of the mixture gave the same dextrorotatory phenylhydrazone from which the acetal had been obtained and the dextrorotatory 2,4-dinitrophenylhydrazone, described above. It is therefore evident that the methyl acetal must be derived from a dextrorotatory component of the adduct.

The crystalline methyl acetal could be obtained directly from the original adduct, although only in poor yield, by heating methanolic solutions containing pyruvic acid, formic acid or 0.02 N hydrochloric acid.

Oxidation of the adduct under mild conditions with hydrogen peroxide gave two monocarboxylic acids. The one was a crystalline compound $C_{19}H_{24}O_2$, m. p. 157°, $[\alpha]_D^{20} = -67°$, and the other an oil with $[\alpha]_D^{20} = +34°$. The acids were boiled with water but no formation of lactones could be detected.

In order to establish the structure and the configuration of the adduct further experimental work will be necessary.

EXPERIMENTAL

α-Phellandrene and maleic anhydride

Optically pure α-phellandrene is rather difficult to obtain as shown by Hancox and Jones [5] who found the rotation to be $[\alpha]_D^{20} = -177°$. In the present case a commercial (−)-α-phellandrene (Eastman) of $[\alpha]_D^{20} = -124$ was used without further purification. The α-phellandrene and an excess of maleic anhydride on keeping for several days at −5° gave in 38 % yield the adduct described by Diels and Alder [2]. After recrystallization from petroleum ether it had m. p. 126°, $[\alpha]_D^{20} = -10°$ ($c = 3$ in chloroform). The adduct (3 g) was boiled with water (1 l) for one hour and the filtered solution then evaporated on the steam-bath to 200 ml in the course of 24 hours. The lactonic acid which had separated (1.6 g) was recrystallized from a mixture of ethyl acetate and ligroin, m. p. 170°, $[\alpha]_D^{20} = -37°$ ($c = 24$ in chloroform). (Found: C 66.65; H 8.08. Equiv. wt. 250. Calc. for $C_{14}H_{20}O_4$: C 66.70; H 8.05. Equiv. wt. for monobasic acid 252). Treatment of the acid m. p. 170° with an ethereal solution of diazomethane gave the corresponding lactonic ester, which after recrystallization from petrol ether had m. p. 105°. West [3] found 104°. $[\alpha]_D^{20} = -18.8°$ (chloroform). (Found: OCH_3 12.51. Calc. for $C_{15}H_{22}O_4$ 11.65).

α-Phellandrene and cinnamaldehyde

The same (−)-α-phellandrene as above (100 g) and cinnamaldehyde (50 g) purified by vacuum fractionation, were heated in sealed tubes for 24 hours at 150°. After removing most of the unreacted α-phellandrene by distillation at 12 mm Hg, the reaction product was fractionated in a high vacuum. The fraction distilling at 114—120°/0.01 mm amounted to about 20 %, based on the quantity of cinnamaldehyde employed in the reaction. The adduct (18 g) was shaken for 2 hours with 25 % sodium hydrogen sulphite (40 ml) and ethanol (20 ml) and the solution then extracted with ether in order to remove impurities. The adduct was regenerated from the bisulphite solution by heating on the steam-bath for 30 min. and was then taken up in ether. The adduct (14 g) distilled at 114—120/0.01 mm $[\alpha]_D^{20} = +17.8°$ ($c = 3$ in chloroform). (Found: C 84.86; H 9.01; Mol.wt. (camphor) 267; 270. Calc. for $C_{19}H_{24}O$: C 85.07; H 8.96. Mol.wt. 268).

By bromination in ether a liquid bromide was formed which contained 35.87 % Br; calc. for 1 double bond 37.33 %.

The adduct (12 g), in methanol (200 ml) to which 0.4 g platinum oxide had been added, absorbed 1 250 ml hydrogen (1.5 atm.). It was thus apparent that both the double bond and the aldehyde group had been reduced. Calc. for 2 moles of hydrogen; 1 460 ml. The hydrogenated product, after distillation at 152°/0.2 mm, had $[\alpha]_D^{20} = 49°$ ($c = 1$, in chloroform). (Found: C 84.12; H 10.34. Calc. for $C_{19}H_{28}O$: C 83.80; H 10.35).

2,4-Dinitrophenylhydrazones

The phosphoric acid method of Johnson [6] was used for the preparation of these hydrazones. A solution of 2,4-dinitrophenylhydrazine (5 g) in 85 % phosphoric acid (60 ml) was heated on the steam-bath, diluted with ethanol (40 ml) and filtered. To a solution of the adduct (1 g) in ethanol (20 ml) the calculated amount of the reagent was added. On standing for some hours at room temperature a mixture of red and yellow crystals separated. These were collected by filtration, washed with water and the mixture was crystallized first from glacial acetic acid and then from petrol ether containing 20 % benzene, when red crystals only were obtained, m. p. 191° $[\alpha]_D^{20} = +272°$ ($c = 1.2$, in chloroform). (Found: C 66.95; H 6.59; N 12.65. Calc. for $C_{25}H_{28}O_4N_4$: C 66.95; H 6.30; N 12.95).

In order to isolate the yellow form a fresh portion of the crystal mixture was prepared, dried at room temperature and refluxed with ether when mainly the yellow crystals dissolved. The filtered solution on cooling gave the yellow hydrazone which after recrystallization from glacial acetic acid had m. p. 176°, $[\alpha]_D^{20} = -210°$ ($c = 0.1$ in chloroform). (Found: C 67.24; H 6.40; N 12.38).

Phenylhydrazone

A solution of the adduct (12 g) and phenylhydrazine (3 g, calc. 4.04 g) in methanol (60 ml) was kept at 0° for 4 hours when colourless needles separated in a yield of 40 %. Recrystallized from methanol, m. p. 112°, $[\alpha]_D^{20} = +96°$ ($c = 1$ in ethanol). (Found: C 83.79; H 8.52; N 7.90. Calc. for $C_{25}H_{30}N_2$: C 83.79; H 8.38; N 7.85).

It should be mentioned that a phenylhydrazone with m. p. 124° and $[\alpha]_D^{20} = +151°$ ($c = 1$ in ethanol) was obtained in some cases when the adduct was prepared by heating to 120°. (Found: C 83.49; H 8.37; N 7.97). The two phenylhydrazones gave the same product when treated with a methanolic solution of pyruvic acid.

Oxidation of the adduct

To a vigorously stirred aqueous solution of sodium hydroxide (0.5 N, 100 ml) containing boric acid (0.1 g) and hydrogen peroxide (10 ml 40 %), a solution of the adduct (10 g) in benzene (20 ml) was added dropwise at room temperature. After 3 hours the

mixture was transferred to a separating funnel, and more benzene added. Next day the aqueous layer was acidified with hydrochloric acid and the oil which separated was washed with water. The oil was dissolved in a small quantity of ethanol and water added until turbidity was produced. On keeping in the refrigerator overnight crystals separated (3 g) which on recrystallization from 75 % methanol gave colourless needles with m. p. 157°, $[\alpha]_D^{20} = -67°$ ($c = 1.5$ in chloroform). (Found: C 79.95; H 8.50; Equiv. wt. 281. Calc. for $C_{19}H_{24}O_3$: C 80.24; H 8.51; Equiv. wt. 284.4).

On the addition of water to the mother liquor from the crystals m. p. 157°, an oil deposited which had $[\alpha]_D^{20°} = +22°$ ($c = 3.5$ chloroform). (Found: Equiv. wt. 279).

A chromatographic fractionation of this oily acid (1.4 g) was attempted on a column of cellulose, using as an eluant a mixture of ethyl acetate, benzene, *n*-propyl alcohol, water (5:1:2:1). Plotting the optical rotation against fraction number a sharp peak in the curve showed that the dextrorotatory acid was concentrated over a few fractions. From these fractions 1.2 g oily acid were recovered which had $[\alpha]_D^{20} = +34.2°$ ($c = 2.5$ in chloroform).

Phenylhydrazone of the adduct with pyruvic acid

A solution of the phenylhydrazone, m. p. 112° (6 g) and pyruvic acid (4 g) in methanol (60 ml) was refluxed for 3 hours. After cooling water (2 ml) was added and the solution kept in a refrigerator overnight when the methyl acetal of the adduct separated as needles (4.5 g). After recrystallization from 80 % methanol the m. p. was 71°, unchanged on recrystallization from a small volume of benzene. $[\alpha]_D^{20} = +68$ ($c = 2$ in chloroform). (Found: C 80.31; H 9.52; OCH_3 19.10. Calc. for $C_{21}H_{30}O_2$; C 80.21; H 9.61; OCH_3 19.72).

When water was added to the mother liquor the phenylhydrazone of pyruvic acid separated. After purification it had m. p. and mixed m. p. 182°.

Hydrogenation of the acetal, m. p. 71°

Platinum oxide (0.29 g) in glacial acetic acid (30 ml) was shaken in an atmosphere of hydrogen until absorption ceased. After adding the methyl acetal (0.564 g) 34.0 ml hydrogen (960 mm, 19°) were absorbed in the course of 100 min, calc. 34.1 ml. The filtered solution was poured into water, the precipitate taken up in ether and the ethereal solution washed with water and dried. After evaporating the ether the crystalline residue was recrystallized from methanol. M. p. 57–60°, $[\alpha]_D^{20} = +63°$ ($c = 3$ in chloroform). (Found: C 79.39; H 10.19; OCH_3 19.98. Calc. for $C_{21}H_{32}O_2$: C 79.68; H 10.19; OCH_3 19.60).

Hydrazones prepared from the acetal

A solution of the methyl acetal (1 g) and 2,4-dinitrophenylhydrazine (0.75 g) in ethanol (50 ml) was heated to boiling. On adding a few drops of conc. hydrochloric acid a reaction immediately took place and on cooling a red crystalline hydrazone precipitated (1.4 g). The hydrazone after recrystallization from petrol ether containing 20 % benzene, had m. p. 189° and $[\alpha]_D^{20} = +262°$ in chloroform. (Found: C 67.10; H 6.44; N 12.40. Calc. for $C_{25}H_{28}O_4N_4$: C 66.95; H 6.30; N 12.95).

The methyl acetal (4 g) was heated with N hydrochloric acid (100 ml) on a water-bath for 20 hours. On cooling a mixture of oil and crystals deposited. The oil was dissolved in 80 % methanol and the solution, after the addition of phenylhydrazine (1 g), was heated for a short time. When the solution was subsequently kept in a refrigerator colourless crystals separated which had $[\alpha]_D^{20} = +97°$ ($c = 0.6$ in ethanol) and m. p. 112° alone and mixed with the phenylhydrazone of the original adduct.

Preparation of acetal directly from adduct

A solution of the oily adduct (1 g) and pyruvic acid (5 g) in methanol (30 ml) was refluxed for 24 hours. After adding water until turbidity was produced the solution was kept in a refrigerator overnight when a small amount of crystalline material separated which, after recrystallization from petrol ether had m. p. 68–70° and $[\alpha]_D^{20} = +65°$ ($c = 1.1$ in chloroform).

Following the same procedure a small amount of the methyl acetal was also obtained when formic acid was used instead of pyruvic acid. Acetic acid had, however, no effect. On using 0.1 ml 5 N hydrochloric acid instead of pyruvic acid, 0.1 g (10 % yield) of the methyl acetal was obtained. It had m. p. 71° alone and mixed with acetal prepared from the phenylhydrazone.

Hydrolysis of the methyl acetal

A solution of the methyl acetal (1 g) in 75 % methanol (150 ml) to which 1.5 ml N hydrochloric acid had been added, was refluxed for 90 min. The methanol was distilled off, and the oil which separated was taken up in ether. The ethereal solution was washed with water and dried over potassium carbonate. After evaporating the ether the residue was dried in a vacuum over calcium chloride. The methoxyl content of the residue (6.1 %) showed that the acetal had not been completely hydrolysed. As the specific rotation of the residue was found to be +39.7° an approximate specific rotation of +27° could be calculated for the aldehyde corresponding to the acetal.

The author wants to express his gratitude to Professor E. Berner for having suggested this investigation and for his kind advice and valuable criticism during the work.

A grant from *Fridtjof Nansen Fond* is gratefully acknowledged.

REFERENCES

1. Northon, J. A. *Chem. Rev.* **31** (1942) 319.
2. Diels, O. and Alder, K. *Ann.* **460** (1928) 104.
3. West, T. F. *J. Chem. Soc.* **1941** 140.
4. Alder, K. and Stein, G. *Angew. Chem.* **50** (1937) 510.
5. Hancox, N. C. and Jones, T. G. H. *Univ. of Queensland Papers Dep. Chem.* **1** (1939) No. 14.
6. Johnson, G. D. *J. Am. Chem. Soc.* **73** (1951) 5888.

Received October 20, 1955.

ACTA CHEMICA SCANDINAVICA 10 (1956) 37—48

Interaction of Pyridine-Nucleotide linked Enzymes

AGNAR P. NYGAARD* and WILLIAM J. RUTTER**

Medicinska Nobelinstitutet, Biokemiska avdelningen, Stockholm, Sweden

The oxidations of lactate by lactic dehydrogenase (LDH), glutamate by glutamic dehydrogenase, and alcohol by liver and yeast alcohol dehydrogenase (ADH) have been found to be somewhat slower with diphosphopyridine nucleotide (DPN) bound to glyceraldehyde-3-phosphate dehydrogenase (TDH) than with free DPN. In contrast, the reduction of pyruvate by LDH and acetaldehyde by liver ADH was faster with reduced DPN (DPNH) bound to TDH than with free DPNH. The equilibrium constants of the systems were in all cases displaced towards the reduced substrate with bound DPN.

The overall kinetics of the liver ADH system using DPN(H) bound to TDH (TDH · DPN and TDH · DPNH) has been studied in some detail. The reaction mechanism appeared to be the same as with free DPN(H).

When liver ADH was added to TDH · DPNH which had been reduced by glyceraldehyde-3-phosphate, the absorption peak of DPNH shifted from 340 mμ to 330 mμ. If the bound DPN was reduced by liver ADH and alcohol, the absorption peak shifted down to 322 mμ, which is in the same region as the absorption peak of ADH·DPNH itself. No complex between liver ADH and TDH · DPNH could be observed in the ultracentrifuge.

Implications of these findings have been discussed.

Most oxidation-reduction reactions at the "substrate" level occur by virtue of pyridine nucleotide-linked (PN) enzymes. In the past it has often been explicitly or implicitly implied that the PN coenzymes themselves act as mobile oxidation-reduction (O/R) carriers between the various dehydrogenase systems. Several lines of evidence, however, allow alternative interpretations. Although these coenzymes are often readily dissociable from their respective apoenzymes, this is by no means always the case. Taylor *et al.*[1] have shown that crystalline triosephosphate dehydrogenase (TDH) contains firmly bound diphosphopyridine nucleotide (DPN) which cannot be removed by dilution or dialysis, but which rapidly exchanges with free DPN. Theorell and Bonnichsen[2] observed that the liver alcohol dehydrogenase, on the other hand, has a very

* Fellow Norwegian Research Council. Present address: Institute for Nutritional Research, University of Oslo, Blindern, Oslo, Norway.

** Fellow U. S. Public Health Service.

high affinity for reduced DPN (DPNH). As a matter of fact, the diversified manners by which pyridine nucleotides are bound may also be inferred from the different spectral manifestations of the coupling reactions of PN and PNH with their various apodehydrogenases [3].

These different types of binding of PN coenzymes could be the reflection of a complicated pattern of interaction between the PN enzymes themselves. In biological systems where the number of binding sites is of the same order of magnitude as the available PN molecules, interactions of apoproteins with bound PN could play a prominent role in physiological oxidation-reduction. It is therefore interesting that DPN-linked enzymes have been found to react with DPN of TDH (TDH · DPN). Cori, Velick and Cori observed [4] that when TDH · DPN was reduced by glyceraldehyde-3-phosphate (G-3-P), it could be reoxidized by addition of pyruvate and lactic dehydrogenase (LDH). The rate of the reaction made the intermediation of dissociated DPNH unlikely. Similar reactions of TDH · DPNH with DPNH cytochrome-c reductase have been reported by Mahler [5], and with various DPN degrading enzymes as well as other dehydrogenases by Astrachan [6]. Under the conditions studied, the rates of reactions were generally somewhat slower than with free DPN(H).

The implications of these data are manifest. The kinetic relations which have been the result of the study of isolated enzymes under the usual assay conditions involving high concentrations of free coenzyme and substrates may well not apply to situations in which apoprotein-holoenzyme interactions predominate. For example, Theorell and Chance [7], and Theorell, Nygaard and Bonnichsen [8] have been able to develop an apparently satisfactory kinetic treatment of the reactions of liver ADH without formal consideration of the formation of complex with the substrate. Under some experimental conditions, association-dissociation reactions of DPN(H) with the apoenzyme seemed to be rate-limiting steps. If, by virtue of interaction with other enzymes, the overall reaction occurred without association and dissociation of coenzyme, or if these reactions occurred at modified rates, then ADH might exhibit quite different reaction properties.

In this paper we wish to present some further information on the nature of the bound DPN(H) of TDH, especially its reactivity with various other dehydrogenases. Using the sensitive recording fluorimetric technique developed in this laboratory, it has been possible to study the kinetics of the interactions with liver ADH rather thoroughly. Some experiments on the mechanism of dehydrogenase interaction are also presented, and the implications of these data are discussed.

MATERIALS AND METHODS

Enzymes. TDH was prepared from rabbit muscle according to Cori *et al.*[9]. The preparation used was recrystallized 4 times, and contained 2.0 moles DPN/mole TDH as determined by reduction with G-3-P as well as with ADH and ethanol. The ratio of light absorption at 280 mμ *vs* 260 mμ was 1.12. This is in agreement with data previously reported by Velick and Hayes [10].

LDH was prepared from bovine heart muscle by the procedure of Straub [11]. It was recrystallized three times and contained both A and B components.

Crystalline preparations of liver ADH and glutamic dehydrogenase were generously supplied by Dr. Roger Bonnichsen. Crystalline yeast ADH was procured from C. F.

Boehringer & Soehne. Crude Zwischenferment was prepared from bottom yeast according to the method of Warburg and Christian [12]. DPN was prepared in this laboratory according to Åkeson and Neilands [13]. The sample used was 88 % pure, as judged by the ADH test. A sample of approximately 90 % pure TPN was obtained from Pabst laboratories. DPNH was prepared enzymatically according to Nygaard and Theorell [14].

Substrates. Glyceraldehyde-3-phosphate (G-3-P) was prepared essentially according to Meyerhof [15]. The other substrates were obtained commercially.

Kinetic measurements. The highly sensitive fluorimetric technique allowed kinetic measurements to be made without using inordinately large amounts of TDH. The experimental procedure is the same as used in the recent study of the ADH system [8]. The calibration of the total amounts of free DPN or bound DPN added in a given experiment was made with yeast ADH and ethanol.

The experiments involving bound DPNH (TDH · DPNH) were carried out in the following manner: The amount of G-3-P necessary to reduce a known amount of TDH · DPN nearly to completion was determined, and that amount was used to form TDH · DPNH for oxidation by the different pyridine-nucleotide systems. To get more than 90 % reduction of TDH · DPN it was not possible to avoid an excess of G-3-P. The initial velocities for oxidation of TDH · DPNH by the various dehydrogenase systems could accordingly never be maximum, because of the counter reaction.

RESULTS

The TDH reaction studied with the fluorescence technique

Before the proposed kinetic studies could be carried out, it was necessary to investigate with the fluorimetric technique certain aspects of the reaction in the presence of TDH. The basis of the technique as applied to the PN enzymes is that DPNH fluoresces while DPN does not. At the outset it was by no means certain that TDH · DPNH would exhibit the same fluorescence properties as free DPNH. It is known that FMN, for example, loses its fluorescence when it is coupled with the old yellow enzyme. Appropriate experiments demonstrated that TDH · DPNH does in fact fluoresce, and that the intensity of fluorescence of TDH · DPNH is the same as for free DPNH within experimental error (—5 %). A similar situation has been found for ADH · DPNH.

It was originally noted by Velick *et al.*[16] that DPNH undergoes a transformation with consequent loss of absorption in the 340 mμ region in the presence of TDH. This interesting fact has been further studied by Krebs *et al.*[17]. Such a "destruction" of DPNH bound to TDH was observed in the fluorescence apparatus. The product(s) of the reaction are therefore non-fluorescent. The reaction cannot represent a simple reoxidation to DPN since further addition of substrate did not elicit additional fluorescence, whereas addition of free DPN resulted in a rapid reaction reflected by an immediate increase in fluorescence. Since no free DPNH was added in these experiments, the reaction probably occurred at the binding site of DPNH on the TDH molecule. There was no observable destruction of DPNH by any of the other dehydrogenases tested.

It was consistently observed that 2 molecules DPN/molecule TDH could be reduced by ADH and ethanol at pH 10. Similar results could be obtained with G-3-P only in the presence of low arsenate concentrations (—10^{-4} M). At higher

concentrations, less than 2 molecules DPN/TDH were reduced (in 0.1 M arsenate the reduction of approximately one of the two DPN molecules on TDH was observed). This effect was not due to a rapid destruction of DPNH [16,17] by a reaction similar to that described above, since such destruction occurred very slowly, if at all, under the conditions of the experiments. High concentrations of arsenate did not inhibit the reduction of 2 DPN per TDH molecule by the ADH. The significance of these observations has not been investigated further, but a relationship to the inhibition of the reaction rate of TDH by arsenate as studied by Bücher [18] is suggested.

Because of the very large effects of pH as well as salts on the binding of FMN to the old yellow enzyme [19], several attempts to dissociate TDH · DPN by dialysis at different pH's in the presence of various salts were made. Whenever dissociation was observed, so also was loss of enzyme activity.

Interaction of LDH with TDH · DPN and TDH · DPNH

The interaction of the LDH system with TDH · DPN and TDH · DPNH first studied by Cori, Velick and Cori [4], has been reinvestigated in an attempt to get more quantitative estimate of the relative reaction rates of LDH with bound and free DPN(H). The 4 times recrystallized TDH preparation used in these experiments exhibited small but definite lactic dehydrogenase activity. Appropriate experiments indicated that "endogenous" LDH had properties different from the crystalline LDH. Figs. 1 and 2 show that the Michaelis constant (K_m) for pyruvate in the two systems is considerably different. Similar results were obtained using TDH · DPNH instead of free DPNH. In addition, the inhibition of activity of crystalline LDH in the presence of high pyruvate concentrations was not observed with "endogenous" LDH at pH 9.0, and was observed only at higher concentrations than with added LDH at pH 7.15. When crystalline LDH was added to the TDH preparation, an intermediate K_m for pyruvate was observed, the Lineweaver-Burk plot being almost the algebraic sum of the plots for the separate enzymes. "Endogenous" LDH activity was not immediately inhibited by 10^{-3} M *p*-chloromercuribenzoate. In this respect it resembles LDH, and contrasts with the known properties of TDH which is sensitive to SH reagents. It is possible that the LDH activity is due to an impurity of muscle LDH, which might have properties different from those of bovine heart muscle LDH.

At high pyruvate concentrations (— 1 mM), the endogenous LDH activity of TDH was great enough to make quantitative evaluation of the effects of added LDH difficult. However, at lower concentrations of the substrate the rate of the reaction due to "endogenous" LDH was much less and could be corrected for. The results with pyruvate concentrations around 20 μM (pH 8.8) showed that LDH oxidized TDH · DPN some 10 % faster than free DPNH. Since the rate of reaction with bound DPNH is submaximum (see materials and methods), this difference is all the more emphasized. An increased reaction rate of LDH with TDH · DPNH observed by Cori, Velick and Cori [4] was attributed to stabilization of LDH by TDH. It is believed that the present results cannot be attributed to such an effect since they are based

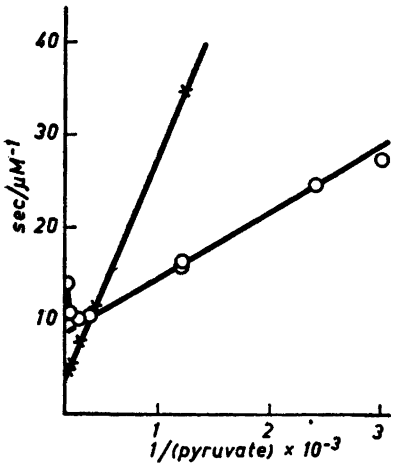


Fig. 1. Pyruvate reduction by 4 times crystallized triosephosphate dehydrogenase (TDH) (xx) and by LDH (oo), pH 9.0.
Conditions of the experiment:
Conc. DPNH: 9.0 μM
Conc. TDH: 0.78 μM
Conc. LDH: 0.0003 μM
Glycine buffer 0.1 M 23° C.
Results:
$K_{(pyruvate,\ TDH)}$: *6 000 μM*
$K_{(pyruvate,\ LDH)}$: *700 μM*

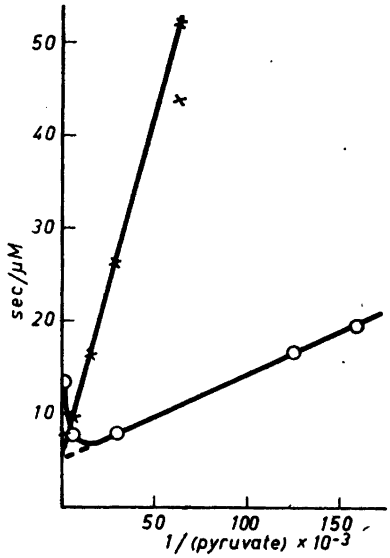


Fig. 2. Pyruvate reduction by 4 times crystallized triosephosphate dehydrogenase (TDH) (xxx) and by LDH (ooo), pH 7.15.
Conditions of the experiment:
Conc. DPNH = 13 μM
Conc. TDH = 0.78 μM
Conc. LDH = 0.00054 μM
Buffer: phosphate, μ = 0.1 + M/1 000 versene
K_M *(pyruvate, TDH) = 150 μM*
K_M *(pyruvate, LDH) = 18 μM*

on the initial rate of the reaction, and the enzyme appeared to be stable at least for 30 seconds after the onset of the reaction.

In the reverse reaction, the oxidation of lactate, LDH definitely reacts with TDH · DPN at a slower rate than with free DPN, and the equilibrium constant is displaced towards lactate. These results are shown in Table 1. In this connection it was of interest to examine the influence of *p*-chloromercuribenzoate (PCMB) on the reaction of LDH and lactate with TDH · DPN, since it has been shown by Racker and Krimsky [20] that —SH— inhibitors affect the binding of DPN to TDP. As shown in Table 1, the reaction of LDH with TDH · DPN treated with PCMB proceeds at the same rate, and gives the same equilibrium constant as the reaction with free DPN. In contrast, incubation with iodoacetate (IAA) produced no effect, although TDH was completely inactivated by treatment with this inhibitor. Since Racker and Krimsky [20] have shown that IAA partially reverses the spectral shift obtained on combination of TDH with DPN, these observations suggest that the DPN nevertheless still remains attached to TDH.

Table 1. Oxidation of lactate by lactic dehydrogenase with free and TDH-bound DPN. The effect of iodoacetate and p-chloromercuribenzoate.

Coenzyme	Inhibitor *	Rate μM/sec	DPNH formed μM
Free	None	0.061	2.6
Free	Iodoacetate	0.065	2.5
Free	*p*-Chloromercuribenzoate	0.065	2.5
Bound	None	0.048	1.9
Bound	Iodoacetate **	0.043	1.8
Bound	*p*-Chloromercuribenzoate incubated 1 min.	0.064	2.5
	5 min.	0.061	2.5

Test conditions: Buffer 0.1 M glycine
DL-lactate: 8.3 mM
DPN, free or bound to TDH 8.2 μM
LDH: 6.8×10^{-9} M
Final pH = 9.0

* To TDH · DPN (25 μl, in phosphate $\mu = 0.1$, pH = 7.2) iodoacetate or *p*-chloromercuribenzoate to 5×10^{-2} M and 4.5×10^{-3} M, respectively, was added. Incubation at 0°. To the solutions with free DPN the same amounts of inhibitors were added.
** TDH was completely unable to oxidize G-3-P after incubation with iodoacetate.

Astrachan [6] has observed that DPN attached to reduced TDH reacts more slowly with a number of dehydrogenases than when attached to TDH in which some of the thiol groups had been oxidized. This is in contrast to our experiments with LDH as well as with those carried out with ADH from yeast and liver. Under our conditions it made no difference whether the solution of TDH was newly prepared, aged, or incubated with cysteine.

Table 2. Rate of oxidation of ethyl alcohol and glutamate by yeast ADH and glutamic dehydrogenase, respectively, using free DPN and DPN bound to TDH.

Enzyme	Concentration of Substrate mM	Concentration of DPN, free and bound μM	Rate of reduction of DPN:μM/sec.		DPNH formed μM	
			Free	Bound	Free	Bound
Yeast ADH	5	8.1	0.058	0.018	1.8	0.84
	50	8.1	—	—	4.6	2.4
Glutamic dehydrogenase	66	8.1	0.035	0.008	5.5	3.2

Buffer: phosphate $\mu = 0.1$ + M/1 000 versene; pH = 7.11; temperature 23.5° C.

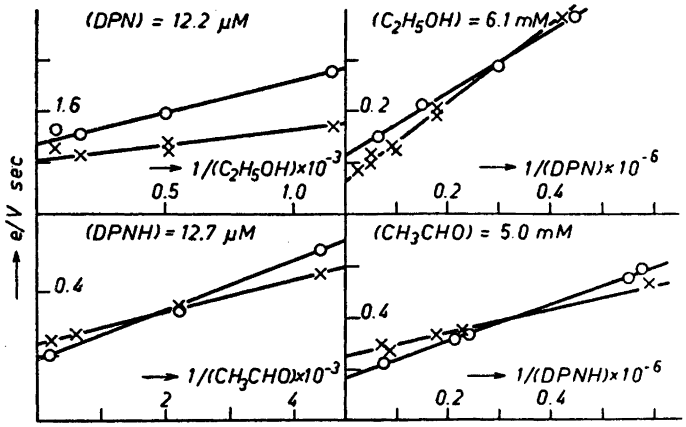


Fig. 3. Liver ADH, pH 8.8, 23° C. × Free DPN(H), O TDH bound DPN(H)

Interaction of yeast ADH and glutamic dehydrogenase with TDH·DPN

Some results obtained with these two enzymes are summarized in Table 2. The rate of reduction for TDH · DPN is much less than for free DPN and the equilibrium is shifted towards oxidized DPN. The reduction of acetaldehyde with bound DPNH was at least as fast as with free DPNH.

Interaction of liver ADH with TDH·DPN and TDH·DPNH

We have investigated the initial rates of the reactions of liver ADH with free and bound DPN(H), with varying concentrations of DPN(H), acetaldehyde, and alcohol. The results are shown in Fig. 3. It can be seen that the reaction with bound DPN(H) can be slower or faster than with free DPN(H), depending upon the concentrations of substrates and coenzyme. TDH · DPN did not oxidize acetaldehyde appreciably under the conditions used in these experiments.

The kinetics of the liver ADH system reacting with free DPN or DPNH have been satisfactorily interpreted according to the following equations [8]:

$$\text{ADH} + \text{DPNH} \underset{k_2}{\overset{k_1}{\rightleftharpoons}} \text{ADH} \cdot \text{DPNH} \qquad (1)$$

$$\text{ADH} \cdot \text{DPNH} + \text{ald} \underset{k_6}{\overset{k_4}{\rightleftharpoons}} \text{ADH} \cdot \text{DPN} + \text{alc.} \qquad (2)$$

$$\text{ADH} \cdot \text{DPN} \underset{k_3}{\overset{k_3}{\rightleftharpoons}} \text{ADH} + \text{DPN} \qquad (3)$$

Table 3. Reaction velocity constants — in the liver ADH system, using free DPN(H) and DPN(H) bound to TDH.

Velocity constants	Bound DPN	Free DPN
$10^{-6} \times k_1$	1.8	2.0
$10^{-6} \times k_5$	0.24	0.24
k_2	1.2	2.0
k_3	7.0	4.9
$10^{-6} \times [H^+]\ k_4$	0.019	0.022
$10^{-4} \times k_6$	0.38	0.58

Buffer: 0.1 M glycine + M/60 arsenate; final pH = 8.8; temperature 23.5° C.

In this scheme, no compound between substrate and enzyme is included. Such a complex is undoubtedly formed, but the kinetic data suggested that it must dissociate more rapidly (into product and ADH · DPN(H)) than does the protein · coenzyme complex, and that it therefore does not effect the kinetic constants indicated above. By means of the experimental data in Fig. 1 and the equilibrium constant we can test whether the above sequence of reactions is possible when the coenzyme is bound to TDH. The method of calculation of the constants k_1 ..... k_6 is the same as outlined previously [8], and the result is tabulated in Table 3. In Table 4 is shown the experimentally determined

Table 4. The equilibrium constant (K_{eq}) as related to reaction velocity constants for different reaction mechanisms [7,8,21].

Slow intramolecular transformation of ternary complex*, affinity of ADH for DPN(H) not influenced by substrate, or *vice versa* [21]. $K_{eq} = \frac{k_3 k_5 k_6}{k_1 k_2 k_4}$		Relative stable ADH·DPN(H) complexes, shortlived ternary complex formed [7,21] $K_{eq} = \frac{k_2 k_5 k_6}{k_1 k_3 k_4}$		A group in the enzyme is oxidized/reduced by substrate(or coenzyme) with the formation of enzyme-substrate intermediates [21]. $K_{eq} = \frac{k_6 k_5}{k_1 k_4}$		K_{eq} (Exptl.)	
Free DPN	Bound DPN	Free DPN	Bound DPN	Free DPN	Bound DPN	Free DPN	Bound DPN
$K \times 10^{11}$							
12	33	2.0	0.76	4.9	5.8	0.9	0.40

* ADH · DPN · alcohol ⇌ ADH · DPNH · aldehyde.

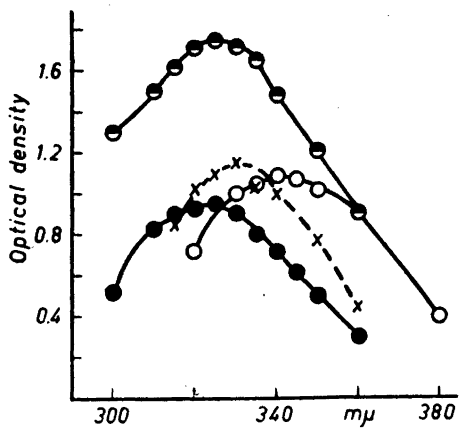


Fig. 4. Difference spectrum.
○ *TDH · DPN (0.05) + G-3-P (5) + arsenate (1)*
● *ADH (0.1) + DPN (0.13) + ethanol. (50)*
× *TDH · DPN (0.05) + ADH (0.1) + G-3-P (5) + arsenate (1)*
◓ *TDH · DPN (0.05) + ADH (0.1) + ethanol (50)*

Buffer: phosphate (100), final pH 7.2, in all experiments. Concentration in micromoles per 3 ml.

equilibrium constants, and the equilibrium constants calculated from k_1..... k_6 on the assumption of different reaction schemes [12].

It is problematic whether in the present system the constants mean what they say, but it is interesting that the association constants k_1 and k_5 of DPNH and DPN, respectively, are not significantly different, while k_2 is *increased* from 4.9 to 7.6 sec^{-1}, and k_3 is *decreased* from 2.0 to 1.2 sec^{-1}. The decrease in k_6 may also be significant, since the ratio k_6/k_4 which determines the equilibrium constant was decreased.

Interaction of Zwischenferment with TDH · DPN

If one dehydrogenase could react with PN bound to another PN-linked enzyme without the PN actually changing proteins during the course of the reaction, then it appears possible that a TPN linked enzyme might utilize bound DPN. The possibility whether a TPN specific enzyme might react with the bound DPN of TDH was therefore experimentally tested. In the presence of glucose-6-phosphate Zwischenferment reduced TPN at a rapid rate. When DPN was substituted for TPN, no reaction was detected. When TDH · DPN was substituted for TPN, still no reaction was detected.

The interaction of liver ADH with TDH · DPNH studied spectrophotometrically

Since liver ADH · DPNH has a markedly different spectrum in the 340 mμ region [2] than TDH · DPN, it was possible to test whether a significant number of DPNH molecules reside on the ADH protein during the reactions

of ethanol and liver ADH with TDH · DPNH. The results are shown in Fig. 4. When TDH · DPN is reduced by G-3-P, it gives a spectrum with a maximum at 340 mμ. When TDH · DPN is reduced by G-3-P in the presence of ADH, however, the maximum is shifted downward to 330 mμ. If ethanol was used as substrate, then the maximum was shifted down to 322 mμ, in the same region as the ADH · DPNH compound itself. Under these latter conditions, therefore, most of the DPNH molecules must have been bound to ADH.

These results indicate ADH can compete successfully with TDH for DPNH and that the substrate may have an effect on the affinity of the coenzyme. The dissociation constant for liver ADH · DPNH has been found to be 4×10^{-7}, the dissociation constant for TDH · DPNH has not been accurately determined, but it is known that it must be larger than the dissociation constant for TDH · DPN whose upper limit according to Velick and Hayes [10] is 2×10^{-7}. Our results suggest that the two dissociation constants (ADH · DPNH and TDH · DPNH) must be of the same order of magnitude.

The interaction of liver ADH with TDH · DPNH studied ultracentrifugally

When small amounts of another dehydrogenase are allowed to react with substrate quantities of TDH · DPN or TDH · DPNH, and the reaction proceeds rapidly, the two proteins must either form a complex which dissociates very readily or it is possible that a more stabile complex is formed and a rapid exchange reaction occurs. The possibility that a more stabile complex is formed in the ADH—TDH · DPNH reaction was tested ultracentrifugally in cooperation with A. Ehrenberg. Approximately equal molar concentrations of ADH and TDH · DPNH, both in 0.1 M phosphate, pH 7.4, were centrifuged at 59 000 RPM in the Spinco Model E ultracentrifuge. The sedimentation patterns were compared with those obtained by running the enzymes separately. Because of the sizeable difference in sedimentation constants of the two proteins, it was estimated that complexes involving 10 % of the molecules would be readily detectable. In actuality the peaks in the combined sample were of the same height and symmetry as in the uncombined single runs, thus indicating no detectable formation of stabile complexes between the two proteins.

DISCUSSION

The results obtained in these studies virtually eliminate the obligatory intermediation of free DPN in the reaction of various dehydrogenases with TDH · DPN and TDH · DPNH. This is obviously so in reactions where the rate of oxidation of TDH · DPNH was faster than with free DPNH, but it is also evident for reactions with TDH · DPN where observed rates were much too fast to be compatible with Velick and Haye's [10] estimate of upper limit of the dissociation constant (2×10^{-7} M). In agreement with interpretations placed by previous investigators in their work, these data are most easily interpretable on the basis of direct interactions of the two dehydrogenases themselves. This is not to say that the PN coenzyme remains immobile during the

reaction. Although our experiments permit no unequivocal conclusions to be drawn on this point, they suggest that the PN switches proteins during the reaction. The spectral shift observed during the reaction of ADH and ethanol with TDH · DPN indicates the formation of ADH · DPNH. The facts that specificity for a particular PN coenzyme is maintained, and also the reaction mechanism of the liver ADH, are most easily interpretable on the basis of a direct exchange of PN from TDH to apodehydrogenase during interaction of the proteins. The ultracentrifugal experiments suggest the complex of the two proteins to be readily dissociated at least for the case of TDH · DPN · ADH.

The kinetics of the reaction of liver ADH with TDH · DPN and TDH · DPNH do not appear to be markedly altered from the kinetics of its reaction with free DPN. The fact that under certain conditions different rate of reaction can be obtained with bound DPN compared with free emphasizes the fact that the turnover rate of the enzyme under usual assay conditions may not correspond to its turnover rate in the living cell.

It must be emphasized that in these experiments, enzymes from widely different sources were employed. In a given physiological system, subtile differences in individual enzymes might well elicit more specific and quantitatively greater effects than those observed. The fact remains, however, that all of the dehydrogenases studied behaved in nearly the same manner, they reacted slower with TDH · DPN and faster with TDH · DPNH compared to the free coenzyme. This indicates some change in the O/R potential of the coupled systems, and together with the observations that the substrate may affect the affinity of dehydrogenase for PN, provides the basis for possible selective interactions under *in vivo* conditions.

But it is perhaps most intriguing to consider the possibility in which certain enzymes along a given metabolic pathway were unable to react with bound PN, either because of structural organization, or chemical disinclination, and were dependent upon free PN for activity. This would provide a reasonable means for selecting important pathways, synthetic, or energy yielding, according to imposed conditions simply by regulating coenzyme levels. This argument needs not be restricted to PN coenzymes but can be extended to all of the so called mobile coenzyme systems.

We are indebted to Professor Hugo Theorell for his interest in this work. Thanks are also due to Miss Ann Louise Swanson for skilful technical assistance.

The expenses connected with this work have been partly covered by grants from *Knut och Alice Wallenbergs Stiftelse, The Rockefeller Foundation, Statens naturvetenskapliga forskningsråd* and *Statens medicinska forskningsråd.*

REFERENCES

1. Taylor, J. F., Velick, S. F., Cori, G. T., Cori, C. F. and Slein, M. W. *J. Biol. Chem.* **173** (1948) 619.
2. Theorell, H. and Bonnichsen, B. *Acta Chem. Scand.* **5** (1951) 1105.
3. Chance, B. in *The Mechanisms of Enzyme Action*, The Johns Hopkins Press 1954, p. 399.
4. Cori, G. T., Velick, S. F. and Cori, C. F. *Biochim. et Biophys. Acta* **4** (1950) 160.
5. Mahler, H. R. and Elowe, D. *Biochim. et Biophys. Acta* **14** (1954) 100.

6. Astrachan, in *The Mechanisms of Enzyme Action*, The Johns Hopkins Press 1954, p. 534.
7. Theorell, H. and Chance, B. *Acta Chem. Scand.* **5** (1951) 1127.
8. Theorell, H., Nygaard, A. P. and Bonnichsen, R. *Acta Chem. Scand.* **9** (1955) 1148.
9. Cori, G. T., Stein, M. W. and Cori, C. F. *J. Biol. Chem.* **173** (1948) 605.
10. Velick, S. F. and Hayes, J. *J. Biol. Chem.* **203** (1953) 545.
11. Straub, F. B. *Biochem. J. London* **32** (1940) 483.
12. Warburg, O. and Christian, W. *Biochem. Z.* **254** (1932) 438.
13. Neilands, J. B. and Åkeson, Å. *J. Biol. Chem.* **188** (1951) 1.
14. Nygaard, A. P. and Theorell, H. *Acta Chem. Scand.* **9** (1955) 1300.
15. Meyerhof, O. *Bull. soc. chim. biol.* **20** (1938) 1032.
16. Velick, S. F., Hayes, J. E. and Harting, J. *J. Biol. Chem.* **203** (1953) 527.
17. Rafter, G. W., Chaykin, S. and Krebs, E. G. *J. Biol. Chem.* **208** (1954) 799.
18. Bücher, T. and Garbade, K.-H. *Biochim. et Biophys. Acta* **8** (1952) 222.
19. Theorell, H. and Nygaard, A. P. *Acta Chem. Scand.* **8** (1954) 1649.
20. Racker, E. and Krimsky, I. *J. Biol. Chem.* **198** (1952) 731.
21. Alberty, R. A. *J. Am. Chem. Soc.* **75** (1953) 1928.

Received October 4, 1955.

ACTA CHEMICA SCANDINAVICA 10 (1956) 49—55

The Rate of Swelling of Ion-Exchange Resin Particles in Different Salt Solutions

CARLOS PULIDO*

Institute of Physical Chemistry, University of Uppsala, Sweden

This note has been published mainly to point out the possibilities of the photographic method used and to show the length of time required for volume changes of ion exchange resin particles due to exchange of ions. Figures 5 to 10 are self-explanatory and it is seen that there is a marked difference in behaviour of the resin for different types of ions and valencies. It is also seen that the time required for these volume changes is such that they can be conveniently followed by the method used. As it seems of interest from many points of view to study the kinetic properties of ionic exchange resins in more detail in this way, a systematic investigation has now been undertaken and it has been found that the pretreatment of the resin is of the greatest importance in determining its behaviour.

Several papers have been presented during the last few years on the study of the swelling of ion-exchange resins, as well as on the diffusion of solutions in these resins. These, however, have dealt with columns or beds of resins.

Thus Boyd *et al.*[1] have used the same shallow bed arrangement used by Domaine *et al.*[2] The amount of exchanger they used was 100 mg or 10 mg depending on the concentration of the solutions. When the amount was 10 mg the shallow bed was a cylinder, roughly three particle diameters deep and about twenty particles in diameter. Hale and Reichenberg[3] have used a modification of Boyd's method[1] or, in the case of sulphonated cross-linked polystyrene, another method in which the hydrogen form of the resin was stirred with a solution in the presence of an indicator. Kressman and Kitchener[4] have employed for their experiments the limited bath method with a large number of particles — about 500.

Many other papers have been published on this subject but in all of them the resins were studied in quantities of at least about a hundred particles.

* Present address: Centros de Estudos da Energia Nuclear, Instituto Superior Técnico, Lisboa, Portugal.

Therefore it should be interesting to study the individual behaviour of the resin particles, and work is being carried on with this aim in view. The purpose of this paper is to present the first results.

RELATION BETWEEN SWELLING AND DIFFUSION

According to Boyd, Adamson and Myers [1], there are three principal stages to be considered in the mechanism of swelling, and each of them may be rate-controlling under appropriate conditions:

I. Diffusion of ions through a thin film of liquid surrounding the particles (or through liquid in macropores inside the particles).

II. Diffusion of ions through the resin material itself.

III. The chemical process of exchange.

However, diffusion in and through the solid material is rate-determining for the more concentrated solutions [1], about 0.1 N.

As the exchange reaction is accompanied by a change of volume, this change should be related to the diffusion inside the particles for concentrations in which this diffusion is rate-controlling. Actually, using 0.5 M solutions, values were found for the swelling of the particles which substantiated this relation.

MATHEMATICAL EQUATIONS

The diffusion of a liquid inside the spherical particles follows the same law as that of the heat transport in spheres [5].

The appropriate equation is

$$\frac{\partial u}{\partial t} = D^i \left(\frac{\partial^2 u}{\partial x^2}\right) \tag{1}$$

where

u $= C^s r$

r = radius of the spherical surface at a concentration C^s in the solid

D^i = internal diffusion coefficient

The solution of this equation was given by Barrer [6] and by Boyd [1]

$$C^s = kC^l + \frac{1}{r}\,(k\ C^l - C^s_0)\,\frac{2r_0}{\pi}\sum_{n=1}^{\infty}\frac{(-1)^n}{n}\sin\frac{n\pi r}{r_0}\cdot e^{-D^i n^2 t / r_0^2} \tag{2}$$

where

k = the distribution coefficient defined by $C^s_e = k\ C^l_e$

C^s_e = the equilibrium concentration in the solid

C^l_e = the equilibrium concentration in the liquid

C^s_0 = the initial concentration of adsorbate in the solid

r = the radius of the spherical adsorbent particle

r_0 = the initial radius of the spherical adsorbent particle.

The rate of permeation, P, *i. e.* the quantity transferred/unit time/unit area of unit thickness under a standard concentration difference is

$$P = -D^i \left(\frac{C^s}{r}\right)_{r=r_0} \tag{3}$$

and the total quantity of solution which crosses the unity of area in the time t is:

$$q = \int_0^t P \, dt \tag{4}$$

Supposing the initial concentration in the solid is zero, we obtain, from eqns. (2), (3) and (4)

$$q = \frac{2r_0}{\pi^2} \, k \, C^1 \left[\sum_{n=1}^{\infty} \frac{1}{n^2} \, e^{-D^i n^2 \pi^2 t / r_0^2} - \sum_{n=1}^{\infty} \frac{1}{n^2} \right] \tag{5}$$

The total quantity adsorbed, will be:

$$Q = 4 \, \pi \, r_0^2 \, q \tag{6}$$

and Q_∞ being the amount adsorbed at equilibrium ($t = \infty$), the expression for the fractional attainment of equilibrium, may be written [1]

$$F = \frac{Q}{Q_\infty} = 1 - \frac{6}{\pi^2} \sum_{n=1}^{\infty} \frac{1}{n^2} \, e^{-D^i \pi^2 n^2 t / r_0^2} \tag{7}$$

since

$$\sum_{n=1}^{\infty} \frac{1}{n^2} = \frac{\pi^2}{6}$$

Boyd [1] also gives the following solution for cases where the adsorbing particles are not spheres but slabs:

$$F = 1 - \frac{8}{\pi^2} \sum_{n=1}^{\infty} \frac{1}{(2n-1)^2} \, e^{-(2n-1)^2 \frac{\pi^2 D^i t}{4 \, x_0^2}}$$

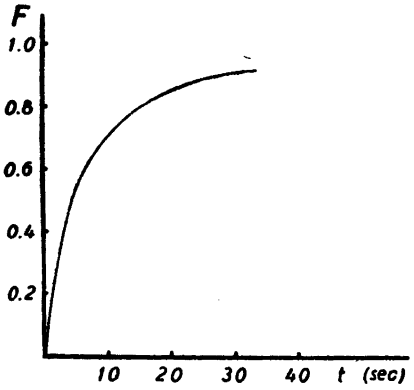
where x_0 is the half-thickness of the slab. However, the equation for the spheres is more in agreement with experimental data.

Fig. 1 shows the curve corresponding to the equation (7) in which $\frac{D^i}{r_0^2}$ has the value 0.74×10^{-2}.

EXPERIMENTAL

a) *Preparation of materials.* A sulphonated cross-linked polystyrene ion-exchanger was employed. This synthetic resin showed great swelling owing to the low level of cross-linkage. The particles were air dried and granulometrically classified and a few spherical grains with diameters between 0.1 and 0.2 mm were taken from it. The following process was used for the choice of these grains:

A few grains were taken and placed on a slanted plate of glass or polished metal. Tapping gently on the plate, the spherical particles rolled down while the others remained on the plate.



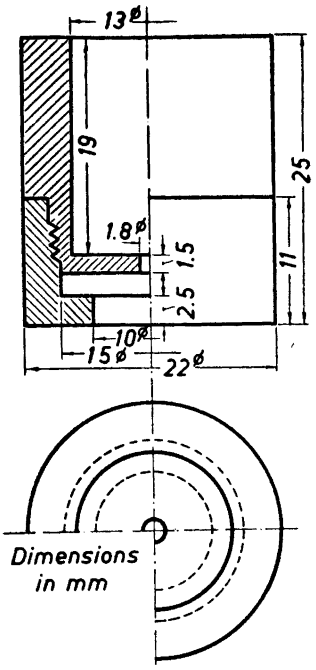


Fig. 1. Curve corresponding to eqn. (7). *Fig. 2. Cylindrical cell containing the resin.*

The spherical particles were gathered into a small container and were prepared as follows: washed, first with HCl, then with distilled water and finally with NaCl. This process was repeated and the particles were then placed in a small cylindrical cell (Fig. 2).

b) *Experimental procedure.* The rate of swelling was determined simply by photographing the particles at regular time intervals. The instrument employed to obtain the values of swelling is shown in Fig. 3.

A known number of spherical particles of resin was placed in the cell. The excess liquid was taken out by means of a curved pipette leaving only enough to cover the resin particles. By means of another pipette HCl was poured into the cell in such a way as to allow the particles to remain unmoved. They were kept there for 6 to 8 hours and then, using the same process the HCl was taken out and NaCl poured into the cell. After another period of 6 to 8 hours the same technique was repeated for three days running. After this preparation the resin was in good condition for measurements.

The concentration of the solutions was 0.5 M for NaCl, KCl, NH_4Cl, $BaCl_2$ and $LaCl_3$, 0.001 M for $BaCl_2$ and 0.5 M for HCl. The technique used was as follows: A photograph was taken of a known number of resin particles placed in the cell, in a given solution (Fig. 4). Afterwards the upper part of the liquid was taken out leaving only the minimum to keep the particles immersed. The solution containing the cation to exchange was then poured into the cell carefully by means of a curved pipette. The time was counted from the moment this solution came into contact with the resin, and two seconds later the first photograph was taken. More photographs were taken at intervals varying according to the reaction under study.

The system has no shutter as it was handled in a dark room and the exposure time was controlled by the lamp S. The diameters of the particles were thus measured in each

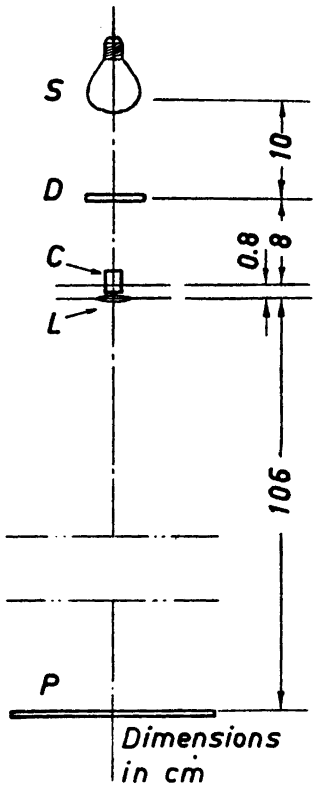


Fig. 3. Arrangement for determination of swelling. S lamp; D diaphragm; C cell containing the resin; L lens; P photographic plate. A 150 w, 220 V normal lamp was used. The lens was a microscope lens which could give a suitable enlargement (about 60 times). The photographic plates used were Gevaert Superchrome 32°. Exposure time about 3/4 sec.

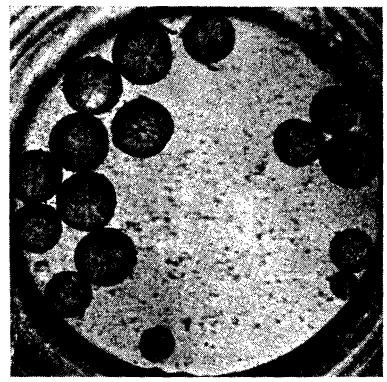


Fig. 4. Resin particles photographed as described in the text.

photograph, provided they had not moved. The average value of the diameters was then computed for each plate. The increasing or decreasing percentage of this average diameter, Δ ø (%), was then plotted against time.

EXPERIMENTAL CURVES

Figures 5 to 10 show the curves obtained, as explained above, with a synthetic resin of the sulphonated cross-linked polystyrene type and the cations mentioned. In each figure there are two curves, one obtained by measuring the diameters of particles which have first adsorbed hydrogen ions from HCl and then cations to be exchanged from the salt. The other curve was obtained

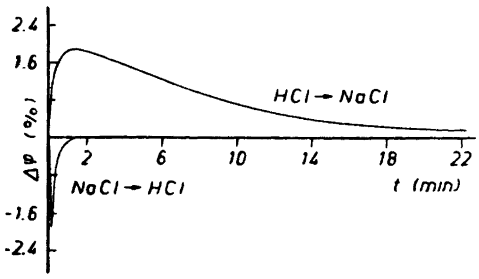


Fig. 5. Particles treated with 0.5 M HCl and 0.5 M NaCl.

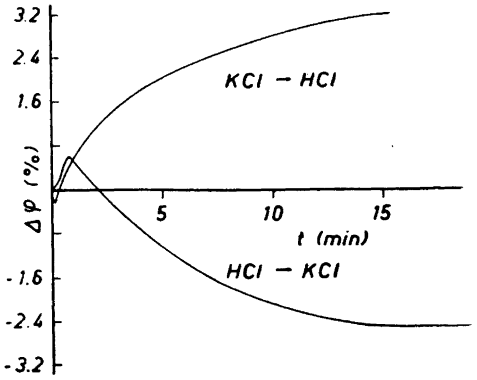


Fig. 6. Particles treated with 0.5 M HCl and 0.5 M KCl.

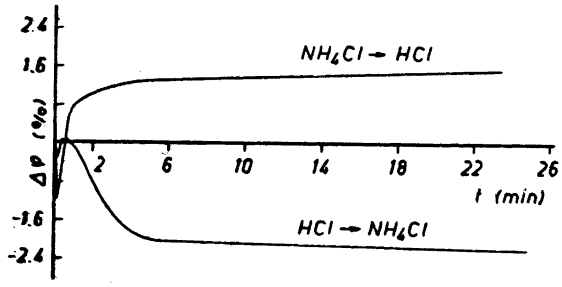


Fig. 7. Particles treated with 0.5 M HCl and 0.5 M NH_4Cl.

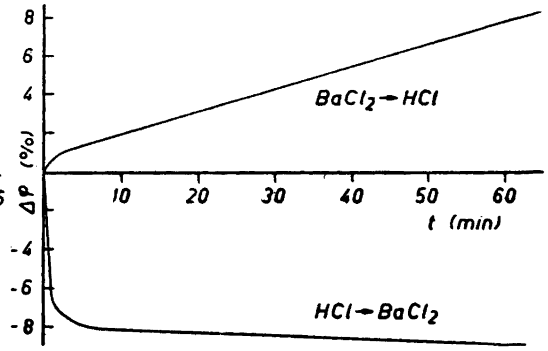


Fig. 8. Particles treated with 0.5 M HCl and 0.5 M $BaCl_2$.

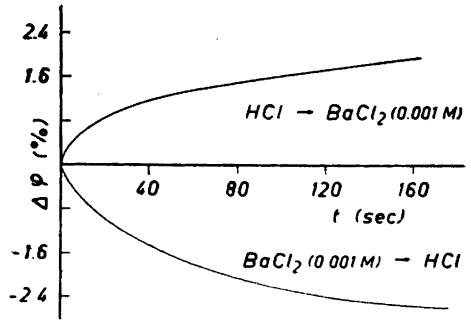


Fig. 9. Particles treated with 0.5 M HCl and 0.001 M $BaCl_2$.

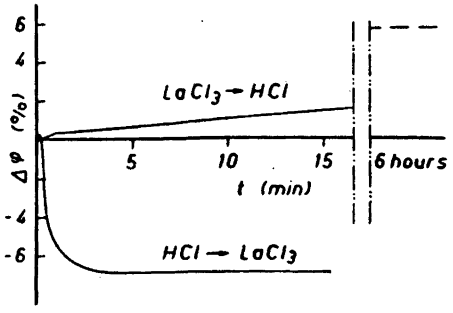


Fig. 10. Particles treated with 0.5 M HCl and 0.5 M $LaCl_3$.

in the opposite way, *i. e.*, the particles were in a salt solution and a hydrochloric acid solution was added. The statistical deviation range is between 0.08 and 0.1 %.

Acknowledgements. The author wishes to express his gratitude to Prof. Stig Claesson, Head of the Institute of Physical Chemistry of the University of Uppsala, and to all the staff of the same institute for their most valuable advice and discussions. He is also very grateful to *Instituto de Alta Cultura*, Lisboa, Portugal, for the fellowship granted to him.

REFERENCES

1. Boyd, G. E., Adamson, A. W. and Myers Jr., L. S. *J. Am. Chem. Soc.* **69** (1947) 2836.
2. du Domaine, J., Swain, R. L. and Hougen, O. A. *Ind. Eng. Chem.* **35** (1943) 546.
3. Hale, D. K. and Reichenberg, D. *Discussions Faraday Soc.* **7** (1949) 79.
4. Kressman, T. R. E. and Kitchener, J. A. *Discussions Faraday Soc.* **7** (1949) 90.
5. Carslaw, H. S. and Jaeger, J. C. *Conduction of Heat in Solids.* Oxford 1947.
6. Barrer, R. M. *Diffusion in and through Solids.* Cambridge Press 1941.

Received October 10, 1955.

ACTA CHEMICA SCANDINAVICA 10 (1956) 56—71

Cholyl-S-CoA as an Intermediate in the Conjugation of Cholic Acid with Taurine by Rat Liver Microsomes

JON BREMER*

Norsk Hydro's Institute for Cancer Research, The Norwegian Radium Hospital, Oslo, Norway

The conjugation of cholic acid with taurine has been investigated.

The conjugation required the presence of coenzyme A (CoA) and adenosinetriphosphate (ATP) and was stimulated by magnesium, manganese, and fluoride and in some cases by cysteine and glutathione.

Cystine, pyrophosphate and adenosine-5-phosphate (AMP) inhibited the conjugation.

When hydroxylamine was added to the incubation medium, cholhydroxamic acid was identified as the reaction product.

A reaction mechanism, involving cholyl-S-CoA as an intermediate and AMP and pyrophosphate as reaction products, has been proposed.

In previous studies [1-3] we have shown that the enzyme system performing the conjugation of cholic acid with taurine or with glycine, was localized in the microsomic particles of the rat liver cell. When isolated microsomes were used, ATP and a heat stable factor in the particle free supernatant were found to be required in the conjugation. This factor was presumed to be CoA.

In the present paper further studies on the reaction mechanism are presented. A preliminary report on the results has been published [4].

MATERIALS AND METHODS

The biological conjugation of cholic acid with taurine was followed by means of ^{35}S-labelled taurine as earlier described [1]. The labelled taurine was synthesized according to Eldjarn [5], and the synthesis was kindly performed by L. Eldjarn and P. Fritzson in this institute.

A 75 % pure CoA, crystalline ATP (potassium salt), and ADP (sodium salt) were obtained from Nutritional Biochemicals Corporation, Cleveland, U. S. A.

A 2 % CoA preparation and tri-(hydroxymethyl)-amino-methane (TRIS) were obtained from Zigma Chemical Company, USA.

* Fellow of the Norwegian Cancer Society.

Preparation of rat liver microsomes

Livers from male rats of a mixed strain were used. The liver weights were usually 6—8 g. After preliminary slicing, the livers were homogenized in four parts 10 % sucrose for approximately 1½ minutes in a glass homogenizer with a plastic pestle doing 1 500 rev/min. Cell debris, nuclei and mitochondria were sedimented by centrifuging at 15 000 —18 000 × g for 15 minutes. The microsomic fraction was then sedimented at 25 000 × g for 110 minutes. The particle free supernatant was discarded, leaving behind the densely packed microsomic particles as a translucent cake of the typical red colour. All isolating operations were performed at 0° C. The sedimented microsomes were stored at —20° C until used.

Preparation of cholhydroxamic acid

The cholhydroxamic acid was synthesized from cholic acid ethyl ester prepared according to Bondi and Müller [6]. The cholic acid ethyl ester was converted to the hydroxamic acid by a modification of the method used by Kornberg and Pricer [7] in their preparation of fatty hydroxamic acids: 2.5 g of ethyl ester and 1 g of hydroxylamine hydrochloride were dissolved in 35 ml of absolute methanol in which 1.2 g metallic sodium had been dissolved beforehand. The mixture was refluxed for 30 minutes on a boiling water bath and neutralized with a mixture of one part concentrated hydrochloric acid in ten parts of absolute ethanol. Two volumes of ethyl ether were added and the precipitated salts filtered off. The filtrate was then evaporated to dryness under reduced pressure. The yellowish residue consisted of almost pure hydroxamic acid. The product was dissolved in 25 ml absolute ethanol, and 150 ml ethyl acetate was added. After storing overnight at 5° C, the precipitate which formed was filtered off and discarded. The clear filtrate was slowly evaporated to 1/5—1/10 of the original volume by passing a stream of air over the surface of the fluid. The hydroxamic acid then started to crystallize in rosettes. After storing overnight at —20° C, 2.15 g of the crystalline compound could be filtered off. When dried at 4 mm pressure and 80° C for 5 hours, the weight decreased by about 10 %. Recrystallization of the product with the same evaporation procedure gave no detectable change in purity as estimated from the colour reaction with ferric ions. The compound decomposed at 117° and was completely melted at 145° C. Elementary analysis showed (theoretical values in brackets): Carbon 68.22 % (68.39), hydrogen 9.54 % (9.39), nitrogen 3.31 % (3.64). When dissolved in concentrated sulphuric acid, the cholhydroxamic acid was shown to have light absorption spectrum and extinction coefficients between 220 and 600 mμ identical with those reported for cholic acid, taurocholic acid and glycocholic acid [8,9]. The compound gave the typical cherry-red colour of hydroxamic acids with ferric ions in acid solution [10]. The elaboration of two spectrophotometric methods for the estimation of biologically formed cholhydroxamic acid were based on these results.

Chromatographic and spectrophotometric estimation of cholhydroxamic acid

To estimate the cholhydroxamic acid formed in the incubation experiments, the acid was extracted from the incubation mixture with 1/3 volume *n*-butanol as described for the isolation of taurocholic acid [1].

Method 1. When the cholhydroxamic acid was estimated from its light absorption in concentrated sulphuric acid, the acid was separated from the unchanged cholic acid using a modification of Sjövall's [11] quantitative paper chromatography for conjugated bile acids. Paper pretreatment and stationary phase were identical with those described by Sjövall [11, 12]. Aliquots of 0.05 ml of butanol extract were put on the paper. Descending chromatography was used. As moving phase a mixture of one part *n*-butanol and two parts petroleum spirit (b. p. above 120° C) saturated with 4 % acetic acid was used. In this system the cholhydroxamic acid moved with an R_F value of 0.20—0.25 and the cholic acid with an R_F value of 0.40—0.45. There was some tailing on the paper, but a complete separation of the compounds was easily obtained. Further details of the method have been described by Sjövall [11].

Table 1. The extraction of cholhydroxamic acid with n-*butanol.*

Each vessel contained 1.5 ml 0.1 M potassium phosphate buffer (pH 7.2) and 0.5 ml *n*-butanol. After equilibration in a shaking machine for 25 minutes, 0.25 ml butanol phase was pipetted off and the content of hydroxamic acid determined according to method 2 (see text).

μmoles cholhydroxamic acid added per vessel		Density read at 525 mμ	
0.19	0.19	0.087	0.090
0.47	0.47	0.184	0.191
1.18	1.18	0.447	0.449
2.36	2.36	0.870	0.873
1.18 + microsomes from 500 mg liver		0.433	0.426

Method 2. As cholic acid gave no colour reaction with ferric ions, no chromatographic separation of the cholic acid and the cholhydroxamic acid was necessary. Aliquots of 0.25 ml of the butanol extract were diluted to 2 ml with the colour reagent, consisting of 0.33 % ferric chloride and 0.2 % perchloric acid in absolute ethanol. The density of the solution was measured in a 1 cm cuvette at 525 mμ. A solution containing 1 μmole hydroxamic acid per ml gave an extinction of 1.26 when measured in a Hilger quartz spectrophotometer, *i. e.* the $\varepsilon^{525}_{\mu mole} = 1\,260$.

The two analytical methods gave results in good agreement as seen from Table 4.

The extraction method had to be calibrated. For this purpose a series of vessels containing 1.5 ml of 0.1 M potassium phosphate buffer (pH 7.2) and 0.5 ml *n*-butanol were prepared. Known amounts of hydroxamic acid were dissolved in the added butanol beforehand. After 25 minutes' equilibration in a shaking machine, the colour developed by 0.25 ml butanol phase was measured in the usual way. As seen from Table 1, the extinction coefficient was proportional to the amount of hydroxamic acid added, and it was not significantly affected by addition of rat liver microsomes in amounts used in the incubation experiments.

EXPERIMENTAL

Before use, the microsomes stored in the frozen condition were thawed at 37° C and resuspended in 10 % sucrose by means of the homogenizer and pipetted as such. Microsomes from 300—500 mg of fresh liver were added to each vessel in the incubation experiments. The following concentrations were maintained in the incubation mixture if not otherwise stated: Potassium phosphate buffer (pH 7.4) 0.0022 M, potassium fluoride 0.2 M, magnesium sulphate 0.001 M, coenzyme A approximately 0.001 M, cysteine 0.0067 M. Cholic acid and ^{35}S-taurine were added as stated under the individual experiments. The incubation was performed at 37° C. Total volume was 1.5 ml per vessel. The results are given as micromoles taurocholate formed per vessel.

The pH-effect was evaluated in the following way: A solution containing all the factors needed for the reaction except the microsomes was prepared, using a phosphate buffer of pH 6.0. This solution was made more and more alkaline by adding normal potassium hydroxide under the control of a pH-meter. Aliquots of 1.4 ml were pipetted off when suitable pH-values were reached. The microsome suspension was later added before incubation without any further adjustment of pH. The diluting effect of the added potassium hydroxide solution did not exceed 2—3 %.

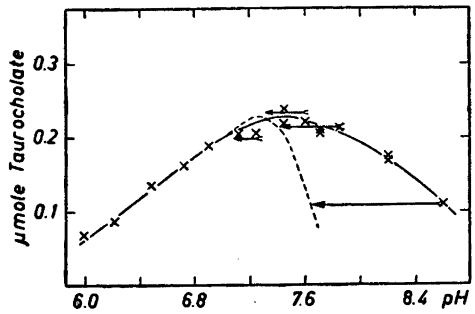


Fig. 1. The effect of pH. Microsomes from approx. 300 mg fresh liver per vessel. ^{35}S-taurine 0.8 µmoles/vessel, cholic acid 2 µmoles/vessel, ATP 4 µmoles/vessel, CoA (2 %) 3 mg/vessel. Potassium phosphate buffer 0.044 M, glutathione 0.0022 M, $MgSO_4$ 0.0025 M, NaF 0.15 M. Incubation time 90 minutes. The arrows indicate the fall of pH during incubation.

RESULTS

Effect of pH

The effect of pH on the conjugation of cholic acid with taurine is shown in Fig. 1. The pH optimum was found to be in the range 7.3—7.6 which is in good agreement with our earlier results when a system of microsomes and particle free supernatant was used [2]. As the buffering capacity of phosphate rapidly decreases at pH values above 7.5, the fall of pH during incubation was measured in some vessels. As indicated by the arrows in Fig. 1, there was a rather large fall in the pH values in the alkaline end of the curve. The decrease in conjugating capacity was therefore probably more abrupt with increasing pH than shown in the curve. A similar pH optimum has been found in the hippuric acid synthesis [13] and in the acetate activation [14]. In all later experiments, the incubation mixtures were adjusted to a pH of 7.40—7.45.

Effect of coenzyme A, glutathione, cysteine and cystine

Fig. 2 shows that there was an absolute requirement for CoA in the conjugation of cholic acid with taurine, and the results obtained with the two different CoA preparations used, showed that probably no other components of the CoA concentrates had any stimulating effect on the process.

Figs. 3 and 4 show that glutathione and cysteine had no significant stimulating effect when the 75 % pure CoA was used. The sulphydryl content of this preparation was titrated according to the method of MacDonnell *et al.*[15]. A sulphydryl content of 1.1 µmoles/mg was found, in good agreement with a content of 75 % CoA in the reduced form. The effect of cysteine and glutathione was therefore probably due to their reducing properties which kept the sulphydryl group of CoA in the reduced form. This sulphydryl group is known to be the functioning group of CoA [16], and other sulphydryl containing com-

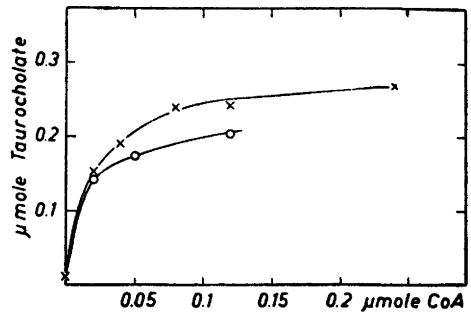


Fig. 2. Effect of CoA. Microsomes from approx. 500 mg liver. ^{35}S taurine 2 µmoles/vessel, cholic acid 2 µmoles/vessel, ATP 4 µmoles/vessel. Potassium phosphate buffer 0.026 M, glutathione 0.0022 M, $MgSO_4$ 0.0025 M, KF 0.15 M. Incubation time 120 minutes. +−+−+−+− *2 % CoA,* O−O−O−O− *75 % CoA.*

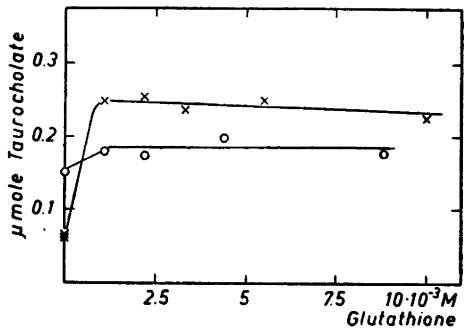


Fig. 3. Effect of glutathione. Microsomes from approx. 500 mg liver. ^{35}S-taurine 2 µmoles/vessel, cholic acid 2 µmoles/vessel, ATP 4 µmoles/vessel, CoA approx. 0.1 µmoles/vessel. Potassium phosphate buffer 0.022 M, $MgSO_4$ 0.0025 M, KF 0.15 M. Incubation time 120 minutes. +−+−+−+−+ *2 % CoA,* O−O−O−O−O *75 % CoA.*

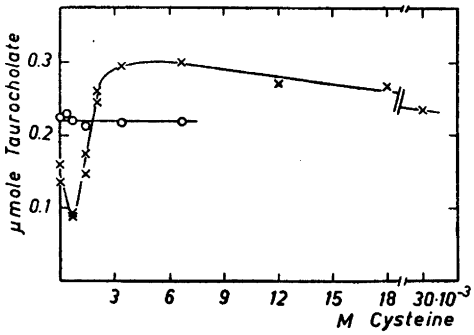


Fig. 4. Effect of cysteine. Microsomes from approx. 500 mg liver. ^{35}S-taurine 2 µmoles/vessel, cholic acid 2 µmoles/vessel, ATP 4 µmoles/vessel, CoA approx. 0.15 µmoles/vessel. Potassium phosphate buffer 0.024 M, $MgSO_4$ 0.0025 M, KF 0.15 M. Incubation time 120 minutes. +−+−+−+−+ *2 % CoA,* O−O−O−O *75 % CoA.*

Table 2. Effect of cysteine and cystine.

Microsomes from 500 mg liver. ^{35}S-taurine 2 μmoles/vessel (= 16 500 c/min/vessel), cholic acid 2 μmoles/vessel, ATP 4 μmoles/vessel, CoA approx. 0.15 μmoles/vessel. Potassium phosphate buffer 0.024 M, $MgSO_4$ 0.0025 M, KF 0.15 M. Incubation time 120 minutes.

Addition	75 % CoA		2 % CoA	
	Net c/min/0.1 ml butanol extract	μmoles taurocholate/vessel	Net c/min/0.1 ml butanol extract	μmoles taurocholate/vessel
None	247 252	0.23	177 151	0.15
Cysteine 6.7×10^{-4} M	242	0.22	104 100	0.09
Cysteine 3.3×10^{-3} M	280 240	0.24	322	0.29
Cystine in substance	65	0.06	78 104	0.08

pounds have been shown to protect it [17, 18]. Fig. 4 shows a peculiar inhibiting effect of cysteine in low concentrations. This inhibition was reversed by cysteine in higher concentrations. A correct explanation of this phenomenon cannot be given with any certainty, but from Table 2 it is seen that cystine had an inhibiting effect of the same magnitude. We have therefore presumed that cysteine in low concentrations catalyzes the oxidation of the CoA sulphydryl groups by some oxidizing contaminant in the 2% CoA preparation.

In higher concentrations both cysteine and glutathione had a weakly inhibiting effect, as is evident also from Table 4.

Effect of fluoride

Fluoride has been used in ATP-dependent reactions to depress ATP-ase and pyrophosphatase activity [19, 20]. Fig. 5 shows that fluoride had a profound stimulating effect in our experiments, and the optimal concentration was found to be astonishingly high (0.15—0.20 M). The ATP-ase activity of microsomes has been reported to be moderate [21]. We have therefore made some experiments to elucidate any possible additional effect of fluoride. Fig. 6 shows the time curves with and without fluoride. The initial reaction rate seemed to be nearly the same in both cases. To exclude the possibility that fluoride prevented an inactivation of the enzyme system, the experiment shown in Table 3 was undertaken. Inactivation could not explain the rapidly de-

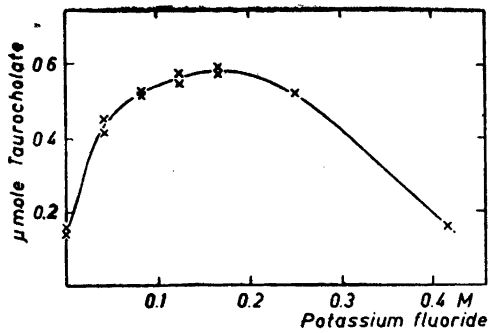


Fig. 5. Effect of fluoride. Microsomes from approx. 500 mg liver. ^{35}S-taurine 2 µmoles/vessel, cholic acid 2 µmoles/vessel, ATP 4 µmoles/vessel, CoA (2 %) approx. 0.1 µmole/vessel. Potassium phosphate buffer 0.020 M, $MgSO_4$ 0.002 M, cysteine 0.0055 M. Total volume 1.8 ml. Incubation time 120 minutes.

creasing reaction rate when fluoride was omitted, as addition of another batch of ATP after 25 minutes resulted in an increased amount of taurocholic acid, whereas addition of another batch of microsomes had no effect. The effect of fluoride therefore seemed to be a saving of ATP, probably through the inhibition of ATP-ase present in the microsomes [21]. In an unpublished experiment an equivalent amount of potassium chloride was added instead of potassium fluoride. No effect on the conjugation was observed, neither stimulating nor inhibiting, showing that the stimulation was due to the fluoride ion, and not to an osmotic effect or to the potassium.

Effect of microsomes

When microsomes from less than approximately 500 mg of fresh liver were added to the vessels, the amount of taurocholate formed was proportional to

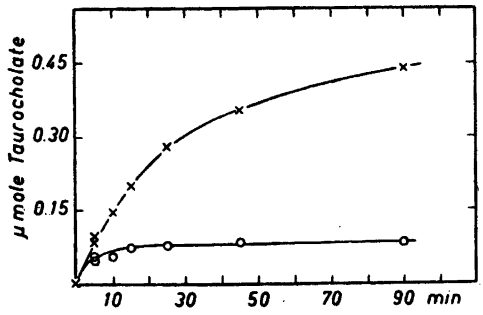


Fig. 6. Time curves with and without fluoride. Microsomes from approx. 500 mg liver. ^{35}S-taurine 0.8 µmoles/vessel, cholic acid 2 µmoles/vessel, ATP 10 µmoles/vessel, CoA (75 %) 0.1 µmole/vessel. Potassium phosphate buffer 0.022 M, $MgSO_4$ 0.001 M. +—+—+—+—+ *0.2 M KF,* O—O—O—O—O *No KF.*

Table 3. Effect of ATP-ase present in the microsomes.

Microsomes from 500 mg liver. ^{35}S-taurine 0.8 μmoles/vessel (= 17 000 c/min/vessel), cholic acid 2 μmoles/vessel, ATP 10 μmoles/vessel, CoA (75 %) 0.15 μmoles/vessel. Potassium phosphate buffer 0.022 M, total volume: first 25 minutes 1.2 ml, next 50 minutes 1.5 ml.

Additions and incubation conditions	Net c/min/0.1 ml butanol extract		μmoles taurocholate formed per vessel	
Reaction stopped after 25 min.	438	441	0.15	0.15
0.3 ml 1.15 % KCl added after 25 min. Reaction stopped after 75 min.	473	495	0.17	0.17
10 μmoles ATP added after 25 min. Stopped after 75 min.	784	843	0.28	0.30
Microsomes from 500 mg liver added after 25 min. Stopped after 75 min.	343	404	0.12	0.14
300 μmoles KF added after 25 min. Stopped after 75 min.	477	524	0.17	0.18

the amount of microsomes added (Fig. 7). Microsomes from 300—500 mg of fresh liver were therefore used in the experiments.

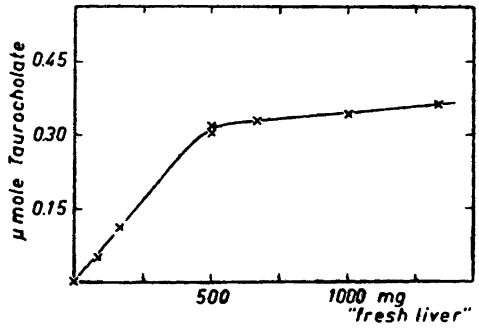


Fig. 7. Effect of microsomes. ^{35}S-taurine 2 μmoles/vessel, cholic acid 2 μmoles/vessel, ATP 4 μmoles/vessel, CoA (75 %) 0.15 μmoles/vessel. Potassium phosphate buffer 0.022 M, KF 0.2 M. Incubation time 120 minutes.

Cholhydroxamic acid formation

The requirement for CoA in the conjugation of cholic acid with taurine made it probable that an "activated cholic acid" in the form of cholyl-S-CoA represented an intermediate in the reaction. As hydroxylamine is known to react spontaneously with acyl-S-CoA at *ca.* pH 7 to form hydroxamic acids [7,19,22] the hydroxylamine represents a trapping agent for such activated carboxyl groups. Table 4 shows that cholhydroxamic acid was formed during the incubation when hydroxylamine was added to the incubation mixture instead of taurine. There was the same dependance on CoA, ATP and fluoride in this reaction as in the formation of taurocholic acid.

As expected cysteine was found to have no effect on the hydroxamic acid formation in this experiment, as the 75 % pure reduced CoA was used.

The same formation of cholhydroxamic acid has been reported in a short communication by Elliott [23].

Effect of preincubation without taurine

Further support for the existence of cholyl-S-CoA as an intermediate was obtained from the experiment cited in Table 5. An intermediate must have

Table 4. The formation of cholhydroxamic acid.

Complete system: Microsomes from approx. 500 mg liver, ATP 0.0067 M, CoA (75 %) 0.0001 M, cysteine 0.0067 M, potassium phosphate buffer 0.022 M, $MgSO_4$ 0.002 M, KF 0.2 M. Expt. I: ^{35}S-taurine 0.8 μmoles/vessel (= 25 000 c/min/vessel), cholic acid 2 μmoles/vessel. Total volume 1.5 ml. Expt. II: Hydroxylamine 50 μmoles/vessel, cholic acid 1 μmole/vessel. Total volume 1.75 ml. Incubation time 90 minutes.

Factor *excluded* from complete system	Experiment 1 μmoles taurocholate formed per vessel		Experiment 2 μmoles hydroxamic acid formed per vessel			
			$FeCl_3$-method		H_2SO_4-method	
None	0.27	0.31	0.73	0.77	0.63	0.65
Cholic acid	0	0	0.07	0.07	0	0
Potassium fluoride	0.12	0.12	0.43	0.43	0.38	0.37
ATP	0	0	0.05	0.05	0	0
CoA	0	0	0.10	0.10	0.06	0.13
Cysteine	0.34	0.35	0.77	0.78	0.77	0.76
Mg^{++}	0.36	0.41	0.68	0.67	0.67	0.66
Hydroxylamine	—	—	0.02	0.02	0	0.05

Table 5. Effect of preincubation without taurine.

Microsomes from approx. 500 mg liver. ^{35}S-taurine 0.8 μmoles/vessel (= 16 900 c/min/vessel), cholic acid 2 μmoles/vessel CoA (75 %) 0.3 μmoles/vessel, ATP 20 μmoles/vessel. Potassium phosphate buffer 0.022 M, KF 0.2 M. Total volume during preincubation 1.4 ml, after preincubation 1.5 ml.

Incubation conditions	Net c/min/0.1 ml butanol extract		μmoles taurocholate formed per vessel	
Complete system incubated for 9 min.	209	219	0.077	0.074
Preincubated for 10 min. without taurine, further for 9 min. with taurine	253	260	0.089	0.092

accumulated during the preincubation, as the reaction rate after addition of taurine was greater in the preincubated vessels. No isolation of the intermediate was attempted, as the amounts accumulated were evidently very small.

Effect of magnesium, manganese and calcium

Table 4 shows that magnesium had no effect when the isolated microsomes were used without any further treatment. This was probably due to magnesium (or manganese) following the microsomes. When the microsomes were dialyzed for 36 hours against 0.0025 M potassium phosphate buffer (pH 7.5), addition of magnesium had a stimulating effect both on the hydroxamic acid — and the taurocholic acid formation (Table 6). Any absolute requirement for

Table 6. Effect of Mg^{++}.

Microsomes from approx. 500 mg liver, dialyzed for 36 hours against 0.005 M potassium phosphate buffer (pH 7.4) at 5° C. ^{35}S-taurine 0.8 μmoles/vessel (= 17 000 c/min/vessel) or hydroxylamine 50 μmoles/vessel, cholic acid 2 μmoles/vessel, ATP 10 μmoles/vessel, CoA 0.15 μmoles/vessel. Potassium phosphate buffer 0.022 M, KF 0.2 M, glutathione 0.003 M. Incubation time 60 minutes.

Additions	μmoles taurocholate formed per vessel		μmoles cholhydroxamic acid formed per vessel	
None	0.16	0.16	0.29	0.31
Mg^{++} 0.4×10^{-3} M	0.23	0.23	0.45	0.44
Mg^{++} 1×10^{-3} M	0.27	0.26	—	—
Mn^{++} 0.4×10^{-3} M	0.17	0.18	0.38	—

Table 7. Effect of Mg^{++}, Mn^{++} and Ca^{++}.

0.8 ml solubilized microsomes dialyzed for 24 hours against 0.005 M potassium phosphate buffer (pH 7.5). ^{35}S-taurine 0.8 μmoles/vessel (= 20 000 c/min/vessel), cholic acid 2 μmoles/vessel, ATP 10 μmoles/vessel, CoA (75 %) 0.15 μmoles/vessel. Potassium phosphate buffer 0.015 M, KF 0.2 M. Incubation time 45 minutes.

Additions	Net c/min/0.1 ml butanol extract	μmoles taurocholate formed per vessel
None	152 153	0.046 0.046
Mg^{++} 0.2×10^{-3} M	245	0.074
Mg^{++} $1 + 10^{-3}$ M	228	0.068
Mn^{++} 0.2×10^{-3} M	265	0.080
Mn^{++} 1×10^{-3} M	223	0.067
Ca^{++} 1×10^{-3} M	115	0.034

magnesium could not be demonstrated, as further prolongation of the dialysis led to increasing inactivation of the enzyme system, and this inactivation could not be reversed by magnesium. It can be seen from Table 7 that manganese had a stimulating effect on the conjugation in contrast to our previously reported results with the microsomes-particle free supernatant system [2]. Solubilized microsomes (see later) dialyzed for approximately 24 hours against 0.0025 M potassium phosphate buffer were used in this experiment. Also in this case increasing inactivation of the enzyme system during dialysis was observed. Calcium had some inhibiting effect.

Effect of ATP, ADP, AMP, pyrophosphate and phosphate

As ATP was required in the reaction, it was found of interest to investigate the effects of the possible reaction products of ATP. Fig. 8 shows that ADP could substitute for ATP in the reaction, but ATP proved to be more than twice as effective in lower concentrations. AMP had, as expected, no effect. From the participation of ATP in the formation of cholyl-S-CoA it may be concluded that either ADP and phosphate or AMP and pyrophosphate must be reaction products. Fig. 9 shows that pyrophosphate had a stronger inhibiting effect on the taurocholate formation than had phosphate. The effect of pyrophosphate was also tested when fluoride was omitted from the incubation

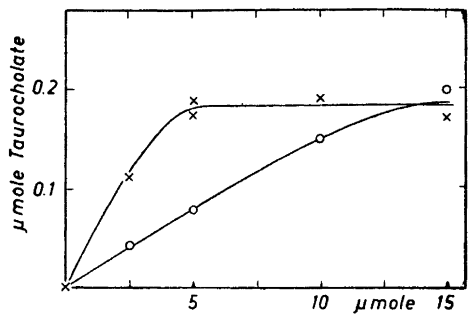


Fig. 8. Effect of ATP, ADP and AMP as energy donors. Microsomes from 300 mg liver. ^{35}S-taurine 0.8 µmoles/vessel, cholic acid 1 µmole/vessel, ATP 5 µmoles/vessel, CoA (75 %) 0.15 µmoles/vessel. TRIS-buffer 0.1 M, KF 0.2 M. Incubation time 60 minutes. +—+—+—+—+ *ATP,* O—O—O—O *ADP,* ▲—▲—▲— *AMP.*

mixture. In this case no inhibiting effect was observed at the pyrophosphate concentration used (0.04 M). As fluoride has been shown to inhibit pyrophosphatase [20, 24], this result indicated that the pyrophosphate ion itself was the inhibiting agent and not the phosphate resulting from its splitting by pyrophosphatase. From Table 8 it is seen that pyrophosphate and AMP together had an inhibiting effect stronger than could be explained by the inhibitions effected by the two compounds when added alone, indicating that the effect of one of them was dependent on the presence of the other. No such effect was observed with ADP and phosphate. These results strongly indicate AMP and pyrophosphate as reaction products. The action of ADP as energy donor (Fig. 8) must then be explained as a result of the myokinase reported to be present in liver [25, 26]. This assumption is contradicted by the fact that liver myokinase is claimed to be inhibited by fluoride [26, 27]. Further purification of the enzyme system is desirable for the clarification of this problem.

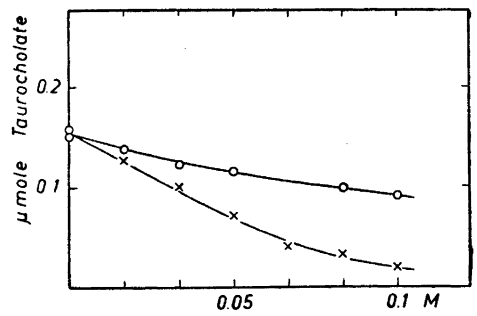


Fig. 9. Effect of orthophosphate and pyrophosphate. Microsomes from approx. 300 mg liver. ^{35}S-taurine 0.8 µmoles/vessel, cholic acid 1 µmole/vessel, ATP 5 µmoles/vessel, CoA (75 %) approx. 0.15 µmoles/vessel. TRIS-buffer 0.1 M, KF 0.2 M. Incubation time 60 minutes. O—O—O—O—O—O *orthophosphate,* +—+—+—+—+ *pyrophosphate.*

Table 8. Effect of AMP, ADP, orthophosphate and pyrophosphate.

Microsomes from approx. 300 mg liver. ^{35}S-taurine 0.8 μmoles/vessel (= 65 000 c/min/vessel), cholic acid 1 μmole/vessel, ATP 5 μmoles/vessel, CoA (75 %) 0.15 μmoles/vessel. TRIS-buffer 0.1 M, KF 0.2 M. Incubation time 60 minutes.

Additions/vessel	Net c/min/0.1 ml butanol extract		μmoles taurocholate formed per vessel	
None	1 485 1 610	1 495 1 690	0.14 0.15	0.14 0.16
20 μmoles ADP	1 595	1 540	0.14	0.14
50 μmoles PO_4^{--}	1 165	1 265	0.11	0.12
20 μmoles ADP 50 μmoles PO_4^{--}	1 240	1 310	0.11	0.12
20 μmoles AMP	1 110	1 225	0.10	0.11
50 μmoles $P_2O_7^{----}$	945	1 080	0.09	0.10
20 μmoles AMP 50 μmoles $P_2O_7^{----}$	375	365	0.03	0.03

Table 9. Solubilization of microsomes.

Microsomes from 5 g liver suspended in 9 ml 0.1 M potassium phosphate buffer (pH 7.4) containing 0.5 % cholic acid. Aliquots of 1.5 ml treated as tabeled and centrifuged at 25 000 × g for 90 minutes. 1.0 *ml* of the slightly turbid supernatant added to the vessels. Other additions: ^{35}S-taurine 2 μmoles/vessel (= 7 600 c/min/vessel), cholic acid (from the microsome suspension) approx. 10 μmoles/vessel, ATP 10 μmoles/vessel, CoA (75 %) 0.15 μmoles/vessel, KF 0.2 M, glutathione 0.002 M. Incubation time 90 minutes.

Treatment of microsomes	Net c/min/0.1 ml butanol extract	μmoles taurocholate formed per vessel
None	178	0.35
Incubated for 40 min. at 37° C	89	0.18
Frozen and thawed once	184	0.36
Frozen and thawed twice	179	0.35
Frozen and thawed three times	227	0.44
Frozen and thawed six times	194	0.38

Stability and solubilization of the enzyme system

For a more careful investigation of the reaction mechanism, a further purification of the enzyme system was considered to be desirable. In preliminary experiments we have apparently succeeded in liberating the enzyme system from the microsomes. We used a method similar to that employed by Wainio *et al.*[28] for the liberation of cytochrome oxidase from cell particles. The microsome fraction was suspended in 0.1 M potassium phosphate buffer (pH 7.4) containing ½—1 % cholic acid. The suspension was frozen at —80° C and re-thawed at 37° C. After freezing and thawing once, the suspension got translucent. When centrifuged at 25 000 × g for 90 minutes, a small colourless sediment and a slightly turbid supernatant were formed, the latter containing at least 70—80 % of the enzyme activity. In Table 9 is shown an experiment where the total enzyme activity was recovered in the supernatant. It must be noted that both phosphate and cholic acid must be added to liberate the enzyme system from the particles. If cholate or phosphate were used alone, a practically inactive supernatant was obtained.

Whether the treatment resulted in a real solubilization or only in a decreased particle size could not be stated, as a faster centrifuge was not available. In preliminary experiments we did not obtain any further purification of the enzyme system, as both ammonium sulphate and acetone precipitation gave almost completely inactive precipitates. Whether this inactivation was due to denaturation or to loss of an unknown co-factor is not known. Thioctic acid has been reported to take part in the acetate activation [29], but this compound did not reactivate our ammonium sulphate — or acetone precipitates.

The enzyme system was very stable in the cold. Storing of the microsomes at —20° C for a fortnight did not lead to any appreciable loss in activity. The microsomes were also lyophilized, and the resulting dry powder showed full activity. Heating to 100° C gave immediately full inactivation.

DISCUSSION AND CONCLUSION

Several biological mechanisms are known by which peptide bonds are formed [30]. CoA is required in the formation of the peptide bond in acetylsulfanilamide [19] and in hippuric acid [31]. Acetyl-S-CoA and benzoyl-S-CoA have been proved to be intermediates in these two reactions [19, 31], and in the acetylation of sulfanilamide two enzymes, one acetate activating and one acetyl transferring enzyme, are involved [19].

In all CoA-dependent reactions, the sulphydryl group of CoA forms thioester bonds with acyl groups [7, 31, 35], and these acyl-S-CoA compounds are known to react spontaneously with hydroxylamine to form hydroxamic acid [7, 18, 22]. The absolute requirement of CoA both in the conjugation of cholic acid with taurine and in the formation of cholhydroxamic acid from cholic acid and hydroxylamine therefore strongly indicates that cholyl-S-CoA is an intermediate in these reactions. The accumulation of an intermediate during the pre-incubation without taurine also supports this conclusion.

Admittedly, hydroxamic acids are also formed in other biological reactions, but in these cases CoA is not required [30, 36, 28].

In the acetate activation the following reaction mechanism has been found in the case of animals [32]

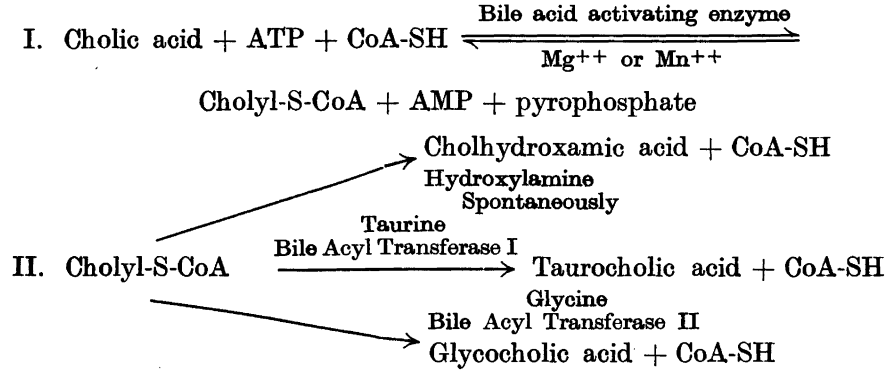
$$\text{Acetate} + \text{ATP} + \text{CoA-SH} \underset{\leftarrow}{\overset{\text{Enzyme} + \text{Mg}^{++}}{\rightleftharpoons}} \text{Acetyl-S-CoA} + \text{AMP} + \text{pyrophosphate}$$

A different reaction mechanism has been found in the activation of succinate [33]

$$\text{Succinate} + \text{ATP} + \text{CoA-SH} \underset{\leftarrow}{\overset{\text{Enzyme} + \text{Mg}^{++}}{\rightleftharpoons}} \text{Succinyl-S-CoA} + \text{ADP} + \text{Phosphate}$$

Both these reactions have been proved to be reversible [32, 33]. The acetate activation is inhibited by AMP and pyrophosphate [14], whereas the succinate activation is inhibited by ADP and orthophosphate [38]. Our results, which showed a much stronger inhibition of the taurocholate formation by AMP and pyrophosphate than by ADP and orthophosphate, therefore indicate a reaction mechanism in this process identical with that found in the acetate activation. This similarity to the acetate activation is also confirmed by the stimulating effect of magnesium ions on the taurocholate- and cholhydroxamic acid formation.

Recently we have carried out experiments indicating that the transfer of the cholyl group from CoA to taurine and glycine is irreversible [39], as the conjugated acids were not converted to cholhydroxamic acid in the presence of microsomes and CoA. We have further shown that rabbit liver microsomes conjugate free bile acids almost exclusively with glycine, whereas chicken liver microsomes conjugate exclusively with taurine. Rat liver microsomes conjugate both with taurine and glycine. These results probably indicate that two different enzymes transfer the cholyl group from CoA to taurine and glycine. The following reaction scheme therefore seems to be a reasonable conclusion on the experimental results:



A further purification of the enzyme system will probably be needed for a closer elucidation of the reaction mechanism. Thioctic acid has been reported to take part in the acetate activation [29], and results have been published which indicate that the acetate activation proceeds with enzyme-AMP and enzyme-S-CoA as intermediates.

REFERENCES

1. Bremer, J. *Acta Chem. Scand.* **9** (1955) 268.
2. Bremer, J. *Ibid.* **9** (1955) 683.
3. Bremer, J. and Gloor, U. *Ibid.* **9** (1955) 689.
4. Bremer, J. *Ibid.* **9** (1955) 1036.
5. Eldjarn, L. *Ibid.* **5** (1951) 677.
6. Bondi, S. and Müller, E. Hoppe-Seyler's *Z. physiol. Chem.* **47** (1906) 499.
7. Kornberg, A. and Pricer, W. E. *J. Biol. Chem.* **204** (1953) 329.
8. Eriksson, S. and Sjövall, J. *Arkiv Kemi* **8** (1955) 303.

9. Eriksson, S. and Sjövall, J. *Ibid.* **8** (1955) 317.
10. Sidgwick, N. V. *The Organic Chemistry of Nitrogen*, Oxford University Press **1949**, p. 198.
11. Sjövall, J. *Arkiv Kemi* **8** (1955) 317.
12. Sjövall, J. *Acta Chem. Scand.* **8** (1954) 345.
13. Cohen, P. P. and McGilvery, R. W. *J. Biol. Chem.* **169** (1947) 119.
14. Eisenberg, M. A. *Biochim. et Biophys. Acta* **16** (1955) 58.
15. MacDonnell, L. R., Silva, R. B. and Feeney, R. E. *Arch. Biochem.* **32** (1951) 288.
16. Lynen, F., Reichert, E. and Rueff, L. *Ann.* **574** (1951) 1.
17. Stern, J. R., Shapiro, B., Stadtman, E. R. and Ochoa, S. *J. Biol. Chem.* **139** (1951) 703.
18. Stadtman, E. R. *Ibid.* **196** (1952) 527.
19. Chou, T. C. and Lipmann, F. *Ibid.* **196** (1952) 89.
20. Jones, M. E., Black, S., Flynn, R. M. and Lipmann, F. *Biochim. et Biophys. Acta* **12** (1953) 141.
21. Novikoff, A. B., Hecht, L., Podber, E. and Ryan, J. *J. Biol. Chem.* **194** (1952) 153.
22. Stadtman, E. R. *J. Cellular Comp. Physiol.* **41 suppl. 1** (1953) 89.
23. Elliott, W. H. *Biochim. et Biophys. Acta* **17** (1955) 440.
24. Lipmann, F., Jones, M. E., Black, S. and Flynn, R. M. *J. Cellular Comp. Physiol.* **41 suppl. 1** (1953) 109.
25. Kotelnikova, A. V. *Doklady Akad. Nauk. SSSR* **59** (1948) 527, *(Chem. Abstracts* **42** (1948) 6388).
26. Barkulis, S. S. and Lehninger, A. L. *J. Biol. Chem.* **190** (1951) 339.
27. Kotelnikova, A. V. *Biokhimiya* **15** (1950) 371. (*Chem. Abstracts* **54** (1950) 198).
28. Wainio, W. W., Cooperstone, S. J., Kollen, S. and Eichel, B. *J. Biol. Chem.* **173** (1948) 145.
29. Seaman, G. R. *J. Am. Chem. Soc.* **76** (1954) 1712.
30. Borsook, H. *Advances in Protein Chemistry* **8** (1953) 127.
31. Schachter, D. and Taggart, J. V. *J. Biol. Chem.* **203** (1953) 925.
32. Jones, M. E., Lipmann, F., Hilz, H. and Lynen, F. *J. Am. Chem. Soc.* **75** (1953) 3285.
33. Kaufman, S., Gilvary, C., Cori, O. and Ochoa, S. *J. Biol. Chem.* **203** (1953) 869.
34. Lynen, F. *The Harvey Lectures*, Series XLVIII, Academic Press, New York 1952–1953, p. 210.
35. Baddiley, J. *Advances in Enzymol.* **16** (1955) 1.
36. Lipmann, F. and Tuttle, L. C. *Biochim. et Biophys. Acta* **4** (1950) 301.
37. Fry, B. A. *Biochem. J. London* **59** (1955) 579.
38. Hift, H., Quellet, L., Littlefield, J. W. and Sanadi, D. R. *J. Biol. Chem.* **204** (1953) 565.
39. Bremer, J. *Biochem. J. London. In press.*

Received October 18, 1955.

ACTA CHEMICA SCANDINAVICA **10** (1956) 72—93

Some Relationships among the Stabilities of Metal Complexes

HARRY IRVING and HAZEL ROSSOTTI

Inorganic Chemistry Laboratory, Oxford, England and Department of Inorganic Chemistry, the Royal Institute of Technology, Stockholm 70, Sweden

The stability constant, K_{ML}, of a first (1:1) metal-ligand complex, ML, can be related to the stability constant of the corresponding proton-ligand complex, HL, and to the partial molar free energies of the various species in solution. The relationship, (6), which is applicable both in water and in mixed aqueous-organic solvents, forms a basis for discussing the linear relationships which have been observed between the following terms:
(i) log K_{ML} and log K_{HL}, for complexes of one metal ion with a series of ligands, (8).
(ii) log K_{YL} and log K_{ZL}, for complexes of two metal ions, Y and Z, with a series of ligands, (12).
(iii) log K_{MP} and log K_{MQ}, for complexes of two ligands, P and Q, with a series of metal ions (13).
The relationships are illustrated using a wide variety of experimental data. Special reference is made to the disturbing effects of steric hindrance, and of differences in the co-ordinating power of the donor atoms in a chelating ligand. The variation of log K_{HL} and log K_{ML} with the organic content of a mixed solvent is also discussed.

The approach may be of use in analytical chemistry for predicting approximate values of stability constants, and for choosing suitable organic reagents for metal ions.

Many complexes, $ML_n^{(z-nJ)+}$ derived from a metal ion, M^{z+}, and an organic reagent H_JL, are of analytical importance. Any discussion of problems of theoretical analytical chemistry, such as the sensitivity or specificity of spot-tests, must take into account both the specific properties of the complex $ML_n^{(z-nJ)+}$ (*e. g.* its absorption spectrum, solubility in water and in organic solvents, etc.) and the position of equilibrium in the reaction

$$M^{z+} + n\ H_JL = ML_n^{(z-nJ)} + n\ H^+ \qquad (1)$$

by which it is produced [1,2].

In this connection it is desirable to know how the equilibrium constant of equation (1) is affected by changes in the metal M, *e. g.* by co-ordination of groups other than L, or by replacing M by a different metal. Can such changes be correlated with independently measurable parameters such as ionisation potential, ionic radius, electronic structure or electronegativity, and could they be predicted theoretically? It is also of interest to know how the equilibrium constant is affected when, for the same metal M, changes are made in the structure of the ligand L, and whether these effects can be correlated with concomitant changes in the acid dissociation constants of the reagent H_jL and in the stereochemistry of the complex system. Finally, it is important to consider the effects on equilibrium in each of these cases when an aqueous-organic mixed solvent replaces water as the reaction medium.

In the last ten years, many stability constants of complexes formed between metal ions and organic ligands have been measured, and numerous qualitative and semi-quantitative relationships between the stability of the complex and of the properties of the metal ion and of the ligand have been discussed (*e. g.* [3–12]). A number of authors have, for example, reported empirical relationships between dissociation constants of reagents, and the stability constants of complexes formed by the same metal ion with various ligands [3,15–19]. These relationships are by no means generally valid, but are usually only applicable to very limited series of closely related ligands. This paper indicates under what conditions relationships of this type are to be expected from considerations of the free energy changes which occur on complex formation, and suggests other types of relationships that may also exist. These conclusions have been tested on stability constants of metal oxinates and similar complexes (published elsewhere [19]) and on data in the literature; in favourable cases the relationships may be used to predict stability constants of complexes which have not yet been studied experimentally.

GENERAL CONSIDERATIONS

Limiting the discussion in the first instance to the first (1:1) metal-ligand and proton-ligand complexes, ML and HL respectively, the equilibrium constant for reaction (1) can be written in the form

$$K = [ML][H]/[M][HL] = {}^cK_{ML} / {}^cK_{HL} \qquad (2)$$

where the stoichiometric stability constants are defined by ${}^cK_{ML} = [ML]/[M][L]$ and ${}^cK_{HL} = [HL]/[L][H]$ and charges are omitted, here and elsewhere, for generality. If ${}^cK_{ML}$ and ${}^cK_{HL}$ are expressed in litres/mole, and if, for each species, S, the partial molar free energy is denoted $\bar{G}^\circ_S$, and the activity coefficient referred to the hypothetical one molar standard state is designated y_S, the following relationship is exact

$$\ln {}^cK_{ML} = \ln {}^cK_{HL} + \frac{1}{RT}(\bar{G}^\circ_M - \bar{G}^\circ_{ML} - \bar{G}^\circ_H + \bar{G}^\circ_{HL}) + \ln (y_M y_{HL} / y_{ML} y_H) \qquad (3)$$

Many organic reagents and their metal complexes are very sparingly soluble in water, and stability constants have often been measured in mixed aqueous-

organic solvents. Equation (3), which refers only to aqueous solution, must therefore be extended. Using heavy (***Clarendon***) type to denote factors which refer to a mixed aqueous-organic solvent, the exact equation corresponding to (3) is

$$\ln {}^{c}\boldsymbol{K}_{\mathbf{ML}} = \ln {}^{c}\boldsymbol{K}_{\mathbf{HL}} + \frac{1}{RT}(\bar{\boldsymbol{G}}^{\circ}_{\mathbf{M}} - \bar{\boldsymbol{G}}^{\circ}_{\mathbf{ML}} - \bar{\boldsymbol{G}}^{\circ}_{\mathbf{H}} + \bar{\boldsymbol{G}}^{\circ}_{\mathbf{HL}}) + \ln (\boldsymbol{\nu}_{\mathbf{M}}\boldsymbol{y}_{\mathbf{HL}}/\boldsymbol{y}_{\mathbf{ML}}\boldsymbol{y}_{\mathbf{H}}) \quad (3a)$$

$\bar{G}^{\circ}_{S}$ and $\bar{G}^{\circ}_{S}$ are related by the expression

$$\bar{G}^{\circ}_{S} - \bar{G}^{\circ}_{S} = \bar{G}^{\circ}_{S(transfer)} = RT \ln y_{S(o)} \quad (4)$$

where $\bar{G}^{\circ}_{S(transfer)}$ is the partial molar free energy of transfer of the solute species, S, at infinite dilution, from water to the binary mixed solvent, and $y_{S(o)}$ is the activity coefficient of the species S, at infinite dilution in the mixed solvent, referred to infinite dilution in water; thus log $y_{S(o)}$ represents the "primary medium effect" defined by Owen [20], *cf.*[21]. The relationship

$$\bar{G}^{\circ}_{S(transfer)} = n_{X} t_{S} \quad (5)$$

where n_X is the molar fraction of the organic component of the mixed solvent, and t_S is a constant for each combination of solute species and organic solvent, has been shown to hold for a number of solutes in water-methanol and water-ethanol mixtures [22–24]. If equation (5) is valid for each species in solution, the stoichiometric stability constants ${}^{c}\boldsymbol{K}_{\mathbf{ML}}$ and ${}^{c}\boldsymbol{K}_{\mathbf{HL}}$ measured in a mixed solvent will be related by the following equation

$$\ln {}^{c}\boldsymbol{K}_{\mathbf{ML}} = \ln {}^{c}\boldsymbol{K}_{\mathbf{HL}} + \frac{1}{RT}\left\{\bar{\boldsymbol{G}}^{\circ}_{\mathbf{M}} - \bar{\boldsymbol{G}}^{\circ}_{\mathbf{ML}} - \bar{\boldsymbol{G}}^{\circ}_{\mathbf{H}} + \bar{\boldsymbol{G}}^{\circ}_{\mathbf{HL}} + \boldsymbol{n}_{\mathbf{X}}(\boldsymbol{t}_{\mathbf{M}} - \boldsymbol{t}_{\mathbf{ML}} - \boldsymbol{t}_{\mathbf{H}} + \boldsymbol{t}_{\mathbf{HL}})\right\} + \ln (\boldsymbol{y}_{\mathbf{M}}\boldsymbol{y}_{\mathbf{HL}}/\boldsymbol{y}_{\mathbf{ML}}\boldsymbol{y}_{\mathbf{H}}) \quad (6)$$

Since the activity coefficients y_S are referred to infinite dilution in a particular mixed solvent, the term (log y_S—log y_S) represents Owen's "secondary medium effect" [20] *cf.*[21].

When the solvent is pure water, $n_X = 0$, ${}^{c}\boldsymbol{K}_{\mathbf{ML}} = {}^{c}K_{ML}$, ${}^{c}\boldsymbol{K}_{\mathbf{HL}} = {}^{c}K_{HL}$, $y_S = y_S$ and equation (6) reduces to (3). For thermodynamic stability constants ${}^{T}K_{ML}$ and ${}^{T}K_{HL}$ measured in water, the equation may be further simplified to

$$\ln {}^{T}K_{ML} = \ln {}^{T}K_{HL} + \frac{1}{RT}(\bar{G}^{\circ}_{M} - \bar{G}^{\circ}_{ML} - \bar{G}^{\circ}_{H} + \bar{G}^{\circ}_{HL}) \quad (7)$$

which was given previously by Duncan [25].

Since $\bar{G}^{\circ}_{H} = 0$, by definition, and values of $\bar{G}^{\circ}_{M}$ are tabulated [26], equation (7) may be used to calculate values of $(\bar{G}^{\circ}_{HL} - \bar{G}^{\circ}_{ML})$, which will be related to the properties of the metal ion and the ligand. For example, the value of $\bar{G}^{\circ}_{ML}$ would be decreased by an increase in the ionisation potential of the metal and, unless steric factors are involved, by a decrease in the radius of the metal ion. It would also depend on the co-ordination number and stereochemistry of the metal ion, and the possibility of favourable hybridisation changes accompanying complex formation. Both $\bar{G}^{\circ}_{HL}$ and $\bar{G}^{\circ}_{ML}$ would be influenced by the number and nature of the donor atoms in the ligand, by the effective charge on them,

by the size and stereochemistry of the ligand molecule and by changes in entropy and resonance energy accompanying the combination of the ligand with a metal ion or a proton.

As values of ${}^{T}K_{ML}$ and ${}^{T}K_{HL}$ have only been measured for a few systems, equation (7) must usually be replaced by the more general equation (6). This equation forms a useful basis for discussing the empirical relationships which have been observed among the stabilities of metal complexes. Four types of relationship are discussed below.

Type I. The relationship between the stabilities of metal-ligand, and proton-ligand complexes

Many authors [3, 15–19] have reported approximately linear relationships between $\log {}^{c}K_{ML}$ and $\log {}^{c}K_{HL}$ for complexes formed by a given metal ion with a series of closely related ligands. The conditions necessary for a relationship of this type may be deduced from equation (6). By rearrangement

$$\ln {}^{c}K_{ML} = \ln {}^{c}K_{HL} + A + B \qquad (8)$$

where

$$A = \frac{1}{RT}\left\{-\bar{G}^{\circ}_{ML} + \bar{G}^{\circ}_{HL} + n_X(-t_{ML} + t_{HL})\right\} - \ln y_{ML} + \ln y_{HL}$$

and

$$B = \frac{1}{RT}\left\{\bar{G}^{\circ}_{M} - \bar{G}^{\circ}_{H} + n_X(t_M - t_H)\right\} - \ln y_H + \ln y_M$$

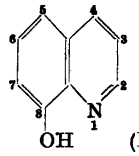
The term B is independent of the nature of the ligand, and is constant for all complexes of a given metal ion, provided that the composition of the solvent, and the ionic strength, are kept constant. Thus, if a plot of $\ln {}^{c}K_{ML}$ against $\ln {}^{c}K_{HL}$ is found to be a straight line of unit slope, the term A must be constant, (or perhaps negligible compared with the term $\ln {}^{c}K_{HL}$). Similarly, if a straight line of non-unit slope is obtained, the term A must itself be a linear function of $\ln {}^{c}K_{HL}$. For dilute solutions in pure water ($n_X = 0$), and the value of A will be determined largely by the difference in magnitude of $\bar{G}^{\circ}_{ML}$ and $\bar{G}^{\circ}_{HL}$; it is unlikely to be negligible in comparison with $\ln {}^{c}K_{HL}$, but may possibly vary with change in HL in some comparatively simple manner (*cf.* p. 76).

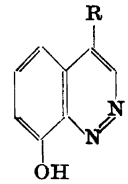
As would be expected, these conditions only hold for series of reagents of very similar structure. For example, a replot of Calvin and Wilson's data for copper complexes of some derivatives of salicylaldehyde [15] (not reproduced) shows that the relationship

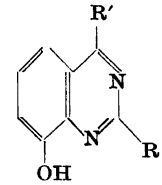
$$\log {}^{c}K_{ML} = a \log {}^{c}K_{HL} + b \quad (a \text{ and } b \text{ constants}) \qquad (9)$$

is approximately applicable only in cases where complex formation would lead to similar changes in resonance energy for each ligand in the series. For these complexes, $a = 1$ and the straight lines are of unit slope. The relationship (9, $a = 1$) is also approximately valid for the iron(III) complexes of some phenol derivatives [27]. As the substituents in the ligands were either *o*- or *p*- to the hydroxyl group, there was no steric hindrance to complex formation among these reagents. The effect of a substituent adjacent to a donor atom in

the ligand is shown in Fig. 1a, in which $\log {}^{c}K_{ML}$ is plotted against $\log {}^{c}K_{HL}$ for magnesium complexes of some derivatives of 8-hydroxyquinoline ("oxine" I) [19].


(I)


(II)


(III)

There are two types of deviation from the best straight line of unit slope. (i) Major deviations, where $\log {}^{c}K_{ML}$ is always smaller than predicted. These are invariably associated with reagents having substituents adjacent to the chelating nitrogen atom, and the stabilities of the metal complexes are clearly decreased by steric hindrance. (ii) Minor deviations, in which $\log {}^{c}K_{ML}$ may be either smaller or larger than predicted from the value of $\log {}^{c}K_{HL}$. Since each ligand has two donor atoms of differing character, *viz.* oxygen and nitrogen, the magnitude of $\log {}^{c}K_{HL}$ (which refers only to the dissociation of the O—H group) is not the only factor which influences $\log {}^{c}K_{ML}$. The observed minor deviations may well be due to differences in the co-ordinating power of the nitrogen atoms in the various ligands (*cf.* [2,19,28]).

Plots of $\log {}^{c}K_{ML}$ against $\log {}^{c}K_{HL}$ for several other series of complexes are straight lines of non-unit slope, indicating that the term A is an approximately linear function of $\log {}^{c}K_{HL}$. Data for the copper(II) complexes of some oxine derivatives [19] are plotted in Fig. 1b, together with the best straight line, which is of slope 2.2. Large deviations from the line are again observed for reagents with substituents adjacent to the chelating nitrogen atom. A similar linear plot [29], of slope 1.3, was obtained for complexes of the uranyl ion, UO_2^{2+}. The importance of steric factors is further emphasised by the fact that plots of $\log {}^{c}K_{ML}$ against $\log {}^{c}K_{HL}$, obtained by Van Uitert *et al.* [17,30] for complexes of 1,3-diketones with nickel(II) and cerium(III) in 74.5% v/v aqueous dioxan, gave three parallel lines, one for diketones with two terminal aromatic groups, a second for diketones with a single terminal methyl group, and the third for diketones with two terminal methyl groups. The complexes of copper(II) and barium behaved similarly; the slopes were always less than unity, and fell in the order Cu(II) > Ni(II) > Ba. The introduction of one or more terminal $-CF_3$ groups had a marked effect in depressing the stability of the copper complexes, somewhat less on the nickel complexes, and very little on the barium complexes. Plots of $\log {}^{c}K_{ML}$ against $\log {}^{c}K_{HL}$ for complexes of the silver(I) ion with ammonia and its derivatives also fall on three parallel lines [16], one for primary (and tertiary heterocyclic) amines and the others for secondary and tertiary aliphatic (or aromatic) amines. An explanation in terms of differences in the degree of hydration of free and co-ordinated amines has been suggested by Trotman-Dickenson [31]; attention has also been drawn to the possibility of steric hindrance [11].

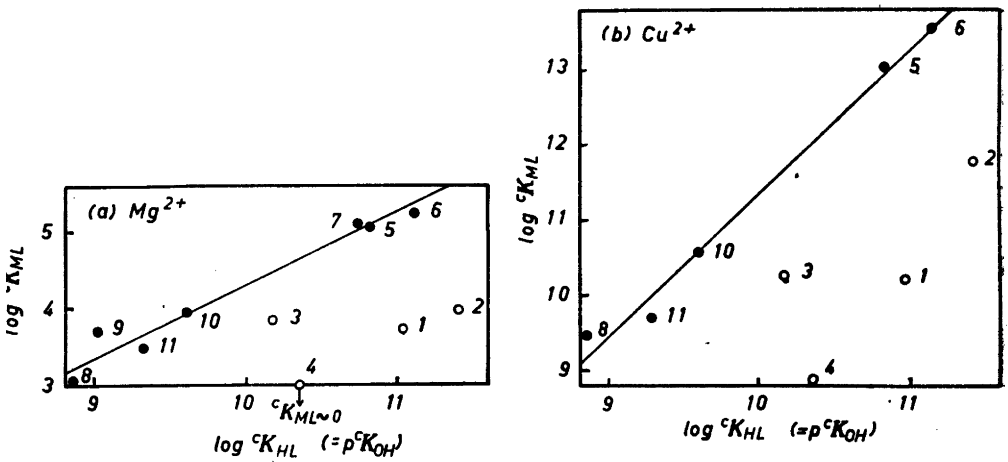


Fig. 1. Log$^cK_{ML}$ as a function of log$^cK_{HL}$ for complexes of oxine derivatives[19] *in 50 % v/v aqueous dioxan (0.3 M sodium perchlorate) at 20° C. Open points refer to reagents with a substituent adjacent to the chelating nitrogen atom: (1) 2-Methyl-oxine (2) 1,2,3,4-Tetrahydro-10-hydroxyacridine (3) 8-Hydroxy-2,4-dimethylquinazoline (4) 8-Hydroxy-4-methyl-2-phenylquinazoline. Full points refer to other reagents: (5) Oxine (6) 5-Methyl-oxine (7) 6-Methyl-oxine (8) 8-Hydroxycinnoline (9) 8-Hydroxy-4-methylcinnoline (10) 8-Hydroxyquinazoline (11) 5-Hydroxyquinoxaline.*

Data for the complexes of magnesium, calcium, strontium, barium and zinc with some aminopolycarboxylic acids indicate that linear plots are only obtained for series of complexes in which the number of rings, and the size of each ring is the same [18,32]; and different lines are obtained for complexes containing purely aliphatic chelate rings, and those in which a benzenoid system is fused to one of the chelate rings, *cf.*[3]. For complexes of substituted iminodiacetic acids $X—CH_2—N(CH_2COOH)_2$ ($X = CO_2^-$, SO_3^-, PO_3^{2-}) the slope of each plot is a linear function of the second ionisation potential, I, of the appropriate metal [18]. Thus, in this series of complexes $^cK_{ML}$ and $^cK_{HL}$ are related by the equation

$$\ln {}^cK_{ML} = \ln {}^cK_{HL}\,(c + dI) + e + B \qquad (10)$$

where c, d and e are constants.

It is not difficult to see why the simple relationship (9) is so seldom exactly followed. With monodentate ligands, differences between the size and deformability of the (solvated) proton and the (solvated) metal ion will lead to steric effects (*cf.* the F-strain discussed by Brown and co-workers [33]). Superimposed steric effects can arise when the spatial geometry of the free ligand is sufficiently modified by co-ordination to the metal (*cf.* Brown's B-strain [33]). With chelating ligands such as the glycinate ion ($L = NH_2CH_2COO^-$), the H—L bond is essentially one between hydrogen and nitrogen, giving the zwitterion $^+NH_3CH_2COO^-$, while in its metal complexes both metal-nitrogen and metal-oxygen bonds are involved. Similar arguments apply to ligands incorporating this basic skeleton within a hetrocyclic structure, *e. g.* 8-hydr-

oxyquinoline, 8-hydroxycinnoline (II, R = H), and 8-hydroxyquinazoline (III, R = R′ = H). Structural changes in L will change the strength of both metal-oxygen and metal-nitrogen bonds, but not necessarily to the same extent, or even in the same direction [2,19]. The greatest deviations from equation (9) will be expected with the metals which show the greatest tendency to form strong bonds, and which exhibit the greatest difference in the relative strength of their bonds to different donor atoms.

Type II. The relationship between the stabilities of complexes of two metal ions with a series of related ligands

The relationship between metal-ligand, and proton-ligand, complexes of a single metal has been discussed in the previous section, with reference to plots of log ${}^{c}K_{ML}$ against log ${}^{c}K_{HL}$. The stabilities of complexes formed by two different metal ions, Y and Z, with a series of ligands may be compared in an analogous way by plotting log ${}^{c}K_{YL}$ as a function of log ${}^{c}K_{ZL}$. Applying equation (6) to each metal ion in turn, and subtracting

$$\ln {}^{c}K_{YL} = \ln {}^{c}K_{ZL} + \frac{1}{RT}\{\bar{G}^{\circ}_{Y} - \bar{G}^{\circ}_{YL} - \bar{G}^{\circ}_{Z} + \bar{G}^{\circ}_{ZL} + n_{X}(t_{Y} - t_{Z} - t_{YL} + t_{ZL})\} + \ln(y_{ZL}y_{Y}/y_{YL}y_{Z}) \quad (11)$$

which can be written in the form

$$\ln {}^{c}K_{YL} = \ln {}^{c}K_{ZL} + C + D \quad (12)$$

where $$C = \frac{1}{RT}\{-\bar{G}^{\circ}_{YL} + \bar{G}^{\circ}_{ZL} + n_{X}(-t_{YL} + t_{ZL})\} - \ln y_{YL} + \ln y_{ZL}$$

and $$D = \frac{1}{RT}\{\bar{G}^{\circ}_{Y} - \bar{G}^{\circ}_{Z} + n_{X}(t_{Y} - t_{Z})\} - \ln y_{Z} + \ln y_{Y}$$

Thus equation (12) corresponds to (8), where the symbols Y, Z, C and D now replace M, H, A and B, respectively. Since D is independent of the nature of the ligand, L, the plot of $\ln {}^{c}K_{YL}$ against $\ln {}^{c}K_{ZL}$ will be a straight line of unit slope if C is a constant or is negligible compared with $\ln {}^{c}K_{ZL}$. A straight line of non-unit slope would result if C were a linear function of $\ln {}^{c}K_{ZL}$. The conditions necessary for a linear relationship between log ${}^{c}K_{YL}$ and log${}^{c}K_{ZL}$ are therefore exactly analogous to those necessary for a linear relationship between log ${}^{c}K_{ML}$ and log${}^{c}K_{HL}$ (see previous section).

As few stability constants for complexes of two closely related metals with the same group of ligands are available, this relationship cannot be tested thoroughly. However, values of log ${}^{c}K_{CuL}$ for fifty six ligands of very varied types are plotted against corresponding values of log ${}^{c}K_{NiL}$ in Fig. 2. The predicted behaviour is approximately followed for complexes ranging in stability from ${}^{c}K_{ML} = 10^{15}$ to $\sim 10^{0}$. Both monodentate and polydentate ligands have been included and while many of the measurements were made in aqueous

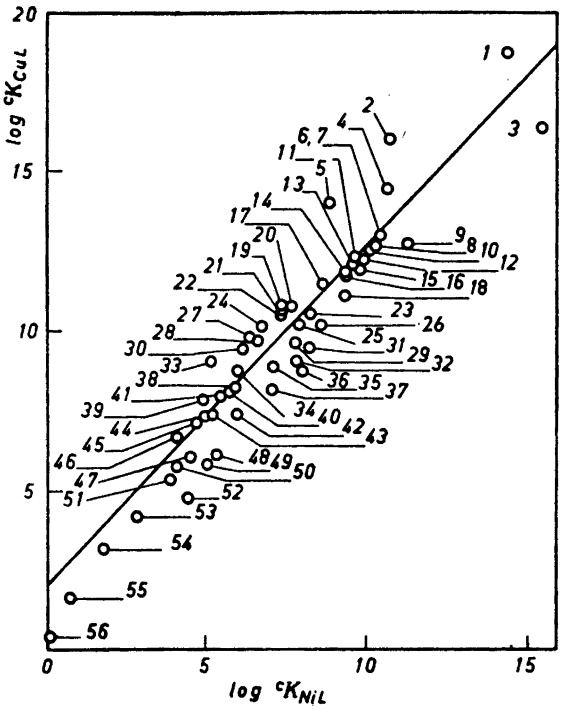


Fig. 2. Log$^cK_{CuL}$ as a function of log$^cK_{NiL}$ for complexes of a wide variety of ligands: (1) β,β',β''-Triaminotriethylamine, cf.[4] *(2) Diethylenetriamine, cf.*[4] *(3) Ethylenediaminediacetic-diproprionic acid*[5] *(4) Tiron (pyrocatechol-3,5-disulphonic acid)*[34] *(5) 1,3-Diaminopropane-2-ammonium ion, cf.*[4] *(6) 8-Hydroxyquinoline*[19] *(7) Dibenzoylmethane*[71] *(8) Thenoylbenzoylmethane*[17] *(9) Nitriloacetic acid*[5] *(10) Benzoylfuroylmethane*[17] *(11) $CH_3CO{\cdot}CH_2{\cdot}CO{\cdot}CH_2{\cdot}CH_2{\cdot}Si(CH_3)_3$ Ref.*[17] *(12) Dithenoylmethane*[17] *(13) Acetylbenzoylmethane*[17] *(14) Acetylacetone*[17] *(15) Furoylthenoylmethane*[17] *(16) Acetylthenoylmethane*[17] *(17) $(CH_3)_3SiC_2H_4{\cdot}CO{\cdot}CH_2{\cdot}CO{\cdot}C_2H_4Si(CH_3)_3$ Ref.*[17] *(18) 1,2,3-Triaminopropane, cf.*[4] *(19) N-Methylethylenediamine*[36] *(20) Ethylenediamine, cf.*[4] *(21) 1,2-Diaminopropane, cf.*[4] *(22) Iminopropionic acetic acid*[5] *(23) Iminodiacetic acid*[5] *(24) N-Ethylethylenediamine*[36] *(25) 8-Hydroxy-2,4-dimethylquinazoline*[19] *(26) 8-Hydroxy-2-methylquinoline*[19] *(27) 1,3-Diaminopropane, cf.*[4] *(28)* sym. *N,N'-Dimethylethylenediamine*[36] *(29) 5-Hydroxyquinoxaline (30) Iminodipropionic acid*[5] *(31) 8-Hydroxycinnoline*[19] *(32) Folic acid, cf.*[4] *(33) N-Propylethylenediamine*[36] *(34) Triethylenetetramine ion, cf.*[4] *(35) Aspartic acid, cf.*[4] *(36) 1,10-Phenanthroline*[37] *(37) 2,2'-Dipyridyl*[37] *(38) α-Alanine, cf.*[4] *(39) Leucine, cf.*[4] *(40) Glycine, cf.*[4] *(41)* Iso-*nicotinic hydrazide*[35] *(42) 2-Methyl-1,10-phenanthroline*[37] *(43) Salicylaldehyde, cf.*[4] *(44) Sarcosine, cf.*[4] *(45) β-Alanine, cf.*[4] *(46) Riboflavin, cf.*[4] *(47) Glycyl-glycine, cf.*[4] *(48) Oxalate ion, cf.*[4] *(49) 2,9-Dimethyl-1,10-phenanthroline*[37] *(50) Malonate ion, cf.*[4] *(51) Salicylaldehyde sulphonic acid, cf.*[4] *(52) 4-Hydroxypteridine, cf.*[4] *(53) Ammonia, cf.*[4] *(54) Pyridine, cf.*[4] *(55) Acetate ion, cf.*[4] *(56) Nitroacetate ion, cf.*[4]. *The full line is of unit slope.*

solution, a number of points refer to water-dioxan mixtures. No attempt has been made to distinguish between points for groups of closely related ligands (*e. g.* 1,3-diketones or 1,2-diamines), although they generally lie more closely

on linear plots. The line in Fig. 2 has a slope of unity. Divergencies will be due, at least in part, to differences in the preferred geometry of nickel and copper and to the fact that the co-ordination number of (planar) copper does not readily rise above four. That the best straight line through all the points should have a slope greater than unity implies that the difference in stability between the copper and nickel complexes increases with the increasing stability of the complexes.

Closer agreement with the predictions of equation (12) is found for complexes of a pair of metals of greater similarity, *e. g.* strontium and barium, and still better agreement would be expected for a pair of tripositive rare earth ions. At present there are insufficient data to subject equation (12) to really exhaustive tests.

Type III. The relationship between the stabilities of two ligands with a series of metal ions

The stabilities of complexes formed by two ligands, P and Q, with a series of metal ions may conveniently be compared by plotting log ${}^{c}K_{MP}$ as a function of log ${}^{c}K_{MQ}$. It has previously been found [19] that the experimental points for closely related pairs of ligands sometimes lie approximately on a straight line of unit slope and of intercept (log ${}^{c}K_{HP}$—log ${}^{c}K_{HQ}$). The theoretical relationship between ln ${}^{c}K_{MP}$ and ln ${}^{c}K_{MQ}$ may be derived from equation (6)

$$\ln {}^{c}K_{MP} - \ln {}^{c}K_{MQ} = \ln {}^{c}K_{HP} - \ln {}^{c}K_{HQ} + \frac{1}{RT}\{-\bar{G}^{\circ}_{MP} + \bar{G}^{\circ}_{MQ} + \bar{G}^{\circ}_{HP} - \bar{G}^{\circ}_{HQ} + n_X(-t_{MP} + t_{MQ} + t_{HP} - t_{HQ})\} + \ln (y_{HP}y_{MQ}/y_{MP}y_{HQ}) \quad (13)$$

$$= \ln {}^{c}K_{HP} - \ln {}^{c}K_{HQ} + E + F + H$$

where

$$E = \frac{1}{RT}\{(\bar{G}^{\circ}_{MQ} - \bar{G}^{\circ}_{MP}) - (\bar{G}^{\circ}_{HQ} - \bar{G}^{\circ}_{HP})\}$$

$$F = \frac{n_X}{RT}\{(t_{MQ} - t_{MP}) - (t_{HQ} - t_{HP})\}$$

and

$$H = \ln y_{MQ}/y_{MP} - \ln y_{HQ}/y_{HP}$$

Thus if the experimental data conform to the linear relationship

$$\log {}^{c}K_{MP} = \log {}^{c}K_{MQ} + (\log {}^{c}K_{HP} - \log {}^{c}K_{HQ}) \quad (14)$$

the term $(E + F + H)$ must be negligible compared with the other terms in equation (13). If $\bar{G}^{\circ}_{MQ} > \bar{G}^{\circ}_{MP}$ it is very probable that $\bar{G}^{\circ}_{HP} > \bar{G}^{\circ}_{HQ}$; hence the value of E, which depends on the difference between two terms which express the magnitude of these changes, will probably be insignificant in comparison with $\ln {}^{c}K_{MQ}$ and will tend rapidly to zero as P and Q approach each other in character. The same argument can be applied to the algebraic sum of the transfer coefficients, t_S, which determine the value of F, and to the activity coefficients included in the term H.

It is therefore not surprising that the relationship (14) is often valid for, though restricted to, very similar pairs of ligands. Values of log ${}^{c}K_{MP}$ for

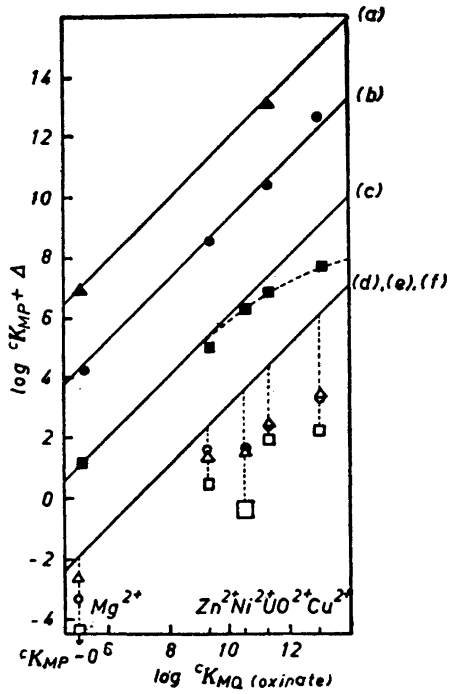


Fig. 3. Log$^cK_{MP}$ for complexes of oxine derivatives as a function of log$^cK_{MQ}$ for the corresponding oxinates. The constants were obtained [19] in 50 % v/v aqueous dioxan (0.3 M sodium perchlorate) at 20° C. The ordinates refer to complexes of: (a) 6-Methyl-oxine, Δ = 2.0 (b) 5-Methyl-oxine, Δ = −1.0 (c) 8-Hydroxycinnoline, (II, R = H), Δ = −2.0 (d) 2-Methyl-oxine (open circles), Δ = −7.0 (e) 8-Hydroxy-2,4-dimethylquinazoline (III, R = R′ = CH_3, open triangles), Δ = −6.3 (f) 8-Hydroxy-4-methyl-2-phenylquinazoline (III, R = phenyl, R′ = CH_3, open squares), Δ = −6.5. The abscissae refer to complexes of oxine. The full lines are of unit slope and of intercept, (log$^cK_{HP}$ − log$^cK_{HQ}$), predicted by equation (14).

complexes of a number of oxine derivatives [19] are plotted as a function of values of log $^cK_{MQ}$ for the corresponding oxinates in Fig. 3. When log $^cK_{MP}$ refers to complexes of 5-methyl-oxine (Fig. 3a) or 6-methyl-oxine (Fig. 3b), the experimental points fall closely on the theoretical lines of unit slope and of intercept (log $^cK_{HP}$— log $^cK_{HQ}$), as might be expected for reagents which differ only slightly from oxine in their structure and values of pK_{NH} (*cf.* [19]) and offer no steric hindrance to complex formation. Similar straight lines are also obtained for complexes of magnesium, zinc, nickel(II), copper(II) and uranyl with pairs of reagents chosen from among 5-fluoro-, 5-chloro-, 5-bromo- and 5-methyl-oxine [38].

The ordinates of Fig. 3d are values of log$^cK_{MP}$ for complexes of 2-methyl-oxine. The experimental points lie from 1 to 3 logarithmic units below the line drawn according to equation (14). This lowering of stability is undoubtedly due to steric hindrance to complex formation. As expected, deviations of the

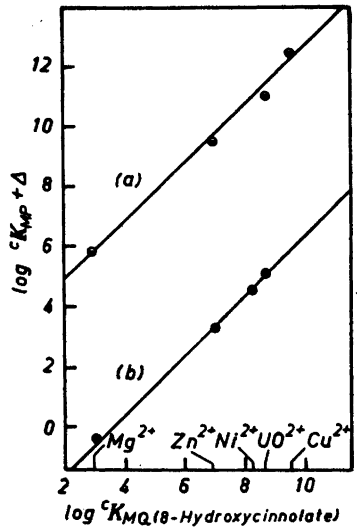


Fig. 4. Log$^cK_{MP}$ for complexes of oxine derivatives as a function of log$^cK_{MQ}$ for the corresponding complexes of 8-hydroxycinnoline. The constants [19] were obtained in 50 % v/v aqueous dioxan (0.3 M sodium perchlorate) at 20° C. The ordinates refer to complexes of (a) 8-Hydroxyquinazoline (III, R = R′ = H), Δ = 2.0 (b) 8-Hydroxy-4-methylcinnoline (II, R = CH_3), Δ = −4.0. The abscissae refer to complexes of 8-hydroxycinnoline (II, R = H). The full lines are of unit slope and of intercept (log$^cK_{HP}$ − log$^cK_{HQ}$), predicted by equation (14).

same order of magnitude are obtained for complexes of 8-hydroxy-2,4-dimethylquinazoline (III, R = R′ = CH_3; Fig. 3e) and 1,2,3,4-tetrahydro-10-hydroxyacridine (IV; graph [29] not reproduced here). When a phenyl group is adjacent to the chelating nitrogen atom (Fig. 3f), there are even greater deviations from the theoretical line, and no complex formation between 8-hydroxy-4-methyl-2-phenylquinazoline (III, R = phenyl, R′ = CH_3) and the magnesium ion could be detected.

Values of log $^cK_{ML}$ for complexes of 8-hydroxycinnoline (II, R = H) form the ordinates in Fig. 3c. The stability constant of the magnesium complex lies on the theoretical line, while that for the copper complex lies well below it. Points for other cations are in intermediate positions. The low value of pK_{NH} of 8-hydroxycinnoline as compared with the value for oxine [19] would be expected to reduce the stability of its copper complex, but to have little effect on the stability of the magnesium complex. Similar plots [29] (not reproduced here) are obtained if values of log $^cK_{MP}$ for complexes of 8-hydroxyquinazoline (III, R = R′ = H) and 8-hydroxy-4-methylcinnoline (II, R = CH_3) form the ordinates. Values of log $^cK_{MP}$ for complexes of both these reagents are plotted against values of log $^cK_{MQ}$ for the corresponding complexes of 8-hydroxycinnoline in Fig. 4. The experimental points lie much nearer the theoretical line than when the stabilities of the oxinates is made the basis of comparison, doubtless because the variation in pK_{NH} among these reagents is much smaller.

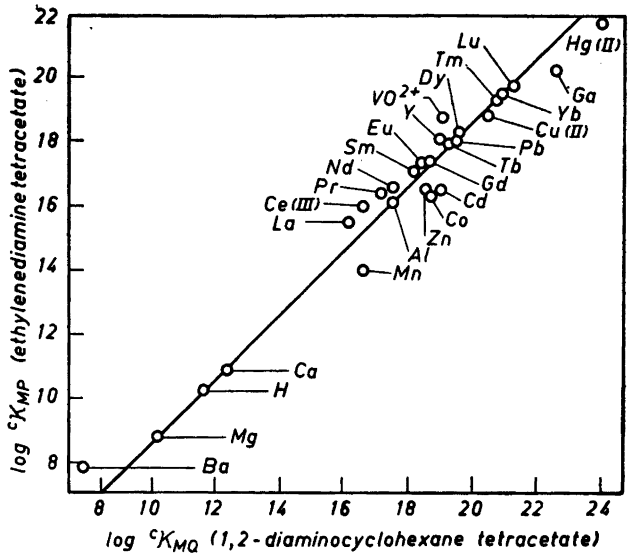
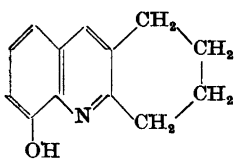
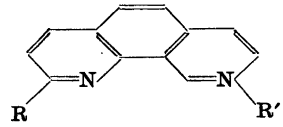


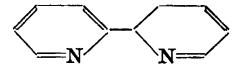
Fig. 5. Log$^cK_{MP}$ for complexes of ethylenediaminetetraacetic acid as a function of log$^cK_{MQ}$ for complexes 1,2-diaminocyclohexanetetraacetic acid. The constants [39,41] were obtained at 20° C (μ = 0.1 M). All the ions shown are in their usual valency state. The straight line is of unit slope and of intercept, (log$^cK_{HP}$ − log$^cK_{HQ}$), predicted by equation (14).



(IV)



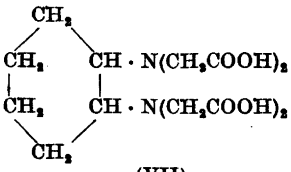
(V)



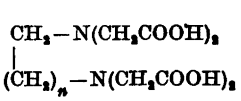
(VI)

Recent measurements [37] have shown that the 1:1 complexes of the divalent transition metals, manganese, iron, cobalt, nickel, copper and zinc with 1,10-phenanthroline (V, R = R′ = H; pK = 4.36) are consistently stronger than those of the stronger base 2-methyl-1,10-phenanthroline (V, R = H, R′ = CH_3; pK = 5.42). On the basis of equation (14) it is possible to calculate the stability constants which would have been expected from the change in basicity, and the instability arising from steric hindrance to complex formation is found to be from 2.5 to 3.5 kcal./mole. For the still less stable complexes of the even more basic reagent 2,9-dimethyl-1,10-phenanthroline (V; R = R′ = CH_3; pK = 5.85) the instability arising from steric factors is 4 to 5.5 kcal./mole. Although 1,10-phenanthroline ("phenan") and 2,2′-dipyridyl (VI; "dipy") are almost identical so far as their mode of chelating is concerned, complexes of the former are always the more stable. A plot of log $^cK_{M.dipy}$ against log $^cK_{M.phenan}$ (not reproduced) gives a good straight line for the transition metals, but the slope is 0.63

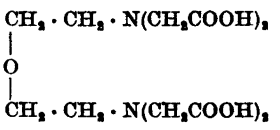
rather than unity; *i. e.* the difference between the stabilities of corresponding complexes of phenanthroline and dipyridyl decreases almost linearly with increasing stability from about 2.2 logarithmic units with manganese to 0.7 with copper. This example shows the limitations of equation (14) and the need for restricting its application to pairs of ligands of the greatest possible similarity.



(VII)



(VIII)



(IX)

Fig. 5 shows values of log ${}^{c}K_{MP}$ for 1:1 complexes of *o*-diaminocyclohexane-tetraacetic acid (VII; pK = 11.70) plotted against values of log ${}^{c}K_{MQ}$ for the corresponding complexes of ethylenediamine-tetraacetic acid [39] (VIII, n = 1; "ENTA"; pK = 10.26). The straight line shown is of unit slope and of theoretical intercept log ${}^{c}K_{HP}$—log${}^{c}K_{HQ}$. Although the complexes include those of monovalent, divalent and trivalent ions, and ions of both A and B subgroups of the periodic table, the general conformity to equation (14) is quite remarkable considering that the individual complexes differ in stability by as much as a factor of 10^{14}. The fact that values of log ${}^{c}K_{ML}$ for ENTA complexes of trivalent rare earth ions do not increase linearly with atomic number has been discussed by Wheelwright *et al.*[40] who first noted that a break in the curve occurs at gadolinium. From Fig. 5 it would appear that the complexes of VII with lanthanons of atomic number 57 to 62 are less stable than would be predicted from the values of log ${}^{c}K_{M.ENTA}$.

For complexes of diaminoethyl ether tetraacetic acid (IX) there is the possibility of co-ordination through the ethereal oxygen atom. Alternatively the 5-atom ring formed by the 1,2-diamine ENTA must be replaced by an 8-membered ring. Now increase of ring-size in the series $A_2N—(CH_2)_n—NA_2$ (A = —CH_2COOH) is reflected in a greatly decreasing stability of its alkaline earth complexes [5]. Thus log ${}^{c}K_{CaL}$ is 10.59, 7.12, 5.05 and 4.60 for n = 2, 3, 4 and 5, respectively. Were the oxygen atom entirely inactive in complex formation, the complexone IX would most closely resemble pentamethylene-tetraacetic acid (VIII, n = 4; pK = 10.58) for which the stability constant of the calcium complex is only $10^{4.6}$. While this complexone VIII is a very slightly weaker acid than ENTA, the complexone IX (pK = 9.49) is a considerably stronger acid, and would therefore be expected to form uniformly weaker complexes. In fact, when values of log ${}^{c}K_{MQ}$ for complexes of ENTA are plotted against values for the corresponding complexes of IX (for data *cf.*[41]) a straight line of unit slope and of theoretical intercept (not reproduced) passes through or close to points for magnesium, calcium, manganese(II), zinc and copper(II). The large ions barium and cadmium form complexes with IX which are 1.2 and 2.4 logarithmic units more stable than would be expected from the stability of the corresponding ENTA complexes. With these exceptions, all the complexes of IX are, as anticipated, weaker than those with ENTA. The anomalous be-

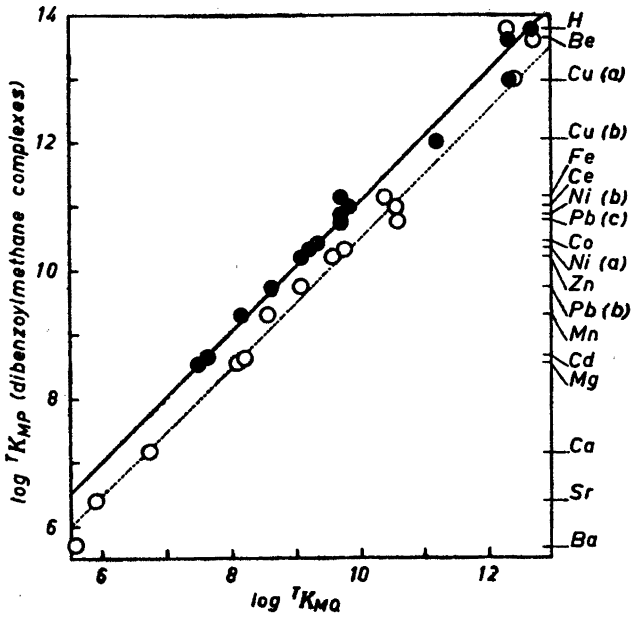


Fig. 6. Log $^{T}K_{MP}$ for complexes of dibenzoylmethane as a function of log $^{T}K_{MQ}$ for complexes of related 1,3-diketones. The thermodynamic constants were obtained [17] in 75 % v/v aqueous dioxan at 30° C. The ordinates refer to complexes of dibenzoylmethane. The abscissae refer to complexes of acetylacetone (full points and line) and of furoyl-thenoylmethane (open circles and dotted line). The full line is of unit slope and of intercept, (log $^{T}K_{HP}$ − log $^{T}K_{HQ}$), predicted by equation (14). The dotted line is the best straight line of unit slope through the open points. The letters (a), (b) and (c) denote chlorides, nitrates and perchlorates respectively; other metals were studied only in the presence of nitrate ions.

haviour of barium can be exploited analytically in a substitution titration of strontium and barium, or in the titration of these alkaline earths and magnesium using Eriochrome Black T as indicator [41].

Good straight lines are often obtained if values of log $^{c}K_{MP}$ are plotted against values of log $^{c}K_{MQ}$ for complexes of pairs of closely related α-diketones. In Fig. 6, complexes of dibenzoylmethane are compared with those of acetylacetone (full circles) and of furoyl-thenoylmethane (open circles). The majority of points for each pair of reagents lie on a straight line of unit slope. However, while the best (full) line for complexes of acetylacetone has the theoretical intercept predicted by equation (14), the best (dotted) line for complexes of furoyl-thenoylmethane has an intercept of 0.6 instead of log $^{c}K_{MP}$—log $^{c}K_{MQ}$ = 1.45. Thus all the complexes of the diketone with two heterocyclic end groups are about 0.8 logarithmic unit more stable than expected; similar, but smaller, deviations from predicted behaviour are observed for complexes of other pairs of 1,3-diketones. The effect of different terminal groups of diketones on the stability of their metal complexes has been discussed by Van Uitert *et al.*[17]; (*cf.* p. 76).

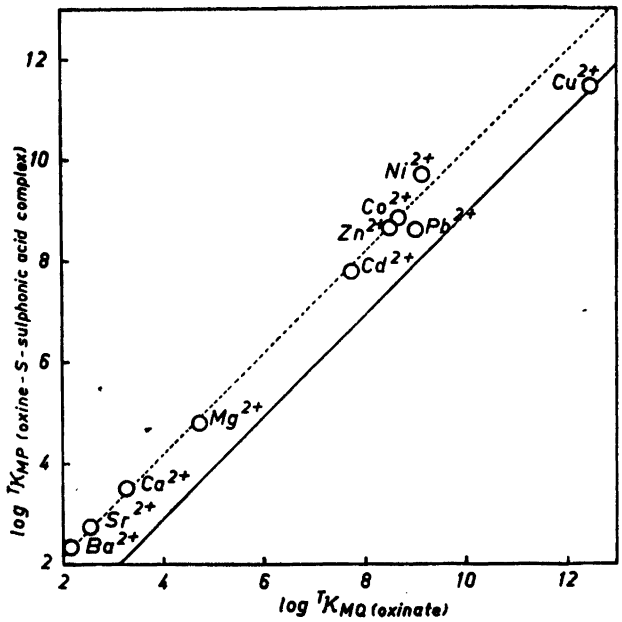


Fig. 7. Log $^{T}K_{MP}$ for complexes of oxine-5-sulphonic acid as a function of log $^{T}K_{MQ}$ for complexes of oxine. The thermodynamic constants were obtained [42-46] in water at 25° C. The full line is of unit slope and of intercept, (log $^{T}K_{HP}$ − log $^{T}K_{HQ}$), predicted by equation (14). The dotted line is the best straight line of unit slope through the experimental points.

The relationship (14) is not always valid, even if there is no possibility of steric hindrance and the ligands are very similar (*e. g.* oxine and oxine-5-sulphonic acid). It is well known that the corresponding complexes of these two ligands are of comparable stability, although the values of log $^{c}K_{HL}$ (= pK_{OH}) for the reagents differ considerably (oxine, pK_{OH} = 9.81; oxine-5-sulphonic acid, pK_{OH} = 8.75) [42,43]. Values of log $^{c}K_{MP}$ for complexes of oxine-5-sulphonic acid [44] are plotted against values of log $^{c}K_{MQ}$ for the corresponding oxinates [45,46] in Fig. 7, together with the theoretical (full) line. Although the complexes of oxine-5-sulphonic acid are much more stable than predicted by equation (14), the experimental points for complexes of many of the metal ions lie approximately on a straight line of unit slope (dotted line in Fig. 7). As the terms (ln $^{c}\mathbf{K}_{HP}$—ln $^{c}\mathbf{K}_{HQ}$) and E are constants for a given pair of reagents, this relationship, *viz.*

$$\log {}^{c}\mathbf{K}_{MP} = \log {}^{c}\mathbf{K}_{MQ} + \text{constant}$$

will only be obtained if the term

$$F = \frac{1}{RT}\{(\bar{G}^{\circ}_{MQ} - \bar{G}^{\circ}_{MP}) + n_{X}(t_{MQ} - t_{MP})\} + \ln y_{MQ}/y_{MP}$$

is negligible, or is a constant for complexes of the two ligands with a series of metal ions.

Type IV. The variation of stability with the composition of the solvent

As many organic reagents and their metal complexes are very sparingly soluble in water, stability constants are often determined in aqueous ethanol or aqueous dioxan and it is of interest to consider how these values would differ from those obtained in water. It has been found[2,21,47] that values of $\log {}^{c}K_{HL}$ for many proton-ligand complexes containing either O—H or N—H groups are approximately linear functions of the molar fraction, n_X, of the organic component of the solvent, at least for low values of n_X. Some plots of this type are shown in Fig. 8.

Now if equation (5) is valid for the species H, L and HL

$$\ln {}^{c}K_{HL'} - \ln {}^{c}K_{HL} = \frac{n_X}{RT}(t_H + t_{L'} - t_{HL'}) + \ln\left(\frac{y_H y_{L'}}{y_{HL'}} \Big/ \frac{y_H y_L}{y_{HL}}\right) \quad (15)$$

and the plot of $\log {}^{c}K_{HL'}$ against n_X will be a straight line of intercept $\log {}^{c}K_{HL}$, provided that the last term in equation (15) is (i) negligible compared with the other terms or (ii) proportional to n_X. The slope of the line is given by

$$\mathrm{d}(\log {}^{c}K_{HL'})/\mathrm{d}(n_X) = \frac{1}{2.303RT}(t_H + t_{L'} - t_L) \quad (16i)$$

or $$\mathrm{d}(\log {}^{c}K_{HL'})/\mathrm{d}(n_X) = \frac{1}{2.303RT}(t_H + t_{L'} - t_{HL'}) + d_H + d_{L'} - d_{HL'} \quad (16ii)$$

for cases (i) and (ii) respectively, where d_S is defined by

$$\ln y_S - \ln y_S = n_X \cdot d_S \quad (17)$$

Fig. 8 shows that the stabilities of complexes containing an O—H link increase with increasing organic content of the solvent, *i. e.* the term $\mathrm{d}(\log {}^{c}K_{HL'})/\mathrm{d}(n_X)$ is positive. However, an increase in the organic content of the solvent causes a decrease in the stabilities of proton-ligand complexes containing an N—H link, and for these compounds $\mathrm{d}(\log {}^{c}K_{HL'})/\mathrm{d}(n_X)$ is negative. An increase in the organic content of the mixed aqueous-organic solvent results in a decrease in the dielectric constant of the medium. This will increase the ionic interaction between a proton and a negatively charged oxygen atom to a greater extent than the ion-dipole interaction between the proton and the solvent. Thus, as n_X increases, the value of $\ln {}^{c}K_{HL'}$ should increase for proton-ligand complexes containing O—H bonds. Conversely, an increase in the organic content of the solvent would be expected to increase the ion-dipole forces between a proton and a nitrogen atom in the ligand to a lesser extent than the ion-dipole forces between a proton and the more electronegative donor oxygen atoms of the solvent (*cf.*[31,52]). A decrease in the value of $\ln {}^{c}K_{HL'}$ would therefore be expected for complexes containing N—H bonds.

The relationship between n_X and $\ln {}^{c}K_{ML'}$ for a metal-ligand complex corresponds exactly to equation (16), where M now replaces H. Thus

$$\ln {}^{c}K_{ML'} - \ln {}^{c}K_{ML} = \frac{n_X}{RT}(t_M + t_{L'} - t_{ML'}) - \ln\left(\frac{y_M y_{L'}}{y_{ML'}} \Big/ \frac{y_M y_L}{y_{ML}}\right) \quad (18)$$

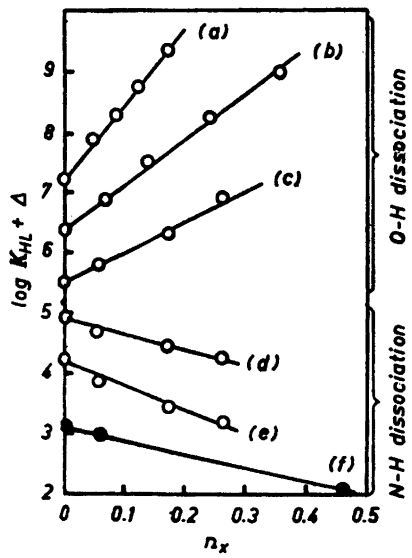


Fig. 8. Log$^cK_{HL}$ (= pK) as a function of the molar fraction, n_X, of the organic content of the solvent. Open and full circles refer to aqueous dioxan and aqueous methanol respectively. (a) to (c); compounds in which an O—H group dissociates: (a) Benzoic acid, Δ = 3.0. Thermodynamic constants [48] were obtained at 25° C. (b) m*-Chlorobenzoic acid, Δ = 2.5. Constants were obtained at 25° C and varying ionic strength [49, 50]. (c) Oxine-5-sulphonic acid, Δ = −3.0. Stoichiometric constants were obtained at 20° C in 0.3 M sodium perchlorate [29].*
(d) to (f); compounds in which an N—H group dissociates: (d) Oxine-5-sulphonic acid, Δ = 1.0. Stoichiometric constants obtained at 20° C in 0.3 M sodium perchlorate [29]. (e) Pyridine, Δ = −1.0. Stoichiometric constants obtained at 20° C in 0.3 M sodium perchlorate [29]. (f) Piperidine, Δ = −8.0. Stoichiometric constants [51] obtained at 25° C and ionic strength 0.1 M.

The conditions necessary for a linear relationship between log $^c\mathbf{K}_{ML}$ and n_X, and the possible values of d(log $^c\mathbf{K}_{ML}$)/d(n_X), are analogous to those given above for proton-ligand complexes. Van Uitert *et al.*[53] have shown that values of log$^c\mathbf{K}_{ML}$ for several acetylacetonates are linear functions of the molar fraction of dioxan in the solvent, and a replot of Maley and Mellor's data [54] (not reproduced here) shows that a similar relationship exists for the magnesium complex of salicylaldehyde. The stability of these complexes, which all contain O-metal links, is increased by an increase in the organic content of the solvent, *i. e.* d(log $^c\mathbf{K}_{ML}$)/d(n_X) is positive.

Combining equations (15) and (18),

$$\ln {}^c\mathbf{K}_{ML} - \ln {}^cK_{ML} = \ln {}^c\mathbf{K}_{HL} - \ln {}^cK_{HL} + \frac{n_X}{RT}(t_M - t_{ML} - t_H + t_{HL}) - \ln\left(\frac{y_{ML}y_H}{y_My_{HL}} \Big/ \frac{y_{ML}y_H}{y_My_{HL}}\right) \qquad (19)$$

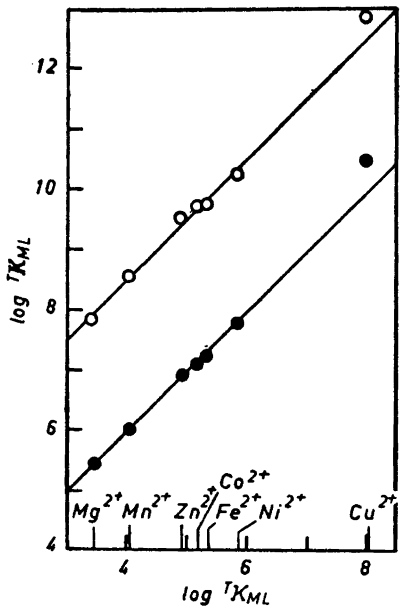


Fig. 9. Thermodynamic stability constants [53] *of metal acetylacetonates in aqueous dioxan at 30° C. The ordinates refer to values obtained in 75 % (open circles) and 50 % (full circles) v/v aqueous dioxan. The abscissae refer to values obtained in water. The lines are of unit slope and of intercept, (log* $^{T}K_{HL}$ *— log* $^{T}K_{HL}$*), predicted by equation (20).*

If the last two terms in equation (19) are negligible compared with the other terms, the equation reduces to

$$\log {}^{c}K_{ML} = \log {}^{c}K_{ML} + \log {}^{c}K_{HL} - \log {}^{c}K_{HL} \qquad (20)$$

and a plot of log $^{c}K_{ML}$ against log $^{c}K_{ML}$ for a series of complexes of different metal ions with the same ligand will be a straight line of unit slope and of intercept (log $^{c}K_{HL}$—log $^{c}K_{HL}$). This relationship is now found to be applicable to many of the data of Van Uitert *et al.*[53] for acetonylacetonates in 50 % and 75 % aqueous dioxan, which are shown in Fig. 9. Thus, for acetylacetone, a change in the composition of the solvent results in parallel changes in log $^{c}K_{ML}$ and log $^{c}K_{HL}$.

No simple relationship between stability and solvent composition would appear to exist for complexes containing N-metal bonds. An increase in the organic content of the solvent has little influence on the stabilities of certain complexes of ammonia [55–59], ethylenediamine [60–62], pyridine [29] and imidazole [63], although the complex $Ag(en)^{+}$ is more stable in pure ethanol and *iso*-propyl alcohol than in water [64].

No one author seems to have investigated the effect of solvent composition on the stabilities of complexes, such as the oxinates, which contain both O-metal and N-metal bonds. By analogy with simpler complexes, an increase in

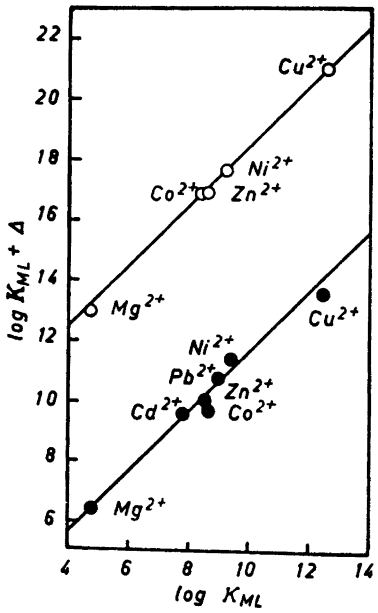


Fig. 10. Stability constants of metal oxinates in aqueous dioxan at 25° C. The ordinates refer to values obtained at varying ionic strengths in 70 % (open circles [54], Δ = 6.0) and 50 % (full circles [65], Δ = 0) v/v aqueous dioxan. The abscissae refer to thermodynamic values obtained in water. The straight lines are of unit slope and of intercept, $(\log^c K_{HL_2} - \log^c K_{HL})$, *predicted by equation (20).*

the organic content of the solvent might be expected to increase the stability of complexes in which the O-metal bond is of predominant importance, but to have less effect on the stability of complexes containing strong N-metal bonds. In Fig. 10, the stabilities of metal oxinates in 50 % and 75 % aqueous dioxan [54,65] are plotted against the corresponding values obtained in water [45,46]. Increased dioxan content leads to a marked increase in stability, in approximate agreement with equation (20). Thus for these complexes the last two terms in equation (19) are negligible compared with the other terms, and the variation of $\log {}^cK_{ML_2}$ with the composition of the solvent merely reflects the variation of $\log {}^cK_{HL}$. It would be of interest to know if this were also true for other complexes containing both O-metal and N-metal links.

APPLICATIONS

Equation (6) has been used above as a basis for discussing the various empirical linear relationships between the stabilities of related complexes. These plots are of interest from both practical and theoretical considerations.

If the stability constants of some closely related complexes have been measured, the stabilities of other complexes in the same series may be predicted by means of equations (9) and (14). For example, although the stability con-

stants of the zinc, nickel(II) and copper(II) 6-methyl-oxinates could not be measured in 50 % aqueous dioxan, on account of the low solubility of the uncharged complexes [19], approximate values, *viz.* 9.2, 10.4 and 12.9, can be estimated using equation (14) in conjunction with values of the stability constants of the corresponding oxinates, and of log ${}^{c}K_{HL}$ of the two reagents [19] (*cf.* Fig. 3b). The estimation of stability constants of very sparingly soluble complexes is especially important for analytical work involving the separation of metal ions by solvent extraction or selective precipitation [2].

It has been shown that plots of log ${}^{c}K_{ML}$ against log ${}^{c}K_{HL}$ are often linear for series of very closely related ligands. If divergent lines of different slope are obtained for different metal ions with the same series of ligands (*e. g.* complexes of magnesium, uranyl and copper(II) ions with derivatives of oxine [19]) a ligand with a high value of ${}^{c}K_{HL}$ will form metal complexes of more varied stability than those formed from a ligand of low ${}^{c}K_{HL}$, and will therefore be a more selective reagent for these metal ions. If only very closely related ligands are considered, deviations from linearity in plots of log ${}^{c}K_{ML}$ against log ${}^{c}K_{HL}$, and in plots of the type (14) indicate any tendencies to selective or specific behaviour. Ligands with bulky substituents adjacent to one of the donor atoms form much less stable metal-ligand complexes than would be expected from the stability of the corresponding proton-ligand complexes (*cf.* Fig. 3d, e, f). As this effect depends on the size of the central group, sterically hindered reagents are of use for the analytical separations of certain metal ions (*cf.* the reactions between 2-methyl-oxine and trivalent aluminium, gallium and indium ions, [66] and refs. therein). Even when no steric hindrance occurs, metal-ligand chelate complexes may deviate appreciably from predicted behaviour (*cf.* Fig. 3c). The formation of a metal chelate involves combination of the metal ion with two or more donor atoms, while the formation of the first proton-ligand complex involves only the atom which has the most basic (donor) character. The observed deviations probably reflect differences in the co-ordinating power of the other donor atoms throughout the series of ligands.

The value of ${}^{c}K_{HL}$ for proton-ligand complexes which are very sparingly soluble in water may be estimated by measuring ${}^{c}K_{HL}$ in a number of water-ethanol or water-dioxan mixtures; log ${}^{c}K_{HL}$ may then be obtained by linear extrapolation of the plot of log ${}^{c}K_{HL}$ against n_X, to the point $n_X = 0$ (*cf.* equation (15) case (i) or (ii)). The value of ${}^{c}K_{ML}$ can be estimated analogously be means of equation (18). If equation (19) is valid, an approximate value of K_{ML} in water may be predicted from the corresponding constant, ${}^{c}K_{ML}$, obtained in a mixed solvent, if the proton-ligand stability constants, ${}^{c}K_{HL}$ and ${}^{c}K_{HL}$, in both solvents are known. Although water has been used as a solvent for most analytical processes in homogeneous systems, a mixed solvent might be of value for absorptiometric work and for certain selective precipitation reactions. Titrations in solvents such as aqueous dioxan, acetic acid, or glycol-*iso*propyl alcohol mixtures are at present being developed extensively but empirically. Progress would be facilitated if more were known of the effect of change of solvent on the stability of proton-ligand and metal-ligand complexes of all types *cf.*[67]. Equations of the type (15), (18) and (19) might then be used to predict approximate values of stability constants in the appropriate solvent. As O-metal bonds appear to be more influenced by the composition of

the solvent than N-metal bonds, the effect of solvent composition on the stability of chelates containing the O-metal-N link might be an indication of the relative importance of these bonds.

Equation (6) and the foregoing discussion refer to the formation of the first metal-ligand complex, and suggest no correlation of the stabilities of complexes which contain more than one ligand group. Although some authors (*e. g.*[15]) have obtained approximate empirical relationships between log ${}^{c}K_{\mathrm{HL}}$ and log $K_{\mathrm{av}} = \frac{1}{2}$ log $[\mathrm{ML_2}]/[\mathrm{M}][\mathrm{L}]^2$ it would be expected that in many cases the formation of the complex ML modifies the properties of the metal ion and ligand group to such an extent that any quantitative comparison of equilibrium constants for reactions of the type

$$\mathrm{ML} + \mathrm{L} = \mathrm{ML_2}$$

would be unjustified.

As so few reliable measurements have been made of the enthalpy and entropy of complex formation, stability constants have been discussed purely in terms of overall changes in free energy. When more precise data become available, a further analysis of heat and entropy changes would be profitable using a similar approach.

Acknowledgements. We would like to thank Dr. James Duncan, University of Melbourne, for stimulating discussion in the early stages of this work, and Professor Lars Gunnar Sillén and Dr. F. J. C. Rossotti, for their helpful comments on the manuscript.

We are also grateful to *A. E. R. E.*, Harwell, and the *Swedish Atomic Energy Commisson*, for financial assistance.

REFERENCES

1. Irving, H. and Williams, R. J. P. *Analyst* **77** (1952) 813.
2. Irving, H. and Rossotti, H. S. *Analyst* **80** (1955) 245.
3. Martell, A. E. and Calvin, M. *Chemistry of the Metal Chelate Compounds*, Prentice Hall Inc. New York 1952.
4. Irving, H. and Williams, R. J. P. *J. Chem. Soc.* **1953** 3192.
5. Irving, H., Williams, R. J. P., Ferrett, D. J. and Williams, A. E. *J. Chem. Soc.* **1954** 3494.
6. Schwarzenbach, G. *Rec. trav. chim. In the press.*
7. Nyholm, R. S. *Rev. Pure Appl. Chem. (Australia)* **4** (1954) 15.
8. Van Uitert, LeG. G. and Fernelius, W. C. *J. Am. Chem. Soc.* **76** (1954) 379.
9. Williams, R. J. P. *J. Chem. Soc.* **1952** 3770.
10. van Eck, C. L. van P. *Rec. trav. chim.* **72** (1953) 50.
11. Bjerrum, J. *Chem. Revs.* **46** (1950) 381.
12. Fyfe, W. S. *J. Chem. Soc.* **1952** 2018.
13. Jørgensen, C. Klixbüll and Bjerrum, J. *Acta Chem. Scand.* **9** (1955) 180.
14. Coulson, C. A. *J. Chem. Soc.* **1955** 2069.
15. Calvin, M. and Wilson, K. W. *J. Am. Chem. Soc.* **67** (1945) 2003.
16. Bruehlman, R. J., and Verhoek, F. H. *J. Am. Chem. Soc.* **70** (1948) 1401.
17. Van Uitert, LeG. G., Fernelius, W. C. and Douglas, B. E. *J. Am. Chem. Soc.* **75** (1953) 457, 2736.
18. Schwarzenbach, G., Ackermann, H. and Ruckstuhl, P. *Helv. Chim. Acta* **32** (1949) 1175.
19. Irving, H. and Rossotti, H. S. *J. Chem. Soc.* **1954** 2910.
20. Owen, B. B. *J. Am. Chem. Soc.* **54** (1932) 1758.
21. Harned, H. S. and Owen, B. B. *Physical Chemistry of Electrolytic Solutions*, Reinhold, 1950.
22. Scatchard, G. *J. Am. Chem. Soc.* **47** (1925) 2098.

23. Åkerlöf, G. *J. Am. Chem. Soc.* **52** (1930) 2353.
24. Butler, J. A. V. and Thomson, D. W. *Proc. Roy. Soc. London* **A 141** (1933) 86.
25. Duncan, J. D. *Private communication; cf.* discussion to paper by Freiser, H. *Analyst* **77** (1952) 830.
26. Rossini, F. D., Wagman, D. D., Evans, W. H., Levine, S. and Jaffe, I. *Selected Values of Chemical Thermodynamic Properties*, U. S. Natl. Bur. Standards, 1952.
27. Milburn, R. M. *J. Am. Chem. Soc.* **77** (1955) 2064.
28. Rossotti, H. S. *Rec. trav. chim. In the press.*
29. Rossotti, H. S. *D. Phil. thesis*, Oxford 1954.
30. Van Uitert, LeG. G. and Fernelius, W. C. *J. Am. Chem. Soc.* **75** (1953) 3862.
31. Trotman-Dickenson, A. F. *J. Chem. Soc.* **1949** 1293.
32. Schwarzenbach, G., Willi, A. and Bach, O. *Helv. Chim. Acta.* **30** (1947) 1303.
33. Brown, H. C., Bartholomay, H. and Taylor, M. D. *J. Am. Chem. Soc.* **66** (1944) **441**; Brown, H. C. and Taylor, M. D. *J. Am. Chem. Soc.* **66** (1944) 846.
34. Willi, A. and Schwarzenbach, G. *Helv. Chim. Acta* **35** (1952) 2353.
35. Albert, A. *Experimentia* **9** (1953) 370.
36. Irving, H. and Griffiths, J. M. M. *J. Chem. Soc.* **1954** 213.
37. Irving, H. and Mellor, D. M. *J. Chem. Soc. To be published.*
38. Irving, H. and Massy-Beresford, P. *J. Chem. Soc. To be published.*
39. Schwarzenbach, G., Gut, R. and Anderegg, G. *Helv. Chim. Acta* **37** (1954) 937.
40. Wheelwright, E. J., Spedding, F. H. and Schwarzenbach, G. *J. Am. Chem. Soc.* **75** (1953) 4196.
41. Schwarzenbach, G. *Die komplexometrische Titration*, Stuttgart 1955.
42. Näsänen, R., Lumme, P. and Mukula, A.-L. *Acta Chem. Scand.* **5** (1951) 1199.
43. Näsänen, R. and Ekman, A. *Acta Chem. Scand.* **6** (1952) 1384.
44. Näsänen, R. and Uusitalo, E. *Acta Chem. Scand.* **8** (1954) 112.
45. Näsänen, R. *Acta Chem. Scand.* **5** (1951) 1293; **6** (1952) 352; *Suomen Kemistilehti* **32** (1953) 11.
46. Näsänen, R. and Penttinen, U. *Acta Chem. Scand.* **6** (1952) 837.
47. Van Uitert, LeG. G., Haas, C. G., Fernelius, W. C. and Douglas, B. E. *J. Am. Chem. Soc.* **75** (1953) 455.
48. Dunsmore, H. S. and Speakman, J. C. *Trans. Faraday Soc.* **50** (1954) 236.
49. Saxton, B. and Meier, H. F. *J. Am. Chem. Soc.* **56** (1934) 1918.
50. Elliot, J. H. and Kilpatrick, M. *J. Phys. Chem.* **45** (1941) 485.
51. Wynne-Jones, W. F. K. and Salomon, G. *Trans. Faraday Soc.* **34** (1938) 1321.
52. Bell, R. P. and Trotman-Dickenson, A. F. *J. Chem. Soc.* **1949** 1288.
53. Van Uitert, LeG. G., Fernelius, W. C. and Douglas, B. E. *J. Am. Chem. Soc.* **75** (1953) 2739.
54. Maley, M. E. and Mellor, D. P. *Austral. J. Sci. Research* **A 2** (1949) 92.
55. Pawelka, F. G. *Z. Electrochem.* **30** (1924) 180.
56. Job, P. *Ann. chim. Paris* **9** (1928) 183.
57. Larrson, E. *Z. physik. Chem.* **A 169** (1934) 207.
58. Bjerrum, J. *Diss. Copenhagen* 1941.
59. Van Uitert, LeG. G. and Fernelius, W. C. *J. Am. Chem. Soc.* **76** (1954) 375.
60. Carlson, G. A., McReynolds, J. P. and Verhoek, F. H. *J. Am. Chem. Soc.* **67** (1945) 1334.
61. Bjerrum, J. and Nielsen, E. J. *Acta Chem. Scand.* **2** (1948) 297.
62. Basolo, F. and Murmann, R. K. *J. Am. Chem. Soc.* **74** (1952) 5243.
63. Li, N. C., White, J. M. and Doody, E. *J. Am. Chem. Soc.* **76** (1954) 6219.
64. Jonassen, H. B., Fagley, T. F., Rolland, C. C. and Yates, P. C. *J. Phys. Chem.* **58** (1954) 286.
65. Johnston, W. B. and Freiser, H. *J. Am. Chem. Soc.* **74** (1952) 5239.
66. Irving, H., Hollinshead, R. G. W. and Harris, G. *Analyst* **80** (1955) 260.
67. Riddick, J. A. *Anal. Chem.* **26** (1954) 77.

Received October 6, 1955.

ACTA CHEMICA SCANDINAVICA 10 (1956) 94—105

On the Chemical State of ^{32}P and ^{33}P in a Sulphur Target

GÖSTA NILSSON

Division of Physical Chemistry, Royal Institute of Technology, Stockholm, Sweden

The yields of ^{32}P, ^{33}P and ^{35}S by the irradiation of sulphur in the Norwegian D_2O-reactor at Kjeller have been determined for different sample positions in the reflector.

It was found that a large amount of ^{32}P and ^{33}P but hardly any ^{35}S followed the insoluble S_μ-fraction of the sulphur samples on dissolving in CS_2. Adsorption can be responsible for this phenomenon but an alternative explanation, assuming S_μ formation in "displacement spikes", is also given.

The initial S_μ content of the sublimated sulphur samples *decreased* on reactor irradiation.

No significant chemical difference was found between ^{32}P and ^{33}P after extraction from a solution of irradiated sulphur in CS_2 to a water phase.

The separation factor for a process where two atoms with recoil ranges r_1 and r_2 recoil from a spherical particle into a catcher phase surrounding the particle has been calculated and applied to the case of ^{32}P and ^{33}P recoiling from colloidal sulphur particles.

For a long time, ^{32}P has been one of the most frequently produced radioisotopes in nuclear reactors and the only isotope used as a radiotracer for phosphorus. Usually the isotope is made by irradiation of sulphur according to the endothermal reaction ^{32}S (n, p)^{32}P (I). Since the threshold energy for the reaction is 954 keV, fast neutrons must be used (Fig. 1).

In 1951, however, the new radioisotope ^{33}P was discovered in reactor-irradiated sulphur and the exothermal reaction ^{33}S (n, p)^{33}P (II) was found to be responsible for its formation [1–4]. Now, ^{33}P possesses properties which make it suitable for tracer applications and it is therefore of interest to produce as pure samples of ^{33}P as possible.

When preparing ^{33}P by irradiation of sulphur with neutrons, the only "impurities" introduced are ^{32}P and a large amount of ^{35}S formed by the exothermal reaction ^{34}S (n, γ) ^{35}S (III). This last "impurity", however, can always be removed chemically. Therefore the main problem is to get a high $^{33}P/^{32}P$ ratio in the irradiated samples.

Now Westermark [3] pointed out that ^{33}P, in contrast to ^{32}P, can be produced also by thermal neutrons, as seen from cross sections pictured in Fig. 1.

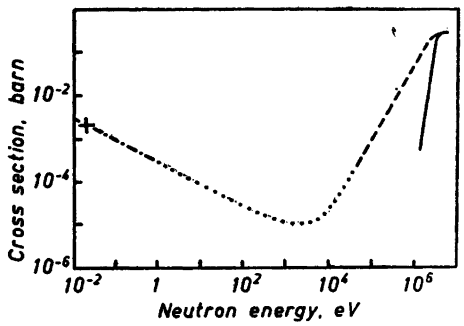


Fig. 1. Cross sections of the reactions ^{33}S (n, p) ^{32}P (I) and ^{33}S (n, p) ^{33}P (II).

———— *experimental cross section of reaction I according to Klema and Hanson* [5].
— — — — *cross section of reaction II calculated from the continuum theory* [6] *by B. Elbek* [7].
\+ *experimental cross section of reaction II according to Westermark* [3].
—·—·— *cross section of reaction II according to the "1/v law" for thermal neutrons.*

The cross sections indicate that an irradiation of a sulphur sample in the peripheral parts of a reactor where the thermal flux is high (compared with the fast flux) would give an optimum value for the $^{33}P/^{32}P$ ratio. One is thus forced to irradiate in a position where the activity of ^{33}P per gram sulphur becomes low. Furthermore, sulphur contains 95.1 % ^{32}S but only 0.75 % ^{33}S. This makes it difficult to establish a high $^{33}P/^{32}P$ ratio at all. Any method, chemical or physical which makes it possible to increase this ratio is therefore of value.

If, in order to get a high $^{33}P/^{32}P$ ratio, a sulphur sample is irradiated in a position where the ratio of thermal to fast flux is high, then the two isotopes are formed by neutrons with essentially different energies. This means that the most probable recoil energies of the isotopes are also different. As a result they might appear in different chemical states in the target, an effect which could be used to increase the $^{33}P/^{32}P$ ratio.

In order to study the $^{33}P/^{32}P$ ratio as a function of the distance from the centre of the reactor and the chemical state of the isotopes, several samples of sulphur were irradiated in the Norwegian D_2O-reactor at Kjeller.

EXPERIMENTAL

Measurement of sample activities

The content of ^{33}P, ^{32}P and ^{35}S in the samples was determined by absorption measurements in a standard geometry using aluminium foils as absorbers and an end-window G.M.-tube as detector (1.4 mg/cm² mica window). A thick aluminium backing established saturation backscattering in all cases and counting rates were corrected for dead time and background. Absorption curves were plotted according to Fig. 2, where I_0 is the extrapolated counting rate at 0 mg/cm². From this plot, the different activities were obtained using standard absorption curves for ^{32}P and ^{33}P. The ^{32}P curve was determined by absorption measurements on a nearly pure ^{32}P sample in the standard geometry. The corresponding ^{33}P curve was the result of measurements on samples containing ^{32}P, ^{33}P and very small amounts of ^{35}S.

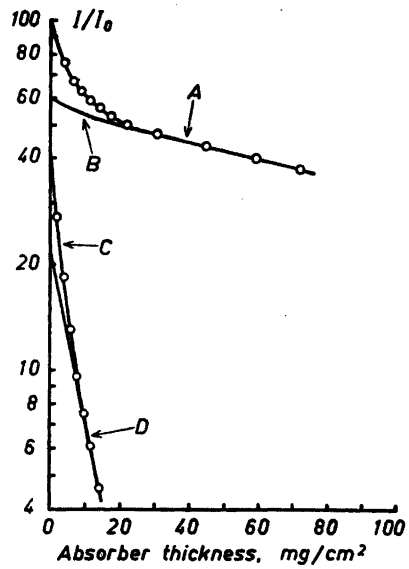


Fig. 2. Absorption curves in the standard geometry.
A = ^{32}P, ^{33}P *and* ^{35}S.
B = ^{32}P *standard curve.*
C = ^{33}P *and* ^{35}S.
D = ^{33}P *standard curve (half thickness 6 mg/cm²).*

The different activities obtained in this way were corrected for half life (*i. e.* the activities compared refer to a common time) and when necessary also for self-absorption in the samples. This method permitted a good comparison of the activities of the different sulphur samples. Since, however, no pure sample of ^{33}P was available, it was only possible to determine the absolute values of the ^{32}P activity with good accuracy.

Yields of the isotopes for different positions in the reactor

Since the ^{35}S activity was very high compared with the ^{33}P activity, it was not possible to determine the ^{33}P and ^{35}S contents by a direct measurement of the activities of the irradiated samples. From such measurements the ^{32}P activity and the sum of the ^{33}P and ^{35}S activities were obtained.

Samples for irradiation in the reactor were, however, prepared from sulphur containing a small amount of S_μ (*i. e.* amorphous sulphur) [6]. When dissolving such a sample in carbon disulphide and centrifuging the solution, it was found that a large amount of the radiophosphorus followed the insoluble S_μ-fraction. Since there was no or only a very small enrichment of ^{35}S in the S_μ-fraction (Table 1), this is a very simple way of separating a large amount of ^{32}P and ^{33}P from ^{35}S, *i. e.* samples were obtained in which the $^{33}P/^{32}P$ ratio could be determined. In addition, these samples had so low a weight per unit area (<1 mg/cm^2) that self-absorption for ^{33}P and ^{35}S could be neglected. If ^{32}P and ^{33}P, as seems reasonable, follow S_μ in proportion to their concentrations, then the $^{33}P/^{32}P$ ratio in the S_μ-fraction and the first measurement (mentioned above) give the amounts of ^{33}P and ^{35}S in the samples. The results are plotted in Fig. 3. They refer to irradiations in the reflector. Samples irradiated in the reactor tank are omitted, since the ^{33}P content was too low to be determined. The samples were irradiated for about 14 days at a reactor effect of 200–250 kW and the results refer to the end of the irradiation.

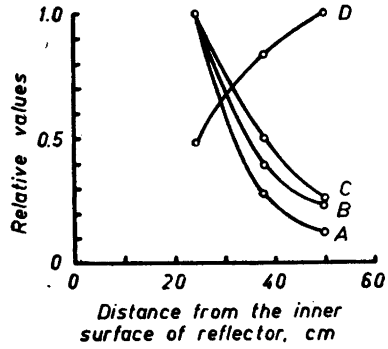


Fig. 3. Yields of the isotopes and the ratio $^{33}P/^{32}P$ for different positions of irradiation in the reflector.

A = ^{32}P	*1.0*	*corresponds to*	*3*	*μC/g*	*sulphur*
B = ^{35}S	*1.0*	»	» *32*	»	»
C = ^{33}P	*1.0*	»	» *0.3*	»	»
D = $^{33}P/^{32}P$	*1.0*	»	» *0.25*		

The carrier action of the S_μ-fraction on ^{32}P and ^{33}P

As previously mentioned, a large part of ^{32}P and ^{33}P was carried by the S_μ-fraction. The separation of S_μ was performed as follows:

Irradiated sulphur (0.5—0.6 g) was dissolved in 10 ml carbon disulphide. The insoluble S_μ was then collected on an aluminium foil by centrifuging in a special centrifuge tube. Before weighing and measuring the activity, the foil was placed for 5 min in pure carbon disulphide. The results are shown in Table 1.

Table 1. The carrier action of the Sμ-fraction of different samples on ^{32}P, ^{33}P and ^{35}S.

Sulphur sample	Distance from centre of reactor cm	% S_μ in sample	% Activity carried by S_μ		
			^{32}P	^{33}P	^{35}S
Subl.	Unirradiated	0.47	—	—	—
Cryst.	»	0.02	—	—	—
Subl.	48	0.08	30	—	0.4
»	60	0.08	32	—	0.3
»	124	0.09	62	59	0.04
»	150	0.09	60	71	0.4
Cryst.	48	0.02	19	—	0.2
»	138	0.02	14	13	0.01

The treatment of the foils with CS_2, as described, resulted in a marked decrease in inactive sulphur and ^{35}S. The influence on ^{32}P and ^{33}P, however, was very small.

Some foils were placed for an additional 24 h in CS_2. Their weights, however, were unchanged and their total activities decreased by only 2—6 %; *i. e.* the results in Table 1 may be regarded as referring to S_μ.

A number of experiments was performed in order to find if ^{32}P and ^{33}P, in the form of phosphorus or a compound of phosphorus, were reversibly adsorbed on S_μ. This was done by studying the displacement of radiophosphorus from S_μ by phosphorus and different

phosphorus compounds added to the carbon disulphide solution. The time interval between adding the compound and centrifugation was about 30 min. The results are shown in Table 2.

Table 2. The displacement action of different substances on ^{32}P adsorbed on S_μ.

Substances added to the CS_2-solution	% of ^{32}P activity carried by S_μ
—	60
—	65
P_2S_3, P_2S_5, P_4S_7	67
P (yellow)	62
»	63
H_3PO_4	56
H_3PO_3	44

The solubilities of H_3PO_4 and H_3PO_3 in CS_2 are small, but certainly the concentrations become sufficient to partly displace the small amounts, if any, of radiophosphorus in the form of H_3PO_4 and H_3PO_3 adsorbed on S_μ.

Sublimated, unirradiated sulphur was added to an irradiated sample of low S_μ content in such an amount that the S_μ-fraction in the sample was doubled. This treatment, however, increased the amount of ^{32}P carried by only 2 %.

Separation of radiophosphorus as magnesium ammonium phosphate

An experiment of this type was performed to determine, if possible, the valency of the phosphorus isotopes in the sulphur target. It was thus necessary to prevent ^{32}P and ^{33}P from being oxidized in the separation process. For this reason, the process was carried out in a nitrogen atmosphere and all solutions added were saturated with nitrogen gas. The separation was performed as follows:

To a solution of irradiated sulphur in CS_2, an aqueous solution containing 0.2 mg/ml of each of H_3PO_4, H_3PO_3 and H_2SO_4 was added. The solution, contained in a tube, was shaken for 2 h in a mechanical shaker. Part of the water phase was separated through a filter and P(V) precipitated as magnesium ammonium phosphate. The addition of H_3PO_3 and H_2SO_4 was made to prevent adsorption of radiophosphorus as phosphite or ^{35}S as sulphate on the precipitate. It also prevented coprecipitation of radiophosphite.

The total amount of radiophosphorus extracted by the water phase was determined by oxidation of phosphite to phosphate by bromine water and precipitating P(V) as before.

Some experiments were carried out in exactly the same way but without protection against oxidation. The results are given in Table 3.

Table 3. The fraction of ^{32}P and ^{33}P extractable from a solution of sulphur in CS_2 to a water phase and the valency of the isotopes in that fraction.

Sulphur sample	Distance from centre of the reactor cm	In nitrogen				In air			
		% ^{32}P extr.	% ^{33}P extr.	%P(V) of extr. ^{32}P	%P (V) of extr. ^{33}P	% ^{32}P extr.	% ^{33}P extr.	%P (V) of extr. ^{32}P	%P (V) of extr. ^{33}P
Cryst.	138	26	19	75	82	40	34	82	87
»	48	51	—	82	—	40	—	91	—
Subl.	150	32	24	88	84	42	24	85	80
»	60	37	—	84	—	35	—	90	—

DISCUSSION

In Fig. 3, A is a graph both of the yield of ^{32}P and also of the decrease of the fast neutron flux in the reflector. This is because reaction I requires fast neutrons. The fast flux, however, decreases more rapidly than the thermal flux and the reactions II and III have relatively large cross sections for thermal neutrons. The yields of ^{33}P (C) and ^{35}S (B), therefore, decrease more slowly and the $^{33}P/^{32}P$ ratio (D) increases with distance from the reactor core.

The most interesting result is that a large amount of radiophosphorus but almost no ^{35}S followed the S_μ-fraction (Table 1). Approximately equal amounts of ^{32}P and ^{33}P follow S_μ but the amounts seem to decrease with decreasing S_μ content of the irradiated sulphur.

At first sight this may be supposed to be due to adsorption of either radiophosphorus or a chemical compound of radiophosphorus on S_μ. However, addition to the CS_2 solution of phosphorus or some of the compounds most probably formed by radiophosphorus in this case had only a small effect (except for H_3PO_3) on the carried activity (Table 2). The increase in amount carried was also small after adding S_μ before dissolving the sample in CS_2. This seems to indicate that adsorption on S_μ of radiophosphorus in these chemical forms cannot alone be responsible for the carrying effect. Adsorption can, however, not be excluded. In any case it may be of value to discuss an alternative explanation:

A recoiling atom is assumed to melt or vaporize a small volume at the end of its track in a solid substance [9]. The local temperature in this "displacement spike" is very high and the quenching is very rapid [10]. This means that "displacement spikes" may also be produced in sulphur by recoiling ^{32}P, ^{33}P and ^{35}S atoms. It is further assumed that small aggregates of S_μ are formed by the rapid quenching of the "displacement spikes", in analogy with the formation of S_μ by the rapid quenching of sulphur vapour or liquid sulphur [8]. Radiophosphorus and ^{35}S trapped in these aggregates are difficult to extract by CS_2 and in the chemical operations the aggregates will follow the macro amounts of S_μ in the sample, *i. e.* the radioisotopes follow the S_μ-fraction.

Only radiophosphorus and hardly any ^{35}S follows the S_μ-fraction (Table 1). As seen from the following calculations, an explanation may be found in the different volumes of the "displacement spikes" produced.

The most probable recoil energies of ^{32}P and ^{33}P can be computed from the equation [11]

$$E_r = \frac{m_p}{M + m_p}\left[E_n\left(1 - \frac{m_n}{M + m_p}\right) + Q\right] \qquad (1)$$

where E_n is the neutron energy, m_n the mass of the neutron, m_p the mass of the proton and M the mass of the recoiling atom. The Q-values of the reactions are 925 (I) and 517 (II) keV [12]. The equation is valid if the compound nucleus has lost its recoil energy before emitting the proton [11]. This may be assumed to happen since the reactions take place in a solid substance [11].

When irradiating in the reflector, the ^{33}P atoms are most probably produced by neutrons having an energy of 0.025 eV, *i. e.* the most probable energy of the

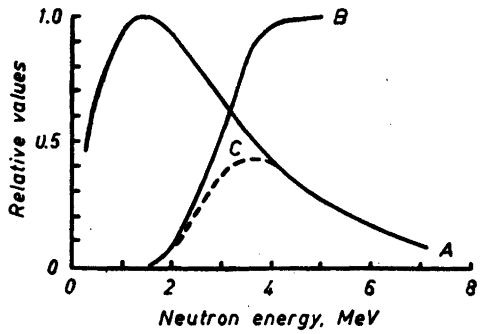


Fig. 4. Graphical determination of the most probable recoil energy of ^{32}P atoms produced in the reaction ^{32}S (n, p) ^{32}P (I) by neutrons of the fission spectrum (fast neutrons).

A = the flux of fission neutrons. The maximum of A is at a neutron energy of 1.4 MeV.
B = cross section of reaction I. The top of B corresponds to about 0.3 barns.
C = the product of flux and cross section. The maximum of C gives the most probable recoil energy of the ^{32}P atoms, i. e. *about 3.5 MeV.*

thermal flux at 20° C. This value gives a most probable recoil energy for the ^{33}P atoms of 15 keV.

It is more difficult to estimate the corresponding energy for ^{32}P. If the fast neutrons had the energy distribution of the fission spectrum [13], a graphical determination (Fig. 4) gives a value of about 3.5 MeV. The maximum of the fast flux in the reflector, however, is very likely at a lower energy. This means that ^{32}P is most probably produced by neutrons having energies between 3.5 and 0.954 MeV (the threshold value). Assuming 2.5 MeV for the neutron energy, the most probable recoil energy is 45 keV.

The recoil energy of the ^{35}S atoms can be calculated from the equation [14]

$$E_r = \frac{536\ E_\gamma^2}{M} \qquad (2)$$

where E_r is the recoil energy in electron volts, M the mass of the recoiling atom in atomic mass units and E_γ the energy of the emitted gamma ray in MeV. The number and the energy of the emitted gamma rays per neutron capture in reaction III, however, have not been determined. By extrapolation from a diagram by Kikuchi *et al.*[15], the maximum energy of the gamma rays is estimated to be 6 MeV, giving the ^{35}S atoms a maximum recoil energy of 0.55 keV. Since the mean number of gammas emitted per neutron capture in even Z-even N nuclei is about 1.7 [16], this value for the recoil energy is too high.

Maximum values of the melted volumes in the three cases can be crudely estimated by assuming that the recoil energy is entirely available for melting (this can be done since the recoil energy is of the same order of magnitude as the transition energy for melting as defined by Brinkman [9]) and that the energy necessary to melt sulphur at atmospheric pressure (about 0.02 eV/atom) [8] can be used. Under these assumptions the melted volumes produced by ^{32}P, ^{33}P and ^{35}S contain about 2×10^6, 8×10^5 and 3×10^4 atoms. Since each

sulphur atom occupies a volume [8] of 26 Å^3, these volumes, assumed to be spherical, would have diameters of about 460, 340 and 110 Å, respectively. Evidently a recoiling ^{32}P atom melts a volume more than ~70 times larger than that melted by a recoiling ^{35}S atom. The resolidification occurs with the surrounding S_α lattice acting as a crystallization nucleus. It is therefore most probable that a S_μ aggregate is formed in the centre of the melted volume — the probability of S_μ-formation increasing with the size of that volume. Assuming that the volumes melted by recoiling ^{35}S atoms are too small to produce S_μ-aggregates will explain why ^{35}S does not follow the S_μ-fraction to any great extent.

It may be pointed out that S_μ is also produced by recoil (knock-on) atoms formed in the slowing down of fast neutrons. An assumed formation of S_μ in these ways seems to conflict with the decrease in S_μ by reactor irradiation, the sublimated samples losing about 80 % of initial S_μ content whereas no change is found in the crystallized samples (Table 1).

In the first case the transformation of S_μ to S_α is evidently more effective than the assumed formation of S_μ in "displacement spikes". It is difficult to estimate the amount of S_μ formed but reasons for being small are:

1. Only a part of the energy of the primary knock-on atoms is effective in melting (*i. e.* their initial energy is larger than the transition energy for melting).

2. Only a small part of a melted volume is assumed to form S_μ.

It is known that S_μ spontaneously transforms to the stable modification [8] S_α. The transformation can be accelerated by heating, irradiation by X-rays and so on [8]. In our case irradiation must be responsible for the transformation since the temperature of the reflector was only 10° C. Maier-Leibnitz [17] and Erbacher [18] found a similar effect in the conversion of white phosphorus to the stable red form by the radiation from a Rn-Be source.

The transformation in the reactor of S_μ to soluble S_α means that a part of the radiophosphorus atoms trapped in S_μ are set free. It can be calculated (Appendix 1) that about 50 % are set free in this way assuming that the amount of S_μ formed can be neglected compared with the initial S_μ amount, *i. e.* that the rate of transformation is that shown by S_μ in the sublimated samples.

From the results given in Table 3 it is seen that the maximum amount of ^{32}P extracted from the CS_2-solution to the water phase was about 50 %. The amount of ^{33}P extracted was found in all cases to be smaller. Owing to the uncertainty in the determination of ^{33}P, it is hard to say whether this has any significance. The amount not extracted probably corresponds to ^{32}P and ^{33}P carried by S_μ.

The valency of extracted ^{32}P and ^{33}P is about the same, *i. e.* the difference in initial recoil energies seems to have no effect on the valency of the isotopes. This is to be expected since the chemical fate of a recoiling atom is determined when most of the recoil energy is lost, the initial energy being too high for any chemical compound to be formed [19].

The valency of the isotopes is not significantly altered by the precautions against oxidation. It is, however, probable that more rigorous precautions would have changed the results.

Thus, despite the difference in recoil energy, one can hardly expect to find ^{32}P and ^{33}P in different chemical states in the sulphur target. There they may exist as ions or atoms trapped within the lattice or in chemical combination with other atoms.

It is often assumed that the recoiling atoms are ionized and trapped as positive ions in the target. A good approximation to the upper limit of the kinetic energy at which a moving atom can be considered as un-ionized is $E = \frac{M}{m} I$ where M is the mass of the atom, m is the electronic mass and I is the ionization energy of the atom. The assumption made is that the atom loses all electrons whose orbital velocities are smaller than that of the recoiling atom. The ionization energy of the 3p electrons of phosphorus atoms is about 11 eV, *i. e.* the recoil energies of ^{32}P and ^{33}P must be at least 640 and 660 keV, respectively, in order to ionize the atoms. Comparing this with the maximum recoil energies ($E_n = 15$ MeV) of ^{32}P and ^{33}P (413 and 443 keV, respectively) shows that the ionic state can be excluded.

Owing to the high "temperature" of the atoms, it is more likely that they enter into chemical combination than that they become trapped as atoms in the target.

The phosphorus compounds most probably found in a sulphur target should be the sulphides. The concentration of radiophosphorus atoms, however, is so low (about 10^{13} atoms/cm^3) that the sulphides (all of them containing more than one P-atom) formed may be supposed not to have a stoichiometric composition. The atoms may also react with impurities in the target. In fact the chemical state of radiophosphorus in the target must to a large extent be a function of its purity and if the intention is to determine this state it must be very well protected in the separation process.

A better way of increasing the $^{33}P/^{32}P$ ratio than the chemical one seems to be a direct utilization of the differences in recoil range of the two isotopes in analogy with the separation of ^{198}Au from ^{197}Au by Magnusson [20] and ^{11}C from ^{12}C by Morinaga and Zaffarano [21]. In our case a similiar experiment is expected to be more difficult since both isotopes recoil.

An expression for the separation factor s has, however, been calculated (Appendix 2) for the case of two atoms with recoil ranges r_1 and r_2 ($r_2 > r_1$) recoiling from a spherical particle of radius R into a catcher phase surrounding the particle. The separation factor is defined as follows:

$$s = \frac{(N_1/N_2)_{\mathrm{I}}\ (\text{When } r_1 \neq 0 \text{ and } r_2 \neq 0)}{(N_1/N_2)_{\mathrm{II}}\ (\text{When } r_1 = r_2 \text{ or } R = \infty)} = \frac{(R + r_1/4)\ (R - r_1/2)^2}{(R + r_2/4)\ (R - r_2/2)^2} \qquad (3)$$

where N_1 and N_2 are the concentrations of the atoms in the particle. The separation factor varies between the R-axis ($r_1 = r_2$) and the solid curve ($r_1 = 0$, $r_2 \neq 0$) in Fig. 5. (The latter case corresponds to the separations made by Magnusson [20] and Morinaga and Zaffarano [21]). When $r_1/2 < R < r_2/2$, then all atoms with recoil range r_2 will leave the particle and the separation factor will be infinity. When $R < r_1/2$ both kinds of atoms will leave the particle. It is seen that s is more sensitive to variations in R than to variations in the value of r_2/r_1.

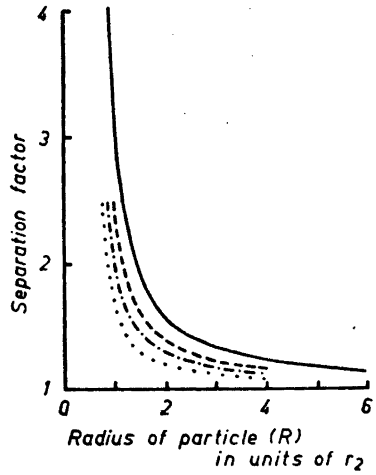


Fig. 5. The recoil separation factor for different values of r_2/r_1 *(the ratio between the recoil ranges) plotted as a function of particle radius. The particle radius is given in units of* r_2.

R — axis	r_2/r_1	$= 1.0$
. . . . .	»	$= 1.5$
—·—·—	»	$= 2.0$
— — —	»	$= 3.0$ *(our case)*
———	»	$= \infty$ $(r_1 = 0,\ r_2 \neq 0)$

The assumptions underlying (3) may be realized when ^{32}P and ^{33}P are produced for example by neutron irradiation of a sulphur sol. To determine s in this case the recoil ranges of ^{33}P and ^{32}P (r_1 and r_2) must be calculated. This can be done from the following equation [22] which is valid for $A_1 > A_2$ and thus probably only gives the right order of magnitude in this case:

$$r = 60 \frac{A_1 + A_2}{A_1} \sqrt{\frac{Z_1^{2/3} + Z_2^{2/3}}{Z_1 Z_2}} A_2 E_r 1/p \qquad (4),$$

where r is the recoil range in Å, E_r is the recoil energy in keV and p is the density of the absorber. (1 refers to recoil atom and 2 to absorber atom). Using the recoil energies calculated above (45 and 15 keV respectively), the most probable recoil ranges of ^{32}P and ^{33}P are 1 230 and 400 Å, respectively, *i. e.* $r_2/r_1 \sim 3$. The separation factor for this case is shown by the dashed curve in Fig. 5. Since sulphur sols with a particle radius of about 2 000 Å can be prepared [8], it would be possible to get a s-value of about 1.6. Trouble may, however, arise from the fact that the size of the particles in a sol increases with time and nothing is known about the behaviour of a sulphur sol in a strong radiation field. A disadvantage is that large volumes must be irradiated since the concentration of sulphur in such a sol is only a few percent. Also a large amount of ^{33}P recoils away from the sulphur particles, the loss being 48 % when $r_2 = 3r_1$ and $R = r_2/2$.

The author wishes to thank Dr. G. Aniansson for calling attention to the possibility of using the recoil phenomenon in a colloidal suspension, Miss Monica Sjöstedt for assistance with the experimental work and *The Swedish Atomic Committee* for financial support.

REFERENCES

1. Sheline, R. K., Holtzman, R. B. and Fan, C. Y. *Phys. Rev.* **83** (1951) 919.
2. Jensen, E. N., Nichols, R. T., Clement, J. and Pohm, A. *Phys. Rev.* **85** (1952) 112.
3. Westermark, T. *Phys. Rev.* **88** (1952) 573.
4. Nichols, R. T. and Jensen, E. N. *Phys. Rev.* **94** (1954) 369.
5. Klema, E. D. and Hanson, A. O. *Phys. Rev.* **73** (1948) 106.
6. Blatt, J. M. and Weisskopf, V. F. *Theoretical Nuclear Physics.* John Wiley & Sons, New York 1952, p. 345.
7. Elbek, B. *Private communication.*
8. Gmelins Handbuch der Anorganischen Chemie. 8 Aufl. System-Nummer 9. Schwefel. Teil A (1953).
9. Brinkman, J. A. *J. Appl. Phys.* **25** (1954) 961.
10. Seitz, F. *Phys. Today* **5** (1952) No. 6, 6.
11. Edwards, R. R. and Davies, T. H. *Nucleonics* **2** (1948) 44.
12. Emdt, P. M. and Kuyver, J. C. *Revs. Mod. Phys.* **26** (1954) 95.
13. Murray, R. L., Keller, M. R. and Hostetler, D. E. *Nucleonics* **12** (1954) 64.
14. Libby, W. F. *J. Am. Chem. Soc.* **69** (1947) 2523.
15. Kikuchi, S., Husima, K. and Aoki, H. *Nature* **137** (1936) 992.
16. Muehlhause, C. O. *Phys. Rev.* **79** (1950) 277.
17. Maier-Leibnitz, H. *Angew. Chem.* **51** (1938) 545.
18. Erbacher, O. *Z. physik. Chem.* **B42** (1939) 137.
19. Willard, J. E. *Ann. Rev. Nuclear Sci.* **3** (1953) 193.
20. Magnusson, L. B. *Phys. Rev.* **81** (1951) 285.
21. Morinaga, H. and Zaffarano, D. J. Z. *Phys. Rev.* **93** (1954) 1422.
22. Nielsen, K. O. *Private communication. Proc. Harwell Conf. on the Production and Utilization of Electromagnetically Enriched Isotopes.*

APPENDIX 1

Assume that R aggregates are formed and kFN are destroyed in the time interval from t to $t + \mathrm{d}t$, then

$$\mathrm{d}N = (R—kFN)\ \mathrm{d}t = (R—KN)\ \mathrm{d}t \qquad (1)$$

where N is the number of aggregates at the time t and F the neutron flux.

Integration gives:

$$N = N_0 \mathrm{e}^{-Kt} + R/K\ (1—\mathrm{e}^{-Kt}) \qquad (2)$$

where N_0 is the initial number of S_μ aggregates.

Assuming that the second term in (2) can be neglected compared with the first, then

$$\mathrm{e}^{-Kt_1} = 1/6 \qquad (3)$$

using the value for the decrease of S_μ in the sublimated samples in a time t_1 (Table 1).

The fraction of radiophosphorus set free in the same time is

$$f = \frac{Rt_1—R/K(1—\mathrm{e}^{-Kt_1})}{Rt_1} = 1—1/Kt\ (1—\mathrm{e}^{-Kt_1}) \qquad (4)$$

Combining with (3) gives $f = 0.54$.

APPENDIX 2

From a spherical particle will escape

$$n = \int C_1 \, w \, \mathrm{d}V \quad \text{recoil atoms/sec} \tag{1}$$

where C_1 is the rate of production of recoil atoms (atoms/cm^3 sec), $\mathrm{d}V$ the volume element and w the solid angle within which recoil atoms produced in $\mathrm{d}V$ escape from the particle.

Now $\mathrm{d}V = r^2 \sin\Theta \mathrm{d}\Theta \mathrm{d}\varphi \mathrm{d}r$ and it can be shown that

$$w = \frac{(r_1+r)^2 - R^2}{4r_1 r}, \quad (0<r_1<2R) \tag{2}$$

where r_1 is the recoil range, r the distance from the centre of the sphere to $\mathrm{d}V$ and R the radius of the particle. Then (1) transforms to

$$n = C_1 \int_0^{\pi} \int_0^{2\pi} \int_{R-r_1}^{R} \frac{(r_1+r)^2+R^2}{4r_1 r} \, r^2 \sin\Theta \mathrm{d}\Theta \mathrm{d}\varphi \mathrm{d}r = \pi C_1 r_1 (R^2 - r_1^2/12) \tag{3}$$

when $0<r_1<R$ and the same result is obtained when $R<r_1<2R$.

If two different atoms with recoil ranges r_1 and r_2 recoil from the particle then the ratio between their concentrations in the particle after a certain time would be

$$(N_1/N_2)_{\mathrm{I}} = C_1/C_2 \, \frac{4/3R^3 - r_1(R^2 - r_1^2/12)}{4/3R^3 - r_2(R^2 - r_2^2/12)}, \quad (0<r_1<r_2<2R) \tag{4}$$

If $r_1 = r_2$ or $R = \infty$, then $(N_1/N_2)_{\mathrm{II}} = C_1/C_2$, *i. e.* no separation would take place and a suitable definition of the separation factor would be

$$s = \frac{(N_1/N_2)_{\mathrm{I}}}{(N_1/N_2)_{\mathrm{II}}} = \frac{4/3R^3 - r_1(R^2 - r_1^2/12)}{4/3R^3 - r_2(R^2 - r_2^2/12)} = \frac{(R+r_1/4)(R-r_1/2)^2}{(R+r_2/4)(R-r_2/2)^2} \tag{5}$$

(It is assumed that the recoil atoms are stable but the same result is obtained for radioactive atoms).

Received October 15, 1955.

ACTA CHEMICA SCANDINAVICA 10 (1956) 106—112

Studies on the Extraction of Metal Complexes

XXII. The Complex Formation of Thorium with 1-Nitroso-2-naphthol and 2-Nitroso-1-naphthol

DAVID DYRSSEN, MARGARETA DYRSSEN and EBBE JOHANSSON

Research Institute of National Defence, Dept. 1. (FOA 1), Sundbyberg 4; Department of Inorganic Chemistry, Royal Institute of Technology, Stockholm 70, Sweden

The extraction of thorium with chloroform or hexone using 1-nitroso-2-naphthol and 2-nitroso-1-naphthol as complexing agents has been studied at 25° C. The perchlorate ion concentration in the aqueous phase was kept constant at 0.1 M.

The mean complexity constants are found to be $10^{8.50}$ for 1-nitroso-2-naphthol and $10^{8.30}$ for 2-nitroso-1-naphthol. These values are lower than for oxine, but higher than for acetylacetone.

It was shown by Fischer [1] in 1940 that the nitroso-naphtholates of transition metal cations like Fe^{2+}, Co^{2+}, Ni^{2+} and Cu^{2+} may be extracted into chloroform. It has also been reported by Harvey *et al.*[2] that plutonium(IV) gives a complex with 1-nitroso-2-naphthol, which is extractable with hexone (methyl *iso*butyl ketone) at pH 2, and we therefore expected that thorium could be extracted from aqueous solutions into chloroform or hexone using either of the two nitroso-naphthols as complexing agents. A study was carried out to confirm whether thorium was extracted in these systems and whether the data for the two-phase distribution of thorium as a function of the nitroso-naphtholate ion concentration would enable us to determine the complex formation between Th^{4+} and the nitroso-naphtholate ions. A summary of our data for thorium with other chelating agents was given in Part XXI [3] of this series.

EXPERIMENTAL

Only a few experimental details will be given here as the general experimental technique has been described in several previous papers of this series, *e. g.* Part VI [4]. In making our solutions we sometimes added 1 ml of 0.1 M sodium acetate per 15 ml to buffer our solutions. This small amount of acetate ion seemed to have no effect on the extraction of thorium. We are not entirely satisfied with our results on these systems as the mass balance ^{234}Th was not always very good (50—100 %; see Table 1, column 2). A possible

Table 1. Distribution of Th-^{234}Th between chloroform and hexone and 0.1 M perchlorate solutions as a function of the nitroso-naphtholate concentration in the aqueous phase at 25° C.
1A. The 1-nitroso-2-naphthol-$CHCl_3$ system.

$[HA]_{org}$	Mass balance %	I_{org} cpm	I_{aq} cpm	log q	$-\log[H^+]$	$-\log[A^-]$
1	2	3	4	5	6	7
0.1	102	412	5 490	−1.11	1.21	10.39
0.1	98	1 140	4 495	−0.58	1.46	10.14
0.1	85	2 416	2 856	−0.06	1.66	9.94
0.1	89	3 861	1 115	+0.56	1.88	9.72
0.1	51	2 830	257	+1.06	2.04	9.56
0.1	54	3 250	57.0	+1.77	2.31	9.29
0.1	73	3 509	3.6	+3.01	2.69	8.91
0.1	75	3 630	0.8	+3.67	3.12	8.48
0.05	90	26.5	8 694	−2.50	1.25	10.65
0.05	88	86.9	8 466	−1.97	1.35	10.55
0.05	94	42.7	11 361	−2.41	1.37	10.53
0.05	79	736	8 824	−1.06	1.67	10.23
0.05	62	2 684	4 803	−0.24	2.04	9.86
0.05	68	3 430	2 987	+0.08	2.31	9.59
0.05	51	5 839	180	+1.53	2.72	9.18

1B. The 1-nitroso-2-naphthol-hexone system.

1	2	3	4	5	6	7
0.1	95	26.8	7 689	−2.47	2.09	9.09
0.1	91	164	7 254	−1.66	2.37	8.81
0.1	87	1 774	5 363	−0.49	2.92	8.26
0.1	94	6 697	722	+0.95	3.95	7.23
0.1	60	4 680	92.9	+1.69	4.75	6.43
0.05	90	0.7	9 007	−4.12	1.82	9.66
0.05	94	7.0	9 336	−3.14	2.02	9.46
0.05	88	356	8 418	−1.39	2.77	8.71
0.05	90	7 894	378	+1.31	4.50	6.98
0.05	99	8 841	195	+1.64	5.20	6.28
0.05	91	8 237	65.0	+2.09	6.37	5.11
0.05	89	8 116	60.1	+2.12	7.38	4.10

1C. The 2-nitroso-1-naphthol-$CHCl_3$ system.

1	2	3	4	5	6	7
0.05	97	256	9 158	−1.54	1.04	9.61
0.05	100	667	9 014	−1.11	1.21	9.44
0.05	94	1 476	8 665	−0.75	1.35	9.30
0.05	81	3 154	4 592	−0.15	1.73	8.92
0.05	71	6 071	553	+1.06	2.22	8.43
0.05	63	6 488	70.7	+1.98	2.83	7.82
0.05	61	6 348	7.4	+2.95	3.20	7.45
0.02	100	7.8	9 169	−3.05	1.04	10.01
0.02	98	27.0	8 926	−2.50	1.19	9.86
0.02	92	259	8 141	−1.48	1.70	9.35
0.02	72	1 145	5 410	−0.66	2.24	8.81

1D. The 2-nitroso-1-naphthol-hexone system.

1	2	3	4	5	6	7
0.1	90	3.6	5 808	−3.22	1.28	9.19
0.1	101	10.8	5 799	−2.74	1.45	9.02
0.1	91	51.7	4 921	−1.99	1.56	8.91
0.1	74	211	4 640	−1.36	1.97	8.50
0.1	103	995	4 963	−0.71	2.25	8.22
0.1	70	2 527	2 066	+0.07	2.68	7.79
0.1	72	3 347	705	+0.66	3.10	7.37
0.1	103	5 341	126	+1.61	4.06	6.41
0.1	104	6 037	33.2	+2.25	5.44	5.03
0.1	94	5 092	79.2	+1.80	5.84	4.63
0.1	97	5 106	34.4	+2.16	6.21	4.26

explanation is that even recrystallized analytical reagents might still contain some solid particles capable of adsorbing radioactivity. However, by centrifuging our solutions after shaking, we assumed that these particles did not interfere with the measurements of the distribution equilibria.

DATA AND EQUILIBRIUM CONSTANTS

The data are given in Table 1, and are plotted in Fig. 1. When the two-parameter method of Dyrssen and Sillén [5] was applied to the data it was found that a templet with a value of $b = 0.70$ fitted the experimental data very well for all of the nitroso-naphthol systems if it was moved parallel to the log q and $-\log[A^-]$ axes. In a plot of log q $-\log \lambda_4$ against $\log[A^-] + a$ (*cf.* Fig. 2 in Part V [5]) all data would consequently fall on the same curve.

Using this templet it was thus possible to determine the second parameter a for the complex-formation, as well as the distribution constants between chloroform and the aqueous phase, λ_4, of the uncharged, extractable thorium nitroso-naphtholate complexes. It is however assumed that complex formation in the aqueous phase is not greatly influenced by the presence of small amounts of the organic solvents.

The complexity constants are defined by

$$k_n = [MA_n]/[MA_{n-1}][A] \text{ or } \varkappa_n = [MA_n]/[M][A]^n$$

and the parameters a and b were so chosen that a defines the mean complexity constant

$$\sqrt{\varkappa_4} = 10^a$$

and $2b$ defines the mean spreading factor

$$k_n/k_{n+1} = 10^{2b}$$

Thus the approximate values of log k_n may be obtained from

$$\log k_n = a + b(5—2n)$$

The following sets of constants determine the distribution curves in Fig. 1:

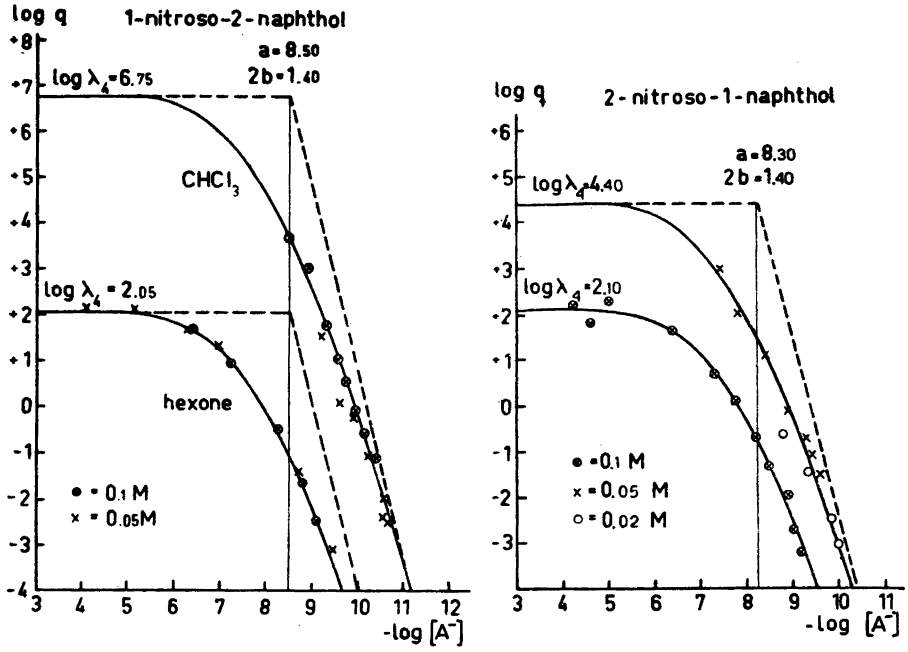


Fig. 1. The distribution ratio of Th-234Th as a function of the nitroso-naphtholate ion concentration in the aqueous phase. The fulldrawn curves are determined by the parameters λ_4, a *and* b, *and the broken lines by the equations log* $q = \log \lambda_4 + 4 \log[A^-]$ *and* $\log q = \log \lambda_4$, *(equations 7 and 8 in Part V[5]).*

For 1-nitroso-2-naphthol

$a = 8.50$; $2b = 1.40$
$\log \lambda_4 = 6.75$ for chloroform
$\log \lambda_4 = 2.05$ for hexone

For 2-nitroso-1-naphthol

$a = 8.30$; $2b = 1.40$
$\log \lambda_4 = 4.40$ for chloroform
$\log \lambda_4 = 2.10$ for hexone

STRENGTH OF COMPLEXES WITH 1-NITROSO-2-NAPHTHOL AND 2-NITROSO-1-NAPHTHOL

It was shown in Part XX[6] of this series that 2-nitroso-1-naphthol ($pk_a = 7.24$) is a stronger acid than 1-nitroso-2-naphthol ($pk_a = 7.63$) and consequently one would expect a lower value of the parameter a for the complex formation of Th with the former derivative. This seems to be the case, although the difference is not definitely outside the experimental error ($\pm$ 0.05 or 0.10).

Jonassen and DeMonsabert [7] studied the zirconyl complexes of the two nitroso-naphthols in 50 % alcohol at pH 3.5 by a spectrophotometric method and concluded: "The d e c r e a s e in stability in the 1-nitroso-2-naphthol complex as compared to the 2-nitroso-1-naphthol is to be expected from a comparison of the reactions of α- and β-naphthols". The relation between the "instability constant", K, of these authors and the complexity constant k_1 defined above is

$$K = [ZrO^{2+}]\ [HA]/[ZrOA^{+}] = [H^{+}]/k_1k_a$$

From Jonassen and DeMonsabert's values of K and $[H^{+}]$ we obtain

$$k_1k_a = 10^{0.1 \pm 0.05} \text{ for 1-nitroso-2-naphthol}$$
$$k_1k_a = 10^{0.6 \pm 0.05} \text{ for 2-nitroso-1-naphthol}$$

The values of k_a are approximately $10^{-7.6-\delta}$ and $10^{-7.2-\delta}$ for the two nitroso-naphthols, respectively, where a value of $\delta \sim 0.5$ may be estimated from a value of $k_a = 10^{-8.7}$ for 1-nitroso-2-naphthol in 96 % alcohol [8]. We then arrive at $k_1 = 10^{8.2 \pm 0.05}$ for the complex formation of ZrO^{2+} with 1-nitroso-2-naphthol and $k_1 = 10^{8.3 \pm 0.05}$ for the 2,1 derivative, *i. e.* again in this case there is no significant difference between the two constants.

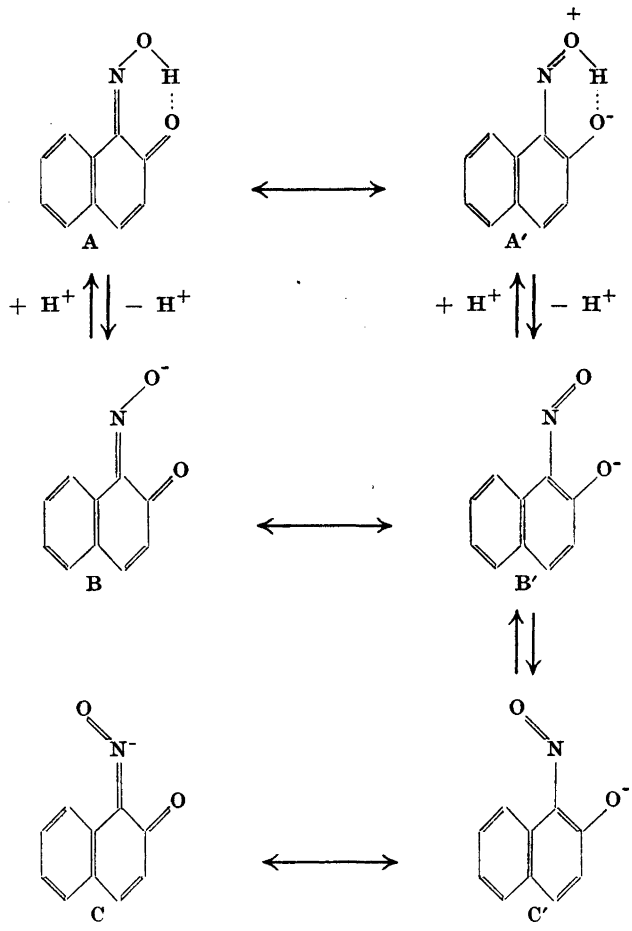
FORM OF THE CHELATE RING

In Part XX [6] we concluded that the two nitroso-naphthols should be regarded as quinone oximes having the structure A. It was also concluded that a structure A′ might contribute to a mesomeric state. Even if it seems to be well established that the proton forms a six-membered chelate ring with the nitroso-naphtholate ion, this does not necessarily have to be the case with metal cations, *i. e.* the nitroso-naphtholate ligand may have the form C$\leftrightarrow$C′ in these complexes. Feigl [9] has critically reviewed various opinions on this topic, and he accepted the form C on the basis of Pfeiffer's studies on nickel with dimethylglyoxime and similar compounds. Godycki *et al.*[10] have proved the existence of a five-membered ring in nickel dimethylglyoxime and have shown that it is stabilized by two short hydrogen bonds. However, such bonds cannot be formed in the case with the nitroso-naphthols. On the basis of the stability of the cobalt(III)complexes with 1-nitroso-2-naphthol and its 3,6-disulfonate in acid Feigl [9] also postulates a pH-dependent tautometric equilibrium. Studies by West [11] indicate, however, that this stability is due to a very slow exchange between cobalt and the proton.

No deductions about the size of the chelate ring can be made from the value of a as it lies between the value for oxine ($a = 9.70$), which forms a five-membered chelate ring (*cf.* Part XXI [3]), and the value for acetylacetone ($a = 6.70$), which forms a six-membered ring. X-ray measurements may settle this question.

CHOICE OF SYSTEM FOR EXTRACTION

The choice of a system for the extraction of thorium is somewhat arbitrary. If the price of the reagent is considered important one would choose 1-nitroso-



2-naphthol, and if one wants an organic solvent that is lighter than water one would choose hexone.

It is probably unimportant which of the nitroso-naphthols one chooses for the separation of metal cations. A few experiments were carried out with 1-nitroso-2-naphthol in order to see if Th^{4+} could be separated from UO_2^{2+} and trivalent ions such as La^{3+} and Sm^{3+}. These experiments revealed that the UO_2^{2+} ion was extractable, but that the trivalent ions were not. Fifty percent of the uranium was extracted at $-\log[H^+] = 3.07$ with an 0.1 M solution of 1-nitroso-2-naphthol in chloroform; the corresponding value for thorium was 1.66. Thus it is possible to separate Th^{4+} and UO_2^{2+} at pH 2, and it is also possible to separate these two ions from the trivalent ions at pH 4. Other metals that have been extracted with either of these nitroso-naphthols [1,2,13] are: Mn(II), Fe(II), Co, Ni, Cu(II), Pd(II), Ag, Cd, Hg(II) and Pu(IV).

In many cases it is important to extract in a low pH-range. This range is approximately defined by

$$\tfrac{1}{4}\log K = \log[H^+] - \log[HA]_{org} = \tfrac{1}{4}\log \lambda_4 + a - pk_a - \log k_d$$

The above equation was discussed in Part VIII [12]. The following values of $\tfrac{1}{4}\log K$ may be calculated for the four systems:

1-nitroso-2-naphthol and chloroform:	−0.41
1-nitroso-2-naphthol and hexone:	−1.17
2-nitroso-1-naphthol and chloroform:	+0.05
2-nitroso-1-naphthol and hexone:	−0.64

For a given value of $[HA]_{org}$ extraction occurs in the lowest pH range for the third system. It is also apparent that chloroform is the better solvent in this respect.

We wish to thank Professor G. Ljunggren and Professor L. G. Sillén for their interest in this work, which has partly been supported by *Atomkommittén*.

REFERENCES

1. Fischer, H. *Mikrochemie ver. Mikrochim. Acta* **30** (1942) 38; *Wiss. Veröffentl. Siemens-Werken* **1940** 217.
2. Harvey, B. G., Heal, H. G., Maddock, A. G. and Rowley, E. L. *J. Chem. Soc.* **1947** 1010.
3. Dyrssen, D. *Acta Chem. Scand.* **9** (1955) 1567.
4. Dyrssen, D. *Svensk Kem. Tidskr.* **65** (1953) 43.
5. Dyrssen, D. and Sillén, L. G. *Acta Chem. Scand.* **7** (1953) 663.
6. Dyrssen, D. and Johansson, E. *Acta Chem. Scand.* **9** (1955) 763.
7. Jonassen, H. B. and DeMonsabert, W. R. *J. Am. Chem. Soc.* **76** (1954) 6025.
8. Treadwell, W. D. and Schwarzenbach, G. *Helv. Chim. Acta* **11** (1928) 386.
9. Feigl, F. *Chemistry of specific, selective and sensitive reactions*, Academic Press, New York, 1949.
10. Godycki, L. E., Rundle, R. E., Voter, R. C. and Bank, C. V. *J. Chem. Phys.* **19** (1951) 1205.
11. West, B. *J. Chem. Soc.* **1952** 3115.
12. Dyrssen, D. and Dahlberg, V. *Acta Chem. Scand.* **7** (1953) 1186.
13. Gorbach, G. and Pohl, F. *Mikrochemie ver. Mikrochim. Acta* **38** (1951) 258.

Received November 3, 1955.

ACTA CHEMICA SCANDINAVICA 10 (1956) 113—117

The Melting Temperatures of 66/6 Copolyamides

SVEN SÖNNERSKOG

A-B Svenskt Konstsilke, Borås, Sweden

A series of 66/6 copolyamides have been prepared by hydrolytic condensation polymerization. Methods of purification and identification of macroscopic melting points are described. Factors, influencing the numerical value of the melting temperature, are discussed. Measurements, carried out on isotropic samples, show appreciable discrepancies from reference values in some cases.

The existence of sharply measurable melting temperatures of polyamides, polyesters and polyurethans is a notable exception from the general behaviour of high polymers. In most cases the melting points of these substances can be observed in the same way and with the same degree of accuracy as on corresponding monomers. This should be compared with the general case, where fusion without decomposition is a rare phenomenon, and, in the best cases, occurs over a range of temperatures. In terms of molecular structure, the temperature of melting is depending on the equilibrium degree of crystallinity. From thermodynamical point of view it is thus convenient to consider the melting as a first order transition where crystallinity completely disappears, and the melting temperature as the highest one, where traces of crystallinity can be detected [1].

Even if this idea is a sound basis for theoretical considerations, experimental difficulties limit the application. The precision of the measurements should be largely depending on the sensitivity of the method employed to detect traces of crystallinity, a circumstance giving preference to combined dilatometric and optical methods. The dilatometric method implies observation of the phase transition in the presence of a diluent. But in the case of polyamides inert, high boiling diluents are uncommon, and, moreover, the 6 polymer releases its equilibrium amount of monomer (caprolactam) at elevated temperature, which interferes with the solvent action of the diluent. It does not seem likely that a dilatometric measurement would give a higher degree of accuracy than a direct observation of the melting process, provided that proper directions are observed to obtain a reproducible structure of the samples. The more important details will be shortly discussed here.

Polyamides and polyesters may show very divergent degrees of crystallinity, even in the isotropic state, but before all in oriented specimens, such as extruded, quenched filaments and cold drawn or annealed fibres. The macroscopic melting point is depending on the difference in crystallinity. This dependence of the prehistory of the polymer has been observed to be valid for many macromolecular substances, but it is especially clearly expressed in a recent investigation on polyester fibres [2], where a gradual increase in melting point of 3° C is observed by a penetrometer technique, when the degree of crystallinity is increased from 38 to 65 %. The simplest way to avoid the influence of the crystallinity is, of course, to prepare all samples in an identical equipment and allow the molten polymers to solidify at rest by rapid cooling. Equivalent result would be obtained by dispersing the polyamide in a good solvent, such as formic acid, and gradually adding a non-solvent (acetone or water) until incipient precipitation occurs. At this stage a large amount of the nonsolvent is added, sufficient to cause a complete separation of the polymer.

An even more important source of error, however, is the inherent sensitivity of polyamides to oxydation in air, even before melting. Chips of 66 nylon melt sharply at 264° C in the absence of air, but as low as 248—256° on a melting block Maquenne [3,4]. Unfortunately 66 nylon shows the highest melting point and the least thermal stability of all the actual polyamides [6]. Pure 6 nylon, poly-(ε-caproamide), melts at 214° C in equilibrium with its monomer, which partly prevents an oxidation on the phase boundary. But the application of an inert atmosphere is necessary even here on prolonged heating.

It seems difficult to find a satisfactory explanation for the large difference in melting temperatures between 6 and 66 nylon. If we start from the general formulation of melting point as a ratio between latent molar heat of fusion and entropy of fusion of the repeating unit, a fairly small difference would be expected, as seen from the following formula of the building sequences:

$$\underbrace{\text{—(CH}_2)_4\text{—CO—NH—(CH}_2)_6\text{—NH—CO—}}_{\text{Repeating unit of 66 nylon}} \qquad \underbrace{\text{—NH—(CH}_2)_5\text{—CO—}}_{\text{Repeating unit of 6 nylon}}$$

The two units show identical ratios between polar and non-polar groups. If any difference exists in the entropy change on fusion, the largest change would occur in the case of 66 nylon with asymmetric distribution of methylene groups.

The question has recently [5] been discussed from other points of view. In short, it seems clear that the "odd-even" effect, known from other homologous series of organic compounds, is of primary importance. At the ends of an odd methylene sequence, the bonds to the amide groups are inclined at an angle of 112°, when the ends of an even sequence are parallell. The analogy with energetic differences, arising from *cis* and *trans* isomerism, is apparent. Even if an exhaustive explanation is still remote, it is sufficient here to establish that steric differences between the structural units makes a mutual space unit cell impossible (isomorphous replacement). Condensation polymerization of caprolactam with increasing amounts of hexamethylenediammonium adipate would thus lead to a decrease in the melting point of the copolymer until a

Table 1. Hydrolytic copolymerization of caprolactam and hexamethylenediammonium adipate.

Comp. of reaction mixture. Per cent, (b. w.) of Lactam — Nylon salt	Lactam content after reaction, % b. w.	Content of 6-unit in *polymer*, as (mole ratio) × 100	Melting points, °C, uncorr.	Viscosity number, at 1 %, conc. in formic acid. Temp. 20.0° C
100 — 0	12.4	100	214	1.1
90 — 10	5.3	95	204	1.1
80 — 20	6.0	91	190	1.2
70 — 30	5.1	83.5	176	1.2
60 — 40	4.0	77	159	1.1
50 — 50	5.1	69	175	1.1
40 — 60	5.0	59.5	188	1.1
30 — 70	4.9	48.5	197	1.2
20 — 80	6.0	35.3	205	0.9
10 — 90	5.1	19.6	234	0.9
66 nylon chips (com. grade)			264	0.9

minimum is reached. At still higher contents of 66 salt, a gradual increase in melting point is expected up to the limit (264° C) found only for the pure 66 polymer.

Copolymers are somewhat rubbery in character before melting, a factor making the temperature of phase transition more difficult to observe. Slow heating is essential. The melt viscosity also appears to be higher than for pure

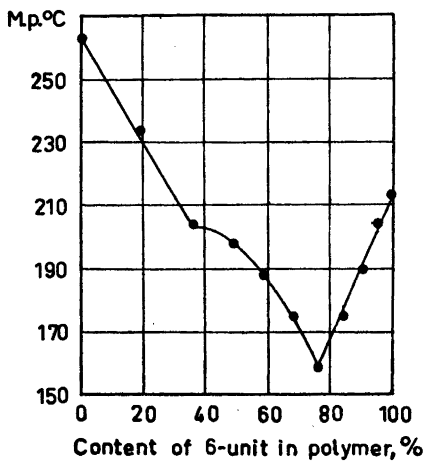


Fig. 1. The melting point of 6/66 copolyamides, according to the present investigation.

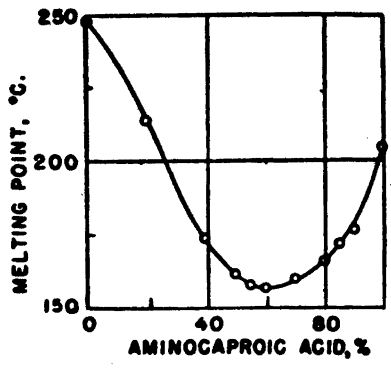


Fig. 2. The melting point of 6/66 copolyamides according to Reynolds [3] and Catlin et al.[4] Reproduced by permission from the Journal of Polymer Science.

polymers in the same range of molecular weight. This is most clearly expressed in the relation, found by Flory [7]:

$$\ln \eta = A + B\ M_w^{1/2} + E/RT$$

where η indicates the melt viscosity in arbitrary units, A and B constants, M_w the weight average molecular weight, E the activation energy of flow, R the gas constant and T the temperature in Kelvin units.

The discussion above has the purpose of searching out the main difficulties in carrying out melting point determinations on polyamides and copolymers. In the experimental part, the preparation and purification of a number of 66/6 copolyamides are described. On determination of their melting points, fairly large deviations are found from the figures in earlier references [3,4]. (Table 1, Figs. 1 and 2). The discussion above may be a guide to find an explanation for this discrepancy.

EXPERIMENTAL

Synthesis of 66/6 copolyamides, including pure 6 polymer.

Apparatus: Tubes of stainless steel, fitted with a cover and a needle valve as an in- or outlet for inert gases and water vapour. The steel tubes are shaped to contain a standard Pyrex test tube with an approximative volume of 50 ml.

Heating device: A cylindrical block of aluminium on an electrically heated plate. The metal cylinder contains six bores for the steel tubes at equidistant positions from the centre, where automatic control of temperature is applied.

Chemicals: *Caprolactam*, recrystallized from ethyl acetate and dried in a slow current of carbon dioxide at room temperature. Added to the reaction mixture as a saturated (80 % b. w.) aqueous solution.

Hexamethylenediammonium adipate. The commercial grade ("nylon salt") was dissolved in distilled water to give a 40 % aqueous solution. After filtering through a Pyrex C glass filter the solution was poured into a large excess of methanol. The transparent, large crystals appeared fairly slow, and only a main fraction was collected and dried in the same manner as the 6 monomer.

Schedule of reaction: Temperature range: 260—265° C. Time of hydrolytic polymerization step: 120 min. Gradual release of pressure and removal of water at atmospheric pressure: 120 min. Cooling to room temperature: 240 min.

Note: The water, removed from the reaction mixture, contains a noticeable amount of caprolactam. It was collected for determination of caprolactam, together with the water used in the subsequent purification of crude polymer.

Purification: The solid polymers are easily knocked free from the test tubes, especially if these earlier had been coated with a thin layer of a silicone oil. The rods were cut into pieces by sawing. The "sawdust" was collected and extracted in hot water for 24 hours together with the residue. After filtering the powder was dried, sieved and used for melting point determination. As a parallel test the large parts were dissolved in formic acid, precipitated with methanol, washed and dried. No difference in melting temperature was detectable even by the mixing of the two fractions. — The mother liquor was evaporated on a waterbath at reduced pressure. The residue was extracted with cold water. This fraction showed the melting point of caprolactam (70 °C) after recrystallization in ethyl acetate. The smaller, insoluble fraction was not studied further in this connection, but according to earlier work [8,9] its main components should be lower cyclic and linear oligomers. The amount of ε-aminocaproic acid formed during the reaction is known to be very low at high degrees of polymerization [8]. In fact, no change in solid content could be observed, when the water soluble fraction was passed over an anion exchanger of the strongly alkaline type. This seems to be in agreement with earlier work [9].

The precipitated polymers were also used for the determination of viscosity number (1 % solutions in 85.0 % formic acid at 20.0° C in an Ubbelohde viscometer).

Melting point determinations: A thin semimicro test tube was placed at the centre of a 50 ml Pyrex tube, containing a light silicone oil. The specimen in the inner tube was observed with a large pocket lens. Heating was carried out by an infrared furnace with a reflecting mirror as a bottom. The rate of heating was less than one degree min^{-1} above 150° C. A calibrated thermometer was selected with such a diameter as would just fill up the remaining volume of the inner test tube. Air was removed by flushing with dry carbon dioxide.

REFERENCES

1. Flory, P. J. *J. Chem. Phys.* **17** (1949) 223.
2. Edgar, O. B. and Hill, R. *J. Polymer Sci.* **8** (1952) 1.
3. Reynolds, R. J. W., in Hill, R. *Synthetic Fibres from High Polymers*, Elsevier Publishing Co., Amsterdam 1953, p. 126.
4. Catlin, W. E., Czerwin, E. P. and Wiley, R. H. *J. Polymer Sci.* **2** (1947) 412.
5. Bunn, C. W. *J. Polymer Sci.* **16** (1955) 323.
6. Meggy, A. B. *J. Appl. Chem. (London)* **4** (1954) 154.
7. Flory, P. J. *J. Am. Chem. Soc.* **62** (1940) 1057.
8. Hanford, W. E. and Joyce, R. M. *J. Polymer Sci.* **3** (1948) 167.
9. Hermans, P. H., Heikens, D. and van Velden, P. F. *J. Polymer Sci.***16** (1955) 451.

Received September 20, 1955.

ACTA CHEMICA SCANDINAVICA 10 (1956) 118—121

Preparation of Flavin Adenine Dinucleotide by Paper Electrophoresis

OTTO WALAAS and EVA WALAAS

Medicinska Nobelinstitutet, Biokemiska avdelningen, Stockholm, Sweden

Satisfactory separation of flavin adenine dinucleotide (FAD), flavin mononucleotide (FMN) and riboflavin has been carried out by paper electrophoresis. By the same method FAD is separated from adenine nucleotides and pyridine nucleotides. Paper electrophoresis has been employed in the final fractionation of FAD from bakers' yeast. The FAD obtained is pure, judging from absorption measurement and enzymatic testing in the D-amino acid oxidase system. The fluorescence of FAD was 20 % of that of pure FMN.

The preparation of pure FAD * from bakers' yeast was originally carried out by Warburg and Christian [1]. Whitby [2,3] and Siliprandi and Bianchi [4] have recently given a summary of the modifications which have been employed later in order to produce a product with a higher yield. The main problem is to separate FAD from other nucleotides in the latter stages of the fractionation. A complete purification has not been achieved by paper chromatography [5], adsorption chromatography on alumina or powder cellulose [2]. A completely pure FAD was prepared by ion exchange chromatography followed by column electrophoresis [4]. As previously mentioned [6], we have prepared pure FAD by using paper electrophoresis in the final purification of FAD extracted from bakers' yeast.

EXPERIMENTAL

Paper electrophoresis. An apparatus similar to that described by Foster [7] has been used. In most experiments Whatman No. 1 filter paper was employed. Three strips of filter paper, 30 cm × 8 cm, were used simultaneously. The material to be separated was applied to the paper by means of an Agla micrometer syringe (Burroughs Wellcome Ltd.) and a volume of 10 μl was applied 5 cm from the end of the paper strip and dried in a stream of air. Repeated applications could be carried out. The strips were wetted with buffer and placed on the glass plate and connected with vessels each containing 400 ml

* Abbreviations: FAD, flavin adenine dinucleotide; FMN, flavin mononucleotide; A-5-P, adenosine-5-phosphate; ADP, adenosine diphosphate; ATP, adenosine triphosphate; DPN, diphosphopyridine nucleotide; TPN, triphosphopyridine nucleotide.

buffer. Each vessel was connected with another by means of a siphon filled with buffer. Carbon electrodes connected to a source of direct current were placed in the latter vessels. The voltage could be regulated by means of a transformer which permitted the use of 200—750 V. Usually 600 volt was employed which gave a potential gradient of 20 V per cm and a current of 5—10 mA, and the experiment was run for 4—5 hours. Cooling was achieved by the circulation of tap water through glass tubes attached to the bottom side of the lower glass plate. This prevented condensation on the upper glass plate covering the apparatus.

After each run the paper was dried in a stream of air. Riboflavin and its derivatives were detected under the fluorescent lamp. Other nucleotides were detected by photography in ultraviolet light [8]. Elution and quantitative estimation of the different products [9] were also carried out. Pieces of paper, 1 × 2 cm, were cut from the starting line and successively in the longitudinal direction of the paper, and each piece eluted with 4 ml of distilled water for 30 min. The spectra of the eluates in the ultra-violet, and near ultra-violet region, were determined using a Beckman spectrophotometer model DU. For the quantitative determination the absorptions at 260 mμ, 375 mμ and 450 mμ were used. By this method 90 % of the material was eluted from the paper. For analytical separation 20—50 μg FAD was applied to each spot. However, as much as 0.5 mg could be purified at the time in this apparatus.

For the preparative purification of larger amount of FAD an apparatus for continuous electrophoresis on paper was employed [10]. Isolation of dry FAD was achieved by freeze-drying the collected fractions.

In the experiments designed to test the possible separation of FAD from other nucleotides, the following materials from "Sigma" Chemical Company were used: A-5-P, ADP, ATP, DPN, TPN, FMN (synthetical product), riboflavin. FAD was prepared from bakers' yeast.

RESULTS

As shown in Fig. 1 complete separation of FAD, FMN and riboflavin was achieved at a pH near neutral both in phosphate buffer and ammonium acetate buffer. Furthermore it appears that the method permits the separation of FAD from DPN, TPN, A-5-P, ADP and ATP. The migration of the two latter compounds was so rapid that they moved off the paper in the time employed.

FAD was prepared from bakers' yeast as described by Warburg and Christian [1]. The main problem in obtaining pure FAD consists of the removal of other nucleotides which contaminate the preparation at a later stage in the fractionation.

Separation by paper electrophoresis was attempted after the stage in which the silver-salt of FAD was decomposed. As shown in Fig. 2 two products with absorption maximum at 260 mμ were found in addition to FAD. FMN was not present. The first peak corresponded to DPN, its presence was verified enzymatically by the alcohol dehydrogenase assay. The fastest moving substance corresponded to the position of TPN and A-5-P. Enzymatic assay with glucose-6-phosphate dehydrogenase gave, however, no evidence for the presence of TPN. FAD was somewhat contaminated by the other components as the ratio R between the light absorption at 260 mμ and 450 mμ was 5.6 calculated from the spectrum. At this stage in the fractionation, however, further purification of FAD was achieved by two-dimensional electrophoresis, initially at pH 3.4 and finally at pH 6.8. It was however more advantageous to continue the fractionation of crude FAD until the extraction with cresol. Electrophoresis at this stage showed the amount of contaminating ultraviolet absorbing

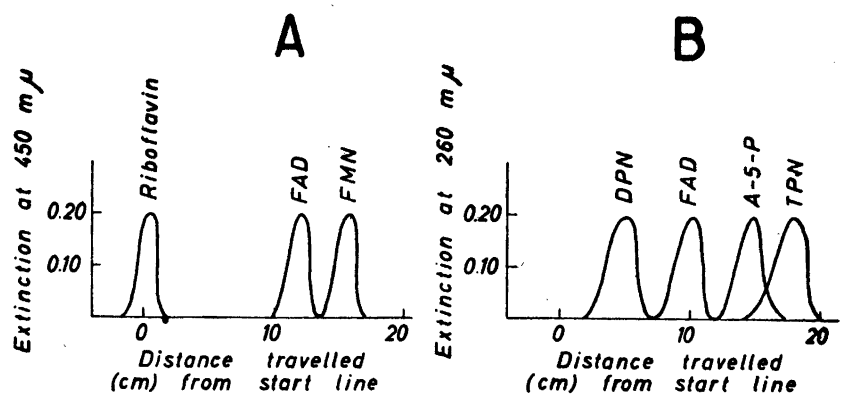


Fig. 1. A: Separation of riboflavin, FAD and FMN by paper electrophoresis. Ammonium acetate pH: 6.8. 5 hours, 600 V, 6 mA. B: Separation of FAD, DPN, TPN, A-5-P by paper electrophoresis. Ammonium acetate pH: 6.7. 4 ½ hours, 600 V, 10 mA.

material to be considerably reduced. Complete purification of FAD was achieved (Fig. 2) in ammonium acetate between pH 6—7, the best results obtained at pH 6.7.

DISCUSSION

As mentioned elsewhere [6] the activity of the D-amino acid oxidase is inhibited by nucleotides. Further, anions strongly dissociate the coenzyme-protein complex in the "old yellow enzyme" [12] and D-amino acid oxidase [6]. Thus in studies on flavin enzymes it is of importance to work with pure coenzymes. The electrophoretic separation of FAD obtained after cresol extraction, in ammonium acetate which is easily removed afterwards by evaporation, solves this problem. The great loss which accompanies the crystallization is avoided, and the method is of value as long as synthetic FAD [13] is not available for

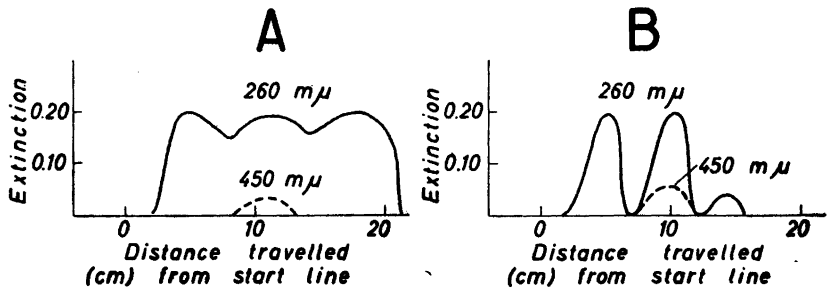


Fig. 2. Purification of FAD extracted from bakers' yeast by paper electrophoresis. A: After decomposition of the silver salt of FAD. Ammonium acetate pH:6.4, 6 hours, 600 V, 12 mA. B: After extraction of FAD with cresol. Ammonium acetate pH: 6.7. 4½ hours, 600 V, 15 mA.

ordinary work. Electrophoresis on paper for the purpose of analytical work also gives better separation of flavin derivatives than by paper chromatography [14].

The FAD prepared was not contaminated with ultraviolet absorbing material. Thus R = 260 mμ/450 mμ was for several samples at pH 7.0 between 3.30 and 3.40. R values previously quoted are 3.38 [1], 3.35 [2] and 3.275 [4]. Enzymatic testing of FAD in the D-amino-acid oxidase system with a highly purified apoenzyme [15] gave $K_M = 1.2 \times 10^{-7}$ M at pH 8.3 and 38° C. This is in accordance with Warburg and Christian [1] who under the same experimental conditions found $K_M = 1.4 \times 10^{-7}$ M.

By reduction of FAD with $Na_2S_2O_4$ the absorption at 450 mμ is reduced by 90 %. The fluorescence of FAD was 20 % of that of FMN purified by paper electrophoresis. 90 % quenching of the fluorescence of FAD occurred when $Na_2S_2O_4$ was added. Previous figures quoted for the fluorescence of FAD as compared to FMN are 20 % [11] and 9 % [7]. In the latter work FAD was not completely pure and the result can be explained by the well known quenching effect of nucleotides on the fluorescence of riboflavin and riboflavin derivatives [18,16].

Acknowledgement. The authors' wish to express their sincere thanks to Professor H. Theorell for stimulating advice and encouragement. The work was supported by a grant from *Norges Almenvitenskapelige Forskningsråd* for one of us (O. W.).

REFERENCES

1. Warburg, O. and Christian, W. *Biochem. Z.* **298** (1938) 150.
2. Whitby, L. G. *Biochem. J. London* **54** (1953) 437.
3. Whitby, L. G. *Biochim. et Biophys. Acta* **15** (1954) 148.
4. Siliprandi, N. and Bianchi, P. *Biochim. et Biophys. Acta* **16** (1955) 424.
5. Burton, K. *Biochem. J. London* **48** (1951) 458.
6. Walaas, O. and Walaas, E. *Acta Chem. Scand.* **8** (1954) 1104.
7. Foster, A. B. *Chemistry & Industry* **1952** 1050.
8. Markham, R. and Smith, J. D. *Biochem. J. London* **45** (1949) 294.
9. Hotchkiss, R. D. *J. Biol. Chem.* **175** (1948) 315.
10. Holdsworth, E. S. *Biochem. J. London* **59** (1954) 340.
11. Kunkel, H. G. and Tiselius, A. *J. Gen. Physiol.* **35** (1951–52) 891.
12. Theorell, H. and Nygaard, A. P. *Acta Chem. Scand.* **8** (1954) 877.
13. Christie, S. M. H., Kenner, G. W. and Todd, A. R. *J. Chem. Soc.* **1954** 46.
14. Crammer, J. L. *Nature* **161** (1948) 349.
15. Negelein, E. and Brömel, H. *Biochem. Z.* **300** (1939) 225.
16. Weber, G. *Biochem. J. London* **47** (1950) 114.
17. Bessey, O. A., Lowry, O. H. and Love, R. H. *J. Biol. Chem.* **180** (1949) 155.
18. Weil-Malherbe, H. *Biochem. J. London* **40** (1946) 363.

Received October 22, 1955.

ACTA CHEMICA SCANDINAVICA 10 (1956) 122—133

Kinetics and Equilibria in Flavoprotein Systems

V. The Effects of pH, Anions and Partial Structural Analogues of the Coenzyme on the Activity of D-Amino Acid Oxidase

EVA WALAAS and OTTO WALAAS

Medicinska Nobelinstitutet, Biokemiska avdelningen, Stockholm, Sweden

The effect of pH, anions and partial structural analogues of flavinadeninedinucleotide (FAD) on the activity of D-amino acid oxidase has been studied. The results suggest that the phosphoryl residues in FAD are linked to the apoenzyme. Furthermore it appears that the adenin residue as well as the ribosyl moiety of FAD takes part in the binding of the coenzyme to the surface of the protein. In contrast to some other flavin enzymes, the NH(3) group in *iso*alloxazine does not appear to be bound, because the D-amino acid oxidase is fluorescent.

The dissociation constant of the enzyme is lower at pH 9.2 ($K_M = 6 \times 10^{-8}$ M) than at pH 8.3 ($K_M = 1.2 \times 10^{-7}$ M). The experiments indicate a closer binding of coenzyme-protein at pH 9.2 than at 8.3. This may be a general phenomenon where flavin enzymes are concerned since the velocity of the association reaction between flavinmononucleotide (FMN) and the protein in the "old yellow enzyme" also increases in the pH region around 9 [1].

FMN and adenin nucleotides exhibit a pronounced inhibition of a competitive type. The inhibition is also shown by anions, the anions of strongly dissociated acids being the most effective inhibitors. The importance of these results on the physiological regulation of the enzyme activity is discussed.

Investigations carried out by Theorell and co-workers have shown that a number of anions affect the binding of coenzyme-apoenzyme, and thereby the velocity of the enzyme reactions. This has been demonstrated in the case of flavin enzymes such as the "old yellow enzyme" [1] and D-amino acid oxidase [2]. The same applies in the case of DPN- or TPN-linked enzymes such as alcohol dehydrogenase [3] and glucose-6-phosphate dehydrogenase [4]. The fact that enzymes are inhibited by partial structural analogues of the coenzyme has been shown in D-amino acid oxidase [5,2] and dehydrogenases [6,7].

A more thorough examination of the inhibitory effect of anions and substances structurally related to the coenzyme FAD on the D-amino acid oxidase has been carried out in the present work. The qualitative and quantitative nature of the inhibition has been characterised. The importance of these facts for the binding of coenzyme-apoenzyme is discussed.

METHODS

A highly purified apoenzyme of the D-amino acid oxidase from pig kidneys was prepared according to the method of Negelein and Brömel [8]. The lyophilized product has retained its activity unchanged for more than one year stored in a desiccator at + 1° C.

FAD was extracted from yeast as reported by Warburg and Christian [9] and purified until the cresol extraction stage. The further purification was carried out by paper electrophoresis [10] as shown in a previous paper. A pure preparation of FAD free from other nucleotides was obtained.

Activity measurements were carried out with D,L-alanin as substrate in the Warburg apparatus. The reaction mixture contained: 20 μg apoenzyme dissolved in 0.02 ml buffer, FAD in varying concentrations, most frequently 0.14 μM, 1 ml buffer, either M/10 pyrophosphate buffer pH 8.3 or M/10 glycine buffer pH 9.2. The reaction was started by introducing 0.2 ml 0.5 M D,L-alanin from the sidearm. Total volume was 3.6 ml. The enzyme activity was measured at 38° C. The O_2-consumption exhibited linear correlation with time for 30 min.

The inhibitors were dissolved in M/20 pyrophosphate buffer pH 8.3 and the pH of the solution adjusted to pH 8.30 when necessary. The final concentration of buffer in the incubation mixture was 0.028 M. A similar procedure was used with glycine buffer at pH 9.2 and other pH values. The inhibition was examined at two or more concentrations of inhibitor and with three or more concentrations of FAD in each experiment.

The following substances were used: FMN, synthetically prepared by "Sigma" Chemical Company. The product was purified by paper electrophoresis. The following preparations were also from "Sigma" Chemical Company: Adenylic acid (A-5-P), adenosine diphosphate (ADP), adenosine triphosphate (ATP), inosinic acid (I-5-P). The Ba-salts were converted to Na-salts by means of a cation-exchanger (Amberlite 120).

Other products used were: Ribose phosphate (R-5-P) (Schwarz), adenine (Hoffman-La Roche), adenosine (Hoffman-La Roche), hypoxanthine (Hoffman-La Roche), cytosine (Dougherty Chemicals), uracil (Eastman Kodak Company), imidazole (Eastman Kodak Company). Riboflavin from Hoffman-La Roche was recrystallised before use. Diphosphopyridine nucleotide (DPN) was prepared by Dr. R. K. Bonnichsen and had a degree of purity of 0.75. The fluorescence measurements were carried out on the apparatus constructed and described by Theorell and Nygaard [11].

Calculations [12,13]. Plotting of the reciprocal value of the reaction velocity (O_2-consumption), v, against the reciprocal value of the molar concentration of FAD resulted in a straight line. "Slope" and "intercept" on the $(1/v)$-axis were thereby determined. When the inhibition is competitive, the two curves which represent the reaction in the presence and absence, respectively, of inhibitor have a common intercept, but different slopes [14]. The inhibition constant K_I was calculated from the equation

$$\text{Slope} = (K_M / v_{Max}) \ (1 + [I] / K_I)$$

where: K_M = Michaelis constant

$1/v_{Max}$ = Intercept of the $(1/v)$-axis

$[I]$ = The molar concentration of inhibitor.

RESULTS

Absorption spectrum and fluorescence of D-amino acid oxidase

The fluorescence of FAD at neutral pH is 20 % of that given by FMN [10]. This quenching of the fluorescence of FAD is assumed to be due to a binding between the NH(3)-group in the *iso*alloxazine ring and the adenine part of the molecule (Bessey, Lowry and Love, 1945) [15]. These authors showed that on titration of FAD to lower pH value, an increase in the fluorescence took place. As seen in Fig. 1 the fluorescence of FAD decreases on titration in the alkaline

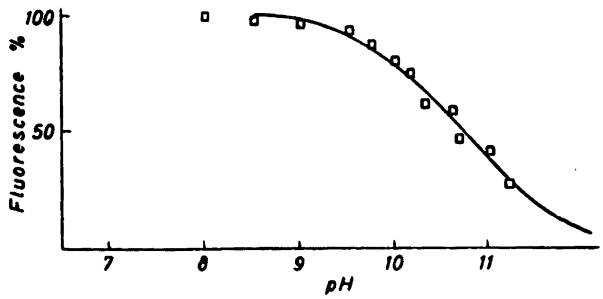


Fig. 1. The fluorescence of FAD at alkaline pH.

□ : *The fluorescence (Expressed in per cent of fluorescence at pH 7)*
———: *Theoretical titration curve* pK' = *10.5*

region. The points fit approximately a titration curve with pK' 10.5. Thus the quenching of the fluorescence at alkaline pH is probably due to the dissociation of the NH(3)-group. Similar results are shown for FMN[1], where the fluorescence decreases according to a titration curve with pK' 10.2.

When combining FAD with the apoenzyme, no quenching of fluorescence in the pH interval 7—9.5 occurred. Thus the D-amino acid oxidase is a fluorescent enzyme. Straub's diaphorase [16] behaves in a similar manner, while the apoenzyme in the "old yellow enzyme" produces quenching of the fluorescence in FMN, probably while the NH(3)-group in the *iso*alloxazine ring is bound [17]. This also applies to most other flavin enzymes [18]. Thus there is no evidence in the case of D-amino acid oxidase to prove that any binding of apoenzyme to free NH(3)-groups takes place.

Under aerobic conditions, no definite changes in the absorption spectrum either at 375 mμ or 450 mμ of FAD were found when combining with the apoenzyme. On the other hand, in accordance with previous investigations [8] a reduction in the absorption at 450 mμ of the reduced enzyme was found under anaerobic conditions.

Dissociation constant for FAD-apoenzyme

The dissociation constant for FAD-apoenzyme has previously been measured by activity determinations and is found [9] at 38° C to be 2.7×10^{-7} M at pH 8.3 in pyrophosphate buffer. It has been recalculated [19] to 1.4×10^{-7} M by taking into account the free amount of FAD which is present at equilibrium. In cases where the apoenzymes are of a greater degree of impurity, values quoted for K_M are [19,12] 4.7×10^{-7} M and 4.6×10^{-7} M, under the same conditions.

A reexamination of K_M at different pH's and in different buffers is carried out in this work. It appears from Fig. 2 that when the apoenzyme is approximately half saturated with FAD the pH-activity curve differs in pyrophosphate buffer and glycine buffer. The statement [20] that the enzyme in pyrophosphate buffer exhibits optimum activity between pH 8 and 9 has been

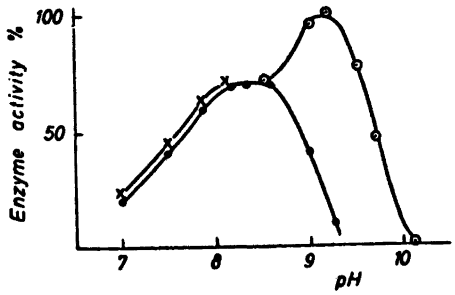


Fig. 2. The effect of pH on D-*amino acid oxidase activity.*
—●—●— : *In pyrophosphate buffer.*
—⊙—⊙— : *In glycine buffer.*
—×—×— : *In glycyl-glycine buffer.*
The concentration of FAD was 1.4×10^{-7} *M.*

confirmed. In glycine buffer however there occurs another optimum in the activity at pH 9.2. The explanation of this difference is that the pyrophosphate anion produces strong inhibition at pH > 9 similar to other anions.

As shown in Fig. 3 by plotting [14] the values for activity in glycine buffer, the curves at pH 8.3 and 9.2 have different slopes but the same intercept. This suggests that the binding between FAD and apoenzyme is stronger at pH 9.2, but probably without new points on the surface of the protein participating in the formation of the holoenzyme. Calculation of K_M gave 1.2×10^{-7} M at pH 8.3 while a lower value 6×10^{-8} M was found at pH 9.2.

It is very interesting to note that the association reaction for FMN and the apoenzyme in the "old yellow enzyme" exhibits a similar pH-dependence in the alkaline region as shown in the present work for the activity of the D-amino acid oxidase in glycine buffer. It is very likely that this is due to a beginning of the dissociation of the imino group in FAD ($pK' = 10.5$) and of the imino

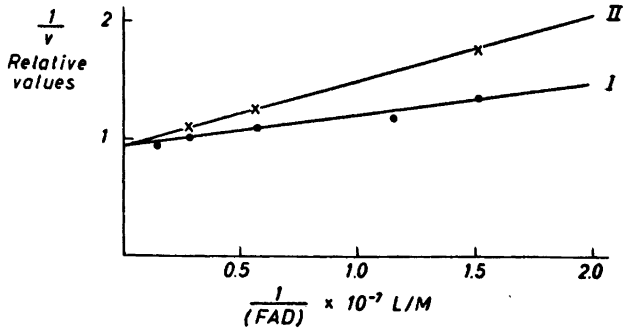


Fig. 3. The activity of D-*amino acid oxidase at different pH and with variation of FAD concentration.*
Curve I: pH 9.2.
Curve II: pH 8.3.

Table 1. Inhibition of D-amino acid oxidase by anions.

Inhibitor	pH	Conc. of Inhibitor	Slope	Intercept	K_I
None *	8.3		0.30	0.90×10^{6}	
Na acetate	8.3	2.0×10^{-1} M	0.44	—»—	4.2×10^{-1} M
» »	—»—	4.0×10^{-1} M	0.64	—»—	3.5×10^{-1} M
Na_2SO_4	8.3	8.0×10^{-2} M	0.42	—»—	2.0×10^{-1} M
»	—»—	1.6×10^{-1} M	0.55	—»—	1.9×10^{-1} M
NaBr	8.3	2.0×10^{-2} M	0.40	—»—	6×10^{-2} M
»	—»—	4.0×10^{-2} M	0.52	—»—	5.5×10^{-2} M
NaCl	8.3	8.6×10^{-2} M	1.12	—»—	3.2×10^{-2} M
Na phosphate	8.3	8.0×10^{-2} M	0.88	—»—	2.7×10^{-2} M
$NaNO_3$	8.3	3.0×10^{-2} M	0.70	—»—	2.3×10^{-2} M
»	—»—	6.0×10^{-2} M	1.25	—»—	1.9×10^{-2} M
None **	9.2		0.15	—»—	
NaCl	9.2	6.0×10^{-2} M	0.72	—»—	1.6×10^{-2} M

* $K_M = 1.2 \times 10^{-7}$ M.
** $K_M = 6.0 \times 10^{-8}$ M.

group in FMN ($pK^1 = 10.2$)[1] at pH> 9, which results in an increased association velocity with the apoproteins in this pH region. The strong reduction in the activity of the D-amino acid oxidase that occurs at pH> 9.5 may be due to an abolishment of the association reaction when the number of positively charged groups on the protein is reduced considerably.

Inhibition of D-amino acid oxidase by anions

Table 1 shows the inhibition of enzyme activity by anions. As also indicated in Table 2, salts of strongly dissociated acids produced the strongest inhibition, while the inhibition by fluoride and acetate was weak. Thus the inhibition can most probably be ascribed to the anions. Furthermore the inhibition was of the same magnitude when potassium salts were used. Ammonium salts

Table 2. Relative inhibitory activity of anions. Pyrophosphate buffer, pH 8.3, concentration of FAD 1.4×10^{-7} M.

Inhibitor	50 % inhibition at	Relative inhibition
NaI	2×10^{-2} M	4.2
NaBr	3×10^{-2} M	2.8
$NaNO_3$	4.5×10^{-2} M	2.0
NaCl	8.5×10^{-2} M	1.0
Na_2SO_4	12×10^{-2} M	0.7
Na phosphate	15×10^{-2} M	0.6
Na acetate	25×10^{-2} M	0.3
NaF	$>30 \times 10^{-2}$ M	<0.3

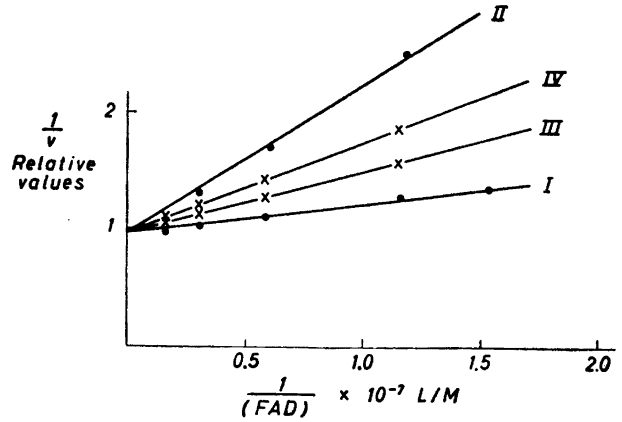


Fig. 4. Inhibition by NaCl.
Curve I: No inhibitor, pH 9.2.
Curve II: 0.06 M NaCl, pH 9.2.
Curve III: No inhibitor, pH 8.3.
Curve IV: 0.06 M NaCl, pH 8.3.

on the other hand gave a stronger inhibition, indicating an effect of the ammonium ion on the protein.

In the experiments with NaI, catalase was added to decompose produced H_2O_2. Without catalase NaI gave complete inhibition in very low concentrations, probably because of the liberation of I_2 by H_2O_2. The competitive nature of the inhibition by anions indicates a competition with the dissociated phosphoryl groups in FAD. In Fig. 4 the inhibition with chloride is given as an example. It is reasonable to assume that negatively charged anions are bound to positively charged groups in the apoenzyme. The inhibition by anions was reversed when increasing the FAD concentration. The quoted experiments were all carried out in pyrophosphate buffer at pH 8.3. In experiments carried out at higher pH values the inhibition was stronger, as shown in Fig. 5.

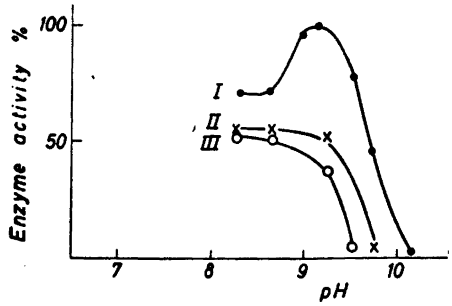


Fig. 5. Inhibition by chloride and phosphate.
Curve I: No inhibitor.
Curve II: 0.06 M NaCl.
Curve III: 0.075 M Na-phosphate.

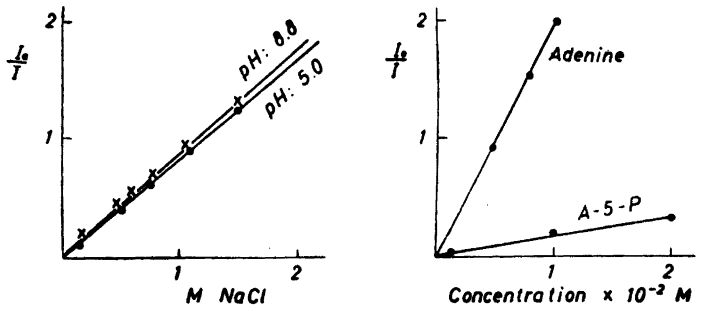


Fig. 6. Quenching effect of NaCl, adenine and A-5-P on the fluorescence of FAD. $\frac{I_0}{I}$: $\frac{\textit{Fluorescence without quencher}}{\textit{Fluorescence with addition of quencher}}$

After the addition of chloride or phosphate in concentrations which at a pH of 8.3 gives moderate inhibition, the inhibition is almost complete at pH 9.2 and the pH optimum of the enzyme activity at this pH almost disappears. Pyrophosphate is without effect at pH 8.3 to 8.6 but gives strong inhibition at higher pH. This explains why the enzyme activity is lost in pyrophosphate buffer at pH > 9. The inhibition by chloride and phosphate is competitive with FAD also at pH 9.2. This suggests that the mechanism of the inhibition is similar to that assumed for the inhibition at pH 8.3.

The activity of the enzyme drops rapidly at pH values above 9.5. This could be due to the fact that the number of positively charged groups in the protein is reduced. In the case of chloride and phosphate the strongly sloping part of the activity curve is shifted towards lower pH. The reason for this may be the well known fact that salts reduce the pK' values of proteins towards the isoionic point.

It is shown that NaCl at a relatively high concentration produces quenching of the fluorescence in FAD (Fig. 6). Provided that a non-fluorescent complex is formed: FAD + Cl^- → (FAD)Cl, the dissociation constant K can be calculated from the equation

$$K = \frac{I}{I_0 - I} \times C$$

C = concentration of NaCl.
I_0 = Fluorescence without NaCl
I = Fluorescence with NaCl

In acetate buffer at pH 5.0 K was 2.5 M and in glycin buffer at pH 8.8 2.2 M. NaCl, however, inhibits the enzyme activity in a concentration interval considerably lower than that producing the quenching effect on the fluorescence of FAD. The fact that the chloride inhibition of D-amino acid oxidase is strongly increased at a pH > 9, could not be explained by assuming that chloride inhibits the dissociation of the NH(3)-group in FAD. Any definite change in the pK of FAD by chloride in the alkaline region could not be detected.

Table 3. Inhibition of D-amino acid oxidase by partial structural analogues of FAD. Experiments performed at pH 8.3.

Inhibitor	Conc. of inhibitor	Slope	Intercept	K_I
FMN	2.5×10^{-4} M	2.86	0.90×10^{6}	3.0×10^{-5} M
A-5-P	4.0×10^{-4} M	0.49	—»—	6.4×10^{-4} M
—»—	8.0×10^{-4} M	1.34	—»—	2.3×10^{-4} M
ATP	8.0×10^{-4} M	0.44	—»—	1.8×10^{-3} M
Riboflavin	5.6×10^{-4} M	0.43	0.98×10^{6}	Non competitive
Adenosine	5.0×10^{-3} M	0.42	1.05×10^{6}	—»—
Hypoxanthine	5.0×10^{-3} M	0.42	1.11×10^{6}	—»—
Adenine	5.0×10^{-3} M	0.45	1.06×10^{6}	—»—
Cytosine	1.5×10^{-2} M	0.34	1.02×10^{6}	—»—
Uracil	1.5×10^{-2} M	0.36	1.09×10^{6}	—»—

Inhibition by partial structural analogues of FAD

Table 3 shows the inhibition by these compounds. Further the relative inhibition by this group of substances is shown in Table 4. The strongest inhibition was produced by FMN, A-5-P and other nucleotides. This group of substances with dissociated phosphoryl groups, all exhibited a competitive, reversible inhibition with FAD. One example is given in Fig. 7. Because of the competitive nature of inhibition, it is probable that the groups in the apoenzyme involved in the formation of the complex with the inhibitor, are the

Table 4. Relative inhibitory activity of partial structural analogues of FAD. Pyrophosphate buffer, pH 8.3, concentration of FAD 1.4×10^{-7} M/L.

Inhibitor	50 % inhibition at	Relative inhibition
FMN	4×10^{-4} M	1.2
A-5-P	5×10^{-4} M	1
ADP	5×10^{-4} M	1
ATP	6×10^{-4} M	0.8
Inosinic acid	5×10^{-4} M	1
DPN	2.5×10^{-3} M	0.2
Adenosine	6×10^{-3} M	0.08
Hypoxanthine	6×10^{-3} M	0.08
Adenine	6×10^{-3} M	0.08
Ribose-5-phosphate	2×10^{-2} M	0.0025
Cytosine	1.5×10^{-2} M	0.003
Uracil	2×10^{-2} M	0.0025
Riboflavin	25 % inhibition at 5.4×10^{-4} M	

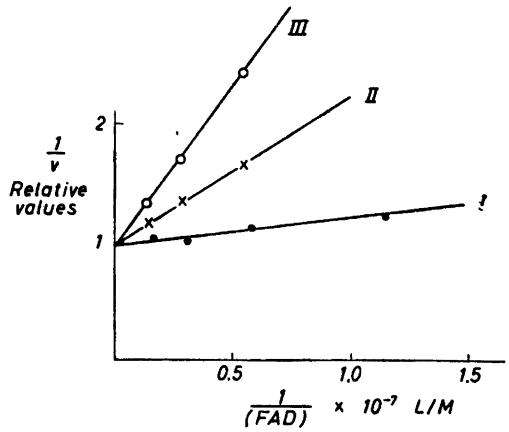


Fig. 7. Inhibition given by FMN and A-5-P.

Curve I: No inhibitor.
Curve II: 0.0008 M A-5-P.
Curve III: 0.00025 M FMN.
The experiments are performed in pyrophosphate buffer, pH 8.3.

same as in the FAD-apoenzyme complex. The experiments indicate that in addition to a binding of the dissociated phosphoryl group, the riboflavin and adenosine part are also linked to the protein.

The inhibition by riboflavin and adenosine was considerably less than in the case of FMN and A-5-P. Other purine and pyrimidine derivatives also produced a weaker inhibition. Furthermore the inhibition in this group was non-competitive with FAD, as shown by an example in Fig. 8. It has previously been shown [21] that the riboflavin analogues *iso*riboflavin, dichloroflavin

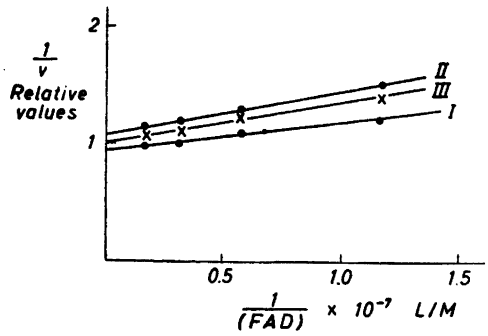


Fig. 8. The inhibition given by riboflavin and adenine.

Curve I: No inhibitor.
Curve II: 0.005 M adenine.
Curve III: 0.00054 M riboflavin.
The experiments are performed in pyrophosphate buffer, pH 8.3.

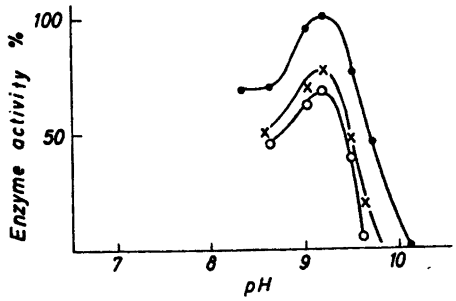


Fig. 9. Inhibition given by FMN and A-5-P.
—●—●—: *No inhibitor.*
—⊙—⊙—: *0.00025 M FMN.*
—×—×—: *0.0004 M A-5-P.*
The concentration of FAD was 1.4 × 10^{-7} M.

and galactoflavin exhibit a competitive inhibition which is, however, not truly reversible. There is some evidence for believing that the ribose part of the molecule is of specific importance in the binding with the protein, since the inhibition with ribose-5-phosphate was considerably stronger than with phosphate. Adenine and adenosine, however, produced the same inhibition. The (6)-NH_2 group in the purine ring was without specific importance, since K_I for adenine and hypoxanthine was of the same magnitude. Likewise there was no difference in K_I for adenylic acid and inosinic acid.

It is known that adenine, adenosine and purines usually produce a quenching of the fluorescence in fluorescent molecules [22]. Quenching of FAD by purines has been demonstrated [23,5]. As shown in Fig. 6 adenine and to a lesser degree adenylic acid produce a quenching of the fluorescence in FAD. At the concentrations used a formation of a complex between adenine and FAD would make the latter inactive as a coenzyme. This might explain the inhibition found in enzyme-activity experiments. Such an explanation however, is not possible in the case of adenylic acid which inhibits at considerably lower concentrations. The inhibition by FMN, A-5-P and ATP were of the same degree at different pH (Fig. 9). This was also the case for the inhibition by riboflavin and adenine.

FMN, riboflavin and DPN could not operate as coenzymes for the D-amino acid oxidase when added in concentrations up to 5 × 10^{-4} M. Neither could FMN + adenylic acid when added in equimolecular concentrations function as a coenzyme.

DISCUSSION

The experiments have indicated that several linkages are involved in the formation of the slightly dissociated coenzyme-apoenzyme complex in the D-amino acid oxidase.

The competitive type of inhibition by anions with the coenzyme molecule, indicates that the phosphoryl residue in FAD is linked to the apoenzyme. The fact that anions of strongly dissociated acids produce the most pronounced

dissociation of the enzyme may be explained by assuming that the negatively charged phosphoryl groups in FAD are linked to positively charged groups in the apoenzyme. The strong inhibition produced by FMN and adenylic acid suggest attachment to the riboflavin part of the FAD molecule as well as to adenosine. There is some evidence to indicate the chemical groups which are of importance for the binding.

It is improbable that the free NH-(3) in *iso*alloxazine participates in a linkage, since the formation of the coenzyme-apoenzyme complex was not followed by a quenching of the fluorescence in FAD. The smaller dissociation constant of FAD at pH 9.2 than at 8.3, is probably due to the fact that the beginning of the dissociation of the NH-(3) group in *iso*alloxazine results in a closer binding to the apoenzyme. A direct binding of the NH-(3) group, however, does not appear to occur since the D-amino acid oxidase is also fluorescent at pH 9.2.

In this connection it should be emphasized, that the effect of pH in the alkaline region on the activity of the D-amino acid oxidase and on the association reaction of FMN and the protein in the old yellow enzyme is completely identical. In both cases the optimal peak of the reaction at pH 9.2 disappears when NaCl is added. Thus it is possible that the dissociation of the NH-(3) group in *iso*alloxazine is of general importance for the formation of the coenzyme-protein complex in flavin enzymes.

The (6)-NH_2 group in the adenin moiety was without specific importance since K_I for adenylic and inosinic acids were of the same magnitude. The importance of the ribosyl group was indicated by the fact that the inhibition by ribose-5-phosphate was considerably stronger than by phosphate. On the other hand K_I for adenine and adenosine were of the same magnitude. In the case of the latter two substances however, the inhibition can be explained by assuming the formation of non-fluorescent complexes with FAD.

In the reduced enzyme new tight bonds appear to occur since the reduced enzyme is almost undissociated [8]. By hydrogenation of *iso*alloxazine in FAD in the reduced enzyme, a reduction in the absorption at 450 mμ occurs. Preliminary investigations indicated that chloride did not dissociate the reduced enzyme. Thus, no detectable effect of NaCl on the formation of the complex coenzyme-apoenzyme occurred as examined by absorption measurements at 450 mμ. Continued investigations on the reduced enzyme are in progress.

It has recently been shown that a number of flavin enzymes are metal enzymes with, *e. g.*, Mo, Fe, or Cu as a component [24]. There is, however, no evidence to show that metal ions are of importance for the activity of the D-amino acid oxidase. Thus it has been shown that cyanide is without effect and in present experiments chelating agents such as versene (2×10^{-3} M) and 8-hydroxyquinoline (2×10^{-4} M) produced no inhibition.

The fact that anions produce dissociation of enzymes, which has been shown where flavin and pyridine nucleotides occur as coenzymes, may be a phenomenon of general importance. The practical result of the presence of anions in buffers has been clearly demonstrated by the fact that D-amino acid oxidase is completely inhibited at pH>9 when pyrophosphate buffer is employed. Furthermore it should be mentioned that tris(hydroxymethyl)aminomethane buffer produced complete inhibition at a concentration of 10^{-3} M.

It is very likely that inhibition of enzyme reactions by anions and by partial structural analogues of coenzymes is of physiological importance in the control of cellular metabolism. Thus it is well known that the optimal reaction velocity for enzyme reactions is greater in extracts and homogenates than in isolated tissue slices of the same organ [25]. It is therefore of interest to bear in mind that the chloride concentration in the extracellular fluid corresponds to a concentration which produces considerable inhibition in the D-amino acid oxidase system. The same applies in the case of the intracellular concentration of adenine nucleotides.

Acknowledgement. The authors' wish to express their sincere gratitude to Professor H. Theorell for stimulating advice and criticism during the work. The kind hospitality of Professor H. Theorell and the staff of the laboratory is greatly appreciated. The work was supported by grants from *Statens Naturvetenskapliga Forskningsråd*, Sweden, and from *Norges Almenvitenskapelige Forskningsråd*, Norway.

REFERENCES

1. Theorell, H. and Nygaard, A. P. *Acta Chem. Scand.* **8** (1954) 877.
2. Walaas, O. and Walaas, E. *Acta Chem. Scand.* **8** (1954) 1104.
3. Theorell, H., Nygaard, A. P. and Bonnichsen, K. *Acta Chem. Scand.* **8** (1954) 1490.
4. Rutter, W. J. and Rolander, B. *Acta Chem. Scand.* **9** (1955) 191.
5. Burton, K. *Biochem. J. London* **48** (1951) 458.
6. Williams, J. N. Jr. *J. Biol. Chem.* **195** (1952) 629.
7. Brink, N. G. *Acta Chem. Scand.* **7** (1953) 1090.
8. Negelein, E. and Brömel, H. *Biochem. Z.* **300** (1939) 225.
9. Warburg, O. and Christian, W. *Biochem. Z.* **298** (1938) 150.
10. Walaas, O. and Walaas, E. *Acta Chem. Scand.* **10** (1956) 118.
11. Theorell, H. and Nygaard, A. P. *Acta Chem. Scand.* **8** (1954) 1649.
12. Hellerman, L., Lindsay, A. and Bovarnick, M. *J. Biol. Chem.* **163** (1946) 553.
13. Massart, L. in Sumner, J. B. and Myrbäck, K. "*The Enzymes*", Vol. I, Part I, Academic Press Inc. New York 1950, p. 307.
14. Lineweaver, H. and Burke, D. *J. Am. Chem. Soc.* **56** (1934) 658.
15. Bessey, O. A., Lowry, O. H. and Love, R. *J. Biol. Chem.* **180** (1949) 755.
16. Straub, F. B. *Biochem. J. London* **33** (1939) 787.
17. Theorell, H. *Biochem. Z.* **278** (1935) 263.
18. Singer, T. P. and Kearney, E. B., in *The Proteins*, Vol. II, Part A, p. 124. Ed. by H. Neurath and K. Bailey, Acad. Press Inc., N. Y. 1954.
19. Stadie, W. C. and Zapp, J. A. Jr. *J. Biol. Chem.* **150** (1943) 165.
20. Krebs, H. A. *Biochem. J. London* **29** (1935) 1620.
21. Kearney, E. B. *J. Biol. Chem.* **194** (1952) 747.
22. Weil-Malherbe, H. *Biochem. J. London* **40** (1946) 363.
23. Weber, G. *Biochem. J. London* **47** (1950) 114.
24. Mahler, H. R. *3ème Congrès International de Biochimie, Bruxelles 1955. Rapports, p. 103.*
25. Potter, V. R., Recknagel, R. O. and Hurlbert, R. B. *Federation Proc.* **10** (1951) 646.

Received October 22, 1955.

ACTA CHEMICA SCANDINAVICA 10 (1956) 134—146

Short Communications

Constitution of Resin Phenols and their Biogenetic Relations

XX *. The Identity of Pseudocubebin and *d*-Sesamin

BERNT CARNMALM

Organisk-kemiska Institutionen, Kungl. Tekniska Högskolan, Stockholm, Sweden

Recently fagarol was found to be identical with *dl*-sesamin [1]. In this paper pseudocubebin the last of the long known lignans of unsettled structure is proved to be *d*-sesamin (*cf.* Erdtman [2]).

In 1896 Peinemann [3] isolated a crystalline colourless substance (m. p. 122°) from the fruits of *Piper Lowong* Bl. From his analyses he calculated the formula $C_{20}H_{20}O_6$ which is the same as that for cubebin which had been isolated 60 years earlier from *Piper cubeba*. Peinemann showed that his substance was different from cubebin and he proposed the name pseudocubebin for the new compound.

Later Halberkann [4] found that pseudocubebin also occurred in the bark of *Ocotea usambarensis* Engl., Ibean Camphor tree, which occurs in East Africa, and on comparison of this substance with Peinemann's original preparation he showed that they were identical.

On oxidation with permanganate Peinemann obtained piperonylic acid. Attempted hydrolysis, transesterification and benzoylation invariably yielded unchanged starting material. Bromination afforded a dibromoderivative melting at 180° and nitration a substance giving the analytical figures for a dinitroderivative although no melting point was reported. From Peinemann's and Halberkann's results it appeared to be likely that pseudocubebin is a lignan most closely resembling sesamin.

Bark of *Ocotea usambarensis* was very kindly put at our disposal by Mr. B. G. Gilchrist, Lushoto Tanganyika.

The isolation of pseudocubebin was carried out mainly according to Halberkann. He reported a yield of about 0.5 % of pseudocubebin but our sample contained much less. The preparation melted at 122—123°, undepressed on admixture with authentic *d*-sesamin. The specific rotation was +64.5° (Halberkann gives +61°) and for *d*-sesamin the highest reported value is +69°. The series of colours developed when the compound was dissolved in sulphuric acid was identical with that for sesamin and also agreed with that given by Halberkann. Further the dibromoderivative of pseudocubebin was found to be identical with dibromo-*d*-sesamin as shown by melting point and mixed melting point determinations. Hence the "pseudocubebin" of *Ocotea usambarensis* is identical with *d*-sesamin.

Experimental. (All melting points uncorrected.) *Isolation of pseudocubebin.* The ground bark of *Ocotea usambarensis* (500 g) was exhaustively extracted with ether. The extract was distilled with steam and the non-volatile portion dissolved in ether and shaken with sodium hydroxide solution (2 N). The ether was evaporated and the oily residue dissolved in petroleum ether. After some time hard crystals (100 mg) deposited at the wall and bottom of the vessel. They were recrystallised from ethanol giving a colourless substance, m. p. 122—123°, $[\alpha]_D^{20}$ + 64.5° (*c* 1.75 in chloroform). The melting point was undepressed on admixture with an authentic sample of *d*-sesamin.

Dibromopseudocubebin. Pseudocubebin was brominated with bromine in chloroform. Crystallisation from ethanol gave very thin

* Part XIX, *Acta Chem. Scand.* 9 (1955) 1111.

needles, m. p. 180—181°, mixed m. p. with dibromo-*d*-sesamin 181—183°.

The author wishes to express his gratitude to *Statens Tekniska Forskningsråd* for financial support.

1. Carnmalm, B., Erdtman, H. and Pelchowicz, Z. *Acta Chem. Scand.* **9** (1955) 1111; Carnmalm, B. and Erdtman, H. *Chemistry & Industry* **1955** 570.
2. Erdtman, H. in Paech, K. and Tracey, M. V. *Moderne Methoden der Pflanzenanalyse*, Springer, Heidelberg, Vol. III, p. 441.
3. Peinemann, K. *Arch. Pharm.* **234** (1896) 204, p. 245.
4. Halberkann, J. *Ibid.* **254** (1916) 246.

Received December 3, 1955.

X-Ray Crystallographic Data on some Nucleic Acid Components

S. FURBERG and A. HORDVIK

Institute of Chemistry, University of Bergen, Bergen, Norway
and

K. TAUGBØL

Joint Establishment for Nuclear Energy Research, Lillestrøm, Norway

X-Ray crystal structure analysis of decomposition products of nucleic acids may be expected to give valuable information on the structure of the macromolecule. The four nucleosides from RNA have earlier been studied by one of us [1]. In this paper the results of a preliminary investigation of some other nucleic acid components are reported.

Weissenberg and oscillation photographs were taken, using Cu$K\alpha$ and Fe$K\alpha$ radiation. Unit cell dimensions and space groups were derived and densities measured by the flotation method. The values given are believed to be accurate to within 1 %.

Crystals of thymine, D-ribose, 2-deoxy-D-ribose, deoxycytidine hydrochloride and thymidine were examined with the following result:

Thymine. Crystals grown from alcohol are needleshaped, elongated along b, with {100} prominent, whereas from water parallelepipeds are obtained, with all faces about equally developed. Both types of crystals are monoclinic with cell dimensions a = 12.87 Å, b = 6.83 Å, c = 6.72 Å and β = 105°. The density was found to be 1.46 g/cm³ and there are four (calculated 3.97) molecules in the unit cell. The only systematic absences occur in the $h0l$ reflections for l odd and in the $0k0$ reflections for k odd. The space group is therefore $P2_1/c$.

D-*Ribose.* Recrystallisation from a number of solvents yielded extremely small crystals, or syrups. From the melt, however, crystals big enough for X-ray work were grown at about 60° C. They had the shape of needles and were elongated along c. The diagrams showed them to be monoclinic twins with (100) as twin-plane. The twinning was difficult to detect, as the cell dimensions happen to be such that the reflections from the two twinned crystals very nearly coincide. The cell dimensions are: a = 6.57 Å, b = 21.59 Å, c = 4.80 Å and β = 113°. The density was found to be 1.59 g/cm³, corresponding to four molecules in the unit cell. The calculated density is also 1.59 g/cm³. The space group is $P2_1$.

Although a great number of simple sugars have been investigated by X-ray crystallographic methods by Cox *et al.*[2], and others, we have found no crystal data on ribose or 2-deoxy-ribose in the literature.

*2-Deoxy-*D-*ribose.* From the melt very thin flakes were obtained, with {100} prominent. The X-ray diagrams were rather poor; however, they showed that the crystals probably are orthorhombic, with a = 11.36 Å, b = 10.65 Å and c = 4.91 Å. The absences indicate the space group $P2_12_12_1$. Four molecules $C_5H_{10}O_4$ per unit cell gives a calculated density of 1.50 g/cm³.

Thymidine. This nucleoside crystallises in well-developed orthorhombic prisms elongated along c, with a = 16.27 Å, b = 13.86 Å and c = 4.86 Å. Four molecules per unit cell corresponds to a density of 1.47 g/cm³. Reflections $h00$ and $0k0$ are absent for odd values of h and k respectively. The $00l$ reflections were not all recorded, but as 001 and 003 appear to be absent, the space group is probably $P2_12_12_1$.

Deoxycytidine hydrochloride. Thin, monoclinic needles elongated along c, with a = 7.03 Å, b = 17.70 Å, c = 5.15 Å and β = 117°. Space group $P2_1$. Two mole-

needles, m. p. 180—181°, mixed m. p. with dibromo-*d*-sesamin 181—183°.

The author wishes to express his gratitude to *Statens Tekniska Forskningsråd* for financial support.

1. Carnmalm, B., Erdtman, H. and Pelchowicz, Z. *Acta Chem. Scand.* **9** (1955) 1111; Carnmalm, B. and Erdtman, H. *Chemistry & Industry* **1955** 570.
2. Erdtman, H. in Paech, K. and Tracey, M. V. *Moderne Methoden der Pflanzenanalyse*, Springer, Heidelberg, Vol. III, p. 441.
3. Peinemann, K. *Arch. Pharm.* **234** (1896) 204, p. 245.
4. Halberkann, J. *Ibid.* **254** (1916) 246.

Received December 3, 1955.

X-Ray Crystallographic Data on some Nucleic Acid Components

S. FURBERG and A. HORDVIK

Institute of Chemistry, University of Bergen, Bergen, Norway
and

K. TAUGBØL

Joint Establishment for Nuclear Energy Research, Lillestrøm, Norway

X-Ray crystal structure analysis of decomposition products of nucleic acids may be expected to give valuable information on the structure of the macromolecule. The four nucleosides from RNA have earlier been studied by one of us [1]. In this paper the results of a preliminary investigation of some other nucleic acid components are reported.

Weissenberg and oscillation photographs were taken, using Cu$K\alpha$ and Fe$K\alpha$ radiation. Unit cell dimensions and space groups were derived and densities measured by the flotation method. The values given are believed to be accurate to within 1 %.

Crystals of thymine, D-ribose, 2-deoxy-D-ribose, deoxycytidine hydrochloride and thymidine were examined with the following result:

Thymine. Crystals grown from alcohol are needleshaped, elongated along b, with {100} prominent, whereas from water parallelepipeds are obtained, with all faces about equally developed. Both types of crystals are monoclinic with cell dimensions a = 12.87 Å, b = 6.83 Å, c = 6.72 Å and β = 105°. The density was found to be 1.46 g/cm³ and there are four (calculated 3.97) molecules in the unit cell. The only systematic absences occur in the $h0l$ reflections for l odd and in the $0k0$ reflections for k odd. The space group is therefore $P2_1/c$.

D-*Ribose.* Recrystallisation from a number of solvents yielded extremely small crystals, or syrups. From the melt, however, crystals big enough for X-ray work were grown at about 60° C. They had the shape of needles and were elongated along c. The diagrams showed them to be monoclinic twins with (100) as twin-plane. The twinning was difficult to detect, as the cell dimensions happen to be such that the reflections from the two twinned crystals very nearly coincide. The cell dimensions are: a = 6.57 Å, b = 21.59 Å, c = 4.80 Å and β = 113°. The density was found to be 1.59 g/cm³, corresponding to four molecules in the unit cell. The calculated density is also 1.59 g/cm³. The space group is $P2_1$.

Although a great number of simple sugars have been investigated by X-ray crystallographic methods by Cox *et al.*[2], and others, we have found no crystal data on ribose or 2-deoxy-ribose in the literature.

*2-Deoxy-*D-*ribose.* From the melt very thin flakes were obtained, with {100} prominent. The X-ray diagrams were rather poor; however, they showed that the crystals probably are orthorhombic, with a = 11.36 Å, b = 10.65 Å and c = 4.91 Å. The absences indicate the space group $P2_12_12_1$. Four molecules $C_5H_{10}O_4$ per unit cell gives a calculated density of 1.50 g/cm³.

Thymidine. This nucleoside crystallises in well-developed orthorhombic prisms elongated along c, with a = 16.27 Å, b = 13.86 Å and c = 4.86 Å. Four molecules per unit cell corresponds to a density of 1.47 g/cm³. Reflections $h00$ and $0k0$ are absent for odd values of h and k respectively. The $00l$ reflections were not all recorded, but as 001 and 003 appear to be absent, the space group is probably $P2_12_12_1$.

Deoxycytidine hydrochloride. Thin, monoclinic needles elongated along c, with a = 7.03 Å, b = 17.70 Å, c = 5.15 Å and β = 117°. Space group $P2_1$. Two mole-

cules in the unit cell gives a calculated density of 1.52 g/cm³.

We wish to thank Dr. S. G. Laland, Institutt for Ernæringsforsking, Universitetet i Oslo, for a sample of 2-deoxy-D-ribose and Dr. P. Reichard, Karolinska Institutet, Stockholm, for samples of thymidine and deoxycytidine hydrochloride.

1. Furberg, S. *Acta Chem. Scand.* 4 (1950) 751.
2. Cox, E. G., Goodwin, T. H. and Wagstaff, A. I. *J. Chem. Soc.* **1935** 978, 1495.

Received December 2, 1955.

Space Groups and Molecular Symmetries of Two Thiocyanates

OLAV FOSS

Institutt for uorganisk kjemi, Norges tekniske høgskole, Trondheim, Norway

The unit cells and space groups of two simple, covalent thiocyanates have been determined from single-crystal oscillation and Weissenberg photographs, using copper radiation, $\lambda(CuK\alpha) = 1.542$ Å.

Sulphur dithiocyanate [1], $S(SCN)_2$. Orthorhombic bipyramidal, $a = 10.12$ Å, $b = 12.83$ Å, $c = 4.34$ Å. Four molecules per unit cell; density, calc. 1.75, found 1.76 g/cm³. Systematic absences, $0kl$ when $k + l$ is odd, $hk0$ when h is odd. The unit cell dimensions, the absences, and the relative intensities of the reflections show that the crystals are isomorphous with those of selenium dithiocyanate[2], $Se(SCN)_2$, and selenium diselenocyanate [3], $Se(SeCN)_2$. The space group is thus D_{2h}^{16}-*Pnma*. From the known structures of the selenium analogues [2,3] it follows that the sulphur dithiocyanate molecule has an unbranched chain structure, with the middle sulphur atom located in a crystallographic mirror plane.

The compound was prepared from sulphur dichloride by reaction with an excess of silver thiocyanate suspended in carbon disulphide, and was recrystallized from the same solvent. Silver thiocyanate was found to react better than mercuric thiocyanate [4]. The crystals occur as plates {010}, bounded by {110} and {111}, and usually very thin. The bulk of crystals became yellow in the course of a day, due to the formation of an insoluble polymer [1,4], but individual crystals could be picked which were sufficiently stable.

Ethylene thiocyanate, $(CH_2SCN)_2$. Orthorhombic bipyramidal, $a = 7.39$ Å, $b = 7.81$ Å, $c = 11.48$ Å. Four molecules per unit cell; density, calc. 1.45, found 1.42 g/cm³. Systematic absences, $0kl$ when k is odd, $h0l$ when l is odd, $hk0$ when h is odd. The space group is thus D_{2h}^{15}-*Pbca*, which has eightfold general positions, and two fourfold sets of symmetry centres as special positions. With four molecules per unit cell, it follows that the ethylene thiocyanate molecules are centrosymmetric in the crystals. This agrees with the finding from infrared measurements [5] that the compound exists in *trans* configuration in the solid state.

Recrystallized from chloroform, the compound was obtained as plates {010}, or as perfect bipyramids {111} with, also here, {010} developed.

Further work on the crystal structures of the two thiocyanates is intended.

1. Lecher, H. and Wittwer, M. *Ber.* **55** (1922) 1481.
2. Ohlberg, S. M. and Vaughan, P. A. *J. Am. Chem. Soc.* **76** (1954) 2649.
3. Aksnes, O. and Foss, O. *Acta Chem. Scand.* **8** (1954) 1787.
4. Baroni, A. *Atti R. Accad. Lincei* [6] **23** (1936) 139.
5. Quagliano, J. V. and Mizushima, S.-I. *J. Am. Chem. Soc.* **75** (1953) 6084.

Received November 30, 1955.

"*Trans*" Naphthodioxan Characterized by its Mercuric Chloride Compound

O. HASSEL and CHR. RØMMING

Universitetets Kjemiske Institutt, Blindern-Oslo, Norway

In 1950 Furberg and Hassel [1] determined the crystal structure of the lower melting compound (m. p. 111° C) found in the reaction between 2,3-dichloro-1,4-dioxan and ethylene glycol. They found

cules in the unit cell gives a calculated density of 1.52 g/cm³.

We wish to thank Dr. S. G. Laland, Institutt for Ernæringsforsking, Universitetet i Oslo, for a sample of 2-deoxy-D-ribose and Dr. P. Reichard, Karolinska Institutet, Stockholm, for samples of thymidine and deoxycytidine hydrochloride.

1. Furberg, S. *Acta Chem. Scand.* 4 (1950) 751.
2. Cox, E. G., Goodwin, T. H. and Wagstaff, A. I. *J. Chem. Soc.* **1935** 978, 1495.

Received December 2, 1955.

Space Groups and Molecular Symmetries of Two Thiocyanates

OLAV FOSS

Institutt for uorganisk kjemi, Norges tekniske høgskole, Trondheim, Norway

The unit cells and space groups of two simple, covalent thiocyanates have been determined from single-crystal oscillation and Weissenberg photographs, using copper radiation, $\lambda(CuK\alpha) = 1.542$ Å.

Sulphur dithiocyanate [1], $S(SCN)_2$. Orthorhombic bipyramidal, $a = 10.12$ Å, $b = 12.83$ Å, $c = 4.34$ Å. Four molecules per unit cell; density, calc. 1.75, found 1.76 g/cm³. Systematic absences, $0kl$ when $k + l$ is odd, $hk0$ when h is odd. The unit cell dimensions, the absences, and the relative intensities of the reflections show that the crystals are isomorphous with those of selenium dithiocyanate[2], $Se(SCN)_2$, and selenium diselenocyanate [3], $Se(SeCN)_2$. The space group is thus D_{2h}^{16}-*Pnma*. From the known structures of the selenium analogues [2,3] it follows that the sulphur dithiocyanate molecule has an unbranched chain structure, with the middle sulphur atom located in a crystallographic mirror plane.

The compound was prepared from sulphur dichloride by reaction with an excess of silver thiocyanate suspended in carbon disulphide, and was recrystallized from the same solvent. Silver thiocyanate was found to react better than mercuric thiocyanate [4]. The crystals occur as plates {010}, bounded by {110} and {111}, and usually very thin. The bulk of crystals became yellow in the course of a day, due to the formation of an insoluble polymer [1,4], but individual crystals could be picked which were sufficiently stable.

Ethylene thiocyanate, $(CH_2SCN)_2$. Orthorhombic bipyramidal, $a = 7.39$ Å, $b = 7.81$ Å, $c = 11.48$ Å. Four molecules per unit cell; density, calc. 1.45, found 1.42 g/cm³. Systematic absences, $0kl$ when k is odd, $h0l$ when l is odd, $hk0$ when h is odd. The space group is thus D_{2h}^{15}-*Pbca*, which has eightfold general positions, and two fourfold sets of symmetry centres as special positions. With four molecules per unit cell, it follows that the ethylene thiocyanate molecules are centrosymmetric in the crystals. This agrees with the finding from infrared measurements [5] that the compound exists in *trans* configuration in the solid state.

Recrystallized from chloroform, the compound was obtained as plates {010}, or as perfect bipyramids {111} with, also here, {010} developed.

Further work on the crystal structures of the two thiocyanates is intended.

1. Lecher, H. and Wittwer, M. *Ber.* **55** (1922) 1481.
2. Ohlberg, S. M. and Vaughan, P. A. *J. Am. Chem. Soc.* **76** (1954) 2649.
3. Aksnes, O. and Foss, O. *Acta Chem. Scand.* **8** (1954) 1787.
4. Baroni, A. *Atti R. Accad. Lincei* [6] **23** (1936) 139.
5. Quagliano, J. V. and Mizushima, S.-I. *J. Am. Chem. Soc.* **75** (1953) 6084.

Received November 30, 1955.

"*Trans*" Naphthodioxan Characterized by its Mercuric Chloride Compound

O. HASSEL and CHR. RØMMING

Universitetets Kjemiske Institutt, Blindern-Oslo, Norway

In 1950 Furberg and Hassel [1] determined the crystal structure of the lower melting compound (m. p. 111° C) found in the reaction between 2,3-dichloro-1,4-dioxan and ethylene glycol. They found

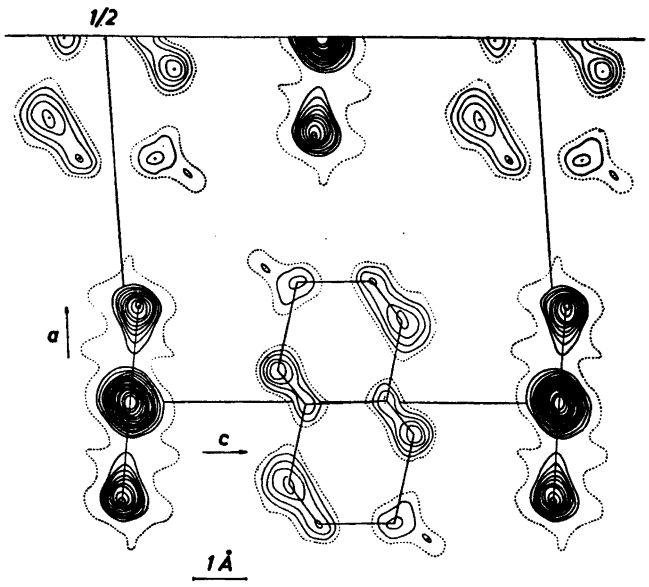


Fig. 1. Electron density map projected along the b-*axis. Intervals between the contour lines for Hg, Cl, C and O are in the ratio 25:10:4:4.*

that this substance is not a naphthodioxan as suggested by Böeseken *et al.*[2], but bi-1, 3-dioxa*cyclo*pentyl(2).

The structure of the higher melting product (m. p. 136° C) had still to be determined although it would of course be expected that this compound is indeed a naphthodioxan and preferably the "*trans*" form. The crystallographic data did not, however, invite to a direct crystal structure investigation [1]. Later on, it was found that addition compounds of the substance with mercury salts are readily formed [3] which might be suited for X-ray determination of the general shape of the organic molecule. We have chosen the mercuric chloride compound which has one short crystal axis (4.46 Å). Zero order layer line Weissenberg diagrams with rotation about the short axis were taken using the multiple film method. The intensities were estimated visually. The general trend of the intensities is a uniform decrease for increasing Bragg angles, which made us believe that the mercury atoms were in unique positions. Anticipating that the projection would contain the appropriate number of symmetry centres a Fourier projection could be worked out without making any assumptions regarding the positions of the chlorine, oxygen or carbon atoms. The resulting electron density map is reproduced in Fig. 1. Besides the projection of a linear symmetrical mercuric chloride molecule the map also contains a centrosymmetrical assembly of ten resolved peaks which corresponds satisfactorily to a picture which may be obtained from a naphthodioxan molecule in the "*trans*" form. The four peaks which in this case must correspond to oxygen atoms are in fact somewhat higher than the six remaining peaks representing carbon atoms.

Without trying to work out further projections which would no doubt exhibit serious overlapping of atoms, we feel entitled to draw the conclusion that the 136° substance is indeed "*trans*" naphthodioxan.

1. Furberg, S. and Hassel, O. *Acta Chem. Scand.* **4** (1950) 1584.
2. Böeseken, J., Tellegen, F. and Cohen Henriques, P. *Rec. trav. chim.* **54** (1935) 733.
3. Hassel, O. and Hvoslef, J. *Acta Chem. Scand.* **8** (1954) 1953.

Received December 13, 1955.

cules in the unit cell gives a calculated density of 1.52 g/cm³.

We wish to thank Dr. S. G. Laland, Institutt for Ernæringsforsking, Universitetet i Oslo, for a sample of 2-deoxy-D-ribose and Dr. P. Reichard, Karolinska Institutet, Stockholm, for samples of thymidine and deoxycytidine hydrochloride.

1. Furberg, S. *Acta Chem. Scand.* 4 (1950) 751.
2. Cox, E. G., Goodwin, T. H. and Wagstaff, A. I. *J. Chem. Soc.* **1935** 978, 1495.

Received December 2, 1955.

Space Groups and Molecular Symmetries of Two Thiocyanates

OLAV FOSS

Institutt for uorganisk kjemi, Norges tekniske høgskole, Trondheim, Norway

The unit cells and space groups of two simple, covalent thiocyanates have been determined from single-crystal oscillation and Weissenberg photographs, using copper radiation, $\lambda(CuK\alpha) = 1.542$ Å.

Sulphur dithiocyanate [1], $S(SCN)_2$. Orthorhombic bipyramidal, $a = 10.12$ Å, $b = 12.83$ Å, $c = 4.34$ Å. Four molecules per unit cell; density, calc. 1.75, found 1.76 g/cm³. Systematic absences, $0kl$ when $k + l$ is odd, $hk0$ when h is odd. The unit cell dimensions, the absences, and the relative intensities of the reflections show that the crystals are isomorphous with those of selenium dithiocyanate[2], $Se(SCN)_2$, and selenium diselenocyanate [3], $Se(SeCN)_2$. The space group is thus D_{2h}^{16}-*Pnma*. From the known structures of the selenium analogues [2,3] it follows that the sulphur dithiocyanate molecule has an unbranched chain structure, with the middle sulphur atom located in a crystallographic mirror plane.

The compound was prepared from sulphur dichloride by reaction with an excess of silver thiocyanate suspended in carbon disulphide, and was recrystallized from the same solvent. Silver thiocyanate was found to react better than mercuric thiocyanate [4]. The crystals occur as plates {010}, bounded by {110} and {111}, and usually very thin. The bulk of crystals became yellow in the course of a day, due to the formation of an insoluble polymer [1,4], but individual crystals could be picked which were sufficiently stable.

Ethylene thiocyanate, $(CH_2SCN)_2$. Orthorhombic bipyramidal, $a = 7.39$ Å, $b = 7.81$ Å, $c = 11.48$ Å. Four molecules per unit cell; density, calc. 1.45, found 1.42 g/cm³. Systematic absences, $0kl$ when k is odd, $h0l$ when l is odd, $hk0$ when h is odd. The space group is thus D_{2h}^{15}-*Pbca*, which has eightfold general positions, and two fourfold sets of symmetry centres as special positions. With four molecules per unit cell, it follows that the ethylene thiocyanate molecules are centrosymmetric in the crystals. This agrees with the finding from infrared measurements [5] that the compound exists in *trans* configuration in the solid state.

Recrystallized from chloroform, the compound was obtained as plates {010}, or as perfect bipyramids {111} with, also here, {010} developed.

Further work on the crystal structures of the two thiocyanates is intended.

1. Lecher, H. and Wittwer, M. *Ber.* **55** (1922) 1481.
2. Ohlberg, S. M. and Vaughan, P. A. *J. Am. Chem. Soc.* **76** (1954) 2649.
3. Aksnes, O. and Foss, O. *Acta Chem. Scand.* **8** (1954) 1787.
4. Baroni, A. *Atti R. Accad. Lincei* [6] **23** (1936) 139.
5. Quagliano, J. V. and Mizushima, S.-I. *J. Am. Chem. Soc.* **75** (1953) 6084.

Received November 30, 1955.

"*Trans*" Naphthodioxan Characterized by its Mercuric Chloride Compound

O. HASSEL and CHR. RØMMING

Universitetets Kjemiske Institutt, Blindern-Oslo, Norway

In 1950 Furberg and Hassel [1] determined the crystal structure of the lower melting compound (m. p. 111° C) found in the reaction between 2,3-dichloro-1,4-dioxan and ethylene glycol. They found

Structure of an Addition Compound Containing two Molecules of Iodine Monochloride and one Molecule of 1,4-Dioxan

O. HASSEL and J. HVOSLEF

Universitetets Kjemiske Institutt, Blindern-Oslo, Norway

It has been assumed that the interaction between an oxygen atom of an ether or a ketone with a halogen molecule results in a symmetrical bond type in which both halogen atoms take an equal part [1]. However, the first X-ray work on a solid addition product — the 1:1 compound between 1,4-dioxan and bromine [2] — revealed that in this case each ether oxygen is linked to *one* bromine atom only. Here the two atoms of a bromine molecule are situated

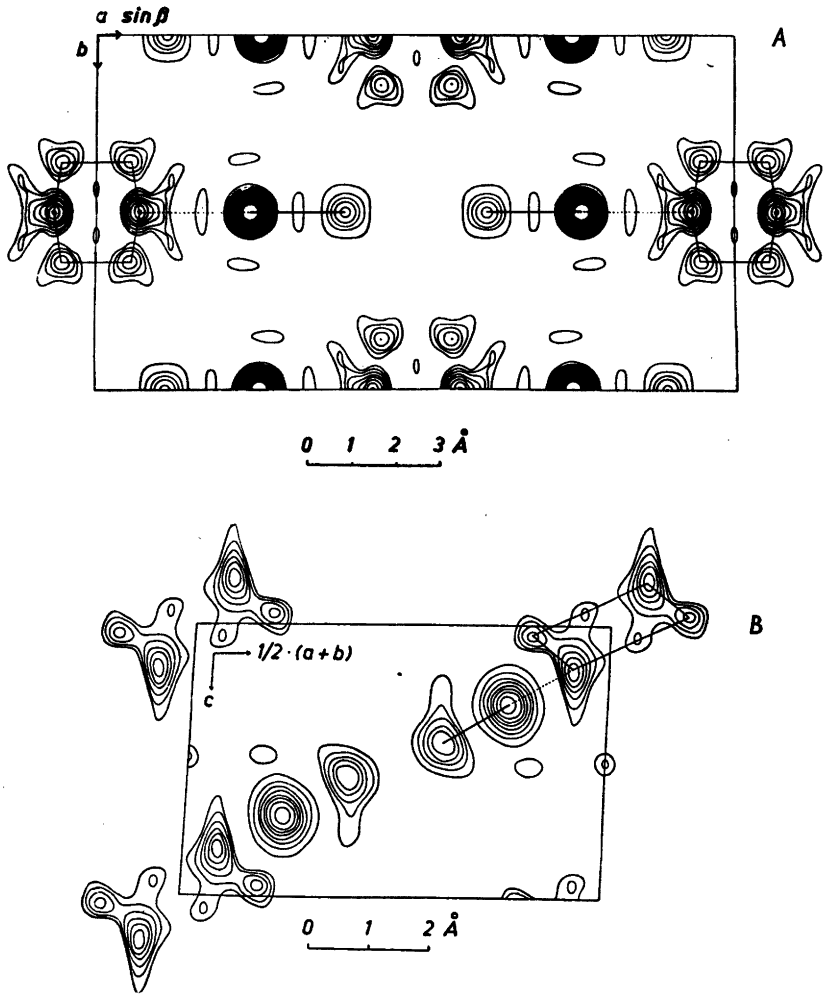


Fig. 1. Electron density maps projected. A) along [001]. Interval between contour lines for I and Cl:100 and between C and O:20. B) along [110]. Corresponding intervals are: I:100, Cl:30, C and O:10.

on the line joining the oxygen atoms of two neighbouring ether molecules. A similar structure is not to be expected if bromine is replaced by iodine monochloride, but we would expect the iodine atom to be directly linked to an ether oxygen and the angle O—I—Cl to be 180°. So far, we have not investigated this compound, but determined the structure of another compound which we obtained in the form of yellow needles (m. p. 103° C) directly from the vapours of the two compounds. Here the ratio of iodine monochloride and dioxan molecules is 2:1 as could easily be shown by dissolving the solid substance in an aqueous solution of potassium iodide and titrating the amount of iodine thereby set free.

The crystals of the new compound are *monoclinic* with $\beta = 95.2°$ and the space group is $C2/m$. The unit cell containing *four* molecules of iodine monochloride and two molecules of 1,4-dioxan have the constants $a = 14.62$, $b = 8.00$, $c = 4.56$. Approximate coordinates of the heavy iodine atoms could easily be found by conventional trial and error methods and Fourier maps computed using the signs of structure factors resulting from these coordinates. Only one refinement was necessary in order to arrive at the final maps reproduced in Fig. 1. The I and Cl coordinates thus obtained are: I: 0.242; 0; −0.290; Cl: 0.389; 0; −0.424. The coordinates of the light atoms derived from the maps are of course less accurate, but it is obvious that the centrosymmetrical dioxan molecules are of the "chair" form and the location of the oxygen atoms are good enough to show that each of them is linked to an iodine atom which has on its opposite side a chlorine atom, the O—I—Cl arrangement being linear or at least very nearly so. The O—I distance may safely be given as 2.6 Å, the I—Cl distance is 2.3 Å. The nearest Cl—Cl-approach, on the other side, is 3.38 Å showing that van der Waals forces only exist between chlorine atoms. The structure of the new compound thus provides a second example of a solid ether-halogen compound displaying a linear arrangement of the type O—Hal—Hal.

1. Mulliken, Robert, S. *J. Am. Chem. Soc.* **72** (1950) 600.
2. Hassel, O. and Hvoslef, J. *Acta Chem. Scand.* **8** (1954) 873.

Received December 13, 1955.

Structure of an Addition Compound Containing *two* Bromine Molecules and one Molecule of Hexamethylene Tetramine

GUNNAR EIA and O. HASSEL

Universitetets Kjemiske Institutt, Blindern-Oslo, Norway

As part of a research programme dealing with crystal structures of addition compounds between ethers, amines *etc.* and inorganic molecules, a bromine compound which, according to analyses, contains two molecules of bromine on every molecule of hexamethylene tetramine has been investigated. The result of the X-ray work shows that each bromine molecule is linked to one of the four tertiary nitrogen atoms, the arrangement of both groups being the same. The N-Br-Br group is *linear* and the line through the three atoms in question is symmetrically situated with respect to the three C—N bonds of the nitrogen atom. Four tetrahedral bonds are thus found by each nitrogen atom involved. The bond angles do not deviate much from the "regular" angle (109.5°). The fact that the N-Br-Br angle is 180° (or at least very nearly so) rules out the possibility that resonance effects in the NBr_2 group based on equivalence of the two bromine atoms are of any significance. The two N-Br-Br groups of a molecular complex are crystallographically independent and the fact that they are found (within the limits of error) to be identical in shape is of considerable interest. The Br-Br distance is found equal to 2.4 Å; for the N-Br distance the value 2.3 Å was obtained. These findings point to a strong interaction between the nitrogen atom and the nearest bromine atom and indicate a very marked weakening of the Br-Br bond. It would appear rather probable that in addition compounds of amines showing markedly stronger basic properties than hexamethylene tetramine, a dissociation of the bromine molecule may even occur. Investigations dealing with addition compounds of such amines are now in progress in our laboratory.

The yellow crystals of the compound between hexamethylene tetramine and two molecules of bromine are *monoclinic* and belong to the space group $P2_1/c$.

on the line joining the oxygen atoms of two neighbouring ether molecules. A similar structure is not to be expected if bromine is replaced by iodine monochloride, but we would expect the iodine atom to be directly linked to an ether oxygen and the angle O—I—Cl to be 180°. So far, we have not investigated this compound, but determined the structure of another compound which we obtained in the form of yellow needles (m. p. 103° C) directly from the vapours of the two compounds. Here the ratio of iodine monochloride and dioxan molecules is 2:1 as could easily be shown by dissolving the solid substance in an aqueous solution of potassium iodide and titrating the amount of iodine thereby set free.

The crystals of the new compound are *monoclinic* with $\beta = 95.2°$ and the space group is $C2/m$. The unit cell containing *four* molecules of iodine monochloride and two molecules of 1,4-dioxan have the constants $a = 14.62$, $b = 8.00$, $c = 4.56$. Approximate coordinates of the heavy iodine atoms could easily be found by conventional trial and error methods and Fourier maps computed using the signs of structure factors resulting from these coordinates. Only one refinement was necessary in order to arrive at the final maps reproduced in Fig. 1. The I and Cl coordinates thus obtained are: I: 0.242; 0; −0.290; Cl: 0.389; 0; −0.424. The coordinates of the light atoms derived from the maps are of course less accurate, but it is obvious that the centrosymmetrical dioxan molecules are of the "chair" form and the location of the oxygen atoms are good enough to show that each of them is linked to an iodine atom which has on its opposite side a chlorine atom, the O—I—Cl arrangement being linear or at least very nearly so. The O—I distance may safely be given as 2.6 Å, the I—Cl distance is 2.3 Å. The nearest Cl—Cl-approach, on the other side, is 3.38 Å showing that van der Waals forces only exist between chlorine atoms. The structure of the new compound thus provides a second example of a solid ether-halogen compound displaying a linear arrangement of the type O—Hal—Hal.

1. Mulliken, Robert, S. *J. Am. Chem. Soc.* **72** (1950) 600.
2. Hassel, O. and Hvoslef, J. *Acta Chem. Scand.* **8** (1954) 873.

Received December 13, 1955.

Structure of an Addition Compound Containing *two* Bromine Molecules and one Molecule of Hexamethylene Tetramine

GUNNAR EIA and O. HASSEL

Universitetets Kjemiske Institutt, Blindern-Oslo, Norway

As part of a research programme dealing with crystal structures of addition compounds between ethers, amines *etc.* and inorganic molecules, a bromine compound which, according to analyses, contains two molecules of bromine on every molecule of hexamethylene tetramine has been investigated. The result of the X-ray work shows that each bromine molecule is linked to one of the four tertiary nitrogen atoms, the arrangement of both groups being the same. The N-Br-Br group is *linear* and the line through the three atoms in question is symmetrically situated with respect to the three C—N bonds of the nitrogen atom. Four tetrahedral bonds are thus found by each nitrogen atom involved. The bond angles do not deviate much from the "regular" angle (109.5°). The fact that the N-Br-Br angle is 180° (or at least very nearly so) rules out the possibility that resonance effects in the NBr_2 group based on equivalence of the two bromine atoms are of any significance. The two N-Br-Br groups of a molecular complex are crystallographically independent and the fact that they are found (within the limits of error) to be identical in shape is of considerable interest. The Br-Br distance is found equal to 2.4 Å; for the N-Br distance the value 2.3 Å was obtained. These findings point to a strong interaction between the nitrogen atom and the nearest bromine atom and indicate a very marked weakening of the Br-Br bond. It would appear rather probable that in addition compounds of amines showing markedly stronger basic properties than hexamethylene tetramine, a dissociation of the bromine molecule may even occur. Investigations dealing with addition compounds of such amines are now in progress in our laboratory.

The yellow crystals of the compound between hexamethylene tetramine and two molecules of bromine are *monoclinic* and belong to the space group $P2_1/c$.

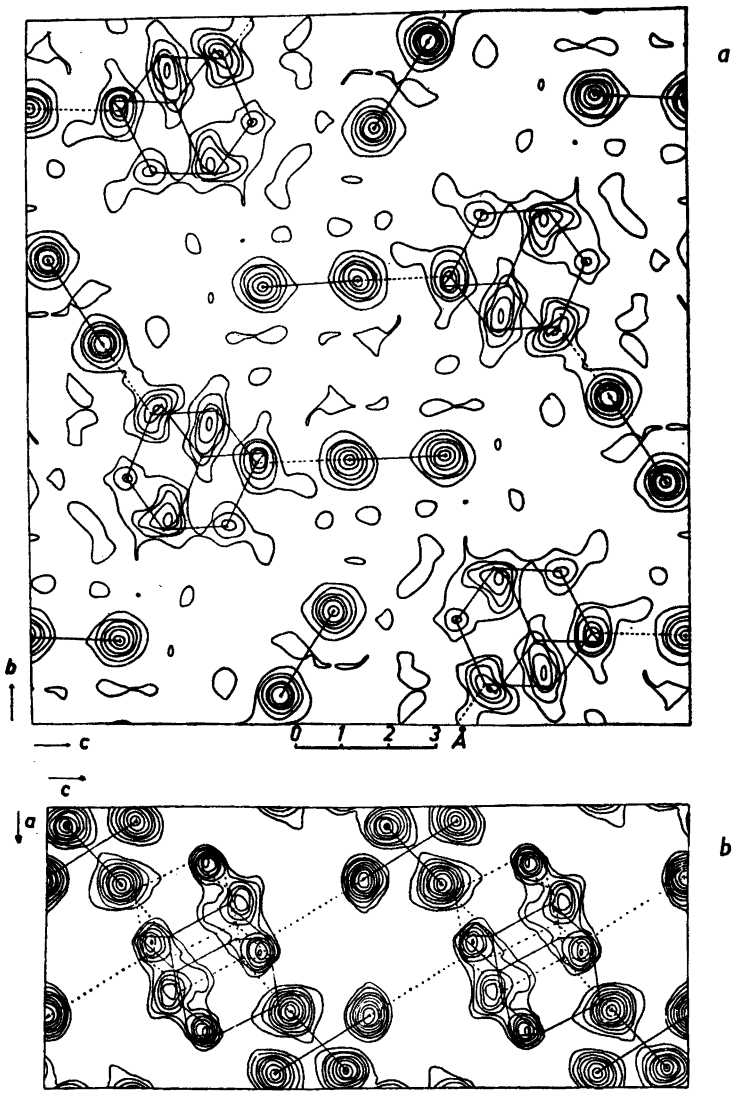


Fig. 1. Electron density maps projected a. along [100], b. along [010]. Interval between drawn contour lines four times larger for bromine than for carbon and nitrogen atoms.

From the observed density (2.35) and the lattice parameters: $a = 6.05$; $b = 14.90$; $c = 13.88$ and $\beta = 91.4°$ follows that the unit cell must contain four molecules of hexamethylene tetramine and eight molecules of bromine. Patterson Charts combined with "trial and error" calculations resulted in approximate values of the bromine parameters which could be used as a basis for two dimensional Fourier syntheses. Reproductions of electron density maps, projected along [100] (Fig. 1 a) and

along [010] (Fig. 1 b) are given. The form of the organic part of the complex necessarily leads to overlapping in any projection. In the [010] projection overlapping of two amine molecules occurs. A difference synthesis — with subtraction of the bromine atoms — led to a chart in which the organic part was better resolved than in Fig. 1 a. All further details of the investigation — now practically finished — will be given in a forthcoming publication.

Received December 13, 1955.

*iso*Thiocyanates XVII. *o*-Methoxybenzyl *iso*Thiocyanate and some Derivatives

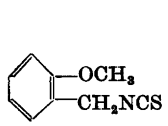
ANDERS KJÆR and ROALD BOE JENSEN

Chemical Laboratory of the University of Copenhagen, Denmark

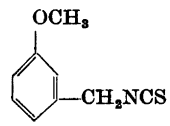
Recently, Ettlinger and Lundeen [1] isolated *m*-methoxybenzyl *iso*thiocyanate (II) from seeds of the American plant *Limnanthes douglasii* R.Br. Coincidently, *p*-methoxybenzyl *iso*thiocyanate (III) was recognised in this laboratory as the aglucone of a glucoside, named glucoaubrietin, occurring in various species of the crucifer genus *Aubrietia* [2]. Both (II) and (III) were synthesised in the course of these investigations.

Ettlinger [4], and used also for the synthesis of (II) [1] and (III) [2]. Contrary to the latter two, which are liquids at ordinary temperature, the mustard oil (I) appeared as a low-melting solid. Its ultra-violet absorption spectrum in 2,2,4-trimethylpentane has a shoulder at about 255 mμ (ε *ca.* 1 550), maxima at 271 mμ (ε 2 400) and 277 mμ (ε 2 400) and minima at 236 mμ (ε 850) and 275 mμ (ε 2 200). These data are in accord with those reported for the *meta*-isomeride (II) [1], but differ considerably from the values determined for (III) in the same solvent, *viz.* shoulders at about 250 mμ (ε 2 300) and 285 mμ (ε 1 000), maxima at 228 mμ (ε 11 600) and 276 mμ (ε 1 730) and a broad minimum around 269 mμ (ε 1 550). In the wave-length region below 11 μ, the infra-red spectrum of (I) was comparable to that of (III), both displaying bands which deviated considerably from those reported for the *meta*-compound [1].

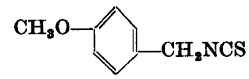
For the purpose of characterisation, (I) was converted into *N*-*o*-methoxybenzyl-thiourea and *N*-benzyl-*N'*-*o*-methoxybenzyl-thiourea on reaction at room temperature with ammonia and benzylamine, respectively. The mustard oil reacted much more sluggishly than generally experienced for *iso*thiocyanates, a fact suggesting a certain sterical influence of the neighbouring methoxy-grouping. In an attempt to enforce the reaction between (I) and benzylamine under more drastic conditions, amine exchange occurred, resulting in the formation of *N*,*N'*-dibenzylthiourea. This reaction presents no novelty in thiourea chemistry. Recently, Ettlinger and Hodg-



I



II



III

On this background it became of interest to prepare the heretofore unknown *o*-methoxybenzyl *iso*thiocyanate (I). The requisite *o*-methoxybenzylamine was obtained by Leuckart-reaction on *o*-methoxybenzaldehyde, according to Lewis [3], but in somewhat better yield (40 %). The amine was converted into (I) by the convenient modification of the Kaluza-synthesis which was recently introduced by Hodgkins and

kins [5] observed the formation of thiocarbanilide in the reaction of *N*-*t*-butyl-*N'*-phenylthiourea with aniline in boiling benzene, and referred to further examples in the literature. In the present case, it seems likely that sterical factors interfere with the usual thiamide-resonance, thus favouring the displacement of *o*-methoxybenzylamine. This view is supported by the infra-red spectra of the thioureas corresponding

along [010] (Fig. 1 b) are given. The form of the organic part of the complex necessarily leads to overlapping in any projection. In the [010] projection overlapping of two amine molecules occurs. A difference synthesis — with subtraction of the bromine atoms — led to a chart in which the organic part was better resolved than in Fig. 1 a. All further details of the investigation — now practically finished — will be given in a forthcoming publication.

Received December 13, 1955.

*iso*Thiocyanates XVII. *o*-Methoxybenzyl *iso*Thiocyanate and some Derivatives

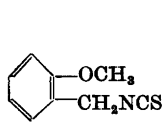
ANDERS KJÆR and ROALD BOE JENSEN

Chemical Laboratory of the University of Copenhagen, Denmark

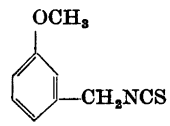
Recently, Ettlinger and Lundeen [1] isolated *m*-methoxybenzyl *iso*thiocyanate (II) from seeds of the American plant *Limnanthes douglasii* R.Br. Coincidently, *p*-methoxybenzyl *iso*thiocyanate (III) was recognised in this laboratory as the aglucone of a glucoside, named glucoaubrietin, occurring in various species of the crucifer genus *Aubrietia* [2]. Both (II) and (III) were synthesised in the course of these investigations.

Ettlinger [4], and used also for the synthesis of (II) [1] and (III) [2]. Contrary to the latter two, which are liquids at ordinary temperature, the mustard oil (I) appeared as a low-melting solid. Its ultra-violet absorption spectrum in 2,2,4-trimethylpentane has a shoulder at about 255 mμ (ε *ca.* 1 550), maxima at 271 mμ (ε 2 400) and 277 mμ (ε 2 400) and minima at 236 mμ (ε 850) and 275 mμ (ε 2 200). These data are in accord with those reported for the *meta*-isomeride (II) [1], but differ considerably from the values determined for (III) in the same solvent, *viz.* shoulders at about 250 mμ (ε 2 300) and 285 mμ (ε 1 000), maxima at 228 mμ (ε 11 600) and 276 mμ (ε 1 730) and a broad minimum around 269 mμ (ε 1 550). In the wave-length region below 11 μ, the infra-red spectrum of (I) was comparable to that of (III), both displaying bands which deviated considerably from those reported for the *meta*-compound [1].

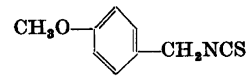
For the purpose of characterisation, (I) was converted into *N*-*o*-methoxybenzyl-thiourea and *N*-benzyl-*N'*-*o*-methoxybenzyl-thiourea on reaction at room temperature with ammonia and benzylamine, respectively. The mustard oil reacted much more sluggishly than generally experienced for *iso*thiocyanates, a fact suggesting a certain sterical influence of the neighbouring methoxy-grouping. In an attempt to enforce the reaction between (I) and benzylamine under more drastic conditions, amine exchange occurred, resulting in the formation of *N*,*N'*-dibenzylthiourea. This reaction presents no novelty in thiourea chemistry. Recently, Ettlinger and Hodg-



I



II



III

On this background it became of interest to prepare the heretofore unknown *o*-methoxybenzyl *iso*thiocyanate (I). The requisite *o*-methoxybenzylamine was obtained by Leuckart-reaction on *o*-methoxybenzaldehyde, according to Lewis [3], but in somewhat better yield (40 %). The amine was converted into (I) by the convenient modification of the Kaluza-synthesis which was recently introduced by Hodgkins and

kins [5] observed the formation of thiocarbanilide in the reaction of *N*-*t*-butyl-*N'*-phenylthiourea with aniline in boiling benzene, and referred to further examples in the literature. In the present case, it seems likely that sterical factors interfere with the usual thiamide-resonance, thus favouring the displacement of *o*-methoxybenzylamine. This view is supported by the infra-red spectra of the thioureas corresponding

to (I), (II) and (III). Whereas the latter two exhibit normal "thioureid" absorption bands at 6.58 μ and 6.57 μ [6], a displacement of the band to 6.38 μ is noticed in the spectrum of *o*-methoxybenzylthiourea.

The three methoxybenzylthioureas were subjected to descending paper chromatography in water-saturated chloroform and the R_{Ph}-values [7] 1.14, 0.99 and 1.02 determined for the *o*-, *m*- and *p*-derivative, respectively. The high value of the *ortho*-compound indicates a rather pronounced chelation of this isomeride in solution. So far, the mustard oil (I) has not been encountered in nature.

Experimental *. o-*Methoxybenzylamine.* *o*-Methoxybenzaldehyde [8] (50 g) was treated with ammonium formate (200 g), and the mixture subsequently hydrolysed with conc. HCl (400 ml) as previously described [3], except that the reaction time was increased to 6 hours. The amine distilled at 114° at 14 mm, yield 20 g (40 %); the previously reported yield was 30 %.

o-*Methoxybenzyl* iso*thiocyanate* (I). The above amine (7.6 g) was converted to (I) by the method formerly used for preparing the corresponding *m*-derivative [1]. The *iso*thiocyanate distilled at 133° and 4 mm, and solidified to a colourless crystalline mass, m. p. 28°, yield 6.8 g (68 %). (Found: C 60.50; H 5.03; N 7.70; S 17.97. Calc. for C_9H_9ONS: C 60.31; H 5.06; N 7.82; S 17.89). The infra-red spectrum, determined in a KBr disc, showed bands at 3.33, 4.65 (very strong, N=C=S), 6.18, 6.57, 6.86, 6.90, 7.40, 7.70, 8.05 (v. s., aryl ether), 8.49, 8.87, 9.45, 9.70, 11.98 and 13.23 μ (v. s.).

N-o-*Methoxybenzylthiourea.* A solution of (I) (500 mg) in ethanol (5 ml), saturated with dry ammonia, was set aside at room temperature for 4 days. The separated thiourea crystallised from water, containing a little ethanol, as colourless needles (361 mg), m. p. 122°. (Found: C 54.90; H 6.35; N 14.12. Calc. for $C_9H_{12}ON_2S$: C 55.05; H 6.17; N 14.27). The infra-red spectrum (KBr pellet) had prominent bands at: 2.93, 3.08, 6.04, 6.38, 6.64 (weak), 6.89, 7.34, 7.51 (w.), 7.68, 7.98, 8.54, 8.87, 9.50, 9.64, 9.86, 10.71, 11.91, 12.74, 13.14 (strong), 13.36 and 14.20 μ.

N-*Benzyl*-N'-o-*methoxybenzyl-thiourea.* An ether solution of (I) (500 mg) and benzylamine (2 ml) was kept at room temperature for 4 weeks. The solvent was removed and the oily residue treated with dilute HCl. After being kept at 0° for some hours the syrup crystallised. After two recrystallisations from 70 % ethanol, an analytical specimen was obtained as colourless needles (494 mg), m. p. 82.5°. (Found: C 66.90; H 6.38; N 9.86. Calc. for $C_{16}H_{18}ON_2S$: C 67.10; H 6.34; N 9.78).

In an attempt to enforce this reaction, (I) (500 mg) was heated to reflux for one hour in benzylamine (10 ml). Excess amine was removed *in vacuo* and the residue triturated with dilute HCl. The now crystalline product was recrystallised twice from ethanol, yielding colourless prisms (329 mg), m. p. 149—150°. (Found: C 70.30; H 6.21; N 10.64. Calc. for $C_{15}H_{16}N_2S$: C 70.29; H 6.29; N 10.93). The composition, in conjunction with reported values for the m. p., *e. g.* 147—148° [9], indicated the identity of the reaction product as *N-N'*-dibenzylthiourea.

Microanalyses were performed in this laboratory by Mr. P. Hansen. The work is part of investigations supported by *Statens Almindelige Videnskabsfond (The Danish State Research Foundation)* and *Carlsbergfondet (The Carlsberg Foundation)*.

1. Ettlinger, M. G. and Lundeen, A. J. *J. Am. Chem. Soc.* **78** (1956). *In press.*
2. Kjær, A., Gmelin, R. and Boe Jensen, R. *Acta Chem. Scand.* **10** (1956), 26.
3. Lewis, K. G. *J. Chem. Soc.* **1950** 2249.
4. Hodgkins, J. E. and Ettlinger, M. G. *J. Org. Chem.* **21** (1956). *In press.*
5. Ettlinger, M. G. and Hodgkins, J. E. *J. Am. Chem. Soc.* **77** (1955) 1831.
6. Ettlinger, M. G. *J. Am. Chem. Soc.* **72** (1950) 4699.
7. Kjær, A. and Rubinstein, K. *Acta Chem. Scand.* **7** (1953) 528.
8. Shoesmith, J. B. and Connor, R. J. *J. Chem. Soc.* **1927** 2230.
9. Dyson, G. M. and George, H. J. *J. Chem. Soc.* **125** (1924) 1702.

Received December 15, 1955.

* Melting points are uncorrected and determined in capillary tubes in a water- or glycerol-bath.

Separation of Saturated Straight Chain Fatty Acids III. Quantitative Paper Chromatography

OLAVI PERILÄ

Finland Institute of Technology, Laboratory for Wood Chemistry, Helsinki, Finland

The lower fatty acids, separated by paper chromatography as their salts, may be determined quantitatively by the area method [1]. The basis of another method of quantitative estimation of the ammonium salts of organic acids is that if an acid is added to a neutralized solution of an acid indicator the anion of which is distinctly coloured, then the depth of the colour due to the anion is inversely proportional to the amount of acid added between 20 and 80 % neutralization [2]. The value of both these methods is somewhat reduced because of the sensitivity of the indicators towards atmospheric (or dissolved) carbon dioxide. As hydroxamic derivatives, the acids may be estimated in more stable conditions. Stadtman [3] describes a method of this kind for the acyl phosphates of C_2. . .C_6, in which the chromatographed hydroxamic derivatives of the acids are extracted from the paper and estimated colorimetrically. Block [4] used a corresponding procedure for the same acids, chromatographing them according to the method of Thompson [5] and estimating them colorimetrically directly on the paper. Wagner [6] describes a quantitative chromatographic method for the long chain acids (C_{12}. . .C_{22}) in which he used the chromatographic procedure of Kaufmann [7] and estimated the amounts of the acids colorimetrically directly on the paper, first converting the acids by the method of Kaufmann into their copper salts and then the copper into the ferrocyanide complex, the amount of which was easily estimated colorimetrically. In the present study corresponding investigations were carried out. The amount of copper was determined colorimetrically by the dithizone method from the ash of the spot cut from the chromatogram. It was found that the amount of combined copper was not quite equivalent to the amount of fatty acid on the paper, but that very small amounts of acids combined with copper in a molar ratio. In the following, procedures now found suitable for the separation and estimation of fatty acids from formic to cerotic acid are described.

The acids from formic to valeric acid may be separated from each other and estimated by converting them into their hydroxamic derivatives and chromatographing with the solvent *n*-butanol:benzene:water (1:1:1, upper layer) by the circular method, which is the most suitable in this case. The acids are located by spraying the paper with $FeCl_3$ solution. The spots are extracted in cuvette solutions containing $FeCl_3$ and the amounts of acids are estimated colorimetrically.

The acids from caproic to pelargonic acid are analysed in the same manner as in the former group, but chromatography is carried out with the solvent benzene: formic acid:water (1:1:1, upper layer).

The acids from capric to cerotic acid may be separated by the method previously described by the author [8]. Quantitative estimation of the acids is achieved by converting them into silver salts on the paper, removing the excess of silver and determining the amount of silver in each spot colorimetrically by the dithizone method.

Experimental: Separation and estimation of the acids from formic to valeric acid. A slight excess of diazomethane dissolved in ether was added at room temperature to the methanol solution of the fatty acids and the excess of diazomethane was evaporated. The methyl esters obtained were converted into hydroxamic derivatives by the method of Thompson [5], adding to the solution of esters obtained alkaline hydroxylamine solution. The reaction was allowed to proceed for half an hour at room temperature, after which the solution was acidified with acetic acid. The sodium acetate precipitate was filtered off and the solution was concentrated in vacuum. Chromatography is most conveniently carried out by the circular method (*cf.* Perilä [8]) using as solvent the upper layer of the mixture *n*-butanol:benzene:water (1:1:1) [9]. Because the solubility of water in the solvent is poor, it is advisable to keep a sheet of filter paper wetted with the water layer of the above-mentioned mixture on the bottom of the chromatographic chamber. Any Whatman double-washed paper is suitable for these analyses. After development, the paper was dried at room temperature and sprayed with $FeCl_3$ solution (*e. g.* 50 grams of $FeCl_3 \cdot 6H_2O$ dissolved in one litre of N HCl in ethanol [3]). For qualitative detection 0.05 micromoles of each acid are sufficient, but for quantitative estimation an acid concentration of 0.1—1 μM/ml is needed. This concentration

then determines the amount of acids to be taken for the chromatography. The spots obtained were cut out, and the ferric complexes of the hydroxamic derivatives of the fatty acids were extracted with a $FeCl_3$ solution (5 g $FeCl_3 \cdot 6H_2O$ + 25 ml conc. HCl + 575 ml water [3]). This solution was then analysed colorimetrically at a wavelength of 5 200 Å. According to Goddu [10] the accuracy of the measurement is ± 2 %. The accuracy is somewhat reduced, however, because of the chromatographic procedure. In the conditions described the following R_F-values were obtained: formic 0.24, acetic 0.34, propionic 0.51, butyric 0.69, valeric 0.83, and caproic acid 0.90.

Separation and estimation of the acids from caproic to pelargonic acid. The analyses were carried out in the same conditions as those of the preceding group, except that the chromatographic solvent was the upper layer of the mixture benzene:formic acid:water (1:1:1) [5]. The following R_F-values were obtained: valeric 0.18, caproic 0.33, oenanthylic 0.49, caprylic 0.62, pelargonic 0.72, and capric acid 0.76.

Separation and estimation of the acids from capric to cerotic acid. The chromatography was carried out by the method previously described by the author [8], using a paper saturated with hydrocarbon and as solvent a mixture of acetic acid and water (9:1) saturated with hydrocarbon. The hydrocarbon was evaporated and the paper treated for half an hour with an 1.5 % aqueous solution of $AgNO_3$. The excess of silver was removed by washing with deionized water, after which the paper was rapidly dried and sprayed with 0.05 % ethanolic *p*-diethylaminobenzylidenrhodanine. After drying, the silver spots were conveniently visible in ultraviolet light. The spots were cut out and the paper was burned in the usual manner with sulfuric acid-perchloric acid-nitric acid. The amount of silver was determined colorimetrically by the dithizone method at a wavelength of 6 250 Å[11]. For qualitative detection with the silver reagent mentioned 0.05 μM of each acid is sufficient, but for quantitative estimation it is advisable to use 0.2—2 μM of each acid. According to several determinations the accuracy of the method is about ± 5 %.

1. Reid, R. L. and Lederer, M. *Biochem. J. London* **50** (1951) 60.
2. Isherwood, F. A. and Hanes, C. S. *Biochem. J. London* **55** (1953) 824.
3. Stadtman, E. R. and Barker, H. A. *J. Biol. Chem.* **184** (1950) 769.
4. Block, R. J., Durrum, E. L. and Zweig, G. *A Manual of Paper Chromatography and Paper Electrophoresis*, Academic Press Inc., Publishers, New York, N. Y. 1955, p. 162.
5. Thompson, A. R. *Australian J. Sci. Research* **B 4** (1951) 180.
6. Wagner, H., Abisch, L. and Bernhard, K. *Helv. Chim. Acta* **38** (1955) 1536.
7. Kaufmann, H. P. and Budwig, J. *Fette u. Seifen* **53** (1951) 390.
8. Perilä, O. *Acta Chem. Scand.* **9** (1955) 864.
9. Inouye, Y. and Noda, M. *J. Agr. Chem. Soc. Japan* **25** (1952) 496.
10. Goddu, R. F., LeBlanc, N. F. and Wright, C. M. *Anal. Chem.* **27** (1955) 1251.
11. Sandell, E. B. *Colorimetric Determination of Traces of Metals*, Interscience Publishers, Inc., New York, N. Y. 1944, p. 394.

Received December 14, 1955.

Purification of Clearing Factor from Postheparin Plasma

ESKO A. NIKKILÄ and RAINER PESOLA

Department of Medical Chemistry, University of Helsinki, Finland

Since the original discovery by Hahn [1] of the lipemia clearing effect of heparin upon injection and the subsequent demonstration of an *in vitro*-active clearing principle in plasma withdrawn after heparin administration [2] much successful work has been done to elucidate the mechanism of this peculiar phenomenon. Evidence has accumulated to show that the clearing factor acts as a lipoprotein lipase [3]. In spite of these advances only a few attempts have so far been made for the purification of the active principle from postheparin plasma. Anfinsen *et al.*[4] showed that the clearing factor falls in Fraction III-1,2,3 in the ethanol fractionation scheme of Cohn and they could thus achieve an about fourteen-fold purification of the activity. Later, Anfinsen and Quigley [5] reported a purification up to 100- to 200-fold by a relatively laborious procedure based on a complex formation between the clearing factor and low density lipoproteins (enzyme-substrate complex). Earlier studies in this laboratory revealed that the clearing activity was precipitated quantitatively from plasma at a low ionic strength at pH 5.6 along with 1/20 to 1/25 of the plasma proteins [6]. This finding was confirmed by Hood *et al.*[7] and the method has since been used by a

then determines the amount of acids to be taken for the chromatography. The spots obtained were cut out, and the ferric complexes of the hydroxamic derivatives of the fatty acids were extracted with a $FeCl_3$ solution (5 g $FeCl_3 \cdot 6H_2O$ + 25 ml conc. HCl + 575 ml water [3]). This solution was then analysed colorimetrically at a wavelength of 5 200 Å. According to Goddu [10] the accuracy of the measurement is ± 2 %. The accuracy is somewhat reduced, however, because of the chromatographic procedure. In the conditions described the following R_F-values were obtained: formic 0.24, acetic 0.34, propionic 0.51, butyric 0.69, valeric 0.83, and caproic acid 0.90.

Separation and estimation of the acids from caproic to pelargonic acid. The analyses were carried out in the same conditions as those of the preceding group, except that the chromatographic solvent was the upper layer of the mixture benzene:formic acid:water (1:1:1) [5]. The following R_F-values were obtained: valeric 0.18, caproic 0.33, oenanthylic 0.49, caprylic 0.62, pelargonic 0.72, and capric acid 0.76.

Separation and estimation of the acids from capric to cerotic acid. The chromatography was carried out by the method previously described by the author [8], using a paper saturated with hydrocarbon and as solvent a mixture of acetic acid and water (9:1) saturated with hydrocarbon. The hydrocarbon was evaporated and the paper treated for half an hour with an 1.5 % aqueous solution of $AgNO_3$. The excess of silver was removed by washing with deionized water, after which the paper was rapidly dried and sprayed with 0.05 % ethanolic *p*-diethylaminobenzylidenrhodanine. After drying, the silver spots were conveniently visible in ultraviolet light. The spots were cut out and the paper was burned in the usual manner with sulfuric acid-perchloric acid-nitric acid. The amount of silver was determined colorimetrically by the dithizone method at a wavelength of 6 250 Å[11]. For qualitative detection with the silver reagent mentioned 0.05 μM of each acid is sufficient, but for quantitative estimation it is advisable to use 0.2—2 μM of each acid. According to several determinations the accuracy of the method is about ± 5 %.

1. Reid, R. L. and Lederer, M. *Biochem. J. London* **50** (1951) 60.
2. Isherwood, F. A. and Hanes, C. S. *Biochem. J. London* **55** (1953) 824.
3. Stadtman, E. R. and Barker, H. A. *J. Biol. Chem.* **184** (1950) 769.
4. Block, R. J., Durrum, E. L. and Zweig, G. *A Manual of Paper Chromatography and Paper Electrophoresis*, Academic Press Inc., Publishers, New York, N. Y. 1955, p. 162.
5. Thompson, A. R. *Australian J. Sci. Research* **B 4** (1951) 180.
6. Wagner, H., Abisch, L. and Bernhard, K. *Helv. Chim. Acta* **38** (1955) 1536.
7. Kaufmann, H. P. and Budwig, J. *Fette u. Seifen* **53** (1951) 390.
8. Perilä, O. *Acta Chem. Scand.* **9** (1955) 864.
9. Inouye, Y. and Noda, M. *J. Agr. Chem. Soc. Japan* **25** (1952) 496.
10. Goddu, R. F., LeBlanc, N. F. and Wright, C. M. *Anal. Chem.* **27** (1955) 1251.
11. Sandell, E. B. *Colorimetric Determination of Traces of Metals*, Interscience Publishers, Inc., New York, N. Y. 1944, p. 394.

Received December 14, 1955.

Purification of Clearing Factor from Postheparin Plasma

ESKO A. NIKKILÄ and RAINER PESOLA

Department of Medical Chemistry, University of Helsinki, Finland

Since the original discovery by Hahn [1] of the lipemia clearing effect of heparin upon injection and the subsequent demonstration of an *in vitro*-active clearing principle in plasma withdrawn after heparin administration [2] much successful work has been done to elucidate the mechanism of this peculiar phenomenon. Evidence has accumulated to show that the clearing factor acts as a lipoprotein lipase [3]. In spite of these advances only a few attempts have so far been made for the purification of the active principle from postheparin plasma. Anfinsen *et al.*[4] showed that the clearing factor falls in Fraction III-1,2,3 in the ethanol fractionation scheme of Cohn and they could thus achieve an about fourteen-fold purification of the activity. Later, Anfinsen and Quigley [5] reported a purification up to 100- to 200-fold by a relatively laborious procedure based on a complex formation between the clearing factor and low density lipoproteins (enzyme-substrate complex). Earlier studies in this laboratory revealed that the clearing activity was precipitated quantitatively from plasma at a low ionic strength at pH 5.6 along with 1/20 to 1/25 of the plasma proteins [6]. This finding was confirmed by Hood *et al.*[7] and the method has since been used by a

number of workers for obtaining a crude preparation of clearing factor.

Because of the irreversible inactivation of clearing factor in concentrated salt solutions its purification by the conventional salting out procedures is not possible. In the search for more effective methods of purification our attention was drawn to the recent findings of Nilsson and Wenckert [8], who demonstrated that heparin is adsorbed to known prothrombin adsorbents and elutable with citrate and that a natural heparin-like anticoagulant occurs in plasma bound to prothrombin. It was thought that also the clearing factor, which most probably contains heparin, might behave like prothrombin against adsorbents, either due to the formation of a complex with the latter or due to its heparin content as such. Thus, the known prothrombin purification methods could possibly be advantageously applied for the purification of lipemia clearing activity as well. This proved in fact to be the case.

The clearing activity of postheparin plasma is completely adsorbed on calcium phosphate gel and can be eluated with 0.1 M citrate. By this means a *40-fold* purification is achieved. Elution of the adsorbate with physiological NaCl removes about half of the proteins adsorbed but none of the clearing activity. Thus, washing of the precipitate with saline before the citrate elution increases the grade of purification up to about *85-fold*. The supernatant liquid of the $Ca_3(PO_4)_2$ adsorbate has the same acceptor-protein activity as untreated plasma and can therefore be used in the assay of clearing activity. In the course of these experiments it was found that citrate is a powerful activator of the clearing reaction, also in oxalated plasma.

Further purification of the clearing factor could be attained by diluting the eluate, after removal of citrate by dialysis, with distilled water and adjusting the pH to 5.5. The precipitate formed contained about 60 % of the original clearing activity purified about *400-fold* over the initial plasma on the protein-tyrosine basis.

Being undialysable the clearing factor differs from the natural heparin-like anticoagulant, which was reported by Nilsson and Wenckert [3] to dissociate from its union with prothrombin during dialysis. The possible identity of clearing factor and the thermolabile anticoagulant described by Fiala [9] remains to be established.

Oxalated plasma was found to have a lower clearing activity than the mere postheparin plasma, thus suggesting that the active principle is adsorbed on calcium oxalate as well (like heparin and prothrombin).

The details of the purification procedure and a description of the properties of the active preparation thus obtained will be published shortly.

1. Hahn, P. F. *Science* **98** (1943) 19.
2. Anderson, N. G. and Fawcett, B. *Proc. Soc. Exptl. Biol. Med.* **74** (1948) 768.
3. Korn, E. D. *J. Biol. Chem.* **215** (1955) 15.
4. Anfinsen, C. B., Boyle, E. and Brown, R. K. *Science* **115** (1952) 583.
5. Anfinsen, C. B. and Quigley, T. W. *Circulation* **8** (1953) 435.
6. Nikkilä, E. *Scand. J. Clin. & Lab. Invest. Suppl.* **8** (1953).
7. Hood, B., Angerwall, G., Isaksson, B. and Welin, G. *Scand. J. Clin. & Lab. Invest.* **6** (1954) 1.
8. Nilsson, I. M. and Wenckert, A. *Acta Med. Scand.* **150** (1954) *Suppl.* 297.
9. Fiala, S. *Nature* **167** (1951) 279.

Received December 19, 1955.

Syntheses of Choline Esters of Monobasic Carbonic Acids

L.-E. TAMMELIN

Research Institute of National Defence, Dept. I, Sundbyberg 4, Sweden

A convenient method which gives good yields of choline esters is shown by the following scheme:

$$(CH_3)_2NCH_2CH_2OH + OC_2O_2R_2 = (CH_3)_2NCH_2CH_2OCOR + RCOOH$$

$$(CH_3)_2NCH_2CH_2OCOR + CH_3I = (CH_3)_3N^+CH_2CH_2OCOR + I^-$$

The first step has been used by Campbell *et al.*[1] in theoretical studies of the amino alcohols. Using this method of synthesis acetylcholine, propionylcholine and butyrylcholine have been prepared in yields of more than 90 % of the theoretical, calculated on the dimethylaminoethanol.

The only step that requires special comment is the first. When the reaction between the alcohol and the anhydride is finished the reaction mixture is distilled

number of workers for obtaining a crude preparation of clearing factor.

Because of the irreversible inactivation of clearing factor in concentrated salt solutions its purification by the conventional salting out procedures is not possible. In the search for more effective methods of purification our attention was drawn to the recent findings of Nilsson and Wenckert [8], who demonstrated that heparin is adsorbed to known prothrombin adsorbents and elutable with citrate and that a natural heparin-like anticoagulant occurs in plasma bound to prothrombin. It was thought that also the clearing factor, which most probably contains heparin, might behave like prothrombin against adsorbents, either due to the formation of a complex with the latter or due to its heparin content as such. Thus, the known prothrombin purification methods could possibly be advantageously applied for the purification of lipemia clearing activity as well. This proved in fact to be the case.

The clearing activity of postheparin plasma is completely adsorbed on calcium phosphate gel and can be eluated with 0.1 M citrate. By this means a *40-fold* purification is achieved. Elution of the adsorbate with physiological NaCl removes about half of the proteins adsorbed but none of the clearing activity. Thus, washing of the precipitate with saline before the citrate elution increases the grade of purification up to about *85-fold*. The supernatant liquid of the $Ca_3(PO_4)_2$ adsorbate has the same acceptor-protein activity as untreated plasma and can therefore be used in the assay of clearing activity. In the course of these experiments it was found that citrate is a powerful activator of the clearing reaction, also in oxalated plasma.

Further purification of the clearing factor could be attained by diluting the eluate, after removal of citrate by dialysis, with distilled water and adjusting the pH to 5.5. The precipitate formed contained about 60 % of the original clearing activity purified about *400-fold* over the initial plasma on the protein-tyrosine basis.

Being undialysable the clearing factor differs from the natural heparin-like anticoagulant, which was reported by Nilsson and Wenckert [3] to dissociate from its union with prothrombin during dialysis. The possible identity of clearing factor and the thermolabile anticoagulant described by Fiala [9] remains to be established.

Oxalated plasma was found to have a lower clearing activity than the mere postheparin plasma, thus suggesting that the active principle is adsorbed on calcium oxalate as well (like heparin and prothrombin).

The details of the purification procedure and a description of the properties of the active preparation thus obtained will be published shortly.

1. Hahn, P. F. *Science* **98** (1943) 19.
2. Anderson, N. G. and Fawcett, B. *Proc. Soc. Exptl. Biol. Med.* **74** (1948) 768.
3. Korn, E. D. *J. Biol. Chem.* **215** (1955) 15.
4. Anfinsen, C. B., Boyle, E. and Brown, R. K. *Science* **115** (1952) 583.
5. Anfinsen, C. B. and Quigley, T. W. *Circulation* **8** (1953) 435.
6. Nikkilä, E. *Scand. J. Clin. & Lab. Invest. Suppl.* **8** (1953).
7. Hood, B., Angerwall, G., Isaksson, B. and Welin, G. *Scand. J. Clin. & Lab. Invest.* **6** (1954) 1.
8. Nilsson, I. M. and Wenckert, A. *Acta Med. Scand.* **150** (1954) *Suppl.* 297.
9. Fiala, S. *Nature* **167** (1951) 279.

Received December 19, 1955.

Syntheses of Choline Esters of Monobasic Carbonic Acids

L.-E. TAMMELIN

Research Institute of National Defence, Dept. I, Sundbyberg 4, Sweden

A convenient method which gives good yields of choline esters is shown by the following scheme:

$$(CH_3)_2NCH_2CH_2OH + OC_2O_2R_2 = (CH_3)_2NCH_2CH_2OCOR + RCOOH$$

$$(CH_3)_2NCH_2CH_2OCOR + CH_3I = (CH_3)_3N^+CH_2CH_2OCOR + I^-$$

The first step has been used by Campbell *et al.*[1] in theoretical studies of the amino alcohols. Using this method of synthesis acetylcholine, propionylcholine and butyrylcholine have been prepared in yields of more than 90 % of the theoretical, calculated on the dimethylaminoethanol.

The only step that requires special comment is the first. When the reaction between the alcohol and the anhydride is finished the reaction mixture is distilled

Table 1.

Compound	Final b. p.	n_D^{20} at final b. p.
Acetic ester	68°/8 mm	1.4309
Propionic ester	70°/8 mm	1.4310
Butyric ester	81°/8 mm	1.4320

Table 2.

Compound	Grams of distillate	Grams of CH_3I	Yield in %, calc. on the alcohol
Acetylcholine	1	2.0	93
Propionyl »	1	1.8	92
Butyryl »	1	1.6	93

Table 3.

Formula	Mol. wt.	C		H		I		M.p. *
		calc	found	calc	found	calc	found	
$C_7H_{16}O_2NI$	273.12	30.8	30.8	5.9	5.8	46.5	47.0	161
$C_8H_{18}O_2NI$	287.15	33.5	33.4	6.3	6.3	44.3	44.7	130
$C_9H_{20}O_2NI$	301.18	36.0	35.8	6.7	6.6	42.3	42.7	87

* Determined with a "Kofler Heizbank".

under reduced pressure. It has been shown that all fractions up to a certain boiling point contain the dimethylaminoethyl ester. Thus all fractions are collected from the beginning of the distillation until temperature exceeds the boiling points given in Table 1.

Experimental: Dimethylaminoethylesters. One mole of acid anhydride was refluxed with 1 mole of dimethylaminoethanol on waterbath overnight. The reaction mixture was distilled at reduced pressure and all fractions collected up to and including the fraction at the temperature given in Table 1.

Choline esters. The combined fractions from the esterifications were dissolved in eight parts of dry ether. Methyl iodide was added in about 100 % excess and the reaction mixture was allowed to stand for three days in a stoppered round-bottomed flask at 25° C. The iodides were obtained as colourless crystalline precipitates which were filtered off and dried in a desiccator. Recrystallisation of the products was found to be unnecessary. Data for the syntheses are given in Table 2 and the analyses are given in Table 3.

My sincere thanks are due to Professor G. Ljunggren, Director of this institute for his kind interest in this work.

1. Campbell, K. N., O'Boyle, C. I. and Campbell, B. K. *Proc. Indiana Acad. Sci.* **58** (1949) 120.

Received December 22, 1955.

ACTA CHEMICA SCANDINAVICA **10** (1956) 147—162

Proceedings of the Swedish Biochemical Society

Papers read at the meeting in Uppsala, January 27—28, 1956.

Purification of Bovine and Human Fibrinogen

Birger Blombäck and Margareta Blombäck

Chemistry Department II, Karolinska Institutet, Stockholm, Sweden

A prerequisite for the study of different coagulation systems is a supply of purified and stable substrates. When studying the inhibition of thrombin by heparin + cofactor we found fibrinogen prepared by salt precipitation or by freezing out [1] to be too impure and unstable. During the course of our work we succeeded in getting a stable and pure fibrinogen by treating fraction I of Cohn's [2] method 6 with glycine.

The effect of glycine on the solubility of proteins has been thoroughly studied by a number of authors [3-6]. As has been pointed out by Cohn *et al.* a polar substance such as glycine strongly reduces the protein-protein interaction. This principle was adopted by Cohn *et al.*[7] in their method 10 of 1950 for the isolation of γ-globulin and β_1-lipoprotein from a human plasma precipitate.

We have found that the salting-in effect on fibrinogen increases sharply in rising the glycine concentration to 0.5 M (at an ionic strength of 0.3) and that at higher glycine concentrations there is a salting-out effect. Thus if Cohn's fraction I is extracted during one hour at —3° C with a solution of 1 M glycine in a citrate buffer of pH 6 and ionic strength 0.3 containing 6.5 % ethanol the fibrinogen and the cold insoluble globulins are almost insoluble. On the other hand the other proteins contaminating fibrinogen in fraction I, including prothrombin, are dissolved and thus removed.

The insoluble fraction is then dissolved at +25° C in a citrate buffer, pH 6.35 and ionic strength 0.3, containing 0.12 M glycine. When this solution is cooled to 0° C and ethanol added to a concentration of 2 % the cold insoluble globulins, described by Edsall [8,9] are precipitated. They are removed and the fibrinogen is precipitated by increasing the ethanol concentration to 6.5 % at —3° C. The final product has a clottable / non clottable ratio of 96—97 %. It is now free of prothrombin, plasmin, heparin-cofactor and the antihemofilic globulin. It is also practically free of plasminogen and of the proactivator of plasminogen. Electrophoresis in the Tiselius apparatus at pH 6.6 showed only one single boundary. The yield was 70 % calculated on the fibrinogen in fraction I, thus considerably higher than in the procedure of Kekwick *et al.*[10]. The technique works equally well on human as on bovine plasma.

1. Ware, A. G., Guest, M. M. and Seegers, W. H. *Arch. Biochem.* **13** (1947) 231.
2. Cohn, E. J., Strong, L. E., Hughes, W. L., Jr., Mulford, D. J., Ashworth, J. N., Melin, M. and Taylor, H. L. *J. Am. Chem. Soc.* **68** (1946) 459.
3. Richards, M. M. *J. Biol. Chem.* **122** (1937) 727.
4. Cohn, E. J., McMeekin, T. L., Ferry, J. D. and Blanchard, M. H. *J. Phys. Chem.* **43** (1939) 169.
5. Ferry, J. D., Cohn, E. J., Oncley, J. L. and Blanchard, M. H. *J. Biol. Chem.* **128** (1939) xxviii.
6. Grönwall, A. *Compt. Rend. Trav. Lab. Carlsberg. Sér. Chim.* **24** (1942) Nos. 8—11.
7. Cohn, E. J. *et al. J. Am. Chem. Soc.* **72** (1950) 465.
8. Morrison, P. R., Edsall, J. T. and Miller S. G. *J. Am. Chem. Soc.* **70** (1948) 3103.
9. Edsall, J. T., Gilbert, G. A. and Scheraga, H. A. *J. Am. Chem. Soc.* **77** (1955) 157.
10. Kekwick, R. A., Mackay, M. E., Nance, M. H. and Record, B. R. *Biochem. J. London* **60** (1955) 671.

Chromatography and Partition of Cells and Cell Fragments

Per-Åke Albertsson

Institute of Biochemistry, Uppsala, Sweden

The adsorption behavior of cells and cell fragments has been studied in order to apply the chromatographic method for their separation. Cells of *Chlorella pyrenoidosa* have been adsorbed on calcium phosphate columns and eluted with phosphate buffers, thus giving fractions with different cell sizes. From disintegrated *Chlorella* cell walls and starch grains have been separated into almost pure fractions by the same procedure. The partition of particles between two liquid phases has also been studied.

The work is in progress and will be published later.

Protein Chromatography on an Anion Exchange Resin

Hans G. Boman

Institute of Biochemistry, Uppsala, Sweden

Serum albumin and different enzymes have been used in order to study the behavior of proteins on columns of Dowex 2. Separations have been carried out both with stepwise elution and displacement technique. A detailed paper is under preparation.

Crystalline Beef Cytochrome c

Stephen A. Kuby, Sven Paléus, Karl-Gustav Paul and Hugo Theorell

Medicinska Nobelinstitutet, Biokemiska avdelningen, and Wallenbergstiftelsens laboratorium för fysiologisk kemi, Stockholm, Sweden

Crystalline precipitates of beef heart cytochrome c have been obtained from slightly ammoniacal ethanol solutions at —20° C. Iron analysis and enzymatic activity agreed favourably with the best preparations obtained by Paléus and Neilands [1].

1. Paléus, S. and Neilands, J. B. *Acta Chem. Scand.* **4** (1950) 1024.

Phenyl *iso*Thiocyanate as a Reagent in Protein Chemistry

Pehr Edman

Department of Physiological Chemistry, University of Lund, Lund, Sweden

Reversible Loss of Enzymatic Activity due to N→O Acyl Migration

Lars Josefsson and Pehr Edman

Department of Physiological Chemistry, University of Lund, Lund, Sweden

It has been found that an N-peptidyl → O-peptidyl rearrangement can be brought about in lysozyme by keeping the enzyme for a few hours in formic acid solution at room temperature. During this treatment the enzyme is gradually inactivated. However, the activity can be completely restored by keeping the inactivated enzyme in aqueous solution at a neutral reaction. Using a pH-stat, it was found that at pH 7.5 the reactivation is accompanied by a consumption of alkali. Both the reactivation and the alkali consumption follows a first order reaction with a specific rate constant at 20° C of 1.15×10^{-2}.

A Comparative Study of Some Methods Used for the Quantitative Determination of Proteins

Bengt von Hofsten

Institute of Biochemistry, University of Uppsala, Sweden

Work on fractionation and metabolism of proteins at this Institute requires methods for protein determination. In many cases it is sufficient with rather approximate values on a large number of samples, whereas more precise methods are required when chromatographic recoveries and protein synthesis are studied.

The following methods have been compared as to relative simplicity, speed, sensitivity and specificity:

Direct turbidimetric method with trichloroacetic acid,

Biuret reaction,
Direct ninhydrin reaction,
Hydrolysis and ninhydrin reaction,
Bromsulfalein method,
Folin reaction according to Lowry *et al.*,
Ultra violet absorption at 280—290 mμ,
Total nitrogen determination (modified Kjeldahl or hypobromite titration).

Certain practical modifications have been introduced in some of these methods. Comparative data are given on protein material of different origin, and the relative merits of the methods are discussed.

Zone Electrophoresis of Low Molecular Weight Compounds in Cellulose Columns

Jerker Porath

Institute of Biochemistry, University of Uppsala, Sweden

The behavior of charged low molecular weight substances in cellulose columns under different conditions has been studied for some time at this Institute. From the experience accumulated, it has been possible to work out suitable methods for effective electrophoretic fractionation of synthetic and natural mixtures of amino acids, peptides and other compounds in quantities ranging from micrograms to 25 grams and more. A description of apparatus, working conditions and results will be given.

Exchange Reactions between D_2O and Proteins or Protein Models

K. Linderstrøm-Lang

Chemical Department, Carlsberg Laboratory, Copenhagen, Denmark

It has been shown by Harrington, Hvidt, Linderstrøm-Lang and Schellman that peptides like clupein, the A-chain of insulin, and oxidized ribonuclease are devoid of secondary and tertiary structures and exist in aqueous solutions in an unfolded state. On the other hand important investigations by Elliot, Doty, Katchalski and Berger have definitely demonstrated the presence of secondary structures in certain synthetic polyamino acids. Thus poly-DL-alanine, copolymers between aspartic acid and lysine and polyglutamic acids seem to form stable α-helices in aqueous solution. This is supported by studies of deuterium exchange carried out by Berger. The reason for the phenomena observed and the possible forces and bonds at play in the stabilization of these helices will be discussed with special reference to sidechain interactions of the following type

a. Electrostatic interaction
b. Hydrophobic forces
c. Hydrogen bonds, 1. neutral, 2. ionic.

Determination of Amino Acids as Phenyl Thiohydantoins

John Sjöquist

Department of Physiological Chemistry, University of Lund, Lund, Sweden

A method for the quantitative determination of amino acids as 3-phenyl-2-thiohydantoin derivatives using partition chromatography was briefly described in a preliminary report [1]. This work has been continued and it is now possible to separate most of the natural amino acid derivatives. The partition system consists of aqueous propionic acid as stationary phase with Celite as an inert support and heptane with increasing concentrations of ethylene chloride as moving phase. Quantitative recoveries from 10—20 μg of each phenyl thiohydantoin are obtained. Through automatic registration of the ultraviolet absorption in the effluent, the composition of the amino acid mixture is obtained directly.

1. Sjöquist, J. *Biochim. et Biophys. Acta* **16** (1955) 283.

Protein Chromatography on Columns of Calcium Phosphate

Arne Tiselius

Institute of Biochemistry, Uppsala, Sweden

A review of recent work at the Institute of Biochemistry regarding the chromatographic separation of a number of proteins and protein mixtures. A detailed paper will be published shortly.

Open Peptide Chains in α-Chymotrypsin

B. Meedom

Chemical Department, Carlsberg Laboratory, Copenhagen, Denmark

After oxidation of either α-chymotrypsin or di-*iso*propyl - phosphat - α - chymotrypsin with performic acid it is in both cases possible to separate the reaction products in three fractions: The reaction mixture is dissolved in alkali, and pH brought down to 6, whereby a precipitate (fraction B) is formed. The supernatant is placed on a small Dowex 50 column (H^+ form). By elution with water fraction A is collected and by subsequent elution with NH_4OH fraction C is obtained. Fraction A is a peptide of 13 amino acids having N-terminal cysteic acid and C-terminal leu. Preliminary experiments seem to indicate that fraction C mainly consists of a peptide of 22 amino acids having N-terminal ala, but no C-terminal residue susceptible to attack by carboxypeptidase. Fraction B seems to be a long peptide chain containing N-terminal leu or ileu, and C-terminal tyr. In the case of DIP-chymotrypsin this fraction contains all the phosphorus. It seems to be possible to correlate the results with the structural model for α-chymotrypsin which has been proposed by Neurath and by Desnuelle.

Dielectric Increment and Dispersion of Tropomyosin — a Highly Polar Protein

L.-G. Allgén

Chemistry Department, Karolinska Institutet, Stockholm, Sweden

A specimen of pure tropomyosin from rabbit skeletal muscle [1] (kindly supplied by Drs Bailey and Tsao, Cambridge) has been studied dielectrically in pure aqueous solution. With concentrations between 0.01 and 0.1 g/100 ml (pH about 6.7) dielectric increments between 1.6 and 7.0 dielectric constant units were obtained. From these values reduced dielectric increments per g per liter, $\Delta\varepsilon/g$, between 4.5 and 7.7 were calculated. There was a slight tendency for the $\Delta\varepsilon/g$ values to increase at low concentrations. As the solutions of tropomyosin showed marked time effects (mainly a decrease of the increment with age of solution) this tendency is not considered significant, however. $\Delta\varepsilon/g$ is thus essentially independent of concentration as has also been found with other simple proteins studied. Such proteins give $\Delta\varepsilon/g$ values between 0 and 2. The $\Delta\varepsilon/g$ obtained for tropomyosin is thus about 3 times higher than with the most polar protein studied so far (β-lactoglobulin).

Dielectric dispersions were obtained for tropomyosin which were markedly influenced by concentration, the critical frequency being displaced towards lower frequencies with decreasing concentration. This is contrary to the case with other simple proteins for which the critical frequency is independent of concentration or displaced towards higher frequencies with decreasing concentration (β-lactoglobulin). The dispersion curve corresponds approximately to a single relaxation time in each case. No further dispersion was obtained down to very low frequencies. The relaxation times calculated varied between 0.75×10^{-7} sec. at 0.10 % concentration and 1.5×10^{-7} sec. at 0.027 %.

The type of dielectric dispersion and the order of the dielectric increments obtained for tropomyosin (and for a nucleotropomyosin previously reported to the Society in 1953) approach those of a number of polyelectrolytes studied dielectrically, but differ markedly from those of other simple proteins. This is probably due to the unusually high content of free ionizable groups [1] (from arginine, lysine and especially glutamic acid residues) and the linear shape [2] (double chain, asymmetry *ca.* 30) of tropomyosin. Tropomyosin shows polyelectrolyte properties also in other respects. The marked viscosity and streaming birefringence of aqueous tropomyosin solutions is sharply reduced by small amounts of simple electrolytes [2]. This has been ascribed to a desaggregation [2], but a contraction of the molecules due to electrostatic screening may also contribute. There is thus a suggestive parallelism between this contractile muscle protein and synthetic mechano-chemical systems obtained by crosslinking acid polyelectrolytes to 3-dimensional networks [3].

1. Bailey, K. *Biochem. J. London* **43** (1948) 271; **49** (1951) 23.
2. Tsao, T.-C. and Bailey, K. *Discussions Faraday Soc.* **13** (1953) 145.
3. Katchalsky, A. *J. Polymer Sci.* **12** (1954) 159.

Application of the pH-Stat for the Measurement of Proteolysis

M. Ottesen

Chemical Department, Carlsberg Laboratory, Copenhagen, Denmark

The methods ordinarily used to follow the opening of peptide bonds in proteins often fail in cases of limited proteolysis due to lack of sensitivity. Provided that the enzymatic reaction takes place at pH-values which are so high that most of the liberated amino groups exist in the unionized form, it is, however, possible to follow the opening of the peptide bonds by continuous titration at a constant pH by means of a Jacobsen-Léonis pH-stat. Different constructions of this device will be discussed. Using the pH-stat it is possible at pH 8 to follow the opening of a single peptide bond in the conversion of ovalbumin to plakalbumin. It has been attempted to correlate the opening of this bond with the change in solubility and crystal form. It was further observed that the salt-free ovalbumin solutions need a small continuous addition of alkali in order to keep pH constant, and the rate of this alkali addition seems to depend on the pH at which the ovalbumin was stored previously to the experiment.

Studies on a Myosin Fragment Obtained by Ammonium Sulphate Treatment of Myosin

Olle Snellman

Institute of Biochemistry, University of Uppsala, Uppsala, Sweden

Some preliminary data about the fragmentation of myosin with neutral ammonium sulphate have been given in another communication [1].

By treatment of the myosin with ammonium sulphate at 20° C two different fragments are obtained in nearly equal amounts by weight. Further studies have now been performed on the water-soluble fragment (H_{20}). This fraction precipitates in the preparation process between 40—50 % saturation of ammonium sulphate but cannot, after having been redissolved, be precipitated again with ammonium sulphate. It does not show any ability to associate with actin. The fragment is unstable and with time it is transformed to a large extent into dialysable pieces. During the deterioration process many different ultraviolet spectra can be obtained by different treatments. The fraction seems at first to break into three different parts as indicated by paper-chromatographic analysis. The final product obtained is dialyzable and has a high positive charge. Amino acids can no longer be obtained from it by acid hydrolysis.

Different means have been tried to stop the deterioration of the H_{20} fragment when it just has been obtained by the ammonium sulphate treatment. It has hereby been found that a treatment of the newly formed fragment with calcium hydroxide can stop the deterioration and a product is obtained which has the ability to associate with actin with an ensuing viscosity increase. This actin complex responses to ATP with a viscosity decrease independent of the salt concentration, and the viscosity increases again after a certain time to the normal level. A treatment with potassium oxalate of the calcium hydroxide-treated H_{20} fragment does not alter this effect. If the calcium hydroxide is added in a later step when the deterioration has begun, no effect of it will be found. As yet no other means have been found to restore the activity. The protein treated with calcium hydroxide shows an UV absorption spectrum with a maximum at 260—270 mμ.

From different experiments it is quite obvious that the myosin molecule must possess a unique structure. Probably some compound containing calcium is of importance in the reactions of the myosin, and when the calcium ions are removed this compound is very labile.

1. Snellman, O. *Biochim. et Biophys. Acta (In press).*

Studies on Human Acute Phase Protein (C-reactive Protein)

Inger Brattsten and Per Hedlund

The Institute of Biochemistry, University of Uppsala, Sweden; The Hospital for Contagious Diseases, and State Bacteriological Laboratory, Stockholm, Sweden

The fractionation of a sample containing sera from two persons in the acute phase of streptococcal pharyngitis and maxillary sinusitis, respectively, has been reported by Hed-

lund and Brattsten [1]. The fractionation was carried out by continuous zone electrophoresis [2] in a starch supporting medium at pH = 8.5 and the ionic strength = 0.03. The presence of acute phase protein in the fractions was determined by the capsular swelling reaction (Löfström [3]). Pneumococci suspensions of type 23 B were used. Reactive substance was found in the γ-globulin fractions exclusively, the capsular swelling titration curve showing a rather striking conformity with the γ-globulin distribution curve.

In order to check these results the same fractions were afterwards analysed against a pneumococci suspension of type 27, which was even more sensitive than type 23 B, and by precipitation with C-reactive protein antiserum (obtained from Schieffelin & Co., New York). Both tests confirmed the findings reported.

In the fractions obtained in the electrophoretic separation the reactive substance was present in mixture with other proteins of the γ-globulin type. This material has been studied as to its solubility in the presence of ammonium sulfate. As judged from the capsular swelling analyses, the reactive substance remains in solution at half saturation of this salt, but some precipitation occurs as the salt content is further increased. However, complete precipitation could not be achieved this way; even at saturation of ammonium sulfate the supernate showed a relatively strong activity reaction.

The initial fractionation experiment also showed that adequate isolation of acute phase protein could be obtained at a considerably lower total resolution than that used. Hence the procedure could be simplified by increasing the rate of fractionation. In subsequent work a quantity corresponding to 1.5 ml of undiluted serum has been fractionated per hour. In all, 65 ml of serum has been worked up. This includes material from three different cases of pneumonia in the acute stage. In order to establish a possible influence of the ionic strength on the mobility of the active material two fractionations have also been carried out at the ionic strength 0.06, other conditions remaining unchanged. After enrichment of the proteins, the fractions have been analysed by the capsular swelling reaction using type 23 B and 27 pneumococci suspensions and the C-reactive protein antiserum test. In all instances complete qualitative agreement with the primary result was obtained, thus showing that acute phase protein, developed in the diseases stated, resembles the γ-globulins in electrophoresis under the reported conditions.

The capsular swelling reaction was found to be more sensitive than the antiserum reaction.

Six months of storage in the frozen state (at —10° C, in Ringer's solution) did not affect the titer of the active substance.

1. Hedlund, P. and Brattsten, I. *Scand. J. Clin. Lab. Invest.* **7** (1955) 99.
2. Svensson, H. and Brattsten, I. *Arkiv Kemi* **1** (1949) 401; Brattsten, I. *Continuous zone electrophoresis by crossed velocity fields in a supporting medium.* Diss. Uppsala 1955.
3. Löfström, G. *Acta med. Scand.* Suppl. 141 (1943).

On the Localization and Composition of Phosphoprotein in *Esherichia coli B*

Gunnar Ågren

Institute of Medical Chemistry, University of Uppsala, Sweden

In an earlier communication the preparation of a new phosphorylated amino acid in *Lactobacillus casei* has been reported [1,2]. Several peptides containing this compound were also found. In attempts to prepare more high molecular phosphoproteins the following experiments were carried out with *E. coli B*.

The bacteria was cultivated on Friedleins synthetic medium containing Na-lactate as the carbon source and NH_4Cl as nitrogen source [3]. To this medium was added 1 mC radioactive phosphate per liter. Procedures for cultivation and separation of bacteria have been described by Palmstierna and Holme [4,5]. In this experiment the initial bacterial density was 1.25×10^9 cells/ml. At the end after 120 minutes of incubation the density was 1.95×10^9 cells/ml. 24 g of freeze-dried bacteria was obtained.

Suspensions containing 0.5 g dry weight bacteria/20 ml in 0.04 M Tris-buffer were shaken in the Raytheon disintegrator for 30 minutes during continous cooling. The cell walls possibly contaminated with some cytoplasmatic debris [6] were removed from the lysed solution by centrifugation at 40 000 r.p.m. One part of

Application of the pH-Stat for the Measurement of Proteolysis

M. Ottesen

Chemical Department, Carlsberg Laboratory, Copenhagen, Denmark

The methods ordinarily used to follow the opening of peptide bonds in proteins often fail in cases of limited proteolysis due to lack of sensitivity. Provided that the enzymatic reaction takes place at pH-values which are so high that most of the liberated amino groups exist in the unionized form, it is, however, possible to follow the opening of the peptide bonds by continuous titration at a constant pH by means of a Jacobsen-Léonis pH-stat. Different constructions of this device will be discussed. Using the pH-stat it is possible at pH 8 to follow the opening of a single peptide bond in the conversion of ovalbumin to plakalbumin. It has been attempted to correlate the opening of this bond with the change in solubility and crystal form. It was further observed that the salt-free ovalbumin solutions need a small continuous addition of alkali in order to keep pH constant, and the rate of this alkali addition seems to depend on the pH at which the ovalbumin was stored previously to the experiment.

Studies on a Myosin Fragment Obtained by Ammonium Sulphate Treatment of Myosin

Olle Snellman

Institute of Biochemistry, University of Uppsala, Uppsala, Sweden

Some preliminary data about the fragmentation of myosin with neutral ammonium sulphate have been given in another communication [1].

By treatment of the myosin with ammonium sulphate at 20° C two different fragments are obtained in nearly equal amounts by weight. Further studies have now been performed on the water-soluble fragment (H_{20}). This fraction precipitates in the preparation process between 40—50 % saturation of ammonium sulphate but cannot, after having been redissolved, be precipitated again with ammonium sulphate. It does not show any ability to associate with actin. The fragment is unstable and with time it is transformed to a large extent into dialysable pieces. During the deterioration process many different ultraviolet spectra can be obtained by different treatments. The fraction seems at first to break into three different parts as indicated by paper-chromatographic analysis. The final product obtained is dialyzable and has a high positive charge. Amino acids can no longer be obtained from it by acid hydrolysis.

Different means have been tried to stop the deterioration of the H_{20} fragment when it just has been obtained by the ammonium sulphate treatment. It has hereby been found that a treatment of the newly formed fragment with calcium hydroxide can stop the deterioration and a product is obtained which has the ability to associate with actin with an ensuing viscosity increase. This actin complex responses to ATP with a viscosity decrease independent of the salt concentration, and the viscosity increases again after a certain time to the normal level. A treatment with potassium oxalate of the calcium hydroxide-treated H_{20} fragment does not alter this effect. If the calcium hydroxide is added in a later step when the deterioration has begun, no effect of it will be found. As yet no other means have been found to restore the activity. The protein treated with calcium hydroxide shows an UV absorption spectrum with a maximum at 260—270 mμ.

From different experiments it is quite obvious that the myosin molecule must possess a unique structure. Probably some compound containing calcium is of importance in the reactions of the myosin, and when the calcium ions are removed this compound is very labile.

1. Snellman, O. *Biochim. et Biophys. Acta (In press).*

Studies on Human Acute Phase Protein (C-reactive Protein)

Inger Brattsten and Per Hedlund

The Institute of Biochemistry, University of Uppsala, Sweden; The Hospital for Contagious Diseases, and State Bacteriological Laboratory, Stockholm, Sweden

The fractionation of a sample containing sera from two persons in the acute phase of streptococcal pharyngitis and maxillary sinusitis, respectively, has been reported by Hed-

lund and Brattsten [1]. The fractionation was carried out by continuous zone electrophoresis [2] in a starch supporting medium at pH = 8.5 and the ionic strength = 0.03. The presence of acute phase protein in the fractions was determined by the capsular swelling reaction (Löfström [3]). Pneumococci suspensions of type 23 B were used. Reactive substance was found in the γ-globulin fractions exclusively, the capsular swelling titration curve showing a rather striking conformity with the γ-globulin distribution curve.

In order to check these results the same fractions were afterwards analysed against a pneumococci suspension of type 27, which was even more sensitive than type 23 B, and by precipitation with C-reactive protein antiserum (obtained from Schieffelin & Co., New York). Both tests confirmed the findings reported.

In the fractions obtained in the electrophoretic separation the reactive substance was present in mixture with other proteins of the γ-globulin type. This material has been studied as to its solubility in the presence of ammonium sulfate. As judged from the capsular swelling analyses, the reactive substance remains in solution at half saturation of this salt, but some precipitation occurs as the salt content is further increased. However, complete precipitation could not be achieved this way; even at saturation of ammonium sulfate the supernate showed a relatively strong activity reaction.

The initial fractionation experiment also showed that adequate isolation of acute phase protein could be obtained at a considerably lower total resolution than that used. Hence the procedure could be simplified by increasing the rate of fractionation. In subsequent work a quantity corresponding to 1.5 ml of undiluted serum has been fractionated per hour. In all, 65 ml of serum has been worked up. This includes material from three different cases of pneumonia in the acute stage. In order to establish a possible influence of the ionic strength on the mobility of the active material two fractionations have also been carried out at the ionic strength 0.06, other conditions remaining unchanged. After enrichment of the proteins, the fractions have been analysed by the capsular swelling reaction using type 23 B and 27 pneumococci suspensions and the C-reactive protein antiserum test. In all instances complete qualitative agreement with the primary result was obtained, thus showing that acute phase protein, developed in the diseases stated, resembles the γ-globulins in electrophoresis under the reported conditions.

The capsular swelling reaction was found to be more sensitive than the antiserum reaction.

Six months of storage in the frozen state (at —10° C, in Ringer's solution) did not affect the titer of the active substance.

1. Hedlund, P. and Brattsten, I. *Scand. J. Clin. Lab. Invest.* **7** (1955) 99.
2. Svensson, H. and Brattsten, I. *Arkiv Kemi* **1** (1949) 401; Brattsten, I. *Continuous zone electrophoresis by crossed velocity fields in a supporting medium.* Diss. Uppsala 1955.
3. Löfström, G. *Acta med. Scand.* Suppl. 141 (1943).

On the Localization and Composition of Phosphoprotein in *Esherichia coli B*

Gunnar Ågren

Institute of Medical Chemistry, University of Uppsala, Sweden

In an earlier communication the preparation of a new phosphorylated amino acid in *Lactobacillus casei* has been reported [1,2]. Several peptides containing this compound were also found. In attempts to prepare more high molecular phosphoproteins the following experiments were carried out with *E. coli B*.

The bacteria was cultivated on Friedleins synthetic medium containing Na-lactate as the carbon source and NH_4Cl as nitrogen source [3]. To this medium was added 1 mC radioactive phosphate per liter. Procedures for cultivation and separation of bacteria have been described by Palmstierna and Holme [4,5]. In this experiment the initial bacterial density was 1.25×10^9 cells/ml. At the end after 120 minutes of incubation the density was 1.95×10^9 cells/ml. 24 g of freeze-dried bacteria was obtained.

Suspensions containing 0.5 g dry weight bacteria/20 ml in 0.04 M Tris-buffer were shaken in the Raytheon disintegrator for 30 minutes during continous cooling. The cell walls possibly contaminated with some cytoplasmatic debris [6] were removed from the lysed solution by centrifugation at 40 000 r.p.m. One part of

Table 1. R_G-values of the two ninhydrin-reacting substances from fraction 3 and 5 of the cell wall after complete hydrolysis. Run in different organic solvents on Munktell OB filter paper. The corresponding values for the hydrolyzed amino acid from L. casei are included.

$$R_G \text{ value} = \frac{R_F \text{ value of unknown substance}}{R_F \text{ value of glycine}}$$

	E. coli		*L. casei*
	Fraction 3	Fraction 5	
Phenol	0.41	0.95	1.26
Pyridine-water	1.77	0.95	1.96
n-Butanol-HAc-water	0.80	1.10	1.81
*Iso*butyric acid-NH_3-water	0.90	1.85	1.00
Pyridine-*iso*amylalcohol-water	1.10	1.50	2.11

centrifugate was fractionated at low temperature with ethanol and Zn-acetate mainly according to Cohn [7] and the other part with acetone [8] and Zn-acetate. From the five fractions of the ethanol and acetone precipitations and the cell wall the Schneider protein was prepared as previously described [1,9]. The partial acid hydrolysates were chromatographed on Dowex 50 columns.

The peaks containing ninhydrin-positive material were analyzed for activity. About 80 % of the total activity was present in the 5 peaks of the cell wall hydrolysate while the remaining 20 % were rather evenly distributed on the 17 peaks of the ethanol and acetone hydrolysates (Table 2). 20 % by weight of the dried bacteria was recovered as cell walls.

After complete hydrolysis all fractions were run on one dimensional chromatogram. The material from the two main peaks of the cell wall hydrolysate (3 and 5) gave one major spot with only traces of other ninhydrin-positive compounds. Table 1 shows the positions of these spots in several solvent systems. It seems probable that these two substances differ from the phosphorylated amino acid in *L. casei*. Furthermore on paper electrophoresis the two new substances behaved as more basic amino acids. With the copper complex method [10] the most basic material reacted like a non α-amino acid. The two new phosphorylated compounds were also present in the ethanol and acetone fractions of the bacterial cytoplasmic material.

Table 2.

Fractions numbered as leaving the Dowex 50 Column	Specific activity in cpm/μg P					
	Cell walls	50 % ethanol	Zn-acetate in 80 % ethanol	40 % acetone	60 % acetone	Zn-acetate in 60 % acetone
1	1 022	1 013	1 030	518	736	—
2	933	835	855	386	640	—
3	1 126	778	451	755	565	—
4	545	496	—	735	405	—
5	658	—	—	455	—	—
6	—	—	—	756	—	—

Table 2 shows the specific activity values of the phosphorylated amino acids and phosphopeptides. The values for the two main fractions of the cell wall are of the same order as the data obtained from the purified phosphorylated amino acid of the *L. casei* at the end of the lag phase.

1. Ågren, G., de Verdier, C.-H. and Glomset, J. *Acta Chem. Scand.* **9** (1955) 196.
2. Ågren, G., de Verdier, C.-H. and Glomset, J. *Acta Soc. Med. Upsaliensis* **60** (1955) 30.
3. Friedlein, F. *Biochem. Z.* **164** (1928) 273.
4. Palmstierna, H. *Acta Chem. Scand.* **9** (1955) 195.
5. Holme, T. and Palmstierna, H. *Acta Chem. Scand.* **9** (1955) 1020.
6. Salton, M. R. J. and Horne, R. W. *Biochim. et Biophys. Acta* **7** (1951) 177.
7. Tullis, J. L. *Blood cells and plasma proteins.* New York 1953.
8. Askonas, B. A. *Biochem. J. London* **48** (1951) 42.
9. Ågren, G., de Verdier, C.-H. and Glomset, J. *Acta Chem. Scand.* **8** (1954) 503.
10. Crumpler, H. R. and Dent, C. H. *Nature* **164** (1948) 441.

Fluorescence of Steroids

S. Arrhenius

Kemiska Avdelningen, Kgl. Veterinärhögskolan, Stockholm, Sweden

It has previously been shown that the Zimmermann reaction cannot be ascribed to the 17-ketosteroids. Thus, the only reaction available at present for the characterization of steroids is their irreversible transformation into lumisteroids [1], *e. g.*, the more stable stereoisomers with the 18-methylgroup in *cis*-position to the hydrogen atom at carbon 14. This reaction, naturally occurring to all steroids, is induced by concentrated sulphuric or phosphoric acid (sometimes alkalies), and by UV light of wave lengths shorter than 3 130 Å.

This fluorescence is generally not observed with other steroids than estrogens and D-substances. It depends on the complicated nature of fluorescence, being a combination of at least five phenomena

1. The absorbtion of light energy by the electrons of one atomic group.

2. The re-emission of light by this or another atomic group.

3. The transformation of energy from the absorbing to the re-emitting group by molecular collisions or intramolecularly.

4. Quenching of energy by other atomic groups transforming the quenched energy into heat or light of unsuitable frequences or dissociation.

5. The re-absorbtion of the re-emitted light by the solutions.

Thus, the formula of Perrin [2] for the total intensity of fluorescence:

$$f = k_1 c \exp(k_2 c) = k_1 c \exp(c/c_{max})$$

will only apply when absorbing and re-emitting groups are combined in the same molecule, and quenching or re-absorbtion may be neglected.

If the principal part of the light energy is absorbed by a molecule which is totally free from the re-emitting atomic group, the intensity of fluorescence is directly proportional to the concentration of this group *e. g.* an amount of fluorescence suitable for quantitative analysis in all regions of concentration. However, the intensity of the absorbed energy must be sufficient for re-emission as well as for quenching to take place. The fluorescence must be measured in a wave length region where the steroid solutions have no absorbtion. An absolute requirement is that the fluorescence is not induced by light of so high frequencies that it will cause dissociation or polymerisation of steroids, *e. g.* UV light.

Both the absorbtion and the fluorescence of a steroid solution will always be spread over a broad wave length region. The maximum of the fluorescence intensity will be recorded by the photo cell when the filter between the light source and the container for the fluorescent medium has transmitted all visible light absorbable by this medium. The filter in front of the photo cell should ideally transmit light of all wave lengths absorbed by the former filter. The only way to approach this ideal filter system is to use certain solutions. Those of nickel sulphate and potassium bichromate have been used in a special type of fluorimeter.

1. Butenandt, A., Karlson-Poschmann, L., Failer, C., Schiedt, U. and Bickert, E. *Ann.* **575** (1951) 123.
2. Perrin, F. *Ann. de Phys.* (X:eme) **12** (1929) 169.

Table 2 shows the specific activity values of the phosphorylated amino acids and phosphopeptides. The values for the two main fractions of the cell wall are of the same order as the data obtained from the purified phosphorylated amino acid of the *L. casei* at the end of the lag phase.

1. Ågren, G., de Verdier, C.-H. and Glomset, J. *Acta Chem. Scand.* **9** (1955) 196.
2. Ågren, G., de Verdier, C.-H. and Glomset, J. *Acta Soc. Med. Upsaliensis* **60** (1955) 30.
3. Friedlein, F. *Biochem. Z.* **164** (1928) 273.
4. Palmstierna, H. *Acta Chem. Scand.* **9** (1955) 195.
5. Holme, T. and Palmstierna, H. *Acta Chem. Scand.* **9** (1955) 1020.
6. Salton, M. R. J. and Horne, R. W. *Biochim. et Biophys. Acta* **7** (1951) 177.
7. Tullis, J. L. *Blood cells and plasma proteins.* New York 1953.
8. Askonas, B. A. *Biochem. J. London* **48** (1951) 42.
9. Ågren, G., de Verdier, C.-H. and Glomset, J. *Acta Chem. Scand.* **8** (1954) 503.
10. Crumpler, H. R. and Dent, C. H. *Nature* **164** (1948) 441.

Fluorescence of Steroids

S. Arrhenius

Kemiska Avdelningen, Kgl. Veterinärhögskolan, Stockholm, Sweden

It has previously been shown that the Zimmermann reaction cannot be ascribed to the 17-ketosteroids. Thus, the only reaction available at present for the characterization of steroids is their irreversible transformation into lumisteroids [1], *e. g.*, the more stable stereoisomers with the 18-methylgroup in *cis*-position to the hydrogen atom at carbon 14. This reaction, naturally occurring to all steroids, is induced by concentrated sulphuric or phosphoric acid (sometimes alkalies), and by UV light of wave lengths shorter than 3 130 Å.

This fluorescence is generally not observed with other steroids than estrogens and D-substances. It depends on the complicated nature of fluorescence, being a combination of at least five phenomena

1. The absorbtion of light energy by the electrons of one atomic group.

2. The re-emission of light by this or another atomic group.

3. The transformation of energy from the absorbing to the re-emitting group by molecular collisions or intramolecularly.

4. Quenching of energy by other atomic groups transforming the quenched energy into heat or light of unsuitable frequences or dissociation.

5. The re-absorbtion of the re-emitted light by the solutions.

Thus, the formula of Perrin [2] for the total intensity of fluorescence:

$$f = k_1 c \exp(k_2 c) = k_1 c \exp(c/c_{max})$$

will only apply when absorbing and re-emitting groups are combined in the same molecule, and quenching or re-absorbtion may be neglected.

If the principal part of the light energy is absorbed by a molecule which is totally free from the re-emitting atomic group, the intensity of fluorescence is directly proportional to the concentration of this group *e. g.* an amount of fluorescence suitable for quantitative analysis in all regions of concentration. However, the intensity of the absorbed energy must be sufficient for re-emission as well as for quenching to take place. The fluorescence must be measured in a wave length region where the steroid solutions have no absorbtion. An absolute requirement is that the fluorescence is not induced by light of so high frequencies that it will cause dissociation or polymerisation of steroids, *e. g.* UV light.

Both the absorbtion and the fluorescence of a steroid solution will always be spread over a broad wave length region. The maximum of the fluorescence intensity will be recorded by the photo cell when the filter between the light source and the container for the fluorescent medium has transmitted all visible light absorbable by this medium. The filter in front of the photo cell should ideally transmit light of all wave lengths absorbed by the former filter. The only way to approach this ideal filter system is to use certain solutions. Those of nickel sulphate and potassium bichromate have been used in a special type of fluorimeter.

1. Butenandt, A., Karlson-Poschmann, L., Failer, C., Schiedt, U. and Bickert, E. *Ann.* **575** (1951) 123.
2. Perrin, F. *Ann. de Phys.* (X:eme) **12** (1929) 169.

On the Synthesis and Breakdown of a Glycogen-like Polysaccharide * in *Escherichia coli B*

T. Holme and H. Palmstierna

Bacteriological Department and Chemical Department I, Karolinska Institutet, Stockholm, Sweden

The following experiment was intended to elucidate the synthesis and breakdown of a glycogen-like polyglucose in bacterial cells.

Experimental. *E. coli* cells were cultivated in Friedleins medium with a restricted nitrogen source in the same way as previously described [1]. During the starvation phase, the cell concentration was 6×10^8 cells per ml, corresponding to 142 mg of cells per liter of culture (corrected dry weight). During this phase no net synthesis of protein occurred but glycogen was synthesized at an initially high rate. At the beginning of this phase, β-labeled ^{14}C-lactate was added. The cells were spun down 45 minutes after the addition of the labeled lactate. Then the cells were suspended in the Friedlein medium devoid of the carbon source. The nitrogen source contained ^{15}N to an excess of 15.6 %. After 90 min. in this medium the cells were harvested. The aeration, the harvesting procedures, and the chemical methods were the same as those previously described [2]. For measuring the radioactivity, the samples were spread on aluminium planchets and counted at infinite thinness in a windowless gas flow counter, flushed with a helium-*iso*butane mixture. Since the layer of material did not exceed 0.05 mg per cm^2, no correction was made for self-absorption.

Results. The specific activity of the glycogen carbon in the cells 45 min. after the addition of the labeled lactate was sixteen times higher than the specific activity of the protein carbon (Table 1, sample II). When these cells had been cultivated for 90 min. in the nitrogen-containing, carbonless medium (sample III), the specific activity of the glycogen carbon had decreased to about one sixth of the value in sample II. The glycogen per liter of culture decreased only to about two thirds of the value in sample II. During the same time there was a net synthesis of protein amounting to 12 % of the amount in sample II. The ^{15}N excess in the protein was 1.3 in sample III. The specific activity of the protein carbon in sample III was eight times the value in sample II.

The results may be interpreted in the same way as the results of Stetten and Stetten [3], working with rats injected once with labeled glucose. When the rats were killed a short time after the injection and their glycogen partially degraded by enzymes, it was found that the specific activity of the limit dextrins was less than the specific activity of the glucose split off. The interpretation may be that those glucose residues, which were the last ones to be formed, were preferentially attached to the ends of the glucose chains in the glycogen. The present results suggest that this "peripheral tier" of glucose residues was the first one to be utilized. Other explanations, taking an inhomogeneity of the glycogen into consideration, are also possible. Part of its carbon was possibly utilized in protein synthesis.

Table 1.

	I	II	III
C.p.m. per milliatom of glycogen carbon	0	110×10^3	17×10^3
C.p.m. per milliatom of protein carbon	0	7×10^3	57×10^3
^{15}N-excess of the protein	0	0	1.32
Protein-nitrogen, per cent of dry weight	6.7	6.4	7.3
Glycogen-glucose, per cent of dry weight	19.7	21.6	15.5

The roman numerals at the top of the table refer to the times at which the samples for analysis were taken. Sample I was taken at the moment of addition of the labeled lactate (205 min. after the inoculation of the nitrogen-deficient culture). Sample II was taken 45 min. after the addition of the labeled lactate, e. g. at the time the cells were spun down and resuspended in the nitrogen-containing, carbon-free medium. Sample III was taken 90 min. after the inoculation into this medium.

1. Holme, T. and Palmstierna, H. *Acta Chem. Scand.* **9** (1955) 1020.
2. Palmstierna, H. *Acta Chem. Scand.* **9** (1955) 195.
3. Stetten, M. R. and Stetten, D. Jr. *J. Biol. Chem.* **213** (1955) 723.

* For the sake of brevity called glycogen.

Kinetics of Hyaluronidase

Svend Olav Andersen and John Graae

Universitetets fysisk kemiske institut, Copenhagen, Denmark

The enzymatic splitting of hyaluronic acid is studied by means of viscometry. The reaction is followed to more than 90 % reduction in the specific viscosity.

The substrate was potassium hyaluronate prepared from umbilical cords according to Jensen [1]. The enzyme was a commercial hyaluronidase "Invasin Lundbeck". The investigations were carried out in a modified Ostwald viscosimeter. All experiments were carried out at 20° C and pH = 7.0 in a McIlvaine phosphate-citrate-sodium chloride buffer solution.

Taking η/η_0 as a reaction parameter and calling $\eta/\eta_0 = y$ we find empirically that the results in the investigated interval fit the chronometric integral

$$E \cdot t = A(1/y—1) + B(1/y^2—1),$$

where t is time, A and B are constants and E is the enzyme concentration which varied by a factor of 4 in different runs.

The concentration of potassium hyaluronate was in all experiments 0.4 %. The above mentioned expression is different from other expressions found in the literature to describe the degradation of hyaluronic acid. Most of these involve a first order decay of the specific viscosity [2] or a Michaelis expression [3].

The interpretation of these results is not obvious. If we accept the Staudinger equation $\eta_{spc} = KMc$, (where K is a constant, M the average number of units in the high molecular substance and c the concentration in weight %) and if we furthermore assume that the enzyme splits a constant number of bonds per time unit, we can derive the expression

$$E \cdot t = K(1/y—1)$$

which accounts for the dominating term in our expression.

More details on these experiments are published at the time of the meeting [4].

1. Jensen, C. E. *Acta Chem. Scand.* **7** (1953) 603.
2. Lundquist, F. *Acta Physiol. Scand.* **17** (1949) 44.
3. Dorfman, A. *J. Biol. Chem.* **172** (1948) 377.
4. Andersen, S. O. and Graae, J. *Acta Chem. Scand.* **9** (1955) 1431.

Biliary Excretion of Cholesterol and Bile Acids in Bile Fistula Rats

Sten Eriksson

Department of Physiological Chemistry, University of Lund, Lund, Sweden

The main metabolic end products of cholesterol in the rat have been shown to be taurocholic and taurochenodeoxycholic acids [1]. Several authors [2,3] have studied the daily excretion of cholic acid and cholesterol in bile fistula rats but due to the lack of a suitable analytical method no detailed analysis of the excretion pattern has so far been undertaken. In the present study bile has been collected from rats with a bile fistula. The amount of bile and its content of taurocholic and taurochenodeoxycholic acid has been determined at various intervals during the 14 days following the operation. The bile acid content was determined by the methods developed by Sjövall [4].

In Table 1 some typical values obtained are shown. The output of bile acids during the first 6 hours after the operation is considerably higher than the output during the subsequent 6 hours periods. A minimum generally occurs between 12 and 18 hours after the operation. The amount of bile acids excreted during the first 6 hours largely represents the amount of bile salts circulating in the intact animal [5]. Following the minimum excretion between 12 and 18 hours there is a rapid increase in the

Table 1. Excretion of Na-taurocholate (TC) and Na-taurochenodeoxycholate (TCD) in bile fistula rats.

Hours after operation	Rat No. 1		Rat No. 2	
	TC mg	TCD mg	TC mg	TCD mg
0— 6	10.4	3.44	13.4	4.9
6— 12	3.86	0.94	3.4	1.5
12— 18	1.97	0.78	1.7	1.0
18— 24	5.25	1.85	2.7	0.95
24— 48	49.1	10.1	33.6	4.0
48— 72	52.2	15.9	39.2	12.0
72— 96	37.6	13.8	31.2	28.0
96—120	35.3	16.5	36.4	12.0
120—144	47.3	19.1	35.8	12.0
144—168	45.2	14.9	26.0	10.8
168—192	39.4	19.2	—	—

amount excreted and a constant level is reached after the second day with a total excretion of bile salts ranging between 50 and 80 mg/day. These amounts have to be compared with the daily synthesis of bile acids in an intact animal. From the turnover time of labelled bile acids [6] and the determinations of the amount of bile acids in the enterohepatic circulation by isotope dilution [5] a daily synthesis of 2—3 mg of bile acids in a 200 g rat has been calculated. In a bile fistula rat there is thus a 20—30 fold increase of the normal bile acid production. This synthesis of bile acids in bile fistula rats is thus the result of a broken enterohepatic circulation. Further studies are in progress to elucidate factors regulating this process and its relation to the metabolism of cholesterol.

1. Bergström, S. and Norman, A. *Proc. Soc. Exptl. Biol. Med.* **83** (1953) 71.
2. Friedman, M., Byers, S. O. and Michaelis, F. *Am. J. Physiol.* **164** (1951) 786.
3. Thompson, J. C. and Vars, H. M. *Proc. Soc. Exptl. Biol. Med.* **83** (1953) 246.
4. Sjövall, J. *Acta Chem. Scand.* **9** (1955) 1034.
5. Bergström, S. and Eriksson, S. *To be published.*
6. Lindstedt, S. and Norman, A. *Acta Chem. Scand.* **9** (1955) 1042.

Urea Solution as a Solvent for the Viscosimetric Determination of Lichenase Activity

Eskil Hultin

Institutet för organisk kemi och biokemi, Stockholm, Sweden

Viscosimetric methods are generally more sensitive than other methods for the determination of the activity of enzymes which are capable of breaking down polymer-homologous substances. It follows as a matter of course that a viscosimetric determination of enzymic activity can only be carried out with such substrates as are completely soluble and give solutions with a high viscosity.

Lichenin is a polysaccharide which is easily soluble only in warm alkaline water solution, and much of it is precipitated if the temperature and the pH are lowered to such values as are suitable for the investigation of the activity of lichenase. A new method for obtaining solutions of lichenin is suggested here.

It has turned out that lichenin is soluble in water solutions of urea.

The viscosimetric determination of lichenase can be carried out as follows. Lichenin is dissolved in a warm urea solution, containing 0.3 to 0.5 g urea for each gram of water. A lichenin concentration of a few per cent may have a viscosity of about 3 or 4 times that of the urea solution, which is convenient.

One ml of an enzyme solution and 1 ml of a buffer solution are transferred to an Erlenmeyer flask. Two ml of the lichenin solution are added, and the contents are thoroughly mixed. Two ml of the reaction mixtures are transferred to a dry Ostwald viscosimeter, and a timer is started. The flow time is measured several times.

The inverse value of the specific viscosity is computed for each flow time by dividing the flow time for the solvent by the flow time of the reaction mixture diminished by the flow time of the solvent.

The inverse values of the specific viscosity are plotted in a diagram *versus* the times, for which they are valid, and a straight line is fitted to the points. The inclination of the line, multiplied by the square of the concentration of lichenin in the reaction mixture, is a measure of the enzyme activity.

By this viscosimetrical method it was shown that sperm of *Paracentrotus lividus* contain lichenase in small quantities.

The method suggested here — dissolving lichenin in a urea solution — has the advantage, that the true solution of even a high molecular fraction of the naturally occurring substrate, and not its hydroxy ethyl or carboxy methyl ether — as is the case with cellulose and chitin — can be used for the assay of enzymes capable of splitting β-1,4 glucoside linkages.

Sialic Acid and Neuraminic Acid

Gunnar Blix

Institute of Medical Chemistry, University of Uppsala, Sweden

The structure of sialic acid and of neuraminic acid is discussed principally on the basis of group analyses and periodate oxidations and with particular regard to the ideas recently put forward by Gottschalk [1]. The structures proposed by this author are in the main in good agreement with our findings.

1. Gottschalk, A. *Nature* **176** (1955) 881.

Kinetics of Hyaluronidase

Svend Olav Andersen and John Graae

Universitetets fysisk kemiske institut, Copenhagen, Denmark

The enzymatic splitting of hyaluronic acid is studied by means of viscometry. The reaction is followed to more than 90 % reduction in the specific viscosity.

The substrate was potassium hyaluronate prepared from umbilical cords according to Jensen [1]. The enzyme was a commercial hyaluronidase "Invasin Lundbeck". The investigations were carried out in a modified Ostwald viscosimeter. All experiments were carried out at 20° C and pH = 7.0 in a McIlvaine phosphate-citrate-sodium chloride buffer solution.

Taking η/η_0 as a reaction parameter and calling $\eta/\eta_0 = y$ we find empirically that the results in the investigated interval fit the chronometric integral

$$E \cdot t = A(1/y—1) + B(1/y^2—1),$$

where t is time, A and B are constants and E is the enzyme concentration which varied by a factor of 4 in different runs.

The concentration of potassium hyaluronate was in all experiments 0.4 %. The above mentioned expression is different from other expressions found in the literature to describe the degradation of hyaluronic acid. Most of these involve a first order decay of the specific viscosity [2] or a Michaelis expression [3].

The interpretation of these results is not obvious. If we accept the Staudinger equation $\eta_{spc} = KMc$, (where K is a constant, M the average number of units in the high molecular substance and c the concentration in weight %) and if we furthermore assume that the enzyme splits a constant number of bonds per time unit, we can derive the expression

$$E \cdot t = K(1/y—1)$$

which accounts for the dominating term in our expression.

More details on these experiments are published at the time of the meeting [4].

1. Jensen, C. E. *Acta Chem. Scand.* **7** (1953) 603.
2. Lundquist, F. *Acta Physiol. Scand.* **17** (1949) 44.
3. Dorfman, A. *J. Biol. Chem.* **172** (1948) 377.
4. Andersen, S. O. and Graae, J. *Acta Chem. Scand.* **9** (1955) 1431.

Biliary Excretion of Cholesterol and Bile Acids in Bile Fistula Rats

Sten Eriksson

Department of Physiological Chemistry, University of Lund, Lund, Sweden

The main metabolic end products of cholesterol in the rat have been shown to be taurocholic and taurochenodeoxycholic acids [1]. Several authors [2,3] have studied the daily excretion of cholic acid and cholesterol in bile fistula rats but due to the lack of a suitable analytical method no detailed analysis of the excretion pattern has so far been undertaken. In the present study bile has been collected from rats with a bile fistula. The amount of bile and its content of taurocholic and taurochenodeoxycholic acid has been determined at various intervals during the 14 days following the operation. The bile acid content was determined by the methods developed by Sjövall [4].

In Table 1 some typical values obtained are shown. The output of bile acids during the first 6 hours after the operation is considerably higher than the output during the subsequent 6 hours periods. A minimum generally occurs between 12 and 18 hours after the operation. The amount of bile acids excreted during the first 6 hours largely represents the amount of bile salts circulating in the intact animal [5]. Following the minimum excretion between 12 and 18 hours there is a rapid increase in the

Table 1. Excretion of Na-taurocholate (TC) and Na-taurochenodeoxycholate (TCD) in bile fistula rats.

Hours after operation	Rat No. 1		Rat No. 2	
	TC mg	TCD mg	TC mg	TCD mg
0— 6	10.4	3.44	13.4	4.9
6— 12	3.86	0.94	3.4	1.5
12— 18	1.97	0.78	1.7	1.0
18— 24	5.25	1.85	2.7	0.95
24— 48	49.1	10.1	33.6	4.0
48— 72	52.2	15.9	39.2	12.0
72— 96	37.6	13.8	31.2	28.0
96—120	35.3	16.5	36.4	12.0
120—144	47.3	19.1	35.8	12.0
144—168	45.2	14.9	26.0	10.8
168—192	39.4	19.2	—	—

amount excreted and a constant level is reached after the second day with a total excretion of bile salts ranging between 50 and 80 mg/day. These amounts have to be compared with the daily synthesis of bile acids in an intact animal. From the turnover time of labelled bile acids [6] and the determinations of the amount of bile acids in the enterohepatic circulation by isotope dilution [5] a daily synthesis of 2—3 mg of bile acids in a 200 g rat has been calculated. In a bile fistula rat there is thus a 20—30 fold increase of the normal bile acid production. This synthesis of bile acids in bile fistula rats is thus the result of a broken enterohepatic circulation. Further studies are in progress to elucidate factors regulating this process and its relation to the metabolism of cholesterol.

1. Bergström, S. and Norman, A. *Proc. Soc. Exptl. Biol. Med.* **83** (1953) 71.
2. Friedman, M., Byers, S. O. and Michaelis, F. *Am. J. Physiol.* **164** (1951) 786.
3. Thompson, J. C. and Vars, H. M. *Proc. Soc. Exptl. Biol. Med.* **83** (1953) 246.
4. Sjövall, J. *Acta Chem. Scand.* **9** (1955) 1034.
5. Bergström, S. and Eriksson, S. *To be published.*
6. Lindstedt, S. and Norman, A. *Acta Chem. Scand.* **9** (1955) 1042.

Urea Solution as a Solvent for the Viscosimetric Determination of Lichenase Activity

Eskil Hultin

Institutet för organisk kemi och biokemi, Stockholm, Sweden

Viscosimetric methods are generally more sensitive than other methods for the determination of the activity of enzymes which are capable of breaking down polymer-homologous substances. It follows as a matter of course that a viscosimetric determination of enzymic activity can only be carried out with such substrates as are completely soluble and give solutions with a high viscosity.

Lichenin is a polysaccharide which is easily soluble only in warm alkaline water solution, and much of it is precipitated if the temperature and the pH are lowered to such values as are suitable for the investigation of the activity of lichenase. A new method for obtaining solutions of lichenin is suggested here.

It has turned out that lichenin is soluble in water solutions of urea.

The viscosimetric determination of lichenase can be carried out as follows. Lichenin is dissolved in a warm urea solution, containing 0.3 to 0.5 g urea for each gram of water. A lichenin concentration of a few per cent may have a viscosity of about 3 or 4 times that of the urea solution, which is convenient.

One ml of an enzyme solution and 1 ml of a buffer solution are transferred to an Erlenmeyer flask. Two ml of the lichenin solution are added, and the contents are thoroughly mixed. Two ml of the reaction mixtures are transferred to a dry Ostwald viscosimeter, and a timer is started. The flow time is measured several times.

The inverse value of the specific viscosity is computed for each flow time by dividing the flow time for the solvent by the flow time of the reaction mixture diminished by the flow time of the solvent.

The inverse values of the specific viscosity are plotted in a diagram *versus* the times, for which they are valid, and a straight line is fitted to the points. The inclination of the line, multiplied by the square of the concentration of lichenin in the reaction mixture, is a measure of the enzyme activity.

By this viscosimetrical method it was shown that sperm of *Paracentrotus lividus* contain lichenase in small quantities.

The method suggested here — dissolving lichenin in a urea solution — has the advantage, that the true solution of even a high molecular fraction of the naturally occurring substrate, and not its hydroxy ethyl or carboxy methyl ether — as is the case with cellulose and chitin — can be used for the assay of enzymes capable of splitting β-1,4 glucoside linkages.

Sialic Acid and Neuraminic Acid

Gunnar Blix

Institute of Medical Chemistry, University of Uppsala, Sweden

The structure of sialic acid and of neuraminic acid is discussed principally on the basis of group analyses and periodate oxidations and with particular regard to the ideas recently put forward by Gottschalk [1]. The structures proposed by this author are in the main in good agreement with our findings.

1. Gottschalk, A. *Nature* **176** (1955) 881.

Information about the Structure of Phthiocerol from Mass Spectral and X-Ray Crystallographic Data

Ragnar Ryhage

Laboratory for mass spectroscopy, Biochemical Institute, Karolinska Institutet, Stockholm

Einar Stenhagen

Department of Medical Biochemistry, Institute of Medical Chemistry, University of Uppsala, Uppsala
and

Erik von Sydow

Institute of Chemistry, University of Uppsala, Uppsala, Sweden

Phthiocerol, the optically active wax alcohol found in the waxes of several types of tubercle bacilli [1,2] has the empirical composition $C_{34}H_{67}(OH)_2OCH_3$. The carbon skeleton of phthiocerol corresponds to 4-methyltritriacontane [3-5]. Recent attempts to determine the structure of phthiocerol by degradative methods have led Demarteau-Ginsburg and Lederer [6], and Hall and Polgar [7] to formulate phthiocerol as 4-methyl-5-methoxy-8,10-dihydroxytritriacontane and 4-methyl-4-methoxy-9,10-dihydroxytritriacontane,respectively.

The above formulations appeared to be at variance with the results of monolayer experiments [8] which suggested that one of the polar groups must be situated near one end of the chain. We have therefore tried to obtain further evidence on the structure of phthiocerol from a study of its mass spectrum and X-ray diffraction pattern [9,10].

A striking feature of mass spectrum is an extremely strong peak at mass number 73. The corresponding fragment must contain one oxygen atom, which in this case means that it must contain the intact methoxyl group. For this to be possible, the methoxyl group must occupy position 2 or 3 in the intact phthiocerol molecule. The strongest peak in the mass spectrum of methyl-*n*-heneicosyl ether is due to the fragment $CH_3—O—CH_2—$; by analogy position 3 appears more probable than position 2 for the methoxyl group in phthiocerol. There is evidence that elimination of methoxyl or hydroxyl groups in the fragmentation process in the mass spectrometer introduces a double bond in α,β-position to the carbon atom initially carrying the oxygen atom. A similar reaction mechanism would explain that Demarteau-Ginsburg and Lederer [6] were able to isolate methyl-*n*-propyl ketone after ozonization of the ene-diol obtained after removal of the methoxyl group.

The mass spectrum of phthiocerol shows further points of interest and may allow a direct determination of the position of the two hydroxyl groups when mass spectral data have been obtained for simple long chain glycols.

The X-ray diffraction pattern of phthiocerol [4] shows a series of orders of a long spacing of 46 Å with a characteristic intensity distribution. Using reasonable assumptions regarding the arrangements of the molecules in the lattice we have calculated the intensities of the 00*l* reflexions for different molecular models with the methoxyl group in position 2, 3, 4 and 5, respectively. Good agreement with experiment was found only when the methoxyl group occupied position 2 or 3.

Details of this work will be published later.

1. Stodola, F. H. and Anderson, R. J. *J. Biol. Chem.* **114** (1936) 467.
2. Cason, J. and Anderson, R. J. *J. Biol. Chem.* **119** (1937) 549.
3. Ställberg-Stenhagen, S., Stenhagen, E., Sheppard, N., Sutherland, G. B. B. M. and Walsh, A. *Nature* **160** (1947) 580.
4. Ställberg-Stenhagen, S. and Stenhagen, E. *J. Biol. Chem.* **173** (1948) 383.
5. Ställberg-Stenhagen, S. and Stenhagen, E. *J. Biol. Chem.* **183** (1950) 223.
6. Demarteau-Ginsburg, H. and Lederer, E. *Compt. rend.* **1955** 815.
7. Hall, J. A. and Polgar, N. *Chemistry & Industry* **1954** 1293.
8. Ställberg-Stenhagen, S. and Stenhagen, E. *J. Biol. Chem.* **143** (1942) 171.
9. The specimen of phthiocerol used was obtained from Professor R. J. Anderson of Yale university several years ago. The infrared spectrum showed the presence of a small amount of ketonic material, *cf.* Ref.[7] and Demarteau-Ginsburg, H., Ginsburg, A. and Lederer, E. *Biochim. et Biophysica Acta* **12** (1953) 587.
10. The mass spectrometer was built by one of us (R.R.). It has a heated intake system, *cf.* O'Neal, M. J. Jr. and Wier, T. P. Jr. *Anal. Chem.* **23** (1951) 830.

Infrared Absorption of Monoketo-Stearic Acid Methylesters

Ingrid Fischmeister

Institute of Medical Chemistry, University of Uppsala, Uppsala, Sweden

The infrared spectra of the monohydroxy- and monoketo-stearic acids and their methyl esters, known from the work of Bergström *et al.*[1], are being investigated in view of the possibility of identification. Out of this group, only the monoketo-stearic acid methylesters are not too complicated with respect to polymorphism; they were therefore investigated first.

The spectra of these positionally isomeric esters — dispersed in the solid state in potassium bromide — show characteristic differences between 7.4 and 15 μ, which allows complete identification. In the region between 7.4 and 8.4 μ there is a sort of band progression, similar to that known from the homologous series of fatty acids. Parallel investigations on methyl esters of keto-fatty acids of varying chain length show that these absorption bands are determined mainly by the chain length between the ester and keto group.

1. Bergström, S., Aulin-Erdtman, G., Rolander, B., Stenhagen, E. and Östling, S. *Acta Chem. Scand.* **6** (1952) 1157.

Quasi-racemic Compounds in Homologous Series of Branched Long Chain Acids

Bo Hallgren

Institute of Medical Chemistry, University of Uppsala, Uppsala, Sweden

We have previously [1] demonstrated the existence of a quasi-racemic compound between optically active forms of isomeric methyl-substituted long chain acids. In the present work quasi-racemic compounds have been found between optically active forms of homologous 3-methyl-substituted long chain acids. When (+)-3D-methyltricosanoic acid [2] of m. p. 62.1—62.3° is mixed in equimolecular proportions with (—)-3L-methyltetracosanoic acid [3] of m. p. 65.4—65.6° it is found that the mixture melts at 68.6°, that is higher than either component. The melting point curve for this binary system shows that mixtures containing from about 10 to about 90 % of one of the enanthiomorphs can exist in two different forms. The stable, higher-melting form corresponds to the racemic compound. The melting point curve of the unstable, low-melting form shows a simple eutectic point only. The melting point diagram of the binary system of (+)-3D-methyltricosanoic acid and (+)-3D-methyltetracosanoic acid also shows the existence of an eutectic point only.

We have recently found that the enanthiomorphs of 3-methyltetracosanoic acid form quasi-racemic compounds with the enanthiomorphs of 3-methyldocosanoic acid [4] and 3-methyloctadecanoic acid [5] having the opposite configuration.

1. Hallgren, B. *Arkiv Kemi. In press.*
2. Ställberg-Stenhagen, S. *Arkiv Kemi* **3** (1951) 117.
3. Ställberg-Stenhagen, S. *Arkiv Kemi, Mineral. Geol.* **26 A** (1948) No. 1.
4. Ställberg-Stenhagen, S. *Arkiv Kemi* **2** (1950) 431.
5. Ställberg-Stenhagen, S. *Arkiv Kemi* **1** (1949) 187.

Adenine Deoxyriboside Polyphosphates

Hans Klenow, Eleanor Lichtler and Bjørn Andersen

Institute of Cytophysiology, University of Copenhagen, Denmark

In the past few years the enzyme catalyzed phosphorylation of a number of nucleoside mono- and diphosphates by nucleoside triphosphates has been recognized. Evidence has also been obtained that deoxyadenylic acid (deoxy-AMP), deoxycytidylic acid and thymidylic acid act as phosphate acceptors in different enzyme systems [1-3].

We have incubated adenosine triphosphate (ATP) with the deoxyribose analogues of adenylic acid (AMP) or guanylic acid in the presence of red bone marrow extract, muscle extract or myokinase. By two dimensional paper chromatography two additional deoxyribose compounds were found to have been formed. The products formed from reactions between ATP and deoxy-AMP have been isolated in preparative scale. This was accom-

plished by chromatography on columns of an anion exchanger. The fractions obtained containing the ultraviolet absorbing peaks were then rechromatographed on cellulose powder columns using an alcoholic borate solution as eluant. The analysis and the chromatographic behaviour of the six adenine compounds isolated suggest that they are AMP, adenosine diphosphate (ADP) and ATP, and their three deoxyribose analogues (deoxy-AMP, deoxy-ADP and deoxy-ATP, respectively).

The deoxy-ADP and deoxy-ATP were tested with some enzyme systems known to react with ADP or ATP. Deoxy-ADP was assayed spectrophotometrically with pyruvate kinase, using phosphopyruvate, reduced diphosphopyridine nucleotide and lactic dehydrogenase. It was found that deoxy-ADP reacted with a rate which was about 10 % of that of the same concentration of ADP. When both compounds were present in equimolar amounts, the reaction rate was reduced to about 80 % of that with ADP alone. When diphosphopyridine nucleotide (DPN) pyrophosphorylase from yeast [4] was tested with deoxy-ATP and nicotinamide mononucleotide (NMN) in the presence of excess inorganic pyrophosphatase, it was found that two compounds were formed. One of them was ortho phosphate, and the other was a compound which in the presence of alcohol and alcohol dehydrogenase or glutamic acid and glutamic acid dehydrogenase gave rise to light absorption at 340 mμ. It is therefore assumed that it is a dinucleotide of NMN and deoxy-AMP.

1. Sable, H. Z., Wilber, P. B., Cohen, A. E. and Kane, M. R. *Biochim. et Biophys. Acta* **14** (1954) 454.
2. Hecht, L. I., Potter, V. R. and Herbert, E. *Biochim. et Biophys. Acta* **15** (1954) 134.
3. Kornberg, A. *J. Biol. Chem.* **182** (1950) 779.
4. Lieberman, I., Kornberg, A. and Simms, E. S. *J. Biol. Chem.* **215** (1955) 429.

Incorporation of ^{32}P into Nucleic Acids of Normal and Synchronized Protozoan Cultures

Otto Scherbaum

Institute of Cytophysiology, University of Copenhagen, Denmark

Cultures of *Tetrahymena pyriformis GL*, grown under controlled conditions [1] were incubated with ^{32}P in different growth phases.

Three parallel cultures were grown up to a density of 5×10^4 cells per ml. They were subjected to intermittent heat treatment to produce synchronized divisions [1]. Each of these cultures was incubated for 20 minutes with ^{32}P at one of the three different growth steps: 1) During normal logarithmic multiplication; 2) after the last of the standard heat treatments, and 3) just prior to the first synchronous division. An acetone powder was prepared as described earlier [2], yielding dry weights of about 150—350 mg for each sample. Nucleic acids were separated and RNA was degraded according to the method of Schmidt-Thannhauser-Schneider. Special consideration was given to the removal of inorganic P. The amounts of DNA and of RNA-ribotides were determined by optical density λ_{260} in the Beckmann Spectrophotometer and the radioactivity per density unit (DU = Vol. (ml) × extinction at 260 mμ) measured. This specific activity indicated the rate of incorporation of ^{32}P during the incubation period. The ribotides of RNA were chromatographed on paper in ammoniumsulphate-propanol solvent, the spots eluted and optical density similarly determined.

The dry weight follows closely the threefold volume increase during treatment, while the estimated content of both nucleic acids, expressed as DU per mg dryweight is almost constant. The specific activity of both nucleic acids is remarkably reduced during the treatment to about 7 % of the control logarithmic phase, but prior to the first synchronous division it rises to about 30—40 % of the values obtained in normal growth. While the overall picture of the specific activity of RNA shows a remarkable decrease after the heat-treatment, also the composition of the RNA, expressed as the ratios of the specific activities of AMP/GMP/UMP+CMP shows changes in the different steps. In Table 1 this is illustrated.

Table 1. Specific activity (SA) of the four ribotides of RNA in different growth phases. The numbers 1, 2 and 3 refer to the earlier mentioned steps of growth.

	1		2		3	
	SA	%	SA	%	SA	%
AMP	1 700	26.2	61	15.9	363	21.3
GMP	2 190	33.8	187	48.5	677	39.8
CMP + UMP	2 590	40.0	137	35.6	663	38.9
		100.0		100.0		100.0

1. Scherbaum, O. and Zeuthen, E. *Exptl. Cell Research, Suppl.* **3** (1955) 31.
2. Plesner, P. *Acta Chem. Scand.* **9** (1955) 197.

Infrared Absorption of Monoketo-Stearic Acid Methylesters

Ingrid Fischmeister

Institute of Medical Chemistry, University of Uppsala, Uppsala, Sweden

The infrared spectra of the monohydroxy- and monoketo-stearic acids and their methyl esters, known from the work of Bergström *et al.*[1], are being investigated in view of the possibility of identification. Out of this group, only the monoketo-stearic acid methylesters are not too complicated with respect to polymorphism; they were therefore investigated first.

The spectra of these positionally isomeric esters — dispersed in the solid state in potassium bromide — show characteristic differences between 7.4 and 15 μ, which allows complete identification. In the region between 7.4 and 8.4 μ there is a sort of band progression, similar to that known from the homologous series of fatty acids. Parallel investigations on methyl esters of keto-fatty acids of varying chain length show that these absorption bands are determined mainly by the chain length between the ester and keto group.

1. Bergström, S., Aulin-Erdtman, G., Rolander, B., Stenhagen, E. and Östling, S. *Acta Chem. Scand.* **6** (1952) 1157.

Quasi-racemic Compounds in Homologous Series of Branched Long Chain Acids

Bo Hallgren

Institute of Medical Chemistry, University of Uppsala, Uppsala, Sweden

We have previously [1] demonstrated the existence of a quasi-racemic compound between optically active forms of isomeric methyl-substituted long chain acids. In the present work quasi-racemic compounds have been found between optically active forms of homologous 3-methyl-substituted long chain acids. When (+)-3D-methyltricosanoic acid [2] of m. p. 62.1—62.3° is mixed in equimolecular proportions with (—)-3L-methyltetracosanoic acid [3] of m. p. 65.4—65.6° it is found that the mixture melts at 68.6°, that is higher than either component. The melting point curve for this binary system shows that mixtures containing from about 10 to about 90 % of one of the enanthiomorphs can exist in two different forms. The stable, higher-melting form corresponds to the racemic compound. The melting point curve of the unstable, low-melting form shows a simple eutectic point only. The melting point diagram of the binary system of (+)-3D-methyltricosanoic acid and (+)-3D-methyltetracosanoic acid also shows the existence of an eutectic point only.

We have recently found that the enanthiomorphs of 3-methyltetracosanoic acid form quasi-racemic compounds with the enanthiomorphs of 3-methyldocosanoic acid [4] and 3-methyloctadecanoic acid [5] having the opposite configuration.

1. Hallgren, B. *Arkiv Kemi. In press.*
2. Ställberg-Stenhagen, S. *Arkiv Kemi* **3** (1951) 117.
3. Ställberg-Stenhagen, S. *Arkiv Kemi, Mineral. Geol.* **26 A** (1948) No. 1.
4. Ställberg-Stenhagen, S. *Arkiv Kemi* **2** (1950) 431.
5. Ställberg-Stenhagen, S. *Arkiv Kemi* **1** (1949) 187.

Adenine Deoxyriboside Polyphosphates

Hans Klenow, Eleanor Lichtler and Bjørn Andersen

Institute of Cytophysiology, University of Copenhagen, Denmark

In the past few years the enzyme catalyzed phosphorylation of a number of nucleoside mono- and diphosphates by nucleoside triphosphates has been recognized. Evidence has also been obtained that deoxyadenylic acid (deoxy-AMP), deoxycytidylic acid and thymidylic acid act as phosphate acceptors in different enzyme systems [1-3].

We have incubated adenosine triphosphate (ATP) with the deoxyribose analogues of adenylic acid (AMP) or guanylic acid in the presence of red bone marrow extract, muscle extract or myokinase. By two dimensional paper chromatography two additional deoxyribose compounds were found to have been formed. The products formed from reactions between ATP and deoxy-AMP have been isolated in preparative scale. This was accom-

plished by chromatography on columns of an anion exchanger. The fractions obtained containing the ultraviolet absorbing peaks were then rechromatographed on cellulose powder columns using an alcoholic borate solution as eluant. The analysis and the chromatographic behaviour of the six adenine compounds isolated suggest that they are AMP, adenosine diphosphate (ADP) and ATP, and their three deoxyribose analogues (deoxy-AMP, deoxy-ADP and deoxy-ATP, respectively).

The deoxy-ADP and deoxy-ATP were tested with some enzyme systems known to react with ADP or ATP. Deoxy-ADP was assayed spectrophotometrically with pyruvate kinase, using phosphopyruvate, reduced diphosphopyridine nucleotide and lactic dehydrogenase. It was found that deoxy-ADP reacted with a rate which was about 10 % of that of the same concentration of ADP. When both compounds were present in equimolar amounts, the reaction rate was reduced to about 80 % of that with ADP alone. When diphosphopyridine nucleotide (DPN) pyrophosphorylase from yeast [4] was tested with deoxy-ATP and nicotinamide mononucleotide (NMN) in the presence of excess inorganic pyrophosphatase, it was found that two compounds were formed. One of them was ortho phosphate, and the other was a compound which in the presence of alcohol and alcohol dehydrogenase or glutamic acid and glutamic acid dehydrogenase gave rise to light absorption at 340 mμ. It is therefore assumed that it is a dinucleotide of NMN and deoxy-AMP.

1. Sable, H. Z., Wilber, P. B., Cohen, A. E. and Kane, M. R. *Biochim. et Biophys. Acta* **14** (1954) 454.
2. Hecht, L. I., Potter, V. R. and Herbert, E. *Biochim. et Biophys. Acta* **15** (1954) 134.
3. Kornberg, A. *J. Biol. Chem.* **182** (1950) 779.
4. Lieberman, I., Kornberg, A. and Simms, E. S. *J. Biol. Chem.* **215** (1955) 429.

Incorporation of ^{32}P into Nucleic Acids of Normal and Synchronized Protozoan Cultures

Otto Scherbaum

Institute of Cytophysiology, University of Copenhagen, Denmark

Cultures of *Tetrahymena pyriformis GL*, grown under controlled conditions [1] were incubated with ^{32}P in different growth phases.

Three parallel cultures were grown up to a density of 5×10^4 cells per ml. They were subjected to intermittent heat treatment to produce synchronized divisions [1]. Each of these cultures was incubated for 20 minutes with ^{32}P at one of the three different growth steps: 1) During normal logarithmic multiplication; 2) after the last of the standard heat treatments, and 3) just prior to the first synchronous division. An acetone powder was prepared as described earlier [2], yielding dry weights of about 150—350 mg for each sample. Nucleic acids were separated and RNA was degraded according to the method of Schmidt-Thannhauser-Schneider. Special consideration was given to the removal of inorganic P. The amounts of DNA and of RNA-ribotides were determined by optical density λ_{260} in the Beckmann Spectrophotometer and the radioactivity per density unit (DU = Vol. (ml) × extinction at 260 mμ) measured. This specific activity indicated the rate of incorporation of ^{32}P during the incubation period. The ribotides of RNA were chromatographed on paper in ammoniumsulphate-propanol solvent, the spots eluted and optical density similarly determined.

The dry weight follows closely the threefold volume increase during treatment, while the estimated content of both nucleic acids, expressed as DU per mg dryweight is almost constant. The specific activity of both nucleic acids is remarkably reduced during the treatment to about 7 % of the control logarithmic phase, but prior to the first synchronous division it rises to about 30—40 % of the values obtained in normal growth. While the overall picture of the specific activity of RNA shows a remarkable decrease after the heat-treatment, also the composition of the RNA, expressed as the ratios of the specific activities of AMP/GMP/UMP+CMP shows changes in the different steps. In Table 1 this is illustrated.

Table 1. Specific activity (SA) of the four ribotides of RNA in different growth phases. The numbers 1, 2 and 3 refer to the earlier mentioned steps of growth.

	1		2		3	
	SA	%	SA	%	SA	%
AMP	1 700	26.2	61	15.9	363	21.3
GMP	2 190	33.8	187	48.5	677	39.8
CMP + UMP	2 590	40.0	137	35.6	663	38.9
		100.0		100.0		100.0

1. Scherbaum, O. and Zeuthen, E. *Exptl. Cell Research, Suppl.* **3** (1955) 31.
2. Plesner, P. *Acta Chem. Scand.* **9** (1955) 197.

The Catabolism of Uracil in Rat Liver Slices

Per Fritzson* and Karl F. Nakken

Norsk Hydro's Institute for Cancer Research, The Norwegian Radium Hospital, Oslo, Norway

Fink *et al.*[1] have clearly established the conversion of dihydrouracil to β-alanine *in vitro*. β-Ureidopropionic acid could be detected [2]. Attempts to demonstrate the formation of dihydrouracil and β-alanine from uracil were unsuccessful.

We have now studied the catabolism of uracil in rat liver slices by means of labeled compounds [3,4].

One μmole of uracil-4-^{14}C, dihydrouracil-4-^{14}C and β-alanine-1-^{14}C, respectively, were incubated with rat liver slices. The incubation mixture was analysed by means of paper chromatography in different systems. The distribution of the activity on the paper strips was determined.

The data recorded in Table 1 together with data from β-alanine catabolism [5] indicate the following pathway of uracil catabolism in the rat: uracil → dihydrouracil → β-ureidopropionic acid → β-alanine → acetic acid + CO_2.

The difficulty in detecting dihydrouracil and β-ureidopropionic acid as intermediates in the uracil catabolism, is probably due to the rapid conversion of dihydrouracil to β-alanine.

1. Fink, R. M., Fink, K. and Henderson, R. B. *J. Biol. Chem.* **201** (1953) 349.
2. Fink, K. and McGaughey, C. *Federation Proc.* **13** (1954) 207.
3. Fritzson, P. *Acta Chem. Scand.* **9** (1955) 1239.
4. Fritzson, P. and Eldjarn, L. *Scand. J. Clin. Lab. Invest.* **4** (1952) 375.
5. Pihl, A. and Fritzson, P. *J. Biol. Chem.* **215** (1955) 345.

* Fellow of the "Norwegian Cancer Society", Oslo, Norway.

Incorporation of ^{32}P into the Purine Ribonucleotides of *Tetrahymena pyriformis* in Heat-treated Cultures

Paul Plesner

Institute of Cytophysiology, University of Copenhagen, Denmark

The incorporation of ^{32}P into synchronized cultures of *Tetrahymena pyriformis* has been investigated by a modification of the technique previously described [1]. In each experiment 3 one liter cultures were simultaneously submitted to intermittent heat-treatment as described by Scherbaum and Zeuthen [2]. 20 minute periods of incubation with isotope were used. 30—20 minutes before the beginning of the

Table 1. Amount of radioactive products after incubation of 1μmole of uracil — 4-^{14}C, dihydrouracil-4-^{14}C and β-alanine-1-^{14}C, with rat liver slices. The results are expressed in per cent of the added activity.

Compound incubated	Time of incubation in hours	Radioactive compounds recovered after incubation (in per cent)				
		Uracil	Dihydro-uracil	β-Ureido-propionic acid	β-Alanine	$^{14}CO_2$
Uracil-4-^{14}C	0.5	87	4 ?	0	6	—
	2	75	3 ?	2 ?	14	6
Dihydro-uracil-4-^{14}C	0.5	0	0	3 ?	94	—
	1	0	0	0	97	3
	2					6
β-alanine-1-^{14}C	2					6

Table 1.

	1	2	3
Total cell number	76×10^6	55×10^6	54×10^6
Total dry weight, mg	147.6	278.2	350.4
^{32}P uptake (% of added)	82.5	48.7	44.7
Total acid soluble fraction, DU *	51	95.5	138
Total counts in acetone-ether extract	59×10^3	21×10^3	81×10^3
Specific activity of adenine nucleotides **	49 400	11 200	16 100
Specific activity of guanine nucleotides	103 500	27 300	53 200

period to be investigated 1 one liter culture was centrifuged in 750 ml tubes with funnel-shaped bottoms at 200 g for 5 minutes, the cells collected, resuspended in 50 ml of proteose-peptone medium and transferred back to the original shaking-aeration-temperature conditions. The isotope was added to this concentrated culture, and at the conclusion of the 20 minute incubation-period acetone powder was made of the ciliates. 1/10 of the powder dried *in vacuo* was submitted to a classical Schmidt-Tannhauser-Schneider procedure. The remaining 9/10 were extracted with 80 % saturated ammonium sulphate and the extract submitted to differential dialysis against Norite [1]. The nucleotides were isolated from the Norite eluate by subsequent chromatography in three different solvent systems.

The results (Table 1) are taken from one experiment, point 1 representing normal growth, point 2 the last 20 minutes of heat-treatment, point 3 the 20 minutes just prior to the first burst of division. The same amount of isotope was added to the cultures.

More detailed results will be presented on other points in support of the following working hypothesis, that the increase in cell size and nucleic acid content [3] in this induced abnormal growth is due to a failure of the cell to produce the normal precursors for nucleic acid synthesis, and that this is not due to a decrease in the permeability of the cell.

1. Plesner, P. *Acta Chem. Scand.* **9** (1955) 197.
2. Scherbaum, O. and Zeuthen, E. *Exptl. Cell Research, Suppl.* **3** (1955) 31.
3. Scherbaum, O. *Acta Chem. Scand.* **10** (1956) 160.

* Density unit = Vol. (ml) × extinction at 260 mμ.

** Counts per minute per density unit.

Aspartate Carbamyl Transferase from *E. Coli*

Peter Reichard

Biochemical Department, Karolinska Institutet, Stockholm, Sweden

Extracts from lyophilized cells of *E. Coli* contain an enzyme which catalyzes the formation of ureidosuccinate (carbamyl aspartate) from aspartate and an "active" carbamyl compound [1]. The recent discovery of carbamyl phosphate as the carbamyl donor in enzymic citrulline synthesis [2] has made possible a further investigation of the mechanism of carbamyl aspartate synthesis. With a 90 fold purified enzyme it was possible to demonstrate the stoichiometric reaction: carbamyl phosphate + aspartate ⇌ carbamyl aspartate + phosphate. The equilibrium of the reaction was shifted far towards synthesis of carbamyl aspartate. In the original bacterial extract ornithine and aspartate served about equally well as acceptors for the carbamyl group. With the purified enzyme, however, only aspartate out of *ca.* 30 different amino acids gave rise to a carbamyl compound.

In the absence of aspartate, there was no enzymic exchange of isotope between ^{32}P-phosphate and carbamyl phosphate. Neither could any enzymic isotope exchange be observed between ^{14}C-aspartate and carbamyl aspartate. These experiments tend to exclude the intermediate formation of a carbamylated enzyme. When the reaction was carried out in H_2O^{18} no isotope was found in the reisolated carbamyl phosphate or in the carbamyl group of the carbamyl aspartate formed. A probable mechanism for the carbamyl transfer reaction will be discussed.

1. Reichard, P. and Hanshoff, G. *Acta Chem. Scand.* **9** (1955) 519.
2. Jones, M. E., Spector, L. and Lipmann, F. *J. Am. Chem. Soc.* **77** (1955) 819.

The Catabolism of Uracil in Rat Liver Slices

Per Fritzson* and Karl F. Nakken

Norsk Hydro's Institute for Cancer Research, The Norwegian Radium Hospital, Oslo, Norway

Fink *et al.*[1] have clearly established the conversion of dihydrouracil to β-alanine *in vitro*. β-Ureidopropionic acid could be detected [2]. Attempts to demonstrate the formation of dihydrouracil and β-alanine from uracil were unsuccessful.

We have now studied the catabolism of uracil in rat liver slices by means of labeled compounds [3,4].

One μmole of uracil-4-^{14}C, dihydrouracil-4-^{14}C and β-alanine-1-^{14}C, respectively, were incubated with rat liver slices. The incubation mixture was analysed by means of paper chromatography in different systems. The distribution of the activity on the paper strips was determined.

The data recorded in Table 1 together with data from β-alanine catabolism [5] indicate the following pathway of uracil catabolism in the rat: uracil → dihydrouracil → β-ureidopropionic acid → β-alanine → acetic acid + CO_2.

The difficulty in detecting dihydrouracil and β-ureidopropionic acid as intermediates in the uracil catabolism, is probably due to the rapid conversion of dihydrouracil to β-alanine.

1. Fink, R. M., Fink, K. and Henderson, R. B. *J. Biol. Chem.* **201** (1953) 349.
2. Fink, K. and McGaughey, C. *Federation Proc.* **13** (1954) 207.
3. Fritzson, P. *Acta Chem. Scand.* **9** (1955) 1239.
4. Fritzson, P. and Eldjarn, L. *Scand. J. Clin. Lab. Invest.* **4** (1952) 375.
5. Pihl, A. and Fritzson, P. *J. Biol. Chem.* **215** (1955) 345.

* Fellow of the "Norwegian Cancer Society", Oslo, Norway.

Incorporation of ^{32}P into the Purine Ribonucleotides of *Tetrahymena pyriformis* in Heat-treated Cultures

Paul Plesner

Institute of Cytophysiology, University of Copenhagen, Denmark

The incorporation of ^{32}P into synchronized cultures of *Tetrahymena pyriformis* has been investigated by a modification of the technique previously described [1]. In each experiment 3 one liter cultures were simultaneously submitted to intermittent heat-treatment as described by Scherbaum and Zeuthen [2]. 20 minute periods of incubation with isotope were used. 30—20 minutes before the beginning of the

Table 1. Amount of radioactive products after incubation of 1μmole of uracil — 4-^{14}C, dihydrouracil-4-^{14}C and β-alanine-1-^{14}C, with rat liver slices. The results are expressed in per cent of the added activity.

Compound incubated	Time of incubation in hours	Radioactive compounds recovered after incubation (in per cent)				
		Uracil	Dihydro-uracil	β-Ureido-propionic acid	β-Alanine	$^{14}CO_2$
Uracil-4-^{14}C	0.5	87	4 ?	0	6	—
	2	75	3 ?	2 ?	14	6
Dihydro-uracil-4-^{14}C	0.5	0	0	3 ?	94	—
	1	0	0	0	97	3
	2					6
β-alanine-1-^{14}C	2					6

Table 1.

	1	2	3
Total cell number	76×10^6	55×10^6	54×10^6
Total dry weight, mg	147.6	278.2	350.4
^{32}P uptake (% of added)	82.5	48.7	44.7
Total acid soluble fraction, DU *	51	95.5	138
Total counts in acetone-ether extract	59×10^3	21×10^3	81×10^3
Specific activity of adenine nucleotides **	49 400	11 200	16 100
Specific activity of guanine nucleotides	103 500	27 300	53 200

period to be investigated 1 one liter culture was centrifuged in 750 ml tubes with funnel-shaped bottoms at 200 g for 5 minutes, the cells collected, resuspended in 50 ml of proteose-peptone medium and transferred back to the original shaking-aeration-temperature conditions. The isotope was added to this concentrated culture, and at the conclusion of the 20 minute incubation-period acetone powder was made of the ciliates. 1/10 of the powder dried *in vacuo* was submitted to a classical Schmidt-Tannhauser-Schneider procedure. The remaining 9/10 were extracted with 80 % saturated ammonium sulphate and the extract submitted to differential dialysis against Norite [1]. The nucleotides were isolated from the Norite eluate by subsequent chromatography in three different solvent systems.

The results (Table 1) are taken from one experiment, point 1 representing normal growth, point 2 the last 20 minutes of heat-treatment, point 3 the 20 minutes just prior to the first burst of division. The same amount of isotope was added to the cultures.

More detailed results will be presented on other points in support of the following working hypothesis, that the increase in cell size and nucleic acid content [3] in this induced abnormal growth is due to a failure of the cell to produce the normal precursors for nucleic acid synthesis, and that this is not due to a decrease in the permeability of the cell.

1. Plesner, P. *Acta Chem. Scand.* **9** (1955) 197.
2. Scherbaum, O. and Zeuthen, E. *Exptl. Cell Research, Suppl.* **3** (1955) 31.
3. Scherbaum, O. *Acta Chem. Scand.* **10** (1956) 160.

* Density unit = Vol. (ml) × extinction at 260 mμ.

** Counts per minute per density unit.

Aspartate Carbamyl Transferase from *E. Coli*

Peter Reichard

Biochemical Department, Karolinska Institutet, Stockholm, Sweden

Extracts from lyophilized cells of *E. Coli* contain an enzyme which catalyzes the formation of ureidosuccinate (carbamyl aspartate) from aspartate and an "active" carbamyl compound [1]. The recent discovery of carbamyl phosphate as the carbamyl donor in enzymic citrulline synthesis [2] has made possible a further investigation of the mechanism of carbamyl aspartate synthesis. With a 90 fold purified enzyme it was possible to demonstrate the stoichiometric reaction: carbamyl phosphate + aspartate ⇌ carbamyl aspartate + phosphate. The equilibrium of the reaction was shifted far towards synthesis of carbamyl aspartate. In the original bacterial extract ornithine and aspartate served about equally well as acceptors for the carbamyl group. With the purified enzyme, however, only aspartate out of *ca.* 30 different amino acids gave rise to a carbamyl compound.

In the absence of aspartate, there was no enzymic exchange of isotope between ^{32}P-phosphate and carbamyl phosphate. Neither could any enzymic isotope exchange be observed between ^{14}C-aspartate and carbamyl aspartate. These experiments tend to exclude the intermediate formation of a carbamylated enzyme. When the reaction was carried out in H_2O^{18} no isotope was found in the reisolated carbamyl phosphate or in the carbamyl group of the carbamyl aspartate formed. A probable mechanism for the carbamyl transfer reaction will be discussed.

1. Reichard, P. and Hanshoff, G. *Acta Chem. Scand.* **9** (1955) 519.
2. Jones, M. E., Spector, L. and Lipmann, F. *J. Am. Chem. Soc.* **77** (1955) 819.

ACTA CHEMICA SCANDINAVICA 10 (1956) 163—173

Studies on the Extraction of Metal Complexes

XVI. Distribution Studies on the Complex Formation of U(VI) with Salicylic Acid and Methoxybenzoic Acid

BRITA HÖK-BERNSTRÖM

Research Institute of National Defence, Dept. 1, (FOA 1), Sundbyberg 4; Institute of Inorganic and Physical Chemistry, University of Stockholm, Sweden

The complex formation of UO_2^{2+} and salicylic acid, H_2A, has been studied by means of distribution data. The solvent system was hexone — 0.1 M $NaClO_4$ and the temperature 25° C. The UO_2^{2+} concentration was varied between 10^{-3} M and 5×10^{-5} M, while the salicylic acid concentration was varied between 1 M and 10^{-2} M. The results indicate that the predominant species in the hexone phase are (for the representation of the complexes, *cf.* Ref.[9]) $UO_2(H_2A)_2(H^+)_{-2}$ and $UO_2(H_2A)_3(H^+)_{-2}$. Complexes formed in appreciable amounts in the aqueous phase in the pH-range 3—5 seem to be $UO_2(H_2A)(H^+)_{-1}$ and $UO_2(H_2A)(H^+)_{-2}$. The equilibrium constants for the formation of these complexes are given in Table 1. Comparative experiments were run with methoxybenzoic acid (HB). The extractable complex is UO_2B_2. In the aqueous phase $UO_2(B)(OH)$ seem to form. The equilibrium constants for the methoxy-complexes are given in Table 2.

Although salicylic acid, H_2A, is known to form complexes with U(VI) and use of this tendency has been made in analytical chemistry [1], no quantitative information can be found regarding how the complexes are built up or about their stability.

Salicylic acid is a dibasic acid. The first dissociation constant $k_a' = 10^{-2.82}$ and the distribution constant $k_d = 10^{2.51}$ of the acid between hexone and water have been determined previously [2]. The second dissociation constant k_a'' due to the phenolic hydrogen, is approximately [3,15] 10^{-13}. In acidic and neutral solutions only undissociated acid, H_2A, and the ion HA^- will be present. However, there are reports in the literature that salicylic acid very often forms chelate compounds with metals [4,5]. The following reaction is therefore conceivable

$$UO_2^{2+} + HA^- \rightleftharpoons UO_2A + H^+ \qquad (1)$$

The ligand may thus be either HA^- or $A^=$. The ability to form a chelate compound by removal of the phenolic hydrogen is lost with methoxybenzoic acid

as the ligand. Since the ligands are very similar, a comparison of these two reagents was made in order to see whether the data indicated that a displacement of the phenolic hydrogen during complex formation took place.

In the present paper extraction data for the system U(VI)-salicylic acid -H_2O-hexone are presented. The data are analysed in order to find which complexes are formed in appreciable amounts and possible equilibrium constants for the formation of these complexes are calculated. Data are also presented for the system U(VI)-methoxybenzoic acid-H_2O-hexone so that comparison of the two ligands can be made.

EXPERIMENTAL

Chemicals. A standard solution of $UO_2(ClO_4)_2$ in 0.1 M $HClO_4$ was prepared by dissolving UO_3 of a very pure quality in a known excess of acid. The concentration of the solution was determined by evaporation of an aliquot and ignition to U_3O_8. Salicylic acid of analytical grade was used without further purification. The hexone used was of technical grade. After filtration it was washed with $HClO_4$ and NaOH in order to remove any basic and acidic impurities and thereafter several times with water.

Procedure. All experiments were carried out at 25° C and the ionic strength was adjusted to 0.1 M with $NaClO_4$. In the experiments a solution of salicylic acid in hexone was shaken for at least 18 hours with an equal volume of an aqueous UO_2^{2+} solution. After equilibration, the two phases were centrifuged and separated. The hydrogen ion concentration of the aqueous phase was measured with a Radiometer valve potentiometer, type 3i. The uranium analyses were made by a fluorimetric method [6] (the fluorimeter used was constructed at *AB Atomenergi*). Only the phase containing the smaller fraction uranium was analysed. The uranium content of the other phase was obtained by difference from the total uranium content. Tests for material balance were only made in a few cases since no precipitate was ever noticed in the solutions. Aliquots of the sample liquid were taken out for analyses and evaporated on a platinum disc. Hexone solutions with high salicylic acid concentration were extremely difficult to evaporate without loss. Furthermore, there was a risk that too large a residue would catch fire in the fusion procedure. 90 % NaF and 10 % Na_2CO_3 was used as mixed flux. Blank determinations were run at the same time and subtracted. A calibration curve was obtained from known $UO_2(ClO_4)_2$-solutions.

The colorimetric determination of uranium by the oxine-extraction method [7] gave no reliable results because of too high blank readings of the salicylic acid.

The experiments were started with constant initial concentration of salicylic acid in the organic phase $[H_2A]_{tot}$. In all experiments $[H_2A]_{tot} \gg [U]_{tot}$ so that the addition of $[U]_{tot}$ does not change the ligand concentration in the solution. The calculation of the concentrations $[HA^-]$ and $[H_2A]_{aq}$ at different pH was made according to eqns. (2) and (3) for equal phase volumes

$$[HA^-] = \frac{k_a\,[H_2A]_{tot}}{[H^+]\,(k_d + 1 + k_a/[H^+])} \tag{2}$$

$$[H_2A]_{aq} = \frac{[H_2A]_{tot}}{(k_d + 1 + k_a/[H^+])} \tag{3}$$

Since k_d is large, the denominator in eqn. (3) is unaffected of the ratio $k_a/[H^+]$ for $[H^+] \geq k_a$; thus $[H_2A]_{aq}$ remains constant in the aqueous phase up to pH $\sim$ 3 after which it starts to decrease with increasing pH.

RESULTS

The U(VI)-salicylic acid system

For mononuclear complex reactions q, the distribution ratio of the metal, must be independent of the metal concentration. For this purpose the initial uranium concentration was varied between 10^{-3} M and 5×10^{-5} M. In Fig. 1 the logarithm of the distribution ratio q is plotted against $-\log[H^+]$ for different initial salicylic acid concentrations. The curves show no systematic spread for uranium concentrations $\leq 2.5 \times 10^{-4}$ M. It may therefore be concluded that the presence of polynuclear complexes can be neglected in solutions of U(VI) and salicylic acid when $[U]_{tot} \leq 2.5 \times 10^{-4}$ M.

For $[U]_{tot} = 10^{-3}$ M the points fall on the curves of the lower uranium concentrations up to a pH about 3 (Fig. 1). However, for $[H_2A]_{tot} = 0.1$ M, the

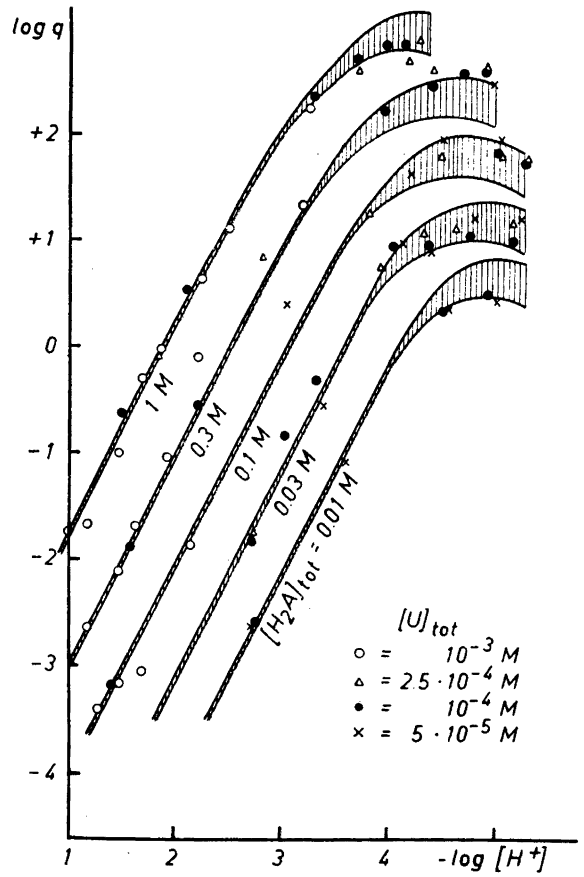


Fig. 1. Variation of the distribution ratio q *of U(VI) with* $-\log [H^+]$ *for different initial salicylic acid concentrations,* $[H_2A]_{tot}$. *The full lines enclosing the shaded area represent the estimated limits of error, when curves are calculated according to eqn. (15).*

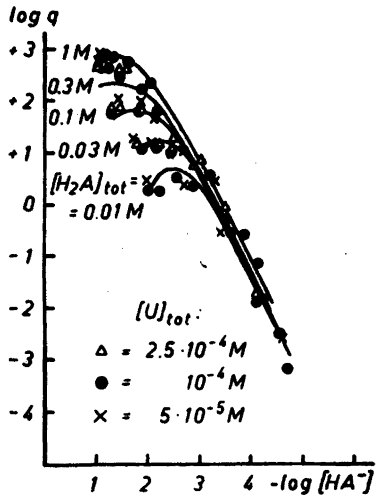


Fig. 2. Variation of the distribution ratio q *of U(VI) with* $-\log [HA^-]$ *for different initial salicylic acid concentrations,* $[H_2A]_{tot}$.

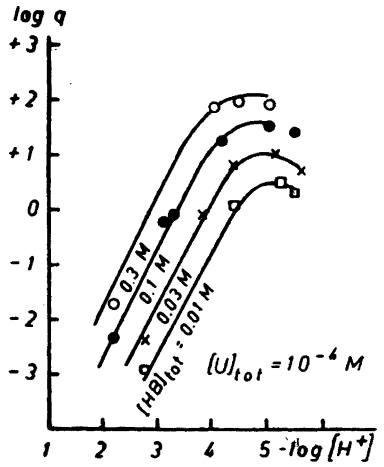


Fig. 3. Variation of the distribution ratio q *of U(VI) with* $-\log [H^+]$ *for different initial methoxybenzoic acid concentrations,* $[HB]_{tot}$.

lowest reagent concentration tested with $[U]_{tot} = 10^{-3}$ M, a marked decrease of the values of q was noticed for pH > 3.5 indicating polynuclear complexes. These data have not been recorded in Fig. 1 for the sake of clarity ($\Delta \log q > 0.3$).

The U(VI)-methoxybenzoic acid system

The investigation was carried out for $[U]_{tot} = 10^{-4}$ M since this concentration could be expected from the experiments with salicylic acid to involve chiefly mononuclear reactions. Because of the lower solubility of methoxybenzoic acid in hexone the highest reagent concentration that was tested was 0.3 M (saturated solutions in hexone ~0.7 M). In order to calculate the anion concentration the ratio k_a/k_d was determined by a two phase titration. Two different titrations gave an average value of $k_a/k_d = 10^{-5.43 \pm 0.01}$. For the same ionic strength (0.1 M) a value of $k_a = 10^{-3.89 \pm 0.01}$ is derived from values reported in the literature [8], whence $k_d = 10^{1.54 \pm 0.02}$. If HB refers to undissociated methoxybenzoic acid, $[B^-]$ is calculated according eqn. (2). The data are represented in Figs. 3—4.

Calculation of the formation constants

In all experiments the uranium concentration was kept smaller than the ligand concentration by a factor of 10^2 or more. The change in ligand concentration due to formation of uranium complexes can therefore be disregarded. Furthermore, only uncharged complexes are believed to dissolve in the organic phase.

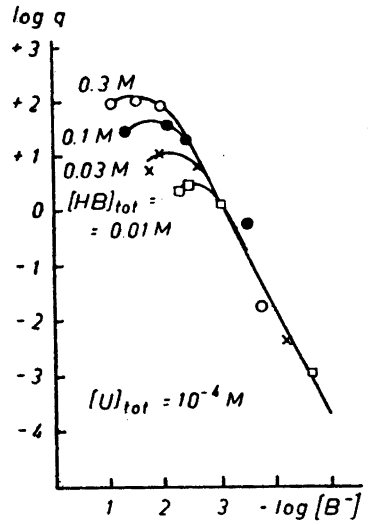


Fig. 4. Variation of the distribution ratio q *with* $-\log [B^-]$ *for different initial methoxybenzoic acid concentrations,* $[HB]_{tot}$.

In Fig. 2 the graphical representation of log q *versus* $-\log [HA^-]$ is given. If q were a function of $[HA^-]$ only all the curves would coincide for varying $[H_2A]_{tot}$ and the data could be explained by the standard approach that the simplest uncharged complex, in this case $UO_2(HA)_2$, dissolves in the organic phase. However, q is observed to increase with increasing $[H_2A]_{tot}$, which indicates that the complex in the organic phase must have H_2A-molecules associated with it.

Let the general formula $UO_2(H_2A)_x(H^+)_{-y}$ describe the complexes present [9]. The complexity product of these complexes is denoted by K_{xy} and the distribution coefficient of the uncharged complexes by Λ_{x2}. The general equation of the distribution ratio q then takes the following form (*cf.* Ref. [9])

$$q = \frac{\Sigma \Lambda_{x2} K_{x2} [H_2A]^x [H^+]^{-2}}{1 + [H^+]^{-1} \Sigma K_{x1} [H_2A]^x + [H^+]^{-2} \Sigma K_{x2} [H_2A]^x + [H^+]^{-3} \Sigma K_{x3} [H_2A]^x + \ldots} \quad (4)$$

As a reasonable assumption the pure hydroxo complex $UO_2(OH)_2$ was not considered to dissolve in the organic phase, which means that $x > 1$ in the numerator in eqn. (4). Furthermore, from the slope of plots of log $q\,[H^+]^2$ against log $[H_2A]_{aq}$ for various pH's it was confirmed that x must be > 2. In Fig. 5 log $q\,[H^+]^2\,[H_2A]^{-2}$ is plotted against log $[H_2A]_{aq}$ for varying pH; values of q were taken from the smooth curves drawn through the experimental points in Fig. 1 at pH 1.0, 1.6, 2.0, etc. With decreasing pH the curves coincide to one curve indicating that $q\,[H^+]^2\,[H_2A]^{-2}$ is independent of the hydrogen ion concentration and approaches the following expression (*cf.* eqn. (4))

$$q\,[H^+]^2\,[H_2A]^{-2} = \Lambda_{22} K_{22} + \Lambda_{32} K_{32} [H_2A] + \Lambda_{42} K_{42} [H_2A]^2 + \ldots \quad (5)$$

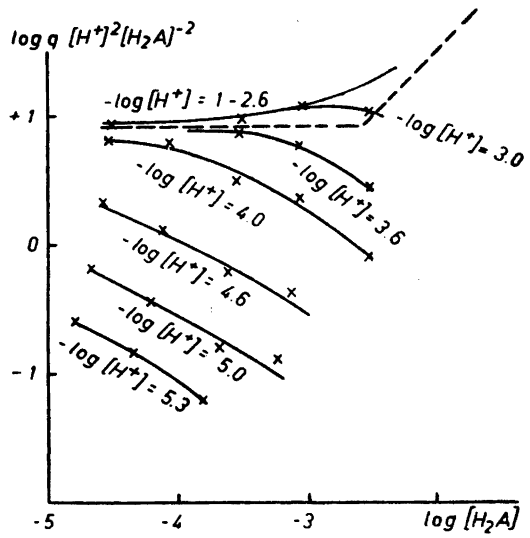


Fig. 5. The calculation of the coefficients $\Lambda_{x2}K_{x2}$ according to eqn. (5).

The unknown constants Λ_{x2} K_{x2} in eqn. (5) can be determined by a graphical procedure recommended by Sillén [10]. The curve for pH 1.0—2.6 in Fig. 5 was first compared with a plot log y (log x) where $y = 1 + x$ to test whether $\Lambda_{42}K_{42} = 0$. Since a good agreement was obtained when the two curves were fitted with each other it was concluded that $\Lambda_{42}K_{42} = 0$ in eqn. (5) and that the polynomial was of the first order. The unknown coefficients $\Lambda_{22}K_{22}$ and $\Lambda_{32}K_{32}$ are obtained from the points of intersection of the asymtotes (dotted lines in Fig. 5)

$$\log \Lambda_{22}K_{22} = 0.92 \pm 0.02 \tag{6}$$

$$\log \frac{\Lambda_{32}K_{32}}{\Lambda_{22}K_{22}} = 2.56 \pm 0.05 \tag{7}$$

$$\therefore \log \Lambda_{32}K_{32} = 3.48 \pm 0.07 \tag{8}$$

For pH $\geq$ 3 the curves in Fig. 5 are no longer independent of the hydrogen ion concentration. The data show that the UO_2^{2+} ions here form complexes in the aqueous phase. In order to find which complexes the following function was set up

$$\varphi = q^{-1}\,[H_2A]^2\,[H^+]^{-2}\,(10^{0.92} + 10^{3.48}\,[H_2A]) \tag{9}$$

Suppose that a stepwise formation of the complexes $UO_2(HA)^+$ and $UO_2(HA)_2$ takes place in the aqueous phase, then φ would be a function of $[H_2A][H^+]^{-1}$ only. Fig. 6 shows that this is not so; φ has been calculated for experimental points obtained with $[U]_{tot} = 10^{-4}$ M. The function ψ defined by eqn. (10) was calculated next

$$\psi = (\varphi - 1)\,[H_2A]^{-1}\,[H^+] \tag{10}$$

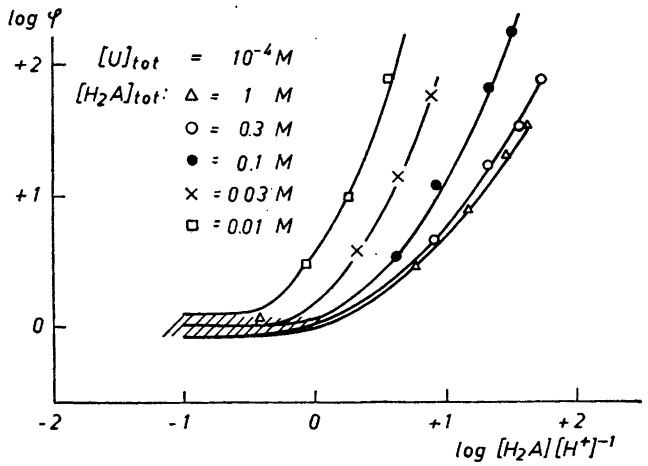


Fig. 6. Variation of log φ with log $[H_2A][H^+]^{-1}$. φ is calculated according to eqn. (9) for experimental points obtained with $[U]_{tot} = 10^{-4}$ M.

In Fig. 7 log ψ has been plotted against $-\log [H^+]$. Now, according to eqn. (4) the function ψ is when developed for $x \geqslant 1$.

$$\psi = K_{11} + K_{12}\,[H^+]^{-1} + \ldots [H_2A]\,(K_{21} + K_{22}\,[H^+]^{-1} + \ldots) + \\ + [H_2A]^2\,(K_{31} + K_{32}\,[H^+]^{-1} + K_{33}\,[H^+]^{-2} + \ldots) + \ldots . \qquad (11)$$

From Fig. 7 it is seen that log ψ increases with $-\log[H^+]$. On the other hand, for a value of $-\log [H^+]$ that is fixed, log ψ appears to decrease if anything with increased $[H_2A]_{tot}$ or $[H_2A]$. This decrease of ψ cannot be real since K_{xy} must be positive because of the law of mass action. It was therefore concluded that the experimental data spread around the curve: $\psi = K_{11} + K_{12}\,[H^+]^{-1}$. From the point of intersection of the asymptotes (dotted lines in Fig. 7) the coefficients K_{11} and K_{12} were estimated

$$\psi = 10^{-0.62 \pm 0.05} + 10^{-4.5 \pm 0.2}\,[H^+]^{-1} \qquad (12)$$

The complexes that seem to form in the aqueous phase are therefore according to eqns. (10) and (11)

$$[U]_{tot\ aq} = [UO_2^{2+}] + [UO_2(H_2A)(H^+)_{-1}] + [UO_2(H_2A)(H^+)_{-2}] \qquad (13)$$

The complexes present in the organic phase are (*cf.* eqns. (6) and (8) with (5))

$$[U]_{tot\ org} = [UO_2(H_2A)_2(H^+)_{-2}] + [UO_2(H_2A)_3(H^+)_{-2}] \qquad (14)$$

The equilibrium constants are summarized in Table 1. With these sets of constants the equation of the distribution ratio follows eqn. (15)

$$q = \frac{[H_2A]^2\,[H^+]^{-2}\,(10^{0.92 \pm 0.02} + 10^{3.48 \pm 0.07}\,[H_2A])}{1 + 10^{-0.62 \pm 0.05}\,[H_2A][H^+]^{-1} + 10^{-4.5 \pm 0.2}\,[H_2A][H^+]^{-2}} \qquad (15)$$

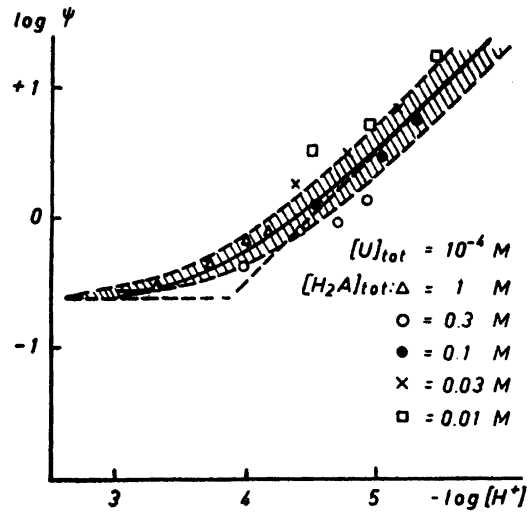


Fig. 7. The calculations of K_{11} *and* K_{12} (cf. *eqn. (11)). Abscissa:* $-\log [H^+]$. *Ordinate* $= \log \psi$, *which is calculated according to eqn. (10) for experimental points obtained with* $[U]_{tot} = 10^{-4}$ *M. The broken lines enclosing the shaded area represent the estimated limits of error for a curve following eqn. (12).*

In Fig. 1 the shaded area represents eqn. (15) with the above uncertainty estimated for the constants. In Fig. 8 the percentage of the different U(VI) complexes in the aqueous phase is plotted as functions of the salicylate concentration, and the hydrogen ion concentration.

Although methoxybenzoic acid was studied in less detail and therefore less reliance can be put on the constants derived, the same treatment of the data was made. In the case of methoxybenzoic acid the only complex extracted

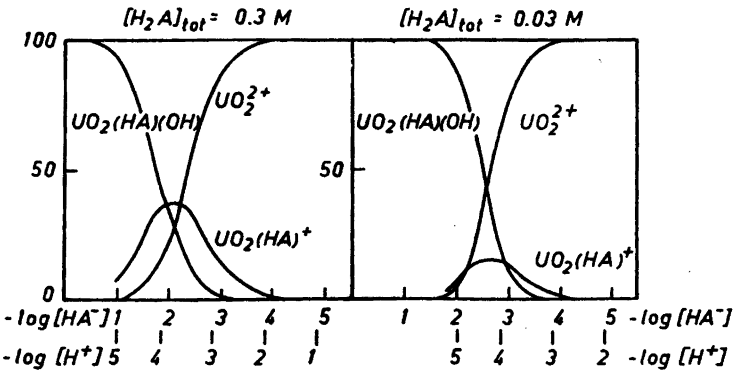


Fig. 8. The fraction of different U(VI) complexes in the aqueous phase. Abscissa: $-\log [HA^-]$ *or* $-\log [H^+]$. *Ordinate: the percentage of a certain complex (the vertical distance of the curve above the zero line represents the percentage).*

into the organic phase seems to be $UO_2(HB)_2(H^+)_{-2}$ or $UO_2(B)_2$. The experimental data can be approximated assuming only the complex $UO_2(HB)(H^+)_{-2}$ or $UO_2(B)(OH)$ in the aqueous phase. With this assumption the equation for q takes the following form

$$q = \frac{10^{-1.56 \pm 0.05}\ [HB]^2[H^+]^{-2}}{1 + 10^{-5.85 \pm 0.10}\ [HB][H^+]^{-2}} \qquad (16)$$

The full curves in Fig. 3 are calculated according to eqn. (16). Estimated values of the equilibrium constants are given in Table 2.

Table 1. Equilibrium constants derived for U(VI) from distribution data with salicylic acid, H_2A, in the system hexone — 0.1 M $NaClO_4$.

$$\Lambda_{22}K_{22} = 10^{0.93 \pm 0.02} \quad \frac{[UO_2(H_2A)_2(H^+)_{-2}]_{org}}{[UO_2(H_2A)_2(H^+)_{-2}]_{org}[H_2A]_{org}} = 10^{0.65 \pm 0.12}$$

$$\Lambda_{32}K_{32} = 10^{3.48 \pm 0.07}$$

$$K_{11} = \frac{[UO_2(H_2A)(H^+)_{-1}]}{[UO_2^{2+}][H_2A][H^+]^{-1}} = 10^{-0.62 \pm 0.05} \frac{[UO_2(HA)^+]}{[UO_2^{2+}][HA^-]} = 10^{2.2}$$

$$K_{12} = \frac{[UO_2(H_2A)(H^+)_{-2}]}{[UO_2^{2+}][H_2A][H^+]^{-2}} = 10^{-4.5 \pm 0.2} \frac{[UO_2(HA)(OH)]}{[UO_2^{2+}][HA^-][OH^-]} = 10^{12.1}$$

Table 2. Equilibrium constants derived for U(VI) from distribution data with methoxybenzoic acid, HB, in the system hexone — 0.1 M $NaClO_4$.

$$\Lambda_{22}K_{22} = 10^{-1.56 \pm 0.05}$$

$$K_{12} = \frac{[UO_2(HB)(H^+)_{-2}]}{[UO_2^{2+}][HB][H^+]^{-2}} = 10^{-5.85 \pm 0.10} \frac{[UO_2(B)(OH)]}{[UO_2^{2+}][B^-][OH^-]} = 10^{11.9}$$

DISCUSSION

Formula of the complexes. In the previous section the salicylate complexes have been described by the general formula $UO_2(H_2A)_x(H^+)_{-y}$ and x and y were determined for the predominant species in the two phases (eqns. (13) and (14)). As was mentioned in the beginning of the present paper the structure of the salicylate complexes can be imagined as nonchelates (the ligand = HA^-) or as chelate compounds (the ligand = $A^=$). Since the complexes ($x = 2$, $y = 2$) and ($x = 3$, $y = 2$) are found in the organic phase, the following isomeric formulae are possible

$UO_2(HA)_2$ and $UO_2(HA)_2 \cdot H_2A$ if the ligand = HA^-

$UO_2A \cdot H_2A$ and $UO_2A \cdot 2\ H_2A$ » » » = $A^=$

In the aqueous phase complexes corresponding to ($x = 1$, $y = 1$) and ($x = 1$, $y = 2$) are shown to form. The former complex ($x = 1$, $y = 1$) is not compatible with $A^=$ as the ligand. The complexes possible in the aqueous phase are therefore $UO_2(HA)^+$ and $UO_2(HA)(OH)$ or UO_2A. To distinguish between the above formulae is not possible. However, the close resemblance of the distribution curve found with methoxybenzoic acid suggests that the salicylate complexes are built up by HA^- ligands. Only two methoxybenzoic acid mole-

cules is found in the extracted uranyl complex. The fact that an additional acid molecule is not found with methoxybenzoic acid may be ascribed to the more limited space around the central group due to the $-CH_3$ (*cf.* the results obtained with Th [11]).

Comparison with earlier work. Weinland and Hager [12] have reported compounds with two and three molecules of salicylic acid attached to the uranium. These compounds were formed in presence of alkali and organic bases and the authors proposed a structure where the uranyl group entered in the anion, as in $C_5H_5N \cdot H[UO_2(HA)_3]$ with three salicylic acid molecules. Migration experiments with uranyl salicylate [13] gave to result that the main part of the uranium migrated towards the cathode even at high concentrations of HA^-. It seems therefore more plausible to assign the following structure to the above complex: $C_5H_5N \cdot [UO_2(HA)_2 \cdot H_2A]$.

Foley and Anderson [14] have studied the complex formation between uranyl and sulfosalicylic acid (H_3R) spectrophotometrically. Some of the measurements were made in acetate buffers, which might invalidate the investigation. The ratio of uranyl to sulfosalicylate was found to be 1:1 in a pH range up to 6.1. The same ratio 1:1 of uranyl to salicylic acid is found by us in the aqueous phase in the present study. Further, the uranyl sulfosalicylate complex shows maximum absorption at a pH $\sim$ 4.7. Since the second dissociation constant [14,15] of sulfosalicylic acid is about $10^{-2.7}$ the main part of the acid will be in the form $HR^=$ at pH = 4.7. The decrease of absorption above pH 4.7 is explained as due to hydrolysis effects. No extraction into benzene or carbon tetrachloride was found. An apparent equilibrium constant $K = \frac{[UO_2^{2+}][R]}{[UO_2R]}$, where [R] stands for sulfosalicylic acid in all forms, was calculated to be 1.9×10^{-4} (25° C).

In Table 1 the equilibrium constant for the formation of $UO_2(HA)^+$ is given, *i. e.* $10^{2.2}$. This value may be compared with the equilibrium constant for the first uranyl acetate complex, which has been determined by Ahrland [16] to $10^{2.6}$.

The hydrolysis of UO_2^{2+}. The data of the present investigation have been treated as if only mononuclear complex formation took place. Now the hydrolysis of the ion UO_2^{2+} has been investigated and discussed as a polymeric process [17]. To find out whether the experiments in the present study were carried out in a concentration range of polynuclear hydrolysis, a value of the function X is needed

$$X = \log [U]_{\text{tot aq}} - 2 \log [H^+] \qquad (16)$$

By comparison with Ahrland's diagram (*cf.* Ref.[17], Fig. 1 or Fig. 5) one sees that for $X < 5$ no appreciable amounts of hydrolysis complexes are formed. Let us calculate a value of X for the lowest H_2A concentration used, *i. e.* $[H_2A]_{tot} = 10^{-2}$ M. A value of $[U]_{\text{tot aq}}$ is estimated from the distribution curves in Fig. 1, since $[U]_{\text{tot aq}} = [U]_{tot}/(q + 1)$. Thus at pH = 5 one obtains a value of $X = 5.4$, which suggests that these distribution experiments might be affected by the hydrolysis of the ion UO_2^{2+}. For H_2A concentrations $> 10^{-2}$ M and $[U]_{tot} = 10^{-4}$ M there is no danger of hydrolysis effects. For $[U]_{tot} =$

10^{-3} M and $[H_2A]_{tot} = 10^{-1}$ M the distribution curve was found to deviate from those obtained with lower $[U]_{tot}$, when pH increased above 3.5. The lower values of q that was obtained, indicate that water soluble polymeric complexes are formed. In this case the value of X is around 5.6.

Polymeric hydroxo complexes have been reported in the reactions of uranyl and organic acids (H_2R) such as citric acid, maleic acid and tartaric acid [18]. The uranium concentration and the concentration of the organic reagent were both 0.05 M. Dimers of the complexes UR held together by oxygen bridges were believed to be formed when the pH was raised to 3.5.

I am indebted to Professor G. Ljunggren, FOA 1, for his continued interest and to Professor L. G. Sillén for his valuable advice and criticism. My thanks are also due to Professor A. Ölander, Dr. J. Rydberg and Dr. D. Dyrssen. The English in this paper has been revised by Dr. F. Rossotti.

This work is part of a program supported by *Atomkommittén*.

REFERENCES

1. Rodden, C. J. *Analytical Chemistry of the Manhattan Project*, McGraw-Hill Book Co. New York 1950.
2. Hök, B. *Svensk Kem. Tidskr.* **65** (1953) 182. (Part XV).
3. Konopik, N. and Leberl, O. *Monatsh.* **80** (1949) 655.
4. Martell, A. E. and Calvin, M. *Chemistry of the Metal Chelate Compounds*, Prentice-Hall, Inc., New York 1952, p. 27, 125, 136.
5. Ågren, A. *Acta Chem. Scand.* **8** (1954) 1059.
6. Price, G. R., Ferretti, R. J. and Schwartz, S. *Anal. Chem.* **25** (1953) 322.
7. Hök, B. *Svensk Kem. Tidskr.* **65** (1953) 105. (Part VII).
8. Dippy, J. F. J. *Chem. Revs* **25** (1939) 151.
9. Rydberg, J. *Arkiv Kemi* **8** (1955) 101. (Part XII).
10. Sillén, L. G. *Acta Chem. Scand.* **10** (1956) 186.
11. Hök-Bernström, B. *Acta Chem. Scand.* **10** (1956) 174 (Part XXIII).
12. Weinland, R. and Hager, K. *Z. anorg. Chem.* **160** (1927) 193.
13. Dittrich, C. *Z. physik. Chem.* **29** (1899) 449.
14. Foley, R. T. and Andersson, R. C. *J. Am. Chem. Soc.* **71** (1949) 909.
15. Ågren, A. *Acta Chem. Scand.* **9** (1955) 49.
16. Ahrland, S. *Acta Chem. Scand.* **5** (1951) 199.
17. Ahrland, S., Hietanen, S. and Sillén, L. G. *Acta Chem. Scand.* **8** (1954) 1907.
18. Feldman, I., Havill, J. R. and Neuman, W. F. *J. Am. Chem. Soc.* **76** (1954) 4726.

Received October 19, 1955.

ACTA CHEMICA SCANDINAVICA 10 (1956) 174—185

Studies on the Extraction of Metal Complexes

XXIII. On the Complex Formation of Thorium with Salicylic Acid, Methoxybenzoic Acid, and Cinnamic Acid

BRITA HÖK-BERNSTRÖM

Research Institute of National Defence, Dept. 1, (FOA 1), Sundbyberg 4; Institute of Inorganic and Physical Chemistry, University of Stockholm, Sweden

The extraction of thorium with salicylic acid H_2A, methoxybenzoic acid HA, and cinnamic acid HA has been studied at 25° C in the solvent systems: methyl *iso*butyl ketone-aqueous solution and chloroform-aqueous solution at a constant ionic strength of 0.1 M.

The complex formation in the aqueous phase between thorium and the acids is described by two parameters a and b [5] which are given in Table 7. The thorium complex extracted into the hexone solution of salicylic acid has been found to have an associated salicylic acid molecule. By comparison with methoxybenzoic acid it seems plausible to write the formula as $Th(HA)_4 \cdot H_2A$.

In our studies of the metal extraction with some phenylcarboxylic acids (Part XXIV [1]) a considerable number of data are reported for thorium.

In the present paper the data for thorium with salicylic acid, methoxybenzoic acid and cinnamic acid are given. Calculations of the data are made in order to draw some conclusions about the complexes formed and if possible to estimate the relevant equilibrium constants.

The distribution of thorium between the organic and aqueous phase was measured radiometrically, using $^{234}Th(UX_1)$ as a tracer for thorium. The distribution was measured after a shaking time of 18 hours at 25° C. The organic solvent was methyl *iso*butyl ketone (hexone) or chloroform and the aqueous phase was made 0.1 M by addition of $NaClO_4$. The hydrogen ion concentration of the aqueous phase was determined with a glass electrode after equilibration. The anion concentration was then calculated by means of the constants given in Part XV [2]. In the experiments the thorium concentration was kept $\sim 10^{-5}$ M by addition of inactive thorium perclorate. Only mononuclear complex formation was assumed to take place at this low metal concentration.

Table 1. Distribution of ^{234}Th $-UX_1$ between hexone and water. H_2A = Salicylic acid.

$[H_2A]_{tot}$ M	$[H_2A]_{aq}$ M	[Th] M	I'_{org}	I'_{aq}	$\log q = \log I'_{org} - \log I'_{aq} - 0.01$	$\log \frac{q}{[H_2A]_{aq}}$	$-\log [H^+]$	$-\log [HA^-]$
1.5	$10^{-2.35}$	10^{-5}	13 706		4		3.83	1.33
»	$10^{-2.34}$	»	13 620	7	+3.28	5.62	3.45	1.71
»	»	»	13 767	44	+2.48	4.82	2.87	2.29
»	»	»	11 687	170	+1.83	4.17	2.47	2.59
»	»	»	11 218	722	+1.18	3.52	2.11	2.94
»	»	»	9 716	2 595	+0.56	2.90	1.86	3.29
»	»	»	4 320	8 113	−0.28	2.06	1.55	3.60
»	»	»	577	11 639	−1.30	1.04	1.28	3.87
1.0	$10^{-2.54}$	»	19 026	29	+2.81	5.35	4.08	1.25
»	»	»	18 653	22	+2.92	5.46	4.06	1.27
»	$10^{-2.53}$	»	19 142	28	+2.82	5.35	3.80	1.53
»	$10^{-2.51}$	»	19 013	119	+2.19	4.70	3.06	2.27
»	»	»	16 029	578	+1.43	3.94	2.61	2.72
»	»	»	14 097	2 833	+0.69	3.20	2.17	3.16
»	»	»	11 542	7 581	+0.17	2.68	1.96	3.38
»	»	$10^{-5.17}$	3 351	3 429	−0.02	2.49	1.90	3.43
»	»	»	2 885	3 882	−0.14	2.37	1.81	3.52
»	»	10^{-5}	519	14 645	−1.44	1.07	1.51	3.83
»	»	»	193	15 409	−1.91	0.60	1.20	4.13
0.50	$10^{-2.87}$	$10^{-5.17}$	4 937	26 ± 5	+2.27	5.14	4.42	1.25
»	$10^{-2.85}$	»	5 431	13 ± 4	+2.60	5.45	4.30	1.36
»	»	»	5 550	30 ± 5	+2.25	5.10	4.18	1.47
»	$10^{-2.83}$	»	5 388	18 ± 4	+2.47	5.30	3.90	1.74
»	$10^{-2.82}$	10^{-5}	8 722	46 ± 4	+2.27	5.09	3.64	1.98
»	»	»	8 196	92 ± 5	+1.94	4.76	3.43	2.20
0.50	$10^{-2.82}$	10^{-5}	9 653	440	+1.33	4.15	3.10	2.53
»	»	»	6 372	2 038	+0.49	3.31	2.64	2.98
»	$10^{-2.81}$	»	3 397	4 847	−0.16	2.65	2.27	3.35
»	»	»	1 884	6 441	−0.54	2.27	2.07	3.56
»	»	»	898	7 375	−0.92	1.89	1.98	3.65
»	»	»	125 ± 9	7 482	−1.79	1.02	1.64	3.99
»	»	»	29 ± 3	7 663	−2.43	0.38	1.48	4.15
0.1	$10^{-3.75}$	10^{-5}	11 292	157	+1.85	5.60	5.19	1.37
»	$10^{-3.61}$	»	9 361	160	+1.76	5.37	4.71	1.70
»	$10^{-3.57}$	»	11 725	232	+1.69	5.26	4.45	1.93
»	»	$10^{-5.17}$	6 261	185	+1.52	5.03	4.35	2.02
»	$10^{-3.55}$	»	6 364	319	+1.29	4.84	4.28	2.09
»	»	10^{-5}	8 941	315	+1.44	4.99	4.23	2.13
»	$10^{-3.54}$	$10^{-5.17}$	5 658	245	+1.35	4.89	4.18	2.18
»	»	»	5 714	308	+1.26	4.80	4.06	2.29
»	$10^{-3.53}$	»	5 651	604	+0.96	4.49	3.85	2.48
»	$10^{-3.52}$	10^{-5}	6 481	1 080	+0.77	4.29	3.72	2.62
»	»	»	7 488	7 336	+0.00	3.52	3.33	3.01
»	$10^{-3.51}$	»	162	14 386	−1.96	1.55	2.51	3.83
»	»	»	34 ± 4	7 184	−2.33	1.18	2.43	3.90

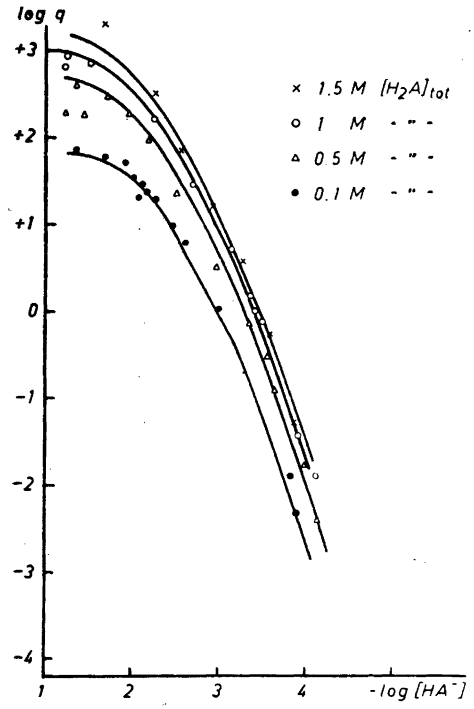


Fig. 1. Plot of log q *against* $-\log [HA^-]$ *for the distribution of* $^{234}Th-UX_1$ *between hexone and* H_2O *with salicylic acid as the organic reagent* (H_2A).

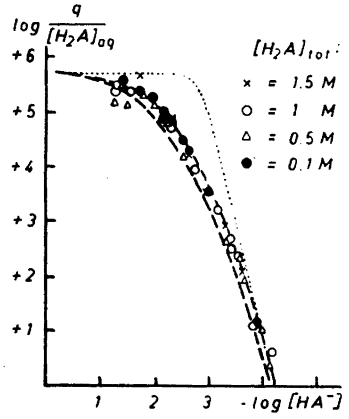
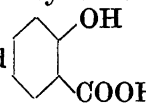


Fig. 2. Plot of $\log(q/[H_2A]_{aq})$ *against* $-\log [HA^-]$ *for the system Th—salicylic acid* (H_2A) *—hexone —*H_2O.

Salicylic acid

In a previous work the distribution of UO_2^{2+} in the system salicylic acid-hexone- 0.1 M $NaClO_4$ was studied (Part XVI [3]). If salicylic acid



is denoted H_2A, it was shown that the complexes formed in appreciable amount in the organic phase are $UO_2(H_2A)_2(H^+)_{-2}$ and $UO_2(H_2A)_3(H^+)_{-2}$, which we presumed to correspond to the formulae $UO_2(HA)_2$ and $UO_2(HA)_2 \cdot H_2A$. In the present study we started to assume that the ligand combining with thorium was HA^-.

The experimental data for the hexone system are given in Table 1. I'_{org} and I'_{aq} represent the radiometric counts obtained from equal aliquots of the organic and aqueous phases. The distribution ratio q involves a correction factor taken from Part X [4] for the density of the sample solution. In Fig. 1 the data are represented by plotting log q against $-\log[HA^-]$. For a given concentration of HA^- the values of q are found to increase when the H_2A concentration is raised. Thus q is a function not only of $[HA^-]$ but also of $[H_2A]_{aq}$.

When log $(q/[H_2A]_{aq})$ is now plotted against $-\log[HA^-]$ for thorium, as in Fig. 2, the curves for varying initial reagent concentrations are found to coincide. The experimental data can therefore be explained by the very simple assumption that the predominant complex in the organic phase is $Th(HA)_4 \cdot H_2A$.

The slope of the curve in Fig. 2 is seen to decrease from 4 to 0; thus at one end Th^{4+}, and at the other $Th(HA)_4$ predominates in the aqueous phase. The curve deviates from the calculated curve (*cf.* Fig. 2, dotted line), where the only thorium species are assumed to be Th^{4+} and $Th(HA)_4$. This clearly shows that intermediate complexes $Th(HA)_n^{4-n+}$ are also formed. For the equilibria in the aqueous phase we shall use an approximation, which has been successfully applied to many of the systems studied in this series [5]. Approximate values of the complexity constants k_n of the successive complexes are obtained from the formulae (1)—(4)

$$k_1\ k_2\ k_3\ k_4 = 10^{4a} = \varkappa_4, \tag{1}$$

$$k_1/k_2 = k_2/k_3 = k_3/k_4 = 10^{2b} \tag{2}$$

$$k_n = \frac{[Th(HA)_n]}{[Th(HA)_{n-1}]\ [HA]} \quad (n = 1,\ 2,\ 3,\ 4) \tag{3}$$

$$\varkappa_n = \frac{[Th(HA)_n]}{[Th]\ [HA]^n} \quad (n = 1,\ 2,\ 3,\ 4) \tag{4}$$

In the organic phase only the species $Th(HA)_4 \cdot H_2A$ need be considered. Presumably the distribution coefficient of $Th(HA)_4$ between the two phases is very low and that of $Th(HA)_4 \cdot H_2A$ very large. Thus $Th(HA)_4$ is not detected in the organic phase, and $Th(HA)_4 \cdot H_2A$ is not detected in the aqueous phase.

In the present case we need only consider the reaction

$$Th(HA)_4(aq) + H_2A(aq) \rightleftharpoons Th(HA)_4 \cdot H_2A\ (org) \tag{5}$$

with the equilibrium constant

$$K = \frac{[Th(HA)_4 \cdot H_2A]_{org}}{[Th(HA)_4]_{aq}\ [H_2A]_{aq}} \tag{6}$$

The equation for q then follows eqn. (7)

$$q = \frac{[Th]_{tot\ org}}{[Th]_{tot\ aq}} = \frac{[Th(HA)_4 \cdot H_2A]_{org}}{[Th]_{tot\ aq}} = \frac{K\varkappa_4\ [HA^-]^4[H_2A]_{aq}}{\sum_0^4 \varkappa_n[HA^-]^n} \tag{7}$$

where $\varkappa_n$ is defined by eqn. (4) ($\varkappa_0 = 1$).

By introducing the parameters a and b in eqn. (7) the curve in Fig. 2 may be described by

$$\log(q/[H_2A]_{aq}) = \log\ K + 4a + 4\ \log\ [HA^-] -$$

$$-\log\ (1 + [HA^-] \times 10^{a+3b} + [HA^-]^2 \times 10^{2a+4b} + [HA^-]^3 \times 10^{3a+3b} +$$

$$+ [HA^-]^4 \times 10^{4a}) \tag{8}$$

Using a similar method as in Part V [5] one can now compare the experimental curve in Fig. 2 with curves calculated for different values of b, *i. e.* log Z (log $y)_b$, where

$$\log Z = 4 \log y - \log (1 + y \times 10^{3b} + y^2 \times 10^{4b} + y^3 \times 10^{3b} + y^4) \quad (9)$$

The two asymptotes to this family of curves are

$$y \to 0 \quad \log Z = 4 \log y \quad (10)$$
$$y \to \infty \quad \log Z = 0 \quad (11)$$

The curve in Fig. 2 is now moved parallel with the log Z- and log y-axes until a position is found, where the experimental curve coincides with one of the curves in the family; then from eqn. (8) and (9)

$$\log Z = \log (q/[H_2A]_{aq}) - \log K \quad (12)$$
$$\log y = a + \log [HA^-] \quad (13)$$

The experimental data in Fig. 2 were found to fall between the calculated curves for $b = 0.40$ and $b = 0.50$ (shown in Fig. 2 by broken lines). One finds from eqn. (12) and Fig. 2 for log $Z = 0$

$$\log K = \log (q/[H_2A]_{aq}) = 5.7 \quad (14)$$

For log $y = 0$, one gets from eqn. (13) and Fig. 2

$$a = -\log [HA^-] = 2.9 \quad (15)$$

The full lines in Fig. 1 are calculated according to eqn. (8) with the values of the constants found above ($a = 2.9$, $b = 0.45$ and log $K = 5.7$).

Table 2. Distribution of $^{234}Th-UX_1$ between $CHCl_3$ and water. H_2A = Salicylic acid.

$[H_2A]_{tot}$ M	[Th] M	I'_{org}	I'_{aq}	log q = logI'_{tot} −logI'_{aq}+0.02	−log [H+]	−log[HA⁻]
0.15	10^{-5}	5 954	946	+0.82	3.33	1.49
»	»	4 901	2 478	+0.32	3.03	1.74
0.10	»	2 248	616	+0.58	3.52	1.46
»	»	1 251	709	+0.27	3.46	1.50
»	»	3 840	1 231	+0.51	3.26	1.65
»	»	5 201	2 083	+0.42	3.10	1.80
»	»	3 667	3 825	0.00	2.93	1.95
0.07	»	87	325	−0.54	3.71	1.45
»	»	610	1 571	−0.39	3.19	1.83
»	»	4 180	2 872	+0.18	3.10	1.91
»	»	3 072	4 080	−0.10	2.93	2.06
»	»	1 940	5 454	−0.63	2.77	2.20
»	»	931	8 761	−0.95	2.58	2.37
»	»	58	8 724	−2.16	2.16	2.78

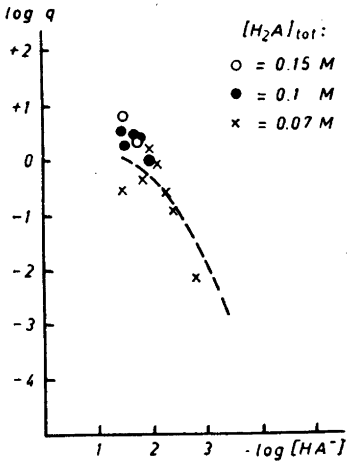


Fig. 3. Plot of log q *against* $-\log [HA^-]$ *for the distribution of* $^{234}Th-UX_1$ *between* $CHCl_3$ *and* H_2O *with salicylic acid as the organic reagent* (H_2A).

The results obtained with chloroform as organic solvent are given in Table 2 and recorded in Fig. 3 by a plot of log q against $-\log [HA^-]$. Because of the low solubility of salicylic acid in chloroform, the highest reagent concentration which could be used in the distribution experiments was $[H_2A]_{tot} = 0.15$ M. If the complex formation in the aqueous phase is assumed to be independent of the organic solvent, the distribution curve in Figs. 2 and 3 ought to have the same shape [6] (broken line in Fig. 3). However, the irregular results obtained with chloroform were not sufficient to confirm the results previously obtained with hexone.

Methoxybenzoic acid

For comparison the distribution of thorium was studied with *o*-methoxybenzoic acid, the methyl ether of salicylic acid, in the same solvent systems. The anion concentration was calculated on the basis of the following constants (log k_d — log k_a was obtained from two-phase titrations)

solvent system	log k_d − log k_a	−log k_a	log k_d
hexone-0.1 M $NaClO_4$	5.43 ± 0.01	3.89 ± 0.01 [7]	1.54 ± 0.02
chloroform-0.1 M $NaClO_4$	5.49 ± 0.01		1.60 ± 0.02

The distribution data are given in Tables 3—4 and plots of log q against $-\log[A^-]$ are recorded in Figs. 4—5. Since a variation of $[HA]_{tot}$ does not affect the distribution curve in the present system, it is concluded that the organic solvent dissolves the uncharged complex ThA_4, while the aqueous phase contains the complexes ThA^{3+}, ThA_2^{2+}, ThA_3^+ and ThA_4. Let us assume as before that the complex formation in the aqueous phase is described by the parameters a and b (eqns. (1) and (2)) and let λ_4 denote the distribution coefficient of ThA_4 between the two phases. To find the constants λ_4, a and b the experimental curves are compared with the family of curves log $Z(\log y)_b$. The parameter b is thus easily determined from the best fitting curve, whereas, in this case, log $\lambda_4 = \log q$ for log $Z = 0$ and $a = -\log [A^-]$ for log $y = 0$. If the

Table 3. Distribution of $^{234}Th-UX_1$ between hexone and water. HA = Methoxybenzoic acid.

$[HA]_{tot}$ M	[Th] M	I'_{org}	I'_{aq}	$\log q = \log I'_{org} - \log I'_{aq} - 0.01$	$-\log[H^+]$	$-\log[A^-]$
0.72	$10^{-5.57}$	24 567	1 154	+1.32	4.31	1.29
»	»	24 184	2 037	+1.06	3.81	1.67
»	»	23 391	4 239	+0.73	3.40	2.17
»	»	20 745	6 924	+0.47	3.09	2.49
»	»	12 686	14 393	−0.07	2.73	2.84
»	»	6 094	19 997	−0.53	2.40	3.17
0.5	$10^{-5.57}$	11 408	908	+1.09	4.59	1.21
»	»	14 485	4 374	+0.51	3.41	2.33
»	»	11 017	7 853	+0.14	3.12	2.62
»	»	4 939	12 822	−0.43	2.66	3.08
»	»	1 281	16 744	−1.13	2.35	3.39
»	»	491	16 640	−1.54	2.18	3.55
0.2	$10^{-5.48}$	4 261	456	+0.96	4.99	1.31
»	»	7 780	736	+1.01	4.53	1.69
»	»	11 798	554	+1.32	4.21	1.98
»	»	10 417	1 030	+1.01	4.11	2.08
»	»	9 650	1 816	+0.72	3.91	2.26
»	$10^{-5.57}$	16 460	2 366	+0.69	3.85	2.33
»	$10^{-5.48}$	8 323	3 623	+0.35	3.63	2.54
»	»	1 177	9 193	−0.90	3.06	3.11
»	»	108	10 180	−1.98	2.56	3.61
»	»	17	11 134	−2.83	2.23	3.94

accuracy admits it and the experimental data approach the two asymptotes (eqns. (10) and (11)), one may determine the unknown λ_4, a and b from the curve $\log Z$ $(\log y)_{b=-\infty}$ (recorded in Figs. 4—7 by a broken line). b is then determined by measuring the vertical distance at $\log y = 0$ between this curve and the experimental one.

The following results were obtained for methoxybenzoic acid

$$a = 2.8 \qquad b = 0.3$$
$$\log \lambda_4 = 1.2 \text{ for the hexone system}$$
$$\log \lambda_4 \sim 1.6 \text{ for the chloroform system}$$

In the chloroform system especially some points fall outside the distribution curves at the lower HA concentrations (Fig. 5). These points correspond to a loss of radioactivity (*cf.* Table 4). After equilibration of the solutions particles are occasionally seen at the boundary between the phases. In such cases the irregularities may be explained by losses of thorium due to adsorption.

Cinnamic acid

The experimental results obtained for thorium with cinnamic acid are given in Tables 5—6 for the two solvent systems studied. The data are plotted in

Table 4. Distribution of $^{234}Th-UX_1$ between $CHCl_3$ and water. HA = Methoxybenzoic acid.

[HA]tot M	[Th] M	I'_{org}	I'_{aq}	log q = $\log I'_{org} - \log I'_{aq} + 0.02$	$-\log[H^+]$	$-\log[A^-]$
0.8	$10^{-5.18}$	15 818	314	+1.72	4.61	0.95
»	»	15 567	323	+1.70	4.46	1.08
»	»	15 739	402	+1.61	4.23	1.30
»	»	16 699	419	+1.62	4.02	1.50
»	»	16 431	1 122	+1.17	3.53	1.99
»	$10^{-5.57}$	14 465	3 187	+0.67	2.99	2.52
»	»	3 036	15 318	−0.68	2.67	2.84
»	»	1 286	17 628	−1.12	2.37	3.14
0.5	$10^{-5.18}$	13 653	956	+1.17	3.64	2.15
»	»	2 191	12 356	+0.77	3.35	2.44
»	»	2 527	13 445	−0.71	2.82	2.97
»	»	469	16 724	−1.53	2.35	3.43
»	»	132	18 107	−2.12	2.14	3.64
0.2	$10^{-5.57}$	14 612	760	+1.30	3.75	2.45
»	»	12 172	4 200	+0.48	3.40	2.80
»	»	423	17 360	−1.59	2.99	3.21
»	»	366	19 017	−1.70	2.63	3.57
0.1	$10^{-5.18}$	2 278	71	+1.53	4.95	1.66
»	»	7 991	187	+1.65	4.33	2.18
»	»	11 839	400	+1.49	3.85	2.65
»	»	7 371	4 246	+0.26	3.67	2.83
»	»	736	13 907	−1.26	3.11	3.38
»	»	41	16 174	−2.58	2.42	4.09

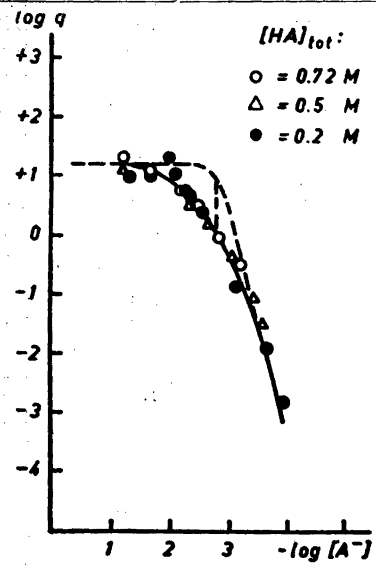


Fig. 4. Plot of log q against $-\log[A^-]$ for the distribution of $^{234}Th-UX_1$ between hexone and H_2O with methoxybenzoic acid as the organic reagent (HA).

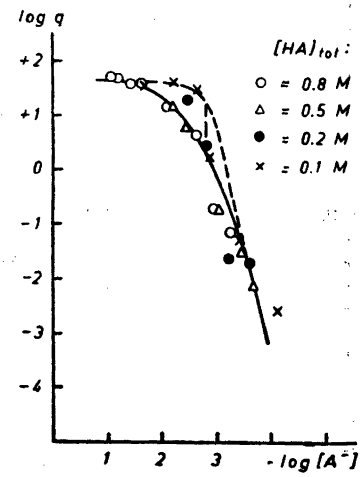


Fig. 5. Plot of log q against $-\log[A^-]$ for the distribution of $^{234}Th-UX_1$ between $CHCl_3$ and H_2O with methoxybenzoic acid as the organic reagent (HA).

Table 5. Distribution of $^{234}Th-UX_1$ between hexone and water. HA = Cinnamic acid.

[HA]tot M	[Th] M	I'_{org}	I'_{aq}	log q = logI'_{org} − logI'_{aq} − 0.01	−log [H+]	−log [A⁻]
0.2	10^{-5}	11 538	20 ± 8	+2.75	5.24	2.08
»	»	12 729	2 ± 8	+3.81	5.16	2.16
»	»	12 258	13 ± 8	+2.97	4.88	2.43
»	»	9 218	12 ± 9	+2.88	4.19	3.11
»	»	1 275	7 542	−0.78	2.95	4.35
»	»	822	10 332	−1.11 ± 0.01	2.68	4.62
»	»	864	10 242	−1.08	2.53	4.77
0.05	»	12 468	8 ± 7	+3.18	5.50	2.44
»	»	11 076	196 ± 12	+1.74	5.24	2.68
»	»	11 374	3 ± 8	+3.41	5.07	2.84
»	»	11 408	10 ± 8	+3.05	4.82	3.09
»	»	11 353	36 ± 8	+2.49	4.34	3.56
»	»	8 251	2 328	+0.54	3.69	4.21
»	»	1 909	7 910	−0.63	3.20	4.70
»	»	347	9 709	−1.46	2.81	5.09

Table 6. Distribution of $^{234}Th - UX_1$ between $CHCl_3$ and water. HA = Cinnamic acid.

[HA]tot	[Th] M	I'_{org}	I'_{aq}	log q = logI'_{org} − logI'_{aq} + 0.02	−log [H+]	−log [A⁻]
0.1	10^{-5}	7 069	3.2 ± 4	+3.36	4.60	2.69
»	»	5 616	5.2 ± 4	+3.05	4.44	2.84
»	»	9 105	30 ± 4	+2.50	4.05	3.23
»	»	8 469	32 ± 4	+2.44	3.87	3.40
»	»	5 676	264	+1.35	3.86	3.41
»	»	8 859	70 ± 5	+2.12	3.90	3.38
»	»	8 633	136 ± 6	+1.82	3.64	3.64
»	»	7 465	921	+0.93	3.38	3.90
»	»	4 756	611	+0.91	3.33	3.95
»	»	2 358	6 443	−0.42	3.04	4.23
»	»	1 583	6 560	−0.60	2.88	4.39
»	»	911	4 488	−0.67	2.64	4.63
»	»	703	8 072	−1.04	2.58	4.69
»	»	162	5 821	−1.53	2.52	4.75
0.05	»	7 839	7 ± 4	+3.07	4.68	2.77
»	»	8 787	38 ± 9	+2.38	3.80	3.65
»	»	8 059	144 ± 6	+1.77	3.74	3.70
»	»	6 679	1 889	+0.57	3.25	4.19
»	»	6 568	2 764	+0.40	3.23	4.21
»	»	1 024	8 676	−0.91	2.79	4.65
»	»	736	8 641	−1.05	2.86	4.58
»	»	388	8 919	−1.34	2.62	4.82
0.01	»	4 241	41 ± 4	+2.04	4.40	3.48
»	»	2 603	2 092	+0.11	3.77	4.09
»	»	732	3 756	−0.69	3.63	4.24
»	»	178	5 327	−1.46	3.25	4.62
»	»	13 ± 4	8 790	−2.81	2.46	5.40

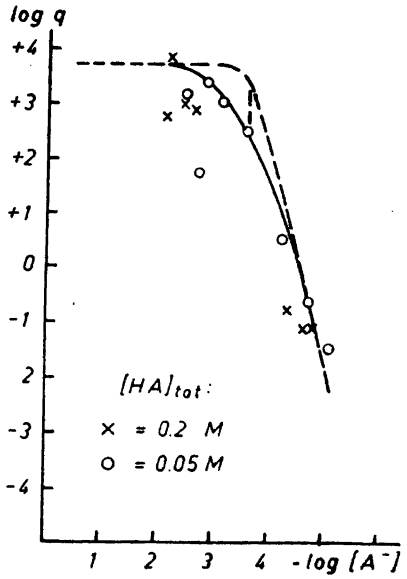


Fig. 6. Plot of log q against −log [A⁻] for the distribution of $^{234}Th-UX_1$ between hexone and H_2O with cinnamic acid as the organic reagent (HA).

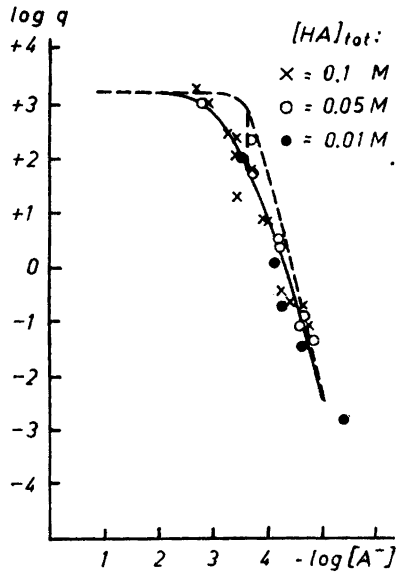


Fig. 7. Plot of log q against −log [A⁻] for the distribution of $^{234}Th-UX_1$ between $CHCl_3$ and H_2O with cinnamic acid as the organic reagent (HA).

Figs. 6—7. The constants, a, b and λ_4, were determined in the same way as before. For cinnamic acid one then obtains

$$a = 3.6 \qquad b = 0.2$$
$$\log\lambda_4 \sim 3.7 \text{ for the hexone system}$$
$$\log\lambda_4 \sim 3.2 \text{ for the chloroform system}$$

A certain spreading of the data is to be seen in Fig. 6. As will be discussed below the effects are probably due to the hydrolysis of thorium.

DISCUSSION

A summary of the constants obtained is given in Table 7, together with the dissociation constants and distribution coefficients of the acids. In the methoxy-compound thorium is only bound to the carboxyl group, while for salicylic acid one also has the possibility that the phenolic hydrogen participates in the reaction. However, the slope in Fig. 2 approaches 4, which suggests, that the salicylic acid ligand is HA^-. It is seen in Table 7 that the parameter a calculated for salicylic acid with the ligand HA^- is about the same as for methoxybenzoic acid.

The salicylate complexes of Cu^{2+}, Be^{2+} and Fe^{3+} have been reported [8-10] as chelate compounds, with the dissociation of the phenolic hydrogen. In the

Table 7.

Organic reagent	$-\log k_2$	log k_d hexone-H_2O	log k_d $CHCl_3$-H_2O	log k_2 $CHCl_3$	Metal	log λ_4 hexone-H_2O	log λ_4 $CHCl_3$-H_2O	log $\varkappa_4$	a	b	log k_1	log k_2	log k_3	log k_4
Salicylic acid H_2A	2.82	2.51	0.5	1.6	Th^{4+}	log K^* = 5.7		11.6	2.9	0.45	4.25	3.35	2.45	1.55
Methoxy-benzoic acid HA	3.89	1.54	1.6		Th^{4+}	1.2	~1.6	11.2	2.8	0.3	3.7	3.1	2.5	1.9
Cinnamic acid (*trans* form) HA	4.27	2.33	1.2	2.2	Th^{4+}	~3.7	~3.2	14.4	3.6	0.2	4.2	3.8	3.4	3.0

* K is defined by eqn. (6).

last work [10] the first complex between Fe^{3+} and salicylic acid H_2A is written as FeA and the complexity constant $\varkappa_1$ is defined

$$\varkappa_1 = \frac{[H^+]\ [FeA]}{[HA]\ [Fe]}$$

The actual complex could equally well be of the isomeric form Fe(OH)(HA) with the following equilibrium constant

$$K = \frac{[Fe(OH)(HA)]}{[Fe][HA][OH]}$$

The weak complex formation between Fe^{3+} and methyl salicylate [11], however, gives evidence for displacement of the phenolic hydrogen in this case. X-ray measurements of salicylates of K, Rb, NH_4 [12] and of Zn [13] have been made. The composition of the latter compound seemed to be $Zn(HA)_2 \cdot 3H_2O$. It might be pointed out in this connection that the parameter a for thorium (*cf.* Table 7) when complexed with the acids studied in this work is much smaller than for typical inner complex formers, such as oxine ($a = 9.8$ [14]), cupferron ($a = 6.8$ [14]) and acetylacetone ($a = 6.7$ [4]; *cf.* also [5]).

The present results give evidence for the association of a salicylic acid molecule to the uncharged complex both for thorium and UO_2^{2+}, *i. e.* the complexes found are written as $Th(HA)_4 \cdot H_2A$ and $UO_2(HA)_2 \cdot H_2A$. When a methyl group replaces the phenolic hydrogen the data indicated no such association of an extra acid molecule, which may be explained by the more limited space available around the central group in this case.

Chloroform is found to be a poor solvent for the salicylate complex. The solubility of the complex is markedly improved when the phenolic group is replaced by a methoxy group (*cf.* Figs. 3 and 5 and Table 7). The distribution of the metal complexes and of the actual acids are roughly parallel (*cf.* Table 7).

Because of the strength of the acids a high anion concentration is attainable at relatively low pH values. Thereby it was thought possible to avoid hydrolysis effects. In a recent publication by Hietanen[15] the hydrolysis of thorium has been discussed. The concentration of total thorium ranged from 2×10^{-2} M down to 10^{-3} M and the data were explained by the formation of successive polynuclear complexes. Under the experimental conditions of the present study the total thorium concentration in the aqueous phase was always $<10^{-5}$ M. Although the hydrolysis process may be chiefly mononuclear at these low metal concentrations one may nevertheless estimate a maximum value of the hydrolysis from Hietanen's data. If the function $X = \log [Th]_{aq\ tot} - 3 \log [H^+]$ is <7 (*cf.* Fig. 3, Ref.[15]) one can state that the experiments will be very little affected by hydrolysis. Since $[Th]_{aq\ tot}$ is obtained from $[Th]_{tot}/(q+1)$ and the hydrogen ion concentration has been measured in each case, it is easy to calculate X. It was found that difficulties due to hydrolysis could be expected for salicylic acid and cinnamic acid at the lowest concentrations studied in the hexone system. A spread of the data was also noticed here with occasional losses of thorium. With methoxybenzoic acid extraction was carried out on the border, where the thorium hydrolysis might start to become appreciable.

The author wishes to thank the head of FOA 1, Professor G. Ljunggren, and Professor A. Ölander for the interest in this work. She also wants to express her gratitude to Professor L. G. Sillén and Dr. D. Dyrssen for valuable and helpful discussions. Dr. F. Rossotti has been kind enough to revise the manuscript.

This work is part of a program supported by *Atomkommittén*.

REFERENCES

1. Hök-Bernström, B. *Svensk Kem. Tidskr.* **68** (1956) 34. Part XXIV.
2. Hök, B. *Svensk Kem. Tidskr.* **65** (1953) 182. Part XV.
3. Hök-Bernström, B. *Acta Chem. Scand.* **10** (1956) 163. Part XVI.
4. Rydberg, J. *Arkiv Kemi* **5** (1953) 413. Part X.
5. Dyrssen, D. and Sillén, L. G. *Acta Chem. Scand.* **7** (1953) 663. Part V.
6. Rydberg, J. *Arkiv Kemi* **5** (1953) 517. Part XI.
7. Dippy, J. F. J. *Chem. Revs.* **25** (1939) 151.
8. Babko, A. K. and Tananajko, M. M. *J. Gen. Chem. (USSR)* **23** (1953) 1459.
9. Meek, H. V. and Banks, C. V. *J. Am. Chem. Soc.* **73** (1951) 4108.
10. Ågren, A. *Acta Chem. Scand.* **8** (1954) 1059.
11. Ågren, A. *Acta Chem. Scand.* **9** (1955) 39.
12. Downie, T. C. and Speakman, J. C. *J. Chem. Soc.* **1954** 787.
13. Clark, G. L. and Kao, H. *J. Am. Chem. Soc.* **70** (1948) 2151.
14. Dyrssen, D. *Svensk Kem. Tidskr.* **65** (1953) 43. Part VI.
15. Hietanen, S. *Acta Chem. Scand.* **8** (1954) 1626.

Received October 19, 1955.

ACTA CHEMICA SCANDINAVICA 10 (1956) 186—202

Some Graphical Methods for Determining Equilibrium Constants II. On "Curve-fitting" Methods for Two-variable Data

LARS GUNNAR SILLÉN

Department of Inorganic Chemistry, Royal Institute of Technology, Stockholm 70, Sweden

A survey is given of graphical methods for determining a number of unknown constants (parameters) p_1, p_2 . . . from a set of data $y(x)$ when the function $y(x, p_1, p_2 \ldots)$ is known. If x, y, and p_i may be so chosen that one or two parameters can be connected with the variables to form "normalized variables" $X = x + p_1$, $Y = y + p_2$, the parameters may be found by fitting normalized curves. Such "curve-fitting" is preferable to numerical or "elimination" methods (see Table 1). For instance, with three parameters, $y(x)$ may be fitted to a family of curves $Y(X, p_3)$; p_1 and p_2 are obtained from the shifts of the coordinate axes, and p_3 from the shape of the curve. — A linear plot is a special case of curve-fitting; linear plots, however, have limitations which often make curved plots preferable.

Some examples are given from the determination of one or two complexity constants, and the determination of coefficients in simple polynomials.

If there are more than 2—3 parameters, "sweeping" and successive approximation may be used; the first procedure should not be used without the second. The use of smoothed curves, instead of the experimental points, requires great caution.

The determination of the equilibrium constants in a complicated system is a special case of the problem of finding a set of unknown constants from a series of experimental data. By choosing as many experimental points as one has unknown parameters, one may obtain a set of equations and solve them straight-forwardly [e.g. 1, 2] or by successive approximations [3, p. 36]. Graphical methods have the advantage over such numerical ones that the information from a much greater number of data may be considered simultaneously.

The usual tendency among chemists who apply graphical methods seems to be that of transforming the experimental data into a diagram of two variables that should give a *straight line*. From the slope and intercept of the best straight line, one may then determine two unknown constants. If there are

more than two unknowns, they may be obtained by a series of successive linear extrapolations, which is a special case of "sweeping" below.

In previous papers by Dyrssen [4] and Sillén [4-6] a somewhat different method has been applied to some special cases, namely fitting a diagram of the experimental data to a family of calculated curves. The shape and position of the curve with the best fit then gives the required information. — In the work on equilibria with polynuclear complexes to be published, various "curve-fitting" methods have proved useful. It has then seemed timely to classify what such methods may achieve.

The present paper will first give a rather general survey of graphical ways of determining one, two, or three unknown parameters from a given collection of experimental data $y(x)$. The application of methods of curve-fitting will then be shown for a number of special cases. A linear plot is only a special case of curve-fitting; it will be argued that the straight line is sometimes, but not always, the best curve.

The way of treatment given below may be common usage in some other branches of pure or applied science. However, it does not seem to be well known to all chemists.

SYMBOLS

a	concentration of free A (6)
b	concentration of free B (6)
f	experimentally determined function in (21) and following
K	equilibrium constant (6)
K_1, K_2	stepwise formation constants of complexes (text above eq. 12)
k_0, k_1, k_2	unknown coefficients in (21) and following
p_1, p_2, p_3	unknown constants (parameters) to be determined
v	auxiliary variable (7, 12a, 23, 27a, 28a)
X, Y	normalized values for x and y (2, 3)
x, y	variables determined experimentally
x_0, y_0	values for x and y coinciding with $X = 0$, $Y = 0$ at best fit (2b, 3a)
Z	average number of A bound per B (7, 12)
β_1, β_2	complexity products (12)
Subscript)$_x$	indicates that x is constant

THE PROBLEM

Table 1 gives a schematic survey of possible ways of treating a collection of experimental data (x, y) in order to determine one or more unknown constants (parameters) $p_1, p_2 \ldots$. If the experimental "points" are sets of two variables (x, y), they may be plotted in a planar diagram $y(x)$. — The case of three experimental variables (x, y, w), which cannot be reduced to a two-dimensional form, will be treated in a following paper.

We shall assume that x and y can be calculated directly from the experimental data, although they may not be the quantities actually measured. Nor need $p_1, p_2 \ldots$ be the equilibrium constants etc. ultimately sought for, although

Table 1. Methods for finding unknown constants p_i *from experimental data* y(x).

Number of parameters	normalized variables	Compare (x, y) graph with calculated graph	Eliminate y to give graph	Two-dimensional projection
1 (p_1)	1(x)	X, y		Curve $y(X)$ and plot $y(x)$
	0		x,p_1	Plot $p_1(x)$
2(p_1,p_2)	2(x,y)	X,Y		Curve $Y(X)$ and plot $y(x)$
	1(x)	X,y,p_2		a) Family of curves $y(X)_{p_2}$ and $y(x)$ plot b) $p_2(X)_y$ and proj. strip $(x)_y$
	0		x,p_1,p_2	a) Horizontal line in family $p_2(x)_{p_1}$ b) Intersection of curves $p_2(p_1)_x$
3(p_1,p_2,p_3)	2 (x,y)	X,Y,p_3		Family of curves $Y(X)_{p_3}$
	1(x)	X,y,p_2,p_3		—
	0		x,p_1,p_2,p_3	—

one must be able to calculate the latter, once the p_i are known. — In fact, it may often require a fair amount of trial to devise the most suitable functions x and y of the primary data, and the most suitable parameters p_i.

For each special problem we know the mathematical relationship between y, x, and the p_i, *e. g.* in the form

$$\begin{aligned} y &= y(x,\ p_1) \\ y &= y(x,\ p_1,\ p_2) \\ \text{or } y &= y(x,\ p_1,\ p_2,\ p_3) \end{aligned} \qquad (1)$$

We shall define our *primary* problem as finding the best possible values for the p_i, assuming that the function (1) is correct, and not as testing the validity of (1).

Table 1 shows two main ways of treating the problem graphically: eliminating one variable (say y), or comparing a plot of $y(x)$ with a calculated "normalized graph".

We shall not discuss graphical methods like that of Scatchard [7] in which the intercepts and slopes of two limiting tangents of a curve give approximate values for four parameters which are, however, then refined numerically. This method does not seem easily adaptable for graphical refinement of the constants.

Eliminating y

One parameter. When the values (x, y) for the experimental points are inserted into $y(x, p_1)$, each point gives a value for p_1. If p_1 is now plotted

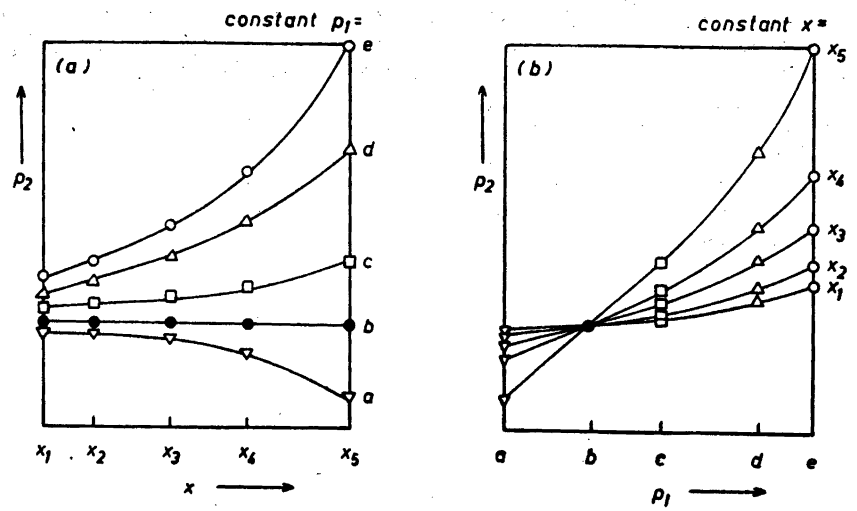


Fig. 1. Finding two parameters from y(x) *data by elimination: a)* $p_2(x)_{p_1}$ *curves: horizontal line for correct value of* p_1*; b)* $p_2(p_1)_x$ *curves: intersection at required point* p_2,p_1.

against x, one would expect to find the points scattered randomly around a horizontal line, since p_1 is really a constant. Usually no plot is made but the average value for p_1 is calculated numerically. The diagram $p_1(x)$ is drawn only if one wants to test for a trend in p_1 (which would show that the equation $y(x, p_1)$ in (1) is not quite correct), or to illustrate the spread in p_1.

Two parameters. The insertion of a pair of experimental values (x, y) into $y(x, p_1, p_2)$ gives a functional relationship between p_1 and p_2, which may be thought of as a planar curve $p_2(p_1)_x$ in (x, p_1, p_2) space. (The subscript "$_x$" indicates that x is kept constant.) A number of these curves would give a three-dimensional surface $p_2(p_1, x)$. Since p_1 and p_2 are constants by definition, the correct set (p_1, p_2) must be possible for all values of x, and thus corresponds to a straight line which is parallel to the x axis and lies entirely on the surface $p_2(p_1, x)$.

This set may be found in two ways:

a) One may plot $p_2(x)_{p_1}$, testing various constant values for p_1, until one finds the value for p_1 that makes $p_2(x)$ a horizontal line (Fig. 1a).

b) One may also plot $p_2(p_1)_x$, each experimental point giving rise to one curve, and find the required set (p_1, p_2) at the common point of intersection of these curves (Fig. 1b). An example of the second method is given in (20) below (Schwarzenbach [8]). It is in general more expedient if one wants accurate values for p_1 and p_2; however, the first method may have advantages if one wants to test for systematic errors in certain parts of the range of x.

Three parameters. Each experimental point $y(x)$, when combined with $y(x, p_1, p_2, p_3)$ in (1), gives rise to a surface $p_1(p_2, p_3)$ in (p_1, p_2, p_3) space; this surface may be thought of as a section at constant x of a four-dimensional super-surface $p_1(p_2, p_3, x)$.

The set (p_1, p_2, p_3) sought for is the common point of intersection of all these surfaces $p_1(p_2, p_3)_x$. If one of the parameters, say p_3, may be estimated rather accurately, so that only two or three values of p_3 need be considered, one might construct a plot $p_1(p_2)_{x,p_3}$ for each of these values of p_3. By studying the range where these curves intersect in each section, one may locate the point of intersection of the surfaces $p_1(p_2, p_3)_x$.

However, in general it seems impractical to vary more than two parameters simultaneously using the elimination procedure. One would then rather resort to successive approximation (see below).

Normalized graphs

The calculations are much simplified if one may normalize one variable or both.

One parameter. Suppose, for instance, that by suitable choice of variables and parameter we may arrange that the function $y(x, p_1)$ contains as the only variable the sum of x and p_1

$$X = x + p_1 \tag{2}$$

The function, which we may thus write

$$y = y(X) \tag{2a}$$

(X = "normalized x"), may then be plotted as a graph (*cf.* Fig. 2a), and moved along the x axis of the experimental diagram $y(x)$ (*cf* Fig. 2b) until the best fit is obtained (cf. Fig. 2c). In this position one reads the x value, x_0, corresponding to $X = 0$, and finds

$$X = 0;\ x = x_0 = -p_1 \tag{2b}$$

as required by (2).

In this laboratory, such curve-fitting is generally made by superimposing the experimental and calculated diagrams, drawn on an ample scale, on a table of opalescent glass, 50 cm × 60 cm, illuminated from below.

Two parameters. If it is possible to normalize both variables

$$X = x + p_1;\ Y = y + p_2 \tag{3}$$

the function $y = y(x, p_1, p_2)$ is reduced to the form $Y = Y(X)$. The curve $Y(X)$ is calculated, and moved on top of the experimental data — this time allowing parallel movement along both coordinate axes — until the best fit is obtained. The coordinates of the point (x_0, y_0) coinciding with the origin of the normalized graph ($X = 0$, $Y = 0$) are read

$$(X = 0,\ Y = 0);\ x = x_0 = -p_1;\ y = y_0 = -p_2 \tag{3a}$$

This procedure provides a great simplification compared with the "elimination" procedure above.

Even if one does not find a suitable way of normalizing two variables, the gain of normalizing one is also considerable. In this case we have a normalized function

$$y = y(X,\ p_2) \tag{4}$$

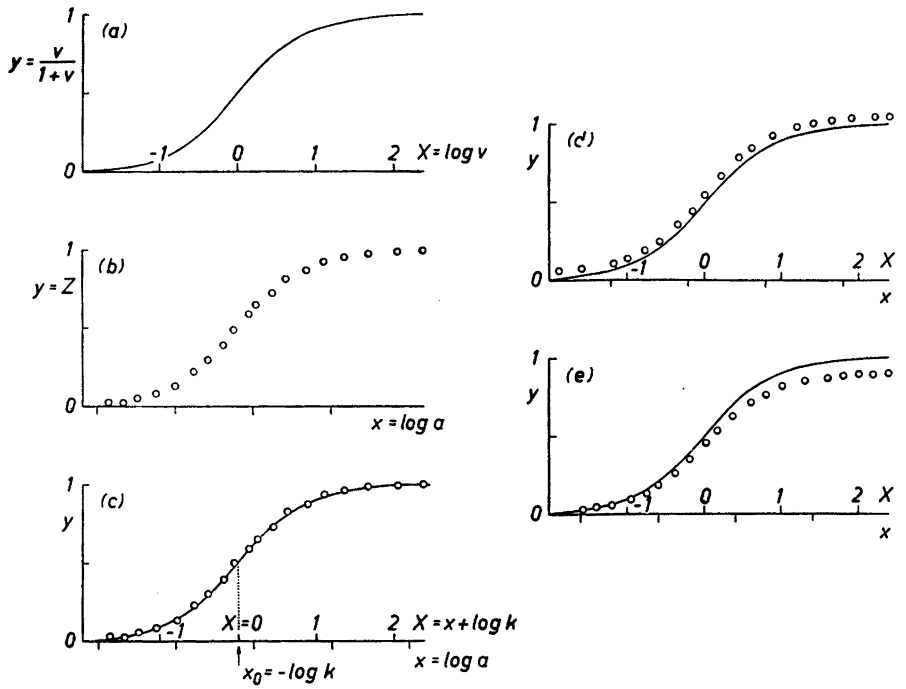


Fig. 2. Single complex: a) calculated curve y(X), *eq (8a) and (8b); b) imaginary experimental data* y(x), *eq (8); c) best fit of a and b; d, e) effect of systematic analytical errors: d) constant error in assumed amount of A, e) constant error in assumed ratio of A to B.*

to which the data $y(x)$ may be fitted. We may imagine $y(X, p_2)$ as a three-dimensional surface, to which the plane curve $y(x)$ may be fitted by shifts along the X and p_2 axes. One might consider working with a three-dimensional model, but two-dimensional plots are more easily handled and represented in print. Two approaches have been attempted:

a) In some earlier papers (Sillén [6], Hietanen and Sillén [9], Rossotti and Rossotti [10], using the "two-parameter" approximation [4]) a family of curves $y(X)_{p_2}$ was compared with the experimental diagram $y(x)$. Then p_2 was obtained from the parameter of the curve that gave the best fit, and $-p_1$ from x_0 at the best position. For improving an approximate value of p_2 one may either draw curves for intermediate values of p_2, or use some characteristic measure of the curve, such as the horizontal distance $x(y_2)$—$x(y_1)$ between two fixed values of y, or the slope dy/dx at a certain value of y.

b) A subsequent paper by Rossotti, Rossotti, and Sillén [11] will show the advantages of constructing curves $p_2(X)_y$ for a series of round values of y, and comparing them with a projection strip $(x)_y$ of the experimental data.

Three parameters, finally, may in principle be determined by fitting $y(x)$ to a three-dimensional surface $Y(X, p_3)$, provided that both x and y can be normalized. Conveniently, $y(x)$ is compared with a family of normalized

curves $Y(X)_{p_s}$: p_1 and p_2 are found from the shifts along the coordinate axes (thus from x_0 and y_0), and p_3 from the shape of the curve. Examples are given in a paper by Dyrssen and Sillén [4], and more will be given below.

If only one variable can be normalized, we have to fit $y(x)$ to a four-dimensional super-surface $y(X, p_2, p_3)$. This problem may be transformed to two-dimensional diagrams, *e. g.* by some method of successive approximation.

Linear plots are a special case of a family of normalized curves. If the two functions y and x are devised so as to give a linear plot, say

$$y = p_2 x + p_1 p_2 = p_2 X \tag{5}$$

the construction of the best line through the data $y(x)$ may be considered as the fitting of $y(x)$ to a family of curves $y(X)_{p_s}$, which are in this special case a bundle of straight lines $y = p_2 X$. In practice they are generally not constructed since a templet (*i. e.* a ruler) for these curves is always available.

Fitting a straight line of a given slope to the $y(x)$ is a special case of fitting a single normalized curve $y(X)$.

In the following sections it will be shown by means of a few simple examples that the use of a suitably chosen set of non-linear normalized curves may have advantages compared with a linear plot. Finally some methods will be discussed — successive approximation, "sweeping" — which are resorted to when the number of parameters is so great that a single two-dimensional diagram will not suffice.

APPLICATIONS TO SIMPLE CASES OF COMPLEX FORMATION

Z (log a) data for single complex

If two reagents, A and B, form the single complex AB, the only constant to be determined is the equilibrium constant K

$$\mathrm{A} + \mathrm{B} \rightleftharpoons \mathrm{AB};\ [\mathrm{AB}] = [\mathrm{A}]\ [\mathrm{B}]\ K = abK \tag{6}$$

(If, for instance, $\mathrm{A} = \mathrm{H}^+$, $\mathrm{B} = \mathrm{Ac}^-$, and $\mathrm{AB} = \mathrm{HAc}$, then $K = K_{\mathrm{acid}}^{-1}$ for HAc.) Let us assume that the concentration a of free A is measured for a series of solutions. For each solution the analytical data, together with a, give us Z, the number of A bound per B. The relationship is

$$Z = \frac{[\mathrm{AB}]}{[\mathrm{B}] + [\mathrm{AB}]} = \frac{aK}{1 + aK} = \frac{v}{1 + v} \tag{7}$$

Data $Z(a)$ are often used for determining complexity constants and acidity constants. As seen from (7), Z is a function of the single variable $v = aK$. Choosing our experimental variables, and the single parameter as

$$x = \log\ a;\ y = Z;\ p_1 = \log\ K \tag{8}$$

we may use a normalized variable (2)

$$X = \log\ v = \log\ a + \log\ K \tag{8a}$$

The normalized curve $y(X)$, which may easily be constructed, is obtained from (7, 8, 8a):

$$y(X) = \frac{v}{1+v} = \frac{10^X}{1+10^X} \tag{8b}$$

This calculated curve $y(X)$, Fig. 2a, is moved parallel with a plot of the experimental data $y(x)$, Fig. 2b, until the best fit is obtained, Fig. 2c. Then one may read, from the value of x coinciding with $X = 0$

$$x_0 = -p_1 = -\log K \tag{8c}$$

Calculated curves of the shape (8b) have been used in several laboratories; *e. g.* Simms [12] mentions the use of a paper mould of this shape for finding acidity constants.

Comparison with alternative methods. One may find K from the same data $Z(\log a)$ by normalized graphs, using the same x and X (8, 8a), but choosing y so as to obtain a linear plot [13]

$$\left.\begin{aligned} x &= \log a;\ X = \log a + \log K \\ y &= \log \frac{Z}{1-Z} = \log aK = X \end{aligned}\right\} \tag{9}$$

Plotting $y = \log Z/(1-Z)$ versus $x = \log a$, one would thus get a straight line of slope 1, which may be fitted to a normalized curve $y = X$. At $X = 0$ one reads $x_0 = -p_1 = -\log K$ as in (8c).

One might also use the elimination method, calculating

$$K = Za^{-1}(1-Z)^{-1} \tag{10}$$

from each experimental point, and taking the average.

In comparison with these methods, the choice of variables in (8) has some real advantages. The variables $\log a$ and Z are so close to the data primarily measured that one may mark out in the diagram how much an experimental point $y(x)$ would be changed by a certain experimental error — say by 0.3 mV in the emf in measuring a, or by 0.5 % in the analysis of A or B. So one may judge whether the deviations from the normalized curve are reasonable in view of the expected experimental accuracy.

Further, systematic analytical errors are easily recognized and corrected for since they give rise to a parallel shift along the y axis (Fig. 2d), or to a small change of scale along the y axis (Fig. 2e). With (9) or (10) such errors would give a trend in K but it would not be as easy to see the cause immediately. Treatment with the least square method, as usual, would do no good in the presence of systematic errors.

If it is found necessary to correct for small analytical errors of both kinds, one may connect these errors in Z with two parameters, one p_2 involving a shift along the y axis, and another p_3 a shift in the y scale. With

$$x = \log a;\ y = Z;\ p_1 = \log K \tag{8}$$

$$X = x + p_1 = \log v;\ Y = y + p_2 = p_3 v(1+v)^{-1} \tag{11}$$

we have a system with two normalized variables and three parameters, which may be solved by means of a set of $Y(X)_{p_2}$ curves. The two other methods are not so easily adapted to correcting for analytical errors.

Z(log a) data for two complexes

If the reactants A and B form two complexes, AB and A_2B, with the overall formation constants ("complexity products") $\beta_1 = K_1$ and $\beta_2 = K_1K_2$ (K_1 and K_2 stepwise formation constants), we have

$$\left.\begin{aligned} [AB] &= \beta_1 ab;\ [A_2B] = \beta_2 a^2 b \\ Z &= \frac{[AB] + 2[A_2B]}{[B] + [AB] + [A_2B]} = \frac{\beta_1 a + 2\ \beta_2 a^2}{1 + \beta_1 a + \beta_2 a^2} \end{aligned}\right\} \quad (12)$$

Setting as before (*cf.* 8, 8a)

$$x = \log\ a;\ y = Z;\ X = x + p_1 = \log\ v \quad (12a)$$

we may normalize log a, leaving one parameter in the expression for y. Two possible ways are, expressing for convenience the relationship $y(X, p_2)$ by means of the auxiliary variable v in (12a)

$$p_1 = \log \beta_1\ ;\ p_2 = \beta_2\beta_1^{-2}\ ;\ y = \frac{v + 2\ p_2v^2}{1 + v + p_2v^2} \quad (13)$$

$$p_1 = \tfrac{1}{2}\ \log \beta_2 = \tfrac{1}{2}\ \log\ K_1K_2\ ;\ p_2 = \beta_1\beta_2^{-\frac{1}{2}} = (K_1K_2^{-1})^{\frac{1}{2}}\ ;\ y = \frac{p_2v + 2\ v^2}{1 + p_2v + v^2} \quad (14)$$

Fig. 3 shows a family of curves $y(X)_{p_2}$, calculated using the second approach (14). They may be regarded as sections of the three-dimensional surface $y(X, p_2)$. — The properties of functions like (12) have been discussed by Auerbach and Smolczyk[14]. A family of curves like Fig. 3 was given by J. Bjerrum[3, p. 26]. Neither seems to have used them for curve-fitting. J. Bjerrum's average constant is 10^{p_1}, and his spreading factor is $\frac{1}{2}\ p_2$, in (14).

To find the required parameters, the experimental data $y(x)$ should be moved along the p_2 and X axes until the best fit is found. By comparison with the family of curves $y(X)_{p_2}$, Fig. 3, one may first test for, and if necessary correct for, systematic analytical errors, like in Figs. 2d and e. Then p_2 can be estimated from the two curves giving the nearest fit; a better value may be found by inserting curves for intermediate values of p_2, or by using some suitable measure (say, the difference between $X(y = 1.5)$ and $X(y = 0.5)$, *cf.* Irving and Rossotti[1]). The other parameter is found from the values of x_0 corresponding to $X = 0$.

For determining the parameters accurately, the method described by Rossotti, Rossotti and Sillén[11] is advantageous: a projection strip $(x)_y$ of the experimental data is moved parallel with the X and p_2 axes to give the best fit with the family of curves $p_2(X)_y$.

Alternative methods

Linear plot. We may transform (12) to the form

$$Z + \beta_1 a(Z - 1) + \beta_2 a^2(Z - 2) = 0 \quad (15)$$

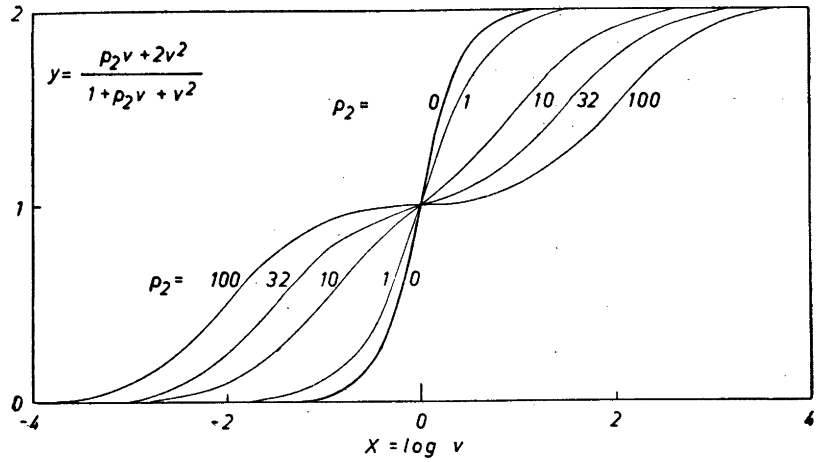


Fig. 3. Two complexes: calculated curves $y(X)_{p_2}$ *(eq (12a) and (14) for various values of* p_2.

Dividing by suitable factors and rearranging, this equation may be reduced to the linear form, with X normalized

$$y = p_2 x + p_1 p_2 = p_2 X \tag{5}$$

by any of six transformations, three of which are given here (in the other three, x and y are only interchanged)

$$a^2(2-Z)Z^{-1} = \beta_1\beta_2^{-1}a(Z-1)Z^{-1} + \beta_2^{-1} \tag{16}$$

$$Za^{-1}(Z-1)^{-1} = \beta_2 a(2-Z)\ (Z-1)^{-1} - \beta_1 \tag{17}$$

$$Za^{-2}(2-Z)^{-1} = -\beta_1 a^{-1}(Z-1)\ (2-Z)^{-1} + \beta_2 \tag{18}$$

For instance, with (16) we have

$$y = a^2(2-Z)Z^{-1}\ ;\ x = a(Z-1)Z^{-1}\ ;\ p_1 = \beta_1^{-1}\ ;\ p_2 = \beta_1\beta_2^{-1} \tag{16a}$$

Equation (16) is essentially identical with that given by Speakman [15] and (17) with that of Irving and Rossotti [1], also used by Rossotti and Rossotti [10].

The method given by Schwarzenbach, Willi, and Bach [8] may be classified as an *elimination* method, using the parameters

$$p_1 = \beta_1^{-1}\ ;\ p_2 = \beta_2\beta_1^{-1} \tag{19}$$

and dividing (17) by β_1 to obtain

$$p_1 \frac{Z}{a(Z-1)} = p_2 \frac{a(2-Z)}{Z-1} - 1 \tag{20}$$

Each experimental point (Z, a) gives a straight line (20) in a plot (p_1, p_2), which is conveniently constructed from the intercepts $-a(Z-1)Z^{-1}$ and $(Z-1)a^{-1}\ (2-Z)^{-1}$. All these lines should intersect at the point (p_1, p_2)

which gives the correct set (β_1, β_2) by means of (19). (For a dibasic acid H_2X, as discussed in Ref.[8], with $A = H^+$ and $B = X^{2-}$, the acid dissociation constants are related to the formation products by $K_{a1} = \beta_1\beta_2^{-1}$ and $K_{a2} = \beta_1^{-1}$).

Linear versus curved plots. The search for the best straight line (5) is a special case of curve-fitting. The advantage of a linear plot is the simplicity of construction. However, considering the time that will usually be spent in getting accurate data, the little extra work of constructing a set of normalized curves is negligible.

There are several limitations to the linear plots, which may often make it worthwhile to try a curved plot.

1) The connection between the functions used and the experimental data will often be so remote in a linear plot that it may be hard to decide whether a certain deviation is compatible with the experimental accuracy. With curved plots one has a greater freedom to choose variables more *directly connected with* the *experimental data*. Compare, for instance, the variables $y = Z$ and $x = \log a$ in the curved plots (Figs. 2 and 3) with the complicated functions of Z and a used in the linear plots (eqns. 16, 17, 18).

2) *Systematic errors* may make a linear plot deviate from linearity; however, such deviations are not always readily explained and corrected for. A curved plot may be devised so that systematic errors to be expected (say, analytical errors) are easily recognized and corrected for. The systematic error may be treated as one or two extra parameters to be determined, as in (11).

3) In studies of chemical equilibria, the concentrations of the reacting species are often varied by several powers of ten — and should be so varied, wherever possible. Then the scale of a linear plot may become awkward: the experimental points being scarce at one end and compressed at the other. A small experimental error may cause much greater deviations in some parts than in others. In estimating the best line, it is difficult to weigh deviations in different parts of the diagram against each other, especially if the variables plotted, y and x, are also rather remote from the measured quantities.

With curved plots this difficulty is overcome by using a *logarithmic concentration scale*, which is also very convenient for normalization. Especially with emf measurements, the accuracy at different parts of a logarithmic scale is approximately the same, and this facilitates the estimation of the best curve.

4) A single linear plot can give only two parameters, whereas a curved plot will allow the simultaneous determination of *three parameters*.

5) Sometimes one may want to use the data for choosing between different hypotheses, each of which gives a different expression (1) for y. If one insists upon linear plots, the various hypotheses will in general give very different variables, and so it is hard to make a good comparison between them. Using curved plots, one has a greater freedom of choice. It is often possible to use a plot of the same variables to *test for several different hypotheses*, *e.g.* in ref [6,9], where mechanisms with a single polynuclear complex, with series of "core + links" polynuclear complexes, and with the formation of a precipitate, could be tested on the same plot $y(x)$; in this case, $y = Z/t$, $x = t \log a + \log B$. Thus it is easier to judge which deviations are really to be considered as essential.

The scale should of course be so chosen that full advantage is made of the experimental accuracy. Thus, for a rather accurate set of data it may prove desirable to use a plot on a much larger scale than would seem necessary for another set of data, otherwise using a plot with the same normalized functions.

DETERMINING THE COEFFICIENTS IN POLYNOMIALS

Suppose that we have measured, over a certain range of the variable a, a number of experimental points (a, f), where f is related to a by

$$f(a) = k_0 + k_1 a + k_2 a^2 \tag{21}$$

k_0, k_1 and k_2 being unknown constants to be determined.

For instance, in studies of systems with complexes A_nB, a may be the concentration of free A, and $-59.16 \log f$ may be the change in the emf of a B electrode; or $a^2 f^{-1}$ may be the distribution ratio of B_{total} between an organic solvent and an aqueous solution of A.

Problems of this kind may be solved by using normalized curves. Setting as experimental variables

$$x = \log\ a;\ y = \log\ f \tag{22}$$

we may use the following normalization

$$\left.\begin{aligned} X &= x + p_1 = \log\ v \\ Y &= y + p_2 = \log(1 + p_3 v + v^2) \end{aligned}\right\} \tag{23}$$

Solving p_1, p_2, and p_3 from (21), (22), and (23) we find

$$\left.\begin{aligned} -x_0 &= p_1 = \tfrac{1}{2} \log\ k_2 - \tfrac{1}{2} \log\ k_0 \\ -y_0 &= p_2 = -\log\ k_0 \\ \log\ p_3 &= \log\ k_1 - \tfrac{1}{2} \log\ k_0 - \tfrac{1}{2} \log\ k_2 \end{aligned}\right\} \tag{23a}$$

Fig. 4a gives a family of curves $Y(X)_{p_3}$ calculated from (23). The curves have two common asymptotes, $Y = 0$ and $Y = 2X$. If a given set of experimental data $y(x)$, eqn. (22), is moved so as to give the best fit (Fig. 4b), the shape of the curve gives p_3, and the coordinates (x_0, y_0) coinciding with $(X = 0, Y = 0)$ give $-p_1$ and $-p_2$.

To refine the value of p_3 one may interpolate in some way between the calculated curves, possibly inserting new curves with intermediate values of p_3. If the accuracy admits it, one may use the vertical distance $y - y_0$ from the experimental curve to (x_0, y_0); at this point $X = 0$, and (23) gives

$$\text{for } X = 0;\ v = 1;\ Y = y - y_0 = \log(2 + p_3) \tag{23b}$$

The required constants are calculated using (23a)

$$\left.\begin{aligned} \log\ k_0 &= -p_2 \\ \log\ k_1 &= p_1 - p_2 + \log\ p_3 \\ \log\ k_2 &= 2p_1 - p_2 \end{aligned}\right\} \tag{23c}$$

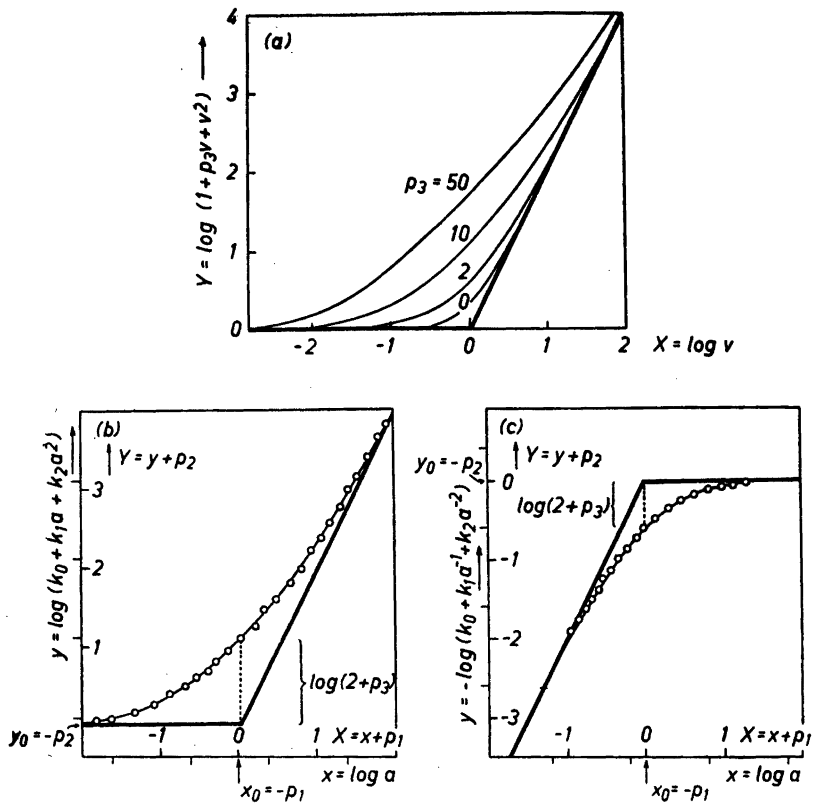


Fig. 4a. Family of curves (23), $X = log\ v$, $Y = log\ (1 + p_3v + v^2)$ *for finding coefficients of polynomials* $k_0 + k_1a + k_2a^2$.

b. Fit of experimental data.

c. Fitting inverted curve, $X = -log\ v$, $Y = -log(1 + p_3v + v^2)$, *eq (26), to data* $x = log\ a$, $y = log\ f = -log(k_0 + k_1a^{-1} + k_2a^{-2})$.

It should be noted that the same set of curves may be used also to find the coefficients of functions of the types

$$f(a) = k_0 + k_1a^{-1} + k_2a^{-2} \quad (24)$$

$$f(a) = (k_0 + k_1a + k_2a^2)^{-1} \quad (25)$$

$$f(a) = (k_0 + k_1a^{-1} + k_2a^{-2})^{-1} \quad (26)$$

One needs only reverse the signs of the X axis for (24), of the Y axis for (25), or of both for (26). For (26) we have for instance (Fig. 4c) $X = -\log v$, $Y = -\log(1 + p_3v + v^2)$.

In practice, the reversal is simply made by rotating the paper, on which the curves have been drawn, by 180° around a vertical or horizontal axis.

Separate curves should be drawn for the values $k_0 = 0$ and $k_2 = 0$ which appear only as limiting cases in the treatment by means of (23). With $k_2 = 0$ we have

$$f(a) = k_0 + k_1 a \tag{27}$$

We may use the same coordinates

$$x = \log\ a;\ y = \log\ f \tag{22}$$

and normalize, using the auxiliary variable v

$$X = x + p_1 = \log\ v;\ Y = y + p_2 = \log(1 + v) \tag{27a}$$

Solving p_1 and p_2 from (22), (27), and (27a) we find

$$p_1 = \log\ k_1 - \log\ k_0;\ p_2 = -\log\ k_0 \tag{27b}$$

With $k_0 = 0$ we have correspondingly

$$f(a) = k_1 a + k_2 a^2 \tag{28}$$

Using the same set of experimental variables (22), and normalizing

$$X = x + p_1 = \log\ v;\ Y = y + p_2 = \log\ (v + v^2) \tag{28a}$$

we would find

$$p_1 = \log\ k_2 - \log\ k_1;\ p_2 = \log\ k_2 - 2\ \log\ k_1 \tag{28b}$$

The curves (27a) and (28a) are shown in Fig. 5; they can of course, like those in Fig. 4a, be applied to functions with inverted values of f or a, just by reversing one coordinate axis or both.

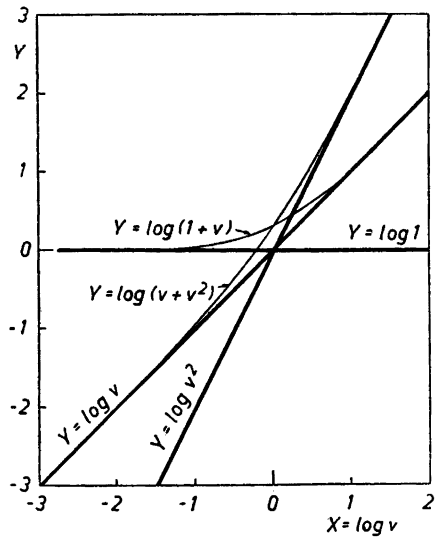


Fig. 5. Normalized curves (27a) and (28a) for finding coefficients in $f = k_0 + k_1 a$ *and* $f = k_1 a + k_2 a^2$.

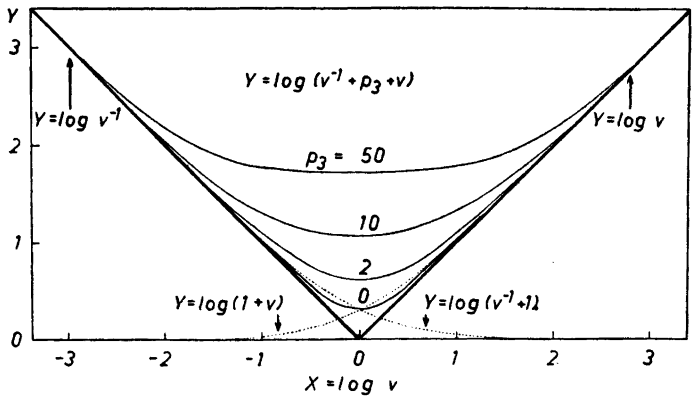


Fig. 6. Normalized curves (29) for finding coefficients of polynomial $k_0 + k_1a + k_2a^2 = f$, *by comparison with log* fa^{-1} *(log a) diagrams. Curves are also drawn for cases with one or two coefficients = 0.*

Using the double-logarithmic plot (22), all three unknowns in $f = k_0 + k_1a + k_2a^2$ may be found by comparing with the curves in Figs. 4a and 5. — It may seem surprising that a curve-fitting method is advocated for problems which have usually been solved by linear plots, and would seem admirably suited to such. However, with experimental data extending over a number of powers of 10, a logarithmic plot may give a better estimate of the real accuracy (see above, p. 196).

The same approach may be used for any polynomial with only three parameters, say $f(a) = k_1a + k_3a^3 + k_4a^4$ etc. It may prove useful in some cases to use as y, not log f but for instance log fa^{-1} or log fa^2. Thus the polynomial (24) may also be treated by considering $y = \log fa^2 = \log (k_2 + k_1a + k_0a^2)$, which may be treated with the curves (23).

Even the polynomial (21) $f = k_0 + k_1a + k_2a^2$ may sometimes preferably be treated using (Fig. 6)

$$\left.\begin{aligned} x &= \log a;\ X = \log v \\ y &= \log fa^{-1};\ Y = \log(v^{-1} + p_3 + v) \end{aligned}\right\} \qquad (29)$$

Equations (23 a, b, c) still hold. Thus p_3 is found from the intersection of the Y axis for $X = 0$: $Y = \log(2 + p_3)$.

SMOOTHED CURVES

It seems a good rule to select such graphical methods as allow one to retain a good feeling for the possible effect of experimental errors. Thus one would like to plot each experimental point as a separate point, with such coordinates that the influence of an experimental error can be readily estimated. In studies of complexity equilibria, this principle has been especially strongly advocated by Leden[e.g. 16].

Thus, it does not seem advisable to draw from the onset a smoothed curve through a set of data, and then to keep strictly to that curve. This approach is

especially dangerous if the data have only intermediate accuracy, and the points are rather scarce in some part of the diagram. On scrutinizing such "smoothed curves" one may find that the position of certain points will unduly influence the way of drawing the curve. If it so happens that from a certain "smoothed curve" one has calculated values for the unknown constants that give a fair agreement with the original smoothed curve, one is too often inclined to think that one has found the right set of parameters, without trying to imagine how wide a domain in parameter space (p_1, p_2 . . .) would also have given an acceptable agreement. Only if a smoothed curve gives constants that fail to reproduce it, it is emphasised that the curve must be incorrectly drawn, *i. e.* that it does not belong to the right family of curves.

Sometimes it may be unavoidable to use a smoothed curve, especially when a differentiation or integration is necessary. To avoid the dangers of smoothing the wrong way, one should use the following precautions:

1) Besides the best "smoothed curve" one should also draw two or more curves that deviate from it but would still give an acceptable agreement with the data. A comparison with constants calculated from these curves will give an indication of the real accuracy.

2) The results obtained with a smoothed curve should be compared with those obtained by other, independent methods.

METHODS FOR SEVERAL PARAMETERS

Successive approximation

The experimental range may often be divided into several parts so that one or two parameters, which give the main effect in one part of the range, give only a small correction in the other. Suppose for instance that we have an experimental quantity $y(x, p_1, p_2, p_3, p_4)$, and that p_1 and p_2 predominate in one range of x whilst p_3 and p_4 give a small correction, whereas in another range it is the other way round. Then p_1 and p_2 may be determined from the first range by one of the methods for a two-parameter problem, using approximate values for p_3 and p_4 or even neglecting them; then p_3 and p_4 are determined by some two-parameter method in the other range, assuming the first approximate values for p_1 and p_2. Using these values for p_3 and p_4 in the first range, better approximations for p_1 and p_2 are found etc.

In this way four or more parameters may be obtained by successive approximation using two-parameter methods. This procedure is not necessarily unsatisfactory, since one need never lose the contact with the experimental data.

"Sweeping" methods

Especially for the determination of consecutive constants of complex formation, another type of method has been used, which may be described as "sweeping" for the parameters. The term will indicate that, just like with a sweeping search-light, the interest is centered on one or two constants at a time, and that the centre of interest is moved along the series of parameters.

The function $y(x, p_1, p_2, p_3, p_4 \ldots)$ is first reduced to a two-parameter problem by neglecting other parameters than p_1 and p_2. In the range where

p_1 and p_2 are predominant, a plot (usually linear) is made from which approximate values for p_1 and p_2 are found. The value for p_1 is accepted and inserted into the function y. Now the function $y(x, p_2, p_3 \ldots)_{p_1}$ is considered, keeping p_1 constant, neglecting p_4 and following parameters, and having p_2 and p_3 as unknown parameters to be determined. This plot gives a value for p_2, which is then used in a new plot with p_3 and p_4 as unknown parameters. The procedure may be speeded up if one accepts both values for p_1 and p_2 obtained from the first plot, and thus gets two parameters from each plot. It is often advantageous to use different experimental functions y and x in different parts of the range.

With such a method there is a danger that errors in the values for the first parameters p_1, p_2 etc will accumulate, making the plots for p_4 and p_5 somewhat unreliable; at any rate, the feeling of contact with the experimental data is definitely lost, and it is very hard to estimate the real accuracy.

The parameters obtained may be checked and improved:

1) by sweeping the series of parameters from both ends; an example is given in part I [10]. The deviations will give an indication of the accuracy.

2) by successive approximation. After a first approximate set of parameters has been obtained, the terms corresponding to the higher parameters are inserted into the first plot for finding p_1 and p_2, which gives better values for these parameters. The process may be repeated, either always from one end, or sweeping from alternate ends of the parameter series, depending on the problem and type of data. As a rule, this simple precaution appears to have been neglected previously.

If curved plots are also considered, one would have a greater freedom of choice.

I wish to thank my friends George Biedermann, David Dyrssen, Brita Hök-Bernström, Gösta Lagerström, Francis Rossotti, Hazel Rossotti, and Jan Rydberg for pleasant cooperation and for many valuable discussions.

This paper is part of a program supported by *Atomkommittén (Swedish Atomic Energy Commission)* and *Statens Naturvetenskapliga Forskningsråd (Swedish Natural Science Research Council)*.

REFERENCES

1. Irving, H. and Rossotti, H. S. *J. Chem. Soc.* **1953** 3397.
2. Block, B. P. and McIntyre, G. H. Jr, *J. Am. Chem. Soc.* **75** (1953) 5667.
3. Bjerrum, J. *Diss.* Copenhagen 1941.
4. Dyrssen, D. and Sillén, L. G. *Acta Chem. Scand.* **7** (1953) 663.
5. Sillén, L. G. *Acta Chem. Scand.* **8** (1954) 299.
6. Sillén, L. G. *Acta Chem. Scand.* **8** (1954) 318.
7. Edsall, J. T., Felsenfeld, G., Goodman, D. S. and Gurd, F. R. N. *J. Am. Chem. Soc.* **76** (1954) 3054.
8. Schwarzenbach, G., Willi, A. and Bach, R. O. *Helv. Chim. Acta* **30** (1947) 1303.
9. Hietanen, S. and Sillén, L. G. *Acta Chem. Scand.* **8** (1954) 1607.
10. Rossotti, F. J. C. and Rossotti, H. S. *Acta Chem. Scand.* **9** (1955) 1166, part I.
11. Rossotti, F. J. C., Rossotti, H. S. and Sillén, L. G. *Acta Chem. Scand.* **10** (1956) 203, part III.
12. Simms, H. S. *J. Am. Chem. Soc.* **48** (1926) 1239.
13. McClendon, J. F. *J. Biol. Chem.* **54** (1922) 647.
14. Auerbach, F. and Smolczyk, E. *Z. physik. Chem.* **110** (1924) 65.
15. Speakman, J. C. *J. Chem. Soc.* **1940** 855.
16. Leden, I. *Diss.* Lund 1943.

Received November 3, 1955.

ACTA CHEMICA SCANDINAVICA 10 (1956) 203—214

Some Graphical Methods of Determining Equilibrium Constants III. A Projection Strip Method for Two-Parameter Systems

F. J. C. ROSSOTTI, HAZEL ROSSOTTI and LARS GUNNAR SILLÉN

Department of Inorganic Chemistry, Royal Institute of Technology, Stockholm 70, Sweden

Experimental data may often be represented by a single curve $y(x)$. It is sometimes possible to describe this function, either rigorously or approximately, in terms of only two parameters, p_1 and p_2, such that the value of p_2 determines the shape of the curve $y(x)$, while the value of p_1 fixes its position on the x axis. Values of p_1 and p_2 may always be obtained by comparing the shape and position of the experimental $y(x)$ curve with theoretical $y(X)_{p_2}$ curves calculated for different values of p_2. It is, however, more convenient to determine them by fitting the data in the form of a projection strip $(x)_y$ to the set of theoretical curves $p_2(X)_y$, where the normalised function $X = x + p_1$. This device is used to calculate equilibrium constants for a number of systems containing polynuclear hydrolysis products, and its application to systems of mononuclear complexes is indicated. The set of curves $p_2(X)_y$ is also useful for the rapid calculation of theoretical $y(x)$ curves for systems in which the values of p_1 and p_2 are known.

In studies of equilibria in a solution containing complexes formed from a central group, M, and a ligand, L, the measurements may often be explained, within the limits of experimental error, in terms of two parameters. For the special case where only the first two mononuclear complexes, ML and ML_2, are formed, two parameters, K_1 and K_2, suffice for a rigorous mathematical description of the system. (Here the stability constant of the species ML_n is given by $K_n = [ML_n]/[ML_{n-1}][L]$ and charges are omitted.) A number of methods for calculating K_1 and K_2 from the experimental data have been described, and are discussed critically elsewhere [1]. When $N > 2$ mononuclear complexes are formed, an exact treatment requires N parameters, $K_1, K_2 \ldots K_N$, which may be determined experimentally if the data are sufficiently precise [2]. However, it may not be possible to obtain more than two independent stability constants from less accurate data, *e. g.* some partition measurements, and it is often convenient to give an approximate description of systems of this type

in terms of only two parameters [3]. A rigid mathematical treatment of a system containing polynuclear complexes, M_qL_p ($1 \leq p \leq P$, $1 \leq q \leq Q$) requires PQ parameters, which could only be determined if a very large number of precise data were available [4]. In practice, it is seldom possible to obtain more than three or four independent constants for these systems, and in many cases the experimental data may again be satisfactorily explained in terms of only two parameters [5-7].

A general discussion of the determination of two or more parameters by curve-fitting, successive extrapolations, or other methods is given elsewhere [2,8]. This paper is restricted to the calculation of equilibrium constants for systems in which the experimental data are of the form $y(x)$, and which may be described in terms of only two parameters, p_1 and p_2, where p_1 fixes the position of the $y(x)$ curve on the x axis, and p_2 determines the shape of the curve. It is always possible to determine the values of p_1 and p_2 by direct curve-fitting [8], using the family of normalised curves $y(X)_{p_2}$, where

$$X = x + p_1 \tag{1}$$

An approximate value of p_2 may be obtained from the parameter of the calculated curve which gives the best fit, and the value of p_1 obtained from the experimental value of x corresponding to $X = 0$. The family of theoretical curves $y(X)_{p_2}$ is useful as a first approach for testing whether the experimental data are compatible with a certain hypothesis, and for recognising and correcting for systematic errors [8].

If the experimental $y(x)$ data are found to fit in with the family of theoretical $y(X)_{p_2}$ curves, the values of p_1 and p_2 may conveniently be refined by comparing a projection strip of the experimental $y(x)$ curve with the family of curves $p_2(X)_y$. The method is used as follows.

The experimental data (yx) are plotted using the same abscissa scale as in the family of curves $p_2(X)_y$. For each value of y tabulated, the corresponding value of x, together with the experimental uncertainty in this value, is marked off on the x axis (*cf.* Fig. 1a). This projection strip $(x)_y$ of the data $y(x)$ is then superimposed on the family of curves $p_2(X)_y$, parallel to the X axis, and in such a position that the best possible fit is obtained for all the values of y shown (*cf.* Fig. 1b).

The value of p_2 is then obtained as the ordinate, corresponding to the best position of the strip. The maximum limits of error in this value may be estimated from the vertical distance through which the projection strip may be moved, whilst allowing the calculated values of $(X)_y$ to remain within the experimental uncertainty. The value of p_1 is obtained as $(-x_0)$ where x_0 is read at the point of intersection of the p_2 axis ($X = 0$) with the projection strip (*cf.* eqn. 1). The maximum error in p_1 is then given by the permissible horizontal displacement of the strip. If data are only available in a very narrow range of y, a number of additional theoretical $p_1(X)_y$ curves may be calculated in this range. The value of p_2 can be found as described above, and the value of p_1 obtained by producing the projection strip to the point of intersection with the line ($X = 0$).

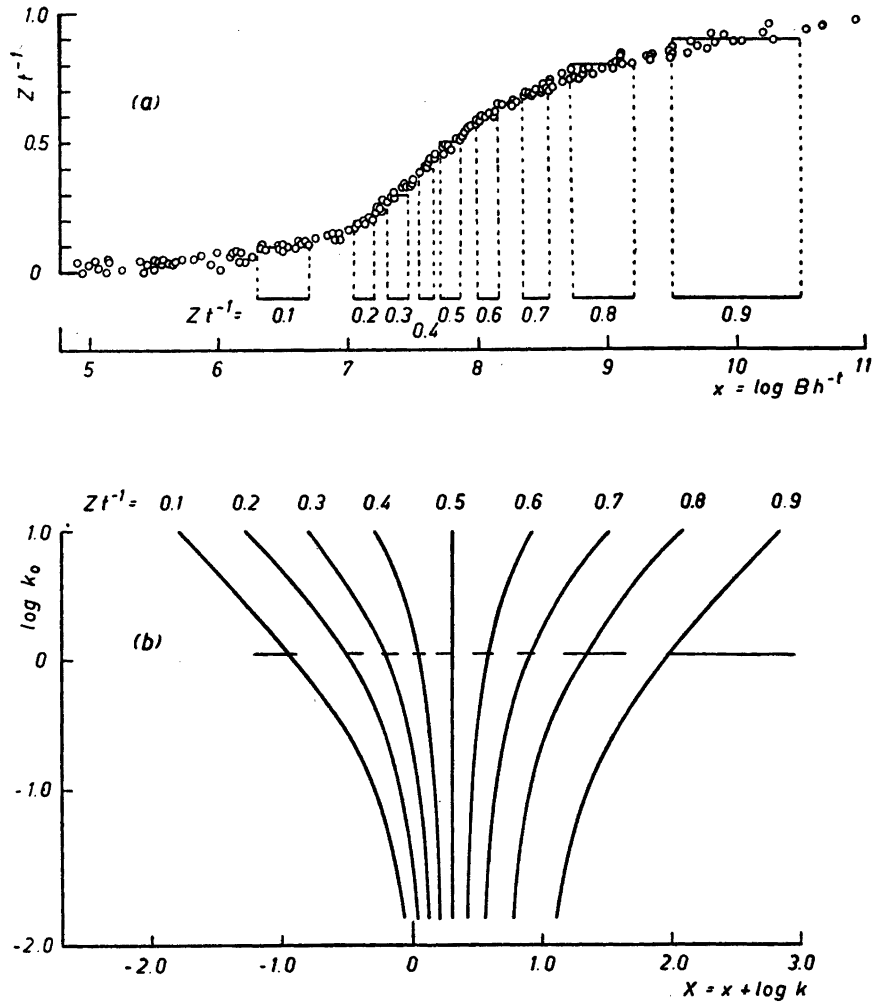


Fig. 1. The determination of the hydrolysis constants of the Th^{4+} ion in a 1.0 M perchlorate medium at 25° C. (a) Experimental curve $y = Zt^{-1}$ *as a function of* $x = \log Bh^{-t}$ *(Hietanen [12]) and projection strip. Points for different total concentrations of metal are not differentiated. (b) Projection strip of the* y(x) *curve superimposed on the family of theoretical curves log* $k_0(X)_y$, *in the position corresponding to log* $k_0 = +0.06$ *and log* $k = -7.53$.

When both p_1 and p_2 are known, the set of curves $p_2(X)_y$ may be used to calculate the theoretical curve $y(x)$. Values of X are obtained as the abscissae corresponding to the value of p_2 previously calculated, for a number of values of y. As p_1 is known, these values of X may then be substituted into equation (1) to give values of x.

The present method for calculating the parameters is no less accurate than those described elsewhere [2,8], and may be used much more rapidly, once

a preliminary check with the $y(X)_{p_2}$ curves has been made. Moreover, it may give a clearer estimate of the limits of error in the values of p_1 and p_2 obtained. Its application to the determination of equilibrium constants in systems of polynuclear hydroxyl complexes is described below. The adaptation of the treatment to other two-parameter systems is also indicated.

LIST OF SYMBOLS

B	total concentration of metal ions
b	concentration of free metal ions
H	total analytical excess concentration of hydrogen ions, assuming no hydrolysis
h	concentration of free hydrogen ions
K_n	stability constant of complex ML_n, defined by $K_n = [ML_n]/[ML_{n-1}][L]$
k	equilibrium constant, defined by $k = k_{n+1}\, k_n^{-1}$ (Hypothesis IIIa)
k_n	equilibrium constant, defined by $[Me((OH)_tMe)_n]/b^{n+1}h^{-t}$
k_0	equilibrium constant, defined by $k_0 = k_n k^{-n}$ (Hypothesis IIIa)
N	maximum value of n (mononuclear systems)
n	number of L groups in complex ML_n, or number of $Me(OH)_t$ "links" in "core + links" complex, $Me((OH)_tMe)_n$
$\bar{n}$	average value of n
P	maximum value of p
p	number of L groups in complex M_qL_p
p_1	parameter determining position of $y(x)$ curve on x axis
p_2	parameter determining shape of $y(x)$ curve
Q	maximum value of q
q	number of M groups in complex M_qL_p
t	number of hydroxyl groups per metal ion in "link", $Me(OH)_t$
$X =$	$x + \log k$
$x =$	abscissa of experimental curve
$x_{\frac{1}{2}} =$	value of x corresponding to $y = \frac{1}{2}$
$y =$	ordinate of experimental curve
Z	average number of hydroxyl groups per metal ion $= (H\text{-}h)B^{-1}$
α_S	fraction of total metal in the form $ML_S = [ML_S]/\sum_{n=0}^{n=N} [ML_n]$
$\eta =$	$\log Bb^{-1}$
$\beta_n =$	$\prod_1^n K_n$

THE CALCULATION OF EQUILIBRIUM CONSTANTS OF POLYNUCLEAR "CORE + LINKS" COMPLEXES

Previous work in this laboratory has indicated that the main products of hydrolysis of many metal ions, Me, are polynuclear "core + links" hydroxyl-complexes, of general formula $Me((OH)_tMe)_n$, where n is variable and t constant (Ref.[9] and refs. therein). A treatment of equilibria involving complexes of this type, together with methods for obtaining the value of t has been given elsewhere [7,10]. The equilibrium constant $k_n = [Me((OH)_tMe)_n]/[Me]^{n+1}[H]^{-t}$ for the formation of the complex $Me((OH)_tMe)_n$ may then be determined if certain

simplifying assumptions are made [7]. Potentiometric measurements for a number of systems, *e. g.*[11-14] may be explained by assuming that complexes with all positive integral values of n are formed, and that the ratio of successive equilibrium constants k_n/k_{n+1}, is constant ([7] hypothesis IIIa). The system may then be approximately described in terms of two parameters, k and k_0, such that

$$p_1 = \log\ k = \log\ k_{n+1} - \log\ k_n \tag{2}$$

and

$$p_2 = \log\ k_0 = \log\ k_n - n\ \log\ k \tag{3}$$

These parameters may readily be determined by the method described above.

Treatment of the data B, H, h

If the total concentrations of metal, B, and hydrogen, H, and the concentration of free hydrogen ions, h, are known, it is convenient to plot $Z = (H\text{-}h)B^{-1}$ as a function of $\log h$. If only "core + links" complexes are formed in appreciable amounts, the curves $Z(\log h)_B$ will be parallel, and the value of t may be determined from the spacing between them [10]. When $y = Z/t$ is plotted against $x = \log Bh^{-t}$, the experimental points fall on a single curve, which may often be approximately represented in terms of two parameters (*cf.* (2) and (3)). The shape of the curve is determined by the value of $\log k_0$ (parameter p_2) and its position on the x axis by the value of $\log k$ (parameter p_1).

If the experimental curve $y(x)$ is found to fit in with a set of theoretical curves, calculated for a few widely separated values of k_0 assuming hypothesis IIIa (*cf.*[7], Fig. 2a), the value of k_0 may be calculated by one of the methods described previously [7]:

a) The shape of the experimental curve may be compared with $y(X)$ curves calculated for different values of k_0,

where

$$X = x + \log\ k \tag{4}$$

This method makes use of the whole range of experimental data, and as it has the further advantage of revealing systematic errors in y, it is a good first approach. For subsequent refining of the parameters it is somewhat time-consuming, as fresh curves will usually have to be calculated for values of k_0 not already available.

b) The value of k_0 may be calculated from corresponding values of y and x, using the equation

$$k_0 = y\ [1-10^X\ (1-y)]^2\ [10^X\ (1-2y)^2]^{-1} \tag{5}$$

where

$$X = \log\ 2 + x-x_{\frac{1}{2}} \tag{6}$$

and where $x_{\frac{1}{2}}$ is the value of x for $y = \frac{1}{2}$. If full use is to be made of the data, k_0 should be calculated for many values of y, and this method would also be rather laborious.

c) The slope of the curve $y(x)$ at the point $y = \frac{1}{2}$ is given by

$$(\mathrm{d}y/\mathrm{d}x)_{y=\frac{1}{2}} = \tfrac{1}{2}\ \ln\ 10 \cdot (1 + 2\sqrt{k_0})^{-1} \tag{7}$$

Even if the data are of the highest precision and extend to values of $y > \frac{1}{2}$, it may be difficult to measure this slope with any great accuracy. Moreover, this method only uses data in one small region of the curve, and does not indicate whether the value of k_0 so obtained gives a good description of the curve as a whole.

The value of log k has previously been calculated from the relationship [7] obtained by combining eqns. (4) and (6)

$$\log k = \log 2 - x_{\frac{1}{2}} \tag{8}$$

but as the value of $x_{\frac{1}{2}}$ is obtained directly from the midpoint of the $y(x)$ curve, this method does not make full use of all the experimental data.

Values of k_0 may be obtained rapidly by the present method, which makes use of the set of theoretical curves log $k_0(X)_y$. Corresponding values of log k_0 and X have been calculated for different values of y, using equation (5), and are shown in Table 1 and Fig. 1b.

Table 1. The function log $k_0 (X)_{Zt^{-1}}$ *for hypothesis IIIa.*

log k_0	$(X)_{0.1}$	$(X)_{0.2}$	$(X)_{0.3}$	$(X)_{0.4}$	$(X)_{0.5}$	$(X)_{0.6}$	$(X)_{0.7}$	$(X)_{0.8}$	$(X)_{0.9}$
−2.000	−0.071	0.033	0.117	0.204	0.301	0.415	0.562	0.766	1.109
−1.699	−0.115	0.005	0.101	0.197	0.301	0.423	0.573	0.792	1.167
−1.301	−0.210	−0.048	0.070	0.182	0.301	0.438	0.608	0.843	1.256
−1.000	−0.303	−0.107	0.035	0.166	0.301	0.454	0.642	0.903	1.356
−1.699	−0.445	−0.189	−0.012	0.143	0.301	0.477	0.693	0.986	1.494
−0.301	−0.684	−0.344	−0.109	0.097	0.301	0.523	0.787	1.140	1.731
0.301	−1.166	−0.708	−0.353	−0.026	0.301	0.646	1.029	1.502	2.208
0.699	−1.529	−1.022	−0.594	−0.162	0.301	0.718	1.274	1.819	2.565
1.000	−1.812	−1.289	−0.823	−0.306	0.301	0.925	1.501	2.088	2.863

As an illustration of the method described above, values of k_0 and k have been calculated for the products of hydrolysis of the ions Th^{4+}, UO_2^{2+} and In^{3+}, and are compared with the values obtained by the original authors, *cf.* pp. 210-211.

When the values of both k_0 and k are known, the theoretical curve $y = Zt^{-1}$ as a function of $x = \log Bh^{-i}$ may be calculated rapidly with the aid of Fig. 1b. For a given value of log k_0, values of X may be obtained from the curves for the values of y tabulated. As log k is also known, these values may be substituted into eqn. (4) to give values of x.

Treatment of the data B, H, b and h

If the free concentrations of both metal ions, b, and hydrogen ions, h, can be measured, the data may be plotted in the form $\eta = \log Bb^{-1}$, as a function of log h. If "core + links" complexes predominate, the curves η (log $h)_B$ are parallel, and the value of t may be obtained from the spacing between them [10]. When $y = \eta$ is plotted as a function of $x = \log Bh^{-i}$, the experimental points will therefore lie on a single curve which may approximately be described in terms of the parameters log k_0 and log k (eqns. (2) and (3)).

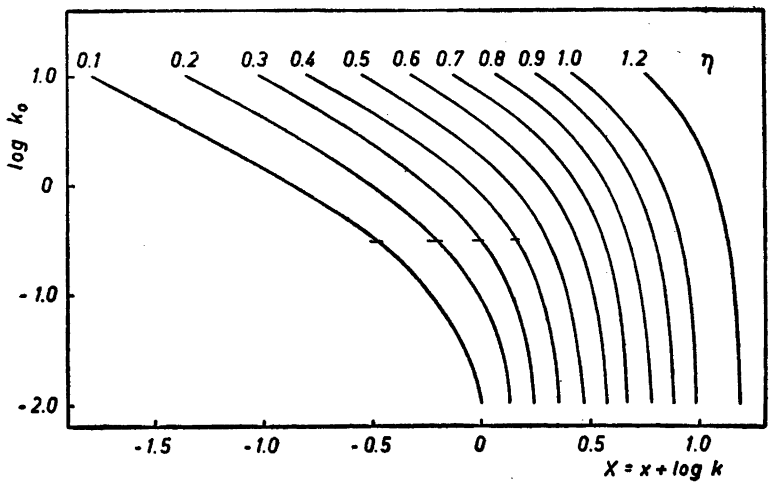


Fig. 2. The determination of the hydrolysis constants of the In^{3+} ion in a 3.0 M perchlorate medium at 25° C. Projection strip of plot of $y = \eta$ *against* $x = \log Bh^{-t}$ *(Biedermann [14]) superimposed on the family of theoretical curves* $\log k_0 (X)_\eta$ *in the position corresponding to* $\log k_0 = -0.50$ *and* $\log k = -4.70$.

The present method for determining these parameters may again be more convenient than that [7] of calculating theoretical curves $\eta(X)$ for hypothesis IIIa to compare with the experimental data $\eta(x)$. Corresponding values of log k_0 and X have been calculated for different values of η, using the equation [7]

$$X = \log \left(1 - \sqrt{\frac{k_0}{10^\eta - 1 + k_0}}\right) + \eta \qquad (9)$$

and are given in Table 2.

The experimental curve $\eta(\log Bh^{-t})$ is plotted using the same abscissa scale as for the curves $\log k_0(X)_\eta$, and a projection strip on the x axis is prepared as before. The values of $\log k_0$ and $\log k$, together with the limits of error, are then obtained by a method exactly analogous to that described above (*cf.* Fig. 2). The method has been applied to the hydrolysis of the In^{3+} ion and the results are given on p. 211.

Fig. 2 may also be used to construct theoretical $\eta(x)$ curves for systems in which k_0 and k are known. From the intersection of the curves with the horizontal line at the required value of $\log k_0$, a number of corresponding values (X, y) are obtained. The corresponding values of x are given by $X = x + \log k$ (eqn. 4).

The experimental data B, H, b and h could also be plotted in the form $\eta(x—\eta)$, and curves of this type could be treated analogously by means of a set of curves $\log k_0(x - \eta)_\eta$.

Table 2. The function $\log k_0\ (X)_\eta$ *for hypothesis IIIa.*

$\log k_0$	$(X)_{0.1}$	$(X)_{0.2}$	$(X)_{0.3}$	$(X)_{0.4}$	$(X)_{0.5}$	$(X)_{0.6}$	$(X)_{0.7}$	$(X)_{0.8}$	$(X)_{0.9}$	$(X)_{1.0}$	$(X)_{1.2}$
−2.000	0.007	0.140	0.254	0.363	0.469	0.574	0.678	0.781	0.883	0.985	1.189
−1.699	−0.035	0.113	0.234	0.347	0.456	0.563	0.668	0.772	0.876	0.979	1.184
−1.301	−0.123	0.057	0.193	0.314	0.429	0.540	0.649	0.756	0.862	0.966	1.174
−1.000	−0.226	−0.009	0.144	0.276	0.397	0.514	0.626	0.737	0.845	0.952	1.163
−0.699	−0.368	−0.105	0.071	0.218	0.351	0.475	0.593	0.708	0.820	0.931	1.147
−0.301	−0.625	−0.293	−0.075	0.100	0.253	0.393	0.524	0.649	0.770	0.887	1.114
0.000	−0.864	−0.487	−0.234	−0.033	0.141	0.298	0.443	0.579	0.710	9.835	1.074
0.301	−1.128	−0.719	−0.438	−0.210	−0.013	0.164	0.326	0.478	0.622	0.759	1.016
0.699	−1.504	−1.008	−0.761	−0.508	−0.284	−0.081	0.107	0.282	0.448	0.605	0.897
1.000	−1.796	−1.353	−1.034	−0.767	−0.530	−0.313	−0.109	0.083	0.265	0.439	0.763

Application of the method to the hydrolysis of some metal ions

It has previously been found [12–14] that the experimental Zt^{-1} (log Bh^{-t}) curves for the ions Th^{4+}, UO_2^{2+} and In^{3+}, and the log Bb^{-1} (log Bh^{-t}) curve for In^{3+} fitted in with the appropriate families of theoretical curves [7], calculated assuming hypothesis IIIa. Values of log k_0 and log k have now been calculated from the theoretical curves by the method described above. The limits of error quoted represent the maximum uncertainly both of individual measurements and of the validity of hypothesis IIIa. The preparation of a projection strip for a system, and the determination of the constants may be carried out in about ten minutes, once the diagrams $y(x)$ and $\eta(x)$ are available.

The Th^{4+} *ion.* The experimental curve [12], $y = Zt^{-1}$ as a function of $x = \log Bh^{-t}$, and the projection strip obtained from it, are shown in Fig. 1a. In Fig. 1b, the strip is superimposed on the family of curves log $k_0(X)_y$. The best fit is obtained with the following values of the constants, which are in satisfactory agreement with those given by Hietanen [12].

Present method	$\log k_0 = +0.06 \pm 0.04$	$\log k = -7.53 \pm 0.05$
Hietanen [12]	$\log k_0 = -0.15 \pm 0.15$	$\log k = -7.50$

The UO_2^{2+} *ion.* The projection strip of the experimental curve, $y = Zt^{-1}$ as a function of $x = \log Bh^{-t}$, for the hydrolysis of the uranyl ion [13] is shown in Fig. 3a. Using Fig. 1b and eqn. (4), the following values were obtained, in good agreement with those previously calculated [13]

Present method	$\log k_0 = 0.3 \pm 0.3$	$\log k = -6.40 \pm 0.18$
Ahrland, Hietanen and Sillén [13]	$\log k_0 = 0.3$	$\log k = -6.35 \pm 0.10$

The In^{3+} *ion.* The projection strip of $y = Zt^{-1}$ as a function of $x = \log Bh^{-t}$ for the hydrolysis of the In^{3+} ion [14] is shown in Fig. 3b, and the constants obtained using the family of curves log $k_0(X)_y$ are given below. As the concentration of free indium ions, b, could be measured, the constants

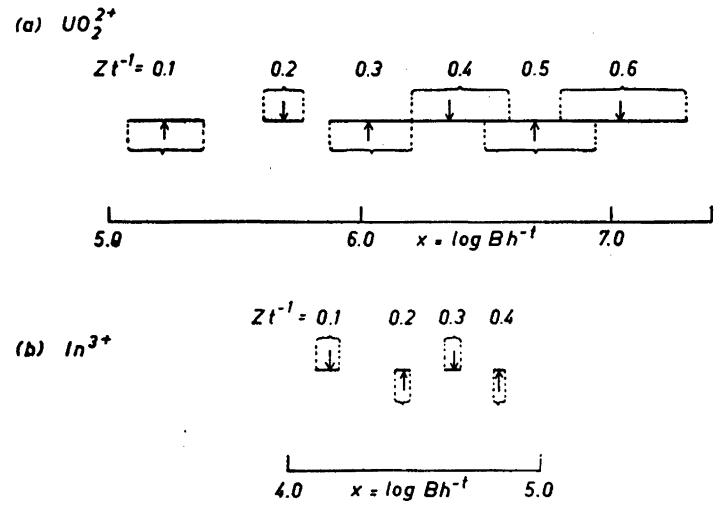


Fig. 3. Projection strips of plots of $y = Zt^{-1}$ *as a function of* $x = \log Bh^{-t}$ *for the hydrolysis of metal ions. (a) The ion* UO_2^{2+} *in a 1.0 M perchlorate medium at 20° C. The experimental curve* y(x) *is taken from Ahrland, Hietanen and Sillén*[13]. *The arrows indicate the points of intersection of the family of theoretical curves log* $k_0(X)_y$ *with the strip in the position corresponding to log* $k_0 = 0.3$ *and log* $k = -6.40$. *(b) The ion* In^{3+} *in a 3.0 M perchlorate medium at 25° C. The experimental* y(x) *curve is taken from Biedermann*[14]. *The arrows indicate the points of intersection of the family of theoretical curves log* k_0 $(X)_y$ *with the strip in the position corresponding to log* $k_0 = -0.5$ *and log* $k = -4.72$.

may also be calculated from the experimental curve $y = \eta$ as a function of $x = \log Bh^{-t}$. The projection strip of this curve is superimposed on the set of curves log $k_0(X)_\eta$ in Fig. 2

	log k_0	log k
Present method Zt^{-1} (x)	-0.5 ± 0.1	-4.72 ± 0.04
Present method η (x)	-0.5 ± 0.1	-4.70 ± 0.05
Biedermann [14]	-0.52	-4.70 ± 0.05

The constants obtained by the present method are in excellent agreement with those calculated by Biedermann [14].

DISCUSSION

Comparison of the sets of curves log $k_0(X)_{Zt^{-1}}$ and log $k_0(X)_\eta$ shown in Figs. 1b and 2b emphasizes that the value of k_0 has a much greater influence on the shape of the former set. Thus, small uncertainties in the experimental curve η (x) lead to much greater uncertainties in k_0 than do small uncertainties in the curve $Zt^{-1}(x)$. If h and b could be determined with equal precision, constants calculated from the curves Zt^{-1} (x) would probably be more reliable than those obtained from $\eta(x)$ curves, although curves of both types are valuable for determining the nature of the species in solution. However, it is sometimes

possible to measure b with much greater accuracy than h, and in such cases the curves Zt^{-1} (x) and $\eta(x)$ may be of comparable value for the determination of the constants.

The shape of the curves $\eta(x-\eta)$ is also influenced by the value of $\log k_0$ to a greater extent than the shape of the curves $\eta(x)$, but the $\eta(x-\eta)$ curves have the disadvantage that any experimental uncertainty in η appears in both the value of the ordinate and the abscissa. The curves are therefore less suitable for determining equilibrium constants than are Zt^{-1} (x) and η (x) curves, especially if the data are not of the highest precision. The present method could also be readily adapted for use with hypotheses other than IIIa provided that not more than two parameters are required to describe a system.

ADAPTATION OF THE METHOD TO OTHER TWO-PARAMETER SYSTEMS

Several other types of experimental curves $y(x)$ may also be described, either rigorously or approximately, in terms of only two parameters, p_1 and p_2, such that p_2 determines the shape of the curve, and p_1 fixes its position on the x axis. If the curve $y(x)$ is found to fit in with the family of theoretical curves $y(X)_{p_2}$, small systematic errors may be corrected for, and approximate values of p_1 and p_2 obtained [8]. These values may be refined by superimposing a projection strip of the experimental $y(x)$ curve on the family of theoretical curves $p_2(X)_y$, as described above.

Systems of mononuclear complexes

If $N>2$ mononuclear complexes are formed, the experimental data may be plotted in the form $y(x)$, where

$$y = \bar{n} = \frac{\sum_{n=1}^{n=N} n[\mathrm{ML}_n]}{\sum_{n=0}^{n=N} [\mathrm{ML}_n]} = \frac{\sum_{n=1}^{n=N} n\beta_n[\mathrm{L}]^n}{\sum_{n=0}^{n=N} \beta_n[\mathrm{L}]^n} \tag{10}$$

or

$$y = \log \alpha_S = \log \frac{[\mathrm{ML}_S]}{\sum_{n=0}^{n=N} [\mathrm{ML}_n]} = \log \frac{\beta_S[\mathrm{L}]^S}{\sum_{n=0}^{n=N} \beta_n[\mathrm{L}]^n} \tag{11}$$

and

$$x = \log [\mathrm{L}] \tag{12}$$

Here $0 \leqslant S \leqslant N$ and $\beta_n = \prod_1^n K_n$. If the species ML_S is distributed between two phases, the term α_S may be obtained from partition data, provided that the value of the partition coefficient $[\mathrm{ML}_S]_{org}/[\mathrm{ML}_S]_{aq}$ can be determined; and if $S = 0$, α_S may be measured potentiometrically by means of an electrode which is reversible to free metal ions.

The present method can only be used if the number of parameters can be reduced to two by some assumption about the relationship between successive stability constants K_n. For example, if the ratio $K_n K_{n+1}^{-1}$ is fixed ($= k$), or a function of n ($= k\ \psi\ (n)$), the parameters p_1 and p_2 may be chosen as

$$p_1 = \frac{1}{N} \sum_{n=1}^{n=N} \log K_N = \frac{1}{N} \log \beta_N \tag{13}$$

and

$$p_2 = \tfrac{1}{2}\log \left\{K_n K_{n+1}^{-1}/\psi(n)\right\} = \log \left\{\beta_n^2 \beta_{n+1}^{-1} \beta_{n-1}^{-1} \,/\, \psi(n)\right\} \tag{14}$$

Then from eqns. (1), (12), and (13)

$$X = \log\ [\mathrm{L}] + \frac{1}{N} \log\ \beta_N \tag{15}$$

Although it would be possible to devise equations for the "statistical" case [15], where

$$\psi\ (n) = \frac{(N-n+1)\ (n+1)}{(N-n)\ n} \tag{16}$$

the present discussion will be limited to Dyrssen and Sillén's simpler approximation [3] that $\psi\ (n) = 1$.
In this case

$$\log\ \beta_n = n\ p_1 + n(N-n)p_2 \tag{17}$$

and from eqns. (13) and (15)

$$\log\ [\mathrm{L}] = X - p_1 \tag{18}$$

Whence

$$\log\ \beta_n\ [\mathrm{L}]^n = n\ \left\{X + p_2\ (N-n)\right\} \tag{19}$$

and y may be expressed in terms of p_2, S and N, and of the normalised variable X.

Thus

$$y = \bar{n} = \frac{\sum_{n=1}^{n=N} n 10^{n\{X+p_2(N-n)\}}}{\sum_{n=0}^{n=N} 10^{n\{X+p_2(N-n)\}}} \tag{20}$$

and

$$\log\ \alpha_S = S\left\{X + p_2(N-S)\right\} - \log \sum_{n=0}^{n=N} 10^{n\{X+p_2(N-n)\}} \tag{21}$$

Approximate values of p_1 and p_2 may be found by direct comparison of the experimental data $y(x)$ with the set of curves $\bar{n}\ (X)_{p_2}$ or $\log\ \alpha_S(X)_{p_2}$, calculated from eqns. (20) and (21) using the appropriate value of N and S. The values of p_1 and p_2 may very conveniently be refined using the projection strip method, and the set of curves $p_2(X)_{\bar{n}}$ or $p_2(X)_{\log\ \alpha_S}$.

If only two mononuclear complexes, ML and ML_2 are formed, the system may be rigorously defined in terms of the two parameters

$$p_1 = \tfrac{1}{2}\ \log\ K_1 K_2 = \tfrac{1}{2}\ \log\ \beta_2 \tag{13a}$$

and

$$p_2 = \tfrac{1}{2}\ \log\ K_1 K_2^{-1} = \log\ \beta_1 \beta_2^{-\frac{1}{2}} \tag{14a}$$

In eqns. (13a) and (14a) $(\frac{1}{2} \cdot 10^{p_2})$ is the spreading factor, and 10^{p_1} is the average constant, defined by J. Bjerrum [15].

When $N = 2$, equation (20) reduces to

$$\bar{n} = \frac{10^{X+p_2} + 2.\ 10^{2X}}{1 + 10^{X+p_2} + 10^{2X}} \tag{20a}$$

If p_2 is defined alternatively as $\sqrt{K_1 K_2^{-1}}$, eqn. (20a) reduces to eqn. (14) in Part II [8].

Accurate values of p_1 and p_2 may be determined using the projection strip method, as described above. A somewhat similar device, which makes use of the symmetrical properties of the $\bar{n}$ (x) curves for systems of this type, has been described previously [1].

We wish to thank the *Swedish Natural Science Research Council* for financial assistance.

REFERENCES

1. Irving, H. and Rossotti, H. S. *J. Chem. Soc.* **1953** 3397.
2. Rossotti, F. J. C. and Rossotti, H. S. *Acta Chem. Scand.* **9** (1955) 1166 (Part I).
3. Dyrssen, D. and Sillén, L. G. *Acta Chem. Scand.* **7** (1953) 663.
4. Hedström, B. O. A. *Acta Chem. Scand.* **9** (1955) 613.
5. Granér, F. and Sillén, L. G. *Acta Chem. Scand.* **1** (1947) 631.
6. Connick, R. E. and Reas, W. H. *J. Am. Chem. Soc.* **73** (1951) 1171.
7. Sillén, L. G. *Acta Chem. Scand.* **8** (1954) 318.
8. Sillén, L. G. *Acta Chem. Scand.* **10** (1956) 186 (Part II).
9. Sillén, L. G. *Rec. trav. chim.* **75** (1956). *In the press.*
10. Sillén, L. G. *Acta Chem. Scand.* **8** (1954) 299.
11. Hietanen, S. and Sillén, L. G. *Acta Chem. Scand.* **8** (1954) 1607.
12. Hietanen, S. *Acta Chem. Scand.* **8** (1954) 1626.
13. Ahrland, S., Hietanen, S. and Sillén, L. G. *Acta Chem. Scand.* **8** (1954) 1907.
14. Biedermann, G. *Arkiv Kemi* **9** (1956) 277.
15. Bjerrum, J. *Diss.* Copenhagen 1941.

Received November 3, 1955.

ACTA CHEMICA SCANDINAVICA 10 (1956) 215—226

Studies on the Interaction of Paraffin Chain Alcohols and Association Colloids

IV. The Effect of Decanol-1 on the Viscosities of Some Association Colloid Solutions

KAAPO PASSINEN and PER EKWALL

Institute of Physical Chemistry, Åbo Akademi, Åbo, Finland

The effect of decanol on the viscosities of solutions of sodium oleate, sodium lauryl sulphate and sodium myristyl sulphate has been studied. When the oleate concentration is low, below about 0.2 *M*, the viscosity increases slowly with the amount of decanol added and the viscosity curve reveals no noticeable irregularities at the turbidity point where a new phase composed of decanol, oleate and water begins to separate. At higher oleate concentrations three ranges can be distinguished in which the effect of decanol on the viscosity differs depending on the amount of decanol added. As long as all the decanol is solubilized in the micelles, the viscosity increases. When the new phase appears, the viscosity decreases at first as decanol is added, then passes through a minimum and begins to increase again when more decanol is added. Some observations on the effect of *p*-xylene on the viscosity of a sodium oleate solution have also been made. The factors which determine the observed variation of the viscosity are discussed. In homogeneous systems at low oleate concentrations the increase in the viscosity caused by decanol (or xylene) can be fairly well explained on the assumption of an increase in the micelle volume; at higher oleate concentrations (above *ca.* 0.2 *M*) large changes in the form and the structure of the micelles must be assumed. The decrease in the viscosity in the heterogeneous systems depends on the decrease in the concentration of the mixed micelles in the aqueous solution caused by the separation of the new phase. When the amount of this new phase becomes so large that it influences strongly the flow of the solution, the viscosity begins to increase rapidly.

The viscosities of solutions of association colloids with and without added inorganic salts have been thoroughly investigated, but the effect of solubilized substances on the viscosities of association colloid solutions has not been systematically studied.

The effect of lower paraffin chain alcohols was investigated by Bose and coworkers [1-5] (methanol to hexanol, different soaps, sodium chloride) and by Rossi and Ragno [6] (ethanol, sodium oleate). The measurements were carried out on clear homogeneous solutions; the alcohol contents used were very high, between 10 and 50 % of the volumes of the soap solutions. The alcohols caused an increase in the viscosity; in some cases Bose observed that the viscosity decreased when greater amounts of alcohol were added. The effect of higher alcohols seems to have been studied only by Klevens [7] (octanol, potassium myristate, potassium chloride), de Jong and van Alphen [8] (methanol to octanol, sodium oleate, potassium chloride) and Ekwall, Passinen and Danielsson [9] (decanol, sodium oleate). The qualitative observations of Klevens show that in myristate solutions containing potassium chloride the viscosity increases with the amount of octanol, passes through a maximum and then begins to decrease; the maximum appears at an octanol content less than that required to effect turbidity. Also Ekwall and coworkers observed a viscosity maximum but this maximum occurs at the point where the system becomes heterogeneous; their solutions contained no added inorganic electrolyte.

The effect of polar-nonpolar compounds other than alkanols has also been studied. Thus, Angelescu and coworkers [10-12] studied the effect of different cresols on the viscosities of some soap solutions. They found that the viscosity increases slowly with the amount of cresol added when the soap concentration is low. At higher soap concentrations, the viscosity increases rapidly to a maximum, then decreases to a minimum and subsequently begins to increase slowly as the amount of cresol is increased further. All the systems studied were homogeneous. The effect of cresols on the viscosities of solutions of soap mixtures was also studied [13]; the viscosity curves were similar in form to those for solutions of the single soaps. Angelescu and coworkers studied also the joint effect of fatty acid and cresol [14] and of electrolytes and cresol [15] and the effect of some other substances [16, 17] (phenol, hydroquinone, resorcinol, nitrophenol, aminophenol, naphthol). In most cases curves similar to those obtained with cresol were obtained, but in some cases no maximum was observed. Philippoff [18] studied the effect of *m*-cresol on the viscosity of a 0.45 *M* sodium oleate solution and found that the viscosity increases with the amount of cresol added, then passes a maximum and begins to decrease. He also established that the addition of cresol effects a pronounced structural viscosity. Ekwall and Henriksson [19] found that the addition of terpineol first effects a pronounced increase in the viscosity of a 0.3 *M* sodium oleate solution, and as more terpineol is added, the system becomes heterogeneous and the viscosity of the system decreases rapidly, goes through a minimum, passes a second less pronounced maximum and finally remains approximately constant. McBain and McHan [20] showed that a 0.10 *M* potassium laurate solution saturated with dimethyl phthalate has a slightly greater viscosity than the pure laurate solution.

Some observations on the effect of solubilized nonpolar compounds have also been made. Hahne [21] and Kiessig and Philippoff [22] studied the effect of benzene on a sodium oleate solution (0.3 *M*) and found that the viscosity first increases rapidly to a maximum when benzene is added, decreases then to a minimum and finally increases slowly. The maximum in the viscosity curve appears at a benzene content much below the solubility value. When the system becomes saturated with benzene, addition of more benzene does not effect any further change of viscosity. No structural viscosity was established in the pure oleate solution, in the solution of maximum viscosity, or in the system saturated with benzene [22]. Stainsby and Alexander [23] found that the addition of chlorobenzene produces marked changes in the viscosities of hexadecyl pyridinium chloride solutions.

It thus seems to be typical of the effect of solubilization on the viscosity that the viscosity attains a maximum when a certain amount of solubilizate has been added. In most cases this maximum occurred in homogeneous systems [7, 10-18, 21, 22] but in two cases it appeared at the point where the system became heterogeneous [9, 19]. The results are complicated by the fact that the systems studied have in most cases contained varying amounts of inorganic electrolytes in addition to association colloid, the solubilized substance and water.

The purpose of the present work was to study the effect of a relatively long paraffin chain alcohol, decanol-1, on the viscosity of association colloid solutions without any other additives and to correlate these data with our previous studies of the solubility of decanol and the effect of decanol on the electrical conductance of these same solutions (Part I [24], Part II [25] and Part III [26] of this series). Some experiments have also been made with the purpose of comparing the effect of solubilization of a hydrocarbon on the viscosity with that of decanol.

MATERIALS AND METHODS

The compounds used were those employed in our previous studies [24-26]. The solutions were prepared in the manner described in Part I[24]. They were shaken at 40° C for periods from three to six days.

The viscosities were measured with an Ostwald viscosimeter. The temperature was held constant at 40° C ± 0.05° C. The viscosity of each solution was measured three times, and the average values were recorded. The viscosities are relative viscosities, η_{rel} (water = 1). The relative viscosity values are accurate to ± 0.5 to 1 %. When the value of $\eta_{rel} = (d_s/d_w)/(t_s/t_w)$, where d_s and d_w are the densities of the solution and water, and t_s and t_w the times of flow of the solution and water, respectively, was calculated, the density ratio d_s/d_w was taken to be unity.

The concentration of the association colloid is given in moles per 1 000 g of solution (denoted by M).

EXPERIMENTAL RESULTS

Sodium oleate solutions containing decanol. The effect of decanol on the viscosities of sodium oleate solutions has been studied at oleate concentrations between 0.05 and 0.3 M (Fig. 1). When the oleate concentration is low, below approximately 0.15 M, the viscosity increases slowly as the amount of decanol is increased. In these dilutions no marked change is observed in the course of the viscosity curve at the point where the addition of decanol effects the separation of a new phase. When the oleate concentration is 0.189 M, the rise of the viscosity curve is slightly arrested in this region. When the oleate concentration is above 0.2 M, the viscosity rises rapidly as long as the decanol added is solubilized in the micelles. When the amount of decanol is so great that the system becomes heterogeneous, the viscosity begins to decrease with increasing amount of decanol added, then passes a minimum and finally increases again rapidly. When more decanol is added the system becomes gel-like.

Thus, at oleate concentrations above 0.2 M, three different regions can be distinguished in which the effect of decanol on the viscosity of the oleate solutions differs. There is first a region where an addition of decanol increases the viscosity, then a region where the viscosity decreases and finally a region where the viscosity increases again as more decanol is added. The boundary between the first and second region coincides with the point where the system becomes heterogeneous owing to the separation of a new phase composed of decanol, oleate and water (turbidity point) and above which the electrical conductance of the solution undergoes an abrupt decrease [25]. The minimum in the viscosity curve appears at a decanol content of approximately 0.3—0.4 mole of decanol per mole of oleate and in the vicinity of the turbidity maximum in the same system [25]; the experimental data are, however, too meagre to permit a

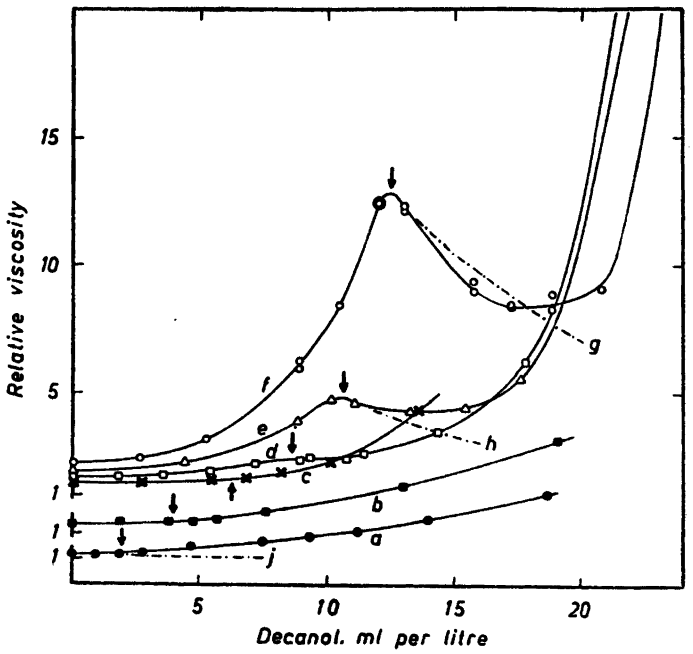


Fig. 1. Relative viscosities of sodium oleate solutions containing decanol. 40° C. The arrows indicate the points where the systems become heterogeneous.

a) 0.0493 M *sodium oleate*
b) 0.0972 M » »
c) 0.143 M » »
d) 0.189 M » »
e) 0.232 M » »
f) 0.275 M » »
g—j) Calculated curves (see text, p. 224)

decision whether viscosity minimum and turbidity maximum always coincide. In every case the viscosity minimum appears at a much lower decanol content than that at which the electrical conductance becomes constant (see Part II[25]); *e. g.* in a 0.232 *M* oleate solution the viscosity minimum occurs when 14 ml of decanol have been added per litre of solution, whereas the conductance becomes constant when approximately 30 ml of decanol have been added per litre.

The curves in Fig. 2 show how the effect of decanol on the viscosity varies with the concentration of oleate. Curve *a* gives the viscosities of the pure oleate solutions and is of the type generally found for the concentration dependence of the viscosity in solutions of association colloids. It increases slowly and linearly to a concentration of about 0.2 *M* and then begins to increase more rapidly. Curve *b* gives the viscosities of the oleate solutions containing decanol at the turbidity point, and curve *c* the viscosities of solutions containing 0.10 mole of decanol per mole of oleate. The difference between the

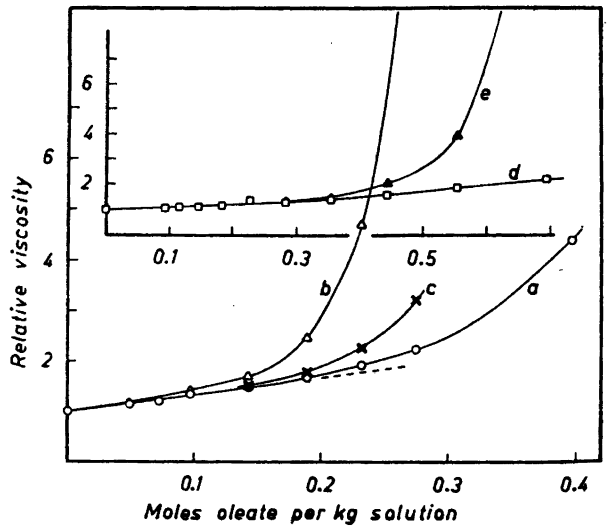


Fig. 2. *a) Relative viscosities of pure sodium oleate solutions. 40° C.*
b) Relative viscosities of sodium oleate solutions containing decanol at the turbidity points. 40° C.
c) Relative viscosities of sodium oleate solutions containing 0.10 mole of decanol per mole of oleate. 40° C.
d) Relative viscosities of pure sodium lauryl sulphate solutions. 40° C.
e) Relative viscosities of sodium lauryl sulphate solutions containing 0.116 mole of decanol per mole of lauryl sulphate. 40° C.

viscosity values of curves *b* and *a*, the increase in viscosity at the turbidity point, is very small up to an oleate concentration of about 0.15 *M*, but above this limit the difference increases rapidly with the oleate concentration. In respect of the oleate concentration there are thus two regions, the first up to a concentration of about 0.15 *M* and the second above this limit where the effect of decanol on the viscosity differs greatly.

Sodium oleate solutions containing p-*xylene.* The viscosities of a series of 0.200 *M* oleate solutions containing various amounts of *p*-xylene were also measured (Fig. 3, curve *a*). The viscosity rises slowly and nearly linearly with increasing additions of xylene up to a point close to the solubility limit of xylene where it becomes approximately constant. The increase of viscosity caused by xylene is much smaller than that caused by the same volume of decanol (Fig. 3, curve *b*).

The specific volumes of sodium oleate solutions containing decanol. In order to determine whether the density ratio d_s/d_w can be taken as unity in the calculation of the relative viscosities, the densities of oleate solutions containing decanol were measured. Fig. 4, curve *a*, shows that the specific volume of a 0.300 *M* solution increases linearly with the amount of decanol added until the new phase is formed; at the latter point the curve changes its slope and continues again as a straight line. The density ratio is seen to be very near unity even for the highest decanol contents. Curve *b* shows the variation of the

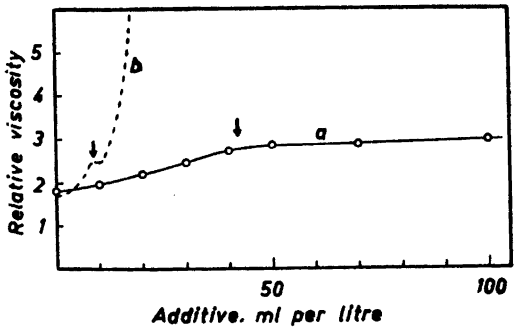


Fig. 3. a) Relative viscosities of 0.200 M *sodium oleate solutions containing p-xylene. 40° C.*
b) Relative viscosities of 0.189 M *sodium oleate solutions containing decanol. 40° C.*
The arrows indicate the points where the systems become heterogeneous.

partial molar volume of decanol with the amount of decanol added. The dotted horizontal line in the figure gives the molar volume of pure decanol, 193.7 ml per mole. In the mixed micelles of oleate and decanol the partial molar volume of decanol is 190.9 ml per mole and in the turbid solutions 196.9 ml per mole. The decanol is thus slightly more densely packed in the mixed micelles than in the pure state, and its partial volume in the two-phase system is greater than that of pure decanol.

Sodium myristyl and sodium lauryl sulphate solutions containing decanol. The effect of decanol on the viscosity of sodium myristyl sulphate solutions has

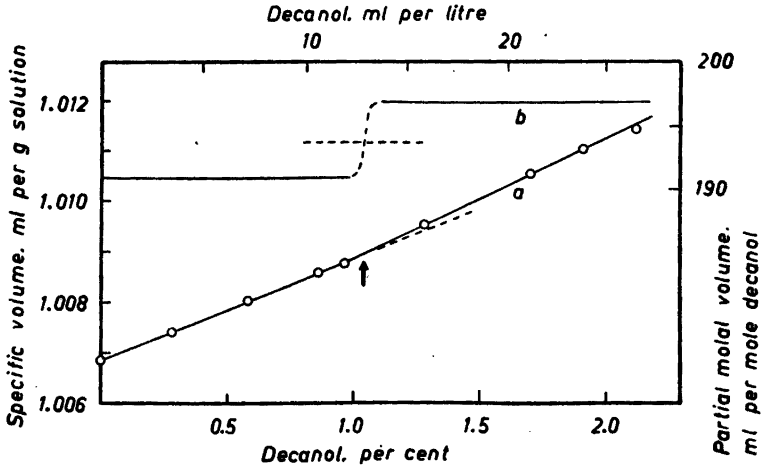


Fig. 4. a) The specific volumes of 0.275 M *sodium oleate solutions containing decanol. 40° C.*
b) The partial molal volume of decanol in the same solutions. 40° C.
The arrow indicates the point where the system becomes heterogeneous.

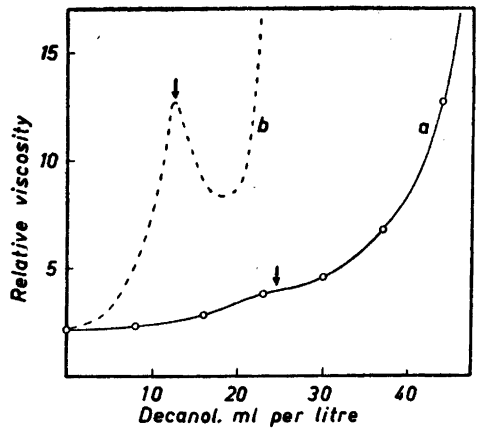


Fig. 5. a) Relative viscosities of 0.300 M *sodium myristyl sulphate solutions containing decanol. 40° C.*
b) Relative viscosities of 0.275 M *sodium oleate solutions containing decanol. 40° C. The arrows indicate the points where the systems become hetrogeneous.*

been studied only at one colloid concentration, 0.300 *M* (Fig. 5, curve *a*). The viscosity increases slowly at first, then more rapidly with the amount of decanol added. In spite of the relatively high concentration of myristyl sulphate, no maximum and minimum values analogous to those observed in equally concentrated decanol-oleate systems were observed. Weak signs of a break point can, however, be noted at the point where the new phase composed of decanol, myristyl sulphate and water begins to separate. The viscosity curve for a decanol-oleate system with approximately the same colloid concentration has been drawn in Fig. 5 (curve *b*) for the sake of comparison; the viscosity of the oleate solution increases appreciably more rapidly than that of a myristyl sulphate solution on adding decanol.

The curves *d* and *e* in Fig. 2 show the variation of the viscosities of pure sodium lauryl sulphate solutions and of solutions containing 0.116 mole of decanol per mole of lauryl sulphate. These systems are homogeneous. The curves are similar in form to the corresponding curves for the decanol-oleate system (Fig. 2, curves *a* and *c*).

DISCUSSION

As we have seen above, the viscosities of pure and decanol-containing oleate solutions increase linearly with the oleate concentration up to the approximately 0.2 *M* concentration. Decanol effects a definitely greater increase in viscosity above the latter limit than below it. We have previously observed [24] that in the higher concentration range the solubility of decanol begins to increase faster than at lower concentrations. The effect of this increase of solubility on the viscosity is, however, very small. We have also found

that the effect of decanol on the conductance is altered at this same concentration (Part III[26], Table 1). Furthermore, the solubility of hydrocarbons undergoes a change [27,28], the conductance of pure oleate solutions passes through a minimum [29,30] and the so-called I band appears in the X-ray diffraction pattern [31] at the same colloid concentration. There is thus strong evidence that the properties of oleate solutions, both in the absence and presence of foreign substances, undergo pronounced variation at about this concentration (0.1—0.2 *M*). There seems to be sufficient reason to speak about a concentration limit in this concentration range; for the lack of a better name, this limit is called the 2nd critical concentration [28,32,33].

We shall first consider the homogeneous systems in which the added substance is solubilized, *i. e.* completely incorporated in the micelles. The increase in viscosity that is observed when decanol (or *p*-xylene) is added to the system may be caused by four factors, 1. the micelle volume increases, 2. changes occur in the electroviscous effect, 3. the micelles become deformed and 4. the degree of aggregation and number of micelles are altered. Actually, of course, these different factors co-operate and depend on each other. Our purpose is, however, to study how great is the effect of each of the factors on the viscosity and to investigate whether any one of them can alone explain the observed increase in viscosity.

The volumes of the micelles increase because the solubilized compound enters the micelles. We have attempted to estimate how much this increase in volume can alter the viscosity. The proportion of the total volume of the solution taken up by the micelles, the volume fraction, can be calculated for a certain concentration from the partial molal volume of the oleate using the data of Ekwall and Smeds [28]. If it is assumed that the incorporated compound effects no other change in the structure of the solution than an increase in the micellar volume, the variation of the specific viscosity with the amount of compound added may be represented by the equation $\eta_{sp} = K \Phi$, where Φ is the combined volume fraction of the micelles and the added compound. The value of the constant K is calculated from the known values of the specific viscosity and volume fraction in pure oleate solutions. The viscosity values calculated for solutions containing solubilized *p*-xylene (0.200 *M* sodium oleate, Fig. 3) are found to be only slightly lower than the experimental values. For 0.3 *M* oleate solutions containing benzene, however, the calculated values are much smaller than the values reported by Kiessig and Philippoff [22] for the range where the viscosity passes through a maximum with increasing benzene content. Also the calculated viscosity values for solutions containing decanol are close to the observed values at low oleate concentrations, but are much too small at higher oleate concentrations. In the concentrated oleate solutions other factors than the increase in the volume of the micelles must thus be responsible for the observed great viscosity changes. This is the case also if the hydration of the alcohol molecules is taken into consideration.

The incorporation of decanol brings about a change in the structure and properties of the micelle surface; among other things the charge density on the micelle surface is altered. This may be expected to effect changes in the electroviscous effect but these changes can be assumed to be insignificant in these systems in view of their high electric conductance.

The interaction between the hydroxyl groups of the solubilized alcohol and the ionized carboxyl groups is known to lead to a denser packing in the palisade layers of the micelles [34,35]. That the solubilized decanol actually is more densely packed than in the bulk is shown by our density measurements (see above). This must obviously influence the form of the micelle. By the light-scattering method it has been found that micelles become more anisodiametric when higher paraffin chain alcohols are solubilized in them [36]. Already a very slight change in the ratio of the axes of the micelle causes a marked increase in viscosity. From Simha's formula for rod-like particles [37] we have computed the degree of deformation that alone can lead to the observed increase in viscosity. From the known viscosities and volume fractions we have computed values of the axis ratio for pure soap solutions and for soap solutions containing solubilized substance. In this way comparatively high axis ratios are obtained for pure oleate solutions (about 10 in the 0.2 *M* concentration range) due to the fact that the viscosity of these solutions is not only caused by the deformation of the micelles and that Simha's formula is strictly valid only at low colloid concentrations. At oleate concentrations below *ca.* 0.2 *M*, a 10—20 % increase in the axis ratio at the turbidity point is sufficient to explain the increase in viscosity caused by decanol (or *p*-xylene). To explain the strong influence of added decanol on the viscosity of concentrated oleate solutions (above *ca.* 0.2 *M*), it is, however, necessary to assume much higher values for the axis ratio (*e. g.* in the 0.275 *M* oleate solution, the axis ratio should increase from about 11 in the pure solution to about 42 in the decanol-containing solution at the turbidity point). This implies that the mixed micelles formed by decanol and oleate at high oleate concentrations are long rod-shaped particles. It seems doubtful, however, whether the relatively small amounts of decanol in question are actually able to effect such great changes in the form of the micelle. We are therefore of the opinion that in the oleate solutions exceeding 0.2 *M* the deformation of the micelles cannot alone explain the observed increase in viscosity.

It has been previously assumed that an aggregation of micelles to larger and more or less anisodiametric lamellar micelles, called large micelles, occurs at higher association colloid concentrations [38,18]. These aggregates have been assumed to be responsible for the appearance of the so-called I band in the X-ray diffraction pattern and for the pronounced structural viscosity [39] of these solutions. Since apparatus for the measurement of structural viscosity was not available, we cannot present any evidence for the occurrence of micelle aggregation in oleate solutions containing decanol. It may be noted, however, that the decrease in the charge density, and the resulting increase in the hydrophobic properties of the surfaces of the micelles, decreases the stability of the micelles in the solution and hence facilitates an aggregation of the decanol-containing micelles. Even if micelle aggregates were not present in a pure 0.275 *M* oleate solution, it is possible that such aggregates might be formed when decanol is solubilized. If lamellar micelles or aggregates of cylindrical micelles are formed, water layers must be located between the hydrophilic layers and this must lead to a marked increase in micellar volume.

As a summary of the discussion of the factors which may cause the observed increases in the viscosity in the homogeneous solutions, the following can

be said. At low oleate concentrations an increase in the volumes of the micelles due to the incorporated decanol (or xylene) can explain nearly the whole observed increase. At higher oleate concentrations (above *ca.* 0.2 *M*) the deformation and aggregation of the micelles are apparently the most important factors.

We shall now proceed to discuss the factors which determine the courses of the viscosity curves in the region above the turbidity point.

When xylene in excess of the amount solubilized is added to an oleate solution, the excess is emulsified in the solution. Conductance measurements (Part III [26]) have shown that the emulsified xylene binds practically no oleate and hence the oleate concentration of the solution is not altered. In accordance with this the viscosity remains practically constant.

As already mentioned, the viscosities of oleate solutions above 0.2 *M* decrease when the new phase containing decanol, oleate and water separates on adding decanol. The new phase is composed of microscopic anisotropic particles of marked stability. Its formation reduces the decanol and oleate contents of the aqueous phase and the number of mixed micelles in this phase therefore decreases. We have estimated the magnitude of the decrease in viscosity which results from the decrease in the concentration in the aqueous phase. We have here assumed that the only changes effected by decanol are that the concentration of the mixed micelles in the aqueous phase decreases and particles of a new phase appear. When only a slight excess of decanol has been added above the turbidity point, the number of these particles is so small that they do not alter the viscosity. With the aid of conductance data (Part II[25]), the concentration of mixed micelles in the aqueous phase can be determined above the turbidity point for different amounts of added decanol.

The calculation will be illustrated by an example. The relative viscosity of a 0.275 *M* oleate solution at the turbidity point is 12.7. A concentration of 0.275 mole of mixed micelles per litre thus gives a specific viscosity equal to 11.7 and hence $\eta_{sp}/c = 11.7 / 0.275 = 42.5$. In the solution containing 0.275 mole of oleate and 15 ml of decanol per litre, the mixed micelle concentration is according to the conductance data 0.221 *M*. If the specific viscosity varied linearly with the mixed micelle concentration, the specific viscosity of the solution should be $42.5 \times 0.221 = 9.40$ and the relative viscosity 10.4. The agreement with the experimental value 9.8 is satisfactory.

The calculated viscosities for concentrated oleate solutions containing varying amounts of decanol are plotted in Fig. 1 (curves *g* and *h*). The agreement with the experimental values is good as long as the excess of decanol (above the turbidity point) is small. For greater excesses, the viscosities are much higher than the calculated values owing to the effect of the particles of the separated phase present in the solution.

At low oleate concentrations below *ca.* 0.15 *M*, no marked variation is observed in the viscosity when the solutions become heterogeneous. The calculated curve *j* in Fig. 1 for the 0.0493 *M* oleate solution shows that the decrease in viscosity is more than compensated for by the increase in viscosity caused by the particles of the new phase, and hence the viscosity curve exhibits no break point when the solution becomes turbid. This is because the specific viscosity due to the micelles that are removed from the solution

is so slight that although their concentration in the water phase diminishes greatly on adding decanol, the viscosity does not undergo any appreciable change. Therefore the particles of the separated phase exert their effect on the viscosity immediately and the viscosity increases gradually and uniformly. The same applies in the case of the 0.300 *M* sodium myristyl sulphate solution, the viscosity curve for which does not either exhibit any pronounced irregularity when the turbidity appears.

The viscosities of concentrated oleate solutions, after passing a minimum, finally begin to increase rapidly with increasing decanol content. The abrupt increase in viscosity begins when the amount of the new phase becomes so large that it begins to influence greatly the flow of the solution.

It is thus possible to connect the changes in viscosity with other phenomena that occur when decanol and *p*-xylene are solubilized by association colloid solutions, *i. e.* to the formation of mixed micelles and the appearance of a new phase. It has also been possible to point out those factors that influence the viscosity. The viscosity phenomena confirm our earlier conclusions that the properties of oleate solutions undergo appreciable changes in the 0.10—0.20 *M* concentration region. Decanol promotes the structural changes which occur in this range also in pure oleate solutions.

As pointed out in the introduction, the solubilization of polar-nonpolar compounds generally results in a more or less marked increase in viscosity. The above conclusions apply to all these cases and are in accordance with the views of other investigators. The factors that cause the viscosity to pass through a maximum in homogeneous systems, as reported by various workers, will not be discussed here. In the systems we have studied no such maxima have been reached, the increase in viscosity being terminated by the appearance of a new phase which leads to a decrease in viscosity due to the decrease in the concentration of micellar substance.

When this publication was already written, we noted an abstract of a study of Markina, Posspelova and Rebinder [40] very similar to ours. As far as it is possible to judge from the abstract, their experimental results and conclusions are in accordance with those presented here.

REFERENCES

1. Bose, A. N. *J. Indian Chem. Soc.* **29** (1952) 43.
2. Bose, A. N. and Misra, J. *Kolloid-Z.* **133** (1953) 108.
3. Bose, A. N. *J. Indian Chem. Soc.* **30** (1953) 496.
4. Bose, A. N. *Z. physik. Chem.* **203** (1954) 113.
5. Bose, A. N. *Z. physik. Chem.* **204** (1955) 16.
6. Rossi, G. and Ragno, M. *Atti accad. Gioenia sci. nat. Catania* [6], Pt. IV, Mem. **14** (1939—40). *Chem. Abstracts* **38** (1944) 2545 [7].
7. Klevens, H. B. *J. Am. Chem. Soc.* **72** (1950) 3780.
8. de Jong, B. H. G. and van Alphen, G. W. H. M. *Koninkl. Ned. Akad. Wetenschap., Proc.* **50** (1947) 1011.
9. Ekwall, P., Passinen, K. and Danielsson, I. *Finska Kemistsamfundets Medd.* **63** (1954) 1.
10. Angelescu, E. and Popescu, D. M. *Kolloid-Z.* **51** (1930) 247.
11. Angelescu, E. and Popescu, D. M. *Kolloid-Z.* **51** (1930) 336.
12. Angelescu, E. and Ciortan, V. *Kolloid-Z.* **82** (1938) 164.
13. Angelescu, E. and Ciortan, V. *Kolloid-Z.* **82** (1938) 304.

14. Angelescu, E. and Ciortan, V. *Kolloid-Z.* **89** (1939) 47.
15. Angelescu, E. and Szász, S. *Kolloid-Z.* **90** (1940) 302.
16. Angelescu, E. and Manolescu, T. *Kolloid-Z.* **94** (1941) 319.
17. Angelescu, E. and Manolescu, T. *Kolloid-Z.* **96** (1941) 75.
18. Philippoff, W. *Kolloid-Z.* **96** (1941) 255.
19. Ekwall, P. *6. Nordiska Kemistmötet, Lund* 1947, p. 179.
20. McBain, J. W. and McHan, H. *J. Am. Chem. Soc.* **70** (1948) 3838.
21. Hahne, A. *Z. deut. Öl- und Fett-Ind.* **45** (1925) 245—310.
22. Kiessig, H. and Philippoff, W. *Naturwiss.* **27** (1939) 593.
23. Stainsby, G. and Alexander, A. E. *Australian J. Chem.* **6** (1953) 123.
24. Ekwall, P. and Passinen, K. *Acta Chem. Scand.* **7** (1953) 1098.
25. Passinen, K. and Ekwall, P. *Acta Chem. Scand.* **9** (1955) 1438.
26. Passinen, K. and Ekwall, P. *Acta Chem. Scand.* **9** (1955) 1450.
27. Ekwall, P., Hasan, A. and Danielsson, I. *Acta Chem. Scand.* **6** (1952) 440.
28. Ekwall, P. and Smeds, K. *Acta Chem. Scand.* **6** (1952) 441.
29. Ekwall, P. *Kolloid-Z.* **101** (1942) 135.
30. Johnston, S. A. and McBain, J. W. *Proc. Roy. Soc. London* **A 181** (1942) 119.
31. Kiessig, H. *Kolloid-Z.* **96** (1941) 252.
32. Ekwall, P. *J. Colloid Sci.* Supplement 1, 1954, p. 66.
33. Ekwall, P. *Kolloid-Z.* **136** (1954) 37.
34. Schulman, J. H. and Hughes, A. H. *Biochem. J. London* **29** (1935) 1242.
35. Harkins, W. D. and Mittelmann, R. *J. Colloid Sci.* **4** (1949) 367.
36. McBain, M. E. L. and Hutchinson, E. *Solubilization and Related Phenomena* Academic Press Inc., New York, 1955, p. 29.
37. Simha, R. *J. Phys. Chem.* **44** (1940) 25.
38. Stauff, J. *Naturwiss.* **27** (1939) 213.
39. Philippoff, W. and Hess, K. *Ber.* **B 70** (1937) 1808.
40. Markina, S. N., Posspelova, K. A. and Rebinder, P. A. *Chem. Zentr.* **126** (1955) 7852.

Received November 24, 1955.

ACTA CHEMICA SCANDINAVICA 10 (1956) 227—236

Studies on the Interaction of Paraffin-Chain Alcohols and Association Colloids

V. The Soap Concentration where Interaction with Decanol-1 Begins and its Dependence on the Chain Length of the Soap

PER EKWALL, OLOF SÖDERBERG and INGVAR DANIELSSON

Institute of Physical Chemistry, Åbo Akademi, Åbo, Finland

Turbidity measurements show that interaction of decanol-1 and fatty acid soaps begins at a clearly defined soap concentration. This concentration is the same as that where the soap begins to interact with its parent fatty acid (the limiting concentration, L. A. C.). The value of the L. A. C. decreases with increasing chain-length of the soap; there is a nearly linear correlation between the logarithm of the L. A. C. and the number of carbon atoms in the hydrocarbon chain of the soap. The value of the L. A. C. increases somewhat with temperature. The L. A. C. lies considerably lower than the C. M. C. of the pure soap and below the concentration where micelle formation begins to increase rapidly in soap solutions that contain added alcohol.

We have previously established [1-5] two separate turbidity maxima in dilute association colloid solutions containing small amounts of decanol-1. The curves showing the variation of the turbidity with the association colloid concentration are similar in form to the schematic curve drawn in Fig. 1.

In the turbidity range I observed at low colloid concentrations, the turbidity is due to emulsified decanol. The turbidity in range II at higher colloid concentrations is caused by a birefringent liquid composed of decanol, association colloid and water which is dispersed in very small droplets. The upper limit of the turbidity range I is sharply defined. It lies considerably below the critical concentration for micelle formation in pure association colloid solutions and it defines the conditions at which interaction between decanol and association colloid begins.

In this and in three following papers of the present series, a considerable body of experimental data relating to the first stages of the above-mentioned interaction will be presented and some of the factors on which this interaction

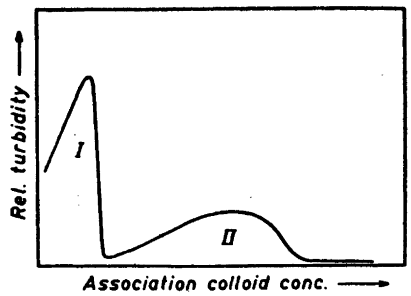


Fig. 1. The turbidity of association colloid solutions containing added decanol. Schematic curve.

depends will be discussed. In the first place, we wish to illustrate how the concentration where interaction between decanol and fatty acid soaps begins depends on the chain length of the soap and on the temperature.

EXPERIMENTAL

The soaps investigated were potassium caprylate, caprate, laurate, myristate, palmitate and stearate, and sodium caprylate, caprate, laurate, and myristate. The soaps were prepared in the usual manner from purest fatty acids and potassium or sodium ethylate.

Dilution series were prepared from each soap in which the molar ratio of decanol-1 (Eastman Kodak Co, Rochester, redistilled) to colloid was constant. Aliquots of the solutions were sealed in glass ampoules and mixed by shaking in a thermostat. The specific conductance of the water employed as solvent was less than 10^{-6} rec. ohm. To suppress the hydrolysis of the soaps, a known quantity of alkali was added to each of the solutions. Care was taken to prevent carbon dioxide from the air from entering the solutions.

In a number of cases it was found more advantageous to add a constant weight of decanol to each of the solutions instead of keeping the molar ratio constant. The decanol was added from an Agla micrometer syringe.

The turbidites were measured directly in the ampoules without opening them. Since the measurements were to be conducted at several temperatures, the shaking of the ampoules was begun and the turbidity first measured at the lowest temperature and then the ampoules were transferred to the next higher temperature and shaken two hours before the turbidity was again measured.

The turbidities were measured with a Zeiss nephelometer fitted to a Pulfrich photometer.

The following series were investigated:

Potassium caprylate + 2, 5, 7.5 and 10 moles of decanol per 100 moles of soap at 20, 30, 40, 50 and 60° C.

Potassium caprate + 1, 2, 3 and 8 moles of decanol per 100 moles of soap at 20, 30, 40, 50 and 60° C.

Potassium laurate + 1, 2, 5, 10 and 15 moles of decanol per 100 moles of soap at 20, 30, 40, 50 and 60° C.

Potassium myristate + 13, 20, 25, 30 and 35 moles of decanol per 100 moles of soap at 20, 30, 40, 50 and 60° C.

Potassium palmitate + 10, 20, 30, 40, 50 and 60 moles of decanol per 100 moles of soap at 50, 55, 60 and 65° C.

Potassium stearate + 0.33 ml of decanol per litre at 47, 59, 72.5, 84 and 97° C.

Sodium caprate + 2, 3, 4 and 6 moles of decanol per 100 moles of soap at 20, 30, 40, 50 and 60° C.

Sodium laurate + 3.2, 5.25, 7.35, 10.5, 15.7 and 21 moles of decanol per 100 moles of soap at 40° C.

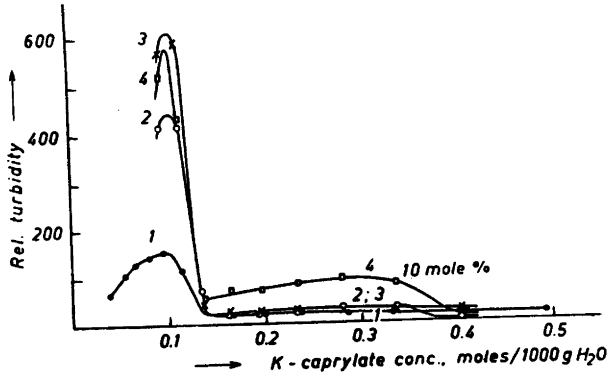


Fig. 2. The turbidities of potassium caprylate solutions containing decanol-1, 20° C. Curve 1 ●—●, 2 moles; Curve 2 ○—○, 5 moles; Curve 3 ×—×, 7.5 moles; Curve 4 □—□, 10 moles decanol per hundred moles caprylate.

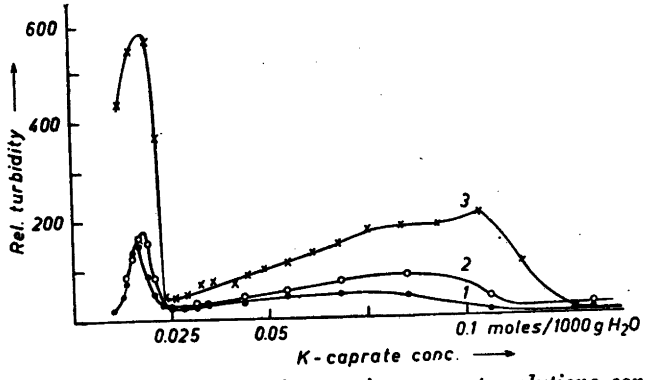


Fig. 3. The turbidities of potassium caprate solutions containing decanol-1. 20° C. Curve 1 ●—●, 2 moles; Curve 2 ○—○, 3 moles; Curve 3 ×—×, 8 moles decanol per hundred moles caprate.

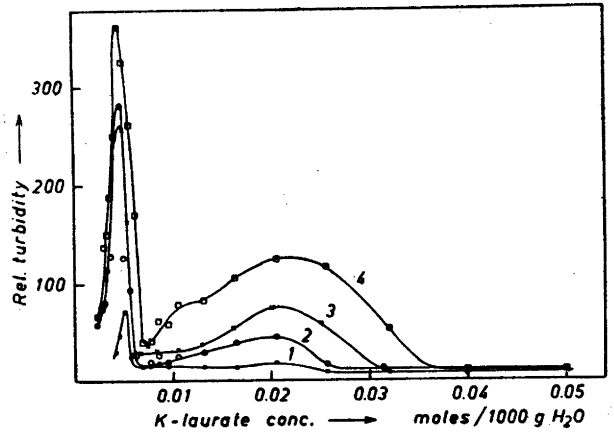


Fig. 4. The turbidities of potassium laurate solutions containing decanol-1. 40° C. Curve 1 ●—●, 2 moles; Curve 2 ○—○, 5.1 moles; Curve 3 ×—×, 10 moles; Curve 4 □—□, 15 moles decanol per hundred moles laurate.

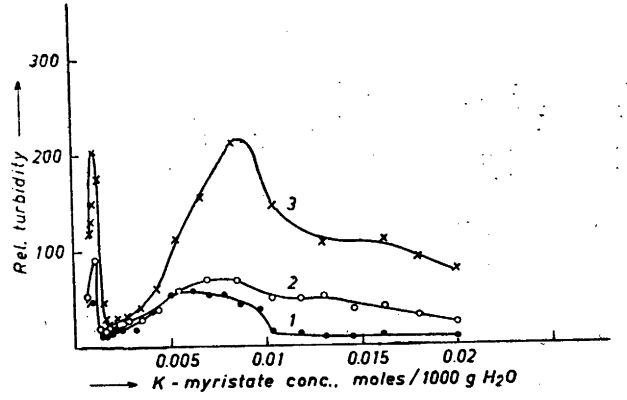


Fig. 5. The turbidities of potassium myristate solutions containing decanol-1. 40° C. Curve 1 ●—●, 20 moles; Curve 2 ○—○, 25 moles; Curve 3 ×—×, 30 moles decanol per hundred moles myristate.

THE RESULTS OF THE MEASUREMENTS

The experimental data have been used to draw curves which plot the relative turbidity as a function of the soap concentration. Figs. 2—6 show typical turbidity curves for several potassium soaps; each curve represents a series of measurements at constant temperature on solutions with different soap concentrations but with a constant mole ratio of added decanol to soap.

It is evident in all the curves that a marked turbidity occurs in relatively high dilutions (turbidity range I) and that this turbidity disappears completely or practically completely when the soap concentration attains a certain level. This concentration level is quite independent of the amount of added decanol as long as this remains within moderate limits. It is obvious that the ability of the soap to bind decanol undergoes a pronounced change at this concentration. Microscopic examination and other studies (*e. g.* conductance measurements) show that below this soap concentration decanol is present in the free form in an emulsified state, while above this concentration decanol interacts with the soap [2, 3, 9, 10]. The decanol-soap complex that is formed in the latter case appears to have a limited solubility in water, and when somewhat larger amounts of decanol are added, a new extremely finely dispersed precipitate is formed which produces a turbidity (turbidity range II) differing from that due to free emulsified decanol observed at low colloid concentrations. The amount of decanol necessary to effect this turbidity varies with the soap. In caprylate solution the turbidity is almost undetectable when 7.5 moles of decanol are added per hundred moles of soap, whereas in the case of caprate and laurate solutions a similar addition produces a quite marked turbidity. This second turbidity range extends to higher soap concentrations when the amount of decanol added is increased until finally, when the amount of the latter is high enough, the turbidity no longer disappears with increasing soap concentration.

As mentioned above the turbidity phenomena were studied at several temperatures. All curves in each of the Figs. 7—11 refer to a constant decanol content (expressed in moles per hundred of soap); they were, however, measured at different temperatures. In range I the intensity of the turbidity increases somewhat with increasing temperature in many cases, but in range II the intensity decreases. The upper limit of the first turbidity range shifts to higher soap concentrations, while the upper limit of the second turbidity range shifts to lower soap concentrations with increasing temperature.

We have observed quite similar turbidity phenomena also in solutions of sodium soaps containing added decanol [1, 2].

DISCUSSION

The reaction that causes the free decanol to disappear from the solution occurs in a narrow concentration range. This range lies between the maximum of the first turbidity range and the somewhat higher concentration where this turbidity disappears. We have used data from all series to determine the limits of this concentration range for the different soaps at different temperatures (Table 1). When doing this, we have taken into consideration that the range

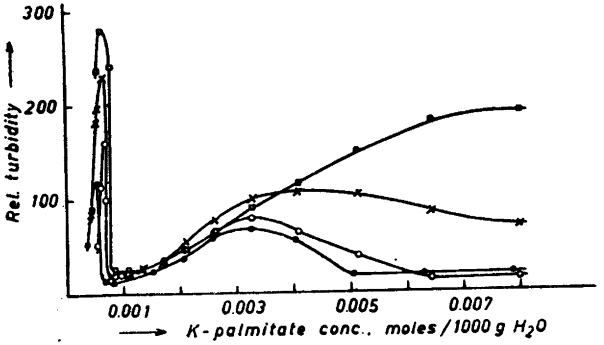


Fig. 6. The turbidities of potassium palmitate solutions containing decanol-1. 60° C. Curve 1 ●—●, 10 moles; Curve 2 ○—○, 30 moles; Curve 3 ×—×, 40 moles; Curve 4 □—□, 50 moles decanol per hundred moles palmitate.

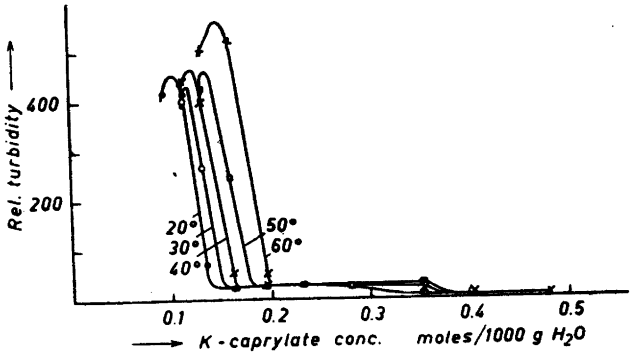


Fig. 7. The turbidities of potassium caprylate solutions containing 5 moles of decanol-1 per hundred moles of soap at different temperatures.

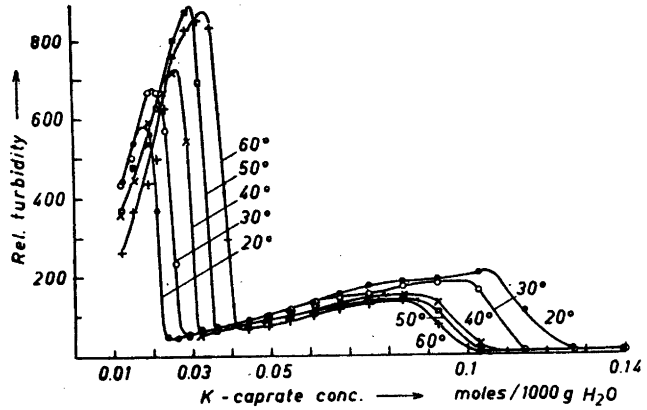


Fig. 8. The turbidities of potassium caprate solutions containing 8 moles of decanol-1 per hundred moles of soap at different temperatures.

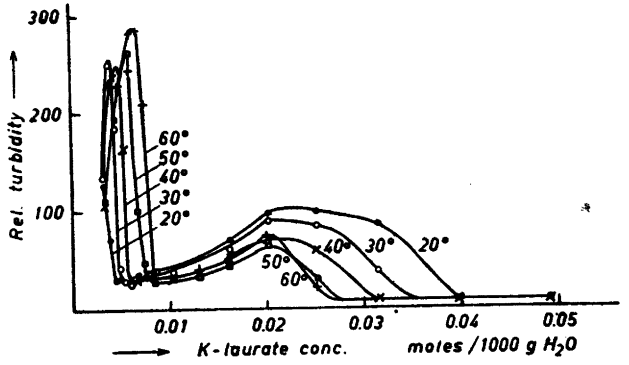


Fig. 9. The turbidities of potassium laurate solutions containing 10 moles of decanol-1 per hundred moles of soap at different temperatures.

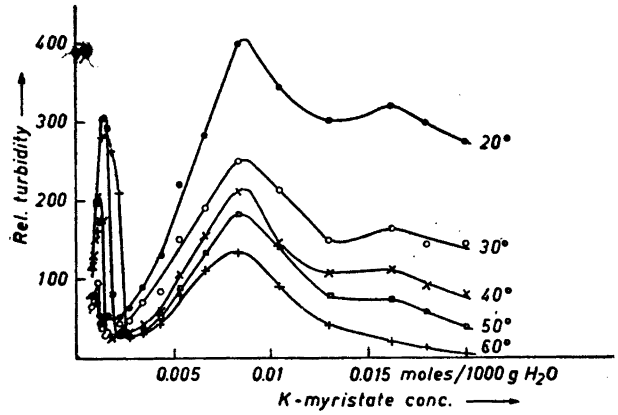


Fig. 10. The turbidities of potassium myristate solutions containing 30 moles of decanol-1 per hundred moles of soap at different temperatures.

certainly becomes more clearly defined when the amount of added decanol increases, but that at high decanol contents a tendency of the range to shift to higher concentrations is observed in some cases. It was in most cases easier to determine the upper limits of the turbidity range than the turbidity maximum. Because of this we shall in the following in general use the concentration at the upper limit to define the conditions where the interaction between soap and decanol begins, although we are fully aware that the interaction actually begins at a somewhat lower concentration.

The interaction begins at about the same soap concentrations in the solutions of the sodium and potassium salts of a fatty acid.

The variation of the upper limit of turbidity range I with increasing temperature is shown in Fig. 12. In most cases the dependence on temperature is practically linear.

From the data in Table 1 it is seen that the soap concentration at which the interaction begins decreases as the length of the hydrocarbon chain of the soap increases. In Fig. 13 the logarithm of the soap concentration at which inter-

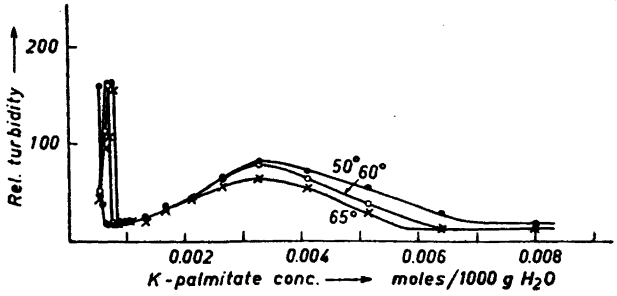


Fig. 11. The turbidities of potassium palmitate solutions containing 30 moles of decanol-1 per hundred moles of soap at different temperatures.

Table 1. The soap concentrations where the interaction between decanol and soap begins. Concentrations in moles per 1 000 g of water.

Soap	°C	Maximum of turbidity range I	Upper limit of turbidity range I
Potassium caprylate	20	0.10—0.11	0.13—0.14
	30	0.11—0.12	0.14—0.15
	40	0.12—0.13	0.15—0.16
	50	0.13—0.15	0.16—0.18
	60	0.15—0.16	0.18—0.19
Potassium caprate	20	0.016—0.019	0.021—0.023
	30	0.020—0.021	0.024—0.027
	40	0.022—0.024	0.026—0.028
	50	0.025—0.029	0.029—0.035
	60	0.028—0.032	0.034—0.037
Potassium laurate	20	0.003—0.004	0.004—0.005
	30	0.003—0.004	0.005—0.006
	40	0.004—0.005	0.006—0.007
	50	0.005—0.006	0.007—0.008
	60	0.006—0.007	0.008—0.009
Potassium myristate	20	~0.0009	~0.0012
	30	~0.0011	0.0012—0.0013
	40	0.0011—0.0012	0.0013—0.0014
	50	0.0012—0.0014	~0.0016
	60	0.0019—0.0020	0.0021—0.0023
Potassium palmitate	50	0.0004—0.0005	0.0005—0.0006
	55	0.0005—0.0006	0.0006—0.0007
	60	0.0006—0.0007	0.0007—0.0008
	65	0.0006—0.0008	0.0008—0.0009
Potassium stearate	47		~0.000080
	59		~0.000085
	72		~0.000090
	84		~0.000096
	97		~0.000102
Sodium caprylate	40	0.12—0.13	0.15—0.16
Sodium caprate	40	0.025—0.027	0.030—0.032
Sodium laurate	40	0.0045—0.0055	0.006—0.007

action with decanol begins is plotted against the number of carbon atoms in the hydrocarbon chain of the soap molecule. These curves are not quite linear; the curvatures are, however, so slight that the interaction concentration can be approximately calculated from the following logarithmic equations, where n indicates the number of carbon atoms in the paraffin chain of the fatty acid.

20° C.: $\log C = -0.364\ n + 1.66$
30° C.: $\log C = -0.345\ n + 1.53$
40° C.: $\log C = -0.334\ n + 1.48$
50° C.: $\log C = -0.326\ n + 1.45$
64° C.: $\log C = -0.310\ n + 1.40$

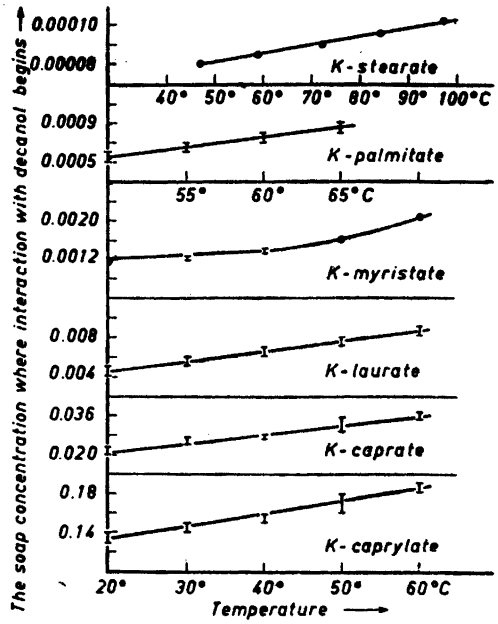


Fig. 12. The temperature dependence of the upper limit of the turbidity range I.

We have noted earlier[1-5] that the concentration at which interaction between decanol and soap begins lies very close to the lowest concentration at which hydrolysis in the soap solution leads to the formation of acid soap or at which the soap forms acid soap when fatty acid is added to the solution. In

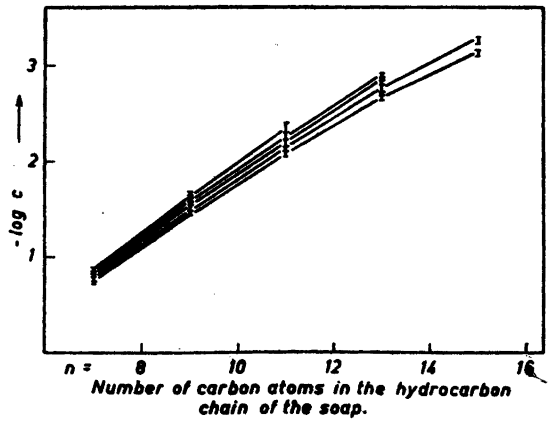


Fig. 13. The dependence of the upper limit of the turbidity range I on the chain length of the soap.

Table 2. Comparison of the soap concentrations where soaps begin to interact with fatty acid and with decanol (the upper limits of the turbidity range I).

Interaction with fatty acid			Interaction with decanol		
Soap	°C	Molarity	Soap	°C	Molarity
Sodium caprate	20	0.020 – 0.025	Potassium caprate	20	0.021 – 0.023
				20 – 60	0.021 – 0.037
Sodium laurate	20	0.005 – 0.0068	Potassium laurate	20	0.004 – 0.005
	20 – 58	0.005 – 0.008		20 – 60	0.004 – 0.009
			Sodium laurate	40	0.006 – 0.007
Sodium myristate	20	0.0010 – 0.0014	Potassium myristate	20	0.0012
	20 – 60	0.001 – 0.002		20 – 60	0.001 – 0.0023
Sodium palmitate	20	0.00025 – 0.0004	Potassium palmitate		
	45 – 65	0.00025 – 0.0007		50 – 65	0.0005 – 0.0009
Sodium stearate	65 – 80	(0.0002 – 0.0005)	Potassium stearate	50 – 77	0.00008 – 0.0001

Table 2 the concentrations at which acid soap is formed are compared with the concentrations at which soap and decanol begin to interact. From these data it is seen that in the case of caprate, laurate and myristate solutions the concentration ranges where interaction begins with fatty acid and with decanol are almost identical. Also for palmitate solutions the two concentration ranges are nearly the same. In the case of the interaction between stearate and stearic acid, only earlier observations on strongly hydrolysed stearate solutions are available and for this and other reasons the upper limit of the first turbidity range is probably too high.

It is thus established that interaction between soap and decanol begins at approximately the same soap concentration as the interaction between a soap and its fatty acid. The concentration in question is that which has been previously termed the limiting concentration or the limiting association concentration (L. A. C.) [6,7,1,2].

Also the location of the critical concentration in decanol-containing soap solutions becomes evident in some cases in the turbidity curves although not always very clearly. The C. M. C. is as usually defined as the concentration where the aggregation to micelles begins to increase rapidly. When the amounts of decanol added are small, the C. M. C. appears at the upper limit of the turbidity range II or at the maximum of the turbidity curve in this range, *i. e.* at that soap concentration where the precipitate of the second turbidity range has just disappeared or begins to disappear because of the formation of soluble decanol-containing mixed micelles. At higher decanol contents however, the turbidity maxima, tend to shift to higher concentrations and above a certain decanol content characteristic for each soap the turbidity does not disappear at all. Because of this and the fact that soap is precipitated from the solution it is difficult to determine exactly where micelle formation begins from the turbidity curve.

The values in the last column of Table 3 are from experiments with small amounts of added decanol, and are the lowest values of the C. M. C. in decanol-

Table 3. The critical concentrations in pure and decanol-containing soap solutions.

	Pure soap solutions		Soap solutions containing decanol	
Soap	°C	C. M. C.	°C	C. M. C.
Caprylate	25	0.40	60	0.24 −0.28
Caprate	20	0.097	60	0.055−0.085
Laurate	20	0.028	60	0.020−0.025
Myristate	30	0.007	60	0.005−0.007
Palmitate	50−60	0.0032	60	0.003

containing soap solutions that we have observed in the turbidity measurements. (They agree rather well with the results of solubility measurements which will be presented in later parts of this series.) These C. M. C. values are somewhat lower than the C. M. C.'s in pure soap solutions, but appreciably higher than the limiting concentrations.

The limiting concentration may be confused with the critical concentration and the appearance of the former may be considered an indication of a displacement of the C. M. C. to very low concentrations due to presence of the added alcohol. This is not correct, however. The phenomena at the critical concentrations and those at the limiting concentrations have been known for more than 25 years and numerous experimental measurements (measurements of surface tension, hydrolysis, and conductance, microscopical observations, determination of the solubility of fatty acids and later also of alcohols, conductometric and potentiometric titrations, *etc.*) have shown that they appear simultaneously in numerous colloid systems, but at different colloid concentrations.

REFERENCES

1. Ekwall, P. *Svensk Kem. Tidskr.* **63** (1951) 277.
2. Ekwall, P. and Danielsson, I. *Acta Chem. Scand.* **5** (1951) 973.
3. Ekwall, P., Passinen, K. and Danielsson, I. *Finska Kemistsamfundets Medd.* **63** (1954) 1.
4. Ekwall, P. *J. Colloid Sci. Suppl.* 1 (1954) 66.
5. Ekwall, P. *Kolloid-Z.* **136** (1954) 37.
6. Ekwall, P. *Kolloid-Z.* **80** (1937) 78.
7. Ekwall, P. *Kolloid-Z.* **77** (1936) 320.
8. Ekwall, P. *Kolloid-Z.* **97** (1941) 71.
9. Passinen, K. and Ekwall, P. *Acta Chem. Scand.* **9** (1955) 1438, 1450.
10. Ekwall, P. and coworkers. *To be published later in this series.*

Received October 29, 1955.

ACTA CHEMICA SCANDINAVICA 10 (1956) 237—243

Studies on the Interaction of Paraffin-Chain Alcohols and Association Colloids

VI. The Sodium Caprate Concentration where Interaction with Long-Chain Alcohols Begins and its Dependence on the Chain Length of the Alcohol

PER EKWALL and CLAES FREDRIK AMINOFF

Institute of Physical Chemistry, Åbo Akademi, Åbo, Finland

Turbidity measurements show that interaction of sodium caprate with hexanol-1, octanol-1, decanol-1, and dodecanol-1 begins at approximately the same concentration of the soap, at the L. A. C., and hence irrespective of the chain-length of the alcohol. Also with tetradecanol-1, hexadecanol-1 and octadecanol-1, at temperatures above their melting points, interaction begins at only slightly higher soap concentrations. The temperature dependence of the interaction concentration is the same for all alcohols. The first step in the interaction is the formation of soluble alcohol-soap aggregates. The part different intermolecular interactions play in determining the L. A. C. is discussed and it is shown that the most decisive factor in determining the position of the L. A. C. is the chain length of the soap.

In the preceding paper of this series [1], it was shown on the basis of extensive experimental data that the soap concentration where interaction between decanol-1 and different fatty acid soaps begins shifts to lower values with increasing chain length of the soap molecule. The interaction concentration was observed to increase slightly with temperature. It was further established that the lowest concentration limit for interaction between soap and decanol is approximately the same as the concentration where the soap begins to react with its parent fatty acid (the limiting concentration, L. A. C.). We have used the same nephelometric technique to determine how the concentration where the soap begins to interact with different long-chain alcohols varies with the chain length of the alcohol and how this concentration depends on the temperature.

EXPERIMENTAL

The soap employed in the experiments was sodium caprate. The interaction with the following alcohols was studied: hexanol-1 (B. D. H. London), octanol-1, decanol-1, dodecanol-1, tetradecanol-1, hexadecanol-1, and octadecanol-1 (Eastman Kodak Company, Rochester). The samples were distilled or recrystallized.

The solutions of soap and alcohols were prepared and their turbidities measured as described in the previous paper [1].

The measurements were conducted at temperatures between 20° and 60° C, but in each case only above the melting point of the alcohol in question. In most cases the amounts of alcohol added were also varied.

The following series were investigated;

Sodium caprate + 0.65 ml of hexanol per litre at 20°, 30°, 40°, 50° and 60° C and with 0.61 ml of hexanol per litre at 20° C.

Sodium caprate + 24.6 and 36 moles of octanol per 100 moles of soap at 20°, 30°, 40°, 50° and 60° C.

Sodium caprate + 2, 3, 4 and 6 moles of decanol per 100 moles of soap at 20°, 30°, 40°, 50° and 60° C.

Sodium caprate + 1.5, 2.5 and 6.1 moles dodecanol per 100 moles of soap at 20°, 30°, 40°, 50° and 60° C.

Sodium caprate + 1.2, 1.9 and 2.8 moles tetradecanol per 100 moles of soap at 40°, 50° and 60° C.

Sodium caprate + 0.65 and 0.95 moles hexadecanol per 100 moles of soap at 60° C.

Sodium caprate + 0.4 moles octadecanol per 100 moles of soap at 60° C.

THE RESULTS OF THE MEASUREMENTS

The measurements gave turbidity curves that are similar in form to those previously found for decanol in which two turbidity ranges are separated by a

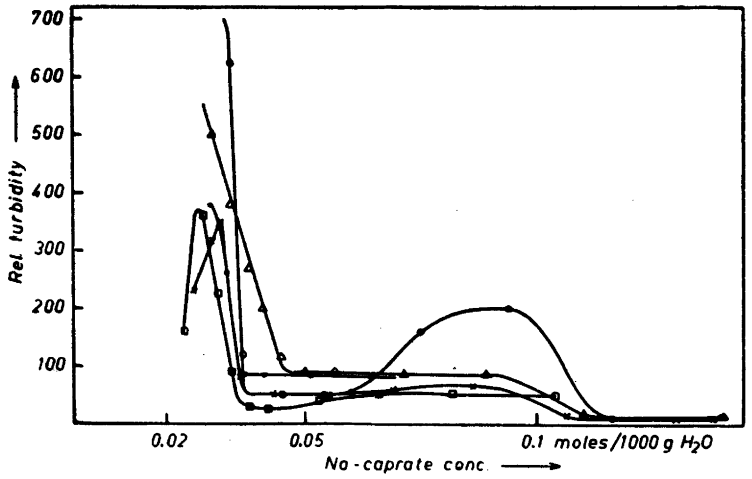


Fig. 1. The turbidity of sodium caprate solutions containing different long-chain alcohols. 50° C.

Curve 1 ●—●, *0.65 ml of hexanol-1 per litre of soap solution.*
Curve 2 ○—○, *24.8 moles of octanol-1 per hundred moles of soap.*
Curve 3 ×—×, *4 moles of decanol-1 per hundred moles of soap.*
Curve 4 □—□, *6.1 moles of dodecanol-1 per hundred moles of soap.*
Curve 5 △—△, *1.9 moles of tetradecanol-1 per hundred moles of soap.*

Table 1. The sodium caprate concentrations where interaction begins with different alcohols. Concentrations in moles per 1 000 g of water.

Alcohol	°C	Maximum of turbidity range I	Upper limit of turbidity range I
Hexanol-1	20	0.024 – 0.027	0.028 – 0.029
	30		0.030 – 0.031
	40		0.032 – 0.033
	50		0.035 – 0.037
	60		0.037 – 0.039
Octanol-1	20	0.023 – 0.026	0.028 – 0.029
	30	0.024 – 0.027	0.030 – 0.031
	40		0.031 – 0.033
	50		0.034 – 0.037
	60		0.036 – 0.039
Decanol-1	20	0.020 – 0.022	0.025 – 0.029
	30	0.023 – 0.025	0.027 – 0.030
	40	0.025 – 0.027	0.030 – 0.032
	50	0.028 – 0.031	0.035 – 0.037
	60	– 0.035	0.039 – 0.041
Dodecanol-1	40	– 0.023	0.029 – 0.031
	50	– 0.028	0.036 – 0.037
	60	– 0.035	0.040 – 0.041
Tetradecanol-1	40	– 0.035	0.042 – 0.044
	50	– 0.035	0.044 – 0.046
	60	– 0.038	0.049 – 0.051
Hexadecanol-1	60	– 0.038	0.049 – 0.052
Octadecanol-1	60	– 0.039	0.057 – 0.059

region of almost clear solutions. The turbidity in the first range (I) is due to emulsified alcohol, in the second range (II) to a birefringent liquid substance composed of alcohol, soap and water. The last-mentioned substance results from the interaction between alcohol and soap that begins in the concentration range between the point of maximum turbidity of the first turbidity range and the upper limit of this range. The purpose of the study was to determine the sodium caprate concentrations at which interaction begins, and hence the complete nephelometric curves were not recorded in all cases. Only one curve recorded at 50° C for each of the alcohols, hexanol, octanol, decanol, dodecanol, and tetradecanol (with different additions of these alcohols) is reproduced in Fig. 1. The results of all the experiments are collected in Table 1.

The caprate concentration at which the turbidity due to emulsified alcohol disappears completely is clearly defined. As previously, we shall use this concentration to define the conditions where interaction begins (last column in Table 1) although the interaction actually begins at a somewhat lower con-

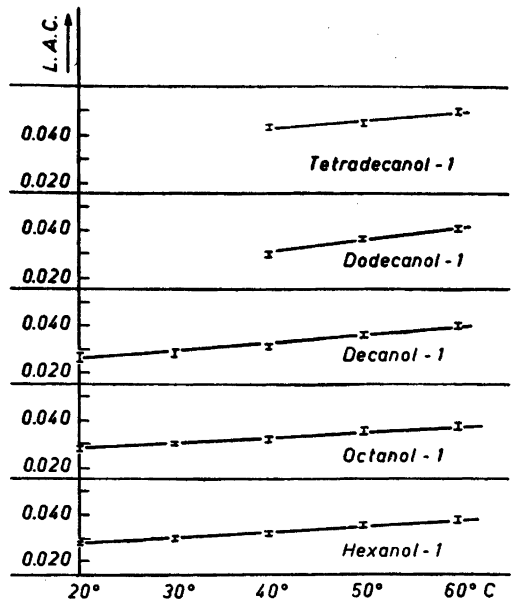


Fig. 2. The temperature dependence of the limiting concentration, L. A. C., of sodium caprate.

centration, *i. e.* at the turbidity maximum. Fig. 2 shows how the concentration mentioned varies with temperature; the curves are seen to be practically linear for all of the alcohols studied.

From the data in Table 1 it is seen that the interaction between the caprate and the four lower alcohols begins at almost the same caprate concentration. This is illustrated by the curves in Fig. 3. With tetradecanol, hexadecanol and octadecanol, the upper limits of the first turbidity range occur at somewhat higher caprate concentrations than with the lower alcohols. In the case of the two highest alcohols, measurements were conducted at only 60° C; only two different additions of hexadecanol and only one of octadecanol were employed (the temperature 60° lies close to the melting point of octadecanol).

DISCUSSION

It is seen that the lower limit for interaction between the soap and the various alcohols, at least for those with 6 to 12 carbon atoms, occurs at approximately the same soap concentration irrespective of the chain length of the alcohol (in the case of the higher alcohols, this soap concentration deviates only slightly from that found for the lower alcohols). As mentioned above, this limit coincides with the lowest concentration at which interaction occurs between the soap and its parent fatty acid. For the fatty acid and all the alcohols the interaction concentration is observed to shift with increasing temperature in a similar manner. We may therefore conclude that this limit is

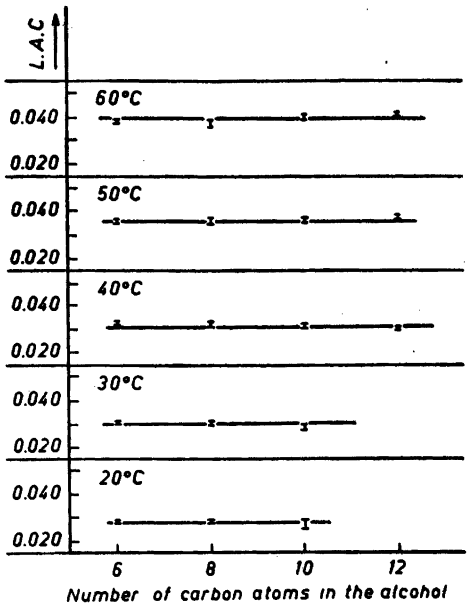


Fig. 3. The dependence of the limiting concentration, L. A. C., of sodium caprate on the chain-length of the alcohol.

fairly well defined and that it thus seems appropriate to refer to it by a special term, the limiting association concentration (L. A. C.) of the soap.

At the maximum of the first turbidity range, the soap solutions contain more alcohol than dissolves in water and in dilute soap solutions. Although the alcohol content increases with the soap concentration, the turbidity disappears completely, *i. e.* the alcohol dissolves in cases where the mole ratio of alcohol to soap is not too high. This shows that the solubility of alcohol increases when the limiting concentration is exceeded. This conclusion has been verified by measurements of the solubility of decanol [2,3]. The increase of the solubility must be due to the formation of complexes between the alcohol molecules and soap ions. The first phenomenon occurring at the limiting concentration is thus the formation of soluble alcohol-soap aggregates and not the formation of a new precipitate. That this is the case also in the interaction between fatty acid and soap has been shown previously [4,5]. The alcohol-soap aggregates (and fatty acid-soap aggregates) formed at the limiting concentration must, however, be rather hydrophobic, for the increase in the solubility is fairly small and the new liquid phase composed of soap, water and alcohol (or of soap, water and fatty acid; in some cases crystalline acid soap is formed) begins to separate when more alcohol (or fatty acid) is added.

When the mole ratio of alcohol to soap exceeds a certain value, the turbidity does not disappear completely but decreases considerably. The new precipitate that is formed effects a much weaker turbidity than emulsified alcohol [3]. In

these cases both factors, the increase in the solubility of the alcohol and the decrease of the opacity of the reaction product together effect the rapid fall in the turbidity curve at the L. A. C.

The association or complex formation above the limiting concentration complies with the law of mass action. The first steps of the interaction may be described by general equations such as (1) and (2);

$$xR'Ac^- + yR''OH = (R''OH)y\ (R'Ac^-)x \quad (1)$$

$$\frac{[(R''OH)y\ (R'Ac^-)x]}{[R'Ac^-]^x \cdot [R''OH]^y} = K \quad (2)$$

In a later paper of this series, when more experimental observations have been published, we will return to a quantitative treatment of the interaction between alcohols and soap. Now we only wish to make some comments.

The same forces that effect the association in pure soap solutions must take an active part also in the formation of the soluble aggregates between soap and polar-nonpolar compounds such as alcohols and fatty acids. In addition, there occurs ion-dipole interaction and probably also formation of hydrogen bonds between the carboxylate groups of the soap ions and the hydroxyl groups of the alcohols or the carboxyl groups of the fatty acids.

An interesting question is the part these different intermolecular interactions play in determining the concentration level where the L. A. C. occurs. Surely the interaction between the ionized carboxyl groups and the alcohol groups determines in some degree the phenomena that are characteristic of the interaction between soaps and alcohols. An interesting fact is, however, that for a certain soap the L. A. C. occurs at almost the same concentration level also when the polar-nonpolar compound is not an alcohol but a fatty acid. This shows that in any case the ion-dipole interaction and the formation of hydrogen bonds do not alone determine the position of the L. A. C. The van der Waals forces between the hydrocarbon chains seem to play a decisive role.

Another interesting fact is that while the L. A. C. is displaced to lower soap concentrations when the chain length of the soap ions increases, the position remains nearly unchanged with increasing chain length of the alcohol (from 6 to 12 carbon atoms). It may be that the lower solubility of the alcohols in water with increasing chain length contributes to this behaviour. The fact remains, however, that according to all our observations made hitherto the most decisive factor in determining the position of L. A. C. is the chain length of the soap ion. This could be interpreted as an indication that the intermolecular forces between the soap ions themselves are decisive for the phenomena that occur at the concentration we have termed the limiting association concentration and that the association tendency between the soap ions is a predominating factor. In the same direction points also the fact that there exists a formally similar relation between the number of carbon atoms in the soap ions and the position of L. A. C. as in the case of the C. M. C. [8,9]; this relation applies up to at least 60° C.

If this last interpretation were correct, it would mean that the phenomena occurring at the L. A. C. are not primarily caused by the alcohol or fatty acid, but must be ascribed to the fact that the association tendency of the soap

anions attains a threshold value at this concentration. The role of the alcohol and fatty acid would then be to promote the association, for instance by decreasing the repulsion between the ionic groups and thus to function like an indicator, which makes the tendency to associate observable.

Whether the phenomena at the limiting concentration only give evidence of the association between soap ions and the molecules of the polar-nonpolar substance or indicate that the tendency to associate has attained a certain level also in the pure soap solution, they must be characterized as deviations from the typical behaviour of normal 1-1 electrolytes, and as far as we know, the first deviations from this behaviour that occur with increasing soap concentration. It seems, however, that the location of the limiting concentration cannot be defined by giving an absolute value for the concentration and it must suffice to report a concentration range within which the first signs of association become evident. Depending on the experimental method employed, the first signs may be observed at somewhat different points in this range. Of importance is, however, that it is possible to detect association phenomena in soap solutions far below the C. M. C's of the pure soaps and also far below the concentrations where the micelle formation occurs in soap solutions containing alcohol or fatty acid.

Our present experimental material relates primarily to fatty acid soap solutions. We have, however, previously found [6,7] that similar phenomena occur also in solutions of alkali metal alkyl sulphates and of alkyltrimethyl ammonium and cetylpyridinium salts; also in these solutions the limiting concentrations (sodium myristyl sulphate 0.0003 M, hexadecyl trimethyl ammonium bromide 0.0004 M) are far below the critical concentrations of the colloids. We believe that a limiting concentration can be determined for all association colloids of the paraffin-chain type.

REFERENCES

1. Ekwall, P., Söderberg, O. and Danielsson, I. *Acta Chem. Scand.* **10** (1956) 227.
2. Ekwall, P., Passinen, K. and Danielsson, I. *Finska Kemistsamfundets Medd.* **63** (1954) 1.
3. Ekwall, P. and Vittasmäki, T. *Unpublished experiments.*
4. Ekwall, P. *Kolloid-Z.* **94** (1941) 42.
5. Ekwall, P. *Kolloid-Z.* **97** (1941) 71.
6. Ekwall, P. *Svensk Kem. Tidskr.* **63** (1951) 277.
7. Ekwall, P. and Danielsson, I. *Acta Chem. Scand.* **5** (1951) 973.
8. Ekwall, P. *Kolloid.-Z.* **8** (1937) 77.
9. Stauff, J. *Z. physik. Chem.* **183** (1938) 55.

Received October 29, 1955.

ACTA CHEMICA SCANDINAVICA 10 (1956) 244—248

On the Reaction between Urea and Formaldehyde in Neutral and Alkaline Solutions

VI. Experimental Studies of the Activation Energy and the Heat of Reaction

NILS LANDQVIST

Rydboholms A.B., Rydboholm, Sweden

The activation energies of the formation and hydrolysis of mono- and dimethylol urea were determined. The activation energies of the reactions between urea — formaldehyde and monomethylol urea — formaldehyde were found to be 15.4 kcal/mole, and the activation energies of the corresponding hydrolysis reactions 20.4 kcal/mole. The heat of reaction of the formation reactions was found to be the same in both cases: 4.9 kcal/mole.

The activation energy of the reaction between urea and formaldehyde at equal concentrations was determined by *e.g.*: (1) Smythe [1]; the amount of unreacted formaldehyde of the 4 M unbuffered reaction solutions was determined by means of the hydroxylamine titration method. The activation energy obtained was 14.7 kcal/mole; (2) Smythe [2]; the reactions in dilute, unbuffered solutions (0.1 M) were studied by means of polarography. Activation energy obtained: 15.3 kcal/mole; (3) Crowe and Lynch [3]; polarographic determinations in 0.05 M LiOH at low concentrations of the reactants. Activation energy: 15.9 kcal/mole.

The activation energy of the reaction between monomethylol urea and formaldehyde was determined by Květoň and Králová [4]. ~2 M reaction solutions and the amount of unreacted formaldehyde determined by means of the hydroxylamine method. Activation energy: 12.2 kcal/mole.

The activation energy of dimethylol urea hydrolysis was also studied by Květoň and Králová [4]. Hydroxylamine method used, activation energy: 16.9 kcal/mole.

As regards the moderate accuracy of the hydroxylamine titration method, reference is given to Landqvist [5].

The purpose of the following paper is to describe experimental studies of the activation energies of mono- and dimethylol urea formation and hydrolysis. The heat of reaction of the forward reactions is given.

Table 1. The activation energy of mono- and dimethylol formation and hydrolysis reactions.

Reaction solution	Buffer	C_{buffer}	pH	Temperature °C	Rate constant $\times 10^5$	E kcal/mole
4.0 M urea + 0.4 M formaldehyde	KH_2PO_4	0.025	6.70	20	6.5	
				30	16.1	16.0
				40	35	14.9
		0.050		20	10.2	
				30	23.1	14.8
				40	54	16.2
		0.100		20	16.0	
				30	38	15.4
				40	84	15.1
	borax	0.050	9.20	20	6.0	
				30	14.0	15.1
				40	32	15.7
						Av. 15.4
	Na_2CO_3	0.050	10.00	20	12.2	
				30	30.0	16.2
				40	73	16.8
1.0 M monomethylol urea + 1.0 M formaldehyde	KH_2PO_4	0.025	6.70	20	2.40	
				30	5.8	15.6
				40	13.1	15.3
		0.050		20	3.8	
				30	8.9	15.1
				40	20.2	15.4
		0.100		20	6.9	
				30	16.0	14.9
				40	37	15.9
	borax	0.050	9.20	20	2.60	14.9
				30	6.0	
				40	13.9	16.1
						Av. 15.4
	Na_2CO_3	0.050	10.00	20	12.2	
				30	30.2	16.8
				40	71	16.4
1.0 M monomethylol urea	KH_2PO_4	0.025	6.70	20	0.221	
				30	0.70	20.5
				40	2.01	19.9
		0.050		20	0.35	
				30	1.10	20.3
				40	3.20	20.3
		0.100		20	0.60	
				30	1.88	20.4
				40	5.7	20.8
	borax	0.050	9.20	20	0.233	
				30	0.74	20.7
				40	2.23	20.4
						Av. 20.4
	Na_2CO_3	0.050	10.00	20	0.46	
				30	1.52	21.0
				40	4.6	21.3

0.5 M dimethylol urea	KH_2PO_4	0.025	6.70	20	0.33	19.7
				30	1.03	
				40	2.99	20.8
		0.050		20	0.53	20.7
				30	1.70	
				40	5.02	20.4
		0.100		20	0.98	20.4
				30	3.11	
				40	9.0	20.1
	borax	0.050	9.20	20	0.302	20.8
				30	0.97	
				40	2.79	20.1
						Av. 20.4
	Na_2CO_3	0.050	10.00	20	1.08	21.6
				30	3.7	
				40	11.9	22.3

* In all cases such an amount of a chloride of the buffer cation was added that a cationic strength corresponding to 0.200 M solutions was maintained.

THE ACTIVATION ENERGIES

The activation energy investigations were carried out as previous studies at 20° C; Landqvist [5]. The temperature interval was 20—40° C. The pH values of the reaction solutions refer to 20° C.

Since the pK of the buffers are dependent on the temperature, and the OH^- catalysis of the reactions is comparatively small, it seems to be most important to keep the concentration of the buffer acid and base as constant as possible (Landqvist [5-8]).

The compositions of the reaction solutions and the reaction rate constants obtained can be found in Table 1. The activation energy, E, from experimental data are included in the table. Examples of the Arrhenius equation relationship are given in Fig. 1.

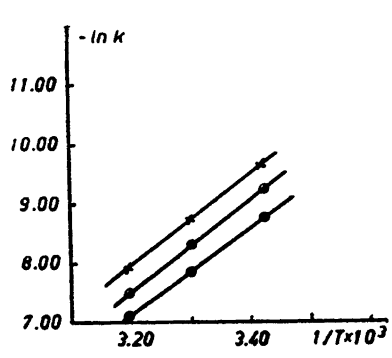


Fig. 1. The relationship between the logarithm of the reaction rate constant and the inverse of the temperature. 4.0 M $CO(NH_2)_2$ + 0.40 M HCHO; $C_{KH_2PO_4}$ = 0.025 (×), 0.050 (○) and 0.100 (●). pH 6.70.

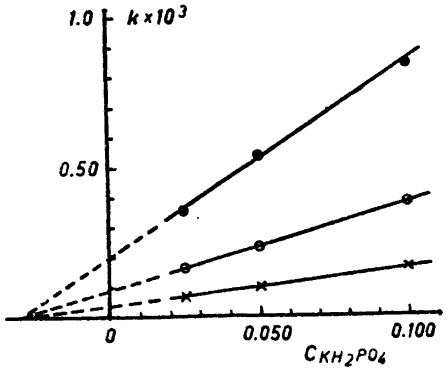


Fig. 2. The relationship between the reaction rate constant and the concentration of the KH_2PO_4 buffer at pH 6.70. The temperatures were: 20° C (×), 30° C (○) and 40° C (●).

At all temperatures and reactions acid — base catalysis as previously reported (Landqvist[5-8]) occurred. An example of the reaction rate constant-buffer concentration (constant cationic strength) relationship is given in Fig. 2. If the curves corresponding to the different temperatures are extrapolated to a reaction rate constant equal to zero, the same (negative) abscissa value was found. These observations support the assumption that the changes in pH due to the change in temperature can be neglected, as regards their influence on the catalysis. The change in the buffer activity is unknown. The activation energies of KH_2PO_4 and borax buffered solutions support an assumption that the influence from this is moderate. In the case of Na_2CO_3 buffers slightly different figures are obtained. The differences between the formation and hydrolysis activation energies are all of the same order, why the carbonate behaviour is probably due to changes in the catalytic properties.

From Table 1 we find reasons to accept the activation energy value 15.4 kcal/mole of the formation reactions; the corresponding hydrolysis figure is 20.4 kcal/mole.

HEAT OF REACTION

The heats of reaction of mono- and dimethylol urea formation were determined calorimetrically. In order to reduce the influence from side reactions; *i. e.* formation of dimethylol urea from urea and formaldehyde and mono- and dimethylol urea hydrolysis, and in order to obtain as complete reactions as possible, the study was made on solutions containing an excess of urea or formaldehyde respectively. In the latter case no formation of tri- and tetramethylol urea is likely to occur, as could be concluded from the consumption of formaldehyde. The catalytic properties were selected to give proper reaction rates. The experiments were carried out as follows.

Monomethylol urea formation. An amount of 500 ml of a 4.0 M urea solution, 0.025 M with respect to Na_2CO_3, pH 11.50, was poured into a Dewar vessel. Through holes in the cork stopper of the vessel a stirrer and a Beckman thermometer were immersed in the urea solution. Through another hole in the stopper a "test tube" was immersed. The tube was made of a polyethylene sheet, and contained 50 ml of a 4 M formaldehyde solution, pH 11.50. When a constant temperature was obtained, 20° C, the tube was torn and the two reactants quickly mixed. Heat transfer through the vessel was corrected for by extrapolation of the time — temperature curve. Corrections for the heats of dilution of the reactants were obtained by replacing the formaldehyde respective urea by distilled water with the same buffers dissolved. The specific heat of the reaction solution was determined by immersing a polyethylene "test tube" containing a known amount of ice. The heat absorption by the calorimeter was determined by the same technique and with distilled water in the vessel.

Dimethylol urea formation. The same technique was used in this case as well. The solution was 500 ml 1.0 M formaldehyde, 0.050 M Na_2CO_3, pH 11.50. The tube contained 4.5 g dry monomethylol urea. Solid monomethylol urea was used in order to prevent influence from hydrolysis reactions. The substance was brought into solution rapidly, and disturbances from this step of the experiment were negligible.

The chemicals used were of A. R. quality, except for the formaldehyde, which was a Merck product containing only traces of methyl alcohol and formic acid ($<4.10^{-4}$ M in solutions containing 380 g/l). The monomethylol urea was prepared in accordance with Walter and Gewing [9]; cryoscopic molecular weight: 90 ± 2.

The heat of reaction was found to be the same for both mono- and dimethylol urea formation, namely 4.9 kcal/mole.

It may be of some interest to compare the activation energy differences ΔE, and the heat of reaction, Q. For processes in solutions we have: $\Delta E \cong Q$. The average difference between the formation and hydrolysis activation energies are 5.0 kcal/mole (Table 1). This figure, as compared with the heat of reaction 4.9 kcal/mole, shows that a good agreement is present.

The author wishes to thank the board of *Rydboholms A. B.* for permission to publish this paper, and is also indebted to Mr G. Johansson and Miss U. Larsson for their valuable assistance in the experimental work.

REFERENCES

1. Smythe, L. *J. Phys. & Colloid Chem.* **51** (1947) 369.
2. Smythe, L. *J. Am. Chem. Soc.* **75** (1953) 574.
3. Crowe, G. and Lynch, C. *J. Am. Chem. Soc.* **71** (1949) 3731.
4. Květoň, R. and Králová, M. *Chem. Listy* **46** (1952) 403.
5. Landqvist, N. *Acta Chem. Scand.* **9** (1955) 1121.
6. Landqvist, N. *Acta Chem. Scand.* **9** (1955) 1459.
7. Landqvist, N. *Acta Chem. Scand.* **9** (1955) 1466.
8. Landqvist, N. *Acta Chem. Scand.* **9** (1955) 1477.
9. Walter, G. and Gewing, M. *Kolloid-Beih.* **34** (1934) 163.

Received October 25, 1955.

ACTA CHEMICA SCANDINAVICA 10 (1956) 249—255

The Configuration of *endo*-Dehydro-norborneol and α-Norborneol

PEKKA HIRSJÄRVI

Institute of Chemistry, University of Helsinki, Finland

The 5-hydroxy-*cyclo*pentane-1,3-*cis*-dicarboxylic acid (5-hydroxy-norcamphoric acid), m.p. 169—170°, prepared by permanganate oxydation and hydrolysis of the so called "*endo*"-dehydro-norbornyl acetate, is a *cis*-hydroxy acid according to the intramolecular hydrogen bonding verified by the author on the infrared absorption spectra of its dimethylester in carbon tetrachloride. From this configuration it follows that "*endo*"-dehydro-norborneol and α-norborneol, its hydrogenation product, have both an *endo*-configuration, as has been generally supposed, but never established. The "*endo*"-dehydro-norbornyl acetate prepared through diene syntheses of vinyl acetate and *cyclo*pentadiene, used as starting material in this work, was catalytically hydrogenated. The hydrolysis product of the hydrogenation product was composed of 75.3 % α-norborneol and 24.7 % β-norborneol on the basis of the infrared spectral analysis. The effect of an addition of boric acid on the electrical conductivity of the solutions of the 5-hydroxy-norcamphoric acid (m.p. 169—170°) in water was investigated. The results are discussed.

In a previous paper [1] a method to investigate the *cis- trans*-configurations of β-hydroxy-*cyclo*pentane-carboxylic acid esters was presented. With this method based on the verification of the intramolecular hydrogen bond formation by means of the infrared absorption spectra, I have now investigated the dimethylester of the 5-hydroxy-norcamphoric acid, prepared by permanganate oxydation of the so called "*endo*"-dehydro-norbornyl acetate*.

The "*endo*"-dehydro-norbornyl acetate is prepared from vinyl acetate and *cyclo*pentadiene through diene syntheses [3]. Owing to the general spectrospecific course (*cf.* Ref. [4]) of the diene syntheses proved by them on other classes of adducts only [5], Alder and Rickert [3] supposed that this compound analogically has *endo*-configuration. The hydrogenation of "*endo*"-dehydro-norborneol yields α-norborneol [6]. Applying their *exo*-addition theory to the catalytic hydrogenation of norcamphor, Alder and Stein [7] drew the conclusion that

* A reaction carried out previously by others in this laboratory [2].

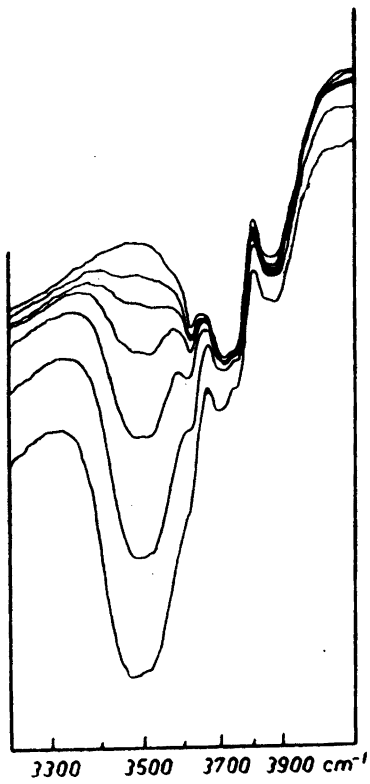


Fig. 1. Infrared absorption spectra of 0.0224—0.0007 M solutions of the 5-hydroxy-norcamphoric acid dimethylester (prepared from the endo*-dehydro-norbornyl acetate) in CCl_4 and that of the solvent in the region of 3 200—3 900 cm^{-1}.*

α-norborneol must have *endo*-configuration, whereas the "*endo*"-dehydro-norborneol and its acetate must have *endo*-configuration. Direct evidence for the configurations of norborneols and dehydro-norborneols has not been presented; Alder and Stein [7], however, have communicated that they are (1936) studying the configuration of α-norborneol in order to prove it. Their method seems possible in theory, but so far no results have been published.

In the Bertram-Walbaum-reaction of a mixture of norbornylene and nortricyclene β-norbornyl acetate is obtained [8]. On the basis of this fact the conclusion may be drawn that the latter has *exo*-configuration (*cf.* Ref. [9]).

According to H. Toivonen [10] the oxydation of α-norborneol with concentrated nitric acid yields norcamphor, whereas β-norborneol in the same circumstances yields nitric acid ester. Further, according to H. Toivonen [11] the *endo*-form of the terpene alcohols for which the *endo-exo*-configurations are chemically explained, *viz.* for borneol, *iso*borneol [12], α-fenchol and β-fenchol [13], is oxidised with nitric acid to the corresponding ketone, while the *exo*-form is esterified. In this reaction thus α-norborneol behaves like the aforementioned *endo*-alcohols and β-norborneol like their *exo*-forms.

To check the steric purity of the starting material in this work a part of the dehydro-norbornyl acetate used was hydrogenated and hydrolysed. Ac-

Table 1. Transmission of the solution of 5-hydroxy-norcamphoric acid dimethylester in CCl_4 on hydrogen bonded O-H-absorption band (3 468 cm^{-1}) (Fig. 1).

Concentration mole · l^{-1}	$\log_{10}\frac{P}{P_0}$	k $l \cdot mole^{-1}$
0.0224	0.150—1	38.0
0.0112	0.574—1	38.0
0.0056	0.789—1	37.7
0.00280	0.8965—1	37.0
0.00140	0.9474—1	37.6
0.00070	0.9731—1	38.5

cording to the infrared spectral analysis[14] the product was composed of 75.3 % α-norborneol and 24.7 % β-norborneol (*cf.* Ref. [4]). 33.9 % of theory of the crystalline, in ether very slightly soluble 5-hydroxy-norcamphoric acid isomer (m.p. 169—170°) was isolated from the permanganate oxydation product of the dehydro-norbornyl acetate. On the basis of the amount of the yield this isomer can arise only from the dehydro-norbornyl acetate of the α-norborneol series.

The infrared absorption spectra of 5-hydroxy-norcamphoric acid dimethylester (0.0224—0.0007 M solutions in carbon tetrachloride) in the region 3 900—3 200 cm^{-1} investigated in this work are given in Fig. 1. The absorption band of the (hydrogen-)bonded hydroxyl group is here broader (double (?) 3 468, 3 515 cm^{-1}) than in the case of the 5-*cis*-hydroxy-*iso*fenchoic acid dimethylester and 5-*cis*-hydroxy-camphoric acid dimethylester [1]. Even in such a small concentration as 0.00070 M one cannot with certainty verify the absorption band of the free hydroxyl group (in the region of 3 600—3 640 cm^{-1}). The values of $\frac{P}{P_0}$ were obtained from the center of the 3 468 cm^{-1} absorption band in the spectra given and the values of the coefficient k in the Beer's law formula $\log_{10}\frac{P}{P_0} = -k \cdot c, (k = a \cdot b)$ were calculated and are given in Table 1. (The same $b = 1.003$ cm quarz cell was used as in the previous work [1]). The value of k is constant in the limits of experimental error. The hydrogen bond absorption band must thus in this case belong to the intramolecular one [1].

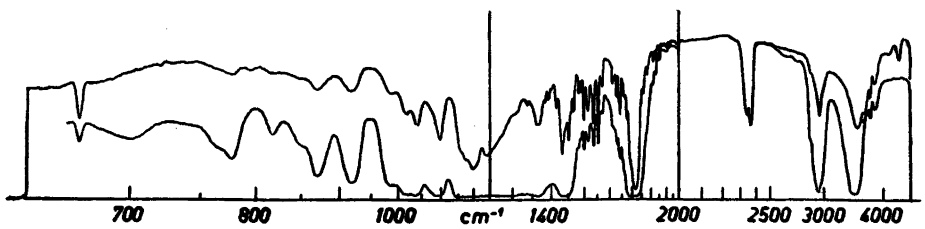
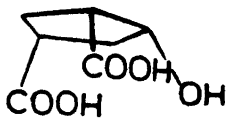
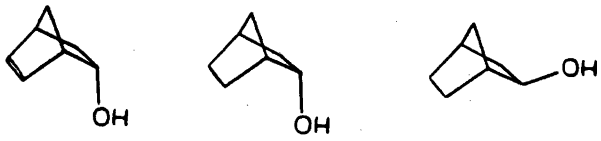


Fig. 2. Infrared absorption spectrum of cis-*5-hydroxy-norcamphoric acid dimethylester (with atmospheric background, upper a capillary film and lower a 0.05 mm thick sample).*

This intramolecular hydrogen bonding on the 5-hydroxy-norcamphoric acid dimethylester is possible only when the (1-)carboxyl group and the (5-) hydroxyl group are in *cis*-position with regard to the five ring; since, further, this is a *cis*-dicarboxylic acid (anhydride formation [2] and preparation by the permanganate oxydation from dehydro-norborneol), the hydroxyl and both carboxyl groups must be on the same side of the five ring plane. This 5-hydroxy-norcamphoric acid isomer is thus 5-*cis*-hydroxy-*cyclo*pentane-1,3-*cis*-dicarboxylic acid (*cf.* Fig. 3).



From this configuration it follows that α-norborneol and "*endo*"-dehydro-norborneol have both *endo*-configuration and that β-norborneol must have *exo*-configuration:



endo-Dehydro-norborneol α-Norborneol β-Norborneol

The absorption band of the bonded O-H-stretching frequency is here broader, as mentioned above, and the value of k is smaller (38.0) than it was in the case of the β-hydroxy-*cyclo*pentane carboxylic acid esters studied in the mentioned previous work [1] (69.0). The 5-*cis*-hydroxy-*cyclo*pentane carboxylic acid dimethylester can form at least four different intramolecular hydrogen bonds (the hydrogen atom of the hydroxyl group is directed either below the molecule or outwards and the bonding occurs either with the carbonyl- or the ether-oxygen atom); *cf.* Fig. 3. The free rotation of the (5-)hydroxyl group and of the (1-)carboxyl group is hindered only by one another. (If the carboxyl group rotated unhindered, the shortest distance between the centers of the oxygen atom of hydroxyl group and of the nearest oxygen atom of (1-)carboxyl group would be *ca.* 2.0 Å. The oxygen-oxygen distance varies in unstrained hydrogen bonds from 2.5 to 2.9 Å). The occurrence of different intramolecular hydrogen bonding possibilities seems to cause a broadening in the absorption band related to the bonded O-H-stretching vibration.

The effect of boric acid on the electrical conductivity of the solution in water of the 5-hydroxy-norcamphoric acid isomer, studied in this work, was also investigated. The method is described elsewhere [1]. The results are given in Table 2. There is no change in the specific conductance when ¼ M boric acid is used as solvent instead of water. Of all β-hydroxy-*cyclo*pentanecarboxylic acids previous studied [1,15,16] boric acid causes an increase in specific conductance of *cis*-hydroxy acid isomers and a slight decrease in that of *trans*-hydroxy acid isomers. In these latter compounds the boric acid complex formation is not possible for steric reasons. On the basis of these facts the results reported in Table 2 can mean boric acid complex formation, though to so very slight an extent that no certain conclusions can be drawn.

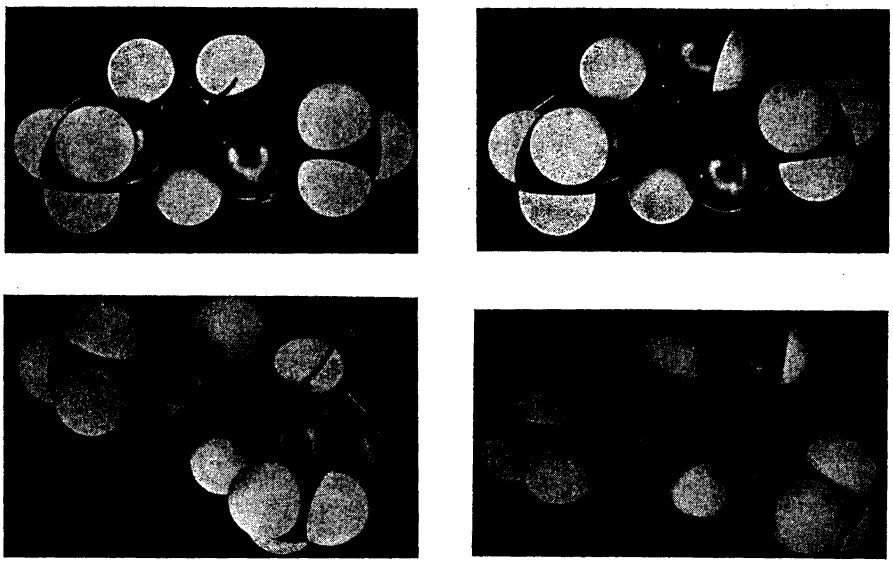


Fig. 3. Stuart-Briegleb models of four different possible intramolecular hydrogen bond types on 5-cis-*hydroxy*-cyclo*pentane-1.3*-cis-*dicarbonic acid dimethylester*

The hydrogen ion activities of the conductivity measurement solutions were compared in pairs. In all concentrations studied, the solution of 5-hydroxy-norcamphoric acid in ¼ M boric acid was more acidic than that of the same concentration in pure water and the difference in pH was greater than that calculated when no boric acid complex formation was taken into consideration. There can thus be weak boric acid complex formation.

Table 2. The electrical conductivity of the solutions of 5-hydroxy-norcamphoric acid (m.p. 169—170°) in water and in ¼ M boric acid—water solution at 25°. The cell constant: 0.283 cm^{-1}. Water $\varkappa^{25}$ 1.42 · 10^{-6}ohm^{-1} · cm^{-1}; ¼ M boric acid—water solution $\varkappa^{25}$ 9.25 · 10^{-6}ohm^{-1} · cm^{-1}.

Concentration mole · l^{-1}	Solvent			
	Water		¼ M boric acid	
	Resistance of the solution ohms	Specific conductance of the solution 10^4 $\varkappa$ ohm^{-1} · cm^{-1}	Resistance of the solution ohms	Specific conductance of the solution 10^4 $\varkappa$ ohm^{-1} · cm^{-1}
1/8	295	9.60	—	—
1/16	407	6.95	405	6.98
1/32	587	4.82	585	4.84
1/64	835	3.39	835	3.39
1/128	1 190	2.38	1 190	2.38
1/256	1 720	1.65	1 720	1.65

As mentioned before, in all previously studied cases the boric acid has caused, in general, a considerable increase in the electrical conductivity of *β-cis*-hydroxy-*cyclo*pentane carboxylic acids and a slight decrease in the conductivity of *β-trans*-hydroxy-*cyclo*pentane carboxylic acids. In this case the possible weak boric acid complex formation can be explained as follows: The intramolecular hydrogen bonding is here very strong and sterically favored, and it competes with success with boric acid complex formation for the not hydrogen bonded hydroxy acid molecules. The magnitude of the equilibrium constants of both reactions and their relation determine the concentration of boric acid complex molecules and the extent of the increase in specific conductance.

EXPERIMENTAL

"endo"-*Dehydro-norbornyl acetate* was prepared from vinyl acetate and di*cyclo*pentadiene by a method similar to that of Alder and Rickert [3]. The product was distilled four times under reduced pressure with an efficient column, and fraction b.p. 67.5° (11.5 mm) was employed. n_D^{20} 1.4693, d_4^{20} 1.0502. A part of this sample of dehydro-norbornyl acetate (4.50 g) was hydrogenated in the presence of a Raney-nickel catalyst at 65° and 100 atm. initial pressure. The product was hydrolysed with sodium hydroxide in water-ethanol. The reaction mixture was extracted with ether-light petroleum mixture (50 + 50) and dried over potassium carbonate. After removal of the ether and light petroleum, 3.68 g of white crystalline powder, m.p. 142.5—145°, was obtained. According to the infrared spectral analysis [14] this is a mixture of 75.3 % α-norborneol and 24.7 % β-norborneol.

5-Hydroxy-norcamphoric acid. To a mixture of 26.6 g of "*endo*"-dehydro-norbornyl acetate, 100.0 g of $MgSO_4 \cdot 7\ H_2O$ and 500 ml of water 73.2 g of potassium permanganate was gradually added during two hours. When the color of the permanganate had disappeared, 450 ml of 2 N sodium hydroxide was added. After 12 hours staying the mixture was filtered, and the filtrate extracted with ether for removal of the neutral materials. The water layer was acidified with sulphuric acid and extracted with ether in a continuous extraction apparatus for 50 hours. A part of the ether extract precipitated during the extraction as a white crystalline powder and was filtered off; 9.87 g, m.p. 165—168°. The ether solution was dried over sodium sulphate, and the ether was removed. Of the oily residue the acetic acid was evaporated in a vacuum and additional 0.45 g of crystals m.p. 165.5—170° was isolated by means of rubbing with ether. The yield of oily product was 10.68 g. In all, 10.32 g (33.9 % of theory) of crystals was obtained. After recrystallisation of water the m.p. was 169—170°. (Found: C 48.15; H 5.84. Calc. for $C_7H_{10}O_5$: C 48.27; H 5.79. The acid was titrated with 0.1 N NaOH: equiv.wt. 87.0. Calc. for twobasic acid $C_7H_{10}O_5$: equiv.wt. 87.1). This 5-hydroxy-norcamphoric acid is very soluble in water and very slightly soluble in ether.

5-Hydroxy-norcamphoric acid dimethylester was prepared in ether of the silver salt and methyl iodide. The product, a colorless, viscous liquid, very soluble in water, was distilled in a high vacuum, n_D^{20} 1.4694. (Found: C 53.60; H 6.88. Calc. for $C_9H_{14}O_5$: C 53.46; H 6.98. Total hydrolysis: equiv.wt. 101.0. Calc. 101.1.) Infrared spectrum in Fig. 2.

REFERENCES

1. Hirsjärvi, P. *Acta Chem. Scand.* **8** (1954) 12.
2. Toivonen, N. J. *Private communication.*
3. Alder, K. and Rickert, H. F. *Ann.* **543** (1940) 1.
4. Roberts, J. D., Trumbull, E. R. Jr., Bennett, W. and Armstrong, R. *J.Am. Chem. Soc.* **72** (1950) 3116.
5. Alder, K. and Stein, G. *Angew.Chem.* **50** (1937) 510.
6. Komppa, G. and Beckmann, S. *Ann.* **512** (1934) 172.

7. Alder, K. and Stein, G. *Ann.* **525** (1936) 183.
8. Pulkkinen, E. *Suomen Kemistilehti A* **27** (1954) 26.
9. Toivonen, N. J. *Suomen Kemistilehti B* **24** (1951) 62.
10. Toivonen, H. *Suomen Kemistilehti B* **26** (1953) 75.
11. Toivonen, H. *Suomen Kemistilehti B* **25** (1952) 69.
12. Toivonen, N. J., Hirsjärvi, P., Melaja, A., Kainulainen, A., Halonen, A. and Pulkkinen, E. *Acta Chem. Scand.* **3** (1949) 991; Asahina, Y., Ishidate, M. and Sano, T. *Ber.* **69** (1936) 343.
13. Toivonen, N. J. *Sjätte Nordiska Kemistmötet, Lund,* 1947, p. 276; Hirsjärvi, P. *Ann. Acad. Sci. Fennicae Ser A. II.* **45** (1952) 1.
14. Hirsjärvi, P. *To be published in another connection.*
15. Böeseken, J., Slooff, G. and Lutgerhorst, A. G. *Proc. Acad. Sci. Amsterdam* **34** (1931) 932.
16. Böeseken, J., Slooff, G., Hoeffelman, J. M. and Hirsch, H. E. *Rec. trav. chim.* **52** (1933) 881.

Received October 31, 1955.

ACTA CHEMICA SCANDINAVICA 10 (1956) 256—260

On the Isomerism of Hydroxyurea

VII. The Reaction of Hydroxylamine with Cyanic Acid in Anhydrous Ether

HELMER KOFOD

Royal Danish School of Pharmacy, Dept. of Organic Chem., Copenhagen, Denmark

By the reaction of hydroxylammonium ion and cyanate ion a mixture of two isomeric hydroxyureas is formed, differing *inter alia* by melting point. In previous work the *lower melting* product was found to predominate, when the reaction was performed in aqueous solution at 0° C.

Experiments reported in the present paper indicate that the corresponding reaction between the uncharged molecules in anhydrous ether solution leads to predominantly the *higher melting* product. A possible correlation of the isomerism with the postulated tautomerism of cyanic acid is briefly discussed.

In part II of the present series [1] it was concluded that the ionic process $HONH_3^+ + {}^-OCN \rightarrow CH_4O_2N_2$ (hydroxyurea) in aqueous solution at 0° C leads to roughly equal amounts of the two known isomerides, which for the sake of brevity will be denoted OU_{72} and OU_{140}, respectively. The index is the characteristic decomposition temperature. The proposed ratio was inferred from the preparative yields, making some allowance for the greater lability of OU_{72}.

More accurate polarographic measurements [2] have indicated that under the said conditions rather more of OU_{72} is formed than of its isomer, the ratio OU_{72}/OU_{140} being probably between 1 and 2.

Although the formation of two isomeric products in a chemical process need not by necessity originate in structural ambiguity of the reactants but may be merely a matter of statistic probabilities, it is, however, striking that both cyanic acid and hydroxylamine display certain dualistic properties.

The structure of cyanic acid has been intensely studied by many investigators and has been a subject of much controversy. The most reliable interpretation is probably that given by Birckenbach and Kolb[3] *cf.* [6] from classical

chemical arguments and by Goubeau [4] from Raman-spectroscopic data. According to these authors cyanic acid exists in the tautomeric equilibrium

$$\underset{a}{H—\underline{N}=C=\underline{\bar{O}}} \rightleftharpoons \underset{b}{|N\equiv C—\underline{\bar{O}}—H},$$

a, which is believed to be the more stable form, predominates in the free cyanic acid and in solutions in "non-polar" solvents, whereas *b* appears to represent the structure of cyanic acid dissolved in "polar" solvents, all provided that equilibrium is attained. The crystalline salts of cyanic acid presumably contain the mesomeric anion

$$\left(\underset{a}{\underline{\bar{N}}=C=\underline{\bar{O}}} \leftrightarrow \underset{b}{|N\equiv C—\underline{\bar{O}}|} \right)^-$$

the actual electron-distribution being close to *a* in the salts of complex-forming metals with a bond type approximating the covalent one and close to *b* in the essentially ionic salts, such as the alkali cyanates. Most salts have been isolated in one form only, corresponding to either structure *a* or *b*, but in a few instances, *e. g.* mercury, individually existing isomeric salts could be isolated by the authors quoted [3].

Let it be assumed that the isomerism of hydroxyurea is somehow the result of the tautomerism of cyanic acid. It is evident, then, that OU_{72}, which is formed in major amounts by the ionic process in aqueous solution, must be associated with cyanic acid of structure *b*, since this electron-distribution is predominant in aqueous solution. As a consequence the reaction of free hydroxylamine-base and cyanic acid in, *e. g.*, ether (structure *a*) should produce exclusively or predominantly the higher melting hydroxyurea OU_{140}.

As a matter of fact this has been experimentally confirmed and some support has therefore been carried to the hypothesis.

The experimentation presented certain difficulties, owing to both reactants being exceedingly unstable. Free hydroxylamine base decomposes rapidly into ammonia, nitrogen and water, and cyanic acid is apt to polymerize and to decompose. After a number of introductory experiments the following procedure was found to work satisfactorily.

The reaction was performed at 0° C in anhydrous ether solution. Under these conditions hydroxylamine is sufficiently soluble and relatively stable, and cyanic acid is very soluble and does not polymerize too rapidly. The reactants were freshly prepared immediately prior to use.

Cyanic acid was obtained [10] by depolymerization of cyanuric acid $(HNCO)_3$; the latter was prepared according to Walther [5] by heating urea with anhydrous zinc chloride at 220° C. The product was recrystallized from water and dried to constant weight at 105° C.

The cyanic acid generator is shown in Fig. 1. A few grammes of cyanuric acid was placed in the quartz combustion tube and a slow stream of dry nitrogen was passed through it, while the part containing the cyanuric acid was heated with a flame until sublimation occurred. The trimer partly sublimes and partly undergoes depolymerization, and the heating and nitrogen flow were regulated in such a way that the sublimate was redeposited within the

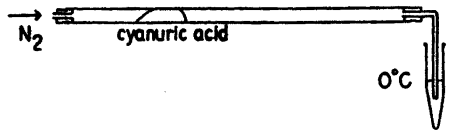


Fig. 1. Cyanic acid generator.

quartz tube and only the gaseous monomer was allowed to leave the outlet. It was absorbed in some milliliters of anhydrous ether in the centrifuge tube, which was immersed in an ice-water bath to retard polymerization of the cyanic acid. By proper operation the contents of the centrifuge tube was a clear solution with the characteristic acetic acid-like smell of cyanic acid.

Hydroxylamine was most conveniently obtained by the method of Hurd [7] with some technical modifications. A solution of sodium butoxide was prepared by refluxing 7.8 g (1/3 mole) of sodium with 100 ml of redistilled butanol-1. The equivalent amount (23 g) of hydroxylammonium chloride (analytical grade, finely ground and thoroughly dried), 3 mg of phenolphthalein and 30 ml of butanol were placed in a 250 ml pyrex-flask fitted with a magnetic stirring device and a delivery funnel containing the butoxide solution. The funnel was heated to about 40° C by exposing it to infra-red radiation in order to prevent crystallization. The butoxide solution was added dropwise with continuous stirring at such a rate that the pink colour never predominated. The "neutralization" required 1.2 hour. Sodium chloride was filtered off and washed with butanol and anhydrous ether and the combined colourless liquids were cooled to —10° C. Hydroxylamine was obtained in good yield as large colourless flakes. It was washed with anhydrous ether and dried *in vacuo* at —10° C to remove solvents; the melting point, taken immediately, was

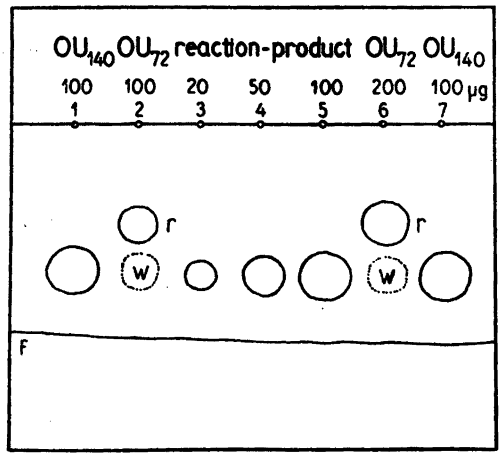


Fig. 2. Descending paper-chromatogram of the reaction product and authentic samples of hydroxyurea isomerides. Whatman paper no. 1; Solvent ethanol-hydrochloric acid; 25.0° C; spray-reagent picryl chloride, subsequent exposure to ammonia vapour. General technique vide *Ref.*[8]*; r means red, other spots orange; w weak.*

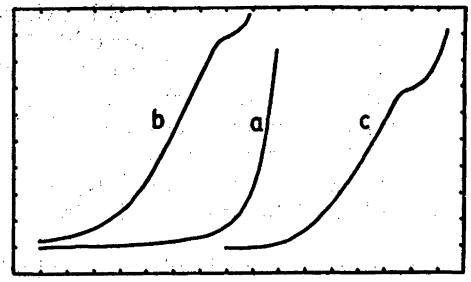


Fig. 3. Polarographic current-voltage curves recorded at 22° C pH 7.2; capillary characteristics of the mercury electrode are height of mercury column h = 24 cm; rate of mercury outflow m = 3.02 mgsec^{-1}; drop time 3.3 sec. One unit on the ordinate equals 0.66 microamps, one unit on the abscissa equals 0.1 volt. All curves begin at −1.0 volt vs. *"saturated calomel electrode".*

a. 0.1 M potassium phosphate buffer[9] pH 7.2 (blank)
b. 3.0 mg reaction product in 5 ml of buffer as under a.
c. 0.25 mg authentic lower melting hydroxyurea (OU_{72}) in 5 ml of buffer.

32° C; Ref.[7] 33° C. The substance was used forthwith for the actual experiment as described below. The remaining crop was stored at 0° C; nevertheless it was completely decomposed the following day.

Anhydrous ether (4 ml) was saturated with hydroxylamine at 0°. A freshly prepared solution of cyanic acid in anhydrous ether (0° C) was added dropwise. A colourless, crystalline precipitate was formed, and the addition of cyanic acid was continued until no further precipitation occurred. The contents of the reaction vessel were centrifuged, and the supernatant ether poured off. The solid was washed with 2 × 1 ml cold anhydrous ether, in which both hydroxyureas are insoluble, and dried *in vacuo*. The product gave the characteristic blue-violet colour produced by OU_{140} on addition of ferric chloride. Paper-chromatographic analysis according to the previously reported technique[8] proved that the product was identical with OU_{140} isolated from the ionic process. In Fig. 2 is reproduced a descending paper-chromatogram of the product (Nos. 3—5) run together with authentic samples of the two known isomerides. The irrigation solvent was a mixture of 70 ml of ethanol and 30 ml of 4 N hydrochloric acid. In this solvent both hydroxyureas are sufficiently stable and the isomerization is very slow[8]. The weak OU_{140}-spot to be seen in the runs 2 and 6 is due to the fact that the sample of OU_{72} was 1 month old, and hence partly isomerized. The spot in run No. 5 is comparable in size to the authentic spot in runs Nos. 1 and 7. As the amount applied to the paper is the same, it may be concluded that the reaction product consists almost entirely of OU_{140}. There was not on the original paper-sheet any trace of the characteristic red OU_{72}-spot to be seen in the runs 3—5.

The still more sensitive polarographic method[9], however, revealed the presence of approximately 10 % OU_{72}. In Fig. 3a is reproduced a blank current-voltage curve of the supporting buffer, pH 7.2 (*vide* Ref.[9]), curve *b* is a polarogram of 3.0 mg reaction product dissolved in 5 ml of the same buffer. It

represents the usual OU_{72}-wave at —1.5 V *vs.* SCE. Curve *c* is a polarogram recorded under identical conditions of a solution of 0.25 mg of authentic OU_{72} in 5 ml of buffer. From the relative heights (linear relationship has been found between concentration and wave height, Ref.[9] Fig. 4) of *b* and *c* it may be estimated, that the 3.0 mg of reaction-product weighed out contain approximately 0.3 mg or 10 % of the lower melting isomer. The identity of the wave *b* was further established by adding authentic OU_{72} to the cell-solution; this caused an increase in wave-height but neither displacement nor distortion of the wave.

The thermal decomposition interval of the product (Kofler hot-stage microscope) was in accordance with the above results. The content of OU_{72} was evidently too small to produce any visible change at 72° C, but decomposition and melting occurred abnormally low and over a large interval, 120—135° C. The decomposition temperature normally found for the pure OU_{140} is 135—140° C, depending upon the rate of heating.

The formation of hydroxyurea isomerides described in the present paper is directly comparable with previous experiments on the ionic process [1,2], in that both reactions were carried out at 0° C and cyanic acid was added to hydroxylamine and not *vice versa*. The observed ratio OU_{72}/OU_{140} was over 1 with the ionic process and approximately 0.1 with the reaction described in this paper. This result strongly suggests that the isomerism of hydroxyurea has some relation to the postulated tautomerism of cyanic acid, a point of view, which is quite interesting, because it means that the isomerism of hydroxyurea is at least formally analogous to that of urea and isourea, which, as far as the parent compounds are concerned, do not seem capable of individual existence. A detailed discussion of formation mechanisms and structure will be presented in a final publication.

REFERENCES

1. Kofod, H. *Acta Chem. Scand.* **7** (1953) 938.
2. Kofod, H. *Acta Chem. Scand. (To be published.)*
3. Birckenbach, L. and Kolb, H. *Ber.* **66** (1933) 1571 p. 1572; *cf. Ber.* **68** (1935) 895.
4. Goubeau, J. *Ber.* **68** (1935) 912 p. 918.
5. Walther, J. *J. prakt. Chem.* (2) **79** (1909) 128.
6. Michael, A. and Hibbert, H. *Ann.* **364** (1909) 130.
7. Hurd, Ch. D. in Booth, H. S. (editor) *Inorganic Syntheses* vol. 1 p. 87, New York and London 1939.
8. Kofod, H. *Acta Chem. Scand.* **9** (1955) 1575.
9. Kofod, H. *Acta Chem. Scand.* **9** (1955) 455 p. 468.
10. Baeyer, A. *Ann.* **114** (1860) 165.

Received November 12, 1955.

ACTA CHEMICA SCANDINAVICA 10 (1956) 261—264

The Structure Parameters of Dimethyldiacetylene

A. ALMENNINGEN, O. BASTIANSEN* and T. MUNTHE-KAAS

Universitetets Kjemiske Institutt, Blindern — Oslo, Norway

Electron diffraction studies have been carried out on the structure of dimethyldiacetylene. The following structure parameters have been obtained, C-H = 1.09 Å, C≡C = 1.208 Å, C_2-C_4 = 1.377 Å, C_1-C_2 = 1.450 Å and HCC = 111.6°

Accurate determinations of bond distances in conjugated systems seem to be of considerable interest. A new electron diffraction apparatus now in operation in Oslo has made it possible to determine internuclear distances with a rather high accuracy. A series of compounds containing conjugated systems is now being studied with the new technique. The investigations include dimethyldiacetylene, vinylacetylene, butadiene and *cyclo*octatetraene. In the present note the results for dimethyldiacetylene will be described.

As the new electron diffraction apparatus and the calculation technique have been described elsewhere [1,2] only a few comments concerning the procedure will be given. The intensity values obtained in this case range from about $s = 1$ up to $s = 60$ Å^{-1}. From the intensity data radial distribution curves have been calculated. Various damping factors have been used. The radial distribution curve presented in Fig. 1. is calculated by applying a damping factor of $e^{-0.0015\,s^2}$. The inner complex of peaks ranging from about 1 Å until 1.6 Å contains the bond distances. The peaks beyond this point contain internuclear distances between atoms which are not directly linked together. In the curve of Fig. 1 the inner complex of peaks is not very well resolved. A better resolution is obtained by applying a smaller damping factor or simply by omitting the damping factor altogether. Detailed studies of this inner complex in the various radial distribution curves, including the use of normal curves, lead to the four first entries in the first column of Table 1. A study of the outer part of the radial distribution curve gives the other internuclear distances listed in the table.

* Present address: Institutt for teoretisk kjemi, Norges tekniske høgskole, Trondheim, Norway.

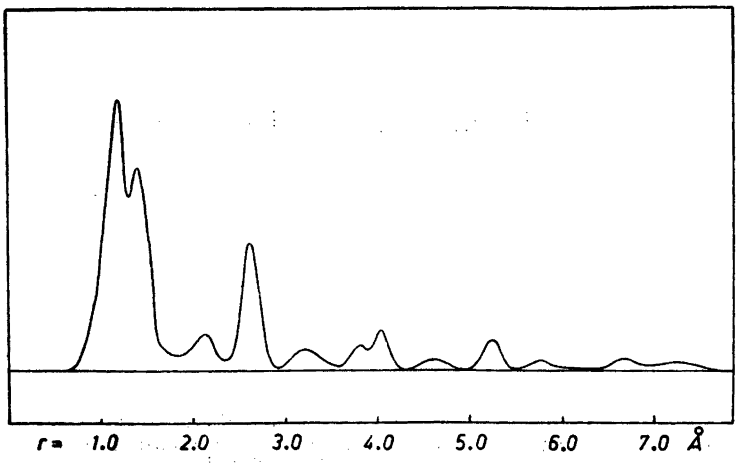


Fig. 1. Radial distribution curve of dimethyldiacetylene.

The geometry of the carbon skeleton is determined by three parameters if a linear arrangement is assumed. These three parameters were obtained from the nine experimental C—C distances by a least-square procedure. The two parameters necessary for the location of the hydrogen atoms were calculated in a similar way. The best structural parameters thus obtained from our experiment are the following: C—H = 1.09 Å, $C_2 \equiv C_3$ = 1.208 Å, C_3—C_4 = 1.377 Å, C_1—C_2 = 1.450 Å and ∠ HCC = 111.6°. These values are in good agreement with those obtained by Jeffrey and Rollett for dimethyltriacetylene [3]. On the basis of the five parameters obtained all the internuclear C—C and C—H distances were calculated. These values are listed in the second column of the table. The correspondence between the values read off from the radial distribution curves and those calculated from the best parameters is in general remarkably good. For the carbon skeleton the average deviation between the two sets of distances is between 0.2 and 0.3 %. This indicates a rather high accuracy in the distance determination, though it does not give any indication concerning the absolute values. Estimations of the various sources of errors, and comparison between results obtained by our electron diffraction procedure and microwave studies seem to indicate that our scale error is about of the same order of magnitude as the deviation observed within a single radial distribution curve [4].

The positions of the hydrogen atoms are not determined with the same degree of accuracy as the carbon atoms. The C—H bond distance does not lead to a resolved peak in the radial distribution curve, and the longer C—H distances are not well suited for accurate determinations of the C—H bond and the HCC angle.

By studying the half widths of the peaks of the radial distribution curves experimental values for the root mean squares of the deviations from the equilibrium distances have been calculated. These values for the C—H bond and

Table 1. Experimental and calculated distances and average displacements from equilibrium, all in Ångstrom units.

	r_{exptl}	r_{calc}	$(\overline{l^2})^{1/2}_{exptl}$	$(\overline{l^2})^{1/2}_{calc}$
C –H	1.08	1.09	0.077	0.075
$C_2 \equiv C_3$	1.210	1.208	0.040	0.036
$C_3 - C_4$	1.379	1.377	0.061	0.044
$C_1 - C_2$	1.452	1.450	0.061	0.045
$C_2 - C_4$	2.590	2.585	0.050	0.049
$C_1 - C_3$	2.661	2.658	0.066	0.049
$C_2 - C_5$	3.778	3.793	0.049	0.053
$C_1 - C_4$	4.026	4.035	0.060	0.057
$C_1 - C_5$	5.228	5.243	0.072	0.059
$C_1 - C_6$	6.661	6.693	0.080	0.065
$H - C_2$	2.110	2.110		
$H - C_3$	3.220	3.222		
$H - C_4$	4.571	4.550		
$H - C_5$		5.734		
$H - C_6$	7.201	7.166		

all the C—C distances are listed in the third column of the table. In the last column of the table are listed the corresponding theoretical values calculated applying the stretching vibrations known from spectroscopical data [5] assuming a temperature of 310°K. As one sees, the correspondence between these sets of values obtained in two entirely different ways is fairly good.

A comparison between the experimental and calculated distances in Table 1 seems to indicate a systematic deviation between the two sets of values for the largest C—C distances. For the four largest C—C distances the experimental values are smaller than the calculated ones, while the opposite is the case for the shorter distances. This fact might be explained by taking into consideration the bending vibrations of the molecule. These vibrations should lead to a decrease in the long distances. If this argument is correct, the longest C—C distances should perhaps have been omitted in the least-square procedure. A correction for this effect, however, would lead only to very small changes in the structure parameters.

Acknowledgement. The authors wish to extend their thanks to Professor E. R. H. Jones for having placed a sample of dimethyldiacetylene at their disposal.

Added in proof: Since this article was submitted for publication an article concerning the structure of dimethylacetylene has been published [6]. In this article a report from Ohio State University has been quoted dealing with the structure of dimethyldiacetylene [7]. Unfortunately the latter was unknown by the present authors. Both compounds were studied by X-ray methods, and the agreement with the present work is very good.

REFERENCES

1. Bastiansen, O. *Det 8. Nordiske Kjemikermöte Oslo* **1953**; Bastiansen, O., Hassel, O. and Risberg, E. *Acta Chem. Scand.* **9** (1955) 232.
2. Almenningen, A. and Bastiansen, O. *Acta Chem. Scand.* **9** (1955) 815.
3. Jeffrey, G. A. and Rollett, J. S. *Proc. Roy. Soc. London* **A 213** (1952) 86.
4. Almenningen, A., Bastiansen, O. and Hansen, L. *Acta Chem. Scand.* **9** (1955) 1306.
5. Ferigle, S. M., Cleveland, F. F. and Meister, A. G. *J. Chem. Phys.* **20** (1952) 1928.
6. Pignataro, E. and Post, B. *Acta Cryst.* **8** (1955) 672.
7. Himes, R. C. and Harris, P. M. *Technical Report No. 3, R. F. Project 355*, Ohio State University, 1953.

Received October 31, 1955.

ACTA CHEMICA SCANDINAVICA 10 (1956) 265—267

The Infrared Spectra of some Modifications of Arsenic Trioxide and Antimony Trioxide

O. BORGEN and J. KROGH-MOE

Institutt for teoretisk kjemi, Norges Tekniske Høgskole, Trondheim, Norway

The infrared spectra of cubic and monoclinic arsenic trioxide and cubic and orthorhombic antimony trioxide have been compared with the spectra of the vitreous modifications. The latter show best agreement with the spectra of the cubic modifications.

The structures of the crystalline modifications of the trioxides of arsenic and antimony are quite well known. The cubic forms are built up of As_4O_6 and Sb_4O_6 molecules [1], whereas the monoclinic arsenic trioxide [2] and the orthorhombic antimony trioxide [3] have chain or layer structures. The existence of other crystalline modifications has been suggested [2].

The structures of the vitreous form are, however, a matter of controversy. Shulman and Shumb [4] inferred from the devitrification of arsenic trioxide glass that it is rather closely related to the cubic form. A comparison of the densities (cubic [5] 3.87, monoclinic [6] 4.14, glass [7] 3.70) seems to strengthen this inference.

As Zachariasen's theory of glass structures [8] seems to be incompatible with the existence of As_4O_6 molecules, Bötticher, Plieth, Reuber-Kürbs and Stranski [9] were led by this and other evidence [10] to carry out an X-ray investigation of the vitreous phase. Their conclusion, the similarity of the vitreous and the monoclinic modifications, seems in the light of later investigations [11] on the errors involved in this kind of determinations rather uncertain.

In order to compare the structures of the above trioxides, their infrared spectra have been obtained in the sodium chloride region.

EXPERIMENTAL

The spectra were obtained on a Perkin-Elmer 21 recording spectrometer in the interval of 2 to 15 microns. The samples were prepared by the potassium bromide technique with 2 or 10 milligrams of oxide in 2 grams discs of about one inch diameter. A pressure of 20 tons was applied for 15 minutes.

The trioxide modifications were prepared from Merck *pro analysi* reagents after recrystallisation. The identities were ascertained by means of the X-ray diffraction patterns.

The samples were as follows

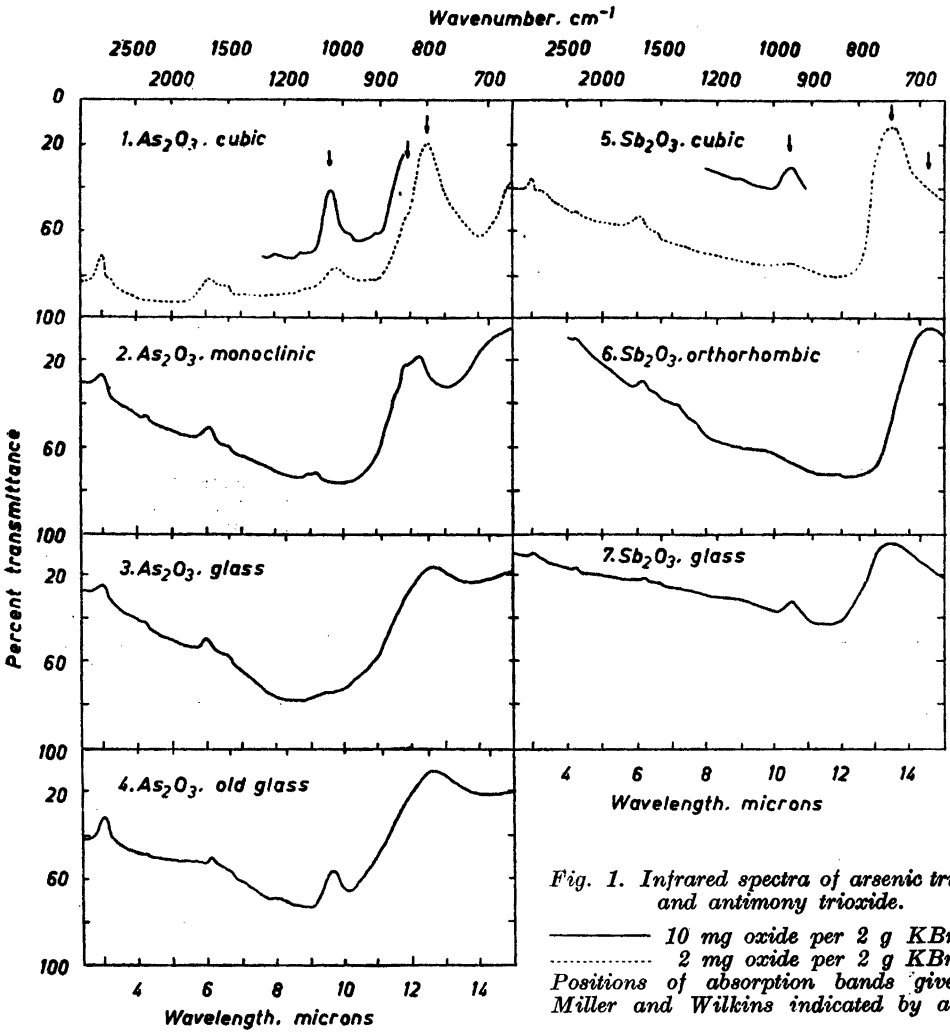


Fig. 1. Infrared spectra of arsenic trioxide and antimony trioxide.
——— *10 mg oxide per 2 g KBr.*
····· *2 mg oxide per 2 g KBr.*
Positions of absorption bands given by Miller and Wilkins indicated by arrows.

Arsenic trioxide: 1) cubic, 2) monoclinic [4], 3) glass, freshly prepared by quenching melted oxide, 4) glass, stored over P_2O_5 for a month after grinding with potassium bromide.

Antimony trioxide: 5) cubic, 6) orthorhombic [12], 7) glass, two days old, prepared by pouring melted oxide into water.

The resulting spectra are shown in Fig. 1.

RESULTS AND DISCUSSION

A number of recurrent absorption bands between 2 and 6.5 microns are caused by water and other impurities. Infrared spectra of arsenic and antimony trioxides of unknown purity have been obtained by Miller and Wilkins [13].

They agree well with our spectra of the cubic forms. These are quite similar in appearance with the bands displaced towards lower wavenumbers in the case of antimony trioxide, as would be expected.

In the spectrum of monoclinic arsenic trioxide the principal band is found at higher wavenumbers than for the cubic form. The corresponding band of orthorhombic antimony trioxide, however, is displaced towards lower wavenumbers. This seems to indicate a structural difference between the modifications of lower symmetry.

For both the vitreous modifications, the principal band is found at the same position as for the cubic modifications. The bands are of less peak intensity and quite broad. Old arsenic trioxide glass and antimony trioxide glass have a secondary band at the same position as found for the cubic modifications. It therefore seems that these samples are partially transformed to the cubic forms. By comparison of all spectra, the vitreous modifications seem to be closer related to the cubic forms than to those of lower symmetry.

The authors are grateful to professor N. A. Sørensen for placing equipment at their disposal.

REFERENCES

1. Bozorth, R. M. *J. Am. Chem. Soc.* **45** (1923) 1621.
2. Becker, K., Plieth, K. and Stranski, I. N. *Z. anorg. allgem. Chem.* **266** (1951) 293.
3. Buerger, M. J. and Hendricks, S. B. *Z. Krist.* **98** (1938) 1.
4. Schulman, J. H. and Schumb, W. C. *J. Am. Chem. Soc.* **65** (1943) 878.
5. Straumanis, M. *Z. Physik* **126** (1949) 49.
6. Groth, P. *Poggendorfs Ann. Physik* **137** (1869) 414.
7. Kordes, E. *Z. physik. Chem.* **B43** (1939) 177.
8. Zachariasen, W. H. *J. Am. Chem. Soc.* **54** (1932) 3841.
9. Bötticher, H., Plieth, K., Reuber-Kürbs, E. and Stranski, I. N. *Z. anorg. allgem. Chem.* **266** (1951) 302.
10. Kürbs , E., Plieth, K. and Stranski, I. N. *Z. anorg. allgem. Chem.* **258** 1949) 238.
11. Borgen, O., Grjotheim, K. and Krogh-Moe, J. *Kgl. Norske Videnskab. Selskabs Forh.* **27** (1954) No. 17.
12. Debray, H. *Compt. rend.* **58** (1864) 1209.
13. Miller, F. A. and Wilkins, C. H. *Anal. Chem.* **24** (1952) 1253.

Received October 17, 1955.

ACTA CHEMICA SCANDINAVICA 10 (1956) 268—272

Ethyl Propenyl Ketone as a ψ-Diene in the Diels-Alder Reaction

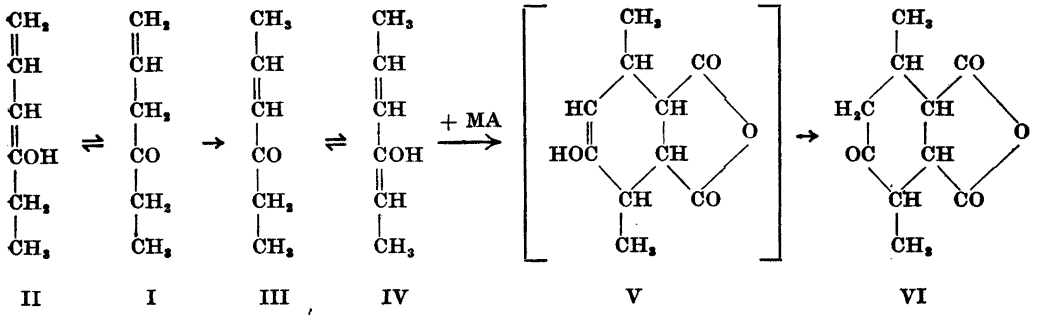
ENDRE BERNER

Universitetets kjemiske institutt, Blindern — Oslo, Norway

A crystalline adduct was formed by heating ethyl allyl ketone with maleic anhydride. The ψ-diene was, however, found to be ethyl propenyl ketone into which the ethyl allyl ketone isomerizes during the heating. The adduct by Clemmensen reduction gave a 3,6-dimethylhexahydrophthalic acid which could be resolved optically.

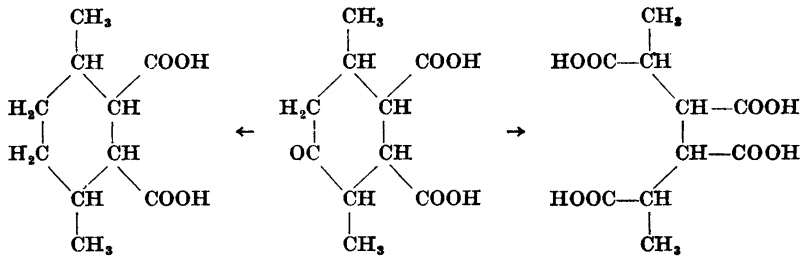
Some years ago the author [1] pointed out that a β-diketone might exist in a dienol form containing conjugated double bonds and accordingly ought to react with maleic anhydride and other dienophilic compounds. It was indeed found that acetylacetone reacted with maleic anhydride but the reaction proceeded in a way quite different from the expected one, an adduct being actually formed from two molecules of maleic anhydride and one of the diketone. Subsequently it was found that also citraconic anhydride reacted with acetylacetone, but neither in this case did the reaction proceed as expected, the reaction product being a furan derivative [2].

From the literature [3] some few examples are known showing that unsaturated aldehydes or ketones can react as ψ-dienes in Diels-Alder reactions. In the present case it was found of interest to investigate the behaviour of ethyl allyl ketone (I) as its enol (II) would contain a conjugated system. The ketone I actually reacted with maleic anhydride when heated for some days to 90°, but the crystalline adduct, although it had the calculated composition, did not behave as expected if the enol II had been the diene component. The adduct was thus completely saturated and had retained the carbonyl function of the ketone. The reason for this is that the ethyl allyl ketone on heating with the maleic anhydride did isomerize to ethyl propenyl ketone (III) the enol of which (IV) reacted with the maleic anhydride (MA) to give the adduct VI. The enolic form V is obviously an unstable intermediate. For the preparation of the adduct it was then of course found practical to isomerize the ethyl allyl ketone in a separate operation and then carry out the Diels-Alder reaction with the pure ethyl propenyl ketone.



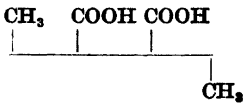
II I III IV V VI

The free dicarboxylic acid (VII) corresponding to the adduct could be resolved into optically active components. By reduction the same acid gave a hydroxy-acid which was easily transformed into a lactone. The acid VII further on Clemmensen reduction gave a 3,6-dimethylhexahydrophthalic acid (VIII) and on oxidation with nitric acid the open-chained hexane-2,3,4,5-tetracarboxylic acid (IX).

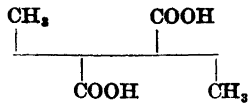


VIII VII IX

As the hexahydrophthalic acid VIII could be resolved optically and the carboxyl groups, due to their origin from maleic anhydride, must be *cis* to each other the methyl groups can only be in *trans* position to each other. The acid VIII ought therefore to be identical with the $3^c,6^t$-dimethyl*cyclo*hexane-$1^c,2^c$-dicarboxylic acid prepared by Alder and Vogt [4] by hydrogenating the adduct of *cis-trans*-1,4-dimethylbutadiene and maleic anhydride. These authors, designating the acid according to their scheme as the Bα-form (X), gave the m. p. as 134°, while we have found 121° for the inactive acid. The discrepancy may most probably be due to dimorphism. It could also be due to a partial spontaneous resolution taking place during the crystallization (we have found m. p. 138° for the active acid), but we have on crystallizing the acid repeatedly from the same solvent as used by Alder and Vogt never observed any deviation of the m. p. from 121°. That the acids m. p. 121° and 134° are identical is, however, evident from the fact that both on isomerization by heating with concentrated hydrochloric acid procured the all-*trans* form XI (Bβ) for which we found the m. p. 185°, while Alder and Vogt gave m. p. 183°.

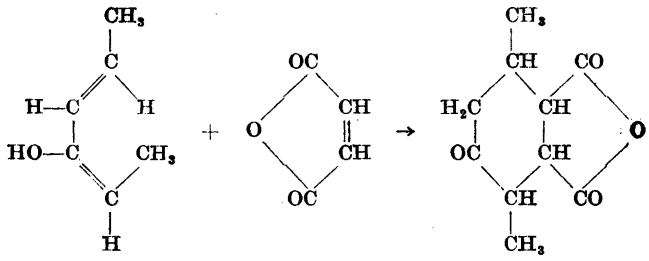


X (Bα)



XI (Bβ)

From the configuration of the acid VIII and the general rules set up by Alder and Schumacher [5], 1) that the diene component reacts according to the "*cis*-principle", 2) that an acyclic diene reacts in its quasi-cyclic form, and 3) that the orientation-complex has maximum congestion of the double bonds, it can be concluded that the enol IV taking part in our reaction must have the configuration *cis-trans* (*cis* referring to the position of the methyl group at the double bond formed by the enolization). The formation of the adduct, which may be designated as the anhydride of 2,5-dimethyl-3,4-dicarboxy*cyclo*hexanone, can therefore be written



IV VI

However, from the experimental data available it is not possible to decide whether the methyl group in position 2 or that in 5 (CO = 1) is the one being in *trans* position to the three other substituents.

EXPERIMENTAL

(Melting points not corrected)

Ethyl allyl ketone and maleic anhydride. Ethyl allyl ketone (25 g), prepared according to Blaise [6], and maleic anhydride (25 g) were mixed and heated for 4 days to 90°, the colour in the end becoming brownish red. After cooling to room temperature the mixture was inoculated with crystals obtained by a preliminary experiment. Next day the adduct was filtered off by suction and washed thoroughly with ethanol when it became practically colourless. It weighed 15.2 g. The mother liquor from this first fraction after heating for three more days gave 4.8 g crystalline adduct. Yield in all 40 %. Recrystallized from ethyl acetate. M. p. 146°. (Found: C 61.38, 61.25; H 6.19, 6.16. Calc. for $C_{10}H_{12}O_4$ (196.2): C 61.21; H 6.17.)

Isomerization of ethyl allyl ketone. Ethyl allyl ketone was mixed with twice its volume of 20 % sulphuric acid and refluxed for one hour. The ketone was taken up in ether and the solution dried with sodium sulphate. After removing the ether the residue was fractionated twice. The fraction boiling at 137—138° consisted of the ethyl propenyl ketone which gave a semicarbazone with m. p. 160° (Blaise [6] found 157°).

Ethyl propenyl ketone and maleic anhydride. The ketone (13.5 g) and maleic anhydride (13.5 g) were heated for 3 days to 90° when a first fraction of adduct (6.0 g) was obtained.

Further heating for 3 days of the mother liquor gave a second fraction of 5.2 g adduct, both fractions washed with ethanol. Yield in all 41.5 %. After recrystallization from ethyl acetate, m. p. as above 146°.

Investigation of the adduct. The adduct could be sublimated unchanged in a high vacuum, after which it had m. p. 145°, recrystallized from ethyl acetate m. p. 146°. A solution of the adduct in chloroform did not add bromine, nor did an aqueous solution react with bromine-water.

The free acid (VII) was obtained by dissolving the adduct in N sodium hydroxide and adding an excess of 2 N sulphuric acid. On standing hard crystals separated which after recrystallization from water had m. p. 206—207°. The same acid was obtained by dissolving the adduct in boiling water and evaporating the solution or by dissolving it in conc. sulphuric acid and pouring the solution on ice. (Found: C 55.93, 55.89; H 6.63, 6.54; M by titration 216.4. Calc. for $C_{10}H_{14}O_5$ (214.4): C 56.07, H 6.59.)

The original adduct was recovered from the acid VII by dehydration. For this purpose the acid (0.5 g) was pulverized and refluxed for 2 hours with acetyl chloride (5 ml). The solution on evaporation in a vacuum desiccator above potassium hydroxide gave a crystalline residue which after recrystallization from ethyl acetate had m. p. and mixed m. p. 145°.

The methyl ester of the acid VII was prepared by means of diazomethane. After evaporating the ethereal solution the ester crystallized spontaneously. It had m. p. 52—53° but was not recrystallized owing to its great solubility in most solvents. For preparation of the hydrazone a solution of 2,4-dinitrophenylhydrazine in hydrochloric acid was added to the ester dissolved in ethanol. The hydrazone separated immediately as an oil which crystallized on scratching. Recrystallized from ethanol, m. p. 177°. (Found: C 51.30; H 5.25; N 13.26. Calc. for $C_{18}H_{22}O_8N_4$: C 51.18; H 5.25; N 13.26.)

Optical resolution of the acid VII. Preliminary experiments gave crystalline salt of the acid with strychnine when used in the molecular ratio 1:1. The acid (2.7 g) and strychnine (4.2 g) were dissolved in water (50 ml) at room temperature and the solution inoculated. The strychnine salt (2.1 g) which had separated during the night was decomposed by adding 10 ml N hydrochloric acid. After removing the strychnine hydrochloride by filtration the active acid was extracted with ether and was obtained as a crystalline mass (0.35 g) which melted at 195—199° and had $[\alpha]_D^{20} = -21.5°$ (water, *c* 3).

Oxidation of the acid VII with nitric acid. To a solution of the adduct (2 g) in water (60 ml) was added conc. nitric acid of sp. gravity 1.4 (11 ml) and the solution heated on the steam-bath. In a few minutes the solution became light blue, the colour soon changing into greenish and then yellow and an evolution of nitric oxide set in. After heating for 20 min. the solution was evaporated slowly at room temperature. The crystalline residue was washed with a small amount of water and crystallized twice from water. A final recrystallization from 2 N hydrochloric acid gave beautifully developed hexagonal prisms, M. p. 202°. (Found: C 45.81; H 5.31. Calc. for $C_{10}H_{14}O_8$ (262.2): C 45.80; H 5.38.)

Esterification: A solution of the acid m. p. 202° (0.2 g) in 20 ml methanol containing 4 % hydrogen chloride was refluxed for 7 hours. A part of the methanol (15 ml) was distilled off and replaced by new methanol containing hydrogen chloride. The refluxing was continued for 4 hours after which most of the methanol was evaporated. The residue was neutralized with sodium carbonate and the ester taken up in ether. From the ethereal solution the ester was obtained as an oil (0.17 g) which after some time crystallized. Recrystallized from dilute methanol. M. p. 50°. (Found: C 52.59; H 7.05; OCH_3 38.90. Calc. for $C_{14}H_{22}O_8$ (318.3): C 52.82; H 6.97; OCH_3 39.00.)

Reduction of the acid VII with sodium amalgam. The adduct (2 g) dissolved in 0.5 N sodium hydroxide (40 ml) was treated with 4 % sodium amalgam at 50—60° until a sample did not give precipitate with dinitrophenylhydrazine. The solution was neutralized and concentrated somewhat on the water-bath. After adding 10 ml 5 N sulphuric acid and standing over night the hydroxy-acid had separated (1.7 g). Recrystallized from water. M. p. 196—197°. (Found: C 55.55; H 7.47. Calc. for $C_{10}H_{16}O_5$ (216.2): C 55.54; H 7.46.)

On refluxing the above 2,5-dimethyl-3,4-dicarboxy*cyclo*hexanol with five times its weight of acetic anhydride for 2 hours it was converted into a lactone. The lactone after being isolated by evaporating the solution in a vacuum was recrystallized twice from ben-

zene. M. p. 135°. Dissolved in dilute ethanol it could be titrated as a monobasic acid. (Found: C 60.52; H 7.14; M 200.0. Calc. for $C_{10}H_{14}O_4$ (198.2): C 60.59; H 7.12.)

Clemmensen reduction of the acid VII. Pieces of zinc sheet (10 g) were treated for half an hour at room temperature with a 5 % solution of mercuric chloride. After washing the zinc with water 15 % hydrochloric acid (20 ml) and adduct (4 g) were added and reduction effected by refluxing for 3 hours. The dimethylhexahydrophthalic acid separated as an oil which crystallized on standing. It was isolated by extraction with ether. Yield 3.0 g. The acid after crystallization from water had m. p. 120°. On recrystallization from acetonitrile the m. p. rose to 121° and this m. p. remained unchanged on recrystallizing the acid repeatedly from the same solvent. (Found: C 59.95, 59.84; H 8.10, 8.07; M by titration 203.7. Calc. for $C_{10}H_{16}O_4$ (200.2): C 59.98; H 8.06.)

Resolution of the acid m. p. 121°. Strychnine and cinchonine did not give crystalline salts. Brucine, however, when used in the ratio 2 moles alkaloid to 1 mole acid was effective. The acid (1 g) and brucine (3.4 g) were dissolved in ethanol (10 ml) by heating gently. On standing at room temperature for 5 days 1.2 g brucine salt had separated. It was dissolved in 2 N hydrochloric acid and the active acid (0.23 g) isolated by extraction with ether. This crude acid which in ethanol had $[\alpha]_D^{20} = -13.0°$ was recrystallized from a small amount of water. The first fraction consisted of practically inactive acid, m. p. 120–121° and $[\alpha]_D^{20} = -1.6°$. Evaporation of the mother liquor gave a laevorotatory acid with m. p. 138° and $[\alpha]_D^{20} = -29.3°$ (ethanol, *c* 2.5). The filtrate from the 1.2 g brucine salt gave a crude dextrorotatory acid with $[\alpha]_D^{20} = +4.2°$.

Isomerization of the acid m. p. 121°. The acid (0.4 g) was heated to 180° in a sealed tube with conc. hydrochloric acid (5 ml) for 5 hours. After diluting with water extraction with ether gave a partly crystallized residue which on a porous tile left 0.2 g crystalline acid. Recrystallized several times from acetonitrile, m. p. 185°.

The author is indebted to *Fridtjof Nansens Fond* for grants.

REFERENCES

1. Berner, E. *J. Chem. Soc.* **1946** 1052.
2. Berner, E. *Acta Chem. Scand.* **6** (1952) 646.
3. *Newer Methods of Prep. Org. Chem.* New York 1948, p. 395.
4. Alder, K. and Vogt, W. *Ann.* **571** (1951) 137.
5. Alder, K. and Schumacher, M. *Ann.* **571** (1951) 87.
6. Blaise, R. E. *Bull. soc. chim. France* [3] **33** (1905) 40.

Received November 12, 1955.

ACTA CHEMICA SCANDINAVICA 10 (1956) 273—278

Some New Benzodifurans and Naphthofurans from Quinones and β-Diketones

ERLING BERNATEK

Universitetets Kjemiske Institutt, Blindern — Oslo, Norway

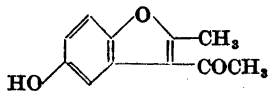
In connection with work on stable ozonides two new benzodifurans and several new naphthofurans have been synthesized from quinones and β-diketones. The reactivity of some substituted naphthoquinones has been tested.

As pointed out by Criegee [1] well-defined ozonides are only rarely encountered in literature. The same author therefore devoted himself to the preparation of stable ozonides as well as to the complete elucidation of their degradative reactions and their rearrangements. He was able to show [2] that in the ozonization of 9,10-octalin no stable ozonide was formed as supposed by Hückel [3], the reaction product turning out to be a dimeric peroxide of *cyclo*decanedione-1,6. Likewise the "ozonide" from 2-phenyl-3-ethyl-indenone described by Frank and collaborators [4] could be shown to consist of a mixed anhydride of *o*-propionylbenzoic acid and benzoic acid.

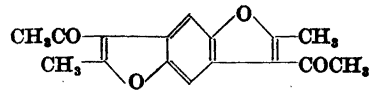
Are thus the stable and well-defined ozonides even more rare than previously supposed, a notable exception is displayed in the ozonides of unsaturated five-membered rings. The reason for this is probably of a steric nature [5]. Such stable ozonides can be prepared from certain steroid derivatives [6,7], indole derivatives [8,9], disubstituted maleic imides [10], *cyclo*pentene [11], cyclic sulphones [12] and 2,3-disubstituted indenones [13]. Recently a new class of compounds has been found to yield stable, monomeric ozonides, *viz.* the benzo [1.2-b, 4.5-b'] difurans [14]. As a preliminary to further work in this field the author has undertaken the synthesis of some new suitably substituted benzodifurans and naphthofurans.

The synthesis of benzofuran and benzodifuran derivatives from quinone and ethyl acetoacetate was established by v. Pechmann [15] and Ikuta [16]. Later Graebe and Levy [17] extended the synthesis to include toluquinone but expressed on the same occasion doubt as to the correctness of some of Ikuta's structural formulae. These, however, seem to have been confirmed by more recent work [18]. Further extensions of the synthesis have been made through the investigation of the reaction between acetylacetone and quinone [18,19].

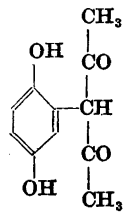
The structure of two new furan derivatives from these works are given in the formulae I and II.



I



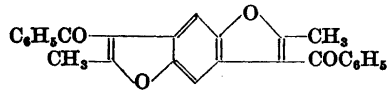
II



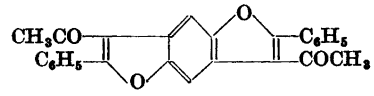
III

These compounds are supposed to be formed by ring closure of intermediate quinols of the type represented by formula III (or its tautomeric form). The determination of the structures I and II was considerably facilitated by the fact that acetylacetone is a symmetrical diketone. Thus the two possible directions of enolization in III are identical and only one product can result from a ring closure. (III will of course give I.)

We now have investigated the reaction between benzoylacetone and quinone in methanolic zinc chloride solution. Only one reaction product could be isolated. Its composition $C_{26}H_{18}O_4$ corresponded to a benzodifuran derivative and in analogy to our earlier results the structure of this product could be either IV or V.



IV



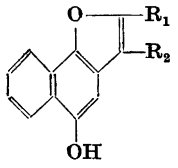
V

The carbonyls in $C_{26}H_{18}O_4$ were relatively unreactive. With ordinary carbonyl reagents, *e. g.* 2,4-dinitrophenylhydrazine, it yielded only a monohydrazone. The iodoform test was negative. In order to decide between IV and V the presumed benzodifuran was treated with methyl magnesium iodide whereby both carbonyls were converted into tertiary alcohol groups, the resulting compound having the composition $C_{28}H_{26}O_4$. The same compound could be prepared by treating II with phenyl magnesium bromide. Consequently the possibility of structure V is ruled out.

Benzoylacetic ester reacted only very sluggishly with quinone under the conditions tried and gave in extremely low yield a substance $C_{28}H_{22}O_4$ which probably is a benzodifuran (V, $COOC_2H_5$ instead of $COCH_3$). This compound was not investigated further.

1,4-Naphthoquinone reacted smoothly with acetylacetone to give a compound $C_{15}H_{12}O_3$ corresponding to one mole of each of the reactants minus one

mole of water. The reaction medium was as usual methanolic zinc chloride solution and only one reaction product could be isolated. With 2,4-dinitrophenylhydrazine it gave a monohydrazone and with acetyl chloride a monoacetate was obtained. The substance was contrary to expectation not soluble in warm 2 N sodium hydroxide. It is supposed to have the naphthofuran structure VI.



VI $R_1 = CH_3$, $R_2 = COCH_3$
VII $R_1 = CH_3$, $R_2 = COOC_2H_5$
VIII $R_1 = C_6H_5$, $R_2 = COOC_2H_5$
IX $R_1 = CH_3$, $R_2 = COC_6H_5$
X $R_1 = CH_3$, $R_2 = C(OH)(CH_3)C_6H_5$

After this part of the investigation was completed it was found in the literature that Ebine [20] also had prepared the substance VI. His findings are in good agreement with ours. In the same paper Ebine reports the synthesis of II and gives the melting point 232—233° which is rather low as compared to our value [19] of 248°. Likewise the found percentage of carbon is by 1.7 smaller than calculated. It is suspected that Ebine has not had the pure compound II in hands but a mixture of II and I. The latter has the melting point 238° and its carbon content is by 1.6 lower than for II[18]. The reason for this contamination is that I and II are always formed together in the condensation of acetylacetone with quinone. Unless I is extracted with alkali (which Ebine has not done) the mixture is very difficult to separate by mere recrystallization. Ebine's dioxime seems to have the correct composition a fact which probably can be explained by different solubilities of the monoxime of the benzofuran and the dioxime of the benzodifuran; the latter most likely being less soluble than the former and therefore separates first from solvents.

In analogy with VI we have prepared VII with ethyl acetoacetate, VIII with benzoylacetic ester, and IX with benzoylacetone. All these compounds could be acetylated to give the monoacetates but were insoluble in 2 N sodium hydroxide. In the case of the benzoyl product there were two structural possibilities, *viz.* one methyl-benzoyl derivative (IX) and one phenyl-acetyl derivative. This question was settled in the same way as for IV by reacting VI with phenyl magnesium bromide and IX with methyl magnesium iodide and obtaining the same tertiary alcohol X in both cases. The identity of the alcohols could not be established by mixed melting point as they readily lost water and melted over a long range. Their infrared spectra were therefore recorded and were found to be absolutely identical.

2-Methyl-1,4-naphthoquinone did not react at all with acetylacetone under the usual reaction conditions while 2-hydroxy-1,4-naphthoquinone gave the corresponding methyl ether and 2-chloro-1,4-naphthoquinone gave bi-1,4-naphthoquinone, $C_{20}H_{10}O_4$.

Naphthazarin and its diacetate were tried as representatives of naphthoquinones with substituents in the benzene ring. In order to avoid alcoholysis the diacetate was treated with acetylacetone in ethereal zinc chloride. Neither the hydroxyquinone nor the diacetate could be induced to react. This is in

agreement with the recent findings of Bruce and Thomson [21] who examined the reactivity of naphthazarin and the diacetate towards several reagents. They conclude that naphthazarin is a relatively unreactive quinone towards nucleophilic and electrophilic reagents (in our reactions we have to deal with the nucleophilic acetylacetonate ion) but reacts normally with substances which add by a radical mechanism (*e. g.* toluene-*p*-thiol) while the diacetate is somewhat, but not markedly, more reactive.

EXPERIMENTAL

(In part with A. Wulff and S. Steinsvik)

p-Benzoquinone and benzoylacetone

p-Benzoquinone (2.0 g) and benzoylacetone (3.0 g) were added to a solution of zinc chloride (10 g) in anhydrous methanol (12.5 ml). The mixture was heated for 7 hours on a water-bath and left overnight at room temperature. Next day a crystalline substance (0.55 g) had separated. Recrystallized twice from glacial acetic acid. M. p. 221°. (Found: C 79.27; H 4.65. Calc. for $C_{26}H_{18}O_4$: C 79.20; H 4.62).

Dinitrophenylhydrazone. Dinitrophenylhydrazine (0.3 g) was dissolved in hydrochloric acid (20 ml, 2 N) to which was added ethanol (10 ml) and IV (0.2 g). The mixture was heated for 7 hours on a water-bath with occasional additions of small amounts of ethanol. Next day the separated crystalline substance was isolated and dissolved in a mixture of chloroform and ligroin (1:1). The solution was passed through a column of silica gel where the dissolved substance was adsorbed in different zones, the predominating one being bright red. This zone was separated from the rest of the column and extracted with chloroform. After evaporation of the chloroform the residue was orange-red and weighed 65 mg. M. p. 249—250°. (Found: N 9.71. Calc. for $C_{32}H_{22}N_4O_7$: N 9.75). The substance seems to be a monohydrazone of the benzodifuran.

Methyl magnesium iodide and IV. To a solution of methyl magnesium iodide (from 0.5 g magnesium) in dry ether (20 ml) was added IV (0.5 g). After the vigorous reaction had subsided the reaction mixture was refluxed for 15 minutes and decomposed with water and dilute hydrochloric acid. The ethereal layer was dried and evaporated, the residue weighing 0.44 g. Recrystallized twice from dilute ethanol. M. p. 194—195°. (Found: C 79.89; H 6.14. Calc. for $C_{28}H_{26}O_4$: C 78.86; H 6.15).

Phenyl magnesium bromide and II

To a solution of phenyl magnesium bromide (from 0.5 g magnesium) in dry ether (20 ml) II (0.5 g) was added. After the moderate reaction had subsided the reaction mixture was refluxed for 25 minutes and decomposed with water and dilute hydrochloric acid. The ethereal layer was dried and evaporated. The residue, which was a yellow plastic mass with a conspicuous smell of biphenyl, was extracted twice with boiling ligroin and recrystallized thrice from dilute ethanol (charcoal). M. p. 197°. Mixed melting point with the substance from the foregoing experiment 197°. (Found: C 80.09; H 6.31. Calc. for $C_{28}H_{26}O_4$: C 78.86; H 6.15).

p-Benzoquinone and benzoylacetic ester

To a solution of zinc chloride (10 g) in anhydrous methanol (15 ml) benzoylacetic ester (3.5 g) was added and thereafter in small portions *p*-benzoquinone (2 g). The mixture was heated on a water-bath for 5.5 hours and placed in a refrigerator. After several days a small amount of a crystalline material had separated. After recrystallization from glacial acetic acid (charcoal) it was yellowish and had m. p. 163°. Due to the very small yield six of the above portions were reacted and worked up. The collected products were

recrystallized five times from glacial acetic acid (charcoal) and then had the constant m. p. of 185—186°. Very small, white needles (45 mg). (Found C 73.66; H 4.82. Calc. for $C_{28}H_{22}O_6$: C 74.00; H 4.88).

1,4-Naphthoquinone and acetylacetone

1,4-Naphthoquinone (1.5 g) and acetylacetone (2 ml) were dissolved in a solution of zinc chloride (5 g) in dry methanol (6 ml). The mixture was refluxed for 5 minutes when it solidified into a crystal mass. Isolated by suction and washed with methanol (0.90 g). Recrystallized twice from glacial acetic acid (charcoal) it had m. p. 262°. (Found: C 74.71; H 5.04. Calc. for $C_{15}H_{12}O_5$: C 74.98; H 5.03).

Dinitrophenylhydrazone. VI (0.2 g) was dissolved in boiling ethanol (25 ml) to which was added a solution of 2,4-dinitrophenylhydrazine (0.2 g) in hydrochloric acid (25 ml, 2 N). Immediately a bright red voluminous precipitate was formed. After 2.5 hours on a water-bath the separated substance was isolated (0.31 g) and recrystallized from glacial acetic acid. M. p. 271—272°. (Found: C 59.82; H 3.94; N 13.22. Calc. for $C_{31}H_{16}N_4O_6$: C 60.01; H 3.84; N 13.33).

Acetate. VI (0.5 g) and acetyl chloride (50 ml) were refluxed for 1.5 hours and the cooled solution poured into icewater (1 l) when a white substance separated. Recrystallized from dilute alcohol and from benzene. White needles. M. p. 152.5—153.5°. (Found: C 72.21; H 4.92. Calc. for $C_{17}H_{14}O_4$: C 72.33; H 5.00).

1,4-Naphthoquinone and ethyl acetoacetate

1,4-Naphthoquinone (5 g) and ethyl acetoacetate (6 ml) were added to a solution of zinc chloride (15 g) in dry methanol (25 ml). The mixture was heated on a steam-bath for 1 hour and cooled to room temperature. The separated crystals (3.5 g) were washed with methanol and recrystallized thrice from glacial acetic acid. White needles. M. p. 208—209° (Kofler bench) (Found: C 70.94; H 5.08. Calc. for $C_{16}H_{14}O_4$: C 71.06; H 5.22).

Acetate. VII (0.6 g) and acetyl chloride (50 ml) were refluxed for 3 hours and poured into ice-water (1 l). The separated, white substance was recrystallized twice from glacial acetic acid. White needles. M. p. 147—148°. (Found: C 68.89; H 5.22. Calc. for $C_{18}H_{16}O_5$: C 69.23; H 5.16).

1,4-Naphthoquinone and benzoylacetic ester

1,4-Naphthoquinone (4 g) and benzoylacetic ester (5 ml) were added to a solution of zinc chloride (25 g) in dry methanol (30 ml) and refluxed for 15 minutes when the reaction mixture solidified to a crystal mass. The crystals (4 g) were washed with methanol and recrystallized thrice from glacial acetic acid (charcoal). M. p. 194—195°. (Found: C 75.88; H 4.94. Calc. for $C_{21}H_{16}O_4$: C 75.90; H 4.85).

Acetate. VIII (0.5 g) and acetyl chloride (20 ml) were refluxed for 2 hours and poured into ice-water (1 l). The separated white substance was recrystallized twice from 80 % ethanol. White needles. M. p. 119.5—120° (Found: C 73.60; H 4.65. Calc. for $C_{23}H_{18}O_6$: C 73.79; H 4.84).

1,4-Naphthoquinone and benzoylacetone

1,4-Naphthoquinone (5 g) and benzoylacetone (7 g) were added to a solution of zinc chloride (25 g) in dry methanol (30 ml) and refluxed for 2.5 hours. After cooling the separated crystals (3.5 g) were washed with warm ethanol and recrystallized thrice from glacial acetic acid. Yellow needles. M. p. 240°, decomp. (Kofler-bench). (Found: C 79.36; H 4.68. Calc. for $C_{20}H_{14}O_3$: C 79.47; H 4.67).

Acetate. IX (0.48 g) and acetyl chloride (50 ml) were refluxed for two hours and poured into ice-water (1 l). The precipitated, white substance was recrystallized thrice from 70 % ethanol. White rhombic crystals. M. p. 144.5—146°. (Found: C 76.38; H 4.70. Calc. for $C_{22}H_{16}O_4$: C 76.70; H 4.68).

VI and phenyl magnesium bromide

The Grignard reagent was prepared from magnesium (1.6 g) and bromobenzene (10 g) in anhydrous ether (25 ml). To a suspension of VI (1 g) in anhydrous toluene (15 ml) were added dropwise 5 ml of the above reagent. The naphthofuran dissolved gradually as the reaction proceeded and to the clear solution an additional amount of dry toluene (35 ml) was added. The solution was heated to 50° for 15 minutes and decomposed with ice and sulphuric acid (20 %). Excess sulphuric acid was neutralized with sodium hydrogen carbonate when a white substance separated on the interface between the aqueous and the toluene layers. This substance was recrystallized twice from dilute alcohol and twice from dilute acetone. No definite melting point. (Found: C 78.70; H 5.79. Calc. for $C_{21}H_{18}O_3$: C 79.20; H 5.71).

IX and methyl magnesium iodide

The Grignard reagent was prepared from magnesium (1 g) and methyl iodide (6 g) in anhydrous ether (10 ml). To a suspension of IX (0.5 g) in dry toluene (15 ml) 6 ml of the reagent were added dropwise. The ensuing reaction led also in this case to a clear solution. From here the procedure was exactly as in the above experiment. The product had no definite melting point. (Found: C 78.83; H 5.81. Calc. for $C_{21}H_{18}O_3$: C 79.20; H 5.71).

The author is indebted to *Fridtjof Nansens Fond* for a grant.

REFERENCES

1. Criegee, R. *Ann.* **583** (1953) 1.
2. Criegee, R. and Wenner, G. *Ann.* **564** (1949) 9.
3. Hückel, W., Danneel, R., Schwartz, A. and Gercke, A. *Ann.* **474** (1929) 121.
4. Frank, R. L., Eklund, H., Richter, J. W., Vannemann, C. R. and Wennerberg, A. N. *J. Am. Chem. Soc.* **66** (1944) 1.
5. Criegee, R. and Lohaus, G. *Ann.* **583** (1953) 9.
6. Miescher, K. and Kägi, H. *Helv. Chim. Acta* **32** (1949) 761.
7. Schmid, H. and Kägi, H. *Helv. Chim. Acta* **33** (1950) 1582.
8. Ockenden, D. W. and Schofield, K. *J. Chem. Soc.* **1953** 612.
9. Witkop, B. and Patrick, J. B. *J. Am. Chem. Soc.* **74** (1952) 3855.
10. Richmond, J. E. and Altman, K. I. *J. Am. Chem. Soc.* **74** (1952) 4368.
11. Criegee, R., Blust, G. and Lohaus, G. *Ann.* **583** (1953) 2.
12. Criegee, R. and Lohaus, G. *Ann.* **583** (1953) 12.
13. Criegee, R., de Bruyn, P. and Lohaus, G. *Ann.* **583** (1953) 19.
14. Bernatek, E. and Thoresen, F. *Acta Chem. Scand.* **9** (1955) 743.
15. v. Pechmann, H. *Ber.* **21** (1888) 3005.
16. Ikuta, M. *J. prakt. Chem.* [2] **45** (1892) 65.
17. Graebe, C. and Levy, S. *Ann.* **283** (1894) 245.
18. Bernatek, E. *Acta Chem. Scand.* **7** (1953) 677.
19. Bernatek, E. and Ramstad, S. *Acta Chem. Scand.* **7** (1953) 1351.
20. Ebine, S. *Sci. Rep. Saitama Univ. Ser. A* **1** (1953) 95.
21. Bruce, D. B. and Thomson, R. H. *J. Chem. Soc.* **1955** 1089.

Received November 8, 1955.

ACTA CHEMICA SCANDINAVICA 10 (1956) 279—287

The Crystal Structure of Tellurium Dibenzenethiosulphonate

PAUL ØYUM and OLAV FOSS

Institutt for teoretisk kjemi and Institutt for uorganisk kjemi, Norges tekniske høgskole, Trondheim, Norway

The crystal structure of tellurium dibenzenethiosulphonate, $Te(S_2O_2C_6H_5)_2$, has been determined from X-ray data, by two-dimensional Patterson and Fourier methods. The crystals are orthorhombic bipyramidal; space group D_{2h}^{14}—*Pbcn*, with $a = 14.46$ Å, $b = 11.18$ Å, $c = 10.48$ Å, and four molecules per unit cell. A twofold axis of molecular symmetry is present.

The molecule contains an unbranched and non-planar S-S-Te-S-S chain, the three middle atoms of which are divalent, whereas to each of the terminal sulphur atoms are attached two oxygen atoms and a phenyl group. The values, 2.08 Å and 2.41 Å, respectively, were found for the S-S and S-Te bond lengths, and 104° and 97°, respectively, for the S-S-Te and S-Te-S bond angles. The molecule occurs in a *trans* form, with a dihedral angle of 79° between the S-S-Te and S-Te-S planes.

The unit cells and space groups of two pentathionic compounds, *viz.*, sulphur dibenzene- and di-*p*-toluenethiosulphonate, were reported by Dawson, Mathieson and Robertson [1] in 1948. The substances, which are also called *bis*-sulphonyl trisulphides, are derived from pentathionic acid by substitution of aryl groups for the hydroxyl groups. The crystals of the two compounds are isomorphous; space group D_4^4—$P4_12_12$ (or the enantiomorph) with four molecules per unit cell, and $a = 7.74$ Å, $c = 26.29$ Å for the benzenethiosulphonate, and $a = 7.70$ Å, $c = 29.50$ Å for the *p*-toluenethiosulphonate. Concerning sulphur dibenzenethiosulphonate the authors said [1 p. 327], "Patterson and Harker projections have been made, but the large number of parameters (31) renders the interpretation difficult. Further work is in progress". No further account has, as far as we know, appeared in literature.

Meanwhile, the selenium and tellurium analogues of the above compounds, *viz.*, selenium and tellurium dibenzene- and di-*p*-toluenethiosulphonate, and triselenium dibenzene- and di-*p*-toluenesulphinate, have been prepared by one of us [2,3], and the unit cells and space groups determined [3]. Of the six new compounds, four are isomorphous with sulphur dibenzene- and di-*p*-toluenethiosulphonate; the two benzene compounds, tellurium dibenzenethiosulphonate and triselenium dibenzenesulphinate, being the only ones which do not crystallize in the tetragonal space group referred to above.

The detailed structure of tellurium dibenzenethiosulphonate has now been worked out, and is reported below. The structure of the molecule, which arises from sulphur dibenzenethiosulphonate by substitution of tellurium for the middle, divalent sulphur atom of the latter, is closely analogous to that of tellurium dimethanethiosulphonate [4], and of the telluropentathionate ion in ammonium telluropentathionate [5]. The three telluropentathionic compounds

$$Te(S_2O_2CH_3)_2; \qquad (NH_4)_2Te(S_2O_3)_2; \qquad Te(S_2O_2C_6H_5)_2$$

have thereby been shown to contain unbranched and non-planar S—S—Te—S—S chains.

EXPERIMENTAL

The yellow crystals of tellurium dibenzenethiosulphonate, $Te(S_2O_2C_6H_5)_2$, are orthorhombic bipyramidal, and show the forms {111} and {100}. The latter is frequently the more predominant, thus giving the crystals the appearance of plates. The axial lengths are [3], $a = 14.46 \pm 0.04$ Å, $b = 11.18 \pm 0.02$ Å, $c = 10.48 \pm 0.02$ Å. There are four molecules per unit cell; density, calc. 1.86, found 1.88 g/cm^3. Systematic absences, $hk0$ when $h + k$ is odd, $h0l$ when l is odd, $0kl$ when k is odd. The space group is therefore uniquely determined as D_{2h}^{14}—*Pbcn*.

The intensities of the $h0l$ and $hk0$ reflections were read visually from Weissenberg photographs about the b and c axes. Unfiltered CuK radiation (α wave-length, 1.54 Å) was used, and crystals having cross-sections of 0.04 × 0.08 mm and 0.07 × 0.08 mm, respectively, in the case of the b and c axis photographs. There are 101 $h0l$ and 114 $hk0$ reflections accessible with Cu$K\alpha$ radiation; of these, 76 and 94, respectively, were recorded on the films with measurable intensities, with values ranging from about thousand to one. The intensities were corrected for the Lorentz and polarization factors, and were converted to relative structure amplitudes, which were eventually put to an approximately absolute scale by comparison with the calculated structure factors. No corrections for absorption were made.

The crystals used for the X-ray photographs had been prepared two years earlier [3], and were still unchanged. On exposure to X-rays, a slight liberation of tellurium took place, which, however, did not appear to affect the intensities of the reflections to any observable degree.

The Patterson and Fourier summations were made at 6° intervals by means of Beevers-Lipson strips.

ANALYSIS OF THE STRUCTURE

The space group, D_{2h}^{14}-*Pbcn*, has eightfold general positions, and the four molecules in the unit cell must accordingly lie in special positions, of which there are three fourfold sets, two having a centre and one a twofold axis of symmetry. Since the molecule cannot reasonably have a centre of symmetry, it must possess a twofold axis, which passes through the tellurium atoms in the positions:

$$0,\ y,\ \tfrac{1}{4};\quad 0,\ \bar{y},\ \tfrac{3}{4};\quad \tfrac{1}{2},\ \tfrac{1}{2}+y,\ \tfrac{1}{4};\quad \tfrac{1}{2},\ \tfrac{1}{2}-y,\ \tfrac{3}{4}.$$

Although the x and z coordinates of tellurium are thus fixed, at $x = 0$, $z = \frac{1}{4}$, a direct solution of the projection along the b axis is not possible, since the tellurium atom does not contribute to $h0l$ reflections having odd h indices.

As the first steps, Patterson and Fourier maps, based on $h0l$ data with even values of h only, and Fourier signs corresponding to the tellurium contributions alone, were prepared. Both maps have mirror planes normal to the

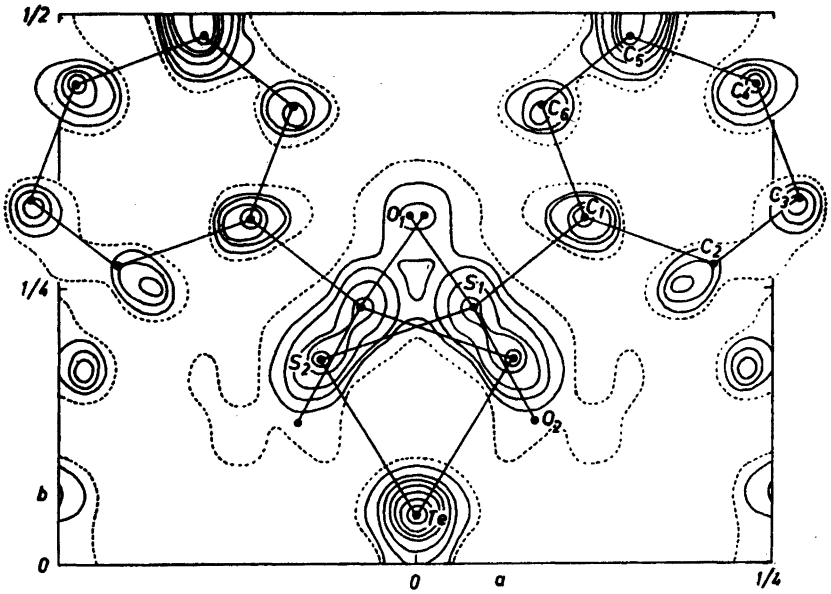


Fig. 1. Electron density projection of $Te(S_2O_2C_6H_5)_2$ *along the c axis, showing two asymmetric units. Contour lines are at intervals of 1 e·Å^{-2} for carbon atoms, 5 e·Å^{-2} for sulphur and oxygen atoms and 15 e·Å^{-2} for the tellurium atom, starting with 6, 10 and 15 e·Å^{-2}, respectively. The 5-electron line is dashed.*

a axis at $x = \frac{1}{4}$, due to the omission of the odd *h* data. The signs used in the Fourier summation were later found to be correct, but for a single reflection, 202. Peaks due to the two sulphur atoms of the asymmetric unit appeared in both maps, and allowed approximate coordinates to be determined for these atoms. The *z* coordinate of S_1 turned out to be equal to or close to $\frac{1}{2}$. With this *z* value, S_1 does not contribute, or contributes very little, to *h*0*l* reflections with *h* odd. Signs of most of the latter reflections were then calculated on the basis of the S_2 contributions alone, and these data when included in the Fourier summation served to remove the false symmetry elements and show S_1 a little displaced from $z = \frac{1}{2}$. The oxygen and carbon positions were uncertain, however, and further work on this projection was not made until the *c* axis projection had been worked out.

In the Patterson projection along the *c* axis, the Te-Te vector at $u = 0$, $v = 2y$ was found to lie close to $v = 0$, and the centre was located through graphical removal of the origin peak, its curvature along $u = 0$ being taken to be the same as along $v = 0$. The *y* coordinate of tellurium, 0.043, found in this way is the same as the final value. In the first Fourier synthesis of the *hk*0 data, signs were calculated from the tellurium contributions alone, and 79 out of the 94 observed terms were included; of these, only one sign was later found to be wrong. Although considerable overlapping of sulphur and oxygen atoms occurs, the resulting map allowed trial coordinates for these atoms to

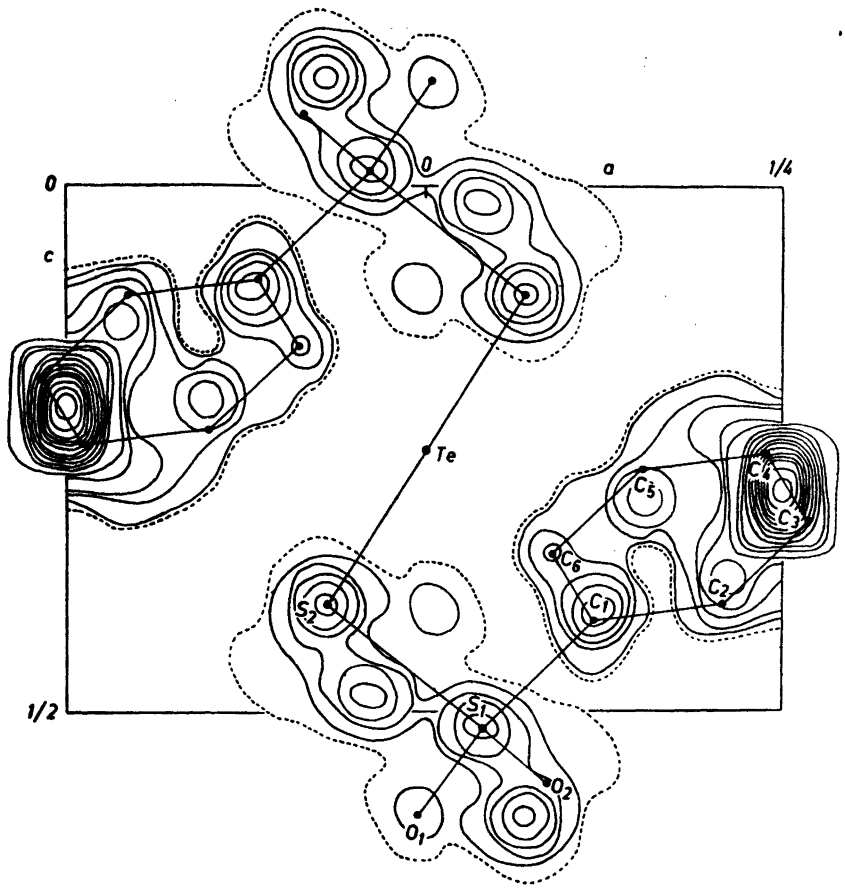


Fig. 2. Electron density projection of $Te(S_2O_2C_6H_5)_2$ *along the* b *axis, with the tellurium atom removed. Two asymmetric units are shown. Contour lines as in Fig. 1.*

be determined and used to calculate signs of the remaining *hk*0 reflections. In the next Fourier map, the benzene ring was recognizable, and the projection was then refined through successive approximations in the usual way.

With the x coordinates of the oxygen and carbon atoms thus known, work on the *h*0*l* data was resumed, and refinement of the b axis projection successfully carried out. In this projection, where the tellurium coordinates are known exactly, the heavy atom diffraction effects were studied through removal of the tellurium peak, by subtracting the calculated, temperature-corrected tellurium contributions from the scaled, observed *h*0*l* structure factors. This procedure needs to be carried out for reflections with even h indices only. The resulting difference map showed better resolved C_6 and O_1 peaks, and lead to an adjustment of the O_1 coordinates which changed the S_1—O_1 distance from 1.39 Å to 1.44 Å and gave a more reasonable value for the $S_2S_1O_1$ angle.

The *hk*0 Fourier map, and the *h*0*l* Fourier map with the tellurium peak removed as described above, are reproduced in Figs. 1 and 2, respectively. The atomic positions are marked with dots, and lines are drawn to show the outline of the molecule.

In both projections, the coordinates of the carbon atoms were adjusted so as to give the best fit with the observed structure factors on the basis of positions defining the corners of a regular hexagon with edges of 1.39 Å, and a linear arrangement of the S_1, C_1 and C_4 atoms.

The position of the tellurium peak in the *c* axis projection corresponds to a tellurium *y* coordinate of 0.046. This coordinate gives a Te-S_2 distance of 2.39 Å and a S_2TeS_2' angle of 99°. It was found, however, that the value, $y = 0.043$, derived from the Patterson map gave a better agreement between observed and calculated *hk*0 structure factors. The displacement of the tellurium peak may be due to diffraction effects, produced by the equivalent atom on the other side of the glide plane *c* at $y = 0$.

Table 1. Atomic coordinates for tellurium dibenzenethiosulphonate, in fractions of cell edges. Origin at a centre of symmetry.

	x	*y*	*z*		*x*	*y*	*z*
Te	0	0.043	0.250	C_1	0.117	0.312	0.413
S_2	−0.068	0.186	0.395	C_2	0.207	0.271	0.396
S_1	0.041	0.233	0.514	C_3	0.268	0.316	0.316
O_1	−0.006	0.316	0.598	C_4	0.238	0.435	0.253
O_2	0.083	0.139	0.566	C_5	0.148	0.476	0.270
				C_6	0.087	0.414	0.349

The final atomic coordinates are listed in Table 1. In Table 4, observed and calculated values of structure factors are compared for all *h*0*l* and *hk*0 reflections within the range of Cu*Kα* radiation. The calculated values are based on the coordinates of Table 1, and the atomic scattering curves of the *International Tables*, with a temperature factor of $B = 2.38$ Å^2 for both zones. The hydrogen atoms of the phenyl group have been ignored. The reliability factor, $R = \Sigma||F_{obs}| - |F_{calc}||/\Sigma|F_{obs}|$, with non-observed reflections included in the difference only when $|F_{calc}|$ in greater than the lowest observable value of $|F_{obs}|$, is 0.157 and 0.172, respectively, for the *h*0*l* and *hk*0 reflections. The largest discrepancy occurs for F_{200}, the observed and calculated values of which are 237 and 352, respectively. This reflection is the strongest one, and is probably subject to extinction. If F_{200} is not included, the *R* values drop to 0.142 and 0.160, respectively, for the two zones.

THE TELLURIUM DIBENZENETHIOSULPHONATE MOLECULE

The present structure is the third to be reported for a telluropentathionic compound, the two earlier ones being those of the methane analogue, tellurium dimethanethiosulphonate [4], and of ammonium telluropentathionate [5]. The compounds are built up of S—S—Te—S—S chains, with the three middle atoms in the divalent state, whereas to each of the terminal sulphur atoms are attached three oxygen atoms, or in the case of the thiosulphonates, two oxygen

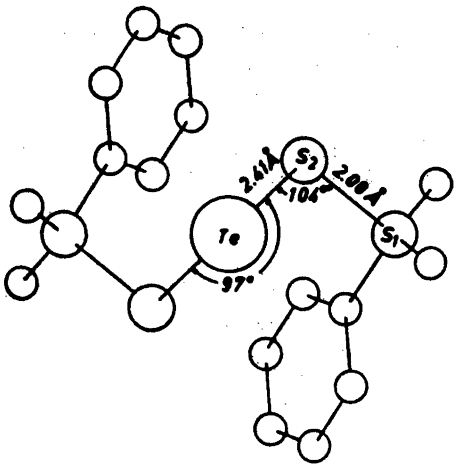


Fig. 3. The tellurium dibenzenethiosulphonate molecule as seen along the twofold axis, showing some bond lengths and angles.

atoms and a methyl or a phenyl group. The chains are non-planar, the terminal sulphur atoms being rotated out of the plane of the three middle atoms, to opposite sides of the plane. This is the *trans* configuration [6] of pentathionic compounds; the *cis* configuration [6], where the terminal atoms are located on the same side of the plane of the three middle atoms, has been found in the crystals of barium pentathionate [7] and selenopentathionate [8] dihydrate.

The shape of the tellurium dibenzenethiosulphonate molecule will appear from the electron density maps of Figs. 1 and 2, which also show the numbering of atoms, and from the line drawing of one isolated molecule in Fig. 3. The principal bond lengths and angles, calculated on the basis of the coordinates of Table 1, are given in Table 2, together with non-bonded Te—S and S—S distances within the molecule. The molecule possesses an exact twofold axis of symmetry, and a prime is used, when relevant, to denote the equivalent of an atom produced by the operation of the twofold axis. In Table 2, data for

Table 2. Dimensions of S-S-Te-S-S chains.

Bond lengths (in Å units) and angles.

Bond or angle	$Te(S_2O_2C_6H_5)_2$	$Te(S_2O_2CH_3)_2$	$(NH_4)_2Te(S_2O_3)_2$
S_1-S_2	2.08	2.13; 2.16	2.11; 2.12
S_2-Te	2.41	2.36; 2.35	2.36; 2.35
$\angle S_1S_2Te$	104°	106°; 104°	105°; 104°
$\angle S_2TeS_2'$	97°	100°	103°
Dihedral angle S_1S_2Te/S_2TeS_2'	79°	81°; 81°	86°; 95°

Non-bonded distances (in Å units).

Distance	$Te(S_2O_2C_6H_5)_2$	$Te(S_2O_2CH_3)_2$	$(NH_4)_2Te(S_2O_3)_2$
S_1-Te	3.54	3.57; 3.55	3.57; 3.52
S_1-S_2'	4.28	4.38; 4.36	4.52; 4.69
S_2-S_2'	3.62	3.60	3.68
S_1-S_1'	5.74	5.74	6.11

Table 4. Observed and calculated values of structure factors for tellurium dibenzenethiosulphonate.

hkl	F_{obs}	F_{calc}	*hkl*	F_{obs}	F_{calc}	*hkl*	F_{obs}	F_{calc}
200	237	+352	8	92	− 93	15	69	+ 61
4	196	+231	9	< 23	− 8	17	37	+ 44
6	51	+ 39	10	86	− 85	020	75	− 75
8	96	+ 75	11	47	− 30	2	37	+ 5
10	77	+ 63	12	78	− 92	4	61	+ 59
12	97	+ 84	13	< 22	− 14	6	125	+144
14	74	+ 83	14	62	− 88	8	148	+155
16	52	+ 51	15	< 17	+ 3	10	103	+ 97
18	24	+ 34	16	42	− 58	12	102	+104
002	114	− 72	008	134	+137	14	56	+ 55
1	58	+ 42	1	< 22	− 8	16	33	+ 32
2	51	+ 11	2	135	+120	18	27	+ 19
3	127	−120	3	< 22	+ 22	130	19	+ 24
4	154	−145	4	114	+105	3	132	+122
5	86	− 73	5	< 19	+ 17	5	155	+166
6	132	−146	6	67	+ 74	7	149	+190
7	41	− 30	7	< 24	− 24	9	141	+143
8	156	−177	8	47	+ 41	11	87	+ 88
9	48	+ 41	9	42	− 46	13	< 28	+ 8
10	105	−102	10	47	+ 25	15	30	+ 32
11	67	+ 65	11	30	− 40	17	22	+ 27
12	116	−114	12	35	+ 30	040	125	+131
13	27	+ 22	13	< 17	+ 1	2	95	+ 86
14	73	− 77	14	36	+ 35	4	118	+124
15	< 22	+ 4	15	< 8	+ 10	6	120	+108
16	44	− 49	00, 10	< 24	− 9	8	44	+ 37
17	< 17	− 14	1	< 24	− 7	10	< 27	− 3
18	27	− 33	2	30	− 22	12	< 29	− 24
004	123	+111	3	33	− 17	14	< 27	+ 8
1	69	− 58	4	46	− 40	16	< 21	+ 8
2	116	+116	5	32	− 33	18	< 14	+ 24
3	74	− 75	6	54	− 55	150	76	+ 79
4	174	+168	7	25	− 16	3	79	+ 66
5	83	− 77	8	55	− 69	5	< 21	− 7
6	167	+160	9	< 17	− 13	7	76	− 67
7	< 18	− 1	10	50	− 50	9	38	− 37
8	123	+124	11	< 15	− 6	11	< 28	− 11
9	< 21	+ 20	12	31	− 56	13	28	+ 28
10	50	+ 20	00, 12	48	+ 73	15	23	+ 5
11	42	+ 48	1	< 19	− 7	17	< 15	+ 15
12	38	+ 25	2	47	+ 52	060	< 21	+ 24
13	< 23	+ 3	3	33	− 40	2	< 21	+ 12
14	< 22	0	4	44	+ 55	4	48	− 34
15	< 20	− 11	5	30	− 23	6	34	− 16
16	20	+ 13	6	37	+ 32	8	< 27	+ 7
17	< 14	− 1	7	19	− 19	10	< 28	+ 12
006	167	−177	8	30	+ 40	12	28	+ 37
1	< 18	+ 5	110	142	+179	14	28	+ 37
2	112	−110	3	191	+215	16	17	+ 24
3	< 19	− 6	5	128	+120	170	71	− 46
4	96	− 82	7	79	+ 68	3	87	− 62
5	< 16	− 7	9	93	+ 70	5	66	− 96
6	81	− 77	11	103	+ 85	7	41	− 35
7	25	− 16	13	78	+ 63	9	< 28	+ 23

hkl	F_{obs}	F_{calc}	*hkl*	F_{obs}	F_{calc}	*hkl*	F_{obs}	F_{calc}
11	< 28	+ 16	9	50	− 43	11	28	− 38
13	< 25	+ 3	11	47	− 50	0, 12, 0	39	− 35
15	< 19	− 8	13	43	− 50	2	51	− 41
080	103	−101	0, 10, 0	57	− 50	4	42	− 41
2	81	− 52	2	63	− 55	6	48	− 50
4	57	− 56	4	82	− 71	8	34	− 41
6	< 28	− 7	6	77	− 63	10	24	− 35
8	49	− 51	8	48	− 46	1, 13, 0	30	− 30
10	36	− 37	10	42	− 32	3	29	− 23
12	50	− 68	12	23	− 21	5	21	− 28
14	35	− 43	1, 11, 0	84	− 86	7	< 15	− 27
190	50	− 38	3	79	− 81	0, 14, 0	38	− 49
3	51	− 25	5	60	− 53	2	29	− 41
5	57	− 38	7	64	− 74	4	< 11	− 29
7	49	− 26	9	45	− 46			

tellurium dimethanethiosulphonate [4] and ammonium telluropentathionate [5] are included for comparison; the latter compounds possess no exact molecular symmetry element in the crystals studied, and the two figures listed for these where one only occurs for the benzenethiosulphonate, refer to the two, here not quite identical halves.

The three structure determinations are probably about equally accurate, with probable errors of about 0.03—0.04 Å for Te—S and S—S distances, and 2—3° for bond angles involving these atoms. It appears that the only differences in dimensions which can be considered significant, are the larger dihedral angles in ammonium telluropentathionate, and the correspondingly larger $S_1—S_2'$ and $S_1—S_1'$ non-bonded distances. These distances, and the dihedral angles, are dependent on rotations about the Te—S bonds, and may vary without change of Te—S and S—S bond lengths and angles.

The benzenesulphonyl groups, data for which are given in Table 3, have dimensions very like those found for the same group in sulphur dibenzenesulphinate [9] and selenium dibenzenesulphinate [10].

Table 3. Dimensions of the benzenesulphonyl groups.

Bond lengths and bond angles.

$S_1—O_1 = 1.44$ Å	$\angle S_2S_1O_1 = 100°$	$\angle O_1S_1O_2 = 120°$
$S_1—O_2 = 1.43$ Å	$\angle S_2S_1O_2 = 110°$	$\angle O_1S_1C_1 = 106°$
$S_1—C_1 = 1.77$ Å	$\angle S_2S_1C_1 = 104°$	$\angle O_2S_1C_1 = 111°$

Non-bonded distances (in Å units).

$O_1—O_2 = 2.49$	$S_2—O_1 = 2.73$
$O_1—C_1 = 2.57$	$S_2—O_2 = 2.90$
$O_2—C_1 = 2.65$	$S_2—C_1 = 3.03$

As mentioned above, the benzene ring has been assumed to be a regular hexagon with C—C bond lengths of 1.39 Å, and with a linear arrangement of the S_1, C_1 and C_4 atoms. Within the benzenesulphonyl group, the shortest oxygen-carbon approaches are $O_2—C_2 = 2.99$ Å and $O_1—C_6 = 3.13$ Å. The

plane of the benzene ring and S_1 makes angles of 5°, 121° and 251°, respectively, with the $O_2S_1C_1$, $S_2S_1C_1$ and $O_1S_1C_1$ planes.

There are no particularly short intermolecular approaches in the crystals; *e. g.*, the shortest Te—S distance of this kind is 4.00 Å and occurs between Te and S_1 atoms.

THE TETRAGONAL ANALOGUES

In the tetragonal crystals of sulphur [1] and selenium [3] dibenzenethiosulphonate, and sulphur [1], selenium and tellurium di-*p*-toluenethiosulphonate and triselenium di-*p*-toluenesulphinate [3], of space group D_4^4—$P4_12_12$ (or the enantiomorph) with four molecules per unit cell, a twofold axis of molecular symmetry is required, as in orthorhombic tellurium dibenzenethiosulphonate. As shown in a note [11] following the preliminary report on the present structure [12], the similarities extend further, there being a close correspondence between the *b* and *c* axis projections of the orthorhombic structure and the *b* axis projection of the tetragonal structure in the centered setting, $C4_122_1$. In fact, the structure of tetragonal tellurium di-*p*-toluenethiosulphonate was solved by means of direct reference to the *b* and *c* axis projections of the orthorhombic benzene analogue. The dimensions found for the S-S-Te-S-S chain of the *p*-toluenethiosulphonate [11] agree well with those reported here for the benzenethiosulphonate.

REFERENCES

1. Dawson, I. M., Mathieson, A. McL. and Robertson, J. M. *J. Chem. Soc.* **1948** 322.
2. Foss, O. *Acta Chem. Scand.* **6** (1952) 508.
3. Foss, O. *Acta Chem. Scand.* **6** (1952) 521.
4. Foss, O. and Vihovde, E. H. *Acta Chem. Scand.* **8** (1954) 1032.
5. Foss, O. and Larssen, P. A. *Acta Chem. Scand.* **8** (1954) 1042.
6. Foss, O. *Acta Chem. Scand.* **7** (1953) 1221.
7. Foss, O. and Zachariasen, H. *Acta Chem. Scand.* **8** (1954) 473.
8. Foss, O. and Tjomsland, O. *Acta Chem. Scand.* **8** (1954) 1701.
9. Mathieson, A. McL. and Robertson, J. M. *J. Chem. Soc.* **1949** 724.
10. Furberg, S. and Øyum, P. *Acta Chem. Scand.* **8** (1954) 42.
11. Foss, O. and Øyum, P. *Acta Chem. Scand.* **9** (1955) 1014.
12. Øyum, P. and Foss, O. *Acta Chem. Scand.* **9** (1955) 1012.

Received October 31, 1955.

ACTA CHEMICA SCANDINAVICA 10 (1956) 288–297

The Crystal Structure of Triclinic Barium Pentathionate Dihydrate

OLAV FOSS and OLAV TJOMSLAND

Institutt for uorganisk kjemi, Norges tekniske høgskole, Trondheim, Norway

The unit cell of triclinic barium pentathionate dihydrate has the dimensions, $a = 5.00$ Å, $b = 10.36$ Å, $c = 11.53$ Å, $\alpha = 109°$, $\beta = 97°$, $\gamma = 90°$. The space group is $C_i^1-P\bar{1}$ with $Z = 2$. Fourier projections along the a and b axes show that the pentathionate ion has an unbranched, *cis* configuration, with $S_1-S_2 = 2.13$ Å, $S_2-S_3 = 2.04$ Å, $S_3-S_4 = 2.04$ Å, $S_4-S_5 = 2.11$ Å (all $\pm$ 0.04 Å), $\angle S_1S_2S_3 = 106°$, $\angle S_2S_3S_4 = 107°$, $\angle S_3S_4S_5 = 105°$ (all $\pm$ 3°), and the dihedral angles, $S_1S_2S_3/S_2S_3S_4 = 108°$ and $S_2S_3S_4/S_3S_4S_5 = 107°$. These values agree within the experimental errors with those found earlier for the orthorhombic dimorph.

The crystals of triclinic and orthorhombic barium pentathionate dihydrate are composed of layers which have the same internal structure in both dimorphs, but are differently arranged relative to each other.

A study of the crystal chemistry of barium salts of pentathionic, selenopentathionic and telluropentathionic acids has recently led to the structure determination of the isomorphous salts, barium pentathionate [1] and selenopentathionate [2] dihydrates. The orthorhombic crystals have four-molecule unit cells based on the space group, $D_{2h}^{16}-Pnma$, with $a = 5.00$ Å, $b = 10.30$ Å, $c = 21.78$ Å for the pentathionate. No orthorhombic dihydrate of barium telluropentathionate has been found, although two dihydrates, one monoclinic and one triclinic, have been characterized and will be described later.

As mentioned earlier [3], a triclinic dimorph of barium pentathionate dihydrate exists. The unit cell dimensions, from oscillation and Weissenberg photographs taken with copper radiation, $\lambda(\mathrm{Cu}K\alpha) = 1.54$ Å, are [3]

$a = 5.00$ Å,	$b = 10.36$ Å,	$c = 11.53$ Å
$\alpha = 109°$	$\beta = 97°$	$\gamma = 90°$

There are two molecules per unit cell, and the space group is the centrosymmetric one, $C_i^1-P\bar{1}$.

It is seen that within the experimental accuracy ($\pm$ 0.5 %) the lengths of the a and b axes of the triclinic and orthorhombic dimorphs are the same, as are also the γ angles. The spacing of the triclinic c plane, $d_{001} = 10.78$ Å,

is close to half the orthorhombic c axis, 10.89 Å. Both dimorphs exhibit perfect cleavage along the c plane, and appear as prisms, elongated along the a axis and with {001} predominant.

In the orthorhombic space group, $00l$ reflections are systematically absent for odd values of l and as many are thus present as in the triclinic crystals. The intensities of the $00l$ reflections of the two dimorphs, with the orthorhombic l indices halved, are very similar. The one-dimensional projections on to a line perpendicular to the c planes of the two unit cells should thus be the same, and the common features noted above indicate further structural similarities.

A preliminary report on the structure of the triclinic crystals has been published [4], giving atomic coordinates and principal bond lengths and angles *.

Barium salts of pentathionic acid were apparently the first salts of the acid to be isolated, over a century ago. Lenoir [5] prepared a barium pentathionate in 1847, one year after the discovery of the acid by Wackenroder [6]. Lenoir crystallized the salt from aqueous solutions containing ethanol, and although he noted that the salt contained ethanol, he described it as a dihydrate. Fordos and Gélis [7], in 1848, stated that the salt always retains some ethanol when precipitated from water by means of ethanol, and said that the best method for the isolation of an ethanol-free salt, a dihydrate, was to crystallize from water by addition of ether containing some ethanol. Lewes [8], in 1881, isolated barium pentathionate without the use of ethanol, but gave the composition as that of a trihydrate, the same water content as he erroneously gave for barium tetrathionate. Debus [9], of the same laboratory as Lewes, in 1888 referred to Lewes' barium pentathionate as but 'nearly pure'. In 1933, Deines and Christoph [10] in a footnote reported on the isolation of barium polythionates, presumably also the pentathionate, from aqueous solutions by addition of ethanol or acetone, but did not give the compositions.

The present authors have isolated trihydrates of barium selenopentathionate and telluropentathionate, but of barium pentathionate, only dihydrates.

Of the earlier authors cited above, it appears that only Fordos and Gélis may have obtained a pure dihydrate. It will be shown later that several organic solvents, among them ethanol and acetone, give solvates when used for the crystallization of barium pentathionate. Lenoir, and Deines and Christoph, probably obtained solvates, and not pure hydrates.

EXPERIMENTAL

The barium pentathionate dihydrates were prepared as follows. A crude salt was obtained by mixing, at a temperature not above 40° C, saturated solutions of potassium pentathionate and a slight excess of barium perchlorate, filtering off the precipitated potassium perchlorate, and addition of ethanol and cooling. The crude preparation, which contained ethanol, was stable for months.

The triclinic dihydrate resulted when an aqueous solution of the crude product, saturated at 40—50° C, was allowed to cool to room or ice temperature. The orthorhombic dihydrate was obtained by addition of methanol to an aqueous solution saturated at 20—30° C. About 0.2 N hydrochloric acid, instead of pure water, was used to dissolve the pentathionates.

No study of the relative stabilities of the dimorphs at various conditions has been made. When pure, they both remain unchanged for months, and appear to be about equally stable.

The salts were analyzed iodometrically by means of the sulphite method [11]. In order to remove the barium as sulphate, so as to prevent the precipitation of barium sulphite which would interfere in the titration with iodine, some sodium sulphate was added to

* In that report [3] and the earlier one [4], values for the α and β angles, respectively, were given which are larger than the present ones, believed to be more correct, by one degree. The change of β from 98° to 97° has led to bond lengths and angles which in a few cases differ slightly from those given in the preliminary report.

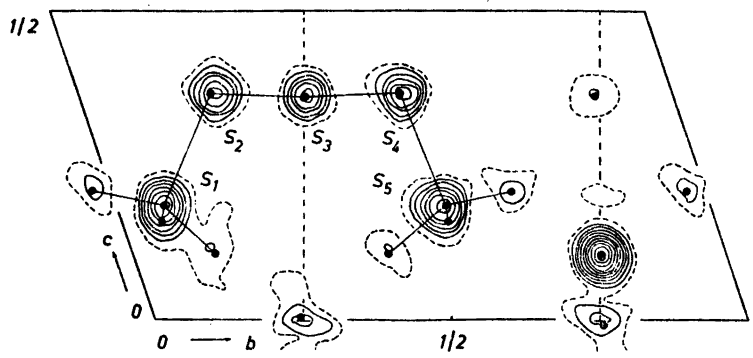


Fig. 1. Electron density projection of triclinic $BaS(S_2O_3)_2 \cdot 2H_2O$ along the a axis. The atomic positions are marked with dots, and lines are drawn to show the outline of the pentathionate ion. The 5-electron line is dashed. Contour intervals: 10 e·Å^{-2} for the barium ion, and 4 e·Å^{-2} for sulphur and oxygen atoms and water molecules.

the barium pentathionate solution before the addition of sodium sulphite reagent. One mole of pentathionate reacts with sulphite to produce two moles of thiosulphate, which is titrated with iodine after masking of excess of sulphite by means of formaldehyde.

Since analytical data have not been included in earlier communications on the salts [1,3], analyses of both modifications are reported here.

Orthorhombic dihydrate. 0.2839 × $\frac{1}{5}$ g substance: 26.20 ml of 0.01010 N iodine.

Triclinic dihydrate. 0.2719 × $\frac{1}{5}$ g substance: 24.88 ml of 0.01019 N iodine.

$BaS(S_2O_3)_2 \cdot 2H_2O$ (429.7) Mol. weights found, 429.2 and 429.0, respectively.

Absence of tetrathionate was checked through control analyses by means of the cyanide method.

The intensities of the 0*kl* and *h*0*l* reflections of triclinic barium pentathionate dihydrate were estimated visually from zero layer Weissenberg photographs taken with copper radiation. Small crystals were used in order to minimize absorption, for which no correction was made. The ready cleavage along the *c* plane made it difficult to cut the crystals for photographs about the *b* axis, and as in the case of the orthorhombic structure [1], the observed intensities of the *h*0*l* reflections are therefore probably less reliable than those of the 0*kl* reflections. The intensities were corrected for the Lorentz and polarization factors, and converted into relative structure factors. They were later put to an approximately absolute scale through comparison with the calculated values.

Patterson and Fourier projections along the *a* and *b* axes were made. The summations were performed by means of Beevers-Lipson strips, the Patterson and first Fourier summations at 12° intervals along the axes, and the final Fourier refinements by summations at 6° intervals along the two longest axes. No great accuracy in bond lengths and angles was aimed at, the chief objective being to establish the relation of the structure to that of the orthorhombic dihydrate.

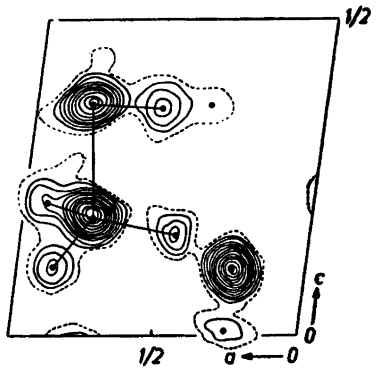


Fig. 2. Electron density projection of triclinic $BaS(S_2O_3)_2 \cdot 2H_2O$ along the b *axis. The 8-electron line is dashed. Contour intervals: 8 e·Å^{-2} for the barium ion, otherwise as in Fig. 1.*

DETERMINATION OF THE STRUCTURE

The 0*kl* Patterson map was prepared first, early in 1953, and on the basis of the barium y and z coordinates derived from the map, signs were calculated and used in a Fourier synthesis of 185 of the 265 observed 0*kl* reflections. The resulting map revealed the positions of the sulphur atoms, in accordance with the barium-sulphur vectors of the Patterson map, and also some of the oxygen atoms. At that phase of the work, attention was shifted from the triclinic to the orthorhombic dihydrate, the latter having a more favourable space group, and work on the former was resumed two years later, with Fourier refinement of the 0*kl* projection through successive approximations in the usual way.

The projection along the b axis was also solved by means of the heavy atom technique, using for the first sign calculation the already known z coordinate of barium and the x coordinate derived from the $h0l$ Patterson map. As was expected from the a axis projection and the orthorhombic structure, sets of two sulphur atoms and three oxygen atoms were found to overlap, having within the experimental accuracy the same x and z coordinates.

The electron density maps are shown in Figs. 1 and 2. The final atomic positions are marked with dots, and lines are drawn to show the sulphur-sulphur and sulphur-oxygen bonds. The coordinates of the positions, in fractions of cell edges and referring to the triclinic axes, are listed in Table 1.

Orthogonal coordinates, in Å, are given in Table 2 under the heading $P\bar{1}$. They refer to the same origin as in Table 1 and to the a, b and c' axes, where, since $\gamma = 90°$, c' is chosen normal to a and b. The coordinates listed in Table 2 under the heading *Pnma*, are those found in the orthorhombic dihydrate, cal-

Table 1. Atomic coordinates. Origin at a centre of symmetry.

	x	y	z		x	y	z
Ba	0.749	0.211	−0.104	O_1	0.462	0.070	0.158
S_1	0.755	0.077	0.186	O_2	0.920	−0.031	0.210
S_2	0.808	0.225	0.366	O_3	0.874	0.140	0.108
S_3	0.564	0.381	0.359	O_4	0.462	0.551	0.158
S_4	0.808	0.542	0.366	O_5	0.920	0.676	0.210
S_5	0.755	0.554	0.186	O_6	0.874	0.432	0.108
$(H_2O)_1$	0.253	0.250	0.007	$(H_2O)_2$	0.603	0.131	−0.363

culated from the fractional coordinates given earlier [1] and referred to a corresponding origin. In the orthorhombic structure, the Ba, S_3 and water oxygen atoms lie in a crystallographic mirror plane of symmetry, at $y = \frac{1}{4}$, and the S_5, S_4, O_4, O_5 and O_6 atoms are related to the S_1, S_2, O_1, O_2 and O_3 atoms, respectively, through this plane.

Table 2. Orthogonal coordinates for the two dimorphs of barium pentathionate dihydrate.

	x'(Å)		y'(Å)		z'(Å)	
	$P\bar{1}$	*Pnma*	$P\bar{1}$	*Pnma*	$P\bar{1}$	*Pnma*
Ba	3.89	3.90	2.58	2.58	−1.12	−1.09
S_1	3.51	3.50	0.10	0.13	2.01	2.05
S_2	3.53	3.58	0.96	0.95	3.96	4.03
S_3	2.32	2.35	2.60	2.58	3.88	3.90
S_4	3.53	3.58	4.24	4.20	3.96	4.03
S_5	3.51	3.50	5.04	5.02	2.01	2.05
O_1	2.09	2.11	0.13	0.08	1.71	1.70
O_2	4.31	4.10	−1.11	−1.12	2.27	2.37
O_3	4.22	4.15	1.05	0.97	1.17	1.09
O_4	2.09	2.11	5.12	5.07	1.71	1.70
O_5	4.31	4.10	6.22	6.27	2.27	2.37
O_6	4.22	4.15	4.07	4.18	1.17	1.09
$(H_2O)_1$	1.26	1.50	2.56	2.58	0.08]	0.04
$(H_2O)_2$	3.53	3.25	2.72	2.58	−3.92	−3.70

In Table 4, observed and calculated values of structure factors are compared for all 0*kl* and *h*0*l* reflections within the range of Cu$K\alpha$ radiation. The calculated values are based on the coordinates of Table 1, and the atomic scattering curves of the *International Tables*, with the xenon curve for the barium ion, and a temperature factor of $B = 2.2$ Å^2 for both zones. The reliability factor, $R = \Sigma \| F_{obs} | - | F_{calc} \| / \Sigma | F_{obs} |$, with non-observed reflections included only when $| F_{calc} |$ is greater than the smallest observable value of $| F_{obs} |$, is 0.18 for the 0*kl* and 0.19 for the *h*0*l* reflections.

DISCUSSION

The average differences between the atomic coordinates of the triclinic and orthorhombic structures, as listed in Table 2, are 0.01 Å for the barium ion, 0.03 Å for the five sulphur atoms, 0.07 Å for the six sulphonate oxygen atoms, and 0.16 Å for the two water oxygen atoms. These differences are considered to be within the probable errors of the two structure determinations.

It follows that the configuration of the pentathionate ion in the triclinic crystals is the same as in the orthorhombic ones, and within the probable errors this applies also to the dimensions. The sulphur chain is unbranched and occurs in a *cis* form. The sulphur-sulphur bond lengths given in Table 3, and angles involving these atoms, are considered to be correct to within 0.04 Å and 3°, respectively.

Table 3. Sulphur-sulphur bond lengths and angles.

$S_1-S_2 = 2.13$ Å	$\angle S_1S_2S_3 = 106°$	$S_4-S_5 = 2.11$ Å
$S_2-S_3 = 2.04$	$\angle S_2S_3S_4 = 107°$	$S_3-S_4 = 2.04$
	$\angle S_3S_4S_5 = 105°$	

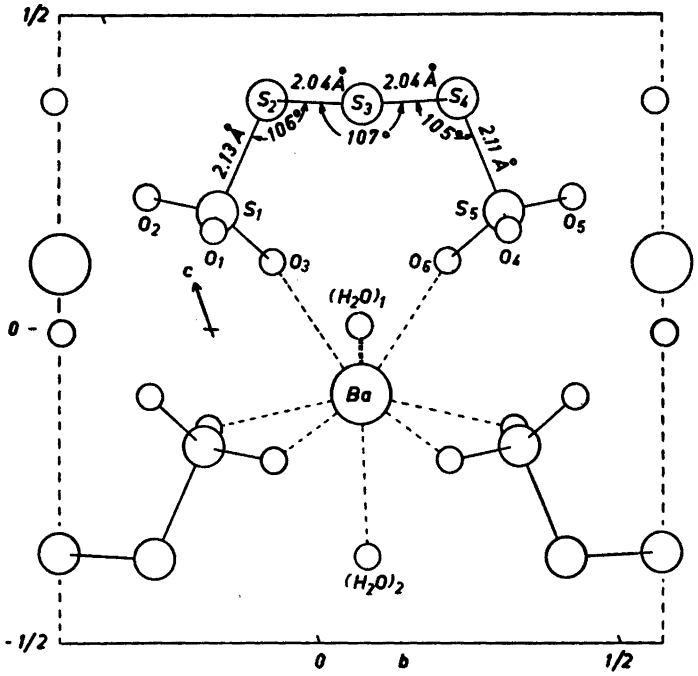


Fig. 3. Arrangement of the ions as seen along the a axis. Origin at the midpoint of the left half of the figure.

The dihedral angles, $S_1S_2S_3/S_2S_3S_4$ and $S_2S_3S_4/S_3S_4S_5$, are 108° and 107°, respectively. The corresponding data for the orthorhombic structure are [1], $S_1-S_2 = S_4-S_5 = 2.14$ Å, $S_2-S_3 = S_3-S_4 = 2.04$ Å, $\angle S_1S_2S_3 = \angle S_3S_4S_5 = 103°$, $\angle S_2S_3S_4 = 106°$, and the dihedral angles, 110°.

The six sulphur-oxygen bonds of the sulphonate groups have an average length of 1.46 ± 0.01 Å. The electron density peaks of the oxygen atoms are rather low and diffuse, and the oxygen atoms were moved within the peaks to give reasonable and uniform S—O distances.

Each barium ion is surrounded by nine oxygen atoms, of which six are sulphonate oxygen atoms and three are water oxygen atoms. The average distance to barium for these nine atoms is 2.78 Å in both dimorphs. The water molecule, $(H_2O)_1$, is coordinated to two barium ions, at distances of 2.89 Å and 2.66 Å, and forms hydrogen bonds to the oxygen atoms O_1 and O_4, at distances of 3.04 Å and 3.15 Å and an angle of 108°.

In the orthorhombic space group, the barium ion and the middle sulphur atom of the pentathionate chain, as well as the two water oxygen atoms, lie in a mirror plane of symmetry. Although the triclinic space group possesses no crystallographic mirror plane of symmetry, an apparent mirror plane is present. From the Fourier maps, and the orthogonal coordinates of Table 2, is seen that the asymmetric unit possesses mirror plane symmetry within the

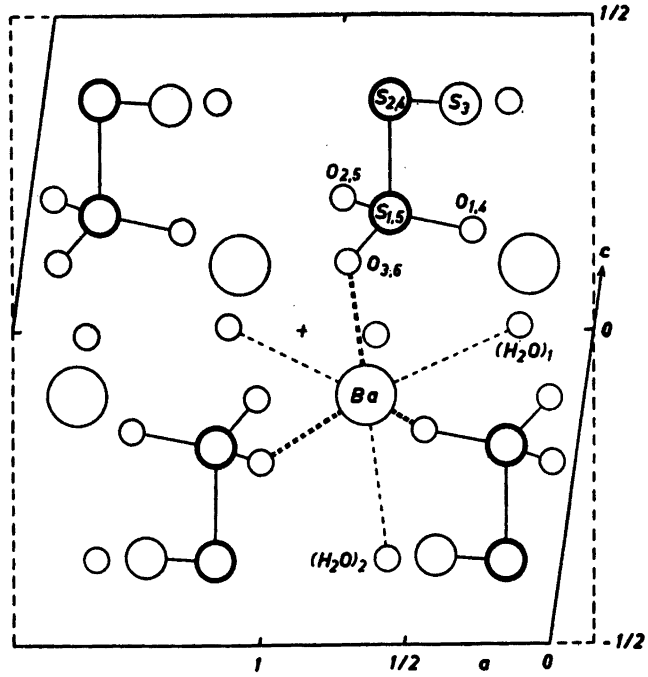


Fig. 4. Arrangement of the ions as seen along the b *axis.*

experimental error. The mirror plane, depicted through broken lines in Fig. 1, is normal to the b axis at $z = 0$, $y = \frac{1}{4}$ and $\frac{3}{4}$, as in the orthorhombic space group, and passes through the same atoms.

The similarity of atomic arrangement in the triclinic and orthorhombic dimorphs extends to within the boundaries of layers parallel to the c planes. The centres of symmetry which have been chosen as the origins of the coordinate systems are located in the middle of a layer, the thickness of which is equal to the triclinic c spacing, $d_{001} = 10.78$ Å, and half the orthorhombic c axis, $c/2 = 10.89$ Å. The line diagrams of Figs. 3 and 4, with boundaries at $z = \frac{1}{2}$ and $-\frac{1}{2}$, cover the thickness of one layer. The similarity of structure within a layer is apparent from a comparison of these diagrams with the corresponding ones for the orthorhombic structure [1].

The triclinic and orthorhombic dimorphs differ in the way in which the layers are arranged relative to each other. In the space group, D_{2h}^{16}-*Pnma*, layers are related to each other through glide planes a in their interface, at $z = \frac{1}{4}$ and $-\frac{1}{4}$, whereas in the space group C_i^1—$P\bar{1}$, the layers are related through symmetry centres in the interface. Since the layer thickness equals the triclinic c spacing, and the α and β angles are different from 90°, the symmetry centres operate to produce a simple repetition of layers, with successive relative displacements in the directions of the a and b axes. A transition from the orthorhombic to the triclinic structure, or *vice versa*, requires a rotation of

Table 4. Observed and calculated values of structure factors for triclinic barium pentathionate dihydrate.

hkl	F_{obs}	F_{calc}	*hkl*	F_{obs}	F_{calc}	*hkl*	F_{obs}	F_{calc}
001	61	+102	0$\bar{2}$1	51	− 33	0$\bar{4}$3	47	+ 44
2	35	− 42	2	43	− 46	4	22	− 23
3	48	− 48	3	88	− 92	5	58	− 58
4	130	−153	4	21	− 32	6	38	− 42
5	20	− 2	5	63	+ 75	7	19	− 7
6	11	+ 11	6	79	+ 88	8	<7	+ 5
7	65	− 58	7	44	+ 51	9	7	− 3
8	37	+ 39	8	7	− 11	10	11	+ 7
9	36	+ 34	9	52	− 60	11	31	+ 26
10	34	+ 35	10	39	− 45	12	31	+ 32
11	53	+ 61	11	18	− 18	13	17	+ 24
12	17	− 12	12	<7	− 9	14	10	− 5
13	23	− 24	13	<6	+ 3	050	78	− 67
010	3	+ 8	14	10	+ 7	1	57	+ 58
1	61	+ 75	030	92	+ 85	2	43	+ 39
2	95	+105	1	82	− 70	3	20	+ 22
3	11	+ 12	2	112	−115	4	49	− 47
4	27	+ 31	3	25	− 39	5	61	− 55
5	16	− 6	4	47	+ 43	6	36	− 30
6	70	− 63	5	32	+ 41	7	21	− 23
7	37	− 32	6	63	+ 66	8	18	+ 13
8	37	− 40	7	36	+ 36	9	25	+ 23
9	17	− 17	8	9	+ 3	10	11	+ 13
10	31	+ 31	9	10	+ 5	11	10	+ 18
11	15	+ 16	10	34	− 29	0$\bar{5}$1	9	+ 8
12	20	+ 18	11	30	− 31	2	6	+ 3
13	16	+ 17	12	11	− 14	3	18	− 18
0$\bar{1}$1	21	+ 3	0$\bar{3}$1	18	− 13	4	82	− 75
2	75	−100	2	100	+ 79	5	61	− 52
3	65	− 79	3	69	+ 66	6	27	− 35
4	12	− 8	4	109	+117	7	<6	− 3
5	22	− 35	5	46	+ 58	8	59	+ 59
6	32	+ 28	6	31	− 39	9	38	+ 47
7	63	+ 59	7	31	− 37	10	24	+ 28
8	33	+ 29	8	20	− 64	11	11	+ 16
9	37	+ 43	9	17	− 45	12	14	− 19
10	12	+ 1	10	7	− 6	13	19	− 18
11	31	− 31	11	<7	− 10	14	14	− 14
12	16	− 12	12	27	+ 23	060	44	− 44
13	23	− 22	13	31	+ 35	1	24	− 27
14	9	− 11	14	11	+ 15	2	79	+ 84
020	39	− 34	040	60	+ 42	3	39	+ 38
1	68	− 63	1	35	− 29	4	39	+ 43
2	79	− 79	2	59	− 56	5	18	+ 21
3	20	+ 21	3	53	− 49	6	50	− 69
4	86	+ 94	4	21	− 7	7	32	− 35
5	68	+ 72	5	10	+ 13	8	23	− 18
6	23	+ 25	6	<7	0	9	21	− 19
7	33	− 40	7	15	+ 8	10	15	+ 20
8	54	− 63	8	35	+ 24	0$\bar{6}$1	12	− 3
9	32	− 30	9	29	+ 29	2	108	− 94
10	9	− 12	10	21	+ 26	3	49	− 31
11	<6	− 3	11	<5	− 3	4	19	− 19
12	9	+ 8	0$\bar{4}$1	116	+109	5	58	− 62
13	10	+ 7	2	117	+103	6	64	+ 60

hkl	F_{obs}	F_{calc}	*hkl*	F_{obs}	F_{calc}	*hkl*	F_{obs}	F_{calc}
$0\bar{6}7$	70	+ 59	093	30	− 29	$0, \bar{1}\bar{2}, 6$	<5	− 1
8	30	+ 33	4	37	− 44	7	<5	+ 6
9	34	+ 49	5	46	− 17	8	18	− 25
10	37	− 47	6	<5	+ 5	9	20	− 20
11	44	− 53	7	8	+ 9	10	5	+ 3
12	9	− 14	$0\bar{9}1$	31	+ 21	$0, \bar{1}\bar{3}, 2$	12	+ 14
13	20	− 28	2	15	+ 18	3	17	+ 21
14	<4	+ 7	3	39	+ 10	4	8	− 8
070	63	+ 54	4	9	− 12	5	9	− 8
1	27	+ 19	5	21	− 11	6	<4	+ 1
2	9	− 8	6	38	− 43	7	17	− 25
3	25	+ 17	7	41	− 44	100	13	+ 1
4	32	+ 27	8	19	− 2	1	57	+ 61
5	<7	+ 4	9	23	+ 16	2	81	− 85
6	39	+ 33	10	32	+ 40	3	77	− 77
7	16	+ 9	11	29	+ 34	4	48	− 47
8	24	− 22	12	<5	+ 3	5	33	− 33
9	19	− 10	13	<4	0	6	56	+ 61
$0\bar{7}1$	99	− 79	0, 10, 0	11	+ 4	7	41	+ 46
2	<6	− 6	1	33	+ 35	8	26	+ 15
3	<6	+ 1	2	30	+ 34	9	24	+ 24
4	68	+ 57	3	<5	+ 2	10	31	− 15
5	61	+ 63	4	10	− 14	11	<23	− 15
6	17	− 14	5	19	− 25	12	<20	− 10
7	9	+ 12	$0, \bar{1}\bar{0}, 1$	11	− 11	13	18	− 25
8	<7	0	2	22	− 21	$\bar{1}01$	49	− 33
9	36	− 32	3	20	− 12	2	82	+ 81
10	12	− 9	4	15	− 8	3	57	+ 54
11	32	− 33	5	33	− 30	4	91	+ 91
12	21	− 19	6	20	− 24	5	24	+ 33
13	21	+ 21	7	9	0	6	95	−117
14	13	+ 10	8	28	+ 26	7	70	− 72
080	31	− 29	9	33	+ 39	8	25	− 21
1	49	− 49	10	47	+ 14	9	24	+ 2
2	32	− 21	11	10	− 9	10	46	+ 53
3	9	+ 2	12	13	− 16	11	23	+ 11
4	9	− 11	0, 11, 0	<6	+ 5	12	<22	− 5
5	15	+ 7	1	9	+ 8	13	30	+ 23
6	26	+ 22	2	18	+ 21	14	<10	+ 4
7	24	+ 22	3	16	+ 15	200	114	−113
8	18	+ 26	$0, \bar{1}\bar{1}, 1$	26	− 23	1	26	− 13
$0\bar{8}1$	<7	− 5	2	36	− 44	2	21	− 3
2	52	+ 57	3	29	− 27	3	46	− 38
3	89	+ 96	4	<7	0	4	49	+ 46
4	40	+ 40	5	27	+ 27	5	<21	+ 9
5	7	− 4	6	35	+ 42	6	31	+ 31
6	31	− 31	7	23	+ 26	7	<24	+ 7
7	38	− 44	8	<6	+ 3	8	25	− 22
8	18	− 12	9	<6	− 4	9	23	− 18
9	12	− 9	10	14	− 18	10	37	− 44
10	15	− 14	11	14	− 17	11	27	− 26
11	8	+ 12	0, 12, 0	23	− 31	12	16	+ 7
12	23	+ 21	1	7	+ 4	$\bar{2}01$	126	−120
13	22	+ 26	$0, \bar{1}\bar{2}, 1$	21	− 18	2	39	− 35
14	10	+ 23	2	<5	+ 1	3	18	+ 3
090	50	− 48	3	<5	0	4	67	+ 69
1	28	+ 22	4	30	+ 47	5	40	+ 51
2	13	− 13	5	27	+ 33	6	24	+ 9

hkl	F_{obs}	F_{calc}	*hkl*	F_{obs}	F_{calc}	*hkl*	F_{obs}	F_{calc}
$\bar{2}07$	29	+ 30	$\bar{3}09$	<25	+ 11	500	23	+ 12
8	<24	− 3	10	24	− 21	1	30	− 24
9	33	− 32	11	27	− 39	2	29	− 29
10	47	− 43	12	19	− 10	3	28	− 17
11	41	− 51	13	14	− 11	4	26	− 39
12	<21	− 3	400	60	+ 60	5	<19	+ 8
13	23	+ 26	1	36	+ 28	6	21	+ 35
300	40	− 47	2	24	+ 34	7	14	+ 18
1	26	+ 23	3	38	− 47	$\bar{5}01$	<25	− 13
2	58	+ 53	4	36	− 39	2	35	+ 29
3	51	+ 43	5	<25	+ 6	3	43	+ 61
4	66	+ 81	6	24	− 20	4	30	+ 13
5	<24	+ 6	7	<22	+ 5	5	<23	+ 9
6	43	− 49	8	<19	+ 9	6	34	− 27
7	38	− 39	9	<14	− 3	7	39	− 54
8	35	− 52	$\bar{4}01$	53	+ 57	8	<19	− 5
9	<22	0	2	26	− 36	9	<16	− 6
10	24	+ 29	3	30	− 11	10	<12	+ 2
11	<13	+ 8	4	32	− 12	600	24	− 36
$\bar{3}01$	23	− 12	5	33	− 35	1	16	− 18
2	34	− 42	6	<25	+ 17	2	<14	+ 1
3	66	− 65	7	<25	− 12	$\bar{6}01$	21	− 31
4	33	− 16	8	<24	− 12	2	<16	+ 5
5	22	− 25	9	27	+ 32	3	17	+ 19
6	39	+ 33	10	26	+ 14	4	20	+ 20
7	73	+ 79	11	24	+ 25	5	16	+ 15
8	33	+ 31	12	12	+ 19	6	<13	+ 1

180° of every second layer about an axis normal to the *c* plane, as well as displacements of layers along the *a* and *b* axes.

In both structures, weak van der Waals contacts only, between sulphur atoms, occur across the layer interfaces, and account for the ready cleavage of the crystals along the *c* plane. The different arrangements of layers lead to different sulphur-sulphur approaches, but the distances of the closest ones are practically the same, *viz.*, 3.61 Å and 3.78 Å in the orthorhombic and 3.51 Å, 3.57 Å, 3.73 Å and 3.74 Å in the triclinic structure.

The work has been aided by grants from *Norges Almenvitenskapelige Forskningsråd* and from *Norges Tekniske Høgskoles Fond.*

REFERENCES

1. Foss, O. and Zachariasen, H. *Acta Chem. Scand.* **8** (1954) 473.
2. Foss, O. and Tjomsland, O. *Acta Chem. Scand.* **8** (1954) 1701.
3. Foss, O. *Acta Chem. Scand.* **7** (1953) 697.
4. Foss, O. and Tjomsland, O. *Acta Chem. Scand.* **9** (1955) 1016.
5. Lenoir, A. *Ann.* **62** (1847) 253.
6. Wackenroder, H. *Ann.* **60** (1846) 189.
7. Fordos, J. and Gélis, A. *J. prakt. Chem.* **43** (1848) 456.
8. Lewes, V. *J. Chem. Soc.* **39** (1881) 68.
9. Debus, H. *J. Chem. Soc.* **53** (1888) 278.
10. Deines, O. and Christoph, E. *Z. anorg. u. allgem. Chem.* **213** (1933) 209.
11. Kurtenacker, A. *Analytische Chemie der Sauerstoffsäuren des Schwefels*, Ferdinand Enke, Stuttgart 1938, pp. 149—155.

Received October 31, 1955.

ACTA CHEMICA SCANDINAVICA 10 (1956) 298—305

On the Hydrolysis of Trialkylphenoxysilanes

EVERT ÅKERMAN

Department of Organic Chemistry, University of Lund, Lund, Sweden

The acid and base catalysed hydrolysis of $R_3SiOC_6H_5$ in aqueous ethanol has been studied for R = methyl, ethyl, *n*-propyl, *n*-butyl and *n*-amyl. The specific rate of reaction follows the equation

$$k = k_a\ [H^+] + k_{sp} + k_b\ [\text{base}]$$

k_a being the catalytic constant for hydrogen ions, k_b that for a mixture of hydroxyl and ethoxide ions, k_{sp} the specific rate of the spontaneous hydrolysis, and [base] the sum of hydroxyl and ethoxide ion concentrations. The first two members are negligible in alkaline solution and the last two members in acid solution. The rate of reaction diminishes with increasing length of the alkyl groups.

Kinetic investigations of the hydrolysis of silanes of the type R_3SiX where R is an alkyl or aryl group and X is a hydrolysable functional group are scarce. Swain, Esteve and Jones [1] found the rate of hydrolysis of triphenylsilylfluoride in 50 % water, 50 % acetone to be proportional to the concentration of silane and that it is not influenced by hydrogen ions but accelerated by hydroxyl ions. From the influence of solvent, neutral salts and substituents they deduced that the hydrolysis possibly proceeded through a pentacovalent silicon intermediate. Krieble and Burkhard [2] found that the acid hydrolysis of dimethyldi-D-2-butoxysilane gave 2-butanol with the same optical activity as the original 2-butanol. This fact indicates that the silicon-oxygen bond is broken and not the carbon-oxygen bond.

As a part of the work in this laboratory five trialkylphenoxysilanes $R_3SiOC_6H_5$ with R = CH_3, C_2H_5, *n*-C_3H_7, *n*-C_4H_9, and *n*-C_5H_{11} have been investigated. The rate of hydrolysis of such compounds can be easily determined spectrophotometrically. In aqueous ethanol with water in great excess over the silane this is hydrolysed according to the formula

$$R_3SiOC_6H_5 + H_2O \rightarrow R_3SiOH + C_6H_5OH$$

in some cases followed by formation of hexaalkyldisiloxanes and in alkaline solutions by the reaction

$$C_6H_5OH + OH^- \rightleftharpoons C_6H_5O^- + H_2O$$

The phenol was identified from its ultraviolet spectrum. Trialkylsilanes and phenol — and the phenolate ion in alkaline solutions — absorb in the ultraviolet region, but the absorption maximum of the silanes is displaced by *ca.* 5 mμ from that of phenol, and the extinction coefficient at the maximum is only half that of phenol. Fig. 1 shows the absorption spectra of phenol, phenolate and trimethylphenoxysilane. The spectra of the other four alkylphenoxysilanes are very similar to that of trimethylphenoxysilane. Trialkylsilanol and hexaalkyldisiloxane do not absorb in this spectral region. The hydrolysis was carried out in water-ethanol mixture, (51.4 weight-% ethanol), since the silanes are insoluble in water, but with water in great excess, thus making the water concentration constant during the run. From the optical density D of the sample the expression log $(D_\infty - D_t)$ was calculated, where D_t is the optical density at the time t and D_∞ is the optical density at infinite time. This expression, when plotted against time, gives a straight line (Fig. 2 shows some typical plots). The reaction is consequently of the first order in silane, following the rate equation

$$k = \frac{1}{t} \log \frac{D_\infty - D_0}{D_\infty - D_t} \qquad (1)$$

D_0 being the optical density at $t = 0$.

The hydrolysis was carried out in diluted HCl or NaOH or buffers of various composition. In the last-mentioned case the concentration of hydrogen and hydroxyl ions was measured electrometrically. In a water-ethanol solution of sodium hydroxide the anions are present partly as ethoxide ions and the

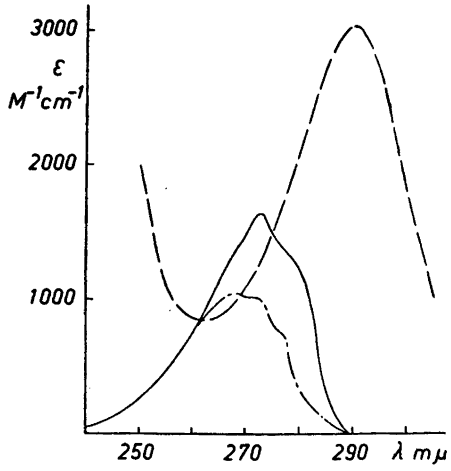


Fig. 1. Molar extinction coefficient ε vs *wavelength*

——— = *phenol*
— — — = *phenolate ion*
—·—·— = *trimethylphenoxysilane*

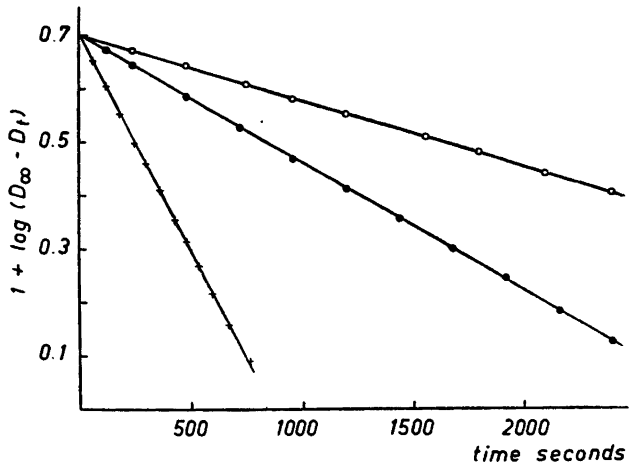


*Fig. 2. Acid hydrolysis of tri-*n*-butyl-phenoxysilane. Log* $(D_\infty - D_t)$ *vs time.*
○ : $[H^+] = 1.52 \times 10^{-3}$ *M*
● : » = 3.03 » »
\+ : » = 10.0 » »

catalytic effect of hydroxyl *and* ethoxide ions is measured. The equilibrium constant for the reaction

$$OH^- + C_2H_5OH \quad \rightleftharpoons \quad H_2O + C_2H_5O^- \qquad (2)$$

has been determined by Caldin and Long [3]. Their values show that in 53 weight-% ethanol at 25° C about 17 % of added hydroxide is converted to ethoxide. If k_{OH} and k_{OEt} are the catalytic constants for hydroxide and ethoxide ions, the rate constant k of the reaction is supposed to be

$$k = k_{OH}\,[OH^-] + k_{OEt}\,[C_2H_5O^-]$$

For stoichiometric reasons the following equation is valid for solutions where the concentration of phenolate ion is negligible.

$$[Na^+] = [OH^-] + [C_2H_5O^-]$$

From equation (2) follows, as ionic strength, solvent and concentrations of water and ethanol are constant,

$$[C_2H_5O^-] = K\,[OH^-]$$

From these three equations follows

$$k = [Na^+]\frac{k_{OH} + Kk_{OEt}}{1 + K} = [Na^+]\,k'$$

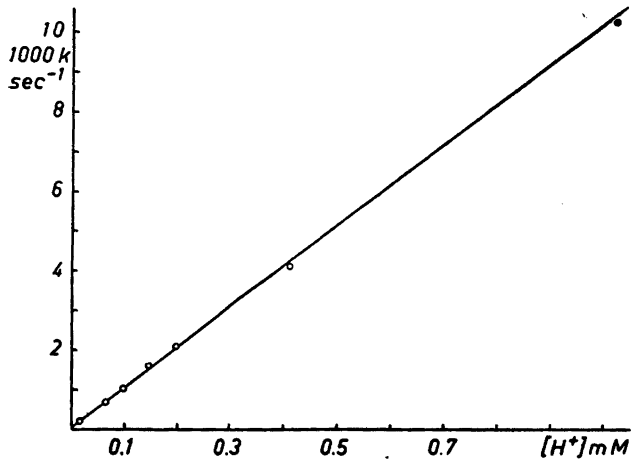


Fig. 3. Acid hydrolysis of trimethylphenoxysilane. Rate constant vs *hydrogen ion concentration.*
○ *: in glycine-HCl buffer.*
● *: in dil. HCl.*

Thus the rate constant of the reaction is proportional to the amount of added sodium hydroxide, *i.e.*, [base].

The values k_a and k_b were calculated (Tables 1, 2) and are found to be constant for each compound. The hydrolysis of trimethylphenoxysilane is very rapid. Fig. 3 shows its acid hydrolysis and the slope of the line is $k_a = 10.4\ M^{-1}\ sec^{-1}$. The alkaline hydrolysis of trimethylphenoxysilane is still more rapid and more complicated. The results obtained from reactions in glycine-NaOH buffers show that the ratio $\frac{k}{[OH^-]}$ is highly dependent on the buffer concentration, but still the reaction seems to be of the first order in hydroxyl ions with $k_b \approx 330\ M^{-1}\ sec^{-1}$. Three runs at the neutral point in a Na_2HPO_4-NaH_2PO_4 buffer seem to indicate a very slow spontaneous hydrolysis of trimethylphenoxysilane with a rate constant $k_{sp} \approx 10^{-5}\ sec^{-1}$, but the rate of reaction here is also dependent on the buffer concentration. Thus the rate of hydrolysis of trimethylphenoxysilane follows the equation

$$k = k_a [H^+] + k_{sp} + k_b [\text{base}]$$

which probably is valid also for the other four compounds, but the spontaneous hydrolysis is too slow to be noticed. The values of k_a and k_b are collected in Table 3.

The investigation will be continued with examination of compounds with other alkyl or aryl groups and with substituents in the phenoxy group.

Table 1. Acid hydrolysis of $R_3SiOC_6H_5$ in 51.4 weight-% ethanol. μ = 0.05 M.

R	[H+] mM	$k \times 10^4$ sec^{-1}	k_a $M^{-1}sec^{-1}$	k_a mean $M^{-1}sec^{-1}$
C_2H_5	1.00	2.02	0.202	0.219
	3.03	6.90	.228	
	8.00	18.0	.225	
	10.0	22.3	.223	
n-C_3H_7	1.00	1.21	0.121	0.115
	3.00	3.65	.121	
	10.0	11.0	.110	
	20.0	21.7	.108	
n-C_4H_9	1.52	1.22	0.080	0.081
	3.03	2.40	.079	
	10.0	8.08	.081	
	20.0	16.5	.082	
n-C_5H_{11}	2.00	1.21	0.061	0.060
	5.00	3.19	.064	
	10.0	6.44	.064	
	14.0	8.25	.059	
	20.0	12.0	.060	
	30.0	17.5	.057	

EXPERIMENTAL

The phenoxysilanes were prepared from phenol and trialkylethoxysilane (in the case of the *n*-propyl compound) or trialkylchlorosilane in the same way as similar compounds were prepared by Larsson [4] and Jörg and Stetter [5]. One example is given.

Tri-n-butylphenoxysilane. 29.3 g (0.125 mole) of tri-*n*-butyl-chlorosilane and 11.8 g (0.125 mole) of phenol were refluxed in a dry atmosphere until no more hydrochloric acid was evolved (60 hours). The product was distilled at reduced pressure in a 33 cm glass helix packed column and gave 23 g (88 % yield) of pure tri-*n*-butylphenoxysilane.

Boiling points, refractive indices (determined with an Abbe refractometer), densities (determined with an Ostwald-Sprengler pycnometer of 1.5 ml), molecular refractivities (calculated from the Lorenz-Lorentz formula) and analyses are given in Table 4. For the calculated molecular refractivities the group refractivities given by Smith [6] have been used. Smith does not give the group refractivity *r*-$SiOC_6H_5$, but from his value of the group refractivity *r*-SiC_6H_5 and the bond refractivities Si-C aromatic, Si-O, and C-O ether given by Vogel [7] and Warrick [8], the group refractivity *r*-$SiOC_6H_5$ was calculated to 28.31 ml. The equivalent weight was determined by hydrolysing the silane in a mixture of glacial acetic acid an 1 N hydrochloric acid for some hours and determining the phenol according to Sprung [9]. Silicon analyses were performed according to Smith [6]. The reactions were carried out in 51.4 weight-% ethanol obtained from 20.00 ml of water made up with redistilled 96 % ethanol to 50.00 ml. Sodium chloride was added to give an ionic strength μ = 0.05 M, calculated from the formula

$$\mu = \frac{1}{2} \sum_i c_i z_i^2$$

Table 2. Alkaline hydrolysis of $R_3SiOC_6H_5$ in 51.4 weight-% ethanol. μ = 0.05 M.

R	Composition of solution	[OH⁺] mM	$k \times 10^4$ sec⁻¹	k_b M⁻¹sec⁻¹	k_b mean M⁻¹sec⁻¹
C_2H_5	0.014 M glycinate 0.0011 M glycine	0.0463	0.954	2.06	2.05
	0.014 M glycinate 0.0018 M glycine	0.0750	1.60	2.13	
	0.01 M Na_2CO_3 0.01 M $NaHCO_3$	0.578	11.2	1.94	
	dil NaOH	1.28	26.5	2.07	
n-C_3H_7	0.01 M Na_2CO_3 0.009 M $NaHCO_3$	0.682	4.55	0.67	0.66
	0.01 M Na_2CO_3 0.005 M $NaHCO_3$	1.27	8.37	0.66	
	0.01 M Na_2CO_3 0.003 M $NaHCO_3$	2.00	13.1	0.65	
	dil. NaOH	4.00	26.3	0.66	
n-C_4H_9	0.01 M Na_2CO_3 0.01 M $NaHCO_3$	0.578	2.30	0.40	0.41
	dil NaOH	1.99	7.96	0.40	
	»	5.00	20.8	0.42	
	»	8.00	33.7	0.42	
n-C_5H_{11}	0.01 M Na_2CO_3 0.01 M $NaHCO_3$	0.585	1.77	0.30	0.30
	dil. NaOH	3.06	8.96	0.29	
	»	8.00	24.7	0.31	
	»	12.0	36.3	0.30	

where c = ion concentrations and z = valency. The concentration of silane was about 10^{-4} M, in some cases of alkaline solutions of low buffer capacity $0.5\ 10^{-4}$ M. (It is not necessary to know the exact concentration, *cf.* eqn. (1)). The optical density was measured in a 1 cm quartz cell with a tight cover in a Beckman DU spectrophotometer provided with a 4 300 photomultiplier attachment. By means of an arrangement designed by the author the walls of the cell compartment were tempered with circulating water from a thermostat. The temperature of the solution was 25.0 ± 0.2° C. The slit width was 0.6 mm and the wave length generally 280 mμ, in some cases of alkaline solutions 290 mμ (see Fig. 1). The first reading D_0 could be made one minute after mixing and the last

Table 3. The acid and base catalysed hydrolysis of $R_3SiOC_6H_5$.

R	k_a M⁻¹sec⁻¹	k_b M⁻¹sec⁻¹
CH_3	10.4	~ 330
C_2H_5	0.22	2.1
n-C_3H_7	.12	0.66
n-C_4H_9	.081	.41
n-C_5H_{11}	.060	.30

one was made after a time equal to ten times the half life. For the reactions with a half life longer than one hour, King's[11] method was used. As a »blank» was used a solution of exactly the same composition as the sample, but where the reaction had started two to three half-lives earlier. The rate equation (1) is in this case transformed to

$$k = \frac{1}{t} \log \frac{D_0'}{Dt'}$$

D' being the optical density read on the photometer. Plotting $D't$ *versus* time gives a straight line, the slope of which is $-k$. The reactions were followed to at least 70 % hydrolysis. All constants were calculated from graphs.

Hydrogen and hydroxyl ion concentrations greater than 0.001 M were obtained by diluting standardized hydrochloric acid and carbonate-free sodium hydroxide solutions. In buffer solutions the concentrations were determined electrometrically using a glass electrode with a saturated calomel electrode as reference electrode and with exclusion of the carbon dioxide of the air. Nernst's equation gives the relation between electromotive force E and activity, but as the ionic strength was constant this relation is supposed to be valid also for concentrations

$$E_{0H} = E - \frac{RT}{F} \ln [H^+] \tag{3}$$

The equation

$$k_w = [H^+] \cdot [OH^-] \tag{4}$$

is supposed to be valid in this ethanol-water mixture. Eqns. (3) and (4) give the equation

$$E_{0OH} = E + \frac{RT}{F} \ln [OH^-] \tag{5}$$

These assumptions are verified in Tables 5 and 6. The electromotive forces were measured in diluted hydrochloric acid and sodium hydroxide and sodium chloride was added to give an ionic strength of 0.05 M. Each value of the electromotive force E is a mean of at least two readings. In the most alkaline solutions the E.M.F measured with the glass electrode does not exactly follow eqn. (5), but these high concentrations were never used for the kinetics. Besides the constancy of E_{0OH} is not very good, although sufficient, especially in poorly buffered solutions.

The author is indebted to Professor Erik Larsson for suggesting the subject of this investigation and his kind interest during its course.

Table 4. Physical constants and analyses of $R_3SiOC_6H_5$.

R	B.p. °C	Pressure mm Hg	n_D^{20}	d^{20}	MR_D		% Si		Equiv. wt.	
					found	calc.	found	calc.	found	calc.
CH_3[1]	68—9	13	1.4787	0.9265	50.89	51.06	16.5	16.9	27.9	27.6
C_2H_5	145	20	1.4883	0.9288	64.69	64.60	13.6	13.5	34.4	34.7
n-C_3H_7	121—2	1.5	1.4837	0.9120	78.54	78.84	11.2	11.2	42.0	41.8
n-C_4H_9	145	3	1.4820	0.8993	92.72	92.74	9.5	9.6	49.0	48.8
n-C_5H_{11}	153	1.5	1.4800	0.8904	106.76	106.65	8.4	8.4	55.7	55.8

1. this compound is previously described by Speier[10].

Table 5. Electromotive forces in dilute hydrochloric acid.

[HCl] M	temp ° C	$-E$ mV	E_{0H} mV
0.0300	22.2	5.9	83.4
.0200	22.0	16.4	83.4
.0120	22.0	29.2	83.5
.0080	22.0	39.3	83.2
.0050	21.9	51.6	83.2
.0030	22.1	64.6	83.3
.0020	22.0	74.4	83.7

Table 6. Electromotive forces in dilute sodium hydroxide.

[NaOH] M	temp ° C	$-E$ mV	E_{0OH} mV
0.0300	22.8	679.4	768.4
.0200	22.0	670.8	770.3
.0120	21.7	661.3	773.7
.0080	22.4	650.3	773.2
.0050	22.0	639.6	774.4
.0030	22.0	625.4	773.2
.0020	22.3	614.2	772.2

REFERENCES

1. Swain, G., Esteve, R. M. and Jones, R. H. *J. Am. Chem. Soc.* **71** (1949) 965.
2. Krieble, R. H. and Burkhard, C. A. *J. Am. Chem. Soc.* **69** (1947) 2689.
3. Caldin, E. F. and Long, G. *J. Chem. Soc.* **1954** 3737.
4. Larsson, E. *Chem. Ber.* **86** (1953) 1382.
5. Jörg, H. and Stetter, J. *J. prakt. Chem.* **117** (1927) 305.
6. Smith, B. *Kiselorganiska studier* (Diss.) Chalmers University of Technology, Gothenburg 1951.
7. Vogel, A. I. *A Textbook of Practical Organic Chemistry*, 2nd Ed., Longmans, Green and Co., London 1951.
8. Warrick, E. L. *J. Am. Chem. Soc.* **68** (1946) 2455.
9. Sprung, M. M. *Ind. Eng. Chem. Anal. Ed.* **13** (1941) 35.
10. Speier, J. L. *J. Am. Chem. Soc.* **74** (1952) 1003.
11. King, E. L. *J. Am. Chem. Soc.* **74** (1952) 563.

Received November 10, 1955.

ACTA CHEMICA SCANDINAVICA 10 (1956) 306–310

Two Volumetric Methods for the Determination of Glyoxal

PENTTI SALOMAA

Department of Chemistry, University of Turku, Turku, Finland

Two different methods have been developed for the quantitative determination of glyoxal. The first method is an alkalimetric titration and is based on the Cannizzaro reaction of glyoxal. In the second method the glyoxal-bisulphite addition reaction has been applied. The development of both methods was based on an investigation of the rates and equilibria of the corresponding reactions under conditions similar to those prevailing during the analysis. Both methods have been found to give identical results, the errors being no greater than the random titration error.

Several methods have been described previously for the quantitative determination of glyoxal. In the semiquantitative gravimetric method used by Glasstone and Hickling [1], glyoxal is precipitated as glyoxal 2,4-dinitrophenylhydrazone. Ariyama [2] has developed a colorimetric method, and Gabrielsson and Samuelsson [3] have presented a method based on the use of ion exchangers. The only volumetric method thus far developed is that described by Friedemann [4]. The method is based on the oxidation of glyoxal to oxalic acid by hydrogen peroxide in alkaline solution and the titration of the excess alkali with standard acid. This method, however, cannot be used in the presence of other oxidizable compounds. In the following, two new volumetric methods for the quantitative determination of low glyoxal concentrations are suggested which have been employed in kinetic investigations [5].

ALKALIMETRIC METHOD

In the presence of alkali, glyoxal is readily converted to glycolic acid by the Cannizzaro reaction:

$$CHO—CHO + OH^- \rightarrow CH_2OH—COO^-$$

When the alkali is present in excess, the reaction goes to completion [5] and glyoxal can be determined by back titration of the excess alkali with a standard acid solution.

For the evaluation of the time required by the reaction to go to completion under the conditions prevailing during the analysis, the results obtained in kinetic investigations [5] may be applied. It was observed that the Cannizzaro

reaction of glyoxal is of the third order, the reaction rate being proportional to the first power of the glyoxal concentration and to the square of hydroxyl ion concentration. The specific rate at 20° C, which corresponds approximately to the conditions of analysis at room temperature, is 87 l^2 $mole^{-2}$ sec^{-1}. The reaction time can be evaluated from the formula for a third order reaction:

$$t = \frac{1}{k(b-a)}\left[\frac{1}{(b-a)}\ln\frac{a(b-x)}{b(a-x)} - \left(\frac{1}{b-x} - \frac{1}{b}\right)\right] \qquad (1)$$

in which k is the specific rate, b and a the initial concentrations of alkali and glyoxal, respectively, and x the concentration of glyoxal reacted during time t. When, for instance, 20 ml of 0.05 N alkali, the excess of alkali corresponding to at least 50 % of the amount of glyoxal present, is added to give a total volume of the reaction solution not exceeding 30 ml, a reaction time of 8 minutes is found to be sufficient for the reaction to proceed nearly to completion at 20° C. After this time less than 0.1 % of the glyoxal initially present remains in the reaction solution.

The above facts lead to the following procedure for the determination of glyoxal:

To a neutral solution containing not more than 0.66 millimoles of glyoxal in a volume not exceeding 10 ml, 20 ml of 0.05 N sodium hydroxide solution are added. After 8 minutes an amount of standard hydrochloric acid equivalent to the amount of sodium hydroxide added initially is run in and the excess acid is titrated with the 0.05 N sodium hydroxide solution using phenol red as indicator. The amount of alkali consumed in the titration corresponds directly to the amount of glyoxal present. All of the operations must be performed in the absence of carbon dioxide.

In case the conditions are not the same as described above it is to be noted that a standing period four times as long is necessary if the volume of the reaction solution is twice that given above. Similarly, the use of concentrations twice as high shortens the reaction time to one fourth of that given.

BISULPHITE METHOD

This method is based on a procedure presented earlier [6,7] by the author for the determination of several other aldehydes. In this procedure the bisulphite addition reaction is carried out at pH 7.3 in a phosphate buffer in order to effect a very rapid addition reaction, after which the excess bisulphite is titrated with standard iodine in a solution acidified to below pH 4.5 in order to prevent the decomposition of the bisulphite compound during the titration. Before the method could be applied for the determination of glyoxal, it was necessary to investigate the kinetics and equilibria of the glyoxal-bisulphite reaction under the conditions of analysis, taking into account that in this case the reaction involves two successive carbonyl additions.

The experiments indicated that in the case of glyoxal the addition to the first carbonyl group takes place almost quantitatively as compared with the addition to the second carbonyl group. If Gl denotes glyoxal, B sulphite present in the solution in any form *cf.* [6], GlB the monobisulphite compound and GlB_2 the dibisulphite compound of glyoxal we have the following equilibria:

$$\frac{[GlB][B]}{[GlB_2]} = K_1 \qquad \frac{[Gl][B]}{[GlB]} = K_2 \qquad (2)$$

in which K_1 and K_2 are, respectively, the first and the second dissociation constants of the glyoxal-dibisulphite compound. When the dissociation of the glyoxal-dibisulphite compound was investigated, it was observed that $K_1 \gg K_2$ and therefore the second dissociation causes no error in analysis. Table 1 contains examples of the experiments. The dissociation constant K_1 has been calculated from the first of the foregoing equations by taking into account that in the present case [GlB] = [B].

Table 1. The dissociation of glyoxal-dibisulphite compound in phosphate buffer at pH 7.3 at 20° C. Analyses of equilibrium solutions.

$[GlB_2]1^{-1}$ mole^1	$[B]1^{-1}$ mole^1	$10^4 \times K_1 1^{-1}$ mole^1
0.01637	0.002095	2.68
0.01216	0.001817	2.71
0.00795	0.001511	2.87
0.00385	0.001009	2.64
		Average K_1 = 0.000272 1^{-1} mole^1.

The value of the equilibrium constant K_1 is approximately the same as that of benzaldehyde [7] under similar conditions. From the analytical viewpoint, the equilibrium is not favourable enough for the formation of the dibisulphite compound and therefore a small correction due to the unreacted monobisulphite compound should be applied when accurate results are required.

The correction may be evaluated as follows. Let x denote the concentration of glyoxal that has reacted with bisulphite and y the concentration of glyoxal-dibisulphite compound present at equilibrium, and b the initial total concentration of sulphite. The first of eqns. (2) can then be written in the form $(x - y)(b - x - y)/y = K_1$, from which it follows that the relative error is approximately $(x - y)/2y = K_1/2\ (b - x - y) = K_1/2\ c$, in which c is the concentration of excess sulphite in the reaction solution. Using the value given above for K_1, 0.000272 1^{-1}mole^1, the correction, which is to be added to the amount of glyoxal found, is thus $0.0136/c$ per cent. Table 2 contains some sample

Table 2. The evaluation of the correction due to unreacted glyoxal-monobisulphite compound in the determination of glyoxal by the bisulphite method. v = ml of glyoxal stock solution (approximately 0.053 M) taken for analysis. V = approximate volume of the reaction solution in ml. ml I = ml of 0.0752 N iodine solution consumed in the titration of excess bisulphite. ml I_g = ml of 0.0752 N iodine equivalent to the amount of glyoxal reacted. p = correction in per cent.

v	ml I	ml I_g	V	p	ml I_g (corr.)	ml I_g (corr.) / v
—	26.82	—	30	—	—	—
1.75	21.87	4.95	32	0.5	4.97	2.84
2.50	19.75	7.07	32	0.6	7.11	2.84
3.25	17.56	9.26	33	0.7	9.32	2.87
4.00	15.61	11.21	34	0.8	11.30	2.82
4.75	13.52	13.30	35	0.9	13.42	2.83
5.50	11.36	15.46	36	1.1	15.63	2.84
6.25	9.40	17.42	36	1.4	17.66	2.83
7.00	7.39	19.43	37	1.8	19.78	2.83
7.50	6.00	20.82	38	2.3	21.30	2.84
8.00	4.70	22.12	38	2.9	22.76	2.84

analyses. The constancy of the values given in the last column of the table shows that conforming analytical results are obtained in experiments with various intial concentrations when the correction is taken into account.

Similarly as in the case of other aldehydes [6,7] the necessary reaction times for the glyoxal-bisulphite addition reaction were evaluated on the basis of results obtained in rate measurements. It was found that the glyoxal-bisulphite reaction is of the second order, the rate at constant pH being proportional to the product of the concentrations of glyoxal and total sulphite. The bisulphite addition to the second carbonyl group was found to take place immeasurably rapidly as compared with the addition to the first carbonyl group which is the rate-determining reaction. In a phosphate buffer at pH 7.3, the second order specific rate of the glyoxal-bisulphite reaction was 6.0 $l^1 mole^{-1}$ sec^{-1} at 20° C, and 4.9 l^1 $mole^{-1}$ sec^{-1} at 18° C. The rate of the glyoxal-bisulphite reaction differs thus only slightly from that of the formaldehyde-bisulphite reaction under similar conditions [6], the specific rate of the latter reaction being 5.2 l^1 $mole^{-1}$ sec^{-1} at pH 7.3 at 18° C. Thus the standing periods evaluated for the formation of the formaldehyde-bisulphite compound are nearly the same in the case of glyoxal.

On the basis of the foregoing discussion, the following procedure is suggested for the determination of glyoxal by the bisulphite method:

To a solution containing not more than 0.75 millimoles of glyoxal 10 ml of phosphate buffer (0.5 mole/l Na_2HPO_4, 0.125 mole/l KH_2PO_4) and 20 ml of approximately 0.1 M sodium bisulphite solution are added. If the total volume of the reaction solution does not exceed 40 ml, a reaction time of three minutes is sufficient, after which 5 ml of 1 N hydrochloric acid are added and the excess of bisulphite is titrated with an approximately 0.1 N standard iodine solution. The titration should be carried out rapidly in order to avoid the decomposition of the bisulphite compound near the end point. The glyoxal content is calculated from the difference between the iodine consumptions corresponding to the amount of bisulphite initially added and to that present after the addition reaction. To the result obtained a correction is added which is $0.0136/c$ % the value directly obtained, in which c is the molar concentration of excess bisulphite in the solution.

When the volumes of the reaction solution or the concentrations of the standard solutions deviate from those proposed above, the reaction time must be changed correspondingly.

EXPERIMENTAL

Glyoxal and glyoxal disodium bisulphite were prepared according to Ronzio and Waugh [8]. For further purification the latter compound was crystallized twice from 40 % ethanol and dried in air. All water used in the experiments was carbon dioxide-free distilled water. The water used in the experiments in which the kinetics and equilibria of glyoxal-bisulphite reaction were investigated, was also freed from dissolved oxygen by passing a stream of nitrogen through it during a period of 24 hours. The water was stored in a nitrogen atmosphere. The kinetic and equilibrium measurements required in the development of the analytical methods were performed as described elsewhere [5,6,7].

Table 3 contains some examples of experiments in which both methods described above were compared with each other. The values given in the table are averages of 3—5 determinations. The values calculated for the concentration of the glyoxal stock solution show that both methods give conforming results, the deviations being no greater than the ordinary titration errors. In cases in which relatively low glyoxal concentrations are analysed, the bisulphite method is more accurate and should be preferred, because the iodine equivalent of glyoxal is one fourth of its sodium hydroxide equivalent.

Table 3. A comparison between the bisulphite and alkalimetric methods for the determination of glyoxal. v = ml of glyoxal stock solution taken for analysis. V = approximate volume of the reaction solution in ml. ml I = ml of 0.0703 N iodine solution consumed in the titration of excess bisulphite. ml I_g = ml of 0.0703 N iodine equivalent to the amount of glyoxal reacted. ml NaOH = ml of 0.0522 N sodium hydroxide equivalent to the amount of glyoxal. [Gl] = calculated glyoxal concentration of the stock solution in moles per liter.

a) Bisulphite method

v	ml I	ml I_g	*V*	ml I_g (corr.)	[Gl]
—	36.72	—	28	—	
5.00	22.62	14.10	33	14.18	0.0498
10.00	8.83	27.89	38	28.37	0.0499

b) Alkalimetric method

v	ml NaOH	[Gl]	*v*	ml NaOH	[Gl]
5.00	4.71	0.0492	15.00	14.25	0.0496
10.00	9.65	0.0504	20.00	19.12	0.0499

REFERENCES

1. Glasstone, S. and Hickling, A. *J. Chem. Soc.* **1936** 824.
2. Ariyama, N. *J. Biol. Chem.* **77** (1928) 359.
3. Gabrielsson, G. and Samuelsson, O. *Svensk Kem. Tidskr.* **62** (1950) 214.
4. Friedemann, T. E. *J. Biol. Chem.* **73** (1927) 331.
5. Salomaa, P. *Acta Chem. Scand.* **10** (1956) 311.
6. Salomaa, P. *Ann. Univ. Turkuensis* **A XIV** (1953).
7. Salomaa, P. *Suomen Kemistilehti* **B 27** (1954) 12.
8. Ronzio, A. R. and Waugh, T. D. *Org. Syntheses* **24** (1944) 61.

Received November 8, 1955.

ACTA CHEMICA SCANDINAVICA 10 (1956) 311—319

The Kinetics of the Cannizzaro Reaction of Glyoxal

PENTTI SALOMAA

Department of Chemistry, University of Turku, Turku, Finland

The kinetics of the Cannizzaro reaction of glyoxal have been investigated in water solution at different temperatures. The reaction is very rapid and is of the third order, the rate being proportional to the first power of the glyoxal concentration and to the square of hydroxyl ion concentration. The reaction is characterized by a very strong positive salt effect. The observed kinetics and salt effect have been discussed and a reaction mechanism has been suggested in which the slow and rate-determining reaction is a reaction between hydroxyl ion and a univalent negative ion which is formed from glyoxal and hydroxyl ion in a primary rapid reaction.

The kinetics of the Cannizzaro reaction of monoaldehydes have been extensively investigated as compared with those of α-dicarbonyl compounds, glyoxal and some of its derivatives, which are known to undergo the Cannizzaro reaction in the presence of alkali. The only observations thus far made, which are to be found in the literature, are those of Ariyama [1] and Alexander [2]. When developing a colorimetric method for the determination of glyoxal Ariyama found that the rate of the Cannizzaro reaction of glyoxal increases more rapidly than the hydroxyl ion concentration of the solution. Alexander found that the conversion of phenyl glyoxal into mandelic acid under the influence of alkali is a first order reaction with respect to both reactants.

It seemed of interest to investigate the kinetics of the Cannizzaro reaction of glyoxal

$$CHOCHO + OH^- \rightarrow CH_2OHCOO^- \qquad (A)$$

more extensively in order to elucidate the reaction mechanism, particularly because, owing to the two carbonyl groups in glyoxal, the reaction involves formally only two reacting molecules, whereas three reacting molecules participate in the Cannizzaro reaction of monoaldehydes. This was expected to give rise to differences in the reaction mechanism.

The order of the reaction

The progress of reaction (A) could be followed by determining both the hydroxyl ion concentration and glyoxal concentration remaining in the reaction solution at different times by methods described in the experimental

part. Both methods gave nearly identical results, but owing to the rapidity of the reaction, relatively low concentrations had to be used in which case the determination of glyoxal concentration was found to give more accurate results *cf.* [3]). Therefore, the latter results were used in the calculation of specific rates.

The results obtained indicate that the rate of reaction (A) is proportional to the first power of glyoxal concentration and to the square of hydroxyl ion concentration. The specific rates were calculated from the integrated form (2) of the differential equation (1)

$$\frac{dx}{dt} = k\ (a - x)\ (b - x)^2 \tag{1}$$

$$k = \frac{1}{t(a-b)}\left[\frac{1}{b-x} - \frac{1}{b} - \frac{1}{a-b}\ln\frac{b(a-x)}{a(b-x)}\right] \tag{2}$$

by applying the initial condition $x = 0$, when $t = 0$. In these equations a and b are the initial concentrations of glyoxal and hydroxyl ion, respectively, and x the concentration of glyoxal reacted at time t, and k is the specific rate. In the experiments, in which equimolar concentrations were employed, *i.e.* $a = b$, eqns. (1) and (2) were replaced by eqns. (1a) and (2a)

$$\frac{dx}{dt} = k\ (a - x)^3 \tag{1a}$$

$$k = \frac{1}{2t}\left[\frac{1}{(a-x)^2} - \frac{1}{a^2}\right] \tag{2a}$$

Table 1 contains results obtained in experiments in which the order of the reaction was determined by using various initial concentrations of the reactants. The values obtained for the specific rate k are nearly the same; the small deviations may be due to experimental errors. The slight increase in the values with increasing hydroxyl ion concentration is probably due to the heat of the reaction which effects a small increase in the temperature of the reaction solution, but this source of error is eliminated when relatively low alkali concentrations are used in which case the reaction is slower and the temperature can be kept constant during the reaction. Tables 2 and 3 give details of two typical runs.

Table 1. Determination of the order of the Cannizzaro reaction of glyoxal in water solution at 25° C using different initial concentrations. Third order specific rates calculated from eqns. (2) and (2a).

a	b	k $l^2\,mole^{-2}\,sec^{-1}$
0.00195	0.01368	169
0.00364	0.01045	170
0.00569	0.00569	170
0.00585	0.00731	164
0.01057	0.00612	162
0.01186	0.00505	161

Table 2. The Cannizzaro reaction of glyoxal in water at 25° C. $a = b = 0.00569$. Specific rates calculated from eqn. (2a).

t (in minutes)	1	2	4	6	9	12	15
$10^3 \times (a - x)$	4.43	3.73	3.03	2.52	2.14	1.90	1.74
k	167	171	163	176	174	171	166

Average k = 170 l^2 mole^{-2} sec^{-1}

Table 3. The Cannizzaro reaction of glyoxal in water at 25° C. $a = 0.01186$, $b = 0.00505$. Specific rates calculated from eqn. (2).

t (in minutes)	0.5	1	1.5	2	2.5	3	3.5
$10^3 \times (a - x)$	10.82	10.09	9.67	9.31	9.11	8.83	8.69
$10^3 \times (b - x)$	4.01	3.28	2.86	2.50	2.30	2.02	1.88
k	152	164	160	164	157	168	164

Average k = 161 l^2 mole^{-2} sec^{-1}

The effect of temperature

The specific rates measured at different temperatures are given in Table 4. In all of these experiments the initial hydroxyl ion concentration was relatively low, about 0.005 N, in order that the reactions would proceed at a measurable rate and to avoid the influence of the heat of reaction. The table contains also the values of the activation energy E and the logarithm of the frequency

Table 4. The effect of temperature on the Cannizzaro reaction of glyoxal in water solution.

°C	0	15	25	35
k l^2 mole^{-2} sec^{-1}	9.28	45.1	161	398

E = 18 200 cal/mole, log A = 15.52

factor A calculated according to the Arrhenius equation from the values of log k at different temperatures by the method of least squares.

The value of the activation energy, 18 200 cal per mole, is considerably lower than the activation energy of the Cannizzaro reaction of formaldehyde in water solution, 22 300 cal per mole, determined by Pajunen [4]. Similarly, the value of log A, 15.52, is considerably higher than the corresponding value for formaldehyde, 11.90, both of which factors effect an enhanced reactivity of glyoxal as compared with formaldehyde.

Salt effect

Table 5 contains results obtained in experiments in which the effect of increase in electrolyte concentration on the reaction rate was investigated in solutions containing added sodium chloride. Table 6 gives details for one of the individual runs. As it is seen from Table 5, the Cannizzaro reaction of glyoxal is characterized by a very pronounced positive salt effect, the specific rate increasing rapidly with increasing electrolyte concentration. The magnitude of the salt effect is of a much higher order of magnitude than that generally observed in reactions between ions and neutral molecules taking place in water solution [5].

Table 5. The effect of added sodium chloride on the rate of the Cannizzaro reaction of glyoxal in water at 25° C.

[NaCl]	—	0.084	0.263	0.572	0.789	1.034	1.316	1.545	1.842
k $l^2 mole^{-2} sec^{-1}$	161	187	212	249	266	295	309	349	377

Table 6. The Cannizzaro reaction of glyoxal in water at 25° C in the presence of added sodium chloride. [NaCl] = 1.545, a = 0.01099, b = 0.00418.

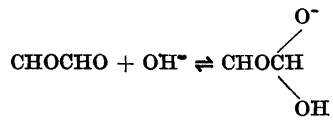
t (in seconds)	22.3	41.2	62.3	98.6	113.8	149.1	167.9
$10^3 \times (a - x)$	9.95	9.44	9.00	8.55	8.46	8.21	8.13
$10^3 \times (b - x)$	3.14	2.63	2.19	1.74	1.65	1.40	1.32
k	341	340	358	363	347	352	344

Average k = 349 $l^2 mole^{-2} sec^{-1}$

DISCUSSION

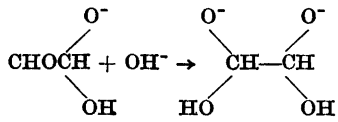
On the basis of the results presented above, a more detailed picture of the Cannizzaro reaction of glyoxal may be attempted. Although the reaction is of the third order, it is highly improbable that an actual termolecular reaction mechanism is involved. Using a method of calculation described by Tommila [6], a value of the order of 2×10^{10} $l^2 mole^{-2} sec^{-1}$ is obtained for the frequency of a ternary collision between two hydroxyl ions and a glyoxal molecule at 25° C. If every collision between activated molecules were to lead to a reaction the frequency factor A should be of this order of magnitude in the case of a termolecular reaction, but actually a lower value for the frequency factor would be expected, because it is improbable that every collision between activated molecules will effect a reaction. The measured value of the frequency factor A is 3.3×10^{15} $l^2 mole^{-2} sec^{-1}$, which is of a much higher order of magnitude than that evaluated for a ternary collision.

It is thus very probable that the reaction takes place in several successive steps, of which the first (B) involves a rapid equilibrium reaction between glyoxal and hydroxyl ion



(fast) (B)

The negatively charged addition product then reacts with another hydroxyl ion in a second step (C), which is slow and rate-determining



(slow) (C)

In the subsequent steps, discussed below, the reactive divalent anion formed in reaction (C) reacts rapidly to yield the final product, the anion of glycolic acid, but these rapid steps do not affect the kinetics of the reaction and cannot be kinetically distinguished.

The reactions (B) and (C) are in good accord with the observed reaction order. For the rate v of the reaction we have

$$v = k' [OH^-] [CHOCH(OH)O^-] \tag{3}$$

in which k' is the specific rate of the rate-determining step (C). For the equilibrium (B) we obtain

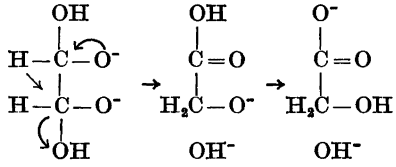
$$\frac{[CHOCH(OH)O^-]}{[CHOCHO][OH^-]} = K \tag{4}$$

in which K denotes the equilibrium constant. From eqns. (3) and (4) we obtain for the reaction rate the expression

$$v = k'K[CHOCHO][OH^-]^2 \tag{5}$$

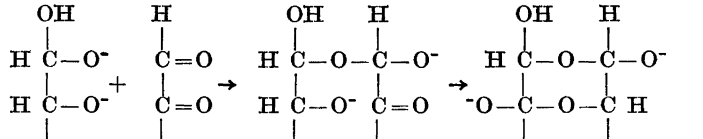
which is the same as that found experimentally if the experimental third order specific rate k is substituted for $k'K$.

The rapid subsequent reaction steps which follow reactions (B) and (C) are probably complicated as in the case of the Cannizzaro reaction of monoaldehydes [6-9]. The subsequent reaction of the anion formed in (C) may take place by an intramolecular hydrogen shift

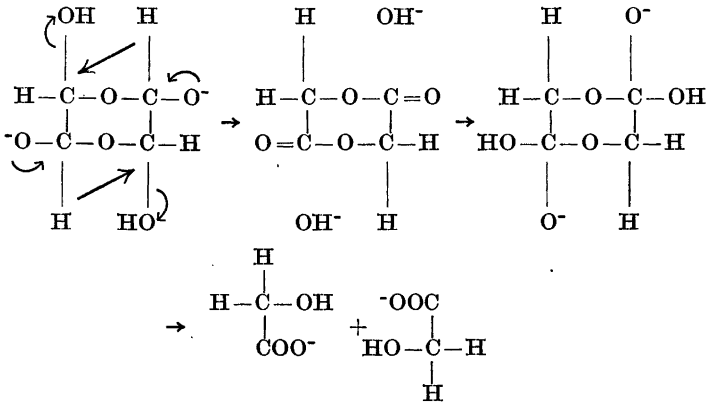


(D)

or, the anion may react first with another glyoxal molecule according to (E), after which the symmetrical product formed is converted to the final product by a mechanism (F) essentially similar to that suggested by Ingold, Wilson and Tommila [6-9] for monoaldehydes



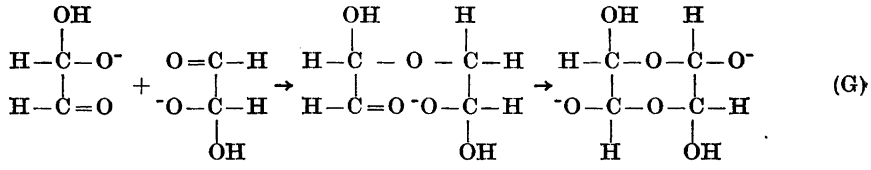
(E)



(F)

The mechanism (D) is in the present case the most probable. In the formation of the symmetrical product in (E) the attainment of the transition state involves a large increase in order, *i.e.* the activation entropy is negative and the frequency factor relatively low as compared with reaction (D). Similarly, the activation energy of the reaction path (D) has probably a much lower value than that of (E), since the latter involves typical carbonyl addition reactions that take place at a measurable speed, whereas in (D) as well as in (F), intramolecular hydrogen shifts take place in which much lower values of the activation energy are to be expected. The rapidity of the subsequent steps following the rate-determining reaction (C) are thus not as readily understood on the basis of mechanism (E) as in the case of the intramolecular mechanism (D). Also Alexander [2] assumed an intramolecular hydrogen shift to take place in the conversion of phenyl glyoxal to mandelic acid under the influence of alkali. The latter reaction was found to be of the second order, the rate being proportional to the first powers of hydroxyl ion and phenyl glyoxal concentrations. In this case the hydrogen shift was assumed to take place directly in the univalent anion corresponding to that formed in reaction (B), in accordance with the observed reaction order. The difference between the reaction mechanisms of glyoxal and phenyl glyoxal can be ascribed to the $-M$ effect of the phenyl group [10] which greatly facilitates the hydrogen shift to the adjacent carbon atom, as a result of which the reaction corresponding to (B) becomes the slowest and hence rate-determining.

If the Cannizzaro reaction of glyoxal were to take place formally similarly as in the case of monoaldehydes [6-9], the rate-determining reaction following (B) would take place between two anions formed in (B) and would lead to a symmetrical product



(G)

The subsequent reactions could be presented by eqn. (F). This type of mechanism is in principle similar to that suggested by Karrer [11] for the Cannizzaro reaction of glyoxal and would lead to fourth order kinetics. If it is taken into account that in the Cannizzaro reaction the step corresponding to (B) generally takes place very rapidly, one must assume that in the case of glyoxal the reaction takes place by an easier and more rapid way than (G). Owing to the presence of two carbonyl groups in glyoxal, there is the possibility that another relatively rapid reaction (C), which in principle is similar to (B), occurs. This would explain the low value of the activation energy for the glyoxal reaction, 18 200 cal per mole, as compared with the formaldehyde reaction, the activation energy of which is 22 300 cal per mole [4]. The fact that reaction (C) is slower than (B) conforms with the mesomeric effect of substituents [10]. The $-M$ influence of the second carbonyl group, which facilitates the addition of hydroxyl ion to the first carbonyl, no longer remains after reaction (B) has occurred.

From the value of log A (Table 4), 15.52, the activation entropy can be calculated according to the theory of absolute reaction rates [12]. From the formula

$$\Delta S^* = R \ln \frac{A h}{e k T} \tag{6}$$

one obtains for the activation entropy, ΔS^*, of the Cannizzaro reaction of glyoxal the value 37.9 cal × deg^{-1}mole^{-1} at 25° C. A is here expressed in cm^{6}mole^{-2}sec^{-1}. Similarly as in the case of formaldehyde [4], the reaction is characterized by a very high positive activation entropy. The corresponding value for formaldehyde is 21.2 cal × deg^{-1}mole^{-1}. A large positive activation entropy corresponds to a large decrease in order in the attainment of the transition state. Pajunen [4] explained the large positive activation entropy of formaldehyde as being due to the hydratation of the carbonyl group, which is not possible in the critical complex; this leads to a decrease in order. This may also be one of the main reason for the large activation entropy of the glyoxal reaction, and its high value as compared with that of the formaldehyde reaction may be ascribed to the presence of two hydrated carbonyl groups in the case of glyoxal.

The fact that in the glyoxal reaction the rate determining stage (C) takes place between two ions is in good accord with the strong positive salt effect observed. In the case of monoaldehydes, as with formaldehyde [4], the influence of electrolytes on the reaction rate is very slight since the rate-determining stage takes place between an ion and a neutral molecule. In Fig. 1 values of log k for the Cannizzaro reaction of glyoxal in sodium chloride solutions are plotted against the ionic strength and against the square root of the ionic strength.

Although the observed salt effect is of nearly the same order of magnitude as is to be expected for reactions between ions, the application of Debye-

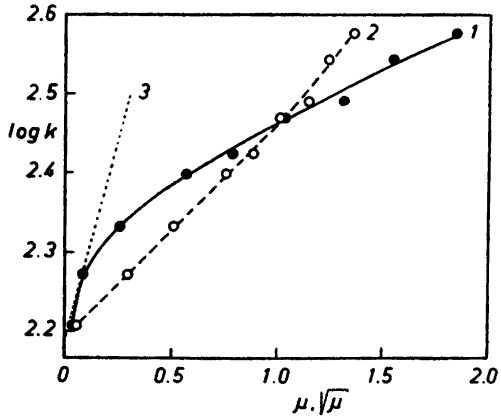


Figure 1. The Cannizzaro reaction of glyoxal in sodium chloride solutions at 25° C. 1. Plot of log k versus *the ionic strength. 2. Plot of log* k versus *the square root of the ionic strength. 3. Debye-Hückel limiting law.*

Hückel theory does not give satisfactory results when the activity coefficient of the critical complex of reaction (C) is taken to be equal to that of a divalent ion. If a_{Gl}, a_{GlOH^-}, a_{OH^-} and a_x denote the activity coefficients of glyoxal, the ion formed in reaction (B), hydroxyl ion, and the critical complex of reaction (C), respectively, we obtain for the specific rate of reaction (C) from the Brönsted rate equation the expression:

$$k' = k_0' \frac{a_{GlOH^-} a_{OH^-}}{a_x} \tag{7}$$

and for the equilibrium constant of the reaction (B):

$$K = K_0 \frac{a_{Gl} a_{OH^-}}{a_{GlOH^-}} \tag{8}$$

in which K_0 is the thermodynamic equilibrium constant. When $k_0' K_0$ is denoted by k_0, and it is taken into account that the measured specific rate k is equal to $k'K$, it follows from eqns. (7) and (8)

$$\log k = \log k_0 + \log a_{Gl} + 2 \log a_{OH^-} - \log a_x \tag{9}$$

If the changes in a_{Gl} effected by changes in the ionic strength are neglected, and the activity coefficients of hydroxyl ion and the critical complex are calculated from the Debye-Hückel theory by considering the critical complex a divalent negative ion, the expression (10) is obtained for the influence of ionic strength on the specific rate at 25° C

$$\log k = \log k_0 + \frac{1.02 \sqrt{\mu}}{1 + a \sqrt{\mu}} - B \mu \tag{10}$$

a and B are constants. Eqn. (10) predicts that in the plot of log k versus the square root of the ionic strength the initial slope should be 1.02. From Fig. 1 it is seen that experimentally determined initial slope is considerably smaller, about 0.25, and the curve shows a slight drift upwards with increasing ionic strength. In many other reactions involving ions of greater charge than one, large deviations from the Debye-Hückel theory have been observed [13]. The Debye-Hückel derivation involves the assumption of a spherical symmetry of the potential field around the ion, which assumption is not justified in the present calculation of the activity coefficient of the doubly charged critical complex of the reaction (C), since in the transition state the two univalent negative charges are situated relatively far apart. Assuming that, as a limiting case, the logarithm of the activity coefficient of the critical complex is the same as that of two univalent ions, the plot of log k versus the ionic strength would be approximately linear owing to the cancellation of the terms containing the square root of the ionic strength. In view of the plot of log k versus the ionic strength shown in Fig. 1, it is also possible that an intermediate case is involved, in which the value of the activity coefficient of the critical complex is somewhere between the values calculated from the Debye-Hückel theory for a divalent ion and for two univalent ions.

EXPERIMENTAL

The solution of glyoxal in water was prepared and purified according to Ronzio and Waugh [14]. For the kinetic experiments, about 0.25 M stock solutions of glyoxal and sodium hydroxide were prepared. All water used in the experiments was distilled water freed from carbon dioxide by boiling.

The kinetic measurements were carried out in electrically heated water thermostats, the temperature of which was kept constant within $\pm$ 0.02° C by a mercury contact regulator. A well stirred ice-water mixture was used as a thermostat at 0° C. All-glass reaction vessels were employed. When the reaction solution, which contained usually about 0.01 mole of glyoxal per liter, had attained the temperature of the thermostat, a volume of sodium hydroxide stock solution was added with vigorous shaking. Except in the experiments in which the order of the reaction was determined, the initial concentration of sodium hydroxide used was relatively low, about 0.005 M, because the rapidity of the reactions at higher sodium hydroxide concentrations did not permit the determination of the specific rates as accurately as when lower concentrations were employed. After the components were mixed, the progress of the reaction was followed by taking 8—11 samples of the reaction mixture with a 20 ml semiautomatic pipette during the course of the reaction. Zero time was the time of taking of the first sample. The samples were run into conical flasks which contained an excess of approximately 0.025 N standard hydrochloric acid solution, and the excess acid was titrated with approximately 0.025 N standard sodium hydroxide solution using phenol red as indicator. This titration gave the hydroxyl ion concentration of the reaction solution at the time of taking of the sample. After this titration, the glyoxal present in the sample was determined by the bisulphite method described in the preceding paper [3] using an approximately 0.05 N standard iodine solution and an approximately 0.05 M bisulphite solution. Both methods, the determination of the hydroxyl ion concentration and the glyoxal concentration gave nearly identical results when applied to the calculation of the specific rates, but owing to the relatively low concentrations used in the experiments, the determination of glyoxal was found to be more accurate *cf.* [3]. For this reason, the results of the latter determination were generally employed in the calculation of the specific rates.

The author wishes to thank Prof. A. Meretoja and Prof. R. Leimu for their interest in this work and for many helpful discussions. The author is also indebted to the authorities of the *University of Turku* for a grant awarded to young scientists by the *Finnish Government.*

REFERENCES

1. Ariyama, N. *J. Biol. Chem.* **77** (1928) 359.
2. Alexander, E. R. *J. Am. Chem. Soc.* **69** (1947) 289.
3. Salomaa, P. *Acta Chem. Scand.* **10** (1956) 306.
4. Pajunen, V. *Ann. Acad. Sci. Fennicae*, **Ser. A II** (1950) No. 37.
5. Amis, E. S. *Kinetics of Chemical Change in Solution*, New York 1949, Chapter VIII.
6. Tommila, E. *Ann. Acad. Sci. Fennicae*, **Ser. A LIX** No. 8 (1942).
7. Ingold, C. K. and Wilson, C. L. *Z. Electrochem.* **44** (1938) 96.
8. Tommila, E. *Suomen Kemistilehti* **A 22** (1949) 27.
9. Ingold, C. K. *Structure and Mechanism in Organic Chemistry*, London 1953, pp. 704—710.
10. Ingold, C. K. *Ibid.* Chapter II.
11. Karrer, P. *Organic Chemistry*, Amsterdam 1947, p. 248.
12. Glasstone, S., Laidler, K. J. and Eyring, H. *The Theory of Rate Processes*, New York 1941, Chapter VIII.
13. Amis, E. S. *Kinetics of Chemical Change in Solution*, New York 1949, p. 74.
14. Ronzio, A. R. and Waugh, T. D. *Org. Syntheses* **24** (1944) 61.

Received November 8, 1955.

ACTA CHEMICA SCANDINAVICA 10 (1956) 320—326

The Mechanism of the Silver(I) Catalyzed Reaction between Cerium(III) and Ammonium Persulphate

STURE FRONÆUS and CARL OTTO ÖSTMAN

Department of Physical Chemistry, Chemical Institute, University of Lund, Lund, Sweden

The kinetics of the decomposition of ammonium persulphate and of the redox reaction with cerium(III), both of them catalyzed by silver(I), are investigated in an acid perchlorate-sulphate ionic medium. From the kinetic laws determined it is found that the two reactions have the same rate determining step. Furthermore, exactly two cerium(III) ions are oxidized for every persulphate ion decomposing in the silver catalyzed reaction, in contrast to what is the case with the corresponding uncatalyzed reaction.

On the basis of different facts a reaction mechanism is proposed, involving the formation of silver(II) and the radical ion SO_4^- in the rate determining step.

It is found that silver(II) reacts more rapidly with ammonium ions than with water, while the reverse is valid for the reactivity of SO_4^-.

In a previous paper the decomposition of ammonium persulphate in aqueous solution and its redox reaction with cerium(III) in the absence of silver ions was investigated by the present authors [1]. There it was found that at the acid concentrations used only a very small part of the decomposing persulphate was operating in the redox reaction. On the other hand, it is well known that in the presence of silver ions the persulphate ion is a much more effective oxidizing agent. Some workers [2–4] have studied the silver ion catalyzed self-decomposition of ammonium persulphate, while in other investigations [5–12] also various reducing agents have been added. In the latter case it has often been postulated *a priori* that practically only the agents supplied were persulphate consuming, and it is remarkable that no one seems to have determined separately the kinetic laws of the self-decomposition and of the redox reactions under identical experimental conditions. From the different results reported it is only clear that in many cases the kinetic laws are of the same form and that the rate constants are of about the same order of magnitude. Thus it is easily understood that the discussions of reaction mechanisms have been very scanty or quite lacking.

It is the aim of the present investigation to study separately the silver ion catalyzed self-decomposition of ammonium persulphate and the redox reaction with cerium(III) in the same ionic medium and at the same temperature. Furthermore, the results arrived at in the previous investigation [1] with silver-free solutions will be taken into consideration in order to obtain a reliable basis for the discussion of the reaction mechanism.

EXPERIMENTAL

Chemicals. Silver perchlorate was prepared by precipitating silver oxide, washing carefully and dissolving in perchloric acid of analytical grade. The concentration of the stock solution was determined by titration according to Volhard.

Other chemicals and stock solutions used were prepared as before [1].

The redox reaction. Equal volumes of two solutions, one containing cerous perchlorate, ammonium persulphate, and perchloric acid and the other containing silver perchlorate, sodium sulphate, and sodium perchlorate, were tempered separately at 25.0 °C and then mixed as quickly as possible. At this temperature the redox reaction is very slow in the absence of silver ions, and thus a well defined starting-time for the reactions to be studied was obtained. Part of the reaction mixture was transferred to a light absorption cell, and at certain intervals the light extinction was determined at the wave length 400 mμ with a Beckman DU Spectrophotometer, modified to keep the cell temperature constant.

Since the decomposition of persulphate is slow at 25 °C even in the presence of silver ions (see below) it was necessary to have sodium sulphate present in advance, otherwise the cerium(IV) formed precipitated. Then, with a practically constant ionic medium it was possible to count on a constant value of the molar extinction of cerium(IV) in a measurement series. The molar extinction was calculated from the final extinction, corresponding to a complete oxidation of cerium(III), and thus the ceric concentrations at the different times were obtained.

The persulphate decomposition. The solutions were prepared and tempered as in the redox measurements above. Then equal volumes were mixed, samples were withdrawn and purified nitrogen was bubbled through them for ten minutes while still in the thermostat. Dilute sulphuric acid, an excess of ferrous sulphate and hot water were added rapidly, the time at the addition of the water being taken as the stop of the self-decomposition of persulphate in the sample. The analysis was completed as in the previous investigation [1].

In those cases where the solutions contained cerium, a correction for the ceric concentration had to be applied. This was easily performed, if the first sample in a run was withdrawn when all of the cerium was oxidized to cerium(IV) according to the measurements above.

THE DETERMINATION OF THE RATE LAWS

Symbols used in the equations below:

a = the initial cerium(III) concentration,
$b(t)$ = the persulphate concentration at the time t,
c = the silver(I) concentration,
x = the cerium(IV) concentration,
y = the concentration of the radical ion SO_4^-,
z = the silver(II) concentration.

Kinetics of the persulphate decomposition. In Fig. 1 $\ln b(t)$ has been plotted against t for different values of the parameters a, $b(0)$, and c and for the ionic medium 500 mM $HClO_4$ + 150 mM Na_2SO_4 + 50 mM $NaClO_4$. The straight

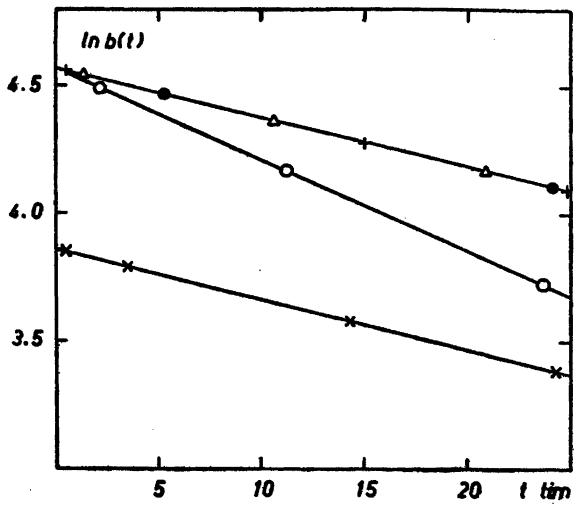


Fig. 1. ln b (t) *as a function of* t *at different values of* a, b(0) *(48.0 and 96.0 mM), and* c. a = *0,* c = *1.20 mM (+ and ×); a = 1.74 mM,* c = *1.20 mM (△); a = 8.69 mM,* c = *1.20 mM (●); a = 0,* c = *2.40 mM (○).*

lines obtained indicate a first order reaction with respect to persulphate. The slope $-k_0'$ of the lines proves to be independent of a and $b(0)$ but almost proportional to c.

Since there is a competition between the silver ion catalyzed decomposition and the one existing in silver-free solutions we can expect the expression for k_0' to be of the form:

$$k_0' = k_0 + k_1' \cdot c \qquad (1)$$

At the acid concentration used k_0 should be approximately equal to the rate constant of the hydrogen ion catalyzed decomposition [1]. For $c = 1.20$ mM $k_0' = (3.20 \pm 0.05) \times 10^{-4}$ min^{-1} while for $c = 2.40$ mM we get $k_0' = (5.90 \pm 0.05) \times 10^{-4}$ min^{-1}. From these values we can calculate $k_0 = (5 \pm 2) \times 10^{-5}$ min^{-1} and $k_1' = 0.225 \pm 0.010$ M^{-1} min^{-1}. Thus k_0 is only a correction term in the present case. If its value is combined with $k_0 = 3.8 \times 10^{-3}$ min^{-1}, determined in the previous work [1] for the same ionic medium but at 61 °C, the activation energy 24 ± 2 kcal is obtained. Kolthoff and Miller [13] give the value 26 kcal for the same reaction.

Kinetics of the redox reaction with cerium (III). In Fig. 2 the ceric concentration x has been plotted against t for different values of the parameters a, $b(0)$, and c and for the same ionic medium as above. It is evident that when the $(a-x)$-values are not very low x is independent of a. Furthermore, since the variation in $b(t)$ is very slight for the short times used in the runs the curves in Fig. 2 consist of approximately straight lines. Thus it is easily found

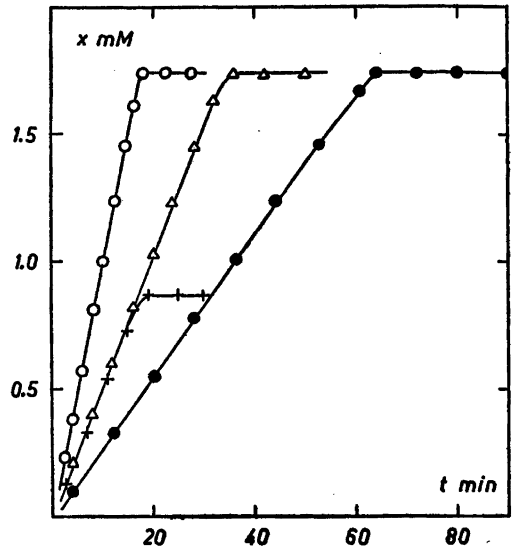


Fig. 2. x *as a function of* t *at different values of* a, b(0), *and* c. a = *0.870 mM*, b(0) = *96.0 mM*, c = *1.20 mM* (+); a = *1.74 mM*, b(0) = *96.0 mM*, c = *1.20 mM* (△); a = *1.74 mM*, b(0) = *47.6 mM*, c = *1.20 mM* (●); a = *1.74 mM*, b(0) = *96.0 Mm*, c = *2.40 mM* (○).

from the slope of the first part of the curves that the reaction rate is proportional to the silver and persulphate concentrations.

$$\frac{dx}{dt} = k\ b(t)\ c \qquad (2)$$

For the rate constant k the different runs give the average value 0.46 ± 0.01 $M^{-1}min^{-1}$. This means that within the limits of experimental random errors the relation $k = 2\ k_1'$ has been found to be valid.

Since $dx/dt = 0$ for $x = a$, it is clear that eqn. (2) cannot be applicable for very small values of $a-x$, and it is very plausible that the first power of $a-x$ enters into the complete differential equation, as was the case with the corresponding equation for the uncatalyzed redox reaction [1].

THE REACTION MECHANISM AND THE COMPLETE RATE LAW

Among the different partial reactions operating in the oxidation of cerium (III) we have the uncatalyzed persulphate decomposition, studied in the previous work [1]. However, preliminary measurements showed that this reaction is quite negligible at 25 °C. Thus the silver(I) catalyzed decomposition is the predominant starting reaction.

For this one Yost [5] was the first to propose the mechanism

$$Ag^+ + S_2O_8^{2-} \rightarrow Ag^{3+} + 2\ SO_4^{2-} \qquad (3)$$

as the rate determining step. However, the experimental evidence for the formation of silver(III) is not very strong, and presumably the real reason for the formulation was the fact that the formation of the radical ion SO_4^- was not known at that time. Since the existence of silver(II) is certain we propose the following formulation of the first step

$$Ag(I) + S_2O_8^{2-} \xrightarrow{k_1'} Ag(II) + SO_4^- + SO_4^{2-} \quad (4)$$

in analogy with the formulation for the uncatalyzed reaction [1]. The formation of SO_4^- according to (4) is supported by the fact that on addition of silver(I) to persulphate this becomes more effective in initiating polymerizations (*cf.* Bacon [14] and Morgan [14]).

In the previous work [1] the rate law obtained proved that in the absence of silver the amount of SO_4^- not consumed in the oxidation of cerium(III) disappeared in a reaction with the rate $k_2[SO_4^-]$, where k_2 is a *constant*. Thus it was concluded that SO_4^- reacted with water giving free oxygen (*cf.* Kolthoff and Miller [13]) and not with the ammonium ions, the concentration of which was not the same in the different runs.

In the presence of silver(I), on the other hand, measurements showed that also in cerium-free solutions practically no oxygen was evolved, even if the persulphate decomposition was considerable. Thus we must conclude that silver(I) reacts more readily than water with SO_4^- according to

$$Ag(I) + SO_4^- \xrightarrow{k_2'} Ag(II) + SO_4^{2-} \quad (5)$$

Furthermore, we have the two simultaneous reactions

$$Ce(III) + SO_4^- \xrightarrow{k_3} Ce(IV) + SO_4^{2-} \quad (6)$$

$$Ce(III) + Ag(II) \xrightarrow{k_3'} Ce(IV) + Ag(I) \quad (7)$$

where (6) is the reaction studied in the previous investigation [1].

Finally, since no oxygen is evolved the amount of silver(II) not consumed in reaction (7) evidently must attack the ammonium ions. According to Marshall [2] ammonium persulphate decomposes in the presence of silver salts with the formation of nitrate ions. Thus we have the stoichiometric formula

$$8\ Ag(II) + NH_4^+ + 3\ H_2O \rightarrow 8\ Ag(I) + 10\ H^+ + NO_3^- \quad (8)$$

Of course the reaction (8) involves several steps, and we can presume, that the reaction is first order with respect to silver(II). Then the reaction rate is equal to $\varphi \cdot z$, where φ may be a function of different concentrations.

If the mechanism (4)—(8) is correct the following system of differential equations should be applicable.

$$\frac{dx}{dt} = (a - x)\ (k_3 y + k_3' z) \tag{9}$$

$$\frac{dy}{dt} = k_1'\ b(t)\ c - \left\{k_2' c + k_3\ (a - x)\right\}\ y \tag{10}$$

$$\frac{dz}{dt} = c\ \left\{k_1'\ b(t) + k_2'\ y\right\} - \left\{\varphi + k_3'\ (a - x)\right\}\ z \tag{11}$$

Referring to the deductions of the previous paper [1] and remembering that $b(t) = b(0)e^{-k_0' t}$ we can establish that if the condition $k_2' \gg k_1'$ (that is $k_2' c \gg k_1' c \approx k_0'$) is fulfilled the steady-state approximation is valid for SO_4^- at all cerous concentrations. Thus we can put $dy/dt = 0$ in eqn. (10) and get an expression for y. When this expression is introduced into eqn. (11) it is found that an equation of a similar type as eqn. (10) is obtained, and the necessary and sufficient condition for the applicability of the steady-state approximation also to silver(II) at all cerous concentrations is that $\varphi \gg k_1' c$.

Applying the steady-state approximations we can easily eliminate the variables y and z, and for dx/dt we get the following complete expression:

$$\frac{dx}{dt} = \frac{k_1'\ (a - x)\ b(t) c}{\varphi + k_3'\ (a - x)} \left\{2\ k_3' + \frac{k_3\ \varphi}{k_2' c + k_3 (a - x)}\right\} \tag{12}$$

If φ is a quantity negligible in comparison with $k_3'\ (a - x)$ this equation becomes identical with the simple eqn. (2) with $k = 2\ k_1'$, which is experimentally verified for not very low cerous concentrations. Thus the mechanism proposed with the reaction (4) as the rate determining step and with the different rate constants fulfilling the conditions stated seems plausible.

According to this mechanism silver(II) reacts more rapidly with ammonium ions than with water, while, as mentioned in the foregoing, the reverse is valid for the reactivity of the radical ion SO_4^-. This state of things could be due to a tendency of silver(II) to form ammine complexes. Then in our acid solutions the equilibrium

$$Ag^{2+} + NH_4^+ \rightleftharpoons AgNH_3^{2+} + H^+ \tag{13}$$

would exist, followed by a rapid decomposition of the ammine complex in a first order reaction involving an electron transfer from the ligand to the central ion. In this case the function φ can be expected to be of the form $\varphi =$ constant$\cdot [NH_4^+]$, since $[H^+]$ is constant.

The measurements of the persulphate decomposition show clearly that c did not vary with time, even if the decrease in $b(t)$ was considerable. This means that z was either very small in comparison with c or a constant fraction of the total silver concentrations. Now, applying the steady-state approximations to the cerium-free solutions and using the expression for φ we get $z/c =$ constant $\cdot\ b(t) / [NH_4^+]$. But from the reactions (4), (5) and (8) it is evident that $b(t) / [NH_4^+]$ decreases with time, and thus z must be $\ll c$ throughout the runs.

After the completion of the present investigation a paper by Bawn and Margerison [16] about the rate of persulphate decomposition has appeared. For the silver catalyzed reaction they have also proposed (4) as the rate determining step. For the uncatalyzed reaction, however, they have accepted the previous mechanism of Bartlett and Cotman [17], which has turned out to be inconsistent with experimental facts [1].

This investigation has been supported by a grant from the *Swedish Natural Science Research Council* which is gratefully acknowledged.

REFERENCES

1. Fronæus, S. and Östman, C. O. *Acta Chem. Scand.* **9** (1955) 902.
2. Marshall, H. *Proc. Roy. Soc. Edinburgh* **23** (1900) 163.
3. Marshall, H. and Inglis, J. K. H. *Proc. Roy. Soc. Edinburgh* **24** (1902) 88.
4. King, C. V. *J. Am. Chem. Soc.* **50** (1928) 2080.
5. Yost, D. M. *J. Am. Chem. Soc.* **48** (1926) 152.
6. Yost, D. M. *J. Am. Chem. Soc.* **48** (1926) 374.
7. King, C. V. *J. Am. Chem. Soc.* **49** (1927) 2689.
8. King, C. V. *J. Am. Chem. Soc.* **50** (1928) 2089.
9. King, C. V. and Griswold, F. L. *J. Am. Chem. Soc.* **52** (1930) 1493.
10. Yost, D. M. and Claussen, W. H. *J. Am. Chem. Soc.* **53** (1931) 3349.
11. Dekker, A. O., Lévy, H. A. and Yost, D. M. *J. Am. Chem. Soc.* **59** (1937) 2131.
12. Cone, W. H. *J. Am. Chem. Soc.* **67** (1945) 78.
13. Kolthoff, I. M. and Miller, I. K. *J. Am. Chem. Soc.* **73** (1951) 3055.
14. Bacon, R. G. R. *Trans. Faraday Soc.* **42** (1946) 140.
15. Morgan, L. B. *Trans. Faraday Soc.* **42** (1946) 169.
16. Bawn, C. E. H. and Margerison, D. *Trans. Faraday Soc.* **51** (1955) 925.
17. Bartlett, P. D. and Cotman, J. D. *J. Am. Chem. Soc.* **71** (1949) 1419.

Received November 28, 1955.

ACTA CHEMICA SCANDINAVICA 10 (1956) 327—340

Short Communications

Small Angle Scattering of X-Rays in Aqueous Solutions of Bile Acid Salts

PER EKWALL and KRISTER FONTELL

Institute of Physical Chemistry, Åbo Akademi, Åbo, Finland

Freezing point determinations, studies on the solubilization of water-insoluble lipophilic dyes, hydrocarbons etc. and electrical conductance measurements have provided conclusive evidence that an association to micelles takes place in aqueous bile acid salt solutions [1-7]. Up to now, however, it has generally been considered that in contrast to the solutions of association colloids of the paraffin chain salt type these solutions do not give long spacing X-ray interferences. The lack of interferences has been taken as evidence that the order in the micelles of the bile salts is of much lesser degree than in the micelles of compounds of the paraffin chain type [8,9].

McBain and Hoffman [8] X-rayed 20 % aqueous solutions of sodium desoxycholate for 12—15 hours with a film-to-sample distance of 200 mm. They reported that there was no suggestion of "a long spacing line, and therefore nothing corresponding to a McBain micelle, a Hess micelle, or an interparticle spacing. Evidently in these solutions the colloid consists of particles too irregular in shape and size and distance from each other to give either a lattice spacing from within the micelles or an interparticle spacing between them".

We have, however, been able to obtain X-ray patterns with aqueous solutions of bile acid salts.

Experimental. The X-ray unit, a Philips Norelco X-ray unit with Cu target, operated at 45 kV, 15 mA; Ni-filtered radiation was employed. Three cameras were used: 1) A small angle vacuum camera with collimator slits, principally of the same design as described by Harkins [10]. Collimator width 0.2 mm, distance between collimators 110 mm, sample-to-film distance 229 mm. 2) A small angle vacuum camera with pinhole collimators of the design described by Kiessig [11]. Sample-to-film distance 212 mm. 3) Pinhole powder camera, diameter 114.6 mm.

Desoxycholic acid (Hoffman La Roche, Basle) was purified by the ether-choleic acid method, dissolved in absolute ethanol and recrystallized twice; m.p. 174—175° C. The acid was dissolved in absolute ethanol, and neutralized with ethanolic sodium ethylate. The crystallized sodium salt was filtered and dried in vacuum over P_2O_5 at 78 °C. All solutions were made by weighing, redistilled water ($\varkappa < 10^{-6}$ mho) being used. The solutions were X-rayed at 25 °C in glass-capillaries, diameter 0.7 mm, wall thickness 0.01 mm. Times of exposure: 1) camera with collimator slits 20 h, 2) camera with pinhole collimators 60 h, 3) powder camera 3 h. The exposed films were measured with a Zeiss nonrecording photometer. Three parallel runs were made on every film, readings being taken at every 0.1 mm of the film.

Results. The diffraction pattern for sodium desoxycholate solutions obtained with the small angle vacuum cameras resembles those for solutions of association colloids of paraffin chain type. We have, however, observed only one intensity maximum in the former patterns; this maximum is not so distinct as the so-called I-band of the last mentioned colloids.

Fig. 1 shows the shape of the photometric curves of the halo obtained with different desoxycholate concentrations. For solutions below the 0.05 M concentration the curves are identical with those for pure water, but already in the 0.06 M solution there occurs a very small difference. With increasing concentration the peak becomes more and more pronounced.

In spite of the long exposure time the patterns in all cases are rather weak. It is difficult to determine the exact position of the intensity maximum. If, however, an attempt is made to determine the maxi-

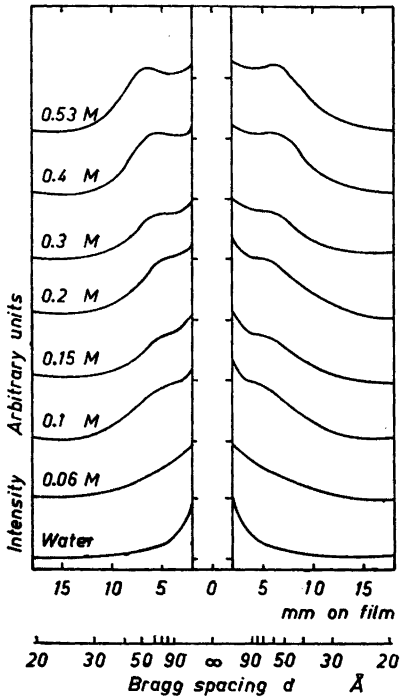


Fig. 1. Photometer traces of the small angle scattering from aqueous solutions of sodium desoxycholate.

mum, and if it is supposed that Bragg's law is valid in this case (compare Guinier's and Fournet's criticism of earlier methods of treating the experimental results [12]), the spacings given in Fig. 2 are obtained. It is seen that the spacing value undergoes a variation with increasing concentration. With the powder camera a short spacing of 6.0—6.2 Å was obtained in addition to the water halo of about 2.7—3.3 Å. This short spacing is not altered by changes in the concentration. We have obtained a pattern of similar character in solutions of sodium cholate.

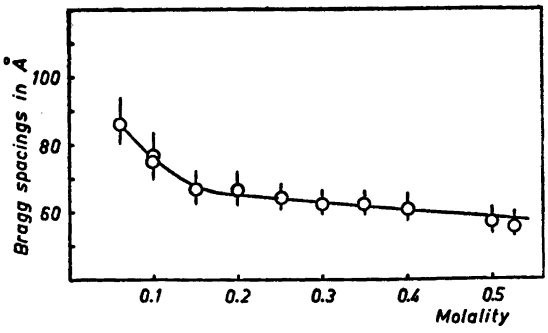


Fig. 2. Graph of the variation of the "band spacing" with sodium desoxycholate concentration.

Previously [5-7] it has been shown that micelle formation begins in sodium desoxycholate solutions at the 0.005 M concentration and becomes fully developed from 0.01 M upwards; a third concentration limit where many of the properties of the desoxycholate solutions are altered lies at 0.045 M. The small angle X-ray patterns thus have been observed in desoxycholate solutions down to the third concentration limit. The spacings in Fig. 2 vary with the colloid concentration in a similar way as the I-band spacing in solutions of association colloids of the paraffin chain type.

The micelles in bile salt solutions are thus regular enough in shape and size to give a small angle X-ray pattern similar in type to those given by micelles in solutions of paraffin chain association colloids. This does not exclude the possibility that the micelles of these two compound groups possess different structures.

1. Johnston, S. A. and McBain, J. W. *Proc. Roy. Soc. London* **181** (1942) 199.
2. Merril, C. R. and McBain, J. W. *J. Phys. Chem.* **46** (1942) 10.
3. Roepke, R. R. and Mason, H. L. *J. Biol. Chem.* **133** (1940) 103.
4. Mellander, O. and Stenhagen, E. *Acta physiol. Scand.* **4** (1942) 349.
5. Ekwall, P. *Acta Acad. Aboensis, Math. Phys.* **XVII** (1951) 4.
6. Ekwall, P. *Koninkl. Vlaamse Acad. v. Wetensk. v. Belgie. Intern. Conference on Biochemical Problems of Lipids.* Brüssel 1953, p. 103.
7. Ekwall, P. *J. Colloid Sci. Suppl.* **1** (1954) 66.
8. McBain, J. W. and Hoffman, O. A. *J. Phys. & Colloid Chem.* **53** (1949) 39.
9. Winsor, P. A. *Solvent Properties of Amphiphilic Compounds.* Butterworths Scientific Publications, London 1954, p. 159.
10. Harkins, W. D., Mattoon, R. W. and Corrin, M. L. *J. Am. Chem. Soc.* **68** (1946) 220.
11. Kiessig, H. *Kolloid-Z.* **98** (1942) 213.

12. Guinier, A. and Fournet, G. *Small-Angle Scattering of X-rays*. John Wiley & Sons, Inc. New York, Chapman & Hall, London, 1955, p. 176.

Received December 27, 1955.

On the Solvent Dependence of the Spectra of Complex Ions

JANNIK BJERRUM, A. W. ADAMSON* and OLE BOSTRUP**

Chemistry Department A, Technical University of Denmark, Copenhagen, Denmark

In recent studies of the absorption spectra of dissolved complexes of transition group elements the so-called crystal field bands are treated as due to electronic transitions between levels caused by the perturbation of the electric fields of the ligands in the first co-ordination sphere. In order to examine the correctness of the assumption of the non-influence of the second sphere we have measured the spectra of some robust complexes of iron(II), chromium(III) and cobalt(III) in other solvents than water. Acetone, nitromethane, chloroform, ethanol, and especially methanol were used as solvents, and in the cases where the complexes were sufficiently soluble the spectra of the solutions were measured at a Cary recording spectrophotometer.

Of the complexes examined dicyano-bis (*o*-phenanthroline)iron(II) was prepared according to Barbieri [1] and recrystallized from chloroform until the spectrum was unchanged by further recrystallization. (Found: Fe 10.81; N 16.32; C 60.90. Calc. for $[Fe(o\text{-phen})_2(CN)_2],3H_2O$: Fe 10.70; N 16.22; C 60.25). Tris(*o*-phenanthroline)-iron(II) bromide was prepared according to Blau [2] and recrystallized once. The Reinecke's salt $K[Cr(NH_3)_2(SCN)_4]$ was prepared after Nordenskjöld [3]. An analyzed preparation of $(NH_4)_3[Cr(SCN)_6]$, $4H_2O$ was kindly made to us and measured in water, methanol and acetone by C. E. Schäffer. Pure samples of Nos. 4—10 in Table 1 were kindly put at our disposal by Professor Fred Basolo, who prepared [4] the compounds during his stay at this laboratory.

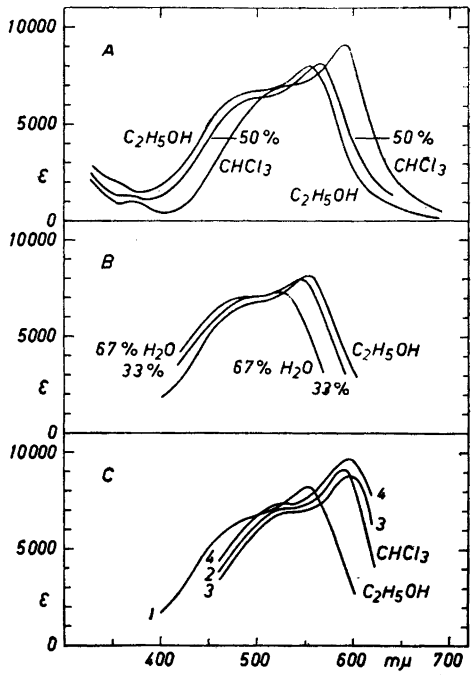


Fig. 1. Extinction curves for $[Fe(o\text{-phen})_2(CN)_2]$ in different solvents.

A. In $CHCl_3$, 50 % $CHCl_3$+50 % C_2H_5OH and C_2H_5OH

B. In C_2H_5OH, 67 % C_2H_5OH+33 % H_2O, 33 % C_2H_5OH+67 % H_2O

C. In C_2H_5OH (curve 1), $CHCl_3$ (curve 2), 50 % $CHCl_3$ + 50 % petrolether (curve 3), 50 % $CHCl_3$ + 50 % CCl_4 (curve 4).

The data for 10 complex salts are summarized in Table 1. For each absorption band are given the value of λ_{max} (wavelengths of maximum in mμ) and ε_{max} (molar extinction coefficient) in water, and for the organic solvents the changes in λ_{max} and ε_{max} as % of values in water. The examples given in the table show that λ_{max} usually is practically independent of the solvent. A significant change of λ_{max} is only found in one case, *viz.* $[Co(en)_2(SCN)_2](SCN)$. This compound has a crystal field band (ε_{max} =

* Present address: Chem. Dept., University of Southern California, Los Angeles, California, USA.

** Present address: Chem. Dept. B, Technical University of Denmark, Copenhagen, Denmark.

12. Guinier, A. and Fournet, G. *Small-Angle Scattering of X-rays*. John Wiley & Sons, Inc. New York, Chapman & Hall, London, 1955, p. 176.

Received December 27, 1955.

On the Solvent Dependence of the Spectra of Complex Ions

JANNIK BJERRUM, A. W. ADAMSON* and OLE BOSTRUP**

Chemistry Department A, Technical University of Denmark, Copenhagen, Denmark

In recent studies of the absorption spectra of dissolved complexes of transition group elements the so-called crystal field bands are treated as due to electronic transitions between levels caused by the perturbation of the electric fields of the ligands in the first co-ordination sphere. In order to examine the correctness of the assumption of the non-influence of the second sphere we have measured the spectra of some robust complexes of iron(II), chromium(III) and cobalt(III) in other solvents than water. Acetone, nitromethane, chloroform, ethanol, and especially methanol were used as solvents, and in the cases where the complexes were sufficiently soluble the spectra of the solutions were measured at a Cary recording spectrophotometer.

Of the complexes examined dicyano-bis (*o*-phenanthroline)iron(II) was prepared according to Barbieri [1] and recrystallized from chloroform until the spectrum was unchanged by further recrystallization. (Found: Fe 10.81; N 16.32; C 60.90. Calc. for $[Fe(o\text{-phen})_2(CN)_2],3H_2O$: Fe 10.70; N 16.22; C 60.25). Tris(*o*-phenanthroline)-iron(II) bromide was prepared according to Blau [2] and recrystallized once. The Reinecke's salt $K[Cr(NH_3)_2(SCN)_4]$ was prepared after Nordenskjöld [3]. An analyzed preparation of $(NH_4)_3[Cr(SCN)_6]$, $4H_2O$ was kindly made to us and measured in water, methanol and acetone by C. E. Schäffer. Pure samples of Nos. 4—10 in Table 1 were kindly put at our disposal by Professor Fred Basolo, who prepared [4] the compounds during his stay at this laboratory.

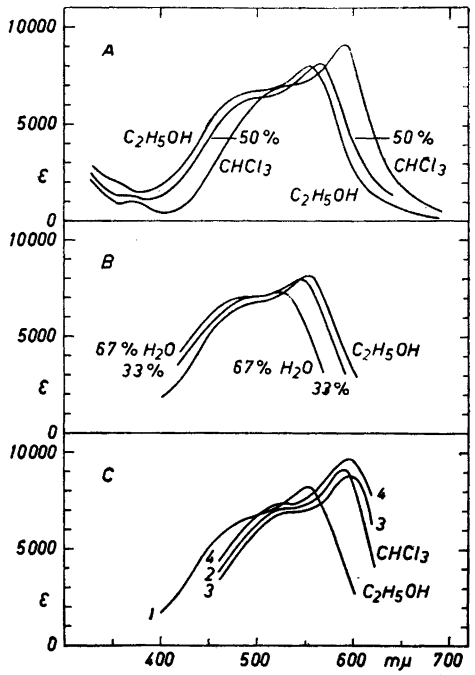


Fig. 1. Extinction curves for $[Fe(o\text{-phen})_2(CN)_2]$ in different solvents.

A. In $CHCl_3$, 50 % $CHCl_3$+50 % C_2H_5OH and C_2H_5OH

B. In C_2H_5OH, 67 % C_2H_5OH+33 % H_2O, 33 % C_2H_5OH+67 % H_2O

C. In C_2H_5OH (curve 1), $CHCl_3$ (curve 2), 50 % $CHCl_3$ + 50 % petrolether (curve 3), 50 % $CHCl_3$ + 50 % CCl_4 (curve 4).

The data for 10 complex salts are summarized in Table 1. For each absorption band are given the value of λ_{max} (wavelengths of maximum in mμ) and ε_{max} (molar extinction coefficient) in water, and for the organic solvents the changes in λ_{max} and ε_{max} as % of values in water. The examples given in the table show that λ_{max} usually is practically independent of the solvent. A significant change of λ_{max} is only found in one case, *viz.* $[Co(en)_2(SCN)_2](SCN)$. This compound has a crystal field band (ε_{max} =

* Present address: Chem. Dept., University of Southern California, Los Angeles, California, USA.

** Present address: Chem. Dept. B, Technical University of Denmark, Copenhagen, Denmark.

Table 1. Data for absorption maxima, and changes in λ_{max} and ε_{max} as per cent of value in water

No.	Compound	Water		Methanol		Nitromethane		Acetone	
		λ_{max}	ε_{max}	$\Delta\lambda$ %	$\Delta\varepsilon$ %	$\Delta\lambda$ %	$\Delta\varepsilon$ %	$\Delta\lambda$ %	$\Delta\varepsilon$ %
1	$[Fe(o\text{-phen})_3]Br_2$	510	11 200	0	+ 5.3				
		266	67 200	0	+ 2				
2	$K[Cr(NH_3)_2(SCN)_4]$	515	107	+1.7	— 5.5	+2	+ 2.8		
		390	96	+1	—15.7	+1	— 8.3		
		303	14 800	+2	+17				
3	$(NH_4)_3[Cr(SCN)_6]$	564	159	—1.7	—28	—0.7	—16.2	—1.4	—35
		420	129	—1.5	—29	—0.5	—17	—1.4	—36
		309	25 000	0	+12				
		234	19 200	(0)	(+33)				
4	*cis*-$[Coen_2(Cl)_2]Cl$	525	72.5	+2	+ 7.2				
5	*trans*-$[Coen_2(Cl)_2]Cl$	617	36	—1.1	~ 2				
		455**	27	(0)	— 7				
		387**	36	(0)	+25				
6	*trans*-$[Coen_2(Br)_2]Br$	648	45	0	+ 9				
7	*cis*-$[Coen_2(SCN)_2]SCN$	487	340	+1	+20			+1	+29 *
		308	2 900	+6	— 4			+7.8	+14 *
8	*cis*-$[Coen_2(NO_2)_2]NO_3$	430	129	+1.8	+13.5				
		323	2 830	+1.3	+21				
9	*trans*-$[Coen_2(NO_2)_2]NO_3$	430	133	+1	+13.2				
		340	2 470	+1	+21				
10	$[Co(NH_3)_3(NO_2)_3]$	435	235	0	+11.3				
		345	4 900	+1.5	+ 7.2				
		258	16 500	+1	— 6				

* Acetone with 10 % CH_3OH.

** A shoulder in H_2O and a peak in CH_3OH. This difference in shape is independent of concentration.

340) as well as an electron transfer band (ε_{max} = 2 900), and it is noteworthy that it is only the last mentioned band which is displaced considerably (6—8 %) by going from water to organic solvent. The influence of the solvent on the intensities of the bands is more varied, and ε_{max} shows some changes in most cases. The data seem to show that compared with water ε_{max} is generally higher for cations and lower for anions in methanol. For one and the same solvent Beer's law was found to be sufficiently obeyed in all cases in which measurements were performed at different concentrations.

$[Fe(o\text{-phen})_3(CN)_2]$ represents a case even more anomalous than *cis*$[Co(en)_2(SCN)_2](SCN)$. The dicyano complex is so insoluble in water, carbon-tetrachloride and ether that measurements cannot be performed in the pure solvents, but it is sufficiently soluble in methanol, ethanol and chloroform. In Fig. 1 extinction curves for this non-electrolyte in different solvents are shown. It is seen that three electron transfer bands are found in visible and near ultraviolet, *e. g.* in chloroform at the wavelengths 591 mμ, 525 mμ (shoulder) and 367 mμ, respectively. The whole appearance of the curves, and the absence

of any isobestic points rule out the possibility of a chemical equilibrium between two forms which shift with solvent composition. *cis*[Coen$_2$(SCN)$_2$](SCN) behaves similarly in water-methanol mixtures. Evidence for a true solvent effect is also found in the fact that light absorption in the various solvents does not show any time effect.

That a crystal field band of a saturated complex ion only to a slight degree is dependent on the solvent can be predicted from the theoretical expression for λ_{max}

$$1/\lambda_{max} = \text{const. } \mu/r^6$$

(see *e. g.* Ballhausen [5]) where μ is the point dipole moment and r the distance of the ligand from the central atom. Denoting the quantities in the first and second spheres by μ', μ'', and r', r'', respectively, the relative contribution of the second sphere to the wavelength is given by

$$\frac{\Delta\lambda_{max}}{\lambda_{max}} = \frac{\mu''}{\mu'} \cdot \left(\frac{r'}{r''}\right)^6$$

Now introducing $\mu' \gtrsim \mu''$ and $r'' = 2r'$, we get

$$\frac{\Delta\lambda_{max}}{\lambda_{max}} \lesssim \frac{1}{64}$$

According to this estimation the displacement of a crystal field band of a saturated complex should always be smaller than 2 % in agreement with what is found experimentally. The greater variability of the electron transfer band found in some cases is quite natural considering that the orbitals of the solvent molecules are closer to the orbitals of the ligands than to the electron systems of the central atom.

1. Barbieri, G. A. *Atti. acad. naz. Lincei. Mem. Classe Sci. fis. mat. e nat. Sez. II*, **20** (1934) 273.
2. Blau, F. *Monatsh.* **19** (1898) 669.
3. Nordenskjöld, O. *Z. anorg. Chem.* **1** (1892) 126.
4. Basolo, F., Ballhausen, C. J. and Bjerrum, J. *Acta Chem. Scand.* **9** (1955) 810.
5. Ballhausen, C. J. *Kgl. Danske Videnskab. Selskab, Mat.-fys. Medd.* **29** (1954) No. 4.

Received January 4, 1956.

On the Proton Conductivity in Water

JAN KROGH-MOE

Department of Physics, University of Missouri, Columbia, Missouri, U.S.A.

It is commonly agreed that the large mobilities of the H_3O^+ and OH^- ions in water must be explained by a proton transfer over hydrogen bridges. By assuming this proton transfer mechanism, Gierer and Wirtz [1,2] derived the following equation to explain the mobility as a function of temperature:

$$u = \frac{C}{T} f(T) \exp\left(-\frac{q}{RT}\right) \qquad (1)$$

Here u is the mobility of the H_3O^+ or OH^- ion in excess of the value expected for ions of that size. C is a factor which incorporates some constants of the system, T is the absolute temperature and q is the activation energy of the rate determining process. $f(T)$ is a function of temperature (and also pressure), which describes the influence of the liquid structure upon the mobility.

If this equation is to be useful, the structural influence $f(T)$ should be known. Gierer and Wirtz used Eucken's structure model of water [3] for their treatment. Eucken assumed that the water structure consisted of a few definite types of molecular species. There is very little evidence to support this assumption, however. An alternative derivation of $f(T)$ from the model of water proposed by Grjotheim and Krogh-Moe [4] shall therefore be suggested.

If the proton transfer across a hydrogen bridge is the rate determining process, one might expect $f(T)$ to be proportional to the total number of hydrogen bonds present in water. Contrary to this assumption the extra mobility increases with temperature in a certain temperature interval, though the number of hydrogen bonds decreases monotonously. By assuming that $f(T)$ is proportional to the number of water molecules with only one hydrogen bond established, consistent results may be derived. This is reasonable if the breaking of the hydrogen bond is the rate determining process. When a proton transfer over a hydrogen bridge has occurred, a reorientation of the water molecule is necessary if the molecule is to participate in further proton transfers. A water molecule

of any isobestic points rule out the possibility of a chemical equilibrium between two forms which shift with solvent composition. *cis*[Coen$_2$(SCN)$_2$](SCN) behaves similarly in water-methanol mixtures. Evidence for a true solvent effect is also found in the fact that light absorption in the various solvents does not show any time effect.

That a crystal field band of a saturated complex ion only to a slight degree is dependent on the solvent can be predicted from the theoretical expression for λ_{max}

$$1/\lambda_{max} = \text{const. } \mu/r^6$$

(see *e. g.* Ballhausen [5]) where μ is the point dipole moment and r the distance of the ligand from the central atom. Denoting the quantities in the first and second spheres by μ', μ'', and r', r'', respectively, the relative contribution of the second sphere to the wavelength is given by

$$\frac{\Delta\lambda_{max}}{\lambda_{max}} = \frac{\mu''}{\mu'} \cdot \left(\frac{r'}{r''}\right)^6$$

Now introducing $\mu' \gtrsim \mu''$ and $r'' = 2r'$, we get

$$\frac{\Delta\lambda_{max}}{\lambda_{max}} \lesssim \frac{1}{64}$$

According to this estimation the displacement of a crystal field band of a saturated complex should always be smaller than 2 % in agreement with what is found experimentally. The greater variability of the electron transfer band found in some cases is quite natural considering that the orbitals of the solvent molecules are closer to the orbitals of the ligands than to the electron systems of the central atom.

1. Barbieri, G. A. *Atti. acad. naz. Lincei. Mem. Classe Sci. fis. mat. e nat. Sez. II*, **20** (1934) 273.
2. Blau, F. *Monatsh.* **19** (1898) 669.
3. Nordenskjöld, O. *Z. anorg. Chem.* **1** (1892) 126.
4. Basolo, F., Ballhausen, C. J. and Bjerrum, J. *Acta Chem. Scand.* **9** (1955) 810.
5. Ballhausen, C. J. *Kgl. Danske Videnskab. Selskab, Mat.-fys. Medd.* **29** (1954) No. 4.

Received January 4, 1956.

On the Proton Conductivity in Water

JAN KROGH-MOE

Department of Physics, University of Missouri, Columbia, Missouri, U.S.A.

It is commonly agreed that the large mobilities of the H_3O^+ and OH^- ions in water must be explained by a proton transfer over hydrogen bridges. By assuming this proton transfer mechanism, Gierer and Wirtz [1,2] derived the following equation to explain the mobility as a function of temperature:

$$u = \frac{C}{T} f(T) \exp\left(-\frac{q}{RT}\right) \qquad (1)$$

Here u is the mobility of the H_3O^+ or OH^- ion in excess of the value expected for ions of that size. C is a factor which incorporates some constants of the system, T is the absolute temperature and q is the activation energy of the rate determining process. $f(T)$ is a function of temperature (and also pressure), which describes the influence of the liquid structure upon the mobility.

If this equation is to be useful, the structural influence $f(T)$ should be known. Gierer and Wirtz used Eucken's structure model of water [3] for their treatment. Eucken assumed that the water structure consisted of a few definite types of molecular species. There is very little evidence to support this assumption, however. An alternative derivation of $f(T)$ from the model of water proposed by Grjotheim and Krogh-Moe [4] shall therefore be suggested.

If the proton transfer across a hydrogen bridge is the rate determining process, one might expect $f(T)$ to be proportional to the total number of hydrogen bonds present in water. Contrary to this assumption the extra mobility increases with temperature in a certain temperature interval, though the number of hydrogen bonds decreases monotonously. By assuming that $f(T)$ is proportional to the number of water molecules with only one hydrogen bond established, consistent results may be derived. This is reasonable if the breaking of the hydrogen bond is the rate determining process. When a proton transfer over a hydrogen bridge has occurred, a reorientation of the water molecule is necessary if the molecule is to participate in further proton transfers. A water molecule

with only one hydrogen bond reorientates readily when the bond breaks.

The description of excess mobility presented here implies a number of assumptions, of which the following are the most important:

1) The model of water applied [3] is assumed adequate for the purpose, though it is only a rough idealization of the real conditions. Hence x, the ratio of the number of established hydrogen bonds to the number of possible bonds, is known.

2) It is assumed that the H_3O^+ ions and the OH^- ions in dilute solutions have the same structural environment as the water molecules.

3) A random distribution of the hydrogen bonds between the molecules will be assumed. The ratio w of one-bonded molecules to the total number of molecules is then given by the following equation:

$$w = 4x(1-x)^3 \qquad (2)$$

Any coupling between the breaking of the bonds is disregarded in deducing this equation.

4) The assumption that the factor $f(T)$ in equation (1) is proportional to the number of molecules with one hydrogen bond is only valid within a limited temperature interval. For instance differences in mean chain lengths for transfers taking place over chains of hydrogen bridges are not taken into account. Coupling between the breaking of bonds is again disregarded.

5) Eqn. (1) is not quite exact, but assumed to be adequate.

In view of these assumptions and approximations the results obtained should be regarded as of only a semiquantitative nature. However, by plotting $\log u + \log T - \log x(1-x)^3$ against $1/T$, using the values of u given for the H_3O^+ ion by Gierer and Wirtz [1] or by Bjerrum [5] and the values of x given by Grjotheim and Krogh-Moe [4], a straight line is obtained for temperatures up to 200° C. The slope of the line corresponds to an activation energy of 1.7 kcal/mole. This value compares favourably with the values 1.3—2.6 kcal/mole obtained by Grjotheim and Krogh-Moe for the breaking of a bond in water. It should be noted that this value for the hydrogen bond includes only the part of the total interaction responsible for the tetrahedral configuration of the water molecules.

The activation energy for the OH^- ion conductivity is shown to be 0.6 kcal/mole higher than that for the H_3O^+ ion [1]. This means that an OH^- ion cannot have quite the same surroundings on average as the H_3O^+ ion. The energy of the hydrogen bond appears to be slightly different in these two cases. Rather than a single energy, however, we have in these systems an energy distribution. A single hydrogen bond energy seems to be a fairly good approximation, however.

The previous considerations enable us to understand why the extra mobility increases with pressure in a certain temperature range. In this temperature range the breaking of a hydrogen bond results in a decrease in volume [4]. Therefore increased pressure means a smaller number of bonds in the liquid. This leads to a larger number of water molecules with only one bond, as may be seen by introducing into eqn. (2) the appropriate values of x. Consequently an increase in extra mobility with pressure is expected. If the factor $f(T)$ of structural influence in eqn. (1) were proportional to the number of established hydrogen bonds, the pressure dependence of extra mobility could not be explained.

1. Gierer, A. and Wirtz, K. *Ann. Physik* **6** (1949) 257.
2. Gierer, A. and Wirtz, K. *J. Phys. Chem.* **56** (1952) 914.
3. Eucken, A. *Gött. Nach. Math.-phys. Kl.* **1946** 38.
4. Grjotheim, K. and Krogh-Moe, J. *Acta Chem. Scand.* **8** (1954) 1193.
5. Bjerrum, N. *Kgl. Danske Videnskab. Selskab, Mat.-fys. Medd.* **27** (1951) No. 1.

Received January 14, 1956.

The Vitamin Content of Pollen after Storing

NIELS NIELSEN

Research Department, AB Kabi, Stockholm, Sweden

In a previous paper [1] the results of an investigation concerning the content of some B-vitamins in pollen from different plants were given. The samples examined were obtained from *Zea mays*, *Alnus glutinosa*, *A. incana* and *Pinus montana*. The following vitamins were determined: riboflavin, nicotinic acid, pantothenic acid, pyridoxine, biotin and inositol. The determinations were carried out during October

with only one hydrogen bond reorientates readily when the bond breaks.

The description of excess mobility presented here implies a number of assumptions, of which the following are the most important:

1) The model of water applied [3] is assumed adequate for the purpose, though it is only a rough idealization of the real conditions. Hence x, the ratio of the number of established hydrogen bonds to the number of possible bonds, is known.

2) It is assumed that the H_3O^+ ions and the OH^- ions in dilute solutions have the same structural environment as the water molecules.

3) A random distribution of the hydrogen bonds between the molecules will be assumed. The ratio w of one-bonded molecules to the total number of molecules is then given by the following equation:

$$w = 4x(1-x)^3 \qquad (2)$$

Any coupling between the breaking of the bonds is disregarded in deducing this equation.

4) The assumption that the factor $f(T)$ in equation (1) is proportional to the number of molecules with one hydrogen bond is only valid within a limited temperature interval. For instance differences in mean chain lengths for transfers taking place over chains of hydrogen bridges are not taken into account. Coupling between the breaking of bonds is again disregarded.

5) Eqn. (1) is not quite exact, but assumed to be adequate.

In view of these assumptions and approximations the results obtained should be regarded as of only a semiquantitative nature. However, by plotting $\log u + \log T - \log x(1-x)^3$ against $1/T$, using the values of u given for the H_3O^+ ion by Gierer and Wirtz [1] or by Bjerrum [5] and the values of x given by Grjotheim and Krogh-Moe [4], a straight line is obtained for temperatures up to 200° C. The slope of the line corresponds to an activation energy of 1.7 kcal/mole. This value compares favourably with the values 1.3—2.6 kcal/mole obtained by Grjotheim and Krogh-Moe for the breaking of a bond in water. It should be noted that this value for the hydrogen bond includes only the part of the total interaction responsible for the tetrahedral configuration of the water molecules.

The activation energy for the OH^- ion conductivity is shown to be 0.6 kcal/mole higher than that for the H_3O^+ ion [1]. This means that an OH^- ion cannot have quite the same surroundings on average as the H_3O^+ ion. The energy of the hydrogen bond appears to be slightly different in these two cases. Rather than a single energy, however, we have in these systems an energy distribution. A single hydrogen bond energy seems to be a fairly good approximation, however.

The previous considerations enable us to understand why the extra mobility increases with pressure in a certain temperature range. In this temperature range the breaking of a hydrogen bond results in a decrease in volume [4]. Therefore increased pressure means a smaller number of bonds in the liquid. This leads to a larger number of water molecules with only one bond, as may be seen by introducing into eqn. (2) the appropriate values of x. Consequently an increase in extra mobility with pressure is expected. If the factor $f(T)$ of structural influence in eqn. (1) were proportional to the number of established hydrogen bonds, the pressure dependence of extra mobility could not be explained.

1. Gierer, A. and Wirtz, K. *Ann. Physik* **6** (1949) 257.
2. Gierer, A. and Wirtz, K. *J. Phys. Chem.* **56** (1952) 914.
3. Eucken, A. *Gött. Nach. Math.-phys. Kl.* **1946** 38.
4. Grjotheim, K. and Krogh-Moe, J. *Acta Chem. Scand.* **8** (1954) 1193.
5. Bjerrum, N. *Kgl. Danske Videnskab. Selskab, Mat.-fys. Medd.* **27** (1951) No. 1.

Received January 14, 1956.

The Vitamin Content of Pollen after Storing

NIELS NIELSEN

Research Department, AB Kabi, Stockholm, Sweden

In a previous paper [1] the results of an investigation concerning the content of some B-vitamins in pollen from different plants were given. The samples examined were obtained from *Zea mays*, *Alnus glutinosa*, *A. incana* and *Pinus montana*. The following vitamins were determined: riboflavin, nicotinic acid, pantothenic acid, pyridoxine, biotin and inositol. The determinations were carried out during October

Table 1.

		Zea mays		*Alnus glutinosa*		*Alnus incana*		*Pinus montana*	
		µg/g	%	µg/g	%	µg/g	%	µg/g	%
Riboflavin	1954	6.2		11.2		12.1		5.6	
	1955	6.6	106	11.4	102	8.9	74	3.5	63
Nicotinic acid	1954	71.8		82.7		82.3		79.8	
	1955	65.7	92	73.1	88	79.0	96	64.9	81
Pantothenic acid	1954	12.7		4.2		5.0		7.8	
	1955	9.9	78	0.6	14	1.9	38	5.6	72
Pyridoxine	1954	5.5		5.7		6.8		3.1	
	1955	5.7	104	5.4	95	6.0	88	3.0	97
Biotin	1954	0.55		0.65		0.69		0.62	
	1955	0.50	91	0.67	103	0.65	94	0.70	113
Inositol mg/g	1954	30		3.0		3.5		9.0	
	1955	30	100	2.8	93	3.5	100	8.0	89

and November 1954, shortly after the pollen samples had been collected. The samples were stored in a cool and dry place immediately after collection.

Now, after one year, the pollen samples have been re-examined to determine, whether the vitamin content had changed. Throughout the year the samples were stored in containers in a cool, dry place. The vitamins determined were the same as in the previous investigation. For the methods employed the reader is referred to the paper mentioned [1].

It is evident from the results presented in Table 1 that the stability of the vitamins in the different pollen samples varies greatly. The pantothenic acid content shows a substantial decrease in all the samples, especially in the pollen taken from the two *Alnus* species. For instance in the sample from *A. glutinosa* only 14 % of the pantothenic acid found in 1954 remains. The biotin and inositol content is practically unaltered in all the samples, the variation being within the limits of the accuracy of the analytical methods. The contents of riboflavin, pyridoxine and nicotinic acid remain the same in some samples and show a decrease in others. With the exception of pantothenic acid, the vitamin content of the pollen from *Zea mays* shows hardly any change. On the other hand, in the pollen from *Alnus incana* a marked decrease is seen not only in the pantothenic acid content but also in the amounts of riboflavin and pyridoxine.

The marked decrease found in the pantothenic acid content may prove to be due to a binding of this vitamin and not to its destruction. For the determination of the pantothenic acid no enzymatic liberation was used.

The previous examination [1] of the pollen samples showed that the two samples from *Zea mays* that were collected in 1953 and 1954 contained different amounts of nicotinic acid. It was assumed that this difference might have been due to the storage of the sample collected in 1953, but the results reported here make this explanation unlikely. Therefore the difference found in 1954 must be due to a variation between different samples.

This repeated investigation shows that the stability of vitamins in pollen (in so far as the six vitamins investigated are concerned) depends on the kind of pollen used. The greatest stability is found in pollen from *Zea mays* in which the contents of five of the vitamins remain practically unchanged. The least stable vitamins are found in pollen from *Alnus incana*.

Pantothenic acid seems to be the most unstable vitamin.

1. Nielsen, N., Grömmer, J. and Lundén, R. *Acta Chem. Scand.* **9** (1955) 1100.

Received January 20, 1956.

Effect of some Metal Ions on the Stability of Natural Vitamin A

KARL BACK

Division of Food Chemistry, Royal Institute of Technology, Stockholm, Sweden

Metal ions have been shown to accelerate the oxidation of fat even when present in very small concentrations. As vitamin A is destroyed when the fat in which it is contained turns rancid through oxidation, some experiments have been carried out to investigate the concentrations of some metal ions required to cause a measurable acceleration of the vitamin A destruction.

Fish liver oil concentrates *, containing about 100 000 IU of vitamin A per g, were used in the experiments. The metal ions of the oil samples were removed by percolating a solution of equal parts of oil and propanol-2 (with some benzene added to ensure complete miscibility) through a cation exchanger in the hydrogen form. Solutions of metal chlorides in absolute ethyl alcohol were then added to the samples so that a final concentration of 2 % ethyl alcohol and 1, 10, or 100 parts per million (ppm) of metal ion was obtained. The metals used in these experiments were Al, Cu, Fe, Ni, Sn and Zn. The samples were distributed in a number of vials which were stored for different lengths of time at a temperature of 34.5° C according to the Schaal oven test modified by Simons *et al.*[1]. At intervals two vials of each sample of oil were removed from the oven and individual determinations of the vitamin A content were immediately made.

Vitamin A was determined by measuring the absorption at 312 mμ, 325 mμ (or the absorption maximum in the interval 325 mμ—328 mμ), and 334 mμ of a solution of the oil in hexane, purified by percolation through a column of defatted bone meal according to Dowler and Laughland [2]. The absorption was corrected using the Morton-Stubbs equation and the content of vitamin A was calculated using a conversion factor of 1 900.

* The oil samples were kindly supplied by Kjellbergs Successors AB, Stockholm.

Table 1. The figures in the table represent the ratios of the time for 50 % destruction of vitamin A in oils containing various concentrations of metal ions, to the time for the same destruction of vitamin A in oil containing no metal ions.

Metal ion	Concentration of metal ion, ppm		
	1	10	100
Al	0.9	0.7	0.5
Cu	0.8	0.5	0.5
Fe	1.0	0.7	0.2
Ni	0.9	0.7	0.4
Sn	0.9	0.9	0.7
Zn	0.9	0.9	0.8

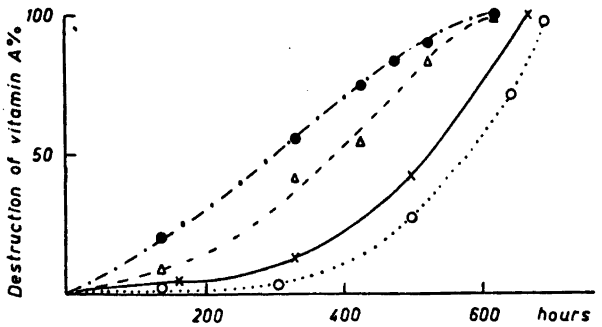


Fig. 1. Destruction of vitamin A in oil from which metal ions had been removed and to which various amounts of Al had been added (as $AlCl_3$). The samples were kept in the dark and exposed to air at 34.5 °C for different lengths of time.

○·····○ *Oil, (metal ions removed)*
×——× " " " " + *1 ppm Al*
△- - - - - -△ " " " " + *10 ppm Al*
●——·——● " " " " +*100 ppm Al*

A typical diagram showing the percentage destruction of vitamin A relative to time is shown in Fig. 1.

The results of the experiments are summarized in Table 1.

It should be emphasized that the figures given in Table 1 are only approximate as they depend on several factors, *e. g.* variations in the composition of different batches of oil, and the storage conditions before testing.

1. Simons, E. J., Buxton, L. O. and Colman, H. B. *Ind. Eng. Chem.* **32** (1940) 706.
2. Dowler, M. W. and Laughland, D. H. *Anal. Chem.* **24** (1952) 1047.

Received February 1, 1956.

*iso*Thiocyanates XVIII. Glucocapparin, a New Crystalline *iso*Thiocyanate Glucoside

ANDERS KJÆR and ROLF GMELIN

Chemical Laboratory of the University of Copenhagen, Denmark

A previous paper of this series [1] described the detection of methyl *iso*thiocyanate as a new natural mustard oil, present in various species of the family *Capparidaceae* as a glucoside, provisionally named *glucocapparin*. We now wish to report on the isolation and characterization of glucocapparin in crystalline condition.

The new glucoside was readily obtained as colourless needles from an extract of seeds of *Cleome spinosa* Jacq., purified as described in the experimental part. The analytical data indicated the composition $C_8H_{14}O_9NS_2K$ for glucocapparin which is the formula expected for a glucoside containing methyl *iso*thiocyanate in the traditional combination with sulphuric acid, potassium and glucose. When glucocapparin was subjected to enzymic hydrolysis, methyl *iso*thiocyanate was liberated and could be identified as *N*-methylthiourea after distillation and treatment with ammonia. The concomitant formation of sulphate and glucose was demonstrated, the latter by paper chromatography in two solvent systems. The ultra-violet absorption spectrum of glucocapparin displayed a maximum at 225 mμ (ε 9 850) in aqueous solution, very similar to the spectra determined in this laboratory for other mustard oil glucosides (Refs. [2,3] and unpublished data). Again, the infra-red absorption spectrum was closely comparable to the spectra of sinigrin [4] and glucoiberin [5], redetermined in this laboratory, a fact suggesting that glucocapparin has a chemical structure closely related to that of other mustard oil glucosides.

For the purpose of further characterization glucocapparin was transformed into a crystalline tetraacetate. That this process was not accompanied by structural changes appeared from the fact that deacetylation with ammonia afforded unchanged glucocapparin as established by the infra-red spectrum and paper chromatography. Recently, acetylation has been successfully employed by Schultz and Wagner [6] for characterizing several mustard oil glucosides as crystalline derivatives.

Glucocapparin adds another representative to the still rather limited group of crystalline *iso*thiocyanate glucosides, heretofore comprising sinigrin, sinalbin, glucocheirolin [7] and glucoiberin [5]. The new glucoside is remarkable in being the first of this type crystallizing without water of crystallization. So far, its known occurrence is limited to species of the family *Capparidaceae*.

Experimental. Isolation. Finely ground seeds (160 g) of *Cleome spinosa* * were extracted with ligroin, containing some *iso*propanol, in order to remove fatty material. The residue (107 g) was subjected to exhaustive extraction, first with 70 % methanol (800 ml) and then with pure methanol (300 ml). The extracts were pooled, a precipitate removed by filtration and the solution concentrated to about 150 ml *in vacuo*. After removal of a new precipitate, the solution was rapidly sucked through a column of neutral aluminium oxide (40 g) in order to remove further impurities. The column was washed with water (100 ml) and the joined filtrate and washing liquid was allowed to flow slowly through another column containing 80 g of anionotropic alumina (Woelm) which quantitatively retained the glucoside [4]. The column was washed with water and then eluted with a 1 % solution of potassium sulphate. The end-point was conveniently estimated by the appearance of a brownish colour in the eluate, emerging simultaneously with the first sulphate ions. The eluate was taken to dryness *in vacuo* and the glucoside separated from traces of inorganic material by repeated

* Commercially obtained from E. Benary, Hann.-Münden, Germany.

A typical diagram showing the percentage destruction of vitamin A relative to time is shown in Fig. 1.

The results of the experiments are summarized in Table 1.

It should be emphasized that the figures given in Table 1 are only approximate as they depend on several factors, *e. g.* variations in the composition of different batches of oil, and the storage conditions before testing.

1. Simons, E. J., Buxton, L. O. and Colman, H. B. *Ind. Eng. Chem.* **32** (1940) 706.
2. Dowler, M. W. and Laughland, D. H. *Anal. Chem.* **24** (1952) 1047.

Received February 1, 1956.

*iso*Thiocyanates XVIII. Glucocapparin, a New Crystalline *iso*Thiocyanate Glucoside

ANDERS KJÆR and ROLF GMELIN

Chemical Laboratory of the University of Copenhagen, Denmark

A previous paper of this series [1] described the detection of methyl *iso*thiocyanate as a new natural mustard oil, present in various species of the family *Capparidaceae* as a glucoside, provisionally named *glucocapparin*. We now wish to report on the isolation and characterization of glucocapparin in crystalline condition.

The new glucoside was readily obtained as colourless needles from an extract of seeds of *Cleome spinosa* Jacq., purified as described in the experimental part. The analytical data indicated the composition $C_8H_{14}O_9NS_2K$ for glucocapparin which is the formula expected for a glucoside containing methyl *iso*thiocyanate in the traditional combination with sulphuric acid, potassium and glucose. When glucocapparin was subjected to enzymic hydrolysis, methyl *iso*thiocyanate was liberated and could be identified as *N*-methylthiourea after distillation and treatment with ammonia. The concomitant formation of sulphate and glucose was demonstrated, the latter by paper chromatography in two solvent systems. The ultra-violet absorption spectrum of glucocapparin displayed a maximum at 225 mμ (ε 9 850) in aqueous solution, very similar to the spectra determined in this laboratory for other mustard oil glucosides (Refs. [2,3] and unpublished data). Again, the infra-red absorption spectrum was closely comparable to the spectra of sinigrin [4] and glucoiberin [5], redetermined in this laboratory, a fact suggesting that glucocapparin has a chemical structure closely related to that of other mustard oil glucosides.

For the purpose of further characterization glucocapparin was transformed into a crystalline tetraacetate. That this process was not accompanied by structural changes appeared from the fact that deacetylation with ammonia afforded unchanged glucocapparin as established by the infra-red spectrum and paper chromatography. Recently, acetylation has been successfully employed by Schultz and Wagner [6] for characterizing several mustard oil glucosides as crystalline derivatives.

Glucocapparin adds another representative to the still rather limited group of crystalline *iso*thiocyanate glucosides, heretofore comprising sinigrin, sinalbin, glucocheirolin [7] and glucoiberin [5]. The new glucoside is remarkable in being the first of this type crystallizing without water of crystallization. So far, its known occurrence is limited to species of the family *Capparidaceae*.

Experimental. Isolation. Finely ground seeds (160 g) of *Cleome spinosa* * were extracted with ligroin, containing some *iso*propanol, in order to remove fatty material. The residue (107 g) was subjected to exhaustive extraction, first with 70 % methanol (800 ml) and then with pure methanol (300 ml). The extracts were pooled, a precipitate removed by filtration and the solution concentrated to about 150 ml *in vacuo*. After removal of a new precipitate, the solution was rapidly sucked through a column of neutral aluminium oxide (40 g) in order to remove further impurities. The column was washed with water (100 ml) and the joined filtrate and washing liquid was allowed to flow slowly through another column containing 80 g of anionotropic alumina (Woelm) which quantitatively retained the glucoside [4]. The column was washed with water and then eluted with a 1 % solution of potassium sulphate. The end-point was conveniently estimated by the appearance of a brownish colour in the eluate, emerging simultaneously with the first sulphate ions. The eluate was taken to dryness *in vacuo* and the glucoside separated from traces of inorganic material by repeated

* Commercially obtained from E. Benary, Hann.-Münden, Germany.

extractions with hot methanol. The organic solvent was removed, leaving a colourless lac which was dissolved in hot 80 % ethanol. Upon cooling and scratching crystals separated (330 mg); pure glucocapparin (271 mg) was obtained as glistening, colourless needles after recrystallization from 80 % ethanol. The above procedure could most likely be modified to give an improved yield of glucocapparin, but no systematic studies were performed with this aim.

Properties of glucocapparin. Glucocapparin decomposes gradually above 198°. Its rotation was determined in aqueous solution, $[\alpha]_D^{25}$ —28.6° ± 1.5° (c = 2.2). (Found: C 25.90; H 3.96; N 3.71; S 17.47. Calc. for $C_8H_{14}O_9NS_2K$: C 25.86; H 3.80; N 3.77; S 17.27). The infra-red spectrum, determined in a KBr pellet, displayed prominent bands at 2.80 (v.s., OH-stretching), 6.28 (m.), 6.93 (m.), 7.17 (w.), 7.31 (w.), 7.51 (m.), 7.72 (s.), 7.82 (s.), 8.14 (v.s., broad), 8.87 (w.) *, 9.00 (w.) *, 9.16 (s.), 9.34 (v.s.), 9.46 (v.s.), 9.74 (s.) **, 10.87 (m.), 11.27 (s.) and 12.43 μ (v.s.).

Glucocapparin (50 mg) was dissolved in a phosphate buffer of pH 6.6 (2 ml) and a drop of a myrosinase solution was added. Next day, the *iso*thiocyanate was removed by distillation and transformed into its thiourea-derivative with ammonia. The thiourea was identified as *N*-methylthiourea on paperchromatographic comparison with an authentic specimen in two solvent systems, *viz.* water-saturated chloroform and *n*-butanol-ethanol-water (4:1:4). Furthermore, the ultra-violet absorption spectrum coincided with that of authentic *N*-methylthiourea. The latter exhibited a maximum at 235 mμ (ε 11 900) and a minimum at 218 mμ (ε 6 300) in water.

An enzymically hydrolyzed solution of glucocapparin (5 mg) was taken to dryness and the residue extracted with methanol. The insoluble part was dissolved in water and the presence of sulphate ions demonstrated as $BaSO_4$. The methanolic extract was chromatographed on paper in two solvent systems, *viz.* *n*-butanol-ethanol-water (4:1:4) and pyridine-amyl alcohol-water (35:30:30), and the presence of glucose established by comparison with authentic specimens.

Glucocapparin-tetraacetate. A solution of glucocapparin in dry pyridine and excess acetic anhydride was kept at 50° for 3 hours. A large volume of ether was added to the pink solution, resulting in precipitation of the crystalline acetyl-derivative, which was recrystallized twice from methanol and separated as tiny, colourless needles, m. p. 209—210° (uncorr., decomp.); $[\alpha]_D^{25}$: —31.0° ± 1.5° (c = 1.82, water). (Found ***: C 35.63; H 4.21; N 2.42; S 11.68. Calc. for $C_{16}H_{22}O_{13}NS_2K$: C 35.62; H 4.21; N 2.60; S 11.88). In aqueous solution the ultra-violet absorption spectrum of the tetraacetate was similar to that of glucocapparin, possessing λ_{max}: 221 mμ (ε_{max} 9 340)[4]. The infra-red spectrum (in KBr) had conspicuous bands at: 5.72 (v.s., ester CO-band), 6.93 (m.), 7.24 (s.), 7.70 (s.), 8.09 (v.s., broad), 9.12 (m.), 9.37 (v.s.), 9.50 (s., plateau), 10.92 (m.), 11.23 (s.) and 12.90 μ (s., broad).

Glucocapparin-tetraacetate (60 mg) was dissolved in anhydrous methanol, saturated with ammonia at 0°, and kept at room temperature. Next day, the solvent was removed and the residue recrystallized from aqueous ethanol to give glucocapparin (33 mg, 80 %), identified by its infra-red spectrum and paperchromatographic comparison. R_F-values of 0.06 and 0.44 were determined in descending paper chromatograms at 24° on Whatman paper No. 1 for glucocapparin and its tetraacetate, respectively, with *n*-butanol-ethanol-water (4:1:4) as a solvent system.

Microanalyses were performed in this laboratory by Mr. P. Hansen. The work is part of investigations supported by *Statens Almindelige Videnskabsfond (The Danish State Research Foundation)* and *Carlsbergfondet (The Carlsberg Foundation)*.

1. Kjær, A., Gmelin, R. and Larsen, I. *Acta Chem. Scand.* **9** (1955) 857.
2. Kjær, A., Gmelin, R. and Boe Jensen, R. *Acta Chem. Scand.* **10** (1956) 26.
3. Kjær, A., Gmelin, R. and Boe Jensen, R. *Acta Chem. Scand. In press.*
4. Gmelin, R. *Präparative und analytische Versuche über Senfölglucoside* (Diss.) University, Tübingen 1954.
5. Schultz, O.-E. and Gmelin, R. *Arch. Pharm.* **287/59** (1954) 404.
6. Schultz, O.-E. and Wagner, W. *Arch. Pharm.* **288/60** (1955) 525.
7. Schneider, W. and Schütz, L. A. *Ber.* **46** (1913) 2634.

* Probably C—O-stretching- (or OH-deformation-)modes of secondary OH-groupings; the bands disappear on acetylation.

** Probably C—O-stretching-(or OH-deformation-) mode of the primary OH-grouping; the band disappears on acetylation.

*** As also experienced elsewhere [6], attempted O-acetyl determinations on this and other glucoside acetates consistently gave too high values.

Received February 18, 1956.

Estimation of Microquantities of Thiocholine Esters

EDITH HEILBRONN

Research Institute of National Defence, Dept. 1, Sundbyberg 4, Sweden

In order to determine the spontaneous hydrolysis and the initial enzymatic hydrolysis of several thiocholine esters an exact method for their quantitative analysis was sought for. The method developed by Hestrin [1] for the estimation of choline esters and other carboxylic acid derivatives was tried and was found to be applicable to the thiocholine esters as well.

This method makes use of the fact that choline esters react quantitatively with hydroxylamine in alkaline solution according to the following scheme

$$RCOOR' + H_2NOH \rightarrow RCONHOH + R'OH$$

The resulting hydroxamic acid can be determined by the coloured complex with ferric chloride in acid solution.

The thiocholine esters used in this investigation, except acetylthiocholine iodide, were synthesized by Hansen [2]. The following esters were used:

acetylthiocholine iodide
acetyl-α-methylthiocholine bromide
acetyl-β-methylthiocholine bromide
propionylthiocholine bromide
butyrylthiocholine bromide
valerylthiocholine bromide
benzoylthiocholine bromide

Experimental. The same reagents as in Hestrin's method [1] for carboxylic acid derivatives were used.

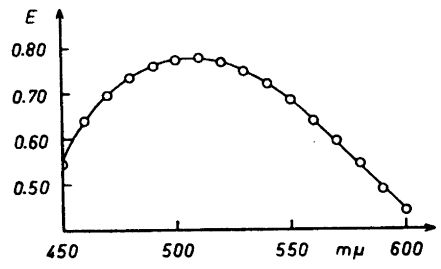


Fig. 1. Absorption curve of the ironhydroxamic acid complex.

Standard solutions: 0.5—10.0 mmole thiocholine ester in Clark and Lubs' [3] phosphate buffer solution at pH 8.00 or in barbital buffer solution [4] at pH 8.07 were used.

The buffer solutions were allowed to reach the thermostat temperature in a volumetric flask. The thiocholine esters were weighed excluding moisture as much as possible and rapidly dissolved in the buffer solution. 1.00 ml of the samples was immediately withdrawn and analysed according to the method developed by Hestrin [1]. The colour was measured in a 10 mm cell with a Beckman B spectrophotometer.

Table 1. Extinction of different concentrations of acetylthiocholine iodide in phosphate buffer solution after varying reaction time with hydroxylamine.

Acetylthiocholine iodide mmole/l	*E* time in min. 1	2	3
10	1.800	1.815	1.807
8	1.441	1.439	1.433
6	1.080	1.072	1.075
4	0.720	0.720	0.741
2	0.365	0.366	0.369
1	0.184	0.186	0.190
0.5	0.093	0.095	0.097

Results. The absorption maximum for the coloured complex was found to be at 510 mμ as shown in Fig. 1.

The reaction with hydroxylamine was carried out for 1, 2 and 3 minutes at room temperature. The extinction appears to be independent of time after 1 minute as can be seen from Table 1. The variation of optical density with ester concentration is shown in Fig. 2 for acetylthiocholine iodide and benzoylthiocholine bromide. It appears from these curves that Lambert Beer's law is obeyed. The lower limit of measurement is about 0.05×10^{-3} mmole of final solution. The upper limit exceeds 2×10^{-3} mmole of final solution. At concentrations of 6×10^{-3} mmole of final solution and above, a precipitate, which is very difficult to centrifuge off, was observed. The precipitate may be sulfur.

The molar extinction coefficient, ε, of the two thiocholine esters was calculated

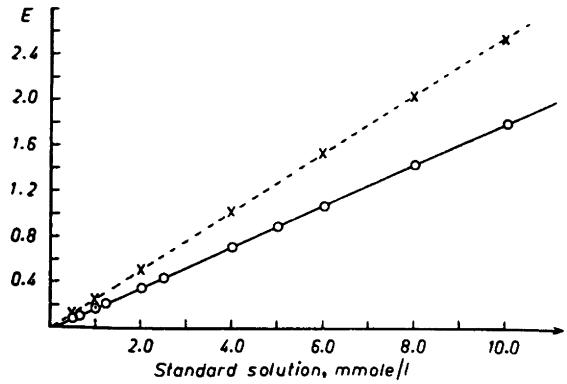


Fig. 2. Density of colour as a function of thiocholine ester concentration.

×--× *benzoylthiocholine bromide*
O—O *acetylthiocholine iodide*

Table 2. Chromogenic activity per thiocholine ester equivalent. Acetylthiocholine iodide = 100.

Compound	Chromogenic activity
Acetyl-α-methyl thiocholine bromide	100
Propionylthiocholine bromide	100
Butyrylthiocholine bromide	104
Valerylthiocholine bromide	104
Benzoylthiocholine bromide	143

from the calibration curves by the equation:

$$E = c \cdot d \cdot \varepsilon$$

where c = mole/l standard solution and d = thickness of the layer in cm. The extinction coefficient was found to be 1.80×10^2 l mole^{-1} cm^{-1} for acetylthiocholine iodide and 2.55×10^2 l mole^{-1} cm^{-1} for benzoylthiocholine bromide. The chromogenic activity of the analysed thiocholine esters is seen from Table 2.

The colour of acetylthiocholine iodide was also determined in barbital buffer solution. The extinction obtained in this case was about 3 % lower than in phosphate buffer solution. Small amounts of protein, enough for determination of enzymatic hydrolysis, did not disturb the reactions.

My sincere thanks are due to Professor G. Ljunggren, Director of the Research Institute of National Defence, Dept. 1, and to Professor A. Tiselius, Director of the Institute of Biochemistry, University of Uppsala, for their kind interest in this work.

1. Hestrin S. *J. Biol. Chem.* **180** (1949) 249.
2. Hansen, B. *To be published.*
3. Clark and Lubs; Kolthoff, J. M. *Die kolorimetrische und potentiometrische pH-Bestimmung*, Berlin 1932, p. 34.
4. Heilbronn, E. *Scand. J. Clin. Lab. Invest.* **5** (1953) 308.

Received February 16, 1956.

Reduction of some Haemo Proteins by Ultraviolet Light

JAN SCHUBERTH

Medicinska Nobelinstitutet, Biokemiska avdelningen, Stockholm, Sweden

During some experiments with oxygen-free solutions of ferrimyoglobin exposed to CO it was noticed that the spectrum of ferrimyoglobin was not stable but slowly changed to that of MgbCO. Apparently ferrimyoglobin was reduced to ferromyoglobin, which subsequently reacted with CO. An examination of the actual conditions revealed that occasional irradiation

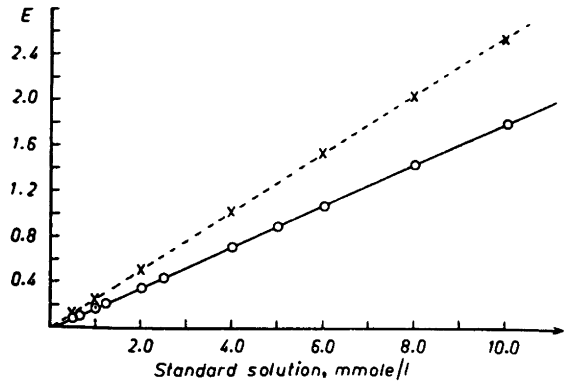


Fig. 2. Density of colour as a function of thiocholine ester concentration.

×--× *benzoylthiocholine bromide*
O—O *acetylthiocholine iodide*

Table 2. Chromogenic activity per thiocholine ester equivalent. Acetylthiocholine iodide = 100.

Compound	Chromogenic activity
Acetyl-α-methyl thiocholine bromide	100
Propionylthiocholine bromide	100
Butyrylthiocholine bromide	104
Valerylthiocholine bromide	104
Benzoylthiocholine bromide	143

from the calibration curves by the equation:

$$E = c \cdot d \cdot \varepsilon$$

where c = mole/l standard solution and d = thickness of the layer in cm. The extinction coefficient was found to be 1.80×10^2 l mole^{-1} cm^{-1} for acetylthiocholine iodide and 2.55×10^2 l mole^{-1} cm^{-1} for benzoylthiocholine bromide. The chromogenic activity of the analysed thiocholine esters is seen from Table 2.

The colour of acetylthiocholine iodide was also determined in barbital buffer solution. The extinction obtained in this case was about 3 % lower than in phosphate buffer solution. Small amounts of protein, enough for determination of enzymatic hydrolysis, did not disturb the reactions.

My sincere thanks are due to Professor G. Ljunggren, Director of the Research Institute of National Defence, Dept. 1, and to Professor A. Tiselius, Director of the Institute of Biochemistry, University of Uppsala, for their kind interest in this work.

1. Hestrin S. *J. Biol. Chem.* **180** (1949) 249.
2. Hansen, B. *To be published.*
3. Clark and Lubs; Kolthoff, J. M. *Die kolorimetrische und potentiometrische pH-Bestimmung*, Berlin 1932, p. 34.
4. Heilbronn, E. *Scand. J. Clin. Lab. Invest.* **5** (1953) 308.

Received February 16, 1956.

Reduction of some Haemo Proteins by Ultraviolet Light

JAN SCHUBERTH

Medicinska Nobelinstitutet, Biokemiska avdelningen, Stockholm, Sweden

During some experiments with oxygen-free solutions of ferrimyoglobin exposed to CO it was noticed that the spectrum of ferrimyoglobin was not stable but slowly changed to that of MgbCO. Apparently ferrimyoglobin was reduced to ferromyoglobin, which subsequently reacted with CO. An examination of the actual conditions revealed that occasional irradiation

with ultraviolet light had caused the reduction. Some preliminary experiments have been performed on ferrimyoglobin, ferrihaemoglobin, ferricytochrome c, and catalase.

Methods. A low pressure water-conditioned mercury lamp was used as the UV source. The solutions were irradiated in a 1 cm Beckman quartz cell connected to the different gas tanks *via* a stopcock system. The specimen was introduced into the cuvette, the system evacuated and flushed with argon 4—5 times. In some experiments argon was replaced by CO in the last filling. The cuvette was kept at a distance of 7 cm from the arc. Na-phosphate buffer (pH 7.1, 0.05 M) was used as solvent.

The concentrations of the haem proteins were for myoglobin 70, haemoglobin 50, cytochrome c 50, and for catalase 20 μM (2 μM for experiments in the Soret band region). During the irradiations readings were taken at regular intervals at suitable wavelengths in a Beckman DU spectrophotometer.

Photoreduction of ferrimyoglobin. After ten minutes 50 % and after 25 min. 90 % of the ferri-Mgb had been reduced and converted to MgbCO, as calculated from the light absorptions at 580 mμ. The addition of dithionite raised the optical density at 580 mμ to the value calculated for complete conversion to MgbCO. If no CO was present a haemochromogene type spectrum was obtained with maxima corresponding to those of $MgbO_2$. The very low concentration of oxygen decreased during irradiation as determined polarographically. This was probably due to the fact that the minute amounts of oxygen present at the beginning of the experiments were gradually taken up by Mgb. There did not seem to be any liberation of oxygen during irradiation. The addition of catalase did not influence the reaction velocity.

Photoreduction of ferrihaemoglobin. Half reduction and conversion to HbCO was obtained after 10 min. and 80 % HbCO after 20 min. Addition of dithionite gave a 7 % too low value, probably due to destruction. Irradiated Hb showed, within the errors of the method, the same affinity for CO as Hb, reduced with dithionite.

Photoreduction of ferricytochrome c. No CO was present in these experiments. Ferricytochrome was half reduced after 12 minutes and 75 % reduced after 20 min. (followed at 549.5 mμ). In this reaction cytochrome c seemed to be highly sensitive even to traces of oxygen. It was in no case possible to obtain the expected light absorption at 549.5 mμ by reduction with dithionite of an irradiated solution. Between 10—15 % of the total cytochrome seemed to have been destroyed. The maxima of the absorption bands of photoreduced cytochrome c were found at 549.5 mμ and 520.5 mμ, exactly in the same positions as those of cytochrome c reduced with dithionite.

Photoreduction of catalase. During the irradiation of liver catalase a change in the absorption spectrum could be noticed and after 45 min. weak absorption bands at 550 mμ and 580 mμ could be observed. In the absence of CO no spectral change was seen. In the presence of dithionite (which does not reduce catalase but acts as an oxygen remover) and without CO a broad absorption band at about 560 mμ appeared. Upon the addition of CO to this solution the same spectrum appeared as obtained without dithionite but with CO initially present. During irradiation in the presence of dithionite the Soret band maximum at 405 mμ shifted to 422 mμ and became somewhat reduced in height. In this case CO partly reversed the shift, from 422 to 418 mμ. The changes of the catalase caused by the irradiation seemed to be fully reversible. Contact with air restored the initial density value at 575 mμ. The activities of a specimen [1] before and after its irradiation with UV light were the same.

A detailed report of these experiments will be published shortly. The investigations are being continued.

1. Bonnichsen, R. K., Chance, B. and Theorell, H. *Acta Chem. Scand.* **1** (1947) 685.

Received February 21, 1956.

The Reaction Between Thiocyanogen and Azide Ions

N. HOFMAN-BANG

Chemistry Department A, Technical University of Denmark, Copenhagen, Denmark

Iodine, as triiodide ions, does not react with azide ions to give nitrogen and iodide ions. However, sulphidic sulphur does catalyze this reaction [1]. Browne *et al.* [2,3] showed that bromine and chlorine give fine analogous bromine- and chlorine-azide reactions, but controlling experiments showed that bromine and chlorine together with sodium azide alone, give slow evolutions of nitrogen. Recently Griffith and Irving [4] have investigated the bromine-azide reaction catalyzed by thiosulphate and by tetrathionate, and the direct reaction between bromine and azide ions.

Taking into consideration that the redox potentials of chlorine, bromine, iodine and thiocyanogen are, respectively, −1.36, −1.07, −0.54 and −0.77 volts, it seems quite possible that thiocyanogen, which often behaves like a halogen, will oxidize azide ions to nitrogen.

Thiocyanogen, $(SCN)_2$, was prepared as a carbon tetrachloride solution according to Söderbäck [5]. This solution, when brought into contact with aqueous sodium azide solution, gave a brisk evolution of gas, while, at the same time, some decomposition of thiocyanogen took place. The gas evolved in the following experiment was analyzed according to Christiansen and Wulff [6]. 25 ml 1 M aqueous solution of sodium azide was allowed to react with 25 ml about 1 M solution of thiocyanogen in carbon tetrachloride. The gas evolved was collected over water and paraffin oil, the latter solvent to extract vapours of carbon tetrachloride in the gas. Analysis of the gas gave the results:

99.6 % N_2 and 0.5 % O_2
99.7 % N_2 and 0.4 % O_2

The reaction is presumably:

$$(SCN)_2 + 2\ N^-_3 \rightarrow 2\ SCN^- + 3\ N_2$$

As thiocyanogen as well as thiocyanate ions catalyze the iodine-azide reaction, it is not unlikely that the above reaction is catalyzed by thiocyanogen as well as by thiocyanate ions. Until now attempts to obtain a homogeneous reaction between thiocyanogen and azide ions in non-aqueous solution have not succeeded.

1. Raschig, F. *Chem. Ztg.* **32** (1908) 1203.
2. Browne, A. W. and Hoel, A. B. *J. Am. Chem. Soc.* **44** (1922) 2315.
3. Browne, A. W., Hoel, A. B., Smith, G. B. L. and Swezey, F. H. *J. Am. Chem. Soc.* **45** (1923) 2541.
4. Griffith, R. O. and Irving, R. *Trans. Faraday Soc.* **45** (1949) 563.
5. Söderbäck, E. *Ann.* **419** (1919) 217.
6. Christiansen, J. A. and Wulff, I. *Kgl. Danske Videnskab. Selskab, Mat.fys. Medd.* **22** (1945) No. 4.

Received February 21, 1956.

ACTA CHEMICA SCANDINAVICA 10 (1956) 341—352

Studies on the Extraction of Metal Complexes

XXXI. Investigations with some 5,7-Dihalogen Derivatives of 8-Quinolinol

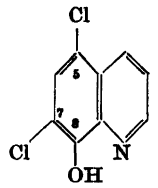
DAVID DYRSSEN, MARGARETA DYRSSEN and EBBE JOHANSSON

Research Institute of National Defence, Dept. 1 (FOA 1), Sundbyberg 4; Department of Inorganic Chemistry, Royal Institute of Technology, Stockholm 70, Sweden

Some equilibrium constants describing the chloroform extraction of La(III), Th(IV) and U(VI) complexes with the 5,7-dichloro, 5,7-dibromo, 5,7-diiodo and 5-chloro-7-iodo derivatives of 8-quinolinol (oxine) have been investigated at 25 °C. The ionic strength in the aqueous phase was kept constant at 0.1 M. The overall equilibrium constant K (eqn. 8) for the extraction of metal complexes is increased by halogen substitution of the reagent (Table 6). This effect, which is very pronounced for thorium, is discussed in terms of the separate dissociation and distribution equilibria (eqns. 2—6). The dihalogen substituted oxines are stronger acids than oxine, but the mean complexity constant, $\sqrt[N]{\varkappa_N} = 10^a$, for the complex formation of thorium ($N = 4$) with dichloro-oxine is about the same ($10^{9.90}$) as with oxine ($10^{9.80}$). The distribution constants of both the reagent, k_d, and of the metal complex, λ_4, are increased by halogen substitution. The molar solubilities of the dihalogen reagents in chloroform are considerably smaller (<0.06 M) than the solubility of oxine (2.63 M), whereas thorium dichloro-oxinate is much more soluble in chloroform (0.0135 M) than is thorium oxinate (0.00088 M). A favorable property of the 5,7-dihalogen derivatives is the fact that they are not extracted as oxinium ions from chloroform by moderately acidic solutions (Fig. 1). Our studies suggest that 5,7-dichloro-oxine may often be preferable to ordinary oxine as a reagent for solvent extraction.

An important aspect of our studies on the extraction of inner complexes of the lanthanides and actinides is to investigate the influence of the structure of the chelating agent. This may be done both by investigating various types of reagents and by studying derivatives of one particular compound. In this paper, the results obtained with some 5,7-dihalogen derivatives of oxine are reported. Moeller and Jackson [1] have previously pointed out that 5,7-dichloro-oxine is preferable to oxine for the extraction of neodymium and er-

bium. Recently Rulfs, De, Lakritz and Elving [2] state that oxine is a better reagent than its dichloro and dibromo derivatives for the extraction of uranium(VI).



5,7-dichloro-oxine

The effect of structural changes in a reagent on the various factors that govern metal extraction has been discussed by Martell and Calvin [3]. We shall extend their discussion somewhat, using our own symbols and apply it to the dihalogenated derivatives of oxine.

One may regard the extraction of a metal ion M^{N+} with an organic reagent HA as a stepwise complex formation of M^{N+} with the ligand ion A^- giving among other complexes an uncharged extractable complex MA_N. If the complexes in the aqueous phase are neglected, the distribution ratio is given by

$$q = [MA_N]_{org}/[M^{N+}] \tag{1}$$

The ligand concentration $[A^-]$ is determined by the reagent concentration and the pH as well as by the two dissociation constants

$$k_1 = [H^+]\,[HA]\,/\,[H_2A^+] \text{ and } k_2 = [H^+]\,[A^-]\,/\,[HA] \qquad (2,\ 3)$$

and the distribution constant

$$k_d = [HA]_{org}\,/\,[HA] \tag{4}$$

The formation of MA_N is determined by the complexity product

$$\varkappa_N = \frac{[MA_N]}{[M^{N+}]\,[A^-]^N} \tag{5}$$

and the distribution of MA_N by the distribution constant

$$\lambda_N = [MA_N]_{org}\,/\,[MA_N] \tag{6}$$

For a given system the main experimental variables governing q are generally the reagent concentration $[HA]_{org}$ and the hydrogen ion concentration $[H^+]$ (pH). Thus using eqns. (3)—(6) we may transform (1) to

$$q = \frac{[HA]^N_{org}}{[H^+]^N} \cdot \varkappa_N \cdot \lambda_N \cdot \left(\frac{k_2}{k_d}\right)^N \tag{7}$$

The overall equilibrium constant K we then define by

$$K = \varkappa_N \cdot \lambda_N \cdot \left(\frac{k_2}{k_d}\right)^N \tag{8}$$

Although halogen substitution would be expected to increase both the dissociation constant k_2 of the reagent, and the distribution constant λ_N of the uncharged metal complex, these changes will probably be offset by an increase in the distribution constant k_d of the reagent (*cf. e. g.* Collander [4]) and possibly also by a decrease in the complexity constant $\varkappa_N$. The total effect on the extraction constant K may therefore be rather small.

Eqn. (7) is based on the approximation that the organic phase contains only the uncharged complex MA_N, and the aqueous phase only the uncomplexed metal ion M^{N+}. As has been pointed out by Dyrssen and Sillén [5], eqn. (7) corresponds to the asymptote

$$\log q = \log \lambda_N + \log \varkappa_N + N \log [A^-] \quad (9)$$

to the distribution curve log q *versus* log $[A^-]$ (see Fig. 2 and 3).

Using eqns. (7) and (8), we may in many cases obtain an approximate value of the pH (— log $[H^+]$) for 50 % extraction ($q = 1$):

$$\log [H^+] = \frac{1}{N} \log K + \log [HA]_{org} \quad (10)$$

Since the tendency for the lanthanide and actinide ions to form inner complexes is rather small compared with their tendency to hydrolyze, it is important to extract in a low pH range; *i. e.* a high value of $\frac{1}{N}$ log K and of the reagent concentration $[HA]_{org}$ is desirable.

EXPERIMENTAL

Many details in the experimental technique are described in previous parts in this series. As usual, the measurements were carried out at 25 °C, and — log $[H^+]$ denotes the hydrogen ion concentration. The ionic strength was kept constant at 0.1 M by the addition of Na^+ or ClO_4^- ions.

Reagents. The chloroform was saturated with water and alcohol-free, and the methyl *iso*butyl carbinol (hexol) was shaken with a 10 % sodium bicarbonate solution. 8-Quinolinols of analytical quality were purchased from Merck-Darmstadt (oxine) and Schuchardt, and were used without further purification. Pure 5,7-dichloro-oxine was however prepared according to Berg [6]. Other reagents were of analytical grade.

Measurements on the oxines. The solubilities in chloroform were obtained by weighing after careful evaporation of the chloroform at 40—50° C. The solubility of 5,7-dichloro-oxine was checked by diluting 1 ml of a saturated solution to 250 ml and determining the concentration by spectrophotometric analysis at 330 mμ. This method gave a solubility of 0.0584 M, which agreed well with the value obtained by weighing (see p. 346).

The values of (pk_2 + log k_d) were obtained by shaking 15 ml of a 0.01—0.05 M chloroform solution of the dihalogen substituted oxine with 15 ml of a 0.1 M sodium borate-perchlorate buffer (— log $[H^+]$ = 9.50—9.60, 0.05 M in boric acid + sodium borate). The oxine concentration in the aqueous phase ($\cong [A^-]$) was determined spectrophotometrically at 350—370 mμ. The values of (pk_1—log k_d) were determined in a similar manner by shaking with 0.1 M perchloric acid. The determination of the oxine concentration in the aqueous phase ($\cong [H_2A^+]$) was carried out at 370 mμ.

The distribution constants k_d were determined by shaking 50 ml of a 0.01—0.05 M chloroform solution of the dihalogen substituted oxine with 900 ml of 0.1 M $NaClO_4$ + 100 ml of 0.1 M phthalate buffer (pH = 5) previously saturated with chloroform. The

Table 1. Distribution of U(VI) between 0.05 M solutions of 5,7-dichloro-oxine in chloroform and 0.1 M $HClO_4$—$NaClO_4$ solutions at 25 °C. Initial concentration of U in the aqueous phase = 1.33 · 10^{-4} M.

A_{390}	log q *	—log [H+]	—log [A⁻] **
0.104	−1.00	1.48	11.09
0.315	−0.42	1.70	10.87
0.514	−0.09	1.88	10.69
0.690	+0.19	2.03	10.54
0.880	+0.53	2.21	10.36
1.07	+1.18	2.53	10.04

* q was calculated from the measured absorbancy A_{390} as $q = A_{390}/(1.140 - A_{390})$.
** —log [A⁻] = log [H+] + 12.57 (eqn. 11).

aqueous phase was centrifuged, 250—750 ml were drawn off and shaken with 10 ml of fresh chloroform. The oxine concentration in this chloroform layer was determined spectrophotometrically at 325—340 mμ.

If 25 cm cuvettes are available, an alternative method is quite useful for the determination of k_d. Ten ml of a 0.01—0.05 M solution of the dihalogen substituted oxines in the organic solvent is shaken with 99 ml of 0.1 M $NaClO_4$ + 1 ml of 0.1 M phthalate buffer (pH = 5). The aqueous phase is centrifuged and acidified to pH = 1 with 1 ml conc. $HClO_4$. The oxine concentration of this solution is determined spectrophotometrically at 370 mμ. This method was used with hexol.

Extraction of the metals. The use of small amounts of buffering substances such as 1 ml of 0.1 M anilinium perchlorate, sodium acetate, hydrazinium perchlorate, or ammonium perchlorate per 15 ml, does not appear to have any

Table 2. Distribution of La(III) between 0.05 M solutions of 5,7-dichloro-oxine in chloroform and 0.1 M $NaClO_4$ at 25 °C. Initial concentration of La—^{140}La in the aqueous phase ~10^{-5} M

I_{org} cpm	I_{aq} cpm	log q *	—log [H+]	—log [A⁻] **
68.0	8 385	−2.01	5.15	7.42
85.4	8 096	−1.90	5.19	7.38
232	7 834	−1.45	5.35	7.22
690	22 075	−1.43	5.16	7.41
1 391	18 679	−1.05	5.42	7.15
872	6 068	−0.76	5.46	7.11
7 821	11 042	−0.07	5.66	6.91
5 865	2 181	+0.51	6.12	6.45
14 521	725	+1.38	6.27	6.30
8 824	389	+1.43	6.51	6.06
5 502	35.5	+2.27	6.94	5.63
8 560	44.4	+2.36	6.61	5.96

* $q = 1.20 \cdot I_{org}/I_{aq}$ (*cf.* Part XVII [16]).
** —log [A⁻] = log [H+] + 12.57 (eqn. 11).

Table 3. Distribution of Th(IV) between chloroform and perchlorate solutions at 25 °C as a function of the concentration of the 5,7-dichloro-oxinate ion in the aqueous phase. Initial concentration of Th— ^{234}Th in the aqueous phase ~10^{-6} M.

$[HA]_{org}$ M	I_{org} cpm	I_{aq} cpm	log q *	—log [H+]	—log [A^-] **
0.05	257	21 104	−1.89	1.02	11.55
»	340	5 207	−1.16	1.21	11.36
»	1 249	4 252	−0.50	1.52	11.05
»	10 863	8 036	+0.16	1.71	10.86
»	3 670	900	+0.64	1.80	10.77
»	4 160	252	+1.25	2.08	10.49
»	4 229	51.4	+1.94	2.37	10.20
»	4 397	8.8	+2.73	3.00	9.57
0.02	11.4	18 143	−3.17	1.11	11.86
»	51.4	17 759	−2.51	1.28	11.69
»	205	16 635	−1.88	1.55	11.42
»	2 522	14 700	−0.74	1.88	11.09
»	7 994	7 667	+0.05	2.15	10.82
»	10 408	5 524	+0.30	2.25	10.72
»	11 302	4 112	+0.47	2.43	10.54
»	14 222	599	+1.40	2.89	10.08
»	12 768	166	+1.91	3.26	9.71
0.01	7.2	7 991	−3.02	1.50	11.77
»	61.0	6 306	−1.99	1.82	11.45
»	196	6 731	−1.51	2.12	11.15
»	422	5 308	−1.07	2.20	11.07
»	1 044	4 930	−0.65	2.38	10.89
»	2 428	2 510	+0.01	2.62	10.65
»	4 361	442	+1.02	2.95	10.32
»	4 396	422	+1.05	3.17	10.10

* $q = (1.067 \pm 0.010) \cdot I_{org}/I_{aq}$ (*cf.* Part XXI[17]).
** $-\log[A^-] = \log[H^+] - \log[HA]_{org} + 11.27$ (eqn. 11).

influence on the extraction. The pH and the volume of the solution were adjusted with 0.1 M $HClO_4$, NaOH and $NaClO_4$.

The distribution ratios of La and Th were measured radiometrically using ^{140}La and ^{234}Th (UX_1) as tracers. The distribution of U(VI), however, was determined spectrophotometrically at 390 mμ with a Beckman DU spectrophotometer with 1 cm cells, using a 0.05 M solution of 5,7-dichloro-oxine of chloroform in the blank cell. With this technique, the following values for the molecular extinction coefficient were obtained:

$\varepsilon \cdot 10^{-4}$ M^{-1}	0.816	0.821	0.855	0.818	0.738	0.646
λ mμ	370	380	390	400	410	420

The absorbancy of the blank became too high below 370 mμ. Moeller and Ramaniah [8] have pointed out that the determinations, which are made on steep parts of the absorption curves, will be very sensitive to small errors in

Table 4. Distribution of Th(IV) between 0.01 M solutions of 5,7-dichloro-oxine in hexol and 0.1 M perchlorate solutions at 25 °C as a function of the 5,7-dichloro-oxinate ion concentration in the aqueous phase. Initial concentration of Th—^{234}Th in the aqueous phase ~$5 \cdot 10^{-6}$ M.

I_{org} cpm	I_{aq} cpm	log q **	—log [H+]	—log [A⁻] ***
16.6	4 237	−2.46	1.59	11.02
50.4	4 522	−2.00	1.71	10.90
194	4 376	−1.40	1.93	10.68
483	4 758	−1.04	2.12	10.49
1 099	3 124	−0.50	2.22	10.39
2 512	2 659	−0.08	2.37	10.24
4 600	717	+0.77	2.78	9.83
5 693	106	+1.68	3.39	9.22
6 631	16.2	+2.56	4.42	8.19
6 457	14.3	+2.60	4.83	7.78
6 861 *	12.5 *	+2.69	5.44	7.17
6 944 *	16.6 *	+2.57	6.27	6.34
8 619 *	12.3 *	+2.80	7.28	5.33
6 791 *	13.5 *	+2.65	7.32	5.29
8 300 *	11.3 *	+2.82	7.39	5.22
8 436 *	12.1 *	+2.79	7.56	5.05

* Values on the plateau used for the calculation of $\lambda_4 = 0.89 \cdot 45\,951/78.3 = 10^{2.72}$.
** $q = 0.89 \cdot I_{org}/I_{aq}$.
*** $-\log[A^-] = \log[H^+] + 12.61$ (eqn. 11).

wave-length setting. This objection is, however, not serious since the wave-length is not altered in shifting from the blank to the sample. The free ligand concentration was calculated from the relationship

$$\log[A^-] = \log[HA]_{org} - \log\,[H^+] - pk_2 - \log\,k_d \qquad (11)$$

SOME PROPERTIES OF THE OXINES

It is clear from the introductory discussion that a high value of $[HA]_{org}$ favors the extraction of the metal. A limit is of course set by the solubility of the reagent in wet chloroform. The following solubilities were obtained at 25° C:

Oxine	(M.W. 145.15):	2.63 ± 0.08 M
5,7-Dichloro-oxine	(M.W. 214.05):	0.0587 ± 0.0003 M
5,7-Dibromo-oxine	(M.W. 302.97):	0.0302 ± 0.0003 M
5,7-Diiodo-oxine	(M.W. 396.97):	0.0109 ± 0.0003 M
5-Chloro-7-iodo-oxine	(M.W. 305.51):	0.0585 ± 0.0003 M

The solubility of 5,7-dichloro-oxine in hexol is only 0.0119 M.

In this respect the dichloro and chloro-iodo compounds are the best extracting agents of these dihalogen substituted oxines. They are, however, about 45 times less soluble in chloroform than is oxine itself.

Table 5. Stoichiometric acid dissociation constants and chloroform/water distribution constants of oxine and some of its 5,7-dihalogen derivatives at 25 °C. Ionic strength in the aqueous phase = 0.1 M.

Constants	5,7-Substituent				
	H, H	Cl, Cl	Br, Br	I, I	Cl, I
$pk_2 + \log k_d$	12.24	*11.27* [c]	*11.47*	*12.15*	*11.79*
$\log k_d$	*2.58* [a]	*3.86±0.06* [d]	*4.15±0.1* [d]	*4.15±0.1*	*3.88±0.1*
pk_2	*9.66* [b]	7.4 [e]	7.3	8.0	7.9
$pk_1 - \log k_d$	+2.42	*−0.92*	*−1.59*	*−1.43*	*−1.20*
pk_1	*5.00* [b]	2.9 [e]	2.6	2.7	2.7

Values determined experimentally are given in italics; where not stated they have an error of ±0.01−0.02 units.

a) This distribution ratio is shown to be somewhat dependent on $[HA]_{org}$: 2.61 at 0.1 M, 2.64 at 0.2 M and 2.70 at 0.5 M.
b) Reported in Part IV [9].
c) A value of 11.28 was obtained by a two-phase titration (*cf.* Part IV [9]).
d) For hexol we obtained 3.14 (dichloro-oxine) and 3.36 ± 0.09 (dibromo-oxine).
e) From thermodynamic dissociation constants given by Näsänen [10] (2.887 and 7.617 at 25 °C) one may calculate $pk_1 = 2.89$ and $pk_2 = 7.47$.

The ligand concentration is also determined by the two-phase dissociation constant k_2/k_d. In the discussion above it is emphasized that an increase in k_2/k_d is desirable, provided the decrease in $\varkappa_N \cdot \lambda_N$ is not too large. Table 5 shows that 5,7-dichloro-oxine has the most favorable value ($10^{-11.27}$); the value for oxine being about 10 times less.

A valuable property of the dihalogen compounds is their very low values of $(pk_1 - \log k_d)$ in comparison with unsubstituted oxine (see Table 5). This means that while oxine is extracted out of the chloroform phase into moderately acidic solutions (pH < 3) as an oxinium salt, its dihalogen derivatives will show this behavior only in very acidic solutions (pH < −0.5; see Fig. 1).

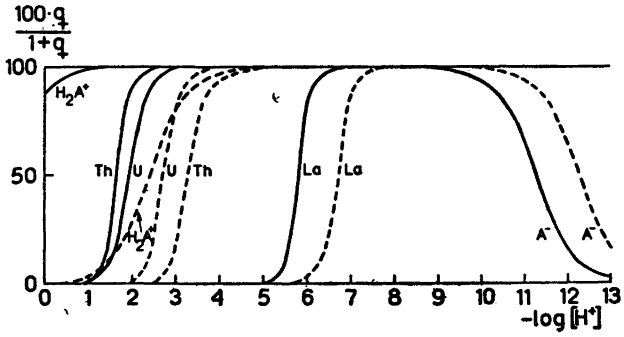


Fig. 1. Comparison of oxine (dashed curves) and 5,7-dichloro-oxine (full curves) as extracting agents. The distribution of La(III), Th(IV) and U(VI) is calculated for the case where a 0.05 M solution of the reagent in chloroform is shaken with an equal volume of an aqueous solution. The H_2A^+ and A^- curves show the extraction of the oxines into the aqueous phase as oxinium and oxinate ions.

The values of the dissociation constants k_1 and k_2 in Table 5 emphasizes the well-known fact (*cf. e. g.* Watson [11]) that the influence of halogen substituents on aromatic nuclei cannot be expressed completely in terms of their inductive effects. The order of pk_1, Br $\sim$ I $<$ Cl, and of pk_2, Br $\sim$ Cl $<$ I, was also found by Feldman and Powell [12] for the 7-halogen derivatives of 8-quinolinol-5-sulfonic acid. It may be assumed from data reported by Minegishi and Nagakura [13] and by Judson and Kilpatrick [14] on monochloro phenols that the lowering of pk_2 of oxine by halogen substitution is primarily due to the 7-substituent.

Since the values of k_d are so very large for the dihalogen compounds, it was very difficult to obtain accurate results for these distribution constants. This uncertainty is reflected in the values of pk_1 and pk_2 calculated from the two-phase dissociation constants $k_1 \cdot k_d$ and k_2/k_d. Table 5, however, shows that there is a more than tenfold increase of k_d on substitution.

EXTRACTION OF La(III), Th(IV) AND U(VI)

The results given in the preceding section show that the 5,7-dihalogen substituted oxines are much stronger acids than unsubstituted oxine. We also found larger distribution constants k_d with the dihalogen substituted compounds. In the introductory discussion it was indicated that one might expect analogous changes for the metal chelate, *i. e.* a decrease in $\varkappa_N$ and an increase in λ_N, thus leaving the overall equilibrium constant K unchanged.

The results of an investigation of UO_2^{2+}, La^{3+} and Th^{4+} with 5,7-dichloro-oxine are given in Tables 1, 2 and 3 and summarized in Table 6 and Fig. 1. These results show that for the same initial concentration of reagent in the chloroform phase (*e. g.* 0.05 M), 5,7-dichloro-oxine extracts in a lower pH range than oxine (Fig. 1); *i. e.*, $\frac{1}{N} \log K$ has increased on halogen substitution (Table 6). The effect ($\Delta \frac{1}{N} \log K$) is in fact so large for Th^{4+} *that it reverses its position in relation to* UO_2^{2+} (Fig. 1).

Eqn. (8) can be written as

$$\frac{1}{N} \log K = \frac{1}{N} \log \varkappa_N \cdot \lambda_N - (pk_2 + \log k_d) \qquad (12)$$

Table 6. Comparison of some chloroform extraction constants for oxine and 5,7-dichloro-oxine.

Metal	N	$\frac{1}{N} \log \varkappa_N \cdot \lambda_N$		$\Delta \frac{1}{N} \log \varkappa_N \cdot \lambda_N$	$\frac{1}{N} \log K$		$\Delta \frac{1}{N} \log K$
		H, H	Cl, Cl		H, H	Cl, Cl	
U (VI)	2	11.03	10.64	−0.39	−1.21 *	−0.63	0.58
La (III)	3	7.02	6.79	−0.23	−5.22 **	−4.48	0.74
Th (IV)	4	10.46	11.05	+0.59	−1.78	−0.22	1.56

* Calculated from data on 0.05 M oxine in Part VIII [15].
** Calculated from data in Part XVII [16].

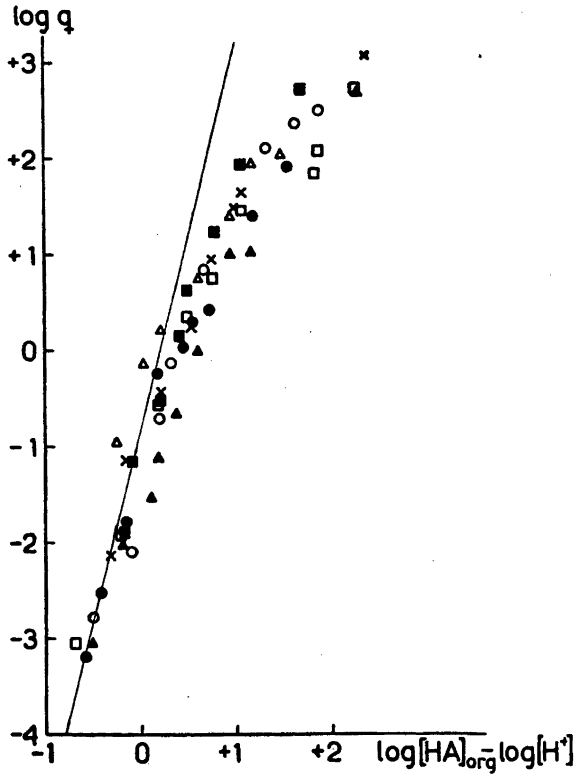


Fig. 2. Comparison of some 5,7-dihalogen substituted oxines as extracting agents for thorium. The distribution ratio of Th—^{234}Th between chloroform and 0.1 M perchlorate solutions is given as a function of $\log[HA]_{org} - \log[H^+]$ *(*$= \log[A^-] + pk_2 + \log k_d$*). Dihalogen derivative and its total concentration in the organic phase (*$[HA]_{org}$*): dichloro: ■ 0.05 M, ● 0.02 M, ▲ 0.01 M; dibromo: □ 0.02 M; diiodo: ○ 0.01 M; chloro-iodo: △ 0.05 M, × 0.02 M.*

and thus values of $\frac{1}{N} \log \varkappa_N \cdot \lambda_N$ may be calculated using the values of ($pk_2 + \log k_d$) given previously in Table 5. The values of $\frac{1}{N} \log \varkappa_N \cdot \lambda_N$ are given in Table 6. As λ_N probably is larger for the 5,7-dichloro-oxinates, it seems as if the complexity products $\varkappa_N$ of UO_2^{2+} and La^{3+} are smaller with dichloro-oxine than with oxine. In order to evaluate $\varkappa_4$ and λ_4 for Th^{4+} a separate investigation was carried out using hexol (methyl *iso*-butyl carbinol) as a solvent. The results are reported below.

Fig. 2 shows the results obtained with Th^{4+} and the various 5,7-dihalogen substituted oxines. The distribution ratio q of Th^{4+} between chloroform and the aqueous phase does not obey eqn. (7) with $\frac{1}{4} \log K = -0.22$, but as was pointed out in the introduction this line should be regarded as an asymptote,

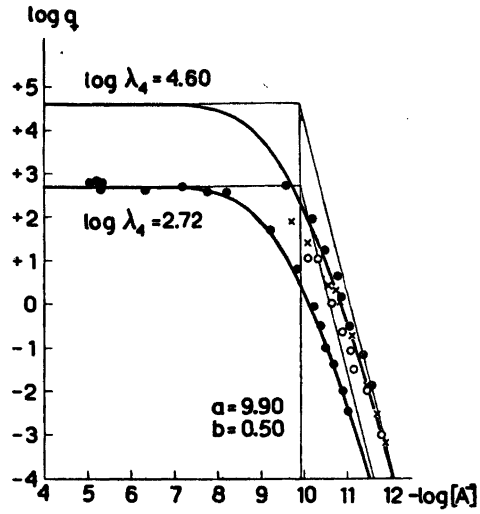


Fig. 3. The distribution ratio of Th as a function of the 5,7-dichloro-oxinate ion concentration in the aqueous phase. Hexol: ● 0.01 M dichloro-oxine; chloroform: ⊗ 0.05 M, × 0.02 M and ○ 0.01 M dichloro-oxine.

and the deviation is undoubtedly due to the presence of Th complexes in the aqueous phase. Values outside log $q = \pm 3.2$ are not included since they are rather unreliable. Furthermore it seems as if there is no significant difference between the dihalogen substituted compounds in this plot. This means that the values of $\frac{1}{4}$ log K are about the same and consequently that according to eqn. (12) the values of $\frac{1}{4}\log \varkappa_4 \cdot \lambda_4$ are shifted by an amount equal to the changes of their ($pk_2 + \log k_d$) values. One might then be tempted to think that equal shifts in the constants for the proton complexes, k_2 and k_d, and in the constants for the thorium complexes, $\sqrt[4]{\varkappa_4} = 10^a$ and $\sqrt[4]{\lambda_4}$, compensate each other.

COMPLEX FORMATION OF THORIUM WITH 5,7-DICHLORO-OXINE

In order to evaluate $\frac{1}{4}$ log $\varkappa_4$ and $\frac{1}{4}$ log λ_4 separately for thorium, 5,7-dichloro-oxine was studied using hexol (methyl *iso*butyl carbinol) as a solvent. Hexol was chosen instead of chloroform so that log λ_4 would be lower and in a measurable range of log q. However, the solubility of 5,7-dichloro-oxine is much lower in hexol (0.0119 M) than in chloroform (0.0587 M). The solubility of hexol in water is only 1.6 % and should not affect $\varkappa_4$ very much.

The results with hexol are given in Table 4 and plotted in Fig. 3 together with the chloroform data. The thick curves in Fig. 3 are calculated with the

parameters (*cf.* Part V[5]) $a = 9.90$, $b = 0.50$, $\log \lambda_4 = 2.72$ (hexol) and $\log \lambda_4 = 4.6$ (chloroform) and have consequently the same shape. The thin lines represent the asymptotes to the distribution curves,

$$\log q = \log \lambda_4 \quad \text{and} \tag{13}$$
$$\log q = \log \varkappa_4 + \log \lambda_4 + 4 \log[A^-] \tag{9a}$$

A reinvestigation of the thorium-oxine-chloroform system (*cf.* Part VI [7]) gave $a = 9.80$, $b = 0.35$ and $\log \lambda_4 = 2.63$. Within a reasonable limit of error in a ($\pm$ 0.05 or 0.10) we may say that there is no significant difference between the mean complexity constants ($= 10^a$) for the thorium complexes of oxine and of 5,7-dichloro-oxine. This result was not expected, and cannot alone form a basis for a theoretical discussion. Future investigations may show if it is merely an exception. We may note that the dichloro-oxinate of thorium is much more soluble in chloroform (0.0135 M) than is the oxinate (0.00088 M).

GENERAL CONCLUSIONS

The extraction properties of the dihalogen substituted oxines investigated here are very much alike. The pH range for the extraction of La(III), Th(IV) and U(VI) with chloroform is lower for dichloro-oxine than for oxine itself. The effect is very large for Th^{4+} (1.56 pH units), but not so large for La^{3+} (0.74) and UO_2^{2+} (0.58). A very favorable property of the 5,7-dihalogen substituted oxines is that they form oxinium ions (H_2A^+) only in very acidic solutions (Fig. 1). Furthermore, the solubility of the thorium complex in chloroform is increased many fold on dichloro substitution.

To summarize, we believe that the 5,7-dihalogen substituted oxines have certain advantages over oxine as solvent extraction agents, and would repay more general use in the future. The 5,7-dichloro compound is preferred because it has the largest solubility in chloroform, and because it is very simple to prepare the pure reagent from oxine [6] with a good yield.

We wish to thank Professor G. Ljunggren and Professor L. G. Sillén for their interest in this work, which has partly been supported by *Atomkommittén*.

REFERENCES

1. Moeller, T. and Jackson, D. E. *Anal. Chem.* **22** (1950) 1393.
2. Rulfs, C. L., De, A. K., Lakritz, J. and Elving, P. J. *Anal. Chem.* **27** (1955) 1802.
3. Martell, A. E. and Calvin, M. *Chemistry of the Metal Chelate Compounds*, Prentice Hall, New York, 1952.
4. Collander, R. *Acta Chem. Scand.* **3** (1949) 717.
5. Dyrssen, D. and Sillén, L. G. *Acta Chem. Scand.* **7** (1953) 663.
6. Berg, R. *Die analytische Verwendung von o-Oxychinolin ("Oxin") und seiner Derivate*, Ferdinand Enke Verlag, Stuttgart 1938.
7. Dyrssen, D. *Svensk Kem. Tidskr.* **65** (1953) 43.
8. Moeller, T. and Ramaniah, M. V. *J. Am. Chem. Soc.* **76** (1954) 5251.
9. Dyrssen, D. *Svensk Kem. Tidskr.* **64** (1952) 213.
10. Näsänen, R. *Suomen Kemistilehti* **26B** (1953) 69.

11. Watson, H. B. *Modern Theories of Organic Chemistry*, Oxford University Press, Oxford, 1941.
12. Feldman, H. B. and Powell, A. L. *J. Am. Chem. Soc.* **62** (1940) 3107.
13. Minegishi, A. and Nagakura, S. *J. Chem. Soc. Japan* **75** (1954) 891.
14. Judson, C. M. and Kilpatrick, M. *J. Am. Chem. Soc.* **71** (1949) 3110.
15. Dyrssen, D. and Dahlberg, V. *Acta Chem. Scand.* **7** (1953) 1186.
16. Dyrssen, D. *Svensk Kem. Tidskr.* **66** (1954) 234.
17. Dyrssen, D. *Acta Chem. Scand.* **9** (1955) 1567.

Received January 21, 1956.

ACTA CHEMICA SCANDINAVICA 10 (1956) 353—359

Studies on the Extraction of Metal Complexes

XXXII. N-Phenylbenzohydroxamic Acid

DAVID DYRSSEN

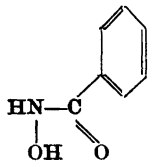
Research Institute of National Defence, Dept 1 (FOA 1), Sundbyberg, Sweden

N-Phenylbenzohydroxamic acid (PBHA) has been investigated at 25 °C as a solvent extraction agent for La(III), Th(IV) and U(VI). Chloroform was used as the organic solvent and the ionic strength in the aqueous phase was kept constant at 0.1 M by addition of $HClO_4$ and $NaClO_4$. The values of $\frac{1}{N}\log K$ (eqn. 3) for La, Th and U are -4.80, -0.17 and -1.57, respectively. Fig. 1 shows that Th and U may easily be separated from La by batch extraction, while a good separation of Th and U would require a simple extraction column.

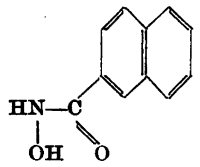
The stoichiometric dissociation constant k_a of PBHA is $10^{-8.15\pm0.01}$ and its distribution constant k_d between chloroform and water is $10^{2.33\pm0.01}$. The mean complexity constant 10^{α} for the formation of Th *tetra*-N-phenylbenzohydroxamate is $10^{9.45}$ and the distribution constant λ_4 of this complex between chloroform and water is $10^{3.45\pm0.03}$.

Benzohydroxamic acid (BHA) and α-naphtohydroxamic acid (NHA) have been used [1] for the extraction of trivalent lanthanide and actinide ions. Shome [2] has pointed out that a stable compound, N-phenylbenzohydroxamic acid (PBHA) was obtained, if the nitroso group in cupferron (N-nitrosophenylhydroxylamine) was substituted with benzoyl, and Lutwick and Ryan [3] have prepared several of these hydroxamic acids (or aromatic hydroxylamines). In Part VIII [4] of this series it was shown that cupferron was a very good reagent for the extraction of the tetravalent ions Hf^{4+} and Th^{4+}.

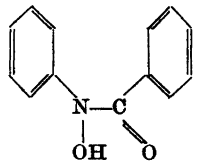
These were the main facts that led to the investigation of N-phenylbenzohydroxamic acid (or N-benzoylphenylhydroxylamine) as a solvent extraction agent for lanthanide and actinide ions. The complex formation and partition of Th phenylbenzohydroxamate was studied in some detail. The dissociation and distribution constants of PBHA were determined so that the free ligand concentration $[A^-]$ could be calculated.



BHA



NHA



PBHA

EXPERIMENTAL

N-Phenylbenzohydroxamic acid (N-benzoylphenylhydroxylamine) was kindly prepared Mr. Bertil Takman and Mr. Sven Lindström, University of Stockholm. They used Shome's modification [2] of Bamberger's [5] method. The product was, however, finally recrystallised from benzene. M. p. 121 °C. (Found: C 73.2; H 5.0; N 6.6. Calc. for $C_{13}H_{11}NO_2$: C 73.2; H 5.2; N 6.6). Chemicals used were of analytical grade, and the chloroform was saturated with water and alcohol-free.

Values of k_a and k_a/k_d were determined by means of the titration technique described in Part IV [6]. However, saturated KCl was used in the reference electrode instead of 0.1 M $NaClO_4$/4 M NaCl. The light absorption curve of PBHA in 0.005 M $HClO_4$ + 0.095 M $NaClO_4$ has a peak at 253 mμ with an extinction coefficient of $0.765 \cdot 10^4$ M^{-1}. Alkaline solutions of PBHA are however yellow. The distribution constants k_d between chloroform and 0.005 M $HClO_4$ + 0.095 M $NaClO_4$ ($-\log[H^+] = 2.30$) were determined for 0.1—0.02 M solutions of PBHA in chloroform by measuring the hydroxamic acid concentration in the aqueous phase at 250—280 mμ with a Beckman Model DU spectrophotometer (1 cm cells).

The radioisotopes ^{140}La and ^{234}Th (UX_1) were employed for the determination of the distribution of La(III) and Th(IV). The distribution of U(VI) was, however, determined in the following way: a 5 ml portion of the 10 ml aqueous phase was removed, and the pH of the solution was adjusted to about 3.3 with 0.1 M sodium acetate. The solution was then shaken with 5 ml of 0.05 M 5,7-dichloro-oxine in chloroform and the absorbancy of the chloroform layer was measured at 390 mμ (*cf.* Part XXXI [7]).

The ionic strength of the aqueous phase was kept constant at 0.1 M by addition of 0.1 M solutions of $HClO_4$, $NaClO_4$ and NaOH. In the distribution measurements of La, Th and U the aqueous phase was sometimes buffered with 1 ml of 0.1 M anilinium perchlorate, sodium acetate or hydrazinium perchlorate per 15 ml. The hydrogen ion concentration, $[H^+]$, was measured with a Radiometer pHM3i potentiometer equipped with glass and calomel electrodes, which were standardized against a 0.01 M $HClO_4$ + 0.09 M $NaClO_4$ buffer ($-\log[H^+] = 2.00$).

All experiments were carried out in thermostated rooms at 25.0 ± 0.3 °C.

THE DISSOCIATION AND DISTRIBUTION CONSTANTS OF PBHA

The dissociation constant k_a and distribution constant k_d of PBHA are given in Table 4 together with the solubilities in chloroform and in 0.005 M $HClO_4$ + 0.095 M $NaClO_4$. The thermodynamic dissociation constant K_a may be calculated as $10^{-8.30}$ using activity coefficients given by Conway [10]. This value seemed much too low in comparison with the value $10^{-6.7}$ for benzohydroxamic acid, reported by Oliveri-Mandalá [11]. Recently Wise [12] has shown, however, that the values calculated from electrical conductance measurements of Oliveri-Mandalá were about a hundred times larger than his potentiometric data. Wise reports $10^{-8.88}$ for the mixed (Brönsted) dissociation constant of benzohydroxamic acid at 20 °C and ionic strength 0.005 M. No values of the dissociation and distribution constants of PBHA have been reported. The value of k_d seemed to increase slightly with the concentration of PBHA in chloroform (0.02—0.1 M). This effect was, however, almost entirely concealed by the experimental error (±0.01) in the determination of log k_d. A two-phase titration (*cf.* Part IV [6]) of 50 ml of 0.01 M PBHA in chloroform gave pk_a + log k_d = 10.46, in good agreement with the separate determinations of pk_a and log k_d. The value of the solubility of PBHA in water, given in Table 4 is in good agreement with the value, 0.40 g/l (0.0019 M), reported by Lutwick and Ryan [3].

Table 1. Distribution of La-^{140}La between 0.1 M solutions of PBHA in chloroform and 0.1 M sodium perchlorate solutions at 25 °C.

Initial conc. of La in the aq. phase M · 10^5	I_{org} cpm	I_{aq} cpm	log q *	—log[H$^+$]	—log [A$^-$]
14.0	36.3	4 959	−2.06	5.04	6.44
14.0	53.8	4 705	−1.86	5.13	6.35
14.0	201	4 429	−1.26	5.42	6.06
0.15	1 774	5 929	−0.44	5.45	6.03
16.4	2 670	15 591	−0.69	5.53	5.95
16.4	6 783	11 189	−0.14	5.81	5.67
7.0	8 241	1 544	+0.81	6.12	5.36
7.0	9 452	387	+1.47	6.35	5.13
14.0	3 791	67.8	+1.83	6.61	4.87
7.0	10 683	126	+2.01	6.62	4.86

* $q = 1.20 \cdot I_{org}/I_{aq}$ (*cf.* Part XVII [8]).

Table 2. Distribution of U(VI) between chloroform and 0.1 M $HClO_4$—$NaClO_4$ solutions at 25 °C as a function of the N-phenylbenzohydroxamate ion concentration in the aqueous phase. Initial concentration of uranium in the aqueous phase 10^{-4} M.

Initial conc. of PBHA in the org. phase M	log q	—log[H$^+$]	—log[A$^-$]
0.2	−1.15	1.71	9.47
0.2	−0.53	2.00	9.18
0.2	−0.35	2.08	9.10
0.2	−0.08	2.22	8.96
0.2	+0.25	2.39	8.79
0.2	+0.45	2.51	8.67
0.2	+0.74	2.65	8.53
0.1	−1.20	2.04	9.44
0.1	−0.95	2.10	9.38
0.1	−0.51	2.23	9.25
0.1	−0.32	2.39	9.09
0.1	+0.11	2.68	8.80
0.1	+0.41	2.89	8.59
0.1	+1.17	3.36	8.12

THE EXTRACTION OF La(III), Th(IV) AND U(VI)

The results for the extraction of La^{3+}, Th^{4+} and UO_2^{2+} are given in Fig. 1 and in Tables 1—3. The ligand concentration [A$^-$] is calculated from the equation

$$-\log [A^-] = \log [H^+] - \log [HA]_{org} + pk_a + \log k_d \qquad (1a)$$

Introducing the values of pk_a and $\log k_d$ from Table 4:

$$-\log [A^-] = \log [H^+] - \log [HA]_{org} + 10.48 \qquad (1b)$$

As the distribution constant k_d for PBHA is so large, the initial reagent concentration in chloroform is $\approx [HA]_{org}$, provided that the pH in the aqueous phase is not too high (<9). Fig. 1 shows that the La, U and Th may be extrac-

Table 3. Distribution of Th—^{234}Th between chloroform and 0.1 M $HClO_4$—$NaClO_4$ solutions at 25 °C as a function of the N-phenylbenzohydroxamate ion concentration in the aqueous phase (—log[A^-]).

Initial conc. of ^{232}Th in the aq.phase [a] M · 10^6	Initial conc. of PBHA in the org.phase M	I_{org} [b] cpm	I_{aq} [b] cpm	log q [c]	—log[H^+]	—log[A^-]
1.33	0.1	831	2 311	−0.42	1.20	10.28
1.33	0.1	1 236	1 675	−0.10	1.22	10.26
1.33	0.1	2 255	815	+0.47	1.57	9.91
2.67	0.1	4 946	284	+1.27	1.91	9.57
1.33	0.1	2 838	68.5	+1.64	2.20	9.28
2.67	0.1	5 242	61.9	+1.96	2.70	8.78
2.67	0.1	5 064	9.4	+2.76	3.39	8.09
2.67	0.1	4 964	8.5	+2.79	3.42	8.06
2.67	0.1	4 911	4.5	+3.07 [d]	4.77	6.71
4	0.1	6 667	1.3	+3.74 [d]	5.18	6.30
4	0.1	6 509	−0.2	— [d]	7.46	4.02
4	0.1	6 250	2.3	+3.46 [d]	8.69	2.78
2.67	0.1	4 906	2.2	+3.38 [d]	8.88	2.59
1.33	0.05	359	16 612	−1.64	1.02	10.76
0.67	0.05	318	10 919	−1.51	1.02	10.76
0.67	0.05	795	10 652	−1.10	1.19	10.59
0.67	0.05	2 077	8 999	−0.61	1.48	10.30
0.67	0.05	6 448	4 384	+0.20	1.88	9.90
0.67	0.05	9 834	1 275	+0.92	2.19	9.59
0.67	0.05	11 278	341	+1.55	2.49	9.29
1.33	0.05	20 218	87.0	+2.39	2.89	8.89
1.33	0.05	20 748	28.4	+2.89	3.11	8.67
1.33	0.05	20 788	14.0	+3.20	3.49	8.29
1.33	0.05	20 272	15.3	+3.15	4.01	7.77
1.33	0.05	17 288	16.7	+3.04	4.19	7.59
1.33	0.05	13 805	7.7	+3.28 [d]	6.76	5.02
1.33	0.05	14 306	4.5	+3.53 [d]	7.26	4.52
1.33	0.05	15 361	5.4	+3.48 [d]	7.86	3.92
0.67	0.025	4.5	10 016	−3.32	1.04	11.04
1.33	0.025	36.4	16 793	−2.64	1.13	10.95
1.33	0.025	27.5	9 707	−2.52	1 28	10.80
1.33	0.025	235	16 210	−1.81	1.49	10.59
1.33	0.025	795	15 472	−1.26	1.69	10.39

a) The measured radioactivity from a 10^{-6} M Th solution is only 0.026 cpm.

b) The standard deviation of I for values <100 cpm is $\sqrt{I}/\sqrt{10}$ cpm.

c) $q = (1.067 \pm 0.010) \cdot I_{org}/I_{aq}$ (*cf.* Part XXI [9]).

d) The distribution constant λ_4 was calculated from these eight measurements:

$$\lambda_4 = \frac{72\,715}{27.7 \pm 1.7} \cdot (1.067 \pm 0.010) = 10^{3.45 \pm 0.03}$$

Table 4. Properties of N-phenylbenzohydroxamic acid (PBHA).

Stoichiometric dissociation constant pk_a in 0.1 M $NaClO_4$	8.15 ± 0.01
Distribution constant log k_d between chloroform and 0.005 M $HClO_4$ + 0.095 M $NaClO_4$	2.33 ± 0.01
Solubility in chloroform (aq)	0.739 M
Solubility in 0.005 M $HClO_4$ + 0.095 M $NaClO_4$	0.00195 M

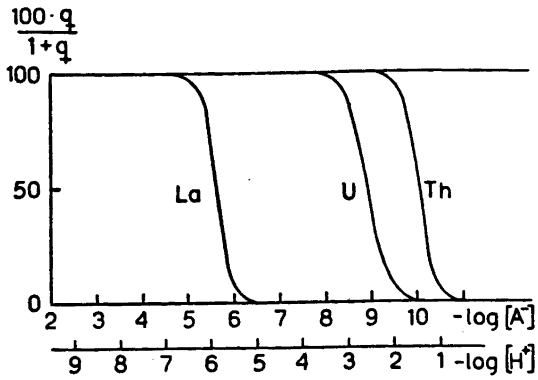


Fig. 1. The distribution of La(III), U(VI) and Th(IV) between chloroform and 0.1 M perchlorate solutions as a function of the N-phenylbenzohydroxamate ion concentration in the aqueous phase. The corresponding values of —log [H⁺] are calculated for 0.1 M PBHA in chloroform.

ted very well with chloroform, using PBHA as a complexing agent. As usual lanthanum is extracted in a much higher pH-range (higher range of log [A⁻]) than uranium and thorium, and may well be separated from the latter elements by a single extraction at pH = 4.5 with a 0.1 M solution of PBHA in chloroform. A good separation of U and Th would however require some degree of fractionation. Compared with cupferron (*cf.* Part VIII[4]) PBHA is a much more stable compound, and the extraction of La(III) and U(VI) is very much better.

If the distribution data on lanthanum (Table 1) and uranium (Table 2) are plotted against log [A⁻], they will fit rather well to straight lines with slopes

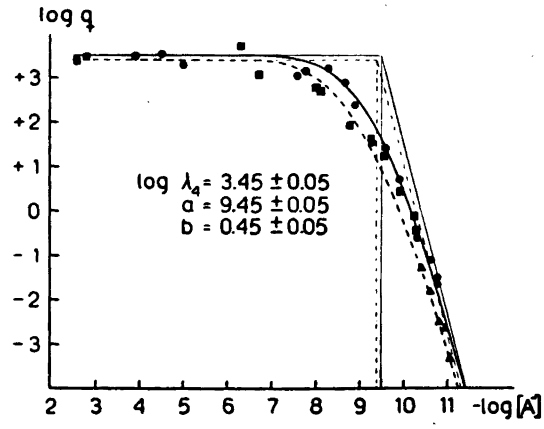


Fig. 2. The distribution ratio of Th(IV) as a function of the N-phenylbenzohydroxamate ion concentration in the aqueous phase. The curves are drawn with two sets of parameters (see text). Total concentration of PBHA in chloroform: ■ 0.1 M, ● 0.05 M, ▲ 0.025 M.

equal to 3 and 2. The general equation for these lines is (eqn. 9 in Part XXXI [7] or eqn. 7 in Part V[13])

$$\log q = \log \varkappa_N \lambda_N + N \log[A^-] \quad (2)$$

Thus for La^{3+} ($N = 3$) one obtains

$$\log \varkappa_3 \lambda_3 = 17.04$$

and for UO_2^{2+} ($N = 2$)

$$\log \varkappa_2 \lambda_2 = 17.82$$

The data for thorium, which are plotted in Fig. 2, cannot be represented by eqn. (2) and this undoubtedly is due to the presence of thorium complexes in the aqueous phase. Using the value of $\log \lambda_4 = 3.45 \pm 0.03$ calculated in Table 3, the two-parameter method described in Part V[13] gave the following values:

$$a = \frac{1}{4} \log \varkappa_4 = 9.45$$

$$b = 0.45$$

The two parameters a and b determine the mean complexity constant 10^a ($= \sqrt[N]{\varkappa_N}$) and the mean spreading factor 10^{2b} ($= k_n/k_{n+1}$).

In order to estimate the limits of error of the parameters two curves are drawn in Fig. 2; the full curve has $a = 9.50$, $b = 0.40$ and $\log \lambda_4 = 3.50$, and the dashed curve has $a = 9.40$, $b = 0.50$ and $\log \lambda_4 = 3.40$. As all of the points do not fall inside these two curves, the errors in each of these constants may be somewhat larger than ± 0.05.

The value of a for PBHA is definitely higher than for tropolone [9] ($a = 8.14$), but somewhat lower than for oxine [1] ($a = 9.80$). All these reagents form five-membered chelate rings. A summary of our work will be published shortly [14], where these values will be discussed together with data for other reagents.

In Part XXXI [7] the overall equilibrium constant K was defined, and it was stated that the pH for 50 % extraction was approximately determined by the terms $\log [HA]_{org}$ and

$$\frac{1}{N} \log K = \frac{1}{N} \log \varkappa_N \lambda_N - (pk_a + \log k_d) \quad (3)$$

The following values of $\frac{1}{N} \log K$ may be calculated using eqn. (3)

La(III):	—4.80
U(VI):	—1.57
Th(IV):	—0.17

If these values are compared with those for other reagents [14], it is found that the values for La(III) and Th(IV) are rather favorable; aromatic N-substituted hydroxamic acids (keto hydroxylamines) may prove to be a very useful group of compounds for the extraction of tri- and tetravalent lanthanide and actinide ions.

The author wishes to thank the head of FOA 1, Professor Gustaf Ljunggren for his interest in these studies, and Mr. Bengt Carlsson and Mr. Ebbe Johansson for their technical assistance.

Part of this work was carried out at the Department of Inorganic Chemistry, Royal Institute of Technology, with financial support from *Atomkommittén*. Sincere thanks are due to Professor Lars Gunnar Sillén for his advice, and to Mrs. Margareta Dyrssen for her technical assistance.

REFERENCES

1. *The Transuranium Elements, N.N.E.S. IV—14B*, p. 166 and 1 359, Mc Graw-Hill Book Co., New York, 1949.
2. Shome, S. C. *Analyst* **75** (1950) 27.
3. Lutwick, G. D. and Ryan, D. E. *Can. J. Chem.* **32** (1954) 949.
4. Dyrssen, D. and Dahlberg, V. *Acta Chem. Scand.* **7** (1953) 1186.
5. Bamberger, E. *Ber.* **52** (1919) 1116.
6. Dyrssen, D. *Svensk Kem. Tidskr.* **64** (1952) 213.
7. Dyrssen, D., Dyrssen, M. and Johansson, E. *Acta Chem. Scand.* **10** (1956) 341.
8. Dyrssen, D. *Svensk Kem. Tidskr.* **66** (1954) 234.
9. Dyrssen, D. *Acta Chem. Scand.* **9** (1955) 1567.
10. Conway, B. E. *Electrochemical Data*, Elsevier Publishing Co., London 1952.
11. Oliveri-Mandalà, E. *Gazz. chim. ital.* **40** (1910) 102; **46** (1916) 298.
12. Wise, W. M. *Hydroxamic acids as analytical reagents* (Diss.) Purdue University, Univ. Microfilms, Publ. No. 11672, Ann Arbor, Mich.; *cf. J. Am. Chem. Soc.* **77** (1955) 1058.
13. Dyrssen, D. and Sillén, L. G. *Acta Chem. Scand.* **7** (1953) 663.
14. Dyrssen, D. *Svensk Kem. Tidskr.* **68** (1956) *In press.*

Received January 31, 1956.

ACTA CHEMICA SCANDINAVICA 10 (1956) 360—377

Mass Distributions of Unfractionated and Fractionated Polymethyl Methacrylates Determined by Ultracentrifugation and Fractional Precipitation

A. FREDRIK V. ERIKSSON

Institute of Physical Chemistry, University of Uppsala, Uppsala, Sweden

A new modification of the analysis of sedimentation curves from a velocity ultracentrifugation has been applied on synthetic high molecular weight samples of very different heterogeneity. The high influence of the hydrostatic pressure on organic solvents has been taken into account. The mass distributions obtained in this way have been found to be in good accordance with the results from other methods.

The purpose of this investigation has been to determine the distribution of mass over the different sedimentation constants occurring in a synthetic high polymer by sedimentation analysis of ultracentrifuge data and to test the validity of the method. This has been done in two ways, by comparing the distributions obtained from sedimentation experiments on two different unfractionated polymers with those obtained by precipitation fractionation and by comparing the results of analyses on mixed fractions with those on the separate fractions.

PREVIOUS THEORIES

A knowledge of the distribution of mass over the different molecular species occurring in a sample of a synthetic high molecular weight polymer is in many cases of importance. For instance a determination of the molecular weight frequency function can give a very good picture of the progress of the polymerization reaction itself, and in studying the polymerization kinetics it provides a means to determine the termination mechanism of the growing molecules. The stop mechanism by which the active radicals will turn to dead molecules can involve either a combination of two radicals to one single polymer molecule or a disproportionation between two radicals. In the latter case a hydrogen atom moves from one growing polymer chain to another, giving

rise to two separate macromolecules. These two kinds of deactivation reactions will give different molecular weight distributions. It is also of interest to know the heterogeneity of an unfractionated or fractionated polymer in connection with such physico-chemical determinations as the measurement of intrinsic viscosity, osmotic pressure, light scattering, and diffusion or sedimentation constant of the polymer in solution. Even in the bulk properties of a polymeric material the polydispersity must be considered. For instance it may influence the mechanical properties and the general behaviour of a synthetic plastic.

For this reason, many attempts have been made to determine how the mass is distributed over the different molecular weights or over the different intrinsic viscosities or sedimentation constants occurring in the polymer. The most commonly used methods are fractionation, turbidimetric titration, determination of different average molecular weights with the aid of an equilibrium ultracentrifuge, dB/dx-measurement or analysis of the sedimentation peak in a velocity ultracentrifuge. In the first method the sample is divided into fractions, usually by fractional precipitation or fractional solution. This procedure gives good results but is very time-consuming because of the necessity of having equilibrium between solution and precipitate for every fraction. For this reason it can take two weeks to a month to complete one single fractionation. It is also easy to lose material during the many manipulations necessary. The turbidimetric method has been used on polymethyl methacrylate with success [1], but as a rule it seems to give results inferior to those obtained by fractional precipitation. This is probably due to the difficulty of getting stable and reproducible values of the turbidity itself. The procedure is valuable when one wants a rapid but rough estimate of the polydispersity of a sample. In the third method, an arbitrarily assumed parametric function is fitted to different observed average ultracentrifuge molecular weights obtained by means of an equilibrium centrifuge. This has been employed in many cases, however, the large deviation from ideality of the polymethyl methacrylate solutions will probably make it impractical for this substance. The dB/dx measurement, first developed by Gralén [2], has been widely used on macromolecular substances with a coiled chain configuration in solution such as occurs with polymethyl methacrylate. In this method, the width (B) of the experimental sedimentation curve is defined as the ratio of area to maximum height of the sedimentation curve:

$$B = \frac{\int_{-\infty}^{+\infty} \frac{dc}{dx}\, dx}{\left(\frac{dc}{dx}\right)_{max.}} \qquad (1)$$

where x is the distance from center of rotation and c is the polymer concentration at a point x and at a given time (t) after full speed of the rotor. This width is plotted as a function of the position x of the peak of the sedimentation curve. It is found to vary in a linear fashion with the distance from center of rotation. The slope dB/dx of this curve is graphically determined for a series of different

concentrations and extrapolated to infinite dilution. This (dB/dx), at zero concentration, is then taken as a measure of the heterogeneity of the polymer. This method has been used among others by Gralén and Rånby [3] on cellulose derivatives. In all these cases it was possible to neglect the influence of diffusion on the spreading of the sedimentation curve. For polymethyl methacrylate the contribution of diffusion to the width of the curve is appreciable because of the high diffusion constant compared with the low sedimentation constant in fractions of moderate molecular weight. An attempt to correct the experimentally measured width for the influence of diffusion in this case has been made by the author [4]. The (dB/dx) method is rapid but it can never reveal details in the distribution and it fails entirely in the case where the frequency function has more than one maximum as can happen for unfractionated polymers prepared by bulk polymerization at high degrees of conversion [5-8].

It is, however, possible to obtain more detailed information about the distribution of mass over the different sedimentation constants contained in a polymer with the aid of a velocity ultracentrifuge. The method of sedimentation analysis was first applied to a high polymer by Signer and Gross [9]. If the polymer solution contains only one species having a constant sedimentation coefficient throughout the entire cell, it is easy to show that the concentration of polymer (c) will be independent of the position in the cell from the boundary between solution and pure solvent down to the bottom. But as a consequence of the sector shape of the centrifuge cell and the increasing strength of the centrifugal field with increasing distance from the center of rotation, the concentration (c) will change with time according to the following square law [10]

$$c = c_0 \ (x_0/x)^2 \tag{2}$$

where c is the actual concentration at the time (t) when the boundary has reached the position (x) in the cell; c_0 is the initial concentration and x_0 the distance from the center of rotation to the position of the meniscus. If the solution consists of more than one component having different but constant sedimentation coefficients, each species will give a separate boundary and a constant concentration in the entire cell from its boundary to the bottom. The square dilution law will still be valid if one uses the x-value of the boundary belonging to the corresponding component.

In the case of a polymer solution with a more or less continuous spectrum of sedimentation constants one can divide the experimental sedimentation curve into a number of strips. The increase of concentration $(dc/dx)dx$ in such an interval $x_1 - dx/2$ to $x_1 + dx/2$, corrected for the dilution effect by multiplication with $(x/x_0)^2$, will then represent the fraction of material having sedimentation constants in the interval $s_1 - ds/2$ to $s_1 + ds/2$, where s_1 is the sedimentation constants for the components having its boundary at the point x_1 at the time of exposure (t).

$$x = x_0 \ e^{\omega^2 ts} \tag{3}$$

We thus have the expressions

$$dx/ds = x \ \omega^2 \ t \tag{4}$$

and

$$g(s) = \frac{dc}{ds} = \left(\frac{dc}{dx}\right) \left(\frac{x}{x_0}\right)^2 x\ \omega^2\ t \qquad (5)$$

with the aid of which we can transform the experimental sedimentation curve to a mass frequency function $g(s)$. This procedure is, however, only valid for the case where the sedimentation coefficients are independent of concentration, that is they are real constants, and where the broadening of the boundary peak is entirely due to the distribution of mass over different sedimentation constants and not at all caused by diffusion of the macromolecules. These conditions were fulfilled in the case of the polystyrene fraction investigated by Signer and Gross. If the contribution from diffusion is great enough, the distributions calculated by the method of Signer and Gross from exposures taken at different times after the start of the experiment will not coincide. The frequency curves determined from earlier exposures are broader than those from later ones.

For the case where diffusion cannot be neglected, Baldwin and Williams [11,12] have developed an extension of the theory by which it is possible to sort out the contribution from sedimentation from that of diffusion. These authors have pointed out that if the concentration is so low that diffusion and sedimentation occur independently of each other the second moment of the experimental sedimentation curve will be equal to the second moment that would have arisen if there had taken place a pure sedimentation process without any diffusion plus the second moment of the curve had there been a pure diffusion without any sedimentation. That is:

$$\sigma^2_{\text{total}} = \sigma^2_{\text{sed.}} + \sigma^2_{\text{diff.}} \qquad (6)$$

where σ^2_{total} = the square of the standard deviation for the experimental curve
$\sigma^2_{\text{sed.}}$ = the square of the standard deviation for an imaginary curve from a pure sedimentation process
$\sigma^2_{\text{diff.}}$ = the square of the standard deviation for the curve from a pure diffusion process.

According to Lamm [13]

$$\sigma^2_{\text{diff.}} = \frac{2Dt}{1 - \omega^2\ st} \qquad (7)$$

where D = the diffusion constant for a homogeneous sample,
s = the sedimentation constant,
ω^2 = the angular velocity of the rotor,
t = time after the start of the combined sedimentation and diffusion process.

Baldwin and Williams calculated the square of the standard deviation of a pure sedimentation curve and found that

$$\sigma^2_{\text{sed.}} = p^2\ \omega^4\ x^2_{\text{m}}\ t^2 \qquad (8)$$

where p^2 = the square of the standard deviation of the distribution of sedimentation constants,

x_m the distance from the center of rotation to the first moment of the gradient curve.

From eqns. (6), (7), and (8) it follows that the fraction of the total standard deviation of the experimental sedimentation curve which is due to the contribution from diffusion will be less important with increasing time (t) and zero when t goes to infinity. In eqn. (7) we have to use average values for the diffusion and sedimentation constants for the inhomogeneous polymer. Baldwin and Williams calculate an apparent distribution $g(s)$ * from each sedimentation curve obtained from the different exposures taken during the same run by means of the equation

$$g(s)^* = \frac{(dc/dx)}{A_{t=0}} \left(\frac{x}{x_0}\right)^2 x\ \omega^2\ t \qquad (9)$$

where $A_{t=0}$ is the area of the sedimentation curve extrapolated to zero time. In order to get the real distribution $g(s)$ undisturbed by the influence of diffusion they then determine $g(s)$ * for a series of fixed s-values and plot these $g(s)$ * values against $1/t$. These values extrapolated to $1/t = 0$ then give the real distribution of sedimentation coefficients. Gosting [14] has examined the question of extrapolation in detail and has found that if t is fairly large $g(s)$ * is a closely linear function of $1/xt$.

Up to this point we have only discussed the problem for the case where the sedimentation is independent of the polymer concentration or the hydrostatic pressure in the cell. The first of these two questions has been treated independently by both Baldwin [15] and Williams [16,17]. If the sedimentation is concentration-dependent, the concentration of each species will no longer be constant throughout the cell as was the case when the sedimentation coefficient was independent of the concentration. Instead, the concentration of the different species will now change with the position in the cell in such a way that a slower component will appear to have a higher and a faster one a lower concentration if calculated in the usual manner. That is, one obtains a so-called Johnston-Ogston effect [18]. Secondly, one does not obtain the distribution of sedimentation constants but rather a distribution of sedimentation coefficients for different concentrations. The concentration is highest for the fastest component and decreases with decreasing sedimentation rate of the species down to zero concentration for the slowest one. Both these effects can be eliminated if we extrapolate the observed distribution function to zero concentration. According to the method of Williams, which is purely graphical, the distributions of sedimentation coefficients derived from a series of concentrations are extrapolated to infinite dilution. This is done by determining the $g(s)$ values for given s values and by plotting these $g(s)$ values as a function of concentration c. The procedure given by Baldwin is, however, analytic. By this method it is possible to calculate the final distribution of sedimentation constants from one single sedimentation run. But this theory requires a knowledge of how the different sedimentation coefficients depend on concentration. This dependence is, however, not identical with the usually determined s—c function as evaluated from the midpoints of the sedimentation peaks. In the

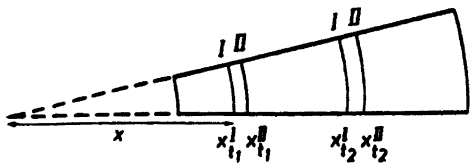


Fig. 1. The centrifuge cell.

Baldwin method one must determine the value of s for a particular species and this value is not identical with that which would be obtained if one could isolate a narrow range of species around the one in question and determine its sedimentation coefficient. Every narrow range of components is influenced by the presence of a much broader distribution of sedimentation coefficients and this is as a rule not symmetrically arranged around the range in question. It is possible to determine the desired function experimentally but because of the large amount of work involved the method has not been used in the present investigation. Both Baldwin and Williams have applied their theories to aqueous solutions of dextran and gelatin [15–17]. Both have obtained good results.

PRESENT IMPROVEMENTS

When organic solvents are used, as is necessary for polymethyl methacrylate, the great influence of the high hydrostatic pressure in the cell on the density and viscosity of the solvent must be taken into account. This pressure varies from about 1 atm. at the meniscus to 200—400 atm. at the bottom of the cell depending on the density of the solvent used and on the speed of the rotor. The sedimentation coefficient has to be reduced to the value of 1 atm. by means of the formula [19]

$$s_1 = s_p \frac{\eta_p(1-V_1\delta_1)}{\eta_1(1-V_p\delta_p)} = s_p \cdot \mathrm{f}(x) \qquad (10)$$

where s and V are the sedimentation coefficient and partial specific volume of the solute, η and δ the viscosity and density of the solvent, and the subscripts 1 and p refer, respectively, to the values at one and p atmospheres. As a rule there is no available data on how the partial specific volume varies with the pressure but it is generally assumed that this variation is small enough that in calculating the correction factor f(x) one may put V_p equal to V_1.

In order to obtain a relation between the concentration of a component (i) and the position coordinate x we may consider two cylindrical surfaces I and II through the centrifugal cell (see Fig. 1). At any given time these two surfaces will move with the same velocities as the (i) components having the same position coordinates. At the time $t = t_1$ the surfaces I and II will be at the points $x^{I}_{t_1}$ and $x^{II}_{t_1}$ and at the time $t = t_2$ at $x^{I}_{t_2}$ and $x^{II}_{t_2}$, respectively. By integration of the equation defining the sedimentation coefficient:

$$\omega^2 \, \mathrm{d}t = \frac{\mathrm{d}x}{x} \frac{\mathrm{f}(x)}{s} \qquad (11)$$

the following expressions are obtained

$$\omega^2 \ (t_2 - t_1) = \int_{x^{I}_{t_1}}^{x^{I}_{t_2}} \frac{f(x)}{x} \frac{dx}{s(c^{I})} = \int_{x^{II}_{t_1}}^{x^{II}_{t_2}} \frac{f(x)}{x} \frac{dx}{s(c^{II})} \tag{12}$$

This equation can be rearranged to

$$\int_{x^{I}_{t_1}}^{x^{II}_{t_1}} \frac{f(x)}{x} \frac{dx}{s(c^{I})} + \int_{x^{II}_{t_1}}^{x^{I}_{t_2}} \frac{f(x)}{x} \frac{dx}{s(c^{I})} = \int_{x^{II}_{t_1}}^{x^{I}_{t_2}} \frac{f(x)}{x} \frac{dx}{s(c^{II})} + \\ + \int_{x^{I}_{t_1}}^{x^{II}_{t_2}} \frac{f(x)}{x} \frac{dx}{s(c^{II})} \tag{13}$$

In these equations, $f(x)$ is the correction factor introduced in order to take into account the influence of the hydrostatic pressure. The surface II will always move in a more concentrated solution than the surface I so it may be valid to assume that

$$c^{I}(x) \leq c^{II}(x) \tag{14}$$

where $c^{II}(x)$ is the total polymer concentration at the point x at the time when the surface II passes this point and $c^{I}(x)$ has a corresponding meaning for the surface I. As a first approximation it can further be assumed that the sedimentation coefficient s of the component (i) decreases with increasing total concentration. We thus obtain the following inequality with the aid of (14)

$$\frac{1}{s \ (c \ (x))} \leq \frac{1}{s \ (c^{II}(x))} \tag{15}$$

This expression and equation (13) give the following inequality

$$\int_{x^{I}_{t_1}}^{x^{II}_{t_1}} \frac{f(x)}{x} \frac{dx}{s(c^{I})} \geq \int_{x^{I}_{t_2}}^{x^{II}_{t_2}} \frac{f(x)}{x} \frac{dx}{s(c^{II})} \tag{16}$$

And if the interval x^{I} to x^{II} is sufficiently small

$$\left\{\frac{f(x)}{x} \frac{dx}{s(x)}\right\}_{x_{t_1}} \geq \left\{\frac{f(x)}{x} \frac{dx}{s(x)}\right\}_{x_{t_2}} \tag{17}$$

Denoting the concentration of component (i) between the two surfaces by c, the volume element between these two surfaces by v and remembering the sector shape of the cell it is possible to write

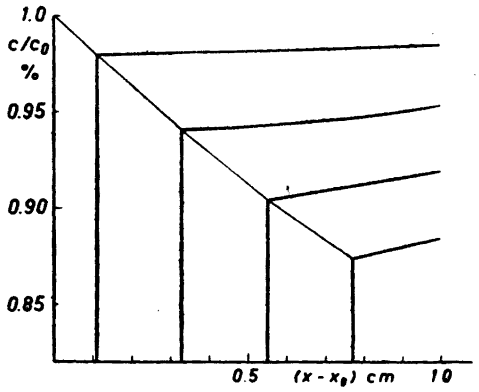


Fig. 2. The relative concentration as a function of $(x-x_0)$ *calculated from equation (19) for different positions of the meniscus.*

$$\frac{c_{t_1}}{c_{t_2}} = \frac{v_{t_2}}{v_{t_1}} = \frac{x_{t_2}(\mathrm{d}x)_{t_2}}{x_{t_1}(\mathrm{d}x)_{t_1}} \leq \frac{(x_{t_2})^2\, \mathrm{f}(x_{t_1})}{(x_{t_1})^2\, \mathrm{f}(x_{t_2})} \frac{s(x_{t_2})}{s(x_{t_1})} \qquad (18)^*$$

As a special case valid without any approximation at all

$$\frac{c_{t_1}}{c_{t_2}} = \frac{(x_{t_2})^2\, \mathrm{f}(x_{t_1})}{(x_{t_1})^2\, \mathrm{f}(x_{t_2})} \qquad (19)$$

if there is no concentration dependence of the sedimentation coefficient. With the aid of this equation the concentration in the cell has been calculated for different positions and at different times for the case of polymethyl methacrylate in ethyl acetate. As can be seen from Fig. 2 the concentration increases with increasing values of x even for sedimentation independent of concentration but dependent on the pressure in the cell **. This increase in concentra-

* This formula is valid for a polydisperse or a monodisperse solute in a solvent, where the influence of the hydrostatic pressure can not be neglected. Working with aqueous solutions Trautman [20] and Schumaker have previously treated the case of no hydrostatic pressure effect. They found that in a region where $(\mathrm{d}c/\mathrm{d}x) = 0$, the dilution will follow the square law

$$c/c_0 = (x/x_0)^2$$

This problem will also be discussed by Moring-Claesson [23] and Kinell [24,25]. Investigating the Ogston effect in a system of a few discrete components Moring-Claesson obtains the same formula as Trautman but in a different way; Kinell will consider in more detail the assumptions made by Trautman *et al.*

** It can be shown that the expression

$$(\partial c/\partial x)_t \equiv 0 \qquad (1)$$

is only possible if the correction function $\mathrm{f}(x)$ fulfils the conditions that

$$\frac{\mathrm{d}\left(x^2\, \frac{1}{\mathrm{f}}\right)}{x\, \mathrm{d}x} = \text{constant} \qquad (2)$$

Cont. on p. 368.

tion is more serious than the corresponding Johnston-Ogston effect caused by the concentration dependence of sedimentation because it can not be eliminated by extrapolation to infinite dilution in the usual way. It will, however, be so small that it will not be further considered here. For the dilution at the boundary one obtains

$$c_0 = c \left(\frac{x}{x_0}\right)^2 \cdot \frac{1}{f(x)} \tag{20}$$

since the pressure correction factor is equal to 1 at the meniscus. Not only will the dilution law change, but it follows from the integrated form of equation (11) that the derivative $\frac{dx}{ds}$ must now be written

$$\frac{dx}{ds} = \frac{1}{f(x)} x \omega^2 t \tag{21}$$

Instead of eqns. (5) and (3) the following expressions are valid for a concentration independent but pressure sensitive sedimentation

$$g(s) = \left(\frac{dc}{dx}\right) \left(\frac{x}{x_0}\right)^2 \frac{1}{f(x)^2} x \omega^2 t \tag{22}$$

$$s = \frac{1}{\omega^2 t} \int_{x_0}^{x} \frac{dx}{x} f(x) \tag{23}$$

When it is impossible to keep the temperature of the centrifuge solution and the angular velocity of the rotor perfectly constant the s-values must be corrected to the same temperature and the same speed of the rotor. The temperature is therefore read at short intervals of time and the sedimentation coefficient calculated for this interval reduced to a temperature of 20° C by means of the formula

$$s_{20} = s_t \frac{\eta_t}{\eta_{20}} \frac{(1 - V_{20}\varrho_{20})}{(1 - V_t \varrho_t)} \tag{24}$$

Cont. from p. 367.

This follows from the equation of continuity

$$\left(\frac{\partial c}{\partial t}\right)_x = - \frac{\omega^2 \partial (x^2 \frac{1}{f} c s)}{x \partial x_t} = - \omega^2 c s \frac{d\left(x^2 \frac{1}{f}\right)}{x\, dx} - \frac{\omega^2 x}{f} \frac{\partial (c s)}{\partial x_t} \tag{3}$$

which in the case of condition (1) reduces to

$$\left(\frac{\partial c}{\partial t}\right)_x = - \omega^2 c s \frac{d\left(\frac{1}{f} x^2\right)}{x\, dx} \tag{4}$$

Equations (1) and (4) can only be simultaneously valid if

$$\frac{d\left(x^2 \frac{1}{f}\right)}{x\, dx} = \text{constant}$$

where all symbols have their usual significance. The subscripts 20 and t refer to the temperature 20 and t °C. Small errors in the determination of temperature or of rotor speed will cause a shift in the whole $g(s)$ curve. This in turn may produce serious errors in the extrapolation of $g(s)$ to infinite time and infinite dilution. For this reason formula (22) has not been used in this investigation. Another procedure to calculate the distribution has therefore been developed. The experimental sedimentation curve dc/dx against x is read at constant x intervals and the dc/dx values corrected for dilution effects with the aid of eqn. (20). This corrected frequency curve is then integrated and starting from the origin the x_p values were determined for successive 10 % increments of the integral distribution curve. The index p refers to an increase of p % in the integral mass distribution. By means of equation (23) the ratio s_p/s_{50} is then calculated from the different x_p. In order to eliminate the contribution from diffusion the ratios s_p/s_{50} from different exposures are plotted against $1/(s_{50} \cdot t)$ and extrapolated to infinite time. The extrapolated values of the ratio s_p/s_{50} have to be converted to s_p-values. This can be done with the aid of eqn. (23) using the experimentally determined values of the integral $\int_{x_0}^{x_{50}} \frac{f(x)}{x} dx$ which are found to be a linear function of time.

This curve crosses the t axis at a small negative value indicating that the sedimentation starts a little before the rotor has reached the operating speed. The s_{50}-values calculated in this way are found to lie close to the $s_{max.}$-value determined in the usual manner from the maximum point of the sedimentation diagram. So in the case of homogeneous fractions it may be preferable to use values of s_{50} calculated from the known relation

$$\frac{1}{s} = \frac{1}{s_{max.}} (1 + kc) \qquad (25)$$

where $s_{max.}$. is the sedimentation constant of the maximum point extrapolated to infinite dilution and k is a constant expressing the concentration dependence of the sedimentation coefficient. Both $1/s_{max.}$ and k have of course been determined by means of the method of least squares from a long series of experimentally found $1/s$, c pairs. In order to obtain the real distribution, $1/s_p$ has to be plotted against c and extrapolated to infinite dilution. This procedure is facilitated by the fact that $1/s_p$ is a closely linear function of c.

EXPERIMENTAL AND RESULTS

Materials. The method of determining the distribution of mass over the different sedimentation constants in a synthetic high polymer has been tested on polymethyl methacrylate in ethyl acetate as solvent. In order to obtain polymers of highly different heterogeneity covering a broad interval of molecular sizes, samples of unfractionated and fractionated polymers as well as mixed fractions have been investigated. The polymethyl methacrylates have been prepared by bulk polymerization with benzoyl peroxide as initiator. Both the concentration of initiator and the degree of conversion have been varied. The reaction conditions will be given in detail later [22]. The polymers were fractionated by precipitation and the sedimentation constants were determined for every

fraction in ethyl acetate. Details of fractionation and sedimentation technique are given in Ref.[12]. The ethyl acetate used was "Baker Analyzed Reagent" and was not further purified.

Influence of the correction factor. The choice of correction factor has only a small influence on the distribution s_p/s_{50} calculated from a sedimentation diagram. This can be seen from Table 1, where the ratio

$$\frac{s_p/s_{50} \text{ corrected with the factor } (x/x_0)^2}{s_p/s_{50} \text{ not corrected for dilution}}$$

has been given for different percents (p) and at five times during the same run. The sample used was an unfractionated polymer /B(714)/ and therefore had an unusually broad massdistribution. The concentration was 0.157 g per 100 ml solution. The dilution-correction will only affect the value of s_{50}. The value of s_{50} calculated by the method of least squares after applying the correction factors, $(x/x_0)^2$ and $(x/x_0)^2 \cdot 1/f(x)$ and no correction, was 13.95 and 13.84 and 13.72, respectively.

Table 1. The ratio $\frac{s_p/s_{50} \text{ corrected with the factor } (x/x_0)^2}{s_p/s_{50} \text{ not corrected for dilution}}$ *for different percents (p) and at five times during the same run in the ultracentrifuge.*

Time after full speed	Percent (p) 10	20	30	40	60	70	80	90
625 sec.	1.007	1.006	1.006	1.000	1.005	1.004	1.000	1.000
935	1.001	1.005	1.001	1.000	1.000	1.000	1.000	0.999
1 285	1.006	1.004	1.000	1.000	1.000	1.002	1.003	1.003
2 400	1.001	1.002	0.999	0.999	0.998	0.997	0.998	0.998
3 025	1.003	1.002	1.000	0.999	0.999	0.998	0.998	0.997
Mean value	1.004	1.004	1.001	1.000	1.000	1.000	1.000	0.999

Extrapolation of s_p/s_{50} to infinite time. With the method used here to get the mass distribution it is not possible to give an unequivocal theoretical justification for the procedure of extrapolating the ratio s_p/s_{50} to infinite time. In two special cases, however, $(s_p - s_{50})^2/s_{50}^2$ will be a linear function of $1/t$, namely if the substance is monodisperse or if the mass is distributed over the different s values in accordance with a Gaussian frequency curve and the diffusion constant is the same for all molecules. In both these cases it can be shown that the experimental sedimentation curves will be Gaussian if diffusion and sedimentation occur independently of each other in the cell. It was experimentally found that for polymethylmethacrylate s_p/s_{50} plotted against $1/(s_{50}t)$ gives a straight line. In order to investigate if different extrapolation methods could give different results, all s_p/s_{50} values for each concentration used (fraction B(712) XIV) were treated in two different ways, in one case s_p/s_{50} and in the other $(s_p/s_{50})^2$ was plotted against $1/(s_{50}t)$. This material has a high diffusion constant but a low sedimentation constant and hence the dependence of s_p/s_{50} on time after the start of the experiment is unusually large. The final distribution extrapolated to zero concentration did not show any systematical trend with the two methods. The mean difference between two corresponding s-values was less than 0.5 % and can be

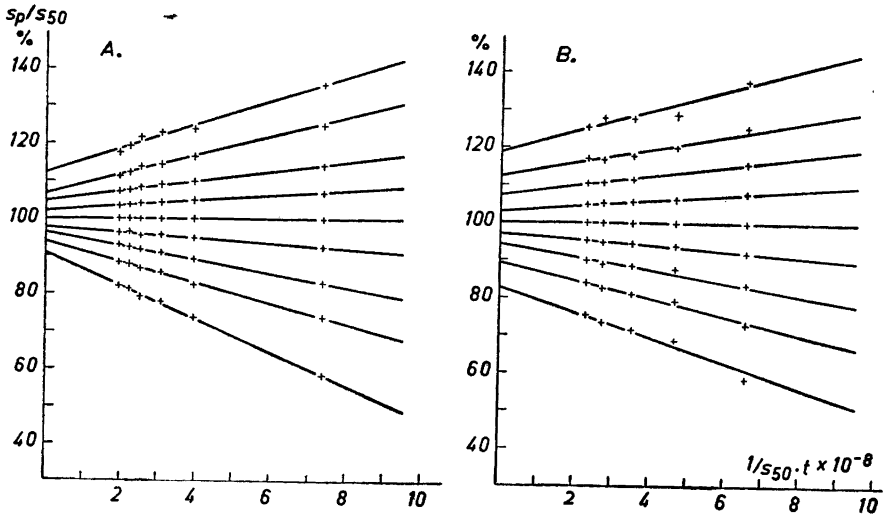


Fig. 3. Extrapolation of s_p/s_{50} to infinite time for two concentrations of B(712) XIV.
A Concentration equal to 0.792 g/100 ml
B Concentration equal to 0.199 g/100 ml

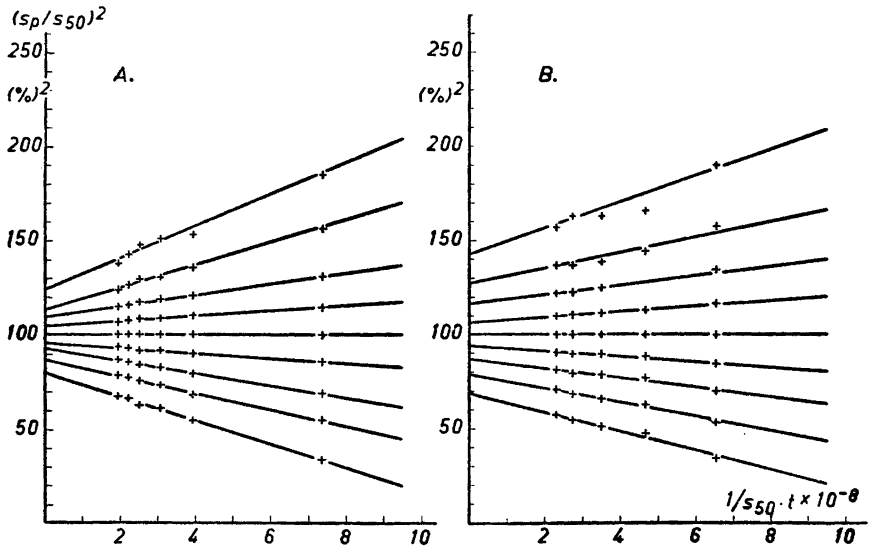


Fig. 4. Extrapolation of $(s_p/s_{50})^2$ to infinite time for the same fraction and at the same concentrations as in figure 3.

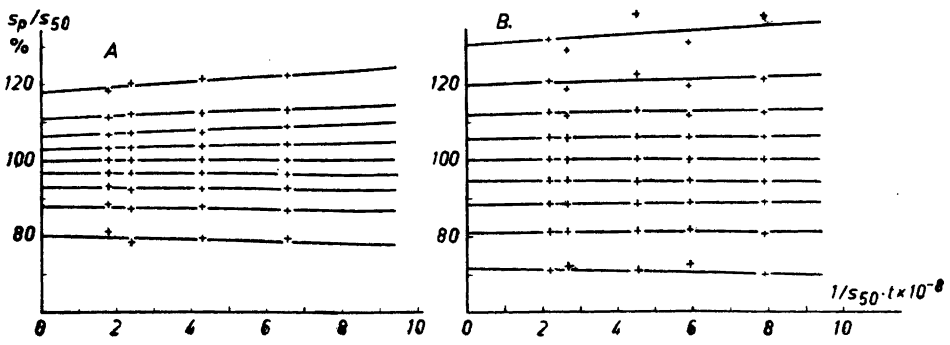


Fig. 5. Extrapolation of s_p/s_{50} to infinite time for the unfractionated polymer B (714) at the concentrations 0.358 (A) and 0.157 (B) g/100 ml.

considered to lie within the experimental accuracy of the procedure. As the difference can be expected to be still less for a more polydisperse substance or fraction with a lower diffusion constant, the method of extrapolating s_p/s_{50} as a linear function of $1/(s_{50}t)$ was chosen in order to save time. The two methods of extrapolation are illustrated in Figs. 3 and 4 for the two concentrations 0.792 and 0.199 g polymethyl metacrylate per 100 ml ethyl acetate solution. The fact that the dependence of s_p/s_{50} on time is much smaller for a more polydisperse sample is shown in Fig. 5 for the two concentrations 0.358 and 0.157 g/ml. The sample used was an unfractionated polymer B(714).

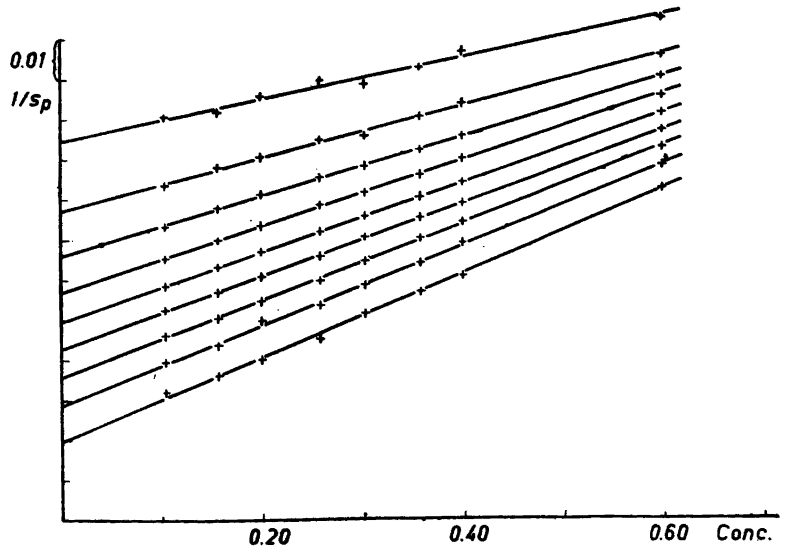


Fig. 6. $1/s_p$ as a function of concentration. In order to spread out the data the lines have been displaced from each other by 0.025 units. Sample B (714).

Comparison of the distributions of mass obtained by means of the velocity ultracentrifuge with those obtained by means of precipitation fractionation. The contribution of diffusion to the total width of the sedimentation peak is relatively small for a polymer with a reasonably heterogeneous composition of different molecular sizes. This is of course quite natural as the spreading from diffusion is determined only by the average diffusion constant and not at all by the width of the distribution of this constant. However, the spreading due to sedimentation is proportional to the mean sedimentation constant multiplied by the standard deviation of the function expressing the mass frequency over this constant. This is the reason why s_p/s_{50} is almost independent of t for all percents (p) except for the last fraction with the highest molecular weight. The function s_p/s_{50} plotted against $1/(s_{50}t)$ was shown in Fig. 5. If the average molecular size is not extremely high it is further possible to use more concentrated solutions in order to minimize the errors from the inaccuracy in the drawing of the base line of the gradient curve, dc/dx against x. The uncertainty in the determination of this line is greatest for polydisperse material and for low concentrations, where the sedimentation peak is very broad and flat. The mass distribution of two unfractionated polymers with an average sedimentation constant of 16.80 and 11.38 have been determined by analysis of the sedimentation diagrams. The first polymer is designed by B(714) and the second by B(712). The $s_{50}(c)$ values used were obtained from an eqn. similar to eqn. 25, the constants being derived by the method of least squares using the experimental s_{50} values for 8 and 5 concs., resp. in the 2 above cases. The coefficients $1/s_p$ were in every case found to lie on a straight line as shown in Fig. 6 for the polymer B(714). The final mass distribution over the sedimentation constant is shown in Fig. 7. In these figures the integral distributions obtained from precipitation fractionation are also given. These have been constructed under the assumption that half the mass of a fraction has a sedimentation constant lower than the average value determined for the fraction. The result is that the curves obtained from the two methods lie close to one another. A part of the small parallel displacement of the curves can possibly be explained by the fact that the sedimentation measurements on the different fractions were performed some years before the determinations on the unfractionated polymer. During this time the thermo-elements giving the rotor temperature have been exchanged and therefore the zero point of the temperature scale re-determined. The method of determining the integral distribution of mass by means of analysis of the sedimentation peaks is considered to be as accurate as the laborious and time-consuming technique of precipitation fractionation. Another advantage with the method of sedimentation analysis is that it can be applied directly on the initial reaction product diluted with the monomer. In this way it will be unnecessary to separate the polymer from the unreacted monomer.

Comparison of the distribution of mass obtained for mixtures of two fractions by means of the velocity ultracentrifuge with those obtained on the separate fractions by means of the same method. In order to get further proof of the usefulness of sedimentation analysis on high polymers, the investigation has been extended to higher molecular sizes and to more homogeneous material composed of one single fraction or mixtures of two fractions in equal parts. The more

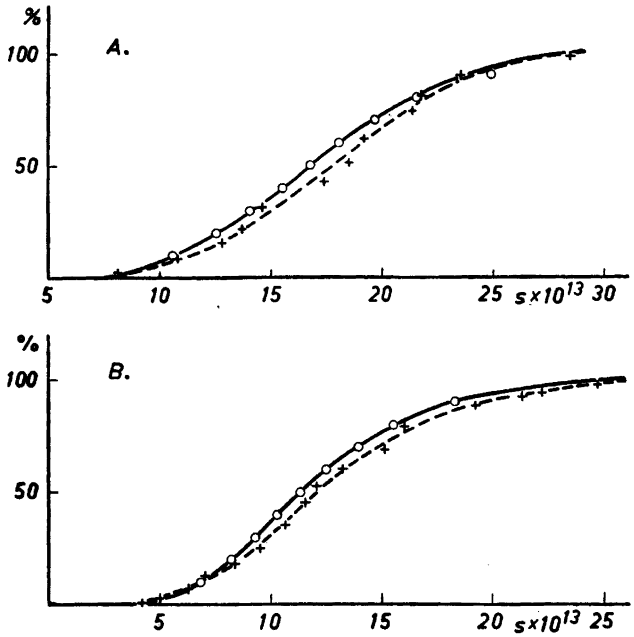


Fig. 7. Integral distributions obtained from sedimentation analyses (fuldrawn lines) and from fractional precipitation (dotted lines). A for B(714) and B for B(712).

essential properties of the fractions used in this study are summarized in Table 2. The values of s_{max} are the sedimentation constant as determined from the maximum point of the sedimentation curve. The experimentally determined relation $1/s = 1/s_{max}\ (1 + k_s c)$ has been used to calculate s_{50}. This has been done because it was found that the s_{50} values for this rather homogeneous sample are very nearly equal to s_{max} and because there was a greater number of data available on which to apply the method of least squares for the determi-

Table 2. Summary of the properties of the polymethyl methacrylate fractions that have been used for the sedimentation analyses.

Fraction		s_{max}	Weight of the fraction in percent of the total weight of the polymer product	Weight of material in the initial polymer product having a higher sedimentation constant than that of the fraction used
B(712)	XIV	6.29	7.68	89.25
B(709)	X	16.38	9.22	69.69
B(709)	XIII	10.50	6.75	90.09
B(709)	X+XIII	13.09 (s_{50})	—	—
B(713)	IV	30.36	4.40	3.40
B(713)	VI	27.05	5.45	10.00
B(713)	IV+VI	28.43	—	—

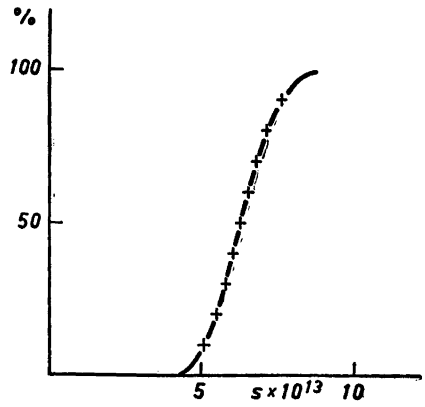


Fig. 8. Integral distribution of B(712) XIV.

nation of the constants $1/s_{max}$ and k_s. The different s_{max} are given in the second column of Table 2. In the next column the amount of each fraction is given in weight percent of the total polymer product, and the last column shows the total amount of material in the initial polymer product having higher sedimentation constant than that of the fractions used. As can be seen from the table, in polymer B(709) the mass of the two fractions between X and XIII was about 11 % of the total polymer. This was enough to give the mixture of the two fractions X and XIII a double peaked sedimentation curve. It was therefore impossible to determine any s_{max}. In this case the observed values of the sedimentation coefficient s_{50} for the five concentrations employed for the sedimentation analysis were used instead to calculate the sedimentation coef-

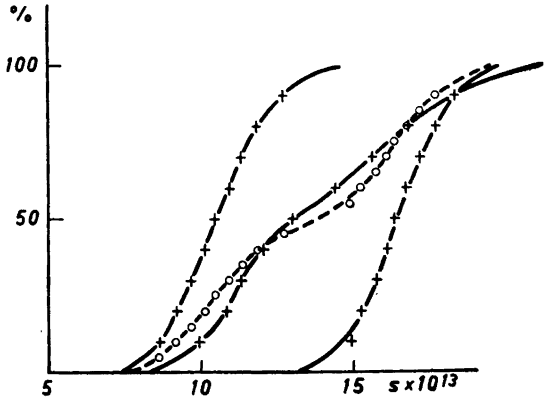


Fig. 9. Integral distributions of B(709) X, B(709) XIII and a mixture of equal parts of these two fractions. The dotted line is the distribution of the mixture calculated from the data of the separate fractions.

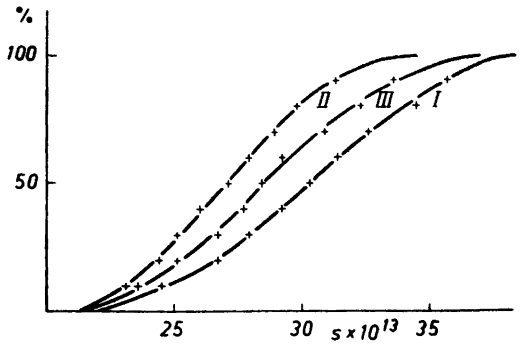


Fig. 10. Integral distributions.
I. of B(713) IV
II. of B(713) VI
III. of the two fractions mixed in equal parts.

ficient at infinite dilution and the constant k_s that expresses the concentration dependence of this coefficient. Five or six concentrations have been used in the sedimentation analysis of each fraction or mixture of fractions. The lowest concentration in each series was about 0.1 g per 100 ml. The upper concentration limit was 1.0, 0.6 and 0.4 g per 100 ml for polymers designated by B(712) B(709) and B(713), respectively. In these concentration intervals it has been possible to extrapolate $1/s_p$ linearly with concentration. The calculated integral distributions of mass are shown in Figs. 8, 9 and 10. The dotted line in Fig. 9 is the mass distribution of the mixture of equal parts of the two fractions B(709) X and B(709) XIII, that has been calculated from the experimentally determined mass distributions of the two fractions separately. As can be seen from the figure this line is in reasonably good accordance with the mass distribution that has been obtained from sedimentation analysis applied directly on the mixture. A part of the small discrepancy may have been caused by errors in the determinations of the different $1/s_{50}$ values at infinite dilution. The result of the sedimentation analysis on the mixture of equal parts of the two fractions B(713) IV and B(713) VI is also very good (Fig. 10). Unfortunately the two fractions lie close together. It is therefore a little difficult to judge the extent to which the good agreement is due only to the reliability of the method. It may be that part of the agreement is due to the fact that the method gives approximately the same errors in all these three cases. It can, however, be concluded from these experiments that the analysis of the sedimentation curves will give integral mass distributions that are at least in broad outline correct even for relatively homogeneous materials.

This investigation has been financially supported by grants from *Statens Tekniska Forskningsråd* och *Stiftelsen Svensk Gummiforskning* (AB. Sieverts Kabelverk, AB. Liljeholmens Kabelfabrik, Goodyear Gummifabriks AB., Svensk Gummifabriks AB., Viskafors Gummifabriks AB.).

The author wishes to acknowledge his indebtness to Professor The Svedberg and Professor Stig Claesson for their kind interest and for the many facilities which have been put at the author's disposal.

The author also wishes to thank Doctor P.-O. Kinell, Doctor K. O. Pedersen and Assistent E. Hellman for their interest in this study.

REFERENCES

1. Harris, I. and Millar, R. G. *J. Polymer Sci.* **7** (1951) 377.
2. Gralén, N. *Sedimentation and Diffusion Measurements on Cellulose and Cellulose Derivatives*, Inaugural Dissertation, Uppsala 1944.
3. Kinell, P.-O. and Rånby, B. G. *Advances in Colloid Sci.* **3** (1950) 194.
4. Eriksson, A. F. V. *Acta Chem. Scand.* **7** (1953) 623.
5. Trommsdorff, E., Köhle, H. and Lagally, P. *Makromol. Chem.* **1** (1948) 165.
6. Kinell, P.-O. *Acta Chem. Scand.* **1** (1947) 832.
7. Smets, G., Masquellier, C. and van Tournot, F. *Bull. soc. chim. Belges* **57** (1948) 493.
8. Eriksson, A. F. V. *Acta Chem. Scand.* **3** (1949) 1.
9. Signer, R. and Gross, H. *Helv. Chim. Acta* **17** (1934) 726.
10. Svedberg, T. and Pedersen, K. O. *The Ultracentrifuge*, Oxford 1940.
11. Baldwin, R. L. and Williams, J. W. *J. Am. Chem. Soc.* **72** (1950) 4325.
12. Williams, J. W., Baldwin, R. L., Saunders, W. H. and Squire, P. G. *J. Am. Chem. Soc.* **74** (1952) 1542.
13. Lamm, O. *Z. physik. Chem.* **143 A** (1929) 177.
14. Gosting, L. J. *J. Am. Chem. Soc.* **74** (1952) 1548.
15. Baldwin, R. L. *J. Am. Chem. Soc.* **76** (1954) 402.
16. Williams, J. W., Saunders, W. M. and Cicirelli, J. S. *J. Phys. Chem.* **58** (1954) 774.
17. Williams, J. W. and Saunders, W. M. *J. Phys. Chem.* **58** (1954) 854.
18. Johnston, J. P. and Ogston, A. G. *Trans. Faraday Soc.* **42** (1946) 789.
19. Mosimann, H. and Signer, R. *Helv. Chim. Acta* **27** (1944) 1123.
20. Trautman, R. and Schumaker, V. *J. Chem. Phys.* **22** (1954) 551.
21. Goldberg, R. J. *J. Phys. Chem.* **57** (1953) 194.
22. Eriksson, A. F. V. *Svensk Kem. Tidskr.* **68** (1956). *In press. Cf. Acta Chem. Scand.* **10** (1956) 378.
23. Moring-Claesson, I. *To be published.*
24. Kinell, P.-O. *Acta Chem. Scand.* **1** (1947) 335.
25. Kinell, P.-O. *To be published.*

Received December 15, 1955.

ACTA CHEMICA SCANDINAVICA 10 (1956) 378—392

Sedimentation, Diffusion and Viscosimetric Measurements on Polymethyl Methacrylate Fractions Obtained at Different Degrees of Conversion

A. FREDRIK V. ERIKSSON

Institute of Physical Chemistry, University of Uppsala, Uppsala, Sweden

It has been found from the nature of the relations between the sedimentation constant s, the intrisic viscosity $[\eta]$ and the molecular weight M that polymethyl methacrylate molecules formed at higher degrees of conversion do not have the same configuration as those molecules obtained during the stationary stage of the polymerisation. The relations between s, $[\eta]$ and M obtained for polymer molecules prepared at low degrees of conversion have been compared with Flory's theory for chain molecules. Slight systematic deviations of the experimental values from the theoretically expected relations have been observed.

The work reported in this paper is a part of an investigation of the molecular weight distribution in polymethyl methacrylate. The purpose of the present part has been to determine empirical relations between the sedimentation constant, the intrisic viscosity and the molecular weight of polymethyl methacrylate molecules.

MATERIAL

The monomer methyl methacrylate has been polymerisated in nitrogen atmosphere with various amounts of benzoylperoxide as initiator. The polymerisation temperature was 60° C for samples B(704) and B(720) and 80° C for samples B(714) and B(712). The degrees of conversion are 18, 72, 14, and 47 % for B(704), B(720), B(714), and B(712), respectively. A detailed account of the polymerisation technique and the method of fractionation will be given elsewhere [1]. Ethyl acetate has been used as solvent for all measurements. The quality of the ethyl acetate was "Baker Analyzed Reagent" and it was used without further purification.

VISCOSITY MEASUREMENTS

The intrinsic viscosity $[\eta]$ has been determined by means of an Ostwald viscometer at 20° C in ethyl acetate. The value of $[\eta]$ was obtained by extrapolating η_{sp}/c to infinite dilution, the reduced viscosity η_{sp}/c being determined for four concentrations (c). The

extrapolation was facilitated by the fact that η_{sp}/c is a linear function of concentration in the concentration range used. All measurements were made at concentrations lower than 0.4 g/100 ml.

SEDIMENTATION MEASUREMENTS

Technique. The sedimentation measurements have been performed in an oilturbine ultracentrifuge of the Svedberg type. A detailed account of the ultracentrifuge process has been given in the monograph by Svedberg and Pedersen [2] so only certain technical data will be mentioned here. The distance between the meniscus and the axis of rotation was 5.9 cm. The speed of the rotor was 800 revs/sec. for all measurements except for those on fractions of the sample B(704). In this latter case the rotor speed was only 600 revs/sec. For the observation of the sedimentation velocity Lamm's [3] scale method was used. The temperature of the rotor was regulated by cooling the turbine oil, and the temperature recorded by means of a thermocouple immediately adjacent to the rotor. The observed sedimentation coefficients have been corrected to 20.0° C and to 1 atm. pressure in the usual manner [4].

In order to test the reliability of the pressure correction formula

$$s_{1\text{ atm.}} = s_p \frac{\eta_p(1-V_1\varrho_1)}{\eta_1(1-V_p\varrho_p)}$$

in the case of the present system of polymer and solvent the sedimentation rate of a polymethyl methacrylate fraction was determined for three different rotor speeds and three different dilutions. The corrected value of the sedimentation coefficient was found to be independent of the rotor speed [5].

Dependence of the sedimentation coefficient on concentration. Because of the large extension of the flexible polymethyl methacrylate molecules the decrease of the sedimentation velocity with increasing concentration is considerable. At a concentration of about 0.8 g per 100 ml all fractions except the ones with molecular weights lower than about two hundred thousand sediment with the same velocity (Fig. 1). This means that they have entirely lost their individuality as molecules and sediment as a clouster. The usual formula

$$\frac{1}{s} = \frac{1}{s_0}(1 + k_s c) \qquad (1)$$

has been used for the extrapolation of the sedimentation coefficient to infinite dilution. It was, however, found that the inverse value of the sedimentation coefficient is a linear function of concentrations only if the dilution is great. This can be seen from Table 1 where the values of s and k_s are given for twelve fractions. For samples with sedimentation constants higher than about 20 the sedimentation coefficient will increase with the dilution more rapidly than is predicted by eqn. (1). For the two fractions with the highest molecular weights the values of s and k_s are considerably greater if calculated from the concentration interval 0.03—0.20 than from the concentration interval 0.15—0.8. All values have of course been obtained by means of the method of least squares. In order to avoid any systematical error from the method of extrapolating $1/s$ to infinite dilution, concentrations higher than 0.20 g per 100 ml have not been used. Six concentrations were used in carrying out the extrapolation.

Reproducibility of the determination of the sedimentation constant. In order to investigate the reliability of the determined values of the sedimentation

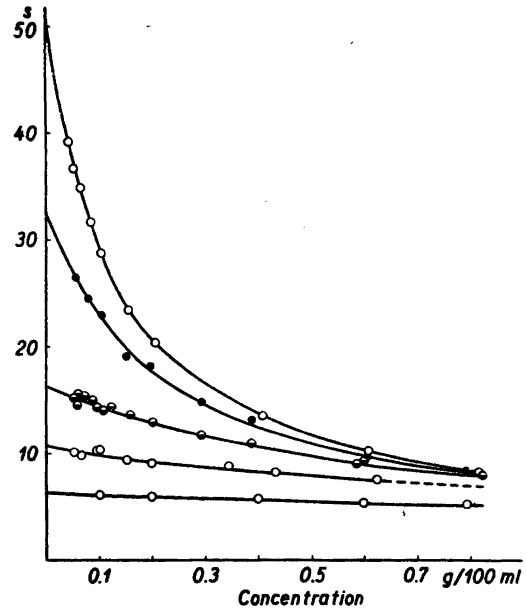


Fig. 1. The dependence of the sedimentation coefficient on concentration for samples B(720) I, B(713) IV, B(709) X, B(709) XIII and B(712) XIV respectively.

Table 1, showing how the value of the sedimentation constant s at infinite dilution and the value of the constant k_s, as obtained from a linear extrapolation of 1/s, depend on the concentration range, from which the extrapolation is performed.

Sample	Concentrations lower than 0.2 g per 100 ml			Concentrations between 0.15 and 0.8 g per 100 ml			Concentrations between 0.4 and 1.0 g per 100 ml			All concentrations		
	s	k_s	No. of conc.	s	k_s	No. of conc.	s	k_s	No. of conc.	s	k_s	No.of conc.
B(720) I	51.1	7.42	7	41.0	4.94	5	—	—	—	46.1	5.78	10
B(720) II	46.8	7.49	10	35.2	4.36	5	—	—	—	43.4	6.15	12
B(709) II	34.8	5.04	8	30.1	3.80	5	—	—	—	33.6	4.53	11
B(713) IV	32.6	4.25	5	28.4	3.11	6	—	—	—	30.4	3.44	9
B(713) VI	26.6	2.94	5	27.6	3.16	5	—	—	—	27.1	3.06	9
B(713) VIII	23.5	2.64	6	21.9	2.02	6	21.8	2.01	3	22.4	2.12	12
B(704) IV	22.9	2.44	7	21.7	1.99	5	—	—	—	22.3	2.10	10
B(720) VIII	22.1	1.99	6	22.2	2.04	6	—	—	—	22.2	2.06	10
B(713) X	20.9	2.01	9	20.4	1.76	5	—	—	—	20.6	1.81	12
B(704) VI	18.3	1.83	6	17.3	1.41	5	—	—	—	17.7	1.48	9
B(709) X	16.3	1.30	10	16.3	1.32	6	16.4	1.34	5	16.4	1.34	16
B(709) XIII	10.7	0.86	6	10.2	0.56	5	10.4	0.62	3	10.5	0.64	10

Table 2, showing the reproducibility of the determination of the sedimentation constant when done at different times and on different parts of the same fraction.

Sample	Sedimentation constant at infinite dilution s_1	s_2	Mean value $\bar{s}$	Mean deviation $\frac{[s_1 - s_2]}{2\,\bar{s}}$ in per cent
B(704) IV	22.0	22.9	22.5	2.0
B(704) VI	18.0	18.3	18.2	0.8
B(720) I	49.0	51.1	50.1	2.1
B(720) II	43.1	46.8	45.0	4.2
B(720) VI	25.4	25.8	25.6	0.8
B(720) VIII	22.3	22.1	22.2	0.5
		Mean error in per cent		1.7

constant, double determinations have been performed for six fractions, the two centrifugal runs for the same sample being made on different parts of the fraction and at a time interval of at least one year. The results are given in Table 2. From this it can be seen that the mean error is less than 2 %. This is, however, not a value of the reproducibility of the sedimentation coefficient itself which is considerably greater. The main part of the deviation is due to inhomogeneity of the sample and variations of the solvent used.

DIFFUSION MEASUREMENTS

Technique. The diffusion coefficient was determined in ethyl acetate at 20° C. The diffusion cell used was of the old Claesson [6] type. (During the course of this investigation a new diffusion cell with increased reproducibility has been constructed by Claesson *et al.*[7]) The diffusion was followed by means of Lamm's scale method [3].

Dependence of the diffusion coefficient on concentration. Because of the strong dependence of the sedimentation velocity on concentration it was considered essential to use as low concentrations as possible for the diffusion measurements. In the initial experiments the highest concentration was 0.4 g/100 ml [5]. Later, however, the concentration range was extended to 0.6 in order to increase the reliability of the determination and to be able to study the concentration dependence of the diffusion coefficient itself. Within the experimental accuracy this coefficient was found to be a linear function of the concentration as can be seen from Fig. 2, where D_m and D_A are plotted against the original concentration of the solution. When the diffusion coefficient is dependent on concentration the experimental curves will no longer be symmetrical around the position of the original boundary between solution and solvent. If, as in this case, the diffusion coefficient increases with increasing concentration the maximum of the diffusion curve must be displaced to the pure solvent side of the boundary [8,9] — the negative side — according to the theory of Boltzmann [8]. The experimentally obtained diffusion curves were also found to be

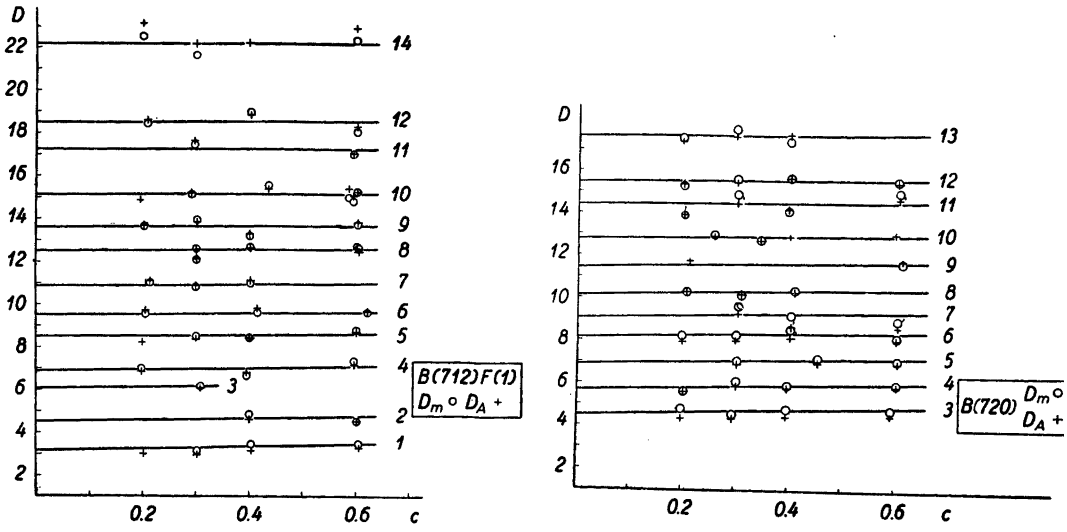


Fig. 2. The dependence of the diffusion coefficient on concentration. Circles represent D_m *and crosses* D_A *values. The figures on the ordinate mark the zero points of the fractions indicated by corresponding numbers on the right. The distance between each scale line is* 10^{-13} *units of* D.

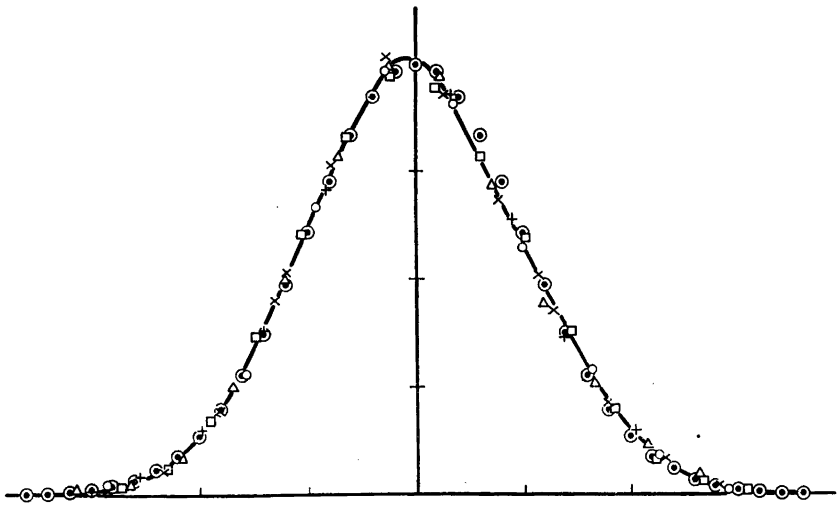


Fig. 3. The normalized diffusion curve. The different symbols represent points from five different exposures taken from 14.6 to 35.6 hours after the start of the diffusion process. The black circles give the Gaussian curve. Sample B(720)VIII. Conc. 0.411 g/100 ml.

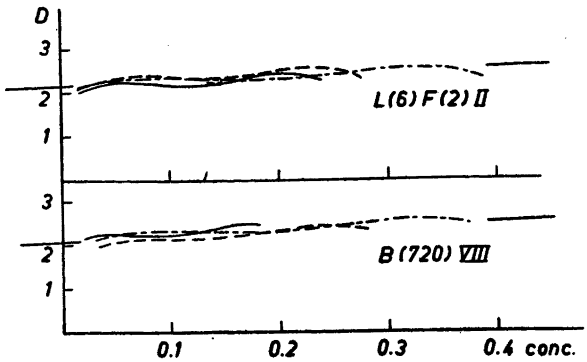


Fig. 4. The dependence of the diffusion coefficient on concentration obtained by Boltzmann analyses. The straight lines at the end of the figures indicate the concentration dependence calculated from the skewness of the diffusion curves according to the method of Gillis et al.

skew and with a negative displacement of the maximum. This is illustrated in Fig. 3 where the normalized diffusion curves [3] from five exposures taken during the same diffusion experiment from 14.6 to 35.6 hours after the start of the diffusion process are given. The experimental points from the five normalized curves fall on the same curve.

Method of extrapolation of the diffusion coefficients. Unfortunately the spread of the D_m and D_A values is rather large at the low concentration — D_m and D_A being, respectively, the diffusion coefficients determined with the method of moments and areas. Two different methods have been used to determine the constant k_D in the equation:

$$D(c) = D_0 \ (1 + k_D c) \tag{2}$$

Method 1. According to the theory of Boltzmann [8-10] it is possible to determine the value of D for every value of the concentration (c) from zero to the initial concentration (c_0) of the solution, $D(c)$ being given by the expression:

$$D(c) = -D_m \cdot \frac{1}{dc/dz} \int_{-\infty}^{z} z \cdot \frac{dc}{dz} \cdot dz \tag{3}$$

where D_m is the obtained value of the diffusion coefficient determined in the usual way by the moment method, dc/dz and z the coordinates of the normalized diffusion curve. In the derivation of eqn. (3) it has been assumed that the diffusing material is monodisperse. As has been shown by Beckmann and Rosenberg [10] the experimentally obtained relation between $D(c)$ and c will show a minimum near the concentration $c = c_0/2$ if eqn. (3) is applied to the diffusion curve of a polydisperse sample.

In Fig. 4 the results of Boltzmann's analyses are shown for two different fractions L(6)F(2) II and B(720) VIII and at three different concentrations. All six curves have minima in the vicinity of $c = c_0/2$. Owing to uncertainty

in the determination of D_m the three curves are also at little displaced parallel to one another. However, they all show the same tendency. An average value of D_0 at infinite dilution and of k_D for the different molecules in the fraction has been defined by the equations

$$D_0 \cdot k_D \frac{c_0}{2} = \frac{\int_{c_0/2}^{c_0} D(c)\mathrm{d}c}{c_0/2} - \frac{\int_{0}^{c_0/2} D(c)\mathrm{d}c}{c_0/2} \tag{4}$$

$$D_m = D_0 \left(1 + k_D \frac{c_0}{2}\right) \tag{5}$$

The last equation [9, 11] can be obtained if one integrates $D(c)$ over the whole concentration interval remembering eqns. (2) and (3).

$$\frac{\int_0^{c_0} D(c)\mathrm{d}c}{c_0} = \frac{\int_0^{c_0} D_0(1+k_D c)\mathrm{d}c}{c_0} = D_0 \left(1 + \tfrac{1}{2} k_D c_0\right) \tag{6}$$

or

$$\frac{\int_0^{c_0} D(c)\mathrm{d}c}{c_0} = \frac{\int_{-\infty}^{+\infty} D_m \mathrm{d}z \int_{-\infty}^{z} z \frac{\mathrm{d}c}{\mathrm{d}z}\mathrm{d}z}{c_0} =$$

$$\frac{D_m}{c_0}\int_{-\infty}^{+\infty} z^2 \frac{\mathrm{d}c}{\mathrm{d}z}\mathrm{d}z - \frac{D_m}{c_0}\left[z \int_{\infty}^{z} z \frac{\mathrm{d}c}{\mathrm{d}z}\mathrm{d}z \right]_{-\infty}^{+\infty} = D_m \tag{7}$$

It may be worth-while to point out that eqn. (7) does not imply that D_m, the diffusion coefficient calculated by the moment method, is a weight average. The whole derivation is strictly valid only for a monodisperse sample. Eqn. (7) expresses only a relation between D_m and the concentration dependence of $D(c)$.

Method 2. The second method used to determine k_D and D_0 is given by Gillis and Kedam [11]. Assuming

$$D(c) = D_0 \left(1 + k_D c\right) \tag{8}$$

they have solved the Fick equation

$$\frac{\partial c}{\partial t} = \frac{\partial}{\partial x}\left(D(c) \frac{\partial c}{\partial x} \right) \tag{9}$$

in an approximate manner and calculated the relation between the product $k_D \times c_0$ and the ratio ϱ of the slope of the diffusion curve at the two points where $\mathrm{d}c/\mathrm{d}z = \frac{1}{2}(\mathrm{d}c/\mathrm{d}z)_{max}$, $(\mathrm{d}c/\mathrm{d}z)_{max}$ denoting the maximum value of the diffusion curve. After having determined k_D from the ratio ϱ one obtains D_0

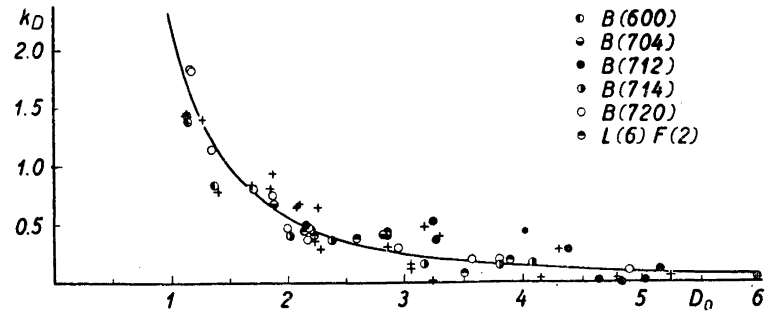


Fig. 5. The dependence of k_D *on the diffusion constant* D_0. *The circles are calculated from the skewness of the diffusion curves, the crosses from analyses according to Boltzmann.*

from eqn. (5). The derivations are rather complicated and cannot be reproduced here; for further details reference must be made to the original work [11]. The derivations are of course only strictly valid for a monodisperse sample. Gillis and Kedam have also calculated the dependence of $(dc/dz)_{max}$ on the ratio ϱ. The results of these calculations are expressed in the form of a table. This table has been used to correct the diffusion coefficients D_A determined in the present investigation. The value of the ratio ϱ has been evaluated from the normalized diffusion curve obtained from about five or six different exposures during the diffusion process.

The results of the two methods to determine k_D and D_0 are given in Fig. 5, where the obtained values of k_D are plotted against the corresponding D_0. The crosses are obtained by method one, the circles by method two. The line corresponds to the equation $k_D = 2.24 \cdot 1/D_0^2$. The constant 2.24 has been determined by applying the method of least squares to the values of k_D and D_0 obtained by method two. After having established this relation between k_D and D_0, the D_0 of each fraction has been calculated by the equation:

$$\frac{\Sigma D_m}{n} = D_0 + \tfrac{1}{2} k_D D_0 \frac{\Sigma c}{n} \tag{10}$$

$$k_D = 2.24 \frac{1}{D_0^2} \tag{11}$$

where $\frac{\Sigma D_m}{n}$ and $\frac{\Sigma c}{n}$ are, respectively, the average value of the diffusion coefficient D_m at finite concentrations and the average concentrations used. The lines drawn in Fig. 2 have been obtained with the aid of eqns. (10) and (11).

MOLECULAR WEIGHT DETERMINATIONS

The molecular weights M_{sD_m} and M_{sD_A} of the different fractions have been calculated with the aid of Svedberg's formula [2]

$$M = \frac{RT\,s}{D(1-V\varrho)} \tag{12}$$

Table 3, summarizing the main properties of the different polymethyl methacrylate fractions. In each series the linear and nonlinear regions in the log s —log [η] plot are separated from each other by a line.

Fraction	[η]	$s_0 10^{13}$	k_s	$M_{sD_m} \times 10^{-3}$	$M_{sD_A} \cdot 10^{-3}$	$(\Phi 1/3P^{-1}) \cdot 10^{-6}$ from M_{sD_m}	from M_{sD_A}	$M_{calc} \times 10^{-3}$	$\frac{M_{calc}}{M_{sD_A}}$	$\frac{k_s}{[\eta]}$
Polymer B(704)										
I	2.10	—	—	—	—	—	—	—	—	—
II	1.83	26.7	2.03	1 425	1 324	2.43	2.55	1 117	0.84	1.11
III	1.44	25.2	2.23	1 200	1 135	2.37	2.46	1 074	0.95	1.55
IV	1.24	22.0	1.78	834	834	2.51	2.51	783	0.94	1.44
V	1.03	19.7	1.53	671	645	2.45	2.50	615	0.95	1.49
VI	0.95	18.0	1.44	506	515	2.63	2.59	521	1.01	1.52
VII	0.81	16.8	1.19	447	462	2.52	2.47	427	0.92	1.47
VIII	0.74	15.0	0.96	402	375	2.34	2.46	324	0.86	1.30
IX	0.65	14.0	0.98	364	357	2.24	2.27	295	0.83	1.51
X	0.54	11.9	0.58	269	269	2.18	2.18	178	0.66	1.07
						Mean for III-X 2.41	Mean for III-X 2.43			
Polymer B(720)										
I	3.73	49.0	7.67	—	—	—	—	5 400	—	2.06
II	3.23	43.1	6.83	—	—	—	—	4 204	—	2.11
III	3.07	34.0	3.61	1 965	2 316	2.97	2.66	2 141	0.92	1.18
IV	2.37	31.0	3.06	1 584	1 634	2.87	2.81	1 717	1.05	1.29
V	1.93	28.8	3.26	1 304	1 395	2.82	2.70	1 587	1.14	1.69
VI	1.65	25.6	2.66	1 021	1 141	2.81	2.61	1 201	1.05	1.61
VII	1.43	—	—	—	—	—	—	—	—	—
VIII	1.21	22.3	2.13	894	898	2.41	2.40	874	0.97	1.76
IX	1.08	19.5	1.46	678	631	2.44	2.56	592	0.94	1.35
X	0.96	18.2	1.12	555	553	2.50	2.50	467	0.84	1.17
XI	0.87	17.4	1.06	433	456	2.73	2.64	425	0.93	1.22
XII	0.68	14.4	0.92	353	356	2.38	2.37	298	0.84	1.35
XIII	0.47	9.86	0.59	180	185	2.26	2.22	135	0.73	1.25
						Mean for VIII— XIII 2.45	Mean for VIII— XIII 2.45			
Polymer B(714)										
I	2.05	28.5	3.53	—	—	—	—	1 625	—	1.72
II	1.34	23.6	2.67	879	907	2.66	2.62	1 065	1.17	1.99
III	1.22	21.8	2.37	—	—	—	—	891	—	1.94
IV	1.09	21.4	2.13	770	763	2.47	2.49	821	1.08	1.95
V	0.92	19.2	1.92	633	621	2.38	2.41	663	1.07	2.09
VI / VII	0.82	18.5	1.89	527	550	2.50	2.43	622	1.13	2.30
VIII	0.81	17.4	1.79	457	461	2.57	2.56	552	1.20	2.21
IX	0.67	14.6	0.85	360	338	2.38	2.48	292	0.86	1.27
X	0.61	13.7	0.98	290	286	2.50	2.52	285	1.00	1.61
XI	0.52	12.8	0.88	264	272	2.35	2.31	244	0.90	1.69
XII	0.43	10.8	0.69	180	182	2.41	2.39	168	0.92	1.60
XIII	0.29	8.11	0.50	103	102	2.30	2.32	93	0.91	1.72
						Mean for IV— XIII 2.43	Mean for IV— XIII 2.43			

Polymer B(712)

I	1.74	24.8	2.03	975	1 082	2.85	2.66	1 000	0.92	1.17
II	1.36	22.3	1.98	753	785	2.82	2.73	842	1.07	1.46
III	1.00	21.4	2.02	590	608	2.86	2.81	800	1.32	2.02
IV	0.95	19.3	1.83	571	578	2.60	2.57	652	1.13	1.93
V	0.74	16.1	1.35	393	408	2.56	2.50	427	1.05	1.83
VI	0.67	15.2	1.50	369	354	2.44	2.50	413	1.17	2.24
VII	0.61	13.3	1.03	291	284	2.42	2.46	280	0.99	1.69
VIII	0.53	12.1	0.68	228	233	2.47	2.43	197	0.85	1.28
IX	0.50	11.6	0.69	214	214	2.42	2.42	187	0.87	1.38
X	0.43	10.7	0.65	177	176	2.41	2.42	161	0.92	1.51
XI	0.38	9.54	0.69	130	128	2.53	2.56	139	1.09	1.82
XII	0.31	8.41	0.43	109	108	2.35	2.36	91	0.84	1.39
XIII	0.28	7.06	—	—	—	—	—	—	—	—
XIV	0.21	6.29	0.29	65	62	2.18	2.25	48	0.77	1.38
						Mean for III—XIV	Mean for III—XIV			
						2.48	2.48			

where T = the absolute temperature
R = the universal gas-constant
V = the partial specific volume of the polymer
ϱ = the density of the solvent
The value [5] 0.787 has been used for V.

The molecular weights calculated from the values of $(D_m)_0$ and $(D_A)_0$ at zero concentration can be found in Table 3.

DISCUSSION

(Relations between intrinsic viscosity, sedimentation constants and molecular weights.) According to the current theories [12] describing the hydrodynamic behaviour of flexible polymer molecules, the dependence of the intrinsic viscosity $[\eta]$ and of the frictional coefficient, f_0, of the chain molecule at infinite dilution on the molecular weight M can be expressed by the equations

$$[\eta] = \Phi \left(\frac{r_0^2}{M}\right)^{3/2} M^{1/2} \alpha_\eta^3 \tag{13}$$

and

$$f_0 = \eta_0 P \left(\frac{r_0^2}{M}\right)^{1/2} M^{1/2} \alpha_f \tag{14}$$

where α_η and α_f represent the ratio of r the effective radius of the molecule in the given solvent to r_0 the root mean square distance between the ends of the polymer chain in a solvent where the second and higher osmotic virial coefficients are zero. Φ and P are universal constants for all flexible polymers irrespective of molecular weight, temperature or solvent used. The sedimentation constant at infinite dilution is further connected with the frictional coefficient f_0 by the expression

$$s_0 = \frac{(1 - V\varrho)M}{Nf_0} \tag{15}$$

where N is Avogadro's number.

Inserting the value of f_0 given by eqn. (14) in eqn. (15) gives

$$s_0 = \frac{(1-V\varrho)}{\eta_0 N\, P} \frac{1}{\left(\frac{r_0^2}{M}\right)^{\frac{1}{2}}} \frac{M^{\frac{1}{2}}}{\alpha_f} \tag{16}$$

By combining (13) and (16) one obtains

$$\frac{s_0[\eta]^{\frac{1}{3}}}{M^{2/3}} \cdot \frac{\eta_0 \cdot N}{(1-V\varrho)} = \Phi^{1/3} P^{-1} \frac{\alpha_\eta}{\alpha_f} \tag{17}$$

In the above equations it is generally assumed that $\alpha_\eta = \alpha_f = \alpha$. A statistical treatment of the long-range intramolecular interaction gives the expression

$$\alpha^5 - \alpha^3 = C_T\, M^{\frac{1}{2}} \tag{18}$$

where C_T is a constant for a given polymer-solvent system. For a not too large molecular weight interval it is therefore possible to assume that

$$[\eta] = K_\eta M^{a_1} \tag{19}$$

and

$$s = K_s M^{a_2} \tag{20}$$

where a_1 and a_2 take into account the extension of the molecule over that which would be obtained by random flight. A log s — log $[\eta]$ plot of the values for the different fractions does not give a straight line as predicted by eqns. (19) and (20), see Fig. 6. The points for the highest molecular weight fractions tend to lie below the straight line. This is most clearly seen for the series B(720) and B(712) for which the polymerization reaction had passed the first stationary stage. The direction of the deviation in the log s — log $[\eta]$ curve indicates that the polymers with the highest molecular weight, which have been formed during the second "explosive" stage of the polymerization, have a more extended configuration. Two explanations are possible, either the molecules are

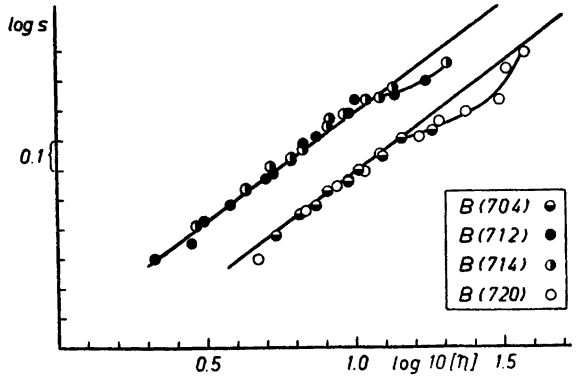


Fig. 6. Log s *plotted against log 10* $[\eta]$. *The upper curve has been displaced 0.2 units upward. The straight lines are drawn with the aid of the equation log* s = *0.74 log* $[\eta]$ + *1.29.*

connected by branching or so tightly entangled with one another that they never behave freely in the dissolved stage. The problem will be treated in detail elsewhere [1] so it will not be discussed further here. The points on the curved part of the line have been excluded in the determination of the constants in the equations describing the relations between sedimentation constant, intrinsic viscosity and molecular weight given in Table 4. In these calculations both M_{sD_m} and M_{sD_A}, the molecular weights obtained from D_m and D_A respectively, have been used. As can be seen from the last row in the table these two kinds of molecular weights give exactly the same relation with s and $[\eta]$ in spite of the fact that for a polydisperse sample D_A must be lower than D_m[3, 9]. The reason for the high values of D_A may be an undercorrection of the concentration effect. In extrapolating the experimentally obtained values of the diffusion coefficients, in accordance with the calculations by Gillis and Kedam, a lower concentration dependence has been assumed for D_A than for D_m. This causes $(D_A)_0$ at infinite dilution to be nearly equal to $(D_m)_0$ although the measured value of the former is lower at finite concentrations (See Fig. 2).

A calculation of $\Phi^{1/3}P^{-1}\frac{\alpha_\eta}{\alpha_f} \times 10^{-6}$ from expression (17) gives lower values for the last fractions in each series. From an analysis of all 34 values in the region where log s is a linear function of log $[\eta]$, one obtains the following mean values 2.37, 2.44 and 2.52 for the molecular weight intervals $< 2.5 \times 10^5$, 2.5×10^5 to 5×10^5 and $> 5 \times 10^5$, respectively. The number of fractions in each region is 9, 13 and 12, respectively. The values of $\Phi^{1/3}P^{-1}$ calculated for polymethyl methacrylate in acetone from data obtained by Meyerhoff show the same trend to increase for the lowest molecular weights [13]. The average value of $\Phi^{1/3}P^{-1}$ calculated from different polymers in different solvents, is $(2.5 \pm 0.1) \times 10^6$. The reason for the low value obtained for the last fractions can be either that these have a different degree of heterogeneity from the others

Table 4, giving the relations between the quantities s, $[\eta]$, M_{sD_m} *and* M_{sD_A}.

	No. of fraction	log s = a log M_{sD_m} − b		log s = a log M_{sD_A} − b		log $[\eta]$ = a log M_{sD_m} − b		log $[\eta]$ = a log M_{sD_A} − b		log s = a log$[\eta]$ + b	
		a	b	a	b	a	b	a	b	a	b
B(704)	8	0.50	1.63	0.51	1.70	0.67	3.89	0.69	3.98	0.74	1.28
B(720)	6	0.51	1.64	0.53	1.76	0.61	3.53	0.63	3.65	0.83	1.28
B(714)	9	0.48	1.51	0.48	1.51	0.65	3.76	0.64	3.75	0.75	1.31
B(712)	11	0.52	1.70	0.51	1.63	0.68	3.92	0.66	3.84	0.78	1.31
All fractions	34	0.48^4	1.51^6	0.48^4	1.51^8	0.65^9	3.82^4	0.65^9	3.82^2	0.73^9	1.29^1

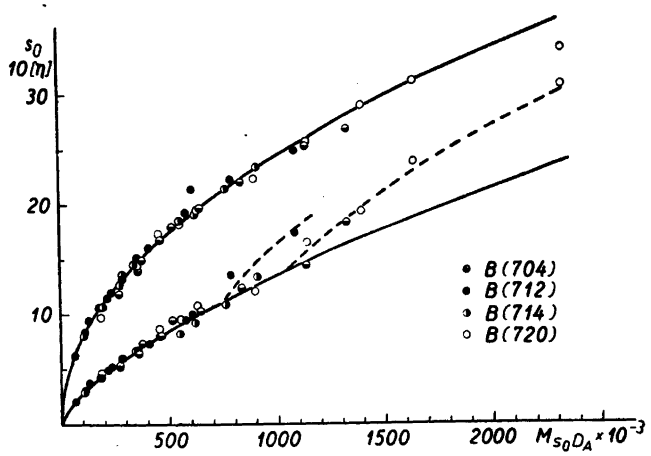


Fig. 7. s_0 *and 10* [η] *as functions of* M_{sD_A}. *The solid lines are the curves obtained from the constants in Table 4. The dotted lines are drawn through points that give a curved log s — log* [η] *line. Upper curve s, lower curve* [η].

or that the shapes of the polymer chains are such that they can not be approximated with an equivalent effective sphere, giving $\alpha_\eta/\alpha_t \neq 1$. (See Ref. 1).

The dependence of the sedimentation constant, the intrinsic viscosity, and the constant $\Phi^{1/3}P^{-1}$ on molecular weight is graphically represented in Figs. 7 and 8. The solid lines in Fig. 7 are the curves obtained from the constants in Table 4. The dotted lines are drawn through points that give a curved log s —log [η] line. This figure shows that the anomalies in intrinsic viscosity occurs at a lower molecular weight for polymers prepared at 80° C — B(712) and B(714) — than those at 60° C — B(704) and B(720). The deviation of the observed sedimentation constants from the solid line at high molecular weights is not so pronounced as in the case of intrinsic viscosity. This must also be expected from eqns. (13) and (16), s being inversely proportional to α and [η] directly proportional to the third power of α.

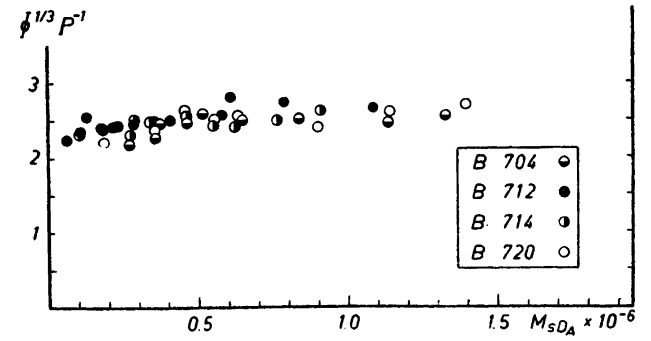


Fig. 8. $\Phi^{1/3}P^{-1}$ *as a function of* M_{sD_A}.

(The concentration dependence of the sedimentation coefficient.) The effect of the concentration on the sedimentation velocity of chain molecules has been investigated by Wales and Holde [14]. In their treatment the coiled polymer is considered as a sphere obeying Stokes' law

$$6\pi\eta_0 \; a = \eta_0 \, P \; r \tag{21}$$

where r is the effective radius of the equivalent sphere and

$$r = r_0 \; \alpha_f \tag{22}$$

The concentration dependence of the sedimentation coefficient of spherical particles is given by Burgers' relation

$$\frac{1}{s} = \frac{1}{s_0}\left(1 + \frac{55}{8} \, n \; v\right) \tag{23}$$

where n is the number of molecules in unit volume and v the volume of a molecule. Eqns. (13)—(15) and (21)—(23) together with the empirically found relation for the concentration dependence of the sedimentation coefficient

$$\frac{1}{s} = \frac{1}{s_0}\left(1 + k_s c\right) \tag{24}$$

give

$$\frac{k_s}{[\eta]} = \frac{\frac{55\,N}{8}\left(\Phi^{1/3} P^{-1}\right)^{-3}}{16\,200\pi^2} \tag{25}$$

and

$$M = \pi N \left(\frac{16\,200}{\frac{55}{8}}\right)^{1/2} k_s^{1/2} \left(\frac{s_0 \eta_0}{(1 - V\varrho)}\right)^{3/2} \tag{26}$$

If the value of $\Phi^{1/3} P^{-1}$ is considered to be 2.5×10^6 one obtains

$$k_s / [\eta] = 1.66 \tag{27}$$

As is seen from Table 3 there is a spread in the individual values of $k_s/[\eta]$ for the different polymethyl methacrylate fractions. However, the average value of $k_s/[\eta]$ in the three molecular weight intervals $< 2.5 \times 10^5$, 2.5×10^5—5×10^5 and $> 5 \times 10^5$ are 1.48, 1.57 and 1.71, respectively, the number of values in each interval being 9, 13 and 12. As can be seen from these figures $k_s/[\eta]$ gives approximately the value predicted by Wales and Holde, but increases slowly with increasing molecular weight. Thus both $k_s/[\eta]$ and $\Phi^{1/3} P^{-1}$ increase with molecular weight contrary to the predictions of eqn. (25).

The molecular weights, M_{calc}, of the different fractions calculated by eqn. (26) are given in Table 3. These are in fairly good agreement with those obtained by direct determination of the molecular weight M_{sD_A}. An analysis of the values in the three molecular weight intervals previously used shows that M_{calc}/M_{sD_A} is about 88, 94 and 103 % and increases with increasing M_{sD_A}. The nature of the average obtained by eqn. (26) is very complicated. It has been

found by the present author that for a symmetrical distribution of s the value of k_s is not very much influenced by the width of the distribution (unpublished work). This means that under the given assumption the average obtained by eqn. (25) would be equal to that calculated by inserting a weight average of s and a weight average of $1/D$ in eqn. (12). As the harmonic mean is less than the arithmetic mean this results in a molecular weight greater than M_{sD} calculated from a weight average of both s and D.

This investigation has been financially supported by grants from *Statens Tekniska Forskningsråd* and *Stiftelsen Svensk Gummiforskning* (Ab. Sieverts Kabelverk, AB. Liljeholmens Kabelfabrik, Goodyear Gummifabriks AB., Svenska Gummifabriks AB., Viskafors Gummifabriks AB.).

The author wishes to acknowledge his indebtness to Professor The Svedberg and Professor Stig Claesson for their very kind interest and for the many facilities which have been put at his disposal.

The author also wishes to thank Dr. P.-O. Kinell and Assistent Evald Hellman for their interest in this study and for many valuable discussions.

REFERENCES

1. Eriksson, A. F. V. *Svensk Kem. Tidskr.* (in English) **68** (1956). *In press.*
2. Svedberg, T. and Pedersen, K. O. *The Ultracentrifuge*, Oxford 1940.
3. Lamm, O. *Nova Acta Regiae Soc. Sci. Upsaliensis* **10** (1937) No. 6.
4. Mosimann, H. and Signer, R. *Helv. Chim. Acta* **27** (1944) 1123.
5. Eriksson, A. F. V. *Acta Chem. Scand.* **7** (1953) 623.
6. Claesson, S. *Nature* **158** (1946) 834.
7. Claesson, S. and Sahlman, Y. *Unpublished.*
8. Boltzmann, L. *Ann. Physik* **53** (1894) 959.
9. Gralén, N. *Sedimentation and Diffusion Measurements on Cellulose and Cellulose Derivatives*, Thesis, Uppsala 1944.
10. Beckmann, C. O. and Rosenberg, Y. L. *Ann. N. Y. Acad. Sci.* **46** (1945) 329.
11. Gillis, J. and Kedem, O. *J. Polymer Sci.* **11** (1953) 545.
12. Flory, P. J. *Principles of Polymer Chemistry*, New York 1953.
13. Fox, T. G. and Mandelkern, L. *J. Chem. Phys.* **21** (1953) 187; Meyerhoff, G. and Schulz, G. V. *Makromol. Chem.* **7** (1952) 294.
14. Wales, M. and van Holde, K. E. *J. Polymer Sci.* **14** (1954) 81.
15. Burgers, J. M. *Proc. Acad. Sci. Amsterdam* **45** (1942) 9.

Received January 24, 1956.

ACTA CHEMICA SCANDINAVICA 10 (1956) 393—396

The Structure of Alpinone

JARL GRIPENBERG, ERKKI HONKANEN and KAJ SILANDER

Department of Chemistry, Institute of Technology, Helsinki, Finland

The seeds of *Alpinia japonica* Miq. contain alpinone and its 3-acetate. The former has been shown to be identical with pinobanksin-7-methylether (V). 3-Hydroxy-5,7-dimethoxy-2-methylflavanone has been synthesised.

In 1936 Kimura and Hoshi [1] advanced the formula (I) for alpinone, a constituent of the seeds of *Alpinia japonica* Miq. The evidence they cited in support of this structure was, however, not very convincing. In particular the very easy loss of the methyl group in position 2, when alpinone was treated with alkali, appears to be extremely improbable. A reinvestigation of the structure of alpinone became even more necessary, when it could be shown that one of the key compounds in Kimura and Hoshi's arguments, namely the so called "apoalpinonemonomethylether" was wrongly formulated [2].

Two different approaches towards the solution of this problem were used. The first was to synthesise a compound with the structure (I) and compare it with alpinone, and the second was a reinvestigation of authentic alpinone. The second approach eventually led to a solution of the problem and the synthetic route was therefore left uncompleted, but the results obtained in the synthesis up to this time are reported in this paper.

When the seeds of *Alpinia japonica* were extracted with light petroleum two crystalline substances were obtained. They could be separated from one another by virtue of their different solubilities in toluene. The less soluble compound had m. p. 179—180°, $[\alpha]_D^{20}$ + 91° (pyridine), —12° (chloroform) and gave a benzoate of m. p. 208—210°. Kimura and Hoshi [1] report for alpinone m. p. 178°;$[\alpha]_D^{29}$ + 79.11 (pyridine), and for its dibenzoate m. p. 208—209°. It is thus evident that this compound is identical with the alpinone of Kimura and Hoshi [1]. Its analysis agrees, however, far better with $C_{16}H_{14}O_5$ than with $C_{17}H_{16}O_5$, as proposed by the Japanese authors. They converted alpinone with alkali into the so called apoalpinone, which upon methylation gave a dimethylether. This was identical with the methylether of a compound which Kimura and Hoshi synthesised and believed to be 3-hydroxy-5,7-dimethoxyflavanone (II) [1]. It has, however, recently been shown that this compound is 2-benzyl-2-hydroxy-4,6-dimethoxycoumaran-3-one (III) [2], from which it follows that "apoalpinone" must be (IV). The formation of (IV) from alpinone under alkaline conditions together with the analytical results mentio-

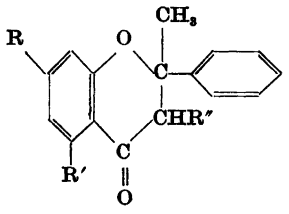
ned above, strongly suggest that alpinone is 3,5-dihydroxy-7-methoxyflavanone (V). It should thus be either identical with pinobanksin-7-methylether [3] or a stereoisomer of this compound. The following comparison clearly establishes that the two compounds are identical, as has been previously reported in a preliminary note [4].

	m. p.	$[\alpha]_D^{20}$ in pyridine	$[\alpha]_D^{20}$ in chloroform	m. p. of dibenzoate
Alpinone	179—180°	+ 91°	— 12°	208—210°
Pinobanksin-7-methylether	181—182° [3]	+ 92°	— 19° [3]	208—210°

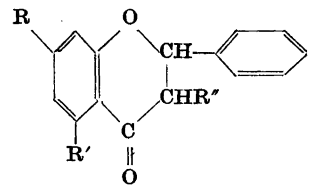
No depression of m.p.s was observed on mixing either the compounds themselves or their dibenzoates.

The same conclusion regarding the structure of alpinone has also been reached by Kotake, Sakan and Kubota [5].

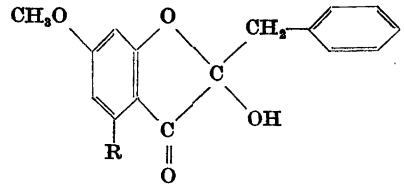
As mentioned above, the extraction of the seeds of *Alpinia japonica* gave in addition to alpinone a second compound, more soluble in toluene. This has m. p. 135°; $[\alpha]_D^{20}$ + 17° (pyridine) and corresponds to the formula $C_{17}H_{13}O_5(OCH_3)$. It gave the same colour reactions with ferric chloride and with magnesium and zinc and hydrochloric acid as alpinone and its U.V.-spectrum is almost indistinguishable from that of alpinone (λ_{max} 292 mμ; log ε 4.28). On hydrolysis with strong acids it gave alpinone and acetic acid. It must thus be a monoacetate of alpinone and its positive colour reaction with ferric chloride places the acetyl group on the hydroxyl in position 3, enabling it to be formulated as (VI). When alpinone was acetylated with acetic anhydride and pyridine the same acetate was obtained. This is, as far as the present authors are aware, the first instance, that a 3-hydroxyflavanone has been found in Nature as its acetate. This compound occurs in an amount about equal to that of alpinone and it is difficult to see why Kimura and Hoshi were unable to isolate it.



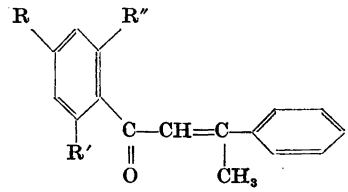
I R = OCH_3; R′ = R″ = OH
IX R = R′ = OH; R″ = H
X R = R′ = OCH_3; R″ = H
XI R = R′ = OCH_3; R″ = OH



II R = R′ = OCH_3; R″ = OH
V R = OCH_3; R′ = R″ = OH
VI R = OCH_3; R′ = OH; R″ = $OCOCH_3$



III R = OCH_3
IV R = OH



VII R = R′ = R″ = OCH_3
VIII R = R′ = OCH_3; R″ = OH

Of the methods available for the synthesis of 3-hydroxyflavanones, the two methods due to Oyamada [6,7] appeared to be most promising for the synthesis of (I). In the first of these [6] bromine is added to the double bond of the acetate of the corresponding chalcone. The dibromide is then treated with silver acetate and the diacetoxydihydrochalcone is submitted to acid hydrolysis giving the 3-hydroxyflavanone. The starting material was in this case 2',4',6'-trimethoxy-β-methylchalcone (VII) obtainable from phloroglucinoltrimethylether and β-methylcinnamoyl chloride under Friedel-Crafts conditions. This was partially demethylated to (VIII) using aluminium bromide in benzene. Addition of bromine to the acetate of (VIII) was, however, unsuccessful. Only intractable tars were obtained.

The second method involves oxidation of the corresponding flavanone with lead tetra-acetate, followed by hydrolysis of the thus formed 3-hydroxyflavanone acetate. The flavanone (IX) has been prepared, although in low yield, by Lindstedt and Misiorny [7] and by Kotake [8]. Because the hydroxyl groups have to be protected during the lead tetra-acetate oxidation it was found more convenient to synthesise its dimethylether (X) from the corresponding chalcone (VIII). The lead tetra-acetate oxidation of (X) gave a very low yield of (IX). For reasons given above, no attempt was made to improve the yield in this step or to carry out the reaction on a larger scale in order to obtain sufficient material for carrying the synthesis to completion.

EXPERIMENTAL

Isolation of alpinone and its 3-acetate. The finely ground seeds of *Alpinia japonica* were extracted in a Soxhlet apparatus with light petroleum for 6 hours. The solvent was distilled off and the residue was steam distilled in order to remove volatile components. The dried residue was boiled with toluene, leaving a green amorphous mass undissolved. Fractional crystallisation of the toluene soluble part gave, as a less soluble component alpinone, m. p. 179—180°, $[\alpha]_D^{20}$ + 91° (*c* 3.46 in pyridine); −12° (*c* 2.64 in chloroform). (Found: C 66.50; H 4.82. $C_{16}H_{14}O_5$ requires C 67.12; H 4.93). The dibenzoate was prepared with benzoyl chloride and pyridine on a water bath; m. p. 208—210°.

The more soluble component was alpinone-3-acetate, m. p. 135°, $[\alpha]_D^{20}$ + 17° (*c* 4.7 in pyridine). (Found: C 66.12; H 4.97; OCH_3 9.60. $C_{17}H_{13}O_5(OCH_3)$ requires C 65.85; H 4.91; OCH_3 9.46).

Alpinone and its 3-acetate have widely different R_F-values (0.42 and 0.76, respectively, in ligroin:water:methanol (100:50:1)).

Hydrolysis of alpinone-3-acetate. Alpinone-3-acetate (330 mg) was boiled in a nitrogen atmosphere for one hour with a solution of hydriodic acid (9 ml) in abs. ethanol (1.5 ml). Water was then added and the precipitate recrystallised from methanol, m. p. 181—182°, undepressed when mixed with alpinone. (Found: C 67.21; H 4.94; OCH_3 10.94. $C_{15}H_{11}O_4(OCH_3)$ requires C 67.12; H 4.93; OCH_3 10.84). The same result was also obtained by using conc. hydrochloric acid or 42 % sulphuric acid. In the last case the volatile acid formed in the reaction was distilled off and its half distillation value (determined according to Virtanen and Pulkki [10]) was found to be 37, which is the value given for acetic acid [10].

Synthesis of alpinone-3-acetate. Pinobanksin-7-methylether [3] (30 mg) was dissolved in acetic anhydride and one drop of pyridine was added. After standing overnight at room temperature water was added. The oil which precipitated crystallised after some time and was recrystallised from methanol. M. p. 135—136°, undepressed when mixed with natural alpinone-3-acetate. (Found: C 65.33; H 5.11. $C_{18}H_{16}O_6$ requires C 65.85; H 4.91).

2',4',6'-Trimethoxy-β-methylchalcone (VII). Phloroglucinoltrimethylether[11] (18.1 g) and β-methylcinnamoylchloride[12] (19.5 g) were dissolved in nitrobenzene (100 ml). The mixture was cooled with ice and stirred, and powdered aluminium chloride (14.0 g) was added in small portions during two hours. Stirring was continued for three hours at room temperature. The precipitate was filtered off, washed with dry ether, and then added in small portions to ice-cold hydrochloric acid. The remaining solid was filtered off, dried, and recrystallised from methanol giving light yellow leaflets, m. p. 127—128°. Yield 16.5 g (50 %). (Found C 72.5; H 6.5. $C_{19}H_{20}O_4$ requires C 73.1; H 6.5).

2'-Hydroxy-4',6'-dimethoxy-β-methylchalcone (VIII). 2',4',6'-Trimethoxy-β-methylcalcone (15.6 g) was dissolved in dry benzene (100 ml) and to this was added during half an hour a solution of aluminium bromide (14.5 g) in benzene (100 ml). The mixture was then refluxed on a water bath for two hours. The solvent was removed in vacuum and the residue was treated with ice-cold hydrochloric acid. The solid was filtered off and recrystallised from methanol. Yellow prisms, m. p. 75—77°. Yield 12.2 g (81 %). (Found: 72.1; H 6.1. $C_{18}H_{18}O_4$ requires C 72.5; H 6.1). Other demethylating agents gave much inferior yields.

The acetate was obtained by boiling the chalcone with acetic anhydride, either in pyridine solution or in the presence of anhydrous sodium acetate. Almost colourless leaflets, m. p. 87—88°. (Found: C 70.04; H 6.47 $C_{20}H_{20}O_5$ requires C 70.57; H 5.92 %).

5,7-Dimethoxy-2-methylflavanone (X). 2'-Hydroxy-4',6'-dimethoxy-β-methylchalcone (6.0 g) was dissolved in hot ethanol (100 ml) and to this was added 2 N sodium hydroxide (50 ml). The mixture was then poured into 400 ml of cold water and allowed to stand for 24 hours. The precipitate was filtered off and recrystallised from ethanol. Colourless crystals, m. p. 135—136°. Yield 5.1 g (85 %). (Found: C 72.2; H 6.1. $C_{18}H_{18}O_4$ requires C 72.5; H 6.1).

3-Hydroxy-5,7-dimethoxy-2-methylflavanone (XI). 5,7-Dimethoxy-2-methylflavanone (3.0 g) was dissolved in glacial acetic acid (50 ml) and lead tetra-acetate (4.7 g) was added. The mixture was kept at 85—90° for 3 hours and then poured into 200 ml of cold water. The precipitate was dissolved in ethanol (100 ml) and conc. hydrochloric acid was added. The mixture was then warmed for half an hour on a water bath in a stream of carbon dioxide, and poured into water (200 ml). This was allowed to stand for 24 hours, whereafter the precipitate was filtered off and recrystallised from methanol. Colourless needles, m. p. 166—167°. Yield 0.06 g. (Found: C 69.1; H 5.8. $C_{18}H_{18}O_5$ requires C 68.8; H 5.8).

The analyses were carried out by Dr. J. Hukki of this Institute, Dr. A. Bernhardt, Mülheim, and Dr. A. Schoeller, Kronach. The authors wish to thank Prof. H. Erdtman, Stockholm, for a generous sample of pinobanksin and Prof. S. Hattori and Dr. Y. Kimura, Tokyo, for providing us with the seeds of *Alpinia japonica*.

REFERENCES

1. Kimura, Y. and Hoshi, M. *Proc. Imp. Acad. Tokyo* **12** (1936 285; *J. Pharm. Soc. Japan* **57** (1937) 147; *Chem. Abstracts* **33** (1939) 531.
2. Gripenberg, J. *Acta Chem. Scand.* **7** (1953) 1323.
3. Lindstedt, G. *Acta Chem. Scand.* **4** (1950) 772.
4. Gripenberg, J. and Silander, K. *Chemistry & Industry* **1955** 443.
5. Kotake, H. Jr., Sakan, T. and Kubota, T. *Chemistry & Industry* **1954** 1562.
6. Oyamada, T. *Ann.* **538** (1939) 44.
7. Oyamada, T. *J. Chem. Soc. Japan* **64** (1943) 331; *Chem. Abstracts* **41** (1947) 3797.
8. Lindstedt, G. and Misiorny, A. *Acta Chem. Scand.* **5** (1951) 971.
9. Kotake, H. *J. Inst. Polytechnics, Osaka City Univ. Ser. C* **4** (1953) 246.
10. Virtanen, A. I. and Pulkki, L. *J. Am. Chem. Soc.* **50** (1928) 3138.
11. Freudenberg, K. *Ann.* **433** (1923) 230.
12. Johnson, J. D. A. and Kon, G. A. R. *J. Chem. Soc.* **1926** 2748.

Received November 11, 1955.

ACTA CHEMICA SCANDINAVICA 10 (1956) 397—407

Essential Groups in DPN-linked Lactic Dehydrogenase

AGNAR P. NYGAARD*

Medicinska Nobelinstitutet, Biokemiska avdelningen, Stockholm, Sweden, and Johan Throne Holst's Institutt for Ernæringsforsking, Blindern, Oslo, Norway

Sulfhydryl groups in lactic dehydrogenase from ox heart (LDH) have been determined both amperometrically with mercuric chloride and spectrophotometrically with *p*-chloromercuribenzoate (PCMB). The enzyme appeared to contain 7—9 SH groups, but only 3 of these reacted with PCMB in the native enzyme. LDH was slowly inhibited by PCMB [4], but rapidly by mercury and silver ions; slowly by periodate, but rapidly by iodine, which oxidized SH groups. Incubation of LDH with acetic anhydride blocked amino groups, increased the reactivity of SH groups to PCMB and caused a strong inhibition. This inhibition was not reversed under conditions which hydrolyzed phenyl acetate and thiol acetate. Also a temporary inhibition by acetic anhydride was observed, which existed while acetic anhydride was present in the solution.

The great majority of DPN-linked ** enzymes contain essential sulfhydryl groups which are susceptible to most SH reagents [1]. In contrast, DPN-linked lactic dehydrogenase from ox heart (LDH) is not readily inhibited by a number of SH reagents [2,3], and was for that reason believed not to require SH groups for activity. Recently, however, *p*-chloromercuribenzoate (PCMB) has been found to react slowly with the enzyme, thus causing inhibition [4]. In this work the reactivity and essentiality of SH groups in LDH have been further investigated.

Many enzymes are known to depend on SH groups for their activity. Less is known about other kinds of functional groups. Ideal reagents are lacking in many cases. Further work may reveal other groups as frequently involved in the regulation of enzyme activity as are SH groups. In this study, the essentiality of amino groups in LDH has been investigated. As carriers of positive charge, these groups could be expected to play a role in the electrostatic interaction of enzyme and coenzyme or substrate. Extensive studies have revealed

---

* Fellow, Norwegian Research Council.

** The following abbreviations are used: DPN: diphosphopyridine nucleotide, DPNH: reduced diphosphopyridine nucleotide, LDH: DPN-linked lactic dehydrogenase from ox heart, PCMB: *p*-chloromercuribenzoate and SH: sulfhydryl (thiol) group.

this kind of interaction between flavin mononucleotide and the apoprotein of the old yellow enzyme [5].

Also included in this work is the detection of what appears to be a very labile acetyl compound of LDH.

A short account on the work with SH groups in LDH has already been published [6].

MATERIALS AND METHODS

Crystalline LDH, containing fractions A and C [3,4] was prepared according to Straub [7]. The enzyme concentration was determined from optical density measurements at 280 mμ. In the calculation, a molar extinction coefficient of 20.1×10^4 and a molecular weight of 135 000 were used [3,4].

Crystalline liver alcohol dehydrogenase was a gift from Dr. R. Bonnichsen.

DPN, 90 % pure, was procured from Sigma Chemical Company, St. Louis, Mo.

DPNH was prepared by enzymatic reduction of DPN [8].

Sodiumpyruvate was made from commercial pyruvic acid [9].

DL-*Lactic acid* was Baker's analyzed reagent.

Oxidoreduction of DPN(H) was measured with a fluorimeter of the type described elsewhere [10,11].

Iodination of the enzyme was carried out at 0° C. The iodinating agent was 0.1 M iodine dissolved in 96 % alcohol.

Acetylation of the enzyme and of cysteine and tyrosine was accomplished by the addition of 1 μl quantities of acetic anhydride to approximately 1 ml of the protein (amino acid) solution buffered with 2.5 M sodium acetate and kept at 0° C [12]. To the control the same amount of acetic anhydride was added to the acetate solution half an hour before the enzyme (amino acid) was added.

Thiol groups were determined both spectrophotometrically with PCMB according to Boyer [13] and amperometrically according to Kolthoff *et al.*[14] In the spectrophotometric determinations the change in optical density at 250 mμ was recorded and a molecular extinction coefficient of 7.6×10^3 was used to calculate the extent of the reaction. Spectrophotometric determinations were carried out both with the native and denatured enzyme. Denaturation was accomplished by incubation of the enzyme in 10 % lauryl sulfate. Foaming prevented amperometric titration of a protein denatured with lauryl sulfate. The amperometric titration had to be carried out within 10 minutes, otherwise the potentials drifted and measurements were impossible. Cysteine treated with acetic anhydride gave no reaction with PCMB or with mercury ions in the amperometric titration. This shows that the thiol groups were blocked and that the acetyl-thiol linkage was stable under the conditions of analysis. Cysteine treated with acetic anhydride will be designated S-acetyl cysteine. Undoubtedly, the amino group was also acetylated in this compound.

Tyrosine was estimated by the Millon-Lugg procedure [15], and the diiodotyrosine formed was calculated from the difference in tyrosine content determined by this procedure before and after iodination [12].

Amino groups were determined by Van Slyke amino nitrogen analysis [16], which was carried out on dialyzed samples containing approximately 15 mg of protein. A 15 minute reaction time was found sufficient to give maximum values.

Phenol groups were estimated by means of Folin's phenol reagent [17], the protein first being denatured with lauryl sulfate [18]. When tyrosine had been treated with acetic anhydride the color reaction was negative, indicating that phenolic hydroxyl was acetylated and that the linkage was stable under the conditions of analysis. Tyrosine treated with acetic anhydride is designated O-acetyl tyrosine. This compound was undoubtedly also acetylated in the amino group.

Hydrolysis of phenol acetate and thiol acetate can be accomplished by incubation at pH 11 for about 5 minutes [12]. The acetyl-amino linkage is stable under these conditions. Therefore, if no reactivation of an acetylated enzyme takes

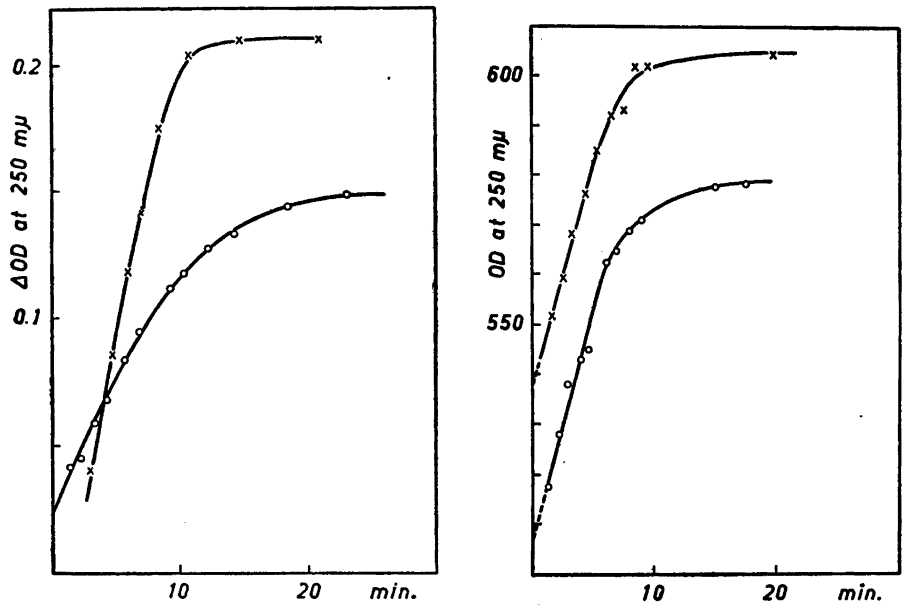


Fig. 1. Reaction of LDH with p-chloromercuribenzoate, before and after treatment of the enzyme with acetic anhydride.

Test conditions: To 2.6 ml 0.2 M phosphate buffer were added 94 mμmoles of PCMB and 14.5 mμmoles of LDH. Final volume 3.0 ml. For unmodified enzyme Δ OD = 0.108 Therefore $\frac{0.108 \times 3 \times 10^6}{7.6 \times 10^3 \times 14.5} = 2.9$ SH groups per mole enzyme.

LDH was acetylated as follows: To 20.1 mμmoles LDH in 0.4 ml 2.5 M sodium acetate pH 7 were added 5 × 1 μl of acetic anhydride at 0° C with one minute's intervals. 290 μl of the solution was allowed to react with PCMB. The enzyme activity decreased 45 % by the acetylation. × × × acetylated LDH O O O LDH, unmodified.

In order to measure total thiol groups, the enzyme dissolved in a few μl solution was allowed to react with 100 μl of 10 % lauryl sulfate before the addition of buffer and PCMB. The denatured enzyme reacted instantaneously with PCMB, as also did cysteine.

Fig. 2. Reaction of liver alcohol dehydrogenase (ADH) with p-chloromercuribenzoate before and after treatment with acetic anhydride.

Test conditions: To 2.66 ml 0.2 M phosphate buffer were added 159 mμmoles PCMB and 8.7 mμmoles ADH. Final pH 6.3. Total volume 3.0 ml Δ OD = 0.070. Therefore $\frac{0.07 \times 3 \times 10^6}{7.6 \times 10^3 \times 8.7} = 3.1$ SH groups per mole ADH.

ADH was acetylated as follows: To 32.6 mμmoles enzyme in 0.4 ml of 2.5 M sodium acetate pH 7 was added 5 × 1 μl acetic anhydride at 0° C with one minute intervals. 106 μl of the solution was allowed to react with PCMB. The enzyme activity decreased 62 % by the acetylation. None of the activity was recovered by incubation in 1 M glycine pH 9.5. × × × acetylated ADH O O O ADH, unmodified

place with incubation at pH 11, essential phenol or thiol groups have probably not been acetylated [19]. However, incubation at pH 11 may cause denaturation of some proteins. We have found that high alkalinity can be avoided by the use of high concentrations of glycine. Thus, O-acetyl tyrosine and S-acetyl cysteine

were found to be hydrolyzed within a few minutes by incubation in 1 M glycine at pH 9.5 but not affected by 0.1 M glycine at pH 9.5. The evidence was that Folin's phenol color (for tyrosine) and the reaction with PCMB (for cysteine) reappeared. LDH, liver alcohol dehydrogenase and the apoenzyme of the old yellow enzyme were perfectly stable in 1 M glycine pH 9.5. The acetyl-amino linkage in acetylated LDH was not hydrolyzed under these conditions, as there was no increase in Van Slyke amino group analysis.

RESULTS

Neilands [3] observed that 10^{-3} M PCMB had no instantaneous effect on LDH activity. However, incubation with the reagent caused inhibition, which was reversed by cysteine [4]. These observations have been confirmed in this study. The reaction between PCMB and LDH, reflecting the inhibition of the enzyme, is shown in Fig. 1. Under the conditions used, 2.8 SH groups reacted with PCMB, whereas Neilands [4] recorded 2 SH groups combining. Also included in Fig. 1 is the more extensive and more rapid reaction between PCMB and an acetylated form of the enzyme. Evidence for specific acetylation of amino groups will be presented later. In contrast to LDH, an acetylated form of liver alcohol dehydrogenase and the unmodified enzyme reacted similarly

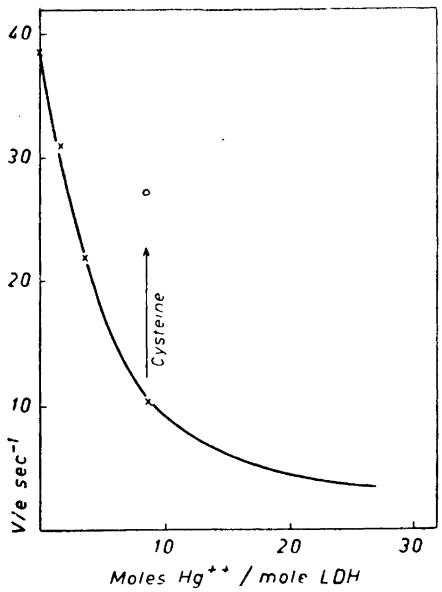


Fig. 3. Inactivation of LDH by $HgCl_2$.

10^{-2} or 10^{-3} M $HgCl_2$ was added to 1.14 mμmoles LDH in 25 μl of 0.02 M phosphate pH 7.2 and the mixture was allowed to react for 2 minutes at 0° C. The solution was then diluted to 500 μl with water and 5 μl were used for testing of activity in 3.0 ml of 0.1 M glycine pH 9.0. Conc. DL-lactate: 8.3 μM. Conc. DPN: 420 μM. To one sample (see figure) 10 μl of 0.5 M neutralized cysteine were added after dilution to 500 μl. The inhibition did not increase with a longer incubation time than 2 minutes.

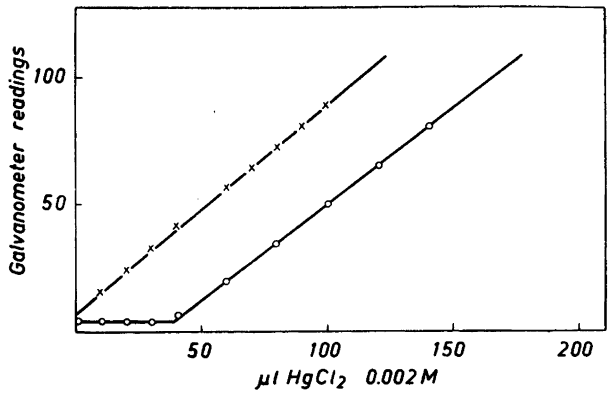


Fig. 4. Amperometric titration of LDH with $HgCl_2$.

The buffer used was 0.01 M in NaH_2PO_4, 0.08 M in Na_2HPO_4 and 0.5 N in KCl [14]. The titration was carried out within 10 min. 11 mμmoles LDH were found to bind 39 μl of 0.002 M $HgCl_2$. That is, 7.1 SH groups per mole LDH reacted with mercuric chloride. × × × blank O O O 11 mμmoles LDH.

with PCMB. This is shown in Fig. 2. For LDH denatured with lauryl sulfate, the reaction with PCMB was too rapid to be followed in a Beckman spectrophotometer; a total of 9.3 SH groups appeared to react.

In contrast to the slow inhibition of LDH by PCMB, mercuric and silver salts have been found to cause a very rapid inactivation of the enzyme. Thus, when 0.018 mμmole of LDH was added to 3.0 ml glycine buffer at pH 9.0, which was 8.3 mM in DL-lactate, 300 μM in DPN and 0.33 μM in Ag_2SO_4, no reduction of DPN was observed. The enzyme must have been inactivated within a few seconds. Inactivation of LDH as a function of added mercuric chloride is illustrated in Fig. 3. The incubation time was 2 minutes. Under the conditions used, 10 moles of mercury per mole of enzyme caused 75 % inhibition. A similar result was observed with Ag_2SO_4. Only 95 % inhibition was obtained with heavy metal ions some five-fold in excess of the total number of thiol groups. Cysteine counteracted the inhibition by $HgCl_2$ and Ag_2SO_4 to varying degrees, apparently depending upon the conditions of the incubation. In one case, a sample which had been completely inhibited by Ag_2SO_4 was reactivated completely. Fig. 4 shows the results of an amperometric titration [14] of LDH with $HgCl_2$ whereby 7 thiol groups were titrated. This is 2 SH groups less than obtained with the spectrophotometric titration with PCMB.

Incubation with iodine resulted in a rapid decrease of the LDH activity. The inhibition illustrated in Fig. 5 was registered within a few minutes after the addition of the reagent, which rapidly lost its color. The following observations suggest strongly that the inhibition was due to oxidation of essential SH groups, mainly to the disulfide stage, and not to substitution of tyrosine [12]: 1) No diiodotyrosine was formed, even in the most iodinated sample (See Fig. 5). 2) The reaction of LDH with PCMB disappeared with iodination of the protein. 3) The amount of iodine necessary for complete inactivation corres-

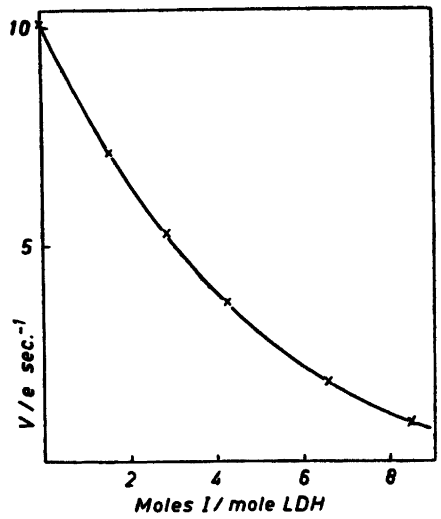


Fig. 5. Inactivation of LDH with iodine.

To 28.2 mμmoles LDH in 0.7 ml of 0.1 M phosphate pH 7.3, 0° C, were added 1 μl quantities of 0.1 M I in alcohol with 5 minute's intervals. To the controls corresponding amounts of alcohol were added. 2 μl of the enzyme solution were used for testing in 3.0 ml of 0.1 M glycine buffer pH 9.0 at 23° C. Conc. DL-lactate: 2.6 mM and conc. DPN 108 μ*M*.

25.8 moles of tyrosine per mole LDH were found with the Millon-Lugg analysis [15] in the most iodinated sample as well as in the control. However, when LDH was iodinated in 0.1 M glycine pH 9.2, 13 % of the iodine was used for substitution of tyrosine to form diiodotyrosine in the most iodinated sample.

ponded roughly to the total number of thiol groups (Fig. 5). 4) Cysteine reactivated the iodinated enzyme. This has also been observed by Neilands [4].

In contrast to the rapid inactivation with iodine, the strong oxidizing reagent, periodate, affected the enzyme only slowly, thus showing that the essential SH groups were unreactive to this reagent. When 5.9 mμmoles LDH were incubated at pH 5.5 with 50 mμmoles periodate in 110 μl 0.6 M acetate, only 25 % of the activity was lost after 1.5 hours incubation. The inactivation took place continuously. Liver alcohol dehydrogenase was inactivated within a few minutes under the same conditions.

The observations reported in the literature [2,3] that LDH is not inhibited by O-iodosobenzoate or iodoacetate have been confirmed.

Acetylation of LDH with acetic anhydride inactivated LDH strongly. Table 1 shows the activity of acetylated LDH as a function of free amino groups. Acetic anhydride has been claimed to be specific for amino groups in all proteins tested [12]. However, the reagent does not necessarily react in the same manner with all proteins. The blocking of SH and phenolic hydroxyl groups appeared as a possibility because ketene, which is a stronger acetylating reagent than is acetic anhydride [12], has been found to acetylate these groups in some proteins. Moreover, acetic anhydride forms O-acetyl tyrosine and S-

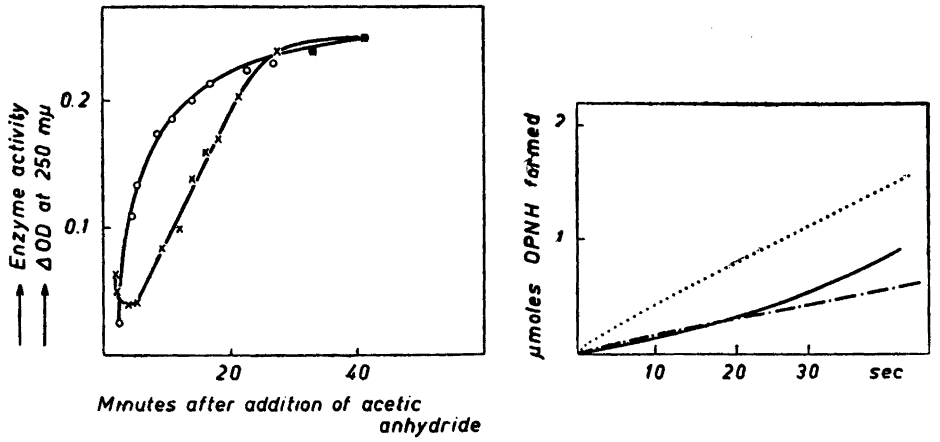


Fig. 6. Reactivation of acetylated LDH and change of optical density of the solution.
a. To 11.1 mμmoles LDH in 0.19 ml buffer (2.5 M in acetate, 0.1 M in Na_2HPO_4) were added 5 × 1 μl acetic anhydride with some seconds intervals. Temp. 0° C. Immediately after the last addition of acetic anhydride, 3.11 ml phosphate buffer (μ = 0.1, pH 7.13) were mixed with the enzyme solution. Final pH: 6.45, temp. 23° C. The change of optical density of this solution at 250 mμ was followed in a Beckman spectrophotometer. Activity measurements of aliquots of the same solution were carried out simultaneously in 0.1 glycine pH 9.75. Conc. DPN: 400 μM and conc. DL-lactate 1.77 mM.
O O O Change in OD_{250} mμ.
× × × Enzyme activity.
b The same experiment as *a*, but now illustrating the activity increase during lactate oxidation, instead of initial velocities used in *a*. ———— 2.5 min. —·—·— 8.5 min. ····· 41 min. after the last addition of acetic anhydride.

acetyl cysteine. Now, if essential SH or phenolic hydroxyl groups in LDH were acetylated, incubation in 1 M glycine at pH 9.5 should reactivate the enzyme to the same degree as these groups were involved (see Methods). But no reactivation of acetylated LDH took place provided the samples were tested at least half an hour after the addition of acetic anhydride *. Furthermore, the Folin's phenol color was not significantly decreased in the acetylated sample, and amperometric titration gave the same result before and after acetylation, around 7 SH groups being titrated in both cases. Therefore, neither phenyl acetate nor thiol acetate appeared to be formed with acetylation of LDH, thus indicating that acetic anhydride was also specific for amino groups in LDH.

Preliminary experiments with formaldehyde and phenylisocyante showed that LDH is sensitive to these amino group reagents. Thus, incubation of a 0.8 % solution of LDH with 0.25 M formaldehyde at pH 7.4 (0° C) decreased the activity by 38 % in one minute and 47 % in 10 minutes. Incubation of 65 μl 0.8 % LDH with 1 μl phenylisocyanate at pH 7.4 (0° C) decreased the activity by 89 % in 3 minutes.

As mentioned above, no reactivation of acetylated LDH took place by incubation with 1 M glycine pH 9.5 provided the samples were tested at least

* For further elaboration on this point, see below.

half an hour after the addition of acetic anhydride. If, however, the activity was tested immediately after the addition of acetic anhydride, reactivation took place within one minute in 1 M glycine at pH 9.5, and within one hour if the enzyme remained in the acetate solution. The same level of enzymatic activity was reached in both cases, some inhibition remaining due to acetylation of amino groups. Fig. 6a shows the reactivation of the enzyme in 2.5 M sodium acetate pH 6. Under these conditions, O-acetyl tyrosine and S-acetyl cysteine were stable. The initial decrease in activity shown in Fig. 6a is probably due to continued acetylation when relatively large amounts of acetic anhydride were still present in the solution. Fig. 6b illustrates reactivation of the same acetylated enzyme during oxidation of DL-lactate in 0.1 M glycine at pH 9.7. A similar reactivation of acetylated LDH was observed during reduction of pyruvate. In an attempt to discover spectral changes of the protein as the activity was restored, we observed that acetic anhydride itself caused a strong spectral absorption in the 250 mμ region, which disappeared upon hydrolysis. In Fig. 6a is included the spectral change that occurred simultaneously with the reactivation. A similar spectral change took place with acetic anhydride in the absence of protein. From the figure it is apparent that reactivation occurs until all acetic anhydride has disappeared from the solution, thus suggesting that this compound prevents the hydrolysis of a labile acetyl compound of LDH.* Also liver alcohol dehydrogenase ** and the apoenzyme of the old yellow enzyme [20] have been incubated with acetic anhydride. Although both proteins were strongly affected by the reagent, apparently by specific acetylation of amino groups, neither of them behaved like LDH with respect to temporary inhibition of acetic anhydride. The activity of liver alcohol dehydrogenase as well as the recombination rate of the apoprotein and FMN were not increased when acetic anhydride disappeared from the solution.

DISCUSSION

The requirements of an ideal inhibitor are that it should react rapidly and specifically with a protein group, and that it should be possible to regenerate the enzyme after treatment with the inhibitor [19]. Silver and mercury ions appear to be ideal inhibitors for SH groups in LDH. PCMB, on the other hand, reacts too slowly, and some of the effects of this reagent may be due to structural alteration. Therefore, the observation that only half or less of the SH groups reacted with PCMB to cause almost complete inactivation [4] does not necessarily imply that the essential SH groups are more reactive to PCMB than are the other SH groups. In the case of mercury and iodine inactivation, the data presented in Figs. 3 and 5 indicate the essential groups to have the same reactivity as the other SH groups toward these reagents.

* Experiments with crystalline LDH from sceletal muscle (C. F. Boehringer & Soehne, Mannheim) and with 80 % pure rat liver LDH (a gift from Dr. Carl S. Vestling, Un. of Illinois) have shown that these enzymes behave in the same manner as ox heart LDH regarding temporary inhibition by acetic anhydride.

** No reactivation of acetylated liver alcohol dehydrogenase took place in 1 M glycine at pH 9.5. See Fig. 2.

Table 1. The decrease of LDH activity with acetylation of amino groups.

pH	Number of free amino groups			
	97 *	76	67	58
	E/V sec	% of the activity of unmodified		
7.1	8.6	57	38	30
9.0	19.7	61	31	29
9.5	25.7	66	36	36

To 95 mμmoles LDH in 0.8 ml of 2.5 M acetate pH 7 were added 1, 3 × 1 or 4 × 1 μl of acetic anhydride at 0° C. The activity was tested one hour after the addition of acetic anhydride, in phosphate buffer (μ = 0.1) pH 7.15, in 0.1 M glycine pH 9.0 and in 0.1 M glycine pH 9.5. Conc. DL*-lactate: 1.7 mM. Conc. DPN: 415 μM.*

The findings that 10 moles of mercury or silver ions per mole of enzyme caused only 75 % inhibition, whereas the number of thiol groups appear to be 7—9, could be the result of high dilution of the enzyme in the activity measurements. Thus, in the titration experiments with mercury the enzyme concentration was about 10^{-6} M, whereas the final dilution in the activity measurements was approximately 10^{-9} M. If a rapid equilibrium were established between SH and the mercury ions, the above discrepancy could perhaps be accounted for in terms of dissociation of the mercaptide. The difference between 7 SH groups per mole enzyme titrated with mercuric chloride and 9.3 SH groups determined spectrophotometrically with PCMB remains unexplained.

The rapid reaction of silver and mercury ions and of iodine with SH groups in LDH, the slow reaction of PCMB and periodate, and the inertness to such SH reagents as O-iodosobenzoate, iodoacetate and N-ethylmaleimide may reflect different permeabilities of molecules of different sizes to the masked SH groups.

The fact that specific acetylation of amino groups inactivated LDH suggest that amino groups are essential for activity. This conclusion is supported by the observation that LDH is inactivated by formaldehyde and phenylisocyanate under conditions where these reagents are fairly specific for protein amino groups. If it is assumed that the extent of inhibition represents the fraction of essential groups which have been acetylated, then the essential amino groups are more reactive to acetic anhydride than are the other amino groups [20]. Table 1 shows that the activity decreases more rapidly than would have been the case if the blocking took place at random. However, the finding that PCMB reacted faster with acetylated enzyme than with the control shows that acetylation beside blocking amino groups also may alter the protein structure so as to increase the reactivity of thiol groups. Unfortunately, the reversibility of this alteration could not be determined. The

* Unmodified.

acetyl-amino linkage can hardly be hydrolyzed without denaturation of the enzyme. The alteration is not likely to be surface denaturation in view of the stability of other proteins to acetic anhydride [12], including liver alcohol dehydrogenase (see Fig. 2).

The activity measurements of acetylated LDH at different hydrogen ion concentrations recorded in Table 1 indicate that the decrease in activity is not due to a general discharge of the protein molecule. At pH 9.5 the number of positive charges of the enzyme should be much less than at pH 7.1, but the relative decrease in activity was roughly the same whether the activity was determined at pH 9.5, 9.0 or 7.1.

The observation that acetic anhydride effected a temporary inactivation of LDH may be explained if it is assumed that essential groups gave readily hydrolyzable acetates. The fact that the activity was regained much faster in 1 M glycine at pH 9.5 than in neutral acetate solution supports this conclusion. N-acetylimidazole has been shown to be a very labile compound [21], and it appears possible that an essential imidazol group in LDH has been acetylated. However, there are other possible explanations. Although S-acetyl cysteine and O-acetyl tyrosine are more stable than the acetyl compound of LDH, these groups may nevertheless be involved. Thus, the sluggishly reactive SH groups could form an acetyl compound more labile than S-acetyl cysteine. Unfortunately, because of the lability of the acetyl LDH compound, measurements for the blocking of these groups were impossible.

The suggestion has been made that thiol groups are involved in the binding of coenzyme or substrate in some DPN-linked enzymes [1]. In view of the low reactivity of SH groups in LDH to PCMB, periodate, iodosobenzoate, iodoacetate and N-ethylmaleimide these groups may not be sufficiently reactive to bind such relatively large molecules as lactate, pyruvate, DPN or DPNH. However, participation of amino groups in the binding could facilitate binding to the SH group(s), in the same way as the reactivity of SH groups increases when amino groups are acetylated. Such an interaction would require a compulsory sequence of reactions between protein, coenzyme and substrate.

Thanks are due to professor Hugo Theorell for his interest in this work, to Dr. Ryo S. Sato for a sample of LDH which started out this work, and to Miss Ann Louise Swanson for valuable technical assistance. A personal grant from *A/S Freias Chocolade Fabriks arbeidsfond for ernæringsforsking* is gratefully acknowledged.

REFERENCES

1. Barron, E. S. G. *Advances in Enzymol.* **2** (1951) 201.
2. Barron, E. S. G. and Singer, T. P. *J. Biol. Chem.* **157** (1945) 221.
3. Neilands, J. B. *J. Biol. Chem.* **199** (1952) 373.
4. Neilands, J. B. *J. Biol. Chem.* **208** (1954) 225.
5. Theorell, H. and Nygaard, A. P. *Acta Chem. Scand.* **8** (1954) 1649.
6. Nygaard, A. P. *Acta Chem. Scand.* **9** (1955) 1048.
7. Straub, F. B. *Biochem. J. London* **34** (1940) 483.
8. Nygaard, A. P. and Theorell, H. *Acta Chem. Scand.* **9** (1955) 1300.
9. Robertson, W. B. *Science* **96** (1942) 93.
10. Theorell, H. and Nygaard, A. P. *Acta Chem. Scand.* **8** (1954) 1489.
11. Theorell, H., Nygaard, A. P. and Bonnichsen, R. *Acta Chem. Scand.* **9** (1955) 1148.

12. Alcott, H. S. and Fraenkel-Conrat, H. *Chem. Revs.* **41** (1947) 151; Putnam, F. W. *The Proteins* 1[b], Acad. Press Inc., New York, 1953, p. 893.
13. Boyer, P. D. *J. Am. Chem. Soc.* **76** (1954) 4331.
14. Kolthoff, I. M., Stricks, W. and Morrens, L. *Anal. Chem.* **26** (1954) 366.
15. Lugg, J. W. H. *Biochem. J. London* **32** (1938) 775.
16. Van Slyke, D. D. *J. Biol. Chem.* **83** (1929) 425.
17. Folin, O. and Ciocalteu, V. *J. Biol. Chem.* **73** (1927) 627.
18. Miller, G. L. *J. Biol. Chem.* **146** (1942) 339.
19. Singer, T. P. *Brewers Dig.* (1945) 42.
20. Nygaard, A. P. and Theorell, H. *Acta Chem. Scand.* **9** (1955) 1587.
21. Stadtman, E. R. and White, F. H. *J. Am. Chem. Soc.* **75** (1953) 2022.

Received November 18, 1955.

ACTA CHEMICA SCANDINAVICA 10 (1956) 408—412

Reaction Velocities of DPN-linked Lactic Dehydrogenase

AGNAR P. NYGAARD*

Medicinska Nobelinstitutet, Biokemiska avdelningen, Stockholm, Sweden, and Johan Throne Holst's Institutt for Ernæringsforsking, Oslo, Norway

Lineweaver-Burk plots of the reaction velocities of crystalline lactic dehydrogenase from ox heart gave straight lines with low concentrations of the reactants. Relationships between Michaelis constants, maximum velocities and the equilibrium constant have been used for selecting a possible mechanism.

The relationships between Michaelis constants, maximum velocities and the equilibrium constant developed for certain mechanisms of enzyme reactions [1–3] have been useful in the determination of the probable mechanism of liver alcohol dehydrogenase [4] and a possible mechanism of yeast alcohol dehydrogenase [5]. In the present study, an attempt has been made to establish a possible reaction mechanism for lactic dehydrogenase from ox heart (LDH) **. The reaction is as follows:

$$\text{pyruvate} + \text{DPNH} + \text{H}^+ \rightleftharpoons \text{lactate} + \text{DPN}^+$$

This enzyme is of particular interest in this connection because the dissociation constant of LDH—DPNH, like that of liver ADH—DPNH, has been determined spectrophotometrically in a single reaction step [6].

MATERIALS AND METHODS

The materials and methods used in this study were the same as those applied in a recent investigation of the essential groups in LDH [7]. L-Lactic acid was procured from Pfahnstil.

RESULTS AND DISCUSSION

Several investigators have determined Michaelis constants and maximum reaction velocities in the DPN-linked LDH system [8–13]. However, the experiments have been carried out under different conditions and with LDH from

* Fellow, Norwegian Research Council.

** The following abbreviations are used: LDH: DPN-linked lactic dehydrogenase from ox heart, DPN: diphosphopyridine nucleotide, DPNH: reduced diphosphopyridine nucleotide, ADH: alcohol dehydrogenase.

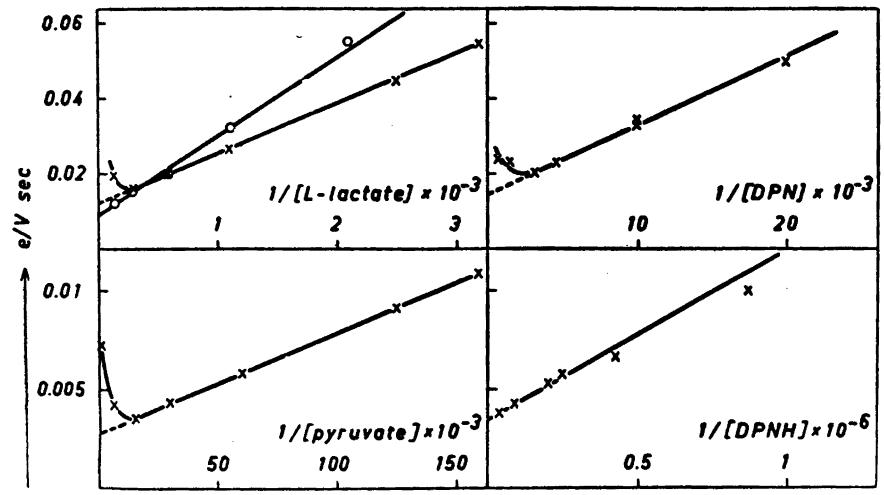


Fig. 1. Reaction velocities of LDH at pH 7.15. Temp. 23° C. Phosphate buffer, μ = 0.1 + M/1 000 versene. O O O DL-*lactate.*

different sources. None of the investigations are extensive enough for calculations of the type described below.

Figs. 1 and 2 illustrate the reaction velocities obtained for LDH at pH 7.15 and 9.0. Straight line Lineweaver-Burk plots were obtained with dilute solutions of the reactants. However, with high concentrations of L-lactate,

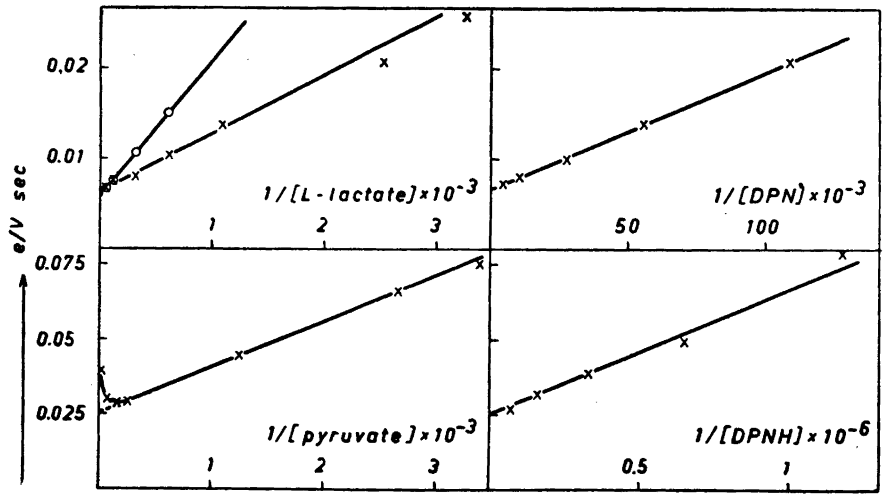


Fig. 2. Reaction velocities of LDH in 0.1 M glycine buffer at pH 9.0. Temp. 23° C. O O O DL-*lactate.*

Table 1. Michaelis constants and maximum reaction velocities for lactic dehydrogenase at 23°. Buffers: phosphate, μ 0.1 + M/1 000 versene, pH 7.15, and 0.1 M glycine, pH 9.0.

Concentration of second reactant		Kinetic Constants		
pH 7.15	pH 9.0	Michaelis constants	pH 7.15	pH 9.0
μM	μM		μM	μM
65	6 600	DPNH	2.5	1.6
12.9	8.9	Pyruvate	18	620
3 300	40 000	DPN	98	22
1 250	416	L-Lactate	1 100	1 100
228	—	»	900	—
1 250	193	DL-Lactate	5 900	5 000
		V_f, sec.$^{-1}$ *	83	177
		V_r sec.$^{-1}$	400	440

* V_f is maximum velocity of lactate oxidation.
V_r is maximum velocity of pyruvate reduction.

pyruvate and DPN at pH 7.15 and with high pyruvate concentration at pH 9.0, the velocities passed through a maximum and then decreased. In all the experiments illustrated in Figs. 1 and 2 the concentration of the second reactant (which was kept constant) was selected so as to be just below the inhibiting concentration of this reactant. At pH 7.15 the inhibiting pyruvate concentration was only three times its Michaelis constant. However, the affinity constants of DPNH and pyruvate at pH 7.3 have been found to be practically independent of the concentration of the second reactant [10].

Table 1 summarizes the maximum velocities (V_f and V_r**) and Michaelis constants calculated from Figs. 1 and 2. In the determination of V_f and V_r the straight lines were extrapolated to infinite concentration and the calculation was made on the basis of infinite concentration of both reactants. All the experimental points in the figures are the average of at least three determinations, which did not vary more than ± 5 % except at the lowest concentrations of DPNH. The velocity determinations with low concentrations of the reactants are less accurate. For that reason, the least square method has not been used in drawing the lines. The kinetic constants in Table 1 are determined within ± 5 % accuracy with the exception of the Michaelis constant of DPNH. This constant is estimated to be within ± 10 %. In Table 2 the data from Table 1 are inserted into formulae representing different reaction mechanisms. Included in the table are the numbers obtained when the errors involved are added up in one direction.

** V_f: maximum velocity of pyruvate reduction.
V_r: maximum velocity of lactate oxidation.

Table 2. Kinetic data from Table 1 inserted into formulae representing different reaction mechanisms.

	I The intramolecular transformation of ternary complex is rate-limiting. General mech. of Alberty[3]	II Special case of I. Affinity of coenzyme for LDH not influenced by substrate, or *vice versa* [3]	III A group in the enzyme is ox/red by substrate or coenzyme with the formation of enzyme-substrate or enzyme-coenzyme intermediates [3]	IV Dissociation of enzyme-coenzyme or enzyme-substrate is rate-limiting [2,3]. Probable mechanism of liver ADH [4]
pH	$K_{eq} = \frac{V_f}{V_r} \cdot A$ ** $\times 10^{12}$	$K_{eq} = \frac{V_f}{V_r} \cdot B$ *** $\times 10^{12}$	$K_{eq} = \left(\frac{V_f}{V_r}\right)^2 \cdot B$ $\times 10^{12}$	$K_{eq} = \left(\frac{V_f}{V_r}\right)^3 \cdot B$ $\times 10^{12}$
7.15	—	6.2 4.1—9.0	1.3 0.76—2.1	0.27 0.14—0.47
9.0		15.6 11—23	5.9 4.0—10.2	2.2 1.4—4.5

$K_{eq} = 4.6 \times 10^{-12}$ over the whole pH range [14].

** $A = \frac{K_m \cdot pyr_{DPNH} \cdot (H^+)}{K_m \cdot lactate_{DPN}}$ For the definition of these constants, see Alberty [3]. A has not been determined, but becomes identical with B when the affinity constants are independent of the concentration of the second reactant.

*** $B = \frac{K_{mDPN} \cdot K_m \text{ pyr} \cdot (H^+)}{K_{mDPN} \cdot K_m \text{ lactate}}$

The mechanism described in column 2, Table 2, agrees rather well with the experimental data. Furthermore, the Michaelis constant of L-lactate at pH 7.15 is nearly independent of the concentration of DPN (see Table 1), and the data of Schwert and Hakala [10] indicate that the affinity constants of DPNH and pyruvate are nearly independent of the concentration of the second reactant at pH 7.3. LDH may therefore follow mechanism 2 at pH 7.15, or nearly so. Mechanisms 3 and 4 are excluded. At pH 9.0, mechanism 2 is excluded and 4 is highly unlikely. Mechanism 3 is improbable for other reasons [7,15]. Experiments by Gibson *et al.*[12] indicate that around this pH the binding of DPN affects the binding of substrate strongly. Mechanism 1 has not been investigated at this pH because of the difficulties in obtaining accurate measurements at very low concentrations of DPNH.

If mechanism 1 or 2 is followed, the rate-limiting reaction in the reduction of pyruvate is the transformation of the ternary complex:

$$\text{LDH—DPNH-pyruvate} + H^+ \rightarrow \text{LDH—DPN-lactate}$$

If the hydrogen ion were taken from the solution, V_r should be proportional to H^+, but V_r was observed to be independent of pH. The enzyme molecule could instead deliver the proton.

If mechanism 2 is followed at pH 7.15, the Michaelis constants represent the dissociation constants of the reactants at this pH. The Michaelis constant of DPNH is 2.5×10^{-6} (23°), as compared to 7×10^{-6} obtained of Chance and Neilands [6] by direct measurements. In view of the uncertainty of the direct measurements [6], the disagreement is not too serious. The 34-fold increase in K_M for pyruvate from pH 7.15 to 9.0 could reflect the discharge of the protein binding site of this substrate, which could be an imidazol group. K_M for lactate is the same at pH 7.15 and 9.0, and may therefore be bound to another site.

The dissociation of Enzyme-DPNH is likely to be the rate-limiting step in the oxidation of alcohol by liver alcohol dehydrogenase [2,4]. LDH oxidizes lactate about 50 times faster than ADH oxidizes alcohol, and the dissociation constant of LDH—DPNH is more than 10 times higher than that of ADH—DPNH. From these observations Chance and Neilands [6] suggested that the dissociation of Enzyme-DPNH was also rate-limiting in the oxidation of substrate in the LDH system, and that a high dissociation constant for Enzyme-DPNH may in general reflect a high rate of oxidation. However, it is evident from Table 2 that mechanism 4, which is probably followed by liver ADH, is not possible for LDH, at least not at pH 7.15. This is supported by the dissociation constant calculated for LDH—DPNH on the assumption that mechanism 4 is followed. It comes out to be $K = \frac{V_f}{V_r} K_{M\ DPNH} = 0.52 \times 10^{-6}$, which is 13—14 times smaller than the measured dissociation constant, and about equal to the dissociation constant of liver ADH found from overall reaction velocities [4].

The fact that DL-lactate has a higher Michaelis constant than has the L-isomer alone suggest that the D-form can also combine on the substrate site without being oxidized, as shown previously [11]. However, the observations that DL gives a higher maximum rate than L alone and that no inhibition is observed with high concentrations of DL show that the D-form also in some other way effects the kinetic constants.

REFERENCES

1. Haldane, J. B. S. *Enzymes*, Longman's Green and Co., London 1930, p. 80.
2. Theorell, H. and Chance, B. *Acta Chem. Scand.* **5** (1951) 1127.
3. Alberty, R. A. *J. Am. Chem. Soc.* **75** (1953) 1928.
4. Theorell, H., Nygaard, A. P. and Bonnichsen, R. *Acta Chem. Scand.* **9** (1955) 1148.
5. Nygaard, A. P. and Theorell, H. *Acta Chem. Scand.* **9** (1955) 1300.
6. Chance, B. and Neilands, J. B. *J. Biol. Chem.* **199** (1952) 383.
7. Nygaard, A. P. *Acta Chem. Scand.* **10** (1956) 397.
8. Straub, F. B. *Enzymologia* **9** (1941) 143.
9. Socquet, I. M. and Laidler, K. J. *Arch. Biochem* **25** (1950) 171.
10. Schwert, G. W. and Hakala, M. T. *Arch. Biochem. and Biophys.* **38** (1952) 55.
11. Kubowitz, F. and Ott, P. *Biochem. Z.* **314** (1943) 94.
12. Gibson, D. M., Davisson, E. O., Bachhawat, B. K., Ray, B. R. and Vestling, C. S. *J. Biol. Chem.* **203** (1953) 397.
13. Meister, A. *J. Biol. Chem.* **184** (1950) 117.
14. Racker, E. *J. Biol. Chem.* **184** (1950) 313.
15. Vennesland, B. and Westheimer, F. H. in *The Mechanism of Enzyme Action*, The Johns Hopkins Press 1954, p. 357.

Received November 19, 1955.

ACTA CHEMICA SCANDINAVICA 10 (1956) 413—415

Constituents of Pollen

I. Low-molecular Carbohydrates in Pollen from *Pinus montana* Mill.

MARTIN NILSSON

Organisk-kemiska Institutionen, Kungl. Tekniska Högskolan, Stockholm, Sweden

Sucrose, glucose, fructose, myo-inositol, sequoitol and pinitol have been isolated from pollen of *Pinus montana* Mill. Of these substances pinitol and sequoitol have not been previously found in pollen.

The literature on pollen chemistry has been recently reviewed by Lundén [1]. Not very much systematic work has been carried out on the low-molecular weight carbohydrates in pollen and only a few substances have been isolated in the crystalline state: sucrose [2], lactose [3] and myo-inositol [4]. However, paper chromatographic investigations indicate the presence of glucose [5], fructose [5], raffinose [6] and stachyose [6] also.

For *Pinus silvestris* various authors (for detailed references and discussion see Ref.[7]) have determined the contents of "reducing" and "non-reducing sugars" as 0—2 % and 8—12 % in uncontaminated pollen. The non-reducing sugars were shown to consist mainly of sucrose. Recently Nielsen, Grömmer and Lundén [8] investigated various pollen using microbiological methods and found after acid hydrolysis 0.9 % myo-inositol in pollen from *Pinus montana*.

The pollen samples used in this investigation were collected in 1954 by *A. B. Cemille*, Vegeholm, Sweden, and contained at least 99 % of pollen from *Pinus montana* Mill.[8] (subgenus Diploxylon). The water-soluble part of the methanol-extract from the pollen was, after a preliminary treatment, fractionated by chromatography on a carbon-celite column [9]. Sucrose (9 %), myo-inositol (0.1 %) and sequoitol (0.05 %) were thus obtained directly in the crystalline state. Pinitol, fructose and glucose could not be separated on the carbon column. From the mixture of these substances pinitol (1.2 %) was separated by crystallisation. The remaining sugars were isolated as *iso*propylidene derivatives as described by Bell [10]. Thus crystalline derivatives of fructose (0.7 %) and glucose (0.3 %) were obtained.

Parts of these sugars might originate from sucrose and other saccharides present by hydrolysis during the storage of the pollen and perhaps also during the extraction and purification process. However, it was found that the first

extracts showed strong spots corresponding to glucose and fructose on paper chromatograms.

Pinitol and sequoitol have not been previously reported to occur in pollen. Pinitol appears to occur in the needles of all conifers [11] and has also been found in the heartwood of pines belonging to the subgenus *Haploxylon* [12]. Sequoitol has only been encountered once in pines; in the heartwood of *Pinus Lambertiana* [13] (Haploxylon).

EXPERIMENTAL

All melting points are uncorrected. Evaporations were carried out *in vacuo* at 40–50°. Paper chromatograms were run in *n*-butanol, ethanol, water (5:1:4) and/or ethyl acetate, acetic acid, water (3:1:1) and developed with the silver nitrate-sodium ethoxide reagent.

Air-dried pollen from *Pinus montana* Mill. (250 g) was extracted with ether in a Soxhlet apparatus for two weeks and then with methanol for three weeks. As the solvent flow through the pollen layer was very slow the extraction temperature was about 25°. The methanol extract on evaporation yielded a semi-solid mass (72 g), which was extracted with water (1.5 l, in portions). The solution was filtered (celite), the filtrate extracted with ether (2 × 300 ml) and purified by the lead acetate method [14]. It was shown by paper chromatography that practically no cyclitols were precipitated or adsorbed under the conditions chosen (pH 5). The aqueous solution was deionized (IR 120 and IR 4 B) and evaporated to dryness. The resulting syrup (42 g) was dissolved in water (400 ml) and fractionated on a carbon-celite column (50 × 6 cm. Ethanol 0–20 %, 15 l, afterwards washed with ethanol, 50 %, 10 l). The eluate was divided into fractions which were investigated by paper chromatography and checked for optical rotation. The first run gave 12.9 g of easily eluted components, 28.0 g of sucrose fraction and 1.3 g of higher sugars. The sucrose fraction on treatment with methanol yielded crystalline sucrose (19.6 g). The easily eluted components were refractionated on the same column (Ethanol 0–10 %, 16 l) giving crystalline myo-inositol (0.23 g), sequoitol (0.12 g) and sucrose (2.2 g). From fractions containing a mixture of pinitol, fructose and glucose (8.1 g), pinitol (3.0 g) was obtained by crystallisations from ethanol. The material in the mother liquors was treated with acetone and sulphuric acid converting the sugars to di*iso*propylidene derivatives, the remaining pinitol being unaffected. Mild hydrolysis of the chloroform-soluble substances and partition of the products obtained gave crystalline 2,3–4,5-di(O-*iso*propylidene)-fructopyranoside (1.2 g) and 1,2-O-*iso*propylidene-glucofuranoside (0.48 g), corresponding to fructose (0.8 g) and glucose (0.4 g).

A reference experiment showed 80 % and 50 % recovery of the fructose and glucose derivatives, respectively, from a mixture of equal parts of pinitol, glucose and fructose. Paper chromatographic investigation of the water-soluble material after the acetone treatment showed the presence of pinitol and glucose only.

The fraction of higher sugars and the sucrose mother liquors were investigated by paper chromatography and were found to contain in addition to sucrose several components with lower R_F-values. Some of the spots could be developed with the anisidine-phosphoric acid reagent and some also with resorcinol-hydrochloric acid. These facts point to the presence of tri- and tetrasaccharides. The isolation of these substances was not, however, attempted.

The *sucrose* m. p. 178–184° was homogeneous on the paper chromatograms. $[\alpha]_D$ +68° (*c* 1.8, water). Octa-acetate (acetic anhydride, pyridine), m. p. and mixed m. p. 89–90°, $[\alpha]_D$ +59° (*c* 6,4, chloroform).

The crude *pinitol* m. p. 180–90° was sublimed and recrystallised from water-ethanol, m. p. and mixed m. p. 188–189°, $[\alpha]_D$ +63° (*c* 6,2, water); pentaacetate (acetic anhydride, perchloric acid), m. p. and mixed m. p. 99–100° $[\alpha]_D$ −6,9 (*c* 6,4, chloroform).

The *myo-inositol* m. p. 219–224° was recrystallised from water-ethanol, m. p. and mixed m. p. 225–228°; hexaacetate (acetic anhydride, perchloric acid) m. p. and mixed m. p. 216–218°.

The *sequoitol* m. p. 233—238° was recrystallised from water-ethanol, m. p. and mixed m. p. 238—239°; pentaacetate (acetic anhydride, perchloric acid), m. p. and mixed m. p. 196—197°.

2,3—4,5-di(O-isopropylidene)-fructopyranoside, m. p. 83—98°, was recrystallised from ether-petrol, m. p. and mixed m. p. 95—96°, $[\alpha]_D$ −21° (*c* 1.4, chloroform).

1,2-O-isopropylideneglucofuranoside, m. p. 100—120°, was recrystallised from ethyl acetate, m. p. and mixed m. p. 159—160°, $[\alpha]_D$ −4.2 (*c* 7.3, ethanol).

Acknowledgements. Thanks are due to Professor H. Erdtman for suggesting the work, to *Statens Tekniska Forskningsråd* for financial support, to *A. B. Kabi* for a generous gift of pollen and to O. Theander and B. Wickberg for valuable discussions.

REFERENCES

1. Lundén, R. *Svensk Kem. Tidskr.* **61** (1954) 201.
2. von Planta, A. *Lantwirtsch. Vers. Sta.* **32** (1886) 215.
3. Kuhn, R. and Löw, I. *Chem. Ber.* **82** (1949) 479.
4. Anderson, R. J. and Kulp, W. L. *J. Biol. Chem.* **50** (1922) 433.
5. Weygand, F. and Hofman, H. *Chem. Ber.* **83** (1950) 405.
6. Sanero Ueno *Kagaku* (Science) **24** (1954) 90; *Chem. Abstracts* **48** (1954) 12242 f.
7. Todd, F. E. and Bretherick, O. *J. Econ. Entomol.* **35** (1942) 312.
8. Nielsen, N., Grömmer, J. and Lundén, R. *Acta Chem. Scand.* **9** (1955) 1100.
9. Lindberg, B. and Wickberg, B. *Acta Chem. Scand.* **7** (1953) 140.
10. Bell, D. J. in Peach, K. and Tracey, M. V. *Moderne Metoden der Pflanzenanalyse*, Berlin 1955, 2. Band Vol. 2, p. 32.
11. Plouvier, V. *Compt. rend.* **234** (1952) 362.
12. Lindstedt, G. *Acta Chem. Scand.* **5** (1951) 135.
13. Ballou, C. E. and Anderson, A. B. *J. Am. Chem. Soc.* **75** (1953) 648.
14. Brieger, R. in Klein, G. *Handbuch der Pflanzenanalyse*, Wien 1931, Bd I, p. 593.

Received December 6, 1955.

ACTA CHEMICA SCANDINAVICA 10 (1956) 416—420

Barium Salts of Telluropentathionic Acid

OLAV FOSS and OLAV TJOMSLAND

Institutt for uorganisk kjemi, Norges tekniske høgskole, Trondheim, Norway

A study has been made of the crystal chemistry of barium telluropentathionate hydrates. On crystallization from water, a monoclinic trihydrate (I) occurs. Two dihydrates were obtained, one triclinic (II) by crystallization from aqueous methanol, and one monoclinic (III) by crystallization from aqueous acetone. The unit cell dimensions and space groups are:

I, $a = 11.16$ Å, $b = 5.24$ Å, $c = 21.30$ Å, $\beta = 107°$; space group, $C_{2h}^5 - P2_1/c$ with $Z = 4$.

II, $a = 4.99$ Å, $b = 10.57$ Å, $c = 12.38$ Å, $\alpha = 106°$, $\beta = 101\frac{1}{2}°$, $\gamma = 90°$; space group, $C_i^1 - P\bar{1}$ with $Z = 2$.

III, $a = 4.99$ Å, $b = 10.59$ Å, $c = 23.61$ Å, $\beta = 98°$; space group, $C_{2h}^3 - A2/m$ with $Z = 4$.

Isomorphism of II with triclinic barium pentathionate dihydrate, and the requirement in III of a mirror plane of molecular symmetry, show that the telluropentathionate ion occurs in a *cis* form in these salts.

The first salts of telluropentathionic acid, those of sodium and potassium, were isolated in 1949 [1]. Later, the ammonium, rubidium and cesium salts were prepared, and unit cells and space groups determined for these and the potassium salt [2]. Detailed crystal structure analyses of ammonium telluropentathionate [3], as well as of orthorhombic [4] and triclinic [5] barium pentathionate dihydrate and orthorhombic barium selenopentathionate dihydrate [6], were subsequently carried out.

Pentathionate chains may occur in two rotational-isomeric forms, which have been termed *cis* and *trans* [7]. The telluropentathionate ion in the ammonium salt occurs in the *trans* form, whereas the *cis* form was found for the pentathionate and selenopentathionate ions in the barium salts. It was of interest to see whether in barium salts also the telluropentathionate ion would have the *cis* form. This has now been found to be the case, in two crystalline modifications of barium telluropentathionate dihydrate. Together with the earlier structure determination of the ammonium salt, the work on barium salts serves to establish the occurrence of different rotational-isomeric forms of the telluropentathionate ion in different salts.

SYNTHESIS OF SALTS

Three distinct barium telluropentathionate hydrates were obtained, on recrystallization under various conditions of crude samples prepared from the sodium salt [1] by metathesis with a slight excess of barium perchlorate. The sodium and barium perchlorates being readily soluble in water, barium telluropentathionate crystallized readily on mixing concentrated solutions of the reactants, and cooling. This procedure was used also for the preparation of crude barium selenopentathionate [6].

When crystallized from water, without the use of an organic solvent to depress the solubility, barium telluropentathionate separates as a trihydrate. Under such conditions also barium selenopentathionate gives a trihydrate, whereas barium pentathionate comes out as a triclinic dihydrate.

From aqueous methanol, barium pentathionate and selenopentathionate separate as orthorhombic dihydrates. Attempts to prepare an orthorhombic barium telluropentathionate dihydrate in this way have failed so far; instead, a triclinic dihydrate, isomorphous with the triclinic pentathionate, was obtained. On crystallization from aqueous acetone, barium pentathionate and selenopentathionate give solvates, whereas barium telluropentathionate crystallized as a monoclinic dihydrate.

The order of decreasing stability of the crystals of the three barium telluropentathionate hydrates, with respect to liberation of tellurium on keeping, appears to be: Trihydrate, monoclinic dihydrate, and triclinic dihydrate. The two former salts are stable for months, and also crystallize readily, with well developed forms free from twinning, whereas the triclinic dihydrate shows a pronounced tendency of irregular growth and twinning. Although crystals of the dihydrates, when moistened, gradually dissolve and recrystallize as the trihydrate, no transition of one crystalline hydrate to another has been observed on keeping at room temperature and ordinary humidity conditions.

The trihydrate has a yellowish green colour, whereas the dihydrates are yellow. The crystals of the monoclinic dihydrate, in daylight and more rapidly on exposure to X-rays, develop an orange colour but give unchanged X-ray photographs.

EXPERIMENTAL

Sodium telluropentathionate dihydrate was prepared from tellurium dioxide and sodium thiosulphate as described earlier [1]. To 25 g of the crude sodium salt, dissolved in 40 ml of 0.2 N hydrochloric acid by gentle heating, and filtered and cooled in ice, was added a solution of 25 g of barium perchlorate trihydrate in 15 ml of water. Crystals of barium telluropentathionate rapidly began to separate out. After a few minutes, the product was filtered off, and washed with methanol and ether. Yield, about 18 g. The recrystallizations were performed as follows.

Trihydrate (I). The crude barium salt was dissolved in four to five times the amount of 0.2 N hydrochloric acid at 40—50° C, and the solution was filtered and allowed to cool, first at room temperature and then in ice.

Triclinic dihydrate (II). To a solution prepared as above, but about half as concentrated, of the crude salt or the trihydrate was added about twice the amount of methanol. The crystallization took place at or slightly above room temperature. If the solution is cooled in ice, the preparation will have a composition intermediate between di- and trihydrate.

Monoclinic dihydrate (III). 1 g of the trihydrate was dissolved in 8 ml of 0.2 N perchloric acid, and the solution was filtered and warmed to 40–50° C. Then 8 ml of acetone was added from a pipet, with stirring, and the solution was allowed to cool to room temperature.

The crops of crystals were filtered with suction on sintered glass filters, and I, II and III were washed with ethanol, methanol and acetone, respectively, and then with ether. They were dried for a short time in a vacuum over sulphuric acid; small crops were dried on a plate in air. On prolonged keeping over sulphuric acid, the water of crystallization is given off.

The salts were analyzed by direct titration with iodine, as described earlier [1]. Absence of tetrathionate was checked through subsequent analysis of the titrated solutions by means of the sulphite method [1].

0.3322 g of I: 24.60 ml of 0.09954 N iodine.
$BaTe(S_2O_3)_2 \cdot 3H_2O$ (543.3). Mol. weight found, 542.6.
0.2744 g of II: 21.01 ml of 0.09954 N iodine.
$BaTe(S_2O_3)_2 \cdot 2H_2O$ (525.3). Mol. weight found, 524.9.
0.1530 g of III: 11.70 ml of 0.09954 N iodine.
$BaTe(S_2O_3)_2 \cdot 2H_2O$ (525.3). Mol. weight found, 525.5.

As mentioned above, barium selenopentathionate on crystallization from water occurs as a trihydrate, like barium telluropentathionate. This trihydrate has not been described, and is therefore included here. Crude barium selenopentathionate [6] was dissolved in about three times the amount of 0.2 N hydrochloric acid at 40–50° C, and the solution was filtered and cooled in ice. It was advantageous, for better crystallization, to add a little barium perchlorate before cooling. The salt was oxidized with potassium bromate and subsequently analyzed iodometrically by means of the Norris and Fay method, as described earlier [6].

0.1989 g substance: 16.10 ml of 0.09954 N sodium thiosulphate.
$BaSe(S_2O_3)_2 \cdot 3H_2O$ (494.6). Mol. weight found, 496.4.

The salt is more stable than the orthorhombic dihydrate [6]; thus, a sample kept in a dark bottle was found unchanged after five years. The pale greenish crystals occur as prisms, of much the same habit as the trihydrate I above, but often flattened almost to leaves and with a tendency of irregular growth. It appears probable that the salt may be isomorphous with I, but no X-ray measurements have been made.

CRYSTALLOGRAPHIC DATA

The crystals of the barium telluropentathionate hydrates were characterized by means of X-ray oscillation and Weissenberg photographs. Copper radiation was used, $\lambda(CuK_\alpha) = 1.542$ Å. The axial lengths recorded below are believed to be accurate to within 0.5 %. The densities of the crystals were determined by flotation in suitable solvents.

Barium telluropentathionate trihydrate, $BaTe(S_2O_3)_2 \cdot 3H_2O$ (I). Monoclinic, $a = 11.16$ Å, $b = 5.24$ Å, $c = 21.30$ Å, $\beta = 107°$. Four molecules per unit cell; density, calc. 3.03, found 3.0 g/cm^3. Systematic absences, $h0l$ when l is odd, $0k0$ when k is odd. The space group is thus C_{2h}^5—$P2_1/c$. The crystals occur as flat prisms, extended along the b axis and with {100} predominant.

Barium telluropentathionate dihydrate, $BaTe(S_2O_3)_2 \cdot 2H_2O$ (II). Triclinic, $a = 4.99$ Å, $b = 10.57$ Å, $c = 12.38$ Å, $\alpha = 106°$, $\beta = 101\frac{1}{2}°$, $\gamma = 90°$. Two molecules per unit cell; density, calc. 2.84, found 2.84 g/cm^3. No systematic absences. The crystals occur as prisms, extended along the a axis and usually flattened along the b axis. There is perfect cleavage along the c plane.

The unit cell dimensions are not far from those of triclinic barium pentathionate dihydrate [5]. The γ angle of 90°, and the characteristic cleavage, are retained, and the b axis and c spacing are a little larger, as may be expected

when tellurium is substituted for sulphur. A comparison of the intensities of the $0kl$ and $h0l$ reflections of the two triclinic dihydrates adds further support to the assumption that the salts are isomorphous. The space group of II has therefore been taken as C_i^1—$P\bar{1}$.

Barium telluropentathionate dihydrate, $BaTe(S_2O_3)_2 \cdot 2H_2O$ (III). Monoclinic, $a = 4.99$ Å, $b = 10.59$ Å, $c = 23.61$ Å, $\beta = 98°$. Four molecules per unit cell; density, calc. 2.82, found 2.80 g/cm^3. Systematic absences, hkl when $k + l$ is odd. The crystals occur as prisms, extended along the a axis and ordinarily flattened along the b axis. The habit is monoclinic prismatic, and the forms {001}, {011} and {110} occur, with the former the more predominant one. There is a pronounced cleavage along the c plane.

On the basis of the systematic absences, three space groups are possible, *viz.*, C_{2h}^3—$A2/m$ and two of lower symmetries. In the crystals of orthorhombic barium pentathionate [4] and selenopentathionate [6] dihydrates, of space group D_{2h}^{16}—$Pnma$ with four molecules per unit cell, $0kl$ reflections are present only when $k + l$ is even, as in III, and the a axis projections of these and of III have also very like dimensions. A comparison of the intensities of the $0kl$ reflections, allowing for the different scattering powers of sulphur, selenium and tellurium, shows that the $0kl$ zone of III has the same intensity distribution as the $0kl$ zones of the orthorhombic dihydrates. The space group and $0kl$ zones of the latter being centrosymmetric, the same applies, beyond reasonable doubt, to the $0kl$ zone of III. The space group is therefore the centrosymmetric one, C_{2h}^3—$A2/m$.

In III, the telluropentathionate ion lies in a crystallographic mirror plane of symmetry, and has thus a *cis* configuration, as contrasted with the *trans* configuration found earlier in the crystals of ammonium telluropentathionate [3]. The crystals of II being isomorphous with those of triclinic barium pentathionate dihydrate, the *cis* configuration occurs also in II. The triclinic space group possesses no crystallographic mirror plane, but the pentathionate ion has mirror plane symmetry also in those crystals [5].

The orthorhombic structure of barium pentathionate and selenopentathionate dihydrate, of space group D_{2h}^{16}—$Pnma$, is built up of layers related to each other through glide planes a in their interface [4,6]. From the correspondence of unit cell dimensions, the cleavage, and the similar intensities of the $0kl$ zones of reflections, it is to be expected that the monoclinic structure of barium telluropentathionate dihydrate, of space group C_{2h}^3—$A2/m$, is built up of layers which have the same internal structure as in the orthorhombic analogues, but are related to each other through twofold rotation axes instead of glide planes. A complete structure determination of III will be made.

The unit cell dimensions of triclinic and monoclinic barium telluropentathionate dihydrate show close correspondence, with $a = 4.99$ Å, $b = 10.57$ Å and 10.59 Å, and $d_{001} = 11.64$ Å and 2×11.69 Å, respectively. The intensities of the $00l$ reflections, with the l indices of III halved, are very similar. The structural difference should be the same as between triclinic and orthorhombic barium pentathionate dihydrate [4,5], and thus consist in a different arrangement of like layers relative to each other.

The work has been aided by grants from *Norges Almenvitenskapelige Forskningsråd* and from *Det Videnskapelige Forskningsfond av 1919.*

REFERENCES

1. Foss, O. *Acta Chem. Scand.* **3** (1949) 708.
2. Foss, O. and Jahr, J. *Acta Chem. Scand.* **4** (1950) 1560.
3. Foss, O. and Larssen, P. A. *Acta Chem. Scand.* **8** (1954) 1042.
4. Foss, O. and Zachariasen, H. *Acta Chem. Scand.* **8** (1954) 473.
5. Foss, O. and Tjomsland, O. *Acta Chem. Scand.* **10** (1956) 288.
6. Foss, O. and Tjomsland, O. *Acta Chem. Scand.* **8** (1954) 1701.
7. Foss, O. *Acta Chem. Scand.* **7** (1953) 1221.
8. Foss, O. *Acta Chem. Scand.* **3** (1949) 435.

Received November 22, 1955.

ACTA CHEMICA SCANDINAVICA 10 (1956) 421—423

Solvates of Barium Pentathionates with Ethanol

OLAV FOSS and OLAV TJOMSLAND

Institutt for uorganisk kjemi, Norges tekniske høgskole, Trondheim, Norway

Barium pentathionate and selenopentathionate crystallize from aqueous ethanol as solvates containing one mole of water and one mole of ethanol per mole of salt. The crystals are isomorphous, and have eight-molecule unit cells based on the space group, D_{2h}^{15}—*Pcab*, with $a = 9.18$ Å, $b = 13.27$ Å, $c = 21.25$ Å for the pentathionate and $a = 9.19$ Å, $b = 13.30$ Å, $c = 21.37$ Å for the selenopentathionate. The solvates are relatively stable.

Barium telluropentathionate gives a solvate which probably contains one mole of ethanol but no water.

In 1847, one year after the discovery of pentathionic acid by Wackenroder [1], Lenoir [2] reported the isolation of barium pentathionate by crystallization from aqueous ethanol. Although the salt by analysis was found to contain 2.93 % of ethanol, the ethanol was regarded as an impurity, and the salt described as a dihydrate. Fordos and Gélis [3], in 1848, stated that barium pentathionate always retain some ethanol when precipitated from water by means of ethanol, but no particular significance was attached to the ethanol content.

It is the purpose of this article to show that barium pentathionate and selenopentathionate, when crystallized from aqueous ethanol, are obtained as solvates containing one mole of water and one mole of ethanol per mole of salt. The formulae are:

$$BaS(S_2O_3)_2 \cdot H_2O \cdot C_2H_5OH; \qquad BaSe(S_2O_3)_2 \cdot H_2O \cdot C_2H_5OH$$

The crystals of the two solvates are isomorphous. Lenoir [2] described his crystals as quadratic prisms, and they are later [4] referred to as tetragonal. In fact, the solvates usually occur as prisms having frequently a quadratic cross-section, but they are orthorhombic bipyramidal, not tetragonal. The correct percentage of ethanol in the pentathionate is 10.1 and thus considerably higher than found by Lenoir.

The ethanol appears to be relatively firmly held in the crystal lattice. When kept in closed bottles, the majority of the individual crystals remain unchanged for months, as revealed by microscopic and X-ray examination, although on opening the bottles, an odour of ethanol is perceptible. With re-

gard to the ordinary decomposition reactions of the pentathionates, *i. e.*, the liberation of sulphur or selenium, the solvates are at least as stable as the corresponding hydrates.

These are apparently the first recorded instances of solvates of barium salts with ethanol. According to Sidgwick [5], "the halides (and sometimes the hydroxide and nitrate as well) of barium will combine with glycerol, sugar alcohols, sugars, carboxylic acids, and aminoacids; strontium halides will also combine with alcohol and acetone". As will be shown later, barium pentathionates form well-defined solvates also with acetone and other simple organic solvents.

EXPERIMENTAL

To solutions of crude barium pentathionate [6] and barium selenopentathionate [7] in about 0.01 N hydrochloric acid, saturated at 40—50° C, and filtered if necessary and still warm, were added about equal volumes of ethanol. On cooling, first at room temperature and afterwards in ice, the solvates slowly crystallized. The crops of crystals were filtered with suction on sintered glass filters, washed with ethanol and then with ether, and dried for less than an hour in a vacuum over sulphuric acid. The same procedure was used for recrystallizations.

The crystals of the pentathionate are colourless and those of the selenopentathionate pale greenish.

The pentathionate was analyzed iodometrically by means of the sulphite method [8], after removal of the barium by addition of sodium sulphate [6]. Two equivalents of iodine correspond to one mole of pentathionate. Through control analyses by means of the cyanide method, the salt was found to be free from tetrathionate.

0.3007 × $\frac{1}{5}$ g substance: 26.04 ml of 0.01010 N iodine.

$BaS(S_2O_3)_2 \cdot H_2O \cdot C_2H_5OH$ (457.8): Mol. weight found, 457.3.

The selenopentathionate was oxidized with potassium bromate and subsequently analyzed iodometrically by means of the Norris and Fay method, as described earlier [9].

0.2011 g substance: 16.10 ml of 0.09954 N sodium thiosulphate.

$BaSe(S_2O_3)_2 \cdot H_2O \cdot C_2H_5OH$ (504.7): Mol. weight found, 501.8.

In order to check the presence of ethanol in the crystals, aqueous solutions were oxidized with chromic acid — sulphuric acid. Acetaldehyde was thereafter distilled off and characterized by means of 2,4-dinitrophenylhydrazine.

Experiments made with barium telluropentathionate have shown that also this salt gives a solvate with ethanol. The yellow crystals, obtained from the trihydrate [10] as described for the above solvates, were small and not suited for single-crystal X-ray work. According to analyses, performed by direct titration with iodine [11], the composition corresponds to one mole of ethanol per mole of barium telluropentathionate, but no water. The presence of ethanol in the crystals was checked as described above.

0.2012 g substance: 15.04 ml of 0.1001 N iodine.

$BaTe(S_2O_3)_2 \cdot C_2H_5OH$ (535.3): Mol. weight found, 534.6.

In lack of X-ray data, there remains some doubt concerning the absence of water in this solvate, since some ethanol or water may have escaped from the crystal lattice before the analysis. Similar analytical results have been obtained with some of the solvates of barium pentathionates with acetone and tetrahydrofuran, and there, isomorphism of the whole series of solvates indicates that the questionable mole of water is present, regardless of the analytical results.

CRYSTALLOGRAPHIC DATA

The solvates of barium pentathionate and selenopentathionate with ethanol are orthorhombic, and ordinarily occur as prisms, elongated in the direction of the *a* axis and bounded by {010} and {001}. The cross-section is frequently quadratic or nearly so. There is perfect cleavage along the *c* plane.

Oscillation and Weissenberg photographs were made on single-crystal specimens, using copper radiation, $\lambda(\mathrm{Cu}K_a) = 1.542$ Å. Densities were measured by a flotation method. The following unit cell dimensions, believed to be accurate to within 0.5 %, were derived.

	a	*b*	*c*
$BaS(S_2O_3)_2 \cdot H_2O \cdot C_2H_5OH$	9.18 Å	13.27 Å	21.25 Å
$BaSe(S_2O_3)_2 \cdot H_2O \cdot C_2H_5OH$	9.19	13.30	21.37

There are eight molecules per unit cell; densities, calc. 2.35 and 2.57 g/cm^3, respectively; found, 2.34 and 2.59 g/cm^3. Systematic absences, $0kl$ when l is odd, $h0l$ when h is odd, $hk0$ when k is odd. The space group is thus unambiguously determined as D_{2h}^{15}—*Pcab*. The unit cell dimensions, the space group extinctions, and the relative intensities of the reflections show that the two salts are isomorphous.

The number of general positions of the space group being eight, the asymmetric unit corresponds to one formula unit. No detailed structure analysis of any of the salts is contemplated at present.

The work has been aided by grants from *Norges Almenvitenskapelige Forskningsråd* and from *Det Videnskapelige Forskningsfond av 1919*.

REFERENCES

1. Wackenroder, H. *Ann.* **60** (1846) 189.
2. Lenoir, A. *Ann.* **62** (1847) 253.
3. Fordos, J. and Gélis, A. *J. prakt. Chem.* **43** (1848) 456.
4. Abegg's *Handbuch der anorganichen Chemie*, Vol. II 2, Leipzig 1905, p. 276; Gmelin-Kraut's *Handbuch der anorganichen Chemie*, 7th Ed., Vol. II 2, Heidelberg 1909, p. 51; Mellor, *A Comprehensive Treatise on Inorganic and Theoretical Chemistry*, Vol. X, Longmans, Green and Co., London 1930, p. 627.
5. Sidgwick, N. V. *The Chemical Elements and Their Compounds*, Vol. I, Oxford 1950, p. 259.
6. Foss, O. and Tjomsland, O. *Acta Chem. Scand.* **10** (1956) 288.
7. Foss, O. and Tjomsland, O, *Acta Chem. Scand.* **8** (1954) 1701.
8. Kurtenacker, A. *Analytische Chemie der Sauerstoffsäuren des Schwefels*, Ferdinand Enke, Stuttgart 1938, pp. 149—155.
9. Foss, O. *Acta Chem. Scand.* **3** (1949) 435.
10. Foss, O. and Tjomsland, O. *Acta Chem. Scand.* **10** (1956) 416.
11. Foss, O. *Acta Chem. Scand.* **3** (1949) 708.

Received November 22, 1955.

ACTA CHEMICA SCANDINAVICA 10 (1956) 424—428

Solvates of Barium Pentathionates with Acetone and Tetrahydrofuran

OLAV FOSS and OLAV TJOMSLAND

Institutt for uorganisk kjemi, Norges tekniske høgskole, Trondheim, Norway

Barium pentathionate and selenopentathionate crystallize from aqueous acetone as solvates containing one mole of water and one mole of acetone per mole of salt. Analogous solvates, containing tetrahydrofuran instead of acetone, occur when barium pentathionate, selenopentathionate and telluropentathionate crystallize from aqueous tetrahydrofuran.

The solvates with acetone and tetrahydrofuran are isomorphous; the space group is C_{2h}^2—$P2_1/m$ with $Z = 2$. The barium ion, the middle atom of the pentathionate chain, the water molecule and the organic molecule lie in a crystallographic mirror plane. Unit cell dimensions are given for the five solvates, and their structure discussed in relation to the structures of barium pentathionate, selenopentathionate and telluropentathionate dihydrates.

In preparations of the solvates, some of the individual crystals give off the acetone or tetrahydrofuran relatively rapidly, while others are more stable.

In earlier papers on the crystal chemistry of barium salts of pentathionic, selenopentathionic and telluropentathionic acids, five dihydrates have been described, which crystallize in three different space groups. The salts are, triclinic barium pentathionate [1] and telluropentathionate [2] dihydrates, space group C_i^1—$P\bar{1}$ with $Z = 2$; orthorhombic barium pentathionate [3] and selenopentathionate [4] dihydrates, space group D_{2h}^{16}—$Pnma$ with $Z = 4$; and monoclinic barium telluropentathionate dihydrate [2], space group C_{2h}^3—$A2/m$ with $Z = 4$. The present paper, on solvates in which one of the water molecules of the dihydrates is replaced by an acetone or tetrahydrofuran molecule, introduces a fourth, closely related structure type, of space group C_{2h}^2—$P2_1/m$ with $Z = 2$.

The solvates of barium pentathionates with acetone and tetrahydrofuran occur very readily, on addition of the solvents to aqueous solutions of the salts. The solvates are relatively stable, although the dissociation pressures of the organic molecules above the solvate crystals appear to be higher than in the case of the corresponding solvates with ethanol [5]. Within a preparation, some individual crystals give off the solvate molecules and become opaque rapidly, while others are quite stable and remain transparent and unchanged for weeks.

The crystals retain the solvate molecules better if immediately after filtering and washing, with the solvate solvent and then with ether, the crop of crystals is spred out on a large surface for drying in air. Crystals, once stable and thus picked and cut for X-ray measurements, mounted on a glass fibre in air in the ordinary way, have not been observed to disintegrate during the exposures to X-rays.

No solvates of barium salts with acetone or tetrahydrofuran appear to have been reported earlier. Deines and Christoph [6] may have had the solvate of barium pentathionate with acetone in their hands, inasmuch as they in 1933 in a footnote reported on the isolation of barium polythionates, presumably also the pentathionate, from aqueous solutions by addition of ethanol or acetone.

EXPERIMENTAL

Solutions of barium pentathionate [1], selenopentathionate [4] and telluropentathionate [5] hydrates, saturated at room temperature, were filtered if necessary and warmed to about 40° C, and from one to two times the volume of acetone or tetrahydrofuran was added with stirring. The solvates crystallized as the solutions were allowed to cool, to room temperature or in ice. Pure water or about 0.2 N perchloric acid was used to dissolve the hydrates, since hydrochloric acid which ordinarily is used to stabilize solutions of the pentathionates, caused contamination of the solvates with barium chloride.

Under the above conditions, the solvates with acetone appear to be less soluble and crystallize more rapidly than those with tetrahydrofuran. As with the hydrates, the solubilities decrease in the order, pentathionate, selenopentathionate and telluropentathionate.

The pentathionates were analyzed iodometrically by means of the sulphite method [7], some sodium sulphate being added to the sample before the addition of the sodium sulphite reagent in order to remove the barium as sulphate. Two equivalents of iodine correspond to one mole of pentathionate. Absence of tetrathionate was checked through control analyses by means of the cyanide method.

0.3048 × $\frac{1}{5}$ g, 0.3442 × $\frac{1}{5}$ g, 0.2820 × $\frac{1}{5}$ g substance: 26.38 ml, 27.10 ml, 24.58 ml of 0.01010 N, 0.01099 N, 0.01010 N iodine, respectively.

$BaS(S_2O_3)_2 \cdot H_2O \cdot (CH_3)_2CO$ (469.8). Mol. weights found, 457.3, 462.3, 454.3.

0.1834 × $\frac{1}{5}$ g, 0.2525 × $\frac{1}{5}$ g, 0.2497 × $\frac{1}{5}$ g substance: 13.99 ml, 18.97 ml, 19.08 ml, respectively, of 0.01099 N iodine.

$BaS(S_2O_3)_2 \cdot H_2O \cdot (CH_2)_4O$ (483.8). Mol. weights found, 477.0, 484.4, 476.3.

The selenopentathionates were titrated with potassium bromate and subsequently analyzed iodometrically by means of the Norris and Fay method, as described earlier [8]. The bromate titration values served as a check on the absence of tetrathionate [8].

0.2808 g, 0.2474 g, 0.2765 g substance: 22.43 ml, 19.15 ml, 21.91 ml, respectively, of 0.09954 N sodium thiosulphate.

$BaSe(S_2O_3)_2 \cdot H_2O \cdot (CH_3)_2CO$ (516.7). Mol. weights found, 503.0, 519.2, 507.1.

0.1983 g, 0.2066 g substance: 15.02 ml, 15.64 ml, respectively, of 0.09954 N sodium thiosulphate.

$BaSe(S_2O_3)_2 \cdot H_2O \cdot (CH_2)_4O$ (530.7). Mol. weights found, 530.6, 530.8.

The telluropentathionate was analyzed by direct titration with iodine, as described earlier [9]. Absence of tetrathionate was checked through subsequent analyses of the titrated solutions by means of the sulphite method [9].

0.3360 g, 0.1500 g, 0.2496 g substance: 24.26 ml, 10.98 ml, 17.70 ml, respectively, of 0.1001 N iodine.

$BaTe(S_2O_3)_2 \cdot H_2O \cdot (CH_2)_4O$ (579.4). Mol. weights found, 553.5, 546.0, 563.4.

Different analyses reported for a substance were on different preparations.

The presence of organic molecules in the solvates was apparent from the strong characteristic odours of acetone or tetrahydrofuran which appeared when the solvates were dissolved in a little water. The acetone was, furthermore, characterized by means of 2,4-dinitrophenylhydrazine.

The solvate of barium selenopentathionate with tetrahydrofuran is the only one which gave consistent analytical results in agreement with the theoretical composition of the solvate. In the case of the other solvates, the results indicate that some water or, more likely, some acetone or tetrahydrofuran may have escaped from the crystal lattices before analysis. There is also a possibility that the solvates are non-stoichiometric, in the sense that, regarding them as derived from dihydrates, a water molecule of the latter is not completely, but only partly replaced by the organic molecule. That is, in the crystal lattice of the solvates some of the acetone or tetrahydrofuran positions are occupied by water.

CRYSTALLOGRAPHIC DATA

The solvates of barium pentathionates with acetone and tetrahydrofuran occur as plates {001}, bounded by {110}. The plates are usually rhomb-shaped and very thin, but do on slow crystallization grow thicker. There is perfect cleavage along (001), and some tendency of cleavage along another plane parallel to the *b* axis, probably (100). Twinning on (001) frequently occurs. The acetone solvates have also been obtained as prisms elongated in the direction of the *a* axis and with, also here, {001} predominant.

The unit cell dimensions were determined from oscillation and Weissenberg photographs about the *a* and *b* axes, using copper radiation. The axial lengths given in Table 1 are based on $\lambda(\mathrm{Cu}K_\alpha) = 1.542$ Å and are believed to be correct to within 0.5 %.

Table 1. Unit cell dimensions of isomorphous acetone and tetrahydrofuran solvates.

	a	*b*	*c*	*β*
$BaS(S_2O_3)_2 \cdot H_2O \cdot (CH_3)_2CO$	5.04 Å	10.47 Å	13.61 Å	104°
$BaSe(S_2O_3)_2 \cdot H_2O \cdot (CH_3)_2CO$	5.02	10.56	13.78	105°
$BaS(S_2O_3)_2 \cdot H_2O \cdot (CH_2)_4O$	5.03	10.56	13.81	104°
$BaSe(S_2O_3)_2 \cdot H_2O \cdot (CH_2)_4O$	5.03	10.69	13.97	105°
$BaTe(S_2O_3)_2 \cdot H_2O \cdot (CH_2)_4O$	5.00	10.82	14.21	106°

The densities of the first and third of the solvates were measured by flotation in bromoform-carbon tetrachloride mixtures and found to be 2.25 and 2.27 g/cm^3, respectively, as compared with the calculated values of 2.24 and 2.26 g/cm^3 for two molecules per unit cell. The only systematic absences are, for all five solvates, $0k0$ when k is odd. A comparison of the intensities of the $0kl$ and $h0l$ zones of reflections, and the close correspondence of unit cell dimensions, leave no doubt that the solvates are isomorphous. The diffraction symmetry being monoclinic, there are two space groups compatible with the systematic absences, of which the centrosymmetric one, C_{2h}^2—$P2_1/m$, has been found to be the correct one through Patterson and Fourier projections along the *a* and *b* axes of the solvate of barium pentathionate with acetone.

With two formula units per unit cell, either centres of symmetry or mirror planes are required as molecular symmetry elements. Since pentathionate ions, water molecules and acetone or tetrahydrofuran molecules cannot reasonably be centrosymmetric, they must lie in mirror planes, as does also the barium ion according to the projections mentioned above.

The work so far done on the crystal structure of the solvate of barium pentathionate with acetone shows, as was expected from the unit cell dimensions and space group and the known structures of barium pentathionate, selenopentathionate and telluropentathionate dihydrates, that the solvate crystals are built up of layers which have the same internal structure as in the dihydrates, but for the substitution of a water molecule by an organic molecule. In the dihydrate structures [1–4], one of the water molecules, $(H_2O)_I$, is firmly bound, being coordinated to two barium ions and forming hydrogen bonds to two oxygen atoms, whereas the other water molecule, $(H_2O)_{II}$, is coordinated to one barium ion only, forms no hydrogen bonds and has a relative spacious environment. It is this water molecule, $(H_2O)_{II}$, of the dihydrates which in the solvates is replaced by acetone or tetrahydrofuran, the internal structure of the layers otherwise being the same.

The dihydrates crystallize in three different space groups [1–4], *viz.*, C_i^1—$P\bar{1}$ with $Z = 2$, D_{2h}^{16}—$Pnma$ with $Z = 4$, and C_{2h}^3—$A2/m$ with $Z = 4$. The space group, C_{2h}^2—$P2_1/m$ with $Z = 2$, of the acetone and tetrahydrofuran solvates represents a fourth structure type. The unit cell dimensions of the dihydrates and the solvates are very like, with $a = 5.0$ Å and $b = 10.3$—10.8 Å, and c spacings as discussed below. The isostructural layers are parallel to the c planes, and the crystals show a corresponding perfect cleavage along this plane. The internal layer symmetry, $2_1/m$, is crystallographically required by all space groups except the triclinic one, but is realized even there [1]. The structure types differ only in the way in which the layers are arranged relative to each other. In the crystals of space group C_i^1—$P\bar{1}$, there is a repetition of layers with relative displacements in the directions of the a and b axes; in C_{2h}^2—$P2_1/m$, there is a repetition with displacements in the direction of the a axis only; in D_{2h}^{16}—$Pnma$, successive layers are related through glide planes a in their interface, and in C_{2h}^3—$A2/m$, through twofold rotation axes parallel to the b axis in the interface.

In the solvates, the oxygen atom of the organic molecule coordinates to the barium ion, like the oxygen atom of the replaced water molecule, and is located between the barium ion and the nearest layer interface, with the rest of the molecule directed towards the interface. It is interesting to compare the space requirements of the water and organic molecules with the observed variations of layer thicknesses. The layer thickness is equal to the c spacing when there are two formula units per unit cell, and half the c spacing when there are four. The distances from the centre of the oxygen atom, along the molecular axis to the van der Waals sphere of the methyl or methylene groups, are calculated as 4.0 Å for acetone and 4.3 Å for tetrahydrofuran, using dimensional data from electron diffraction studies [10,11] and taking the van der Waals radius of methyl and methylene groups [12] as 2.0 Å. For water, the corresponding distance is 1.8 Å. The observed c spacings of the solvates with tetrahydrofuran are, in fact, a little larger than of those with acetone, *viz.*, 0.19 Å for the pentathionates and 0.18 Å for the selenopentathionates. Also, the c spacings of the solvates are larger, by 2.0—2.4 Å, than the c spacings, or half these values, of the corresponding dihydrates [1–4]. Although the molecules probably do not point directly towards the layer interface, but are more or less inclined to it in the direction of the a axis, it appears that there is a

dependence of layer thickness on the space requirements of the replaceable molecules.

The work has been aided by grants from *Norges Almenvitenskapelige Forskningsråd* and from *Det Videnskapelige Forskningsfond av 1919.*

REFERENCES

1. Foss, O. and Tjomsland, O. *Acta Chem. Scand.* **10** (1956) 288.
2. Foss, O. and Tjomsland, O. *Acta Chem. Scand.* **10** (1956) 416.
3. Foss, O. and Zachariasen, H. *Acta Chem. Scand.* **8** (1954) 473.
4. Foss, O. and Tjomsland, O. *Acta Chem. Scand.* **8** (1954) 1701.
5. Foss, O. and Tjomsland, O. *Acta Chem. Scand.* **10** (1956) 421.
6. Deines, O. and Christoph, E. *Z. anorg. u. allgem. Chem.* **213** (1933) 209.
7. Kurtenacker, A. *Analytische Chemie der Sauerstoffsäuren des Schwefels.* Ferdinand Enke, Stuttgart 1938, pp. 149–155.
8. Foss, O. *Acta Chem. Scand.* **3** (1949) 435.
9. Foss, O. *Acta Chem. Scand.* **3** (1949) 708.
10. Beach, J. Y. *J. Chem. Phys.* **9** (1941) 54.
11. Allen, P. W., Bowen, H. J. M., Sutton, L. E. and Bastiansen, O. *Trans. Faraday Soc.* **48** (1952) 991.
12. Pauling, L. *The Nature of the Chemical Bond.* Cornell University Press, Ithaca, New York 1945, p. 190.

Received November 31, 1955.

ACTA CHEMICA SCANDINAVICA 10 (1956) 429—431

The Infrared Spectrum of 1,2-Butylene Oxide

An Azeotropic System (1,2-Butylene Oxide/Chloroform) with a Maximum Boiling Point

BERTIL NYCANDER and CARL OLOF GABRIELSON

Research Laboratory, Mo och Domsjö AB, Örnsköldsvik, Sweden

Pure 1,2-butylene oxide has been obtained by fractional distillation of a mixture rich in isomeric butylene oxides. The infrared spectrum of the pure substance is recorded. 1,2-butylene oxide forms with chloroform an azeotrope with a maximum boiling point of 69.0° C at atmospheric pressure. The azeotrope contains 39.4 % by weight of the oxide.

In connection with an investigation of impurities in raw technical ethylene chloride obtained as a by-product during the manufacture of ethylene oxide by the ethylene chlorohydrin process, it was found that 1,2-butylene oxide forms with chloroform an azeotropic system with a maximum boiling point. This azeotrope does not seem to have been described in literature before.

EXPERIMENTAL

Distillation apparatus. A Podbielniak Hyper-Cal apparatus, Cat. No. HC-701-A, Series "D", has been used for all distillations. Butylene oxide or mixtures of this and other substances have been fractionated in a 25 mm I. D. × 72″ long Heli-Grid packed column. The chloroform was distilled in the same kind of column which in this case was only 36″ long. The distillation temperature was measured with an iron-constantan thermocouple which was calibrated against a standardized thermometer.

Analysis. Butylene oxides were analysed by a method given by Swern *et al.*[1] using the reaction of epoxides with hydrochloric acid in absolute ethyl ether.

1,2-Butylene oxide. In order to obtain this substance in a pure form, a fraction was used which had been enriched in butylene oxides during a technical distillation of raw ethylene chloride which contained butylene oxides as impurities. The mixture was fractionated in the above mentioned apparatus with a reflux ratio of 100:1. When the distillation temperature reached the boiling point of ethylene chloride, the distillation was stopped. The distillate was redistilled with a reflux ratio of 200:1. Three main fractions were obtained in the second distillation.

The first one had a boiling point of 54° C at atmospheric pressure, which is close to the value 53.5° C that Winstein and Lucas [2] found for *trans*-2,3-butylene oxide. The identi-

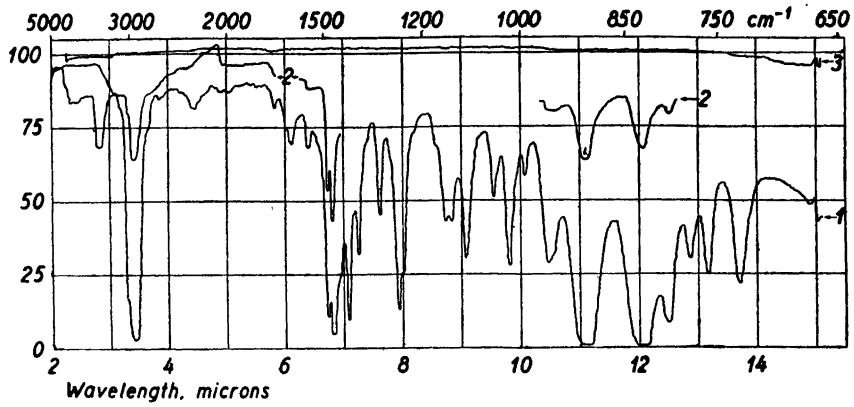


Fig. 1. Infrared spectrum of 1,2-butylene oxide. Phase: Liquid. Thickness: 1 = 0.05 mm; 2 = cap. Prism: NaCl. Resolution: 895. Response: 1. Gain: 6. Speed 2. Suppression: 1; 3 = Example of compensation with the same adjustments. Ordinate: Transmittance (% Transmission).

fication was confirmed by recording the infrared spectrum of the fraction and comparing this with the spectrum of *trans*-2,3-butylene oxide published by Patterson [3].

The second fraction boiled at 58–60° C, indicating that it consists of *cis*-2,3-butylene oxide since, according to Winstein and Lucas [2], the boiling point of this compound is 59.7 ° C. The identification was also in this case confirmed when the infrared spectrum was found to be identical with the one published by Patterson [3].

The third main fraction boiled at 65° C and ought to consist of 1,2-butylene oxide. Analysis of this fraction gave 99.8 (99.6, 99.8, 100.1) % butylene oxide. Its infrared spectrum (Fig. 1) shows that it does not contain any *cis*- or *trans*-2,3-butylene-oxide.

In order to confirm that it really was 1,2-butylene oxide, this substance was synthetized from ethyl bromide and monochloro acetaldehyde by a method used by Andersson [4]:

$$C_2H_5MgBr + OHC \cdot CH_2Cl \rightarrow C_2H_5CH(OH)CH_2CL \xrightarrow{OH^-} C_2H_5CH \cdot CH_2$$
$$\qquad\qquad\qquad

The azeotrope contained 39.4 (39.4, 39.4) % by weight of 1,2-butylene oxide.

The boiling point was determined by boiling the azeotrope slowly under reflux in a Claisen flask and the temperature was read on a standardized thermometer graduated to 0.1° C. At 769 mm Hg the boiling point was 69.0° C.

In the same way the boiling points of the pure 1,2-butylene oxide and chloroform was found to be 63.2 and 61.2° C, respectively, at 763 mm Hg. The boiling point of chloroform at atmospheric pressure is given [5] as 61.2° C and that of 1,2-butylene oxide [6] as 63.7° C at 767 mm Hg.

The infrared spectrum of the pure 1,2-butylene oxide was recorded on a Perkin-Elmer Model 21 Double Beam Infrared Spectrometer at Uppsala University *. The positions of the strongest absorption maxima are 3.39, 6.72, 6.80, 7.07, 7.93, 11.08, 12.06 μ. The wave lengths of the absorption maxima were determined by calibration against the spectrum of polystyrene [7].

REFERENCES

1. Swern, D., Findley, T. W., Billen, G. N. and Scanlan, J. T. *Anal. Chem.* **19** (1947) 414.
2. Winstein, S. and Lucas, H. J. *J. Am. Chem. Soc.* **61** (1939) 1576.
3. Patterson, W. A. *Anal. Chem.* **26** (1954) 823.
4. Andersson, S. *The Reaction between Ethylene Oxides and Ammonia*, Diss., Lund 1955, p. 14.
5. Timmermans, J. *Physico-Chemical Constants of Pure Organic Compounds*, Elsevier Publishing Company, New York, Amsterdam, London, Brussels 1950, p. 219.
6. Reference 4, p. 18.
7. Plyer, E. K. and Peters, C. W. *J. Research Natl. Bur. Standards* **45** (1950) 462.

Received December 14, 1955.

* We are much obliged to Mr. Andreas Rosenberg at the Biochemical Institution of Uppsala University for his kind service in this matter.

ACTA CHEMICA SCANDINAVICA 10 (1956) 432—438

*iso*Thiocyanates XVI. Glucoconringiin, the Natural Precursor of 5,5-Dimethyl-2-oxazolidinethione

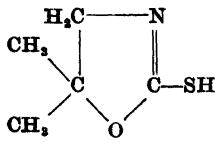
ANDERS KJÆR, ROLF GMELIN and ROALD BOE JENSEN

Chemical Laboratory of the University of Copenhagen, Denmark

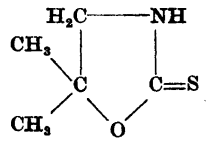
Seed of the crucifer *Conringia orientalis* (L.) Andrz. has been shown to contain a new glucoside, *glucoconringiin*, characterised as a crystalline tetraacetate (IV) and affording glucose, sulphuric acid and 2-hydroxy-2-methyl-propyl *iso*thiocyanate (V) on enzymic hydrolysis. The mustard oil cyclises spontaneously to 5,5-dimethyl-2-oxazolidinethione (II), a fact accounting for the previously reported isolation of (II) from the same seed.

A modified synthesis of the heterocyclic compound is described. A paperchromatographic method has disclosed the presence of glucoconringiin also in three species of the genus *Cochlearia*, further substantiated by the isolation from *Cochlearia officinalis* L. of crystalline 5,5-dimethyl-2-oxazolidinethione after enzymic hydrolysis. Evidence is available of the existence of additional 2-oxazolidinethione-producing glucosides in plants.

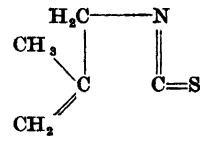
In 1938 Hopkins [1] reported the isolation of 5,5-dimethyl-oxazoline-2-thiol (I) from seed of the common Canadian weed *Conringia orientalis* L. (Dumort) *.



I



II



III

The structure of (I) followed from its identity with a synthetic sample, prepared by Bruson and Eastes [2]. On the basis of infra-red studies, Ettlinger [3] later provided evidence in favour of the thione structure (II). It appeared from Hopkins' studies that the heterocyclic compound was formed by enzymic cleavage of a parent glycoside, the aglycone of which was considered to be

* The species should be more correctly designated as *Conringia orientalis* (L.) Andrz. (= *Erysimum orientale* Mill.).

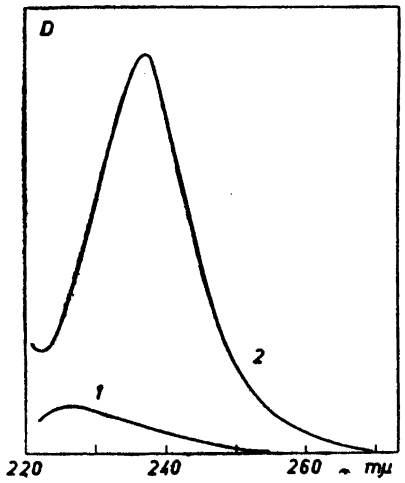


Fig. 1. Ultra-violet absorption spectra of: 1. an aqueous solution of glucoconringiin; 2. an aqueous solution of the ether-soluble product, (II), formed by enzymic cleavage of glucoconringiin.

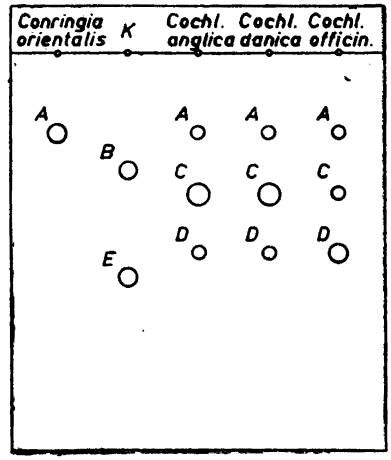


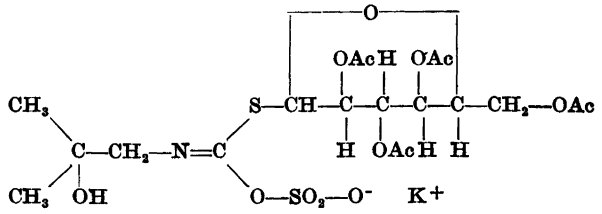
Fig. 2. Descending paper chromatogram, run in n-butanol: acetic acid : water. Sprayed with ammoniacal silver nitrate solution. K: control solution; A: glucoconringiin; B: sinigrin; C: glucoputranjivin; D: glucocochlearin; E: glucotropaeolin.

2-methylallyl *iso*thiocyanate (III). Addition of water to the *iso*thiocyanate-grouping of the latter, followed by spontaneous cyclisation of the intermediate thiocarbamic acid to (I) was regarded as a likely mode of formation. When synthetic 2-methylallyl *iso*thiocyanate became available in this laboratory [4], it was established that no such tendency to water addition and ring-closure existed.

As pointed out in a previous paper of this series [5], seed of *Conringia orientalis* yielded no volatile *iso*thiocyanates on enzymic hydrolysis. Paper chromatography [6] of a seed extract has now, however, disclosed the presence of a single glucoside, giving a spot in the lower R_F-region (Fig. 2). The glucoside solution exhibited an absorption spectrum of the usual type (Fig. 1), as known for, *e. g.*, sinigrin [7], a fact precluding the presence of chromophors, such as the heterocyclic ring system (II), in the *Conringia*-glucoside, for which the name *glucoconringiin* is proposed.

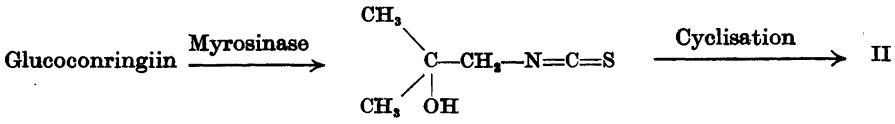
Upon enzymic hydrolysis of glucoconringiin an ether-soluble substance arose, with spectroscopical characteristics (Fig. 1) similar to those reported for (II) by Hopkins [1] and Astwood *et al.*[8] The concomitant formation of glucose and sulphate was established. During the summer of 1955, *Conringia orientalis* (L.) Andrz. was cultivated on a larger scale in the Botanical Garden of the University of Copenhagen. The seed material thus obtained was employed for the isolation of further quantities of glucoconringiin, which did not show signs of crystallisation, but could be transformed into a crystalline acetyl-derivative with the composition $C_{19}H_{28}O_{14}NS_2K$. Analytical data indicated the presence of four O-acetyl groupings; on the assumption that these are

located in the glucose moiety, as rendered highly probable by model preparation of the analogous tetraacetyl-sinigrin, and provided sulphuric acid is bound as generally believed in this type of glucosides, the structure (IV) appears to account for the properties of acetylglucoconringiin.



IV

As expected, the hydroxy-grouping of the side-chain escaped acetylation due to its tertiary character. The derivative (IV) was not attacked by myrosinase. Its infra-red spectrum was determined in the solid state and found very similar to that of acetylsinigrin. Probably due to association, no band attributable to the tertiary hydroxy-function was observed in the spectrum of (IV). That acetylation was not accompanied by secondary changes appeared from the fact that (IV) could be smoothly deacetylated to glucoconringiin, the identity of which followed from its rapid enzymic hydrolysis, resulting in the formation of (II). There can be little doubt, therefore, that (II) is to be considered as a secondary product, arising from the initially formed 2-hydroxy-2-methyl-propyl *iso*thiocyanate (V) by spontaneous cyclisation.



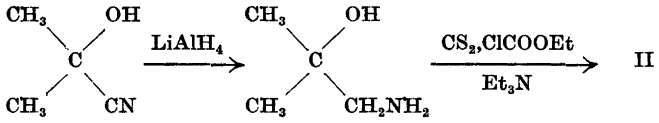
V

The cyclisation proceeds at a measurable rate. It was spectroscopically established that a partly purified glucoconringiin preparation, subjected to enzymic hydrolysis for four hours at room temperature, afforded the cyclic product in a yield of only about 40 %; about 24 hours were required for the cyclisation to go to completion. From analogous cases it appeared very unlikely that the enzymic hydrolysis is the rate-determining step in the present reaction.

For further studies a synthetic sample of (II) became desirable. As in previously described syntheses [2,9,10] of this compound, 1-amino-2-methyl-2-propanol (VI) was selected as a starting material. Several methods have been described [11,12] for the preparation of this aminoalcohol, which has recently been isolated from the phospholipid fraction of *Neurospora crassa* [13] and established as the amine moiety of sanshoamide, an amide isolated from *Zanthoxylum piperitum* [14]. Whereas Meisenheimer and Chou [15] were unsuc-

cessful in attempts to reduce acetone cyanohydrin catalytically, a mixture of amines, with unstated yield of the desired primary derivative, was formed by high-pressure reduction with Raney-nickel as a catalyst, according to a patent claim [16]. We found that acetone cyanohydrin could be reduced to (VI) with lithium aluminium hydride. Analogous reductions of the cyanohydrins of benzaldehyde [17] and *cyclo*hexanone [18] have been reported previously.

Several methods of converting 1,2-aminoalcohols into 2-oxazolidinethiones have been proposed, all proceeding *via* dithiocarbamates by means of reagents, traditionally employed for converting the latter into *iso*thiocyanates [10,19,20]. The Kaluza method of *iso*thiocyanate synthesis, modified according to Hodgkins and Ettlinger [21], belongs to this type of reaction and has proved to be useful for the preparation of 2-oxazolidinethiones also *. We subjected (VI) to this reaction in a non-aqueous system with triethylamine as a base and obtained (II) in 78 % yield. Several attempts to isolate the intermediate *iso*thiocyanate (V) proved unsuccessful, probably due to the cyclisation being facilitated under basic conditions. The identity of the final product was established by comparison with an authentic specimen of (II), kindly furnished by Dr. Ettlinger.



VI

In the course of our systematic studies on the distribution of *iso*thiocyanates in plants, it was found that oxazolidinethiones could be separated by paper chromatography in the solvent system heptane: *n*-butanol: 90 % formic acid, introduced by Sjöquist [22] for the separation of phenylthiohydantoins. By this technique, oxazolidinethiones were recognised in other plants also. For example, glucoside chromatography disclosed the presence in *Cochlearia anglica* (L.) Asch. & Grb., *C. danica* L. and *C. officinalis* L. of three glucosides (Fig. 2), two of which were recognised as the previously known species glucoputranjivin and glucococchlearin, affording *iso*propyl [23] and *sec*-butyl [5] *iso*thiocyanate, respectively, on enzymic hydrolysis. The third glucoside spot could be attributed to glucoconringiin because of its enzymic cleavage to a compound, indistinguishable from (II) by paper chromatography in the heptane system. Final proof of its identity was provided when a crystalline specimen was obtained from a seed sample of *C. officinalis* L. The natural product was found to be identical with an authentic specimen of (II).

It should be noticed that the structurally analogous *l*-5-vinyl-2-oxazolidinethione has been recognised as a constituent of several species of the important genus *Brassica* [8]. We have spectroscopical evidence that this compound is formed in a similar way from an analogous genuine glucoside of more wide-

* Applied by Dr. Ettlinger in a synthesis of 4-vinyl-2-oxazolidinethione (private communication).

spread occurrence than previously reported and derivable from one of the stereoisomeric 2-hydroxy-3-butenyl *iso*thiocyanates.* Additional natural representatives of the class of oxazolidinethione-progenitors have been discovered and are at present being further studied. An account of the results will form the subject of forthcoming communications.

EXPERIMENTAL

Melting points are uncorrected and determined in capillary tubes in a glycerol bath, if not otherwise stated. Infra-red spectra were determined in potassium bromide discs on a Beckman IR-2 instrument.

Detection and nature of glucoconringiin. Seed of *Conringia orientalis* (L.) Andrz. (1 g) was extracted with hot methanol and the solvent was removed by evaporation. The residue was taken up in water, the solution filtered and a drop of the filtrate used for descending paper chromatography in *n*-butanol:acetic acid:water (4:1:3), essentially as described by Schultz and Gmelin[6]; a single glucoside-spot of glucoconringiin appeared (Fig. 2).

The glucoside solution was purified by exchange on a small column of acidic aluminium oxide, eluted with a 1 % solution of K_2SO_4 and a sample withdrawn for ultra-violet absorption measurement (Fig. 1). A few drops of a myrosinase preparation were added to the eluate which was set aside for 24 hours. The now turbid solution was extracted three times with ether; the solvent was removed, the residue dissolved in water (200 ml) and the ultra-violet absorption spectrum determined (Fig. 1). A high-extinction band was observed at 239 mμ, displaced in alkali to 232 mμ, and a minimum at about 222 mμ, both values agreeing well with those previously published [8].

Samples of the aqueous phase were chromatographed for sugars in *n*-butanol:acetic acid:water and in pyridine:amyl alcohol:water. In both solvent systems, the presence of glucose was established upon comparison with control spots. A separate sample of glucoconringiin, which had not been purified by ion exchange, served to establish the presence of sulphate after the enzymic fission.

Preparation and properties of acetylglucoconringiin **. *Conringia* seed (100 g) was extracted with two portions (each 500 ml) of hot 70 % methanol and the solution taken to dryness *in vacuo*. The residue was dissolved in water (300 ml) and impurities precipitated by adding excess lead acetate solution. After filtration and removal of excess lead salt as PbS, the solution was again taken to dryness *in vacuo*, leaving glucoconringiin as an almost colourless, glassy mass.

After thorough drying the product was dissolved in a mixture of dry pyridine (25 ml) and acetic anhydride (25 ml) and set aside for 24 hours. Volatile reagents were then removed *in vacuo* and the brown residue dissolved in a large volume of hot ethanol. The solution was treated with charcoal, filtered and chilled. A slight amount of amorphous material was removed and the filtrate concentrated, whereupon the crystalline acetyl-derivative (663 mg) separated. Two recrystallisations from 96 % ethanol, containing a little methanol, afforded an analytical specimen (397 mg) as tiny, colourless needles, m. p. 152° (decomp.) on rapid heating. The acetyl-derivative is easily soluble in water, moderately soluble in methanol and slightly soluble in ethanol. $[\alpha]_D^{24}$ −5.3° (H_2O, c = 5.3). (Found: C 37.95; H 4.85; N 2.25; S 10.80; CH_3CO 30.9. Calc. for $C_{19}H_{23}O_{14}NS_2K$: C 38.18; H 4.73; N 2.34; S 10.73; 4 CH_3CO 28.8). The infra-red spectrum had characteristic bands

* *Note added in proof:* After this paper was submitted for publication, Greer [26] announced the isolation of this glucoside, "progoitrin", as a crystalline sodium salt. The composition and provenance of the glucoside "glukorapiferin", recently characterized by Schultz and Wagner [27] as a crystalline pentaacetate, strongly indicate the identity of "progoitrin" and "glukorapiferin".

** According to a personal communication to one of us (R.G.) from Prof. O.-E. Schultz, Tübingen, acetylation has been used in his laboratory for the purpose of characterising *iso*thiocyanate glucosides, *cf.* Ref.[27]

at: 5.67 (very strong, C = O stretching vibration), 5.99 (weak), 7.24 (strong), 7.97, 8.10 (split peak, v. s.), 8.46 (w.), 8.80 (w.), 9.06 (w.), 9.40 (v. s.), 10.10 (w.), 10.92 (medium), 11.12 (m.), 11.45 (w.), 11.95 (w.) and 12.60 μ (s.).

A solution of acetylglucoconringiin in ethanolic ammonia was kept at room temperature for five days. The solvent was then removed and a sample of the residue subjected to paper chromatography in *n*-butanol:acetic acid:water. A single spot was observed, indistinguishable from that of glucoconringiin. The remaining part of the reaction product was hydrolysed enzymically, and the ether-soluble reaction product was identified as 5,5-dimethyl-2-oxazolidinethione by its absorption spectrum and by paperchromatographic comparison with an authentic sample.

Acetylsinigrin. In a model experiment, sinigrin was subjected to acetylation by a similar procedure. Previously, Gadamer [24] reported failure in obtaining a crystalline derivative by treatment of sinigrin with acetic anhydride.

Sinigrin (200 mg) was dissolved in hot pyridine (4 ml), and acetic anhydride (2 ml) added after cooling. After 4 hours, the separation of acetylsinigrin started and was completed by careful addition of ether. The crude product was recrystallised twice from aqueous ethanol and once from methanol to give pure tetraacetylsinigrin as thin, colourless needles (77 mg), m. p. 192–93° (dec.), determined in an electrically heated block. The solubility properties were the same as those of acetylglucoconringiin. $[\alpha]_D^{24}$ −18.6° (H_2O, c = 3.6). (Found: C 38.15; H 4.36; N 2.30. Calc. for $C_{18}H_{24}O_{13}NS_2K$: C 38.24; H 4.28; N 2.48). The infrared spectrum had conspicuous bands at 5.67 (v. s., C = O stretching vibration), 6.00 (w.), 7.24 (s.), 7.76 (s.), 7.97 (v. s. —C—O-vibration), 8.62 (w.), 9.39 (v. s.), 10.43 (w.), 10.64 (w.), 10.84 (w.), 11.20 (medium) and 12.60 μ (s.).

1-Amino-2-methyl-2-propanol (VI). To a well-stirred solution of $LiAlH_4$ (9.1 g) in dry ether (200 ml) was slowly added a solution of acetone cyanohydrin (8.9 g) in dry ether (100 ml). The reaction was performed in a nitrogen atmosphere, and completed upon heating to reflux temperature for 30 minutes. Then water (10 ml) and 15 % NaOH (25 ml) were cautiously added, the precipitate filtered off and thoroughly washed with ether, and the ether solution dried over KOH. The ether was removed and the colourless, viscous amine (4.6 g, 50 %) distilled, b. p. 150°, in agreement with several literature values. No attempts were made to raise the yield by systematic variations of the conditions. It was found, however, that reduction in the presence of $AlCl_3$, a recently introduced modification in the reduction of ordinary nitriles [25], gave a much lower yield (25 %), due to cleavage of the cyanhydrin. In this case, a rather large proportion of pinacol was also isolated as a secondary product.

5,5-Dimethyl-2-oxazolidinethione (II). The above amine was converted into (II) by a recently published method of *iso*thiocyanate synthesis [21]. To a stirred solution of (VI) (4.6 g) in dioxan (7.5 ml) and triethylamine (7.5 ml), kept at −10°, carbon disulphide (3.1 ml) was slowly added and the solution allowed to come to room temperature. After cooling again, ethyl chlorocarbonate (5.6 ml) was added very slowly, and the mixture again brought to room temperature. Triethylammonium chloride was removed by filtration and washed with a little dioxan. A solution of triethylamine (7.5 ml) in chloroform (15 ml) was then added and the solution heated shortly to 50°. After removal of all volatile constituents at 50° and 12 mm, crystalline (II) remained (5.31 g, 78 %). A pure sample was obtained as colourless platelets by recrystallisation, first from ether and then from benzene, m. p. 107°, alone or in admixture with an authentic specimen, kindly furnished by Dr. Ettlinger.

Isolation of (II) from seed of Cochlearia officinalis *L.* When a seed sample of *C. officin.* L. was assayed by the method described for the determination of 5-vinyl-2-oxazolidinethione in plant tissues [8], a content of about 45 mg per 100 g of seed was found.

500 g of seed were employed for isolation of the heterocyclic compound. With minor modifications, the procedure was the same as that used for the isolation of the vinyl-derivative [8]. The mainly crystalline, crude product (100 mg) was purified by recrystallisation, first from ether and then from benzene. Thus, colourless flat prisms were obtained (22 mg), m. p. 105°. A mixture of this compound and the synthetic specimen of (II) melted at 106°. (Found: C 46.05; H 7.25; N 10.18. Calc. for C_5H_9ONS: C 45.78; H 6.91; N 10.68). As further proof of identity, the infra-red spectra of the two products were determined and found to coincide. The spectral pattern was essentially the same as that previously reported for (II) [3].

Microanalyses were performed in this laboratory by Mr. P. Hansen. We wish to thank the *Botanical Garden of the University of Copenhagen* for the cultivation of *Conringia orientalis* (L.) Andrz. on a larger scale, and for various seed samples.

The work is part of investigations supported by *Statens Almindelige Videnskabsfond (The Danish State Research Foundation)* and *Carlsbergfondet (The Carlsberg Foundation)*.

REFERENCES

1. Hopkins, C. Y. *Can. J. Research* **16B** (1938) 341.
2. Bruson, H. A. and Eastes, J. W. *J. Am. Chem. Soc.* **59** (1937) 2011.
3. Ettlinger, M. G. *J. Am. Chem. Soc.* **72** (1950) 4699.
4. Kjær, A., Rubinstein, K. and Jensen, K. A. *Acta Chem. Scand.* **7** (1953) 518.
5. Kjær, A., Conti, J. and Larsen, I. *Acta Chem. Scand.* **7** (1953) 1276.
6. Schultz, O.-E. and Gmelin, R. *Z. Naturforsch.* **7b** (1952) 500.
7. Kjær, A., Gmelin, R. and Boe Jensen, R. *Acta Chem. Scand.* **10** (1956) 26.
8. Astwood, E. B., Greer, M. A. and Ettlinger, M. G. *J. Biol. Chem.* **181** (1949) 121.
9. Hopkins, C. Y. *Can. J. Research* **20B** (1942) 268.
10. Rosen, A. A. *J. Am. Chem. Soc.* **74** (1952) 2994.
11. Cairns, T. L. *J. Am. Chem. Soc.* **63** (1941) 871.
12. Krassuski, K. *Compt. rend.* **146** (1908) 236.
13. Ellman, G. L. and Mitchell, H. K. *J. Am. Chem. Soc.* **76** (1954) 4028.
14. Aihara, T. *J. Pharm. Soc. Japan* **71** (1951) 1112. *Cf. Chem. Abstracts* **46** (1952) 4994.
15. Meisenheimer, J. and Chou, L.-H. *Ann.* **539** (1939) 70.
16. *Brit. Pat. 598984. Cf. Chem. Abstracts* **42** (1948) 6377.
17. Nystrom, R. F. and Brown, W. G. *J. Am. Chem. Soc.* **70** (1948) 3738.
18. Nace, H. R. and Smith, B. B. *J. Am. Chem. Soc.* **74** (1952) 1861.
19. Sergeev, P. G. and Ivanova, S. N. *J. Gen. Chem. (U.S.S.R.)* **7** (1937) 1495. *Cf. Chem. Abstracts* **32** (1938) 2534.
20. Ettlinger, M. G. *J. Am. Chem. Soc.* **72** (1950) 4792.
21. Hodgkins, J. E. and Ettlinger, M. G. *J. Org. Chem.* **21** (1956). *In press.*
22. Sjöquist, J. *Acta Chem. Scand.* **7** (1953) 447.
23. Kjær, A. and Conti, J. *Acta Chem. Scand.* **7** (1953) 1011.
24. Gadamer, J. *Arch. Pharm.* **235** (1897) 44 (p. 82).
25. Nystrom, R. F. *J. Am. Chem. Soc.* **77** (1955) 2544.
26. Greer, M. A. *J. Am. Chem. Soc.* **78** (1956) 1260.
27. Schultz, O.-E. and Wagner, W. *Arch. Pharm.* **288/60** (1955) 525.

Received December 15, 1955.

ACTA CHEMICA SCANDINAVICA 10 (1956) 439—444

Double Bond Migration and Dehydrogenation of Squalene on Hydrogenation Catalysts *

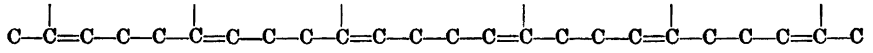
JOHANNES DALE and TORSTEIN ÅRTUN

Forsvarets Forskningsinstitutt, Kjeller, Norway

From infrared spectroscopic evidence it has been concluded that considerable double bond migration takes place during the catalytic hydrogenation of squalene. Dehydrogenation has been observed after treating the olefin with catalysts, in particular with Raney nickel. Ultraviolet spectra indicate the presence of chromophores consisting of 2, 4, and 6 conjugated double bonds, but none with 3, 5, or 7, which suggests a reversed 1,4-addition as a possible mechanism.

Catalytic dehydrogenation has also been achieved with esters of oleic acid.

In the course of a study of the catalytic hydrogenation of the triterpenoid hydrocarbon squalene,



it was observed that the partially hydrogenated product showed infrared absorption bands that were not present either in the starting material, natural squalene, or the completely saturated product, squalane. Thus, in the C=C double bond stretching region a new band had developed at 6.07 μ in addition to the original band at 6.01 μ. Stronger bands had developed at 10.35 μ and at 11.27 μ (only weak in natural squalene); also a weak band appeared at 14.4 μ. These latter bands are generally attributed to the out-of-plane deformation vibrations of ethylenic C—H bonds [2] and are characteristic for the various types of alkyl substitution at a double bond, as indicated in Fig. 1. The obvious conclusion was therefore that the double bonds had in part migrated from the trisubstituted position (absorption at 12.0 μ) and along the chain to give *trans*- or *cis*-disubstituted double bonds, or to the methyl groups to give asymmetrically disubstituted double bonds.

* This work has been preliminarily mentioned in a survey article on squalene [1].

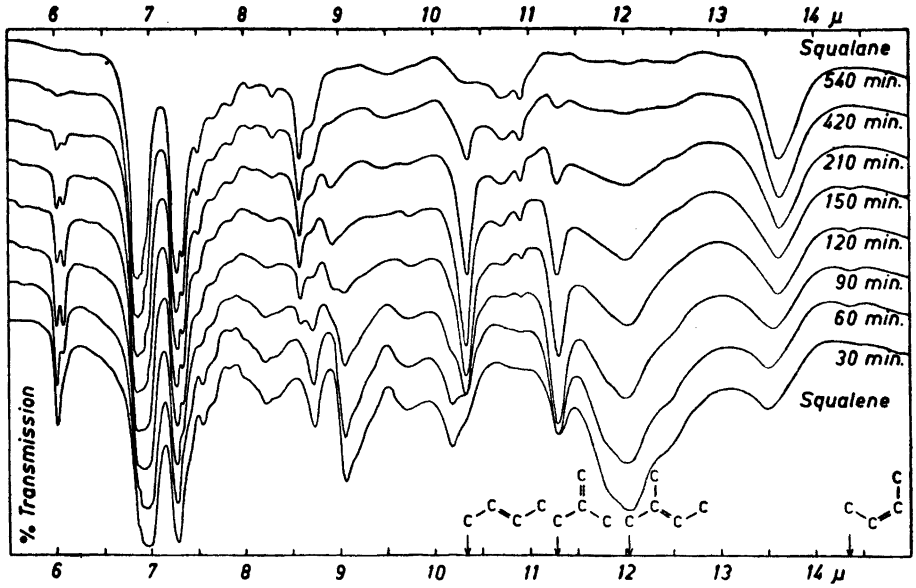


Fig. 1. Infrared spectra taken at intervals during an ordinary hydrogenation of squalene with Raney nickel. Cell thickness: 0.055 mm.

Further systematic studies revealed that this *double bond migration* is quite general and always takes place during the hydrogenation of squalene, irrespective of reaction velocity, temperature, pressure, and of activity and type of catalyst used (nickel, platinum, palladium). Fig. 1 shows the gradual change in the infrared spectrum that occurs during a typical hydrogenation experiment using Raney nickel as a catalyst. The variation in the amount of

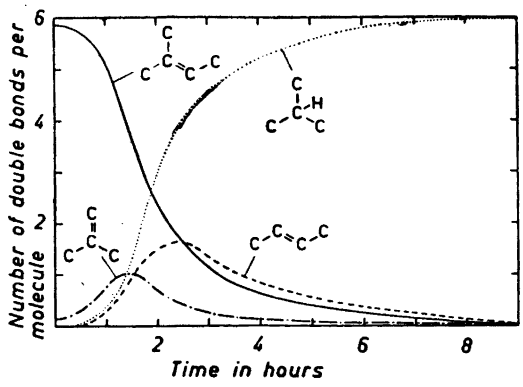


Fig. 2. Approximate amounts of the various types of double bonds during hydrogenation of squalene as estimated from the spectra in Fig. 1. The increase of tertiary hydrogen (absorption at 8.57 μ) has been included for comparison.

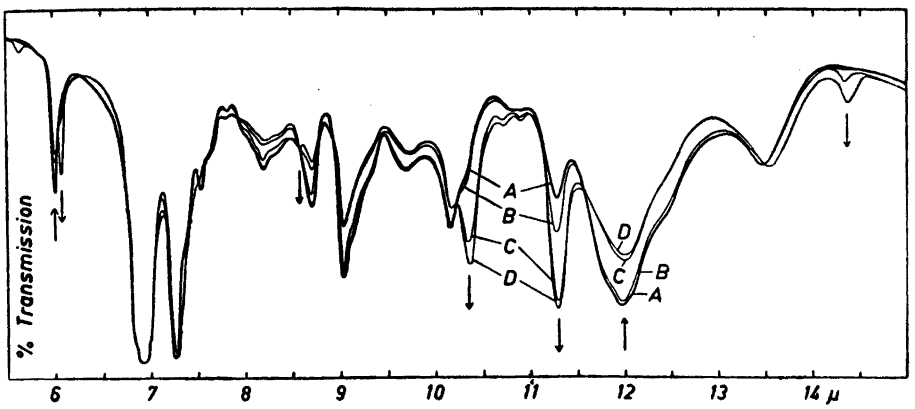


Fig. 3. Changes in the infrared spectrum of squalene during treatment with a Raney nickel catalyst (no hydrogen).
Curve A: heavy line: starting material.
Curve B: after 15 hours.
Curve C: 72 hours.
Curve D: 158 hours. Cell thickness: 0.055 mm.

the various types of double bonds during hydrogenation has been estimated from these spectra using approximate extinction values known from other systems [3], and the results are given graphically in Fig. 2. As can be seen from these curves the *trans*-disubstituted bonds tend to lag behind and are the last ones to become saturated.

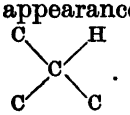
It is here interesting to note that Heilbron, Hilditch and Kamm concluded, from the course of the hydrogenation of squalene, that it was strongly selective [4]. From our results, however, it is more likely that the change in reaction velocity is merely a secondary effect, and not due to real differences in hydrogenation velocity of the original double bonds. That these authors have actually had to do with double bond migration is shown by the oxidation products which were obtained from partially hydrogenated squalene (5/6 saturation) [5]. Together with reasonable cleavage products, there were also isolated C_{19}- and C_{24}-ketones and C_6- and C_{11}-acids which cannot be expected from ozonization of the original double bonds. Furthermore, the corresponding products were not obtained by oxidation of squalene itself [6].

Dehydrogenation has also been observed on hydrogenation catalysts. In one case, evolution of hydrogen started immediately after mixing squalene with a Raney nickel catalyst that had been prepared in a somewhat abnormal manner (see Experimental Part). When the gas evolution slowed down, heat, vacuum, and stirring were applied, and the reaction was made to proceed for many days. The colourless oil became yellow, then orange, and eventually red, and a greenish fluorescence developed. The corresponding changes in the infrared spectrum are shown in Fig. 3, and are strikingly similar to the changes observed during hydrogenation.

The red oil was chromatographically separated into fractions that, when examined for ultraviolet absorption, showed the maxima characteristic for two, four, and six conjugated double bonds, the yields decreasing rapidly in the given order. There was no indication of the formation of chromophores consisting of three, five, or seven conjugated bonds.

Considering the structure of squalene, it may be seen that the exclusive formation of chromophores with an even number of double bonds must result if the assumption is made that the dehydrogenation proceeds as a sort of reversed 1,4-addition; that is, the hydrocarbon may be adsorbed on the catalyst *via* the double bond, and then desorbed, while one hydrogen atom on each side of the double bond is retained by the catalyst. This idea receives some support from the observation that chemisorption of ethylene on nickel films is accompanied by dehydrogenation to give an acetylene complex [7]. In squalene acetylene formation is not possible and may be replaced by diene formation.

By comparing the number of double bonds (~10 %) that are in conjugation, as estimated from ultraviolet absorption, and the decrease in trisubstituted double bonds estimated from infrared absorption (~30 %), it is evident that the main effect is still double bond migration. This is confirmed by the appearance of an absorption band at 8.57 μ which is due [3] to the grouping



. Also, no significant increase in iodine number, determined by hydrogenation [8], could be detected, so apparently most of the hydrogen released is used for the saturation of other double bonds.

At first it was found surprising that there was no detectable displacement or doubling of the new infrared absorption bands due to conjugation, like that reported for the simpler conjugated olefins [2,9]. However, recently reported spectra of polyenes with a similar isoprenoid skeleton, show that the bands have in many cases reverted to the isolated position [10-12]. Also, a slight displacement might be obscured by the strong absorption of isolated double bonds.

When *ethyl oleate* was tried, and later *triolein*, to make possible the use of higher temperatures and lower pressure, the main effect was a rapid elaidinization. Whether it was accompanied by migration, could not be decided from the infrared spectra, but migration is known to occur during hydrogenation [13]. An increase in ultraviolet absorption at 232 mμ, due to the diene chromophore, indicated that some dehydrogenation had taken place, in accordance with the results of Forbes and Neville [14]. In the infrared spectrum the stretching frequency underwent a normal displacement from 6.05 μ to 6.22 μ.

It is an open question, which deserves consideration, whether double bond migration on contact with catalysts might actually proceed *via* dehydrogenation and subsequent partial hydrogenation (1,2-addition) of the diene formed. One indication of such a mechanism is the fact that the double bonds of squalene migrate from trisubstituted to disubstituted positions. The general tendency is for double bonds to migrate towards higher substitution. Furthermore, alkali treatment is quite ineffective in conjugating the double bonds of squalene [15].

Unfortunately, it was not possible to reproduce a catalyst with such a high activity as the Raney nickel catalyst we first tried. A systematic search revealed that there is some dehydrogenating effect with all types of hydrogenation catalysts. However, even the least active catalyst in this respect caused extensive double bond migration when used for hydrogenation. This is in accord with earlier findings that the presence of adsorbed hydrogen promotes isomerization [16] and disproportionation [17].

EXPERIMENTAL

Materials. The squalene used for the experiments was prepared from a concentrate obtained by technical distillation of basking-shark liver oil. Ethyl oleate and triolein were prepared by esterification of oleic acid that had been carefully purified through its urea adduct.

For most of the hydrogenations and dehydrogenations a W-6 Raney nickel catalyst [18] was used. In cases where washing with water had to be interrupted, the catalyst could not later be washed free from alkali in the continuous apparatus without too much loss, and a discontinuous process was used. In one particular case several days were needed, and this was the one catalyst that proved to be especially efficient for dehydrogenation.

Hydrogenation experiments. These were usually performed with about 2.5 litres of purified squalene and 50 g Raney nickel in an autoclave fitted with stirrer and cooling coil. With a hydrogen pressure of 90 atm and initial temperature of 155° C, complete saturation was obtained within 3 minutes, whereby the temperature rose to 210° even with full cooling. At 10 atm and 170° C, saturation was obtained in about 3 hours.

Sometimes the hydrogen uptake ceased before complete saturation. This we believe is a poisoning effect due to CO, and can be avoided by repeatedly expelling the gas with fresh hydrogen. When working at atmospheric pressure by bubbling hydrogen through the oil-catalyst mixture, the hydrogenation was always complete.

Dehydrogenation experiments. These were performed on 100 g squalene and 20 g Raney nickel under a vacuum of 1 mm Hg and with vigorous shaking. The temperature was gradually increased to keep the gas evolution constant, and stayed at 140—150° C most of the time. After 160 hours there was little further change in the infrared spectrum (Fig. 3), and the oil was chromatographed from petrol ether on zinc carbonate. Most of the oil passed through the column; it showed a strong U. V. maximum at 238 mμ (diene). The lower part of the column contained a broad colourless, blue-fluorescent zone with U. V. maxima at 334, *317*, and 302 mμ (tetraene). Above this was a narrow yellow, blue-fluorescent zone with U. V. maxima at 397, *379*, and 352 mμ (hexaene), and on the top were several coloured zones without distinct spectral maxima. The eluted polyene fractions were very easily autoxidized.

Ultraviolet spectra were measured in hexane with a Beckman spectrophotometer, Model DU. Infrared spectra were recorded in a Perkin-Elmer instrument, Model 21.

REFERENCES

1. Dale, J. *Tidsskr. Kjemi, Bergvesen Met.* **15** (1955) 162.
2. Sheppard, N. and Simpson, D. M. *Quart. Revs.* **6** (1952) 1.
3. McMurry, H. L. and Thornton, V. *Anal. Chem.* **24** (1952) 318.
4. Heilbron, I. M., Hilditch, T. P. and Kamm, E. D. *J. Chem. Soc.* **1926** 3131.
5. Heilbron, I. M. and Thompson, A. *J. Chem. Soc.* **1929** 883.
6. Heilbron, I. M., Owens, W. M. and Simpson, I. A. *J. Chem. Soc.* **1929** 873.
7. Jenkins, G. I. and Rideal, E. *J. Chem. Soc.* **1955** 2490.
8. Kuhn, R. and Möller, E. F. *Angew. Chem.* **47** (1934) 145.
9. Jackson, J. E., Paschke, R. F., Tolberg, W., Boyd, H. M. and Wheeler, D. H. *J. Am. Oil Chemists' Soc.* **29** (1952) 229.

10. Farrar, K. R., Hamlet, J. C., Henbest, H. B. and Jones, E. R. H. *J. Chem. Soc.* **1952** 2567.
11. Oroshnik, W. and Mebane, A. D. *J. Am. Chem. Soc.* **76** (1954) 5719.
12. Lunde, K. and Zechmeister, L. *J. Am. Chem. Soc.* **77** (1955) 1647.
13. Boelhouwer, C., Gerckens, J., Lie, O. T. and Waterman, H. I. *J. Am. Oil Chemists' Soc.* **30** (1953) 59.
14. Forbes, W. C. and Neville, H. A. *Ind. Eng. Chem.* **32** (1940) 555.
15. Farmer, E. H. *Trans. Faraday Soc.* **38** (1942) 356.
16. Lie, J. and Spillum, E. *J. Am. Oil Chemists' Soc.* **29** (1952) 601.
17. Braude, E. A., Linstead, R. P. and Mitchell, P. W. D. *J. Chem. Soc.* **1954** 3578.
18. Adkins, H. and Billica, H. R. *J. Am. Chem. Soc.* **70** (1948) 695.

Received December 9, 1955.

ACTA CHEMICA SCANDINAVICA 10 (1956) 445—446

Pinoresinol and its Dimethyl Ether from *Araucaria angustifolia* *

ELISABETH DRYSELIUS and BENGT LINDBERG

Träkemiska avdelningen, Svenska Träforskningsinstitutet and Institutionen för Träkemi, Kungl. Tekniska Högskolan, Stockholm, Sweden

Pinoresinol and its dimethyl ether have been isolated from the coniferous wood *Araucaria angustifolia*, order *Araucariales*.

The resin obtained by ethanol extraction of "ligno-tubers" (outgrowths from the roots, the sap wood of which had decayed) from *Araucaria angustifolia*, was investigated some years ago at this Institute. In connection with this work a colourless, crystalline substance, m. p. 106—107°, was isolated by chromatography on aluminium oxide but was not further investigated.

We have now reinvestigated the extract and found that the same substance is easily obtained from the neutral fraction. It melted at 107—109° and had a specific rotation of +65° in chloroform. These values agree with those of the lignan derivative pinoresinol dimethylether [1], m. p. 107—108°, $[\alpha]_D$ +65°, and the melting point was undepressed on admixture with that substance. From the phenolic fraction pinoresinol was isolated in a low yield and characterised as its diacetate. Pinoresinol dimethylether has not been found in Nature before but its optical antipode, eudesmine, has been isolated from several *Eucalyptus* species [2]. The phenol, pinoresinol, has been isolated from several pine and spruce species (*Pinus* and *Picea*, order *Pinales*) and the pinoresinol type of lignans is widespread in Nature. (*Cf.* Ref.[3]). It is of interest that these lignans have now been found in another order of *Coniferae*, *Araucariales*.

EXPERIMENTAL

The resin (55 g) was triturated with ether (3 × 100 ml). The ether was distilled off, the residue (9.2 g) dissolved in ethanol (15 ml) and a solution of potassium hydroxide (10 g) in water (4 ml) was added. Yellow crystals slowly deposited and after 24 hours the salt (0.7 g) was collected and recrystallised from ethanol. The potassium salt was acetylated by heating with acetic anhydride (5 ml) for 2 hours on the steam bath, the solution

* Also XXI. contribution on the Constitution of resin phenols and their biogenetic relations. Part XX, this journal 10 (1956) 134.

was poured into ice water and the precipitate collected and crystallised twice from ethanol. Yield, 80 mg. M. p. 162—163°, undepressed on admixture with authentic pinoresinol diacetate.

The alkaline mother liquors were concentrated under reduced pressure, water was added and the solution extracted with ether. The ether solution was washed with water, dried over anhydrous sodium sulphate and concentrated. The residue (0.8 g) partly crystallised on standing and was purified by crystallisations from methanol. Yield, 240 mg. M. p. 107—109° (corr.). $[\alpha]_D^{20}$ + 65° (*c* 2.0 in chloroform). A mixture of the substance and authentic pinoresinol dimethyl ether showed no depression of m. p.

We are indebted to Professor T. Streyffert, Stockholm, for the identification of the wood sample.

REFERENCES

1. Erdtman, H. *Ann.* **516** (1935) 162.
2. Robinson, R. and Smith, G. *Proc. Roy. Soc. N. S. Wales* **48** (1915) 449.
3. Erdtman, H. *Lignans*, in Paech, K. and Tracy, M. W. *Modern Methods of Plant Analysis*, Vol. III, p. 441, Berlin 1955.

Received December 23, 1955.

ACTA CHEMICA SCANDINAVICA 10 (1956) 447—450

The Change in Reduced Diphosphopyridine Nucleotide (DPNH) Fluorescence upon Combination with Liver Alcohol Dehydrogenase (ADH)

P. D. BOYER and HUGO THEORELL

Medicinska Nobelinstitutet, Biokemiska avdelningen, Stockholm, Sweden

Measurement of the intensity of fluorescence at different wave lengths has shown that the fluorescence of DPNH is shifted from a maximum at about 450 millimicrons to about 415 millimicrons and increased in intensity upon combination of the DPNH with liver alcohol dehydrogenase.

Previous communications from this laboratory have described a fluorescence recorder and its application to the study of the combination of riboflavin phosphate with the old yellow enzyme and the velocity of the formation or disappearance of DPNH [1-3]. The measurements had shown that DPNH gave the same intense fluorescence whether it was free in solution or combined with liver alcohol dehydrogenase (ADH). In view of the shift in absorption spectra shown by DPNH when it is bound to ADH [4] together with the known spectral shifts of many dyes upon binding to proteins, it seemed possible that DPNH might show some change in the intensity of fluorescent light emitted at different wavelengths upon binding to ADH. Simple modifications of the apparatus previously used allowed test of this possibility. The results obtained are given in this paper. They show that the binding of DPNH by ADH results in a definite lowering of the wavelength for the fluorescence maximum and an increase in the intensity of the fluorescence.

EXPERIMENTAL

The apparatus previously described [1] was modified by removing the exit filter and placing before the phototube a suitable, covered compartment for insertion of various interference filters in the exit beam.

The ADH was prepared essentially as described by Bonnichsen [5], with final crystallization from dilute phosphate buffer at pH 7. The colorless preparation used was recrystallized twice, and was approximately 70 % pure based on activity tests assuming that

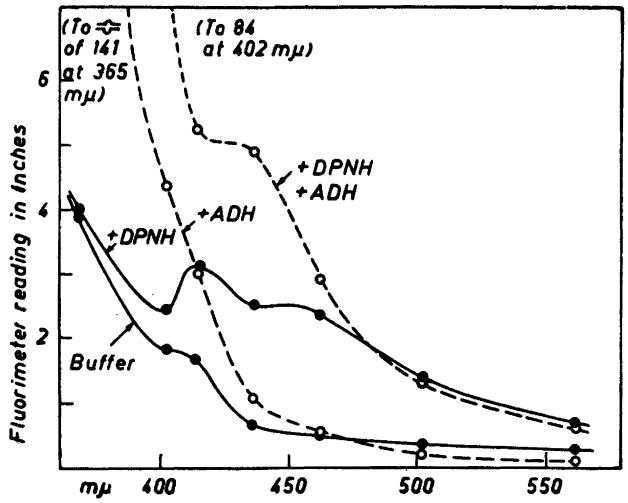


Fig. 1. Observed fluorimeter readings at different wavelengths. [DPNH] at 4 × 10⁻⁶ M [ADH] at approximately 4 × 10⁻⁶ M, in 0.09 M phosphate buffer, pH 7.0, 0.01 M semicarbazide and 0.03 M ethanol. Inlet slit at 7 mm, exist slit at 6 mm, and potentiometer sensitivity at 0.1 volt per 10 inches. (Expt. F-13).

all the material absorbing at 280 mμ was ADH [4]. The DPNH was a preparation of Sigma Chemical Company with a ratio of absorption at 260 mμ to that at 340 mμ of 2.59. It was over 98 % reduced as measured by treatment with ADH and ethanol in the presence of semicarbazide, and the absorption at 340 mμ was nearly completely abolished by treatment with ADH and acetaldehyde.

In the experiments reported herein the DPNH was dissolved in 2.65 ml of 0.1 M phosphate buffer, pH 7.0, 0.3 ml of 0.1 M semicarbazide pH 8, and 0.05 ml of 1:10 ethanol. A small catalytic amount of ADH was added and the solutions allowed to stand for one hour to reduce the final traces of DPN. This insured that any observed shifts in fluorescence in later experiments were not the result of reduction of DPN.

Comparisons of fluorescence were made with the same buffer mixture as that used for dissolving the DPNH, with addition of appropriate small volumes of ADH crystal suspension or solution in approximately 0.01 M phosphate buffer, pH 7.0.

RESULTS AND DISCUSSION

In Fig. 1 are shown the observed fluorimeter readings at different wavelengths for the buffer mixture, buffer + DPNH, and buffer + ADH, and buffer + DPNH and ADH. The amount of ADH was in excess of that of the DPNH as ADH contains two active combining sites per mole [4].

In Fig. 2 are shown the fluorescence increments for free and ADH-bound DPNH.

The data show clearly that the combination of the DPNH with ADH results in a rather pronounced increase in fluorescence intensity together with a decrease in the wave-length for the maximum observed fluorescence. This shift in observed fluorescence likely results from changes in the properties of the

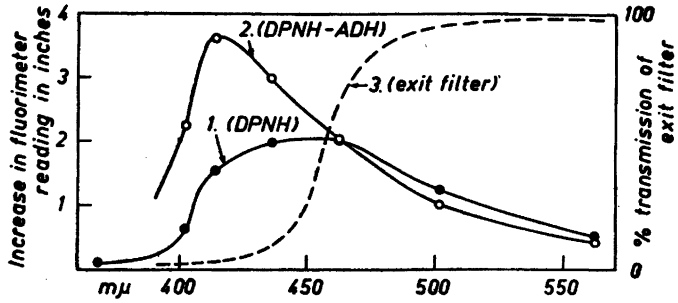


Fig. 2. Increase in fluorimeter reading at different wavelengths for DPNH (1) and DPNH—ADH (2), corrected for the fluorescence of ADH. The points represent the averages of these experimental series under conditions as for Fig. 1. Also shown is the per cent transmission of the exit filter used in the apparatus as previously described (3).

DPNH molecule upon binding, but the possible formation of a new fluorescent grouping by the combination of DPNH with ADH also merits consideration.

Previously it was reported that combination of ADH with DPNH did not result in any change in the measured fluorescence [6]. This observation was entirely valid under the experimental conditions used in those experiments. The exit filter of the original apparatus was chosen primarily for measurement of flavin fluorescence. As noted in Fig. 2, the light transmission by this exit filter was fortuitously of such characteristics as to completely mask the change in the DPNH fluorescence.

The observed fluorescence increase as given in Fig. 1 may be corrected for the known sensitivity of the photomultiplier tube used (RCA IP21) to give a closer approximation of the actual relative intensity of the emitted fluorescence. Such corrections only increased the observed maximum of the DPNH fluorescence by about 5 mμ and did not change that of the ADH-bound DPNH.

Titrations of the approximate combining capacity of ADH for DPNH based on the fluorimetric shift gave values in the range expected from the activity and the absorption at 280 mμ of the ADH. However, further instrumental modifications are necessary for accurate measurement of combining proportions based on fluorescence changes.

Possible instrumental modifications which would facilitate more accurate measurements of the fluorescence shift and use of the shift for stoichiometric and kinetic measurements should be mentioned. A particularly troublesome difficulty was the high fluorescence given by ADH in the lower wavelength region (see Fig. 1). In part this difficulty may be decreased by use of exciting light such that none of the light can pass through the exit filter and thus reach the photocell by reflection. The inlet filter of the present instrument allows some light in the 400—430 mμ region to pass and this results in variations in fluorescence due to the presence of dust particles in the solutions used or small amounts of turbidity in the ADH preparations. Also by the judicious selection of filters or use of suitable monochromators it may be possible to

decrease the fluorescence of the ADH by eliminating the lower wavelengths of light which brings about the fluorescence of ADH.

A definite limitation in the use of filters and monochromators is the decreased sensitivity of the measurements. For example, the data reported in Figs. 1 and 2 were obtained employing the maximum sensitivity of the instrument.

The results with the liver alcohol dehydrogenase suggest further experiments, preferably with improved experimental conditions, to find if the combination of DPNH with other dehydrogenases will result in fluorescence shifts or if the shift is limited to liver alcohol dehydrogenase. Also, other fluorescent coenzymes and substrates may show shifts in fluorescence upon combination with their respective apoenzymes. Measurement of such fluorescent shifts may become a valuable experimental tool.

Mr. B. Hellström and Mr. L. Salomonsson gave valuable assistance in modification of the apparatus. One of us (P.D.B.) is indebted to a grant from the *Guggenheim Foundation* which made this work possible.

REFERENCES

1. Theorell, H. and Nygaard, A. P. *Acta Chem. Scand.* **8** (1954) 877.
2. Theorell, H. and Nygaard, A. P. *Acta Chem. Scand.* **8** (1954) 1649.
3. Theorell, H., Nygaard, A. P. and Bonnichsen, R. *Acta Chem. Scand.* **8** (1954) 1490.
4. Theorell, H. and Bonnichsen, R. *Acta Chem. Scand.* **5** (1951) 1105.
5. Bonnichsen, R. *Acta Chem. Scand.* **4** (1950) 715.
6. Theorell, H., Nygaard, A. P. and Bonnichsen, R. *Acta Chem. Scand.* **9** (1955) 1148.

Received December 30, 1955.

ACTA CHEMICA SCANDINAVICA 10 (1956) 451—458

Polarographic Investigation of Oximes as an Indication of the Polarographic Behaviour of Hydroxamic Acids

TH. ØSTERUD and MILDA PRYTZ

Universitetets Kjemiske Institutt, Blindern-Oslo, Norway

The polarographic behaviour of several oximes has been investigated.

The oximes were readily reduced at the dropping mercury electrode giving well defined, reproducible waves.

The pH of the buffer used as supporting electrolyte influences the position of the half wave by shifting the half wave potential towards more negative values with increasing pH.

The form of the curves, and studies using the log plot method and the Ilkovic equation for determining the number of electrons consumed by the reaction, show that the reduction waves are irreversible.

The height of the polarographic waves decreases as the pH increases, indicating that neutral and alkaline buffers have insufficient protons for the reduction process.

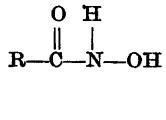
For some oximes double waves have been obtained within certain pH limits. Of the simple aliphatic monoximes only ethanal oxime gave a series of unmistakable double waves but in the case of 2,3-butanedione dioxime a number of polarograms exhibited pronounced double waves.

In the application of the polarographic method to organic problems greater difficulties are encountered than in the inorganic field. Consequently, the practical study of the polarographic reduction of organic compounds is still somewhat incomplete and many problems remain unsolved — among these is the determination of aliphatic esters. Although a direct polarographic reduction of simple saturated aliphatic esters seems out of the question, several attempts have been made. Thus Stackelberg and Stracke [1] investigated different types of organic compounds and found that ethyl acetate caused no rise of the polarographic curve as distinct from ethyl benzoate which gave a reduction wave with the half wave potential $E_{\frac{1}{2}} = -2.14$. Brdicka [2] concluded that ethyl acetoacetate is not reducible at the dropping mercury electrode. The present authors have endeavoured to obtain polarographic reduction with various saturated aliphatic esters by increasing the applied voltage as far as

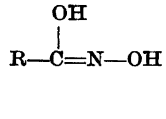
possible, but have concluded that such esters are not reducible within the potential range of the dropping mercury electrode.

Since direct polarographic reduction of the esters was impracticable an attempt was made to find readily prepared derivatives which would give well-defined reduction waves. The polarographic determination of these compounds might then be used to estimate the corresponding esters.

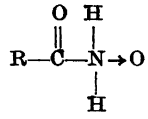
Primarily we were interested in the hydroxamic acids. The colour reaction between hydroxamic acids and ferric chloride was introduced by Feigl [3] as a spot test, but gives equally good results in macro analysis [4,5]. The hydroxamic acids with the molecular formula R—CO—NHOH are generally assumed to be tautomeric substances to which may be assigned the hydroxyamide structure (I) and the hydroxy-oxime structure (II). They may also be interpreted [6,4] as amide oxides (III).



(I)



(II)



(III)

Both the hydroxy-amide group —CO—NHOH and the oxime group >C=N—OH have been chemically reduced by a variety of methods giving the corresponding amide, resp. amine for instance:

$$R-CO-NHOH + 2H \rightarrow R-CO-NH_2 + H_2O$$
$$R-CH=N-OH + 4H \rightarrow R-CH_2-NH_2 + H_2O$$

The hydroxamic acids, containing these groups, may, accordingly, be expected to undergo similar reductions. Moreover, if a simple oxime can be polarographically reduced yielding a distinct reduction wave it is possible that the hydroxamic acids themselves may also be polarographically reduced.

In order to test the above assumptions we first studied the polarographic behaviour of some simple aliphatic oximes, *viz.* ethanal oxime, $CH_3CH=N-OH$, and propanal oxime, $CH_3CH_2CH=N-OH$. The diketone oxime, 2,3-butanedione dioxime, $H_3C-C(=N-OH)-C(=N-OH)-H_3C$, was also tested. All these compounds gave very well defined polarographic waves. As supporting electrolyte McIlvaine buffers were used within the pH limits 2.2 → 6.0. The reduction of two aromatic oximes, *viz.* the salicylaldehyde oxime, $HO-C_6H_4-CH=N-OH$, and the ketoxime benzoin-1-oxime, $C_6H_5-CHOH-C(=N-OH)-C_6H_5$, was also examined, and both of them were shown to give distinct waves.

The above mentioned measurements were carried out with a mercury pool anode, but some polarograms were also recorded using a saturated calomel electrode as external anode. Since the primary interest is in the aliphatic oximes these were re-examined in the case of ethanal oxime and propanal oxime and the investigation was supplemented by a study of 2-methylpropanal oxime.

EXPERIMENTAL PROCEDURE

A recording polarograph (Radiometer, Copenhagen) was used in these experiments and for some of the records use was made of its counter current compensation arrangement. The usual precautions against oxygen interference were taken, the solutions in the electrolysis vessel being kept under an inert gas, the flow of which was stopped during the recording of the polarogram.

The molar concentrations of the oxime solutions were of the order 10^{-3} to 10^{-4}. The McIlvaine buffer solutions were prepared in the usual way and the oximes were not added until a polarogram showed that the buffer solution was oxygen-free — a suitable amount of the oxime solution in 50 % ethanol was then transferred to the polarographic cell. The pH of the solution was always determined at the start and controlled at the completion of the experiment.

EXPERIMENTAL RESULTS

The records made applying counter current compensation gave very distinct polarographic waves. The aliphatic monoximes, however, showed a tendency towards the formation of maxima at pH values lower than 3; but when the pH values approached 4 the curves became completely regular. Conversely, the formation of maxima in solutions of aromatic oximes only appears at values of pH where the solutions can no longer be characterized as acid.

In addition to the chief wave some of the oximes show a small second wave with $E_{\frac{1}{2}}$ at more negative voltages. This was the case for ethanal oxime within the pH limits 5.4 → 6 but for propanal oxime, and for the two aromatic oximes, salicylaldehyde oxime and benzoin-1-oxime, only one wave was obtained. On the other hand 2,3-butanedione dioxime gives well pronounced second waves within the pH limits 3.7 → 5.4. Polarographic records of these experiments are given in Figs. 1—4.

The polarographic records for which the counter current compensation was omitted did not give such pronounced reduction waves as those already tabulated but they nevertheless confirmed the previous results. Since a saturated calomel electrode was used as external reference anode the half-wave

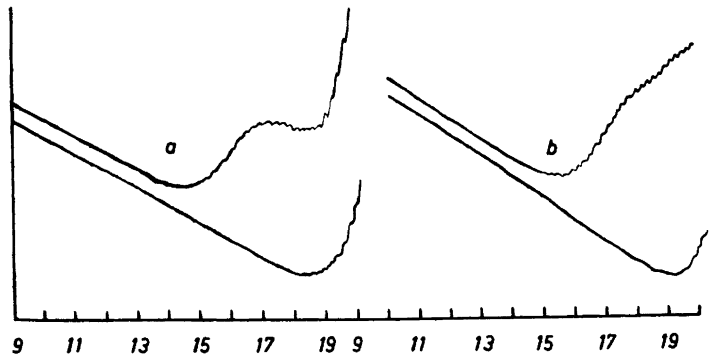


Fig. 1. Electro-reduction of ethanal oxime at pH = 4 and pH = 5.6, c = 6.5 × 10⁻³, v_{appl} = 2 V. Mercury pool anode, counter current. Only two of the polarograms are reproduced but data from the whole series are given in Table 1.

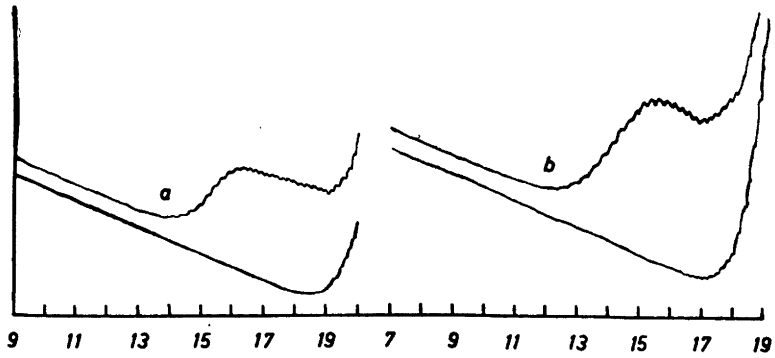


Fig. 2. Electro-reduction of propanal oxime at pH = 4 and pH = 5.6, c = 6.3 × 10⁻³, $v_{appl.}$ = 2 V. Mercury pool anode, counter current. Complete data are given in Table 2.

Table 1. Half-wave potential and height of wave at different pHs for ethanal oxime, c = 6.5 × 10⁻³. McIlvaine buffer. 1/sens = 300.

pH	$E^1_{1/2}$	$E^2_{1/2}$	h_1	h_2
2.2	1.54		41	
3.0	1.54		44	
3.6	1.58		48	
4.0	1.58		37	
5.0	1.68		33	
5.4	1.69	1.92	20	2.7
5.6	1.68	1.90	15	1.7
6.0	1.63	1.84	7	1.2

Table 2. Half wave potential and height of wave at different pHs for propanal oxime, c = 6.3 × 10⁻³. McIlvaine buffer. 1/sens = 300.

pH	$E_{1/2}$	h
2.2	1.50	38
3.0	1.50	30
4.0	1.52	27
5.0		18.7
5.4		11.3
5.6		10.5
6.0		5.3

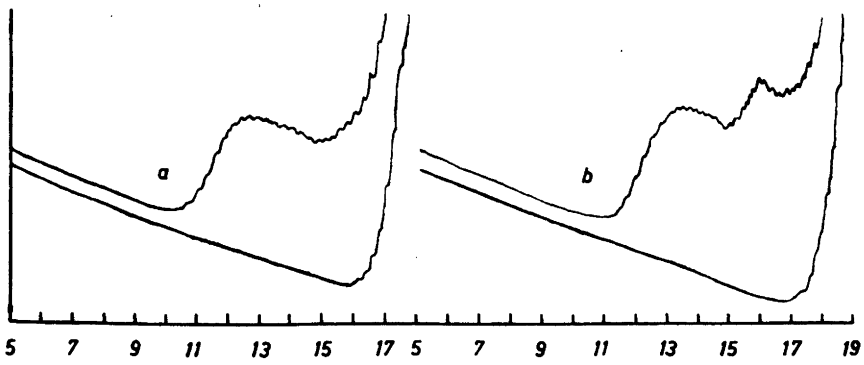


Fig. 3. Electro-reduction of 2,3-butanedione dioxime at pH = 3 and pH = 4, c = 2 × 10⁻⁴, v_{appl} = 2 V. Mercury pool anode, counter current. Complete data are given in Table 3.

Table 3. Half wave potential and height of wave at different pHs for 2,3-butanedione dioxime, c = 2 × 10⁻⁴. Measured at 1/sens = 15.

pH	$E^1_{1/2}$	$E^2_{1/2}$	h_1	h_2
2.2	1.08		65	
3.0	1.15		43	
3.6	1.22		46	
3.7	1.22	1.57	42	8
3.8	1.22	1.57	39	10
3.9	1.22	1.57	43	11.5
4.0	1.22	1.55	48	18
5.0	1.30	1.53	26	6
5.4	1.32	1.52	19	2
5.6	1.36		24	
6.0	1.38		21	

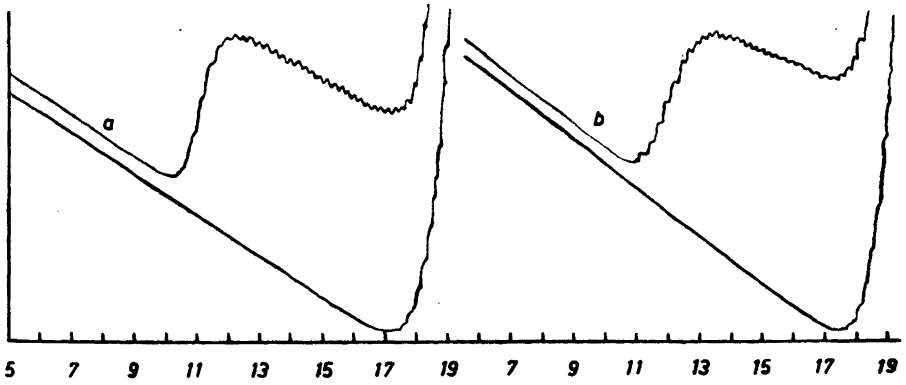


Fig. 4. Electro-reduction of salicylaldehyde oxime and of benzoin-1-oxime at pH = 4, $c_a = 10^{-3}$, $c_b = 2 \times 10^{-4}$. 1/sens for a = 30, for b = 5.

Table 4. Half wave potential and height of wave at different pHs for salicylaldehyde oxime, c = 1 × 10⁻³. Measured at 1/sens = 30.

pH	$E_{1/2}$	h
2.2	1.17	50
4.0	1.12	62
5.4	1.14	28
6.0	1.15	19

Table 5. Half wave potential and height of wave at different pHs for benzoin-1-oxime, calculated for c = 2 × 10⁻⁴ and 1/sens = 5.

pH	$E_{1/2}$	h
2.2	1.07	62
3.0	1.05	53
4.0	1.17	62
5.0	1.17	64
6.0	1.22	38

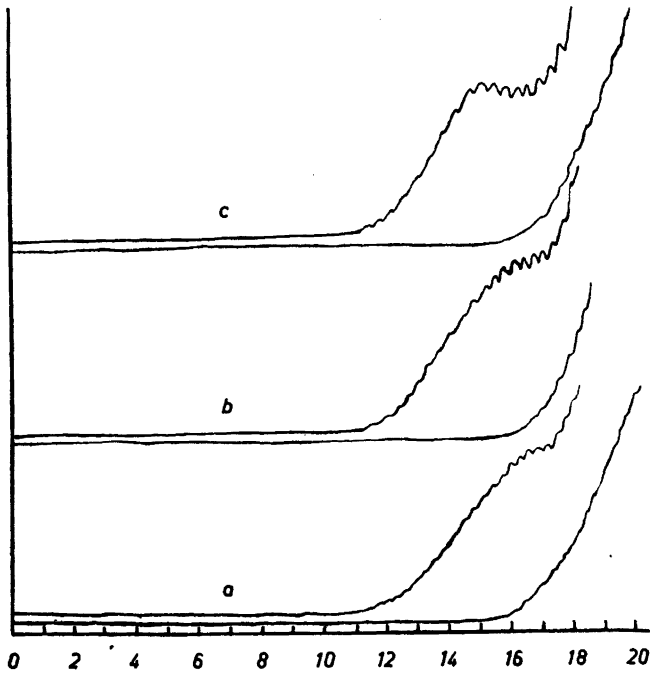


Fig. 5. Electro-reduction of ethanal oxime, propanal oxime and 2-methylpropanal oxime at pH = 5. $c_a = 6.4 \times 10^{-3}$, $c_b = 5.7 \times 10^{-3}$, $c_c = 6.2 \times 10^{-3}$. *S.C.E. as reference electrode.*

potentials were less negative in these latter curves than in the earlier ones and the tendency to form maxima was present at higher values of pH. The aliphatic oximes, ethanal oxime, propanal oxime and 2-methyl-propanal oxime, were examined in this way. A curve is given for each of these oximes (Fig. 5).

DISCUSSION

The polarographic records show that the electrolytic reduction of both aliphatic and aromatic oximes readily takes place in buffered solutions using the customary applied e.m.f. s and that very well defined waves are produced. Carruthers [7] obtained the same result when using salicylaldehyde oxime for the indirect determination of Cu, and good oxime curves were obtained by Kolthoff and Langers [8] during amperometric titrations of Ni^{++} with dimethylglyoxime (2,3-butanedione dioxime) and by Langers [9], in the amperometric titration of copper with α-benzoin oxime.

With increasing values of pH our half wave potentials showed a slight but regular shift towards more negative values indicating that the ease of reduction decreases slightly as the supporting electrolyte becomes less acid. Some of the oximes give a second wave as the acidity of the medium grows less.

Thus, as might be expected, the diketone dioxime shows double waves within certain pH limits. At pH = 3.7 the half wave potential values (against mercury anode) are —1.22 V. and —1.57 V. respectively, while at pH = 5.4 the heights of both waves have decreased, the second wave being hardly discernible and disappearing entirely at still higher pH values.

Double waves in connection with the polarographic reduction of organic substances occur frequently, and these are sometimes attributed to tautomerism or isomerism. Since oximes can show tautomerism as well as *cis-trans* isomerism these properties may be instrumental in producing anomalous waves. However, of the simple aliphatic aldehyde oximes, only ethanal oxime gave pronounced double waves and these did not appear until a pH of at least 5.4 was reached. Propanal oxime gave a very indistinct second wave at pH = 5.6.

It is a well known fact that both the buffer system and the pH of the buffer influence the ease of reduction of organic substances. Thus many organic compounds which are weak bases may add protons from acid buffers and give more easily reducible compounds; this seems to be the case for the oximes inasmuch as the half wave potentials increase with increasing pH. It is to be expected that the ease of reduction of the oximes, which have both weakly acid and weakly basic properties, may depend on the pH of the solution, and it is possible that the substituted hydroxylamines exhibit auto-ionization corresponding to the well known autoionization of hydroxylamine itself:

$$NH_2OH + NH_2OH \rightleftharpoons NH_3OH^+ + NHOH^-$$

In acid solution the hydroxylammonium form will predominate and it is not inconceivable that this form is the one most easily reduced since the wave height decreases with increasing pH of the supporting electrolyte, *i. e.* with a decreasing concentration of the hydroxylammonium form.

The fact that protons are used in the reduction of organic compounds also contributes to a more facile reduction in solutions of high hydrogen ion concentration.

For the reduction of organic substances one may write the general equation:

$$R + n\ H^+ + n\ e^- \rightleftharpoons RH_n$$

There are several methods for the determination of n. When the electrode reaction is reversible the log plot method has proved suitable. In our case, however, the form of the curves indicated that the electrolytic reduction of the oximes was an irreversible electrode reaction; calculations of $\frac{V}{\log [i/(i_d - i)]}$ gave exceptionally high values while the slope of the log plot was much greater than that calculated for any probable value of n. Similarly, attempts to estimate n from the Ilkovic equation did not give reliable values with this method although Hartnell and Bricker [10] appear to have been successful in their calculations for methyl-4,5-diketo-2-pentenoate-5-oxime.

The authors are indebted to Bjørn Hansen and K. Maartmann-Moe for the recording of the polarograms.

REFERENCES

1. Stackelberg, M. V. and Stracke, W. Z. *Z. Elektrochem.* **53** (1949) 118.
2. Brdicka, R. *Chem. Listy* **39** (1945) 35.
3. Feigl, F. *Tüpfelreaktionen, Leipzig* (1938), p. 402.
4. Davidson, D. *J. Chem. Educ.* **17** (1940) 81.
5. Buckles, R. and Thelen, Ch. *Anal. Chem.* **22** (1950) 676.
6. Yale, H. L. *Chem. Revs.* **33** (1943) 207.
7. Carruthers, Ch. *Ind. Eng. Chem. Anal. Ed.* **17** (1945) 398.
8. Kolthoff, I. M. and Langer, A. J. *J. Am. Chem. Soc.* **62** (1942) 283.
9. Langer, A. J. *Ind. Eng. Chem. Anal. Ed.* **14** (1942) 283.
10. Hartnell, E. D. and Bricker, C. E. *J. Am. Chem. Soc.* **70** (1948) 3385.

Received November 21, 1955.

ACTA CHEMICA SCANDINAVICA 10 (1956) 459—465

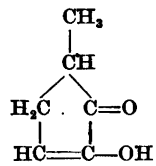
Über isomere Dithiosemicarbazone von Methyl*cyclo*pentenolonen

G. R. GUMMERUS und TERJE ENKVIST

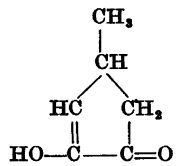
Chemisches Institut der Universität Helsinki, Helsinki, Finland

Es wurden je zwei isomere Dithiosemicarbazone der beiden Methyl*cyclo*pentenolone I bzw. II dargestellt. Die Art der Isomerie dieser Dithiosemicarbazone sowie ein Fall der Überführung einer Form in eine andere über die Bleiverbindung (Fig. 2) werden diskutiert. Eines der Isomeren hat starke tuberkulostatische Wirkung, ist aber nicht weniger toxisch als das Conteben.

Die vorliegende Arbeit bezieht sich auf die Darstellung isomerer Thiosemicarbazone von zwei strukturisomeren Methyl*cyclo*pentenolonen, nämlich 1-Methyl-*cyclo*penten-(3)-ol-(3)-on-(2) (Formel I)[1-3] und 1-Methyl-*cyclo*penten-(2)-ol-(3)-on-(4) (Formel II), sowie die Prüfung der tuberkulostatischen Eigenschaften dieser Thiosemicarbazone.



I

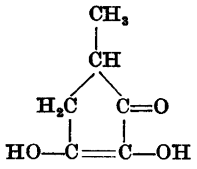


II

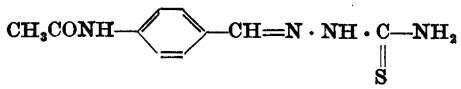
Die genannten Methyl*cyclo*pentenolone reduzieren wie Aldehyde ammoniakalische Silberlösung und bilden mit Carbonylreagenzien wie Hydroxylamin, Semicarbazid und 2,4-Dinitrophenylhydrazin keine Monoderivate, sondern ausschliesslich Derivate der entsprechenden Diketone. Die Verbindungen I und II sind also in gewisser Hinsicht eigenartige Ketone, die in ihrer Struktur sogar Ähnlichkeit mit solchen physiologisch stark wirksamen Verbindungen wie die Methylreduktinsäure (III) aufweisen, die ein Hauptbestandteil des nordafrikanischen Pfeilgiftes ist[4].

Es wurden die Thiosemicarbazone der Methylcyclopentenolone I und II dargestellt, zunächst in der Hoffnung, hierdurch vielleicht zu tuberkulosta-

tisch wirkenden Verbindungen zu kommen, die weniger toxisch wären als das bekannte Conteben (IV).



III



IV

Diese Hoffnung wurde nicht erfüllt. Die erhaltenen Thiosemicarbazone, die in der Arzneifabrik Medica in Helsinki untersucht wurden, hatten zwar tuberkulostatische Wirkung, und der Effekt eines von ihnen gegen einige Stämme von *Mycobacterium tuberculosis* war sogar etwa ebenso stark wie der des Contebens oder des Isoniazids (Tab. 3), seine Toxizität war jedoch nicht geringer als die des Contebens *. Die Verbindungen erbieten ein stereochemisch interessantes Problem, da sie in mehreren isomeren Formen auftreten. Bisher sind von den Thiosemicarbazonen der Methyl*cyclo*pentenolone I und II je zwei isomere Formen isoliert worden, die sich von einander in Bezug auf Schmelzpunkt, Lage des Absorptionsmaximums in ultraviolettem Licht und vor allem in der Löslichkeit unterscheiden, wie Tabelle 1 näher zeigt.

Tabelle 1.

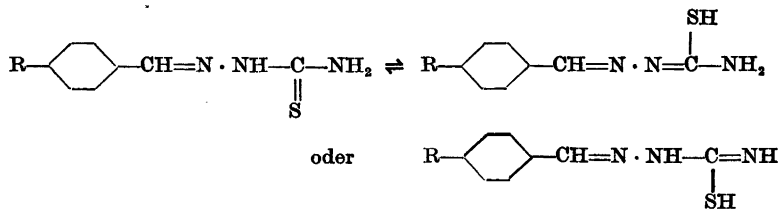
	I a	I b	II a	II b	
Schmelzpunkt	225–227°	242–244°	222–223°	231–232°	(Zers.)
U. V. Absorpt. max. mμ	340	355	354	349	
Löslichkeit					
Wasser	–	+	–	+	
Äthylalkohol	–	+	+	+	
Chloroform	–	–	+	+	
Dioxan	+	+	+	+	

Ia und Ib: Die Thiosemicarbazone der Verbindung I.
IIa und IIb: Die Thiosemicarbazone der Verbindung II.

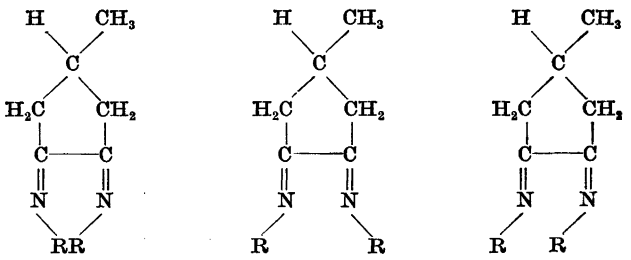
Die Verhältnisse sind sowohl experimentell als auch theoretisch recht kompliziert und die Untersuchung ist noch nicht abgeschlossen. Der im Folgenden gemachte Versuch, den verschiedenen Isomeren eine gewisse Konfiguration zuzuerteilen ist daher teilweise noch als Arbeitshypothese zu betrachten.

Nach Spinks [6] bilden einige Thiosemicarbazone von substituierten Benzaldehyden in Lösungen Strukturisomere, wenn die Lösungen mit ultraviolettem Licht bestrahlt werden:

* Toxizitätsbestimmungen von Dr. G. Östling.



Die von uns hergestellten Isomeren konnten durch Bestrahlung mit ultraviolettem Licht nicht ineinander übergeführt werden (Fig. 3). Man hat darum an andere Arten der Isomerie zu denken. Die vorliegenden Dithiosemicarbazone sind Derivate von Diketonen und daher besteht hier Analogie mit den Verhältnissen bei den bekannten geometrischen Isomeren des Benzildioxims. Danach wären z. B. von der Verbindung II die folgenden Isomeren in Betracht zu ziehen: eine Synform (V), eine Antiform (VI) und eine Amphiform (VII).



V VI VII

Ein Studium an Stuartschen Molekülmodellen (Fig. 1) zeigt jedoch, dass die Synform hier nicht möglich ist, weil die Atome in einer solchen Form nicht Raum genug finden. Es sind nur die Anti- und die Amphiform denkbar.

Bei Zusatz einer methylalkoholischen Bleiacetat-Lösung zu Lösungen der isomeren Dithiosemicarbazone des Methyl*cyclo*pentenolons II in organischen Lösungsmitteln wird eine rote, kristallinische Bleiverbindung gefällt, die unter Zersetzung bei 245—246° schmilzt. Sie ist in Wasser löslich und zeigt im Ultraviolett ein Absorptionsmaximum bei denselben Wellenlängen (340 mμ) wie die höherschmelzende Form des Dithiosemicarbazons. Beide isomere Formen scheinen dieselbe Bleiverbindung zu liefern und zwar so, dass die höherschmelzende Form momentan die Bleiverbindung bildet, während die niedrigschmelzende Form erst nach einiger Zeit ausfällt. Bei der Zersetzung des Bleiniederschlags mit Schwefelwasserstoff wird die höherschmelzende Form erhalten. Dieses Verhalten könnte vorläufig mit folgendem Schema erklärt werden (Fig. 2):

Die Bleiverbindung wäre also ein Komplexsalz der Antiform, und die Amphiform liesse sich über dieses in die Antiform umlagern.

Von dem Thiosemicarbazon des Methyl*cyclo*pentenolons I sollten zwei Amphiformen möglich sein (VIII und IX). Sie sind noch nicht isoliert worden,

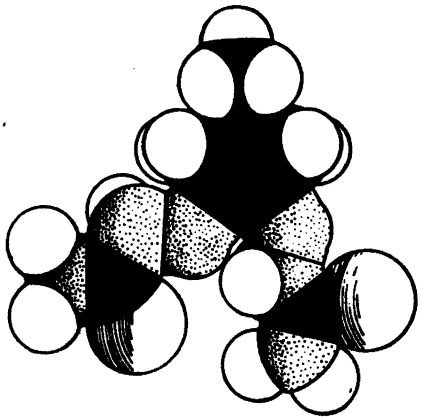
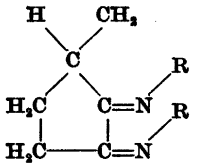
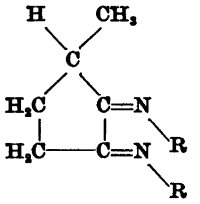


Fig. 1. Modell der Amphiform VII.

aber das Verhalten der bei der Reaktion entstehenden, niedrig schmelzenden Substanz deutet die Möglichkeit an, dass diese noch in zwei Formen aufgespaltet werden könnte.



VIII



IX

Es ist vielleicht von gewissem, allgemeinem Interesse, dass die Isomerenpräparate der Thiosemicarbazone Unterschiede in der tuberkulostatischen Wirkung zu haben scheinen (Tabelle 3). Ein physiologischer Unterschied geometrisch isomerer Formen von Thiosemicarbazonen ist unseren Wissens bisher noch nicht bekannt, gibt aber Anlass zu fortgesetzten Studien.

VERSUCHSTEIL

Thiosemicarbazone der Verbindung I

0,448 g 1-Methyl-*cyclo*penten-(3)-ol-(3)-on-(2) (aus Blasenteer nach Hellström isoliert [5]) wurden in 20 ml 50 %igem Äthylalkohol gelöst und mit einer Lösung von 0,730 g Thiosemicarbazid in 40 ml Wasser versetzt. Nach einstündigem Sieden auf dem Wasserbad war die anfangs farblose Lösung schwach gelblich und nach 7 Stunden stark gelb. Es wurde in allem 20 Stunden lang erhitzt. Nach Abkühlen der Lösung wurden die gebildeten, gelben Kristalle abfiltriert. Schmp. ca. 220° (Zers). Die Kristalle lösten sich in Dioxan und Eisessig völlig, in heissem Wasser und Alkohol teilweise, waren aber unlöslich in Benzol, Aceton und Chloroform. Beim Behandeln der Kristalle mit viel kochendem Wasser löste sich ein Teil. Die ungelöst verbliebenen, gelben Kristalle wurden sogleich aus der Lösung abfiltriert und mit viel heissem Wasser gewaschen. Schmp. 225—

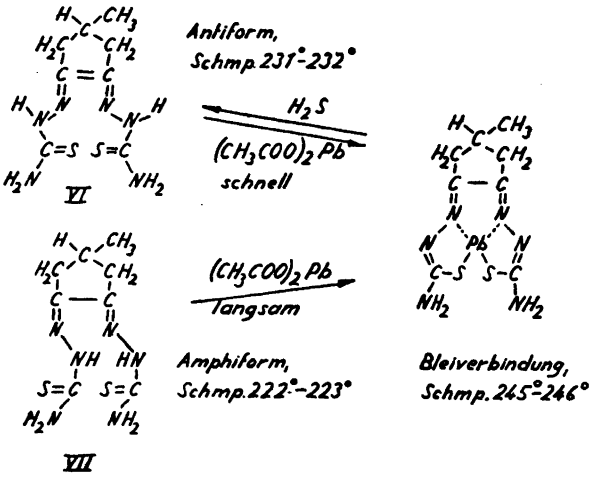


Fig. 2.

227° (Zers.) (Substanz Ia). Versuche, die Substanz umzukristallisieren, waren vergeblich. Über Löslichkeit siehe Tab. 1. — Aus dem warmen Filtrat begannen bald bräunliche Kristalle auszufallen (Substanz Ib), die abfiltriert wurden. Das Filtrat war jetzt farblos. Schmp. 237—238° (Zers.), nach Umkristallisation aus Äthylalkohol 242—244° (Zers.). Über Löslichkeit siehe Tab. 1. — Der Mischschmelzpunkt der Substanzen Ia und Ib betrug ca. 220° (Zers.), zeigte also Depression. Analysen, siehe Tab. 2.

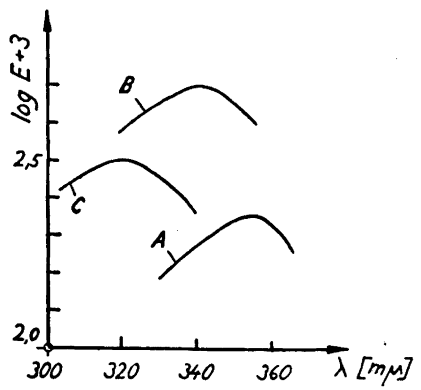


Fig. 3. Einige U.V.-Absorptionsspektren.

A: Verbindung IIa 10 mg/l in Dioxan, Absorpt. Max. bei $\lambda = 340$ mμ
B: Verbindung IIb 10 » » » » » » $\lambda = 354$ mμ
C: Verbindung IIa wurde in Chloroform gelöst 15 Stunden mit U.V.-Licht bestrahlt. Es wurde eine Substanz erhalten, die jetzt wasserlöslich war. C stellt das Absorpt. spektrum dieser neuen Substanz in Dioxan dar. Absorpt. Max. bei $\lambda = 320$ mμ. Als Verbindung IIb auf dieselben Weise belichtet wurde, wurde ihr Spektrum nicht verändert.

Tabelle 2. Analysen.

Substanz	C %	H %	N %	S %
$C_8H_4N_6S_2$, ber.	37,18	5,46	32,53	24,84
Substanz Ia, gef.	37,62	5,32	32,60	25,42
» Ib, »	37,68	5,22	32,95	24,48
» IIa, »	37,33	5,16	32,30	25,31
» IIb, »	37,18	5,01	32,10	24,61

Thiosemicarbazone der Verbindung II

0,700 g 1-Methyl-*cyclo*penten-(2)-ol-(3)-on-(4) (durch Verseifung von 1-Methyl-*cyclo*pentandion-3,4-dicarbonsäure-2,5-diäthylester bereitet) wurden in 40 ml 50 %igem Äthylalkohol mit einer Lösung von 1,140 g Thiosemicarbazid in 50 ml Wasser versetzt und auf dem Wasserbad erwärmt. Die Farbe der Lösung schlug bald nach gelb um und gelbe Kristalle begannen sich abzuscheiden. Nach einstündigem Sieden wurden die hellgelben Kristalle abfiltriert. Schmp. ca. 215° (Zers.) Löslichkeit siehe Tab. 1. — Beim Behandeln der Kristalle mit viel siedendem Wasser löste sich nur ein kleiner Teil. Die heiss abfiltrierten Kristalle wurden mit viel heissem Wasser gewaschen. Schmp. 220—222° (Zers.), nach Umkristallisation aus Methylalkohol 222—223° (Substanz IIa). Löslichkeit, siehe Tab. 1. — Das gelbbräunliche Filtrat wurde konzentriert. Aus der erkalteten Lösung kristallisierten hellbräunliche Kristalle, die bei 231—232° unter Zersetzung schmolzen (Substanz IIb). Das Filtrat war noch deutlich gelblich. Eine Umkristallisation wurde nicht unternommen, da die Ausbeute so gering war. Der Mischschmelzpunkt der Substanzen IIa und IIb betrug 212—215° (Zers.), zeigte also Depression. Analysen, siehe Tab. 2.

Tabelle 3. Tuberkulostatische Wirkung der Thiosemicarbazone Ia, Ib, IIa und IIb. *

+++ Schneller, ++ guter, + schwacher, — kein Zuwachs.

Konzentration, µg/ml	0	0,05	0,5	5	50	500
Bakterienkultur		*Mycobact.*	*tuberculosis*	*106*		
Substanz Ia	+++	+++	+++	++	—	—
Substanz Ib	+++	+++	++	++	—	—
Substanz IIa	+++	+++	++	+	—	—
Substanz IIb	+++	++	+	—	—	—
Bakterienkultur		*Mycobact.*	*tuberculosis*	*Parv.*		
Substanz Ia	+++	+++	++	+	—	—
Substanz Ib	+++	+++	+++	+++	—	—
Substanz IIa	+++	+++	+++	++	—	—
Substanz IIb	+++	++	—	—	—	—

Bleiverbindungen

0,8 g der Verbindung IIa wurden in 100 ml Methylalkohol und 50 ml Dioxan gelöst. Zu dieser Lösung wurde eine Lösung von 1,1 g Bleiacetat in 50 ml Methylalkohol hinzugefügt. Nach einiger Zeit fiel ein roter, kristallinischer Niederschlag aus, der abfiltriert und bei 70° getrocknet wurde. Schmp. 245—246° (Zers.). Die Substanz war löslich in Wasser und Methylalkohol, spärlich löslich in Chloroform, praktisch unlöslich in Benzol.

* Versuche von Dr. N. Oker-Blom mit aus Patienten des Sanatoriums Nummela isolierten Stämmen.

Analyse: Aus 72,4 mg Substanz wurde das Blei als Chromat gefällt und jodometrisch titriert. 46 ml 0,100 N Natriumthiosulfat wurden verbraucht. 1 ml 0,100 N Natriumthiosulfat entspricht 0,6907 mg Pb. Gefunden 31,8 mg Pb oder 43,9 %. Ber. für $C_8H_{12}N_6S_2Pb$ 44,7 % Pb.

Aus der Verbindung IIb (Schmp. 231—232°) wurde mit Bleiacetat in derselben Weise wie oben sofort ein bei 245—246° (Zers.) schmelzender Niederschlag erhalten, der in Bezug auf Farbe, Aussehen und Löslichkeit in Wasser, Methylalkohol, Chloroform und Benzol der oben analysierten Bleiverbindung (aus Verbindung IIa erhalten) völlig ähnlich war.

LITERATUR

1. Meyerfeld, J. *Chem. Ztg.* **36** (1912) 549.
2. Rojahn, C. A. und Rühl, F. *Arch. Pharm.* **264** (1926) 211.
3. Enkvist, T. *Acta Chem. Scand.* **8** (1954) 51.
4. Hesse, G. und Böckmann, K. *Ann.* **563** (1949) 53.
5. Hellström, N. *Kgl. Tek. Högskol. Handl.* **1947** No. 4.
6. Spinks, A. *Brit. J. Pharmacol.* **6** (1951) 35.

Eingegangen am 14. Dezember, 1955.

ACTA CHEMICA SCANDINAVICA 10 (1956) 466—494

Short Communications

Note on the Preparation of Phenyl Thiohydantoins from Glutamine, S-Carboxymethyl Cysteine and Cysteic Acid

PEHR EDMAN and KONRAD LAUBER

Department of Physiological Chemistry, University of Lund, Lund, Sweden

In an earlier paper [1] the preparation of the phenyl thiohydantoins (PTH) from most of the natural amino acids has been described. Some of these amino acids did not yield the expected thiohydantoins owing to decomposition during the preparation, which involved prolonged refluxing of the phenyl thiocarbamyl (PTC) amino acids in N hydrochloric acid. Under these conditions PTC-cystine and PTC-cysteine gave off hydrogen sulfide and formed undefined products. The PTC derivatives of the β-hydroxyamino acid lost water and became α-β-unsaturated which at least for serine led to polymerization. However, since then Ingram [2] has described a satisfactory synthesis of PTH-serine and PTH-threonine using milder conditions for the cyclization. It has now been found that two derivatives of cysteine, cysteic acid and S-carboxymethyl cysteine, form normal thiohydantoins of sufficient stability for identification purposes in the amino acid sequence determination [3]. By appropriate treatment of the peptide under investigation it should be possible to form these derivatives [4,5]. The preparation of PTH-glutamine is also described *.

To avoid side reactions ring closure of the PTC-amino acids was brought about under mildest possible conditions in respect to concentration of acid and temperature. It was then helpful to follow the ring closure by measuring the ultraviolet absorption (in ethanol) of a sample, since the PTC-amino acids have two maxima at approx. 248 mμ and 268 mμ whereas the PTH-amino acids show only one maximum at approx. 268 mμ. At pH 1—2 and room temperature the ring closure was generally completed in less than 48 hours.

Experimental. Elementary analyses except micro-Kjeldahl were made at the Analytical Laboratory, Department of Chemistry, University of Lund and at the Chemical Laboratory, University of Copenhagen.

Melting points were determined on a heating block (Fisher-John) and are uncorrected.

Paper chromatography was carried out as described by Sjöquist [6]. All R_F-values are referred to PTH-glycine, R_F for PTH-X / R_F for PTH-glycine = q.

3-Phenyl-2-thio-5-hydantoinpropionamide. A suspension of L-glutamine (1.46 g) in pyridine-water (3:2, 30 ml) was brought to pH 8.6 by the addition of N sodium hydroxide. Under stirring phenyl *iso*thiocyanate (5 ml) was added and pH was kept at 8.6 by the continuous addition of N sodium hydroxide. After two hours the reaction mixture was extracted three times with 1 vol. of benzene, which was then discarded. The aqueous solution was brought to pH 1 by the addition of 4 N hydrochloric acid and left overnight at room temperature. The crystals (1.9 g) were filtered off and crystallized and recrystallized from boiling glacial acetic acid. M. p. 201—211° (decomp.).

Paper chromatography: Solvent A, q=0.23; solvent B, q = 0.08; solvent C, q = 0.82.

Analyses. N (Kjeldahl) 15.87; S (Zimmermann [7]) 12.2. $C_{12}H_{13}O_2N_3S$ requires: N 15.95; S 12.2.

5-(Carboxymethylmercaptomethyl)-3-phenyl-2-thiohydantoin. L-β-(Carboxymethylmercapto)-alanine (S-carboxymethyl cysteine) was prepared essentially as described by Dickens [5]. This preparation (1.79 g) was dissolved in

* Recently Ramachandran *et al.*[9] have reported the preparation of this compound.

pyridine-water (3:2, 30 ml) and pH was adjusted to 8.4 by the addition of N sodium hydroxide. Phenyl *iso*thiocyanate (4 ml) was added with stirring and pH was kept at 8.4 by the addition of N sodium hydroxide. After seven hours the reaction mixture was extracted three times with equal volumes of benzene, which were then discarded. The aqueous phase was brought to pH 2.7 and exhaustively extracted with ethyl acetate (90 ml). The extracts were combined and the ethyl acetate was evaporated *in vacuo* (temperature not above 30° C). To the oily residue water (20 ml) was added and pH was adjusted to 8 by the addition of N sodium hydroxide. A small precipitate was removed and the filtrate then extracted with ethyl acetate (30 ml), which was discarded. The solution was acidified to pH 2 by the addition of 4 N hydrochloric acid which resulted in an oily precipitate. After 24 hours the oil had crystallized (1.8 g). Recrystallization twice from ethanol-petroleum ether. M. p. 164°.

Paper chromatography: Solvent A, decomposition with the appearance of several spots; solvent B, $q = 0.23$; solvent C, $q = 0.98$.

Analyses. N (Dumas) 9.30; S (Cuck and Grim [8]) 21.3. $C_{12}H_{12}O_3N_2S_2$ requires: N 9.45; S 21.6.

5 - (Potassiummethylsulfonate) - 3 - phenyl - 2-thiohydantoin. A solution of L-cysteic acid (1.7 g) in pyridine-water (3:2, 30 ml) was brought to pH 8.6 by the addition of N potassium hydroxide. Under stirring phenyl *iso*thiocyanate (4 ml) was added and pH was then kept at 8.6 by the continuous addition of N potassium hydroxide. After three hours the reaction mixture was extracted three times with equal volumes of benzene, which were then discarded. The aqueous phase was brought to pH 1 by the addition of 4 N hydrochloric acid and the solution was left overnight at room temperature. The solution was then brought to pH 4.2 with N potassium hydroxide and concentrated *in vacuo* to dryness. The residue was dried in a desiccator over phosphorus pentoxide and the dry product extracted with aqueous acetone which left the potassium chloride undissolved. The acetone solution was concentrated *in vacuo* to a viscous solution. On addition of acetone crystallization set in and was completed in the ice box (2.2 g). The product was taken up in a small volume of water and pH adjusted to 5 with potassium hydroxide. On the addition of abs. ethanol the preparation crystallized in fine needles. Recrystallization twice from water-ethanol. The product was highly hygroscopic and was dried *in vacuo* over phosphorus pentoxide at 110°. M. p. 193—7° (decomp.).

Paper chromatography: Solvent A, $q = 0$; solvent B, $q = 0$; solvent C, $q = 0.11$.

Analyses: N (Dumas) 8.62; S (Cuck and Grim [8]) 19.4. $C_{10}H_9O_4N_2S_2K$ requires: N 8.64; S 19.8.

This investigation has been supported by grants to one of us (P.E.) from Eli Lilly and Company and from *Statens medicinska forskningsråd*, which is gratefully acknowledged.

1. Edman, P. *Acta Chem. Scand.* **4** (1950) 277.
2. Ingram, V. M. *J. Chem. Soc.* **1953** 3717.
3. Edman, P. *Acta Chem. Scand.* **4** (1950) 283.
4. Sanger, F. *Nature* **160** (1947) 295.
5. Dickens, F. *Biochem. J. London* **27** (1933) 1141.
6. Sjöquist, J. *Acta Chem. Scand.* **7** (1953) 447.
7. Zimmermann, W. *Mikrochemie* **31** (1943) 15.
8. Cuck, J. A. and Grim, E. *Mikrochemie ver. Microchim. Acta* **1954** 201.
9. Ramachandran, L. K., Epp, A. and McConnell, W. B. *Anal. Chem.* **27** (1955) 1734.

Received February 25, 1956.

Note on the Reaction between Linear Polyamides and Ethylene Carbonate

SVEN SÖNNERSKOG

A-B Svenskt Konstsilke, Borås, Sweden

In connection with an investigation on the interaction between polyamides and cyclic esters the observation was made, contrary to earlier statements elsewhere [1] that ethylene carbonate may act, under particular conditions, as a hydroxyethylating agent upon homopolymers of ε-aminocaproic acid or hexamethylenediammonium adipate. The reaction is observable just in the temperature range, where the polymers are dissolved by the cyclic ester (approximately 180—185° C). At still higher temperatures (200—220° C) *water soluble* derivatives are obtained by heating the polymer in a tenfold excess of ethylene carbonate for 4 hours. An inert gas, such as dry carbon dioxide, should be present to prevent side reactions (oxidation, depolymerization).

In a system, containing an unstabilized polymer, no simple kinetic scheme can be

pyridine-water (3:2, 30 ml) and pH was adjusted to 8.4 by the addition of N sodium hydroxide. Phenyl *iso*thiocyanate (4 ml) was added with stirring and pH was kept at 8.4 by the addition of N sodium hydroxide. After seven hours the reaction mixture was extracted three times with equal volumes of benzene, which were then discarded. The aqueous phase was brought to pH 2.7 and exhaustively extracted with ethyl acetate (90 ml). The extracts were combined and the ethyl acetate was evaporated *in vacuo* (temperature not above 30° C). To the oily residue water (20 ml) was added and pH was adjusted to 8 by the addition of N sodium hydroxide. A small precipitate was removed and the filtrate then extracted with ethyl acetate (30 ml), which was discarded. The solution was acidified to pH 2 by the addition of 4 N hydrochloric acid which resulted in an oily precipitate. After 24 hours the oil had crystallized (1.8 g). Recrystallization twice from ethanol-petroleum ether. M. p. 164°.

Paper chromatography: Solvent A, decomposition with the appearance of several spots; solvent B, $q = 0.23$; solvent C, $q = 0.98$.

Analyses. N (Dumas) 9.30; S (Cuck and Grim [8]) 21.3. $C_{12}H_{12}O_3N_2S_2$ requires: N 9.45; S 21.6.

5 - (Potassiummethylsulfonate) - 3 - phenyl - 2-thiohydantoin. A solution of L-cysteic acid (1.7 g) in pyridine-water (3:2, 30 ml) was brought to pH 8.6 by the addition of N potassium hydroxide. Under stirring phenyl *iso*thiocyanate (4 ml) was added and pH was then kept at 8.6 by the continuous addition of N potassium hydroxide. After three hours the reaction mixture was extracted three times with equal volumes of benzene, which were then discarded. The aqueous phase was brought to pH 1 by the addition of 4 N hydrochloric acid and the solution was left overnight at room temperature. The solution was then brought to pH 4.2 with N potassium hydroxide and concentrated *in vacuo* to dryness. The residue was dried in a desiccator over phosphorus pentoxide and the dry product extracted with aqueous acetone which left the potassium chloride undissolved. The acetone solution was concentrated *in vacuo* to a viscous solution. On addition of acetone crystallization set in and was completed in the ice box (2.2 g). The product was taken up in a small volume of water and pH adjusted to 5 with potassium hydroxide. On the addition of abs. ethanol the preparation crystallized in fine needles. Recrystallization twice from water-ethanol. The product was highly hygroscopic and was dried *in vacuo* over phosphorus pentoxide at 110°. M. p. 193—7° (decomp.).

Paper chromatography: Solvent A, $q = 0$; solvent B, $q = 0$; solvent C, $q = 0.11$.

Analyses: N (Dumas) 8.62; S (Cuck and Grim [8]) 19.4. $C_{10}H_9O_4N_2S_2K$ requires: N 8.64; S 19.8.

This investigation has been supported by grants to one of us (P.E.) from Eli Lilly and Company and from *Statens medicinska forskningsråd*, which is gratefully acknowledged.

1. Edman, P. *Acta Chem. Scand.* **4** (1950) 277.
2. Ingram, V. M. *J. Chem. Soc.* **1953** 3717.
3. Edman, P. *Acta Chem. Scand.* **4** (1950) 283.
4. Sanger, F. *Nature* **160** (1947) 295.
5. Dickens, F. *Biochem. J. London* **27** (1933) 1141.
6. Sjöquist, J. *Acta Chem. Scand.* **7** (1953) 447.
7. Zimmermann, W. *Mikrochemie* **31** (1943) 15.
8. Cuck, J. A. and Grim, E. *Mikrochemie ver. Microchim. Acta* **1954** 201.
9. Ramachandran, L. K., Epp, A. and McConnell, W. B. *Anal. Chem.* **27** (1955) 1734.

Received February 25, 1956.

Note on the Reaction between Linear Polyamides and Ethylene Carbonate

SVEN SÖNNERSKOG

A-B Svenskt Konstsilke, Borås, Sweden

In connection with an investigation on the interaction between polyamides and cyclic esters the observation was made, contrary to earlier statements elsewhere [1] that ethylene carbonate may act, under particular conditions, as a hydroxyethylating agent upon homopolymers of ε-aminocaproic acid or hexamethylenediammonium adipate. The reaction is observable just in the temperature range, where the polymers are dissolved by the cyclic ester (approximately 180—185° C). At still higher temperatures (200—220° C) *water soluble* derivatives are obtained by heating the polymer in a tenfold excess of ethylene carbonate for 4 hours. An inert gas, such as dry carbon dioxide, should be present to prevent side reactions (oxidation, depolymerization).

In a system, containing an unstabilized polymer, no simple kinetic scheme can be

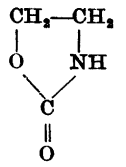
suggested *a priori*. At least the following five steps must be considered:

1. Decomposition of ethylene carbonate into ethylene oxide and carbon dioxide.
2. Etherification of the polyamide at unstabilized end groups.
3. Formation of graft polymers by etherification at the amide links.
4. Ester interchange between polymer and solvent. (The incorporation of small amounts of carbonate ester unit is already reported from an analysis of infrared spectra [1]).
5. The formation of pure polyethylene oxide (linear polyether) by thermal or ionic polymerization in the anhydrous system.

Preliminary studies have been carried out on the water soluble compounds obtained from nylon 6 and nylon 66 polymer. Solubility is not limited to pure water, in fact it seems clear that when once water solubility is reached, a similar solubility in organic solvents such as methanol, acetone, and several aliphatic esters is also obtained, which is in contrast to the insolubility of the parent polymers. Fractional precipitation with a nonsolvent has thus not been feasible up to now. The only successful method for the separation of polymer has been the addition of strong sodium hydroxide solution until the polymer appears as a *coacervate*, which can be collected as an upper layer. Since homopolymers of ethylene oxide of the moderate molecular weight possible in a synthesis carried out at the actual high temperature do not show this behaviour, it is believed that the coacervate (in the most complex case) represents a mixture of graft polymer and block copolymer (steps 2 and 3 in the scheme above). The remaining part of the sodium hydroxide is easily removed from the polymer phase by separating the two layers in a small funnel, adding water and deionising with a hydrogen saturated ion exchanger.

Water soluble ethylene oxide "adducts" from fatty alcohols, fatty amines and alkyl phenols are known to give well defined precipitates with ferrocyanic acid [2]. The actual derivatives from nylon 6 and nylon 66 show the same behaviour. If the purified aqueous solution of the coacervate, mentioned above, is acidified with hydrochloric acid, a slight yellow precipitate is immediately obtained on adding potassium ferrocyanide. Nylons of low molecular weight give a highly dispersed precipitate, passing most filter papers. At higher molecular weight (*e. g.* plastic grades of polymer) the precipitate gradually coalesces to a yellow mass of pronounced rubbery character. A modified Zeisel analysis (according to Morgan [3]) indicates large, but varying amounts of accessible hydroxyethyl groups in the polymers, and it remains to be seen if a more detailed picture of the distribution of the etherifying agent can be obtained.

In this connection it should be mentioned that oxazolidone (I) dissolves polyamides above 80° C. On heating to 170° C it slowly decomposes into carbon dioxide and ethylene imine [4], thus representing a potential source for the analogous grafting of the polyamide with ethylene imine monomer. In this case, however, solubility in water is never reached, but water soluble polyethylene imine can be isolated by condensing the escaping gases on a "cold finger". The carbon dioxide apparently serves as a gaseous phase activator, similar to its action in aqueous systems [5].



I

1. Haas, H. C., Cohen, S. G., Oglesby, A. C. and Karlin, E. R. *J. Polymer Sci.* **15** (1955) 427.
2. Schönfeldt, N. *J. Am. Oil Chemists Soc.* **32** (1955) 77.
3. Morgan, P. W. *Ind. Eng. Chem., Anal. Ed.* **18** (1946) 500.
4. Swed. Pat. 148559.
5. Jones, G. D., Langsjoen, A., Neuman, M. M. C. and Zomlefer, J. *J. Org. Chem.* **9** (1944) 125.

Received February 28, 1956.

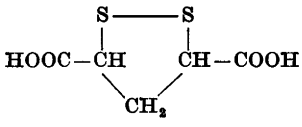
Polarographic Studies on Cyclic Disulphides

BENGT NYGÅRD and
LENNART SCHOTTE

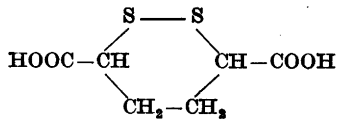
Chemical Institute, University of Uppsala
Uppsala, Sweden

In the course of recent work by one of the authors (L.S.) on cyclic disulphides related mainly to glutaric [1,2] and pimelic [3,4] acid it seemed to be of interest to examine the polarographic behaviour of analogous compounds, especially as very little attention has hitherto been devoted to this subject in polarography. It has recently been shown that the disulphide linkage in 6,8-thioctic acid (α-lipoic acid) is reducible at the dropping mercury electrode [5]. However, no conclusions were drawn about the ring system.

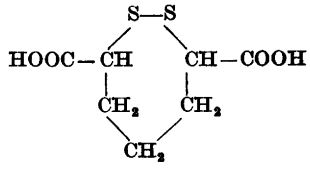
The α,α′-disubstituted dicarboxylic acids, *racem*-1,2-dithiolane-3,5-dicarboxylic acid (I), 1,2-dithiane-3,6-dicarboxylic acid (II) and 1,2-dithiepane-3,7-dicarboxylic acid (III) have been investigated together with the related dimercaptans. For (II) and (III) both the diastereomers were examined. The substances have all been studied in standard buffer solutions and at a concentration of 1.00×10^{-3} M.



(I)



(II)



(III)

Racem-(I) gives in acid solution a very good wave, reversible in character, with a half-wave potential of −0.330 V *vs.* the sat. calomel electrode (S.C.E.) at pH = 2.2. In neutral medium, on the other hand, the wave is quite deformed and at higher pH no waves are found.

Racem- and *meso*-(II) give polarographic waves only in acid solution. The waves are rather drawn out indicating irreversible electroreduction. The half-wave potential value is −0.75 V.

Analogous behaviour, as compared with (II) exists for *racem*- and *meso*-(III). The corresponding value for the half-wave potentials is −0.92 V.

The wave height and the relation log $[i/(i_d - i)]$ *vs.* the applied potential E for *racem*-(I) suggest a two electron reduction. Analogous to the polarographic behaviour of a number of aliphatic disulphides (cystine, glutathione) the wave obtained seems to be due to the reduction of Hg-complexes, which are formed on the drop at the rupture of the S−S linkage. The pronounced irreversible appearance of (II) and (III) in acid solution indicates that the primary reaction — the cleavage of the S−S group — in these cases does not proceed so readily as with *racem*-(I). A greater ring stability for the six- and seven-membered cyclic disulphides as compared with the 1,2-dithiolane derivative is apparent. This is in agreement with data from spectrochemical studies [6-8] and from the characteristics of the unsubstituted heterocycles [9].

An interesting analogy supporting our interpretation can be found *i. a.* in the behaviour of dithio- and diseleno-diglycolic acid. Leussing and Kolthoff [10] have shown that dithio-diglycolic acid gives only irreversible polarographic waves. On the other hand, one of us (B.N.) [11] has found that the corresponding diselenide is characterized by reversible effects over the whole pH range. Thus the radical cleavage necessary for the formation of electroreducible Hg-complexes on the mercury drop is more easily realized for the selenium compound. Fredga [12] has already established a striking difference between the aliphatic S−S and Se−Se groups in reactivity against Hg.

The α,α′-dimercapto dicarboxylic acids related to (I), (II) and (III) have been found to give polarographic effects, the qualitative nature of which resemble each other. Thus a double wave is obtained in acid and neutral media; the smaller one remains in basic solution. Its half-wave potentials vary with pH.

It is obvious from the foregoing that the polarographic effects of the 1,2-dithiolane derivatives may be of special interest. For a closer investigation of this disulphide system a number of 4-substituted com-

pounds [7] (originally prepared by Backer and co-workers) were also examined. They all gave good polarographic waves over the whole pH range indicating a two electron reduction. Especially in acid solution the agreement between their half-wave potentials and that of *racem*-(I) is excellent. — In this connection the polarographic method has been used to further emphasize the improbability of coordinated sulphur-sulphur bonds [8].

This general polarographic character of the five-membered cyclic disulphide has also been found to include that of 6,8-thioctic acid.

Experimental. The investigation was performed at 25° C with a Leybold Polarograph model 54. In order to minimize the influence of the cathodic mercury on the solution a special type of polarographic cell according to Schwabe and Berg was used.

In connection with a current polarographic investigation of a number of aliphatic diseleno dicarboxylic acids a closer examination of the above subject will be undertaken.

The authors are indebted to Professor Mark von Stackelberg for valuable discussions and for making it possible for one of us (B.N.) to carry out this preliminary study at the Institute of Physical Chemistry, University of Bonn, Germany. — Thanks are also due to Professor Arne Fredga for kind interest in our work and for placing certain materials at our disposal. The sample of 6,8-thioctic acid was kindly supplied by Docent Stig Sunner.

Grants from the *Swedish Natural Science Research Council* are gratefully acknowledged.

1. Schotte, L. *Acta Chem. Scand.* **8** (1954) 130.
2. Schotte, L. *Arkiv Kemi* **9** (1956) No. 36.
3. Schotte, L. *Acta Chem. Scand.* **8** (1954) 131.
4. Schotte, L. *Arkiv Kemi* **9** (1956) No. 34.
5. Reed, L. J., Gunsalus, I. C., Schnakenberg, G. H. F., Soper, Q. F., Boaz, H. E., Kern, S. F. and Parke, T. V. *J. Am. Chem. Soc.* **75** (1953) 1267.
6. Schotte, L. *Arkiv Kemi* **8** (1955) No. 56.
7. Schotte, L. *Arkiv Kemi* **9** (1956) No. 24.
8. Schotte, L. *Arkiv Kemi* **9** (1956) No. 29.
9. Affleck, J. G. and Dougherty, G. *J. Org. Chem.* **15** (1950) 865.
10. Leussing, D. L. and Kolthoff, I. M. *J. Electrochem. Soc.* **100** (1953) 334.
11. Nygård, B. *To be published.*
12. Fredga, A. *Arkiv Kemi, Mineral. Geol.* **11 B** (1934) No. 44.

Received February 28, 1956.

Carotene Isomers in some Red Algae

BJØRN LARSEN and ARNE HAUG

Norwegian Institute of Seaweed Research, Trondheim, Norway

According to previous investigations, β-carotene is the only carotene isomer present in most red algae (Table 1). An investigation of the unsaponifiable matter of *Rhodymenia palmata*, carried out at the Institute of Organic Chemistry at the Norwegian Technical University in Trondheim, seemed to indicate the presence of both α- and β-carotene in this alga. As this was contrary to previous observations of Heilbron *et al.* [1] (Table 1), it was decided to carry out a further investigation of the carotene isomers in red algae.

Samples of the more common red algae were collected in the Trondheimsfjord during the months of May to August 1955. The samples were blanched with steam at 100° C as soon as possible after harvesting and dried at approximately 35° C overnight. This proved to be the best procedure, since quantitative extraction of the carotene from fresh material was difficult to accomplish and no carotene breakdown was observed during the steam-treatment and drying [2]. After having been ground to pass a 60 mesh sieve, 1 g of the sample was moistened with 5 ml of water, and extracted overnight with 25 ml of acetone. The extraction was repeated until the extract was colourless. The carotene was extracted from the acetone solution, after addition of more water, with light petroleum, and the light petroleum extract concentrated to a small volume on a water bath. The carotenes were separated from chlorophylls and other carotenoids by chromatography on magnesium oxide — Hyflo Super-Cel (1:3). The carotene zones were washed through the column with light petroleum containing 0.5 % acetone, the eluate made up to 50 ml and the carotene concentration determined by reading the optical density at 436 mμ in a Beckman spectrophotometer.

In the case of *Rhodymenia palmata*, two zones were observed on the column, apart from the stationary chlorophyll and carotenoid zones: A fast moving yellow zone, and a slower moving brick-red zone. Complete separation of the two pigments was

pounds [7] (originally prepared by Backer and co-workers) were also examined. They all gave good polarographic waves over the whole pH range indicating a two electron reduction. Especially in acid solution the agreement between their half-wave potentials and that of *racem*-(I) is excellent. — In this connection the polarographic method has been used to further emphasize the improbability of coordinated sulphur-sulphur bonds [8].

This general polarographic character of the five-membered cyclic disulphide has also been found to include that of 6,8-thioctic acid.

Experimental. The investigation was performed at 25° C with a Leybold Polarograph model 54. In order to minimize the influence of the cathodic mercury on the solution a special type of polarographic cell according to Schwabe and Berg was used.

In connection with a current polarographic investigation of a number of aliphatic diseleno dicarboxylic acids a closer examination of the above subject will be undertaken.

The authors are indebted to Professor Mark von Stackelberg for valuable discussions and for making it possible for one of us (B.N.) to carry out this preliminary study at the Institute of Physical Chemistry, University of Bonn, Germany. — Thanks are also due to Professor Arne Fredga for kind interest in our work and for placing certain materials at our disposal. The sample of 6,8-thioctic acid was kindly supplied by Docent Stig Sunner.

Grants from the *Swedish Natural Science Research Council* are gratefully acknowledged.

1. Schotte, L. *Acta Chem. Scand.* **8** (1954) 130.
2. Schotte, L. *Arkiv Kemi* **9** (1956) No. 36.
3. Schotte, L. *Acta Chem. Scand.* **8** (1954) 131.
4. Schotte, L. *Arkiv Kemi* **9** (1956) No. 34.
5. Reed, L. J., Gunsalus, I. C., Schnakenberg, G. H. F., Soper, Q. F., Boaz, H. E., Kern, S. F. and Parke, T. V. *J. Am. Chem. Soc.* **75** (1953) 1267.
6. Schotte, L. *Arkiv Kemi* **8** (1955) No. 56.
7. Schotte, L. *Arkiv Kemi* **9** (1956) No. 24.
8. Schotte, L. *Arkiv Kemi* **9** (1956) No. 29.
9. Affleck, J. G. and Dougherty, G. *J. Org. Chem.* **15** (1950) 865.
10. Leussing, D. L. and Kolthoff, I. M. *J. Electrochem. Soc.* **100** (1953) 334.
11. Nygård, B. *To be published.*
12. Fredga, A. *Arkiv Kemi, Mineral. Geol.* **11 B** (1934) No. 44.

Received February 28, 1956.

Carotene Isomers in some Red Algae

BJØRN LARSEN and ARNE HAUG

Norwegian Institute of Seaweed Research, Trondheim, Norway

According to previous investigations, β-carotene is the only carotene isomer present in most red algae (Table 1). An investigation of the unsaponifiable matter of *Rhodymenia palmata*, carried out at the Institute of Organic Chemistry at the Norwegian Technical University in Trondheim, seemed to indicate the presence of both α- and β-carotene in this alga. As this was contrary to previous observations of Heilbron *et al.* [1] (Table 1), it was decided to carry out a further investigation of the carotene isomers in red algae.

Samples of the more common red algae were collected in the Trondheimsfjord during the months of May to August 1955. The samples were blanched with steam at 100° C as soon as possible after harvesting and dried at approximately 35° C overnight. This proved to be the best procedure, since quantitative extraction of the carotene from fresh material was difficult to accomplish and no carotene breakdown was observed during the steam-treatment and drying [2]. After having been ground to pass a 60 mesh sieve, 1 g of the sample was moistened with 5 ml of water, and extracted overnight with 25 ml of acetone. The extraction was repeated until the extract was colourless. The carotene was extracted from the acetone solution, after addition of more water, with light petroleum, and the light petroleum extract concentrated to a small volume on a water bath. The carotenes were separated from chlorophylls and other carotenoids by chromatography on magnesium oxide — Hyflo Super-Cel (1:3). The carotene zones were washed through the column with light petroleum containing 0.5 % acetone, the eluate made up to 50 ml and the carotene concentration determined by reading the optical density at 436 mμ in a Beckman spectrophotometer.

In the case of *Rhodymenia palmata*, two zones were observed on the column, apart from the stationary chlorophyll and carotenoid zones: A fast moving yellow zone, and a slower moving brick-red zone. Complete separation of the two pigments was

Table 1.

	α-Carotene	β-Carotene	Refs.	Total amount of carotene, p.p.m.
Ahnfeltia plicata (Huds.) Fries	+ (+?)	+ (+)	3	69
Ceramium rubrum (Huds.) Ag.	+ (+)	+ (+)	5, 6, 3	326
Chondrus crispus Stackh.	+ (+?)	+ (+)	3	84
Delesseria sanguinea (L.) Lamour.	+ (—)	+ (+)	4	270
Dumontia incrassata (Müll.) Lamour.	+	+		222
Furcellaria fastigiata (Huds.) Lamour.	+ (—)	+ (+)	4	135
Gigartina stellata (Stackh.) Batt.	+ (+?)	+ (+)	3	86
Membranoptera alata (Huds.) Stackh.	+	+		67
Ptilota plumosa (L.) Ag.	+	+		65
Phycodrys sinuosa (Good. et Woodw.) Kütz.	+	?		
Rhodymenia palmata (L.) Grev.	+ (—)	+ (+)	1	360
Callithamnion arbuscula (Dillw.) Lyngb.	—	+		200
Corallina officinalis L.	— (—)	+ (+)	3, 5	
Polysiphonia fastigiata (Roth.) Grev.	— (—)	+ (+)	3	245
Polysiphonia urceolata (Dillw.) Grev.	—	+		
Porphyra sp.	— (—)	+ (+)	3, 4	85

The signs in brackets refer to earlier investigations.
References are given in the third column.

obtained by chromatography on calcium hydroxide from light petroleum, and developing with the solvent mentioned above. The two zones were cut out of the column and the pigments extracted with acetone. After filtering off the adsorbent, the acetone was removed by evaporation *in vacuo* and the pigments redissolved in carbon disulphide (spectroscopic grade). The absorption spectra were read in a Beckman spectrophotometer. The pigment from the yellow zone showed an absorption pattern in carbon disulphide identical with that of α-carotene, with the peaks at 509 and 477 mμ (Fig. 1). Further identification was carried out by means of carotene isolated from carrots. This well known mixture of α- and β-carotene showed exactly the same picture as that from *Rhodymenia* when chromatographed on the same adsorbent. Both isomers were isolated from carrots and a "misch"-chromatogram with the corresponding zones from *Rhodymenia* was run on calcium hydroxide. Both mixtures behaved as homogeneous substances. In order to rule out the possibility of the first zone being a *cis-trans* isomer of the second, the pigments from the yellow zone of *Rhodymenia* and carrots were isomerised by boiling under reflux in light petroleum. Chromatography of the isomerised pigments showed exactly the same zones in

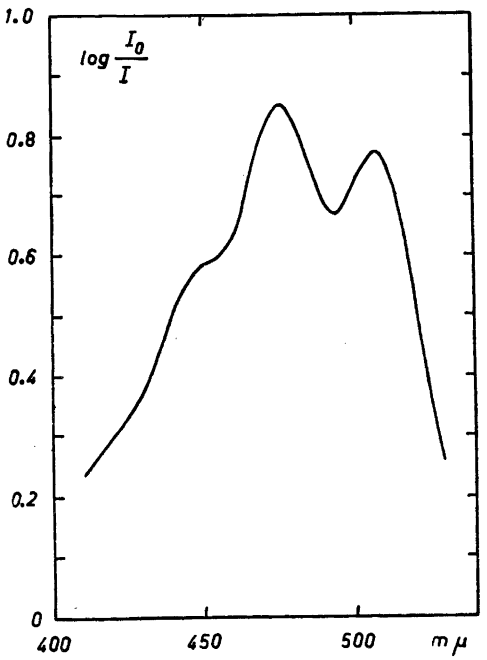


Fig. 1. Absorption spectrum of the pigment from the yellow zone.

both cases, and no brick-red zone could be observed above the yellow one.

Since Carter *et al.*[3] and Kylin [5] state that *Ceramium rubrum* contains both α- and β-carotene, we also carried out a comparison between this alga and *Rhodymenia*. Chromatography of the light petroleum extract on magnesium oxide and calcium hydroxide showed exactly the same picture for both species, and the isolated pigments were indistinguishable with respect to their absorption spectra in carbon disulphide. According to these experiments, therefore, we find it safe to conclude that *Rhodymenia palmata* contains both α- and β-carotene.

Several other species of *Rhodophyceae* were investigated along the same lines. The results are given in Table 1. The results from earlier investigations are shown in the same table. As the table shows, 11 of the 16 investigated species were found to contain α-carotene.

The table also shows the total amounts of carotene (α + β) given as mg per 1 000 g dry matter. The amounts were found to depend strongly on the season and the treatment of the samples. The figures given here should, however, give a fairly correct picture of the variation between the species during the summer months.

The relative amounts of α- and β-carotene were determined in 6 species. The results are given in Table 2 as the amount of α-carotene divided by the amount of β-carotene. The amounts are calculated from the optical densities in carbon disulphide and the molar extinction of α- and β-carotene in the same solvent. As the table shows, the amount of α-carotene in the investigated species was of the same order of magnitude as that of β. *Delesseria sanguinea* was found to be particularly rich in α-carotene. Contrary to the total amounts of carotene, the relative amounts seemed to be approximately constant, independent of the season (samples from the winter months were not investigated) and the treatment of the samples.

Phycodrys sinuosa differed markedly from the other investigated species, as in this alga we were not able to show the presence of β-carotene. Samples from different localities and collected at different seasons gave the same result. We are thus forced to conclude that *Phycodrys sinuosa* either has a specific mechanism for a rapid destruction of β-carotene, or that the amount of β-carotene, if this is present at all, was very small compared with α-carotene. Whatever the explanation may be, this species seems to deserve a further investigation.

Table 2.

	α/β
Delesseria sanguinea	3.1
Rhodymenia palmata	1.4
Furcellaria fastigiata	1.3
Ceramium rubrum	0.5
Gigartina stellata	0.5
Dumontia incrassata	0.4

Acknowledgements. This work forms part of the research program of the *Norwegian Institute of Seaweed Research.* We are indebted to professor N. A. Sørensen for inspiring interest and helpful suggestions, to one of the algologists of the Institute, Dr. E. Baardseth, for collecting and identifying the material, and to Miss S. Svendsen for skilful assistance with the analyses.

1. Heilbron, I. M., Parry, E. G. and Phipers, R. F. *Biochem. J. London* **29** (1935) 1376.
2. Haug, A. and Larsen, B. *Acta Chem. Scand.* **10** (1956) 472.
3. Carter, P. W., Heilbron, I. M. and Lythgoe, B. *Proc. Roy. Soc. London* **128B** (1940) 82.
4. Seybold, A. und Egle, K. *Jahrb. wiss. Botan.* **86** (1938) 50.
5. Kylin, H. *Hoppe-Seyler's Z. physiol. Chem.* **74** (1911) 105.
6. Kylin, H. *Ibid.* **166** (1927) 39.

Received February 24, 1956.

Carotene Breakdown in *Rhodymenia palmata* (L.) Grev.

ARNE HAUG and BJØRN LARSEN

Norwegian Institute of Seaweed Research, Trondheim, Norway

During an investigation of the carotene breakdown in some Norwegian seaweeds and seaweed meals an extraordinary rapid loss of carotene was observed in the red alga *Rhodymenia palmata*. This alga, therefore, seemed to be a convenient object for further studies of the breakdown mechanism. The carotene present in *Rhodymenia palmata* was found to consist of about equal amounts of the α- and β-isomers [1].

both cases, and no brick-red zone could be observed above the yellow one.

Since Carter *et al.*[3] and Kylin [5] state that *Ceramium rubrum* contains both α- and β-carotene, we also carried out a comparison between this alga and *Rhodymenia*. Chromatography of the light petroleum extract on magnesium oxide and calcium hydroxide showed exactly the same picture for both species, and the isolated pigments were indistinguishable with respect to their absorption spectra in carbon disulphide. According to these experiments, therefore, we find it safe to conclude that *Rhodymenia palmata* contains both α- and β-carotene.

Several other species of *Rhodophyceae* were investigated along the same lines. The results are given in Table 1. The results from earlier investigations are shown in the same table. As the table shows, 11 of the 16 investigated species were found to contain α-carotene.

The table also shows the total amounts of carotene (α + β) given as mg per 1 000 g dry matter. The amounts were found to depend strongly on the season and the treatment of the samples. The figures given here should, however, give a fairly correct picture of the variation between the species during the summer months.

The relative amounts of α- and β-carotene were determined in 6 species. The results are given in Table 2 as the amount of α-carotene divided by the amount of β-carotene. The amounts are calculated from the optical densities in carbon disulphide and the molar extinction of α- and β-carotene in the same solvent. As the table shows, the amount of α-carotene in the investigated species was of the same order of magnitude as that of β. *Delesseria sanguinea* was found to be particularly rich in α-carotene. Contrary to the total amounts of carotene, the relative amounts seemed to be approximately constant, independent of the season (samples from the winter months were not investigated) and the treatment of the samples.

Phycodrys sinuosa differed markedly from the other investigated species, as in this alga we were not able to show the presence of β-carotene. Samples from different localities and collected at different seasons gave the same result. We are thus forced to conclude that *Phycodrys sinuosa* either has a specific mechanism for a rapid destruction of β-carotene, or that the amount of β-carotene, if this is present at all, was very small compared with α-carotene. Whatever the explanation may be, this species seems to deserve a further investigation.

Table 2.

	α/β
Delesseria sanguinea	3.1
Rhodymenia palmata	1.4
Furcellaria fastigiata	1.3
Ceramium rubrum	0.5
Gigartina stellata	0.5
Dumontia incrassata	0.4

Acknowledgements. This work forms part of the research program of the *Norwegian Institute of Seaweed Research.* We are indebted to professor N. A. Sørensen for inspiring interest and helpful suggestions, to one of the algologists of the Institute, Dr. E. Baardseth, for collecting and identifying the material, and to Miss S. Svendsen for skilful assistance with the analyses.

1. Heilbron, I. M., Parry, E. G. and Phipers, R. F. *Biochem. J. London* **29** (1935) 1376.
2. Haug, A. and Larsen, B. *Acta Chem. Scand.* **10** (1956) 472.
3. Carter, P. W., Heilbron, I. M. and Lythgoe, B. *Proc. Roy. Soc. London* **128B** (1940) 82.
4. Seybold, A. und Egle, K. *Jahrb. wiss. Botan.* **86** (1938) 50.
5. Kylin, H. *Hoppe-Seyler's Z. physiol. Chem.* **74** (1911) 105.
6. Kylin, H. *Ibid.* **166** (1927) 39.

Received February 24, 1956.

Carotene Breakdown in *Rhodymenia palmata* (L.) Grev.

ARNE HAUG and BJØRN LARSEN

Norwegian Institute of Seaweed Research, Trondheim, Norway

During an investigation of the carotene breakdown in some Norwegian seaweeds and seaweed meals an extraordinary rapid loss of carotene was observed in the red alga *Rhodymenia palmata*. This alga, therefore, seemed to be a convenient object for further studies of the breakdown mechanism. The carotene present in *Rhodymenia palmata* was found to consist of about equal amounts of the α- and β-isomers [1].

Table 1.

Drying conditions		Carotene content as per cent of the content of the fresh samples		
		23/2	23/3	25/4
	Fresh	100(197)	100(217)	100(259)
Indoors	1 week, dark	74		
	2 days, diffuse light		79	
	1 week, » »	65		73
	2 days, u.v.-light		79	
Open air	2 days, protected against rain		64	
	3 » » » »			57
	3 » subjected to rain			15
	1 week, » » »	0		
	2 hours at 80° C			86
	Steam blanched 5 min., dried, milled			109

The analytical procedure used for the quantitative determination of carotene has been described in a previous paper [1]. Estimation of the carotene content in fresh samples needed special attention. The quantitative extraction of carotene from fresh *Rhodymenia palmata* was found to be difficult to accomplish. The highest values for fresh algae were obtained when the material was ground in a mortar with quartz sand and solid carbon dioxide, followed by immediate extraction with acetone. However, as will be shown below, still higher values for the initial carotene content in the samples, and which we think are more reliable, were obtained when the samples were steam blanched and dried overnight.

In order to determine the influence of light, heat and rain on the breakdown rate, three series of simple drying experiments were carried out. The results are shown in Table 1. The figures in brackets refer to the carotene content in fresh samples given as mg carotene per 1 000 g dry matter. The amount of carotene in the samples increased from February to April due to seasonal variation.

It will be seen that the breakdown rate was approximately the same for samples dried in darkness, in diffuse light or in ultraviolet light, while samples dried in open air, subjected to direct sunlight, showed a more rapid breakdown. The results seem to indicate that the reaction is slightly photosensitive, and that the active part of the spectrum is in the visible region. This observation is in good agreement with observations by Griffith and Thompson [2] for the carotene breakdown in alfalfa during drying.

When the samples were dried at 80° C only a slight breakdown was observed, while steam blanching led to no carotene loss. The steam blanched samples could be dried overnight without any breakdown taking place. That the figure for the steam blanched sample is higher than for the fresh material is supposed to be due to incomplete extraction of the latter and to small losses of dry matter during the steam blanching.

The samples dried in open air and subjected to rain during the drying period lost their carotene content very rapidly compared with samples protected against rain.

The results from the drying experiments indicated that the carotene breakdown in *Rhodymenia palmata* might be of enzymatic nature. To further establish this, some experiments with fresh material were carried out.

If the fresh alga was stored before carotene determination a considerable carotene loss was observed. A sample blanched within 1 hour after harvesting was found to contain 280 mg carotene per 1 000 g dry matter. When the sample was stored for 20 hours before blanching only 135 mg per 1 000 g dry matter (48 %) was found.

If the sample was ground as described above, and allowed to thaw before acetone was added, the breakdown was extremely rapid as shown in Table 2. Attempts were made to inhibit this breakdown by means of enzyme inhibitors. The inhibitors were ground together with the samples in the mortar in concentrations of approximately

Table 2.

Treatment		Carotene content as per cent of the content of the fresh samples	
		23/3	25/4
Acetone added immediately		100(217)	100(259)
» »	after 1 hour		63
» »	» 20 hours	0	16
Acetone added after 20 hours	Ground with 0.5 % KCN		78
	» » 0.5 » Na_2S		91
	» » 0.5 » $HgCl_2$		30
	» » 0.5 » NaF		0
	Vacuum desiccator, 20 mm Hg		29

0.5 % and the samples set aside for 20 hours before acetone was added. It will be seen from Table 2 that sodium fluoride had no effect and that mercury chloride was only slightly effective. A slight inhibition was also observed when the sample was stored in a vacuum desiccator at a pressure of approximately 20 mm Hg. On the other hand, both potassium cyanide and sodium sulphide were fairly effective. The inhibition obtained with sodium sulphide may be due to the anaerobic conditions set up by this substance. In the case of potassium cyanide, however, the effect must be due to the inhibition of an enzymatic reaction. It seems, therefore, to be safe to conclude, that an enzymatic reaction must be involved in the carotene breakdown in *Rhodymenia palmata*.

A similar inhibition of the carotene breakdown by means of potassium cyanide was observed in alfalfa by Mitchell and Hauge in 1946 [3]. The enzyme system responsible for the carotene breakdown in alfalfa has later been found to be lipoxidase. The carotene is oxidised by some of the intermediate reaction products formed in the enzymatic oxidation of unsaturated fatty acids. Whether a similar reaction is responsible for the destruction of carotene in *Rhodymenia palmata* has not been established.

Acknowledgements. This work forms part of the research program of the *Norwegian Institute of Seaweed Research*. We are indebted to professor N. A. Sørensen for inspiring interest and helpful suggestions, and to Miss S. Svendsen for skilful assistance with the analyses.

1. Larsen, B. and Haug, A. *Acta Chem. Scand.* **10** (1956) 470.
2. Griffith, R. B. and Thompson, C. R. *Botan. Gaz.* **111** (1950) 165.
3. Mitchell, H. L. and Hauge, S. M. *J. Biol. Chem.* **163** (1946) 7.

Received February 24, 1956.

Demonstration of Reichstein's Substance S in Dog Adrenal Vein Blood by Countercurrent Distribution

HANS CARSTENSEN

Institute of Physiology, University of Upsala, Upsala, Sweden

The two major corticosteroids of dog adrenal vein blood, from a quantitative point of view, are cortisol and corticosterone, as demonstrated by several physical and chemical methods [1-4]. Among other possible components, the presence of minor amounts of Reichstein's substance S (Δ^4-pregnene-17*a*,21-diol-3,20-dione) seems to have considerable interest [5] (*cf.* Eberlein *et al.*[6]).

Further evidence of its occurrence in dog adrenal vein blood is provided here by its demonstration after countercurrent distribution. A sample of 330 ml blood was collected from the left adrenal of a mongrel male dog weighing 18 kg during 60 minutes and extracted with ethyl acetate as previously outlined [4]. The common corticosteroid fraction was recovered from the polar phase after double distribution between *n*-hexane and 50 % ethanol in water and subjected to successive countercurrent distributions (Table 1).

Table 2.

Treatment		Carotene content as per cent of the content of the fresh samples	
		23/3	25/4
Acetone added immediately		100(217)	100(259)
» »	after 1 hour		63
» »	» 20 hours	0	16
Acetone added after 20 hours	Ground with 0.5 % KCN		78
	» » 0.5 » Na_2S		91
	» » 0.5 » $HgCl_2$		30
	» » 0.5 » NaF		0
	Vacuum desiccator, 20 mm Hg		29

0.5 % and the samples set aside for 20 hours before acetone was added. It will be seen from Table 2 that sodium fluoride had no effect and that mercury chloride was only slightly effective. A slight inhibition was also observed when the sample was stored in a vacuum desiccator at a pressure of approximately 20 mm Hg. On the other hand, both potassium cyanide and sodium sulphide were fairly effective. The inhibition obtained with sodium sulphide may be due to the anaerobic conditions set up by this substance. In the case of potassium cyanide, however, the effect must be due to the inhibition of an enzymatic reaction. It seems, therefore, to be safe to conclude, that an enzymatic reaction must be involved in the carotene breakdown in *Rhodymenia palmata*.

A similar inhibition of the carotene breakdown by means of potassium cyanide was observed in alfalfa by Mitchell and Hauge in 1946 [3]. The enzyme system responsible for the carotene breakdown in alfalfa has later been found to be lipoxidase. The carotene is oxidised by some of the intermediate reaction products formed in the enzymatic oxidation of unsaturated fatty acids. Whether a similar reaction is responsible for the destruction of carotene in *Rhodymenia palmata* has not been established.

Acknowledgements. This work forms part of the research program of the *Norwegian Institute of Seaweed Research*. We are indebted to professor N. A. Sørensen for inspiring interest and helpful suggestions, and to Miss S. Svendsen for skilful assistance with the analyses.

1. Larsen, B. and Haug, A. *Acta Chem. Scand.* **10** (1956) 470.
2. Griffith, R. B. and Thompson, C. R. *Botan. Gaz.* **111** (1950) 165.
3. Mitchell, H. L. and Hauge, S. M. *J. Biol. Chem.* **163** (1946) 7.

Received February 24, 1956.

Demonstration of Reichstein's Substance S in Dog Adrenal Vein Blood by Countercurrent Distribution

HANS CARSTENSEN

Institute of Physiology, University of Upsala, Upsala, Sweden

The two major corticosteroids of dog adrenal vein blood, from a quantitative point of view, are cortisol and corticosterone, as demonstrated by several physical and chemical methods [1-4]. Among other possible components, the presence of minor amounts of Reichstein's substance S (Δ^4-pregnene-17*a*,21-diol-3,20-dione) seems to have considerable interest [5] (*cf.* Eberlein *et al.*[6]).

Further evidence of its occurrence in dog adrenal vein blood is provided here by its demonstration after countercurrent distribution. A sample of 330 ml blood was collected from the left adrenal of a mongrel male dog weighing 18 kg during 60 minutes and extracted with ethyl acetate as previously outlined [4]. The common corticosteroid fraction was recovered from the polar phase after double distribution between *n*-hexane and 50 % ethanol in water and subjected to successive countercurrent distributions (Table 1).

Table 1. Countercurrent distribution data of steroids in dog adrenal vein blood (24 transfers at 20°—21° C).

A: 20 % Ethanol + 80 % H_2O; 0.05 % (w/v) NaCl/ 50 % $CHCl_3$ + 50 % *n*-hexane
B: 20 % Ethanol + 80 % H_2O; 0.05 % (w/v) NaCl/ 90 % CCl_4 + 10 % $CHCl_3$
C: 50 % 2-Butanol + 50 % *n*-hexane/ H_2O
D: 75 % 2-Butanol + 25 % *n*-hexane/ H_2O
E: 20 % Ethanol + 80 % (w/v) H_2O; 0.05 % NaCl/ CCl_4
F: 15 % 2-Butanol + 85 % *n*-hexane/ H_2O

Partition coefficients (K)				Quantities estimated by different methods *, μg				
	K	*Followed by*	*Steroid identified*	*UV*	*BT*	*PS*	*SA*	*An*
A	0.33	B			(404)			
	2.13	C	Cortisol (K = 2.58)	573	720			
	8	D		—	(748)			
B**	?	E		+				
	0.79	F	Corticosterone (K = 0.82)	133				
	3.2		Cortisone (K = 3.5)	19		+		
	12			—	(64)	+	+	
C	3.0		Cortisol (K = 2.9)	265				
D	0.11				(41)			
	1.17				(22)			
	24				(12)			
E	0.1			(25)				1.5
	0.92		Substance S (K = 0.88)	77		28	45	
F	0.24		Corticosterone (K = 0.25)	68				

* Figures in brackets indicate cortisone equivalents. If no figure is stated, a positive reaction is denoted + and a negative reaction —.
UV: Specific extinction at 240 mμ in ethanol.
BT: Reduction of blue tetrazolium [12].
PS: Porter-Silber reaction [7].
SA: Sulfuric acid chromogen at 280 mμ [8].
An: Anthrone reaction with specific extinction at 600 mμ [9].
** Ketonic fraction after Girard separation.

The identity with substance S is suggested by the following criteria:

1) identical partition coefficient within the limits of the method,

2) specific extinction at 240 mμ in ethanol (α,β-unsaturated ketone),

3) positive Porter-Silber reaction, carried out according to Wilson and Fairbanks [7] (dihydroxy acetone side chain at C_{17}),

4) pink sulfuric acid chromogen with the typical second peak in the region at about 550 mμ, as well as the peak at 280-290 mμ indicative of a Δ^4-3-keto configuration [8].

The final amount recovered was 28 μg. This is probably much less than the original amount owing to repeated losses during the many different steps preceding the last determination. The higher values obtained by estimating the specific ultraviolet extinction at 240 mμ (77 μg) and the sulfuric acid chromogen at 280 mμ (45 μg) may be explained by the simultaneous occurrence of some Δ^4-pregnene-21-ol-3,11,20-trione (K = 0.75). — The other component of System E (K = 0.1) may contain a very small amount of cortexone (Δ^4-pregnene-21-ol-3,20-dione), having a specific extinction at 600 mμ with the anthrone reagent [9]. At the same time a very sharp and high peak appeared at 418 mμ, indicating the presence of a constituent which was not further characterized.

Besides cortisol, corticosterone and a small amount of cortisone, several other

components are demonstrated which have not yet been identified. The use of countercurrent distribution for separating corticosteroids has previously been described [10] but a more detailed discussion will appear elsewhere [11].

1. Reich, H., Nelson, D. H. and Zaffaroni, A. *J. Biol. Chem.* **187** (1950) 411.
2. Bush, I. E. *Biochem. J. London* **50** (1951) 370.
3. Zaffaroni, A. and Burton, R. B. *Arch. Biochem. and Biophys.* **42** (1953) 1.
4. Carstensen, H. *Acta Chem. Scand.* **9** (1955) 1238.
5. Farrell, G. L. and Lamus, B. *Proc. Soc. Exptl. Biol. Med.* **84** (1953) 89.
6. Eberlein, W. R. and Bongiovanni, A. M. *J. Clin. Endocrinol. and Metabolism* **15** (1955) 1531.
7. Wilson, H. and Fairbanks, R. *Arch. Biochem. and Biophys.* **53** (1954) 71.
8. Zaffaroni, A. *Recent Progr. Hormone Research* **8** (1953) 51.
9. Graff, M. M., McElroy, J. T. and Mooney, A. L. *J. Biol. Chem.* **195** (1952) 351.
10. Carstensen, H. *Acta Chem. Scand.* **9** (1955) 1026.
11. Carstensen, H. *Acta Soc. Med. Upsaliensis* **61** (1956). *In press.*
12. Mader, W. J. and Buck, R. R. *Anal. Chem.* **24** (1952) 666.

Received March 9, 1956.

On the Hydrolysis of the Bi^{3+} Ion — a Preliminary Note

FREDRIK GRANÉR, ÅKE OLIN and LARS GUNNAR SILLÉN

Department of Inorganic Chemistry, Royal Institute of Technology, Stockholm 70, Sweden

In 1947, Granér and Sillén [2] studied the hydrolysis of bismuth(III) in 3 M $NaClO_4$ medium, measuring $[H^+]$ with quinhydrone and glass electrodes, and $[Bi^{3+}]$ with bismuth amalgam electrodes. A mechanism was proposed which seemed to agree well with their data, which covered the range $[Bi]_{tot}$ = 10 to 50 mM.

One of us (Å.O.) has now undertaken a study with similar methods, but with total Bi concentrations ranging from 0.1 to 50 mM, thus a factor of 1 : 500 instead of 1 : 5. The present data can be explained by assuming the presence of only two complexes, the mononuclear $BiOH^{2+}$ and the hexanuclear $Bi_6(OH)_{12}^{6+}$ (as usual, plus or minus an unknown amount of water) with the preliminary equilibrium constants:

$$Bi^{3+} + H_2O \rightleftharpoons BiOH^{2+} + H^+ \qquad K_{1,1} = 0.026 \text{ M}$$

$$6\ Bi^{3+} + 12\ H_2O \rightleftharpoons Bi_6(OH)_{12}^{6+} + 12\ H^+ \qquad K_{12,6} = 2.14 \text{ M}^7$$

This result agrees with the findings of Kraus, Holmberg and Johnson [2] in so far as their "equilibrium ultracentrifugations suggest predominance of a low molecular weight polymer (N = *ca.* 5 or 6)". In a more narrow concentration range Souchay and Peschanski [3] concluded that there is only one complex present; they ascribed to it the formula, $Bi_4O_4^{4+}$.

The old data of Granér and Sillén were slightly distorted by the fact, then unknown, that quinone is a base and attracts protons at the highest acidities (Biedermann and Sillén [4]). After a correction for this effect, the present data are in general found to agree well with those of Granér and Sillén. This little deviation, however, sufficed (together with the narrowness of the $[Bi]_{total}$ range) to indicate an incorrect mechanism.

Attempts are now being made, in collaboration with Professor Cyrill Brosset, to study the structure of the complex by means of X-ray diffraction on aqueous solutions.

This work has been supported by Statens Tekniska Forskningsråd *(Swedish Technical Research Council)*.

A detailed paper will be published elsewhere.

1. Granér, F. and Sillén, L. G. *Acta Chem. Scand.* **1** (1947) 631.
2. Kraus, K., Holmberg, R. W. and Johnson, J. S. *(unpublished)*, quoted by Johnson, J. S., Kraus, K. and Holmberg, R. W. *J. Phys. Chem.* **58** (1954) 325.
3. Souchay, P. and Peschanski, D. *Bull. soc. chim. France* **1948** 439.
4. Biedermann, G. and Sillén, L. G. *Arkiv Kemi* **5** (1952) 425.

Received March 19, 1956.

components are demonstrated which have not yet been identified. The use of countercurrent distribution for separating corticosteroids has previously been described [10] but a more detailed discussion will appear elsewhere [11].

1. Reich, H., Nelson, D. H. and Zaffaroni, A. *J. Biol. Chem.* **187** (1950) 411.
2. Bush, I. E. *Biochem. J. London* **50** (1951) 370.
3. Zaffaroni, A. and Burton, R. B. *Arch. Biochem. and Biophys.* **42** (1953) 1.
4. Carstensen, H. *Acta Chem. Scand.* **9** (1955) 1238.
5. Farrell, G. L. and Lamus, B. *Proc. Soc. Exptl. Biol. Med.* **84** (1953) 89.
6. Eberlein, W. R. and Bongiovanni, A. M. *J. Clin. Endocrinol. and Metabolism* **15** (1955) 1531.
7. Wilson, H. and Fairbanks, R. *Arch. Biochem. and Biophys.* **53** (1954) 71.
8. Zaffaroni, A. *Recent Progr. Hormone Research* **8** (1953) 51.
9. Graff, M. M., McElroy, J. T. and Mooney, A. L. *J. Biol. Chem.* **195** (1952) 351.
10. Carstensen, H. *Acta Chem. Scand.* **9** (1955) 1026.
11. Carstensen, H. *Acta Soc. Med. Upsaliensis* **61** (1956). *In press.*
12. Mader, W. J. and Buck, R. R. *Anal. Chem.* **24** (1952) 666.

Received March 9, 1956.

On the Hydrolysis of the Bi^{3+} Ion — a Preliminary Note

FREDRIK GRANÉR, ÅKE OLIN and LARS GUNNAR SILLÉN

Department of Inorganic Chemistry, Royal Institute of Technology, Stockholm 70, Sweden

In 1947, Granér and Sillén [2] studied the hydrolysis of bismuth(III) in 3 M $NaClO_4$ medium, measuring $[H^+]$ with quinhydrone and glass electrodes, and $[Bi^{3+}]$ with bismuth amalgam electrodes. A mechanism was proposed which seemed to agree well with their data, which covered the range $[Bi]_{tot}$ = 10 to 50 mM.

One of us (Å.O.) has now undertaken a study with similar methods, but with total Bi concentrations ranging from 0.1 to 50 mM, thus a factor of 1 : 500 instead of 1 : 5. The present data can be explained by assuming the presence of only two complexes, the mononuclear $BiOH^{2+}$ and the hexanuclear $Bi_6(OH)_{12}^{6+}$ (as usual, plus or minus an unknown amount of water) with the preliminary equilibrium constants:

$$Bi^{3+} + H_2O \rightleftharpoons BiOH^{2+} + H^+ \qquad K_{1,1} = 0.026 \text{ M}$$

$$6\ Bi^{3+} + 12\ H_2O \rightleftharpoons Bi_6(OH)_{12}^{6+} + 12\ H^+ \qquad K_{12,6} = 2.14 \text{ M}^7$$

This result agrees with the findings of Kraus, Holmberg and Johnson [2] in so far as their "equilibrium ultracentrifugations suggest predominance of a low molecular weight polymer (N = *ca.* 5 or 6)". In a more narrow concentration range Souchay and Peschanski [3] concluded that there is only one complex present; they ascribed to it the formula, $Bi_4O_4^{4+}$.

The old data of Granér and Sillén were slightly distorted by the fact, then unknown, that quinone is a base and attracts protons at the highest acidities (Biedermann and Sillén [4]). After a correction for this effect, the present data are in general found to agree well with those of Granér and Sillén. This little deviation, however, sufficed (together with the narrowness of the $[Bi]_{total}$ range) to indicate an incorrect mechanism.

Attempts are now being made, in collaboration with Professor Cyrill Brosset, to study the structure of the complex by means of X-ray diffraction on aqueous solutions.

This work has been supported by Statens Tekniska Forskningsråd *(Swedish Technical Research Council)*.

A detailed paper will be published elsewhere.

1. Granér, F. and Sillén, L. G. *Acta Chem. Scand.* **1** (1947) 631.
2. Kraus, K., Holmberg, R. W. and Johnson, J. S. *(unpublished)*, quoted by Johnson, J. S., Kraus, K. and Holmberg, R. W. *J. Phys. Chem.* **58** (1954) 325.
3. Souchay, P. and Peschanski, D. *Bull. soc. chim. France* **1948** 439.
4. Biedermann, G. and Sillén, L. G. *Arkiv Kemi* **5** (1952) 425.

Received March 19, 1956.

Constitution of Resin Phenols and their Biogenetic Relations

XXII *. On the Absolute Configuration of Lignans

BERNT CARNMALM

Organisk-kemiska Institutionen, Kungl. Tekniska Högskolan, Stockholm, Sweden

The sterical relationships between the known members of the lignan series are largely established (for references see Erdtman [1] and Hearon and MacGregor [2]). If therefore the absolute configuration of one of the lignans could be determined this would simultaneously establish the confiration of all the interrelated lignans.

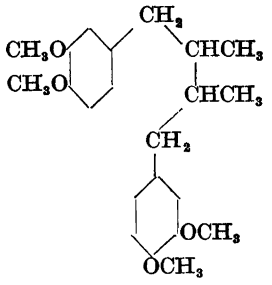
The work of Bijvoet *et al.*[3] has shown that the absolute configuration of glyceraldehyde is the same as that arbitrarily adopted by Fischer. In order to correlate the lignans with glyceraldehyde the conversion of dextrorotatory bis(hydroxymethyl)-succinic acid dilactone, obtained from pinoresinol, into compounds of known configuration has been investigated. These experiments have hitherto been unsuccessful, however, a promising route for the solution of the problem has now been found.

(−)-Dihydroguaiaretic acid dimethylether(I) afforded a weakly dextrorotatory dimethyladipic acid (II) on ozonolysis followed by oxidation with hydrogen peroxide. This acid was very readily converted into a dimethyl*cyclo*pentanone which shows a very high negative rotation. The formation of the *cyclo*pentanone demonstrates that the ozonolysis in fact has given the expected acid (II).

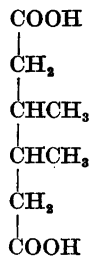
Work is in progress to correlate this acid with dimethylsuccinic acid (III) both by synthetic and degradative methods. By removing the carboxyl group of the half-ester of the dimethylsuccinic acid it is hoped to obtain α-methylbutyric acid (IV) which has already been correlated with glyceraldehyde (*cf.* Crombie and Harper [4]). The details of these correlation experiments and a discussion of the results will be published shortly.

The author is indebted to *Statens Tekniska Forskningsråd* for financial support.

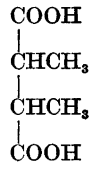
1. Erdtman, H. in Paech, K. and Tracey, M. V. *Moderne Methoden der Pflanzenanalyse*, Springer, Heidelberg, Vol. III.
2. Hearon, W. M. and MacGregor, W. S. *Chem. Rev.* **55** (1955) 957.



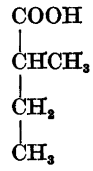
I



II



III



IV

3. Bijvoet, J. M., Peerdeman, A. F. and van Bommel, A. J. *Nature* **186** (1951) 271.
4. Crombie, L. and Harper, S. H. *J. Chem. Soc.* **1950** 2685.

Received March 14, 1956.

* Part XXI *Acta Chem. Scand.* **10** (1956). *In press.*

Optical Resolution of α-Phenylglutaric Acid

ARNE FREDGA and LARS WESTMAN

Chemical Institute, University of Uppsala, Uppsala, Sweden

In connection with current work on steric relationships, the authors have resolved α-phenylglutaric acid into its

optical antipodes. Quinine in ethanol and brucine in methanol were found to give the best results.

The racemic acid, prepared through the anhydride [1], had the m.p. 100–102°. The value 82–83° reported by previous authors [2] obviously refers to an unstable modification. The optically active acid melted at 129–131°.

Experimental. The anhydride was prepared by conventional methods [1]. After distillation *in vacuo* and recrystallisation from ethyl acetate + hexane, it melted at 94–95°. It was hydrolysed with boiling water (30 minutes); after extraction with ether and evaporation of the solvent, the acid was obtained as a gradually crystallising syrup. After recrystallisation from formic acid, it melted at 98–101°; further recrystallisation from ether + petrol ether raised the m.p. to 100–102°.

33.5 g racemic acid and 104 g quinine were dissolved together in 800 ml 96-% ethanol. The salt obtained after standing over-night was recrystallised seven times from the same solvent. The activity of the acid was practically constant from the fourth recrystallisation. The salt obtained (32.8 g) was decomposed with dilute sulphuric acid and the phenylglutaric acid isolated by extraction with ether. M. p. 129–131°. (Found: equiv.wt 104.7. $C_{11}H_{12}O_4$ requires 104.1. $[\alpha]_D^{25} = +85.8°$, $[M]_D^{25} = +178.5°$ in ethanol solution.)

The mother liquor from the first crystallisation of the quinine salt was evaporated and the acid liberated. 13.7 g with $[\alpha]_D^{25} = -46.8°$ was obtained. It was dissolved with 62 g brucine in 150 ml methanol. The salt obtained after 24 hours was recrystallised seven times from the same solvent; after five recrystallisations, the activity of the acid was constant and had practically the same maximum value as the antipode. The yield of salt was 27.9 g.

A grant from the *Swedish Natural Science Research Council* is gratefully acknowledged.

1. *Org. Syntheses* **30** (1950) 81.
2. Fichter, F. and Merckens, O. *Ber.* **34** (1902) 4174.

Received March 5, 1956.

Synthesis of Racemic Methyl Phthienoate

CECILE ASSELINEAU, JEAN ASSELINEAU* and STINA STÄLLBERG-STENHAGEN

Institute of Medical Biochemistry, University of Gothenburg, Gothenburg, Sweden, and

EINAR STENHAGEN

Department of Medical Biochemistry, Institute of Medical Chemistry, University of Uppsala, Uppsala, Sweden

In the lipids of a human strain of the tubercle bacillus Anderson and Chargaff in 1929 [1,2] found a dextrorotatory, branched chain fatty acid which they called phthioic acid. When injected into animals, this acid was found [3] to produce epitheloid cell tissue reaction characteristic of tuberculosis. The elucidation of the chemical structure of the compound proved difficult and has been achieved only recently, mainly as a result of work by Polgar *et al.*[4–6] at Oxford and by Cason *et al.*[7–9] at Berkeley. After the α,β-unsaturation of the acid had been recognized [4,7] the new names mycolipenic acid-I[b] and C_{27}-phthienoic acid [8] were suggested. According to Cason and Sumrell [8] several homologues of C_{27}-phthienoic acid are present in the lipids of tubercle bacilli.

On the basis of the above-mentioned degradation studies at Oxford and Berkeley, and synthetic work performed at Uppsala, Ställberg-Stenhagen [10] suggested that C_{27}-phthienoic acid ** is *trans*-2,4L, 6L-trimethyl-$\Delta^{2:3}$-tetracosenoic acid. This conclusion has been strengthened by Fray and Polgar's recent synthesis [11] of (+)-2L,4L-dimethyldocosanoic acid, a degradation product of the natural compound. The synthesis of the *cis*- and *trans*-DL-erythro isomers of methyl 2,4,6-trimethyl-$\Delta^{2:3}$-tetracosenoate has now been performed through the following sequence of reactions:

* Rockefeller Foundation fellow.

** We prefer this name because of its similarity with the name originally proposed by R. J. Anderson.

Constitution of Resin Phenols and their Biogenetic Relations

XXII *. On the Absolute Configuration of Lignans

BERNT CARNMALM

Organisk-kemiska Institutionen, Kungl. Tekniska Högskolan, Stockholm, Sweden

The sterical relationships between the known members of the lignan series are largely established (for references see Erdtman [1] and Hearon and MacGregor [2]). If therefore the absolute configuration of one of the lignans could be determined this would simultaneously establish the confiration of all the interrelated lignans.

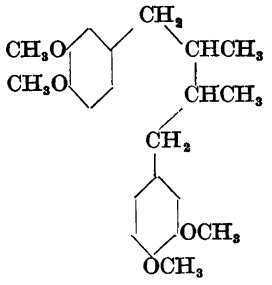
The work of Bijvoet *et al.*[3] has shown that the absolute configuration of glyceraldehyde is the same as that arbitrarily adopted by Fischer. In order to correlate the lignans with glyceraldehyde the conversion of dextrorotatory bis(hydroxymethyl)-succinic acid dilactone, obtained from pinoresinol, into compounds of known configuration has been investigated. These experiments have hitherto been unsuccessful, however, a promising route for the solution of the problem has now been found.

(−)-Dihydroguaiaretic acid dimethylether(I) afforded a weakly dextrorotatory dimethyladipic acid (II) on ozonolysis followed by oxidation with hydrogen peroxide. This acid was very readily converted into a dimethyl*cyclo*pentanone which shows a very high negative rotation. The formation of the *cyclo*pentanone demonstrates that the ozonolysis in fact has given the expected acid (II).

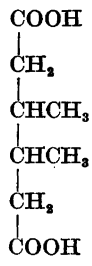
Work is in progress to correlate this acid with dimethylsuccinic acid (III) both by synthetic and degradative methods. By removing the carboxyl group of the half-ester of the dimethylsuccinic acid it is hoped to obtain α-methylbutyric acid (IV) which has already been correlated with glyceraldehyde (*cf.* Crombie and Harper [4]). The details of these correlation experiments and a discussion of the results will be published shortly.

The author is indebted to *Statens Tekniska Forskningsråd* for financial support.

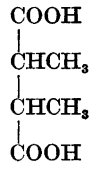
1. Erdtman, H. in Paech, K. and Tracey, M. V. *Moderne Methoden der Pflanzenanalyse*, Springer, Heidelberg, Vol. III.
2. Hearon, W. M. and MacGregor, W. S. *Chem. Rev.* **55** (1955) 957.



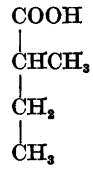
I



II



III



IV

3. Bijvoet, J. M., Peerdeman, A. F. and van Bommel, A. J. *Nature* **186** (1951) 271.
4. Crombie, L. and Harper, S. H. *J. Chem. Soc.* **1950** 2685.

Received March 14, 1956.

* Part XXI *Acta Chem. Scand.* **10** (1956). *In press.*

Optical Resolution of α-Phenylglutaric Acid

ARNE FREDGA and LARS WESTMAN

Chemical Institute, University of Uppsala, Uppsala, Sweden

In connection with current work on steric relationships, the authors have resolved α-phenylglutaric acid into its

optical antipodes. Quinine in ethanol and brucine in methanol were found to give the best results.

The racemic acid, prepared through the anhydride [1], had the m.p. 100–102°. The value 82–83° reported by previous authors [2] obviously refers to an unstable modification. The optically active acid melted at 129–131°.

Experimental. The anhydride was prepared by conventional methods [1]. After distillation *in vacuo* and recrystallisation from ethyl acetate + hexane, it melted at 94–95°. It was hydrolysed with boiling water (30 minutes); after extraction with ether and evaporation of the solvent, the acid was obtained as a gradually crystallising syrup. After recrystallisation from formic acid, it melted at 98–101°; further recrystallisation from ether + petrol ether raised the m.p. to 100–102°.

33.5 g racemic acid and 104 g quinine were dissolved together in 800 ml 96-% ethanol. The salt obtained after standing over-night was recrystallised seven times from the same solvent. The activity of the acid was practically constant from the fourth recrystallisation. The salt obtained (32.8 g) was decomposed with dilute sulphuric acid and the phenylglutaric acid isolated by extraction with ether. M. p. 129–131°. (Found: equiv.wt 104.7. $C_{11}H_{12}O_4$ requires 104.1. $[\alpha]_D^{25} = +85.8°$, $[M]_D^{25} = +178.5°$ in ethanol solution.)

The mother liquor from the first crystallisation of the quinine salt was evaporated and the acid liberated. 13.7 g with $[\alpha]_D^{25} = -46.8°$ was obtained. It was dissolved with 62 g brucine in 150 ml methanol. The salt obtained after 24 hours was recrystallised seven times from the same solvent; after five recrystallisations, the activity of the acid was constant and had practically the same maximum value as the antipode. The yield of salt was 27.9 g.

A grant from the *Swedish Natural Science Research Council* is gratefully acknowledged.

1. *Org. Syntheses* **30** (1950) 81.
2. Fichter, F. and Merckens, O. *Ber.* **34** (1902) 4174.

Received March 5, 1956.

Synthesis of Racemic Methyl Phthienoate

CECILE ASSELINEAU, JEAN ASSELINEAU* and STINA STÄLLBERG-STENHAGEN

Institute of Medical Biochemistry, University of Gothenburg, Gothenburg, Sweden, and

EINAR STENHAGEN

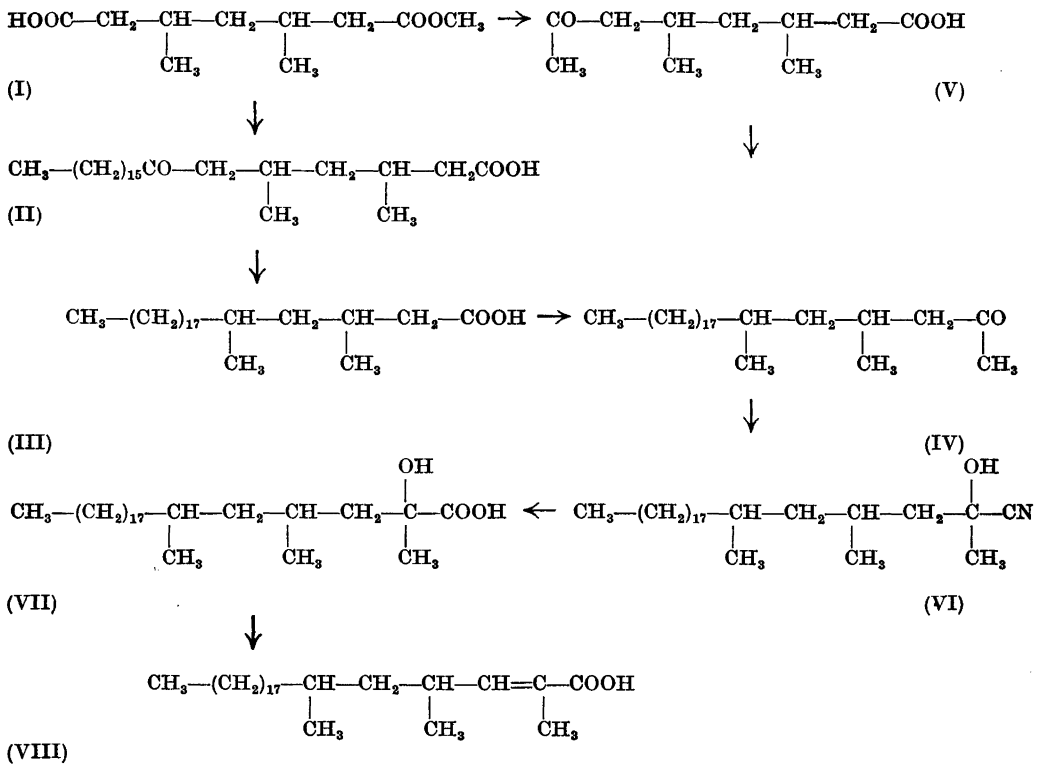
Department of Medical Biochemistry, Institute of Medical Chemistry, University of Uppsala, Uppsala, Sweden

In the lipids of a human strain of the tubercle bacillus Anderson and Chargaff in 1929 [1,2] found a dextrorotatory, branched chain fatty acid which they called phthioic acid. When injected into animals, this acid was found [3] to produce epitheloid cell tissue reaction characteristic of tuberculosis. The elucidation of the chemical structure of the compound proved difficult and has been achieved only recently, mainly as a result of work by Polgar *et al.*[4–6] at Oxford and by Cason *et al.*[7–9] at Berkeley. After the α,β-unsaturation of the acid had been recognized [4,7] the new names mycolipenic acid-I[b] and C_{27}-phthienoic acid [8] were suggested. According to Cason and Sumrell [8] several homologues of C_{27}-phthienoic acid are present in the lipids of tubercle bacilli.

On the basis of the above-mentioned degradation studies at Oxford and Berkeley, and synthetic work performed at Uppsala, Ställberg-Stenhagen [10] suggested that C_{27}-phthienoic acid ** is *trans*-2,4L, 6L-trimethyl-$\Delta^{2:3}$-tetracosenoic acid. This conclusion has been strengthened by Fray and Polgar's recent synthesis [11] of (+)-2L,4L-dimethyldocosanoic acid, a degradation product of the natural compound. The synthesis of the *cis*- and *trans*-DL-erythro isomers of methyl 2,4,6-trimethyl-$\Delta^{2:3}$-tetracosenoate has now been performed through the following sequence of reactions:

* Rockefeller Foundation fellow.

** We prefer this name because of its similarity with the name originally proposed by R. J. Anderson.



Experimental. The starting material, *meso*-3,5-dimethylpimelic acid, has been prepared from 3,5-dimethyl*cyclo*hexanone: free acid m. p. 98.6—99.8°; monomethyl ester (I) n_D^{25} 1.4438, d_4^{25} 1.037; dimethyl ester n_D^{22} 1.4334, d_4^{22} 1.002. By means of Bowman's synthesis 3,5-dimethyl-7-oxotricosanoic acid (II), m. p. 51.3—52.2° and 29.0—29.3° (dimorphism) was prepared (semicarbazone m. p. 104—109° (decomp.)). Reduction of this acid, either by Huang-Minlon's modification [12] of the Wolff-Kishner procedure or by treatment of the ethylene mercaptal with Raney nickel [13] gave 3,5-dimethyltricosanoic acid (DL-erythro form) (III), m. p. 46.4—48.4° and 27.0—27.3° (dimorphism). Methyl ester: m. p. 18.3—18.8°, $n_D^{21.5}$ 1.4500, $d_4^{21.5}$ 0.858; ethyl ester: m. p. 14.8—15.3°, n_D^{22} 1.4495, d_4^{22} 0.854. Through reaction of the acid chloride of the last mentioned acid with methyl cadmium [14] 4,6-dimethyltetracosanone-2 (IV) was obtained, m. p. 20.9—21.4°, n_D^{20} 1.4530, d_D^{20} 0.846 (semicarbazone m. p. 82—83°). The same ketone was also obtained from 3,5-dimethyl-7-oxooctanoic acid (V) (n_D^{22} 1.4494, d_4^{22} 0.9988) and stearic acid through the Kolbe reaction. Treatment of the ketone with hydrocyanic acid gave the cyanhydrin (VI) which without further purification was hydrolyzed to 2,4,6-trimethyl-2-hydroxytetracosanoic acid (VII), m. p. 51.2—52.5° (mixture of diastereoisomers) (methyl ester: m. p. 22.5—23.1°, n_D^{25} 1.4527; I. R. spectrum: bands at 2.85 and 5.77 μ). Pyrolysis of the free hydroxy-acid gave a mixture from which, after methylation and chromatography on alumina, *cis*- and *trans*-isomers of methyl DL-erythro-2,4,6-trimethyl-$\Delta^{2,3}$-tetracosenoate (VIII) were isolated: *cis*-isomer m. p. 35.2—36.6° and 16.3—16.6° (dimorphism), n_D^{25} 1.4587, U. V. spectrum: λ_{max} 217 mμ, ε = 10.240; *trans*-isomer m. p. 14.3—14.7°, n_D^{25} 1.4600, U. V. spectrum: λ_{max} 215 mμ, ε = 12.930 (hexane).

The assignment of geometrical configuration of 2-methyl-2-alkenoic acids has been discussed by Ställberg-Stenhagen [10]

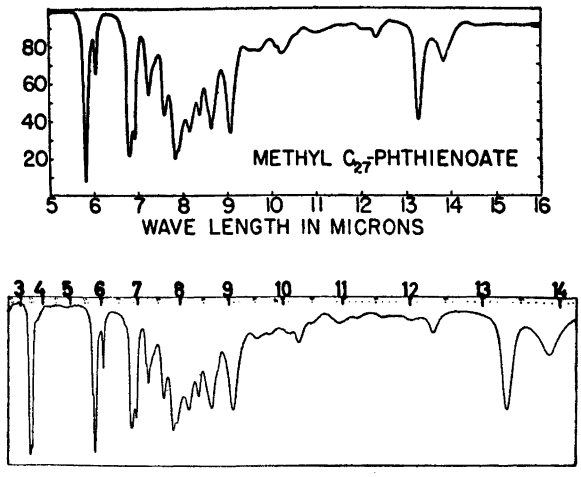


Fig. 1. Infrared absorption spectra.

Upper curve: Methyl C_{27}-phthienoate according to Cason et al.[9]
Lower curve: Synthetic methyl trans-DL-*erythro-2,4,6-trimethyl-$\Delta^{2:3}$-tetracosenoate (liquid, cell 0.02 mm thick).*

and Cason and Kalm [15]. The results of these authors are supported by the X-ray crystallographic work of Robertson and Porte [16] on angelic and tiglic acid.

The infrared absorption spectra of the *cis-* and *trans-*isomers in liquid state are considerably different especially in the region 10 to 15 μ. The spectrum of the *trans-*isomer proved identical with that of a specimen of methyl C_{27}-phthienoate recently isolated by one of us (J.A.) from the strain test of the tubercle bacillus. As shown in Fig. 1 the spectrum also appears identical with that for methyl C_{27}-phthienoate published by Cason *et al.*[9]. The *trans-*configuration of the ester derived from bacterial sources [10,15] is thus confirmed.

Methyl hydrogen 3,5-dimethylpimelate(I) has been resolved into the antipodes, $[\alpha]_D^{25} \pm 1.5°$, and we are now engaged in the synthesis of the optically active *cis-* and *trans-*isomers.

Acknowledgements: We are indebted to Mr. L. Ahlquist for skilled assistance in the preparative work and to Dr. I. Fischmeister for the infrared absorption spectra. This work has been supported by grants from *Statens Medicinska Forskningsråd.*

1. Anderson, R. J. and Chargaff, E. *J. Biol. Chem.* **85** (1929—30) 77.
2. Anderson, R. J. *J. Biol. Chem.* **97** (1932) 639.
3. Sabin, F. R. *Physiol. Rev.* **12** (1932) 141.
4. Chanley, J. D. and Polgar, N. *Nature* **166** (1950) 693.
5. Polgar, N. and Robinson, R. *Chemistry & Industry* **1951** 685.
6. Polgar, N. *J. Chem. Soc.* **1954** 1008.
7. Cason, J. and Sumrell, G. *J. Am. Chem. Soc.* **72** (1950) 4837.
8. Cason, J. and Sumrell, G. *J. Biol. Chem.* **192** (1951) 405.
9. Cason, J., Freeman, N. K. and Sumrell, G. *J. Biol. Chem.* **192** (1951) 415.
10. Ställberg-Stenhagen, S. *Arkiv Kemi* **6** (1954) 537.
11. Fray, G. I. and Polgar, N. *Chemistry & Industry* **1956** 22.
12. Huang-Minlon *J. Am. Chem. Soc.* **68** (1946) 2487.
13. Hauptmann, H. *J. Am. Chem. Soc.* **69** (1947) 565.
14. Cason, J. *Chem. Revs.* **40** (1947) 15.
15. Cason, J. and Kalm, M. J. *J. Org. Chem.* **19** (1954) 1947.
16. Robertson, J. M. and Porte, A. L. *Nature* **176** (1955) 1116.

Received March 16, 1956.

The Ethylenic Bond in Dihydroabietic Acid

HENRIK H. BRUUN*

Department of Medical Biochemistry, Institute of Medical Chemistry, University of Uppsala, Sweden

The position of the double bond in the isomeric dihydroabietic acids has not been established. The suggested sites are Δ 7, 8(14), 9(14) and 13 (Fig. 1) **. For two dihydroabietic acids prepared by partial hydrogenation of abietic acid, the α- and β-dihydroabietic acids of Lombard [5,6], Simonsen and Barton [7] have proposed the position 9(14) and 13, respectively. This proposal is supported by the recent molecular rotation studies of Klyne [8].

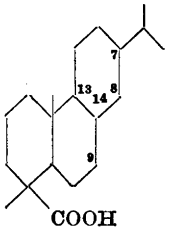


Fig. 1.

Trisubstituted ethylenic bonds ($R_1R_2C=CHR_3$) can generally be distinguished from the tetrasubstituted bonds ($R_1R_2C=CR_3R_4$) by infrared absorption measurements by means of the C—H out-of-plane deformation vibrations in the spectra of the former. Complex molecules studied by this method are triterpenes (Ruzicka, Jeger *et al.*[9,10] and a number of sterols (Hirschmann [11]). For sterols the absorption band occurs at a wavelength of 12.5 μ. In the present study, the infrared absorption in this range has been recorded for dihydroabietic acid and for several other abietic and pimaric acids of known structure. The aim has been to determine whether the infrared spectrum of dihydroabietic acid shows the band in question or not. A negative result would suggest that the double bond is tetrasubstituted, *i. e.* the position is at 13; however, this would not be fully conclusive in view of the frequently weak and varying intensity of the band. A positive result would imply without reservation that the double bond is of the trisubstituted type, *i. e.* it would be situated somewhere else in the molecule.

Experimental. The infrared absorption spectra were recorded with a double beam spectrophotometer (built by Dr. M. Skogh) of the type described by Hornig, Hyde and Adcock [12]. The samples were prepared by the potassium bromide technique, the tablets were 0.8 mm thick and 13 mm in diameter, and contained 3—3.2 mg of the acid per 300 mg of potassium bromide.

The samples of the dihydro-, tetrahydro- and dehydroabietic acids and *iso*dextropimaric acid were obtained from the Research Laboratory of Hercules Powder Company, Wilmington, Delaware. According to Dr. C. G. Harris of that laboratory, the dihydroabietic acid had been prepared by partial hydrogenation of abietic acid and was a mixture of isomeric acids, but otherwise pure. M. p. 133.8—136.8, $[\alpha]_D^{20}$ + 19° ± 2°. Tetrahydroabietic acid, m.p. 149.4—152.4, $[\alpha]_D^{20}$ + 11° ± 2°; dehydroabietic acid, m. p. 173.3—174.6, $[\alpha]_D^{20}$ + 66° ± 1°; *iso*dextropimaric acid, m. p. 162.9—164.9, $[\alpha]_D^{20}$ 0°.

The dextropimaric acid was obtained from Dr. O. Jeger at the Eidg. Techn. Hochschule, Zürich.

The abietic acid was obtained in the form of its butylamine salt from Dr. E. Back of the Swedish Forest Products Research Laboratory, Stockholm. Before use, the acid was liberated from its salt with an aqueous boric acid solution. M. p. 170.2—172.7, $[\alpha]_D^{20}$ —104° ± 1°.

The melting points were determined by the capillary method (diameter of the capillary tubes 1 mm). The values were corrected. The optical rotations in absolute alcohol (0.01 g per ml) were measured with a Lippich polarimeter.

For monolayer data relating to the same samples of rosin acids, see Ref. [13].

Results. The infrared absorption spectra of the rosin acids for the range 12—13 μ are shown in Fig. 2. There is a band at 12.5 μ in the spectrum of dihydroabietic acid (*a*). The two pimaric acids have a trisubstituted etylenic bond at 8(14) and the corresponding band is evident in the spectra. For *iso*dextropimaric acid (*b*), the band is of a relatively high intensity,

* Address: Institute of Physical Chemistry, Åbo Akademi, Åbo, Finland.

** For reviews, see *e. g.* Refs. [1-4].

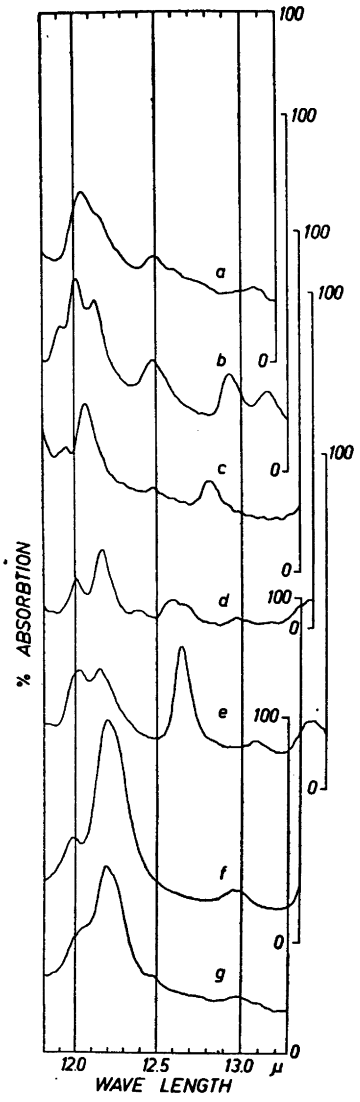


Fig. 2.

while that for dextropimaric acid (*c*) is of much lower intensity. The band is not evident in the spectrum of the fully saturated tetrahydroabietic acid (*d*), in the spectrum of the abietic acid (*e*) with conjugated double bonds or in the spectrum of the hydroaromatic dehydroabietic acid (*f*). In a mixture containing equal parts of the last mentioned and dihydroabietic acid (*g*) the band at 12.5 μ is still observed.

Discussion. The evidence presented above strongly suggests that the dihydrobietic acid studied contains a trisubstituted ethylenic bond. If we assume provisionally that the sample is a mixture of Lombard's α- and β-acids (*cf.* Refs. [7,8]), the appearance of the band in the spectrum of the mixture in spite of the strong background absorption implies that the α-acid content in the sample is relatively high. This conclusion is supported by the optical rotation value of the sample; a comparison with the values for Lombard's α- and β-acids ($-26°$ and $+128°$, respectively) points to a concentration of about 70 %.

I wish to express my sincere gratitude to Professor Einar Stenhagen for placing the facilities of the department at my disposal. I am indebted to Dr. Ingrid Fischmeister for assistance with the spectrophotometric measurements. This work has been made possible by a grant from the *Committee for the Advancement of Natural Sciences* appointed by the Finnish Government.

1. Zeiss, H. H. *Chem. Revs.* **72** (1948) 163.
2. Barton, D. H. R. *Quart. Revs. London* **3** (1949) 36.
3. Fieser, L. F. and Fieser, M. *Natural Products Related to Phenanthrene*, New York, 1949.
4. Simonsen, J. and Barton, D. H. R. *The Terpenes III*, Cambridge 1952, p. 374.
5. Lombard, R. *Bull. soc. chim. France* **9** (1942) 833.
6. Lombard, R. *Ibid.* **11** (1944) 526.
7. Simonsen, J. and Barton, D. H. R. *The Terpenes III*, Cambridge 1952, p. 408.
8. Klyne, W. *J. Chem. Soc.* **1953** 3072.
9. Meyer, A., Jeger, O. and Ruzicka, L. *Helv. Chim. Acta* **33** (1950) 672.
10. Koller, E., Hiestand, A., Dietrich, P. and Jeger, O. *Helv. Chim. Acta* **33** (1950) 1050.
11. Hirschmann, H. *J. Am. Chem. Soc.* **74** (1952) 5357.
12. Hornig, D. F., Hyde, G. E. and Adcock, W. A. *J. Opt. Soc. Amer.* **40** (1950) 498.
13. Bruun, H. H. *Surface Balance Studies of Rosin Acid Monolayers* (Diss.), *Acta Acad. Aboensis, Math. et Phys.* **19** (1954) No. 3.

Received March 16, 1956.

Organic Hydroxylamine Compounds Formed from Nitrite in *Torulopsis utilis*. II. Acetylhydroxamic Acid

ARTTURI I. VIRTANEN and NILS-ERIK SARIS

Laboratory of the Foundation for Chemical Research, Biochemical Institute, Helsinki, Finland

In an earlier paper [1] we reported results which showed that "bound hydroxylamine", which is formed in small amounts in the cells of *Torulopsis utilis* suspended in a nitrite-containing nutrient solution, contains oximes of α-keto acids. In all experiments the amount of the oxime of pyruvic acid was highest, next came the oxime of α-ketoglutaric acid, the smallest amounts being those of the oximes of oxypyruvic, oxalacetic, and glyoxalic acids. The amounts and mutual relations of different oximes varied appreciably in different experiments, as can be expected since the amount of the corresponding keto acids varies in the cells and is dependent on many different factors.

When continuing our investigations special attention was given to hydroxamic acids which could possibly be formed in addition to oximes. In the experiment described in our first paper about 70 % of "bound hydroxylamine" was reduced by sodium amalgam to amino acids. The rest of the "bound hydroxylamine" could thus consist of hydroxamic acids. In most experiments practically all the "bound hydroxylamine" passed through the Dowex 50 column. On the basis of this *Torulopsis* cells do not contain noticeable amounts of the hydroxamic acids of amino acids. The hydroxamic acids of such carboxylic acids which do not contain basic groups were instead to be expected in the solution emerging from the Dowex column. In our very first experiments we found this to be the case, as in fact a reddish spot was obtained with ferric chloride on the paper chromatogram of the solution. The chemical nature of the compound remained obscure, however, and was not therefore dealt with in our earlier paper.

A closer investigation has now been made on the nature of the hydroxamic acid formed when *Torulopsis* reduces

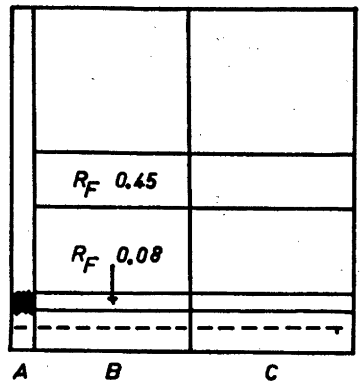


Fig. 1. Paper chromatogram of »bound hydroxylamine» in Torulopsis *cells. Solvent: amylacetate/formic acid/water (4:1:1). Dotted line = starting line.*

A. Paper strip sprayed with ferric chloride solution. Reddish spot with R_F *0.08.*

B. After hydrolysis hydroxylamine could be found mostly in the zones with R_F *0.08 and 0.45.*

C. The corresponding zones were analyzed. The zone with R_F *0.45 gave on reduction with sodium amalgam alanine and accordingly contained the oxime of pyruvic acid. The zone with* R_F *0.08 contained acetylhydroxamic acid (*cf. *Fig. 2).*

nitrite. The extract obtained from the cell mass was passed through a cellulose powder column with butanol-acetic acid as solvent (Dowex treatment was omitted). "Bound hydroxylamine" passed through comparatively quickly. The combined fractions containing "bound hydroxylamine" were evaporated to a small volume. The solution obtained was spread along a starting line at the bottom of a Whatman No. 4 paper, and using amylacetate/formic acid/water (4:1:1) as solvent the chromatogram was developed. A narrow strip cut off from the margin of the paper was sprayed with a solution of ferric chloride upon which the reddish spot appeared, R_F 0.08 (Fig. 1 A). The sheet was then cut in two lengthwise and one of the halves again was cut crosswise into 16 strips which were extracted with water (Fig. 1 B). The solutions obtained were hydrolyzed with sulphuric acid and hydroxylamine was determined by the method of Csàky. The values showed that "bound

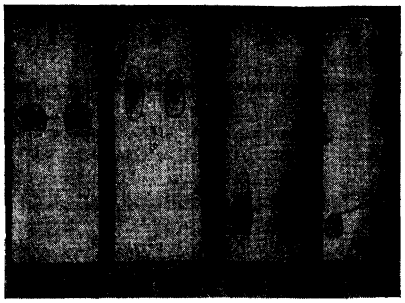


Fig. 2. Comparison between synthetic acetylhydroxamic acid and the hydroxamic acid found in Torulopsis *cells. A. Synthetic acetylhydroxamic acid. X. Hydroxamic acid found in* Torulopsis *cells. Solvents: 1 butanol/acetic acid/water (63:27:10), 2) amylacetate/formic acid (80 %)/water (4:1:1), 3) ethylacetate/butanol/water (8:2:1), 4) ethylacetate/propanol/acetic acid/water (5:2:2:1).*

hydroxylamine" had mostly divided into two zones: R_F 0.08 and R_F 0.45. From the other half of the paper (Fig. 1 C) the zones corresponding to hydroxylamine maxima were cut off and eluted with water. From the zone corresponding to R_F 0.45 alanine was obtained by reduction with sodium amalgam (identified by paper chromatography). This zone accordingly contained the oxime of pyruvic acid. The hydroxylamine compound obtained from the strip with R_F 0.08, which corresponded to the red spot, was used for several paper chromatograms with different solvents: butanol/acetic acid/water (63:27:10), amylacetate/formic acid (80 %)/water (4:1:1), ethylacetate/butanol/water (8:2:1), and ethylacetate / propanol / acetic acid / water (5:2:2:1) (Fig. 2). Corresponding paper chromatograms were made for comparison with synthetic acetylhydroxamic acid.

The synthetic acid was prepared from ethylacetate and hydroxylamine-HCl in an alkaline methanol solution at 30° C. The solution was neutralized with HCl upon which KCl precipitated. The precipitate was filtered off and the solution evaporated to dryness *in vacuo*. The residue was dissolved in ethanol, ether was added, and the precipitate was filtered off. The clear solution was evaporated to dryness and the residue crystallized from acetone. M.p. 88—89 °C. According to the determination of hydroxylamine in the preparation it is pure acetylhydroxamic acid. It gives an intensely red colour with ferric chloride.

The hydroxamic acid found in *Torulopsis* cells is according to chromatographic analyses, presented in Fig. 2, acetylhydroxamic acid.

Acetylhydroxamic acid is not reduced by sodium amalgam (1.5 %), whereas oximes are reduced quantitatively to the corresponding amino acids. On the basis of this the following experiment was performed: from the alcoholextract of the cell mass of *Torulopsis* alcohol was evaporated, and the oximes in the solution were reduced with sodium amalgam. The amount of hydroxylamine which disappeared on reduction indicated the amount of oximes. The difference between the total "bound hydroxylamine"-N and the reduced oxime-N indicates the amount of acetylhydroxamic acid. In two different experiments 30 and 50 %, respectively, of the total "bound hydroxylamine" was acetylhydroxamic acid, whereas 50—70 % of "bound hydroxylamine" thus corresponded to the oximes of keto acids, mainly to that of pyruvic acid.

In the earlier paper we reported that appreciable amounts of "bound hydroxylamine" were formed in nitrite solution only at low oxygen concentration. We have now found that *Torulopsis* cells with low N-content form "bound hydroxylamine" both from nitrate and nitrite in aerated suspensions. At best about 10—20 μg NH_2OH-N/g fresh yeast was accumulated in the cells during the first ten to twenty minutes.

Our results indicate that "bound hydroxylamine" is accumulated in *Torulopsis utilis* cells suspended in a nitrate or nitrite containing nutrient solution. In this nitrogen fraction the oximes of α-keto acids as well as acetylhydroxamic acid are found. The oximes are obviously formed through a chemical reaction between hydroxylamine and α-keto acids [2]. Acetylhydroxamic acid is probably formed either from hydroxylamine and acetyl-CoA [3] or from hydroxylamine and acetylphosphate [4].

Since the amount of oximes rapidly decreases in *Torulopsis* cells there must be some mechanism through which "bound hydroxylamine" is either reduced or hydrolyzed in the cells. Virtanen has earlier advanced the hypothesis that the oximes of α-keto acids should be reduced to the corresponding amino acids. For the present we have not been able to demonstrate this reduction. The observations made by

Yamafuji [5] on this point cannot be regarded as conclusive evidence. The question is thus still open. The other possibility that the oximes formed are hydrolyzed, and that the free hydroxylamine is then reduced to ammonia also lacks experimental evidence.

At the moment it seems very likely that the physiological function of the formation of "bound hydroxylamine" is the "trapping" of hydroxylamine in case it is not reduced to ammonia quickly enough. On the other hand, it is still unsettled if the formation of oximes at the same time constitutes a special pathway for amino acid synthesis. The significance of acetylhydroxamic acid is also obscure.

1. Virtanen, A. I. and Saris, N.-E. *Acta Chem. Scand.* **9** (1955) 337.
2. Virtanen, A. I. and Alfthan, M., *unpublished*, Ref. Virtanen, A. I. *Ann. Acad. Sci. Fennicae, Ser. A. II, Chem.* **1952** No. 43.
3. Chou, T. C. and Lipmann, F. *J. Biol. Chem.* **196** (1952) 89.
4. Lipmann, F. and Tuttle, C. *J. Biol. Chem.* **159** (1945) 21.
5. Yamafuji, K. *Nature* **167** (1951) 770; Yamafuji, K. and Omura, H. *Enzymologia* **15** (1952) 296.

Received February 15, 1956.

Activation Energies in the Alkaline Hydrolysis of Saturated Aliphatic Esters

EERO A. HALONEN

Institute of Chemistry, University of Helsinki, Finland

The volatility and low solubility of saturated aliphatic esters in water may lead to appreciable errors in the determination of the rates of hydrolysis.

In the present study, the air volume above the solution was kept small by using two ampoules, one of about 6 ml capacity and the other of about 10.5 ml, which were connected by a short length of rubber tubing. 5 ml of an 0.02 M aqueous solution of the ester was measured into the larger ampoule and 5 ml of 0.02 M aqueous sodium hydroxide into the other. After the rubber tubing was closed with a screw fastener, the ampoules were placed alongside each other in the thermostat; in this way evaporation of the ester into the alkali solution was avoided. After both ampoules had attained the thermostat temperature, the tubing was opened, the alkali was transferred into the ester solution with vigorous shaking, and the tubing was closed again. The ampoules were taken from the thermostat after suitable intervals, the tubing was removed, and the reaction mixture poured rapidly into an ice-cold hydrochloric acid solution. The excess of hydrogen chloride was titrated with baryta solution using phenolphtalein as indicator. The rate constants were calculated from the second-order rate equation. The values of the ate constants obtained are given in Table 1 (the values for ethyl formate from a publication of Tommila and Maltamo [1] have been included for comparison).

The rate constants for all the esters studied are in good agreement with the values reported by Salmi and Leimu [2], and those for ethyl acetate with the values published by Tommila and coworkers [3,4]. From the calculated activation energy and frequency factor values given in the table it is seen that for the last three esters the decrease in the rate is mainly due to a decrease in the frequency factor, and that the activation energy increases from ethyl formate to ethyl acetate and then decreases slowly in the series ethyl acetate, ethyl propionate and ethyl *iso*butyrate. On the other hand, the activation energies for ethyl propionate and ethyl *n*-butyrate do not differ from each other. The rate falls greatly from ethyl formate to ethyl acetate and the difference between the rates of ethyl propionate and ethyl butyrate is abnormally large (*cf.* Ref.[4]). The rate decreases only slightly from ethyl acetate to ethyl propionate in the temperature range studied (as calculated from the Arrhenius plot, ethyl propionate hydrolyses more rapidly than ethyl acetate at temperatures below $-3°$ C).

The differences in the rates of hydrolysis can be explained by assuming that the activation energy differences are mainly determined by hyperconjugation and that the differences in the inductive and steric effects appear mainly in the frequency factors. In a previous study [5], it was concluded that the conjugation between the

Yamafuji [5] on this point cannot be regarded as conclusive evidence. The question is thus still open. The other possibility that the oximes formed are hydrolyzed, and that the free hydroxylamine is then reduced to ammonia also lacks experimental evidence.

At the moment it seems very likely that the physiological function of the formation of "bound hydroxylamine" is the "trapping" of hydroxylamine in case it is not reduced to ammonia quickly enough. On the other hand, it is still unsettled if the formation of oximes at the same time constitutes a special pathway for amino acid synthesis. The significance of acetylhydroxamic acid is also obscure.

1. Virtanen, A. I. and Saris, N.-E. *Acta Chem. Scand.* **9** (1955) 337.
2. Virtanen, A. I. and Alfthan, M., *unpublished*, Ref. Virtanen, A. I. *Ann. Acad. Sci. Fennicae, Ser. A. II, Chem.* **1952** No. 43.
3. Chou, T. C. and Lipmann, F. *J. Biol. Chem.* **196** (1952) 89.
4. Lipmann, F. and Tuttle, C. *J. Biol. Chem.* **159** (1945) 21.
5. Yamafuji, K. *Nature* **167** (1951) 770; Yamafuji, K. and Omura, H. *Enzymologia* **15** (1952) 296.

Received February 15, 1956.

Activation Energies in the Alkaline Hydrolysis of Saturated Aliphatic Esters

EERO A. HALONEN

Institute of Chemistry, University of Helsinki, Finland

The volatility and low solubility of saturated aliphatic esters in water may lead to appreciable errors in the determination of the rates of hydrolysis.

In the present study, the air volume above the solution was kept small by using two ampoules, one of about 6 ml capacity and the other of about 10.5 ml, which were connected by a short length of rubber tubing. 5 ml of an 0.02 M aqueous solution of the ester was measured into the larger ampoule and 5 ml of 0.02 M aqueous sodium hydroxide into the other. After the rubber tubing was closed with a screw fastener, the ampoules were placed alongside each other in the thermostat; in this way evaporation of the ester into the alkali solution was avoided. After both ampoules had attained the thermostat temperature, the tubing was opened, the alkali was transferred into the ester solution with vigorous shaking, and the tubing was closed again. The ampoules were taken from the thermostat after suitable intervals, the tubing was removed, and the reaction mixture poured rapidly into an ice-cold hydrochloric acid solution. The excess of hydrogen chloride was titrated with baryta solution using phenolphtalein as indicator. The rate constants were calculated from the second-order rate equation. The values of the ate constants obtained are given in Table 1 (the values for ethyl formate from a publication of Tommila and Maltamo [1] have been included for comparison).

The rate constants for all the esters studied are in good agreement with the values reported by Salmi and Leimu [2], and those for ethyl acetate with the values published by Tommila and coworkers [3,4]. From the calculated activation energy and frequency factor values given in the table it is seen that for the last three esters the decrease in the rate is mainly due to a decrease in the frequency factor, and that the activation energy increases from ethyl formate to ethyl acetate and then decreases slowly in the series ethyl acetate, ethyl propionate and ethyl *iso*butyrate. On the other hand, the activation energies for ethyl propionate and ethyl *n*-butyrate do not differ from each other. The rate falls greatly from ethyl formate to ethyl acetate and the difference between the rates of ethyl propionate and ethyl butyrate is abnormally large (*cf.* Ref.[4]). The rate decreases only slightly from ethyl acetate to ethyl propionate in the temperature range studied (as calculated from the Arrhenius plot, ethyl propionate hydrolyses more rapidly than ethyl acetate at temperatures below $-3°$ C).

The differences in the rates of hydrolysis can be explained by assuming that the activation energy differences are mainly determined by hyperconjugation and that the differences in the inductive and steric effects appear mainly in the frequency factors. In a previous study [5], it was concluded that the conjugation between the

Table 1. Alkaline hydrolysis of esters in water.

Ester	k l mol.$^{-1}$ sec.$^{-1}$				E cal	log A
	0.00°	20.00°	25.00°*	40.00°		
$H—CO_2Et$	5.07	—	—	—	9.680	8.46
$CH_3—CO_2Et$	0.0177	0.0764	0.109	0.284	11.790	7.68
$CH_3—CH_2—CO_2Et$	0.0170	0.0657	0.0880	0.206	10.590	6.71
$CH_3—CH_2—CH_2—CO_2Et$	0.00906	0.0361	0.0477	0.111	10.660	6.49
$(CH_3)_2CH—CO_2Et$	0.00621	0.0226	0.0300	0.0678	10.170	5.93

* Computed from the Arrhenius equation.

carboxyl carbonyl group and the α,β-unsaturated bond is an important factor determining the activation energy in alkaline ester hydrolysis. As compared with ethyl formate, ethyl acetate contains a methyl group which enters into conjugation with the carboxyl carbonyl group and also possesses weak inductive and steric effects. The ethyl group in the acid part of ethyl propionate possesses stronger inductive and steric effects, but a weaker hyperconjugative effect, than the methyl group in ethyl acetate. The decreased hyperconjugation lowers the activation energy and hence increases the hydrolysis rate, which is in accordance with the fact that the ethyl propionate hydrolyses more rapidly than ethyl acetate at low temperatures. This increase in the hydrolysis rate is opposed by the strengthened inductive and steric effects. In ethyl *iso*butyrate the inductive and steric effects are even larger, but there is no hyperconjugation. If the hyperconjugation alone determined the differences in the activation energies, the activation energy should be the same for both ethyl *iso*butyrate and ethyl formate. Since the observed difference is 490 cal, it must be concluded that also the inductive and steric effects increase the activation energy in some degree.

The hyperconjugation is the same in both ethyl propionate and ethyl *n*-butyrate, and so also are the activation energies. The change in the inductive effect is slight, and hence the observed abnormal fall in the rate is due to a marked steric effect in ethyl *n*-butyrate. The steric effect may evidently be considered to involve geometrical hindrance, since there is no difference in the activation energies. Quantitatively this steric effect is comparable with the difference in the rates of hydrolysis of the methyl and ethyl esters of acids in general. The mean ratios of the rates of both pairs are both approximately 1.8 (see Table 1 and the data of Leimu and Salmi [2]). The decisive influence of the steric effect is also apparent from the observation that the ratio of the rates of hydrolysis of the methyl and ethyl esters increases rapidly as the degree of branching increases in the acid component of the ester [2].

This work was made possible by a grant from the *Finnish Academy*.

1. Tommila, E. and Maltamo, S. *Suomen Kemistilehti* **B 28** (1955) 73.
2. Salmi, E. J. and Leimu, R. *Suomen Kemistilehti* **B 20** (1947) 43.
3. Tommila, E., Koivisto, A., Lyyra, J. P., Antell, K. and Heimo, S. *Ann. Acad. Sci. Fennicae* **A II** (1952) 47.
4. Tommila, E. and Hietala, S. *Acta Chem. Scand.* **8** (1954) 257.
5. Halonen, E. A. *Acta Chem. Scand.* **9** (1955) 1492.

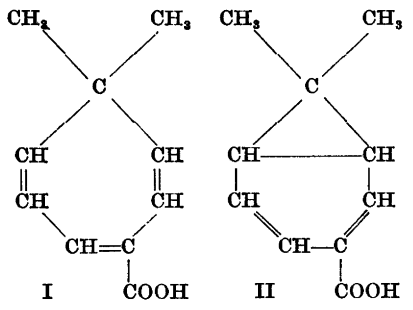
Received March 27, 1956.

Confirmation of the Structure of Thujic Acid by Nuclear Magnetic Resonance

JARL GRIPENBERG

Department of Chemistry, Institute of Technology, Helsingfors, Finland

In a previous paper [1] it was pointed out that there are two likely structures for thujic acid, namely (I) and (II).



Degradation and synthesis [1,2] were definitely in favour of (I), which has therefore been regarded as the correct structure of thujic acid.

Confirmation of this structure by some independent means, preferably by a method not involving chemical reactions appeared, however, to be very desirable. Corey *et al.*[3] have recently solved a similar problem in the eucarvone series by the use of nuclear magnetic reasonance [4].

Dr. J. N. Shoolery of Varian Associates has been kind enough to measure the N M R spectrum of thujic acid methylester, which is reproduced in Fig. 1.

The shift in resonance is expressed as mgauss relative to benzene as zero standard, with an applied magnetic field of 7 050 gauss. There are three different bands of absorption. The very complex one at A is due to the ethylenic hydrogens. The sharp peak at B is due to the ester methyl group, while the *gem*-dimethyl hydrogens absorb at C. There is no absorption at about 35 mgauss, where the tertiary bridge hydrogens of (II) should absorb [3]. Furthermore the area under A is close to that under C, but much greater than that under B, which is also in agreement with structure (I) with five ethylenic hydrogens.

There is thus no doubt that (I) correctly represents thujic acid.

The author wishes to express his thanks to Dr. J. N. Shoolery, Varian Associates, Palo Alto, California, for taking the N M R spectra and for his comments on them.

1. Gripenberg, J. *Acta Chem. Scand.* **5** (1951) 995.
2. Gripenberg, J. *Acta Chem. Scand.* **3** (1949) 1137.
3. Corey, E. J., Burke, H. J. and Remers, W. A. *J. Am. Chem. Soc.* **77** (1955) 4941.
4. Purcell, E. M. *Science* **118** (1953) 431.

Received March 3, 1956.

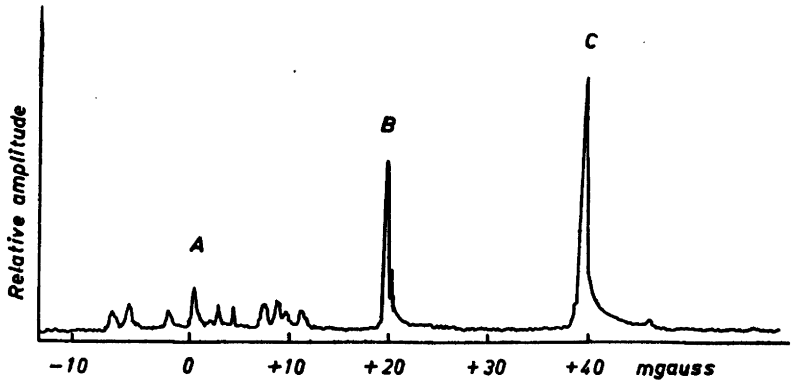


Fig. 1.

A Method for the Determination of the Content of Glycogen-like Polysaccharides in Small Amounts of Bacteria

H. PALMSTIERNA and R. ELIASSON

Chemistry Department I, Karolinska Institutet, Stockholm, Sweden

In order to obtain a survey of the amount of glycogen-like polysaccharides * present in bacterial cells at different times of growth and under different cultivation conditions, it was found desirable to use a less time-consuming and less elaborate method than that previously employed [1,2]. The method described in the following involves no precipitation of the polysaccharides and it is therefore possible to use small amounts of cells. The test organism was *Escherichia coli* B.

Method: Between 5 and 20 mg of lyophilized cells were hydrolysed in 0.2 ml 3 N KOH for two hours in small Pyrex glass test tubes (Length 100 mm, inner diameter 6 mm). The upper end of the test tube was drawn to a capillary in order to avoid losses of fluid. After the alkaline hydrolysis, the pH was adjusted to about 1 with 4 N sulfuric acid and hydrolysed for thirty minutes. Both hydrolyses were performed on a boiling water-bath. The glucose was isolated from the hydrolysate by means of ion-exchangers. The hydrolysate was first passed through Dowex 50 in the H^+-form, and thereafter through Dowex 2 in the acetate-form; both were thoroughly washed. It is necessary to use the ion-exchangers in the order mentioned, since the reverse order seriously affects the yield of glucose. The ion-exchangers were placed in a column between thin layers of Pyrex glass wool. The inner diameter of the column was 6 mm and the length of each of the ion-exchange layers was 90 mm. The mesh size of the ion-exchangers was between 20 and 40. The level of the fluid in the column was kept constant at the top of the ion-exchangers. The hydrolysate was slowly washed through the column. The total volume of the effluent amounted to 15 ml. When required, the volume was reduced by blowing thoroughly filtered air over the fluid, which was heated to between 50 and 60° C. It is necessary to keep the temperature at this high level, since the yield of glucose might otherwise be reduced by bacterial contaminations. The glucose was determined by a modification of Dische's carbazol method [3].

Results. The effluent from the column contained no ninhydrin positive substances, and was free from ultraviolet absorption between 240 and 320 mμ. Ascending paper chromatograms (butanol saturated with water) were performed. Slight traces of ribose were found in most instances. For the same reasons as mentioned previously, the presence of galactose could not be excluded [2].

Forty determination were performed. The results are shown in Table 1.

Table 1.

Sample	Glycogen-glucose in per cent of the dry weight. Precipitation method.	Glycogen-glucose in per cent of the dry weight. Method described in this paper.
A	1.2	1.7 ± .5
B	2.9	3.2 ± .7
C	3.5	3.5 ± .6
D	7.4	7.9 ± .9
E	8.0	8.9 ± 1.2
F	9.3	9.4 ± .7
G	10.1	10.8 ± 1.2
H	15.0	16.2 ± 1.0

As previously shown by the isotope dilution method [2], the values obtained by the precipitation method are about 5 per cent too low.

Discussion. If other bacteria than *E. coli* B are under examination, it is necessary to ascertain that the glucose obtained is substantially free from other carbohydrates. The method is not as accurate as that previously used by the authors, but since the variations in the glycogen content of *E. coli* B are very large, the method described gives useful information. It is easily performed on small amounts of bacteria and is not as time-consuming as methods involving precipitation of the alkalistable polysaccharides.

* For the sake of brevity called glycogen in the following.

1. Palmstierna, H. *Acta Chem. Scand.* **9** (1955) 195.
2. Palmstierna, H. *Acta Chem. Scand.* **10** (1956). *In press.*
3. Gurin, S. and Hood, D. B. *J. Biol. Chem.* **131** (1939) 211.

Received March 27, 1956.

Isolation of ^{32}P-Labeled Phosphoserine from a Yeast Hexokinase Preparation, Incubated with Labeled ATP or Glucose-6-Phosphate

GUNNAR ÅGREN and LORENTZ ENGSTRÖM

Institute of Medical Chemistry, University of Uppsala, Sweden

In earlier communications from this laboratory we reported the incorporation of radioactive inorganic phosphate into phosphoserine isolated from the Schneider protein residues of several rat organs [1]. The maximum incorporation for all organs investigated occurred at approximately three hours after injection of radioactive phosphate [2]. This seemed to infer that some intracellular phosphoproteins may function as transphosphorylating enzymes.

The incorporation of radioactive inorganic phosphate into a new phosphorylated amino acid [3], prepared from the protein of *Lactobacillus casei*, was also compared with the phosphorus uptake of nucleotide and nucleic acid fractions in an attempt to trace the source and the destination of the amino acid phosphorus [4]. However, all these measurements can only give an average value for presumably different kinds of phosphoproteins of different loci within the cell.

As an alternative it seemed of interest to study pure phosphoproteins, as hexokinase or phosphoglucomutase, which are known to be involved in the transfer of phosphorus. The possibility that this transfer might include the formation of an enzyme-phosphate intermediate has been suggested by many authors [5]. Recently this hypothesis received support from the demonstration by Najjar and Pullman [6], that phosphoglucomutase exists in two states, a phosphoenzyme and a dephosphoenzyme. The former transfers phosphate to glucose-1-phosphate or glucose-6-phosphate. Glucose-1,6-diphosphate is formed in the process.

In the present study we have shown the formation of an enzyme -phosphate intermediate in the hexokinase reaction by isolating phosphoserine from the acid hydrolysate of the enzyme, incubated with ^{32}P-labeled ATP [7] in the presence of glucose. In another experiment we also obtained phosphoserine from the enzyme incubated with glucose-6-phosphate isolated from the reaction mixture of the enzyme and AT^{32}P.

The enzyme was purified according to the first six steps of the methods of Berger *et al.*[8] and contained one per cent of glucose *. About 20 mg of this protein was incubated for a few seconds with 1—2 mg ATP, containing about 1—2 mC of phosphorus activity and in the presence of 0.01 M $MgCl_2$. The enzyme was precipitated with 10 % trichloroacetic acid. The protein was hydrolysed and fractionated on a Dowex 50-column according to Ågren *et al.*[1]. The peak eluted after the inorganic phosphate in the expected position of phosphoserine weighed less than 0.1 mg. A part of this material was run through a Dowex 1 formate column according to Busch *et al.*[9] with the addition of non-labeled phosphoserine. The ninhydrin colour from the non-labeled phosphoserine and the activity from the isolated fraction were eluted in the same column volume. Other parts of the activity together with non-labeled phosphoserine were analyzed with one-dimensional paper chromatography using *iso*butyric acid-ammonia and benzene-propionic acid systems. After development of the ninhydrin colour, the paper strips were scanned in the apparatus previously described [2]. The ninhydrin colour from the non-labeled phosphoserine and the activity from the isolated fraction completely agreed.

The trichloroacetic acid centrifugate from the reaction mixture of enzyme and AT^{32}P was run through a Dowex 1 formate column according to Siekevitz and Potter[10], and the column volume containing the radioactive glucose-6-phosphate was incubated with more enzyme solution, con-

* The enzyme was kindly furnished by professor O. Lindberg, Wenner-Gren Institute, Stockholm.

1. Palmstierna, H. *Acta Chem. Scand.* **9** (1955) 195.
2. Palmstierna, H. *Acta Chem. Scand.* **10** (1956). *In press.*
3. Gurin, S. and Hood, D. B. *J. Biol. Chem.* **131** (1939) 211.

Received March 27, 1956.

Isolation of ^{32}P-Labeled Phosphoserine from a Yeast Hexokinase Preparation, Incubated with Labeled ATP or Glucose-6-Phosphate

GUNNAR ÅGREN and LORENTZ ENGSTRÖM

Institute of Medical Chemistry, University of Uppsala, Sweden

In earlier communications from this laboratory we reported the incorporation of radioactive inorganic phosphate into phosphoserine isolated from the Schneider protein residues of several rat organs [1]. The maximum incorporation for all organs investigated occurred at approximately three hours after injection of radioactive phosphate [2]. This seemed to infer that some intracellular phosphoproteins may function as transphosphorylating enzymes.

The incorporation of radioactive inorganic phosphate into a new phosphorylated amino acid [3], prepared from the protein of *Lactobacillus casei*, was also compared with the phosphorus uptake of nucleotide and nucleic acid fractions in an attempt to trace the source and the destination of the amino acid phosphorus [4]. However, all these measurements can only give an average value for presumably different kinds of phosphoproteins of different loci within the cell.

As an alternative it seemed of interest to study pure phosphoproteins, as hexokinase or phosphoglucomutase, which are known to be involved in the transfer of phosphorus. The possibility that this transfer might include the formation of an enzyme-phosphate intermediate has been suggested by many authors [5]. Recently this hypothesis received support from the demonstration by Najjar and Pullman [6], that phosphoglucomutase exists in two states, a phosphoenzyme and a dephosphoenzyme. The former transfers phosphate to glucose-1-phosphate or glucose-6-phosphate. Glucose-1,6-diphosphate is formed in the process.

In the present study we have shown the formation of an enzyme -phosphate intermediate in the hexokinase reaction by isolating phosphoserine from the acid hydrolysate of the enzyme, incubated with ^{32}P-labeled ATP [7] in the presence of glucose. In another experiment we also obtained phosphoserine from the enzyme incubated with glucose-6-phosphate isolated from the reaction mixture of the enzyme and AT^{32}P.

The enzyme was purified according to the first six steps of the methods of Berger *et al.*[8] and contained one per cent of glucose *. About 20 mg of this protein was incubated for a few seconds with 1—2 mg ATP, containing about 1—2 mC of phosphorus activity and in the presence of 0.01 M $MgCl_2$. The enzyme was precipitated with 10 % trichloroacetic acid. The protein was hydrolysed and fractionated on a Dowex 50-column according to Ågren *et al.*[1]. The peak eluted after the inorganic phosphate in the expected position of phosphoserine weighed less than 0.1 mg. A part of this material was run through a Dowex 1 formate column according to Busch *et al.*[9] with the addition of non-labeled phosphoserine. The ninhydrin colour from the non-labeled phosphoserine and the activity from the isolated fraction were eluted in the same column volume. Other parts of the activity together with non-labeled phosphoserine were analyzed with one-dimensional paper chromatography using *iso*butyric acid-ammonia and benzene-propionic acid systems. After development of the ninhydrin colour, the paper strips were scanned in the apparatus previously described [2]. The ninhydrin colour from the non-labeled phosphoserine and the activity from the isolated fraction completely agreed.

The trichloroacetic acid centrifugate from the reaction mixture of enzyme and AT^{32}P was run through a Dowex 1 formate column according to Siekevitz and Potter[10], and the column volume containing the radioactive glucose-6-phosphate was incubated with more enzyme solution, con-

* The enzyme was kindly furnished by professor O. Lindberg, Wenner-Gren Institute, Stockholm.

taining glucose. $MgCl_2$ was added as before. From the hydrolysed enzyme phosphoserine was identified in the same manner as previously described.

Our present method to show that the phosphorus atom is linked to the protein molecule consists in the isolation of a phosphorylated amino acid as phosphoserine from the hydrolysed protein. It therefore seems that the transfer of phosphorus in the hexokinase system is at least a two-step reaction. The phosphorus atom is first transferred from the donator molecule to the enzyme and secondly donated from the enzyme to the acceptor. We therefore consider that our results suggest that an enzyme-phosphate is an intermediate in the hexokinase reaction. Hexokinase and phosphoglucomutase are examples of phosphoproteins functioning as transphosphorylases. It is highly possible that other phosphoprotein-enzymes may be engaged in the transfer of phosphorus in a similar way. This assumption is in line with the previously published high values for the incorporation of radioactive phosphate in the proteins from different cells [3].

This investigation was supported by grants from the *Swedish Medical Research Council* and the *Wallenberg Foundation*.

1. Ågren, G., de Verdier, C.-H. and Glomset, J. *Acta Chem. Scand.* **8** (1954) 503.
2. Ågren, G., de Verdier, C.-H. and Glomset, J. *Acta Chem. Scand.* **8** (1954) 1570.
3. Ågren, G., de Verdier, C.-H. and Glomset, J. *Acta Soc. Med. Upsaliensis* **9** (1955) 30.
4. Ågren, G., de Verdier, C.-H. and Glomset, J. *Acta Chem. Scand.* **9** (1955) 1041.
5. Boyer, P. D. and Harrison, W. H. *Mechanism of enzyme action, Baltimore* 1945, p. 658.
6. Najjar, V. A. and Pullman, M. E. *Science* **119** (1954) 631.
7. Beyer, R. E., Glomset, J. and Beyer, T. *Biochem. et Biophys. Acta* **18** (1955) 292.
8. Berger, L., Slein, M. W., Colowick, S. P. and Cori, C. F. *J. Gen. Physiol.* **29** (1945) 379.
9. Busch, H., Hurlbert, R. B. and Potter, V. R. *J. Biol. Chem.* **196** (1952) 717.
10. Siekevitz, P. and Potter, V. R. *J. Biol. Chem.* **215** (1955) 237.

Received March 28, 1956.

An Absolute Determination of the Rate of the Exchange Reaction between Cadmium Amalgam and Cadmium Cyanide Solutions

STURE FRONÆUS

Department of Physical Chemistry, Chemical Institute, University of Lund, Lund, Sweden

The kinetics and mechanism of the heterogeneous exchange reaction at equilibrium electrode potential between cadmium amalgams and cadmium cyanide solutions containing sodium cyanide in excess was investigated by a radioactive tracer method in a previous work [1]. Preliminary measurements showed that the rate of exchange in this system was not controlled by the diffusion of cadmium in the solution phase, as was the case in perchlorate solutions [2] or in solutions containing cadmium complexes of moderate strength [3].

In order to attain sufficiently high accuracy in the isotopic exchange determinations, the main measurements were performed according to a procedure where the amalgam and the solution were shaken under reproducible conditions. For an activation-controlled exchange process a relationship of the following form should be obtained

$$r = k\, c^{1-\alpha}\, q^{\alpha}\, [CN^-]^{-j(1-\alpha)} \qquad (1)$$

where r denotes the rate of exchange, c the total concentration of cadmium in the solution, q the total concentration in the amalgam and k a constant. The exponent α is also a constant, fulfilling the condition $0<\alpha<1$, and j is the number of cyanide ligands in the complex that predominates in the exchange process. Actually an expression of the form (1) for r was obtained in the investigation with the values $\alpha = 0.34 \pm 0.02$ and $j = 2.2 \pm 0.1$. Thus the measurements indicated that under the existing concentration conditions the exchange reaction is activation-controlled and that the predominating reversible transfer reaction is the following one:

$$Cd(CN)_2 + 2e^-(\text{electrode}) \rightleftharpoons Cd(\text{amalgam}) + 2CN^- \qquad (2)$$

taining glucose. $MgCl_2$ was added as before. From the hydrolysed enzyme phosphoserine was identified in the same manner as previously described.

Our present method to show that the phosphorus atom is linked to the protein molecule consists in the isolation of a phosphorylated amino acid as phosphoserine from the hydrolysed protein. It therefore seems that the transfer of phosphorus in the hexokinase system is at least a two-step reaction. The phosphorus atom is first transferred from the donator molecule to the enzyme and secondly donated from the enzyme to the acceptor. We therefore consider that our results suggest that an enzyme-phosphate is an intermediate in the hexokinase reaction. Hexokinase and phosphoglucomutase are examples of phosphoproteins functioning as transphosphorylases. It is highly possible that other phosphoprotein-enzymes may be engaged in the transfer of phosphorus in a similar way. This assumption is in line with the previously published high values for the incorporation of radioactive phosphate in the proteins from different cells [3].

This investigation was supported by grants from the *Swedish Medical Research Council* and the *Wallenberg Foundation*.

1. Ågren, G., de Verdier, C.-H. and Glomset, J. *Acta Chem. Scand.* **8** (1954) 503.
2. Ågren, G., de Verdier, C.-H. and Glomset, J. *Acta Chem. Scand.* **8** (1954) 1570.
3. Ågren, G., de Verdier, C.-H. and Glomset, J. *Acta Soc. Med. Upsaliensis* **9** (1955) 30.
4. Ågren, G., de Verdier, C.-H. and Glomset, J. *Acta Chem. Scand.* **9** (1955) 1041.
5. Boyer, P. D. and Harrison, W. H. *Mechanism of enzyme action, Baltimore* 1945, p. 658.
6. Najjar, V. A. and Pullman, M. E. *Science* **119** (1954) 631.
7. Beyer, R. E., Glomset, J. and Beyer, T. *Biochem. et Biophys. Acta* **18** (1955) 292.
8. Berger, L., Slein, M. W., Colowick, S. P. and Cori, C. F. *J. Gen. Physiol.* **29** (1945) 379.
9. Busch, H., Hurlbert, R. B. and Potter, V. R. *J. Biol. Chem.* **196** (1952) 717.
10. Siekevitz, P. and Potter, V. R. *J. Biol. Chem.* **215** (1955) 237.

Received March 28, 1956.

An Absolute Determination of the Rate of the Exchange Reaction between Cadmium Amalgam and Cadmium Cyanide Solutions

STURE FRONÆUS

Department of Physical Chemistry, Chemical Institute, University of Lund, Lund, Sweden

The kinetics and mechanism of the heterogeneous exchange reaction at equilibrium electrode potential between cadmium amalgams and cadmium cyanide solutions containing sodium cyanide in excess was investigated by a radioactive tracer method in a previous work [1]. Preliminary measurements showed that the rate of exchange in this system was not controlled by the diffusion of cadmium in the solution phase, as was the case in perchlorate solutions [2] or in solutions containing cadmium complexes of moderate strength [3].

In order to attain sufficiently high accuracy in the isotopic exchange determinations, the main measurements were performed according to a procedure where the amalgam and the solution were shaken under reproducible conditions. For an activation-controlled exchange process a relationship of the following form should be obtained

$$r = k\, c^{1-\alpha}\, q^{\alpha}\, [CN^-]^{-j(1-\alpha)} \qquad (1)$$

where r denotes the rate of exchange, c the total concentration of cadmium in the solution, q the total concentration in the amalgam and k a constant. The exponent α is also a constant, fulfilling the condition $0<\alpha<1$, and j is the number of cyanide ligands in the complex that predominates in the exchange process. Actually an expression of the form (1) for r was obtained in the investigation with the values $\alpha = 0.34 \pm 0.02$ and $j = 2.2 \pm 0.1$. Thus the measurements indicated that under the existing concentration conditions the exchange reaction is activation-controlled and that the predominating reversible transfer reaction is the following one:

$$Cd(CN)_2 + 2e^-(\text{electrode}) \rightleftharpoons Cd(\text{amalgam}) + 2CN^- \qquad (2)$$

Since in the present case there is no transfer of electrons through the rigid part of the electrode double layer but a transfer of cadmium ions free from all ligands, the same process can also be denoted

$$Cd(CN)_2 \rightleftharpoons Cd^{2+}(amalgam) + 2CN^- \quad (3)$$

By electrode impedance measurements, giving the exchange current density i_0 of the transfer step, Gerischer [4] also has arrived at the result that $j \approx 2$ at low values of the cyanide ion excess, though the exponent 0.25 ± 0.02 of q diverges somewhat from our α-value.

In the investigation with the radioactive tracer it was possible to keep the average area of the interface constant, as was indicated by the measurements [1], but, since it was not possible by the method used to determine this area, the value of the constant k in eqn. (1) could not be obtained. However, a comparison between the resultant rate of the exchange r and the exchange current density i_0, measured by Gerischer, is of great interest, and for this reason the present complementary investigation was performed.

The experimental procedure was the same as in the preliminary measurements of the previous investigation [1], *viz.* to let a stream of small amalgam droplets pass at a great velocity through the radioactive cadmium cyanide solution, containing sodium cyanide in excess. For a description of the apparatus used and other experimental details about the exchange measurements the reader is referred to an earlier work [2]. In another paper [3] it was shown how this apparatus was calibrated, so that the surface area of the droplets and the time of contact between the phases was known, and accordingly absolute values of the rate r were obtained.

Since the kinetic law (1) has already been verified, a determination of r for a single set of values of c, q, and $[CN^-]$ is sufficient to obtain the value of the constant k. In the experiments of the present investigation the concentrations $c = 7.0 \times 10^{-3}$ M, $q = 1.2$ M (1 % by weight) and $[CN^-] = 2.7 \times 10^{-2}$ M were used, and the ionic strength was 1 M with sodium perchlorate as an additional electrolyte. The rate of exchange measured was $r = 3.2 \times 10^{-8}$ mole cm^{-2} sec^{-1}. Thus we have

$$r = 1.5 \times 10^{-7}\, c^{0.66}\, q^{0.34}\, [CN^-]^{-0.46} \quad (4)$$

if r is expressed in mole cm^{-2} sec^{-1} and the concentrations in M. From the figures in the paper by Gerischer [4], it is found that for $c = 2 \times 10^{-3}$ M, $q = 2 \times 10^{-2}$ M, and $[CN^-] = 2 \times 10^{-2}$ M and at the ionic strength 5 M with sodium chloride as an additional electrolyte the exchange current density is $i_0 = 0.5 \times 10^{-3}$ A · cm^{-2}. If i_0 is divided by $2F$, we get the rate 0.3×10^{-8} mole · cm^{-2} · sec^{-1} of the transfer reaction (3).

Now, if the expression (4) determined refers to the same partial reaction, we can use eqn. (4) for the calculation of the rate of this step for the last-mentioned values of c, q, and $[CN^-]$, even if the tracer method would possibly have given another kinetic law for the over-all exchange reaction for such a low value of the amalgam concentration q. Then we find $r = 0.4 \times 10^{-8}$ mole · cm^{-2} · sec^{-1}. Of course, this good agreement with the value obtained from i_0 is somewhat changed for varying values of c and q, since the exponents in eqn. (4) are not exactly the same as those found by Gerischer, but in any case the two methods give the same order of magnitude of r. Thus it is conclusively proved that for the ranges of concentrations used in the previous investigation [1] the over-all exchange reaction is controlled by the charge transfer between the phases.

In a paper about the kinetics of electrode processes, Vetter [5] has discussed among other things the transfer reaction (3) above. He assumes that the two cyanide ions form a complex $(CN)_2^{2-}$ without any bond energy (in German "Begegnungskomplex" according to a notation of Weller [6]), which coordinates to the cadmium ion, leaving the amalgam. However, the assumption does not seem very plausible, especially if a corresponding conception is meant to be applicable to the transfer reaction for high values of the cyanide ion excess, where the third complex $Cd(CN)_3^-$ predominates in this step (*cf.* Gerischer [4]).

According to the opinion of the present author it may be assumed that when the "naked" cadmium ion leaves the amalgam, two cyanide ions are coordinated consecutively without an intermediate coordination of water. First after this the more loosely bound water ligands are coordinated, forming an activated, hydrated complex with the central ion in the rigid part of the electrode double layer. For the reverse process, where all ligands are split off, we may assume the same stages, occurring in the reverse order.

Thus, since no other hydrated complex of the system is formed intermediately in the charge transfer reaction, it is justifiable to say that this step proceeds by way of the hydrated complex $Cd(CN)_2$, though in all probability the ligands cannot be coordinated or split off simultaneously.

1. Fronæus, S. and Östman, C. O. *Acta Chem. Scand.* **8** (1954) 961.
2. Fronæus, S. *Acta Chem. Scand.* **7** (1953) 764.
3. Fronæus, S. *Acta Chem. Scand.* **8** (1954) 412.
4. Gerischer, H. *Z. Elektrochem.* **57** (1953) 604.
5. Vetter, K. J. *Z. Elektrochem.* **59** (1955) 596.
6. Weller, A. *Z. physik. Chem.* N.F. **3** (1955) 238.

Received March 29, 1956.

Chemically Induced Mutation and Sterility in Barley

L. EHRENBERG, Å. GUSTAFSSON, and U. LUNDQVIST

Institute for Organic Chemistry and Biochemistry, University, Stockholm; Forest Research Institute, Stockholm, and Institute of Genetics, University, Lund, Sweden

This paper gives some preliminary results from investigations concerning the induction, by chemical means, of mutations in higher plants. The experiments are complementary to treatments of the material with ionizing radiations [1], which seem rather unspecific since they always cause mutation as well as sterility, the latter effect especially at higher ion densities. A variation within wide limits of the linear energy transfer and irradiation conditions gives only small changes as regards relative frequencies of mutation types, possibly except the erectoides case [2]. It was, therefore, our hope that an application of (a) chemically reactive compounds affecting biological materials differently, and (b) biochemically active compounds interfering with processes important to the synthesis of the gene material would, apart from an elucidation of the radiation induced mutation process, increase our possibilities to direct the mutation process.

In treatments of wet tissue with "radiomimetic" chemical agents [3], also when these are specifically nucleotoxic, it is extremely difficult to establish quantitative relationships based on a dosimetry. As compared to radiations, where active ions and radicals are formed anywhere in the tissue, diffusing molecules form gradients of change from outside towards inside of the tissue, cell, or cell nucleus. To some degree such difficulties might be overcome when dry resting seeds, which are in fact very insensitive to toxic agents, are treated with gaseous reactive chemicals. The imbibition of water and, in consequence, at least part of the final steps of the reactions will then follow afterwards. In the present study barley seeds containing 10–11 % H_2O were treated with a gas phase containing ethylene oxide, iodine, or chlorine. — Non-volatile compounds have to be applied in solution. Either resting seeds, or presoaked seeds, the germination process of which had been initiated by soaking in water for 24 hours, were immersed for different times in solutions of the agents studied.

All treatments were done at 20° C. Afterwards the seeds were sown in the field, and the mature plants obtained were analysed for survival, mutation, and sterility according to standard methods (*cf.* Ehrenberg and Nybom [1]). Below, "sterility" is defined as the frequency of spikes with more than 10 % empty spikelets.

Tested compounds; results. The following subdivision as to the expected mode of action can be made (*cf.* Table 1):

(a) *Alkylating agents*, which after radicalization or ionization react with nucleophilic groups, such as amino and ionized acid groups. Effects of *mustards* have been described earlier [1,4]. — *Ethylene oxide*, earlier found mutagenic in other organisms [5,6], was in part given, for 6 days, in the gas phase with 20 % air; in this treatment seeds survive if they contain less than 10 % H_2O; partly presoaked seeds were treated for 2 hours with solutions (0.5 % kills the seeds). — *Formaldehyde*, which, attacking amino and other groups, induces methylene groups and bridges, gives according to Favret [7] mutations in barley. Under Favret's conditions, as well as in presence [6] of H_2O_2 it was found inactive, however, although some sterility appeared.

(b) *Oxidizing agents. Chlorine* (24 h, 80 % being lethal) and *iodine* (saturated vapours, 48 hour's treatment lethal, 24 h used; washing in 10 % KI has to follow treatment) might oxidize (or substitute) almost everything.

Thus, since no other hydrated complex of the system is formed intermediately in the charge transfer reaction, it is justifiable to say that this step proceeds by way of the hydrated complex $Cd(CN)_2$, though in all probability the ligands cannot be coordinated or split off simultaneously.

1. Fronæus, S. and Östman, C. O. *Acta Chem. Scand.* **8** (1954) 961.
2. Fronæus, S. *Acta Chem. Scand.* **7** (1953) 764.
3. Fronæus, S. *Acta Chem. Scand.* **8** (1954) 412.
4. Gerischer, H. *Z. Elektrochem.* **57** (1953) 604.
5. Vetter, K. J. *Z. Elektrochem.* **59** (1955) 596.
6. Weller, A. *Z. physik. Chem.* N.F. **3** (1955) 238.

Received March 29, 1956.

Chemically Induced Mutation and Sterility in Barley

L. EHRENBERG, Å. GUSTAFSSON, and U. LUNDQVIST

Institute for Organic Chemistry and Biochemistry, University, Stockholm; Forest Research Institute, Stockholm, and Institute of Genetics, University, Lund, Sweden

This paper gives some preliminary results from investigations concerning the induction, by chemical means, of mutations in higher plants. The experiments are complementary to treatments of the material with ionizing radiations [1], which seem rather unspecific since they always cause mutation as well as sterility, the latter effect especially at higher ion densities. A variation within wide limits of the linear energy transfer and irradiation conditions gives only small changes as regards relative frequencies of mutation types, possibly except the erectoides case [2]. It was, therefore, our hope that an application of (a) chemically reactive compounds affecting biological materials differently, and (b) biochemically active compounds interfering with processes important to the synthesis of the gene material would, apart from an elucidation of the radiation induced mutation process, increase our possibilities to direct the mutation process.

In treatments of wet tissue with "radiomimetic" chemical agents [3], also when these are specifically nucleotoxic, it is extremely difficult to establish quantitative relationships based on a dosimetry. As compared to radiations, where active ions and radicals are formed anywhere in the tissue, diffusing molecules form gradients of change from outside towards inside of the tissue, cell, or cell nucleus. To some degree such difficulties might be overcome when dry resting seeds, which are in fact very insensitive to toxic agents, are treated with gaseous reactive chemicals. The imbibition of water and, in consequence, at least part of the final steps of the reactions will then follow afterwards. In the present study barley seeds containing 10–11 % H_2O were treated with a gas phase containing ethylene oxide, iodine, or chlorine. — Non-volatile compounds have to be applied in solution. Either resting seeds, or presoaked seeds, the germination process of which had been initiated by soaking in water for 24 hours, were immersed for different times in solutions of the agents studied.

All treatments were done at 20° C. Afterwards the seeds were sown in the field, and the mature plants obtained were analysed for survival, mutation, and sterility according to standard methods (*cf.* Ehrenberg and Nybom [1]). Below, "sterility" is defined as the frequency of spikes with more than 10 % empty spikelets.

Tested compounds; results. The following subdivision as to the expected mode of action can be made (*cf.* Table 1):

(a) *Alkylating agents*, which after radicalization or ionization react with nucleophilic groups, such as amino and ionized acid groups. Effects of *mustards* have been described earlier [1,4]. — *Ethylene oxide*, earlier found mutagenic in other organisms [5,6], was in part given, for 6 days, in the gas phase with 20 % air; in this treatment seeds survive if they contain less than 10 % H_2O; partly presoaked seeds were treated for 2 hours with solutions (0.5 % kills the seeds). — *Formaldehyde*, which, attacking amino and other groups, induces methylene groups and bridges, gives according to Favret [7] mutations in barley. Under Favret's conditions, as well as in presence [6] of H_2O_2 it was found inactive, however, although some sterility appeared.

(b) *Oxidizing agents. Chlorine* (24 h, 80 % being lethal) and *iodine* (saturated vapours, 48 hour's treatment lethal, 24 h used; washing in 10 % KI has to follow treatment) might oxidize (or substitute) almost everything.

Table 1.

Group	Compound	Concn. %	Sterility %	Mutations %	Mutations No. of spikes analysed	Relative frequencies of chlorophyll mutation types, % *albina*	*viridis*	*xantha*	others	Total no. of cases
	Control	—	4	0.054	15 861	35	35	10	20	20
a	N-Mustard (Mac Key [1])	0.7	24	0.25	729	26	52	2	19	42
	Ethylene oxide	80 (gas)	22.1	1.8	989					
	Do (presoaked)	0.12	9.5	0.75	1 872	50	39	3	8	36
	Do Do	0.03	5.7	0.20	2 510					
b	Chlorine	20 (gas)	18.4	0.3	696		100			2
	Iodine	sat. (gas)	6.1	0.6	908		100			5
	Dioxan	1—5	6	0.24	5 500	29	71			14
c	Nebularine (presoaked)	0.025	1.4	0.8	1 293					
	Do	0.05	0	0.1	1 361					
	Do (resting)	0.025	1.6	0.2	1 373	8	85	4	4	26
	Do	0.05	1.5	0.6	1 289					
	Ethoxycaffeine	0.2	4—57	0.1	2 930	33	67			3
X-rays for comparison (1 000 r on resting seeds)		—	15	0.6	∞	51	34	6	10	∞

Sacharoff [8] found the latter compound mutagenic in *Drosophila*. — Due to the role ascribed to peroxides in radiation action, *peroxide*-containing *p-dioxan* was used (resting and presoaked seeds stand 24 h soaking in 5 % solution; 2—8 h used in experiments).

(c) *Purine derivatives* might be supposed to interfere specifically with nucleic acid metabolism. The *8-ethoxycaffeine* was found by Kihlman to break chromosomes in plant roots, the action being coupled to oxidative phosphorylation [9]. *Nebularine*, the tuberculostatic principle from *Clitocybe nebularis*, was used since it was found by Löfgren and Lüning [10] to be purine-9-D-riboside, *i. e.*, a nucleoside not occurring in nucleic acids of higher plants. — Resting or presoaked seeds were treated for 24 h with these compounds, the ethoxycaffeine at different oxygen tensions [9].

(d) In a comprehensive experiment we tested the mutagenicity of *acridines* claimed by D'Amato [11]. When applied as described by this author as well as under other conditions, *acridine orange* and *acriflavine* gave in 20 000 spike progenies only 4 mutation cases, *i. e.*, not different from the spontaneous rate.

When discussing the results (Table 1) it should be remembered that the third generation has not yet been studied. Since we are dealing with agents not tested before in barley, the induction of *Dauer*-modifications or plasmon mutations is not excluded offhand.

The experiments prove with full evidence that sterility (dependent on chromosomal rearrangements) and mutation are not induced by the same mechanism: Ethoxycaffeine gives rise to sterilities corresponding to those obtained by a treatment with up to 6 000 r, without any significant increase of the mutation frequency (at this sterility X-rays give about 4 %

chlorophyll mutations). With the reservations just expressed, the nebularine, on the other hand, gives a fairly high mutation rate without any simultaneous induction of sterility. In addition, this compound gives a distribution of mutation types (*virides* being dominating) quite different from that obtained in other treatments. It seems probable, therefore, that the application of agents disturbing the metabolism (incl. synthesis) of nucleic acids causes effects much more specific than those obtained with radiations.

The alkylating and oxidizing agents are, as expected, more unspecific, causing sterility as well as mutation. Ethylene oxide gives about the same distribution of mutation types as is obtained in X-ray experiments, whereas deviations from this distribution is indicated in other cases.

It should be added that optimum conditions for mutation induction by means of the compounds studied is not yet worked out. Therefore some series are omitted from the table. The fact that nebularine is most active at low concentrations (0.1 % which gives lower mutation frequencies, is omitted) indicates that the action of the compound is only manifested when metabolism is fairly undisturbed. Ethylene oxide, on the other hand, acts proportionally to concentration.

We are indebted to Dr. Nils Löfgren for supplying us with nebularine.

1. Review in: *Acta Agr. Scand.* IV:3 (1954).
2. Ehrenberg, L., Granhall, I. and Gustafsson, Å. *Intern. Conf. Peaceful Uses Atomic Energy* (1955) P/ 793.
3. Haddow, A. *Ibid.* P/ 898.
4. Gustafsson, Å. and Mac Key, J. *Hereditas* **34** (1948) 371.
5. Rapoport, I. A. *Doklady Akad. Nauk SSSR* **60** (1948) 469.
6. Kölmark, G. and Westergaard, M. *Hereditas* **39** (1953) 209.
7. Favret, E. A. *Rev. argentina agron.* **17** (1950) 260.
8. Sacharoff, W. *Biol. Zhur.* **1**:3 (1932) 1.
9. Kihlman, B. *Exptl. Cell Research* **8** (1955) 345, 404.
10. Löfgren, N. and Lüning, B. *Acta Chem. Scand.* **7** (1953) 225; Löfgren, N., Lüning, B. and Hedström, H. *Ibid.* **8** (1954) 670.
11. D'Amato, F. *Caryologia* **3** (1950) 211.

Received April 5, 1956.

ACTA CHEMICA SCANDINAVICA 10 (1956) 495—499

On the Use of the Senses of Taste and Smell in Determining the End Point of an Acid-Base Titration

E. RANCKE-MADSEN and J. A. KROGH

Chemistry Department A, Technical University of Denmark, Copenhagen, Denmark

While the sense of taste is hardly applicable to the fixation of the end point of a titration, the examination reported in the following shows that the sense of smell is quite applicable. Five different smell indicators are mentioned: Sodium butyrate, sodium sulphide, quinoline, pyridine, and ammonium chloride, the first four of which are applicable in the strong acid/strong base titration with an uncertainty on the single determination of 0.2 % or less.

The recognition of the end point of a titration is based either on a visual impression or on a measurement of a physical quantity which is altered at or in the neighbourhood of the equivalence point. In the former case use is made of the sense of sight, but the question forces itself on one as to whether other senses could be used. In ancient chemistry the senses of taste and smell were used as much as possible; in the 18th century it was customary to use the taste of a substance — among other criteria — as a qualitative test, and also the smell of the substance was observed whenever possible.

Also when neutralizing with preparative purposes the sense of taste was used. By way of example may be quoted de Lassone [1], who wished to prepare ammonium acetate: "Lorsque par le mélange successif de l'esprit acéteux et de l'alkali volatile, on est parvenu à une saturation exacte et complète, ce que la saveur et les autres indices font reconnoître."

However, the estimation of the sense of taste as a chemical help decreased, and the use of it became extinct. Thus already Bergmann (quoted from Tabor's German translation of Bergmann's Latin text) [2] wrote as follows in "Meditationen über das System der Fossilien":

"*Geschmack.* Dieser hängt von der Empfindlichkeit der Zunge ab, und ist, wie die Erfahrung lehret, sehr verschieden, denn was bey dem einen die Nerven=Wärzgen mercklich reizet, reizet sie bey einem andern nicht. Man kann also auf diese Eigenschaft nur sehr wenig bauen."

In 1898, however, Richards [3] made the question of the possible applicability of the sense of taste in titrations the subject of a debate. He found

that the taste of a 0.001 N strong acid can be recognized, and that it should therefore be possible to fix the end point of a strong acid/strong base titration with an accuracy of 1—2 %. He reported a few experiments with still better results (greatest deviation 0.9 %).

We have tested the strong acid/strong base titration (25 ml 0.1 M hydrochloric acid with 0.1 M sodium hydroxide and *vice versa*) and found that it is not possible with any certainty to taste the difference between solutions with pH between just under 3 and just under 11 (*i. e.* that OH^- can be tasted in a little lower concentration than H_3O^+). We did find that the end point in such a titration cannot be fixed by means of the sense of taste with deviation of less than 2 or 3 %. Even though individual differences are attached to the sense of taste, it can be established that the taste cannot with any reasonable accuracy be used in this way as indication in the strong acid/strong base titration.

As, for various reasons, any method based upon the taste must be inadequate, we have not wished to continue working in this direction. We may add only that the sole possibility of obtaining results of any reasonable accuracy by means of the sense of taste will probably be to add a taste indicator, *i. e.* a weak acid-base system, in which the weak acid has a different taste from that of the corresponding weak base.

As to the use of the sense of smell in titrations an article on this subject was written in 1913 by Sacher [4]. He titrated *iso*valeric acid with an excess of sodium hydroxide and titrated back with hydrochloric acid, since the appearance of the smell of *iso*valeric acid is more easily recognizable than the disappearance. He further titrated ammonia with hydrochloric acid until the disappearance of the smell of ammonia. He also tried to titrate acetic acid and phenol. In all cases he obtained results that group themselves around the theoretical results, but with rather great deviations (up to 6 %).

We are of the opinion, however, that if the sense of smell has to be used in connection with a titration, it must be done by adding to the titration system a smell indicator, which in an acid-base titration should be a weak acid-base system in which the weak acid has a different smell from that of the corresponding weak base.

As indicators of this type the following substances have been examined: 1) Sodium butyrate, 2) sodium sulphide, 3) quinoline, 4) pyridine, and 5) ammonium chloride. Of all five indicators a weak acid-base system can be made, one component of which is odourless, and the other has a characteristic smell. In all experiments mentioned in the following, titrations were carried out until the appearance of a smell.

0.1 M sodium hydroxide, free from carbon dioxide, was used in the experiments, and the solution was standardized against hydrazine sulphate. Further 0.1 M hydrochloric acid was used (the same hydrochloric acid in the experiments in connection with the first two indicators and a different hydrochloric acid in connection with the last three indicators). *Ca.* 25 ml titrand was used and to this was added 21—22 ml titrator. It was not till then that the indicator was added, and titration was made by dropwise addition of titrator.

1) *Indicator 0.01 M sodium butyrate* ($pK_s = 4.8$ for butyric acid). Titrand NaOH; titrator HCl. The molarity of the hydrochloric acid was found to be

Table 1. Determination of the molarity of a hydrochloric acid by means of titration of standard sodium hydroxide and with a 0.01 M sodium butyrate as smell indicator.

Expt. series	Number of expts.	Quantity of indicator ml	Molarity of HCl (found)	Greatest deviation from mean value	Uncertainty in % on single determination	Uncertainty in % on mean value
I	10	0.10	0.1002	0.0005	0.3	0.10
II	10	0.10	0.1001	0.0005	0.4	0.13
III	10	0.05	0.1002	0.0005	(0.3)	(0.11)
IV	10	0.10	0.10020	0.0003	0.2	0.07

0.10046, if methyl red was used as indicator. (Mean value of 10 determinations; greatest deviation from mean value 0.00010; uncertainty on a single determination 0.07 %; uncertainty on the mean value 0.02 %.)

The results are given in Table 1. In series I a smelling liquid was used for comparison, whereas the other series of experiments were performed without such a liquid. In series III, three of the experiments were unsuccessful owing to the small quantity of indicator; the calculations of uncertainty were carried out for the remaining 7 experiments. Series IV was carried through exactly as No. II, and it is seen that training in the recognition of the smell of butyric acid may increase the accuracy.

Besides, the butyric acid was found to be easily liberated by local excess of a strong acid, which fact may lead to a wrong estimation of the end point; the hydrochloric acid should therefore be added carefully and the addition be accompanied by vigorous shaking.

Conclusion: After some training in the use of the method, 0.10 ml 0.01 M sodium butyrate can be used as a smell indicator in the titration of strong acid/strong base; uncertainty on a single determination *ca.* 0.2 %.

2) *Indicator 0.01 M sodium sulphide* ($pK_s = 7.2$ for hydrogen sulphide). Titrand NaOH; titrator HCl. The molarity of the hydrochloric acid was found to be 0.10068 when bromothymol blue (6.0—7.6 in pH) was used as the indicator. (Mean value of 10 determinations; greatest deviation from mean value 0.00011; uncertainty on a single determination 0.06 %; uncertainty on the mean value 0.02 %.)

The results are given in Table 2. In series I and III, but not in series II and IV, a smelling liquid was used for comparison. It is seen that this comparison liquid is unnecessary. Liberation of hydrogen sulphide in connection

Table 2. Determination of the molarity of a hydrochloric acid by means of titration of standard sodium hydroxide and with a 0.01 M sodium sulphide as smell indicator.

Expt. series	Number of expts.	Quantity of indicator ml	Molarity of HCl (found)	Greatest deviation from mean value	Uncertainty in % on single determination	Uncertainty in % on mean value
I	6	0.10	0.10068	0.00023	0.15	0.06
II	6	0.10	0.10074	0.00025	0.15	0.06
III	6	0.05	0.10079	0.00018	0.15	0.06
IV	6	0.05	0.10077	0.00019	0.14	0.06

Table 3. Determination of the molarity of a hydrochloric acid by means of titration with standard sodium hydroxide and with a 0.01 M quinoline as smell indicator.

Expt. series	Number of expts.	Quantity of indicator ml	Molarity of HCl (found)	Greatest deviation from mean value	Uncertainty in % on single determination	Uncertainty in % on mean value
I	6	0.10	0.1002	0.0004	0.29	0.12
II	6	0.10	0.1002	0.0002	0.19	0.08
III	6	0.20	0.10023	0.00030	0.20	0.08
IV	6	0.20	0.10029	0.00018	0.14	0.06

with local excess of acid during the titration did not take place to any disturbing degree — in contradistinction to what was the case with butyric acid.

Conclusion: Without special training sodium sulphide can be used as a smell indicator in the titration of a strong acid/strong base; uncertainty on a single determination *ca.* 0.15 %.

3) *Indicator 0.01 M quinoline* dissolved in 20 % ethanol ($pK_s = 4.9$ for quinolinium ion). Titrand HCl; titrator NaOH. The results are given in Table 3. A smelling liquid was used for comparison in series I and III, but not in

Table 4. Determination of the molarity of a hydrochloric acid by means of titration with standard sodium hydroxide and with a 0.01 M pyridine as smell indicator.

Expt. series	Number of expts.	Quantity of indicator ml	Molarity of HCl (found)	Greatest deviation from mean value	Uncertainty in % on single determination	Uncertainty in % on mean value
I	6	0.10	0.10019	0.00019	0.14	0.06
II	6	0.10	0.10039	0.00028	0.14	0.06
III	6	0.20	0.10021	0.00025	0.13	0.05
IV	6	0.20	0.10029	0.00023	0.15	0.06

series II and IV; it is seen that this liquid is unnecessary. Liberation of quinoline in local excess of base during the titration did not take place to any disturbing degree. About one half of the experiments with addition of only 0.05 ml 0.01 M quinoline were unsuccessful.

In the titrated solutions pH (electrometrically found) was 6.1 on an average; the deviations from the mean value of pH corresponded well to the deviations of the results from the mean value of these.

Conclusions: Quinoline is quite applicable as a smell indicator in the titration of strong acid/strong base; uncertainty on a single determination *ca.* 0.2 %.

4) *Indicator 0.01 M pyridine* dissolved in water ($pK_s = 5.2$ for pyridinium ion). Titrand HCl; titrator NaOH. The results are given in Table 4. In series I and III a comparison smelling liquid was used; it is seen that this liquid is superfluous. The sense of smell appears to be somewhat dulled by pyridine if the experiments are carried out one immediately after the other. In the experiments reported here the titrations were performed with intervals of about 7 minutes. Eight out of ten experiments with addition of only 0.05 ml 0.01 M pyridine were unsuccessful. In the titrated solutions pH was 6.9 on an average.

Table 5. Determination of the molarity of a hydrochloric acid by means of titration with standard sodium hydroxide and with a 0.01 M ammonium chloride as smell indicator.

Expt. series	Number of expts.	Quantity of indicator ml	Molarity of HCl (found)	Greatest deviation from mean value	Uncertainty in % on single determination	Uncertainty in % on mean value
I	6	0.20	0.1007	0.0001	0.10	0.04
II	6	0.20	0.1012	0.0006	0.49	0.20

Conclusion: Pyridine is quite applicable as a smell indicator in the titration of strong acid/strong base; uncertainty on a single determination *ca.* 0.15 %.

5) *Indicator 0.01 M ammonium chloride* ($pK_s = 9.3$ for ammonium ion). Titrand HCl; titrator NaOH. The results of the experiments are shown in Table 5. In series I a comparison smelling liquid was used, which was not the case in series II. The comparison liquid is useful here, but the sense of smell should be accustomed beforehand to the smell of ammonia. A smaller quantity than 0.20 ml 0.01 M NH_4Cl could not be used; with 0.10 ml most of the experiments were unsuccessful. In the titrated solutions pH was 10.0 on an average.

Conclusion: Ammonium chloride can be used as a smell indicator, even though its applicability does not come up to that of the indicators mentioned above.

Consequently, it is possible to carry out acid-base titrations using smell indicators. In the titration of weak acids or bases an indicator system with a suitable pK_s should be used. The titrations can be carried out in coloured solutions and require here no special apparatus (as *e. g.* ultraviolet radiation when using fluorescence indicators, conductance cells, *etc.*).

REFERENCES

1. de Lassone, *Mem. Acad. Roy. Sci. Paris* **1775** 40.
2. Bergmann, T. *Kleine Physische und Chymische Werke, IV*, Frankfurt am Main 1788, 224–350.
3. Richards, T. W. *Am. Chem. J. Baltimore* **20** (1898) 121.
4. Sacher, J. F. *Chem. Ztg.* **37** (1913) 1222.

Received December 21, 1955.

ACTA CHEMICA SCANDINAVICA 10 (1956) 500—517

Complexes of the 4d- and 5d-Groups

I. Crystal Field Spectra of Rhodium(III) and Iridium(III)

CHR. KLIXBÜLL JØRGENSEN

Chemistry Department A, Technical University of Denmark, Copenhagen, Denmark

In octahedral complexes with six d-electrons and singlet (*i. e.* diamagnetic) ground state, the crystal field theory predicts transitions to two singlet and two triplet levels. Several authors have studied the case of cobalt(III), and in this paper the four bands are found in rhodium(III) and iridium(III) complexes, *e. g.* with six bromide or chloride ligands. The slow aquation of these complexes in HCl and $HClO_4$ is studied, and rhodium(III) aquo ions prepared in $HClO_4$. The solutions of $Rh(OH)_3$ in acids show a high ultraviolet absorption, which disappears slowly, presumably owing to acidolysis of polymer hydroxo complexes. The hexammine and nitro-, iodo-, bromo-, chloro-, hydroxo-, and aquo-pentammine rhodium complexes of S. M. Jørgensen and the oxalato and ethylenediamine complexes exhibit the shifts predicted from the spectrochemical series, as also $Ir(NH_3)_5Cl^{++}$ and $Ir\ en_3^{+++}$. The relative intensities of singlet and triplet transitions are explained by the deviations from the Russell-Saunders coupling, which are important in the heavy atoms. Later papers of the series will discuss why the concept of molecular orbitals is compatible with the approximate validity of the electrostatic model using $(E_1 - E_2)$ as empirical parameter.

Nearly all the applications of the crystal field theory [1–17] to the absorption spectra of the complexes with partly filled d-shells have concerned the first transition group with 3d-electrons. The $4d^3$-system molybdenum(III) in $MoCl_6^{---}$ was investigated by Schmidt [18] who found that the energy differences in the 4d-case are *inter alia* larger than in the 3d-case. Similar conclusions were drawn by Orgel [13] from qualitative observations of the colours of the platinum group complexes, compared to cobalt(III). In the present paper the complexes of rhodium(III) and iridium(III) will be compared to the diamagnetic cobalt(III) complexes, which are all regularly octahedral. The ground state [6, 9–11] is ${}^1\Gamma_1$ from the closed shell configuration γ_5^6, and the next electron distribution $\gamma_5^5\gamma_3$ has the four levels ${}^3\Gamma_4$, ${}^3\Gamma_5$, ${}^1\Gamma_4$ and ${}^1\Gamma_5$. All authors agree that the two relatively strong bands with $\varepsilon \sim 100$ are due to the transitions to ${}^1\Gamma_4$ and ${}^1\Gamma_5$. It is not yet certain which of the bands corresponds to ${}^1\Gamma_4$, but the theory of Tanabe and Sugano [10] with pure 3d-configura-

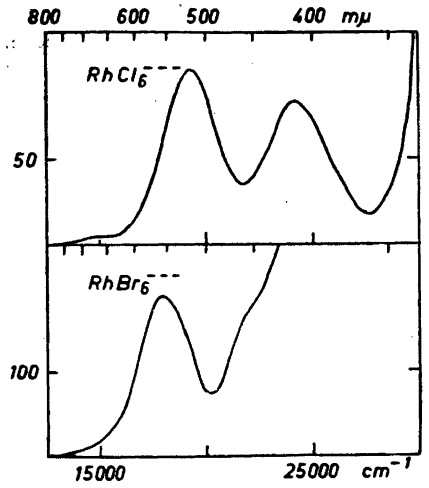


Fig. 1. Absorption spectra of hexachloro- and hexabromo-rhodium (III) ions.

From 0.01 M to 0.3 M Na_3RhCl_6 in 4 M HCl and H_2O, immediately measured. 0.01 M $RhBr_6^{---}$ in 4M HBr.

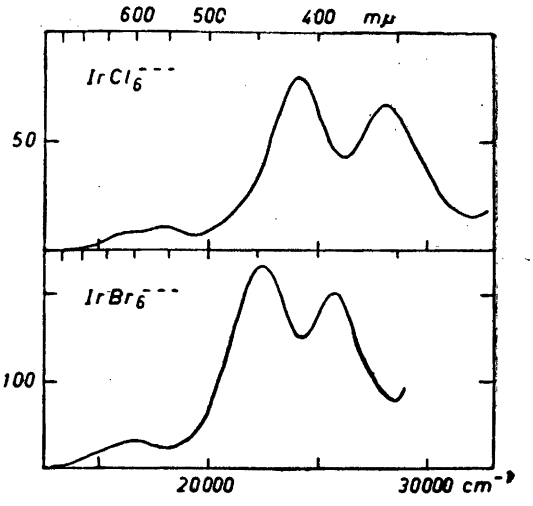


Fig. 2. Absorption spectra of hexachloro- and hexabromo-iridium (III) ions.

From 0.01 M to 0.1 M K_3IrCl_6 in 4 M HCl and H_2O, immediately measured. 0.005 M to 0.015 M $IrBr_6^{---}$ in 4 M HBr.

tions imply that it is the band with lowest wavenumber. The present author [8] and Kondo [10] have found a weak band with $\varepsilon \sim 0.4$ of $Co(NH_3)_6^{+3}$ and $Co\,en_3^{+3}$ in the far red. This must be due to either $^3T_4$ (which has the lowest energy [10]) or $^3T_5$. This band is found here with relatively higher intensity in rhodium(III) and iridium(III) complexes.

HEXACHLORO- AND HEXABROMO-COMPLEXES

Fig. 1 gives the absorption spectra of $RhCl_6^{---}$ and $RhBr_6^{---}$, and Fig. 2 those of $IrCl_6^{---}$ and $IrBr_6^{---}$, while Tables 1 and 2 give the wavenumbers, wavelengths, and molar extinction coefficients of the maxima [19] and the half-widths and oscillator strengths of the bands [16, 19].

Samuel and Uddin [20] have measured $RhCl_6^{---}$ in H_2O (partly aquated, with maxima at 503 and 393 mμ), in a saturated solution of NaCl (at 520 and 409 mμ, nearly as here) and in saturated KBr (at 540 and 420 mμ) probably transformed into bromo complexes. Babaeva [21] has found maxima at 499 and 390 mμ of $RhCl_6^{---}$ and at 480, 418 and 359 mμ of $IrCl_6^{---}$. The first complex must be aquated, while the second is slightly oxidized. As discussed in the next paper of this series, $IrCl_6^{--}$ has 40 times higher bands than $IrCl_6^{---}$. Inamura and Kondo [22] have measured $IrCl_6^{---}$ and several other iridium(III) complexes.

It is seen from Figs. 1 and 2 that the second band is lower than the first in all four complexes. According to C. E. Schäffer of this laboratory, similar be-

Table 1. Absorption bands of rhodium(III) complexes.

Wavelength λ_n wavenumber ν_n and molar extinction coefficient ε_n of each maximum, halfwidths $\delta(-)$ towards smaller and $\delta(+)$ towards higher wavenumbers, and the oscillator strength P of each band [19]. Transitions from $^1\Gamma_1$ to one of the levels $^3\Gamma_4$ or $^3\Gamma_5$ are marked (a) and (b) and from $^1\Gamma_1$ to $^1\Gamma_4$ and $^1\Gamma_5$ is marked (c) and (d).

		λ_n mμ	ν_n cm^{-1}	ε_n	$\delta(-)$ cm^{-1}	$\delta(+)$ cm^{-1}	$P \cdot 10^{-5}$
$RhBr_6^{---}$	(c)	553	18 100	190	1 500	1 400	250
	(d)	450	22 200	180	—	—	250
$RhCl_6^{---}$	(a)	680	14 700	3	1 200	—	3
	(c)	518	19 300	102	1 500	1 500	140
	(d)	412	24 300	82	1 600	1 900	130
$Rhox_3^{---}$	(a)	520	19 200	8	1 000	—	8
	(c)	398	25 100	290	2 000	—	540
	(d)	333	30 000	—	—	—	—
$Rh(H_2O)_6^{+++}$	(c)	393	25 500	47	2 600	—	110
	(d)	305	32 800	55	3 000	—	140
$Rh(NH_3)_5I^{++}$	(c_1)	416	24 100	270	2 100	—	700
	(c_2)	388	25 800	230	—	—	
	(d?)	278	36 000	3 200	2 500	—	7 400
$Rh(NH_3)_5Br^{++}$	(a)	424	23 600	25	1 100	—	25
	(c)	359	27 800	122	2 000	2 600	260
$Rh(NH_3)_5Cl^{++}$	(c)	349	28 700	100	2 000	2 600	210
	(d)	277	36 100	103	2 800	2 900	270
$Rh(NH_3)_5OH^{++}$	(c)	321	31 200	124	2 800	—	500
	(d)	278	36 000	108	—	—	
$Rh(NH_3)_5H_2O^{+++}$	(c)	316	31 600	105	2 800	—	260
	(d)	263	38 100	89	—	2 800	230
$Rh(NH_3)_6^{+++}$	(c)	306	32 700	135	2 300	—	300
	(d)	256	39 100	100	—	2 700	250
$Rhen_3^{+++}$	(c)	301	33 200	210	2 400	—	480
	(d)	253	39 600	190	—	—	460
$Rh(NH_3)_5NO_2^{++}$	(c)	296	33 800	330	3 000	—	900
	(d?)	246	40 600	1 030	3 400	—	3 200

Table 2. Absorption bands of iridium(III) complexes. Nomenclature as in Table 1.

		λ_n mμ	ν_n cm^{-1}	ε_n	$\delta(-)$ cm^{-1}	$\delta(+)$ cm^{-1}	$P \cdot 10^{-5}$
$IrBr_6^{---}$	(b)	597	16 800	27	2 200	1 500	43
	(c)	447	22 400	232	1 800	1 700	370
	(d)	387	25 800	198	1 500	2 000	320
$IrCl_6^{---}$	(a)	615	16 300	7.5	1 200	800	7
	(b)	560	17 900	10	900	1 500	11
	(c)	415	24 100	76	1 800	—	125
	(d)	356	28 100	64	—	2 100	120
$Ir(NH_3)_5Cl^{++}$	(b)	360	27 800	10	1 800	—	17
	(c)	286	35 000	71	3 500	—	230
$Ir\,en_3^{+++}$	(b)	302	33 100	28	2 200	—	57
	(c)	249	40 200	170	2 800	—	400

haviour is found for nearly all chromium(III) and cobalt(III) complexes except the aquo ions and a few others. The small, spin-forbidden bands are discussed below in a special section. In the tables, the two transitions to the triplet levels are denoted a and b, while the stronger transitions to singlet levels are denoted c and d with increasing wavenumber.

THE AQUATION OF HEXACHLORO-COMPLEXES

It has been known for many years that rhodium(III) occurs in brownish-red and orange complexes containing less chloride than the raspberry-red $RhCl_6^{---}$. Thus, Meyer and Kawczyk [22] recognized the non-ionized red $RhCl_3(H_2O)_3$ and the yellow ion $Rh(H_2O)_6^{+++}$ in solutions of $Rh(OH)_3$ in HCl, and these authors stressed the analogy with the chromium complexes $Cr(H_2O)_6^{+++}$, $CrCl(H_2O)_5^{++}$, and $CrCl_2(H_2O)_4^{+}$ investigated by N. Bjerrum [24]. Delépine [25, 26] studied the reversible transformations of $RhCl_6^{---}$ to $RhCl_5(H_2O)^{--}$ and $IrCl_6^{---}$ to $IrCl_5(H_2O)^{--}$.

The chloro complexes of the platinum metals are often assumed to have high formation constants [27]. Even if they are robust, *i. e.* their reaction velocities are very low, they seem to have rather small formation constants, at least for the last chloride ligands. The latter effect is partly due to statistical reasons and to the electrostatic part of the residual effect [28].

Table 3 gives the wavelengths of the maxima, as well as points with half the maximum value of ε, and minima of the absorption spectra of $RhCl_6^{---}$ in 1 M HCl and 1 M $HClO_4$ as function of time at room temperature 18 ± 2° C. It is seen that the two absorption bands move towards shorter wavelengths, corresponding to the exchange of chloride with water. In 1 M HCl, a steady state seems to be reached within some weeks, while the reaction continues in 1 M $HClO_4$ where the total chloride concentration is due only to the original

Table 3. The aquation of $RhCl_6^{---}$.

	$\lambda\left(\varepsilon = \frac{\varepsilon_1}{2}\right)$	λ_{max}	ε_1	λ_{min}	λ_{max}	ε_2	$\lambda\left(\varepsilon = \frac{\varepsilon_2}{2}\right)$	λ_{min}
6 M HCl:								
immediately	561	518	100	460	412	81	381	361
7 days after	560	519	100	460	411	81	382	362
60 days after	560	518	100	459	411	81	382	360
4 M HCl:								
9 months after	559	513	101	457	410	90	380	360
1 M HCl:								
2 minutes after	559	513	105	453	405	99	376	355
4 minutes after	556	510	104	453	406	101	376	357
12 minutes after	554	508	103	451	402	105	375	354
2 days after	545	495	92	441	392	101	362	346
14 days after	541	494	90	439	391	99	361	348
28 days after	541	494	89	441	391	98	362	347
57 days after	541	495	90	440	392	97	362	348
1 M $HClO_4$:								
2 minutes after	559	513	102	457	410	95	379	360
8 minutes after	555	510	101	452	404	102	375	355
10 minutes after	552	508	101	451	403	104	375	355
120 minutes after	548	500	94	414	396	101	368	350
2 days after	537	490	89	438	390	100	361	344
14 days after	529	481	79	431	384	90	351	341
28 days after	525	478	79	426	380	90	349	339
57 days after	526	477	79	425	379	89	—	344

Table 4. The aquation of $IrCl_6^{---}$.

	$\lambda\left(\varepsilon=\frac{\varepsilon_1}{2}\right)$	λ_{max}	ε_1	λ_{min}	λ_{max}	ε_2	$\lambda\left(\varepsilon=\frac{\varepsilon_2}{2}\right)$
1 M HCl:							
2 hours after	448	413	79	383	356	66	330
4 days after	444	403	87	374	346	91	320
20 days after	440	398	83	360	340	87	316
1 M $HClO_4$:							
10 minutes after	449	415	76	380	355	64	331
4 days after	445	402	85	372	344	90	—
30 days after	438	395	79	366	338	85	—

0.018 M Na_3RhCl_6. In 6 M HCl, there seems to be no change in a month, and a stock solution in 4 M HCl, which has been stored for nine months, is not more aquated than the solution in 1 M HCl after 3 minutes. The reciprocal process of $Rh(OH)_3$ dissolved in 1 M HCl is extremely slow at room temperature, and even by boiling with 4 M HCl the colour is only changed from yellow to orange after 10 minutes.

It is seen from Table 3 that by the aquation the second maximum increased strongly, while the first is somewhat decreased. It is interesting to note that the halfwidths of the bands are not greatly increased. Generally, a mixture of several complexes tends to have higher halfwidths, *i. e.* the bands are blurred out. In this particular case, the reaction rates for expelling chloride ions, k_{-6}, k_{-5}, ... seem to be highly decreasing with decreasing number of chloride ligands at constant pH. Thus, the system may contain mainly two complexes at the same time, as it gives not so levelled a spectrum as a mixture of many components. Definite maxima of $RhCl_n(H_2O)_{6-n}^{3-n}$, have not yet been assigned but if the maxima are a linear function of n, *e. g.* their wavenumber

$$\nu = \frac{n}{6}\nu(RhCl_6^{---}) + \frac{6-n}{6}\nu(Rh(H_2O)_6^{+++}) \qquad (1)$$

then the steady state obtained in 1 M HCl corresponds to $n \doteq 4.4$ from the first band and 4.5 from the second, while the state in 1 M $HClO_4$ after four weeks corresponds to $n = 3.5$ and 3.7.

Sundram and Sandell [29] have shown that the four first consecutive formation constants of palladium(II) with Cl^- are higher than 500, while the fifth and sixth constants are about 1. Palladium(II) is strongly tetragonal [12] analogously to Cu(II) and has probably anomalously high constants for the four first ligands, while the next two should be much more loosely bound. In the regular octahedral Rh(III), the constants were expected to be more nearly equal, but owing to the higher external charge, higher affinity for halide ions would be predicted than for Pd(II). However, the sixth formation constant in the rhodium(III)-chloride system cannot be larger than 0.5. The enhanced stability of $RhCl_6^{---}$ in stronger HCl can be ascribed to the activity conditions in this medium [30]. Mr. C. E. Schäffer has kindly pointed out to me that the crystal field stabilization [12] is negative for anion complexes with less crystal field strength than the aquo ions. Thus, each of the six consecutive

formation constants of $RhCl_6^{---}$ should be decreased by a factor 10^5 of this cause. However, this large effect is probably somewhat counter-acted by intermixing of other molecular orbitals than the 4d-electrons, *viz.* the 5s- and 5p-orbitals.

Table 4 shows that $IrCl_6^{---}$ is also slightly aquated in 1 M HCl or 1 M $HClO_4$ during some weeks. In stronger HCl, the ion is either stable or much more slowly reacting. In 10 M HCl, a 0.013 M K_3IrCl_6 was changed in five days from the pale olive-green colour to brownish red. This was due to oxidation to $IrCl_6^{--}$, the spectrum of which demonstrated the presence of 0.0001 M. As discussed in the experimental section, ascorbic acid reduces momentaneously iridium(IV). The intensity of the second band of $IrCl_6^{---}$ increases also during the aquation, but here the formation of hydroxo complexes cannot be excluded as easily as in the case of rhodium(III). Delépine [25] described the curious change of visible colour of $IrCl_6^{---}$ with increasing concentration: from lemon yellow over olive-green and reddish brown to black. The spectra were measured of several concentrated solutions in H_2O, which are only slowly aquating. $IrCl_5(H_2O)^{--}$ is more brownish yellow [25]. A similar effect of the sensitivity of the eye is observed with $RhBr_6^{---}$, which changes from greyish green to cherry red by increasing concentration or by use of tungsten light in the place of daylight. Two or more absorption bands of different intensity or with nearly complementary colours produce this type of dichroism.

THE HYDROXO AND AQUO COMPLEXES OF RHODIUM(III)

Analogously to the behaviour [31] of chromium(III), the exchange reactions of rhodium(III) complexes are highly catalyzed by hydroxyl ions.* Thus, $RhCl_6^{---}$ and the other chloro complexes form purple intermediates and after some minutes a yellow precipitate of $Rh(OH)_3$. This precipitate is weakly amphoteric and dissolves in NaOH with pale yellow colour. The weaker base $BaCO_3$ precipitates $Rh(OH)_3$ quantitatively by boiling.

Moderately strong acids dissolve the hydroxide to yellow solutions, which can be assumed to contain the hexaaquo ion. Fig. 3 shows a titration curve of a 0.01 M Rh(III) in 1 M $NaClO_4$ with NaOH and $HClO_4$. This preliminary experiment shows that pH is a reversible function of added and consumed amounts of hydrogen ions per Rh. The hydroxide is seen to be soluble in one equivalent of hydrogen ions, as also found by Grube and Kesting [32]. The pK for this process is 5.0, and the acid product formed must be $Rh(OH)_2(H_2O)_4^+$ or some polymer with lower content of water. It cannot be seen from the curve whether the di-hydroxo complex takes up further hydrogen ions **, but in any case pK is less than 2.5.

Thus, it is useful to study the absorption spectra of rhodium hydroxide, dissolved in 0.01 M—10 M $HClO_4$. A solution of 0.015 M Rh in 0.06 M $HClO_4$

* However, preliminary experiments seem to show that the aquation of $RhCl_6^{---}$ has the same velocity in 0.1 M as in 1 M HCl.

** The hexaaquo ion does not seem to be a very strong acid, since the aqueous solution of $CsRh(SO_4)_2$, 12 H_2O is only weakly acidic, according to Krauss and Umbach[62]. The electric conductance of the hexaaquo ion is of the same magnitude [23] as that of $Cr(H_2O)_6^{+++}$.

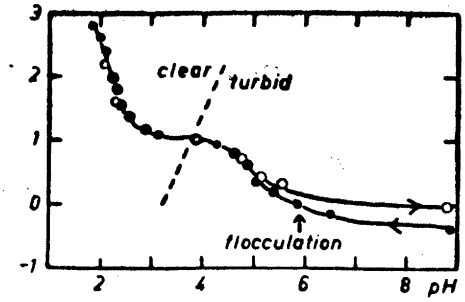


Fig. 3. Titration curve of rhodium (III) hydroxide in 1 M $NaClO_4$ at 20° C. 0.01 M Rh.

pH as function of added hydrogen ions (or consumed hydroxyl ions) per rhodium atom. Empty circles titration from acid range with NaOH and filled circles titration from alkaline range with $HClO_4$. Turbidity appears at pH over 3.8 and disappears below this value, marked on the figure.

was measured and $HClO_4$ added in small quantities until a concentration of 0.4 M was reached. Fig. 4 gives the nearly identical absorption spectra of these two solutions. This might have been an argument for the two first pK-values of $Rh(H_2O)_6^{+++}$ being less than 0.3. But when the spectrum was measured two days later (the original operations lasted two hours), the high absorption in the near ultraviolet was somewhat decreased, and much more so after 12 days. As seen in Fig. 4, a similar preparation from $BaCO_3$ + $Rh(OH)_3$ exhibited similar properties. Since the reactions between monomeric hydroxo complexes and hydrogen ions presumably are very fast, the high absorption below 400 mμ is probably due to a hydroxo complex with at least two rhodium atoms. This can be compared with the dimeric $Fe(OH)_2Fe^{+4}$ found by Mulay and Selwood [33], which also has a strong electron transfer spectrum at lower wavenumbers than $FeOH(H_2O)_5^{++}$. Many rhodium(III) complexes have electron transfer spectra below 300 mμ, *e. g.* $RhCl_6^{---}$ has a shoulder at 242 mμ with $\varepsilon \sim 14\,000$ (it is decreased to 7 000 at 270 mμ). In strongly alkaline solution, the polymer hydroxo complexes seem to disappear — two bands of ordinary intensity are observed at 415 and 326 mμ.

The high absorption in the ultraviolet of hydroxo complexes can hardly be due to higher oxidation states of rhodium, since ascorbic acid has no influence, except reducing a trace of iridium(IV) with absorption at 480 mμ. If rhodium (III) is oxidized in alkaline solution, blue solutions of Rh(VI) and green of Rh(IV) can be obtained, as studied by Grube and Autenrieth [34]. The present author has measured the green solution in 1 M $HClO_4$ and found a broad absorption band around 770 mμ. *Cf.* the measurements by Ayres [64].

If the solution in 0.4 M $HClO_4$ mentioned above is added to stronger $HClO_4$, only small changes are observed, but the strong absorption limit decreases faster in 5 M $HClO_4$. If the solutions are boiled, the second crystal field band appears as a shoulder ~320 mμ. The best way found to eliminate the polymers is to boil Na_3RhCl_6, 12 H_2O with 5 M $HClO_4$ for half an hour. The hydrochloric acid is evaporated, and the yellow solution exhibits two distinct

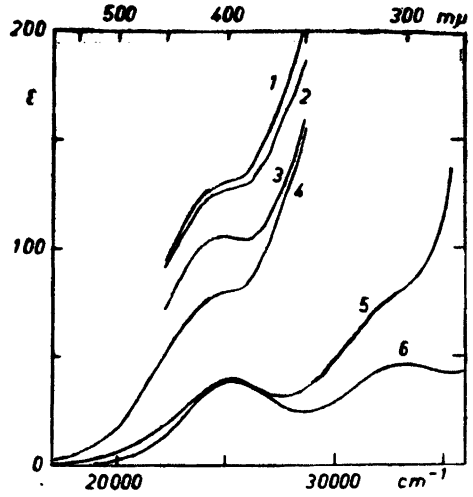


Fig. 4. Absorption spectra of aquo and hydroxo complexes of rhodium (III).

Curve 1. 0.015 M Rh in 0.06 M $HClO_4$.
Curve 2. 0.015 Rh in 0.4 M $HClO_4$, immediately measured.
Curve 3. The solution of curve 2 after two days.
Curve 4. 0.01 M Rh in 2 M $HClO_4$, from $Rh(OH)_3$ precipitated by $BaCO_3$.
Curve 5. The solution of curve 4 after longer time of boiling.
Curve 6. 0.015 M Rh in 1 M $HClO_4$, from Na_3RhCl_6 boiled with $HClO_4$.

crystal field bands at 393 and ~305 mμ (Fig. 4) when diluted to 1 M $HClO_4$. It is highly probable that these maxima correspond to $Rh(H_2O)_6^{+++}$. The half-width of the first band is not very large, and the position in the spectrochemical series is that predicted (Table 1) as compared to $Rhox_3^{---}$ with the maximum at 398 mμ; and the sulphato complexes (prepared from metal and $HNO_3 + H_2SO_4$ boiled nearly down) with maximum at 401 mμ and a shoulder ~320 mμ.

It has not been possible by similar methods to find the crystal field bands of $Ir(H_2O)_6^{+++}$, which most likely is a strong acid. If K_3IrCl_6 is boiled with $HClO_4$, black-red K_2IrCl_6 precipitates at first, owing to oxidation. It redissolves with bluish purple colour, which does not change by dilution of the cooled solution to 1 M $HClO_4$. This can be reduced by ascorbic acid, except for small precipitate of blue IrO_2, to a straw-yellow solution. This solution has only steeply increasing absorption in ultraviolet, as $Irox_3^{---}$ discussed below. Marino [35] prepared alums of iridium(III) and found yellow crystals and solutions. These are oxidizable by air to a purple colour, but can be reduced with H_2S. This reagent precipitates the solution in 1 M $HClO_4$ mentioned above.

TRIS(OXALATO) COMPLEXES

The orange $Rhox_3^{---}$ and the yellow $Irox_3^{---}$ have been much studied, owing to their optical activity and extreme robustness. Lifschitz and Rosenbohm [36] found that $Rhox_3^{---}$ has a low band at 25 000 and a higher band at 35 000 cm^{-1}.

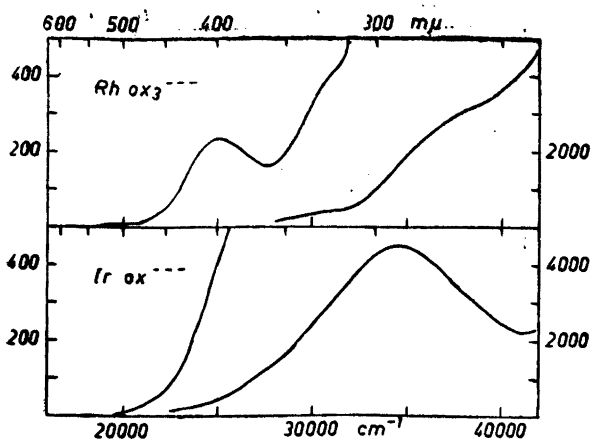


Fig. 5. Absorption spectra of tris-oxalato complexes of rhodium (III) and iridium (III).

0.1 M $Rhox_3^{---}$ in 0.6 M K_3ox, warmed at 100° C for 4 hours, and subsequently diluted. 0.01 M $Irox_3^{---}$ from similar method, and 0.0005 M to 0.02 M K_3Irox_3 from Professor Marcel Delépine.

Fig. 5 shows that the first band is the first crystal field band, while the other is a strong electron transfer band, as expected of an oxalato complex. The second crystal field band can be seen as a shoulder on the red side of this band. Delépine [37] has described the extremely slow reactions of $IrCl_6^{---}$ with one, two, and three oxalate ions. The third consecutive reaction takes ten hours at 130° C. Fig. 5 gives the spectrum of a solution which contains mainly $Irox_3^{---}$. It has also high absorption in the ultraviolet, but a shoulder can be observed at 360 mμ. This is a very reasonable place for the first crystal field band estimated from the value for $Rhox_3^{---}$ and the hypsochromy of iridium(III) complexes compared to rhodium(III).

HEXAMMINE AND PENTAMMINE COMPLEXES

S. M. Jørgensen [38] found an analogy to the chromium(III) and cobalt(III) ammine complexes in the rhodium(III) complexes, and prepared the hexammine and iodo-, bromo-, chloro-, and nitro-pentammine complexes used for this study. Palmær [39] studied the similar iridium(III) complexes, of which only $IrCl(NH_3)_5^{++}$ is examined here. The aquopentammine rhodium(III) salt, which with base gives the hydroxopentammine ion, was made from one of S. M. Jørgensen's preparations as a perchlorate by Brønsted and Volqvartz [40]. These authors found $pK = 6.3$.

Fig. 6 gives the spectra of the rhodium(III) complexes. The hexammine is remarkable by its very deep minimum at 220 mμ, which shows the absence of both an electron transfer spectrum and of impurities. The two high bands resemble very much the spectrum of $Co(NH_3)_6^{+++}$, displaced towards higher wavenumbers, and the first band is highest as in $RhCl_6^{---}$.

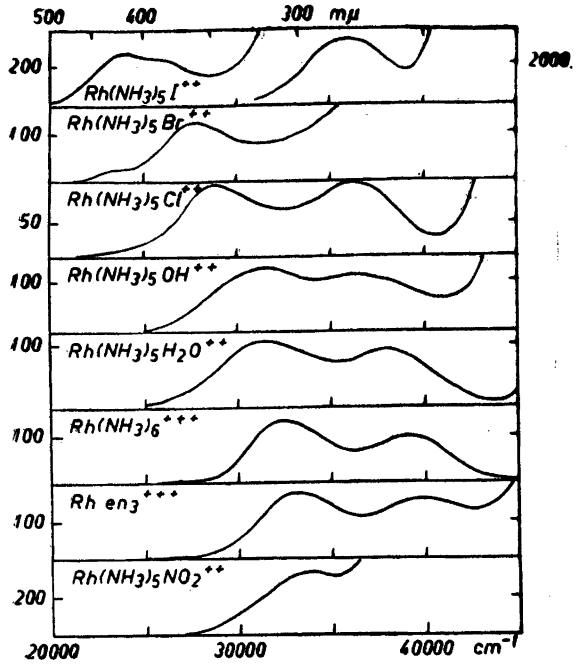


Fig. 6. Absorption spectra of hexammine and pentammine complexes of rhodium (III).

0.001 M to 0.01 M $[Rh(NH_3)_5I]Cl_2$ in H_2O.
0.01 M $[Rh(NH_3)_5Br]Br_2$ in H_2O.
0.01 M $[Rh(NH_3)_5Cl]Cl_2$ in H_2O.
0.01 M $[Rh(NH_3)_5H_2O](ClO_4)_3$ in 0.1 M Na_2CO_3 (forming $Rh(NH_3)_5OH^{++}$) and in 0.05 M $HClO_4$.
0.01 M $[Rh(NH_3)_6]Cl_3$ in H_2O.
0.008 M $Rh\ en_3^{+++}$ in 0.1 M en.
0.003 M $[Rh(NH_3)_5NO_2]Cl_2$ and 0.06 M $[Rh(NH_3)_5NO_2](NO_3)_2$ in H_2O.

$Rh(NH_3)_5H_2O^{+++}$ shows the same displacement towards lower wavenumbers as all "roseo" salts, compared to "luteo" salts, and $Rh(NH_3)_5OH^{++}$ has a smaller distance between the two bands, as usually found. The halidopentammine complexes were expected to have tetragonal splittings, since the two ligands are so distant in the spectrochemical series [14]. It cannot be excluded that the first band of $RhCl(NH_3)_5^{++}$ is slightly split by tetragonal field effects, producing the flat minimum between the two bands as in $Rh(NH_3)_5OH^{++}$. The second band is masked by the electron transfer spectrum in $RhBr(NH_3)_5^{++}$ and $RhI(NH_3)_5^{++}$. In the former ion, a weak shoulder is observed on the red side of the first band, while the shoulder is larger on the blue side in the latter case. The band in the bromo complex is presumably one of the triplet transitions which are intermixed with the strong singlet transitions [16]. If the double band in the iodo complex is not due to a similar intermixing, it is a

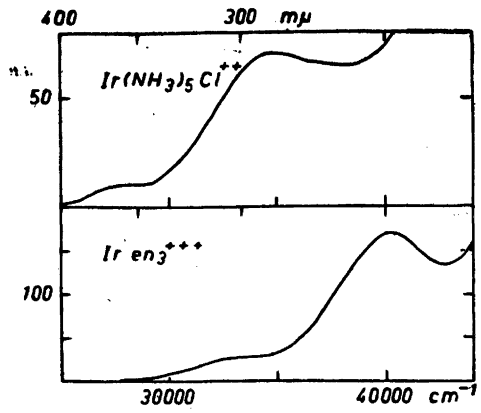


Fig. 7. Absorption spectra of chloropentammine- and tris(ethylenediamine)iridium (III) ions.

0.015 M $[Ir(NH_3)_5Cl]Cl_2$ and 0.004 M $[Iren_3]Br_3$, $2H_2O$ in H_2O, from J.-P. Mathieu's preparations.

genuine tetragonal splitting. But the theory for this splitting [4, 7, 14, 17] is not easy to correlate with the observations.

The ammine complexes of rhodium(III) are exceedingly robust, as shown by Christiansen and Asmussen [41], who in nearly all cases found the salts prepared fifty years before by S. M. Jørgensen undecomposed. The halide ions in the pentammine complexes exchange very slowly with water and even with hydroxyl ions, as found to a higher degree for iridium(III) pentammines by Palmær [39] and Lamb and Fairhall [42].

It has been assumed by Grünberg [43] that $Rh(NH_3)_6^{+++}$ is a weak acid with $pK \sim 11.2$, forming the amidopentammine complex $Rh(NH_2)(NH_3)_5^{++}$. The present author has measured $Rh(NH_3)_6^{+++}$ in 5 M and 1 M NaOH and $Rh\ en_3^{++}$ and $Rh(NH_3)_5OH^{++}$ in 1 M NaOH and found no observable deviation from the ordinary spectrum; especially are the band maxima displaced less than 1 mμ. Since the amido complexes presumably would be displaced much more towards the red, the pK for their formation seems to be > 15, *i. e.* they are not formed to a high degree in any aqueous solution. There is evidence [44] from reaction kinetics that the base hydrolysis of cobalt(III) complexes proceeds by an acid-base equilibrium followed by dissociation of the amido complex.

In the third paper of this series, which will concern the complexes prepared by M. Delépine, it will be shown that the base [45] assumed to be $Ir(NH_2)(NH_3)_3py_2^{++}$ has the same pK, *viz.* 5.1, as $Ir(OH)(NH_3)_3py_2^{++}$ and thus probably does not have the presumed composition. Thus, Rh(III) and Ir(III) do not seem to exhibit amine acidity in aqueous solution contrary to Pt(IV) discussed in the second paper of this series.

In Figure 7, $Ir(NH_3)_5Cl^{++}$ exhibits a rather narrow and weak band at 360 mμ, which can be ascribed to the first transition to a triplet level, while the second band at 286 mμ is due to the first excited singlet level with some

evidence for tetragonal splitting. These two positions are displaced toward shorter wavelengths compared to $Rh(NH_3)_5Cl^{++}$ as can be extrapolated from the behaviour of $IrCl_6^{--}$ and $RhCl_6^{--}$.

The first crystal field band can also be distinguished in $Rh(NH_3)_5NO_2^{++}$, while the second is hidden by or intermixed with electron transfer absorption. The intensity of the first band is not exceedingly large, as also observed in nitropentamminecobalt(III) ions. $Rh(NO_2)_6^{---}$ has a band at 270 mμ with $\varepsilon \sim 17\,000$, which cannot reasonably be described as a crystal field band.

TRIS(ETHYLENEDIAMINE) COMPLEXES

The colourless Rh en_3^{+++} was studied by Werner[46] and Jaeger[47]. Lifschitz and Rosenbohm[36] give the two absorption bands at $\sim$ 33 000 and $\sim$ 39 500 cm^{-1}, as also Mathieu[48]. The two crystal field bands are seen from Fig. 6 to be slightly hypsochromic, compared to $Rh(NH_3)_6^{+++}$.

The very robust Ir en_3^{+++} has according to Lifschitz and Bosenbohm[36], shoulders at 32 500 and $\sim$ 38 000 cm^{-1}, while Mathieu[48] found a broad shoulder at 31 000 cm^{-1}. Both bands are observed here in Mathieu's preparation, but with smaller intensity (Fig. 7 and Table 2). Thus, the first shoulder must be a triplet band. This band is $\sim$15 % singlet-like as in the other iridium(III) complexes and the distance between the first triplet and first singlet level of the configuration $\gamma_5^5\gamma_3$ seems to remain rather constant at increasing crystal field strength.

COMPARISON OF COBALT(III), RHODIUM(III) and IRIDIUM(III).

In Table 5 are given the evolution of the spectrochemical series and the distances between the two singlet levels of the electron configuration $\gamma_5^5\gamma_3$, represented by the two band maxima. The energy difference (E_1—E_2) between

Table 5. Comparison of crystal field strength in nickel (II), chromium (III), cobalt (III), rhodium (III) and iridium (III) complexes.

ν/ν_{aq} is the wavenumber of the first band of the complex, divided with the wavenumber of the first band of the aquo ion. $\Delta\nu$ is the difference in wavenumber between the two first bands, which are not spin-forbidden. The measurements of Cr(III) and Co(III) are made by Mr. C. E. Schäffer, and those of Ni(II) taken from Ref. 16.

	Ni(II)	Cr(III)		Co(III)		Rh(III)		Ir(III)	
Complex	ν/ν_{aq}	ν/ν_{aq}	$\Delta\nu$	ν/ν_{aq}	$\Delta\nu$	ν/ν_{aq}	$\Delta\nu$	ν/ν_{aq}	$\Delta\nu$
Br_6	—		—		—	0.71	4 100	0.71	3 400
Cl_6	—	0.78	5 200		—	0.76	5 000	0.76	4 000
ox_3	—	1.00	6 600	0.99	7 300	0.98	~4 900		—
$(H_2O)_6$	1.00	1.00	7 300	1.00	8 300	1.00	7 400		—
$(NH_3)_5J$	—	1.06	—	1.05	—	0.95	—		—
$(NH_3)_5Br$	—	1.10	7 400	1.11	—	1.09	—		—
$(NH_3)_5Cl$	—	1.12	7 200	1.15	8 500	1.13	7 400	1.11	—
$(NH_3)_5OH$	—	1.12	6 600	1.20	7 200	1.22	4 800		—
$(NH_3)_5H_2O$	—	1.19	6 900	1.24	8 800	1.24	6 500		—
$(NH_3)_6$	1.27	1.24	7 000	1.28	8 400	1.28	6 400		—
en_3	1.36	1.26	6 600	1.31	8 000	1.30	6 400	1.28	—
$(NH_3)_5NO_2$	—		—	1.32	—	1.32	—		—
$(CN)_6$	—	1.51	5 900	1.95	6 600		—		—

a γ_3- and a γ_5-electron corresponds directly to the first band in octahedral d^3- and d^8-systems, therefore chromium(III) and nickel(II) complexes [16] are also considered in Table 5. Since the distance between the two bands of the same first-order electron configuration has considerable interest for the theory of intermixing of molecular orbitals, *i. e.* beginning covalency, the wavenumber difference has been given not only for all three diamagnetic d^6-systems, but also for $\gamma_5^2\gamma_3$ of chromium(III). Mr. C. E. Schäffer has kindly informed me about all his measurements of chromium(III) and cobalt(III) complexes.

In the case of d^6-systems, $(E_1—E_2)$ is undoubtedly [10] somewhat larger than the wavenumber of the first singlet band. This is due to different energies of electrostatic interaction between the electrons in the groundstate $^1\Gamma_1$ and the excited state, which according to Tanabe and Sugano [10] is $^1\Gamma_4$ and not $^1\Gamma_5$. But since the exact meaning of $(E_1—E_2)$ in the diamagnetic d^6-complexes is rather dispersed, owing to the interaction with other electron configurations, the wavenumber of the first band will be used as reference here.

The hexaaquo ion is chosen as standard for each element with 8 500 cm^{-1} in nickel(II), 17 400 cm^{-1} in chromium(III), 16 600 cm^{-1} in cobalt(III), and 25 500 cm^{-1} in rhodium(III). Since $Ir(H_2O)_6^{+++}$ is not known, it has been assigned the hypothetical value 31 500 cm^{-1}, which makes the ratios between the wavenumbers of hexachloro and hexaaquo ions equal in rhodium(III) and iridium(III). As already proposed by Tsuchida [49], $CrCl_6^{---}$ is represented by the anhydrous $CrCl_3$, in which the environment of each chromium ion is a regular octahedron of six chloride ions [50].

While Table 5 illustrates the relative crystal field strengths of different ligands for the same ion, it is also possible to investigate the relative tendency of high crystal field strengths, *i. e.* hypsochromy, for the three related central ions, Co^{+3}, Rh^{+3}, and Ir^{+3}. Since the deviations of the ratios in Table 5 are rather small and scattered without a pronounced tendency, the assumed values of the hexaaquo ions can be applied as constants: If a given ligand gives the crystal field strength 1.00 in a cobalt(III) complex, the same ligand will within a few per cent uncertainty give 1.54 in rhodium(III) and 1.90 in iridium(III). Since Ir^{+3} does not have a much larger ionic radius than Rh^{+3}, owing to the lanthanide contraction, there seems to be a specific difference between the 3d-, 4d-, and 5d-electrons, which probably evolves from the different interaction with the molecular orbitals. The purely electrostatic model with hydrogenic d-wave functions [3,7] can hardly explain these facts and the strong increase of $(E_1—E_2)$ with the external charge [9].

THE INTERMIXING OF SINGLET AND TRIPLET LEVELS

In the pure Russell-Saunders coupling [51], the levels of the free ions can be classified in the multiplet terms with a given combination of S (the total spin quantum number) and L (the total angular momentum quantum number). These are quantized vector sums of the quantum numbers of the individual electrons, denoted by small letters: s (always $= \frac{1}{2}$) and l ($= 0$ for s-, 1 for p-, 2 for d-, 3 for f-electrons . . . .). In the heavy atoms, the levels deviate from the Russell-Saunders coupling, as shown *e. g.* by Rasmussen [52] or by the author from the absorption spectra of lanthanide and actinide ions [53]. The vector sum

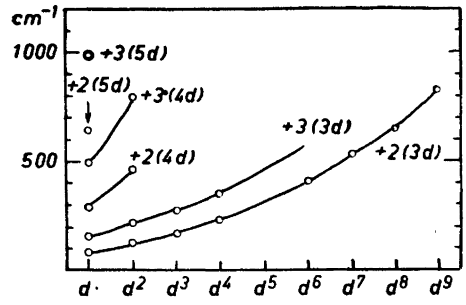


Fig. 8. Lande's multiplet splitting factor ζ_{nd} as function of the number of electrons in the partly filled nd-shell.

Divalent and trivalent ions of the 3d-, 4d- and 5d-groups [54]. The steep increase of the curve for *e. g.* trivalent $4d^n$-ions can be interpolated from the value $\zeta_{4d} = 2\,325$ cm^{-1} in Cd^{+++}, which has nine 4d-electrons.

J of L and S of each level is preserved when the q levels of a given electron configuration with the same J intermix, and the energy levels produced can be described by the eigen-values of a matrix of degree q. The elements of this matrix consist of the energies of the centres of the multiplet terms; and of constants multiplied by the Lande's multiplet splitting constant ζ_{nl} where n and l are the quantum numbers characteristic for each electron. The deviations from the Russell-Saunders coupling can be quantitatively described by increasing values of ζ_{nl}. For isoelectronic species, ζ_{nl} increases roughly proportionally to the square of Z_0^2 (the external charge is $= Z_0 - 1$), and varies much with the value of the principal quantum number n, *i. e.* in the second and third transition group compared to the first [54]. Fig. 8 gives the values of ζ_{nl}, known from atomic spectroscopy, as function of the number of nd-electrons.

The crystal field theory, when applied to d^n-systems, assumes that the crystal field strength is much larger than ζ_{nl}. Then, the total spin S is "a good quantum number", and the levels can be described by the combination Γ_n and S in the theory of Bethe [55]. The energies of the levels develop as a function of the crystal field strength as the q eigen-values of a matrix of q'th degree, if q levels present the same combinations [11] of Γ_n and S. This matrix can have either as diagonal elements the weak-field energies [1, 13, 15] with defined L from the free ion, or the strong-field energies [6, 10, 14] with defined electron configurations $\gamma_5^a\gamma_3^b$. The final results are of course equal, but the former type of matrix has exclusively crystal field strengths in the non-diagonal elements, while the latter type has exclusively electrostatic interaction energies (from multiplet distances in the free ions) in the non-diagonal elements. In both types of matrices, the diagonal elements are linear combinations of electrostatic interactions and crystal field strengths.

But as seen from Fig. 8, the assumption of much larger $(E_1 - E_2)$ than ζ_{nl} is weakened in the ends of each transition group, and especially in the later groups with 4d- and 5d-electrons. Unfortunately, atomic spectroscopy has no information about Co^{+3} and most $4d^n$- and $5d^n$-systems, while most other

$3d^n$-systems are well known [56]. In Ni^{++}, the absorption spectra [16] demonstrate an interaction of the level $^1\Gamma_3$ with $^3\Gamma_5$ and $^3\Gamma_4(F)$ with the non-diagonal elements 500 and 800 cm^{-1}, while $\zeta_{3d} = 600$ cm^{-1}. Generally, the intermixing in the squares of the wave functions is approximately $\left(\frac{k\zeta_{nl}}{E_a - E_b}\right)^2$, where k in the non-diagonal element $k\zeta_{nl}$ is a small number near 1, and $(E_a - E_b)$ is the energy distance between the two interacting levels. The selection rule that transitions are only allowed between levels with the same S, is weakened exactly to the extent, the two levels (originally with different S) have the same S, owing to intermixing effects. This is the explanation [5] of the observation of spin-forbidden bands [1, 8, 10, 53]. In cobalt(III) complexes, where the weak triplet bands [8] demonstrate an intermixing ~ 0.005, the value of $k\zeta_{nl}$ is thus 500 cm^{-1}, if the nearest singlet is the only cause of intermixing. From Fig. 8 ζ_{3d} can be extrapolated to 600 cm^{-1}. The groundstate $^1\Gamma_1$ is presumably intermixed with triplet states ~ 0.001, which perhaps causes the temperature-independent paramagnetism of some cobalt(III) complexes [57]. Sloth and Garner [58] have found relatively strong paramagnetism of $IrCl_6^{--}$ and $IrCl_5(H_2O)^{--}$, agreeing well with the large ζ_{5d}.

In the hexachloro complexes of rhodium(III) and iridium(III), the intermixing of singlet character in the triplet levels is about 0.03 and 0.12, corresponding to $k\zeta_{4d} = 900$ cm^{-1} and $k\zeta_{5d} = 2\,000$ cm^{-1}, respectively. The evolution

$$\zeta_{5d} \cong 2\ \zeta_{4d} \cong 5\ \zeta_{3d} \tag{2}$$

is predicted from Fig. 8, analogous to the relation $\zeta_{5f} = 2\ \zeta_{4f}$ found in the actinides and lanthanides [53].

$IrCl_6^{--}$ has evidently two weak triplet bands with the distance 1 700 cm^{-1} (Table 2), and $RhCl_6^{--}$ seems also to have two triplet bands, since the shoulder towards the red is so broad (Fig. 1). The two bands are probably due to transitions to $^3\Gamma_4$ and $^3\Gamma_5$ with increasing energy [10]. It cannot be excluded that the splitting in the weak band of $IrCl_6^{--}$ is due to different levels of the Γ_J type discussed below, since their distance is not larger than ζ_{5d}; but it is a quite paradoxical fact that such a splitting has never as yet been observed in a band with a defined Γ_n except in the tetrahedral $CoCl_4^{--}$ [59].

Tanabe and Sugano [10] pointed out that the quantum numbers of the levels must be written Γ_J, where the ordinary Bethe-level (S, Γ_n) split into the class of Γ_J given by the internal vector product [14]

$$C(\Gamma_J) = C(\Gamma_n) \times C(S) \tag{3}$$

For integral numbers of S, $C(S)$ is equal to the usual [14] $C(L)$ with $S = L$, *e. g.* Γ_1 for $S = 0$; Γ_4 for $S = 1$; $\Gamma_3 + \Gamma_5$ for $S = 2$; *etc.* For half-numbered values of S, the double-groups Γ_6, Γ_7, and Γ_8 must be used [55].

Thus [16], the triplet levels $^3\Gamma_4$ and $^3\Gamma_5$ should each divide into four levels with distances which are of the order of magnitude ζ_{nl}, as calculated for γ_5^a by Kotani [60] and Griffiths, Owen and Ward [61]. Absorption bands due to transitions [8,10], where one electron changes from γ_5 to γ_3 have a halfwidth between 1 000 and 2 000 cm^{-1}. Thus, it should be possible in many cases to distinguish the Γ_J components. Especially Mr. Schäffer has continued the investigations

of Gaussian shape of absorption bands [19] and found no sign of extra bands, except those due to intermixing of other values of S. The two sharp lines of Cr^{+++} in the ruby are due to $^2\Gamma_3$ and the broader band groups with higher wavenumber due to $^2\Gamma_4$ in the red and $^2\Gamma_5$ in the blue. The two latter groups are perhaps each divided into two Γ_J-bands, but it cannot easily be decided.

In the next paper of this series, the influence of other molecular orbitals than the γ_5 and γ_3 (from d-electrons) will be discussed for the octahedral complexes of the second and third transition groups.

EXPERIMENTAL

The measurements of absorption spectra were performed on a Cary spectrophotometer, ~25° C. The titration curve of $Rh(OH)_3$ was measured with a glass electrode pH-meter Radiometer M 22.

Na_3RhCl_6, $12H_2O$. Rhodium metal from S. M. Jørgensen's collection (partly from Johnson and Matthew, London) was mixed with 10 moles sodium chloride per Rh and treated with chlorine for six hours at 600 – 700° C in a pyrex tube, electrically heated. The cooled mass was perfectly soluble in 4 M HCl, except for a few per cent of anhydrous $RhCl_3$ formed. By addition of ethanol to such a solution, most rhodium crystallizes after some days as Na_3RhCl_6, $12H_2O$. But this method is disadvantageous, since metal tends to precipitate from the filtrate when boiled. Rather, fractionated crystallization of the melted mass in dilute HCl can be recommended. $Rh(OH)_3$ can be regenerated from the solutions with NaOH or $BaCO_3$.

The iridium content was found to 0.4 % and 0.2 % in two samples, from the absorption spectra in HCl + Cl_2. There were found 17 % Rh from precipitation of the metal by $TiCl_3$ and 37 % Cl from Mohr's titration of the filtrate from $BaCO_3$ (calc. 17.1 % Rh and 35.1 % Cl).

$RhBr_6^{---}$ was prepared in solution by prolonged boiling of Na_3RhCl_6, $12H_2O$ with 6 M HBr till the spectrum of different solutions did not change. Even though Poulenc [63] has prepared solid salts of $Rh_2Br_9^{-3}$, $RhBr_5^{-2}$ and $Rh_2Br_{11}^{-5}$, it is here assumed that these complexes with bromide bridges are not abundant in strong HBr.

$Rh(H_2O)_6^{+++}$ was made by boiling 0.5 g Na_3RhCl_6, $12H_2O$ with 50 ml 5 M $HClO_4$ in a 100 ml beaker, covered with a watch-glass. The dark-red colour turns first orange, then a red-brown precipitate is formed, which redissolves to a dark brown solution. By dilution of the residual 4 ml to 50 ml with water, a clear yellow solution is obtained.

$Rh\,ox_3^{---}$ was made by heating 4 hours to 100° C of a solution, originally 0.1 M $RhCl_6^{---}$ and 0.6 M K_2ox.

$Rh(NH_3)_6Cl_3$, *$[Rh(NH_3)_5NO_3](NO_3)_2$*, *$[Rh(NH_3)_5I]Cl_2$*, *$[Rh(NH_3)_5Br]Br_2$ and $[Rh(NH_3)_5Cl]Cl_2$* were taken from the collection of S. M. Jørgensen. The last salt was prepared for the determination of the atomic weight of Rh.

$[Rh(NH_3)_5H_2O](ClO_4)_3$ of Brønsted and Volqvartz [40] was kindly furnished by Professor J. A. Christiansen. It was measured in 0.05 M $HClO_4$ and in H_2O, giving the aquo form, and in 0.1 M Na_2CO_3 and 1 M NaOH, giving the hydroxo ion. Further, it was compared with the solution of sodium aquopentammine rhodium(III) pyrophosphate (S. M. Jørgensen) in 1 M HCl and in 5 M NH_3.

$Rh\,en_3^{+++}$ was prepared by Werner [46] by reacting Na_3RhCl_6, $12H_2O$ with 50 % ethylenediamine. If the solution is more dilute, a yellow precipitate ($Rh(OH)_3$?) is formed by warming, and the quantitative reaction is slow. For the experiments, 0.5 g Na_3RhCl_6, $12H_2O$ was dissolved in 2 ml H_2O and added a solution of 0.5 ml ethylenediamine hydrate (Merck's No. 946) in 10 ml 0.2 M HCl. The solution was evaporated cautiously to 1 ml under stirring.

In the next paper of this series the preparation of iridium compounds from the metal will be described. Here, it can be mentioned that $IrCl_6^{--}$ was reduced by H_2S or ascorbic acid for some repeated measurements. In most cases were used:

K_3IrCl_6, $3H_2O$, supplied from Dansk Hollandsk Ædelmetal (H. Drijfhout and Zoon).

IrBr$_6^{---}$, prepared by boiling this salt with 6 M HBr.

Ir ox$_3^{---}$, made by warming 30 hours at 110° C of a solution 0.05 M K_3IrCl_6, $3H_2O$ and 0.8 M K_2ox, in a stoppered bottle. Professor Marcel Delépine, Collège de France, has kindly presented me with a series of iridium(III) and rhodium(III) complexes, which will be the subject of the third paper of this series. K_3Irox_3, $4.5H_2O$ of this collection has a spectrum similar to that given in Fig. 5.

[Ir (NH$_3$)$_5$Cl]Cl$_2$ and [Ir en$_3$]Br$_3$, 2H$_2$O (the l-form), kindly furnished by Professor Jean-Paul Mathieu. The spectrum of Ir en$_3^{+++}$ was also measured in 0.3 M NaOH and showed no change.

Acknowledgments. I am very much indebted to Professor J. Bjerrum for his interest in the work. Further, I thank Mr. C. E. Schäffer for interesting discussions and valuable information about his measurements of chromium(III) and cobalt(III) complexes, and Miss Bodil Friis for assistance with the preparation of Na_3RhCl_6, $12H_2O$. Finally, I thank Professor Jean-Paul Mathieu of Université de Paris for the valuable samples of iridium(III) amine complexes.

REFERENCES

1. Finkelstein, R. and Van Vleck, J. H. *J. Chem. Phys.* **8** (1940) 790.
2. Abragam, A. and Pryce, M. H. L. *Proc. Roy. Soc. London* **206** *A* (1951) 173.
3. Ilse, F. E. and Hartmann, H. *Z. physik. Chem.* **197** (1951) 239.
4. Hartmann, H. and Ilse, F. E. *Z. Naturforsch.* **6a** (1951) 751.
5. Hartmann, H. and Schläfer, H. L. *Z. Naturforsch.* **6a** (1951) 754.
6. Orgel, L. E. *J. Chem. Soc.* **1952** 4756.
7. Ballhausen, C. J. *Kgl. Danske Videnskab. Selskab, Mat.-fys. Medd.* **29** (1954) No. 4 and **29** (1955) No. 8.
8. Jørgensen, C. Klixbüll *Acta Chem. Scand.* **8** (1954) 1502.
9. Owen, J. *Proc. Roy. Soc. London* **227** *A* (1955) 183.
10. Tanabe, Y. and Sugano, S. *J. Phys. Soc. Japan* **9** (1954) 753 and 766.
11. Jørgensen, C. Klixbüll *Acta Chem. Scand.* **9** (1955) 116.
12. Jørgensen, C. Klixbüll and Bjerrum, J. *Acta Chem. Scand.* **9** (1955) 180.
13. Orgel, L. E. *J. Chem. Phys.* **23** (1955) 1004 and 1819.
14. Ballhausen, C. J. and Jørgensen, C. Klixbüll *Kgl. Danske Videnskab. Selskab, Mat. fys. Medd.* **29** (1955) No. 14.
15. Hartmann, H. and Fischer-Wasels, H. *Z. physik. Chem.* **4** (1955) 297.
16. Jørgensen, C. Klixbüll *Acta Chem. Scand.* **9** (1955) 717 and 1362.
17. Basolo, F., Ballhausen, C. J. and Bjerrum, J. *Acta Chem. Scand.* **9** (1955) 810.
18. Hartmann, H. and Schläfer, L. *Angew. Chem.* **66** (1954) 768.
19. Jørgensen, C. Klixbüll *Acta Chem. Scand.* **8** (1954) 1495.
20. Samuel, R. and Uddin, M. *Trans. Faraday Soc.* **31** (1935) 423.
21. Babaeva, A. V. *Bull. Acad. Sci. URSS Cl. Sci. Chim.* **1943** 171.
22. Inamura, Y. and Kondo, Y. *J. Chem. Soc. Japan* **72** (1951) 787.
23. Meyer, J. and Kawczyk, M. *Z. anorg. Chem.* **228** (1936) 297.
24. Bjerrum, N. *Z. physik. Chem.* **59** (1907) 336.
25. Delépine, M. *Ann. chimie* [9] **7** (1917) 277.
26. Delépine, M. *Bull. soc. chim. Belg.* **36** (1927) 108.
27. Charlot, G. and Gauguin, R. *Les methodes d'analyse des reactions en solution.* Paris. 1951.
28. Bjerrum, J. *Metal Ammine Formation in Aqueous Solution.* Copenhagen 1941.
29. Sundram, A. K. and Sandell, E. B. *J. Am. Chem. Soc.* **77** (1955) 855.
30. Bjerrum, J. *Kgl. Danske Videnskab. Selskab, Mat.-fys. Medd.* **22** (1946) No. 18.
31. Bjerrum, N. *Kgl. Danske Videnskab. Selskabs Skrifter, Nat. math. Afd.* [7] **4** (1907) No. 1.
32. Grube, G. and Kesting, E. *Z. Elektrochem.* **39** (1933) 948.
33. Mulay, L. N. and Selwood, P. W. *J. Am. Chem. Soc.* **77** (1955) 2693.
34. Grube, G. and Autenrieth, H. *Z. Elektrochem.* **43** (1937) 880 and **44** (1938) 296.
35. Marino, L. *Z. anorg. Chem.* **42** (1904) 213.
36. Lifschitz, J. and Rosenbohm, E. *Z. physik. Chem.* **97** (1920) 1.

37. Delépine, M. *Bull. soc. chim. France* [4] **21** (1917) 157.
38. Jørgensen, S. M. *J. prakt. Chem.* [2] **27** (1883) 461, **34** (1886) 440, and **44** (1891) 42 and 63.
39. Palmær, W. *Z. anorg. Chem.* **10** (1895) 320 and **13** (1897) 211.
40. Brønsted, J. N. and Volqvartz, K. *Z. physik. Chem.* **134** (1928) 97.
41. Christiansen, J. A. and Asmussen, R. W. *Kgl. Danske Videnskab. Selskab, Mat.-fys. Medd.* **12** (1934) No. 1.
42. Lamb, A. B. and Fairhall, L. T. *J. Am. Chem. Soc.* **45** (1923) 384.
43. Grünberg, A. A. and Faerman, G. P. *Z. anorg. Chem.* **193** (1930) 193.
44. Adamson, A. W. and Basolo, F. *Acta Chem. Scand.* **9** (1955) 1261.
45. Delépine, M. *Z. physik. Chem.* **130** (1927) 222.
46. Werner, A. *Ber.* **45** (1912) 1228.
47. Jaeger, F. M. *Rec. trav. chim.* **38** (1919) 171.
48. Mathieu, J.-P. *J. chim. phys.* **33** (1936) 85.
49. Tsuchida, R. *Bull. Chem. Soc. Japan* **13** (1938) 388 and 436.
50. Wooster, N. *Z. Kryst.* **74** (1930) 363.
51. Condon, E. U. and Shortley, G. H. *Theory of Atomic Spectra.* Cambridge 1953.
52. Rasmussen, E. *Serier i de ædle Luftarters Spektre.* Thesis. Copenhagen 1931.
53. Jørgensen, C. Klixbüll *Kgl. Danske Videnskab. Selskab, Mat.-fys. Medd.* **29** (1955) No. 7 and 11.
54. Jørgensen, C. Klixbüll *J. Inorg. Nucl. Chem.* **1** (1955) 301.
55. Bethe, H. *Ann. Physik* [5] **3** (1929) 133.
56. Moore, C. E. *Nat. Bur. Stand. Circ.* No. 467, Vol. II, 1952.
57. Asmussen, R. W. *Magnetokemiske Undersøgelser.* Thesis. Copenhagen 1944.
58. Sloth, E. N. and Garner, C. S. *J. Chem. Phys.* **22** (1954) 2064.
59. Ballhausen, C. J. and Jørgensen, C. Klixbüll *Acta Chem. Scand.* **9** (1955) 397.
60. Kotani, M. *J. Phys. Soc. Japan* **4** (1949) 293.
61. Griffiths, J. H. E., Owen, J. and Ward, I. M. *Proc. Roy. Soc. London* **219** *A* (1953) 526.
62. Krauss, F. and Umbach, H. *Z. anorg. Chem.* **182** (1929) 411.
63. Poulenc, P. *Compt. rend.* **190** (1930) 639.
64. Ayres, G. H. *Anal. Chem.* **25** (1953) 1622.

Received December 22, 1955.

ACTA CHEMICA SCANDINAVICA 10 (1956) 518—534

Complexes of the 4d- and 5d-Groups

II. Crystal Field and Electron Transfer Spectra of Ruthenium(II) and (III), Iridium(IV) and Platinum(IV)

CHR. KLIXBÜLL JØRGENSEN

Chemistry Department A, Technical University of Denmark, Copenhagen, Denmark

The octahedral complexes of the platinum metals often exhibit relatively strong absorption bands. The electron transfer bands with the lowest wavenumbers are assumed to be due to π-electrons from the ligands, which are transferred to holes in the 4d- and 5d-shells. In the halido complexes of ruthenium(III) and platinum(IV), the crystal field bands of d^5- and d^6-systems, respectively, can be observed. The acidity of $Pt(NH_3)_6^{+4}$ and $Pt(NH_3)_5Cl^{+3}$ is measured; the formations of the monoamido complexes have $pK = 7.75$ and 8.7, respectively. The theory of molecular orbitals is compared to the explanation by the crystal field theory of the energy difference between γ_3- and γ_5-electrons. Probably, it will be necessary to consider the interaction between different configurations of molecular orbitals.

In the first paper [1] of this series, the regularly octahedral complexes of the d^6-systems rhodium(III) and iridium(III) were studied. Their absorption spectra can be explained as the crystal field bands, also found of the complexes of cobalt(III). However, this proves by no means that the electrostatic model of the crystal field, acting on the d-electrons [2] is a very good approximation for the actual states of the transition group complexes. Van Vleck [3] has pointed out that the theory of molecular orbitals of Mulliken [4] gives several of the results of the crystal field theory, thus the 10-fold degenerate d-shell in an octahedral complex is split to four γ_3-electrons with higher energy and six γ_5-electrons with lower energy. This analogy has been extended further by Hartmann [5], Orgel [6,7], Owen [8], Tanabe and Sugano [9]. Experimental evidence for the intermixing of molecular orbitals with the γ_5-electrons was found by paramagnetic reasonance measurements of $IrCl_6^{--}$ and $IrBr_6^{--}$ by Owen and Stevens [10] and Griffiths and Owen [11]. The present paper is a contribution to the discussion of molecular orbitals, applied to the electron transfer spectra.

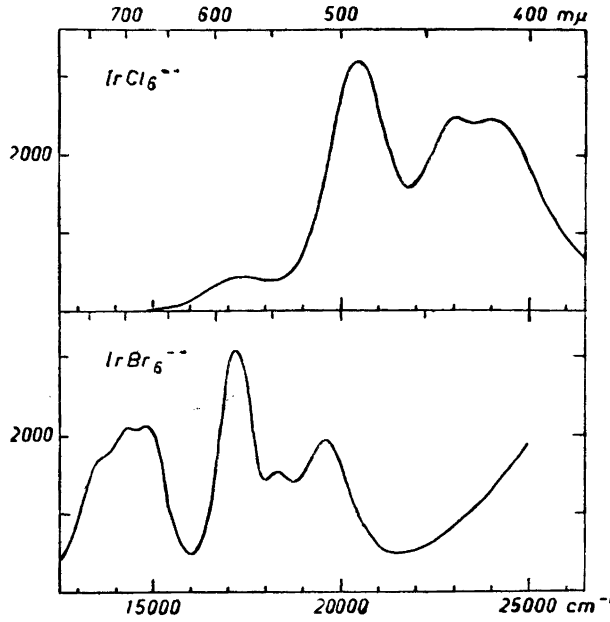


Fig. 1. Absorption spectra of hexachloro- and hexabromo-iridium(IV) ions.

0.0005 M Na_2IrCl_6, measured in different solutions in water and dilute hydrochloric acid, which was not changed by addition of free chlorine, and from $K_3IrCl_6 + Cl_2$. 0.0005 M $IrBr_6^{--}$ from Na_2IrCl_6 in 0.1 M HBr.

HEXACHLORO- AND HEXABROMO-COMPLEXES OF IRIDIUM(IV).

The absorption spectra of the red-brown $IrCl_6^{--}$ and violet-blue $IrBr_6^{--}$ are given in Fig. 1 and Table 1. The band maxima of $IrCl_6^{--}$ have been found by Babaeva [12] at 490, 424 and 286 mμ. The doublet structure of the second band was found by Inamura and Kondo [13]. The complex $IrBr_6^{--}$ is only stable under special conditions of temperature and concentrations. Thus, the dark-blue crystals of tetramethylammonium hexabromo iridate(IV) dissolves under complete decomposition in 6 M hydrobromic acid, which contains some free bromine. Only quite dilute solutions of HBr do not favorize the trivalent anion $IrBr_6^{---}$ so much, and $IrBr_6^{-}$ has been measured here. Therefore, the values of ε in Table 1 may be uncertain minimum values, but the relative heigth of the peaks is reproducible in many different solutions, since the decomposition product $IrBr_6^{---}$ is much less coloured [1].

There are six discernible absorption bands in the visible range of $IrBr_6^{--}$, but only four of $IrCl_6^{--}$. This can be ascribed to the larger energy differences between the two lowest levels $^2P_{3/2}$ and $^2P_{1/2}$ in the free halogen atom (404 cm^{-1} in F, 881 cm^{-1} in Cl, 3 685 cm^{-1} in Br and 7 603 cm^{-1} in I[14]) *i. e.* increasing ζ_{np} with increasing principal quantum number n[1]. This was early found by Scheibe [15] from the double absorption band in the far ultraviolet of Br^- and I^-, compared to Cl^-.

Table 1. Absorption bands of iridium(IV) complexes.

Wavelength λ_n, wavenumber ν_n and molar extinction coefficient ε_n of each maximum, halfwidths $\delta(-)$ towards smaller and $\delta(+)$ towards higher wavenumbers, and the oscillator strength P of each band [27].

	λ_n mμ	ν_n cm^{-1}	ε_n	$\delta(-)$ cm^{-1}	$\delta(+)$ cm^{-1}	$P \cdot 10^{-5}$
$IrCl_6^{--}$	575	17 400	460	1 200	—	500
	489	20 450	3 200	900	—	2 600
	431	23 200	2 540	—	—	4 000
	414	24 200	2 480	—	1 400	
$IrBr_6^{--}$	737	13 600	1 550	600	—	2 000
	698	14 300	2 050	—	—	
	675	14 800	2 100	—	—	
	583	17 200	3 070	500	500	1 400
	544	18 400	1 500	—	—	1 500
	511	19 600	1 800	—	800	

The absorption spectrum of $IrCl_6^{--}$ (Fig. 1) resembles much the spectrum of $IrCl_6^{---}$ (Ref. 1, Fig. 2) multiplied in height by 40 and displaced 4 000 cm^{-1} towards the red. This might perhaps suggest that iridium has the oxidation state +3 in $IrCl_6^{--}$, involving as ligands the resonance structure of five chloride ions and one chlorine atom. Hovewer, this is impossible, since Owen and Stevens [10] found the magnetic hole (the missing electron in the γ_5^5-shell) is on an average, to 80 % near the iridium nucleus and to 3 % near each of the six chloride nuclei, *i. e.* about 20 % intermixing of the molecular orbitals with symmetry γ_5. The question may be raised whether the oxidation state of Ir is an integral number, *e. g.* +3 or +4. In the author's opinion it is not deciding that the number of electrons within a volume defined as "the central atom" is some decimal fraction. Rather, the oxidation state of the central ion can be defined from the number of electrons in the highest γ_3- and γ_5-orbitals, which would have been pure d-electrons, if no intermixing occurred. *E. g.*, iridium is trivalent with γ_5^6 and quadrivalent with γ_5^5 as groundstate. This has nearly an exact meaning, since the interaction between different electron configurations is small in strong crystal fields, and since by chance the groundstates in weak crystal fields often contain an integral number of γ_3- and γ_5-electrons (*cf.* Santen and Wieringen [16]). It is known from applications of molecular orbital theory that the electron configurations can be highly intermixed by increasing nuclear distances and correspondingly weaker bonding, as pointed out by Slater [53] and Mc Weeny [54].

Thus, the absorption spectra of $IrCl_6^{--}$ and $IrBr_6^{--}$ must be interpreted as transitions of one electron from the ligands to the central ion, which achieve the oxidation state +3, as defined above. The orbitals between which the electron moves, will be discussed below in a special section. The bathochromic effects of chloro-, bromo- and iodo-complexes (*cf.* platinum(IV) below) is qualitatively well understood. Thus, by a constant electron affinity of Ir^{+4}, less energy is necessary to remove an electron from the most reducing ligand [17], *i. e.* the heaviest halide ion. But the effect is larger than expected (one electron

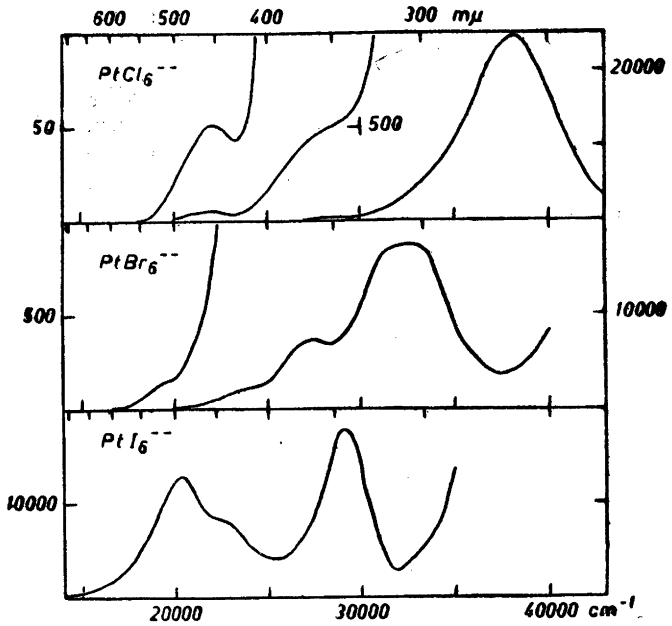


Fig. 2. Absorption spectra of hexachloro-, hexabromo- and hexaiodo-platinum(IV) ions.
0.0001 M to 0.05 M $[N(C_2H_5)_4]_2PtCl_6$ in 1 M HCl.
0.0001 M to 0.05 M $[N(C_2H_5)_4]_2PtBr_6$ in 0.1 M HBr.
0.0001 M PtI_6^{--} from $PtCl_6^{--}$ in 0.1 M KI.

volt corresponds to 8 067 cm^{-1}). However, the electron affinities of free halogen atoms are not easily compared with the conditions in aqueous solution, and are further influenced by the stabilization by resonance of the excited state of the iridium(IV) complexes.

Table 2. Absorption bands of platinum(IV) complexes. Notation as in Table 1.

	λ_n mμ	ν_n cm^{-1}	ε_n	$\delta(-)$ cm^{-1}	$\delta(+)$ cm^{-1}	$P \cdot 10^{-5}$
$PtCl_6^{--}$	453	22 100	50	1 900	—	90
	353	28 300	490	1 700	—	700
	262	38 200	24 500	2 750	2 300	57 000
$PtBr_6^{--}$	525	19 100	140	—	—	~150
	435	23 000	1 500	—	—	~2 000
	364	27 500	7 400	2 200	—	15 000
	311	32 200	17 800	2 800	2 600	44 000
PtI_6^{--}	494	20 250	12 800	1 700	—	20 000
	446	22 400	8 300	—	—	12 000
	343	29 150	17 700	1 600	1 350	24 000

HEXACHLORO-, HEXABROMO-, AND HEXAIODO COMPLEXES OF PLATINUM(IV)

The colourless PtF_6^{--}, yellow $PtCl_6^{--}$, red-orange $PtBr_6^{--}$, and dark purple-red PtI_6^{--} was already measured by Schlesinger and Tapley [18], and Wheeler, Perros and Naeser [19] have later re-examined the two weak bands ($\varepsilon \sim 50$) of PtF_6^{--} at 318 and 275 mμ. Babaeva [12] has found bands of $PtCl_6^{--}$ at 440, 348 and 254 mμ. Fig. 2 and Table 1 give the measurements by the present author of $PtCl_6^{--}$, $PtBr_6^{--}$ and PtI_6^{--}.

Platinum(IV) is a d^6-system with strong tendency of forming diamagnetic complexes with regularly octahedral configuration. Thus, the crystal field bands analogous to these of cobalt(III), rhodium(III) and iridium(III) [1] may be predicted. They are present as the relatively weak shoulders in the spectra of $PtCl_6^{--}$ and $PtBr_6^{--}$. The weakest bands at 453 and 525 mμ, respectively, are identified as the transition from $^1\Gamma_1$ (γ_5^6) to one of the triplet levels $^3\Gamma_4$ or $^3\Gamma_5$ ($\gamma_5^5\gamma_3$); and the stronger bands at 353 and 435 mμ, respectively, with the lowest singlet level, *viz.*[9] $^1\Gamma_4$ ($\gamma_5^5\ \gamma_3$). The ratio between the wave-number of this band and the corresponding band in the iridium(III) complexes [1] will then have the values:

	$PtCl_6^{--}/IrCl_6^{---}$	$PtBr_6^{--}/IrBr_6^{---}$
Triplet level	1.24	1.14
Singlet level	1.17	1.03

This is reasonable evolution for two isoelectronic species with increasing oxidation state. The energy difference (E_1—E_2) between γ_3- and γ_5-electrons is thus at least double as large in platinum(IV) complexes as in cobalt(III) complexes *inter alia* as discussed earlier [1]. This explains the high tendency of magnetic anomaly in the platinum metal complexes ($S = 0$ for even and $S = \frac{1}{2}$ for odd number of electrons) since the distances in the free ion of terms with different S in the heavy elements is either less or equal to the distances in the first transition group, and they seem decreased in the complexes, relative to gaseous ions [7,8,9].

The two bands in PtF_6^{--} are presumably the transitions to the two singlet levels of $\gamma_5^5\ \gamma_3$. The three electron transfer bands in PtI_6^{--} are superposed the predicted places of the crystal field bands, which may show some intermixing effects.

AMMINE PLATINUM(IV) COMPLEXES

Like other d^6-systems, platinum(IV) forms very robust hexammine complexes. They have been difficult to prepare before Tronev and Shumilina [20] recently demonstrated that $Pt(NH_2)(NH_3)_5Cl_3$ is formed by the action at room temperature of liquid NH_3 on $(NH_4)_2PtCl_6$. This base reacts with hydrogen ions and forms the normal "luteo" ion:

$$Pt(NH_2)(NH_3)_5^{+++} + H^+ \rightleftharpoons Pt(NH_3)_6^{++++} \qquad (1)$$

The titration curve, Fig. 3, shows that pK for this process is 7.75. Grünberg and Faerman [55] determined pK = 8.9 by the more uncertain method of dis-

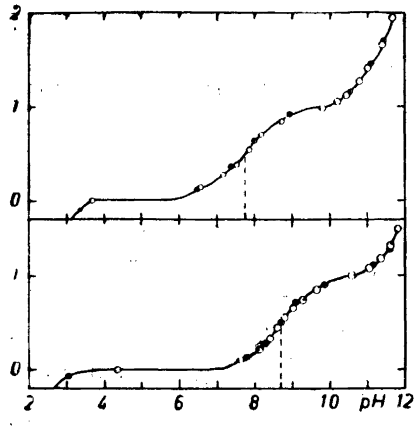


Fig. 3. Titration curve of hexammine and chloropentammine complexes of platinum(IV) at 20° C.

pH as function of consumed hydrogen ions per platinum atom. 0.02 M $Pt(NH_3)_6Cl_4$ and 0.025 M $[Pt(NH_3)_5Cl](NO_3)_3$ in H_2O titrated with 0.1 M NaOH (empty circles) and titrated backwards with 0.1 M HCl.

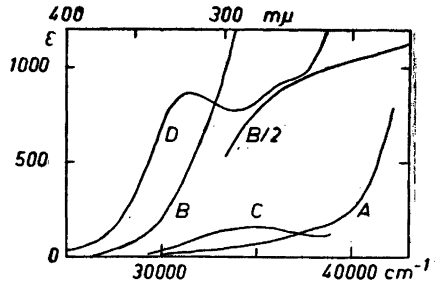


Fig. 4. Absorption spectra of hexammine-, amido- and chloropentammine-platinum(IV) ions.

A. 0.01 M $[Pt(NH_3)_6]Cl_4$ in H_2O
B. 0.001 M $[Pt(NH_3)_6]Cl_4$ in 1 M NH_3
C. 0.01 M $[Pt(NH_3)_5Cl](NO_3)_3$ in H_2O
D. 0.002 M $[Pt(NH_3)_5Cl](NO_3)_3$ in 1 M NH_3

solving the pure $Pt(NH_3)_6Cl_4$ in water and inserting the measured pH in Ostwald's square-root formula for the dissociation of a weak acid. Already Grünberg and Faerman [55] demonstrated the change of absorption spectrum of $Pt(NH_3)_6^{+4}$ by addition of one equivalent of OH^-, the absorption limit is displaced towards longer wavelengths. Fig. 4 gives the spectra of $Pt(NH_3)_6^{+4}$ $Pt(NH_3)_5NH_2^{+3}$, $Pt(NH_3)_5Cl^{+3}$ and $Pt(NH_3)_4(NH_2)Cl^{+2}$. The spectrum of $Pt(NH_3)_5NH_2^{+3}$ is not further displaced in 1 M NaOH, and the titration curve Fig. 3 demonstrates that the next proton does not dissociate with pK lower than 12. Thus there might be involved an electrostatic effect, which separates the two consecutive values of pK by more than 5 units. However, $Pt(NH_3)_5Cl^{+3}$ is not a much weaker acid than $Pt(NH_3)_6^{+4}$. The titration curve in the lowest part of Fig. 3 gives pK = 8.7. The reversible titration demonstrates that the chloride ligand is not exchanged by OH^- during the measurements. Grünberg and Faerman [55] found pK = 9.0. Before this investigation was made, Professor F. Basolo informed me kindly that Pt en_3^{+4} is also a weak acid, forming amido complexes with the absorption band displaced towards lower wavenumbers.*

Sidgwick's concept of complexes as having "inert gas configurations" is in some way exemplified by the whitest of all ammonia complexes with partly filled d-shells $Pt(NH_3)_6^{+4}$. The characteristic property of an inert gas with

* Grünberg has later determined the consecutive values of pK for Pt en_3^{+4}, *viz.* 5.5, 9.7, and 10.7; of $Pt(NH_3)_6^{+4}$, *viz.* 7.9 and 10.1; and of Pt $(NH_3)_5Cl^{+3}$, *viz.* 8.1 and 10.3.

a closed shell-groundstate is that the excited states have much higher energy than the ground-state. The singlet levels of $\gamma_5^5\gamma_3$ are hidden by the electron transfer band below 240 mμ, but the triplet level can perhaps be observed as the shoulder at 300 mμ.

RUTHENIUM(III) COMPLEXES

A most unsual discussion was once made of the oxidation states of ruthenium. Howe [22] prepared a rose-red isomer of the dark-brown K_2RuCl_5, H_2O, and maintained [23] that these two salts and the yellow-brown anhydrous K_2RuCl_5 do all contain trivalent ruthenium. Charonnat [24] demonstrated that the dark-brown salt really was $K_2RuCl_5(OH)$ with quadrivalent Ru, and finally Howe [25] agreed.

By a profound investigation, Charonnat [26] demonstrated the many analogies between ruthenium(III) and rhodium(III). Thus, two red complexes $RuCl_6^{---}$ and $RuCl_5(H_2O)^{--}$ are known, of which the first is only stable in very strong HCl, and the brownish green Ru ox_3^{---} forms salts, which are isomeric with those of Rh ox_3^{---} and many other tris(oxalato) complexes of trivalent metals. The octahedral configuration of ruthenium(III) is thus evident, even though Charonnat [26] proposes octa-coordination in several complexes. Since the d^5-systems with $S = \frac{1}{2}$ are liable to rhombic distortion [27] while d^6-systems with $S = 0$ are regularly octahedral, a distortion is predicted as found [28] in the corresponding $Fe(CN)_6^{---}$. Thus, the anhydrous K_2RuCl_5 and the orange pentanitrites as $K_2Ru(NO_2)_5$ may be penta-coordinated, but they are rather under suspicion for being dimeric with two anion bridges.

Wehner and Hindman [29] have later investigated the solutions of ruthenium (III) and (IV) in $HClO_4$, where hydroxo- and aquo-complexes are expected. Since the spectrum of the trivalent form is equal in 9 M and 1 M $HClO_4$ (one peak at 300 mμ with $\varepsilon \sim 2\,000$), it is assumed to be due to the hexaaquo ion. This might very well have been a stronger acid; the tendency for deviation from regularly octahedral complexes gives higher affinity for the two first hydroxyl ions (*cf.* copper(II) and manganese(III) compared to the regular neighbors nickel(II), zinc(II), chromium(III) and iron(III)) [27].

Fig. 5 and Table 3 give the spectra of ruthenium(III) in strong HCl and HBr, which can be assumed to contain $RuCl_6^{---}$ and $RuBr_6^{---}$. Mr. K. G. Poulsen has kindly pointed out to me that metallic silver is a good reducing agent in these media for providing the oxidation state +3; and even a green solution, containing a trace of + 2 can be produced. However, upon standing in the air, a strawberry-red solution is obtained in HCl. This is slowly oxidized over a period of weeks to a yellow-brown solution with increasing amounts of +4. When the solution does not contain much ruthenium, less than 0.001 M, it is almost colourless in +3, while oxidation to +4 produces a strong colour. At this concentration, ruthenium(IV) has the same characteristic brownish orange colour as dilute $IrCl_6^{--}$ and nearly the same absorption spectrum, which is rather curious for this d^4-system. The solution of ruthenium (III) in 4 M HBr is dark purple-brown.

It is seen from Fig. 5 and Table 3 that the chloro complex has much higher absorption in the near ultraviolet (as also has the aquo ion [29]) and the bromo

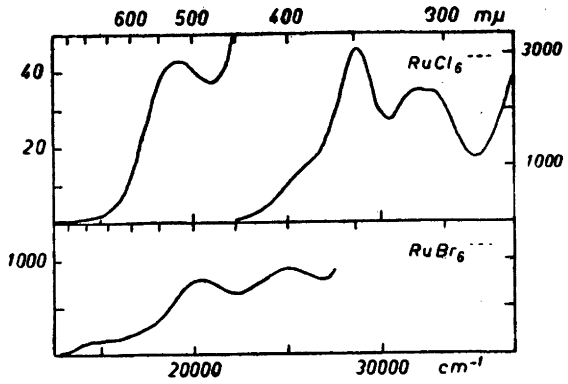


Fig. 5. Absorption spectra of chloro and bromo complexes of ruthenium(III).
0.0005 M to 0.05 M ruthenium(III) in 10 M HCl, reduced with Ag powder.
0.002 M to 0.05 M ruthenium(III) in 6 M HBr, reduced with Ag powder.

complex in the visible than found for rhodium(III)[1]. These bands are undoubtedly due to electron transfer and will be discussed below. But there are also signs of crystal field bands: the relatively weak band at 521 mμ and the shoulder at 388 mμ in the chloro complex and perhaps also the shoulder at 653 mμ in the bromo complex. The intensity of these bands classify them as spin-allowed transitions from the groundstate $^2\Gamma_5(\gamma_5^5)$ to one of the doublet levels[30] of $\gamma_5^4\,\gamma_3$. If they were spin-forbidden, the asymmetry of the ruthenium(III) complex must be so large that the hemiedric crystal field[31] have made the spin-allowed crystal field bands nearly as allowed as electron transfer band. The present author has sought for spin-forbidden bands out to 1 100 mμ, but found at most a background with $\varepsilon \sim 1$.

According to Tanabe and Sugano's calculation on pure d^n-configurations[9] the order of energy of $\gamma_5^4\,\gamma_3$-levels in strong crystal fields will be

$$^4\Gamma_4,\ ^4\Gamma_5,\ ^2\Gamma_2,\ ^2\Gamma_4,\ ^2\Gamma_5,\ ^2\Gamma_3 \cdots\cdots \qquad (2)$$

Table 3. Absorption bands of ruthenium(III) and (II) complexes. Notation as in Table 1.

	λ_n mμ	ν_n cm^{-1}	ε_n	$\delta(-)$ cm^{-1}	$\delta(+)$ cm^{-1}	$P \cdot 10^{-5}$
$RuCl_6^{---}$?	521	19 200	43	2 000	—	70
	388	25 800	800	—	—	~1 000
	349	28 700	3 000	1 400	1 300	3 700
	313	32 000	2 300	—	—	~5 000
	307	32 600	2 300	—	—	
$RuBr_6^{---}$?	655	15 300	130	1 500	—	180
	485	20 600	770	1 600	—	1 100
	400	25 000	900	—	—	—
Ru(II) in 2 M HCl	660	15 200	1 250	—	—	~5 000
	570	17 600	1 130	—	—	

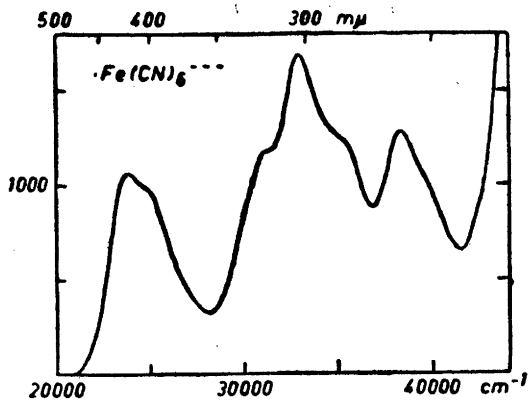


Fig. 6. Absorption spectrum of iron(III)hexacyanide ions.
0.001 M $K_3Fe(CN)_6$ in H_2O.

within a relatively narrow range of energy, about 50 B, where the Racah parameter B presumably is about 1 000 cm^{-1} in the gaseous ion, but is decreased in complexes [7,8,9]. Since the four bands in d^6-systems should be placed [9]:

$$\begin{aligned} {}^3\Gamma_4 &: (E_1 - E_2) - 3\ C \\ {}^3\Gamma_5 &: (E_1 - E_2) + 8\ B - 3\ C \\ {}^1\Gamma_4 &: (E_1 - E_2) - C \\ {}^1\Gamma_5 &: (E_1 - E_2) + 16\ B - C \end{aligned} \qquad (3)$$

with $C \cong 4.5$ B, the first singlet band in $RhCl_6^{---}$ corresponds to $(E_1 - E_2) =$ 21 000 cm^{-1} and the distance between the two singlet bands *, which is somewhat less than 16 B due to the influence of non-diagonal elements, implies B = 400 cm^{-1} for $RhCl_6^{---}$. If similar values are applied to $RuCl_6^{---}$, Tanabe and Sugano's theory predicts the first quartet band at 11 800 cm^{-1} and the first doublet band at 18 000 cm^{-1}.

For comparison with the electron transfer bands of ruthenium(III), Fig. 6 gives the spectrum of $Fe(CN)_6^{---}$. The six strong bands agree with the measurements of Kiss, Abraham and Hegedüs [32], and the present author has also found the very weak, broad band at 550 mμ with $\varepsilon \sim 0.3$. This seems to be a spin-forbidden crystal field band, even if it is tempting to ascribe it to impurities of the Turnbull's blue type. Gleu *et al.*[33–35] have prepared robust ruthenium(III) ammine complexes with nearly the same colours as the corresponding rhodium(III) ammines:

* It will be shown later that the values of B in d^n-complexes are only compatible with an average radius of the d-shell larger than the ionic radius. Thus, the partly occupied orbitals must be localized also on the ligands, eventhough a decreased central field relative to the gaseous ion (produced by the presence of some electrons donated from the ligands) co-operates in decreasing B.

$Ru(NH_3)_6^{+++}$	colourless
$Ru(NH_3)_5H_2O^{+++}$	colourless
$Ru(NH_3)_5Cl^{++}$	yellow
$Ru(NH_3)_5Br^{++}$	dark yellow
cis-$Ru(NH_3)_4Cl_2^+$	orange
trans-$Ru(NH_3)_4Cl_2^+$	red-orange
cis-$Ru(NH_3)_4Br_2^+$	red
trans-$Ru(NH_3)_4Br_2^+$	purple
$Ru(NH_3)_4\ ox^+$	yellow
$Ru(NH_3)_3\ Cl_3$	red

These colours demonstrate a bathochromic influence which is larger for bromide than for chloride, and which is slightly larger for *trans*- than for *cis*-complexes. The latter fact is of interest for the theory of tetragonal complexes. Since the spectrochemical series of crystal fields $Br^- < Cl^- < ox^{--} < H_2O < NH_3$ varies nearly as the decreasing tendency to give electrons off, it cannot be said with certainty if the colours are due to crystal field or electron transfer bands.

When sufficient ammonium chloride is added to prevent the precipitation of $Ru(OH)_3$, solutions of $Ru\ Cl_6^{---}$ in HCl reacts with concentrated ammonia water under formation of a clear, pink solution. It is difficult to separate the colourless hexammines and pentammines, probably formed in this reaction, from the traces of highly coloured ruthenium red. The constitution of the latter compound is not yet elucidated; it is diamagnetic [35] and probably a polynuclear complex with hydroxo bridges. Its formation in the solution mentioned above is reversible.

RUTHENIUM(II) COMPLEXES

Already Claus [36] observed a dark blue solution of ruthenium with strong reducing agents. This solution contains ruthenium(II) as shown by titrations with sodium amalgam (authors who assumed K_2RuCl_5OH to be $K_2RuCl_5(H_2O)$ found of course +1). The present author can add but a few new arguments to the vivid debate about the green colour formed, when yellow ruthenium solutions (with traces of +4?) are reduced with zinc amalgam or other metals, and which turn lavender blue with excess of reducing agent [37–43]. Grube and Nann [44] found that the actual oxidation state +1 in few minutes disproportionates to the metal and +2; and that +2 in 2 M HCl in two days is 5 % disproportionated to metal and +3. Grube and Fromm [45] later investigated $RuCl_3$ and its hydrates and found the emerald-green $RuCl_2^+$, which may resemble the green isomer of $RuCl_4(H_2O)_2^-$ (the other isomer is red) which Gall and Lehmann [41] assume to be a mixture of +2 and +3.

The reaction between yellow +4 and blue +2 requires some minutes, so that a green intermediate colour can be observed. Besides this the blue solution has only been measured in solutions 1 M to 4 M in HCl. In stronger hydrochloric acid, the spectrum of the solution is displaced towards red with resulting green colour: The maximum at 660 mμ to 710 mμ and the shoulder at 568 mμ to 578 mμ. The influence of the halide ion was studied by reduction of a chloride-free ruthenium(III) solution in 4 M HBr (see experimental section). Similar blue and green solutions with broad bands in the red are obtained.

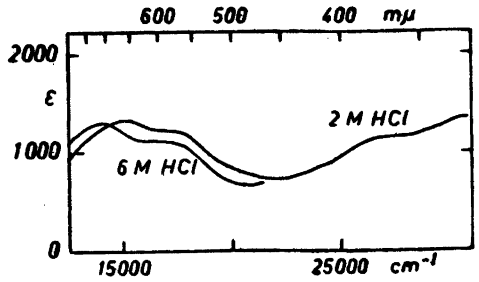


Fig. 7. Absorption spectra of ruthenium (II) complexes.

0.001 M ruthenium in 2 M and 6 M HCl, reduced with zinc amalgam.

The absolute extinction coefficients cannot be determined exactly, due to the impurities of +3 and the metal. But the value of $\varepsilon \sim 1\,100$ is too high for an ordinary crystal field band. Thus, it is probably an electron transfer band. It cannot be excluded *a priori* that ruthenium(II) is a stronger oxidizing agent, *i. e.* has larger electron affinity, than ruthenium(III). The disproportionation [44] supports this possibility, analogous to the behaviour of copper(I).

Ruthenium(II) is a d^6-system and may thus be expected to form diamagnetic complexes ($S = 0$). But only the colourless $Ru(CN)_6^{-4}$ and several sulphito-ammine complexes [46] are known to be six-coordinated, while the blue complexes are often assumed to be $RuCl_4^-$. If they have a planar configuration, they have probably the groundstate $\gamma_5^5\,\gamma_3$ with $S = 1$. Even if Tanabe and Sugano [9] have proven that no groundstate of an octahedral complex has $S = 1$ in d^6 and $S = \frac{3}{4}$ in d^5-systems, tetragonal complexes may stabilize the intermediate values of S.

ELECTRON TRANSFER FROM MOLECULAR ORBITALS

In Mulliken's theory of molecular orbitals [4], the symmetry of the distribution of atomic nuclei in the molecule determines the possible quantum numbers of the orbitals, analogous to the symmetry of the crystal field from the ligands, acting on the central ion [2]. In this paper the notation of Bethe [2] will be used also for molecular orbitals of octahedral complexes. The translation table is:

Mulliken:	a_1	a_2	e	t_1	t_2	(4)
Bethe:	γ_1	γ_2	γ_3	γ_4	γ_5	

While small letters denote the states of electrons, the corresponding states of whole systems, here molecules, are denoted by capital letters $A_1 = \Gamma_1$. In a complex with a centre of symmetry, the states can further be divided into two classes with different parity: odd and even. This is denoted by the small letters u (ungerade) and g (gerade) after the numbers: γ_{1g}, Γ_{3u}. The parity of a system is equal to the sum of parities of the electrons, defined by the addition rules:

$$\begin{aligned} g + g &= g \\ u + g = g + u &= u \\ u + u &= g \end{aligned} \qquad (5)$$

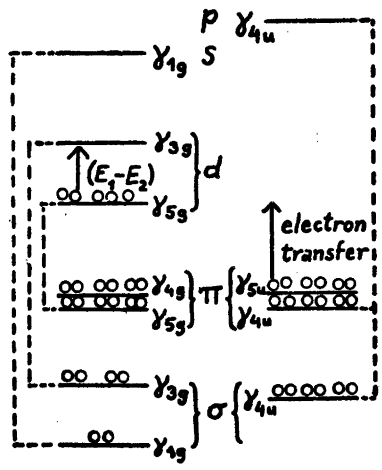


Fig. 8. Molecular orbitals of an octahedral complex MX_6 with partly filled d-shell in M. Even orbitals (g) at left-hand and odd (u) at right-hand side. Arrows denote possible interactions between orbitals with the same Γ_n and parity.

In a single atom or ion, an electron has the quantum number 1, and the parity is g for even values of 1, *i. e.* for s-, d-, g-electrons *etc.* and u for odd values of 1, *i. e.* for p-, f-, h-electrons etc. Thus, all the values of γ_n and Γ_n encountered in the theory for pure d^n-configurations are even, and the "g" is often neglected in the quantum numbers.

The electrons of the six ligands of an octahedral complex can be classified as σ-electrons, π-electrons, etc. according to their angular momentum around the straight line connecting central ion-ligand's centre being 0 or 1, etc. The chemical bonds between the ligands and the central ion can be described by the intermixing of orbitals having the same γ_n and parity, from the ligands and the central ion. Thus, the chemical bonds can be classified as σ-bonds, π-bonds *etc.* according to the electrons, participating from the ligands.

Van Vleck [3] pointed out the σ-bonds in an octahedral complex with an unfilled nd-shell is due to the three pairs of intermixing orbitals:

$$\begin{aligned} &\gamma_{3g} \text{ with } \gamma_{3g}(\mathrm{nd}) \\ &\gamma_{4u} \text{ with } \gamma_{4u}(\mathrm{n}+1\mathrm{p}) \\ &\gamma_{1g} \text{ with } \gamma_{1g}(\mathrm{n}+1\mathrm{s}) \end{aligned} \qquad (6)$$

The three types of orbitals can accumulate 4, 6, and 2 electrons, respectively, 12 bonding and 12 anti-bonding electrons (six electron-pairs in the localized valence picture). According to Hartmann [5], the energy of the bonding orbitals decrease in the order, given in eqn. 6. It is evident that the d^2sp^3-hybridization discovered by Pauling [47,48] is equivalent to complete intermixing of the three pairs of orbitals. The molecular orbital theory has the advantage that the electrostatic crystal field model and Pauling's hybridization can be described as two limiting cases [5] with, respectively, pure d^n-configurations and complete intermixing (which is 50 % in the squares of the wavefunctions). Owen [8] pointed out that the intermixing coefficients can be different for the three orbital types γ_{3g}, γ_{4u} and γ_{1g}. Thus, the evolution from the "ionic" to "co-

valent" structure [48] must be described by three independent parameters. In all cases of intermixing, the parameter may happen to exceed 50 % in the squares, corresponding in this case to higher energy of the original σ-electrons than of the electron of the central ion.

The 24 π-electrons from six monatomic ligands of the type Cl^- are distributed in the four orbitals (*cf.* Orgel [7]) of which two are intermixed [8]:

$$\begin{aligned} \gamma_{4u} &\text{ — with } \gamma_{4u} \text{ (n +1 p)} \\ \gamma_{4g} &\text{ —} \\ \gamma_{5u} &\text{ —} \\ \gamma_{5g} &\text{ — with } \gamma_{5g}\text{(nd)} \end{aligned} \qquad (7)$$

There are no orbitals in the central ions of the type γ_{4g} and γ_{5u}, and the ligand orbitals are thus non-bonding (*cf.* Fig. 8).

The effect of intermixing of orbitals [3,8] is to increase (E_1—E_2) by σ-bonding (which increases the energy of γ_{3g}(d)) and to decrease (E_1—E_2) by π-bonding (which increases the energy of the relatively low γ_{3g}(d)). This type of intermixing is connected with the non-orthogonality of the orbitals in the central ion and the ligands, which thus have "overlap" integrals contrary to the orbitals used in monatomic problems. Another type of intermixing can be found between two levels of the system with the same Γ_n, due to two configurations with a different distribution of electrons in the molecular orbitals. The latter type of intermixing gives generally smaller effects [49,50], but it must be realized that the molecular orbital theory does not give a detailed picture, when more levels are possible from a given configuration: the four levels $^3\Gamma_4$, $^3\Gamma_5$, $^1\Gamma_4$ and $^1\Gamma_5$ of the d^6-systems $\gamma_5^5\,\gamma_3$ have different energies even in a strong crystal field, while the distribution of electrons in the molecular orbitals is identical in the four levels. The concept of molecular orbitals is more distinct in the compounds outside the transition groups, where most configurations of interest do only contain one level.

The crystal field bands, which are characteristic for the complexes with partly filled d-shells are thus in the molecular orbital language due to transitions between the possible levels Γ_n of the electrons in γ_{5g} and γ_{3g}, while the other molecular orbitals are invariably filled or empty during the transition. The low intensities demonstrate [31] that the parity "g" is at least a 99 % good quantum number; and the orbital quantum numbers γ_{5g} and γ_{3g} are only affected by relatively small intermixings with other configurations, while Γ_n is only intermixed by (L, S) coupling effects. But the orbitals γ_{5g} and γ_{3g} cannot be seen from the absorption spectra to be pure d-electrons; they may contain considerable amounts of π- and σ-antibonding character, respectively. Owen [8] concludes from the decreased values of ζ_{3d} in the first transition group complexes, found by paramagnetic measurements, that the σ-intermixing of γ_{3g} varies between 17 % in $Ni(H_2O)_6^{++}$ to 37 % in $Cr(H_2O)_6^{+++}$. By the more direct method of measuring the contribution of nuclear fine-structure of Ir, Cl and Br to the paramagnetic reasonance curves of $IrCl_6^-$ and $IrBr_6^-$, Owen and Stevens [10] found 20 % π-intermixing of γ_{5g} in these much more distinctly "covalent" complexes, while the σ-intermixing is assumed to be rather complete, *i. e.* 50 % in the platinum group complexes.

In d^5-systems, the excited states of the electron transfer bands correspond presumably to the closed shell γ_5^6, which can be only in one state, $^1\Gamma_{1g}$. Since $\gamma_{5g}^5\gamma_{3g}$ in iridium(III) is situated [1] about 25 000 cm^{-1} above γ_{5g}^6, the next type of excited state $\gamma_{5g}^5\gamma_{3g}$ will be far in the ultraviolet. Besides (L, S) coupling effects, each band should thus correspond to one type of hole in the molecular orbitals, which have lower energy than the partly filled γ_{5g}-shell (if this is not be case, the electron transfer would be spontaneous). It can be presumed that these orbitals of highest energy are of the π-electron type, while the stronger bonding σ-orbitals have lower energy. This is supported by the observed intensities in iridium(IV) and ruthenium(III) complexes (see Tables 1 and 3). The intensity of a transition is increasing with the coincident presence in space of the groundstate ψ_1 and the excited state ψ_2, *i. e.* proportional to [51]:

$$\left(\int \psi_1 \; r \; \psi_2 \; dr\right)^2 \tag{8}$$

The π-electrons which are mainly removed from the central ion, has a relatively low value of this integral, corresponding to the oscillator strength $P \sim 0.02$. When the σ-electrons are excited to anti-bonding states, much higher values of P are expected at higher wavenumbers. Since γ_{4u} is weakly bonding, while γ_{5u} is not bonding at all, the configuration $\gamma_{5g}^6\gamma_{4u}^{-1}$ (π) has probably slightly higher energy than $\gamma_{5g}^6\gamma_{5u}^{-1}$ (π), when a hole in a molecular orbital is denoted $\gamma_u^{-1}(\pi)$ or (σ).

The two high bands with $\varepsilon \sim 2\,000$ in $RuCl_6^{---}$, $RuBr_6^{---}$ and $IrCl_6^{--}$ should thus correspond to $^2\Gamma_{5u}$ at lower and $^2\Gamma_{4u}$ at higher wavenumber. By effects of intermediate coupling, the two bands should each divide into two bands:

$$\begin{aligned} {}^2\Gamma_5 \times \Gamma_6 &= \Gamma_7 + \Gamma_8 \\ {}^2\Gamma_4 \times \Gamma_6 &= \Gamma_6 + \Gamma_8 \end{aligned} \tag{9}$$

Due to deviations from the cubic symmetry, the band Γ_8 can further divide into two, but Kramer's degeneracy permits only three levels to be formed from the six states in $^2\Gamma_4$ or $^2\Gamma_5$. This accounts for $IrBr_6^{---}$ exhibiting six bands with a splitting, comparable to $\zeta_{4p} = 2\,458$ cm^{-1} in atomic Br, while the smaller $\zeta_{3p} = 588$ cm^{-1} in Cl is only indicated by the splitting in $IrCl_6^{--}$ at 23 200 and 24 200 cm^{-1}.

Since the even $\gamma_{4g}(\pi)$ and $\gamma_{5g}(\pi)$ presumably have similar energy as the odd π-orbitals, the observation of weak electron transfer bands from these states is not very probable. But the weak shoulder of $IrCl_6^{--}$ at 17 400 cm^{-1} is not yet identified; it resembles very much a spin-forbidden band as discussed above, but quartet levels are only possible in configurations with at least two partly filled shells with each an electron or a hole. It may be a crystal field band $^2\Gamma_{ng}$ of the type discussed above for ruthenium(III) complexes, highly intermixed by hemiedric fields with the odd levels of electron transfer. However, this necesitates interactions between two levels, which are mainly different by two electrons.

In the platinum(IV) and other d^6-systems, the excited configuration of an electron transfer band must be $\gamma_{5g}^6\gamma_{3g}$. The relatively high energy of this configuration explains very well the lower oxidizing character of platinum(IV),

compared to iridium(IV) and of rhodium(III), compared to ruthenium(III). The electron transfer bands seem to be about 10 times higher in the d^6-systems than in the d^5-systems, suggesting the transfer of $\gamma_{4u}(\sigma)$.

In the first transition group, the d^6-systems of cobalt(III) exhibit similar very strong electron transfer bands, as shown by Linhard and Weigel [52]. Smaller bands with $\varepsilon \sim 1\,000$ occur only in the case of ligands with internal transitions, *e. g.* SCN^- or NO_2^-. An analogy to ruthenium(III) and iridium(IV) with one hole in a closed shell, which moves by the transition, can be found in the d^9-system copper(II). Besides the strong absorption in the far ultraviolet, a band of $CuCl_4^{--}$ can be distinguished at 26 000 cm^{-1} with $\varepsilon \sim 1\,500$. In the dark-red solutions of copper(II) in HBr, presumably containing $CuBr_4^{--}$, a double band is found by the author at 588 mμ ($\varepsilon = 1\,000$) and 512 mμ ($\varepsilon = 2\,100$). These bands are probably due to transfer of a γ_{t5u} electron. This level is the only tetragonal one, which can split due to intermediate coupling, maintaining Kramer's degeneracy. Belford [56] has recently applied the molecular orbital theory to copper(II) complexes, especially with two acetylacetonates in the plane and different solvents perpendicular to the plane. Ito and Kuroda [57] have published four papers on the molecular intermixing of d-orbitals in general. Only the japanese text of the three first has been available to the present author, but Ito and Kuroda seem to place the bonding σ-orbitals γ_3 and γ_{4u} very close below γ_5 (3d), thus exaggerating their influence. Rather, the crystal field splitting must constitute roughly 50 % of $(E_1 - E_2)$, as pointed out by Belford [56] who calculated the influence of the crystal field on a Hartree's self-consistent field copper ion, rather than the unprobable hydrogen-like 3d-electron [5] with $Z = 7.85$.

Fig. 6 gives the spectrum of $Fe(CN)_6^{---}$, one of the few $3d^5$-systems with $S = \frac{1}{2}$. The six bands found may be compared to those of $IrBr_6^{--}$. However, in this case the diatomic ligands have empty molecular orbitals to which γ_{5g}-electrons from the central ion can be excited. The triple bond between carbon and nitrogen in CN^- is equivalent to one σ- and two π-orbitals of anti-bonding type, which are empty in the ground-state. The excited states in this ion must have high energy, since ε first exceeds 1 at 265 mμ and $\varepsilon = 10$ at 215 mμ.

EXPERIMENTAL

The spectra were measured on a Cary spectrophotometer, furnished with a tungsten lamp in the range 800 – 325 mμ and with a hydrogen lamp 400 – 220 mμ; 1 cm absorption cells were used. While the Beckman spectrophotometer has its optimum accuracy at optical densities in the range 0.3 to 0.6, the similar range seems to be 0.8 to 1.5 on the Cary.

Preparation of the solutions of ruthenium complexes. Ruthenium metal powder from "Dansk Hollandsk Ædelmetal" (H. Drijfhout and Zoon) was melted with the ten-fold weight of Merck's potassium hydroxide in a nickel dish. Air-oxidation produces K_2RuO_4, but KNO_3 or $KClO_3$ mixed with the metal finishes the reaction in ten minutes. For preparation of the ruthenium(III) bromide solution, $KBrO_3$ was used as oxidizing agent. In all cases the cooled, tomato-red mass was dissolved in water (small gas-bubbles were evolved) and a few ml 96 % ethanol was added. After some seconds, the ruthenium is quantitatively reduced and precipitated as a black tetrahydroxide from a greenish, intermediate colour. It was washed several times with water and soon (to evade ageing) dissolved by boiling for 30 minutes with 6 M HCl or HBr. The clear, dark-brown solution

in HCl can be reduced with excess of precipitated silver powder to a strawberry-red solution of $RuCl_6^{--}$ and $RuCl_5(H_2O)^{--}$, while further reduction with stronger reducing agents (Zn, Al) gives green and finally blue-violet ruthenium(II), as described above. $Ru(OH)_4$ boiled with HBr liberates Br_2 and a dark purple-brown solution is formed.

Preparation of the solutions of iridium(IV) complexes. Iridium metal powder from "Dansk Hollandsk Ædelmetal" was more difficult to oxidize. 3.3 g was mixed with 10 g NaCl and heated to 600–700° C in a vitreosil tube in a stream of chlorine. The cooled mass yielded only 1.3 g Ir soluble in water as $IrCl_6^{--}$. The coarse crystalline residue was melted six hours with NaOH + $NaNO_3$ in a nickel crucible; only 0.4 g was dissolved. Then, it was melted with 5 g BaO_2 + 5 g $Ba(NO_3)_2$, dissolving 0.5 g. The main portion of the rest was dissolved by melting with pure barium dioxide in the same crucible at 700° C for two hours. In all cases, the alkaline solutions precipitated, on boiling and dilution, most iridium as blue tetrahydroxide, which could be washed and dissolved in 10 M HCl. This gives a dark-blue colour, which after four days at room temperature or by boiling turns red-brown. The alkaline filtrate is pale lavender-blue and is unchanged by addition of acids. The absorption spectrum exhibits maxima at 575 mμ (very broad, often with a shoulder at 740 mμ) and a shoulder at 356 mμ. If boiled with $BaCO_3$, the acid solution precipitates $Ir(OH)_4$.

Na_2IrCl_6, $6H_2O$. A sample of fine quality from the laboratory's collection was used. K_2IrCl_6 of unknown origin was found to contain much Pt; "Crude IrO_2" of S. M. Jørgensen had a high content of Os, *etc.*

The purple chloride-free solutions of iridium(IV) have been made [1] from Na_2IrCl_6 boiled with $HClO_4$. Ayres and Quick [58] have investigated the solutions in mixtures of $HClO_4$, H_3PO_4, and HNO_3 and demonstrated the oxidation state to be +4. The maximum at 564 mμ has ε = 2 650 and is displaced, when pH increases over 3 to 584 mμ at pH = 5. The analytical method does not seem to be more advantageous than the determination of $IrCl_6^{--}$ in strong HCl + Cl_2 and seems to have the same drawbacks: Ru and Os interfere strongly, while Rh, Pd and Pt in both cases have ε only a few per cent of Ir. Although $Ir(OH)_4$ forms blue and purple, colloidal solutions [59,60], it cannot be regarded as certain, if the purple solutions in strong acids (which already were discovered by Vauquelin [61]), are not simply monomer or dimer hydroxo-aquo complexes.

$[N(C_2H_5)_4]_2PtCl_6$, K_2PtBr_6 and $[N(C_2H_5)_4]_2PtBr_6$ were taken from S. M. Jørgensen's collection. PtI_6^{--} was prepared several times from different solutions of $PtCl_6^{--}$ and KI and always showed identical spectra.

$[Pt(NH_3)_6]Cl_4$ was prepared according to Tronev and Shumilina [20]. $(NH_4)_2PtCl_6$ of the laboratory's collection was treated with liquid ammonia in a test tube, surrounded by a steel micro-autoclave. The pale yellow powder was extracted with water and made 5 M in HCl, which precipitated the white chloride. Since nearly all salts of $Pt(NH_3)_6^{++++}$ are feebly soluble, the ionic strength was maintained at only 0.1 during the titration with the glass-electrode pH-meter Radiometer M22.

$[Pt(NH_3)_5Cl](NO_3)_3$ was kindly furnished by Professor J. A. Christiansen. For study of the influence of nitrate ions the spectra were compared with $[Pt(NH_3)_4(NH_2)Cl]Cl_2$ dissolved in HCl, which exhibited also the weak band at 286 mμ.

$K_3Fe(CN)_6$ was recrystallized from "Anala R" by Miss Lene Rasmussen.

Acknowledgments. I am very much indebted to Professor J. Bjerrum for his interest in the work. Further, I thank Miss Bodil Friis for assistance with preparation of ruthenium complexes.

REFERENCES

1. Jørgensen, C. Klixbüll *Acta Chem. Scand.* **10** (1956) 500.
2. Bethe, H. *Ann. Physik* [5] **3** (1929) 133.
3. Van Vleck, J. H. *J. Chem. Phys.* **3** (1935) 803 and 807.
4. Mulliken, R. S. *J. Chem. Phys.* **3** (1935) 375, 506, 517 and 586.
5. Hartmann, H. *Theorie der chemischen Bindung auf quanten-theoretischer Grundlage* Springer Verlag 1954.
6. Orgel, L. *J. Chem. Soc.* **1952** 4756.
7. Orgel, L. *J. Chem. Phys.* **23** (1955) 1004, 1819 and 1824.

8. Owen, J. *Proc. Roy. Soc. London* **227 A** (1955) 183.
9. Tanabe, Y. and Sugano, S. *J. Phys. Soc. Japan* **9** (1954) 753 and 766.
10. Owen, J. and Stevens, K. W. H. *Nature* **171** (1953) 836.
11. Griffiths, J. H. E. and Owen, J. *Proc. Roy. Soc. London* **226 A** (1954) 96.
12. Babaeva, A. V. *Bull. Acad. Sci. URSS Cl. Sci. Chim.* **1943** 171.
13. Inamura, Y. and Kondo, Y. *J. Chem. Soc. Japan* **72** (1951) 840.
14. Landolt-Börnstein Tables Ed. Vol I, part 1, p. 165.
15. Scheibe, G. *Z. physik. Chem.* **5B** (1929) 355.
16. van Santen, J. H. and van Wieringen, J. S. *Rec. trav. chim.* **71** (1952) 420.
17. Jørgensen, C. Klixbüll *Acta Chem. Scand.* **8** (1954) 1502.
18. Schlesinger, H. and Tapley, M. *J. Am. Chem. Soc.* **46** (1924) 276.
19. Wheeler, Th. E., Perros, Th. P. and Naeser, C. R. *J. Am. Chem. Soc.* **77** (1955) 3488.
20. Tronev, V. G. and Shumilina, M. E. *Doklady Akad. Nauk. SSSR* **101** (1955) 499.
21. Lifschitz, J. and Rosenbohm, E. *Z. physik. Chem.* **97** (1920) 1.
22. Howe, J. L. *J. Am. Chem. Soc.* **26** (1904) 543.
23. Howe, J. L. and Haynes, L. P. *J. Am. Chem. Soc.* **47** (1925) 2920.
24. Charonnat, R. *Compt. rend.* **180** (1925) 1271.
25. Howe, J. L. *J. Am. Chem. Soc.* **49** (1927) 2381.
26. Charonnat, R. *Ann. Chim.* [10] **16** (1931) 5 and 123.
27. Jørgensen, C. Klixbüll and Bjerrum, J. *Acta Chem. Scand.* **9** (1955) 180.
28. Howard, J. B. *J. Chem. Phys.* **3** (1935) 813.
29. Wehner, P. and Hindman, J. C. *J. Am. Chem. Soc.* **72** (1950) 3911.
30. Jørgensen, C. Klixbüll *Acta Chem. Scand.* **9** (1955) 116.
31. Jørgensen, C. Klixbüll *Acta Chem. Scand.* **9** (1955) 405.
32. Kiss, A v, Abraham, J. and Hegedüs, I. *Z. anorg. Chem.* **244** (1940) 98.
33. Gleu, K. and Rehm, K. *Z. anorg. Chem.* **227** (1936) 237.
34. Gleu, K. and Cuntze, W. *Z. anorg. Chem.* **237** (1938) 187.
35. Gleu, K. and Breuel, W. *Z. anorg. Chem.* **237** (1938) 197, 326, 335 and 350.
36. Claus, C. *J. prakt. Chem.* **34** (1845) 431.
37. Remy, H. *Z. anorg. Chem.* **113** (1920) 229.
38. Remy, H. and Lührs, A. *Ber.* **61** (1928) 917.
39. Remy, H. and Wagner, Th. *Ber.* **61** (1928) 151.
40. Zintl, E. and Zaimis, Ph. *Ber.* **60** (1927) 842.
41. Gall, H. and Lehmann, G. *Ber.* **59** (1926) 2856, **60** (1927) 2491; **61** (1928) 1573.
42. Krauss, F. and Kückenthal, H. *Z. anorg. Chem.* **137** (1924) 33.
43. Remy, H. *Angew. Chem.* **42** (1929) 289 and 291.
44. Grube, G. and Nann, H. *Z. Elektrochem.* **45** (1939) 874.
45. Grube, G. and Fromm, G. *Z. Elektrochem.* **46** (1940) 661 and **47** (1941) 208.
46. Gleu, K., Breuel, W. and Rehm, K. *Z. anorg. Chem.* **235** (1938) 201 and 211.
47. Pauling, L. *J. Am. Chem. Soc.* **53** (1931) 1367.
48. Pauling, L. *The Nature of the Chemical Bond*, Ithaca, 1944.
49. Jørgensen, C. Klixbüll *Acta Chem. Scand.* **9** (1955) 717.
50. Jørgensen, C. Klixbüll *Acta Chem. Scand.* **9** (1955) 1362.
51. Condon, E. U. and Shortley, G. H. *Theory of Atomic Spectra*. Cambridge 1953.
52. Linhard, M. and Weigel, M. *Z. anorg. Chem.* **266** (1951) 49.
53. Slater, J. C. *Electronic Structure of Atoms and Molecules*. Technical Report No. 3, Solid-State and Molecular Theory Group. Massachusetts Institute of Technology, 1953.
54. McWeeny, R. *Electronic Structure of Molecules. Some recent Developments*. Technical Report No. 7. Solid-State and Molecular Theory Group. Massachusetts Institute of Technology. 1955.
55. Grünberg, A. A. and Faerman, G. P. *Z. anorg. Chem.* **192** (1930) 193.
56. Belford, R. L. *Bonding and Spectra of Metal Chelates*. University of California. Radiation Laboratory. 1955. UCRL-3051.
57. Ito, K. and Kuroda, Y. *J. Chem. Soc. Japan* **76** (1955) 545, 762, 766 and 934.
58. Ayres, G. H. and Quick, Q. *Anal. Chem.* **22** (1950) 1403.
59. Wöhler, L. and Witzmann, W. *Z. anorg. Chem.* **57** (1908) 323.
60. Ruff, O. and Fischer, J. *Z. anorg. chem.* **179** (1929) 177.
61. Vauquelin, L. N. *Ann. Chim.* **90** (1814) 260.

Received December 22, 1955.

ACTA CHEMICA SCANDINAVICA 10 (1956) 535—539

The Solubility of Silver Iodide in Aqueous Solutions of Silver Perchlorate

IDO LEDEN and CURT PARCK

Department of Inorganic Chemistry, Chalmers Institute of Technology, Göteborg, Sweden

The reaction between solid silver iodide and silver ions (*vide* formula (2) below) was studied at 25° C and at an ionic strength of 4 M by saturating 4 M solutions of silver perchlorate and sodium perchlorate and mixtures of these two solutions with silver iodide. The concentration of silver perchlorate in the mixtures ranged from 10^{-5} M to 3 M. The solubility of silver iodide in aqueous solutions of silver salts has been determined by previous authors only at rather high silver ion concentrations (for literature, *vide* Sillén [1]).

Solubilities above 5×10^{-4} M (molar silver ion concentration, $[Ag^+]$, >0.5) were determined by diluting the saturated solutions with hot water to a silver ion concentration of 0.025 M, where the solubility ($\sim 2 \times 10^{-6}$ M at 25° C) of silver iodide is negligible compared with the solubility at those high silver ion concentrations. The silver iodide, precipitated by the dilution, was filtered off from the solution after cooling and then weighed. The method was controlled by dissolving known (~0.1 g) amounts of silver iodide in a 4 M solution of silver perchlorate, which was then diluted as mentioned above. Three such experiments were made and the difference between the weights of silver iodide dissolved and recovered was in all three cases less than 0.05 %. It was determined by analyses that no solid phases other than AgI were formed by contact with any of the silver perchlorate solutions.

In the range $10^{-5} < [Ag^+] < 10^{-1}$ the solubilities were determined by using silver iodide labelled with ^{131}I (from Harwell). Radioactive silver iodide was prepared by mixing an aqueous solution of carrier-free iodide ^{131} with a solution of inactive sodium iodide to a known concentration of iodide, say 10^{-2} M, and precipitating the silver iodide with silver perchlorate. Before the precipitation a small part of the active solution of sodium iodide was diluted 10^3 or 10^5 times (with inactive iodide), so that its activity could be conveniently determined in a 10-ml G. M. tube for liquids (Type M6 from 20th Century Electronics Ltd., combined with a Predetermined Count Scaler PW 4035 from Philips). The precipitate of labelled silver iodide was washed carefully first with water and then with the solution, in which its solubility was finally de-

Table 1. The solubility of silver iodide in silver perchlorate solutions. Ionic strength 4 M ($NaClO_4$). Concentrations in M.

c_{AgClO_4}	$l_{exp.}$	$l_{calc.}$
0	$(9 \pm 3) \times 10^{-9}$	13×10^{-9}
10^{-5}	$(7 \pm 1) \times 10^{-9}$	6×10^{-9}
10^{-4}	$(6 \pm 1) \times 10^{-9}$	6×10^{-9}
10^{-3}	$(8 \pm 1) \times 10^{-9}$	8×10^{-9}
10^{-2}	$(8 \pm 1) \times 10^{-8}$	9×10^{-8}
10^{-1}	$(12 \pm 1) \times 10^{-6}$	11×10^{-6}
0.5	$(62 \pm 1) \times 10^{-5}$	64×10^{-5}
1	$(427 \pm 1) \times 10^{-5}$	4.3×10^{-3} *
2	$(298 \pm 3) \times 10^{-4}$	28×10^{-3} *
3	$(951 \pm 3) \times 10^{-4}$	85×10^{-3} *
4	0.2137 ± 0.0003	0.15 *

* These four values are calculated for the silver ion concentrations 0.99, 1.91, 2.78, and 3.37, respectively, which would be the values of $[Ag^+]$, if all complexes formed contain only one iodide atom.

termined by shaking in a thermostat. About 10 mg precipitate were used to prepare 100 ml of solution. Samples were taken from the solution after 8, 24, and 48 hrs and filtered under pressure at 25° C through a collodion filter in a Thiessen apparatus. During this time no other change of the activity of the saturated solution could be detected than that depending on the decay of ^{131}I (half-life 8.0 days), although the silver iodide darkened obviously in a few hours and was quite black after 2 days. The specific activity of the solid silver iodide had to be at least 100 millicuries per gram, when the lowest solubilities were measured. Further experimental details are given elsewhere [2].

The results are listed in Table 1. The accuracy (*vide* Table 1) of the radio assay method is rather low, mainly because of the low specific activity of the solutions, which corresponded to 10 to 30 cpm for the lowest solubilities, measured with a 30 cpm background count.

The solubility, l can be described by the equation

$$l = \sum_{n=-1}^{N} K_n [Ag^+]^n \qquad (1)$$

if the activity constants maintain constant values in all the solutions, and if the silver iodide is dissolved according to the reactions

$$m\ AgI(s) + n\ Ag^+ \rightleftharpoons Ag_{m+n}I_m^{n+} \qquad (2)$$

i. e., to produce species with the charges n (*cf.* Ref. [3]). By graphical methods or by trial and error the following constants are easily calculated ($N = 3$): $K_0 = 6 \times 10^{-9}$, $K_1 = 10^{-6}$, $K_2 = 7 \times 10^{-4}$, $K_3 = 3.7 \times 10^{-3}$. For K_{-1} the value 4.5×10^{-17} has been used, which is the value of the solubility product of silver iodide in a 4 M solution of sodium perchlorate, as determined in this laboratory by e.m.f. measurements. The experimental values of the solubility

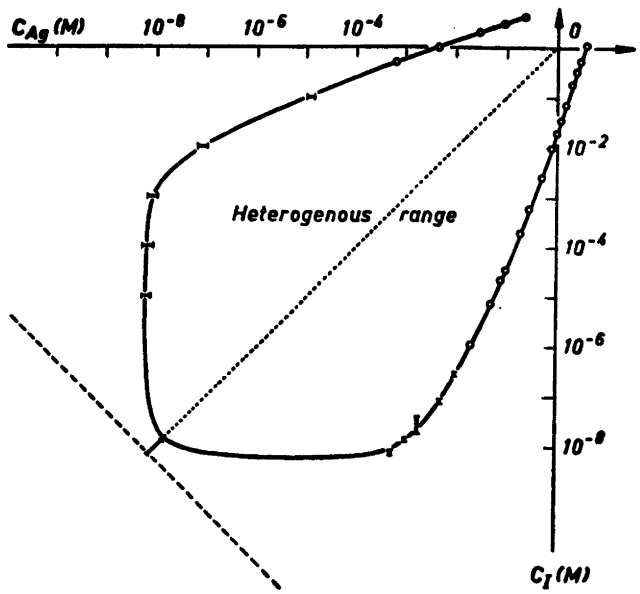


Fig. 1. The solubility of silver iodide in aqueous silver perchlorate and sodium iodide at 25° C. Ionic strength 4 M ($NaClO_4$).

are compared with those computed from eqn. (1) in Table 1. The concentration of free silver ions may be considered to be equal to the concentration of silver perchlorate in the solvent except for the pure sodium perchlorate, where the value $\sqrt{K_{-1}}$ has been used, and for the last four determinations in Table 1. In these latter cases the solubility can be neglected no longer, when compared with the contents of silver perchlorate. For the calculation of $[Ag^+]$ of these four solutions the constants K_n have been used, and it has been assumed that every complex contains only one iodide atom, *i. e.*, that the dominating species are Ag_4I^{3+} and Ag_3I^{2+}. As is seen from Table 1 the solubility is described well by eqn. (1) in all solutions except three, *viz.*, those of pure sodium perchlorate and 3 and 4 M silver perchlorate. In sodium perchlorate the reproducibility is also less than elsewhere, being dependent perhaps on the difficulty in washing away the silver perchlorate from the precipitate so carefully that its remaining concentration becomes small compared with 10^{-8} M. In the two last solutions with high silver ion concentrations the lack of success in describing the results with eqn. (1) can depend on any or all of the following reasons: (a) changes of activity factors, as most of the sodium perchlorate is here substituted by silver perchlorate; (b) formation of complexes with charges higher than 3, *i. e.*, $N > 3$ in eqn. (1), which would then contain more than five terms; (c) formation of complexes with several iodide atoms, *e. g.* $Ag_6I_3^{3+}$ instead of Ag_4I^{3+}, which would cause a smaller decrease of the free silver ions of the silver perchlorate than that calculated at the bottom of Table 1 and hence higher values of l_{calc}.

Fig. 1 is a graphical representation of the data of Table 1 and contains also the solubility of silver iodide in solutions of sodium iodide as determined in this laboratory. The curve above the line $c_{Ag} = c_I$, (dotted in Fig. 1) is calculated from the constants K_n and thus represents eqn. (1). The part of the curve under the same line describes the solubility in sodium iodide solutions. c_{Ag} and c_I are the t o t a l contents of silver and iodide of a system. Every point outside the curve signifies an unsaturated solution, the composition of which is given by the co-ordinates of the point. A point inside the curve signifies a heterogeneous system, containing both solid silver iodide and a saturated solution, the composition of which can be obtained easily from the diagram in the following way. Let Δ be the difference between the known total contents of silver and iodide of the heterogeneous system. Then the intersection of the solubility curve in Fig. 1 and the curve $c_{Ag}-c_I = \Delta$ gives the composition of the saturated solution. It is to be noted that $c_{Ag}-c_I = \Delta \neq 0$ is not a straight line, if drawn in a l o g a r i t h m i c diagram like Fig. 1. The dashed line to the left of Fig. 1 would describe the solubility of silver iodide, if no complexes were formed between silver and iodide ions.

From the constants K_n the distribution of iodide on the different complexes in a saturated solution can be calculated. If α_n is that fraction of the dissolved iodide, which is contained in a species with the charge n, the following expression is valid (*cf.* Ref.[4])

$$\alpha_n = \frac{K_n\,[Ag^+]^n}{l} \qquad (n = 0,\ 1,\ 2,\ \text{or}\ 3) \tag{3}$$

The distribution of iodide as calculated from eqn. (3) is given in Fig. 2, from which the values of α_n at a given silver ion concentration are obtained by drawing a vertical line through the corresponding abscissa. The curves divide this line in parts, each of which is equal to that α_n, whose number n has been written in the area between two curves. A remarkable feature of the distribution diagram is the almost complete predominance of uncharged molecules in a broad range of silver ion concentrations.

From solubility measurements alone it is not possible to conclude, whether the species formed contain one or several iodide atoms (*vide* Ref. [3]). As the solubility of silver iodide is very small in most of the solutions studied, it seems rather probable, however, that the species with the charges 0, 1, 2, and 3 simply are AgI, Ag_2I^+, Ag_3I^{2+}, and Ag_4I^{3+}. If this be the case, the distribution shown by Fig. 2 is also valid for u n s a t u r a t e d solutions containing silver iodide dissolved in aqueous silver perchlorate.

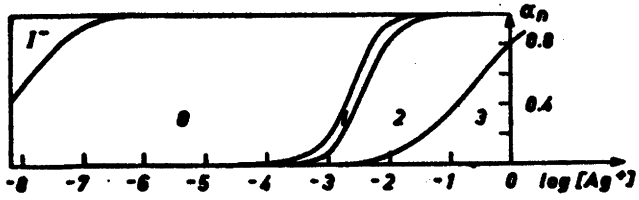


Fig. 2. The distribution of dissolved iodide on species with charges 0, 1, 2, and 3 in aqueous solutions of silver perchlorate saturated with silver iodide. Ionic strength 4 M ($NaClO_4$).

Obviously silver iodide is a very weak electrolyte. The degree of ionic dissociation of silver iodide in a pure aqueous solution is only about 50 % in spite of the low concentration. (See Fig. 2, which starts to the left with a solution of silver iodide in pure aqueous sodium perchlorate.) The dissociation constant for $AgI \rightleftharpoons Ag^+ + I^-$ (referring to d i s s o l v e d silver iodide) is $K_{-1}/K_0 = 7.5 \times 10^{-9}$, if the silver-iodide molecules are monomeric. The corresponding dissociation constants for silver chloride and silver bromide are about 8×10^{-4} and 4×10^{-5}, respectively (*vide* Refs.[2,4]).

Our thanks are due to Professor C. Brosset, who kindly permitted the use of the equipment of his laboratory for the G. M. measurements reported in this paper. We also wish to thank Professor J. Pepper, Saskatoon, Canada, for his work at our manuscript to make it more readable. The work was financially supported by *Statens Naturvetenskapliga Forskningsråd.*

REFERENCES

1. Sillén, L.-G. *Solubility of Silver Halides.* Prel. Report to the Int. Union of Pure and Applied Chem., Stockholm 1953 (mimeographed).
2. Berne, E. and Leden, I. *Z. Naturforsch.* **8a** (1953) 719.
3. Leden, I. *Svensk Kem. Tidskr.* **64** (1952) 249.
4. Berne, E. and Leden, I. *Ibid.* **65** (1953) 88.

Received December 7, 1955.

ACTA CHEMICA SCANDINAVICA 10 (1956) 540—547

A Potentiometric Study of the Complex Formation between Silver and Iodide Ions

IDO LEDEN

Department of Inorganic Chemistry, Chalmers Institute of Technology, Göteborg, Sweden

The e.m.f. of the cell (1) below was measured at 25° C in the range $0.003 < c_{Ag} < 0.08$ and with enough sodium iodide (<4 M) to prevent solid silver iodide from being precipitated. In this range the solutions contained significant amounts of four silver iodide species, *viz.* AgI_3^{2-}, AgI_4^{3-}, $Ag_2I_6^{4-}$, and $Ag_3I_8^{5-}$. The corresponding equilibrium constants were computed (Table 2) and the solubility product of silver iodide at the given ionic strength 4 M ($NaClO_4$) was determined.

The following cell, e. m. f. E mV, was measured at 25° C. All concentrations throughout the paper are given in gram formula weight per litre (M)

$$+\ \mathrm{Ag,AgI}\left|\begin{array}{l}c_{Ag}\ \mathrm{M\ AgClO_4}\\(4-c_{Ag})\ \mathrm{M\ NaClO_4}\end{array}\right|\mathrm{NaNO_3\ (sat.)}\left|\begin{array}{l}\mathrm{4\ M\ NaI}\end{array}\right|\begin{array}{l}c_{Ag}\ \mathrm{M\ AgClO_4}\\c_I\ \mathrm{M\ NaI}\\(4-c_{Ag}-c_I)\ \mathrm{M\ NaClO_4}\end{array}\Bigg|\ \mathrm{Ag}\quad(1)$$

The solutions of the right hand half-cell were obtained by mixing an original solution in the electrode vessel, containing c_{Ag} M $AgClO_4$ and $(4-c_{Ag})$ M NaI, with a solution from a burette containing c_{Ag} M $AgClO_4$ and $(4-c_{Ag})$ M $NaClO_4$. Portions of this latter solution were added until silver iodide was precipitated in the vessel. In some cases E was determined by measuring the two halves of the cell above against a reference electrode, $Hg,Hg_2Cl_2\,|\,4\ M\ NaCl\,|\,NaNO_3$ (sat.). The silver electrodes consisted of silver plated platinum wires, from which the silver-silver iodide electrodes were produced by anodic oxidation in a solution of sodium iodide acidified with hydrogen perchlorate (*cf.* Brown[1]). The sodium iodide was of *pro analysi* quality. Other chemicals used are described elsewhere (Ref. [2,3]), and here also the experimental details may be found.

The results of the measurements are given in Table 1. If the concentration of uncomplexed silver ions in the right hand solution of cell (1) is $[Ag^+]$, Nernst's formula gives

$$E = 59.16\ \log \frac{c_{Ag}}{[Ag^+]} \qquad (2)$$

Table 1. The potentiometric measurements.

$c_{Ag} = 0.08$ ●					$c_{Ag} = 0.02$ ○				
c_I	$[I^-]$	E	$10^{14} \times F_4$	$-\log [Ag^+] - 2 \log [I^-]$	c_I	$[I^-]$	E	$10^{14} \times F_4$	$-\log [Ag^+] - 2\log [I^-]$
3.92	3.63	987.1	2.75	16.66	3.98	3.90	988.3	2.19	17.23
3.63	3.34	979.4	2.88	16.60	3.69	3.61	979.9	2.14	17.14
3.38	3.09	972.5	3.02	16.56	3.43	3.35	972.8	2.19	17.09
3.16	2.87	966.2	3.16	16.51	3.21	3.13	966.0	2.24	17.04
2.80	2.52	954.9	3.44	16.44	3.02	2.94	960.0	2.30	16.99
2.58	2.31	947.7	3.64	16.39	2.84	2.76	954.3	2.35	16.95
2.39	2.12	941.2	3.98	16.35	2.62	2.54	946.0	2.35	16.88
2.23	1.97	935.8	4.37	16.33	2.43	2.36	939.1	2.40	16.82
2.09	1.83	930.2	4.68	16.30	2.26	2.19	931.9	2.46	16.77
1.92	1.67	923.7	5.25	16.27	2.12	2.05	926.1	2.58	16.74
1.78	1.53	916.8	5.83	16.22	1.95	1.87	918.5	2.70	16.68
1.66	1.42	911.9	6.47	16.21	1.81	1.74	911.5	2.76	16.63
					1.66	1.59	904.3	3.03	16.59
1.61	1.39	911.3	$L = 4.4 \times 10^{-17}$		1.53	1.46	897.2	3.25	16.54
1.56	1.34	910.7	$L = 4.3 \times 10^{-17}$		1.42	1.35	891.2	3.48	16.50
1.51	1.29	910.5	$L = 4.2 \times 10^{-17}$		1.31	1.24	883.6	3.64	16.45
					1.28	1.21	881.6	3.73	16.43
					1.17	1.10	874.2	4.08	16.40
					1.08	1.01	868.0	4.48	16.36
					0.996	0.93	863.6	$L = 4.7 \times 10^{-17}$	
					0.926	0.86	862.2	$L = 4.6 \times 10^{-17}$	

From the solutions below the lines silver iodide has been precipitated. Hence the solubility product, L, can be computed from the values of E, measured in these solutions.

●, ○, □, +: These signs are used in Figs. 1 and 2 to distinguish the four titration series.

As the variation of $c_{Ag}/[Ag^+]$ is about 1000:1 within a titration series, it is more practical to use the function (*cf.* Ref.[3])

$$F_4 = \frac{c_{Ag}}{[Ag^+]\ [I^-]^4} \tag{3}$$

for the graphical representation as the range of variation of F_4 is only 3:1 at most. F_4, drawn as a function of $1/[I^-]$, gives some of the equilibrium constants more directly than does a logarithmic representation.

To calculate F_4 and on the whole to analyse the data of Table 1, it is necessary to compute the concentration of the f r e e iodide ions of the solution. This has been done (*cf.* columns c_I and $[I^-]$ of Table 1) by reducing c_I with the small term of correction $\bar{n} \cdot c_{Ag}$, where $\bar{n}$, defined by the well-known eqn. (4), is the mean number of iodide ions bound per silver ion in the solution.

$$[I^-] = c_I - \bar{n} \cdot c_{Ag} \tag{4}$$

Table 1. Continued.

c_{Ag} = 0.01 □					c_{Ag} = 0.00333 +				
c_I	$[I^-]$	E	$10^{14} \times F_4$	$-\log [Ag^+] - 2 \log [I^-]$	c_I	$[I^-]$	E	$10^{14} \times F_4$	$-\log [Ag^+] - 2\log [I^-]$
3.99	3.95	988.8	2.14	17.52	4.00	3.99	989.7	2.10	18.01
3.69	3.65	980.7	2.14	17.46	3.45	3.44	974.5	2.10	17.88
3.44	3.40	973.7	2.14	17.40	3.23	3.22	967.9	2.14	17.82
3.22	3.18	966.7	2.14	17.34	3.03	3.02	961.2	2.10	17.76
3.02	2.98	960.6	2.20	17.30	2.86	2.85	954.6	2.10	17.71
2.63	2.59	946.5	2.24	17.17	2.63	2.62	946.6	2.14	17.64
2.43	2.39	939.0	2.30	17.11	2.44	2.43	939.7	2.19	17.59
2.27	2.23	932.4	2.35	17.06	2.27	2.26	932.2	2.20	17.53
2.12	2.08	925.9	2.40	17.01	2.13	2.12	926.1	2.24	17.48
1.96	1.92	917.6	2.40	16.94	1.96	1.95	918.1	2.30	17.44
1.81	1.77	910.4	2.52	16.89	1.82	1.81	911.2	2.35	17.38
1.66	1.62	902.9	2.64	16.84	1.67	1.66	902.3	2.35	17.31
1.60	1.56	898.7	2.64	16.80	1.60	1.59	898.6	2.46	17.27
1.53	1.49	895.4	2.76	16.79	1.54	1.53	894.7	2.40	17.23
1.43	1.39	888.8	2.82	16.74	1.43	1.42	887.8	2.52	17.19
1.29	1.25	879.2	3.03	16.67	1.29	1.28	878.2	2.58	17.11
1.17	1.13	871.5	3.31	16.62	1.08	1.07	861.3	2.76	16.98
1.08	1.04	863.0	3.32	16.56	1.00	0.99	854.1	2.82	16.93
0.998	0.963	857.0	3.56	16.52	0.909	0.897	845.4	3.03	16.86
0.907	0.873	849.2	3.90	16.47	0.833	0.822	837.9	3.17	16.81
0.832	0.798	842.9	4.37	16.44	0.769	0.758	831.2	3.40	16.77
					0.667	0.656	818.4	3.72	16.68
					0.615	0.614	811.7	3.72	16.57
0.798	0.766	841.0 $L = 4.6_5 \times 10^{-17}$							
0.768	0.736	839.5 $L = 4.7_5 \times 10^{-17}$			0.533	0.522	803.2 $L = 4.6 \times 10^{-17}$		

A sufficiently accurate value of $\bar{n}$ can be deduced from Bodländer's formula, approximated to (*cf.* Ref.[4])

$$\frac{\Delta E}{\Delta \log c_I} = 59.16\ \bar{n} \qquad (5)$$

where ΔE and Δc_I are the differences between two consecutive values of E and c_I in a titration series of Table 1. Though this approximation is certainly far from accurate, especially as the solutions contain polynuclear complexes, it gives values of $[I^-]$ from eqn. (4), which agree in all cases to within 1 % with the final values computed below. Hedström [5] has recently given an exact and general method to calculate the concentration of free ligands of a complex system, but in the present case a sufficient number of titration series has not been measured in order to make it possible to carry out the graphical integration necessary in Hedström's method.

The complex formation can be described by the equilibria

$$m\ Ag^+ + n\ I^- \rightleftharpoons Ag_mI_n^{m-n} \qquad (6)$$

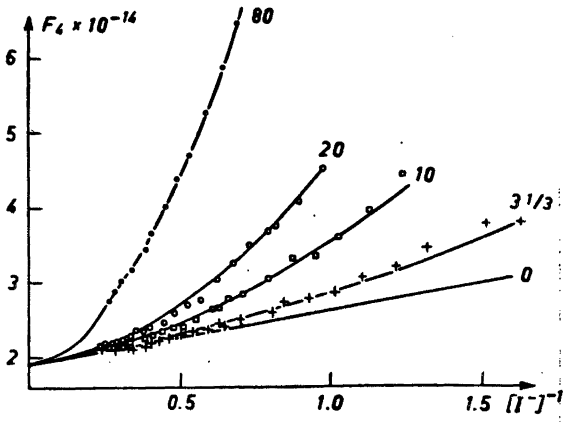


Fig. 1. F_4 *as a function of* $1/[I^-]$. *The numbers at the curves denote* $10^3 \times c_{Ag}$. *The ordinates of the points are obtained from the experiments by means of eqn. (3). The curves are calculated from the values of* $\beta_{m,m+n}$ *in Table 2 with the aid of eqns. (11) and (12).*

with the over-all complexity constants $\beta_{m,n}$. The law of mass action then gives ($\beta_{1,0} = 1$)

$$c_{Ag} = \sum_{m=1}^{M} \sum_{n=0}^{N} m\,[Ag_m I_n^{m-n}] = \sum_{m=1}^{M} \sum_{n=0}^{N} m\beta_{m,n}[Ag^+]^m[I^-]^n \qquad (7)$$

and hence F_4 can be written as

$$F_4 = \sum_{n=0}^{N} \beta_{1,n}[I^-]^{n-4} + \sum_{m=2}^{M} \sum_{n=1}^{N} m\beta_{m,n}[Ag^+]^{m-1}[I^-]^{n-4} \qquad (8)$$

where the first sum of the right hand member originates from the mononuclear and the double sum from the polynuclear species. Obviously

$$\lim_{c_{Ag} \to 0} F_4 = F_4^\circ = \sum_{n=0}^{N} \beta_{1,n}[I^-]^{n-4} \qquad (9)$$

F_4 is drawn as a function of $1/[I^-]$ in Fig. 1, from which it is seen that the curves for the two series with lowest silver contents coincide for low values of $1/[I^-]$. This gives immediately F_4°, which can be described by a straight line, *i. e.*

$$F_4^\circ = \beta_{1,4} + \beta_{1,3} / [I^-] \qquad (10)$$

for sufficiently high values of $[I^-]$. $\beta_{1,3} = (7 \pm 2) \times 10^{13}$ is obtained as the slope and $\beta_{1,4} = (19 \pm 1) \times 10^{13}$ as the extrapolated ordinate of this line. In Fig. 1 F_4° is drawn as a straight line in all that range, where potentiometric measurements have been made. This could be done, as some measurements of the solubility of silver iodide in aqueous sodium iodide, carried out in this

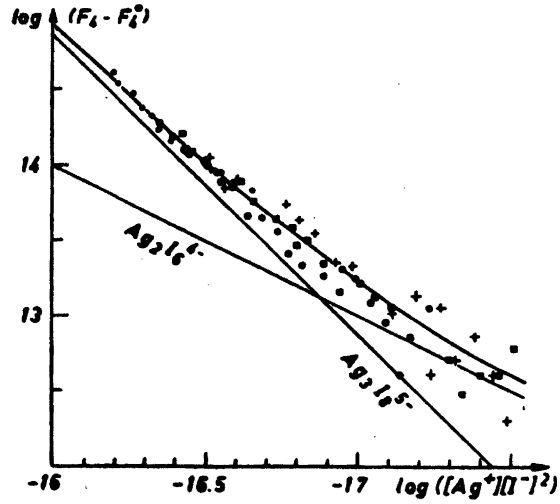


Fig. 2. (F_4—F_4°) *is a function of* $[Ag^+][I^-]^2$ *solely for all the four series measured. The straight lines show how* (F_4—F_4°) *can be separated into two terms, corresponding to the two complexes marked.*

laboratory, show definitely that the succeeding terms of F_4°, *viz.* $\beta_{1,2}/[I^-]^2$ and so on, are quite negligible, when $[I^-] > 0.5$.

The polynuclear species and their strength can be obtained by studying the difference (F_4—F_4°), F_4° now being known from eqn. (10). This has been done in Fig. 2, where log (F_4—F_4°) has been drawn as a function of log ($[Ag^+][I^-]^2$) (*cf. e.g.* Hietanen and Sillén [6]). In this diagram the points from all the four series measured fall on one single curve. This means that the only terms to be considered in the double sum of eqn. (8) are those of the form $\beta_{m,\,2m+2}$ $([Ag^+][I^-]^2)^m$, corresponding to one or several of the species $Ag_mI_{2m+2}^{(m+2)-}$. At the higher values of (F_4—F_4°) the curve of Fig. 2 is described rather well by a straight line with slope —2, which means that the species $Ag_3I_8^{5-}$ dominates. At lower values the accuracy is small, as (F_4—F_4°) is small compared with F_4. At all events it seems obvious that the points here lie over the line mentioned, and hence a term of first degree in $[Ag^+]$ $[I^-]^2$ has been introduced, representing the silver tied up in $Ag_2I_6^{4-}$. Hence the only polynuclear complexes to be considered are $Ag_2I_6^{4-}$ and $Ag_3I_8^{5-}$. The distribution of the silver between those is shown by the two straight lines in Fig. 2. Their positions are settled by the over-all complexity constants $\beta_{2,6} = (5 \pm 3) \times 10^{29}$ and $\beta_{3,8} = (25 \pm 5) \times 10^{45}$, which have been obtained from the straight line resulting, when (F_4—F_4°) · $[Ag^+]^{-1}$ $[I^-]^{-2}$ is drawn in a diagram as a function of $[Ag^+]$ $[I^-]^2$. From such a diagram the accuracy of the constants can also be judged.

From the discussions above it follows, that only four complexes, *viz.* AgI_3^{2-}, AgI_4^{3-}, $Ag_2I_6^{4-}$, and $Ag_3I_8^{5-}$, are to be considered in the range, where e.m.f. measurements have been carried out. Hence eqn. (7) is simplified in this range to

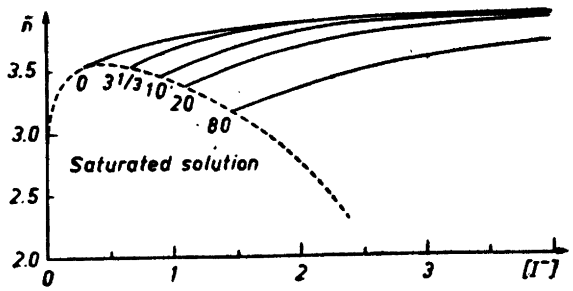


Fig. 3. The mean number, $\bar{n}$, of iodide ions bound per silver ion in unsaturated solutions with total silver contents marked as $10^3 \times c_{Ag}$ at the corresponding curves. The dashed curve is calculated from the solubility of AgI in aqueous solutions of NaI.

$$c_{Ag} = \beta_{1,3}[Ag^+][I^-]^3 + \beta_{1,4}[Ag^+][I^-]^4 + 2\beta_{2,6}[Ag^+]^2[I^-]^6 + 3\beta_{3,8}[Ag^+]^3[I^-]^8 \quad (11)$$

and correspondingly

$$c_I - [I] = 3\beta_{1,3}[Ag^+][I^-]^3 + 4\beta_{1,4}[Ag^+][I^-]^4 + \\ + 6\beta_{2,6}[Ag^+]^2[I^-]^6 + 8\beta_{3,8}[Ag^+]^3[I^-]^8 \quad (12)$$

where the pertinent constants $\beta_{m,n}$ are now known from the graphical computations, described above. Hence $\bar{n}$, representing the value of the right hand member of eqn. (12) divided by the right hand member of eqn. (11), may be calculated for each titration series, by solving for $[Ag^+]$ and $[I^-]$ from eqns. (11) and (12) for some values of c_I. The same values of $[Ag^+]$ and $[I^-]$ have also been used to calculate the F_4-curve of Fig. 1. The corresponding $\bar{n}$-curves are to be seen in Fig. 3, which has been used to calculate the values of $[I^-]$ in Table 1 from eqn. (4). On the whole this computation gives the same result as the first approximation from Bodländer's formula, eqn. (5), and the same values of $[I^-]$ were also obtained by several other approaches, tried by the author to describe the complex formation. The reason for this is of course that c_I is in all cases so much larger than c_{Ag} that even a very rough approximation of $\bar{n}$ gives a rather correct value of $[I^-]$ from eqn. (4).

The two polynuclear complexes found above are formed quite reasonably by the two consecutive condensation reactions

$$2AgI_4^{3-} \rightleftharpoons Ag_2I_6^{4-} + 2I^- \text{ and } Ag_2I_6^{4-} + AgI_4^{3-} \rightleftharpoons Ag_3I_8^{5-} + 2I^- \quad (13)$$

with the equilibrium constants $b_{2,6} = \beta_{2,6} \cdot (\beta_{1,4})^{-2} = 15 \pm 10$ and $b_{3,8} = \beta_{3,8} \cdot (\beta_{2,6} \cdot \beta_{1,4})^{-1} = 250 \pm 150$, respectively. It seems rather probable that analogous condensation reactions continue to produce larger species of the form $Ag_mI_{2m+2}^{(m+2)-}$ with increasing total silver concentrations. It could certainly be possible to draw the curve of Fig. 2 less rectilinear in its upper part and so make room for more highly condensed species at the expense of $Ag_3I_8^{5-}$. Such an increased curvature would be rather arbitrary, however. It is known (Sillén [7]) that the method used in the present paper is "a rather un-

favourable case, as $[Ag^+]$ is measured, but the difference $(c_I - [I^-])$ cannot be calculated with enough accuracy to be of much help". Hence there is not much reason to speculate about the higher condensation products. Perhaps it could be said that it is rather probable that the equilibrium constant, $b_{4,10}$, of the next member of the series, $Ag_4I_{10}^{6-}$, is less than $b_{3,8}$, as $b_{4,10} > b_3$ would give a quite pronounced curvature to the upper part of the curve of Fig. 2. The description above of the silver-iodide system is in better agreement with the experimental data than an infinite series of complexes would be, in which all the equilibrium constants $b_{m,2m+2}$ have the same value for $m > 2$. There is also the possibility that a reaction, *e. g.* a ring closure:

$$Ag_mI_{2m+2}^{(m+2)-} \rightleftharpoons Ag_mI_{2m}^{m-} + 2I^- \qquad (14)$$

cuts off the series at some step in the postulated continuing condensation.

The results obtained from the e.m.f. measurements agree quantitatively with those from the solubility determinations already mentioned. These latter measurements moreover gave some information about the silver iodide species with negative charges less than —2. They also proved the existence of complexes with negative charges higher than —5 in solutions with silver contents larger than those studied in the present paper.

Table 2. The over-all complexity constants $\beta_{m,m+n}$ for the reaction (6) and $k_{m,n}$ for the reaction (16). $L = 4.5 \times 10^{-17}$.

Complex	$\beta_{m,m+n}$	$k_{m,n}$
AgI_3^{2-}	$\beta_{1,3} = (7 \pm 2) \times 10^{13}$	$k_{1,2} = (3 \pm 1) \times 10^{-3}$
AgI_4^{3-}	$\beta_{1,4} = (19 \pm 2) \times 10^{13}$	$k_{1,3} = (9 \pm 1) \times 10^{-3}$
$Ag_2I_6^{4-}$	$\beta_{2,6} = (5 \pm 3) \times 10^{29}$	$k_{2,4} = (10 \pm 6) \times 10^{-4}$
$Ag_2I_8^{5-}$	$\beta_{2,8} = (25 \pm 5) \times 10^{45}$	$k_{2,5} = (23 \pm 5) \times 10^{-4}$

The solubility product, L, of silver iodide in 4 M sodium perchlorate could be computed from the values of E in those solutions at the end of the titration series (*vide* Table 1), where solid silver iodide was formed. It was also determined by measuring the e.m.f. of the following cell

$$+ \text{Ag,AgI} \left| \begin{matrix} 0.016 \text{ M } AgClO_4 \\ 3.98 \text{ M } NaClO_4 \end{matrix} \right| 4 \text{ M } NaClO_4 \left| \begin{matrix} c_I \text{ M NaI} \\ (4 - c_I) \text{ M } NaClO_4 \end{matrix} \right| \text{Ag,AgI} - \qquad (15)$$

The e.m.f. was 723.8 mV for $c_I = 0.005$ and 801.7 for $c_I = 0.1$, which gives $L = 4.6_6 \times 10^{-17}$, respectively $4.5_0 \times 10^{-17}$. The average of all the determinations is $L = (45 \pm 1) \times 10^{-18}$. This value has been used in Table 2 to calculate the equilibrium constants, $k_{m,n}$, valid for the reactions between solid silver iodide and iodide ions

$$m \text{ AgI(s)} + n \text{ } I^- \rightleftharpoons Ag_mI_{m+n}^{n-} \qquad (16)$$

Hence

$$k_{m,n} = L_m \times \beta_{m,m+n} \qquad (17)$$

The author is grateful to Professor J. Pepper for his revision of the English of the manuscript and to L. E. Marthén for experimental assistance. *Statens Naturvetenskapliga Forskningsråd* supported the work financially.

REFERENCES

1. Brown, A. S. *J. Am. Chem. Soc.* **56** (1934) 646.
2. Leden, I. and Schöön, N.-H. *Acta Polytechnica* **155** (1954).
3. Leden, I. and Berne, E. *Z. Naturforsch.* **8a** (1953) 719.
4. Leden, I. *Diss.* Lund (1943), 13.
5. Hedström, B. *Acta Chem. Scand.* **9** (1955) 613.
6. Hietanen, S. and Sillén, L. G. *Ibid.* **8** (1954) 1607.
7. Sillén, L. G. *Ibid.* **8** (1954) 314.

Received January 5, 1956.

ACTA CHEMICA SCANDINAVICA 10 (1956) 548—566

Aspartate Carbamyl Transferase from *Escherichia coli*

PETER REICHARD and GUNNAR HANSHOFF

Biochemical Department, Karolinska Institutet, Stockholm, Sweden

Carbamyl phosphate was found to be an intermediate in the biosynthesis of carbamyl aspartic acid (= ureidosuccinic acid). Strong evidence was obtained that enzymically prepared and purified compound X was identical with synthetic carbamyl phosphate.

An enzyme was purified *ca.* 100 fold from extracts of lyophilized *E. coli* which catalyzed the following stoichiometric reaction:
Carbamyl phosphate + L-aspartate → L-carbamyl aspartate + P_i

The name aspartate carbamyl transferase is proposed for this enzyme. The equilibrium of the reaction was shifted very far towards synthesis of CA-aspartate.

Out of 31 tested amino acids only L-aspartic acid served as acceptor for the carbamyl group. The enzyme is distinct from the citrulline forming enzyme and the enzyme forming β-ureidopropionic acid.

The enzyme was inhibited by *p*-chloromercuribenzoate and the inhibition could be completely reversed by glutathione. Aspartate + carbamyl phosphate protected the enzyme from the inhibition, while each substrate alone had no effect.

Inorganic ^{32}P showed no enzymic exchange with the phosphate moiety of carbamyl phosphate in the absence of aspartate, and the enzyme catalyzed no exchange of isotope between L-aspartate-^{14}C and carbamyl aspartate.

When the reaction was carried out in $H_2{}^{18}O$ no isotope was found in the carbamyl group of carbamyl aspartate or carbamyl phosphate.

A probable mechanism for the reaction is discussed.

Extracts from various organs of the rat and from lyophilized *E. coli* contain an enzyme which has the ability to catalyze the formation of carbamyl asparacid (= ureido succinic acid *) from aspartic acid and an activated carbamyl compound, called compound X[1,2]. This reaction shows a close analogy to the previously demonstrated formation [3] of citrulline from ornithine + compound X. With a partially purified enzyme from *E. coli* we could demonstrate the stoichiometric formation of one molecule of CA-aspartate ** per one molecule

*. In earlier communications the name ureidosuccinic acid was used instead of the synonym carbamyl aspartic acid. The enzymic mechanism involved in the formation of this substance makes us now prefer the latter name.

**. The following abbrevations are used in this paper: ATP, adenosine triphosphate; CA, carbamyl; CAP, carbamyl phosphate; CMBA, *p*-chloromercuribenzoate; P_i, inorganic phosphate; tris, trishydroxymethylaminomethane; PCA, perchloric acid.

of aspartate and one molecule of compound X. Since it was believed [3] that compound X contained acetylglutamate and phosphate as well as the carbamyl group, the reaction was tentatively formulated as follows:

$$\text{Compound X} + \text{L-aspartate} \rightleftharpoons \text{CA-aspartate} + \text{acetyl glutamate} + P_i \quad (1)$$

Jones *et al.*[4] have recently synthesized carbamyl phosphate and have presented very strong evidence that this compound is the carbamyl donor in enzymic citrulline synthesis and therefore identical with compound X. Their work prompted us to reinvestigate the formation of CA-aspartate with the bacterial enzyme. It was found that the earlier enzymically prepared and purified compound X was identical with synthetic CAP. The easy availability of the latter compound made feasible a further purification and a closer study of the CA-aspartate forming enzyme and the mechanism of its action. The enzyme was found to catalyze the transfer of a carbamyl group from phosphate to L-aspartate in a stoichiometric manner:

$$\text{Carbamyl phosphate} + \text{L-aspartate} \rightarrow \text{L-carbamyl aspartate} + P_i \quad (2)$$

The name aspartate carbamyl transferase is proposed for this enzyme.

EXPERIMENTAL

L-Acetyl glutamic acid was synthesized according to Karrer *et al.*[5], the labeled *L-aspartic acids* according to Wu and Rittenberg [6], and *carbamyl phosphate* according to Jones *et al.*[4] *DL-CA-aspartate* was synthesized according to Nyc and Mitchell [7]. Since the L-isomer does not crystallize readily it was purified by chromatography as described below, lyophilized and utilized directly for the demonstration of the back reaction. *Compound X* was prepared enzymically as described earlier [8,1].

Enzyme assay. Method 1: L-Aspartate-^{15}N was used as substrate and the CA-aspartate formed was determined after addition of carrier DL-CA-aspartate as described earlier [9]. The reaction was terminated by acidification with PCA instead of heat denaturation used in previous studies. In this way it was possible to avoid significant non-enzymic formation of CA-aspartate at substrate concentrations below 0.1 M. When conditions were the same as described for method 2, identical results were obtained with both methods. In most cases, however, only 0.03 M aspartate-^{15}N was used in order to preserve isotope. Under those conditions the obtained value for CA-aspartate formation could be multiplied by a factor of 1.5 in order to obtain a comparison with standard conditions.

Method 2: This method depended on the direct determination of the inorganic phosphate formed during the enzyme reaction. It was the method of choice with the purified enzyme whenever, in a set of experiments, it was possible to work with a relatively low and constant concentration of CAP, and no substances were present which interfered with phosphate analysis.

The enzyme was added to a solution containing 100 μmoles of L-aspartate, 20—30 μmoles of CAP and 150—500 μmoles of tris buffer, pH 7.5, the final volume being 1.0 ml *. Incubation was carried out for 15 minutes at 37°. The reaction was stopped by immersion of the sample in an ice bath and P_i determined directly on aliquots by the Lowry-Lopez [10] method. A blank containing the same constituents with the exception of aspartate (or enzyme) was carried through the same procedure in order to make possible a correction for the non-enzymic decomposition of CAP. The P_i value of the blank was subtracted from that of the complete sample. Under those conditions proportionality

*. The lithium salt of CAP and the potassium salt of L-aspartic acid were used in all experiments. Li-CAP was dissolved immediately before use in each experiment. No difference was found in the reaction rate when sodium aspartate was used instead of the potassium salt.

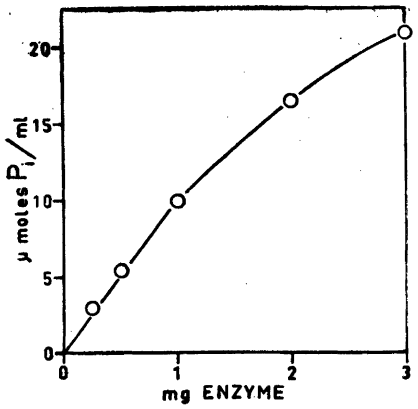


Fig. 1. Formation of P_i from CAP with different amounts of enzyme (ammonium sulfate fraction).

The solutions contained per ml: 100 μmoles of L-aspartate, 25 μmoles of CAP and 150 μmoles of tris buffer, pH 7.5. Incubation for 15 minutes at 37°.

between amount of enzyme added and P_i formed was observed up to *ca.* 10 μmoles (Fig. 1).

One unit of enzyme activity was defined as the amount of enzyme which formed one μmole of P_i or CA-aspartate under the above conditions. The specific activity of the enzyme was defined as units per mg protein. Up to and including the ammonium sulfate fractionation step protein concentration was determined by nitrogen analysis of the PCA precipitate, assuming a nitrogen content of 16 %. Subsequently protein was determined by light absorption measurements at 280 and 310 mμ. It was found that 1 mg of protein of the lyophilized ammonium sulfate fraction dissolved in 1 ml of water showed a value for $E_{280}-E_{310}$ of 0.60. This value was used for calculation of protein concentrations during and after the chromatographic purification step.

The activity of the *citrulline forming* enzyme was measured under identical conditions as described above for CA-aspartate, except that ornithine was substituted for aspartate. The citrulline formed was determined colorimetrically according to Koritz and Cohen [11].

Purification of the enzyme. Lyophilized *E. coli* were handled as forty grams samples. The first steps including extraction, protamine precipitation and ammonium sulfate fractionation were carried out as described earlier [1] with one exception. Incomplete precipitation with protamine was encountered in a few cases. Therefore this precipitation was performed in an ice bath and the solution allowed to stand for 30 minutes in the cold room prior to centrifugation in the Spinco centrifuge (30 000 g for 10 minutes). In this way less than 15 % of the enzyme activity remained in the supernatant in all cases. After the ammonium sulfate step a 7—12 fold purification of the enzyme had been achieved. The enzyme could be lyophilized and stored at —15° without appreciable loss of activity for at least 6 months.

Further purification of the enzyme was carried out by chromatography [13] on DEAE columns *. The column (diameter 2 cm) was prepared from 12 g of DEAE-cellulose (0.9—1.0 % nitrogen, prepared from Whatman's standard grade paper powder). It was washed first with *ca.* 500 ml M KCl, followed by 200 ml of 0.01 M imidazole : HCl buffer, pH 6.5, containing KCl at 0.02 M concentration. The last wash and all the following operations were carried out at 2—4°.

The dialyzed enzyme, after the ammonium sulfate step (from 40 g of bacteria, dissolved in 15—20 ml of 0.01 M phosphate buffer, pH 6.5), was then adsorbed on the column, which was connected with a 1 000 ml mixing flask containing 0.01 M imidazole buffer (pH 6.5) : 0.02 M KCl. This flask received 0.75 M KCl from a reservoir flask. The protein was eluted by gradient chromatography (*cf.* Ref [13]). Half hour fractions with a volume of *ca.* 10 ml were collected.

*. We wish to thank Drs. E. A. Peterson and H. A. Sober who most generously made available to us a manuscript of their work prior to publication.

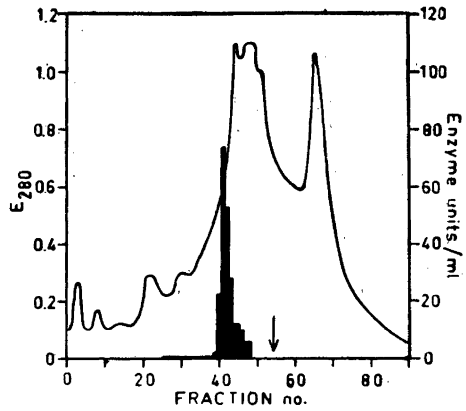


Fig. 2. Chromatography of transferase (560 mg, 5 300 units) on DEAE cellulose.

KCl concentration changed to 2 M at arrow. Stepped curve = enzyme activity, continuous curve = E_{280}.

Protein concentration was determined in each fraction by direct measurement of the light absorption at 280 mμ in a Beckman spectrophotometer, model DU. Furthermore, aliquots from each fraction (usually 0.1 ml) were analyzed for transferase activity according to method 2. A typical diagram obtained in this way is shown in Fig. 2.

The total recovery of enzyme activity after chromatography was *ca.* 75 %. More than 60 % of the recovered activity was located in two or three middle fractions. By chosing only these fractions for further work the chromatographic step resulted in a 8—13 fold purification of the enzyme with a recovery of 45—50 % of the total activity.

To the combined chromatographic fractions were added 1 ml of M K_2HPO_4 and 100 μmoles of neutralized reduced glutathione. The enzyme was then precipitated by addition of solid ammonium sulfate to 65 % saturation. The solution was first attached to a water pump for 15 minutes in order to remove most of the dissolved air and then centrifuged. The resulting precipitate was suspended in 2 ml of 0.1 M tris buffer, pH 7.5, and centrifuged. The supernatant contained 80—100 % of the transferase activity of the combined chromatographic fractions. It was frozen and stored at −15°. Lyophilization could not be carried out at this point without heavy losses. During storage different preparations showed a varying decline of enzyme activity. Addition of glutathione (final concentration 0.05 M) seemed to preserve enzyme activity for a longer time (at least 2—3 weeks).

The results obtained by the chromatographic step were very reproducible. The enzyme could always be localized in an approximate way from the E_{280} curve, since it coincided with a more or less pronounced "shoulder" of this curve before the first large peak.

A summary of a typical purification procedure is given in Table 1.

Table 1. Purification of transferase.

	mg protein	total units	specific activity	recovery %
Extract from lyophilized bacteria (40 g)	12 300	13 900	1.13	100
Extract from protamine precipitate	2 350	12 200	5.2	88
Ammonium sulfate fraction (30—45 % sat.)	675	7 800	11.6	57
After chromatography and ammonium sulfate precip.	28	3 550	127	25

Chromatographic separations. CA-aspartate and aspartate were separated by gradient elution from a Dowex-2 formate column. This separation was carried out both during the demonstration of the back reaction of the enzyme and during the chemical synthesis of L-CA-aspartate. In the latter case the solution (pH 9—10) was applied to a 3 cm^2 × 10 cm column connected with a 500 ml mixing flask containing water. Gradient elution with M formic acid separated aspartate (emerging after *ca.* 6 column volumes) from CA-aspartate (after *ca.* 13 column volumes). A small peak, which appeared at 9 column volumes and coincided with the position of 5-acetic acid hydantoin was completely separated from the other substances. The peaks were localized by their radioactivity and by spot tests with ninhydrin (aspartate) and *p*-dimethylaminobenzaldehyde (CA-aspartate [14]). For the separation of CA-aspartate from aspartate during the demonstration of the back reaction four columns, 0.63 cm^2 × 10 cm, connected with one 500 ml mixer flask were chromatographed simultaneously as described above.

Separation of CAP and P_i by gradient elution was carried out during the isotope exchange experiments. Four columns of Dowex-2 formate, 0.62 cm^2 × 10 cm, were connected with one 1 000 ml mixing flask containing water. During chromatography the mixing flask received M ammonium formate, pH 5.0. P_i appeared after *ca.* 16 column volumes completely separated from CAP, which appeared after *ca.* 24 column volumes. The peaks were localized by determination of radioactivity and by phosphate analysis. The chromatography was carried out at +4°.

Isotope determinations. ^{15}N and ^{13}C were measured as N_2 and CO_2, respectively, in the mass spectrometer. ^{14}C and ^{32}P were determined on infinite thin samples in a Tracerlab SC-18 windowless flow counter.

^{18}O*-analyses* were performed directly on CAP and CA-aspartate. For this purpose *CAP* was isolated from the incubation mixture in the following way. After cooling in an ice bath the solution was acidified with M PCA and evacuated with an oil pump to remove CO_2 as completely as possible. The solution was neutralized with M NaOH (CO_2-free) with phenolphtalein as internal indicator. Then 0.25 ml of 2 M barium acetate were added and the resulting precipitate removed by centrifugation at 0°. Two volumes of alcohol were added to the supernatant and after standing for 5 minutes the resulting barium salt of CAP was collected by centrifugation, washed twice with 2 ml of 50 % alcohol and dried in a desiccator.

The Ba-CAP was finely ground and poured into a glass tube of 3 mm internal diameter which was sealed at one end. It was directly attached to the inlet system of the mass spectrometer by a ground glass joint. After evacuation of the system the bottom of the tube was immersed in a metal bath of 350°. At this temperature Ba-CAP decomposed thermally, while $BaCO_3$ was relatively stable. This was important since CO_2, during incubation, equilibrated with the isotope of $H_2{}^{18}O$ and since Ba-CAP might contain some $BaCO_3$. To ascertain the maximum amount of possible contamination a mixture of 2.5 mg of $Ba^{13}CO_3$ (32 % excess) and 10 mg of non-labeled Ba-CAP were analyzed under the described conditions. The CO_2 contained 0.14 % excess ^{13}C, indicating that less than 0.5 % was derived from the $BaCO_3$.

CA-aspartate for ^{18}O *analyses* was isolated directly from the incubation mixture by chromatography as described earlier. After addition of carrier (DL-form) it was crystallized from water.

CA-aspartate could be thermally decomposed at 200° *in vacuo* in the same way as described for CAP. Since the purpose was to analyze the ^{18}O content of the carbamyl group, it was necessary to determine the contribution of this group to the CO_2 evolved during the thermal decomposition. Thus ^{13}CA-aspartate was synthesized [15,7] from $K^{13}CN$ (atom per cent excess = 5.0) and the gas mixture resulting from the decomposition of ^{13}CA-aspartate was analyzed in a mass spectrometer [16] (Table 2). It can be seen that by far the most intensive peak had a mass number of 44 (CO_2). In a separate experiment the excess ^{13}C was accurately determined from the mass ratio 44/45 and found to be 4.91. This result demonstrated that within experimental error all the carbon of the CO_2 obtained by thermal decomposition of ^{13}CA-aspartate was derived from the carbamyl carbon. Therefore half of the oxygen from this peak corresponded to the carbamyl oxygen.

In the same experiment measurements of the ratio 28/29 (CO and/or N_2) were performed. On the assumption that the ratio was completely due to CO a ^{13}C-value of 4.65 atom per cent excess was obtained (as compared to the theoretical value of 5.0). The presence of either nitrogen or CO arising from another source than the carbamyl group

would have lowered the ^{13}C-value. The observed value therefore demonstrated that 90—95 % of the peaks with a mass number of 28 and 29 consisted of CO derived from the carbamyl group of CA-aspartate. In the case of CO all oxygen arose from the carbamyl oxygen.

Table 2. Thermal decomposition of ^{13}CA-aspartate.

Mass number	Intensity of peak
16	4.1
17	2.2
18	7.7
22	0.9
28	5.6
29	0.4
44	100.0
45	7.0
46	0.47

The analysis of the gas mixture was carried out in a recording mass spectrometer [16]. The carbamyl group of CA-aspartate contained 5.0 per cent excess ^{13}C. Decomposition was carried out at 200° in a high vacuum. The intensity of the peak with a mass of 44 is arbitrarily chosen as 100.

In the actual experiments both the 44/46 and 28/30 ratios were used for the calculations of ^{18}O.

Attempts to characterize the non volatile products of this interesting thermal decomposition have not been successful.

RESULTS

CAP as substrate for CA-aspartate formation

Our earlier experiments [1] had been carried out with enzymically prepared compound X and for further work it was of the greatest interest to establish the possible identity of this substance with synthetic CAP [4], especially in view of differences of opinion in the literature concerning this point [17,18].

For this purpose compound-X-^{14}C was prepared enzymically from labeled $NaHCO_3$ and purified as earlier. It was then co-chromatographed on paper with synthetic nonlabeled CAP in two different solvents and subjected to paper electrophoresis (Table 3). In each experiment one radioactive spot was obtained which coincided with one spot obtained by a phosphate spray [19].

When a small amount of compound-X-^{14}C was co-chromatographed with CAP on Dowex-2 as described in the experimental part for CAP, radioactivity emerged from the column simultaneously with CAP (by phosphate analysis), and a constant ^{14}C/phosphate ratio was obtained in the different fractions (Table 4).

The identity of the two substances was also established in enzyme experiments. Using aspartate-^{14}C and ^{13}CAP as substrates the amount of CA-aspartate formed from each precursor could be calculated by the isotope dilution method. Identical amounts were formed from each precursor. In different experiments increasing amounts of compound-X-carbamyl-^{15}N were added simultaneously with constant amounts of ^{13}CAP and aspartate-^{14}C. When the amount of CA-aspartate formed in the different experiments was calculated independently from the three different isotopes the results demonstrated in Fig. 3 were obtained. The total amount of CA-aspartate formed (calc. from

Table 3. Paper chromatography and paper electrophoresis of CAP and compound-X-carbamyl-^{14}C.

Solvent system	cm from start		Front cm
	radioactive spot	phosphate spot	
n-Propanol:water:conc.NH_3:versene [20] 6 : 10 : 3 : 0.01	3.5 – 8.5	3.7 – 8.3	28
Methanol: 2 N NH_3 : versene [22] 7 : 3 : 0.01	22.5 – 27.5	23 – 27	30
Paper electrophoresis (saturated tetraborate in 0.01 M versene) [21]	13.0 – 16.0	13.4 – 15.6	

In each experiment 0.5 – 2 μmoles of CAP were chromatographed together with 0.05 μmoles of labeled compound X (60 000 ct/μmole). At the end of the experiment the position of the radioactive spots was first determined, and then the paper sprayed with a phosphate reagent [19].

Electrophoresis (12 volts/cm) was carried out for 4 hours. All operations were performed at temperatures between 0 and +4°.

^{14}C) was constant in all experiments and equalled the sum of the amounts formed from CAP (calc. from ^{13}C) and from compound X (calc. from ^{15}N). Furthermore, with increasing amounts of compound X, increasing amounts of CA-aspartate were formed from ^{15}N and decreasing amounts from ^{13}C. The two curves were the mirror images of each other. These results are explained, if compound X and CAP are freely interchangeable with each other in the enzyme reaction.

The same type of behaviour was observed when the concentrations of compound X and aspartate were kept constant, while increasing amounts of CAP were added (Fig. 4).

The intermediate position of CAP in the synthesis of CA-aspartate from NH_3, CO_2, aspartate and ATP could be demonstrated in extracts from rat liver mitochondria. In different experiments CA-aspartate was synthesized from constant amounts of $^{15}NH_4Cl$, $NaHCO_3$, aspartate-^{14}C, ATP and acetyl-

Table 4. Ion exchange chromatography of CAP (25 μmoles) + compound-X-carbamyl-^{14}C (1 μmole, 60 000 ct/μmole).

Fraction No.	ct/ml	μmoles of phosphate/ml	ct/μmole
30	1 200	0.52	2 300
31	6 200	2.78	2 230
32	4 100	1.71	2 400
33	1 050	0.47	2 230
34	100	—	—

Phosphate analysis [10] was carried out after heating for 5 minutes in a boiling water bath. For the determination of radioactivity samples of 0.05 ml + 0.05 ml of 0.1 M NaOH were dried and counted.

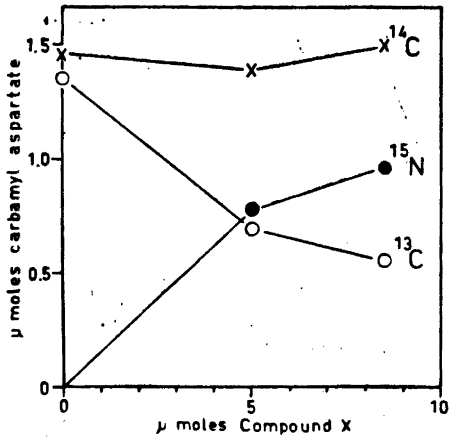


Fig. 3. Influence of compound-X-^{15}N on the synthesis of CA-aspartate from ^{13}CAP.

Substrate (per ml): 30 μmoles of L-aspartate-^{14}C (12.000 ct/μmole), 5 μmoles of CAP (31 atom per cent excess ^{13}C), 150 μmoles of tris buffer, pH 7.5, and 3 units of transferase (spec. activity 10). Compound-X-^{15}N (atom per cent excess $^{15}N = 32$) as indicated on abscissa. Incubation for 15 minutes at 37°.

In each experiment 160 μmoles of carrier DL-CA-aspartate were added, and the content of the different isotopes in the reisolated CA-aspartate was determined.

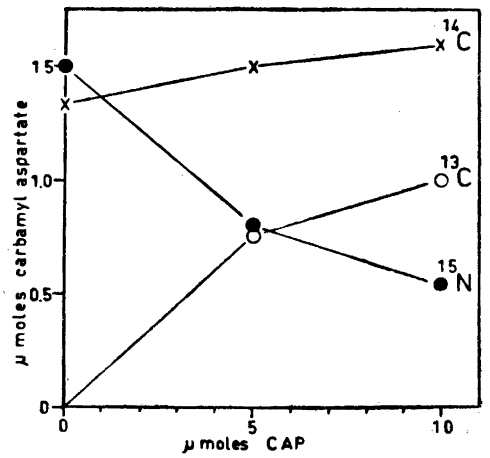


Fig. 4. Influence of ^{13}CAP on CA-aspartate synthesis from compound-X-^{15}N..

Substrate (per ml): 30 μmoles of L-aspartate-^{14}C, 5 μmoles of Compound-X-^{15}N, 150 μmoles of tris buffer, pH 7.5, and 3 units of transferase. ^{13}CAP as indicated on abscissa.. The experiments were conducted as in Fig. 3.

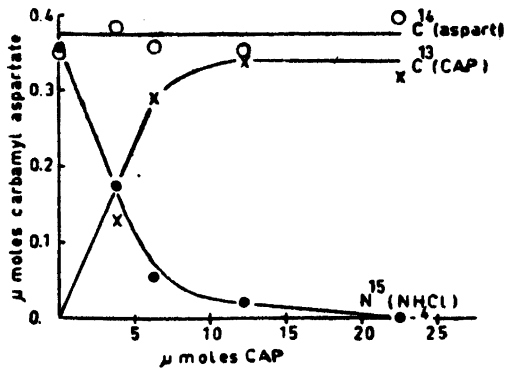


Fig. 5. Influence of ^{13}CAP on CA-aspartate synthesis from $^{15}NH_4Cl$, $NaHCO_3$, ATP and L-aspartate-^{14}C in an extract from rat liver mitochondria.

Substrate (per 3 ml): 20 μmoles of L-aspartate-1,4-^{14}C (12 000 ct/μmole), 20 μmoles of $^{15}NH_4Cl$ (32 atom per cent excess), 100 μmoles of $NaHCO_3$, 10 μmoles of ATP, 60 μmoles of 3-phosphoglycerate, 20 μmoles of acetylglutamate, 100 μmoles of $MgSO_4$, 200 μmoles of phosphate buffer, pH 7.5, and 5 mg of a muscle protein fraction (Ratner, S. and Pappas, A. *J. Biol. Chem* **179** (1949) 1183). ^{13}CAP (31 atom per cent excess) as indicated on the abscissa.

The mitochondrial enzyme (1.51 mg nitrogen per experiment) was prepared as described earlier [1].

Incubation for 60 minutes at 37°. Carrier added as in Fig. 3.

glutamate, while increasing amounts of ^{13}CAP were added. When the formation of CA-aspartate from the different isotopic substances was studied (Fig. 5), the results demonstrated that CAP had a large dilution effect on the ^{15}N-incorporation. At the highest CAP concentration studied practically no CA-aspartate was formed from ammonia, while identical amounts were formed from CAP and aspartate.

The experiments are in full agrement with the idea that CAP is the active carbamyl compound in the bacterial enzyme reaction and that it is also an intermediate in CA-aspartate formation in rat liver.

Properties of the transferase reaction

The *stoichiometry* of reaction (2) could be demonstrated with the ammonium sulfate fractionated enzyme (Table 5). The slightly larger formation of P_i than CA-aspartate is fully explained by some non-enzymic decomposition of CAP under the experimental conditions.

Isolation of L-CA-aspartate. Only L-aspartate could act as substrate (see below) and the CA-aspartate formed during the reaction was also the L-isomer. This was demonstrated by the isolation of its barium salt from a large scale experiment. Two mmoles of L-aspartate and 3 mmoles of CAP were incubated with 520 units of enzyme (specific acitivity = 11) at 37° for 60 minutes. After chromatography on Dowex-2 the fractions containing CA-aspartate were combined and the formic acid was removed by evaporation *in vacuo*. The

Table 5. Stoichiometry of transferase reaction.

Expt. No.		CAP	P_i	L-aspartate	CA-aspartate
			μmoles		
1	Initial	31.2	3.0	30.0	0
	Final	11.9	23.1	13.6	16.8
	Δ	19.3	20.1	16.4	16.8
2	Initial	31.2	2.1	30.0	0
	Final	26.9	6.8		
	Δ	4.3	4.7		

Incubation was carried out at 37° for 15 minutes in 1 ml volume.

Experiment 1: 1.5 mg of ammonium sulfate fractionated enzyme, experiment 2: no enzyme.

CAP + P_i was determined by heating an aliquot of the sample in 0.01 N HCl at 100° for 1 minute [4] before phosphate analysis [18].

L-Aspartate (32 atom per cent excess ^{15}N in substrate) was determined by the isotope dilution method. One mmole of carrier L-aspartate was added to an aliquot of the solution. After acidification the aspartic acid was crystallized to a constant isotope content.

CA-aspartate was determined by method 1 and according to Koritz and Cohen [11].

residue was dissolved in a minimum amount of water and the barium salt (160 mg) prepared as described earlier [23]. It showed $[\alpha]_D^{25} = +25.7°$ (as compared to the earlier obtained value of +24.1° for synthetic L-CA-aspartate).

A *time curve* of the reaction is given in Fig. 6.

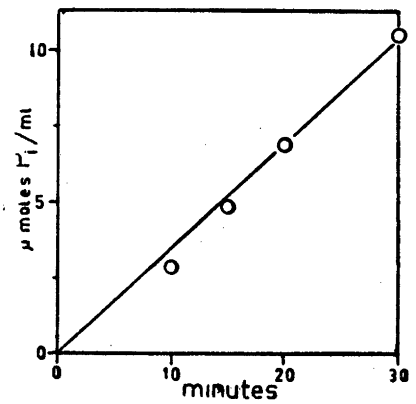


Fig. 6. Time curve of transferase action.

In each experiment volume = 1.0 ml. 5 units of transferase (spec. activity = 11) were incubated with 100 μmoles of L-aspartate, 30 μmoles of CAP and 150 μmoles of tris buffer, pH 7.5. Enzyme assay according to method 2.

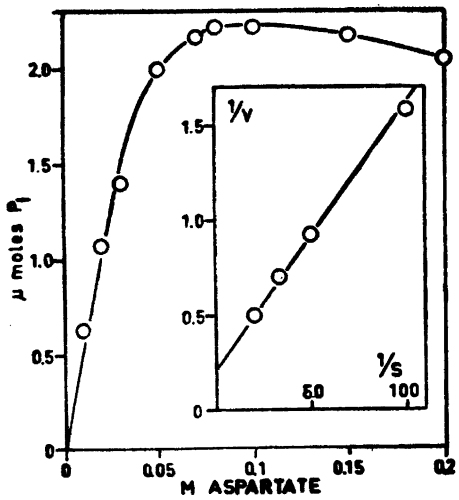


Fig. 7. Influence of aspartate concentration.

Transferase (2 units, spec. activity = 90) was incubated for 15 min. at 37° with 8 μmoles of CAP, 150 μmoles of tris buffer, pH 7.5, and L-aspartate as indicated on the abscissa. Final volume = 1.0 ml. Enzyme assay by method 2.

Dependance on substrate concentration. The influence of *aspartate concentration* on the reaction rate is shown in Fig. 7. As indicated earlier [1] large amounts of substrate were necessary for enzyme saturation. Furthermore, at concentrations above 0.1 M a clear inhibition by aspartate did take place. When a Lineweaver-Burk plot was made from the values obtained below 0.05 M aspartate concentration a value of $K_M = 0.065$ was obtained. In a different experiment at higher CAP concentration (0.1 M) and using method 1 for the determination of reaction rate the value for K_M was 0.060.

The influence of *CAP concentration* is demonstrated by Fig. 8. No inhibition was observed up to 0.3 M concentration. $K_M = 0.45 \times 10^{-3}$.

The *pH-curve* of the reaction is shown in Fig. 9. This curve differs significantly from the one given earlier [1], which had been obtained under somewhat different conditions. The reason for the discrepancy is not understood. In the present investigation a pH optimum of 7.5 was obtained in five different experiments with both methods of enzyme assay, using tris or imidazole buffer.

Specificity of the reaction. Ureidopropionic, ureidoglutaric and ureidosuccinic acids, citrulline and urea could not serve as carbamyl donors in place of carbamyl phosphate.

With a 90 fold purified enzyme L-aspartate alone could serve as acceptor for the carbamyl group of CAP. 31 amino acids and related compounds were tested for their ability to bring about the enzymic dephosphorylation of CAP. Furthermore, the appearance of a new carbamyl compound was sought by the method of Koritz and Cohen[11]. Those non reacting compounds were: L-α-alanine, β-alanine, DL-α-aminoadipic acid, α, β, and γ-aminobutyric acids,

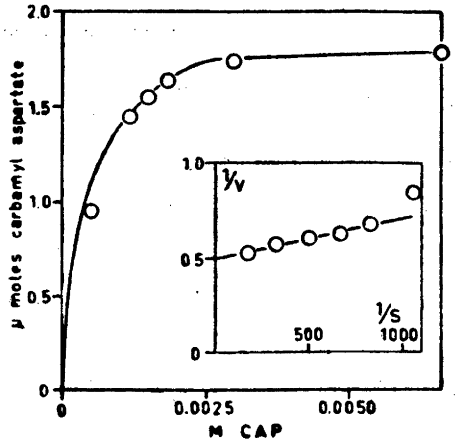


Fig. 8. Influence of CAP concentration.

Incubation (volume = 3.0 ml): 2 units of transferase (spec. activity = 90) were incubated for 15 min. at 37° with 300 µmoles of L-aspartate-^{15}N (32 atom per cent excess ^{15}N), 400 µmoles of tris buffer, pH 7.5, and CAP as indicated on abscissa. Enzyme assay by method 1.

L-arginine, L-asparagine, D-aspartic acid, L-citrulline, L-cysteic acid, L-cysteine, L-glutamic acid, L-glutamine, glycine, L-histidine, DL-homoserine, L-hydroxylysine, L-*iso*leucine, L-leucine, L-lysine, L-methionine, L-ornithine, L-phenylalanine, L-proline, L-serine, taurine, L-threonine, L-tryptophane and L-valine*.

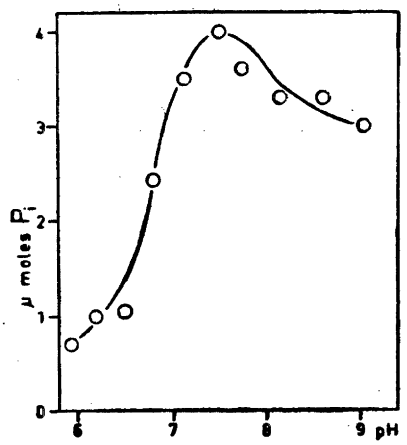


Fig. 9. pH curve.

Transferase (4 units, spec. act. 90) was incubated for 15 min. at 37° with 100 µmoles of L-aspartate, 20 µmoles of CAP and 300 µmoles of tris (pH range 7—9) or imidazole (pH range 6—7.5) buffers. Volume = 1.0 ml. Enzyme assay by method 2.

*. The amino acids were commercial products. We wish to thank Drs. G. Ågren and Z. Bánhidi for gifts of some of these amino acids.

Table 6. Aspartate and ornithine carbamyl transferase activity during enzyme fractionation

	μmoles CA-aspartate formed per ml	μmoles citrulline formed per ml
Bacterial extract	18	14
Supernat. from protamine	3.4	5.6
Extract of protamine precipitate	22	9.4
Ammonium sulfate 0—30 %	9	0
» » 30—45 »	87	10
» » >45 »	0	4.2
After DEAE chromatography	52	0

The CA-aspartate forming enzyme was determined by method 1.
The substrate for the citrulline forming enzyme contained 60 μmoles of DL-ornithine. instead of 30 μmoles of L-aspartate, but apart from this conditions were the same.
Protamine precipitation in this preparation was performed at room temperature.

The ammonium sulfate fractionated enzyme showed activity in catalyzing the reaction between CAP and L-ornithine to form citrulline. It was thought of interest to make a comparison between CA-aspartate formation and citrulline formation at various stages of purification of the enzyme. The result, summarized in Table 6, clearly demonstrated the existence of two different carbamyl transferases, one forming CA-aspartate and the other forming citrulline.

Inhibition of transferase activity. Several amino acids showing structural relationship to L-aspartate were investigated as possible inhibitors of the reaction. In these experiments 30 μmoles of L-aspartate and 20 μmoles of CAP were used as substrate together with 5—10 units of transferase. Usually 150 μmoles of the substance under investigation were added and the formation of P_i measured by method 2. No inhibition was observed with, α-, β- or γ-aminobutyric acids, L-asparagine, D-aspartate, L-cysteic acid, L-glutamate and DL-homoserine.

Table 7. Inhibition of transferase reaction.

Inhibitor	concentration (M)	% inhibition
NaCN	0.01	
Versene	0.05	
Arsenate	0.1	
Phosphate	0.1	
Hydroxylamine	0.1	
Phenylhydrazine	0.01	0
Semicarbazide	0.01	
Bisulfite	0.01	
Arsenite	0.01	
Ethyldichloroarsin	0.0005	
Iodosobenzoate	0.004	
Iodoacetate	0.01	5—10
CMBA	0.003	90—95
CMBA	0.001	45

The inhibitor was added to the buffered enzyme solution (5—10 units, spec. activity 90) at room temperature (volume 0.8 ml). After 10 minutes the solution was cooled in an ice bath for 5 minutes. Then 100 μmoles of L-aspartate + 25 μmoles of CAP were added, final volume 1.0 ml. Incubation for 15 minutes at 37°.

Table 8. Protection from CMBA-inhibition by substrates.

Added at time 0 min.	Added at time 15 min.	μmoles P_i formed	% inhibition
Enz.	CAP + asp.	7.9	
Enz. + CMBA	CAP + asp	4.0	49
Enz. + CAP	asp.	8.1	
Enz. + CAP + CMBA	asp.	4.0	51
Enz. + asp.	CAP	7.6	
Enz. + asp. + CMBA	CAP	4.1	46
Enz. + CAP + asp.	—	8.8	
Enz. + CAP + asp. + CMBA	—	7.3	17

The experimental conditions were as described in Table 7 with additions as indicated. Final CMBA concentration = 0.001 M.

Table 7 demonstrates the results obtained with different types of inhibitors. In all cases, except with versene, phosphate and arsenate, method 2 was used for enzyme assay. Significant inhibition was only observed with CMBA and only at relatively high concentration of the inhibitor.

When, in an experiment at 0.001 M CMBA concentration, 5 μmoles of reduced glutathione were added 5 minutes before the start of the incubation at 37° (*cf.* conditions of Table 7), no inhibition was observed. This experiment demonstrates that inhibition with CMBA could be completely reversed by glutathione.

No protection of the enzyme wat observed by CAP or L-aspartate alone However, a mixture of both substrates partially protected the enzyme from the action of the inhibitor (Table 8).

Reversibility of transferase reaction. The equilibrium of the reaction was shifted very far towards synthesis of CA-aspartate. Unsuccessful attempts

Table 9. Formation of aspartate from CA-aspartate.

Experimental conditions	total counts in aspartate fractions	μmoles aspartate formed
Complete	730	0.76×10^{-2}
No enzyme	515	0.54×10^{-2}
No phosphate	525	0.55×10^{-2}
No enzyme or phosphate	540	0.56×10^{-2}

The complete experiment was carried out with 30 μmoles of CA-aspartate-^{14}C (0.96×10^5 ct/μmole), 50 μmoles of phosphate buffer, pH 7.5, 100 μmoles of tris buffer, pH 7.5, and 80 units of transferase (spec. activity 130). Final volume: 1.0 ml. Incubation for 30 minutes at 37°. The reaction was terminated by addition of 0.4 ml of M PCA. Three ml of water were added together with 30 μmoles of non-labeled aspartate. The pH was adjusted to 9—10 (phenolphtalein). Chromatographic separation of aspartate and CA-aspartate was then carried out as described in the experimental part. Aspartate was localized in the effluent by spot tests with ninhydrin. The total radioactivity in the pooled aspartate fractions was determined, and the amount of aspartate formed calculated from this value.

were made to measure the enzymic formation of aspartate from CA-aspartate and P_i (back reaction) by coupling the reaction with glutamo-oxaloacetic-transaminase [24] and malic dehydrogenase [25] after addition of α-ketoglutarate and DPNH.

The reversibility of the reaction could be demonstrated and measured by the use of carboxyl labeled CA-aspartate-^{14}C as substrate. It could be demonstrated that maximum amounts of aspartate-^{14}C were formed only in the presence of both enzyme and P_i (Table 9). The "background" formation of aspartate resulted from the presence of small amounts of this amino acid in the synthetic CA-aspartate and to a lesser extent from non enzymic breakdown during experiments of long duration. A further complication for any quantitative determinations of the equilibrium position was the chemical lability of CAP, the other product formed during the back reaction. Attempts to determine the equilibrium constant for the transferase action from the back reaction using CA-aspartate-^{14}C did not show conclusive results. It was evident, however, that the equilibrium position was shifted very far towards synthesis of CA-aspartate.

The mechanism of the reaction

Isotope exchange experiments. It was thought possible that the carbamyl group of CAP was first transferred to the enzyme, followed by a carbamyl transfer from the enzyme to aspartate:

$$\text{CAP} + \text{Enzyme} \rightleftharpoons \text{CA-Enzyme} + P_i \quad (3)$$

$$\text{CA-Enzyme} + \text{L-aspartate} \rightleftharpoons \text{L-CA-aspartate} + \text{Enzyme} \quad (4)$$

This mechanism was tested by isotope exchange experiments. According to reaction (3) an enzymic exchange of $^{32}P_i$ with phosphate in CAP should take place in the absence of aspartate. Table 10 demonstrates that such an *enzymic* exchange does not take place. Some ^{32}P was found in CAP in the absence of the enzyme, and addition of enzyme did not increase the specific acticity of the

Table 10. Isotope exchange experiments with $^{32}P_i$.

	Reisolated P_i		Reisolated CAP	
	μmoles	ct/μmole	μmoles	ct/μmole
Complete	59	0.62×10^6	10	2.6×10^3
No aspartate	48	0.77×10^6	18	1.3×10^3
No enzyme	47	0.71×10^6	23	1.5×10^3
No enzyme and asp.	50	0.70×10^6	16	1.7×10^3

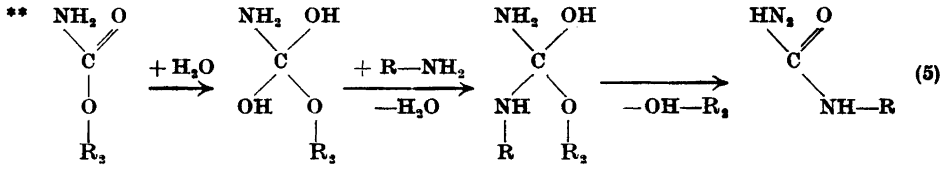
The complete experiment contained 35 μmoles of CAP, 40 μmoles of $^{32}P_i$ (0.83×10^6 ct/μmole), 15 units of transferase (spec. act. 90), and 250 μmoles of tris buffer, pH 7.5. Incubation for 15 min. at 37°. The solution was then cooled in ice, adsorbed directly on a Dowex-2-formate column and chromatographed (see experimental part). Fractions containing P_i and CAP respectively were pooled, and the radioactivity and phosphorus content were determined on aliquots.

reisolated CAP. However, after addition of L-aspartate a small but significant increase was observed. Table 10 demonstrates results typical of 5 different experiments at pH 7.5 and 6.5. The enzymic isotope exchange in the presence of aspartate again demonstrated the reversibility of the reaction while the absence of enzymic isotope exchange without aspartate made reaction (3) seem unlikely.

Further evidence against reaction (3) was obtained from experiments with arsenate. If reaction (3) took place in the presence of arsenate one might expect that the CA-enzyme formed would give rise to CA-arsenate, which in turn would decompose to carbamate + arsenate. The net effect would be an accelerated breakdown of CAP in the presence of enzyme and arsenate. Such an effect was not observed when 40 μmoles of CAP, 50 units of transferase and 100 μmoles of arsenate were incubated for 15 minutes at 37° *.

Reaction (4) was made improbable by an exchange experiment with L-aspartate-2,3-^{14}C (50 μmoles, 19 000 ct/μmole), CA-aspartate (48 μmoles) and enzyme (50 units). After incubation for 1 hour at 37° no radioactivity was found in the reisolated CA-aspartate.

Experiments with $H_2{}^{18}O$. Another possible mechanism involved the hydration of CAP as a first step, followed by condensation of the hydrate with aspartate by removal of water and subsequent dephosphorylation of the formed intermediate to give rise to CA-aspartate:



(5)

The participation of water in such a mechanism could be investigated by carrying out the transferase reaction in $H_2{}^{18}O$. In such an experiment no ^{18}O was incorporated into the carbamyl group of CA-aspartate, nor was there any significant enzymic exchange of the oxygen of water with that of CAP (Table 11).

DISCUSSION

CA-aspartic acid is known to be an intermediate in the biosynthesis of orotic acid both in microbial[26,27] and mammalian[21,28] systems. The demonstration that L-aspartate and the carbamyl group of CAP are the two groups from which the pyrimidine ring originates links together pyrimidine synthesis with both the tricarboxylic acid cycle and the urea cycle. The occurrence of the enzyme in various mammalian organs and in microbial extracts together with the fact that the equilibrium of the reaction is shifted far towards synthesis of

*. The decomposition of CAP in these experiments was measured by the formation of ammonia. The reaction was stopped by acidification with PCA. After neutralization the mixture was adsorbed on a small Dowex-2-formate column (0.62 cm² × 5 cm). The column was washed with 15 ml of water and aliquots of the eluant were analyzed for ammonia.

**. $R_2 = H_2PO_3$; $R—NH_2$ = L-aspartic acid.

Table 11. Transferase reaction in $H_2{}^{18}O$.

	Atom per cent excess ^{18}O in		
	CAP	Carbamyl group of CA-aspartate	
		from CO	from CO_2
Complete	0.003	0.000	0.001
No aspartate	0.001		
No enzyme	0.005		

Complete experiment: 100 μmoles of CAP, 100 μmoles of L-aspartate-^{14}C (10^3 ct/μmole), 125 μmoles of tris buffer, pH 7.5, 30 units of transferase (spec. act. 130). Incubation for 15 min. at 37° in 1 ml of $H_2{}^{18}O$ (1.4 atom per cent excess).

Two complete experiments were conducted, one for the isolation of CAP, the other for the isolation of CA-aspartate.

Ba-CAP was isolated and analyzed for ^{18}O as described in the experimental part.

CA-aspartate was separated by chromatography and localized by its radioactivity (26 μmoles of L-CA-aspartate). After addition of 80 μmoles of carrier DL-CA-aspartate, the substance was crystallized from water, decomposed and analyzed for ^{18}O.

CA-aspartate makes it very likely that this reaction represents a general first step in pyrimidine biosynthesis.

The purified enzyme showed the very specific capacity to catalyze a transfer of a carbamyl group attached to phosphate in "high energy" linkage to the amino group of L-aspartate. The extreme position of the equilibrium towards CA-aspartate synthesis together with the low affinity of the enzyme for aspartate and the instability of CAP made it impossible to measure the equilibrium constant of the transferase reaction. The existence of a back reaction could be demonstrated with the aid of $^{32}P_i$ (Table 10) and CA-aspartate-carboxyl-^{14}C (Table 9). Although a quantitative determination of the equilibrium position could not be carried out, it is clear from the data of Tables 9 and 10 that the back reaction proceeds at a very slow rate, and that the transferase reaction greatly favours synthesis of CA-aspartate.

Only one enzyme seemed to be involved in the reaction and no evidence could be obtained for the participation of a prosthetic group or an activator. The enzyme was named aspartate carbamyl transferase since this name seems to describe its function properly, although previously described transferases do not generally show such extreme equilibrium positions. The enzyme is distinct from the citrulline forming enzyme[3] and the enzyme forming β-ureidopropionic acid[29]. The latter two enzymes have as yet not been described in detail, but it seems highly probable that they also belong to the class of carbamyl transferases.

The isotope exchange experiments gave no evidence for the formation of a carbamylated enzyme. The experimental conditions allowed the demonstration of the reversibility of the sum of reactions (3) and (4), *i.e.* enzymic exchange of ^{32}P between P_i and CAP in the presence of aspartate. This makes

it improbable that the failure to find evidence from isotope exchange experiments for reaction (3) *or* reaction (4) depended on a limited reversibility of these two reactions, but rather argues against the actual existence of reactions (3) and (4).

The experiments with $H_2{}^{18}O$ speak against the participation of water and the formation of a phosphorylated intermediate as depicted in reaction (5). Such a type of mechanism can, however, not be completely ruled out if the whole reaction sequence were to be considered as taking place with enzyme bound intermediates and if the same molecule of water were first added and then removed.

It would appear, however, that the most probable explanation for all of the experimental results is that the transferase reaction involves a single displacement mechanism of the same type as earlier suggested for phosphate transferases[30]. According to this view both CAP and L-aspartate are first attached to the enzyme. By a nucleophilic attack of the nitrogen atom of aspartic acid on the carbon atom of CAP the carbon-oxygen bond is broken simultaneously with the formation of the new carbon-nitrogen bond.

Inhibition of the enzyme by CMBA could be demonstrated. Glutathione completely reversed the inhibition, which was probably due to the interaction of CMBA with active SH-groups. The absence of inhibition by less powerful SH-reagents does not necessarily speak against the concept that inhibition by CMBA was due to combination with SH groups (*cf.* Refs. [31,32]). Of interest for the understanding of the transferase mechanism was the finding that CAP + aspartate showed the ability to protect the enzyme against inhibition, while CAP or aspartate alone showed little effect. This finding is explained if both substrates compete with CMBA for SH groups of the enzyme. The results therefore tentatively indicate that both aspartate and CAP, during the action of the enzyme, are attached to SH groups.

Acknowledgement. This work has been supported by a grant from *Riksföreningen för Kräftsjukdomarnas bekämpande.*

REFERENCES

1. Reichard, P. and Hanshoff, G. *Acta Chem. Scand.* **9** (1955) 519.
2. Lowenstein, J. M. and Cohen, P. P. *J. Biol. Chem.* **213** (1955) 689.
3. Grisolia, S. and Cohen, P. P. *J. Biol. Chem.* **198** (1952) 561.
4. Jones, M. E., Spector, L. and Lipmann, F. *J. Am. Chem. Soc.* **77** (1955) 819.
5. Karrer, P., Escher, K. and Widmer, R. *Helv. Chem. Acta* **9** (1926) 301.
6. Wu, H. and Rittenberg, D. *J. Biol. Chem.* **179** (1949) 847.
7. Nyc, J. F. and Mitchell, H. K. *J. Am. Chem. Soc.* **69** (1947) 1382.
8. Grisolia, S. and Marshall, R. O. in Mc Elroy, W. D. and Glass, B. *Amino acid metabolism* (1954) 258.
9. Reichard, P. *Acta Chem. Scand.* **8** (1954) 795.
10. Lowry, O. H. and Lopez, J. *J. Biol. Chem.* **162** (1946) 421.
11. Koritz, S. B. and Cohen, P. P. *J. Biol. Chem.* **209** (1954) 145.
12. Peterson, E. A. and Sober, H. A. *J. Am. Chem. Soc.* **78** (1956) 751.
13. Hurlbert, R. B., Schmitz, H., Brumm, A. F. and Potter, V. R. *J. Biol. Chem.* **209** (1954) 23.
14. Phillips, D. M. P. *Biochim. et Biophys. Acta* **13** (1954) 560.
15. Gall, H. and Lohman, G. *Ber.* **61B** (1928) 670.
16. Ryhage, R. *To be published.*

17. Marshall, R. O., Hall, L. M. and Cohen, P. P. *Biochim. et Biophys. Acta* **17** (1955) 279.
18. Grisolia, S., Grady, H. J. and Wallach, D. P. *Biochim et Biophys. Acta* **17** (1955) 277.
19. Hanes, C. S. and Isherwood, F. A. *Nature* **164** (1949) 1107.
20. Deutsch, A. and Nilsson, R. *Acta Chem. Scand.* **7** (1953) 858.
21. Reichard, P., Smith, H. L., Jr. and Hanshoff, G. *Acta Chem. Scand.* **9** (1955) 1010.
22. Burrows, S., Grylls, F. S. M. and Harrison, J. S. *Nature* **170** (1952) 800.
23. Reichard, P. and Lagerkvist, U. *Acta Chem. Scand.* **7** (1953) 1207.
24. Cammarata, P. S. and Cohen, P. P. *J. Biol. Chem.* **193** (1951) 53.
25. Straub, F. B. *Hoppe-Seylers Z. physiol. Chem.* **275** (1942) 63.
26. Wright, L. D., Huff, J. W., Skeggs, H. R., Valentik, K. A. and Bosshardt, D. K. *J. Am. Chem. Soc.* **72** (1950) 2312.
27. Lieberman, I. and Kornberg, A. *J. Biol. Chem.* **207** (1954) 911.
28. Weed, L. L. and Wilson, D. W. *J. Biol. Chem.* **207** (1954) 439.
29. Grisolia, S. and Wallach, D. P. *Biochim. et Biophys. Acta* **18** (1955) 449.
30. Boyer, P. D. and Harrison, W. H. in Mc Elroy, W. D. and Glass, B. *Mechanism of Enzyme Action* (1953) 658.
31. Barron, E. S. G. and Singer, T. B. *J. Biol. Chem.* **157** (1945) 221.
32. Neilands, J. B. *J. Biol. Chem.* **208** (1954) 225.

Received January 11, 1956.

ACTA CHEMICA SCANDINAVICA 10 (1956) 567—577

Glycogen-like Polyglucose * in *Escherichia coli B* during the First Hours of Growth

H. PALMSTIERNA

Chemical Department I, Karolinska Institutet, Stockholm, Sweden

A method is described by which it is possible to estimate the mean dry weight of bacterial cells.

A polysaccharide occurring in *Escherichia coli B* is shown to be of a glycogen-like nature. This glycogen accumulated before the cells began to divide, and the glycogen content of the culture diminished when the nitrogen-containing cell constituents per litre of culture increased at the highest rate the culture conditions allowed.

It is shown that during the period of growth observed, the incorporation of ^{14}C from β-labeled lactate into the glycogen was smaller than could have been expected if all the glycogen had been synthesized from lactate in the medium only.

It is shown that the glycogen incorporated some carbon from carbon dioxide.

If is shown that glycogen could be synthesized from intracellular carbon sources as well as from carbon sources supplied with the medium.

The glycogen increased in the cells during the lag phase and decreased during the log phase in both glucose medium and broth, in the same way as in lactate medium. An increase of the same magnitude was noted in all culture volumes and at all cell concentrations used.

Escherichia coli B contains an alkalistable polyglucose as previously reported [1]. An alkalistable polysaccharide has also been observed in enteric bacteria by Levine *et al.*, detected by means of infra-red spectrophotometry [2]. Isolations of glycogen-like polysaccharides from *Mycobacterium tuberculosis* [3], *Neisseria perflava* [4] and *Bacillus megaterium* [5] have also been reported.

In the present paper the glycogen content of the cells was studied at different phases of growth. A very rapid increase in the glycogen content of the cells was noted to occur before the first cell divisions, followed by a decrease when the cells began to divide.

* For the sake of brevity called glycogen in the present paper.

BACTERIOLOGICAL METHODS

Media. The salt medium with sodium lactate as the sole source of carbon was that originally described by Friedlein [9]. The salt medium with glucose as the sole source of carbon was the one used by Hook and co-workers [10].

The broth was prepared in the usual way and buffered to pH 7.0 with 0.1 M phosphate buffer and sodium chloride was added up to a concentration of 0.5 g per litre. The medium was stored for 24 hours at 0 °C. The precipitate was filtered off and the medium sterilized in steam under pressure (1.5 kg/cm^2). This procedure was repeated twice. In this way it was possible to get a clear broth in which hardly any precipitate was formed during growth and during the cooling down of the culture.

The nitrogen-free medium was that used by Friedlein, from which the ammonium chloride was omitted. In the lactate- and nitrogen-free medium both ammonium chloride and lactate were left out. A completely nitrogen- and carbon-free medium was prepared by using this last-mentioned medium and filtering the air through an "Ascarite" filter, two flasks containing 50 % KOH and one flask containing saturated barium hydroxide. The air was dispersed by means of sintered glass discs.

Cultivation technique. The cultivation techniques are modifications of the techniques used by Cavanna *et al*[6]. Lyophilized cells, grown from one and the same culture of *E. coli B* were used in all the experiments. The cells were spread onto two agar slants and incubated for 24 hours at 37° C. Then the cells were suspended in 5 ml of culture medium. The suspension was inoculated into a 6 litre Erlenmeyer flask containing 4 or 5 litres of medium. The medium in this praeculture was of the same composition as that of the medium in the final culture. The praeculture was grown for 18 hours at 37° C and the cells were spun down at 0 °C in an International refrigerated centrifuge at 2 000 × g for 90 min. The cups were thoroughly rinsed, but not sterilized, before centrifugation. The loss of cells into the supernatant was too small to be estimated in a Beckman spectrophotometer, equipped with turbidimetric facilities. The cells were washed in fresh medium and suspended again in 200 ml of medium. The cell concentration was determined by counting the cells in the Bürker chamber under the phase contrast microscope. The final culture was inoculated with an appropriate amount of the suspension. The cultures were kept at 36.5—36.7 °C by means of a water-bath (volume 1 m^3) and shaken vigourously. The aeration current was filtered through tightly packed, sterilized cotton-wool and dispersed by sintered glass filters. The rate of aeration was 1 litre per minute and litre of medium as estimated by means of rotameters. The media were aerated for at least five minutes prior to inoculation. The air entering the praeculture was moistened by passing it through sterile, distilled water at 37 °C. From a culture of 5 litres, the loss of fluid from the praeculture did not exceed 0.2 litres in 18 hours.

Harvesting procedure. Aliquots of the culture were withdrawn by suction and the samples immediately cooled down to 4 °C by means of a sling of stainless steel tubing through which alcohol of −40 °C circulated. The time taken from the commencement of the suction to the finish of the cooling did not exceed 4.5 minutes, with the samples ranging from 1 to 12 litres. The samples called 0 were taken from the suspension used for inoculation. The samples were stored at 0 °C and centrifuged within 12 hours. It was found, however, that they could be stored for three days at 0 °C without any detectable change in the glycogen content occurring.

Determination of the mean dry weight of the cells. The volume of the cell suspension was determined, and the number of cells per ml estimated in a Bürker chamber under the phase contrast microscope. The cells were spun down at 0 °C and 2 000 × g for two hours in the afore mentioned centrifuge. In order to prevent the cells from whirling up again when the centrifuge slowed down, the bottoms of the centrifuge tubes were covered with a double layer of fine mesh stainless steel netting. The tubes were divided up into four chambers by means of baffles. The losses of cells were checked by estimating the amount of cells in the supernatant with the turbidimeter mentioned. (The supernatant was compared with a sample of the original suspension, diluted 25—50 times with fresh medium, to which formaldehyde was added to give a final concentration of approximately 0.3 %). The losses were lower than 2.4 % when the original suspension contained 10^8 to 5×10^8 cells per ml. When the cell concentration was higher than 5×10^8 cells per ml, the losses were too small to be estimated by the method used. All the data presented have been corrected for the losses of cells during centrifugation.

The cells were washed twice with fresh medium. The centrifugations were performed in an International refrigerated centrifuge typ PR-1 with a multispeed attachment (0 °C, 4 minutes, 24 000 × g at the bottom). The losses amounted to 3 000 cells per ml of washing fluid. This estimate was arrived at by counting the number of colonies produced on endo agar plates. The volume of the washing fluid was less than 60 ml. No corrections were introduced for these small losses.

The cells were washed in medium, since they lost appreciable amounts of ultra-violet absorbing substances into the washing fluid when they were treated with water or 0.9 % sodium chloride. This was especially the case with cells harvested during the last part of the lag phase and the first part of the log phase of growth. No losses of ultraviolet absorbing matter were observed when the cells were washed in fresh medium.

The washed samples were weighed in wet state and lyophilized. All analyses were performed on this freeze-dried material, with the exception of the nitrogen determinations. These determinations were performed on 15 to 25 mg of the material dried to constant dry weight over P_2O_5 at 90 °C *in vacuo*.

The difference between the wet weight and the constant dry weight was taken as medium water. All values presented were corrected for the amount of medium constituents, that is contained in the corresponding amount of medium.

The sum of the corrections amounted to between 8 and 15 % of the freeze dry weight.

The mean dry weight of the cells was calculated by dividing the corrected dry weight of the cell material per unit volume of culture by the number of cells per unit volume of culture.

All cultures were tested for purity by means of blood and endo agar cultures. In no case were any contaminations observed.

CHEMICAL METHODS

Isolation of the glycogen-like polysaccharide. Between 80 and 150 mg of the lyophilized material was treated with 0.1 ml of 30 % KOH per 10 mg of lyophilized material for three hours on a boiling water-bath. Immediately after the hydrolysis, three volumes of water and 8 volumes of 99 % ethanol were added. The precipitate was washed twice with 60 % ethanol and dried with ethanol and ether. When it was expected that the cells would contain small amounts of the polysaccharide only, they were treated with boiling ether prior to the alkaline hydrolysis, in order to remove most of the lipids which go down with the polysaccharide at the first precipitation with alcohol.

The polysaccharide obtained in this way is called here crude glycogen.

When deemed necessary, the crude glycogen was purified in the following way: 100 mg of the crude glycogen was dissolved in 1 ml of water, cooled down to 0 °C and precipitated again by adding glacial acetic acid to a final concentration of 80 %. This procedure was repeated twice. The precipitate was again dissolved and precipitated by adding alcohol to a final concentration of 60 %. The precipitate was dried with ethanol and ether. The glycogen purified by the acetic acid treatment is called here purified glycogen. Analyses of this glycogen are presented in the following.

The preparation and quantitative determination of glucose from the glycogen-like polysaccharide. The crude glycogen was submitted to hydrolysis in either 0.6 N HCl, or N H_2SO_4, for three hours on a boiling water-bath. No difference between the yields of glucose in the two kinds of hydrolysis could be observed. The glucose thus obtained was purified by passing the hydrolysate through a column of "Dowex 50" in the H^+-form and "Dowex 2" in the acetate-form. The columns had a length of 20 cm and an inner diameter of 0.7 cm. The ion exchange resins (40—100 mesh) were thoroughly washed with distilled water prior to use.

The purified glucose solutions were brought to dryness by heating to about 50° C in a strong air current.

Glucose (2, 4, and 10 mg in 10 ml of water) was passed through the columns, and 103 %, 99 % and 97 %, respectively, of the glucose were recovered.

All estimations of glucose were performed according to a modification of Disches' method [7].

Table 1. Isotopic dilution of glycogen in E. coli B.

Recovery of the glycogen (Chemical method) percentage	95.2	97.1	96.4	97.3
Recovery according to the dilution of the isotope, percentage	92.9	96.0	97.5	96.9

^{14}C-glycogen was added to samples of lyophilized cells (ranging between 50 and 100 mg) with a known content of glycogen. The glycogen was isolated and determined as glucose according to a modification of Dische's colorimetric method. The dilution of the isotope ranged between 10 and 60 per cent. Aqueous solutions of the hydrolyzed glycogen was spread directly on aluminium planchets and counted with a windowless gas flow counter, flushed with a helium-*iso*butane mixture. Since the layer of the material on the planchets did not exceed 0.03 mg/cm^2, no correction was made for self-absorption.

Protein isolation and nitrogen determination. Protein was isolated from the cells according to Schneider [8]. The nitrogen determinations were performed according to the micro-Kjeldahl method.

The isolation of glycogen and the determination of glucose checked by isotope dilution. In order to obtain ^{14}C-glycogen of bacterial origin, a culture was performed with sodium lactate, labeled in the β-carbon with ^{14}C, as the sole source of carbon. The isotopic lactate was synthesized by L. Reio and purified by ion exchange chomatography by S. Aqvist [15]. The culture volume was 5 litres, the initial cell concentration 5.5×10^8 cells per ml and the cultivation time 90 min. The concentration of the lactate was one-third of the concentration in the experiments mentioned in the following. The yield of glycogen was 13.1 % of the cells in the lyophilized state. The specific activity of the purified glycogen was 58.7 c.p.m. per microgram of glucose carbon. This ^{14}C-glycogen was used for determinations by the isotope dilution method. (Table 1.)

RESULTS

Analysis of the glycogen. Apart from glucose, no other sugar could be observed on the routine paper chromatograms (butanol saturated with water). The separation of glucose and galactose in this solvent is not satisfactory.

In order to exclude the presence of any sugar other than glucose in the polysaccharide, the purified glycogen was hydrolysed in N sulfuric acid for ten hours and chromatographed according to a modification of the method of Gardell [11], introduced by himself. (Butanol, propanol and water were used in the proportions 3:2:1 instead of in the proportions 4:1:1, and the column was heated to 40° C.) With this kind of hydrolysis, the polysaccharide sugar was destroyed to an extent of between 7.1 and 10.2 %. When hydrolysed and chromatographed in this way, 92.2, 91.7, and 91.3 % of the polysaccharide were recovered as glucose. If a correctior is allowed for the amount of sugar destroyed during hydrolysis, this would mean that between 99 and 105 % of the polysaccharide was revocered after chromatography. No traces of mannose, galactose or any other sugar were found. It is possible, however, that there were other sugars besides glucose present in the polysaccharide, and that these sugars were selectively destroyed during hydrolysis, since the linkages in the polysaccharide might influence the effect of the acid on the sugar itself.

Table 2. The content of glycogen-glucose in E. coli B *at different times after inoculation.* (Friedleins sodium lactate medium. culture volume 40 litres.)

Exp.	Time after inoculation in minutes	Number of cells $\times 10^{-8}$, per ml	Mean dry weight of cells, mg $\times 10^{-10}$	Glycogen-glucose			Protein-nitrogen per litre of culture, mg
				per cell mg $\times 10^{-12}$	in per cent of dry weight	per litre of culture, mg	
A	0	1.3	1.5	3.5	2.3	0.5	1.8
	10	1.3	1.7	28.9	16.9	3.8	1.8
	20	1.3	1.9	34.9	18.3	4.6	2.0
	30	1.3	2.2	38.5	17.5	5.1	2.1
	50	1.3	2.3	48.3	21.1	6.4	2.2
	70	1.6	2.5	49.9	19.9	8.0	3.0
	90	1.9	2.5	46.3	18.5	8.8	3.8
	130	3.2	2.7	26.2	9.7	8.4	6.7
	180	6.7	2.3	8.5	3.7	5.7	14.1
	240	22.8	1.6	1.1	0.7	2.5	31.9
	360	52.3	1.4	1.3	0.9	6.6	73.2
	960	— **	—	—	1.3	12.2 *	—
B	0	1.3	2.4	4.3	1.8	0.6	3.0
	30	1.3	2.5	26.9	10.8	3.5	2.6
	60	1.4	3.6	38.2	10.6	5.2	3.6
	90	1.5	3.5	36.7	10.4	5.5	4.4
	120	2.8	3.0	17.1	5.7	4.7	7.3
	240	20.1	1.5	1.0	0.7	2.0	28.1
	360	43.7	1.3	1.1	0.8	4.8	56.8
	960	— **	—	—	0.5	6.2 *	—

* In experiment A no precautions were taken to prevent loss of water from the culture. In experiment B loss of water was prevented by moistening the air entering the culture.

** It was not possible to get a reliable estimate of the cell concentration due to scanty contrast in the cells.

When glucose was added to the hydrolysate, a single symmetrical peak was observed on the chromatogram. When galactose was added, two distinctly separated peaks were obtained.

The polysaccharide was partly degradable with β-amylase and gave the same reddish-brown colour with iodine as that obtained with rabbit and rat liver glycogen.

Due to the difficulty of obtaining a clear solution of the bacterial glycogen, even when purified glycogen was used, the specific optical rotation could not be determined exactly (*cf.* Ref.[2].) It lies somewhere between $+185°$ and $+200°$ (rat liver glycogen $+198°$ to $+200°$).

The polysaccharide had a slight reducing power prior to hydrolysis. After hydrolysis for ten hours in N sulfuric acid it gave a yield of 91 % of the theoretically expected value.

The phosphorus content of three different batches of purified glycogen was 0.8, 0.8, and 0.7 %, the nitrogen content 0.1, 0.15, and 0.3 %, respectively. These values are calculated on the ash-free polysaccharide. The ash content

was 2.4, 1.9, and 2.0 %, respectively. The carbon content of the ash-free polysaccharide was 43.7 ± 0.7 % (four determinations).

The glycogen content of the cells at different intervals after inoculation. The results from the cultures in sodium lactate medium are shown in Figs. 1 and 2, and in the Tables 2, 3 and 4.

The glycogen-glucose content of the cells increased very rapidly during the lag phase of growth. The increase was most pronounced during the first ten minutes after inoculation. The increase in glycogen accounted for most of the increase in dry weight of the cells during the first part of the lag phase.

In the time between ten minutes after inoculation and the time of the first cell divisions (70—90 min. after inoculation) the increase in glycogen-glucose per unit weight of cells was less pronounced. The glycogen-glucose per dryweight and litre of culture, still showed a rapid increase during the same period. This difference is due to the increasing synthesis of other cell constituents during the last part of the lag phase (*cf.* the protein per litre values, Table 2). During the log phase * the glycogen-glucose per cell decreased up to 240 minutes after inoculation, after which it remained constant at a value of the same magnitude as the zero time value. This was also the case with the glycogen-glucose per unit weight value. The glycogen-glycose per dryweight and litre of culture (in the following called total glycogen) also decreased up to 240 minutes after inoculation. The decrease coincided with the time at which the culture attained its highest cell division rate (Fig. 2). The total glycogen-glucose increased again when the cell division rate began to slow down (about 240 min. after the inoculation). This increase in total glycogen-glucose was due to an increase in the cell concentration, without any significant increase in the glycogen-glucose per cell.

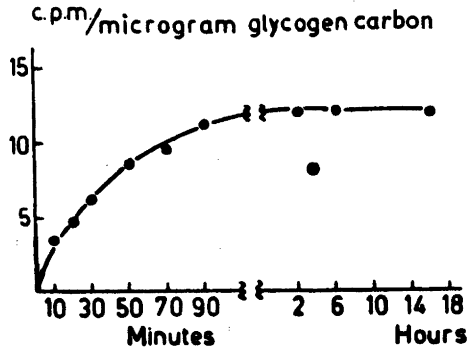


Fig. 1. In experiment A (Table 2) the cells were cultivated in Friedlein's medium in which the lactate was labeled in the β-carbon with ^{14}C. The specific activity was 32.2 c.p.m. per microgram of lactate carbon, as estimated by diluting a sample of the original, highly active sodium lactate. The radioactivity measurements were performed in the same way as described under Table 1. The ^{14}C-lactate used was to a slight extent contaminated with ^{14}C-alanine.

* The log phase is here defined as follows: beginning when the first cell divisions are found and lasting until the cells have stopped dividing, as checked by counting the cells in the Bürker chamber under the phase contrast microscope.

Table 3. Glycogen-glucose of E. coli B *cells incubated into Friedlein's medium from which nitrogen source has been left out.*

Exp.	Carbon source	Time after inoculation, in minutes	Number of cells × 10^{-8} per ml	Glycogen-glucose in per cent of the dry weight
H	Lactate and CO_2	0	1.3	1.7
		90	1.4	7.1
J	CO_2	0	1.0	1.3
		60	1.0	3.8
		90	1.0	3.5
K	None	0	1.6	2.1
		90	1.7	1.4
L	Lactate No CO_2	0	1.2	1.2
		90	1.2	9.3

In these experiments, Friedlein's lactate medium was used, but the usual source of nitrogen, ammonium chloride, was omitted. The carbon dioxide is that present in the air entering the culture. In experiments K and L the carbon dioxide was absorbed before the air entered the culture.

Incorporation of labeled lactate into bacterial glycogen. When sodium lactate, labeled in the β-carbon with ^{14}C, was used as the sole source of carbon, the specific activity of the glycogen carbon increased rapidly during the whole lag phase. Thereafter the specific activity remained constant at a value of about one-third of the specific activity of the substrate carbon (Fig. 1).

The glycogen content of the cells when cultivated in other media. When the cells were incubated in the Friedlein medium from which the nitrogen source had been omitted, they were still able to synthesize glycogen for at least 90 min. The glycogen-glucose content increased from 1.7 % to 7.1 % of the dry weight. The increase in glycogen-glucose was considerably lower when both the nitrogen source and the lactate were omitted, but there was still an increase (from 1.3 % at zero time to 3.5 % at 90 min.). If the air entering the culture was freed from carbon dioxide, and both the nitrogen and the lactate were excluded from the medium, no glycogen was formed by the cells. When lactate was present, and the carbon dioxide supply to the culture was prevented, the glycogen-glucose increased from 1.2 to 9.3 % of the dry weight (Table 3).

When the cells were cultivated in a glucose medium, the glycogen-glucose increased during the lag phase and decreased during the log phase in the same way as when the cells were grown in Friedlein's medium (Table 4, expt. G). The major difference consisted in a higher glycogen-glucose content of the cells at the moment of inoculation compared with cells grown in a lactate medium. The glycogen-glucose content of cells grown in broth also behaved in the same way (Table 4, expt. F). The increase in glycogen-glucose was however not so pronounced during the lag phase as in the lactate medium. This may be due to the difficulty of obtaining cells free from medium constituents tending to precipitate at the harvest.

Table 4. The glycogen-glucose content of E. coli B, *varying the size of the culture, the initial cell concentration and the composition of the medium.*

Exp.	Time after inoculation in minutes	Number of cells × 10^{-6} per ml	Glycogen-glucose in per cent of dry weight
C	0	1.0	2.1
	60	1.1	14.2
	360	—	2.2
D	0	10.5	2.1
	90	12.1	9.2
E	70	5.1 *	11.3
F	0	0.9	2.4
	60	0.9	8.0
	360	66.7	1.6
G	0	1.4	6.2
	60	1.8	12.1
	360	12.0	4.7

The cultures C, D, and E were performed in Friedlein's lactate medium. The size of the culture was 5 litres in exp. C and D. In exp. E the culture volume was 70 litres. This culture was performed in a stainless steel tank. Culture F was performed in a broth medium, culture G in a glucose medium. The culture volumes in both F and G was 5 litres.

The influence of cell concentration and culture volume on the increase in glycogen during the lag phase. The culture volume did not affect the increase in glycogen during the lag phase. Cultures performed in 5, 40, and 70 litres (Expts. A—E) all showed a glycogen increase of the same magnitude during the lag phase.

The initial cell concentration did not affect the increase in glycogen during the first 60 to 90 minutes after inoculation (Table 4, expts. C, D and E).

DISCUSSION

The observation that glycogen had accumulated in lactate, glucose as well as in broth cultures during the lag phase of growth, and that in all these media the glycogen decreased during the log phase, shows that the changes in glycogen were not due to specific actions of the various carbon sources. As shown in Table 2 and Fig. 2 there was a decrease in total glycogen during the first part of the log phase, coinciding with high rates of synthesis of the nitrogen-containing cell constituents. The lag phase may in respect of the glycogen be pictured as an endergonic phase of growth and the first part of the log phase as an exergonic phase.

During the last part of the log phase there was an increase in total glycogen, but there was no significant increase in the low amount of glycogen per cell.

* The initial cell concentration was 5.3 × 10^6 cells per ml as estimated from the cell concentration in the praeculture.

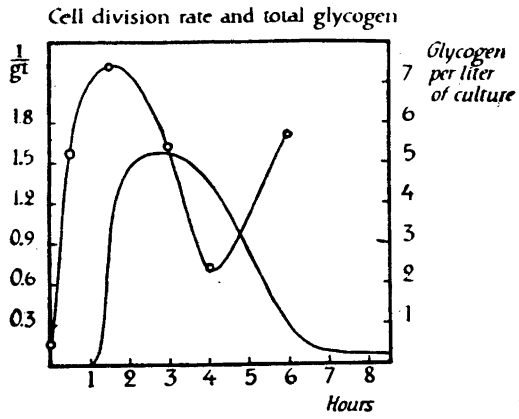


Fig. 2. The cell division rate was estimated by taking the reciprocal value of the mean generation time in hours (gt). Samples for counting were taken every 15 minutes until 6 hours after inoculation. After that the intervals were 40 minutes. The glycogen-glucose (in mg) per litre of culture is shown by the open circles. The rate of formation of nitrogen-containing compounds showed its maximum at the same time as the cell division rate was at its maximum.

It might be suggested that the small residual amount of glycogen left in the cells be considered as a primer for glycogen synthesis.

Hershey and Bronfenbrenner [12], observing the uptake of oxygen in relation to the phase of growth in *E. coli*, found that the uptake of oxygen per hour and gram of bacterial nitrogen was constant during all phases of growth. No observations were made during the first 150 minutes of growth. It is, however, evident that the oxygen uptake per unit weight of bacterial nitrogen and hour was the same at the beginning of the log phase as at the end of this phase. This means that the oxygen uptake was the same whether the synthesis of nitrogen-containing compounds proceeded at a high rate or at a low rate. It seems justifiable to conclude that the aerobic mechanisms functioned at the same rate throughout all phases of growth. Since the high rate of synthesis of nitrogen-containing compounds during the first part of the log phase was not accompanied by a high rate of oxygen consumption, the energy, necessary for these syntheses, may partly have been made available by anaerobic breakdown of carbohydrate. An auxiliary source of this carbohydrate was the glycogen accumulated during the lag phase.

The experiments C and D (Table 4) were performed in order to rule out the possibility that the decrease in glycogen during the first part of the log phase was caused by anaerobic conditions in the medium. Anaerobic or semi-anaerobic conditions might have been induced by high cell concentrations. If a high cell mass per unit volume of culture were to produce oxygen deficiency in the medium, this would cause an inhibition of the glycogen synthesis from lactate. No significant lowering of glycogen per unit weight of bacteria was observed, even though the initial cell concentration was increased ten times. Furthermore, preliminary experiments have shown that it was possible to diminish the aeration to 100 ml per minute and litre of culture, without any changes in

the length of the lag phase and the mean generation time occurring. These results seem to exclude the possibility that the decrease in glycogen during the first part of the log phase was caused by oxygen deficiency in the medium.

Roberts *et al.*[13], observing the incorporation of ^{14}C from various sources, concluded that in the case of proliferating *E. coli* cultures, the tricarboxylic acid cycle furnishes 50 % of the carbon required for protein synthesis, but is relatively unimportant as an oxidative mechanism. They express the view that the function of the tricarboxylic acid cycle is mainly a synthetic one[14] in this case. It might be suggested that the energy derived from the oxidative breakdown is sufficient for the syntheses during the lag phase, but that the capacity of the cycle is insufficient to furnish the carbon for the syntheses and the energy required during the first part of the log phase. The energy output from the cycle may be less at this time, due to the disappearance of considerable amounts of tricarboxylic acid components in the form of nitrogen containing compounds. This would imply that less energy-rich bonds were produced by the cycle, and consequently the situation would be favourable for the formation of these compounds by means of glycolysis. It should however not be overlooked that there may be other ways of oxidative breakdown in *E. coli* than that of the tricarboxylic acid cycle.

An attempt was made to get some more information about the oxygen consumption of cells in the lag phase by the Warburg "indirect" manometric method. No reproducible results could be obtained.

In the experiment performed in ^{14}C-lactate medium, the specific activity of the glycogen carbon showed a very sharp increase during the lag phase and thereafter remained at a level of about one-third of the specific activity of the lactate carbon in the medium. If every glucose molecule in the glycogen had been synthesized from two lactate molecules only, the specific activity of the glycogen carbon would have shown a still sharper increase during the lag phase, and would have reached approximately the same specific activity during the log phase as that of the medium lactate. The dilution of the glycogen carbon during the lag phase may at least in part be ascribed to dilution from cellular carbon already present at the moment of inoculation. That such was the case is indicated by the results presented in Table 3, which show that glycogen was synthesized to some extent, even when there was no carbon source except CO_2 in the medium. Hammarsten, Palmstierna, Reio and Åqvist[15] have shown that the glycogen in cells praecultured for 18 hours in β-labeled ^{13}C-lactate medium contained increasing amounts of ^{13}C during the lag phase when cultivated in a medium free from ^{13}C. This proves that the glycogen carbon was diluted by carbon of cellular origin during this phase.

A synthesis of glycogen from internal carbon sources was made probable also by the experiments described in Table 3. The role of carbon dioxide in this synthesis was also made evident. If carbon dioxide was available a synthesis of glycogen from cellular carbon sources occurred (expt. J), in this case in the absence of the organic carbon source. No such synthesis occurred if both carbon dioxide and the organic carbon source were excluded, indicating that the mechanism of the synthesis of glycogen from cellular carbon was sensitive to carbon dioxide deficiency. The result that the glycogen synthesis

was uninhibited if lactate but no carbon dioxide was provided, may be explained by a production of carbon dioxide from lactate-carbon (expt. L).

Ehrensvärd and Palmstierna [16] have shown that certain amounts of ^{14}C were incorporated into bacterial glycogen when the culture was aerated with $^{14}CO_2$-containing air. This finding agrees with the results obtained by Hastings *et al.*[17] when working with rats. The incorporation of CO_2-carbon does not explain the low specific activity of this substance when grown on β-labeled lactate, since the CO_2 was incorporated into C_3 and/or C_4. The β-carbon from lactate may be expected in the positions C_1 and C_6.

The observation that glycogen had accumulated to an approximately equal extent in lactate, glucose or broth cultures during the lag phase, and that in all of these media the glycogen decreased during the first part of the log phase, shows that the changes in glycogen were not due to a specific action of the lactate.

REFERENCES

1. Palmstierna H. *Acta Chem. Scand.* **9** (1955) 195.
2. Levine, S. *et al. J. Bacteriol* **6** (1953) 664.
3. Chargaff, E. and Moore, D. H. *J. Biol. Chem.* **155** (1944) 493.
4. Hehre, E. J. and Hamilton, D. N. *J. Bacteriol.* **55** (1948) 197.
5. Barry, C. *et al. Compt. rend.* **235** (1952) 1062.
6. Cavanna, R., Chain, E. B., Hedén, C. G., Malmgren, B., Elianson, N. A., Hammarsten, E. and Åqvist, S. *Rendiconti dell Instituto Superiore di Sanita (English ed.)* Vol. **XVII.** 168.
7. Gurin, S. and Hood, D. B. *J. Biol. Chem.* **131** (1939) 211.
8. Schneier, W. C. *J. Biol. Chem.* **161** (1945) 293.
9. Friedlein, F. *Biochem. Z.* **164** (1928) 273.
10. Hook, A. E., Beard, D., Taylor, A. R., Sharp, D. G. and Beard, J. W. *J. Biol. Chem.* **165** (1946) 241.
11. Gardell, S. *Acta Chem. Scand.* **7** (1953) 201.
12. Hershey, A. D. and Bronfenbrenner, J. *J. Gen. Physiol.* **21** (1937–38) 721.
13. Roberts, R. B. *et al. Proc. Natl. Acad. Sci. U. S.* **39** (1954) 1013.
14. Roberts, R. B. *et al. Yearbook Carnegie Institution,* Washington 1955.
15. Hammarsten, E., Reio, L., Palmstierna, H. and Åqvist, S. *In preparation.*
16. Ehrensvärd, G. and Palmstierna, H. *In preparation.*
17. Solomon, A. K., Vennesland, B., Klemper, F. W., Buchanan, J. M. and Hastings, A. B. *J. Biol. Chem.* **140** (1941) 171.

Received January 11, 1955.

ACTA CHEMICA SCANDINAVICA 10 (1956) 578—586

Changes in Glycogen and Nitrogen-containing Compounds in *Escherichia coli B* during Growth in Deficient Media

I. Nitrogen and Carbon Starvation

T. HOLME and H. PALMSTIERNA

Bacteriological Department and Chemical Department I, Karolinska institutet, Stockholm, Sweden

When *Escherichia coli B* was cultivated in media deficient either in the nitrogen or in the carbon source, there was no increase in the nitrogen-containing compounds in the cells during the phase of constant cell concentration, which was caused by exhaustion of the limiting factor.

During this starvation phase an increase of glycogen in the cells was observed.

During the phase of rapid cell division following the addition of the limiting factor in the nitrogen-deficient culture with sodium lactate as the carbon source, the glycogen per litre of culture decreased rapidly.

When the cells were cultivated in nitrogen-deficient media, substances causing an absorption in the ultra-violet region poured into the medium. During the period of growth following the addition of the nitrogen source, the ultra-violet absorption of the culture fluid decreased rapidly.

In earlier experiments it was shown that the total glycogen in *Escherichia coli B* cultures increased considerably during the lag phase of growth, and decreased abruptly when the cells began to divide[1]. By the use of a synthetic medium deficient in one essential nutrient it is possible to arrest cell division after a certain number of generations in the logarithmic phase of growth[2]. In this paper experiments are described in which this technique is used in order to obtain additional information regarding glycogen synthesis in non-dividing cells. The experiments also include the addition of the limiting factor after a certain period of starvation, as well as observations concerning the phase of cell division that followed.

METHODS

Media. The medium used in all experiments but one was Friedlein's synthetic sodium lactate medium [3]. In one experiment a medium with glucose as the carbon source was used [4]. The nitrogen source was ammonium chloride in all experiments. Praecultures were grown in these media. In the final cultures, media of the same composition as in the praecultures were used, except that they were deficient either in the carbon or in the nitrogen source. In the experiments in which the nitrogen source was the limiting factor, the initial concentration of ammonium chloride was 0.75×10^{-3} M. In the experiment with the carbon source as the limiting factor, the initial sodium lactate concentration was 1.67×10^{-2} M.

Cultivation technique. Praecultures were grown as previously described [1]. The final cultures were inoculated with an amount of cells sufficient to give a concentration of about 10^{8} cells per ml. Prior to inoculation the cells were washed once with the deficient medium. One and a half hour after the cells had ceased dividing in the nitrogen-deficient cultures, and four hours later in the carbon-deficient one, a quantity of the limiting factor was added in order to give approximately the same concentration of those factors as in the complete media, *e. g.* 0.02 M in respect of ammonium chloride and 0.1 M in respect of sodium lactate. In all other respects the techniques were the same as previously described.

Chemical methods. The isolation of glycogen and the estimation of the glycogen-glucose were performed as described in a preceding article [1]. The trichloro-acetic acid (TCA) extractions were performed according to Schneider [5]. The "hot TCA"-extraction was always performed on the material already TCA-extracted in the cold. The micro-Kjeldahl method was used for the nitrogen determinations.

Table 1. Experiment A. Nitrogen starvation. Carbon source: sodium lactate.

Time after inoculation in min.	Number of cells per ml $\times 10^{-8}$	Dry weight of cells per litre of culture (mg)	Dry weight per cell (mg $\times 10^{-10}$)	Glycogen-glucose % of dry weight	Glycogen-glucose per litre of culture (mg)	Glycogen-glucose per cell (mg $\times 10^{-12}$)	Cold TCA-N % of dry weight	Cold TCA-N per litre of culture (mg)	Cold TCA-N per cell (mg $\times 10^{-12}$)	Hot TCA-N % of dry weight	Hot TCA-N per litre of culture (mg)	Hot TCA-N per cell (mg $\times 10^{-12}$)	Protein-N % of dry weight	Protein-N per litre of culture (mg)	Protein-N per cell (mg $\times 10^{-12}$)
0	0.75	13.5	1.8	2.1	0.3	3.8	0.6	0.1	1.1	2.6	0.4	4.8	10.1	1.4	18.3
15	0.75	18.2	2.4	5.0	0.9	12.1				2.3	0.4	5.5	7.1	1.3	17.2
30	0.8	18.9	2.4	8.8	1.7	20.8				2.5	0.5	5.9	7.0	1.3	16.5
60	1.1	26.3	2.4	8.8	2.3	21.1				2.8	0.7	6.7	7.2	1.9	17.1
90	1.5	38.6	2.6	8.4	3.2	22.0	0.6	0.2	1.6	3.2	1.2	8.1	7.6	2.9	19.5
140	2.7	79.5	3.0	6.1	4.8	17.9				3.3	2.6	9.7	7.8	6.2	23.1
180	4.5	111.4	2.5	9.3	10.4	23.1				3.1	3.5	7.8	7.3	8.2	18.2
220	4.6	111.1	2.4	12.2	13.6	29.5	0.5	0.6	1.3	3.0	3.3	7.2	7.0	7.8	17.0
240	5.0	119.1	2.4	13.6	16.2	32.4	0.6	0.7	1.4	2.6	3.1	6.1	7.0	8.3	16.6
260	4.9	119.0	2.4	15.3	18.2	37.2				2.5	3.0	6.1	6.9	8.3	16,8
265	addition of ammonium chloride.														
270	5.3	124.8	2.4	13.8	17.2	32.4	0.7	0.9	1.6	2.6	3.3	6.1	6.8	8.4	15.9
280	5.7	132.6	2.3	13.0	17.3	30.4				2.7	3.6	6.3	7.1	9.4	16.5
295	6.8	152.9	2.3	9.9	15.2	22.3	0.6	1.0	1.5	3.0	4.6	6.8	7.3	11.2	16.5
325	8.5	190.0	2.2	7.5	14.2	16.7	0.6	1.2	1.4	3.4	6.4	7.6	7.9	14.9	17.5
355	12.0	295.0	2.5	3.5	10.4	8.7	0.6	1.8	1.5	3.5	10.3	8.6	8.8	25.8	21.5
475	—	833.2	—	0.4	3.5	—	0.6	5.4	—	3.1	25.7	—	9.3	77.2	—
630	—	1 224.0	—	0.6	7.5	—				2.9	35.3	—	9.7	118.4	—

The cells were washed with fresh medium free of the nitrogen source. TCA: trichloro-acetic acid.

RESULTS

Nitrogen starvation. In the nitrogen-deficient cultures (expts. A, C and D), the lag phase was of the same duration as in the complete media. After an initial multiplication period, the cells ceased dividing on account of the deficiency in the medium (Fig. 1, Tables 1, 3 and 4).

In order to obtain a cell concentration of about 5×10^8 cells per ml during the starvation phase, the initial concentration of ammonium chloride in the medium had to be 0.75×10^{-3}M.

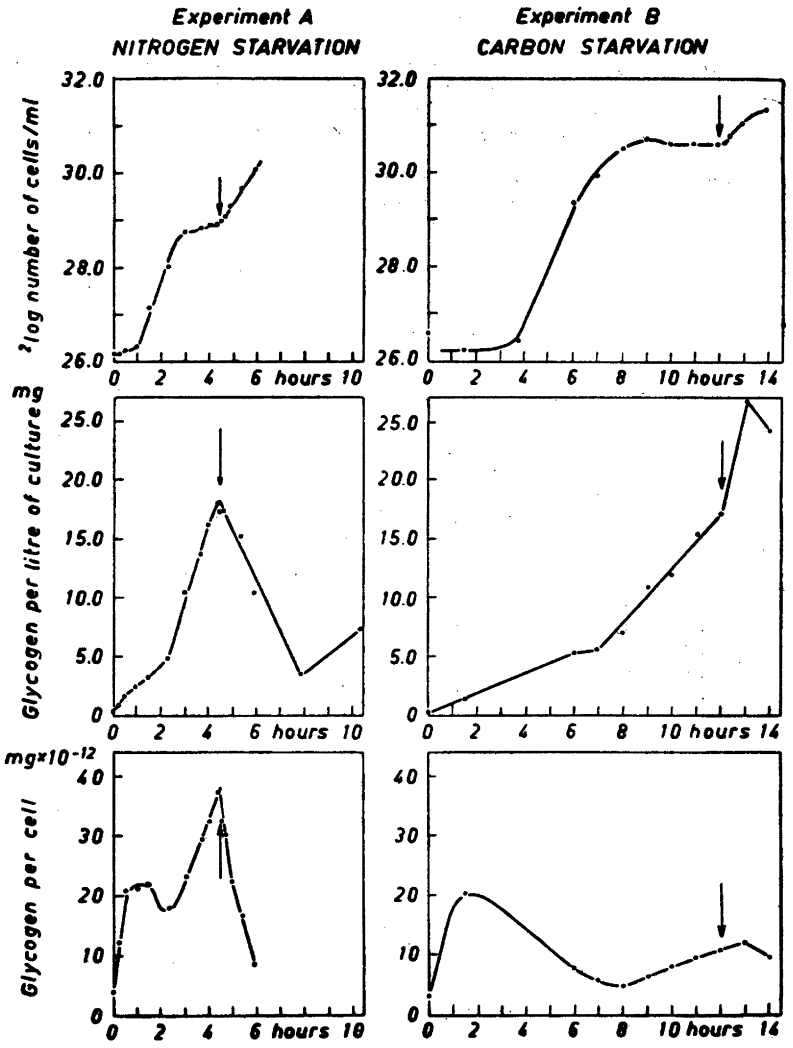


Fig. 1. Experiments A (nitrogen starvation) and B (carbon starvation). The arrows indicate the moment when ammonium chloride and sodium lactate respectively were added.

In one experiment (D, Table 4) it was noted that the glycogen content of the cells had reached a value near maximum in about two hours from the beginning of the starvation phase.* Consequently, when the starvation phase had lasted for that period in expts. A and C, ammonium chloride was added to obtain a concentration of 0.02 M, in order to initiate a second multiplication phase with the cells loaded with glycogen.

After the addition of ammonium chloride, the cells began to divide immediately (Fig. 1).

Glycogen per cell. The glycogen per cell increased during the lag phase and decreased during the first part of the logarithmic phase of growth in the same way as when the cells were cultivated in a complete medium (Fig. 1). However, when the division rate began to decrease, the glycogen per cell increased again. This increase continued linearly during the starvation phase until ammonium chloride was added. In experiment A, where lactate was the carbon source, the glycogen per cell increased from 17.9 to 37.2 $\times 10^{-12}$ mg (Table 1). The same course of development was noted in expt. C, with glucose as the carbon source, and the corresponding figures for the glycogen increase per cell were 26.0 and 75.7 $\times 10^{-12}$ mg, respectively, showing as in earlier experiments that the amount of glycogen was higher in cultures with glucose as the carbon source (Table 3). In both experiments (A and C) the addition

Table 2. Experiment B. Carbon starvation. Carbon source: sodium lactate.

Time after inoculation in min.	Number of cells per ml $\times 10^{-8}$	Dry weight of cells per litre of culture (mg)	Dry weight per cell (mg $\times 10^{-10}$)	Glycogen-glucose % of dry weight	Glycogen-glucose per litre of culture (mg)	Glycogen-glucose per cell (mg $\times 10^{-12}$)	Cold TCA-N % of dry weight	Cold TCA-N per litre of culture(mg)	Cold TCA-N per cell (mg $\times 10^{-12}$)	Hot TCA-N % of dry weight	Hot TCA-N per litre of culture(mg)	Hot TCA-N per cell (mg $\times 10^{-12}$)	Protein-N % of dry weight	Protein-N per litre of culture (mg)	Protein-N per cell (mg $\times 10^{-12}$)
0	1.0	12.0	1.2	2.1	0.3	2.5									
90	0.7	19.1	2.6	7.8	1.5	20.3	5.1	1.0	13.2	1.8	0.3	4.6	8.0	1.5	20.7
225	0.9														
360	7.0	133.5	1.9	4.1	5.4	7.7	2.6	3.5	5.0	1.8	2.3	3.4	8.6	11.4	16.3
420	10.0	212.4	2.1	2.7	5.7	5.7	2.2	4.7	4.7	2.0	4.1	4.1	8.9	18.9	18.9
480	15	250.6	1.7	2.8	7.0	4.7	2.4	6.1	4.1	1.6	3.9	2.6	9.0	22.5	15.0
540	17	283.7	1.7	3.9	10.9	6.4	2.5	7.0	4.1	1.5	4.3	2.6	9.1	25.7	15.1
600	16	276.2	1.7	4.6	12.8	8.0	2.3	6.4	4.0	1.7	4.6	2.9	9.5	26.4	16.5
660	16	272.2	1.7	5.7	15.5	9.7	2.1	5.7	3.6	1.6	4.3	2.7	8.9	24.3	15.2
720	16	267.9	1.7	6.4	17.2	10.7	2.2	5.8	3.6	1.4	3.8	2.4	8.8	23.6	14.8
721	addition of sodium lactate														
735	16														
745	18														
780	22	388.4	1.8	6.9	26.8	12.2	1.0	3.7	1.7	2.4	9.4	4.3	8.4	32.8	14.9
840	26	466.9	1.8	5.4	25.2	9.7	0.9	4.0	1.5	2.5	14.8	5.7	8.8	41.2	15.9

The cells were washed with fresh medium free of the carbon source.

The cold TCA-N values are corrected for the amount of nitrogen originating from the washing fluid.

* The starvation phase is considered to have begun when the cell division rate decreases owing to a deficiency in the medium.

Table 3. Experiment C. Nitrogen starvation. Carbon source: glucose.

Time after inoculation in minutes	Number of cells per ml × 10^{-6}	Dry weight of cells per litre of culture (mg)	Dry weight per cell (mg × 10^{-10})	Glycogen-glucose % of dry weight	Glycogen-glucose per litre of culture (mg)	Glycogen-glucose per cell (mg × 10^{-12})
0	1.2	19.0	1.6	6.6	1.3	10.4
60	1.2	23.9	2.0	13.4	3.2	26.7
150 *	1.7	51.1	3.0	11.0	5.6	33.0
300	2.8	101.4	3.6	21.0	21.2	75.8
305	addition of ammonium chloride					
375	5.9	207.1	3.5	11.9	24.6	41.6

* After 200 minutes the number of cells remained constant at 2.8 × 10^6 cells per ml.

of ammonium chloride caused an immediate and rapid decrease in glycogen per cell.

T o t a l g l y c o g e n. In experiments performed in complete media, glycogen per dry weight and litre of culture (total glycogen) began to decrease two hours after inoculation. In the deficient cultures the starvation phase had already begun at the time when this decrease was expected and the total glycogen began instead to increase at this point. This increase was linear and continued during the starvation phase.

After the addition of ammonium chloride the total glycogen decreased rapidly in the culture with lactate as its carbon source, showing that the glycogen synthesis was too small to compensate for the utilization. The lowest figure was noted at the beginning of the stationary phase (3.5 mg per litre o culture). The slight increase in total glycogen that followed in this experiment was primarily due to the increase in the cell mass (Table 1). The culture with glucose as its carbon source (expt. C) did not show the same immediate decrease in total glycogen after the addition of ammonium chloride, but the rate of increase slowed down (Table 3).

The protein-nitrogen per cell decreased slightly at the beginning of the starvation phase, and then remained constant (Table 1).

Ultra-violet absorption of the culture fluid. In cultures grown in an unmodified Friedlein's medium, the UV absorption of the cell-free culture fluid never exceeded an extinction of 0.15 at 260 mμ (read against fresh medium, 1 cm cuvettes). The case was the same in the carbon-starved culture (expt. B). In nitrogen-starved cultures grown in lactate medium, as described above (expt. A), substances poured from the cells into the medium, causing an absorption in the UV region (Figs. 2 and 3). At 260 mμ the absorption increased from 0.15 at 90 min. after inoculation to 0.6 at 5 hours after inoculation. By that time the starvation phase had lasted for about 2 hours (Fig. 2). When the ammonium chloride was added, the UV absorption of the culture fluid decreased rapidly. The same results were obtained in three different experiments, two in 5 litre cultures, and one in a 200 ml culture.

Carbon starvation. One carbon-deficient culture (expt. B) was also investigated (Fig. 1, Table 2). In lactate-deficient media there was a considerable increase in the duration of the lag phase when the sodium lactate concentration

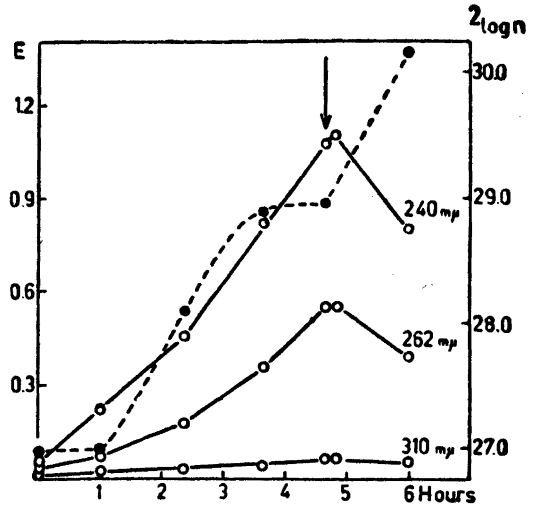


Fig. 2. Ultra-violet absorption of the cell-free medium in a nitrogen-starved culture. Broken curve: ^{2}log number of cells per ml. Unbroken curves: specific absorption (E) of the medium. The arrow indicates the moment when ammonium chloride was added.

was lower than 3.0×10^{-2} M. The initial concentration of lactate in expt. B was 1.67×10^{-2} M, giving a lag phase of about three hours' duration. The cell concentration during the starvation phase reached rather a high level, 1.6×10^9 bacteria per ml, which was about three times as much as the cell concentration during this phase in the nitrogen-starved cultures. The period of constant cell

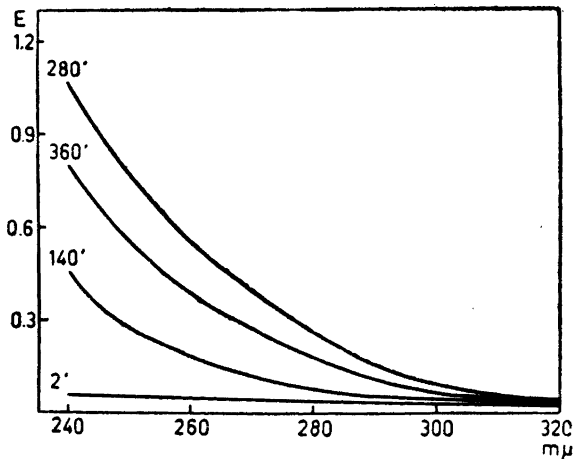


Fig. 3. The same experiment as in Fig. 2. Absorption curves obtained at different times, indicated by the figures at the end of each curve. The extinction was determined at intervals of 5 mμ except in the region 250—270 mμ, where the intervals were 2 mμ.

Table 4. Experiment D. Nitrogen starvation. Carbon source: sodium lactate. No addition of the limiting factor.

Time after inoculation in minutes	Number of cells per ml $\times 10^{-8}$	Dry weight of cells per litre of culture (mg)	Dry weight per cell (mg $\times 10^{-10}$)	Glycogen-glucose % of dry weight	Glycogen-glucose per litre of culture (mg)	Glycogen-glucose per cell (mg $\times 10^{-12}$)
0	1.1	14.3	1.3	1.9	0.3	2.5
90	1.1					
140	2.1	69.3	3.3	5.4	3.7	17.7
240	6.0					
300	6.3	96.5	1.5	18.2	17.5	27.8
540	5.7 *	117.5	2.1	21.4	25.2	44.1

* Difficult to count in the Buerker chamber because of the scanty contrast.

concentration due to starvation in experiment B was not interrupted as early as in the nitrogen-starved cultures. The time chosen in each case corresponded roughly to that of the lag phase.

After the addition of sodium lactate (12 hours after inoculation) there was a short lag before the cells began to divide (Fig. 1). The increase in cell numbers was small, and the division rate low, during the period of multiplication that followed, probably because the cell concentration was near its maximum value in the medium used. Two hours after the addition, the cell concentration was 2.6×10^9 bacteria per ml.

Glycogen per cell. The glycogen per cell reached a value of about 20×10^{-12} mg during the lag phase (Table 2). During the logarithmic phase it decreased to a minimum value of 4.7×10^{-12} mg eight hours after inoculation. At this point the division rate slowed down, due to the deficiency in the medium, and the glycogen began to increase again. Compared with the nitrogen-starved cultures, this increase proceeded at a very slow rate, the glycogen per cell amounting twelve hours after inoculation to 10.7×10^{-12} mg. Since the dry weight per cell was constant during the whole starvation phase, the same rate of increase was found in glycogen per mg of dry cells. During the first hour after the addition of sodium lactate, the glycogen per cell showed a slight increase, followed by a decrease.

The "per cell" values do not of course account for different types of cells that may be present in a culture. No attempt has been made as yet to study more closely the differences between cells belonging to the same population.

Total glycogen. Glycogen per dry weight and litre of culture increased throughout the lag, logarithmic, and starvation phases in approximately the same way as in the nitrogen-starved cultures. The rate of increase, however, was much slower (Fig. 1).

In spite of the low content of glycogen in the carbon-starved cells, the values of total glycogen are similar to those in the nitrogen-starved cultures. This is due to the fact that the dry weight of cells per unit volume during the starvation phase was about 2.5 times greater in the carbon-starved culture (B) than in the nitrogen-starved cultures.

After the addition of lactate in expt. B, the total glycogen increased considerably within the first hour, followed by a decrease during the second hour.

Influence of carbon dioxide. Carbon deficient cultures (lactate starvation) were aerated with an air-CO_2-mixture. One per cent CO_2 increased the rate of glycogen synthesis 1.8 times and 4 per cent CO_2 increased the rate 2.5 times that in experiment B (aerated with common air).

DISCUSSION

Several authors have reported experiments dealing with the chemical composition of bacteria cultivated in deficient media[6-8]. When cultivated in media with high carbohydrate and low nitrogen content, *Escherichia coli* and *Aerobacter aerogenes* showed a high polysaccharide content in the stationary phase[7].

Dagley and Dawes[8] determined the total polysaccharides of *E. coli* cells cultivated in deficient media. The interpretation of their results is rendered difficult because of the inhomogeneity of the substances determined. Evidently the polysaccharide material that accumulates during prolonged nitrogen starvation represents different kinds of carbohydrates which may be more or less actively participating in the metabolism.

In a later article, Dagley, Dawes and Morrison[9] describe experiments with *Aerobacter aerogenes*, in which pyruvate was determined in the medium under different conditions of growth.

As reported previously[1], the glycogen accumulation and utilization seems to be correlated to the synthesis of the nitrogen-containing compounds in the

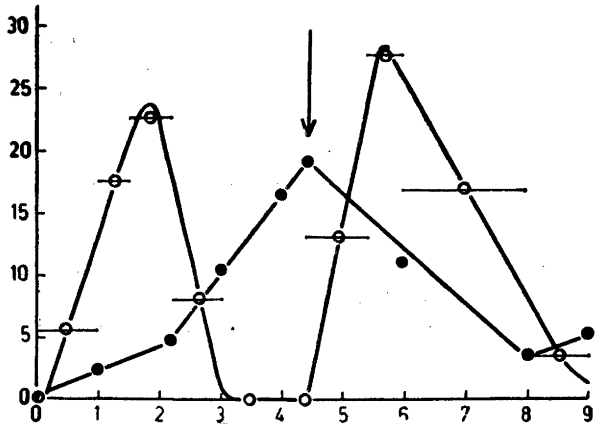


Fig. 4. Total glycogen and rate of protein synthesis in a nitrogen-starved culture. Abscissa: Time in hours. Ordinate: Glycogen per litre of culture in mg and *per cent increase in protein-nitrogen per litre of culture in 10 minutes. The arrow indicates the moment when ammonium chloride was added. The net synthesis of protein was arrived at by estimating the increase in protein nitrogen per litre of culture in per cent of the preceding value. The curve* O——O *was drawn through the midpoint of these time intervals. The curve* ●——● *represents the glycogen per litre values in mg. The curves show that the glycogen increased relatively slowly during the time when the net synthesis of protein showed its first maximum, and that the net synthesis of glycogen increased at a higher rate when there was no protein synthesis due to nitrogen starvation. After the addition of ammonium chloride, the net synthesis of protein increased very rapidly. The glycogen decreased sharply at the same time.*

cells. This view is supported by our present results. In the experiments presented in this paper, as well as in those previously reported a low net synthesis of nitrogen-containing compounds was accompanied by a high net synthesis of glycogen. During a phase of growth in which the synthesis of nitrogen-containing compounds was limited by nitrogen starvation (the starvation phase), glycogen accumulated rapidly.

The high rate of synthesis of nitrogen-containing compounds observed immediately after the addition of ammonium chloride was accompanied by a sharp decrease in the total glycogen in the culture, which also lends support to the view expressed. (Fig. 4.) In one experiment described by Dagley *et al.*[9], the addition of the nitrogen source to a nitrogen-starved culture caused an arrest in the pyruvate production from the cells. This may be explained by a high rate of utilization of the pyruvate, presumably for the synthesis of protein.

The fact that there was no lag before the cell concentration began to increase logarithmically after the addition of ammonium chloride shows that the cells were well prepared for cell division.

The material that poured into the medium during nitrogen starvation causing an absorption in the UV region (Fig. 2), was probably not of protein or nucleic acid origin. The fact that these compounds were dialysable to at least 90 % as measured by the absorption, showed that the UV absorption in the medium was not caused by non-dialysable protein or polynucleotides from autolysed cells. Furthermore, no maximum in the absorption at 260 mμ was recorded (Fig. 3), which would have been the case if cellular material of nucleic acid origin had been released to the medium.

The immediate decrease in the UV absorption in the medium after the addition of ammonium chloride shows that as soon as a nitrogen source was available, the cells were able to take up, or possibly, destroy the substances causing the absorption.

During the starvation phase in the carbon-deficient culture (expt. B) there was no increase in nitrogen-containing compounds (cold and hot TCA fractions, and protein). There was in fact a slight decrease (Table 2). In spite of the low concentration of the carbon source in the medium, there was still an accumulation of glycogen. The reactions involved in cell division and in the synthesis of the nitrogen-containing compounds are apparently more sensitive to a lowering of the concentration of the organic carbon source than is the synthesis of glycogen.

REFERENCES

1. Palmstierna, H. *Acta Chem. Scand.* **10** (1956) 567.
2. Monod, J. *Ann. Rev. Microbiol.* **3** (1949) 371.
3. Friedlein, F. *Biochem. Z.* **164** (1928) 273.
4. Hook, A. E., Beard, D., Taylor, A. R., Sharp, D. G. and Beard, J. W. *J. Biol. Chem.* **165** (1946) 241.
5. Schneider, W. C. *J. Biol. Chem.* **161** (1945) 293.
6. Lockhart, W. and Powelson, D. *J. Cellular Comp. Physiol.* **44** (1954) 177.
7. Wilkinson, J. F., Duguid, J. P. and Edmunds, P. N. *J. Gen. Microbiol.* **11** (1954) 59.
8. Dagley, S. and Dawes, E. E. *Biochem. J. London* **45** (1949) 331.
9. Dagley, S. Dawes, E. E. and Morrison, G. A. *J. Bacteriol* **61** (1951) 433.

Received January 11, 1956.

ACTA CHEMICA SCANDINAVICA 10 (1956) 587—590

Studies on Pyrazolones

X. Reactions of Pyrazole Blue with Cyanoacetamide and Malononitrile

GUNNEL WESTÖÖ

Institute of Organic Chemistry, University of Lund, Lund, Sweden

Cyanoacetamide and malononitrile add to pyrazole blue by normal Michael additions with formation of compounds V and VII. The malononitrile derivative (VII) rearranges readily to the cyclic compound VI.

In a previous paper [1] it was shown that ethyl cyanoacetate reacts with pyrazole blue (I) with the formation of two different adducts (II and III). Both adducts were readily hydrolysed by alkali with the formation of IV.

In the present investigation, one adduct only, a monobasic acid for which the structure V is proposed, was obtained from the reaction of pyrazole blue with cyanoacetamide. Compound V showed no tendency to ring closure and in this behaviour resembled IV and contrasted with II. The UV absorption curve of V (Fig. 1) showed a striking resemblance to the corresponding curves of II and IV.

Addition of malononitrile to pyrazole blue in the presence of a small amount of piperidine furnished mainly a product, which was obviously the iminolactone VI (a, b, c), since it had a neutral reaction and a UV absorption very similar to that of III [1]. In the absence of a catalyst, a mixture of VI and a dibasic acid was obtained. The same dibasic acid was formed on treatment of VI with excess of dilute alkali at room temperature. It had a UV absorption curve quite analogous to the corresponding curves of II, IV and V (Fig. 1). Hence structure VII is proposed for this compound.

As in the case of II, VII could be easily transformed into the corresponding cyclization product. Thus a solution of VII in ethanol was slowly isomerized to form VI. The transformation was rapid when a small amount of piperidine was added. Dry hydrogen chloride reacted with VII in ether solution with the formation of a hydrochloride of VI.

The IR spectrum of V showed a distinct C≡N stretching band at 2 240±15 cm^{-1}, whereas in VII the nitrile band was very weak in spite of the two C≡N

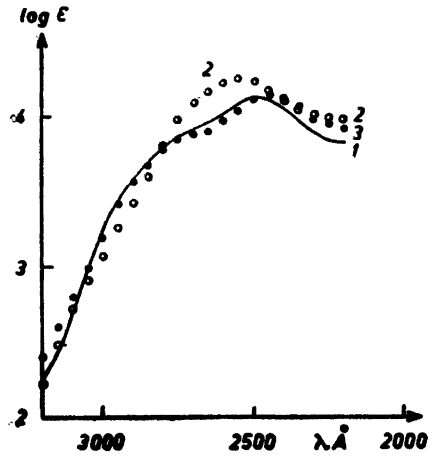


Fig. 1. UV absorption curves of compound V (1), VI (2) and VII (3) in ethanol solutions.

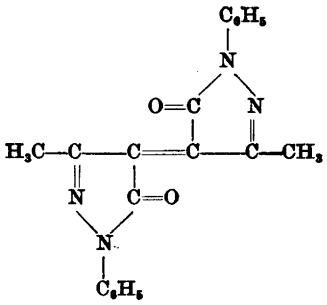
groups present in the molecule. A similar weakening of a C≡N band was described in 1952 by Kitson and Griffith [2], particularly in molecules with oxygen-containing groups. With compound IV the same effect was observed [1].

The spectrum of VI exhibited an intense C≡N absorption. The band was, however, situated at 2 190±15 cm^{-1}. This indicates that the C≡N group is in conjugation and hence that the structure of VI is essentially that of VI b. According to Kitson and Griffith the IR absorption of a nitrile group in conjugation with an olefinic double bond is found at 2 225±8 cm^{-1}. Thus the extension of the resonance to the free electron pairs of the oxygen and nitrogen atoms in the β-position of the cyano group in VI b gives rise to a marked shift of the nitrile band towards longer wavelengths.

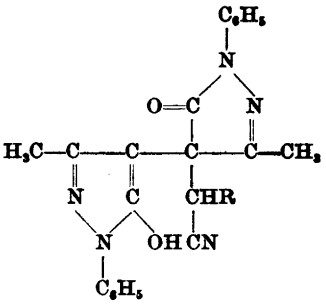
The acidic strength of the hydrogen atoms in the α-position of the cyano groups in II, IV, V and VII is rather different. In ethanol-water solution using alizarine yellow indicator the α-hydrogen atom is neutral in compounds IV and V. In II it can be titrated with barium hydroxide solution (alizarine yellow indicator), though with a very poor end point. It is possible, however, to titrate compound VII with a sharp end point using thymolphthalein indicator. Thus in II and VII the acidifying effect of the bispyrazolonyl group, which is electron attracting and hence stabilizes the carbanion, is striking, for ethyl cyanoacetate exhibits very weakly acidic properties under the above conditions, and the ionization constant of malononitrile is 6.5×10^{-12} according to Pearson and Dillon [3].

In dimethylformamide solution, using azo violet indicator, the effect of the bispyrazolonyl group is not noticeable on titration with sodium methoxide [4]. Both malononitrile, ethyl cyanoacetate and their bispyrazolonyl derivatives are accurately titrated. Cyanoacetamide and compound V can be titrated, though with a very poor end point. In cyanoacetic acid as in compound IV the α-hydrogen has no acidic properties on titration.

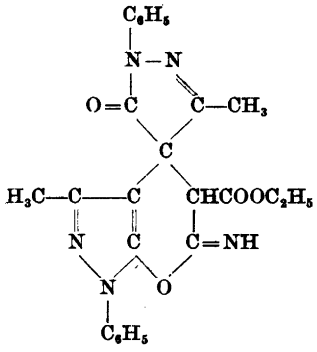
Thus compounds II and VII differ from IV and V both in their greater tendency to ring closure and in the greater acidity of the hydrogen atoms in the α-position of the nitrile groups. One reason for these properties is the grea-



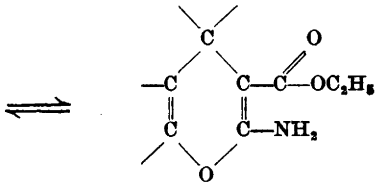
I



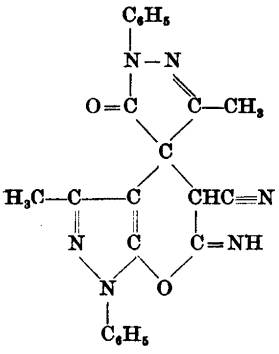
II R=$COOC_2H_5$
IV R=COOH
V R=$CONH_2$
VII R=CN



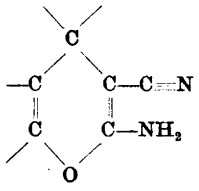
III a



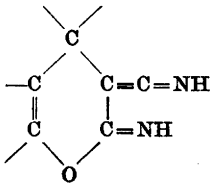
III b



VI a



VI b



VI c

ter resonance interaction with conjugated groups or free electron pairs of the carbethoxy group of II and still more of the cyano group of VII, compared to the carboxyl and amide groups of IV and V. The resonance causes stabilization of the ring compounds III b and VI b. It also stabilizes the anions of II and VII.

EXPERIMENTAL

Preparation of compound V from pyrazole blue and cyanoacetamide. A mixture of cyanoacetamide (4.0 g), pyrazole blue (16.2 g), chloroform (70 ml), ethanol (10 ml) and piperidine (0.4 ml) was shaken overnight. The colourless precipitate formed was filtered off and washed with ethanol. Yield of air-dried product: 20.0 g. It was purified by crystallization from ethanol. The compound adsorbed the solvent strongly. It was dried at 0.1 mm Hg, 78°, over phosphoric anhydride and was afterwards hygroscopic. (Found: C 64.0; H 4.6; N 19.4; equiv. wt. 430. $C_{23}H_{20}N_6O_3$ requires C 64.5; H 4.7; N 19.6; equiv. wt. 428.5.) For UV absorption curve, see Fig. 1.

Preparation of VI from pyrazole blue and malononitrile. Malononitrile (3.15 g), pyrazole blue (15.6 g), chloroform (90 ml) and piperidine (0.3 ml) were mixed together. Decolorization took place in a few minutes, and crystals of VI separated. After cooling with iced water, the precipitate was filtered off and washed with cold ethanol. Yield: 17.2 g of air-dried product. It was purified by recrystallization from ethanol and dried *in vacuo* (0.1 mm Hg) at 100°, m. p. about 240° (decomp.). The product was rapidly isomerized into VII even by 0.1 N alkali solution. (Found: C 67.1; H 4.5; N 20.5. $C_{23}H_{16}N_6O_2$ requires C 67.3; H 4.4; N 20.5.) UV absorption curve see Fig. 1.

Transformation of VI into VII by addition of alkali. A mixture of compound VI (7.0 g), ethanol (35 ml) and 2.5 N sodium hydroxide solution (35 ml) was kept overnight and then poured into N hydrochloric acid. The product which separated (6.9 g) was collected by filtration, washed with water and air-dried. After extraction of impurities with ethyl acetate it was dried under reduced pressure (0.1 mm Hg) at 78° over phosphoric anhydride. The product melted at 230–240° (decomp.). (Found: C 67.3; H 4.5; N 20.4; equiv. wt. 203. $C_{23}H_{16}N_6O_2$ requires C 67.3; H 4.4; N 20.5; equiv. wt. 205.) The UV absorption curve is seen in Fig. 1.

Transformation of VII into VI using piperidine as a catalyst. A solution of compound VII (0.85 g) and two drops of piperidine in ethanol (25 ml) was kept overnight at room temperature. The product formed was precipitated by addition of N hydrochloric acid and water, filtered and washed with water. It was purified by crystallization from ethanol. The neutral product obtained was easily hydrolysed by alkali in a similar manner to compound VI. UV absorption curve and analyses were identical with the data of VI.

Transformation of VII into VI by hydrogen chloride. A suspension of VII in ether was treated with dry hydrogen chloride, and the resulting salt was filtered off and washed with ether. (Equiv. wt. of the air-dried product on titration using bromophenolblue indicator: 470. Calc. for $C_{23}H_{16}N_6O_2$, HCl: 447.) The free base was isolated by precipitation of the ethanol solution of the salt with water. According to analyses, UV absorption curve and melting point, it was identical with compound VI.

The analyses were performed by Miss M. Westerdahl, Department of Analytical Chemistry, University of Lund. Dr. Andreas Rosenberg, University of Uppsala, carried out the IR measurements.

The author wishes to thank *Statens naturvetenskapliga forskningsråd* for financial support.

REFERENCES

1. Westöö, G. *Acta Chem. Scand.* **10** (1956) 9.
2. Kitson, R. E. and Griffith, N. E. *Anal. Chem.* **24** (1952) 334.
3. Pearson, R. G. and Dillon, R. L. *J. Am. Chem. Soc.* **75** (1953) 2439.
4. Fritz, J. S. *Anal. Chem.* **24** (1952) 674.

Received January 14, 1956.

ACTA CHEMICA SCANDINAVICA 10 (1956) 591—593

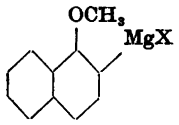
Methoxy Substituted Naphthylmagnesium Halides and Carbon Dioxide

GUST.-AD. HOLMBERG

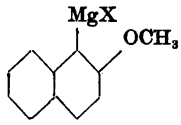
Institutet för organisk kemi, Åbo Akademi, Åbo, Finland

The rules for the anomalous reactivity of *o*-methoxy substituted phenylmagnesium bromides are also valid for methoxy substituted naphthylmagnesium halides, if the condensed ring is considered to be a substituent.

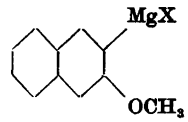
If the rules which are valid for the anomalous reactivity of *o*-methoxy substituted phenylmagnesium bromides [1] also are valid for the corresponding naphthalene derivatives, it may be expected that 1-methoxy-2-naphthylmagnesium halide (I) and 2-methoxy-1-naphthylmagnesium halide (II) will react with carbon dioxide to give only the corresponding acid, while 3-methoxy-2-naphthylmagnesium halide (III) under the same conditions will give both the corresponding acid and the corresponding ketone.



I



II



III

These predictions were fulfilled when the Grignard reagents prepared from 1-bromo-2-methoxynaphthalene, 2-iodo-1-methoxynaphthalene, and 3-iodo-2-methoxynaphthalene were allowed to react with carbon dioxide.

The iodine compounds were used since they can be more easily transformed into the corresponding Grignard reagents. The fact that different halogen compounds have been used has scarcely any significance, because the nature of the halogen does not seem to influence the anomalous reactivity. This I have found to be true in the case of *o*-methoxyphenylmagnesium bromide and *o*-methoxyphenylmagnesium iodide.

Table 1. Yields of naphthoic acids and neutral substances.

Naphthalene derivative	Acid isolated				Neutral substances g
	g	M. p.	*p*-Nitrobenzyl ester Calc. N 4.15		
			M. p.	Found N	
1-Bromo-2-methoxy-	0.84	175–176	117–118	4.25	2.35
2-Iodo-1-methoxy-	1.26	123–125	93–94	4.28	3.42
3-Iodo-2-methoxy-	1.07	131–133	123–124	4.20	2.48

EXPERIMENTAL

1-Bromo-2-methoxynaphthalene was prepared according to Franzen and Stäuble [2] through bromination of β-naphthol and methylation of the resulting 1-bromo-2-naphthol.

2-Iodo-1-methoxynaphthalene. α-Naphthylamine was nitrated and the reaction product was treated with potassium hydroxide according to Burkhardt and Wood [3]. The crude potassium 2-nitro-1-naphthoxide thus obtained was treated with methyl sulphate according to Clemo, Cockburn, and Spence [4] in order to give 2-nitro-1-methoxynaphthalene. This compound was reduced to the corresponding amine by stannous chloride in the way previously used in the synthesis of 5-amino-3-bromoveratrole [5]. The yield of 1-methoxy-2-naphthylamine after distillation under reduced pressure at 158–159°/9 mm was 71.5 %. This amine was converted into 2-iodo-1-methoxynaphthalene according to Clemo, Cockburn, and Spence. The crude product was, however, finally purified by distillation under reduced pressure. The yield of material boiling at 166–167°/10 mm and melting after recrystallization from ethyl alcohol at 41–42° was 81.4 %.

3-Iodo-2-methoxynaphthalene. 3-Hydroxy-2-naphthoic acid was successively converted into 3-methoxy-2-naphthoic acid, ethyl 3-methoxy-2-naphthoate, 3-methoxy-2-naphthoic hydrazide, ethyl 3-methoxy-2-naphthylcarbamate, and 3-methoxy-2-naphthylamine according to Jambuservala, Holt and Mason [6]. From the last mentioned substance, 3-iodo-2-methoxynaphthalene was prepared according to Clemo and Spence [7]. The yield of material boiling at 186–189°/10 mm and melting, after recrystallization from methyl alcohol, at 64.5–65.5° was 39.5 %.

The reactions between Grignard reagents and carbon dioxide were examined as has previously been described [1]. Because the halomethoxynaphthalenes used are not volatile with steam, the steam distillation was omitted. The neutral substances thus contain unreacted halomethoxy compound and perhaps methoxynaphthalenes derived from Grignard reagent that has not reacted with carbon dioxide. The results are collected in Table 1.

Only unreacted halogen compounds could be isolated from the neutral substances obtained in the experiments with Grignard reagents prepared from 1-bromo-2-methoxynaphthalene and 2-iodo-1-methoxynaphthalene. No ketone was detected.

When the neutral substances isolated from the experiment with Grignard reagent prepared from 3-iodo-2-methoxynaphthalene were treated with ether, di-3-methoxynaphthylketone was isolated. After recrystallization from ethyl alcohol, it melted at 154–155°. (Found: C 80.45; H 5.45. Calc. for $C_{23}H_{18}O_3$: C 80.68; H 5.30). Its 2,4-dinitrophenylhydrazone melted at 240–241°. (Found: N 10.87. Calc. for $C_{29}H_{22}O_6N_4$: N 10.72.)

A solution of *o*-methoxyphenylmagnesium iodide was prepared by reacting *o*-iodoanisole [8] (4.68 g) with magnesium (0.49 g) in dry ether (30 ml). Carbon dioxide was led into the solution, and when the reaction products were isolated, *o*-methoxybenzoic acid (0.55 g) and 2,2'-dimethoxybenzophenone (2.27 g) were obtained.

REFERENCES

1. Holmberg, G. A. *Acta Chem. Scand.* **9** (1955) 555.
2. Franzen, H. and Stäuble, G. *J. prakt. Chem.* **103** (1922) 352.
3. Burkhardt, G. N. and Wood, H. *J. Chem. Soc.* **1929** 141.
4. Clemo, G. R., Cockburn, J. G. and Spence, R. *J. Chem. Soc.* **1931** 1265.
5. Holmberg, G. A. *Acta Chem. Scand.* **8** (1954) 728.
6. Jambuservala, G. B., Holt, S. and Mason, F. A. *J. Chem. Soc.* **1931** 373.
7. Clemo, G. R. and Spence, R. *J. Chem. Soc.* **1928** 2811.
8. Jannasch, P. and Hinterskirch, W. *Ber.* **31** (1898) 1710.

Received February 2, 1956.

ACTA CHEMICA SCANDINAVICA 10 (1956) 594—598

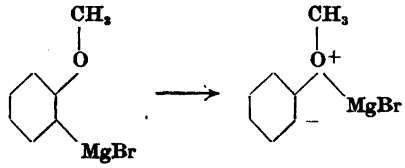
The Effect of Different Alkoxy Groups on the Anomalous Reactivity of *o*-Alkoxyphenylmagnesium Bromides

GUST.-AD. HOLMBERG

Institutet för organisk kemi, Åbo Akademi, Åbo, Finland

The reactions between carbon dioxide and 2-alkoxy-5-methylphenylmagnesium bromides containing ethoxy, *n*-propoxy, *n*-butoxy, *iso*propoxy, and *iso*butoxy groups as alkoxy groups have been studied. As in the case of the methoxy homologue both the corresponding acids and the corresponding ketones are formed in these reactions, the yield of ketone being the lowest in the case of 2-*iso*propoxy-5-methylphenylmagnesium bromide. This fact is associated with steric effects that probably cancel the anomalous reactivity of *o*-methoxyphenylmagnesium bromides with a methyl group, methoxy group or a condensed benzene ring in the ortho position relative to the original methoxy group.

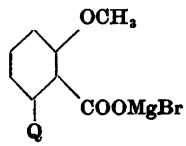
Some time ago the author proposed a reaction mechanism to explain the anomalous reactivity of *o*-methoxyphenylmagnesium bromides [1]. The mechanism in question involves an intramolecular ring formation by replacement of one of the two "etherate" ether molecules of the Grignard reagent by the methoxy group. The strained rings were expected to favour the polarization of the carbon-to-magnesium bonds:



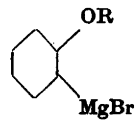
The anomalous reactivity of the *o*-methoxyphenylmagnesium bromides is cancelled by a methyl or methoxy group in the ortho position relative to the magnesium or oxygen atom [2,3]. The same rule is also valid in the naphthalene series if the condensed ring is considered to be a substituent [4]. In the former case, *i. e.* when the substituent is in the ortho position relative to the magnesium atom, it is believed that the first reaction product (I) is sterically hindered in the same way as certain mesityl derivatives. A molecular study of the

latter case (the substituent and the oxygen atom in the ortho position relative each other) shows that the methoxy group is unable to rotate freely. It may thus be prevented from occupying the proper position for ring formation. If this is right, it may be expected that the anomalous reactivity would even be cancelled when the steric effect is produced in another way.

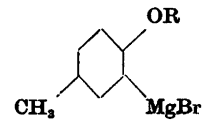
A substance with the required properties is 2-*tert.*-butoxyphenylmagnesium bromide (IIg). Unfortunately, 2-*tert.*-butoxybromobenzene, which is needed for its preparation, is very difficult to synthesize. For this reason other substances had to be used although they were not as well adapted. In 2-*iso*propoxyphenylmagnesium bromide (IIe) the rotation of the alkoxy group is not quite prevented, but is nevertheless obstructed to some extent. In this case a decrease in the yield of the corresponding ketone may be expected.



I



II



III

Q = —CH_3 or —OCH_3 R = (a) —CH_3, (b) —CH_2CH_3, (c) —$CH_2CH_2CH_3$, (d) —$CH_2CH_2CH_2CH_3$ (e) —$CH(CH_3)_2$, (f) —$CH_2CH(CH_3)_2$, or (g) —$C(CH_3)_3$

o-Alkoxyphenylmagnesium bromides with a primary carbon atom attached to the oxygen ought to possess an anomalous reactivity of about the same order as that of the methoxy homologue, although substances in which the β carbon atom in the alkoxy group is secondary as in 2-*iso*butoxyphenylmagnesium bromide (IIf) should perhaps give a somewhat lower yield of the corresponding ketone.

For the preparation of the 2-alkoxyphenylmagnesium bromides the corresponding 2-alkoxybromobenzenes are required. These substances are most conveniently obtained through alkylation of *o*-bromophenol, which, however, is very difficult to purify. Consequently 3-bromo-4-hydroxytoluene was chosen as the starting material, because it is easily prepared and purified [5], and because the methyl group, at least in the methoxy derivative (IIIa) did not cancel the anomalous reactivity. The bromocresol was alkylated to give the ethoxy, *n*-propoxy, *n*-butoxy, *iso*propoxy, and *iso*butoxy derivatives (IIIb, c, d, e, and f). From the latter the corresponding Grignard reagents were then prepared and reacted with carbon dioxide.

The formation of an acid in the reaction between a Grignard reagent and carbon dioxide is considered to be the normal reaction. In the formation of one molecule of the corresponding ketone, one molecule of the Grignard reagent reacts normally to form a derivative of an acid (I or its homologue). Another molecule of the Grignard reagent then reacts with this first reaction product. This latter reaction is considered a consequence of the anomalous reactivity of the Grignard reagent. According to this the number of moles of the Grignard reagent, which react normally, is equal to the sum of the moles of acid and

ketone which have been formed during the reaction. The number of moles which react anomalously is equal to those of the ketone. In order to obtain comparable values, the ratios

$$\frac{\text{moles of ketone}}{\text{moles of ketone} + \text{moles of acid}}$$

have been calculated and used as a measure of the anomalous reactivity. From Table 1 in which these values have been collected it is to be seen that the anomalous reactivity of the *iso*propoxy homologue is considerably, and that of the *iso*butoxy derivative slightly lower than those of the other Grignard reagents. Also in the series methoxy, ethoxy, *n*-propoxy, and *n*-butoxy a slight decrease of the anomalous reactivity can be observed.

Table 1. The anomalous reactivity of 2-alkoxy-5-methylphenylmagnesium bromides.

Alkoxy group	$\frac{\text{Moles of ketone}}{\text{Moles of ketone + moles of acid}}$
Methoxy	0.46 [a]
Ethoxy	0.47
n-Propoxy	0.44
n-Butoxy	0.41
*Iso*propoxy	0.07
*Iso*butoxy	0.32

[a] According to previously published results [2]

The results show that the anomalous reactivity of *o*-alkoxyphenylmagnesium bromides is influenced by steric effects which prevent or restrict the free rotation of the alkoxy group, *i. e.* which prevent the alkoxy group from occupying the proper position for the formation of a complex bond between the oxygen and magnesium atoms.

EXPERIMENTAL

3-Bromo-4-ethoxytoluene was prepared by alkylation of 3-bromo-4-hydroxytoluene with ethyl *p*-toluenesulphonate in the following way. Sodium (3.85 g) was dissolved in absolute ethyl alcohol (77 ml) and to this solution 3-bromo-4-hydroxy-toluene (31.33 g) was added. After cooling, a solution of ethyl *p*-toluenesulphonate (33.50 g) in ethyl alcohol (30 ml) was gradually added. When the addition was complete, the mixture was heated on a boiling water bath for 1 hour. The solvent was then evaporated under reduced pressure and the residue was treated with a mixture of water and ether. The ether phase was separated and washed with a dilute solution of sodium hydroxide and finally with water. After drying with anhydrous sodium sulphate, the solvent was evaporated and the residue was distilled under reduced pressure. The yield of 3-bromo-4-ethoxytoluene, b. p. 117–118.5°/11 mm, was 87.8 % (31.62 g). Found: Br 37.10; Calc. for $C_9H_{11}OBr$: Br 37.15).

Table 2. Yields, boiling points, and analyses of 3-bromo-4-alkoxytoluenes.

Alkoxy group	Yield, %	B. p.	Br	
			Found	Calc.
n-Propoxy	82.4	121.5—122.0°/11 mm	34.80	34.88
n-Butoxy	63.7	139.0—140.0°/12 mm	32.70	32.87
*Iso*propoxy	62.8	108.0—109.0°/ 8 mm	34.81	34.88

Table 3. Reactions between carbon dioxide and 2-alkoxy-5-methylphenylmagnesium bromides.

Alkoxy group	Acid, isolated			Ketone, isolated		
	g	M. p. °C	M. p. of *p*-nitrobenzyl ester	g	M. p. °C	M. p. of 2,4-dinitrophenylhydrazone, °C
Ethoxy	1.01	44—45	104—105	1.51	78—79	165—166
n-Propoxy	1.26	21—22	63—64	1.68	46—47	*
n-Butoxy	1.35	54—55	59—60	1.63	71.5—72.5	124.5—125.5
*Iso*propoxy	2.48	Oil	52—53	0.31	62—63	175—176
*Iso*butoxy	1.81	Oil	46—47	1.31	59—60	121—122

* Melted after a rapid heating at 131—132°, and after a slow heating at 151—152°. On the "Kofler Heizbank" the substance melted at 131—132°. On further heating it solidified and melted again at 151—152°.

Table 4. Analyses of prepared substances.

Alkoxy group	2-Alkoxy-5-methylbenzoic acid						2,2′-Dialkoxy-5,5′-dimethylbenzophenone					
	Found		Calc.		*p*-Nitrobenzyl ester N		Found		Calc.		2,4-Dinitrophenylhydrazone N	
	C	H	C	H	Found	Calc.	C	H	C	H	Found	Calc.
Ethoxy	66.75	6.78	66.65	6.71	4.53	4.44	76.60	7.50	76.48	7.43	11.66	11.71
n-Propoxy	68.18	7.35	68.02	7.27	4.32	4.25	77.41	8.13	77.27	8.03	11.12	11.06
n-Butoxy	69.35	7.85	69.21	7.74	4.20	4.08	78.05	8.62	77.93	8.53	10.58	10.48
*Iso*propoxy	a				4.31	4.25	77.45	8.20	77.27	8.03	11.11	11.06
*Iso*butoxy	a				4.22	4.08	78.05	8.65	77.93	8.53	10.57	10.48

[a] Not sufficiently pure.

3-Bromo-4-isobutoxytoluene was prepared in the same way using *iso*butyl bromide as alkylating agent except that the reaction mixture was heated 4.5 hours on the boiling water bath. The yield of pure 3-bromo-4-*iso*butoxytoluene, b. p. 124.5—125.5°/8 mm, was 48.9 %. (Found: Br 32.81; Calc. for $C_{11}H_{15}OBr$: Br 32.87).

3-Bromo-4-n-propoxytoluene, *3-bromo-4-isopropoxytoluene*, and *3-bromo-4-n-butoxytoluene* were prepared in the same way using the corresponding bromides as alkylating agents. In these cases the reaction mixture was heated in an autoclave to 120—130° for one hour. The yields, boiling points, and analyses are collected in Table 2.

The Grignard reagents were prepared from 0.02 equivalents of magnesium and 3-bromo-2-alkoxytolene in dry ether (30 ml).

The reaction between Grignard reagents and carbon dioxide were examined as previously described [2]. The results are collected in Tables 3 and 4.

REFERENCES

1. Holmberg, G. A. *Acta Chem. Scand.* **9** (1955) 555.
2. Holmberg, G. A. *Acta Chem. Scand.* **6** (1952) 1137.
3. Holmberg, G. A. *Acta Chem. Scand.* **8** (1954) 728.
4. Holmberg, G. A. *Acta Chem. Scand.* **10** (1956) 591.
5. *Organic Syntheses* **23** (1946) 11.

Received February 2, 1956.

ACTA CHEMICA SCANDINAVICA 10 (1956) 599—616

The Crystal Structure of $U(SO_4)_2 4H_2O$

PEDER KIERKEGAARD

Institute of Inorganic and Physical Chemistry, University, Stockholm, Sweden

$U(SO_4)_2 4H_2O$ has an orthorhombic unit cell containing four formula units and with the dimensions

$$a = (14.674 \pm 0.005)\ \text{Å}$$
$$b = (11.093 \pm 0.005)\ \text{Å}$$
$$c = (5.688 \pm 0.005)\ \text{Å}$$
$$V = 925.8_9\ \text{Å}^3$$

A structure is proposed with atomic positions in the space group No. 62 *Pnma*. The positions of the uranium and sulphur atoms were determined with Fourier methods. The parameters of the oxygen atoms were deduced from geometrical considerations, using interatomic distances from previously determined structures. The crystals are built up of layers parallel to the *yz* plane and formed by uranium atoms and sulphate groups. The layers are held together by water molecules, so that each sulphate tetrahedron has two oxygen atoms linked with hydrogen bonds to adjacent water molecules. Every uranium atom is in contact with four sulphate groups and four water molecules, so that the coordination of oxygen atoms around uranium is eightfold in the shape of a square Archimedean antiprism.

Uranium(IV)sulphate-tetrahydrate was first prepared by Ebelmen [1] by a photochemical reduction of U_3O_8 in the presence of ethanol and diluted sulphuric acid.

Meyer and Nachod [2] obtained the salt as a green crystalline precipitate when concentrated sulphuric acid was added slowly to a uranium(IV)-solution, keeping the temperature between 0 °C and 70 °C. The crystals formed star-shaped needles and were according to Ebelmen [1] and Kohlschütter [3] insoluble in ethanol and ether and were not reactive towards the water vapor and oxygen of the air.

The crystallographic results are summarized by Groth [4] as: orthorhombic bipyramidal, $b:a:c = 0.7563:1:0.3805$ (with the orientation of the axes in agreement with the present investigation).

PREPARATION OF THE CRYSTALS

A saturated solution of uranium(IV)sulphate in 1.0 M H_2SO_4 was prepared. When 30 ml of this solution was sealed and heated in a thick-walled glass tube (Pyrex) to 90° C in an oven for about a week, good crystals for X-ray work were obtained. (The method according to Lundgren [5]). After cooling, the glass tube was opened and the crystals were filtered off, washed with water and dried in air.

The crystals were dark green and most of them formed rather thin plates about 0.05—0.2 mm in length. Some crystals of more needle-shaped form were however also obtained and sometimes the crystals had grown together into clusters of varying appearance.

Analysis. A sample was dissolved in hot nitric acid (1:1) and the *uranium* was precipitated with 8-hydroxyquinoline according to Hecht and Donau [6]. The precipitate was filtered off, washed with water, ignited and weighed as U_3O_8. The amount of *sulphate* in the filtrate was determined gravimetrically by precipitation as $BaSO_4$.

The *water* was determined by Hartwig-Bendig's [7] modification of Brush [8] and Penfield's [9] method.

The *density* of the crystals was determined from the loss of weight in benzene.

	Calculated for $U(SO_4)_2 4H_2O$	Found	
% UO_2	53.77	53.9	54.0
% SO_3	31.87	32.0	31.9
% H_2O	14.36	14.2	14.0
Density	3.60	3.6_3 *	3.59

The density is calculated for 4 formula units per cell.

UNIT CELL AND SPACE GROUP

From rotation and Weissenberg photographs (zero, first and second layer), taken with CuK-radiation, of two small crystals of different shapes, (one needle rotated around the needle axis, [001], and one plate rotated around a diagonal in the plane of the plate, [010]), it was concluded that the crystals are orthorhombic and that the dimensions of the unit cell are about 14.5_5 Å, 10.9_7 Å and 5.6_4 Å.

The reflections were recorded photographically with the multiple film technique and the relative intensities were estimated visually by comparison with an intensity scale obtained by photographing a reflection with different exposure times. The values of F^2 were then calculated by division with the expression $(1 + \cos^2 2\Theta)/\sin 2\Theta$.

More accurate values for the unit cell dimensions were calculated from a powder photograph, taken with monochromatized Cu$K\alpha$-radiation in a focussing camera of Guinier type, *cf.* Table 1.

$$a = (14.674 \pm 0.005) \text{ Å}$$
$$b = (11.093 \pm 0.005) \text{ Å}$$
$$c = (5.688 \pm 0.005) \text{ Å}$$
$$V = 925.8_9 \text{ Å}^3$$

The value (3.60) found for the density gives 4 formula units in the unit cell.

* This density determination was made with small amounts of substance and thus this value is more uncertain than the second one.

The reflections systematically absent are

$$hk0 \text{ with } h = \text{odd}$$
$$0kl \text{ with } k+l = \text{odd}$$

This is characteristic of the two space groups No. 62 *Pnma* and No. 33 $Pn2_1a$. At first only the space group of higher symmetry (*Pnma*) was considered and since it was possible to find a plausible structure assuming this space group, the low-symmetrical ($Pn2_1a$) was not taken into account.

In No. 62 *Pnma* the following point positions are possible

4(*a*): 000; $0\frac{1}{2}0$; $\frac{1}{2}0\frac{1}{2}$; $\frac{1}{2}\frac{1}{2}\frac{1}{2}$; 4(*b*): $00\frac{1}{2}$; $0\frac{1}{2}\frac{1}{2}$; $\frac{1}{2}00$; $\frac{1}{2}\frac{1}{2}0$;

4(*c*): $\pm(x,\frac{1}{4},z)$; $\pm(\frac{1}{2}+x,\frac{1}{4},\frac{1}{2}-z)$

8(*d*): $\pm(x,y,z)$; $\pm(\frac{1}{2}+x,\frac{1}{2}-y,\frac{1}{2}-z)$; $\pm(\bar{x},\frac{1}{2}+y,\bar{z})$; $\pm(\frac{1}{2}-x,\bar{y},\frac{1}{2}+z)$.

Table 1. Powder photograph of $U(SO_4)_2 4H_2O$. CuKa-radiation. $\lambda_{CuK\alpha} = 1.5418$ Å.

hkl	$10^4\sin^2\Theta$ calc	$10^4\sin^2\Theta$ obs	pF^2 calc	*I* obs	*hkl*	$10^4\sin^2\Theta$ calc	$10^4\sin^2\Theta$ obs	pF^2 calc	*I* obs
200	110	110	19	m	212	894	—	0	—
210	159	160	24	st	511	922	923	34	w+
020	193	192	16	m	022	928	—	0	—
101	211	211	2	v v w	122	956	954	110	v v st
011	232	231	28	s t	302	983	984	10	v v w
111	260	259	74	v v st⁻	141	984		7	
201	294	293	44	v st	600	994	995	23	w
220	304	304	18	w+	312	1032	1031	148	v v st
211	342	342	18	w+	222	1038	—	0	—
121	405	404	30	m+	610	1042	—	4	—
301	432	432	13	w	431	1060	1059	13	v v w
400	442	442	23	m	241	1067	1069	37	st
311	480	—	0	—	521			26	
221	487	488	12	v w	402	1176	—	0	—
410	490	490	40	st	322			2	—
230	545	545	90	v v st	601	1177	—	0	—
031	618	617	72	v st	620	1187	1186	45	m
401	625	625	46	v v st	132	1197	1198	41	m
321			131		341	1205	1205	74	v st
420	635	—	0	—	440	1214	1214	12	v v w
131	646	649	19	v w	412	1225	1226	0	v st
411	674	—	6	—	611	1226		77	
231	729	729	14	w	232	1280	—	0	—
002	735	—	0	—	531	1308	1309	42	m
102	762	759	9	v v w	250	1318	1317	11	v v w
040	773	772	16	w	422	1370	—	0	—
112	811	808	9	v v w	621	1371	—	1	—
421	819	822	20	w	051	1391	1391	31	m
202	845	—	0	—	441	1398	1398	20	v w
331	867	—	3	—	332	1418	1419	109	v v st
501	874	877	7	m+	151	1419		39	
430	876		34		502	1425		21	
240	883	883	8	v w	630	1428	—	0	—

The powder photograph has been measured and interpreted to $\sin^2\Theta = 0.48$.
Reflections systematically absent in space group no. 62 *Pnma* have been omitted.

POSITIONS OF THE URANIUM ATOMS

In order to find the four uranium positions, the Patterson functions $P(uvp)$ and $P(upw)$ were calculated (Figs. 1 and 2).

The four uranium atoms in the unit cell must occupy one of the fourfold positions, *i. e.* 4(*a*), 4(*b*) or 4(*c*). If they were situated in 4(*a*) or 4(*b*), $P(uvp)$ should have high peaks at $u = 0$, $v = \frac{1}{2}$, at $u = \frac{1}{2}$, $v = 0$, and at $u = \frac{1}{2}$, $v = \frac{1}{2}$, and $P(upw)$ should have high maxima at $u = 0$, $w = 0$, and at $u = \frac{1}{2}$, $w = \frac{1}{2}$. $P(uvp)$ has, however, no maximum at $u = 0$, $v = \frac{1}{2}$ and $P(upw)$ has no maximum at $u = \frac{1}{2}$, $w = \frac{1}{2}$. Thus the uranium atoms are situated in 4(*c*).

In the point position 4(*c*) the U—U distances would be

$$\pm (\tfrac{1}{2},0,\tfrac{1}{2} \pm 2z)$$
$$\pm (\tfrac{1}{2} \pm 2x,\tfrac{1}{2},\tfrac{1}{2})$$
$$\pm (\pm 2x,\tfrac{1}{2},2z)$$

The Patterson projections on the *uv* and *uw* plane would thus show (besides the origin maxima) the following maxima

in the uv *plane*		*in the* uw *plane*	
I. $\pm (\frac{1}{2},0)$	weight 4	IV. $\pm (\frac{1}{2},\frac{1}{2}-2z)$	weight 2
II. $\pm (\frac{1}{2}-2x,\frac{1}{2})$	weight 2	V. $\pm (\frac{1}{2}-2x,\frac{1}{2})$	weight 2
III. $\pm (2x,\frac{1}{2})$	weight 2	VI. $\pm (\pm 2x, 2z)$	weight 1

Now there are two high peaks in $P(uvp)$ at $u = 0.15_8$, $v = \frac{1}{2}$ (A in Fig. 1) and at $u = 0.34_2$; $v = \frac{1}{2}$ (B in Fig. 1) and one peak at $u = \frac{1}{2}$, $v = 0$, whose height is about double that of the other two. (All maxima have been located by the interpolation table given by Booth [10]). These maxima certainly correspond to the U—U vectors I, II, and III and if the peak A corresponds to the vector II above (and B to III) we get $x_U = 0.17_1$. However, if the peak A corresponds to the vector III (and B to II) we get $x_U = 0.07_9$. (It is sufficient to consider the range $0 \leq x \leq \frac{1}{4}$, $0 \leq z \leq \frac{1}{4}$).

The projection $P(upw)$ must have one high peak at $w = \frac{1}{2}$ (corresponding to the vector V above) and if $x_U = 0.17_1$ this maximum should be at $u = 0.15_8$ or if $x_U = 0.07_9$ at $u = 0.34_2$. Now the projection $P(upw)$ has a pronounced peak at $u = 0.15_8$, $w = \frac{1}{2}$ (C in Fig. 2) and a considerably lower maximum at $u = 0.33_1$, $w = \frac{1}{2}$ (3 in Fig. 2). Of these two peaks, the first one (C) has the correct height in comparison with the other maxima in this projection (see below) and with the calculated weights above, and thus certainly corresponds to the vector V above. (In fact, the lower peak (3) was found to correspond to a U—S vector, see p. 605). Thus we conclude $x_U = 0.17_1$.

Moreover the projection $P(upw)$ has two more peaks, one at $u = \frac{1}{2}$, $w = 0.25_4$ (D in Fig. 2) and one at $u = 0.34_2$, $w = 0.25_4$ (E in Fig. 2). If we identify the vectors IV and V with the high maxima D and C (giving the coordinates $x_U = 0.17_1$, $z_U = 0.12_3$), the projection must have one peak at

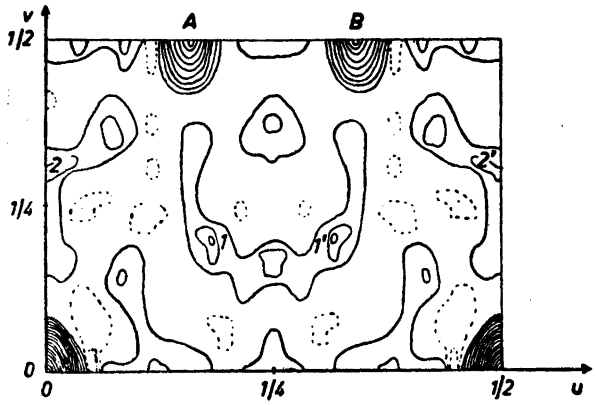


Fig. 1. The Patterson function P (uvp) *for* $U(SO_4)_2 4H_2O$. *Dotted lines indicate negative values. The figures 1,1', 2 and 2' denote peaks due to U—S vectors (see text p. 602).*

$u = 0.34_2$, $w = 0.25_4$ (corresponding to the vector VI above), whose height should be half that of the other two. Since the height and the position of E correspond to these calculated values we thus conclude:

4 U in No. 62 *Pnma* 4(*c*) with $x \approx 0.171$, $y = \frac{1}{4}$, $z \approx 0.123$.

POSITIONS OF THE SULPHUR ATOMS

Electron density projections. For a salt like $U(SO_4)_2 4H_2O$ the electron density projections could rather easily be calculated, since the signs of all the *F*-values could be determined from the contributions given by the uranium atoms, because of their dominant scattering factors. In this way, $\varrho(xyp)$ and $\varrho(xpz)$ were calculated and the results are given in Figs. 3 and 4.

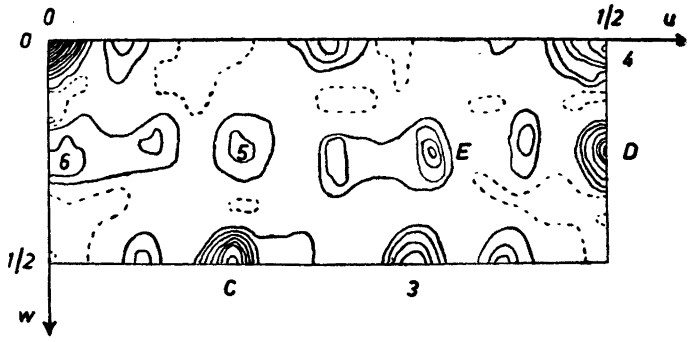


Fig. 2. The Patterson function P (upw) *for* $U(SO_4)_2 4H_2O$. *Dotted lines indicate negative values. The figures 3—6 denote peaks due to U—S vectors (see text p. 602).*

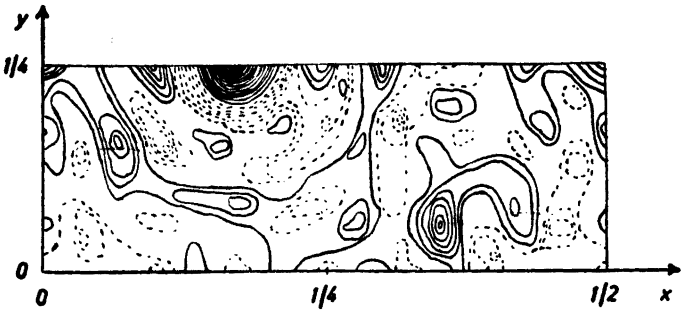


Fig. 3. Electron density of $U(SO_4)_2 4H_2O$ projected on the xy *plane. Dotted lines indicate negative values. In the uranium peak only every second contour has been marked out.*

From Fig. 3 we see, that there is, besides the very high maximum at $x = 0.171$, $y = 0.250$ giving the position of the uranium atom at this quadrant, a lower one at $x = 0.35$, $y = 0.05$. The electron density projected on the xz plane (Fig. 4) also shows, apart from the uranium maximum at $x = 0.171$, $z = 0.121$, a quite high peak at $x = 0.15$, $z = 0.37$. If the lower peaks in these projections are real maxima and not false formed by errors, diffraction effects or errors in the observed intensities due to absorption in the crystal [11], the only atoms, which could give peaks of this height, are the sulphur atoms.

In order to find out, if the lower maxima from $\varrho(xyp)$ and $\varrho(xpz)$ really correspond to sulphur positions in the unit cell, the uranium atoms were subtracted from the Fourier maps in Figs. 3 and 4 and thus two new electron density projections were calculated by the expressions

$$\varrho_s(xyp) = \sum_h \sum_k F_{\mathrm{obs}(hk0)} \cdot \cos 2\pi\,(hx + ky) - \sum_h \sum_k F_{\mathrm{U}(hk0)} \cdot \cos 2\pi\,(hx + ky)$$

$$\varrho_s(xpz) = \sum_h \sum_l F_{\mathrm{obs}(h0l)} \cdot \cos 2\pi\,(hx + lz) - \sum_h \sum_l F_{\mathrm{U}(h0l)} \cdot \cos 2\,(hx + lz)$$

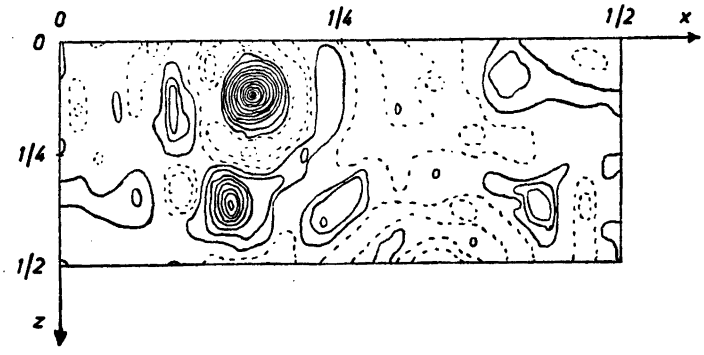


Fig. 4. Electron density of $U(SO_4)_2 4H_2O$ projected on the xz *plane. Dotted lines indicate negative values. In the uranium peak only every second contour has been marked out.*

In these new electron density projections, F_{obs} are the observed structure factors and F_U are the calculated uranium contributions to the structure factors normalized by multiplication

with the constant $\dfrac{\sum_{h,k} |F_{obs(hk0)}|}{\sum_{h,k} |F_{calc\ U(hk0)}|}$ at $\varrho_s(xyp)$ and

with the constant $\dfrac{\sum_{h,l} |F_{obs(h0l)}|}{\sum_{h,l} |F_{calc\ U(h0l)}|}$ at $\varrho_s(xpz)$.

The effect of the temperature factor, calculated by the ordinary procedure, was found to be negligible.

From Fig. 5, which shows $\varrho_s(xyp)$, we see that the uranium atoms have disappeared and that there is a rather distinct maximum at $x = 0.351$, $y = 0.054$, which should give the position of the sulphur atom. In the unit cell there are eight sulphur atoms and, with the parameters above, they must occupy the point position 8(*d*), if they belong to the space group No. 62 *Pnma* which was presumed, when $\varrho_s(xyp)$ was calculated. Since this projection really shows distinct maxima, this assumption seems to be very probable.

If the sulphur atoms are situated in 8(*d*), two sulphur maxima overlap in the *xz* projection of the electron density, and thus we get a ratio between the heights of the sulphur and the uranium peaks of about twice the ratio of the sulphur and uranium maxima obtained from the electron density projected on the *xy* plane. Fig. 6 shows $\varrho_s(xpz)$ and, as is seen, the uranium atom and most of its diffraction effects have disappeared, but there is, however, a pronounced maximum at $x = 0.149$, $z = 0.379$, which could be ascribed to sulphur atoms, and moreover this peak has the correct height corresponding to eight sulphur atoms in No. 62 *Pnma* 8(*d*).

Thus from the electron density projections the following set of parameters could be obtained

4 U in No. 62 *Pnma* 4(*c*) with $x = 0.171$, $y = \frac{1}{4}$, $z = 0.121$

8 S in No. 62 *Pnma* 8(*d*) with $x = 0.351$, $y = 0.054$, $z = 0.879$

Using these parameters, the U—S distances were calculated and the remaining maxima in the Patterson projections (Figs. 1—2) were compared with the U—S vectors. They were found to correspond to the maxima 1,1′, 2 and 2′ in *P*(*uvp*) and to 3, 4 and 5 and 6 in *P*(*upw*) and moreover the heights of the peaks also corresponded to the calculated weights. The remaining maxima in the Patterson projections may correspond to U—O vectors but, since the peaks due to some U—S and all U—O vectors are of about the same height as the false maxima [11], the remaining peaks were not considered.

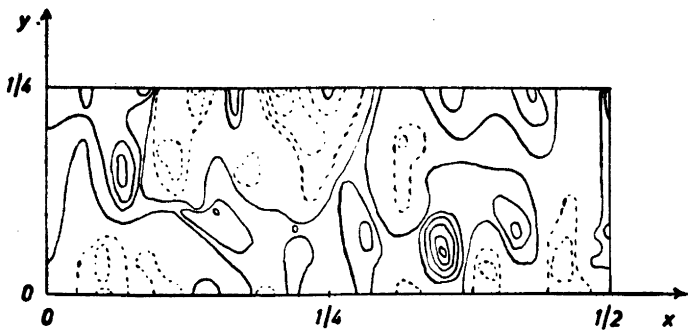


Fig. 5. Electron density of $U(SO_4)_2 4H_2O$ projected on the xy plane and with the uranium atom substracted. Dotted lines indicate negative values.

POSITIONS OF THE OXYGEN ATOMS

General remarks. The light hydrogen and oxygen atoms do not make any appreciable contribution to the intensities of the reflections and their positions had thus to be found from considerations of the interatomic distances. The following assumptions were then made

1. The U—O distance was assumed to be not less than that found[12–14] in UO_2, *i. e.* 2.3_6 Å.

2. The sulphate ion was considered to be a regular tetrahedron with the sulphur atom situated at its centre and with the bond lengths S—O = 1.4_7 Å and O—O = 2.4_0 Å. These distances are mean values of those published[15,16] for S—O and O—O in SO_4^{2-} and also in $S_2O_5^{2-}$ and $SO_3NH_2^-$.

3. The distance between two oxygen atoms, not belonging to the same sulphate group, was assumed to be not less than 2.6_0 Å.

With these assumptions the space free for oxygen atoms will be reduced as follows.

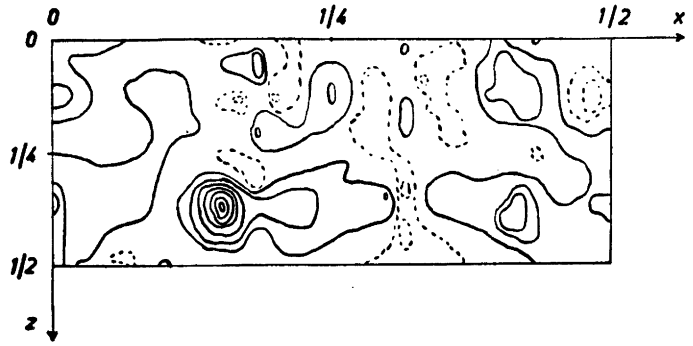


Fig. 6. Electron density of $U(SO_4)_2 4H_2O$ projected on the xz plane and with the uranium atom subtracted. Dotted lines indicate negative values.

There are two symmetry planes in the unit cell at $y = \pm \frac{1}{4}$. If an oxygen atom is not situated exactly in a symmetry plane, it must be at a distance of at least 1.3_0 Å from it. Accordingly, the y coordinates of the atoms should be either $y = \frac{1}{4}$ and $y = \frac{3}{4}$ or within the limits: $-0.13_3 \leq y \leq 0.13_3$, $0.36_7 \leq y \leq 0.63_3$. Moreover there are eight symmetry centres per unit cell (the point positions 4(*a*) and 4(*b*)). If an oxygen centre does not coincide with a symmetry centre, it must be situated outside a sphere of radius 1.3_0 Å around it. For the same reason spheres, of radii 2.6_0 Å around each oxygen atom which has been located and of radii 2.3_6 Å around each uranium atom, enclose domains forbidden for the centres of other oxygen atoms.

Positions of the sulphate oxygen atoms. For the sulphate oxygen atoms it seems probable that they are strongly attracted by the highly charged uranium ions. With the assumptions made above, the distance U—S should be $\leq 3.8_3$ Å, if a sulphate oxygen atom is in contact with a uranium atom. Now, in the structure found above, the uranium atoms are surrounded by four sulphur atoms at a distance of 3.6_9 Å, and each of the sulphur atoms has two uranium atoms at the same distance (Fig. 7). The angle, U—S—U, between the sulphur and the two neighbouring uranium atoms is 128°. Thus it is possible for at most two sulphate oxygen atoms, belonging to the same sulphate group, to be in contact with two different uranium atoms. Assuming this, which seems to be very probable, and regarding the sulphur positions as definite, we obtain an approximate position of the sulphate tetrahedron according to the following:

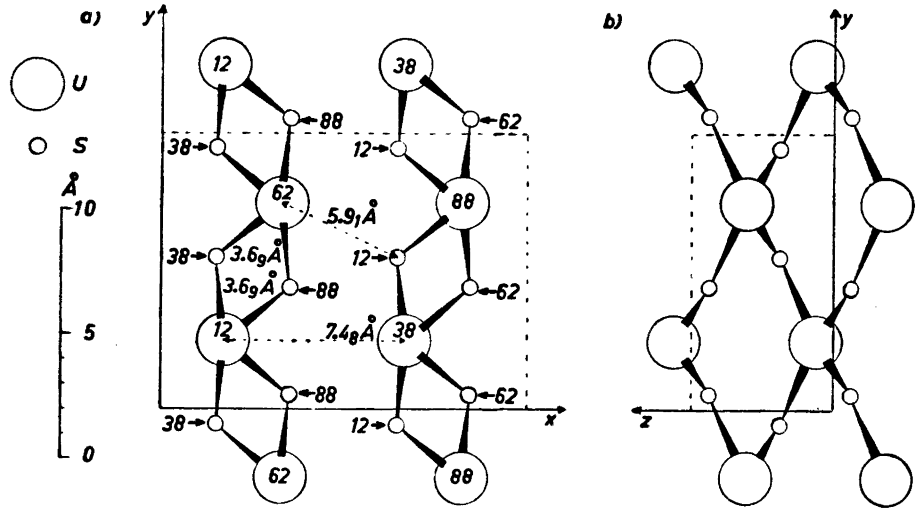


Fig. 7. Contacts (via oxygen atoms, which have not been indicated) between the uranium and the sulphate ions. a) Projection on the xy *plane. The figures denote the height of the atoms in percentages of* c. *b) Projection on the* yz *plane showing the contact in the* $U(SO_4)_2$*-layers. Only one layer has been indicated, i. e. uranium and sulphur atoms with* x *parameters between* 0 *and* $\frac{1}{2}$.

8 O_1 in 8(d) in contact with uranium; *i. e.* the oxygen centre should be situated on a circle with radius 0.5_6 Å and with the centre at $x = 0.28_4$, $y = 0.12_7$ and $z = 0.96_9$.

8 O_2 in 8 (d) in contact with uranium; *i. e.* the oxygen centre situated on a circle with radius 0.5_6 Å and with the centre at $x = 0.34_3$, $y = 0.94_1$, $z = 0.78_3$.

8 O_3 and 8 O_4 in 8(d).

However, there are 16 more oxygen atoms in the unit cell and to determine the positions of the sulphate groups more exactly, it seemed necessary at this state of the investigation to determine the positions of these non-sulphate oxygen atoms using the sulphate group position concluded above.

Positions of the non-sulphate oxygen atoms. For the non-sulphate oxygen we note, as before for the sulphate oxygen atoms, that they must be strongly attracted by the tetravalent uranium ions and consequently should be situated as close to them as possible.

Now, we have found contacts U—4O, *i. e.* four sulphate oxygen atoms in contact with each uranium, and if all of the non-sulphate oxygen atoms are in contact with uranium, we obtain the coordination U—8O. Now, in UO_2, which has CaF_2 structure [17] every uranium is surrounded by eight oxygen atoms and this is also to be expected for ions of this radius ratio [18]. It seems thus reasonable that the coordination U—8O also occurs in $U(SO_4)_2 4H_2O$ and hence we investigate the possibility that all of the non-sulphate oxygen atoms in the unit cell are in contact with uranium. This will eliminate the point positions 4(a) and 4(b) for the non-sulphate oxygen atoms and a careful survey shows that the only possibility of obtaining contact between uranium and all of the non-sulphate oxygen atoms is with

4 O_5 in 4(c)
4 O_6 in 4(c)
8 O_7 in 8(d).

Now we have to find the position of O_7. It is situated in an eightfold position and, with the assumptions made (see p. 606), reasonable interatomic distances were only obtained assuming:

8 O_7 in 8(d); $x = 0.08_3$, $y = 0.12_4$, $z = 0.87_5$.

In order to determine the x and z coordinates of O_5 and O_6 the section $y = \frac{1}{4}$ in the unit cell was drawn and domains forbidden for oxygen atoms were marked out (Fig. 8). From the figure we see that there are only two small arcs of the U—O circles, left free for the centres of O_5 and O_6. The coordinates of these oxygen atoms would then be

4 O_5 in 4(c); $x = 0.04_2$, $y = \frac{1}{4}$, $z = 0.36_8$.

4 O_6 in 4(c); $x = 0.30_0$, $y = \frac{1}{4}$, $z = 0.36_8$.

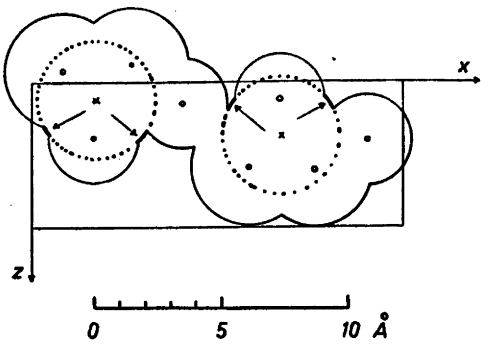


Fig. 8. Section at y = ¼ *through the unit cell showing the areas forbidden for the non-sulphate oxygen atoms* (O_5 *and* O_6) *in this plane. Thick circles indicate U—O contacts and thin circles enclose domains forbidden around the sulphate oxygen atoms and the oxygen atoms* O_7. *The arrows point out the only arcs of the U—O circles left free for the centres of* O_5 *and* O_6.
+ = *centre of uranium* ○ = *centre of oxygen*

Thus for the non-sulphate oxygen atoms we conclude

4 O_5 in No. 62 *Pnma* 4(*c*) with $x = 0.04_2$, $y = \frac{1}{4}$, $z = 0.36_8$

4 O_6 in No. 62 » 4(*c*) with $x = 0.30_0$, $y = \frac{1}{4}$, $z = 0.36_8$

8 O_7 » » 62 » 8(*d*) with $x = 0.08_3$, $y = 0.12_4$, $z = 0.87_5$.

FINAL POSITIONS OF THE LIGHT ATOMS

Now, when the positions of the atoms O_5—O_7 had been determined, the parameters of the sulphate oxygen atoms could be obtained from space considerations. It was concluded above that two of the four oxygen atoms in a sulphate group are in contact with uranium. We had also found that the centres of these two oxygen atoms (O_1 and O_2) should be situated on two circles with radii and centres given above. In fact, we can get their position still more exactly, if we notice that the distance O_1—O_2 shall be 2.4_0 Å and that the y coordinates of each of the sulphate oxygen atoms shall be within the limits $-0.13_3 \leq y \leq 0.13_3$ or $0.36_7 \leq y \leq 0.63_3$. Since the parameters of the non-sulphate oxygen atoms (O_5, O_6 and O_7) are known, it is easy to determine the orientations of the regular sulphate tetrahedra so that all O—O distances (oxygen atoms not belonging to the same sulphate group) are $\geq 2.6_0$ Å and so that U—O_1 = U—O_2 = 2.3_6 Å. In this way the coordinates of the oxygen atoms O_1 and O_2 were obtained. Finally the positions of the remaining sulphate oxygen atoms in SO_4 tetrahedra follow immediately from the parameters for S, O_1 and O_2. Thus we obtain

8 O_1 in No. 62 *Pnma* 8(*d*) with: $x = 0.26_5$ $y = 0.12_4$ $z = 0.89$
8 O_2 » » 62 » 8(*d*) with: $x = 0.33_0$ $y = 0.92_1$ $z = 0.88$
8 O_3 » » 62 » 8(*d*) with: $x = 0.40_4$ $y = 0.08_1$ $z = 0.09$
8 O_4 » » 62 » 8(*d*) with: $x = 0.40_2$ $y = 0.08_4$ $z = 0.66$

The oxygen positions are not free from assumptions. Thus we have assumed that the oxygen atoms belong to the space group No. 62 *Pnma*, but since the uranium and sulphur atoms really belong to this group, it seems plausible to assume the same for the oxygen atoms. Moreover, the positions of the uranium and sulphur atoms cannot be far from the truth and this will make the determination of the positions of the sulphate groups rather probable. The remaining non-sulphate oxygen atoms were concluded to be in contact with uranium and the positions were obtained from space considerations. This will give a coordination figure, the square Archimedean antiprism, which is found in previously determined crystal structures of uranium salts [19-23] (see below, p. 611).

Now, there are in the unit cell four uranium atoms, eight sulphur atoms and forty-eight oxygen atoms. The signs of the structure factors were determined from the uranium contributions, but of course, the magnitudes will be influenced by the sulphur and oxygen contributions. Table 2 shows some reflections, where this influence is more pronounced and it will appear that the sulphur and the oxygen contributions lead to better agreement between observed and calculated structure factors and this is noticeable with most of the reflections, when the scattering power of these atoms was taken into account.

Table 2. Comparison between calculated and observed structure factors of some reflections from Weissenberg photographs of $U(SO_4)_2 4H_2O$ CuK-radiation.

h k l	F_U calc	F_S calc	$F_U + F_S$ calc	F_O calc	F calc	F obs
6 0 0	+76	+17	+93	−25	+68	67
14 0 0	−43	+12	−31	− 9	−40	43
2 1 0	−74	+ 7	−67	+18	−49	49
4 2 0	+33	−15	+18	−17	+ 1	—
4 3 0	−71	−11	−82	+24	+58	60
0 4 0	+79	+ 4	+83	−26	+57	57
2 4 0	−43	− 1	−44	+15	−29	33
2 5 0	−61	+19	−42	+ 9	−33	33
4 5 0	+64	−11	+53	+11	+64	62
0 6 0	−70	− 8	−78	−35	−113	124
4 6 0	+27	+ 7	+34	+11	+45	43
4 8 0	−24	+12	−12	+11	− 1	—
6 8 0	+58	−11	+47	− 8	+39	34
2 9 0	−49	+ 1	−48	+19	−29	35
4 9 0	+53	− 1	+52	−21	+31	34
1 0 2	−69	+18	−51	+21	−30	30
7 0 2	−64	+ 4	−60	+17	−43	42
4 0 3	+47	+ 8	+55	+13	+68	74
0 0 4	−64	−16	−80	−35	−115	116
6 1 1	−51	+ 4	−47	−15	−62	61
7 1 1	−49	− 1	−50	+14	−36	34
3 2 1	+58	+12	+70	+11	+81	71
4 2 1	−49	+ 7	−42	+10	−32	28
0 3 1	+55	+14	+69	+16	+85	86
1 3 1	+51	−11	+40	− 9	+31	27
1 6 1	−24	+ 3	−21	+ 7	−14	12

Thus it seems probable that the sulphur and oxygen coordinates concluded above are correct.

In the unit cell there are also thirty-two hydrogen atoms, which must be situated at the oxygen atoms O_5, O_6 and O_7, *i. e.* H_2O molecules. The structure would otherwise be built up of UO_2 or $U(OH)_4$ groups and neutral H_2SO_4 molecules (or HSO_4^--ions), which does not seem very probable. The hydrogen atoms may then form hydrogen bonds with the neighbouring sulphate oxygen atoms. However, it is not possible to determine the parameters of the hydrogen atoms.

FINAL STRUCTURE PROPOSITION

The following structure is thus proposed for $U(SO_4)_2 4H_2O$. Space group: No. 62 *Pnma*. 4 formula units per unit cell.

		x	y	z
4 U	in 4(*c*)	0.171 ± 0.003	¼	0.121 ± 0.003
8 S	in 8(*d*)	0.351 ± 0.005	0.054 ± 0.005	0.879 ± 0.005
8 O_1	in 8(*d*)	0.27	0.12	0.89
8 O_2	in 8(*d*)	0.33	0.92	0.88
8 O_3	in 8(*d*)	0.40	0.08	0.09
8 O_4	in 8(*d*)	0.40	0.08	0.66
4 O_5 (H_2O)	in 4(*c*)	0.04	¼	0.37
4 O_6 (H_2O)	in 4(*c*)	0.30	¼	0.37
8 O_7 (H_2O)	in 8(*d*)	0.08	0.12	0.88

4(*c*): $\pm(x, \frac{1}{4}, z)$; $\pm(\frac{1}{2}+x, \frac{1}{4}, \frac{1}{2}-z)$

8(*d*): $\pm(x,y,z)$; $\pm(\frac{1}{2}+x, \frac{1}{2}-y, \frac{1}{2}-z)$; $\pm(\bar{x}, \frac{1}{2}+y, \bar{z})$; $\pm(\frac{1}{2}-x, \bar{y}, \frac{1}{2}-z)$

The accuracy of the oxygen parameters is estimated to be about ±0.01, the *z* parameters being perhaps a little more uncertain. Using these parameters the structure factors for *hk*0, *hk*1 and *h*0*l* were calculated and compared with the observed structure factors from the corresponding Weissenberg photographs (Table 3). Taking into account that, in spite of the choice of two crystals with different longitudinal directions, there is an absorption effect [11] in the reflections, the agreement between observed and calculated intensities is rather good.

DESCRIPTION OF THE STRUCTURE

In the structure of $U(SO_4)_2 4H_2O$ the uranium atoms are surrounded by eight oxygen atoms, a coordination, which is to be expected for ions of this radius ratio [18]. The coordination figure is a somewhat distorted square Archimedean antiprism, which according to Pauling [18] gives a more satisfactory ionic coordination than the cube. The same configuration around uranium is also found in $U(OH)_2SO_4$ [19] and $U_6O_4(OH)_4(SO_4)_6$ [20] and further around thorium in $Th(OH)_2CrO_4H_2O$ [21] and $Th(OH)_2SO_4$ [22] and around cerium in $CeOSO_4H_2O$ [23].

In the crystals of $U(SO_4)_2 4H_2O$ every uranium ion is in contact with four sulphate ions and every sulphate ions with two uranium ions, *i. e.* the crystals

Table 3. Comparison between calculated and observed structure factors from Weissenberg photographs of $U(SO_4)_2 4H_2O$. Cu-K radiation.

h k l	*F* calc	*F* obs	*h k l*	*F* calc	*F* obs	*h k l*	*F* calc	*F* obs
2 0 0	−62	34	2 5 0	−33	33	2 11 0	+36	34
4 0 0	−68	49	4 5 0	+64	62	4 11 0	−49	40
6 0 0	+68	67	6 5 0	−29	15	6 11 0	+17	—
8 0 0	−47	47	8 5 0	−46	38	8 11 0	+39	34
10 0 0	−22	33	10 5 0	+52	48			
12 0 0	+74	90	12 5 0	−24	41	10 11 0	−42	43
14 0 0	−40	43	14 5 0	−25	31			
16 0 0	−24	18	16 5 0	+65	76	0 12 0	+50	48
18 0 0	+39	36				2 12 0	−32	24
			0 6 0	−113	124	4 12 0	−22	15
2 1 0	−49	49	2 6 0	+39	39	6 12 0	+47	42
4 1 0	+63	50	4 6 0	+45	43	8 12 0	−39	31
6 1 0	−20	25	6 6 0	−65	67	10 12 0	+ 2	—
8 1 0	−67	78	8 6 0	+44	33			
10 1 0	+70	90	10 6 0	+11	—	2 13 0	−36	48
12 1 0	−21	31	12 6 0	−57	72	4 13 0	+53	43
14 1 0	−30	41	14 6 0	+44	51	6 13 0	− 3	—
16 1 0	+51	59	16 6 0	+16	—			
18 1 0	−27	34				0 14 0	−44	38
			2 7 0	+65	57	2 14 0	+25	17
0 2 0	−57	66	4 7 0	−58	52	4 14 0	+13	—
2 2 0	+42	44	6 7 0	+ 4	—			
4 2 0	+ 1	—	8 7 0	+63	54	1 0 1	+14	17
6 2 0	−67	64	10 7 0	−58	54	2 0 1	−66	70
8 2 0	+47	66	12 7 0	+ 6	—	3 0 1	−36	34
10 2 0	+ 7	—	14 7 0	+33	42	4 0 1	+68	76
12 2 0	−42	53	16 7 0	−39	32	5 0 1	+26	30
14 2 0	+49	63				6 0 1	+ 6	—
16 2 0	− 7	—	0 8 0	+55	55	7 0 1	− 1	—
18 2 0	−42	44	2 8 0	−32	22	8 0 1	−54	62
			4 8 0	− 1	—	9 0 1	−38	38
2 3 0	+95	67	6 8 0	+39	34	10 0 1	+36	39
4 3 0	−58	60	8 8 0	−44	34	11 0 1	+45	46
6 3 0	− 5	—	10 8 0	− 5	—	12 0 1	− 1	—
8 3 0	+47	55	12 8 0	+42	52	13 0 1	− 4	—
10 3 0	−45	50	14 8 0	−43	46	14 0 1	−32	36
12 3 0	+10	—				15 0 1	−25	31
14 3 0	+45	58	2 9 0	−29	35	16 0 1	+39	42
16 3 0	−49	56	4 9 0	+31	34	17 0 1	+31	37
18 3 0	+ 6	—	6 9 0	− 3	—	18 0 1	− 9	—
			8 9 0	−29	24			
			10 9 0	+50	43	0 0 2	+ 5	—
0 4 0	+57	57	12 9 0	−23	20	1 0 2	−30	30
2 4 0	−29	33	14 9 0	−32	27	2 0 2	− 4	—
4 4 0	−34	22				3 0 2	−31	30
6 4 0	+76	80	0 10 0	−69	60	4 0 2	− 1	—
8 4 0	−60	40	2 10 0	+35	34	5 0 2	+46	43
10 4 0	−17	—	4 10 0	+30	22	6 0 2	+ 4	—
12 4 0	+48	49	6 10 0	−66	52	7 0 2	−43	42
14 4 0	−32	52	8 10 0	+33	32	8 0 2	− 1	—
16 4 0	− 4	—	10 10 0	+27	18	9 0 2	+34	33
18 4 0	+33	22	12 10 0	−42	50	10 0 2	− 3	—

Table 3.
(cont.)

h k l	*F* calc	*F* obs	*h k l*	*F* calc	*F* obs	*h k l*	*F* calc	*F* obs
11 0 2	+17	17	10 0 5	−27	33	9 2 1	+51	57
12 0 2	+ 4	—	11 0 5	−34	31	10 2 1	−36	46
13 0 2	−61	67	12 0 5	+ 5	—	11 2 1	−31	37
14 0 2	− 1	—	13 0 5	+ 3	—	12 2 1	+18	22
15 0 2	+31	48				13 2 1	−15	—
16 0 2	− 1	—	0 0 6	−10	—	14 2 1	+18	22
17 0 2	+29	31	1 0 6	+23	31	15 2 1	+33	41
18 0 2	+ 2	—	2 0 6	+ 6	—	16 2 1	−39	50
			3 0 6	− 7	—	17 2 1	−22	23
1 0 3	−20	24	4 0 6	+ 3	—	18 2 1	+20	21
2 0 3	−52	54	5 0 6	−30	29			
3 0 3	+33	48	6 0 6	− 8	—	0 3 1	+85	86
4 0 3	+68	74	7 0 6	+38	33	1 3 1	+31	27
5 0 3	−14	12	8 0 6	+ 3	—	2 3 1	−26	27
6 0 3	− 6	—	9 0 6	−20	12	3 3 1	−13	—
7 0 3	+ 4	—	10 0 6	+ 7	—	4 3 1	−25	25
8 0 3	−57	68	11 0 6	−18	12	5 3 1	−46	36
9 0 3	+26	24				6 3 1	+43	36
10 0 3	+35	33	1 0 7	+12	12	7 3 1	+52	38
11 0 3	−42	42	2 0 7	+37	24	8 3 1	−27	26
12 0 3	+ 3	—	3 0 7	−21	20	9 3 1	−17	13
13 0 3	+ 3	—	4 0 7	−48	36	10 3 1	−17	15
14 0 3	−29	33	5 0 7	+10	12	11 3 1	−24	16
15 0 3	+25	38	6 0 7	+ 5	—	12 3 1	+36	49
16 0 3	+39	38				13 3 1	+43	54
17 0 3	−26	26	0 1 1	−53	49	14 3 1	−21	21
			1 1 1	−61	57	15 3 1	−25	36
0 0 4	−115	116	2 1 1	+30	31	16 3 1	−10	—
1 0 4	+ 9	—	3 1 1	+ 2	—	17 3 1	−19	21
2 0 4	+42	43	4 1 1	+17	—	18 3 1	+22	21
3 0 4	0	—	5 1 1	+41	36			
4 0 4	+47	44	6 1 1	−62	61	1 4 1	+19	19
5 0 4	+ 4	—	7 1 1	−36	34	2 4 1	−43	44
6 0 4	−61	53	8 1 1	+40	51	3 4 1	−61	50
7 0 4	− 8	—	9 1 1	+ 9	—	4 4 1	+32	37
8 0 4	+37	38	10 1 1	+ 8	—	5 4 1	+42	36
9 0 4	+ 3	—	11 1 1	+37	42	6 4 1	+ 2	—
10 0 4	+23	28	12 1 1	−32	36	7 4 1	+13	10
11 0 4	+ 2	—	13 1 1	−40	50	8 4 1	−38	39
12 0 4	−59	60	14 1 1	+34	44	9 4 1	−38	40
13 0 4	− 4	—	15 1 1	+ 8	—	10 4 1	+41	47
14 0 4	+32	29	16 1 1	0	—	11 4 1	+30	31
15 0 4	+ 3	—	17 1 1	+18	17	12 4 1	−11	—
			18 1 1	−31	31	13 4 1	+ 5	—
1 0 5	− 9	—				14 4 1	−22	30
2 0 5	+43	38	1 2 1	−39	43	15 4 1	−36	39
3 0 5	+29	17	2 2 1	+24	31	16 4 1	+28	30
4 0 5	−35	38	3 2 1	+81	71	17 4 1	+35	33
5 0 5	−27	29	4 2 1	−32	28	18 4 1	−12	—
6 0 5	− 1	—	5 2 1	−36	31			
7 0 5	− 4	—	6 2 1	+ 8	14	0 5 1	−56	67
8 0 5	+32	39	7 2 1	−26	23	1 5 1	−44	52
9 0 5	+36	31	8 2 1	+28	31	2 5 1	+27	31

Table 3.
(cont.)

h k l	F calc	F obs	h k l	F calc	F obs	h k l	F calc	F obs
3 5 1	− 2	—	11 7 1	−24	22	6 10 1	− 2	—
4 5 1	+ 6	—	12 7 1	+30	37	7 10 1	− 3	—
5 5 1	+57	56	13 7 1	+39	39	8 10 1	+36	29
6 5 1	−35	37	14 7 1	−23	18	9 10 1	+29	27
7 5 1	−44	39	15 7 1	−16	15	10 10 1	−30	31
8 5 1	+38	40	16 7 1	− 6	—	11 10 1	−33	28
9 5 1	+ 1	—				12 10 1	+ 1	—
10 5 1	+ 1	—	1 8 1	+32	41	13 10 1	+ 1	—
11 5 1	+33	44	2 8 1	−17	29			
12 5 1	−35	54	3 8 1	−59	56	0 11 1	+41	37
13 5 1	−32	52	4 8 1	+33	21	1 11 1	+31	31
14 5 1	+36	53	5 8 1	+22	16	2 11 1	−20	16
15 5 1	+ 4	—	6 8 1	−10	12	3 11 1	0	—
16 5 1	− 3	—	7 8 1	+21	12	4 11 1	− 9	—
17 5 1	+21	20	8 8 1	−21	16	5 11 1	−37	29
			9 8 1	−46	45	6 11 1	+29	20
1 6 1	−14	12	10 8 1	+27	21	7 11 1	+32	19
2 6 1	+49	54	11 8 1	+31	20	8 11 1	−28	15
3 6 1	+41	36	12 8 1	−15	19	9 11 1	− 4	—
4 6 1	−44	48	13 8 1	+14	12	10 11 1	− 4	—
5 6 1	−30	32	14 8 1	−16	15	11 11 1	−24	17
6 6 1	− 1	—	15 8 1	−28	19			
7 6 1	− 8	—				1 12 1	+15	—
8 6 1	+40	42	0 9 1	−36	38	2 12 1	−27	19
9 6 1	+34	38	1 9 1	−42	38	3 12 1	−41	32
10 6 1	−39	39	2 9 1	+18	22	4 12 1	+23	18
11 6 1	−30	31	3 9 1	+ 5	—	5 12 1	+25	18
12 6 1	+ 9	—	4 9 1	+14	—	6 12 1	− 4	—
13 6 1	− 1	—	5 9 1	+34	31	7 12 1	+16	9
14 6 1	+26	27	6 9 1	−37	31	8 12 1	−22	25
15 6 1	+26	29	7 9 1	−36	31	9 12 1	−31	23
16 6 1	−35	31	8 9 1	+25	16			
			9 9 1	+ 8	—			
0 7 1	+52	46	10 9 1	+ 5	—	0 13 1	−46	36
1 7 1	+36	32	11 9 1	+31	27	1 13 1	−19	11
2 7 1	−27	19	12 9 1	−24	24	2 13 1	+22	11
3 7 1	− 6	—	13 9 1	−37	29	3 13 1	+ 6	—
4 7 1	−23	20	14 9 1	+27	22	4 13 1	+17	10
5 7 1	−23	15				5 13 1	+22	19
6 7 1	+56	47	1 10 1	−12	—	6 13 1	−37	29
7 7 1	+30	31	2 10 1	+37	22	7 13 1	−29	26
8 7 1	−28	22	3 10 1	+33	22			
9 7 1	−14	15	4 10 1	−36	31	1 14 1	−17	10
10 7 1	−17	22	5 10 1	−26	22	2 14 1	+24	—

are built up of $U(SO_4)_2$-layers parallel with the *yz* plane (Fig. 7 b). Between these layers there is water of crystallization, so that every uranium atom is in contact with four water molecules and each of them is in contact with one uranium atom. The two sulphate oxygen atoms (O_3 and O_4), which are not bound to uranium, are in contact with the water oxygen atoms (O_5, O_6 and O_7). These O—O distances vary between 2.7 and 2.9 Å, and are similar to

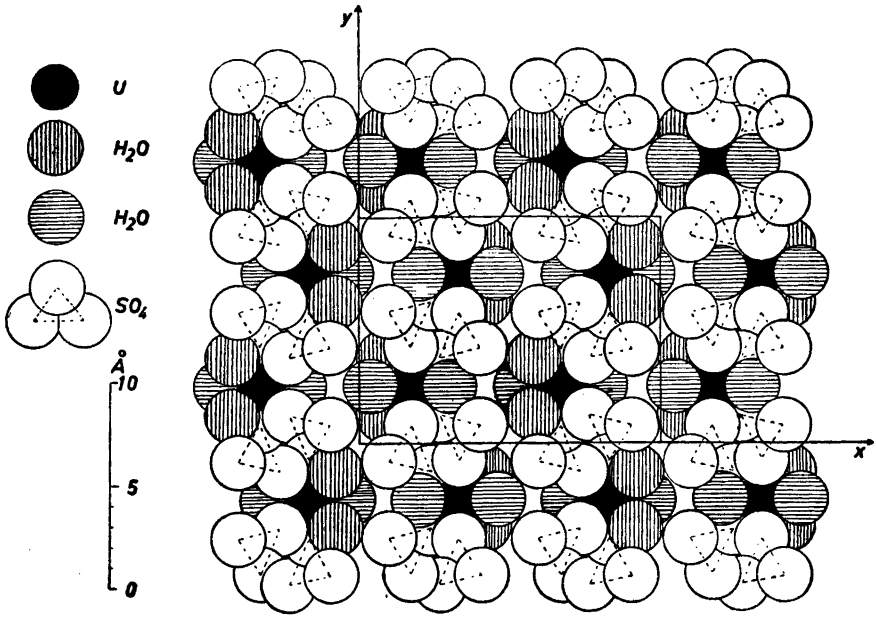


Fig. 9. Projection on the xy *plane of the structure of* $U(SO_4)_2 4H_2O$.

those found in several hydrates of oxy-salts containing O—H—O-bonds [24]. It seems therefore very probable that the layers, mentioned above, are joined by hydrogen bonds between the water oxygen atoms and the sulphate oxygen atoms O_3 and O_4.

The *xy* projection of the structure is shown in Fig. 9.

The distances U—O, S—O and O—O (within a sulphate group) were assumed to be 2.3_6 Å, 1.4_7 Å and 2.4_0 Å. The distances between the oxygen atoms, not belonging to the same sulphate group, will be (in Å)

O_1-O_1	$= 2.8_0$	O_3-O_5; O_5-2O_3	$= 2.7_7$	
O_1-2O_2; O_2-2O_1	$= 2 \times 3.1_5$; $2 \times 3.2_5$	O_3-O_6; O_6-2O_3	$= 2.8_8$	
O_1-2O_6; O_6-4O_1	$= 3 \times 3.1_3$; $3 \times 3.3_0$	O_3-O_7; O_7-O_3	$= 2.7_9$	
O_1-O_7; O_7-O_1	$= 2.6_7$	O_4-O_6; O_6-2O_4	$= 2.9_0$	
O_2-O_5; O_5-2O_2	$= 2.7_7$	O_4-O_7; O_7-2O_4	$= 2 \times 2.7_9$	
O_2-O_6; O_6-2O_2	$= 2.7_9$	O_5-4O_7; O_7-2O_5	$= 3 \times 3.1_9$; $3 \times 3.2_6$	
O_2-2O_7; O_7-2O_2	$= 2 \times 3.1_6$; $2 \times 3.1_5$	O_7-O_7	$= 2.7_9$	
O_3-O_4	$= 3.2_3$			

The O—O distances are all within the normal range, showing that the lattice is also supported by O—O contacts. However, they may be in error by a few tenths of an Ångström unit.

The author wishes to thank Professor Arne Ölander for his kind interest and Docent Bengt Aurivillius and Fil. lic. Karin Aurivillius for their helpful interest and for valuable discussions.

Thanks are also due to Dr. Arne Magnéli and Fil. lic. Georg Lundgren for the very great interest they have shown in this work and for the many valuable discussions, which the author had with them.

REFERENCES

1. Ebelmen, *Ann.* **43** (1842) 310; *Ann. Chim. Phys.* (3) **5** (1842) 214.
2. Meyer, R. J. and Nachod, H. *Ann.* **440** (1924) 191.
3. Kohlschütter, V. *Ber.* **34** (1901) 3629.
4. Groth, P. *Chemische Krystallographie*, Leipzig 1906—19, Vol. 2, p. 477.
5. Lundgren, G. *Private communication.*
6. Hecht, F. and Donau, J. *Anorganische Mikrogewichtsanalyse*, Wien 1940, p. 205.
7. Hartvig-Bendig, M. *Z. angew. Mineral.* **3** (1941) 195.
8. Brush, G. J. *Am. J. Sci.* **460** (1868) 240.
9. Penfield, S. L. *Am. J. Sci.* (3) **48** (1894) 30.
10. Booth, A. D. *Fourier Technique in X-Ray Organic Structure Analysis*, Cambridge 1948, p. 64.
11. Wells, A. F. *Z. Krist.* **96** (1937) 451.
12. Zachariasen, W. H. *Phys. Rev.* **73** Ser. II (1948) 1104.
13. Rundle, R. E., Baenziger, N. C., Wilson, A. S. and McDonald, R. A. *J. Am. Chem. Soc.* **70** (1948) 99.
14. Magnéli, A. and Kihlborg, L. *Acta Chem. Scand.* **5** (1951) 578.
15. Brown, C. J. and Cox, E. G. *J. Chem. Soc.* **1940** 1.
16. Wells, A. F. *J. Chem. Soc.* **1848** 55.
17. Goldschmidt, V. M. and Thomassen, L. *Videnskapselskapets Skrifter Mat. Naturv. Kl.* Kristiania **1923** No. 2; *Strukturbericht* **1** 212.
18. Pauling, L. *The Nature of the Chemical Bond*, 2 ed. New York 1940, p. 381.
19. Lundgren, G. *Arkiv Kemi* **4** (1952) 421.
20. Lundgren, G. *Arkiv Kemi* **5** (1953) 349.
21. Lundgren, G. and Sillén, L. G. *Arkiv Kemi* **1** (1949) 277; *Naturwiss.* **36** (1949) 345.
22. Lundgren, G. *Arkiv Kemi* **2** (1950) 535.
23. Lundgren, G. *Arkiv Kemi* **6** (1954) 59.
24. Wells, A. F. *Structural Inorganic Chemistry*, Oxford 1945, p. 252, 368.

Received January 17, 1956.

ACTA CHEMICA SCANDINAVICA 10 (1956) 617—622

A Protease Inhibitor in Ox Lung Tissue

TAGE ASTRUP and AGNETE STAGE

Biological Institute, Carlsberg Foundation, Copenhagen, Denmark

Procedures are described for the isolation and partial purification of a protease inhibitor from ox lung tissue. The active compound has a characteristic thermostability. It is most stable at acid reaction, and is destroyed at neutral and alkaline reaction. The inhibitor differs from heparin and shows similarity with pancreatic trypsin inhibitors.

Ox lung tissue inhibits the proteolytic effect of a number of proteases [1]. The present paper describes the isolation of a powerful protease inhibitor from ox lung tissue. The inhibitor differs from heparin and appears similar to the trypsin inhibitor present in pancreatic tissue. The active compound has been termed *pulmin* [2].

EXPERIMENTAL

1. *Estimation of inhibitory effect.* Trypsin (crystalline, Armour, containing less than 50 % $MgSO_4$) was used in estimating the inhibitory effect. The proteolytic activities of appropriate mixtures of enzyme solution (1 vol.) and inhibitor dilutions (1 vol.) were estimated by the fibrin plate method and recorded as the products in mm^2 of two diameters of the lysed zones (average of 3 determinations) [3]. In the first part of this work [4] the activity was estimated at pH 6.5 or 7.2 and at 32°. Later when the improved fibrin plate method (pH 7.8; 37°) was available [7], this was used.

Though the form of the inhibition curves does not allow a precise quantitative estimation of the inhibitory activity at low concentrations of inhibitory compounds, the fibrin plate method has important advantages in preparative work. The presence of salts at different concentrations, of dissolving or precipitating agents, of small amounts of alcohol, or even of solid matter in suspension, does not significantly interfere with the estimations. This makes the estimation of the inhibitory effects of the preparations obtained very simple. Thiocyanate (1 M) had no influence on the trypsin activity or on the inhibitory effect, and was therefore preferred as dissolving medium in the estimation of the activity of the preparations. In order to increase the accuracy of the estimations during the final steps of the purification procedure, the inhibitory effect towards chymotrypsin (crystalline, Armour) was also measured, because the curves obtained here were more suitable for interpolation. The yields given below are approximate. They vary from batch to batch of crude material, and the amount of total substances in a given preparation is not always easily estimated (see later).

2. *Crude material.* The ox lung tissue was freed from water-soluble proteins by repeated treatment of the ground tissue with 0.9 % NaCl and water, followed by dehydration with acetone [1]. The aqueous phase was removed through gauze instead of by centrifug-

ing, and the final treatment with ether was omitted. One kg of ground lung tissue produced about 70 g of dried tissue containing about 13.3 % N. The inhibitory effects of these preparations were compared by shaking a trypsin solution with varying amounts of the dried tissue, followed by estimation of the protease activity retained in the solution [1]. Larger amounts, prepared according to our description, were kindly placed at our disposal by the *Løvens kemiske Fabrik*, Copenhagen.

3. *Crude extract.* Extraction of the inhibitory compound was accomplished with thiocyanate, as used by Snellman, Jensen and Sylvén [14], in the isolation of heparin. Because of considerable swelling of the lung tissue an amount of 5 g dried tissue per 100 ml solution was found most convenient.

The dried tissue (100 g) was stirred for 2 hours at room temp. with 2 000 ml M potassium thiocyanate and then passed through a double layer of gauze, yielding about 1 650 ml extract. The nitrogen content was estimated to 0.2 mg/ml (Micro-Kjeldahl) after removal of thiocyanate by dialysis (discarding a small inactive sediment). This gave about 350 mg N in the extract from 100 g dried tissue.

Low yields were obtained in extraction experiments with secondary phosphate (M), NH_4OH, sodium salicylate (50 %), dextrose (50 %), thiosulphate (M) and pyridine (5 %). Urea (50 %) gave potent solutions but inconsistent results. Treatment with NaOH yielded very potent solutions, but produced also an extreme swelling of the lung tissue, resulting in poor yields. Potassium thiocyanate (M) produced potent solutions without too much swelling. Treatment for 2, 6 and 20 hours (at room temp.) gave the same potencies of the extracts, but the content of impurities increased with time. Best yields were obtained with 0.5—1.0 M potassium thiocyanate. Extraction at room temp. produced slightly higher activity than at 0°, but also a higher N content. The turbid thiocyanate extract could be clarified without loss of activity by passing through a Seitz clarification filter (asbestos filter pad). Dialysis produced a slight, inactive sediment and from the resulting solution the active compound could be precipitated with acetone or ethanol. Repeated treatment of the lung tissue with thiocyanate did not significantly increase the yield of soluble inhibitor, though a certain amount of inhibitor effect still remained in the lung tissue. Extraction of the washed lung tissue before dehydration yielded inferior results because of an immense swelling of the tissue, and because of the presence of large amounts of inert material in the resulting solution. The activity and N content of the crude extract varied considerably with the sample of lung tissue used.

4. *Fractional precipitation.* Large amounts of inactive proteins could be removed by means of sulphosalicylic acid whereafter the inhibitory fraction could be precipitated by addition of tungstic acid. The procedure finally adopted was as follows:

Five ml of 0.1 M sodium sulphosalicylate was added to each 100 ml of undialyzed thiocyanate extract. The mixture was stirred mechanically, and N HCl was added until pH 2.8 was attained. An inactive precipitate (amounting to 150 mg N per 100 g dried tissue) was removed by centrifugation. 10 ml of 0.1 M sodium tungstate were added to each 100 ml of the supernatant followed by 10 ml N HCl (mechanical stirring). The pH was now about 1.3. After standing in the icebox for 2 hours for complete sedimentation, the mixture was centrifuged and the inactive supernatant discarded. The precipitate could be redissolved in about 100 ml H_2O per 100 g tissue by addition of solid sodium bicarbonate to neutral reaction. The solution had about 200 mg N per 100 g of tissue, and contained most of the activity of the crude extract. The methods used in this fractional precipitation were derived from previous studies on the precipitation of proteins with anions [5,6]. If the precipitation was carried out on a dialyzed extract the precipitate with sulphosalicylic acid contained the active material.

5. *Acetone precipitation.* When the solution containing the dissolved tungstic acid precipitate was dialyzed against tap water (24 hours), a precipitate containing part of the inhibitory activity was formed. In order to retain this substance in solution it was found necessary to add an equal volume of 1 M potassium thiocyanate to the dialyzed mixture. Some insoluble matter (amounting to 50 mg N per 100 g tissue) was removed by centrifugation and discarded. The supernatant was still turbid and had to be clarified by passing through a thin layer of diatomaceous earth (Kieselguhr) in a Büchner funnel. After this treatment the solution contained about 125 mg N per 100 g tissue. After dialysis against tap water (24 hours) and addition of a few drops of saturated NaCl solution an active precipitate was obtained in the cold with 3 volumes of acetone. After treatment with acetone and ether it amounted to about 1 g (~ 120 mg N) per 100 g tis-

sue. This preparation was soluble in water after addition of alkali and contained almost the total activity of the crude extract.

Further purification was attempted by fractionation with ethanol. The thiocyanate solution of the tungstic acid precipitate was clarified and dialyzed as described. Then 0.6 vol. of 96 % ethanol and a few drops of saturated NaCl solution were added. An active precipitate was isolated by centrifugation, and dried with ethanol and ether (*pulmin I*). It amounted to about 0.9 g per 100 g tissue. A re-precipitation was performed by dissolving pulmin I in 0.9 % NaCl (16 mg per ml) and adding 0.5 vol. of 96 % ethanol. The centrifugate was again inactive, and the active precipitate was dried with abs. ethanol and ether *(pulmin II)*. It amounted to about 250 mg per 100 g tissue.

6. *Purification of the thiocyanate solution.* The good solubility of the precipitates in M thiocyanate suggested a fractional precipitation of such solutions.

100 mg of an ethanol precipitated product (pulmin II) was dissolved in 20 ml M potassium thiocyanate and precipitated with 50 ml of 96 % ethanol. The precipitate was inactive and was discarded. The centrifugate was freed from ethanol by evaporation *in vacuo*, diluted to the original volume with water, and 6 g solid ammonium sulphate per 10 ml solution was added. The active precipitate obtained was extracted twice by stirring for half an hour with a mixture of 12.5 ml ethanol and 5 ml H_2O per 10 ml original volume. The united extracts were freed from ethanol *in vacuo* and the resulting solution dialyzed for a short time against 0.9 % NaCl in a rapid dialyser. The solution was precipitated slowly by addition to 10 volumes of abs. ethanol, and the precipitate was washed and dried with ethanol and ether *(pulmin III)*.

This procedure was based on preliminary experiments about which the following could be stated: The solubility of the ethanol precipitated product (pulmin II) in thiocyanate solutions is of great advantage, because the presence of thiocyanate completely changes the order of precipitation. Without thiocyanate active components precipitate at low ethanol concentrations (see Section 5). In the presence of thiocyanate considerable amounts of inert matter (80 % of the material) could be precipitated at low ethanol concentration. However, the subsequent separation of the active components was not possible even with excess of ethanol. The removal of thiocyanate was difficult. Dialysis of the solutions produced a considerable loss of activity. Slight losses had also been observed in the preparation of the previous products, but had been thought to be caused by losses during the procedures. With the more pure preparations the losses were so large that they could not be accounted for in this way. Dialysis against a number of different solutions was tried. Apparently the loss only depended upon time, and some activity could be recovered from the outer fluid. Best results were obtained by rapid dialysis in a dipping dialyser. These results suggest that the inhibitor has a fairly low molecular weight, and this possibility has to be taken into consideration when preparing larger quantities. Losses were not encountered during storage of the solutions.

Because of the difficulties involved in removing thiocyanate by dialysis without losing inhibitor activity, other ways were sought for the isolation of active compounds. It was found that the solution could be evaporated to dryness *in vacuo* (bath temp. $<50°$) without losing activity. Complete removal of thiocyanate by extraction of the residue with ethanol could not be accomplished without loss of activity. Removal of free thiocyanic acid was attempted by addition of glacial acetic acid and water during the evaporation. No loss in activity was encountered, but difficulties arose in the subsequent removal of potassium acetate. After evaporation of ethanol *in vacuo* the active components in the thiocyanate solution could be precipitated by addition of ammonium sulphate. Addition of 6 g solid ammonium sulphate per 10 ml solution produced a precipitate containing all activity in addition to inorganic components. Most of the activity could be extracted with a mixture of ethanol and water in the proportion 25:10. After removal of ethanol *in vacuo* and concentration to a smaller volume, a short dialysis could be performed and an active precipitate obtained by dropwise addition to 10 vol. abs. ethanol.

The yields during these last steps were not high. Losses were encountered during dialysis as already mentioned, and the extraction of the ammonium sulphate precipitate was far from quantitative. However, the precipitates as finally obtained (pulmin III) were extremely potent powders.

7. *Properties.* The experiments described above have revealed some interesting properties of the active component. It is extremely stable at acid reaction, tolerating treatment for several days at a pH between 1 and 2. The active substance appears to have

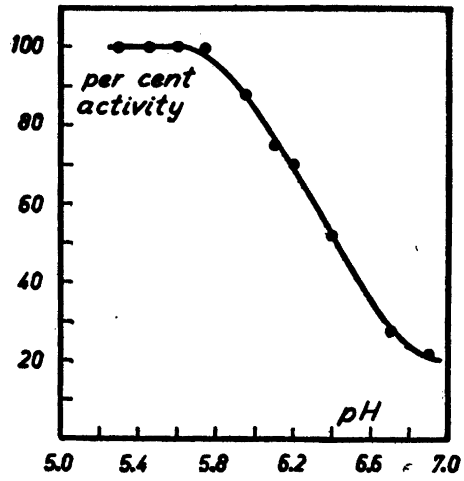


Fig. 1. Thermostability of ox lung inhibitor. (Acetone precipitated preparation). Appropriate solutions were made in a dilute maleic acid buffer. After heating in a boiling water bath for 1 hour the activity against trypsin was estimated on fibrin plates, and read on a dilution curve of the inhibitor. A b s c i s s a: pH during heating. O r d i n a t e: Remaining activity in per cent of untreated solution.

a fairly low molecular weight, disappearing slowly by diffusion during dialysis. This ability to diffuse appears to be especially pronounced in more pure preparations. Less pure preparations do not dialyze. In these solutions proteins probably combine with the active substance, preventing diffusion. When a dialysis is incorporated into the procedure, a certain loss is therefore encountered in all excepting the first few steps. The necessity of using thiocyanate solutions makes it impossible to follow the purification steps accurately by nitrogen estimations and the amount of dry matter isolated at different steps has to be used as an approximate measure of the total amount of substance present. In the first steps the amounts of nitrogen have been estimated after dialysis; the figures recorded represent a good estimate of the compounds present, because the active, dialysable component in these steps is only a small fraction of the total amount of solid matter. Because of the high solubility of the active components in alcohol-water mixtures, it was impossible in all intermediate steps to isolate the products quantitatively as a dry powder.

The preparation isolated as pulmin I contained about 11 % N and 6 % P. Pulmin II contained about 10 % N and 5 % P. The preparation isolated as pulmin III contained a large amount of inorganic salts so that the nitrogen content was reduced. It contained also thiocyanate if the dialysis had not been sufficient. The inactive product removed during the step leading to pulmin III (fractional precipitation of the thiocyanate solution with ethanol) contained about 12 % N and 7 % P, which by re-precipitation could be increased to about 8.9 % P. Measurements of ultraviolet absorption of solutions of this compound indicated that it consisted mainly of nucleic acids. Because of the high salt content in pulmin III, the solutions were analysed for N and P and the proportion P/N compared with that obtained from other products. For pulmin I and pulmin II P/N (mg/mg) was between 0.4 and 0.5. For pulmin III it was below 0.01 because of removal of most of the phosphorus. A rough idea of the degree of purification could be obtained from the amounts of nitrogen in the different preparations which produced complete inhibition of a chymotrypsin solution. One mg of chymotrypsin was inhibited by the following amounts: pulmin I, 0.9 mg N; pulmin II, 0.3 mg N; pulmin III, <0.1 mg N.

The lung inhibitor is a rather stable compound. Solutions of pulmin heated for 2 hours at 56° (pH between 1.6 and 9.7) did not lose activity. At acid reaction the com-

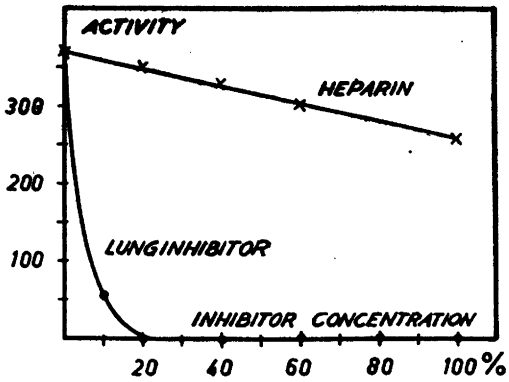


Fig. 2. Inhibitory effect of heparin and the ox lung inhibitor on streptokinase activated human globulin. In each case 20 mg substance were dissolved in 10 ml physiol. NaCl. Dilutions of the inhibitors were prepared and samples added to equal volumes of the active solution. The resulting activities were estimated by means of the fibrin plate method at pH 7.2 and 32°. A b s c i s s a: Concentration of inhibitor in per cent of stock solution. O r d i n a t e: Fibrinolytic activity recorded as the product of two diameters of the lyzed zones. The lung inhibitor was an acetone precipitated preparation (Section 5).

pound tolerates heating for 1 hour at 100°, but at neutral and alkaline reactions it is destroyed (see the thermostability curve, Fig. 1).

A comparison was made between the inhibitory effects of heparin (obtained from Løvens kemiske Fabrik, Copenhagen) and the acetone precipitated lung inhibitor on a solution of human globulin activated by streptokinase. This solution contains plasmin as well as an activator of plasminogen. The results are presented in Fig. 2. It can be seen that the lung inhibitor is a much more powerful inhibitor of fibrinolysis than heparin.

DISCUSSION

The method described here for the isolation and preparation of a protease inhibitor from ox lung tissue makes it possible to obtain this antiproteolytic agent as a stable, watersoluble dry powder of high potency. The losses encountered during dialysis indicate that the inhibitor is not a protein, but that it has a rather low molecular weight, possibly less than 10 000. The heat stability curve shows a characteristic optimum at rather acid reaction and in this respect the compound resembles trypsin inhibitors isolated from pancreas and colostrum (Laskowski and Laskowski, Jr.[13]). The yield of inhibitory compounds from the pancreas is low. Green and Work [11] mention a figure of 1 mg pure inhibitor per kg of fresh pancreas, and they obtained only 10 g of a product about 50 % pure from 100 kg dried pancreas residues. The results with ox lung show that this organ is extremely rich in inhibitory substance. Apart from the pancreas it is the only organ in the animal organism, which has been found to contain large amounts of a protease inhibitor, though it may be mentioned that urine contains an inhibitor of apparently similar nature (Astrup and Sterndorff [8]). It is of interest that the inhibitor is absent from the lungs of most other mammalian species, including man. Lung tissue is usually a

potent plasminogen activator. Even calf embryo lung is a potent plasminogen activator and does not contain the inhibitor.

Ox lung serves as a source for the production of heparin (Charles and Scott [10]; Kuizenga and Spaulding [12]). Initially we thought that the substance might contain heparin bound to protein. We have tried to prepare heparin from the lung inhibitor after methods devised by Charles and Scott [9] and Wilander [15] for the extraction of heparin from tissues. Only traces were obtained. A search for sulphuric acid residues after hydrolysis with HCl revealed only insignificant amounts. The comparison in Fig. 2 of heparin with a purified lung inhibitor shows definitely that the inhibitor is different from heparin, and we have therefore suggested the term *pulmin* for the ox lung inhibitor. Larger amounts of this compound are being prepared in order to study its properties and physiological effects.

The participation of A. S. in this work was made possible by means of a fellowship from *Det teknisk-videnskabelige Forskningsraad*, Copenhagen. It was also aided by a grant from the *Josiah Macy Jr. Foundation*, New York. Mr. Chr. Pedersen, M. Sc., and Mrs. Alice Kjær, M. Sc., assisted in some of the experiments.

REFERENCES

1. Astrup, T. *Acta Physiol. Scand.* **26** (1952) 243.
2. Astrup, T. *Acta Haematol.* **7** (1952) 271.
3. Astrup, T. and Alkjærsig, N. *Nature* **168** (1951) 565.
4. Astrup, T. and Alkjærsig, N. *Arch. Biochem. and Biophys.* **37** (1952) 99.
5. Astrup, T. and Birch-Andersen, A. *Nature* **160** (1947) 570, 637.
6. Astrup, T., Birch-Andersen, A. and Schilling, K. *Acta Chem. Scand.* **8** (1954) 901.
7. Astrup, T. and Müllertz, S. *Arch. Biochem. and Biophys.* **40** (1952) 346.
8. Astrup, T. and Sterndorff, I. *Scand. J. Clin. Lab. Invest.* **7** (1955) 239.
9. Charles, A. F. and Scott, D. A. *J. Biol. Chem.* **102** (1933) 425, 437.
10. Charles, A. F. and Scott, D. A. *Trans. Roy. Soc. Can.* 3. *V.* **28** (1934) 55.
11. Green, N. M. and Work, E. *Biochem. J. London* **54** (1953) 257.
12. Kuizenga, M. H. and Spaulding, L. B. *J. Biol. Chem.* **148** (1943) 641.
13. Laskowski, M. and Laskowski, M. Jr. *Advances in Enzymol.* **9** (1954) 203.
14. Snellman, O., Jensen, R. and Sylvén, B. *Nature* **161** (1948) 639.
15. Wilander, O. *Skand. Arch. Physiol.* **81** (1938) Suppl. No. 15.

Received January 18, 1956.

ACTA CHEMICA SCANDINAVICA 10 (1956) 623—628

Studies on Vanadium Oxides

II. The Crystal Structure of Vanadium Dioxide

GEORG ANDERSSON

Institute of Chemistry, University of Uppsala, Uppsala, Sweden

The crystal structure of VO_2 has been investigated by X-ray methods. It has been found to belong to the space-group $P2_1/c$. The unit cell dimensions and the parameters of the metal and oxygen atoms are given. The structure is shown to be of a deformed rutile type with the metal atoms within the strings of VO_6 octahedra occurring in doublets as in the MoO_2 structure type. The interatomic distances and angles in the VO_6 octahedra are compared with those in the TiO_6 octahedra (rutile).

In a recent report [1] on a phase analysis of the vanadium-oxygen system carried out at this Institute it was stated that the crystal structure of the dioxide is not of the simple rutile type proposed by Goldschmidt [2] but constitutes a monoclinic deformation of this structure type. The unit cell dimensions obtained from powder photographs in a Guinier focussing camera using Cr$K\alpha$ radiation and sodium chloride, added as an internal standard (a_{NaCl}= 5.640 Å), were thus found to be

$$a = 5.743 \text{ Å}, \; b = 4.517 \text{ Å}, \quad c = 5.375 \text{ Å}, \quad \beta = 122.61°$$

The observed density of 4.65 corresponds to a cell content of 4 formula units of VO_2 (calculated density 4.67).

The dimensions of the rutile type cell reported by Goldschmidt [2] were

$$a_r = 4.54 \text{ Å}, \quad c_r = 2.88 \text{ Å}$$

Evidently the following relations exist between the monoclinic cell and the rutile type subcell:

$$\underline{a} = 2c_r, \quad \underline{b} = a_r, \quad \underline{c} = a_r - c_r$$

Crystals grown by heating vanadium trioxide-vanadium pentoxide mixtures of the gross composition $VO_{2.00}$ in evacuated sealed silica tubes at 900° C for about a week were used for the single crystal X-ray investigations. The blue-black crystals showed prismatic form elongated along the *a* direction.

MoK radiation was used throughout for the single crystal photographs. Weissenberg diagrams were registered with the prism axis as rotation axis (layer lines $h = 0$—6). The intensity scales of these photographs were correlated by means of precession photographs of the layer lines $h0l$, $h1l$ and $h2l$ taken with a Buerger camera.

The intensities of the reflections were estimated using a calibration scale of reflections of known relative intensities. The structure factor values were derived using the curves of Lu [3] for the Weissenberg photographs and those of Waser [4] and of Burbank *et al.*[5,6] for the precession diagrams.

All reflections $h0l$ with l odd were found to be absent while reflections $0k0$ were only observed for k even. This is characteristic of the space-group $P2_1/c$ (No. 14), the symmetry of which thus is very likely to be that of vanadium dioxide.

The crystal structure of the isomorphous dioxides of molybdenum and wolfram are known to be of deformed rutile type [7]. Their unit cell dimensions are similar to those of vanadium dioxide and show the same relation to the basic rutile-type subcell as does the latter. This observation suggested the possibility of structural similarities between vanadium dioxide and the MoO_2-type. However, due to the lower symmetry [$P2_1$ (No. 4)] observed for the latter the structure problem for vanadium dioxide was attacked without postulating the existence of such a structural relation.

DETERMINATION OF THE STRUCTURE

The space-group $P2_1/c$ contains a general point position 4(e): x, y, z; $\bar{x}$, $\bar{y}$, $\bar{z}$; $\bar{x}$, $\frac{1}{2}+y$, $\frac{1}{2}-z$; x,$\frac{1}{2}-y$,$\frac{1}{2}+z$ and four sets of twofold point-positions corresponding to the symmetry centers of the cell. The occurrence of the glide plane and the twofold screw axis in this space-group suggested that the Harker sections $P(0v\frac{1}{2})$ and $P(u\frac{1}{2}w)$ should be investigated. The former was found to contain only one major maximum ($v=\frac{1}{2}$) which shows that all the metal atoms are situated close to the planes $y = 0$ and $y = \frac{1}{2}$. The latter section shows a heavy maximum in $u = 0$, $w=\frac{1}{2}$ and peaks of about half the height of the maximum in $u = 0.48$, $w = 0.55$ and $u = 0.52$, $w = 0.45$ and in addition a few maxima of considerably lower magnitude. This observation excludes the possibility of the vanadium atoms occupying specialized point positions. An arrangement of four vanadium atoms in 4(e) with y close to 0 (and $\frac{1}{2}$), however, requires the following maxima in the section $P(u\frac{1}{2}w)$:

(1)	$u = 2x$,	$w = 2z + \frac{1}{2}$	(weight = 1)
(2)	$u = -2x$,	$w = -(2z + \frac{1}{2})$	(weight = 1)
(3)	$u = 0$,	$w = \frac{1}{2}$	(weight = 2)

This immediately gives the approximate arrangement of the vanadium atoms

4 V in 4(e): $x \approx 0.24$, $y \approx 0$, $z \approx 0.025$.

After deriving the signs of the structure factors $F(h0l)$ from these vanadium positions the projection parallel to the b axis of the electron density function was calculated. It was found to show high peaks very close to the positions

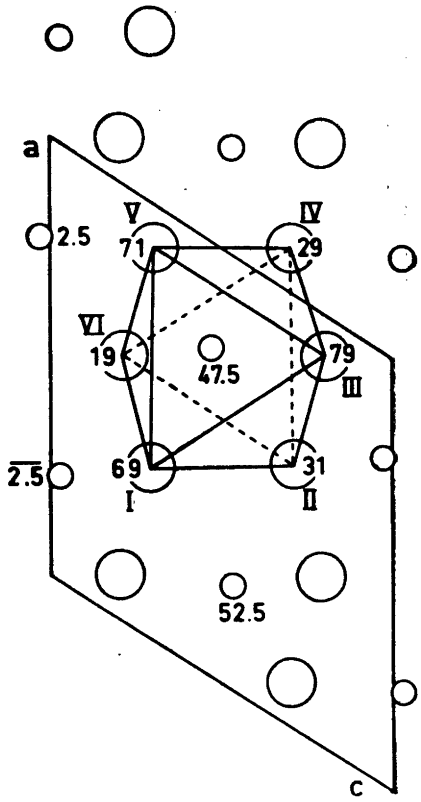


Fig. 1. VO_2. Projection of the structure on (010). The large circles denote O atoms and the small circles V atoms. The arabic numerals give the levels of the atoms in per cent of b. *One VO_6 octahedron is marked out and its O atoms are denoted with roman numerals (*cf. *Table 2).*

assumed for the vanadium atoms and minor maxima, the heights and arrangement of which suggested that they corresponded to the oxygen atoms. The oxygen atoms were found to have no influence on the signs of the structure factors $F(h0l)$.

Atoms situated in the planes $y = 0$ and $y = \frac{1}{2}$ do not contribute to the intensities of reflections $0kl$ with $k + l =$ odd. As several reflections of this type were found with too high intensities to be accounted for by mere influence of the oxygen atoms, it was concluded that the y parameter of vanadium was slightly different from zero. The signs of the structure factors $F(hkl)$ were thus calculated from a y_V value of —0.02 obtained by a rough trial and error estimation. The values of the y parameters of vanadium and oxygen were then finally obtained from the bounded projection $\varrho_{12}(y,z) = \int_{x_1}^{x_2} \varrho(x,y,z) a \, dx$ evaluated between the planes $x_1 = 0$ and $x_2 = \frac{1}{2}$.

In this way the following structure was arrived at:

Space-group: $P2_1/c$ (No. 14)

Unit cell content: 4 VO_2

Table 1. VO_2. *Comparison between observed and calculated* $|F|$ *values for reflections* 0kl, 3kl *and* 4kl. *Weissenberg photographs with Mo*K *radiation.*

hkl	|F| obs.	|F| calc.	hkl	|F| obs.	|F| calc.	hkl	|F| obs.	|F| calc.
0,0,2	67	63	3,1,4	—	7	3,6,0	—	1
0,0,4	102	108	3̄,1,4	—	11	3̄,6,1	48	58
0,0,6	54	51	3̄,1,5	83	83	3̄,6,2	—	31
0,1,1	156	191	3̄,1,6	—	10	3̄,6,3	38	44
0,1,2	49	40	3̄,1,7	64	75	4,0,0	74	72
0,1,3	98	95	3̄,1,8	—	0	4,0,2	99	109
0,1,4	54	49	3,2,0	—	19	4̄,0,2	142 *	173
0,1,5	73	75	3,2,1	34	38	4,0,4	68	63
0,1,6	—	20	3̄,2,1	36	31	4̄,0,4	40	35
0,2,0	68	67	3,2,2	—	20	4̄,0,6	46	47
0,2,1	47	45	3̄,2,2	59	56	4̄,0,8	—	14
0,2,2	166	168	3,2,3	—	24	4,1,0	—	27
0,2,3	40	37	3̄,2,3	33	36	4,1,1	87	92
0,2,4	64	65	3,2,4	—	25	4̄,1,1	103	115
0,2,5	—	15	3̄,2,4	71	70	4,1,2	33	33
0,2,6	45	40	3,2,5	—	14	4̄,1,2	—	14
0,3,1	100	95	3̄,2,6	72	75	4,1,3	81	85
0,3,2	40	34	3̄,2,7	—	11	4̄,1,3	93	98
0,3,3	106	110	3,2,8	55	65	4,1,4	—	23
0,3,4	—	5	3,3,0	46	42	4̄,1,4	—	15
0,3,5	—	26	3,3,1	—	3	4,1,5	46	44
0,3,6	—	43	3̄,3,1	36	29	4̄,1,6	46	45
0,4,0	110	102	3,3,2	46	46	4̄,1,7	—	31
0,4,1	57	51	3̄,3,2	47	50	4̄,1,8	—	17
0,4,2	68	69	3,3,3	—	27	4,2,0	120	130
0,4,3	—	2	3̄,3,3	61	58	4,2,1	—	16
0,4,4	66	58	3,3,4	—	28	4̄,2,1	37	40
0,4,5	—	37	3̄,3,4	—	34	4,2,2	72	68
0,5,1	79	74	3̄,3,5	74	65	4̄,2,2	56	52
0,5,2	—	18	3̄,3,6	—	13	4,2,3	—	2
0,5,3	—	28	3̄,3,7	54	61	4̄,2,3	—	6
0,5,4	—	32	3,4,0	—	14	4,2,4	57	56
0,5,5	62	60	3,4,1	44	48	4̄,2,4	110	97
0,6,0	65	56	3̄,4,1	49	59	4̄,2,5	38	39
0,6,1	—	37	3,4,2	—	8	4̄,2,6	—	23
0,6,2	—	35	3̄,4,2	36	30	4̄,2,7	—	21
3,0,0	34	14	3,4,3	48	45	4,3,0	—	3
3,0,2	—	10	3̄,4,3	38	42	4,3,1	91	99
3̄,0,2	77 *	65	3,4,4	58	59	4̄,3,1	77	78
3,0,4	38	42	3̄,4,5	—	32	4,3,2	—	12
3̄,0,4	95	83	3,4,6	47	47	4̄,3,2	—	22
3̄,0,6	85	84	3,5,0	65	68	4,3,3	—	39
3̄,0,8	60	65	3,5,1	—	1	4̄,3,3	59	60
3,1,0	—	23	3̄,5,1	—	17	4̄,3,4	48	46
3,1,1	—	4	3,5,2	48	42	4̄,3,5	63	67
3̄,1,1	45	43	3̄,5,2	42	48	4̄,3,6	—	16
3,1,2	—	16	3,5,3	—	13	4̄,3,7	—	6
3̄,1,2	—	16	3̄,5,3	38	34	4,4,0	64	59
3,1,3	—	25	3̄,5,4	36	40	4,4,1	—	23
3̄,1,3	84	73	3,5,5	48	45	4̄,4,1	—	15

* These reflections are obtained from a Buerger camera photograph.

Table 1. (contd.)

hkl	|*F*| obs.	|*F*| calc.	*hkl*	|*F*| obs.	|*F*| calc.	*hkl*	|*F*| obs.	|*F*| calc.
4,4,2	65	62	4,5,0	—	12	$\bar{4}$,5,3	53	61
$\bar{4}$,4,2	79	76	4,5,1	—	31	$\bar{4}$,5,4	—	40
4,4,3	—	17	$\bar{4}$,5,1	65	60	$\bar{4}$,5,5	—	6
$\bar{4}$,4,3	61	58	4,5,2	—	7	$\bar{4}$,6,1	48	46
$\bar{4}$,4,4	—	38	$\bar{4}$,5,2	—	27	$\bar{4}$,6,2	55	45
$\bar{4}$,4,5	—	22	4,5,3	61	65	$\bar{4}$,6,3	—	11
$\bar{4}$,4,6	—	28						

4 V in 4(*e*): $x, y, z;\ \bar{x}, \bar{y}, \bar{z};\ \bar{x}, \frac{1}{2}+y, \frac{1}{2}-z;\ x, \frac{1}{2}-y, \frac{1}{2}+z$
$x = 0.242, \quad y = 0.975, \quad z = 0.025$
4 O in 4(*e*): $x = 0.10, \quad y = 0.21, \quad z = 0.20$
4 O in 4(*e*): $x = 0.39, \quad y = 0.69, \quad z = 0.29.$

The oxygen-oxygen vectors required by this atomic arrangement will give rise to maxima in the Patterson function with v not far from $\frac{1}{2}$ and u and w values close to those of the minor maxima found in the section $P(u\frac{1}{2}w)$.

The agreement between observed and calculated structure factor values is illustrated in Table 1. The reliability factor $R = \frac{\Sigma||F_{obs}| - |F_{calc}||}{\Sigma|F_{obs}|}$ for all observed reflections was found to be 0.10.

DISCUSSION OF THE STRUCTURE

The structure thus derived corresponds to reasonable interatomic distances throughout (*cf.* Table 2). The vanadium-oxygen distances of 1.76—2.05 Å are comparable with those found in, *e. g.*, paramontroseite (a metastable, naturally occurring form of VO_2) 1.88—2.13 Å [8], in V_6O_{13} 1.85—2.50 Å [9], and in V_2O_5 1.54—2.02 Å [10].

The structure of vanadium dioxide may be described as built up of distorted VO_6 octahedra joined by edges to form strings, which are mutually connected by corners to a three-dimensional network of deformed rutile type. As in the MoO_2 structure type the metal atoms within the strings are grouped pairwise to form doublets. The fundamental analogy between the structures of vanadium dioxide and molybdenum dioxide and the higher symmetry of the former suggest that the vanadium dioxide structure be considered as representing the idealized form of the "MoO_2 structure type", which also comprises the dioxides of wolfram, technetium and rhenium [11].

The metal-metal atom distances within the strings of octahedra are 2.959 Å in titanium dioxide (rutile), 2.65 and 3.12 Å in vanadium dioxide and 2.50 and 3.10 Å in molydebdenum dioxide. The sequence 2.959, 2.65 and 2.50 Å demonstrates the influence of the number of valence electrons of the metal on the formation of metal atom doublets (*cf.* Ref. [11]).

Table 2 gives a survey of the geometry of the MeO_6 octahedra of titanium dioxide (rutile) [12] and vanadium dioxide. The vanadium-oxygen distances are

Table 2. Interatomic distances (Å) and angles in MeO_6 octahedra of VO_2 and TiO_2 (rutile) [12].

Me—O	VO_2	TiO_2	O—O	VO_2	TiO_2	∧(OMeO)	VO_2	TiO_2
Me—O_I	2.03	1.944	O_I —O_{II}	2.56	2.520	O_I MeO_{II}	79°	80.8°
—O_{II}	2.01	1.944	O_I —O_{III}	2.76	2.780	O_I MeO_{III}	85°	90.0°
—O_{III}	2.05	1.988	O_I —O_V	2.90	2.959	O_I MeO_V	96°	99.2°
—O_{IV}	1.86	1.944	O_I —O_{VI}	2.73	2.780	O_I MeO_{VI}	93°	90.0°
—O_V	1.87	1.944	O_{II} —O_{III}	2.62	2.780	O_{II} MeO_{III}	80°	90.0°
—O_{VI}	1.76	1.988	O_{II} —O_{IV}	2.84	2.959	O_{II} MeO_{IV}	94°	99.2°
			O_{II} —O_{VI}	2.74	2.780	O_{II} MeO_{VI}	93°	90.0°
			O_{III}—O_{IV}	2.72	2.780	O_{III}MeO_{IV}	88°	90.0°
			O_{III}—O_V	2.71	2.780	O_{III}MeO_V	87°	90.0°
			O_{IV} —O_V	2.62	2.520	O_{IV} MeO_V	89°	80.8°
			O_{IV} —O_{VI}	2.66	2.780	O_{IV} MeO_{VI}	95°	90.0°
			O_V —O_{VI}	2.77	2.780	O_V MeO_{VI}	99°	90.0°

probably correct within ±0.05 Å while the oxygen-oxygen distances are likely to be better than ±0.08 Å. The error in the interatomic angles is estimated to a few degrees.

It is evident that the shapes of the oxygen octahedra of titanium dioxide (rutile) and vanadium dioxide differ little in spite of the distortion of the rutile type of the latter structure. Thus the oxygen atoms forming the edge common to the two VO_6 octahedra of a metal atom pair are somewhat forced apart. The corresponding distance in molybdenum dioxide is considerably longer, *viz.* 3.1 Å which is accounted for by the very close molybdenum-molybdenum contact. The conservation of the fairly regular arrangement of the oxygen atoms implies that the metal atom in vanadium dioxide is somewhat removed from the center of gravity and approaching one face of the VO_6 octahedron.

Acknowledgements. The author wishes to express his thanks to Professor G. Hägg for the facilities placed at his disposal. Thanks are also due to Dr. A. Magnéli for valuable discussions and continued interest in this investigation. A grant from the *Swedish Natural Science Research Council* is gratefully acknowledged.

REFERENCES.

1. Andersson, G. *Acta Chem. Scand.* **8** (1954) 1599.
2. Goldschmidt, V. M. *Skrifter Norske Videnskaps-Akad. Oslo, I. Mat. Naturv. Kl.* **1926** No. 1.
3. Lu, C. S. *Rev. Sci. Instr.* **14** (1943) 331.
4. Waser, J. *Ibid.* **22** (1951) 563.
5. Burbank, R. D. *Ibid.* **23** (1952) 321.
6. Greenville-Wells, H. J. and Abrahams, S. C. *Ibid.* **23** (1952) 328.
7. Magnéli, A. *Arkiv Kemi Mineral. Geol. A* **24** (1946) No. 2.
8. Evans, H. T. Jr. and Mrose, M. E. *Am. Mineralogist* **40** (1955) 861.
9. Aebi, F. *Helv. Chim. Acta* **31** (1948) 8.
10. Byström, A., Wilhelmi, K.-A. and Brotzen, O. *Acta Chem. Scand.* **4** (1950) 1119.
11. Magnéli, A. and Andersson, G. *Ibid.* **9** (1955) 1378.
12. Baur, W. *Naturwiss.* **42** (1955) 295.

Received January 20, 1956.

ACTA CHEMICA SCANDINAVICA 10 (1956) 629—632

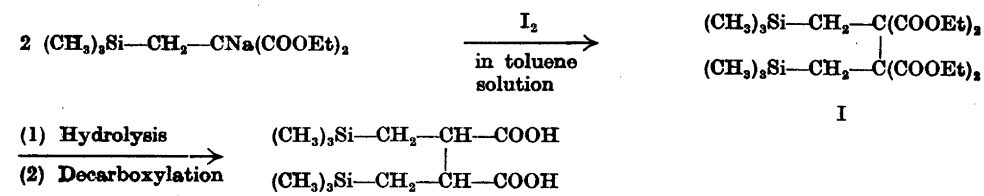
The Synthesis of Some Aliphatic Organosilicon Dicarboxylic Acids. III *

LENNART EBERSON

Department of Organic Chemistry, Chemical Institute, University of Lund, Sweden

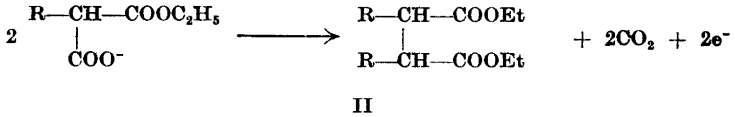
The preparation of α,α′-bis-[trimethylsilylmethyl]-succinic acid by electrolysis of monoethyl trimethylsilylmethylmalonate is described. The acid is found to exist in two forms, corresponding to the *meso* and racemic forms.

During attempts to prepare α,α′-bis-[trimethylsilylmethyl]-succinic acid by the following sequence of reactions



it was found [1] that the intermediate tetraester (I) could not be hydrolyzed under conditions which did not cause cleavage of methyl groups from the silicon atoms.

Another method for the preparation of α,α′-dialkylsubstituted succinic acids is the Crum Brown-Walker modification of the Kolbe electrolytic synthesis [2], namely the electrolysis of a half ester of an alkylmalonic acid according to the formula



II

* Part II: see Ref.[1].

In this paper the application of this reaction to monoethyl trimethylsilylmethylmalonate will be described.

The half ester was readily obtained in the crude state by half saponification of the corresponding diester, but could not be purified by distillation on account of its thermal instability. When heated to a temperature above 120° it decomposed into ethyl β-trimethylsilylpropionate, similarly to other monoethyl alkylmalonates. Attempts to purify the half ester by conversion into its calcium salt and recrystallization were not successful, as there was considerable loss of material during this procedure. However, the use of the crude ester in the electrolyses gave reasonably good yields and therefore no other purification methods were tried.

The electrolysis was carried out in anhydrous methanolic solution, where the conditions for optimum yields are not so critical as in aqueous solution. In water solution the yield of diester was much smaller, and besides which large amounts of polymeric material were obtained. The latter was probably polyacrylic ester, which could be formed by β-elimination of an intermediate radical. The presence of this polymer made the separation of the reaction products very difficult. In methanolic solution the reaction proceeded smoothly and a 40 % yield of the diester (II), R = $(CH_3)_3Si—CH_2$-, was obtained. (II) was then readily hydrolyzed by boiling with ethanolic potassium hydroxide to give a mixture of the *meso* and racemic forms of α,α'-bis-[trimethylsilylmethyl]-succinic acid. The separation of the diastereoisomers was easily affected by a simple crystallization from acetone, in which the high-melting acid was rather insoluble. The acids were finally recrystallized from 70 % acetic acid, giving the pure isomers of the melting points 241—244° (decomp.) and 160—162°, respectively.

The two forms could readily be converted into their anhydrides by boiling them with acetyl chloride. The anhydride of the high-melting acid melted at 74—76°, while the other was obtained as an oil, which did not crystallize. The anhydrides were hydrolyzed by boiling aqueous sodium hydroxide to form the corresponding acids. The above-mentioned decomposition of the high-melting acid at its melting point was found to be due to an elimination of water with the formation of the anhydride of the *low*-melting acid. The low-melting acid, in turn, on heating to 80—100° above its melting point gave its own anhydride. This was in line with the behavior of other α,α'-dialkyl-substituted succinic acids, *e. g.*, α,α'-diethylsuccinic acid [3].

With the preparation of these two acids the series of α,α'-bis-[trimethylsilylmethyl]-substituted *n*-dicarboxylic acids from the succinic to the suberic acid derivative has been completed. The work on these acids is now being continued to determine which of the forms can be resolved into optically active acids.

EXPERIMENTAL

Monoethyl trimethylsilylmethylmalonate. 49.2 g (0.2 mole) of diethyl trimethylsilylmethylmalonate was added to a solution of 11.2 g (0.2 mole) of potassium hydroxide in 250 ml of absolute ethanol, and the mixture was allowed to stand at room temperature for two hours. Then 100 ml of water was added and the ethanol was distilled off on a water-bath. The aqueous solution was extracted four times with 30 ml portions of ether

to remove unreacted diester and then acidified with concentrated hydrochloric acid with cooling in an ice-bath. (The recovered diester amounted to 7.2 g, 14 %). The organic layer was taken up in ether and the ether solution was washed twice with water, the ether distilled off and 100 ml of benzene was added. By distilling the benzene the contaminating water was removed from the half ester and a dry product was obtained. During the distillation the temperature of the flask content was not allowed to exceed 100° in order to prevent decarboxylation. The yield of crude ester was 85 % (based on unrecovered material) and it could be used directly in the electrolysis experiments.

Diethyl α,α'-bis-[trimethylsilylmethyl]-succinate. 21.8 g (0.1 mole) of monoethyl trimethylsilylmethylmalonate and 2 g of potassium hydroxide were dissolved in 100 ml of dry methanol. The solution was placed in a cell consisting of a 200 ml beaker fitted with a platinum spiral anode (surface area 3.0 cm²), a platinum net cathode (total surface area *ca.* 50 cm²), and a thermometer reaching into the liquid. The cell was cooled by immersion in an ice-bath (internal temperature of cell was kept all the time about 30°) and a current of 1.5 amp. was passed until the electrolyte became approximately neutral. This required *ca.* 20 % longer time than that calculated on the basis of the current and the amount of half ester employed.

The product was isolated by dilution of the cell contents with water, distilling off the methanol on a water-bath and taking up the organic layer in ether. The extract was washed with very dilute (2 %) sodium hydroxide solution to remove small amounts of starting material, then with water and finally dried with anhydrous magnesium sulphate. After evaporation the remaining oil was distilled in *vacuo*, b.p. 136—138°/4 mm, n_D^{20} 1.4448, d_4^{20} 0.9363, yield 6.9 g (40 %). (Found: C 55.3; H 9.8; Si 16.0; r_D 0.2841. Calc. for $C_{16}H_{34}O_4Si_2$: C 55.4; H 9.9; Si 16.2; r_D 0.2843.)

α,α'-Bis-[trimethylsilylmethyl]-succinic acid. 5.1 g (0.015 mole) of the above diester was hydrolyzed by boiling with excess 10 % ethanolic potassium hydroxide for 24 hours. The solution was diluted with water and the ethanol distilled off on a water-bath. Acidification with 5 N hydrochloric acid precipitated the mixture of the diastereoisomers. The crystals were filtered, washed thoroughly with water and air-dried. They were dissolved in 100 ml of boiling acetone, filtered to remove insoluble matter and left to crystallize. A yield of 1.4 g melting at 235° (decomp.) was obtained. The filtrate was evaporated to a volume of 10 ml and then gave an additional 0.4 g with the same melting point. The two fractions were combined and recrystallized from 70 % acetic acid giving a product, m. p. 242—244° (decomp.), which was not increased by further recrystallization. Yield 1.5 g.

The mother-liquor from the second filtration was evaporated to dryness and the residue recrystallized twice from 70 % acetic acid to give 1.4 g of the low-melting acid, m. p. 160—162°. The yields of the pure isomers were 34 and 32 %, respectively. (Found for the high-melting acid: C 49.3; H 9.1; Si 19.2; equiv. wt. 145.2. Found for the low-melting acid: C 49.8; H 9.1; Si 19.3; equiv. wt. 145.0. Calc. for $C_{12}H_{26}O_4Si_2$: C 49.6; H 9.0; Si 19.3; equiv. wt. 145.3.)

Preparation and hydrolysis of the anhydrides. I. 0.5 g of the high-melting acid was boiled with 3 ml of acetyl chloride until the crystals had completely dissolved, which required about 20 hours. Evaporation of the excess acetyl chloride and the acetic acid formed gave a residue which soon solidified, m. p. 71—76°, yield 0.4 g. The crude product was recrystallized from petroleum ether, to give the m. p. 74—76°. Upon hydrolysis with hot sodium hydroxide solution the high-melting acid was quantitatively recovered.

II. After treating the low-melting acid in the same manner as above an oil was obtained which did not solidify. It was vacuum-distilled, b. p. 130—135°/12 mm. The product gave the low-melting acid on hydrolysis as before. (Found for the anhydride, m. p. 74—76°: C 52.7; H 8.8; Si 20.6. Found for the liquid anhydride: C 52.9; H 8.8; Si 20.5; Calc. for $C_{12}H_{24}O_3Si_2$: C 52.9; H 8.9; Si 20.6.)

Anhydrization of the acids by heat. 160 mg of the high-melting acid was heated in a small test-tube to 250° in an oil-bath for 15 minutes. The crystals melted and drops of water condensed in the upper end of the test-tube. The product was liquid and consisted of the anhydride of the low-melting acid, as identified by its almost quantitative conversion into the low-melting acid by hydrolysis. (150 mg, m. p. 159—162°).

The low-melting acid on the same treatment gave exclusively its own anhydride.

The author wishes to express his sincere gratitude to Professor Erik Larsson for his kind interest in this work.

REFERENCES

1. Eberson, L. *Acta Chem. Scand.* **9** (1956) 1711.
2. Brown, A. C. and Walker, J. *Ann.* **274** (1893) 41.
3. Bischoff, C. A. *Chem. Ber.* **21** (1888) 2103.

Received January 23, 1956.

ACTA CHEMICA SCANDINAVICA 10 (1956) 633—637

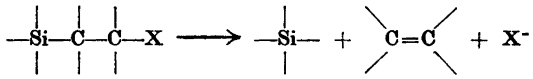
On Diethyl Trimethylsilylmethylhalogenomalonates

LENNART EBERSON

Department of Organic Chemistry, Chemical Institute, University of Lund, Sweden

The diethyl trimethylsilylmethylchloro- and bromomalonates have been prepared and the chemical properties of the bromo compound have been studied in some detail. It has been allowed to react with aqueous base, ethanolic base, diethyl sodiomalonate, and bromine, and subjected to pyrolysis. In the first three reactions it has been found that β-elimination is wholly or partially absent, whereas in the last two reactions β-elimination occurs.

Organosilicon compounds in which a halogen atom is situated on the carbon atom β to the silicon atom have received much attention [1–13]. Their most important chemical property is the so-called β-elimination which occurs more or less readily under the influence of various reagents (alcoholic bases, aqueous alkali, water, methyl magnesium bromide, bromine, silver nitrate, anhydrous aluminium chloride, and heat alone) according to the formula



A few general rules of the influence of structure upon β-elimination have been established.

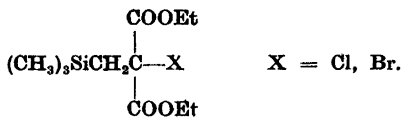
1. Electronegative substituents, *e. g.*, halogen, situated on the silicon atom give an increased rate of the reaction [6].

2. The β-elimination is hindered by alkyl substituents on the β carbon atom [11,13].

3. The order of reactivity of the β halogen is I>Br>Cl [13].

4. β-Halovinylsilanes do not undergo β-elimination [9].

This communication is a report of the preparation and the investigation of some chemical properties of the chloro and bromo derivatives of diethyl trimethylsilylmethylmalonate (I).



X = Cl, Br.

I

This type of β-haloalkylsilanes is substituted by two carbethoxy groups on the β-carbon and it was of interest to investigate if the presence of these groups has any remarkable influence on the β-elimination reaction. No β-haloalkylsilane simultaneously containing functional groups other than halogen on the β-carbon atom has hitherto been investigated.

When diethyl trimethylsilylmethylmalonate was boiled with an excess of sulphuryl chloride the chloroester (I), X = Cl, was obtained in a 62 % yield. The corresponding bromoester was prepared by adding one mole of bromine dropwise with stirring to one mole of diethyl trimethylsilylmethylmalonate. The reaction was started by adding a few ml of bromine and heating the mixture to 40—50 °. When the reaction once had begun each new drop of bromine reacted almost instantaneously. The stirring had to be very efficient to avoid partially high bromine concentrations in the reaction mixture (see below).

Diethyl trimethylsilylmethylbromomalonate was quite stable towards aqueous bases. Thus, it could be boiled with 10 % aqueous potassium hydroxide without being affected. However, when treated with 10 % ethanolic potassium hydroxide, in which the compound was soluble, the bromine atom was rapidly split off as bromide ion and there were formed small amounts of hexamethyldisiloxane together with an alkali-soluble silicon-containing polymer. The minute amount of hexamethyldisiloxane formed and the fact that the polymer contained silicon indicated that β-elimination was only a side-reaction under these conditions. The nature of the polymer was not further investigated.

On reaction with diethyl sodiomalonate the bromoester behaved like other alkylbromomalonic esters [14], *i. e.*, diethyl trimethylsilylmethylmalonate and tetraethyl ethylenetetracarboxylate were formed according to the formula

$$2\ (CH_3)_3Si{-}CH_2{-}\underset{\displaystyle COOEt}{\overset{\displaystyle COOEt}{\overset{|}{\underset{|}{C}}}}{-}Br\ +\ 2\ NaCH(COOEt)_2 \longrightarrow$$

$$2\ (CH_3)_3Si{-}CH_2{-}CH(COOEt)_2\ +\ (EtOOC)_2C{=}C(COOEt)_2\ +\ 2\ NaBr$$

No traces of products which could have resulted from a β-elimination could be detected. The relative stability of (I) against β-elimination in the above reaction might be ascribed to the tendency of dissociating into a positive bromine ion and a negative diethyl trimethylsilylmethylmalonate ion [15].

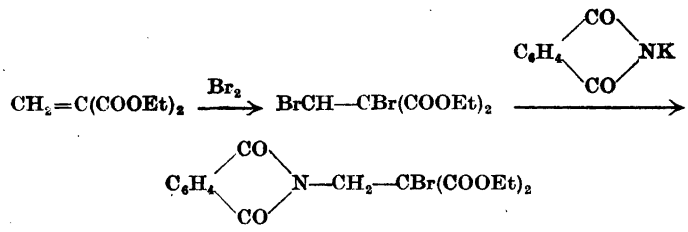
$$(CH_3)_3Si{-}CH{-}CBr(COOEt)_2 \longrightarrow (CH_3)_3Si{-}CH{-}C^{-}(COOEt)_2\ +\ Br^{+}$$

This ion is stable under the conditions employed.

Decomposition of I by heat occurred at 190—200° with the formation of trimethylbromosilane and diethyl methylenemalonate.

$$(CH_3)_3Si{-}CH_2{-}CBr(COOEt)_2 \xrightarrow{Heat} (CH_3)_3SiBr\ +\ CH_2{=}C(COOEt)_2$$

The diethyl methylenemalonate was identified by addition of bromine and reaction of the resulting dibromoester with potassium phthalimide [16].



The product did not depress the melting point of an authentic sample.

Diethyl trimethylsilylmethylbromomalonate reacted with bromine with the formation of trimethylbromosilane and diethyl bromomethylbromomalonate according to

$$(CH_3)_3Si—CH_2—CBr(COOEt)_2 + Br_2 \longrightarrow (CH_3)_2SiBr + BrCH_2—CBr(COOEt)_2$$

The last-mentioned compound was identified as before.

Preliminary experiments in order to brominate the free trimethylsilylmethylmalonic acid were not successful, as the bromination product was very unstable and decomposed rapidly on standing. Likewise the bromination of β-trimethylsilylpropionic acid gave decomposition products, among which trimethylbromosilane could be identified. The residue was probably a complex mixture of polybrominated propionic acids.

EXPERIMENTAL

Chlorination of diethyl trimethylsilylmethylmalonate. In a 100 ml flask equipped with a reflux condenser and a dropping funnel there was placed 24.6 g (0.1 mole) of diethyl trimethylsilylmethylmalonate. A few ml of freshly distilled sulphuryl chloride were added and the solution was heated to 60°. When the reaction had started as indicated by the evolution of hydrogen chloride the rest of the sulphuryl chloride (total amount 13.5 g) was added during a period of 30 minutes. The reaction was completed by heating at 70—80° for two hours. Then excess sulphuryl chloride and dissolved gases were evaporated under reduced pressure at room temperature and at last the residue was fractionated *in vacuo*. From this was obtained 17.3 g (0.062 mole) of diethyl trimethylsilylmethylchloromalonate, b. p. 131—133°/11 mm, n_D^{20} 1.4463, d_4^{20} 1.0553. (Found: C 47.1; H 7.6; Cl 12.4; Si 10.0; r_D 0.2528. Calc. for $C_{11}H_{21}O_4ClSi$: C 47.1; H 7.5; Cl 12.6; Si 10.0; r_D 0.2516.)

Bromination of diethyl trimethylsilylmethylmalonate. In a 250 ml flask equipped with an efficient stirrer, a reflux condenser, and a dropping funnel 98.4 g (0.4 mole) of diethyl trimethylsilylmethylmalonate was heated with a few ml of bromine to *ca.* 40°. The reaction soon began and the bromine colour disappeared. Bromine (a total of 64 g = 0.4 mole) was then added so slowly that the solution never assumed more than a faint brown colour. The stirring was rapid to avoid partially too high bromine concentrations. The hydrogen bromide evolved was absorbed in alkali. After the gas evolution had ended the reaction mixture was washed twice with water, once with saturated sodium carbonate solution, and with water again. After drying with anhydrous calcium chloride the product was fractionated under reduced pressure. From this was obtained 99.0 g (0.304 mole) of diethyl trimethylsilylmethylbromomalonate, b. p. 118—120°/4 mm, n_D^{20} 1.4597, d_4^{20} 1.2033, a yield of 76 %. (Found: C 40.4; H 6.5; Br 24.6; Si 8.5; r_D 0.2275. Calc. for $C_{11}H_{21}O_4BrSi$: C 40.6; H 6.5; Br 24.6; Si 8.6; r_D 0.2261.)

Reactions of diethyl trimethylsilylmethylbromomalonate. A. With aqueous base. 3.25 g of the bromo compound (0.01 mole) was boiled for 30 minutes with 20 ml of 10 % aqueous

potassium hydroxide. Only traces of bromide ion could be detected in the aqueous layer after cooling and extraction with ether. The ether solution was dried with anhydrous calcium chloride and gave upon distillation nearly all the starting material in recovery.

B. With ethanolic base. To a solution of 6.7 g (0.12 mole) of potassium hydroxide in 3 ml of water and 10 ml of ethanol was added 6.5 g (0.02 mole) of diethyl trimethylsilylmethylbromomalonate. The mixture was gradually heated and suddenly a violent reaction occurred. The flask was cooled in ice water, when necessary. At last the solution was heated under reflux for three hours, after which time it was acidified with hydrochloric acid and 50 ml of water was added. The organic layer was taken up in ether and the ether solution washed thoroughly with water to remove ethanol. After drying with anhydrous sodium sulphate fractionation gave 0.2 g of hexamethyldisiloxane, b. p. 99°, n_D^{20} 1.3774, a 12 % yield. None of the other lowboiling products contained silicon. The residue (3.3 g) was a very viscous, alkali-soluble polymer, which on titration with standard alkali solution showed an equivalent of 172. The silicon content was 10.5 %, corresponding to 62 % of the silicon present in the starting material.

C. With diethyl sodiomalonate. In a 25 ml three-necked flask equipped with a stirrer, a reflux condenser, and a dropping funnel 0.46 g (0.02 mole) of sodium was dissolved in 10 ml of absolute ethanol, followed by 3.2 g (0.02 mole) of diethyl malonate. 6.50 g (0.02 mole) of the bromoester was added cautiously. This was followed by refluxing for one hour, after which time the mixture was slightly acidified with glacial acetic acid and the ethanol distilled off. The residue was poured into 20 ml of water and worked up as usual. From this was obtained 3.0 g of diethyl trimethylsilylmethylmalonate (0.012 mole) and 1.8 g of tetraethyl ethylenetetracarboxylate (0.0057 mole), m. p. after recrystallization from ligroin 52—53°, mixed m. p. with an authentic specimen 52—53° [17].

The diethyl trimethylsilylmethylmalonate was identified by conversion into its diamide according to the method of Russell [18]. The authentic compound which was prepared from diethyl trimethylsilylmethylmalonate prepared otherwise melted at 161—162°. It contained one mole of water of crystallization which was removed by heating the compound before being analyzed in air at 110° for 20 hours. (Found C 45.5; H 8.7; Si 14.9; Calc. for $C_7H_{16}O_2N_2Si$: C 45.6; H 8.7; Si 14.9.)

D. Decomposition by heat. In a 25 ml flask equipped with a short column and a thermometer reaching into the flask there was placed 8.1 g (0.025 mole) of diethyl trimethylsilylmethylbromomalonate. The flask was slowly heated. When the temperature of the liquid reached 190° the compound began to decompose and a liquid distilled over, b. p. 75—77°. It was redistilled and was found to be trimethylbromosilane, b. p. 78—80°, 3.0 g, a yield of 79 %. (Found: Br 52.0. Calc. for C_3H_9BrSi: Br 52.2.)

The residue in the reaction flask was a dark oil with the characteristic odour of diethyl methylenemalonate, which was distilled at atmospheric pressure, b. p. 195—198°, 3.0 g, a yield of 70 %. For identification it was dissolved in 10 ml of carbon tetrachloride, 2.8 g of bromine was slowly added, the solvent was evaporated, and at last 3.2 g of potassium phthalimide was added. This mixture was heated at 150° for two hours, and then cooled. The solid mass was washed with water and finally recrystallized twice from ethanol, giving beautiful crystals, m. p. 135.5—136.5° undepressed on admixing with an authentic sample [16].

Reaction with bromine. To 8.1 g (0.025 mole) of diethyl trimethylsilylmethylbromomalonate 4.0 g (0.025 mole) of dry bromine was slowly dropped. The mixture warmed and soon began to reflux. After standing for an hour the trimethylbromosilane formed was distilled over, b. p. 76—78°, 3.1 g, a yield of 81 %. It was redistilled over a small amount of red phosphorus in order to remove traces of bromine. (Found: Br 52.1. Calc. for C_3H_9BrSi: 52.2.)

The residue was distilled under reduced pressure. From this was obtained 6.7 g of diethyl bromomethylbromomalonate, b. p. 125—126/5 mm, n_D^{20} 1.4838, d_4^{20} 1.6268, a yield of 80 %. It was identified as in the foregoing experiment.

The author wishes to express his sincere gratitude to Professor Erik Larsson for his kind interest in this work.

REFERENCES

1. Ushakov, S. N. and Itenberg, A. M. *J. Gen. Chem. S.S.S.R.* **7** (1937) 2495.
2. Sommer, L. H. and Whitmore, F. C. *J. Am. Chem. Soc.* **68** (1946) 485.
3. Sommer, L. H., Dorfman, E. Goldberg, G. M. and Whitmore, F. C. *J. Am. Chem. Soc.* **68** (1946) 488.
4. Sommer, L. H., Goldberg, G. M. and Whitmore, F. C. *J. Am. Chem. Soc.* **68** (1946) 1083.
5. Sommer, L. H., Bailey, D. L., Strong, W. A. and Whitmore, F. C. *J. Am. Chem. Soc.* **68** (1946) 1881.
6. Sommer, L. H., Bailey, D. L. and Whitmore, F. C. *J. Am. Chem. Soc.* **70** (1948) 2869.
7. Sommer, L. H., Tyler, L. J. and Whitmore, F. C. *J. Am. Chem. Soc.* **70** (1948) 2872.
8. Tyler, L. J., Sommer, L. H. and Whitmore, F. C. *J. Am. Chem. Soc.* **70** (1948) 2876.
9. Agre, C. L. *J. Am. Chem. Soc.* **71** (1949) 300.
10. Sommer, L. H., Bailey, D. L., Goldberg, G. M., Buck, C. E., Bye, T. S., Evans, F. J. and Whitmore, F. C. *J. Am. Chem. Soc.* **76** (1954) 1613.
11. Petrov, A. D. and Mironov, V. F. *Doklady Akad. Nauk S.S.S.R.* **75** (1950) 707.
12. Petrov, A. D. and Mironov, V. F. *Doklady Akad. Nauk S.S.S.R.* **80** (1951) 761.
13. Petrov, A. D. and Mironov, V. F. *Izvest. Akad. Nauk S.S.S.R., Otdel. Khim. Nauk* (1952) 635.
14. Ruhemann, S. *Ber.* **26** (1893) 2356.
15. Fresenius, Ph. *Angew. Chem.* **64** (1952) 470.
16. Elks, F., Elliott, D. F. and Hems, B. A. *J. Chem. Soc.* **1944** 626.
17. Corson, B. B. and Benson, W. L. *Org. Syntheses, Coll. Vol. II*, p. 273.
18. Russell, P. B. *J. Am. Chem. Soc.* **72** (1950) 1853.

Received January 23, 1956.

ACTA CHEMICA SCANDINAVICA 10 (1956) 638—642

The Identification of Organic Compounds

I. The Preparation of *p*-Bromophenacyl Esters of Carboxylic Acids

JØRGEN BERGER

Department of Organic Chemistry, Royal Danish School of Pharmacy, Copenhagen, Denmark

The melting points of twenty *p*-bromophenacyl esters are given. The melting points taken from the literature of the *p*-bromophenacyl esters of formic acid (92° C, 99—100 °C, 134.5° C, 135.2° C and 140° C), oxalic acid (242° C) and fumaric acid (197° C) are discussed and revised by the author to 101° C, 244—245° C and 256—257° C, respectively. Further, the melting point of the oxalate and the fumarate determined on Koflers Heizbank are found to 256° C and 266° C, respectively. An improved method for the preparation of the *p*-bromophenacyl formate and the *p*-bromophenacyl oxalate is given.

It is known to be convenient to identify carboxylic acids as their esters of *p*-halogenophenacyl alcohol and in this paper and in a subsequent paper some new esters will be reported. Judefind and Reid [1] have prepared the *p*-bromophenacyl esters of many acids but they found that some acids did not give derivatives, such as oxalic acid and formic acid. However, Moses and Reid [2] later prepared the *p*-bromophenacyl formate with m. p. 135.2° C. Hurd and Christ [3] reported the m. p. as 140° C, which was confirmed by Summerbell and Bauer [4].

In 1950 Kubota and Matsuura [5] pointed out that the compound widely used as a derivative for the identification of formic acid was the *p*-bromophenacyl alcohol and not the ester, and in addition they found that the *p*-iodophenacyl and the *p*-chlorophenacyl formate reported by Moses and Reid [2] were also the corresponding alcohols. They reported the m. p. of the *p*-bromophenacyl formate as 99—100° C, but they recommended the use of another derivative for the identification of formic acid.

Similary Grove and Suter [6] in 1950 found the m. p. to be 99° C for the formate, but they could only obtain the pure derivative after chromatography of a benzene solution on activated alumina. In 1952 Neish and Lemieux [7] stated that the *p*-bromophenacyl formate had a m. p. of 92° C. The ester was

prepared by refluxing equivalent amounts of the reactants in ethanol for 30 minutes giving a yield of 80 %. By refluxing longer the ester was hydrolysed and the derivative was the alcohol with m. p. varying from 137° C to 142° C depending on the rate of heating.

In order to explain some of these discrepancies we have prepared the *p*-halogenophenacyl formates and the m. p. were 87° C, 101° C and 124° C for the *p*-chloro-, *p*-bromo- and *p*-iodophenacyl ester, respectively; these values are in accordance with those given by Kubota and Matsuura [5]. The special procedure used is described in the experimental part; the *p*-bromo phenacyl formate is recommended as an excellent derivative of formic acid.

We found that the derivative, prepared according to the method of Neish and Lemieux [7] had a m. p. of 92° C, but this was increased to 101° C by repeated recrystallisation from ethanol. The derivative is extremely difficult to purify because of the presence of *p*-bromophenacyl alcohol and unconverted *p*-bromophenacyl bromide.

In 1951 Erickson, Dechary and Kesling [8] described a new method for the preparation of the *p*-bromophenacyl esters; the acid being converted by *p*-bromo-*α*-diazoacetophenone in dioxan solution. Apparently this procedure also gives the *p*-bromophenacyl alcohol, as they reported the m. p. of the formic ester as 134.5° C.

Hydrolysis of the p-*bromophenacyl esters.* Neish and Lemieux [7] state that the hydrolysis of the formic ester appears to be catalysed by salts of carboxylic acids and that in general it is to be recommended for the preparation of *p*-substituted phenacyl esters that equivalent amounts of reactants should be used and that the reaction time should be kept to a minimum. Procedures in many textbooks for the preparation of the derivatives, prescribe the use of about equal amounts (weight/weight) of the acid and the *p*-bromophenacyl bromide and consequently there will usually be an excess of the salt and this might cause hydrolysis of the ester formed.

However, we have found that by using an excess of the salt — two or three times the equivalent amount — a pure derivative was always obtained after recrystallisation. Furthermore, the refluxing period has been varied and again a pure derivative was isolated after recrystallisation even if the reaction mixture was refluxed for four hours. Certainly a hydrolysis occurs but the crude product can be purified. This hydrolysis can be observed for those derivatives which melt below the melting point of the *p*-bromophenacyl alcohol (143° C) as a derivative contaminated with the *p*-bromophenacyl alcohol only melts partially near the expected m. p. and on further heating it melts completely in the proximity of 143° C. The conclusion must be that in general it is advisable to keep the refluxing period below four hours.

An extensive hydrolysis of a derivative only occurs in carboxylic acids of which the esters are known to be highly sensitive to hydrolytic conditions; for example formic acid. Also in the preparation of the *p*-bromophenacyl oxalate some alcohol appears and has been isolated (see later).

It was also observed that in order to obtain a pure derivative it is essential that the reaction mixture should be adjusted to a pH of approximately 5 or below. At higher pH values the reaction mixture acquires a more intense yellow to red colour. The further addition of 10—15 drops of 0.5 N hydro-

chloric acid after the red colour of the indicator has disappeared is therefore suggested in the general procedure given in the experimental part.

The p-*bromophenacyl oxalate.* Mowry and Brode [9] have prepared the oxalate, the m. p. of which was 242° C (decomp.); this was determined by using a thermometer of the Anschütz type. However, it is very difficult to prepare this derivative according to Mowry and Brode and we have worked out a special procedure. Due to a decomposition the m. p. was found to be highly dependent on the time in which the substance is in the silicone bath before melting. By introducing the capillary tube into the bath at *ca.* 235° C, the m. p. is found to be 244—245° C (rate of heating: 1—2° C per minute). Determined on Kofler Heizbank the m. p. was 256° C ± 2° and no decomposition was observed when it melted; destruction occurred after some seconds.

The p-*bromophenacyl fumarate.* The melting point of this derivative is given in the textbook by Shriner and Fuson [10,p.225] as 197° C but is has not been possible to find it in the original literature or in other textbooks on organic analysis; only the phenacyl fumarate is found (m. p. 197° C) [11,p.80]. We have now prepared the fumarate by the general method, given later in the text, and the m. p. was found to be 256—257° C (decomp.). On Kofler Heizbank no decomposition of the melt was observed, and the m. p. was 266° C ± 2°.

Melting points and microanalysis of twenty *p*-bromophenacyl esters are given in Table 1.

Table 1. Corrected capillary melting points of p-*bromophenacyl esters.*

Acid	Melting point, °C	Formula	% C		% H	
			calc.	found	calc.	found
Formic	101	$C_9H_7BrO_3$	44.47	44.40	2.90	2.96
Vinylacetic	60.5	$C_{13}H_{11}BrO_3$	50.90	50.87	3.92	3.79
β,β-Dimethylacrylic	101	$C_{13}H_{13}BrO_3$	52.54	52.74	4.41	4.43
Oxalic	244—245 d	$C_{16}H_{12}Br_2O_6$	44.66	44.75	2.50	2.72
Fumaric	256—257 d	$C_{20}H_{14}Br_2O_6$	47.08	47.20	2.77	2.97
d-Camphoric	142.5	$C_{26}H_{26}Br_2O_6$	52.54	52.61	4.41	4.42
Diphenylacetic	112	$C_{22}H_{17}BrO_3$	64.56	64.75	4.19	4.21
3,4-Dichlorobenzoic	123	$C_{15}H_9BrCl_2O_3$	46.42	46.20	2.34	2.25
4-Bromophenylacetic	100.5	$C_{16}H_{12}Br_2O_3$	46.63	46.48	2.94	3.04
d,l-Mandelic	113	$C_{16}H_{13}BrO_4$	55.03	54.85	3.75	3.72
o-Cresotic	172	$C_{16}H_{13}BrO_4$	55.03	54.85	3.75	3.74
p-Cresotic	142	$C_{16}H_{13}BrO_4$	55.03	54.80	3.75	3.93
4-Ethoxybenzoic	141	$C_{17}H_{15}BrO_4$	56.21	56.20	4.16	4.26
Veratric	124	$C_{17}H_{15}BrO_5$	53.84	53.71	3.99	4.02
Piperonylic	165.5	$C_{16}H_{11}BrO_5$	52.91	52.78	3.05	3.23
2-Chlorophenoxyacetic	95.5	$C_{16}H_{12}BrClO_4$	50.09	50.00	3.15	3.32
4-Chloro-3,5-dinitrobenzoic	153	$C_{15}H_8BrClN_2O_7$	40.61	40.65	1.82	1.85
3-Nitrophthalic	166	$C_{24}H_{15}Br_2NO_8$	47.63	47.50	2.50	2.67
3,4,5-Trimethoxybenzoic	129	$C_{18}H_{17}BrO_6$	52.83	52.84	4.19	4.23
1-Naphthylacetic	112.5	$C_{20}H_{15}BrO_3$	62.68	62.72	3.95	3.99

EXPERIMENTAL PART *

The capillary melting points are determined in an electrically heated silicone bath with mechanical stirrer. The temperature at which the compound melts completely are registered. The thermometers used were of the Anschütz type calibrated in 0.1 of a degree. The results are corrected melting points to about 0.5° C. Rate of heating *ca.* 1° C/per minute; it is found that generally the melting points are almost independent of the rate of heating. The derivatives have been recrystallised to constant melting points.

Preparation of the *p*-bromophenacyl esters

The procedure used for the preparation of the esters given in Table 1, except the ester of formic acid and oxalic acid, is that given by Judefind and Reid [1] with some modifications. The detailed description is given below.

Procedure. An amount corresponding to 0.004 equivalents of the acid is dissolved in 5 ml of ethanol (by heating if necessary). The solution is neutralised with 2 N sodium hydroxide to phenolphthalein as indicator. To this solution is added 3 ml of water and 0.5 N hydrochloric acid to remove the red colour and then further 10—15 drops hydrochloric acid. It is important that the solution of the sodium salt is faintly acid in order to prevent the formation of coloured by-products in the subsequent reaction. 1 g of *p*-bromophenacyl bromide, 5 ml of ethanol and some porous plate are added and the solution is heated under reflux for one or two hours according to whether the acid is mono- or dibasic.

If the reaction mixture is not clear on heating to boiling, a little more ethanol is added (10—30 ml). After boiling for 5—10 minutes a precipitate sometimes is formed but the boiling is continued nevertheless.

The solution is immediately cooled under the tap; if an appreciable amount is not precipitated by cooling a little water is added. The ester is removed by suction and washed on the filter with a few ml of ethanol (*ca.* 50 %). Generally the yield of the crude product is 60—80 %, and this is satisfactory as the aim is purity rather than large yields.

The derivative is recrystallised from ethanol or from aqueous ethanol (*ca.* 50 %). Usually one or two recrystallisations are sufficient. If the ester is insoluble in ethanol, glacial acetic acid should be used.

The p-*bromophenacyl formate.* The procedure above is followed except that the refluxing period is reduced to 30 minutes. The crude product melts at *ca.* 90° C; it should be recrystallised one to three times from ethanol. The *p*-chloro- and the *p*-iodophenacyl formate can be prepared in the same way.

The p-*bromophenacyl oxalate.* The procedure above could not be used; after refluxing for two hours unreacted sodium oxalate and *p*-bromophenacyl bromide were the main products. Other solvents were tried (dioxan, methyl cellosolve and butyl cellosolve) and by using methyl cellosolve the preparation of the oxalate was successful. The method above is modified so that the oxalic acid is dissolved in 5 ml of methyl cellosolve and the solution is adjusted as above. 1 g of *p*-bromophenacyl bromide, 15 ml of methyl cellosolve and some porous plate are added and the reaction mixture is refluxed for only one hour. After cooling under the tap, the ester is removed by suction and washed on the filter with a little ethanol (50 %). A pure derivative usually is obtained; it can be recrystallised from glacial acetic acid (sparingly soluble).

The *p*-bromophenacyl oxalate is readily hydrolysed to the *p*-bromophenacyl alcohol. By varying the refluxing period it is found that the largest yield of the *p*-bromophenacyl oxalate was obtained by refluxing for about one hour (yield *ca.* 40 %). Also by heating for 30 minutes the oxalate was obtained in good yield but unreacted *p*-bromophenacyl bromide was recovered. By boiling for two hours the yield of the oxalate was about 30 % and the main product was the *p*-bromophenacyl alcohol; this was precipitated by addition of water to the filtrate (yield 50—60 %; m. p. 143° C Kofler Heizbank). When the reaction mixture was boiled for only one hour the filtrate did not give an immediate precipitation upon dilution with water.

* Microanalysis by Mr. W. Egger or Mr. P. Hansen, Department of Organic Chemistry, University of Copenhagen, Denmark.

The author is greatly indebted to the Head of the Department, Professor, Dr. H. Baggesgaard Rasmussen.

REFERENCES

1. Judefind, W. L. and Reid, E. E. *J. Am. Chem. Soc.* **42** (1920) 1043.
2. Moses, C. G. and Reid, E. E. *J. Am. Chem. Soc.* **54** (1932) 2101.
3. Hurd, C. D. and Christ, R. E. *J. Am. Chem. Soc.* **57** (1935) 2007.
4. Summerbell, R. K. and Bauer, L. N. *J. Am. Chem. Soc.* **57** (1935) 2366.
5. Kubota, T. and Matsuura, T. *J. Inst. Polytech. Osaka City Univ. Ser. C*, **1** (1950) 49.
6. Grove, J. F. and Suter, P. J. *J. Chem. Soc.* **1950** 3350.
7. Neish, A. C. and Lemieux, R. U. *Cand. J. Chem.* **30** (1952) 454.
8. Erickson, J. L. E., Dechary, J. M. and Kesling, M. R. *J. Am. Chem. Soc.* **73** (1951) 5301.
9. Mowry, D. T. and Brode, W. R. *J. Am. Chem. Soc.* **63** (1941) 2281.
10. Shriner, R. L. and Fuson, R. C. *The Systematic Identification of Organic Compounds*, 3rd Ed., John Wiley Sons, Inc., New York, 1948.
11. Rather, J. B. and Reid, E. E. *J. Am. Chem. Soc.* **41** (1919) 75.

Received February 7, 1956.

ACTA CHEMICA SCANDINAVICA 10 (1956) 643—646

Kinetics of the Splitting of Hyaluronic Acid by Streptococcal Hyaluronidase

JOHN GRAAE and C. E. JENSEN

Københavns Universitets Fysisk-kemiske Institut, Copenhagen, Denmark

The splitting of hyaluronic acid by streptococcal hyaluronidase was investigated viscometrically. This degradation can be described by either of the following two expressions:

$$Et = A(1/y-1) + B(1/y^3-1) \quad (1)$$
$$Et = C(e^{D/y}-e^{D}) \quad (2)$$

where y is a measure of the remaining viscosity, and E the total enzyme concentration. These expressions are of the same form as those previously found for the splitting of hyaluronic acid by a preparation of testicular enzyme. In the present case expression (2) by insertion of the experimental values yields a closer fit than expression (1), the constant D being 0.165.

The source of streptococcal hyaluronidase was a strain of group A hemolytic streptococcus type 24 (A. 24 N.W.).

The solution of enzyme was prepared by Dr. Viggo Faber, Statens serum-institut, Copenhagen, in the following way:

0.1 ml of an 18 hours culture was inocculated into 1 l of Todd-Hewitt substrate [1]. After incubation for 24 hours at 37°C the culture was centrifuged, the supernatant Seitz-filtered, and the pH adjusted to 6.0. The solution was stored at —20° C until use. This solution contains 25 turbidity-reducing units per ml as measured with a modification of the turbidity-reducing method described by Faber [2].

The experimental conditions of the kinetic investigations reported here were identical with those used by Andersen and Graae [3], with the only exception that the substrate concentration was lowered to 0.2 %.

The stability of the enzyme was checked as described by Andersen and Graae [3]. The result was that the enzyme was stable at 20 °C for more than 4 hours.

It was established that the time necessary to reach a given degree of reaction varies approximately inversely proportional to the enzyme concentration. A similar result was obtained by Hale [4], Madinaveitia and Quibell [5], and in this laboratory [3].

Table 1. a means degree of reaction; t_1, t_2 and t_3 times necessary to reach the given degree of reaction for three different enzyme concentrations. Times are determined by graphical interpolation from the measured figures indicated in Tables 2 and 3.

a	t_1 min	t_2 min	t_3 min	t_2/t_1	t_3/t_1	t_3/t_2
0.491	(4.7)	7.9	12.5	(1.68)	(2.65)	1.58
0.564	(6.3)	11.0	17.4	(1.75)	(2.76)	1.58
0.636	(8.9)	15.0	24.8	(1.69)	(2.79)	1.65
0.709	12.0	22.0	36.5	1.83	3.04	1.66
0.781	19.5	36.5	60	1.87	3.08	1.64
0.854	39.0	73.5	122	1.88	3.13	1.66

Mutually interdependent values of time and degree of reaction for three different enzyme concentrations, are recorded in Table 1. The figures given in parenthesis are estimated to be erroneous, because the time is determined under the wrong condition that a linear relationship exists between time and decrease in viscosity [3]. The constant value of the proportions seems to indicate that the chronometric integral is of the ordinary form $Et = f(y)$. The directly measured values are recorded in Table 2.

Table 2. The table gives the measured values of time and the difference Δ between the flow time for the solution and the flow time for water (45.0 sec.).

Expt. 1		Expt. 3	
t_1 min.	Δ flow time, sec.	t_3 min	Δ flow time, sec.
0	275	0	274
3.33	171	3.77	210
6.91	110	8.58	164
10.15	89	12.62	139
12.92	77	16.20	124
18.96	62	21.32	107
27.11	49.5	27.05	95
31.72	45.0	37.58	78.5
39.13	40.0	52.75	65.0
45.90	36.2	60.70	60.0
54.53	33.0	74.17	53.3
60.52	31.3	86.17	48.8
70.61	28.5	100.75	44.7
72.46	28.0	112.25	42.3
80.20	26.5	122.15	39.3
90.55	24.8	131.43	38.8
100.21	23.1	155.72	35.3
103.09	23.2	171.98	33.6
114.51	22.1	185.55	32.5
125.82	21.1	207.60	30.9
139.42	20.3	224.92	29.4
149.99	20.0	235.73	28.9
188.00	18.0	247.93	28.0
223.56	16.7	263.60	27.4

Table 3. The table indicates the measured values of time and Δ flow time for exp. No. 2. y is $\eta_{spc}/\eta^{\circ}_{spc}$ where η_{spc} is the specific viscosity at time t and η°_{spc} is the specific viscosity at zero time, and Δ_1 and Δ_2 is the difference between calculated and measured times for the chronometric integrals 1 and 2, respectively.

t min	Δ flow time sec	y	Δ_1	Δ_2
0	276	1	0	0
3.25	189	0.6848	0.13	0.29
7.65	137.5	0.4982	0.21	0.42
11.63	114.1	0.4134	0.05	0.10
14.92	100.0	0.3623	0.12	0.09
21.78	81.5	0.2953	0.01	−0.06
28.70	69.3	0.2511	0.18	−0.42
53.52	48.0	0.1739	0.29	−0.58
73.17	40.1	0.1453	−0.34	−0.20
86.15	36.6	0.1326	−1.14	0.24
98.80	34.0	0.1232	−2.53	0.64
114.17	33.0	0.1196	−12.89	−8.81
116.33	31.6	0.1145	−7.27	−1.47
117.10	31.0	0.1123	−4.36	2.33
144.08	28.1	0.1018	−10.69	2.16
173.28	25.9	0.0938	−19.71	1.24
211.97	24.0	0.0870	−37.03	−5.17
244.78	22.6	0.0819	−50.46	−6.49
255.07	22.0	0.0797	−51.24	−0.60
1 181	13.7	0.0496	−707	−175

As will be seen from Table 3, the two expressions earlier found [3], fit in this case too. These were

$$Et = A(1/y - 1) + B(1/y^2 - 1) \quad (1)$$

and

$$Et = C(e^{D/y} - e^{D}) \quad (2)$$

In the experiment calculated in Table 2 the values of the constants are: A = 5.05, B = 0.93, C = 37.71 and D = 0.165. It is obvious from these experiments that expression (2) is the best one. It should be noticed that it could be expected that the constant D only depends of the nature of the enzyme and neither of enzyme nor substrate concentration.

The amount of reducing sugar liberated from a given substrate is much greater with pneumococcal hyaluronidase than with testicular hyaluronidase as enzyme [6]. Other bacterial hyaluronidases, especially streptococcal enzymes, show a similar behaviour, *cf.* Rapport, Linker and Meyer [6].

The fact that chronometric integrals of the same form fit both testicular and streptococcal hyaluronidases strongly suggests that the pathways of the reactions are the same. However, in a viscometric investigation it is impossible to distinguish between a reaction resulting in a disaccharide as endproduct and one resulting in other oligosaccharides as endproducts. Therefore the experimental results reported here do not necessarily contrast those obtained by Rapport *et al.*[6]

We wish to thank professor J. A. Christiansen for his interest and help in this investigation.

REFERENCES

1. Todd, E. W. and Hewitt, L. F. *J. Pathol. Bacteriol* **35** (1932) 973.
2. Faber, V. *Acta Pathol. Microbiol. Scand.* **31** (1952) 345.
3. Andersen, S. O. and Graae, J. *Acta Chem. Scand.* **9** (1955) 1431.
4. Hale, C. W. *Biochem. J. London* **38** (1944) 368.
5. Madinaveitia, J. and Quibell, T. H. H. *Biochem. J. London* **34** (1940) 625.
6. Rapport, M. M., Linker, A. and Meyer, K. *J. Biol. Chem.* **192** (1951) 283.

Received January 26, 1956.

ACTA CHEMICA SCANDINAVICA 10 (1956) 647—654

Dihydrofurocoumarins

Synthesis of some Long Chain 4-*n*-Alkyl Substituted Dihydroxanthotoxins, 4-Phenyl-dihydroxanthotoxin and Methyl 8-(Dihydroxanthotoxin-4)-*n*-octanoate

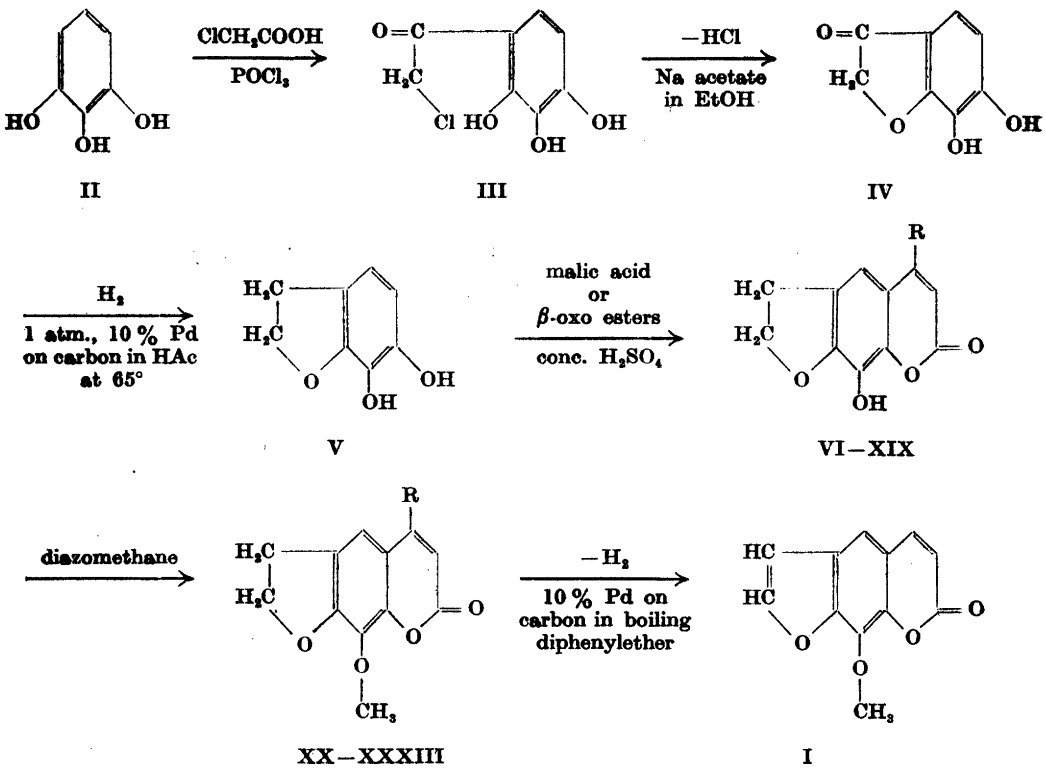
CARL LAGERCRANTZ

Institute of Medical Chemistry, University of Uppsala, Sweden

A number of long chain 4-*n*-alkyl substituted dihydroxanthotoxols and dihydroxanthotoxins have been synthesized together with some other substituted dihydroxanthotoxols and dihydroxanthotoxins. Xanthotoxin has been prepared by a modification of the method described by Späth and Pailer [4].

Since old times in Egypt a drug obtained from the plant *Ammi majus* L. has been used as treatment for *leucoderma idiopathicum*. The active principle of this drug was crystallized by Fahmy and Abushady [1] and was shown by Schönberg and Sina [2] to be identical with the methoxyfurocoumarin xanthotoxin (I) previously isolated by Thoms [3] from the fruits of *Fagara xanthoxyloides*. The total synthesis of xanthotoxin was performed by Späth and Pailer [4].

For the knowledge of the etiology of *leucoderma idiopathicum*, it would seem important to study the effect of furocoumarins and related compounds on the pigment metabolism. In this connection a number of new derivatives of dihydroxanthotoxin has been prepared. This report describes the synthesis of some 4-alkyl substituted dihydroxanthotoxols and dihydroxanthotoxins, 4-phenyl-dihydroxanthotoxol and 4-phenyl-dihydroxanthotoxin and methyl 8-(dihydroxanthotoxin-4)-*n*-octanoate. Xanthotoxin was prepared according to Späth and Pailer [4] with some minor modifications of the original method. The accompanying chart shows the route by which the synthesis of xanthotoxin and the derivatives of dihydroxanthotoxin were carried out.



In this chart R is equal to: VI and XX = H, VII and XXI = methyl, VIII and XXII = ethyl, IX and XXIII = *n*-pentyl, X and XXIV = *n*-hexyl, XI and XXV = *n*-heptyl, XII and XXVI = *n*-octyl, XIII and XXVII = *n*-nonyl, XIV and XXVIII = *n*-hendecyl, XV and XXIX = *n*-tridecyl, XVI and XXX = *n*-pentadecyl, XVII and XXXI = *n*-heneicosyl, XVIII and XXXII = phenyl, XIX and XXXIII = *n*-heptyl-7-methoxycarbonyl.

Späth and Pailer [4] carried out the conversion of 6,7-dihydroxy-coumaran-3-one (IV) to the corresponding 6,7-dihydroxy-coumaran (V) by low pressure hydrogenation at elevated temperature using a palladium on carbon catalyst. The calculated amount of hydrogen was absorbed, but the yield of (V) was only about one third of the theoretical one, indicating that other reactions than conversion of the carbonyl group to a methylene group took place. Attempting to convert 6-hydroxy-coumaran-3-one to 6-hydroxy-coumaran, Horning and Reisner [5] completely failed to isolate the desired product, and they noted that an excess of about 40 % hydrogen was absorbed in the reaction. After acetylation of the free hydroxy group, however, 6-acetoxy-coumaran was obtained in nearly quantitative yield, indicating that the free hydroxy group is involved in these side reactions. However, reduction of the carbonyl group

of hydroxy-coumaran-3-ones and their acetoxy derivatives is perhaps still more complex. Davies and Deegan [6] have shown that acetylation of 6,7-dihydroxy-coumaran-3-one (IV) with acetyl chloride in ethyl acetate solution gives two different products, *i. e.* 6,7-diacetoxy-coumaran-3-one and 3,6,7-triacetoxy-coumarone. The last compound was successfully hydrogenated to give 6,7-diacetoxy-coumaran. Thus, in this case acetylation involves an enolization on the carbonyl group with introduction of a double bond in the heterocyclic ring prior to the hydrogenation reaction. Similar conditions seem to be valid for the acetylated product of 6-hydroxy-coumaran (Davies *et al.*[7]).

When converting 6,7-dihydroxy-coumaran-3-one (IV) to 6,7-dihydroxy-coumaran (V), the overall yield appears to be about the same, either direct hydrogenation is used, or the route is followed which includes acetylation of IV, hydrogenation of the acetylated product and finally deacetylation of the hydrogenated compound. Consequently, the present author preferred to carry out the reaction in one step. In order to avoid poisoning of the catalyst, it is essential that the 6,7-dihydroxy-coumaran-3-one is very pure (recrystallization several times with active carbon), and that efficient stirring is employed when dissolving the substance in the acetic acid used as solvent in the hydrogenation reaction. With these precautions fulfilled, the theoretical amount of hydrogen is rapidly absorbed on hydrogenation at 65° and one atmosphere pressure with 10 % palladium on carbon as catalyst. Very constant yields are obtained, which are somewhat higher than those reported by Späth and Pailer [4].

The condensation of 6,7-dihydroxy-coumaran with malic acid in the presence of concentrated sulphuric acid at 114° gives dihydroxanthotoxol (VI). In this reaction the present author obtained a yield of about 38 % of the theoretical in good agreement with the result reported by Späth and Pailer [4]. In this connection it may be remarked that condensation of phenols with malic acid generally gives lower yields than those obtained when condensating the same phenols with a β-oxo ester as ethyl acetoacetate (*cf.* Sethna and Phadke[8]). Horning and Reisner [5] got pure dihydropsoralene only in a yield of 11 % condensing 6-hydroxy-coumaran with malic acid.

Condensation of phenols with β-oxo esters in the presence of sulphuric acid almost always produces coumarins (*cf.* Sethna and Phadke [8]) and consequently γ-substituted β-oxo esters form coumarins substituted in position 4. Long chain β-oxo esters do not seem to have been used for such condensation to any large extent. The reactivity of the β-oxo esters is generally assumed to decrease with increasing length of the carbon chain. When condensing 6,7-dihydroxy-coumaran (V) with a number of β-oxo esters, which have straight chains of a length varying from four to twenty-four carbon atoms, however, 4-*n*-alkyl substituted dihydroxanthotoxols (VII—XVII) were obtained as crystalline products in rather good yields. The condensation between 6,7-dihydroxy-coumaran and the higher β-oxo esters were generally carried out as follows. After dissolving the phenol and the β-oxo ester in each other by heating, the solution was slowly poured into concentrated sulphuric acid and the mixture was kept at room temperature for three to five days before the product was isolated. Condensing methyl 3-oxo-hendecane-1, 11-dioate with 6,7-dihydroxy-coumaran yielded 8-(dihydroxanthotoxol-4)-*n*-octanoic

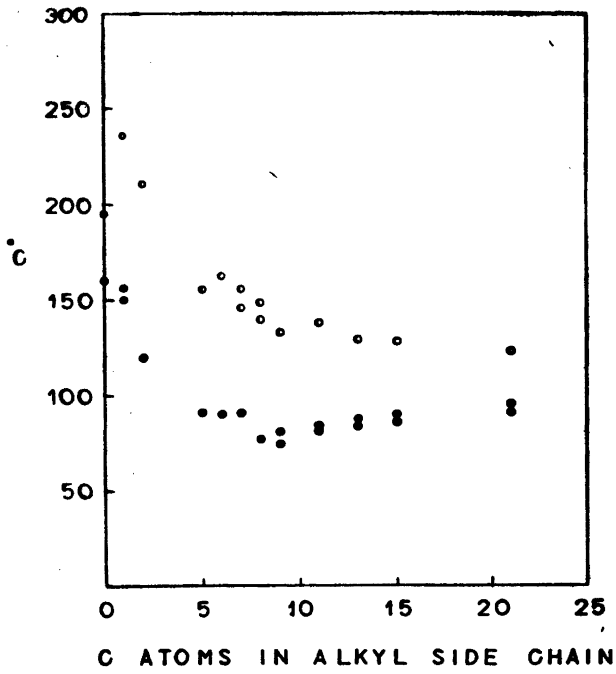


Fig. 1. Melting points of 4-n-alkyl substituted dihydroxanthotoxols, O, and 4-n-alkyl substituted dihydroxanthotoxins, ●, as a function of the number of carbon atoms in the side chain.

acid together with the corresponding methyl ester (XVIII) due to partial hydrolysis during the condensing reaction.

Methylation of the phenolic hydroxy group with diazomethane converted the dihydroxanthotoxols to the corresponding dihydroxanthotoxins (XX—XXXIII). Many of the alkyl substituted dihydroxanthotoxols and dihydroxanthotoxins are dimorphous and possess two melting points. Fig. 1 gives the melting points of these substances as a function of the number of carbon atoms in the alkyl side chain. The melting points of the alkyl substituted dihydroxanthotoxols are generally much higher than the corresponding dihydroxanthotoxins and decrease with increasing length of the side chain. An increase of the alkyl side chain of the dihydroxanthotoxins to about eight carbons continously depresses the melting points. With further lengthening of the side chain the melting points are slowly raised in a rather regular manner.

The last step in the preparation of xanthotoxin involves a dehydrogenation of the dihydrofuran ring. By heating a mixture of dihydroxanthotoxin and a palladium catalyst at 170° Späth and Pailer [4] carried out this reaction with a yield of about 10 % of the theoretical one. Horning and Reisner [9] successfully dehydrogenated dihydropsoralene (2′,3′-dihydrofurocoumarin) to psoralene with a yield of about 50 % by refluxing the substance during four hours together with a 5 % palladium on carbon catalyst in a high boiling medium,

viz. diphenyl ether (b. p. 259°). By employing this technique, the present author could dehydrogenate dihydroxanthotoxin to xanthotoxin in a yield of 37 % of the theoretical. An attempt to dehydrogenate 4-methyl-dihydroxanthotoxin (XXI) with the same technique was unsuccessful. The corresponding xanthotoxin could not be isolated and the starting material had almost completely decomposed. When mesitylene (b. p. 165°) was used as an indifferent medium, only an almost quantitative recovery of 4-methyl-dihydroxanthotoxin was obtained.

EXPERIMENTAL *

6,7-Dihydroxy-coumaran-3-one (IV) was prepared by the method of Davies and Deegan [9]. In the reaction leading to ω-chloro-gallacetophenone (III), a minimum of tarry products was obtained when the temperature was kept below 61° (Davies and Deegan give 60—70°). The overall yield of 6,7-dihydroxy-coumaran-3-one crystallized twice (charcoal) from water was about 16 % of the theoretical calculated on the pyrogallol used.

6,7-Dihydroxy-coumaran (V). 6,7-Dihydroxy-coumaran-3-one (36 g) was dissolved in hot acetic acid (850 ml) with careful stirring. The yellow solution was transferred to a hydrogenation vessel previously filled with hydrogen and containing 15 g 10 % palladium on carbon (*Organic Syntheses*, Vol. 26, method D). The vessel, which was placed in a large flask shaker, was equipped with a jacket through which water maintained at 65° was circulated from a thermostat. The gas burette and other devices for supply of hydrogen gas were of a construction similar to those described by Parrette [10]. The theoretical amount of hydrogen was absorbed in about two hours, but in some runs it was necessary to add more catalyst in order to complete the reaction. After removal of the catalyst and evaporation of the acetic acid, the residue (a brown oil) was distilled at 125—132° at 0.05 mm pressure to give a nearly colourless oil (25 g) that immediately solidified on cooling. This material was redistilled to give a colourless substance (24 g) that was further purified by crystallization from a mixture of light petroleum (b. p. 20—40°) and benzene (1:1 by volume) as follows. The finely powdered substance was extracted with 500 ml light petroleum-benzene by refluxing with stirring for 15 minutes. The liquid was decanted off and discarded. The remaining amount of substance was dissolved in about 3 000 ml light petroleum-benzene. After being kept at —8° overnight, 6,7-dihydroxy-coumaran (16.8 g) crystallized as long beautiful needles. Melting point 112° (Kofler "Heizbank"). The yield was about 50 % of the theoretical.

Dihydroxanthotoxol (VI) (*cf.* Späth and Pailer [4]). A mixture of 6,7-dihydroxy-coumaran (5 g), malic acid (5 g), and concentrated sulphuric acid (25 ml) was kept at 114° in an oil bath with constant stirring until foaming stopped (about 7 minutes). After cooling the mixture was poured with stirring into 250 ml of cold water to give a dark tarry product suspended in the aqueous layer. After extraction with eight 100 ml portions of chloroform, the combined organic solutions were dried over anhydrous sodium sulphate and the solvent evaporated to yield 3.5 g of a yellow powder. Crystallization from water (charcoal) gave 2.3 g (38 % of the theoretical) of slightly yellow long beautiful needles. The melting point was 195° (Kofler "Heizbank", odour of coumarin) and could not be raised after sublimation *in vacuo*. Späth and Pailer [4] reported a melting point of 202°.

4-n-Alkyl-dihydroxanthotoxols (VII—XVII) and 4-phenyl-dihydroxanthotoxol (XVIII). 6,7-Dihydroxy-coumaran was condensed with a number of β-oxo esters in the presence of concentrated sulphuric acid. The data of these preparations are collected in Table 1. Generally the condensation was performed as follows.

* If not otherwise stated, the melting points up to about 200 °C recorded in this paper were taken in sealed capillary tubes using calibrated Anschütz type thermometers completely immersed in a well stirred bath of silicon oil (DC 710 Fluid, Dow Corning Co.). The heating was carried out very slowly (1° per 3 minutes). The melting points over 200 °C were taken by use of a Kofler type hot stage microscope.

Table 1. Dihydroxanthotoxols substituted in position 4.

β-Oxo ester condensed with 6,7-dihydroxy-coumaran	Time of reaction h = hours d = days	Substituent	No.	Yield %	Empirical formula	Composition, %				Melting point °C	
						Calc.		Found			
						C	H	C	H		
Ethyl 3-oxo-butanoate	1 h	4-methyl-	VII	43	$C_{13}H_{10}O_4,H_2O$*	61.01	5.12	60.96	5.13	236	—237
Ethyl 3-oxo-pentanoate	1 h	4-ethyl-	VIII	44	$C_{13}H_{12}O_4$	67.23	5.21	67.07	5.30	210	—212
Methyl 3-oxo-octanoate	1 h	4-*n*-pentyl-	IX	44	$C_{16}H_{18}O_4$	70.05	6.61	69.89	6.57	155.7	—157.0
Methyl 3-oxo-nonanoate	1 h	4-*n*-hexyl-	X	66	$C_{17}H_{20}O_4$	70.81	6.99	70.83	6.55	162.0	—163.3
Methyl 3-oxo-decanoate	1 h	4-*n*-heptyl-	XI	54	$C_{18}H_{22}O_4$	71.50	7.33	71.50	7.40	145.7 156.2	—147.2 —157.3
Methyl 3-oxo-hendecanoate	2 h	4-*n*-octyl-	XII	51	$C_{19}H_{24}O_4$	72.12	7.65	72.34	7.69	139.6 148.6	—140.6 —149.6
Methyl 3-oxo-dodecanoate	3 d	4-*n*-nonyl-	XIII	32	$C_{20}H_{26}O_4$	72.70	7.93	72.93	7.97	132.2	—134.2
Methyl 3-oxo-tetradecanoate	3 d	4-*n*-hendecyl-	XIV	27	$C_{22}H_{30}O_4$	73.71	8.44	73.44	8.47	138.2	—138.8
Methyl 3-oxo-hexadecanoate	3 d	4-*n*-tridecyl-	XV	33	$C_{24}H_{34}O_4$	74.57	8.87	75.11	8.85	128.6	—130.0
Methyl 3-oxo-octadecanoate	5 d	4-*n*-pentadecyl	XVI	18	$C_{26}H_{38}O_4$	75.32	9.24	75.21	9.38	127.2	—128.4
Methyl 3-oxo-tetracosanoate	5 d	4-*n*-heneicosyl-	XVII	11	$C_{32}H_{50}O_4$	77.06	10.11	77.26	10.51	123.7	—124.5
Ethyl 3-oxo-3-phenyl-propionate	1 h	4-phenyl-	XVIII	29	$C_{17}H_{18}O_4$	72.85	4.32	73.13	4.39	245.5	—247.0

* When crystallized from aqueous methanol, one mole of substance VII contains one mole of water that could be quantitatively removed after drying overnight at 120°.

A mixture of 6,7-dihydroxy-coumaran and an excess (10—20 %) of the β-oxo ester was dissolved by heating. The solution was poured into concentrated sulphuric acid with constant stirring. The mixture was kept standing at room temperature for one hour to five days (see Table 1) and was then slowly poured with stirring into ice water. The precipitate formed was collected and suspended in water. The excess of ester was removed by steam distillation. The material collected was recrystallized several times from acetone and from methanol (charcoal).

Table 2. Dihydroxanthotoxins substituted in position 4.

Compound	No.	Empirical formula	Composition, %				Melting point °C
			Calc.		Found		
			C	H	C	H	
4-Methyl-dihydroxanthotoxin	XXI	$C_{13}H_{12}O_4$	67.23	5.21	67.44	5.35	149.5—151.2 156.2—157.1
4-Ethyl- »	XXII	$C_{14}H_{14}O_4$	68.26	5.73	68.44	5.79	119.6—121.4
4-*n*-Pentyl- »	XXIII	$C_{17}H_{20}O_4$	70.81	6.99	70.73	7.06	90.2— 91.6
4-*n*-Hexyl- »	XXIV	$C_{18}H_{22}O_4$	71.50	7.33	71.22	7.44	90.3— 91.9
4-*n*-Heptyl- »	XXV	$C_{19}H_{24}O_4$	72.12	7.65	72.21	7.71	91.2— 92.6
4-*n*-Octyl- »	XXVI	$C_{20}H_{26}O_4$	72.70	7.93	72.66	7.91	75.6— 78.1
4-*n*-Nonyl- »	XXVII	$C_{21}H_{28}O_4$	73.20	8.19	73.55	8.20	74.0— 75.0 80.4— 81.9
4-*n*-Hendecyl- »	XXVIII	$C_{23}H_{32}O_4$	74.16	8.66	74.34	8.71	80.6— 81.5 83.8— 84.7
4-*n*-Tridecyl- »	XXIX	$C_{25}H_{36}O_4$	74.96	9.06	74.88	9.07	83.6— 84.5 87.4— 88.8
4-*n*-Pentadecyl- »	XXX	$C_{27}H_{40}O_4$	75.66	9.41	75.68	9.52	86.5— 86.9 89.6— 89.9
4-*n*-Heneicosyl- »	XXXI	$C_{33}H_{52}O_4$	77.29	10.22	77.04	10.44	91.2— 92.3 95.1— 96.4
4-Phenyl- »	XXXII	$C_{18}H_{14}O_4$	73.46	4.80	73.60	4.93	198 —199
Methyl 8-(dihydroxanthotoxin-4)-*n*-octanoate	XXXIII	$C_{21}H_{26}O_6$	67.36	7.00	67.42	7.06	71.8— 73.2 76.6— 77.8

Ethyl 3-oxo-pentanoate was prepared as described by Brändström [11]. The higher β-oxo esters were those prepared by Mrs. Ställberg-Stenhagen (Ställberg-Stenhagen [12]).

Methyl 8-(dihydroxanthotoxol-4)-n-octanoate (XIX). 6,7-Dihydroxycoumaran (5 g) was dissolved by heating in methyl 3-oxo-hendecane-1,11-dioate (10 g, prepared by the author as described by Ställberg-Stenhagen [12]) and was poured with stirring into 25 ml of concentrated sulphuric acid. The reaction mixture was kept at room temperature for three days. Proceeding as usual gave 3.65 g (about 30 % of the theoretical) of a crystalline material melting between 80 and 95° (recrystallized once from acetone, twice from methanol, charcoal). This substance is most likely a mixture of the ester and the corresponding free acid. No attempts were made to separate the substances.

Derivatives of dihydroxanthotoxin. The 4-substituted dihydroxanthotoxols were converted to the corresponding dihydroxanthotoxins by methylation with diazomethane in a mixture of methanol and ether (1:1 by volume). The solutions were chilled to about +15° before an excess of cold solution (−5°) of diazomethane in ether was added. The reaction mixtures were kept at room temperature overnight. After evaporating the solvent, the methylated products were recrystallized from methanol. The yields were in general between 70 and 85 % of the theoretical. The analytical figures and the melting points of these substances are collected in Table 2. After methylation the mixture of free acid and ester (XIX) was converted to a homogeneous substance, methyl 8-(dihydroxanthotoxin-4)-*n*-octanoate of m. p. 71.8—73.2° and 76.6—77.8° (for analytical figures see Table 2 XXXIII).

Xanthotoxin (I) (*cf.* Späth and Pailer [4]). A mixture of dihydroxanthotoxin (XX) (0.165 g) (m. p. 160.4—161.2°, obtained by methylating VI), 10 % palladium on carbon catalyst (0.165 g), and diphenyl ether (11 g) was heated under reflux for four hours. The catalyst was removed by filtration and washed with hot diphenyl ether (20 g). After removing the diphenyl ether with steam distillation, the hot aqueous solution was filtered. Crystalline xanthotoxin was obtained from the chilled solution as slightly yellow needles. Recrystallization from methanol (charcoal) yielded 0.061 g (37 % of the theoretical) of colourless needles of m. p. 145.7—146.2° in good agreement with that given by Späth and Pailer [4] (146°).

4-Methyl-xanthotoxin. 4-Methyl-dihydroxanthotoxin (XXI) (0.3 g), 10 % palladium on carbon catalyst (0.3 g), and diphenyl ether (17 g) were heated under reflux with mechanical stirring for four hours. Proceeding as just described only 0.08 g of a substance could be isolated that was identical with the starting material. When the same procedure was performed with mesitylene as an indifferent solvent, only a nearly quantitative yield of the starting material was obtained.

Acknowledgements. The author is very much indebted to Mrs. Stina Ställberg-Stenhagen and Professor Einar Stenhagen for the long chain β-oxo esters used in the synthesis described, and to Miss Ulla-Britt Dahlberg in the microanalytical laboratory of this institute for the analyses.

The author would like to thank Notarie S. Haeger and *Statens Medicinska Forskningsråd* for financial support.

REFERENCES

1. Fahmy, I. R. and Abushady, H. *Quart. J. Pharm. and Pharmacol.* **20** (1947) 281.
2. Schönberg, A. and Sina, A. *Nature* **161** (1948) 481.
3. Thoms, H. *Ber.* **44** (1911) 3325.
4. Späth, E. and Pailer, M. *Ber.* **69** (1936) 767.
5. Horning, E. C. and Reisner, D. B. *J. Am. Chem. Soc.* **70** (1948) 3619.
6. Davies, J. S. H. and Deegan, T. *J. Chem. Soc.* **1950** 3202.
7. Davies, J. S. H., Mc Crea, P. A., Norris, W. L. and Ramage, G. R. *J. Chem. Soc.* **1950** 3206.
8. Sethna, S. and Phadke, R. *Org. Reactions* **7** (1953) 1—58.
9. Horning, E. C. and Reisner, D. B. *J. Am. Chem. Soc.* **72** (1950) 1514.
10. Parrette, R. *Anal. Chem.* **26** (1954) 237.
11. Brändström, A. *Acta Chem. Scand.* **5** (1951) 820.
12. Ställberg-Stenhagen, S. *Arkiv Kemi, Mineral. Geol.* **A 20** (1945) No. 19.

Received January 28, 1956.

ACTA CHEMICA SCANDINAVICA 10 (1956) 655—666

The Isotopic Exchange between Hydrogen and Water on Platinum. Relative Rates of Exchange of Isotopic Hydrogen Molecules

KÅRE HANNERZ

Department of Physical Chemistry, Royal Institute of Technology, Stockholm, Sweden

The isotopic exchange between deuterium- and tritiumcontaining hydrogen and ordinary water vapor on platinum has been investigated using mass spectrometric and radiotracer techniques. A certain amount of HD is formed when D_2 exchanges with deuterium-free water vapor. The rate of HD formation shows that the exchange cannot be due to the interaction of a D_2 molecule, from the gas phase or from the van der Waals layer, with a chemisorbed hydrogen atom or hydroxyl radical. It is necessary to assume that both the hydrogen molecule and the water undergo a dissociative chemisorption on the surface. The ratio of the rates of chemisorption of HD and D_2 has approximately the value given by the simple collision theory for a reaction without activation energy. This points to the possibility that hydrogen is chemisorbed without activation energy on bare dual sites on the surface, formed by the desorption of water or hydrogen.

The isotopic exchange between water and hydrogen has been studied by a large number of investigators. Most of the work has been done with liquid water with a view to elucidating the phenomena involved in the electrolytic discharge of molecular hydrogen. During the war, the exchange reaction between water vapor and hydrogen acquired technical importance as the basis for a method of producing heavy water. The mechanism of the exchange reaction was extensively studied by Farkas in the middle of the thirties [1,2]. From a comparison of the rates of the exchange reaction and the *para-ortho*-hydrogen conversion, Farkas concluded that the exchange must involve a dissociative chemisorption of the hydrogen as atoms. Later, doubts were cast on the correctness of this mechanism, based mainly on the high heats of chemisorption of hydrogen on clean metal surfaces, which seemed to preclude the occurrence of desorption near room temperature. Eley suggested a mechanism where the interaction of a hydrogen molecule from the gas phase or the van der Waals layer with a chemisorbed hydroxyl or hydrogen atom was responsible for the exchange [3]. Recently, the validity of the early measurements of the heat of adsorption of hydrogen on clean metal surfaces has been questioned,

and Rideal and Trapnell have been able to show that the heat of adsorption on tungsten falls to quite low values at full coverage of the surface, in contradiction to previous results [4]. Recent considerations of the effect of the electric double layer formed in chemisorption predict a large variation in heat of adsorption with coverage to be quite common, independent of any neighbour interactions [5]. These new findings make the arguments against Farkas's original mechanism appear less serious.

In the early work with deuterium exchange, heat conductivity measurements were generally used for the determination of deuterium. Since then, the mass spectrometer has become generally available. With it, much more detailed and accurate information about the composition of the hydrogen can be obtained than was possible before. The discovery of the radioactive tritium provides another important tool for investigations of this kind.

With these new experimental resources at hand, an investigation of the exchange reaction has been made in an attempt to test the correctness of the different mechanisms proposed. The rate of the tritium exchange has been used as a measure of the activity of the catalyst, thereby making it unnecessary to assume that the activity of the catalyst is unchanged between successive experiments. In this way the ratio of the exchange rates of D_2 and HD has been obtained, and this in turn makes possible a determination of the amount of HD formed when D_2 exchanges with an excess of light water. As shown below this provides important information about the mechanism of the exchange.

EXPERIMENTAL

Reaction apparatus

The exchange reaction was studied in a static system. To eliminate any influence of diffusion on the reaction rate the reacting gas was circulated over the catalyst. The apparatus is shown in Fig. 1. It contains about 50 ml of specially purified water and has a total volume of about 2 l. During an experiment, most of the water is at A in the figure. From A, the water flows through a capillary constriction to a heated piece of asbestos at B, where it is evaporated without risk for explosive boiling. The vapor passes to the jet at C, which it leaves with a high velocity, thus circulating the gas in the rest of the apparatus. Thermostated water circulates through the condensers. Most of the excess water vapor is condensed on the downward path of the gas and only a little in the lower part of the upward condenser. In the upper part of the latter, there is a constriction. Any water condensing above this constriction would have therefore been visible. The fact that no water was observed shows that the water vapor pressure of the gas, when it left the condensers, was the equilibrium pressure corresponding to the temperature of the water circulating through the condensers. After leaving the condensers, the gas enters the bulb D, which constitutes most of the volume of the reaction apparatus. It is inserted in a thermostat set at a temperature higher than that of the gas circulating through the condensers. On its way out from the bulb the gas comes into contact with the platinized platinum catalyst at E. A thermocouple inside the glass tube carrying the catalyst indicates the temperature at which the exchange reaction takes place. The stopcock F and the ground joint G are lubricated with apiezon L high vacuum grease which is considered to have an immeasurably low vapor pressure at room temperature. Before being installed, the reaction apparatus was heated in oxygen in an oven to 550 °C to burn out any organic impurities. The efficiency of the gas circulation was checked by cooling at E when the apparatus was running with about equal pressures of hydrogen and water vapor. A very rapid condensation took place and continued as long as the cooling was applied. This could not have been due to diffusion of water vapor through the hydrogen, but showed that the circulation in the apparatus was very efficient.

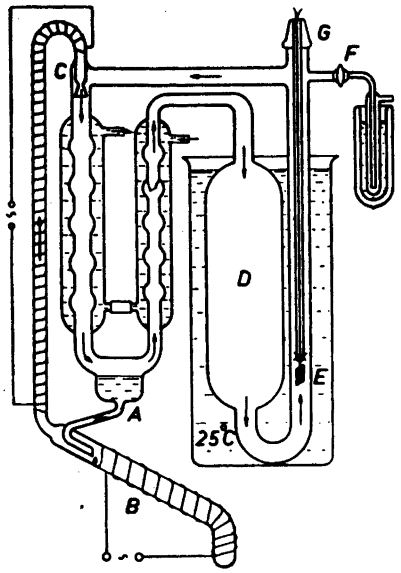


Fig. 1. Reaction apparatus. A: About 50 ml light water. B: Heated asbestos fabric. C: Jet nozzle. D: 1.5 l bulb. E: Platinized platinum catalyst and thermocouple. F: Stopcock. G: Ground joint.

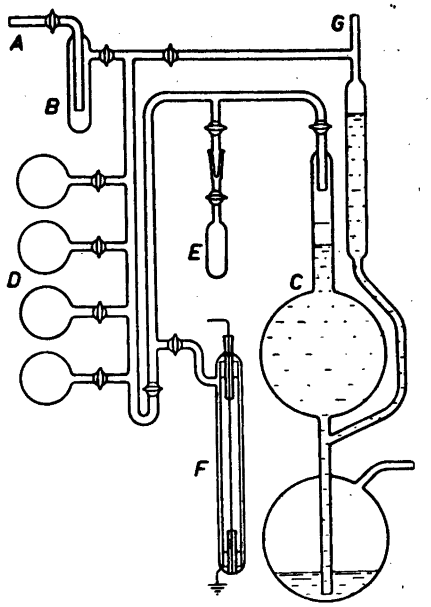


Fig. 2. Gas analysis section. A: From reaction apparatus. B: Liquid air trap. C: Toepler pump. D: Sample storage bulbs. E: Ampoule for masspectrometric deuterium determination. F: Proportional counter. G: To vacuum.

Materials

The catalyst consisted of a piece of platinum foil, 20 × 10 × 0.05 mm, platinized by 60 mA, 2—3 min. After platinizing, the foil was purified using cathodically evolved hydrogen in a dilute sulfuric acid bath, carefully rinsed with distilled water and kept in doubly distilled water overnight before use.

The water used for the exchange experiments was purified by double distillation, and finally the vapor was passed through a quartz tube kept at 800° C to destroy any volatile organic impurities.

Commercial cylinder hydrogen was used and purified before use by passing through a pyrex tube filled with platinized asbestos at 500 °C and a liquid air trap.

Deuterium was prepared by electrolysis of 99.6 % heavy water and purified as the hydrogen above. Deuterium was circulated over the platinized asbestos for three hours before the gas from the electrolysis cell was sent to the deuterium storage bulb.

Tritium, about 0.1 mC as hydrogen gas, was obtained from A.E.R.E., Harwell, England.

Determination of deuterium

Deuterium was determined in a 90°, Nier type mass spectrometer. The pressure before the leak was kept constant during all analyses. The spectrometer was calibrated with gas samples of known composition. These were prepared by diluting deuterium gas from the storage bulb with hydrogen. An aliquot of the gas was analyzed in the mass spectrometer and another part burned in dry oxygen and the deuterium content in the resulting water

determined by means of the gradient-tube method. In this way a calibration for D_2 was obtained. Still another part of the gas mixture was equilibrated over a glowing platinum wire, previously outgassed by prolonged heating in a high vacuum, and then analyzed in the spectrometer. This gave a calibration curve for HD. There was very little mass 2 background in the spectrometer, and background on masses 3 and 4 from previous samples was never observed. In the range of HD and D_2 percentages used it was found that peak heights and percentages were always proportional within experimental errors, when the 2 peak was corrected for background, so that there was no fractionation in the spectrometer. The percentage of HD and D_2 was consequently obtained directly from the peak heights on the recorder diagram. When the HD content of a sample was below 0.5 %, the value obtained was discarded and not used in the calculation of the reaction rate constant, since the spectrometer was not calibrated below this percentage. The standard deviation obtained when making repeated measurements on several samples taken from the same storage bulk was 3 % of the measured HD or D_2 percentage.

Determination of tritium

Tritium analyses were made in a proportional counter. The counter consisted of a 20 mm diam. copper tube, enclosed in a pyrex tube. The anode was a 0.05 mm tungsten wire. It hung freely and was stretched by a 20 g weight at the lower end, and could thus easily be removed. The distance between the sleeves, *i. e.* the active length of the wire, was 25 cm. The total volume of the counter was 200 ml. The high voltage was supplied by an EKCO power unit type 1033/7. The pulses were amplified in an EKCO amplifier type 1008 and counted with an EKCO scaler type 1009 A. The counter had a plateau with a slope of 4 % per 100 volt between 1 900 and 2 100 volt. When measurements were made, the sample gas was first allowed to expand into the previously evacuated counter. Ordinary hydrogen was then added to a total pressure of 40 mm Hg. Finally, methane was added to a total pressure of 200 mm Hg. The counter was left for 15 min. to allow the gases to mix completely. Counting was made at 4 to 5 different voltages with each sample. The precision of the method was tested by counting ten different mixtures of a gas of known activity and ordinary hydrogen. These samples underwent exactly the same treatment as the samples taken during exchange experiments. The standard deviation of the activity of the original T-containing gas was obtained as 3 % of the mean value. The counter did not show any detectable memory effects. After some use, the plateau became steeper and narrower, probably as a result of the deposition of hydrocarbon residues from the methane on the anode, caused by the discharges [6]. Replacement of the anode wire restored the original plateau.

Procedure

Before each experiment, the whole apparatus was evacuated by means of a mercury diffusion pump to less than 10^{-5} mm Hg. The water in the reaction apparatus was frozen in a solid CO_2 bath during the evacuation.

The stopcock leading to the reaction apparatus was closed, and the water heated and distilled to position A (Fig. 1). A constant flow of water passed through the capillary and entered the heated zone, where it was evaporated. When the vapor jet circulation was working, the predetermined mixture of tritium, deuterium and hydrogen was admitted *via* a liquid air trap. The mixing of the gases was performed in a special bulb and if desired the mixture could be equilibrated over a glowing platinum filament. After admission of the gas, the total pressure in the reaction apparatus was measured on a mercury manometer placed outside the apparatus while the stopcock was kept open. As mentioned above the water vapor pressure could be taken as the saturation pressure corresponding to the temperature of the water circulating through the condensers. The hydrogen pressure was obtained as the difference. The number of moles of water taking part in the exchange reaction was about 2 000 times the number of moles of hydrogen, so that the increase in deuterium and tritium content of the water after completed exchange could be neglected.

The exchange reaction was allowed to go on for 5 min. during which the liquid air trap (volume about 20 ml) was evacuated. Then the first sample was taken. After the

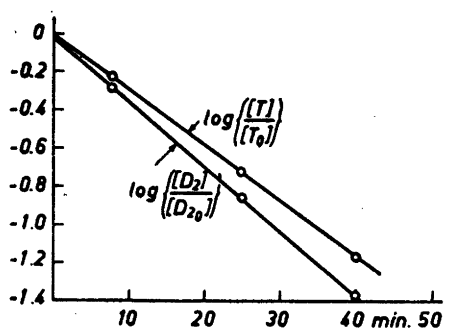


Fig. 3. Reaction of hydrogen containing tritium and a few per cent D_2 with light water vapor. (Exp. 6).

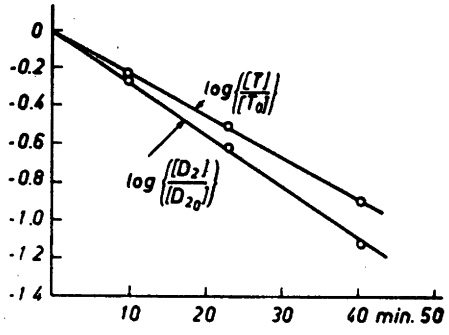


Fig. 4. Reaction of tritium containing, D_2-rich hydrogen with light water vapor. (Exp. 4).

water vapor had been frozen out, the sample was sent to a storage bulb *via* a Toepler pump. Four or five samples at intervals of about 10 min. were taken in each experiment.

From the sample storage bulb, part of the gas was forced into an ampoule, which was removed from the apparatus, and the gas contained submitted to mass spectrometric analysis.

The rest of the gas was forced into a gas burette by means of the Toepler pump, and the mercury adjusted to a constant marked level (Fig. 2). The pressure of the gas was then measured on the other arm of the manometer by means of a cathetometer. The temperature at the gas burette was noted. The gas was then allowd to expand into the counter, and the mercury level in the Toepler pump adjusted to the lower end of the outlet tube (B, Fig. 2). When corrected for temperature variations, the amount of hydrogen in the counter was thus proportional to the pressure of the gas in the burette. Counting was then done as described, and gave the relative specific activity of the gas. Absolute determination of the specific activity was of course not necessary.

RESULTS

All measurements were made at a water vapor pressure of 14 mm Hg, a hydrogen pressure of 22 mm Hg and a reaction temperature of 25 °C.

All successful experiments are reported in Table 1, where the apparent monomolecular reaction constants of the different hydrogen molecules are given. The plot of the logarithm of the tritium content in the hydrogen against time generally gave excellent straight lines, showing that the reaction was of first order. When a gas mixture containing a few per cent D_2 and very little HD was exchanged, the plot of log (D_2) *vs.* time was also strictly linear (Fig. 3). When hydrogen with a high D_2 content was exchanged, however, there seemed to be a tendency for the half life to decrease slightly as the deuterium content of the hydrogen decreased (Fig. 4). The number of samples taken is too small to allow anything more than a qualitative observation of this effect.

In a few experiments, first order kinetics were not obtained, instead the exchange tended to become slower with time. This was attributed to some impurity in the reaction gas, which caused poisoning of the catalyst. When this was observed, the reaction apparatus was heated in an oven to 500 °C for several hours to burn out any impurities, and the catalyst replatinized.

The D_2, HD and HT concentrations were generally observed over a range of 10 or more. If four points are taken on each curve, and the logarithm of a concentration value is considered as derived from a sample taken from a normal distribution of concentration values with a coefficient of variation of 3 %, the ratio of the reaction constants of HD and D_2 is obtained from six experiments (5—10) with a coefficient of variation of 4 %. This means that in present case, where the ratio is near unity, there is only one chance in twenty that the obtained ratio is in error by more than 0.08.

DISCUSSION

Before undertaking a discussion of the mechanism of the exchange reaction it must be shown that the kinetics are not obscured by the influence of diffusion.

The adsorption of water on a blank platinum surface has been examined by Bowden and Throssell [7]. At the relative saturation of the water vapor used in the present experiments, they have found an adsorbed amount corresponding to as much as 50 molecular layers. By means of an optical method they found that the water was not uniformly distributed but must have been localized as microscopic droplets on certain contaminated parts of the surface. On almost the whole surface the adsorbed layer was only about 2 molecules thick. If it is still assumed for the moment that the water is adsorbed as a layer 50 molecules thick, the diffusion through this layer would approximately account for the observed reaction rates with a roughness factor of unity for the surface. However, from the measurements of Bowden and Rideal [8], confirmed by numerous polarization measurements, it is evident that the roughness factor of platinized platinum is of the order of 10^3. It is thus quite clear that diffusion through the adsorbed layer of water cannot have influenced the reaction rate in any way. As mentioned earlier the mixing of the reaction gases was very rapid, so that the gas could at all times be regarded as homogeneous and the water vapor as deuterium-free.

The various mechanisms proposed for the exchange reaction will now be discussed in the light of the experimental findings.

I. The fact that HD is formed during the exchange of D_2 with H_2O shows at once that the deuterium atoms are not transferred simultaneously to the water, so that the reduction of a surface oxygen atom by a hydrogen molecule cannot be responsible for the exchange.

II. The electrolytic mechanism proposed for the hydrogen electrode

$$H_2O + H—M \rightarrow M^- + H_3O^+ \qquad (1)$$

where M means a surface metal atom, cannot be expected to occur in such a thin water layer as was present in these experiments. The incomplete solvation of the ions would increase the activation energy for the process considerably above the value in the presence of liquid water [1].

III. Rideal and Eley have suggested a mechanism for the *para-ortho*-hydrogen conversion where the interaction of a hydrogen molecule from the van der Waals layer and a chemisorbed hydrogen atom is the rate determining step [9]

$$p\text{-}H_2 + H—M \rightarrow o\text{-}H_2 + H—M \qquad (2)$$

Table 1.

Experiment No.	Initial content in hydrogen			k_{D_2}	k_{HD}	k_T	$\frac{k_{D_2}}{k_T}$	$\frac{k_{HD}}{k_T}$
	% D_2	% HD	% H_2	min $^{-1}$	min $^{-1}$	min $^{-1}$		
1	74.7	10.2	15.1	0.122		0.097	1.26	
2	83.4	7.5	9.1	0.063		0.051	1.23	
3	65.3	15.1	19.6	0.136		0.099	1.37	
4	66.6	13.9	19.5	0.099		0.078	1.27	
5	6.3	0.31	93.4	0.157		0.123	1.27	
6	4.7	0.26	95.1	0.081		0.066	1.24	
7	4.1	0.21	95.7	0.118		0.083	1.30	
8	0.03	3.0	96.9		0.187	0.163		1.15
9	0.04	3.9	96.1		0.085	0.078		1.09
10	0.04	3.8	96.2		0.094	0.083		1.14

It has been shown by Farkas [1] that the *p-o*-conversion and the exchange of deuterium occur with similar rates under conditions such as used here; the small difference in rate seems to be due to an isotopic effect. Therefore, if the *p-o*-conversion proceeds at all according to eqn. (2) it must be assumed that the chemisorbed D atom produced according to the same mechanism:

$$D_2 + H—M \rightarrow HD + D—M \quad (3)$$

is rapidly transferred to the water. The chemisorbed hydrogen atoms would then consist exclusively of light hydrogen.

In experiments 8—10 (Table 1), the ratio of the following two reaction constants were measured:

$$HD + H_2O \rightarrow HDO + H_2,\ k_2 \quad (4)$$
$$HT + H_2O \rightarrow HTO + H_2,\ k_3 \quad (5)$$

In experiments 5—7 the ratio k_1/k_3 was measured:

$$D_2 + H_2O \rightarrow HDO + HD,\ k_1 \quad (6)$$

In these experiments there must be very little chemisorbed deuterium on the surface, and according to the above mechanism the reaction constants represent the rate of reaction of HD, HT and D_2 with chemisorbed H atoms.

If it is now assumed that the surface is free from chemisorbed deuterium even when pure D_2 is undergoing exchange, it is easy to calculate the concentration of HD in the hydrogen in terms of the remaining D_2 from the formulae for consecutive reactions, because the ratio of their reaction constants is known from experiments 5—10.

In experiment 4 (Fig. 4) the rate constant for D_2 is taken from the slope of the straight line of best fit for the experimental values of log (D_2). In Fig. 5 are shown the curves for the calculated (curve I) and actually observed (curve II) HD concentration. Curve III would be obtained if no HD formation

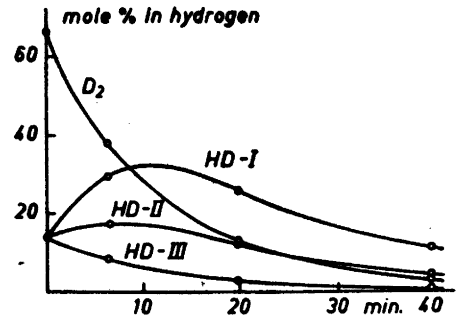


Fig. 5. The formation of HD in the exchange of D_2 with H_2O (Exp. 4).

from D_2 occurred. Clearly much smaller amounts of HD are formed than those required by the postulated mechanism.

If chemisorbed D atoms are actually present on the surface, the rates of D_2 and HD disappearance are governed by the following expressions:

$$\frac{-\mathrm{d(D_2)}}{\mathrm{d}t} = k_1(\mathrm{D_2})\,\sigma_\mathrm{H} - k_4\,(\mathrm{HD})\,\sigma_\mathrm{D} \qquad (7)$$

$$\frac{-\mathrm{d(HD)}}{\mathrm{d}t} = k_2\,(\mathrm{HD})\sigma_\mathrm{H} + k_4(\mathrm{HD})\sigma_\mathrm{D} - k_1(\mathrm{D_2})\sigma_\mathrm{H} - k_5(\mathrm{H_2})\sigma_\mathrm{D} \qquad (8)$$

Here σ_D = fraction of deuterium among the chemisorbed hydrogen atoms, σ_H = that for light hydrogen, σ_T = that for tritium.

$$\sigma_\mathrm{H} + \sigma_\mathrm{D} + \sigma_\mathrm{T} = 1 \qquad (9)$$

where, of course, $\sigma_\mathrm{T} \ll 1$.
The ratio

$$\frac{-\mathrm{d(HD)}/\mathrm{d}t}{\mathrm{d(D_2)}/\mathrm{d}t} = \frac{k_1(\mathrm{D_2})\sigma_\mathrm{H} - k_4(\mathrm{HD})\sigma_\mathrm{D} + k_5(\mathrm{H_2})\sigma_\mathrm{D} - k_2(\mathrm{HD})\sigma_\mathrm{H}}{k_1(\mathrm{D_2})\sigma_\mathrm{H} - k_4(\mathrm{HD})\sigma_\mathrm{D}} \qquad (10)$$

is seen to have its lowest value for $\sigma_\mathrm{D} = 0$, which gives the above-mentioned curve I in Fig. 5. Consequently, for $\sigma_\mathrm{D} > 0$, the HD concentration must at all times be *higher* than that given by curve I. The fact that the experimental curve is considerably below curve I definitely rules out a Rideal-Eley mechanism as the preliminary step in the exchange of molecular hydrogen with water.

IV. A mechanism suggested by Eley [3] involves interaction between a D_2 molecule and a chemisorbed OH radical

$$\mathrm{D_2 + HO{-}M \rightarrow HDO + D{-}M} \qquad (11)$$

which must be followed either by

$$\mathrm{H_2O + D{-}M \rightarrow HD + HO{-}M} \qquad (12)$$

or

$$\mathrm{H_2O + D{-}M \rightarrow H_2 + DO{-}M} \qquad (13)$$

In eqn. (13) the D atom in the hydroxyl group can then exchange rapidly with the water. If reaction (12) occurs, it gives rise to the same kinetics as mechanism III above and is thus excluded for the same reasons. The correct rate of HD formation from D_2 could, however, result if reactions (12) and (13) occurred simultaneously. As they must involve quite dissimilar transition states this is very unlikely. Besides, reaction (13) seems improbable as such, since it involves the simultaneous breaking and formation of three bonds. It is also unable to explain the exchange between hydrogen and alcohols, which occurs with about the same rate as with water [1].

V. Finally, Farkas has presented evidence for a mechanism in which the hydrogen is chemisorbed as hydrogen atoms on the platinum surface [1].

If the exchange occurs *via* chemisorption of hydrogen it is necessary that the chemisorption of water is also reversible. It is now generally agreed that chemisorption of simple hydrides involves a splitting of the bond between the central atom and a hydrogen atom [3]. In the case of water this leads to formation of hydroxyl radicals on the surface. If the hydroxyls are irreversibly adsorbed, they will eventually cover the surface completely if they are mobile, and the exchange comes to a standstill. If they are immobile on the surface, some isolated hydrogen atoms will be left which could be active in mechanisms III and IV but not in the one discussed here. As the former mechanisms have been shown to be inapplicable, the dissociative chemisorption of water must necessarily be reversible. It is then reasonable to assume that the chemisorbed hydrogen atoms are transferred to the water *via* desorption of a hydrogen atom and an adjacent hydroxyl radical. The disappearance of the various hydrogen molecules is then governed by the following equations:

$$\frac{-\mathrm{d}(\mathrm{D_2})}{\mathrm{d}t} = k_1(\mathrm{D_2}) - k'_1\sigma_{\mathrm{D}}^2 \tag{14}$$

$$\frac{-\mathrm{d}(\mathrm{HD})}{\mathrm{d}t} = k_2(\mathrm{HD}) - k'_2\sigma_{\mathrm{H}}\sigma_{\mathrm{D}} \tag{15}$$

$$\frac{-\mathrm{d}(\mathrm{H_2})}{\mathrm{d}t} = k_3(\mathrm{H_2}) - k'_3\sigma_{\mathrm{H}}^2 \tag{16}$$

$$\frac{-\mathrm{d}(\mathrm{HT}+\mathrm{DT})}{\mathrm{d}t} = k_4(\mathrm{HT}) + k_5(\mathrm{DT}) - k'_4\sigma_{\mathrm{H}}\sigma_{\mathrm{T}} - k'_5\sigma_{\mathrm{D}}\sigma_{\mathrm{T}} \tag{17}$$

The above equations involve two assumptions:

a) That the amount of chemisorbed hydrogen is independent of the isotopic composition of the molecular hydrogen. In view of what is now known about the generally occurring large variation in heat of adsorption with coverage it is very unlikely that the necessarily small difference in heat of adsorption between the different isotopes can give rise to any noticeable change in coverage.

b) That surface diffusion of the adsorbed hydrogen atoms is rapid compared with desorption, so that the composition of the desorbed hydrogen is statistically governed by the amount of the different hydrogen isotopes chemisorbed on the surface.

It is evident that by choosing a suitable value of the ratio k'_2/k_1, this mechanism can be made to account for any observed rate of HD formation.

Using the above equations and some additional ones describing the chemisorption and desorption of the water on the surface, Farkas has calculated the composition of the adsorbate from a comparison of the rates of *p*-*o*-hydrogen conversion and deuterium exchange [1]. He then had to assume that $k_1 = k_2 = k_3$ and $k'_1 = k'_2 = k'_3$.

If the preliminary step is the chemisorption of hydrogen molecules as atoms, and the exchange is made with water containing only light hydrogen, it is obviously correct to write:

Rate of transfer of chemisorbed deuterium to the water = net rate of exchange $= k_D\sigma_D$ (18)

whilst that for tritium $= k_T\sigma_T$ (19)

From eqns. (15) and (17) it is seen that, in the exchange of HD and HT with light water, first order kinetics will always be obtained since the amount of chemisorbed deuterium and tritium will be proportional to the fraction of HD and HT, respectively, in the hydrogen gas. In the exchange of D_2 with light water, on the other hand, eqn. (14) shows that the kinetics will not be simple first order. The deviation from first order kinetics depends on the ratio k'_1/k_1. In all cases where the exchange of hydrogen with a high D_2 content was observed, there is in fact a slight downward curvature of the log (D_2) *vs.* time lines, as required by eqn. (14) (Fig. 4). However, the number of samples taken in each exchange experiment is too small to permit an evaluation of the σ_D^2-term.

If a mixture of small amounts of almost HD-free D_2 with H_2 is undergoing exchange the disappearance of D_2 represents directly the rate of chemisorption of D_2 if assumption b) above is correct.

If HD in low concentration is present in the hydrogen, on the other hand, some HD will desorb from the surface. The probability of escape to the hydrogen gas of a chemisorbed D-atom will be constant as long as σ_D is small, resulting in first order kinetics. When the deuterium in the hydrogen gas is present as D_2 this probability is determined by measuring the rate of formation of HD. In experiments 5 to 7, the rate of HD formation was obtained from a knowledge of the mean value of the ratio of the reaction constants of D_2 and HD, obtained from experiments 5 to 10 as 1, 14. The probability of desorption of a D atom as HD enters the calculations as a parameter. If this probability is given the value 0.23, the experimental points give the best agreement with the theoretical curve. Evidently, then, the rate of chemisorption of HD is 1/1—0.23 = 1.30 times larger than the actual rate of disappearance of HD. The ratio of the rates of chemisorption of HD and D_2 at equal concentration is then 1.30/1.14 = 1.14.

If it is assumed for the moment that the probability of escape to the hydrogen as HT of a chemisorbed tritium atom is the same as that for deuterium as HD at low D concentrations, the relative rates of chemisorption of HD, D_2 and HT are obtained as 1.14:1:1.03. It is interesting to note that this is quite close to what would be expected from the simple collision theory for a process without activation energy (1.16:1:1).

It is now known that hydrogen is chemisorbed immeasurably fast on many clean metal surfaces even at liquid air temperatures, so that the energy of activation of the adsorption must be very low. This process may therefore well be a case where the assumption of equilibrium between reactants and activated complex in the theory of absolute reaction rates is not valid. The ratio of the adsorption velocities of different isotopic hydrogen molecules may then be expected to be equal to the ratio of the collision frequencies with the surface. If this is true the obtained ratios of adsorption velocities seem to indicate that the chemisorption of a hydrogen molecule on a bare dual site occurs without appreciable energy of activation even when the surface is largely covered with adsorbate.

If the relative rate of chemisorption of H_2 can be obtained analogously from the simple collision theory, the *p-o*-conversion of light hydrogen can be calculated to proceed 1.8 times faster than the deuterium exchange. Farkas [1] generally obtained a conversion rate 2—3 times higher than the exchange rate. If the disagreement is real, the explanation may be that there is a certain probability that a hydrogen molecule adsorbed on a dual site may desorb before the atoms are separated by surface diffusion. Assumption b) is then no longer valid, and the arguments based on it break down. Whether such an immediate desorption actually occurs could have been tested by observing the *ortho-para*-conversion of the unexchanged deuterium in the experiments with D_2-rich gas.

In conclusion it has been shown that of the mechanisms so far suggested for the isotopic exchange between hydrogen and water vapor on platinum, the only one in agreement with the reported experimental results involves a simultaneous dissociative chemisorption of both hydrogen and water on the surface. This is followed by desorption of the same molecular species. The hydrogen is chemisorbed as atoms, the water as a hydrogen atom and a hydroxyl radical. The chemisorption of hydrogen probably occurs without any appreciable activation energy and its rate is governed by the production of bare dual sites on the surface by the desorption of water or hydrogen.

A consequence of this mechanism is that in order for a metal to be an efficient catalyst for the isotopic exchange between hydrogen and water, the heat of adsorption of hydroxyl radicals must be low. The heat of adsorption of hydroxyl should run roughly parallel to the tendency of the metal to combine with oxygen. Among the metals commonly used in hydrogen catalysis, platinum has the lowest affinity for oxygen, and it is thus not surprising to find that it is by far the most efficient catalyst for the exchange reaction [10-12].

Acknowledgement. The author wishes to thank professor Ole Lamm for his kind interest and supervision and Stockholms Superfosfatfabriks AB for a grant that made the work possible.

REFERENCES

1. Farkas, A. and Farkas, L. *Trans. Faraday Soc.* **33** (1937) 678.
2. Farkas, A. *Trans. Faraday Soc.* **32** (1936) 922.
3. Eley, D. D. *Advances in Catalysis* **1** (1948) 183.
4. Rideal, E. K. and Trapnell, B. M. W. *J. Chim. Phys.* **47** (1950) 126.
5. Boudart, M. *J. Am. Chem. Soc.* **74** (1952) 3556.

6. Koester, L. and Maier-Leibnitz, H. *Sitzber. Heidelberg. Akad. Wiss., Math.-naturw. Kl.* **1951** 22, 5 Abh.
7. Bowden, F. P. and Throssell, W. R. *Proc. Roy. Soc. London* **209 A** (1951) 297.
8. Bowden, F. P. and Rideal, E. K. *Proc. Roy. Soc. London* **129 A** (1928) 24.
9. Eley, D. D. and Rideal, E. K. *Proc. Roy. Soc. London* **178 A** (1941) 429.
10. Hannerz, K. *Unpublished results.*
11. Hirota, K. and Horiuti, J. *Sci. Papers Inst. Phys. Chem. Research, Tokyo* **30** (1936) 151.
12. Murphy, G. M. *Production of Heavy Water, Natl. Nucl. En. Series III—4F*, **1955** 228.

Received February 7, 1956.

ACTA CHEMICA SCANDINAVICA 10 (1956) 667—672

Infrared Spectroscopic Investigations of some Hydrazides

J. BUUR JENSEN*

Leo Pharmaceutical Products, Copenhagen, Denmark

The infrared spectra of some hydrazides in the solid state and in chloroform solution have been investigated in the 6 μ region. Characteristic frequencies in the solid state are found at 1 630—1 660 cm^{-1}, 1 620 cm^{-1} and between 1 570 and 1 530 cm^{-1}. Corresponding bands in the solutions are found around 1 670, 1 620 and 1 500 cm^{-1}. The assignment of the bands to different group frequencies is discussed. Investigations in the 3 μ region on phenylacetic acid hydrazide make it evident that hydrogen bonding takes place in the solid state and in concentrated solutions.

Furthermore it is shown, that the spectrum of cinnamic acid hydrazide synthesized by Godtfredsen and Vangedal [1] is in agreement with the spectra of the other hydrazides, while the spectrum of the compound which Muckermann [2] believed to be cinnamic acid hydrazide shows essential differences.

In a recent publication from this laboratory Godtfredsen and Vangedal [1] have proved, that the compound synthesized by Muckermann [2] was 3-phenyl-5-pyrazolidone and not, as hitherto believed, cinnamic acid hydrazide. This observation caused the author to investigate the infrared spectra of some hydrazides. The present publication deals mainly with the spectra in the 6 μ region, but measurements in the 3 μ region are also reported.

Only few spectra of hydrazides are found in the literature; thus Lenormant [3] in a work on amides has recorded the spectrum of acetic acid hydrazide, while Mattu and Pirisi [4] have recorded that of *iso*nicotinic acid hydrazide.

EXPERIMENTAL

All spectra are absorption spectra measured on a Beckman infrared spectrophotometer model IR 2 equipped with rock salt optics and automatic recorder. A computing device, as described by Foreman and Jackson [5] was used for the purpose of eliminating background absorption. Spectra of solids were recorded in KBr-discs. The KBr employed was prepared as described by Clauson-Kaas *et al.*[6] The discs contained 0.5 % hydrazide, weighed about 0.2 g and were prepared in a pressing device and under experimental

* Present address: Specialitetskontrollen, Copenhagen, Denmark.

conditions as described elsewhere [7]. Spectra of chloroform solutions were recorded in rock salt cells. The employed chloroform was Merck a.g.

All the hydrazides were synthesized in this laboratory. With the exeption of cinnamic acid hydrazide, which was synthesized by the method of Godtfredsen and Vangedal [1], they were all prepared by the reaction of the corresponding ethyl ester with hydrazine. Melting points agreed with those found in the literature.

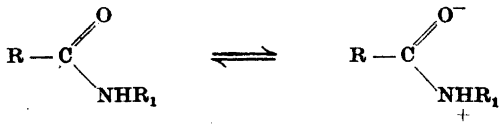
RESULTS AND DISCUSSION

Figs. 1 and 2 show, respectively, the spectra of the solid hydrazides and those of the chloroform solutions. In addition the spectrum of 3-phenyl-5-pyrazolidone is given. Among the spectra of the solids acetic acid hydrazide is absent, as it was impossible to prepare a sufficiently transparent disc with this compound, presumably due to its low melting point. However, the spectrum given by Lenormant [3] is in comparatively good agreement with those given in Fig. 1.

One observes at once that the transition from the solid state to dilute solution is associated with distinct changes in the spectra. In the solid state the hydrazides absorb strongly between 1 630 and 1 660 cm^{-1}, while this absorption in chloroform solution is shifted to frequencies about 20 cm^{-1} higher. Likewise the hydrazides in the solid state show medium absorption in the region around 1 530—1 570 cm^{-1}. This absorption is found in the solutions at essentially lower frequencies around 1 500 cm^{-1}. The absorption of the phenyl groups can be observed [8] around 1 500 and 1 600 cm^{-1}, and finally is a medium to strong band found in the neighbourhood of 1 620 cm^{-1} in the spectra of the dissolved hydrazides. In the spectra of the solid hydrazides this absorption may be overlapped by the strong band at 1 630—1 660 cm^{-1}, but the absorption pattern makes it evident, that this band also is present in the spectra of the solid hydrazides.

In the following it is attempted to assign the absorption bands to different groups in the molecule. It should be noted at once that the spectra of the hydrazides resemble those of the N-monosubstituted amides. Considerable contribution to the understanding of the spectra of the amides is offered by among others Richards and Thompson [9], Lenormant [3] and latest by Gierer [10].

The strong absorption of the hydrazides around 1 650 cm^{-1} in the solid state and 1 670 cm^{-1} in chloroform solution in analogy with the N-monosubstituted amides must be ascribed to the carbonyl group. Normally one would expect its absorption at a somewhat higher frequency around 1 710 cm^{-1}. The reason for the low frequency is explained by a weakening of the double bond, due to the following resonance:



In the spectra of the N-monosubstituted amides Richards and Thompson [9] observed, that the absorption of the carbonyl group is dependant on the state

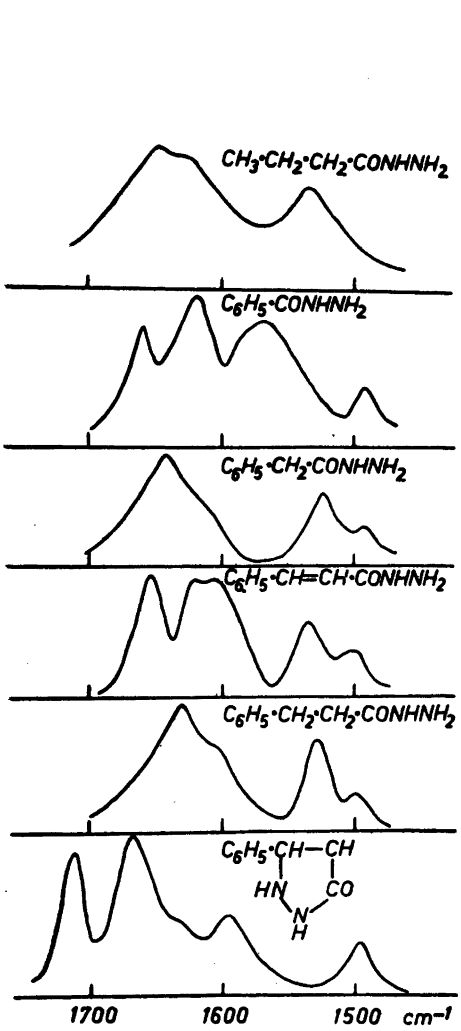


Fig. 1. I.R.-spectra of solid hydrazides (KBr discs containing 0.5 % hydrazide).

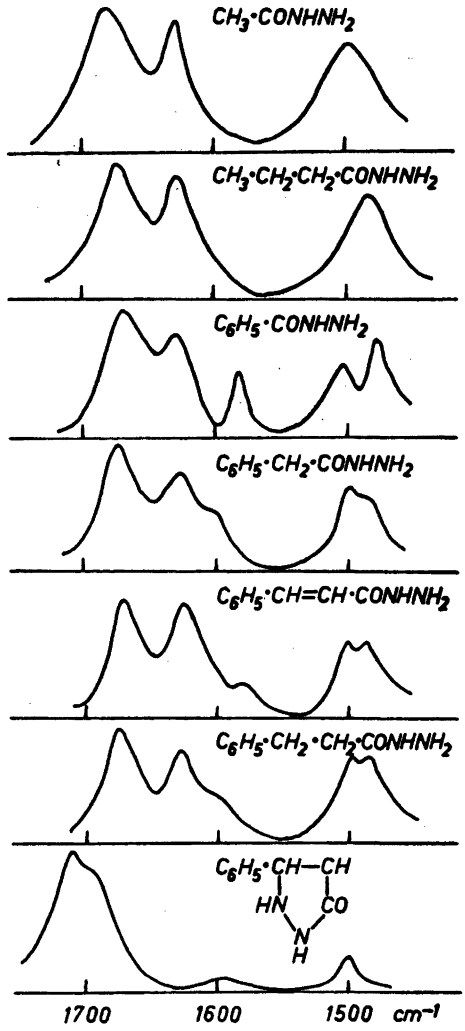
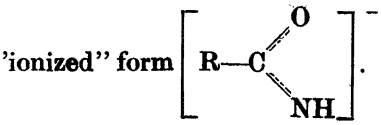
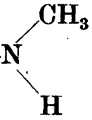


Fig. 2. I.R.-spectra of hydrazides (1 % in $CHCl_3$)

in the same manner as here observed for the absorption of the carbonyl group in the hydrazides.

The medium band observed between 1 530 and 1 570 cm^{-1} in the solid hydrazides is also found in the spectra of solid N-monosubstituted amides [9], and in both cases this absorption is shifted to lower frequencies in the spectra of the solutions [9]. There are yet different opinions on the causes of this absorption. In the N-monosubstituted amides Richards and Thompson assign this absorption to NH deformation frequency, while Lenormant is of the opinion that

the absorption can be attributed to an "ionized" form  .

Finally Gierer assigns the band in N-metylacetamide to a deformation of the group  . A final explanation of this problem is still missing, and it will only be brought to attention, that the spectra of the hydrazides also on this point resemble the N-monosubstituted amides.

Absorption around 1 600 cm^{-1} and 1 500 cm^{-1} is found in the hydrazides containing a phenyl group, and must be due to this [8]. Only the assignment of the medium or strong band around 1 620 cm^{-1} is remaining. Absorption at this frequency is due most often to C=C stretching, C=N stretching or NH_2 deformation [8]. As absorption of the carbon-carbon double bond is most often weak, and as only cinnamic acid hydrazide contains this bond, absorption can not originate here. If the absorption is assigned to a C=N group it must involve a ketone-enol equilibrium in the solid state, which is most unlikely. It is therefore most reasonable to assign the absorption around 1 620 cm^{-1} to a NH_2 deformation frequency in conformity with what is observed in primary amines [8]. This assignment may be further evidenced by the fact, that this band is absent in the spectra of the hydrohalides [3].

From Figs. 1 and 2 it is seen that the spectrum of cinnamic acid hydrazide synthesized by the method of Godtfredsen and Vangedal [1] is in exact agreement with the spectra of the other hydrazides, while 3-phenyl-5-pyrazolidone, which Muckermann [2] believed to be cinnamic acid hydrazide, differs in essential degree. This may be regarded as a further proof of the structure determinations of these compounds accomplished by Godtfredsen and Vangedal [1].

The variations mentioned in the spectra on passing from dilute chloroform solution to solids may be ascribed to association of the molecules in the solid state under the formation of hydrogen bonds. A concrete proof of this can be derived from the spectra in the 3 μ region, as it is well established that free —NH-groups give rise to narrow bands in the region 3 500—3 300 cm^{-1} while the bonded groups give rise to broader bands at somewhat lower frequencies [8]. The employed rock salt optics, however, are not suitable for measurements in this region due to low resolution, and the experimental technique in recording the spectra of solids is complicated by scattering.

For this reason, reference is made only to the measurements which are performed on phenylacetic acid hydrazide. Although they cannot be regarded as exhaustive, they form a basis sufficient to verify that association takes place in concentrated solutions and in the solid state.

Figs. 3 and 4 show the spectra of phenylacetic acid hydrazide in the solid state and in chloroform solution, respectively. The spectrum of the chloroform solution shows a narrow band of high intensity at approximately 3 450 cm^{-1}, and a weaker broad one at approximately 3 340 cm^{-1}. An eventual absorption at lower frequency is difficult to measure due to the background absorption of the chloroform. The spectrum of the solid substance lacks ab-

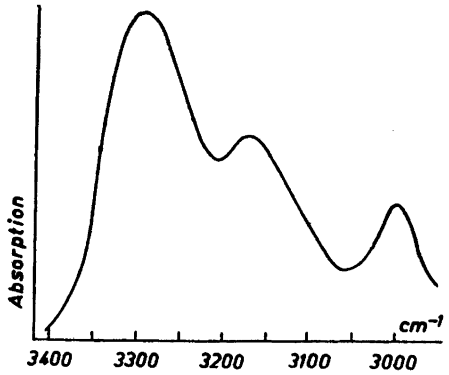


Fig. 3. I.R.-spectrum of phenyl acetic acid hydrazide in the solid state (0.5 % in KBr).

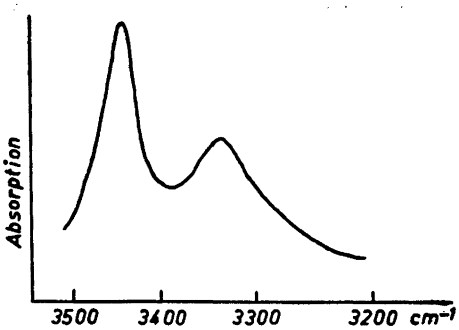


Fig. 4. I.R. spectrum of phenylacetic acid hydrazide (1 % in $CHCl_3$).

sorption at 3 450 cm^{-1}, instead an intense band is found centered around 3 300 cm^{-1}, a weaker broad band around 3 175 cm^{-1}, and furthermore a weak band at approximately 3 000 cm^{-1}. There is no doubt that a complete association takes place in the solid state, as the narrow band in the solution must be assigned to a free —NH-group, while the broad band in the spectrum of the solid substance is due to a bonded —NH-group.

The absorption at 3 340 cm^{-1} found in the chloroform solution may consist of two bands unresolved by the available spectrograph. However, the absorption at this frequency increases more rapidly at increasing concentrations than the absorption at 3 450 cm^{-1}. This fact may be explained by association in concentrated solutions.

On the basis of the measurements carried out here it is, however, difficult to determine in which form association takes place. It may be mentioned that during the time this work was done, a publication by Jensen [11] on X-ray crystallographic investigations of *iso*nicotinic acid hydrazide appeared, in which the author claims the existence of hydrogen bonds of the type NH---N. However it seems most unreasonable not to consider hydrogen bonds of the NH---OC type, solely because the frequency of the carbonyl group in the 6 μ region is displaced significantly to higher frequencies when passing from the solid state to dilute solutions.

Acknowledgment. The author is indebted to W. O. Godtfredsen and I. S. Vangedal for supplying the compounds, and to L. Fleischer-Olsen and G. Bay-Christiansen for assistance in recording the spectra.

REFERENCES

1. Godtfredsen, W. O. and Vangedal, I. S. *XIVth International Congress of Pure and Applied Chemistry, Zürich 1955, Congress Handbook*, p. 232.
2. Muckermann, E. *Ber.* **42** (1909) 3449.
3. Lenormant, H. *Bull. soc. chim. France* [5] **15** (1948) 33.
4. Mattu, F. and Pirisi, E. *Ann. Chim. Rome* **43** (1953) 580.

5. Foreman, R. W. and Jackson, W. Jr. *Instruments* **22** (1949) 497.
6. Clauson-Kaas, N., Nedenskov, P., Bak, B. and Rastrup-Andersen, J. *Acta Chem. Scand.* **8** (1954) 1088.
7. Jensen, J. B. *Ibid.* **8** (1954) 393.
8. Bellamy, J. L. *The infrared spectra of complex molecules*, Methuen, London 1954.
9. Richards, R. E. and Thompson, H. W. *J. Chem. Soc.* **1947** 1248.
10. Gierer, A. *Z. Naturforsch.* **8 b** (1953) 644.
11. Jensen, L H. *J. Am. Chem. Soc.* **76** (1954) 4663.

Received August 18, 1955.

ACTA CHEMICA SCANDINAVICA 10 (1956) 673—680

X-Ray Investigations on Uranyl Hydroxides

I. The Crystal Structure of β-$UO_2(OH)_2$

GUNILLA BERGSTRÖM and GEORG LUNDGREN

Research Institute of National Defence, Dpt. 1, Sundbyberg 4; Department of Inorganic Chemistry, Royal Institute of Technology, Stockholm 70; Institute of Inorganic and Physical Chemistry, University, Stockholm, Sweden

β-$UO_2(OH)_2$ has a face-centered orthorhombic cell with the dimensions $a = 6.295 \pm 0.005$ Å, $b = 5.636 \pm 0.005$ Å, and $c = 9.92_9 \pm 0.01$ Å. The unit cell contains four formula units. The atomic positions can be described by the space group No. 69 *Fmmm* as given on p. 678. The structure is built up of pseudotetragonal layers connected by van der Waals contact between the UO_2^{2+} groups. Every uranium atom is joined through four atoms to its neighbouring U atoms. The positions of the oxygen atoms were inferred from geometrical arguments and considerations of the strength of the U—O bonds.

In connection with an X-ray investigation of "uranates" undertaken at these institutes by Bergström and Sillén [1], it was of interest to know the crystal structure of a pure uranyl hydroxide. However, in the literature only a preliminary structure determination of a uranyl hydroxide, *viz.* α-$UO_2(OH)_2$, has been published (Zachariasen) [2]. The positions of the uranium atoms in the unit cell are given, but the parameters of the oxygen atoms are not discussed. Other investigations [2] are mainly concerned with the identification of different phases of $UO_2(OH)_2(H_2O)_x$. Thus, since no complete structure determination seems to have been published, we thought that an investigation of such a structure would be worth while.

In Gmelin's Handbuch some papers on the preparation of crystalline uranyl hydroxides are cited. The best of the methods described seemed to be thermal hydrolysis of uranyl acetate solutions [3,4]. In this way we were able to prepare some different uranyl hydroxides in a crystalline form suitable for single crystal X-ray work. The structure determination of one of them is dealt with here. It has been called β-$UO_2(OH)_2$ for reasons to be given at the end of this paper. Structure studies on some of the other phases will be published in subsequent papers.

PREPARATION OF THE CRYSTALS

A solution of uranyl acetate containing 1 g $UO_2(CH_3COO)_2$ in 100 ml water was heated in a sealed glass tube at 105—110° C for about 120 hours, after which a yellow, crystalline precipitate had formed. The crystals were filtered off and dried in air. Under the microscope they proved to be either yellow, transparent, six-sided plates or yellow needles about 0.1—0.2 mm in length. They often grew together in clusters.

X-ray powder photographs were taken with focussing cameras of the Phragmén type, first of the original mixture of plates and needles, and then only of picked-out plates. The same patterns were obtained. However, on comparing the observed values of $\sin^2\Theta$ with those calculated from the cell dimensions obtained from single crystal photographs, we found that some of the weaker lines of the powder photograph did not fit in. As no indication of a superstructure was found in the single crystal photographs, we concluded that the preparation contained one or more phases as impurities. We also tried to index the extra lines assuming the impurity to be α-$UO_2(OH)_2$ [2], but the attempt was not successful.

Analysis. Since the crystals were prepared from a solution of uranyl acetate we tested them for acetate ions with lanthanum nitrate and iodine before they were analysed quantitatively [5]. The result was negative and we concluded that the compound contained only uranium, oxygen, and hydrogen. The uranium content was determined by igniting the sample at 750° C and weighing the residue as U_3O_8. The water was determined by Brush [6] and Penfield's [7] method, described by Kolthoff and Sandell [8].

	Found		Calculated for $UO_2(OH)_2$
% UO_2	93.0	93.2	94.08
% H_2O	5.9	6.1	5.92
Density	5.72	5.72	5.73

The analyses indicate the formula $UO_2(OH)_2$. Since, however, the powder photographs show that the preparation contains more than one phase the analytical data alone do not allow a definite conclusion. As will be shown below, the geometrical arguments for the positions of the oxygen atoms also support the formula $UO_2(OH)_2$.

UNIT CELL AND SPACE GROUPS

A crystal was set with the longest diagonal of the plate as rotational axis; it was called the a axis. Using CuK radiation, rotation and the following Weissenberg photographs were taken: $0kl$ (with 4 × 23 reflections registered), $1kl$ (with 4 × 16 reflections registered) and $2kl$ (with 4 × 19 reflections registered). From these photographs the following approximate cell dimensions of the orthorhombic unit cell were found: $a = 6.2_9$ Å, $b = 5.6_3$ Å, and $c = 9.9_3$ Å. The c axis is perpendicular to the plate. Rotation and Weissenberg photographs were also taken of the needles, which proved to have the same cell dimensions and symmetry as the plates. The axis of the needles was [110].

From the powder photographs (*cf.* Table 1) more accurate cell dimensions were calculated:

$$a = 6.295 \pm 0.005 \text{ Å}$$
$$b = 5.636 \pm 0.005 \text{ Å}$$
$$c = 9.92_9 \pm 0.01 \text{ Å}$$
$$V = 352.4 \text{ Å}^3$$

All reflections hkl with $h + k$ = odd or $k + l$ = odd are systematically absent. This is characteristic of the space groups No. 69 $Fmmm$, No. 42

Table 1. Powder photographs of β-$UO_2(OH)_2$. CrK radiation $\lambda_{CrK\alpha} = 2.2909$ Å.

h k l	$10^4\sin^2\Theta$ calc	$10^4\sin^2\Theta$ obs	*I* obs	*h k l*	$10^4\sin^2\Theta$ calc	$10^4\sin^2\Theta$ obs	*I* obs
1 1 1	877	870	m	4 0 0	5298	5297	vw
—	—	962	vw	—	—	5658	vvw
—	—	1125	w	4 0 2	5831	5844	vw
2 0 0	1324	1323	w	2 0 6	6118	6121	m
—	—	1493	vvw	—	—	6209	w
0 2 0	1652	(1642)	w	—	—	6296	w
2 0 2	1857	1851	vw	0 2 6	6446	(6443)	w+
1 1 3	1943	1933	w	0 4 0	6608	(6607)	vw
—	—	1969	w—	3 1 5	6722	6725	w
—	—	1981	m	3 3 1	6830	6822	w
0 0 4	2131	2129	m	4 2 0	6950	6957	vvw
0 2 2	2185	2182	vw—	0 4 2	7141	—	—
—	—	2924	vw	1 1 7	7269	7262	s
2 2 0	2976	2983	vw—	1 3 5	7377	7377	vw
—	—	3070	vw	4 0 4	7429	7440	w
—	—	3218	vw	4 2 2	7483	—	—
—	—	3307	vw	2 2 6	7780	7771	w+
2 0 4	3455	3457	w+	3 3 3	7896	7884	vvw
2 2 2	3509	3519	vw	2 4 0	7932	—	—
3 1 1	3526	3534	vw	—	—	7963	w+
0 2 4	3783	3782	w—	—	—	8150	w
—	—	3893	vvw	—	—	8228	w
1 1 5	4073	4068	s	—	—	8418	w
1 3 1	4181	4186	vvw	2 4 2	8465	—	—
—	—	4290	w	0 0 8	8523	8511	m
—	—	4433	w—	0 4 4	8739	8740	vw—
—	—	4492	m	5 1 1	8824	8837	vvw
3 1 3	4592	4597	vw	—	—	9051	vvw
0 0 6	4794	4789	m	4 2 4	9081	9082	vw—
2 2 4	5107	5098	vw	—	—	9533	vw
1 3 3	5245	5248	vw	—	—	9686	vw

The horizontal lines mark the boundaries between the angular ranges of the three different focussing cameras used. Reflections systematically absent in the space group *Fmmm* have been omitted. Reflections coinciding with β reflections are given in brackets. Reflections having no corresponding $\sin^2\Theta$ are assumed to belong to the phase not investigated. In the powder photographs there is an absorption and orientation effect favouring reflections with high *l* indices.

*Fmm*2, and No. 22 *F*222. The reflections recorded in the Weissenberg photographs were all strong and of much the same intensity, apart from the general decrease in intensity always found with increasing Θ.

Positions of the uranium atoms

The plausible space groups demand that there should be $4n$ uranium atoms in the unit cell (where n is an integer). From the volume of the cell we can calculate that, for $n = 1$, $d_{calc} = 5.73$ (assuming the formula as $UO_2(OH)_2$). As the observed density is 5.72 and as the major part of the preparation seems to consist of the phase investigated, we could then safely say that there are

4 U atoms per unit cell. We may arbitrarily choose their positions as 4(*a*) in *Fmmm*, 4(*a*) in *F*222 or 4(*a*) with $z = 0$ in *Fmm*2. All these positions have the coordinates 000; $\frac{1}{2}\frac{1}{2}0$; $\frac{1}{2}0\frac{1}{2}$; $0\frac{1}{2}\frac{1}{2}$, corresponding to a face-centered uranium lattice.

Previous data on uranium-oxygen coordination

In addition to the uranium atoms there are oxygen and hydrogen atoms in the unit cell. The positions of these light atoms could not be determined from the intensities of the reflections, and thus they had to be inferred from considerations of the interatomic distances and the bond strength of the U—O bond.

All oxygen compounds of U(VI) hitherto studied by X-ray methods, except α-UO_3, seem to contain uranyl ions UO_2^{2+}. In the "uranates" investigated ($CaUO_4$, $SrUO_4$, $BaUO_4$, Li_2UO_4, Na_2UO_4, K_2UO_4, $MgUO_4$) [9-11], the uranium atoms are connected by oxygen bridges forming $(UO_2O_2)_\infty^{2n-}$-layers or chains perpendicular, or almost perpendicular, to the uranyl groups.

In $BaUO_4$ and $MgUO_4$ each oxygen bridge connects two neighbouring uranyl groups, resulting in pseudo-tetragonal $(UO_2O_2)_\infty^{2n-}$-layers with single oxygen bridges for $BaUO_4$ [10] and $(UO_2O_2)_\infty^{2n-}$-chains with double oxygen bridges for $MgUO_4$.[11] The distances U—O_{bridge} are 2.12—2.22 Å.

In the other "uranates" mentioned each UO_2^{2+} group is connected with its next six UO_2^{2+} neighbours by oxygen atoms, each of which is shared between three uranyl groups, and thus a pseudo-hexagonal lattice is formed. In these compounds the distances U—O_{bridge} are 2.3 Å.

In α-UO_3 the coordination uranium-oxygen is the same as in the pseudo-hexagonal "uranates". However, the "uranyl" oxygen atoms are shared between two uranium atoms forming chains of U—O—U—. . . . instead of discrete UO_2^{2+} groups.

A compilation of all observed U—O distances has been given by Zachariasen [12]. He found that they all lay on a smooth curve when they were plotted as a function of the bond strength s of the U—O bond.

Positions of the oxygen atoms

The positions of the oxygen atoms were discussed from geometrical arguments without assuming any special space group. We felt it justified to assume that the O—O distances are not less than 2.6 Å and that the distances between interacting U and O atoms are within the limits 1.6—2.5 Å (*cf.* Zachariasen [12]).

If none of the oxygen atoms were shared between two or more uranium atoms, the structure would be built up of separate molecules and every uranium should be surrounded by only four oxygen atoms. This is not very probable as the coordination number of U is 6—8. Moreover, crystals of $UO_2(OH)_2$ built up of separate molecules should be easily soluble in water, as, for instance, is H_2SO_4. The crystals are, however, very sparingly soluble in water, and from this reason too the configuration seems rather improbable. Thus it is likely that the uranium atoms are joined by oxygen (or OH^-) bridges to form infinite chains, layers, or a three-dimensional framework, as they are in the "uranates", which are difficult to bring in solution.

Now, every uranium atom is surrounded by four other uranium atoms at a distance of 4.22 Å $= \sqrt{\left(\frac{a}{2}\right)^2 + \left(\frac{b}{2}\right)^2}$, all other U—U distances being larger than 5.63 Å.

If the oxygen atoms in the bridges were to be shared between three or more uranium atoms, the U—O distances would be larger than 2.8 Å, *i. e.* too long for a U—O interaction. We thus concluded that each of them is in contact only with two uranium atoms.

The shared oxygen atoms (O_{II}) are then probably situated between the uranium atoms, 4.22 Å apart, as the U—O_{II} distances would otherwise be longer than 2.8 Å. The uranium atoms could then be joined either by double oxygen bridges leading to the formation of chains, as in $MgUO_4$[11], or by single oxygen bridges leading to the formation of pseudo-tetragonal layers, as in $BaUO_4$[10].

In the first case the distances U—O_{II} would be 2.48 Å, if the oxygen atoms were situated 2.60 Å apart. According to Zachariasen [12], this would indicate a U—O bond strength of about 0.45 units. As there are four such bonds we would have 6—4 × 0.45 = 4.2 units left for bonds to the remaining oxygen atoms O_I in the coordination polyhedron, leading to the very short bond distances U—O_I = 1.6 Å. (The shortest experimentally determined [13] distance U—O_I is 1.76 Å in $K_3UO_2F_5$ corresponding to a bond strength of 1.63. The distance U—O_I = 1.58 Å in $RbUO_2(NO_3)_3$ was estimated and is therefore very uncertain [14].)

In the second case when the uranium atoms are joined by single oxygen bridges the distance U—O_{II} would be $\frac{1}{2}$ × 4.22 Å = 2.11 Å corresponding to a bond strength of about 0.95. The bond strength left for bonds to the two remaining oxygen atoms O_I in the coordination polyhedron would then be 2.2, giving a distance U—O_I = 2.0 Å, which is close to those observed for the uranyl groups in the "uranates" mentioned above.

From these considerations the second case with single oxygen bridges seemed to be the most plausible and we concluded that the bridging oxygen atoms are situated in the following way:

8 O_{II} in *Fmmm* 8(*e*): $(0,0,0;\ 0,\frac{1}{2},\frac{1}{2};\ \frac{1}{2},0,\frac{1}{2};\ \frac{1}{2},\frac{1}{2},0) \pm (\frac{1}{4},\frac{1}{4},0;\frac{1}{4},\frac{1}{4},\frac{1}{2})$

Thus the crystals contain pseudo-tetragonal layers similar to those in $BaUO_4$.

In all the "uranates" previously determined there are UO_2^{2+} ions with U—O = 1.76—2.08 Å, and thus it is plausible that our crystals also contain uranyl groups, perpendicular, or almost perpendicular, to the sheets. As we have found the unit cell to contain four uranium atoms there must be eight uranyl oxygen atoms (O_I) in addition to the eight bridging oxygen atoms (O_{II}), the approximate positions of which we have already found. The O_I atoms should then be arranged as follows:

8 O_I in *Fmmm* 8(*i*): $(0,0,0;\ 0,\frac{1}{2},\frac{1}{2};\ \frac{1}{2},0,\frac{1}{2};\ \frac{1}{2},\frac{1}{2},0) \pm (0,0,z)$ with $z = 0.20$

The parameter $z = 0.20$ was determined from the distance U—O_I = 2.0 Å expected from the bond strength $s = 1.1$ in the uranyl bond (*cf.* above).

In this way we have found the positions of 4 U and 16 O atoms in the unit cell, corresponding to the formula $UO_2(OH)_2$, as indicated by the analysis. However, since the chemical analysis was not quite conclusive as the sample contained some impurities, and since the structure seemed to be very open we concluded to investigate whether there could be more oxygen atoms present in the unit cell.

We found then that the most favourable positions for any additional O atoms (O_{III}) would be at $(0,0,0; \frac{1}{2},\frac{1}{2},0; 0,\frac{1}{2},\frac{1}{2}; \frac{1}{2},0,\frac{1}{2}) \pm(\frac{1}{4},\frac{1}{4},\frac{1}{4})$. An investigation showed, however, that even if the structure would be distorted a little some $O—O_{III}$ distances came out rather short (2.4 Å or less) and thus it did not seem probable that the unit cell contained any additional oxygen atoms at all. This also supports the conclusion made from the analytical data that the formula of the compound should be $UO_2(OH)_2$

Positions of the hydrogen atoms

As there are 4 O atoms per U(VI) atom electrical neutrality demands 2 H atoms per U, and thus the cell must contain 8 H. They can be situated close to the uranyl oxygen atoms (O_I) or close to the bridging oxygen atoms (O_{II}). From the considerations of the bond strength of the U—O bond the first seems to be rather plausible as the total bond strength for O_I is 1.1 when the total bond strength for O_{II} is 1.9. On the other hand, investigations on the hydrolysis of uranyl ions [15,16] show that UO_2^{2+} groups do not seem to attract protons in acidic solutions, which would demand that in the crystals of $UO_2(OH)_2$ we would have the hydrogen atoms situated at the O_{II} atoms forming OH^- ions.

At present we could not say which of the two possibilities is the correct one even if the argument in the second case seems to be the most convincing.

In both cases the hydrogen atoms may form hydrogen bonds to the neighbouring oxygen atoms.

Final structure proposition

We thus consider that the crystals have the following structure:

Space group: No. 69 *Fmmm* with

$(0,0,0; 0,\frac{1}{2},\frac{1}{2}; \frac{1}{2},0,\frac{1}{2}; \frac{1}{2},\frac{1}{2},0) \pm$

4 U in 4(*a*): 0,0,0

8 O_I in 8(*i*): 0,0,*z* with $z = 0.20$

8 O_{II} in 8(*e*): $\frac{1}{4},\frac{1}{4},0; \frac{1}{4},\frac{1}{4},\frac{1}{2}$

DISCUSSION OF THE STRUCTURE

Projections of the structure on the *xy* and *xz* planes are shown in Figs. 1 and 2. The structure is built up of layers $UO_2(OH)_2$ consisting of linear UO_2^{2+} ions (perpendicular to the sheets) joined to each other through oxygen atoms, two uranyl ions sharing one O atom. The layers are perpendicular to the *c*

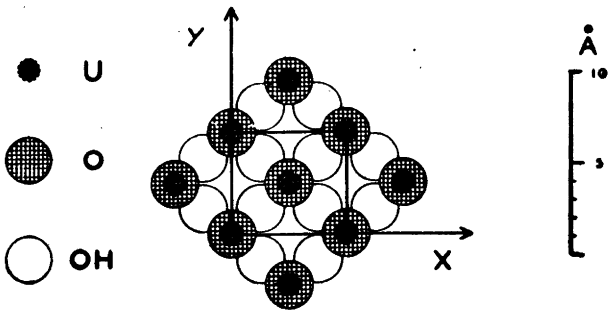


Fig. 1. Part of the structure of β-$UO_2(OH)_2$ projected on the xy *plane. Only atoms with* z *within the limits* $-0.25 \leqq z \leqq 0.25$ *have been marked out.*

axis, and they are connected to each other by van der Waals forces between the uranyl groups.

The distances between the atoms in the same layer would be:

$$\begin{aligned} &U\ -2\ O_I\ ,\ O_I\ -U && = 2.0\ \text{Å} \\ &U\ -4\ O_{II},\ O_{II}-2\ U && = 2.11\ \text{Å} \\ &O_I\ -4\ O_{II},\ O_{II}-2\ O_I && = 2.8_4\ \text{Å} \\ &O_{II}-4\ O_{II} && = 2 \times 2.82,\ 2 \times 3.15\ \text{Å} \end{aligned}$$

The layers support each other by:

$$O_I-4\ O_I = 2 \times 3.0_5,\ 2 \times 3.3_6\ \text{Å}$$

These figures are all within the normal range, showing that O—O interaction also occurs in the lattice. However, the bond lengths may be inaccurate by one or a few 0.1 Å since the positions of the oxygen atoms have been inferred from geometrical arguments.

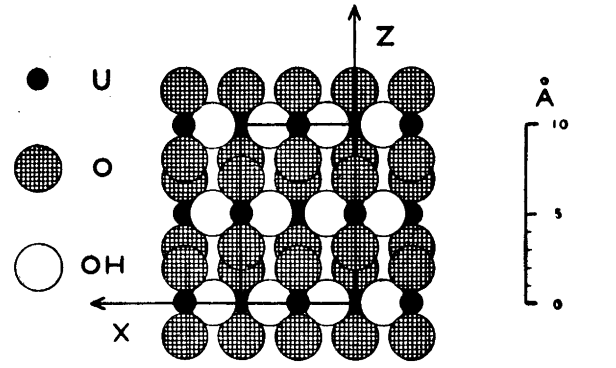


Fig. 2. The structure of β-$UO_2(OH)_2$ projected on the xz *plane.*

During the Manhattan project Zachariasen [2] made a preliminary structure determination of an orthorhombic uranyl hydroxide, α-$UO_2(OH)_2$. Its cell dimensions were found to be $a = 6.86 \pm 0.03$ Å, $b = 4.27 \pm 0.03$ Å, $c = 10.19 \pm 0.06$ Å, $V = 299$ Å^3 and the phase is thus different from ours. Zachariasen determined the positions of its uranium atoms but not those of its oxygen atoms. He found that every uranium is surrounded by six others at distances 4.05—4.27 Å in pseudohexagonal layers. Zachariasen's α-$UO_2(OH)_2$ structure then seems to resemble the hexagonal "uranates", whereas our structure is closely related to the tetragonal "uranates", where every uranium atom is surrounded by four others at the distance 4.22 Å.

In *"The Chemistry of Uranium"* [2] four phases of $UO_2(OH)_2$ are described. Two of them (α and β) are said to be orthorhombic, and as Zachariasen's crystals were called α-$UO_2(OH)_2$, the phase described in our paper should be β-$UO_2(OH)_2$. However, the data are very meagre, and the identity between our crystals and the β phase there could not be definitely stated.

We wish to thank Professor Lars Gunnar Sillén and Dr. Arne Magnéli for many valuable discussions in connection with this work. We are also very much indebted to Professor Gustaf Ljunggren, FOA 1, and Professor Arne Ölander, University of Stockholm, for their kind interest.

REFERENCES

1. Bergström, G. and Sillén, L. G. *To be published.*
2. Katz, J. J. and Rabinowitch, E. *National Nulear Energy Series* VIII-5:1, New York 1951, pp. 281—289.
3. Riban, J. *Compt. rend.* **93** (1881) 1141; *Bull. soc. chim. France* (2), **38** (1882) 157.
4. Zehenter, J. *Monatsh.* **21** (1900) 241.
5. Vogel, A. I. *Qualitative Chemical Analysis*, p. 307.
6. Brush, G. J. *Am. J. Sci.* **460** (1868) 240.
7. Penfield, S. L. *Am. J. Sci.* (3), **48** (1894) 30; *Z. anorg. Chem.* **7** (1894) 22.
8. Kolthoff, I. M. and Sandell, E. B. *Textbook of Quantitative Inorganic Analysis*, New York, 1943, p. 753.
9. Zachariasen, W. H. *Acta Cryst.* **1** (1948) 281.
10. Samson, S. and Sillén, L. G. *Arkiv Kemi Mineral. Geol.* **25** (1947) No. 21.
11. Zachariasen, W. H. *Acta Cryst.* **7** (1954) 788.
12. Zachariasen, W. H. *Acta Cryst.* **7** (1954) 795.
13. Zachariasen, W. H. *Acta Cryst.* **7** (1954) 783.
14. Hoard, J. L. and Stroupe, J. D. in Dieke, G. H. and Duncan, A. B. F. *National Nuclear Energy Series* III-2, New York 1949, p. 13.
15. Ahrland, S. *Acta Chem. Scand.* **3** (1949) 374.
16. Ahrland, S., Hietanen, S. and Sillén, L. G. *Acta Chem. Scand.* **8** (1954) 1907.

Received January 2, 1956.

ACTA CHEMICA SCANDINAVICA 10 (1956) 681—704

Short Communications

Some Differences between Solubilization in Bile Salt and Paraffin Chain Salt Solutions

PER EKWALL, ARMAS STEN and ARNE NORMAN*

Institute of Physical Chemistry, Åbo Akademi, Åbo, Finland

Similarly as other association colloids, the bile acid salts are good solubilizers of lipophilic substances, but there exist clear differences between the solubilization processes in solutions of the bile salts and the association colloids of the paraffin chain salt type. In both cases solubilization of hydrocarbons begins at a well-defined low colloid concentration and proceeds stepwise as the colloid concentration is increased [1-4]. The concentrations separating the solubility ranges are more or less clearly definable even when substances other than hydrocarbons are solubilized (but in some cases slightly displaced owing to the interaction between the solubilized substance and the colloid). In other respects marked differences are noted when polar-nonpolar substances such as straight-chain alcohols and fatty acids are solubilized. Whereas the solubilization of these substances begins in the bile salt solutions at the same concentration as the solubilization of hydrocarbons, in paraffin chain salt solutions the solubilization begins, although in a limited degree, at a concentration, the L.A.C., that is far below that where the hydrocarbon solubilization begins [4-6]. In the bile salt solutions the solubilization of alcohol continues until the micelles become saturated with alcohol, after which the excess of alcohol separates in the free form. In the paraffin chain salt solutions the solubilization in many cases ends when a mesomorphic phase composed of alcohol, association colloid and water separates. The added long-chain alcohols do not influence the conductances of the bile salt solutions (as far as we have investigated), but do alter the conductances of the paraffin chain salt solutions (Fig. 1 A). In the latter case even small amounts of alcohol bound by the micelles in the solutions alter the conductance, but a rapid decrease in the conductance occurs as soon as the system becomes heterogeneous [6-7]. Similar differences are also noted when fatty acids are solubilized by bile salt and fatty acid soap solutions.

The fact that the conductances of bile salt solutions are not altered by the alcohols (in any case not by small amounts of the additive) suggests that the charge distribution on the surface of the bile salt micelle does not change when alcohols are incorporated in the micelles, whereas the charge distribution is, however, altered when the alcohols are incorporated in fatty acid soap and alkyl sulphate micelles. That the mesomorphic phase does not separate from bile salt solutions may possibly be due to the fact that hydrophilic properties of the micelle surface of the bile salt micelles are not diminished to the same extent by alcohols and fatty acids as when the latter are incorporated in the paraffin chain salt micelles.

The polar-nonpolar compounds mentioned are known to increase the power of paraffin chain colloids to solubilize hydrocarbons [5,8]. This is illustrated by the curves 1 a and 1 b in Fig. 1 B which shows that the solubility of *p*-xylene in 0.04 M sodium myristate solution increases as much as 60—70 % when increasing amounts of decanol or myristic acid are added to the solution. In bile salt solutions the effect of the addition is the opposite. This is evident from curve 2 which shows the influence of added decanol on the solubility of *p*-xylene in a 0.1 M sodium cholate solution, and from curves 3 a and 3 b (in Fig. 1 B) which

* Present address: Department of Physiological Chemistry, University of Lund, Lund, Sweden.

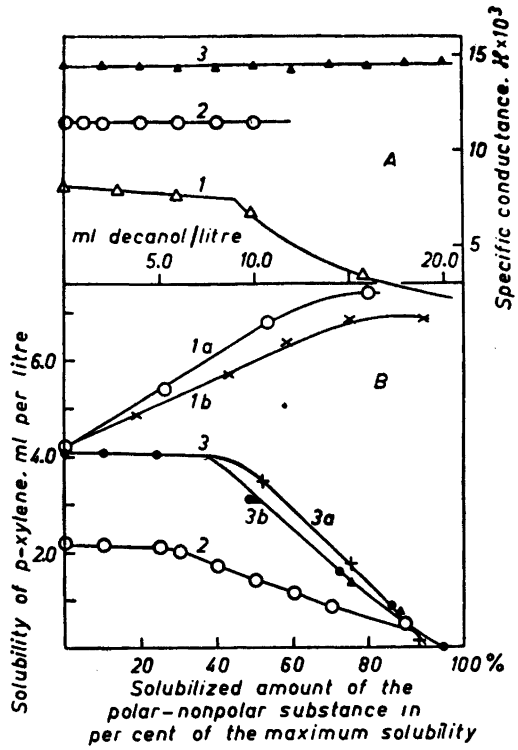


Fig. 1 A. The effect of added decanol-1 on the conductance of association colloid solutions. 40° C

1. *0.207 M sodium oleate solution containing decanol-1*
2. *0.180 M sodium cholate solution containing decanol-1*
3. *0.250 M sodium desoxycholate solution containing decanol-1*

Fig. 1 B. Solubility of p-*xylene at 40° C in association colloid solutions.*

1. *0.04 M potassium myristate solutions containing*
   a) decanol-1 O—O
   b) myristic acid ×—×
2. *0.10 M sodium cholate solutions containing decanol-1*
3. *0.09 M sodium taurodesoxycholate solutions containing*
   a) decanol-1 +—+
   b) nonylic acid ●—●
   heptylic acid ▲—▲

show the influence of decanol, nonylic acid and heptylic acid on the solubility of *p*-xylene in 0.09 M sodium taurodesoxycholate solution. As long as the amount of polar-nonpolar additive is relatively small, the xylene solubility either remains constant or decreases slowly, but when the amount added exceeds a certain value, the solubility of xylene decreases rapidly. (In order to facilitate the comparison, the content of the polar-nonpolar compound has been expressed as a percentage of the maximum solubility of the compound in the pure colloid solution in question).

It has, as known, been concluded (above all on the basis of X-ray studies) that the solubilized hydrocarbon molecules are built in between the palisade layers of the paraffin chain colloid micelles (or in the centre of the

spherical or spheroidal micelles); the molecules of the alcohols and fatty acids are, however, incorporated between the colloid molecules in the palisade layers and thus increase the amount of micelle-forming matter. Solubilization data of the type on which curves 1 a and 1 b in Fig. 1 B are based have been considered to support this view and to prove the existence of two loci of solubilization in the micelles [8,9].

The experiments described in curves 2 and 3 in Fig. 1 B show that the alcohols and fatty acids on one hand and hydrocarbons on the other, are initially solubilized quite independently by the bile salt micelles. This can be considered to indicate that the polar-nonpolar compounds and hydrocarbons are solubilized in different loci in the bile salt micelles. A marked difference as compared with the paraffin chain colloids is, however, that the polar-nonpolar compounds are built in the bile salt micelles in such a manner that the power of the micelles to solubilize hydrocarbons is not increased; on the contrary, the incorporation of larger amounts of the polar-nonpolar compounds progressively diminishes the power to solubilize hydrocarbons. It is thus evident that the mode in which the polar-nonpolar compounds are built in the micelles differs for the bile and paraffin chain salts.

One of the present authors has called attention to the fact that the maximum amounts of fatty acids that sodium taurocholate solutions are able to solubilize are so great [3] (from about 2 moles of nonylic acid to 5 moles of caproic acid per mole of taurocholate in 0.09 M solution) that it must be assumed that the structure of the micelles is altered to such an extent that mixed micelles with completely new properties are formed. Also the maximum amounts of long-chain alcohols solubilized by bile salt micelles are fairly large (1—2 moles per mole of the bile salt). According to the data presented here altered properties of the micelles become apparent only after the mole ratio of polar-nonpolar compound and bile salt exceeds a certain value, which is about 0.14 for decanol and sodium cholate, 0.34 for decanol and sodium taurodesoxycholate, and 0.8 for nonylic and 1.3 for heptylic acid and sodium taurodesoxycholate. A change in micellar structure apparently occurs only after these values of the ratio are exceeded.

All the above mentioned data show that there exist important differences in the solubilization mechanism in the case of bile salts and paraffin chain salts, particularly in regard to the location of solubilized molecules in the micelles and the interaction between the solubilizer and solubilizate. This is evidently connected with essential differences in the structures of the micelles of the two types of association colloids.

1. Ekwall, P. *Acta Acad. Aboensis, Math. Phys.* **XVII** (1951) 8.
2. Ekwall, P. *Svensk Kem. Tidskr.* **63** (1951) 973.
3. Ekwall, P. *Koninkl. Vlaam. Acad. Vetenschap. Intern. conference on Biochemical Problems of Lipids.* Brussels 1953, p. 103.
4. Ekwall, P. *J. Colloid Sci. Suppl.* **1** (1954) 66.
5. Ekwall, P. and Danielsson, I. *Acta Chem. Scand.* **5** (1951) 973.
6. Ekwall, P., Passinen, K. and Danielsson, I. *Finska Kemistsamfundets Medd.* **63** (1954) 1.
7. Passinen, K. and Ekwall, P. *Acta Chem. Scand.* **9** (1955) 1438, 1450.
8. Klevens, H. B. *J. Chem. Phys.* **17** (1944) 1004.
9. Klevens, H. B. *J. Am. Chem. Soc.* **72** (1950) 3581, 3780.

Received April 14, 1956.

Can Micelles be Treated as Ideal Mixtures of Ions and Neutral Molecules?

JÜRI SEIM, LARS GUNNAR SILLÉN and ULF ULFVARSON

Department of Inorganic Chemistry, Royal Institute of Technology, Stockholm 70, Sweden

In the last few years, attempts have been made in this Institution to study equilibria involving micelles of carboxylic acids such as lauric acid, $C_{11}H_{23}COOH$ = HL, and amines like dodecyl amine $C_{12}H_{25}NH_2$ = D. Emf titrations have been made (using glass or hydrogen electrodes, sometimes Ag, AgL electrodes) with a practically constant ionic medium, in order to keep the activity factors constant. In each titration, the total concentration $B = [HL]_t + [L^-]_t$ or $[D]_t + [DH^+]_t$ has been kept constant, and the data have been given in the shape of a plot $Z(\log h)_B$,

spherical or spheroidal micelles); the molecules of the alcohols and fatty acids are, however, incorporated between the colloid molecules in the palisade layers and thus increase the amount of micelle-forming matter. Solubilization data of the type on which curves 1 a and 1 b in Fig. 1 B are based have been considered to support this view and to prove the existence of two loci of solubilization in the micelles [8,9].

The experiments described in curves 2 and 3 in Fig. 1 B show that the alcohols and fatty acids on one hand and hydrocarbons on the other, are initially solubilized quite independently by the bile salt micelles. This can be considered to indicate that the polar-nonpolar compounds and hydrocarbons are solubilized in different loci in the bile salt micelles. A marked difference as compared with the paraffin chain colloids is, however, that the polar-nonpolar compounds are built in the bile salt micelles in such a manner that the power of the micelles to solubilize hydrocarbons is not increased; on the contrary, the incorporation of larger amounts of the polar-nonpolar compounds progressively diminishes the power to solubilize hydrocarbons. It is thus evident that the mode in which the polar-nonpolar compounds are built in the micelles differs for the bile and paraffin chain salts.

One of the present authors has called attention to the fact that the maximum amounts of fatty acids that sodium taurocholate solutions are able to solubilize are so great [3] (from about 2 moles of nonylic acid to 5 moles of caproic acid per mole of taurocholate in 0.09 M solution) that it must be assumed that the structure of the micelles is altered to such an extent that mixed micelles with completely new properties are formed. Also the maximum amounts of long-chain alcohols solubilized by bile salt micelles are fairly large (1—2 moles per mole of the bile salt). According to the data presented here altered properties of the micelles become apparent only after the mole ratio of polar-nonpolar compound and bile salt exceeds a certain value, which is about 0.14 for decanol and sodium cholate, 0.34 for decanol and sodium taurodesoxycholate, and 0.8 for nonylic and 1.3 for heptylic acid and sodium taurodesoxycholate. A change in micellar structure apparently occurs only after these values of the ratio are exceeded.

All the above mentioned data show that there exist important differences in the solubilization mechanism in the case of bile salts and paraffin chain salts, particularly in regard to the location of solubilized molecules in the micelles and the interaction between the solubilizer and solubilizate. This is evidently connected with essential differences in the structures of the micelles of the two types of association colloids.

1. Ekwall, P. *Acta Acad. Aboensis, Math. Phys.* **XVII** (1951) 8.
2. Ekwall, P. *Svensk Kem. Tidskr.* **63** (1951) 973.
3. Ekwall, P. *Koninkl. Vlaam. Acad. Vetenschap. Intern. conference on Biochemical Problems of Lipids.* Brussels 1953, p. 103.
4. Ekwall, P. *J. Colloid Sci. Suppl.* **1** (1954) 66.
5. Ekwall, P. and Danielsson, I. *Acta Chem. Scand.* **5** (1951) 973.
6. Ekwall, P., Passinen, K. and Danielsson, I. *Finska Kemistsamfundets Medd.* **63** (1954) 1.
7. Passinen, K. and Ekwall, P. *Acta Chem. Scand.* **9** (1955) 1438, 1450.
8. Klevens, H. B. *J. Chem. Phys.* **17** (1944) 1004.
9. Klevens, H. B. *J. Am. Chem. Soc.* **72** (1950) 3581, 3780.

Received April 14, 1956.

Can Micelles be Treated as Ideal Mixtures of Ions and Neutral Molecules?

JÜRI SEIM, LARS GUNNAR SILLÉN and ULF ULFVARSON

Department of Inorganic Chemistry, Royal Institute of Technology, Stockholm 70, Sweden

In the last few years, attempts have been made in this Institution to study equilibria involving micelles of carboxylic acids such as lauric acid, $C_{11}H_{23}COOH$ = HL, and amines like dodecyl amine $C_{12}H_{25}NH_2$ = D. Emf titrations have been made (using glass or hydrogen electrodes, sometimes Ag, AgL electrodes) with a practically constant ionic medium, in order to keep the activity factors constant. In each titration, the total concentration $B = [HL]_t + [L^-]_t$ or $[D]_t + [DH^+]_t$ has been kept constant, and the data have been given in the shape of a plot $Z(\log h)_B$,

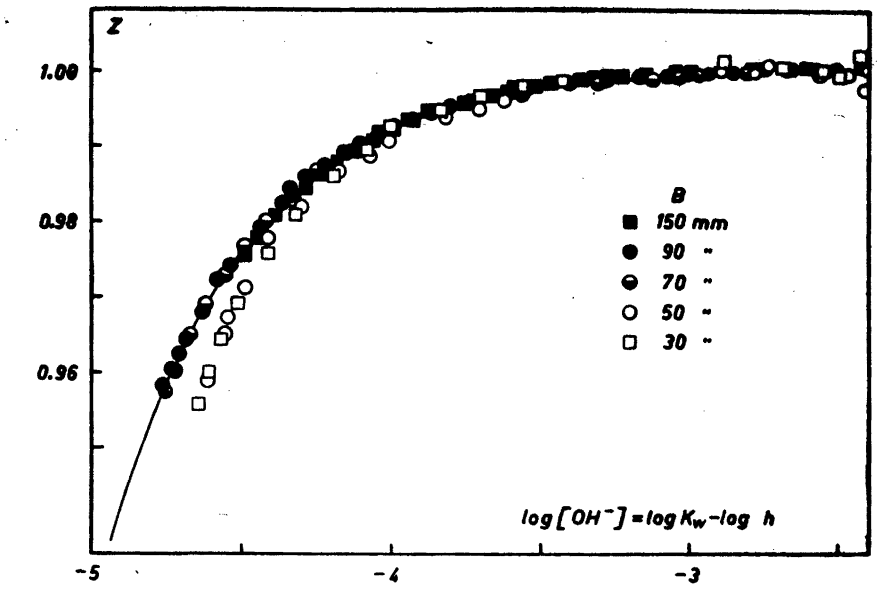


Fig. 1. Z (log K_w *—log* h)$_B$ *for potassium laurate solutions in 1 m* KNO_3 *at 25° C. Points: experimental points for five total concentrations. Curve: calculated for monoprotic acid with* $pK_w - pK_a = 6.11$.

where $h = [H^+]$ and Z is the average charge per unit, thus $BZ = [L^-]_t$ or $[DH^+]_t$. These experiments have met with many difficulties and are still in progress. We would however like to draw attention to one of the results obtained.

Fig. 1 gives the data $Z(\log h)_B$ for lauric acid, obtained by one of us (J.S.). Ionic medium 1 m $K^+(NO_3^-)$, 25° C, glass electrode. The abscissa is really $\log [OH^-] = \log K_w - \log h$. In the range $Z = 1.0$ to 0.95, reversible equilibria were achieved since the same curves were obtained when HNO_3 or KOH was added; for lower values of Z, precipitates appeared which dissolved but slowly on addition of KOH. For lower values of B, there were also difficulties with the equilibria.

In the concentration range given, 30 to 150 mm, the major part of the laurate groups would be present in the form of micelles. Using the method of Ekwall and Harva [1], we found the maximum concentration of free L^- to be about 6 mm at 50° C. From data of Corrin and Harkins [2], one may estimate the critical concentration to be about 2.5 mm.

One may calculate what the shape of $Z(\log h)_B$ would have been under various simple assumptions concerning the phases and dissolved species present. At equilibrium between two solid phases of constant composition, such as KL(s) + HL(s), or KL(s) + KHL_2(s), $\log h$ would be constant. If the main reaction is equilibrium between L^- in solution and KHL_2(s) or HL(s), the slope of $Z(\log h)$ would also have been much steeper than that actually found. Moreover, the curve would have shifted with varying values of B.

Assuming equilibrium between KL(s) and HL or HL_2^- in solution, one would get curves of the right shape, but the curves would have been shifted with an amount equal to the shift in log B. According to experiment, the points for 70, 90, and 150 mm practically coincide, and the deviations for 30 and 50 mm are only about 0.1 units, whereas log 150/30 = 0.7. Thus, none of these assumptions is valid.

However, a very good fit is found with the simple curve $Z = K_a h^{-1} (1 + K_a h^{-1})^{-1}$, calculated for the dissociation of a monoprotic acid, with $pK_w - pK_a = 6.11$. Assuming $pK_w \approx 13.7$ one obtains $pK_a \approx 7.6$. The simple explanation that the solution

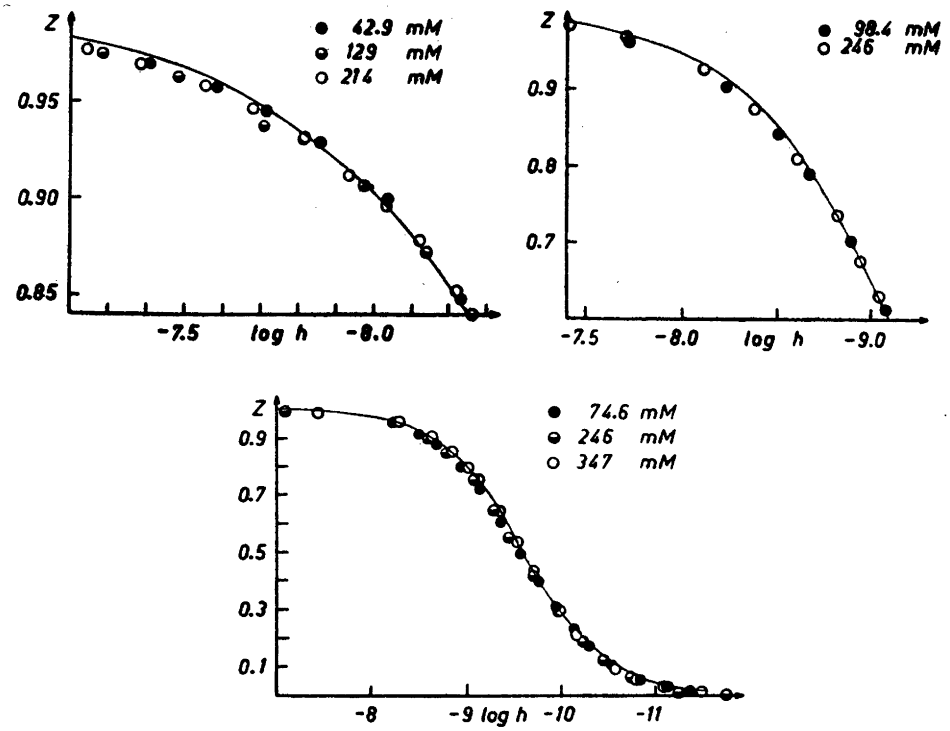


Fig. 2 a—c. $Z(\log h)_B$ *for dodecyl ammonium chloride solutions in 0.5 M NaCl at 25° C with a) 1.70, b) 4.75, c) 6.78 M* C_2H_5OH. *Curves: calculated for simple equilibrium* $DH^+ \rightleftharpoons D + H^+$, *with a)* $pK_a = 8.97$, $pK_w = 13.96$; *b)* $pK_a = 9.27$, $pK_w = 14.03$; *c)* $pK_a = 9.62$, $pK_w = 14.09$.

would contain only single molecules HL and L^- is ruled out already by the fact that, for lower values of B, the curves $Z(\log h)_B$ break away from the curve in Fig. 1. Nor would it be consistent with what is known about the micellar behavior.

The simplest way of expressing our results is perhaps treating the micelles formally as a separate phase, a mixture of L^- and HL (perhaps also K^+, NO_3^-, and H_2O from the ionic medium). Then our results would imply that, in the range where this phase is stable ($x_{HL} = 0$ to 0.05), it is approximately an ideal mixture of L^- and HL. A similar picture has been given by Stainsby and Alexander [3]; at that time it was supported only by measurements of the hydrolysis of pure soap solutions with varying ionic strength.

One might speculate on why the acid is so much less willing to give off a proton than normal carboxylic acids in aqueous solution ($pK_a = 4$ to 5). A related fact is the observation of Ekwall [4] that monolayers of myristic acid show a large ionization effect around pH ≈ 8—10.

Fig. 2 gives analogous results, obtained by one of us (U.U.), for dodecyl ammonium chloride (DH^+Cl^-). The ionic medium was 0.5 M (Na^+)Cl^-, with three different concentrations of C_2H_5OH (1.70, 4.75, and 6.78 M). For each concentration of C_2H_5OH, two or three different total concentrations B were used, all in a range in which the micelles would predominate, even without adding NaCl, according to the conductivity data of Ralston and Hoerr [4].

In this case too, the $Z(\log h)$ curves seem to be independent of the total concentration B, and to coincide surprisingly well with those calculated for a simple equi-

librium between dissolved B and BH^+, with $pK_a \approx 8.9$ to 9.6. If the previous conductivity data have been interpreted correctly, we are once more brought to the approximation of the micelle as an ideal mixture; for D and DH^+, the range of Z is moreover much wider than it was for lauric acid.

The work on lauric acid has been supported by a grant from *Statens Naturvetenskapliga Forskningsråd (Swedish Natural Science Research Council)*.

1. Ekwall, P. and Harva, O. *Finska Kemistsamfundets Medd.* **52** (1943) 257.
2. Corrin, M. L. and Harkins, W. D. *J. Am. Chem. Soc.* **69** (1947) 683.
3. Stainsby, G. and Alexander, A. E. *Trans. Faraday Soc.* **45** (1949) 585.
4. Ekwall, P. *Svensk Kem. Tidskr.* **63** (1951) **277.**
5. Ralston, A. W. and Hoerr, C. W. *J. Am. Chem. Soc.* **68** (1946) 851.

Received April 19, 1956.

Preparation of Di-*p*-nitrobenzylphosphoryl chloride *via* the Corresponding Phosphite

GEORG FÖLSCH

Department of Medical Biochemistry, University of Gothenburg, Gothenburg, Sweden

The very promising phosphorylating reagents recently introduced by Leonidas Zerwas and collaborators, *e. g.* di-*p*-nitrobenzylphosphoryl chloride, were originally synthesized by procedures involving silver salt esterifications [1]. For preparation of these reagents in large batches it seems to be preferable to use the phosphite route [2,3]. In connection with syntheses of phosphopeptides [4] we have obtained di-*p*-nitrobenzyl phosphite in good yield from *p*-nitrobenzyl alcohol and phosphorus trichloride. This phosphite gives, as expected, the desired phosphoryl chloride quantitatively by chlorination with sulphuryl chloride.

Experimental. Di-p-nitrobenzyl phosphite. To a vigorously stirred solution of 27.6 g phosphorus trichloride (1 mole) in 600 ml dry benzene of room temperature a warm solution of 61.2 g *p*-nitrobenzyl alcohol (2 moles) and 48.4 g dimethylanilin (2 moles) in 200 ml benzene was added in small portions within one hour. After an additional hour of stirring, 30.6 g *p*-nitrobenzyl alcohol (1 mole) in 200 ml benzene was added within 20 minutes. The mixture was stirred for a further two hours and then left overnight. The benzene solution was washed with water (3 × 200 ml), 5 N ammonia (2 × 200 ml), water (2 × 200 ml) and dried over anhydrous sodium sulphate. By addition of light petroleum, di-*p*-nitrobenzyl phosphite separated as white crystals. The yield was 43.5 g (62 % of the theoretical). The phosphite was recrystallized from ethanol or chloroform-cyclohexane. M. p. 75°. (Found: C 47.70; H 3.70; N 7.91; P 9.00. Calc. for $C_{14}H_{13}O_7N_2P$: C 47.70; H 3.72; N 7.96; P 8.81).

Chlorination. To a suspension of 35.3 g phosphite in 250 ml carbon tetrachloride 8 ml sulphuryl chloride was added dropwise with shaking. Dry nitrogen was slowly bubbled through the mixture and the temperature was held under 20°. After 20 minutes the solvent was removed *in vacuo* and the solid dissolved in chloroform. Addition of light petroleum gave white crystals of di-*p*-nitrobenzylphosphoryl chloride (36.0 g = 93 %) with the m. p. 107—108°. The mixed melting point with phosphoryl chloride prepared according to Zerwas [1] showed no depression. (Found: P 7.91; Cl 8.89. Calc. for $C_{14}H_{12}O_7N_2PCl$: P 8.00; Cl 9.16).

1. Zerwas, L. and Dilaris, I. *J. Am. Chem. Soc.* **77** (1955) 5354.
2. Atherton, F. R., Openshaw, H. T. and Tood, A. R. *J. Chem. Soc.* **1945** 382.
3. Miyano, M. and Funahashi, S. *J. Am. Chem. Soc.* **77** (1955) 3522.
4. Fölsch, G. *Acta Chem. Scand.* **9** (1955) 1039.

Received May 8, 1956.

librium between dissolved B and BH^+, with $pK_a \approx 8.9$ to 9.6. If the previous conductivity data have been interpreted correctly, we are once more brought to the approximation of the micelle as an ideal mixture; for D and DH^+, the range of Z is moreover much wider than it was for lauric acid.

The work on lauric acid has been supported by a grant from *Statens Naturvetenskapliga Forskningsråd (Swedish Natural Science Research Council)*.

1. Ekwall, P. and Harva, O. *Finska Kemistsamfundets Medd.* **52** (1943) 257.
2. Corrin, M. L. and Harkins, W. D. *J. Am. Chem. Soc.* **69** (1947) 683.
3. Stainsby, G. and Alexander, A. E. *Trans. Faraday Soc.* **45** (1949) 585.
4. Ekwall, P. *Svensk Kem. Tidskr.* **63** (1951) **277.**
5. Ralston, A. W. and Hoerr, C. W. *J. Am. Chem. Soc.* **68** (1946) 851.

Received April 19, 1956.

Preparation of Di-*p*-nitrobenzylphosphoryl chloride *via* the Corresponding Phosphite

GEORG FÖLSCH

Department of Medical Biochemistry, University of Gothenburg, Gothenburg, Sweden

The very promising phosphorylating reagents recently introduced by Leonidas Zerwas and collaborators, *e. g.* di-*p*-nitrobenzylphosphoryl chloride, were originally synthesized by procedures involving silver salt esterifications [1]. For preparation of these reagents in large batches it seems to be preferable to use the phosphite route [2,3]. In connection with syntheses of phosphopeptides [4] we have obtained di-*p*-nitrobenzyl phosphite in good yield from *p*-nitrobenzyl alcohol and phosphorus trichloride. This phosphite gives, as expected, the desired phosphoryl chloride quantitatively by chlorination with sulphuryl chloride.

Experimental. Di-p-nitrobenzyl phosphite. To a vigorously stirred solution of 27.6 g phosphorus trichloride (1 mole) in 600 ml dry benzene of room temperature a warm solution of 61.2 g *p*-nitrobenzyl alcohol (2 moles) and 48.4 g dimethylanilin (2 moles) in 200 ml benzene was added in small portions within one hour. After an additional hour of stirring, 30.6 g *p*-nitrobenzyl alcohol (1 mole) in 200 ml benzene was added within 20 minutes. The mixture was stirred for a further two hours and then left overnight. The benzene solution was washed with water (3 × 200 ml), 5 N ammonia (2 × 200 ml), water (2 × 200 ml) and dried over anhydrous sodium sulphate. By addition of light petroleum, di-*p*-nitrobenzyl phosphite separated as white crystals. The yield was 43.5 g (62 % of the theoretical). The phosphite was recrystallized from ethanol or chloroform-cyclohexane. M. p. 75°. (Found: C 47.70; H 3.70; N 7.91; P 9.00. Calc. for $C_{14}H_{13}O_7N_2P$: C 47.70; H 3.72; N 7.96; P 8.81).

Chlorination. To a suspension of 35.3 g phosphite in 250 ml carbon tetrachloride 8 ml sulphuryl chloride was added dropwise with shaking. Dry nitrogen was slowly bubbled through the mixture and the temperature was held under 20°. After 20 minutes the solvent was removed *in vacuo* and the solid dissolved in chloroform. Addition of light petroleum gave white crystals of di-*p*-nitrobenzylphosphoryl chloride (36.0 g = 93 %) with the m. p. 107—108°. The mixed melting point with phosphoryl chloride prepared according to Zerwas [1] showed no depression. (Found: P 7.91; Cl 8.89. Calc. for $C_{14}H_{12}O_7N_2PCl$: P 8.00; Cl 9.16).

1. Zerwas, L. and Dilaris, I. *J. Am. Chem. Soc.* **77** (1955) 5354.
2. Atherton, F. R., Openshaw, H. T. and Tood, A. R. *J. Chem. Soc.* **1945** 382.
3. Miyano, M. and Funahashi, S. *J. Am. Chem. Soc.* **77** (1955) 3522.
4. Fölsch, G. *Acta Chem. Scand.* **9** (1955) 1039.

Received May 8, 1956.

The Preparation of 1,2-Dithiolane-4-carboxylic Acid

LENNART SCHOTTE and HOLGER STRÖM

Chemical Institute, University of Uppsala, Uppsala, Sweden

In order to complete an investigation of the substituent influence on the spectral behaviour of the disulphide group in 1,2-dithiolane derivatives [1,2], it seemed important to include 1,2-dithiolane-4-carboxylic acid.

The related dimercaptan, β,β′-dimercapto-*iso*butyric acid, was first obtained in 1948 by Jansen [3] upon reduction of a sulphur-containing polymeric material isolated from asparagus juice. The mercapto acid appeared to be the first dithiol substance reported from a natural source. The structural proof involved identification of the methylated compound with authentic β,β′-di-methylmercapto-*iso*butyric acid (obtained from the related di-iodo acid and methyl mercaptan). Recently the preparation of β,β′-dimercapto-*iso*butyric acid was described by Corse and Jansen [4]. Reduction of β,β′-dibenzylmercapto-*iso*butyric acid with sodium in liquid ammonia yielded the expected substance, whereas hydrolysis of the related di-*iso*thiuronium salt was unsuccessful.

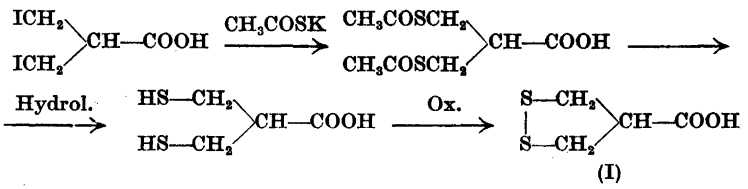
1,2-Dithiolane-4-carboxylic acid (I) has now been prepared from the mercaptan (without intermediate isolation) by oxidation with oxygen [5]. The β,β′-dimercapto-*iso*butyric acid was obtained from the corresponding di-iodo compound [3,6] and potassium thiolacetate with subsequent hydrolysis of the bis-acetyl substance formed.

The spectrochemical (UV and IR) and polarographic properties of (I) have been discussed in a previous communication [2] where also comparison was made with the 3-isomer, prepared by Claeson [7].

The presence of disulphide in asparagus juice has been qualitatively shown by Jansen. His results might suggest that the disulphide material present in asparagus is of polymeric nature but the experience of the present authors indicates that the conditions used by Jansen [3] were not mild enough to ensure the isolation of a possible monomer. As the 1,2-dithiolane system is reactive (*cf.* 6-thioctic acid) and cleavage of the S—S bond with formation of polymers readily occurs, it seems reasonable to assume the presence of (I) in the plant. In view of the properties of 6-thioctic acid it will therefore be very interesting to find out if the occurrence of the reactive ring system is in some way important for the biochemical processes in the rapidly growing asparagus.

Both the monomeric disulphide and the polymer give β,β′-dimercapto-*iso*butyric acid when reduced according to Fredga [8] with zinc in ammoniacal solution. The data of the mercapto acid coincide with those previously reported.

Experimental. 1,2-Dithiolane - 4 - carboxylic acid. 11 g (0.032 mole) of β,β′-diiodo-*iso*butyric acid was suspended in 40 ml of water and neutralized with an aqueous solution (40 ml) of 2.1 g (0.032 mole) of 86 % KOH. A solution of 5.2 g (0.0685 mole) of thiolacetic acid and 4.45 g (0.0685 mole) of 86 % KOH in 40 ml of water was added dropwise, and the mixture heated in an oil bath at 80° for 8 hours. Acidification with dilute H_2SO_4 caused precipitation of the bis-acetylmercapto acid as a heavy oil. After its separation the product



(I)

was dissolved in 100 ml of KOH water solution (containing 10 g (0.154 mole) of 86 % KOH). The mixture was kept at room temperature for 16 hours and then acidified (dil. H_2SO_4). The mercapto acid was extracted five times with ether. The substance remaining after spontaneous evaporation of the dried solvent was

The disulphide acid obtained was contaminated with polymeric material, which, however, could be removed by treatment with benzene in which the polymers are insoluble. Recrystallized from benzene-*cyclo*hexane (I) was obtained as transparent yellow prisms.

dissolved (without previous purification) in 400 ml of aqueous $NaHCO_3$ solution (containing 8.5 g (0.10 mole) of $NaHCO_3$). A small amount of $FeCl_3$ was added as a combined catalyst and indicator and oxygen bubbled through the mixture until the violet colour disappeared (about two hours). After acidification (dil. H_2SO_4) and removal of small amounts of polymeric material by filtration the product was extracted with ether (6 × 75 ml). The ether solution was dried with anhydrous Na_2SO_4 and the solvent evaporated *(in vacuo)*. 1.3 g (27 %) of crude acid (mixture of monomer and polymer) with m. p. 60—70° was obtained; after treatment with benzene for some minutes at room temperature it left an insoluble viscous substance. Evaporation of the solvent yielded 0.8 g (16.5 %) of dry acid (monomer) with m. p. 75—77°. This product was now recrystallized from benzene-*cyclo*hexane and obtained as transparent yellow prisms with m. p. 76.5—77.5°. (Found: Equiv. wt. 151.1; C 31.96; H 3.92; S 42.72; Mol.wt. 146. Calc. for $C_4H_6O_2S_2$ (150.22): Equiv. wt. 150.2; C 31.98; H 4.03; S 42.68; Mol.wt. 150).

β,β'-Dimercapto-isobutyric acid. 0.5 g of (I) or the related polymer (insoluble in benzene) was dissolved in 20 ml of 4 M ammonia, and the solution sucked through a layer of zinc powder four times. The reaction mixture was neutralized with dil. H_2SO_4 and the precipitated zinc mercaptide filtered. The acid was liberated and extracted with ether. Evaporation of the solvent gave the dimercapto acid, which crystallized after being kept for some days at —15°. M. p. 57—60°. (Found: Equiv. wt. 75.7. Calc. for $C_4H_8O_2S_2$ (152.22): 76.1).

The authors are indebted to Professor Arne Fredga for valuable discussions. A grant from the *Swedish Natural Science Research Council* is gratefully acknowledged.

1. Schotte, L. *Arkiv Kemi* **9** (1956) No. 24.
2. Schotte, L. *Arkiv Kemi* **9** (1956) No. 37.
3. Jansen, E. F. *J. Biol. Chem.* **176** (1948) 657.
4. Corse, J. and Jansen, E. F. *J. Am. Chem. Soc.* **77** (1955) 6632.
5. Bullock, M. W., Brockman Jr., J. A., Patterson, E. L., Pierce, J. V., von Saltza, M. H., Sanders, F. and Stokstad, E. L. R. *J. Am. Chem. Soc.* **76** (1954) 1828.
6. Glattfeld, J. W. E. and Schneider, J. M. *J. Am. Chem. Soc.* **60** (1938) 415.
7. Claeson, G. *Acta Chem. Scand.* **9** (1955) 178.
8. Fredga, A. *Arkiv Kemi, Mineral. Geol.* **12A** (1938) No. 27.

Received April 21, 1956.

Ein Beispiel für die Variationsmöglichkeiten in der Zusammensetzung der freien Aminosäuren in einer Pflanzenart

BARBARA BRAMESFELD und ARTTURI I. VIRTANEN

Laboratorium der Stiftung für chemische Forschung, Biochemisches Institut, Helsinki, Finnland

Im Sommer 1954 isolierten Virtanen, Uksila und Matikkala [1] α-Amino-γ-hydroxy-pimelinsäure aus *Asplenium septentrionale*. Das Pflanzenmaterial war in den Monaten Mai, Juni, Juli und August gesammelt und gesondert auf seinen Aminosäuregehalt geprüft worden. Alle Alkoholextrakte zeigten im zwei-dimensionalen Papierchromatogramm (Butanol-Essigsäure-H_2O und Phenol-Ammoniak) die in Fig. 1 A dargestellte Zusammensetzung. Vom gleichen Standort wurde im August 1955—Juni und Juli waren ausser-gewöhnlich trocken — *Asplenium septentrionale* geerntet und der Alkoholextrakt dieses Materials ergab das Chromatogramm in Fig. 1 B, auf dem zwischen Asparaginsäure und Glutaminsäure ein Ninhydrin-positiver Fleck sichtbar ist.

Die Trennung dieser Aminosäure von Asparaginsäure und Glutaminsäure gelang zum Teil an Dowex 50 (200—400 mesh) mit 0.2 M Natriumcitratpuffer pH 3,48 [2]. Die Lage der Aminosäure im Chromatogramm deutete auf die von Steward *et al.*[3] aus *Adiantum pedatum* und von Virtanen und Berg [4] aus *Phyllitis scolopendrium* isolierte γ-Hydroxy-γ-methylglutaminsäure hin.

Die Reduktion mit 66 % HJ (d = 1.9) und rotem Phosphor bei 130° C für 4 Stdn. ergab Methylglutaminsäure. Nach Oxydation mit $KMnO_4$ in saurer Lösung erhielten wir im Chromatogramm einen gelben Flecken im Bereich der neutralen Aminosäuren, den wir bisher nicht identifiziert haben. Die reine Substanz enthält Kristallwasser, welches durch Erhitzen auf 105° C für 16 Stdn. mit ½ H_2O pro Mol. bestimmt wurde. Dies stimmt mit dem von Steward nach Elementaranalyse gefundenen Wert überein.

Der Perjodat-test auf nachbarständige Hydroxy- und Aminogruppe war negativ. N-Bestimmung: gef. 8.03 %; theor. 7.53 %. Die Substanz verkohlt ab 165°. Papier-

dissolved (without previous purification) in 400 ml of aqueous $NaHCO_3$ solution (containing 8.5 g (0.10 mole) of $NaHCO_3$). A small amount of $FeCl_3$ was added as a combined catalyst and indicator and oxygen bubbled through the mixture until the violet colour disappeared (about two hours). After acidification (dil. H_2SO_4) and removal of small amounts of polymeric material by filtration the product was extracted with ether (6 × 75 ml). The ether solution was dried with anhydrous Na_2SO_4 and the solvent evaporated *(in vacuo)*. 1.3 g (27 %) of crude acid (mixture of monomer and polymer) with m. p. 60—70° was obtained; after treatment with benzene for some minutes at room temperature it left an insoluble viscous substance. Evaporation of the solvent yielded 0.8 g (16.5 %) of dry acid (monomer) with m. p. 75—77°. This product was now recrystallized from benzene-*cyclo*hexane and obtained as transparent yellow prisms with m. p. 76.5—77.5°. (Found: Equiv. wt. 151.1; C 31.96; H 3.92; S 42.72; Mol.wt. 146. Calc. for $C_4H_6O_2S_2$ (150.22): Equiv. wt. 150.2; C 31.98; H 4.03; S 42.68; Mol.wt. 150).

β,β'-Dimercapto-isobutyric acid. 0.5 g of (I) or the related polymer (insoluble in benzene) was dissolved in 20 ml of 4 M ammonia, and the solution sucked through a layer of zinc powder four times. The reaction mixture was neutralized with dil. H_2SO_4 and the precipitated zinc mercaptide filtered. The acid was liberated and extracted with ether. Evaporation of the solvent gave the dimercapto acid, which crystallized after being kept for some days at —15°. M. p. 57—60°. (Found: Equiv. wt. 75.7. Calc. for $C_4H_8O_2S_2$ (152.22): 76.1).

The authors are indebted to Professor Arne Fredga for valuable discussions. A grant from the *Swedish Natural Science Research Council* is gratefully acknowledged.

1. Schotte, L. *Arkiv Kemi* **9** (1956) No. 24.
2. Schotte, L. *Arkiv Kemi* **9** (1956) No. 37.
3. Jansen, E. F. *J. Biol. Chem.* **176** (1948) 657.
4. Corse, J. and Jansen, E. F. *J. Am. Chem. Soc.* **77** (1955) 6632.
5. Bullock, M. W., Brockman Jr., J. A., Patterson, E. L., Pierce, J. V., von Saltza, M. H., Sanders, F. and Stokstad, E. L. R. *J. Am. Chem. Soc.* **76** (1954) 1828.
6. Glattfeld, J. W. E. and Schneider, J. M. *J. Am. Chem. Soc.* **60** (1938) 415.
7. Claeson, G. *Acta Chem. Scand.* **9** (1955) 178.
8. Fredga, A. *Arkiv Kemi, Mineral. Geol.* **12A** (1938) No. 27.

Received April 21, 1956.

Ein Beispiel für die Variationsmöglichkeiten in der Zusammensetzung der freien Aminosäuren in einer Pflanzenart

BARBARA BRAMESFELD und ARTTURI I. VIRTANEN

Laboratorium der Stiftung für chemische Forschung, Biochemisches Institut, Helsinki, Finnland

Im Sommer 1954 isolierten Virtanen, Uksila und Matikkala [1] α-Amino-γ-hydroxy-pimelinsäure aus *Asplenium septentrionale*. Das Pflanzenmaterial war in den Monaten Mai, Juni, Juli und August gesammelt und gesondert auf seinen Aminosäuregehalt geprüft worden. Alle Alkoholextrakte zeigten im zwei-dimensionalen Papierchromatogramm (Butanol-Essigsäure-H_2O und Phenol-Ammoniak) die in Fig. 1 A dargestellte Zusammensetzung. Vom gleichen Standort wurde im August 1955—Juni und Juli waren ausser-gewöhnlich trocken — *Asplenium septentrionale* geerntet und der Alkoholextrakt dieses Materials ergab das Chromatogramm in Fig. 1 B, auf dem zwischen Asparaginsäure und Glutaminsäure ein Ninhydrin-positiver Fleck sichtbar ist.

Die Trennung dieser Aminosäure von Asparaginsäure und Glutaminsäure gelang zum Teil an Dowex 50 (200—400 mesh) mit 0.2 M Natriumcitratpuffer pH 3,48 [2]. Die Lage der Aminosäure im Chromatogramm deutete auf die von Steward *et al.*[3] aus *Adiantum pedatum* und von Virtanen und Berg [4] aus *Phyllitis scolopendrium* isolierte γ-Hydroxy-γ-methylglutaminsäure hin.

Die Reduktion mit 66 % HJ (d = 1.9) und rotem Phosphor bei 130° C für 4 Stdn. ergab Methylglutaminsäure. Nach Oxydation mit $KMnO_4$ in saurer Lösung erhielten wir im Chromatogramm einen gelben Flecken im Bereich der neutralen Aminosäuren, den wir bisher nicht identifiziert haben. Die reine Substanz enthält Kristallwasser, welches durch Erhitzen auf 105° C für 16 Stdn. mit ½ H_2O pro Mol. bestimmt wurde. Dies stimmt mit dem von Steward nach Elementaranalyse gefundenen Wert überein.

Der Perjodat-test auf nachbarständige Hydroxy- und Aminogruppe war negativ. N-Bestimmung: gef. 8.03 %; theor. 7.53 %. Die Substanz verkohlt ab 165°. Papier-

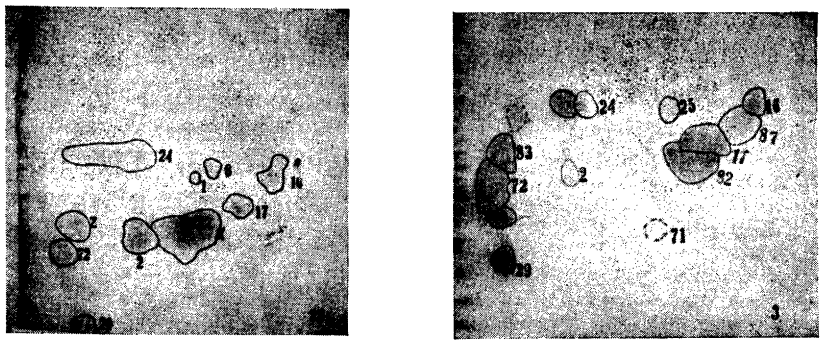


Fig. 1. Zwei-dimensionale Papierchromatogramme (Butanol-Essigsäure-H_2O und Phenol-NH_3) der freien Aminosäuren in Asplenium septentrionale.

A: Sommer 1954 [1]. B: August 1955.
1 = Glycin, 2 = Alanin, 8 = Serin, 16 = Asparaginsäure, 17 = Glutaminsäure, 24 = Glutamin, 29 = γ-Aminobuttersäure, 71 = α-Aminopimelinsäure, 72 = Acetylornithin, x = 82 = α-Amino-γ-hydroxypimelinsäure, z = 83 = Lakton der α-Amino-γ-hydroxypimelinsäure, 87 = γ-Hydroxy-γ-methylglutaminsäure.

chromatographisch war die Aminosäure identisch mit der aus *Phyllitis scolopendrium* isolierten. Aus den Ergebnissen ist zu schliessen, dass es sich um γ-Hydroxy-γ-methylglutaminsäure handelt. Ein Versuch, die Aminosäure zu decarboxylieren, verlief sowohl mit *Escherichia coli* als auch mit einem Extract aus *Asplenium nidus*-Blatt negativ. Glutaminsäure wird unter gleichen Bedingungen von *Escherichia coli* quantitativ und von *Asplenium nidus*-Extrakt zum grössten Teil decarboxyliert. Wie Virtanen und Hietala [5] gezeigt haben, wird auch γ-Hydroxyglutaminsäure von *Escherichia coli* decarboxyliert.

Da keine Spuren von dieser Aminosäure im Pflanzenmaterial von Mai, Juni, Juli und August 1954 papierchromatographisch zu finden waren, scheint es, dass die Aminosäure in den *Asplenium*-Proben des Sommers 1954 entweder total fehlte oder in so kleinen Mengen vorkam, dass sie keinen sichtbaren Flecken auf dem Chromatogramm bildete. Zu bemerken ist, dass γ-Methyl-γ-hydroxyglutaminsäure bedeutend schwächere Farbe mit Ninhydrin gibt als Glutaminsäure, γ-Hydroxyglutaminsäure und γ-Methylglutaminsäure. Unsere Befunde zeigen wie vorsichtig man sein muss bei der Beurteilung der Aminosäurezusammensetzung einer Pflanzenart auf Grund der Befunde einer einzigen Wachstumsperiode.

Im Mai 1956 wurden nochmals *Asplenium septentrionale* Proben vom gleichen Standort in der Nähe Helsinkis und ausserdem eine kleine Menge *Aspl. septentrionale* aus Locarno (Schweiz) auf ihren Aminosäuregehalt untersucht. In beiden Proben liess sich γ-Hydroxy-γ-methylglutaminsäure nachweisen; es scheint also, dass γ-Hydroxy-γ-methylglutaminsäure meistens in *Aspl. septentrionale* vorkommt.

1. Virtanen, A. I., Uksila, E. and Matikkala, E. J. *Acta Chem. Scand.* **8** (1954) 1091.
2. Moore, S. and Stein, W. H. *J. Biol. Chem.* **192** (1951) 663.
3. Grobbelaar, N., Pollard, J. K. and Steward, F. C. *Nature* **175** (1955) 703.
4. Virtanen, A. I. and Berg, A.-M. *Acta Chem. Scand.* **9** (1955) 553.
5. Virtanen, A. I. and Hietala, P. K. *Acta Chem. Scand.* **9** (1955) 549.

Eingegangen am 17. April 1956.

Infrared Conformational Analysis of 1,2-Dichloro-4,5-dibromo*cyclo*hexane (*a,a-e,e* ⇌ *e,e-a,a*)

K. LUNDE

Universitetets Kjemiske Institutt, Blindern — Oslo, Norway

Some years ago the compound 1,2-dichloro-4,5-dibromo*cyclo*hexane (*a, a—e, e* ⇌ *e, e—a, a*) was prepared in this laboratory [1] in order to see which of the two possible conformations, a or b (Fig. 1), would be the preferred one. According to an X-ray investigation by Hassel and Wang Lund [2] the bromine atoms are in the *e, e* position (Fig. 1a) in the solid state. Using the electron diffraction method Bastiansen and Hassel [3] demonstrated that this conformation was the only detectable also for the molecules in the vapour phase.

This latter result has now been confirmed by the present investigation, using the general assumption that no large shift in the conformational equilibrium should be expected on going from the vapour to the liquid phase. The infrared spectra of the solid compound (nujol mull) and that of the liquid (dissolved in carbon disulphide) were practically identical. Considering the very small quantities of molecular species which can be detected by infrared analysis this result seems remarkable. It indicates a much lower energy content for the free molecules of conformation a than of conformation b (Fig. 1).

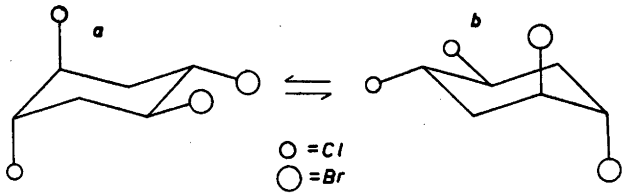


Fig. 1.

Furthermore, it is quite interesting to compare the X-ray results for the solid 1,2-dibromo-4,5-dichloro compound with a recent infrared investigation of the *trans* 1,2-dichloro- and *trans* 1,2-dibromo-*cyclo*hexane [4]. These dihalogeno*cyclo*hexanes can be regarded as the two "halves" of the 1,2-dichloro-4,5-dibromo-*cyclo*hexane molecule. They crystallize, however, according to the infrared investigation in inversed conformations: The dichloro-*cyclo*hexane has the conformation *e, e* and the dibromo-*cyclo*hexane the conformation *a, a* in the solid state. It will be seen that this is just the inverted geometrical direction of the halogen atoms in the crystalline 1,2-dichloro-4,5-dibromo*cyclo*hexane. The explanation of this phenomenon may be simple: When the energy difference between two conformations of a molecule is small, the lattice packing forces may become the determining factor. Thus, the question of which conformation is present in the crystals will be the question of which conformation gives the most favourable lattice packing.

This argument can, of course, not be used when considering the molecules in their free state. It is therefore surprising to compare the conformational equilibria of the two *trans* 1,2-dihalogeno*cyclo*hexanes with the data for the 1,2,4,5-tetrahalogeno compound. In the liquid dihalogeno*cyclo*hexanes there are almost equal quantities of the two possible conformations, whereas only *one* conformation has been observed in the case of the tetrahalogeno compound. This unexpected finding cannot be accounted for by simple considerations involving steric interactions.

The author wishes to thank *Sentralinstitutt for Industriell Forskning* for cooperation in recording the spectra and *Norges almenvitenskaplige forskningsråd* for financial support.

1. Hassel, O., Wang Lund, E. and Lunde, K. *Acta Chem. Scand.* **6** (1952) 426.
2. Hassel, O. and Wang Lund, E. *Acta Chem. Scand.* **6** (1952) 238.
3. Bastiansen, O. and Hassel, O. *Acta Chem. Scand.* **5** (1951) 1404.
4. Klæboe, P., Lothe, J. and Lunde, K. *To be published shortly.*

Received April 21, 1956.

A Simple Method for Preparation of Glucose-3,4-^{14}C

H. PALMSTIERNA and G. EHRENSVÄRD

Chemical Department, Karolinska Institutet Stockholm; Department of Physiological Chemistry, Wenner-Grens Institut, Stockholm, Sweden

As shown before [1] *Escherichia coli B* accumulates a glycogen-like polysaccharide during the lag phase of growth. This finding could be used to label the glycogen-glucose preponderantly in the position C_3 and C_4. One way of obtaining such a labeling would be to grow the cells on lactate-1-^{14}C, expecting the pyruvate formed to enter the classical Embden-Meyerhof pathway towards glucose. Another possibility would be to circumvent the cumbersome synthesis of labeled lactate and cultivate the cells on non-labeled lactate in the presence of $^{14}CO_2$, expecting a CO_2-incorporation by way of the Wood-Werkman reaction and the tricarboxylic acid cycle to occur. Our experiments were carried out with this last assumption in mind.

Method: The cells were precultivated aerobically under shaking in a 6-litre Erlenmeyer flask containing 5 l of Friedleins lactate medium [2] (medium I) and harvested in the cold after 18 hours. About 4 g of cells (wet weight) were inoculated into a 6-litre Erlenmeyer flask containing 4 l of the medium mentioned, from which, however, the ammonium chloride had been omitted (medium II). It should be stressed that the cells must be kept in the cold until the moment of inoculation. A slight underpressure was effected in the vessel and a quantity of ^{14}C-labeled carbon dioxide was introduced corresponding to 2 g of barium carbonate. This will give an atmosphere containing about 10 % of carbon dioxide. After closing, the flask was vigorously shaken for 15 minutes before the inoculation. For practical reasons the cells were introduced by means of a syringe containing the cells suspended in 50 ml of cold medium II. The cells were allowed to grow for 60 minutes under very vigorous shaking.

Growth may either be interrupted by cooling the content of the flask to 4° or by adding formaldehyde to a final concentration of 0.5 %. The cells were harvested by centrifugation in the cold [1] and lyophilized. The glycogen was isolated and hydrolysed as previously described [1]. After purification by chromatography according to Gardell [3], the glucose was subjected to biological degradation in order to determine the ^{14}C-content in the separate carbon atoms of the glucose molecule * [4].

Results. The yield of glucose varied between 80 and 126 mg. In one experiment the distribution of the activity in the glucose obtained was as follows:

Carbon atoms 3,4	116 c.p.m. per μg
Carbon atoms 2,5	1.8 c.p.m. per μg
Carbon atoms 1,6	2.6 c.p.m. per μg

More than 95 % of the activity has thus entered carbon atoms 3 and 4. It must be stressed that the method of degradation used does not differentiate between the carbon atoms 3 and 4. Further work is in progress to find the ratio between the specific activities incorporated into C_3 and C_4. The isotope entering the positions 3 and 4 was diluted between 10 and 15 times. The specific activity of the protein carbon was in one experiment 21 c.p.m. per μg protein carbon. The specific activity of the glycogen carbon was in the same experiment 198 c.p.m. per μg of glucose carbon, showing that very little of the activity was lost to the protein. The remaining $^{14}CO_2$ in the atmosphere and the culture medium may be trapped by conventional methods and reutilized for further cultures of the same type as described, thus stepping up the actual yield of glucose-3,4-^{14}C considerably. The limiting factor is the amount of CO_2 expired by the cells. According to preliminary experiments it does not seem impossible to step up the yield to 20 %.

1. Palmstierna, H. *Acta Chem. Scand.* **9** (1955) 195.
2. Friedlein, F. *Biochem. Z.* **194** (1928) 273.
3. Gardell, S. *Acta Chem. Scand.* **7** (1953) 201.
4. Wood, H. G., Lifson, N. and Lorber, V. *J. Biol. Chem.* **159** (1945) 475.

* We are indebted to Mr. R. Stjernholm, Dept. of Biochemistry, Medical School, Western Reserve University, Ohio, for carrying out this analysis.

Received April 24, 1956.

Difficulties at the Infrared-Spectrophotometric Identification and Estimation of Pure Compounds and Mixtures by Use of Potassium Bromide Disk Technique

BØRGE BAK and DANIEL CHRISTENSEN

Chemical Laboratory of the University of Copenhagen, Copenhagen, Denmark

Spectra of a number of biologically active compounds such as urea, D-glucose, D-fructose, amino acids etc. have been studied in the infrared, using pressed KBr-disk technique. Examples show that identification of the compounds of even simple mixtures of compounds of this type meets with difficulties of unexpected magnitude.

With the advent of the KBr-disk technique [1,2] new fields of research were opened up. Since strong, discrete spectra are obtainable from a mixture of 0.2—2.0 mg crystalline material and 500 mg KBr, evaporation residues from rather small amounts of reaction mixtures, blood serum, tissue liquids etc. can now be examined spectrophotometrically in the infrared. In this connection it is of interest to know how well-defined a KBr-disk spectrum of a *pure compound* is. Also, the spectra of *mixtures* may or may not obey the 'superposition principle' to the same extent as for mixtures of liquids and mixtures of gases. We want to illuminate these problems by practical examples from an investigation of blood serum crystalloids in which we are engaged. No complete treatment of the subject is intended.

Experimental. All our spectra were recorded on a Beckmann IR 2 instrument with NaCl optics. Water vapor and CO_2 had effectively been removed from the spectrograph by flushing with air from a liquid-air container. The quantity of sample to be mixed with 500 mg KBr never exceeded *ca.* 2 mg. Table 1 gives the results of seven experiments with glycine. The method of disk preparation marked with an '*a*' in Table 1 consisted in mixing the quantity of crystalline glycine indicated with 500 mg KBr, shaking the mixture in a conventional von Ardenne vibrator [3], and finally pressing the disk *in vacuo*. The recorded spectra were quite comparable in quality with spectra of liquids and gases. Lines in the region where the spectrograph has high resolving power (667—1 000 cm^{-1}) appear typically with a width of about 10 cm^{-1} at the 'foot' and very sharp maxima with D (optical density) = 0.3—0.4 for 1 mg samples.

In many types of experiment it is, however, impossible or impractical to use the '*a*' procedure. In such cases we dissolve 300 mg KBr in 1—2 ml of an aqueous solution of the compound(s) to be investigated, whereafter the water is removed by freeze-drying. The resulting voluminous crystalline powder is slightly compressed in order to decrease the volume, 200 mg KBr is added, a five minutes treatment in the vibrator follows and a disk is pressed (procedure *b*).

The results in Table 1 show that method *b* gives spectral lines at 894 and 912 cm^{-1} of *equal* peak intensity in contrast to the lines of *different* intensity observed with

Table 1. Optical density at maximum of some of the spectral lines observed for KBr-disks containing glycine.

Experiment number	Glycine quantity (mg)	Method of disk preparation	Optical density of disk at top of absorption line at (cm^{-1}) 700	894	912	934
1	1.170	*a*	0.25	0.32	0.26	No line
2	1.210	*b*	0.25	0.31	0.30	» »
3	1.180	*b*	0.33	0.37	0.36	» »
4	1.150	*c*	0.37	0.38	0.38	» »
5	0.818	*b*	0.21	0.27	0.26	» »
6	0.414	*b*	0.06	0.13	0.11	0.05
7	0.400	*b*	0.06	0.12	0.10	0.04

the *a* procedure. In method *c* an aqueous glycine solution (1 ml) was freeze-dried. The resulting glycine was mixed with 500 mg KBr, vibrated and pressed. The spectrum only deviates from *b*-spectra in the astonishing high intensity of the band at 700 cm^{-1}. Since the glycine particle size is probably more uniform in freeze-drying experiments (*b*) then by 'dry mixing' (*a*), freeze-drying is likely to mean a step towards a standardization of the disk-spectra. But a glance at the results in expts. Nos. 2 and 3 (Table 1) shows that no simple relationship between spectral band intensity and compound quantity exists. Expts. 3, 5 and 6 in which the freeze-drying was carried out simultaneously do show a very rough Beer's law agreement. But as will be noted, expt. 6 (successfully repeated in expt. 7) presents the surprising feature that a new line is observed! The remaining part of the glycine spectrum has the same not too well defined character but we chose the examples in Table 1 in order to speak of bands that could be observed with optimum resolving power. Since we know now with what kind of uncertainties we are dealing in the disk-spectrum of a pure compound we shall see what happens with mixtures.

Glycine and L-*alanine* form relatively well-behaving mixtures. Spectra of disks prepared by *a* and *b* procedure are almost identical. Roughly, they are a superposition of a glycine and an alanine spectrum. But the absorption intensities are wrong. For the line at 894 cm^{-1} in the spectrum of a mixture (glycine 0.87 mg; alanine 0.619 mg) we would expect $D = 0.27$ at the maximum (Table 1). We found $D = 0.20$. But inspite of similar defaults throughout the spectrum nobody would doubt that one sees the spectrum of a mixture of glycine and alanine since no bands of medium and high intensity from these components are missing and *no* extra bands are found.

In the disk-spectrum of mixtures of *urea and* D-*glucose* prepared by method *a* and *b*, *no* bands corresponding to the strong absorption at 1 481 and 1 716 cm^{-1} in urea occur (urea quantity 0.5 mg; D-glucose 1.5 mg). In return, both disks have an extra line at 1 460 cm^{-1} (which may be a displaced 1 481-band (urea)). A band, corresponding to the urea band at 1 169 cm^{-1} is observed in the 'dry' disk (proc. *a*), but hardly in the 'wet' (*b*). The freeze-dried disk has a band at 1 083 cm^{-1} neither to be found in the spectrum of pure D-glucose, nor in the urea spectrum. A superficial glance at the disk-spectrum of the urea-glucose spectrum immediately makes one suspect what the components are. But closer inspection reveals features quite incompatible with the superposition principle, even if this is reduced to being of only qualitative validity.

A third case may be mentioned in which the identification of the components is even more difficult. We studied mixtures of *glycine and* L-*aspartic acid.* Between 863 and 953 cm^{-1} glycine has bands at 894 and 912 cm^{-1}. Aspartic acid has bands at 875 ($D = 0.06$), 900 ($D = 0.11$), and 940 ($D = 0.03$) (sample quantity 1.156 mg). A 'dry-mixed' disk with 0.987 mg aspartic acid and 0.532 mg glycine roughly shows the four bands to be expected from superposition, namely, at 875; $(894 + 900)/2 = 897$; 912, and 940 cm^{-1}. If 3/5 of the disk is treated by the 'wet' procedure (*b*), a spectrum results with only one pronounced maximum at 904 cm^{-1}. Also a band at 700 cm^{-1} which would indicate the presence of glycine, is completely missing. From the spectrum of the freeze-dried disk one can probably conclude that the disk contains two or more *amino acids.* But it seems impossible to deduct that a simply glycine-aspartic acid mixture is present.

No simple explanation covers the glycine-aspartic acid case. If it is suggested that hydrogen ions are transferred from the latter (being the stronger acid) to the former this would mean that we should 'see' the ion $H_3\overset{+}{N}-CH_2-COOH$. But the spectrum of this ion we know from a study of glycine hydrochloride which has dominant lines at 807 and 859 cm^{-1} where no lines are observed by us in any glycine-aspartic acid mixture.

Discussion. Ebert and Gottlieb [4] found pronounced differences in the spectra of *polymorphic* compounds (in Nujol), but it seems impossible to assume any kind of polymorphism in our cases. Kirkland [5] has emphasized that caution must be used when attempting to apply the disk technique to systems containing solid solutions or mixed crystals, but no examples of the effect to be expected were given by him. The findings by Brockmann and Musso [6] seem more interesting in the present connection. They demonstrated that differences exist between the spectra of optical isomers and the spectrum of the racemate, provided that the optical isomer and the racemate differ sufficiently in melting

point and solubility. Also, they claim that mixtures of optical isomers can be converted to the racemate if the KBr disk technique is applied (see also Right [7]). Therefore, the optical isomers can 'find' each other inspite of the great quantity of KBr, consistent with our result on the 'dry' D-glucose-urea mixture. Brockmann and Musso state that probably hydrogen bonding is responsible for the effects they found. The same explanation may be valid here, but further experiments are undoubtedly necessary to verify this interpretation. Therefore, although KBr disk spectra are of great value to the analyst they must be used with some reservation in view of the present incomplete experimental coverage of the field and the lack of adequate theoretical insight.

1. Stimson, M. *J. Am. Chem. Soc.* **74** (1952) 1805.
2. Schieds, U. *Z. Naturforsch.* **76** (1952) 270.
3. v. Ardenne, M. *Angew. Chem.* **54** (1941) 144.
4. Ebert, A. and Gottlieb, H. B. *J. Am. Chem. Soc.* **74** (1952) 2806.
5. Kirkland, J. J. *Anal. Chem.* **27** (1955) 1537.
6. Brockmann, H. and Musso, H. *Ber.* **89** (1956) 241.
7. Right, N. *J. biol. Chem.* **127** (1939) 137.

Received April 25, 1956.

On Sialic Acid in Brain Tissue

LARS SVENNERHOLM

Department of Medical Biochemistry, University of Gothenburg, Gothenburg, Sweden

Gangliosides were isolated from brains by exhausted extraction with methanol-chloroform (2:1, v/v). After evaporation of the solvent *in vacuo* and drying the residue with ethanol the lipids were redissolved in waterfree solvent of the same composition. An insoluble rest remained, and it was considerably larger when the tissue was extracted directly with methanol-chloroform without previous drying with acetone. It was composed of low molecular substances, such as amino acids, purines and salts but also substances of high molecular weight. The low molecular substances were removed by repeated dialysis against distilled water. The total amount of carbohydrates (hexose, hexosamine and sialic acid) was high (20–50 % in different samples) in the dialysed material. After hydrolysis several amino acids were also identified with paper chromatography. If strandin prepared according to procedure C of Folch, Arsove and Meath [1] was redissolved in methanol-chloroform (2:1) a substance containing hexosamine and sialic acid remained undissolved.

Only a few similar observations have been found in the literature. Klenk and Lauenstein [2] isolated a substance from methanol-chloroform extract of erythrocyte stroma which was only soluble in hot pyridine and contained a high amount of hexosamine. Rosenberg, Howe and Chargaff [3] have recently identified several amino acids after hydrolysis of strandin prepared by procedure C of Folch *et al.*

The observations described indicate that amino sugar and sialic acid are not only occurring in the lipopolysaccharides (gangliosides) but also in other substances in brain.

A quantitative estimation of sialic acid with Bial's reagent [4] in brain tissue, from which the lipids had been extracted, demonstrated that the amount of 'protein-bound' sialic acid was higher than that of lipid-bound. The amount of sialic acid was higher in old brains than in young ones and about twice as high in grey as compared with white matter. In adult brain the content was about 0.6 %, calculated on lipid-free brain tissue. N-Acetyl-sialic acid has now been isolated from lipid-free brain tissue and its X-ray diagram compared with that of sialic acid from gangliosides and serum proteins.

Analytical methods. Nitrogen was determined by the Kjeldahl micromethod. Hexose was determined with an orcinol-sulphuric acid method [5] and calculated as galactose. Hexosamine was assayed with a modified Elson and Morgan method [6], and glucosamine was separated by the procedure outlined by Gardell [7]. The determination of sialic acid was performed with Bial's reagent and calculated as N-acetyl sialic acid (mol.wt. 309) [4]. The X-ray powder diagrams were taken with a Guinier camera using copper $K\alpha$-radiation.

Materials. Brains from old people were freed from membranes and blood vessels. Grey matter was dissected free from the main part of white matter and water removed by two successive treatments with 4 vol. of acetone at 0°. The dried brain powder was extracted with

point and solubility. Also, they claim that mixtures of optical isomers can be converted to the racemate if the KBr disk technique is applied (see also Right [7]). Therefore, the optical isomers can 'find' each other inspite of the great quantity of KBr, consistent with our result on the 'dry' D-glucose-urea mixture. Brockmann and Musso state that probably hydrogen bonding is responsible for the effects they found. The same explanation may be valid here, but further experiments are undoubtedly necessary to verify this interpretation. Therefore, although KBr disk spectra are of great value to the analyst they must be used with some reservation in view of the present incomplete experimental coverage of the field and the lack of adequate theoretical insight.

1. Stimson, M. *J. Am. Chem. Soc.* **74** (1952) 1805.
2. Schieds, U. *Z. Naturforsch.* **76** (1952) 270.
3. v. Ardenne, M. *Angew. Chem.* **54** (1941) 144.
4. Ebert, A. and Gottlieb, H. B. *J. Am. Chem. Soc.* **74** (1952) 2806.
5. Kirkland, J. J. *Anal. Chem.* **27** (1955) 1537.
6. Brockmann, H. and Musso, H. *Ber.* **89** (1956) 241.
7. Right, N. *J. biol. Chem.* **127** (1939) 137.

Received April 25, 1956.

On Sialic Acid in Brain Tissue

LARS SVENNERHOLM

Department of Medical Biochemistry, University of Gothenburg, Gothenburg, Sweden

Gangliosides were isolated from brains by exhausted extraction with methanol-chloroform (2:1, v/v). After evaporation of the solvent *in vacuo* and drying the residue with ethanol the lipids were redissolved in waterfree solvent of the same composition. An insoluble rest remained, and it was considerably larger when the tissue was extracted directly with methanol-chloroform without previous drying with acetone. It was composed of low molecular substances, such as amino acids, purines and salts but also substances of high molecular weight. The low molecular substances were removed by repeated dialysis against distilled water. The total amount of carbohydrates (hexose, hexosamine and sialic acid) was high (20–50 % in different samples) in the dialysed material. After hydrolysis several amino acids were also identified with paper chromatography. If strandin prepared according to procedure C of Folch, Arsove and Meath [1] was redissolved in methanol-chloroform (2:1) a substance containing hexosamine and sialic acid remained undissolved.

Only a few similar observations have been found in the literature. Klenk and Lauenstein [2] isolated a substance from methanol-chloroform extract of erythrocyte stroma which was only soluble in hot pyridine and contained a high amount of hexosamine. Rosenberg, Howe and Chargaff [3] have recently identified several amino acids after hydrolysis of strandin prepared by procedure C of Folch *et al.*

The observations described indicate that amino sugar and sialic acid are not only occurring in the lipopolysaccharides (gangliosides) but also in other substances in brain.

A quantitative estimation of sialic acid with Bial's reagent [4] in brain tissue, from which the lipids had been extracted, demonstrated that the amount of 'protein-bound' sialic acid was higher than that of lipid-bound. The amount of sialic acid was higher in old brains than in young ones and about twice as high in grey as compared with white matter. In adult brain the content was about 0.6 %, calculated on lipid-free brain tissue. N-Acetyl-sialic acid has now been isolated from lipid-free brain tissue and its X-ray diagram compared with that of sialic acid from gangliosides and serum proteins.

Analytical methods. Nitrogen was determined by the Kjeldahl micromethod. Hexose was determined with an orcinol-sulphuric acid method [5] and calculated as galactose. Hexosamine was assayed with a modified Elson and Morgan method [6], and glucosamine was separated by the procedure outlined by Gardell [7]. The determination of sialic acid was performed with Bial's reagent and calculated as N-acetyl sialic acid (mol.wt. 309) [4]. The X-ray powder diagrams were taken with a Guinier camera using copper $K\alpha$-radiation.

Materials. Brains from old people were freed from membranes and blood vessels. Grey matter was dissected free from the main part of white matter and water removed by two successive treatments with 4 vol. of acetone at 0°. The dried brain powder was extracted with

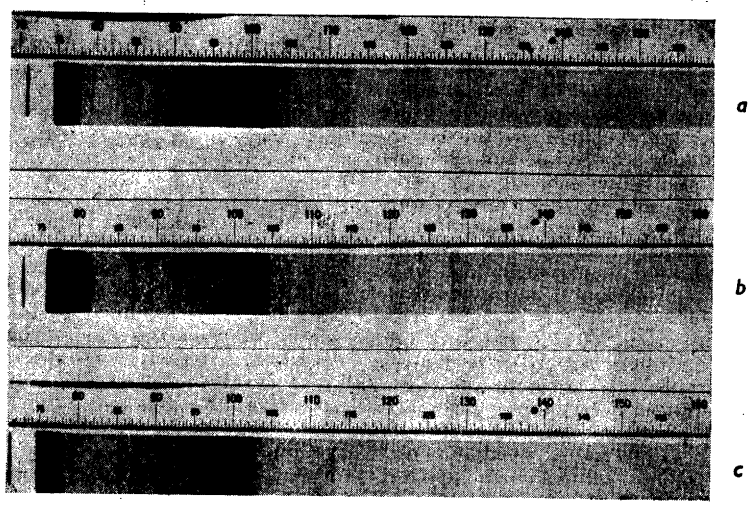


Fig. 1. X-ray powder diagram of N-acetyl-sialic acid isolated from (a) serum, (b) gangliosides and (c) lipid-free brain tissue.

methanol-chloroform (2:1, v/v) in a modified Soxhlet apparatus during 24 hours.

Gangliosides were prepared from the lipid extract by chromatography on cellulose columns [8]. Analysis of the potassium salt of gangliosides gave the following composition: nitrogen 2.70 %, chondrosamine (base) 6.45 %, hexose 27.5 %, N-acetyl-sialic acid 25.2 %.

Lipid-free substance. Portions of 100 g extracted tissue were suspended in about 3 l of 0.01 N sulphuric acid at 0° and shaken for at least 4 hrs. The liquid was filtered off and the treatment of the tissue was repeated until pH of the filtrate did not exceed 2.5. The substance was then hydrolysed as described below. *Analysis* (figures calculated on dry weight). Hexosamine 0.7 % (ratio glucosamine: galactosamine = 3:1), N-acetyl-sialic acid 0.9 %.

Serum. Pooled human serum was added four volumes of ethanol and brought to boiling. The precipitate was then treated as described for lipid-free brain substance. *Analysis* (calc. on dry weight). Hexose 1.8 %, hexosamine 1.3 % (glucosamine:galactosamine = 12:1), N-acetyl-sialic acid 1.0 %.

Isolation of N-acetyl-sialic acid. The procedure used [9] for isolation of N-acetyl-sialic acid has in the main been the same as that described by Zilliken, Braun and György [10] for the isolation of gynaminic acid from human milk.

The yield of crystalline acid was 40—50 % calculated from the quantitative estimation of N-acetyl-sialic acid with Bial's reagent on the starting material.

The isolated acids were tested by partition chromatography on Whatman paper No. 1. The solvents used were *n*-butanol-acetic acid-water (4:1:5), *sec*-butanol-acetic acid-water (4:1:5) and *sec*-butanol-acetone-acetic acid-water (3:3:1.5:2.5). After drying of the chromatograms the sialic acids were detected by spraying with [10]: orcinol-trichloroacetic acid [11]. All the crystallized acids ran as only one spot and had the same R_F-values. The X-ray diffraction patterns of the acids were identical (Fig. 1). The X-ray diagrams were also identical with that of ovine sialic acid [12].

Conclusion. N-Acetyl-sialic acid ($C_{11}H_{19}NO_9$) has been isolated from brain gangliosides and lipid extracted brain tissue.

The methods worked out for the quantitative estimation of gangliosides are based on determinations of sialic acid in lipid extracts. But a minor part of the non-lipid-bound sialic acid is extracted together with the lipids by methanol-chloroform mixtures containing some water. So when fresh tissues are extracted

directly with methanol-chloroform mixtures too high values for gangliosides are obtained.

Rittenberg, Howe and Chargaff [8] have suggested the existence of both gangliosides and mucolipids (strandin) in brain tissue, as they found that strandin contained amino acids, which was not the case of gangliosides. When strandin, prepared by the method used by them, was chromatographed on a cellulose column [9] with chloroform-methanol mixtures, gangliosides were isolated in the effluents, while on the top of the column a substance remained which gave strong positive reactions for sialic acid (Bial's reagent) and amino-acids (ninhydrin). After hydrolysis of the substance all the common amino acids were indicated by paper chromatography. A further evidence for the heterogenity of strandin is that Folch *et al.*[1] showed only amino acids in strandin prepared with the partition dialysis method (procedure C) but not in strandin prepared by two other procedures.

Until further data are given for strandin we have to consider it is a ganglioside to which other substances are associated. Gangliosides consist of a hydrophobic and a hydrophilic portion and may be able to act as protecting colloids for, *e.g.*, polypeptides in organic solvents and cerebrosides in water.

Acknowledgment. The author is indebted to Dr. E. von Sydow, Kemiska Institutionen, Uppsala, for performing the X-ray diagrams.

1. Folch, J., Arsove, S. and Meath, J. A. *J. Biol. Chem.* **191** (1951) 819.
2. Klenk, E. and Lauenstein, K. *Hoppe-Seylers Z. physiol. Chem.* **291** (1953) 249.
3. Rosenberg, A., Howe, C. and Chargaff, E. *Nature* **175** (1956) 234.
4. Svennerholm, L. *Colloque sur les Lipidoses du Système Nerveux Central*, Anvers 1955.
5. Svennerholm, L. *J. Neurochem.* 1 (1956) 42.
6. Svennerholm, L. *Unpublished.*
7. Gardell, S. *Acta Chem. Scand.* **7** (1953) 207.
8. Svennerholm, L. *Ibid.* **8** (1954) 1108.
9. Svennerholm, L. *Acta Soc. Med. Uppsaliensis* **61** (1956) 00.
10. Zilliken, F., Braun, G. A. and György, P. *Arch. Biochem. and Biophys.* **54** (1955) 564.
11. Klevstrand, R. and Nordahl, A. *Acta Chem. Scand.* **4** (1950) 1320.
12. Blix, G., Lindberg, E., Odin, L. and Werner, I. *Nature* **175** (1955) 340.

Received April 28, 1956.

Structure of the 1:1 Compound Pyridine — Iodo Monochloride

O. HASSEL and CHR. RØMMING

Universitetets Kjemiske Institutt, Blindern-Oslo, Norway

It has been suggested that the 1:1 complexes probably present in the liquids containing pyridine and halogens are non-planar: The halogen atom directly linked to nitrogen is assumed to lie in the ring plane whereas the second halogen atom (bearing a negative charge) was expected to form an electrostatic link with the (positive) nitrogen atom and to lie outside the ring plane [1,2]. Unfortunately the yellow precipitate obtained by adding water to a solution of iodine in pyridine has been shown to contain water and the very unstable compound obtained in the absence of water does not appear to have the 1:1 composition [3]. Our X-ray work has therefore started with the iodo monochloride compound [4], the yellow, needle-shaped crystals of which (m. p. 132° C) turned out to be monoclinic — space group $P2_1/c$ — with the parameters $a = 4.25$, $b = 12.29$, $c = 14.07$, $\beta = 94.4°$. Using trial and error methods approximate y and z parameters of the iodine atoms (occupying a fourfold position) could easily be determined and signs of the structure factors evaluated which made possible a preliminary Fourier synthesis referring to the $(0kl)$-zone.

In Fig. 1a the refined electron density map is reproduced. The pyridine ring drawn in the figure is derived not from the direct synthesis but is slightly modified according to the results of a difference synthesis with subtraction of the contribution to structure factors from the halogen atoms. The $(h0l)$-synthesis in its final form is given in Fig. 1b. Here the overlapping of *two* pyridine rings forms an obstacle to a more precise determination especially of the carbon coordinates. A difference synthesis with subtraction of the contribution of the *iodine* atoms led to a z coordinate of the nitrogen atom which did not deviate more than 0.004 from the value obtained in the first projection. Neglecting not observed reflexions, the R factors for the two zones are 0.12 and 0.14, respectively.

From the above results it may safely be

directly with methanol-chloroform mixtures too high values for gangliosides are obtained.

Rittenberg, Howe and Chargaff [8] have suggested the existence of both gangliosides and mucolipids (strandin) in brain tissue, as they found that strandin contained amino acids, which was not the case of gangliosides. When strandin, prepared by the method used by them, was chromatographed on a cellulose column [9] with chloroform-methanol mixtures, gangliosides were isolated in the effluents, while on the top of the column a substance remained which gave strong positive reactions for sialic acid (Bial's reagent) and amino-acids (ninhydrin). After hydrolysis of the substance all the common amino acids were indicated by paper chromatography. A further evidence for the heterogenity of strandin is that Folch *et al.*[1] showed only amino acids in strandin prepared with the partition dialysis method (procedure C) but not in strandin prepared by two other procedures.

Until further data are given for strandin we have to consider it is a ganglioside to which other substances are associated. Gangliosides consist of a hydrophobic and a hydrophilic portion and may be able to act as protecting colloids for, *e.g.*, polypeptides in organic solvents and cerebrosides in water.

Acknowledgment. The author is indebted to Dr. E. von Sydow, Kemiska Institutionen, Uppsala, for performing the X-ray diagrams.

1. Folch, J., Arsove, S. and Meath, J. A. *J. Biol. Chem.* **191** (1951) 819.
2. Klenk, E. and Lauenstein, K. *Hoppe-Seylers Z. physiol. Chem.* **291** (1953) 249.
3. Rosenberg, A., Howe, C. and Chargaff, E. *Nature* **175** (1956) 234.
4. Svennerholm, L. *Colloque sur les Lipidoses du Système Nerveux Central*, Anvers 1955.
5. Svennerholm, L. *J. Neurochem.* 1 (1956) 42.
6. Svennerholm, L. *Unpublished.*
7. Gardell, S. *Acta Chem. Scand.* **7** (1953) 207.
8. Svennerholm, L. *Ibid.* **8** (1954) 1108.
9. Svennerholm, L. *Acta Soc. Med. Uppsaliensis* **61** (1956) 00.
10. Zilliken, F., Braun, G. A. and György, P. *Arch. Biochem. and Biophys.* **54** (1955) 564.
11. Klevstrand, R. and Nordahl, A. *Acta Chem. Scand.* **4** (1950) 1320.
12. Blix, G., Lindberg, E., Odin, L. and Werner, I. *Nature* **175** (1955) 340.

Received April 28, 1956.

Structure of the 1:1 Compound Pyridine — Iodo Monochloride

O. HASSEL and CHR. RØMMING

Universitetets Kjemiske Institutt, Blindern-Oslo, Norway

It has been suggested that the 1:1 complexes probably present in the liquids containing pyridine and halogens are non-planar: The halogen atom directly linked to nitrogen is assumed to lie in the ring plane whereas the second halogen atom (bearing a negative charge) was expected to form an electrostatic link with the (positive) nitrogen atom and to lie outside the ring plane [1,2]. Unfortunately the yellow precipitate obtained by adding water to a solution of iodine in pyridine has been shown to contain water and the very unstable compound obtained in the absence of water does not appear to have the 1:1 composition [3]. Our X-ray work has therefore started with the iodo monochloride compound [4], the yellow, needle-shaped crystals of which (m. p. 132° C) turned out to be monoclinic — space group $P2_1/c$ — with the parameters $a = 4.25$, $b = 12.29$, $c = 14.07$, $\beta = 94.4°$. Using trial and error methods approximate y and z parameters of the iodine atoms (occupying a fourfold position) could easily be determined and signs of the structure factors evaluated which made possible a preliminary Fourier synthesis referring to the $(0kl)$-zone.

In Fig. 1a the refined electron density map is reproduced. The pyridine ring drawn in the figure is derived not from the direct synthesis but is slightly modified according to the results of a difference synthesis with subtraction of the contribution to structure factors from the halogen atoms. The $(h0l)$-synthesis in its final form is given in Fig. 1b. Here the overlapping of *two* pyridine rings forms an obstacle to a more precise determination especially of the carbon coordinates. A difference synthesis with subtraction of the contribution of the *iodine* atoms led to a z coordinate of the nitrogen atom which did not deviate more than 0.004 from the value obtained in the first projection. Neglecting not observed reflexions, the R factors for the two zones are 0.12 and 0.14, respectively.

From the above results it may safely be

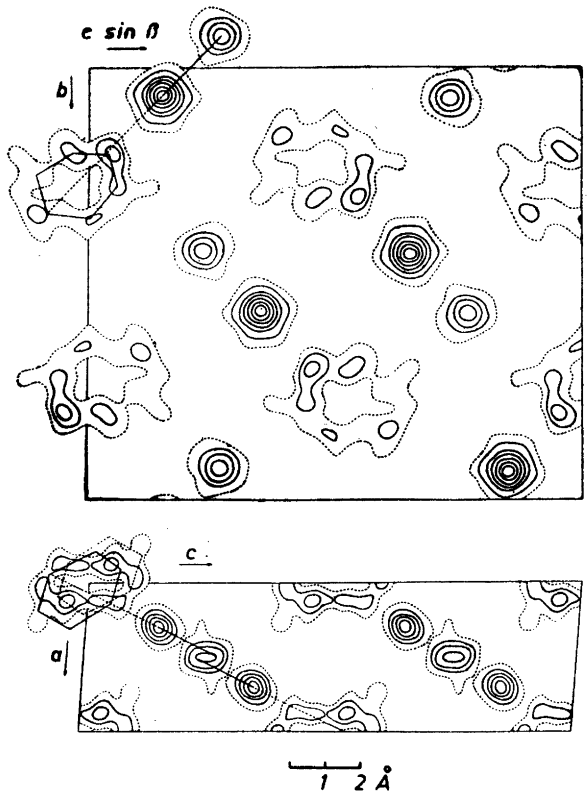


Fig. 1. a. Fourier projection along a-*axis. b. Fourier projection along* b-*axis. Approximate relative position of two overlapping pyridine rings is indicated. In both projections the ratio of contour line distances is: N(C): Cl : I = 1 : 2 : 5.*

concluded that the I, Cl and N atoms are situated at least very nearly on a straight line. The projection 1a together with considerations of ring dimensions [5] strongly suggest that the carbon atom opposite to the nitrogen atom is also situated on this line. The I, Cl and N parameters are: I(0.298, 0.068, 0.151); Cl(0.509, 0.072, 0.268) and N(0.141, 0.201, 0.047). From these values the following distances result: I—Cl = 2.51 Å, N—Cl = 2.2$_6$ Å.

Published structure analyses of addition compounds of ethers and amines with halogens [6-8] show a linear arrangement O (or N)—Hal.—Hal. in contrast to suggestions earlier made. The experimental findings do not appear to strengthen the suggestion that the "outer" halogen atom attains a strong negative charge. In the case of *ethers* a small lengthening only of the Hal.—Hal. bond is observed, whereas in the case of amines the lengthening is considerably greater. This lengthening may at least partly be due to a weakening of the double bond character [9] of the Hal.-Hal. bond present in the free molecules. The strong interaction between the oxygen (nitrogen) atom and the nearest halogen atom is evident from the short separation between these atoms, this effect being greatest in the case of nitrogen. It appears probable that electrons associated with the atoms forming an O-Hal. or N-Hal. bond are partially promoted to d orbitals.

We wish to express our sincere gratitude towards *The Rockefeller Foundation* for financial aid.

1. Mulliken, R. S. *J. Am. Chem. Soc.* **72** (1950) 600.
2. Mulliken, R. S. *J. Am. Chem. Soc.* **76** (1954) 3869.
3. Chatelet, M. *Ann. Chim.* [11] **2** (1934) 12.
4. Zappi, E. V. and Fernandez, M. *Anales asoc. quim. argentina* **27** (1939) 102.
5. Almenningen, A., Bastiansen, O. and Hansen, L. *Acta Chem. Scand.* **9** (1955) 1306.
6. Hassel, O. and Hvoslef, J. *Acta Chem. Scand.* **8** (1954) 872.
7. Hassel, O. and Hvoslef, J. *Acta Chem. Scand.* **10** (1956) 138.
8. Eia, G. and Hassel, O. *Acta Chem. Scand.* **10** (1956) 139.
9. Mulliken, R. S. *J. Am. Chem. Soc.* **77** (1955) 884.

Received May 5, 1956.

Electrophoresis of the Red Beet Pigments

GÖSTA LINDSTEDT

Food Chemistry Laboratory, National Institute of Public Health, Tomteboda, Sweden

The chemical nature of the red beet pigments is still unknown, and they have not yet been isolated in a pure state. They have been classified as "nitrogenous anthocyanins" since the pioneer investigation by Schudel [1], who discovered the nitrogen content and the glycosidic character of the pigments. Other workers have isolated different preparations of "betanin chloride", which all differ in their composition [2-5]. The formulae hitherto proposed are all based on the assumption that "betanin" really is an anthocyanin derivative. So far, there has been no proof of that assumption.

The complexity of the red beet pigments was later demonstrated by the aid of adsorption chromatography [6]. At least eleven coloured zones (yellow, orange, and red) could be observed on the column. The absorption spectra of the different components were determined, but no chemical investigations were made.

A similar separation of the red beet pigments can be effected by means of paper electrophoresis. Within the pH interval 2—7, they form relatively stable, *negatively* charged ions. A typical electrophoresis strip from fresh red beet sap is shown on Fig. 1. In a 0.1 M citrate buffer of pH 5.5, a good separation is obtained in 3—4 hours (Munktell 20/150 paper strips of size 5 × 35 cm; 220 V). At least seven coloured zones can be observed, of which one red and one bright yellow are always the strongest ones. The different zones seem to separate in roughly the same order as on an adsorption column [6]. The main yellow component is very easily destroyed and appears only in fresh beet sap. Different varieties of the red beet seem to contain the same coloured components, though differing in their relative amounts.

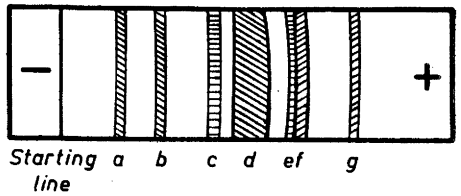


Fig. 1. Typical electrophoresis strip of fresh red beet sap in 0.1 M citrate buffer at pH 5.5. Paper: Munktell 20/150; 220/35 volts/cm; 3 hours at room temperature. Visible zones: a: *red, very weak;* b: *red, weak;* c: *orange, very weak;* d: *red, very strong;* e: *orange, weak;* f: *yellow, strong;* g: *yellow, very weak.*

At pH values below 2, a weak tendency to migrate towards the cathode can be observed, but observation is made difficult by the rapid destruction of the beet pigments in strongly acid solution. Thus, the pigments seem to have an isoelectric point at about pH 2. The exact position of the isoelectric point has not been determined, but it seems to be about the same for all the coloured fractions. In their behaviour during electrophoresis, the beet pigments differ from the common anthocyanins, which form positively charged ions except in alkaline solution. The extremely low value of the isoelectric point indicates that the molecule is dominated by strongly acidic groups, such as carboxyls. From methylation experiments, previous workers have concluded that the "betanin" molecule must contain one or two carboxyl groups [2,4].

The results obtained on electrophoresis have been confirmed by experiments with ion exchange resins. The red colour of beet

1. Mulliken, R. S. *J. Am. Chem. Soc.* **72** (1950) 600.
2. Mulliken, R. S. *J. Am. Chem. Soc.* **76** (1954) 3869.
3. Chatelet, M. *Ann. Chim.* [11] **2** (1934) 12.
4. Zappi, E. V. and Fernandez, M. *Anales asoc. quim. argentina* **27** (1939) 102.
5. Almenningen, A., Bastiansen, O. and Hansen, L. *Acta Chem. Scand.* **9** (1955) 1306.
6. Hassel, O. and Hvoslef, J. *Acta Chem. Scand.* **8** (1954) 872.
7. Hassel, O. and Hvoslef, J. *Acta Chem. Scand.* **10** (1956) 138.
8. Eia, G. and Hassel, O. *Acta Chem. Scand.* **10** (1956) 139.
9. Mulliken, R. S. *J. Am. Chem. Soc.* **77** (1955) 884.

Received May 5, 1956.

Electrophoresis of the Red Beet Pigments

GÖSTA LINDSTEDT

Food Chemistry Laboratory, National Institute of Public Health, Tomteboda, Sweden

The chemical nature of the red beet pigments is still unknown, and they have not yet been isolated in a pure state. They have been classified as "nitrogenous anthocyanins" since the pioneer investigation by Schudel [1], who discovered the nitrogen content and the glycosidic character of the pigments. Other workers have isolated different preparations of "betanin chloride", which all differ in their composition [2-5]. The formulae hitherto proposed are all based on the assumption that "betanin" really is an anthocyanin derivative. So far, there has been no proof of that assumption.

The complexity of the red beet pigments was later demonstrated by the aid of adsorption chromatography [6]. At least eleven coloured zones (yellow, orange, and red) could be observed on the column. The absorption spectra of the different components were determined, but no chemical investigations were made.

A similar separation of the red beet pigments can be effected by means of paper electrophoresis. Within the pH interval 2—7, they form relatively stable, *negatively* charged ions. A typical electrophoresis strip from fresh red beet sap is shown on Fig. 1. In a 0.1 M citrate buffer of pH 5.5, a good separation is obtained in 3—4 hours (Munktell 20/150 paper strips of size 5 × 35 cm; 220 V). At least seven coloured zones can be observed, of which one red and one bright yellow are always the strongest ones. The different zones seem to separate in roughly the same order as on an adsorption column [6]. The main yellow component is very easily destroyed and appears only in fresh beet sap. Different varieties of the red beet seem to contain the same coloured components, though differing in their relative amounts.

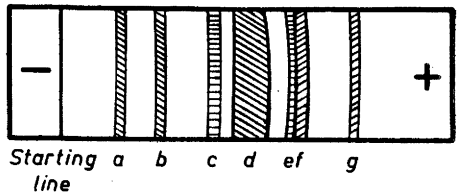


Fig. 1. Typical electrophoresis strip of fresh red beet sap in 0.1 M citrate buffer at pH 5.5. Paper: Munktell 20/150; 220/35 volts/cm; 3 hours at room temperature. Visible zones: a: *red, very weak;* b: *red, weak;* c: *orange, very weak;* d: *red, very strong;* e: *orange, weak;* f: *yellow, strong;* g: *yellow, very weak.*

At pH values below 2, a weak tendency to migrate towards the cathode can be observed, but observation is made difficult by the rapid destruction of the beet pigments in strongly acid solution. Thus, the pigments seem to have an isoelectric point at about pH 2. The exact position of the isoelectric point has not been determined, but it seems to be about the same for all the coloured fractions. In their behaviour during electrophoresis, the beet pigments differ from the common anthocyanins, which form positively charged ions except in alkaline solution. The extremely low value of the isoelectric point indicates that the molecule is dominated by strongly acidic groups, such as carboxyls. From methylation experiments, previous workers have concluded that the "betanin" molecule must contain one or two carboxyl groups [2,4].

The results obtained on electrophoresis have been confirmed by experiments with ion exchange resins. The red colour of beet

sap is firmly adsorbed on an anion exchanger, but rather little on a cation exchanger. Anthocyanins from fruits or berries behave in the opposite way.

In practice, paper electrophoresis can be used to detect the addition of red beet sap to fruit juices, as only the beet pigments migrate towards the anode in weakly acid solution. An addition of 10 % of red beet sap is easily detected.

Electrophoresis on cellulose columns has been used with some success in attempts to isolate the beet pigments. A very simple apparatus built after the same principle as that described by Porath [7] was used. The buffer solutions were volatile, consisting of 0.1 M formic acid and 0.1 M pyridine in varying proportions. The separation was generally carried out at a pH about 3.5, because the pigments then can be separated from most proteins and amino acids, which move in the opposite direction. The "main red zone" was eluted from the electrophoresis column and further purified by adsorption on a talc column [6]. Lyophilisation (evaporation from a frozen solution) was generally used for concentration of the solutions, since the pigments are easily changed even during vacuum distillation at low temperature. The dark red solid fractions obtained by this method are at present being further investigated.

The author is indebted to Mrs. G. Ageby for skilful experimental assistance.

1. Schudel, G. *Diss., Zürich* (1918).
2. Ainley, A. D. and Robinson, R. *J. Chem. Soc.* **1937** 446.
3. Schmidt, O. T. *Naturwiss.* **25** (1937) 284.
4. Chmielevska, I. *Roczniki Chem.* **18** (1938) 1.
5. Pucher, G. W., Curtis, L. C. and Vickery, H. B. *J. Biol. Chem.* **123** (1938) 61.
6. Aronoff, S. and Aronoff, E. M. *Food Research* **13** (1948) 59.
7. Porath, J. *Acta Chem. Scand.* **8** (1954) 1813.

Added in proof: In a recent communication (*Naturwiss.* **43** (1956) 159). O. T. Schmidt and W. Schönleben have arrived at similar results, and, in addition, shown that the beet pigments do not contain nitrogen.

Received May 7, 1956.

The Cuprous Salts of some N,N-Disubstituted Dithiocarbamic Acids and their Degree of Polymerisation

STIG ÅKERSTRÖM

Department of Organic Chemistry, Chemical Institute, University of Uppsala, Sweden

Among the cuprous salts of the N,N-disubstituted dithiocarbamic acids, only the diethyl compound is mentioned in the literature. It was first prepared by Cambi and Coriselli [1]. They treated the sodium salt of diethyldithiocarbamic acid in inert atmosphere with cuprous oxide, stirring for about twelve hours; the salt was recrystallized from chloroform + petroleum ether. Fredga [2] prepared cuprous diethyldithiocarbamate by shaking thiuramdisulphide with copper bronze in chloroform solution, at room temperature. The compound isolated by him consisted of yellow, glistening needles, with a molecular weight of about 1 000 (determined in boiling chloroform). At about the same time, Tamminen and Hjelt [3] obtained a mixture of the cupri- and cuprous compounds, by boiling tetraethylthiuramdisulphide in benzene solution with metallic copper.

It was the author's intention to synthesize more of such compounds, and examine their polymerity. An X-ray examination of the cuprous diethyldithiocarbamate was begun in The Inorganic Department of this Institute by Hesse [4]; about the same time a molecular weight determination in boiling carbon disulphide was made, and later, an ultracentrifugation according to Archibald's method. It appeared that the true molecule consists of four formula units. The determination of the structure of the complex now completed, evidently shows that the molecule is tetrameric and that the four copper atoms are situated in the corners of a tetrahedron.

When the cuprous dithiocarbamates were prepared, the thiuramdisulphide was shaken with an excess of copper bronze in carbon disulphide until the colour of the solution became yellow or yellow-brown. After the copper bronze had settled, the solution was filtered and the cuprous complexes were isolated by means of their different solubilities. Several

sap is firmly adsorbed on an anion exchanger, but rather little on a cation exchanger. Anthocyanins from fruits or berries behave in the opposite way.

In practice, paper electrophoresis can be used to detect the addition of red beet sap to fruit juices, as only the beet pigments migrate towards the anode in weakly acid solution. An addition of 10 % of red beet sap is easily detected.

Electrophoresis on cellulose columns has been used with some success in attempts to isolate the beet pigments. A very simple apparatus built after the same principle as that described by Porath [7] was used. The buffer solutions were volatile, consisting of 0.1 M formic acid and 0.1 M pyridine in varying proportions. The separation was generally carried out at a pH about 3.5, because the pigments then can be separated from most proteins and amino acids, which move in the opposite direction. The "main red zone" was eluted from the electrophoresis column and further purified by adsorption on a talc column [6]. Lyophilisation (evaporation from a frozen solution) was generally used for concentration of the solutions, since the pigments are easily changed even during vacuum distillation at low temperature. The dark red solid fractions obtained by this method are at present being further investigated.

The author is indebted to Mrs. G. Ageby for skilful experimental assistance.

1. Schudel, G. *Diss., Zürich* (1918).
2. Ainley, A. D. and Robinson, R. *J. Chem. Soc.* **1937** 446.
3. Schmidt, O. T. *Naturwiss.* **25** (1937) 284.
4. Chmielevska, I. *Roczniki Chem.* **18** (1938) 1.
5. Pucher, G. W., Curtis, L. C. and Vickery, H. B. *J. Biol. Chem.* **123** (1938) 61.
6. Aronoff, S. and Aronoff, E. M. *Food Research* **13** (1948) 59.
7. Porath, J. *Acta Chem. Scand.* **8** (1954) 1813.

Added in proof: In a recent communication (*Naturwiss.* **43** (1956) 159). O. T. Schmidt and W. Schönleben have arrived at similar results, and, in addition, shown that the beet pigments do not contain nitrogen.

Received May 7, 1956.

The Cuprous Salts of some N,N-Disubstituted Dithiocarbamic Acids and their Degree of Polymerisation

STIG ÅKERSTRÖM

Department of Organic Chemistry, Chemical Institute, University of Uppsala, Sweden

Among the cuprous salts of the N,N-disubstituted dithiocarbamic acids, only the diethyl compound is mentioned in the literature. It was first prepared by Cambi and Coriselli [1]. They treated the sodium salt of diethyldithiocarbamic acid in inert atmosphere with cuprous oxide, stirring for about twelve hours; the salt was recrystallized from chloroform + petroleum ether. Fredga [2] prepared cuprous diethyldithiocarbamate by shaking thiuramdisulphide with copper bronze in chloroform solution, at room temperature. The compound isolated by him consisted of yellow, glistening needles, with a molecular weight of about 1 000 (determined in boiling chloroform). At about the same time, Tamminen and Hjelt [3] obtained a mixture of the cupri- and cuprous compounds, by boiling tetraethylthiuramdisulphide in benzene solution with metallic copper.

It was the author's intention to synthesize more of such compounds, and examine their polymerity. An X-ray examination of the cuprous diethyldithiocarbamate was begun in The Inorganic Department of this Institute by Hesse [4]; about the same time a molecular weight determination in boiling carbon disulphide was made, and later, an ultracentrifugation according to Archibald's method. It appeared that the true molecule consists of four formula units. The determination of the structure of the complex now completed, evidently shows that the molecule is tetrameric and that the four copper atoms are situated in the corners of a tetrahedron.

When the cuprous dithiocarbamates were prepared, the thiuramdisulphide was shaken with an excess of copper bronze in carbon disulphide until the colour of the solution became yellow or yellow-brown. After the copper bronze had settled, the solution was filtered and the cuprous complexes were isolated by means of their different solubilities. Several

Table 1.

No.	Cu[I]-dithiocarbamates	M.p.[1], °C	Crystal solvent	Mol.wt.	Postulated polymerity	Part. spec. volume in toluene at 25°C	Crystalline form colour
1	$(CH_3)_2NCS_2Cu$	270° d		831, 865 [2]	?	0.600	yellow needles
2	$(C_2H_5)_2NCS_2Cu$	190° d		970 [3]	tetrameric		yellow needles
3	$(nC_3H_7)_2NCS_2Cu$	200° d	½ $CHCl_3$, ½ CS_2 ½ C_6H_6	684, 725, 705, 733 [3] 869, 834, 880, 839 [4]	trimeric	0.686	yellow needles or hexagonal crystals
4	$(nC_4H_9)_2NCS_2Cu$	113—114°		783, 793 [4]	trimeric	0.724	hexagonal yellow crystals
5	$(nC_5H_{11})_2NCS_2Cu$	106—107°		1070 [3], 857 [4]	trimeric	0.765	yellow leaves
6	$(isoC_3H_7)_2NCS_2Cu$	300° d		polymeric ?	high		yellow powder
7	$(isoC_4H_9)_2NCS_2Cu$	165° d			?		yellow crystals
8	$(isoC_5H_{11})_2NCS_2Cu$	146—147°		861 [4] 970 [3]	trimeric	0.775	hexagonal yellow crystals
9	C_2H_5 / nC_3H_7 >NCS_2Cu	190° d		950 [3]	tetrameric	0.632	yellow crystals
10	$(C_6H_5CH)_2NCS_2Cu$	284—286°			?		yellow needles
11	CH_3 / C_4H_7 >NCS_2Cu	245° d	½ $CHCl_3$		?		yellow needles
12	NCS_2Cu	290° d	½ $CHCl_3$		?		yellow needles or hexagonal crystals
13	NCS_2Cu				?		yellow needles

1. Uncorrected.
2. Determined in boiling CS_2.
3. Determined by ultracentrifugation according to Archibald's method.
4. Determined in boiling C_6H_6.

solvents were examined as a reaction medium for the above mentioned reaction. However, carbon disulphide proved to be the most suitable. As the cuprous compounds are easily oxidized in solution, and also have a tendency to absorb various impurities on the surface of the newly-formed crystals, repeated recrystallisation is required for their purification.

The compounds hitherto prepared are listed in Tables 1 and 2, together with some data. As seen from these tables, some of the compounds are postulated tetrameric

Table 2.

Substance No.	Cu (calc.)	Cu (found)	H (calc.)	H (found)	C (calc.)	C (found)
3	* 21.21	21.25	4.88	4.44	30.06	30.00
			** 5.66	5.49	34.32	34.13
4	23.72	23.37				
5	21.47	21.10				
10	—	—	4.20	3.99	53.62	53.46
12	28.40	28.33	4.5	4.0	32.20	32.50

* Calculated for $(nC_3H_7)_2NCS_2Cu \frac{1}{2} CHCl_3$.
** » » $(nC_3H_7)_2NCS_2Cu \frac{1}{8} CS_2$.

and some are postulated trimeric. The latter may possibly be built up of copper triangles. Preliminary data from a recently commenced X-ray examination [4] of one of the postulated trimeric compounds, $(nC_4H_9)_2NCS_2Cu$, seem to support the postulate of its trimerity. It should also be observed here, that several of these trimeric cuprous compounds crystallized with solvents (see Table 1). These solvents could be removed by careful heating *in vacuo* without the crystals being deformed, as far as could be seen. Obviously, these trimeric compounds are so packed that a crystal structure with "hollow spaces" could be well imagined. These "hollow spaces" can thus, partly or entirely, be filled out by the organic carbon chains, provided that these chains are large enough (*e. g.* $(nC_4H_9)_2NCS_2Cu$). They can also be filled by solvents (*e. g.* $(nC_3H_7)_2NCS_2Cu.1/2\ CHCl_3$).

It is remarkable that a change from a tetrameric to a trimeric structure takes place in the series of cuprous *n*-dialkyl-dithiocarbamates if the carbon chain is increased by one carbon atom. It should be observed that the only trimeric copper compounds which, up to this time, have been published, are some esters of phosphoric acid [5] (*e. g.* $CuClP(OPr\text{-}iso)_3$). The cuprous di-*iso*propyl-dithiocarbamate may possibly be high polymeric.

Acknowledgements. The author is greatly indebted to Professor Arne Fredga and Fil.lic. Rolf Hesse for valuable discussions. He also wishes to express his gratitude to Dr. Kai Pedersen for valuable help with the ultracentrifugation.

1. Gambi, L. and Coriselli, C. *Gazz. chim. ital.* **66** (1936) 779.
2. Fredga, A. *Rec. trav. chim.* **69** (1950) 416, 949.
3. Tamminen, V. and Hjelt, E. *Suomen Kemistilehti* **23B** (1950) 39.
4. Hesse, R. *To be published.*
5. Arbuzov, B. A. and Shavska, T. G. *Doklady Akad. Nauk. S.S.S.R.* **84** (1952) 507; *Chem. Abstracts* **64** (1952) 10729 g.

Received May 3, 1956.

Determination of Small Amounts of Deuterium Oxide in Water by Infra-red Spectroscopy

ULLA BERGLUND-LARSSON

Nobel Institute of Chemistry, Stockholm 50, Sweden

In studies of isotope effects it was of interest to know the absolute deuterium concentration of various deuterium substituted organic compounds. For that reason the compounds were burned to water and the deuterium content of the water was determined by means of infra-red spectroscopy. A method, similar to that of Thornton and Condon [1], but more accurate, has been worked out.

Table 2.

Substance No.	Cu (calc.)	Cu (found)	H (calc.)	H (found)	C (calc.)	C (found)
3	* 21.21	21.25	4.88	4.44	30.06	30.00
			** 5.66	5.49	34.32	34.13
4	23.72	23.37				
5	21.47	21.10				
10	—	—	4.20	3.99	53.62	53.46
12	28.40	28.33	4.5	4.0	32.20	32.50

* Calculated for $(nC_3H_7)_2NCS_2Cu \frac{1}{2} CHCl_3$.
** » » $(nC_3H_7)_2NCS_2Cu \frac{1}{8} CS_2$.

and some are postulated trimeric. The latter may possibly be built up of copper triangles. Preliminary data from a recently commenced X-ray examination [4] of one of the postulated trimeric compounds, $(nC_4H_9)_2NCS_2Cu$, seem to support the postulate of its trimerity. It should also be observed here, that several of these trimeric cuprous compounds crystallized with solvents (see Table 1). These solvents could be removed by careful heating *in vacuo* without the crystals being deformed, as far as could be seen. Obviously, these trimeric compounds are so packed that a crystal structure with "hollow spaces" could be well imagined. These "hollow spaces" can thus, partly or entirely, be filled out by the organic carbon chains, provided that these chains are large enough (*e. g.* $(nC_4H_9)_2NCS_2Cu$). They can also be filled by solvents (*e. g.* $(nC_3H_7)_2NCS_2Cu.1/2\ CHCl_3$).

It is remarkable that a change from a tetrameric to a trimeric structure takes place in the series of cuprous *n*-dialkyl-dithiocarbamates if the carbon chain is increased by one carbon atom. It should be observed that the only trimeric copper compounds which, up to this time, have been published, are some esters of phosphoric acid [5] (*e. g.* $CuClP(OPr\text{-}iso)_3$). The cuprous di-*iso*propyl-dithiocarbamate may possibly be high polymeric.

Acknowledgements. The author is greatly indebted to Professor Arne Fredga and Fil.lic. Rolf Hesse for valuable discussions. He also wishes to express his gratitude to Dr. Kai Pedersen for valuable help with the ultracentrifugation.

1. Gambi, L. and Coriselli, C. *Gazz. chim. ital.* **66** (1936) 779.
2. Fredga, A. *Rec. trav. chim.* **69** (1950) 416, 949.
3. Tamminen, V. and Hjelt, E. *Suomen Kemistilehti* **23B** (1950) 39.
4. Hesse, R. *To be published.*
5. Arbuzov, B. A. and Shavska, T. G. *Doklady Akad. Nauk. S.S.S.R.* **84** (1952) 507; *Chem. Abstracts* **64** (1952) 10729 g.

Received May 3, 1956.

Determination of Small Amounts of Deuterium Oxide in Water by Infra-red Spectroscopy

ULLA BERGLUND-LARSSON

Nobel Institute of Chemistry, Stockholm 50, Sweden

In studies of isotope effects it was of interest to know the absolute deuterium concentration of various deuterium substituted organic compounds. For that reason the compounds were burned to water and the deuterium content of the water was determined by means of infra-red spectroscopy. A method, similar to that of Thornton and Condon [1], but more accurate, has been worked out.

Experimental. The measurements were carried out on a Perkin-Elmer infra-red spectrometer, model 112, with a NaCl-prism. The cell thickness was about 0.05 mm and its windows were made of CaF_2. The slit width used was 0.050 mm. A number of standard samples were made from deuterium water containing 99.84 % D_2O, $d_4^{20} = 1.10521$ (Norsk Hydro), and ordinary distilled water. Care was taken to prevent undue dilution by exchange with atmospheric moisture.

At each determination, the whole absorption band at 3.98 μ (2 513 cm^{-1}) was recorded to eliminate a possible error in the wavelength setting, but the reading was always taken at exactly 3.98 μ. The absorption of ordinary distilled water in the same cell was always checked between the analyses. After each recording the cell was washed with acetone and dried by blowing dry nitrogen through it. No memory effect was found in the cell even when the D_2O concentration exceeded 5 % D_2O.

A calibration curve was drawn and a straight line was obtained by the method of least squares. As there will always be an error both in the determination of the absorption of ordinary water, I_0, and in that of the sample, I, the line need not pass the origin but has a small intercept on the ordinate. The equation of the line was found to be:

$$\log \frac{I_0}{I} = 0.3174c - 0.0034$$

where c is the concentration measured in per cent by weight. In Table 1 we see the true concentrations compared with those calculated from the equation. $\Delta = c_{true} - c_{found}$; e = mean error in a single determination $= \sqrt{\frac{\Sigma\Delta^2}{n-2}} = 6 \times 10^{-3}$ wt %.

Table 1. Weighed out quantities of D_2O (wt %) in ordinary water, c_{true}, compared with the values obtained from the equation, c_{found}. $\Delta = c_{true} - c_{found}$.

c_{true}	c_{found}	$\Delta 10^{-3}$
0.0163	0.0107	+5.6
0.3053	0.3091	—3.8
0.5466	0.5436	+3.0
0.8707	0.8804	—9.7
1.1161	1.1130	+3.1
1.3515	1.3547	—3.2
1.6497	1.6442	+5.5

Corrections were made for the natural occurrence of heavy water in distilled water assuming [2] its concentration to be 0.0163 wt %.

In the present investigation, Beer's law is obeyed and a straight line is obtained when plotting optical density against concentration. In a work of Gaunt [3], Beer's law was not obeyed since he used a too large slit width. This also caused some overlapping from the absorption band of the carbon dioxide at 4.25 μ (2 353 cm^{-1}). Under these conditions the accuracy of Gaunt's experiments cannot be as high as 1 % as he claimed, even if he included only concentrations up to 0.8 % D_2O. With the method of least squares (straight line), the mean error in his experiments is found to be 2 %. The assumption of a straight line was made as all the points up to concentrations of about 0.6 % fall on a straight line, but at concentrations higher than this the curvature begins, and after 0.8 % it will be appreciable.

In the present work the absorption band of HOD at 3.98 μ was well separated from other absorbtion bands and no overlapping could be observed. The absolute mean error in a single determination is found to be ± 0.006 wt % for concentrations up to 1.3 % D_2O.

The author is indebted to Docent Lars Melander for his kind interest in this investigation. The *Swedish Natural Science Research Council* has contributed to the acquirement of the infra-red spectrographic equipment.

1. Thornton, V. and Condon, F. E. *Anal. Chem.* **22** (1950) 690.
2. Kirshenbaum, I. *Physical Properties and Analysis of Heavy Water*, New York 1951, p. 396.
3. Gaunt, J. *Analyst* **79** (1954) 580.

Received May 15, 1956.

The Configuration of the *aa'*-Dimethylpimelic Acids

ARNE FREDGA and BÖRJE ÖSTMAN

Department of Organic Chemistry, Chemical Institute, University of Uppsala, Sweden

The diastereomeric *aa'*-dimethylpimelic acids melting at 81–81.5° and 76–76.5° have been investigated by several authors. They have been designated as the *para*- and *anti*-form, respectively, but no attempts to determine the configuration have been reported [1,2,3]. The present authors have found that the *low-melting* acid can be resolved into optically active forms using strychnine. On the other hand, the *high-melting* form gives a strychnine salt, from which the inactive compound can be regenerated with unchanged m. p. This indicates that the latter acid is the pure *meso*-form.

The separation of the diastereomeric acids is rather tedious and time-consuming. Kipping has performed it through the anilides [3], and in spite of extensive experiments no better method could be found. Owing to lack of material, the optical antipodes have not yet been prepared in a state of purity. The acid from the first crystallisation of the strychnine salt had $[\alpha]_D^{25} = -20°$ (abs. ethanol). In the same solvent, dimethylglutaric and dimethyladipic acid show 36.5° and 30.3° [4], respectively. The maximum activity of the dimethylpimelic acid can be assumed to be somewhat lower, probably near 25°. The strychnine salt thus gives a fairly good resolution.

Experimental. The inactive acids were prepared according to Kipping [3].

0.250 g of the *low-melting* acid and 0.445 g of strychnine were dissolved together in hot dilute ethanol. After standing for several days, the salt was filtered off and the acid liberated. M. p. of the crude acid 67–68°. 0.0235 g dissolved in abs. ethanol to 10.00 ml: $2\alpha_D^{25} = -0.09°$. $[\alpha]_D^{25} = -20°$.

The mother liquor from the strychnine salt was evaporated to dryness and the acid liberated. 0.0293 g dissolved in abs. ethanol to 10.00 ml: $2\alpha_D^{25} = +0.105°$. $[\alpha]_D^{25} = +18°$.

Levorotatory aa'-dimethylglutaric acid was prepared according to Möller [5]. 0.4586 g dissolved in abs. ethanol to 10.00 ml: $2\alpha_D^{25} = -3.345°$. $[\alpha]_D^{25} = -36.5°$.

1. Kipping, F. S. and McKenzie, J. E. *J. Chem. Soc.* **59** (1891) 569.
2. Zelinsky, N. *Ber.* **24** (1891) 3997.
3. Kipping, F. S. *J. Chem. Soc.* **67** (1895) 139.
4. Hedlund, I. *Arkiv Kemi* **8** (1955) 89.
5. Möller, E. *Diss.* Lund 1918; *Chem. Centr.* **1919:I** 606.

Received May 8, 1956.

Iron Transport through the Lymph Stream

G. von EHRENSTEIN

Institute of Organic Chemistry and Biochemistry, University of Stockholm, Sweden

In the course of one hour about 30 μg of iron leaves the circulation of the rabbit. Most of this iron is ultimately utilized in the formation of hemoglobin, but a fraction before doing so is lead into the "depots" and utilized at a later stage only.

The iron circulating in the plasma is bound to β_1-globulin and has prior to passing the capillary wall to be split off from that compound [1].

The writer found the thoracic lymph of the rabbit to contain 73 μg/100 ml of iron (range 40–115 μg/100 ml, S.D. 27 μg/100 ml), all this iron being bound to β_1-globulin. It is probable that the same is the case for the iron of the whole extracellular fluid. The iron of the depots and that of the extracellular fluid has to enter the vascular bed prior to reaching the hemopoetic organs, and thus the problem occurs in which way these fractions reach the circulation.

Thirty minutes after injecting intraperitoneally or subcutaneously labelled iron-β_1-globulin to the rabbit, 1 ml of thoracic lymph was found by the writer to contain more than 150 times as much labelled iron than does 1 ml of plasma. This observation suggests that much of the iron of the interspaces and thus also the iron released from the depots, as far it is bound to β_1-globulin, is transported into the circulation with the lymph stream.

To test this conclusion, the influx of a large part of the lymph stream into the

Table 1. Change of iron content of the plasma of rabbits with ligated thoracic duct and of sham operated rabbits.

		Iron content, μg / 100 ml	
		Time 0	after 4 h
Seven rabbits with ligated thoracic duct	mean	196±17 *	151±12 *
	range	115—260	95—197
	S. D.	45	32
Seven sham operated rabbits	mean	178±10 *	159±13 *
	range	145—210	112—208
	S. D.	27	35

* Standard deviation of the mean.

circulation was obstructed by ligating the thoracic duct and the *truncus jugularis sinister*. The effect of this obstruction on the iron content of the plasma of operated and of sham operated rabbits was then determined. The results of these experiments are seen in Table 1. They show a significant decrease of the iron content of the plasma following obstruction of much of the lymph flow.

Thus ligation of much of the lymph stream reduces the influx of iron into the plasma by 3.8 μg/h. The total iron loss by the plasma amounts to 30 μg/h. Thus 1/8 of the total iron loss by the plasma is compensated by iron lead into the circulation by the lymph stream. The share of iron carried by the lymph stream in the iron replacement is, however, much larger, if we consider the amount of iron lead from the depots into the circulation alone. This amounts to 4.5 μg/h. Thus the amount of iron lead into the plasma by the lymph stream makes out a very appreciable part of the iron carried from the depots into the circulation.

From the decrease of the plasma iron content due to obstruction of the lymph flow and from the iron content of the lymph we can calculate the volume of lymph lead hourly into the circulation. We arrive at a volume of up to 5.2 ml/kg body weight. This compares with the values of 1.4—6.8 ml/kg/h found by Forker *et al*,[2] for the rat, and 0.2—3.0 ml/kg/h measured by Paine *et al.*[3] in the dog.

As the lymph iron is bound to β_1-globulin we have to expect that a corresponding amount of β_1-globulin, making out 2.8 %/h of the total plasma content, will reach the circulation with the lymph stream as well. This is about in the case of the rat (2.8 % / h) and of the dog (2 % / h) [2,4]. Forker *et al.*[2] found, that at least about half of the plasma proteins of the dog are daily replaced by the lymph proteins. A result which suggests, among other things, that about 2.8 % of the plasma iron passes the capillary wall without being dissociated.

Three experiments carried out with growing pigs also brought out the fact, that ligation of the thoracic duct appreciably depresses the plasma iron level.

The author wishes to express his thanks to Professor George de Hevesy for the promoting interest taken in this work.

1. Holmberg, C. G. and Laurell, C. B. *Acta Physiol. Scand.* **10** (1945) 327.
2. Forker, L. L., Chaikoff, I. L. and Reinhardt, W. O. *J. Biol. Chem.* **197** (1952) 625.
3. Paine, R., Butcher, H. R., Howard, F. A. and Smith, I. R. *J. Lab. Clin. Med.* **34** (1949) 1576.
4. Forker, L. L. and Chaikoff, I. L. *J. Biol. Chem.* **196** (1952) 829.

Received May 18, 1956.

The Configuration of the *aa'*-Dimethylpimelic Acids

ARNE FREDGA and BÖRJE ÖSTMAN

Department of Organic Chemistry, Chemical Institute, University of Uppsala, Sweden

The diastereomeric *aa'*-dimethylpimelic acids melting at 81–81.5° and 76–76.5° have been investigated by several authors. They have been designated as the *para*- and *anti*-form, respectively, but no attempts to determine the configuration have been reported [1,2,3]. The present authors have found that the *low-melting* acid can be resolved into optically active forms using strychnine. On the other hand, the *high-melting* form gives a strychnine salt, from which the inactive compound can be regenerated with unchanged m. p. This indicates that the latter acid is the pure *meso*-form.

The separation of the diastereomeric acids is rather tedious and time-consuming. Kipping has performed it through the anilides [3], and in spite of extensive experiments no better method could be found. Owing to lack of material, the optical antipodes have not yet been prepared in a state of purity. The acid from the first crystallisation of the strychnine salt had $[\alpha]_D^{25} = -20°$ (abs. ethanol). In the same solvent, dimethylglutaric and dimethyladipic acid show 36.5° and 30.3° [4], respectively. The maximum activity of the dimethylpimelic acid can be assumed to be somewhat lower, probably near 25°. The strychnine salt thus gives a fairly good resolution.

Experimental. The inactive acids were prepared according to Kipping [3].

0.250 g of the *low-melting* acid and 0.445 g of strychnine were dissolved together in hot dilute ethanol. After standing for several days, the salt was filtered off and the acid liberated. M. p. of the crude acid 67–68°. 0.0235 g dissolved in abs. ethanol to 10.00 ml: $2\alpha_D^{25} = -0.09°$. $[\alpha]_D^{25} = -20°$.

The mother liquor from the strychnine salt was evaporated to dryness and the acid liberated. 0.0293 g dissolved in abs. ethanol to 10.00 ml: $2\alpha_D^{25} = +0.105°$. $[\alpha]_D^{25} = +18°$.

Levorotatory aa'-dimethylglutaric acid was prepared according to Möller [5]. 0.4586 g dissolved in abs. ethanol to 10.00 ml: $2\alpha_D^{25} = -3.345°$. $[\alpha]_D^{25} = -36.5°$.

1. Kipping, F. S. and McKenzie, J. E. *J. Chem. Soc.* **59** (1891) 569.
2. Zelinsky, N. *Ber.* **24** (1891) 3997.
3. Kipping, F. S. *J. Chem. Soc.* **67** (1895) 139.
4. Hedlund, I. *Arkiv Kemi* **8** (1955) 89.
5. Möller, E. *Diss.* Lund 1918; *Chem. Centr.* **1919:I** 606.

Received May 8, 1956.

Iron Transport through the Lymph Stream

G. von EHRENSTEIN

Institute of Organic Chemistry and Biochemistry, University of Stockholm, Sweden

In the course of one hour about 30 μg of iron leaves the circulation of the rabbit. Most of this iron is ultimately utilized in the formation of hemoglobin, but a fraction before doing so is lead into the "depots" and utilized at a later stage only.

The iron circulating in the plasma is bound to β_1-globulin and has prior to passing the capillary wall to be split off from that compound [1].

The writer found the thoracic lymph of the rabbit to contain 73 μg/100 ml of iron (range 40–115 μg/100 ml, S.D. 27 μg/100 ml), all this iron being bound to β_1-globulin. It is probable that the same is the case for the iron of the whole extracellular fluid. The iron of the depots and that of the extracellular fluid has to enter the vascular bed prior to reaching the hemopoetic organs, and thus the problem occurs in which way these fractions reach the circulation.

Thirty minutes after injecting intraperitoneally or subcutaneously labelled iron-β_1-globulin to the rabbit, 1 ml of thoracic lymph was found by the writer to contain more than 150 times as much labelled iron than does 1 ml of plasma. This observation suggests that much of the iron of the interspaces and thus also the iron released from the depots, as far it is bound to β_1-globulin, is transported into the circulation with the lymph stream.

To test this conclusion, the influx of a large part of the lymph stream into the

ACTA CHEMICA SCANDINAVICA 10 (1956) 705—718

On the Complex Chemistry of the Uranyl Ion

VIII. The Complexity of Uranyl Fluoride

STEN AHRLAND, RAGNAR LARSSON and KJELL ROSENGREN

Department of Inorganic and Physical Chemistry, Chemical Institute, University of Lund, Lund, Sweden

The complexity of the uranyl fluoride system has been determined by measurements of $[H^+]$ in fluoride buffers. A perchlorate medium of ionic strength 1 M was used at a temperature 20° C. In the concentration range investigated ($C_M \leqq 100$ mM; $C_A \leqq 400$ mM) a strong mononuclear complex formation takes place between UO_2^{2+} and F^-, with $UO_2F_4^{2-}$ as the upper limit (Table 7). Neither polynuclear complexes, nor complexes containing HF_2^- seem to exist in this range. — The constants of the hydrogen fluoride system in the present medium were also obtained.

In the systems of complexes investigated so far, the uranyl ion is usually able to coordinate with not more than three ligands. This is the case for the acetate [1], chloroacetate [2] and glycolate [3] systems in aqueous solution and also for the nitrate systems in ketonic solvents [4]. These results are also corroborated by the existence of compounds in the solid state evidently containing groups such as $UO_2(CH_3 \cdot COO)_3^-$ and $UO_2(CO_3)_3^{4-}$ (*e. g.* Ref. [5, p. 158]).

The only exception seems to be the fluoride system, where a complex $UO_2F_4^{2-}$ has been reported in solution [6]. The same group is moreover present [7] in solid $K_3UO_2F_5$. As has already been reported [8] preliminarily, the present measurements confirm that four F^- can be taken up as ligands. In fact four should most probably be regarded as the maximum coordination number of the uranyl ion as this number would be displayed by the fluoride system on account of the high stability of the complexes and the small size of the ligand.

CALCULATION OF THE COMPLEXITY CONSTANTS FROM MEASUREMENTS OF $[H^+]$ OF FLUORIDE BUFFERS

A good method for investigating systems of strong complexes is the determination of the free ligand ion concentration [A], with subsequent calculation

of the complex formation function * $\bar{n} = f([A])$. From this function the complexity constants and the composition of the system for a given value of [A] can always be calculated according to established methods [2] using the function X, here denoted X_M.

In a system like the present one where the ligand is the anion of a weak acid, [A] can be found from potentiometric measurements of $[H^+]$ in a buffer solution of the ligand and its corresponding acid. This method has also been used for the aqueous uranyl systems mentioned above. For these systems, the connection between $[H^+]$ and [A] is very simple, for the fluoride system it is somewhat more complicated owing to the peculiar property of F^- to form HF_2^- and possibly also H_2F_2 beside HF. Moreover HF_2^- may be able to form complexes with UO_2^{2+}, thus competing with the complex formation of F^-.

On the other hand no hydrolytic reactions are likely to occur under the conditions chosen for the present measurements. Those solutions which contained only little fluoride were so acid that no hydrolysis was possible and as the pH gradually rose to fairly high values, ≈ 5, with increasing concentration of fluoride, UO_2^{2+} was probably well protected by the simultaneous strong complex formation with F^- (*cf.* Ref.[1]). This was confirmed experimentally since the formation function was independent of $[H^+]$ (see p. 713).

The measurements were carried out as titrations (*cf.* Ref. [9, p. 383]). Portions of a fluoride solution were added to a certain volume of perchloric acid solution and $[H^+]$ of the resulting solution measured by means of the quinhydrone electrode. In the main series, the solutions also contained a uranyl concentration C_M, but measurements had also to be performed with solutions free from uranyl ions. As in the previous parts of this series, all solutions had a constant ionic strength $I = 1$ M, sodium perchlorate being used as the supplementary neutral salt. The temperature was also the same as before, 20° C.

The half-cell containing buffer was connected with the same reference electrode RE as used before [9]. The emf of the cell thus formed is given by

$$E = E_d + \frac{RT}{F} \ln \frac{[H^+]_0}{[H^+]} \tag{1a}$$

In the initial perchloric acid solution before the addition of fluoride, $[H^+] = C_H$. For this special case eqn. (1 a) becomes

$$E^{(i)} = E_d^{(i)} + \frac{RT}{F} \ln \frac{[H^+]_0}{C_H} \tag{1b}$$

Hence

$$E - E^{(i)} - E_d + E_d^{(i)} = E_H = \frac{RT}{F} \ln \frac{C_H}{[H^+]} \tag{2}$$

As the difference of the liquid junction potentials $E_d - E_d^{(i)}$ can be estimated in separate experiments (p. 711), eqn. (2) permits the calculation of $[H^+]$ (or $C_H/[H^+]$). Hence [A] is calculated in the following way.

If all complexes which are mentioned above are considered as possibly existing, C_H can be written as

$$C_H = [H^+] + [HA] + [HA_2] + 2[H_2A_2] + \sum_{q=1}^{Q} q\,[M(HA_2)_q]$$

* Unless stated otherwise, the same symbols are used as in the previous parts I—VII of this series.

where $A = F^-$ and $M = UO_2^{2+}$. Introducing

$$[HA] = \delta_1[H^+][A] \quad (3) \qquad [HA_2] = \delta_2[H^+][A]^2 \quad (4)$$

$$[H_2A_2] = \delta_2''[H^+]^2[A]^2 \quad (5) \qquad [M(HA_2)_q] = \eta_q[M][H^+]^q[A]^{2q} \quad (6)$$

we obtain

$$C_H/[H^+] = 1 + \delta_1[A] + \delta_2[A]^2 + 2[H^+]\delta_2''[A]^2 + [M]\sum_{q=1}^{Q} q \cdot \eta_q[H^+]^{q-1}[A]^{2q} \quad (7)$$

The function experimentally determined from eqn. (2) thus generally depends upon [A], $[H^+]$ and [M]. If complexes containing HF_2^- do not exist in perceptible amounts, then the function will be independent of [M], and [A] can be calculated from eqn. (7) provided the constants δ are known.

Still more complicated complexes could be conceived, *e. g.* mixed complexes containing both F^- and HF_2^- as ligands, or polynuclear HF_2^--complexes. But this would introduce no new variable and therefore no further essential complication. The function (7) may thus be regarded as the general case.

If on the other hand values of [A] are calculated from eqn. (7) on the assumption that HF_2-complexes do not exist and they in fact do, then the computed values of [A] will be in error. However, the error will decrease as [M] (i. e. C_M) decreases and will finally disappear when $C_M \to 0$. It should therefore in any case be possible to obtain the right values of [A] by a method of extrapolation.

From the values of [A] found, the corresponding values of the ligand number of the metal ion $\bar{n}_M$, *i. e.* the complex formation function of the UO_2^{2+}—F^- system, are calculated according to

$$\bar{n}_M = \frac{C_A - [A] - \bar{n}_H \cdot C_H}{C_M} \quad (8)$$

where $\bar{n}_H$ is the ligand number of the hydrogen ion. This quantity, defined as the mean number of fluoride ions bound by each hydrogen ion is generally given by:

$$\bar{n}_H = \frac{\delta_1[A] + 2\delta_2[A]^2 + 2[H^+]\delta_2''[A]^2 + 2[M]\sum_{q=1}^{Q} q \cdot \eta_q [H^+]^{q-1}[A]^{2q}}{1 + \delta_1[A] + \delta_2[A]^2 + 2[H^+]\delta_2''[A]^2 + [M]\sum_{q=1}^{Q} q \cdot \eta_q [H^+]^{q-1}[A]^{2q}} \quad (9)$$

Thus the same condition applies to the calculation of $\bar{n}_H$ from eqn. (9) as to that of [A] from eqn. (7): if no HF_2^--complexes exist $\bar{n}_H$ may be calculated directly, if on the contrary such complexes exist, eqn. (9) gives the correct values of $\bar{n}_H$ when $C_M \to 0$. When [A] and $\bar{n}_H$ are known, $\bar{n}_M$ can be calculated from (8).

Therefore, if no HF_2^--complexes exist, all values of C_M will give the correct complex formation function, and if such complexes really do exist the correct values can in any case be calculated when $C_M \to 0$. In such a case however, we will find the complex formation function dependent on C_M when formally calculated on the assumption that $\eta = 0$.

As has been repeatedly pointed out before, even the true complex formation curve is dependent upon C_M, if polynuclear complexes exist [10, 11, 9]. Therefore if the function is found to depend upon C_M there may be two different reasons. On the other hand if it is found to be independent of C_M we may safely conclude that neither complexes of HF_2^- nor polynuclear ones exist as it is most improbable that these two factors would just compensate each other over the whole ranges of [A] and C_M used.

The constants δ necessary for the calculation of [A] and $\bar{n}_H$ are determined by separate titration series with solutions containing no uranyl ions. The symbols referring to those are denoted by primes in the following. For a solution of the same C_H as above, the emf, E_H', corresponding to E_H of eqn. (2) is given by

$$E'—E^{(i)} — E_d' + E_d^{(i)} = E_H' = \frac{RT}{F} \ln \frac{C_H}{[H^+]'} \tag{10}$$

In this case we obtain

$$C_H/[H^+]' = 1 + \delta_1[A]' + \delta_2([A]')^2 + 2[H^+]'\delta_2''([A]')^2 \tag{11}$$

The function $C_H/[H^+]'$ determined experimentally is thus generally dependent upon [A]' and $[H^+]'$. If however H_2F_2 does not exist in the solution, $C_H/[H^+]'$ will be a function of [A]' only. In any case, this will be true when $C_H \to 0$ and, consequently, $[H^+] \to 0$. Thus the limiting function will be

$$\lim_{C_H \to 0} C_H/[H^+]' = 1 + \delta_1[A]' + \delta_2([A]')^2 = X_H \tag{12}$$

When corresponding values of $(C_H/(H^+]')_{C_H=0}$ and [A]' are known δ_1 and δ_2 can be calculated from eqn. (12) (*cf.* Ref.[2, p. 787]).

The determination of the limiting function (12) is carried out by the Fronaeus' method [11 p. 18], *i. e.* corresponding values of E_H' and C_A for series of different values of C_H are plotted and the resulting family of curves is cut at a number of values of E_H'. The corresponding values of C_H and C_A thus found are now plotted with E_H' as parameter. The resulting lines when extrapolated to $C_H = 0$ give $C_A = [A]'$ corresponding to $(C_H/[H^+]')_{C_H=0}$ for each line. Moreover, this value of (A]' will remain constant along the line of constant E_H' (*i. e.* constant $C_H/[H^+]'$) if H_2F_2 does not exist, as seen from eqns. (10) and (11). The ligand number $\bar{n}_H'$ of these solutions free from uranyl ions is, according to the definition of p. 707 given by the formula

$$\bar{n}_H' = (C_A — [A]')/C_H \tag{13}$$

and if H_2F_2 does not exist it is connected with [A]' according to (*cf.* eqn. (9))

$$\bar{n}_H' = \frac{\delta_1[A]' + 2\delta_2([A]')^2}{1 + \delta_1[A]' + \delta_2([A]')^2} \tag{14}$$

Therefore $\bar{n}_H'$ is constant too along a line of constant [A]'. The C_A, C_H lines of constant E_H' will therefore in such a case be straight ones with the slope $k_E = \bar{n}_H'$, as evident from eqn. (13).

If on the other hand H_2F_2 really exists in perceptible amounts then neither [A]' nor $\bar{n}_H'$ are constant along a line of constant E_H'. The slope k_E will then

not be $\bar{n}_H'$, but another quantity $< \bar{n}_H'$ (*cf.* Fronæus [11, p. 21]). A comparison between the values of $\bar{n}_H'$ calculated from eqn. (14) using the values of δ_1 and δ_2 found from eqn. (12) and the slope k_E of the C_A, C_H lines will therefore reveal if H_2F_2 really does exist. In fact it does not, and in the following calculations of $\bar{n}_M = f([A])$ the terms referring to this complex are therefore omitted.

It is however necessary to exercise some care when using the values of δ_1 and δ_2 so found for calculating [A] in the way described on p. 707. Unfortunately, δ_1 and δ_2 vary perceptibly as the medium is altered by the exchange of perchlorate for fluoride. The values of δ_1 and δ_2 found apply to a perchlorate medium, and are therefore not sufficiently exact when C_A is high, especially as [A] must be determined as precisely as possible at high C_A on account of the gradual decrease of the difference C_A—[A] relative to [A] which always makes the computation of high values of $\bar{n}_M$ rather uncertain (*cf.* Refs.[1, 3]).

Therefore high values of [A] should be calculated using values of δ valid at these [A]. It is however not necessary to carry out a formal calculation of these values, instead [A] may be found by an appropiate modification of the method used previously [1-3] for simple acid systems.

From eqns. (10) and (2) the difference E_A is given by

$$E_H' - E_H = E_A = \frac{RT}{F} \ln \frac{[H^+]}{[H^+]'} \tag{15}$$

Combining eqns. (15) and (4) and setting $[HA_2]/[HA_2]' = \alpha_2/\alpha_2'$ ($\alpha_2 = [HA_2]/C_H$ and $\alpha_2' = [HA_2]'/C_H$, *cf.*[2]) we obtain

$$2\ln \frac{[A]'}{[A]} = \frac{E_A}{RT/F} + \ln \frac{\alpha_2'}{\alpha_2} \tag{16}$$

Combining eqns. (15) and (3) we obtain analogously

$$\ln \frac{[A]'}{[A]} = \frac{E_A}{RT/F} - \ln \frac{\alpha_1}{\alpha_1'} \tag{17}$$

where $\alpha_1 = [HA]/C_H$ and $\alpha_1' = [HA]'/C_H$. At high values of [A], $[H^+]$ is negligible compared with [HA] and $[HA_2]$. Therefore

$$\alpha_1 + \alpha_2 = 1 \tag{18}$$

Moreover the following connection exists (*cf.* eqn. (14))

$$\alpha_1 + 2\alpha_2 = \bar{n}_H \tag{19}$$

Hence $\alpha_2 = \bar{n}_H - 1$ and $\alpha_1 = 2 - \bar{n}_H$ which when combined with eqns. (16) and (17) give

$$2\ln \frac{[A]'}{[A]} = \frac{E_A}{RT/F} + \ln \frac{\bar{n}_H' - 1}{\bar{n}_H - 1} \tag{20}$$

and

$$\ln \frac{[A]'}{[A]} = \frac{E_A}{RT/F} - \ln \frac{2 - \bar{n}_H}{2 - \bar{n}_H'} \tag{21}$$

Hence [A] can be calculated by a series of approximations utilizing the fact that $[A]' = C_A - \bar{n}_H' \cdot C_H \approx C_A$ at high values of C_A. A sufficiently good value of [A]′ can therefore be found by successive approximations using values of $\bar{n}_H'$ obtained from eqn. (14) with the values of δ calculated previously. As [A] is not too far from [A]′, $\bar{n}_H \approx \bar{n}_H'$ and an approximate value of [A] can thus be calculated from eqn. (20) (if $\bar{n}_H' > 1.5$) or eqn. (21) (if $\bar{n}_H' < 1.5$). From this value of [A] a better value of $\bar{n}_H$ is obtained. Inserted in eqns. (20) or (21) the new $\bar{n}_H$will yield a better value of [A] and so by successive approximations the true value of [A] will finally be found.

In practice all values of [A] are first calculated according to the method first mentioned and then, starting with highest ones, recalculated by the more laborious method of E_A using eqns. (20) and (21) until this method gives a value of [A] identical with that found from δ_1 and δ_2.

EXPERIMENTAL

Chemicals: Uranyl perchlorate was prepared as before [9]. Its purity was proved by the fact that the solution had an extinction curve identical to that of the carefully purified preparation used before. The exact concentration of the stock solution (C_M = 334 mM) was determined cerimetrically.

The excess of perchloric acid in the present preparation was determined potentiometrically. A sample of the stock solution, suitably diluted, was titrated with a perchloric acid solution, and $[H^+]$ of the solutions thus obtained was measured by means of a quinhydrone electrode connected with the usual reference electrode RE of $[H^+]_0$ = 10.06 mM. As I = 1 M throughout the cell $[H^+]$ can be calculated directly from the emfs measured provided a correction is applied for the liquid junction potentials between solutions of different $[H^+]$ (*cf.* p. 711). The differences between the values of $[H^+]$ thus found and those stoichiometrically calculated from the amounts of perchloric acid added will give the acid content of the uranyl salt, provided the hydrolysis of the uranyl ion is negligible. This is the case [9] when $[H^+] > 10$ mM and in fact a constant difference = 8.3 ± 0.3 mM was found in the present titration where the value of $[H^+]$ measured increased from 8.2 to 67.2 mM while C_M was kept constant = 33.4 mM. The amount of free acid in the stock solution is thus 83 mM. This method of determining free acid in the presence of the fairly acidic uranyl ion is much more satisfactory than the method of potentiometric titration with alkali used previously.

Perchloric acid was of analytical grade and *sodium perchlorate*, Ciba *purum*, was purified and tested as described before [9].

Sodium fluoride: First a preparation "Bakers analyzed", lot No 3593, was used. A stock solution with C_A = 600 mM and I = 1 M was prepared. Such a solution should have pH ≈ 8.4. The present one contained excess alkali and perchloric acid was therefore added until phenolphtalein was decolourized. The solution was kept in a polythene bottle where its pH remained constant. (The pH soon rose perceptibly when the solution came into contact with glass.) During the measurement the fluoride solution had to be added from a glass burette. The titrations therefore had to be completed within about two hours; during this time no perceptible increase of pH had occurred. By use of this stock solution series of titrations with C_H = 5, 10, 15, and 25 mM, with no uranyl ions present, were first performed in order to investigate the hydrogen fluoride system. After that three uranyl ion titrations were carried out with C_M' = 10 mM, C_H = 10 mM; C_M' = 25 mM, C_H = 10 mM; and C_M' = 25 mM, C_H = 25 mM respectively * yielding three sets of values of the formation function $\bar{n}_M$ = f([A]).

At this stage it became desirable to extend the search for polynuclear complexes by using higher values of [M]. Another preparation of sodium fluoride "Baker analyzed", lot No. 5093, had then to be used. As a check, the uranyl free titrations of C_H = 10 and

* C_M' = initial value of C_M in a series of measurements (*cf.* p. 711).

25 mM were repeated with a stock solution of this preparation. In spite of the fact that this solution did not contain any free alkali, as shown by its pH, perceptibly higher values of E_H were found than before, especially for the lower value of C_H = 10 mM. The difference became greater with increasing C_A, finally reaching ≈ 3.5 mV for C_H = 10 mM. Evidently the presence of a base much stronger than F^- must be suspected but on the other hand it cannot be very strong as shown by the pH of the solution. A potentiometric titration of the fluoride stock solution also revealed that it possessed a buffering region around pH 7. The amount of the foreign base could be estimated as ≈ 0.4 mole %. This prompted us to investigate a sample left of the first stock solution, and we found that it also contained the same basic impurity but in only about half the amount. It could therefore be assumed that E_H and hence the constants of the hydrogen fluoride system are slightly in error as determined by use of the first stock solution. The figures of the uranyl system on the other hand should not be much affected as they are calculated from the difference between two series of measurements of the same C_H, one with and the other without uranyl ions, which both ought to contain the same error in their emfs.

The foreign basic substance is evidently connected with the hydrolysis of the fluosilicate, present as an impurity in the fluoride preparations. It should however be possible to remove its influence by repressing this hydrolysis in advance. In fact the titration curve of the stock solution shows a minimum of buffer capacity at pH ≈ 6.3. An adjustment of pH to this value will therefore prevent further consumption of H+ by the fluosilicate, while F^- is still left unaffected by H^+.

When the check titrations of C_H = 10 and 25 mM were repeated with such a solution, E_H had in fact decreased and moreover to a value lower than that found with the first stock solution, as could be expected. This difference is at most only 2 mV and the new constants of the hydrogen fluoride system are therefore only slightly different from those previously determined. Series of measurements were then made with uranyl solutions of C_M = 50 and 100 mM, both having C_H = 25 mM. As expected the formation function $\bar{n}_M$ = f ([A]) hence obtained does not deviate essentially from that found by the previous measurements (*cf.* p. 713).

Apparatus: The electrode vessel used for the fluoride buffers was made from methacrylate plastic (»plexiglas»). The stems of the electrodes, the burette tips and other parts which might come into contact with these solutions were also made from plastic (»perspex» tubing). These plastics are completely resistant towards the solutions used. The plexiglas especially has a good transparancy and both are moreover easily worked. The solutions are mixed by a stream of nitrogen gas free from oxygen [9], and the gas inlet tube could also be used to remove the last drop from the burette tips.

Procedure: To a known volume of a solution of known C_M and C_H present in the electrode vessel initially fluoride stock solution was added from one burette and perchloric acid was added from another, in order to keep C_H of the buffer constant during the titration. In the later measurements, the acid solution of the second burette also contained uranyl ions so as to keep also C_M constant. This is not necessary but simplifies the calculations somewhat.

The potentials measured were reproducible within ±0.2 mV and they attained their final values almost at once.

MEASUREMENTS

The solutions are so acid at the outset that perceptible liquid junction potentials must exist. Approximately these potentials are determined merely by $[H^+]$. They may therefore be determined by separate titrations of 1 M

Table 1. The liquid junction potential E_d *as a function of* E. $[H^+]_0$ = *10 mM.*

E mV	>40	30	20	10	0	−10	−20	−30
E_d mV	−0.6	−0.5	−0.3	−0.2	0	0.3	0.9	1.7
$[H^+]$ mM	<2.0	3.0	4.5	6.7	10	15	23	35

sodium perchlorate with a perchloric acid solution. The difference between the emfs found and those calculated stoichiometrically are considered to be liquid junction potentials, the activity conditions assumed to be constant as usual. In Table 1, smoothed values of E_d (or E_d') for some round E (or E') are tabulated together with the corresponding values of $[H^+]$. From these figures all resulting liquid junction potentials for the calculation of E_H (or E_H') are easily found (*cf.* eqns. (2) and (10)).

The measurements of the hydrogen fluoride system then performed are tabulated in Table 2 A for the first fluoride preparation and in Table 2 B for the second one. The C_H, C_A function of Table 2 A are straight lines, the slopes of which agree fairly well with the ligand number $\bar{n}_H'$ calculated from (14) Fig. 1. In fact k_E is for some reason even a little higher than $\bar{n}_H'$. Thus H_2F_2 does not exist at the concentrations used here. The constants found are slightly higher for the first preparation than for the second one. For δ_1, the

Table 2. The complexity constants of the hydrogen fluoride system.

C_H mM	25	15	10	5	0	X_H	X_{1H}	X_{2H}	k_E
E_H mV	C_A mM				$C_A=[A]$		M^{-1}	M^{-2}	
A. First fluoride preparation $\delta_1 = 870 \pm 30$ M^{-1} $\delta_2 = 3\,300 \pm 300$ M^{-2}									
25	18.4	12.1	8.7	5.2	1.95	2.69	870		0.66
40	25.5	17.1	13.0	8.7	4.4	4.88	880		0.85
55	32.8	23:2	18.4	13.6	8.7	8.84	900	3 500	0.96
70	42.4	31.9	26.7	21.2	15.9	15.95	940	4 400	1.06
85	57.2	45.8	40.3	34.8	29.2	29.0	960	3 100	1.11
100	80.5	67.7	61.8	56.2	49.8	52.5	1 035	3 300	1.22
110	103.3	89.5	83.5	76.8	70.1	78.1	1 100	3 300	1.35
120	132.0	118.5	111.2	104.4	97.3	115.7	1 180	3 200	1.60
130	172.0	155.7	147.2	138.5	130.0	171.9	1 320	3 500	
140	222	204	196	185	177	256	1 440	3 200	
150	287	265	257	242	234	380	1 620	3 200	
B. Second fluoride preparation $\delta_1 = 850 \pm 30$ M^{-1} $\delta_2 = 2\,600 \pm 300$ M^{-2}									
50	31.2		16.7		7.0	7.25	890		0.97
70	43.7		27.6		16.9	15.95	890		1.07
90	65.9		48.4		36.7	35.4	940	2 460	1.17
100	83.5		65.2		53.0	52.5	970	2 260	1.22
110	107.3		87.6		74.5	78.1	1 040	2 550	1.31
120	138.4		117.3		103.2	115.7	1 120	2 620	1.41
130	179.4		155.8		140.1	171.9	1 220	2 650	1.57
140	232.5		207		190	256	1 350	2 640	
150	298		271		253	380	1 500	2 570	
155	339		309		289	464	1 600	2 600	
160	389		355		332	564	1 700	2 560	

difference is within the experimental error, but for δ_2 it is just beyond. For reasons mentioned above the second set is thought to be the best one. As the series with the two preparations were so close together, measurements with the second one were confined to the two values of C_H already mentioned. The values of k_E obtained from the lines through the two points at each E_H agree however tolerably well with the $\bar{n}_H'$ calculated from δ_1 and δ_2, Fig. 1. — For the same medium Sundén [12] has found $\delta_1 = 840$ M^{-1} and $\delta_2 \approx 1700$ M^{-2}.

The three uranyl series performed with the first stock solution are tabulated in Tables 3 and 4. Table 3 contains the series of the same $C_H = 10.17$ mM having $C_M = 10$ and 25 mM at the outset. The formation functions, shown in Fig. 2, coincide completely within the experimental errors (which are most marked at high [A], *cf.* p. 709). This proves that neither polynuclear complexes nor complexes containing HF_2 exist in the solutions measured (*cf.* p. 708). Table 4 contains the series of $C_H = 25.43$ mM, $C_M = 25$ mM. The formation function found coincides with those already obtained, Fig. 2, thus proving that no noticeable hydrolysis exists in the solutions [1].

The two uranyl titrations performed with the second stock solution have both $C_H = 25.00$ mM. They are tabulated in Table 5 and the values of $\bar{n}_M$ and [A] are plotted in Fig. 2. The formation function of $C_M = 50$ mM coincides very well with that of lower C_M. Perhaps a slight deviation downwards could be traced for the very lowest values of [A]. For the series of $C_M = 100$ mM a deviation for low [A] is quite perceptible, but nevertheless the coincidence is complete for this series also as soon as [A] > 0.2 mM.

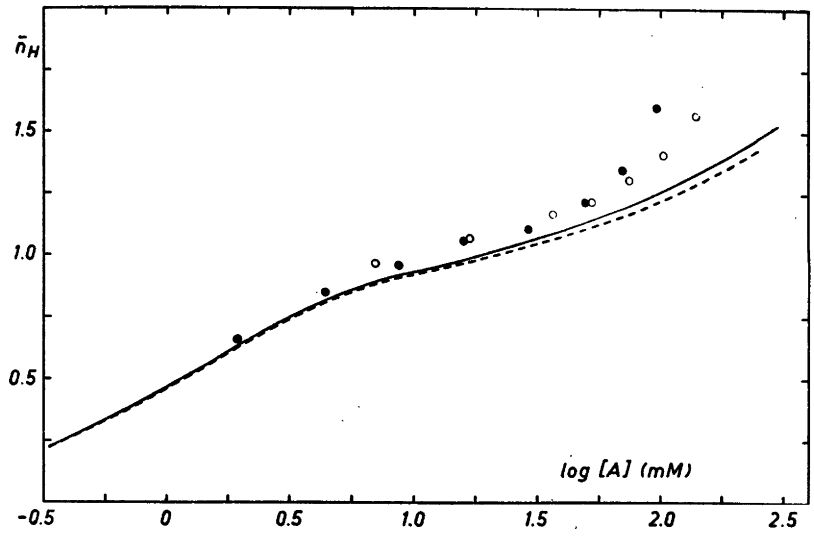


Fig. 1 Complex formation function of the hydrogen fluoride system. —

Curves calculated from (14) with the values of δ_1 and δ_2 found, circles obtained from the slopes k_E of the C_H, C_A-lines of constant E_H'. First fluoride preparation: fulldrawn curve and filled circles; second preparation: dashed curve and open circles.

This deviation at high C_M cannot be attributed to a formation of polynuclear complexes as this would cause the formation curve to move upwards instead of downwards as here (*cf.* Refs.[9, 11, p. 16]). The most probable explanation is a considerable change in the activity conditions caused by the high uranyl concentration since the uranyl salt is responsible for 1/3 of the ionic strength of the solution. Alternatively a small change in the liquid junction potentials might be the cause. E_H is <3.5 mV in this region and a quite small systematic error in the emf measured will therefore have a very marked effect.

Thus a mononuclear complex formation between UO_2^{2+} and F^- is the only reaction involving UO_2^{2+} which takes place in the present solutions. From the bend of the complex formation curve towards $\bar{n}_M = 4$ it is plain that $UO_2F_4^{2-}$ is the upper limit of this complex formation, at least within the range investigated here ([A] $<$ 300 mM).

From the complex formation function thus found the complexity constants were calculated [2], Table 6. As $\bar{n}_M/[A]$ increases very rapidly for low [A] a finite value $[A]_0 = 0.04$ mM was chosen as the lower limit of integration when $X_M([A])$ was computed. The values of β found are given in Table 7 together with the ligand number and the composition of the system calculated [2] for some values of [A]. The formation curve thus found is introduced in Fig. 2 (full-drawn). As seen it fits the experimental points very well *.

Table 7 also contains the consecutive constants [3] b and the ratios b_n/b_{n+1}. Especially the first and third ratios have unusually high values [3, 10, 11] indicating a remarkable stability of the first and third complexes. Consequently the maximum values of α_1 and α_3 (at $\bar{n}_M = 1$ and 3) are unusually high. High values of b_n/b_{n+1} seems to be a common feature of many strong fluoride systems, (for ref. see [13]) but it is quite contrary to that displayed by other uranyl systems [3], especially the acetate.

COMPARISON WITH PREVIOUS WORK

The strong complexity of uranyl fluoride was recognized during the early work on atomic energy but the first quantitative investigation is due to Kraus [14], who found $\beta_1 = 2.1 \times 10^4$ M^{-1} by an ion exchange method in an ionic medium not stated. The spectrophotometric work of Blake, Lowrie and Brown [6] gave $\beta_1 \approx 3 \times 10^5$ M^{-1} and moreover evidence was found for $UO_2F_4^{2-}$, with a value of $\beta_4 \approx 10^8$ M^{-4}. The method used was not very accurate nor was a constant ionic medium maintained. The results are therefore very approximate, and the authors themselves give the uncertainty as one power of ten. Day and Powers [15] have investigated the fluoride complexes in perchlorate medium at several temperatures and ionic strengths by means of TTA-extraction. Owing to the strong complexity a conveniently measurable partition was obtained only for low C_A. Only the first constant $[UO_2F^+][H^+]/[UO_2^{2+}][HF]$ can therefore be computed. For 20° C, $I = 1$ M a value ≈ 34 is found by inter-

* The values of β given here deviate slightly from those of the preliminary note [8]. It has been found that the formation curve obtained from the present values gives a somewhat better fit to the experimental points than did the curve from the previous ones.

Table 3. Determination of $\bar{n}_M$ *as a function of* [A] *for* $C_M = 10$ *and 25 mM,* $C_H = 10.17$ *mM.*

C_M' mM	10					25				
$E^{(i)}$ mV	0.0					0.1				
C_A mM	C_M mM	E_H mV	X_H	[A] mM	$\bar{n}_M$	C_M mC	E_H mV	X_H	[A] mM	$\bar{n}_M$
8.83	9.81	1.3	1.053	0.061	0.843	24.5	0.3	1.012	0.014	0.355
17.3	9.62	6.9	1.314	0.361	1.51	24.05	1.0	1.040	0.046	0.73
25.5	9.44	17.6	2.007	1.15	2.04	23.6	2.4	1.100	0.115	1.04
33.4	9.27	32.9	3.68	3.05	2.47	23.15	5.3	1.234	0.269	1.35
40.9	9.10	48.8	6.89	6.60	2.79	22.75	9.4	1.451	0.518	1.63
55.9	8.78	71.6	17.05	17.3	3.18	21.95	22.7	2.456	1.66	2.17
75.0	8.33	90.4	35.8	36.0	3.35	20.65	50.8	7.47	7.24	2.84
104.0	7.70	106.9	68.7	64.4	3.58	19.25	84.5	28.4	28.5	3.36
128.6	7.14	116.9	101.5	90.5	3.57	17.85	101.3	55.3	53.4	3.56
168.7	6.25	129.3	167.0	133.1	3.54	15.6	119.6	114.0	99.2	3.64
200.0	5.56	136.7	223	166.0	3.60	13.9	129.6	168.3	135.0	3.70
225	5.00	141.9	274	193	3.5	12.5	136.1	219	163.5	3.8
262.5	4.17	148.6	360	234	3.3	10.42	144.4	303	209	3.75
300	3.33	154.2	452	272.5	3.8	8.33	151.3	399	252	3.95
338	2.50	158.9	537	311	4.6	6.25	157.2	505	298	3.9

polation, corresponding to $\beta_1 \approx 2.9 \times 10^4$ M^{-1} if $\delta_1 = 850$ M^{-1}. This result thus agrees fairly well with ours as does qualitatively also the previous ones.

Johnson and Kraus [16], and Johnson, Kraus and Young [17] have determined mean activity coefficients for uranyl fluoride by freezing point depression and

Table 4. Determination of $\bar{n}_M$ *as a function of* [A] *for* $C_M' = 25$ *mM;* $C_H = 25.4$ *mM.* $E^{(i)} = -22.3$ *mV.*

C_A mM	C_M mM	E_H mV	X_H	[A] mM	$\bar{n}_M$
8.83	24.5	0.4	1.016	0.018	0.343
17.3	24.05	0.9	1.036	0.041	0.682
25.5	23.6	2.2	1.091	0.105	0.99
33.4	23.15	4.2	1.181	0.208	1.27
40.9	22.75	7.0	1.319	0.367	1.51
55.3	21.95	15.5	1.847	0.973	1.94
75.0	20.65	34.9	3.98	3.38	2.53
104.0	19.25	70.9	16.5	16.8	3.23
128.6	17.85	92.0	38.2	38.9	3.47
168.7	15.6	113.1	88.1	82.3	3.54
200.0	13.9	124.0	135.2	116.5	3.64
225	12.5	131.2	181	144.5	3.7
262.5	10.42	140.1	256	188.5	3.65
300	8.33	147.3	342	232.5	3.7
338	6.25	153.6	438	278	3.45

Table 5. Determination of $\bar{n}_M$ *as a function of* $[A]$ *for* $C_M = 50$ *and* 100 *mM*; $C_H = 25$ *mM.*

C_M mM	50				100				
$E^{(i)}$ mV	−22.1				−23.1				
C_A mM	E_H mV	X_H	[A] mM	$\bar{n}_M$	C_A mM	E_H mV	X_H	[A] mM	$\bar{n}_M$
22.8	0.5	1.020	0.024	0.446	22.6	0.4	1.016	0.019	0.22
43.6	1.7	1.070	0.082	0.838	42.8	0.7	1.028	0.033	0.42
62.5	3.8	1.162	0.190	1.176	60.9	1.1	1.044	0.052	0.599
79.9	6.6	1.298	0.350	1.484	77.3	1.6	1.065	0.076	0.759
95.9	10.6	1.522	0.614	1.73	92.1	2.3	1.095	0.112	0.899
110.5	15.4	1.840	0.987	1.96	112.0	3.5	1.149	0.175	1.086
137.0	27.3	2.948	2.28	2.365	137.3	5.6	1.248	0.292	1.322
159.8	40.8	5.03	4.67	2.692	158.8	8.0	1.373	0.439	1.514
189.0	60.2	10.85	11.21	3.088	189.0	12.4	1.634	0.747	1.78
213	75.6	20.0	24.2	3.27	213	17.3	1.984	1.15	1.99
240	89.8	35.0	40.3	3.45	240	24.1	2.597	1.87	2.23
271	102.8	58.8	63.2	3.58	271	34.4	3.91	3.39	2.49
308	114.7	94.0	94.1	3.67	300	42.7	5.42	5.13	2.74
361.5	127.6	156.5	143.2	3.72	343	60.6	11.05	11.42	3.08
400	134.8	208	179.6	3.73	369	72.3	17.5	22.8	3.21

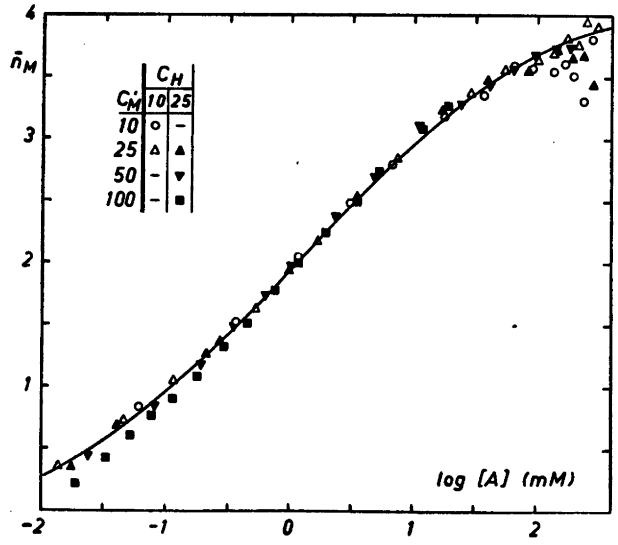


Fig. 2 Complex formation function of the uranyl fluoride system. —

The signs refer to titrations with different values of C_M and C_H according to the scheme given in the fig. The curve is obtained from the values of β found (Table 7).

Table 6. Computation of the complexity constants of the uranyl fluoride system.

[A] mM	$\frac{X([A])}{X(4\cdot10^{-5})}$	$X_{1M}\cdot10^{-4}$ M^{-1}	$X_{2M}\cdot10^{-7}$ M^{-2}	$X_{3M}\cdot10^{-10}$ M^{-3}	$X_{4M}\cdot10^{-11}$ M^{-4}
0	*0.39*	*3.5*	*7.8*	*2.9*	*6.5*
0.04	1.000	3.90			
0.06	1.330	4.05			
0.08	1.684	4.15	8.1		
0.1	2.060	4.30	8.0		
0.15	3.139	4.70	8.0		
0.2	4.411	5.15	8.25		
0.3	7.500	6.07	8.55		
0.5	16.30	8.13	9.26	2.9	
0.75	32.47	10.96	9.96	2.9	
1	55.82	14.20	10.70	2.9	
1.5	128.0	21.8	12.2	2.9	
2	241.5	30.9	13.7	3.0	
3	624	53.3	16.6	2.9	
5	2 340	119.6	23.3	3.1	
10	$1.67\cdot10^4$	427	42.3	3.45	
20	$14.7\cdot10^4$	1 880	93.8	4.3	
30	$54.9\cdot10^4$	4 690	156.0	4.94	6.7
50	$3.16\cdot10^6$	$1.616\cdot10^4$	316	6.16	6.5
100	$37.3\cdot10^6$	$9.55\cdot10^4$	955	9.47	6.6
150	$165.2\cdot10^6$	$28.2\cdot10^4$	1 880	12.48	6.4
200	$490\cdot10^6$	$62.7\cdot10^4$	3 140	15.7	6.4
300	$2300\cdot10^6$	$196.5\cdot10^4$	6 540	21.8	6.3

ultracentrifugation experiments. They interpret their results by assuming that the main equilibrium of the solution is $2\ UO_2F_2 \rightleftharpoons (UO_2F_2)_2$. We have here in fact found no polynuclear complexes for $C_M \leqq 100$ mM but of course

Table 7. The constants found. The ligand number and the percentage composition of the system as calculated for some values of [A] with these constants.

$\beta_1 = (3.5\pm0.4)\cdot10^4\ M^{-1}\ \beta_2 = (7.8\pm0.8)\cdot10^7\ M^{-2}\ \beta_3 = (2.9\pm0.4)\cdot10^{10}\ M^{-3}\ \beta_4 = (6.5\pm1.5)\cdot10^{11}\ M^{-4}$

$b_1 = \beta_1 \qquad b_2 = 2\,200\ M^{-1} \qquad b_3 = 370\ M^{-1} \qquad b_4 = 22\ M^{-1}$

$b_1/b_2 = 16 \qquad b_2/b_3 = 6 \qquad b_3/b_4 = 17$

[A] mM	$\bar{n}_M$	a_0	a_1	a_2	a_3	a_4
0.01	0.26	74	26	0	0	0
0.03	0.56	47	49.5	3.5	0	0
0.1	0.96	19	66	14.5	0.5	0
0.3	1.39	5	54.5	36.5	4	0
1	1.94	0.5	24.5	54.5	19.5	0.5
3	2.46	0	6.5	43	47	3
10	2.96	0	1	18.5	66	15
30	3.34	0	0	5	56.5	38.5
100	3.68	0	0	1	30.5	68.5
300	3.87	0	0	0	13	87

this does not exclude the formation of such complexes in more concentrated uranyl solutions. The result that this dimerisation is increasing when excess fluoride is added is however very surprising. One would have expected that an increase of [A] would have favoured the formation of complexes richer in A, such as $UO_2F_3^-$ and $UO_2F_4^{2-}$. As shown above these complexes are in fact the predominating species of solutions which are not very different from those investigated by Johnson, Kraus and Young.

This work has been supported by grants from *Atomkommittén (The Swedish Atomic Committee)* and *Statens naturvetenskapliga forskningsråd (Swedish Natural Science Research Council)*. We wish to thank Dr. F. J. C. Rossotti whose reading of our manuscript has resulted in improvements of both language and content.

REFERENCES

1. Ahrland, S. *Acta Chem. Scand.* **5** (1951) 199 (= IV).
2. Ahrland, S. *Acta Chem. Scand.* **3** (1949) 783 (= II).
3. Ahrland, S. *Acta Chem. Scand.* **7** (1953) 485 (= VII).
4. Kaplan, L., Hildebrandt, R. A. and Ader, M. *ANL*-4520 (1950).
5. *The Actinide Elements, NNES IV-14A* New York 1954.
6. Blake, C. A., Lowrie, R. S. and Brown, K. B. *AECD*-3212 (1951).
7. Zachariasen, W. H. *Report CK*-2737 (1945) (quoted in Katz, J. J. and Rabinowitch, E. *The Chemistry of Uranium, NNES VIII-5* New York 1951, p. 575).
8. Ahrland, S. and Larsson, R. *Acta Chem. Scand.* **8** (1954) 354.
9. Ahrland, S. *Acta Chem. Scand.* **3** (1949) 374 (= I).
10. Leden, I. *Potentiometrisk undersökning av några kadmiumsalters komplexitet*, Thesis, Lund 1943.
11. Fronæus, S. *Komplexsystem hos koppar*, Thesis, Lund 1948.
12. Sundén, N. *Svensk Kem. Tidskr.* **66** (1954) 50.
13. McKay, H. A. C., *A.E.R.E.* C/R 884 (1952).
14. Kraus, K. A. *ORNL*-795 (1950) (quoted in Ref. 6)
15. Day, R. A. Jr. and Powers, R. M. *J. Am. Chem. Soc.* **76** (1954) 3895.
16. Johnson, J. S. and Kraus, K. A. *J. Am. Chem. Soc.* **74** (1952) 4436.
17. Johnson, J. S., Kraus, K. A. and Young, T. F. *J. Am. Chem. Soc.* **76** (1954) 1436.

Received January 23, 1956.

ACTA CHEMICA SCANDINAVICA 10 (1956) 719—722

Über den Abbau von Lignin und Ligninmodellsubstanzen mit Hypochlorit. III. Mitteilung

HERMANN RICHTZENHAIN und BO ALFREDSSON

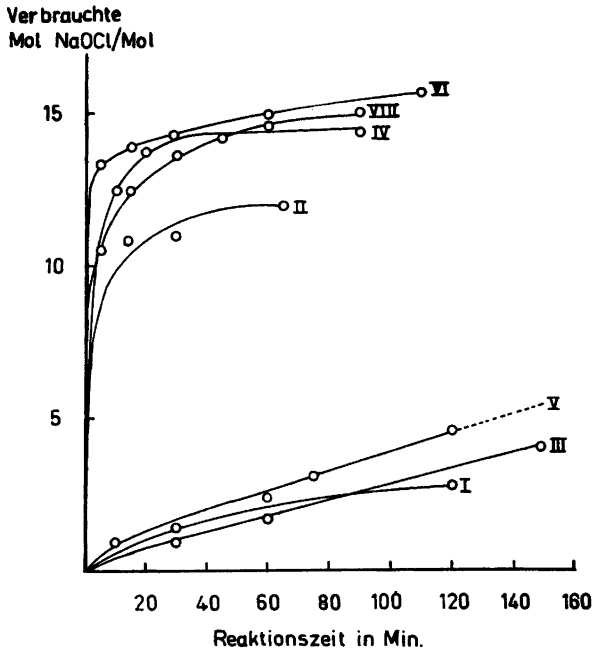
Holzchemische Abteilung der Schwedischen Holzforschungsanstalt, Stockholm, Schweden

Die Einwirkung von Hypochlorit auf β-Guajacyläther von Guajacylpropaneinheiten wurde kinetisch untersucht. Das Verhalten dieser Modellsubstanzen dürfte die Auffassung stützen, dass im Lignin entsprechende Gruppierungen in grösserer Menge vorkommen.
Die Synthese einiger Modellsubstanzen wird beschrieben.

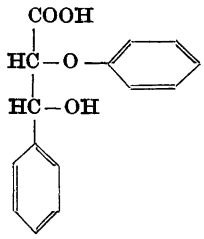
In zwei vorangehenden Mitteilungen [1,2] wurde über das Verhalten von Lignin bzw. von einer grösseren Anzahl von Ligninmodellsubstanzen gegen Hypochlorit berichtet. Diese Modellsubstanzen unterschieden sich im wesentlichen dadurch, dass sie einen Guajacolrest phenolätherartig an das α-, β- oder γ-Kohlenstoffatom einer 4-Propylguajacol- bzw. einer 4-Propylveratroleinheit gebunden enthielten. Unter diesen Modellsubstanzen zeigten einige mit einem in α-Stellung gebundenen Guajacolrest — insbesonders der von K. Freudenberg und Hübner [3] dargestellte Dehydrodiconiferylalkohol — insofern eine recht gute Übereinstimmung mit dem Verhalten des Lignins, als nicht nur der phenolische Rest, sondern auch ein Teil des phenolätherartig gebundenen Guajacolrestes durch Hypochlorit oxydiert wurde. Während in der Gruppe der β-Äther bisher nur solche von Propylveratroleinheiten auf ihr Verhalten gegen Hypochlorit geprüft wurden, wird in der vorliegenden Mitteilung nun auch der Abbau von β-Äthern von Guajacylpropanderivaten beschrieben.

Die Gruppe der β-Äther gewann in den letzten Jahren gesteigertes Interesse, nachdem Adler und Yllner [4] die Ähnlichkeit solcher Verbindungen mit dem Lignin in Bezug auf Sulfitierung und Alkoholyse erkannt und nachdem Freudenberg und Mitarbeiter [5] bei der enzymatischen Dehydrierung von Coniferylalkohol den β-Äther VII isoliert und als wichtiges Zwischenprodukt bei der Bildung der ligninähnlichen Dehydrierungspolymerisate des Coniferylalkohols erkannt hatten.

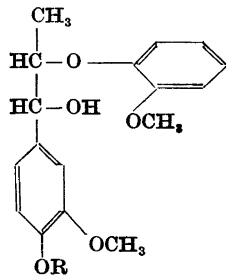
Von den untersuchten Verbindungen erwies sich die nach Stoermer und Kippe [6] dargestellte Verbindung I als ziemlich stabil gegen Hypochlorit bei 90°. Wie aus der folgenden Figur hervorgeht, ist der Hypochloritverbrauch von I so gering, dass der Ätherrest in β-Stellung sicher nur sehr langsam abge-



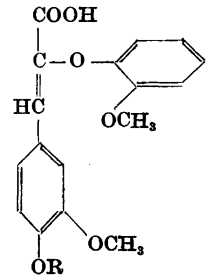
spalten werden kann. Immerhin konnte beim Abbau eine geringe Menge Benzoesäure nachgewiesen werden. Ein Vergleich des Verhaltens der phenolischen Verbindung II und ihres Methyläthers III, welche beide von Adler und Delin [7] dargestellt wurden, zeigt, dass III analog zu I nur relativ wenig Hypochlorit verbraucht. Dagegen ist bei II der Verbrauch mit 11 Mol Hypochlorit pro Mol innerhalb von 40 Min. so gross, dass bei II ausser dem phenolischen Rest auch schon der ätherartig gebundene Guajacolrest in gewissem Umfang oxydiert werden muss.



I



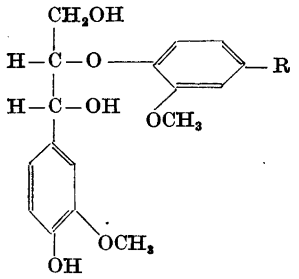
II: R = H
III: R = CH_3



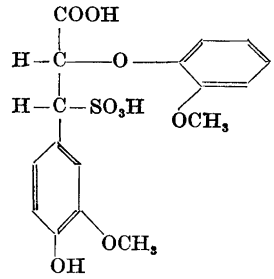
IV: R = H
V: R = CH_3

In der Verbindung IV, welche durch Kondensation von Vanillinacetat mit 2-Methoxyphenoxyessigsäure dargestellt wurde, werden beide Kerne bei einem Verbrauch von etwa 14 Mol Hypochlorit innerhalb von 20 Min. rasch abgebaut. Dass tatsächlich beide Kerne angegriffen werden, geht aus der Bestimmung der abgespaltenen Methanolmenge hervor. Aus einem Ansatz von 14 Mol Hypochlorit pro Mol IV lassen sich 1,7—1,8 Mol Methanol abdestillieren. Die IV entsprechende, methylierte Verbindung V — durch Kondensation von Veratrumaldehyd mit dem Natriumsalz der 2-Methoxyphenoxyessigsäure dargestellt — verbraucht im Verlauf von 60 Min. weniger als 3 Mol Hypochlorit. Es findet demnach nur ein langsamer Abbau des ätherartig gebundenen Guajacolrestes statt, wobei eine geringe Menge Veratrumsäure gebildet wird.

Ganz analog werden beim β-Guajacyläther des Guajacylglycerins (VI) beide Kerne rasch abgebaut. Auch in der Sulfosäure VIII werden die beiden Kerne rasch abgebaut. Nach einem Hypochloritverbrauch von etwa 14 Mol im Verlauf von 30 Min. erhält man 1,5—1,6 Mol Methanol. Die Sulfosäure lässt sich durch Erhitzen von IV mit neutraler Sulfitlösung auf 135° herstellen und wurde als Bariumsalz isoliert. Auch V lässt sich in gleicher Weise sulfitieren. Das UV-Absorptionsspektrum des Bariumsalzes von VIII zeigt Maxima bei 225 und 277 mμ sowie ein Minimum bei 253 mμ. Die Sulfosäure VIII zeigt keine Tendenz, beim Kochen ihrer wässrigen Lösung Guajacol abzuspalten.



VI: R = H
VII: R = CH : CH · CH_2OH



VIII

Aus den Kurven des Hypochloritverbrauchs geht klar hervor, dass in den Verbindungen IV, VI und VIII die ätherartig gebundenen Guajacolreste rasch und ziemlich vollständig abgebaut werden. Diese Modellversuche stehen demnach in gutem Einklang mit der Vermutung, dass ein wesentlicher Teil der Lignineinheiten durch derartige Ätherbindungen an der β-Stellung der Guajacylpropanseitenkette miteinander verknüpft sind.

Herrn Prof. E. Adler danken wir für die freundliche Überlassung einiger Präparate. Frau S. Safwat danken wir für die Ausführung der Methanolbestimmungen.

EXPERIMENTELLER TEIL

α-(2-Methoxyphenoxy)-ferulasäure (IV). 9,7 g Vanillinacetat, 10,2 g gut getrocknetes Natriumsalz der 2-Methoxyphenoxyessigsäure und 50 ml Essigsäureanhydrid werden unter Rühren 24 Stunden auf 105—110° erwärmt. Nach dieser Zeit wird ein Teil des

Essigsäureanhydrids im Vacuum abdestilliert und der Rückstand in Wasser gegossen. Das sich zuerst ölig ausscheidende Reaktionsprodukt erstarrt allmählich und wird abgenutscht. Nun wird das Rohprodukt mehrmals mit Äther ausgezogen, wobei das Acetat von IV in Lösung geht, während die Hauptmenge der als Nebenprodukt gebildeten Acetylferulasäure ungelöst zurückbleibt. Der Ätherlösung wird das Acetat von IV durch Ausschütteln mit Sodalösung entzogen, welche in verdünnte Salzsäure gegossen wird. Das kristallin ausfallende Produkt wird durch Umkristallisieren aus Benzol rein erhalten. Schmp. 164—166°. Ausbeute 1,6 g. (Gef. C 63,76; H 5,57; OCH_3 16,82. Ber. für $C_{19}H_{18}O_7$ (358,3): C 63,69; H 5,06; OCH_3 17,30.)

Nach dreistündigem Erwärmen des Acetats mit N Natronlauge erhält man beim Ansäuern IV, welches nach Umkristallisieren aus Benzol bei 152—153° schmilzt. (Gef. C 64,50; H 5,30; OCH_3 19,13. Ber. für $C_{17}H_{16}O_6$ (316,3): C 64,55; H 5,10; OCH_3 19,60.)

Sulfitierung von IV. 2,04 g IV werden mit 40 ml neutraler Natriumsulfitlösung (10 % Schwefeldioxyd, pH 6,4) 25 Stunden auf 135° erhitzt. Aus der Reaktionslösung wird eine kleine Menge öliger Substanz mit Äther ausgeschüttelt. Nach längerem Stehen scheiden sich aus der wässrigen Lösung 0,68 g des Natriumsalzes der gebildeten Sulfosäure ab, welches in das Bariumsalz übergeführt wurde. Aus der Mutterlauge wurde nach Katjonenaustausch, Entfernung der schwefligen Säure und Neutralisation mit Bariumcarbonat eine weitere Menge Bariumsalz erhalten. Die Ausbeute an reinem Bariumsalz betrug 1,49 g (44 % der Theorie). (Gef. S 6,18; OCH_3 11,24. Ber. für $C_{17}H_{16}O_9SBa$ (533,7): S 6,01; OCH_3 11,63).

α-(Methoxyphenoxy)-3,4-dimethoxyzimtsäure (V). Wird analog der bei IV beschriebenen Kondensation aus Veratrumaldehyd und dem Natriumsalz der 2-Methoxyphenoxyessigsäure erhalten. Schmilzt nach Umkristallisieren aus verdünntem Alkohol bei 199—201°. (Gef. OCH_3 28,41. Ber. für $C_{18}H_{18}O_6$ (330,3): OCH_3 28,19).

LITERATUR

1. Richtzenhain, H. und Alfredsson, B. *Acta Chem. Scand.* **7** (1953) 1177.
2. Richtzenhain, H. und Alfredsson, B. *Acta Chem. Scand.* **8** (1954) 1519.
3. Freudenberg, K. und Hübner, H. *Chem. Ber.* **85** (1952) 1181.
4. Adler, E. und Yllner, S. *Acta Chem. Scand.* **7** (1953) 570; *Svensk Papperstidn.* **57** (1954) 78.
5. Freudenberg, K., Schlüter, H. und Eisenhut, W. *Naturwiss.* **41** (1954) 576. Freudenberg, K. und Schlüter, H. *Chem. Ber.* **88** (1955) 617.
6. Stoermer, R. und Kippe, O. *Ber.* **38** (1905) 1955.
7. Adler, E. und Delin, S. *(unveröffentlicht).*

Eingegangen am 24. Januar 1956.

ACTA CHEMICA SCANDINAVICA 10 (1956) 723—726

The Stability of Metal Halide Complexes in Aqueous Solution

I. The Stability of Metal Halide Complexes in Relation to the Position of the Metal in the Periodic System

STEN AHRLAND

Department of Inorganic and Physical Chemistry, Chemical Institute, University of Lund, Lund, Sweden

With respect to the strength of their halide complexes central ions may be divided into two groups. The first group shows decreasing stability in the order $F^- \gg Cl^- > Br^- > I^-$, the second one in the reversed order $F^- \ll Cl^- < Br^- < I^-$. The extension of the two groups within the Periodic System is discussed.

As pointed out previously by Ahrland and Larsson [1] central ions may be divided into two distinct groups with respect to their ability to form halide complexes. The ions of the first group form fluoride complexes which are much stronger than the complexes formed with the heavier halide ions. The strength of these decreases in the order $Cl^- > Br^- > I^-$. On the contrary, the ions of the second group form fluoride complexes which are much weaker than the complexes formed with the heavier halide ions. Moreover the strength of these always increases in the order $Cl^- < Br^- < I^-$.

The strength of the halide complexes is thus completely reversed between the two groups. In both cases however, the complexity varies monotonicly with the atomic number of the halogen and there is moreover always a difference in the order of magnitude between the complexity of the fluoride and that of the other halide ions.

The first group is the more numerous one. It certainly contains * H^+, Ce^{3+}, U^{4+}, UO_2^{2+}, Zr^{4+}, Fe^{3+}, and In^{3+}, most probably also Be^{2+}, Th^{4+}, Pu^{4+}, Cu^{2+}, Zn^{2+}, Al^{3+}, and Sn^{2+}. In the latter cases many desirable data are admittedly still lacking but the trend nevertheless seems obvious. In the case of Be^{2+} and Al^{3+} where only the fluoride systems have been quantitatively measured supplementary evidence is provided by the fact that the chlorides [9, 10, p. 573] are typical strong electrolytes, quite unlike the fluorides. This is also the case for aluminium bromide [11].

* A very comprehensive list of references has been compiled by Carleson and Irving [2]. Further references: U^{4+}, see [3]; Be^{2+}, see [4]; Pu^{4+}, see [5,6]; Hg^{2+}, see [7]; Pb^{2+}, see [8].

The less numerous second group certainly contains Pt(II), Cu^+, Ag^+, Cd^{2+}, Hg^{2+} and Pb^{2+}. The complexes of Pt(II) are as a rule inert and their equilibria therefore difficult to measure. In the olefin complexes however, the bond *trans* to the olefin position becomes labilised [12] and measurements of equilibria involving this ligand are therefore feasible, as shown by Leden and Chatt [13]. These measurements prove definitely that Pt(II) belongs to the second group and this could also be expected from preparative data known previously. Thus Pt(II) forms very stable chloro and bromo salts while the corresponding fluoro compounds do not even seem to exist [14]. For Pb^{2+}, the order $Cl^- < Br^-$ has recently also been confirmed by ion exchange measurements [15].

Most probably Pd(II), Pd(IV), Pt(IV), Au(III), and Tl^{3+} also belong to the second group. For Pd(II), Pd(IV) and Au(III) this conclusion is based on preparative data similar to those quoted for Pt(II) above (*cf.*[16,17] and references quoted therein). For Pt(IV), semi-quantitative measurements of Schlesinger and Palmateer [18] unequivocally indicate the second group order $Cl^- < Br^- < I^-$ of complex stability.

Now the striking fact is that all the central ions of the second group are derived from neighbouring elements around the end of the transition series. Moreover these elements seem to form a roughly triangular figure with the apex at Cu and the base stretching from somewhere to the left of Pt to the right of Pb.

The right borderline of the triangle seems fairly well established. It certainly runs between the pairs Cu—Zn, Zn—Cd, Cd—In, In—Tl, and Sn—Pb; only the last part of its course is still unknown.

On the other hand the left borderline is only roughly known at present. Fe is definitely outside the triangle and there is no doubt that the border runs between Cu and Ni, as the heavy halides of Ni^{2+} are typical strong electrolytes. Thus the activity coefficients of nickel chloride resemble those of barium and calcium chlorides [10, p. 423] and the absorption spectrum of the solution is practically identical with that of nickel perchlorate [19], both solutions evidently containing the same absorbing species, Ni^{2+}. Thus Cu^+ is the only central ion of the 4th period belonging to the second group, and the triangular area has an apex at copper. Unlike Cu^+, Cu^{2+} belongs to the first group. Copper is the only element where different valency states have been found to belong to different groups. It would be interesting if a method of investigating halide complexes of Ag(II) could be found, to see whether silver behaved analogous to copper in this respect. As to the further course of the left borderline, it may be supposed that the remaining platinum metals are also inside the triangle on account of their resemblance to Pd and Pt. However, it is not known at present if there is a further extension to the left of the second group area. The known facts are that Zr^{4+} and Ce^{3+} (and certainly the other lanthanides as well) are outside it, as are also the actinides of the 7th period.

The relative strength of the halide complexes of central ions belonging to the first group, outside the triangle, is just the one which would be expected if the complex formation is due to essentially electrostatic forces. In such a case strong bonds should be formed by ligands combining slight polarizability with small ionic radius. These quantities both decrease monotonicly from

I^- to F^-, but F^- occupies a unique position as the differences between F^- and Cl^- are much greater than those between the heavy halides. Therefore the sequence of halide complexity should be $F^- \gg Cl^- > Br^- > I^-$ as is also found for the first group.

The strength of the complex formation will also depend upon the central ion, and strong electrostatic bonds should be formed by central ions of high ionic charge and small radius. As pointed out by Connick and Tsao [20] the strength of the fluoride complexes just follow this pattern thus indicating their essentially electrostatic character.

The reversal of the relative strength of the halide complexes for the central ions within the triangle has been explained by Leden and Chatt [13] as being due to a formation of partial double bonds of an essentially covalent character between the metal ion and the heavy halide donor. In their penultimate shells, the elements at the end of the transition series have filled d-orbitals of an energy close to that of the ordinary valency hybrids. These orbitals might therefore be incorporated in the bond system of the complex provided the ligand is able to accomodate the extra bonding electrons thus offered. The three heavier halides have vacant d-orbitals in their outer shells and are therefore able to participate in a double bond while the fluoride ions has no such orbitals and thus cannot form any double bond. If the strength of the complexes is determined by a covalent double bond formation, the fluoride complexes should therefore be much weaker than those of the heavier halide ions. The order between these will be determined by their donating properties, which show a smooth increase from Cl^- to I^-. The expected order will therefore be $F^- \ll Cl^- < Br^- < I^-$, or just the one found within the second group.

Leden and Chatt [13] also point out that those metals which show a strong complexity of the chloride relative to the fluoride are also characterized by the much greater stability of thio-ether complexes relative to ether complexes, and trialkylphosphine complexes relative to trialkylamine complexes. In these cases too the formation of strong complexes might be attributed to the formation of double bonds with those ligands which possess vacant d-orbitals in their outer shells.

The existence of multiple metal to ligand bonds involving d-orbitals of the metal was first postulated by Pauling [21] in order to account for the remarkable stability of carbonyl, nitrosyl and cyano complexes of the later transition metals. In these cases it was assumed that the additional bonding electrons are accommodated in the ligand by means of an electronic rearrangement leading to a decrease in bond order of the internal ligand bond. Later Dewar [22] and Chatt [23, 24] have explained the formation of olefin complexes along similar lines. In all those cases there is also strong physical evidence (from measurements of bond lengths and infrared stretching frequencies) that the bonds of the complexes are really of the orders postulated by the multiple bond theory. Evidence of that kind is admittedly still lacking for the halide complexes.

Measurements on further halide systems are now in progress in order to see whether they all fit into the above scheme. In the first hand systems on the supposed borderlines are being investigated as they will give the information required about the exact extension of the triangular area. Such systems will possibly also show some interesting transitional properties.

This work is part of an investigation supported by *Statens naturvetenskapliga forskningsråd (Swedish Natural Science Research Council)*. My thanks are due to Dr. J. Chatt, Dr. Sture Fronæus, Dr. Ido Leden and Dr. F. J. C. Rossotti for interesting discussions and useful comments.

REFERENCES

1. Ahrland, S. and Larsson, R. *Acta Chem. Scand.* **8** (1954) 354.
2. Carleson, B. G. F. and Irving, H. *J. Chem. Soc.* **1954** 4390.
3. Day, R. A. Jr., Wilhite, R. N. and Hamilton, F. D. *J. Am. Chem. Soc.* **77** (1955) 3 180.
4. Dodgen, H. W. and Yates, L. M. presented at Fall Meeting of Am. Chem. Soc. at Atlantic City 1952 (from a quotation in 20).
5. Hindman, J. C. *The Transuranium Elements NNES IV—14B*, New York 1949, p. 405.
6. Mc Lane, C. K. *The Transuranium Elements*, p. 414.
7. Connick, R. E. presented at Fall Meeting of Am. Chem. Soc. at New York 1954.
8. Biggs, A. I., Parton, H. N. and Robinson, R. A. *J. Am. Chem. Soc.* **77** (1955) 5844.
9. Sidgwick, N. V. and Lewis, N. B. *J. Chem. Soc.* **1926** 1287.
10. Harned, H. S. and Owen, B. B. *The Physical Chemistry of Electrolytic Solutions*, New York 1950.
11. Kablukov, I. and Sachanov, A. *Z. physik. Chem.* **69** (1909) 419.
12. Chernyaev, I. I. and Hel'man, A. D. *Compt. rend. acad. sci., U.R.S.S.* **4** (1936) 181 (from a quotation in 13).
13. Leden, I. and Chatt, J. *J. Chem. Soc.* **1955** 2936.
14. *Gmelins Handbuch*, 8th ed., **68 Pt C**, 1939—40.
15. Karlsson, C. *To be published.*
16. *Gmelins Handbuch*, 8th ed., **62 Au**, 1950—54.
17. *Gmelins Handbuch*, 8th ed., **65 Pd**, 1942.
18. Schlesinger, H. I. and Palmateer, R. E. *J. Am. Chem. Soc.* **52** (1930) 4316.
19. Fronæus, S. *Private communication.*
20. Connick, R. E. and Tsao, Maak-Sang *J. Am. Chem. Soc.* **76** (1954) 5311.
21. Pauling, L. *The Nature of the Chemical Bond*, New York 1939.
22. Dewar, J. S. *Bull. soc. chim. France* **1951** C 79.
23. Chatt, J. *J. Chem. Soc.* **1949** 3340.
24. Chatt, J. and Duncanson, L. A. *J. Chem. Soc.* **1953** 2939.

Received February 13, 1956.

ACTA CHEMICA SCANDINAVICA 10 (1956) 727—734

The Stability of Metal Halide Complexes in Aqueous Solution

II. The Fluoride Complexes of Divalent Nickel, Copper, and Zinc

STEN AHRLAND and KJELL ROSENGREN

Department of Inorganic and Physical Chemistry, Chemical Institute, University of Lund, Lund, Sweden

The stabilities of the fluoride complexes of Ni^{2+}, Cu^{2+}, and Zn^{2+} have been determined. In the solutions studied ($[F^-] \leqq 200$ mM; $C_M \leqq 100$ mM; perchlorate medium of ionic strength 1 M at 20° C) only the first mononuclear complex exists in appreciable concentrations. The following values of the constant $\beta_1 = [MF^+] / [M^{2+}] [F^-]$ have been found:

Ni^{2+}: 4.6 ± 0.5 M^{-1}; Cu^{2+}: 9 ± 1 M^{-1}; Zn^{2+}: 5.9 ± 0.6 M^{-1}

The stability order of these complexes, as well as their strength relative to the complexes formed by the same metal ions with the other halide ions is in accordance with the views advanced in the first paper [1] of this series.

According to the views developed in part I of this series of papers [1], the fluoride complexes of Ni^{2+}, Cu^{2+}, and Zn^{2+} should be much stronger than the complexes formed by these ions with the other halides. However, even the fluoride complexes will be of moderate strength as the central ions are only divalent and do not have especially small ionic radii. The stability of the fluoride complexes will vary inversely with the ionic radii, *i. e.* in the order $Ni^{2+} < Cu^{2+} > Zn^{2+}$ (*cf.* Connick and Tsao [2]).

The aim of the present investigation was to test these views experimentally. The systems were studied in the same way as the uranyl fluoride [3] system. The ionic medium (perchlorate of ionic strength $I = 1$ M) and the temperature (20° C) were also the same as in the previous measurements.

From the emf E_H obtained experimentally * by means of the quinhydrone electrode the free ligand concentration [A] may be calculated using the equation

* The same symbols are used as in the paper on uranyl fluoride [3].

$$\text{antilog}\ \frac{E_H}{RT/F} = \frac{C_H}{[H^+]} = 1 + \delta_1\,[A] + \delta_2\,[A]^2 = X_H \qquad (1)$$

where the constants δ_1 and δ_2 of the hydrogen fluoride system have been determined previously [3]. Then the ligand number $\bar{n}_M$ can be calculated from the relationship

$$\bar{n}_M = \frac{C_A - [A] - \bar{n}_H \cdot C_H}{C_M} \qquad (2)$$

where the value of $\bar{n}_H$ corresponding to the appropriate value of [A] is found from the known [3] complex formation function of the hydrogen fluoride system. Once the complex formation function $\bar{n}_M = f([A])$ has thus been found, the complexity constants can be calculated in the usual way [4].

The calculation of [A] and $\bar{n}_H$ described above presupposes however that neither the dimer H_2F_2 nor metal complexes with HF_2^- as ligand exist in the range of concentration used. It has previously [3] been shown that no H_2F_2 is formed and that HF_2^- does not compete appreciably with F^- in the formation of complexes with UO_2^{2+}. It was therefore assumed in the first instance that no complexes with HF_2 are formed by the present cations. This assumption may be tested experimentally in the same way as for UO_2^{2+}, *viz.* by determining the formation function for different values of total concentration of metal C_M. If this function is independent of C_M it may be concluded not only that no complexes of HF_2^- exist but also that the complex formation is entirely mononuclear [3].

It is well known that the present cations are not hydrolysed at low pH. This is also confirmed by the analysis performed (p. 729) in order to check if the preparations of perchlorates used contain any free perchloric acid. No buffering due to Cu^{2+} could be detected below a pH of 4 or 5; and the hydrolysis of Zn^{2+} and Ni^{2+} becomes perceptible only at still higher pH. Nevertheless series of measurement were performed at two different values of total concentration of acid, C_H, in order to ensure that complex formation is really independent of $[H^+]$ (*cf.* Ref.[3]).

The calculation of the complex formation function from δ_1 and δ_2 also presupposes that the values of these constants do not change appreciably in the range of C_A used. To judge from previous measurements this is true for $C_A \lessapprox 200$ mM. For $C_A \gtrapprox 200$ mM a fairly tedious method of calculation must be used in order to find $\bar{n}_M = f([A])$. For the present systems however no measurements are performed in this upper range, as they are not likely to give further information justifying the work involved. The systems are so unstable that only the first complex MF^+ can be shown to exist with certainty when $C_A \lessapprox 200$ mM. Even at the highest value of C_A, ≈ 400 mM, which can be reached by adding a fluoride solution almost saturated with respect to NaF, the concentration of the second complex must therefore be low. In view of the further uncertainty inherent in the change of the medium, a calculation of the stability constant of this complex is not really possible even if the measurements are extended to $C_A = 400$ mM.

EXPERIMENTAL

Chemicals. The preparations of *nickel perchlorate* and *copper perchlorate* were the same as used by Fronæus [5,6]. *Zinc perchlorate* was prepared by adding the equivalent amount of a solution of sodium hydroxide (EKA *puriss*) to a solution of zinc nitrate (Bakers analyzed), washing the precipitate free from nitrate ions and then dissolving it in a slight excess of perchloric acid (Bakers analyzed). When excess water was driven off nice crystals of the zinc perchlorate hexahydrate were obtained.

Stock solutions of the perchlorates, of an ionic strength I = 1 M, were prepared and their exact concentrations then determined by electroanalysis (according to the methods described by Vogel [7]).

The amounts of free perchloric acid possibly present in the stock solutions were determined by adding a known amount of acid to a sample which was then titrated potentiometrically with alkali. The metal ions present are all so weakly acidic that they do not interfere with the determination of the free acid. The stock solutions of Ni^{2+} and Zn^{2+} did not contain any free acid. For Cu^{2+} a small concentration of acid was found (= 1.0 % of the total perchlorate concentration) and taken into account when solutions were mixed for the fluoride titrations.

Table 1. Determination of the complex formation function of the nickel fluoride system.

A. C_M = 50 mM; C_H = 10 and 25 mM.

C_H mM →	10				25			
C_A mM	E_H mV	X_H	[A] mM	$n\bar{}_M$	E_H mV	X_H	[A] mM	$\bar{n}_M$
22.8	59.3	10.46	10.78	0.054	31.6	3.49	2.91	0.036
43.6	82.7	26.4	27.5	0.116	66.9	14.13	14.78	0.093
62.5	95.0	43.0	43.6	0.160	84.3	28.2	29.3	0.142
79.9	103.2	59.5	58.2	0.208	95.2	43.3	43.9	0.172
95.9	109.3	75.7	72.1	0.242	102.6	58.1	57.1	0.210
110.5	114.3	92.3	85.2	0.27	108.4	73.1	69.8	0.234
137.0	121.6	123.2	108	0.33	116.8	101.9	92.6	0.28
160	127.0	152.6	128	0.38	122.7	128.7	112	0.34
189	132.9	192.8	153	0.45	129.1	165.9	137	0.40
213	137.1	227.7	174	0.51	133.8	199.8	158	0.45

B. C_M = 100 mM; C_H = 10 mM.

C_A mM	E_H mV	X_H	[A] mM	$\bar{n}_M$
22.6	55.6	9.04	9.20	0.042
42.8	78.7	22.6	23.6	0.090
60.9	90.9	36.6	37.5	0.127
77.3	98.9	50.2	50.2	0.160
92.1	104.7	63.1	61.6	0.187
112.0	111.3	82.0	77.1	0.231
137.3	118.3	108.2	97.2	0.28
159	123.4	132.4	114	0.32
189	129.5	168.5	138	0.38
213	133.7	199.0	157	0.42

Table 2. Determination of the complex formation function of the copper fluoride system.

A. C_M = 50 mM; C_H = 10 and 25 mM.

C_H mM →	10				25			
C_A mM	E_H mV	X_H	[A] mM	$\bar{n}_M$	E_H mV	X_H	[A] mM	$\bar{n}_M$
22.8	56.7	9.44	9.64	0.079	31.0	3.41	2.81	0.044
43.6	79.8	23.6	24.7	0.174	64.5	12.85	13.38	0.126
62.5	92.2	38.5	39.3	0.248	81.6	25.3	26.4	0.206
79.9	100.5	53.5	53.1	0.31	92.3	38.6	39.5	0.27
95.9	106.5	67.8	65.4	0.38	99.7	51.8	51.5	0.33
110.5	111.4	82.3	77.4	0.43	105.2	64.4	62.7	0.38
137.0	118.8	110.3	98.6	0.52	113.6	89.8	83.3	0.48
160	124.4	137.7	118	0.58	119.6	113.9	101	0.55
189	130.4	174.6	142	0.68	126.1	147.3	125	0.66
213	134.8	207.8	163	0.74	130.8	177.4	144	0.73

B. C_M = 100 mM; C_H = 10 mM.

C_A mM	E_H mV	X_H	[A] mM	$\bar{n}_M$
22.6	51.9	7.81	7.83	0.058
42.8	74.3	18.95	19.8	0.130
60.9	86.3	30.5	31.6	0.190
77.3	94.3	41.8	42.5	0.239
92.1	100.1	52.6	52.3	0.28
112.0	106.5	67.8	65.4	0.35
137.3	113.5	89.4	83.1	0.42
159	118.6	109.4	98.1	0.48
189	124.7	139.3	119	0.57
213	129.1	165.9	137	0.63

The *sodium fluoride* was of the second preparation used for the uranyl fluoride measurements [3]. The *other chemicals* were also the same as used in this investigation.

Procedure. For each central ion three titrations were performed, the first two with C_M = 50 mM and C_H = 10 and 25 mM, the third with C_M = 100 mM and C_H = 10 mM. The values of C_M and C_H were kept constant throughout every titration. The titrations were all performed with the same reference electrode RE (with $[H]_0$ = 10 mM) as was used before [3].

The quinhydrone electrode functioned well in the present solutions. Even at the highest concentrations of metal ions used, C_M = 100 mM, the potentials differed only slightly from the values calculated from known values of $[H^+]$. Thus the emf $E^{(i)}$ measured initially which should be zero for the series of C_H = 10 mM is found to be 1—2 mV for C_M = 100 mM. This deviation may be caused by several factors which probably co-operate. The changes of the ionic medium may produce changes in the activity coefficients and the liquid junction potentials and some complex formation between the metal ion and the hydroquinone may occur. These slight deviations certainly have very little influence on the calculation of [A] (and $\bar{n}_M$) as E_H is the emf of a cell with the same value of C_M in both half-cells. The potentials measured reached equilibrium almost at once and as a rule they could be reproduced within 0.2 mV.

Table 3. Determination of the complex formation function of the zinc fluoride system.

A. C_M = 50 mM; C_H = 10 and 25 mM.

C_H mM	10				25			
C_A mM	E_H mV	X_H	[A] mM	$\bar{n}_M$	E_H mM	X_H	[A] mM	$\bar{n}_M$
22.8	58.2	10.00	10.27	0.065	31.4	3.46	2.68	0.052
43.6	81.8	25.5	26.7	0.133	65.8	13.53	14.12	0.109
62.5	94.0	41.3	42.1	0.190	83.0	26.7	27.9	0.174
79.9	102.2	57.2	56.4	0.244	93.6	40.7	41.4	0.226
95.9	108.5	73.4	70.1	0.28	100.8	54.1	53.6	0.28
110.5	113.5	89.4	83.0	0.31	106.6	68.1	65.8	0.32
137.0	120.9	119.9	105.8	0.38	115.1	95.3	87.5	0.39
160	126.2	147.9	125	0.44	121.0	120.4	106	0.45
189	132.1	186.8	150	0.52	127.4	155.1	130	0.54
213	136.4	222	171	0.58	132.1	186.8	150	0.61

B. C_M = 100 mM; C_H = 10 mM.

C_A mM	E_H mV	X_H	[A] mM	$\bar{n}_M$
22.6	53.8	8.41	8.50	0.050
42.8	76.6	20.8	21.8	0.109
60.9	88.8	33.6	34.7	0.156
77.3	96.8	46.2	46.6	0.197
92.1	102.6	58.1	57.1	0.237
112.0	109.4	76.0	72.3	0.28
137.3	116.3	99.9	91.0	0.34
159	121.5	122.8	108	0.38
189	127.6	156.3	131	0.45
213	131.8	184.6	148	0.51

RESULTS

The complex formation functions are given in Tables 1—3 and plotted in Figs 1 and 2. For the three ions measured, this function is seen to be independent of both C_M and C_H within the experimental errors. It must be remembered that the errors are fairly large when weak complexes are determined by measurements of [A]. Thus no polynuclear complexes, no complexes containing HF_2^- and no hydroxo complexes exist in perceptible amounts in the solutions investigated. The mononuclear complex formation between metal ion and F^- is therefore the only process which need be considered.

The complexity constants are calculated from the complex formation functions in the same way as before [4]. When integrating the function $\bar{n}_M/[A]$ in order to find X_M it is suitable to choose [A] = 10 mM as the lower limit of integration. The results are in Table 4. As seen the function X_{1M} is virtually constant over the whole range of [A] for all the systems measured, with the

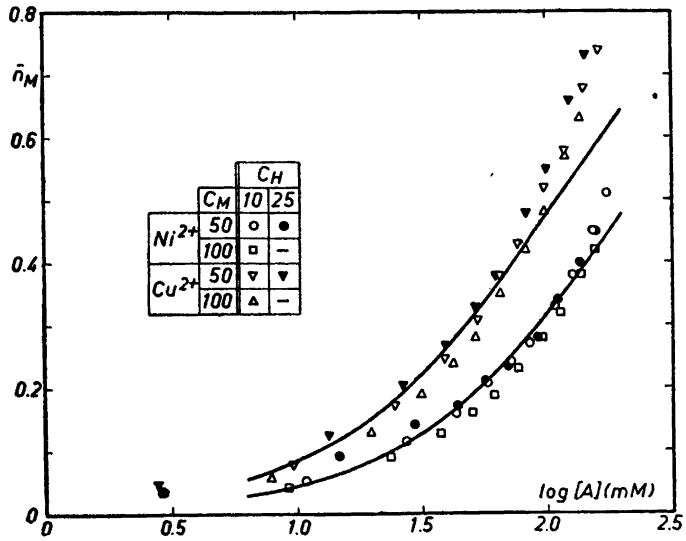


Fig. 1. The complex formation functions of the nickel and copper fluoride systems. The signs refer to different titrations as indicated by the scheme given in the fig. The curves are obtained from the values of β_1 found.

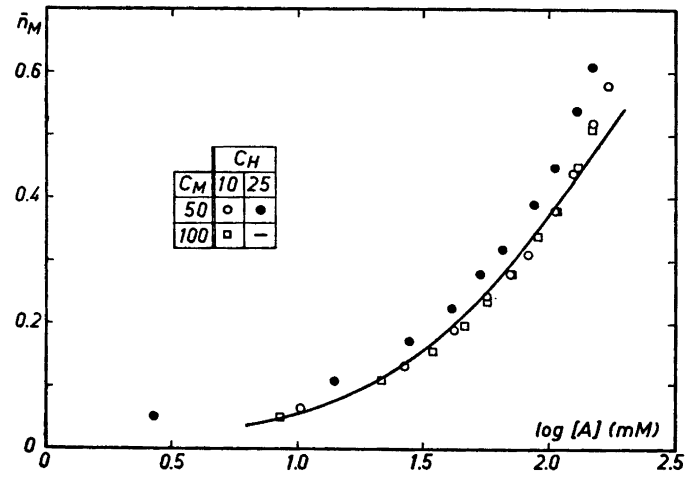


Fig. 2. The complex formation function of the zinc fluoride system. The signs refer to different titrations as indicated by the scheme. The curve is obtained from the value of β_1 found.

Table 4. Computation of the first complexity constant β_1 for the three systems measured.

M →	Ni^{2+}		Cu^{2+}		Zn^{2+}	
[A] mM	$\frac{X_M([A])}{X_M(0.01)}$	X_{1M} M^{-1}	$\frac{X_M([A])}{X_M(0.01)}$	X_{1M} M^{-1}	$\frac{X_M([A])}{X_M(0.01)}$	X_{1M} M^{-1}
0	0.956		0.920		0.945	
10	1.000	4.6	1.000	8.7	1.000	5.8
25	1.071	4.8	1.120	8.3	1.087	6.0
40	1.136	4.7	1.238	8.7	1.168	5.9
60	1.219	4.6	1.396	8.6	1.275	5.8
80	1.301	4.5	1.561	8.7	1.383	5.8
100	1.383	4.5	1.736	8.9	1.493	5.8
120	1.467	4.5	1.921	9.1	1.608	5.8
140	1.555	4.5	2.116	9.3	1.727	5.9
160	1.645	4.5	2.324	9.6	1.853	6.0
180	1.739	4.5	2.545	9.8	1.985	6.1
200	1.837	4.6	2.782	10.2	2.124	6.2
β_1 M^{-1} →	4.6 ± 0.5		9 ± 1		5.9 ± 0.6	

exception of the highest values of Cu^{2+}, where a slight upward trend is found. Thus the first complex MF^+ is the only one existing in measurable amounts in the present solutions. Therefore the value of β_1 is taken for each ion as the mean of the values of X_{1M} over the whole range of [A] (with the highest values for Cu^{2+} left out). The values of β_1 thus found are given in Table 4, with the random errors indicated.

As could be foreseen from their charge and ionic radii, Ni^{2+}, Cu^{2+}, and Zn^{2+} form only weak fluoride complexes with the stability order $Ni^{2+} < Cu^{2+} > Zn^{2+}$. Nevertheless the fluoride complexes are all, as expected, much stronger than the complexes formed by the other halides. Thus in the case of Cu^{2+} and Zn^{2+}, β_1 of the fluoride system is 10 times greater than β_1 of the next strongest system, the chloride [8,9]. In the case of Ni^{2+}, there are no quantitative data about the other halides, but they are typical strong electrolytes (*cf.*[1] and references therein). From the sequence of ionic radii one would rather expect them to be less stable than the corresponding complexes of Cu^{2+}.

The results of this investigation thus agree in all respects with the predictions made on the basis of the views put forward in I. Moreover the ions Ni^{2+}, Cu^{2+}, and Zn^{2+}, which were previously considered as only probable members of the first group of central ions (as defined in I), are now shown as certainly belonging to this group.

This investigation has been generously supported by *Statens naturvetenskapliga forskningsråd (Swedish Natural Science Research Council)*. We are further indebted to Dr. Sture Fronæus for the gift of the preparations of nickel and copper perchlorate.

REFERENCES

1. Ahrland, S. *Acta Chem. Scand.* **10** (1956) 723.
2. Connick, R. E. and Tsao, Maak-Sang *J. Am. Chem. Soc.* **76** (1954) 5311.
3. Ahrland, S., Larsson, R. and Rosengren, K. *Acta Chem. Scand.* **10** (1956) 705.
4. Ahrland, S. *Acta Chem. Scand.* **3** (1949) 783.
5. Fronæus, S. *Acta Chem. Scand.* **6** (1952) 1200.
6. Fronæus, S. *Komplexsystem hos koppar* (Diss.) University, Lund, 1948.
7. Vogel, A. I. *Quantitative Inorganic Analysis*, 2nd Ed., Longmans, Green and Co, London 1951.
8. Bjerrum, J. *Kgl. Danske Videnskab. Selskab, Mat.-fys. Medd.* **22** (1946) No 18.
9. Sillén, L. G. and Liljeqvist, B. *Svensk Kem. Tidskr.* **56** (1944) 85.

Received March 2, 1956.

ACTA CHEMICA SCANDINAVICA 10 (1956) 735—738

Synthesis of Compounds Related to Muscarufin I

HOLGER ERDTMAN and MARTIN NILSSON

Organisk-kemiska institutionen, Kungl. Tekniska Högskolan, Stockholm, Sweden

The synthesis and properties of 2,5-dimethoxy-1,4-bis-(2-carbomethoxyphenyl)-benzene (II), 2,5-bis-(2-carbomethoxyphenyl)-benzoquinone (III) and some related compounds is reported. These compounds embrace parts of the structure proposed by Kögl and Erxleben for muscarufin (I).

From the common fly-agaric, *Amanita muscaria*, Kögl and Erxleben [1] isolated in 1930 a red pigment muscarufin for which, as a result of elegant degradative work carried out with very small quantities of material, they were able to advance structure I. This formula appears to have met with general acceptance.

Other products of fungal metabolism which exhibit structural relationships to muscarufine include polyporic acid [2], atromentin [3] and leucomelone [4] which all possess the terphenyl system in common with muscarufin. The unsaturated side chain of muscarufin recurs in the widespread fungus and lichen pigment telephoric acid [5] and is somewhat reminiscent of polyenoid pigments of fungal origin, *e. g.* corticrocin [6], cortisalin [7], fumigallin [8] and limocrocin [9]. Among natural products from higher plants compounds of the piperic acid type are worthy of mention.

Some of these compounds have been synthesised and the bis-phenyl-dihydroxybenzoquinones in particular have been the subject of a number of investigations.

Since the work of Kögl and Erxleben, however, no further publications on muscarufin have appeared and a synthetic confirmation of the proposed structure is still lacking.

In order to obtain information about the synthetic pathways to, and the properties of, 2,5-bis-(2-carboxyphenyl)-benzoquinone and related compounds the present investigation was undertaken.

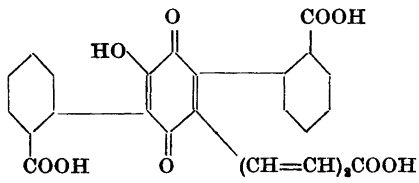
In view of the successful application of the Ullmann reaction for the preparation of tri- and tetraquinone [10] we have explored this approach for the synthesis of muscarufin-like substances.

The mixed Ullmann coupling of methyl 2-bromobenzoate and 2,5-diiodohydroquinone dimethylether afforded 2,5-dimethoxy-1,4-bis-(2-carbomethoxyphenyl)-benzene (II) in good yield (50 %). On treatment with nitric acid it furnished the yellow 2,5-bis-(2-carbomethoxyphenyl)-benzoquinone (III).

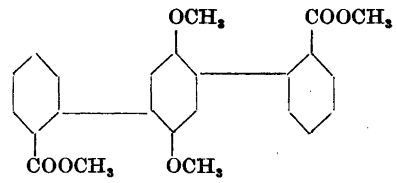
We have investigated the possibilities of introducing various substituents into the central nucleus of these terphenyl systems. All attempts to brominate the terphenyl derivative II failed and the reaction between the quinone III and hydrogen bromide afforded the dilactone IV (R = H); the hydrogen bromide thus simply reduced the quinone. The same dilactone resulted from demethylation of II with pyridinium chloride and was even obtained on attempted reductive acetylation of the quinone. This fact is of interest since Kögl and Erxleben report that muscarufin under similiar conditions did not undergo lactonisation but yielded a *triacetate*. The addition of hydrogen chloride to III was more successful but lactonisation again occurred with formation of the chlorodilactone (IV, R = Cl). These lactones are very high melting, sparingly soluble substances and it is therefore sometimes difficult to isolate them in a state of complete purity. They can be dissolved in hot, strong alkali but on acidification the dilactones are recovered. Repeated treatment of the dilactone IV (R = H) with potassium hydroxide and methyl iodide afforded the monolactone methyl ether methyl ester (V).

Thiele acetylation of the quinone III using sulphuric acid as a catalyst failed. However, when perchloric acid was employed a complex reaction product was obtained, from which 2,3,5-triacetoxy-1,4-bis-(2-carbomethoxyphenyl)-benzene (VI) could be isolated although in poor yield. This compound contains all the characteristic features of *leuco*-muscarufin except the unsaturated side chain.

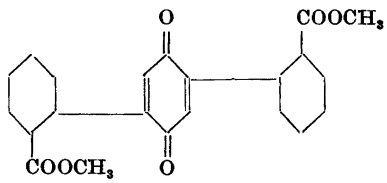
Further work on this subject is in progress and will be published shortly in this journal.



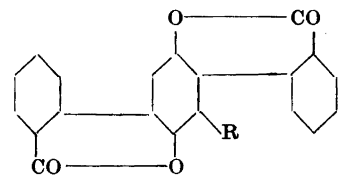
I



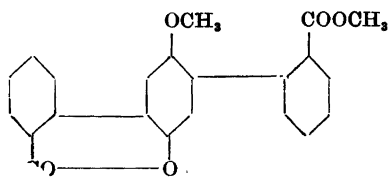
II



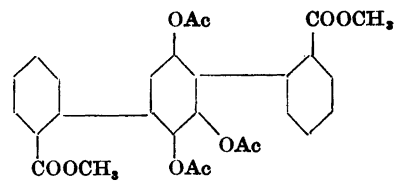
III



IV



V



VI

EXPERIMENTAL

All melting points are uncorrected. Melting points above 300° were determined by dropping a few crystals on a preheated bloc; the very strong sublimation of the substances in question prohibited the use of ordinary methods.

2,5-Dimethoxy-1,4-bis-(2-carbomethoxyphenyl)-benzene (II). 2,5-Diiodohydroquinone dimethylether (25 g, 0.1 mole) and methyl 2-bromobenzoate (84 g, 0.4 mole) were heated in a 300 ml flask until a homogeneous solution was obtained. This was thoroughly mixed with copper bronze (240 g) and then slowly heated in a salt bath. At *ca.* 200° a considerable heat of reaction developed and the temperature rose to *ca.* 300°. After cooling to room temperature the hard mass was desintegrated and exhaustively extracted with chloroform in a Soxhlet apparatus. The solvent was removed and the residual oil (A) distilled *in vacuo* yielding a small amount of methyl benzoate, dimethyl diphenate and an oily fraction b. p. 200—285° (1 mm) the bulk of which passed over at about 240°. On trituration with methanol the fraction b. p. 200—285° crystallised (12 g, 48 %). Alternatively methanol (50 ml) was added to the crude oil (A) and after keeping in the refrigerator overnight most of the terphenyl derivative crystallised leaving the dimethyl diphenate in the mother liquors. Recrystallisation from glacial acetic acid gave the pure compound as small colourless prisms, m. p. 174—175°. (Found: C 70.9; H 5.5; CH_3O 30.9. Calc. for $C_{24}H_{22}O_6$: C 70.9; H 5.5; CH_3O 30.5.)

2,5-Bis-(2-carbomethoxyphenyl)-benzoquinone (III). 2,5-Dimethoxy-1,4-bis-(2-carbomethoxyphenyl)-benzene (10 g) was slowly added to nitric acid (150 ml, *d* 1.42). The initial dark colouration rapidly disappeared and nitrous fumes were evolved. The suspension was allowed to stand for 15 minutes and was then poured into water (500 ml). After standing overnight the yellow precipitate was collected and recrystallised from methyl-ethyl ketone giving the pure quinone as yellow prisms, m. p. 188—189°. (Found: C 70.0; H 4.4; CH_3O 16.2. Calc. for $C_{22}H_{16}O_6$: C 70.2; H 4.3; CH_3O 16.5.)

2,5-Dihydroxy-1,4-bis-(2-carboxyphenyl)-benzene dilactone (IV, R = H). (a). The quinone III (0.20 g) was dissolved in chloroform (20 ml) and a rapid stream of hydrogen bromide passed into the solution. After an initial dark coloration white crystals began to separate. When the precipitation appeared complete the crystals were collected (0.19 g) and recrystallised from diacetone alcohol giving needles, m. p. *ca.* 410°, subliming readily above 390°. Qualitative tests showed the abscence of bromine.

(b). Attempted reductive acetylation of III using acetic anhydride, zinc dust and a trace of pyridine or fused sodium acetate led to the formation of a white flocculent precipitate, which was separated from excess zinc by decantation. Recrystallisation from very large volumes of acetic anhydride afforded small white needles, m. p. *ca.* 410°, alone or in admixture with the substance obtained in experiment (a). Determination of the acetyl content (about 2 %) indicated the almost complete abscence of acetoxyl groups.

(c). Treatment of the terphenyl derivative II with excess pyridinium chloride at 200° for 2 h resulted in the formation of the same dilactone as in experiments (a) and (b) as shown by melting point and mixed melting point determinations. (Found: C 75.9; H 3.2. Calc. for $C_{20}H_{10}O_4$: C 76.4; H 3.2.)

2,5-Dihydroxy-3-chloro-1,4-bis-(2-carboxyphenyl)-benzene dilactone (IV, R = Cl). The quinone III (0.25 g) was dissolved in chloroform and a stream of hydrogen chloride passed into the solution. The product soon separated as white crystals (0.16 g), which were recrystallised from diacetone alcohol (needles), m. p. *ca.* 385°. (Found: C 68.2; H 2.6; Cl 10.7. Calc. for $C_{20}H_9O_4Cl$: C 68.9; H 2.6; Cl 10.2.)

2-Hydroxy-5-methoxy-1-(2-carboxyphenyl)-4-(2-carbomethoxyphenyl)-benzene lactone (V). The dilactone IV (R = H) (0.9 g), potassium hydroxide (0.9 g) and methanol (10 ml) were heated on a water bath until a clear solution was obtained (0.5 h). Methyl iodide (4.3 g) was added and the mixture refluxed for 6 h. Additional quantities of potassium hydroxide (0.1 g) and methyl iodide (1 g) were introduced and the heating continued for a further 6 h. The solvent was removed and the solid residue (A) extracted several times with boiling chloroform. The extract was evaporated to dryness and the product (0.4 g) recrystallised from methanol (small needles), m. p. 197—198°. (Found: C 73.5; H 4.6. Calc. for $C_{22}H_{16}O_5$: C 73.3; H 4.5.) From the chloroform insoluble part of A unchanged starting material was recovered.

2,3,5-Triacetoxy-1,4-bis-(2-carbomethoxyphenyl)-benzene (VI). Perchloric acid (15 ml, *d* 1.67) was slowly added to acetic anhydride (300 ml), cooled in an ice bath. The temperature of the solution was then allowed to rise to *ca.* 20° and the quinone III (7.4 g) introduced with stirring. After about 5 h it had dissolved giving a brownish red solution, which was kept overnight and then poured onto ice (1 kg). Water (2 l) was added and the suspension stirred for 24 h. The dried precipitate (A) (8.5 g) was dissolved in benzene (a small amount of insoluble amorphous material being removed by filtration), and the solution evaporated to a small volume. On standing some crystalline material was deposited (B), which was, however, found to be a difficultly resolvable mixture. (M. p. of the components *ca.* 160° and *ca.* 180°.) The mother liquor was *rapidly* (compare below) passed through a column of activated alumina (15 × 2 cm), which was then thoroughly washed with benzene. Evaporation of the purified solution yielded an oil, which on treatment with benzene afforded unchanged starting material. Addition of ligroin to the mother liquor precipitated a yellowish mixture of crystals yielding on fractional crystallisation from methanol and benzene-ligroin mixtures small amounts of starting material, a mixture of higher melting compounds (B) and the desired product (*ca.* 2 g). The last named formed colourless prisms finally purified by recrystallisation from methyl *cyclo*hexane, m. p. 144—146°. (Found: C 64.1; H 4.5. Calc. for $C_{28}H_{24}O_{10}$: C 64.6; H 4.6.)

If the reaction was carried out at a slightly elevated temperature (30°) or for a prolonged time the amount of starting material recovered decreased, the amount of triacetate remained approximately constant but that of the higher melting unidentified compounds (B) increased.

In preliminary experiments the crude reaction product (A) was treated with dimethyl sulphate and alkali giving, in poor yield, a compound which according to its properties and the analytical result was a *dilactone of 2,3,5-trihydroxy-1,4-bis-(2-carboxyphenyl)-benzene methyl ether* (*e. g.* IV, R = OCH_3). On recrystallisation from acetic anhydride the dilactone was obtained as needles, m. p. *ca.* 310°. (Found: C 73.2; H 3.3; CH_3O 9.8. Calc. for $C_{21}H_{13}O_5$: C 73.4; H 3.5; CH_3O 9.0.) In another experiment A was subjected to acid methanolysis affording again in poor yield a compound, m. p. *ca.* 355°, after recrystallisation (needles) from acetic acid. This substance apparently was a *dilactone of 2,3,5-trihydroxy-1,4-bis-(2-carboxyphenyl)-benzene, e. g.* IV, R = OH). (Found: C 72.9; H 3.2. Calc. for $C_{20}H_{10}O_4$: C 72.7; 3.1.) Attempts were also made to separate the components of A by chromatography on activated alumina but on prolonged contact with the alumina the triacetate was apparently hydrolysed and the product strongly adsorbed.

REFERENCES

1. Kögl, F. and Erxleben, H. *Ann.* **479** (1930) 11.
2. Kögl, F. *Ann.* **447** (1925) 78.
3. Kögl, F. and Becker, H. *Ann.* **465** (1928) 211.
4. Akagi, M. *J. Pharm. Soc. Japan.* **62** (1942) 129. *Cf. Chem. Abstracts* **45** (1951) 2898.
5. Kögl, F., Erxleben, H. and Jänecke, L. *Ann.* **482** (1930) 105.
6. Erdtman, H. *Acta Chem. Scand.* **2** (1948) 209.
7. Gripenberg, J. *Ibid.* **6** (1952) 580.
8. Brockman H. and Maö H.-U. *Chem. Ber.* **88** (1955) 419.
9. Schenck, J. R., Hargie, M. P., Tarbell D. S. and Hoffman, P. *J. Am. Chem. Soc.* **75** (1953) 2274.
10. Erdtman, H., Granath, M. and Schultz, G. *Acta Chem. Scand.* **8** (1954) 1442.

Received February 18, 1956.

ACTA CHEMICA SCANDINAVICA 10 (1956) 739—743

The Action of Enterokinase on Trypsinogen *

IKUO YAMASHINA

Chemistry Department II, Karolinska Institutet, Stockholm, Sweden, and Department of Physiological Chemistry, University of Lund, Lund, Sweden

Using Edman's phenyl*iso*thiocyanate method, valine and *iso*leucine were identified as the N-terminal amino acids of trypsinogen and of trypsin formed by autoactivation, respectively.

The activation of trypsinogen by enterokinase was followed by determining the N-terminal amino acids. *Iso*leucine was detected in increasing quantity during the course of the activation, the amount being directly related to the appearance of tryptic activity.

Enterokinase seems to be a peptidase with a high specificity for trypsinogen.

By means of kinetic studies Kunitz [2] showed that enterokinase is an enzyme which activates trypsinogen to trypsin. No studies have, however, been carried out on the chemical nature of the reaction.

Davie and Neurath [3] investigated the mechanism of autoactivation, the activation by trypsin itself, and showed that a valylpeptide was split off, the amount being proportional to the tryptic activity developed. Thus trypsinogen is activated to trypsin by means of a limited hydrolysis giving rise to a new N-terminal amino acid.

As to the N-terminal amino acids of trypsinogen and of trypsin formed by autoactivation, Rovery, Fabre and Desnuelle [4] have identified valine as the N-terminal amino acid of trypsinogen by using Sanger's dinitrofluorobenzene method, and *iso*leucine as that of DIP-trypsin (di*iso*propylphosphoryl trypsin) by using both Sanger's method and Edman's phenyl*iso*thiocyanate method.

Thus, if enterokinase acts as a peptidase on trypsinogen as trypsin does, the reaction may be followed by determining free amino groups which are liberated during the hydrolysis of peptide bonds. The present paper will show that this is the case.

In the first instance, the N-terminal amino acids of trypsinogen and of trypsin formed by autoactivation were determined by Edman's method and results were obtained which confirm the findings already mentioned. The

* A short communication [1] was presented at the meeting of the Swedish Biochemical Society, January 27, 1956.

activation by enterokinase was then followed by determining the N-terminal amino acids. *Iso*leucine was detected in increasing amount paralleling the appearance of tryptic activity.

EXPERIMENTAL

Trypsinogen was prepared from beef pancreas according to the method of Northrop and Kunitz [5]. The crystalline product was purified further by treatment with trichloroacetic acid. Enterokinase was prepared from swine duodenal fluid contents according to the author's method [6,7]. It has an activity of 2 000 units per mg dry substance, which indicates a high degree of purity. The estimation of the tryptic activity was performed according to Anson's hemoglobin method [5].

The N-terminal amino acid of trypsinogen. Rovery, Fabre and Desnuelle [4] have detected valine as the N-terminal amino acid of trypsinogen by using the dinitrofluorobenzene (DNFB) method. However, alkaline conditions under which the coupling between protein and DNFB takes place are quite favourable to the autoactivation and autodigestion due to an unavoidable trace of trypsin present in the trypsinogen preparation.

Several amino acids including valine and *iso*leucine were in fact detected when a non-denatured and soluble trypsinogen preparation was used instead of the denatured and insoluble one used by the French workers. The pre-treatment of the trypsinogen preparation by di*iso*propyl fluorophosphate (DFP) eliminated amino acids other than valine.

The use of Edman's method simplified the situation. By this method, both DFP-treated and non-treated trypsinogen preparations gave, due to the rapid reaction between phenyl*iso*thiocyanate and the terminal amino group as demonstrated by Edman [8,9], only one single amino acid, identified as valine.

The N-terminal amino acid of trypsin formed by autoactivation. The trypsinogen preparation was activated at 0° C and pH 5.6 using 0.1 M triethylammonium acetate buffer which contains 0.05 M $CaCl_2$. 10 mg of trypsinogen was dissolved per ml, giving a concentration of trypsin of 0.05 mg per ml without any further addition of pure trypsin. Under these conditions 100 % activation could be obtained after 22 hours. The reaction mixture was then adjusted to pH 2.5 by the addition of 1 N HCl. Aliquots were taken, diluted with water and to these solutions an equal volume of pyridine was added. To 2 ml of the pyridine-water solutions containing trypsin corresponding to 4 mg trypsinogen, 20 μl of phenyl*iso*thiocyanate was added with vigorous stirring. The pH was then adjusted to 9.0 by the addition of a few drops of triethylamine. The reaction was allowed to continue for two hours at room temperature with occasional stirring and the further addition of triethylamine in order to keep the pH between 8.5 and 9.0. After the completion of the coupling, the reaction mixture was washed with benzene (3 × 5 ml) in order to remove pyridine and an excess of phenyl*iso*thiocyanate. To the aqueous layer, 8 ml of acetone was added and the precipitate of phenylthiocarbamyl derivatives was collected by centrifugation and dried *in vacuo*. The dried material was then suspended in 1 ml of 1 N HCl and heated for one hour in boiling water with occasional stirring. The phenylthiohydantoin derivatives of the amino acids were then extracted with ethyl acetate (3 × 2 ml) and the combined extracts were washed with 0.8 ml of water. 2.0 ml of the extract was diluted to 5 ml with 95 % ethanol and the ultraviolet absorption measured. From the shape of the curve, the formation of phenylthiohydantoin derivatives of amino acids was confirmed. The yield, referred to the amount of trypsinogen, was 170 % based on the optical density at 269 mμ. For the molecular weight of trypsinogen and the molecular extinction coefficient of phenylthiohydantoin derivatives of the amino acid, 23 800 and 16 000 were used, respectively.

The rest of the extract was evaporated to dryness, dissolved in ethylene chloride and aliquots used in the identification experiments.

For this purpose paper chromatography was used according to the directions of Sjöquist and Edman [10,11]. A starch-treated Whatman No. 1 paper was dipped into a mixture of acetone and formamide (3 : 1 by volume) and dried at room temperature until the acetone had evaporated. The test solution was then applied to the paper and developed with xylene. Two spots, derived from valine and *iso*leucine, were observed either by

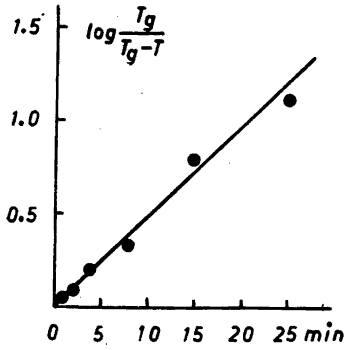


Fig. 1. Reaction of enterokinase at high trypsinogen concentration. T_g: Initial concentration of trypsinogen. T: Tryptic activity at any time. The line shows the theoretical relationship for a first order reaction and the points are the experimental values obtained.

ultraviolet absorption with the aid of a fluorescence screen or by spraying with the KI-NaN_3 reagent. Since no spots other than these two were observed, it is evident that *iso*leucine is an N-terminal amino acid of trypsin formed by autoactivation.

The N-terminal amino acid of trypsin formed by the action of enterokinase. The experimental conditions cause some difficulties in the study of the activation of trypsinogen by means of enterokinase. The standard conditions for the estimation of enterokinase activity established by Kunitz are quite inconvenient for the present purpose because of the extremely low concentration of trypsinogen (65 μg per ml). The use of a high concentration of trypsinogen is accompanied by autoactivation, autodigestion or formation of inert protein due to trypsin. In this case, the kinetics do not correspond to those of a first order reaction as has been thoroughly demonstrated by Kunitz [5].

These disadvantages could be overcome by the use of a high concentration of enterokinase together with the use of triethylammonium acetate buffer which seems to stabilize trypsin. In a series of test tubes, 5 mg of trypsinogen and 0.8 mg of enterokinase preparation having an activity of 2 000 units per mg were dissolved in 12.5 ml of 0.1 M triethylammonium acetate buffer (pH 5.6). The reaction was carried out at 0° C. Under these conditions it corresponds to a first order reaction as shown in Fig. 1, which indicates that there are no appreciable signs of autoactivation or autodigestion.

The activation was stopped at intervals by adding 1 ml of 1 N HCl to 12.5 ml of reaction mixture. To this acid solution an equal volume of pyridine, containing phenyl-*iso*thiocyanate in a concentration of 50 μl per ml was added. The pH was then adjusted to 9.0 by the addition of a few drops of triethylamine.

As to the stability of trypsin in pyridine-water (1:1) in which the coupling reaction takes place, it was found that 60 % of the activity is recovered after 2 hours at room temperature. When both trypsinogen and trypsin were present in an equal concentration of 0.1 mg per ml in this solvent, corresponding to 50 % activation where the autoactivation shows the highest velocity, 20 % of trypsinogen was converted to trypsin after 2 hours at room temperature. However, when phenyl*iso*thiocyanate was present in the above-mentioned concentration, tryptic activity was very quickly blocked, 95 % of the activity being lost 5 min. after the addition of pyridine containing phenyl*iso*thiocyanate. Consequently, the risk of autodigestion or autoactivation due to trypsin under the coupling conditions could be excluded.

The coupling was continued for 2 hours at room temperature, the pH being maintained between 8.5 and 9.0 by occasional addition of triethylamine. The reaction mixture was then washed with benzene (5 × 20 ml) and the aqueous layer was then lyophilized. The dried material was suspended in 3 ml of 1 N HCl and heated at 100° C for one hour. The phenylthiohydantoin derivatives of the amino acids were extracted with ethyl acetate (3 × 2 ml). The combined extracts were then washed by 0.8 ml of water and evaporated to dryness. The residue was dissolved in 40 μl of ethylene chloride and 5 μl of the solution was used for a single paper chromatography run.

The paper chromatogram which was prepared as described above and made visible by spraying with KI-NaN_3 reagent is shown in Fig. 2. In this figure, the amount of valine

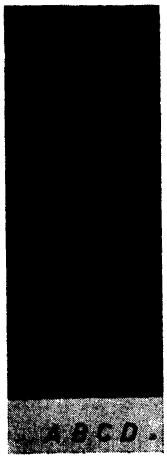


Fig. 2. Paper chromatogram demonstrating the development of isoleucine *as a new N-terminal amino acid during the activation. A: Standard substances, phenylthiohydantoins of valine and* isoleucine. *B: Zero time activation. C: 38 % activation after 4 minutes. D: 79 % activation after 15 minutes.*

remains almost constant throughout the whole course of activation whereas the amount of *iso*leucine increases with the progress of activation. The spots localized at the original point and those of low R_F values were considered to have no relation to the activation reaction.

For the quantitative evaluation of the developed spots on the chromatogram, the elution technique was applied. Thus, the spots identified by ultraviolet absorption with the aid of a fluorescence screen were cut off, eluted with 1 ml of 95 % ethanol for one hour at room temperature and the ultraviolet absorption at 269 mμ determined. The amount of valine was practically constant and that of *iso*leucine increased throughout the activation process. Since the phenylthiohydantoin derivatives of valine, *iso*leucine and alanine can be eluted just as effectively (about 80 % of the substance applied on the paper [12]), the amounts of *iso*leucine were corrected with reference to those of valine in each run. In Fig. 3, the percentages of *iso*leucine found and corrected are shown at each step of activation.

It could be concluded that there is a quantitative relationship between the degree of the activation of trypsinogen caused by enterokinase and the amount of *iso*leucine appearing as N-terminal amino acid.

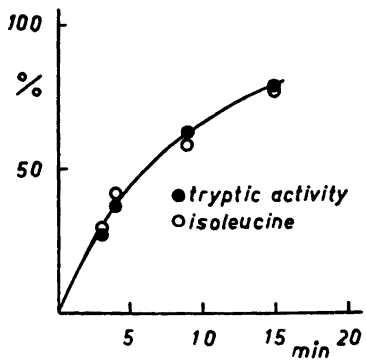


Fig. 3. Relation between the percentages of isoleucine *as referred to valine and those of activation.*

DISCUSSION

Since valine and *iso*leucine are the N-terminal amino acids of trypsinogen and trypsin, respectively, as found by Rovery *et al.*[4] and by the present author, the appearance of *iso*leucine as N-terminal amino acid and the constant presence of valine suggest that enterokinase acts as a peptidase splitting off a valylpeptide from the amino end of trypsinogen, a reaction similar to that in the case of autoactivation. The good agreement of the percentages of *iso*-leucine referred to valine and those of activation throughout the whole activation process excludes the possibility of a transitory formation of an active form of trypsinogen.

Although enterokinase acts as a peptidase in this respect its action is highly specific. Since trypsin acts on esters of lysine and arginine, the activity of the enterokinase preparation was tested on tosylarginine methyl ester and lysin ethyl ester. A slight activity was observed at a pH of between 6 and 9. Judging from the low activity and the peak of the activity curve at pH 7.5 it is very likely that the activity was caused by a contamination by trypsin.

This work was made possible by a research grant to Professor Erik Jorpes from the *Swedish State Medical Research Council.* The author's thanks are also due to Dr. Pehr Edman for his help during the progress of the work.

REFERENCES

1. Yamashina, I. *Biochim. et Biophys. Acta. In print.*
2. Kunitz, M. *J. Gen. Physiol.* **22** (1939) 429.
3. Davie, E. W. and Neurath, H. *J. Biol. Chem.* **212** (1955) 515.
4. Rovery, M., Fabre, C. and Desnuelle, P. *Biochim. et Biophys. Acta* **12** (1953) 547.
5. Northrop, J., Kunitz, M. and Herriot, R. M. *Crystalline Enzymes*, 2nd Edition, New York 1948.
6. Yamashina, I. *Arkiv Kemi* **7** (1954) 539.
7. Yamashina, I. *Arkiv Kemi*, **9** (1956) 225.
8. Edman, P. *Acta Chem. Scand.* **4** (1950) 277.
9. Edman, P. *Acta Chem. Scand.* **4** (1950) 283.
10. Sjöquist, J. *Acta Chem. Scand.* **7** (1953) 447.
11. Edman, P. *Unpublished.*
12. Edman, P. and Arvidsson, O. E. *Unpublished.*

Received February 21, 1956.

ACTA CHEMICA SCANDINAVICA 10 (1956) 744—746

Apparatus for Simple Laboratory Batch Distillation

NIELS CLAUSON-KAAS

Department of Chemistry, Israel Institute of Technology, Haifa, Israel
and
FRANZ LIMBORG

Centrallaboratoriet, Sadolin & Holmblad A/S, Copenhagen, Denmark

A rugged and versatile setup for distillation of charges up to 5 liter volume is described. The setup is intended mainly for work in organic chemical and biochemical laboratories. It has been in daily use for seven years and has been tested in four different laboratories. All simple laboratory distillations, at pressures above 0.1 mm, can be carried out in this, or one of the two other setups, described previously by us (*Acta Chem. Scand.* 8 (1954) 1579).

This communication describes a distillation setup intended for (a) the purification of solvents (b) the removal of solvents and (c) the distillation of amounts larger than 100 ml of liquid organic compounds.

The setup (Fig. 1), which is mounted at the end of a laboratory bench, is especially simple and rapid to operate. After putting the distillation flask in place, outside of the water bath, the steel support rod is lifted, and the whole apparatus turned, so that the distillation flask may be immersed in the bath. *Since the three clamps supporting the glass part of the apparatus are directly aligned, there is no risk of breakage, or of leakage at the ground joints, being caused by the strain of mounting.*

Owing to the large diameter of the tube leading from the distillation flask to the condenser, distillations can be carried out rapidly and at low pressure. Table 1 shows three representative distillations illustrating the capacity of the setup.

The construction and use of the setup is described in detail below.

The distillation and the receiver flasks have either glass hooks (sizes 100, 250, 500 and 1 000 ml) or metal holders (sizes 2, 3 and 5 liters) permitting attachment of springs. When distilling under vacuum no springs are used to hold the distillation flask, but the flask is held by hand until immersed in the water bath. When solvents are distilled

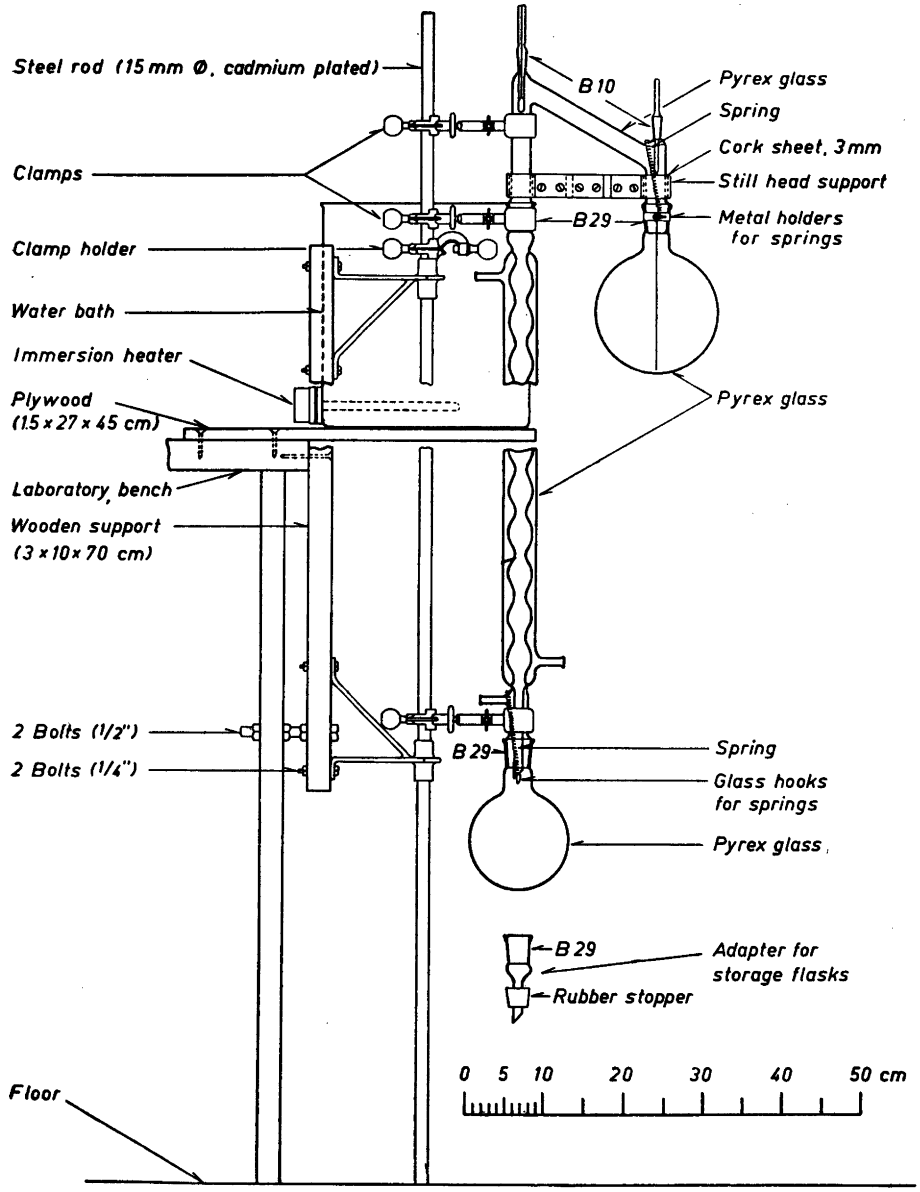


Fig. 1. Setup for simple distillation of up to 5 liters, viewed from rear.

under atmospheric pressure directly into storage flasks, an adapter as shown in Fig. 1 should be used.

The still support (3 mm iron or brass) is made of three parts to prevent breakage of the head due to strain. It is fixed to the glass by first tightening the two pairs of screws

Table 1. Representative distillations. In the case of the distillation of water, the still head was insulated with a cloth and the receiver flask cooled with ice.

Compound	B. p. at 760 mm °C	Charge ml	Yield of distillate ml	Distillation temp. °C	Bath temp. °C	Back pressure mm Hg	Distillation time min.
Acetone, crude	56	2 000	1 974	55–61	81–94	757	72
Water	100	1 000	940	36–38	75–78	26–29	64
1-Methyl-naphthalene	245	100.0	98.2	58–59	87	0.1	22

at the ends, and then the pair in the middle. The still head can carry a distillation flask weighing 5 kg without its breaking.

Suitable clamps for supporting the glass part of the setup are utility clamps (large size, rubber sleeve) from *Fisher Scientific Company*, Pittsburgh, U.S.A.

The water bath is designed for distillation flasks up to 5 liters. It is heated by a 1 500 watt immersion heater connected with the network through a bimetal regulator. In order to minimize evaporation of water, the bath is covered with a lid, slotted to receive the neck of the distillation flask. The height of the distillation flask is adjusted by use of the clamp holder, which is attached directly above the upper support for the steel rod. In general, the distillation flask should be immersed up to its neck in the water bath in order to prevent foaming. If required, the flask can easily be shaken by hand while in the bath during a distillation.

For the distillation of very high-boiling liquids, the water bath is replaced by some other heating device.

The supports for the steel rod are 40 mm wide and screwed symmetrically on to the wooden support. The wooden support is fixed to the laboratory bench in such a way that the center line of the support is 42 cm from the front of the bench. The plywood plate carrying the water bath is fixed in line with the front of the bench.

Rubber tube connections to cooling water and vacuum pumps should be mounted so that they do not disturb the lifting and turning of the apparatus.

Cleaning of the still head and the condenser is best accomplished by sucking a suitable solvent once or twice from a 50 ml beaker through the socket of the joint on to which the distillation flask fits.

Received February 21, 1956.

ACTA CHEMICA SCANDINAVICA 10 (1956) 747—755

Reactions between Carbon Dioxide and Amino Alcohols

III. Diethanolamine

ERIK JØRGENSEN

The Royal Danish School of Pharmacy, Copenhagen, Denmark

When carbon dioxide reacts with diethanolamine in aqueous solutions the product formed is a mixture of carbamate and monoalkyl carbonate. The previous conclusion of carbamate being the main product was verified for not too alkaline solutions. In strongly alkaline solution, however, the amount of monoalkyl carbonate formed was big enough for evaluating velocity constants for the formation and decomposition.

For the determination of carbonate a complexometric method was used, which was based on the reaction between barium ion and versenate ion.

1. Carbon dioxide reacts with amino alcohols containing primary and secondary amino groups to yield carbamate and monoalkyl carbonate. Previous experiments [1] show that carbamate is the main product in the case of ethanolamine and diethanolamine.

The present paper reports additional experiments with diethanolamine in order to disclose the formation of monoalkyl carbonate.

2. The method of analysis was in principle as in previous investigations. Added barium chloride precipitates carbonate, but not carbamate or monoalkyl carbonate. The barium carbonate is separated by centrifugation. In the previous method the supernatant was heated until the carbamate and monoalkyl carbonate had been decomposed and been precipitated as barium carbonate, which was titrated acidimetrically. In the numbered experiments of this publication a slightly modified method was used.

To make the separation faster, the electric centrifuge was replaced by a hand-driven one and the sample size was diminished from 100 to 8 ml. The possibility of titrating barium ion [2] with reasonable accuracy suggested the determination of excess barium ion in the supernatant. The details are as follows:

8.00 ml of the specimen is run into a centrifuge tube (15 ml) containing 1.000 ml 0.25 M barium chloride. To mix the contents the tube is inverted twice before centrifugation. 5.00 ml of the supernatant are run into 15.00 ml 0.01 M sodium versenate + 10

drops of phthaleinpurpur-I. To neutralize the sodium hydroxide a slight excess of ammonium chloride is added. After an addition of 10 ml concentrated ammonia and 50 ml 96 % ethanol the excess of versenate is titrated with 0.005 M barium chloride.

The method is tested by titration of carbonate in solutions of potassium bicarbonate in 0.2 N sodium hydroxide. To make sure that diethanolamine does not enhance supersaturation this substance was added to some of the solutions. The results are in Table 1.

The precision of the method is comparable to the precision of the previous method, maybe slightly less, which, however, is amply compensated by the increased speed. 30 seconds suffice to separate the barium carbonate from the liquid.

Table 1. Complexometric determination of carbonate.

mM CO_3^{--}/litre	found				mean	deviation
	without diethanolamine					
6.54	6.59	6.79	6.47	6.41	6.57	+0.03
8.06	8.26	7.90	8.24	8.10	8.13	+0.07
9.86	9.87	10.00	10.03	9.94	9.96	+0.10
14.95	14.87	14.82	15.00	15.09	14.95	0.00
20.34	20.28	20.30	20.37	20.48	20.36	+0.02
27.52	27.52	27.34	27.34	27.43	27.41	−0.11
	with diethanolamine					
10.43	10.26	10.49	10.40	10.58	10.43	0.00
15.17	15.17	15.28	15.15	15.26	15.22	+0.05
24.29	24.38	24.32	24.20	24.11	24.25	−0.04

3. The problem of simultaneous formation of carbamate and monoalkyl carbonate is attacked in two ways.

One is to determine, how the carbon dioxide is shared instantaneously between carbonate and non-carbonate, when it is dissolved in aqueous solutions of varying concentration of sodium hydroxide and diethanolamine. The term, non-carbonate, stands for the sum of monoalkyl carbonate and carbamate.

A second is to determine the rate of the decomposition of the non-carbonate. Monoalkyl carbonates usually decompose with a higher rate and deviation from a first order reaction should be expected.

4. The experiments were carried out at 0° and 18° C. Velocity constants are calculated by means of Briggs' logarithms, which shall be thus understood: In the integrated expressions the base e is substituted by 10 without any compensation. As in previous publications the velocity constants are to be multiplied by $\log_e 10$ for correction. As the reactions take place between neutral molecules or neutral molecules and monovalent ions disregard of activity coefficients is used as a working approximation.

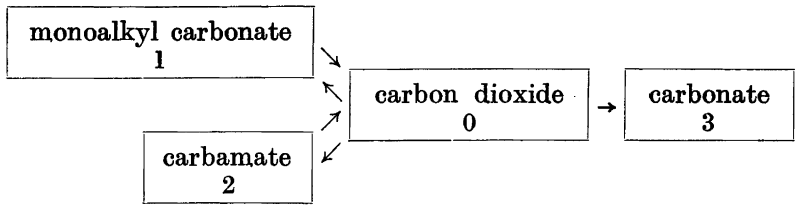
5. To simplify the necessary calculations the velocity constants previously used are substituted by symbols introduced by Christiansen [3].

When carbon dioxide reacts with alkaline solutions of amine and alcohol and during the decomposition of the non-carbonate formed the following processes compete:

$$CO_2 + RO^- \rightleftharpoons ROCOO^- \quad (01)$$
$$CO_2 + RNH_2 \rightleftharpoons RNHCOOH \rightleftharpoons RNHCOO^- + [H^+] \quad (02)$$
$$CO_2 + OH^- \rightarrow HCO_3^- \rightarrow CO_3^{--} + [H^+] \quad (03)$$

RO^- and RNH_2 meaning alcoholate ion and amine, respectively. The hydrogen ions are removed by hydroxyl ions.

The reactions may diagrammatically be represented by:



x_0, x_1, x_2, x_3 and x will be used for the concentrations of carbon dioxide, monoalkyl carbonate, carbamate, carbonate and non-carbonate, respectively.

The velocities are:

$$s_{10} = x_1 \cdot w_{10} - x_0 \cdot w_{01}$$
$$s_{20} = x_2 \cdot w_{20} - x_0 \cdot w_{02}$$
$$s_{03} = x_0 \cdot w_{03}$$

where, introducing the previously used symbols

$$w_{01} = k_{CO_2 \cdot RO^-} \cdot c_{RO^-} = k' \cdot c_{ROH} \cdot c_{OH^-}$$
$$w_{02} = k_{CO_2 \cdot Am} \cdot c_{RNH_2}$$
$$w_{03} = k_{CO_2 \cdot OH^-} \cdot c_{OH^-}$$
$$w_{10} = k_{ROCOO^-}$$
$$w_{20} = k_{RNHCOO^- \cdot H^+} \cdot c_{H^+}$$

ADDITION OF CARBON DIOXIDE TO SOLUTIONS OF DIETHANOLAMINE

1. The carbon dioxide introduced is shared between non-carbonate and carbonate within a small fraction of a second. The reactions (10) and (20) may be disregarded and thus the quotient non-carbonate: carbonate is equal to $(w_{01} + w_{02})$: w_{03}.

w_{01} and w_{03} are proportional to the concentration of hydroxyl ion while w_{02} is independent.

$$\frac{w_{01}+w_{02}}{w_{03}} \text{ multiplied by } \frac{c_{OH^-}}{c_{\text{amino alcohol}}}$$

gives us

$$\frac{k'}{k_{CO_2 \cdot OH^-}} \cdot c_{OH^-} + \frac{k_{CO_2 \cdot Am}}{k_{CO_2 \cdot OH^-}}$$

This expression being linearly dependent on the concentration of hydroxyl ion, we can calculate k' and $k_{CO_2 \cdot Am}$ from two experiments with different concentration of hydroxyl ion (log $k_{CO_2 \cdot OH^-}$ being fixed at 4.39 and 5.02 at 0° and 18° C, respectively).

2. A preliminary experiment (4) is performed on a solution, which besides sodium hydroxide contains an amine (diethylamine) without alcohol groups and an alcohol (triethanolamine) without primary or secondary amino groups.

In Table 2 this experiment (4) is compared with experiments (1—3) where only one of the compounds is present in the alkaline solution. From the velocity constant calculated from the experiments 1—3, it was calculated that 21.9 % monoalkyl carbonate and 39.8 % carbamate should be formed. The sum agrees reasonably with the found percentage of non-carbonate.

Table 2. Carbon dioxide in amine + alcohol + NaOH. 18°.

No.	Initial solution			Absorbed CO_2/litre	% non-carbonate		log k'	log $k_{CO_2 \cdot Am}$
	c_{NaOH}	$c_{Triethanol-amine}$	$c_{Diethyl-amine}$		% monoalkyl carbonate	% carbamate		
1	0.2	0.4		0.0250	54.0		5.49	
2	0.2	0.2		0.0269	35.6		5.47	
3	0.2		0.06	0.0205		50.8		5.56*
4	0.2	0.2	0.06	0.0230	experimental 65.2 calculated 21.9 + 39.8			

* Vibeke Lund and Carl Faurholt [4] find 5.46 applying 10 % CO_2.

3. In Table 3 are listed experimental values for addition of carbon dioxide to solutions of diethanolamine and sodium hydroxide at 0° C. The velocity constants have been calculated and the division of non-carbonate into monoalkyl carbonate and carbamate is estimated.

Table 3. Carbon dioxide in diethanolamine + NaOH. 0°.

Initial solution		Absorbed CO_2/litre	% non-carbonate experimental	$\frac{w_{01} + w_{02}}{w_{03}} \cdot \frac{c_{OH^-}}{c_{Diethanolamine}}$	log k' [1]	log $k_{CO_2 \cdot Am}$ [2]	% non-carbonate calculated	
c_{NaOH}	$c_{Diethanolamine}$						% monoalkyl carbonate	% carbamate
0.1	0.1	0.0192	52.9	1.02		4.25	15.4	38.8
	0.2	0.0196	71.0	1.11		4.29	20.2	50.2
	0.3	0.0198	78.9	1.13		4.30	22.6	55.6
0.2	0.1	0.0205	41.2	1.34	4.80	4.23	19.5	23.0
	0.2	0.0200	61.5	1.53	5.04	4.33	27.7	32.2
	0.3	0.0210	71.6	1.61	5.11	4.37	32.0	37.1
0.3	0.1	0.0210	34.9	1.57	4.78	4.15	21.3	16.3
	0.2	0.0215	52.7	1.63	4.83	4.18	31.2	23.7
	0.3	0.0203	65.9	1.89	4.99	4.33	36.8	27.8
				Mean:	4.94	4.28		

[1] Calculated from the mean of the first three determinations.
[2] Calculated from the mean of k'.

Evidently a fairly high proportion of monoalkyl carbonate is found.

In judging the velocity constants found one must, however, as previous work [5] on the subject has shown, bear in mind that the experimental results are to no small extent dependent on the way in which carbon dioxide has been added. In all the experiments present, atmospheric air, of which 30 % was substituted by carbon dioxide, has been applied. In a 1-litre flask, containing 250 ml of the reaction mixture, 250 ml of the gas phase were substituted by carbon dioxide from a gasometer. The flask was immediately shaken vigorously for about one minute.

It should be noticed that the fifth column of Table 3 shows for constant concentration of hydroxyl ion a slight increase with an increasing concentration of diethanolamine, which might be due to a perceptible amount of hydroxyl ions being consumed by the alcohol groups of diethanolamine. Glass electrode measurements on 0.04 N NaOH and various amounts of diethanolamine, ranging from 0.0 to 0.3 M, showed no difference in potential, however.

THE CONVERSION: NON-CARBONATE → CARBONATE

1. Before mentioning the experiments on the velocity of decomposition the mathematical and calculatory aspects should be examined.

The following differential equations:

$$s_{10} = -\mathrm{d}x_1/\mathrm{d}t = x_1 \cdot w_{10} - x_0 \cdot w_{01}$$
$$s_{20} = -\mathrm{d}x_2/\mathrm{d}t = x_2 \cdot w_{20} - x_0 \cdot w_{02}$$

combined with the stationarity condition for the free carbon dioxide

$$s_{10} + s_{20} = s_{03} = x_0 \cdot w_{03}$$

yield solutions of the form

$$\begin{aligned} x_1 &= a_1 \cdot \exp(-k_1 \cdot t) + b_1 \cdot \exp(-k_2 \cdot t) \\ x_2 &= a_2 \cdot \exp(-k_1 \cdot t) + b_2 \cdot \exp(-k_2 \cdot t) \\ \hline x = x_1 + x_2 &= A \cdot \exp(-k_1 \cdot t) + B \cdot \exp(-k_2 \cdot t) \end{aligned}$$

$-k_1$ and $-k_2$ being roots in the auxiliary equation

$$R^2 + \frac{w_{10} \cdot (w_{02} + w_{03}) + w_{20} \cdot (w_{01} + w_{03})}{w_{01} + w_{02} + w_{03}} \cdot R + \frac{w_{10} \cdot w_{20} \cdot w_{03}}{w_{01} + w_{02} + w_{03}} = 0$$

The solution is

$$k_1 = \frac{w_{10} \cdot (w_{02} + w_{03}) + \varepsilon}{w_{01} + w_{02} + w_{03}} \qquad k_2 = \frac{w_{10} \cdot w_{20} \cdot w_{03}}{w_{10} \cdot (w_{02} + w_{03}) + \varepsilon}$$

where ε is a root in

$$\varepsilon^2 + [w_{10} \cdot (w_{02} + w_{03}) - w_{20} \cdot (w_{01} + w_{03})]\, \varepsilon - w_{10} \cdot w_{20} \cdot w_{01} \cdot w_{02} = 0$$

Now the assumption is made:

$$w_{10} \cdot w_{0i} >> w_{20} \cdot w_{0j} \text{ (i and j = 1, 2 or 3)}$$

i. e. the monoalkyl carbonate is decomposed very fast compared with the carbamate, and w_{01}, w_{02} and w_{03} are of the same order of magnitude. This assumption is supported by the fact that the experiments clearly reveal the presence of two processes, k_1 and k_2 thus differing in order of magnitude.

Choosing ε as the positive root of the above equation, the following inequalities hold:

$$0 < \varepsilon < w_{20} \cdot (w_{01} + w_{03}) \ll w_{10} \cdot (w_{02} + w_{03})$$

When the total carbon dioxide concentration is C the initial

$$x_1 = \frac{w_{01}}{w_{01} + w_{02} + w_{03}} \cdot C \text{ and } x_2 = \frac{w_{02}}{w_{01} + w_{02} + w_{03}} \cdot C$$

Inserting these concentrations as boundary conditions we get for A and B:

$$A = \frac{w_{10} \cdot w_{01} \cdot w_{03} - w_{20} \cdot w_{01} \cdot (w_{01} + w_{02} + w_{03}) + \varepsilon \cdot (w_{01} + w_{02})}{(w_{01} + w_{02} + w_{03}) \cdot [w_{10} \cdot (w_{02} + w_{03}) - w_{20} \cdot (w_{01} + w_{03}) + 2\,\varepsilon]} \cdot C$$

$$B = \frac{w_{10} \cdot w_{02} \cdot (w_{01} + w_{02} + w_{03}) - w_{20} \cdot w_{02} \cdot w_{03} + \varepsilon \cdot (w_{01} + w_{02})}{(w_{01} + w_{02} + w_{03}) \cdot [w_{10} \cdot (w_{02} + w_{03}) - w_{20}\,(w_{01} + w_{03}) + 2\,\varepsilon]} \cdot C$$

Disregarding ε and $w_{20} \cdot w_{0i}$ in sums and differences of $w_{10} \cdot w_{0j}$ reduces k_1, k_2, A and B to

$$k_1 \sim w_{10} \cdot \frac{w_{02} + w_{03}}{w_{01} + w_{02} + w_{03}}$$

$$k_2 \sim w_{20} \cdot \frac{w_{03}}{w_{02} + w_{03}}$$

$$A \sim \frac{w_{03}}{w_{02} + w_{03}} \cdot \frac{w_{01}}{w_{01} + w_{02} + w_{03}} \cdot C$$

$$B \sim \frac{w_{02}}{w_{02} + w_{03}} \cdot C$$

The significance of the approximated expressions is directly seen from the diagram, imagining the monoalkyl carbonate being quickly decomposed partly to carbamate and partly to carbonate while the carbamate slowly decomposes to carbonate. k_1 is a fraction of w_{10} corresponding to the carbon dioxide from 10 not reverting along 01. k_2 is a fraction of w_{20} corresponding to the carbon dioxide from 20 not reverting along 02 and neglecting the reaction 01. A is the fraction of the initial monoalkyl carbonate, which is temporarily not converted to carbamate. B is the amount of carbamate that was formed initially when no alcohol groups were present.

w_{03} ($= k_{CO_3} \cdot {}_{OH^-} \cdot c_{OH^-}$) is known, hence B, A, k_2 and k_1 give us w_{02}, w_{01}, w_{20} and w_{10}, successively.

To get the parameters A, B, k_1 and k_2 of each experiment, the results are subjected to a linear regression analysis in two steps. From the experimental values where the contribution of $A \cdot \exp(-k_1 \cdot t)$ is vanishing, $\log x$ is taken as

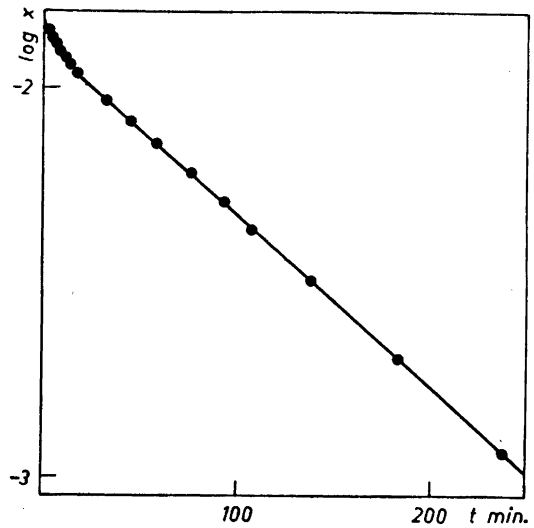


Fig. 1. The decomposition of the non-carbonate from solution 4.

the dependent variable and t as the independent variable. We then have an estimate of B and k_2. The contribution from the term $B \cdot \exp(-k_2 \cdot t)$ is extrapolated back to the first values and the differences are formed. The differences are subjected to a similar analysis and we have an estimate of A and k_1.

We proceeded on the lines laid down by A. Hald [6]. x is assumed to have a normal distribution with constant variance. Hence the variance on log x is inversely proportional to the square of x. Therefore, to each value of x a weight has been ascribed proportional to the square of the value.

2. The decomposition of the non-carbonate in the solutions from Table 2 is investigated. The three first solutions which either contain alcohol groups or amino groups give a first order rate as expected. The last, however, containing both alcohol groups and amino groups, deviates distinctly in the beginning of the experiment, *cf.* Fig. 1.

Table 4. Decomposition of non-carbonate from Table 2. Experimental part.

No.	A *	B	C	k_1	k_2
1	0.0135		0.0250	0.0302	
2	0.0096		0.0269	0.0445	
3		0.0104	0.0205		0.00392
4	0.0021	0.0129	0.0230	0.0665	0.00436

* Regarding the significance of symbols, see text.

Table 5. Decomposition of non-carbonate from Table 2. Calculated part.

No.	log k'	log $k_{CO_3} \cdot Am$	k_{ROCOO^-}	$k_{RNHCOO^-} \cdot H^+ \cdot K_{H_2O}$	% monoalkyl carbonate	% carbamate
1	5.49		0.066		54.0	
2	5.47		0.069		35.6	
3		5.56		0.00135		50.8
4	5.50	5.65	0.084	0.00160	20.6	44.6

In Tables 4 and 5 the experimental values, *i. e.* the parameters calculated from the experimental values by the regression analysis, and the calculated velocity constants are listed, respectively. The results from the mixture of the amine and alcohol are seen to agree with the experiments where only one of the groups is present.

To get a comparison between parameters from the regression analysis and the concrete, experimental values, Table 6 has been constructed.

Table 6. Comparison between experimental values from solution No. 4 and the corresponding regression analysis.

Experimental		$A \cdot \exp(-k_1 \cdot t) + B \cdot \exp(-k_2 \cdot t)$ *			Deviation
t	x				
0	(0.01498)	0.00207	+	0.01291	
2.1	0.01409	0.00150	+	0.01264	+0.00005
4.0	0.01355	0.00112	+	0.01241	−0.00002
6.3	0.01296	0.00079	+	0.01212	−0.00005
8.3	0.01235	0.00058	+	0.01188	+0.00011
11.0	0.01192	0.00038	+	0.01156	+0.00002
13.7	0.01154	0.00025	+	0.01125	−0.00004
17.0	0.01095	0.00015	+	0.01089	+0.00009
31.9	0.00928	0.00002	+	0.00937	+0.00011
45.1	0.00826	0.00001	+	0.00821	−0.00004
58.3	0.00722	0.00000	+	0.00719	−0.00003
76.0	0.00606	0.00000	+	0.00602	−0.00004
93.1	0.00513	0.00000	+	0.00507	−0.00006
107.5	0.00434	0.00000	+	0.00439	+0.00005
137.6	0.00321	0.00000	+	0.00324	+0.00003
183.2	0.00203	0.00000	+	0.00205	+0.00002
236.8	0.00115	0.00000	+	0.00120	+0.00005

* Numerical values of A, B, k_1 and k_2 are found in Table 4.

3. Finally, similar experiments were made on diethanolamine at 18° C. Here also a deviation from a first order reaction was found which clearly showed the formation of monoalkyl carbonate. Experimental and calculated results are listed in Tables 7 and 8, respectively.

The author wishes to express his thanks to the head of the department, Professor C. Faurholt, for his kind and stimulant discussions concerning the experiments.

Table 7. Formation and decomposition of non-carbonate of diethanolamine. 18°. Experimental part.

No.	Initial solution		A *	B	C	k_1	k_2
	c_{OH^-}	$c_{diethanolamine}$					
5	0.2	0.2	0.0009	0.0106	0.0199	0.065	0.00084
6	0.3	0.1	0.0014	0.0063	0.0245	0.070	0.00103
7	0.3	0.3	0.0019	0.0108	0.0206	0.047	0.00057

* Regarding the significance of symbols, see text.

Table 8. Formation and decomposition of non-carbonate of diethanolamine. 18°. Calculated part.

No.	log k'	log $k_{CO_2 \cdot Am}$	k_{ROCOO^-}	$k_{RNHCOO^- \cdot H^+} \cdot K_{H_2O}$	%monoalkyl carbonate	% carbamate
5	5.06	5.05	0.072	0.00033	9.1	48.3
6	5.09	5.02	0.076	0.00035	7.8	23.8
7	5.25	4.99	0.058	0.00031	19.2	42.4
Mean	5.14	5.02	0.069	0.00033		

REFERENCES

1. Jensen, M. B., Jørgensen, E. and Faurholt, C. *Acta Chem. Scand.* **8** (1954) 1137.
2. Flaschka, H. *Fortschr. chem. Forsch.* **3** (1955) 289.
3. Christiansen, J. A. *Advances in Catalysis* **5** (1953) 311.
4. Lund, V. and Faurholt, C. *Dansk Tidskr. Farm.* **22** (1948) 109.
5. Jensen, A., Jensen, M. B. and Faurholt, C. *Acta Chem. Scand.* **8** (1954) 1129.
6. Hald, A. *Statistiske metoder*, Det Private Ingeniørfond, Copenhagen 1948, p. 398.

Received February 22, 1956.

ACTA CHEMICA SCANDINAVICA 10 (1956) 756—760

Potentiometric Study on the Formation of Perboric Acids

P. J. ANTIKAINEN

Institute of Chemistry, University of Helsinki, Helsinki, Finland

The influence of hydrogen peroxide on the ionization of boric acid in aqueous potassium chloride solutions at 25° C has been studied by means of a potentiometric method. Apparently mainly two different peracids exist in solutions of boric acid and hydrogen peroxide. The complex formation constants of these perboric acids in potassium chloride solutions of different concentrations were calculated. The corresponding thermodynamic complex formation constants and the parameters of the Debye-Hückel equation have also been determined.

The formation of perboric acid in solutions containing boric acid and hydrogen peroxide has been the object of only few investigations. According to Menzel [1] conductivity measurements show that the complex acid $H_3BO_3 \cdot H_2O_2$ or $(H_3BO_3 \cdot H_2O_2)_2$ exists in solutions of this kind, the equilibrium constants for the reactions

$$\text{a)} \quad H_3BO_3 + H_2O_2 = H^+ + (H_2BO_3 \cdot H_2O_2)^- \qquad (1)$$
$$\text{b)} \quad 2H_3BO_3 + 2H_2O_2 = H^+ + (H_2BO_3 \cdot H_3BO_3 \cdot 2H_2O_2)^-$$

being of the order of 10^{-8}—10^{-7}. On the other hand, pH measurements carried out by Edwards [2] do not confirm the assumption that the peroxide complex is a definite compound. The author of this paper has in a recent preliminary study [3] reported a potentiometric method and its application to the investigation of perboric acid formation. The object of the investigation to be reported here was to complete this preliminary work.

EXPERIMENTAL

The potentiometric titrations were carried out at 25° C, employing a differential potentiometric method [4]. A tube potentiometer Type PHM 3 manufactured by Radiometer and a Beckmann Glass Electrode Type 4990—83 were used. The reading accuracy of the apparatus was about 0.2 mV. The measurements were carried out in 0.1—1.5 M potassium chloride solutions, the concentrations of boric acid and hydrogen peroxide being varied between 0.025—0.1 M and 0.1—8.0 M, respectively. Other details of apparatus and measurement technique have previously [5] been described. All reagents used were of reagent grade. The concentration of boric acid stock solutions was determined by titration with sodium hydroxide using mannitol and phenolphthalein [6]. The hydrogen peroxide stock solutions were titrated with permanganate.

THEORY

Recent investigations [5,7-9] have shown that boric acid in its dilute solutions can be considered as a weak monobasic acid. Since according to cryoscopic measurements carried out by Menzel [1] it is apparent that the amount of any peracid formed is very small, the concentrations of boric acid and hydrogen peroxide in the solutions of boric acid-hydrogen peroxide can be exchanged for the corresponding stoicheiometric concentrations C_1 and C_2, respectively, especially when it is noted that the insignificiant ionization of boric acid does not affect conditions. Thus for the apparent ionization constant K^* of boric acid in solutions containing hydrogen peroxide an equation

$$K^* = K_1' \cdot K_k \cdot C_2^n + K_1 = K_m \cdot C_2^n + K_1 \quad (2)$$

can be derived on the basis of the experimental method [4] and its applications to boric acid [5] and telluric acid [10-11]. In this equation K_1' denotes the first ionization constant of perboric acid, here considered as a monobasic acid, and K_k the equilibrium constant of the following assumed reaction:

$$H_3BO_3 + nH_2O_2 \rightleftharpoons H_3BO_3 \cdot nH_2O_2 \quad (3)$$

In addition K_1 is the first ionization constant of orthoboric acid. Further, the value of n is the number of hydrogen peroxide molecules, which combine with each molecule of boric acid. If in this case several complexes occur, n then indicates the average of this number. In such cases it is often possible to calculate the two main complex formation constants using the equation [12]

$$K^* = k_1 \cdot C_2^{n_1} + k_2 \cdot C_2^{n_2} + K_1 \quad (4)$$

where k_1 and k_2 are the complex formation constants corresponding to K_m in eqn. (2), where it is assumed that the value of n is the average of two different values. For the determination of the constants k_1 and k_2 in eqn. (4) it is necessary to know the values of the apparent ionization constants at least two different concentrations of hydrogen peroxide. Further, the most obvious values of n_1 and n_2 should be used in these calculations as shown in a recent investigation [12] concerning the complex formation of boric acid with mannitol.

RESULTS

In Table 1 the values for the apparent ionization constants of boric acid are given at constant ionic strength and different concentrations of hydrogen peroxide. Using these results the average value of n and the complex formation constant K_m can be calculated using eqn. (2). If a complex acid really exists the values of $p(K^*—K_1)$ as a function of log C_2 should lie on a straight line with the slope n. This line should intersect the $p(K^*—K_1)$-axis at the point pK_m. However, as can be seen from Fig. 1 the linearity is only approximate and two different limiting slopes for this curve can be obtained. Here the value 8×10^{-10} for the constant K_1 has been used when the concentration

Table 1. Potentiometric data for the influence of the concentration of hydrogen peroxide on the apparent ionization constant of boric acid for different concentrations of boric acid in about 0.0996 M potassium chloride solutions at 25° C.

C_1	C_2	Pm × 10^4	pK *
0.02498	0.09670	4.105	8.409
0.04985	0.09668	5.730	8.510
0.09975	0.2413	1.405	8.032
0.09982	0.4830	1.982	7.750
0.09950	0.7155	2.640	7.483
0.09950	0.9450	3.340	7.279
0.04971	0.9643	2.465	7.242
0.02490	0.9645	1.527	7.357
0.09965	1.446	4.852	6.958
0.02495	2.432	4.021	6.516
0.04991	2.432	5.520	6.542
0.09961	2.425	8.035	6.516
0.009965	3.280	3.721	6.185
0.09943	4.810	18.95	5.731
0.009945	5.730	8.165	5.452
0.009982	6.746	11.99	5.161
0.09802	8.930	43.30	5.034

of potassium chloride is about 0.1 M and that of boric acid [5] 0.1 M. Consequently one might assume that mainly two different peracids exist in these solutions. Furthermore, it appears that the most obvious values of n_1 and n_2

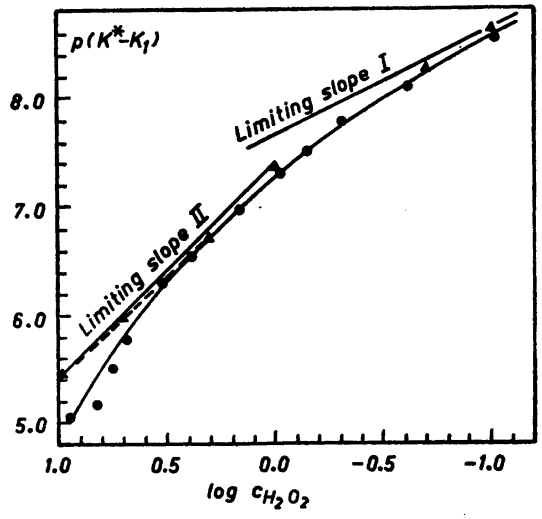


Fig. 1. The dependence of the apparent ionization constant of boric acid on the concentrations of hydrogen peroxide in about 0.1 M potassium chloride solutions. ● *Experimental results.* ▲ *Values calculated from the observed values of* pk_1 *and* pk_2 *using the theoretical eqn. (4).*

Table 2. Determination of the complex formation constants k_1 *and* k_2 *of perboric acids in about 0.0996 M potassium chloride solutions using the interpolated values from Table 1 at 25° C (*cf. *p. 757 and Eqn. 4).*

C_2'	C_2''	$K' \times 10^9$	$K'' \times 10^7$	pk_1
0.2	3.0	6.32	5.02	7.665
0.2	2.0	6.32	2.24	7.644
0.2	1.5	6.32	1.20	7.627
0.2	1.0	6.32	0.632	7.624
0.4	3.0	15.8	5.02	7.703
0.4	2.0	15.8	2.24	7.660
0.4	1.5	15.8	1.20	7.605
0.4	1.0	15.8	0.632	7.624

Average $pk_1 = 7.645 \pm 0.025$
$pk_2 = 7.40$

in eqn. (4) are 1 and 2, respectively. Using these values it is possible to calculate the corresponding complex formation constants for reactions (1a) and

$$H_3BO_3 + 2H_2O_2 \rightleftharpoons H^+ + (H_2BO_3 \cdot H_2O_2)^- \qquad (5)$$

as already has been stated. The results of these calculations are given in Table 2. Thus the corresponding values for pk_1 and pk_2 are about 7.645 and 7.40, respectively, in about 0.1 M potassium chloride solution. In this connection it should be noted that owing to the slight apparent ionization of boric acid the electrolyte concentration of this acid can be neglected. In Table 3 the values for pk_1 and pk_2 in potassium chloride solutions of different concentrations are calculated using the corresponding values for the apparent ionization constants of boric acid in these solutions. Thus the values 7.914 ± 0.04 and 7.71 ± 0.04 for the thermodynamic complex formation constants $pk_{1,0}$ and

Table 3. Determination of the complex formation constants k_1 *and* k_2 *of perboric acids in different potassium chloride solutions at 25° C (*cf. *p. 757 and Eqn. 4).*

$I^{\frac{1}{2}}$	C_2	pK^*	$(K^* - K_1) \times 10^8$	pk_1	pk_2
0.333	—	—	—	7.645	7.40
0.706	0.0800	8.393	0.305	7.472	7.22
0.705	0.9640	7.059	8.64		
1.181	0.0800	8.378	0.311	7.467	7.28
1.168	0.8802	7.119	7.50		

The average thermodynamic pk-values $pk_{1,0} = 7.914 \pm 0.04$
$pk_{2,0} = 7.71 \pm 0.04$

$pk_{2,0}$ were obtained. The values for the parameters of the Debye-Hückel equation were also calculated using the values in Table 3, with the following results:

pk_1: $\alpha = 0.525$ and $B = 0.160$
pk_2: $\alpha = 0.450$ and $B = 0.200$

CONCLUSIONS

It should be noted that the results obtained agree very well with eqns. (1a) and (5). Only the values for the apparent ionization constants measured at high concentrations of hydrogen peroxide differ markedly from the theoretically calculated values. This might be due to the formation of the next complex peracid in very concentrated hydrogen peroxide solutions, but more likely it is caused by the great variations of the dielectric constants of such solutions, which recent investigations have revealed [13]. According to these observations it can be assumed that the variation of the dielectric constants in less than 3 M H_2O_2 solutions is so small that it does not affect results (*cf.* Tables 2 and 3). On the other hand the existence of a complex acid formed according to eqn. (1b) seems most unlikely, since in this case the values of the apparent ionization constants should vary with the concentration of boric acid (*cf.* eqn. 2 and Table 1).

Using the above-mentioned values for the complex formation constants the thermodynamic complex formation constants $K_{n,1,0}$ and $K_{n,2,0}$ of the reactions

$$\begin{aligned} &\text{a)} \quad H_2BO_3^- + H_2O_2 \rightleftharpoons (H_2BO_3 \cdot H_2O_2)^- \\ &\text{b)} \quad H_2BO_3^- + 2H_2O_2 \rightleftharpoons (H_2BO_3 \cdot 2H_2O_2)^- \end{aligned} \tag{6}$$

can also be calculated [5,10,11]. Thus we get

$$\begin{aligned} &\text{a)} \quad K_{n,1,0} = \frac{c_{(H_2BO_3 \cdot H_2O_2)^-}}{c_{H_2BO_3^-} \cdot c_{H_2O_2}} = \frac{k_{1,0}}{K_{1,0}} = 21.1 \\ &\text{b)} \quad K_{n,2,0} = \frac{c_{(H_2BO_3 \cdot 2H_2O_2)^-}}{c_{H_2BO_3^-} \cdot (c_{H_2O_2})^2} = \frac{k_{2,0}}{K_{1,0}} = 33.6 \end{aligned} \tag{7}$$

The author is indebted to the *Finnish Academy Government Grant for Young Scientists* for a research scholarship.

REFERENCES

1. Menzel, H. *Z. anorg. u. allgem. Chem.* **164** (1927) 1.
2. Edwards, J. O. *J. Am. Chem. Soc.* **75** (1953) 6154.
3. Antikainen, P. J. *Suomen Kemistilehti* **B 28** (1955) 159.
4. Kilpi, S. *J. Am. Chem. Soc.* **74** (1952) 5296.
5. Antikainen, P. J. *Ann. Acad. Sci. Fennicae, Ser. A* II 56 (1954).
6. Heberlein, K. B. *Diss.* Basel 1898, p. 64.
7. Owen, B. B. *J. Am. Chem. Soc.* **56** (1934) 1685.
8. Hahn, F. L. and Klockmann, R. *Z. physik. Chem.* **151** (1930) 80.
9. Thomson, J. *Ann. Physik.* **20** (1870) 505.
10. Antikainen, P. J. *Suomen Kemistilehti* **B 28** (1955) 135.
11. Antikainen, P. J. *Ibid.* **B 29** (1956) 14.
12. Antikainen, P. J. *Acta Chem. Scand.* **9** (1955) 1008.
13. Guthberton, A. C. and Maas, O. *J. Am. Chem. Soc.* **52** (1930) 489.

Received February 22, 1956.

ACTA CHEMICA SCANDINAVICA 10 (1956) 761—768

On the Mechanism of the Phenyl *Iso*thiocyanate Degradation of Peptides

PEHR EDMAN

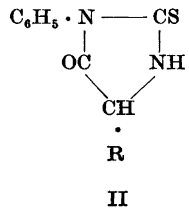
Department of Physiological Chemistry, University of Lund, Lund, Sweden

A study of the reaction mechanism has revealed that the N-terminal amino acid is split off in the form of its 2-anilino-5-thiazolinone derivative. The latter is very unstable and can be converted along two different routes — thermal or hydrolytic — to the isomeric 3-phenyl-2-thiohydantoin derivative. The bearings of these findings on the degradation method are discussed.

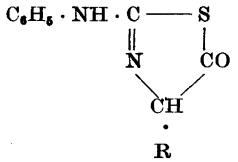
A formal analogy has earlier been assumed for the phenyl *iso*cyanate [1,2] and the phenyl *iso*thiocyanate [3,4] degradation of peptides. However, some observations and in particular the great difference in the rate of formation of phenyl thiohydantoin (PTH) in aqueous [5,6] and non-aqueous media [4,7] indicated a peculiarity in the mechanism of the phenyl *iso*thiocyanate degradation which required closer investigation. With the introduction of the paper chromatographic procedure for the identification of phenyl thiohydantoins [8] this became possible.

$C_6H_5 \cdot NH \cdot CS \cdot NH \cdot CHR \cdot CO \cdot NH \cdot CHR' \cdot COOH$

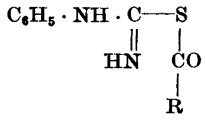
I



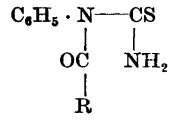
II



III



IV



V

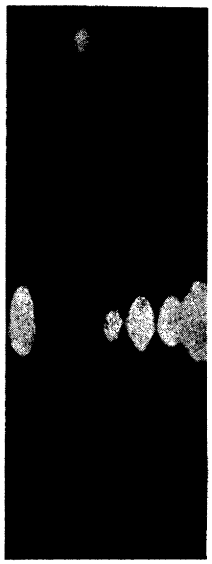


Fig. 1. Paper chromatogram of products resulting from the cleavage of PTC-leucylglycine in nitromethane-hydrogen chloride. From left to right: PTH-leucine, "crude product", PTC-leucylglycine, 1st, 2nd and 3rd fraction of recrystallised product, PTH-leucine. Solvent A.

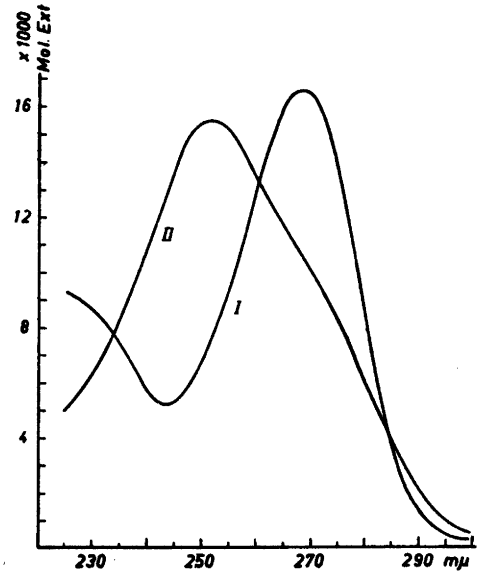


Fig. 2. Ultraviolet absorption curves of 5-isobutyl-3-phenyl-2-thiohydantoin (I) and 2-anilino-4-isobutyl-5-thiazolinone (II) in ethanol.

Paper chromatography of the reaction mixture resulting from cleavage of phenyl thiocarbamyl (PTC)-DL-leucylglycine (I; R = $CH_2 \cdot CHMe_2$; R′ = H) in nitromethane-hydrogen chloride, revealed a hitherto unobserved substance, whereas the expected PTH-leucine (II; R = $CH_2 \cdot CHMe_2$) was lacking (Fig. 1). However, on mere recrystallization the new compound was completely transformed into PTH-leucine. Obviously the N-terminal amino acid of the peptide was split off in the form of a labile derivative which was easily convertible to the phenyl thiohydantoin. The nature of this intermediate and the conditions for its conversion have been studied.

Avoiding heat and moisture the intermediate could be recrystallized as its salt with strong acids. Elementary analyses showed it to be an isomeride of the corresponding phenyl thiohydantoin from which it however differed in paper chromatographic behaviour (Fig. 1) and in ultraviolet absorption (Fig. 2).

It could be demonstrated that two different ways are open for the conversion of the intermediary compound into the corresponding phenyl thiohydantoin. At elevated temperature the transformation takes place as an intramolecular rearrangement (Figs. 3 and 4). On the other hand, in the presence of water, the intermediate compound is rapidly hydrolysed to the correspond-

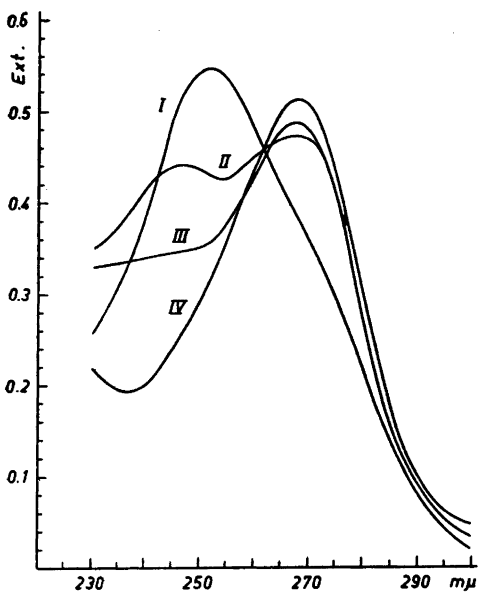


*Fig. 3. Conversion of 2-anilino-4-*isobutyl*-2-thiazolinone hydrochloride into PTH-leucine in the dry state at 115° C. Ultraviolet absorption curves of samples at zero time (I) and after 10 min. (II), 25 min. (III) and 60 min. (IV).*

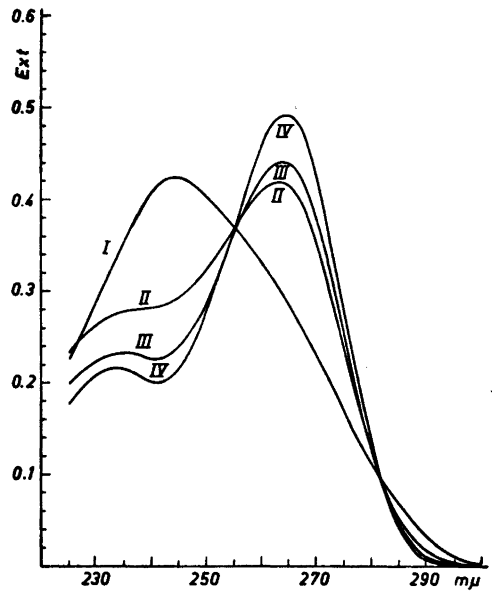


*Fig. 4. Conversion of 2-anilino-4-*isobutyl*-5-thiazolinone hydrochloride into PTH-leucine in glacial acetic acid at 93° C. Ultraviolet absorption curves of samples at zero time (I) and after 10 min. (II), 19 min. (III) and 39 min. (IV).*

ing PTC-amino acid which then slowly undergoes ringclosure to the PTH-amino acid (Fig. 6). The rate of this ringclosure was followed at pH 3 and the temperatures 30° C and 50° C (Fig. 5).

A striking similarity exists between these reactions and those displayed by S-acylated thioureas. The latter have been extensively investigated by Dixon and his coworkers [9–11]. They obtained the hydrochloride of S-acetyl-N-phenyl thiourea * (IV; R = Me) by reacting phenyl thiourea with acetyl chloride in the cold. On heating, this compound was rapidly converted first to the N-acetyl-N-phenyl thiourea (V; R = Me) and later to the N′-acetyl-N-phenyl thiourea. On the other hand water hydrolysed the thiolester linkage with the formation of phenyl thiourea and acetic acid. By analogy our intermediate should then be formulated as a 2-anilino-5-thiazolinone (III).

Several attempts were made at an independent synthesis of the labile intermediate compound but of these only an approach analogous to the one used by Dixon *et al.* for preparing the open-chain S-acylated thioureas was successful. The acid chloride of phenyl thiocarbamyl-L-leucine was prepared and

* Dixon *et al.*[10] prefer to formulate these compounds as sulfonium chlorides.

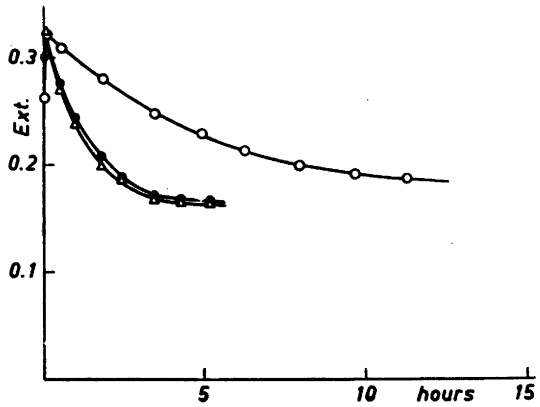


*Fig. 5. Conversion of 2-anilino-4-*isobutyl*-5-thiazolinone hydrochloride* via *PTC-leucine (initial rapid rise) into PTH-leucine in aqueous solution at pH 3 and 30° C (—○—○—) and 50° C (—●—●—) followed through change in extinction at 243 mμ. For comparison the conversion of PTC-leucine into PTH-leucine at pH 3 and 50° C (—△—△—).*

this spontaneously converted itself to the hydrochloride of 2-anilino-4-*iso*-butyl-5-thiazolinone:

$$C_6H_5 \cdot NH \cdot CS \cdot NH \cdot CH(CH_2 \cdot CHMe_2)COONa \xrightarrow{POCl_3} [C_6H_5 \cdot NH \cdot CS \cdot NH \cdot CH(CH_2 \cdot CHMe_2)COCl]$$

$$\longrightarrow C_6H_5 \cdot NH \cdot C(=S) \cdot N(CH)(CO) \cdot CH(CH_2 \cdot CHMe_2) \quad Cl^-$$

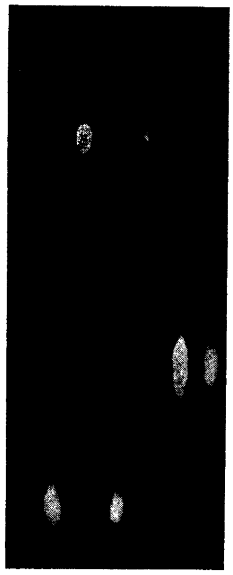


*Fig. 6. Paper chromatogram of products formed in the cleavage of PTC-leucylglycine in 4 N hydrochloric acid. From left to right; PTC-leucylglycine, 2-anilino-4-*isobutyl*-5-thiazolinone hydrochloride, PTC-leucine, samples of reaction mixture after 1 min., 15 min., 80 min., and PTH-leucine. Solvent A.*

EXPERIMENTAL

Elementary analyses (except micro-Kjeldahl) were made at the Analytical Laboratory, Department of Chemistry, University of Lund, and at the Chemical Laboratory, University of Copenhagen.

Melting points were determined on a heating block (Fisher-John) and are uncorrected.

Paper chromatography was carried out as described by Sjöquist [8].

*Cleavage of phenyl thiocarbamyl-*DL*-leucylglycine in nitromethane-hydrogen chloride.* Phenyl thiocarbamyl-DL-leucylglycine [4] (200 mg) was suspended in dry nitromethane (10 ml) saturated with dry hydrogen chloride. The reaction mixture was left at room temperature for 15 min. and the crystals of glycine hydrochloride were filtered off. The mother liquor was evaporated *in vacuo* to dryness without heating. The crude, crystalline product (157 mg) was subjected to paper chromatography in solvent A (Fig. 1) and the U.V.-absorption was measured in abs. ethanol * where a broad absorption with a maximum at 252 mμ ($\varepsilon_{252} = 59$; $C = 1$ g/l) was observed.

Part of the crude product (70 mg) was dissolved in abs. ethanol (1 ml) and a small insoluble residue filtered off. The preparation was then fractionally crystallized in the cold by the gradual addition of petroleum ether. Melting points, R_F-values in solvent A (Fig. 1) and U.V.-absorption curves were determined on the separate fractions (Table 1).

Table 1.

	M. p.	R_F-value in solvent A	Abs. max.
Crude product	126—135°	0.80	$\varepsilon_{252} = 59$
Fract. I (10 mg)	178°	0.59	$\varepsilon_{268} = 63$
Fract. II (31 mg)	178°	0.59	$\varepsilon_{268} = 63$
Fract. III (4 mg)	140—144°	0.59	$\varepsilon_{268} = 59$
PTH-leucine	178°	0.59	$\varepsilon_{268} = 64$

*Cleavage of phenyl thiocarbamyl-*DL*-leucylglycine in glacial acetic acid-hydrogen chloride* [7]. Phenyl thiocarbamyl-DL-leucylglycine (0.65 g) was dissolved in glacial acetic acid saturated with hydrogen chloride (5 ml). Almost immediately crystals began to appear and they were filtered off after a few minutes (0.21 g). Paper chromatography in pyridine-amyl alcohol [12] and in acetic acid-butanol [13] showed identity with glycine.

To the mother liquor ten vols. of dry ethyl ether were added. Needleshaped crystals were collected (0.47 g). Recrystallization from glacial acetic acid — hydrogen chloride and ethyl ether. M. p. 128—31°. For U.V.-absorption curve see Fig. 2. (Found: N 9.64. $C_{13}H_{17}ON_2ClS$ requires: N 9.83).

The product was taken up in a small volume of glacial acetic acid-sulfuric acid (1 M) and ethyl ether added to crystallization. The crystals melted at 133° C. (Found: C 44.4; H 5.30; N 8.03; S 18.2. $C_{13}H_{18}O_5N_2S_2$ requires: C 45.0; H 5.25; N 8.08; S 18.5).

*Sodium salt of phenyl thiocarbamyl-*L*-leucine.* L-Leucine (2.7 g) was dissolved in pyridine-water (3:2, 50 ml) and 2 N sodium hydroxide added to pH 9. Phenyl *iso*thiocyanate (5 ml) was added and pH was kept at 9 during the reaction by the continuous addition of sodium hydroxide. After one hour the reaction mixture was extracted several times with equal volumes of benzene and finally with ethyl ether and the extracts discarded. A small insoluble residue was filtered off and pH was again adjusted to 9 with sodium hydroxide. The solution was concentrated *in vacuo* to a thick syrup. This was repeatedly

* Since the 5-thiazolinone slowly reacts with ethanol all measurements were made immediately after dissolution.

extracted first with acetone and then with ethyl ether and finally dried *in vacuo* (4.95 g). (Found: N 9.15. $C_{13}H_{17}O_3N_2SNa \cdot 1\ H_2O$ requires: N 9.15).

2-Anilino-4-isobutyl-5-thiazolinone. The sodium salt of PTC-L-leucine (2.3 g) was suspended in ethylene chloride (10 ml). Phosphorus oxychloride (0.6 ml) was added slowly under cooling in ice and the reaction mixture then left for two hours at room temperature. The precipitated salts were removed and the solvent then evaporated in a current of dry air. To the oily residue several vols. of dry ethyl ether were added and a stream of hydrogen chloride passed through the solution for a short while. Crystals appeared which were filtered off and recrystallized three times in quick succession from glacial acetic acid-sulfuric acid (1 M) and ethyl ether (0.8 g). M. p. 133°. R_F-value in solvent A and U.V.-absorption curve identical with that of the initial product obtained from the degradation of PTC-leucylglycine (see above). (Found: C 44.5; H 5.30; N 8.02; S 18.3. $C_{13}H_{16}O_2N_2S_2$ requires: C 45.0; H 5.25; N 8.08; S 18.5).

Attempted conversion of 5-isobutyl-3-phenyl-2-thiohydantoin into 2-anilino-4-isobutyl-5-thiazolinone. 5-*iso*butyl-3-phenyl-2-thiohydantoin (0.25 g) was dissolved in dry nitromethane (10 ml) and the solution saturated in the cold with dry hydrogen chloride. After 15 min. the solvent was removed *in vacuo*. Paper chromatography in solvents A and B and U.V.-absorption showed that the original product had been recovered unchanged.

Conversion of 2-anilino-4-isobutyl-5-thiazolinone into 5-isobutyl-3-phenyl-2-thiohydantoin by heat. Dry samples of 2-anilino-4-*iso*butyl-5-thiazolinone hydrochloride were heated at 115° C for varying times. The products were then dissolved in abs. ethanol and the U.V.-absorption measured (Fig. 3).

A solution of 2-anilino-4-*iso*butyl-5-thiazolinone hydrochloride (1 mg/ml) in glacial acetic acid was heated at 93° C. At intervals samples were diluted with abs. ethanol (1:100) and the U.V.-absorption measured (Fig. 4).

Conversion of 2-anilino-4-isobutyl-5-thiazolinone into 5-isobutyl-3-phenyl-2-thiohydantoin in aqueous acid. Solutions of 2-anilino-4-*iso*butyl-5-thiazolinone hydrochloride in acetone (10 mg/ml) were diluted with 4 N hydrochloric acid (1:10). Paper chromatograms in solvent A were run on samples taken after various times along with authentic samples of PTC-leucine and of PTH-leucine *. Already after 1 min. the spot corresponding to the 5-thiazolinone had almost completely disappeared and been substituted by a strong spot corresponding to PTC-leucine. After 5 min. a spot corresponding to PTH-leucine began to appear. The latter spot grew at the expense of the other spots and it was the only one to persist after 90 min.

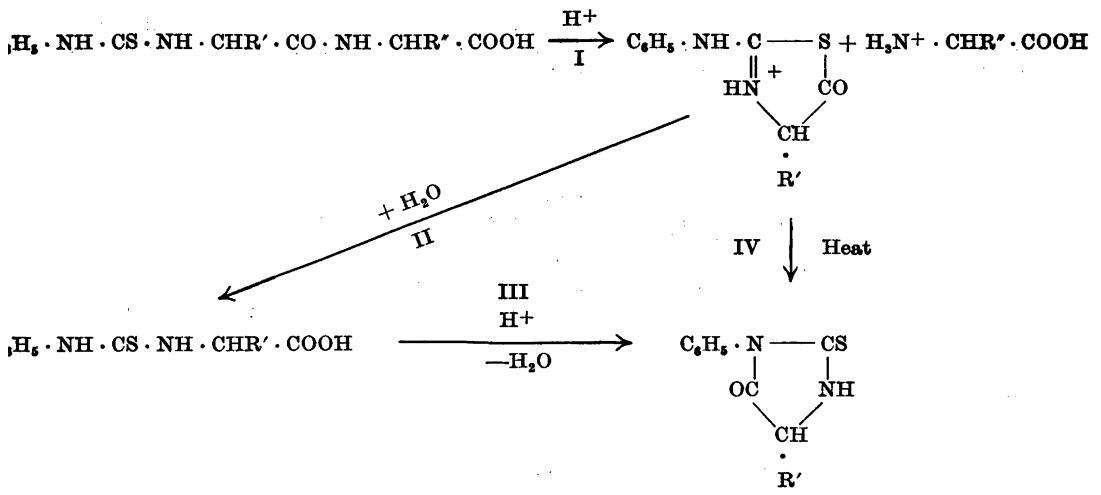
Solutions of 2-anilino-4-*iso*butyl-5-thiazolinone hydrochloride and PTC-leucine (approx. 10 mg/ml) were made up in dry acetone. These solutions were diluted (1:1 000) with water previously adjusted to pH 3 and equilibrated at 30° and 50° C. The change in the U.V.-absorption at 243 mμ was then followed. The results were recalculated for equimolar concentrations (Fig. 5).

Cleavage of phenyl thiocarbamyl-DL-leucylglycine in aqueous acid. Solutions of PTC-DL-leucylglycine (15 mg/ml) in acetone were diluted with 4 N hydrochloric acid (1:10). Paper chromatograms in solvent A were run on samples withdrawn after various times along with authentic samples of PTC-leucylglycine, 2-anilino-4-*iso*butyl-5-thiazolinone, PTC-leucine and PTH-leucine (Fig. 6) *. After 1 min. a strong spot corresponding to the 5-thiazolinone and a weak spot corresponding to PTC-leucine were visible, after 15 min. PTH-leucine began to appear and this was the only substance present after 80 min.

DISCUSSION

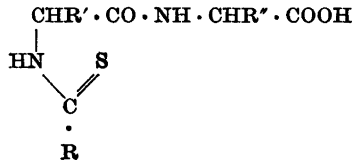
The reaction sequences observed can be summarized in the following way:

* The 5-thiazolinone tends to react with the paper at the point of application and it was therefore necessary to develop the chromatogram without delay.



This reaction mechanism helps to clarify several hitherto obscure points. Thus the considerable difference in the rate of cleavage of PTC-peptides in nonaqueous [4,7] and in aqueous solution [5,6] is only apparent since the reactions observed were not the same. In the former case only reaction I was followed whereas in the latter instance measurements were made on the reaction sequence I—II—III of which reaction III is by far the slowest (Fig. 5). Furthermore, the frequently noted appearance of multiple spots on paper chromatograms as the result of a single step in the degradation has most likely often been due to the presence of intermediates. For the same reason the extent of cleavage of the peptide may have appeared low if calculated from the yield of thiohydantoin.

A unified aspect can be laid on several of the reactions for the degradation of peptides from the N-terminal. The reactive N-substituted peptide derivatives can be formulated:



where R represents various substituents such as C_6H_5NH- [3,4], HS- [14] or alkoxy groups [15] and the cleavage of the peptide bond ensues on the establishment of the —CO—S— linkage.

It is interesting to note that in aqueous medium the —CO—S-linkage has only a transient existence since the thiocarbamyl configuration is rapidly reestablished through hydrolysis after fission of the peptide bond. One may therefore be justified in designating the role of the thioketonic grouping (or its enolic form) as catalytic. Apparently, the nature of the neighboring R group greatly influences this catalytic activity.

This investigation has been supported by a grant from the Eli Lilly and Company which is gratefully acknowledged. The author is also indebted to Mr. K. Lauber for his skilful assistance in the experimental work.

REFERENCES

1. Bergmann, M., Kann, E. and Miekeley, A. *Ann.* **458** (1927) 56.
2. Abderhalden, E. and Brockmann, H. *Biochem. Z.* **225** (1930) 386.
3. Edman, P. *Arch. Biochem.* **22** (1949) 475.
4. Edman, P. *Acta Chem. Scand.* **4** (1950) 283.
5. Ottesen, M. and Wollenberger, A. *Nature* **170** (1952) 801.
6. Fraenkel-Conrat, H. and Fraenkel-Conrat, J. *Acta Chem. Scand.* **5** (1951) 1409.
7. Edman, P. *Acta Chem. Scand.* **7** (1953) 700.
8. Sjöquist, J. *Acta Chem. Scand.* **7** (1953) 447.
9. Dixon, A. E. and Hawthorne, J. *J. Chem. Soc.* **91** (1907) 122.
10. Dixon, A. E. and Taylor, J. *J. Chem. Soc.* **101** (1912) 2502.
11. Dixon, A. E. and Taylor, J. *J. Chem. Soc.* **117** (1920) 720.
12. Edman, P. *Arkiv Kemi, Mineral. Geol.* **A 22** (1945) No. 3.
13. Partridge, S. M. *Biochem. J. London* **42** (1948) 238.
14. Levy, A. L. *J. Chem. Soc.* **1950** 404.
15. Kenner, G. W. and Khorana, H. C. *J. Chem. Soc.* **1952** 2076.

Received February 25, 1956.

ACTA CHEMICA SCANDINAVICA 10 (1956) 769—778

The Mechanism of the Exchange Reaction between Cerium(III) and Cerium(IV) at Platinum Surfaces

STURE FRONÆUS and CARL OTTO ÖSTMAN

Department of Physical Chemistry, Chemical Institute, University of Lund, Lund, Sweden

The heterogeneous electron exchange reaction between cerium(III) and cerium(IV) at platinum surfaces under equilibrium electrode potential is investigated in a perchlorate ionic medium by means of a radioactive tracer. A general relationship for the combination of rates of consecutive steps in exchange reactions is given. From the kinetic law obtained in the present case it is established that at 0° C and in approximately 3 M perchloric acid the resultant rate of the reaction is controlled both by the electron transfer step and by the diffusion of cerium(IV) up to the interface.

The measurements indicate that the uptake of electrons from platinum by cerium(IV) takes place *via* a dimer of cerium(IV). Thus this species together with the corresponding mixed cerium(III)—cerium(IV) product, operating in the reverse process, are directly potential adjusting, although the concentrations of both species are very low in comparison with the total concentrations of cerium.

The mechanism proposed is discussed in connection with other facts about some homogeneous redox reactions in which cerium is involved.

Few kinetic investigations on the mechanisms of electrode reactions of inorganic redox systems have been reported in the literature, and electrical methods alone have been used in these studies. In some cases, *e. g.* the redox systems Fe^{3+} / Fe^{2+}, Mn^{3+} / Mn^{2+}, and Ce(IV) / Ce(III), it has been found [1–4] that the electron transfer step and the over-all electrode reaction are the same, while for other systems [5], *e. g.* Mn^{4+}/Mn^{3+}, they may be different, even though the over-all electrode reaction is very simple.

In the investigation of the cerium(IV) / cerium(III) system Vetter [4] used sulphuric acid as an additional electrolyte. However, it is known that both the cerium(III) ion (Fronæus [6]) and especially the cerium(IV) ion (Hardwick and Robertson [7]) can form three mononuclear sulphate complexes and that the hydrolysis of cerium(IV) is suppressed by this complex formation. For this reason it is probable that the electron transfer step found [4] in sulphuric acid refers to sulphate complexes.

On the other hand it has been shown by Hardwick and Robertson [8] that hydrolysis of the cerium(IV) ion occurs in perchloric acid solutions, partly with the formation of a dinuclear species. Furthermore, Gryder and Dodson [9] found that the rate of the homogeneous exchange reaction between cerium(III) and cerium(IV) is a linear function of the reciprocal of the perchloric acid concentration.

It was therefore to be expected that the electron transfer step of the heterogeneous exchange reaction in perchloric acid at platinum surfaces would be less simple than in sulphuric acid solutions. Thus the present investigation was started with the aim of elucidating the mechanism of this exchange reaction by the use of a radioactive cerium isotope.

In those cases where the electron transfer step is not very rapid in comparison with the rate of diffusion of the exchanging species up to the interface, the radioactive tracer method can give the rate of the first-mentioned step at equilibrium potential. The method has the advantage over electrical methods of being uninfluenced by small amounts of other redox systems present as impurities or formed from the solvent, and which are in redox equilibrium with the main system. The tracer method has been successfully employed by us in a previous investigation [10] of an electrode reaction of a different type.

THEORETICAL

The following notation is used for total concentrations.

c_a, q_a = concentrations of radioactive cerium(IV) and cerium(III).

c_i, q_i = concentrations of inactive cerium(IV) and cerium(III).

$c = c_a + c_i$

$q = q_a + q_i$

The kinetic law for the electron transfer step

According to Hardwick and Robertson [8] cerium(IV) is present as a mixture of Ce^{4+}, $CeOH^{3+}$, and a dimer, denoted Ce_2O^{6+}, in perchlorate solutions containing perchloric acid. Thus, to make a general treatment of the over-all electrode reaction

$$Ce(IV) + e^- \text{ (electrode)} \rightleftharpoons Ce(III) \tag{1}$$

we must presuppose that we have a set of simultaneous one-electron transfer steps of the type

$$\overset{IV}{Ce}_j(OH)_n^x + e^- \text{ (electrode)} \rightleftharpoons \overset{III\ IV}{CeCe}_{j-1}(OH)_n^{x-1} \tag{2}$$

combined with the hydrolytic equilibria

$$\overset{IV}{Ce}_j(OH)_n^x + nH^+ \rightleftharpoons jCe^{4+} + nH_2O \tag{3}$$

$$\overset{III\ IV}{CeCe}_{j-1}(OH)_n^{x-1} + nH^+ \rightleftharpoons Ce^{3+} + (j-1)Ce^{4+} + nH_2O \tag{4}$$

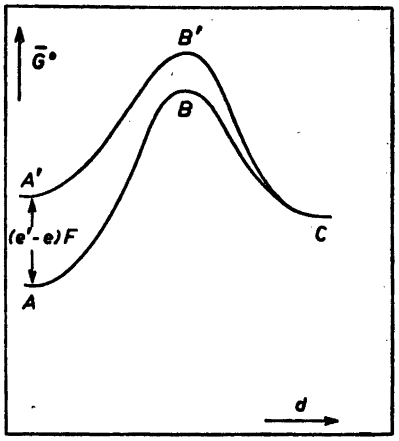


Fig. 1. The standard electrochemical free energy $\bar{G}^\circ$ during the electron transfer as a function of the distance d of the electron from the electrode surface.

Here $n \geqq 0$ for $j = 1$ and $n \geqq 2$ for $j = 2$. Within a limited range of values of q and c and at a fixed value of the perchloric acid concentration we can assume that the rates $\vec{r}$ and $\overleftarrow{r}$ of one of the reactions of type (2) predominate, and then these rates are practically equal to the total rates of the electron transfer in both directions. It should be emphasised that the concentrations of the species responsible for the electron transfer may be very small in comparison with q and c (*cf.* Fronæus and Östman [10]).

In Fig. 1 the standard electrochemical free energy during the electron transfer, $\bar{G}^0$, is represented as a function of the distance d of the electron from the electrode surface. The value of $\bar{G}^0$ at A refers to the left-hand side of (2) at a fixed value e' of the electrode potential while the value at C is that of the right-hand side of (2) just outside the rigid part of the electrode double layer. The steepness of the curve AB depends upon the so-called image force between the electrode and the electron(*cf.* Pitzer [11]).

When the electrode potential is decreased from e' to e the new energy barrier A'B'C is obtained, the increase in $\bar{G}^0$ at A being $(e'—e)F$ and for the activated state $\alpha(e'—e)F$, where $0<\alpha<1$. Thus it is evident that the electrochemical free energy of activation of the forward reaction of (2) decreases by the quantity $(1—\alpha)\ (e'—e)F$ and that of the reverse reaction increases by the quantity $\alpha(e'—e)F$. Then if e is the equilibrium electrode potential we have $\vec{r} = \overleftarrow{r} = r_0$ and for r_0 the following expressions are obtained

$$r_0 = k_1\ [\overset{IV}{Ce}_j(OH)_n^s]\ \exp\left\{\frac{(1—\alpha)\ (e'—e)\ F}{RT}\right\} \tag{5}$$

$$r_0 = k_2\ [\overset{III\ IV}{CeCe}_{j-1}(OH)_n^{s-1}]\ \exp\left\{-\frac{\alpha(e'—e)\ F}{RT}\right\} \tag{6}$$

where k_1 and k_2 denote the specific rates of the forward and reverse reactions at the electrode potential e'. For a survey of deductions of equations of the types (5) and (6) in the literature the reader is referred to a paper by Vetter [12].

Variations in the ζ-potential are suppressed in the presence of perchloric acid at a high and constant concentration as an additional electrolyte [13], and then the concentrations of the electron transferring species in the diffuse double layer are proportional to the corresponding concentrations in the bulk of the solution. Then if the latter concentrations are introduced in (5) and (6) the coefficients k_1 and k_2 should still be constants, provided, of course, that the state of the electrode surface is reproducible.

Furthermore, if, as usual, we presuppose that the inner potential in the solution phase varies linearly with d through the rigid part of the double layer, the transfer coefficient α should be a constant and, in the case of a symmetrical energy barrier, have the value 0.5.

Eliminating $e' - e$ from (5) and (6) we get

$$r_0 = \text{constant} \cdot [\overset{\text{IV}}{\text{Ce}}_j(\text{OH})_n^x]^{\alpha} \; [\overset{\text{III IV}}{\text{CeCe}}_{j-1}(\text{OH})_n^{x-1}]^{1-\alpha} \tag{7}$$

Then we apply the law of mass action to the equilibria (3) and (4), and the expressions obtained are combined with (7) giving

$$r_0 = \text{constant} \cdot [\text{Ce}^{4+}]^{j-1+\alpha} \; [\text{Ce}^{3+}]^{1-\alpha} \tag{8}$$

since $[\text{H}^+]$ is kept constant.

From the known effect of temperature on the equilibrium constants of the hydrolytic reactions [8] of Ce^{4+} it can be calculated that the concentration of the dimer is $\leqq 2.5$ % of c at 0° C, in 2.82 M perchloric acid as ionic medium, and at c-values $\leqq 8.5$ mM (the conditions for the measurements in the present investigation). The concentration of $\overset{\text{III IV}}{\text{CeCe}}(\text{OH})_n^{x-1}$ is also certainly very small, since an extinctiometric investigation by King and Pandow [14] indicates that the system cerium(III)/cerium(IV) in perchloric acid solutions does not exhibit "interaction absorption".

Thus the mononuclear species predominate, and we have $[\text{Ce}^{4+}] \approx 0.86\, c$ throughout the measurements at our acid concentrations. Furthermore, since no hydrolysis of Ce^{3+} occurs in perchloric acid solutions [6] $[\text{Ce}^{3+}] = q$, and introducing these expressions into (8) we finally obtain

$$r_0 = k_0 \; c^{j-1+\alpha} q^{1-\alpha} \tag{9}$$

where k_0 is a constant.

The resultant rate of the heterogeneous reaction

The rate r of the heterogeneous reaction is composed of the rates of at least three consecutive steps; the rate r_1 of the diffusion of cerium(III) to and from the electrode surface, the rate r_0 of the electron transfer in both directions, and the rate r_2 of the diffusion of cerium(IV) to and from the electrode, expressed in moles per unit surface area and unit time.

Of r_1 moles of cerium(III) diffusing to the electrode surface only r' moles take part in the electron transfer reaction. Now, since the fraction $r_0/(r_0+r_1)$

of all cerium(III) appearing and disappearing at the electrode is due to the electron transfer reaction we have the relation $r'/r_1 = r_0/(r_0 + r_1)$ or

$$\frac{1}{r'} = \frac{1}{r_0} + \frac{1}{r_1} \tag{10}$$

Evidently r' is the rate of transfer of cerium(III) from the solution outside the diffusion layer to cerium(IV) at the electrode surface. As the deduction is independent of the mechanisms of the two steps, the resultant rate r can be obtained by combination of r' and r_2 in the same way, and we get

$$\frac{1}{r} = \frac{1}{r_0} + \frac{1}{r_1} + \frac{1}{r_2} \tag{11}$$

If the reversible reactions (3) and (4) are not extremely rapid these steps must also be taken into consideration, and the reciprocals of their rates added to the sum on the right side of (11). Thus the reciprocals can be treated as kinetic resistances.

Obviously this fundamental law for the combination of rates of consecutive steps is *generally* applicable to exchange reactions, where all concentrations are independent of time and consequently for every step the rates are equal in both directions. For heterogeneous reactions (not exchange reactions) composed of a diffusion step and a reaction at an interface it has been shown previously [15,16] that a law of the type (10) is valid in the simplest case with a first order surface reaction.

For the diffusion rates r_1 and r_2 we have the following expressions

$$r_1 = \frac{D_1\, q}{\delta} \tag{12}$$

$$r_2 = \frac{D_2\, c}{\delta} \tag{13}$$

where δ is the thickness of the diffusion layer and D_1 the diffusion coefficient of the cerium(III) ion. D_2 is an average diffusion coefficient [17] of cerium(IV) valid at the fixed concentration ratios of the mononuclear cerium(IV) species.

EXPERIMENTAL

Chemicals. Radioactive cerium(III) perchlorate (containing some ^{141}Ce from Harwell, England) and inactive cerium(III) and cerium(IV) perchlorate solutions were prepared and analysed in the way described in previous papers [6,18]. All the stock solutions used were 2.82 M with respect to perchloric acid. The concentration of cerium(IV) was redetermined every day since the solution of cerium(IV) perchlorate was not stable but slowly oxidized water.

A 4.5 M solution of nitric acid was freed from oxides of nitrogen by bubbling air through for some hours at 60—80° C, and it was checked that the solution had no reducing effect on cerium(IV).

Diethyl ether was distilled once and stored in contact with sodium.

Exchange measurements. Cerium(III) perchlorate, cerium(IV) perchlorate and perchloric acid were mixed and tempered in a thermostat at 0° C. 15 ml of the mixture were introduced into a reaction vessel, which could be shaken in the thermostat, and 1.00 ml of the radioactive cerium(III) perchlorate solution was added quickly. After a certain

time, varying from 2 to 30 minutes, 10 ml of the solution were withdrawn and added to a mixture of 25 ml 4.5 M nitric acid and 50 ml ether. In the presence of the nitric acid cerium(IV) is rapidly extracted into the ether and this is a satisfactory and convenient method for the separation of the exchanging species, given by Gryder and Dodson [9]. After extraction the ether phase was washed once with 25 ml of the nitric acid, and the cerium(IV) was reduced with 10 ml aqueous hydrogen peroxide, causing a re-extraction of all the cerium into the aqueous phase. The gamma radioactivity of a fixed volume of the last-mentioned phase was determined with a scintillation detector (Tracerlab P-20) under reproducible geometry.

For every set of values of c and q two series of measurements were performed, one in the absence of platinum, giving the rate of the homogeneous exchange, and another with a platinum wire of 40 cm^2 surface area in the reaction vessel. In the last-mentioned case the solution was shaken so that the diffusion layer at the electrode had a fixed thickness throughout the measurements. Furthermore, the platinum wire was heated in an alcohol flame just before use, since it was very important to have the surface of the electrode in a reproducible state.

The radioactivity of cerium(IV) when approximate equilibrium with respect to isotopic mixing had been attained was determined on separate solutions, where the homogeneous exchange had proceeded for at least ten half reaction times, by the procedure described above.

It should be mentioned here that the reaction between cerium(IV) and water is so slow at 0° C, even in the presence of platinum, that it could have no influence on the exchange measurements during the reaction times used.

THE EXPERIMENTAL OVER-ALL RATE OF EXCHANGE

The differential equation for the total radioactive exchange

$$\overset{*}{\mathrm{Ce}}(\mathrm{III}) + \mathrm{Ce}(\mathrm{IV}) \rightleftharpoons \overset{*}{\mathrm{Ce}}(\mathrm{IV}) + \mathrm{Ce}(\mathrm{III}) \tag{14}$$

has the following general form [10]

$$\frac{\mathrm{d}c_a}{\mathrm{d}t} = \left(\frac{sr}{v} + R\right)\frac{c_i q_a - c_a q_i}{c\,q} \tag{15}$$

where s (= 40 cm^2) is the surface area of the platinum, v (= 16 ml) the volume of the reaction mixture, and R the rate of the homogeneous exchange reaction. If the measured radioactivity of cerium(IV) is denoted x at time t and x_∞ when the isotopic mixing has attained equilibrium the fraction exchanged will be equal to x/x_∞. If we further note that c_i and q_i are practically equal to the total concentrations c and q, integration of (15) gives

$$\ln\left(1-\frac{x}{x_\infty}\right) = -\left(\frac{sr}{v} + R\right)\cdot\frac{c+q}{qc}\cdot t \tag{16}$$

When $\ln(1-x/x_\infty)$ is plotted against t a straight line should be obtained, from the slope of which the value of R (in the absence of platinum) or $sr/v+R$ can be calculated. Since the separation with ether was performed in exactly the same way for all the solutions in a series of measurements, corresponding

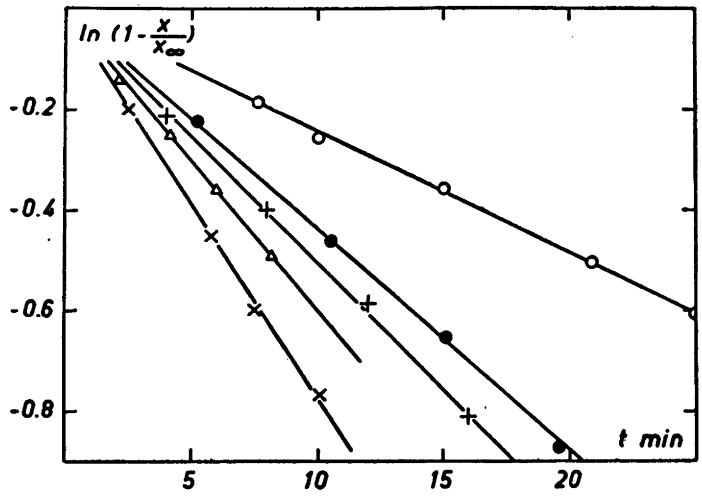


Fig. 2. $\ln(1-x/x_\infty)$ as a function of t in the homogeneous exchange for various values of c and q. —— *c = 2.18 mM, q = 2.18 mM (○); c = 2.18 mM, q = 5.43 mM ●; c = 2.18 mM, q = 10.34 mM (×); c = 4.25 mM, q = 6.14 mM (+); c = 8.21 mM, q = 4.85 mM (△).*

to fixed values of c and q, the fraction x/x_∞ should be independent of any slight incompleteness in the separation of cerium(IV).

The graphs in Fig. 2 represent the measurements of R for different values of c and q. An extrapolation of the straight lines obtained shows that $x = 0$ for $t = 0$, proving that the separation procedure does not induce any exchange. In passing it can be mentioned that R/q is a linear function of c, as found also by Gryder and Dodson [9]. The measurements with platinum in the reaction solution are represented in Figs. 3 and 4. Straight lines are also obtained in this case if very small values of t are not used in the runs corresponding to the lowest values of the rate r of the heterogeneous exchange.

It was necessary to keep $c \cdot q < 4 \times 10^{-5}$ M² in order to make the exchange rate conveniently measureable. On the other hand, the specific activity of the radioactive cerium(III) preparation available set the lower limit to the ranges of values of c and q.

Introducing the expressions (9), (12), and (13) for r_0, r_1, and r_2 into (11) we get the following relationship

$$\frac{q}{r} = \frac{q^a}{k_0\, c^{j-1+a}} + \frac{\delta}{D_1} + \frac{\delta\, q}{D_2\, c} \qquad (17)$$

From (17) it is evident that for $j = 1$ the quantity q/r should be a function of q/c only and increase monotonicly for increasing values of q/c. However, an inspection of Table 1, where the results from the exchange measurements are given, shows that this is not the case under the experimental conditions used. There remains the alternative $j = 2$, and the possibility of determining

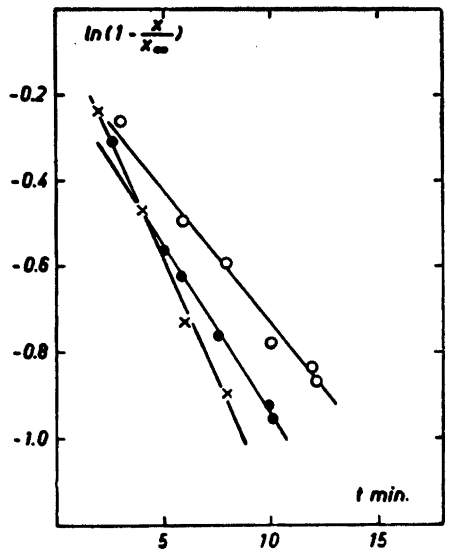


Fig. 3. $\ln(1-x/x_\infty)$ as a function of t in the mixed heterogeneous and homogeneous exchange for c = 2.18 mM and various values of q. —— q = 2.18 mM (○); q = 5.43 mM (●); q = 10.34 mM (×).

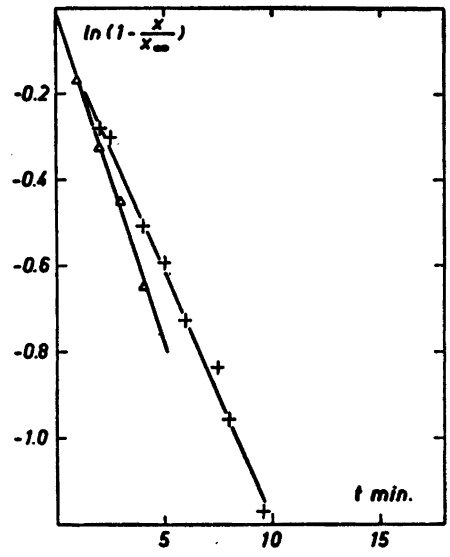


Fig. 4. The same function as in Fig. 3 for various values of c and q. —— c = 4.25 mM, q = 6.14 mM (+); c = 8.21 mM, q = 4.85 mM (△).

values of the parameters k_0, α, δ/D_1, and δ/D_2 by this approach will be investigated.

At the highest value of c and the lowest value of q/c the ratio q/r becomes so small that we can conclude that the constant term δ/D_1 is negligible. In a perchloric acid medium, where no complexing anions are present, the cerium (IV) ion is more strongly hydrated than the cerium(III) ion. Thus the difference between D_1 and D_2 should be greater than *e. g.* in a sulphuric acid medium [4], where complex formation certainly reduces the hydration of especially the cerium(IV) ion.

Table 1. The rates R and r of the homogeneous and heterogeneous exchange reactions for different values of the total cerium (III) and cerium (IV) concentrations.

c mM	q mM	$\frac{q}{c}$	R mM. min^{-1}	$\frac{sr}{v}+R$ mM · min^{-1}	$r \times 10^8$ mole · cm^{-2}.min^{-1}	$\frac{q}{r}$ cm^{-1} · min	$\frac{q}{r_{calc}}$ cm^{-1}.min
2.18	2.18	1.00	0.026	0.067	1.65	130	130
2.18	5.43	2.49	0.068	0.125	2.30	235	235
2.18	10.34	4.75	0.137	0.205	2.70	380	370
4.25	6.14	1.45	0.129	0.285	6.25	98	107
8.21	4.85	0.59	0.185	0.470	11.4	42.5	39.5

The following procedure was applied to determine the other parameters. For different values of α between 0 and 1, the quantities k_0 and δ/D_2 were calculated from corresponding values of q/r, c, and q in the first two lines of Table 1. With every set of parameters, q/r was calculated for the other c- and q-values, and it was found that the best fit with all the measurements was obtained for $\alpha = 0.50 \pm 0.05$. Then the relationship

$$\frac{1}{r} = \frac{211}{c^{1.5}\, q^{0.5}} + \frac{33}{c} \tag{18}$$

is obtained when c and q are expressed in mM and r in mM · cm · min^{-1}. In the last column of Table 1 the values of q/r have been calculated from this formula, and it is seen that they are in good agreement with the measured values. It is easily checked that no fit with all measurements can be obtained for $j > 2$. At the lowest cerium(IV) concentrations used $r_0 < r_2$, and for the highest c-values r_0 and r_2 are practically equal. Thus r_0 has a considerable influence on the resultant rate r.

We further obtain $D_2/\delta = (0.50 \pm 0.10) \times 10^{-3}$ cm · sec^{-1} from the measurements. A value of the average diffusion coefficient D_2 in the acid medium used is not known, but we can presuppose it to be of the order of magnitude 10^{-6} cm^2 · sec^{-1} (*cf.* Vetter [4]), giving us $\delta \approx 10^{-3}$ cm. This is a very plausible δ-value [19] at low relative velocities between the platinum and the solution, and there is nothing in the measurements that indicates an influence of the rates of the reactions (3) and (4) upon the total rate of the heterogeneous exchange.

DISCUSSION

We arrive at the following conclusions from the results of the present investigation.

(a) Within the concentration ranges of cerium(III) and cerium(IV) used and in approximately 3 M perchloric acid as an ionic medium the rate of the heterogeneous exchange reaction is controlled both by the electron transfer step and by the diffusion of cerium(IV), whereas the diffusion of cerium(III) seems to be too rapid to influence markedly the rate of exchange. Thus the tracer method is very suitable for the investigation of the mechanism of the electrode reaction.

(b) The hydrated cerium(IV) ion and its mononuclear hydrolysis products do not take up electrons appreciably from the platinum. This process takes place solely by way of a *dinuclear hydrolysis product*, although its concentration is only between 0,5 and 2.5 % of the total cerium (IV) concentration. As mentioned above the concentration of the corresponding mixed cerium(III)—cerium(IV) hydrolysis product, formed as an intermediate in the taking up of one electron and operating in the reverse process, must also be very low. The two dinuclear hydrolysis products mentioned are evidently the cerium species *directly* involved in the adjustment of the equilibrium electrode potential.

The results of some investigations of homogeneous reactions make conclusion (b) above very plausible. Thus Heidt and Smith [20] have investigated

the photochemical oxidation of water by cerium(IV) perchlorate in perchloric acid solutions and Kolp and Thomas [21] have studied the corresponding thermal reaction, and in both cases the measurements indicate that the oxidation is caused by a reactive dimer of cerium(IV).

It should also be mentioned that in a previous work by the present authors [18], dealing with the reaction between cerium(III) and persulphate, it was found that the rate of electron transfer is increased considerably by the coordination of sulphate ions to the cerium(III) ion. From the results of the present investigation it is evident that the coordination of a mononuclear hydrolysis product of cerium(IV) to the cerium(III) ion with the liberation of hydrogen ions has a similar effect in the electrode reaction studied. Also here the effect may be caused by a decrease in the energies of hydration (*cf.* Ref.[18]) or by a promotion of the 4*f* electron to a higher energy level. In this way we obtain a plausible explanation of the difference between the mechanisms of the electrode reactions in sulphuric acid [4] and in perchloric acid.

This investigation has been supported by a grant from the *Swedish Natural Science Research Council* which is gratefully acknowledged. We are most grateful to Dr. F. J. C. Rossotti for his revision of the English text in this paper.

REFERENCES

1. Gerischer, H. *Z. Elektrochem.* **54** (1950) 362.
2. Gerischer, H. *Z. Elektrochem.* **54** (1950) 366.
3. Vetter, K. J. and Manecke, G. *Z. physik. Chem.* **195** (1950) 270.
4. Vetter, K. J. *Z. physik. Chem.* **196** (1951) 360.
5. Vetter, K. J. and Manecke, G. *Z. physik. Chem.* **195** (1950) 337.
6. Fronæus, S. *Svensk Kem. Tidskr.* **64** (1952) 317.
7. Hardwick, T. J. and Robertson, E. *Can. J. Chem.* **29** (1951) 828.
8. Hardwick, T. J. and Robertson, E. *Can. J. Chem.* **29** (1951) 818.
9. Gryder, J. W. and Dodson, R. W. *J. Am. Chem. Soc.* **73** (1951) 2890.
10. Fronæus, S. and Östman, C. O. *Acta Chem. Scand.* **8** (1954) 961.
11. Pitzer, K. S. *Quantum Chemistry*, Prentice-Hall Inc., New York 1953, p. 300.
12. Vetter, K. J. *Z. Elektrochem.* **59** (1955) 596.
13. Parsons, R. *Trans. Faraday Soc.* **47** (1951) 1332.
14. King, E. L. and Pandow, M. L. *J. Am. Chem. Soc.* **74** (1952) 1966.
15. Fischbeck, K. *Z. Elektrochem.* **39** (1933) 316.
16. Frank-Kamenetskii, D. A. *Diffusion and Heat Exchange in Chemical Kinetics*, Princeton University Press, Princeton, New Jersey 1955, p. 49.
17. Fronaæs, S. *Acta Chem. Scand.* **8** (1954) 412.
18. Fronæus, S. and Östman, C. O. *Acta Chem. Scand.* **9** (1955) 902.
19. Brunner, E. *Z. physik. Chem.* **47** (1904) 56.
20. Heidt, L. J. and Smith, M. E. *J. Am. Chem. Soc.* **70** (1948) 2476.
21. Kolp, D. and Thomas, H. C. *J. Am. Chem. Soc.* **71** (1949) 3047.

Received February 28, 1956.

ACTA CHEMICA SCANDINAVICA 10 (1956) 779—792

Studies on the Hydrolysis of Metal Ions

XV. Partition Equilibria in the System ^{114}In/TTA/benzene

F. J. C. ROSSOTTI and HAZEL ROSSOTTI

Department of Inorganic Chemistry, the Royal Institute of Technology, Stockholm 70, Sweden *

The mononuclear hydrolysis constants of indium have been determined by studying the distribution of tracer concentrations of the indium-TTA complex, InL_3, between benzene and aqueous 3M (sodium) perchlorate solutions at 25° C. When allowance was made for TTA complexes in the aqueous phase, the data could be approximately explained in terms of the single hydroxo-complex $In(OH)_2^+$. However, agreement is improved by also taking into account the first hydrolysis product, $InOH^{2+}$. The best values of the hydrolysis constants so obtained

$$\varkappa_1 = [InOH^{2+}]\,[H^+] / [In^{3+}] = 10^{-4.4}$$

$$\varkappa_2 = [In(OH)_2^+][H^+]^2 / [In^{3+}] = 10^{-8.8}$$

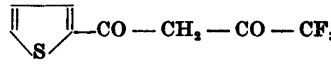
are in very satisfactory agreement with those obtained potentiometrically by Biedermann [7].

Although the potentiometric method is the most accurate for studying the hydrolysis of metal ions, it can only be used for total concentrations of metal between 10^{-1} M and 10^{-3} or 10^{-4} M. Since many metal ions form predominantly polynuclear hydrolysis products in this concentration range [1,2], it may be difficult, or even impossible, to obtain reliable values of mononuclear hydrolysis constants from potentiometric measurements.

A number of stability constants have recently been measured by studying the influence of a secondary ligand on the distribution of a metal chelate between an organic and an aqueous phase. Since the partition equilibria may often be followed radiometrically using tracer concentrations of metal, the method would seem to be suitable for the determination of mononuclear hydrolysis constants. Although the effect of hydrogen ion concentration on the partition of *e. g.* 2-thenoyltrifluoroacetone (TTA, I) complexes of zirconium [3,4], thorium [5] and neptunium (IV) [6] has led to qualitative deductions about the hydrolysis of these ions, no hydrolysis constants were calculated.

* Present address: Department of Chemistry, University of Edinburgh, Scotland.

The possibility of using the method to determine mononuclear hydrolysis constants was therefore tested by studying the ^{114}In / TTA / benzene system under the same conditions as were used by Biedermann [7] in his potentiometric investigation.



I.

LIST OF SYMBOLS

a	number of hydrogen atoms in the species $H_aInL_n^{(3+a-n)+}$, $(n>1)$; negative values refer to hydroxyl groups
A	value of a for complex in organic phase
$\overline{A}$	mean value of A
C_I	initial concentration of TTA in benzene
C_M	initial concentration of indium in aqueous phase
E	measured potential in mV
E_o	$= E - 16.5\ h - 59.16 \log h$ (equation 4)
f_p	$= \varkappa_p + \sum_{n=1} K_{n-p,n} L^n$ (equation 22)
h	concentration of free hydrogen ions
J	$= \sum_{a \gtrless 0} \sum_{n=1} K_{a,n} h^{a-n} L^n$ (equation 17)
k	equilibrium constant for the reaction $H^+ + L^- \rightleftharpoons HL$
$K_{a,n}$	$= \beta_{a,n} k^{-n} (P_{HL} + 1)^{-n}$ (equation 9)
K_w	ionic product of water
l	concentration of free L^- ions in the aqueous phase
L	sum of concentrations of uncomplexed TTA in both phases (equations 6 and 7)
M	mole / l
n	number of TTA groups in species $H_aInL_n^{(3+a-n)+}$ (> 1)
$\overline{n}$	mean value of n
N	value of n for complex in organic phase
$\overline{N}$	mean value of N
p	number of hydroxyl groups in species $In(OH)_p^{(3-p)+}$
$P_{A,N}$	partition coefficient, $[H_AInL_N]_o$ / $[H_AInL_N]$
P_{HL}	partition coefficient $[HL]_o$ / $[HL]$
q	distribution ratio of indium (equations 3 and 5)
R	counting rate of equilibrated aqueous phase
R_i	counting rate of initial aqueous phase
R_o	counting rate of equilibrated organic phase
X	normalised log h, defined by equations (14) and 14a)
y, y_0, y'	defined by equations (12), (13) and (20)
Y	normalised y, y_0 and y', defined by equations (15) and (15a)
$\beta_{a,n}$	equilibrium constant for the reaction $aH^+ + In^{3+} + nL^- \rightleftharpoons H_aInL_n^{(3+a-n)+}$
$\varkappa_p$	equilibrium constant for the reaction $In^{3+} + pH_2O \rightleftharpoons In(OH)_p^{(3-p)+} + pH^+$
K_p	equilibrium constant for the reaction $In(OH)_{p-1}^{(4-p)+} + OH^- \rightleftharpoons In(OH)_p^{(3-p)+}$
Λ	radiometric absorption ratio (equation 2)
τ	$\varkappa_1 \cdot \varkappa_2^{-\frac{1}{2}}$ (equation 16) or $f_1 \cdot f_2^{-\frac{1}{2}}$ (equation 16a)
[ ]	equilibrium concentration in aqueous phase
[ ]$_o$	equilibrium concentration in organic phase

All species may be combined with sodium or perchlorate ions, or with molecules of benzene or water. Concentrations and equilibrium constants will be expressed using the molar scale.

METHOD

The variation of the distribution ratio

$$q = \frac{\text{total concentration of indium in organic phase}}{\text{total concentration of indium in aqueous phase}}$$

with the concentration, h, of free hydrogen ions was studied at 25° C for a number of initial concentrations of TTA (C_L) in benzene and of indium (C_M) in the aqueous phase in the range $-2.7 > \log h > -4.5$, $-2.3 > \log C_L > -3.0$ and $-5.24 > \log C_M > -5.65$. The aqueous phase was made 3 M with respect to the perchlorate ion, by the addition of sodium perchlorate. Since the combined concentrations of indium, hydrogen and ligand ions never exceeded 0.1 % of the concentration of perchlorate ions, the activity coefficients of all species in the aqueous phase may be assumed to remain constant [8]. King and Reas [9] have shown that the activity coefficient of TTA in benzene is effectively constant if $C_L \leq 10^{-2}$ M. Huffman and Iddings [10] have found that the solubility (and hence the activity coefficient) of the uncharged TTA complex of zirconium in benzene is independent of C_L if $C_L \leq 0.08$ M, and it is probable that the activity coefficient of the corresponding indium complex in benzene is also constant in the ranges of concentration studied. Thus it may be assumed that there is no variation of activity coefficients in either phase, and that true stoichiometric equilibrium constants may be calculated from the partition measurements.

The distribution ratio, q, was obtained radiometrically, using ^{114}In. Since equal phase volumes were used throughout, and no volume changes occurred on equilibration,

$$q = \Lambda R_o / R \qquad (1)$$

where R_o and R are the counting rates of the equilibrated organic and aqueous phases, and

$$\Lambda = \frac{\text{absorption of } ^{114}\text{In radiation in benzene}}{\text{absorption of } ^{114}\text{In radiation in 3M } NaClO_4}$$

Assuming 100 % mass balance

$$\Lambda = (R_i - R) / R_o \qquad (2)$$

(*cf.* Ref.[11]) where R_i is the counting rate of the initial aqueous phase, and the initial organic phase is not radioactive. Values of q and Λ were calculated from the measured values of R_i, R_o and R, using the relationship

$$q = (R_i - R) / R \qquad (3)$$

and eqn. (2). The standard deviation in the value of Λ is a measure of the standard deviation in the overall mass balance (*cf.* p. 783).

The equilibrium hydrogen ion concentration in the aqueous phase was obtained using a glass electrode in combination with the half-cell

$$RE = Ag \,/\, 0.01 \text{ M } AgClO_4,\ 2.99 \text{ M } NaClO_4 \,/\, 3 \text{ M } NaClO_4$$

For the cell

$$RE \,/\, h \text{ M } HClO_4,\ (3 - h) \text{ M } NaClO_4 \,/\, \text{Glass} \qquad 25° \text{ C}$$

Table 1. Log q *as a function of log* h.

$C_L = 10^{-3}$ M				$C_L = 2 \times 10^{-3}$ M, $C_M = 4.46 \times 10^{-6}$ M			$C_L = 3 \times 10^{-3}$ M, $C_M = 4.46 \times 10^{-6}$ M			$C_L = 5 \times 10^{-3}$ M, $C_M = 2.67 \times 10^{-6}$ M		
-log *h*	log *q*	$C_M \times 10^6$	-*y'*	-log *h*	log *q*	-*y'*	-log *h*	log *q*	-*y'*	-log *h*	log *q*	-*y'*
3.090	—2.39	5.34	2.66	2.914	—1.93	2.57	2.880	—1.51	2.58	2.681	—1.46	2.60
3.110	—2.32	2.67	2.64	3.210	—1.13	2.66	3.071	—1.02	2.67	2.830	—1.08	2.66
3.142	—2.13	4.46	2.55	3.412	—0.47	2.61	3.294	—0.34	2.65	3.002	—0.51	2.67
3.280	—1.76	2.67	2.60	3.546	—0.13	2.66	3.440	0.08	2.67	3.022	—0.48	2.64
3.288	—1.64	4.46	2.50	3.673	0.17	2.74	3.580	0.59	2.57	3.059	—0.39	2.66
3.413	—1.36	4.46	2.60	3.758	0.38	2.79	3.734	0.87	2.75	3.085	—0.33	2.67
3.428	—1.30	5.76	2.59	3.903	0.81	2.79	3.781	0.98	2.78	3.254	0.20	2.63
3.489	—1.12	2.67	2.59	4.042	1.09	2.95	3.866	1.29	2.72	3.494	0.86	2.66
3.534	—1.11	4.46	2.71	4.170	1.54	2.84	3.974	1.49	2.71	3.673	1.30	2.71
3.580	—0.80	4.46	2.53	4.386	1.97	3.06	3.979	1.47	2.88	3.846	1.71	2.72
3.660	—0.70	5.76	2.67	4.491	2.14	3.20	4.065	1.61	3.00	3.860	1.71	2.78
3.714	—0.57	4.46	2.70	4.552	2.28	3.23	4.144	1.84	3.00	4.079	2.02	3.06
3.748	—0.50	5.73	2.73				4.232	2.12	2.97	4.084	2.09	2.96
3.756	—0.39	2.67	2.65	$C_L = 4 \times 10^{-3}$ M, $C_M = 4.46 \times 10^{-6}$ M			4.336	2.29	3.10	4.324	2.39	2.67
3.800	—0.32	4.46	2.70							$C_L = 5 \times 10^{-3}$ M, $C_M = 4.46 \times 10^{-6}$ M		
3.801	—0.22	5.34	2.60	-log *h*	log *q*	-*y'*						
3.906	—0.02	2.67	2.72							-log *h*	log *q*	-*y'*
3.969	0.22	4.46	2.66	2.879	—1.11	2.55						
3.970	0.15	2.67	2.74	3.308	0.24	2.56						
4.040	0.18	4.46	2.91	3.403	0.41	2.58				2.956	—0.72	2.66
4.119	0.50	2.23	2.82	3.874	1.53	2.76				3.229	0.11	2.66
4.130	0.47	5.76	2.87	4.184	2.28	2.75				3.446	0.74	2.65
4.192	0.58	5.73	2.95	4.300	2.42	3.06				3.702	1.37	2.71
4.232	0.86	2.23	2.89							4.050	1.99	3.00
4.320	0.96	5.73	2.92							4.091	2.12	2.92
										4.268	2.40	2.99
										4.298	2.45	2.98

the relationship between the measured potential, E (in mV), and the concentration of free hydrogen ions is given by

$$E = E_0 + 16.5\ h + 59.16 \log h \qquad (4)$$

where the term E_0 includes the standard potentials of the electrodes and the asymmetry potential of the glass electrode. The term 16.5 h represents the liquid junction potential [12]. Before each measurement, the glass electrode was immersed in two standard solutions of perchloric acid ($h = 0.231$ M and $h = 0.023$ M); the two values of E_0 which were calculated from the measured potentials by means of equation (4) always agreed within 0.1 mV. The distribution experiments were carried out at such low acidities ($h < 0.002$ M) that $E_0 \gg 16.5\ h$, and log h could be directly calculated from the expression

$$\log h = (E - E_0) / 59.16 \qquad (4a)$$

The partition measurements are given in Table 1, and are plotted in the form log q $(\log h)_{C_L}$ in Fig. 1.

EXPERIMENTAL DETAILS

Indium perchlorate. Indium—114 (half-life 49 days) was obtained by irradiation of a known weight of "Specpure" indium wire (Johnson Matthey, Ltd.) at A.E.R.E., Harwell. The irradiated wire was dissolved in warm 3M perchloric acid, to which a drop of hydrogen peroxide had been added to prevent the formation of chloride or chlorate ions [13]. The solution was boiled to decompose the excess of hydrogen peroxide, cooled, and diluted to a known volume.

Solutions of *sodium hydroxide, perchloric acid, sodium perchlorate* and *silver perchlorate* were prepared and standardised as described elsewhere [12, 14].

TTA. The reagent obtained from Dow Chemical Company was not purified further, as the melting point (43.5° C) was the same as that given by Day and Powers [5]. Known weights of the solid were dissolved in benzene (Merck *p. a.*) which had been presaturated with aqueous 3 M perchlorate. This ensured that the equilibrium concentration ($\sim$ 10 %) of the keto-hydrate was present [16] and reduced the time required for partition equilibrium. The solutions were stored in the dark, over a small volume of 3 M perchlorate to remove any traces of trifluoroacetic acid formed by decomposition of the TTA.

Apparatus

The radioactivity was assayed using a 20th. Century Electronics Ltd. M6 liquid counter, in conjunction with a Tracerlab scalar.

The hydrogen ion concentrations were measured in a 25 ml beaker, using a Radiometer glass electrode (type G 202 B), which had been tested as described before [14]. The reference half-cell, RE, and the valve potentiometer, were the same as used in previous work [14].

Procedure

The equilibrations and measurements were carried out in a room thermostated at 25° $\pm$ 1° C. All aqueous solutions were made 3 M with respect to the perchlorate ion by the addition of sodium perchlorate, and were presaturated with benzene.

For each distribution experiment, a known volume of a solution of radioactive indium perchlorate ($\sim 1.6 \times 10^{-5}$ M) in perchloric acid ($\sim 2 \times 10^{-4}$ M) was diluted to 25.0 ml, using sufficient perchloric acid ($\sim 1.5 \times 10^{-2}$ M) or sodium hydroxide ($\sim 2 \times 10^{-4}$ M) to give the required hydrogen ion concentration. 15.0 ml of this solution, and 15.0 ml of a solution of TTA (concentration C_L) in benzene were pipetted into a 50 ml centrifuge tube. The remaining initial aqueous solution was acidified with one drop of concentrated perchloric acid to prevent adsorption losses on the glass. The centrifuge tube was closed with a ground glass stopper, which was wetted with a solution of collodion in ether and placed firmly in position. The tube was shaken mechanically at 30 revolutions per minute for 16 hours, which had been shown to be sufficient for equilibration, even at the lowest acidities studied ($\log h \sim -4.5$). After centrifugation, the two phases were carefully separated by pipetting.

10 ml portions of the initial aqueous solution, and of the two equilibrated phases, were assayed radiometrically. The counting rates were corrected for the background activity ($\sim$ 15 counts min.$^{-1}$). Correction for the paralysis time of the counting assembly was found to be unnecessary at the counting rates used ($\leqslant$ 10 000 counts min.$^{-1}$) and no correction was needed for the decay of the 49-day indium, as aliquots from any one experiment were assayed consecutively. Whenever possible, the duration of the counting was chosen to give a standard deviation of $\pm$ 1 %. The mean value of the absorption ratio, A, was calculated using eqn. (2) and found to be 0.90; the standard deviation in this value, and hence in the overall mass balance (including statistical variations, and fluctuations in the counting efficiency), was $\pm$ 6.3 %.

The hydrogen ion concentration in the aqueous phase was determined after the radioactivity of the solution had been measured.

At values of $\log h < -4.5$, or of $\log C_L < -3.0$, low mass balances ($\leqslant$ 80 %, assuming $A = 0.90$) were obtained, and it is possible that some invisible precipitate was present. When $\log h \leqslant -5$, a visible precipitate collected at the phase boundary.

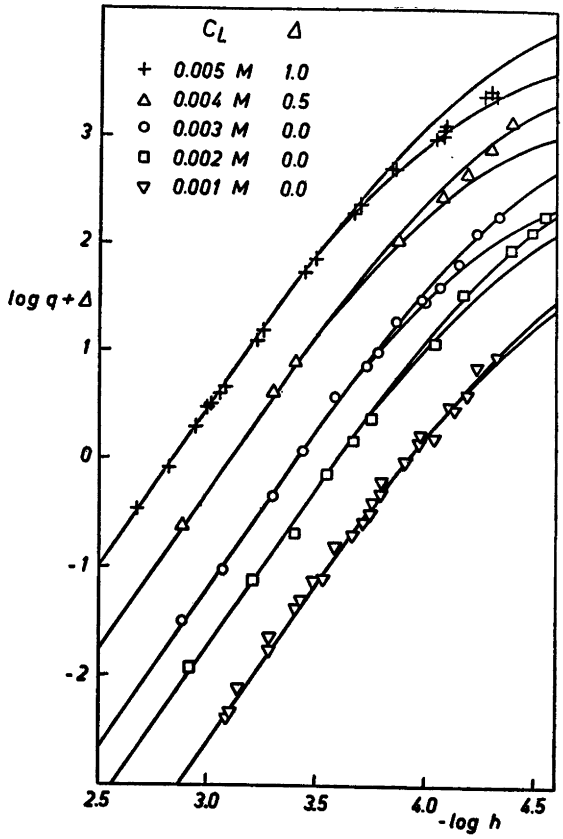


Fig. 1. Log q *as a function of log* h. +, △, ○, □ *and* ▽ *are experimental points for different initial concentrations,* C_L, *of TTA; points for different initial concentrations of metal in the range* $-5.24 \leqslant \log C_M \leqslant -5.65$ *are not differentiated. The full curves are calculated for* $\log P_{0,2}K_{0,2} = -2.60$, $\log \varkappa_1 = -4.4$, $\log \varkappa_2 = -8.8$ *and* $\log K_{0,2} = -3.4$ *(upper curves) or* -3.0 *(lower curves).*

INTERPRETATION OF THE DATA

Since the distribution curves shown in Fig. 1 are independent of the total concentration, C_M, of indium, the system is homonuclear; and as $C_M \leqslant 6 \times 10^{-6}$ M, it may be assumed that only mononuclear complexes are present in appreciable amounts. If the species H_AInL_N are present in the organic phase

$$q = \sum_{A \gtrless 0} \sum_{N=1} [H_AInL_N]_o \,/\, \{[In] + \sum_{p=1} [In(OH)_p] + \sum_{a \gtrless 0} \sum_{n=1} [H_aInL_n]\}$$

$$= \sum_{A \gtrless 0} \sum_{N=1} P_{A,N}\beta_{A,N}h^A l^N \,/\, \{1 + \sum_{p=1} \varkappa_p h^{-p} + \sum_{a \gtrless 0} \sum_{n=1} \beta_{a,n} h^a l^n\} \qquad (5)$$

where charges are omitted, and [ ]$_o$ and [ ] refer to concentrations in the organic and aqueous phases respectively; l is the concentration in the aqueous

phase of the anion L derived from TTA (HL), and $P_{A,N}$, $\varkappa_p$ and $\beta_{a,n}$ are defined by

$$P_{A,N} = [H_A InL_N]_o\,[H_A InL_N]^{-1}$$
$$\varkappa_p = [In(OH)_p]h^p\,[In]^{-1}$$
and
$$\beta_{a,n} = [H_a InL_n]\,[In]^{-1}\,h^{-a}l^{-n}$$

Values of a and A will be negative for mixed TTA-hydroxo-complexes.

For equal volumes of the phases at equilibrium, the sum of the concentrations of uncomplexed TTA in both phases is given by

$$L = C_L - \sum_{A \gtrless 0} \sum_{N=1} N[H_A InL_N] - \sum_{a \gtrless 0} \sum_{n=1} n[H_a InL_n] \quad (6)$$

As the last term is negligible compared with C_L under the experimental conditions used (see p. 788)

$$L = C_L - \overline{N}[H_{\overline{A}} InL_{\overline{N}}]_o = C_L - \overline{N}C_M q(q+1)^{-1} \quad (6a)$$

where $\overline{A}$ and $\overline{N}$ are the average numbers of hydrogen and TTA groups attached to each indium ion in the organic phase. In this work, $\overline{N}[H_{\overline{A}} InL_{\overline{N}}]_o \leqslant 0.02\,C_L$. Now

$$L = [HL]_o + [HL] + l = l\{kh(P_{HL} + 1) + 1\} \quad (7)$$

where
$$k = [HL]h^{-1}l^{-1}$$

and
$$P_{HL} = [HL]_o\,[HL]^{-1}$$

If $k \sim 10^6$ (Ref.[3]) and $P_{HL} \sim 40$ (Ref.[9]), then $kh(P_{HL}+1) \gg 1$ at values of $h > 10^{-5}$ M, and

$$l = L\,/\,kh(P_{HL}+1) \quad (7a)$$

Combining eqns. (5) and (7a)

$$q = \sum_{A \gtrless 0} \sum_{N=1} P_{A,N}K_{A,N}h^{A-N}L^N\,/\,\{1 + \sum_{p=1} \varkappa_p\,h^{-p} + \sum_{a \gtrless 0} \sum_{n=1} K_{a,n}\,h^{a-n}L^n\} \quad (8)$$

where
$$K_{a,n} = \beta_{a,n}\,k^{-n}(P_{HL}+1)^{-n} \quad (9)$$

At high acidities, no indium complexes will be formed in the aqueous phase, and moreover, $L \to C_L$; then [3,17]

$$\lim_{h \to \infty} (\partial \log q\,/\,\partial \log h)_{C_L} = \overline{A} - \overline{N} \quad (10)$$

$$\lim_{h \to \infty} (\partial \log q\,/\,\partial \log C_L)_h = \overline{N} \quad (11)$$

From the data $\log q$ $(\log h)_{C_L}$ shown in Fig. 1, it was found that $\overline{A}-\overline{N} = -3.0$. Values of $\log q$ at given values of $\log h$ were interpolated from Fig. 1, and the function $\log q$ $(\log C_L)_h$ is plotted in Fig. 2; whence a value of $\overline{N} = 3.0$ was obtained.

Since $\overline{A} = 0.0$ and $\overline{N} = 3.0$, InL_3 is the sole species extracted, and the function

$$y = \log q - 3\log L + 3\log h = \log P_{0,3}K_{0,3} - \log\{1 + \sum_{p=1} \varkappa_p\,h^{-p} + \sum_{a \gtrless 0} \sum_{n=1} K_{a,n}h^{a-n}L^n\} \quad (12)$$

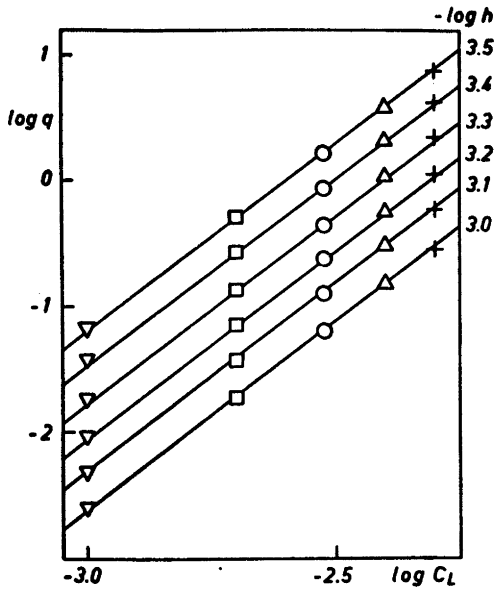


Fig. 2. Interpolated values of log q *as a function of log* C_L *for different values of log* h, *together with the best straight lines of slope 3.0. The symbols are those used in Fig. 1.*

derived from eqn. (8) will have a constant value, log $P_{0,3}K_{0,3}$, if all the metal in the aqueous phase is in the form of free indium ions. If hydroxo-complexes, but no TTA complexes, are present, y will be a function of h only, and independent of L, while if TTA complexes are formed, y will be a function of both h and L.

At hydrogen ion concentrations $> 7 \times 10^{-4}$ M, y is constant (-2.60 ± 0.03) within the experimental error, confirming that InL_3 is the species extracted. At lower acidities, the curves y (log $h)_{C_L}$ are not coincident, indicating that TTA complexes are formed in the aqueous phase. Approximate values of the hydrolysis constants, $\varkappa_p$, may be obtained by extrapolating the term y to zero concentration of TTA, and used to calculate preliminary values of the constants $K_{a,n}$; both sets of constants may then be refined by successive approximations, using eqn. (12).

Preliminary values of the hydrolysis constants. Smooth curves were drawn through the points y(log $h)_{C_L}$ and, for each value of C_L, values of y were interpolated at a number of values of h. Curves y $(C_L)_h$ were then plotted, and extrapolated to $C_L = 0$ to give values of

$$y_0 = \log P_{0,3}K_{0,3} - \log \{1 + \sum_{p=1} \varkappa_p h^{-p}\} \qquad (13)$$

which are given in Table 2 and Fig. 4. The extrapolated function y_0(log h) lies only slightly above the points y (log h) for $C_L = 10^{-3}$ M.

Table 2. Values of y_0 as a function of log h.

-log h	3.50	3.60	3.70	3.80	3.90	4.00	4.10	4.20	4.30	4.40	4.50
$-y_0 \pm 0.04$	2.59	2.63	2.64	2.69	2.74	2.78	2.84	2.89	2.96	3.02	3.13

If the uncharged complex $In(OH)_3$ is not present in appreciable amounts, preliminary values of the hydrolysis constants $\varkappa_1$ and $\varkappa_2$ may conveniently be obtained by superimposing the family of theoretical curves [18] $Y(X)_\tau$ on the extrapolated function $y_0(\log h)$. The normalised variables X and Y are given by

$$X = \log h - \tfrac{1}{2} \log \varkappa_2 \qquad (14)$$

$$Y = y_0 - \log P_{0,3}K_{0,3} = -\log (1 + \tau\, 10^{-X} + 10^{-2X}) \qquad (15)$$

where $$\log \tau = \log \varkappa_1 - \tfrac{1}{2} \log \varkappa_2 \qquad (16)$$

The required value of τ is that used to calculate the theoretical curve of the same shape as the experimental function, and the values of $\log P_{0,3}K_{0,3}$ and $\frac{1}{2} \log \varkappa_2$ are obtained from the corresponding co-ordinates of the theoretical and experimental curves, in the position of best fit (equations 14 and 15). Within the limits of experimental error, the data $y_0(\log h)$ could be described by the curve $Y(X)$ calculated for $\tau = 1$ (see Fig. 4). Thus there is no evidence for the presence of $In(OH)_3$, as would be expected from its low solubility [19]. The best fit was obtained with $\log P_{0,3}K_{0,3} = -2.6$ and $\frac{1}{2} \log \varkappa_2 = -4.45$; whence $\log \varkappa_1 = -4.45$ (eqn. 16) and $\log \varkappa_2 = -8.9$.

Final values of the constants. Substituting the preliminary values of $P_{0,3}K_{0,3}$, $\varkappa_1$ and $\varkappa_2$ into eqn. (12), values of

$$J = P_{0,3}K_{0,3} \cdot 10^{-y} - \{1 + \sum_{p=1} \varkappa_p h^{-p}\} = \sum_{a \gtrless 0} \sum_{n=1} K_{a,n} h^{a-n} L^n \qquad (17)$$

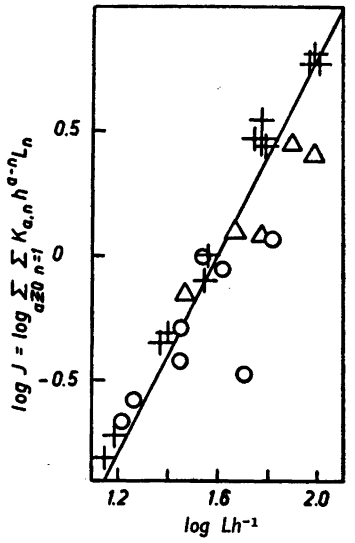


Fig. 3. Log J = log $\sum_{a \gtrless 0} \sum_{n=1} K_{a,n} h^{a-n} L^n$ as a function of log $L\,h^{-1}$. The symbols are those used in fig. 1 and the straight line is of slope 2.0 and of intercept −3.2.

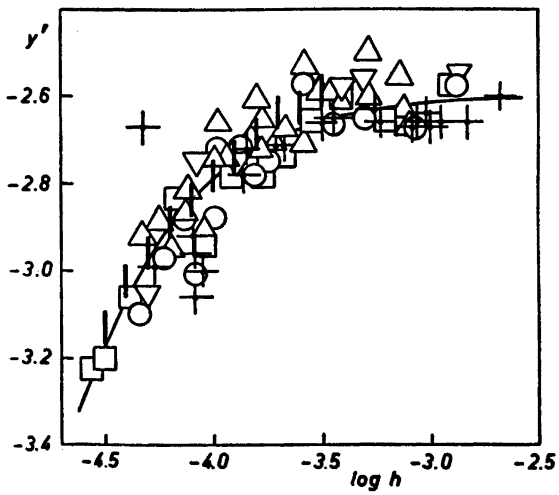


Fig. 4. Values of y′ *(points) and* y_0 *(vertical lines) as a function of log* h. *The symbols are those used in Fig. 1. The full curve is that calculated for log* $\tau = 0$, *in the position corresponding to log* $P_{0,3}K_{0,3} = -2.60$ *and* $\frac{1}{2}$ *log* $\varkappa_2 = -4.4$.

were calculated for each point $y(h,L)$. If the TTA complexes in the aqueous phase are all of the type InL_n (i.e. $a = 0$), J will be a function of Lh^{-1} only, and

$$\mathrm{d}\ \log\ J\ /\ \mathrm{d}\ \log\ Lh^{-1} = \bar{n} \qquad (18)$$

where $\bar{n}$ is the average number of TTA groups in the complex InL_n ($n > 1$). Log J is plotted as a function of log Lh^{-1} in Fig. 3; within the limits of experimental error, the points for $C_L > 3 \times 10^{-3}$ M can be represented by the equation

$$\log\ J = 2\ \log\ Lh^{-1} - 3.2 \pm 0.2 \qquad (19)$$

indicating that InL_2^+ is the predominant TTA complex in the aqueous phase in the range $1.2 < \log\ Lh^{-1} \leqslant 2.0$, and that $\log\ K_{0,2} = -3.2 \pm 0.2$. Thus the assumption that $\sum_{a \gtrless 0} \sum_{n=1} n[H_aInL_n] \ll C_L$ (see p. 785) is justified. If $\log\ k(P_{HL} + 1) \sim 7.8$ (refs.[3,9]), then from eqn. (9) the overall stability constant of InL_2^+, $\beta_{0,2} \sim 12.4$.

Values of

$$y' = \log\{qh^3L^{-3} - P_{0,3}K_{0,3}K_{0,2}^{-1}h^2L^{-2}\} = \log P_{0,3}K_{0,3} - \log\{1 + \sum_{p=1} \varkappa_p\ h^{-p}\} \qquad (20)$$

were calculated for each experimental point $q(h,L)$ using the values of $P_{0,3}K_{0,3}$ and $K_{0,2}$ given above, and are shown in Table 1 and Fig. 4. Within the experimental error (± 0.1 log unit), the function $y'(\log\ h)$ is independent of L, and is coincident with the function $y_0(\log\ h)$ obtained by extrapolation to $L = 0$ (eqn. 13). Thus no refinement of the constants is necessary. The limits of error in $\varkappa_1$, $\varkappa_2$ and $P_{0,3}K_{0,3}$ were obtained by curve-fitting using the set of

normalised $Y(X)_\tau$ curves, as described above. Although the data could be approximately explained in terms of the single hydroxo-complex $In(OH)_2^+$, represented by the curve for $\log \tau = -\infty$ and $\frac{1}{2} \log \varkappa_2 = -4.2$, the agreement is more satisfactory if the first hydroxo-complex, $InOH^{2+}$ is also taken into account. The best fit was obtained with $\log \tau = 0.0 \pm 0.1$ and $\log P_{0,3}K_{0,3} = -2.60 \pm 0.03$; for this case, $\frac{1}{2} \log \varkappa_2 = -4.4 \pm 0.1$.

The step stability constant of the species $In(OH)_p$ is given by

$$K_p = [In(OH)_p][In(OH)_{p-1}]^{-1} [OH]^{-1} = \varkappa_p / \varkappa_{p-1}. K_w \qquad (21)$$

Values of K_p were calculated assuming that the ionic product of water, $K_w = 10^{-14.22}$ in a 3 M (sodium) perchlorate medium [20].

Table 3. Equilibrium constants.

	$\log \varkappa_1$	$\log \varkappa_2$	$\log K_1$	$\log K_2$	$\log P_{0,3}K_{0,3}$
This work	-4.4 ± 0.1	-8.8 ± 0.3	9.8	9.8	-2.60 ± 0.03
Biedermann [7]	-4.42 ± 0.05	-8.3 ± 0.1	9.80	10.3	—

Curves $\log q$ ($\log h)_{C_L}$ were calculated by successive approximations, using eqns. (7) and (12), the values of the equilibrium constants given in Table 3, and the two extreme possible values of $K_{0,2}$. The calculated curves, which are shown in Fig. 1, are in very good agreement with the experimental data.

ALTERNATIVE TREATMENT OF THE DATA

The above interpretation of the data was checked using a method of curve-fitting developed by Sillén [21]. Eqn. (12) may be rewritten

$$y = \log P_{0,3}K_{0,3} - \log \{1 + (\varkappa_1 + K_{0,1}L + K_{1,2}L^2 \cdots)h^{-1} + (\varkappa_2 + K_{-1,1}L + K_{0,2}L^2 \cdots)h^{-2} \cdots\}$$

$$= \log P_{0,3}K_{0,3} - \log \{1 + \sum_{p=1} f_p h^{-p}\} \qquad (12a)$$

where

$$f_p = \varkappa_p + \sum_{n=1} K_{n-p,n}L^n \qquad (22)$$

Provided that $p \leqslant 2$, the parameter $P_{0,3}K_{0,3}$ and the coefficients f_1 and f_2 may be found by comparing the experimental data $y(\log h)_L$ with the family of normalised curves $Y(X)_\tau$. In this case (*cf.* Ref.[18])

$$X = \log h - \tfrac{1}{2} \log f_2 \qquad (14a)$$

$$Y = y - \log P_{0,3}K_{0,3} \qquad (15a)$$

and

$$\log \tau = \log f_1 - \tfrac{1}{2} \log f_2 \qquad (16a)$$

As before, it was found that the value of $\log P_{0,3}K_{0,3}$ (-2.60 ± 0.03) was independent of L, indicating that InL_3 is the extracted species. Since the value of f_1 obtained ($< 10^{-4}$) is independent of L within the experimental error, it may be assumed that this term represents only the first hydrolysis constant

$\varkappa_1$. The term f_2 is a function of L, indicating that at least one indium-TTA complex, $H_{n-2}InL_n$, is present in the aqueous phase. If $n<2$, the function $\log f_2(\log L)$ may also be analysed by curve-fitting [18]. Although the presence of appreciable concentrations of $In(OH)L^+$ cannot definitely be excluded, the variation of f_2 with L may best be explained in terms of the two species $In(OH)_2^+$ ($\log \varkappa_2 = -8.7 \pm 0.3$) and InL_2^+ ($\log K_{0,2} = -3.2 \pm 0.2$). These conclusions are in satisfactory agreement with those reached above.

DISCUSSION

The hydrolysis constants given in Table 3 may be obtained by extrapolating the experimental data to zero concentration of TTA, and are almost independent of any assumption about the nature of the TTA complexes in the aqueous phase. However, from the variation of extraction with the concentration of reagent, it appears that InL_2^+ ($\log K_{0,2} = -3.2 \pm 0.2$, corresponding to $\log \beta_{0,2} \sim 12.4$) is the predominant TTA complex present under the experimental conditions used. No polynuclear complexes could be detected, as would be expected, since the total concentration of metal in the aqueous phase, $C_M(q+1)^{-1}$, never exceeded 3×10^{-6} M in the range $\log h < -3.5$ in which hydrolysis occurs (*cf.* Ref. [7]).

Previous work on the hydrolysis of indium. As the molar fraction of benzene in the aqueous phase was less than 1.8×10^{-3}, the present hydrolysis constants should be strictly comparable with those obtained potentiometrically by Biedermann [7] (see Table 3). The best value of $\varkappa_1$ obtained from the partition data is in excellent agreement with Biedermann's value, and the difference between the two values of $\varkappa_2$ is not surprising in view of the limited accuracy both of the radiometric measurements and of the potentials of indium amalgam electrodes [7] in solutions of indium $\sim 5 \times 10^{-4}$ M.

Earlier work on the hydrolysis of indium was restricted to measurements of the pH of solutions of indium salts at different concentrations. Hepler and Hugus [22] calculated

$$\varkappa_1 = \lim_{C_M \to 0} (C_M - h)\, h^{-2} \sim 10^{-3.9}$$

from Moeller's data for the indium halides [23], and the same value at infinite dilution may also be obtained from Hattox and De Vries' and Moeller's data [24, 25] for indium sulphate. Since the measurements were made in the concentration range where indium forms predominantly polynuclear hydrolysis products [7], this value is probably unreliable. However, a decrease in the hydrolysis constant with increasing ionic strength is in accordance with the extended Debye-Hückel equation, and has also been observed for iron(III) [26] and scandium [27]. The difference in the values of $\log \varkappa_1$ at infinite dilution and in a 3 M perchlorate medium is the same (0.5 log unit) for indium as that reported for iron(III) [26].

Comparison with other trivalent metals. Mattock [2] has shown that the stability constants, K_1, of the hydroxo-complexes often follow the same order as the ratios of the negative heats of hydration, $-\Delta H_{aq}$ of the metal ions, to their characteristic co-ordination numbers, N. The same correlation is valid for the Group III B metals.

	Ga^{3+}	In^{3+}	Tl^{3+}
log K_1 (medium)	11.4 (μ = O) [a]	9.8 (3 M $NaClO_4$)	13.08 (3 M $NaClO_4$) [29]
Δ H_{aq} / N [b]	187.3	165.8	246.0
χ [c]	1.6	1.5	1.9

[a] Ref.[28] and refs. therein [b] values taken from Refs. [30, 31] [c] Ref.[32]

The stabilities of the hydroxo-complexes follow the same order (Tl>Ga>In) as Pritchard and Skinner's "best" values, χ, of the electronegativities [32].

When $P_{HL} \gg 1$ and $\bar{A} = 0$, $P_{A,N}K_{A,N}$ approximates to the extractability constant [33], $\boldsymbol{K} = [MeL_N]_o\,[H]^N / [Me][HL_o^N]$. Although values of $\boldsymbol{K}$ for the extraction of TTA complexes of trivalent metals into benzene have been obtained under different experimental conditions, it seems that indium is extracted less readily than iron(III) and scandium, but more readily than bismuth, aluminium, thallium(III), americium, yttrium, dysprosium, praeseodynium, lanthanum and actinium (Ref[34]. and refs. therein, Refs.[35–37]).

The choice of a chelating ligand for studies of hydrolysis. Although it has been shown that the partition method may be used for quantitative investigation of the hydrolysis of metal ions, the difficulty of obtaining accurate distribution measurements, and the introduction of unknown parameters associated with the extracting reagent, lowers the precision of the hydrolysis constants obtained. Even if a suitable radionuclide is available, the choice of a chelating ligand may be somewhat restricted. In studies of many other types of complexes (*e. g.* if the secondary ligand is the conjugate base of a strong acid, or is an anion which may be added to a strongly acidic solution in the form of the corresponding weak acid) the concentration of the secondary ligand may be varied almost independently of h, and hence of the concentration, l, of chelating ligand; but if the secondary ligand is the hydroxyl ion, its concentration, $K_w h^{-1}$, cannot be varied independently of l (*cf.* eqn. 8). As accurate values of the distribution ratio may only be obtained radiometrically if $2.5 \geqslant \log q \geqslant -2.5$, the reagent and solvent should be chosen so that

$$\log P_{A,N}K_{A,N} = (N - A) \log h - N \log C_L \pm 2.5 \qquad (23)$$

(assuming H_AMeL_N is the only species extracted, *cf.* eqn. 9). If possible, measurements should be made over the whole range of hydrogen ion concentration in which hydrolysis occurs, and also at somewhat higher acidities, so that a reliable value of log $P_{A,N}K_{A,N}$ can be obtained. In order to detect, and correct for, the presence of chelate complexes in the aqueous phase, series of experiments should be carried out using different concentrations of reagent (*cf.* eqn. 12). However, even within the limits imposed by eqn. (23), it is not always desirable to vary this quantity over a very wide range; at high values of C_L, the activity coefficient of the reagent in the organic phase may vary with concentration [9] and at low concentrations such that $C_L < 10\,N\,C_M$, uncertainties in the distribution measurements may result in appreciable uncertainties in the total concentration, L, of the uncomplexed reagent (*cf.* eqn. 7). Thus the TTA / benzene system could not be used to study the polynuclear hydrolysis of indium. A reagent / solvent system for which log $P_{0,3}K_{0,3} \sim -8$ would be

necessary, since measurements would be required for $C_M \leq 5 \times 10^{-2}$ M and $h \leq 10^{-2}$ M (*cf.* Ref. [7]).

We are grateful to Professor Lars Gunnar Sillén for his helpful comments on the manuscript, and to the *Swedish Atomic Energy Commission* and the *Swedish Natural Science Research Council*, for financial assistance.

REFERENCES

1. Sillén, L. G. *Rec. trav. chim.* **75** (1956) 705.
2. Mattock, G. *Acta Chem. Scand.* **8** (1954) 777.
3. Connick, R. E. and McVey, W. H. *J. Am. Chem. Soc.* **71** (1949) 3182.
4. Connick, R. E. and Reas, W. H. *J. Am. Chem. Soc.* **73** (1951) 1171.
5. Zebroski, E. L., Alter, H. W. and Heumann, F. K. *J. Am. Chem. Soc.* **73** (1951) 5646.
6. Sullivan, J. C. and Hindman, J. C. *J. Am. Chem. Soc.* **76** (1954) 5931.
7. Biedermann, G. *Arkiv Kemi* **9** (1956) 271.
8. Biedermann, G. and Sillén, L. G. *Arkiv Kemi* **5** (1953) 425.
9. King, E. L. and Reas, W. H. *J. Am. Chem. Soc.* **73** (1951) 1804.
10. Huffman, E. H. and Iddings, G. M. *U.C.R.L.* 377 (1949).
11. Dyrssen, D. *Svensk Kem. Tidskr.* **65** (1953) 43.
12. Rossotti, F. J. C. and Rossotti, H. S. *Acta Chem. Scand.* **10** (1956) *In the press.*
13. Carleson, B. G. F. and Irving, H. M. *J. Chem. Soc.* **1954** 4390.
14. Rossotti, F. J. C. and Rossotti, H. S. *Acta Chem. Scand.* **9** (1955) 1177.
15. Day, R. A. and Powers, R. M. *J. Am. Chem. Soc.* **76** (1954) 3895.
16. King, E. L. and Reas, W. H. *J. Am. Chem. Soc.* **73** (1951) 1806.
17. Irving, H. M., Rossotti, F. J. C. and Williams, R. J. P. *J. Chem. Soc.* **1955** 1906.
18. Sillén, L. G. *Acta Chem. Scand.* **10** (1956) 186.
19. Moeller, T. *J. Am. Chem. Soc.* **63** (1941) 2625.
20. Frydman, M., Lagerström, G., Sillén, L. G. and Ulfvarson, U. *Unpublished work.*
21. Sillén, L. G. *Acta Chem. Scand.* **10** (1956) 803.
22. Hepler, L. G. and Hugus, Z. Z. *J. Am. Chem. Soc.* **74** (1952) 6115.
23. Moeller, T. *J. Am. Chem. Soc.* **63** (1941) 1206; **64** (1942) 953.
24. Hattox, E. M. and De Vries, T. *J. Am. Chem. Soc.* **58** (1936) 2126.
25. Moeller, T. *J. Phys. Chem.* **45** (1941) 1235.
26. Milburn, R. M. and Vosburgh, W. C. *J. Am. Chem. Soc.* **77** (1955) 1352.
27. Kilpatrick, M. and Pockras, L. *J. Electrochem. Soc.* **101** (1954) 39.
28. Wilson, A. S. and Taube, H. *J. Am. Chem. Soc.* **74** (1952) 3509.
29. Biedermann, G. *Arkiv Kemi* **5** (1953) 441.
30. Quill, L. L. "*Chemistry and Metallurgy of Miscellaneous Materials: Thermodynamics*", McGraw Hill 1950.
31. Bjerrum, J. *Chem. Revs.* **46** (1950) 381.
32. Pritchard, H. O. and Skinner, H. A. *Chem. Revs.* **55** (1955) 745.
33. Kolthoff, I. M. and Sandell, E. B. *J. Am. Chem. Soc.* **63** (1941) 1906.
34. Keenan, T. K. and Suttle, J. F. *J. Am. Chem. Soc.* **76** (1954) 2184.
35. Hagermann, F. *J. Am. Chem. Soc.* **72** (1950) 768.
36. Cornish, F. W. *A. E. R. E. C/R* 891 (1952).
37. Werner, L. B. *AECD* 2729 (1948).

Received March 3, 1956.

ACTA CHEMICA SCANDINAVICA 10 (1956) 793—802

Studies on Apurinic and Reduced Apurinic Acids — the Hydrogen Ion Dissociation Curves

E. HURLEN and S. G. LALAND

Johan Throne Holst's Institutt for Ernæringsforskning, Blindern-Oslo, Norway

and

R. A. COX and A. R. PEACOCKE

Chemistry Department, The University, Edgbaston, Birmingham, England

A method for the reduction of the aldehyde groups in apurinic acid derived from sodium deoxyribonucleate and the chemical and dissociation properties of the reduced apurinic acid are described. Comparison of the titration curves of this material with that of the sodium deoxyribonucleate from which it was derived has enabled the dissociation ranges of the titratable groups in the deoxyribonucleate to be estimated.

Apurinic acid has been obtained from deoxyribonucleic acid by removal of its purine bases but with retention of an unchanged proportion of pyrimidines and has proved to be a useful substance for the study of the chemical structure of the original deoxyribonucleate. When apurinic acid was degraded by alkali [1] a decrease was observed in the intensity of the colour produced in the Dische test, probably because the sugar moieties containing free aldehyde groups were partly destroyed by the alkali. Hence it seemed likely that if the aldehyde groups in apurinic acid could be reduced, a more stable product would result. A suitable reducing agent would have to leave the pyrimidine bases unchanged and preliminary experiments with sodium borohydride showed that it did not reduce thymidine. In the following the reduction of the free aldehyde groups of apurinic acid to primary alcoholic groups by sodium borohydride is described together with the chemical and dissociation properties of the reduced apurinic acid so obtained. The greater stability of this reduced form made it particularly useful for titration purposes. Comparison of the titration curves of the reduced apurinic acid, which contained only thymine and cytosine bases, with those of the parent deoxyribonucleate, which in addition contained adenine and guanine, has enabled the dissociation ranges of the various groups in the deoxyribonucleate to be elucidated.

EXPERIMENTAL

Materials and preparations. Sodium deoxyribonucleate was isolated both from herring and cod roes. The herring sample used in this investigation has been described elsewhere [2] and has also been employed in concurrent titration studies [3,11]. Two samples of apurinic acid were prepared from the herring deoxyribonucleate by treatment with an acidic ion exchange resin, as previously described [4,11]. The first sample (APA—H1) of apurinic acid was isolated as the free acid by drying in the frozen state. A second sample (APA—H2) was first neutralized and isolated as the sodium salt, again by drying in the frozen state. Reduced apurinic acid (RAPA—H2) was then prepared in the form of its sodium salt from APA—H2 and was isolated after dialysis and drying in the frozen state. A second reduced apurinic acid sample (RAPA—C) was similarly obtained from apurinic acid (APA—C) which had been prepared from cod roe deoxyribonucleate by the resin method. Ribonucleoprotein was removed from the cod roes by extraction with 0.14 M sodium chloride solution. Deoxyribonucleoprotein was obtained by extraction with a stronger salt solution (1 M sodium chloride) followed by precipitation with 96 % ethanol. The protein was then removed by the use of chloral hydrate [5]. The sodium deoxyribonucleate was precipitated with ethanol, dissolved in water, dialysed against water and finally dried in the frozen state.

Reduction of apurinic acid. The course of the reduction of apurinic acid by the borohydride was studied in the following way. Apurinic acid (0.1 g of APA—C) was dissolved in distilled water (5 ml) and small amounts (0.05 ml and 0.025 ml) of this solution were withdrawn for use in the Schiff's and Dische test, respectively. Weighed amounts of solid sodium borohydride were then added successively. After each addition the mixture was shaken and half an hour was allowed to elapse before further samples were withdrawn for Dische and Schiff's tests. From these experiments (reported in Fig. 1) the following procedure for reducing apurinic acid was deduced. Apurinic acid (0.052 g of APA—H2) was dissolved in water (2 ml) and sodium borohydride (0.01 g) was added. The mixture was left at room temperature for nearly 4 hours. The absence of aldehyde groups in the product was always confirmed by Schiff's test, since control experiments showed that there was a linear relation between the amount of apurinic acid and the intensity of Schiff's colour. After reduction, the mixture which had a pH of 9 was neutralized with dilute hydrochloric acid and dried in the frozen state. Ethanol (10 ml, 96 %) was added to the white residue and the mixture was left to stand at room temperature for several days. The solid was separated by centrifugation, dried with ether, dissolved in distilled water (20 ml, pH 6.8) and dialysed at 2 °C against distilled water (300 ml). The dialysed solution was dried in the frozen state to yield the reduced apurinic acid (0.038 g). The ultraviolet absorption at 260 mμ of the dialysate indicated that negligible amounts of apurinic acid had passed through the dialysis tubing.

Chromatographic analysis. The purine and pyrimidine contents of the materials under examination were determined by hydrolysis of the samples (5 mg), previously dried at 110° C, with anhydrous trifluoroacetic acid (0.2 ml) [6] at 155° C for 1 hour, separation of the bases on paper chromatograms using *iso*propanol-hydrochloric acid [7] as the solvent system, elution of the spots and corresponding blanks with 0.1 N hydrochloric acid (5 ml) at 37° C for 12 hours, followed by examination of their ultraviolet absorption *. To obtain a more correct ultraviolet absorption of the bases at peak absorption the following formula was used [8]

$$\varepsilon_{net} = \text{net reading of base extinction} = \varepsilon_{\text{Spot at peak of base}} - \left[\varepsilon_{\text{Blank at peak}} \times \frac{\varepsilon_{\text{Base Spot at 320 m}\mu}}{\varepsilon_{\text{Blank at 320 m}\mu}} \right]$$

ε_{net} was used for the calculation of the amounts of bases present in the eluates.

Schiff's test. Schiff's reagent was prepared according to Tobie [8]. To a sample (0.05 ml) of the reduction mixture were added 0.1 N hydrochloric acid (0.05 ml), to destroy

* Eluates of spots and blanks were examined against 0.1 N hydrochloric acid in a Beckman Spectrophotometer DU.

excess borohydride, water (3 ml) and Schiff's reagent (1 ml). The mixture was left at room temperature for 135 minutes and its extinction at 560 mμ was measured in a Coleman spectrophotometer.

Dische test. The reagent was prepared according to Dische [9]. Water (2 ml) containing the material to be tested was heated with Dische reagent (5 ml) in a boiling water bath for 15 minutes. After cooling its extinction at 600 mμ was measured in a Coleman spectrophotometer.

Ultraviolet absorption measurements. The ultraviolet spectra of apurinic and reduced apurinic acid were determined at pH 7.0 in phosphate buffer and at pH 1.0 in 0.1 N hydrochloric acid. The phosphorus contents of the solutions were obtained by analysis according to the method of Jones *et al.*[10]

Titration methods. The procedures used were the same as those employed in parallel studies on the nucleic acids [11]. Solutions of the apurinic or reduced apurinic acids were prepared by dissolving the air-dry samples in sodium chloride (usually 0.05 M) and were titrated at 25 °C with acid and alkali using a cell consisting of a "Doran" Alkacid glass electrode and a saturated calomel electrode connected by a saturated potassium chloride bridge. During the titration hydrogen was passed through the cell in order both to stir the solution and to keep out carbon dioxide. The pH was measured with a Cambridge pH meter, previously standardized with 0.05 M potassium hydrogen phthalate (pH = 4.008) and 0.05 M sodium borate decahydrate (pH = 9.18) to give readings on the "saturated calomel scale" of Hitchcock and Taylor [12]. The determination of pH and of the number of equivalents of acid bound per 4 g-atoms of phosphorus had maximum errors of ± 0.01 and ± 0.03, respectively. "Water corrections" were made by the usual blank titrations.

RESULTS AND DISCUSSION

A. The preparation and properties of reduced apurinic acid

The decrease in Schiff's colour on the addition of increasing amounts of sodium borohydride continued until a total of about 20 mg of this reagent had been added to every 100 mg of apurinic acid (APA—C, Fig. 1). After this no Schiff's colour could be obtained so the aldehyde groups of the apurinic acid must have been completely reduced *. It is noteworthy that addition of 5 % of the total apurinic acid to an acidified reaction mixture could be detected by the Schiff's test. The completion of the reduction was further confirmed by the following tests. Spraying of a solution of *m*-phenylene diamine dihydrochloride on to a spot of the reaction product (400 μg) on filter paper failed to produce any fluorescence [13] in ultraviolet light as it did with apurinic acid, 20 μg of which could be readily detected by this method. Furthermore, Tollen's reagent [14], which could detect 20 μg of apurinic acid, produced a negative result with 500 μg of the reaction product, which must therefore be regarded as reduced apurinic acid. Apurinic acid in amounts of 1 mg is strongly reduced upon heating with Fehling solution. Under corresponding conditions, reduced apurinic gave only a very slight reduction. In quantities of 3 mg there was somewhat more reduction but considerably less than that given by 1 mg apurinic acid. The absence of reducing aldehyde groups is amply demonstrated by the other chemical tests and this latter observation is probably explained by the breakdown at 100° C of the 2-deoxy-D-ribitol moieties to reducing fragments by the very strong alkali in the Fehling solution. This latter view

* We have also reduced apurinic acid prepared by Chargaff's method.

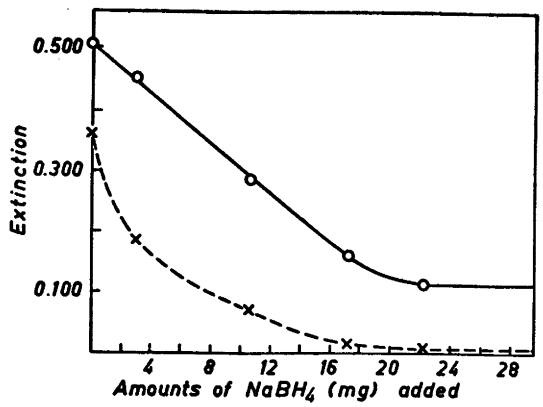


Fig. 1. Reduction of cod roe DNA (APA—C) with $NaBH_4$. The dotted line shows the decrease in the intensity of the colour produced by Schiff's reagent when added after various amounts of $NaBH_4$. The continuous line shows the decrease in the colour produced in the Dische test.

was confirmed by the fact that in a more concentrated Fehlings solution the reduction by reduced apurinic acid was greater.

On reducing apurinic acid (APA—C) there is a drop in the intensity of the colour developed with Dische's reagent. This is seen from Fig. 1 which gives the Dische colour of the reaction mixture following the addition of increasing amounts of reducing agent. It is noticeable that a constant Dische colour is obtained at a point where a negative Schiff's test indicates a complete reduction. The absorption spectrum of the Dische colour produced with reduced apurinic acid is identical with that given by apurinic acid. Comparative values (based on equal amounts of phosphorus) with cod roe sodium deoxyribonucleate, apurinic acid (APA—C) and reduced apurinic acid (RAPA—C) were 100, 83 and 15, respectively.

Chargaff [1] reported that the free aldehydo sugar in apurinic acid was unstable towards alkali, the Dische colour, for example, falling to 7 % of its original value after treatment with 2 N sodium hydroxide at 37° C for 24 hours. The reduction of the aldehydo group renders the sugar moiety stable to alkali for the Dische colour of reduced apurinic acid was almost unchanged after treatment with 2 N sodium hydroxide at 37° C for 24 hours.

Since the reduction of apurinic acid takes place in slightly alkaline solution (pH not above 9) a control experiment was carried out by keeping apurinic acid at room temperature in 0.01 M NaOH. The Dische colour of the solution was tested before and after three days and found to be the same. Thus the very slight alkalinity of the reduction mixture could not have affected the aldehydo sugar in apurinic acid.

The ultraviolet absorption spectra of apurinic and reduced apurinic acid from cod roe deoxyribonucleate are given in Fig. 2. The minima and maxima of absorption occurred at the same wavelengths. In Table 1 are given ε_{268} (P) for the different preparations. These data suggest that the reduction of apurinic acid with sodium borohydride does not affect the pyrimidines. This

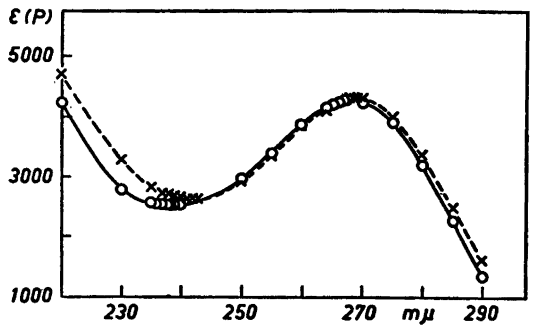


Fig. 2. The ultraviolet absorption spectra of apurinic acid (dotted line) and reduced apurinic acid (drawn line) from cod roe DNA at pH 7.

is further confirmed by the chromatographic analyses, which show no significant difference in cytosine and thymine content between a reduced apurinic acid and the apurinic acid from which it was obtained (*e. g.*, Table 2, 2nd and 4th columns).

B. The dissociation of apurinic and reduced apurinic acids

Typical titration curves in 0.05 M sodium chloride of herring apurinic and reduced apurinic acid are shown in Fig. 3 together with the reversible back titration of the herring sperm deoxyribonucleate from which they were derived [11]. The ordinate represents the acid or alkali bound by a unit amount of these substances containing 4 g-atoms of phosphorus so that, in spite of varying molecular weights, direct comparison between the curves is possible. No titration "anomaly" of the type found with sodium deoxyribonucleate was observed with either the apurinic or reduced apurinic acid, the forward and back titration curves being identical. All hydrogen bonds involving titratable groups must therefore have been ruptured in the course of the preparations.

Comparison of the apurinic and reduced apurinic acids. Comparison of the titration curves of these two substances is best effected by subtracting the alkali bound along the reduced apurinic acid curve (II) from that bound at the same pH's along the apurinic acid curve (I). The resulting comparison curve

Table 1. Ultraviolet absorption of apurinic and reduced apurinic acids. Extinctions (ε_{268}(P)) per g-atom of phosphorus per litre at λ = 268 mμ.

Source	Apurinic acid	Reduced apurinic acid
Cod roes	5 000 (APA—C)	5 100 (RAPA—C)
Herring roes	4 270 (APA—H 2)	4 290 (RAPA—H 2)

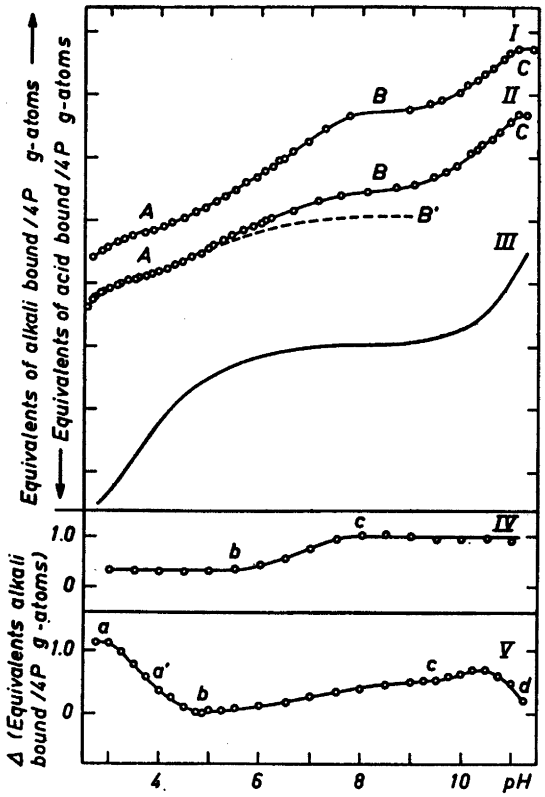


Fig. 3. Titration curves of herring apurinic, reduced apurinic and deoxyribonucleic acids. At 25° C in 0.05 M sodium chloride.

I. Herring apurinic acid (APA—H 2). Circles-experimental points.
II. Herring reduced apurinic acid (RAPA—H 2). Circles-experimental points.
III. Back titration curve of herring sodium deoxyribonucleate (from Ref. 11). Divisions on ordinate scale for curves I, II, III represent one equivalent of acid or alkali bound per 4 P g-atoms. Curves I, II, III separated vertically for clarity. Comparison curves:
IV. Alkali bound by apurinic acid, APA—H 2, along I, minus alkali bound by reduced apurinic acid, RAPA—H 2, along II.
V. Alkali bound by reduced apurinic acid, RAPA—H 2, along II, minus alkali bound by sodium deoxyribonucleate along III.

(IV) shows that only over the pH range 5.5—8.5 (*bc*) is there any significant difference in the number of titratable groups in the two derivatives. The groups titrating in this pH range are secondary phosphoryl end groups ($pK_a' = 6$—7) [15] and cytosine 6-amino groups ($pK_a' = 4.6$ according to Hurst *et al.*[15], but see below where $pK_a' = 5.0$ in 0.05 M salt is suggested). Since the analytical evidence (Table 2) indicates that the cytosine contents (in moles/4 P g-atoms) of apurinic and reduced apurinic acids are almost identical, and

equal to that of the original deoxyribonucleate, the shape of curve IV must be attributed to a larger proportion of titratable end groups in the apurinic acid than in the reduced form. This may well arise because smaller fragments, which would contain a higher proportion of end groups, were removed from the reduced apurinic acid preparation by dialysis but not from the apurinic acid preparation. In confirmation of this some of the APA—H 2 sample did appear to be dialysable after long storage.

The curves I, II and IV therefore show that in the reduction of apurinic acid there has been no structural modification of the molecule which affects the cytosine and thymine components.

Comparison of titration and analytical results. The chromatographic analytical evidence (Table 2) shows that the method of preparation of apurinic acid has entirely eliminated the purine bases, guanine and adenine, from the original nucleate structure, leaving only cytosine and thymine in the same ratio as before. Hence the titration curves I and II of apurinic and reduced apurinic acids must be interpreted in terms of the dissociations of the following groups only: primary phosphoryl groups ($pK_a' = 1—2$) [15]; cytosine 6-amino groups ($pK_a' = 4.6—5.0$, see above); secondary phosphoryl end groups ($pK_a' = 6—7$); and the —NH—CO-systems of thymine ($pK_a' \sim 10$)[15].

Curves I and II (Fig. 3) exhibit inflexion points at A (pH = 3.7), B (pH = 8.5) and an incipient one at C (pH = 11). In view of the evidence given above, the groups titrating in the various regions must be: below pH 3.7, the primary phosphoryl groups only; between pH 3.7 and 8.5 (AB), the cytosine amino groups and secondary phosphoryl groups; and between pH 8.5 and 11 (BC), the —NH—CO-systems of thymine. The difference between the alkali bound at the inflexion points B and C should be equal to the number of thymine

Table 2. Comparison of analytical and titration data. The numbers are the composition in moles or equivs/4 P—g atoms.

Preparation	Herring DNA	RAPA—H 2 [c]		APA—H 2	APA—H 1	
Method	Analysis [b]	Analysis	Titration [d]	Titration[d,e]	Analysis [f]	Titration [g]
Adenine	1.09	0	0	0	0	
Guanine	0.88	0	0	0	0	
Cytosine [a]	0.88	0.88	0.90	0.92	0.85	?
Thymine	1.08	1.07	1.14	1.02	1.06	1.1
Sec. phosphoryl groups			0.40	0.96		0.88

(a) Including 5-methylcytosine
(b) Analysis of Dr. G. E. Marsh (*Thesis*, University of Birmingham 1954)
(c) Prepared from APA—H 2
(d) In 0.05 M NaCl solution
(e) Analysis not available
(f) Analysis by Dr. S. Letham, Chemistry Department, University of Birmingham
(g) In 0.15 M NaCl solution

residues per 4 P g-atoms since there is only one —NH—CO-dissociation in each thymine molecule. The proportion of thymine residues so deduced from the titration curves is in good agreement with that obtained from chromatographic analysis (Table 2) both for the samples whose titration curves are given in Fig. 3 and for APA—Hl, which was titrated in 0.15 M sodium chloride solution.

It has recently been concluded [11,16] that the modern analytical and titration data show evidence for the presence in the original herring sodium deoxyribonucleate of no more than a negligible proportion of secondary phosphoryl end groups. Hence the difference curve (V) between the titration curve of reduced apurinic acid and of the original nucleate in the region of pH 5—8.5 (*bc*) must be entirely due to the (extra) secondary phosphoryl groups in the former. The estimates in Table 2 of the proportion of these end groups were obtained in this way.

If these arguments are valid, the curve (dotted line AB′, Fig. 3) obtained by subtraction of the alkali bound along *bc* of curve V from AB of curve II should be the dissociation curve of the cytosine amino groups in the reduced apurinic acid. The difference in the alkali bound at the inflexion points A and B′ should then be equal to the number of cytosine residues per 4 P g-atoms. The agreement between the amount of cytosine so determined from titration and that given by direct analysis is very satisfactory (Table 2, 2nd and 3rd columns of numbers) and demonstrates the validity of this method of deduction from the titration data.

Comparison of reduced apurinic acid and sodium deoxyribonucleate and the pK_a' *values of the dissociable groups.* Since there is no titration anomaly with the reduced apurinic acid, comparison must be made with the titration curve of non-hydrogen bonded deoxyribonucleate, *i. e.*, with its back titration curve (III). It has already been concluded that in the difference curve V (obtained by subtracting the alkali bound along III from that bound along II) the section *bc* represents the dissociation of the (extra) secondary phosphoryl groups in the reduced apurinic acid. No cytosine amino groups are involved in *bc* since analysis shows the same number of these groups in the two materials (Table 2) and therefore they cancel out in the subtraction which gives V. The section *ab* of V represents extra groups titrating in the deoxyribonucleate which are not present in the reduced apurinic acid and must be attributed to the amino groups of guanine and adenine in the former. The part *a′b* of V must be predominantly the dissociation of the adenine group and, knowing the amount of adenine present the deoxyribonucleate (1.09 moles/4 P g atoms) an estimate of the pK_a' of this group can be made. Similarly, the pK_a' of cytosine 6-amino groups in a polynucleotide can be obtained from AB′ of II, that of secondary phosphoryl groups from bc of IV and V, and that of the thymine —NH—CO-system from BC of II. Reliable values for the pK_a' of the guanine —NH—CO-group cannot be obtained from cd of V since its shape suggests some difference in pK_a' of this group as between curves II and III. The pK_a' values derived for the other groups in 0.05 M sodium chloride are given in Table 3 together with the values of some other authors [15–17]. The pK_a' for the cytosine amino group appears to increase slightly with its degree of dissociation. This may be due to the cumulative errors of the above

Table 3. pK_a' in 0.05 M sodium chloride of the dissociable groups of herring roe deoxyribonucleate. Obtained by comparison with the corresponding reduced apurinic acid.

Degree of acid dissociation of the group in 0.05 M NaCl	pK_a' values			
	Thymine —NH—CO—	Cytosine Amino	Adenine Amino	Secondary Phosphoryl
0.20	10.1	4.95	3.65 (approx.)	6.75 (approx.)
0.30	10.1	4.98		
0.50	10.1	5.10		
0.75	10.1	5.19		
0.80	10.1	5.20		
In deoxyribonucleotides, absence of salt (Ref. 15)	10.0	4.6	4.4	6.5
From analysis of DNA titration curves, at zero ionic strength.[a] (Table 1, Ref. 16)		4.85	3.65	6.0 [b]
From spectrophotometric back titration curves at ionic strength of 0.008 (Table 1, Ref. 17) [c]		5.3		

(a) DNA concentration of 0.139 mgm P/ml = 0.001125 equiv. 4P/l.
(b) By interpolation.
(c) The other figures quoted in Table 1, Ref. 17, refer to the forward titration curve of DNA, which corresponds not to a reversible dissociation but to a simultaneous ionisation and irreversible denaturation.

procedure but, on the other hand, it may also be a genuine decrease of acidity consequent upon the increasing negative charge of the deoxyribonucleate anion. However the change of pK_a' is much less than that observed with synthetic polyacids (*e. g.*, changes [18] of pK_a' of the order of 0.8 units over the degree of dissociation range of Table 3; this relative suppression of the polyelectrolyte effect by the sodium gegenions has been discussed elsewhere [11]). The mean value for the pK_a' of the cytosine amino group (*viz.*, 5.0 in 0.05 M salt) is higher than would have been expected from earlier data [15] and this has important consequences [11, 19] for the interpretation of the deoxyribonucleate titration curve over pH 5.5—9. It accords with the value of 5.3 in 0.008 M salt obtained by spectrophotometric titration of thymus DNA [17]. The values obtained by Jordan *et al.*[16] (and quoted in Table 3 for comparable conditions) are more open to doubt since they depend on an analysis of the back titration curves of thymus DNA where the dissociation ranges of various groups overlap and the allocation of pK_a' values is more ambiguous [3] than in the spectrophotometric method [17], and the method reported here.

C. Conclusion

The titration results indicate that the same proportion of pyrimidine dissociable groups are present in the apurinic and reduced apurinic acid. The reduction of the free aldehyde groups in apurinic acid by sodium borohydride has therefore been effected with no major structural change and has increased the stability of the sugar ring to alkali. The proportion of end groups is relatively high in both derivatives and suggests that considerable degradation has occurred relative to the original deoxyribonucleic acid. The apurinic acid (APA—H2, undialysed) contained 1 secondary phosphoryl group for every 4 phosphorus atoms, which implies that it was on the average about 4 nucleotides long, assuming every fragment carried one secondary phosphoryl group. The reduced apurinic (RAPA—H2, dialysed) contained 1 secondary phosphoryl group every 10 phosphorus atoms, implying an average chain length of 10 nucleotides. These are lower in molecular weight than the apurinic acid obtained by Tamm *et al.* which were thought to contain about 45 nucleotides but whose titration behaviour and end-group content were not obtained *. Any difference may arise not only because different preparative reactions were employed but also because the preparation of Tamm *et al.* was carried out under conditions of continuous dialysis during the acid hydrolysis, thereby concurrently removing all except the larger fragments.

One of us (S. G. L.) wishes to thank the *Rockefeller Foundation* for financial support.

REFERENCES

1. Tamm, C., Hodes, M. E. and Chargaff, E. *J. Biol. Chem.* **195** (1952) 49.
2. Laland, S. G., Lee W. A., Overend, W. A. and Peacocke, A. R. *Biochem. et Biophys. Acta* **14** (1954) 356.
3. Peacocke, A. R. *Proc. Inter. Symp. Macromol. Chem.* Milan-Turin, Sept. 1954; *Ricerca Scientifica* **25** (1955) 812.
4. Laland, S. G. *Acta Chem. Scand.* **8** (1954) 449.
5. Jones, A. S. and Marsh, G. E. *Biochem. et Biophys. Acta* **14** (1954) 559.
6. Jones, A. S. and Stacey, M. *J. Gen. Microbiol.* **4** (1956) 160; Marsh, G. E. *Thesis, University of Birmingham* 1954.
7. Wyatt, G. R. *Biochem. J. London* **48** (1951) 584.
8. Tobie, W. C. *Ind. Eng. Chem. Anal. Ed.* **14** (1942) 405.
9. Dische, Z. *Mikrochemie* **8** (1930) 4.
10. Jones, A. S., Lee, W. A. and Peacocke, A. R. *J. Chem. Soc.* **1951** 623.
11. Cox, R. A. and Peacocke, A. R. *J. Chem. Soc.* **1956** 2499.
12. Hitchcock, D. I. and Taylor, A. C. *J. Am. Chem. Soc.* **59** (1937) 1812.
13. Chargaff, E., Levine, C. and Green, C. *J. Biol. Chem.* **175** (1948) 67.
14. Porter, C. W. and Stewart, T. D. *Organic Chemistry for the Laboratory* Gehm & Co., Boston 1943, p. 216.
15. Hurst, R. O., Marko, A. M. and Butler, C. G. *J. Biol. Chem.* **204** (1953) 847.
16. Jordan, D. O., Mathieson, A. R. and Matty, S. *J. Chem. Soc.* **1956** 158.
17. Cavalieri, L. F. and Stone, A. L. *J. Am. Chem. Soc.* **77** (1955) 6499.
18. Katchalsky, A., *et al. J. Polymer Sci.* **13** (1954) 69.
19. Cox, R. A. and Peacocke, A. R. *Informal Conference on Nucleic Acids*, Culoz, France, July 1955.

Received March 1, 1956.

* *Note added in proof.* We have now titrated APA prepared from herring roe DNA using the method of Tamm *et al.*[1] The titration curve was identical with that of RAPA-H2 between pH 2.6-9. Hence the number of secondary phosphoryl groups in RAPA-H2 and the APA prepared by the method of Tamm *et al.*[1] must be identical, which means the number average chain length must be the same.

ACTA CHEMICA SCANDINAVICA 10 (1956) 803—811

Some Graphical Methods for Determining Equilibrium Constants. IV. On Methods for Three-Variable Data $w(x, y)$

LARS GUNNAR SILLÉN

Department of Inorganic Chemistry, Royal Institute of Technology, Stockholm 70, Sweden

The treatment in part II [1] is extended to indicate graphical methods of determining a number of unknown constants (parameters) $p_1, p_2 \ldots$ from a set of three-variable data (w, x, y) when the function $w(x, y, p_1, p_2 \ldots)$ is known.

Sometimes, by transformation of variables a true reduction to a two-variable problem is possible. In other cases the function can be transformed to $w(x, f_1(y), f_2(y) \ldots)$. By considering sections at constant values of y, the parameters may then be found by two successive two-variable treatments. The method is illustrated by application to extraction equilibria of complexes of the general formula $B(HA)_p(H)_{-n}$.

When a reduction to two variables is not possible, methods of "surface-fitting" may be applied, if the parameters can be eliminated by normalizing the variables. For instance, with two variables and two parameters one may fit a calculated projection map $Y(X)_w$ to an experimental projection map $y(x)_w$. Convenient normalized variables are given for a system with species B, AB, and A_PB_Q, as an example.

Applications will be given in following papers on hydrolysis equilibria.

In part II of this series [1] various ways were discussed of treating two-variable experimental data, *i. e.* data that can be represented by a planar diagram $y(x)$, where y and x are functions that can be obtained directly from the experimental data.

More complicated cases arise if the experimental points are sets of three variables. For example, in the study of polynuclear complexes formed between two reagents A and B, the average number of A bound per B, Z, is often measured together with a, the concentration of free A, and B, the total concentration of B, so that each experimental point is a set (Z, a, B). The data can thus be represented by a curved surface in three-dimensional space, $Z(a, B)$.

We shall consider a general case where the variables determined experimentally are w, x, and y (we shall not use the symbol z to avoid confusion with Z), and the constants to be determined (parameters) are denoted by p_1, p_2 ... . We know in advance the function

$$w = w(x,\ y,\ p_1,\ p_2 \ldots) \tag{1}$$

relating the experimental variables with the parameters. As in part II, w, x, and y need not be the quantities directly determined, although it should be possible to calculate them from the data; nor need the p_i be the constants ultimately required. The most suitable functions w, x, y and parameters p_i for each case may not be immediately obvious.

SYMBOLS

a, b	concentrations of free A and B
B	total concentration of B
c	concentration of free HA (5)
f_i, f_n	functions (2), (8)
h	concentration of H^+ (5)
j	constant (16)
K_{pn}, K_{11}, K_{PQ}	equilibrium constants (3), (12)
L_{pN}	distribution constants (4)
N	charge of metal ion B^{N+}
n, p, P, Q	integer numbers (3), (12)
p_1, p_2, p_3	unknown constants (parameters) to be determined
q	over-all distribution ratio of B between organic and aqueous phase
u, v	auxiliary functions (15), (16)
w, x, y	variables determined experimentally
W, X, Y	normalized values for w, x, y
x_0, y_0	values for x and y coinciding with $X = 0$, $Y = 0$ at best fit (18, 19)
Z	average number of A bound per B

subscript)$_x$ indicates that x is constant

REDUCTION TO A TWO-VARIABLE PROBLEM

True reduction

In some cases an analysis of the data shows that one may definitely reduce the problem to one with only two variables. Three simple examples will be given.

In the formation of mononuclear complexes A_nB by a central group B and a ligand A, the experimental variables may be, for instance, (Z, a, B) or (a, b, B). Now, if only mononuclear complexes are formed, it is easily shown (N. Bjerrum [2]) that both Z and bB^{-1} are functions of a only. (Also for "homonuclear" complexes [3] Z (but not bB^{-1}) is a function of a only.) So the total concentration B is eliminated, and we are left with the two-variable problem of finding the equilibrium constants from the functions $Z(a)$ or bB^{-1} (a). For refined mathematical treatment, further transformations of the variables are usually necessary [1,4].

If, again, all complexes formed are polynuclear and can be written in the "core + links" form, $B(A_tB)_n$, then Z and bB^{-1} can be written [3,5] as functions of the single variable $x = t \log a + \log B$.

Another example is the distribution of a metal ion B, between an aqueous solution and an organic solvent, in the presence of an acid HA, forming complexes like A_nB. We shall denote by q the ratio between the total concentrations of B in the organic and aqueous phases. One might first consider this as a problem of four variables, say q (the distribution ratio), B (the total concentration of B in the aqueous phase), and the concentrations of free H^+ and HA in the aqueous phase. If only mononuclear complexes are formed, the total concentration B should, however, have no influence on $q([H^+], [HA])$. If, moreover, all complexes in the aqueous phase are of the form A_nB and only the uncharged A_NB is extracted, then q should be a function of the concentration of free A only, $a = [A] = [HA][H^+]^{-1}K_a$, so that we really have the two-variable problem [6,7] of studying $q(a)$. If, on the other hand, not A_NB but a single complex $A_NB(HA)_{p-N}$ is extracted, then $q[HA]^{N-p}$ is a function of a only.

For each of these cases, one may apply the methods for two-variable data given in part II [1].

Reduction to two-variable sections

Sometimes it proves impossible by any transformation, truly to reduce three-variable data (w, x, y) to two variables. However one may cut sections at constant values of y (say) and treat each of these as a two-variable problem. Suppose that we can transform equation (1) to the form

$$w = w(x, f_1(y), f_2(y), \ldots) \tag{2}$$

where the functions $f_i(y)$ contain the variable y, and usually a number of unknown constants. If a section $w(x)_y$ at a constant value of y is considered, the functions f_i are constants, which can be found by some method for two-variable problems given in part II[1]. Thus one may determine the values of f_1, f_2 *etc.* for a number of values of y. Finally, the functions $f_i(y)$ are treated separately; each of these functions contains one or more parameters, which can now be determined by some two-variable method.

As an example, we shall consider a case previously treated somewhat differently by Rydberg [8]. A metal ion B is distributed between an aqueous solution and an organic solvent, in the presence of an acid HA, which may form complexes with B. All those complexes present may be written in the form $B(HA)_p(H)_{-n}$, since their content of organic solvent, water or ions from the ionic medium cannot be determined by equilibrium measurements. (We replace Rydberg's symbols x and y by p and n to avoid confusion in the present paper.)

If the charge of the ion B is N^+, it is reasonable to assume that only uncharged complexes, with $n = N$, are extracted by the organic solvent. We may then write, assuming only mononuclear complexes:

$$[B(HA)_p(H)_{-n}]_{aq} = [B][HA]^p[H]^{-n}K_{pn} = bc^p h^{-n}K_{pn} \tag{3}$$

$$[B(HA)_p(H)_{-N}]_{org} = [B][HA]^p[H]^{-N}K_{pN}L_{pN} = bc^p h^{-N}K_{pN}L_{pN} \tag{4}$$

where K_{pn} are the formation constants, and L_{pN} the distribution constants of the complexes, and

$$c = [HA] \text{ and } h = [H^+] \tag{5}$$

The over-all distribution ratio q is given by

$$q = \frac{\Sigma[B(HA)_p(H)_{-N}]_{org}}{\Sigma\Sigma[B(HA)_p(H)_{-n}]_{aq}} = \frac{\Sigma c^p h^{-N} K_{pN} L_{pN}}{\Sigma\Sigma c^p h^{-n} K_{pn}} \tag{6}$$

Thus $q(c, h)$ is a function of c and h. We may, however, obtain two-variable sections by studying instead the variable

$$q^{-1}h^{-N} = \frac{\Sigma\Sigma h^{-n} c^p K_{pn}}{\Sigma c^p K_{pN} L_{pN}} = \Sigma h^{-n} f_n(c) \tag{7}$$

$$f_n(c) = \frac{\Sigma c^p K_{pn}}{\Sigma c^p K_{pN} L_{pN}} \; ; \; f_0(c) = \frac{\Sigma c^p K_{p0}}{\Sigma c^p K_{pN} L_{pN}} \tag{8}$$

If c is kept constant, (7) gives a polynomial in h^{-1}. Each section can thus be used to find the values for the functions $f_n(c)$ at the value of c chosen. Rydberg [8] has used a single "sweep" [1], with successive linear extrapolations. However, it may be preferable to study the function $w(x)_c$

$$w = \log(q^{-1}h^{-N}) = \log \Sigma h^{-n} f_n; \; x = \log h \tag{9}$$

and find the best values of $f_n(c)$ by use of the curve-fitting methods for polynomials, described in part II [1].

The treatment of the data $f_n(c)$ so obtained, will depend on the accuracy of the data and the range of concentrations studied.

It seems a reasonable assumption [8] that complexes $B(HA)_p^{N+}$ can be neglected, so that $K_{p0} = 0$ for $p \neq 0$. By definition, $K_{00} = 1$. Then, as indicated by Rydberg (whose symbols are slightly different), it is profitable to study the functions

$$f_0^{-1}(c) = \Sigma K_{pN} L_{pN} c^p \tag{10}$$

$$f_n(c) f_0^{-1}(c) = \Sigma K_{pn} c^p \tag{11}$$

To find the individual * constants K_{pn} and L_{pN} one may use the curve-fitting methods for polynomials, for instance preparing plots of $\log f_0^{-1}$ (or, say, $\log(c^{-N} f_0^{-1})$), and $\log f_n f_0^{-1}$ (or, say, $\log(c^{-n} f_n f_0^{-1})$, as functions of $\log c$, and comparing them with families of normalized curves for polynomials [1]. Such methods seem preferable to linear plots, for the same reasons as given in part II [1]. Hök-Bernström [9] has recently applied this method to extraction data for UO_2^{2+}.

As a rule, partition data will allow an independent determination of only a few equilibrium constants, and it may be wise to start by searching for the *smallest set* of complexes $B(HA)_p(H)_{-n}$ needed to explain the data. With the curve-fitting methods given, one may compare the same graphical representa-

* If $[A_pBH_{p-N}]$ is important in the organic phase but negligible in the aqueous solution, only the product $K_{pN}L_{pN}$ may be obtained.

tion of the data with curves for a number of possible combinations. One may then judge — more directly than with linear plots — which combinations can be excluded, which are just compatible with the data, and which will give the best fit.

METHODS WITHOUT REDUCTION

Elimination

If one is not successful in reducing a three-variable problem to two-variable plots, the problem becomes slightly more complicated. A survey of the possible methods is given in Table 1, which is analogous to Table 1 of part II [1].

With only one parameter, p_1, a value for this parameter is obtained by inserting the coordinates of each experimental point (w, x, y) into eqn. (1). To test for the spread and any trend in the values of p_1, one would need a three-dimensional diagram (x, y, p_1), which could be given in the form of curves $p_1(x)_y$. If p_1 is really a constant, then these curves will all coincide in a single horizontal line.

Similarily, with two or three parameters, the graphs will not be more complicated than for two-variable data with two or three parameters, provided one does not want to test for a trend. With two parameters, one may for instance use curves $p_2(p_1)_{x,y}$.

Normalized graphs

With three variables, more serious complications occur in using normalized graphs, as indicated in Table 1. For instance, with two parameters, and two normalized variables, one can no longer use a single curve $Y(X)$ to compare with the data $y(x)$, but must instead compare a curved surface in space $w(x, y)$ with another, $w(X, Y)$. In practice this is done by preparing a *projec-*

Table 1. Methods for finding unknown constants p_i *from experimental data* w(x, y).

Number of		Compare (w, x, y) graph with calculated graph	Eliminate w to give graph	Two-dimensional projections, e. g.
parameters	normalized variables			
1 (p_1)	1 (x) 0	w, X, y	x, y, p_1	$y(X)_w$ and $y(x)_w$ $p_1\ (x)_y$
2(p_1, p_2)	2 (x, y) 1 (x) 0	w, X, Y w, X, y, p_2	x, y, p_1, p_2	$Y(X)_w$ and $y(x)_w$ — intersection of curves $p_2\,(p_1)_{x,y}$
3(p_1, p_2, p_3)	3 (w, x, y) 2 (x, y) 1 (x) 0	W, X, Y w, X, Y, p_3 w, X, y, p_2, p_3	x, y, p_1, p_2, p_3	$Y(X)_W$ and $y\,(x)_w$ — — —

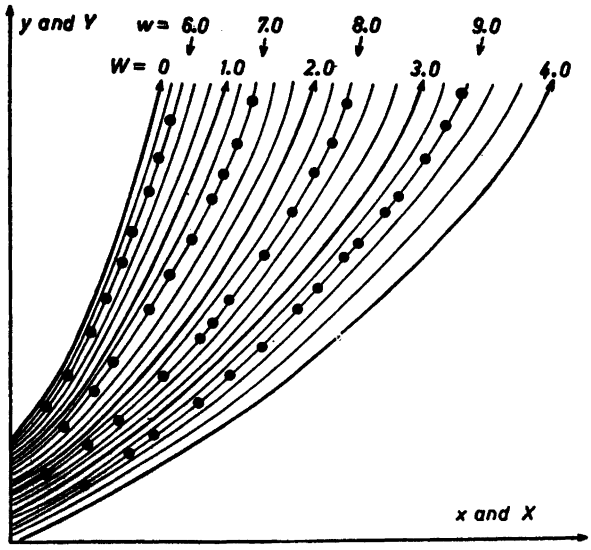


Fig. 1. "Surface-fitting" with three parameters. Curves = calculated projection map $Y(X)_W$ *for* $W = 0, 1, 2, 3, 4$ *(thick curves) and intermediate values, with a spacing of 0.2 units (thin curves). Circles: experimental points* $y(x)_w$ *for* $w = 6.0, 7.0, 8.0,$ *and 9.0, in the position of best fit. The parameter* $p_3 = W - w$ *in this case is around* -5.6. *— From the differences between normalized and experimental variables one could also find the two other parameters,* $p_1 = X - x$ *and* $p_3 = Y - y$. *These coordinate scales have not been marked out in the figure.*

tion map with $Y(X)_w$ curves for a number of values of w, and comparing it with the experimental data, given as curves $y(x)_w$ with the same values for w. The additional work involved should be a strong incentive to reduce the problem to a two-variable one. However, it will be shown in subsequent papers that if necessary such "surface-fitting" operations may be carried through successfully.

With three variables, a problem with one parameter and one normalized variable also requires the "surface-fitting" of a projection map $y(x)_w$ of the data and a normalized one $y(X)_w$ with calculated curves.

With three parameters and three normalized variables, one should fit a normalized surface $W(X, Y)$ to the plot $w(x, y)$ of the experimental data. This could possibly be carried out on three-dimensional models. When one tries to find the best fit of two-dimensional projections $Y(X)_W$ for a number of values of, W and $y(x)_w$ for a number of values of w, a difficulty arises: in the best fit, the experimental points may in general fall somewhere midway between the calculated curves. It might be practical to use a constant spacing of w in the experimental plot, and draw a set of thicker calculated curves with the same spacing in W; between these one may insert a series of thinner calculated curves for intermediate values of W (Fig. 1).

The other types of systems in Table 1 lead us to consider four-dimensional or five-dimensional super-surfaces, so that successive approximations and "sweeping" must be resorted to [1].

Application to systems with two equilibrium constants

As a simple example, let us assume that the reagents A and B form the two complexes AB and A_PB_Q, where P and Q are known, and that we want to determine the formation constants K_{11} and K_{PQ} from experimental data $Z(a, B)$.

From the definitions of B and Z, and the law of mass action we have

$$B = [B] + [AB] + Q[A_PB_Q] = b + abK_{11} + Qa^Pb^QK_{PQ} \quad (12)$$

$$BZ = [AB] + P[A_PB_Q] = abK_{11} + Pa^Pb^QK_{PQ} \quad (13)$$

Now, it is convenient to use the experimental variables

$$w = Z;\ x = \log\ a;\ y = \log\ B \quad (14)$$

and the normalized variables

$$X = x + p_1;\ Y = y + p_2 \quad (15)$$

Let us first introduce the auxiliary variables

$$u = 10^X = a \cdot 10^p;\ v = bj \quad (16)$$

where j is a constant. We wish to give such values to p_1, p_2 and j that all equilibrium constants are removed from (12) and (13), thus

$$Y = \log(v + uv + Qu^Pv^Q) \quad (12a)$$

$$Y + \log\ w = \log(uv + Pu^Pv^Q) \quad (13a)$$

Comparison with equations (12) to (16) gives us

$$p_1 = \log\ K_{11};\ p_2 = \frac{1}{Q-1}\ (\log\ K_{PQ} - P\ \log\ K_{11}) = \log\ j \quad (17)$$

The procedure is then to construct a map $Y(X)_w$ for a series of values of w, using (12a), (16), and (13a), and to plot the experimental data $y(x)_w$, *i. e.* $\log\ B(\log\ a)_Z$, for the same values of w. The plots are moved parallel to the coordinate axes until the best fit is found. One may then read the coordinates of the point (x_0, y_0) coinciding with $(X = 0, Y = 0)$, which give us

$$x_0 = -p_1 = -\log\ K_{11} \quad (18)$$

$$y_0 = -p_2 = -\frac{1}{Q-1}\ (\log\ K_{PQ} - P\ \log\ K_{11}) \quad (19)$$

The curve $Y(X)_w$ may be calculated in two ways. One may plot curves $w(v)_u$ and $Y(v)_u$ inserting a series of values for u and v into (12a) and (13a). Then, for each value of w considered one may take sets of corresponding values $v(u)_w$, and insert them into the

Y plot which gives $Y(u)_w$ or $Y(X)_w$ since $X = \log u$ (16). One may also eliminate v from (12a) and (13a), which gives

$$(Q-1)Y = (Q-1)\log(P+u(P-Q)) + \log(w+uw-u) - Q\log(P-Qw) - P\log u \quad (20)$$

Thus for each set of values of w and $X = \log u$ one may calculate Y directly.

If experimental data (a, b, B) are available instead, we may use the same experimental, normalized and auxiliary variables as in (14, 15, 16, 17) with the exception of w:

$$x = \log a;\ X = x + p_1;\ p_1 = \log K_{11} \quad (21)$$

$$y = \log B;\ Y = y + p_2;\ p_2 = \frac{1}{Q-1}(\log K_{PQ} - P \log K_{11}) \quad (22)$$

$$u = 10^X = a \cdot 10^{p_1};\ v = bj = b \cdot 10^{p_2} \quad (23)$$

$$Y = \log(v + uv + Qu^P v^Q) \quad (12a)$$

As the third experimental variable it is convenient to use the dimensionless quantity $\log(Bb^{-1})$ denoted by η in previous papers [3,5]. From (22), (23), and (12a)

$$w = \log \frac{B}{b} = y + p_2 - \log v = Y - \log v \quad (24)$$

$$w = \log(1 + u + Qu^P v^{Q-1}) \quad (25)$$

The normalized curve $Y(X)_w$ may be constructed by inserting a series of values of $X = \log u$ and w into (25); this gives v immediately, and Y is obtained from (24): $Y = w + \log v$.

The projection map $y(x)_w$ of the experimental data is then moved parallel to the axes until the best fit with the normalized projection map $Y(X)_w$ is found, which gives p_1 and p_2, and thus K_{11} and K_{PQ}.

One may proceed similarily for any set of equilibria with only two equilibrium constants, thus either free B and two complexes, or three complexes and a negligible concentration of free B. With four species containing B, thus three equilibrium constants, one may draw a series of projection maps, in each of which the ratio between two equilibrium constants (or some other suitable expression) is kept constant.

An advantage of the choice (14; 21, 22, 24) of $\log a$ and $\log B$ as planar coordinates and Z or $\log \frac{B}{b}$ as "height" in the experimental maps is that several alternative explanations may be compared directly on the same plot of experimental data.

Examples will be given in subsequent papers on hydrolysis equilibria.

This paper is part of a program supported by *Atomkommittén (Swedish Atomic Energy Committee)* and *Statens Naturvetenskapliga Forskningsråd (Swedish Natural Science Research Council)*. I wish to thank my friends George Biedermann, David Dyrssen, Brita Hök-Bernström, Hidetake Kakihana, Gösta Lagerström, Hazel Rossotti, Francis Rossotti, and Jan Rydberg for many valuable discussions.

REFERENCES

1. Sillén, L. G. *Acta Chem. Scand.* **10** (1956) 186 (part II).
2. Bjerrum, N. *Kgl. Danske Videnskab. Selskab. Skrifter, Naturvidenskab. math. Afdel.* (7) **12** (1915) 206.
3. Sillén, L. G. *Acta Chem. Scand.* **8** (1954) 299.
4. Rossotti, F. J. C. and Rossotti, H. S. *Acta Chem. Scand.* **9** (1955) 1166 (part I).
5. Sillén, L. G. *Acta Chem. Scand.* **8** (1954) 318.
6. Rydberg, J. *Acta Chem. Scand.* **4** (1950) 1503.
7. Dyrssen, D. and Sillén, L. G. *Acta Chem. Scand.* **7** (1953) 663.
8. Rydberg, J. *Arkiv Kemi* **8** (1955) 101, 113.
9. Hök-Bernström, B. *Acta Chem. Scand.* **10** (1956) 163.

Received March 10, 1956.

ACTA CHEMICA SCANDINAVICA 10 (1956) 812—821

Anionic Silver Iodide Complexes in Aqueous Solutions

IDO LEDEN

Departments of Inorganic and Nuclear Chemistry, Chalmers Institute of Technology, Göteborg, Sweden

The reaction between solid silver iodide and iodide ions was studied by solubility measurements at 25° C and at an ionic strength of 4 M ($NaClO_4$). The results have been interpreted by assuming that the mononuclear species AgI_n^{1-n} (n = 1, 2, 3, and 4) and the polynuclear species $Ag_2I_6^{4-}$ and $Ag_3I_8^{5-}$ were formed. At the highest iodide concentrations the saturated solutions also contained other more highly charged species. Their composition could not be determined exactly, but they are of the form $(AgI_2^-)_m$ or closely similar, most probably $Ag_mI_{2m+2}^{(m+2)-}$, with rather high average values of m (~10).

Earlier measurements of the solubility, l, of silver iodide have been summarized by Sillén [1], and a survey of equilibrium constants for the silver iodide system is given by Kratohvil, Težak, and Vouk [2]. King, Krall, and Pandow [3] are the only authors who have used a constant ionic strength (2 M $NaClO_4$). Their method was a direct titration analysis, which could only be used when $l > \sim 10^{-4}$. Their results can be described by eqn. (2) below. The constants in this equation have been calculated by the author for the range of their data, *vide* Table 2. They agree, after making a reasonable allowance for the difference in ionic strength, with those I have now determined.

The solubility of silver iodide in the solvent c_{NaI} M NaI + $(4 - c_{NaI})$ M $NaClO_4$, where c_{NaI} ranged from 5×10^{-4} to 4, was determined in the following ways: by electroanalyses after addition of sodium cyanide, when $l > 10^{-3}$; by potentiometric microtitrations with bromide (*vide* Ref.[4]) in the range $10^{-6} < l < 10^{-2}$; and by a radio assay technique, with silver iodide labelled with ^{110}Ag (from Harwell), when $l < 10^{-4}$. The solubility equilibria were in all cases established in less than one day. Experimental details are given elsewhere (Refs.[5-8]). The results are collected in Table 1. The accuracy has been judged from the reproducibility of the experiments. Every solubility given in Table 1 has been determined at least three times, several of them more than five times. The poor accuracy at low solubilities depends mainly on the small specific activity. When the solubility could be determined by two methods they were always in agreement. The original concentrations of sodium iodide in the solvent were corrected for the change in volume at saturation. This correction became significant at the highest solubilities measured.

Table 1. The solubility, s (in M), of silver iodide in aqueous sodium iodide. Ionic strength of the solvent 4 M ($NaClO_4$) except in the last one (6 M NaI).

c_{NaI}	s	c_{NaI}	$[I^-]$ **	s
5×10^{-4}	$(7 \pm 1) \times 10^{-9}$	0.8 *	0.78	$(198 \pm 1) \times 10^{-4}$
10^{-3}	$(13 \pm 1) \times 10^{-9}$	1.00 *	0.95	$(187 \pm 5) \times 10^{-4}$
2×10^{-3}	$(3 \pm 1) \times 10^{-8}$	1.20 *	1.12	$(347 \pm 1) \times 10^{-4}$
5×10^{-3}	$(8 \pm 2) \times 10^{-8}$	1.50 *	1.35	$(696 \pm 3) \times 10^{-4}$
0.01	$(33 \pm 3) \times 10^{-8}$	1.75 *	1.51	0.110 ± 0.001
0.02	$(112 \pm 5) \times 10^{-8}$	2.00 *	1.65	0.168 ± 0.001
0.05	$(77 \pm 1) \times 10^{-7}$	2.25	1.78	0.238 ± 0.001
0.08	$(214 \pm 5) \times 10^{-7}$	2.46	1.85	0.323 ± 0.001
0.1	$(35 \pm 1) \times 10^{-6}$	2.74	1.97	0.437 ± 0.002
0.2	$(20 \pm 1) \times 10^{-5}$	2.93	2.03	0.528 ± 0.003
0.3	$(59 \pm 2) \times 10^{-5}$	3.85	2.23	1.08 ± 0.01
0.5 *	$(24 \pm 1) \times 10^{-4}$	5.46	2.37	2.41 ± 0.01

* In these 7 solutions the concentration of free iodide ions could be determined by e. m. f. measurements, which gave the following results for $[I^-]$: 0.49_5, 0.78, 0.95, 1.11, 1.35, 1.50, 1.7 respectively.

** Calculated from eqn. (5).

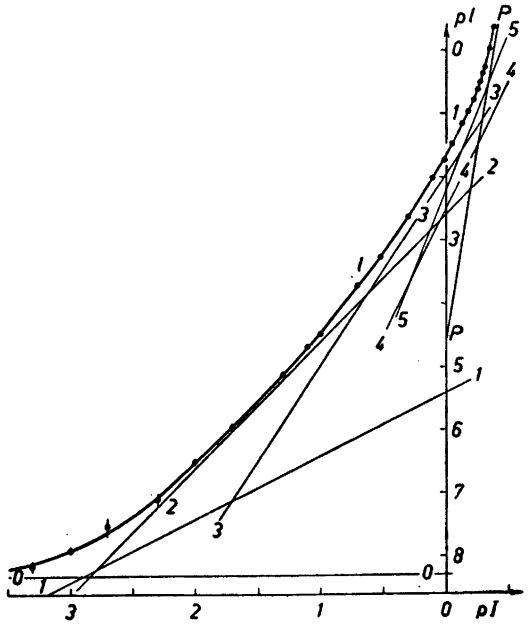


Fig. 1. The solubility, s, of silver iodide in aqueous sodium iodide. The numbered straight lines give the concentration of silver in the respective complexes as follows: 0:AgI, 1:AgI_3^-, 2:AgI^{2-}, 3:AgI_4^{3-}, 4:$Ag_2I_6^{4-}$, 5:$Ag_3I_8^{5-}$. P signifies the entire silver contents in species of ionic weight greater than $Ag_3I_8^{5-}$. Ionic strength 4 M ($NaClO_4$).

The dissolution of solid silver iodide in aqueous sodium iodide depends on reactions of the type

$$m\ \mathrm{AgI(s)} + n\ \mathrm{I^-} \rightleftharpoons \mathrm{Ag}_m\mathrm{I}_{m+n}^{n-} \qquad (1)$$

where m and n are integers to be determined by experiment. Hence the solubility is described by (*cf.* Ref.[4])

$$l = \sum_{n=-1}^{N} K_n\,[\mathrm{I^-}]^n \qquad (2)$$

If there is only one species of charge $-n$, it follows that

$$K_n = m \cdot k_{m,n} \qquad (3)$$

where $k_{m,n}$ is the equilibrium constant for reaction (1). If there are several species with the same charge, eqn. (3) would become $K_n = \sum_{m=1}^{M} m \cdot k_{m,n}$.

Computation of the constants K_n. K_0 has been determined previously from measurements of the solubility of silver iodide in aqueous silver perchlorate at 25° C and at an ionic strength of 4 M ($NaClO_4$), Ref.[8]; the value $K_0 = (6 \pm 1) \times 10^{-9}$ was found. This value ought to be confirmed by corresponding measurements with ^{110}Ag at low iodide concentrations, but the maximum specific activity of the silver obtainable at Harwell, is just insufficient to measure concentrations in the range 10^{-9} M with the apparatus at my disposal. The first term, $K_{-1}/[\mathrm{I^-}]$, of eqn. (2) is negligible in all solutions studied in this paper as the solubility product $K_{-1} = 4.5 \times 10^{-17}$ (*cf.* Refs. [8,9]).

In the range $5 \times 10^{-3} \leq [\mathrm{I^-}] \leq 5 \times 10^{-2}$, l is rather well described by a straight line of slope 2 in a logarithmic diagram (*vide* Fig. 1), which means that the term $K_2[\mathrm{I^-}]^2$ of eqn. (2) is dominant. Hence $K_2 = (25 \pm 1) \times 10^{-4}$ is immediately found. When $[\mathrm{I^-}] < 10^{-2}$, $l \simeq K_0 + K_1[\mathrm{I^-}] + K_2[\mathrm{I^-}]^2$ is a very good approximation to eqn. (2) and, as K_0 and K_2 are known, one value of K_1 can be computed from every value of l determined in this range. For K_0

Table 2. Comparison of the equilibrium constants from the e.m.f. measurements with those from solubility determinations. Temperature 25° C.

Reference	Ref. [9]	This paper	Ref. [3]
Ionic strength	4 M	4 M	2 M
$\mathrm{Ag}_m\mathrm{I}_{m+n}^{n-}$	$k_{m,n}$ (e. m. f.)	K_n/m (sol.)	K_n/m (sol.)
$\mathrm{AgI_2^-}$	—	$(4 \pm 2) \times 10^{-6}$	—
$\mathrm{AgI_3^{2-}}$	$(3 \pm 1) \times 10^{-3}$	$(25 \pm 1) \times 10^{-4}$	4×10^{-3}
$\mathrm{AgI_4^{3-}}$	$(9 \pm 1) \times 10^{-3}$	$(11 \pm 1) \times 10^{-3}$	5×10^{-3}
$\mathrm{Ag_2I_6^{4-}}$	$(10 \pm 6) \times 10^{-4}$	$(15 \pm 5) \times 10^{-4}$	5×10^{-4}
$\mathrm{Ag_3I_8^{5-}}$	$(23 \pm 5) \times 10^{-4}$	$(20 \pm 3) \times 10^{-4}$	17×10^{-4}
$\mathrm{Ag_{12}I_{24}^{12-}}$	—	4×10^{-6}	—

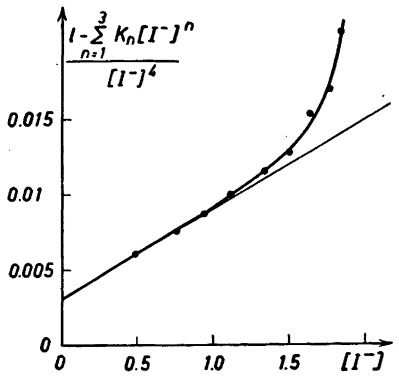


Fig. 2. The computation of K_4 *and* K_5.

the value 5×10^{-9} has been used, as this gives a better constancy to K_1 than does the mean value, 6×10^{-9}, from Ref.[8]. $K_1 = (4 \pm 2) \times 10^{-6}$ is thus obtained. Analogously, $l \simeq K_2[I^-]^2 + K_3[I^-]^3$ in the range $0.05 < [I^-] < 0.3$ and hence one value of K_3 can be calculated from every determination of l; a mean value, $K_3 = (11 \pm 1) \times 10^{-4}$, was found. In all solutions hitherto mentioned the solubility is so small that $[I^-] \simeq c_{NaI}$ with sufficient accuracy.

The equilibrium constants $k_{1,2}$ and $k_{1,3}$ have been determined recently by e.m.f. measurements (Ref.[9]). These values are compared with the values of K_n above in Table 2, from which it is evident that $K_2 = k_{1,2}$ and $K_3 = k_{1,3}$ within experimental error. Hence it follows that the only significant silver iodide species with the charges —2 and —3 are AgI_3^{2-} and AgI_4^{3-}.

When the iodide concentrations are greater than 0.3 M, the solutions contain anionic species which have charges larger than 3 and are no longer negligible in quantity. In order to determine the coefficients of the corresponding terms of degree higher than 3 in eqn. (2), $(l - \sum_{n=1}^{3} K_n[I^-]^n) / [I^-]^4$ is plotted as a function of $[I^-]$ for numerators >15 % of l (*vide* Fig. 2). As is seen from the graph, this function is very well described by a straight line in the range $0.5 \leq [I^-] \leq 1.5$. The slope of this line gives $K_5 = (6 \pm 1) \times 10^{-3}$, and its intersection with the ordinate axis gives $K_4 = (3 \pm 1) \times 10^{-3}$. These values have been compared with $k_{2,5}$ and $k_{2,4}$ from the e.m.f. measurements in unsaturated solutions (Ref.[9]) in Table 2. It is evident that $k_{2,4} = \frac{1}{2}K_4$ and $k_{3,5} = \frac{1}{3}K_5$ within experimental error, as required by eqn. (3) when there is only one species with each sharge. As the e.m.f. measurements have been made in a range $0.003 < c_{Ag} < 0.1$ corresponding to the range $0.002 < l < 0.1$, where the curve in Fig. 2 is with good approximation a straight line, it is evident that the only polynuclear complexes significant at these silver concentrations are $Ag_2I_6^{4-}$ and $Ag_3I_8^{5-}$, which thus are the only species in the saturated solutions with the charges —4 and —5.

In this range the solubility is no longer negligible compared with the concentration of sodium iodide. The concentration of free iodide ions had therefore to be determined from the e.m.f. (E mV) of the following cell:

+ Ag, AgI	0.3 M NaI 3.7 M $NaClO_4$	4 M NaI	c_{NaI} M NaI $(4-c_{NaI})$ M $NaClO_4$	Ag, AgI −

where the right hand solutions are those listed in Table 1 with $c_{NaI} > 0.3$. The concentration, $[I^-]$, of free iodide in these solutions can be calculated from Nernst's formula

$$E = 59.16 \log \frac{[I^-]}{0.3} \tag{4}$$

In order to confirm that the results from eqn. (4) are in accordance with the known concentrations of sodium iodide, $[I^-]$ was recalculated by inserting the values of $[I^-]$ from eqn. (4) in the right hand member of eqn. (5).

$$[I^-] = c_{NaI} - 2K_2[I^-]^2 - 3K_3[I^-]^3 - 2K_4[I^-]^4 - \frac{5}{3}K_5[I^-]^5 - [P] \tag{5}$$

The negative terms of this equation represent the concentration of iodide used in the formation (1) of the complexes, if these are AgI_3^{2-}, AgI_4^{3-}, $Ag_2I_6^{4-}$, and $Ag_3I_8^{5-}$, as has been found by e.m.f. measurements (Ref.[9] and see above). The term —[P], discussed below, is negligible, when $[I^-]<1.5$. The results from eqns. (4) and (5) (*vide* Table 1) agree, when the solubility is less than 0.2 M. At higher silver concentrations eqn. (4) gives absurdly high values of $[I^-]$, *e. g.* $[I^-] = 2.83$ for $c_{NaI} = 3.85$, in all probability because of increasing liquid junction potentials and changed activity factors.

At higher iodide concentrations the curve of Fig. 2 becomes increasingly steeper, which means that anionic complexes are formed with charges higher than 5. To analyse this region, it is again necessary to compute values of $[I^-]$, which can no longer be determined by e.m.f. measurements (see above). This computation has been done as follows. It can be deduced (*vide* Ref.[10]) from Erber's [11] determinations of the solubility of silver iodide in highly concentrated solutions of hydrogen iodide that the complexes formed, either have the composition $Ag_mI_{2m}^{m-}$ (with a rather high value of m, say at least 8), or a composition which comes close to this, *e. g.* $Ag_mI_{2m+2}^{(m+2)-}$ for large values of m. Erber himself claimed that the ion $Ag_2I_6^{4-}$ predominates in his concentrated solutions, but he arrived at this false conclusion by assuming that $c_{NaI} = [I^-]$ within the accuracy of his experiments. Erber, however, used this approximation for very high solubilities where it does not hold, *e. g.* for $c_{NaI} \simeq 7$ and $l \simeq 5$ (hence $[I^-] \simeq 2$, *i. e.* $[I^-]^4 \ll c^4_{NaI}$). Hence it follows that the concentration of free iodide ions must be calculated from eqn. (5), where [P] means the concentration of silver, present in complexes with ionic weights larger than that of $Ag_3I_8^{5-}$. The solubility is described by

$$l = \sum_{n=2}^{5} K_n[I^-]^n + [P] \tag{6}$$

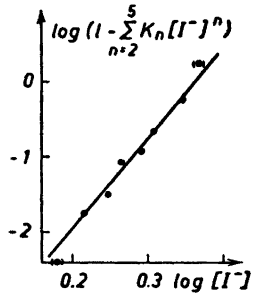


Fig. 3. The concentration, $[P] = l - \sum_{n=2}^{5} K_n [I^-]^n$, *of silver present in species of ionic weight greater than* $Ag_3I_8^{5-}$.

in this range. Values of [P] and [I^-], which satisfy both eqn. (5) and eqn. (6) are easily found for each known pair of l and c_{NaI}. The resulting values of [I^-] are given in Table 1. This approach ought to give rather good values of [I^-], as, according to Erber's measurements, the highly condensed complexes, dominant when [P] is large, are either exactly of the form $Ag_mI_{2m}^{m-}$ or very close to it, which means that the amount of iodide ions used in the formation of these complexes (*vide* reaction (1)) is equal to [P], as required by eqn. (5). On the other hand, when [P] is less, the iodide bound in complex species is presumably a little larger than [P], as the complexes are probably of the form $Ag_mI_{2m+2}^{(m+2)-}$. Fortunately in this case [P] is such a small correction term in eqn. (5), that it does not matter that this term ought strictly to be replaced by the slightly greater term $\frac{m+2}{m} \cdot [P]$, $(m \geq 4)$.

The result of the computation is shown in Fig. 3. Log [P] is seen to be a rectilinear function of log [I^-] with the slope 12 in the whole range, where [P] is sufficiently large to be calculated from eqn. (6). This connection is approximately valid even for the last solution of Table 1, in spite of the change in ionic strength from 4 M to 6 M.

SURVEY OF THE SILVER IODIDE SYSTEM

A. *Uncharged and cationic complexes.* These have been studied by the dissolution of silver iodide in aqueous solutions of silver perchlorate [8]. The complexes are probably of the form Ag_nI^{n-1} with $n = 1$, 2, 3, and 4. At high concentrations of silver perchlorate small amounts of complexes containing more than one iodide ion are probably formed. King, Krall, and Pandow [3] came to the same conclusion, because their measurements of the light absorption at the wave length 300 mμ showed that Beer's law is not obeyed exactly in solutions of silver perchlorate, undersaturated with silver iodide.

B. *Mononuclear complexes,* AgI_n^{1-n}. The existence of the species AgI_3^{2-} and AgI_4^{3-} has been shown both by e.m.f. measurements and solubility determinations. The two methods gave complexity constants, which were in agreement. The solubility measurements have also given evidence of species of charge 0 and —1. These species exist in noticeable concentration only when the solubility is small ($\sim 10^{-8}$ M), which makes it rather probable that these

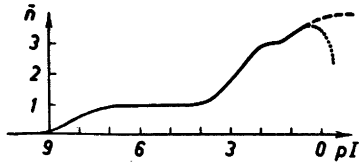


Fig. 4. The formation curves, $\bar{n}$, for saturated solutions of AgI (dotted curve) and for solutions containing so little silver, that polynuclear complexes can be neglected (dashed curve). When these two curves coincide they have been full-drawn.

species are mononuclear, *i. e.* of the form AgI and AgI_2^-. This cannot, however, be established by e.m.f. measurements because of the small total silver concentrations. The formation curve, $\bar{n}$, of the mononuclear complexes is shown in Fig. 4. A remarkable feature is the relatively high stability of the first and — to a less extent — of the third complex of the series.

This is in accordance with the idea of a dative π-bond between transition metals with filled d-orbitals and ligands with vacant d-orbitals of suitable size and energy level, as discussed by Chatt [12,13] and Chatt and Wilkins [14], who also give further literature. That the co-ordination number of silver can sometimes be 3 with strongly bound ligands containing a donor atom with vacant d-orbitals has been shown by Ahrland and Chatt [15] in their study of some complexes of silver ion with a tertiary phosphine. In the silver iodide case the strength of the first complex, AgI, relative to the second, AgI_2^-, is even still more pronounced than in the phosphine complexes studied by Ahrland and Chatt. There is a distinct "stop" in the formation curve of Fig. 4 at $\bar{n} = 3$, though the complex formation continues to the 4th complex at high iodide concentrations. This could perhaps mean that the species, written above as AgI_3^{2-}, actually has this formula and the possible fourth co-ordination place is not occupied by a molecule of water. This accords with Strock's [16] study of the high temperature form of solid silver iodide, α-AgI. Strock claims that α-AgI contains as well as two-, three- and four-co-ordinated silver ions in its iodide lattice.

In the silver thiocyanate [7] and azide systems [17] the complex AgA_2^- is more stable than the other members of the mononuclear series. From Fig. 4 it is evident that AgI_2^- is the least stable intermediate species. It is known [5,6] from the other silver halides that the activity factors at high ionic strength do not favour AgA_2^- relative to the other mononuclear species. It seems probable, therefore, that an $\bar{n}$-curve for the iodide system at zero ionic strength would show a "stop", *i. e.* a point of inflexion with a low slope of the tangent, at $\bar{n} = 2$, too. This means that the equilibrium constants, $b_{1,n}$, of the successive steps (Table 3) will differ markedly from the thermodynamic constants. In spite of this, however, the silver iodide system seems to be rather abnormal ($b_{1,1} / b_{1,2}$ being very great even after a correction for the activity factors) and this might suggest that different types of bonding occur at the different steps.

C. *Polynuclear anionic complexes.* The existence of $Ag_3I_8^{5-}$ is conclusively shown by the agreement between the results of the e.m.f. and solubility measurements. There can be little doubt about $Ag_2I_6^{4-}$, even if the silver present in this species never exceeds 20 % of the total silver concentration. It is reasonable to suppose that the two species are formed by the two condensations reactions written at the bottom of Table 3. This would indicate that the silver ion is four-co-ordinated in these species just as it is in the normal solid silver iodide, γ-AgI. The solubility measurements have shown that anionic

Table 3. The step reactions, their equilibrium constants, $b_{m,n}$, *and their over-all complexity constants,* $\beta_{m,n} = k_{m,n}/K_{-1}$. *Ionic strength 4 M* ($NaClO_4$). *Temperature 25° C.*

$Ag^+ + I^-$	$\rightleftharpoons AgI$	$b_{1,1} \gtrsim 10^{8}$	$\beta_{1,1} \gtrsim 10^{8}$
$AgI + I^-$	$\rightleftharpoons AgI_2^-$	$b_{1,2} \gtrsim 10^{3}$	$\beta_{1,2} \gtrsim 10^{11}$
$AgI_2^- + I^-$	$\rightleftharpoons AgI_3^{2-}$	$b_{1,3} \gtrsim 600$	$\beta_{1,3} = (6 \pm 1) \times 10^{13}$
$AgI_3^{2-} + I^-$	$\rightleftharpoons AgI_4^{3-}$	$b_{1,4} \gtrsim 4$	$\beta_{1,4} = (21 \pm 2) \times 10^{13}$
$2\ AgI_4^{3-}$	$\rightleftharpoons Ag_2I_6^{4-} + 2\ I^-$	$b_{2,6} \gtrsim 15$	$\beta_{2,6} = (6 \pm 2) \times 10^{29}$
$AgI_4^{3-} + Ag_2I_6^{4-}$	$\rightleftharpoons Ag_3I_8^{5-} + 2\ I^-$	$b_{3,8} \gtrsim 250$	$\beta_{3,8} = (24 \pm 2) \times 10^{45}$

complexes are formed with (negative) charges larger than 5. As is shown by Fig. 3 the solubilities can be interpreted assuming that only one such species, *viz.* $Ag_{12}I_{24}^{12-}$, is formed. It does not prove that this is the only highly condensed species in these concentrated solutions or that this particular species exists at all. It merely shows that $Ag_{12}I_{24}^{12-}$ can be regarded as a summarizing mean of the anionic complexes with high ionic weight. (For criticism of the propensity for selecting rather arbitrary species to describe complex systems, *vide* Hietanen and Sillén [18], Sillén [19], or Ahrland, Hietanen, and Sillén [20].) In the range where e.m.f. measurements [9] have been carried out, the silver concentration of the complexes, summarized as [P], *i. e.* formally $12[Ag_2I_{24}^{12-}]$, in Fig. 3, would be quite negligible, in agreement with the fact that no other species than $Ag_2I_6^{4-}$ and $Ag_3I_8^{5-}$ were needed to describe the potentiometric measurements.

An attempt [10] to describe the solubility measurements by assuming an infinite series of complexes, $Ag_mI_{2m+2}^{(m+2)-}$, formed by condensation reactions, of which all, except the first one, had the same equilibrium constant, accommodated all except the two last determinations of Table 1. E. m. f. measurements in the silver iodide system [9] might also be described by assuming an infinite series of complexes, $Ag_mI_{2m+2}^{(m+2)-}$, but the equilibrium constants calculated from the e. m. f.s on this assumption did not agree very well with those calculated from the solubility measurements. A quantitative description of the higher condensation products by such an infinite series was therefore abandoned. The most probable hypothesis is that the condensation reactions continue to some rather high value of m in $Ag_mI_{2m+2}^{(m+2)-}$, but with increasing charge the reaction with new AgI_4^{3-} becomes more difficult. It is also possible that a reaction, *e. g.* a ring-closure,

$$Ag_mI_{2m+2}^{(m+2)-} \rightleftharpoons Ag_mI_{2m}^{m-} + 2I^- \qquad (7)$$

occurs at some condensation step. It would be very difficult to decide between an infinite series and a series, cut off by a reaction such as (7) with a high value of m. In the former case the curve $\log l = f(\log[I^-])$ would have a vertical asymptote, in the latter one an asymptote with the large slope m. Perhaps the structure of the species with high ionic weights can be obtained from an X-ray analysis of solutions of silver iodide. A concentrated aqueous solution of lithium iodide, saturated with silver iodide gives X-ray photograms with distinct refraction patterns, which show that the polynuclear complexes are built up by tetrahedral AgI_4-links (Nilsson [21]). Chains of such links sharing corners have been found in solid K_2AgI_3 (Brink and Kroese [22]) and double chains of the same links sharing edges in $CsAg_2I_3$ (Brink, Binnendijk, and van de Linde [23]).

Although it has not been possible to determine the composition of the species, summarized as P above, certain forms can be excluded. They cannot be dinuclear, $Ag_2I_4^{2-}$—$Ag_2I_7^{5-}$, as Bodländer and Eberlein [24] have claimed, as

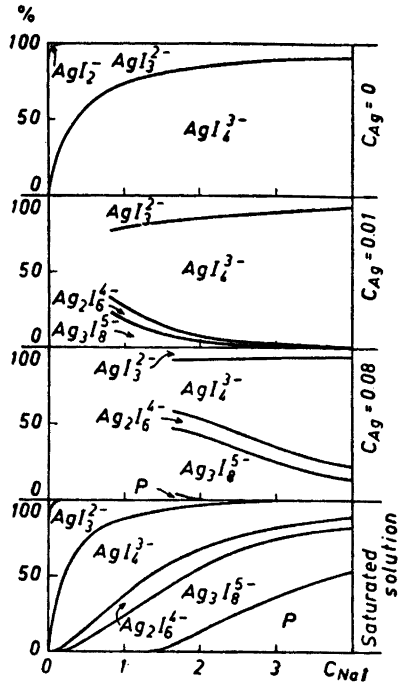


Fig. 5. The distribution of silver in anionic species in saturated solutions, in solutions containing a constant total silver concentration $c_{Ag} = 0.08$ *or* $0.01\ M$ *respectively, and in the limiting case* $c_{Ag} = 0$.

all species with the charges —2 to —5 have been quantitatively determined both by e.m.f. and solubility measurements. Similarly $Ag_4I_6^{2-}$, which Mackor [25] has found in a solvent of acetone and water is excluded. The silver iodide system seems to be completely different in organic solvents because AgI_2^- appears to be the limit of mononuclear complex formation both in acetone (Mackor [25]) and in ether (Alin, Evers, and Sillén [26]).

There is an obvious difference between the condensation reactions above and the corresponding "core + link"-description used by Sillén's school in studying hydrolysis of metal ions, as the link is uncharged in those hydrolyses — except in that of thorium — where an infinite series of hydrolysis products is formed. (The hydrolysis of bismuth seems to be under revision, *vide* Hietanen and Sillén [18,p.1622]. Hence the ionic charges of hydrolysis products do not increase with increasing ionic weight (*cf.* Rossotti and Rossotti [27]).

Data relating to the anionic complexes are summarized in Table 3, which contains the most probable values of the equilibrium constants for the stepwise formation of the complexes. Fig. 5 shows the distribution of silver in the different complexes, in saturated as well as in unsaturated solutions containing 0.08 or 0.01 M silver. In the two latter cases the curves cannot be continued to the left because the point of saturation has been reached. The figure also shows the distribution of silver at such low silver concentrations that polynuclear complexes are not formed. The calculation of the curves and directions for reading the diagrams are described elsewhere [4,7,8]. The distribution

of silver at low iodide concentration can be judged from Fig. 4. An $\bar{n}$-curve for saturated solutions for iodide concentrations higher than 0.1 M, drawn in larger scale than that of Fig. 4, is to be seen in Fig. 3 of Ref.[9]. This latter curve would be only slightly changed (and at the highest iodide concentrations only), if an infinite series of complexes were used instead of the description above. The equilibrium constants of the cationic complexes and the distribution of silver among these are given elsewhere [8].

The author is grateful to Dr. J. Chatt for valuable discussions, and to him and Dr. G. A. Gamlen for their efforts to make my manuscript readable. E. Berne and R. Nilsson carried out the G. M.-measurements and L. E. Marthén assisted at all stages of the experimental work. *Statens Naturvetenskapliga Forskningsråd* gave liberal financial support.

REFERENCES

1. Sillén, L. G. *Solubility of Silver Halides.* Prel. report to I. U. P. A. C., Stockholm (1953), mimeographed.
2. Kratohvil, J., Težak, B. and Vouk, V. B. *Arhiv Kem.* **26** (1954) 191.
3. King, E., Krall, H. and Pandow, M. *J. Am. Chem. Soc.* **74** (1952) 3492.
4. Leden, I. *Svensk Kem. Tidskr.* **64** (1952) 249.
5. Berne, E. and Leden, I. *Ibid.* **65** (1953) 88.
6. Berne, E. and Leden, I. *Z. Naturforsch.* **8a** (1953) 719.
7. Leden, I. and Nilsson, R. *Ibid.* **10a** (1955) 67.
8. Leden, I. and Parck, C. *Acta Chem. Scand.* **10** (1956) 535.
9. Leden, I. *Acta Chem. Scand.* **10** (1956) 540.
10. Leden, I. *Symposium on Co-ordination Chemistry,* Copenhagen (1953) 80.
11. Erber, W. *Z. anorg. u. allgem. Chem.* **248** (1941) 36.
12. Chatt, J. *ICI Report No. BRL/105,* Welwyn (1950), mimeographed.
13. Chatt, J. *Nature* **165** (1950) 637.
14. Chatt, J. and Wilkins, R. G. *J. Chem. Soc.* **1952** 4300.
15. Ahrland, S. and Chatt, J. *Chemistry & Industry* **1955** 96.
16. Strock, L. *Z. physik. Chem.* **B 25** (1934) 441.
17. Leden, I. and Schöön, N.-H. *Acta Polytechnica* **155** (1954).
18. Hietanen, S. and Sillén, L. G. *Acta Chem. Scand.* **8** (1954) 1623.
19. Sillén, L. G. *Ibid.* **8** (1954) 299.
20. Ahrland, S., Hietanen, S. and Sillén, L. G. *Ibid.* **8** (1954) 1913.
21. Nilsson, R. *Private communication.*
22. Brink, C. and Kroese, H. A. C. *Acta Cryst.* **5** (1952) 433.
23. Brink, C., Binnendijk, N. F. and van de Linde, J. *Ibid.* **7** (1954) 176.
24. Bodländer, G. and Eberlein, W. *Z. anorg. u. allgem. Chem.* **39** (1904) 197.
25. Mackor, E. L. *Rec. trav chim.* **70** (1951) 457.
26. Alin, B., Evers, L. and Sillén, L. G. *Acta Chem. Scand.* **6** (1952) 959.
27. Rossotti, F. J. C. and Rossotti, H. S. *Ibid.* **9** (1955) 1191.

Received March 20, 1956.

ACTA CHEMICA SCANDINAVICA 10 (1956) 822—830

Kinetics of the Hydrolysis and Formation of Dimethylmaleic Anhydride in Solvent Mixtures

JOUKO KOSKIKALLIO

Institute of Chemistry, University of Helsinki, Finland

In a study of the rate of attainment of the equilibrium between dimethylmaleic anhydride and the acid in various acetone-water mixtures it has been established that the molecularity with respect to water is about three for the hydrolysis of the anhydride and about two for the reverse reaction. The rate of anhydride formation from dimethyl maleic acid has been investigated also in non-aqueous solvents as in acetone, dioxan and various diethyl ether-benzene mixtures. In benzene the rate was more than a thousand times as fast as in pure ether. The reaction was kinetically of second order and the rate constant was found to vary approximately as $1/c^2_{ox}$, where c_{ox} is the molar concentration of the solvent component which contains oxygen. The value of the rate constant obtained in dioxan fulfils the same relation fairly well if c_{ox} is taken to be equal to half the molar concentration of dioxan.

The activation energy for the hydrolysis reaction 13.4 kcal in 50 vol. % acetone-water is smaller than that for the reverse reaction, 16 kcal, and the hydrolysis reaction is exothermic by 2.6 kcal. The entropies of activation are for the hydrolysis -30.2 cal/degree and for the anhydride formation -18.7 cal/degree. These large differences in the entropies more than counterbalances the difference in the activation energies, and hence the rate of hydrolysis is smaller than the rate of the reverse reaction, and the equilibrium lies more on the side of the anhydride.

In a previous paper [1] are given data of the equilibrium constant for the reaction

$$\text{Dimethylmaleic acid} \underset{k_{-1}}{\overset{k_1}{\rightleftharpoons}} \text{Dimethylmaleic anhydride} + \text{Water} \qquad (1)$$

in various acetone-water mixtures. The composition of the solvent was found to influence the equilibrium only slightly. On the other hand, previous work [2] had shown that the rates of hydrolysis of acetic, succinic, and glutaric anhydrides decrease considerably when acetone is added to water. For com-

parison, kinetic measurements on the formation and hydrolysis of dimethylmaleic anhydride have been performed in acetone-water and diethyl ether-benzene mixtures and in dioxan.

EXPERIMENTAL

The dimethylmaleic anhydride was prepared as described previously [1]. The disodium-salt of dimethylmaleic acid was obtained by shaking a concentrated acetone solution of the anhydride with an approximately 20 % aqueous sodium hydroxide solution. The precipitated salt was washed with acetone and dried *in vacuo*.

For the kinetic experiments, a weighed quantity of the disodium salt was dissolved in a small volume of water, the solution cooled to 0°, and slightly less than the calculated amount of 30 % hydrochloric acid added. The liberated dimethylmaleic acid was dissolved in a small volume of one of the solvent components used in the kinetic experiments. After shaking with anhydrous sodium sulphate, the nearly anhydrous solution was warmed to 20° and pipetted to the solvent mixture previously temperated to 20° to make the mixture desired. The disadvantage of the method was that, in spite of the drying with sodium sulphate, small amounts of water were still present in the reaction mixture (especially when acetone and dioxan were used). Experiments made with diethyl ether saturated with water showed an about 5 % increase in the rate at 60° as compared with experiments made in previously dried ether solution. The values of the rate constants given in Table 5 are therefore probably all higher than the values for the corresponding dry solvents, but in no case more than about 1—2 %.

In all the organic solvents and their mixtures the conversion of dimethylmaleic acid into anhydride went to completion. Samples were titrated with 0.05 N sodium methylate, the consumption of which decreases as the acid is converted into anhydride because the anhydride consumes only one equivalent of methylate (anhydride + MeONa → monoester salt), whereas the acid consumes two equivalents. When titrated with baryta, both the acid and the anhydride consume two equivalents of base, and at the end of the reaction the consumption should be twice the methylate value if the reaction goes to completion. This was found to be the case in the dry organic solvents. Second-order kinetics were obeyed, and the rate constants were calculated from the following equation

$$k_2 = \frac{100}{at}\left(\frac{1}{100-\mathrm{p}} - \frac{1}{100}\right) \qquad (2)$$

where a is the initial concentration of the acid, t time in seconds and p the percentage of the acid changed into anhydride. Table 1 shows an example of a typical kinetic run.

In water, the hydrolysis of dimethylmaleic anhydride was followed conductometrically. In order to calculate the concentration of the acid, the conductances of the acid at various dilutions had to be measured separately. In aqueous solution the anhydride is

Table 1. Conversion of dimethylmaleic acid into anhydride in diethyl ether solution at 20°.

Time in seconds	$c_{anhydride}$ mole/l	c_{acid} mole/l	% reacted	$10^3 \times k_2$ $l \cdot mole^{-1}sec^{-1}$
0	0.0254	0.0309	0	
6 060	0.0318	0.0245	20.7	1.40
9 120	0.0344	0.0219	29.1	1.46
13 680	0.0370	0.0193	37.5	1.42
25 020	0.0414	0.0149	51.8	1.39
70 200	0.0488	0.0075	75.7	1.43
96 780	0.0504	0.0059	80.9	1.37

Table 2. Hydrolysis of dimethylmaleic anhydride in water at 0°.

Conductance data		Kinetic experiment				
$10^4 \times c_{acid}$ mole/l	$10^4 \times 1/R$ ohm^{-1}	Time in sec.	$10^4 \times 1/R$ ohm^{-1}	$10^4 \times c_{acid}$ mole/l	% reacted	$10^4 \times (k_1 + k_{-1})$ sec^{-1}
19.8	16.62	0	7.24	7.1	0	
14.9	13.40	61	8.52	8.5	9.4	16.2
9.9	9.71	92	9.23	9.3	14.8	17.5
3.96	4.33	137	10.00	10.2	20.8	17.0
2.97	3.14	192	10.83	11.3	28.2	17.0
1.98	2.09	261	11.74	12.3	34.9	16.6
		351	12.73	13.8	45.0	17.0
		477	13.81	15.3	55.0	16.7
		688	15.00	17.3	68.5	17.3
		7 200	17.62	22.0	100	

in equilibrium with the acid. This equilibrium is disturbed on dilution since the concentration of unionized acid is changed, and hence the values of conductances had to be extrapolated to zero mixing time. The conductances thus obtained are proportional to the acid concentrations, and the concentrations required in calculating the rate constants may be obtained with the aid of a graph. Because of the acid-anhydride equilibrium, rate constants were calculated using the following equations

$$k_1 + k_{-1} = \frac{2.303}{t} \log \frac{c_o - c_{eq}}{c_t - c_{eq}} \tag{3}$$

$$K = \frac{k_1}{k_{-1}} = \frac{c_o - c_{eq}}{c_{eq}} \tag{4}$$

where k_1 and k_{-1} are the first-order rate constants (see eqn. 1), t the time and c_o, c_t, c_{eq} the concentrations of acid at the beginning of the experiment, at time t, and at equilibrium, respectively. The conductances of different dilutions of a stock solution con-

Table 3. Conversion of dimethylmaleic acid into anhydride in 90 % acetone-water at 20°. 5-ml samples were analysed by adding 5 ml of 0.0508 M MeONa and titrating with 0.0202 N HCl. A sample titrated with 0.0205 N baryta consumed 11.1 ml which corresponds to 0.0114 mequiv.

Time in min.	HCl 0.0202 N ml	Anhydride mequiv.	Acid mequiv.	% reacted	$10^5 \times k_1$ sec^{-1}	$10^5 \times (k_1 + k_{-1})$	$10^3 \times k_2$ $l \cdot$mole^{-1} sec^{-1}	$10^5 \times k_1$ sec^{-1} $\beta = 0.5$
0	1.90	0.012	0.102	0				
25	2.45	23	91	10.8	7.54	8.15	4.23	4.91
71	3.10	37	77	24.5	6.60	7.15	4.03	3.78
117	3.65	48	66	35.3	6.19	6.70	4.20	4.00
182	4.25	60	54	47.1	5.82	6.39	4.50	3.77
250	4.75	70	44	56.9	5.63	6.19	4.96	3.78
326	5.20	79	35	65.7	5.46	6.13	5.78	3.92
358	5.30	81	33	67.6	5.26	5.92	5.81	3.83
1 270	6.50	105	9	91.2	3.18	4.54	20.0	3.68
4 000		108	6	94				

taining 19.8×10^{-4} mole/l of acid and anhydride are given in Table 2. With aid of these values, using a graph, the conductances obtained in a kinetic run may be converted into concentrations, and values for the sum of rate constants are obtained. An example of a typical kinetic run is given in Table 2. The mean of the sum of rate constants is 16.9×10^{-4} sec^{-1} and when the value $K = 2.6$ taken from the previous paper [1] is used, it is found that $k_{-1} = 12.2 \times 10^{-4}$ and $k_1 = 4.7 \times 10^{-4}$ sec^{-1}. As already mentioned the acid concentrations and conductances given in Table 2 are only values proportional to the true values. The constancy of the sum $k_1 + k_{-1}$ in this typical run indicates that first-order kinetics are well obeyed.

In the case of all acetone-water mixtures, the samples were analysed as in the previous work [1] by titrating with 0.05 N sodium methylate and 0.02 N baryta. The experimental data for acetone-water mixture containing 90 vol. % acetone were not found to fit either first-order or the second-order rate equation. The reaction does not proceed to completion and at equilibrium at 20° 95 % of acid has been converted into anhydride. In order to simplify the calculations, the reverse reaction was disregarded and the constants were calculated by assuming two reactions, one of first-order and one of second-order to occur simultaneously:

$$-\frac{dx}{dt} = k_1 (a-x) + k_2 (a-x)^2 \qquad (5)$$

which gives on integration

$$k_1 = \frac{2.303}{t} \log \frac{a-\beta x}{a-x} \; ; \; \beta = \frac{k_1 + ak_2}{ak_2} \qquad (6)$$

where a is the initial acid concentration, x the reacted amount of acid, t time in seconds and β a constant.

Rate constants calculated in different ways, from the rate equation for an overall first-order reaction disregarding the equilibrium (Table 3, column 6), from the first-order rate equation taking into account the equilibrium (Table 3, column 7, eqn. 3), from the second-order rate equation disregarding the equilibrium (column 8, eqn. 2) and from the rate equation for simultaneous first-order and second-order reactions assuming the value 0.5 for β (column 9, eqn. 6). Only in this last case are fairly good constants obtained. In pure acetone, the reaction is solely of the second-order, and thus a transition from first-order into second-order kinetics occurs in the acetone-water mixture containing about 90 % acetone.

RESULTS AND DISCUSSION

The rate constants obtained are summarized in Tables 4 and 5. The hydrolysis of dimethylmaleic anhydride in aqueous solution is considerably slower than the hydrolysis of maleic anhydride [2], the respective first-order rate constants at 0° being 4.7×10^{-4} and 34.3×10^{-4} sec^{-1}, but somewhat faster than the hydrolysis of succinic anhydride [2] for which the first-order rate constant at 0° is 3.34×10^{-4}. The hydrolysis of maleic anhydride is only slightly faster than the hydrolysis of methylmaleic anhydride [3]: the rate constants at 25° are 26.6×10^{-4} and 17.6×10^{-4} sec^{-1}, respectively. These differences in the rates are in the direction predicted by steric and inductive effects [6].

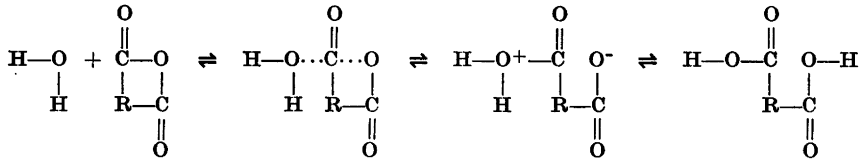
In acetone-water mixtures, the hydrolyses of all anhydrides studied previously [2] and the conversion of dimethylmaleic acid into anhydride are greatly retarded as the acetone content of the aqueous solvent is increased (Table 4). When log k is plotted against log c_{H_2O}, fairly constant slopes are obtained for the cyclic anhydrides, but not for acetic anhydride [2] (Table 6). For succinic, glutaric and dimethylmaleic anhydrides, the slope is about three, while for acetic anhydride the slope decreases continously from about four to one.

In 99.93 wt.% dioxan-water the hydrolysis of acetic anhydride is of the first-order with respect to water [2]. The rate of conversion of dimethylmaleic acid into anhydride is approximately proportional to the second power of the water concentration, while the rate of hydrolysis varies as the third power of the water concentration. Similar solvent effects are found for reactions occurring by the S_N2 mechanism [4].

It is interesting to note that the equilibrium constant

$$K = \frac{[\text{dimethylmaleic anhydride}]\ [\text{water}]}{[\text{dimethylmaleic acid}]} = \frac{k_1}{k_{-1}} \qquad (7)$$

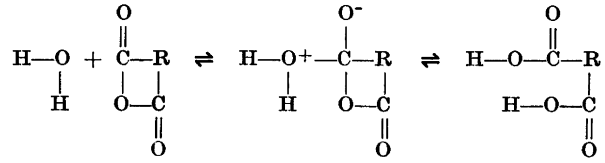
remains fairly constant in acetone-water mixtures, at least up to the 90 vol.% acetone-water mixture [1]. Thus both k_1 and k_1/c_{H_2O} should decrease to about the same extent in acetone-water mixtures as is also obtained. Consequently the reactants and products should be similar, and in this case neutral molecules. The S_N2 mechanism usually written for the hydrolysis of anhydrides gives as the primary reaction products two ions of opposite charge which are formed from the anhydride and water [6,2]. Thus the hydrolysis of the anhydride should be retarded when acetone is added to water, but the reverse reaction should simultaneously be greatly accelerated.



(8)

In this equation R denotes the group $CH_3\dot{C}{=}\dot{C}CH_3$, while for monocarboxylic acids and their anhydrides R denotes two alkyl groups, *e. g.* two methyl groups in the case of acetic anhydride.

A mechanism analogous to the Lowry mechanism for the ester hydrolysis would give better agreement with the solvent effects observed in the reversible hydrolysis of dimethylmaleic anhydride:



(9

The main difference between these mechanism is that in eqn. (8) the proton shift does not occur simultaneously as the C—O bond is broken, whereas in eqn. (9) the proton shift occurs at the same time as the C—O bond is broken, *i. e.* in the rate-determining slow step. The addition of a water molecule to the carbonyl carbon involves a loosening of the O—H bonds in the water molecule, and it can be assumed that a kind of hydrogen bond is developed between one of the protons of the water and the "etheral oxygen" atom of the an-

Table 4. Conversion of dimethylmaleic acid into anhydride in acetone-water mixtures. The equilibrium values are from a previous paper [1].

H_2O vol. %	c_{H_2O} mole/l	$t°$	$10^4 \times k_1$ sec^{-1}	$10^4 \times k_{-1}$ sec^{-1}	$10^4 \times k_2$ $l \cdot mole^{-1}$ sec^{-1}	Equilibrium c_{anh}/c_{acid}
100	55.4	0	12.2	4.7		2.6
50	29.1	0	2.03	0.70		2.9
50		20	15.2	3.8		4.0
10	11.2	20	0.38	0.020	17.7	18
1		20			6.52	

hydride. The breaking of the C—O bond will thus occur more easily and the reaction products will not carry any charges. The acid formed may of course ionize later. About the transition state between reactants and products, it can only be said that it is more polar than either the reactants or products because both the hydrolysis and the reverse reaction are retarded in solvents of low ionizing power (acetone).

In acetone, diethyl ether and dioxan and their mixtures with benzene, dimethylmaleic acid is, as far as can be determined, spontaneously and completely changed into its anhydride, and it is not possible to measure the position of the equilibrium. The rate of reaction is slow in all solvents but benzene which, when added to ether, increases the rate more than a thousand times. The reaction is of second order with respect to the acid in all the nonaqueous solvents studied, but of first order with respect to the acid in acetone-water mixtures containing less than 90 vol. % acetone. The conversion of dimethylmaleic acid into anhydride is thus probably acid-catalysed in solvents containing no, or only small amounts of, hydroxylic solvents. The hydrolysis of succinic anhydride is catalysed by acids in acetone-water mixtures containing

Table 5. Conversion of dimethylmaleic acid into anhydride in acetone, dioxan and diethyl ether-benzene mixtures.

Solvent	Benzene	$c_{ox.}$ mole/l	$10^2 \times k_2$ $l \cdot mole^{-1}$ sec^{-1}				E kcal.	log A
			0°	20°	40°	60°		
Ether-benzene	0	9.63	0.0180	0.141	0.82	4.35	16.49	9.44
	50	4.85	0.0566	0.386	0.232	1.09	16.17	9.67
	75	2.41		1.12				
	90	0.964		4.95	27.7		15.7	10.42
	95	0.482		16.05	66.3		12.9	8.85
	98.5	0.144		48.3	168		11.4	8.17
	99.6	0.0385		113	324		10.1	7.35
	99.9	0.0096		200				
Dioxan-benzene	0	23.5		0.0242				
	98.8	0.247		30.4				
Acetone	0	13.55		0.065				

Table 6. The order of the hydrolysis reaction with respect to water in acetone-water mixtures at 20°.

Acetone wt. %	Order of reaction with respect to water = $\Delta\log k/\Delta\log c_{H_2O}$				
	in hydrolysis of				conversion of DiMe-maleic acid into anhydride
	Acetic anhydride	Succinic anhydride	Glutaric anhydride	DiMe-maleic anhydride	
0 –40		3.47			
0 –43.9				2.46	2.32
0 –50	4.04		3.12		
40 –70		3.17			
43.9–87.8				3.04	2.18
50 –70	3.06		3.12		
70 –90	2.30	3.22	3.25		
90 –99	1.40				

small amounts of water, as is also the case for the ethanolysis in ethanol-benzene mixtures containing small amounts of ethanol [2]. The hydrolysis and alcoholysis of acetic anhydride was found to be slow in acetone, dioxan and ether, but fast in benzene [2]. Thus the solvent effects are very similar to those found in the present study (Table 5).

In Fig. 1, log k_2 (second order rate constant for the conversion of dimethylmaleic acid into anhydride) is plotted against log c_{ox} the molar concentration of the oxygen-containing solvent component, (in the case of dioxan the molar concentration divided by two). A linear relationship is found in mixtures containing less than 90 % benzene. The values for the pure solvents acetone, ether and dioxan fit the same curve too, but in case of dioxan only when the molar concentration is divided by two in order to take into account the two oxygen atoms in the molecule. The slope of the linear part of the curve is slightly less than two. All these effects suggest that the reactant, the acid molecule, forms an addition product with the oxygen-containing solvent molecules by hydrogen bond formation [5], which retards the rate of reaction:

$$\text{Acid} + \text{solvent} = \text{addition product} \tag{10}$$

$$c_{\text{free acid}} = K' \frac{c_{\text{add. prod.}}}{c_{\text{solvent}}} \tag{11}$$

$$-\frac{dc}{dt} = k_2 \cdot c^2_{\text{free acid}} = k_2 K'^2 \frac{c^2_{\text{add. prod.}}}{c^2_{\text{solvent}}} \tag{12}$$

In solvent mixtures containing a high proportion of the oxygen-containing solvent the addition of solvent to acid molecules may be regarded as complete and $c_{\text{add. prod.}}$ equals the total acid concentration (in curve 1 the linear part up to 90 vol. % benzene). In pure benzene the association between acid molecules and the solvent can be neglected, and hence a limiting value will be obtai-

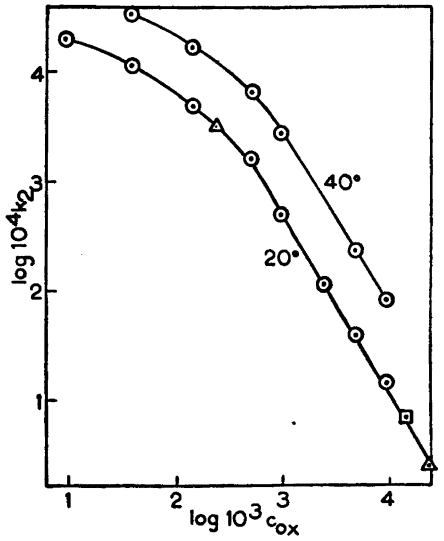


Fig. 1. Graphs showing the correlation between log k_2 *(the second-order rate constant of anhydride formation from dimethylmaleic acid) and log* c_{ox} *(the concentration of the oxygen-containing solvent component in moles per liter). Circles: diethyl ether-benzene mixtures; triangles: dioxan-benzene mixtures and square: pure acetone.*

ned for the rate constant. According to eqn. (12), the rate constant k_2 should vary inversely as the square of the concentration of the oxygen-containing solvent component; this is approximate true for the different solvents studied.

The high activation energy found in ether (16.5 kcal, Table 5) is partly due to the heat of addition or to the variation of K' in eqn. (10) with temperature. The activation energy, 10.1 kcal, found in 99.6 vol % benzene-ether, should be fairly close to the true activation energy. The reaction mechanism for the acid catalysed hydrolysis and the reverse reaction can be written in the same manner as for the uncatalysed reaction (eqn. (9)) with the difference that an additional proton is attached to the "etheral oxygen" of the anhydride before reacting. That the reaction is not acid catalysed in hydroxylic solvents may be due to hydrogen bonding at the "etheral oxygen" of the anhydride which has a similar catalysing effect as a proton addition.

From the differences in the activation energies for the hydrolysis and the reverse reaction in 50 vol. % acetone-water (13.4 and 16 kcal, respectively, calculated from the values in Table 4) and also from the equilibrium data published previously [1], it is seen that the hydrolysis is an exothermic reaction. In spite of this, the anhydride form is favoured because of the greater effect of the entropy factor. The first-order frequency factors of the hydrolysis and the reverse reaction in the same solvent mixture are log $A_{-1} = 6.61$ and log $A_1 = 9.12$. The activation entropies calculated [7] from frequency factors by means of the following eqn. (13)

$$A = e \frac{kT}{h} e^{\Delta S^*/R} \qquad (13)$$

are $\Delta S_{-1} = -30.2$ and $\Delta S^*_1 = -18.7$ e.u. The hydrolysis reaction is probably bimolecular, and by writing $k_{-2} = k_{-1}/c_{H_2O}$ an even more negative value is obtained for the entropy of activation, *viz.* $\Delta S^*_{-2} = -37.4$ e.u. In the for-

mation of anhydride from dimethylmaleic acid, the entropy increases by 18.7 e.u., and therefore the equilibrium lies more on the side of the anhydride in spite of the fact that this reaction is endothermic. From the difference in the activation entropies, it can be deduced that the geometry of the transition state between reactants and products is closer to that of the acid than of the anhydride form. From the great differences between both ionization constants of maleic and methylmaleic acids and from other facts, it is deduced that the two carboxyl groups are situated close to each other. The additional methyl group in dimethylmaleic acid should still effect a decrease of the distance between carboxyl groups. The high rate of conversion of dimethylmaleic acid into anhydride is due to the closely situated carboxyl groups and the resulting greater entropy of activation, which makes the anhydride form unusually stable against hydroxylic reagents. The rates and the energies and entropies of activation of the hydrolysis reaction are, however, of the same order as those found for other anhydrides [2].

REFERENCES

1. Koskikallio, J. *Suomen Kemistilehti* **B 29** (1955) 5.
2. Koskikallio, J. *Ann. Acad. Sci. Fennicae A II* (**1954**) 57.
3. Rivett, A. C. D. and Sidwick, N. V. *J. Chem. Soc.* **97** (1910) 1677, 732.
4. Tommila, E., Tiilikainen, M. and Voipio, A. *Ann. Acad. Sci. Fennicae A II* (**1955**) 65; Tommila, E. *Acta. Chem. Scand.* **9** (1955) 975; Tommila, E. and Nieminen, A. *Acta Chem. Scand.* **9** (1955) 989.
5. Mecke, R. *Discussions Faraday Soc.* **9** (1950) 161.
6. Ingold, C. K. *Structure and Mechanism in Organic Chemistry.* London 1955, p. 345, 752.
7. Glasstone, S., Laidler, K. J. and Eyring, H. *The Theory of Rate Processes* New York 1941, p. 417.

Received March 10, 1956.

ACTA CHEMICA SCANDINAVICA 10 (1956) 831—839

Incorporation of Radioactive Phosphate into Thiamine Phosphates in Yeast

KARL-HEINZ KIESSLING

Institute of Zoophysiology, Uppsala, Sweden

The incorporation of radioactive phosphate into thiaminetri-, di-, and monophosphate in baker's yeast has been examined. Yeast containing only its natural content of thiaminephosphates was used as well as yeast made rich in these compounds by preincubation with excess of thiamine.

In both cases radioactive phosphate was incorporated to a higher degree into thiamine triphosphate than into the other thiamine phosphates. The incorporation into thiamine triphosphate was localized especially to the terminal phosphate.

No appreciable synthesis of thiamine phosphates was going on during incorporation. Therefore the high turnover rate of radioactivity in the terminal phosphate of thiamine triphosphate with glucose as a substrate has been interpreted as caused by the compound in question taking part in the phosphate transport in the metabolism.

Yeast has a considerable ability of transforming added thiamine into thiamine diphosphate * (cocarboxylase) [1-4].

The role of TDP has long been known to be that of a decarboxylating coenzyme. Moreover Kiessling and Lindahl [5] found a turnover of the phosphate groups in TDP with a liver cyclophorase system when pyruvate was the substrate. Bartley [6] could not verify these results when using a kidney system and adding TDP, differing thereby from our experiments without added TDP. In a paper by Ogata *et al.*[7], however, it was shown that a rapid transfer of phosphate occurred from ^{32}P labelled TDP into ATP by a rat liver homogenate as well as by a cyclophorase system.

In 1954 it was shown that baker's yeast synthesizes besides TDP also thiamine triphosphate [8]. TTP exists likewise in yeast not preincubated with an excess of thiamine, but to a very small extent as compared with TDP.

* Abbreviations: T thiamine, TMP thiamine monophosphate, TDP thiamine diphosphate, TTP thiamine triphosphate, ATP adenosine triphosphate, ADP adenosine diphosphate, DPN diphosphopyridine nucleotide, Pi inorganic phosphate.

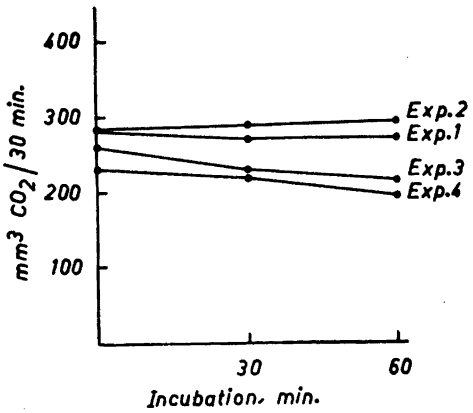


Fig. 1. TDP content of yeast during incubation with glucose and ^{32}P. The yeast had been preincubated with excess of thiamine.

Samples of 2 ml were taken at 0, 60 and 120 minutes, and added to 5 ml 0.1 M HCl at 100°, boiled for 1 minute, cooled, and centrifuged. The clear extracts were neutralized to pH 6, and TDP determined according to Westenbrink *et al.* with the Warburg method [13].

The question soon arose whether TTP could replace TDP in a decarboxylating system. Up to now only a system decarboxylating pyruvate has been examined. It has been shown by Gertrudes de la Fuente [9] * that chemically synthesized TTP, and by Kiessling [10] that both chemically synthesized TTP and TTP isolated from baker's yeast could not replace TDP as a coenzyme in this enzyme system from yeast.

In the present paper the incorporation of radioactive phosphate into yeast TTP is studied and compared with that into TDP, TMP, and ATP. The experiments have been carried out partly with yeast containing only its natural amount of thiamine phosphates, partly with yeast enriched in thiamine phosphates by preincubation with thiamine.

EXPERIMENTAL

Special chemicals. TDP and T were commercial samples (Roche products Ltd.). TMP was prepared by 20 minutes' hydrolysis of TDP at 100°. Paper chromatography proved all TDP to be transformed into TMP.

Chemical estimations. Phosphate was determined according to Berenblum and Chain [11] in a Beckman spectrophotometer. Measurements of radioactivity were made on samples of the diluted, wet ashed material. A M-6 liquid counter (20th Century Electronics) was used.

Enzyme preparation. Potato apyrase was prepared by Dr. W. Bartley according to Lee and Eiler [12].

* Recently a paper appeared by Rossi-Fanelli *et al.* (*Arch. Biochem. Biophys.* **58** (1955) 237) where the results of de la Fuente were confirmed.

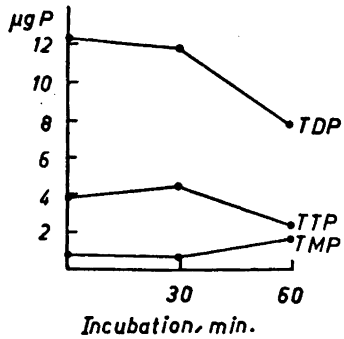


Fig. 2. TTP, TDP, and TMP in yeast rich in thiamine phosphates during incubation with glucose and inorganic phosphate.

Samples were taken at 0, 30 and 60 minutes, the thiamine phosphates isolated, and the phosphate determined after wet ashing.

Preparation and incubation of the particulate suspensions. The content of TTP in biological material in general is very low, but yeast is in my experience a better source than animal tissues. Furthermore, the TTP content of yeast can be very much increased. Preliminary experiments by the present author with animal tissues (liver, heart, brain) never showed any analogous accumulation. Thus yeast has been used in this investigation **. The first part of this paper deals with the naturally occurring TTP in yeast with regard to its capacity of incorporating radioactive phosphate. But even when starting with large amounts of yeast (1 kg) the content of TTP was so small that never sufficient TTP could be isolated to allow an enzymatic analysis of the incorporation of ^{32}P into its different phosphate groups. Thus for the carrying out of such analyses as is treated in the later part of this paper, yeast was used which by preincubation with an excess of T had been made rich in TTP and of course also in TDP and TMP [10]. This preincubation was allowed to go on for 20 hours, after which only a very slow synthesis of thiamine phosphates still occurred. To eliminate this remaining synthesis, the yeast was centrifuged down, mixed with NaCl (20 %), and washed once with succinate buffer pH 5 and twice with distilled water. The NaCl treatment was intended to cause a slight destruction of the cell surface. Excess of T could thus be washed away from the cells, and when yeast pretreated in this way with glucose and phosphate at 27° was incubated in a succinate buffer pH 6, no synthesis of TDP took place (Fig. 1). On the contrary a slight breakdown occurred. The purpose of eliminating the synthesis was to make sure that a possibly occurring incorporation of ^{32}P during the following incubation was not caused by further synthesis of thiamine phosphates from thiamine.

The concentration of TTP, TDP, and TMP throughout an experiment can be seen in Fig. 2. Phosphate was determined after wet ashing. During the first 60 minutes the concentrations are rather constant, but between 60 and 120 minutes TTP and TDP are decomposed (in this experiment TDP was decomposed more rapidly than in the experiments of the same type shown in Fig. 1), and a slight accumulation of TMP takes place.

When examining the incorporation of ^{32}P into the different phosphate groups of the thiamine phosphates 200 g of yeast pretreated as described above was incubated with 0.5 mC inorganic radioactive phosphate and 4 g glucose. Samples containing 50 g yeast were taken at 0, 10, 30, and 60 minutes, and trichloroacetic acid added to a final concentration of 9 %. Then TTP, TDP, and TMP were isolated according to Kiessling [10], and ATP and Pi according to Krebs *et al.*[15]

** The yeast was a baker's yeast from Uppsala Ångkvarn Ltd, Sweden.

When studying the incorporation of ^{32}P into TTP in yeast only containing its natural amount of TTP, fresh baker's yeast was used without adding T and treating it with NaCl, but otherwise with the same additions as to the NaCl treated yeast.

Paper chromatographic separation of thiamine phosphates. For the separation of TTP from other phosphates different paper chromatographic methods have been developed, and the author considers one using *iso*butyric acid-ammonia-versene the most suitable [10]. However, during the first part of this investigation, *viz.* that with yeast only containing its natural amount of TTP, this solvent was not yet known to separate also TTP from other compounds. Instead the method described by Siliprandi and Siliprandi [14] was used. Here ATP and ADP have the same R_F value as TTP, and had to be eliminated prior to chromatography. This was done by adsorbing the thiamine phosphates on Fuller's earth at pH 6, as described before [10]. No ATP, ADP, or other nucleotides then contaminated the thiamine phosphates as was proved by using a paper chromatographic method of Burrows *et al.*[16], separating nucleotides from thiamine phosphates, but not TTP, TDP, and TMP from each other (Fig. 3 A).

Enzymatic hydrolysis of γP and βP from TTP. Lee and Eiler [12] found that a potato apyrase, when incubated with ATP at 0° only splits off the γP, and at 40° both γ and βP. When incubating TTP with this enzyme, Kiessling demonstrated that TTP was attacked in the same way [10]. This enzyme was therefore used in the present investigation to split off the different phosphate groups from TTP in order to compare the incorporation of ^{32}P into them.

RESULTS

Incorporation of ^{32}P into thiamine phosphates in yeast not preincubated with thiamine

In fresh baker's yeast incubated with glucose and radioactive inorganic phosphate the incorporation into TTP, TDP, and TMP is clear from chromatograms reproduced in Fig. 3 B.

It is obvious that the incorporation of ^{32}P into TTP is much more rapid than that into TDP or TMP. No synthesis of TDP occurred during the incubation as evidenced by measurements with the Warburg manometric method.

The incorporation into TTP was dependent on the presence of a substrate. In the experiment shown in Fig. 3 B no substrate was added before the lapse of 20 minutes, and the incorporation of ^{32}P into TTP was very slow. At 20 minutes glucose was added, and the incorporation rate increased immediately.

Hydrolysis of TTP to TDP and TMP. When keeping a TTP sample at room temperature it decomposes only slowly to TDP and TMP. After 15 minutes in N HCl at 100° C it is nearly completely broken down to TMP, but shorter hydrolyzing times give mixtures of TDP and TMP.

A TTP sample isolated from yeast which had been incubated as described above was put as two spots on a chromatogram. A drop of diluted HCl was then added to one of the spots, and dried with hot air. This was repeated until total hydrolysis of the TTP of the spot was supposed to have taken place. Fig. 3 C shows the results. TTP was hydrolyzed, and in its place TDP and TMP spots were formed. The radioactivity of the TDP spot was low, and no appreciable activity was found of the TMP spot. On the other hand the ^{32}P was recovered as inorganic phosphate. From Fig. 3 C it appears that chiefly the γP of TTP becomes radioactive during 20 minutes incubation with substrate.

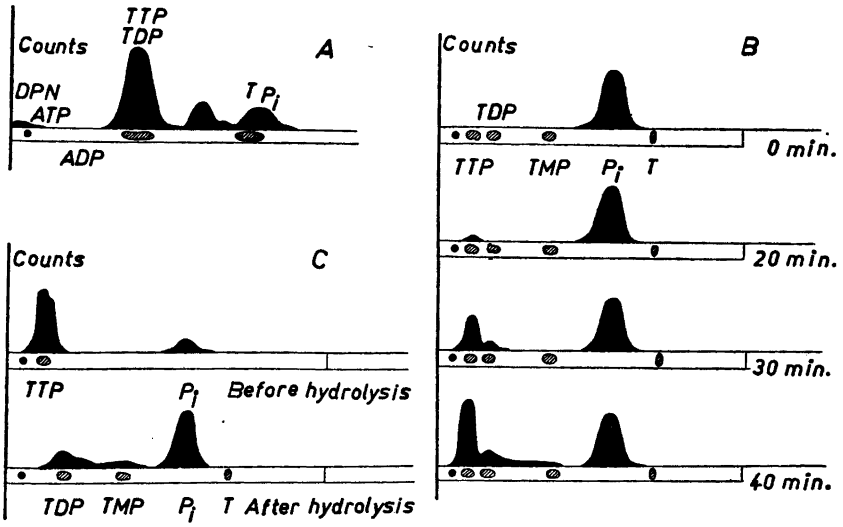


Fig. 3 A. Paper chromatographic separation of thiamine phosphates after removal of ATP, ADP, and DPN.

The chromatographic method is one described by Burrows *et al.*[16] in a solvent containing 60 vol. acetone and 40 vol. 35 % v/v formic acid. The chromatogram shows the absence of radioactivity in the spots corresponding to the R_F-values of the nucleotides. Moreover, when examinating the chromatograms in UV-light 260 mμ no dark spots could be seen. The thiamine phosphates could, however, be detected easily in UV-light after spraying the chromatograms with alcaline $Fe(CN)_6^{3-}$. They are marked out as dark spots in the figure.

B. Paper chromatographic separation of TTP, TDP, TMP, and Pi from yeast.

The yeast was incubated with ^{32}P and glucose in a succinate buffer pH 6. Glucose was not added until after the lapse of 20 minutes. Samples were taken at 0, 20, 30, and 40 minutes, and the thiamine phosphates separated. The paper chromatographic method is one described by Siliprandi and Siliprandi [14]. The thiamine compounds were made visible in UV-light as described in fig. 3 A, and marked out as dark spots.

C. TTP from a yeast sample taken after 40 minutes incubation as described in Fig. 3 B before and after hydrolysis.

As seen from the upper figure this gives only a single spot without hydrolysis. The lower figure shows the same, only here the TTP was hydrolyzed on the paper chromatogram with HCl in hot air before starting the second chromatography. TTP is transformed into TDP and TMP, and the radioactivity is mainly recovered as inorganic phosphate.

The determination of radioactivity on the strips was done according to Lindberg and Hummel [17].

A rough analysis of the radioactivity per μg P was made on TTP and ATP collected from several chromatograms (Table 1). The radioactivity of TTP was about half that of ATP.

Incorporation of ^{32}P into thiamine phosphates in yeast preincubated with an excess of thiamine

In order to obtain in the yeast an amount of TTP sufficient for a real analysis of ^{32}P in the different phosphate groups preincubation with an excess

Table 1. Radioactivity of TTP and ATP from yeast incubated with radioactive phosphate and glucose in a succinate buffer pH 6. The yeast contained only its natural amount of thiamine phosphates, i. e. *no preincubation with thiamine had been carried out before the addition of ^{32}P and substrate. TTP was isolated by paper chromatography (Siliprandi and Siliprandi)* [14], *and ATP according to Krebs and Hems* [15]. *After wet ashing of the isolated compounds radioactivity was determined, and expressed as counts / μg P.*

Exp. 1.	TTP	1 717
	ATP	3 145
Exp. 2.	TTP	1 350
	ATP	3 480

of T was started with, as described above. This preincubation was carried on until no appreciable synthesis occurred, and the thiamine not yet used up was then washed out of the cells. Thereafter the yeast, rich in TTP, TDP, and TMP, was incubated in the same way as described for the fresh yeast containing only its naturally occurring TTP. Glucose was, however, present from the beginning. Fig. 4 shows the ^{32}P per *ug* acid hydrolysable phosphate in TTP and TDP at different intervals. The incorporation into TDP was slow, and ceased after 30 minutes. Into TTP it was much more rapid, and even at 60 minutes ^{32}P was still being incorporated.

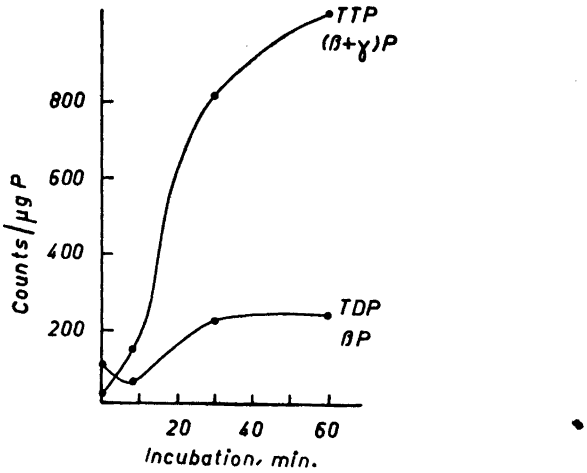


Fig. 4. Radioactivity of hydrolysable phosphate in TTP and TDP from yeast after incubation with ^{32}P and glucose in a succinate buffer pH 6.

The content of thiamine phosphates in the yeast was very high as the yeast had been incubated with an excess of thiamine for 20 hours before ^{32}P and glucose were added. The values are given as counts / μg P, and for TTP this means both βP and γP together, for TDP only βP.

Table 2. Radioactivity of α, β, and γ P of TTP and ATP from yeast after incubation with glucose and radioactive phosphate. Before the addition of ^{32}P and glucose the yeast had been preincubated with excess of thiamine, and thus was very rich in thiamine phosphates during the following incubation. The different phosphate groups were split off by means of a potato apyrase, except for ATP in exp. II, where βP and γP are determined together after acid hydrolysis. The values are given as counts / μg P.

Exp.	Time of incubation (minutes)	TTP			ATP		P_i
		αP	βP	γP	βP	γP	
I	0	0	0	0	0	0	6 310
	10	16	128	280	—	—	—
	30	250	1 102	1 860	3 290	3 820	—
	60	960	1 140	2 400	3 260	2 865	4 070
					(β + γ)P		
II	0	0	0	0	0		39 360
	30	600	1 200	7 320	17 800		—
	60	2 080	2 432	6 992	16 480		20 143

Enzymatic hydrolysis of TTP. When TTP is incubated with potato apyrase at 0° only the γ P is split off, at 40° both the γ and the βP[10]. TTP isolated from samples taken at different intervals of the ^{32}P-incubation was treated with apyrase, and then analyzed for radioactive phosphate (Table 2). In expt. I, Table 2 also ATP is treated in the same way as TTP. In expt. 2, Table 2 β P and γ P from ATP are determined together after acid hydrolysis. Also TDP and TMP (Table 3) were analysed for ^{32}P by acid hydrolysis and wet ashing.

DISCUSSION

This work was started with yeast containing only its natural amount of TTP, *i. e.* no thiamine was added after the yeast left the factory. From yeast TTP could be isolated in amounts detectable on a paper chromatogram. With the chromatographic method used in this part of the investigation only small amounts of yeast extract could be added on the paper to allow a good separation of TTP and TDP. After collecting TTP from several chromatograms it was, however, possible to make preliminary analyses as seen from Table 1. When hydrolyzing the TTP directly on the chromatogram it could be transformed into TDP and TMP. Thus TTP isolated from yeast incubated with ^{32}P and glucose in a succinate buffer gave a spot on the chromatogram which was rather radioactive, whereas the TDP and TMP formed by hydrolysis gave spots exhibiting only very feeble radioactivity (Fig. 3 B and C). It thus seems as if during the comparatively short incubation only the γP of TTP was exchanged. Glucose is necessary for this exchange as is shown in Fig. 3 B. Here no substrate was added until after 20 minutes, and TTP did not incorporate any noteworthy amount of ^{32}P until glucose was present.

Table 3. Radioactivity of α and βP of TDP and αP of TMP from yeast after incubation with glucose and radioactive phosphate. The yeast was the same as that used for investigating TTP and ATP (Table 2). The phosphate groups were split off by acid hydrolysis and wet ashing. The values are given as counts / μg P.

Exp.	Time of incubation (minutes)	TDP		TMP
		αP	βP	αP
II	0	0	0	0
	30	324	490	301
	60	332	408	482

When yeast is incubated with an excess of thiamine in a pyrophosphate buffer a strong synthesis of thiamine phosphates occurs [10]. TTP accumulates to a greater extent in this buffer than for example in a succinate or monophosphate buffer. After about 24 hours the synthesis has almost ceased, and on the removal of most of the remaining thiamine it comes to an end. The use of yeast rich in thiamine phosphates, especially TTP, has certain advantages with regard to the investigation into the rate of incorporation of ^{32}P into the different phosphate groups during the metabolism of glucose. A much greater amount of TTP can be isolated making possible an enzymatic hydrolysis of the different phosphate groups. From Tables 2 and 3 and Fig. 4 it is seen that there is a higher turnover rate of phosphate in TTP than in TDP or TMP. When incubating only for a short time (10 or 30 minutes) mainly the two terminal phosphate groups of TTP are radioactive, and γP in a higher degree than βP. After 60 minutes the radioactivity of αP nearly equals that of βP (Table 3). From this it can be concluded that TTP takes part in the phosphate transport during the metabolism, and this mainly by the turnover of its terminal phosphate. The radioactivity of the most active phosphate group of TTP, the γP, never reaches that of inorganic phosphate or ATP. This may be explained by the hypothesis that during the preincubation with excess of thiamine, the yeast synthesizes more TTP than can take a share in the phosphate transport. This is not the case when using yeast containing only its natural source of TTP. In Table 1 the values of TTP are about half those of ATP, but as is seen from the chromatograms in Fig. 3 C, only γP exhibits a remarkable radioactivity after 20 minutes' incubation. In ATP both βP and γP are nearly equally labelled after this incubation time. Consequently the terminal P of TTP and ATP may be labelled to about the same extent.

Acknowledgements. I am indebted to Prof. P. E. Lindahl for the kind interest he has shown in my work, to Dr. W. Bartley for the preparation of potato apyrase, and to Mrs. M. Aunver for valuable technical assistance.

This work was made possible by a grant from the *Swedish Natural Science Research Council.*

REFERENCES

1. Fink, H. and Just, F. *Biochem. Z.* **308** (1941) 15; **309** (1941) 1, 219, 212; **311** (1942) 61, 287.
2. Sperber, E. *Naturwiss.* **29** (1941) 765.
3. Sperber, E. and Renwall, S. *Biochem. Z.* **310** (1941) 160.
4. Westenbrink, H. G. K., Steyn-Parvé, E. P. and Veldman, H. *Biochim. et Biophys. Acta* **1** (1947) 154.
5. Kiessling, K.-H. and Lindahl, P. E. *Arkiv Kemi* **4** (1952) 285.
6. Bartley, W. *Biochem. J. London* **56** (1954) 379.
7. Ogata, K., Nohara, H., Morita, T. and Kawai, K. *J. Biochem. Japan* **42** (1955) 13.
8. Kiessling, K.-H. *Nature* **172** (1953) 1187.
9. de la Fuente, G. and Diaz-Cadavieco, R. *Nature* **174** (1954) 1014.
10. Kiessling, K.-H. *Biochim. et Biophys. Acta* **20** (1956) 293.
11. Berenblum, I. and Chain, F. *Biochim. J. London* **32** (1938) 295.
12. Lee, K. H. and Eiler, J. J. *Science* **114** (1951) 393.
13. Westenbrink, H. G. K. and Steyn-Parvé, E. *Vitaminforsch.* **21** (1949—50) 461.
14. Siliprandi, D. and Siliprandi, N. *Biochim. et Biophys. Acta* **14** (1954) 52.
15. Krebs, H. A. and Hems, R. *Biochim. et Biophys. Acta* **12** (1953) 172.
16. Burrows, S., Grylls, F. S. M. and Harrison, J. S. *Nature* **170** (1952) 800.
17. Lindberg, O. and Hummel, J. P. *Arkiv Kemi* **1** (1949) 17.

Received March 24, 1956.

ACTA CHEMICA SCANDINAVICA 10 (1956) 840—851

The Infra-Red Absorption Spectra of Some Amino Acid-Metal Chelates at Liquid Air Temperature

ANDREAS ROSENBERG

Institute of Biochemistry, Uppsala, Sweden

A method for obtaining infra-red absorption spectra at low temperatures is described. The infra-red spectra of some amino acid-metal chelates are examined and evidence presented in support of the concept that the carboxyl groups and the metal ions in certain chelates tend to form bonds of different, probably more covalent, character than the usual ionic carboxyl-metal ion linkage.

The use of infra-red (IR) absorption measurements for the investigation of coordination compounds has been scarce. Recently, however, a number of investigations on metal chelate compounds have been published. In these studies changes in IR absorption have been used in order to gain information about the behaviour of chelate forming groups in the molecule and thus even about the nature of the bond with the metal ion. Such spectral changes have also been used as a means of distinguishing between different geometrical isomers of the same chelate. Thus, for example, Bryant, Parriaud and Fernelius [1] have studied the effect of metal ions on the position of the carbonyl frequency of tropolone and its derivatives. They have observed shifts of about 20 cm^{-1} towards lower wavenumbers for the carbonyl frequency after chelate formation. On the other hand differences between shifts caused by various metal ions were negligible. This seems to confirm the conclusion arrived at by Bellamy and Branch [2] from investigations on the metal chelates of diketones. They found that the values for the carbonyl frequency of acetylacetone chelates are essentially the same for all the metals investigated. The shift in carbonyl frequency in this case is probably mostly influenced by an increase in the resonance effects of the *p*-diketone molecule and not by any difference in the type of linkage with the metal ion. That this kind of behaviour is not general is shown by the same authors with salicylaldehyde. The chelates of this compound with different metal ions do show significant differences in the position of the carbonyl frequency. A slightly different way of applying IR absorption was used by Merrit and Wiberley [3] who showed that differences exist in IR absorption between *cis* and *trans* isomers of Co^{+++} chelates.

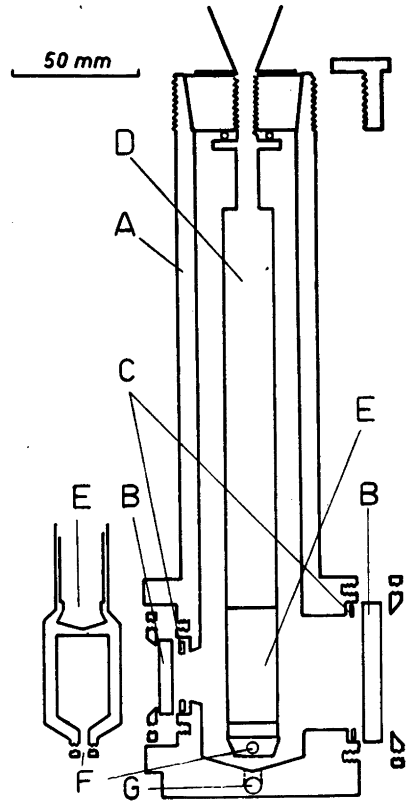


Fig. 1. Low-temperature cell. For explanations, see the text.

The aim of the present study was to examine the possibilities of using the IR methods for investigating biochemically interesting metal chelates. The investigation of complicated compounds can only be successful provided that the behaviour of the important chelate forming groups, such as NH_2, has been studied in simple molecules with established configurations. Previously Lenormant [4] has published some IR curves for such compounds and recently Sen *et al.*[5] have studied Cu^{++} and Ni^{++} chelates of glycine. The present investigation of amino acid-metal chelates was carried out as a necessary introduction to further studies of metal-ion peptide complexes. Pt^{++}, Cu^{++} and Ni^{++} were used since these ions form chelates of the same square-planar type[6].

EXPERIMENTAL

A Perkin-Elmer model 21 spectrophotometer equipped with a CaF_2 prism was used for the IR measurements. The substances, all in the solid state, were mixed with powdered KBr and pressed to transparent discs according to the method developed by Schiedt and Reinwein [7]. Earlier investigations [5] and preliminary experiments made here showed that the changes in the spectra were such that the NaCl prism was not able to give the required resolution. The important regions around 3 and 6 μ showed broad absorption

bands strongly influenced by the presence of the water of crystallization. Even with the use of a CaF_2 prism the resolution was not always sufficient. In search for a method giving still better resolution, the low-temperature approach seemed to be most promising. In recent years low-temperature IR spectroscopy has been the subject of some controversy. It is generally accepted that cooling a substance so that it changes its state of aggregation, causes changes in its IR absorption. On the other hand the effects produced by continued cooling of a given crystalline phase are open to discussion. King, Hainer and Mc Mahon [8], for example, have investigated a number of high-molecular-weight substances and conclude that very little is gained by the use of low temperatures. However, work reviewed by Hornig [9] indicate that the low-temperature method is very effective when used for low-molecular-weight substances. The main difficulty encountered in the present work was to obtain definite bands from regions with broad non-specific absorption. Thus even if the results obtained by low-temperature measurements were only caused by an increased transparency giving new peaks in the region of non-specific absorption, the use of low temperatures would be justified. The next step was the construction of a simple low-temperature cell suitable for work with crystalline substances. The main obstacle in low-temperature work with crystals is the heat transfer from the substance to the refrigerant. For this reason the KBr-disc method was utilized. The crystals investigated were mixed with powdered KBr and pressed to rectangular plates which were firmly attached to metal frames. The only problem of heat transport was thus the transfer from the metal frame to the metal reservoir containing liquid air and this was easily solved. Fig. 1 shows a schematic drawing of the cell. The outer case (A) is made of Perspex. The windows (B) are standard Perkin Elmer cell windows made of NaCl which are tightened with rubber washers (C). The metal container (D) for the liquid air is made of brass. Its lower part (E) is formed as a holder for the metal frame of the KBr disc. Good contact between the frame and the holder is obtained by tightening with a screw at (F). The cell is connected to a vacuum pump *via* (G). When the pressure was maintained below 0.5 mm Hg, no fogging of the windows could be detected after approximately 100 runs. The following procedure was used to control the effectiveness of the cell. A copper-constantan thermocouple was embedded in powdered KBr and pressed into the disc. When liquid air was introduced in the container by means of a siphon the temperature sank rapidly reaching an equilibrium value of $-170°$ after approx. 8 minutes and it remained constant as long as the reservoir contained liquid air.

Cu^{++} and Ni^{++} chelates were prepared by mixing aqueous solutions of Na salts of amino acids with solutions of $CuCl_2$ and $NiCl_2$, respectively. The water-soluble chelates were recrystallized from water, the insoluble chelates washed extensively with water and alcohol. The Pt^{++} chelates were prepared from K_2PtCl_4 and glycine according to Refs [11,12]. The *cis* and *trans* forms were separated by fractional crystallization.

Table 1. Analyses.

Chelate	% N		% Metal	
	Calc.	Found	Calc.	Found
$Cu(NH_2CH_2COO)_2H_2O$	12.20	12.27		
$Cu(CH_3CHNH_2COO)_2H_2O$	10.87	10.95		
$Ni(NH_2CH_2COO)_22H_2O$	11.54	11.67		
$Ni(CH_3CHNH_2COO)_22H_2O$	10.34	10.20		
$Cu((CH_3)_2CHCH_2CH(NH_2)COO)_2$	8.65	8.50	Cu 19.62	Cu 19.85
$Ni((CH_3)_2CHCH_2CH(NH_2)COO)_2$	8.78	8.43	Ni 18.40	Ni 18.76
$Pt(NH_2CH_2COO)_2$ *cis*	8.16	8.06		
$Pt(NH_2CH_2COO)_2$ *trans*	8.16	8.20		
$KPtCl_3(NH_2CH_2COO)$	3.69	3.84		

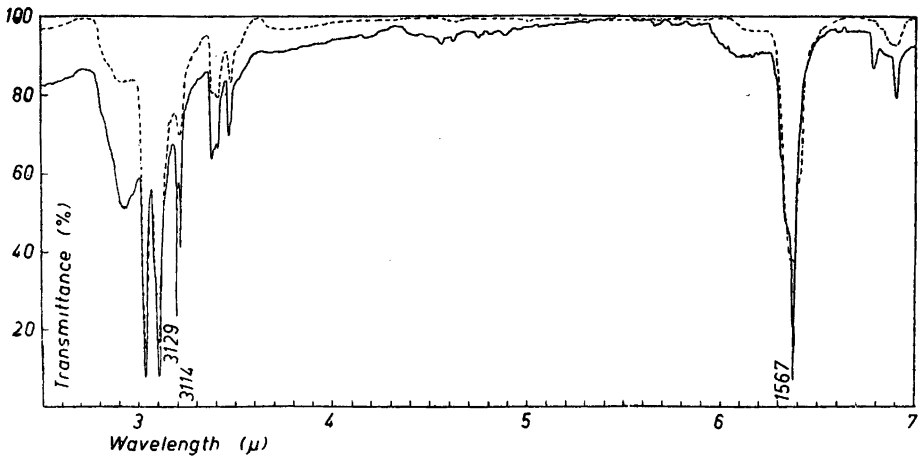


Fig. 2. IR absorption of ethylenediamine Cu++ $CuCl_4$.
..... *at 25°*
——— *at —170°*

RESULTS OF THE ABSORPTION MEASUREMENTS

In order to illustrate the effect of low temperature on the IR absorption, the IR spectra of a group of substances were recorded both at room temperature and at —170°. The substances were deliberately chosen among those closely related to the compounds which were to be investigated. The effects obtained vary with different substances. Figs. 2 and 3 show two possibilities

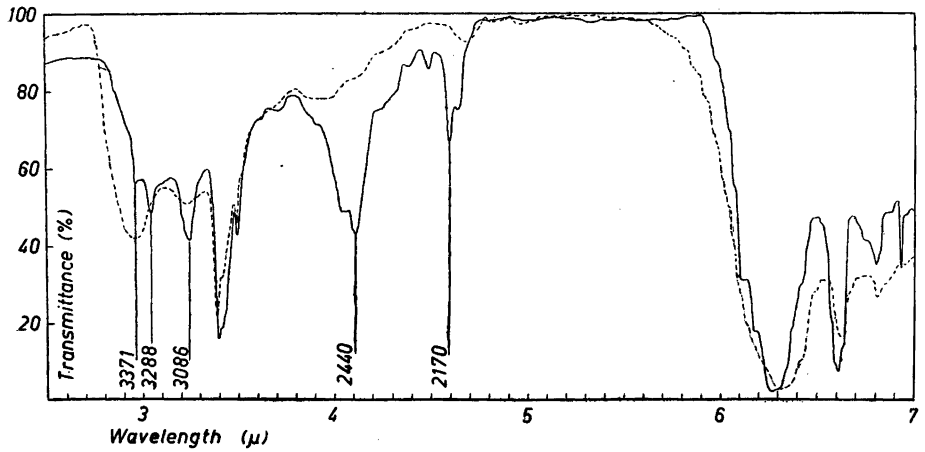


Fig. 3. IR absorption of Na+ leucine.
..... *at 25°*
——— *at —170°*

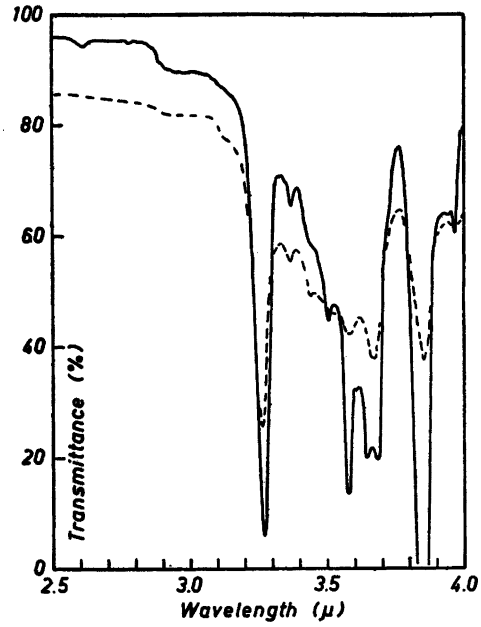


Fig. 4. IR absorption of DL-*alanine.*
..... *at 25°*
——— *at −170°*

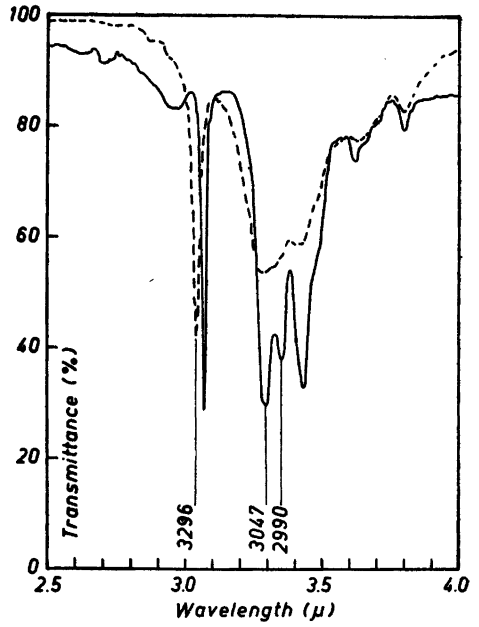


Fig. 5. IR absorption of glycylglycine.
..... *at 25°*
——— *at −170°*

of an extreme nature. $EDA_2Cu \cdot CuCl_4$ (Fig. 2), prepared according to Chattaway and Drew [10], shows a simple and well-defined spectrum already at normal temperatures. The only effects obtained by the low temperature were the splitting of one band into two at 3 129 cm^{-1} (3.196 μ) and 3 114 cm^{-1} (3.211 μ) besides the narrowing of the 1 567 cm^{-1} (6.380 μ) band. In sharp contrast stands the behaviour of Na DL-leucine (Fig. 3) where the effects are considerable. The NH_2 bands at 3 371 cm^{-1} (2.966 μ) and 3 288 cm^{-1} (3.041 μ) emerge from a broad band of continuous absorption. The bands at 3 086, 2 440 and 2 170 cm^{-1} (3.240, 4.10 and 4.61 μ) are most likely due to water molecules present in the crystals as these bands vanish completely after heating to 120° over P_2O_5. The NH_2 bands remain unperturbed with the exception of a slight shift. That the effects obtained by the low temperature are not entirely due to the presence of water molecules is shown by Figs. 4 and 5, displaying the IR absorption spectra of DL-alanine and glycylglycine from 2.5 μ to 4 μ. In this connection it is of interest to note that while the absorption bands due to the NH_3^+ group of glycylglycine at 3 047 cm^{-1} and 2 990 cm^{-1} (3.282 and 3.344 μ) scarcely show any shifts due to the temperature change, the band at 3 296 cm^{-1} (3.034 μ) ascribed to the NH of the amid linkage shows a shift of approximately 25 cm^{-1} towards lower wavenumbers.

Before further discussion some words ought to be said about the effects due to moisture. As it is difficult to keep KBr powder absolutely dry and as

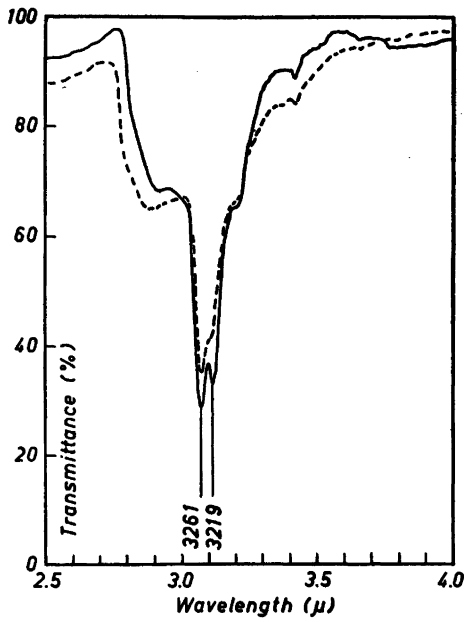


Fig. 6. IR absorption of $KPt^{++}Cl_2$ glycine.
..... *at 25°*
——— *at −170°*

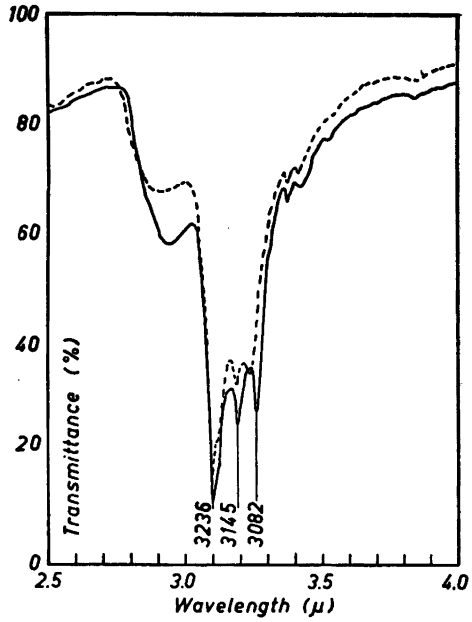
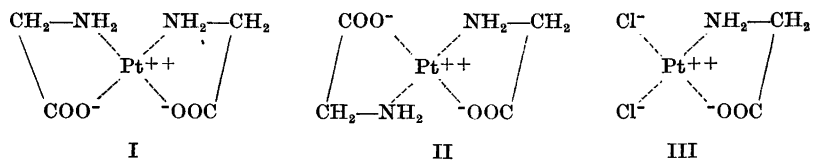


Fig. 7. IR absorption of Pt^{++} glycine$_2$(cis).
..... *at 25°*
——— *at −170°*

during the low-temperature run a certain amount of water vapour condenses on the KBr disc, a relatively weak and broad absorption appears at 2.95 μ (3 400 cm^{-1}). This kind of absorption has very little effect on the sharp and well defined bands of NH_2 and no special effort was made to compensate for it.

In general all the metal-amino acid chelates investigated showed different and highly individual absorptions in the "fingerprint region" (8—15 μ). As the purpose of this investigation was to study the behaviour of NH_2 and COOH groups the discussion is limited to the regions around 3 and 6 μ where well-defined absorption bands of these groups appear. The first question to be answered was if the difference between geometric isomers of the same chelate has any influence on the IR absorption of NH_2 and COOH vibrations. For this purpose the three possible forms of Pt^{++} glycine chelates were prepared according to Grünberg and Pitzyn [11] and Ficken and Ley [12]. Figs. 6—8 show the IR absorption in the 3 μ region of Pt^{++} glycine$_2$*cis* (I), Pt^{++} glycine$_2$*trans* (II) and $KPt^{++}Cl_2$-glycine (III).



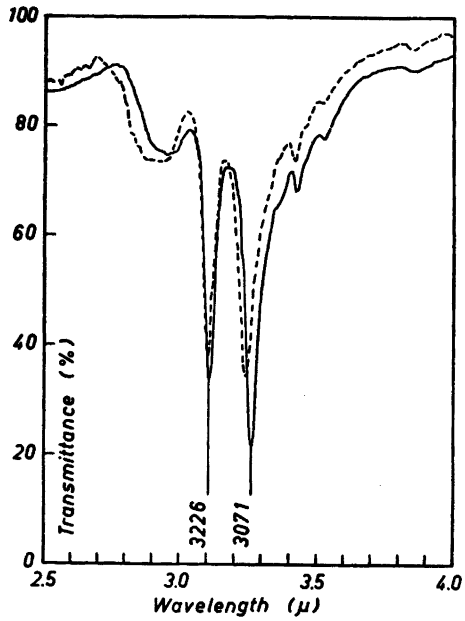


Fig. 8. IR absorption of Pt++ glycine$_2$ (trans).
..... *at 25°*
——— *at −170°*

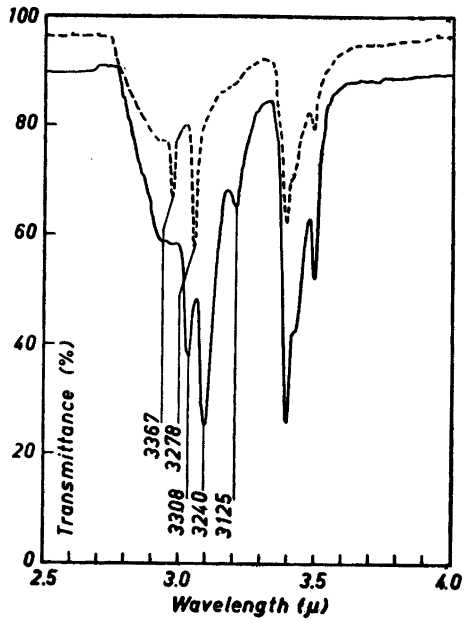


Fig. 9. IR absorption at −170° of
..... *Ni++ leucine$_2$*
——— *Cu++ leucine$_2$*

Low-temperature values are given in Table 2 as the absorption curve of monoglycine shows inadequate resolution at normal temperatures.

Table 2.

	NH_2 frequencies in wavenumbers (cm^{-1})		
$KPt^{++}Cl_2$-glycine	3 261	3 219	
Pt^{++}-diglycine *cis*	3 236	3 145	3 082
Pt^{++}-diglycine *trans*	3 226	3 071	

The same kind of differences are present in the 6 μ region. Here both the *mono* and *trans* chelates display a well-defined absorption band of great intensity at 1 655 cm^{-1} (6.04 μ) and 1 644 cm^{-1} (6.08 μ), respectively. These bands are naturally not as sharp as those in the NH region so that an uncertainty of $\pm$ 5 cm^{-1} must be taken into account. They can with certainty be ascribed to the carboxyl group. The NH bending mode is found at 1 582 cm^{-1} (6.321 μ) for the *mono*chelate and at 1 608 cm^{-1} (6.220 μ) for the *trans* isomer of the dichelate. The *cis* form displays a broad band of overlapping carbonyl frequencies with distinct maxima at 1 681 (5.95 μ) 1 661 cm^{-1} (6.02 μ) and 1 639 cm^{-1} (6.10 μ). The region of NH bendings also shows two peaks at 1 610 cm^{-1} (6.208 μ) and 1 570 cm^{-1} (6.370 μ), respectively. These perturbations in the

Table 3.

	NH_2 frequencies in wavenumbers (cm^{-1})		
Na^+ leucine	3 378.	3 289	
Ni^{++} $leucine_2$	3 367	3 278	
Cu^{++} $leucine_2$	3 308	3 240	3 125

spectrum are not due to the presence of water molecules since the spectrum remains unchanged after the substance is dried at 120° over P_2O_5. The same conclusion can be drawn from the analytical data. The next step was to investigate the influence of different metal ions on the NH_2 and COOH frequencies. The presence of water molecules in most of the Cu^{++} and Ni^{++} chelates greatly complicates the spectra. Although these effects can be reduced by drying it seemed advisable to avoid such complications in the beginning. For this reason the salts of DL-leucine with Na^+, Ni^{++} and Cu^{++} were compared. Both the Cu^{++} and Ni^{++} chelates of leucine contain no water, the spectrum remaining unchanged after heating over P_2O_5. Fig. 9 presents the IR absorption of Ni^{++} and Cu^{++} chelates of DL-leucine. The NH_2 frequencies of Ni^{++}, Cu^{++} and a dried sample of Na^+ leucine are presented in Table 3.

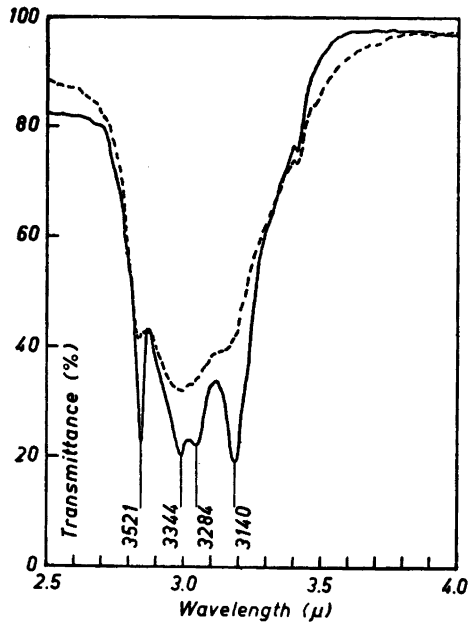


Fig. 10. IR absorption of KMg^{++} nitrilotriacetic acid.
..... *at 25°*
——— *at −170°*

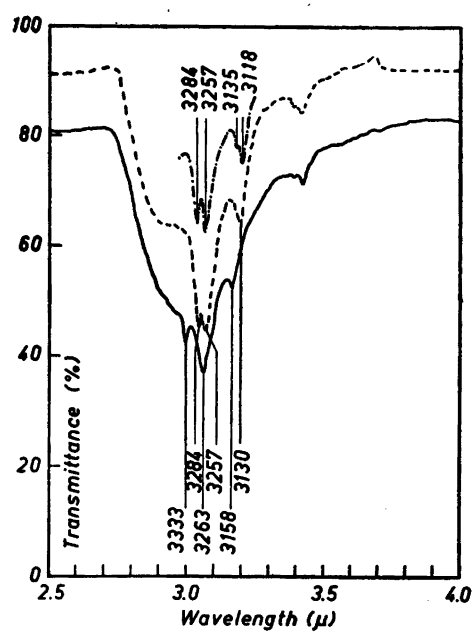


Fig. 11. IR absorption of Cu^{++} $glycine_2$ H_2O ——— at −170° and Cu^{++} $glycine_2$
..... *at 25°*
—·—·— *at −170°*

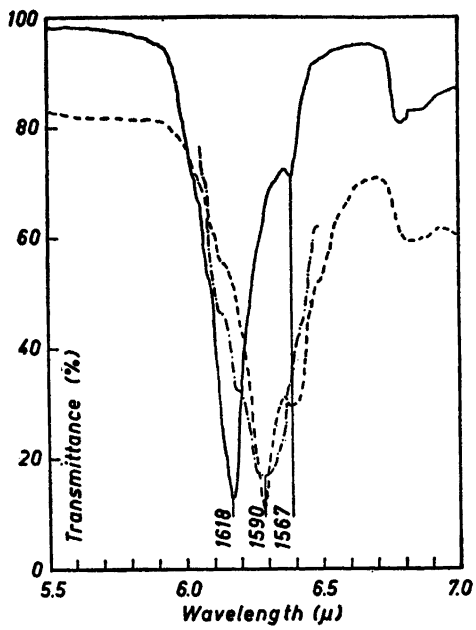


Fig. 12. IR absorption at −170° of
..... *Cu++ leucine₂*
——— *Ni++ leucine₂*
—·—·—· *Na+ leucine*

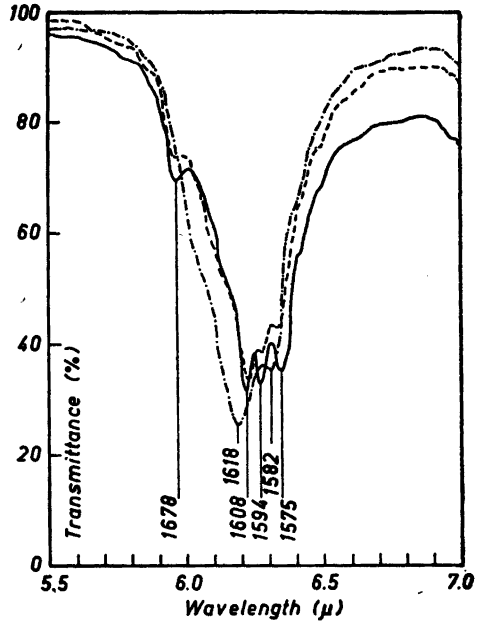


Fig. 13. IR absorption of Cu++ glycine₂ H_2O.
..... *at 25°*
——— *at −170°*
Cu++ glycine₂ —·—·—· *at −170°*

All the values in Table 3 are low-temperature values. As the low temperature curves of Ni^{++} and Cu^{++} chelates showed no shifts of absorption bands when compared to the curves at normal temperature, Fig. 9 shows only one, the low-temperature curve of each substance. The IR spectra of glycine and alanine chelates in this region are rather complicated due to hydration. That water molecules itself may possess, well defined and sharp bands in the neighbourhood of 3 μ can conveniently be demonstrated by the IR absorption spectrum of KMg-nitrilotriacetic acid prepared according to Schwarzenbach [13]. This salt of a substituted amino acid has no NH or OH groups of its own. But as it crystallizes with several molecules of water the IR spectrum shown in Fig. 10 has several sharp absorption peaks reminding of the frequencies of NH_2. The different absorption curves of Cu^{++} $glycine_2$ are shown in Fig. 11. It is difficult to decide without further investigations if the absorption maximum at 3 333 cm^{-1} (3.000 μ) being NH frequency is shifted to 3 248 cm^{-1} (3.045 μ) after drying or if this frequency belongs to the water of hydration. The behaviour of Cu^{++}DL-$alanine_2$ is analoguous. The spectra of dried substances, however, show the same kind of differences with varying metal ions as leucine chelates. For exampel Ni^{++} $alanine_2$ has its NH_2 frequencies at 3 361 cm^{-1} (2.975 μ) and 3 284 cm^{-1} (3.045 μ) whereas the Cu^{++} chelate of alanine shows

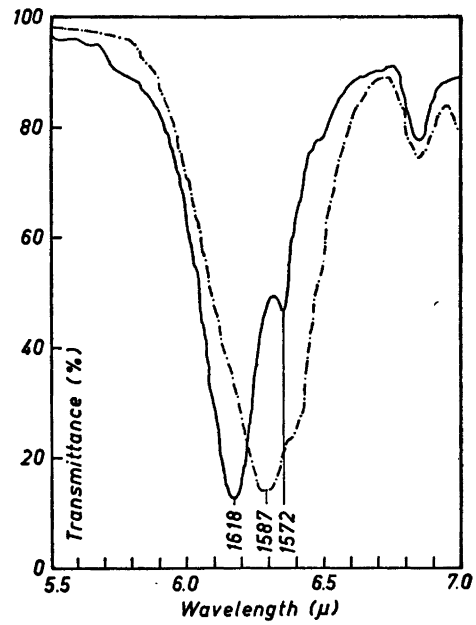


Fig. 14. IR absorption at −170° of Cu^{++} *alanine*$_2$ ———— Ni^{++} *alanine*$_2$ —·—·—·

two strong bands at 3 263 and 3 231 cm^{-1} (3.065 and 3.095 μ) with an additional weak band at 3 145 cm^{-1} (3.180 μ).

The behaviour of the carboxyl frequencies at about 6 μ of different salts of DL-leucine is demonstrated by Fig. 12. The general picture resembles that of NH_2 stretchings. The Ni^{++} chelate shows a frequency practically identical with the frequency of the Na^+ salt whereas the carboxyl absorption band of the Cu^{++} chelate is shifted towards higher wavenumbers. The water of crystallization in Ni^{++} and Cu^{++} chelates has an effect, even more pronounced than in the 3 μ region. Fig. 13 shows the absorption bands of Cu^{++} glycine$_2$ before and after drying. The four distinct peaks present yield when the chelate is dried a single intense band at 1 618 cm^{-1} (6.18 μ) with a shoulder at 1 582 cm^{-1} (6.32 μ) probably due to the NH bending. These changes are reversible and the original spectrum can be restored through recrystallization from water. These water effects were probably the reason why Sen *et al.*[5] only observed one broad band between 1 639 and 1 563 cm^{-1} (6.10 and 6.40 μ) for Cu^{++} and Ni^{++} chelates of glycine. The differences between Ni^{++} and Cu^{++} chelates are further illustrated by Fig. 14 which shows the spectra of dried chelates of DL-alanine. The behaviour of the carboxyl frequencies of Na salts and water-free chelates is summarized in Table 4.

Table 4. The carboxyl frequency in wavenumbers (cm^{-1}).

Na^+ leucine	1 590	Na^+ glycine	1 588	Na^+ alanine	1 590
Ni^{++} leucine$_2$	1 590	Ni^{++} glycine$_2$	1 587	Ni^{++} alanine$_2$	1 587
Cu^{++} leucine$_2$	1 618	Cu^{++} glycine$_2$	1 618	Cu^{++} alanine$_2$	1 618

The Cu^{++} chelates of valine, sarcosine, proline and serine showed the same position of the carboxyl frequency which confirms the conclusion that the shift to 1 618 cm^{-1} seems to be characteristic of Cu^{++} chelates.

The frequencies of NH_2 and COOH were unchanged when L-amino acids were used instead of DL-acids.

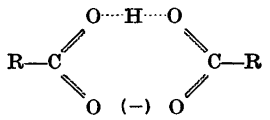
DISCUSSION

When compared to the NH_2 frequencies of Na glycine at 3 400 and 3 360 cm^{-1} (2.941 and 2.975 μ) all the chelates of Pt^{++} show a definite shift towards lower wavenumbers. The slight trend of NH_2 frequencies from *mono* to *trans* form can be explained by the assumption that the *trans* form is most favourable for the formation of a symmetric bond structure. Another feature of interest here is the fact that the *cis* form shows a far more complicated spectrum than the *trans* form. There is more than one plausible explanation for this. In the first place the stretching vibrations of NH_2 groups may be coupled due to a rigid structure and as the *trans* form is more symmetrical some of its vibrations may be IR-inactive. Another possibility is that due to the unsymmetrical position of the chelate forming groups the bonds formed by the two NH_2 groups with the metal ion are not identical. Even a change in the system of hydrogen bonds between NH_2 and the oxygen of the carboxyl group between different molecules of the chelate may render a possible explanation. The existence of such a system of hydrogen bonds has been demonstrated by Stosick [14]. The NH_2 groups of Cu^{++} and Ni^{++} chelates show differences in position of frequencies resembling those of the different forms of Pt^{++} glycine chelates. The NH_2 frequencies of Cu^{++} chelates are found at lower wavenumbers than the frequencies of Ni^{++} chelates. This, together with the fact that Pt^{++} chelates have their NH_2 frequencies at still lower wavenumbers, may indicate that the magnitude of the shift towards lower wavenumbers is dependent on the strength of the covalent linkage between nitrogen and metal ion. The pattern of NH_2 frequencies together with the single and well-defined carboxyl group frequency when compared with the different forms of Pt^{++} glycine, support the conclusion from the X-ray work of Stosick [14] that the Cu^{++} and Ni^{++} chelates with amino acids are the *trans* forms of the coplanar structure. This conclusion is naturally valid only for the dehydrated forms of glycine and alanine chelates. The behaviour of the carboxyl frequency is of special interest. Previous investigators [5] came to the conclusion that the carboxyl group retains its ionic character and does not partake in bond formation with the central metal ion. If this were the case the carboxyl frequency should lie unchanged at approx. 1 590 cm^{-1} as in salts with alkali metals. This is the case with Ni^{++} chelates. Cu^{++} and Pt^{++} chelates, on the other hand, do show a definite shift. The behaviour of the carboxyl frequency with different metals can be summarized for glycine chelates.

Na^{+} glycine 1 590 cm^{-1}, Ni^{++} $glycine_2$ 1 590 cm^{-1}, Cu^{++} $glycine_2$ 1 618 cm^{-1}, Pt^{++} $glycine_2$ (*trans*) 1 644 cm^{-1}. This gives a shift of 28 cm^{-1} for the Cu^{++} chelate and of 54 cm^{-1} for the Pt^{++} chelate.

It is suggested that a shift of this magnitude and direction can be correlated with covalent bond formation. A parallel case is that of K acetate and

acetic acid. K acetate and acetic acid form, when present in equimolar amounts a wellknown addition compound. For this investigation the addition compound between chloroacetic acid and K chloroacetate was used as the acid in this case is crystalline and the separation of the addition compound is simple. Pure chloroacetic acid shows a carboxyl frequency at 1 735 cm^{-1} and the K-salt the normal frequency for ionized carboxyl at 1 590 cm^{-1}. The addition compound showed no trace of either of these bands. The only band present in this region was an intense band at 1 645 cm^{-1}. It is doubtful that the structure in question may be represented by a configuration involving a symmetrical H-bond (IV),



IV

but that the carboxyl groups in this case are connected through covalent bonds with a H atom is very plausible. Thus it seems probable that the shift of the carboxyl group frequency observed with Cu^{++} and Pt^{++} chelates really indicates that the carbonyl group partakes in bond formation with the central metal ion, while in the Ni^{++} chelates it shows no such tendency. This is naturally restricted to the crystalline state as the situation in aqueous solutions may be different due to the fact that the water molecules can to a certain extent replace the carboxyl groups in bond formation with the central ion. Likewise it is clear that the results are valid only for the waterfree chelates as the role played by water molecules is not sufficiently elucidated.

Acknowledgements. The author wants to express his gratitude to Professor Arne Tiselius for encouraging interest and to make grateful acknowledgement to Mr. Stig Bergwall for able technical assistance. This investigation is a part of a program of infra-red research financially supported by grants from the *Royal Swedish Academy of Sciences*, *the State Technical Research Council* and the *Rockefeller Foundation.*

REFERENCES

1. Bryant, B. F., Pariaud, J. C. and Fernelius, W. C. *J. Org. Chem.* **19** (1954) 1889.
2. Bellamy, L. J. and Branch, R. F. *J. Chem. Soc.* **1954** 4491.
3. Merrit, P. E. and Wiberley, S. E. *J. phys. Chem.* **59** (1955) 55.
4. Lennormant, H. *J. Chim. phys.* **43** (1946) 327.
5. Sen, D. N., Mizushima, S. J., Curran, C. and Quagliano, J. V. *J. Am. Chem. Soc.* **77** (1955) 211.
6. Martell, A. E. and Calvin, M. *Chemistry of the Metal Chelate Compounds*, New York 1952.
7. Schiedt, U. und Reinwein, H. *Z. Naturforsch.* **7b** (1952) 270.
8. King, G. W., Hainer, R. M. and McMahon, H. Q. *J. appl. Phys.* **20** (1949) 559.
9. Hornig, D. F. *Discussions Faraday Soc.* **9** (1950) 115.
10. Chattaway, F. W. and Drew, H. D. K. *J. chem. Soc.* **1937** 947.
11. Grünberg, A. A. and Ptizyn, B. W. *J. prakt. Chem.* **136** (1933) 143.
12. Ley, H. and Ficken, K. *Ber.* **45** (1912) 377.
13. Schwarzenbach, G., Kampitsch, E. and Steiner, R. *Helv. Chim. Acta* **28** (1945) 828.
14. Stosick, A. J. *J. Am. Chem. Soc.* **67** (1945) 365.

Received February 10, 1956.

ACTA CHEMICA SCANDINAVICA 10 (1956) 852—866

The Crystal Structure of Mercury(II)oxide Studied by X-Ray and Neutron Diffraction Methods

KARIN AURIVILLIUS

Institute of Inorganic and Physical Chemistry, University of Stockholm, Stockholm, Sweden; Joint Establishment for Nuclear Energy Research, Kjeller, Norway

The crystal structure of mercury(II)oxide has been investigated by X-ray and neutron diffraction methods. The symmetry has been found to be *Pnma* (No. 62) and the unit cell twice the one reported by previous authors. The positions of the mercury and oxygen atoms have been determined. The structure is built up of infinite, planar zig-zag chains —O—Hg—O— running parallel to the *a*-axis and lying in the *ac* plane. Within the chains the Hg—O distance is 2.03 ± 0.10 Å and the angles O—Hg—O and Hg—O—Hg 179° ± 3° and 109° ± 1°, respectively.

In connection with studies of the crystal chemistry of mercury in various mercury oxide halides [1], knowledge of the mercury-oxygen distance was of fundamental importance for the discussion of the spatial arrangement of the atoms. No exact value of this distance could be obtained from the literature and it was thus found appropriate to undertake a detailed investigation of the crystal structure of mercury(II)oxide.

A previous study of this substance carried out in 1927 by Zachariasen [2] by means of X-ray powder photographs indicated an orthorhombic structure with the unit cell dimensions $a = 3.303$ Å, $b = 3.520$ Å, $c = 5.515$ Å.

The following positions of the mercury atoms were given:

Space group *Pmmn*, No. 59 *, 2 Hg in 2(*a*): 0, 0, z; $\frac{1}{2}$, $\frac{1}{2}$, $\bar{z}$; $z \sim \frac{1}{4}$
or space group $Pmn2_1$, No. 31*, 2 Hg in 2(*a*): 0, y, z; $\frac{1}{2}$, $\bar{y}$, $\frac{1}{2}+z$; $y \sim \frac{1}{4}$ $z = \frac{1}{4}$

Three possible arrangements for the oxygen atoms were discussed but it was not possible to decide between them. The mercury-oxygen distances were 2.15 Å for two of the alternative structures and 2.41 Å for the third.

The considerable difference in scattering power for X-rays between mercury and oxygen makes it almost a hopeless enterprise to locate the latter atoms in mercury(II)oxide. On the other hand the relative scattering power

* Notations rearranged to conform with *International Tables for X-ray Crystallography*, Birmingham 1952.

of the two elements for neutrons is much more favourable. The author was thus very happy in having the privilege of performing a neutron diffraction study at the *Joint Establishment for Nuclear Energy Research*, Kjeller, Norway, in addition to the X-ray investigation performed at the University of Stockholm.

X-RAY DIFFRACTION STUDIES

For the X-ray studies, three samples of various origins were used, *viz.* commercial mercury(II)oxide (Baker's Analysed), a sample obtained by carefully heating mercury(II)nitrate in air and naturally occurring montroydite from Terlingua, Texas. All the samples gave identical powder photographs. Tiny rods and thin plates were observed in the samples of the synthetic materials while the natural substance showed only rods. The registering of single crystal reflexions was accompanied by considerable difficulties, due to the extreme delicacy of the crystals. The very slight mechanical stress applied when mounting the crystals often gave rise to serious damage noticeable by the occurrence of multiple spots or even powder lines in the Weissenberg photographs. In some cases, however, it was possible to register the diffraction patterns of obvious single crystals and all calculations were based on data obtained in this way.

CELL DIMENSIONS AND SPACE-GROUP

The powder photographs were taken in a Guinier focussing camera of 80 mm diameter using monochromatic Cu-$K\alpha_1$ radiation and potassium chloride ($a = 6.2930$ Å[3]) added as an internal standard. The powder pattern is given in Table 1. Normally exposed photographs (30 minutes) were found to be in fair agreement with that given by Zachariasen but, in amply exposed ones (3 hours), several extra lines were found which were also observed in single crystal photographs (see below). The unit cell was thus found to have the dimensions $a = 6.612_1$ Å, $b = 5.520_1$ Å, $c = 3.521_3$ Å, corresponding to a doubling of the a axis of the orthorhombic cell reported by Zachariasen.

The observed density of 11.3 indicates a cell content of 4 formula units of HgO per unit cell. The calculated density is 11.2.

Cu-K radiation was used for the single crystal photographs. Rotation diagrams were taken around all the three axes and also Weissenberg photographs registering the reflexions $h0l$—$h3l$, $0kl$—$3kl$, $hk0$—$hk3$. Weak interspacing layer lines in the rotation photograph around [100] showed the a axis to be twice that reported by Zachariasen. This was confirmed by the powder patterns (see above) and by the Weissenberg photographs. The layer line $1kl$ showed no less than 4×18 reflexions.

The Laue symmetry mmm was confirmed. The following spectra were systematically missing: $0kl$ with $k+l =$ odd and $hk0$ with $h =$ odd, which is characteristic of the space groups No. 33, $Pn2_1a$ * and No. 62, $Pnma$.

* Orientation analogous to that of No. 62 but different from that given in the *International Tables*.

Table 1. Powder photograph of HgO. CuKa$_1$ radiation. a (KCl) = 6.2930 Å. Time of exposure 3 hours.

hkl	$10^4 \times \sin^2\Theta$ obs	$10^4 \times \sin^2\Theta$ calc	I_{obs}	I_{calc} *
200	544	543	vw	14
101	615	614	vw	11
011	673	673	vst	1700
210	737	737	vst	1500
020	778	779	vst	1100
111	807	809	vvw	5
201	1021	1021	vst	1800
211	1215	1216	w	59
220	1320	1322	vw	23
121	1393	1393	vw	13
301	1704	1700	vvw	6
221	1798	1800	vst	3000
311	—	1895	—	0.2
002	1914	1914	st	1300
102	2047	2050	vvw	10
400	2170	2171	st	1400
031	2231	2231	st	660
112	—	2244	—	0.1
230	2295	2295	st	1100
410	2363	2366	w	90
131		2366		1
202	—	2457	—	22
321	—	2479	—	10
401	2651	2650	vst	700
212		2651		2500
022	2692	2693	st	1100
231	2772	2774	vw	42
122	—	2829	—	15
411	2846	2844	vst	2100
420	2951	2950	st	1200
040	3116	3115	m	630
302	—	3135	—	7
222	3230	3236	vw	39
312	—	3330	—	0.1
421	3246	3428	w	130
331	—	3452	—	0.0
240	—	3658	—	16
141	—	3729	—	6
132	—	3802	—	0.4
501	—	3871	—	2
430	3919	3923	w	69
511	—	4066	—	1
402	4085	4085	m	900
241	4138	4137	vst	1800
232	4208	4209	vst	2000
412	4277	4280	w	110
431	4402	4402	vst	1700
103	—	4442	—	4
013	4501	4501	m	600

* $I_{calc} = 6.25 \cdot 10^{-3}(pF^2)_{calc}$.

The intensities of the reflexions, which were visually estimated, were considerably influenced by the high absorption in the crystal. Unfortunately, a source of harder radiation than Cu-K radiation was not available at that time. Attempts to cut or grind the crystals to a cylindrical form were not successful due to the extreme delicacy of the material (*cf.* above). However, the absorption was minimized by using as small crystals as possible.

POSITIONS OF THE MERCURY ATOMS

The projections *P(pvw)*, *P(uvp)* and *P(upw)* of the Patterson function were calculated on the basis of F^2 values derived in the usual way. The maps thus obtained were of a rather simple appearance, indicating the existence of the heavy maxima listed in Table 2.

Table 2. Observed maxima in the Patterson functions.

u	v	w	Relative weight obs.	calc.
$\frac{1}{2}$	0	0	2.0	2
$\frac{1}{4}$	$\frac{1}{2}$	$\frac{1}{2}$	2.0	2

In the space-groups $Pn2_1a$ and *Pnma*, the following positions are possible for the four mercury atoms:

$Pn2_1a$: 4(a): $x, y, z;\ \bar{x}, \frac{1}{2}+y, \bar{z};\ \frac{1}{2}-x, \frac{1}{2}+y, \frac{1}{2}+z;\ \frac{1}{2}+x, y, \frac{1}{2}-z$

Pnma: 4(a): 0,0,0; $0,\frac{1}{2},0$; $\frac{1}{2},0,\frac{1}{2}$; $\frac{1}{2},\frac{1}{2},\frac{1}{2}$

4(b): $0,0,\frac{1}{2}$; $0,\frac{1}{2},\frac{1}{2}$; $\frac{1}{2},0,0$; $\frac{1}{2},\frac{1}{2},0$

4(c): $x,\frac{1}{4},z;\ \bar{x},\frac{3}{4},\bar{z};\ \frac{1}{2}-x,\frac{3}{4},\frac{1}{2}+z;\ \frac{1}{2}+x,\frac{1}{4},\frac{1}{2}-z$

All the maxima of Table 2 are undoubtedly due to mercury-mercury interactions. This excludes the possibility that the positions 4(a) and 4(b) in *Pnma* are the sites of the metal atoms.

If the mercury atoms occupy the point positions 4(a) in $Pn2_1a$ or 4(c) in *Pnma*, the following set of interatomic vectors will occur in the Patterson function in addition to the trivial peak at the origin (Table 3).

Table 3. Expected maxima in the Patterson functions.

u	v	w	Relative weight
$\pm 2x$	$\frac{1}{2}$	$\pm 2z$	1
$\pm(2x \pm \frac{1}{2})$	$\frac{1}{2}$	$\frac{1}{2}$	2
$\frac{1}{2}$	0	$\pm(2z \pm \frac{1}{2})$	2

A comparison of this set of vectors with the Patterson function derived from experimental data immediately gives the following approximate parameter values:

$Pn2_1a$: 4 Hg in 4(a): $x = \frac{1}{8}$ and $z = \frac{1}{4}$

Pnma: 4 Hg in 4(c): $x = \frac{1}{8}$, $y = \frac{1}{4}$, $z = \frac{1}{4}$.

The y parameter for the former space-group may be arbitrarily chosen equal to $\frac{1}{4}$ — the two possibilities will thus become identical, making possible the use of the second space group with its higher symmetry.

The approximate arrangement of the metal atoms thus derived is actually bodycentered with the symmetry identical with that proposed by Zachariasen [2]. However, it does not account for several reflexions observed in the Weissenberg diagrams, *e. g. hkl* with $h = 2n + 1$ and $h0l$ with $\frac{h}{2} + l = 2m + 1$ (n, m are integers). The F^2 values of these reflexions are too high to be ascribed only to the influence of the oxygen atoms. The parameters of the mercury atoms must thus be somewhat different from the values given above. By trial methods it was found that a slight shift of the metal atoms to the position (I) with $x = 0.115$ and $z = 0.245$ (or, which is equivalent, (II) with $x = 0.115$ and $z = 0.255$) was enough to give a better agreement between observed and calculated X-ray intensities (*cf.* Table 4). The former alternative (I) was arbitrarily chosen as giving the sites of the mercury atoms.

NEUTRON DIFFRACTION STUDIES

A comparison of the coherent scattering amplitudes of the mercury and oxygen atoms for neutrons and for X-rays shows the great advantage in investigating mercury(II)oxide by neutron diffraction.

Scattering amplitude (10^{-12} cm)[4]

	Neutron	X-ray ($\Theta = 0°$)
Hg	1.31	22.5
O	0.58	2.25

While the amplitude values for neutrons are independent of the scattering angle, those for X-rays decrease with Θ—relatively more so for oxygen than for mercury.

Due to the relatively low neutron flux of the pile, which was run at an effect of 200—250 kW, it was necessary to use a large single crystal. A beautiful crystal of montroydite ($1.5 \times 1.5 \times 14$ mm) from Terlingua in Texas was kindly lent by Drs. W. F. Foshag and G. Switzer, Smithsonian Institution, U.S. National Museum, Washington, D. C. The absorption of the radiation in the crystal was neglected for the wavelength of 1.01 Å applied. X-Ray photographs confirmed that this specimen is a single crystal.

The crystal was mounted in a thinwalled glass capillary tube to prevent mechanical injury and oriented on the spectrometer table with rotation around the longest edge (the a direction). With the strongest reflexion 020 as a starting point, the diffraction peaks of the reflexions $0kl$ were measured at counter intervals of 0.5° scattering angle. The monitor counter serving as a measure of the incident monochromatic beam intensity was set at 40 000 counts for the weaker reflexions and 20 000 for the stronger ones. The ap-

Table 4 a.

Calculated structure factor values and observed intensities *h0l*, *h1l* and *h2l* from Weissenberg photographs of HgO. Cu*K* radiation.

I. $I = 6.25 \cdot 10^{-3} (f_{Hg} \cdot A_{Hg})^2$, II. $I = 6.25 \cdot 10^{-3} (f_{Hg} \cdot A_{Hg} + f_O \cdot A_O)^2$

The reflexions *h0l*

The dotted line indicates the range of heaviest absorption.

l ↓ / *h* →		0	1	2	3	4	5	6	7	8
0	I			8		312		30		127
	II			7		354		28		138
	obs			—		vw		—		m
1	I		0.3	417	0.1	19	0.2	181	0.0	37
	II		3	453	2	18	0.5	190	0.4	35
	obs		—	w	—	—	—	w	—	m
2	I	350	0.5	5	0.7	230	0.2	25		
	II	328	2	6	2	218	1	26		
	obs	vst	vw	vvw	vvw	m	—	w		
3	I		1	217	0.5	12	1	137		
	II		1	196	0.5	13	1	125		
	obs		vw	st	vvw	m	vvw	st		
4	I	171	1	3	2					
	II	162	0.5	3	1					
	obs	st	vvw	w	vw					

The reflexions *h1l*

l ↓ / *h* →		0	1	2	3	4	5	6	7	8
0	I			452		20		187		37
	II			375		23		171		41
	obs			m		vvw		w		vw
1	I	472	0.2	7	0.2	279	0.1	28	0.1	122
	II	429	0.6	7	0.0	262	0.2	29	0.0	116
	obs	vst	—	—	—	w	—	vvw	—	m
2	I		0.7	298	0.3	15	0.6	158	0.1	
	II		0.0	316	0.0	14	0.1	164	0.0	
	obs		—	st	—	vvw	—	w	—	
3	I	160	0.8	3	1	120	0.3	15		
	II	141	0.8	3	1	108	0.3	16		
	obs	vst	—	vvw	vvw	st	—	w		
4	I		2	160						
	II		3	168						
	obs		vw	vst						

The reflexions *h*2*l*

l ↓ \ *h* →		0	1	2	3	4	5	6	7	8
0	I			7		272		28		121
	II			6		306		25		132
	obs			vvw		st		vw		st
1	I		0.2	350	0.1	17	0.2	167	0.0	
	II		2	376	1	16	0.5	175	0.4	
	obs		vvw	vst	—	vw	—	m	—	
2	I	300	0.5	5	0.6	209	0.1	24		
	II	283	2	5	2	199	1	25		
	obs	vst	vw	w	vvw	st	vvw	w		
3	I		1	200	0.5	11	1			
	II		1	182	0.5	12	1			
	obs		vw	vst	vvw	w	vvw			
4	I	163	1	3						
	II	155	1	3						
	obs	vst	vvw	w						

Table 4 b

Calculated structure factor values and observed intensities 1*kl* from a Weissenberg photograph of HgO. Cu*K* radiation.

I. $I = 0.625\ (f_{Hg} \cdot A_{Hg})^2$ II. $I = 0.625\ (f_{Hg} \cdot A_{Hg} + f_O \cdot A_O)^2$

l ↓ \ *k* →		0	1	2	3	4	5	6
1	I	24	18	20	13	13	8	9
	II	269	58	166	14	73	2	35
	obs	st	m	m	—	—	—	—
2	I	53	66	46	51	33	37	25
	II	239	2	187	5	108	6	75
	obs	st	—	st	—	m	w	m
3	I	106	80	97	67	80	55	
	II	110	77	99	65	82	54	
	obs	m	m	m	m	m	m	
4	I	127	162	121	147			
	II	36	255	55	229			
	obs	m	st	m	st			

pearance of the curves obtained by plotting the intensities against the angles is given in Fig. 1. The observed intensities obtained by measuring the areas under the peaks with a planimeter and corrected for the Lorentz factor are given in Table 5. Because of the mechanical arrangement of the

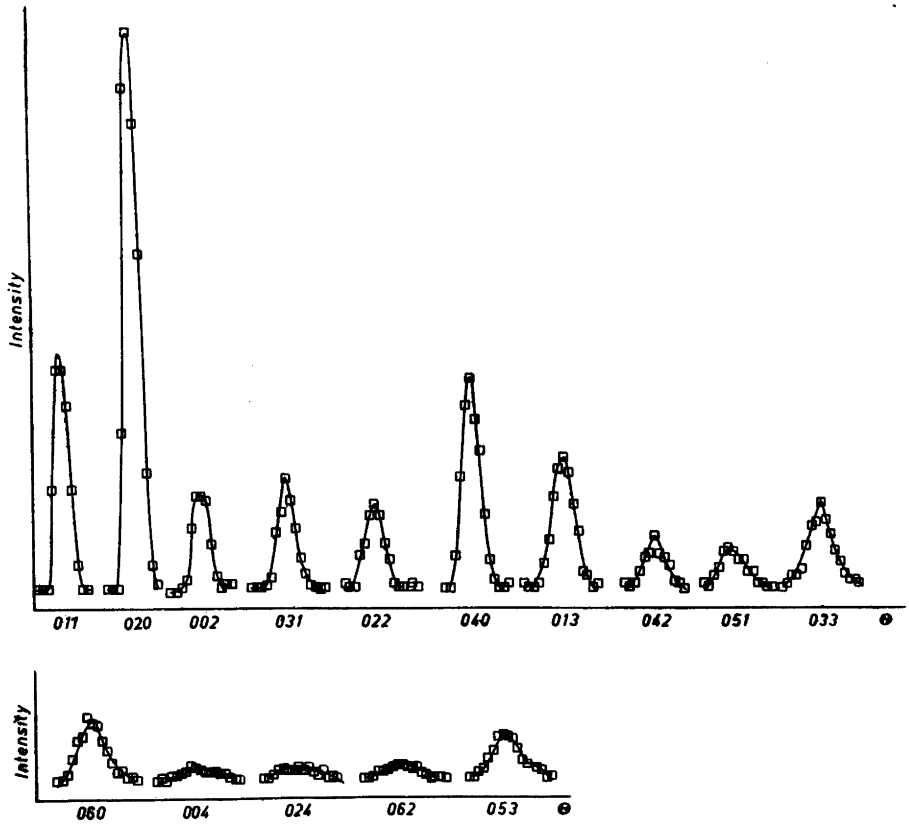


Fig. 1. Neutron reflexions 0kl *from the single crystal investigation. Counts for angular intervals of 0.5°.*

apparatus it was only possible to measure the intensities of the reflexions of the 0*kl* layer line.

Neutron diffraction powder diagrams were also taken using both a cylindrical and a flat container for the sample.

Positions of the oxygen atoms

On the basis of the neutron reflexions 0*kl* from the single crystal diagram, the projection $P(pvw)$ of the Patterson function was calculated. As the degree of mosaic character of the crystal was not known, the two extreme possibilities, *viz.* that the observed intensities are proportional to F^2 or to $|F|$, were considered. The Patterson functions derived from these two assumptions were, however, found to be of a closely similar character. The positions of the maxima were thus exactly the same in both cases and the relative heights were only moder-

Table 5. Calculated and observed neutron intensities 0kl from the single crystal investigation. The observed intensity was considered proportional to F^2.

hkl	F^2_{obs}	F^2_{calc}
011	52	63
020	143	171
002	45	48
031	55	48
022	46	42
040	123	142
013	103	108
042	38	28
051	36	28
033	83	83
060	67	70
004	15	20
024	14	17
062	20	14
053	55	47

ately different. The appearance of $P(pvw)$ calculated on the basis of $F^2(0kl)$ is given in Fig. 2. The mercury-mercury vector is superimposed on the origin maximum in this picture. The discussion of the oxygen arrangement is based on the positions of the mercury atoms derived from the X-ray investigation described above. The following sets of projections of the mercury-oxygen vectors correspond to the possible arrangements of the four oxygen atoms in the space-groups $Pn2_1a$ and $Pnma$.

	Mercury-oxygen vectors v	w	Relative weight obs.	calc.
$Pn2_1a$: 4 O in 4(a):	$\frac{1}{4}-y$	$\pm(0.245-z)$	1	1
	»	$\pm(0.255-z)$	1	1
	$\frac{3}{4}-y$	$\pm(0.245+z)$	1	1
	»	$\pm(0.255+z)$	1	1
Pnma: 4 O in 4(a) or 4(b):	$\frac{1}{4}$	$\pm$ 0.255	—	1
	»	$\pm$ 0.245	—	1
	$\frac{3}{4}$	$\pm$ 0.255	—	1
	»	$\pm$ 0.245	—	1
Pnma: 4 O in 4(c):	0	$\pm(0.245-z)$	1	1
	»	$\pm(0.255-z)$	1	1
	$\frac{1}{2}$	$\pm(0.245+z)$	1	1
	»	$\pm(0.255+z)$	1	1

Since the maxima of $P(pvw)$ only occur at $v = 0$ and $\frac{1}{2}$, the y parameter of the oxygen atoms must be $\frac{1}{4}$ which excludes alternatives *Pnma*, 4(a) and 4(b) for the arrangement of the oxygen atoms. It also makes the two alternatives

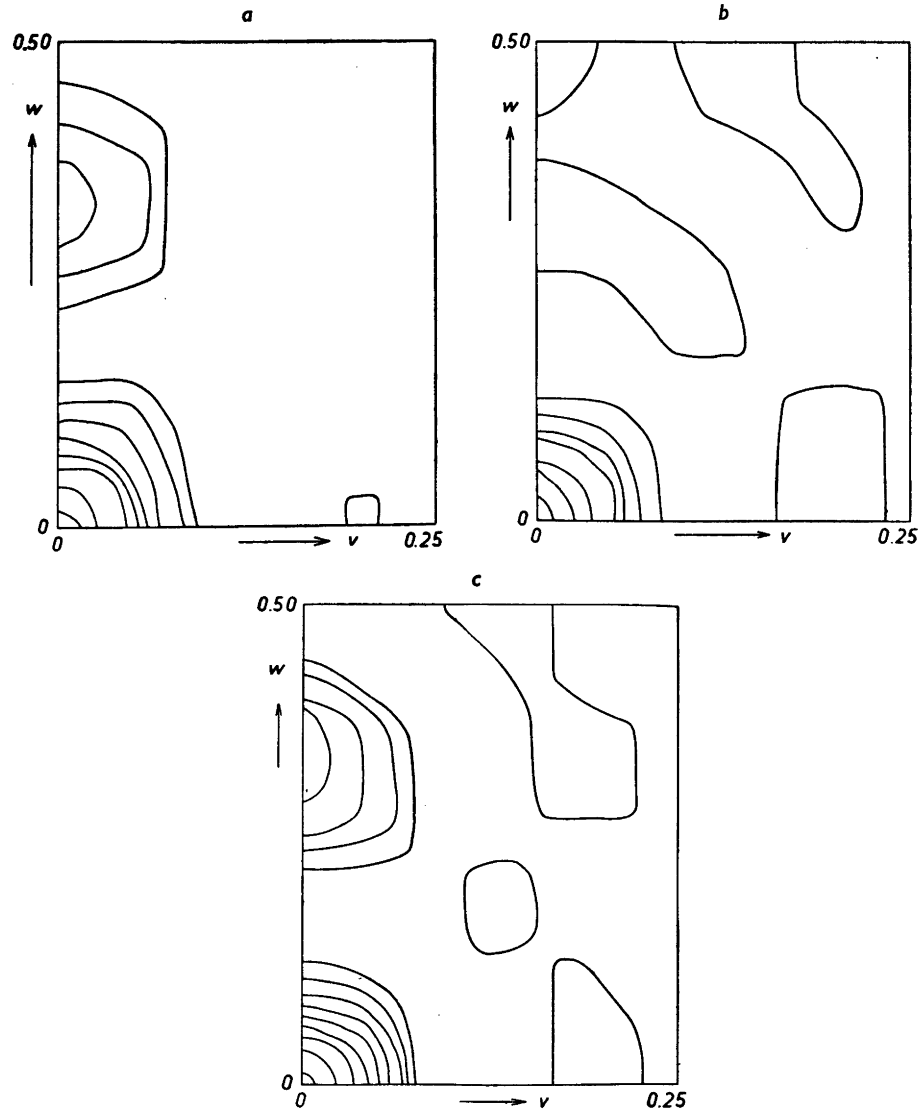


Fig. 2. a) The Patterson function P(pvw) *based on observed neutron intensities* 0kl, *b)* P(pvw) *based on calculated values* $(A_{Hg} \cdot b_{Hg})^2$, *c)* P(pvw) *based on calculated values* $(A_{Hg} \cdot b_{Hg} + A_O \cdot b_O)^2$ (cf. *Ref. 4)*

$Pn2_1a$, 4(*a*) and *Pnma*, 4(*c*) coincide and evidently shows that the structure of mercury oxide has the symmetry *Pnma* at least as far as can be judged from the present experimental data.

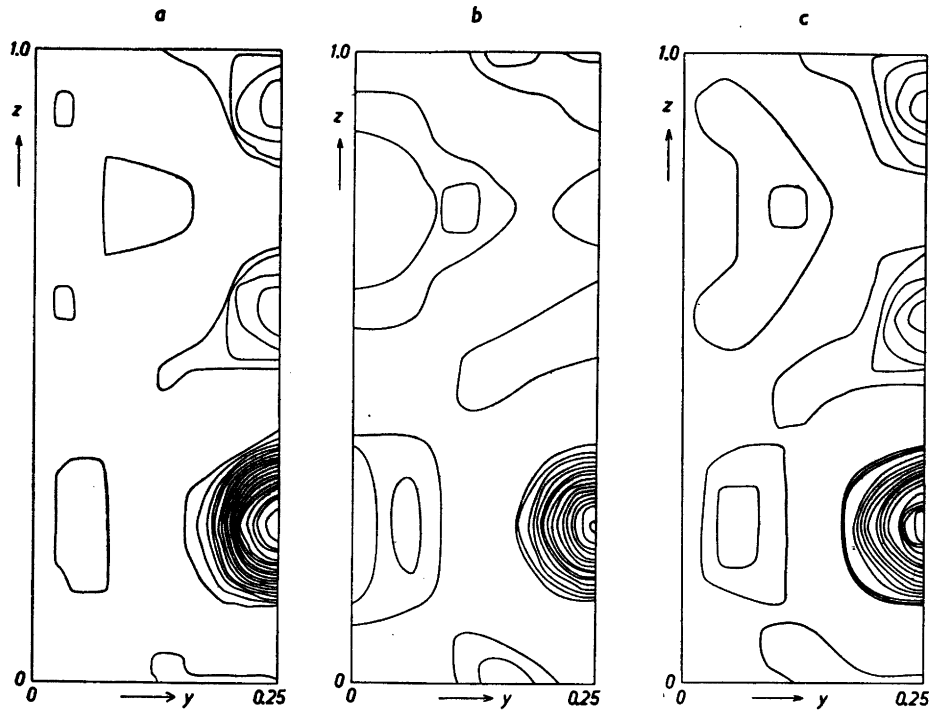


Fig. 3. a) The Fourier projection ϱ(pyz) *based on neutron intensities* 0kl *(the observed intensity considered proportional to* F^2*),*
b) ϱ(pyz) *based on calculated values* $A_{Hg} \cdot b_{Hg}$,
c) ϱ(pyz) *based on values* $A_{Hg} \cdot b_{Hg} + A_O \cdot b_O$.

The mercury-oxygen peaks in $P(pvw)$ at $v = 0$, $w = \frac{1}{3}$ give the following two alternatives for the arrangement of the oxygen atoms:

$$A: \quad 4\ \mathrm{O}\ \text{in}\ 4(c): \quad x,y = \tfrac{1}{4},\ z = 0.58$$
$$B: \quad 4\ \mathrm{O}\ \text{in}\ 4(c): \quad x,y = \tfrac{1}{4},\ z = 0.92$$

Due to the slight displacement of the mercury atom positions from ($x = \frac{1}{8}$, $y = \frac{1}{4}$, $z = \frac{1}{4}$) with $|\Delta x| = 0.010$ and $|\Delta z| = 0.005$, these two alternatives are not identical. However, the difference between them is not big enough to affect the signs of the structure factor values $F(0kl)$ for neutron diffraction. The projection of the electron density function $\varrho\ (pyz)$ thus derived, on the assumption that the observed intensity is proportional to F^2, is represented in Fig. 3. The mercury maximum in this projection (corresponding to two superimposed atoms) appears in $y = 0.250$, $z = 0.250$ and the oxygen maxima in $y = 0.250$, $z = 0.585$ and $z = 0.915$ respectively. Functions $P(pvw)$ based on F^2 $(0kl)$ values and $\varrho\ (pyz)$ based on $F(0kl)$ values calculated for the mercury atoms only and also for both the mercury and oxygen

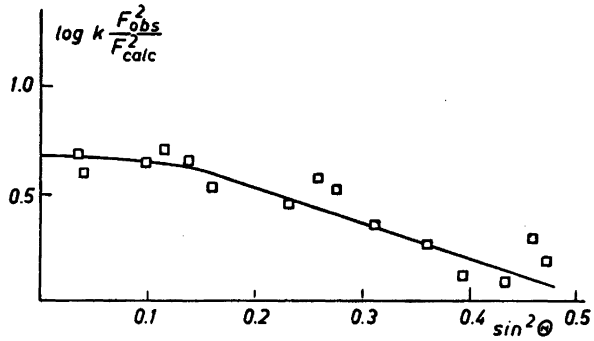


Fig. 4. Temperature correction curve. Log $k \frac{F^2_{obs}}{F^2_{calc}}$ *plotted against* $\sin^2\Theta$.

atoms in the positions derived above are of reasonable appearance with the heights and positions of the various maxima in accordance with those of the experimentally derived functions (*cf.* Figs. 2 and 3).

Calculated and observed neutron intensities $0kl$ are given in Table 5. For each reflexion a temperature factor correction was calculated from the curve in Fig. 4. The reliability index

$$R = \frac{\Sigma \| F_{obs}| - |F_{calc} \|}{\Sigma |F_{obs}|}$$

was calculated to be 6.8 %.

CORRELATION OF X-RAY AND NEUTRON DIFFRACTION DATA

The intensities of the $1kl$ X-ray reflexions were found to be greatly influenced by the oxygen atom positions and allowed a decision to be made between the two alternatives *A* and *B* for the oxygen atom arrangement. As a matter of fact, only *A* was found to be compatible with the arbitrarily chosen position I for the mercury atoms. However, the structure thus obtained was identical with the combination of the mercury arrangement II with the oxygen arrangement *B*.

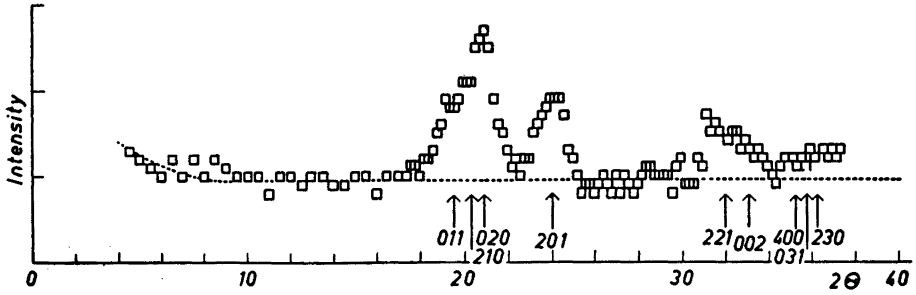


Fig. 5. Neutron diffraction powder diagram of a sample of HgO in a flat container.

Table 6. Observed and calculated neutron intensities of a few reflexions from a powdered sample of HgO.

I. Flat sample. II. Cylindrical sample.

Calculations according to G. E. Bacon, *Neutron Diffraction*, Oxford 1955.

hkl	I		II	
	F^2_{obs}	F^2_{calc}	F^2_{obs}	F^2_{calc}
011	58	35	114	75
210		16		34
020	49	50	103	108
201	49	55	118	118

The accuracy of the resolution of the area under the first observed peak into its components, the reflexions 011, 210, and 020 may be rather low. The separate intensities have not been used for any further calculation.

Systematic variation of the x parameter of the oxygen atom position gave the best agreement between observed and calculated structure factor values for adjacent reflexions of comparable absorption when x_O was equal to 0.36 ± 0.02 (*cf.* Table 4).

The spots in the Weissenberg photograph $3kl$ were highly elongated. It was not possible to estimate their intensities with the accuracy needed for quantitative calculations.

Due to the considerable absorption for several reflexions, the R-index for the X-ray data lacks significance.

The atomic positions thus derived are in accordance with the neutron diffraction powder diagrams. The low resolution of the latter, however, makes these diagrams less reliable than the X-ray data for the determination of the parameter values (*cf.* Fig. 5 and Table 6).

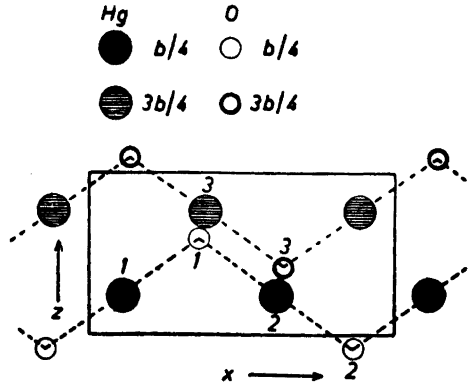


Fig. 6. xz *projection of the structure of HgO. The diagram shows the coordination of the atoms. The small circles show the O atoms and the larger ones the Hg atoms. The distances Hg→Hg, Hg→O and O→O are listed in the text. The dotted lines indicate the bonds of one zig-zag chain.*

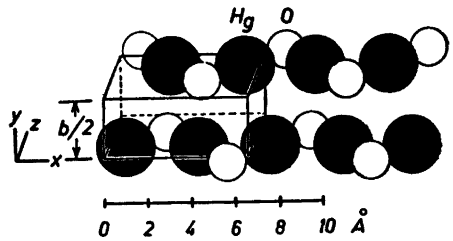


Fig. 7. Diagram showing the infinite zig-zag chain —O—Hg—O— lying in the ac plane and running parallel to the a axis.

DESCRIPTION OF THE STRUCTURE

The following structure of mercury(II)oxide has thus been arrived at:

Cell content: 4 HgO
Space group: *Pnma*, No. 62
4 Hg in the point position 4(*c*): $x,\frac{1}{4},z;\ \bar{x},\frac{3}{4},\bar{z};\ \frac{1}{2}-x,\ \frac{3}{4},\ \frac{1}{2}+z;\ \frac{1}{2}+x,\frac{1}{4},\frac{1}{2}-z$
$x = 0.115,\ z = 0.245$
4 O in the point position 4(*c*): $x = 0.36_5,\ z = 0.58_5$

The structure is built up of infinite, planar zig-zag chains —O—Hg—O— running parallel to the *a* axis and lying in the *ac* plane (*cf.* Figs. 6 and 7).

The distances and angles within the chains are:

Hg(1) — O(1)	2.03 ± 0.10 Å
Hg(2) — O(1)	2.03 ± 0.10 Å
Hg(1) — Hg(2)	3.30 Å
The angle Hg(1) — O(1)—Hg(2)	109° ± 1°
The angle O(1) — Hg(2)—O(2)	179° ± 3°

The distances between the chains are:

Hg(3) — O(1)	2.82 Å
Hg(2) — O(3)	2.82 Å
Hg(2) — Hg(3)	3.59 Å
O(1) — O(3)	3.39 Å

The distance from a mercury atom to an adjacent oxygen atom should be [5,6]:

for ionic bonds 2.18 Å (coordination number 2)
for covalent sp^3 bonds 2.16 Å
for covalent sp bonds 2.0_1 Å

The Hg—O distances, actually found within the chain, 2.03 Å, and the values of the angles suggest that the bond between Hg and O within the chains is mainly homopolar. Between the chains, the forces are far weaker since the interatomic distances are considerably longer than those within the chains. The chains probably support each other by means of the Hg—O contacts.

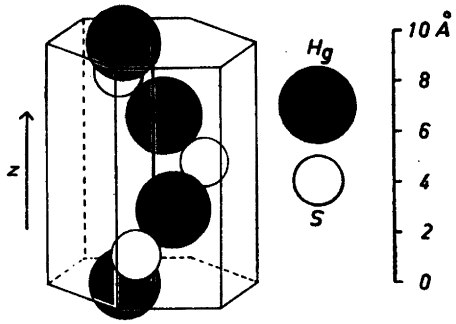


Fig. 8. Diagram showing one spiral chain —S—Hg—S— of the cinnabar structure. The spiral chain extends indefinitely through the crystal in a vertical direction.

A comparison between the structures of mercury(II)oxide and the hexagonal modification of mercury(II)sulphide (cinnabar) [7] (*cf.* Figs. 7 and 8) indicates the existence of similar building principles in these two structures. The infinite zig-zag chains —O—Hg—O— of the former correspond to infinite spiral chains —S—Hg—S— running parallel to the *c* axis of the latter. The angles —X—Hg—X— do not differ much from 180° in either case. The decrease in the angle Hg—X—Hg when going from oxygen (109° ± 1°) to sulphur (105° ± 2°) is in analogy to previously reported structural data.

A recent report by Roth [8] on an X-ray and neutron diffraction study of mercury(II)oxide gives a structure considerably different from that found in the present investigation. The doubling of the *a* axis and thus also the primitive character of the unit cell were not observed. The oxygen atom arrangement suggested by Roth and leading to a different system of Hg—O chains and to O—Hg—O angles of 105° is likewise inconsistent with the experimental data obtained by the present author.

The author wishes to thank Professor A. Ölander for his kind interest in this work. The author is also much indebted to Dr. A. Magnéli for many valuable discussions. Thanks are also due to Dr. G. Randers, head of the *Joint Establishment for Nuclear Energy Research*, Kjeller, Norway, for his kind hospitality and to Dr. J. A. Goedkoop, head of the Neutron Physics Department and to Dr. A. F. Andresen for very valuable help in the neutron diffraction work.

These studies form part of a research program on metal oxides and fluorides financially supported by the *Swedish Natural Science Research Council.*

REFERENCES

1. Aurivillius, K. *Acta Chem. Scand.* **8** (1954) 523.
2. Zachariasen, W. *Z. physik. Chem.* **128** (1927) 421.
3. Hambling, P. G. *Acta Cryst.* **6** (1953) 98.
4. Bacon, G. E. *Neutron Diffraction*, Oxford 1955.
5. Wells, A. F. *Structural Inorganic Chemistry*, Oxford 1950.
6. Pauling, L. *Z. Krist.* **87** (1934) 205.
7. Aurivillius, K. *Acta Chem. Scand.* **4** (1950) 1413.
8. Roth, W. L. *Acta Cryst.* **9** (1956) 277.

Received March 14, 1956.

ACTA CHEMICA SCANDINAVICA 10 (1956) 867—886

Short Communications

A Preliminary X-Ray Investigation of Naphthazarin

O. BORGEN

Institutt for teoretisk kjemi, Norges Tekniske Høgskole, Trondheim, Norway

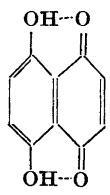
Naphthazarin has been isolated in three modifications at room temperature. Two of these have been reported previously by Palacios and Salvia [1] and Rogers [2].

Our approximate X-ray data are as follows:

Modification	I	II	III
a (Å)	3.81	8.09	5.46
b (Å)	7.63	7.27	6.35
c (Å)	14.52	15.26	11.71
β (°)	97.2	115	91.5
Space group	$P2_1/c$	$P2_1/c$	$P2_1/c$
Molecules in unit cell	2	4	2
Colour	green metallic lustre	red	dark red

The physical properties, especially the colours, of the various modifications are appreciably different. An investigation has therefore been commenced in order to study the influence of intermolecular forces and molecular orientation.

The structure of naphthazarin, based on chemical evidence, is given as 5,8-dihydroxy-1,4-naphthoquinone.



The space group of the modifications I and III is $P2_1/c$, and the unit cells contain 2 molecules. The molecules therefore have a centre of symmetry. This is incompatible with the above formula.

There exist a number of possible explanations, of which we may mention some.

1) The compound may be of the form 4,8-dihydroxy-1,5-naphthoquinone, in spite of certain chemical evidence.
2) The hydrogen bonds may be symmetrical, although such bonds are not known in any organic compound.
3) The protons of the hydrogen bonds may change positions between neighbouring oxygen atoms, giving a quasi-centrosymmetric structure.
4) The benzo- and keto-parts of the molecules may be statistically distributed in the lattice, giving a quasicentrosymmetric structure.

In the three later cases we would expect to find the four C—O distances equal.

The electron-density projection of naphthazarin I on (100) is shown in Fig. 1. The signs of the structure amplitudes have been determined from a model based on a Patterson projection.

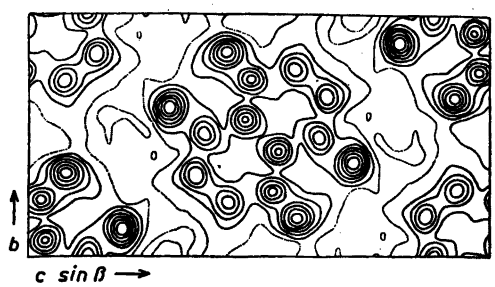


Fig. 1. Electron-density projection on (100) of naphthazarin I.

The molecules are oriented nearly parallel to the (100) plane, and a rough calculation of the atomic positions indicates short intramolecular O—H...O distances and rather close intermolecular approach. The length of the hydrogen bond is of great interest in connection with the recent studies of the infrared spectra of hydroxy-quinones [3-5], but further discussion will have to await the final refinements of the calculations.

1. Palacios, J. and Salvia, R. *Anales soc. espan. fis. y quim.* **32** (1934) 49.
2. Rogers, M. T. *J. Am. Chem. Soc.* **69** (1947) 1506.
3. Josien, M.-L., Fuson, N., Lebas, J.-M. and Gregory, T. M. *J. Chem. Phys.* **21** (1953) 331.
4. Hadzi, D. and Sheppard, N. *Trans. Faraday Soc.* **50** (1954) 911.
5. Flett, M. St. C. *J. Chem. Soc.* **1948** 1441.

Received May 28, 1956.

X-Ray Crystallographic Data on Sodium and Potassium Thiosulphonates

OLAV FOSS

Chemical Institute, University of Bergen, Bergen, Norway

A study of unit cells and space groups of some alkali methane- and *p*-toluenethiosulphonates has been made, with the following results. The axial lengths, from oscillation and Weissenberg photographs taken with copper radiation, $\lambda(CuK\alpha) = 1.542$ Å, are probably correct to within 0.5 %. Densities were determined by a flotation method.

Sodium methanethiosulphonate monohydrate, $CH_3SO_2SNa \cdot H_2O$. Orthorhombic, $a = 6.49$ Å, $b = 5.55$ Å, $c = 16.23$ Å. Four formula units per unit cell; density, calc. 1.73, found 1.72 g/cm³. Systematic absences, $0kl$ when $k + l$ is odd, $hk0$ when h is odd. These absences are characteristic of the space groups, $D_{2h}^{16}-Pnma$ and $C_{2v}^{9}-Pn2_1a$. If the former is the correct one, the carbon and both sulphur atoms of the methanethiosulphonate ion lie in a crystallographic mirror plane of symmetry.

From water, the salt crystallized as plates {001} with plate edges parallel to the a and b axes. There is perfect cleavage along the plate face, and also a pronounced tendency of cleavage along another, not identified plane parallel to the a axis.

Potassium methanethiosulphonate, CH_3SO_2SK. Monoclinic prismatic, $a = 8.76$ Å, $b = 8.12$ Å, $c = 7.42$ Å, $\beta = 92°$. Four formula units per unit cell; density, calc. 1.89, found 1.88 g/cm³. Systematic absences, $h0l$ when l is odd, $0k0$ when k is odd. The space group is thus $C_{2h}^{5}-P2_1/c$.

The salt crystallized from water or methanol as thick plates {100} bounded by {011}, {010} and occasionally {111}. There is perfect cleavage along the plate face.

Potassium p-*toluenethiosulphonate monohydrate*, $C_7H_7SO_2SK \cdot H_2O$. Monoclinic, $a = 8.56$ Å, $b = 9.67$ Å, $c = 13.01$ Å, $\beta = 95°$. Four formula units per unit cell; density, calc. 1.51, found 1.49 g/cm³. Systematic absences, hkl when $h + k$ is odd. The monoclinic prismatic morphology [1,2] of the crystals points to the centrosymmetric space group, $C_{2h}^{3}-C2/m$, the correctness of which would imply that the *p*-toluenethiosulphonate ion possesses mirror plane symmetry in the crystals.

The salt was first prepared by Blomstrand [3] and Wahlstedt [4], and by these authors noted to crystallize particularly well. Brugnatelli [1,2] described the crystals as monoclinic prismatic, with $a : b : c = 0.8854 : 1 : 1.5436$ and $\beta = 119° 52'$. Transforming according to the matrix, 100/010/$\bar{1}0\bar{1}$, these data become $a : b : c = 0.8854 : 1 : 1.344$; $\beta = 94.9°$, as compared with $a : b : c = 0.8853 : 1 : 1.345$; $\beta = 95°$ from the X-ray data.

There is perfect cleavage along the c plane.

Sodium p-*toluenethiosulphonate*, $C_7H_7SO_2SNa$. Monoclinic, $a = 7.36$ Å, $b = 9.72$ Å, $c = 12.96$ Å, $\beta = 93°$. Four formula units per unit cell; density, calc. 1.51, found 1.51 g/cm³. Systematic absences, hkl when $h + k$ is odd.

Except for the length of the a axis, the cell dimensions are close to those found for potassium *p*-toluenethiosulphonate monohydrate. The systematic absences are the same, and the intensity distribution of the $0kl$ reflections of the two salts are very similar. It appears likely that the space group of the sodium salt is that of the potassium salt, and thus probably $C_{2h}^{3}-C2/m$.

Crystallized from 96 % ethanol above room temperature, the salt occurred as

The molecules are oriented nearly parallel to the (100) plane, and a rough calculation of the atomic positions indicates short intramolecular O—H...O distances and rather close intermolecular approach. The length of the hydrogen bond is of great interest in connection with the recent studies of the infrared spectra of hydroxy-quinones [3-5], but further discussion will have to await the final refinements of the calculations.

1. Palacios, J. and Salvia, R. *Anales soc. espan. fis. y quim.* **32** (1934) 49.
2. Rogers, M. T. *J. Am. Chem. Soc.* **69** (1947) 1506.
3. Josien, M.-L., Fuson, N., Lebas, J.-M. and Gregory, T. M. *J. Chem. Phys.* **21** (1953) 331.
4. Hadzi, D. and Sheppard, N. *Trans. Faraday Soc.* **50** (1954) 911.
5. Flett, M. St. C. *J. Chem. Soc.* **1948** 1441.

Received May 28, 1956.

X-Ray Crystallographic Data on Sodium and Potassium Thiosulphonates

OLAV FOSS

Chemical Institute, University of Bergen, Bergen, Norway

A study of unit cells and space groups of some alkali methane- and *p*-toluenethiosulphonates has been made, with the following results. The axial lengths, from oscillation and Weissenberg photographs taken with copper radiation, $\lambda(CuK\alpha) = 1.542$ Å, are probably correct to within 0.5 %. Densities were determined by a flotation method.

Sodium methanethiosulphonate monohydrate, $CH_3SO_2SNa \cdot H_2O$. Orthorhombic, $a = 6.49$ Å, $b = 5.55$ Å, $c = 16.23$ Å. Four formula units per unit cell; density, calc. 1.73, found 1.72 g/cm³. Systematic absences, $0kl$ when $k + l$ is odd, $hk0$ when h is odd. These absences are characteristic of the space groups, $D_{2h}^{16}-Pnma$ and $C_{2v}^{9}-Pn2_1a$. If the former is the correct one, the carbon and both sulphur atoms of the methanethiosulphonate ion lie in a crystallographic mirror plane of symmetry.

From water, the salt crystallized as plates {001} with plate edges parallel to the a and b axes. There is perfect cleavage along the plate face, and also a pronounced tendency of cleavage along another, not identified plane parallel to the a axis.

Potassium methanethiosulphonate, CH_3SO_2SK. Monoclinic prismatic, $a = 8.76$ Å, $b = 8.12$ Å, $c = 7.42$ Å, $\beta = 92°$. Four formula units per unit cell; density, calc. 1.89, found 1.88 g/cm³. Systematic absences, $h0l$ when l is odd, $0k0$ when k is odd. The space group is thus $C_{2h}^{5}-P2_1/c$.

The salt crystallized from water or methanol as thick plates {100} bounded by {011}, {010} and occasionally {111}. There is perfect cleavage along the plate face.

Potassium p-*toluenethiosulphonate monohydrate*, $C_7H_7SO_2SK \cdot H_2O$. Monoclinic, $a = 8.56$ Å, $b = 9.67$ Å, $c = 13.01$ Å, $\beta = 95°$. Four formula units per unit cell; density, calc. 1.51, found 1.49 g/cm³. Systematic absences, hkl when $h + k$ is odd. The monoclinic prismatic morphology [1,2] of the crystals points to the centrosymmetric space group, $C_{2h}^{3}-C2/m$, the correctness of which would imply that the *p*-toluenethiosulphonate ion possesses mirror plane symmetry in the crystals.

The salt was first prepared by Blomstrand [3] and Wahlstedt [4], and by these authors noted to crystallize particularly well. Brugnatelli [1,2] described the crystals as monoclinic prismatic, with $a : b : c = 0.8854 : 1 : 1.5436$ and $\beta = 119° 52'$. Transforming according to the matrix, 100/010/$\bar{1}0\bar{1}$, these data become $a : b : c = 0.8854 : 1 : 1.344$; $\beta = 94.9°$, as compared with $a : b : c = 0.8853 : 1 : 1.345$; $\beta = 95°$ from the X-ray data.

There is perfect cleavage along the c plane.

Sodium p-*toluenethiosulphonate*, $C_7H_7SO_2SNa$. Monoclinic, $a = 7.36$ Å, $b = 9.72$ Å, $c = 12.96$ Å, $\beta = 93°$. Four formula units per unit cell; density, calc. 1.51, found 1.51 g/cm³. Systematic absences, hkl when $h + k$ is odd.

Except for the length of the a axis, the cell dimensions are close to those found for potassium *p*-toluenethiosulphonate monohydrate. The systematic absences are the same, and the intensity distribution of the $0kl$ reflections of the two salts are very similar. It appears likely that the space group of the sodium salt is that of the potassium salt, and thus probably $C_{2h}^{3}-C2/m$.

Crystallized from 96 % ethanol above room temperature, the salt occurred as

fatty leaves or thin plates {001}. There is perfect cleavage along (001) and along planes parallel to the *ab* diagonals.

Sodium p-toluenethiosulphonate dihydrate, $C_7H_7SO_2SNa \cdot 2H_2O$. Monoclinic prismatic, $a = 13.59$ Å, $b = 6.47$ Å, $c = 12.95$ Å, $\beta = 91\frac{1}{2}°$. Four formula units per unit cell; density, calc. 1.44, found 1.43 g/cm³. Systematic absences, $h0l$ when l is odd, $0k0$ when k is odd. The space group is thus $C_{2h}^5 - P2_1/c$.

The dihydrate [3,5] was obtained by crystallization from 96 % ethanol at low room temperature, and occurred as plates {100} which were often prismatic along the *b* axis. There is a pronounced tendency of cleavage along the plate face. In air, the crystals keep well at temperatures below 10° C, but give off the water of crystallization rapidly above 20° C.

A salt, originally [6] listed as sodium *p*-toluenethiosulphonate dihydrate but later [2] reported to be the monohydrate, was described by Weibull [2,6] as monoclinic prismatic with $a : b : c = 0.8869 : 1 : 2.774$ and $\beta = 103° 52'$. With the transformation, $\bar{1}00/0\bar{1}0/\frac{1}{2},0,\frac{1}{2}$, Weibull's data become $a : b : c = 0.8869 : 1 : 1.351$; $\beta = 94.6°$, which do not agree with the X-ray data for the dihydrate nor the anhydrous salt. A monohydrate has not been observed in the present work. Weibull's transformed data are almost identical with those which apply to potassium *p*-toluenethiosulphonate monohydrate.

Further work on the crystal structures of some of the salts will be made, with a view of determining the length of a thiosulphonate sulphur-sulphur bond. As pointed out earlier [7], this bond is probably a predominantly double bond.

1. Brugnatelli, L. *Ber.* **24** (1891) 494.
2. Groth, P. *Chemische Krystallographie* Bd. 4, Leipzig 1917, p. 424.
3. Blomstrand, W. *Ber.* **3** (1870) 957.
4. Wahlstedt, A. *Acta Univ. Lund.* **16** (1879—80) Part II No. 2.
5. Otto, R. and Rössing, A. *Ber.* **24** (1891) 3874. Footnote pp. 3877—8.
6. Weibull, M. *Z. Kryst.* **15** (1889) 234.
7. Foss, O. *Acta Chem. Scand.* **4** (1950) 404.

Received June 13, 1956.

Structure of Thiuret Hydroiodide

OLAV FOSS and OLAV TJOMSLAND

Chemical Institute, University of Bergen, Bergen, Norway

Thiuret hydroiodide, or 3,5-diimino-1,2,4-dithiazolidine hydroiodide, occurs on oxidation of dithiobiuret with iodine [1], and is a five-membered cyclic disulphide [1,2].

The unit cells and space groups of some simple 1,2,4-dithiazolidine derivatives, including thiuret hydroiodide, were reported by one of us in a preceding note [3]. The preliminary results of a complete crystal structure determination of thiuret hydroiodide are given here. The disulphide group has been found to lie across a crystallographic mirror plane of symmetry, and is thus exactly planar. This appears to be the first crystal structure determination reported for a cyclic disulphide, and the first recorded instance of a planar disulphide group.

Open-chain disulphides, X—S—S—X, have always been found to be non-planar *cf.*[4] with a dihedral angle of about 90° between the X—S—S and S—S—X planes, there being a barrier to internal rotation about an S—S bond of from 10 to 14 kcal/mole [5-7]. The formation of a five-membered cyclic disulphide requires the rotation of the S—S bond to a dihedral angle of nearly 0°, where the barrier probably has its highest value. The nevertheless relatively high stabilities of unsaturated five-membered cyclic disulphides, such as 1,2-dithiacenaphthene [8] and the trithiones [9,10], and of 1,2,4-dithiazolidine derivatives with double-bonded substituents in the 3 and 5 positions, must be due to some extent to resonance stabilization of the ring, a resonance involving the unshared *p* electron pairs of the sulphur atoms. The barrier to internal rotation about an S—S bond being thought to be due principally to the mutual repulsion of these electron pairs [11], one on each sulphur atom, their participation in π bonding with the adjacent carbon atoms would tend to lower the barrier height.

The yellow crystals of thiuret hydroiodide, $S_2(C{:}NH)_2NH \cdot HI$, occur as prisms, bounded by {001} and {011} and showing perfect cleavage along the *c* plane. The four-molecule unit cell has the dimensions [3], $a = 5.38$ Å, $b = 9.24$ Å, $c = 13.98$ Å, and the space group is $D_{2h}^{16} - Pnma$. The intensities of the $0kl$ reflections were

fatty leaves or thin plates {001}. There is perfect cleavage along (001) and along planes parallel to the *ab* diagonals.

Sodium p-toluenethiosulphonate dihydrate, $C_7H_7SO_2SNa \cdot 2H_2O$. Monoclinic prismatic, $a = 13.59$ Å, $b = 6.47$ Å, $c = 12.95$ Å, $\beta = 91\frac{1}{2}°$. Four formula units per unit cell; density, calc. 1.44, found 1.43 g/cm³. Systematic absences, $h0l$ when l is odd, $0k0$ when k is odd. The space group is thus $C_{2h}^5 - P2_1/c$.

The dihydrate [3,5] was obtained by crystallization from 96 % ethanol at low room temperature, and occurred as plates {100} which were often prismatic along the *b* axis. There is a pronounced tendency of cleavage along the plate face. In air, the crystals keep well at temperatures below 10° C, but give off the water of crystallization rapidly above 20° C.

A salt, originally [6] listed as sodium *p*-toluenethiosulphonate dihydrate but later [2] reported to be the monohydrate, was described by Weibull [2,6] as monoclinic prismatic with $a : b : c = 0.8869 : 1 : 2.774$ and $\beta = 103° 52'$. With the transformation, $\bar{1}00/0\bar{1}0/\frac{1}{2},0,\frac{1}{2}$, Weibull's data become $a : b : c = 0.8869 : 1 : 1.351$; $\beta = 94.6°$, which do not agree with the X-ray data for the dihydrate nor the anhydrous salt. A monohydrate has not been observed in the present work. Weibull's transformed data are almost identical with those which apply to potassium *p*-toluenethiosulphonate monohydrate.

Further work on the crystal structures of some of the salts will be made, with a view of determining the length of a thiosulphonate sulphur-sulphur bond. As pointed out earlier [7], this bond is probably a predominantly double bond.

1. Brugnatelli, L. *Ber.* **24** (1891) 494.
2. Groth, P. *Chemische Krystallographie* Bd. 4, Leipzig 1917, p. 424.
3. Blomstrand, W. *Ber.* **3** (1870) 957.
4. Wahlstedt, A. *Acta Univ. Lund.* **16** (1879—80) Part II No. 2.
5. Otto, R. and Rössing, A. *Ber.* **24** (1891) 3874. Footnote pp. 3877—8.
6. Weibull, M. *Z. Kryst.* **15** (1889) 234.
7. Foss, O. *Acta Chem. Scand.* **4** (1950) 404.

Received June 13, 1956.

Structure of Thiuret Hydroiodide

OLAV FOSS and OLAV TJOMSLAND

Chemical Institute, University of Bergen, Bergen, Norway

Thiuret hydroiodide, or 3,5-diimino-1,2,4-dithiazolidine hydroiodide, occurs on oxidation of dithiobiuret with iodine [1], and is a five-membered cyclic disulphide [1,2].

The unit cells and space groups of some simple 1,2,4-dithiazolidine derivatives, including thiuret hydroiodide, were reported by one of us in a preceding note [3]. The preliminary results of a complete crystal structure determination of thiuret hydroiodide are given here. The disulphide group has been found to lie across a crystallographic mirror plane of symmetry, and is thus exactly planar. This appears to be the first crystal structure determination reported for a cyclic disulphide, and the first recorded instance of a planar disulphide group.

Open-chain disulphides, X—S—S—X, have always been found to be non-planar *cf.*[4] with a dihedral angle of about 90° between the X—S—S and S—S—X planes, there being a barrier to internal rotation about an S—S bond of from 10 to 14 kcal/mole [5-7]. The formation of a five-membered cyclic disulphide requires the rotation of the S—S bond to a dihedral angle of nearly 0°, where the barrier probably has its highest value. The nevertheless relatively high stabilities of unsaturated five-membered cyclic disulphides, such as 1,2-dithiacenaphthene [8] and the trithiones [9,10], and of 1,2,4-dithiazolidine derivatives with double-bonded substituents in the 3 and 5 positions, must be due to some extent to resonance stabilization of the ring, a resonance involving the unshared *p* electron pairs of the sulphur atoms. The barrier to internal rotation about an S—S bond being thought to be due principally to the mutual repulsion of these electron pairs [11], one on each sulphur atom, their participation in π bonding with the adjacent carbon atoms would tend to lower the barrier height.

The yellow crystals of thiuret hydroiodide, $S_2(C{:}NH)_2NH \cdot HI$, occur as prisms, bounded by {001} and {011} and showing perfect cleavage along the *c* plane. The four-molecule unit cell has the dimensions [3], $a = 5.38$ Å, $b = 9.24$ Å, $c = 13.98$ Å, and the space group is $D_{2h}^{16} - Pnma$. The intensities of the $0kl$ reflections were

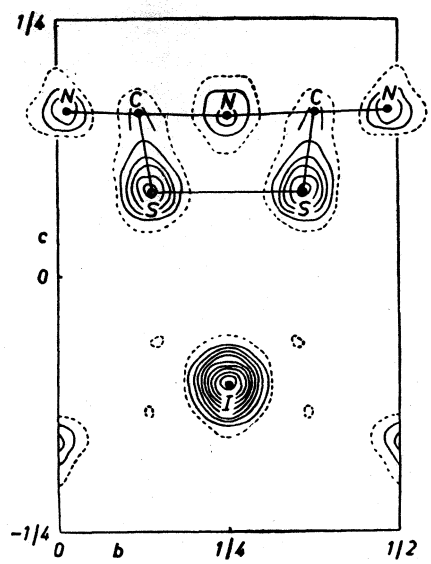


Fig. 1. Electron density projection of thiuret hydroiodide along the a *axis, showing two asymmetric units. The 4-electron line is dashed. Contour intervals: 10 e · Å^{-2} for the iodide ion, 4 e · Å^{-2} for the sulphur atoms and 2 e · Å^{-2} for the carbon and nitrogen atoms.*

estimated visually from zero layer Weissenberg photographs about the *a* axis. A crystal with cross-section 0.07 × 0.08 mm was used, and copper radiation. A Patterson synthesis based on the 0*kl* data gave the *y* and *z* coordinates of the iodide ion and the sulphur atom of the asymmetric unit, and subsequent Fourier syntheses lead to the electron density map reproduced in Fig. 1.

At the present stage of refinement, the *y* and *z* coordinates are as listed in Table 1. These coordinates, with appropriate temperature and scale factors, give a reliability factor of $R = 14.4$ % for the 0*kl* reflections.

The sulphur *y* coordinate and the iodide *z* coordinate give a S—S bond length of 2.05 Å and a closest I—I approach of 4.82 Å, respectively. The former of these distances agrees well with the S—S bond length in orthorhombic sulphur [12], 2.04 Å, and the latter is 0.5 Å larger than twice the ionic radius of iodine [13].

Table 1. Atomic coordinates, in fractions of corresponding cell edges. Origin at a centre of symmetry.

	y	*z*
I	0.250	—0.107
N_1	0.250	0.156
S	0.139	0.081
C	0.120	0.160
N_2	0.014	0.162

The 1,2,4-dithiazolidine ring is intersected by a crystallographic mirror plane, which passes through the nitrogen atom and midway between the sulphur atoms, and it follows that the disulphide group, including the two sulphur atoms and the adjacent carbon atoms, is planar. The ring as a whole, however, need not be planar, and as far as can be judged from the 0*kl* electron density map, the nitrogen atom of the 1,2,4-dithiazolidine ring is displaced from the plane of the sulphur and carbon atoms.

The work will be continued, and details published later. Also, it is intended to study the crystal structures of 1,2-dithiacyclohepta-3,6-diene derivatives [14,15], with a view of determining the degree of planarity of the disulphide group in unsaturated seven-membered rings.

Note added in proof, Sept. 3, 1956. — Refinement by difference syntheses of the *a* axis projection of thiuret hydroiodide has led to a reliability factor of $R = 7.6$ % and a S—S bond length of 2.09 Å.

The authors wish to express their thanks to *Norges Almenvitenskapelige Forskningsråd* for a grant.

1. *Dithiobiuret*, Technical Data Sheet, American Cyanamid Company, New York, 1947.
2. Preisler, P. W. and Bateman, M. M. *J. Am. Chem. Soc.* **69** (1947) 2632.
3. Foss, O. *Acta Chem. Scand.* **10** (1956) 868.
4. Foss, O. *Acta Chem. Scand.* **8** (1954) 469.
5. Scott, D. W., Finke, H. L., Gross, M. E., Guthrie, G. B. and Huffman, H. M. *J. Am. Chem. Soc.* **72** (1950) 2424.
6. Scott, D. W., Finke, H. L., McCullough, J. P., Gross, M. E., Pennington, R. E. and Waddington, G. *J. Am. Chem. Soc.* **74** (1952) 2478.
7. Guthrie, G. B. Jr., Scott, D. W. and Waddington, G. J. *Am. Chem. Soc.* **76** (1954) 1488.
8. Price, W. B. and Smiles, S. *J. Chem. Soc.* **1928** 2372.
9. Böttcher. B. and Lüttringhaus, A. *Ann.* **557** (1947) 89.
10. Lüttringhaus, A. and Cleve, W. *Ann.* **575** (1951) 112.
11. Pauling, L. *Proc. Natl. Acad. Sci. U. S.* **35** (1949) 495.

12. Abrahams, S. C. *Acta Cryst.* **8** (1955) 661.
13. Pauling, L. *Nature of the chemical bond*, Ithaca 1945, p. 346.
14. Arndt, F., Nachtwey, P. and Pusch, J. *Ber.* **58** (1925) 1633.
15. Arndt, F. and Traverso, G. *Ber.* **89** (1956) 124.

Received June 13, 1956.

X-Ray Crystallographic Data on Certain Five-membered Cyclic Disulphides

OLAV FOSS

Chemical Institute, University of Bergen, Bergen, Norway

A survey has been made of unit cells and space groups of some simple 1,2,4-dithiazolidine derivatives. The compounds studied are, xanthan hydride [1-3] (3-imino-1,2,4-dithiazolidine-5-thione), rhodan hydrate [4,5] (3-imino-1,2,4-dithiazolidine-5-one), and three thiuret (3,5-diimino-1,2,4-dithiazolidine) hydrohalides. The latter compounds are oxidation products of dithiobiuret; the hydrochloride [6] and hydroiodide [7] have been mentioned in literature earlier, but apparently not the hydrobromide. The hydrobromide and hydroiodide used in the present work were obtained by adding an excess of aqueous potassium bromide or iodide to a warm aqueous solution of the hydrochloride.

Oscillation and Weissenberg photographs were taken using copper radiation, $\lambda(CuK\alpha) = 1.542$ Å. The axial lengths given below are believed to be correct to within 0.5 %. Densities were determined by flotation in bromoform-carbon tetrachloride mixtures.

Xanthan hydride, $S_2(C{:}NH)(C{:}S)NH$. Monoclinic prismatic, $a = 4.05$ Å, $b = 10.59$ Å, $c = 12.78$ Å, $\beta = 97°$. Four molecules per unit cell; density, calc. 1.83, found 1.84 g/cm³. Systematic absences, $h0l$ when l is odd, $0k0$ when k is odd. The space group is thus $C_{2h}^5-P2_1/c$.

From 60 % acetic acid the compound crystallized as long prisms, extended along the a axis and flattened along the b axis.

Rhodan hydrate, $S_2(C{:}NH)(C{:}O)NH$. Monoclinic, $a = 12.50$ Å, $b = 5.24$ Å, $c = 14.67$ Å, $\beta = 95\frac{1}{2}°$. Eight molecules per unit cell; density, calc. 1.86, found 1.87 g/cm³. Systematic absences, hkl when $h + k$ is odd, $h0l$ when l is odd. The space group is thus either C_{2h}^6-C2/c or C_s^4-C/c.

From water, the compound crystallized as flat prisms, extended along the b axis and with {100} predominant. There is perfect cleavage along (001). The morphology of the crystals indicates the presence of a twofold axis and thus the correctness of the centrosymmetric space group, C_{2h}^6-C2/c.

Thiuret hydrochloride, $S_2(C{:}NH)_2NH \cdot HCl \cdot \frac{1}{2}H_2O$. Monoclinic, $a = 19.58$ Å, $b = 5.47$ Å, $c = 14.34$ Å, $\beta = 114\frac{1}{2}°$. Eight formula units per unit cell; density, calc. 1.70, found 1.71 g/cm³. Systematic absences, hkl when $h + k$ is odd, $h0l$ when l is odd. Space group, C_{2h}^6-C2/c or C_s^4-C/c.

The density, and the statement by Preisler and Bateman [6] that 5 % water remain after drying over calcium chloride, point to the presence of half a mole of crystal water per mole of hydrochloride.

From water, the compound crystallized as prisms extended along the b axis. As in the case of rhodan hydrate, the morphology is in favour of the former of the two possible space groups. The water molecules would then lie on twofold axes.

Thiuret hydrobromide, $S_2(C{:}NH)_2NH \cdot HBr$. Monoclinic prismatic, $a = 5.11$ Å, $b = 12.76$ Å, $c = 10.47$ Å, $\beta = 110°$. Four formula units per unit cell; density, calc. 2.22, found 2.22 g/cm³. Systematic absences, $h0l$ when l is odd, $0k0$ when k is odd. The space group is thus $C_{2h}^5-P2_1/c$.

The compound crystallized from water as large plates {010} or as prisms extended along the a axis with, also here, {010} predominant.

Thiuret hydroiodide, $S_2(C{:}NH)_2NH \cdot HI$. Orthorhombic bipyramidal, $a = 5.38$ Å, $b = 9.24$ Å, $c = 13.98$ Å. Four formula units per unit cell; density, calc. 2.50, found 2.49 g/cm³. Systematic absences, $0kl$ when $k + l$ is odd, $hk0$ when h is odd. Of the two space groups compatible with these absences, the centrosymmetric one, $D_{2h}^{16}-Pnma$, has been found to be the correct one through Patterson and Fourier projections along the a axis [8]. The thiuret-H^+ ion lies across a crystallographic mirror plane of symmetry, and also the iodide ion is located in the mirror plane.

From water, the compound crystallized as prisms extended along the a axis and bounded by {001} and {011}. There is perfect cleavage along (001), and a rather pronounced tendency of irregular growth and twinning.

Further work on the crystal structures of some of the compounds will be made.

12. Abrahams, S. C. *Acta Cryst.* **8** (1955) 661.
13. Pauling, L. *Nature of the chemical bond*, Ithaca 1945, p. 346.
14. Arndt, F., Nachtwey, P. and Pusch, J. *Ber.* **58** (1925) 1633.
15. Arndt, F. and Traverso, G. *Ber.* **89** (1956) 124.

Received June 13, 1956.

X-Ray Crystallographic Data on Certain Five-membered Cyclic Disulphides

OLAV FOSS

Chemical Institute, University of Bergen, Bergen, Norway

A survey has been made of unit cells and space groups of some simple 1,2,4-dithiazolidine derivatives. The compounds studied are, xanthan hydride [1-3] (3-imino-1,2,4-dithiazolidine-5-thione), rhodan hydrate [4,5] (3-imino-1,2,4-dithiazolidine-5-one), and three thiuret (3,5-diimino-1,2,4-dithiazolidine) hydrohalides. The latter compounds are oxidation products of dithiobiuret; the hydrochloride [6] and hydroiodide [7] have been mentioned in literature earlier, but apparently not the hydrobromide. The hydrobromide and hydroiodide used in the present work were obtained by adding an excess of aqueous potassium bromide or iodide to a warm aqueous solution of the hydrochloride.

Oscillation and Weissenberg photographs were taken using copper radiation, $\lambda(CuK\alpha) = 1.542$ Å. The axial lengths given below are believed to be correct to within 0.5 %. Densities were determined by flotation in bromoform-carbon tetrachloride mixtures.

Xanthan hydride, $S_2(C{:}NH)(C{:}S)NH$. Monoclinic prismatic, $a = 4.05$ Å, $b = 10.59$ Å, $c = 12.78$ Å, $\beta = 97°$. Four molecules per unit cell; density, calc. 1.83, found 1.84 g/cm³. Systematic absences, $h0l$ when l is odd, $0k0$ when k is odd. The space group is thus $C_{2h}^5-P2_1/c$.

From 60 % acetic acid the compound crystallized as long prisms, extended along the a axis and flattened along the b axis.

Rhodan hydrate, $S_2(C{:}NH)(C{:}O)NH$. Monoclinic, $a = 12.50$ Å, $b = 5.24$ Å, $c = 14.67$ Å, $\beta = 95\frac{1}{2}°$. Eight molecules per unit cell; density, calc. 1.86, found 1.87 g/cm³. Systematic absences, hkl when $h + k$ is odd, $h0l$ when l is odd. The space group is thus either C_{2h}^6-C2/c or C_s^4-C/c.

From water, the compound crystallized as flat prisms, extended along the b axis and with {100} predominant. There is perfect cleavage along (001). The morphology of the crystals indicates the presence of a twofold axis and thus the correctness of the centrosymmetric space group, C_{2h}^6-C2/c.

Thiuret hydrochloride, $S_2(C{:}NH)_2NH \cdot HCl \cdot \frac{1}{2}H_2O$. Monoclinic, $a = 19.58$ Å, $b = 5.47$ Å, $c = 14.34$ Å, $\beta = 114\frac{1}{2}°$. Eight formula units per unit cell; density, calc. 1.70, found 1.71 g/cm³. Systematic absences, hkl when $h + k$ is odd, $h0l$ when l is odd. Space group, C_{2h}^6-C2/c or C_s^4-C/c.

The density, and the statement by Preisler and Bateman [6] that 5 % water remain after drying over calcium chloride, point to the presence of half a mole of crystal water per mole of hydrochloride.

From water, the compound crystallized as prisms extended along the b axis. As in the case of rhodan hydrate, the morphology is in favour of the former of the two possible space groups. The water molecules would then lie on twofold axes.

Thiuret hydrobromide, $S_2(C{:}NH)_2NH \cdot HBr$. Monoclinic prismatic, $a = 5.11$ Å, $b = 12.76$ Å, $c = 10.47$ Å, $\beta = 110°$. Four formula units per unit cell; density, calc. 2.22, found 2.22 g/cm³. Systematic absences, $h0l$ when l is odd, $0k0$ when k is odd. The space group is thus $C_{2h}^5-P2_1/c$.

The compound crystallized from water as large plates {010} or as prisms extended along the a axis with, also here, {010} predominant.

Thiuret hydroiodide, $S_2(C{:}NH)_2NH \cdot HI$. Orthorhombic bipyramidal, $a = 5.38$ Å, $b = 9.24$ Å, $c = 13.98$ Å. Four formula units per unit cell; density, calc. 2.50, found 2.49 g/cm³. Systematic absences, $0kl$ when $k + l$ is odd, $hk0$ when h is odd. Of the two space groups compatible with these absences, the centrosymmetric one, $D_{2h}^{16}-Pnma$, has been found to be the correct one through Patterson and Fourier projections along the a axis [8]. The thiuret-H^+ ion lies across a crystallographic mirror plane of symmetry, and also the iodide ion is located in the mirror plane.

From water, the compound crystallized as prisms extended along the a axis and bounded by {001} and {011}. There is perfect cleavage along (001), and a rather pronounced tendency of irregular growth and twinning.

Further work on the crystal structures of some of the compounds will be made.

The author wishes to express his thanks to the American Cyanamid Company, New York, for a sample of thiuret hydrochloride.

1. Vöckel, C. *Ann.* **43** (1842) 74.
2. Klason, P. *J. prakt. Chem.* [2] **38** (1888) 366.
3. Hantzsch, A. and Wolvekamp, M. *Ann.* **331** (1904) 265.
4. Söderbäck, E. *Ann.* **419** (1919) 217.
5. Söderbäck, E. *Ann.* **465** (1928) 184.
6. Preisler, P. W. and Bateman, M. M. *J. Am. Chem. Soc.* **69** (1947) 2632.
7. *Dithiobiuret*, Technical Data Sheet, American Cyanamid Company, New York, 1947.
8. Foss, O. and Tjomsland, O. *Acta Chem. Scand.* **10** (1956) 869.

Received June 13, 1956.

Kinetics of the Heterogeneous Reaction of Calcium Bicarbonate Formation, with Special Reference to Copper Ion Inhibition

O. ERGA and S. G. TERJESEN

Chemical Engineering Laboratory, Technical University of Norway, Trondheim, Norway

The system $CaCO_{3(s)}-CO_{2(g)}-H_2O_{(l)}$ is of considerable geological, physiological and technical importance. The reaction between solid calcium carbonate and aqueous carbon dioxide has therefore been discussed extensively in literature [1]. However, the published papers deal mainly with the thermodynamics of the reaction whereas the kinetic aspects seem to have been largely neglected.

Calcite of natural origin was used in the present investigation. When giving the ground material a repeated treatment with aqueous carbon dioxide, the reactivity of the calcite particles used for the experiment, did not change from one run to another. The experiments were carried out at 25° C in an agitated vessel made of stainless steel and designed to keep the solid particles well suspended in the liquid during the runs. The carbon dioxide-air mixture was blown into the suspension of calcite particles, and the reaction was followed by conductivity measurements.

The reaction was found to be strongly inhibited by very small amounts of copper ions. In Fig. 1 are shown the results of three runs, all carried out with 100 g of calcite suspended in 10 litres of distilled water. The particle size was 295—422 μ, corresponding to a surface area of approximately 125 cm² per g². The carbon dioxide pressure was 0.95 atm. In the first experiment traces of copper inevitably present in the solution were screened by adding 4×10^{-5} moles per litre of disodium - ethylenediamin - tetraacetic acid (EDTA) [2]. The middle curve shows that less than 2×10^{-7} moles per litre of copper ions, accidentally present due to contamination of the surface of the particles and the distilled water, has a significant effect on the reaction rate. The third run was carried out in the presence of 10^{-5} moles per litre of cupric chloride. The inhibition was now so strong that the reaction gave the appearance of approaching a new equilibrium concentration, 20—30 % below the real one.

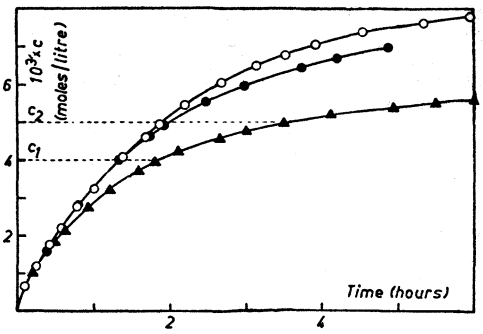


Fig. 1. Time-concentration curves showing the inhibiting effect of copper ions.
○: *No active copper present*
●: $2 \cdot 10^{-7}$ *moles copper/l*
▲: 10^{-5} » »

With the object of investigating whether the bulk of the added copper ions was adsorbed on the calcite surface or remained dissolved in the water, the following experiment was carried out: Initially, the liquid contained 10^{-5} moles per litre of cupric chloride, but when the concentration of calcium bicarbonate reached c_1 in Fig. 1, the experiment was stopped, the liquid decanted and used for another run with a fresh portion of calcite. The concentration then continued to rise along the lower curve. At c_2 this experiment was stopped, the solution removed by decantation and

The author wishes to express his thanks to the American Cyanamid Company, New York, for a sample of thiuret hydrochloride.

1. Vöckel, C. *Ann.* **43** (1842) 74.
2. Klason, P. *J. prakt. Chem.* [2] **38** (1888) 366.
3. Hantzsch, A. and Wolvekamp, M. *Ann.* **331** (1904) 265.
4. Söderbäck, E. *Ann.* **419** (1919) 217.
5. Söderbäck, E. *Ann.* **465** (1928) 184.
6. Preisler, P. W. and Bateman, M. M. *J. Am. Chem. Soc.* **69** (1947) 2632.
7. *Dithiobiuret*, Technical Data Sheet, American Cyanamid Company, New York, 1947.
8. Foss, O. and Tjomsland, O. *Acta Chem. Scand.* **10** (1956) 869.

Received June 13, 1956.

Kinetics of the Heterogeneous Reaction of Calcium Bicarbonate Formation, with Special Reference to Copper Ion Inhibition

O. ERGA and S. G. TERJESEN

Chemical Engineering Laboratory, Technical University of Norway, Trondheim, Norway

The system $CaCO_{3(s)}-CO_{2(g)}-H_2O_{(l)}$ is of considerable geological, physiological and technical importance. The reaction between solid calcium carbonate and aqueous carbon dioxide has therefore been discussed extensively in literature [1]. However, the published papers deal mainly with the thermodynamics of the reaction whereas the kinetic aspects seem to have been largely neglected.

Calcite of natural origin was used in the present investigation. When giving the ground material a repeated treatment with aqueous carbon dioxide, the reactivity of the calcite particles used for the experiment, did not change from one run to another. The experiments were carried out at 25° C in an agitated vessel made of stainless steel and designed to keep the solid particles well suspended in the liquid during the runs. The carbon dioxide-air mixture was blown into the suspension of calcite particles, and the reaction was followed by conductivity measurements.

The reaction was found to be strongly inhibited by very small amounts of copper ions. In Fig. 1 are shown the results of three runs, all carried out with 100 g of calcite suspended in 10 litres of distilled water. The particle size was 295—422 μ, corresponding to a surface area of approximately 125 cm² per g². The carbon dioxide pressure was 0.95 atm. In the first experiment traces of copper inevitably present in the solution were screened by adding 4×10^{-5} moles per litre of disodium - ethylenediamin - tetraacetic acid (EDTA) [2]. The middle curve shows that less than 2×10^{-7} moles per litre of copper ions, accidentally present due to contamination of the surface of the particles and the distilled water, has a significant effect on the reaction rate. The third run was carried out in the presence of 10^{-5} moles per litre of cupric chloride. The inhibition was now so strong that the reaction gave the appearance of approaching a new equilibrium concentration, 20—30 % below the real one.

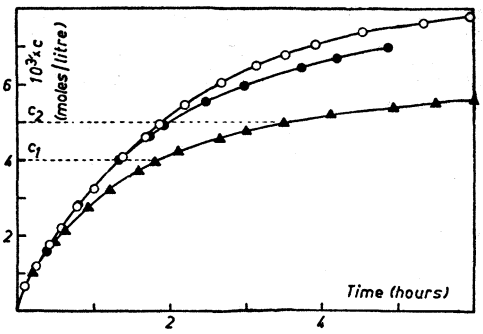


Fig. 1. Time-concentration curves showing the inhibiting effect of copper ions.
○: *No active copper present*
●: $2 \cdot 10^{-7}$ *moles copper/l*
▲: 10^{-5} » »

With the object of investigating whether the bulk of the added copper ions was adsorbed on the calcite surface or remained dissolved in the water, the following experiment was carried out: Initially, the liquid contained 10^{-5} moles per litre of cupric chloride, but when the concentration of calcium bicarbonate reached c_1 in Fig. 1, the experiment was stopped, the liquid decanted and used for another run with a fresh portion of calcite. The concentration then continued to rise along the lower curve. At c_2 this experiment was stopped, the solution removed by decantation and

a new experiment started with the same particles but with fresh water. The reaction now followed the middle curve. These experiments strongly indicate that the copper was present mainly in the bulk of the liquid and that very little could have been adsorbed at the surface of the particles.

The inhibition by copper ions provides a reasonable explanation for the difficulties encountered by many investigators in reaching a final state of equilibrium. Frear and Johnston [4] found it necessary to allow weeks and Shtermina and Frolova [5] even months for the establishment of equilibrium. It is shown here that this excessive delay can be eliminated by additions of small quantities of EDTA, an expedient which might prove useful also in other cases involving solid calcium carbonate.

In Fig. 2, the rate of reaction is plotted against the concentration of calcium bicarbonate for partial pressures of carbon dioxide of 0.952, 0.664, 0.392 and 0.135 atm. The amount and size of the calcite particles were exactly as for the runs shown in Fig. 1, and 4×10^{-5} moles per litre of EDTA was added. Except for a short period after the start of the experiments, the relation between the concentration of calcium bicarbonate and the rate of reaction is linear. Furthermore, the points of intersection of these lines with the abscissa, give the respective equilibrium concentrations. These are 6.2 to 9.8 % lower than

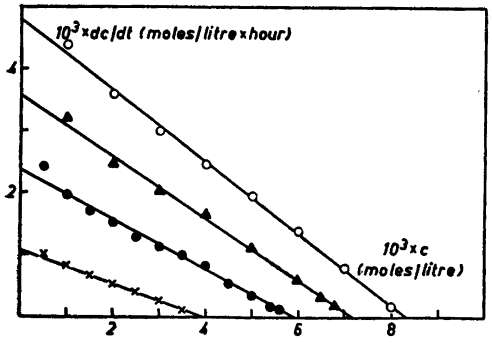


Fig. 2. A plot of the rate of the unhibited reaction against concentration of calcium bicarbonate for different partial pressures of carbon dioxide.

○: p_{CO_2} = *0.952 atm*
▲: p_{CO_2} = *0.664* »
●: p_{CO_2} = *0.392* »
×: p_{CO_2} = *0.135* »

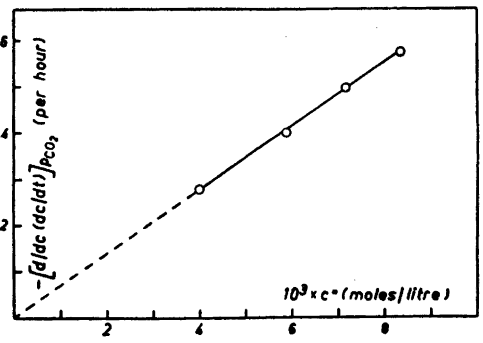


Fig. 3. A plot of the slope of the rate-concentration lines of Fig. 2 against the respective equilibrium concentrations.

the values reported by Frear and Johnston [4], who used finely powdered material, but 4 to 0 % higher than those of Miller [1], obtained with coarser crystalline aggregates of natural calcite.

The slope of the lines in Fig. 2 have been plotted against the corresponding equilibrium concentrations in Fig. 3, and it can be seen that the relationship is a straight line through origo. This means that the results of the experiments without inhibition can be described by the following kinetic equation:

$$\frac{dc}{dt} = k \cdot c^* \ (c^* - c)$$

where c^* = concentration of calciumbicarbonate at equilibrium in moles per litre; c = concentration of calciumbicarbonate at a time t after start of the reaction; k = a constant, independent of c^*, but shown below to be proportional to the surface area of the particles per unit volume of suspension.

In an attempt to localise the rate determining steps, experiments were carried out with various gas velocities, intensities of agitation and quantities of particles, but with the same particle size as above and with a partial pressure of carbon dioxide of 0.95—0.97 atm. The rate of reaction was found to be strictly proportional to the surface area of the particles, but independent of the gas velocity in the range investigated. This shows that the rate of reaction is affected neither by the transfer of carbon dioxide from the gas to the liquid, nor by any chemical reaction in the bulk

of the liquid. Consequently, the rate determining steps are localised at the solid-liquid interface or in the liquid film in immediate contact with it.

The effect of the rate of stirring can be expressed by the coefficient of stirring, a, defined by the relationship: dc/dt proportional to $(\text{r.p.m.})^a$. The average value of this coefficient was found to be 0.22 over the range investigated, *i. e.* 280—555 r.p.m. This is much smaller than the value of 0.5—1.0 generally reported for heterogeneous processes controlled by diffusion [4], indicating that chemical reactions are among the rate determining steps.

Further work is in progress in an endeavour to elucidate the reaction mechanism both in the absence and presence of inhibiting metal ions.

1. Miller, J. P. *Am. J. Sci.* **250** (1952) 161.
2. Brown, G. G. *Unit Operations*, John Wiley & Sons, Inc., New York 1950, p. 21.
3. Schwarzenbach, G. *Die Komplexometrische Titration*, Ferdinand Enke Verlag, Stuttgart 1955.
4. Frear, G. L. and Johnston, J. *J. Am. Chem. Soc.* **51** (1929) 2082.
5. Shtermina, E. B. and Frolova, E. V. *Doklady Akad. Nauk. SSSR* **21** (1952) 271; *Chem. Abstracts* **48** (1954) 6224 [a].
6. Bircumshaw, L. L. and Riddiford, A. C. *Quart. Rev. London* **6** (1952) 157.

Received June 9, 1956.

Action of Ionizing Radiation on Insulating Plastics

L. EHRENBERG and K. G. ZIMMER

Institute for Organic Chemistry and Biochemistry, University, Stockholm, Sweden, and Max-Planck-Institut für physikalische Chemie, Göttingen, Germany

The action of ionizing radiation on insulating plastics is of great interest from various points of view, such as (i) the selection of most suitable materials for the construction of measuring equipment, (ii) the elucidation of the mechanism of induced conductivity and also (iii) as a model for the action of radiation on biologically important macromolecules [1,2]. By making use of a new experimental method [3] it has been possible to demonstrate that induced conductivity during beta irradiation (from Ce-Pr-144) as well as the so called after-effects are generally very different when part of the volume only is irradiated (leaving the insulating surface completely untouched by radiation) or when directing the radiation on the insulating surface [4]. From a theoretical point of view volume effects seem more interesting but for practical purposes surface effects are sometimes very important. They are often so pronounced as to make an otherwise excellent insulator practically useless. It seemed of interest, therefore, to investigate these surface effects somewhat further.

Insulating surfaces are in most cases in contact with atmospheric air and we thought it likely that, amongst other things, the deterioration might be caused by oxidation under the action of radiation. Oxidation would be expected to lead to the formation of hydrophilic groups and, consequently, to an increase in wettability. This would tend to decrease the usefulness of any insulator as small changes of temperature will always occur and may, on a wettable surface, enable a continuous and conducting layer of water to be formed. The formation of hydrophilic groups we were able to demonstrate in several ways:

(a) Specimens of insulating plastics were exposed to gamma-radiation from a ^{60}Co source of 70 Curies and the contact angle of small drops of 0.1 N NaOH measured on freshly machined surfaces. For machining we used a tool carefully washed in benzene and alcohol, for measuring a simple device made from a microscope. The data compiled in Table 1 show a considerable decrease of contact angle (increase in adhesion [5]).

(b) The formation of hydrophilic groups can be demonstrated very easily using liquid paraffin which has been shown to undergo much the same change of properties under irradiation as does polyethylene [6]. A drop of a paraffin of standard weight put onto a clean surface of 0.1 N aqueous NaOH forms a lens with a well defined diameter [7] which increases due to increased number of hydrophilic groups as the material is irradiated by ionizing radiation (previous to putting drops onto the aqueous alkali). We used 180 kV X-rays for irradiation in this case. A series of measurements is shown in Fig. 1.

(c) The effect can also be demonstrated in another way, lending itself more easily

of the liquid. Consequently, the rate determining steps are localised at the solid-liquid interface or in the liquid film in immediate contact with it.

The effect of the rate of stirring can be expressed by the coefficient of stirring, a, defined by the relationship: dc/dt proportional to $(\text{r.p.m.})^a$. The average value of this coefficient was found to be 0.22 over the range investigated, *i. e.* 280—555 r.p.m. This is much smaller than the value of 0.5—1.0 generally reported for heterogeneous processes controlled by diffusion [4], indicating that chemical reactions are among the rate determining steps.

Further work is in progress in an endeavour to elucidate the reaction mechanism both in the absence and presence of inhibiting metal ions.

1. Miller, J. P. *Am. J. Sci.* **250** (1952) 161.
2. Brown, G. G. *Unit Operations*, John Wiley & Sons, Inc., New York 1950, p. 21.
3. Schwarzenbach, G. *Die Komplexometrische Titration*, Ferdinand Enke Verlag, Stuttgart 1955.
4. Frear, G. L. and Johnston, J. *J. Am. Chem. Soc.* **51** (1929) 2082.
5. Shtermina, E. B. and Frolova, E. V. *Doklady Akad. Nauk. SSSR* **21** (1952) 271; *Chem. Abstracts* **48** (1954) 6224 [a].
6. Bircumshaw, L. L. and Riddiford, A. C. *Quart. Rev. London* **6** (1952) 157.

Received June 9, 1956.

Action of Ionizing Radiation on Insulating Plastics

L. EHRENBERG and K. G. ZIMMER

Institute for Organic Chemistry and Biochemistry, University, Stockholm, Sweden, and Max-Planck-Institut für physikalische Chemie, Göttingen, Germany

The action of ionizing radiation on insulating plastics is of great interest from various points of view, such as (i) the selection of most suitable materials for the construction of measuring equipment, (ii) the elucidation of the mechanism of induced conductivity and also (iii) as a model for the action of radiation on biologically important macromolecules [1,2]. By making use of a new experimental method [3] it has been possible to demonstrate that induced conductivity during beta irradiation (from Ce-Pr-144) as well as the so called after-effects are generally very different when part of the volume only is irradiated (leaving the insulating surface completely untouched by radiation) or when directing the radiation on the insulating surface [4]. From a theoretical point of view volume effects seem more interesting but for practical purposes surface effects are sometimes very important. They are often so pronounced as to make an otherwise excellent insulator practically useless. It seemed of interest, therefore, to investigate these surface effects somewhat further.

Insulating surfaces are in most cases in contact with atmospheric air and we thought it likely that, amongst other things, the deterioration might be caused by oxidation under the action of radiation. Oxidation would be expected to lead to the formation of hydrophilic groups and, consequently, to an increase in wettability. This would tend to decrease the usefulness of any insulator as small changes of temperature will always occur and may, on a wettable surface, enable a continuous and conducting layer of water to be formed. The formation of hydrophilic groups we were able to demonstrate in several ways:

(a) Specimens of insulating plastics were exposed to gamma-radiation from a ^{60}Co source of 70 Curies and the contact angle of small drops of 0.1 N NaOH measured on freshly machined surfaces. For machining we used a tool carefully washed in benzene and alcohol, for measuring a simple device made from a microscope. The data compiled in Table 1 show a considerable decrease of contact angle (increase in adhesion [5]).

(b) The formation of hydrophilic groups can be demonstrated very easily using liquid paraffin which has been shown to undergo much the same change of properties under irradiation as does polyethylene [6]. A drop of a paraffin of standard weight put onto a clean surface of 0.1 N aqueous NaOH forms a lens with a well defined diameter [7] which increases due to increased number of hydrophilic groups as the material is irradiated by ionizing radiation (previous to putting drops onto the aqueous alkali). We used 180 kV X-rays for irradiation in this case. A series of measurements is shown in Fig. 1.

(c) The effect can also be demonstrated in another way, lending itself more easily

Table 1. Contact angles of drops of aqueous alkali on various plastics before and after irradiation.

Material	Contact angle after irradiation with 0 Mrad	8 Mrad	16 Mrad
Polyethylene * ("Alkathene")	85°	76°	75°
Polysterene ("Trolitul")	98°	86°	77°
Polymethylmethacrylate ("Plexiglas")	84°	72°	52°
Polytetrafluorethylene ("Teflon")	90°	86°	82°
Polymonochlortrifluorethylene ("Kel F")	74°	55°	50°
Polyethyleneterephthalate ("Melinex")	71°	62°	55°

* Paraffin wax was measured for comparison. A dose of 2 Mrad gave a change of contact angle from 100° to 95°.

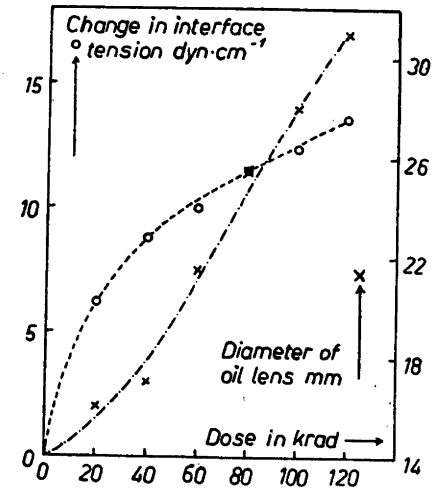


Fig. 1. Equilibrium values of interfacial tensions (24 hours) and oil lens diameters (10 mins. after surface contact). Latter values average 10 measurements. 20° C.

to quantitative evaluation, by measuring the interfacial tension between liquid paraffin and water by means of a Du-Noüy-balance (Fig. 1).

Another series of irradiations was conducted in an atmosphere of purified nitrogen admitted after prolonged evacuation of the vessels containing the specimens of plastic. Contact angles were measured by method (a) in air. They showed a decrease of the same order as had been found after irradiation in air. Though this result seems to disagree with the above explanation it must be kept in mind that irradiation of many substances in the absence of air produces long lived radicals which react with oxygen rapidly as soon as the latter becomes available [8].

The fact that the materials studied were of technical grade has to be borne in mind. This does not detract from the practical value of the results though side effects due to unspecified additions cannot be excluded.

It is a pleasure to express our gratitude to the *Knut and Alice Wallenberg Foundation* and to the *Agricultural Research Council* for grants which made this work possible, and to Prof. Å. Gustafsson, Genetics Department, Forest Research Institute, Stockholm, for permission to use the X-ray and the Cobalt-sources of this institute.

1. Fowler, J. F. and Farmer, F. T. *Brit. J. Radiol.* **29** (1956) 118.
2. Bacq, Z. M. and Alexander, P. *Fundamentals of Radiobiology*, London 1955.
3. Rosman, I. M. and Zimmer, K. G. *Z. Naturforsch.* **11 b** (1956) 55.
4. Rosman, I. M. and Zimmer, K. G. *Zhur. Eksptl. Teort. Fiz. In press since 1954.*
5. Adam, N. K. *The Physics and Chemistry of Surfaces*, Oxford 1944.
6. Charlesby, A. *Proc. Roy. Soc. London* **A 222** (1954) 60.
7. Stenström, W. and Vigness, I. *Am. J. Roentgenol.* **40** (1938) 427.
8. Gordy, W., Ard, W. B. and Shields, H. *Proc. Natl. Acad. Sci. U. S.* **41** (1955) 983.

Received August 9, 1956.

On the Presence of Phosphoproteins in Erythrocyte Ghosts

GUNNAR ÅGREN and LORENTZ ENGSTRÖM

Institute of Medical Chemistry, University of Uppsala, Sweden

In a previous paper it has been demonstrated that the main part of the phosphoproteins in *E. coli* cells are located in the cell wall preparations [1]. It was therefore of interest to carry out a similar investigation with some animal cells. The erythrocytes seemed to offer a suitable material. This paper deals with the isolation of phosphoserine from erythrocyte ghosts.

After some preliminary work with earlier methods the ghosts were finally prepared in the following manner. 500 ml samples of blood were washed with cold physiological sodium chloride solution at least twice in a centrifuge taking 4 liters. After each washing the leucocytes were removed by decantation and suction. 3 volumes of cold distilled water were added. After haemolysis the remaining leucocytes were removed by centrifugation in a Spinco centrifuge with rotor 21 at 6 000 r.p.m. for 20 min. The suspension of erythrocyte ghosts was decanted and centrifuged for 20 min. at 18 000 r.p.m. in the same rotor. The voluminous precipitate was washed once with distilled water and at least 3 times with a 0.1 % sodium chloride solution.

The ghosts were suspended to a final volume of 100 ml in 0.1 M Tris (tris-(hydroxymethyl)aminomethane) at pH 7.4, and in the presence of 0.01 M $MgCl_2$. 5 mC ^{32}P was added and the incubation was finished after different times by the addition of trichloroacetic acid to a final concentration of 10 %. Lipids and nucleic acids were removed as previously described [2]. The residue from this treatment, taken as the Schneider protein fraction weighed about 2 g. This fraction was partially hydrolysed according to Lipmann [3]. Radioactive phosphoserine could be isolated both from pig and human erythrocyte ghosts in the same manner as previously described [4].

A ghost suspension was quickly heated to and kept at 80° C for about 1 minute, followed by rapid cooling. After incubation with ^{32}P it was not possible to detect more than traces of activity in the isolated phosphoserine fractions. A similar result was obtained when the ghosts were incubated with ^{32}P in the presence of monoiodoacetate to a final concentration of 0.01 M.

For the determination of the specific activity the effluents from the Dowex 50−8X columns were run through Dowex 1−X2 columns according to Busch *et al* [5]. The specific activity of the pure phosphoserine isolated from pig erythrocyte ghosts incubated with ^{32}P for 20 min. at room temperature was 3 550 cpm per μg P. It may be of interest that the specific activity of the pure phosphoserine isolated in earlier experiments [7] from rat liver fractions was about 4 500 cpm per μg P.

The trichloroacetic acid centrifugate from the reaction mixtures of erythrocyte ghosts and ^{32}P were run through Dowex 1−X2 formate columns according to Siekevitz and Potter [7]. Several peaks of radioactivity could be observed, but so far they have not been identified. Ultraviolet absorbing peaks could not be found in the eluates.

These experiments demonstrate that the ghosts contain phosphoproteins which may be active in the phosphorus metabolism of the erythrocytes. A metabolic pontential of erythrocyte ghosts has recently been recorded by Lionetti [8]. He used ghost plasma suspensions and studied the effect of adenosine on plasma inorganic phosphorus.

This investigation was supported by grants from *the Swedish Medical Research Council* and *the Wallenberg Foundation.*

1. Ågren, G. *Acta Chem. Scand.* **10** (1956) 152.
2. Ågren, G., de Verdier, C.-H. and Glomset, J. *Acta Chem. Scand.* **8** (1954) 503.
3. Lipmann, F. *Biochem. Z.* **262** (1933) 2.
4. Ågren, G. and Engström, L. *Acta Chem. Scand.* **10** (1956) 489.
5. Busch, H., Hurlbert, R. B. and Potter, V. R. *J. Biol. Chem.* **196** (1952) 717.
6. Siekevitz, P. and Potter, V. R. *J. Biol. Chem.* **215** (1955) 237.
7. Ågren, G., de Verdier, C.-H. and Glomset, J. *Acta Chem. Scand.* **8** (1954) 1570.
8. Lionetti, F. *Biochim. et Biophys. Acta* **18** (1955) 443.

Received June 28, 1956.

On the Phosphorus Linkage in a Muscle Phosphorylase Preparation

LORENTZ ENGSTROM and GUNNAR ÅGREN

Institute of Medical Chemistry, University of Uppsala, Sweden

Recently we reported the isolation of ^{32}P-labeled phosphoserine from a yeast hexokinase preparation [1] incubated with radioactive adenosinetriphosphate or glucose-6-phosphate. It was concluded that hexokinase was a phosphoprotein functioning as a phosphotransferring enzyme with an incorporation of phosphate from the substrate to the enzyme molecule or an exchange between substrate and enzyme phosphate.

This paper deals with the isolation of ^{32}P-labeled phosphoserine from a muscle phosphorylase preparation incubated with glycogen and radioactive ^{32}P. The following different types of experiments were carried out with the same amount of enzyme in each experiment.

100 mg of a commercial muscle phosphorylase preparation (Delta Chemical Works, Inc.) and 150 mg of glycogen (Merck) were dissolved in 5 ml of a freshly prepared cysteine-glycerophosphate buffer [2]. 5 mC carrierfree ^{32}P was added. The solution was kept at room temperature. After 30 minutes the enzyme was precipitated with trichloroacetic acid to a final concentration of 10 %. The protein was hydrolyzed according to Lipmann [3]. ^{32}P-labeled phosphoserine was identified as previously described [1]. The specific activity calculated as cpm per μg P was 72 186. This is the highest value so far recorded by us for any phosphorylated amino acid isolated from animal or plant tissue proteins. When glycogen was present the addition of 5 mg of adenosinemonophosphate (AMP) did not seem to increase the incorporation of radioactive phosphate into the enzyme molecule. The specific activity of the isolated phosphoserine was 32 977.

Next the enzyme was incubated with ^{32}P without the addition of glycogen. The phosphoserine was isolated in the usual way. It was only slightly labeled. The specific activity was 182. Finally when the enzyme was incubated with ^{32}P and AMP the specific activity of the isolated phosphoserine was 2 626 cpm per μg P.

The results seem to indicate that muscle phosphorylase is a phosphoprotein according to our definition, since we have been able to isolate phosphoserine from the partially hydrolysed enzyme. In the enzyme reaction there is probably an exchange between enzyme and substrate phosphate. Glycogen appears to play an essential role in this mechanism. The small exchange which takes place when no polysaccharide is added to the system may depend on traces of glycogen present in the enzyme preparation.

The bearing of our results to those obtained by Sutherland and coworkers [4] is difficult to discuss at present time. The possibility of an exchange with glucose-1-phosphate without addition of glycogen will be examined later. When possible, the results will also be controlled by repeated experiments with a more purified enzyme preparation.

This investigation was supported by grants from *the Gustav and Tyra Svenssons Memorial Foundation* and *the Wallenberg Foundation.*

1. Ågren, G. and Engström, L. *Acta Chem. Scand.* **10** (1956) 489.
2. Cori, G. T., Illingworth, B. and Keller, P. J. *Methods in Enzymology*, New York 1955, Vol. 1, p. 200.
3. Lipmann, F. *Biochem. Z.* **262** (1933) 2.
4. Rall, T. W., Sutherland, E. W. and Wosilait, W. D. *J. Biol. Chem.* **218** (1956) 483.

Received June 28, 1956.

On the Presence of Phosphoproteins in Baker's Yeast

LORENTZ ENGSTROM and GUNNAR ÅGREN

Institute of Medical Chemistry, University of Uppsala, Sweden

In previous reports from this laboratory it has been demonstrated that phosphoproteins are present in several microorganisms [1,2]. It has now been possible to demonstrate the presence of phosphoproteins in yeast.

The cells were washed twice in distilled water and cultured in the medium of Juni *et al.*[3] for different times. Non-labeled inorganic phosphate was excluded from the

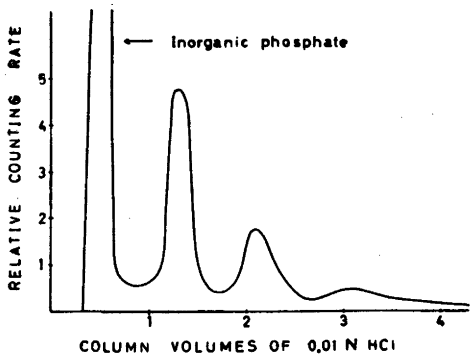


Fig. 1. Radioactivity curve from the hydrolysate of baker's yeast.

medium. About 2—3 mC radioactive phosphate per liter medium was added at the beginning of each experiment. Very heavy inocculum was used in order to obtain large amounts of phosphorylated products. At the end of the experiments trichloroacetic acid was added to a final concentration of 10 %. After centrifugation the precipitate was washed twice with 5 % trichloroacetic acid at 90° C for 15 minutes and hydrolyzed in the usual way [4].

The acid hydrolysate was run through a Dowex 50—X8 column with 0.01 N HCl. In Fig. 1 the first part of a typical elution curve is demonstrated.

A small part of the material from the first peak after the inorganic phosphate was run through a Dowex 1—X2 formate column according to Busch *et al.*[5] with the addition of non-labeled phosphoserine. The main part of the activity run parallel with the non-labeled phosphoserine. Two small peaks containing peptides of phosphoserine were also isolated from the eluate. In this way about 80 mg of crystalline radioactive phosphoserine was obtained from about 4 kg of fresh yeast cultured for about two hours at 37° C in the presence of 2 mC radioactive phosphate per liter of medium. The X-ray powder diagram of the crystals was identical with a sample isolated from casein.

The crystalline precipitate was analyzed. (Found: C 21.4; H 3.91; N 7.50; P 16.30. Calc. for $C_3H_8O_6NP$: C 19.5; H 4.32; N 7.57; P 16.76.)

Altogether about 10 column volumes of effluent from the Dowex 50 column were analyzed for radioactivity. Only one rather high peak immediately after the phosphoserine peak could be observed. In this respect the elution curve is of the same type as previously reported in experiments with partial hydrolysates of animal tissues [6], and in contrast to the findings in other microorganisms where other peaks of phosphorylated amino acids and peptides are dominating the diagram [7,2]. The peak following the phosphoserine peak is at present purified for further analysis. In hydrolysates from animal tissues the corresponding peak contains phosphothreonine.

This investigation was supported by grants from *the Swedish Cancer Society* and *the Wallenberg Foundation*.

1. Ågren, G., de Verdier, C.-H. and Glomset, J. *Acta Chem. Scand.* **9** (1955) 30.
2. Ågren, G. *Acta Chem. Scand.* **10** (1956) 152.



Fig. 2. X-ray powder diagram of phosphoserine from baker's yeast.

3. Juni, E., Kamen, M. D., Reiner, J. M. and Spiegelman, S. *Arch. Biochem.* **18** (1948) 387.
4. Lipmann, F. *Biochem. Z.* **262** (1933) 2.
5. Busch, H., Hurlbert, R. B. and Potter, V. R. *J. Biol. Chem.* **196** (1952) 717.
6. Ågren, G., de Verdier, C.-H. and Glomset, J. *Acta Chem. Scand.* **8** (1954) 503.
7. Ågren, G., de Verdier, C.-H. and Glomset, J. *Acta Soc. Med. Upsaliensis* **60** (1955) 30.

Received June 28, 1956.

On the Phosphorus Linkage in a Muscle Phosphorylase Preparation

LORENTZ ENGSTROM and GUNNAR ÅGREN

Institute of Medical Chemistry, University of Uppsala, Sweden

Recently we reported the isolation of ^{32}P-labeled phosphoserine from a yeast hexokinase preparation [1] incubated with radioactive adenosinetriphosphate or glucose-6-phosphate. It was concluded that hexokinase was a phosphoprotein functioning as a phosphotransferring enzyme with an incorporation of phosphate from the substrate to the enzyme molecule or an exchange between substrate and enzyme phosphate.

This paper deals with the isolation of ^{32}P-labeled phosphoserine from a muscle phosphorylase preparation incubated with glycogen and radioactive ^{32}P. The following different types of experiments were carried out with the same amount of enzyme in each experiment.

100 mg of a commercial muscle phosphorylase preparation (Delta Chemical Works, Inc.) and 150 mg of glycogen (Merck) were dissolved in 5 ml of a freshly prepared cysteine-glycerophosphate buffer [2]. 5 mC carrierfree ^{32}P was added. The solution was kept at room temperature. After 30 minutes the enzyme was precipitated with trichloroacetic acid to a final concentration of 10 %. The protein was hydrolyzed according to Lipmann [3]. ^{32}P-labeled phosphoserine was identified as previously described [1]. The specific activity calculated as cpm per μg P was 72 186. This is the highest value so far recorded by us for any phosphorylated amino acid isolated from animal or plant tissue proteins. When glycogen was present the addition of 5 mg of adenosinemonophosphate (AMP) did not seem to increase the incorporation of radioactive phosphate into the enzyme molecule. The specific activity of the isolated phosphoserine was 32 977.

Next the enzyme was incubated with ^{32}P without the addition of glycogen. The phosphoserine was isolated in the usual way. It was only slightly labeled. The specific activity was 182. Finally when the enzyme was incubated with ^{32}P and AMP the specific activity of the isolated phosphoserine was 2 626 cpm per μg P.

The results seem to indicate that muscle phosphorylase is a phosphoprotein according to our definition, since we have been able to isolate phosphoserine from the partially hydrolysed enzyme. In the enzyme reaction there is probably an exchange between enzyme and substrate phosphate. Glycogen appears to play an essential role in this mechanism. The small exchange which takes place when no polysaccharide is added to the system may depend on traces of glycogen present in the enzyme preparation.

The bearing of our results to those obtained by Sutherland and coworkers [4] is difficult to discuss at present time. The possibility of an exchange with glucose-1-phosphate without addition of glycogen will be examined later. When possible, the results will also be controlled by repeated experiments with a more purified enzyme preparation.

This investigation was supported by grants from *the Gustav and Tyra Svenssons Memorial Foundation* and *the Wallenberg Foundation.*

1. Ågren, G. and Engström, L. *Acta Chem. Scand.* **10** (1956) 489.
2. Cori, G. T., Illingworth, B. and Keller, P. J. *Methods in Enzymology*, New York 1955, Vol. 1, p. 200.
3. Lipmann, F. *Biochem. Z.* **262** (1933) 2.
4. Rall, T. W., Sutherland, E. W. and Wosilait, W. D. *J. Biol. Chem.* **218** (1956) 483.

Received June 28, 1956.

On the Presence of Phosphoproteins in Baker's Yeast

LORENTZ ENGSTROM and GUNNAR ÅGREN

Institute of Medical Chemistry, University of Uppsala, Sweden

In previous reports from this laboratory it has been demonstrated that phosphoproteins are present in several microorganisms [1,2]. It has now been possible to demonstrate the presence of phosphoproteins in yeast.

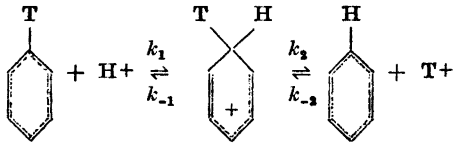
The cells were washed twice in distilled water and cultured in the medium of Juni *et al.*[3] for different times. Non-labeled inorganic phosphate was excluded from the

Kinetic Isotope Effect in Isotopic Exchange. Electrophilic Exchange of Hydrogen in Benzene and Toluene

LARS MELANDER and STIG OLSSON

Nobel Institute of Chemistry, Stockholm 50, Sweden

The existence of two heavy isotopes of hydrogen, deuterium and tritium, offers the possibility of determining the kinetic isotope effect in hydrogen exchange. As the reaction is symmetric except for the mass of the hydrogen, it is believed to be useful for examining the mechanism of electrophilic aromatic substitution [1]. If the reaction is represented by



and the intermediate is assumed to be present in a very small amount, the rate factor

$$\frac{k_2}{k_{-1} + k_2} = \frac{1}{k_{-1}/k_2 + 1}$$

will determine the isotope effect in the forward reaction. This holds irrespective of whether a hydrogen acceptor is involved in reactions -1 and 2 and also irrespective of whether the reaction proceeds *via* a low-stability intermediate of the π-complex type as assumed by Gold and Satchell [2]. If the σ-complex intermediate shown above behaves like an ordinary molecule, the ratio k_{-1}/k_2 could be supposed to be of the order of 7—10 for the tritium-protium and 4—6 for the deuterium-protium exchange. Consequently the following observable isotope effect could be expected

$$\frac{k_T}{k_D} = \frac{(k_{-1}/k_2)_D + 1}{(k_{-1}/k_2)_T + 1} \approx 0.6$$

This is indeed found.

As in previous experiments [3] 3 ml of the labelled hydrocarbon was shaken with 20 ml of aqueous sulphuric acid (this time

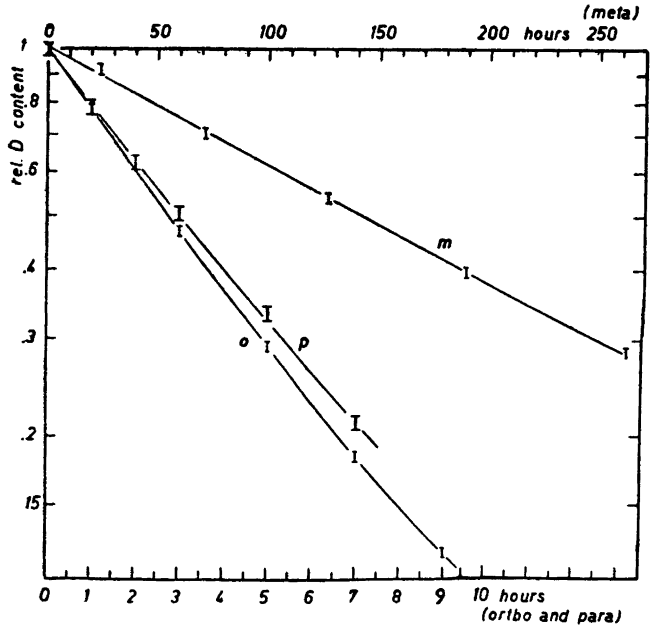


Fig. 1. Semilogarithmic plot of relative deuterium content of toluene-2-t (o), -3-t (m), and -4-t (p) as a function of time (note different time scales). For conditions, see the text.

80.8 %) at 25° C for different time intervals. In special experiments it was checked that the shaking frequency was without measurable influence on the observed rate, that the reaction took place in the acid phase, and that sulphonation was negligible. The deuterium derivatives were present in a few percent and the tritium derivatives in tracer concentrations, and the exchange of both isotopes was studied in the same experiments in each other's presence. In the analytical procedures (infrared spectrography and Geiger-Müller counting, respectively) the isotopes did not interfere. Fig. 1 shows the exchange curve for deuterium in the three nuclear positions of toluene. The limits of error were slightly less in the case of tritium. The exchange rates were determined from the initial slopes of the semilogarithmic curves [4].

The relative exchange rates for tritium in the individual positions of toluene are *o:m:p* = (47 ± 2):(1.00 ± 0.04):(41 ± 2) and for deuterium (51 ± 2):(1.00 ± 0.04):(46 ± 3). The former result differs from that obtained earlier [3] owing to insufficient shaking speed in the preliminary experiments. The results with deuterium are in agreement with similar and somewhat more approximate results obtained by Gold and Satchell in a homogeneous system (private communication).

Experiments on benzene have also been carried out in this laboratory, but the partial rate factors for the toluene positions cannot be obtained from these heterogeneous systems until the relative solubilities of the hydrocarbons have been determined.

It is seen that the directive influence of the methyl group is not exactly the same for the two exchange reactions, *i. e.* the isotope effect is not the same in the three positions. In Fig. 2 the initial slopes are represented on a reduced time scale such that all deuterium curves coincide. The results for benzene have also been included. The slopes of the tritium curves relative to the single deuterium curve give the isotope effects. The results are given in Table 1, and an idea of the accuracy could be obtained from a comparison of Fig. 2 with the typical experimental curve in

Table 1. Isotope effects in hydrogen exchange for different aromatic positions. For conditions, see the text.

Position	k_T/k_D
Toluene, *ortho*	0.53
Toluene, *meta*	0.59
Toluene, *para*	0.52
Benzene	0.65

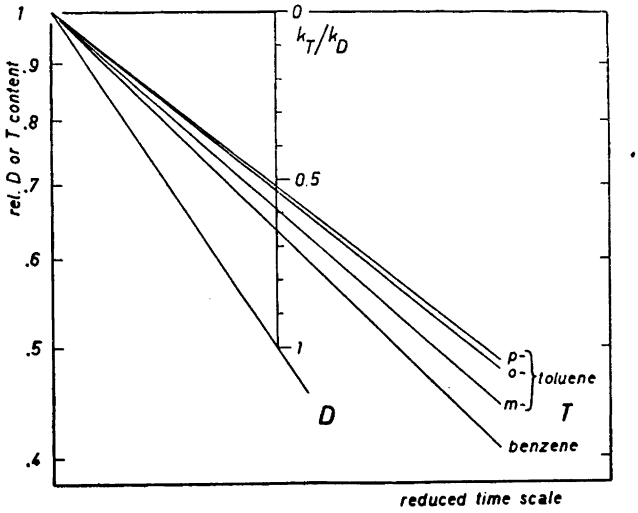


Fig. 2. Isotope effect in hydrogen exchange for different aromatic positions, cf. the text.

Fig. 1. All differences between the isotope effects except that between the *ortho* and *para* positions in toluene are believed to be significant. Differences in solubility between isotopic molecules are believed to be negligible and without importance for the present conclusions.

From the work privately communicated by Gold and Satchell it is evident that the *meta* position in toluene is somewhat more reactive than a single position in benzene, just as with the common electrophilic substitutions. Thus, it appears that the ratio k_T/k_D increases with decreasing reactivity, but whether this is a general rule cannot, of course, be inferred from the present very limited experimental material.

The *Swedish Natural Science Research Council* has contributed to the infrared spectrographic equipment used in this investigation.

1. Melander, L. *Svensk Kem. Tidskr.* **67** (1955) 51.
2. Gold, V. and Satchell, D.P.N. *J. Chem. Soc.* **1955** 3609.
3. Olsson, S. and Melander, L. *Acta Chem. Scand.* **8** (1954) 523.
4. Melander, L. *Arkiv Kemi* **7** (1955) 287.

Received July 2, 1956.

Open Peptide Chains in Chymotrypsinogen and α-Chymotrypsin

BODIL MEEDOM

Carlsberg Laboratorium, Copenhagen, Denmark

The principle of breaking S—S linkages in proteins by oxidation has been used extensively and with considerable success in the study of the chemical constitution of the peptide chains in these substances [1].

Upon the suggestion of M. Ottesen the author has applied this method to the study of α-chymotrypsin and chymotrypsinogen. Part of this work was reported in a paper read at a meeting in Uppsala in January 1956 [2] and in the following the further development of these investigations is briefly described.

The opening of the disulfide bridges by oxidation [3] causes the α-chymotrypsin molecule to fall apart essentially into three peptides which were separated as follows:

The oxidized enzyme was dissolved in alkali and pH brought down to 6 whereby a precipitate (fraction B) was formed. The supernatant was placed on a small Dowex 50 column (H^+ form). By elution with water, fraction A was collected, and by subsequent elution with NH_4OH, fraction C was obtained.

Fractions A, B, and C could also be separated by dialysis (removal of A) followed by free electrophoresis at pH-values higher than 7.5 (separation of B and C).

Amino acid analysis and end-group determinations were carried out on the fractions using the Sanger method [4] for amino-endgroup determination and digestion by carboxypeptidase [5] for the carboxyl-end-group estimation. The results were as follows:

Fraction A is a peptide composed of 13 amino acids, *viz.* 1 cysteic acid, 1 serine, 1 glutamic acid, 1 alanine, 2 glycine, 2 valine, 1 *iso*leucine, 2 leucine, and 2 proline. The N-terminal amino acid is cysteic acid and the C-terminal leucine.

Fraction C is a larger peptide containing about 50 amino acids. Of the species present in chymotrypsin only histidine and arginine are missing in C. Alanine is the N-terminal amino acid and tyrosine the C-terminal.

Fraction B seems to be a long peptide chain with an N-terminal *iso*leucine and a C-terminal tyrosine.

It is rather surprising that all three separated peptides are attacked by carboxypeptidase inasmuch as native α-chymotrypsin only contains two C-terminal end-groups as estimated by degradation with this enzyme [5].

The higher susceptibility of oxidized α-chymotrypsin to the action of carboxypeptidase may be due to an "unmasking" of a group which, although it conforms to the specific requirements of the enzyme, is inaccessible to it in native α-chymotrypsin under normal conditions.

The same effect would naturally be observed if a peptide bond had been broken during the oxidation procedure, but we feel justified in ruling out this possibility since no new N-terminal group seems to be formed.

The presence of a hidden C-terminal group in α-chymotrypsin suggests that of an identical group in chymotrypsinogen.

Oxidized, dialyzed chymotrypsinogen was therefore incubated with carboxypeptidase and the reaction mixture analyzed for free amino acids in the usual way.

Fig. 1. All differences between the isotope effects except that between the *ortho* and *para* positions in toluene are believed to be significant. Differences in solubility between isotopic molecules are believed to be negligible and without importance for the present conclusions.

From the work privately communicated by Gold and Satchell it is evident that the *meta* position in toluene is somewhat more reactive than a single position in benzene, just as with the common electrophilic substitutions. Thus, it appears that the ratio k_T/k_D increases with decreasing reactivity, but whether this is a general rule cannot, of course, be inferred from the present very limited experimental material.

The *Swedish Natural Science Research Council* has contributed to the infrared spectrographic equipment used in this investigation.

1. Melander, L. *Svensk Kem. Tidskr.* **67** (1955) 51.
2. Gold, V. and Satchell, D.P.N. *J. Chem. Soc.* **1955** 3609.
3. Olsson, S. and Melander, L. *Acta Chem. Scand.* **8** (1954) 523.
4. Melander, L. *Arkiv Kemi* **7** (1955) 287.

Received July 2, 1956.

Open Peptide Chains in Chymotrypsinogen and α-Chymotrypsin

BODIL MEEDOM

Carlsberg Laboratorium, Copenhagen, Denmark

The principle of breaking S—S linkages in proteins by oxidation has been used extensively and with considerable success in the study of the chemical constitution of the peptide chains in these substances [1].

Upon the suggestion of M. Ottesen the author has applied this method to the study of α-chymotrypsin and chymotrypsinogen. Part of this work was reported in a paper read at a meeting in Uppsala in January 1956 [2] and in the following the further development of these investigations is briefly described.

The opening of the disulfide bridges by oxidation [3] causes the α-chymotrypsin molecule to fall apart essentially into three peptides which were separated as follows:

The oxidized enzyme was dissolved in alkali and pH brought down to 6 whereby a precipitate (fraction B) was formed. The supernatant was placed on a small Dowex 50 column (H^+ form). By elution with water, fraction A was collected, and by subsequent elution with NH_4OH, fraction C was obtained.

Fractions A, B, and C could also be separated by dialysis (removal of A) followed by free electrophoresis at pH-values higher than 7.5 (separation of B and C).

Amino acid analysis and end-group determinations were carried out on the fractions using the Sanger method [4] for amino-endgroup determination and digestion by carboxypeptidase [5] for the carboxyl-end-group estimation. The results were as follows:

Fraction A is a peptide composed of 13 amino acids, *viz.* 1 cysteic acid, 1 serine, 1 glutamic acid, 1 alanine, 2 glycine, 2 valine, 1 *iso*leucine, 2 leucine, and 2 proline. The N-terminal amino acid is cysteic acid and the C-terminal leucine.

Fraction C is a larger peptide containing about 50 amino acids. Of the species present in chymotrypsin only histidine and arginine are missing in C. Alanine is the N-terminal amino acid and tyrosine the C-terminal.

Fraction B seems to be a long peptide chain with an N-terminal *iso*leucine and a C-terminal tyrosine.

It is rather surprising that all three separated peptides are attacked by carboxypeptidase inasmuch as native α-chymotrypsin only contains two C-terminal end-groups as estimated by degradation with this enzyme [5].

The higher susceptibility of oxidized α-chymotrypsin to the action of carboxypeptidase may be due to an "unmasking" of a group which, although it conforms to the specific requirements of the enzyme, is inaccessible to it in native α-chymotrypsin under normal conditions.

The same effect would naturally be observed if a peptide bond had been broken during the oxidation procedure, but we feel justified in ruling out this possibility since no new N-terminal group seems to be formed.

The presence of a hidden C-terminal group in α-chymotrypsin suggests that of an identical group in chymotrypsinogen.

Oxidized, dialyzed chymotrypsinogen was therefore incubated with carboxypeptidase and the reaction mixture analyzed for free amino acids in the usual way.

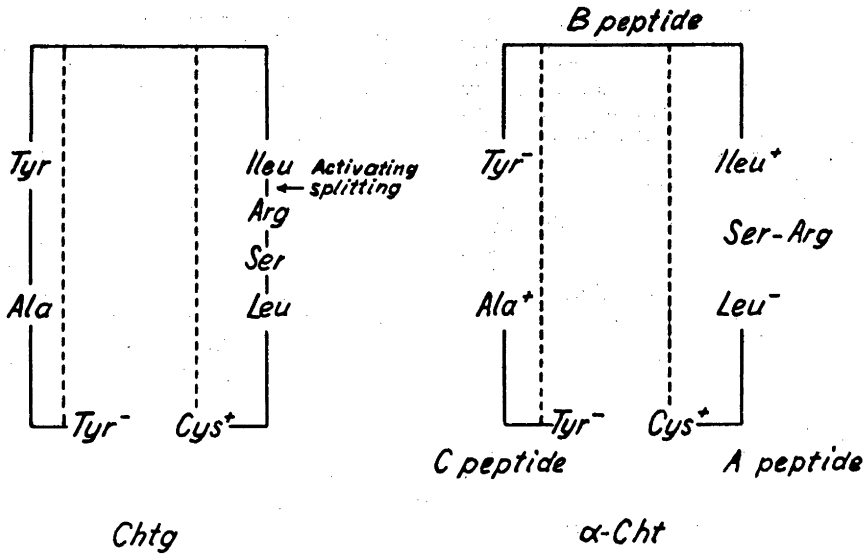


Fig. 1. Schematic drawing of chymotrypsinogen and α-chymotrypsin. The S—S bridges which link the peptide chains together are symbolized by the dotted lines. The A peptide is arbitrarily connected to the B peptide.

Paperchromatograms revealed that tyrosine and leucine were released as the first two amino acids, followed by valine, alanine, and serine.

Also in this case oxidation produced no new N-terminal groups in stoichiometrically significant amounts and in agreement herewith only one boundary was formed in free electrophoresis of the oxidized protein.

In an attempt to unmask the C-terminal group in a milder way than by oxidation, carboxypeptidase was allowed to act on chymotrypsinogen in 6 M urea [6]. In one of the experiments 0.8 mole of tyrosine, 0.7 mole of leucine, and 0.4 mole of valine were liberated per mole of chymotrypsinogen together with smaller quantities of phenylalanine, serine, and alanine (quantitative estimation by chromatography on Moore and Stein columns [7]).

On the basis of these experiments it may be stated with considerable certainty that the third C-terminal group found in oxidized α-chymotrypsin is not formed by rupture of a peptide bond during oxidation but is a hitherto not identified terminal group in chymotrypsinogen.

This result together with Bettelheim's discovery of the N-terminal half cystine [8] establishes chymotrypsinogen as an open peptide chain with a C-terminal tyrosine. This fact is easily brought in relation to previous considerations concerning the structure of α-chymotrypsin and its precursors [3,5]. This is seen in Fig. 1. It will be observed that in the model assumed here the activating splitting should take place at a distance of 15 amino acids from the N-terminal group (peptide A + ser-arg).

A more detailed report of the experiments will appear in *Comptes Rendus des Travaux du Laboratoire Carlsberg.*

1. Sanger, F. *Biochem. J. London* **44** (1949) 126.
2. Meedom, B. *Acta Chem. Scand.* **10** (1956) 150.
3. Hirs, C. H. W. *J. Biol. Chem.* **219** (1956) 611.
4. Sanger, F. *Biochem. J. London* **39** (1945) 507.
5. Gladner, J. A. and Neurath, H. *J. Biol. Chem.* **205** (1953) 345.
6. Halsey, Y. D. and Neurath, H. *J. Biol. Chem.* **217** (1955) 247.
7. Moore, S. and Stein, W. H. *J. Biol. Chem.* **192** (1951) 663.
8. Bettelheim, F. R. *J. Biol. Chem.* **212** (1955) 235.
9. Rovery, M., Poilroux, M., Curner, A. and Desnuelle, P. *Biochim. et Biophys. Acta* **16** (1955) 590.

Received July 9, 1956.

The Synthesis of Some Organosilicon Alcohols.

SUNE BRYNOLF

Chemical Institute of the University, Department of Organic Chemistry, Lund, Sweden

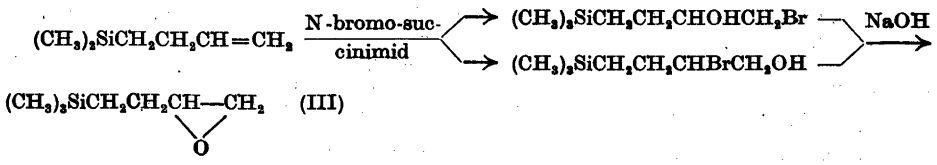
In order to prepare some organosilicon alcohols with their hydroxyl groups attached to carbon atoms the reaction between epichlorohydrin and trimethylsilylmethylmagnesium bromide was investigated. The only silicon-containing alcohol (A) that could be isolated was 4-trimethylsilyl-1-chlorobutanol-2. The constitution of this compound was proved by transforming it into the corresponding epoxy-compound, 4-trimethylsilylbutylene-1,2-oxide, which was compared with an authentic sample.

The two chlorohydrins that theoretically may be obtained from epichlorohydrin and trimethylsilylmethylmagnesium bromide must have either constitution (I) or (II)

$(CH_3)_3SiCH_2CH_2CHOHCH_2Cl$
(I)

$(CH_3)_3SiCH_2CH(CH_2Cl)CH_2OH$
(II)

The obtained chlorohydrin (A) must have the constitution (I) because it gave on alkaline hydrolysis an oxide (B), identical with the oxide (III) that was obtained from 4-trimethylsilylbuten-1, prepared by Hauser and Hance [1], on interaction with N-bromosuccinimide and alkali, analogously to a method described by Guss and Rosenthal [2]. The synthesis may be described by the following formulas:



$(CH_3)_3SiCH_2CH_2CH{-}CH_2$ (III)
O

The identity between (B) and (III) was demonstrated by the fact that the crystalline amine alcohols resulting from interaction between the oxides and aniline had the same melting points.

Oxide	Addition product with aniline. M. p.	B.p. 20 mm Hg
(B)	52.5—53° *	58—59°
(III)	53 —53.5°	58—60°

(A) was characterized as its phenylurethan.

Experimental. 4-Trimethylsilyl-1-chlorobutanol-2 (A). 92.5 g (1.0 mole) of epichlorohydrin were dropped with stirring into the Grignard reagent prepared from 83.5 g (0.5 mole) of bromomethyltrimethylsilane, 12.0 g magnesium and 100 ml of absolute ether in a 1-litre flask equipped with a stirrer, a reflux condenser and a dropping funnel, and immersed in an ice-bath. When all the oxide had been added the ice-bath was removed, whereupon the temperature of the mixture generally rose enough to cause boiling. When this ceased the mixture was warmed on a water bath (45—46°) for 5—6 hours. The reaction mixture was decomposed with ice-water. Simultaneously the ether and tetramethylsilane were distilled over. *Ca.* 10 g (0.13 mole) of tetramethylsilane could be recovered from the distillate by dropping it into concentrated sulphuric acid, cooled in an ice-and-salt bath.

The magnesium hydroxide precipitated by hydrolysis was dissolved by adding a sufficient quantity of dilute hydrochloric acid. The organic layer was separated and the water layer extracted with ether. The combined ether solutions were washed with a small quantity of water and dried with anhydrous sodium sulphate. After removal of the ether, fractionation at 20 mm Hg yielded 49 g (0.39 mole) of glyceroldichlorohydrin at 74—75°, 34 g (0.20 mole) glycerolchlorobromohydrin at 88—89° and 45.5 g (0.25 mole) 4-trimethylsilyl-1-chlorobutanol-2 at 103—104°. Practically no higher boiling products were obtained. $n_D^{20} = 1.4562$, $d_4^{20} = 0.9790$. (Found: C 46.4; H 9.6; Si 15.3, MR_D 50.2; equiv. wt 180.* Calc.

* mixed m. p. with (III). 53—53.5°.

for $C_7H_{17}OClSi$: C 46.5; H 9.5; Si 15.5; MR_D 50.5; equiv.wt. 181).

N-Phenylurethan. 2.3 g (0.019 mole) of phenyl *iso*cyanate and 2.6 g (0.015 mole) of (A) were warmed for 5 minutes on a boiling water bath. The mixture was allowed to stand at room temperature until crystallization occurred. The crystal cake was boiled with 10 ml of petroleum ether (b.p. 100—110°) and the insoluble diphenylurea removed by filtration. The filtrate was cooled in ice and the obtained crystals were collected on a filter and recrystallized from petroleum ether. The yield of crystals melting at 77.5—78° was 3.2 g (0.011 mole). (Found: C 56.3; H 7.4; Si 9.3; equiv.wt. 298 *. Calc. for $C_{14}H_{22}O_2ClNSi$: C 56.1; H 7.4; Si 9.3; equiv.wt. 300.)

4-Trimethylsilylbutylene-1,2 oxide (B) from (A). 100 g (0.55 mole) of (A) were dissolved in 200 ml of ether and refluxed for 3 h with 80 g (2.0 moles) of finely powdered sodium hydroxide. The mixture was filtered and the precipitate washed several times with ether. The ether was removed by distillation and the residue was fractionated at 20 mm Hg. 56 g (0.39 mole) of 4-trimethylsilylbutylene-1,2-oxide were collected at 58—59°. $n_D^{20} = 1.4276$, $d_4^{20} = 0.8452$. (Found: C 58.2; H 11.3; Si 19.0; MR_D 43.9. Calc. for $C_7H_{16}OSi$: C 58.2; H 11.2; Si 19.5; MR_D 43.9.)

Addition product with aniline. 2.0 g of (B) dissolved in 30 ml of ethanol were dropped into a stirred solution of 14.0 g of freshly distilled aniline in 50 ml of ethanol and 15 ml of water. The mixture was allowed to stand for 3 days. The ethyl alcohol was distilled off until two layers were formed. After cooling to room temperature the organic layer was separated and the water layer extracted with ether. The ether and the remaining ethanol were removed from the combined ether layers by distillation at ordinary pressure and the excess of aniline at 2 mm Hg. The residue solidified on cooling and was crystallized four times from petroleum ether (b. p. 30—50°). 2.0 g (60 %) of crystals melting at 52.5—53° were obtained. (Found: C 64.8; H 9.7; Si 11.8. Calc. for $C_{13}H_{23}NOSi$: C 65.8; H 9.8; Si 11.8.)

4-Trimethylsilylbutylene-1,2-oxide from 4-trimethylsilylbutene-1. (III). 16.2 g (0.091 mole) of N-bromosuccinimide and 11.6 g (0.091 mole) of 4-trimethylsilylbutene-1 were shaken with 100 ml of water until all the N-bromosuccinimide had dissolved. The solution was extracted with ether and the combined ether portions were treated with alkali according to the method above. 4.2 g (0.030 mole) of (III) were obtained.

The *addition product with aniline* was prepared in the same way as above for the oxide (B). M. p. 53—53.5°.

The author wishes to express his appreciation to Professor Erik Larsson for his kind interest in this work.

1. Hauser, C. R. and Hance, C. R. *J. Am. Chem. Soc.* **74** (1952) 5091.
2. Guss, C. O. and Rosenthal, R. *Ibid.* **77** (1955) 2549.

Received July 31, 1956.

* The equivalent weights were determined by hydrolysis with ethanolic sodium hydroxide and titration of the formed chloride ions with silver nitrate solution.

Corrected Heats of Combustion of Organic Iodine Compounds

LENNART SMITH

Chemical Institute, University of Lund, Sweden

In his dissertation [1] Karlsson * has shown convincingly that combustion in a calorimetric bomb of iodine containing compounds forms only elemental iodine besides carbon dioxide and water **. He further estimated that the heats of sublimation and solution of the iodine under his experimental conditions (liquid phase in the bomb 20 ml water) were very small (0.05 and 0.1 cal, respectively) and considered them negligible. For the heats of solution of the carbon dioxide appropriate corrections, however, were not applied, since the method of calculation of these was worked out and described after the publication of Karlssons dissertation (Smith *et al.*[3]).

Owing to the experimental conditions used by Karlsson, and the iodine compounds chosen by him, the last mentioned corrections are mostly very small as will be shown below. Thus his values of combustion are more accurate than should be expected from the considerable quantity of water present in the bomb during the

* Now Karrman.

** Concerning other investigations of this problem, see Ref.[2].

for $C_7H_{17}OClSi$: C 46.5; H 9.5; Si 15.5; MR_D 50.5; equiv.wt. 181).

N-Phenylurethan. 2.3 g (0.019 mole) of phenyl *iso*cyanate and 2.6 g (0.015 mole) of (A) were warmed for 5 minutes on a boiling water bath. The mixture was allowed to stand at room temperature until crystallization occurred. The crystal cake was boiled with 10 ml of petroleum ether (b.p. 100—110°) and the insoluble diphenylurea removed by filtration. The filtrate was cooled in ice and the obtained crystals were collected on a filter and recrystallized from petroleum ether. The yield of crystals melting at 77.5—78° was 3.2 g (0.011 mole). (Found: C 56.3; H 7.4; Si 9.3; equiv.wt. 298 *. Calc. for $C_{14}H_{22}O_2ClNSi$: C 56.1; H 7.4; Si 9.3; equiv.wt. 300.)

4-Trimethylsilylbutylene-1,2 oxide (B) from (A). 100 g (0.55 mole) of (A) were dissolved in 200 ml of ether and refluxed for 3 h with 80 g (2.0 moles) of finely powdered sodium hydroxide. The mixture was filtered and the precipitate washed several times with ether. The ether was removed by distillation and the residue was fractionated at 20 mm Hg. 56 g (0.39 mole) of 4-trimethylsilylbutylene-1,2-oxide were collected at 58—59°. $n_D^{20} = 1.4276$, $d_4^{20} = 0.8452$. (Found: C 58.2; H 11.3; Si 19.0; MR_D 43.9. Calc. for $C_7H_{16}OSi$: C 58.2; H 11.2; Si 19.5; MR_D 43.9.)

Addition product with aniline. 2.0 g of (B) dissolved in 30 ml of ethanol were dropped into a stirred solution of 14.0 g of freshly distilled aniline in 50 ml of ethanol and 15 ml of water. The mixture was allowed to stand for 3 days. The ethyl alcohol was distilled off until two layers were formed. After cooling to room temperature the organic layer was separated and the water layer extracted with ether. The ether and the remaining ethanol were removed from the combined ether layers by distillation at ordinary pressure and the excess of aniline at 2 mm Hg. The residue solidified on cooling and was crystallized four times from petroleum ether (b. p. 30—50°). 2.0 g (60 %) of crystals melting at 52.5—53° were obtained. (Found: C 64.8; H 9.7; Si 11.8. Calc. for $C_{13}H_{23}NOSi$: C 65.8; H 9.8; Si 11.8.)

4-Trimethylsilylbutylene-1,2-oxide from 4-trimethylsilylbutene-1. (III). 16.2 g (0.091 mole) of N-bromosuccinimide and 11.6 g (0.091 mole) of 4-trimethylsilylbutene-1 were shaken with 100 ml of water until all the N-bromosuccinimide had dissolved. The solution was extracted with ether and the combined ether portions were treated with alkali according to the method above. 4.2 g (0.030 mole) of (III) were obtained.

The *addition product with aniline* was prepared in the same way as above for the oxide (B). M. p. 53—53.5°.

The author wishes to express his appreciation to Professor Erik Larsson for his kind interest in this work.

1. Hauser, C. R. and Hance, C. R. *J. Am. Chem. Soc.* **74** (1952) 5091.
2. Guss, C. O. and Rosenthal, R. *Ibid.* **77** (1955) 2549.

Received July 31, 1956.

* The equivalent weights were determined by hydrolysis with ethanolic sodium hydroxide and titration of the formed chloride ions with silver nitrate solution.

Corrected Heats of Combustion of Organic Iodine Compounds

LENNART SMITH

Chemical Institute, University of Lund, Sweden

In his dissertation [1] Karlsson * has shown convincingly that combustion in a calorimetric bomb of iodine containing compounds forms only elemental iodine besides carbon dioxide and water **. He further estimated that the heats of sublimation and solution of the iodine under his experimental conditions (liquid phase in the bomb 20 ml water) were very small (0.05 and 0.1 cal, respectively) and considered them negligible. For the heats of solution of the carbon dioxide appropriate corrections, however, were not applied, since the method of calculation of these was worked out and described after the publication of Karlssons dissertation (Smith *et al.*[3]).

Owing to the experimental conditions used by Karlsson, and the iodine compounds chosen by him, the last mentioned corrections are mostly very small as will be shown below. Thus his values of combustion are more accurate than should be expected from the considerable quantity of water present in the bomb during the

* Now Karrman.

** Concerning other investigations of this problem, see Ref.[2].

combustion. It may be mentioned here that his values are not published elsewhere than in his dissertation.

For the recalculation of his data I have applied eqn 2 in Ref.[3]. This equation, the result of experiments with chlorine compounds, in which a HCl-containing bomb solution is formed, was nevertheless used even here, as considered exact enough for the very small corrections occurring in this case.

In Karlssons *calibration* experiments also the above mentioned quantity of water was present in the bomb. The standard being benzoic acid and almost all the compounds burnt aromatic, the errors in the heat equivalent and in the heats of combustion of the compounds tend to cancel. Among the aromatic compounds the iodotoluenes have the maximum-correction (0.4 cal/g). For the only non-aromatic compound, iodo*cyclo*hexane, the correction has been calculated to 0.7 cal/g.

In Table 1 developed heat is considered *positive*, as done in the dissertation. Notations in the table: In the first column "No." refers to the table numbers in Ref.[1]; in the second the names of the compounds are given, "l" = liquid, "s" = solid, and in the third the heats of combustion (cal/g; const. volume) determined by Karlsson. In the fourth column "Corr.CO_2" denotes the calculated correction (cal/g) for the heat of solution of carbon dioxide; the fifth contains the correction to weight in vacuum ("Corr. vac.") and the sixth ("Heats of comb, corr.") the final corrected heats. Temperature 20°. — For computing the heats of combustion in the gaseous state of the compounds, the heats of vaporization and sublimation in Ref.[1], Tables 89 and 90, can be used.

Compounds, which are liquid at 20°, were burnt with cellophane cover. This method gives too low results (see Ref.[3], p. 79). The resulting errors will of course diminish with rising boiling points of the compounds (see also Ref.[4], p. 196).

The table shows that the corrections caused by the heat of solution of carbon dioxide, especially for the solid compounds, are very small and negligible, this, as already mentioned, depending on the fact that the errors in the determination of the heat equivalent and the heat of combustion of the compounds mostly almost cancel.

Table 1. Heats of combustion of iodine compounds.

No.	Compound	Heat of comb. uncorr. cal/g [a]	Corr. CO_2 cal/g	Corr.[b] vac. cal/g	Heat of comb. corr. cal/g
41	Iodobenzene (l)	3 738.9 ± 0.6	0.2	—1.9	3 737.2 ± 0.6
42	*o*-Iodotoluene (l)	4 199.9 ± 0.6	0.4	—2.4	4 197.9 ± 0.6
43	*m*- » (l)	4 200.8 ± 0.4	0.4	—2.4	4 198.8 ± 0.4
44	*p*- » (l)	4 188.1 ± 1.2	0.3	—2.3	4 186.0 ± 1.2
45	*o*-Iodobenzoic acid (s)	3 052.8 ± 0.4	—0.05	—1.2	3 051.5 ± 0.4
46	*m*- » » (s)	3 039.0 ± 0.6	—0.1	—1.2	3 037.7 ± 0.6
47	*p*- » » (s)	3 039.5 ± 0.8	—0.1	—1.2	3 038.2 ± 0.8
48	*o*-Iodomethylbenzoate (l)	3 562.2 ± 1.5	0.1	—1.8	3 560.5 ± 1.5
49	*m*- » (s)	3 530.6 ± 0.6	0.1	—1.8	3 528.9 ± 0.6
50	*p*- » (s)	3 523.0 ± 0.9	0.0	—1.8	3 521.2 ± 0.9
51	*o*-Diiodobenzene (l)	2 259.1 ± 0.4	0.1	—0.8	2 258.4 ± 0.4
52	*o*- » (s)	2 248.8 ± 1.2	0.1	—0.8	2 248.1 ± 1.2
53	*m*- » (s)	2 259.3 ± 1.7	0.1	—0.8	2 258.6 ± 1.7
54	*p*- » (s)	2 240.2 ± 1.0	0.1	—0.8	2 239.5 ± 1.0
55	*o*-Iodophenol (s)	3 237.0 ± 1.4	0.1	—1.5	3 235.6 ± 1.4
56	*m*- » (s)	3 238.2 ± 1.2	0.1	—1.5	3 236.8 ± 1.2
57	*p*- » (s)	3 237.6 ± 1.0	0.1	—1.5	3 236.2 ± 1.0
58	*α*-Iodonaphthalene (l)	4 793.5 ± 1.5	0.2	—2.7	4 791.0 ± 1.5
59	*β*- » (s)	4 777.8 ± 1.8	0.2	—2.7	4 775.3 ± 1.8
60	Iodo*cyclo*hexane (l)	4 360.1 ± 0.9	0.7	—2.6	4 358.2 ± 0.9

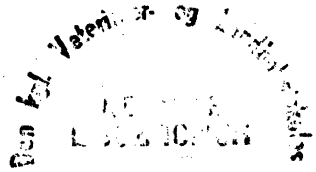
[a] Not corrected to weight in vacuum.

[b] These corrections are given by Karlsson only for the heat of combustion per mole.

Compounds with an appreciable carbon dioxide correction are in the liquid state and Karlssons values (see above) of the heats of combustion are certainly somewhat too low (perhaps except for α-iodonaphthalene with a very high boiling point). The plus-correction in the heats for the liquid compounds thus will diminish the error in question.

1. Karlsson, K. J. *Zur Thermochemie einiger chlor- und jodhaltiger Benzolderivate*, Diss. Lund 1941.
2. Smith, L. *Combustion in a bomb of organic iodine compounds*, in Rossini, F. D. *Experimental Thermochemistry*, 1956.
3. Smith, L., Bjellerup, L., Krook, S. and Westermark, H. *Acta Chem. Scand.* **7** (1953) 65.
4. Smith, L. and Hubbard, W. N. *Combustion in a bomb of organic chlorine compounds*, in *Experimental Thermochemistry*, 1956.

Received August 4, 1956.



ACTA CHEMICA SCANDINAVICA 10 (1956) 887—910

Comparative Crystal Field Studies II. Nickel(II) and Copper(II) Complexes with Polydentate Ligands and the Behaviour of the Residual Places for Co-Ordination

CHR. KLIXBÜLL JØRGENSEN

Chemistry Department A, Technical University of Denmark, Copenhagen, Denmark

The complexes of nickel(II) and copper(II) with ethylenediaminetetraacetate, nitrogentriacetate and β,β',β''-tris(ethylamino)amine have one or more residual places left for co-ordination. The absorption spectra of such complexes containing either water, ammonia, ethylenediamine, glycinate or cyanide were determined. The wavenumbers of the bands illustrate the regular behaviour of paramagnetic octahedral nickel(II) complexes, whereas the intensities vary. Some copper(II) complexes are much more tetragonally distorted than others. The "chelate" effect in formation constants is not only due to the different dependence on dilution of the degree of formation of polydentate ligands' complexes, but can be estimated from the spectra in some cases to contain actual stabilization energies. The different crystal field strength of six nitrogens in nickel(II) amine complexes is further illustrated, *e.g.* by 1,3-diaminopropane. The bonding of cyanide in paramagnetic complexes is not very strong and the complexes slowly react to form yellow, diamagnetic nickel(II) and colourless copper(I) cyanides. β,β',β''-tris(ethylamino)amine does not form a tetrahedral complex with nickel(II), since the water in *cis*-position of the octahedral complex can be exchanged with ammonia, ethylenediamine or glycinate. The last complex has a very hypsochromic spectrum corresponding to a high stabilization energy. The absorption spectra of nickel(II) complexes demonstrate intermediate coupling and decreased values of the Racah parameters of electrostatic interaction between d-electrons, relative to the gaseous ion.

The first paper of this series [1] treated nickel(II) complexes with increasing crystal field strength, corresponding to yellow, green, blue, purple and red colours. The four strongest absorption bands can be interpreted as transitions from the groundstate $^3\Gamma_2$ (F) to $^1\Gamma_3$ (D), $^3\Gamma_5$ (F), $^3\Gamma_4$ (F) and $^3\Gamma_4$ (P) in the notation of Bethe [2]. It was shown that the singlet state $^1\Gamma_3$ (D) is intermixed with $^3\Gamma_5$ (F) and $^3\Gamma_4$ (F) by effects of intermediate coupling. In the present paper, nickel(II) is studied in different environments, supplied partly by polydentate ligands. Further, characteristic properties of copper(II), compared to nickel(II) complexes will be discussed [1].

Empirically, the absorption spectra of mixed complexes have led to the idea of averaged environment. For example, except for very small solvent effects, the six atoms in the first co-ordination sphere of an octahedral complex determine the absorption spectrum. The position of the absorption bands can be predicted mainly from one parameter, expressing the average of the positions of the ligands in the spectrochemical series. Thus, Mead [3] studied mixed ethylenediamine- and oxalate complexes of chromium (III) and cobalt(III); Tsuchida [4] investigated many complexes of the same two metals, *e.g.* acido-pentammines. Mathieu [5] investigated the influence of amino-acids on the two residual places in *cis*-bis(ethylenediamine)cobalt(III) ions. Linhard and Weigel studied the halogenopentammines [6] and the *cis*- and *trans*-tetrammines and pentammines of cobalt(III) with carboxyl groups on the residual places [7]. Copper(II) complexes with ethylenediamine and other ligands have been studied by Jonassen *et al.*[8], copper(II) bis(acetylacetonate) with different solvents by Belford [9] and cobalt(III) complexes by Basolo, Ballhausen and Bjerrum [10]. In some cases crystal fields of pronounced tetragonal symmetry produce new bands by splitting as in *trans*-Co $en_2Cl_2^+$. In the second and third transition group, Delépine's complexes of rhodium(III) and iridium(III) exhibit similar behaviour [11]. Since water is exchanged without change of the co-ordination number, the consecutive uptake of six ammonia molecules to nickel(II), studied by J. Bjerrum [12], or of three ethylenediamine molecules, measured by Ballhausen [13], can also be cited as examples of mixed complexes with water as one of the ligands.

Table 1 gives the absorption spectra measured here of nickel(II) complexes and Table 3 of copper(II) complexes. Table 2 collects the band maxima of nickel(II) and gives also the results of the first paper [1].

The following abbreviations will be used for the ligands:

en	= ethylenediamine = 1,2-diaminoethane
tn	= trimethylenediamine = 1,3-diaminopropane
bdn	= 1,3-diaminobutane
ptn	= 1,2,3-triaminopropane
tren	= β,β',β''-tris(ethylamino)amine
trien	= triethylenetetramine
den	= diethylenetriamine
tetren	= tetraethylenepentamine
temeen	= C,C,C′,C′-tetramethyl-ethylenediamine
dip	= α,α'-dipyridyl = 2,2′-bipyridine
phen	= *o*-phenanthroline = 1,10-phenanthroline
gly^-	= glycinate = aminoacetate
ata^{-3}	= ammoniatriacetate * = nitrilotriacetate = nitrogentriacetate
$enta^{-4}$	= ethylenediaminetetraacetate.

NICKEL(II) ETHYLENEDIAMINETETRAACETATES

Schwarzenbach [14] studied the colour reactions of Ni $enta^{---}$ with NH_3, en and CN^-. He pointed out that the formation constant of Ni $enta^{---}$ is so large that the other ligands do not decompose this complex. While this has a somewhat limited validity in the case of Ni $enta^{---}$ + en, as discussed below, the ligands must be assumed to exchange with the water present in the first co-ordination sphere of Ni enta, H_2O^{---}. The latter complex has a free carboxyl group, which can take up protons[15] with $pK = 3$, forming Ni enta H, H_2O^{--}. In Table 1, two forms are given of nickel(II) ethylenediaminetetraacetate, denoted α and β. The latter form corresponds to the intermediate form which is observed [1] during the slow formation reactions. However, at low pH $\sim$ 3,

* As proposed by Martell and Calvin in *The Chemistry of the Metal Chelate Compounds*, New York 1952. Professor K. A. Jensen has proposed the name "nitrogentriacetate".

Table 1. Absorption bands of nickel(II) complexes. Wavelength λ_n, wavenumber ν_n and molar extinction coefficient ε_n of the maxima; δ (−) and δ (+) the half-width towards lower and higher wavenumbers, and P *the oscillator strength for each band.*

	Excited level	λ_n mμ	ν_n cm^{-1}	ε_n	$\delta(-)$ cm^{-1}	$\delta(+)$ cm^{-1}	P · 10^{-5}
α-Ni enta^{--}	$^3\Gamma_5$ (*F*)	990	10 100	31.0	1 400	1 300	38
	$^1\Gamma_3$ (*D*)	790	12 700	5.4	—	—	3
	$^3\Gamma_4$ (*F*)	587	17 000	8.4	1 700	1 500	12
	$^3\Gamma_4$ (*P*)	382	26 200	12.6	1 700	2 100	22
β-Ni enta^{--}	$^3\Gamma_5$ (*F*)	1 010	9 900	26	—	1 400	34
	$^1\Gamma_3$ (*D*)	780	13 000	3	—	300	1
	$^3\Gamma_4$ (*F*)	592	16 900	8.2	1 700	1 500	12
	$^3\Gamma_4$ (*P*)	379	26 400	13.8	1 600	1 900	22
Ni entaNH$_3^{--}$	$^3\Gamma_5$ (*F*)	980	10 200	16.6	—	1 500	23
	$^1\Gamma_3$ (*D*)	785	12 700	3.4	—	—	2
	$^3\Gamma_4$ (*F*)	582	17 200	10.9	2 000	1 900	19
	$^3\Gamma_4$ (*P*)	372	26 900	20.2	1 600	1 700	30
Ni enta en^{--}	$^3\Gamma_5$ (*F*)	995	10 050	25	—	1 400	32
	$^1\Gamma_3$ (*D*)	796	12 550	4.7	—	—	4
	$^3\Gamma_4$ (*F*)	579	17 300	8.1	1 800	1 600	13
	$^3\Gamma_4$ (*P*)	368	27 100	10.8	2 400	~3 000	27
Ni enta CN^{-3}	$^3\Gamma_5$ (*F*)	955	10 500	14	—	1 700	22
	$^1\Gamma_3$ (*D*)	800	12 500	5.4	—	—	6
	$^3\Gamma_4$ (*F*)	570	17 500	12	2 100	1 600	20
Ni ata$^-$	$^3\Gamma_5$ (*F*)	1 050	9 500	16.0	—	1 400	21
	$^1\Gamma_3$ (*D*)	753	13 300	2.5	—	—	1
	$^3\Gamma_4$ (*F*)	625	16 000	6.6	1 900	1 400	10
	$^3\Gamma_4$ (*P*)	391	25 600	12.8	1 800	2 000	22
Ni ata$_2^{-4}$	$^3\Gamma_5$ (*F*)	960	10 400	5.4	1 400	1 500	7
	$^1\Gamma_3$ (*D*)	770	13 000	1.5	—	—	1
	$^3\Gamma_4$ (*F*)	575	17 400	4.3	2 600	1 400	8
	$^3\Gamma_4$ (*P*)	370	27 000	6.4	2 000	—	15
		350	28 600	6.0	—	—	
Ni ata(NH$_3$)$_2^-$(?)	$^3\Gamma_5$ (*F*)	1 045	9 600	11.0	—	1 600	16
	$^1\Gamma_3$ (*D*)	761	13 100	2.3	—	—	2
	$^3\Gamma_4$ (*F*)	607	16 500	9.3	2 000	1 600	15
	$^3\Gamma_4$ (*P*)	375	26 600	16.2	1 800	2 000	28
Ni ata en$^-$	$^3\Gamma_5$ (*F*)	1 060	9 400	11	—	1 700	18
	$^1\Gamma_3$ (*D*)	772	13 100	2.3	—	—	2
	$^3\Gamma_4$ (*F*)	592	16 900	7.7	2 300	1 900	15
	$^3\Gamma_4$ (*P*)	367	27 200	13.2	2 200	2 200	27
Ni ata gly$^-$	$^3\Gamma_5$ (*F*)	1 010	9 900	9.8	—	1 800	16
	$^1\Gamma_3$ (*D*)	771	13 000	2.9	—	—	3
	$^3\Gamma_4$ (*F*)	584	17 100	7.0	2 300	1 500	12
	$^3\Gamma_4$ (*P*)	381	26 200	11.1	1 800	2 900	24
Ni ata den$^-$	$^3\Gamma_5$ (*F*)	915	10 900	7.4	1 700	1 900	12
	$^1\Gamma_3$ (*D*)	798	12 500	5.1	—	—	—
	$^3\Gamma_4$ (*F*)	568	17 600	6.8	2 200	2 000	13
	$^3\Gamma_4$ (*P*)	348	28 700	8.8	2 200	—	17
Ni tren(H$_2$O)$_2^{++}$	$^3\Gamma_5$ (*F*)	950	10 500	15.5	1 400	1 800	23
	$^1\Gamma_3$ (*D*)	782	12 800	6.3	—	—	
	$^3\Gamma_4$ (*F*)	561	17 800	9.3	1 800	1 700	15
	$^3\Gamma_4$ (*P*)	360	27 800	12.0	2 200	—	24
Ni$_2$tren$_3^{+4}$	$^3\Gamma_5$ (*F*)	935	10 700	9.4	1 400	1 800	14
	$^1\Gamma_3$ (*D*)	800	12 500	4.6	—	—	
	$^3\Gamma_4$ (*F*)	548	18 300	7.2	2 000	1 600	12
	$^3\Gamma_4$ (*P*)	348	28 700	9.3	1 700	—	15

Ni tren$(NH_3)_2$++	$^3\Gamma_5$ (*F*)	910	11 000	12.5	1 600	1 800	19
	$^1\Gamma_3$ (*D*)	784	12 750	7.0	—	—	
	$^3\Gamma_4$ (*F*)	549	18 200	10.1	1 700	1 600	15
	$^3\Gamma_4$ (*P*)	354	28 200	13.0	2 200	2 200	26
Ni tren en++	$^3\Gamma_5$ (*F*)	910	11 000	11.0	1 400	—	16
	$^1\Gamma_3$ (*D*)	800	12 500	8.1	—	—	
	$^3\Gamma_4$ (*F*)	534	18 700	8.8	2 400	2 400	19
	$^3\Gamma_4$ (*P*)	345	29 000	14.2	3 000	—	38
Ni tren gly+	$^3\Gamma_5$ (*F*)	890	11 200	14.0	1 300	—	19
	$^1\Gamma_3$ (*D*)	794	12 600	9.8	—	—	
	$^3\Gamma_4$ (*F*)	532	18 800	11.0	1 800	1 600	17
	$^3\Gamma_4$ (*P*)	354	28 200	11.0	2 400	—	24
Ni en gly_2	$^3\Gamma_5$ (*F*)	955	10 500	8.7	1 700	1 700	14
	$^1\Gamma_3$ (*D*)	770	13 000	2.6	—	—	3
	$^3\Gamma_4$ (*F*)	577	17 300	8.0	1 800	1 700	13
	$^3\Gamma_4$ (*P*)	356	28 100	12.7	1 800	2 200	23
Ni en_2gly+	$^3\Gamma_5$ (*F*)	922	10 800	9.2	1 400	1 800	14
	$^1\Gamma_3$ (*D*)	790	12 650	4.2	—	—	
	$^3\Gamma_4$ (*F*)	560	17 900	8.7	1 700	1 700	14
	$^3\Gamma_4$ (*P*)	350	28 600	12.0	1 800	—	20
Ni py_6++(?)	$^3\Gamma_5$ (*F*)	985	10 150	3.7	—	1 900	6
	$^1\Gamma_3$ (*D*)	743	13 500	1.2	—	—	1
	$^3\Gamma_4$ (*F*)	607	16 500	5.4	1 700	1 600	8
	$^3\Gamma_4$ (*P*)	371	27 000	9.9	1 600	1 700	15
Ni tn_3++	$^3\Gamma_5$ (*F*)	920	10 900	5.9	1 600	1 600	9
	$^1\Gamma_3$ (*D*)	798	12 500	2.7	—	—	
	$^3\Gamma_4$ (*F*)	563	17 800	7.7	1 600	1 500	11
	$^3\Gamma_4$ (*P*)	354	28 200	10.8	2 500	2 800	26
Ni bdn_3++	$^3\Gamma_4$ (*F*)	915	10 950	6.5	1 400	—	8
	$^1\Gamma_3$ (*D*)	790	12 700	3.0	—	—	
	$^3\Gamma_4$ (*F*)	556	18 000	7.0	1 600	1 500	10
	$^3\Gamma_4$ (*P*)	350	28 600	10.0	1 800	—	17
Ni ptn_2++	$^3\Gamma_5$ (*F*)	890	11 200	4.7	1 600	—	8
	$^1\Gamma_3$ (*D*)	800	12 500	3.8	—	—	
	$^3\Gamma_4$ (*F*)	526	19 000	4.5	1 800	1 700	7
	$^3\Gamma_4$ (*P*)	337	29 700	4.6	1 900	—	8
Ni den_2++	$^3\Gamma_5$ (*F*)	872	11 500	12.9	1 500	1 800	20
	$^3\Gamma_4$ (*F*)	535	18 700	7.7	1 900	1 400	12
	$^3\Gamma_4$ (*P*)	344	29 100	10.8	1 900	—	19
Ni tetren++	$^3\Gamma_5$ (*F*)	920	10 900	12.3	1 700	1 900	21
	$^1\Gamma_3$ (*D*)	792	12 600	7.7	—	—	—
	$^3\Gamma_4$ (*F*)	543	18 400	6.8	2 200	1 700	12
	$^3\Gamma_4$ (*P*)	351	28 500	9.8	2 100	—	19
Ni tetren NH_3++	$^3\Gamma_5$ (*F*)	902	11 100	13	1 500	—	18
	$^1\Gamma_3$ (*D*)	800	12 500	9	—	—	—
	$^3\Gamma_4$ (*F*)	536	18 700	8.3	1 900	1 500	13
	$^3\Gamma_4$ (*P*)	350	28 600	11	2 200	—	22

the β-form is stable and can be formed by addition of acids to the α-form. This cannot be due to a partly decomposition to hexaaquo ions, since the fourth band of the β-form is higher and shifted towards higher wavenumbers than of the α-form, while the other three bands show a different behaviour *. Since two isomers are possible [1] for the complex Ni enta (H_2O), with water in *cis*- or *trans*-position to one of the nitrogen atoms, α- and β-may represent two

* Plumb, Martell and Bersworth [58] measured the spectra of some enta^{-4}-complexes. The height of the first band indicate the β-structure of their Ni enta^{--}.

different equilibrium mixtures, where the equilibrium is changed by the formation of Ni enta H, H_2O^-. But the change might also be due to a variable number of water molecules in the environment. An anhydrous complex analogous to Co enta$^-$, would be promoted by high pH and might thus participate in the α-form.

It is seen from Table 1 that the enormously high intensity of the first band of α-Ni enta^{--} decreases for the addition compounds of NH_3, en and CN^-, while the other bands show mainly increasing intensities. The fourth band of Ni enta en^{--} is not high, but rather broad. This may be ascribed to tetragonal splitting [16] or to the presence of more isomers. Although enta^{-4} probably occupies only four co-ordination positions in this complex, the question might be raised as to whether one or two NH_3 are bound in the ammonia complex. If ammonia is added to 0.1 M Ni enta^{--} the ε values of the fourth band are, respectively:

α-Ni enta^{--}	12.6
β-Ni enta^{--}	13.8
1 NH_3: 1 Ni	16.0
2 NH_3: 1 Ni	18.1
3 NH_3: 1 Ni	19.5
10 NH_3: 1 Ni	20.2

This suggests a formation constant for Ni enta NH_3^{--} of about 20, leaving 0.05 M free NH_3 at its 50 % formation. The small band-width (Table 1) does not suggest the presence of more complexes, but this can of course not be excluded. The intensity demonstrates that the decomposition to enta-free ammonia complexes cannot be advanced. log $K = 1.3$ resembles much the average value [12] in the nickel(II)-ammonia system, *viz.* log $K_{av} = 1.43$, whilst log $K_6 = 0.01$.

If 1 M potassium cyanide is gradually added to 0.1 M Ni enta$^-$, a more intense blue-violet colour is observed. The colour becomes distinctly more lilac at the ratio 3 CN^-: 1 Ni. These solutions do not change for several weeks at room temperature. They are, however, slightly decomposed due to local excess concentrations during the preparation as shown by the high absorption in the ultraviolet due to ~1 % Ni $(CN)_4^{--}$. Therefore, the fourth absorption band can only be observed as a shoulder. Solutions in the ratio 5 CN^-: 1 Ni decompose in a few seconds to the yellow colour of diamagnetic nickel(II). The formation constants of the paramagnetic, violet forms are not exceedingly large, as shown by the slow variation of the spectrum with the ratio x CN^-: 1 Ni. A similar behaviour was found by Schwarzenbach [14] for Co enta SCN^{-3} which has the formation constant $K = 0.7$.

NICKEL(II) NITROGENTRIACETATES

Schwarzenbach and Biedermann [17] found two nitrogentriacetate complexes of several metal ions, *e. g.* Ni ata$^-$ and Ni ata$_2^{-4}$ with log $K_1 = 11.26$ (as later determined by Schwarzenbach and Freitag [59]) and log $K_2 = 4.7$. As seen in Table 1, the first band of blue-green Ni ata$^-$ is not as high as that of Ni enta^{--} and the band intensities of the violet-blue Ni ata$_2^{-4}$ are low, suggesting the presence of a centre of inversion [10,18]. It is not known whether ata^{-3} functions

as a tri- or tetradentate ligand, but this will not be of great importance to the spectra, since H_2O and $RCOO^-$ are nearly adjacent in the spectrochemical series. In the Ni ata_2^{-4}, one would for symmetry reasons expect bonding of one nitrogen and two carboxyl groups from each ligand. The two nitrogen atoms may be in *cis*- or *trans*-configuration. The *cis*-form does not seem very likely, since the intensity relations are different from Ni $enta^{-2}$ with two *cis*-nitrogens. The fourth band of Ni ata_2^{-4} has a shoulder on the side of high wavenumbers, and the second band a less pronounced shoulder towards the lower wavenumbers. This may be ascribed to tetragonal effects (of the rare "compressed" type [11,16] in the *trans*-complex) or to the presence of different isomers.

The uptake of ammonia and ethylenediamine in Ni ata^- does not lead to very high displacements towards higher wavenumbers (Table 1) whereas glycinate in Ni ata gly^- has a stronger effect. The first absorption band is particularly difficult to move, and the direction of change is even opposite to that expected for Ni ata en^-. Ni ata^- decomposes very rapidly upon addition of CN^- probably due to more positions for "attack" than in Ni $enta^-$. Ni ata den^- has broad bands with relatively very high wavenumbers.

NICKEL(II) tren-COMPLEXES

Cox and Webster [19] investigated the crystal structure of Ni $tren(SCN)_2$, which could either be a *cis*-octahedral or a tetrahedral complex. Mr. C. J. Ballhausen and the present author have a year ago measured the spectrum of Ni $tren^{++}$ which is similar to that of Ni en_2^{++}, strongly supporting the *cis*-diaquo configuration. Mr. S. E. Rasmussen has kindly presented me with a sample of anhydrous Ni $tren(SCN)_2$ which in 0.03 M aqueous solution has an identical spectrum. In solution, the thiocyanate ions are thus exchanged with water.

Data in Table 1 show that Ni $tren^{++}$ reacts with dilute NH_3 and one mole of en with a slight displacement of the bands towards lower wavenumbers, as expected for the exchange of H_2O by NH_3 and en in an octahedral complex. Most surprising is the behaviour of the purplish red Ni tren gly^+, which is much more hypsochromic than either Ni $tren^{++}$, Ni gly_3^- or Ni_2 $tren_3^{+4}$. This deviation from the rule of average environment can be ascribed to an actual chelate effect, or to the electrostatic effect of binding one glycinate and thus decreasing the external charge. On the other hand Ni en_2 gly^+ is not so strongly hypsochromic.

With excess tren, Ni $tren^{++}$ forms the complexes $Ni_2tren_3^{+4}$ or Ni $tren_2^{++}$ with a crystal field strength similar to that of Ni en_3^{++}. Similar behaviour was found by Jonassen and Douglas [20] for nickel(II) complexes of triethylenetetramine = trien. The spectra found for Ni $trien^{++}$ and Ni_2 $trien_3^{++}$ have the absorption bands at almost the same wavenumbers as do Ni en_2^{++} and Ni en_3^{++}, respectively. Jonassen and Douglas [20] have measured the double band, corresponding to the intermixing [1] of ${}^1\Gamma_3$ (*D*) and ${}^3\Gamma_5$ (*F*), but did not draw the curves through the points. In the case of Hg $tren^{++}$, Prue and Schwarzenbach [42] demonstrated the existence of mixed complexes with chloride and bromide ions on the residual places. *Cf.* also the observations by Mann [66] of hexaco-ordinated Pt $trenI_2$ and Pt ptn_2^{++}.

NICKEL(II) COMPLEXES OF ETHYLENEDIAMINE AND GLYCINATES

Ballhausen [13] determined the spectra of Ni en$(H_2O)_4^{++}$ and Ni $en_2(H_2O)_2^{++}$ from the observed spectra of Ni^{++}-en-mixtures treated by the method of J. Bjerrum [12]. However, Ballhausen did not observe the weak singlet transition ^{1} to $^1\Gamma_3$ (D). In mixtures of 1 Ni : 1 en, a narrow band can be distinguished at 734 mμ with an effective $\varepsilon = 2.1$. Since the mixed spectrum of Ni^{++} + Ni en_2^{++} is approximately a horizontal line in this wavelength range [13], the measured band occurs at the same place for pure Ni en^{++} as it does for the mixture (18 % each of Ni^{++} and Ni en_2^{++} and 64 % Ni en^{++} at $\bar{n} = 1$).

Ni en_2 gly^+ was measured (Table 1) for comparison with Ni tren gly^+. The spectrum of Ni en_2 gly^+ is not changed noticeably with excess of gly^-. However, the formation constants with en are so large [12] relative to glycinate [21] that no appreciable disproportionation occurs.

Further the spectrum of Ni en gly_2 was determined in solution (Table 1), which for similar reasons does not deviate much from that of the pure complex. The spectra agree well with the interpolation between Ni en_3^{++} and Ni gly_3^-.

NICKEL(II) COMPLEXES OF VARIOUS AMINES

In the first paper [1], several nickel(II) complexes were studied with six nitrogen atoms surrounding the central ion, *viz.* Ni$(NH_3)_6^{++}$, Ni en_3^{++}, Ni dip_3^{++} and Ni $phen_3^{++}$. The crystal field strength (E_1—E_2) varies from 10 800 to 12 200 cm^{-1} in this series. Since the groundstate is stabilized 1.2 (E_1—E_2) by the $\gamma_5^6\gamma_3^2$-configuration [22], this represents a considerable range of energy differences, relative to (E_1—E_2) = 8 500 cm^{-1} in Ni$(H_2O)_6^{++}$. J. Bjerrum and the present author pointed out [23] that these stabilizations actually can be found in the values of ΔG for formation of nickel(II) complexes, compared with the similar values of Ca^{++}, Mn^{++} and Zn^{++} without crystal field stabilization. There has been much discussion [24] as to whether the large formation constants for complexes with chelates are only due to effects of entropy, leaving ΔH nearly constant, or if a real "chelate effect" exists also in the bond strength. Since the absorption spectra demonstrate stronger stabilization of ethylenediamine than of ammonia complexes, the chelate effect according to I. Poulsen and J. Bjerrum [25] must be partly real in the complexes with unfilled d-shells, while it may be due to entropy alone in complexes with closed shells. I. Poulsen and J. Bjerrum [25] also investigated ΔG and ΔH of nickel(II) and copper(II) complexes with tn. Trimethylenediamine was found to be distinctly weaker bound to these metal ions than ethylenediamine. As seen from Tables 1 and 2 the place of tn in the spectrochemical series is between NH_3 and en, and rather near to NH_3. Except for the first absorption band of Ni tn_3^{++}, the bands are higher than that of Ni en_3^{++}, as often found by increasing size of the organic ligand [18].

Similar behaviour is found in Ni bdn_3^{++}, as by C-methylsubstituted ethylenediamine complexes studied by F. Basolo. The position of bdn in the spectrochemical series is between tn (of which it is the methyl substitute) and en.

Table 2. The four strong absorption bands in nickel(II) complexes, classified according to the number of nitrogen atoms in the first co-ordination sphere. Wavenumbers of maxima in cm^{-1}.

	$^3\Gamma_5$ (F)	$^1\Gamma_2$ (D)	$^3\Gamma_4$ (F)	$^3\Gamma_4$ (P)
0 nitrogen:				
$Ni(H_2O)_6^{++}$	8 500	(13 500)	(15 400)	25 300
1 nitrogen:				
Ni ata$(H_2O)_2^-$	9 500	13 300	16 000	25 600
2 nitrogens:				
Ni en$(H_2O)_4^{++}$	9 800	13 600	15 800	26 800
α-Ni enta$(H_2O)^{--}$	10 100	12 700	17 000	26 200
β-Ni enta$(H_2O)^{--}$	9 900	12 800	16 900	26 400
Ni ata gly^{--}	9 900	13 000	17 100	26 200
Ni ata_2^{-4}	10 400	13 000	17 400	27 000
3 nitrogens:				
Ni ata$(NH_3)_2^-$(?)	9 600	13 100	16 500	26 600
Ni ata en^-	9 400	13 100	16 900	27 200
Ni enta$(NH_3)^-$	10 200	12 700	17 200	26 900
Ni gly_2^-	10 100	13 100	16 600	27 600
Ni enta$(CN)^-$	10 500	12 500	17 500	—
4 nitrogens:				
$Ni(NH_3)_4(H_2O)_2^{++}$	—	—	16 700	—
Ni enta en^{--}	10 050	12 550	17 300	27 100
Ni en gly_2	10 500	13 000	17 300	28 100
Ni tren$(H_2O)_2^{++}$	10 500	12 800	17 800	27 800
Ni $en_2(H_2O)_2^{++}$	10 500	—	17 900	28 100
Ni ata den^-	10 900	12 500	17 600	28 700
5 nitrogens:				
$Ni(NH_3)_5(H_2O)^{++}$	—	—	17 250	—
Ni en_2gly^+	10 800	12 650	17 900	28 600
Ni tetren^{++}	10 900	12 600	18 400	28 500
Ni tren gly^+	11 200	12 600	18 800	28 200
6 nitrogens:				
Ni py_6^{++}(?)	10 150	13 500	16 500	27 000
$Ni(NH_3)_6^{++}$	10 750	13 150	17 500	28 200
Ni tn_3^{++}	10 900	12 500	17 800	28 200
Ni bdn_3^{++}	10 950	12 700	18 000	28 600
Ni en_3^{++}	11 200	12 400	18 350	29 000
Ni tren$(NH_3)_2^{++}$	11 000	12 750	18 200	28 200
$Ni_2tren_3^{+4}$	10 700	12 500	18 300	28 700
Ni tren en^{++}	11 000	12 500	18 700	29 000
Ni tetren NH_3^{++}	11 100	12 500	18 700	28 600
Ni den_2^{++}	11 500	—	18 700	29 100
Ni ptn_2^{++}	11 200	12 500	19 000	29 700
Ni dip_3^{++}	(11 500)	(12 650)	19 200	—
Ni $phen_3^{++}$	(11 550)	(12 700)	19 300	—

Prue and Schwarzenbach [26] have studied the complex formation with 1,2,3-triaminopropane. It is found here that at least two complexes are formed in solutions with up to three moles ptn per nickel ion. The purple complex finally formed (presumably Ni ptn_2^{++}) has about 1 % higher value of $(E_1—E_2)$ than Ni en_3^{++}, but has lower band maxima. The upper limit of $(E_1—E_2)$ for aliphatic amines does not seem to be more than 1 % higher than that of en, as exemplified by tren, trien and ptn, while larger alkyl radicals and larger chelate rings, as in tn and to a lesser degree in bdn have an decreasing influence on bonding strength.

Another aliphatic amine with a high crystal field strength is C,C,C′,C′-tetramethyl-ethylenediamine of which Basolo, Chen and Murmann report [27] diamagnetic, planar yellow ions Ni temeen$_2^{++}$ (with only one absorption maximum [27] at 23 000 cm^{-1}, while the reflection spectrum of the salmon-pink [16] solid [Ni en$_2$] [AgBrI]$_2$ shows a band at 20 800 cm^{-1}). Basolo and the present author observed that solid [Ni temeen$_2$] Cl$_2$ reacts with concentrated aqueous ammonia to a violet solution *. It was obvious to suppose the existence of a paramagnetic ion Ni temeen$_2$ (NH$_3$)$_2^{++}$. However, the solution shows bands at nearly the same place as Ni (NH$_3$)$_6^{++}$, and a solution, 0.05 M Ni^{++}, 6 M NH$_3$, 0.12 M temeen, which contains less than 2 % of the yellow form, is decomposed by addition of 50 volume % 0.4 M temeen to a mixture of about 60 % Ni temeen$_2^{++}$ and 40 % of the violet form. It is not a reasonable behaviour for a mixed ammonia complex, but is rather caused by the sudden break-down of the chelate complex at increasing ammonia concentration, as discussed below. Basolo, Chen and Murmann [27] found that Ni temeen$_3^{++}$ cannot be formed, due to steric hindrance; and Ni temeen$_2$ Cl$_2$ has the same absorption spectrum in water and absolute ethanol, showing no tendency of solvation or association of chloride ions in the first co-ordination sphere. Neither has it been possible to identify a purple *cis*-Ni temeen$_2$ en^{++} in mixed solutions.

Although the heterocyclic diamines as α,α'-dipyridyl and *o*-phenanthroline have even larger crystal field strengths [1] than ethylenediamine, the heterocyclic monamine pyridine has a smaller crystal field strength than ammonia. It is not easy to identify the hypothetical Ni py$_6^{++}$ in solution. The solutions of nickel(II) nitrate in pyridine with a small water content may still contain nitrato complexes [28], which perhaps also were important in the system *n*-butylamine-water-copper(II) nitrate, studied by Bjerrum and Lamm [23]. Robust complexes of cobalt(III) and rhodium(III) are only known with at most four molecules of pyridine. Nevertheless, the results in Table 1 and 2 demonstrate a low crystal field strength of pyridine, compared to other amines agreeing well with the observed weak tendency to complex formation [51].

Table 1 gives also the spectra of Ni den$_2^{++}$, Ni tetren^{++}, and Ni tetren NH$_3^{++}$, demonstrating the regular behaviour of nickel(II), compared to copper(II), of which Table 3 gives Cu den^{++}, Cu den NH$_3^{++}$, Cu den$_2^{++}$, and Cu tetren^{++}. The latter series of complexes resembles much the spectra of Cu(NH$_3$)$_n$ (H$_2$O)$_{6-n}^{++}$ with n = 3, 4, 6, and 5, respectively, exhibiting pentammine effect in the two last cases [32]. Haendler [67] measured the absorption spectra of Cu^{++} and Ni^{++} with 1 and 2 moles of den. While K_1/K_2 is so large in the first case that Cu den^{++} disproportionates only to the extent $10^{-5.4}$, 5 % each of Ni^{++} and Ni den$_2^{++}$ occur for n = 1. The complex formation with the "guirlande" chain amines den, trien, tetren with H$_2$O and NH$_3$ on the residual places will be discussed later.

* However, Basolo isolated a violet solid from the action of liquid ammonia. Since this solid returns to the original yellow complex upon standing in the air, Basolo assumes the solid to be the mixed complex [Ni temeen$_2$ (NH$_3$)$_2$]Cl$_2$. *(Private communication).*

Table 3. Absorption bands of copper(II) complexes. Notation as in Table 1.

	λ_n mμ	ν_n cm^{-1}	ε_n	$\delta(-)$ cm^{-1}	$\delta(+)$ cm^{-1}	$P \cdot 10^{-5}$
Cu enta^{--}	734	13 600	91	2 000	2 200	185
Cu enta NH_3^{--}	722	13 800	38		2 200	75
Cu ata$^-$	880	11 400	60	2 400	—	170
	775	12 900	54	—	2 600	
Cu ata_2^{-4}	658	15 200	37	2 700	2 400	90
Cu tren++	860	11 600	117	2 600	3 300	320
Cu $tren(NH_3)_2$++	785	12 700	134	2 500	3 300	360
Cu den++	611	16 300	74	2 300	2 600	170
Cu den NH_3++	576	17 400	84	2 600	2 600	200
Cu den_2++	~850	11 800	~70	1 800	—	310
	630	15 900	106	—	2 600	
Cu tetren++	~840	11 900	~100	1 700	—	520
	643	15 600	165	—	2 400	
Cu tn_2++	568	17 600	111	2 700	2 300	250
Cu bdn_2++	566	17 700	125	2 500	2 300	280
Cu ptn_2++	559	17 900	66	2 300	2 200	140
Cu en_2++	549	18 200	63	2 400	2 400	140
Cu $temeen_2$++	547	18 300	120	2 700	2 500	290

COPPER(II) ETHYLENEDIAMINETETRAACETATES

It was shown above that the absorption spectra of paramagnetic nickel(II) complexes can be described roughly by only one parameter, which may be identified with the energy difference (E_1—E_2) between γ_3- and γ_5-electrons in a regularly octahedral complex [13,16,30,31]. In copper(II) complexes, one further parameter is necessary to describe the relative tetragonality [2] varying from a regular octahedron to square planar complexes with decreasingly weaker ligands on the perpendicular axis. Empirically, the ratio ν_{Cu}/ν_{Ni} between the principal band of the copper(II) complex and the first band of the corresponding nickel(II) complex is proposed [1]. This ratio is roughly 1 in copper (II) complexes with cubic symmetry, increasing to about 1.8 in the most extremely tetragonal cases.

J. Bjerrum, Ballhausen and the author [32] discussed previously the ligands ammonia and ethylenediamine, which form the distinctly tetragonal planar complexes $Cu(NH_3)_4^{++}$ and $Cu\ en_2^{++}$ with two weakly bound water molecules, resulting in $\nu_{Cu}/\nu_{Ni} = 1.7$. If stronger bound ligands such as ammonia, replace water on the z-axis, a pentammine effect is observed to decrease the value of this ratio. Recently Linford [9] studied the solvates of copper(II) bis(acetylacetonate) and similar planar complexes with chloroform, acetone, dioxan, alcohols, pyridine and piperidine solvates, arranged according to increasing z-axis contribution. Most of the results obtained are readily explained except for the absorption band of $Cu\ en_2^{++}$ which is shifted 800 cm^{-1} in the wrong direction by solvation with ethanol [33]. This effect is much larger than the solvation effects of the second co-ordination sphere, studied by J. Bjerrum, Adamson, and Bostrup [34].

A series of copper(II) complexes with much lower values of ν_{Cu}/ν_{Ni} have been investigated [1]. The behaviour of amines as ligands is rather capricious,

some form "cubic" and some "tetragonal" complexes without conspicuous regularities. The polydentate amino-acids, however, form only weakly tetragonal copper(II) complexes whenever, of steric reasons, the carboxyl groups cannot be bound in the plane of four strongly bound atoms. In the case [1] of Cu enta$(H_2O)^{--}$ we have $\nu_{Cu}/\nu_{Ni} = 1.36$.

Bonnett and Schmidt [35] found that the less coloured Cu enta$(OH)^{-3}$ is formed with pK = 11.35 in 1 M Na_2SO_4 and with higher pK at lower ionic strength. Schwarzenbach and Heller [36] found pK = 7.39 for the acidity of Cr enta$(H_2O)^{-}$ and 7.49 for the first proton of Fe enta$(H_2O)^{-}$. It is known from pK of $Cu(H_2O)_6^{++}$ and from the formation [32] of $Cu(NH_3)_3OH^{+}$ that copper(II) complexes generally are more acidic than those of nickel(II) and zinc(II). Even though the external charge and the oxidizing power (the intermixing of electron transfer states stabilizes perhaps the groundstate of the hydroxo complexes) make an important contribution to the acidity, there is, *inter alia*, an evident effect of deviation from cubic symmetry for metal ions with unfilled d-shells [22]. This is especially evident for the tetragonal d^4- and d^9-systems.

Data in Table 3 show that the band of Cu entaNH_3^{--} has much lower intensity than that of Cu entaH_2O^{--}. This cannot be ascribed to the formation of Cu enta OH^{--} in aqueous ammonia, since addition of a large amount of NH_4NO_3 has no effect on the spectrum. The maximum in Cu entaNH_3^{--} is only shifted 2 % towards higher wavenumbers, relative to Cu entaH_2O^{--}. Thus, the ammonia molecule must be placed on the axis, perpendicular to the plane containing the two *cis*-nitrogen atoms of enta $^{-4}$.

Upon addition of KCN to 0.02 M Cu enta^{-3}, the maximum at 734 mμ is displaced to 719 mμ with 1 CN^- : 1 Cu and to 706 mμ with 3 CN : 1 Cu. The corresponding violet colours can be changed even further towards brownish purple. Such solutions are very unstable (the lowest maximum measured is 695 mμ) and change in a minute to colourless copper(I) cyanide complexes. It is interesting to note that a high electron transfer spectrum in the violet is present in the intermediate copper(II) complex. Representative values of the effective ε are 16 at 400 mμ, 75 at 375 mμ and 280 at 350 mμ, while the decomposed solution has only $\varepsilon = 9$ at 350 mμ and $\varepsilon = 20$ at 325 mμ. Also Cu enta^{--} has an electron transfer spectrum [1] with $\varepsilon = 46$ at 350 mμ, and similar values are found for Cu enta NH_3^{--}.

Thus, the intrinsic tendency of a redox process in Cu enta$(CN)^{-3}$ is depicted by the electron transfer spectrum, as is also the case of $CuCl_4^{--}$ and $CuBr_4^{--}$. Duke and Courtney [37] demonstrated the strong colour produced in copper(II) solutions in ammonia water by CN^-, which contained rather stable complexes of the type $Cu(NH_3)_3CN^+$. Analogously, Cu en^{++} forms purple and reddish intermediate complexes with CN^-, probably corresponding to high values of the tetragonality. The position of CN^- is at the extreme end of the spectrochemical series. For example the first band of tris(ethylenediamine) complexes of cobalt(III), rhodium(III) and iridium(III) [38] has 1.30 times as large a wavenumber as in the corresponding hexaaquo ions. The similar ratio is 1.96 for $Co(CN)_6^{---}$.

Pfeiffer and Schmitz [39] maintain the existence of enta-complexes with two metal ions in the solid compound Ca Cu enta, 3.5 H_2O. Although such complexes would be very

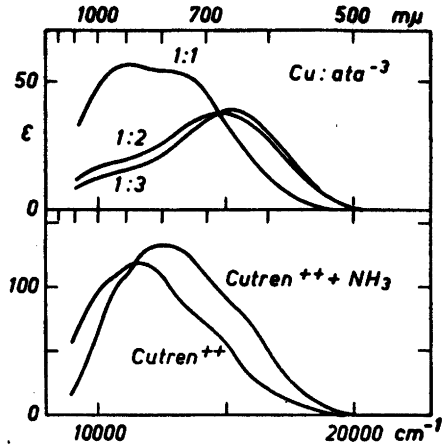


Figure 1. Upper part: Absorption spectra, demonstrating the consecutive formation of Cu ata⁻ and Cu ata₂⁻⁴. The solutions measured were:
0.04 M Cu++, 0.04 M ata⁻³
0.04 M Cu++, 0.08 M ata⁻³
0.04 M Cu++, 0.12 M ata⁻³

Lower part: Absorption spectra of the two complexes Cu tren $(H_2O)_3$++ and Cu tren $(NH_3)_2$++ (or perhaps Cu tren $(NH_3)(H_2O)$++) from solutions:
0.01 M Cu++, 0.01 M tren
0.01 M Cu++, 0.01 M tren. 1 M NH_3

interesting it would not appear that there is any good evidence for their existence. Pfeiffer and Schmitz [39] found that $Cu(OH)_2$ is precipitated with NaOH from CaCu enta, while Na_2Cu enta is not decomposed. But this may be a consequence of the presence of calcium ions, removing enta⁻⁴ from the equilibria by formation of Ca enta⁻⁻ with log $K = 10.59$, while Cu enta⁻⁻ has log $K = 18.4$. Mixtures of Ni enta⁻⁻ and Ni++ do not react, according to the spectra, and in alkaline solution, Ni $(OH)_2$ is precipitated. The second formation constant of Ca $enta_2^{-6}$ is [61] less than 20, but the investigation is rendered difficult by the relatively low value of $pK = 11.39$ for formation of Ca(OH) enta⁻³. The intention of Pfeiffer and Schmitz [39] to prepare isomeric enta-salts, differing only in the free metal ion, is more apt to occur with robust species, *e.g.* $[Cr(H_2O)_6]_2$ [Ni enta]$_3$ and $[Ni(H_2O)_6][Cr\ enta]_2$.

COPPER(II) NITROGENTRIACETATES

The robin-egg's blue Cu ata⁻ reacts with an excess of ata⁻ to form darker blue complexes. It is seen from Fig. 1 that the formation of Cu ata_2^{-4} is not totally complete at the ratio 2 ata⁻³ : 1 Cu^{+2} but the spectrum is a linear combination of that of Cu ata⁻ with the new complex.

The intensity of Cu ata_2^{-4} is much lower than of Cu ata⁻, analogous to the nickel(II) complexes. Since ν_{Cu}/ν_{Ni} goes from 1.25 for Cu ata⁻ to 1.45 for Cu ata_2^{-4}, the two nitrogens in the latter complex determine the tetragonal plan. The development has the opposite direction [1] in Cu gly_2 with $\nu_{Cu}/\nu_{Ni} = 1.60$, which decreases in Cu gly_3^-. The complex formation necessitates in the latter case relatively large free concentrations of the ligand.

Cu ata$^-$ has two absorption bands (Table 3) with a distance of 1 500 cm^{-1} between the maxima, while Cu ata$_2^{-4}$ has only an extreme large half-width towards the infra-red. The former phenomenon resembles Cuphen$_2$(H$_2$O)$_2^{++}$ and Cudip$_2$(H$_2$O)$_2^{++}$, both of which are presumed to have *cis*-configuration [1]. R. Linn and Geneva Belford [9] assume that the broad bands of copper (II) complexes can be resolved into three Gaussian curves [40] with three different half-widths, but with $\delta(-) = \delta(+)$ for each band [40]. While the existence of three bands may be theoretically justified [9], the determination of their positions is certainly near to the limits of experimental uncertainty. However, at least two bands are constituents of most of the spectra of copper(II) complexes [1,32], and three are observed in Fig. 1 of Cu tren $^{++}$.

COPPER(II) tren-COMPLEXES

Cu tren^{++} is sea-blue with the same tint as the hexaaquo ion and the high band is displaced to 860 mμ, compared to Cu(H$_2$O)$_6^{++}$ at 790 mμ. Hence the crystal field is strong in Ni tren (H$_2$O)$_2^{++}$, ν_{Cu}/ν_{Ni} is only = 1.08, the lowest value found in any copper(II) complex. Thus, a *cis*-diaquo configuration for Cu tren(H$_2$O)$_2^{++}$ can be proposed. In aqueous ammonia a flat maximum is obtained at 785 mμ. This increases the ratio ν_{Cu}/ν_{Ni} only slightly to 1.11.

Thus, the tendency of forming cubic copper(II) complexes is not restricted to heterocyclic diamines, but can also be found in aliphatic amines with steric resistance against formation of planar complexes. However, in the discussion of copper(II) complexes of polydentate ligands a special precaution must be taken: Contrary to most calculational assumptions [9,16], the six atoms in an octahedral complex are not bound to the axes of a Cartesian co-ordinate system, but instead may have a triclinic symmetry. Geometrically a *cis*-complex MA$_4$B$_2$ with loosely bound B can smoothly transform to a tetrahedral complex MA$_4$, first of non-regular and later of regular symmetry. During this process, the cubic contribution [16] will change in sign, and the energies of the five d-orbitals, if calculated from the electrostatic model [41] will cross in a very complicated way. The most stable configuration is obtained when the average energy of the d-electrons is relatively low and the interaction energies of the ligands low, while the highest d-orbital has a relatively high energy. The latter orbital contains only one electron in Cu^{++}. A further complication arises, because the regularly tetrahedral symmetry of copper(II) is unstable, due to the Jahn-Teller effect [22]. Actually, bonding of tren to Cu^{++} is rather strong: Prue and Schwarzenbach [42] determined log K = 14.65 for Zn tren^{++}, 18.8 for Cu tren^{++} and 14.8 for Ni tren^{++}. Contrary to this behaviour, the heterocyclic diamines have their formation constants in the order [23] Ni>Cu>Zn. However, the profound analogy (Fig. 1) between the spectra with two shoulders at nearly the same place strongly supports the *cis*-configuration of mainly octahedral Cu tren(H$_2$O)$_2^{++}$ and Cu tren(NH$_3$)$_2^{++}$ (or Cu tren(NH$_3$)(H$_2$O)$^{++}$).

COPPER(II) COMPLEXES WITH ALIPHATIC DIAMINES

I. Poulsen and J. Bjerrum [25] found the formation heats for copper(II) amine complexes for the four first co-ordination places the series NH_3<tn <en. As seen from Table 3, ν_n of Cu tn_2^{++} occurs between that of Cu $(NH_3)_4^{++}$ and Cu en_2^{++} and ν_{Cu}/ν_{Ni} is therefore ~1.7. The stabilization energy is probably also roughly proportional to the wavenumber of the principal band in tetragonal complexes.

The highest wavenumber observed yet in a copper(II) complex occurs in Cu $temeen_2^{++}$ (Table 3), 1/2 % larger than that of Cu en_2^{++}. The diamagnetism of Ni $temeen_2^{++}$ corresponds to an even higher tendency of tetragonality [27] with the highly destabilized orbital γ_{t3} which is empty [16].

The tridentate ptn does not utilize the possibility of forming a nearly cubic, hexa-coordinated copper(II) complex such as dip and phen. On the other hand Cu ptn_2^{++} is dark violet with $\nu_{Cu}/\nu_{Ni} = 1.6$ and must be assumed to bind only four nitrogen atoms, as already proposed by Mann and Pope [65]. It would be interesting to know, if the residual amine group has affinity to silver ions, forming perhaps the bi-nuclear complex Cu ptn_2 Ag^{+3} with linear environment of the silver [12,60].

While the tridentate amines ptn and den (of which the latter has one secondary amine group) form similar nickel(II) complexes, is Cu den_2^{++} distinctly hexa-(or penta-)co-ordinated, and has high intensity of the double band, as also Cu $tetren^{++}$ has.

The band intensity of Cu ptn_2^{++} is of the same magnitude as for Cu en_2^{++}, while Cu $temeen_2^{++}$, Cu tn_2^{++}, and Cu bdn_2^{++} are much stronger coloured. In the bis(diamine) complexes, the absorption band vanishes in the infra-red. the values of ε being:

	800 mμ	900 mμ	1 000 mμ
Cu en_2^{++}	2.7	0.7	0.3
Cu tn_2^{++}	13.0	4.1	1.4
Cu ptn_2^{++}	7.2	3.4	1.5
Cu $temeen_2^{++}$	9.6	4.0	2.4
Cu bdn_2^{++}	19.6	6.0	2.0
Cu den^{++}	11.5	3.4	1.0

CHELATE STABILIZATION EFFECTS

In Table 2, the wavenumbers of the four strong absorption bands of paramagnetic nickel(II) complexes are classified, according to the number of nitrogen atoms in the first co-ordination sphere. The formulae of Ni py_6^{++}, Ni $ata(NH_3)_2^-$, Ni $enta(NH_3)^{--}$ and Ni enta CN^{-3} are tentative.

The last complex is classified as a system with three N.

It is a rather good approximation except for the highly polarizable anions as SCN^-, NO_2^-, and CN^- to write the spectrochemical series according to the elements alone as:

$$Br < Cl < F < O < N$$

In the amino-acid complexes, the active atoms in the first co-ordination sphere are O from carboxyl groups and water and N from the amine groups. The oxygen atoms are not very different. The oxalate ion is nearly coincident

with water in the spectrochemical series [4], but has a similar position among carboxyl groups as ethylenediamine has among the amines. The other carboxyl groups are slightly bathochromic, as found by Linhard and Weigel [7] and for nickel(II) propionates etc. by Pestemer and Alslev-Klinker [44]. The results reported in this paper show the following spreading of the amines in the spectrochemical series:

$$py < NH_3 < tn < bdn < \left\{ \begin{matrix} en \\ temeen \\ trien \\ tren \end{matrix} \right\} < den < ptn < dip < phen.$$

Already Russell, Cooper and Vosburgh [57] found empirically that the formation constants of nickel(II) amine complexes increase with the hypsochromic effect of the ligand.

It is easily seen from Table 2 that the polydentate amino-acids generally are further removed in the spectrochemical series than interpolated directly from the rule of average environment. Thus, one N in Ni ata^- and two N in Ni $enta^{-2}$ function as 2.5 NH_3 and 4.5 NH_3, respectively, if the visible band is compared to the spectra of Ni $(NH_3)_n$ $(H_2O)_{6-n}{}^{++}$ found by J. Bjerrum [12]. Since the crystal field strength is roughly proportional [9,41,45,46] to R^{-5}, where R is the distance to the negative charge of the ligand, this observation can easily be explained by a slightly tighter bonding. It is interesting [1] that even the anhydrous Co $enta^-$ is 2.5 % hypsochromic in the first band, compared to Co enta H_2O^-. As seen from the method of preparation [14], the latter complex must be highly thermodynamically unstable in aqueous solution.

Even if ΔG and ΔH cannot be calculated from the spectrochemical series, ignoring the many unknown factors in the case of closed-shells as Zn^{++}, considerable correlation can be found between the relative values for ΔG and ΔH. For example, the differences between negative and neutral ligands are particularly large. The exchange with water of chloride ions has formation constants slightly below 1, whereas the relative crystal field strength [38] of Cl^- and H_2O is 0.76 and the corresponding ratio for amines and H_2O is $\sim$1.3. Thus, the high formation constants for $enta^{-4}$-complexes are partly due to electrostatic effects.

J. Bjerrum and the author [23] discussed the ethylenediaminetetraacetates of the divalent ions of the first transition group, log K varies [15] from 10.96 for Ca^{++} over 14.04 for Mn^{++} to 16.50 for Zn^{++}. If Ni^{++} had a closed d-shell, log K would extrapolate 15.5 instead of the observed value 18.62. The stabilization of 2.8 in log K corresponds to 3.8 kcal/mole = 1 300 cm^{-1}. Analogously, the formation constants for lanthanide-enta complexes vary smoothly from log K = 15.50 for La $enta^-$ over 17.37 for Gd $enta^-$ to 19.83 for Lu $enta^-$. These half- and closed shell structures represent the standard state of electrostatic behaviour while all the other complexes are stabilized between 0.2 and 0.3 units in log K, due to the smaller influence of the crystal field on f- than on d-electrons.

In Table 4, a series of stabilization energies are compiled for Fe^{++}, Co^{++}, Ni^{++} and Cu^{++}, when the non-stabilized values of log K_n are assumed to vary linearly with the number of d-electrons between Mn^{++} and Zn^{++}. Most examples are taken from the article of Schwarzenbach [24] on the chelate effect,

Table 4. Crystal field stabilization of complexes of the second half of the first transition group. Most formation constants refer to 20° C and the ionic strength ~0.1. ϱ is the stabilization parameter [22] valid for regularly octahedral complexes, viz. energy decrease = 0.2 ϱ (E_1—E_2). Ref. 63 considers N-substituted iminodiacetates $RN(CH_2COO^-)_2$, here denoted Rada. The consecutive formation constants are considered in cases, where the formulae indicate the binding of the second or the third ligand.

Ref. No. Ligands beside water	log K_n		Stabilization found from the hypothesis of linear variation of log K_n with the number of d-electrons from 5 to 10			
	Mn++	Zn++	Fe++	Co++	Ni++	Cu++
62 py	0.14	0.95	0.41	0.68	1.15	1.62
24 en	2.8	6.0	1.0	1.9	3.2	5.4
24 en_2	2.1	3.3	1.0	2.4	3.8	6.3
24 en_3	0.9	2.0	0.9	1.9	3.1	—1.7
24 tren	5.8	14.6	1.2	3.5	3.7	6.0
24 trien	4.9	12.1	1.5	3.2	4.8	9.7
24 penten	9.4	16.2	0.4	3.7	5.8	7.6
59 ata	7.44	10.45	0.8	2.0	2.0	2.8
17 ata_2	3.7	3.0	—	0.5	1.6	—
15 enta	14.04	16.50	~0	1.3	3.1	2.8
63 CH_3ada	5.40	7.66	0.80	1.32	1.97	3.88
63 $(CH_3ada)_2$	4.16	6.43	0.76	1.24	1.70	0.85
63 C_6H_5ada	1.58	3.22	0.10	0.66	0.97	3.68
63 HOC_2H_4ada	5.55	8.33	0.67	1.23	2.07	4.09
63 $(HOC_2H_4ada)_2$	3.76	3.69	—0.53	0.46	1.25	1.31
63 $NH_2C_2H_4$ada	7.71	11.93	1.25	2.37	3.50	4.82
ϱ =	0	0	2	~4	6	3

and from the recent measurements by Schwarzenbach, Anderegg, Schneider and Senn [63] on substituted iminodiacetates $R(CH_2COO^-)_2 \equiv$ R ada. It is seen that the stabilization for iron(II), cobalt(II), and nickel(II) complexes are roughly proportional to the stabilization parameter [22]ϱ, *viz.* 2, 4 and 6. In some cases, *e. g.* the third en or the second HOC_2H_4ada the steric conditions for bonding are better in Mn^{++} than in Zn^{++}, but here also the evolution of stabilization energies is rather regular. On the other hand, the strong tendency of tetragonal distortion in copper(II) complexes produces an enormous stabilization of ligands on the four planar places, *e. g.* in en_2 and trien. The effective value of ϱ for Cu^{++} in Table 4 can exceed the value 10, whereas values ~3 ν_{Cu}/ν_{Ni} ~5 might have been expected.

In nickel(II) complexes the crystal field stabilization can be compared to the theoretical value 1.2 (E_1—E_2). However, as seen from Table 2, the value of (E_1—E_2) cannot be found accurately from the absorption spectra, since the relative positions of the bands vary some hundred cm^{-1} in an irregular way. If the energies of the two lowest levels are defined:

$$^3\Gamma_2\ (F) = -1.20\ (E_1-E_2)$$
$$^3\Gamma_5\ (F) = -0.20\ (E_1-E_2)$$

then the Orgel diagram of nickel(II) complexes [1] can be approximately described by the three other lines in the range of our interest:

$$^3\Gamma_4\ (F) = 2\,800\ cm^{-1} + 0.155\ (E_1-E_2)$$
$$^3\Gamma_4\ (P) = 15\,100\ cm^{-1}$$

and after correction for the intermixing of triplet character:

$$^1\Gamma_3\,(D) = 16\,500 \text{ cm}^{-1} - 1.55\,(E_1 - E_2)$$

These equations demonstrate that either are the term distances to ^3P, ^1D, and ^1G decreased from the values, found from the gaseous ion, or other electron configurations are intermixed in the states of the complexes. The former alternative explanation is discussed below in the last section.

If $(E_1 - E_2)$ is assumed to be the wavenumber of the first band 10 100 cm^{-1} in α-Ni enta^{-1} and 8 500 cm^{-1} in $Ni(H_2O)_6^{++}$ the predicted stabilization is 1 900 cm^{-1}. The similar numbers are:

Ni ata$^-$	1 200 cm^{-1}	3.4 kcal/mole	2.5 units in log K
Ni gly$_3^-$	1 900	5.4	4.0
$Ni(NH_3)_6^{++}$	2 700	7.7	5.7
Ni tn$_3^{++}$	3 300	9.3	6.9
Ni tren^{++}	2 900	8.2	6.1
Ni en^{++}	3 700	10.5	7.8
Ni phen$_3^{++}$	4 400	12.5	9.3
Ni en$_2$gly$^+$	3 100	8.8	6.5
Ni tren gly$^+$	3 800	10.8	8.0

It must be remembered that these quantities are found from the spectra by subtraction of the even larger stabilization of the hexaaquo ion, relative to the free Ni^{++} *in vacuo*. This quantity is 10 200 cm^{-1} ≡ 29 kcal/mole ≡ (log K = 22). Orgel [47] pointed out that this stabilization can actually be observed as a part (~ 5 %) of the absolute heat of hydration of metal ions. I. Poulsen and J. Bjerrum [25] found ΔH = 21.0 kcal/mole for $Ni(NH_3)_6^{++}$, 21.3 kcal/mole for Ni tn$_3^{++}$ and 27.9 kcal/mole for Ni en$_3^{++}$. If these values are corrected for the stabilization mentioned above, the residual "closed shell" case gives 13.3, 12.0 and 17.4 kcal/mole, respectively, for $Ni(NH_3)_6^{++}$, Ni tn$_3^{++}$ and Ni en$_3^{++}$. Besides the d-orbital stabilization, the σ-bonding of even γ_1 and odd γ_4-electrons[48-50] may be stronger in the ethylenediamine complexes where the ligands have comparatively smaller distances due to the γ_3-bonding.

The entropy effects in chelate complexes are rather peculiar, inducing the irregular behaviour of ΔG, compared to ΔH. The discussion that follows is concerned only with the importance of chelating number L in reactions of a complex with a polydentate, *viz.* of the type

$$\text{Ni enta}^{--} + 6\ NH_3 \rightleftharpoons Ni(NH_3)_6^{++} + \text{enta}^{-4}$$

It is seen from the mass action law that this process is half complete when

$$\frac{[NH_3]^6}{[\text{enta}]} = \frac{K_{\text{Ni enta}}}{K_{\text{Ni (NH}_3)_6}}$$

Thus, if a buffer concentration of free [enta] = 0.01 M is maintained, the free [NH_3] will be 20 M. If a similar experiment is performed with [enta] = 0.01 M and the nickel complex is destroyed with tn or en, respectively, [tn] = 28 M and [en] = 0.24 M are necessary for 50 % decomposition to Ni tn$_3^{++}$ or Ni en$_3^{++}$. Any formation of mixed complexes, as Ni enta NH_3^{--} and Ni enta en^{--} studied above, will of course delay the actual destruction of the bonding between Ni^{++} and enta^{-4}.

Even though log $K_{1\text{-}3}$ = 12.0 for Ni tn$_3^{++}$, and log $K_{1\text{-}6}$ = 8.6 for Ni $(NH_3)_6^{++}$, it is seen that tn and NH_3 in high concentrations are nearly equally effective for decomposing Ni enta^{--}. This is a result of the occurrence of a sixth power term in the mass action law for NH_3, but only a third power term for tn. Roughly speaking, a dilute solution of a polydentate amine resembles "coarsegrained" aqueous ammonia. The prob-

ability of finding a high number of amine groups (L groups per molecule) within reach of a certain metal ion is very high, and it is proportional to C^{-1}, whereas, in a monodentate amine like NH_3, the corresponding probability is proportional to C^{-L}.

Inversely, a polydentate complex is affected very little by dilution of the free ligand. Although 0.01 M free enta^{-4} encountered 20 M free NH_3 above, 10^{-5} M free [enta] will still afford 6 M free NH_3 for half decomposition of Ni enta^{--}, and $10^{-9.6}$ M enta^{-4} is sufficient against 1 M NH_3. Now, it is easily understood why the yellow diamagnetic Ni temeen$_3^{++}$ suddenly breaks down at a rather high ammonia concentration:

$$\text{Ni temeen}_3^{++} + 6\ NH_3 \rightleftharpoons Ni(NH_3)_6^{++} + 2\ \text{temeen}$$

with the constants [27] log $K_{1-3} = 14.68$ for Ni temeen$_3^{++}$ and log $K_{1-6} = 8.6$ for $Ni(NH_3)_6^{++}$, 50 % decomposition is predicted at $[NH_3] = 4.8$ M when [temeen] = 0.1 M. At slightly higher ammonia concentration, the decomposition is practically complete, owing to the sixth power dependence.

Reversely, the presence of a mixed complex Cu tren en^{++} can definitely be proven by the absorption spectrum of a solution, 0.001 M Cu, 0.001 M tren, 0.8 M en, which shows the presence of only ~50 % of the copper as Cu en$_3^{++}$. From the formation constants of Cu en$_3^{++}$ and Cu tren^{++}, the constant for the reaction en + Cu tren^{++} → Cu tren en^{++} can be estimated to ~4.10^4.

By comparison of ligands with different chelating number L, it might be reasonable to choose a scale of apparent activity, proportional to C^3/L. Since the standard state of chemical compounds is often chosen as the pure compounds, the formation constants referring to 1 M solutions are from this point of view exaggerated for polydentate ligands. For instance, tren is less affected by dilution than is NH_3. J. Bjerrum [51] pointed out for monodentate ligands that the exchange with water might be treated by defining $[H_2O] = 55$ M in the dilute solutions. Adamson [43] later demonstrated that most of the ΔS by chelate formation [24] vanishes, if a new $\Delta G'$ is defined

$$\Delta G' = \Delta G + \Delta \mu\, RT \ln 55$$

when $\Delta\mu$ is the number of produced moles minus reacted moles, except of the solvent. Actually, the activities of different ligands in dilute solution, compared to the pure compounds, ought to be determined by partial vapour pressures. Adamson's proposal [43] is equivalent to the assumption of activities, proportional to the mole fraction. An alternative proposal will be the molar concentration of the ligand in solution divided with the molar concentration of the pure ligand. In ideal gas mixtures, the two concepts based on number and partial volumes, are identical, and in dilute solutions the two concepts are only different by a proportionality constant, characteristic for the solvent and the ligand. In stronger solutions, the two proposals may differ somewhat. The molar concentration of the anhydrous, liquid amines at 25° C are 38 M NH_3, 15 M en and 12 M tn. Thus the formation constants of nickel(II) complexes can be corrected by the factors 38^6, 15^3, and 12^3, respectively, resulting in log $K'_{1-6} = 18.1$ for $Ni(NH_3)_6^{++}$, log $K'_{1-3} = 21.8$ for Ni en$_3^{++}$ and log $K'_{1-3} = 15.3$ for Ni tn$_3^{++}$. By this method, there appear small residual entropy effects [25], and the crystal field stabilization in ΔH will of course still subsist in the values of $\Delta G'$, corresponding, *e.g.*, to the predicted difference 2.1 between log K_{1-6} for $Ni(NH_3)_6^{++}$ and log K_{1-3} for Ni en$_3^{++}$.

THE INTERMIXING OF SINGLET AND TRIPLET LEVELS BY INTERMEDIATE COUPLING

The validity of sharply defined total spin S and total angular moment L in the free atoms and ions, corresponding [2] to S and Γ_n in crystal fields, is weakened by increasing values [52] of Landé's multiplet factor ζ_{nl}. In systems in crystal fields, states with the same Γ_J (found from the internal vector product [16] of $C(S)$ and $C(\Gamma_n)$) are intermixed with nondiagonal elements of energy

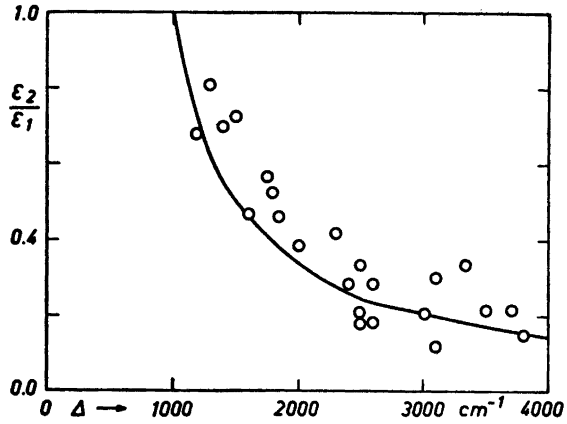


Figure 2. The ratio $\varepsilon_2/\varepsilon_1$ between the directly observed heights of the two first absorption bands of nickel(II) complexes as function of the difference Δ between the wavenumbers of the two maxima. The curve represents the function $\frac{a}{1-a}$ with $a = \frac{500\ cm^{-1}}{\Delta}$ discussed in the text.

$= k\,\zeta_n$, where the constants k are not very different from 1. Thus, the usual description of levels in d^n-systems as having definite S and Γ_n breaks down, when $k\,\zeta_{nl}$ is sufficiently large [1] and the distance Δ between the interacting levels small. The intermixing in the squares of the wavefunctions is approximately $\left(\frac{k\,\zeta_{nl}}{\Delta}\right)^2$.

The most conspicuous case [1] of intermixing of S in the nickel(II) complexes occurs between the lowest singlet level $^1\Gamma_3(D)$ and the two lowest excited triplet levels $^3\Gamma_5(F)$ and $^3\Gamma_4(F)$ with the values of $k\,\zeta_{nl} = 500$ cm^{-1} and 800 cm^{-1}, respectively. The numerical results of Tables 1 and 2 are used in Fig. 2 to estimate the former intermixing. The oscillator strength P is divided between the two interacting levels proportional to their triplet character ($S = 1$) since the groundstate for the transition has $S = 1$ to a high degree of precision. But the ratio between the values of P for the two components is not easily accessible from the measurements. Rather, it is assumed that the observed maximum ε_n is proportional to the numerical value of intermixing a, *viz.*

$$\frac{\varepsilon_2}{\varepsilon_1} = \frac{a}{1-a} \text{ with } a = \frac{k\zeta_{nl}}{\Delta}$$

This is equivalent to assume the half-widths of the bands to be also proportional to ε_n. This is a good approximation, since the pure singlet bands $^1\Gamma_3(D)$ are very narrow.

Fig. 2 gives the ratio $\varepsilon_2/\varepsilon_1$ as function of the distance Δ between the two maxima. Further the curve for the function $\frac{a}{1-a}$ with $k\,\zeta_{nl} = 500$ cm^{-1} is given. It is seen to represent the somewhat scattered points reasonably well.

The influence of the second triplet level $^3\Gamma_4(F)$ is important for large values of Δ (over 2 000 cm^{-1}) raising the degree of intermixing. On the other side, the non-vanishing half width for $\alpha \rightarrow 0$ should decrease the position of the right-hand side points.

The statistical distribution of the points of mixed complexes demonstrates that no particular deviation from cubic symmetry is necessary for making $k\zeta_{nl}$ large. Fig. 2 demonstrates also the lower limit of $\Delta = 2\ k\ \zeta_{nl}$. The two bands are actually repulsed from each other by this impenetrable barrier. Mr. C. E. Schäffer [53] has found a similar variation of relative intensities of quartets and doublets with Δ in chromium(III) complexes. Also iridium(III) complexes [38] prove that $k\ \zeta_{nl}$ is rather invariant (= 2 000 cm^{-1}) in so different ions as $IrBr_6^{---}$, $IrCl_6^{---}$, $Ir(NH_3)_5Cl^{++}$, Ir en_3^{+++} but here Δ is nearly constant (= 7 000 cm^{-1}) as function of the crystal field strength, because the singlet and triplet level belong to the same electron configuration [31] of γ_n.

The other singlet levels of nickel(II) give much lower intensities to the bands. Therefore, it is necessary to measure strong solutions of pure complexes, and the detection is often impossible in the ranges of the triplet bands. Besides $^1\Gamma_3$ (D), the two levels $^1\Gamma_5$ (D) and $^1\Gamma_1$ (G) should be the next excited singlets, as discussed by Tanabe and Sugano [54], Ballhausen and Klixbüll Jørgensen [16], and Orgel [49]. $^1\Gamma_3(D)$ and $^1\Gamma_1$ (G) have the configuration $\gamma_5^6\gamma_3^2$ common [31] with the groundstate $^3\Gamma_2$ (F) and thus should produce narrow bands [54,55], while $^1\Gamma_5$ (D) analogous to $^1\Gamma_4$ (G), $^3\Gamma_5$ (F) and $^3\Gamma_4$ (F) in strong crystal fields are $\gamma_5^5\gamma_3^3$ with broader transitions from the groundstate. The concept of a single distribution of electrons in molecular orbitals seems nevertheless to be rather inadequate [50] for the description of a given level (S, Γ_n).

Already Gielessen [56] found a great number of small bands in solid salts of $Ni(H_2O)_6^{++}$. In solutions, small bands are found [49] at 18 400 cm^{-1} and 22 000 cm^{-1}. In Ni en_3^{++}, a weak band can be distinguished at 24 000 cm^{-1} in Ref. 40, Fig. 5. It is not easily decided from the half-widths, which band is the "narrow" $^1\Gamma_1(G)$, but there is some evidence that it is the band at 18 400 cm^{-1} in the hexaaquo ion, contrary to primitive electrostatic calculations [16]. It can interact [1] by intermediate coupling with $^3\Gamma_4$, but not with $^3\Gamma_5$. While most of the absorption bands in Table 1 are very regular, and do not exhibit signs of tetragonal splitting except the fourth band of Ni ata_2^{-4}, there is a tendency of the third band to have a shoulder towards lower wavenumbers (see the half-widths in Ni $en\ gly_2$, Ni enta NH_3^{---}, α-Ni $enta^{---}$, Ni ata gly^{---} and Ni ata^{---}). While this may very well depend on tetragonal splitting and in a few cases be due to presence of more isomers, it is quite suspicious that the phenomenon prevails in a narrow range of the Orgel diagram near $(E_1—E_2)$ = 10 000 cm^{-1}. It cannot be excluded that $^1\Gamma_1$ (G) is going down in the Orgel diagram along a line of the type 23 000 cm^{-1}—1.7 $(E_1—E_2)$.

THE DECREASE OF THE PARAMETERS OF ELECTROSTATIC INTERACTION BETWEEN d-ELECTRONS IN COMPLEXES

For a complex with regularly octahedral configuration, the energy levels can be given in the Orgel diagram as function of the crystal field strength $(E_1—E_2)$. Tanabe and Sugano [54] and Owen [48] emphasized that term differen-

Table 5. Crystal field strength (E_1-E_2) and effective term distances for various nickel(II) complexes. The value of (E_1-E_2) is derived from ν_1 and the energies (^3P) and $\frac{4}{7}$ (^1D) + $\frac{3}{7}$ (^1G) from $\nu_3 + \nu_4$ and ν_2, respectively. In all cases, the values of ν_n from Table 2 are corrected for effects of intermediate coupling (important for ν_1 and ν_2) and for asymmetry of the bands (usually significant for ν_3). Finally are given the calculated and observed values of the perturbation energy ΔE between $^3\Gamma_4$ (F) and $^3\Gamma_4$ (P), as defined p. 908. All the energies are given in the unit cm^{-1}.

Complex	(E_1-E_2)	$(^3P) = 15\,B$	$\frac{4}{7}(^1D)+\frac{3}{7}(^1G)$ $=8B+2C$	ΔE, calc.	ΔE, obs.
Free Ni++	0	16 900	17 900	—	—
$Ni(H_2O)_6$++	8 500	14 100	14 800	1 080	1 000
Niata$^-$	9 500	12 800	13 300	1 690	1 400
a-Nienta^{--}	10 100	13 000	12 700	1 980	1 300
Ni gly_3^-	10 100	13 900	13 100	1 730	1 600
Ni py_6++ (?)	10 200	13 000	13 500	1 910	1 900
Ni enta NH_3^{--}	10 200	13 500	12 700	1 950	1 200
Ni ata_2^{-4}	10 400	13 400	13 000	1 900	1 900
Ni en gly_2	10 700	13 500	12 800	2 060	1 750
$Ni(NH_3)_6$++	10 800	13 400	13 100	2 380	1 950
Ni en_2 gly+	11 300	12 600	12 200	2 460	2 450
Ni tren$(H_2O)_2$++	11 300	11 700	12 000	2 720	2 550
Ni tn_3++	11 400	11 900	12 000	2 640	2 650
Ni en_3++	11 600	12 600	12 000	2 590	2 550
Ni ptn_2++	11 700	12 800	12 000	2 700	2 400
Ni tren$(NH_3)_2$++	11 700	11 300	12 000	3 030	2 900
Ni tren en++	11 700	12 600	11 800	2 720	2 400
Ni tren gly+	11 800	11 500	11 900	2 500	2 500

ces might also change in complexes from the values for the gaseous ion. Thus, it might be necessary to apply more than one parameter in the Orgel diagram. Actually, the agreement with observed absorption bands can be highly improved by the assumption of decreased term distances in the complexes. Especially, the decrease is larger for many anion complexes than for complexes with neutral ligands.

The energy differences between multiplet terms of a given d^n-configuration can be expressed as multipla of the Slater-Condon-Shortley [52] parameters F_2 and F_4. Racah [64] applies the linear combinations $B = F_2 - 5F_4$ and $C = 35F_4$. In nickel(II)complexes, the distance from the ground term ^3F to the other triplet term ^3P is $15B$. Table 5 gives this distance inferred from the diagonal sum rule:

$$\nu_3 + \nu_4 = 3(E_1 - E_2) + (^3P)$$

The wavenumbers ν_3 and ν_4 of the third and fourth absorption band are corrected for asymmetry by taking the average of $\nu_n - \delta(-)$ and $\nu_n + \delta(+)$ from Table 1. It is seen from Table 5 that B actually decreases to ~70 % of the original value, but not as a monotoneous function of $(E_1 - E_2)$. Since three excited triplet levels occur in paramagnetic nickel(II)complexes, it is of interest to see whether the two parameters $(E_1 - E_2)$ and B are sufficient for their description. The two $^3\Gamma_4$ levels have energies, which are the roots E_a and E_b of the secular determinant [49]:

$$\begin{vmatrix} E_{33}-E & E_{34} \\ E_{34} & E_{44}-E \end{vmatrix} = 0$$

with $E_{33} = 0.6\ (E_1-E_2)$; $E_{44} = (^3P)$; and $E_{34} = 0.4\ (E_1-E_2)$.

We define the perturbation energy ΔE by $E_a = E_{33}-\Delta E$ and $E_b = E_{44} + \Delta E$. The observed and calculated values of ΔE are seen to agree except for the ethylenediaminetetraacetate complexes.

Finally, Table 5 gives the values of $\frac{4}{7}(^1D) + \frac{3}{7}(^1G) = 8B + 2C$, which is the asymptotical[16,54] energy of $^1\Gamma_3\ (D)$ above $^3\Gamma_2\ (F)$. The wavenumber ν_2 is corrected for the influence of intermediate coupling. It is seen that C decreases slightly more than B in the complexes. This can be interpreted as an expansion of the 3d-wavefunction into a larger volume. For isomorphous wavefunctions, both F_2 and F_4 are inversely proportional to the average radius; whereas in the case of spreading from, *e. g.*, the concentration on a spherical surface, F_2/F_4 increases with resulting decrease of the ratio C/B. Owen[48] assumes that the decrease of B in complexes is caused by covalent bonding. However, it is not easily decided if this is the only possible explanation. It is interesting to compare nickel(II) with other metal ions. Thus, Schäffer[53] investigates many chromium(III) complexes, where the distance $\sim 12B$ between $^4\Gamma_5\ (F)$ and $^4\Gamma_4\ (P)$ implies values of B in the range 500—750 cm^{-1} while $B = 950\ cm^{-1}$ in Cr^{+++}. The distance $\sim 16B$ between $^1\Gamma_4$ and $^1\Gamma_5$ of cobalt(III) complexes[54] gives slightly smaller values of B. Diamagnetic d^6-systems of the two next transition groups[38] have even smaller values of B: $RhCl_6^{-3}$ has 310 cm^{-1}, $Rh(NH_3)_6^{+++}$ and $Rhen_3^{+++}$ both 400 cm^{-1}, and $IrCl_6^{-3}$ has $B = 250\ cm^{-1}$. On the other hand, manganese(II) complexes have values of B and C, which are not much less than the values for Mn^{++}. Thus, only 7 % decrease is observed[55] in $Mn(H_2O)_6^{++}$ and 11 % in Mn enta^{--}, as will be discussed in the third paper of this series. While it might seem somewhat unsatisfactory to describe four absorption bonds of nickel(II) complexes by three parameters, (E_1-E_2), B, and C, ten bands of manganese(II) can also be described by the three parameters. The crystal field theory can be applied to all d^n-systems, giving a much more unified picture than earlier sharp distinctions between "ionic" and "covalent" complexes.

EXPERIMENTAL

The absorption spectra were measured in the range 800—325 mμ with a Cary recording spectrophotometer at room temperature, 20° C, and in the range 800—1 080 mμ with a Beckman DU spectrophotometer. 1 cm absorption cells were always used, and the measurements in the infra-red performed with a maximum interval of 20 mμ.

1.07 M $Ni(NO_3)_2$ (AnalaR) and 0.050 M $CuSO_4$ were transferred to measuring flasks with a Krogh's 1.00 ml syringe pipette. The ligands were added in solutions from microburettes, and finally diluted with water. In cases of rarer ligands, 10 ml measuring flasks were shown to be sufficiently precise for the measurement of the spectra.

H_4enta (complexon II) and H_3ata (Prof. Schwarzenbach's sample and complexon I) were dissolved in water with 2 and 1.5 moles of Merck's Na_2CO_3 per mole amino-acid, respectively, and diluted.

tren H_3Cl_3, ptn H_3Cl_3 and temeen$_2H_2Cl_2$ were weighed off and dissolved in stoichiometric amounts of NaOH solution.

H gly was dissolved with 1 equiv. of KOH in water.

Dilute solutions of ammonia and ethylenediamine (Merck's No. 946) were titrated. tn and bdn were supplied by Shapley Co. den was purified from the commercial product by fractional distillation and tetren by standing two weeks of the 1 M solution with norite coal, removing the yellow colour. Cu den NH_3^{++} was measured in 0.4 M NH_3 and Ni tetren NH_3^{++} in 1 M and 2 M NH_3.

Redistilled pyridine was kindly furnished by Mr. F. Woldbye.

The concentration of nickel(II) was usually 0.107 M, but more dilute solutions (0.02 M) were made of Ni enta^{--} and addition compounds for measurement of the high first band.

The concentration of copper(II) solutions varied between 0.04 M and 0.01 M.

Acknowledgments. I am very much indebted to Professor Jannik Bjerrum for his interest in the work. Further, I thank Mr. C. E. Schäffer for valuable discussions and information about the analogies with absorption spectra of chromium(III) and cobalt(III) complexes. Finally, I express my gratitude to Professor G. Schwarzenbach, Zürich, for samples of H_2ata, ptnH_3Cl and tren H_3Cl_3, and to Professor Fred Basolo, Northwestern University, Evanston, Illinois, for samples of temeen H_2Cl_2, Ni temeen$_2Cl_2$ and of tren H_3Cl_3, and to Dr. F. G. Mann, Cambridge, for samples of Ni ptn$_2SO_4$ and several tren-complexes presented to this study of energy levels.

REFERENCES

1. Jørgensen, C. Klixbüll *Acta Chem. Scand.* **9** (1955) 1362.
2. Bethe, H. *Ann. Physik* [5] **3** (1929) 133.
3. Mead, A. *Trans. Faraday Soc.* **38** (1934) 1055.
4. Tsuchida, R. *Bull. Chem. Soc. Japan* **13** (1938) 388, 436 and 471.
5. Mathieu, J.-P. *Bull. soc. chim. France* [5] **3** (1935) 463, 476 and **5** (1938) 105.
6. Linhard, M. and Wiegel, M. *Z. anorg. Chem.* **266** (1951) 49.
7. Linhard, M. and Weigel, M. *Z. anorg. Chem.* **264** (1951) 321.
8. Jonassen, H. B., Reeves, R. E. and Segal, L. *J. Am. Chem. Soc.* **77** (1955) 2667 and 2748.
9. Belford, R. L. *Bonding and Spectra of Metal Chelates.* Thesis 1955. University of California UCRL—3051.
10. Basolo, F., Ballhausen, C. J. and Bjerrum, J. *Acta Chem. Scand.* **9** (1955) 810.
11. Jørgensen, C. Klixbüll *Acta Chem. Scand.* **10** (1956) *in press.*
12. Bjerrum, J. *Metal Ammine Formation in Aqueous Solution.* Thesis, Copenhagen 1941.
13. Ballhausen, C. J. *Kgl. Danske Videnskab. Selskab, Mat.-fys. Medd.* **29** (1955) No. 8.
14. Schwarzenbach, G. *Helv. Chim. Acta* **32** (1949) 839.
15. Schwarzenbach, G., Gut, R. and Anderegg, G. *Helv. Chim. Acta* **37** (1954) 937.
16. Ballhausen, C. J. and Jørgensen, C. Klixbüll *Kgl. Danske Videnskab. Selskab, Mat.-fys. Medd.* **29** (1955) No. 14.
17. Schwarzenbach, G. and Biedermann, W. *Helv. Chim. Acta* **31** (1948) 331.
18. Jørgensen, C. Klixbüll *Acta Chem. Scand.* **9** (1955) 405.
19. Cox, E. G. and Webster, K. C. *Z. Kristallogr.* **92** (1935) 478.
20. Jonassen, H. B. and Douglas, B. E. *J. Am. Chem. Soc.* **71** (1949) 4094.
21. Flood, H. and Lorås, V. *Tidsskr. Kjemi, Bergvesen Met.* **6** (1945) 83.
22. Jørgensen, C. Klixbüll and Bjerrum, J. *Acta Chem. Scand.* **9** (1955) 180.
23. Bjerrum, J. and Jørgensen, C. Klixbüll *Rec. trav. chim.* **75** (1956) 658.
24. Schwarzenbach, G. *Helv. Chim. Acta* **35** (1952) 2344.
25. Poulsen, I. and Bjerrum, J. *Acta Chem. Scand.* **9** (1955) 1407.
26. Prue, J. E. and Schwarzenbach, G. *Helv. Chim. Acta* **33** (1950) 995.
27. Basolo, F., Chen, Y. T. and Murmann, R. K. *J. Am. Chem. Soc.* **76** (1954) 956.
28. Jørgensen, C. Klixbüll and Bjerrum, J. *Nature* **175** (1955) 426.
29. Bjerrum, J. and Lamm, C. G. *Acta Chem. Scand.* **4** (1950) 997.
30. Jørgensen, C. Klixbüll *Acta Chem. Scand.* **8** (1954) 1502.
31. Jørgensen, C. Klixbüll *Acta Chem. Scand.* **9** (1955) 116.
32. Bjerrum, J., Ballhausen, C. J. and Jørgensen, C. Klixbüll *Acta Chem. Scand.* **8** (1954) 1275.
33. Jørgensen, C. Klixbüll *Acta Chem. Scand.* **8** (1954) 175.
34. Bjerrum, J., Adamson, A. W. and Bostrup, O. *Acta Chem. Scand.* **10** (1956) 329.

35. Bennett, M. C. and Schmidt, N. O. *Trans. Faraday Soc.* **51** (1955) 1412.
36. Schwarzenbach, G. and Heller, J. *Helv. Chim. Acta* **34** (1951) 576.
37. Duke, F. R. and Courtney, W. G. *J. Phys. Chem.* **56** (1952) 19.
38. Jørgensen, C. Klixbüll *Acta Chem. Scand.* **10** (1956) 500.
39. Pfeiffer, P. and Schmitz, E. *Z. anorg. Chem.* **258** (1949) 247.
40. Jørgensen, C. Klixbüll *Acta Chem. Scand.* **8** (1954) 1495.
41. Ballhausen, C. J. *Kgl. Danske Videnskab. Selskab, Mat.-fys. Medd.* **29** (1954) No. 4.
42. Prue, J. E. and Schwarzenbach, G. *Helv. Chim. Acta* **33** (1950) 963.
43. Adamson, A. W. *J. Am. Chem. Soc.* **76** (1954) 1578.
44. Pestemer, M. and Alslev-Klinker, A. *Z. Elektrochem.* **53** (1949) 387.
45. Polder, D. *Physica* **9** (1942) 709.
46. Ilse, F. E. and Hartmann, H. *Z. physik. Chem.* **197** (1951) 239.
47. Orgel, L. E. *J. Chem. Soc.* **1952** 4756.
48. Owen, J. *Proc. Roy. Soc. London* **227** *A* (1955) 183.
49. Orgel, L. E. *J. Chem. Phys.* **23** (1955) 1004 and 1819.
50. Jørgensen, C. Klixbüll *Acta Chem. Scand.* **10** (1956) 518.
51. Bjerrum, J. *Chem. Revs.* **46** (1950) 381.
52. Condon, E. U. and Shortley, G. H. *Theory of Atomic Spectra.* Cambridge 1953.
53. Schäffer, C. E. *Acta Chem. Scand. To be published.*
54. Tanabe, Y. and Sugano, S. *J. Phys. Soc. Japan* **9** (1954) 753 and 766.
55. Orgel, L. E. *J. Chem. Phys.* **23** (1955) 1824 and 1958.
56. Gielessen, J. *Ann. Physik* [5] **22** (1935) 537.
57. Russell, C. D., Cooper, G. R. and Vosburgh, W. G. *J. Am. Chem. Soc.* **65** (1943) 1301.
58. Plumb, R. C., Martell, A. E. and Bersworth, F. C. *J. Phys. Chem.* **54** (1950) 1208.
59. Schwarzenbach, G. and Freitag, E. *Helv. Chim. Acta* **34** (1951) 1492.
60. Schwarzenbach, G., Ackermann, H., Maissen, B. and Anderegg, G. *Helv. Chim. Acta* **35** (1952) 2337.
61. Schwarzenbach, G. and Ackermann, H. *Helv. Chim. Acta* **30** (1947) 1798.
62. Bjerrum, J. *Tables of Complexity Constants . . . (In press).*
63. Schwarzenbach, G., Anderegg, G., Schneider, W. and Senn, H. *Helv. Chim. Acta* **38** (1955) 1147.
64. Racah, G. *Phys. Rev.* **62** (1942) 438.
65. Mann, F. G. and Pope, W. J. *J. Chem. Soc.* **1926** 2675 and 2681.
66. Mann, F. G. *Symposium on Co-ordination Chemistry.* Copenhagen 1953, p. 71.
67. Haendler, H. M. *J. Am. Chem. Soc.* **64** (1942) 686.

Received March 2, 1956.

ACTA CHEMICA SCANDINAVICA 10 (1956) 911—916

Chromatographic Separation of Anomeric Glycosides

III. Crystalline Methylfuranosides of L-Fucose, D-Ribose, and L-Rhamnose

INGVALD AUGESTAD and ENDRE BERNER

Universitetets Kjemiske Institutt, Blindern-Oslo, Norway

Three crystalline methylfuranosides of L-fucose, D-ribose, and L-rhamnose, respectively, have been prepared by column chromatography. The rates of hydrolysis of these and some previously prepared furanosides have been measured at 20° in N hydrochloric acid. The rule seems to exist that furanosides having *cis*-configuration at C_1 and C_2 are more easily hydrolyzed than the anomeric forms with *trans*-configuration.

Since the publication of part II [1] of this series Watkins [2] has described the isolation of crystalline α-methyl-L-fucofuranoside. Already before his publication appeared we had obtained the same crystalline fucoside, but although our results agree with those of Watkins we find it appropriate to include them here. Barker and Smith [3] have described the chromatographic separation on a column of "Solkafloc" of the four isomeric methyl-D-ribosides, but they did not obtain any of the furanosides in the crystalline state. Using a similar procedure as described in part II of this series we succeeded in isolating the crystalline β-methyl-D-ribofuranoside. By the same method we have also prepared the crystalline α-methyl-L-rhamnofuranoside. The melting points and rotations of the new crystalline furanosides are as follows:

α-Methyl-L-fucofuranoside	M.p.	126°	$[\alpha]_D^{20}$	−111.4° (in water)
β-Methyl-D-ribofuranoside	"	80°	"	− 49.8° "
α-Methyl-L-rhamnofuranoside	"	62°	"	− 98.6° "

The rates of hydrolysis of the furanosides in N hydrochloric acid at 20° have been calculated from measurements of free sugar. As the rates of hydrolysis given in part II were measured only at room temperature we have redetermined them at exactly 20°. For comparison the rates of hydrolysis of a few other methylfuranosides have been included. The results are collected in

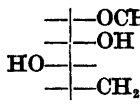
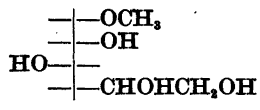
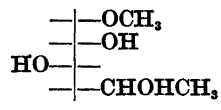
Table 1 in which the rate constants are calculated from the equation $k = 1/t \cdot \ln(a/a—x)$ with time in minutes. As some authors, *e. g.* Riiber and Sørensen [4] and Isbell and Frush [5] have calculated the rates of hydrolysis of glycosides from the equation $k_{10} = 1/t \log (a/a—x)$, we have also given the figures for k_{10}.

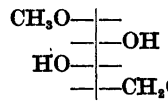
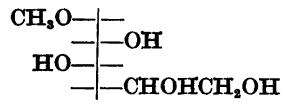
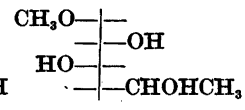
Table 1. Rates of hydrolysis in N HCl at 20°.

	$[\alpha]_D^{20}$	k	k_{10}	Half life
β-Methyl-D-ribofuranoside	−49.8°	0.0067	0.0029	1 h 44 m
α-Methyl-L-rhamnofuranoside	−98.6°	0.00050	0.00022	23 » 6 »
α-Methyl-D-xylofuranoside	+182°	0.0128	0.0056	0 » 54 »
β- » »	−89°	0.0075	0.0033	1 » 32 »
α-Methyl-L-arabofuranoside	−127°	0.000206	0.000089	56 » 5 »
β- » »	+118°	0.00140	0.00061	8 » 15 »
α-Methyl-D-arabofuranoside	+128°	0.000206	0.000089	56 » 5 »
β- » »	−119°	0.00120	0.00052	9 » 38 »
α-Methyl-D-galactofuranoside	+104°	0.00104	0.00045	11 » 7 »
β- » »	−112°	0.000123	0.000053	93 » 55 »
α-Methyl-L-fucofuranoside	−111.4°	0.00049	0.00021	23 » 35 »
β- » » (syrup)	+113°	0.00015	0.000065	76 » 50 »

As the ring in the furanosides is most probably plane a relationship between configuration and physical constants is more likely to be found for these glycosides than in the case of the pyranosides in which the six-membered ring may have different conformations (see, *e. g.*, the discussion recently by Edward [6]). In the following consideration of this question we have, besides our own experimental data, made use of the figures for rotation and hydrolysis of the α- and β-ethyl-D-glucofuranosides determined by Haworth, Porter, and Waine [7]. Their values for k were measured at 55—60° in 0.01 N hydrochloric acid.

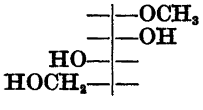
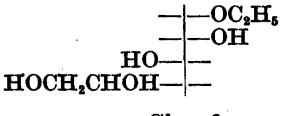
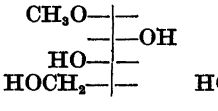
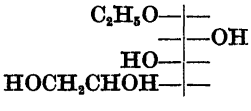
Using the periodic oxidation method Jackson and Hudson [8] have shown that, in the case of the methylpyranosides of aldopentoses and aldohexoses, the α-forms of D-sugars in all cases investigated have the same configuration at C_1, *viz.* the methoxyl group falling to the right in the conventional projection formulae. In a single case they oxidized a furanoside, *viz.* α-methyl-D-arabofuranoside, and found that also this glycoside had the same configuration at C_1 as the α-pyranosides. Assuming now that this hold for the other α-furanosides as well, it will be seen from the simplified projection formulae below that the anomeric form having *cis*-configuration at C_1 and C_2 always is more easily hydrolyzed than the corresponding anomer with *trans*-configuration. In the case of D-fucose it is assumed that enanthiomeric glycosides have the same rate of hydrolysis and that their optical rotations differ in sign only. The molecular rotation given are calculated in the usual way as one hundreth of the product of specific rotation and molecular weight.

			
	β-L-Arabofurano-side	α-D-Galactofurano-side	α-D-Fucofurano-side
$[M]_D$	+194°	+202°	+198°
$k^{20°}$	0.00140	0.00104	0.00049

			
	α-L-Arabofurano-side	β-D-Galactofurano-side	β-D-Fucofurano-side
$[M]_D$	−209°	−218°	−201°
$k^{20°}$	0.000206	0.000123	0.00015

The molecular rotations of the configurationally corresponding methylosides of the three sugars are as will be seen very nearly the same, indicating that the influence on the optical rotation of the size of the substituent at C_4 is insignificant.

In the case of the methyl-D-xylo- and the ethyl-D-glucofuranosides again the anomers having *cis*-configuration at C_1 and C_2 are hydrolyzed more easily than those with *trans*-configurations, although the ratio *cis*:*trans* is considerably less than by the three sugars above. The latter fact might be due to the different configuration at C_4. In the case of D-xylose and D-glucose the furanosides which are more easily hydrolyzed have *trans*-configurations of the substituents at C_1 and C_4, while in the case of the three other sugars the more easily hydrolyzable furanosides have the groups at C_1 and C_4 in *cis*-position.

				
	α-D-Xylofuran-oside	α-D-Glucofuran-oside	β-D-Xylofuran-oside	β-D-Glucofuran-oside
$[M]_D$	+299°	+210°	−146°	−179°
$k^{20°}$	0.0128	$k^{60°}$ 0.0230	$k^{20°}$ 0.0075	$k^{60°}$ 0.0124

The experimental material is still too small for a further discussion of these questions, and it must be hoped that additional data will soon be available.

Added in proof: The α- and β-methyl-D-mannofuranosides have been isolated by means of column chromatography, the β-form, however, only as a syrup. The rates of hydrolysis in N hydrochloric acid at 20° were found to be in agreement with the results in the case of the other anomeric furanosides described above: α-Methyl-D-mannofuranoside, m. p. 120°, $[\alpha]_D^{20} = +109°$, $k = 0.000327$ ($k_{10} = 0.000142$), half life 35 h 21 m. β-Methyl-D-mannofuranoside (syrup) $[\alpha]_D^{20} = -86.5°$, $k = 0.00471$ ($k_{10} = 0.00205$), half life 2 h 27 m.

EXPERIMENTAL

Methyl-L-fucofuranosides

Watkins [2] using the method described by us succeeded in preparing crystalline α-methyl-L-fucofuranoside with m. p. 125—126° and $[\alpha]_D$ −108° (c = 2 in water). The corresponding β-furanoside was obtained as a clear syrup with $[\alpha]_D$ +113°.

In the present case a 2 % solution of L-fucose in methanol containing 0.014 % HCl (0.0039 N) was refluxed for 2 hours. After removing the hydrogen chloride with silver carbonate the solution was evaporated to a syrup. On leaving the syrup from 3.1 g fucose in a vacuum desiccator for a week some crystalline material (0.37 g) had separated which was found to be α-methyl-L-fucopyranoside having m. p. 156° and $[\alpha]_D$ −190° (water). This separation of the α-pyranoside was found to be advantageous for the subsequent separation on the cellulose column. As mobile phase was used a mixture of butanol-1, methyl ethyl ketone, and water (1:1:1) and the effluent was collected automatically in tubes. At certain intervals paper chromatograms were run (using methyl ethyl ketone saturated with water) in order to check the degree of separation. The pyranosides necessary for this purpose were prepared according to Minsaas [9]. The tubes 1—19 contained only β-furanoside, and the solution on evaporation gave a clear syrup (1.08 g) which has not yet crystallized; $[\alpha]_D^{20}$ +113° (c = 2 in water). From the tubes 28—39 was obtained the pure α-methyl-L-fucofuranoside (0.5 g) which recrystallized from ethyl acetate had m. p. 126° and $[\alpha]_D^{20}$ −111.4° (c = 3 in water). (Found: C 47.33; H 7.71. Calc. for $C_7H_{14}O_5$: C 47.19; H 7.92.)

β-Methyl-D-ribofuranoside

Barker and Smith [3] prepared a mixture of the four ribosides by treatment of ribose at room temperature with methanol containing 1 % hydrogen chloride. The separation of the ribosides was effected on a column of cellulose using butanol-water as eluant. The ribosides finally distilled in a high vacuum were obtained as syrups except in the case of the β-pyranoside which had also previously been prepared in the crystalline state.

In the present investigation a syrup rich in furanosides was obtained by refluxing for 70 min. a methanolic solution containing 2.6 % D-ribose and 0.0108 % HCl (0.003 N). Under these conditions the sugar was transformed completely into glycosides. After removing the hydrogen chloride in the usual way and evaporating the methanol a clear syrup was obtained. The syrup (4.04 g) dissolved in a small quantity of the eluant was placed on top of a column of powdered cellulose and eluted with a mixture of ethyl acetate, propanol-1, and water (5:3:2) which left the column at a rate of 28 ml per min, 7 ml being collected in each tube. The following fractions were obtained:

Fraction	Tube No.	Weight
A	2—12	1.44 g
B	13—18	1.30 »
C	19—25	0.73 »
D	26—46	0.40 »
		3.87 g (95 % recovered)

On a new column, using butanol-1 saturated with water as eluant, fraction A was separated into two fractions A_1 and A_2 of 0.73 and 0.57 g respectively. Fraction A_1 was dissolved in 30 ml dry ethyl acetate, treated for one hour at room temperature with charcoal, filtered and then 25 ml of the solvent was removed by distillation. After the concentrated solution had been kept for a few days above calcium chloride at −20° the β-methyl-D-ribofuranoside had crystallized. On inoculating A_2 with the new crystalline riboside also this fraction crystallized. Fractions B and C were each fractionated a second time on cellulose columns, using butanol-1 saturated with water as eluant. In both cases

the first fractions on inoculation gave some crystalline β-furanoside. The yield of crystalline β-furanoside was in all 2.34 g (58 %). After recrystallization from ethyl acetate, m. p. 80° and $[\alpha]_D^{20}$ −49.8° (c = 4.2 in water).

The second fractions of B and C had the specific rotations +100° and +121°, respectively, but the quantities were too small for further treatment.

α-Methyl-L-rhamnofuranoside

Of the L-rhamnosides the α- and β-pyranosides have been known in the crystalline state since the days of Emil Fischer. They also represent the pair of anomeric glycosides which was for the first time separated by a chromatographic method; see Hough, Jones, and Wadman [10]. In the present case a mixture of methylrhamnosides rich in furanosides was prepared by refluxing for 4 1/2 hours a solution of anhydrous L-rhamnose (10 g) in methanol (500 ml) containing 0.02 % hydrogen chloride (0.0055 N). After treatment first with lead carbonate and then with silver carbonate the solvent was evaporated at room temperature. The syrup was redissolved in some methanol and shaken with charcoal in order to remove traces of colloidal silver. Finally the filtered clear solution on evaporation in a vacuum above calcium chloride gave a syrup with $[\alpha]_D$ −39° (in water).

The first fractionation of the syrup (10 g) was carried out on three columns of powdered cellulose, each loaded with about 3 g. The eluant was a mixture of butanol-1, ethyl acetate, and water (7:5:2) and the general procedure by the separation as described before. As an example may serve the fractionation in one of the columns:

Fraction	Tube No.	Weight
A	1—15	1.92 g
B	16—20	0.27 »
C	21—25	0.15 »
D	36—60	0.29 »
E	61—71	0.07 »

Paper chromatograms showed that A contained mainly α-furanoside, and actually the tubes 1—6 from one of the columns on evaporation gave a syrup which crystallized spontaneously. In order to achieve a better separation the rest of fraction A from the same column and the whole of the fractions A from the other two columns were put together and the syrup obtained from them fractionated for a second time on a column. The new first fraction (AII) together with the above tubes 1—6 gave 3.05 g which were dissolved in ethyl acetate (20 ml), treated with charcoal and filtered. After distilling off half of the solvent the solution was placed at −20° overnight and then inoculated whereby the glycoside separated in crystals. On recrystallization from benzene this new α-methyl-L-rhamnofuranoside was obtained in needles with m. p. 62° and $[\alpha]_D^{18}$ −98.6° (c = 3.8 in water). A paper chromatogram gave a single spot only.

The fractions B and C from the first and BII and CII from the second fractionation contained mixtures of the other rhamnosides. The fractions D were rich in β-pyranoside and on evaporation crystallized partly. In order to obtain more of the β-pyranoside all fractions B and C were collected and their content subjected to a new fractionation. The β-methyl-L-rhamnopyranoside thus isolated was recrystallized from ethyl acetate and obtained in needles with m. p. 138° and $[\alpha]_D^{22}$ +96.4° (c = 2.2 in water). On the paper chromatogram a single spot only appeared.

REFERENCES

1. Augestad, I. and Berner, E. *Acta Chem. Scand.* **8** (1954) 251.
2. Watkins, W. M. *J. Chem. Soc.* **1955** 2054.
3. Barker, G. R. and Smith, D. C. C. *J. Chem. Soc.* **1954** 2151.
4. Riiber, C. N., and Sørensen, N. A. *Kgl. Norske Videnskab. Selskabs Skrifter* **1938**, No. 1.

5. Isbell, H. S. and Frush, H. L. *J. Research Natl. Bur. Standards* **24** (1940) 125.
6. Edward, J. T. *Chemistry & Industry* **1955** 1102.
7. Haworth, W. N., Porter, C. R. and Waine, A. C. *J. Chem. Soc.* **1932** 2257.
8. Jackson, E. L. and Hudson, C. S. *J. Am. Chem. Soc.* **59** (1937) 994.
9. Minsaas, J. *Rec. trav. chim.* **51** (1932) 475.
10. Hough, L., Jones, J. K. N. and Wadman, W. H. *J. Chem. Soc.* **1950** 1702.

Received March 10, 1956.

ACTA CHEMICA SCANDINAVICA 10 (1956) 917—927

On Vitamins in Sewage Sludge

IV. Isolation of New Vitamin B_{12}-like Factors

HALINA Y. NEUJAHR

Royal Institute of Technology, Division of Food Chemistry, Stockholm, Sweden

Of eleven vitamin B_{12}-like factors isolated from digested sewage sludge three behave as nucleotide-containing compounds and show considerable activity towards *Ochromonas malhamensis*. One of them (the most abundant) has been identified as cyanocobalamin, another may be identical with Factor III (Bernhauer) but the third has not, as yet, been identified with any known factor.

Eight of the isolated factors show behaviour typical of the factors lacking a nucleotide component. Three of them have considerable activity towards *E. coli* and one of these factors has been identified as factor B; the other two, or at least one of them, are probably identical with factor C. The microbiological activity of the remaining five factors is practically negligible.

Some properties of the isolated factors are given, and their behaviour during the isolation process discussed.

The abundance and variety of known vitamin B_{12}-like factors has increased considerably during the last two years. In particular, faecal sources — raw faeces of different animals and treated sewage sludges — have been found to contain many new factors suggesting that hitherto unknown forms of this vitamin may occur in nature..

At the same time there arose the problem of a rational method of nomenclature. At present several authors use individual systems of their own invention when describing factors isolated by them — a fact which complicates the naming of new factors when isolated by other workers. In previous work on vitamin B_{12}-activity in sewage sludge [1–3] the present author adapted the terminology of the Reading-[4–7] and Glaxo-[8,9] groups, and of Pfiffner *et al.*[10] who isolated a series of vitamin B_{12}-like factors from the faeces and rumen contents of certain ruminants. The factors found in sewage sludge (in addition to cyanocobalamin) were designated A, B, C, (C_1 and C_2) and pseudovitamin B_{12} after their identification by bioautography and paper electrophoresis with samples of the respective factors kindly provided by the above mentioned authors. Such identification was in most cases performed on crude sludge extracts or concentrates.

Armitage and co-workers [11] have described two series of vitamin B_{12}-like factors obtained by the hydrolytic cleavage of cyanocobalamin and have shown that those factors lacking a nucleotide component form stable *violet* * dicyanocomplexes at pH 6.5, while those containing a nucleotide component factors yield *red* monocyanocomplexes at this pH. Bernhauer and co-workers [12,13] have used this property and have characterized factors isolated from sewage sludge as "complete" (containing nucleotide) or "incomplete" (lacking nucleotide). Among several vitamin B_{12}-like factors isolated by them from sewage sludge was the previously unknown Factor III ("complete") which was later shown by two independent groups [14,15] to differ from cyanocobalamin in containing 5(6)-hydroxybenzimidazole instead of 5,6-dimethyl-benzimidazole. Bernhauer and co-workers [12] have also isolated from sewage sludge a substance, originally called "Factor V", which on electrophoresis was resolved into five different factors ** corresponding to the five nucleotide-lacking carboxylic acids described by Armitage *et al.*[11] (*cf.* Bernhauer [12]).

From portions of digested sewage sludge totalling 100 l (containing 10 % dry solids) 11 vitamin B_{12}-like factors of which three are red and eight violet in the presence of cyanide at pH 6.5, have now been isolated together with an orange substance of similar R_F-value to the slow moving vitamin B_{12}-like factors. Thus repeated chromatographic and electrophoretic separations have shown "factor A + pseudovitamin B_{12}"[1-3] to be a mixture of six factors with R_F-values close to those of factor A and pseudovitamin B_{12} but differing in their microbiological activities and spectrophotometric characteristics. Since most of these substances have not, as yet, been identified with known factors they may be conveniently described as: factor B, cyanocobalamin, factors V and W, factors X1, X2, X3 and X4, factors Z1, Z2, Z3, and factor Y which is not, however, a vitamin B_{12} factor. The investigation of the nature of these factors is continued with a view to their identification with similar substances isolated from other sources. Factor Z3 appears to be identical with factor C [6,7]. In the earlier stages of purification by chromatography, it behaved as factor C_2[1,2] (or B_{12s} [18,19]), while after numerous chromatographic and electrophoretic separations its behaviour changed to that of factor C_1[1,2].

EXPERIMENTAL

Isolation of factors

2–3 l portions of digested sludge (10 % total solids) were diluted (4:1) with water boiled at pH 6 for 15 min. in the presence of KCN (100 mg/l) and centrifuged. The combined supernatants (1 % total solids) were subjected to absorption on activated charcoal (Norit. 2 % w/v) at pH 6 and 3° C for 2 hours in 10 l portions. The charcoal suspension (together with 2 % w/v filteraid (Hyflo-Super Cel)) was removed by filtration through

* The term "violet" as used in this paper corresponds to the term "purple" used by the above mentioned authors.

** The electrophoretic separation of these factors was performed by the author in Professor Bernhauers laboratory, using the two zone electrophoresis apparatus described by Flodin [16] and Carlsson [17].

filteraid layers of 2—3 cm thickness in large Büchner funnels and then washed with a 5 % (w/v) solution of phenol in water. Considerable amounts of brown impurities, but negligible amounts of vitamin B_{12}-active material, were removed by the washing. Every filtercake was washed with 2—3 l of the phenolic solution. The washed filtercakes were boiled for 5 minutes under reflux with a volume of 70 % ethyl alcohol equal to about four times that of the filtercake and quickly filtered. This operation was repeated four times. The filtrates were cooled rapidly and the alcohol distilled *in vacuo*. The remaining liquid was concentrated by further evaporation *in vacuo* and the precipitated material was removed by filtration at 80° C with some filteraid. The red-brown liquid was then extracted with an equal volume of *iso*propanol containing 30 % $(NH_4)_2SO_4$ and the emulsions and precipitates formed were reextracted until the solution was only very slightly coloured and showed negligible vitamin B_{12} activity. The combined purple extracts were concentrated *in vacuo* in order to remove *iso*propanol and about half the water and the concentrate was subjected to a series of extractions with *p*-chlorophenol solutions the vitamin B_{12} activity being finally precipitated on kieselguhr as described by Bernhauer [12]. Each extraction was repeated until the red material passed completely into the extracting phase and until microbiological tests (mainly cup plate assay with *E. coli* 113—3) showed the almost total absence of vitamin B_{12} activity in the extracted phase. In some cases as many as 10—15 extractions were necessary.

For the final stages of purification and separation of the different factors the vitamin B_{12} preparation was subjected to partition chromatography on cellulose powder columns and on Whatman 3MM filterpaper using, as solvents, water saturated *sec.* and *n*-butanols containing 0.01 % KCN and saturated with $KClO_4$ [20]. The height of the columns varied between 8—12 cm; the filter paper sheets were 50 cm long and 20 cm broad.

Although in earlier experiments the vitamin B_{12} material was dissolved in few ml of the eluting solvent and applied directly to the top of the column it was later found more convenient to apply the kieselguhr concentrate itself as described by Friedrich and Bernhauer [20].

The first stage of chromatography was performed with *sec.* butanol on cellulose columns when the vitamin B_{12} material resolved into four bands. The fastest, a violet band (I), was followed by a red band (II) which in turn was followed by a very slow violet band (III) and another, almost immobile, violet band (IV). The degree of separation was poor and considerable amounts of yellow and brown impurities could be seen in the column moving both faster than (I) and as slow as or slower than (IV). The kieselguhr layer on the top of the column retained a large amount of brown immobile material. Although (I) and (II) could easily be eluted and collected in two distinctly separated fractions the bands (III) and (IV) could not be eluted even after an extended period of time. The cellulose column was then extruded and the two violet bands cut off, extracted with water, evaporated to small volumes in *vacuo* and the vitamin B_{12} activity precipitated on kieselguhr as before. The remainder of the column including the kieselguhr layer was cut in sections and analyzed for vitamin B_{12} activity. Only that extract corresponding to the top of the column, including the kieselguhr layer, contained noteworthy amounts of vitamin B_{12}-activity. This extract was evaporated to dryness and rechromatographed several times on thick Whatman paper using, respectively, *sec.* and *n*-butanol but the separation of the vitamin B_{12} activity from the yellow and brown impurities was not successful (*cf.* p. 926). The four kieselguhr preparations were then rechromatographed on cellulose columns with *n*-butanol. All four preparations contained besides the main band smaller amounts of the three other bands and of brown or yellow impurities which could be separated from the vitamin B_{12}-active substances; (III) divided into two poorly separated violet bands (IIIa) and (IIIb). Again (I) and (II) could be easily eluted, while (IIIa), (IIIb) and (IV) were cut from the columns and treated as before. After repeated precipitation on kieselguhr the five fractions were rechromatographed on cellulose columns using *n*-butanol for (I), (II) and (IIIa) and *sec.* butanol for (IIIb) and (IV). After this third fractionation (I) appeared to have divided into two bands, one of which was a weak violet, faster-moving band (Ia) poorly separated from the main violet band (I). Fraction Ia was collected but could not be thoroughly investigated due to an accident. Its R_F value (relative to that of cyanocobalamin) was about 1.5 while the corresponding R_F-value of (I) was 1.35 and on mixed bioautograms the two fractions appeared as distinct zones. In the following, fraction Ia will be referred to as factor B1. When fraction (I) was again chromatographed on thick Whatman paper with *n*-butanol it appeared as a

single violet band free of yellow impurities. Ionophoretic test confirmed the homogeneity of the fraction but an attempt to crystallize it from aqueous acetone gave only a precipitate. It could be identified by bioautography and paper electrophoresis as factor B, its other properties can be seen in Tables 1 and 2 referred to as factor B.

Fraction II appeared as a distint single red band on the column but to ensure its purity it was rechromatographed on thick Whatman paper with *n*-butanol. It was then crystallized from aqueous acetone and identified as cyanocobalamin.

Fraction (IIIa) appeared as a broad violet band which could be removed from the column only by protracted elution. Spectrophotometric measurements of the eluate fractions indicated the presence of three different factors in this band but repeated chromatography on thick Whatman paper did not lead to a satisfactory separation. On paper electrophoresis at pH 3.0 (0.5 N HAc containing 0.01 % KCN) the mixture separated into three zones: one basic (X2), one neutral (W) and one strongly acidic (X1). The degree of separation of zones X2 and W was not quite satisfactory but could be improved by electrophoresis at pH 6.5 (phosphate, $\mu = 0.1$). The three factors thus obtained were rechromatographed on thick Whatman paper with *n*-butanol. Factor W appeared as a single distinct red band, while factors X1 and X2 moved as violet zones. Considerable amounts of factor B separated from each of these two latter factors.

Fraction IIIb appeared on the column as a broad violet band. Spectrophotometric measurements of the eluate fractions gave no indication of its heterogeneity but to ensure its purity it was rechromatographed on thick Whatman paper with *n*-butanol. After a considerable time it appeared to separate into three very close zones but a satisfactory separation of the factors could not be obtained. Paper electrophoresis of the mixture at pH 3.0 led to separation into one neutral (V) and two basic zones (X3 and X4) and the three factors were rechromatographed on thick Whatman paper with *n*-butanol. Factor V gave a single, rather wide pink zone while factors X3 and X4 appeared as distinct violet bands. As in the case of the factors isolated from (IIIa) considerable amounts of factor B could be separated from factors X3 and X4 during this final purification.

Fraction (IV) appeared on the column as a very broad violet band and the presence of several factors was confirmed by spectrophotometric measurements of the eluate fractions. The degree of separation was very poor and the band appeared to contain considerable amounts of yellow substances. Paper-electrophoresis at pH 6.5 followed three times by chromatography on thick Whatman paper with *n*-butanol resulted in the isolation of three violet factors (Z1, Z2 and Z3) and one orange factor (Y). Again, considerable amounts of factor B could be separated at the same time.

All chromatographically pure factors were tested for their homogeneity by paper electrophoresis and further purified in that way if necessary. Attempts to crystallize the isolated factors were unsuccessful except in the case of cyanocobalamin. The amounts isolated were in most cases too small to be weighed and they are listed in Table 2 on the basis of the optical density of their solutions. The factors were desalted and kept in 70 % EtOH at $-20°$ C.

Characterization of factors

Absorption spectra. For determination of spectra appropriate amounts of the alcoholic solutions were evaporated to dryness and dissolved in 5 ml water. 1 drop of 0.1 % KCN solution was added and the pH adjusted to 6.5 with HAc or NH_4OH; in most cases these additions were negligible. The pH of the solution was also measured after each determination and in no case did the pH change exceed 0.2 pH units. The measurements were performed on a Beckman Spectrophotometer Model DU. Although the spectrophotometric data on the non-crystalline factors listed in Table 2 must be taken with reserve, it is hoped that they can help to elucidate the relationships between these factors and those previously identified.

Partition coefficients were determined in the solvent pair 20 % *p*-chlorophenol in trichloroethylene-water. The amount of vitamin B_{12}-like factor in each phase was measured spectrophotometrically.

Paper electrophoresis was performed with two buffer systems; at pH 3 with HAc and at pH 6.5 with $K_2HPO_4-KH_2PO_4$, both containing 0.01 % KCN and having an ionic strenght of 0.1. Voltage gradients of 10 V/cm at $+4°$ C during 18 hours were standard experimental conditions using LKB Paper Electrophoresis Apparatus Type 3276 B.

Both the bioautographic technique using *E. coli* 113—3 and the technique with visible spots were used in detection.

Microbiological tests were performed with *E. coli* 113—3 in both cup plate and tube assays and with *Ochromonas malhamensis*. Using Ford's technique most tests were repeated on 3—5 different days and the values listed in Table 2 are averages of all determinations. The microbiological potency of the factors is calculated on the basis of the optical density of their solutions at λ = 361 mμ for the red and at λ = 367 mμ for the violet factors.

Bioautography was used to determine the R_F-values of the factors and in certain cases visible spots were chromatographed for comparison. Chromatograms (descending technique) were run for 48 h at 21° C in water-saturated *sec.* butanol containing 3 % HAc and 0.01 KCN, and developed on *E. coli* 113—3 plates; authentic specimens were run as standards. The R_F-values listed in Table 1 are calculated in relation to that of cyanocobalamin and will be referred to as R_c-values. Mixtures of known and unknown factors as well as of groups of unknown factors were chromatographed but usually little information was obtained regarding the relationships between different factors (Table 1). The R_c-values appeared to be influenced by the impurities present in the samples and usually increased with the degree of purity.

RESULTS AND DISCUSSION

The factors isolated are listed in Table 1 and are grouped vertically according to their ability to form violet (di)cyano complexes at neutral pH, and horizontally according to their R_c-values. The horizontal arrangement yields four main groups (left column in Table 1), with R_c-values 1.6—1.3 (I), 1.0 (II), 0.7—0.6 (III) and 0.5—0.4 (IV), respectively. The R_c-values of the factors within each group have been determined at least six times in each case giving variations of up to $\pm$0.05. Although the values listed in Table 1 agree

Table 1. Vitamin B_{12} factors isolated from sewage sludge. (Behaviour at pH 6.5 in the presence of CN^-.)

Group of factors	R_c * interval	Red factors	R_c *	Violet factors	R_c *	Other factors not yet defined	R_c *	Known (unisolated) factors	R_c *
I	1.6—1.3	—	—	factor B	1.35	factor B1 ** red or violet?	ca 1.5	factor B	1.4
II	1.0	cyanocobalamin	1.00	—	—	—	—	cyanocobalamin	1.0
a	(0.70—0.65)	W	0.69	X1	0.67	—	—	"factor A	
				X2	0.66	—	—	+pseudo-	0.7
III	0.7—0.6							vitamin	
				X3	0.62	—	—	B_{12}"	
b	(0.65—0.60)	V	0.61	X4	0.60	—	—		
				Z1	0.46	Y(orange)	0.46	factor $C_{(1)}$	0.4
IV	0.5—0.4	—	—	Z2	0.43				
				Z3	0.40			factor $C_{(2)}$	0.0

* $R_c = \frac{R_F \text{ of factor}}{R_F \text{ of cyanocobalamin}}$; solvent system: water-saturated *sec.* butanol + 3 % HAc + 0.01 % KCN, 48 h, descending technique.

** This factor could be found in many sludge preparations. No further investigation has, however, been made.

Table 2. Some properties of Vita-

Factor *	Physical properties			
	Absorption maxima	Points of inflexion	Electrophoretic behaviour	
	H_2O, pH 6.5, in presence of CN^-		pH 3.0	pH 6.5
cyanoco-balamin	278 (306 323) 361 (523) 550. —	—	neutral	slightly acidic
W	278 — — 361 — 550 —	288 410 526	neutral	slightly basic (>factor A)
V	275 — — 361 — 550 —	—	neutral	slightly basic (<W)
B	278 (306) — 368 — 540 580	—	basic	neutral
X1	? — — 366 — 540 580	350 440	strongly acidic	slightly acidic
X2	277 — — 366 — 540 —	300	basic	slightly acidic (<X1)
X3	— — — 367 — 540 580	270 300	basic(<B)	slightly acidic (>X1)
X4	277 (305) — 367 — 540 580	350 415 510	basic ≈B)	acidic(≈X3)
Z1	— — — 368 — 540 580	512	basic(≈X4)	acidic(≈X4)
Z2	276 (304) — 368 — 540 580	350 415	basic(<Z1)	acidic(>Z1)
Z3	280 — — 367 — 540 580	512	neutral	acidic(<Z1)
Y	264 — — — — — —	530		

* for the corresponding R_c values see Table 1.

** $C_W/C = \frac{\text{concentration of the factor in water phase}}{\text{concentration of the factor in solvent phase}}$
solvent: 20 % *p*-chlorophenol in trichloroethylene.

fairly well with the order in which the factors moved on chromatograms during the isolation procedure (*cf.* p. 920) it is evident that R_c-values are of limited use in the characterization of these factors unless they are well differentiated. It is possible that group III can be divided into two subgroups with R_c-values 0.70—0.65 (IIIb), respectively.

Some properties of these factors are listed in Table 2. The four main groups (left column in Table 1) are in full agreement with earlier findings [1] (*cf.* right column in Table 1) except in the case of "factor C_2".

Factors "Z". The presence in sewage sludge of a virtually immobile B_{12}-like factor ($R_c = 0.0$) has been noted in this laboratory before [1-3]. In the present isolation experiment such a factor was detected by bioautography in the original sludge and after repeated purification by chromatography it appeared as a very distinct, immobile, violet band at the top of the column (*cf.* p. 919). Its behaviour was similar to that of "factor C_2" or B_{12a} [18,19] and was unchanged after being twice chromatographed on

min B_{12} factors from sewage sludge.

Partition coefficients Cw/Cs **		Microbiological activities *** $\frac{\mu g}{D}$			Identified as	Amount isolated from 100 l sludge, ml of a soln. of optic dens.	
		Escherichia coli 113—3		*Ochromonas malhamensis*			
CN^-	no CN^-	plate assay	tube assay	tube assay			
		49	49	49	cyanocobalamin	40 mg	
1.5	1.0	300	50	25		10	1.0
		50	45	20	Factor III?	10	0.9
		200	25	1	factor B ††	10 mg	
		10—50†	1—3†	2		3	0.4
1.5	1.0	10—50†	5—50†	4		3	0.8
2.5	0.5	10—80†	5—50†	1		3	0.8
3.0	0.5	15	5	0		25	7.0
4.5	2.0	5—15†	0.2—2†	0		25	0.9
1.5	1.0	100—200†	15—45†	0		25	0.5
		100—500†	10—300†	0	factor C?		
		traces	traces				

*** Calculated as cyanocobalamin on the basis of optical densities of the solutions

$\frac{\mu g}{D}$ {at 361 mμ for red factors / at 367 mμ for violet factors} {Beckman spectrophotometer Modell DU

† non linear response

†† by chromatography, electrophoresis and spectra

cellulose powder columns although there was then some indication that this factor was, in fact, not homogeneous. After further chromatography (on thick Whatman paper) and electrophoresis this factor could be separated into three violet factors (Z1, Z2, Z3) and one orange factor (Y), all of which had R_c values within the range 0.5—0.4. This R_c range corresponds to "factor C_1" (*cf.* right column in Table 1). The explanation of this fact is not yet known. It appears that the immobile violet factor has been transformed to other violet forms during the extended time of isolation.

Similarly it is difficult to decide whether the orange factor (Y) was initially present in the sludge or merely formed during the transformation of the original immobile violet material into the violet factors of R_c 0.5—0.4. The slight microbiological activity of this factor may be due to traces of impurities; its absorption spectrum indicates that it is not a vitamin B_{12}-like factor. The "intermediate" character of "factors C_2" and "C_1" which are present only in

the initial stages of bacterial fermentation, "factor C_2" being the first one to disappear, has already been noted [2]. Assuming that "Fraction IV" (p. 920), the source of the three factors "Z", corresponds to the "factor C_2" of bioautograms then the present investigation offers further confirmation of the labile nature of this factor. Similarly the labile nature of "factor C_1" may be confirmed by the separation of considerable amounts of factor B at each of the numerous chromatographings of "Fraction IV" (*cf.* p. 920).

It is difficult to decide which, if any, of the factors "Z" most closely resembles factor C but on the basis of microbiological activity it cannot be Z1 whose activity for *E. coli* is insignificant and probably due only to traces of the other two factors "Z" still present.

Earlier information on the electrophoretic behaviour of factor C (C_1 and C_2) or B_{12s} concerns mostly crude extracts or concentrates. Holdsworth [21] reports the mobility of factor C in 0.5 N acetic acid containing KCN; as -1.4×10^{-5}. According to Ericson [19] vitamin B_{12s} should move to the anode under these conditions as should factors C_1 and C_2. Brown and coworkers have determined the acidic character of factor C by electrophoresis in neutral and alkaline buffers [9].

As can be seen in Table 2 all three factors "Z" show acidic electrophoretic behaviour at pH 6.5 but at pH 3.0 factor Z3 is neutral while factors Z1 and Z2 behave as bases. This corresponds to the findings of Brown and coworkers [9] on factor C but is contrary to the earlier information [19] on the electrophoretic behaviour of this factor at pH 3.0.

However, it should be remembered that some determinations were carried out on crude extracts whose content of salts and other impurities may have influenced the electrophoretic behaviour of the B_{12}-like factors. Again if "factor C" has "changed" during the isolation procedure, this would explain its changed electrophoretic behaviour. (*cf.* p. 923).

It is, therefore, probably factor Z3 which most closely resembles the earlier description of factor C (C_1), both in its microbiological activity and in its chromatographic and electrophoretic behaviour.

Factors X. The four violet factors of R_c values 0.7—0.6 occurred together with two red factors V and W on the bioautograms (see Table 2). On mixed chromatograms (bioautograms) with standard substances — factor A, ψ B_{12}, and factor III — they gave in most cases single spots. In a few cases the spots were oval suggesting the presence of at least two components. It is evident, therefore, that this method of identifying B_{12} factors must be used only with very great caution. The "incomplete" character of these factors is shown by their ability to form violet (di)cyano complexes at neutral pH. Not only is their R_c range distinct from that of "factors C" but their microbiological activity for *E. coli* is also extremely low — this slight activity, together with the low activity for *O. malhamensis*, may be explained by the presence of traces of factors V and W (*cf.* Table 2). Although the electrophoretic behaviour of factors X2, X3 and X4 resembles that of factors Z, insofar as they are acidic at pH 6.5 and basic at pH 3.0; factor XI differs markedly from the rest of the group in being strongly acidic at both pH's although much less so at pH 6.5. (*cf.* Table 2).

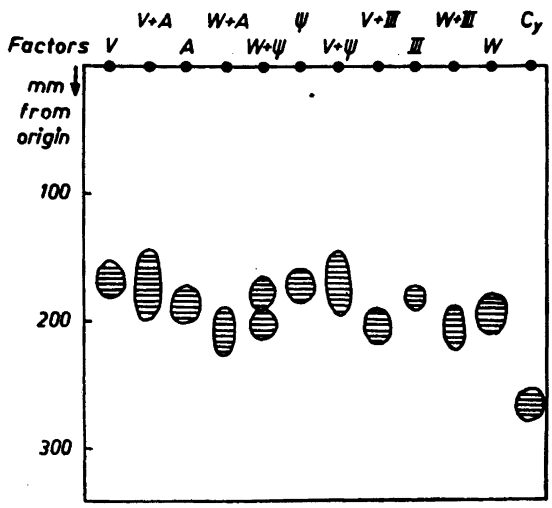


Fig. 1. Mixed bioautograms of factors W and V with known factors. Solvent system: water satur. sec. BuOH containing 3 % HAc and 0.01 % KCN; 21° C, 48 h. run. Developed with E. coli 113—3.

ψ = pseudovitamin B_{12}
C_y = cyanocobalamin

Factors V and W. These two red factors with R_c-values 0.7—0.6 have absorption spectra closely resembling that of cyanocobalamin. They are neutral at pH 3.0 and slightly basic at pH 6.5 (*cf.* Table 2). In order to establish their identity with known factors, bioautography, electrophoresis and, in the case of Factor III, spectrophotometric measurements were carried out several times on mixed solutions in order to compare them with known standards.

Since a mixture of factor W and ψ B_{12} is resolved by paper chromatography (Fig. 1) it is obvious that the two substances are not identical. Although other mixed solutions gave single spots these have a markedly oval shape, except in the case of V+III, while the single spots of pure solutions are more circular. It seems likely therefore that factor W is not identical with any of the three factors A, ψ B_{12}, and III available for comparison, while factor V is possibly identical with Factor III.

It was not possible to identify the factors V and W with the above mentioned known standards by electrophoresis or by spectrophotometric measurements. The spectrophotometric data for ψ B_{12} were unavailable. The band at 295 mμ characteristic for the monocyano complex of Factor III could not be detected in either factor W or V but the monocyano complexes of these factors showed, instead, bands at 275 mμ and 278 mμ, respectively. The absence of a band in this region may not be incompatible with the postulate of a relationship to Factor III, since the measurements were performed on a non-crystalline product. Moreover factor V resembles Factor III in its microbiological activity towards *E. coli* by both the cup plate and tube methods. The activity towards *O. malhamensis* is about 40 % of that of cyanocobalamin.

Factor W shows a strikingly high microbiological activity towards *E. coli* in plate assay. Its activity towards *E. coli* in tube assay is of the same order as that of cyanocobalamin. Although Factor H, isolated by Brown and coworkers [9] also has a very high activity towards *E. coli* in plate assay its activity in tube assay is lower than that of factor W and the activity towards *O. malhamensis* is very small. Further differences between these two factors are found in their absorption spectra [9] (*cf.* Table 2).

GENERAL CONSIDERATIONS

Violet factors. Of the 8 violet factors only three (B, Z2 and Z3) have a pronounced microbiological activity (Table 2) while the remaining five factors (X1, X2, X3, X4 and Z1) can be considered as inactive, (*cf.* p. 924). They form violet (di)cyanocomplexes at pH 6.5 which show the characteristic maxima at 367—368, 540 and 580 mμ. They exhibit acidic properties upon electrophoresis at the same pH. When acidified to pH 4.0 the colour of the solutions changes rapidly to orange, presumably due to the formation of hydroxo (or aquo) compounds.

The microbiologically active factors Z2 and Z3 (as well as factor B) were identical with the inactive factors in the formation of (di)cyano and hydroxyforms, respectively, and in their electrophoretic behaviour (*cf.* Table 2 and p. 924). In cup-plate assay with *E. coli* these factors showed characteristically *diffuse* growth zones which may account for their high microbiological potencies when calculated by this method. The phenomenon was much more pronounced in the case of factors Z2 and Z3 than in the case of factor B.

Behaviour of the different factors during some isolation steps. It is possible that the inactive factors, like the violet factors (Z2 and Z3) of high activity, tended to remain in precipitates, emulsions *etc.* during extraction. For this reason the solutions were exhaustively extracted beyond the point judged necessary by the behaviour of the red-brown substances (*cf.* p. 919) but constant microbiological testing is essential if the yellow hydroxo (or aquo) compounds formed by the active violet factors at pH 4.0—5.0 are not to be mistaken for "impurities" (most of which are also yellowish) and lost during the isolation procedure. Although these factors can be easily detected in solution by the violet colour formed immediately upon addition of CN^- this may not be the case in emulsions and precipitates. However, such extended extractions may give impure preparations necessitating repeated chromatography in later purification. It is not clear, whether the microbiological activity contained in the "kieselguhr layer" (p. 919) was due to still another factor or to the "tail" of the immobile violet factor which later resolved into factors Z1, Z2 and Z3 (*cf.* p. 919). Furthermore, the factors apparently differ in their ability to form the phenolic complexes described by Bernhauer since they behaved in different ways during extractions with phenolic solutions; some preliminary values for partition coefficients in one solvent system are given (Table 2). Unfortunately in many cases the amount of material available was insufficient to allow a thorough investigation of the problem.

It has been pointed out above (*cf.* p. 920) that considerable amounts of factor B could be separated from the violet factors upon repeated chromato-

graphy. This phenomenon suggests the possibility that the violet factors (or some of them) correspond merely to some different cyanide complexes of factor B. However, the relatively stable character of these factors during the process of determination of their spectrophotometric and electrophoretic properties rather points against this possibility. The problem was not further investigated.

Acknowledgements. The author wishes to thank Professor H. Lundin, Head of the Division, for his encouraging interest and valuable advice in performing this work. The author is grateful to Professor Dr. K. Bernhauer, Aschaffenburger Zellstoffwerke, Stockstadt/Main, Germany, for the stimulating experience acquired during her stay in his laboratory in the summer of 1954 and for samples of factor III and factor B, and to Dr. E. Lester Smith, Glaxo Laboratories, England, for spectrophotometric data on factor B. Valuable information on electrochromatography was given by Dr. L. Carlsson, King Gustaf V:s Research Institute, Stockholm, and Dr. P. Flodin, The Institute of Biochemistry, Upsala.

Thanks are due to Mrs. M. Jonason, Mr. I. T. Okine, and Mr. Th. Kirsipuu for technical assistance. The financial support of *Statens Tekniska Forskningsråd* is gratefully acknowledged.

REFERENCES

1. Sjöström, A. G. M., Neujahr, H. Y. and Lundin, H. *Acta Chem. Scand.* **7** (1953) 1036.
2. Neujahr, H. Y. *Acta Chem. Scand.* **9** (1955) 622.
3. Neujahr, H. Y. *Acta Chem. Scand.* **9** (1955) 803.
4. Ford, J. E. *Brit. J. Nutrition* **6** (1952) 324.
5. Ford, J. E. *Nature* **171** (1953) 148, 149.
6. Ford, J. E., Kon, S. K. and Porter, J. W. G. *Chemistry & Industry* **1952** 495.
7. Ford, J. E. and Porter, J. W. G. *Brit. J. Nutrition* **7** (1953) 326.
8. Gant, D. E., Smith, E. L. and Parker, L. F. J. *Biochem. J. London* **56** (1954) xxxiv.
9. Brown, I. C. Cain, Gant, D. E., Parker, L. F. J. and Smith, E. L. *Biochem. J. London* **59** (1955) 82.
10. Pfifner, J. J., Dion, H. W. and Calkins, D. G. *Federation Proc.* **11** (1952) 269.
11. Armitage, J. B., Cannon, J. R., Johnson, A. W., Parker, L. F. J., Smith, E. L., Stafford, W. H. and Todd, A. R. *J. Chem. Soc.* **1953** 3849.
12. Bernhauer, K. und Friedrich, W. *Angew. Chem.* **66** (1954) 776.
13. Friedrich, W. und Bernhauer, K. *Angew. Chem.* **65** (1953) 627.
14. Friedrich, W. und Bernhauer, K. *Angew. Chem.* **67** (1955) 619.
15. Robinson, F. M., Miller, J. M., Mc Pherson, J. F. and Folkers, K. *J. Am. Chem. Soc.* **77** (1955) 5192.
16. Flodin, P. and Porath, J. *Biochim. et Biophys. Acta* **13** (1954) 175.
17. Carlson, L. A. *Acta Chem. Scand.* **8** (1954) 510.
18. Ericson, L.-E. and Lewis, L. *Arkiv Kemi* **6** (1953) 427.
19. Ericson, L.-E. *Acta Chem. Scand.* **7** (1953) 703.
20. Friedrich, W. und Bernhauer, K. *Z. Naturforsch.* 106 (1955) 755.
21. Holdsworth, E. S. *Nature* **171** (1953) 148.

Received March 15, 1956.

ACTA CHEMICA SCANDINAVICA 10 (1956) 928—934

Reversible Enzymatic Synthesis of Guanosine Diphosphate Mannose from Guanosine Triphosphate and Mannose-1-Phosphate

AGNETE MUNCH-PETERSEN

Universitetets cytofysiologiske Institut, Copenhagen, Denmark

From brewer's yeast an enzyme is isolated and purified, which catalyzes a pyrophosphorylation of guanosine diphosphate mannose. This reaction is demonstrated spectrophotometrically, and the reversibility of the process is proved by means of paper chromatography. Separation of guanosine diphosphate mannose from uridine diphosphate glucose on a cellulose column is described.

A number of enzyme systems, catalyzing processes which involve guanosine compounds have recently been demonstrated [1–4] and guanosine nucleotides have been isolated from liver, brain, tumor and muscle tissue [5,6]. An interesting compound, guanosine diphosphate mannose (GDPM) *, was isolated from yeast and identified by Leloir and Cabib [7]. This compound is probably identical with the mannose-containing nucleotide, noticed by Buchanan *et al.*[8] in their investigations of phosphorus compounds as intermediates in photosynthesis.

In the present paper the existence of an enzymatic pathway for the synthesis of GTP from GDPM and P—P is reported, and the reversibility of the process is proved. The reaction consists in a pyrophosphorolytic cleavage of GDPM according to the following equation:

$$\text{GDPM} + \text{P—P} \rightleftharpoons \text{GTP} + \text{M—1—P} \qquad (1)$$

and the process seems analogous to the earlier described pyrophosphorolytic cleavages of DPN [9], UDPG [10] and UDPAG [11].

* The following abbreviations are used: GDPM for guanosine diphosphate mannose; GMP, GDP, GTP for guanosine mono-, di- and triphosphate; DPN, TPN for di- and triphosphopyridine nucleotide; UMP, UDP, UTP for uridine mono-, di- and triphosphate; UDPG for uridine diphosphoglucose; UDPAG for uridine diphosphate N-acetyl glucosamine; AMP, ADP, ATP for adenosine mono-, di- and triphosphate; M-1-P for mannose-1-phosphate; G-6-P for glucose-6-phosphate and Tris for tris(hydroxymethyl)aminomethane.

The enzyme, for which the name GDPM pyrophosphorylase is proposed, has been prepared and purified from brewer's yeast, and its presence has been demonstrated in a number of microorganisms. A preliminary report of the work has appeared earlier [12].

EXPERIMENTAL

M-1-P was prepared synthetically according to Colowick [13]. Hexokinase, G-6-P dehydrogenase and nucleoside diphosphokinase were obtained as previously described [14].

GTP, isolated from muscle tissue, was a gift from Dr. Adam Deutsch, University of Lund, Sweden.

GDPM was prepared from baker's yeast using a method similar to the one described by Cabib and Leloir [7] with a few modifications in the column technique. Baker's yeast, 10 kg, was used as starting material, and the solution of nucleotides obtained by decomposition of the mercury salts (*cf.* Ref.[7]) was run through a Dowex-1 anion exchange column, which was eluted according to the principle described by Alm *et al.*[15], by gradually increasing the concentration of the eluting agent.

The column used for this purpose had a length of 25 cm and a bed volume of 64 cm^3. About 2 000 μmoles (200 ml) of the nucleotide mixture was applied in a run, and after rinsing with 25 ml H_2O the column was subjected to gradient elution. The apparatus was similar to that described by Hurlbert *et al.*[16], starting with 250 ml H_2O in the mixing flask and 800 ml 0.03 M HCl, containing 0.03 M NaCl, in the reservoir. Under these conditions nucleosides, AMP, UMP and ADP were eluted from the column. When the reservoir was empty, elution was continued by adding 500 ml 0.03 M HCl, containing 0.3 M NaCl, to the reservoir without changing the content of the mixing flask. During this step GDPM, UDPAG, UDPG, UDP and finally the nucleoside triphosphates are eluted from the column. The identity of the different peaks mentioned here was established by adsorption of each fraction on norite followed by paper chromatography together with known compounds. The eluted fractions were concentrated by adsorption on norite and subsequent elution with 50 % ethanol.

By this method GDPM is obtained, contaminated with varying amounts of UDPAG and UDPG. Complete separation of these nucleotides is difficult to accomplish on a Dowex-1 column, whereas paper chromatography in the ethanol-ammonium acetate solvent [17] at pH 7.5 yields a good separation. Separation of the compounds on a somewhat

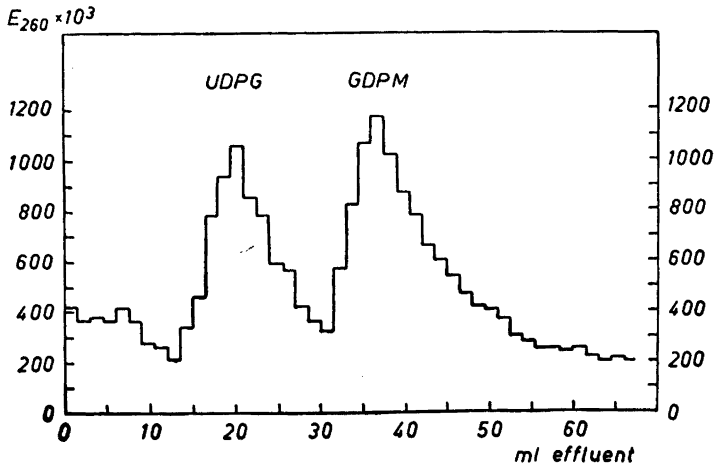


Fig. 1. Separation of GDPM from UDPG on a cellulose column.
Eluting agent: 1 M ethanol-ammonium acetate, pH 7.5 (17).

larger scale was obtained by using a cellulose column (standard grade Whatman cellulose powder), 20 cm high, with a bed volume of 22 cm^3. A solution of 10–15 μmoles of nucleotides in a volume of about 100 μl was placed on top of the column, and the column was washed with 2–3 ml ethanol. Elution was effected with 1 M ethanol-ammonium acetate, pH 7.5, the same solvent as used for paper chromatography [17]. Fig. 1 shows the separation of GDPM from UDPG by this method. The peaks were identified by paper chromatography.

The combined eluates containing the GDPM were evaporated to a small volume, and this solution was used directly in the enzymatic experiments. A salt free solution, if desired, was obtained by treating the mixture once more with norite, and subsequent elution of the norite. The technique used for adsorption of the nucleotides on norite and elution with 50 % ethanol was as earlier described [14].

Assay of enzyme activity. During the purification procedure enzyme activity was estimated by determining the GTP formed in reaction (1). The method is similar to the one used [14] for determination of UTP by pyrophosphorylation of UDPG or UDPAG. In the assay system the following reactions take place:

GDPM + P–P ⇌ GTP + M–1–P	(GDPM pyrophosphorylase)
GTP + ADP ⇌ GDP + ATP	(nucleoside diphosphokinase)
ATP + glucose ⇌ ADP + G–6–P	(hexokinase)
G–6–P + TPN + H_2O ⇌ 6-phosphogluconic acid + TPNH + H+	(G–6–P dehydrogenase)

and the reduction of TPN is followed in the Beckman spectrophotometer at 340 mμ. 1 ml quartz cells were used, and the components of the system were as follows: 100 μl GDPM, 0.002 M; 800 μl Tris, 0.05 M, pH 7.3; 5 μl $MgCl_2$, 1 M; 20 μl ADP (0.002 M); 25 μl glucose (0.01 M); 25 μl hexokinase (12 mg/ml protein); 15 μl TPN (10 mg/ml); 15 μl G–6–P dehydrogenase (1 mg/ml protein) and 5–10 μl GDPM pyrophosphorylase. 10 μl P–P (0.1 M) was added to start the reaction (*cf.* Fig. 4).

A unit of enzyme activity was defined as the amount causing the splitting of 0.1 μmole/min. Specific activity is defined as units per mg protein. A rise in extinction of 0.622 per 0.1 μmole at 340 mμ was used as basis for the calculation [18].

Protein determinations were carried out according to Bücher [19].

RESULTS

Purification of enzyme. 50 g of dried brewer's yeast (A/S Tuborgs Fabriker) was autolyzed and extracted overnight with 200 ml 0.07 M $(NH_4)_2HPO_4$ at 25° C. After centrifugation the proteins in the supernatant (150 ml) were precipitated by addition of 280 ml saturated ammonium sulphate. The mixture was left for 30 min. at 2° C before centrifugation. The supernatant was discarded, and the precipitate was dissolved in 75 ml chilled H_2O, and pH adjusted to 7.5 (volume 90 ml). To this was added 150 ml saturated ammonium sulphate. After 30 min. at 2° C the precipitate was collected by centrifugation, dissolved in 25 ml 0.02 M phosphate buffer, pH 7.5, and subjected to ethanol fractionation.

Table 1. Purification of GDPM pyrophosphorylase from brewer's yeast.

	Total units	volume ml	specific activity units / mg protein
Crude extract	145	150	0.01
Ammonium sulphate at pH 7.5	96	90	0.02
Ethanol fractionation	53	35	0.11
Calcium phosphate gel eluate	21	5	0.50

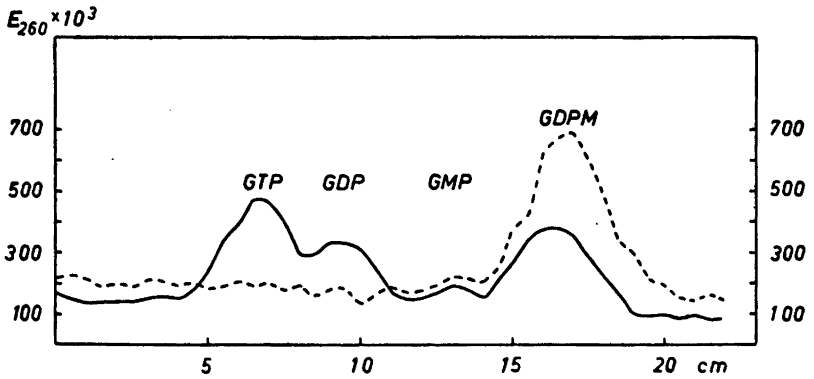


Fig. 2. Diagram of paper chromatogram from GDPM pyrophosphorylase digest.

Reaction mixture: 0.3 μmoles GDPM; 2 μmoles P—P (8 280 cts/min/μmole); 1 ml Tris; 0.05 M, pH 7.3; 0.5 μmoles $MgCl_2$.
Control: same without P—P
After 60 min. incubation the digest was acidified, adsorbed on norite and eluted with 50 % ethanol. Chromatographed 22 hours. Chromatogram scanned in the Beckman spectrophotometer at 260 mμ.

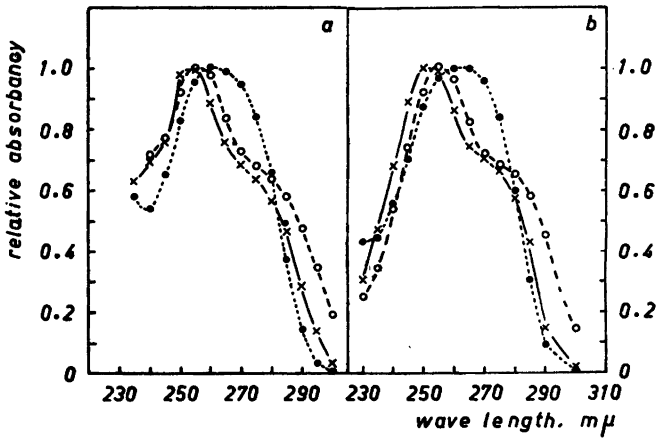


Fig. 3a. Ultraviolet absorption curves for GTP eluted from paper chromatogram.

For comparison with Hotchkiss' data [20] the relative absorbing value is used (maximum absorbancy taken as equal to 1). The values were corrected for absorption originating from the paper.

Fig. 3b. Spectra obtained for guanosine as reported by Hotchkiss [20].

Legend: O····O····O acid solution
×—×—× neutral solution
●····●····● alkaline solution

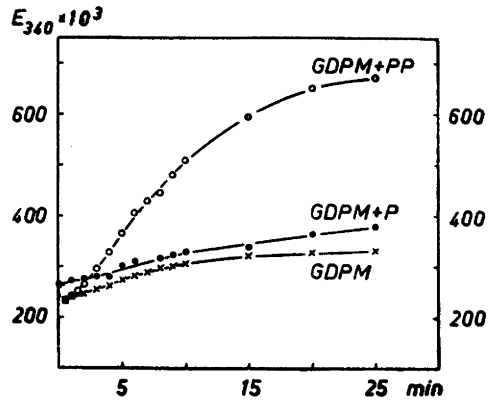


Fig. 4. Spectrophotometric demonstration of the GTP formed by pyrophosphorylation of GDPM.

Reaction mixture O—O—O: 50 µl GDPM, 0.002 M; 20 µl ADP, 0.002 M; 25 µl glucose, 0.01 M; 25 µl hexokinase (12 mg/ml); 15 µl TPN (10 mg/ml); 15 µl G—6—P dehydrogenase (0.5 mg/ml); 10 µl pyrophosphorylase; 10 µl P—P, 0.1 M and 800 µl Tris, 0.05 M, pH 7.3; 5 µl $MgCl_2$, 1 M.
Control 1 ×—×—× same without P—P.
Control 2 ●—●—● same with 2 µmoles inorganic P instead of P—P.

To 40 ml solution, cooled to —1° C were added dropwise 80 ml 50 % ethanol. During this addition the solution was stirred mechanically, and the temperature of the surrounding bath was gradually lowered to —12° C. The mixture was centrifuged 5 min. at —15° C in a previously cooled centrifuge. The supernatant was left 20 min. at —15° C and centrifuged again. The last precipitate contained the bulk of activity and was stored overnight at —20° C.

Next morning the precipitate was dissolved in 35 ml chilled Tris buffer, 0.001 M, pH 7.3, 35 ml calcium phosphate gel (16 mg/ml dry weight) was added, and the solution thoroughly mixed. After centrifugation and removal of the supernatant the precipitate was treated with 50 ml 0.05 M phosphate buffer, pH 7.2. The mixture was spun, and to the supernatant was added 80 ml ammonium sulphate. The mixture was left overnight at 2° C, and the precipitate collected by centrifugation. Stored at —20° C, this preparation retained its activity for several weeks. The preparation was soluble in 0.05 M Tris buffer. The activity was about 40 times that of the crude extract, and the overall yield was 14 % (Table 1).

The purified preparation showed no pyrophosphorolytic activity towards UDPG, but contained traces of UDPAG pyrophosphorylase.

Pyrophosphorolysis of GDPM. If GDPM, prepared from yeast, as described in Methods, was incubated with ^{32}P-labelled pyrophosphate and the enzyme, paper chromatography of the reaction mixture showed that a new ultraviolet absorbing substance had appeared (Fig. 2). The new spot was eluted with H_2O, and the ultraviolet absorption spectrum of the substance in neutral, alkaline and acid solution was determined, as presented in Fig. 3. The curves

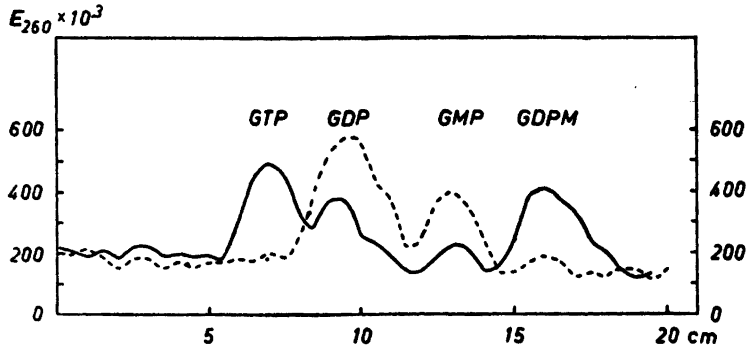


Fig. 5. Diagram of paper chromatogram from GTP—M—1—P pyrophosphorylase digest.

Reaction mixture (solid line): 0.2 μmoles GTP; 0.4 μmoles M—1—P; 1 ml Tris, 0.05 M, pH 7.3 and 25 μl GDPM pyrophosphorylase.
Control mixture (broken line): same as above, except that 0.2 μmoles GDP is substituted for GTP. After 60 min. incubation the digests were acidified and treated as described in Fig. 2.

are almost identical to those found for guanosine by Hotchkiss [20], and the changes in acid and alkaline solution are the same.

Aliquots of the solution were deposited on planchets, dried and counted in a Geiger-Müller counter. Counts per min. per μmole of the new compound (μmoles calculated from the absorption value at 257 mμ) and of the ^{32}P-labelled pyrophosphate used in the experiment were 7 800 and 8 270, respectively, and thus agree with the assumption that a pyrophosphorolysis of GDPM has occurred with simultaneous formation of GTP. The GTP formed in the reaction may be demonstrated spectrophotometrically as described in Methods (Fig. 4). As seen in Fig. 4 addition of inorganic phosphate instead of pyrophosphate causes no formation of GTP.

Reversibility of the reaction. Incubation of GTP with M-1-P and the enzyme results in formation of a compound which moves on the paper chromatogram with the same rate as known GDPM (Fig. 5). Incubation of GDP with the same M-1-P solution yields a very faint spot at the GDPM site. It is possible that a reaction exists by which GTP and GMP are formed from GDP, but this possibility has not been further investigated.

Judging from the curves in Figs. 2 and 5 the equilibrium of the reaction is at around 50 % conversion, similar to what is found for the UDPG pyrophosphorylase [14].

DISCUSSION

Nucleotidyl transferases, the group of enzymes to which the GDPM-pyrophosphorylase belongs, have been demonstrated in a number of tissue and in several microorganisms, and it is assumed that their role in the cell is the synthesis of nucleoside diphosphate glycosyl compounds from nucleoside triphosphates and glycosyl phosphates.

The function of the nucleoside diphosphate glycosyl compounds as donors of glycosyl groups has been experimentally demonstrated in the case of

UDPG[21–23] and UDPGlucuronic acid [24]. GDPM has been suggested to be active in the synthesis of mannan in the yeast cell-walls [7], but no proof of this hypothesis has so far been obtained. The abundance of mannose-containing polysaccharides in brown algae suggests these as a suitable material for further investigations on the function of GDPM.

This work has been supported by the *Danish State Research Foundation, Carlsbergfondet, Nordisk Insulinfond* and the *Lilly Foundation.*

REFERENCES

1. Sanadi, D. R., Gibson, D. M. and Ayengar, P. *Biochim. et Biophys. Acta* **14** (1954) 434.
2. Strominger, J. L. *Federation Proc.* **13** (1954) 307.
3. Strominger, J. L. *Biochim. et Biophys. Acta* **16** (1955) 616.
4. Ochoa, S. and Greenberg-Manago, M. *J. Am. Chem. Soc.* **77** (1955) 3165.
5. Schmitz, H., Hurlbert, R. B. and Potter, V. R. *J. Biol. Chem.* **209** (1954) 41.
6. Bergkvist, R. and Deutsch, A. *Acta Chem. Scand.* **8** (1954) 1889.
7. Cabib, E. and Leloir, L. F. *J. Biol. Chem.* **206** (1954) 779.
8. Buchanan, J. G., Bassham, J. A., Benson, A. A., Bradley, D. F., Calvin, M., Daus, L. L., Goodman, M., Hayes, P. M., Lynch, V. H., Norris, L. T. and Wilson, A. T. in McElroy and Glass: *Phosphorus Metabolism* **II** (1952) p. 440.
9. Kornberg, A. *J. Biol. Chem.* **182** (1950) 779.
10. Kalckar, H. M. and Cutolo, E. IIe *Congr. Internat. de Biochimie*, Paris 1952, p. 260.
11. Smith, E. E. B. and Mills, G. T. *Biochim. et Biophys. Acta* **13** (1954) 386.
12. Munch-Petersen, A. *Arch. Biophys.* **55** (1955) 592.
13. Colowick, S. P. *J. Biol. Chem.* **124** (1938) 557.
14. Munch-Petersen, A. *Acta Chem. Scand.* **9** (1955) 1523.
15. Alm, R. S., Williams, R. J. B. and Tiselius, A. *Acta Chem. Scand.* **6** (1952) 826.
16. Hurlbert, R. B., Schmitz, H., Brum, A. F. and Potter, V. R. *J. Biol. Chem.* **209** (1954) 23.
17. Paladini, A. C. and Leloir, L. F. *Biochem. J. London* **51** (1952) 426.
18. Horecker, B. L. and Kornberg, A. *J. Biol. Chem.* **175** (1948) 385.
19. Bücher, Th. *Biochim. et Biophys. Acta* **1** (1947) 292.
20. Hotchkiss, R. D. *J. Biol. Chem.* **175** (1948) 315.
21. Leloir, L. F. and Cardini, C. E. *J. Am. Chem. Soc.* **75** (1953) 6084.
22. Leloir, L. F. and Cabib, E. *J. Am. Chem. Soc.* **75** (1953) 5445.
23. Leloir, L. F. and Cardini, C. E. *J. Biol. Chem.* **214** (1955) 157.
24. Dutton, G. J. and Storey, I. D. E. *Biochem. J.* **57** (1954) 275.

Received April 18, 1956.

ACTA CHEMICA SCANDINAVICA 10 (1956) 935—942

On the Instantaneous Polarographic Current

I. Automatic Recording of Selected Parts of the Current-time Curve of the Individual Mercury Drop

ERIK WÅHLIN and ÅKE BRESLE

Royal Institute of Technology, Stockholm, Sweden

A method of measuring the instantaneous polarographic current within an accuracy of ± 0.2 per cent is described. The apparatus includes a polarograph, a recording potentiometer and a device with the double purpose of knocking off the mercury drops and of periodically connecting the recording pen.

In polarography calculations are usually based, not on the instantaneous diffusion current, but on a mean value, evaluated in some way. This seems satisfactory for analytical purposes, but it is a serious drawback in theoretical studies. A method which gives the instantaneous current must, however, also have great advantages in analytical work. The correct evaluation of a polarographic curve is often very difficult and for practical reasons the recording instrument is damped. However the damping often conceals small polarographic waves and thus the sensitivity is reduced. Furthermore Lingane [1] has pointed out that the damping of the polarographic current results in a registered mean current; the deviation from the theoretical current depends on the degree of damping. In analytical work there is also a tendency to use shorter drop times in order to get smoother curves, but the gain in simplicity of evaluation is lost on account of interference from other sources.

In an earlier communication [2] Wåhlin has given a short description of an apparatus which makes it possible to measure a selected part of the diffusion-time curve. The present paper describes the apparatus fully and gives some tests of its performance.

List of Symbols used

C = concentration of depolarizer, millimoles liter^{-1}
D = diffusion constant, cm^2 sec^{-1}
$\bar{i}$ = mean diffusion current, microamperes

i_τ = instantaneous current, microamperes
i_t = instantaneous current immediately before the drop falls
K = a constant in eqn. (1)
n = number of faradays of electricity required per mole of electrode reaction
m = rate of flow of mercury from the capillary, mg sec^{-1}
τ = age of drop, sec
t = τ_{max}, sec
h = the distance between the upper and lower mercury surface (cm).

APPLICATIONS

The characteristic features of our apparatus make it suitable for measurements of the following types.

1. Checking the revised Ilkovic equations

The measurements on which the polarographic theory is based are mostly done with the mean diffusion current method. It would be more logical and closer to facts to use the instantaneous polarographic current for checking the modified Ilkovic equation[3,4]. Several investigators are of the opinion that the formula is as follows:

$$i_\tau = 709\ nD^{\frac{1}{2}}Cm^{2/3}\tau^{1/6} + KnDC(m\tau)^{1/3} \qquad (1)$$

The mean diffusion current is derived from eqn. (1) and is only valid if eqn. (1) is correct

$$\bar{i} = 607\ nD^{\frac{1}{2}}Cm^{2/3}t^{1/6} + \frac{3}{4}KnDCm^{1/3}t^{1/3} \qquad (2)$$

However the theoretical value of the constant K is still discussed in the literature[3-6], and furthermore Hans *et al.*[7] do not consider K a constant, but a function of τ and t. Sufficiently accurate measurements of i_τ are still very rare and therefore it is natural that values of the constant K as different as 17 and 39 may be found in the literature. Precision measurements of the instantaneous current are only given by Hans, Henne and Meurer [7], Taylor, Smith and Cooter [8], and Khalafalla [9]. The lack of data is due to the difficulty of making measurements of the complete course of the instantaneous current/time curve, owing to the discontinuity of the polarographic current obtained when the mercury drop falls and the rapid increase of current during the first second after the formation of a new drop.

Oscillographic measurements are of course quick enough, but the accuracy is only around ± 2 % which means that the second term of eqn. (1) can only be determined within approximately ± 20 %. Some research has also been done with undamped galvanometers. These instruments are, however, very delicate, and according to Strehlow [10] the results obtained are subject to certain limitations.

The fact that the polarographic current during the life-time of an individual mercury drop is approximately proportional to $\tau^{1/6}$ means that while the age of the drop increases from 0 to 1 second the current increase is 76 units, but from 4.0 to 5.0 seconds the increment is only 3.5 units. A polarograph cannot record this complete curve with its sharp discontinuity when the drop falls, but records instead some kind of "damped" curve, which is sometimes undesirable. Especially at long drop times the conventional polarograph gives curves with big oscillations and it is doubtful whether these curves have any relation to the true polarographic current.

Accurate measurements of the later parts of the current-time curve can be used for investigating the symbol K. Our method is well adapted for supplying such data and furthermore the measurements can be made very quickly.

2. Analytical precision polarography

For analytical polarography it may seem satisfactory to measure the mean diffusion current, but experience in this field has shown that correct evaluation of the curves requires a skilled analyst. As mentioned above the curves obtained with our apparatus are undamped and still very easy to evaluate (Fig. 1)

When prewave compensation is used on conventional polarographs, the results are not very accurate because of the big oscillations. With the present method straight lines are obtained, and the results are much more reproducible.

3. Extending the lower limit in analytical polarography

When determining micro quantities of depolarizer with the mean current method the diffusion controlled part of the measured current is only a minor constituent beside the main component, the condenser current. This restricts the possibility of determining very small quantities of depolarizer with any reasonable degree of accuracy. As the diffusion current increases with the

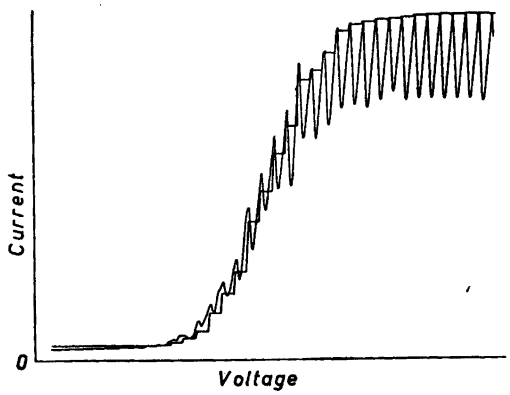


Fig. 1. Polarograms obtained in the conventional way (lower curve) and with the apparatus described in the text (upper curve).

age of the drop, while the condenser current decreases, the most favourable conditions for determining small diffusion currents occur immediately before the drop falls. Thus, if the instantaneous current is measured in this way the accuracy is increased and the lower limit of detection is depressed.

APPARATUS

1) *Capillary.* Length: 253 mm, drop time: 5.2 seconds in 0.1 M potassium chloride solution at a mercury pressure of 60 cm and at 0.90 volts *vs* the silver anode. The capillary was made from Pyrex glass rod [11].

2) *Polarographic vessel* including de-aerating tube and a tube to keep the oxygen out by blowing nitrogen gas over the surface. The nitrogen was purified by passing it over activated copper absorbed on diatomaceous earth according to Meyer and Ronge [12]. In this way the partial pressure of the oxygen was reduced to less than 3×10^{-4} mm of mercury.

3) *Anode,* a silver sheet of 8 cm^2. This anode proved to be much more convenient to handle than the conventional calomel electrode [13,14].

4) *Hammer for knocking off the mercury drops* at predetermined intervals. The hammer was actuated by an electromagnet [15] and the intervals were timed with an accuracy of ± 0.01 seconds by a rotating cam.

5) *Disconnector and interval selector for balancing motor.* The intervals were timed in the same way as above with the exception that the circuit could be also connected for longer periods. The cams were both attached to the same shaft, driven by a constant speed electric motor.

6) *Potentiometer recorder,* Speedomax Type G, Model S, Leeds and Northrup Comp. USA. The essential part of the recorder for this application is a phase sensitive balancing motor, which moves the pen to its correct position.

7) *Polarograph,* both an electronic polarograph, LKB Type 3266 B LKB-produkter, Fabriks AB, Sweden, and a Heyrovsky type polarograph, Polarograph 38, F. Leybold Nachfolger, Germany. Both types contain damping capacitors, which were disconnected in order to obtain the correct value of the polarographic current.

OPERATING PRINCIPLES

Fig. 2 illustrates the construction of the apparatus schematically and Fig. 1 shows a typical current/voltage curve. The operating principle of the apparatus is as follows:

The mercury drop is knocked off by the hammer for example every 5.02 seconds. The current is recorded while the age of the drop increases from *e.g.*, 4.5 to 5.0 seconds. Immediately before the drop falls the balancing motor circuit is broken and so the pen rests in the 5.0 second position until the next drop is 4.5 seconds old, and the same process is then repeated. In this way it is possible to record accurately the instantaneous value of the diffusion current (not the mean diffusion current), as a mean value from a suitable number of drops.

Especially at long drop times, the i/V curves of this apparatus will be smooth and easily evaluated. During the periods when the polarographic curve is not being recorded calibrated resistors may be connected in place of the polarographic cell, and the resulting current can be measured. This provides calibration of the polarograph.

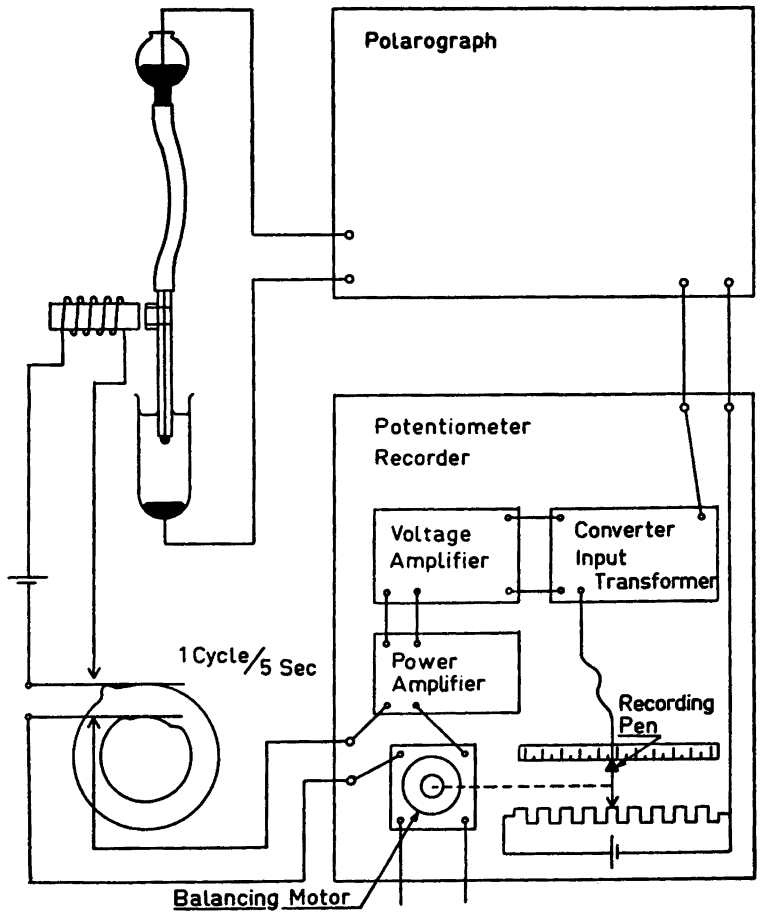


Fig. 2. Diagram of the assembly used in the experiments.

TESTS

1. It is essential to prove that the apparatus really records the true current. The following experiments were carried out in order to demonstrate that the recording pen always moves to its correct position.

A deaerated cadmium solution in potassium chloride was polarographed at constant voltage (−0.90 volts *vs* the silver anode). The mercury drops were knocked off every 5.0 seconds and the recorder was first connected during the whole drop life a) in Fig. 3. At b) the recorder was disconnected at a pen position corresponding to 4.7 seconds. As the timer had been adjusted to have the pen connected between 2.0—2.2 seconds, the pen moved downwards a small distance every time it was connected and reached its final position after about 4 drops. Then the paper was wound back and the pen was placed in a position

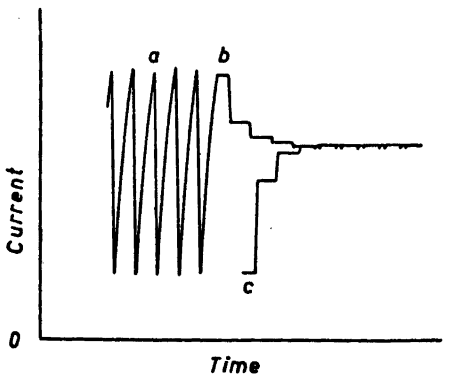


Fig. 3. Precision polarogram obtained at a constant potential. For explanation of a) b) and c) see p. 939.

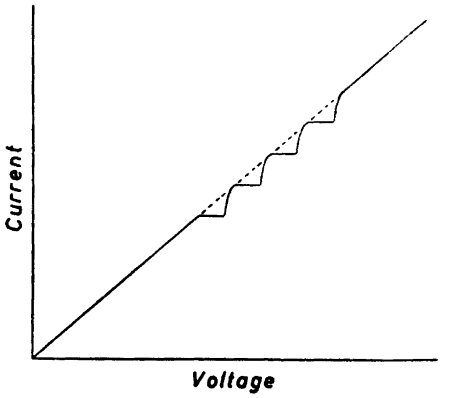


Fig. 4. Current-voltage diagram showing the ability of the apparatus to give a definite current for the short period of operation of the recorder.

corresponding to $\tau = 0.9$ sec, c) in Fig. 3. When connected, the pen now moved up to the same final value as before. This experiment proves that the apparatus records a definite current value corresponding to every value of τ during the drop life independently of the initial pen position.

2. In order to check the ability of the apparatus to record the true instantaneous current the following experiment was carried out. The polarographic cell was replaced by a resistor, and the voltage was increased at constant rate beginning at 0 volt. Under these conditions the recorded current should be a straight line. (Fig. 4). At the beginning the recorder was connected registering a straight line. Then the timer was started making the recorder to be connected and disconnected at predetermined intervals. Fig. 4 shows that when connected only 0.5 sec of a 5.0 sec period the pen moves to a position that coincides with the straight line. Of course this is only true when the i/V curve is not too steep, but the experiment shows that the apparatus is quick enough for the present investigation.

3. All revised formulae suggested for the polarographic current agree on one point, *viz.* the proportionality between current and concentration of depolarizer. All precision measurements up to now have proved this to be true within very close limits [16]. It was therefore considered important to use this well-known fact as a method of testing the apparatus. The following experiments were carried out: The timer was adjusted to give the undamped, instantaneous current after about 4.0 seconds. Drop time 5.2 sec. The cadmium concentration was varied according to Table 1. Background solution was 0.1 molar potassium chloride and 0.009 % gelatine. The height of the mercury reservoir was 60 cm above the capillary orifice and the temperature was 25.0 ± 0.1 °C.

Table 1 shows that our measurements of i_τ / C are constant within ±0.24 %, which lies within the experimental errors.

Table 1. The linear correlation between the diffusion current and the depolarizer concentration.

mM Cd	μA	μA_{corr}	μA_{corr} / mM Cd
0.000	0.041	0.000	—
0.892	7.410	7.369	8.261
1.115	9.240	9.199	8.250
1.337	11.08	11.04	8.257
1.783	14.78	14.74	8.267
2.229	18.44	18.40	8.255
2.786	23.11	23.07	8.280

Mean value: μA_{corr} / mM Cd = 8.26 ± 0.02.

4. In order to get a comparison between the polarographic current obtained from an electronic and from a non-electronic polarograph a polarogram was taken from the same solution with Polarograph LKB and Leybold Polarograph 38. The result is shown in Table 2. Under LKB is listed the instantaneous current obtained with the electronic polarograph and under LEYBOLD the same is given for the non-electronic instrument. The symbol Δ % is the percentage deviation of the current from the calculated mean value. As can be seen, the difference never exceeds 0.2 %.

Table 2. Comparison between currents obtained with an electronic and a non-electronic polarograph.

Sec	μA		Δ %
	LKB	LEYBOLD	
3.12	10.570	10.542	0.13
3.47	10.806	10.767	0.09
3.82	11.031	11.006	0.02
4.16	11.245	11.205	0.18

m = 2.024 mg Hg pr sec. h = 70 cm.
C = 1.315 mmoles/l. T = 25 °C.

REFERENCES

1. Lingane, J. J. *Ind. Eng. Chem. Anal. Ed.* **18** (1946) 734.
2. Wåhlin, E. *Radiometer Polarographics* **1** (1952) 113.
3. Strehlow, H. and v. Stackelberg, M. *Z. Elektrochem.* **54** (1950) 51; v. Stackelberg, *Ibid.* **57** (1953) 338.
4. Lingane, J. J. and Loveridge, B. A. *J. Am. Chem. Soc.* **72** (1950) 438.
5. Kambara, T., Suzuki, M. and Tachi, I. *Bull Chem. Soc. Japan* **23** (1950) 219; Kambara, T. and Tachi, I. *Ibid.* **23** (1950) 225.
6. Müller, O. H. *Natl. Bur. Standards Circ.* **524** (1953) 289.
7. Hans, W., Henne, W. and Meurer, E. *Z. Elektrochem.* **58** (1954) 836.

8. Taylor, J. K., Smith, R. E. and Cooter, I. L. *J. Research Natl. Bur. Standards* **42** (1949) 387.
9. Khalafalla, S. **Publ. 5542** *Univ. Microfilm, Ann Arbor, Mich.* (1953).
10. Strehlow, H. *Z. Elektrochem.* **55** (1951) 420.
11. Ferrett, D. J. and Phillips, C. S. G. *Analyst* **78** (1953) 564.
12. Meyer, F. R. and Ronge, G. *Z. angew. Chem.* **52** (1939) 637.
13. Lydersen, D. *Acta Chem. Scand.* **3** (1949) 259.
14. Meites, L. *Polarographic Techniques*, Interscience Publ. New York 1955, p. 18.
15. Airey, L. and Smales, A. A. *Analyst* **75** (1950) 287.
16. Kolthoff, I. M. and Lingane, J. J. *Polarography*, Interscience Publ. New York 1952, p. 68.

Received April 13, 1956.

ACTA CHEMICA SCANDINAVICA 10 (1956) 943—946

On the Instantaneous Polarographic Current

II. Measurements of the Rate of Flow of Mercury

ÅKE BRESLE

Institute of Inorganic and Physical Chemistry, University, Stockholm; Royal Institute of Technology, Stockholm, Sweden

The variation of the rate of flow of mercury from a polarographic capillary during the lifetime of a drop is given. The results are based upon measurements of the instantaneous rate of flow obtained by a special technique described earlier. The agreement between the experimental data and those calculated from the theoretical formula is shown, the deviation being about 0.3 %.

The polarographic diffusion current is a function of the age of the mercury drop, the rate of flow of mercury through the capillary and some characteristics of the electrolyzed solution, *i. e.* the concentration, the valency and the diffusion constant of the depolarizer. In ordinary polarographic work, for instance in analytical polarography where the mean diffusion current is measured, the mean value of the rate of flow of mercury is determined, but in investigations on the instantaneous current it is necessary to know the corresponding instantaneous value of the rate of flow.

As a part of an investigation on the instantaneous polarographic current data concerning the flow of mercury were collected and the theoretical and experimental results were compared.

List of symbols

m = instantaneous rate of mercury flow at the time τ (mg · sec $^{-1}$)
$\overline{m}$ = mean value of the rate of mercury flow, measured from the time zero to τ (mg · sec^{-1})
M = constant rate of mercury flow obtained when the capillary tip is immersed in mercury (mg · sec^{-1})
τ = age of the drop at a certain moment (sec)
r = radius of the drop at the time τ (cm)
r_c = inner radius of the capillary (cm)

l = length of the capillary (cm)
d = density of mercury (g · ml^{-1})
η = viscosity coefficient of mercury (dynes · sec · cm^{-2})
σ = interfacial tension between mercury and the electrolyte (dynes · cm^{-1})
h = distance between the upper and lower mercury surfaces (cm)
P_{tot} = total applied pressure (dynes · cm^{-2})
P_{eff} = effective pressure (dynes · cm^{-2})
P_b = back pressure (dynes · cm^{-2})
ω = weight of the drop at the time τ
k_1, k_2, k_3, α, β = constants

THEORETICAL

When mercury flows through a capillary and forms a growing drop at the capillary tip, the rate of flow varies during the life of the drop. The relation between the dimensions of the drop and the variables m and τ is expressed by the equation

$$\frac{4}{3}\pi r^3 = \frac{\overline{m}\,\tau}{d} = \frac{\omega}{d} \tag{1}$$

or

$$r = k_1 \cdot (\overline{m}\,\tau)^{1/3} = k_1 \cdot \omega^{1/3} \tag{2}$$

and the rate of flow is given by the Poiseuille relation

$$m = \frac{\pi\, r_c^4 d\, P_{eff}}{8\, l\, \eta} = k_2\, P_{eff} \tag{3}$$

Owing to the back pressure, produced by the interfacial tension at the surface of the growing drop, the effective pressure varies during the life of the drop. The back pressure [1] is related to the geometry of the drop by the equation

$$P_b = \frac{2\,\sigma}{r} \tag{4}$$

and the effective pressure can be written

$$P_{eff} = P_{tot} - P_b \tag{5}$$

If eqns. (2), (3), (4), and (5) are combined the instantaneous rate of flow is given by

$$m = k_2 P_{tot} - \frac{2\, k_2\, \sigma}{k_1\, (\overline{m}\,\tau)^{1/3}} = M - \frac{k_3}{(\overline{m}\,\tau)^{1/3}} \tag{6}$$

This equation cannot be tested experimentally as the rate of flow is not explicitly expressed. It may, however, be transformed. The instantaneous and mean rates of flow are related to the weight of the drop by the equations

$$m = \frac{d\omega}{d\tau} \tag{7}$$

and

$$\overline{m} = \frac{\omega}{\tau} \tag{8}$$

After substituting these equations into eqn. (6) and solving for ω and differentiating the following expression is obtained [2]

$$m = M - \frac{2}{3} \cdot \frac{1.5\ M^{2/3}\ \delta\ \tau^{-1/3}}{172.7\ h} - \frac{1}{3} \cdot \frac{1.5\ M^{1/3}\ \sigma^2\ \tau^{-2/3}}{(172.7\ h)^2} \tag{9}$$

The corresponding formula of the mean rate of flow is

$$\overline{m} = M - \frac{1.5\ M^{2/3}\ \sigma\ \tau^{-1/3}}{172.7\ h} - \frac{1.5\ M^{1/3}\ \sigma^2\ \tau^{-2/3}}{(172.7\ h)^2} \tag{10}$$

In these equations the first term on the right hand side is equal to the rate of flow obtained when there is no back pressure. It can be measured by determining the rate of flow when the capillary tip is immersed in a pool of mercury [3]. The quantities M, σ, τ and h in the equations are known, or can easily be determined. With a technique described below the instantaneous rate of flow can be measured, thus making it possible to check eqn. (9) experimentally.

Table 1. Comparison between measured and calculated values of the instantaneous rate of flow of mercury.

Sec	Expt. a, −0.8 volts		Expt. b, −0.9 volts		Expt. c, −1.0 volts		Expt. d, −1.1 volts		Expt. e, −1.2 volts	
	m calc.	*m* meas.	*m* calc.	*m* meas.	*m* calc.	*m* meas.	*m* calc.	*m* meas.	*m* calc.	*m* meas.
0.432	1.648	1.652	1.649	1.655	1.651	1.647	1.655	1.663	1.659	1.658
0.864	1.675	1.669	1.676	1.681	1.678	1.665	1.681	1.682	1.684	1.687
1.296	1.688	1.681	1.689	1.698	1.691	1.685	1.694	1.695	1.696	1.697
1.723	1.696	1.694	1.697	1.698	1.699	1.700	1.701	1.702	1.703	1.701
2.592	1.707	1.705	1.708	1.713	1.709	1.710	1.711	1.712	1.713	1.712
3.447	1.713	1.714	1.714	1.717	1.715	1.719	1.717	1.717	1.718	1.720
3.889	1.716	1.709	1.716	1.719	1.717	1.723	1.719	1.717	1.721	1.723
5.160	1.721	1.720	1.722	1.724	1.723	1.720	1.724	1.724	1.726	1.726

EXPERIMENTAL

The method of determining the rate of flow is as follows.

For a given capillary and at a constant mercury pressure the weight of mercury droplets falling naturally from the dropping mercury electrode can be determined in a well-known manner. If now the individual droplets are disengaged from the capillary at a moment shortly before the natural drop time is reached, the difference between the weights of a natural and forced drop gives a mean value of the rate of flow during this last interval of the life of the drop. If this interval is chosen to be sufficiently short, the mean rate of flow can be taken as the instantaneous value during the interval.

This process is repeated for other selected intervals of the life of the drop, giving the instantaneous rate of flow of mercury from the capillary for any time.

The mercury drops are disengaged using an electromagnetically operated hammer described in a previous paper in this series [4]. The solution used in the experiments was 0.1 M potassium chloride with 0.009 % of gelatine, deaerated with purified nitrogen [5]. The anode consisted of a silver sheet and the applied potential, constant during each experiment, was varied from 0.8 to 1.2 volts *vs* the silver anode. The vessel and apparatus used for collecting the mercury drops has been described by Lingane and Kolthoff [6]. The temperature was held at 25 ± 0.1° C, the height of the upper mercury level above the capillary orifice was 57.0 cm and for M a value of 1.776 mg mercury per second was obtained.

With the technique described above a series of experiments has been carried out and the results are given in Table 1, where the measured values of m are listed together with those calculated according to eqn. (9). The values of the interfacial tension used in the calculations have been taken from Grahame [7].

The empirical results show a very good agreement with those calculated. The deviation of the measured value from the calculated value does not exceed 0.3 %, a figure that is of the same order of magnitude as for example the accuracy of the measurements of the age of the drop. Thus, eqn. (9) is shown to give a correct value of the instantaneous rate of flow of mercury from the measured data.

REFERENCES

1. Kucera, G. *Ann. Physik* **11** (1903) 529.
2. Smith, G. S. *Trans. Faraday Soc.* **47** (1951) 63.
3. Müller, O. H. *J. Am. Chem. Soc.* **66** (1944) 1019.
4. Wåhlin, E. and Bresle, Å. *Acta Chem. Scand.* **10** (1956) 935.
5. Meyer, F. R. and Ronge, G. *Z. anorg. Chem.* **52** (1939) 637.
6. Lingane, J. J. and Kolthoff, I. M. *J. Am. Chem. Soc.* **61** (1939) 825.
7. Grahame, D. C. *Chem. Revs.* **41** (1947) 448.

Received April 13, 1956.

ACTA CHEMICA SCANDINAVICA 10 (1956) 947—950

On the Instantaneous Polarographic Current

III. Accurate Measurements of the Residual Current

ÅKE BRESLE

Institute of Inorganic and Physical Chemistry, University, Stockholm; Royal Institute of Technology, Stockholm, Sweden

With an apparatus described by Wåhlin and Bresle the instantaneous residual polarographic current has been measured. Data from these measurements are presented in this paper. The measured values show that the residual current can quantitatively be divided into a condenser and a faradaic current. From the condenser current the capacity constant is calculated giving the value of 19.7 ± 0.2 microfarads · cm^{-2}.

The instantaneous diffusion current is not a primary quantity found experimentally, but is a calculated difference between the measured limiting current and the measured residual current. The accuracy of the calculated diffusion current, as a consequence, depends on the accuracy of measurement of these quantities. Several theoretical considerations on the form of the mathematical expression for the diffusion current are to be found in the literature, but there are few accurate experimental data on the instantaneous currents.

This paper gives experimental data and calculations on the instantaneous residual current obtained in a common electrolyte under ordinary polarographic conditions. The measurements are intended to be used later in presenting instantaneous values of the diffusion current from measurements of the limiting current.

THEORETICAL

The instantaneous condenser current produced by the dropping mercury electrode can be written [1]

$$i_c = k \cdot \frac{dF}{d\tau} \cdot \Delta E \qquad (1)$$

where F is the area of the drop at the time τ, ΔE the potential difference between the electrocapillary maximum and the actual constant potential for the experiment, τ the age of the drop, and k the capacity constant. If the

drop is assumed to be spherical [2,3], the area can be expressed using the symbols m (the rate of flow of mercury from the capillary in mg per sec) and τ, eqn. (1) being transformed to

$$i_c = k \cdot 0.0057 \cdot m^{2/3}\ \tau^{-1/3}\Delta E \qquad (2)$$

As it is very difficult to remove the last traces of oxygen and mercury ions from the solution [4] the current obtained is always a sum of the condenser current and a faradaic current, i_F, caused by the reduction of the above-mentioned elements and sometimes of other impurities. Thus the measured current i_{res} can be written

$$i_{res} = i_c + i_F \qquad (3)$$

or, as the condenser current is proportional to $\tau^{-1/3}$ and the faradaic current is proportional to $\tau^{1/6}$

$$i_{res} = A\tau^{-1/3} + B\tau^{1/6} \qquad (4)$$

This can be transformed to

$$\frac{i_{res}}{\tau^{1/6}} = A\tau^{-\frac{1}{2}} + B \qquad (5)$$

The value of the true condenser current is obtained graphically if the experimental data, $i_{res}/\tau^{1/6}$, are plotted against $\tau^{-\frac{1}{2}}$ and the constant A is evaluated.

EXPERIMENTAL

The apparatus used in the experiments was Polarograph Type 3266 B, LKB-Produkter Fabriks AB, Sweden, furnished with a device for knocking the mercury drop off the capillary, described earlier by Wåhlin and Bresle [5].

The solution was 0.1 M potassium chloride with 0.09 % of gelatine in ion-free water. Deaeration was carried out for two hours with oxygen-free nitrogen gas, purified according to Meyer and Ronge [6]. The chemicals used, mercury, potassium chloride, and gelatine, were of Polaritan reagent grade in all experiments. The temperature was 25 ± 0.1 °C. The mean rate of flow of mercury from the capillary was measured and the corresponding instantaneous value was calculated as described in a previous paper in this series [7]. The calculations justified the use of a constant value of m for the last 2/3 of the life of the drop without any great error. The potential at the electrocapillary maximum was obtained by evaluating the maximum drop time from observed values of the drop time at different potentials. The value thus obtained was −0.45 ± 0.02 volts *vs* the silver anode. The potential in all the experiments was −0.94 volts *vs* the silver anode.

The rates of flow of mercury in the experiments are given in Table 1 and corresponding values of time and residual current in Table 2. With the aid of eqn. (5) the constants A and B are calculated [8] and listed in Table 3 together with the values of the capacity constant, calculated according to eqn. (2). Table 4, finally, gives a comparison between the residual current measured directly, and the calculated as the sum of a condenser and a faradaic current using Table 3 and eqn. (4).

CONCLUSIONS

The reproducibility of the measurements can be studied in Table 2. The experiments number 1 and 2 listed in this table are made under the same conditions. The values of the residual current differs somewhat, those in expt. 1

Table 1. Values of the rate of flow of mercury.

Expt.	m mg / sec
1	2.024
2	2.024
3	1.716
4	1.487
5	1.280

Table 2. Instantaneous values of the residual current.

Sec	i_{res} measured				
	No. 1	No. 2	No. 3	No. 4	No. 5
1.383	0.1005	0.0967	0.0855	0.0784	0.0703
1.729	0.0942	0.0917 *	0.0811 *	0.0745 *	0.0669 *
2.075	0.0908	0.0867	0.0774	0.0701	0.0630
2.421	0.0882	0.0852 *	0.0753 *	0.0687 *	0.0614 *
2.766	0.0865	0.0829	0.0730	0.0663	0.0594
3.112	0.0845	0.0807 *	0.0715 *	0.0646 *	0.0580 *
3.458	0.0825	0.0792	0.0694	0.0632	0.0566
3.804	0.0811	0.0776 *	0.0682 *	0.0615 *	0.0550 *
4.150	0.0794	0.0764	0.0672	0.0606	0.0542

* interpolated

Table 3. The capacity constant for different parameters.

Expt.	A	B	k
1	0.0873	0.0200	19.9
2	0.0872	0.0175	19.9
3	0.0748	0.0164	19.1
4	0.0705	0.0133	19.5
5	0.0647	0.0111	20.1

always exceeding those in expt. 2 by about 4 %. The explanation for this difference is given in Table 3, where it can be seen that the condenser current part in these two experiments is the same, as the values of A are practically identical. The different values of the constant B, however, indicate that the faradaic component, due to impurities, is somewhat smaller in the latter experiment.

The capacity constant of the expanding mercury drop calculated from values of the current for different rates of flow assumes the value of 19.7 ± 0.2 microfarads $\cdot$ cm^{-2}. The value given by other authors obtained by different methods are: Philpot [9], 21.8 microfarads $\cdot$ cm^{-2}; Ilkovic [1], 22.3 microfarads $\cdot$ cm^{-2}.

There is good agreement between the measured residual current, and that calculated on the assumption that this current can be divided into a condenser part and a faradaic part. The deviation is about 1 % at the beginning of the life of the drop, but is then diminished to some tenths of a per cent, as can be seen from Table 4.

Table 4. Comparison between calculated and measured values of the instantaneous residual current obtained in experiment No 1.

Sec	i_c calc.	i_F calc.	$i_c + i_F$	
			calc.	meas.
1.383	0.0784	0.0211	0.0995	0.1005
1.729	0.0727	0.0219	0.0946	0.0942
2.075	0.0684	0.0226	0.0910	0.0908
2.421	0.0650	0.0232	0.0882	0.0882
2.766	0.0622	0.0237	0.0859	0.0865
3.112	0.0598	0.0242	0.0840	0.0845
3.458	0.0578	0.0246	0.0824	0.0825
3.804	0.0560	0.0250	0.0810	0.0811
4.150	0.0544	0.0254	0.0798	0.0794

REFERENCES

1. Ilkovic, D. *Collection Czechoslov Chem. Communs.* **8** (1936) 170.
2. Smith, G. S. *Trans. Faraday Soc.* **47** (1951) 63.
3. Hans, W., Henne, W. and Meurer, E. *Z. Elektrochem.* **58** (1954) 836.
4. Kolthoff, I. M. and Lingane, J. J. *Polarography* 2nd Ed., Interscience Publ. Inc. New York 1952, p. 151.
5. Wåhlin, E. and Bresle, Å. *Acta Chem. Scand.* **10** (1956) 935.
6. Meyer, F. R. and Ronge, G. *Z. anorg. Chem.* **52** (1939) 637.
7. Bresle, Å. *Acta Chem. Scand.* **10** (1956) 943.
8. Scarborough, B. J. *Numerical mathematical analysis*, 2nd Ed. Baltimore 1950, p. 446.
9. Philpot, Y. St. I. *Phil. Mag.* **13** (1932) 775.

Received April 13, 1956.

ACTA CHEMICA SCANDINAVICA 10 (1956) 951—956

On the Instantaneous Polarographic Current

IV. Measurements of the Diffusion Controlled Current

ÅKE BRESLE

Royal Institute of Technology, Stockholm, Sweden

The instantaneous diffusion current has been measured by means of a special method which makes use of an externally controlled drop time of the dropping mercury electrode. The results are shown to be very reproducible. Attempts to correlate the experimental data with the revised Ilkovic relationship support the assumption this equation is inadequate in its present form.

It is well-known that the Ilkovic formula gives a relatively clear picture of the mathematical relationship between the fundamental polarographic variables. However, more quantitative attempts to correlate the empirical values of the diffusion current using the Ilkovic formula have lead to the addition of a correction term to this expression, based upon theoretical considerations neglected in the original formula. The nature of this correction term has been widely discussed in the literature. As there are few sufficiently accurate measurements of the instantaneous diffusion current, the different proposals cannot be rigorously checked.

Such precise diffusion current data can only be obtained from reliable measurements of the following polarographic quantities, *viz.* the instantaneous rate of flow of mercury from the capillary, the instantaneous residual current and the instantaneous limiting current.

Using a method, described by Wåhlin and Bresle [1], the rate of flow of mercury [2] and the residual current [3] have been investigated. The results obtained show that it is possible to measure values of these variables with an accuracy of the same order of magnitude as the accuracy of, *e. g.*, the temperature constancy and the measurements of the concentration of the depolarizer in the experiments.

The instantaneous limiting diffusion current of cadmium ions in potassium chloride solution has been determined with the techniques mentioned above. This paper gives results of these measurements together with some calculations of the diffusion current according to the revised Ilkovic formula. The results are compared with those obtained by other investigators.

EXPERIMENTAL

The measurements were made with the same apparatus and the same techniques as described earlier [3]. The depolarizer was cadmium sulphate of ANALAR quality. A stock solution of this reagent was made and standardized with the aid of an ion exchanger resin (Dowex 50). Potassium chloride and gelatine were added to known volumes of this solution which was then diluted to give the final solutions used in the experiments.

For the calculations the value of the diffusion constant of cadmium ions in 0.1 M potassium chloride was assumed to be 7.17×10^{-6} cm^2 sec^{-1}, a value determined experimentally by v. Stackelberg *et al* [4].

THE REPRODUCIBILITY OF THE MEASUREMENTS

In order to check the reproducibility of the measurements some experiments have been repeated under identical conditions. The values of the currents measured in three experiments are given under No. 1, No. 2, and No. 3 in Table 1. The two first experiments are made with an electronic polarograph and the last with a non-electronic instrument. The deviation from the calculated mean of these values of the current is about 0.2 % indicating that there is no significant difference in the results obtained using the two types of polarograph.

List of symbols

i_{lim} = instantaneous limiting current microamps
i_τ = instantaneous diffusion current microamps
τ = age of the drop, sec
n = number of electrons taking part in the electrode reaction
D = diffusion constant, cm^2 · sec^{-1}
m = rate of flow of mercury from the capillary, mg · sec^{-1}
C = concentration of the depolarizer, millimoles · liter^{-1}
K,α = constants

THE RELATION BETWEEN i AND C

According to the fundamental polarographic law

$$i_\tau = \alpha \cdot C \qquad (1)$$

the ratio of the instantaneous diffusion current and the concentration of the depolarizer is a constant for fixed values of m and τ. Using values of the residual instantaneous current [3] published earlier and of the limiting instantaneous current, given in Tables 1 and 2 in this paper, this ratio has been calculated.

The results are given in Table 3, together with the mean value and the percentage deviation of the three measurements for every value of τ.

The divergence from the mean value is about 1 % up to the first second of the life of the drop; it gradually diminishes as the drop grows older and is only some tenths of a per cent at the later part of the life of the drop. There is a slight increase of the ratio α with increasing concentrations of the depolarizer; this is probably due to some contribution of the migration current in the total measured current in the experiments with the highest depolarizer concentration.

Table 1. Measured values of the instantaneous limiting current.

Sec	i_{lim} (μA)				Percentage error	i_{lim} (μA)			Percentage error
	No. 1	No. 2	No. 3	Mean value		No. 4	No. 5	Mean value	
1.038	3.1894	3.2012	3.2171	3.2026	0.5	7.9489	7.9693	7.9591	0.1
1.383	3.4542	3.4449	3.4460	3.4484	0.2	8.5814	8.5792	8.5803	0.1
1.729	3.6730	3.6815	3.6908	3.6818	0.3	9.1174	9.1494	9.1334	0.2
2.075	3.8418	3.8448	3.8585	3.8484	0.3	9.5462	9.5605	9.5534	0.1
2.421	3.9915	3.9867	3.9888	3.9890	0.1	9.9482	9.9384	9.9433	0.1
2.766	4.1335	4.1287	4.1325	4.1316	0.1	10.2590	10.2566	10.2578	0.0
3.112	4.2372	4.2351	4.2470	4.2398	0.2	10.5699	10.5417	10.5558	0.1
3.458	4.3446	4.3440	4.3454	4.3447	0.1	10.8058	10.7671	10.7865	0.2
3.804	4.4310	4.4386	4.4412	4.4369	0.1	11.0309	11.0058	11.0184	0.1
4.150	4.5173	4.5309	4.5317	4.5266	0.1	11.2453	11.2047	11.2250	0.2

No. 1: 0.5256 mM Cd^{2+}, LKB polarograph (electronic)
No. 2: 0.5256 mM Cd^{2+}, —»—
No. 3: 0.5256 mM Cd^{2+}, Heyrovsky type polarograph (non-electronic)
No. 4: 1.3152 mM Cd^{2+}, LKB polarograph
No. 5: 1.3152 mM Cd^{2+}, Heyrovsky type polarograph

Nos. 1—5: —0.93 volts *vs* the silver anode, m = 2.024 mg Hg pr sec, supporting electrolyte: 0.1 M KCl with 0.009 % gelatine, temperature: 25 °C

Table 2. Measured values of the instantaneous limiting current.

Sec	i_{lim} (μA)			
	No. 6	No. 7	No. 8	No. 9
1.038	0.7262	2.8382	2.5465	2.2798
1.383	0.7681	3.0838	2.7768	2.4985
1.729	0.8100	3.2661	2.9591	2.6674
2.075	0.8393	3.4273	3.1049	2.7979
2.421	0.8630	3.5655	3.2220	2.9073
2.766	0.8905	3.6883	3.3371	3.0071
3.112	0.9124	3.8035	3.4350	3.0973
3.458	0.9324	3.8994	3.5310	3.1779
3.804	0.9506	3.9954	3.6116	3.2604
4.150	0.9664	4.0587	3.6538	3.3160

No. 6: 0.1049 mM Cd^{2+}, m = 2.024 mg Hg pr sec
No. 7: 0.5256 mM Cd^{2+}, m = 1.716 mg Hg pr sec
No. 8: 0.5256 mM Cd^{2+}, m = 1.487 mg Hg pr sec
No. 9: 0.5256 mM Cd^{2+}, m = 1.280 mg Hg pr sec
Nos. 6—9: —0.93 volts *vs* the silver anode, upporting electrolyte: 0.1 M KCl with 0.009 % gelatine, temperature: 25 °C.

Table 3. Relation between instantaneous diffusion current and concentration.

Sec	$i_\tau/C = a$						Mean value	Percentage deviation
	No. 6	No. 1	No. 2	No. 3	No. 4	No. 5		
1.038	5.878	5.860	5.882	5.912	5.961	5.976	5.916	1.0
1.383	6.364	6.381	6.363	6.365	6.448	6.447	6.395	0.8
1.729	6.824	6.820	6.825	6.843	6.861	6.885	6.843	0.6
2.075	7.135	7.137	7.142	7.168	7.189	7.200	7.162	0.5
2.421	7.386	7.426	7.417	7.421	7.497	7.490	7.440	0.7
2.766	7.664	7.700	7.667	7.698	7.735	7.733	7.700	0.5
3.112	7.892	7.901	7.897	7.920	7.952	7.951	7.922	0.4
3.458	8.102	8.109	8.108	8.111	8.153	8.124	8.118	0.2
3.804	8.289	8.276	8.291	8.295	8.326	8.310	8.298	0.3
4.150	8.456	8.443	8.469	8.471	8.460	8.459	8.465	0.3

MATHEMATICAL INTERPRETATION OF THE MEASURED DIFFUSION CURRENT

The revised Ilkovic equation can be written according to v. Stackelberg-Strehlow [5], Lingane-Loveridge [6] and Kambara *et al.*[7]

$$i_\tau = 709\ n\ D^{\frac{1}{2}}\ C\ m^{2/3}\ \tau^{1/6} + KnDC\ m^{1/3}\ \tau^{1/3} \qquad (2)$$

where different values are given to the symbol K by the various investigators. Eqn. (2) may be rewritten in a form more easily handled and more suitable for studying the symbol K:

$$i_\tau - 709\ n\ D^{\frac{1}{2}}\ C\ m^{2/3}\ \tau^{1/6} = P = KnDCm^{1/3}\ \tau^{1/3} \qquad (3)$$

$$K = \frac{P}{nDC\ m^{1/3}\ \tau^{1/3}} \qquad (4)$$

Taking the available values of the diffusion current given by Taylor *et al.*[8], Khalafalla [9], Hans *et al.*[10] and in Table 3 in this paper, K has been calculated and the different values are presented in Table 4. The variation of K with time can be studied in Fig. 1. The agreement between the results obtained from the data of the different investigators shows the term K to be a function of τ. It has large negative values in the beginning of the life of the drop, passes through the value zero when the drop is about 1 second old and then increases, more and more slowly, until the maximum drop time is reached. This indicates that the revised Ilkovic equation in the form given in eqn. (2) does not describe the experimental data exactly. The variation of i_τ with m has been studied in experiments Nos. 1, 7, 8, and 9 given in Tables 1 and 2. According to eqn. (2) the diffusion current for fixed values of C and τ should depend on

Table 4. Comparison between different calculated values of the symbol K in the revised Ilkovic equation.

Taylor			Khalafalla			Hans			The author		
τ	i_τ	K	τ	i_τ	K	τ	i_τ	K	τ	i_τ	K
0.100	8.26	−200 300	0.4	5.50	−55 600	0.10	1.308	−201 000	1.038	5.916	−10 700
0.200	12.14	− 93 200	0.5	6.05	−32 100	0.40	2.867	− 46 200	1.383	6.395	− 740
0.384	15.59	− 34 200	1.0	7.25	− 6 500	0.60	3.350	− 20 200	1.729	6.843	+ 8 440
0.495	16.98	− 5 250	1.5	7.95	+ 2 600	0.80	3.718	− 4 600	2.075	7.162	13 060
0.719	19.06	+ 3 900	2.0	8.55	10 700	1.00	3.994	+ 4 700	2.421	7.442	16 340
1.062	21.17	17 700	2.5	9.03	16 200	1.50	4.428	13 600	2.766	7.700	19 630
1.468	23.02	27 100	3.0	9.40	19 100	2.00	4.794	21 000	3.112	7.922	21 990
2.014	24.64	38 000				3.00	5.320	29 000	3.458	8.118	23 500
2.410	25.85	36 100				4.00	5.720	33 400	3.804	8.298	25 050
2.990	26.98	36 800				4.60	5.902	34 900	4.150	8.465	26 100
3.488	27.70	36 400									

the rate of flow, m, raised to a power of between one third and two thirds, or mathematically expressed

$$\frac{1}{3} < \left(\frac{\delta \log i_\tau}{\delta \log m}\right)_{c,\tau} < \frac{2}{3} \qquad (5)$$

The plot of log i_τ *vs* log m (not reproduced here) for values obtained in the experiments described above, shows that the individual points lie very well together, but, somewhat surprisingly on a straight line of slope 0.7 rather than

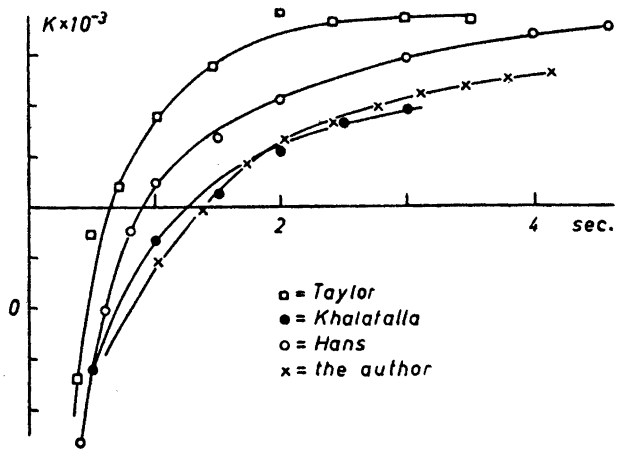


Fig. 1. The variation of the symbol K *in the revised Ilkovic equation.*

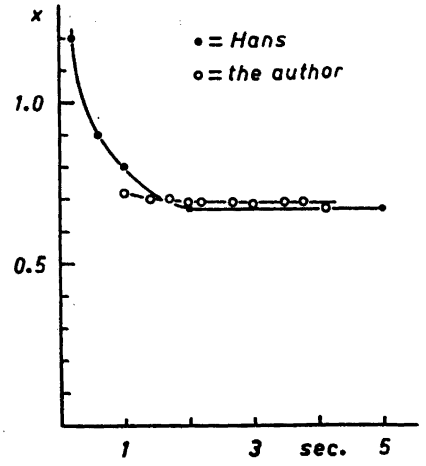


Fig. 2. The slope of the line log $i_\tau = x \log \tau + \log A$ *for different values of the age of the drop.*

on a curve. For a comparison the corresponding values from the measurements of Hans *et al.*[10] have been studied, and the same result was obtained: for fixed values of C and τ, log i_τ can be expressed as a linear function of log m. In Fig. 2 the slopes of these lines are plotted *vs* the age of the drop. The result indicates that the diffusion current is a function of m raised to a power, not between 1/3 and 2/3, but greater than 2/3, or approaching it asymptotically. To explain this fact it is necessary to reconsider whether the best revision of the Ilkovic equation is to add a correction term as done by the authors cited above, or whether the theoretical principles underlying the original Ilkovic equation should be critically re-examined.

The author wishes to acknowledge his great gratitude to Dr. Axel Johansson for his interest and encouragement and to Dr. Erik Wåhlin for many valuable discussions.

REFERENCES

1. Wåhlin, E. and Bresle, Å. *Acta Chem. Scand.* **10** (1956) 935.
2. Bresle, Å. *Acta Chem. Scand.* **10** (1956) 943.
3. Bresle, Å. *Acta Chem. Scand.* **10** (1956) 947.
4. von Stackelberg, M. Pilgram, M. and Toome, V. *Z. Electrochem.* **57** (1953) 342.
5. Strehlow, H. and von Stackelberg, M. *Z. Electrochem.* **54** (1950) 51.
6. Lingane, J. J. and Loveridge, B. *J. Am. Chem. Soc.* **72** (1950) 438.
7. Kambara, T., Suzuki, M. and Tachi, I. *Bull. Chem. Soc. Japan* **23** (1950) 219.
8. Taylor, J. K., Smith, R. E. and Cooter, I. L. *J. Research Natl. Bur. Standards* **42** (1949) 387.
9. Khalafalla, S. **Publ. 5542**, *Univ. Microfilm, Ann Arbor, Mich.* (1953).
10. Hans, W., Henne, W. and Meurer, E. *Z. Electrochem.* **58** (1954) 836.

Received April 13, 1956.

ACTA CHEMICA SCANDINAVICA 10 (1956) 957—984

Equilibrium Studies of Polyanions

I. Isopolyvanadates in Acidic Media

F. J. C. ROSSOTTI and HAZEL ROSSOTTI

Department of Inorganic Chemistry, The Royal Institute of Technology, Stockholm 70, Sweden *

The following equilibria have been assigned to the isopolyvanadate system in the range $-0.5<\mathrm{pcH}<6.5$, on the basis of spectrophotometric and potentiometric measurements (with glass electrodes) made in perchlorate media at 25°C:

$10VO_2^+,\mathrm{aq.} + 8\,H_2O \rightleftharpoons H_2V_{10}O_{28}^{4-},\mathrm{aq.} + 14\,H^+$; $\varkappa_{14,10}$

$H_2V_{10}O_{28}^{4-},\mathrm{aq.} \rightleftharpoons HV_{10}O_{28}^{5-},\mathrm{aq.} + H^+$; $K_{15,10}$

$HV_{10}O_{28}^{5-},\mathrm{aq.} \rightleftharpoons V_{10}O_{28}^{6-},\mathrm{aq.} + H^+$; $K_{16,10}$

The cation $VO_2^+,\mathrm{aq.}$ is the sole species in solutions $-0.5<\mathrm{pcH}<1.3$ (for a 1 M perchlorate medium in which sodium is the predominant cation), and the isoelectric point is given by:

$$\mathrm{pcH} = 0.803 - 0.643 \log B \text{ and}$$
$$\mathrm{pcH} = 0.715 - 0.643 \log B$$

for 1 M and 3 M perchlorate media, respectively. The values of the equilibrium constants are evaluated as:
$\log \varkappa_{14,10} = -6.75 \pm 0.15$; $\log K_{15,10} = -3.6 \pm 0.3$; and $\log K_{16,10} = -5.8 \pm 0.1$ in the 1 M medium, and $\log \varkappa_{14,10} = -5.5 \pm 0.15$; and $\log K_{15,10} = -3.5 \pm 0.3$ in the 3 M medium. The application of the "core + links" treatment to the data is indicated in an appendix.

PREVIOUS WORK ON THE HYDROLYSIS OF VANADIUM(V)

Considerable uncertainty exists as to the nature of the orange-yellow vanadium(V) species which occur in acidic solution. The existence of the cation, VO_2^+, is well established, but it is not clear if less hydrolysed cations also exist. The nature of the polyvanadates in acidic media appears to be completely in doubt.

Düllberg [1] demonstrated the existence of cationic species by transport measurements in strongly acidic solutions, and the redox potentials between vanadium(V) and (IV) were first interpreted in terms of an equilibrium between

* Present address: Department of Chemistry, University of Edinburgh, Scotland.

VO_2^+ and VO^{2+} by Foerster and Böttcher [2]. Although this interpretation has been confirmed by many other workers (*cf.* Hart and Partington [3] and refs. therein) several authors have mentioned the possible existence of species less hydrolysed than VO_2^+. The existence of VO^{3+} has been discussed by Meyer and Pawletta [4], Britton and Welford [5] and Jander and Jahr [6]. More recently, the existence of VO^{3+} has been proposed by Trujillo and Rios [7] and of $V(OH)_3^{2+}$ by Ramsey, Colichman and Pack [8], in order to explain the kinetics of reduction of vanadium(V) by iodide ions. The diffusion data of Jander and Jahr [6] indicate that the cations, whatever they may be, are not polymerised. No distinction can be made between alternative formulae such as VO_2^+ or $V(OH)_4^+$ by conventional equilibrium methods, but LaSalle and Cobble [9] have recently shown that the former formula is more probable on the basis of structure-entropy considerations. For simplicity, all formulae will be written here in a form stripped of the maximum possible number of molecules of water.

An isoelectric point [6,10] occurs in the region of pcH = 2 *. The orange-yellow *iso*polyvanadic acid which is then formed has been variously considered to contain 2, 4, 5, 6 and 10 vanadium atoms. The main experimental support for most of these formulations has been the occurrence of a point of inflexion in pH titration curves, or a break in conductimetric titration curves in the region $3<\text{pcH}<6$. Thus Ducret [10] considers that the inflexion corresponds to the uptake of one hydroxyl ion per molecule of V_2O_5, and that the orange-yellow colour is due to $H_3V_2O_7^-$. Düllberg [1] had realised that this evidence alone cannot give the degree of polymerisation of the acid, and chose instead the formula $HV_6O_{17}^{3-}$ on the basis of molecular weight determinations and by analogy with an orange solid $Na_4V_6O_{17}$, aq. However, solid vanadates corresponding to a wide variety of ratios of $Na_2O:V_2O_5$ are claimed (see p. 978), and the molecular weights determined by a combination of cryoscopic and conductivity measurements are of doubtful validity. Nevertheless, the existence of hexavanadic acid has been supported by Bray and Tihenko [12], Carpéni and Souchay [13,14], and by Trujillo [15] mainly on the basis of the point of inflexion obtained in titration curves.

However, Britton and Robinson [16], Britton and Welford [5], and Hazel, McNabb and Santini [17] consider that the point of inflexion corresponds to the uptake of only 0.8 hydroxyl ions per molecule of V_2O_5, and formulate the species in solution as $V_{10}O_{27}^{4-}$. This choice was also supported by the existence of the salt $Na_4V_{10}O_{27}$, aq. Although the interpretation of Robinson and Sinclair's vapour pressure measurements [18] is not unequivocal, the data indicate that the molecular weight of the polyvanadate ion existing in acidic solutions is of the order of 1 000, and point to a degree of polymerisation greater than 6 and of the order of 10.

Jander and Jahr [6] assumed that the stable polyvanadate at pcH$\sim$3 is $Na_2H_4V_5O_{16}^-$, by analogy with a salt which was considered to be a pentatantalate [19], but which Lindqvist and Aronsson have subsequently shown to be a hexatantalate [20]. This erroneous assumption forms the basis of Jander and Jahr's interpretation of diffusion data for the polyvanadate system [6] in terms

* The symbol pcH denotes $-\log h$, where h is the free concentration of hydrogen ions *cf. Ref.* [11].

of Riecke's law, which is itself of doubtful validity in these systems [21]. Moreover, as Carpéni and Souchay [14] have pointed out, Jander and Jahr's titration data [6] do not, in fact, appear to support these authors' interpretation of the diffusion data. Ottar [22] has recently reinterpreted the diffusion data on the basis of a kinetic theory, and has obtained the formula $V_4O_{13}^{6-}$ for the polyvanadates existing in acidic solutions. This interpretation is based on the supposition that all polyvanadates consist of chains of VO_4^{3-} tetrahedra, which share one corner, (see p. 978), and involves assumptions about the formation of hydrogen bonds between solute and solvent. Consequently, the diffusion data must still be considered to be of only qualitative interest.

It appears to be generally agreed [17] that the polyvanadates stable in acidic media depolymerise with increasing pcH to trimeric or tetrameric metavanadates, $(VO_3^-)_n$; pyrovanadates, $V_2O_7^{4-}$; and finally to monomeric orthovanadates, VO_4^{3-}. These equilibria, however, are outside the scope of the present work.

List of symbols

A		Total concentration of A
a		concentration of free A
A_s		optical absorbancy
B		total concentration of B, or of metal
$\boldsymbol{B}$		normalised variable defined by (25) or (31)
b		concentration of free B
c_j	=	$[B(A_{st}B_s)_j]$ (51)
E		measured potential in mV
E_j		liquid junction potential
E_0	=	$E - E_j - 59.16 \log h$ (2)
g	=	$\Sigma\ K_j u^{sj}$ (48)
H		total concentration of hydrogen ions, assuming all vanadium to be in the form VO_2^+ (4)
H'		total concentration of hydrogen ions, assuming all vanadium to be in the form V^{5+} (3)
h		concentration of free hydrogen ions
$\boldsymbol{h}$		normalised variable, variously defined by (13), (28) and (36)
j		variable number of polynuclear links, $(A_{st}B_s)$, per complex $B(A_{st}B_s)_j$
$\bar{j}$		average number of polynuclear links per complex, $B(A_{st}B_s)_j$
K_j		equilibrium constant for $(1 + sj)B + sjt\ A \rightleftharpoons B(A_{st}B_s)_j$ (49)
k_0, k		parameters defined by $K_j \rightleftharpoons k_0 k^{sj}$ (54)
$K_{p,q}$		equilibrium constant for $(VO_2)_q(OH)_p^{(p-q)-} + H_2O = (VO_2)_q(OH)_{p+1}^{(p+1-q)-} + H^+$
K_w	=	$[H^+][OH^-]$
l	=	$K_{16,10}K_{15,10}^{-1}$ (29)
M		mole/l
N		unique value of n
n		variable number of mononuclear links, (A_tB), per complex $B(A_tB)_n$
P		unique value of p
p		number of hydroxyl groups in complex $(VO_2)_q(OH)_p$
pcH	=	$-\log h$
Q		unique value of q
q		number of VO_2^+ groups in complex $(VO_2)_q(OH)_p$
s		smallest integer such that product st is also integral
t		number of A groups per B group in mononuclear link (A_tB)
u	=	bh^{-t} (48)
V	=	v^s (55)

v = ku (56)
$V_{\frac{1}{2}}$ = value of V corresponding to $y = \frac{1}{2}$
$X^{\frac{1}{2}}$ normalised variable defined by (60)
x = $\log B - t \log h$ (7)
$x_{\frac{1}{2}}$ = value of x corresponding to $y = \frac{1}{2}$
y = Zt^{-1} (8)
Z average number of hydroxyl groups per VO_2^+ group = $(h-H)B^{-1}$ (1)
Z_q = $\Sigma\, p[A_pB_q] \,/\, q\,\Sigma\,[A_pB_q]$ (19) and (34)
$\boldsymbol{Z}$ = ZZ_{10}^{-1}
$\alpha_{p,q}$ = $100q[A_pB_q]B^{-1}$ (42) and (43)
$\beta_{p,q}$ = $[A_pB_q]a^{-p}b^{-q}$ (41)
ε = $\frac{1}{9}(1 + \log \varkappa_{14,10} - 14 \log K_{15,10})$ (30)
η = $\log \frac{B}{b}$ (45)
ϑ = $P\varkappa_{P,Q}b^{Q-1}h^{-P}$ (12)
$\varkappa_{p,q}$ equilibrium constant for $q\ VO_2^+ + pH_2O \rightleftharpoons (VO_3)_q(OH)_p^{(p-q)-} + p\ H^+$

METHOD

A series of potentiometric titrations of vanadium(V) perchlorate solutions of differing concentrations, in an excess of perchloric acid, was carried out at 25° C. In each titration, the total concentration of metal, B, was held constant, and the hydrogen ion concentration was varied by additions of sodium hydroxide or sodium hydrogen carbonate. In the main series of titrations, all solutions were made 1 M with respect to perchlorate ions by the addition of sodium perchlorate. Preliminary titrations were also made in a 3 M perchlorate medium. As the concentration of metal ions and hydrogen ions never exceeded 2 % and 10 %, respectively, in the former medium, and 0.33 % and 3.3 %, respectively, in the latter medium, it may be assumed that the activity coefficients of all species remain constant. Although McKay has questioned this type of assumption [23], the simplest explanation of Biedermann and Sillén's results [24] appears to be that the activity coefficients remain constant, within the experimental error, for changes in the medium of this order of magnitude. Accordingly, it has been assumed that true stoichiometric equilibrium constants may be calculated from the measurements in each medium.

Since the hydrolysis of vanadium(IV) in a 3 M perchlorate medium has previously been reported [25], the possibility exists of interpreting vanadium (IV/V) redox equilibria as a function of hydrogen ion concentration in terms of the hydrolysis of vanadium(V). Unfortunately, equilibrium values of the redox potential could not be achieved in periods of up to 30 hours, using a number of different platinum, palladium and gold electrodes in conjunction with various potential mediators (*cf.* Refs.[3,26]). Therefore, only the equilibrium hydrogen ion concentration, h, was measured. Although this quantity may often be determined most accurately with hydrogen or quinhydrone electrodes, these cannot be used in vanadium(V) solutions [27]. A glass electrode was therefore used in combination with the reference half-cells, RE_1 or RE_3, where

RE_1 = Ag/0.01M $AgClO_4$ + 0.99M $NaClO_4$/1.00M $NaClO_4$

for titrations in 1 M perchlorate media, and

RE_3 = Ag/0.01 M $AgClO_4$ + 2.99M $NaClO_4$/3.00M $NaClO_4$

for titrations in the 3 M medium. Since equilibrium was achieved in 2 to 15 minutes with these cells (see below), it is considered that the failure to attain equilibrium redox potentials was due to some cause other than a slow hydrolysis reaction.

The average number of hydroxyl ions bound per central group may be calculated for each point of titration, using the relationship

$$Z = (h—H) / B. \quad (1)$$

where H is the total analytical concentration of hydrogen ions, defined by eqn. (4). Thus both H and B are known from the analyses of stock solutions. The data for Z as a function of log h at different total concentrations of metal were analysed by number of methods.

The potentiometric study was supplemented by a spectrophotometric investigation of the species existing in strongly acidic solution.

EXPERIMENTAL

Reagents

Vanadium (V) perchlorate solutions were prepared by dissolving vanadium pentoxide in perchloric acid. One batch of the pentoxide was prepared by dissolving sodium vanadate (*p.a.*) in hot water, and acidifying with perchloric acid. After the solution had stood overnight, more pentoxide was precipitated by evaporating the solution to half its bulk. The product was washed by decantation, centrifuged, and washed free from sodium ions. In other cases, commercial pentoxide (*p.a.*) which had been shown by analysis for vanadium(V) to be >99.9 % pure, was used. The solubility of vanadium pentoxide in perchloric acid is very low (*e.g.* ~0.06 M in 0.2 M acid), and equilibration is slow, *cf.* Ref. [9]. An excess of the oxide was allowed to stand in contact with ~0.2 M perchloric acid for about 4 weeks, and the yellow solution filtered through a very fine sintered glass disc. The concentration of vanadium(V) in the stock solution was determined as described previously [25]. The total concentration of perchlorate ions was found by titrating the eluate of aliquots passed through the hydrogen form of the resin Amberlite IR 120. Acidic solutions of vanadium(V) are reduced during passage through cation exchange resins [28] and the results were not reproducible. Accordingly, vanadium(V) was reduced to vanadium(IV) before passing aliquots through the ion-exhange column. Hydrogen sulphide was passed into the hot solution, excess of the gas expelled and sulphur coagulated by boiling, and the solution filtered.

Sodium hydroxide was freed from carbonate by allowing a 50 % solution of AnalaR grade reagent to stand for 4 weeks in a polythene bottle. Under nitrogen, the solution was filtered through a fine sintered glass disc, diluted with carbon dioxide-free water, and stored in polythene bottles. These solutions were standardised by potentiometric titration with perchloric acid, using Gran's method for calculating the end-point [29].

Sodium perchlorate solutions. One batch was prepared as described elsewhere [25]. A further stock solution was made by filtering a solution of the G. F. Smith Co. product, which had been shown to be free from iron, chlorate, hypochlorite and chloride ions. The solutions were analysed as described previously [25].

Other reagents were prepared and standardised by methods described elsewhere [25].

Procedure

The titration vessel, liquid junction, electrodes and potentiometer have also been described elsewhere [25]. The correct functioning of the Blomgren glass electrode was also tested by comparison with the quinhydrone electrode [25]. For the cell

$$RE/HClO_4 + NaClO_4/glass$$

at 25°C the relationship between the measured potential, E (in mV), and the concentration, of free hydrogen ions is given by

$$E = E_0 + E_j + 59.16 \log h \qquad (2)$$

The term E_0 includes the standard potentials of the electrodes, and the asymmetry potential of the glass electrode. E_j is the liquid junction potential, which was found to be a linear function of h in the range of acidity studied ($h \leq 0.1$ M) and in a given medium. The values of E_0 and of $E_j(h)$ were determined for each titration in the region where no hydrolysis of the ion VO_2^+ occurs (see below), and where h is identical to H.For each point, H is known from the analyses of the solution so that ($E - 59.16 \log h$) may be plotted as a function of h. The values of E_j so found

$$E_j = -16.5h \pm 0.5 \text{ mV/mole in 3 M perchlorate}$$
$$E_j = -63h \pm 2 \text{ mV/mole in 1 M perchlorate}$$

are in good agreement with the values of Biedermann and Sillén [24] and of Biedermann (quoted by Hietanen) [30].

In preliminary work, values of E_0 and of $E_j(h)$ for each titration were found by first titrating acid and base in the absence of metal. However, a change of $\lesssim 0.5$ mV in E_0 usually occurred when some of the acid-base mixture was withdrawn from the titration vessel and metal solution added.

When E_0 and $E_j(h)$ are known, values of h corresponding to the measured potentials E can be found by successive approximation, using eqn. (2).

Measurements were carried out at 25.0 ± 0.1°C in a paraffin oil thermostat placed in a room also thermostated at 25°C. In a particular titration, 18.0 ml of a solution A, containing 0.04 M vanadium(V) perchlorate and 0.12 M perchloric acid was added to 18.0 ml of 0.08 M perchloric acid. This mixture was titrated with equal volumes of 0.2 M sodium hydroxide, and of solution A. (All these solutions were 1 M with respect to perchlorate ions.) Thus, the total concentration of vanadium was 0.02 M throughout the titration. A total volume of 32 ml of each titrant was added stepwise. A value of $E_0 = -314.6$ mV was obtained from the points corresponding to the addition of the first 5.0 ml of each solution. Lower concentrations of perchloric acid and of sodium hydroxide were used for measurements with lower concentrations of vanadium. Series of titrations were carried out at least in duplicate with vanadium concentrations of 0.02, 0.01, 0.005 and 0.0025 M in a 1 M perchlorate medium. Titrations at the three lowest concentrations of metal were repeated in a 3 M perchlorate medium. Higher concentrations of metal could not be used, as vanadium pentoxide is precipitated from initial solutions ($h \sim 0.1$ M) in this medium. The equilibrium hydrogen ion concentration was varied from 10^{-1} to $10^{-6.5}$ M by additions of sodium hydroxide in the 1 M medium ,and of sodium hydrogen carbonate in the 3 M medium. Local excesses of hydroxyl ions were avoided by the use of the latter reagent, and it was shown by alternately bubbling nitrogen and carbon dioxide [31] that the measurements were not invalidated by complex formation between carbonate and vanadium(V) ions. The similarity between the $\bar{Z}$ $(\log h)_B$ data obtained in the two media using the different bases provides a further indication of the absence of such an effect.

A steady potential was usually reached between 2 and 15 minutes after the addition of alkali; the longer times were required for high values of d $\bar{Z}$/d log h. When a steady potential had been obtained, the same value was always found when measured again after an interval of 3 hours. Individial titrations appeared to be reversible. Thus, the pcH of a 0.01 M solution of vanadium(V) was raised from ~1.0 to ~4.3 during the course of 6½ hours. After an interval of 1 hour, the pcH was lowered stepwise to pcH ~1. Points for $\bar{Z}(\log h)_B$ lay on the same curve for the forward and backward titration (*cf.* Fig. 2). For this reason, it is considered that the failure to achieve an equilibrium redox potential was due to some cause other than a slow hydrolytic reaction. Britton and Welford [5] have previously found that equilibrium is rapid below, but slow above, pcH ~5, *cf.* Ref. [17].

The spectrophotometric measurements were made at 25 ± 1°C with a Beckman DU Spectrophotometer, using matched 1.00 cm silica cells, and minimum slit widths.

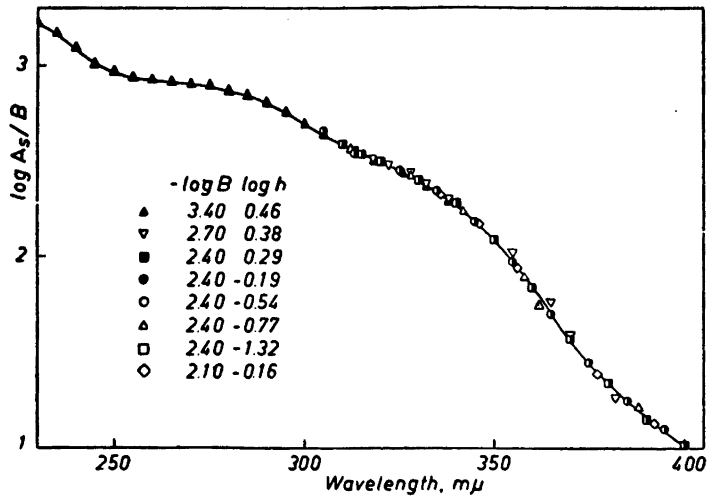


Fig. 1. Absorption spectrum of vanadium(V) perchlorate in acidic solutions 3 M with respect to perchlorate ion.

VANADIUM(V) PERCHLORATE IN STRONGLY ACIDIC SOLUTION

The total analytical hydrogen ion concentration, H', in the stock solution of vanadium(V) perchlorate and perchloric acid was first calculated assuming that all the vanadium(V) was unhydrolysed. Then

$$H' = [ClO_4^-] - 5\ B \qquad (3)$$

Preliminary titrations based on this assumption indicated that 4 hydroxyl ions are bound to each metal atom in the range 0.1 M$\geq h \gtrsim$0.04 M (for 0.01 M vanadium in the 3 M perchlorate medium), *i. e.* the species present is $[V(OH)_4^+]_x$ or $[VO_2^+]_x$.

The effect of higher acidities on the nature of this species was investigated for a range of metal concentrations by comparing the optical absorbancy, A_s, of a series of solutions, 3 M with respect to perchlorate ion. It was found that the plot of A_s/B against wavelength was independent of B in the range 0.008 M$\geq B \geq$0.0004 M, and of h in the range 2.89 M$\geq h \geq$0.048 M. The spectrum (see Fig. 1) is substantially the same as that recently obtained in ~0.2 M perchloric acid by LaSalle and Cobble [9]. As the ratio A_s/B is independent of the value of B, the vanadium cation may be assumed to be the monomeric species, VO_2^+,aq.

It is therefore convenient to discuss subsequent results in terms of the combination of hydroxyl ions to a central VO_2^+ group. H is now defined as the total analytical concentration of hydrogen ions, assuming all the vanadium to be in the form VO_2^+. Thus for the stock solution of vanadium (V) perchlorate

$$H = [ClO_4^-] - B \qquad (4)$$

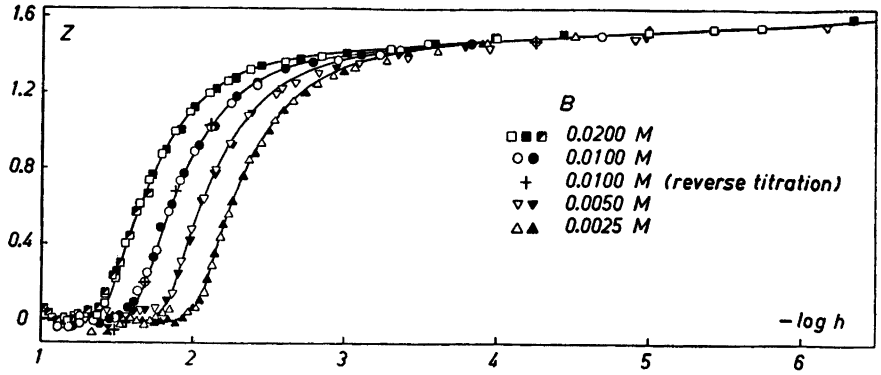


Fig. 2. The average number of hydroxyl groups, Z, bound to each VO_2^+ ion as a function of pcH for different total concentrations of vanadium, B. The lines represent theoretical formation curves calculated for: $\varkappa_{14,10} = 10^{-6.75}$, $K_{15,10} = 10^{-3.6}$ and $K_{16,10} = 10^{-5.8}$

Similarly, Z is now defined as the average number of hydroxyl ions bound to, or protons dissociated from, the VO_2^+ ion.

THE HYDROLYSIS OF THE VO_2^+ ION

Identification of the initial product of hydrolysis

In the first instance, discussion will be restricted to the potentiometric measurements made in the 1 M perchlorate medium. The data $Z(\log h)_B$ calculated for ten titrations using eqns. (1), (2) and (4) are shown in full in Fig. 2. The data for four representative titrations at different total metal concentrations, B, are also given in Table 1.

The upper limit of 0.02 M for the metal concentrations used was imposed by the limited solubility of vanadium(V) in the perchlorate medium; and the lower limit of 0.0025 M by the limited accuracy of the glass electrode in solutions of $0.1\ M \geqslant h \geqslant 0.05\ M$. The random scatter about $Z = 0$ at the base of the curves lies within the experimental error of $\pm$ 0.2 mV.

As the curves referring to different values of B are not coincident, it is apparent that at least one polynuclear complex, $(VO_2)_q(OH)_p^{(q-p)+}$ is formed. The curves pass through an isoelectric point (represented by $Z = 1.0$), and each VO_2^+ ion evidently combines with a maximum of $\sim$1.6 hydroxyl ions in the range studied (pcH$<$6.5). The high values of $(-\partial Z/\partial \log h)_B$ for $Z<1.0$ indicate the formation of polynuclear species which contain a relatively high number of vanadium atoms, *cf.* Fig. 1 in Ref.[32]. For $Z \gtrsim 1.5$, and pcH$>$4, the system is again homonuclear, since curves for different values of B are coincident.

For values of $Z \lesssim 1.2$, the curves $Z(\log h)_B$ appear to be parallel, so that Sillén's "core + links" hypothesis [32,33] may be applied. In this range, the complex, or complexes, $(VO_2)_q(OH)_p$ may be written in the form

Table 1. $Z(\log h)_B$ for four representative titrations. The symbols are those used in Fig. 2.

$B = 2\times10^{-3}$ M		$B = 10^{-3}$ M		$B = 5\times10^{-3}$ M		$B = 2.5\times10^{-3}$M	
$-\log h$	□ Z	$-\log h$	● Z	$-\log h$	▼ Z	$-\log h$	▲ Z
1.00	0.05	1.14	−0.05	1.27	0.00	1.34	0.00
1.05	0.08	1.18	−0.05	1.29	0.01	1.39	0.06
1.11	0.01	1.22	−0.03	1.34	−0.06	1.45	−0.05
1.16	−0.01	1.26	−0.01	1.39	−0.01	1.50	−0.01
1.21	0.01	1.30	−0.02	1.44	−0.04	1.55	0.01
1.26	0.00	1.34	−0.01	1.50	−0.02	1.61	0.06
1.43	0.130	1.39	−0.02	1.55	0.02	1.67	0.00
1.48	0.234	1.43	0.02	1.61	0.05	1.74	−0.01
1.56	0.411	1.48	0.00	1.68	0.06	1.78	0.00
1.63	0.576	1.52	0.02	1.75	0.07	1.83	0.01
1.71	0.742	1.56	0.07	1.83	0.114	1.88	−0.01
1.79	0.880	1.61	0.117	1.90	0.250	1.93	0.02
1.88	1.00	1.68	0.201	1.97	0.420	1.98	0.07
1.98	1.10	1.73	0.336	2.05	0.595	2.04	0.107
2.11	1.20	1.79	0.486	2.14	0.776	2.09	0.220
2.12	1.21	1.85	0.608	2.25	0.933	2.14	0.356
2.23	1.26	1.93	0.774	2.38	1.09	2.20	0.508
2.37	1.32	2.03	0.920	2.58	1.22	2.26	0.631
2.60	1.36	2.14	1.05	2.94	1.34	2.32	0.764
2.84	1.39	2.28	1.17	3.36	1.40	2.40	0.885
3.29	1.43	2.41	1.25	3.79	1.44	2.49	0.998
3.54	1.46	2.60	1.32	4.98	1.50	2.59	1.11
3.99	1.49	2.78	1.36			2.73	1.20
5.00	1.52	3.10	1.40			2.99	1.31
5.74	1.55	3.36	1.43			3.41	1.40
		3.82	1.46			3.92	1.46
		4.69	1.50			5.00	1.53

$VO_2((OH)_t(VO_2))_n$, where t is a constant (not necessarily integral) and where n may be a unique integer, N, or a series of integers such that the product nt is also integral. Charges are omitted for clarity. Hence, the parameter t is defined by

$$t = p/(q-1) \tag{5}$$

and p is a linear function of q. Sillén [33] has shown that

$$t = (\partial \log B / \partial \log h)_Z \tag{6}$$

The function $\log B\ (\log h)_Z$, which is derived from the data in Fig. 2, is plotted in Fig. 3, and it is found that $t = 1.50 \pm 0.07$. Accordingly, the different $Z(\log h)_B$ curves may be made to coincide by transforming the $\log h$ axis to

$$x = \log B - t \log h \tag{7}$$

For convenience, the Z axis is simultaneously transformed to

$$y = Z / t \tag{8}$$

The plot of $Z/1.5$ against $(\log B - 1.5 \log h)$ is not reproduced here, but as in the similar plot shown in the Appendix (Fig. 8), all points lie on a single curve, within experimental error. Now a curve $y(x)$ is analogous to the

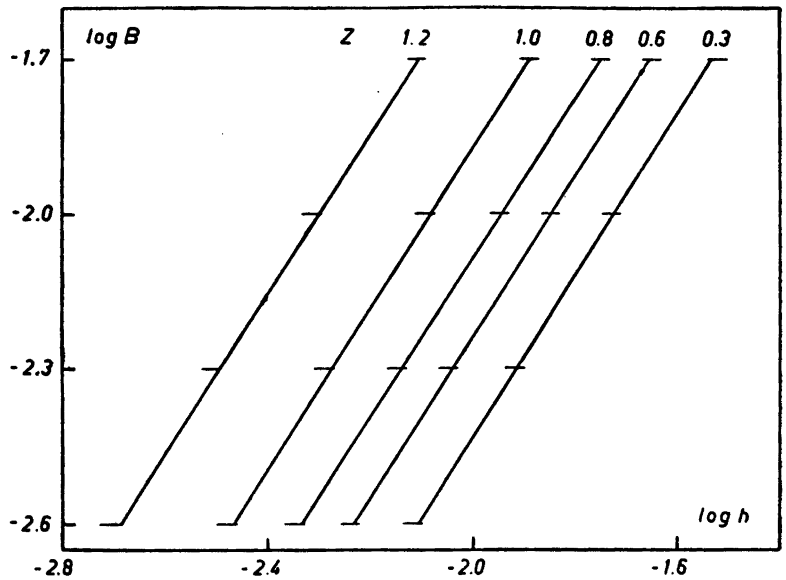


Fig. 3. Log B *as a function of log* h *for different values of* Z. *The lines are calculated for* $\varkappa_{14,10} = 10^{-6.75}$.

single curve $Z(\log h)$ which obtains for a system of mononuclear hydroxyl complexes. Thus, as a first approximation, the products of the reaction between VO_2^+ ions and hydroxyl ions may be represented by the formula $VO_2((OH)_{1.5}(VO_2))_n$.

By comparing the experimental curve $y(x)$ with families of normalised curves $y(X)$ calculated for certain simplifying assumptions, the value or values of n may be found, and the formation constants for the system described in terms of two parameters. Sillén [32] has given a number of normalised curves calculated on the assumptions that:

I, no soluble complexes are formed, but an insoluble complex precipitates,
II, a unique complex $B(A_tB)_N$ is formed in solution,
III, a series of complexes $B(A_tB)_n$ is formed in solution, with values of n ranging from unity to infinity.

Although the curves given elsewhere [32] for hypotheses I and II are valid irrespective of whether t is integral or non-integral, the curves given for hypothesis III are only valid for integral values of t (*cf.* Appendix).

For $y \lesssim 0.5$, the curve $y(x)$ was found to fit in with the family of normalised curves for hypothesis II, with a value of $N = 8$ or 10 (odd values of N are excluded from consideration, since the product $Nt = P$ must be integral). It could therefore be tentatively inferred that the initial reaction product is a single polynuclear species $VO_2^+((OH)_{1.5}VO_2)_8^{4-}$ or $VO_2^+((OH)_{1.5}VO_2)_{10}^{5-}$, and that this species undergoes some further reaction. Even if the value of t is not exactly 1.5, it is likely that the above formulae approximate to the com-

position of the complex. Other possible combinations of values of t (within the range 1.5 ± 0.07) and of N were found by trial and error, and are given in Table 2, together with the two combinations discussed above.

Table 2. Possible initial reaction products, $(VO_2)_Q(OH)_P$ or $VO_2((OH)_2(VO_2))_N$

t	N	Q	P	Range fitted by hypothesis II
1.444	9	10	13	$Z \lesssim 0.6$
1.455	11	12	16	0.6
1.500	8	9	12	1.0
1.500	10	11	15	1.1
1.545	11	12	17	0.8
1.556	9	10	14	1.3

Now for the reaction

$$Q\ VO_2^+ + P\ H_2O \rightleftharpoons (VO_2)_Q(OH)_P^{(P-Q)-} + P\ H^+ \quad (9)$$

$$B = b + Q\ [(VO_2)_Q(OH)_P] \quad (10)$$

$$\text{and } BZ = P\ [(VO_2)_Q(OH)_P] \quad (11)$$

where b is the concentration of free VO_2^+ ions. Introducing the following auxiliary variables into eqns. (10) and (11)

$$\vartheta = Q\ [(VO_2)_Q(OH)_P]\ b^{-1} = Q\varkappa_{P,Q} b^{Q-1} h^{-P} \quad (12)$$

where $\varkappa_{P,Q}$ is the equilibrium constant for reaction (9) and

$$\log h = \frac{1}{P} \log Q\varkappa_{P,Q} + \frac{Q-1}{P} \log B - \log h = \frac{1}{P} \log \vartheta + \frac{Q-1}{P} \log (1+\vartheta) \quad (13)$$

it may be shown that

$$Z = \frac{P}{Q} \frac{\vartheta}{1+\vartheta} \quad (14)$$

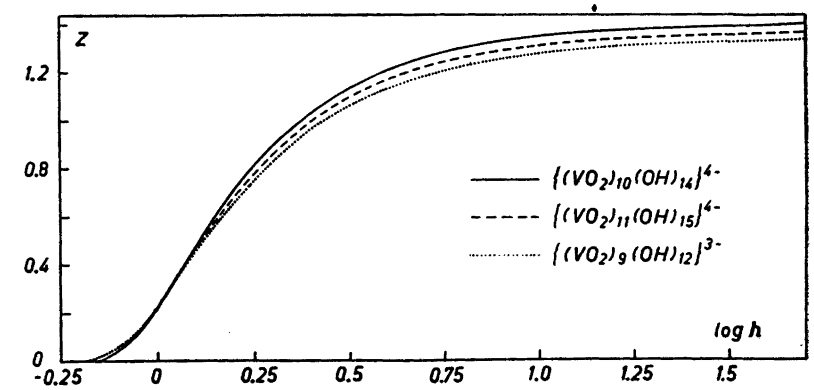


Fig. 4. Normalised curves $Z(\log h)_B$ for the single species $(VO_2)_Q(OH)_P$

Thus a normalised set of $Z(\log h)_B$ curves may be calculated using eqns. (12) and (13), together with the values of P and Q given in Table 2, and compared with the experimental data shown in Fig. 2. Some of the normalised curves are shown in Fig. 4. A good fit could be obtained, within the limits of experimental error, with all the curves, for values of Z less than those listed in column 4 of Table 2. None of the curves fitted particularly well for values of $Z<0.05$, but this is to be expected from the large experimental error in this region. For values of $Z\lesssim 0.8$, the data appear to be consistent with the formation of $(VO_2)_9(OH)_{12}^{3-}$, $(VO_2)_{10}(OH)_{14}^{4-}$, $(VO_2)_{11}(OH)_{15}^{4-}$ or of $(VO_2)_{12}(OH)_{17}^{5-}$, and there seems to be no reliable criterion for distinguishing with certainty between these possibilities with the present data. However, since the data are consistent with the existence of $(VO_2)_{10}(OH)_{14}^{4-}$ over the biggest range of values of Z ($\lesssim 1.3$), the simplest and most likely explanation of the hydrolysis of the VO_2^+ ion may be given in terms of the initial formation of this species.

The hydrolysis constant of $(VO_2)_{10}(OH)_{14}^{4-}$

The equilibrium constant $\varkappa_{14,10}$ for the initial reaction

$$10\ VO_2^+ + 14\ H_2O \rightleftharpoons (VO_2)_{10}(OH)_{14}^{4-} + 14\ H^+ \qquad (9a)$$

may be calculated in many ways from the data in the range where no further reaction is detectable.

(a) *Direct curve fitting.* Values of $\varkappa_{14,10}$ may be obtained directly from corresponding coordinates of experimental and theoretical curves $Z(\log h)_B$ placed in the position of best fit in the region $Z<1.3$ (*cf.* Figs 2 and 4). When the right hand side of eqn. (13) is zero,

$$\log \varkappa_{14,10} = 14\ \log h - 9\ \log B - \log 10 \qquad (13a)$$

whence is obtained $\log \varkappa_{14,10} = -6.75 \pm 0.15$

(b) *Linear extrapolation.* It has been shown elsewhere [25] that

$$\log\{P^{Q-1}Z(P-QZ)^{-Q}\} = (Q-1)\ \log B - P\ \log h + \log \varkappa_{P,Q} \qquad (15)$$

for reaction (9). The data for 26 titration points in the range $0.1<Z<1.3$, but otherwise selected at random, were plotted in the form of $\log\{14^9 Z(14-10Z)^{-10}\}$ against $(9\ \log B - 14\ \log h)$; *cf.* Table 3. Since the points lie on a straight line (not reproduced here) of unit slope, and of intercept -6.8 ± 0.1, the data are consistent with the initial formation of $(VO_2)_{10}(OH)_{14}^{4-}$ with a hydrolysis constant of $\log \varkappa_{14,10} = -6.8 \pm 0.1$.

(c) *Methods based on the "core + links" hypothesis.* Values of

$$\log \varkappa_{14,10} = -6.75 \pm 0.03$$
$$\text{and} \qquad -6.75 \pm 0.07$$

were obtained by integration, and by curve fitting, respectively, of the plot of $Z/1.556$ against $(\log B - 1.556\ \log h)$. Discussion of the application of the "core + links" hypothesis [32] to the present data will be deferred to an appendix to this paper.

Table 3. Data for determining $\varkappa_{14,10}$ by linear extrapolation according to eqn. (15).

$-\log B$	$-\log h$	Z	$\log\{14^9 Z(14-10Z)^{-10}\}$	$9\log B - 14\log h$
1.70	1.63	0.576	0.92	7.59
	1.79	0.880	3.09	9.75
	1.98	1.10	5.58	12.51
	2.01	1.13	6.04	12.91
	2.12	1.21	7.62	14.44
	2.37	1.32	10.70	17.91
2.00	1.83	0.569	0.88	7.60
	1.91	0.732	1.44	8.77
	2.00	0.887	3.16	10.03
	2.11	1.02	4.53	11.53
	2.24	1.14	6.32	13.35
	2.28	1.17	6.76	13.87
	2.42	1.24	8.36	15.84
2.30	1.87	0.140	−1.54	5.45
	1.99	0.480	0.36	7.10
	2.06	0.643	1.33	8.12
	2.14	0.792	2.37	9.32
	2.25	0.930	3.57	10.75
	2.37	1.08	5.29	12.43
	2.55	1.19	7.17	14.94
2.60	2.09	0.220	−1.07	5.86
	2.14	0.356	−0.32	6.60
	2.20	0.508	0.52	7.34
	2.32	0.764	2.16	9.12
	2.49	0.998	4.28	11.40
	2.59	1.11	5.70	12.87
	2.73	1.20	7.37	14.85

Straight lines of unit slope are also obtained in certain ranges for plots using the other values of P and Q listed in table 2. However, the data may be represented by equation (15) over the biggest range of values of Z ($\leqslant 1.3$) with $P = 14$ and $Q = 10$.

The secondary products of hydrolysis

If $(VO_2)_{10}(OH)_{14}^{4-}$ were the sole product of hydrolysis of VO_2^+, the plots $Z(\log h)_B$ would coincide at $Z = 1.4$, and $dZ / d\log h$ would then be zero. On the contrary, the curves do not coincide until $Z > 1.4$, and Z increases to approximately 1.6 in the range $3 \leqslant pcH \leqslant 6.5$. Within the accuracy of the experimental measurements, it appears possible to describe the upper parts of the Z $(\log h)_B$ curves mathematically in one of two ways:

(a) further hydrolysis of $(VO_2)_{10}(OH)_{14}^{4-}$ to $(VO_2)_{10}(OH)_{15}^{5-}$ and $(VO_2)_{10}(OH)_{16}^{6-}$, or

(b) formation of a series of more condensed isopolyvanadates, $(VO_2^+)_q(OH^-)_p$ where $q > 10$.

The former explanation is preferable on grounds of simplicity and in view of recent preliminary crystallographic studies of isopolyvanadates, which will be discussed later.

If $(VO_2)_{10}(OH)_{16}^{6-}$ is the ultimate decavanadate, the three isopolyvanadates may arbitrarily be assigned the formulae $H_2V_{10}O_{28}^{4-}$, aq., $HV_{10}O_{28}^{5-}$, aq., and $V_{10}O_{28}^{6-}$, aq. The dissociation constants of the first two species may be denoted

by $K_{15,10}$ and $K_{16,10}$, and the overall hydrolysis constants of the last two species by $\varkappa_{15,10}$ and $\varkappa_{16,10}$. Thus

$$\varkappa_{15,10} = \varkappa_{14,10} \cdot K_{15,10} \tag{16a}$$

$$\varkappa_{16,10} = \varkappa_{15,10} \cdot K_{16,10} \tag{16b}$$

Accordingly, for a system consisting of VO_2^+, $H_2V_{10}O_{28}^{4-}$, aq., $HV_{10}O_{28}^{5-}$, aq. and $V_{10}O_{28}^{6-}$, aq. in equilibrium

$$B = b + 10b^{10} \sum_{p=14}^{p=16} \varkappa_{p,10} h^{-p} \tag{17}$$

and

$$h - H = BZ = 10b^{10} Z_{10} \sum_{p=14}^{p=16} \varkappa_{p,10} h^{-p} \tag{18}$$

where Z_{10}, the average number of additional hydroxyl groups per VO_2 group in the decavanadates is defined by

$$Z_{10} = \frac{\sum_{p=14}^{p=16} p[(VO_2)_{10}(OH)_p]}{10 \sum_{p=14}^{p=16} [(VO_2)_{10}(OH)_p]} \tag{19}$$

where charges are omitted for clarity. Now

$$Z = \frac{10\varkappa_{14,10} b^{10} h^{-14} \ (1.4 + 1.5K_{15,10}h^{-1} + 1.6K_{15,10}K_{16,10}h^{-2})}{b + 10\varkappa_{14,10} b^{10} h^{-14} \ (1 + K_{15,10}h^{-1} + K_{15,10}K_{16,10}h^{-2})} \tag{20}$$

so that the function $Z(\log h)_B$ may be described in terms of the two variables b and h and the three parameters $\varkappa_{14,10}$, $K_{15,10}$ and $K_{16,10}$. Moreover

$$Z_{10} = \frac{1.4 + 1.5K_{15,10}h^{-1} + 1.6K_{15,10}K_{16,10}h^{-2}}{1 + K_{15,10}h^{-1} + K_{15,10}K_{16,10}h^{-2}} \tag{21}$$

so that Z_{10} (log h) may be described in terms of the single variable h and the two parameters $K_{15,10}$ and $K_{16,10}$. Combining eqns. (17) and (18)

$$\frac{b}{B} = \frac{Z_{10} - Z}{Z_{10}} \tag{22}$$

whereby b may be eliminated from eqn. (18). Thus

$$Z = 10B^9 \ (Z_{10} - Z)^{10} (Z_{10})^{-9} \sum_{p=14}^{p=16} \varkappa_{p,10} h^{-p} \tag{23}$$

By introducing auxiliary variables into this equation, it is possible to calculate theoretical (or normalised) curves, which may be superimposed on the experimental data. The required equilibrium constants are found from the differences between the coordinates of these curves in the position of best fit. This approach is analogous to that used by Lagerström and Sillén for interpreting measurements of equilibria in silicate solutions [34].

Evaluation of the decavanadate hydrolysis constants

(a) *Normalised curves log B (log Z).*

Introducing the auxiliary variables

$$\log Z = \log Z - \log Z_{10} \tag{24}$$

and

$$\log B = \log B + \frac{1}{9}\left(1+\log \sum_{p=14}^{p=16} \varkappa_{p,10} h^{-p}\right) \tag{25}$$

eqn. (23) may be rewritten in the form

$$\log B = \frac{1}{9} \log Z - \frac{10}{9} \log (1-Z) \tag{26}$$

The normalised curve log B (log Z) may be calculated from eqn. (26) and fitted to each of the experimental curves log B (log $Z)_h$ by movement parallel to the axes, *cf.* Fig. 5. Then, for each particular value of h, the differences between the coordinates of the theoretical and experimental curves give values of Z_{10} and $\sum_{p=14}^{p=16} \varkappa_{p,10} h^{-p}$ according to eqns. (24) and (25). The internal consistency of the values so obtained may be checked since it may be shown from eqn. (21) that

$$\frac{\mathrm{d} \log \sum_{p=14}^{p=16} \varkappa_{p,10} h^{-p}}{\mathrm{d} \log h} = -10 Z_{10} \tag{27}$$

The equilibrium constants may be found from the functions $\sum_{p=14}^{p=16} \varkappa_{p,10} h^{-p}$ (h) or $10 Z_{10}(h)$ by standard methods, *cf.* Ref.[35] and parts (c) and (d) of this section.

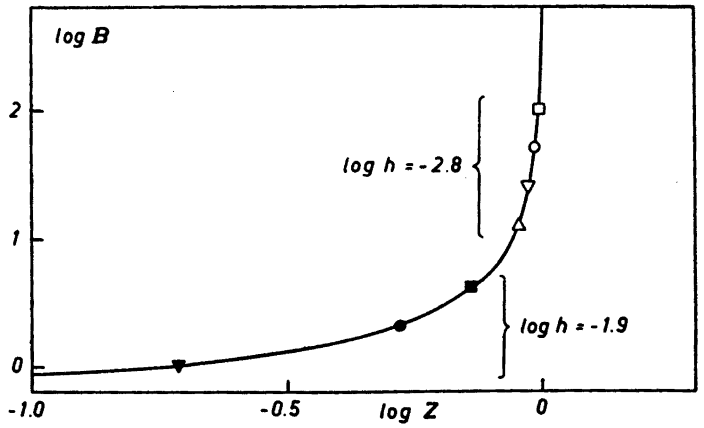


Fig. 5. Normalised curve log B (log Z) for the series of complexes $(VO_2)_{10}(OH)_p$. The lower and upper groups of experimental points show log B$(\log Z)_h$ *for* h = $10^{-2.8}$ *and* $10^{-1.9}$ *M in the positions of best fit.*

In the present case, reliable experimental data for log $B(\log Z)_h$ can only be derived from the data log Z (log $h)_B$ in the range $1.6 \leqslant \text{pcH} \leqslant 2.8$. Throughout this range it is found that

$$Z_{10} = 1.4$$
$$\text{and } \log \varkappa_{14,10} = -6.7 \pm 0.2$$

In the range $2.8 \leqslant \text{pcH} \leqslant 4.0$, d log B/d log $h \to \infty$ so that experimental curves cannot be obtained, and fitted to the normalised curves, with any great accuracy. Nevertheless, it is evident that Z_{10} increases from 1.4 to 1.5 in this region.

(b) *Normalised curves log B (log h)$_{Z,l}$.*

Alternatively, the following auxiliary variables and parameters may be introduced into eqn. (23):

$$\log \boldsymbol{h} = \log K_{15,10} - \log h \tag{28}$$

$$\log l = \log K_{16,10} - \log K_{15,10} \tag{29}$$

$$\log \varepsilon = \frac{1}{9}(1 + \log \varkappa_{14,10} - 14 \log K_{15,10}) \tag{30}$$

$$\log \boldsymbol{B} = \log B + \log \varepsilon \tag{31}$$

and it may be shown that

$$\log \boldsymbol{B} = \log Z + \log (1.4 + 1.5\boldsymbol{h} + 1.6\ \boldsymbol{h}^2 l) - \frac{14}{9} \log \boldsymbol{h} - \frac{10}{9} \log [(1.4 - Z) + (1.5 - Z)\ \boldsymbol{h} + (1.6 - Z)\boldsymbol{h}^2 l] \tag{32}$$

A family of normalised curves log $\boldsymbol{B}$ (log $\boldsymbol{h})_{Z,l}$ may be calculated from eqn. (32) for a number of values of Z ($\leqslant 1.42$). For each family of curves, it is also necessary to assume some value of l, defined by eqn. (29), *cf.* Fig. 6. The experimental curves log B (log $h)_Z$ are moved over the families of normalised curves, calculated for different values of l. In the position of best fit, the differences between the coordinates of the experimental and normalised curves give log $K_{15,10}$ according to eqn. (28), and

$$\log \boldsymbol{B} - \log B = \frac{1}{9}(1 + \log \varkappa_{14,10} - 14 \log K_{15,10}) \tag{33}$$

according to eqns. (30) and (31). Log $K_{16,10}$ is found from eqn. (29).

Comparison of the experimental data log B (log $h)_Z$ with families of normalised curves calculated for a few different values of l indicated that the best fit could be obtained with values of $l < 0.01$, *i.e.* in the range $Z < 1.4$, the species $V_{10}O_{28}^{6-}$,aq. is scarcely detectable. Hence a simplified form of eqn. (32) was used, with $l = 0$. From the coordinates in the position of best fit, the following equilibrium constants were evaluated: —

$$\log \varkappa_{14,10} = -6.75 \pm 0.15$$
$$\log K_{15,10} = -3.6 \pm 0.3$$

Moreover, log $K_{16,10} < -5.6$

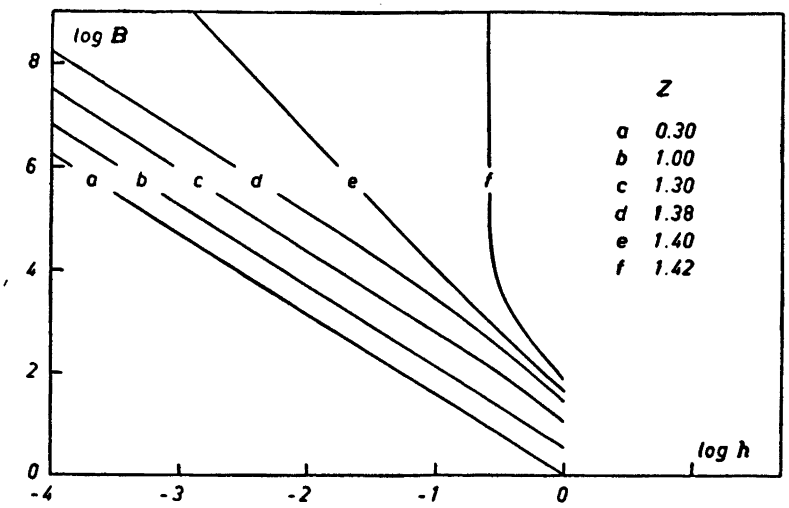


Fig. 6. Normalised curves log B $(\log h)_{Z,l}$ for $l = 0$.

(c) *Normalised curves* $10Z_{10}$ $(\log h)_l$

For a system consisting of a metal ion Me and of two mononuclear complexes MeOH and $Me(OH)_2$

$$Z_1 = \frac{\sum_{p=1}^{p=2} p\varkappa_{p,1}h^{-p}}{\sum_{p=0}^{p=2} \varkappa_{p,1}h^{-p}} \tag{34}$$

where $\varkappa_{0,1} = 1$.

Similarly, for the species $H_2V_{10}O_{28}^{4-}$ and its dissociation products $HV_{10}O_{28}^{5-}$ and $V_{10}O_{28}^{6-}$, eqn. (21) may be rewritten

$$10Z_{10}-14 = \frac{K_{15,10}h^{-1} + 2K_{15,10}K_{16,10}h^{-2}}{1 + K_{15,10}h^{-1} + K_{15,10}K_{16,10}h^{-2}} \tag{21a}$$

Thus, eqn. (21a) is of the same form as eqn. (34). The family of curves $10Z_{10}(\log h)_{K_{15,10}/K_{16,10}}$ will be the same shape as the formation function Z_1 $(\log h)_{K_{1,1}/K_{2,1}}$ for a mononuclear system, but will be displaced 14 units up the ordinate axis. As $b \to 0$ in the homonuclear range pcH>4, Z_{10} may be obtained as the value of Z in this region.

Introducing the auxiliary parameters and variables

$$\gamma = \tfrac{1}{2}\ (\log\ K_{15,10} + \log\ K_{16,10}) \tag{35}$$

$$l\ = K_{16,10}\ /\ K_{15,10} \tag{29a}$$

$$\log\ h = \gamma - \log\ h \tag{36}$$

into eqn. (21a)

$$10Z_{10} - 14 = \frac{l^{\frac{1}{2}}h + 2h^2}{1 + l^{\frac{1}{2}}h + h^2} \tag{37}$$

Normalised curves $10Z_{10}$ (log h)$_l$ were calculated for a number of values of $l^{\frac{1}{2}}$, using eqn. (37) (*cf.*[36]), and fitted to the experimental function $10Z_{10}$(log h), by movement along the log h axis. The parameter l is that value used to calculate the curve of appropriate shape, and γ is obtained from the differences between the coordinates, according to eqn. (36). The following values of the dissociation constants of $H_2V_{10}O_{28}^{4-}$ and $HV_{10}O_{28}^{5-}$ were obtained

$$\log K_{15,10} = -3.6 \pm 0.3$$

$$\log K_{16,10} = -5.8 \pm 0.1$$

(d) *Linear Extrapolation.*

Eqn. (17) may be rewritten as

$$\frac{B-b}{10b^{10}h^{-14}} = \varkappa_{14,10} + \varkappa_{15,10}h^{-1} + \varkappa_{16,10}h^{-2} \tag{17a}$$

or

$$\frac{B-b}{10b^{10}h^{-16}} = \varkappa_{16,10} + \varkappa_{15,10}h + \varkappa_{14,10}h^2 \tag{17b}$$

Hence, if the concentration of free VO_2^+ ions, b, were known, the equilibrium constants could be found by successive extrapolations, *cf.* Ref.[35]. In the absence of direct measurements of b, this quantity may be calculated. Hedström [37] has shown that

$$\left(\frac{\partial \ln b}{\partial \ln h}\right)_B = \left(\frac{\partial H}{\partial B}\right)_h \tag{38}$$

Combining eqns. (1) and (38), it may be shown that

$$\ln\frac{B}{b} = \left[\int\left\{Z + \left(\frac{\partial Z}{\partial \ln B}\right)_h\right\}\mathrm{d}\ln h\right]_B \tag{39}$$

for a system which is mononuclear at the lower limit of integration, *cf.* Lagerström and Sillén [34]. Values of $\left(\frac{\partial Z}{\partial \log B}\right)_{h,B}$ were obtained by graphical differentiation of plots of Z (log B)$_h$, and the right hand side of eqn. (39) was evaluated by graphical integration of plots of $\left\{Z + \left(\frac{\partial Z}{\partial \log B}\right)_h\right\}_B$ against log h. Corresponding values of B, b and h were substituted into eqns. (17 a) and (17 b) and the polynomials plotted both as a function of h and of h^{-1}. The following mean values of the overall hydrolysis constants were obtained:

$$\log \varkappa_{14,10} = -\ 6.82 \pm 0.17$$

$$\log \varkappa_{15,10} = -\ 9.9\ \pm 0.6$$

$$\log \varkappa_{16,10} = -\ 15.7\ \pm 0.6$$

Table 4. The determination of $\varkappa_{p,10}$, by successive linear extrapolations according to eqns. (17a) and (17b): an example of the calculations for $B = 2 \times 10^{-2}$ M.

$-\log h.$	Z	$\left(\frac{\partial Z}{\partial \ln B}\right)_h$	$\log \frac{B}{b}$	$-\log b.$	$-\log \frac{B-b}{10b^{10}h^{-14}}$
1.3	0	0	0	1.698	—
1.4	0.08	0.20	0.012	1.710	6.66
1.5	0.26	0.50	0.059	1.757	7.03
1.6	0.49	0.724	0.161	1.859	7.02
1.7	0.71	0.68	0.292	1.990	6.90
1.8	0.89	0.55	0.432	2.130	6.80
1.9	1.016	0.35	0.575	2.273	6.71
2.0	1.10	0.25	0.718	2.416	6.63
2.5	1.356	0.075	1.438	3.136	6.35
3.0	1.41	0.053	2.166	3.864	6.06
3.5	1.452	0.019	2.901	4.599	5.71
4.0	1.484	0.007	3.642	5.340	5.30
4.5	1.50	0.0	4.394	6.092	4.78
5.0	1.52	0.0	5.149	6.847	4.22
5.5	1.55	0.0	5.914	7.612	3.58
6.0	1.564	0.0	6.687	8.385	2.85
6.5	1.59	0.0	7.471	9.169	2.01
7.0	1.60	0.0	8.258	9.956	1.14

Hydrolysis constants found: $\log \varkappa_{14,10} = -6.8$, $\log \varkappa_{15,10} = -9.3$, $\log \varkappa_{16,10} = -15.07$.

The large errors associated with $\varkappa_{15,10}$ and $\varkappa_{16,10}$ arise from a systematic drift in the values of the left hand side of eqns. (17a) and (17b) obtained using different total concentrations of vanadium, B. Such discrepancies are scarcely surprising as high powers of b and h are involved, and neither of these variables can be obtained very accurately from measurements made with a glass electrode of high resistance.

POTENTIOMETRIC TITRATIONS IN A 3 M MEDIUM

The preliminary titrations (like the spectrophotometric work) were carried out in a 3 M perchlorate medium in which sodium was the predominant cation, and in the region $1 < \text{pcH} < 4$, only. This work was discontinued owing to the limited solubility of vanadium(V) perchlorate in the medium. The curves, Z ($\log h)_B$, (not reproduced here) were of the same shape as those obtained in the 1 M medium, but for identical vanadium concentrations were displaced by —0.1 pcH units. Assuming the same products of reaction as in the 1 M medium the following equilibrium constants were obtained for this medium:

$$\log \varkappa_{14,10} = -5.5 \pm 0.15$$
$$\log K_{15,10} = -3.5 \pm 0.3$$

DISCUSSION

Potentiometric and absorptiometric studies indicate that vanadium(V) exists as the VO_2^+, aq. ion in the range of acidity 2.9 M$> h >$0.05 M. No evidence was found of less hydrolysed cations, which have been suggested by

previous investigators [4–8]. Although the interpretation of the potentiometric data in the range $1.3<\text{pcH}<6.5$ is not unequivocal, these data are clearly incompatible with the formation of hexavanadates [1,12–15], pentavanadates [6], or other smaller polyanions [10,22], which have also been proposed by earlier workers, and which are described in contemporary text-books. The present data may most simply be explained by assuming that the decavanadates $H_2V_{10}O_{28}^{4-}$, aq., $HV_{10}O_{28}^{5-}$, aq., and $V_{10}O_{28}^{6-}$, aq. are successively formed in solution from VO_2^+, aq. The species $H_2V_{10}O_{28}^{4-}$ corresponds to $V_{10}O_{27}^{4-}$, which has been suggested by Britton and Welford [5], and by Hazel, McNabb and Santini [17], although this species has now been shown to give rise to further decavanadates. The present data provide no evidence for the equilibrium

$$VO_2^+ \rightleftharpoons (VO_2^+)_q(OH^-)_p \rightleftharpoons V_{10}O_{27}^{4-} \text{ (where } q>10)$$

suggested by the latter workers. At higher vanadium concentrations than have been used in the present work, the pentoxide precipitates in the region of the isoelectric point, which is given by

$$\text{pcH} = 0.803—0.643 \log B \quad \text{and} \tag{40a}$$

$$\text{pcH} = 0.715—0.643 \log B \tag{40b}$$

in 1 M and 3 M (sodium) perchlorate media, respectively.

Since few quantitative studies of step-equilibria of the type

$$10VO_2^+, \text{ aq.} + 8H_2O \rightleftharpoons H_2V_{10}O_{28}^{4-}, \text{ aq.} + 14H^+ \qquad \varkappa_{14,10}$$

$$H_2V_{10}O_{28}^{4-}, \text{ aq.} \rightleftharpoons HV_{10}O_{28}^{5-}, \text{ aq.} + H^+ \qquad K_{15,10}$$

$$HV_{10}O_{28}^{5-}, \text{ aq.} \rightleftharpoons V_{10}O_{28}^{6-}, \text{ aq.} + H^+ \qquad K_{16,10}$$

have been reported, values of the equilibrium constants have been obtained using a variety of methods, and are given below.

Table 5. Hydrolysis constants valid at 25°C in a 1 M perchlorate medium, in which sodium is the predominant cation.

Method		$-\log \varkappa_{14,10}$	$-\log K_{15,10}$	$-\log K_{16,10}$
Curve fitting:	Z ($\log h$)$_B$	6.75±0.15	—	—
	Z/1.556 ($\log B - 1.556 \log h$)	6.75±0.07	—	—
	$\log B$ ($\log h$)$_Z$	6.7 ±0.2	—	—
	$\log B$ ($\log Z$)$_h$	6.75±0.15	3.6±0.3	>5.6
	$10Z_{10}$ ($\log h$)	—	3.6±0.3	5.8±0.1
Linear extrapolation	eqn. (15)	6.8 ±0.1	—	—
	eqns. (17a), (17b)	6.82±0.17	3.1±0.6	5.8±0.1
Integration Z/1.556 ($\log B - 1.556 \log h$)		6.75±0.03	—	—
Proposed values		6.75±0.15	3.6±0.3	5.8±0.1

The hydrolysis of vanadium(V) is somewhat greater in a 3 M (sodium) perchlorate medium than in a 1 M medium, and the following equilibrium constants have been obtained;

$$\log \varkappa_{14,10} = —5.5 \pm 0.15$$

$$\log K_{15,10} = —3.5 \pm 0.3$$

The overall stability constant, $\beta_{q,p}$, for the hydroxo-complex $Me_q(OH)_p$ is related to the corresponding hydrolysis constant, $\varkappa_{q,p}$, by the expression

$$\beta_{q,p} = \frac{[Me_q(OH)_p]}{[Me]^q[OH]^p} = \varkappa_{q,p}K_w^{-p} \tag{41}$$

where K_w is the ionic product for water. Using values $K_w = 10^{-13.8}$ and $10^{-14.22}$ (Ref. 38) $\log \beta_{14,10} = 186$ and 194 in the 1 M and 3 M media, respectively. An increase in the overall hydrolysis constant of $Fe_2(OH)_2^{4+}$ with increasing ionic strength has recently been reported by Milburn and Vosburgh [39].

In order to calculate the proportions of the various species present in solution, it is convenient to combine eqn. (17) with the auxiliary variables defined by eqns. (29) and (30).

$$\frac{100\ [VO_2]}{B} = 100\left[1 + 10\varkappa_{14,10}B^9h^{-14}\left(1 - \frac{Z(1+h)}{1.4+1.5\ h}\right)^9\ (1+h)\right]^{-1} \tag{42}$$

$$\frac{100\ [H_{16-p}V_{10}O_{28}]}{B} = \frac{10^3\varkappa_{14,10}B^9h^{-p}\left(1 - \frac{Z(1+h+lh^2)}{1.4+1.5\ h+1.6lh^2}\right)^9}{1 + 10\varkappa_{14,10}B^9h^{-14}\left(1 - \frac{Z(1+h+lh^2)}{1.4+1.5h+1.6lh^2}\right)^9(1+h+lh^2)} \tag{43}$$

The proportions of the different species, $\alpha_{p,q}$, have been calculated as percentages of the total vanadium present for the highest (2×10^{-2} M) and lowest (2.5×10^{-3} M) vanadium concentrations used in the 1 M medium. These are plotted as functions of pcH in Fig. 7. The curves for VO_2^+ and $H_2V_{10}O_{28}^{4-}$, which are in heteronuclear equilibrium, are unsymmetrical. However, the curves $\alpha_{p,10}$ (pcH) for $HV_{10}O_{28}^{5-}$ and $V_{10}O_{28}^{6-}$, which are substantially in homonuclear equilibrium, are symmetrical (*cf.* mononuclear systems).

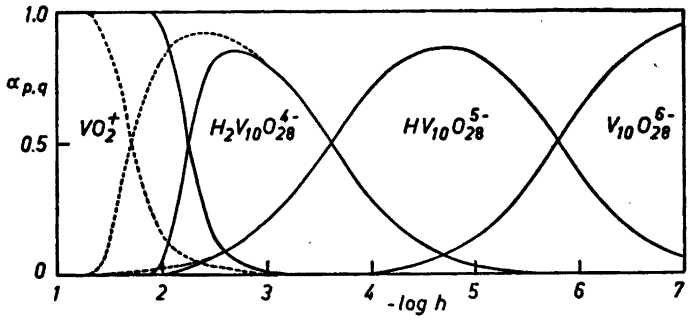


Fig. 7. The relative amounts of the hydrolysis products of vanadium (V) as a function of pcH in a 1 M perchlorate medium at 25°C expressed as percentages of the total vanadium. ——— B = 2.5×10^{-3} *M and* — — — B = 2×10^{-2} *M.*

Polyvanadates in the solid state

Orange polyvanadates crystallise from solutions of pcH<7. The analytical ratios Me(I)/V(*V*) reported in the literature [40] include; 5/6, 4/5, 5/8, 2/3, 3/5, 4/7, 1/2, 3/7, 2/5, 1/3, 1/4, 2/9. Previous formulae suggested for the polyvanadates have been in accordance with one or other of these ratios. If solid vanadates of the VO_2^+ ion can be obtained from acidic solutions, as Jahr and Jander [41] have suggested, a number of these ratios may represent distinct compounds. However, in the absence of further evidence, it is somewhat doubtful whether all these ratios can represent different compounds.

Lindqvist [42], and Evans, Mrose, and Marvin [43] have recently examined crystallographically a number of orange polyvanadates, which were crystallised at pcH ~ 6.5. Analytical data were in good agreement with the formulae listed in Table 6, and the salts have all been shown to contain ten, or multiples of ten, vanadium atoms per unit cell.

Table 6. Polyvanadates examined structurally.

Analytical formula	V atoms per unit cell.	Ref.
$(NH_4)_6V_{10}O_{28},6H_2O$	20	Lindqvist[42]
$K_6V_{10}O_{28},9H_2O$	20	Evans, Mrose & Marvin [43]
$K_6V_{10}O_{28},10H_2O$	40	»
$Ca_3V_{10}O_{28},16H_2O$ (pascoite)	20	»
$K_2Mg_2V_{10}O_{28},16H_2O$ (hummerite)	10	»
$K_2Zn_2V_{10}O_{28},16H_2O$	10	»

Although attempts to solve these structures have so far failed [42,43], it seems likely that anions which contain ten vanadium atoms exist in the solid phase.

The coordination number of vanadium(V) may be 4, 5 or 6, in solid vanadates depending upon the pcH at which the compound is obtained. Vanadium pentoxide (which precipitates at pcH ~ 2) is considered to consist of chains of distorted trigonal bipyramids (Byström, Wilhelmi and Brotzen [44]) or of distorted octahedra (Magnéli and Oughton [45]). Metavanadates, $(VO_3)_n^{n-}$, crystallise from solutions of 6.5<pcH<8.0, and for KVO_3, H_2O, Christ, Clark and Evans [46] have shown that the basic structural unit is again the trigonal bipyramid. The metal-oxygen coordination is octahedral in the polyanions $Nb_6O_{19}^{8-}$ (Lindqvist [47]) and $Ta_6O_{19}^{8-}$ (Lindqvist and Aronsson [20]). Since, moreover, tetrahedral coordination [48] is only found in the orthovanadates, $MeVO_4$, which crystallise at pcH> 10, it is probable that vanadium is coordinated to 5 or 6 oxygen atoms in the decavanadates, which are obtained at pcH ~ 6.5 (however, *cf.* Ottar [22]).

APPENDIX

The experimental data obtained in the 1 M medium are now discussed with reference to the "core + links" hypothesis [32,33]. When the parameter t is non-integral, the basic formulae [32] are still valid, but those concerned with continuous polymerisation (hypothesis III) must be modified, since some terms in the summation are now equal to zero. The "core + links" complexes

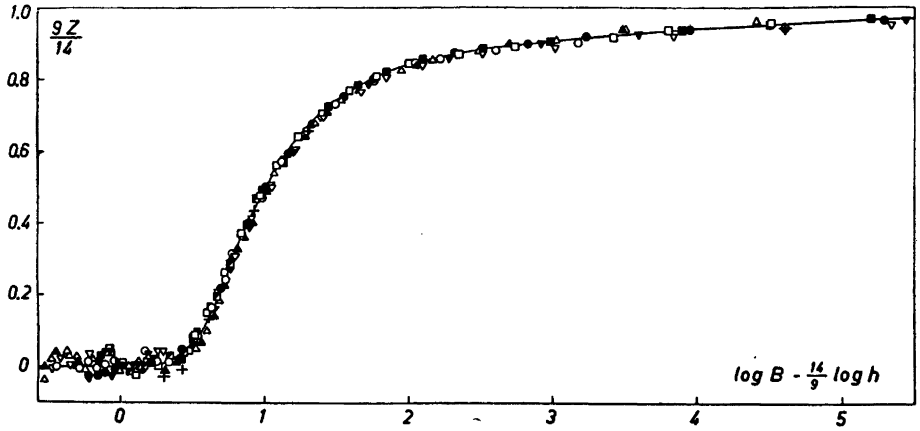


Fig. 8. y(= Z/*1.556*) *as a function of* x(= *log* B − *1.556 log* h). *The symbols are those used in Fig. 2. The curve is calculated from equations (59) and (60) with the two parameters, log* k_0 = *2.0 and 9 log* k = −*8.75.*

$B(A_tB)_n$ only have a physical meaning when the product nt is also integral. If s is the smallest positive integer such that the product st is also integral, the possible complexes may be written as $B(A_{st}B_s)_j$, where j is either a single integer or a series of integers, and

$$n = sj \tag{44}$$

The spacing of the curves Z (log $h)_B$ indicates that the predominant complexes may be written in the form $VO_2((OH)_tVO_2)_n$, and it has been shown that the best value of t (within the experimental limit of 1.50 ± 0.07) is 14/9, or 1.556. By plotting the data in the form $y(x)$, where

$$y = 9\ Z\ /\ 14 \tag{8a}$$

and

$$x = \log\ B - \frac{14}{9} \log\ h \tag{7a}$$

the separate curves may be made to coincide (see Fig. 8). Hence $s = 9$, and the system may be considered as a series of complexes $VO_2((OH)_{14}(VO_2)_9)_j$. The points for $x < 2.5$ fit the curve calculated for the first complex with $sj = N = 9$ (hypothesis II, Ref. [32]) in a position corresponding to log $\varkappa_{14,10} = -6.75 \pm 0.07$ for the complex $(VO_2)_{10}(OH)_{14}$. This conclusion has been reached by other methods; but the upper part of the curve $y(x)$ with $x > 2.5$ could now be interpreted in terms of continuous polymerisation.

Integration of the curve $y(x)$

Combining eqns. (5a), (8a) and (14) in Ref. [32], it may be shown that

$$\eta = \log \frac{B}{b} = \int_{-\infty}^{x} y\ dx + y\ \log\ e \tag{45}$$

The function $y(x)$ may be used to calculate

$$\log\ (1 + g) = \log\ (1 - y) + \eta \tag{46}$$

and

$$\log\ u = x - \eta \tag{47}$$

Here

$$g = \Sigma\ K_j u^{sj}, \qquad u = bh^{-t} \tag{48}$$

and K_j is the equilibrium constant for the reaction

$$(1 + sj)\ \mathrm{B} + sjt\mathrm{A} \rightleftharpoons \mathrm{B}(\mathrm{A}_{st}\mathrm{B}_s)_j \tag{49}$$

The average number, $\bar{j}$, of polynuclear links, $(\mathrm{A}_{st}\mathrm{B}_s)$, per complex is given by

$$\bar{j} = \frac{\Sigma\ j\ c_j}{\Sigma\ c_j} = \frac{\bar{n}}{s} = \frac{1}{s} \cdot \frac{\mathrm{d}\ \log\ g}{\mathrm{d}\ \log\ u} \tag{50}$$

$$\text{where } c_j = [\mathrm{B}(\mathrm{A}_{st}\mathrm{B}_s)_j] \tag{51}$$

As an alternative to finding $\bar{j}$ by graphical differentiation of the function $\log\ g$ ($s\ \log\ u$), it may be shown that

$$\bar{j} = \frac{y}{s\ (1 - y - 10^{-\eta})} \tag{52}$$

A smooth curve was drawn through the experimental points of Z / 1.556 plotted against ($\log B - 1.556\ \log h$), and a set of values of $\int_{-\infty}^{z} y\,dx$ was obtained by graphical integration. The residual integral $\int_{-\infty}^{0.35} y\,dx$ was assumed to be zero *cf.* Fig. 8. Corresponding values of $\log\ g$ and $\log\ u$ were calculated using eqns. (46) and (47), and are given in Table 7, together with values of $\bar{j}$, calculated from eqn. (52). The function $\bar{j}(x)$ is plotted in Fig. 9.

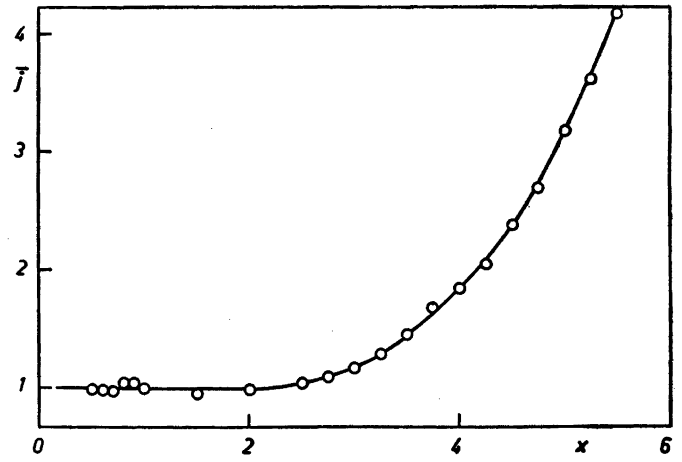


Fig. 9. The average number $\bar{j}$ *of* $((OH)_{14}(VO_2)_8)$ *links per complex as a function of* x.

Table 7. Integration of the smoothed curve $y(x)$.

x	y	$\int_{-\infty}^{x} y\,dx$	$\log g$	$\log u$	$\bar{j}$
0.50	0.040	0.0024	−2.301	0.480	0.99
0.60	0.116	0.0097	−1.824	0.540	0.98
0.70	0.212	0.0252	−1.495	0.583	0.96
0.80	0.324	0.0520	−1.276	0.607	1.04
0.90	0.420	0.0893	−1.076	0.628	1.03
1.00	0.500	0.135	−0.900	0.647	0.99
1.50	0.746	0.455	−0.277	0.721	0.94
2.00	0.844	0.856	0.205	0.777	0.98
2.50	0.884	1.289	0.649	0.827	1.03
2.75	0.896	1.511	0.861	0.850	1.09
3.00	0.906	1.736	1.067	0.871	1.17
3.25	0.916	1.964	1.263	0.889	1.28
3.50	0.926	2.194	1.450	0.904	1.44
3.75	0.936	2.427	1.629	0.917	1.67
4.00	0.942	2.661	1.827	0.930	1.83
4.25	0.948	2.898	2.022	0.940	2.04
4.50	0.955	3.136	2.201	0.949	2.38
4.75	0.960	3.375	2.393	0.958	2.68
5.00	0.966	3.616	2.566	0.964	3.17
5.25	0.970	3.858	2.802	0.970	3.60
5.50	0.974	4.101	2.939	0.976	4.17

Since $\bar{j}$ is approximately unity for $x<2.5$, the single complex $VO_2((OH)_{14}(VO_2)_9)$ predominates in this region. From eqn. (48)

$$\log K_1 = \log g - 9 \log u \tag{53}$$

whence the value

$$\log K_1 = \log \varkappa_{14,10} = -6.75 \pm 0.03$$

was obtained, in good agreement with values obtained by other methods.

Curve fitting of the function $y(x)$

It is evident from Fig. 9 that $\bar{j}$ increases to values >4 at $x = 5.5$ (corresponding to pcH $\sim$ 5 for 5×10^{-3} M vanadium). Thus within the accuracy that the data may be represented by a single curve $y(x)$, the "core + links" treatment would indicate that polymers containing at least 37 vanadium atoms are formed. This system may be described in terms of two parameters k_0 and k, provided that some assumption is made about the ratio of successive hydrolysis constants. For simplicity, attention is restricted to the hypothesis (IIIa, Ref.[32]) that this ratio is constant, and that complexes with all positive integral values of j may be formed. Sillén's treatment may be modified by defining

$$K_j = k_0 k^{sj} \tag{54}$$

and

$$V = v^s \tag{55}$$

where

$$v = ku = ka^t b \tag{56}$$

On the reasonable assumption that $|V| < 1$, then

$$g = k_0 \Sigma V^j = k_0 V (1-V)^{-1} \quad (57)$$

and

$$v \frac{dg}{dv} = sV \frac{dg}{dV} = sk_0 V (1-V)^{-2} \quad (58)$$

The coordinates of normalised curves $y(X)$ are found by substituting eqns. (57) and (58) into eqns. (8a) and (9a) of Ref.[32]. For convenience, the X coordinate is defined so that the family of curves $y(X)$ passes through the point (log 2, $\frac{1}{2}$). Then

$$y = sk_0 V [(1-V)^2 + k_0 V (1 + s - V)]^{-1} \quad (59)$$

$$X = x + \log 2 - x_{\frac{1}{2}}$$

$$= \frac{1}{s} \log V + \log [(1-V)^2 + k_0 V (1 + s - V)] - 2 \log (1-V) - \log sk_0$$

$$- (1 + \frac{1}{s}) \log V_{\frac{1}{2}} + 2 \log (1-V_{\frac{1}{2}}) \quad (60)$$

where

$$x_{\frac{1}{2}} = \log 2sk_0 - \log k + (1 + \frac{1}{s}) \log V_{\frac{1}{2}} - 2 \log (1-V_{\frac{1}{2}}) \quad (61)$$

and $V_{\frac{1}{2}}$ is given by eqn. (59) when $y = \frac{1}{2}$.

Hence the value of log k may be found from the x coordinate of the point ($x_{\frac{1}{2}}$, $\frac{1}{2}$) of the experimental curve $y(x)$, when the normalised curve $y(X)$ of the same shape has been found. The value of k_0 is that used to calculate the appropriate curve $y(X)$.

It would thus be incorrect to compare experimental curves $y(sx)$ for systems with non-integral values of t and in which continuous polymerisation is suspected, with normalised curves calculated on the assumption that t was integral. This procedure was inadvertantly used in an earlier paper on the hydrolysis of aluminium [49]. Families of curves are required for different values of s; when $s = 1$, eqns. (59), (60) and (61) reduce to equations given previously by Sillén [32]. As $k_0 \to 0$, the curves for all values of s tend to the limiting curve calculated [32] assuming that precipitation occurs, but that no complexes are detectable in solution (hypothesis I). As $k_0 \to \infty$ then each family of curves tends to a limiting curve calculated [32] assuming that a single species is present in solution (hypothesis II, $N = s$).

The normalised curve $y(X)$, calculated using eqns. (59) and (60) with $s = 9$ and $k_0 = 100$, is shown in the position of best fit in Fig. 8. From eqn. (61) the value of 9 log $k = -8.75$ is obtained, and hence from eqn. (54), log $K_1 = -6.75$, log $K_2 = -15.5$, log $K_3 = -24.25$ . . . . . The large value of k_0 implies that the formation of the first complex with $j = 1$ dominates the first stages of the reaction.

If more accurate experimental data in the range $Z > 1.3$ were available, it might be possible to distinguish between the hypothesis of a further hydrolysis of the first decavanadate ion $(VO_2)_{10}(OH)_{14}^{4-}$, and that of a repeated "core + links" mechanism. The former would give a single curve Z (log h), indepen-

dent of B, and the latter would give a single curve $y(x)$, also independent of B, in the region $1.4 \leq Z \leq 1.6$. However, although the repeated mechanism cannot be excluded with the present data, it appears to be physically much less plausible.

The authors are indebted to Professor Lars Gunnar Sillén for helpful discussions, to Professor Sillén and Civ.ing. Gösta Lagerström for communicating to them some methods of evaluating equilibrium constants prior to publication; to Docent Ingvar Lindqvist of Uppsala University and Dr. Howard T. Evans, Jr. of the U.S. Geological Survey for crystallographic data and to the *Swedish Natural Science Research Council* for financial assistance.

REFERENCES

1. Düllberg, P. *Z. physik. Chem.* **45** (1903) 129.
2. Foerster, F. and Böttcher, F. *Z. physik. Chem.* **151A** (1930) 321.
3. Hart, A. B. and Partington, J. R. *J. Chem. Soc.* **1940** 1532.
4. Meyer, J. and Pawletta, A. *Z. physik. Chem.* **125** (1927) 49.
5. Britton, H. T. S. and Welford, G. *J. Chem. Soc.* **1940**, 764.
6. Jander, G. and Jahr, K. *Z. anorg. Chem.* **212** (1933) 1.
7. Trujillo, R. and Rios, R. *Anales fis. y quim. Madrid* **49B** (1953) 473.
8. Ramsey, J. B., Colichman, E. L. and Pack, L. C. *J. Am. Chem. Soc.* **68** (1946) 1695.
9. LaSalle, M. J. and Cobble, J. W. *J. Phys. Chem.* **59** (1955) 519.
10. Ducret, L. P. *Ann. Chim.* **6** (1951) 705.
11. Bates, R. G. *Electrometric pH Determinations.* John Wiley & Sons Inc. New York 1954.
12. Bray, W. C. and Tihenko, V. J. quoted in Latimer, W. M. *Oxidation Potentials*, 2nd Ed. Prentice-Hall, Inc. New York, 1952.
13. Carpéni, G. and Souchay, P. *J. Chim. Phys.* **42** (1945) 149.
14. Souchay, P. and Carpéni, G. *Bull. soc. chim. France.* **1946** 160.
15. Trujillo, R. *Anales fis. y. quim. Madrid* **50B** (1954) 553.
16. Britton, H. T. S. and Robinson, R. A. *J. Chem. Soc.* **1932** 1955.
17. Hazel, J. F., McNabb, W. M. and Santini, R. *J. Phys. Chem.* **57** (1953) 681.
18. Robinson, R. A. and Sinclair, D. A. *J. Chem. Soc.* **1934** 642.
19. Jander, G. and Schulz, H. *Z. anorg. Chem.* **144** (1925) 225.
20. Lindqvist, I. and Aronsson, B. *Arkiv Kemi* **7** (1954) 49.
21. Souchay, P. *Bull. soc. chim. France* **1947** 914; Carpéni, G. *Bull. soc. chim. France.* **1947** 492; Anderson, J. S. and Saddington, K. *J. Chem. Soc.* **1949** (Suppl.) 381.
22. Ottar, B. *Acta Chem. Scand.* **9** (1955) 344; *Tidsskr. Kjemi Bergvesen Met.* **15** (1955) 92.
23. McKay, H. A. C., *Proceedings of International Conference on Coordination Compounds*, Amsterdam 1955.
24. Biedermann, G. and Sillén, L. G. *Arkiv Kemi* **5** (1953) 425.
25. Rossotti, F. J. C. and Rossotti, H. S. *Acta Chem. Scand.* **9** (1955) 1177.
26. Coryell, C. D. and Yost, D. M. *J. Am. Chem. Soc.* **55** (1933) 1909.
27. Britton, H. T. S. and Robinson, R. A. *J. Chem. Soc.* **1930** 1261.
28. Salmon, T. E. and Tietze, H. R. *J. Chem. Soc.* **1952** 2329.
29. Gran, G. *Analyst* **77** (1952) 661.
30. Hietanen, S. *Acta Chem. Scand.* **8** (1954) 1626.
31. Hedström, B. O. A. *Arkiv Kemi* **6** (1953) 1.
32. Sillén, L. G. *Acta Chem. Scand.* **8** (1954) 318.
33. Sillén, L. G. *Acta Chem. Scand.* **8** (1954) 229.
34. Lagerström, G. and Sillén, L. G. *Unpublished work.*
35. Rossotti, F. J. C. and Rossotti, H. S. *Acta Chem. Scand.* **9** (1955) 1166.
36. Bjerrum, J. *Metal Ammine Formation in Aqueous Solution* (Diss.) Copenhagen **1941**
    Sillén, L. G. *Acta Chem. Scand.* **10** (1956) 186.
37. Hedström, B. O. A. *Acta Chem. Scand.* **9** (1955) 613.
38. Harned, H. S. and Owen, B. B. *Physical Chemistry of Electrolytic Solutions*, 2nd ed. Reinhold Publ. Corpn., New York 1950.
    Frydman, M., Lagerström, G., Sillén, L. G. and Ulfvarson, U. *Private communication.*

39. Milburn, R. W. and Vosburgh, W. C. *J. Am. Chem. Soc.* **77** (1955) 1352.
40. Mellor, J. W. *Comprehensive Treatise on Inorganic and Theoretical Chemistry*, Vol IX., Longmans, London 1929.
Jander, G. and Jahr, K. *Kolloid Beih.* **41** (1934) 1.
Robinson, R. A., Jones, G. B., Wylie, A. W. and Brundell, J. E. *Trans. Roy. Soc. New Zealand.* **68** (1938) 390.
41. Jahr, K. and Jander, G. *Z. anorg. Chem.* **220** (1934) 201.
42. Lindqvist, I. *Private communication.*
43. Evans, H. T., Mrose, M. E. and Marvin, R. *Am. Mineralogist.* **40** (1955) 314; Evans. H. T. *Private communication.*
44. Byström, A., Wilhelmi, K. A. and Brotzen, O. *Acta Chem. Scand.* **4** (1950)1119.
45. Magnéli, A. and Oughton, B. M. *Acta Chem. Scand.* **5** (1951) 581.
46. Christ, C. L., Clark, J. R. and Evans, H. T. *Acta Cryst.* **7** (1954) 801.
47. Lindqvist, I. *Arkiv Kemi* **5** (1953) 247.
48. Milligan, W. O. and Vernon, L. W. *J. Phys. Chem.* **56** (1952) 145.
49. Brosset, C., Biedermann, G. and Sillén, L. G. *Acta Chem. Scand.* **8** (1954) 1917.

Received March 28, 1956.

ACTA CHEMICA SCANDINAVICA 10 (1956) 985—1005

Studies on the Hydrolysis of Metal Ions

XVI. The Hydrolysis of the Beryllium Ion, Be^{2+}

HIDETAKE KAKIHANA* and LARS GUNNAR SILLÉN

Department of Inorganic Chemistry, The Royal Institute of Technology, Stockholm 70, Sweden

The hydrolysis of the ion Be^{2+} has been studied by electrometric titrations at constant ionic medium (3 M ClO_4^-), using quinhydrone and hydrogen electrodes. A mathematical analysis was made of the curves Z (log h)$_B$ giving Z, the average number of OH bound per Be, as a function of log h, at various total beryllium concentrations B. It was concluded that the main product is $Be_3(OH)_3^{3+}$; for the equilibrium constant of the reaction $3Be^{2+} + 3H_2O \rightleftharpoons Be_3(OH)_3^{3+} + 3H^+$, $\log K_{33} = -8.66 \pm 0.03$ was obtained. No evidence was found of the complexes $(BeOH)_2^{2+}$ and $(BeOH)_4^{4+}$ proposed by previous workers.

Deviations at low values of B and Z indicate the presence of Be_2OH^{3+} and $Be(OH)_2$. The best value for the equilibrium constants were: $2Be^{2+} + H_2O \rightleftharpoons Be_2OH^{3+} + H^+$, $\log K_{12} = -3.24 \pm 0.02$; $Be^{2+} + 2H_2O \rightleftharpoons Be(OH)_2 + 2H^+$, $\log K_{21} = -10.9 \pm 0.2$. Slight deviations at $Z > 0.9$ where equilibrium is achieved very slowly may be due to precipitation or to higher complexes.

Solutions of beryllium salts are acidic, and Berzelius [1] noticed that a solution of beryllium sulfate can dissolve considerable quantities of beryllium hydroxide. Thus the existence of beryllium hydroxo or oxo complexes seems very probable. Several quantitative investigations of the hydrolysis of Be^{2+} have been reported. Most workers agree [2-10] that clear solutions can be obtained up to $Z = 1.0$ (Z = average number of OH^- bound per Be^{2+}). At higher values of Z, precipitation begins. With halogenide ions [2] it is completed by $Z = 2.0$. With other ions precipitation is complete by $Z = 1.8$ to 1.9, which indicates that in these cases the precipitate is not pure $Be(OH)_2$ but contains sulfate [2,8], nitrate [7] or perchlorate [7] ions as well.

The fact that the precipitate appears only when Z exceeds 1.0 suggests the formula $(BeOH)_n^{n+}$ for the soluble complexes. The main reaction would then be (*cf.* eqn. 4 below)

$$n\ Be^{2+} + n\ H_2O \rightleftharpoons (BeOH)_n^{n+} + n\ H^+;\ K_{nn} = [(BeOH)_n^{n+}]\ h^n[Be^{2+}]^{-n} \quad (1)$$

* Associate professor of chemistry, University of Nagoya, Japan

Prytz [2-4] has compared pH titrations carried out with different beryllium concentrations in the presence of various anions. Testing for $n = 1$ and $n = 2$, she found a variable value for K_{11} whereas K_{22} seemed to be fairly constant. The average value of 10^7 K_{22} was 1.4 for sulfate [2], 1.7 for chloride [2], 5.9 for bromide [3], and 4.4 for iodide [3] solutions. According to Prytz, the complex would then not be $BeOH^+$ but $(BeOH)_2^{2+}$ or Be_2O^{2+}; as usual, equilibrium data cannot distinguish between species containing different amounts of the solvent.

In connection with his work on metal ammine complexes, J. Bjerrum [5, p. 173] studied solutions containing Be^{2+} and NH_3 in 2 M NH_4NO_3. He concluded that his data should rather be explained by the formation of OH complexes than of NH_3 complexes. Following Prytz, he also assumed the equilibrium (1) with $n = 2$, but since his values of K_{22} varied, he suggested that in addition to Be_2O^{2+} also Be_2OH^{3+} and small amounts of a trimer are present.

From pH titration curves for total beryllium concentrations from 10 to 100 mM, and with the ionic medium 1 M $NaClO_4$ or 1 M KNO_3, Schaal and Faucherre [6,7] concluded that n should rather be 4. Teyssèdre and Souchay [8] made a mathematical analysis of the titration curves of 200 and 40 mM Be in 1 M Na_2SO_4 between $Z = 1.0$ (clear solution) and 1.9 (complete precipitation). They also concluded that $n = 4$ in the solution with $Z = 1$. Souchay [9] titrated $BeSO_4$ with NaOH in a solution saturated with Na_2SO_4, and measured the change in temperature of formation of solid $Na_2SO_4(H_2O)_{10}$. From these data he also concluded that $n = 4$. Faucherre [7] studied the depression of the NH_4NO_3-ice eutectic point in the presence of beryllium hydroxo complexes; no figures seem to be given, but he claims that the tetramer, with $n = 4$, is formed. Thus, according to the French workers, the predominant complex would be $(BeOH)_4^{4+}$ or $Be_4O_2^{4+}$.

The existence of ions $(BeOH)_n^{n+}$ is confirmed by the finding of Puche and Josien [10] that $Be(OH)_2$ dissolves in $Be^{2+}SO_4^{2-}$ solutions until the ratio OH/Be becomes 1, and by the thermometric titration of Haldar [11]. Ion exchange data obtained by Honda [12] were explained in terms of the species $(BeOH)_2^{2+}$ in solution. However, Honda's data may equally well be explained by assuming the presence of any species $(BeOH)_n^{n+}$.

Diffusion and conductivity measurements by Heukeshoven and Winkel [13] give an almost linear transition from Be^{2+} to the region with one OH per Be; these data give no evidence for complexes with less than one OH group per Be.

Using a glass electrode, Mattock[14] made "static" titrations of $Be(ClO_4)_2$ solutions of concentration from 1 mM to 30 mM, with NaOH using the ionic medium 1 M $NaClO_4$. He seems to have had considerable difficulties with irreversible equilibria, and his data differ in some respects from those obtained by ourselves and other workers. His conclusions are that there are rapid equilibria up to $Z = 0.5$ whereas the equilibria between $Z = 0.5$ and 1.0 are reached only after about two months at 25°C. Equilibrium constants are given for the formation of $BeOH^+$ and Be_2OH^{3+}: $[BeOH^+][H^+][Be^{2+}]^{-1} = (3 \pm 1) \cdot 10^{-7}$; $[Be_2OH^{3+}]\,[H^+][Be^{2+}]^{-2} = (3.1 \pm 0.6) \cdot 10^{-4}$.

From all other data, including our own, it seems that equilibrium is established very rapidly, as long as a clear solution is obtained. When a precipitate of $Be(OH)_2$ has already been formed, *e.g.* by local high pH, it can only be redissolved rather slowly, and the attainment of equilibrium is retarded. Mattock's equilibrium constants were calculated from data in the lowest pH region, where equilibrium was rapidly obtained, and his value for log K_{12} (−3.5) is in fair agreement with ours (−3.24).

The present work was carried out to throw a little more light on the hydrolysis of Be^{2+}, using the techniques previously developed in this laboratory [15-31].

Symbols

B	total concentration of Be
$\mathbf{B}$	normalized value of B (29)
b	concentration of free Be^{2+} (9a)
c_{pq}; c_n	concentration of complex $Be_q(OH)_p$ (4); of n:th complex (10)
E	emf; E_0 constant, E_j liquid junction emf (2)
F, F_r, F_q	functions of experimental data (7), (19), (22), (23)
g	defined in (9b)
H	total (analytical) excess concentration of H^+
h	concentration of free H^+
j	constant in $E_j = -jh$
k, k_0	constants in hypotheses "II" and "IIIa" (14) and ff
K_{nn} K_{pq},	equilibrium constants (1) (4)
k_n	$= K_{tn,\ n+1}$, equilibrium constants (9)
N	singular value of n in (1) or (9c); (14)
n	integer (1); number of links in "core + links" complex (9c)
$\bar{n}$	average number of links (10)
p_1, p_2	constant parameters to be determined (29)
p, q	integers: number of OH and Be in complex (4)
r	integer (19)
s_n	constants (18)
t	number of OH in "link" (5)
u	auxiliary functions (9a), (17) or (30)
X, Y	normalized x and y (29)
x, y	experimental functions (6a, b) or (28)
Z	average number of OH bound per Be
α	auxiliary function (29), (30)
δ	residual integral in (12)

In the calculations and especially in the equilibrium constants, M (mole/l) is used as unit throughout. Sometimes in the text or headings, however, the convenient unit mM (millimole/l) is used.

METHOD

The present investigation consisted of a series of potentiometric titrations at 25° C. In each titration, the total concentration of beryllium, B, was kept constant, while the total concentration of acid in the system was varied. All solutions were made to contain 3 M ClO_4^- by the addition of $NaClO_4$. Since the concentrations of hydrogen and beryllium ions were low, Be at most 48 mM, H^+ usually much less, compared with the concentrations $\approx$ 3 000 mM of Na^+ and ClO_4^-, it can be assumed with good approximation that the activity factors of all reacting species remain constant [17], and hence that true stoichiometric constants may be calculated from the measurements.

It would be desirable to know the concentrations of both free H^+ and free Be^{2+}. However, no electrode reversible to Be^{2+} is known, so the titrations were followed only by measuring h, the free hydrogen ion concentration. A quinhydrone electrode was used, in combination with the reference electrode

$$SE// = Ag \,/\, 0.01\ M\ AgClO_4,\ 2.99\ M\ NaClO_4 \,/\, 3\ M\ NaClO_4$$

To check that no error is introduced by the use of quinhydrone, the hydrogen electrode was used in a few titrations.

Thus the cells for measuring h may be written:

$$\mathrm{SE//H^+}\ (h),\ \mathrm{QH_2},\ \mathrm{Q/Pt} \qquad (25^\circ\,\mathrm{C})$$

or

$$\mathrm{SE//H^+}\ (h)\ /\ \mathrm{H_2(g)},\ \mathrm{Pd} \qquad (25^\circ\,\mathrm{C})$$

For each of these cells, the measured emf, E, is related to h by

$$E = E_0 + E_j + 59.16\ \log\ h \qquad (2)$$

Here E_0 is a constant, different for each type of cell, and E_j is the liquid junction potential [17], which is approximately given by $E_j = -jh$, where j is a constant, around 0.018 ± 0.001 mV $\mathrm{mM^{-1}}$. The values for E_0 and j were checked for each titration, either by a preliminary acid-base titration in the absence of beryllium, or by titration in the presence of a small amount of beryllium ($B = 1.00$ or 2.56 mM) in the range $0.1\ \mathrm{M} > h > 0.01\ \mathrm{M}$, where the hydrolysis is negligible.

When E_0 and j are known, and E is measured, h can be obtained from equation (2). From the composition of the solution, the total beryllium concentration B is known, and the analytical excess of hydrogen ions H can be obtained (assuming all beryllium to be present as $\mathrm{Be^{2+}}$). Z, the average number of OH per Be, may then be calculated for any point of the titration:

$$Z = (h - H)\ B^{-1} \qquad (3)$$

(part 8[20], eqn. 6; $[\mathrm{OH^-}]$ is negligible in all beryllium solutions studied here).

The data may conveniently be discussed in terms of the variation of Z with $\log h$.

EXPERIMENTAL DETAILS

Reagents

Beryllium perchlorate solutions were prepared as follows: Beryllium carbonate (Kebo puriss) was moistened with water and dissolved in dilute HCl, and sufficient water was added to make $[\mathrm{Be^{2+}}] \approx 0.1$ M and $[\mathrm{H^+}] \approx 0.1$ M. The solution was passed through a column containing the $\mathrm{H^+}$ form of the cation exchange resin, Amberlite IR-120. In the effluent beryllium was obtained completely free from impurities such as aluminium, iron and calcium, which have a far stronger affinity for the cation exchange resin than beryllium ion [33]. An excess of dilute $\mathrm{NH_3}$ was added dropwise to the effluent. The precipitate was centrifuged, dissolved in dilute $\mathrm{HNO_3}$ (p.a.), and reprecipitated with dilute $\mathrm{NH_3}$, freshly prepared from $\mathrm{NH_3}$ gas. This precipitate was again centrifuged, washed free from $\mathrm{NO_3^-}$ ions, and dried at 300°C for 12 hours. Each batch of the porous oxide contained about 2 % of water; it was divided into three portions.

The purity of the first portion was checked by the alizarin drop test for aluminium and the thiocyanate test for iron [33]; both tests were negative. The second portion was weighed and ignited at 1 200°C for 8 hours; the accurate content of BeO in the batch was obtained from the constant weight. The third portion was weighed and dissolved in a weighed excess of perchloric acid. The clear solution was completely transferred into a standard flask, and made up to a known volume. The concentration of beryllium in the solution was checked by gravimetric determination as BeO. The result agreed with the expected value within the experimental error. Dilute solutions of $\mathrm{Be(ClO_4)_2}$ for titration were prepared by weight.

Perchloric acid solutions were prepared from perchloric acid (p.a.) and standardized against potassium hydrogen carbonate (Merck p.a.) which was free from $\mathrm{Na^+}$, and had been dried in an atmosphere of $\mathrm{CO_2}$.

Sodium hydrogen carbonate solutions were prepared from the p.a. product of Merck. The concentrations were determined against standard $\mathrm{HClO_4}$, both by potentiometric titration using Gran's method for calculating the end-point [34], and by visual titration to the methyl-red end-point.

Sodium perchlorate was prepared by neutralising a solution of $HClO_4$ with $NaHCO_3$. The solutions were analysed by evaporating and drying to constant weight at 125°C. No chloride, chlorate, aluminium or iron could be detected in the product.

Silver perchlorate solutions were prepared by adding an excess of Ag_2O to a boiling solution of $HClO_4$. The solution was filtered, and the concentration of Ag^+ determined by Volhard's method.

Quinhydrone (Merck p.a.) was used without purification since no positive reaction was found for acid, alkali, or iron.

Apparatus

The titration cell was of the "Wilhelm" type described by Forsling, Hietanen, and Sillén [16]. It was kept in a paraffin oil thermostat, 25.0 ± 0.1°C, which was placed in a room thermostated at approximately 25°C.

In the cells with quinhydrone, a Pt foil was used as the inert electrode. It was first cleansed in HNO_3 (1:1), washed with water, and ignited in an alcohol flame. The hydrogen electrodes were lightly palladinated Pt foil [35]. The silver reference electrodes were first prepared as recommended by Brown [36] and then coated with AgCl by electrolysis for half an hour in 0.1 M HCl with a current of 0.3 mA per electrode. The emfs (E) were measured with a Jensen compensator, type 10A, or a Vernier potentiometer. Hundredths of a mV were estimated in each case.

The solutions were introduced into the titration cell from burets which had been calibrated by weighing, using 3 M $NaClO_4$ solution. When a quinhydrone electrode was used, the titration solution was stirred by means of nitrogen which had passed through 10 % H_2SO_4, 10 % NaOH, and 3 M $NaClO_4$ solutions. When a hydrogen electrode was used, the solution in the cell was stirred by a stream of hydrogen which had passed through a column filled with activated copper [37], and then through 10 % H_2SO_4, 10 % NaOH, and 3 M $NaClO_4$ solutions.

Titration procedure

In the following it will be tacitly understood that all solutions contained 3 M ClO_4^-, and in addition Na^+.

Preliminary titrations with NaOH (0.1 M) showed that local precipitation occurred. To avoid this, $NaHCO_3$ (Hedström [19]) was used as the base. To get preliminary values for E_0 and j (eqn. 2), 25.0 or 50.0 ml of 24.92 or 99.43 mM $HClO_4$ was titrated with 100.65 mM $NaHCO_3$. In the main experiments, eleven titrations were made with B = 48.7_4, $19{,}2_7$, 10.02_5, 5.05_7, 2.56_0, and 1.00 mM.

Almost all titrations were carried out as follows: 25.0 ml of "neutral medium" (3 M $NaClO_4$), or of 24.92 mM $HClO_4$ was added to 25.0 ml of a solution T_1, containing Be^{2+} (concentration 2 B) and H^+. This mixture, solution S, was titrated, always adding equal volumes of 100.65 or 30.25 mM $NaHCO_3$(T_2), and of solution T_1. In a few cases, the experiment was continued with a back titration, adding equal volumes of 24.92 mM H^+ and of solution T_1, to confirm that equilibrium had been obtained (see below). The total concentration of beryllium, B, always remained constant throughout the titration.

For the highest value of B, 48.7_4 mM, a different procedure was adopted. To 25.0 ml of a solution T_1, containing Be^{2+} (concentration 2 B) and 113.5 mM H^+, 25.0 ml of 100.65 mM $NaHCO_3$(T_3) was at first added in portions. This mixture was titrated with equal volumes of 264.0 mM $NaHCO_3$(T_3) and solution T_1.

At the end of one titration, with 10 mM Be, the equilibrium emf was noted, and the stream of nitrogen replaced by a stream of CO_2. The system was left for an hour, and then nitrogen was bubbled through the solution for two minutes. The emf was the same as before, indicating that the measurements are not invalidated by complex formation between beryllium and carbonate ions.

A steady E was usually attained within half an hour for $Z \leqq 0.8$, thus in the main part of the range studied. When hydrolysed solutions (with $Z \leqq 0.8$) were back-titrated with acid, the points $Z(\log h)$ fell on the same curve as points obtained by forward titration with HCO_3^-, indicating that the equilibria are reversible in this region. (Fig. 1, 19 mM and 48 mM). In solutions with $0.8 < Z < 0.9$, equilibrium was reached more slowly. A steady E was obtained within one or two hours, and remained constant for at least four

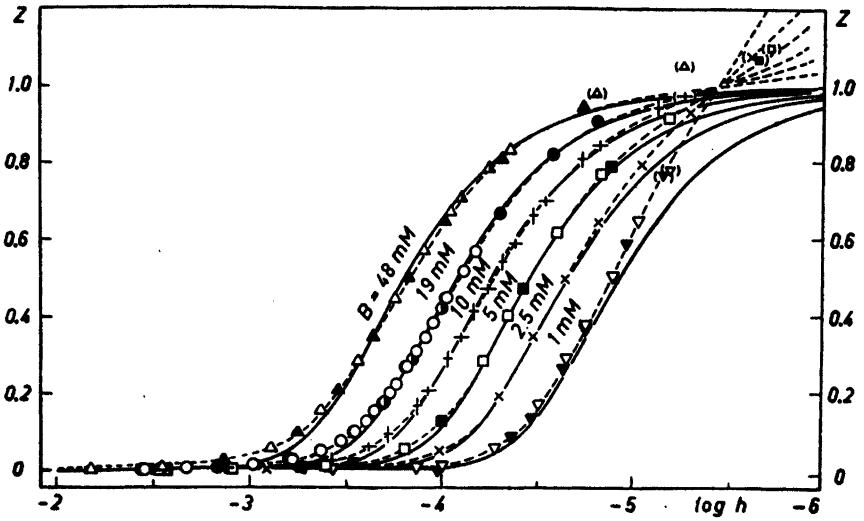


Fig. 1. Average number, Z, of OH bound per Be, as a function of log h. *All experimental points are given. Filled or open symbols represent points from different titrations, half-filled symbols from backtitrations. Total Be concentration B:* ▲ Δ ◭ *48.7, mM;* ● ○ ◑ *19.2, mM;* + *10.0, mM;* ■ □ *5.05, mM;* × *2.5, mM;* ▼ ▽ *1.00 mM. Hydrogen electrode used for* ● *and* ■, *quinhydrone for other symbols. Full curve: calculated for* $K_{21} = K_{12} = 0$, $\log K_{22} = -8.66$. *Broken curves: calculated for* $\log K_{12} = -3.25$, $\log K_{21} = -10.87$, $\log K_{22} = -8.66$.

hours. With $Z \geq 1$, E was always unsteady, even before a visible precipitate appeared, so that titration was discontinued. With the lowest metal concentration, $B = 1$ mM, a steady emf was only obtained up to $Z = 0.6$; with higher values of Z, E kept drifting even after three hours; it seems practically impossible to get accurate values in this region.

With hydrogen electrodes, the $Z(\log h)$ curves for $B = 19$ and 5 mM agreed, within 0.15 mV, with those obtained with quinhydrone electrodes throughout the whole region of hydrolysis (see Fig 1). Hence, there is no reason to assume an appreciable error due to beryllium-quinhydrone complexes.

THE MAIN PRODUCT OF HYDROLYSIS

Fig. 1 gives the data $Z(\log h)_B$, calculated from the potentiometric measurements, using eqns. (2) and (3). Table 1 gives the values of $\log h$ and Z for one titration at each of the six values of B, and for one titration with a hydrogen electrode. If only mononuclear complexes were formed, Z would be a function of h only, and all points would lie on the same Z ($\log h$) curve, regardless of the value of B. As this is not the case, at least one polynuclear hydroxo complex must be formed.

The polynuclear species may be written in the general form $Be_q(OH)_p^{(2q-p)+}$, where p and q are positive integers; we shall by K_{pq} denote the equilibrium constant of the reaction

$$pH_2O + qBe^{2+} \rightleftharpoons Be_q(OH)_p^{(2q-p)+} + pH^+, \quad K_{pq} = c_{pq}h^p b^{-q} \qquad (4)$$

Table 1. Experimental data Z (log h)$_B$ for typical titrations.

Titration 1.
B = 48.74 mM

−log h	Z
2.170	0.005
3.100	0.057
3.366	0.153
3.554	0.277
3.753	0.442
3.907	0.569
4.047	0.671
4.104	0.706 *
4.251	0.784 *
4.360	0.831
(4.816)	(0.976)
(5.276)	(1.054)

Titration 3.
B = 19.27 mM

−log h	Z
2.445	0.000
2.664	0.004
3.011	0.013
3.213	0.027
3.365	0.049
3.468	0.075
3.542	0.101
3.599	0.127
3.646	0.152
3.692	0.177
3.728	0.201
3.761	0.224
3.818	0.267
3.865	0.308
3.911	0.346
3.953	0.382
4.029	0.447
4.112	0.518
4.175	0.568
3.999	0.418 *
3.848	0.288 *
3.695	0.173 *

Titration 4 **
B = 19.27 mM

−log h	Z
2.444	0.000
2.828	0.006
3.199	0.028
3.540	0.102
3.810	0.267
4.025	0.447
4.304	0.667
4.582	0.821
4.818	0.907

Titration 5.
B = 10.02$_5$ mM

−log h	Z
2.483	0.000
2.884	0.004
3.619	0.062
3.931	0.206
4.103	0.344
4.244	0.472
4.388	0.588
4.544	0.698
4.824	0.844
(5.264)	(0.975)

Titration 7
B = 5.05$_7$ mM

−log h	Z
2.564	0.000
2.900	0.003
3.393	0.011
3.799	0.056
4.214	0.287
4.340	0.401
4.599	0.617
4.834	0.771
5.183	0.916
(5.709)	(1.100)

Titration 9
B = 2.56$_0$ mM

−log h	Z
2.571	0.000
3.086	0.001
3.990	0.049
4.298	0.192
4.474	0.375
4.640	0.496
4.816	0.646
5.047	0.796
5.293	0.936
(5.615)	(1.080)

Titration 10
B = 1.00$_3$ mM

−log h	Z
2.916	0.000
3.424	0.002
3.868	0.006
4.006	0.013
4.281	0.064
4.509	0.169
4.653	0.287
4.754	0.316
4.897	0.503
5.031	0.651
(5.193)	(0.776)

* Values of back-titration.
** Hydrogen electrodes were used. ( ) no steady potential obtained.

A quite general method for computing the various K_{pq}, which has been suggested by Hedström [27] could not be used in the present work, since the data have not the extreme accuracy needed. Therefore, two other approaches were attempted: the "core + links" approach and the assumption that all complexes are $(BeOH)_n^{n+}$. When the main product of hydrolysis had thus been determined, the secondary products were considered.

"Core + links" approach

It has previously been found that the main hydrolysis products of a number of metal ions [20-23] may be written in a general "core + links" form $Me((OH)_tMe)_n$, where t is a constant, and n is a constant or variable integer; then $p = t\,(q-1)$. If all the complexes present in appreciable amounts can be written in such a "core + links" form, a set of parallel $Z(\log h)_B$ curves should be obtained [25, 20], and the value of t is given by

$$t = (\partial \log B / \partial \log h)_Z \qquad (5)$$

Indeed, the data in Fig. 1 for the hydrolysis of Be^{2+} seem to lie on parallel curves $Z\,(\log h)_B$, in the range $0.1 < Z < 0.8$. In Fig. 2, $\log B$ is plotted against $\log h$ for values of Z between 0.05 and 0.8. From the slope, and (5), a value of $t = 1.5$ may be obtained, neglecting the slight deviations at high and low values of Z.

Again, if only "core + links" species $Be((OH)_tBe)_n$ are formed, all experimental points should lie on the same curve $y\,(x)$ with the coordinates [26, 20]

$$x = \log B - t \log h; \quad y = Z / t \qquad (6a, b)$$

The experimental plot of $y = Z/1.5$ against $x = \log B - 1.5 \log h$ is shown in Fig. 3. It is seen that the points for 48 mM $\geqq B \geqq$ 5 mM lie on a single curve except these for very low values of Z. Small deviations are observed for the lowest values of B, 2.5 and 1 mM, which may indicate the presence of mononuclear complexes.

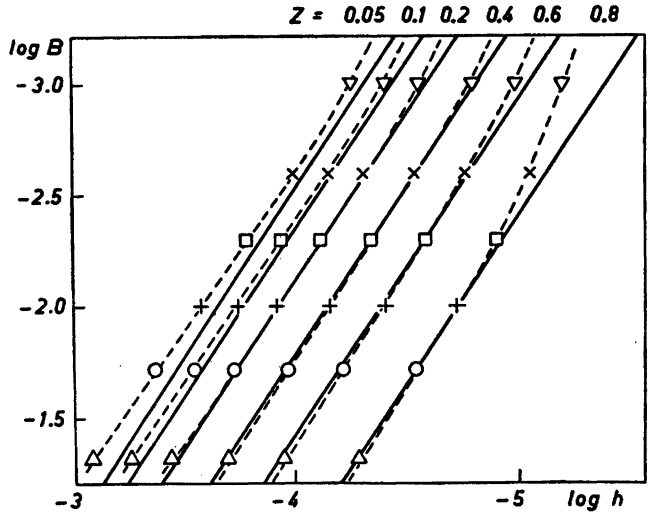


Fig. 2. Log B *as a function of log* h, *for different values of* Z. *Full lines are calculated for log* $K_{33} = -8.66$, *and no other complexes than* $(BeOH)_3^{3+}$. *Broken curves are calculated for same set of constants as in Fig 1; they also represent the best fit with the "normalized projection map" (29).*

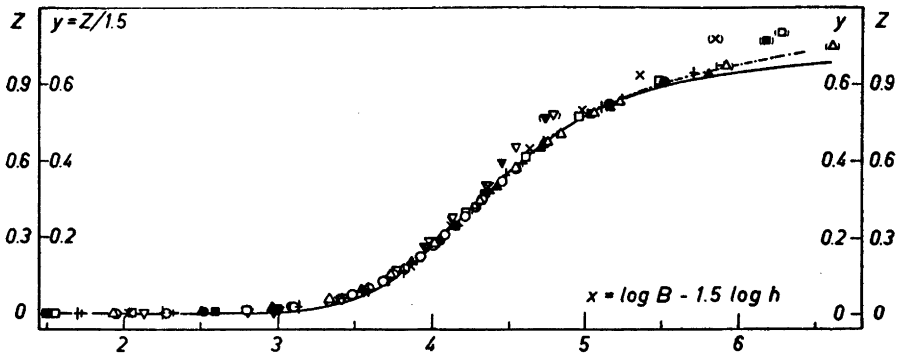


Fig. 3. Z, *or* y = Z/*1.5, as a function of* x = *log* B − *1.5 log* h. *All experimental points are shown using the same symbols as in Fig. 1. Full curve: calculated for log* $K_{33} = -8.66$; *dot-dash curve: calculated for log* $K_{33} = -8.68$, *log* $K_{56} = -19.14$ *etc (IIIa,* $k_0 = 60$).

Although these deviations for low values of Z or B seem to be beyond the experimental errors, it seems reasonable to postpone a discussion of them, and to start by discussing the main reaction in the range where the y (x) curves coincide for $t = 1.5$.

To test for the other values of t, plots were made of $Z/2$ against (log B − 2 log h), of $3Z/5$ against (log $B - \frac{5}{3}$ log h) and of $3Z/4$ against (log $B - \frac{4}{3}$ log h). With $t = 2$, the spread of the points was too severe. With $t = \frac{5}{3}$ and $\frac{4}{3}$, the spread of the points was not so bad as with $t = 2$, but far worse than with $t = 1.5$.

With $t = 1.5$, the complexes formed in appreciable amounts would be of the type $\mathrm{Be}((\mathrm{OH})_{1.5}\mathrm{Be})_n^{(2+0.5n)+}$. To decide whether n is a constant or a variable, the curve y (x) must be investigated further.

Direct analysis of the curve y (x)

It may be shown (AB II [26], eqns. 14 and 15) that from data y (x) one can calculate

$$\log F = y \log e + \int_{-\infty}^{x} y \, dx \qquad (7)$$

$$u = 10^x F^{-1}; \qquad g = F(1-y)-1; \qquad (8a, b)$$

where in our case

$$u = [\mathrm{Be}^{2+}]h^{-1.5} = bh^{-1.5}; \quad g = \Sigma k_n u^n \qquad (9a, b)$$

and k_n is the equilibrium constant for the reaction

$$(n+1)\mathrm{Be}^{2+} + 1.5\,n\,\mathrm{H_2O} \rightleftharpoons \mathrm{Be}((\mathrm{OH})_{1.5}\mathrm{Be})_n^{(2+0.5n)+} + 1.5\,n\,H^+; \quad k_n = K_{1.5n,n+1} \qquad (9c)$$

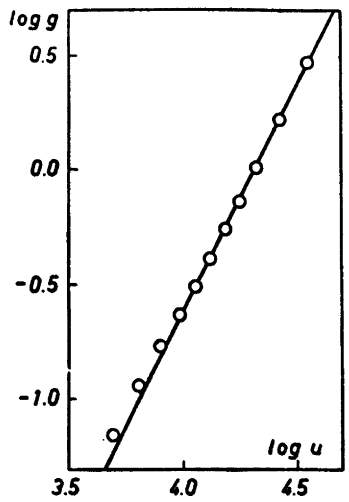


Fig 4. Direct analysis of the curve y(x) *in Fig. 3: log* g *as a function of log* u*, together with the best straight line of slope 2.*

(In passing we may note that $\log F = \log \frac{B}{b}$ and is thus identical with the quantity that has been denoted by η in other papers [20, 25 etc]).

The average number of $((OH)_{1.5}Be)$ links per complex is defined by

$$\bar{n} = \Sigma n c_n / \Sigma c_n \qquad (10)$$

where c_n is the equilibrium concentration of the complex with n links. One may calculate $\bar{n}$ either by differentiating log g (log u), or directly [29] from y and F:

$$\bar{n} = \frac{\mathrm{d}\ \log\ g}{\mathrm{d}\ \log\ u} = \frac{y}{1 - y - F^{-1}} \qquad (11a,\ 11b)$$

A smooth curve was drawn through the experimental points (y, x); where deviations occurred at low y, the lowest value of y was always used for each

Table 2. Direct analysis of curve $y(x)$

y	x	$\int_a^x y\,dx$	F	$\delta = 0$ log u	log g	$\bar{n}$	-log k_2	$\delta = -0.05$ $\bar{n}$	-log k_2
0.1	3.760	0.0323	1.190	3.685	−1.149	1.67	8.52	4.35	8.99
0.15	3.925	0.0531	1.313	3.807	−0.935	1.71	8.55	2.68	8.80
0.2	4.070	0.0786	1.464	3.904	−0.767	1.71	8.58	2.15	8.72
0.25	4.200	0.1077	1.646	3.983	−0.631	1.76	8.60	2.03	8.70
0.3	4.330	0.1424	1.874	4.058	−0.506	1.81	8.62	1.97	8.70
0.35	4.455	0.1844	2.170	4.119	−0.387	1.85	8.63	1.97	8.68
0.4	4.600	0.2388	2.585	4.187	−0.259	1.88	8.63	1.94	8.68
0.45	4.745	0.3006	3.134	4.249	−0.140	1.95	8.64	1.99	8.67
0.5	4.930	0.3888	4.037	4.324	+0.008	1.98	8.66	2.01	8.66
0.55	5.200	0.5312	5.890	4.430	+0.218	1.96	8.64	1.97	8.66
0.6	5.550	0.7329	9.853	4.556	+0.468	2.01	8.64	2.01	8.65

value of x. By graphical integration from $x = 2$ and using (7), (8), and (11 b), the values of F, log g, log u and $\bar{n}$ in Table 2 were calculated. The residual integral

$$\delta = \int_{-\infty}^{2.0} y \mathrm{d}x \tag{12}$$

was assumed to be zero. In Fig. 4, log g is plotted against log u; a straight line of slope 2.0 was obtained in almost the whole range, which according to (11a) means that only the complex with $n = 2$, *i. e.* $Be_3(OH)_3^{3+}$, is formed. The same conclusion is drawn from the values for $\bar{n}$ calculated directly and given in Table 2. If the residual integral δ is assumed to be —0.05, a still better constancy of $\bar{n}$ is obtained. (Last two columns of Table 2). Since at low values of x there are also secondary reactions, we need not be surprised at a negative value of δ.

If higher complexes were formed, the slope d log g/d log u should increase with increasing log u; however, no such curvature can be observed in the region with $y \leqq 0.6$ ($Z \leqq 0.9$). In the range $y \leqq 0.25$, where $\bar{n}$ is very sensitive to small errors in y, a slight deviation from the straight line is observed, which may be due to the presence of other complexes.

If only the complex with $n = 2$ is formed, then from equation (9b)

$$\log g - 2 \log u = \log k_2 \tag{13}$$

and a value of log k_2 can be obtained for each point (log g, log u) from eqn. (13). The average values

$$\log k_2 = \log K_{33} = -8.64 \pm 0.02 \text{ (for } \delta = 0)$$
$$= -8.67 \pm 0.03 \text{ (for } \delta = -0.05)$$

were obtained using points in the range $0.25 \leqq y \leqq 0.60$ (Table 2).

Comparison with simple mechanisms

Following AB II [26] and part 8 of this series [20], the experimental curve $y(x)$, Fig. 3, was compared with families of cures $y(X)$, calculated for the simple mechanisms I—III. With hypothesis I (no soluble complex, precipitate formed), no agreement was found.

With hypothesis II (only one complex formed, with $n = N$), only $N = 2$ gave an acceptable agreement in the main part of the curve (even then small deviations were seen for high and low values of y) (Fig. 3). This agreement again makes it very probable that the main complex is $Be_3(OH)_3^{3+}$. Thus we may apply AB II[26], eqn. (24).

$$x_{\frac{1}{2}} = \log 2 - \log k + \log N - (1 + N^{-1}) \log (N - 1) = \log 4 - \log k \tag{14}$$

From the value $x_{\frac{1}{2}} = 4.93 \pm 0.015$, where $y = \frac{1}{2}$, eqn. (14) gives log k = —4.33 ± 0.015. Since the equilibrium constant $k_2 = k^2$, we find

$$\log k_2 = \log K_{33} = -8.66 \pm 0.03$$

With a repeated mechanism like IIIa, the equations in AB II[26] must be modified because n must be even to give an integral number of atoms per complex. Curves were constructed of the $y(X)$ functions calculated for the modified hypothesis IIIa and various values of k_0. Suitable equations are given in the appendix of a paper of Rossotti and Rossotti [31]. For $k_0 \approx 60$, the agreement for high values of y was improved (dot-dash curve in Fig. 3). For $y < 0.53$ ($Z < 0.8$) the curve practically coincides with the full curve for a single complex; the first complex $Be_3(OH)_3^{3+}$ would predominate over all the following complexes $Be((OH)_3Be_2)_{\frac{1}{2}n}^{(\frac{1}{2}n+2)+}$, with $n = 4$, 6 etc. Since the equilibria are very slow for high Z, we do not consider the existence of the higher complexes as certain. The value obtained for log K_{33}, -8.68 ± 0.03, is the same as with other methods.

Although they do not give coincident curves, the experimental diagrams $y(x)$, assuming $t = \frac{4}{3}$ and $\frac{5}{3}$, were also compared with calculated curves for mechanisms I, II and IIIa. No agreement could be found.

Approach assuming polymers $(BeOH)_n^{n+}$

It is remarkable that the present work has indicated $(BeOH)_3^{3+}$ as the main product, whereas previous workers have decided upon either $(BeOH)_2^{2+}$ (Prytz [2-4]), or $(BeOH)_4^{4+}$ (Faucherre [6,7], Souchay [8,9]). It thus seemed worthwhile to test the assumption that all complexes formed are of the general formula $(BeOH)_n^{n+}$. This approach might give an independent check on our conclusion about the main complex ($n = 3$), and also test to what extent complexes $(BeOH)_n^{n+}$ with $n = 2$ or 4 might be formed. (These complexes would not be covered by the "core + links" formula with $t = 1.5$.)

We shall develop this approach along lines given in AB I[25], p. 313. If we have a series of equilibria

$$n\ Be^{2+} + n\ H_2O \rightleftharpoons (BeOH)_n^{n+} + n\ H^+;\ [(BeOH)_n^{n+}] = K_{nn}b^n h^{-n} \quad (1)$$

we find

$$BZ = \Sigma\, nK_{nn}b^n h^{-n};\quad B = b + \Sigma\, nK_{nn}b^n h^{-n} \quad (15)$$

hence

$$b = B\ (1 - Z) \quad (16)$$

We introduce the auxiliary variable u and a series of constants s_n:

$$u = bh^{-1};\ s_n = nK_{nn} \quad (17)$$

From (15), (16) and (17) we obtain

$$BZ = \Sigma\, s_n u^n;\quad u = B(1-Z)h^{-1} \quad (18)$$

We may find the constants s_n by the aid of a family of functions F_r which can be obtained from the experimental data:

$$F_r = BZu^{-r} = BZ[B(1-Z)h^{-1}]^{-r} = \Sigma\, s_n u^{n-r} \quad (19)$$

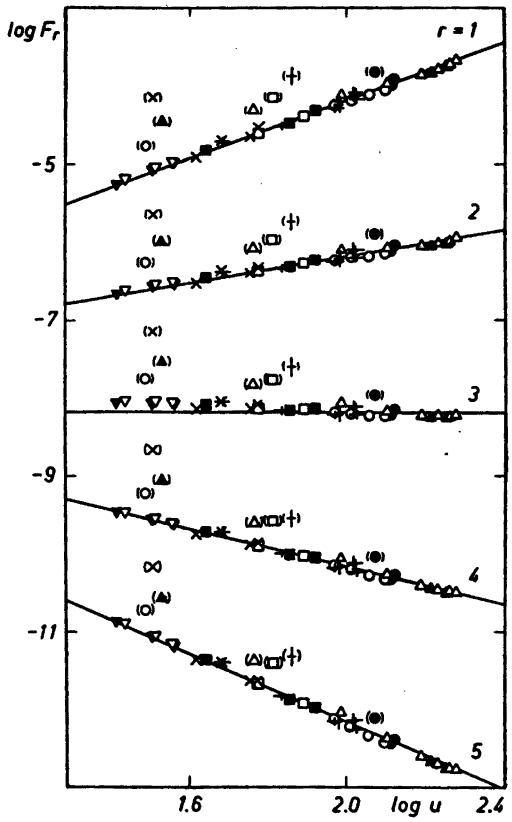


Fig 5. Log F_r, *eqn (19), for* r = *1 to 5, as functions of log* u, *eq (18), and best lines of slope 3 — N. About one half of the experimental points, which were chosen at random, are given.*

If only one complex $(BeOH)_N^{N+}$ is formed, log $F_N(\log u)$ should be a horizontal line at log $F_N = \log s_N$.

Fig. 5 gives plots of log F_1 to log F_5 against log u. Indeed, log F_3 gives a horizontal line, indicating that the main complex formed in the solution is $(BeOH)_3^{3+}$, but not $(BeOH)_2^{2+}$ or $(BeOH)_4^{4+}$. If the two latter complexes were present in appreciable amounts, (19) would give $F_3 = s_2u^{-1} + s_3 + s_4u$. One would then expect the log F_3 plot to form a single curve, independent of B, with upward bends at one or both ends. This is, however, not observed. There are deviations at $Z < 0.15$ and $Z > 0.9$, but they are not independent of B and should be due either to experimental errors (the function in rather sensitive to small errors) or to other complexes than the polymers $(BeOH)_n^{n+}$.

From the constant value of log $F_3 = \log 3 + \log K_{33}$ we obtained

$$\log K_{33} = -8.68 \pm 0.05$$

Likewise, from the straight lines log $F_1 = \log s_3 + 2 \log u$ and log $F_2 = \log s_3 + \log u$, the same value was obtained from both lines

$$\log K_{33} = -8.66 \pm 0.05$$

Conclusion on K_{33}

For the main reaction, $3\ Be^{2+} + 3\ H_2O \rightleftharpoons Be_3(OH)_3^{3+} + 3\ H^+$, the equilibrium constant K_{33} has been found by a number of methods, which give values that agree very well:

Method	log K_{33}	
Direct analysis	-8.64 ± 0.02	($\delta = 0$); -8.67 ± 0.02 ($\delta = -0.05$)
Curve-fitting	-8.66 ± 0.03	(hyp. II); -8.68 ± 0.03 (IIIa, $K_0 = 60$)
Polymer approach	-8.66 ± 0.05	(F_1 or F_2); -8.68 ± 0.05 (F_3)
Normalized proj.map (see below)	-8.65 ± 0.03	

As an average we may use the value log $K_{33} = -8.66 \pm 0.03$.

THE SECONDARY REACTIONS

Although the main part of the Z (log $h)_B$ curves is compatible with the existence of a single complex $Be_3(OH)_3^{3+}$, there are deviations, especially at low values of Z and B, indicating the presence of secondary products. To find the formulas of these products we shall use a method which will be discussed by Kakihana [38] in a subsequent paper.

Formulas of complexes

Let us first assume that besides $Be_3(OH)_3^{3+}$ there is only one more complex, $Be_q(OH)_p$, and try to find the values of p and q. The equilibrium constants of formation are K_{pq} and K_{33} and

$$B = [Be^{2+}] + q[Be_q(OH)_p] + 3[Be_3(OH)_3] = b + qh^{-p}b^qK_{pq} + 3h^{-3}b^3K_{33} \quad (20)$$

$$BZ = ph^{-p}b^qK_{pq} + 3h^{-3}b^3K_{33} \quad (21)$$

For small values of Z, where the deviations are most pronounced, we may approximately set $b \approx B$ in (21) and study the function

$$F = Zh^3B^{-2} - 3K_{33} \approx ph^{3-p}B^{q-3}K_{pq} \quad (22)$$

Fig. 6 gives a plot log h(log $F)_B$ calculated using log $K_{33} = -8.66$. As h increases the curves tend to straight lines with d log F/d log $h = 3 - p = 2$;

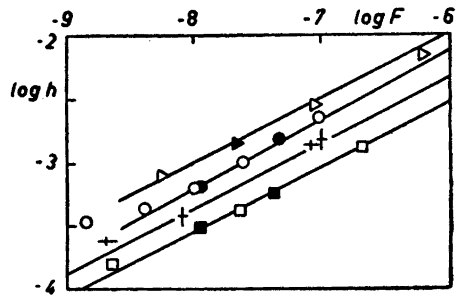


Fig 6. Log F, *eqn.* (22) versus *log* h. *Straight lines of slope* ½, *calculated with log* $K_{11} = -3.25$. *All experimental points are given within the range shown.*

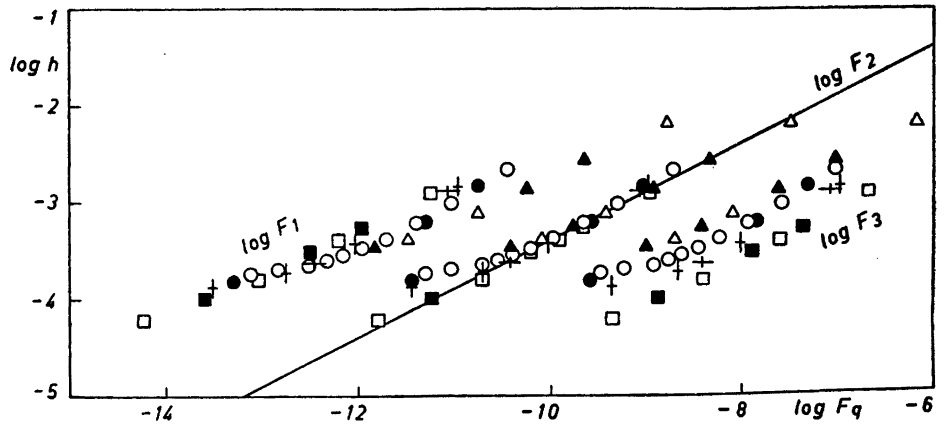


Fig 7. Log F_1, *log* F_2, *and log* F_3, *eqn. (23)* versus *log* h. *Straight line: log* h (*log* F_2) *calculated using log* $K_{12} = -3.25$. *All experimental points are given within the range shown.*

from the spacing between the lines for various values of B, between 48.74 and 5.06 mM, we may calculate $q - 3 = -1.0$. Changes in log K_{33} by $\pm$ 0.03 do not affect the values obtained for p or q.

We might then conclude that the most important complex in this range, next to $Be_3(OH)_3^{3+}$, is Be_2OH^{3+}; from the position of the curves in Fig. 6 we may calculate log $K_{12} = -3.25 \pm 0.07$.

To check this result we may try another approximation in (21), namely $b \approx B(1-Z)$; in fact in most of our solutions $B > b > B(1-Z)$. We may then study the function

$$F_q = [Z(1-Z)^{-3}h^3B^{-2} - 3K_{33}][B(1-Z)]^{3-q} \approx pK_{pq}h^{3-p} \qquad (23)$$

We have inserted in turn $q = 1, 2, 3$ and used the data to plot in Fig. 7 log F_q *versus* log h. With $q = 2$ the data with B between 5 and 48 mM fitted a straight line with d log F_2/d log $h = 3$ — $p = 2.0$. With $q = 1$ or 3, points with different values of B spread out considerably. Thus we once more conclude $p = 1$ and $q = 2$; the position of the line gives log $K_{12} = -3.25 \pm 0.05$.

It still remains to explain the deviations as to the two lowest values of B, 2.56 and 1.00 mM. The only reasonable explanation (besides experimental errors) would be the presence of one or more mononuclear complexes $Be(OH)_n$. We would then have

$$BZ = \Sigma n[Be(OH)_n] + [Be_2OH] + 3[Be_3(OH)_3] = \Sigma nh^{-n}bK_{n1} + h^{-1}b^2K_{12} + 3h^{-3}b^3K_{33} \qquad (24)$$

Again, we may approximately set $b \approx B(1-Z)$ in (24) and calculate the function $F = Z(1-Z)^{-1} - K_{12}(1-Z)h^{-1}B - 3K_{33}(1-Z)^2h^{-3}B^2 \approx \Sigma nK_{n1}h^{-n}$ (25)

Inserting the previously determined values of log $K_{33} = -8.66$ and log $K_{12} = -3.25$, in (25) log F was calculated as a function of log h (Fig. 8).

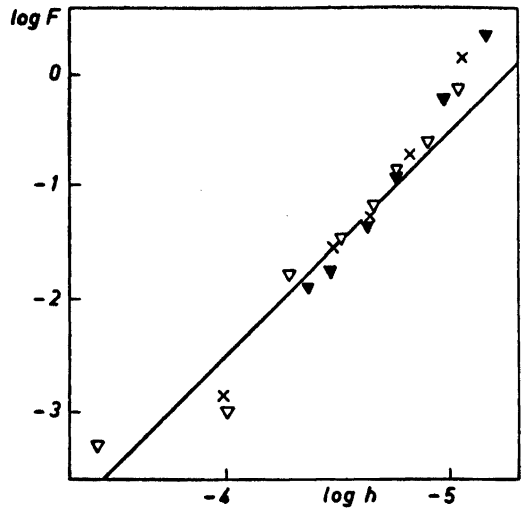


Fig 8. Log F, *eqn. (25), as a function of log* h. *Straight line: calculated for* $K_{11} = 0$, *log* $K_{21} = -10.8$.

Even up to $Z \approx 0.65$, the points seem to fall on a straight line of slope —2, in a position corresponding to log $K_{21} = -10.8$. We may conclude that the main mononuclear complex formed is $Be(OH)_2$; however, the spread of the data certainly does not permit one to exclude the presence of small amounts of $BeOH^+$.

This is not so surprising. For several ions, mercury(II) [15], thallium(III) [18], iron(III) [19], indium(III) [23, 24] the intermediate complex MOH has a remarkable tendency to split up to M and $M(OH)_2$, in marked contrast to the intermediate ion of most dibasic acids.

Calculation of equilibrium constants with normalized projection maps

Now that the formulas of the main and secondary products of hydrolysis were known, we set out to refine the values of the constants, using the method of normalized projection maps for three-variable data [30, 28].

In the present case, the quantities directly measured are h, B, and Z. We have

$$B = b + K_{21}h^{-2}b + 2K_{12}h^{-1}b^2 + 3K_{33}h^{-3}b^3 \tag{26}$$

$$BZ = 2K_{21}h^{-2}b + K_{12}h^{-1}b^2 + 3K_{33}h^{-3}b^3 \tag{27}$$

It is convenient to compare projection maps $y(x)_Z$ of the experimental variables

$$x = -\log h; \qquad y = \log B \tag{28}$$

with calculated normalized projection maps $Y(X)_z$ of the normalized variables

$$X = \log a = -\log h + p_1; \quad Y = \log B = \log B + p_2 \tag{29}$$

From the best fit of the maps one may obtain $X—x = p_1$ and $Y—y = p_2$. We shall introduce the auxiliary variables ("normalized h^{-1} and b")

$$a = h^{-1} \cdot 10^{p_1}; \quad u = b \cdot 10^{p_2} \tag{30}$$

In order to get simple formulas for calculation, we want to choose the constants p_1 and p_2 so that all equilibrium constants are eliminated except for a constant k, which replaces the smallest correction term K_{21}. We thus set

$$B = B \cdot 10^{p_2} = u + ka^2u + 2au^2 + 3a^3u^3 \tag{31}$$

$$BZ = 2ka^2u + au^2 + 3a^3u^3 \tag{32}$$

Inserting (30) into (31) and comparing with (26) we find

$$\log K_{33} = 3p_1 + 2p_2; \quad \log K_{12} = p_1 + p_2; \quad \log K_{21} = 2p_1 + \log k \tag{33}$$

To construct the necessary graphs $Y(X)_Z$ we used the formulas, derived from (31) and (32).

$$(2—Z)B = u(2 + 3au + 3a^3u^2) \tag{34}$$

$$Z = 2 - (2 + 3au + 3a^3u^2)\ (1 + ka^2 + 2au + 3a^3u^2)^{-1} \tag{35}$$

Auxiliary diagrams were constructed: $\log [(2—Z)B]$ $(\log u)_a$ which is independent of k, and Z $(\log u)_a$ for a number of different values of k. From these diagrams, $Y(X)_Z$ or $\log B$ $(\log a)_Z$ was constructed for various values of k, namely $10^7k = 0$, 2, 3, 5 and 10.

The best agreement was found for $k = 3.10^{-7}$, thus $\log k \approx -6.5_3$. In the position of the best fit, the parameters were

$p_1 = \log a + \log h = -2.17 \pm 0.01$; $p_2 = \log B - \log B = -1.07 \pm 0.01$; $\log k = -6.5_3 \pm 0.2$

whence with (33)

$\log K_{33} = 3p_1 + 2p_2 = -8.65 \pm 0.03$.
$\log K_{12} = p_1 + p_2 = -3.24 \pm 0.02$
$\log K_{21} = 2p_1 + \log k = -10.9 \pm 0.2$.

The value for $\log K_{33}$ agrees well with the average —8.66 obtained by several methods in the previous sections. Also the values for $\log K_{12}$ and $\log K_{21}$ are in good agreement with the values obtained from the diagrams in Figs. 6—8. We shall accept the values for $\log K_{12}$ and $\log K_{21}$ from the projection maps as our final values.

The dashed curves Z $(\log h)_B$ in Fig. 1 were calculated with $\log K_{33} = -8.66$, $\log K_{12} = -3.25$ and $\log K_{21} = -10.87$, thus practically the final set of constants K_{33}, K_{12} and K_{21}. The agreement seems to be as good as can be expected except in the region with $Z > 0.9$. However, in this region the equilibrium emf was obtained much more slowly than for lower values of Z, which may be explained by the presence of either higher species (*e. g.* according to hypothesis IIIa above), or of an invisible precipitate; both might give rise to

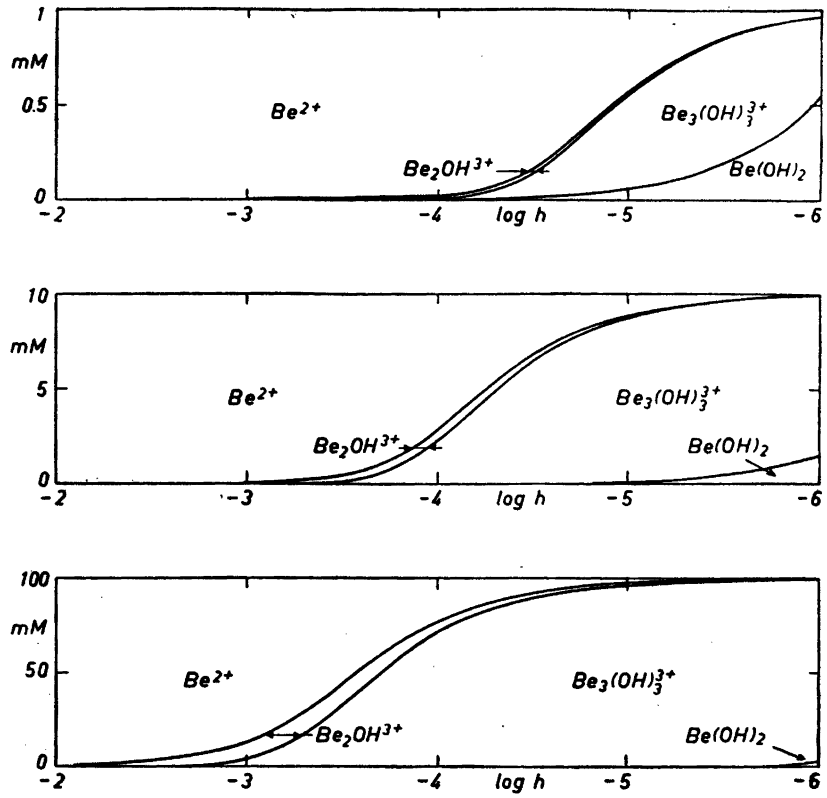


Fig 9. Distribution of complexes for total beryllium concentration B = 1, 10, and 100 mM, as a function of log h. *If a vertical line is drawn for a given value of* h, *the segment of this line falling in a certain area, e.g.* Be_2OH^{3+}, *represents the concentration of Be present as this complex in the solution at equilibrium.*

the slight positive deviation in the observed value of Z. The accuracy of the present work does not permit any certain conclusion.

Fig. 9 shows the distribution of the total beryllium over the various species, as a function of log h, for the total concentrations B = 1 mM, 10 mM and 100 mM, assuming the equilibrium constants obtained here.

ON THE STRUCTURE OF THE COMPLEXES

Four-coordination of Be^{2+}

Two- or three-coordinated beryllium occurs in some organoberyllium compounds like $Be(C_6H_5)_2$ and $Be(C_6H_5)_3^-$, but with O and F, the coordination always appears to be tetrahedral. The proof of this is to be found in certain simple crystal structures, since beryllium is light and thus rather difficult

to locate with X-ray methods. For complicated structures, it has generally been taken for granted that Be is in the centre of a BeO_4 or BeF_4 tetrahedron.

Phenakite, Be_2SiO_4, has a rhombohedral structure built up of SiO_4 and BeO_4 tetrahedra [39]; Be_2GeO_4 is isomorphous [40]. The structure of hambergite, Be_2BO_3OH, is built up of BO_3 triangles and BeO_3OH tetrahedra, sharing corners [41]. In β-$Be(OH)_2$, each Be is surrounded [42] by a somewhat distorted tetrahedron of 4 OH. The structure of $BeSO_4(H_2O)_4$, is built up [43] of tetrahedra $Be(H_2O)_4^{2+}$ and SO_4^{2-}. The stable complexes with organic acids, $Be_4O(OCOR)_6$, where R = CH_3, C_2H_5, C_6H_5 etc., have a symmetrical structure [44] with a central O surrounded by 4 Be. Each Be is in contact with the central O, and with 3 O from three different RCOO groups. The two oxygen atoms of a RCOO group are parallel with an edge of the Be_4 tetrahedron and in contact each with one Be.

With the exception of these volatile substances, which are rather rapidly hydrolysed by water, with the formation of RCOOH, and the rather special Be_2BO_3OH, no structures of beryllium hydroxo- or oxo-compounds seem to be known that would give an easy clue to the structure of the soluble complexes.

In the fluoride complexes, Be and F are very often found to give compounds isomorphous to corresponding compounds with Si and O. For instance, BeF_2 seems to be isomorphous with cristobalite [45], $BaBeF_4$ with $BaSO_4$ [46], the five forms of Na_2BeF_4 with different forms of Ca_2SiO_4 (Thilo and Liebau [47]), and $NaBeF_3$ with β-$CaSiO_3$ [48]. It may thus be expected that the structures contain BeF_4 tetrahedra connected by sharing corners (but not edges), just like the SiO_4 tetrahedra in the corresponding silicon compounds.

Similarly, in Be-OH complexes one may expect the BeO_4 tetrahedra to share corners but not edges.

In the older literature, a number of "basic" beryllium salts have been described. Later work has thrown considerable doubt on their existence as well-defined compounds [49]. Slavvo [50] has recently prepared halogenomercurates as hygroscopic crystals. In addition to $Be(H_2O)_5HgCl_4$ and $Be(H_2O)_5HgBr_4$, he also prepared crystalline $BeOH(H_2O)_2HgCl_3$, $BeOH(H_2O)_2HgBr_3$, and $Be_3(OH)_3(H_2O)_6Hg_2I_7$. It is interesting to note that the three last mentioned salts may all contain the ringshaped complex $Be_3(OH)_3(H_2O)_6^{3+}$ proposed below.

Possible structure of the hydrolysis products

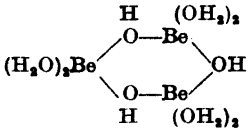
From what is known on the structure of other beryllium compounds it seems reasonable that the complex Be_2OH^{3+} consists of two BeO_4 tetrahedra, sharing a corner, which is very probably OH. The complex would thus be: $(H_2O)_3BeOHBe(OH_2)_3$

The mononuclear complex $Be(OH)_2$ is probably also a tetrahedron, $(H_2O)_2Be(OH)_2$. There is, however, a possibility that the molecule may be linear, forming *sp* bonds: HOBeOH. Alternation between tetrahedral to linear coordination may occur in some Hg^{2+}-complex systems [51] and might be related to the unusually small stability of the complex with one ligand.

The equilibrium constant for the formation of the main complex, $Be_3(OH)_3^{3+}$ from the mono- and dinuclear complexes is

$Be_2OH^{3+} + Be(OH)_2 \rightleftharpoons Be_3(OH)_3^{3+}$; $K_{33}K_{12}^{-1}K_{21}^{-1} = 10^{5.5}$.

The very high value of this constant, and the predominance of $Be_3(OH)_3^{3+}$ make it extremely unlikely that this complex would have an open chain structure. The most likely structure seems to be a six-membered ring, three tetrahedra being linked by sharing OH corners:



If the tetrahedra are filled out with water, one would get the formula $Be_3(OH)_3(OH_2)_6^{3+}$, which corresponds very well to the formulas of the halogenomercurates prepared by Slavvo [50].

This work is part of a program, financially supported by *Statens Naturvetenskapliga Forskningsråd* (*Swedish Natural Science Research Council*) and *Atomkommittén* (*Swedish Atomic Energy Committee*). We are indebted to Dr. George Biedermann for valuable advice, to Dr G. Mattock for giving us access to his primary data, to Drs. Francis and Hazel Rossotti for discussions of the manuscript and to Mr Frans Ericson for practical aid in many ways.

REFERENCES

1. Berzelius, J. J. *Schweiggers J.* **15** (1815) 296.
2. Prytz, M. *Z. anorg. allgem. Chem.* **180** (1929) 355.
3. Prytz, M. *Z. anorg. allgem. Chem.* **197** (1931) 103.
4. Prytz, M. *Z. anorg. allgem. Chem.* **231** (1937) 238.
5. Bjerrum, J. *Diss.* Copenhagen (1941).
6. Schaal, R. and Faucherre, J. *Bull. soc. chim. France* **1947** 927.
7. Faucherre, J. *Diss.* Paris (1954).
8. Teyssèdre, M. and Souchay, P. *Bull. soc. chim. France* **1951** 945.
9. Souchay, P. *Bull. soc. chim. France* **1948** 143.
10. Puche, F. and Josien, M. L. *Bull. soc. chim. France* **1940** 755.
11. Haldar, B. C. *J. Indian Chem. Soc.* **25** (1948) 439; *Chem. Abstracts* **1949** 4967 g.
12. Honda, M. *J. Chem. Soc. Japan* **72** (1951) 361.
13. Heukeshoven, W. and Winkel, A. *Z. anorg. allgem. Chem.* **213** (1933) 1.
14. Mattock, G. *J. Am. Chem. Soc.* **76** (1954) 4835.
15. Hietanen, S. and Sillén, L. G. *Acta Chem. Scand.* **6** (1952) 747 (part 2).
16. Forsling, W., Hietanen, S. and Sillén, L. G. *Acta Chem. Scand.* **6** (1952) 901 (part 3).
17. Biedermann, G. and Sillén, L. G. *Arkiv Kemi* **5** (1953) 425 (part 4).
18. Biedermann, G. *Arkiv Kemi* **5** (1953) 441 (part 5).
19. Hedström, B. O. A. *Arkiv Kemi* **6** (1953) 1 (part 7).
20. Hietanen, S. and Sillén, L. G. *Acta Chem. Scand.* **8** (1954) 1607 (part 8).
21. Hietanen, S. *Acta Chem. Scand.* **8** (1954) 1626 (part 9).
22. Ahrland, S., Hietanen, S. and Sillén, L. G. *Acta Chem. Scand.* **8** (1954) 1907 (part 10).
23. Biedermann, G. *Arkiv Kemi* **9** (1956) 277 (part 14).
24. Rossotti, F. J. C. and Rossotti, H. *Acta Chem. Scand.* **10** (1956) 779 (part 15).
25. Sillén, L. G. *Acta Chem. Scand.* **8** (1954) 299 (AB I).
26. Sillén, L. G. *Acta Chem. Scand.* **8** (1954) 318 (AB II).
27. Hedström, B. O. A. *Acta Chem. Scand.* **9** (1955) 613 (AB III).
28. Biedermann, G. and Sillén, L. G. *Acta Chem. Scand.* **10** (1956) 1011 (AB IV).
29. Sillén, L. G. *Mimeographed sheet for Amsterdam symposium*, April 1955.

30. Sillén, L. G. *Acta Chem. Scand.* **10** (1956) 803.
31. Rossotti, F. J. C. and Rossotti, H. *Acta Chem. Scand.* **10** (1956) 957.
32. Kakihana, H. *J. Chem. Soc. Japan* **72** (1951) 200.
33. Feigl, F. *Qualitative Analyse mit Hilfe von Tüpfel-Reaktionen*, 2 Auflage, Leipzig 1935, p. 219 and 237.
34. Gran, G. *Analyst* **77** (1952) 661.
35. Hamer, W. J. and Acree, S. F. *J. Research Natl. Bur. Standards* **33** (1944) 87.
36. Brown, A. S. *J. Am. Chem. Soc.* **56** (1934) 646.
37. Meyer, F. R. and Ronge, G. *Angew. Chem.* **52** (1939) 637.
38. Kakihana, H. *To be published.*
39. Bragg, W. and Zachariasen, W. H. *Z. Krist.* **72** (1930) 518.
40. Schütz, W. *Z. physik. Chem.* **B 31** (1936) 292.
41. Zachariasen, W. H. *Z. Krist.* **76** (1931) 289.
42. Seitz, A., Rösler, U. and Schubert, K. *Z. anorg. Chem.* **261** (1950) 94.
43. Beevers, C. A. and Lipson, H. *Z. Krist.* **82** (1932) 297.
44. Pauling, L. and Sherman, J. *Proc. Natl. Acad. Sci* **20** (1934) 336.
45. Brandenberger, E., *Schweiz. mineralog. petrog. Mitt.* **12** (1932) 243.
46. Ray N.N. *Z. anorg. allgem. Chem.* **201** (1931) 289.
47. Thilo, E. and Liebau, F. *Z. physik. Chem.* **199** (1952) 125.
48. O'Daniel, H. and Tscheischwili L. *Neues Jahrb. Mineral.Geol. Monatsh.* **48 A** (1945) 56, (*Chem. Abstracts 1949* 5253a).
49. Venturello, G. *Gazz. chim. ital.* **69** (1939) 73.
50. Slavvo, A. V. *Zhur. Obshchei Khim.* **22** (1952) 361, 368, 374.
51. Sillén L. G. *Acta Chem. Scand.* **3** (1949) 539.

Received April 3, 1956.

ACTA CHEMICA SCANDINAVICA 10 (1956) 1006—1010

The Reaction between Phenols and Orthoesters. A New Synthesis of Aryl Alkyl Ethers

BENGT SMITH

Institutionen för Organisk Kemi, Chalmers Tekniska Högskola, Göteborg, Sweden

It has been shown that alkyl orthocarbonates and phenols react under very mild conditions with the formation of aryl alkyl ethers. The reaction between phenols and ethyl orthoacetate and ethyl orthoformate was also studied in some detail. Only by the former reaction were aryl alkyl ethers formed as the ultimate products.

In an attempt to prepare some carbon analogues of the phenoxyalkoxysilanes from alkyl orthocarbonates and phenol it was found that the reaction produced phenyl alkyl ethers, dialkyl carbonates, and alcohols instead of the expected phenyl alkyl orthocarbonates.

$$(RO)_4C + C_6H_5OH \rightarrow C_6H_5OR + (RO)_2CO + ROH \quad (1)$$

This reaction seems, with certain exceptions, to be a general one for phenols. The yield of ethers from phenol is good (80—90 %), but methyl groups in the *ortho* position to the hydroxyl group diminish the yield appreciably. In the case of 2,6-di-*tert.*-butyl-*p*-cresol no reaction took place. This is certainly caused by the shielding of the hydroxyl group by the butyl groups.

Among the dihydric phenols investigated resorcinol reacted regularly yielding the mono- and diethers while no ethers were formed in the reaction between pyrocatechol and methyl orthocarbonate. Instead *o*-phenylene dimethyl orthocarbonate resulted.

$$C_6H_4(OH)_2 + (CH_3O)_4C \rightarrow C_6H_4\begin{smallmatrix}O\\ \diagup\ \diagdown\\ O\end{smallmatrix}C(OCH_3)_2 + 2CH_3OH \quad (2)$$

The mode of reaction between phenols and some other types of orthoesters was also examined in some detail. Phenol and ethyl orthoacetate reacted with the formation of phenyl diethyl orthoacetate

$$CH_3C(OC_2H_5)_3 + C_6H_5OH \rightarrow CH_3C(OC_6H_5)(OC_2H_5)_2 + C_2H_5OH \quad (3)$$

and a small amount of diphenyl ethyl orthoacetate. Depending on the conditions used for the synthesis smaller or larger amounts of decomposition products were also formed.

Phenyl diethyl orthoacetate was previously prepared by McElvain and Kundiger [1] from ketene diethyl acetal and phenol. They reported that it decomposed on distillation at atmospheric pressure yielding phenetole and phenyl acetate *. The phenetole and the ethyl acetate probably originate from the reaction **.

$$CH_3C(OC_6H_5)(OC_2H_5)_2 \rightarrow C_6H_5OC_2H_5 + CH_3COOC_2H_5 \quad (5)$$

The particular reactions by which the ethyl alcohol, phenol and phenyl acetate are formed are obscure as yet. The reaction between *p*-nitrophenol and ethyl orthoacetate furnished directly *p*-nitrophenetole in fair yield. This result is in accordance with the observation made by McElvain and Kundiger [1] that aryl alkyl ethers were formed in high yields from ketene diethyl acetale and phenols with negative substituents, while no aryl diethyl orthoacetates could be isolated.

Phenol reacted with ethyl orthoformate in much the same way as with ethyl orthoacetate; the main product being phenyl diethyl orthoformate. Contrary to the decomposition of phenyl diethyl orthoacetate the phenyl diethyl orthoformate yielded no phenetole on distillation at atmospheric pressure. Only ethyl formate, ethyl alcohol, and a black brittle resin were isolated.

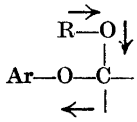
The course of the reaction between phenols and ethyl orthoacetate throws some light on the related reaction between phenols and alkyl orthocarbonates. It must be assumed that a labile phenyl alkyl orthocarbonate is formed,

$$C_6H_5OH + (RO)_4C \rightarrow [C_6H_5OC(OR)_3] + ROH \quad (6)$$

which decomposes according to eqn. 7 ***

$$[C_6H_5OC(OR)_3] \rightarrow C_6H_5OR + (RO)_2CO \quad (7)$$

The instability of a structure containing one aryloxy group and three alkoxy groups bonded to a carbon atom must be due mainly to the presence of the aryloxy group since alkyl orthocarbonates are quite stable compounds at moderate temperatures. The resonance in the aryloxy group is likely to originate an electron displacement in the manner denoted by the arrows in the following formula,



* No mention is made in the cited paper of the simultaneous formation of ethyl alcohol, phenol, and ethyl acetate. (See the experimental part).

** In an attempt to prepare ketene acetals by thermal decomposition of orthoesters at 250—300°, Staudinger and Rathsam [2] observed the following reaction

$$RC(OC_2H_5)_3 \rightarrow C_2H_5OC_2H_5 + RCOOC_2H_5 \quad (4)$$

for ethyl orthoformate, ethyl orthoacetate and ethyl orthopropionate.

*** In 1911 Einhorn and Rothlauf [3] snowed that certain aryl alkyl ethers could be prepared from the corresponding aryl alkyl carbonates (ArOCOOR) by heating them to 200—300° for long periods.

thereby causing the decomposition according to eqn. 7. The proximity of the R-group and the oxygen atom of the aryloxy group is probably also of significance for the decomposition. The existence of phenyl diethyl orthoacetate and the corresponding orthoformate shows that the stability increases when a methyl group or a hydrogen atom is substituted for an ethoxy group in the hypothetic phenyl triethyl orthocarbonate. This fact can be ascribed to the increased electron density at the central carbon atom, whereby the electron withdrawal from the R-group is opposed. Again, the presence of a *p*-nitro group on the benzene ring enhances the pull exercised by the aryloxy group on the electrons, thus making the *p*-nitrophenyl alkyl orthoester (*e. g.* orthoacetate) more susceptible to decomposition.

Orthoesters and especially alkyl orthocarbonates might be valuable in certain instances as alkylating agents for phenols because of the mild conditions under which the reaction proceeds. The orthocarbonates may be prepared conveniently from thiocarbonylperchloride (Cl_3CSCl) and sodium alkoxides [4].

It is interesting to note the difference in their reaction with phenols of alkyl orthocarbonates and the corresponding organosilicon compounds, the tetraalkoxysilanes. In the latter case quite stable aryloxyalkoxysilanes are formed; no thermal decomposition of these compounds has been observed [5]. A contributive reason for this circumstance is, undoubtedly, the non-existence of compounds with silicon-oxygen double bonds [6].

EXPERIMENTAL

Phenol and methyl orthocarbonate. A mixture of methyl orthocarbonate (27.2 g, 0.2 mole) and phenol (18.8 g, 0.2 mole) was slowly heated at atmospheric pressure. An azeotrope (10.2 g) mixture of methyl alcohol and dimethyl carbonate was distilled over between 62–64°, $n_D^{20} = 1.348$. Further distillation yielded dimethyl carbonate (9.7 g) b.p. 90–91°, $n_D^{20} = 1.369$, and a mixture (5.6 g) of the latter compound and methyl orthocarbonate b.p. 91–113°, $n_D^{20} = 1.377$. The residue, after removal of some phenol by alkali, was distilled under vacuum yielding *anisole* (18.8 g, 87 %) b.p. 46° (12 mm). (Found: OCH_3 28.4. Calc. for C_7H_8O: OCH_3 28.7).

Phenol and ethyl orthocarbonate. Ethyl orthocarbonate (38.5 g, 0.2 mole) and phenol (18.8 g, 0.2 mole) yielded on treatment as above a mixture (10.0 g) of ethyl alcohol and a small amount of diethyl carbonate, b.p. 78–79°, $n_D^{20} = 1.368$, and diethyl carbonate (20.1 g) b.p. 125–126°, $n_D^{20} = 1.384$. From the residue, after removal of some phenol, was obtained *phenetole* (20.7 g, 85 %) b.p. 55° (10 mm) $n_D^{20} = 1.507$. (Found: OC_2H_5 36.7. Calc. for $C_8H_{10}O$: OC_2H_5 36.9).

Alkylation of various phenols using methyl orthocarbonate. The general procedure for the alkylation of phenols using methyl orthocarbonate was the following. The phenol and methyl orthocarbonate were mixed in the molar ratio 1:1.2 for monohydric phenols and 1:2.5 for dihydric phenols. Gentle heating of the mixture was continued as long as any methyl alcohol was being distilled after which the dimethyl carbonate and residual methyl orthocarbonate were distilled rapidly. The residue was taken up in ether and this solution extracted with dilute sodium hydroxide to remove any phenol. After drying the solution and distilling the ether, the residue was fractionated under vacuum.

In this way there was obtained: From *o*-cresol (10.8 g, 0.1 mole) o-*cresyl methyl ether* (6.6 g, 54 %) b.p. 68° (18 mm). (Found: OCH_3 25.3. Calc. for $C_8H_{10}O$: OCH_3 25.4.). From *m*-cresol (10.8 g, 0.1 mole) m-*cresyl methyl ether* (7.0 g, 57 %) b.p. 71–72° (17 mm). (Found: OCH_3 25.5. Calc. for $C_8H_{10}O$: OCH_3 25.4). From 2,6-xylenol (12.2 g, 0.1 mole)

2,6-xylyl methyl ether (3.0 g, 22 %) b.p. 72° (15 mm). (Found: OCH_3 22.8. Calc. for $C_9H_{12}O$: OCH_3 22.8). From resorcinol (11.0 g, 0.1 mole) *resorcinol monomethyl ether* (2.0 g, 16 %) b.p. 137° (18 mm). (Found: OCH_3 25.0. Calc. for $C_7H_8O_2$: OCH_3 25.0) and *resorcinol dimethyl ether* (9.1 g, 66 %) b.p. 103° (18 mm). (Found: OCH_3 44.8. Calc. for $C_8H_{10}O_2$: OCH_3 44.9). The last two ethers were separated by extracting the former with alkali. No reaction could be traced between methyl orthocarbonate and 2,6-di-*tert.*-butyl-*p*-cresol.

Pyrocatechol and methyl orthocarbonate. Pyrocatechol (11.0 g, 0.1 mole) and methyl orthocarbonate (34.0 g, 0.25 mole) were treated in the usual way. There was obtained methyl alcohol (6.4 g) b.p. 64—65°, n_D^{20} = 1.334 and methyl orthocarbonate (18.4 g) b.p. 111—113°, n_D^{20} = 1.384. Further fractionation under vacuum yielded *o-phenylene dimethyl orthocarbonate* * (16.5 g, 91 %) b.p. 115—116° (19 mm), n_D^{20} = 1.4978, d_4^{20} = = 1.1959, MR_D = 44.64. (Found: OCH_3 33.6, H 5.61, C 59.4. Calc. for $C_9H_{10}O_4$: OCH_3 34.0, H 5.53, C 59.33). Guaiacyl methyl carbonate which has the same composition as *o*-phenylene dimethyl orthocarbonate might also be formed in the reaction above. The proof that *o*-phenylene dimethyl orthocarbonate was actually obtained was given by the hydrolysis of the reaction product in a mixture of dilute hydrochloric acid and methyl alcohol to yield pyrocatechol quantitatively. Furthermore the refractive index of guaiacyl methyl carbonate is reported as $n_D^{15.7}$ = 1.51736.[7]

Phenol and ethyl orthoacetate. A mixture of phenol (18.8 g, 0.2 mole) and ethyl orthoacetate (32.4 g, 0.2 mole) was heated to 70—110° at 70 mm pressure. A liquid (7.8 g), distilled over between 26 and 49°. It was composed mainly of ethyl alcohol but also contained some ethyl acetate and ethyl orthoacetate. On continuation of the distillation at 15 mm there was obtained a fraction (8.9 g) boiling between 50 and 100° and comprising unchanged starting materials and decomposition products. The main fraction, phenyl diethyl orthoacetate (24.2 g, 58 %), distilled at 104—105° (15 mm), n_D^{20} = 1.4801, d_4^{20} = = 1.0099, MR_D = 59.16. (According to McElvain and Kundiger [1] n_D^{25} = 1.4783). Found: Equiv. wt.** 35.0. Calc. for $C_{12}H_{18}O_3$: Equiv. wt. 35.04). A small amount of diphenyl ethyl orthoacetate * (3.5 g, 7%) was obtained at 135—136° (4 mm), n_D^{20} = 1.5369, d_4^{20} = 1.0934, MR_D = 73.77. (Found: OC_2H_5 17.1, equiv.wt. * 21.9. Calc. for $C_{16}H_{18}O_3$: OC_2H_5 17.4, equiv. wt. 21.5).

A better yield of phenyl diethyl orthoacetate was obtained if the ethyl orthoacetate was used in excess. In a synthesis performed as above but with phenol and ethyl orthoacetate in the molar ratio 1:3 the yield of phenyl diethyl orthoacetate was 92 %.

When the initial stage of the reaction between phenol and ethyl orthoacetate was allowed to proceed at atmospheric pressure instead of at 70 mm, the yield of phenyl diethyl orthoacetate dropped to about 30 % as the higher bath temperature (140—160°) caused an increased decomposition of the latter compound.

Thermal decomposition of phenyl diethyl orthoacetate. The thermal decomposition of this compound was previously studied by McElvain adn Kundiger [1] who reported the formation of phenetole and phenyl acetate. Here it was of principal interest to determine the amount of phenetole formed.

Phenyl diethyl orthoacetate (21.0 g, 0.1 mole) was heated to 170—180°. A mixture of ethyl alcohol and ethyl acetate (6.0 g), n_D^{20} = 1.370, containing about 80 % of the latter distilled between 72—78°. Further heating afforded a mixture (10.2 g) of phenetole, phenyl acetate and some phenol all boiling at about 170°. On redistillation under vacuum it distilled between 63—86° (13 mm), n_D^{20} = 1.510. Boiling this fraction with ethanolic sodium hydroxide produced pure phenetole (7.6 g, 62 %) b.p. 62° (15 mm), n_D^{20} = 1.507.

As phenyl diethyl orthoacetate under favourable conditions may be prepared in about 90 % yield from phenol and ethyl orthoacetate it appears that the overall yield of phenetole from phenol by this method is at best about 50 %.

---

* New compound.

** Titration with 0.1 N bromide-bromate solution.

p-*Nitrophenol and ethyl orthoacetate.* *p*-Nitrophenol (13.9 g, 0.1 mole) and ethyl orthoacetate (24.3 g, 0.15 mole) were heated together to 140—160°. A liquid (13.5 g) containing principally ethyl alcohol and ethyl acetate distilled at 77°. Further distillation under vacuum afforded, along with other products, *p*-nitrophenetole (11.2 g, 67 %) b.p. 112—115° (3 mm). After recrystallization from light petroleum m.p. 59—60°. (According to Jaeger [8] m.p. 60°. Found: OC_2H_5 27.0. Calc. for $C_8H_9NO_3$: OC_2H_5 26.96).

Phenol and ethyl orthoformate. A mixture of phenol (18.8 g, 0.2 mole) and ethyl orthoformate (29.6 g, 0.2 mole) was heated at 140—170° until 9.2 g of a liquid boiling at 78—79° had distilled. It was composed mainly of ethyl alcohol, but contained also some ethyl formate. By continued fractionation under vacuum there was obtained unchanged starting materials and phenyl diethyl orthoformate * (22.4 g, 57 %), b.p. 111° (11 mm), n_D^{20} = = 1.4799, d_4^{20} = 1.0185, MR_D = 54.72. (Found: Equiv. wt. ** 32.7, H 8.28, C 67.4 Calc. for $C_{11}H_{16}O_3$: Equiv. wt. 32.71, H 8.22, C 67,32). A small amount of a black resin remained in the distillation flask.

Thermal decomposition of phenyl diethyl orthoformate. Phenyl diethyl orthoformate (18.5 g, 0.094 mole) was heated to about 200°. A mixture (6.9 g) of ethyl alcohol and ethyl formate distilled over between 53 and 73°. At the end of the heating period carbon dioxide and other gases were evolved. A black brittle resin (9.3 g) remained in the distillation flask. The losses amounted to 2.3 g.

If the heating were discontinued before all of the material in the distilling flask had resinified, fractions boiling between 40 and 80° at 10 mm could be isolated. They were composed mainly of ethyl orthoformate and phenol. No phenetole was found.

REFERENCES

1. McElvain, S. M. and Kundiger, D. *J. Am. Chem. Soc.* **64** (1942) 254.
2. Staudinger, H. and Rathsam, G. *Helv. Chim. Acta* **5** (1921) 645.
3. Einhorn, A. and Rothlauf, L. *Ann.* **382** (1911) 237.
4. Smith, B. and Delin, S. *Svensk Kem. Tidskr.* **65** (1953) 10.
5. Smith, B. *Acta Chem. Scand.* **9** (1955) 1337.
6. Gilman, H. and Dunn, G. E. *Chem. Revs.* **52** (1953) 102.
7. Morel, A. *Bull. soc. chim. France* [3] **21** (1899) 823.
8. Jaeger, F. M. *Z. anorg. Chem.* **101** (1918) 131.

Received April 7, 1956.

* New compound.
** Titration with 0.1 N bromide-bromate solution.

ACTA CHEMICA SCANDINAVICA 10 (1956) 1011—1019

On Equilibria in Systems with Polynuclear Complex Formation

IV. The Transition from Polynuclear to Mononuclear Products

GEORGE BIEDERMANN and LARS GUNNAR SILLÉN

Department of Inorganic Chemistry, Royal Institute of Technology, Stockholm 70, Sweden

The behavior of Z (average number of A bound per B) as a function of log a and log B is discussed for a system, where both mononuclear complexes A_tB and polynuclear "core + links" complexes $B(A_tB)_n$ exist. At high values of B, the family of curves $Z(\log a)_B$ are parallel with a constant spacing. With decreasing values of B they approach to a limiting curve $Z(\log a)$, the "mononuclear wall". The transition range from a predominantly polynuclear to a predominantly mononuclear mechanism may be only about two units in log B.

"Normalized projection maps" and numerical methods are given for finding the first or first two mononuclear constants. The corresponding treatment of the function η is indicated.

In our studies of hydrolysis equilibria [1], the data have often indicated the formation of "core + links" complexes, *i. e.* complexes that can be written in the general form $B(A_tB)_n$, where t is a constant and n may have one or several values. For B = cation, and A = OH^-, examples of this type of complex are $UO_2((OH)_2UO_2)_n^{2+}$ and $In((OH)_2In)_n^{(3+n)+}$. The occurrence of such complexes was one reason for treating them rather thoroughly in the papers "AB I"[2] and "AB II"[3]; in the following we shall use, as a rule, the notation of these papers. (See "Symbols" below).

When "core + links" complexes of the type $B(A_tB)_n$ predominate, the curves $Z(\log a)_B$ are parallel, and Z (the average number of A bound per B) is a function of (AB I, eqn. 26)

$$x = t \log a + \log B \qquad (1)$$

A plot of Z against log a^tB may thus be used as an experimental test of this type of mechanism; if the correct value of t has been chosen, the points should fall on a single curve, irrespective of the value of B.

In several systems, the data for high values of B are explained by a "core + links" mechanism, within the experimental accuracy, whereas for low values

of B deviations are observed which might be explained by the formation of species richer in A than $B(A_tB)_n$, such as $AB(A_tB)_n$ and $B(A_{t+1}B)_n$.

If B is made sufficiently low, one may always expect that the concentrations of *mononuclear complexes* A_iB will become appreciable in comparison with those of polynuclear complexes, and finally predominate completely. The aim of the present paper is to discuss the behavior of the experimental quantities Z and $\eta = \log (B\, b^{-1})$ in a transition range where both mononuclear and polynuclear "core + links" complexes exist in comparable amounts, and to indicate methods for the evaluation of data from such a transition range.

Symbols

a, b	concentrations of free A and B
B	total concentration of B
$\mathbf{B}$	normalized B (12)
$g(v)$	function for polynuclear complexes (7)
i	number of ligands in mononuclear complex A_iB (3)
k	constant, ratio k_{n+1}/k_n with hypothesis IIIa (18)
k_0	constant, k_1/k in hypothesis IIIa (18)
k_n	equilibrium constant (2)
l	$\beta_2\beta_1^{-2}$ (27)
n	number of links in polynuclear complex $B(A_tB)_n$ (2)
t	number of A in link A_tB
u	auxiliary function, a^tb (2a)
v	$= ka^tb$ (6)
X, Y	normalized values for x and y, particularly (13), (14)
x, y	variables determined experimentally, particularly (1), (15)
Z	average number of A bound per B
α	normalized a (10)
β_i	equilibrium constant for mononuclear complexes (3)
η	$= \log B - \log b$

General equations

Let us assume that A and B form two series of complexes: polynuclear species $B(A_tB)_n$ and mononuclear species A_iB, and that the equilibrium constants of their formation are k_n and β_i, thus

$$nt\ \mathrm{A} + (n+1)\ \mathrm{B} \rightleftharpoons \mathrm{B(A_tB)_n};\quad [\mathrm{B(A_tB)_n}] = bk_nu^n \tag{2}$$

$$u = a^tb \tag{2a}$$

and

$$i\ \mathrm{A} + \mathrm{B} \rightleftharpoons \mathrm{A_iB};\qquad [\mathrm{A_iB}] = b\beta_ia^i \tag{3}$$

The total concentration of B, and the concentration of A bound to B, will be expressed by

$$B = [\mathrm{B}] + \Sigma[\mathrm{A_iB}] + \Sigma(n+1)\,[\mathrm{B(A_tB)_n}] = b(1 + \Sigma\beta_ia^i + \Sigma(n+1)k_nu^n) = b10^\eta \tag{4}$$

$$BZ = \Sigma i\ [\mathrm{A_iB}] + \Sigma nt\ [\mathrm{B(A_tB)_n}] = b\ (\Sigma i\beta_ia^i + t\ \Sigma nk_nu^n) \tag{5}$$

Introducing from AB II [3] the symbols

$$v = ku = ka^tb \tag{6}$$

$$g(v) = \Sigma\ k_nu^n;\qquad v\frac{\mathrm{d}g}{\mathrm{d}v} = vg' = \Sigma\ nk_nu^n \tag{7}$$

we obtain from (4) and (5)

$$B = b\ (1 + \Sigma\beta_i a^i + g + vg') \tag{8}$$

$$BZ = b\ (\Sigma i\beta_i a^i + tvg') \tag{9}$$

In AB II[3], expressions for $g(v)$ have been derived for a few simple hypotheses: I (no soluble complex, precipitate formed), II (a single complex formed, with $n = N$), and III (complexes with all values of n are formed, three different simple assumptions about the k_n). In the following we shall treat the simple cases, where only one or two mononuclear complexes are formed, and shall calculate diagrams for the additional simple assumption that the polynuclear complexity constants follow "hypothesis IIIa" [3], with an integer t. On these assumptions it seems possible to explain approximately the experimental data for the hydrolysis of scandium(III)[4,5] and uranium(IV)[6]. Even in more complicated cases the behavior should be analogous, and a similar mathematical treatment could be applied.

ONLY ONE MONONUCLEAR COMPLEX

If only one mononuclear complex, AB, is formed, all $\beta_i = 0$ except β_1. To eliminate the constant β_1 we introduce the auxiliary "normalized" variable

$$\alpha = \beta_1 a \tag{10}$$

Then (8) and (9) take the form

$$B = b\ (1 + \alpha + g + vg'); \qquad BZ = b\ (\alpha + tvg') \tag{8a, 9a}$$

Hence

$$Z = \frac{\alpha + tvg'}{1 + \alpha + g + vg'} \tag{11}$$

Multiplying B by $k\,\beta_1^{-}$ we obtain a new function, $\mathcal{B}$, which like Z is a function of v and α only and does not contain the constants k and β_1 (8a, 10, 6):

$$\mathcal{B} = B\ k\ \beta_1^{-t} = v\ \alpha^{-t}\ (1 + \alpha + g + vg') \tag{12}$$

If the constant t and the function $g(v)$ (including constants like k_0 below) are known, one may use (11) and (12) and suitable values of the auxiliary variable v to calculate corresponding values of α and $\mathcal{B}$ for a series of fixed values of Z. These figures may be used for plotting projection maps $Y(X)_Z$, for the variables

$$X = \log\ (B\ a^t) = \log\ B + t\ \log\ a + \log\ k = x + \log\ k \tag{13}$$

$$Y = \log\ \mathcal{B} = \log\ B + \log\ k\ -\ t\ \log\ \beta_1 = y + \log\ k - t\ \log\ \beta_1 \tag{14}$$

As seen from (13) and (14) X and Y are normalized variables [7,8] corresponding to the experimental variables

$$x = \log\ B + t\ \log\ a; \qquad y = \log\ B \tag{15}$$

Fig. 1 and Fig. 2. Variation of Z with other variables for a system A—B with a single mononuclear complex AB, and polynuclear "core + links" complexes $B(A_2B)_n$, hypothesis IIIa, $k_0 = 5$.

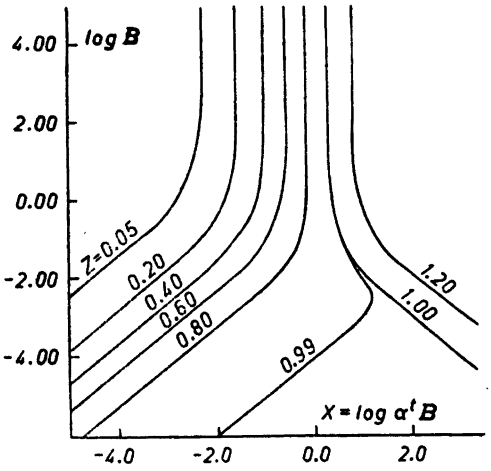


Fig. 1a. Projection map of $Y(X)_Z$, with $Y = \log B$ and $X = \log(\alpha^t B)$.

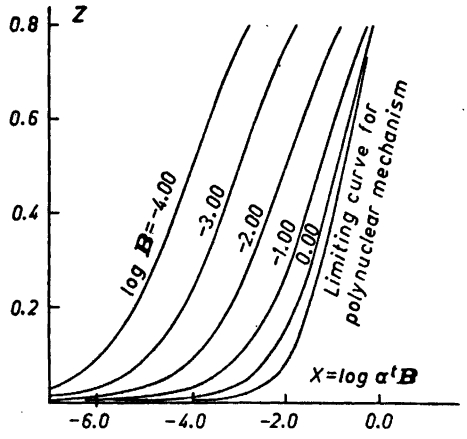


Fig. 1b. Family of curves $Z(X)_B$. For $\log B > 1$, the curves practically coincide with the limiting curve.

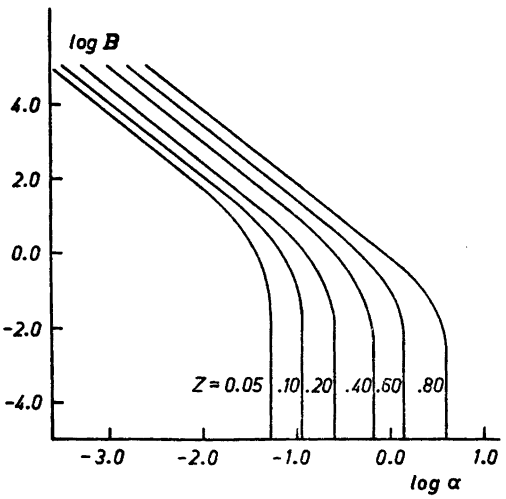


Fig. 2a. Projection map log $B(\log \alpha)_Z$.

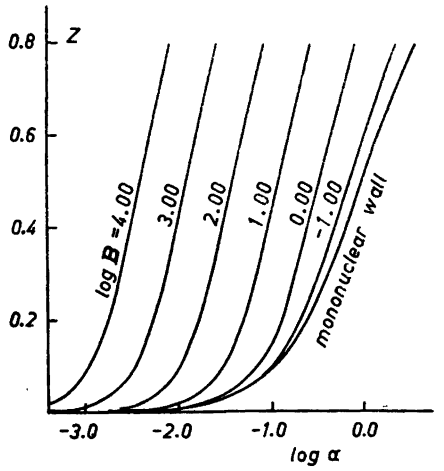


Fig. 2b. Family of curves $Z(\log \alpha)_B$. For $\log B < -1.5$, the curves practically coincide with the limiting curve, the "mononuclear wall".

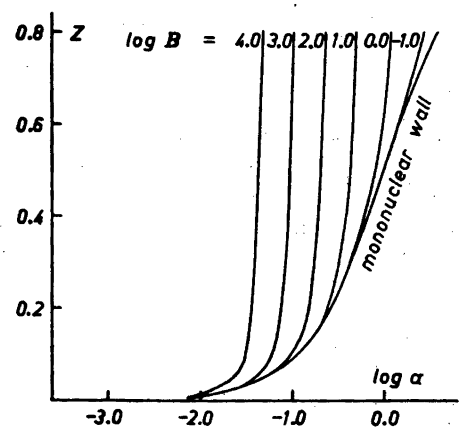


Fig. 3. Family of curves $Z(\log \alpha)_B$ *calculated for single mononuclear complex + polynuclear "IIIa" complexes with* $t = 3$, $k_0 = 0.06$.

The following formulas are useful for the calculations, (11, 12, 13)

$$\alpha = \frac{Z}{1-Z}(1 + g + v\,g') - \frac{t\,v\,g'}{1-Z} \tag{16}$$

$$X = \log v + \log [1 + g - v\,g'\,(t-1)] - \log (1-Z) \tag{17}$$

Diagrams for single mononuclear complex + hypothesis IIIa

In Fig. 1a, a projection map is given of $\log B(X)_Z$ calculated using (13, 14, 16, 17) assuming "hypothesis IIIa" [3],

$$k_n = k_0\,k^n \tag{18}$$

with $t = 2$ and $k_0 = 5$. These values give a good agreement with the data for scandium(III) [4,5].

Hypothesis IIIa with integer t would give (AB II[3], eqn. 31)

$$g(v) = k_0 v\,(1-v)^{-1}; \qquad vg'(v) = k_0 v(1-v)^{-2} \tag{18a}$$

The irregular shape of the curves for $Z = 0.99$, 1.00, and 1.20 in Fig. 1a should be disregarded. It is due to the fact that with the reactions assumed, the mononuclear complex can give at most $Z = 1$, whereas with polynuclear complexes, higher values of Z can be achieved. The case of a non-integer t has been treated by Rossotti and Rossotti [9].

The same values of t and k_0 have been used to construct the diagrams $Z(X)_B$ (Fig. 1b), $\log B(\log \alpha)_Z$ (Fig. 2a), and $Z\,(\log \alpha)_B$ (Fig. 2b). When considering these diagrams one should remember that the normalized variables $X = \log (\alpha^t B)$, $\log B$, and $\log \alpha$ differ from the experimental variables $x = \log (a^t B)$, $\log B$, and $\log a$, only by constant terms (13, 14, 10).

For high total concentrations B, the polynuclear complexes predominate and Z is a function of x only (vertical lines in upper part of Fig. 1a, limiting curve $Z(X)$ to the right of Fig. 1b, constant spacing in Fig. 2b). For very low

values of B, on the other hand, the polynuclear complexes become negligible in comparison with the mononuclear complexes. Then Z is effectively a function of a only (vertical lines in lower part of Fig. 2a, lines of slope 1 in lower part of Fig. 1a). The limiting curve $Z(\log a)$ is referred to as the "mononuclear wall", (Fig. 2b), since with decreasing B the curves Z $(\log a)_B$ approach to it indefinitely but never pass it. For intermediate values of B there is a transition range, of a breadth of 2—3 units in log B. This range of transition from a practically mononuclear reaction (within ordinary experimental errors) to a practically pure "core + links" reaction may seem surprisingly narrow, which may partly be due to the fact that in Fig. 2b the polynuclear and mononuclear curves have a rather similar shape.

Fig. 3 shows $Z(\log a)_B$ calculated for $t = 3$ and hypothesis IIIa with $k_0 = 0.06$; these values describe approximately the hydrolysis of uranium(IV)[6]. Here the polynuclear curves are steeper, and the transition range in log B is much broader.

Similar behavior would be expected for the function $Z(\log a)_B$ on transition between a mononuclear reaction and polynuclear reactions of other types, and also for the function $\eta(\log a)_B$, where $\eta = \log \frac{B}{b}$ (see (4)).

Evaluation of data by normalized projection map

In very favorable systems, the experiments cover a range of B such that at low values of B the mononuclear, at high values of B the polynuclear processes predominate. Then approximate equilibrium constants for both processes can be calculated separately, and refined values may be obtained by considering, at each end, the other process as a small disturbance. Such a procedure was possible for the hydrolysis of iron(III) (Hedström[10]) and indium(III) (Biedermann[11]). These cases were additionally favorable in that both the free concentrations a and b could be measured.

In other systems, the polynuclear process certainly predominates at high values for B, so that one may use the methods in AB II[3] to find a mechanism that gives a good agreement, and an approximate value for log k. At low values for B, deviations from the "core + links" curve are observed; however, the mononuclear process is too small a disturbance to be treated independently.

In such cases, the accuracy of the data may not allow one to determine more than one equilibrium constant for the mononuclear reactions; it has seemed reasonable to start by assuming that the first mononuclear complex AB is formed and testing this assumption by "surface-fitting", using projection maps.

To find the formation constant β_1 for this complex, and a refined value of log k, one may plot the experimental data in the form $y(x)_Z$, (15), and move this projection map parallel with the axes on a calculated normalized plot $Y(X)_Z$, (13, 14), until the best agreement is found. From the coordinates $x_0 = x—X$ and $y_0 = y—Y = \log B—\log B$ of the points coinciding with the point $X = 0$, $Y = 0$, one may then find the best values for log k and log β_1, using (13) and (14). An example is given in Fig. 4a, where the experimental values of Kilpatrick and Pokras[4] (dots) are shown in the position of best fit with calculated

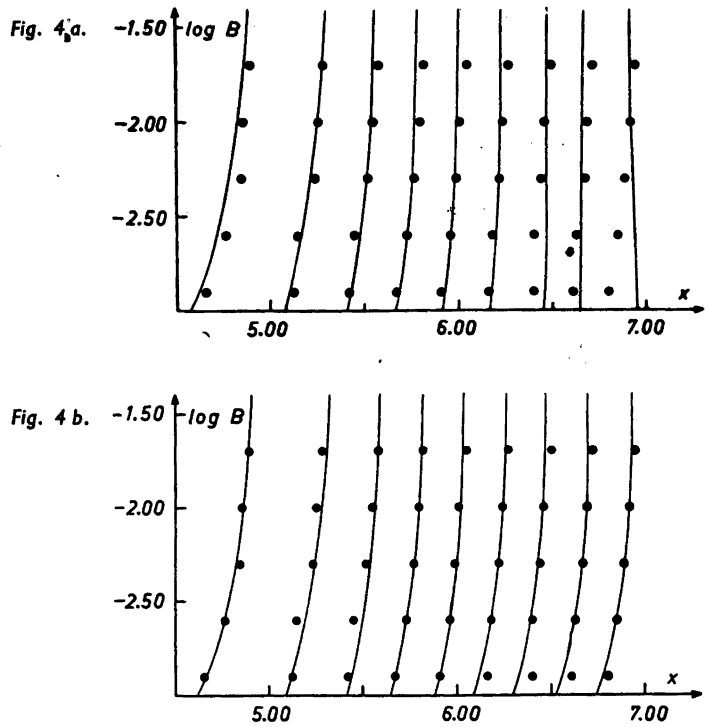


Fig. 4. "Surface-fitting" of Kilpatrick's and Pokras' data for scandium(III) hydrolysis [4] *(dots), plotted as log* $B(\log h^{-2} B)_Z$. *Curves :projection map log* $B(X)_Z$ *in best fit; a) only one mononuclear complex,* $k_0 = 5$: $\log \beta_1 = -5.02$ *and log* $k = -6.85$. *The curves are the same as in Fig. 1a but on a larger scale. b) two mononuclear complexes* $1 = 1$: $\log \beta_1 = -5.1$, $\log \beta_2 = -10.2$ *and log* $k = -6.87$.

curves for a single mononuclear complex + hypothesis IIIa with $k_0 = 5$. In this case, $x_0 = 6.85$ and $y_0 = -3.15$, which give $\log k = -6.85$ and $\log \beta_1 = -5.0$.

Numerical approach

One may use a numerical approach to find β_1 if the equilibrium constants k_n of the polynuclear reactions are known, or, which is the same, if k and $g(v)$ are known. If there is only one mononuclear complex, one may conveniently start with (8a), (9a) and (6) and eliminate b and a to find

$$a^t B(1-Z) = k^{-1}v(1 + g-(t-1)vg') \qquad (19)$$

Thus $a^t B$ $(1-Z)$ is a function of v only. Using the known k and $g(v)$ one may calculate and plot the expression to the right of (19) as a function of v. For each experimental point one may then calculate $a^t B$ $(1-Z)$ from the experim-

ental data, read off the value of v from the plot of (19), and use it to calculate (9a, 6)

$$\beta_1 = a^{-1}\,(a^i\ B\ Z\ k\ v^{-1}\text{—}t\ v\ g') \tag{20}$$

This can be done for a series of experimental points, and the average value of β_1 is taken. This method was used in the study of the Cu^{2+} hydrolysis [12].

Treatment of data (a, b, B)

If both a and b are measured and t is known, one may calculate $u = a^i b$ for each point. Now from (4)

$$\eta = \log \frac{B}{b} = \log\ (1 + \Sigma\ \beta_i\ a^i + \Sigma(n+1)\ k_n\ u^n) \tag{21}$$

In this case, one may also treat mechanisms with more than one mononuclear complex in a comparatively simple manner. Assuming, however, that we need consider only one mononuclear complex, AB, (21) takes the form

$$\eta = \log\,(1 + \alpha + g + v\ g') \tag{22}$$

If $g(v)$ is known, one may easily calculate a normalized projection map $\log v(\log \alpha)_\eta$ for a set of values of η and $\log v$. This could be fitted to an experimental diagram $\log u(\log a)_\eta$. The position of best agreement gives (6, 10)

$$\log k = \log v\text{—}\log u; \qquad \log \beta_1 = \log \alpha\text{—}\log a \tag{23}$$

Alternatively one may calculate $X(\log \alpha)_\eta$ and compare with the experimental $x(\log a)_\eta$. From (13), and (8)

$$X = \log v + \eta = x + \log k; \qquad \alpha = 10^\eta\text{—}(1 + g + vg') = \beta_1 a \tag{24}$$

So, by keeping η constant and varying v we may obtain sets of corresponding values for X and α.

To construct $\log u(\log a)_\eta$ one may draw the primary graphs $\eta(\log a)_B$ and $\log u(\log a)_B$, read the $\log a$ values for round values of η in the first diagram, mark out these points on corresponding curves in the second diagram, and finally join the points with the same η values in the latter diagram. The plot $x(\log a)_\eta$ is constructed in an analogous way.

TWO MONONUCLEAR COMPLEXES

Graphical method

If, in addition to AB, the second mononuclear complex A_2B must also be considered, there will be an additional term $b\beta_2 a^2$ in (8) and $2\,b\beta_2 a^2$ in (9). Defining the normalized functions α and B as before, (10, 12), we find from (8) and (9)

$$B = v\alpha^{-t}(1 + \alpha + l\ \alpha^2 + g + vg') \tag{25}$$

$$BZ = v\alpha^{-t}(\alpha + 2\ l\ \alpha^2 + tvg') \tag{26}$$

$$l = \beta_2\beta^{-2} \tag{27}$$

We may construct one normalized projection map log $B(X)_Z$ for each value of l to be tested, and search for the best fit with the experimental data log $B(x)_Z$, or alternatively construct log B (log $a)_Z$ and compare it with log B (log $a)_Z$.

Elimination of B from (25) and (26) leads to a second-degree equation in a, from which we get an explicit expression for $a(v,Z)$. Inserting this into (25) we find explicit expressions for $B(v,Z)$ and $X = \log Ba^l(v,Z)$. If the values of these functions are calculated for a series of values of v and Z, one may obtain the plots log $B(X)_Z$ and log $B(\log a)_Z$.

Alternatively we may construct intermediate plots of curves $X = \log Ba^l(v)_Z$, log $B(v)_a$ and $Z(v)_a$, by means of (25) and (26), and read off corresponding values of B, Z, and X or a.

Fig. 4 gives the projection map log $B(X)_Z$ for $k_0 = 5$ and $l = 0$ (Fig. 4a) or $l = 1$ (Fig. 4b) and the data for scandium(III). The agreement is improved by introducing the second complex.

It is true that we will have to construct as many projection maps as we want to test values for l. On the other hand, once this work is done, the "surface fitting" has several advantages over other methods (such as successive approximation) which might be devised. The normalized projection maps may be compared with a plot of experimental data, like log $B(\log a)_Z$, where one may still retain a feeling for the influence of experimental errors, so that one may see whether a certain agreement is satisfactory or not. It is an important advantage with this method that the same experimental plot log $B(\log a)_Z$ may also be used for testing other mechanisms that might be considered. One may then see where the significant differences between the various mechanisms arise, and whether the data suffice to make a certain decision between them.

This work is part of a program supported by *Atomkommittén (Swedish Atomic Energy Commission)* and *Statens Naturvetenskapliga Forskningsråd (Swedish Natural Science Research Council)*. We are indebted to Dr. Sirkka Hietanen and Dr. Gösta Lagerström for valuable discussions in the course of our work and to Drs. Francis and Hazel Rossotti for reading and discussing the manuscript.

REFERENCES

1. Sillén, L. G. *Rec. trav. chim.* **75** (1956) 705.
2. Sillén, L. G. *Acta Chem. Scand.* **8** (1954) 299 (AB I).
3. Sillén, L. G. *Acta Chem. Scand.* **8** (1954) 318 (AB II).
4. Kilpatrick, M. and Pokras, L. *J. Electrochem. Soc.* **100** (1953) 85; **101** (1954) 39.
5. Biedermann, G., Kilpatrick, M., Pokras, L. and Sillén, L. G. *Acta Chem. Scand.* **10** (1956).
6. Hietanen, S. *Acta Chem. Scand.* **10** (1956). *In press.*
7. Sillén, L. G. *Acta Chem. Scand.* **10** (1956) 186 (G II).
8. Sillén, L. G. *Acta Chem. Scand.* **10** (1956) 803 (G IV).
9. Rossotti, F. J. C. and Rossotti, H. S. *Acta Chem. Scand.* **10** (1956) 957.
10. Hedström, B. O. A. *Arkiv Kemi* **6** (1953) 1.
11. Biedermann, G. *Arkiv Kemi* **9** (1956) 277.
12. Berecki-Biedermann, C. *Arkiv Kemi* **9** (1956) 175.

Received April 9, 1956.

ACTA CHEMICA SCANDINAVICA 10 (1956) 1020—1023

Dehalogenation of Bromothiophenes with Butyllithium

SVEN-OLOV LAWESSON

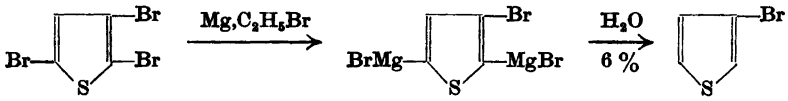
Department of Organic Chemistry, Chemical Institute, University of Uppsala, Sweden

Two new methods of preparing 3-bromothiophene and the preparation of a new compound, 3,5-dibromo-2-thiophencarboxylic acid, are described.

A possible route to 2,4-dibromothiophene is outlined.

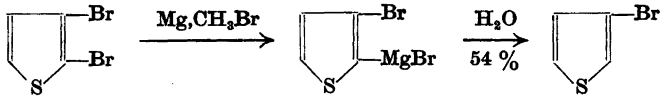
The author, who is investigating thiopheneboronic acids, needs as intermediates all isomers of the bromothiophenes. Some of these are troublesome to synthesize and the identity and purity of the product are not certain and, therefore, some preliminary experiments have been made in order to work out better methods. This paper deals with the preparation of 3-bromothiophene and 2,4-dibromothiophene.

As early as 1934, Steinkopf [1] prepared 3-bromothiophene according to the following reaction:



(Method I)

The yield was very low, but he did not abandon the method, neither did he try to improve it, strange to say. Instead, he prepared 3-bromothiophene by reacting 2,3-dibromothiophene with methylmagnesium bromide [2], *viz.*



(Method II)

Gronowitz [3] has recently improved both the methods of Steinkopf. By refluxing 2,3,5-tribromothiophene with magnesium for 49 hours, using ethyl bromide as entraining agent and then hydrolysing the Grignard reagent, he got 3-bromothiophene in a yield of 51 %. Using Steinkopf's method II, Gronowitz got 3-bromothiophene in a good yield.

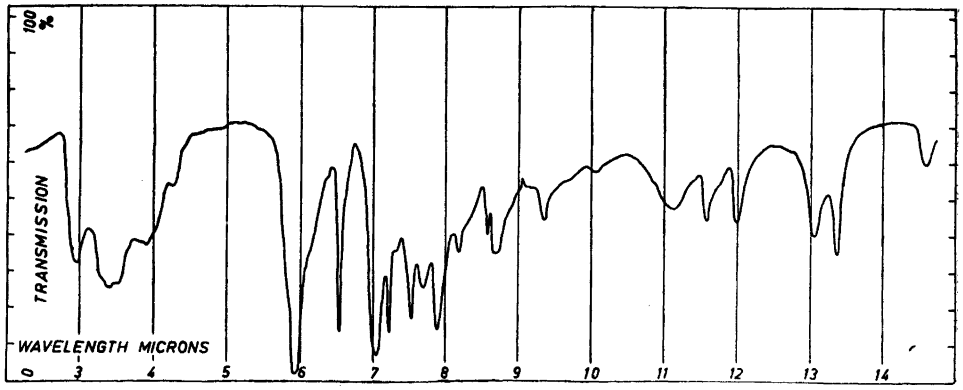


Fig. 1. The infrared spectrum of 4,5-dibromo-2-thiophenecarboxylic acid (in pressed KBr).

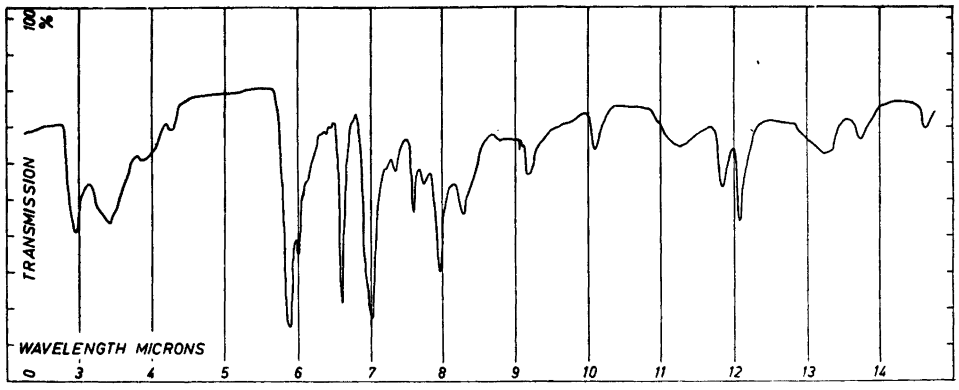
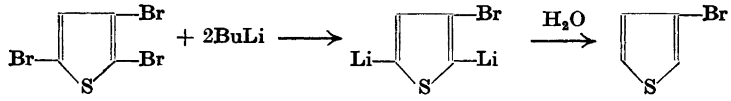


Fig. 2. The infrared spectrum of 3,5-dibromo-2-thiophenecarboxylic acid (in pressed KBr).

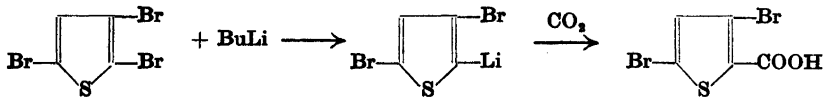
All these methods seem to be tedious and very time-consuming. We have instead brought together one mole of 2,3,5-tribromothiophene [4] and two moles of butyllithium [5] and obtained, after hydrolysing the lithium compound, 3-bromothiophene, through the reaction:



(Method III)

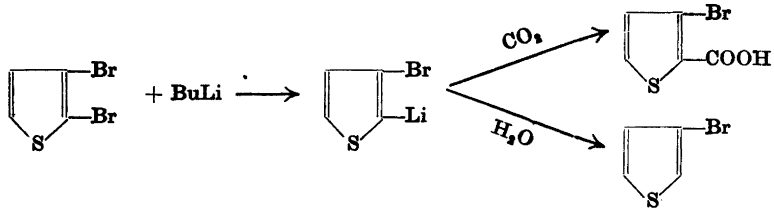
If the reaction was carried out with a 1 : 1 molar ratio of the 2,3,5-tribromothiophene and the butyllithium, at —70°, we obtained, after pouring the solution onto dry ice, a substance with a melting point 15° lower than that of 4,5-dibromo-2-thiophenecarboxylic acid [1]. The IR spectra (Figs. 1 and 2) showed

great differences in the finger-print region between 4,5-dibromo-2-thiophenecarboxylic acid, prepared by brominating 2-thiophenecarboxylic acid, and the new compound. Even in chloroform solution the differences remained, and consequently, the possibility of polymorphism is excluded. As a matter of fact, the occurrence of the following reaction is proposed:



From this it is seen that if instead of pouring the monolithium reagent on dry ice, we hydrolyse it, 2,4-dibromothiophene should be obtained. Investigation in this field is in progress at this Institute.

By treating 2,3-dibromothiophene[6] with an equimolar amount of butyllithium, 3-bromothiophene was obtained in good yields after hydrolysis. If the lithium reagent was poured onto dry ice, 3-bromo-2-thiophenecarboxylic acid[1] was isolated, as a result of the reaction:



(Method IV)

The infrared spectra were recorded with a Perkin-Elmer spectrophotometer (model 21) equipped with NaCl optics.

EXPERIMENTAL

3-Bromothiophene (*Method III*). A solution of 0.2 mole of butyllithium in 250 ml dry ether was added dropwise, over a period of 90 minutes, to an ice-cold solution of 2,3,5-tribromothiophene (32 g, 0.1 mole) in 200 ml of dry ether. The reaction was carried out under nitrogen, with stirring. The resulting yellow suspension was poured into ice-water. The organic layer was separated off and the water phase shaken several times with ether. The combined extracts were washed once with water, dried over sodium sulfate, and then concentrated. The residue was distilled, yielding 10.5 g of 3-bromothiophene, b.p. 58°/20 mm Hg, (identified by means of the IR spectrum), and 2 g of dibromothiophenes, b.p. 94°–96°/15 mm Hg. Yield of 3-bromothiophene: 65 %.

3,5-Dibromo-2-thiophenecarboxylic acid. 21 ml of 1.5 M butyllithium in dry ether was added, in a slow stream, to 10 g of 2,3,5-tribromothiophene in 100 ml of ether, at −70°. The solution was stirred for 5 minutes and then treated all at once with an excess of powdered solid carbon dioxide. After the dry ice had evaporated, the mixture was hydrolysed with water, the organic layer separated off, the water solution extracted with ether, and the combined ether layers extracted with dilute sodium hydroxide. Upon acidification of the alkaline solution, a white powder precipitated; this, after recrystallisation from water-ethanol solution, yielded small, faintly yellow-coloured, needles. Weight: 3.2 g, yield 36 %. M.p. 210–212°C.

Anal Subst. 44.30 mg; 3.11 ml of 0.0495 M NaOH
27.60 mg; 9.88 ml of 0.00978 M $Hg(NO_3)_2$
$C_5H_2Br_2O_2S$ Calc. Equiv. wt. 285.95 Br 56.19
Found » » 288.0 Br 55.98

3-Bromothiophene (*Method IV*). Butyllithium (0.09 mole) in 150 ml of dry ether was added with stirring over a 45-minute period to 20 g (0.083 mole) of 2,3-dibromothiophene in 150 ml of ether at 0°C. The solution was hydrolysed, and after being worked up as usual was distilled, giving 7.9 g of 3-bromothiophene (b.p. 44°—46°/11 mm Hg). Yield 58 %.

The yield ought to be better, but the optimum conditions have not been worked out, since this method is inferior to method III and more time-consuming.

3-Bromo-2-thiophenecarboxylic acid. Into 10 g of 2,3-dibromothiophene in 50 ml of ether, at −40°, was poured 23 ml of 1.5 M butyllithium. The reaction was carried out under nitrogen, with stirring; after 7 minutes, the solution was poured onto dry ice and worked up in the usual way. Recrystallisation from water-ethanol solution gave white needles with m.p. 193°—195°C. Weight: 6 g; yield 70 %.

Anal. Subst., 24.30 mg; 2.37 ml of 0.0495 M NaOH. Equiv. wt. Calc. 207.1; Found 207.2.

Indebtedness is expressed to Professor A. Fredga for his kind interest, and to Dr. A. Rosenberg for taking the IR spectra.

A grant from the *Swedish Natural Science Research Council* is gratefully acknowledged.

REFERENCES

1. Steinkopf, W., Jacob, H. and Penz. H. *Ann.* **512** (1934) 136.
2. Steinkopf, W. *Ibid.* **543** (1940) 128.
3. Gronowitz, S. *Arkiv Kemi* **7** (1954) 267.
4. Lawesson, S.-O. *To be published.*
5. Wittig, G. *Angew. Chem.* **53** (1940) 241.
6. Steinkopf, W. and Köhler, W. *Ann.* **532** (1937) 250.

Received April 9. 1956.

ACTA CHEMICA SCANDINAVICA 10 (1956) 1024—1034

Enzymic Synthesis of Carbamylaspartate from Citrulline in Extracts from Rat Liver Mitochondria

LLOYD H. SMITH JR.* and PETER REICHARD

Biochemical Department, Karolinska Institutet, Stockholm, Sweden

The formation of carbamylaspartate from citrulline and aspartate has been demonstrated to proceed in at least two steps. First, carbamylphosphate was formed from the carbamyl group of citrulline and ATP. Secondly, carbamylphosphate and aspartate formed carbamylaspartate. The formation of carbamylphosphate from citrulline required ATP, acetylglutamate and Mg^{++}. Ornithine was identified as the second product of the reaction. The reaction was very strongly inhibited by ornithine.

The carbamyl group of citrulline was found to be utilized for the biosynthesis of polynucleotide pyrimidines in pigeon liver by Schulmann and Badger [1]. These authors could not demonstrate the specific incorporation of this group into polynucleotide pyrimidines of the rat. Later work indicated, however, that rat liver slices formed orotic acid-^{14}C from carbamyl labeled citrulline [2]. Since orotic acid is formed from aspartic acid *via* CA-aspartate ** in rat liver slices [4], it seemed likely that the utilization of citrulline took place by a transfer of its carbamyl moiety to aspartic acid. The possibility of such a mechanism has been considered earlier and argininosuccinate [4,5] was suggested as an intermediate in the formation of CA-aspartate from citrulline and aspartate.

The enzymic formation of CA-aspartate in rat liver has recently been shown to proceed in at least two steps[6-8]:

$$(1)\ NH_3 + CO_2 + ATP \xrightarrow[\text{acetylglutamate}]{Mg^{++}} \text{Compound X} + ADP$$

$$(2)\ \text{Compound X} + \text{L-aspartate} \longrightarrow \text{L-carbamylaspartate} + \text{phosphate}$$

* Fellow of U. S. Public Health Service. Present address: Mass. General Hospital, Boston, Mass. USA. Requests for reprints should be addressed to Stockholm.

** The following abbreviations are used in this paper: CA = carbamyl; CAP = carbamylphosphate; ATP, ADP and AMP = adenosine tri-, di- and monophosphate, respectively; PGA = 3-phosphoglyceric acid; MP = muscle protein fraction for regeneration of ATP from ADP + PGA[15]; PCA = perchloric acid; P_i = inorg. phosphate.

Reaction (1) has been described earlier by Grisolia and Cohen [9] as the first step in citrulline synthesis, the second being:

(3) Compound X + ornithine ⟶ Citrulline + phosphate

The recent work of Jones *et al.*[10] has demonstrated the identity of compound X with carbamylphosphate in reaction (3).

The investigations described here were carried out to determine if CA-aspartate could be formed from citrulline through these known enzymic mechanisms. Using preparations from rat liver mitochondria, evidence has been obtained for a reaction by which carbamylphosphate (CAP) and ornithine are formed from citrulline and ATP in the presence of acetylglutamate and Mg^{++}:

$$\text{(4) Citrulline} + \text{ATP} \xrightarrow[\text{acetylglutamate}]{Mg^{++}} \text{carbamylphosphate} + \text{ornithine (+ADP)}$$

When aspartate was included during the reaction the formation of CA-aspartate could be demonstrated. Some of these experimental results have been briefly published earlier [11,12].

MATERIALS AND METHODS

L-*Citrulline-carbamyl-*^{14}C was synthesized according to Smith [13]. *CAP* was prepared according to Jones *et al.*[10] and L-*acetylglutamate* according to Karrer *et al.*[14] ATP, ADP, AMP and PGA were commercial products (Schwartz and Sigma). A muscle protein fraction [15] was prepared for the regeneration of ATP from ADP and PGA. ATP-^{32}P (labeled in the two terminal phosphate groups) was prepared from AMP through oxidative phosphorylation [16].

Ion exchange chromatography of CAP was carried out by gradient elution at 5°. Two columns of Dowex-2-formate (0.8 cm^2 × 10 cm) were connected with a 1 000 ml mixing flask, containing water, which received 2.25 M ammonium formate, pH 5.0, from a reservoir flask. P_i (10 column volumes), CAP (15 column volumes), ADP (34 column volumes) and ATP (45 column volumes) were completely separated (*cf.* also Ref.[8]).

Preparation of enzymes. The enzymes carrying out the overall synthesis of CA-aspartate from citrulline and aspartate were prepared by freezing and thawing rat liver mitochondria in 0.1 M $NaHCO_3$[7].

The enzyme preparation which was used for the study of reaction (4) was made in a slightly different manner. Mitochondria from *ca.* 40 g rat liver were prepared in 0.25 M sucrose-0.01 M versene (*cf.* Ref.[6]) suspended in 50 ml of distilled water, and quickly frozen in dry ice. The frozen mass was lyophilized directly, and the dry powder stored in a desiccator at 0°. Immediately before use the powder was extracted with 0.02 M glycylglycine buffer, pH 8.0, for 5 minutes in an ice bath and centrifuged at 20 000 g for 15 minutes at 0°. The supernatant was used for the experiments. The lyophilized powder could be stored for several days with a slow decrease of activity. When in solution the enzyme deteriorated in a few hours, even at 0° and despite the addition of glutathione.

Assay of enzyme activity. The *over all reaction* (formation of CA-aspartate) was determined by the isotope dilution method as described earlier [6,8].

Reaction (4). A convenient determination of CAP formation was based on its decomposition to release free CO_2 in the presence of a strong mineral acid. The amount of CAP formed during an experiment was calculated from the total radioactivity of the liberated $^{14}CO_2$ and the specific activity of the precursor citrulline-carbamyl-^{14}C. Incubations were carried out in stoppered 25 ml Warburg vessels, containing 0.5 ml of 12 N H_2SO_4 in the side arm, and 0.5 ml of 6 N NaOH in the center well. At the end of the experiment 100 μmoles of $NaHCO_3$ were added to the incubation mixture, the flask was

stoppered again, and the sulfuric acid added from the side arm. The flask was then shaken at 37° for 30 minutes, during which time all of the CAP was decomposed and the liberated CO_2 was collected in the center well. The completeness of CO_2 collection under these conditions was established in model experiments with radioactive CAP.

The carbonate in the center well was precipitated with saturated $Ba(OH)_2$, washed twice with hot water, filtered on to a paper disk of standard size, and counted as an infinitely thick sample in an end window Geiger-Müller counter. The number of μmoles $^{14}CO_2$ liberated could then be calculated from an experimentally determined conversion factor.

In this way all CAP formed during the experiment (including CAP broken down to CO_2 during the incubation) was determined. The assay method, of course, also determined any $^{14}CO_2$ formed from citrulline without the intermediate formation of CAP. Under the proper conditions this "background formation" of CO_2, however, did not amount to more than 10—15 % of the total amount of CO_2 formed from citrulline (*cf.* Fig. 1).

RESULTS

Over-all formation of CA-aspartate from citrulline

The over-all reaction was first demonstrated in rat *liver slices*. The conditions were the same as those described for orotic acid synthesis [3] except for the use of 200 μmoles of citrulline-carbamyl-^{14}C and a carrier of 100 μmoles of non-labeled CA-aspartate. From the isotope content of the reisolated CA-aspartate it was calculated that approximately two μmoles of CA-aspartate had been formed during the 4-hour incubation period.

In liver homogenates CA-aspartate synthesis from citrulline could also be demonstrated, though only to a small and varying extent. The homogenates were centrifuged at 100 g for 10 minutes at 0° to remove most of the cell nuclei and then for 15 minutes at 15 000 g (*cf.* Ref. [6]). Activity for CA-aspartate formation from citrulline per mg nitrogen was roughly five times larger in the sediment (mitochondria) than in the supernatant (cell sap + microsomes). All subsequent experiments were carried out with mitochondrial preparations.

Non-involvement of free CO_2. It has previously been shown [7] that the carbamyl carbon of CA-aspartate is derived from CO_2. Rat liver preparations contain a "citrullinase" which liberates CO_2 from the carbamyl group of citrulline, possibly unrelated to CAP formation [17] (see also below). It was possible, therefore, that "free CO_2" released from citrulline by this enzyme was then incorporated into CA-aspartate *via* the known enzymic pathways described as reactions (1) and (2) above. Experiments were therefore designed to test whether the carbamyl carbon of citrulline equilibrated with bicarbonate in the system or was transferred to CA-aspartate over a "closed circuit". For this purpose the synthesis of ^{14}C-labeled CA-aspartate by mitochondria was compared in tightly stoppered flasks containing either (a) citrulline-^{14}C + non-labeled $KHCO_3$, or (b) $KHCO_3$-^{14}C + non-labeled citrulline. At the end of the incubation CO_2 was liberated by the addition of PCA and collected and counted as $BaCO_3$ at infinite thickness. The amount of CA-aspartate-^{14}C formed from the respective ^{14}C precursors was then measured by the isotope dilution technique. The results summarized in Table 1 demonstrate that considerably more CA-aspartate was formed from citrulline-^{14}C than from bicarbonate-^{14}C, even though the specific activity of the bicarbonate at the end of the incubation in experiment 1 (citrulline-^{14}C) was only about one tenth as great as that in

Table 1. Non involvement of "free CO_2" in CA-aspartate synthesis from citrulline-CA-^{14}C.

Experimental conditions	+ acetylglutamate		no acetylglutamate	
	specific activity of $BaCO_3$	μmoles ^{14}CA-aspartate formed	specific activity of $BaCO_3$	μmoles ^{14}CA-aspartate formed
Citrulline-^{14}C $KHCO_3$ Phosphate buffer	13 400	0.16	7 700	0.09
Citrulline $KHCO_3$-^{14}C Phosphate buffer	142 000	0.02	132 000	0.00
Citrulline-^{14}C $KHCO_3$ Glycylglycine buffer	2 300	0.24		

Each vessel contained 100 μmoles of citrulline, 300 μmoles of L-aspartate, 1 000 μmoles of buffer, pH 7.4, 180 μmoles of succinate, 10 μmoles of ATP, 100 μmoles of $MgSO_4$, 200 μmoles of $KHCO_3$ and KCl to give isotonicity. Where indicated the vessels contained 100 μmoles of L-acetylglutamate. Volume 16 ml. Incubation for 60 minutes at 37° with rat liver mitochondria (8.7 mg nitrogen). The carbamyl labeled citrulline contained 60 000 ct/min/μmole; $KH^{14}CO_3$ contained 8 000 ct/min/μmole.

experiment 2 (bicarbonate-^{14}C). When glycylglycine was used instead of phosphate buffer (to decrease the phosphorolysis of citrulline) the specific activity of the bicarbonate at the end of the experiment was considerably decreased, but the formation of ^{14}CA-aspartate was not materially affected. When acetylglutamate was excluded from the reaction mixture there was a decrease of ^{14}CA-aspartate formation. This effect will be described more fully below.

The same general results were obtained when extracts of mitochondria were used rather than intact mitochondria. In these experiments the influence of increasing amounts of non-labeled ammonium carbonate on the formation of ^{14}CA-aspartate from labeled citrulline was studied. No dilution effect was observed.

Table 2. Requirements over-all reaction.

	μmoles CA-aspartate formed
Complete	0.26
no acetylglutamate	0.07
no aspartate	0.00
no ATP, PGA and MP	0.05
no phosphate	0.23

The complete system contained 20 μmoles of citrulline-^{14}C, 15 μmoles of L-aspartate, 10 μmoles of ATP, 60 μmoles of PGA, 2 mg MP, 40 μmoles of $MgCl_2$ and 100 μmoles of potassium phosphate buffer, pH 7.4. Volume = 3 ml. Incubation for 60 minutes at 37° with 40 mg of a lyophilized mitochondrial extract.

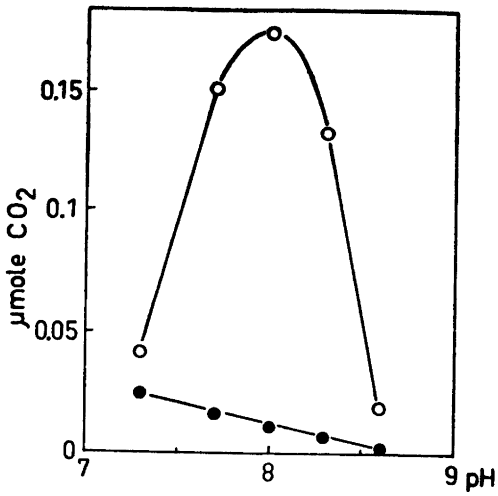


Fig. 1. pH curve of $^{14}CO_2$ formation from citrulline-^{14}C.

5 µmoles of citrulline-^{14}C, 5 µmoles of ATP, 30 µmoles of PGA, 5 mg MP, 50 µmoles of $MgSO_4$, 250 µmoles of glycyl-glycine buffer and 20 µmoles of acetyl glutamate were incubated with enzyme (1.1 mg nitrogen) for 20 minutes at 37° at pH values indicated (open circles). The full circles represent experiments where acetyl glutamate was excluded.

Requirements for over-all reaction. After the enzyme was brought into solution by freezing and thawing the rat liver mitochondria in 0.1 M $NaHCO_3$, the requirements for the over-all reaction were established (Table 2). CA-aspartate formation from citrulline was dependent on the presence of L-aspartate, and was strongly stimulated by acetylglutamate*, Mg^{++}, and ATP (and an ATP regenerating system). The addition of phosphate was not necessary. The strong stimulation by acetylglutamate suggested the intermediate formation of CAP, which in liver preparations requires the presence of acetylglutamate.

Formation of CAP from citrulline

Since it was demonstrated that free CO_2 was not involved in the reaction, CAP could not be formed from citrulline by way of reaction (1), described above. This suggested a direct transfer of the carbamyl group from citrulline to a phosphate group to form CAP. This reaction was studied directly in soluble extracts from lyophilized mitochondria by the omission of aspartate from the system. The enzyme assay was based on the measurement of the acetylglutamate dependent release of $^{14}CO_2$ from citrulline-carbamyl-^{14}C, following the addition of strong acid to break down CAP. In confirmation of the work of Krebs *et al.*[17] it was found that our enzyme preparation contained a "citrullinase" which released CO_2 from the carbamyl group of citrulline inde-

* Stimulation by acetyl glutamate was much more pronounced in mitochondrial extracts than in intact mitochondria. The amount of stimulation varied considerably with different preparations.

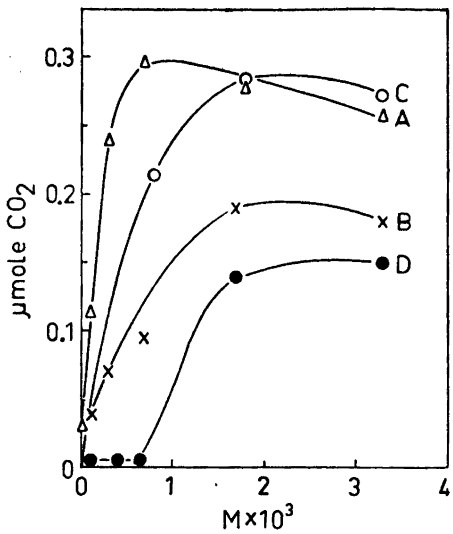


Fig. 2. Dependence of CAP formation on citrulline (curve A), acetylglutamate (curve B) and ATP (curves C and D).

Incubation for 20 minutes at 37°. 50 µmoles of $MgSO_4$ and 250 µmoles of glycylglycine buffer, pH 8.0, in a volume of 3.0 ml for each curve.

Curve A: 10 µmoles of ATP, 20 µmoles of acetyl glutamate, enzyme (1.1 mg nitrogen) and citrulline-^{14}C as indicated on abscissa.

Curve B: 10 µmoles of ATP, 5 µmoles of citrulline-^{14}C, enzyme (0.9 mg nitrogen), and acetyl glutamate as indicated.

Curve C: 5 µmoles of citrulline-^{14}C, 20 µmoles of acetyl glutamate, enzyme (1.1 mg nitrogen), 30 µmoles of PGA, 5 mg MP, and ATP as indicated.

Curve D: 5 µmoles of citrulline-^{14}C, 20 µmoles of acetyl glutamate, enzyme (1.1 mg nitrogen), and ATP as indicated.

All values are given for one experimental point in each curve.

pendent of acetylglutamate concentration. This background release of CO_2 was greatly diminished by the exclusion of phosphate from the system, which did not affect CAP formation. The citrullinase activity was furthermore sharply decreased by carrying out the reaction at pH 8.0, the pH optimum for CAP formation from citrulline (Fig. 1). The pH optimum for citrullinase is 6.8 [17]. The closed circles in Fig. 1 represent the release of carbamyl-CO_2 from citrulline in the absence of added acetyl glutamate, *i.e.* the maximum value for citrullinase in the present system under our experimental conditions.

Requirements of the reaction. Fig. 2 demonstrates the dependence of the reaction on acetylglutamate, citrulline, and ATP. As the different curves were not obtained with the same enzyme preparation, no significance should be attached to the absolute height of the curves, with the exception of curves C and D. These two curves show that the presence of an ATP regenerating system gives better synthesis than ATP alone, presumably because of the presence of ATP-ases. The S-shaped curve D was observed in several experi-

Table 3. Comparison of ATP, ADP, AMP and phosphate in the synthesis of CAP from citrulline-^{14}C.

Additions	μmoles of $^{14}CO_2$ formed	
	+ acetylglutamate	no acetylglutamate
None	0.008	—
20 μmoles of phosphate	0.006	0.011
20 μmoles of ATP	0.105	0.002
20 μmoles of ADP	0.033	0.004
20 μmoles of AMP	0.001	0.001
20 μmoles of ATP + 30 μmoles of PGA + 5 mg MP	0.163	—

5 μmoles of citrulline-^{14}C, 50 μmoles of $MgSO_4$, 250 μmoles of glycyl-glycine buffer, pH 8.0 and additions as indicated were incubated with enzyme (1.3 mg nitrogen) in 3 ml volume for 20 minutes at 37°.

ments and maximum synthesis was sometimes not achieved below 3×10^{-3} M concentration of ATP.

The reaction was also found to be dependent on the presence of Mg^{++}. Enzyme saturation was achieved between 6×10^{-3} — 3×10^{-2} M concentration of $MgSO_4$ without apparent inhibition at higher concentration. Some "versene" was always left in the enzyme (from the preparation of the mitochondria) and undoubtedly influenced the amount of Mg^{++} necessary for optimum synthesis.

The specific requirement for ATP is also demonstrated by Table 3. A small amount of synthesis was observed also with ADP (myokinase action), while AMP or phosphate were without effect. Best synthesis was obtained when ATP was regenerated by addition of PGA and a muscle enzyme fraction.

Fig. 3 represents a time curve of the reaction. The dependance on the amount of enzyme is shown in Fig. 4.

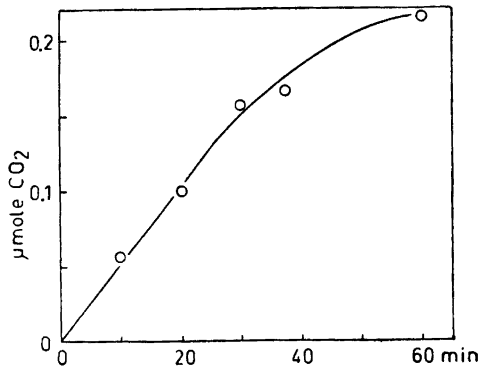


Fig. 3. Time curve of CAP formation.

Substrate and conditions as in Fig. 1 (pH 8.0). 1.1 mg of enzyme nitrogen.

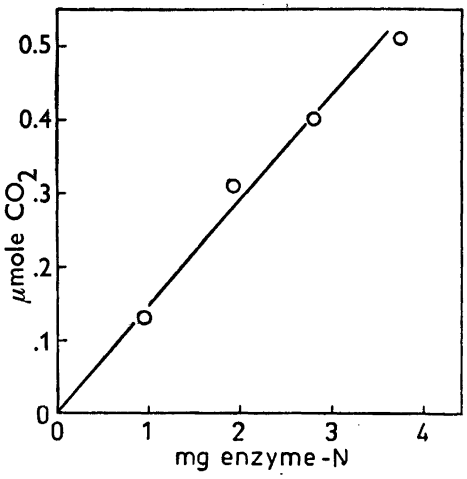


Fig. 4. Dependence of CAP formation on the amount of enzyme. Substrate and conditions as in Fig. 1 (pH 8.0).

Products of the reaction. The presence of CAP at the end of an experiment was demonstrated by the enzymic formation of CA-aspartate after addition of an excess of L-aspartate and aspartate carbamyl transferase from *E. coli* [8]. This enzyme catalyzed the formation of CA-aspartate from CAP and aspartate, but was incapable of forming CA-aspartate from citrulline + aspartate. From several such experiments it was calculated that a minimum of one fourth to one half of the $^{14}CO_2$ released by the addition of acid in the enzyme assay corresponded to CAP present at the end of the incubation. The rest of the $^{14}CO_2$ corresponded presumably to CAP broken down chemically and enzymically [18] during the course of the incubation.

Further evidence for the formation of CAP was obtained by paper chromatography and paper electrophoresis. Citrulline-^{14}C (750 000 ct/min/µmole in the carbamyl group) was incubated under the conditions described in Fig. 3. At the end of the incubation the reaction mixture was chilled and 20 µmoles of synthetic CAP were added as carrier. All subsequent steps were carried out at 0—5°. Protein was precipitated by the addition of 0.5 N PCA to pH 1—2 and the supernatant after centrifugation was neutralized to pH 8.0 with M NaOH (phenolphthalein). Then 0.5 ml of M barium acetate were added and the resulting precipitate was discarded after centrifugation. Two volumes of alcohol were added and the Ba-CAP was centrifuged and dried.

The barium salt was extracted with 0.25 ml of water + 0.05 ml of M sodium sulfate in the cold. After centrifugation aliquots of 0.01 ml of supernatant were subjected to paper electrophoresis[12] (saturated sodium tetraborate containing 0.01 M versene, 4 hours at 0°, 12 volts/cm) and ascending paper chromatography with three different solvents (methanol: 2 M NH_3: versene [19], 7:3:0,01;

5 % K_2HPO_4: *iso*amyl alcohol [20]; propanol: water; conc. NH_3: versene [21], 6:1:3:0.01). After drying the paper strips were scanned for radioactivity.

In all four solvents the CAP obtained by the carrier technique from the citrulline-^{14}C incubation showed a radioactive spot which coincided with that obtained from synthetic CAP (*cf.* Ref. [8]). When acetylglutamate or ATP was not included during the incubation no radioactivity appeared in the chromatograms at the place of CAP. The best separation was obtained by paper electrophoresis and results with this method have been published in a preliminary communication [12]. After paper electrophoresis one more radioactive spot was observed whose presence depended on the inclusion of acetylglutamate and ATP during the incubation. This compound moved faster towards the anode than CAP and it could also be obtained from carbamylglutamate-^{14}C. It was therefore suggested that the compound was CAP bound to a glutamic acid derivative [12].

The incorrectness of this idea has now been demonstrated by experiments in which CAP was formed in the presence of ^{32}P labeled ATP and ^{32}P labeled inorganic phosphate, respectively (conditions as in Fig. 3, but including 100 μmoles of K_2HPO_4 and excluding PGA and MP). When added carrier CAP was reisolated and subjected to electrophoresis as described above no radioactivity was found in the position of the fast moving band.

Ion exchange chromatography of the reisolated CAP showed that this substance had received ^{32}P from ATP while in the experiment with labeled inorganic phosphate only a very small incorporation of isotope into CAP was observed (*ca.* 12 % of that found in the ATP experiment).

Ornithine was demonstrated as a product of the reaction by ion exchange chromatography by the method of Hirs *et al.*[22] In one experiment when 0.80 μmoles of $^{12}CO_2$ were liberated after acid treatment (corresponding to CAP), 1.04 μmoles of ornithine were formed, thus demonstrating a rough stoichiometry for the two products of the reaction. In the absence of acetylglutamate ornithine formation was negligible.

Ornithine was a very potent inhibitor of CAP formation from citrulline and ATP. At 1.7×10^{-3} M concentration of citrulline a 50 % inhibition of the reaction rate was observed at *ca.* 0.7×10^{-4} M concentration of ornithine. No similar inhibition was observed with CAP.

DISCUSSION

It is evident from the present investigation that the utilization of citrulline for the biosynthesis of pyrimidines in rat liver represents a relatively small fraction of the total pyrimidines formed. In liver slices it was found that only 0.14 μmoles of orotic acid were synthesized from citrulline-CA-^{14}C under conditions that permitted synthesis of 3—5 μmoles of orotic acid from ammonia. This low rate of pyrimidine synthesis from citrulline was the reason why in earlier experiments with citrulline-CA-^{15}N it was concluded that the utilization of ammonia for pyrimidine synthesis did not proceed *via* citrulline.[6]

The present experiments demonstrate that in rat liver preparations the carbamyl group of citrulline can be utilized for the synthesis of CA-aspartate. This process could be separated into at least two enzymic steps. In the first

step the CA-group of citrulline gave rise to CAP, which in the second step reacted with aspartate to form CA-aspartate. Since the second step has been described earlier [6-8], this paper is mainly concerned with the first step, *i.e.* the formation of CAP.

Using intact mitochondria and comparing the utilization of labeled bicarbonate and citrulline for CA-aspartate synthesis it could be clearly demonstrated that the carbamyl group of citrulline was used relatively directly and not after breakdown to ammonia and CO_2 (Table 1). The dilution experiments with non-labeled ammonium carbonate — which in solution is in equilibrium with ammonium carbamate — also made the participation of free carbamate in the reaction unlikely.

In addition to citrulline the formation of CAP required ATP, acetylglutamate, and Mg^{++}. Addition of phosphate either did not influence or slightly decreased CAP formation as measured in our enzyme assay. This fact, together with the specific requirement for ATP and the pH optimum of 8.0, makes it unlikely that the phosphorolytic cleavage of citrulline [17], which might represent a reversion of reaction (3), was involved in the formation of CAP from citrulline *.

The requirement for acetylglutamate also differentiates this enzyme system from citrullinase. Acetylglutamate, or a similar compound, was previously shown to be required by rat liver preparations for CAP synthesis from CO_2, NH_3 and ATP. The function of acetylglutamate in CAP formation is not understood at the present time. Our earlier evidence for the existence of an intermediate compound, containing CAP bound to acetylglutamate [12] has been invalidated by the present finding that the proposed compound does not contain phosphate.

Two of the products of the reaction have been identified as CAP and ornithine. It seems likely that ADP was also formed but the presence of ATP-ase and myokinase in the mitochondrial extracts made it impossible to demonstrate the specific formation of ADP. Because of the unusual instability of the enzyme activity attempts to purify the enzyme by ammonium sulfate precipitation were not successful.

CAP formation from citrulline in other rat organs than liver could not be demonstrated **. The apparent low activity in mitochondrial extracts together with the high inhibition by ornithine would seem to indicate that the formation of CAP from citrulline in the rat is of minor quantitative importance for pyrimidine biosynthesis.

Acknowledgement. This investigation has been supported by grants from *Riksföreningen för Kräftsjukdomarnas bekämpande.*

The authors gratefully acknowledge the valuable technical assistence of Miss B. Carlsson and Mr. G. Hanshoff.

* *Added in proof:* We have recently extensively purified ornithine carbamyl transferase (the enzyme catalyzing reaction (3)) from rat liver and found that the citrullinase of Krebs *et al.*[17] in all probability is identical with this enzyme. Reversal of reaction (3) therefore represents an alternative way for CAP formation from citrulline which — unlike the reaction demonstrated in this paper — does not involve the participation of acetyl glutamate or ATP.

** An acetylglutamate stimulated release of $^{14}CO_2$ from citrulline-carbamyl-^{14}C was, however, observed with washed cells of *E.coli*.

REFERENCES

1. Schulman, M. P. and Badger, S. J. *Federation Proc.* **13** (1954) 292.
2. Smith, L. H. Jr. and Stetten, D. Jr. *J. Am. Chem. Soc.* **76** (1954) 3864.
3. Reichard, P. and Lagerkvist, U. *Acta Chem. Scand.* **7** (1953) 1207.
4. Walker, J. B. and Myers, J. *J. Biol. Chem.* **203** (1953) 143.
5. Ratner, S., Anslow, W. P. Jr. and Petrack, B. *J. Biol. Chem.* **204** (1953) 115.
6. Reichard, P. *Acta Chem. Scand.* **8** (1954) 795.
7. Reichard, P. and Hanshoff, G. *Acta Chem. Scand.* **9** (1955) 519.
8. Reichard, P. and Hanshoff, G. *Acta Chem. Scand.* **10** (1956) 548.
9. Grisolia, S. and Cohen, P. P. *J. Biol. Chem.* **198** (1952) 561.
10. Jones, M. E., Spector, L. and Lipmann, F. *J. Am. Chem. Soc.* **77** (1955) 819.
11. Reichard, P. and Smith, L. H. Jr. *Acta Chem. Scand.* **9** (1955) 194.
12. Reichard, P., Smith, L. H. Jr. and Hanshoff, G. *Acta Chem. Scand.* **9** (1955) 1010.
13. Smith, L. H. Jr. *J. Am. Chem. Soc.* **77** (1955) 6691.
14. Karrer, P., Escher, K. and Widmer, R. *Helv. Chem. Acta* **9** (1926) 301.
15. Ratner, S. and Pappas, A. *J. Biol. Chem.* **179** (1949) 1183.
16. Lindberg, O. and Ernster, L. *Nature* **173** (1954) 1038.
17. Krebs, H. A., Eggleston, L. V. and Knivett, V. A. *Biochem. J. London* **59** (1955) 185.
18. Grisolia, S. and Marshall, R. O. *Biochim. et Biophys. Acta* **14** (1954) 446.
19. Burrows, S., Grylls, F. S. M. and Harrison, J. S. *Nature* **170** (1952) 800.
20. Carter, C. E. *J. Am. Chem. Soc.* **72** (1950) 1466.
21. Deutsch, A. and Nilsson, R. *Acta Chem. Scand.* **7** (1953) 858.
22. Hirs, C. H. W., Moore, S. and Stein, W. H. *J. Biol. Chem.* **195** (1952) 669.

Received April 12, 1956.

ACTA CHEMICA SCANDINAVICA 10 (1956) 1035—1037

Short Communication

Synthesis of Racemic Methyl C_{27}-Phthienoate. Part II.

CECILE ASSELINEAU*, JEAN ASSELINEAU* **, and STINA STÄLLBERG-STENHAGEN

Institute of Medical Biochemistry, University of Gothenburg, Gothenburg, Sweden,

and

EINAR STENHAGEN

Department of Medical Biochemistry, Institute of Medical Chemistry, University of Uppsala, Uppsala, Sweden

A synthesis of racemic methyl *erythro*-2,4,6-trimethyl-$\Delta^{2:3}$-tetracosenoate was described in a previous communication [1]. The route which was used gave, as major product, the *cis*-isomer. The *trans*-isomer also obtained had the same infra-red absorption curve as the methyl ester of C_{27}-phthienoic acid isolated from tubercle bacilli [2,3].

In the present communication, a new method of synthesizing racemic methyl *erythro*-2,4,6-trimethyl-$\Delta^{2:3}$-tetracosenoate is described, which gives almost solely the *trans*-isomer. The starting material, the monomethyl ester of *meso*-3,5-dimethylpimelate (I), is the same as that used in the previous synthesis [1]. The sequence of reactions involved is shown in the following chart.

The acid chloride of (I) was treated with the calculated amount of CH_3MgI in the cold, and the neutral product obtained (II) was acetylated by boiling with acetic anhydride: methyl 3,5,7-trimethyl-7-acetoxyoctanoate (III) was isolated as a colourless liquid, b. p. 92—94°, 0.2 mm, $n_D^{25} = 1.4358$, $d_4^{25} = 0.965$. By cautious saponification, the acid (IV) was obtained. Kolbe reaction [4] of 3,5,7-trimethyl-7-acetoxyoctanoic acid (IV) with stearic acid and isolation of the reaction products by distillation gave 2,4,6-trimethyltetracosene-1 (V), m. p. 10.2—10.6°, $n_D^{20} = 1.4549$, $d_4^{20} = 0.811$ ($C=CH_2$ I.R. out of plane deformation vibration at 11.26 μ).

The formation of the unsaturated hydrocarbon (V) (instead of the expected long-chain acetoxy-compound) is due to thermal decomposition of an intermediary trimethyltetracosanyl-2 stearate arising from a transesterification of trimethyltetracosanyl-2 acetate (X) when distilled in the presence of free stearic acid. 2,4,6-Trimethyl-2-acetoxytetracosane (X) can be distilled without decomposition, whereas slow distillation of a mixture of the same acetoxy-compound (X) together with free stearic acid gives trimethyltetracosene-1 in excellent yield.

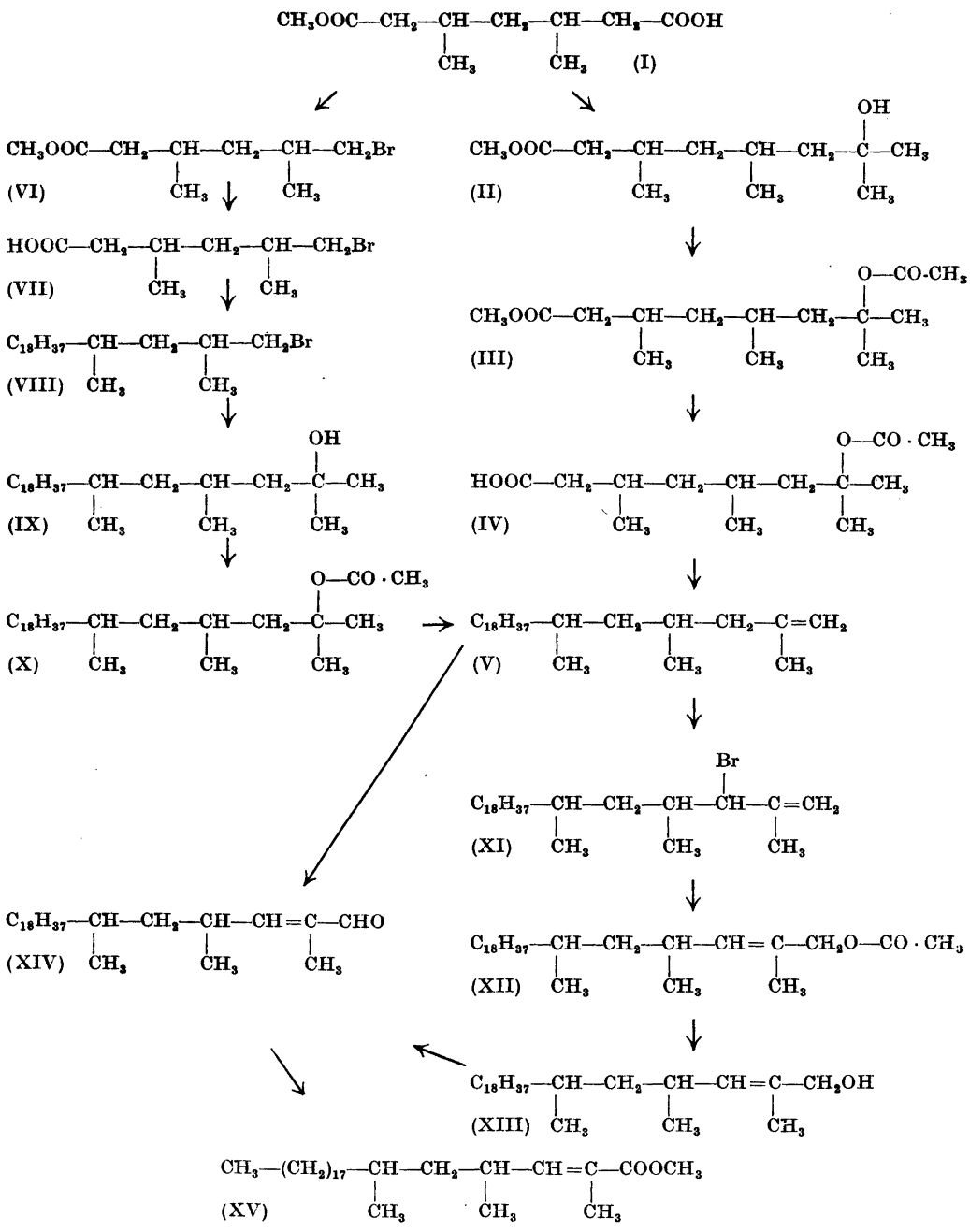
The same hydrocarbon (V) was also prepared from methyl hydrogen 3,5-dimethylpimelate (I) by bromine degradation of its silver salt according to Hunsdiecker [5], hydrolysis of the bromo-ester (VI) thus obtained to the bromo-acid (VII) (colourless liquid, $n_D^{21} = 1.4750$, $d_4^{21} = 1.298$), and transformation of this bromo-acid through Kolbe reaction with stearic acid * into 2,4-dimethyldocosanyl bromide (VIII) (colourless liquid, $n_D^{20} = 1.4635$, $d_4^{20} = 0.950$). 2,4-Dimethyldocosanyl magnesium bromide was obtained in low yield by the

---

* On leave of absence from the Centre National de la Recherche Scientifique, Paris, France.

** Rockefeller Foundation fellow, 1955—56. Present address: Institut de Biologie physico-chimique, 13, Rue Pierre Curie, Paris.

* In a recent paper [10], the behaviour of straight chain ω-halogenocarboxylic acids in the Kolbe reaction was studied; it was concluded that "only with a chain length of eleven or greater did normal coupling occur". In our case, the main chain consisted of only six carbon atoms.


CH3OOC—CH2—CH(CH3)—CH2—CH(CH2)—CH2—COOH (I)
CH3OOC—CH2—CH(CH3)—CH2—CH(CH2Br)—CH3 (VI)
HOOC—CH2—CH(CH3)—CH2—CH(CH2Br)—CH3 (VII)
C18H37—CH(CH3)—CH2—CH(CH3)—CH2Br (VIII)
C18H37—CH(CH3)—CH2—CH(CH3)—CH2—C(OH)(CH3)—CH3 (IX)
C18H37—CH(CH3)—CH2—CH(CH3)—CH2—C(O—CO·CH3)(CH3)—CH3 (X)
CH3OOC—CH2—CH(CH3)—CH2—CH(CH3)—CH2—C(OH)(CH3)—CH3 (II)
CH3OOC—CH2—CH(CH3)—CH2—CH(CH3)—CH2—C(O—CO·CH3)(CH3)—CH3 (III)
HOOC—CH2—CH(CH3)—CH2—CH(CH3)—CH2—C(O—CO·CH3)(CH3)—CH3 (IV)
C18H37—CH(CH3)—CH2—CH(CH3)—CH2—C(=CH2)—CH3 (V)
C18H37—CH(CH3)—CH2—CH(CH3)—CHBr—C(=CH2)—CH3 (XI)
C18H37—CH(CH3)—CH2—CH(CH3)—CH=C(CH2O—CO·CH3)—CH3 (XII)
C18H37—CH(CH3)—CH2—CH(CH3)—CH=C(CH2OH)—CH3 (XIII)
C18H37—CH(CH3)—CH2—CH(CH3)—CH=C(CHO)—CH3 (XIV)
CH3—(CH2)17—CH(CH3)—CH2—CH(CH3)—CH=C(COOCH3)—CH3 (XV)

method of Geiger-Berschandy [6] and after reaction with acetone, 2,4,6-trimethyltetracosanol-2 (IX) was isolated (m. p. 23.1—24.1° and 27.5—29.0° (dimorphism)), $n_D^{24} = 1.4554$, $d_4^{24} = 0.842$. 2,4,6-Trimethyl-2-acetoxytetracosane (X) (m. p. 8.6—9.2°, $n_D^{23} = 1.4498$, $d_4^{23} = 0.853$) was prepared by boiling the free alcohol with acetic anhydride. Distillation of this acetate with stearic acid gave 2,4,6-trimethyltetracosene-1 (V) ($n_D^{23} = 1.4533$, $d_4^{23} = 0.808$).

Allylic bromination of the unsaturated hydrocarbon (V) with N-bromo-succinimide [7] gave a bromo-compound (XI) which was transformed into 2,4,6-trimethyl-1-acetoxytetracosene (XII) under conditions which favoured the allylic transposition. The free primary alcohol (XIII) was obtained after $LiAlH_4$ reduction of its acetate. CrO_3-pyridine oxidation [8] gave the unsaturated aldehyde (XIV) (phthienoic aldehyde) (crude product: λ_{max} 225 mμ, $\varepsilon = 7\,280$ in hexane; I.R. spectrum: aldehydic C—H stretching vibration at 3.72 μ and C=O stretching vibration at 5.92 μ). Silver oxide oxidation [9] of the unsaturated aldehyde and chromatographic purification of the acidic fraction as methyl ester gave the *trans*-isomer of methyl *erythro*-2,4,6-trimethyl-$\Delta^{2:3}$-tetracosenoate (XV) (m. p. 14.1—14.6°, $n_D^{25} = 1.4598$, λ_{max} 216 mμ, $\varepsilon = 12\,850$ in hexane); no *cis*-isomer could be detected.

The transformation of 2,4,6-trimethyltetracosene-1 (V) into C_{27}-phthienoic aldehyde (XIV) was also directly performed by SeO_2 oxidation [11]; the α,β-unsaturated aldehyde chromatographically purified had m. p. 29.5—35.0°, λ_{max} 225 mμ, $\varepsilon = 15\,550$ (hexane). Silver oxide oxidation lead to a sample of slightly impure *trans*-isomer of methyl *erythro*-2,4,6-trimethyl-$\Delta^{2:3}$-tetracosenoate (XV): m. p. 16.8—17.6°, $n_D^{25} = 1.4597$, λ_{max} 217 mμ, $\varepsilon = 11\,900$ in hexane.

The infra-red absorption curves of both preparations of the *trans*-form of racemic methyl *erythro*-2,4,6-trimethyl-$\Delta^{2:3}$- tetracosenoate described in the present paper are identical with that of the *trans*-isomer described previously [1], and with that of the methyl ester of naturally occurring C_{27}-phthienoic acid.

In this synthetic route, the carboxyl group of phthienoic acid is introduced on the side of the free acid group of the methyl hydrogen 3,5-dimethylpimelate (I) whereas in the route previously described [1] it is introduced on the ester side of the half ester (I). For the synthesis of the optically active natural acid it is therefore necessary to start with different enantiomorphs of (I) in the two routes.

We are indebted to Dr. I. Fischmeister for the infra-red spectra. The expenses involved in this work were defrayed by grants from *the Swedish Medical Research Council* to S. Ställberg-Stenhagen.

1. Asselineau, C., Asselineau, J., Ställberg-Stenhagen, S. and Stenhagen, E. *Acta Chem. Scand.* **10** (1956) 478.
2. Polgar, N. *J. Chem. Soc.* **1954** 1008.
3. Cason, J. and Sumrell, G. *J. Biol. Chem.* **192** (1951) 405.
4. Weedon, B. C. L. *Quart. Rev.* **6** (1952) 380.
5. Hunsdiecker, H. and Hunsdiecker, C. *Ber.* **75** (1942) 291.
6. Geiger-Berschandy, S. *Bull. soc. chim. France* **1955** 994.
7. Ziegler, K., Späth, A., Schaaf, E., Schumann, W. and Winkelmann, E. *Ann.* **551** (1942) 80.
8. Poos, G. I., Arth, G. E., Beyler, R. E. and Sarett, L. H. *J. Am. Chem. Soc.* **75** (1953) 422.
9. Delépine, M. and Bonnet, P. *Bull. soc. chim. France* **5** (1909) 879.
10. Pattison, F. L. M., Stothers, J. B. and Woolford, R. G. *J. Am. Chem. Soc.* **78** (1956) 2255.
11. Guillemonat, A. *Ann. chim. Paris* **11** (1939) 143.

Received July 31, 1956.

ACTA CHEMICA SCANDINAVICA 10 (1956) 1038—1060

Proceedings of the Norwegian Biochemical and Physiological Society

Papers read at the joint meeting of the Scandinavian Biochemical Societies in Oslo, June 4—5, 1956

Structural Factors Involved in the Reduction of External DPN * by Mitochondrial Systems

L. Ernster and F. Navazio **

The Wenner-Gren Institute for Experimental Biology, Stockholm, Sweden

Previous studies [1] of the mitochondrial organization of DPN-linked oxidative systems have indicated the involvement of reversibly alterable structural factors in the availability of external DPN for intramitochondrial dehydrogenase reactions. The present report constitutes a complement to these studies, dealing with the effects of aging and subsequent structural reconstruction by ATP and Mn^{++} on the capacity of mitochondria to oxidize glutamate with external DPN as the terminal hydrogen acceptor.

Twice washed mitochondria from one rat liver, prepared in 0.25 M sucrose, were suspended in 20 ml 0.15 M KCl, containing 24 mg AMP, 174 mg K_2HPO_4 and 216 mg glucose (pH 7.5); the suspension was supplemented with 0.6 ml 0.1 M $MgCl_2$ and an excess of hexokinase, and diluted with 0.25 M sucrose to 30 ml. The suspension was aged at 30° C in a 200 ml Erlenmeyer flask under shaking in the presence of air. 0.2 ml aliquots were removed before and during aging and transferred to Beckman cuvettes containing 1.1 ml 0.05 M potassium phosphate buffer (pH 7.5), including 2.7 μmoles DPN, 1 μmole KCN and other additions to be tested. Silica plungers, reducing the light path to 1 mm, were placed in the cuvettes and optical density was measured at 340 mμ. After the zero time reading, 0.2 ml 0.1 M glutamate was added and the readings repeated each minute. The increase, proportional to the formation of DPNH, was virtually linear during the first five minutes. The blank contained all components but glutamate, which was replaced by 0.2 ml 0.05 M phosphate buffer.

In experiments entailing a determination of respiration and phosphorylation, 1.5 ml aliquots of the mitochondrial suspension were transferred to Warburg vessels and supplemented with 0.2 ml 0.1 M glutamate, as well as desired individual additions, to a final volume of 2 ml. The analytical procedures have been described elsewhere [2]. All experiments were performed at 25° C.

Table 1 shows that the rate of DPNH formation markedly increases upon aging and reaches a maximum after about 80 minutes. This increase can be prevented by Mn^{++} (Table 2), or reversed to the level prevailing in the intact system by the addition of ATP

Table 1. Effect of aging on DPNH formation. Values referred to mitochondria derived from 100 mg liver.

Aging time minutes	μmoles DPNH/5min.
0	0.68
20	1.16
40	1.33
60	1.91
80	2.32
100	2.11

Table 2. Prevention of aging effect by Mn^{++}. Time of aging: 60 minutes. Mn^{++}, 0.5 mM. Values referred to mitochondria derived from 100 mg liver.

System	μmoles DPNH/5min.
intact	0.47
aged	1.26
aged with Mn^{++}	0.49

* Abbreviations: DPN, diphosphopyridinenucleotide; DPNH, reduced diphosphopyridinenucleotide; AMP, adenosine-5-phosphate; ADP, adenosinediphosphate; ATP, adenosine triphosphate.

** Postgraduate Research Fellow of the Rotary Club of Rome. Permanent address: Institute of Biological Chemistry, Univ. of Rome.

Table 3. Restoration of aging effect. Time of aging: 60 minutes. Additions: AMP, ADP and ATP, 2.4 mM; Mn++, 0.5 mM. Values referred to mitochondria derived from 100 mg liver.

System	Additions	μmoles DPNH/5min
intact	—	0.62
aged	—	2.31
	AMP	2.24
	ADP	1.43
	ATP	0.82
	Mn++	2.35
	ATP+Mn++	0.65

and Mn++ (Table 3). In the latter case, Mn++ alone is without effect, while ATP alone or, to a lesser extent, ADP, but not AMP, may exhibit a certain action.

In the experiment presented in Table 4, it is shown that the effect of ATP and Mn++ is not due to an inhibition of the oxidation of glutamate, but rather to a structural reconstruction of the mitochondrial system, also involving a restoration of the phosphorylative ability.

The results support the previous postulate [1] that the availability of cytoplasmic DPNH is controlled by the structural state of the mitochondria.

1. Ernster, L. *Exptl. Cell Research* **10** (1956) 704, 721.
2. Ernster, L. and Löw, H. *Exptl. Cell Research, Suppl.* **3** (1955) 133.

The Effect of Thyroxine on Mitochondrial Stability

Robert E. Beyer*, Hans Löw and Lars Ernster

Wenner-Gren's Institute, Stockholm, Sweden

It has been demonstrated repeatedly that thyroxine, either administered *in vivo* [1-3] or applied *in vitro* [1,2,4-8], may lower the P/O ratio of isolated rat liver mitochondria. The action of thyroxine applied *in vitro* can be obliterated by Mg++, and more efficiently [7] by Mn++. These ions had been shown previously to protect mitochondria against the action of calcium [9,10]. Using phosphorylative ability [10] and optical density [11] as criteria, it has been shown that under suitable conditions the stability of the enzymic and morphological integrity of isolated mitochondria is an inverse function of the concentration ratio of Ca++/Mg++ and/or Ca++/Mn++ in the system. It was therefore visualized that the action of thyroxine may be reflected primarily in a labilization of mitochondria rather than in a direct action on oxidative phosphorylation. Optical density studies of liver mitochondrial preparations derived from normal and thyroxine treated rats have lent support to this concept [8]. A labilization of the system has been demonstrated to occur even at doses of thyroxine where a direct effect on oxidative phosphorylation could not be ascertained.

All rats used were of the Wistar strain weighing between 125 and 150 g. Hyperthyroidism

* United States Public Health Service Postdoctoral Research Fellow of The National Cancer Institute. Present address: Physiology Dept., Tufts University Medical School, Boston, Massachusetts. U.S.A.

Table 4. DPNH formation and oxidative phosphorylation in aged and restored systems. Additions: DPN, 1.8 mM; ATP, 2.4 mM; Mn++, 0.5 mM. Values referred to mitochondria derived from 100 mg liver.

Aging time minutes	Additions	μmoles DPNH/5 min. (in presence of KCN)	μat. O_2/5 min. (in absence of KCN)	P/O
0	—		1.57	2.84
	DPN	0.88		
30	—		0.45	
	DPN	1.94	1.81	0.33
	DPN, ATP, Mn++	0.69	1.35	1.65
60	—		0.12	
	DPN	2.81	1.09	0.25
	DPN, ATP, Mn++	0.92	1.09	1.86

Table 3. Restoration of aging effect. Time of aging: 60 minutes. Additions: AMP, ADP and ATP, 2.4 mM; Mn++, 0.5 mM. Values referred to mitochondria derived from 100 mg liver.

System	Additions	μmoles DPNH/5min
intact	—	0.62
aged	—	2.31
	AMP	2.24
	ADP	1.43
	ATP	0.82
	Mn++	2.35
	ATP+Mn++	0.65

and Mn++ (Table 3). In the latter case, Mn++ alone is without effect, while ATP alone or, to a lesser extent, ADP, but not AMP, may exhibit a certain action.

In the experiment presented in Table 4, it is shown that the effect of ATP and Mn++ is not due to an inhibition of the oxidation of glutamate, but rather to a structural reconstruction of the mitochondrial system, also involving a restoration of the phosphorylative ability.

The results support the previous postulate [1] that the availability of cytoplasmic DPNH is controlled by the structural state of the mitochondria.

1. Ernster, L. *Exptl. Cell Research* **10** (1956) 704, 721.
2. Ernster, L. and Löw, H. *Exptl. Cell Research, Suppl.* **3** (1955) 133.

The Effect of Thyroxine on Mitochondrial Stability

Robert E. Beyer*, Hans Löw and Lars Ernster

Wenner-Gren's Institute, Stockholm, Sweden

It has been demonstrated repeatedly that thyroxine, either administered *in vivo* [1-3] or applied *in vitro* [1,2,4-8], may lower the P/O ratio of isolated rat liver mitochondria. The action of thyroxine applied *in vitro* can be obliterated by Mg++, and more efficiently [7] by Mn++. These ions had been shown previously to protect mitochondria against the action of calcium [9,10]. Using phosphorylative ability [10] and optical density [11] as criteria, it has been shown that under suitable conditions the stability of the enzymic and morphological integrity of isolated mitochondria is an inverse function of the concentration ratio of Ca++/Mg++ and/or Ca++/Mn++ in the system. It was therefore visualized that the action of thyroxine may be reflected primarily in a labilization of mitochondria rather than in a direct action on oxidative phosphorylation. Optical density studies of liver mitochondrial preparations derived from normal and thyroxine treated rats have lent support to this concept [8]. A labilization of the system has been demonstrated to occur even at doses of thyroxine where a direct effect on oxidative phosphorylation could not be ascertained.

All rats used were of the Wistar strain weighing between 125 and 150 g. Hyperthyroidism

* United States Public Health Service Postdoctoral Research Fellow of The National Cancer Institute. Present address: Physiology Dept., Tufts University Medical School, Boston, Massachusetts. U.S.A.

Table 4. DPNH formation and oxidative phosphorylation in aged and restored systems. Additions: DPN, 1.8 mM; ATP, 2.4 mM; Mn++, 0.5 mM. Values referred to mitochondria derived from 100 mg liver.

Aging time minutes	Additions	μmoles DPNH/5 min. (in presence of KCN)	μat. O_2/5 min. (in absence of KCN)	P/O
0	—		1.57	2.84
	DPN	0.88		
30	—		0.45	
	DPN	1.94	1.81	0.33
	DPN, ATP, Mn++	0.69	1.35	1.65
60	—		0.12	
	DPN	2.81	1.09	0.25
	DPN, ATP, Mn++	0.92	1.09	1.86

was induced by intraperitoneal injections of 0.1 mg DL-thyroxine (F. Hoffmann-La Roche and Co. A. G., Basel) for five days, thyrotoxicosis by intraperitoneal injections of 2 mg of DL-thyroxine for various periods. Control animals were injected with suitable sodium chloride solutions. Mitochondria were prepared essentially after Schneider and Hogeboom [12] and suspended in the Mg^{++} free aging medium of Ernster and Löw [10]. Optical density measurements were performed as previously described [11] at room temperature. Phosphorylation was determined according to a modification [13,14] of the Martin and Doty [15] method. Succinate oxidation was measured by the conventional Warburg technique.

Since the *potential* phosphorylative ability of a mitochondrial system may be studied by following the optical density loss during aging in a Mg^{++} free, substrate free, incubation medium supplemented with hexokinase [11], such experiments were performed on liver mitochondria derived from thyrotoxic and control rats. Mitochondria from a thyrotoxic rat liver swell more rapidly than control mitochondria, *i. e.* the former mitochondria become swollen at an earlier stage of the aging process. When the "aging index" is expressed as the time required for 1/2 minimum optical density to be attained, the mean value of 12 experiments for the thyrotoxic mitochondria is 6.5 minutes, for the control, 17.8. The probability that this difference will occur through chance alone is 14 in 10 000. Preliminary data indicate that liver mitochondria from hyperthyroid rats have an aging index intermediate between the control and the thyrotoxic. Further preliminary experiments indicate that the phosphorylation coupled to the oxidation of succinate in mitochondria from thyrotoxic rats possesses a greater sensitivity to calcium ions than does the normal preparation. Table 1 presents an experiment illustrating this point. Phosphorylation became uncoupled from oxidation at the 0.5 mM level in the thyrotoxic series while the P/O ratio remained above 1 at considerably higher levels of calcium in the control flasks. It may also be seen that no uncoupling of oxidative phosphorylation occurred in the thyrotoxic flask when calcium was not added. Unpublished experiments indicate that a preincubation, or equilibration period, may cause a preferential uncoupling of oxidative phosphorylation in the thyrotoxic system, and that this effect may be restored by the addition of ATP and Mn^{++}.

These data are interpreted as follows: Thyroxine, or its active principle, renders the mitochondria, *in vivo*, more susceptible to factors or mechanisms which may lower their phosphorylative efficiency. Upon isolation of the particles and incubation in routinely employed medium this increased susceptibility may elude detection since the incubation media used in studies of oxidative phosphorylation have been systematically developed with the highest possible phosphorylative efficiency as a goal. The lability of the mitochondria, or the potential aging capacity, remains, however. Thus, aging under controlled conditions [10,11], *i. e.* supplying artificial regulatory mechanisms, reveals that the difference between the thyroxine treated and normal animals is the *degree of lability* of the oxidation-phosphorylation systems.

Table 1. Calcium sensitivity of thyrotoxic and control mitochondria.

mM Ca^{++} added	P/O ratios	
	Control	Thyrotoxic
0	1.69	1.67
0.4	1.85	1.24
0.5	2.23	0.16
0.6	1.72	0.10
0.7	1.53	0.06
0.8	1.05	0.03

Each Warburg vessel contained: Mitochondria, 1/20 rat liver; KCl, 150 μmoles; orthophosphate, 50 μmoles; adenylic acid, 4.3 μmoles; glucose, 60 μmoles; sucrose, 125 μmoles; succinate, 30 μmoles; Mg^{++}, 7.5 μmoles; hexokinase, in excess. Final volume, 2.0 ml. Gas phase, air. Temperature, 30° C. Time of incubation, 20 minutes.

1. Martius, C. and Hess, B. *Arch. Biochem.* **33** (1951) 486.
2. Martius, C. in *Hormone und ihre Wirkungsweise*, Springer-Verlag, Berlin, 1955, p. 143.
3. Maley, G. F. and Lardy, H. A. *J. Biol. Chem.* **215** (1955) 377.
4. Hoch, F. L. and Lipmann, F. *Proc. Natl. Acad. Sci.* **40** (1954) 909.
5. Klemperer, H. G. *Biochem. J. London* **60** (1955) 122.
6. Maley, G. F. and Lardy, H. A. *J. Biol. Chem.* **204** (1953) 435.
7. Mudd, S. M., Park, J. H. and Lipmann, F. *Proc. Natl. Acad. Sci.* **41** (1955) 571.
8. Tapley, D. F., Cooper, C. and Lehninger, A. L. *Biochim. et Biophys. Acta* **18** (1955) 597.

9. Lindberg, O. and Ernster, L. *Nature* **173** (1954) 1038.
10. Ernster, L. and Löw, H. *Exptl. Cell Research, Suppl.* **3** (1955) 133.
11. Beyer, R. E., Ernster, L., Löw, H. and Beyer, T. *Exptl. Cell Research* **8** (1955) 586.
12. Schneider, W. C. and Hogeboom, G. H. *J. Biol. Chem.* **183** (1950) 123.
13. Ernster, L., Zetterström, R. and Lindberg, O. *Acta Chem. Scand.* **4** (1950) 942.
14. Lindberg, O., Ljunggren, M., Ernster, L. and Révész, L. *Exptl. Cell Research* **4** (1953) 243.
15. Martin, J. M. and Doty, D. M. *Anal. Chem.* **21** (1949) 965.

The Action of a Mitochondrial Protein Fraction on Mitochondrial ATP-ase and Oxidative Phosphorylation

Robert E. Beyer* and John Glomset

Wenner-Gren's Institute, University of Stockholm, Stockholm, and Institute of Medical Chemistry, University of Uppsala, Uppsala, Sweden

A protein fraction has been extracted from rat liver mitochondria which stimulates "latent" mitochondrial ATP-ase activity without exhibiting ATP-ase itself and which stimulates the oxidation of succinate in a mitochondrial system containing AMP as the terminal phosphate acceptor. The fraction, in 0.1 M Tris (tris(hydroxymethyl)aminomethane), pH 7.4, has its spectroscopic peak in the Soret region at 414 mμ; in the visible region at 548 mμ and 576 mμ. The mitochondrial ATP-ase stimulating activity is proportional to the concentration of the fraction added.

The mitochondrial fraction (fraction 60) is prepared as follows. Rat liver mitochondria are prepared essentially according to Schneider and Hogeboom [1] using 0.25 M sucrose-0.001 M versene, pH 7.4, as the homogenizing medium. The mitochondrial pellet is washed twice in 0.25 M sucrose and then suspended in Na_2CO_3 which has been adjusted to pH 8.4 with HCl and diluted to 0.1 M. The suspension is then shaken for 12—18 hours at 0—4° C, followed by centrifugation in a Spinco Model L Centrifuge for 7 979 400 *g*-minutes (3 hours, 21 000 RPM, head $\neq$21). The resulting pinkish-yellow supernate is then adjusted to pH 6.5 with acetic acid. The slight cloudy precipitate which forms is centrifuged down. Chilled acetone is added to the supernate in a dropwise fashion with constant stirring to 10 % and maintained in an acetone-dry ice bath made by producing a thick slurry of 9 % acetone and powdered dry ice. The precipitate is spun down in an International Refrigerated Centrifuge at the temperature of the acetone-dry ice bath. Additional fractions are collected at 20, 30, 40 and 60 % acetone, adjusting the acetone-dry ice bath to 19, 29, 39 and 59 % acetone at each subsequent precipitation. The centrifuge is also adjusted accordingly until its lower limit is reached. The pink precipitate resulting from the 40—60 % fraction, called fraction 60, is completely soluble in Tris buffer, pH 7.4, resulting in a cherry red solution. From approximately 100 g of rat liver 10 ml of a solution with an optical density reading at 280 mμ (Beckman DU spectrophotometer) of 1.7 through a 1 cm path length have been obtained. Preliminary experiments indicate that fraction 60 may also be prepared by the above method from "acetone mitochondria" which have been stored *in vacuo* at —15° C for several weeks.

The preparation of a mitochondrial fraction with an action on mitochondrial ATP-ase processes provides a basis for hypotheses which implicate the fraction in oxidative phosphorylation. A protein factor, called mitochrome-I, has been reported briefly [2-4] which appears to have an action similar to fraction 60. Attempts to prepare mitochrome-I, however, have not been successful in our hands. Furthermore, since the only datum of a chemical nature reported for mitochrome-I is its approximate molecular weight, a direct comparison of the two factors has been impossible.

It must be added that fraction 60 is probably not homogeneous. Attempts are in progress to further purify the active principle of fraction 60 by zone electrophoresis and chromatography on cellulose ion exchange columns, as well as to gain some insight into its role in the transfer of high energy phosphate.

* United States Public Health Service Postdoctoral Research Fellow of the National Cancer Institute. Present address: Physiology Dept., Tufts University Medical School, Massachusetts, U.S.A.

1. Schneider, W. C. and Hogeboom, G. H. *J. Biol. Chem.* **183** (1950) 123.
2. Shmukler, H. W. and Polis, B. D. *Abstracts Div. Biol. Chem. Am. Chem. Soc.*, Sept. 1953, p. 13c.
3. Polis, B. D. and Shmukler, H. W. *Ibid.* p. 72c.
4. Polis, B. D. and Shmukler, H. W. *Ibid.* p. 19c.

9. Lindberg, O. and Ernster, L. *Nature* **173** (1954) 1038.
10. Ernster, L. and Löw, H. *Exptl. Cell Research, Suppl.* **3** (1955) 133.
11. Beyer, R. E., Ernster, L., Löw, H. and Beyer, T. *Exptl. Cell Research* **8** (1955) 586.
12. Schneider, W. C. and Hogeboom, G. H. *J. Biol. Chem.* **183** (1950) 123.
13. Ernster, L., Zetterström, R. and Lindberg, O. *Acta Chem. Scand.* **4** (1950) 942.
14. Lindberg, O., Ljunggren, M., Ernster, L. and Révész, L. *Exptl. Cell Research* **4** (1953) 243.
15. Martin, J. M. and Doty, D. M. *Anal. Chem.* **21** (1949) 965.

The Action of a Mitochondrial Protein Fraction on Mitochondrial ATP-ase and Oxidative Phosphorylation

Robert E. Beyer* and John Glomset

Wenner-Gren's Institute, University of Stockholm, Stockholm, and Institute of Medical Chemistry, University of Uppsala, Uppsala, Sweden

A protein fraction has been extracted from rat liver mitochondria which stimulates "latent" mitochondrial ATP-ase activity without exhibiting ATP-ase itself and which stimulates the oxidation of succinate in a mitochondrial system containing AMP as the terminal phosphate acceptor. The fraction, in 0.1 M Tris (tris(hydroxymethyl)aminomethane), pH 7.4, has its spectroscopic peak in the Soret region at 414 mμ; in the visible region at 548 mμ and 576 mμ. The mitochondrial ATP-ase stimulating activity is proportional to the concentration of the fraction added.

The mitochondrial fraction (fraction 60) is prepared as follows. Rat liver mitochondria are prepared essentially according to Schneider and Hogeboom [1] using 0.25 M sucrose-0.001 M versene, pH 7.4, as the homogenizing medium. The mitochondrial pellet is washed twice in 0.25 M sucrose and then suspended in Na_2CO_3 which has been adjusted to pH 8.4 with HCl and diluted to 0.1 M. The suspension is then shaken for 12—18 hours at 0—4° C, followed by centrifugation in a Spinco Model L Centrifuge for 7 979 400 *g*-minutes (3 hours, 21 000 RPM, head $\neq$21). The resulting pinkish-yellow supernate is then adjusted to pH 6.5 with acetic acid. The slight cloudy precipitate which forms is centrifuged down. Chilled acetone is added to the supernate in a dropwise fashion with constant stirring to 10 % and maintained in an acetone-dry ice bath made by producing a thick slurry of 9 % acetone and powdered dry ice. The precipitate is spun down in an International Refrigerated Centrifuge at the temperature of the acetone-dry ice bath. Additional fractions are collected at 20, 30, 40 and 60 % acetone, adjusting the acetone-dry ice bath to 19, 29, 39 and 59 % acetone at each subsequent precipitation. The centrifuge is also adjusted accordingly until its lower limit is reached. The pink precipitate resulting from the 40—60 % fraction, called fraction 60, is completely soluble in Tris buffer, pH 7.4, resulting in a cherry red solution. From approximately 100 g of rat liver 10 ml of a solution with an optical density reading at 280 mμ (Beckman DU spectrophotometer) of 1.7 through a 1 cm path length have been obtained. Preliminary experiments indicate that fraction 60 may also be prepared by the above method from "acetone mitochondria" which have been stored *in vacuo* at —15° C for several weeks.

The preparation of a mitochondrial fraction with an action on mitochondrial ATP-ase processes provides a basis for hypotheses which implicate the fraction in oxidative phosphorylation. A protein factor, called mitochrome-I, has been reported briefly [2-4] which appears to have an action similar to fraction 60. Attempts to prepare mitochrome-I, however, have not been successful in our hands. Furthermore, since the only datum of a chemical nature reported for mitochrome-I is its approximate molecular weight, a direct comparison of the two factors has been impossible.

It must be added that fraction 60 is probably not homogeneous. Attempts are in progress to further purify the active principle of fraction 60 by zone electrophoresis and chromatography on cellulose ion exchange columns, as well as to gain some insight into its role in the transfer of high energy phosphate.

* United States Public Health Service Postdoctoral Research Fellow of the National Cancer Institute. Present address: Physiology Dept., Tufts University Medical School, Massachusetts, U.S.A.

1. Schneider, W. C. and Hogeboom, G. H. *J. Biol. Chem.* **183** (1950) 123.
2. Shmukler, H. W. and Polis, B. D. *Abstracts Div. Biol. Chem. Am. Chem. Soc.*, Sept. 1953, p. 13c.
3. Polis, B. D. and Shmukler, H. W. *Ibid.* p. 72c.
4. Polis, B. D. and Shmukler, H. W. *Ibid.* p. 19c.

Enzymic Synthesis of Xanthosine- and Guanosine-5-phosphate

Ulf Lagerkvist

Biochemical Department, Karolinska Institutet, Stockholm, Sweden

Extracts of pigeon liver acetone powder catalyze the following reactions: [1]

$$\text{Inosine-5-phosphate} \xrightarrow{\text{DPN}^*} \text{Xanthosine-5-phosphate} \quad (1)$$

$$\text{Xanthosine-5-phosphate} \xrightarrow[\text{L-glutamine}]{\text{ATP}} \text{Guanosine-5-phosphate} \quad (2)$$

Abrams and Bentley [2] have independently demonstrated the occurrence of reactions (1) and (2) in extracts of rabbit bone marrow while Gehring and Magasanik found reaction (1) in *Aerobacter aerogenes* [3].

* The following abbreviations are employed: ATP = adenosine triphosphate, DPN = diphosphopyridine nucleotide, DEAE = diethylaminoethyl.

The enzyme (or enzymes) catalyzing reaction (2) has been purified by fractionation with ammonium sulfate, adsorption on Cγ gel and chromatography on DEAE-cellulose according to Peterson and Sober *et al.* [4,5]. The stoichiometry and mechanism of reaction (2) will be discussed.

1. Lagerkvist, U. *Acta Chem. Scand.* **9** (1955) 1028.
2. Abrams, R. and Bentley, M. *J. Am. Chem Soc.* **77** (1955) 4179.
3. Gehring, L. B. and Magasanik, B. *J. Am. Chem. Soc.* **77** (1955) 4685.
4. Peterson, E. A. and Sober, H. A. *J. Am. Chem. Soc.* **78** (1956) 751.
5. Sober, H. A., Gutter, F. J., Wyckhoff, M. M. and Peterson, E. A. *J. Am. Chem. Soc.* **78** (1956) 756.

Incorporation of Radioactive Phosphate into Thiamine Phosphate in Yeast

Karl-Heinz Kiessling

Zoophysiological Institute, Uppsala, Sweden

Besides thiamine diphosphate yeast contains small amounts of thiamine triphosphate. When incubating yeast with an excess of thiamine under special conditions the amount of thiamine triphosphate can be considerably increased. The incorporation of ^{32}P into thiamine triphosphate in yeast has been studied and compared with that into thiamine di- and monophosphate and adenosine triphosphate. The experiments have been carried out partly with yeast containing only its natural amount of thiamine phosphates, partly with yeast enriched in thiamine phosphates. In both cases ^{32}P was incorporated to a higher degree into thiamine triphosphate than into the other thiamine compounds. The incorporation into thiamine triphosphate was localized especially to the terminal phosphate.

Studies on a Thrombin-coagulable Protein in Blood Platelets

Kristian Grette

The Physiological Institute, University of Oslo, Norway

Reports on the effect of thrombin on washed platelet suspensions and platelet extracts indicate the presence of a thrombin-coagulable protein [1,2].

A preliminary report is given of experiments in which these observations were verified. Extraction and partial purification of the coagulable material is described, together with observations of some of its characteristics. The effects of thrombin on intact blood platelets are discussed in relation to these results.

A detailed report will be published later.

1. Ware, A. G., Fahey, J. L. and Seegers, W. H. *Am. J. Physiol.* **154** (1948) 140.
2. Schneider, C. L., Claxton, E. B., Hughes, C. H. and Johnson, S. A. *Am. J. Physiol* **179** (1954) 236.

Nucleotide Metabolism in the Surviving Rat Diaphragm

Aa. Rye Alertsen, O. Walaas and E. Walaas

Institute of Physiology, University of Oslo, Norway

The metabolism of acid-soluble nucleotides in the isolated rat diaphragm has been studied by aid of ion exchange chromatography on Dowex-1 Resin according to the method of Hurlbert *et al.*[1]. 9 major compounds have been isolated, the predominant nucleotides being AMP, ADP, ATP and DPN. In incubation experiments the interconversion of nucleotides within the diaphragm and the liberation of nucleotides to the medium have been studied. Experiments under aerobic and anaerobic conditions have been performed. The effect of 2,4-dinitrophenol, insulin and adrenaline on nucleotide metabolism has been studied. The mechanism of glucose uptake by muscle is discussed.

1. Hurlbert, R. B., Schmitz, H., Brumm, A. F. and Potter, V. R. *J. Biol. Chem.* **209** (1954) 23.

The Interaction of Rat Muscle Hexokinase with the Mg-ATP Complex

E. Walaas and O. Walaas

Institute of Physiology, University of Oslo, Norway

In experiments on partly purified rat muscle hexokinase the role of Mg^{2+} and ATP on the enzyme activity have been studied. The effects of cations, anions, inorganic pyrophosphate, ITP, UTP, GTP and CTP on the rate of the reaction have been investigated. Indication of the nature of the Mg-ATP complex with hexokinase has been obtained.

The Breakdown of Adenosine Triphosphate in Human Blood

Søren Jørgensen

Department of Pharmacology, University of Copenhagen, Denmark

Using an enzymic spectrophotometric method elaborated according to Kalckar's principles, the concentrations of the adenosine mononucleotides ATP, ADP and AMP were followed in shed human blood during standing.

In freshly withdrawn blood the total concentration of these three nucleotides was about 600 μmole per liter of blood; 85 % of this was ATP. The amount of ADP was higher than AMP. During storage at 37° C the ATP decreased gradually and had disappeared in 24 hours. ADP and AMP showed an intermittent 2—5 fold increase compared to the initial concentration. During the 24 hours storage the concentration of hypoxanthine and xanthine increased about 100 fold from 5 to 500 μmole/l. The total molar sum of the adenine nucleotides, hypoxanthine and xanthine, was nearly constant during the whole period.

In mechanically haemolysed blood the ATP disappeared completely within 4 hours. In the same period the ADP and AMP increased about 3 and 10 fold, respectively, and disappeared from the blood within 8 hours. The concentration of hypoxanthine and xanthine showed a concomitant increase from 5 to 500 μmole/l. In this case also, the sum of all the measured compounds remained constant.

By adding ATP, AMP and IMP (inosinic acid) to blood these nucleotides were degraded into hypoxanthine with increasing velocity in the mentioned sequence. Adenosine and inosine were transformed with greater but uniform velocity.

The breakdown of added ATP in whole blood takes place extracellularly and consists of a stepwise dephosphorylation. From the course of the curves for ATP, ADP and AMP in the plasma of the whole blood, it is concluded that the splitting off of all three phosphate groups is catalysed by one and the same enzyme mainly localised on the blood cells.

In plasma without blood corpuscles the breakdown of ATP takes place with a much smaller velocity than in whole blood.

The breakdown of AMP and IMP is initiated by a dephosphorylation.

Hypoxanthine formation in plasma takes place with equal velocity from added AMP, IMP, adenosine and inosine. It is therefore concluded that the splitting of inosine is the velocity determining reaction.

Biosynthetic Preparation of ^{14}C-labelled 2-Deoxy-D-ribose and Thymidine by Means of *Thiobacillus denitrificans*

K. Baalsrud and S. Laland

Institute of Marine Biology and Biochemistry Department, University of Oslo, Norway

In connection with studies on the metabolism of 2-deoxy-D-ribose and thymidine, it became desirable to perform experiments with labelled material. The possibility of obtaining ^{14}C uniformly labelled DNA as a source for these substances has been considered. It was concluded that the use of an autotrophic organism like *Thiobacillus denitrificans* which can be grown in the dark on a large scale in deep culture under controlled conditions, would offer a simple and satisfactory solution. The strain of *Thiobacillus denitrificans* used was isolated from the fresh water mud of an Oslo lake. The medium and technique used for the large scale cultivation of this organism has been described previously [1]. The organism was grown in the presence of $Na_2{}^{14}C\,O_3$ and utilized 98 % of the total activity present. The cells were harvested from a 50 % ethanol solution and the supernatant contained 20 % of the total activity. The cell residue was treated with 96 % ethanol and, after drying, extracted twice with 10 % NaCl at 100° C. The nucleic acids were precipitated with ethanol, redissolved in 10 % NaCl and reprecipitated. From 17 g of dried cells, 26 mg DNA (as estimated by the Dische test) and 58.4 mg RNA (as estimated by the Euler and Hahn test) were obtained. DNA was separated from RNA by treatment with KOH and acid precipitation. 2-Deoxy-D-ribose and thymidine were isolated from DNA by a method described previously [2]. The mixture of labelled thymidine and 2-deoxy-D-ribose was separated by paper chromatography and isolated by the elution of the appropriate areas of the chromatogram. There was isolated 0.625 mg thymidine (2.58 μM) and 0.347 mg (2.59 μM) of 2-deoxy-D-ribose, with a total activity of 0.93×10^6 c/min and 0.51×10^6 c/min, which corresponds to an activity of 0.36×10^5 c/min/μM carbon and 0.32×10^5 c/min/μM carbon respectively. The total activity of 2-deoxy-D-ribose and thymidine together represented 0.2 % of that taken up by the cell residue.

1. Baalsrud, K. and Baalsrud, K. S. *Phosphorus Metabolism* **2** (1952) 544.
2. Jones, A. S. and Laland, S. G. *Acta Chem. Scand.* **8** (1954) 603.

Kinetics of Fatty Acid Dehydrogenation

J. G. Hauge

Central Institute for Industrial Research, Blindern, Oslo, Norway

Four flavoproteins are involved in the first dehydrogenation step of the fatty acid cycle in pig liver [1-3]. Some of the kinetic properties of this system have now been investigated with 2,6-dichlorophenolindophenol as electron acceptor. From these studies the following three step mechanism of reaction appears likely: Electrons are passed from substrate to a primary dehydrogenase; thence to a specific electron transferring flavoprotein; and finally to indophenol. The interaction of the two enzymes concerned with their respective substrates, *i. e.* fatty acyl CoA and reduced primary dehydrogenase, follows Michaelis-Menten behaviour. In the primary dehydrogenation reaction a pronounced product inhibition was observed. The pH optima ranged from 7.6 to 8.4 for the three primary dehydrogenases, when these enzymes were rate limiting. When the transfer step was rate limiting, the optimum was at pH 6.8.

Theoretical considerations reveal that oxidation enzyme systems with tightly bound prosthetic groups, such as the system studied, have special kinetic properties. Michaelis constants and turnover numbers of these enzymes cannot be obtained when overall reactions are measured. The observed apparent Michaelis constants and turnover numbers give the kinetic characteristics of the total substrate-enzyme-acceptor system.

1. Crane, F. L. and Beinert, H. *J. Biol. Chem.* **218** (1956) 717.
2. Crane, F. L., Mii, S., Hauge, J. G., Green, D. E. and Beinert, H. *J. Biol. Chem.* **218** (1956) 701.
3. Hauge, J. G., Crane, F. L. and Beinert, H. *J. Biol. Chem. In press.*

The Fractionation of the Phosphorus-containing Proteins of Rat Liver Cell Sap

John Glomset

Institute of Medical Chemistry, Uppsala, Sweden

The occurrence of phosphoserine and phosphothreonine in partial hydrolysates of liver protein has been demonstrated in previous reports from this laboratory [1,2]. Moreover, phosphoserine was also found in hydrolysates of rat liver nuclear, mitochondrial, microsomal and supernatant protein. Attempts are now in progress to isolate the native, phosphorus-containing proteins of these liver cell fractions. The fractionation of the proteins of the rat liver supernatant fraction is the subject of this communication.

2—4 hours after the intraperitoneal injection of radioactive phosphate into non-fasted male, Wistar rats, the animals were sacrificed by cervical dislocation. The livers were perfused with ice-cold isotonic saline followed by 0.25 M sucrose *via* the hepatic portal vein. The pH of both solutions had been adjusted to 7.4 and both contained 0.01 M versene. After mincing and homogenizing the livers in the versene-sucrose solution the supernatant fraction was prepared essentially according to Hogeboom [3]. The proteins of this fraction were then subjected to a preliminary fractionation by precipitation with either a modification of the method of Cohn *et al.*[4] or with ammonium sulfate. The various precipitates were subsequently dissolved in tris buffer (tris hydroxymethyl aminomethane) pH 7.8, dialyzed at 0—1° for 1—2 hours and then further fractionated by zone electrophoresis in tris buffer according to Porath [5] on 100—150 cm cellulose powder columns. After the completion of the electrophoresis the effluent from the column was followed by spectrophotometric reading at 260 and 280 mμ and by measurement of the ^{32}P content of the effluent tubes. The identity of the phosphoprotein fractions was established by hydrolysis followed by the chromatographic isolation of phosphoserine using the methods described previously [1,2]. A detailed paper will be published shortly.

1. Ågren, G., de Verdier, C.-H. and Glomset, J. *Acta Chem. Scand.* **8** (1954) 503.
2. Ågren, G., de Verdier, C.-H. and Glomset, J. *Acta Chem. Scand.* **8** (1954) 1570.
3. Hogeboom, G. H. in *Methods in Enzymology*, Vol. 1 p. 16 Academic Press Inc., New York, 1955.
4. Cohn, E. J. *et al.*, *Enzymes and Enzyme Systems*, Harvard University Press 1951.
5. Porath, J. *Biophys. et Biochim. Acta. In press.*

Partition Chromatography of some C_{27}-Steroids

H. Danielsson

Department of Physiological Chemistry, University of Lund, Lund, Sweden

With reversed-phase partition chromatography using *iso*propanol/water (165/135 ml) as mobile and chloroform/heptane (10/40 ml) as stationary phase, it is possible to separate hydroxy- and keto-C_{27}-steroids. Substances with hydroxyls in the 3-, 7- and 12-position and 3-ketones have been used and are separated into groups of compounds containing 3, 2 and 1 hydroxyl, respectively, and one with 3-ketones. Those with a double bond in the 5,6-position can be separated from the saturated ones. Furthermore, by increasing the content of water in the mobile phase a separation of 3α,7α-dihydroxy from 3α,12α-dihydroxy coprostane is obtained.

Table 1 shows the result of a run with the phases mentioned above. 4 ml of the stationary phase was supported on 4.5 g of Hyflo Supercel, made completely hydrophobic with dichlorodimethylsilane [1].

Compound	Appearance of compound Beginning	Peak	End
3α,7α,12α-Trihydroxy-coprostane	17	22	26
7α-Cholesterol	22	28	38
3α,7α-Dihydroxy-coprostane	36	45	70
3α,12α-Dihydroxy-coprostane	36	48	70
Cholesterol	75	89	110
Cholestenone	118	132	143
Cholestanone	150	175	200

Some other separations will be discussed.

1. Howard, G. A. and Martin, A. J. P. *Biochem. J. London* **46** (1950) 532.

The Conjugation of 2-Aminoethanesulfinic Acid (Hypotaurine) with Cholic Acid by Rat Liver Microsomes

Lorentz Eldjarn and Jon Bremer*

Norsk Hydro's Institute for Cancer Research, Det Norske Radiumhospital, Oslo, Norway

Hypotaurine seems to be the main immediate precursor of taurine in the organism [1]. Taurine is conjugated with cholic acid by an enzyme system in rat liver microsomes [2]. In the present report we have demonstrated that hypotaurine as well is conjugated with cholic acid by this enzyme system, with the formation of "hypotaurocholic acid".

Hypotaurine-^{35}S was synthesized according to Eldjarn, Pihl and Sverdrup [3]. The preparation of rat liver microsomes and the incubation experiments were performed as earlier described [2].

The reaction was stopped and the proteins precipitated by adding 0.15 ml N perchloric acid to the vessels, followed by 0.15 ml N KOH. The reaction mixture was extracted with 0.6 ml *n*-butanol. Aliquots of the butanol extract were plated for radioactivity measurements or chromatographed on paper according to Sjövall [4].

* Fellow of the Norwegian Cancer Society, Oslo.

The paper chromatography showed that mainly taurocholic acid (R_F 0.25) had been formed after incubation of hypotaurine with cholic acid, but in addition a radioactive compound with R_F 0.75 was found. This presumably was hypotaurocholic acid, since no radioactivity was found at this R_F when hypotaurine was incubated without cholic acid. The identity of the unknown compound was confirmed by the following experiment: The radioactive compound at R_F 0.75 was eluted from the paper with ethanol. The eluate was made alkaline with a few drops of N KOH and stored for 24 hours at 37° C. The eluate was then brought to dryness and the residue was extracted twice with 0.1 ml ethanol. The eluate was again chromatographed according to Sjövall [4]. Approximately 60 % of the radioactivity of the unknown compound at R_F 0.75 reappeared at the R_F of taurocholic acid after this treatment, *i. e.* the hypotaurocholic acid had been oxidized to taurocholic acid.

As the sulfinic groups is a less polar group than the sulfonic group, the coefficient:

$$\frac{\text{concentration in butanol phase after extraction}}{\text{concentration in } H_2O \text{ before extraction}}$$

of hypotaurocholic acid presumably is greater than the coefficient of taurocholate which is known [5] to be 2.0. As a coefficient of 3.5 corresponds to quantitative extraction, the coefficient of hypotaurocholate was presumed to be 3.0. From this coefficient, the extractable radioactivity and from the radioactivity on the paper chromatograms the results of Table 1 were calculated.

The table shows that addition of taurine almost completely abolished the formation of

Table 1.

Substrates	Net counts/min/ 0.05 ml butanol extract	µmole taurocholate formed per vessel	µmole hypotaurocholate formed per vessel
0.5 µmole hypotaurine-^{35}S = 340 000 c/min	0	0	0
0.5 µmole hypotaurine-^{35}S + 1 µmole cholate	4 150	0.082	0.019
0.25 µmole hypotaurine-^{35}S = 170 000 c/min + 1 µmole cholate	3 905 3 660	0.075	0.014
0.25 µmole hypotaurine-^{35}S + 2.4 µmoles inactive taurine + 1 µmole cholate	460 400	—	0.001
0.8 µmole taurine-^{35}S = 105 000 c/min + 1 µmole cholate	2 330 2 220	0.307	0
0.8 µmole taurine-^{35}S + 2.4 µmoles inactive hypotaurine + 1 µmole cholate	1 960 1 820	0.275	—

Microsomes from approximately 500 mg rat liver per vessel, CoA 0.001 M, ATP 0.006 M, KF 0.15 M, sucrose 0.05 M, potassium phosphate buffer (pH 7.4) 0.033 M. Gas phase air, incubation time 90 min., temp. 37° C, total volume 1.5 ml.

hypotaurocholate, whereas addition of hypotaurine had no significant effect on the taurocholate formation. Our experiments therefore show that rat liver microsomes can conjugate hypotaurine with cholic acid, but that taurine is preferred as substrate in the reaction. Since rat liver is known to contain great amounts of free taurine [5], the conjugation with hypotaurine can only be of limited physiological importance in the rat.

Whether the conversion of hypotaurine to taurine is enzymatic or spontaneous in our system is not known.

1. Chatagner, F. and Bergeret, B. *Ann. nutrition et aliment.* **9** (1955) 93.
2. Bremer, J. *Acta Chem. Scand.* **10** (1956) 56.
3. Eldjarn, L., Pihl, A. and Sverdrup, A. *J. Biol. Chem. In press.*
4. Sjövall, J. *Acta Chem. Scand.* **8** (1954) 339.
5. Bremer, J. *Acta Chem. Scand.* **9** (1955) 683.

Formation of Itaconic Acid from the Krebs Cycle Tricarboxylic Acids by Extracts of *Aspergillus terreus*

Elizabeth Brigham Jenssen, Helge Larsen and John G. Ormerod

Department of Biochemistry, The Technical University of Norway, Trondheim, Norway

Evidence has been presented that citric acid [1,2] and *cis*-aconitic acid [3] are intermediates and close precursors to itaconic acid in the formation of itaconic acid from sugars by *Aspergillus terreus*.

Cell-free extracts of *A. terreus* can be prepared by crushing rapidly frozen mycelium in the Hughes' bacterial press and extracting the paste with water. Such extracts, when prepared from itaconic acid producing mycelia (*i. e.*, mycelia grown under acid conditions [4]), will catalyze a conversion of citric, *cis*-aconitic and *iso*citric acids to itaconic acid and carbon dioxide. *cis*-Aconitic acid is by far the most readily converted; citric and isocitric acids were in some experiments converted to itaconic acid only to a negligible extent. The optimum pH is about 5.7. Molecular oxygen does not affect the conversions. Extracts prepared from mycelia grown under neutral conditions (*i. e.*, mycelia not producing itaconic acid from sugars [4]), will not catalyze a conversion of the aforementioned tricarboxylic acids to itaconic acid. This finding is in agreement with the previously presented hypothesis that the itaconic acid forming enzyme system is dependent upon acid conditions for its formation [4].

Active extracts decarboxylate 1 mole of *cis*-aconitic acid to give close to 1 mole of carbon dioxide and 1 mole of itaconic acid. Correspondingly, the yield of carbon dioxide from citric acid is close to 1 mole per mole of citric acid converted, whereas the yield of itaconic acid is usually much lower, *viz.* 0.3—0.6 moles per mole of citric acid converted.

Synthetic monofluorocitrate in a concn. of 10^{-4} M causes an appreciable inhibition in the rate of itaconic acid production from citric acid and a slight inhibition in the rate of itaconic acid production from isocitric acid. 10^{-4} M fluorocitrate does not inhibit the rate or lower the yield of itaconic acid formation from *cis*-aconitic acid; there is rather a slight stimulation. Aconitase has been shown to be present in the extract. Assuming the aconitase to be fluorocitrate sensitive [5], the results would indicate that itaconic acid is formed by decarboxylation of *cis*-aconitic acid.

The reversibility of the decarboxylating system has been tested by incubating itaconic acid producing extracts in the presence of *cis*-aconitic acid and $^{14}CO_2$ at pH 5.3. Itaconic acid and residual *cis*-aconitic acid were isolated and tested for radioactivity. Both compounds were found to be non-radioactive. The lack of radioactivity in the *cis*-aconitic acid does not necessarily imply that the conversion is irreversible; it might equally well indicate an extreme slowness in the mixing of the *cis*-aconitic acid supplied and its biologically activated counterpart [6].

The work was supported by grants from the *Royal Norwegian Council for Scientific and Industrial Research*. We are indebted to Professor R. A. Peters for a gift of synthetic tri sodium monofluorocitrate.

1. Corzo, R. H. and Tatum, E. L. *Federation Proc.* **12** (1953) 470.
2. Eimhjellen, K. E. and Larsen, H. *Biochem. J. London* **60** (1955) 139.
3. Bentley, R. and Thiessen, C. P. *Science.* **122** (1955) 330.
4. Larsen, H. and Eimhjellen, K. E. *Biochem. J. London* **60** (1955) 135.
5. Morrison, J. F. and Peters, R. A. *Biochem. J. London* **58** (1954) 473.
6. Swim, H. E. and Krampitz, L. O. *J. Bact.* **67** (1954) 419.

hypotaurocholate, whereas addition of hypotaurine had no significant effect on the taurocholate formation. Our experiments therefore show that rat liver microsomes can conjugate hypotaurine with cholic acid, but that taurine is preferred as substrate in the reaction. Since rat liver is known to contain great amounts of free taurine [5], the conjugation with hypotaurine can only be of limited physiological importance in the rat.

Whether the conversion of hypotaurine to taurine is enzymatic or spontaneous in our system is not known.

1. Chatagner, F. and Bergeret, B. *Ann. nutrition et aliment.* **9** (1955) 93.
2. Bremer, J. *Acta Chem. Scand.* **10** (1956) 56.
3. Eldjarn, L., Pihl, A. and Sverdrup, A. *J. Biol. Chem. In press.*
4. Sjövall, J. *Acta Chem. Scand.* **8** (1954) 339.
5. Bremer, J. *Acta Chem. Scand.* **9** (1955) 683.

Formation of Itaconic Acid from the Krebs Cycle Tricarboxylic Acids by Extracts of *Aspergillus terreus*

Elizabeth Brigham Jenssen, Helge Larsen and John G. Ormerod

Department of Biochemistry, The Technical University of Norway, Trondheim, Norway

Evidence has been presented that citric acid [1,2] and *cis*-aconitic acid [3] are intermediates and close precursors to itaconic acid in the formation of itaconic acid from sugars by *Aspergillus terreus*.

Cell-free extracts of *A. terreus* can be prepared by crushing rapidly frozen mycelium in the Hughes' bacterial press and extracting the paste with water. Such extracts, when prepared from itaconic acid producing mycelia (*i. e.*, mycelia grown under acid conditions [4]), will catalyze a conversion of citric, *cis*-aconitic and *iso*citric acids to itaconic acid and carbon dioxide. *cis*-Aconitic acid is by far the most readily converted; citric and isocitric acids were in some experiments converted to itaconic acid only to a negligible extent. The optimum pH is about 5.7. Molecular oxygen does not affect the conversions. Extracts prepared from mycelia grown under neutral conditions (*i. e.*, mycelia not producing itaconic acid from sugars [4]), will not catalyze a conversion of the aforementioned tricarboxylic acids to itaconic acid. This finding is in agreement with the previously presented hypothesis that the itaconic acid forming enzyme system is dependent upon acid conditions for its formation [4].

Active extracts decarboxylate 1 mole of *cis*-aconitic acid to give close to 1 mole of carbon dioxide and 1 mole of itaconic acid. Correspondingly, the yield of carbon dioxide from citric acid is close to 1 mole per mole of citric acid converted, whereas the yield of itaconic acid is usually much lower, *viz.* 0.3—0.6 moles per mole of citric acid converted.

Synthetic monofluorocitrate in a concn. of 10^{-4} M causes an appreciable inhibition in the rate of itaconic acid production from citric acid and a slight inhibition in the rate of itaconic acid production from isocitric acid. 10^{-4} M fluorocitrate does not inhibit the rate or lower the yield of itaconic acid formation from *cis*-aconitic acid; there is rather a slight stimulation. Aconitase has been shown to be present in the extract. Assuming the aconitase to be fluorocitrate sensitive [5], the results would indicate that itaconic acid is formed by decarboxylation of *cis*-aconitic acid.

The reversibility of the decarboxylating system has been tested by incubating itaconic acid producing extracts in the presence of *cis*-aconitic acid and $^{14}CO_2$ at pH 5.3. Itaconic acid and residual *cis*-aconitic acid were isolated and tested for radioactivity. Both compounds were found to be non-radioactive. The lack of radioactivity in the *cis*-aconitic acid does not necessarily imply that the conversion is irreversible; it might equally well indicate an extreme slowness in the mixing of the *cis*-aconitic acid supplied and its biologically activated counterpart [6].

The work was supported by grants from the *Royal Norwegian Council for Scientific and Industrial Research*. We are indebted to Professor R. A. Peters for a gift of synthetic tri sodium monofluorocitrate.

1. Corzo, R. H. and Tatum, E. L. *Federation Proc.* **12** (1953) 470.
2. Eimhjellen, K. E. and Larsen, H. *Biochem. J. London* **60** (1955) 139.
3. Bentley, R. and Thiessen, C. P. *Science.* **122** (1955) 330.
4. Larsen, H. and Eimhjellen, K. E. *Biochem. J. London* **60** (1955) 135.
5. Morrison, J. F. and Peters, R. A. *Biochem. J. London* **58** (1954) 473.
6. Swim, H. E. and Krampitz, L. O. *J. Bact.* **67** (1954) 419.

On the Isolation of Gangliosides

Lars Svennerholm

Department of Medical Biochemistry, University of Gothenburg, Gothenburg, Sweden

Gangliosides in a high yield have been isolated on a small scale by partition chromatography on cellulose columns [1]. A disadvantage with the method is the low capacity. When larger amounts of lipids are applied to the column, part of the gangliosides is eluted together with the main bulk of other lipids. Other methods have therefore been tried. Reversed phase chromatography on hydrophobic kieselguhr did not separate gangliosides from the other lipids. Zone electrophoresis in a capillary system with pyridinium-formic acid buffer in 80 % methanol was suitable only for preparations containing 50 % or more of gangliosides. A good separation was achieved on anion exchange resins. Radin, Lavin and Brown [2] have in a recent work used the same type of resins for the separation of cerebrosides from other glycolipids.

Chloroform-methanol extracts of brain lipids were passed on a strong cation exchanger in hydrogen form (Amberlite IR-120 or Dowex 50-X8, 50—100 mesh). The solution was then percolated through a column packed with a weak anion exchange resin in hydroxyl form (Duolite A-7, 40—60 mesh) or through a strong one in bicarbonate form (Dowex 1, 50—100 mesh). Cerebrosides, cholesterols and part of the phospholipids passed through the column. The rest of the phospholipids, cerebroside sulphuric acid and gangliosides were taken up by the resin and eluted with 0.1—1.0 N formic acid in chloroform--methanol mainly in the order mentioned. The fractions containing gangliosides were evaporated to a small volume. Formic acid and contaminating lipids were removed by partition dialysis as described by Folch *et al* [3]. The anion exchange resins are capable to bind considerable amounts of gangliosides. A Duolite column of the dimensions 25 × 250 mm removed about 90 % of the gangliosides from a total lipid extract of one kilogram of fresh brains.

1. Svennerholm, L. *Acta Chem. Scand.* **8** (1954) 1108.
2. Radin, N. S., Lavin, B. F. and Brown, J. R. *J. Biol. Chem.* **217** (1955) 789.
3. Folch, J., Arsove, S. and Meath, J. A. *J. Biol. Chem.* **191** (1951) 819.

Determination of Glycolipids in Plasma

Elisabet Svennerholm and Lars Svennerholm

Departments of Medical Clinic II and Medical Biochemistry, University of Gothenburg, Gothenburg, Sweden

Only few quantitative estimations of the glycolipids in plasma have earlier been performed [1,2]. They have been based on the determination of the reducing power of a lipid extract before and after hydrolysis. The difference has been attributed to cerebroside sugar, but no attempt has been made to isolate the corresponding lipid. Large variations in the cerebroside content (0—167 mg/100 ml) have been reported. The methods used are unsatisfactory because other reducing substances than sugars are released during the hydrolysis. If gangliosides occur in addition to cerebrosides they will be included in the cerebroside value.

In the method worked out the lipid extract is purified through partition between chloroform and methanol-water. Cerebrosides will go into the chloroform phase, while gangliosides and low molecular contaminants will go into the methanol-water phase.

Experimental. Blood is drawn into a centrifuge tube containing sodium citrate. Plasma is separated from blood cells in a refrigerated centrifuge at 0° and lyophilized. The lipids are extracted with chloroform-methanol (2:1, v/v) under reflux boiling. After evaporation *in vacuo* the lipids are redissolved in the same solvent and quantitatively filtered down into a volumetric cylinder. 1/4 volume of 0.1 % sodium chloride in water is added and the cylinder is shaken thoroughly. On the resulting two phases hexose is determined in the chloroform phase with an orcinol method and sialic acid from gangliosides is determined in the methanol-water phase with Bial's reagent. The mean value of 8 normals was for cerebrosides 4.8 mg/100 ml (range 3.5—5.7) and for gangliosides 2.5 mg/100 ml (range 2.0—3.8). Cerebrosides were isolated from the chloroform phase by the method of Klenk and Leupold [3].

1. Kirk, E. *J. Biol. Chem.* **123** (1938) 637.
2. Ericksson, B. N., Souders, H. J., Shepherd, M. L., Teague, D. M. and Williams, H. H. *Proc. Soc. Exptl. Biol. Med.* **45** (1940) 153.
3. Klenk, E. and Leupold, F. *Hoppe-Seyler's Z. physiol. Chem.* **281** (1944) 208.

Bacterial Dissimilation of Acetylene Dicarboxylic Acid

Kjell Eimhjellen*

Department of Biochemistry, The Technical University of Norway, Trondheim, Norway

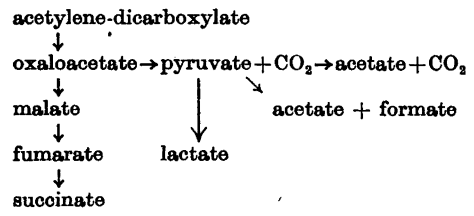
Very little is known about the biological conversion of acetylenic compounds. As part of an investigation of the biosynthesis and dissimilation of organic compounds containing acetylenic bonds, a facultative anaerobic bacterium has been isolated from sewage. The bacterium has been identified as a member of the family of *Enterobacteriaceae*. The organism grows on acetylene dicarboxylic acid as the only carbon source and ammonium-N as the only nitrogen source.

Acetylene dicarboxylic acid is converted by resting cell suspensions under anaerobic conditions to CO_2, lactate, succinate, acetate, formate and ethanol; the latter compound is produced in relatively small amounts. H_2 is hardly detectable. Occasionally fumarate will accumulate. The fermentation of glucose leads to the same end products, but relatively larger amounts of ethanol and H_2 are produced.

The non-gaseous products of the fermentations have been isolated either in the pure state or as the derivatives of *p*-bromophenacylbromide. The volatile products have been further identified by Duclaux distillation, ethanol as acetic acid after oxidation by chromic acid.

When the CO_2-evolution from acetylene dicarboxylic acid by resting cell suspensions is followed manometrically, a sharp break in reaction velocity is observed, at which time pyruvate can easily be detected. The pyruvic acid has been isolated and characterized as the 2,4-dinitrophenylhydrazone.

The results indicate that acetylene dicarboxylic acid is dissimilated by this bacterium according to the following scheme:



* Fellow of the Technical University of Norway.

Fumarate and malate are fermented anaerobically by resting cells with CO_2 production in correspondance with the above scheme.

The CO_2 output from acetylene dicarboxylic acid is completely inhibited by 2×10^{-2} M KF. Lower concentrations of KF, *viz.* 10^{-3}—10^{-2} M, cause a greater total output of CO_2 from the same substrate, concomitantly with a smaller total production of succinate.

In view of the above results it would appear that the initial reaction in the metabolism of acetylene dicarboxylic acid is a conversion to oxaloacetate followed by known pathways of metabolism of the latter substance.

The Mechanism of Formation of Bile Acids from Cholesterol

S. Bergström and S. Lindstedt

Department of Physiological Chemistry, University of Lund, Lund, Sweden

A short review of recent work on the transformation of cholesterol into bile acids will be given.

Recent results have brought further support to the view that the steroid ring system is modified before the side chain degradation is completed [1], thus 3α,7α-dihydroxycoprostane is transformed into both cholic and chenodesoxycholic acid in the rat [2], whereas earlier work [3] has shown that chenodesoxycholic acid cannot be 12α-hydroxylated into cholic acid.

Furthermore 7α-hydroxycholesterol has been found to give rise to cholic acid as well as to chenodesoxycholic acid [4].

In this connection results obtained in studies on hydroxylated coprostanic acids and their possible role as intermediates in the formation of bile acids from cholesterol will be discussed [5,6].

1. Bergström, S. *Record of Chem. Progr. Kresge-Hooker Sci. Lib.* **16** (1955) 63.
2. Bergström, S. and Lindstedt, S. *Biochim. et Biophys. Acta* **19** (1956) 556.
3. Bergström, S. and Sjövall, J. *Acta Chem. Scand.* **8** (1954) 611.
4. Lindstedt, S. *Biochim. et Biophys. Acta. To be published.*
5. Bridgewater, Y. and Lindstedt, S. *Acta Chem. Scand. To be published.*
6. Bergström, S. and Gloor U. *To be published.*

Carbon Dioxide Fixation in *Rhodospirillum rubrum*

J. G. Ormerod*

Department of Microbiology, The University, Sheffield 10, England

Rhodospirillum rubrum is a photosynthetic bacterium which uses simple organic compounds as electron donors in photosynthesis. During the oxidation of these compounds under anaerobic conditions in the light, CO_2 may be fixed in the photosynthetic process, but at the same time CO_2 may be produced as a result of the oxidation of the electron donor. Depending on the state of oxidation of these substrates the net result of these processes may be an uptake or an output of CO_2. In either case, it is impossible to determine by manometric methods alone the actual amounts of CO_2 fixed or produced. An attempt was therefore made to measure the CO_2 fixation by washed suspensions in the presence of various organic compounds as electron donors by means of $^{14}CO_2$.

In the light the endogenous incorporation of isotopic CO_2 proceeds at a fairly high rate and corrections were therefore made for this. With acetate as substrate the amount of $^{14}CO_2$ incorporated was less than in the control without substrate, indicating that acetate inhibits the endogenous fixation of CO_2 (*cf.* Glover and Kamen [1]). Butyrate was the only substrate which caused a $^{14}CO_2$ incorporation equal in amount to the CO_2 fixation as measured manometrically. It seems likely that no CO_2 is produced in the photometabolism of this substrate. The quantity of $^{14}CO_2$ incorporated with propionate was more than twice as great as the net fixation measured manometrically. It is possible that the photometabolism of propionate involves carboxylation to succinate as in the green sulphur bacterium *Chlorobium thiosulphatophilum* [2]. When succinate was the substrate the $^{14}CO_2$ incorporation was the same as expected on theoretical grounds [3]. Malate, fumarate and lactate all gave results higher than expected on the basis of theory. Manometric measurements showed that there was a net output of CO_2 with each of these substrates. A possible explanation of these discrepancies is that certain substrates may stimulate exchange reactions involving CO_2, leading to an incorporation of isotope but without affecting the net fixation of CO_2. In view of the probable occurrence of these reactions methods involving isotopic CO_2 are not suitable for measuring CO_2 fixation in photosynthetic systems of this type.

* Present address: Department of Biochemistry, The Technical University of Norway, Trondheim, Norway.

1. Glover, J. and Kamen, M. D. *Fed. Proc.* **10** (1951) 190.
2. Larsen, H. *J. Biol. Chem.* **193** (1951) 167.
3. Elsden, S. R. and Ormerod, J. G. *Biochem. J. London In press.*

Sulfhydryl Groups in Serum Proteins During Influence of Cortisone

B. Larsen

Rheumatic Research Laboratory, University Institute for Pathological Anatomy, Copenhagen, Denmark

It has previously been shown that cortisone restores the lowered sulfhydryl values in patients with polyarthritis [1]. Several investigations seem to indicate that cortisone when it acts inhibitively on cell activity and protein synthesis does so through the mediation of sulfhydryl dependent systems [2].

These investigations have been continued in experiments *in vitro*. The sulfhydryl determinations are carried out by means of amperometric methods, using a rotating platinum electrode and mercuric acetate as the titrator.

The results so far reached show that cortisone is capable of increasing sulfhydryl values in albumin by 15—20 % depending on incubation conditions.

Work is in progress and a detailed paper is in preparation.

1. Larsen, B. and Bent-Hansen, K. *J. Lab. Clin. Med. In press.*
2. Anderson, G. E., Wiesel, L. L., Hillmann, R. W. and Stumpe, W. M. *Proc. Soc. Exptl. Biol. Med.* **76** (1951) 825.

Quantitative Determination of Bile Acids in Human Bile

Jan Sjövall

Department of Physiological Chemistry, University of Lund, Lund, Sweden

The methods used for the determination of bile acids in bile have usually been based on different colour reactions. These methods have mostly been limited to the determination of only one or a few of the bile acids in the bile. Since the different bile acids under various conditions may be excreted independently of each other it is desirable to have a method where all the bile acids can be determined simultaneously.

Synthetic mixtures of bile acids can be determined after separation by paper chromatography [1]. A preliminary note on the application of this method to bile acids in bile has been published [2]. The method has been used for the determination of bile acids in rat bile [3] and has now been adapted to the determination of bile acids in gall-bladder bile, fistula bile and duodenal contents of man.

The fluid to be analyzed is applied directly on the starting line of the chromatogram as described for synthetic bile acids [1]. Bile from the gall-bladder usually has to be diluted.

Taurine conjugated bile acids are separated with ascending chromatography. *Iso*amyl acetate:heptane 85:15 saturated with an equal volume of 70 % (v/v) formic acid is used as moving phase. The papers are equilibrated for 1/2 hour in the atmosphere of the moving phase. The chromatograms are then run for 20 hours. This procedure gives well defined spots of the bile acids even when large amounts of other bile constituents are present.

After localization the spots are cut out and eluted [1]. Taurocholic acid (TC) is determined in 65 % sulfuric acid as described [1]. Since taurodeoxycholic (TD) and taurochenodeoxycholic (TDC) acids often occur together in human bile and since they do not separate in these chromatograms they are determined as the sum TD+TCD. This is done by heating the acids 15 minutes at 50° C in 65 % sulfuric acid when TD and TCD show the same molar extinction at their maximum at 305 mμ. This is reproducible within ±5 % with synthetic acids and the acids follow Beer's law singly and in mixtures.

Bile constituents other than bile acids (mainly bile pigments) also contribute to the light absorption of the samples in sulfuric acid. When this contribution is between 10 and 20 % of the total light absorption it can be corrected for by subtracting the light absorption of a corresponding sample in 80 % ethanol where bile acids have no absorption at the wave lengths used.

Glycine conjugated bile acids are separated with descending chromatography using ethylene chloride:heptane 50:50 as moving phase [4]. The filter paper used for the chromatography is cut as described but since the bile acids travel different distances on the different strips in descending chromatography one strip on each side of the strip to be eluted has to be sprayed in order to localize the bile acids. Glycocholic (GC), glycochenodeoxycholic (GCD) and glycodeoxycholic (GD) acids are separated and can be eluted and determined. Synthetic mixtures of GCD and GD are determined within ±5 %. Except in cases with extraordinarily large amounts of bile pigments no ethanol correction has to be made.

Within the errors of the method (approximately ±15 % for each bile acid in biological material) the ratio of glycine to taurine conjugation was the same for trihydroxy- as for dihydroxycholanic acids. In most human samples the glycine conjugated bile acids dominated. No free bile acids were detected It has been confirmed that cholic and chenodeoxycholic acids are the main hydroxycholanic acids in human bile. In several bile samples no conjugated deoxycholic acid could be found. With the method used glycodeoxycholic acid would have been detected when present as 2 % of the total amount of bile acids.

1. Sjövall, J. *Arkiv Kemi* **8** (1955) 317.
2. Sjövall, J. *Acta Chem. Scand.* **9** (1955) 1034.
3. Eriksson, S. *Acta Chem. Scand.* **10** (1956) 156.
4. Sjövall, J. *Arkiv Kemi* **8** (1955) 299.

Quantitative Aspects of Bile Acid Formation in Man

Sven Lindstedt

Department of Physiological Chemistry, University of Lund, Lund, Sweden

Our knowledge of the amount of bile acids taking part in the enterohepatic circulation is incomplete and based on determinations of concentration of bile acids in bladder or fistula bile. For a review see Josephson [1].

We have attempted to determine the total amount of circulating cholic acid by an isotope dilution *in vivo*. By determining the fall of specific activity with time information has been gained on the rate of formation of this compound. 3—4 μC of cholic acid-24-^{14}C was given orally as sodium salt to healthy male medical students. At different time intervals bile was obtained through a duodenal tube after administration of 1—3 mg of a purified pancreozymine-cholecystochinine preparation (kindly supplied by Professor Erik Jorpes, Stockholm). Cholic acid was isolated and the specific activity determined. A bile sample was used for a quantitative determination with a paperchromatographic technique of the concentration of various bile acids. These determinations were kindly carried out by Dr. J. Sjövall [2]. By the use of the figures thus obtained the total amount of circulating acids was calculated. In the table the results obtained in three subjects are given:

Subject	Cholic acid g	Total amount of of bile acids g	"Half-life" of cholic acid in days
B	0.575	1.85	1.2
P	0.92	3.65	2.5
S	1.29	3.55	3

1. Josephson, B. *Physiol. Rev.* **21** (1941) 463.
2. Sjövall, J. *Acta Chem. Scand. To be published.*

On the Metabolism of Bile Acids in Germ-free Rats

B. Gustafsson, S. Bergström, S. Lindstedt and A. Norman

Section of research on germ-free animals, Department of Histology and Department of Physiological Chemistry, University of Lund, Lund, Sweden

The bile of rats contains taurocholic and taurochenodeoxycholic acids [1]. With the aid of 24-^{14}C-labelled acids it has been shown that these acids are extensively modified during the passage down the intestinal tract [2]. When the fecal acids were chromatographed these modifications were found to include:

1) a splitting of the peptide bond,
2) an attack on the bile acid moiety leading to a variety of mostly less hydrophilic compounds.

It has been found [3] that in rats treated with intestinal chemoterapeutics no such modifications occur making it highly probable that microbial enzymes are responsible for the reactions. Furthermore several strains of bacteria that can split the conjugated bile acid *in vitro* have been isolated from the rat intestine [4]. We have earlier reported on the turnover of bile acids in normal rats and in animals treated with chemoterapeutics [5]. The half-lives were found to be about 2.5 and 6—7 days, respectively. In order to study the importance of intestinal microorganism for the elimination of bile acids we have administered 24-^{14}C-labelled cholic acid to germ-free rats and to a rat that had been infected with *Aspergillus niger* and then further with *Clostridium perfingens* type E. The rats were reared with slight modifications in the technique of Gustafsson [6]. The time course of excretion was followed and the acids in the feces fractionated with chromatography. One rat was finally transferred from the apparatus to normal environments and the elimination rate investigated.

The germ-free rats were found to excrete unchanged taurocholic acid in their feces. This was also the case in the rat infected with the mould. When the same rat was also infected with the *Clostridium* strain, however, about 25 % of the labelled acids appeared in the feces in the free form, mainly as cholic acid. The chromatographic pattern was in this case similar to that found after *in vitro* incubation of taurocholic acid with the same strain of bacterium [4].

In all rats studied the excretion rate was quite slow with a half life-time of about 7 days. It may be concluded that the state of the intestinal flora greatly influences the rate of elimination from the enterohepatic circulation. As, however, neither the mould nor the peptide bond-splitting *Clostridium* increases the excretion rate it seems probable that other microorganisms are of importance for the rate of elimination of bile acids.

1. Bergström, S. and Sjövall, J. *Acta Chem. Scand.* **8** (1954) 611.
2. Lindstedt, S. and Norman, A. *Acta Physiol. Scand.* **34** (1955) 1.
3. Norman, A. *Acta Physiol. Scand.* **33** (1955) 100.
4. Norman, A. and Grubb, R. *Acta Pathol. Microbiol. Scand.* **36** (1955).
5. Lindstedt, S. and Norman, A. *Acta Chem. Scand.* **9** (1955) 1042.
6. Gustafsson, B. *Acta Pathol. Microbiol. Scand.* Suppl. **73** (1948).

Quantitative Determination of Bile Acids in Human Bile

Jan Sjövall

Department of Physiological Chemistry, University of Lund, Lund, Sweden

The methods used for the determination of bile acids in bile have usually been based on different colour reactions. These methods have mostly been limited to the determination of only one or a few of the bile acids in the bile. Since the different bile acids under various conditions may be excreted independently of each other it is desirable to have a method where all the bile acids can be determined simultaneously.

Synthetic mixtures of bile acids can be determined after separation by paper chromatography [1]. A preliminary note on the application of this method to bile acids in bile has been published [2]. The method has been used for the determination of bile acids in rat bile [3] and has now been adapted to the determination of bile acids in gall-bladder bile, fistula bile and duodenal contents of man.

The fluid to be analyzed is applied directly on the starting line of the chromatogram as described for synthetic bile acids [1]. Bile from the gall-bladder usually has to be diluted.

Taurine conjugated bile acids are separated with ascending chromatography. *Iso*amyl acetate:heptane 85:15 saturated with an equal volume of 70 % (v/v) formic acid is used as moving phase. The papers are equilibrated for 1/2 hour in the atmosphere of the moving phase. The chromatograms are then run for 20 hours. This procedure gives well defined spots of the bile acids even when large amounts of other bile constituents are present.

After localization the spots are cut out and eluted [1]. Taurocholic acid (TC) is determined in 65 % sulfuric acid as described [1]. Since taurodeoxycholic (TD) and taurochenodeoxycholic (TDC) acids often occur together in human bile and since they do not separate in these chromatograms they are determined as the sum TD+TCD. This is done by heating the acids 15 minutes at 50° C in 65 % sulfuric acid when TD and TCD show the same molar extinction at their maximum at 305 mμ. This is reproducible within ±5 % with synthetic acids and the acids follow Beer's law singly and in mixtures.

Bile constituents other than bile acids (mainly bile pigments) also contribute to the light absorption of the samples in sulfuric acid. When this contribution is between 10 and 20 % of the total light absorption it can be corrected for by subtracting the light absorption of a corresponding sample in 80 % ethanol where bile acids have no absorption at the wave lengths used.

Glycine conjugated bile acids are separated with descending chromatography using ethylene chloride:heptane 50:50 as moving phase [4]. The filter paper used for the chromatography is cut as described but since the bile acids travel different distances on the different strips in descending chromatography one strip on each side of the strip to be eluted has to be sprayed in order to localize the bile acids. Glycocholic (GC), glycochenodeoxycholic (GCD) and glycodeoxycholic (GD) acids are separated and can be eluted and determined. Synthetic mixtures of GCD and GD are determined within ±5 %. Except in cases with extraordinarily large amounts of bile pigments no ethanol correction has to be made.

Within the errors of the method (approximately ±15 % for each bile acid in biological material) the ratio of glycine to taurine conjugation was the same for trihydroxy- as for dihydroxycholanic acids. In most human samples the glycine conjugated bile acids dominated. No free bile acids were detected It has been confirmed that cholic and chenodeoxycholic acids are the main hydroxycholanic acids in human bile. In several bile samples no conjugated deoxycholic acid could be found. With the method used glycodeoxycholic acid would have been detected when present as 2 % of the total amount of bile acids.

1. Sjövall, J. *Arkiv Kemi* **8** (1955) 317.
2. Sjövall, J. *Acta Chem. Scand.* **9** (1955) 1034.
3. Eriksson, S. *Acta Chem. Scand.* **10** (1956) 156.
4. Sjövall, J. *Arkiv Kemi* **8** (1955) 299.

Quantitative Aspects of Bile Acid Formation in Man

Sven Lindstedt

Department of Physiological Chemistry, University of Lund, Lund, Sweden

Our knowledge of the amount of bile acids taking part in the enterohepatic circulation is incomplete and based on determinations of concentration of bile acids in bladder or fistula bile. For a review see Josephson [1].

We have attempted to determine the total amount of circulating cholic acid by an isotope dilution *in vivo*. By determining the fall of specific activity with time information has been gained on the rate of formation of this compound. 3—4 μC of cholic acid-24-^{14}C was given orally as sodium salt to healthy male medical students. At different time intervals bile was obtained through a duodenal tube after administration of 1—3 mg of a purified pancreozymine-cholecystochinine preparation (kindly supplied by Professor Erik Jorpes, Stockholm). Cholic acid was isolated and the specific activity determined. A bile sample was used for a quantitative determination with a paperchromatographic technique of the concentration of various bile acids. These determinations were kindly carried out by Dr. J. Sjövall [2]. By the use of the figures thus obtained the total amount of circulating acids was calculated. In the table the results obtained in three subjects are given:

Subject	Cholic acid g	Total amount of of bile acids g	"Half-life" of cholic acid in days
B	0.575	1.85	1.2
P	0.92	3.65	2.5
S	1.29	3.55	3

1. Josephson, B. *Physiol. Rev.* **21** (1941) 463.
2. Sjövall, J. *Acta Chem. Scand. To be published.*

On the Metabolism of Bile Acids in Germ-free Rats

B. Gustafsson, S. Bergström, S. Lindstedt and A. Norman

Section of research on germ-free animals, Department of Histology and Department of Physiological Chemistry, University of Lund, Lund, Sweden

The bile of rats contains taurocholic and taurochenodeoxycholic acids [1]. With the aid of 24-^{14}C-labelled acids it has been shown that these acids are extensively modified during the passage down the intestinal tract [2]. When the fecal acids were chromatographed these modifications were found to include:

1) a splitting of the peptide bond,
2) an attack on the bile acid moiety leading to a variety of mostly less hydrophilic compounds.

It has been found [3] that in rats treated with intestinal chemoterapeutics no such modifications occur making it highly probable that microbial enzymes are responsible for the reactions. Furthermore several strains of bacteria that can split the conjugated bile acid *in vitro* have been isolated from the rat intestine [4]. We have earlier reported on the turnover of bile acids in normal rats and in animals treated with chemoterapeutics [5]. The half-lives were found to be about 2.5 and 6—7 days, respectively. In order to study the importance of intestinal microorganism for the elimination of bile acids we have administered 24-^{14}C-labelled cholic acid to germ-free rats and to a rat that had been infected with *Aspergillus niger* and then further with *Clostridium perfingens* type E. The rats were reared with slight modifications in the technique of Gustafsson [6]. The time course of excretion was followed and the acids in the feces fractionated with chromatography. One rat was finally transferred from the apparatus to normal environments and the elimination rate investigated.

The germ-free rats were found to excrete unchanged taurocholic acid in their feces. This was also the case in the rat infected with the mould. When the same rat was also infected with the *Clostridium* strain, however, about 25 % of the labelled acids appeared in the feces in the free form, mainly as cholic acid. The chromatographic pattern was in this case similar to that found after *in vitro* incubation of taurocholic acid with the same strain of bacterium [4].

In all rats studied the excretion rate was quite slow with a half life-time of about 7 days. It may be concluded that the state of the intestinal flora greatly influences the rate of elimination from the enterohepatic circulation. As, however, neither the mould nor the peptide bond-splitting *Clostridium* increases the excretion rate it seems probable that other microorganisms are of importance for the rate of elimination of bile acids.

1. Bergström, S. and Sjövall, J. *Acta Chem. Scand.* **8** (1954) 611.
2. Lindstedt, S. and Norman, A. *Acta Physiol. Scand.* **34** (1955) 1.
3. Norman, A. *Acta Physiol. Scand.* **33** (1955) 100.
4. Norman, A. and Grubb, R. *Acta Pathol. Microbiol. Scand.* **36** (1955).
5. Lindstedt, S. and Norman, A. *Acta Chem. Scand.* **9** (1955) 1042.
6. Gustafsson, B. *Acta Pathol. Microbiol. Scand.* Suppl. **73** (1948).

Conjugation of Cholic Acid in Human Liver Homogenates

Urs Gloor and Per-Hugo Ekdahl

Department of Physiological Chemistry and Department of Surgery, University of Lund, Lund, Sweden

Cholic acid is the end-product of cholesterol metabolism, that is, no further oxidation of the steroid nucleus takes place. We therefore used it as a model substance for conjugation studies. In liver homogenates human bile acids are conjugated with taurine and glycine in different proportions [1].

We have now developed this procedure further both as a macro and a micro method for homogenizing human liver biopsies. For macro experiments we used 1 ml 20 % homogenate in a medium similar to that described by Bucher [2] containing 11 g KH_2PO_4, 4 g KOH (85 % pure), 1 g $MgCl_2$, $6H_2O$ and 3.7 g nicotinamide per liter. The pH was 7.4. A loose fitting pestle and a short homogenisation time are essential. We used a gap between tube and pestle of 1 mm, a motor of 1 500 RPM and 1 min homogenisation time. To 1 ml medium we added 100 μg (= 40 000 counts per minute, end window tube) cholic acid-24-^{14}C and 2 mg adenosine triphosphate (crystalline, Pabst Laboratories, Milwaukee 5, Wisc.) and incubated in air for 2 hours at 37° after which time we stopped the reaction by adding 5 volumes of ethanol and proceeded as described earlier [3]. The time between surgical operation and incubation of the homogenate should not exceed 2 hours and care has to be taken that no part of the liver piece becomes dry. For micro experiments, that is liver pieces obtained by punction through the abdominal wall, we used the same buffer solution and 15 μg cholic acid + 200 μg adenosine triphosphate in a total of 0.25 ml. The liver (20—40 mg) was transferred directly from the biopsy needle into the homogenisation tube where all further operations were performed. We proceeded with methods similar to those described earlier [3].

Some results are compiled in Table 1. Glyco- + tauro-conjugation = 100 %. The variations of the extent of conjugation (1—50 %) had no influence on the ratio between glycine and taurine coupling.

The patients in all three of the groups had different clinical test values and exact diagnosis may result in a further specification. Yet, the values for patients with cirrhosis are much lower than for the other groups. In this group a deficiency of glycine could be at least a partial explanation. In two experiments glycine and taurine (5 mole per mole acid) alone or together were added. In the case of single additions glyco- respectively tauro-conjugation was increased, whereas with both together the ratio between the conjugates did not differ from that without amino acids added.

Table 1. Per cent glyco-cholic acid formed of total conjugated acids from 1 ml 20 % human liver homogenate with different patients.

Diagnosis		
Liver cirrhosis shunt operations	Gall-bladder and bile duct diseases	Ulcus duodeni Ulcus ventriculi
10	43	57
18	43	35
25	40	54
16	25	54
17	47	56
28	46	46
	39	36
	45	58
	48	57
	45	47
	47	56

In a few cases we made macro and micro experiments from the same liver and found the results the same within limits of ± 10 %, *i. e.* the same deviation as among different macro experiments on the same liver.

1. Bergström, S. and Gloor, U. *Acta Chem. Scand.* 8 (1954) 1109.
2. Bucher, N. L. R. *J. Am. Chem. Soc.* **75** (1953) 498.
3. Bergström, S. and Gloor, U. *Acta Chem. Scand.* 8 (1954) 1373.

Studies on the Formation of Mixed Disulphides of Biological Importance

L. Eldjarn and A. Pihl

Norsk Hydro's Institute for Cancer Research, The Norwegian Radium Hospital, Oslo

Previously we have shown that cystamine interacts *in vivo* as well as *in vitro* with the free SH groups of proteins and other body constituents to form considerable amounts of mixed disulphides [1-3]. This raises the question as to the chemistry of mixed disulphide formation in general.

A study has now been made of the chemical kinetics of the reaction of cystamine and cysteamine with various thiols and disulphides. A method has been worked out for the direct determination of the mixed disulphide formation. Use is made of the fact that the disulphide-thiol interaction is negligible below pH 2. ^{35}S-labeled cystamine or cysteamine is incubated with the thiol or disulphide, the reaction stopped by acidification, the mixed disulphide separated by rapid paper electrophoresis at pH 2, and the amount of mixed di sulphide measured by direct counting on paper.

In general the reaction proceeds according to the equations:

$$\mathrm{XSH} + \mathrm{R{-}SS{-}R} \underset{v_2}{\overset{K_1\ v_1}{\rightleftharpoons}} \mathrm{XSSR} + \mathrm{RSH} \qquad K_1 \qquad \text{I}$$

$$\mathrm{XSSR} + \mathrm{XSH} \underset{v_4}{\overset{v_3}{\rightleftharpoons}} \mathrm{XSSX} + \mathrm{RSH} \qquad \text{II}$$

When XSH = glutathione and RSH = cysteamine a rapid and extensive formation of mixed disulphide takes place. The $K_4 = K_2/K_3$ has been found to be greater than 130. This high K_4 value makes difficult the accurate determination of K_2 and K_3 from equilibrium data. The equilibrium values for the mixed disulphide were found to be independent of temperature (0 to 37° C), and of pH (5 to 7.4).

The velocity constants k_{v_1} and k_{v_4} were measured separately. Their pH dependence showed that $-S^-$ is the reactive form of the thiol. With equimolar amounts of the reactants, equilibrium at pH 7.4 and 37° C is attained in less than 45 seconds and 3 minutes in reactions I and II respectively.

The striking fact emerging from the present experiments is that at equilibrium nearly 80 % of glutathione (and of cysteine) exist as the mixed disulphide when incubated, in the absence of oxygen, with equimolar amounts of cystamine at 37° C, pH 7.4. Recently Kolthoff *et al.*[4] have calculated, from cystine solubility data, the equilibrium constants for the reactions of cystine with reduced glutathione and thioglycolic acid respectively. It can be calculated from these constants that in equimolar concentrations and under conditions comparable to ours, 41 % of the glutathione exist as mixed disulphides at equilibrium.

The rapid reaction velocities demonstrated in the present study and the high equilibrium values for the mixed disulphides would seem to have considerable interest with regard to the chemistry of protein sulphur groups. We have previously studied the formation of mixed disulphides between protein SH groups and cystamine [1-3]. In recent experiments we have found that cysteamine, as expected, forms mixed disulphides with accessible protein SS groups (serum albumin, desoxyribonuclease, cytochrom c).

Our data strongly suggest that the accessible protein SH and SS groups exist in a dynamic equilibrium with the thiols and disulphides of the surrounding medium. Thus, depending on the conditions, one particular protein sulphur group may conceivably exist either as a free SH group, in a mixed disulphide with a smaller compound, in an intramolecular disulphide, or occasionally in a protein-SS-protein linkage. Accordingly, the number of titratable SH groups of a protein may depend on the exact conditions of its pretreatment with thiols and/or disulphides (pH, temperature, chemical nature, concentrations). This view might offer an explanation of the numerous controversies concerning the number of free SH groups of various proteins.

It is suggested, on the basis of the above evidence, that the accessible sulphur groups of a protein should be classified as a) single SH groups, b) adjacent sulphur groups capable of forming intramolecular disulphides. It seems probable that in the case of proteins, the formation of intermolecular disulphides is of minor significance.

1. Eldjarn, L., Pihl, A. and Shapiro, B. *Internat. Conf. on the Peaceful Uses of Atomic Energy* (1955). *In press.*

2. Eldjarn, L. and Pihl, A. In Radiobiology Symposium, Cambridge, Oliver and Boyd, Edinburgh (1955).
3. Eldjarn, L. and Pihl, A. *J. Biol. Chem.* (1956) *In press.*
4. Kolthoff, I. N., Stricks, W. and Kapoor, R. C. *J. Am. Chem. Soc.* **77** (1955) 4733.

Influence of Thyroid Hormone on the Formation of Bile Acids

Sten Eriksson

Department of Physiological Chemistry, University of Lund, Lund, Sweden

It has long been recognized that an inverse relationship exists between plasma cholesterol level and thyroid activity [1]. As the bile acids have been shown [2,3] to be the main metabolic end-products of cholesterol in the rat we have studied the influence of thyroid activity on the excretion of bile acids in bile fistula rats. Thompson and Vars [4] studying the same problem found lower values of cholic acid in the hyperthyroid and hypothyroid rats than in the euthyroid animals. In their experiments they did not determine taurochenodesoxycholic acid, the second bile acid of quantitative importance in the rat [5]. In the present work taurocholic and taurochenodesoxycholic acids have been determined with the technique used in a previous work from this laboratory in which the quantitative excretion of bile acids in normal bile fistula rats were studied [6]. The rats were made hyper- and hypothyroid by including 0.4 % thyroid or 0.5 % propyltiouracil, respectively, in the diet. The bile was collected for five days following operation. In Table 1 are given the values obtained for the excretion of taurocholic and taurochenodesoxycholic acids during the time of collection. In the hypothyroid group there is a large reduction of the total excretion of bile acids. In the hyperthyroid group the total excretion remains unchanged as compared to the control rats. In the hypothyroid group the excretion of taurochenodesoxycholic acid is less than 10 % of the total excretion, whereas the normal rats had about 20 %. On the other hand in the hyperthyroid group taurochenodesoxycholic acid constitutes between 70 and 80 % of the total excretion. Thus the excretion of bile acids in hyperthyroid rats is not decreased but the composition is changed in that taurocholic acid is markedly decreased but taurochenodesoxycholic acid increased.

Further data will be presented.

1. Peters, J. P. and Van Slyke, D. D. *Quantitative clinical chemistry*, 1, 2nd ed. Baltimore: Williams and Wilkins (1946).
2. Bergström, S. *Kgl. Fysiograf. Sällskap Lund Förh.* **22** (1952) No. 16.
3. Byers, S. O. and Biggs, M. W. *Arch. Biochem. Biophys.* **39** (1952) 301.
4. Thompson, J. C. and Vars, H. M. *Am. J. Physiol.* **179** (1954) 405.
5. Bergström, S. and Sjövall, J. *Acta Chem. Scand.* **8** (1954) 611.
6. Eriksson, S. *Acta Chem. Scand.* **10** (1956) 156.

Table 1. Excretion of Na-taurocholate (TC) and Na-taurochenodesoxycholate (TCD). The total excretion (TC+TCD) is given as mg per 100 g body weight. The rats weighed 180—250 g.

Hours After operation	Hypothyr. (4 rats)		Controls (4 rats)		Hyperthyr. (4 rats)	
	TC+TCD Mg	TCD % of total excretion	TC+TCD Mg	TCD % of total excretion	TC+TCD Mg	TCD % of total excretion
0—6	10.4	6.5	8.5	12.6	15.5	50.6
6—12	5.7	12.5	3.1	14.7	4.9	48.9
12—18	1.4	15.7	2.8	11.8	3.5	72.0
18—24	1.2	5.5	2.1	15.4	5.0	80.5
24—48	8.7	4.1	20.4	18.4	25.2	69.5
48—72	12.7	6.2	22.8	28.6	22.2	71.3
72—96	13.7	12.7	17.3	24.8	19.9	70.0
96—120	10.2	6.5	19.7	22.9	19.8	67.7

2. Eldjarn, L. and Pihl, A. In Radiobiology Symposium, Cambridge, Oliver and Boyd, Edinburgh (1955).
3. Eldjarn, L. and Pihl, A. *J. Biol. Chem.* (1956) *In press.*
4. Kolthoff, I. N., Stricks, W. and Kapoor, R. C. *J. Am. Chem. Soc.* **77** (1955) 4733.

Influence of Thyroid Hormone on the Formation of Bile Acids

Sten Eriksson

Department of Physiological Chemistry, University of Lund, Lund, Sweden

It has long been recognized that an inverse relationship exists between plasma cholesterol level and thyroid activity [1]. As the bile acids have been shown [2,3] to be the main metabolic end-products of cholesterol in the rat we have studied the influence of thyroid activity on the excretion of bile acids in bile fistula rats. Thompson and Vars [4] studying the same problem found lower values of cholic acid in the hyperthyroid and hypothyroid rats than in the euthyroid animals. In their experiments they did not determine taurochenodesoxycholic acid, the second bile acid of quantitative importance in the rat [5]. In the present work taurocholic and taurochenodesoxycholic acids have been determined with the technique used in a previous work from this laboratory in which the quantitative excretion of bile acids in normal bile fistula rats were studied [6]. The rats were made hyper- and hypothyroid by including 0.4 % thyroid or 0.5 % propyltiouracil, respectively, in the diet. The bile was collected for five days following operation. In Table 1 are given the values obtained for the excretion of taurocholic and taurochenodesoxycholic acids during the time of collection. In the hypothyroid group there is a large reduction of the total excretion of bile acids. In the hyperthyroid group the total excretion remains unchanged as compared to the control rats. In the hypothyroid group the excretion of taurochenodesoxycholic acid is less than 10 % of the total excretion, whereas the normal rats had about 20 %. On the other hand in the hyperthyroid group taurochenodesoxycholic acid constitutes between 70 and 80 % of the total excretion. Thus the excretion of bile acids in hyperthyroid rats is not decreased but the composition is changed in that taurocholic acid is markedly decreased but taurochenodesoxycholic acid increased.

Further data will be presented.

1. Peters, J. P. and Van Slyke, D. D. *Quantitative clinical chemistry*, 1, 2nd ed. Baltimore: Williams and Wilkins (1946).
2. Bergström, S. *Kgl. Fysiograf. Sällskap Lund Förh.* **22** (1952) No. 16.
3. Byers, S. O. and Biggs, M. W. *Arch. Biochem. Biophys.* **39** (1952) 301.
4. Thompson, J. C. and Vars, H. M. *Am. J. Physiol.* **179** (1954) 405.
5. Bergström, S. and Sjövall, J. *Acta Chem. Scand.* **8** (1954) 611.
6. Eriksson, S. *Acta Chem. Scand.* **10** (1956) 156.

Table 1. Excretion of Na-taurocholate (TC) and Na-taurochenodesoxycholate (TCD). The total excretion (TC+TCD) is given as mg per 100 g body weight. The rats weighed 180—250 g.

Hours After operation	Hypothyr. (4 rats)		Controls (4 rats)		Hyperthyr. (4 rats)	
	TC+TCD Mg	TCD % of total excretion	TC+TCD Mg	TCD % of total excretion	TC+TCD Mg	TCD % of total excretion
0—6	10.4	6.5	8.5	12.6	15.5	50.6
6—12	5.7	12.5	3.1	14.7	4.9	48.9
12—18	1.4	15.7	2.8	11.8	3.5	72.0
18—24	1.2	5.5	2.1	15.4	5.0	80.5
24—48	8.7	4.1	20.4	18.4	25.2	69.5
48—72	12.7	6.2	22.8	28.6	22.2	71.3
72—96	13.7	12.7	17.3	24.8	19.9	70.0
96—120	10.2	6.5	19.7	22.9	19.8	67.7

The Incorporation of Methyl and Carboxyl Labelled Acetate into the Purine-Bound Sugars of Nucleic Acids in Liver Slices

S. Laland and I. Smith-Kielland

Biochemistry Department, The University, Oslo

The incorporation of carbon-labelled acetate into ribose has been the subject of several investigations. Thus it was shown that in chicks carboxyl labelled acetate was incorporated into the purine-bound ribose of RNA [1]. Löw [2] using rats found that when given $^{13}CH_3$ $^{14}COOH$ both isotopes were present in the ribose of RNA and that the methyl carbon was incorporated to a considerable greater extent than the carboxyl. However, studies on the incorporation of labelled acetate into the purine-bound 2-deoxy-D-ribose has not been reported. The present study concerns this problem together with an investigation of the simultaneous incorporation of isotope into the purine-bound ribose. Liver slices obtained from regenerating rat liver were incubated in Krebs-Hensleit medium at pH.7.4 containing glucose together with labelled sodium acetate for 3 hours at 37° C. The nucleic acids were isolated from the liver slices by the method of Brown *et al.*[3] The purine-bound 2-deoxy-D-ribose was isolated from the DNA by a slight modification of a method described previously[4]. The sugar was finally purified by paper chromatography, eluted, estimated and counted. D-Ribose was isolated from the RNA after acid hydrolysis, followed by passage of the hydrolysate through a column of mixed resins (IR 120(H) and IR4B(OH)) and finally paper chromatography. The sugar was eluted from the chromatogram, estimated and counted. In both cases results obtained from three different chromatographic solvent systems were found to agree satisfactorily and the figures quoted in the table below represent the mean of the three figures.

Acetate incubated	2-Deoxy-D-ribose c/min/μmole	D-Ribose c/min/μmole
$^{14}CH_3COONa$	147	790
$CH_3{}^{14}COONa$	292	300

It thus appears that in regenerating liver slices both the methyl and carboxyl carbon of acetate can be incorporated into the purine-bound 2-deoxy-D-ribose. Experiments performed with liver slices from non regenerating liver showed as expected no incorporation of carboxyl labelled acetate. Furthermore it is seen that in the case of the methyl labelled acetate the incorporation of isotope is 5 times as large in the case of the purine-bound D-ribose, as for the purine-bound 2-deoxy-D-ribose. With carboxyl-labelled acetate there is however the same degree of incorporation of isotope.

1. Bernstein, I. A. *J. Biol. Chem.* **205** (1953) 317.
2. Löw, B. *Acta Chem. Scand.* **6** (1952) 304.
3. Bendich, Aa., Russel, P. J. and Brown, G. B. *J. Biol. Chem.* **203** (1953) 306.
4. Jones, A. S. and Laland, S. G. *Acta Chem. Scand.* **8** (1954) 603.

Studies on the Regulation of Bile Acid Formation in Bile Fistula Rats

S. Bergström, H. Danielsson and U. Gloor

Department of Physiological Chemistry, University of Lund, Lund, Sweden

When a bile fistula is made in a rat the excretion of bile acids increases 20—40 fold over the normal daily synthesis to 40—60 mg per day!

In order to study the influence of the bile acids in the enterohepatic circulation on the bile acid production in the liver, we have used two experimental approaches.

We have prepared fistula rats as normal but also inserted a cannula into the lower part of the severed bile duct and continuously injected 0.5 ml of saline per hour containing the synthetic bile salt investigated.

In order to follow the taurocholic acid production we have injected sodium-taurochenodesoxycholate. It is known that this substance does not give rise to cholic acid but to relatively small amounts of higher hydroxyla-

ted compounds, that can be differentiated from cholic acid by partition chromatography [2,3]. The amount of cholic acid in the hydrolysed bile was then calculated from the titration values of the cholic acid band.

It was found, that the injection of 2.5 mg of sodium-taurochenodesoxycholate per hour scarcely influenced the cholic acid production, 5 mg per hour reduced the daily production to about 4 mg, whereas 10 mg per hour caused a reduction down to the normal daily synthesis of 1—2 mg.

If the amount of bile salts in a 200 g rat is about 15 mg the bile acids have to circulate 15—20 times per day in the enterohepatic circulation to maintain a concentration in the portal blood similar to that in the last mentioned experiment.

The daily formation of 40—60 mg of bile acids corresponds to about three times the amount cholesterol present in the liver. We have therefore injected ^{14}C-acetate intraperitoneally and followed the appearance of ^{14}C in the secreted bile.

In a typical experiment about 1 mg of sodium acetate (1.9×10^6 c.p.m.) in 1.5 ml of saline was injected intraperitoneally into fistula rats at the time indicated after the operation. The percentage of the administered isotope that was recovered in the bile during the following 6 hours is shown in the second column below.

Hours after operation	% injected isotope recovered in bile
16	0.13
64	0.61
112	1.41

According to paper chromatography about 80 % of the isotope was contained in the bile salts.

The correlation of data of this type with the bile acid formation will be exemplified and discussed. The method has been found useful for studying the regulation of the synthesis of bile acids under different experimental conditions.

1. Eriksson, S. *Acta Chem. Scand. In press.*
2. Bergström, S., Rottenberg, M. and Sjövall, I. *Hoppe Seylers Z. physiol. Chem.* **295** (1953) 278.
3. Norman, A. *Acta Chem. Scand.* **7** (1953) 1413.

Increase of Cholinesterase Content in Mouse Liver Homogenates after Incubation

Karl Håkon Skramstad

The Norwegian Defence Research Establishment, Toxicological group, Kjeller, Norway

The rate of hydrolysis of acetylcholine by mouse liver homogenates increases by about 100 % when the homogenates are left either overnight at room temperature (20° C) or two to three hours at 37° C.

Of the organs investigated (brain, kidney, plasma, erythrocytes and liver) only the liver presented a real "autoactivation". This increase in activity takes place in liver homogenates from mice of different ages and both sexes, but seems to be more progressive in the female. There seems to be a greater "activation" in liver homogenates from infantile mice than mature ones, although there are large fluctuations.

The "activation" does not disappear with dialysis and seems to be localized to the particles of the liver cell upon "high speed" centrifuging. Calcium ions have no influence, neither is the increase in activity dependent on the isotonicity of the medium.

Kinetic experiments with a selective inhibitor of "pseudo"-cholinesterase [1], Nu 683, suggest that one and the same enzyme, *viz.* a "pseudo"-cholinesterase, is responsible for the major part of the activity with acetylcholine as substrate, both prior to and after the "activation".

The increase of hydrolysis takes place with acetylcholine and butyrylcholine as substrates, while deactivation results when tributyrin and benzoylcholine are employed. With acetyl-β-methyl-choline the rate of hydrolysis is quite slow, but has a slight tendency to increase with time; too small, however, to be of any experimental significance. These experiments indicate that we are dealing with a butyrocholinesterase [2].

Benzoylcholine, often used as a specific substrate for "pseudo"-cholinesterase [3], is not hydrolysed at an increased rate after incubation. On the contrary, the hydrolysis decreases with time. Thus there might perhaps be two "pseudo"-cholinesterases in the mouse liver; one butyrocholinesterase and one "benzoylcholinesterase". As known, "benzoylcholinesterases" are occasionally found in the plasma of rabbits [4] and in the liver of guinea pigs [5,6].

The Incorporation of Methyl and Carboxyl Labelled Acetate into the Purine-Bound Sugars of Nucleic Acids in Liver Slices

S. Laland and I. Smith-Kielland

Biochemistry Department, The University, Oslo

The incorporation of carbon-labelled acetate into ribose has been the subject of several investigations. Thus it was shown that in chicks carboxyl labelled acetate was incorporated into the purine-bound ribose of RNA [1]. Löw [2] using rats found that when given $^{13}CH_3$ $^{14}COOH$ both isotopes were present in the ribose of RNA and that the methyl carbon was incorporated to a considerable greater extent than the carboxyl. However, studies on the incorporation of labelled acetate into the purine-bound 2-deoxy-D-ribose has not been reported. The present study concerns this problem together with an investigation of the simultaneous incorporation of isotope into the purine-bound ribose. Liver slices obtained from regenerating rat liver were incubated in Krebs-Hensleit medium at pH.7.4 containing glucose together with labelled sodium acetate for 3 hours at 37° C. The nucleic acids were isolated from the liver slices by the method of Brown *et al.*[3] The purine-bound 2-deoxy-D-ribose was isolated from the DNA by a slight modification of a method described previously[4]. The sugar was finally purified by paper chromatography, eluted, estimated and counted. D-Ribose was isolated from the RNA after acid hydrolysis, followed by passage of the hydrolysate through a column of mixed resins (IR 120(H) and IR4B(OH)) and finally paper chromatography. The sugar was eluted from the chromatogram, estimated and counted. In both cases results obtained from three different chromatographic solvent systems were found to agree satisfactorily and the figures quoted in the table below represent the mean of the three figures.

Acetate incubated	2-Deoxy-D-ribose c/min/μmole	D-Ribose c/min/μmole
$^{14}CH_3COONa$	147	790
$CH_3{}^{14}COONa$	292	300

It thus appears that in regenerating liver slices both the methyl and carboxyl carbon of acetate can be incorporated into the purine-bound 2-deoxy-D-ribose. Experiments performed with liver slices from non regenerating liver showed as expected no incorporation of carboxyl labelled acetate. Furthermore it is seen that in the case of the methyl labelled acetate the incorporation of isotope is 5 times as large in the case of the purine-bound D-ribose, as for the purine-bound 2-deoxy-D-ribose. With carboxyl-labelled acetate there is however the same degree of incorporation of isotope.

1. Bernstein, I. A. *J. Biol. Chem.* **205** (1953) 317.
2. Löw, B. *Acta Chem. Scand.* **6** (1952) 304.
3. Bendich, Aa., Russel, P. J. and Brown, G. B. *J. Biol. Chem.* **203** (1953) 306.
4. Jones, A. S. and Laland, S. G. *Acta Chem. Scand.* **8** (1954) 603.

Studies on the Regulation of Bile Acid Formation in Bile Fistula Rats

S. Bergström, H. Danielsson and U. Gloor

Department of Physiological Chemistry, University of Lund, Lund, Sweden

When a bile fistula is made in a rat the excretion of bile acids increases 20—40 fold over the normal daily synthesis to 40—60 mg per day!

In order to study the influence of the bile acids in the enterohepatic circulation on the bile acid production in the liver, we have used two experimental approaches.

We have prepared fistula rats as normal but also inserted a cannula into the lower part of the severed bile duct and continuously injected 0.5 ml of saline per hour containing the synthetic bile salt investigated.

In order to follow the taurocholic acid production we have injected sodium-taurochenodesoxycholate. It is known that this substance does not give rise to cholic acid but to relatively small amounts of higher hydroxyla-

ted compounds, that can be differentiated from cholic acid by partition chromatography [2,3]. The amount of cholic acid in the hydrolysed bile was then calculated from the titration values of the cholic acid band.

It was found, that the injection of 2.5 mg of sodium-taurochenodesoxycholate per hour scarcely influenced the cholic acid production, 5 mg per hour reduced the daily production to about 4 mg, whereas 10 mg per hour caused a reduction down to the normal daily synthesis of 1—2 mg.

If the amount of bile salts in a 200 g rat is about 15 mg the bile acids have to circulate 15—20 times per day in the enterohepatic circulation to maintain a concentration in the portal blood similar to that in the last mentioned experiment.

The daily formation of 40—60 mg of bile acids corresponds to about three times the amount cholesterol present in the liver. We have therefore injected ^{14}C-acetate intraperitoneally and followed the appearance of ^{14}C in the secreted bile.

In a typical experiment about 1 mg of sodium acetate (1.9×10^6 c.p.m.) in 1.5 ml of saline was injected intraperitoneally into fistula rats at the time indicated after the operation. The percentage of the administered isotope that was recovered in the bile during the following 6 hours is shown in the second column below.

Hours after operation	% injected isotope recovered in bile
16	0.13
64	0.61
112	1.41

According to paper chromatography about 80 % of the isotope was contained in the bile salts.

The correlation of data of this type with the bile acid formation will be exemplified and discussed. The method has been found useful for studying the regulation of the synthesis of bile acids under different experimental conditions.

1. Eriksson, S. *Acta Chem. Scand. In press.*
2. Bergström, S., Rottenberg, M. and Sjövall, I. *Hoppe Seylers Z. physiol. Chem.* **295** (1953) 278.
3. Norman, A. *Acta Chem. Scand.* **7** (1953) 1413.

Increase of Cholinesterase Content in Mouse Liver Homogenates after Incubation

Karl Håkon Skramstad

The Norwegian Defence Research Establishment, Toxicological group, Kjeller, Norway

The rate of hydrolysis of acetylcholine by mouse liver homogenates increases by about 100 % when the homogenates are left either overnight at room temperature (20° C) or two to three hours at 37° C.

Of the organs investigated (brain, kidney, plasma, erythrocytes and liver) only the liver presented a real "autoactivation". This increase in activity takes place in liver homogenates from mice of different ages and both sexes, but seems to be more progressive in the female. There seems to be a greater "activation" in liver homogenates from infantile mice than mature ones, although there are large fluctuations.

The "activation" does not disappear with dialysis and seems to be localized to the particles of the liver cell upon "high speed" centrifuging. Calcium ions have no influence, neither is the increase in activity dependent on the isotonicity of the medium.

Kinetic experiments with a selective inhibitor of "pseudo"-cholinesterase [1], Nu 683, suggest that one and the same enzyme, *viz.* a "pseudo"-cholinesterase, is responsible for the major part of the activity with acetylcholine as substrate, both prior to and after the "activation".

The increase of hydrolysis takes place with acetylcholine and butyrylcholine as substrates, while deactivation results when tributyrin and benzoylcholine are employed. With acetyl-β-methyl-choline the rate of hydrolysis is quite slow, but has a slight tendency to increase with time; too small, however, to be of any experimental significance. These experiments indicate that we are dealing with a butyrocholinesterase [2].

Benzoylcholine, often used as a specific substrate for "pseudo"-cholinesterase [3], is not hydrolysed at an increased rate after incubation. On the contrary, the hydrolysis decreases with time. Thus there might perhaps be two "pseudo"-cholinesterases in the mouse liver; one butyrocholinesterase and one "benzoylcholinesterase". As known, "benzoylcholinesterases" are occasionally found in the plasma of rabbits [4] and in the liver of guinea pigs [5,6].

1. Hawkins, R. D. and Gunter, J. M. *Biochem. J. London* **40** (1946) 192.
2. Whittaker, V. P. *Physiol. Rev.* **31** (1951) 312.
3. Mendel, B., Mundell, D. B. and Rudney, H. *Biochem. J. London* **37** (1943) 473.
4. Koelle, G. B. *Biochem. J. London* **53** (1953) 217.
5. Augustinsson, K. B. *Acta Physiol. Scand.* **15** *Suppl.* **52** (1948).
6. Blaschko, H., Chou, T. C. and Wajda, I. *Brit. J. Pharmacol.* **2** (1947) 108, 116.

On the Question of a Cysteinyl-glycinase Activity of RNA

G. Semenza

Institute of Biochemistry, University of Uppsala, Sweden

Binkley [1] reported that cysteinyl-glycinase should be a protein-free RNA and put forward the hypothesis that RNA should interfere in protein synthesis through this activity.

Because of the remarkable implications of these statements (among others, that an enzyme should be non-protein in nature), an attempt was made at purifying further the cysteinyl-glycinase (through chromatography on calcium phosphate, Dowex 2 and DEAE cellulose) and at studying some of its chemical properties.

A separation of cysteinyl-glycinase activity from RNA was achieved, and Folin-positive, orcinol-negative, P-negative, chloroform-sensitive preparations of enzyme were obtained, showing a maximum in UV absorption spectrum at about 280 mμ.

1. Binkley, F. *Nature* **167** (1951) 888; *Exptl. Cell Research Suppl.* **2** (1952) 145.

A Method for the Isolation of 2-Deoxy-D-ribose from Thymidine

S. Laland and E. Roth

Biochemistry Department, The University, Oslo

It has always been assumed that the sugar component of thymidine is in analogy with the purine nucleosides 2-deoxy-D-ribose. Good evidence in support of this assumption has recently been provided [1-3], although the conclusive chemical proof was lacking. The present work describes the isolation of crystalline 2-deoxy-D-ribose from thymidine, and also provides a very convenient micro-method for the isolation of this sugar for tracer studies, which was the main purpose of this work. Thymidine is reduced by 3 % NaHg in aqueous solution at room temperature. The reduction mixture was shown by paper electrophoresis to contain two acidic 2-deoxy-D-ribosyl components formed by breakage of the reduced pyrimidine ring under the prevailing alkaline conditions. Removal of alkali in the reduction mixture with Amberlite IR 120(H) followed by gentle acid hydrolysis with dilute sulphuric acid and passage through a column of weakly basic resin such as Amberlite IR 4B(OH) afforded crystalline 2-deoxy-D-ribose. The yield was almost 100 %. For tracer work it is advisable to purify it by recrystallization or paper chromatography.

1. Macnutt, W. S. *Biochem. J. London* **50** (1952) 384.
2. Burke, D. C. *Chemistry and Industry* **1954** 1393.
3. Michelson, A. M. and Todd, A. R. *J. Chem. Soc.* **1955** 816.

Glucose Inhibition of Respiration in Ascites Tumor Cells

Elling Kvamme

Ullevål Sykehus, Centrallaboratoriet, Oslo, Norway

Glucose exerts a pronounced inhibitory effect upon the respiration of ascites tumor cells, a phenomenon also called the Crabtree effect. In an attempt to approach this problem the glycolysis and the tricarboxylic acid cycle of the ascites tumor cells were studied under various conditions.

Ascites cells (30—40 mg protein) incubated in phosphate buffer for 1 h at 37° with excess glucose as substrate were found to accumulate 1—2 μM of a barium insoluble fructose ester, assumed to be fructose-diphosphate.

In the presence of glucose (10 μM/ml), the removal of inorganic phosphate (20 μM/ml) from the medium increased the oxygen uptake by 25—50 % and decreased the glucose uptake

1. Hawkins, R. D. and Gunter, J. M. *Biochem. J. London* **40** (1946) 192.
2. Whittaker, V. P. *Physiol. Rev.* **31** (1951) 312.
3. Mendel, B., Mundell, D. B. and Rudney, H. *Biochem. J. London* **37** (1943) 473.
4. Koelle, G. B. *Biochem. J. London* **53** (1953) 217.
5. Augustinsson, K. B. *Acta Physiol. Scand.* **15** *Suppl.* **52** (1948).
6. Blaschko, H., Chou, T. C. and Wajda, I. *Brit. J. Pharmacol.* **2** (1947) 108, 116.

On the Question of a Cysteinyl-glycinase Activity of RNA

G. Semenza

Institute of Biochemistry, University of Uppsala, Sweden

Binkley [1] reported that cysteinyl-glycinase should be a protein-free RNA and put forward the hypothesis that RNA should interfere in protein synthesis through this activity.

Because of the remarkable implications of these statements (among others, that an enzyme should be non-protein in nature), an attempt was made at purifying further the cysteinyl-glycinase (through chromatography on calcium phosphate, Dowex 2 and DEAE cellulose) and at studying some of its chemical properties.

A separation of cysteinyl-glycinase activity from RNA was achieved, and Folin-positive, orcinol-negative, P-negative, chloroform-sensitive preparations of enzyme were obtained, showing a maximum in UV absorption spectrum at about 280 mμ.

1. Binkley, F. *Nature* **167** (1951) 888; *Exptl. Cell Research Suppl.* **2** (1952) 145.

A Method for the Isolation of 2-Deoxy-D-ribose from Thymidine

S. Laland and E. Roth

Biochemistry Department, The University, Oslo

It has always been assumed that the sugar component of thymidine is in analogy with the purine nucleosides 2-deoxy-D-ribose. Good evidence in support of this assumption has recently been provided [1-3], although the conclusive chemical proof was lacking. The present work describes the isolation of crystalline 2-deoxy-D-ribose from thymidine, and also provides a very convenient micro-method for the isolation of this sugar for tracer studies, which was the main purpose of this work. Thymidine is reduced by 3 % NaHg in aqueous solution at room temperature. The reduction mixture was shown by paper electrophoresis to contain two acidic 2-deoxy-D-ribosyl components formed by breakage of the reduced pyrimidine ring under the prevailing alkaline conditions. Removal of alkali in the reduction mixture with Amberlite IR 120(H) followed by gentle acid hydrolysis with dilute sulphuric acid and passage through a column of weakly basic resin such as Amberlite IR 4B(OH) afforded crystalline 2-deoxy-D-ribose. The yield was almost 100 %. For tracer work it is advisable to purify it by recrystallization or paper chromatography.

1. Macnutt, W. S. *Biochem. J. London* **50** (1952) 384.
2. Burke, D. C. *Chemistry and Industry* **1954** 1393.
3. Michelson, A. M. and Todd, A. R. *J. Chem. Soc.* **1955** 816.

Glucose Inhibition of Respiration in Ascites Tumor Cells

Elling Kvamme

Ullevål Sykehus, Centrallaboratoriet, Oslo, Norway

Glucose exerts a pronounced inhibitory effect upon the respiration of ascites tumor cells, a phenomenon also called the Crabtree effect. In an attempt to approach this problem the glycolysis and the tricarboxylic acid cycle of the ascites tumor cells were studied under various conditions.

Ascites cells (30—40 mg protein) incubated in phosphate buffer for 1 h at 37° with excess glucose as substrate were found to accumulate 1—2 μM of a barium insoluble fructose ester, assumed to be fructose-diphosphate.

In the presence of glucose (10 μM/ml), the removal of inorganic phosphate (20 μM/ml) from the medium increased the oxygen uptake by 25—50 % and decreased the glucose uptake

as well as the lactic acid formation by 30—50 %, while the blank respiration was unaffected. In this experiment the cells were incubated in trisbuffer with and without phosphate, and special care was taken to maintain the same ionic concentrations of sodium and potassium. The oxygen uptake was measured in a Warburg apparatus for 1 h at 37°. This experiment is in apparent contrast to the results reported by Ibsen, Mc Carty and Mc Kee [1]. These authors operated with glucose concentrations of less than 3 μM/ml and measured the oxygen uptake during a 3 h period. The small glucose concentrations employed may explain the discrepancy, because in the presence of phosphate (20 μM/ml) more than twice as much glucose was taken up after 1 h by the cells (13—15 mg protein) in our experiments.

In iodoacetate (10^{-4} M) treated cells phosphate on the contrary slightly stimulated the respiration and exerted no appreciable effect upon glucose uptake or lactic acid formation.

Increasing amounts of iodoacetate (0—1.5×10^{-4} M final concn.) successively enhanced the oxygen uptake of ascites cells incubated with glucose as substrate in a way fairly parallel to the normalization of the pH, while the blank respiration decreased slightly. Judged from the glucose uptake and the formation of fructose-diphosphate and lactic acid, an excess of adenosinediphosphate is likely to be formed extramitochondrially in IAA poisoned cells. The still existent Crabtree effect may be explained in accordance with Rackers shuttling theory [2] if one presumes a rate difference as to the permeation of adenine nucleotides in and out of the mitochondria.

Dinitrophenol (DNP, 10^{-4} M) increased the glucose uptake and lactic acid formation markedly. DNP initially stimulated the oxygen uptake more than the blank when glucose was substrate, but fell off earlier.

Excess fumarate completely abolished the glucose inhibition of the respiration in malonate treated cells. The oxygen uptake was also unaffected by malonate in the presence of glucose and fumarate. Glucose did not appreciably affect the citrate formation from fumarate in these cells. Glucose increased the concentration of α-ketoglutarate and reduced the formation of succinate when the cells were incubated in the presence of excess citrate and malonate. Under similar conditions glucose markedly inhibited the oxygen uptake in the presence of excess citrate or α-ketoglutarate.

Hence there was found no evidence for an inhibition of the tricarboxylic acid cycle between fumarate and citrate by glucose. The results may be explained by assuming a partial block of the cycle between α-ketoglutarate and succinate and that this step is rate limiting of the overall mitochondrial respiration in the presence of glucose.

1. Ibsen, K., Mc Carty, B. and Mc Kee, R. W. *Federation Proc.* **15** (1956) 279.
2. Racker, E. *Annals New York Acad. Sci.* **63** (1956) 1017.

Estimation of Corticosteroid Metabolites in Urine

L.-O. Plantin, E. Diczfalusy and G. Birke

King Gustaf V:th Research Institute and Hormone Laboratory, The Womens Clinic, Karolinska sjukhuset, Stockholm 60, Sweden

During the last decade the importance of adequate methods for evaluation of the adrenocortical function has been more clearly recognized. We have compared the methods most used for corticosteroid determinations in urine and related them to the structure of the steroid hormones and their metabolites. We have worked especially with the method developed by Norymberski and coworkers which we think is superior to other methods [1,2]. This method converts, by an oxidation with sodium bismuthate, corticosteroids of certain types called 17-ketogenic steroids (17-KGS) to 17-ketosteroids (17-KS). Apart from the desired oxidative effect of the sodium bismuthate on the side chain at carbon atom 17, other effects appear which can cause faulty results. That is especially the case with dehydro*epi*androsterone, which is almost completely transformed to other products by the combined effects of sodium bismuthate and acid hydrolysis. The bismuthate probably causes an oxidation to the 5,6-epoxide which is then further rearranged by the acid hydrolysis. This deleterious effect can be minimised by using short oxidation time and it can be completely avoided by using the modification proposed by Appleby *et al.*[3]

A system has been worked out for the separation and estimation of the different more important corticosteroid metabolites in urine. It employs enzymatic hydrolysis of the corticosteroid conjugates with β-glucuronidase, oxidation of corticosteroids to 17-KS with sodium bismuthate, reduction of ketonic groups to

1. Hawkins, R. D. and Gunter, J. M. *Biochem. J. London* **40** (1946) 192.
2. Whittaker, V. P. *Physiol. Rev.* **31** (1951) 312.
3. Mendel, B., Mundell, D. B. and Rudney, H. *Biochem. J. London* **37** (1943) 473.
4. Koelle, G. B. *Biochem. J. London* **53** (1953) 217.
5. Augustinsson, K. B. *Acta Physiol. Scand.* **15** *Suppl.* **52** (1948).
6. Blaschko, H., Chou, T. C. and Wajda, I. *Brit. J. Pharmacol.* **2** (1947) 108, 116.

On the Question of a Cysteinyl-glycinase Activity of RNA

G. Semenza

Institute of Biochemistry, University of Uppsala, Sweden

Binkley [1] reported that cysteinyl-glycinase should be a protein-free RNA and put forward the hypothesis that RNA should interfere in protein synthesis through this activity.

Because of the remarkable implications of these statements (among others, that an enzyme should be non-protein in nature), an attempt was made at purifying further the cysteinyl-glycinase (through chromatography on calcium phosphate, Dowex 2 and DEAE cellulose) and at studying some of its chemical properties.

A separation of cysteinyl-glycinase activity from RNA was achieved, and Folin-positive, orcinol-negative, P-negative, chloroform-sensitive preparations of enzyme were obtained, showing a maximum in UV absorption spectrum at about 280 mμ.

1. Binkley, F. *Nature* **167** (1951) 888; *Exptl. Cell Research Suppl.* **2** (1952) 145.

A Method for the Isolation of 2-Deoxy-D-ribose from Thymidine

S. Laland and E. Roth

Biochemistry Department, The University, Oslo

It has always been assumed that the sugar component of thymidine is in analogy with the purine nucleosides 2-deoxy-D-ribose. Good evidence in support of this assumption has recently been provided [1-3], although the conclusive chemical proof was lacking. The present work describes the isolation of crystalline 2-deoxy-D-ribose from thymidine, and also provides a very convenient micro-method for the isolation of this sugar for tracer studies, which was the main purpose of this work. Thymidine is reduced by 3 % NaHg in aqueous solution at room temperature. The reduction mixture was shown by paper electrophoresis to contain two acidic 2-deoxy-D-ribosyl components formed by breakage of the reduced pyrimidine ring under the prevailing alkaline conditions. Removal of alkali in the reduction mixture with Amberlite IR 120(H) followed by gentle acid hydrolysis with dilute sulphuric acid and passage through a column of weakly basic resin such as Amberlite IR 4B(OH) afforded crystalline 2-deoxy-D-ribose. The yield was almost 100 %. For tracer work it is advisable to purify it by recrystallization or paper chromatography.

1. Macnutt, W. S. *Biochem. J. London* **50** (1952) 384.
2. Burke, D. C. *Chemistry and Industry* **1954** 1393.
3. Michelson, A. M. and Todd, A. R. *J. Chem. Soc.* **1955** 816.

Glucose Inhibition of Respiration in Ascites Tumor Cells

Elling Kvamme

Ullevål Sykehus, Centrallaboratoriet, Oslo, Norway

Glucose exerts a pronounced inhibitory effect upon the respiration of ascites tumor cells, a phenomenon also called the Crabtree effect. In an attempt to approach this problem the glycolysis and the tricarboxylic acid cycle of the ascites tumor cells were studied under various conditions.

Ascites cells (30—40 mg protein) incubated in phosphate buffer for 1 h at 37° with excess glucose as substrate were found to accumulate 1—2 μM of a barium insoluble fructose ester, assumed to be fructose-diphosphate.

In the presence of glucose (10 μM/ml), the removal of inorganic phosphate (20 μM/ml) from the medium increased the oxygen uptake by 25—50 % and decreased the glucose uptake

as well as the lactic acid formation by 30—50 %, while the blank respiration was unaffected. In this experiment the cells were incubated in trisbuffer with and without phosphate, and special care was taken to maintain the same ionic concentrations of sodium and potassium. The oxygen uptake was measured in a Warburg apparatus for 1 h at 37°. This experiment is in apparent contrast to the results reported by Ibsen, Mc Carty and Mc Kee [1]. These authors operated with glucose concentrations of less than 3 μM/ml and measured the oxygen uptake during a 3 h period. The small glucose concentrations employed may explain the discrepancy, because in the presence of phosphate (20 μM/ml) more than twice as much glucose was taken up after 1 h by the cells (13—15 mg protein) in our experiments.

In iodoacetate (10^{-4} M) treated cells phosphate on the contrary slightly stimulated the respiration and exerted no appreciable effect upon glucose uptake or lactic acid formation.

Increasing amounts of iodoacetate (0—1.5×10^{-4} M final concn.) successively enhanced the oxygen uptake of ascites cells incubated with glucose as substrate in a way fairly parallel to the normalization of the pH, while the blank respiration decreased slightly. Judged from the glucose uptake and the formation of fructose-diphosphate and lactic acid, an excess of adenosinediphosphate is likely to be formed extramitochondrially in IAA poisoned cells. The still existent Crabtree effect may be explained in accordance with Rackers shuttling theory [2] if one presumes a rate difference as to the permeation of adenine nucleotides in and out of the mitochondria.

Dinitrophenol (DNP, 10^{-4} M) increased the glucose uptake and lactic acid formation markedly. DNP initially stimulated the oxygen uptake more than the blank when glucose was substrate, but fell off earlier.

Excess fumarate completely abolished the glucose inhibition of the respiration in malonate treated cells. The oxygen uptake was also unaffected by malonate in the presence of glucose and fumarate. Glucose did not appreciably affect the citrate formation from fumarate in these cells. Glucose increased the concentration of α-ketoglutarate and reduced the formation of succinate when the cells were incubated in the presence of excess citrate and malonate. Under similar conditions glucose markedly inhibited the oxygen uptake in the presence of excess citrate or α-ketoglutarate.

Hence there was found no evidence for an inhibition of the tricarboxylic acid cycle between fumarate and citrate by glucose. The results may be explained by assuming a partial block of the cycle between α-ketoglutarate and succinate and that this step is rate limiting of the overall mitochondrial respiration in the presence of glucose.

1. Ibsen, K., Mc Carty, B. and Mc Kee, R. W. *Federation Proc.* **15** (1956) 279.
2. Racker, E. *Annals New York Acad. Sci.* **63** (1956) 1017.

Estimation of Corticosteroid Metabolites in Urine

L.-O. Plantin, E. Diczfalusy and G. Birke

King Gustaf V:th Research Institute and Hormone Laboratory, The Womens Clinic, Karolinska sjukhuset, Stockholm 60, Sweden

During the last decade the importance of adequate methods for evaluation of the adrenocortical function has been more clearly recognized. We have compared the methods most used for corticosteroid determinations in urine and related them to the structure of the steroid hormones and their metabolites. We have worked especially with the method developed by Norymberski and coworkers which we think is superior to other methods [1,2]. This method converts, by an oxidation with sodium bismuthate, corticosteroids of certain types called 17-ketogenic steroids (17-KGS) to 17-ketosteroids (17-KS). Apart from the desired oxidative effect of the sodium bismuthate on the side chain at carbon atom 17, other effects appear which can cause faulty results. That is especially the case with dehydro*epi*androsterone, which is almost completely transformed to other products by the combined effects of sodium bismuthate and acid hydrolysis. The bismuthate probably causes an oxidation to the 5,6-epoxide which is then further rearranged by the acid hydrolysis. This deleterious effect can be minimised by using short oxidation time and it can be completely avoided by using the modification proposed by Appleby *et al.*[3]

A system has been worked out for the separation and estimation of the different more important corticosteroid metabolites in urine. It employs enzymatic hydrolysis of the corticosteroid conjugates with β-glucuronidase, oxidation of corticosteroids to 17-KS with sodium bismuthate, reduction of ketonic groups to

hydroxyl groups with potassium borohydride, separation with Girards reagent T of ketones from alcohols, chromatographic separation of the 17-KS formed and infrared spectrographic identification of the 17-KS. This indirect identification system will be more completely worked out with the help of radioactive steroids and applied to different clinical problems.

1. Norymberski, J. K., Stubbs, R. D. and West, H. F. *Lancet* **1** (1953) 1276.
2. Diczfalusy, E., Plantin, L.-O., Birke, G. and Westman, A. *Acta Endocrinol.* **18** (1955) 356.
3. Appleby, J. I., Gibson, G., Norymberski, J. K. and Stubbs, R. D. *Biochem. J. London* **60** (1955) 453.

ACTA CHEMICA SCANDINAVICA 10 (1956) 1061—1067

The Amino Acid Composition of a Melanophore-expanding Peptide from Pig Pituitary Gland

PAUL ROOS

Institute of Biochemistry, University of Uppsala, Uppsala, Sweden

The amino acid composition of a melanophore-expanding peptide isolated from pig pituitaries has been investigated by chromatography on Dowex 50 columns. Tryptophan was determined spectrophotometrically. The analyses indicate the following 18 amino acid residues in the molecule (mol. wt. 2176):

Asp_2 Glu_2 Gly_2 Ser Met Pro_2 Phe Tyr Try His Lys_2 Arg.

In a previous communication [1] the isolation from acetone-dried pig posterior lobe powder, of an electrophoretically homogeneous fraction, a peptide, possessing a high melanophore-expanding activity, has been reported. Isolation and amino acid analysis of a melanophore-expanding hormone from pig pituitary gland have also been reported by Lerner and Lee [2], and by Benfey and Purvis [3]. Their substances differed considerably in the amino acid composition, and this disagreement prompted the publication of the present investigation.

In the following experiments acid hydrolysates of the peptide have been analyzed by chromatography on columns of Dowex 50—X4 and of Dowex 50—X8, using the methods of Moore and Stein [4,5]. The concentrations of the amino acids in the effluent fractions were in all experiments determined by the modified reagent described by Moore and Stein [6]. Tyrosine and tryptophan have been determined spectrophotometrically according to Goodwin and Morton [7], and the occurrence of cystine and cysteine have been tested by paper electrophoresis of a sample previously oxidized with performic acid according to Thompson [8] and then hydrolyzed with 6 N hydrochloric acid.

The investigation was started with chromatography on columns of Dowex 50—X4. This method, however, did not give satisfying separations of all the present acids, and, furthermore, difficulties arose in the determination of the correct base-line (caused by ammonia) in the vicinity of the lysine and histidine peaks. Complementary analyses were therefore performed according to the older method of Moore and Stein on Dowex 50 of the stronger crossed-linked type. All the methods mentioned above have given a satisfactory determination of the amino acid composition.

EXPERIMENTAL

From a pure specimen, dried over phosphorus pentoxide *in vacuo*, samples weighing about 2 mg were taken for analysis. The peptide was dissolved in 1.0 ml 6 N hydrochloric acid and hydrolyzed in a sealed Pyrex tube. The hydrolytic conditions were varied (see Table 1) in order to make sure that all peptide linkages were split and in order to obtain indications of the reaction orders of the amino acids being decomposed. The hydrolysate was quantitatively transferred to a small beaker (5 ml) and the hydrochloric acid removed over sodium hydroxide pellets in a vacuum desiccator. The dry residue was dissolved in 1 ml buffer solution, according to the directions given by Moore and Stein. When using Dowex 50-X4, the column was 0.9 × 150 cm; for the separations on Dowex 50-X8, the column used for the acidic and neutral acids was 0.9 × 115 cm; and that used for the basic amino acids was 0.9 × 15 cm. The fractions were collected by means of an automatic fraction collector and analyzed for the amino acids with ninhydrin. The optical density readings were made with a Beckman B spectrophotometer. The integration for each amino acid was performed by simple addition of the ninhydrin color values (in leucine equivalents in micromoles), after subtracting the base-line value near the amino acid peak. With the modified ninhydrin reagent an investigation of the color yields of the amino acids was carried out. The acids were dissolved in the buffer solutions, in which they emerge from columns of Dowex 50—X4 and of Dowex 50—X8 in the current chromatographic procedures. The found values agree, within the experimental errors, with those which have been given by Moore and Stein [6] when using the buffers described by them for Dowex 50—X4.

The substances in the different peaks of the column chromatograms were identified by paper chromatography, paper electrophoresis, or specific reactions, according to the following procedure. In order to locate the different peaks, 0.5 ml of every other fraction (1 ml) was boiled with ninhydrin. All fractions which belonged to the same peak were then desalted on ion exchange resin according to Drèze, Moore and Bigwood [9], using columns of 0.9 × 10 cm. The salt-free eluates were then evaporated to dryness. For the identification of the acidic and neutral amino acids paper chromatography was used, and for that of the basic amino acids paper electrophoresis was used. In addition, the Pauli test, modified according to Sanger and Tuppy [10], and the reaction of Sakaguchi, as described by Jepson and Smith [11], gave an additional identification method for histidine and arginine respectively.

The presence of methionine could only be demonstrated in one of the methods of Moore and Stein [4,5], and therefore it was necessary to confirm the presence of this amino acid by an independent method. One sample of the intact hormone and one of methionine were oxidized with performic acid according to Thompson [8]. The oxidized hormone, free from hydrogen peroxide, was hydrolyzed for 30 hours at 120° with 6 N hydrochloric acid. A first separation of the acids was achieved by paper electrophoresis in 0.05 M borate buffer (pH = 8.7), when using an apparatus constructed by Porath and Jerstedt [12], which permits electrophoresis in one direction and succeeding chromatography in the perpendicular direction. After the electrophoresis the paper was dried, the oxidized methionine was put on near the edge of the paper as a reference, and the acids were separated by descending chromatography in a system of eighty parts of pyridine and twenty parts of the 0.05 M borate buffer.

An independent investigation of the occurrence of cysteine and cystine was also made. One sample of the peptide and one of cystine were simultaneously oxidized with performic acid according to Thompson. The peptide hydrolysate was subjected to paper electrophoresis at pH 4.9, using 0.1 M pyridine-acetic acid buffer. The oxidized cystine and a mixture of cysteic acid, aspartic acid, glutamic acid, and lysine were used as references.

For the analysis for tyrosine and tryptophan [7], 1.5 mg of the peptide was dissolved in 5 ml 0.1 M NaOH. Readings of the ultraviolet absorption at 280 and 294.5 mμ were made with a Beckman DU spectrophotometer using 1 cm quartz cells. The molar extinction coefficients for tyrosine and tryptophan were determined at the same wave-lengths, and from the measurements it was possible to calculate the molar ratio of tyrosine to tryptophan.

In order to find out if the ammonia in the total hydrolysate originated from amide nitrogen or from another source, the amide nitrogen of the peptide was determined by the Conway microdiffusion technique. The Conway vessels were provided with a liquid seal according to Öbrink [13], and the procedure was essentially the same as that of Hirs, Stein and Moore [14]. 3.28 mg of the peptide was dissolved in 1.00 ml of 1 N H_2SO_4. The solution was divided into two equal parts and heated in sealed Pyrex tubes at 100°, one tube for 4 hours, the other for 8 hours. 0.2 ml aliquots were transferred from the tubes to the Conway vessels containing 0.4 ml of 0.02 N H_2SO_4 in the inner chamber. The sample in the outer chamber was brought to pH 10 to 11 by addition of 1 ml of the alkaline solution (see Hirs *et al.*[14]), which was also used in the seal of liquid. After standing overnight at room temperature, 0.15 ml aliquots from the inner chamber were analyzed for NH_3 with the modified ninhydrin reagent [6]. The technique was checked on an electrophoretically homogeneous preparation of asparagine.

RESULTS AND DISCUSSION

The elution curve obtained from a run on a column of Dowex 50—X4 is presented in Fig. 1. The time of hydrolysis was 30 hours at 120°. The separation of the acids was not as good as was expected. This was especially the case for tyrosine and phenylalanine, which emerged together as one symmetric peak. There was no separate ammonia peak, but ammonia caused an elevated base-line color in the region of lysine and histidine, which made the exact determination of these acids difficult. The ninhydrin-positive peak X, only given by this method and not by the Dowex 50—X8 method, could not be identified as one of the common amino acids.

A two-dimensional chromatogram run with a hydrolysate of the peptide prepared under identical conditions to those mentioned above gave no spot which could account for X. The system used was *n*-butanol-acetic acid-water, followed by phenol, pH 9.3 borate buffer [15].

In Figs. 2 and 3 the results obtained, respectively, with a long and short column of Dowex 50—X8 are shown. The time of hydrolysis was 40 hours at 120°. The amino acids were all completely separated except tyrosine and phenylalanine. A peculiarity, however, was that this method did not give any methionine.

The check of methionine as methionine sulfone (see Experimental) gave a distinct spot, which in color and position agreed with the only spot given by the simultaneously oxidized methionine. The occurrence of methionine was further confirmed by the sulphur content and by the absence of cysteine and cystine. The peptide was found to contain 1.47 % S, which corresponds to one gram atom sulphur per mole (molecular weight approximately 2 500, as obtained by a recent determination at this Institute by the method of Archibald [16]), and as the test of cysteine and cystine gave a negative result (see Fig. 4), the total sulphur must come from methionine.

In Table 1 the analytical data from various experiments on Dowex 50 columns are collected. From the values in the table it appears that 15 hours at 115° is too short a time for complete hydrolysis, and that a hydrolysis for 50 hours at 120° is rather long. Especially serine is decomposed to a large extent.

The runs on short columns of Dowex 50—X8 gave a separate ammonia peak (Fig. 3). If the ammonia values in the table are corrected for ammonia

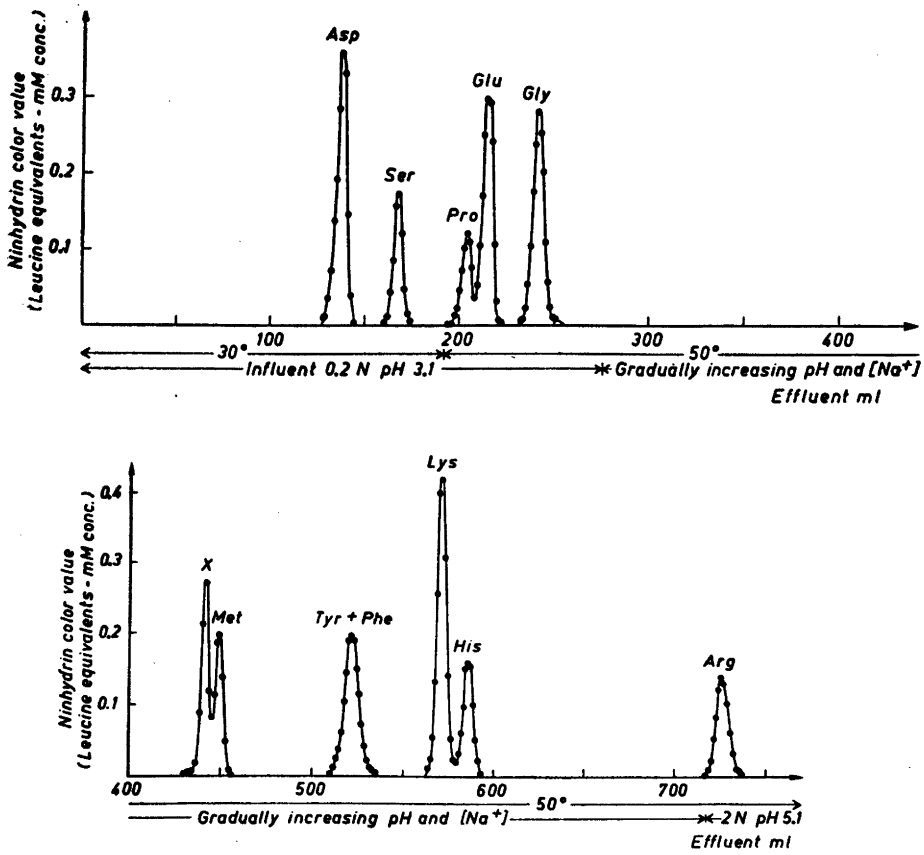


Fig. 1. Elution curve for a 30 hour hydrolysate of the peptide at 120° on a 0.9 × 150 cm column of Dowex 50—X4. For the run shown 1.874 mg of peptide hydrolysate was used.

from the destruction of serine, they indicate the presence of one amide group in the molecule. When using the Conway microdiffusion technique, however, the found ammonia values, after 4, respectively 8 hours of hydrolysis, were 3.8 and 4.4 μmoles per 100 mg of the peptide, which is only about 0.1 amide group per molecule. The check of the method on asparagine gave after 4 hours of hydrolysis 1.0 ± 0.1 amide group per molecule. Thus it seems necessary to assume another source of the ammonia in the total hydrolysate than amide nitrogen.

The molar ratio of tyrosine to tryptophan was found to be [7] 1.07, and this together with the values in the table give the following empirical formula of the peptide:

$$Asp_2\ Glu_2\ Gly_2\ Ser\ Met\ Pro_3\ Phe\ Tyr\ Try\ His\ Lys_2\ Arg.$$

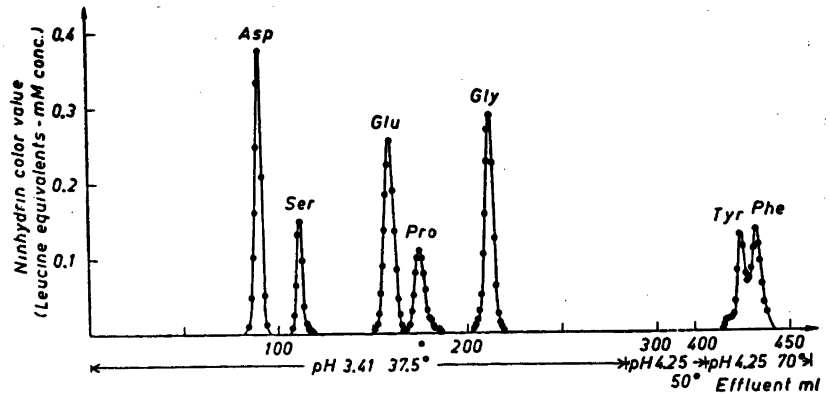


Fig. 2. Elution curve for the determination of the acidic and neutral amino acids on a 0.9 × 115 cm column of Dowex 50—X8. The time of hydrolysis was 40 hours at 120°. For the run illustrated 1.990 mg of peptide hydrolysate was used.

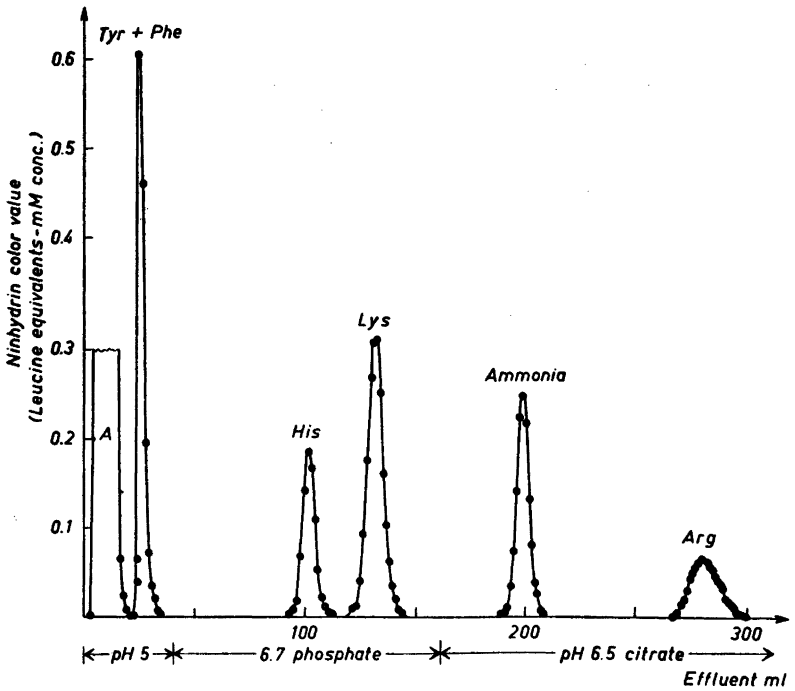


Fig. 3. Elution curve for the determination of the basic amino acids and ammonia on a 0.9 × 15 cm column of Dowex 50—X8. The time of hydrolysis was 40 hours at 120°. For the run illustrated 1.851 mg of peptide hydrolysate was used. The large peak, A, comprised all the amino acids emerging before tyrosine and phenylalanine.

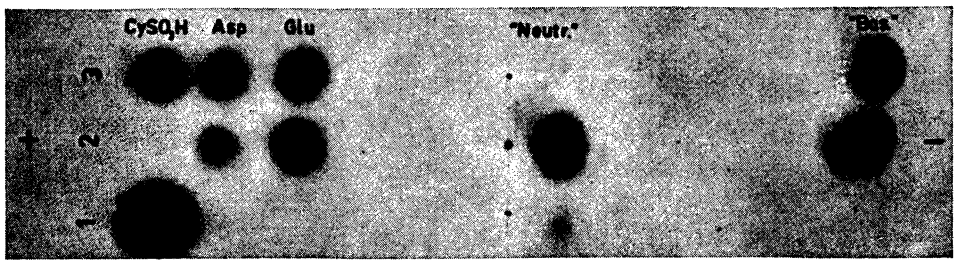


Fig. 4. Electrophoretic patterns of 1) cystine oxidized according to Thompson, 2) the active peptide oxidized according to Thompson and then hydrolyzed for 20 hours at 120°, 3) a mixture of cysteic acid, aspartic acid, glutamic acid, and lysine.

The results in this analysis differ considerably from those given by Lerner and Lee [2], who reported the presence of alanine, valine, cystine, leucine and threonine, which were not found in this investigation. Furthermore, they did not find histidine and did not analyze for methionine. Benfey and Purvis [3] reported the same amino acids as found in this work, but their minimum number of residues per molecule were twice those in Table 1 for all acids except glycine, methionine and proline.

Table 1. Analytical data from various experiments on Dowex 50 columns.

Ion exchange	Dowex 50−X4			Dowex 50−X8				Calculated integral numbers of residues for mol. wt. 2 500 *
Dimension of the column	0.9 × 150 cm			0.9 × 115 cm		0.9 × 15 cm		
Hydrolytic conditions	15 h at 115°	30 h at 120°	50 h at 120°	40 h at 120°	40 h at 120°	30 h at 120°	40 h at 120°	
Amount of hydrolysate	1.974 mg	1.874 mg	1.865 mg	1.832 mg	1.990 mg	1.832 mg	1.851 mg	
Amino acids	Micromoles/100 mg peptide							
Aspartic acid	83.6	90.6	81.0	84.3	84.6			2
Glutamic acid	75.4	83.9	86.1	88.2	86.6			2
Glycine	84.9	85.1	84.5	86.2	85.4			2
Serine	38.9	36.7	20.2	22.3	28.9			1
Methionine	34.5	42.3	36.5					1
Proline	126.5	129.6	124.0	113.7	133.6			3
Phenylalanine	29.3	37.0			43.2	} 73.5	} 79.1	1
Tyrosine	30.3	37.0			36.3			1
Histidine	42.1	43.6	46.8			41.8	42.0	1
Lysine	77.2	90.0	88.7			85.9	91.2	2
Arginine	41.5	41.4	42.7			38.8	43.3	1
Ammonia						53.2	69.0	

* The approximative value found in the ultracentrifuge. The molecular weight calculated on the basis of the integral numbers of residues including the tryptophan residue, amounts to 2 176.

The author wishes to thank Professor A. Tiselius for kind interest in this work. The author is also indebted to Dr. J. Porath for advice and encouragement.

This work has been supported by a grant from the *Swedish Natural Science Research Council.*

Added in proof: Since this manuscript was submitted for publication the amino acid analysis has been repeated on a Dowex 50—X4 column. The results obtained were in complete agreement with those reported in the text, except that in this case the unidentified component X did not appear. The author is indebted to Mr. M. Rees, Department of Biochemistry, Cambridge, for his assistance in carrying out this analysis.

REFERENCES

1. Porath, J., Roos, P., Landgrebe, F. W. and Mitchell, G. M. *Biochim. et Biophys. Acta* **17** (1955) 598.
2. Lerner, A. B. and Lee, T. H. *J. Am. Chem. Soc.* **77** (1955) 1066.
3. Benfey, B. G. and Purvis, J. L. *J. Am. Chem. Soc.* **77** (1955) 5167.
4. Moore, S. and Stein, W. H. *J. Biol. Chem.* **211** (1954) 893.
5. Moore, S. and Stein, W. H. *J. Biol. Chem.* **192** (1951) 663.
6. Moore, S. and Stein, W. H. *J. Biol. Chem.* **211** (1954) 907.
7. Goodwin, T. W. and Morton, R. A. *Biochem. J., London* **40** (1946) 628.
8. Thompson, E. O. P. *Biochim. et Biophys. Acta* **15** (1954) 440.
9. Drèze, A., Moore, S. and Bigwood, E. J. *Anal. Chim. Acta* **17** (1954) 554.
10. Sanger, F. and Tuppy, H. *Biochem. J., London* **49** (1951) 463.
11. Jepson, J. B. and Smith, I. *Nature* **172** (1953) 1100.
12. Porath, J. and Jerstedt, S. *To be published.*
13. Öbrink, K. J. *Biochem. J. London* **59** (1955) 134.
14. Hirs, C. H. W., Stein, W. H. and Moore, S. *J. Biol. Chem.* **211** (1954) 941.
15. Levy, A. L. and Chung, D. *Anal. Chem.* **25** (1953) 396.
16. Archibald, W. *J. Phys. & Colloid Chem.* **51** (1947) 1204.

Received March 24, 1956.

ACTA CHEMICA SCANDINAVICA 10 (1956) 1068—1070

Syntheses of Dimethylhydrazoniumethyl Esters of Aliphatic Dicarboxylic Acids

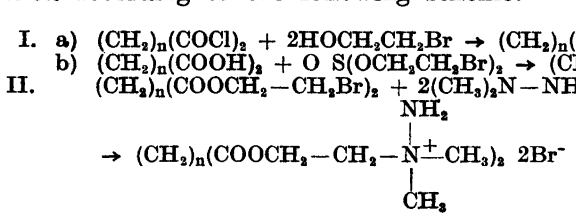
L.-E. TAMMELIN

Research Institute of National Defence, Dept. 1, Sundbyberg 4, Sweden

The choline analogue N′,N′-dimethyl-N′-hydroxyethylhydrazonium bromide has been prepared.

The bis-(ω-bromoethyl)-esters of oxalic, malonic, succinic, glutaric and adipic acids have been prepared. It is shown that these esters, except the oxalic ester, react with unsym. dimethylhydrazine in ether at 25° C yielding a product which is a bis quaternary ammonium compound of the N′,N′-dialkyl-N′-amino-ammonium type. The compounds are analogous to choline esters and have neuro-muscular blocking effects.

It has been shown by Renouf[1] that unsym. dimethylhydrazine reacts with alkyl halogenides to form N′,N′-dimethyl-N′-alkyl-N′-amino-ammonium halogenides, compounds having most of the properties of ordinary tetra alkyl ammonium compounds. An analogue of the acetylcholine has been synthesized by Schuler *et al.*[2] which contains the N′,N′-dimethyl-N′-amino-ammonium group. The purpose of this paper is to report methods of syntheses of similar analogues of succinylcholine and its homologues. The synthesis was performed according to the following scheme:



I. a) $(CH_2)_n(COCl)_2 + 2HOCH_2CH_2Br \rightarrow (CH_2)_n(COOCH_2CH_2Br)_2 + 2HCl$

b) $(CH_2)_n(COOH)_2 + O\ S(OCH_2CH_2Br)_2 \rightarrow (CH_2)_n(COOCH_2CH_2Br)_2 + H_2SO_3$

II. $(CH_2)_n(COOCH_2-CH_2Br)_2 + 2(CH_3)_2N-NH_2 \rightarrow$

$\rightarrow (CH_2)_n(COOCH_2-CH_2-\overset{NH_2}{\underset{CH_3}{\overset{|}{\underset{|}{N^+}}}}-CH_3)_2\ 2Br^-$

According to II the resulting product is analogous to a choline ester, except that choline is substituted for N′,N′-dimethyl-N′-hydroxyethyl-hydrazonium bromide. This compound was also synthesized.

EXPERIMENTAL

Bis-(ω-bromoethyl) esters of the aliphatic dicarboxylic acids

Unsym. dimethylhydrazine was prepared according to H. H. Hatt [3].

a) The bis-(ω-bromoethyl)esters of oxalic, malonic, succinic, glutaric and adipic acids were prepared as follows. 1 Mole of acid dichloride in 500 ml of benzene was added to 3 moles of ethylenebromhydrine and 1 mole of potassium carbonate in 500 ml of benzene. Nitrogen was bubbled through the reaction mixture and the reaction vessel was fitted with a reflux condenser and sealed with calcium chloride to eliminate moisture. The reaction was complete in 2 hours after which the potassium chloride was filtered off, the solution treated with calcium chloride, filtered again and finally fractioned by distillation. The esters were distilled *in vacuo*. For data see Table 1.

b) *A method according to Voss and Blanke* [4] was also tested for the preparation of bromoethyl esters of aliphatic dicarboxylic acids. The esters of oxalic and glutaric acids were prepared. For data see Table 1.

Table 1.

ω-Bromo-ethyl-ester of	Formula	M	Method of preparation	b. p. °C/mm Hg	m. p. °C	n_D^{20}	d_4^{20}	MR		% Br		Yield calc. on acid in %
								calc.	found	calc.	found	
Oxalic acid	$C_6H_8O_4Br_2$	304.0	a, b	122—124/0.25	54—55	—	—	—	—	52.8	52.7	(a) 45 (b) 60
Malonic acid	$C_7H_{10}O_4Br_2$	318.0	a	152/1	<20	1.5000	1.7393	53.1	53.7	—	—	(a) 57
Succinic acid	$C_8H_{12}O_4Br_2$	332.0	a	161/1	<20	1.5012	1.6990	57.7	57.7	—	—	(a) 63
Glutaric acid	$C_9H_{14}O_4Br_2$	346.0	a, b	148/0.3	<20	1.4962	1.6293	62.4	62.1	—	—	(a) 30 (b) 63
Adipic acid	$C_{10}H_{16}O_4Br_2$	360.1	a	156—161/0.3	<20	1.4928	1.5612	67.1	67.0	—	—	(a) 64

Bis-(ω-bromoethyl) ester of oxalic acid. 3.3 Moles of bis-(ω-bromoethyl)sulfite and 1 mole of oxalic acid [$(COOH)_2$, $2H_2O$] were mixed and heated on a steam bath for two hours. The reaction mixture was extracted with ether and the ether solution washed twice with water and finally with a sodium bicarbonate solution. The solution was dried with sodium sulfate and fractionated by distillation. The ester was distilled *in vacuo*. For data see Table 1.

Bis-(ω-bromoethyl) ester of glutaric acid. 1.1 Moles of bis-(ω-bromoethyl)sulfite, 1 mole of glutaric acid and one drop of conc. sulfuric acid were mixed and heated for two hours on a steam bath. The reaction mixture was extracted with ether and the ether solution was washed twice with water and finally with a sodium bicarbonate solution. The solution was dried with sodium sulfate and fractionated by distillation. The ester was distilled *in vacuo*. For data see Table 1.

Dimethyl-hydrazoniumethyl esters of the aliphatic dicarboxylic acids

1 Mole of the bis-(ω-bromoethyl)ester and 2.2 moles of unsym. dimethylhydrazine were mixed with about eight volume parts of dry ether in a glass stoppered round bottomed flask. After three weeks at 25° C a crystalline or viscous precipitate was filtered off from the ether. When viscous products occurred the preparation was stored for a few

Table 2.

Acid esterified by N′,N′-dimethyl-N′,-hydroxyethyl hydrazonium bromide	Formula	M	m. p. °C	% Br		% C		% H		Yield in % of theoretical
				calc.	found	calc.	found	calc.	found	
Malonic acid	$C_{11}H_{26}O_4N_4Br_2$	438.2	80—100	36.5	35.9	30.2	30.2	6.0	6.0	55
Succinic »	$C_{12}H_{28}O_4N_4Br_2$	452.2	158—164	35.4	34.6	31.8	31.6	6.2	6.1	62
Glutaric »	$C_{13}H_{30}O_4N_4Br_2$	466.2	104	34.3	34.4	33.6	33.7	6.5	6.6	50
Adipic »	$C_{14}H_{32}O_4N_4Br_2$	480.3	108	33.3	33.8	35.0	35.0	6.7	6.5	57

days in a desiccator for crystallization. The compounds were recrystallized from ethanol. For data see Table 2.

N′,N′,-dimethyl-N′-hydroxyethylhydrazonium bromide

1 Mole of ethylenebromhydrine and 1.1 moles of unsym. dimethylhydrazine were mixed with about eight volume parts of dry ether in a glass stoppered round bottomed flask. After three days the colourless precipitate was filtered off. (Yield 76 %; m. p. < 50°, hygroscopic). (Found: C 25.8; H 7.0; Br 43.6. Calc. for $C_4H_{13}N_2OBr$ (185.1) C 25.9; H 7.1; Br 43.2).

The ω-bromo-ethyl esters of the aliphatic dicarboxylic acids have been shown to react with unsym. dimethylhydrazine with the formation of N′,N′-dimethyl-N′-amino-ammonium-ethyl ester bromides, although the reaction does not seem to be possible with the oxalic ester, yielding precipitates which differ in composition from the end product of reaction II. The esters of malonic, succinic, glutaric and adipic acids are all colourless crystalline compounds of salt character. They are easily soluble in water and the bromine content has been determined by means of directly applied argentometric titration. Since this was possible the compounds are completely dissociated in bromine ions and the organic cations. By means of pH-measurements and potentiometric titrations the amino groups have been shown to fail in protolytic properties in ordinary water solutions and seem even in this respect to correspond to the third methyl group in choline. A report on the pharmacological properties of these compounds will be given elsewhere.[5] It might be worth mentioning, however, that they possess neuromuscular blocking activity, but are less potent than the corresponding choline esters.

My sincere thanks are due to the Director of this Institute, Professor G. Ljunggren, for his kind interest in this work.

REFERENCES

1. Renouf, E. *Ber.* **13** (1880) 2172.
2. Schuler, F. W. and Calvin, H. *Arch. intern. pharmacodynamie* **88** (1951) 351.
3. Hatt, H. H. *Org. Syntheses Coll. Volume* **II** (1946) 211.
4. Voss, V. and Blanke, E. *Ann.* **485** (1931) 258.
5. Fredriksson, T. *Acta Pharmacol. Toxicol.* (1957), *in press.*

Received April 13, 1956.

ACTA CHEMICA SCANDINAVICA 10 (1956) 1071—1076

Determination of the Distribution Constant of a Compound Reacting with One of the Phases

LENNART LARSSON

Research Institute of National Defence, Dept 1, Sundbyberg 4, Sweden

A formula has been deduced for calculation of the distribution constant of a compound which reacts with one of the phases according to a first order reaction. The application of the formula is illustrated by the distribution of 2-methoxy-ethyl nicotinate between xylene and water. Another formula has been deduced in the case of association of the compound in one phase in addition to its decomposition in the other.

The distribution constant of a compound which reacts with one of the phases can be accurately determined if the concentrations of the solute are determined in each phase. Distribution constants, however, are generally evaluated from determinations of the concentration of the solute in one phase, the concentration in the other being obtained as a difference. In the case of reaction between the compound and one of the phases the total amount of compound is reduced ,and an erroneous concentration in the unanalysed phase is obtained. Hence the error of the distribution constant will be considerable. In this investigation it has been found that the distribution constant of a compound can also be calculated from measurements of its reaction rate in the phase in question.

Let us consider the concentrations in the two phases of a compound distributed between an organic solvent and water, when the compound hydrolyses in the aqueous phase according to a first order reaction.

The following symbols will be used:

$[\ ]_{aq}$ or $[\ ]_{org}$ = concentrations in aqueous and organic phases, respectively;
α = slope of the line, when log $[A]_{aq}$ is plotted against t;
A = unhydrolysed compound;
A_2 = double molecule of A;
D = optical density;
k = reaction rate constant of A in water;
k_{ass} = association constant of A in organic phase;
k_d = distribution constant of A between organic and aqueous phase;

P = one of the hydrolysis products;
t = time;
v = phase volume.

Assuming that at a given moment the concentration of the hydrolysis product is

$$[P]_{aq} = \int_0^t k \cdot [A]_{aq} dt \tag{1}$$

Then the total amount of the compound and its hydrolysis product is

$$v_{org}[A]_{org} + v_{aq}[A]_{aq} + v_{aq}[P]_{aq} = \text{const.} \tag{2}$$

Further the distribution constant is

$$k_d = \frac{[A]_{org}}{[A]_{aq}}$$

On differentiating eqn. (2) we obtain

$$v_{org}d[A]_{org} + v_{aq}d[A]_{aq} + v_{aq}d[P]_{aq} = 0 \tag{4}$$

and on substitution of $d[P]_{aq}$ which according to eqn. (1) is

$$d[P]_{aq} = k \cdot [A]_{aq} dt \tag{5}$$

in eqn. (4), we get

$$\frac{v_{org}}{v_{aq}} \cdot \frac{d[A]_{org}}{dt} + \frac{d[A]_{aq}}{dt} = -k \cdot [A]_{aq} \tag{6}$$

From eqn. (3) we obtain on differentiating with respect to time

$$\frac{d[A]_{org}}{dt} = k_d \frac{d[A]_{aq}}{dt} \tag{7}$$

On introduction of this expression into eqn. (6) we get

$$\frac{d[A]_{aq}}{dt}\left(\frac{v_{org}}{v_{aq}} k_d + 1\right) = -k \cdot [A]_{aq} \tag{8}$$

When this equation is integrated, we obtain

$$\frac{k \cdot t}{\frac{v_{org}}{v_{aq}} k_d + 1} = \ln \frac{[A]^0_{aq}}{[A]_{aq}} \tag{9}$$

where $[A]^0_{aq}$ is the concentration of A in the aqueous phase at distribution equilibrium, at which time no hydrolysis is assumed to have occurred.

By plotting log $[A]_{aq}$ against t we get a straight line the slope of which is

$$|\alpha| = \frac{0.4343 \cdot k}{\frac{v_{org}}{v_{aq}} k_d + 1} \tag{10a}$$

or

$$k_d = \frac{v_{aq}}{v_{org}}\left(\frac{0.4343 \cdot k}{|\alpha|} - 1\right) \tag{10b}$$

If the compound is associated to some extent into double molecules in the organic phase, a straight line would not be obtained. On the assumption that such an association occurs, the distribution constant can be calculated from eqn. (11) which can be deduced analogously to eqn. (9).

$$k \cdot t = \left(\frac{v_{org}}{v_{aq}}\, k_d + 1\right) \overline{\ln} \frac{[A]^0_{aq}}{[A]_{aq}} + 4k_{ass} \cdot k_d^2 \frac{v_{org}}{v_{aq}} ([A]^0_{aq} - [A]_{aq}) \qquad (11)$$

where $k_{ass} = \dfrac{[A_2]_{org}}{[A]^2_{org}}$

EXPERIMENTAL

The application of the method is illustrated by determination of the distribution constant of 2-methoxy-ethyl nicotinate between xylene and a buffer solution at pH 9.15. At this pH the nicotinic ester may be regarded as completely unionized. The two phases are nearly insoluble in each other. Hydrolysis of the ester proceeds as a first order reaction, when the pH remains constant. In order to verify the result obtained with this method the distribution constant was also determined in the conventional manner from the concentrations of the ester in the aqueous phase before and after shaking to equilibrium. The hydrolysis of this compound is negligible during the time required for this experiment.

Materials. 2-Methoxy-ethyl nicotinate: To 17.7 g (0.10 mole) of the hydrochloride of nicotinyl chloride, prepared from nicotinic acid and thionyl chloride [1], was gradually added 22.8 g (0.30 mole) of 2-methoxy-ethanol. The reaction mixture was refluxed for two hours in a water bath. After cooling, the mixture was neutralized with a saturated solution of potassium carbonate and extracted three times with ether. After drying of the ether extract overnight the ether was evaporated, and the ester was distilled under reduced pressure; b.p. 80–83°/0.20–0.25 mm Hg. A solid, colourless product was obtained which was recrystallized from acetone. Yield 11.0 g (61 %). (Found: C 59.5; H 6.0, Calc. for $C_9H_{11}O_3N$: C 59.7 ;H 6.1.)

Buffer solution: A borax buffer solution with pH 9.15 was used. It was standardized at 25°C against 0.05 M solution of potassium hydrogen *o*-phthalate, pH 4.01[2], with a Radiometer pH-meter, type 3.

Xylene: Reagent grade; b.p. 139–140°; $n_D^{20} = 1.4957$.

Procedure I. All experiments were carried out in a thermostat at 25°C. Each series of experiments consisted of 6–8 samples with the same concentration. The 2-methoxy-

Table 1. The distribution constant of 2-methoxy-ethyl nicotinate calculated from the hydrolysis rate of the ester. $[A]_{org}$ *denotes the original ester concentration in xylene.*

v_{org}/v_{aq}	$[A]_{org}$ mmole/l	$a \times 10^3$ hours^{-1}	k_d
1:2	8.73	7.16	4.15
	6.57	6.90	4.38
1:1	8.01	4.11	4.35
	5.75	4.20	4.24
2:1	8.26	2.24	4.42
	5.45	2.25	4.39
		Mean value	4.32 ± 0.10

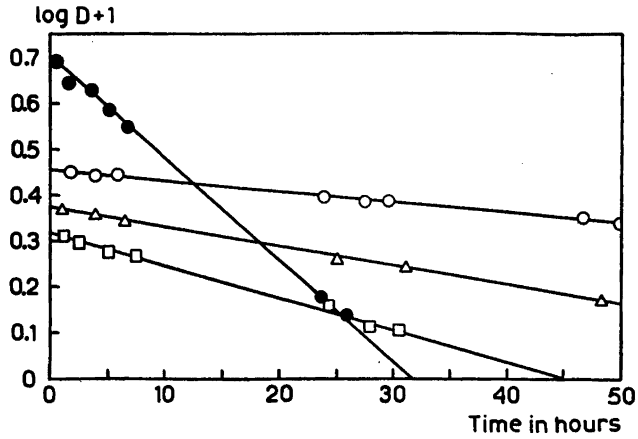


Fig. 1. Hydrolysis of 2-methoxy-ethyl nicotinate in buffer solution (●) *and in mixtures of xylene — buffer solution* v_{org}/v_{aq} *= 1:2* (□), v_{org}/v_{aq} *= 1:1* (△) *and* v_{org}/v_{aq} *= 2:1* (○).

ethyl nicotinate was dissolved in xylene; in this way a smaller amount of the compound came into contact with water, before equilibrium was attained, than if the compound was dissolved in buffer solution. The buffer solution was added at zero time. The mixtures were shaken mechanically in sealed ampoules which were withdrawn from the thermostat at annotated times. After separation and filtration, the concentration of unhydrolysed ester in the aqueous phase was determined colorimetrically with the method reported by Hestrin [3]. The colour intensities of the samples were measured in a 10 mm cell at 5 200 Å with a Beckmann B Spectrophotometer. In the different series both the concentration of ester and the ratio of the volumes of xylene to buffer solution were varied as shown in Table 1. The total volume of each sample was 30 ml. Preliminary mutual saturation of the immiscible layers was unnecessary, since it was found to have no effect on the distribution constant. The pH of the solutions was determined at the beginning and end of hydrolysis, and was found to remain constant within 0.01 pH unit. Because Beer's law was obeyed, the logarithm of the optical density rather than that of the concentration of unhydrolysed ester was plotted against time. This is illustrated in Fig. 1. From the slope of the line obtained the distribution constant was calculated by means of eqn. (10b).

The rate constant of hydrolysis of the ester in buffer solution alone was determined colorimetrically as described above and calculated from the first order equation

$$k = \frac{1}{t} \ln \frac{D^\circ}{D} \qquad (12)$$

Table 2. The rate constant for the hydrolysis of 2-methoxy-ethyl nicotinate.

$[A]_{aq}$ mmole/l	$k \times 10^2$ hours^{-1}
2.96	5.10
3.39	5.02
3.71	5.09

Mean value 5.07×10^{-2}

Table 3. The distribution constant of 2-methoxy-ethyl nicotinate calculated from the concentrations of the ester in both phases. $[A]_{aq}$ denotes the original ester concentration in the buffer solution.

v_{org}/v_{aq}	$[A]_{aq}$ mmole/l	D'	D	k_d
1:2	10.39	1.712	0.545	4.28
	5.33	0.884	0.273	4.48
	5.08	0.862	0.270	4.39
1:1	11.27	1.798	0.337	4.33
	7.53	1.316	0.253	4.20
	5.67	0.962	0.182	4.28
2:1	11.50	1.830	0.193	4.24
	6.17	1.070	0.114	4.19
	5.33	0.884	0.096	4.10
			Mean value	4.28 ± 0.11

where $D°$ and D are the optical densities at zero time and t time, respectively. The values obtained are given in Table 2.

Procedure II. Buffer solutions in which the ester was dissolved, were shaken with xylene for about 5 minutes. The concentration of ester and the ratio of the volumes were varied as in the previous experiment. The concentration of ester in the aqueous phase before and after shaking was determined colorimetrically as described in procedure I. The unshaken buffer solutions had to be diluted four times before they were analysed. The values of the optical density, D', given in Table 3 have been converted for this dilution. Mixtures shaken for 3, 6, 9, and 12 minutes showed that equilibrium was already attained after 3 minutes. As Beer's law proved to be valid, the distribution constant was calculated from

$$k_d = \frac{[A]_{org}}{[A]_{aq}} = \frac{v_{aq}}{v_{org}} \cdot \frac{D'-D}{D} \qquad (13)$$

where D' and D are the optical densities before and after shaking, respectively.

RESULTS AND DISCUSSION

From Tables 1 and 3 it will be seen that the distribution constant calculated from kinetic data is in close agreement with that obtained from analysis of the aqueous phase before and after shaking, and that the precision of the two methods is approximately the same. When the logarithm of the optical density is plotted against time (Fig. 1), straight lines are obtained, indicating that no appreciable association occurs in the xylene phase. Further confirmation of this is that the distribution constant is independent of concentration.

The kinetic method is of course more time-consuming than the other, but it is far more reliable. Eqn. (9) is, however, not exactly valid, because no account has been taken of the distribution rate of the solute. The internal controlling factor in this process is the rate of solute diffusion across the interfacial stationary films [4], but the thicknessses and surfaces of the interfacial films vary considerably with the experimental conditions. The rate of distribution will consequently be very difficult to determine. However, since equi-

librium is generally attained very rapidly [5], the method can be applied in all cases where the reaction rate is relatively low, or where the concentration of the solute in the indifferent phase is high compared to that of the reacting phase. The assumption made in eqn. (9) concerning $[A]^0_{aq}$, on the other hand, does not influence the accuracy, because zero time can just as well be taken as the moment when equilibrium is attained.

The method described may also be used in the study of rapid reactions, for the reaction rate can be reduced appreciably by adding a suitable solvent which must be immiscible with the reacting phase and readily dissolve the solute. One must consider that errors may arise from neglecting the rate of distribution and, in this case, from $[A]^0_{aq}$ too, if this value is used for determination of the distribution constant.

My thanks are due to the Director of the Research Institute of National Defence, Dept. 1, Professor G. Ljunggren, for the kind interest he has shown in this investigation.

REFERENCES

1. Späth, E. and Spitzer, H. *Ber.* **59** (1926) 1477.
2. Bates, R. G. *Electrometric pH Determinations.* John Wiley & Sons, Inc., New York, 1954, p. 81.
3. Hestrin, S. *J. Biol. Chem.* **180** (1949) 249.
4. Hunter, T. G. and Nash, A. W. *J. Soc. Chem. Ind.* **51** (1932) 285.
5. Barry, G. T., Sato, Y. and Craig, L. C. *J. Biol. Chem.* **174** (1948) 209.

Received April 12, 1956.

ACTA CHEMICA SCANDINAVICA 10 (1956) 1077—1082

Chromatography of Human Serum Cholinesterase

B. G. MALMSTRÖM, Ö. LEVIN and H. G. BOMAN

Institute of Biochemistry, Uppsala, and the Research Institute of National Defence, Department 1, Sundbyberg, Sweden

Human serum cholinesterase has been purified by chromatography on calcium phosphate and on the anion exchange resin Dowex 2. One milligram of the most highly active material, obtained by calcium-phosphate chromatography alone, hydrolyzes 13 000 micromoles of acetylcholine in 1 h at 37.5°. The chromatographic experiments show that this is not a homogeneous protein but that further purification can be achieved by rechromatographing on the same adsorbents.

Several methods for the partial purification of serum cholinesterase (ChE) have been developed [1]. The most active preparation from human serum has been obtained by low-temperature alcohol fractionation according to Surgenor and Ellis [2]. In the present communication, experiments will be described showing that an additional purification of the enzyme material can be achieved by chromatography on calcium phosphate [3,4] and on an anion exchange resin (Dowex 2) [5].

MATERIALS AND METHODS

Enzyme. A partially purified preparation of human serum ChE, fraction IV-6-3 of Surgenor and Ellis [2] (prepared by AB. Kabi, Stockholm), was used as the starting material for the chromatographic experiments.

Chromatographic Techniques. The preparation of calcium phosphate (hydroxylapatite) and details of the chromatographic procedure have been described [3,4]. Sodium phosphate buffers, pH 6.83, were used in all experiments. The enzyme was adsorbed at low ionic strength and eluted with increasing buffer concentrations.

An extensive description of protein chromatography on the anion exchange resin Dowex 2 has been published recently [5]. With this adsorbent, tris(hydroxymethyl) aminomethane (THAM)-HCl buffers, pH 7.3, were used. As in the case of calcium phosphate, adsorption of the protein was effected at low ionic strength and elution by increasing buffer concentrations.

All chromatographic runs have been performed at +4°.

The protein concentration of the eluate fractions was determined by ultraviolet absorption measurements at 280 mμ in the Beckman DU spectrophotometer using 1 cm cells. The protein components of the separate fractions were identified by paper electrophoresis; the solutions were concentrated by pressure dialysis before application to the paper.

Measurement of Enzyme Activity. For determining the ChE activity of the fractions, an indicator method was used. The substrate mixture employed had the following composition: (a) 0.01 M Na barbital; (b) 0.02 M KH_2PO_4; (c) 0.3 M KCl; (d) 0.0014 M HCl; (e) 0.05 M butyrylcholine iodide; and (f) 0.005 % bromothymol blue. To 3 ml of this solution, 0.1 ml of the sample was added, and the optical density at 610 mμ was immediately determined in a Beckman B spectrophotometer using 1 cm cells. The solution was then allowed to stand at 22° for 30 min. after which time the optical density was read again. The measured change in optical density allowed the estimation of the activity from a standard curve constructed by carrying serial dilutions of a solution of fraction IV-6-3 through the entire procedure. The activity unit was defined as the activity obtained when a solution containing 1 mg of IV-6-3/ml was used as sample.

The simplicity of the method described made it suitable for following the activity in the eluate fractions, but it could not be employed for accurate determinations of the specific activity of the starting material and purified fractions. For this purpose, the method of Hestrin [6] was used, and the activity was expressed as the number of micromoles of acetylcholine (AcCh) hydrolyzed in 1 h at 37.5° per mg of protein.

RESULTS

Fig. 1 gives part of the elution curve from an experiment with 360 mg of IV-6-3 on a column (15 × 4 cm) with 190 ml of calcium phosphate in equilibrium with 0.01 M phosphate buffer. The sample was dissolved in 35 ml of the same buffer and applied to the column. Elution was first carried out with 0.05 M buffer and fractions of about 5 ml volume were collected. The two zones that are obtained in this elution range are the ones shown in Fig. 1. They account for about 40 % of the added activity but contain only 10 % of the protein material applied. The remainder of the adsorbed proteins could be eluted with 0.3 M buffer but the specific activity in the zones obtained in this elution range was never higher than that of the starting material.

Fractions 40—44 from the experiment illustrated in Fig. 1 were combined (fraction A) and used for rechromatographing both on calcium phosphate and

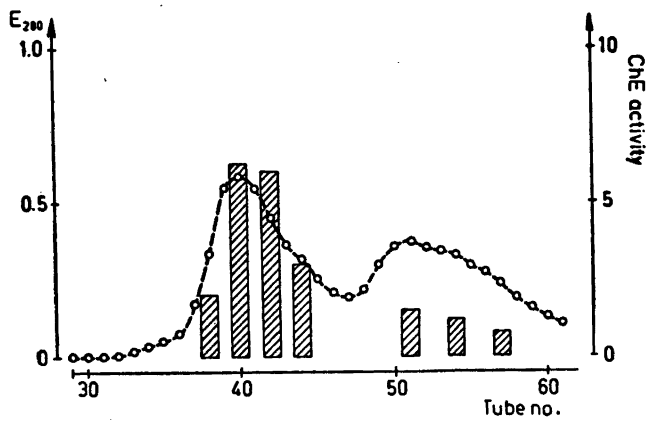


Fig. 1. The first part of a chromatogram obtained with 360 mg of IV-6-3 on a column with 190 ml of calcium phosphate. Elution was here carried out with 0.05 M phosphate buffer, pH 6.83. Open circles denote extinction at 280 mμ, and the blocks show the ChE activity.

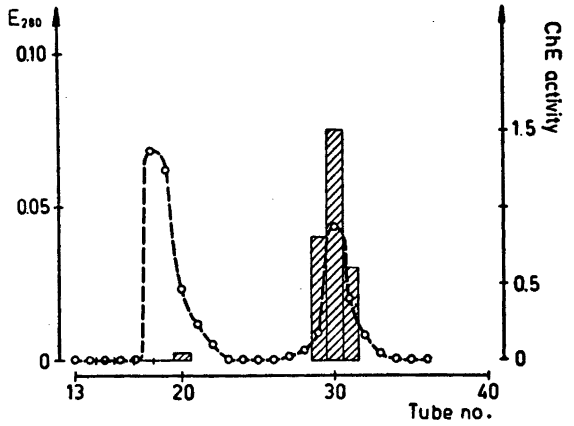


Fig. 2. Rechromatographing of fractions 40—44 from the experiment shown in Fig. 1 on a column with 7.5 ml of calcium phosphate. The first zone (tubes 18—22) was eluted with a gradient and the second one (tubes 29—32) with 0.1 M phosphate buffer, pH 6.83. Open circles denote extinction at 280 mμ, and the blocks show the ChE activity, zero acitivity being marked with a line.

on Dowex 2; the specific activity in the combined sample was about 10 times that of the starting material. The distribution of ultraviolet-absorbing material and activity seen in Fig. 1 indicate that a separation of the enzyme from contaminating proteins by step-wise elution would offer difficulties. Thus, gradient elution [7] was tried, but it was found that the enzyme zone was too wide to allow accurate measurements of concentration and activity. Instead the

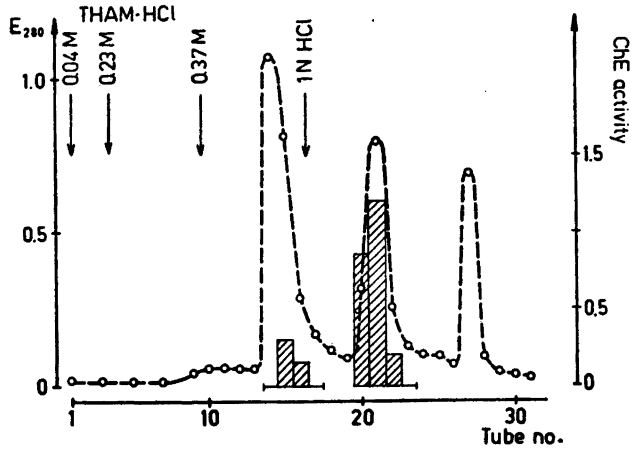


Fig. 3. Chromatography of 40 mg of IV-6-3 on a column with 180 ml of Dowex 2. The arrows indicate the start at the top of the column of the different elution agents. Open circles denote extinction at 280 mμ, and the blocks show the ChE activity, zero activity being marked with a line.

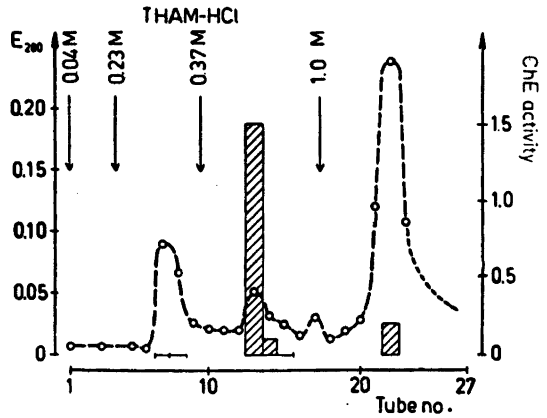


Fig. 4. Rechromatographing of fractions 40—44 from the experiment shown in Fig. 1 on a column with 34 ml of Dowex 2. The second zone (tubes 13—14), containing most of the activity, was eluted with 0.37 M THAM-HCl, pH 7.3. Open circles denote extinction at 280 mμ, and the blocks show the ChE activity, zero activity being marked with a line.

following procedure was adopted: After dialysis against 0.01 M phosphate buffer, 4.5 ml of the combined sample was applied to a column (9.5 × 1.0 cm) with 7.5 ml of calcium phosphate. Elution was first carried out with a linear gradient (discussed by Drake[7] as "case 4") between 0.03 and 0.08 M phosphate buffer, pH 6.83. The fraction volumes were 3.8 ml. When the first zone (tubes 18—22 in Fig. 2) had emerged (at about 0.04 M phosphate), the gradient was interrupted and elution with 0.1 M buffer was started. With this concentration a second zone (tubes 29—31 in Fig. 2) was eluted containing about 70 % of the activity applied. The most highly purified fraction (tube 29) was about 70 times more active than fraction IV-6-3.

Fig. 3 illustrates an experiment with 40 mg of IV-6-3 on a column with 180 ml of Dowex 2 in equilibrium with 0.04 M THAM—HCl. In this figure, as well as in Fig. 4, the arrows indicate the start at the top of the column of the different eluting agents. As can be seen, most of the material added is adsorbed at 0.04 M buffer concentration while three separate zones are obtained for the other three steps. Both the first and the second zone contain activity but most of it is present in the second one, the recovery being about 50 %.

Fig. 4 gives the results of an experiment in which ChE chromatographed once on calcium phosphate is run on Dowex 2. Five milliliters of the same solution used in the experiment in Fig. 2 were applied directly to a column with 34 ml of the resin. The first and last zone together account for about 80 % of the ultraviolet absorbing material while approximately 50 % of the activity applied was found in the second zone. The specific activity in tube 13 is approximately 40 times higher than that of IV-6-3.

The identification of the protein components is illustrated in Fig. 5, which shows a paper electrophoresis run on the starting material (denoted "0") and on material from the first two zones of an experiment similar to that in Fig. 3. The starting material is seen to be made up mainly of α_2-globulin with smaller

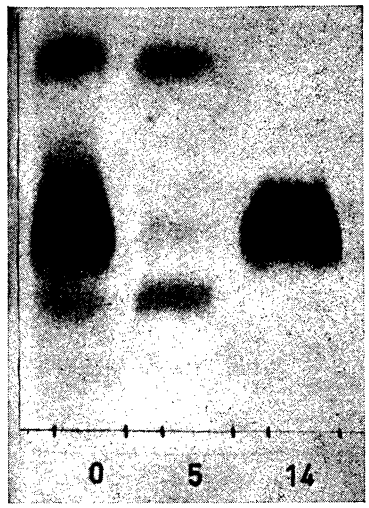


Fig. 5. Paper electrophoresis of IV-6-3 ("0") together with the first ("5") and second zone ("14") from a chromatographic experiment on Dowex 2, comparable to the one shown in Fig. 3.

amounts of albumin and β-globulin. The latter two components, with small amounts of α_2-globulin, are obviously eluted in the first zone ("5"), while most of the α_2-globulin, together with the enzyme, appears in the second zone ("14"). In the most highly purified fractions, the only protein component that could be identified had a mobility close to that of α_1-globulin. However, zone electrophoresis on cellulose columns (unpublished experiments) showed that the enzyme activity migrates somewhat slower than α_2-globulin, so that this component cannot be ChE.

Table 1 summarizes the maximum specific activities obtained in the experiments described herein.

The enzyme can also be purified directly from human serum using stepwise elution on Dowex 2 as described for the experiment illustrated in Fig. 3.

Table 1. Specific activity of ChE fractions.

Fraction	Maximum specific activity (μM AcCh hydrolyzed per mg of protein in 1 h at 37.5°)
Starting material (Cohn fraction IV-6-3)	175
One chromatographic run on calcium phosphate (tube 42, Fig. 1)	1 940
One chromatographic run on Dowex 2 (tube 20, Fig. 3)	423
Rechromatographing of "fraction A" on Dowex 2 (tube 13, Fig. 4)	7 700
Rechromatographing of "fraction A" on calcium phosphate (tube 29, Fig. 2)	13 000

The specific activity of the enzyme obtained after one chromatographic run is about 50 times that of human serum. The purification directly from serum can also be carried out by a displacement technique as described by Boman and Westlund [5].

DISCUSSION

Mutual displacement phenomena play an important role in chromatography [4,5] both on calcium phosphate and on Dowex 2. This is shown in Figs. 2 and 3, where it can be seen that the zones of the major part of the ultraviolet-absorbing material and of the enzymic activity do not coincide. This also demonstrates that even the most highly purified material is not homogeneous. The small amounts obtained prohibited the use of other purity criteria, such as electrophoresis and ultracentrifugation.

It should be stressed that the exact elution concentrations given here for the calcium phosphate experiments apply only to hydroxylapatite. Thus, the detailed directions for the preparation of the adsorbent [4] must be strictly adhered to. It is recommended that, before a new batch of calcium phosphate is used in a preparative chromatographic run, the elution concentrations are determined in an orientating experiment with a smaller column and smaller amounts of protein.

While the uneven distribution of protein and activity demonstrates inhomogeneity, it also indicates that further purification can be obtained by additional rechromatographing on these same adsorbents. On Dowex 2, ChE and α_2-globulin are eluted in the same range of THAM—HCl concentration, while these substances can be separated on calcium phosphate columns. Thus, it may be possible to use calcium phosphate alone for the purification of the enzyme, and, in any case, the procedure must start with chromatography on this adsorbent. It is, however, impossible as yet to decide which adsorbent is capable of giving the highest degree of purification on rechromatographing. A possible advantage of combining the two methods is the fact that the eluate from the calcium phosphate column can be applied directly to Dowex 2, thus obviating the need for dialysis. The main difficulty in carrying the purification further appears to be the fact that the concentration of ChE in serum is very low compared that of contaminating proteins. Thus, considerably larger amounts of starting material than those employed here would be necessary.

Acknowledgment. The authors are indebted to Professor A. Tiselius for helpful discussions. They also wish to thank Professor G. Ljunggren for his stimulating interest and generous support.

REFERENCES

1. Nachmansohn, D. and Wilson, I. B. in Colowick, S. P. and Kaplan, N. O. *Methods in Enzymology*, Academic Press, New York 1955, Vol. 1, p. 642.
2. Surgenor, D. M. and Ellis, D. *J. Am. Chem. Soc.* **76** (1954) 6049.
3. Tiselius, A. *Arkiv Kemi* **7** (1954) 443.
4. Tiselius, A., Hjertén, S. and Levin, Ö. *Arch. Biochem. and Biophys.*, Oct. (1956).
5. Boman, H. and Westlund, L. E. *Arch. Biochem. and Biophys.* **64** (1956) 217.
6. Hestrin, S. *J. Biol. Chem.* **180** (1949) 249.
7. Drake, B. *Arkiv Kemi* **8** (1955) 1.

Received April 26, 1956.

ACTA CHEMICA SCANDINAVICA 10 (1956) 1083—1096

New Spectrophotometric Methods for Investigation of the Respiratorical Enzymes of Yeast

H. LUNDEGÅRDH

Penningby, Sweden

Modern photo multiplier tubes have made it possible to observe the state of oxidation-reduction of respiratorical enzymes in living objects on the basis of accurate measurements of the extinction in the whole range of the spectrum. Leading principles for the construction of a new recording spectrophotometer, especially built for this purpose, are briefly presented. A survey is also given of the corrections by means of which the obstacles arising from optical interference of the pigments and from the turbidity of the object may be eliminated. A special technique has been elaborated for the observation of rapid changes in the steady states of the respiratorical enzymes of yeast.

The results regarding observed start lags and apparent velocity constants of reduction and reoxidation elucidate the order of activation of the following enzymes: cytochromes a_3, a, c, c_1, and b, flavoprotein (FP), diphosphopyridine nucleotide (DPN) and its combination with alcohol dehydrogenase (ADH). Besides of its far-going inactivation of cytochrome b antimycin A is shown to reduce the operating activities of cytochrome c_1, FP and DPN to about 50 % but leave the group a + a_3 and c nearly unaffected. Cytochrome b and one fraction of the total FP are closely cooperating in equimolar quantities.

EXPERIMENTAL TECHNIQUE AND PROCEDURE

A new recording spectrophotometer. Sensitive recording photometers were introduced only a few years ago [1,2]. The instruments constructed by the author are primarily built for the purpose of *accurate measurements of the extinction in distinct wave-length intervals.* The figures for the reference and the sample are separately recorded. The new construction eliminates the inertia of the recording millivoltmeter and secures the attainment of precise wave-length positions, a fact of fundamental importance for accurate calculations of extinction values. One of the author's instruments is shown in Fig. 1. It automatically plots extinction values of reference beam and sample for a series of wave-lengths, the intervals of which may be chosen at will. Sufficient for most purposes are intervals of 2 mμ. A record in 2 mμ intervals of the range

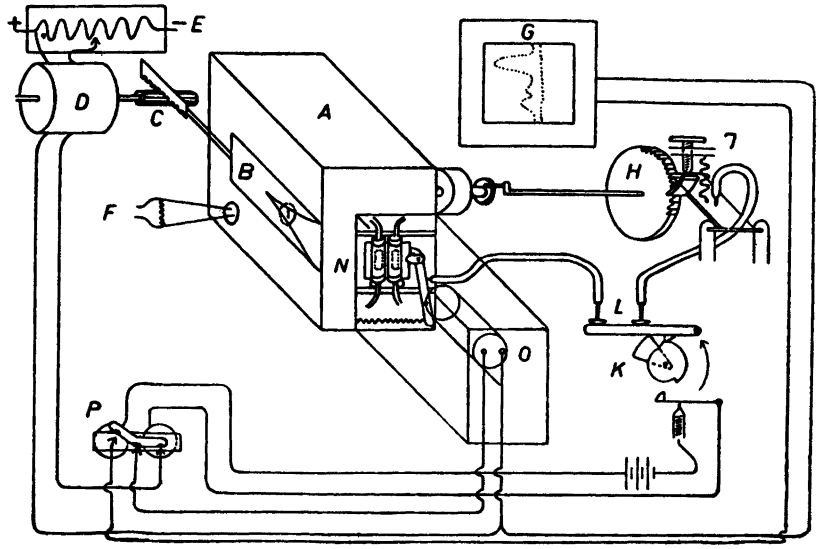


Fig. 1. Scheme of the recording spectrophotometer. A *grating monochromator (Bausch and Lomb 60 cm),* B *screen with triangular opening for adjusting the intensity of the in-going light beam,* C *gear,* D *balancing motor for adjustment of the position of* B, E *potentiometer, balancing against the photo cell,* F *light source (6 volt bulb or hydrogen lamp),* G *recording millivoltmeter,* H *toothed wheel (one cog = 1 mμ) steering the wave-length drum,* I *device for moving* H *in distinct intervals,* K *cam wheel driven by a motor of constant speed, the wheel at will making one turn in 2, 4, or 6 seconds,* L *lever transmitting the movement of the lower cam of* K *to* I *and* N *(transmission by means of steel cables),* N *sliding object holder facing the out-going beam of the monochromator and alternately exposing the tube with the reference substance and the tube with the sample to the beam,* O *photo multiplier tube,* P *relay for switching over the current from* O *alternately to* G *or* D, *the relay being put in action by the high cam of* K. — *At one revolution of* K *in 4 seconds the schedule of operating is the following: 0—0.8 sec. high cam of* K *closing the circuit through* P *and bringing* O *in connection with* D *(adjustment of the light intensity to a fixed value), 0.8—2.4 sec. relay put out of action and* O *connected to* G *(recording of the reference), 2.4—4.0 sec. lever* L *lifted by the low cam of* K, *thus moving* N *to the left (recording of the sample), 4.0 sec.* L *falling down again thereby releasing the tension of* I *and instantaneously moving the wheel* H *one step.*

between 400 and 620 mμ takes 3 to 6 minutes, a single band may be recorded in 10—20 seconds. A high degree of accuracy is attained, enabling optical resolution of bands lying 3—4 mμ apart (*cf.* Refs. [3,4]).

Rapid recording of bands. Complete records of larger spectral regions may be used for the study of more slowly changing steady states. For a more incisive analysis of the kinetics, however, still more rapidly working procedures must be applied. Some bands, *e. g.* the α-band of cytochrome c, may be measured from the difference in extinction between 550 and 546 mμ, which in the case of a difference spectrum (ε reduced-ε oxidized, *cf.* Fig. 4) corresponds to approximately 50 % of the total height. Some authors prefer to compute such measurements by means of a device implying rapid oscillation between the two wave-lengths [2]. According to my experience with yeast constant

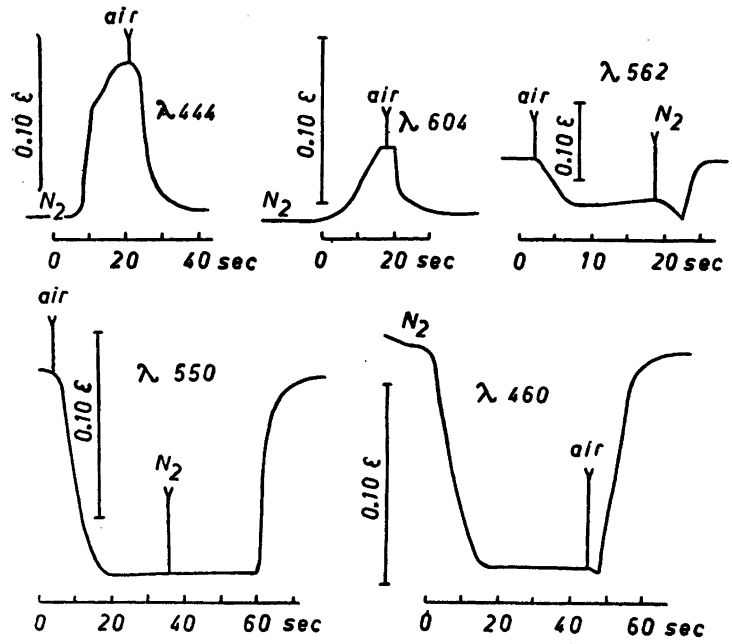


Fig. 2. Direct records of the top of the main bands of the cytochromes a_3 (444 mμ), a (604 mμ), c (550 mμ), b (562 mμ), and flavoprotein (460 mμ), at alternating reduction in N_2 and reoxidation in air.

recording of the top of the band, *viz.* in the case of cytochrome c at 550 mμ, serves the same purpose. With a sensitive and rapid millivoltmeter, *e. g.* Speedomax G supplied with A. C. 60 periods, changes in time intervals of *ca.* 0.5 seconds are within the reach of the operator (see Fig. 2).

Corrections for interfering bands. Accurate knowledge of the variations of the background of the spectrum constitutes the basis of all measurements. Baker's yeast, fortunately, lacks pigments which are interfering with the respiratorical enzymes, but the spectra of the different cytochromes and FP are partly overlapping, a fact necessitating a number of corrections. There is little hope for reliable results unless the spectral behaviour of the chosen object is thoroughly known. For successful calculation the observed spectrum has to be carefully compared with spectra of known preparations of the single enzymes, which must be recorded on the same instrument, because variations in dispersion and slit width may to some extent affect the shape of the bands. Good preparations of riboflavin, DPN and ADH are commercially available. Preparations of peroxydase and cytochrome c have been kindly afforded by Professor Keilin and Dr. Hill in Cambridge. Professor Kiese in Marburg kindly sent a preparation of cytochrome oxidase and recommended a method for the preparation of cytochrome b from beef heart. The spectrum of this preparation was carefully compared with the spectrum of the same cyto-

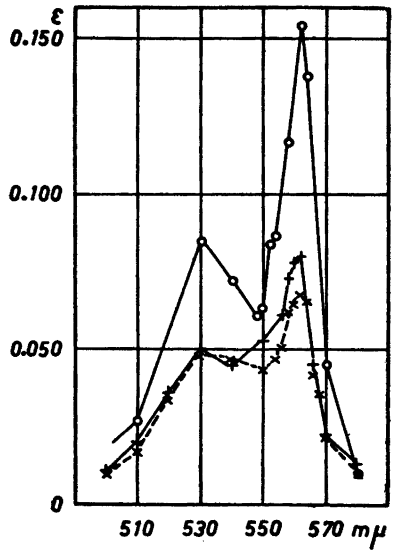


Fig. 3. Direct *spectrograms (with filter paper as reference substance) of 15 % aerated yeast in a 17 mm wide quartz tube.* ×----× *aqua destillata,* +———+ *0.1 m malonate pH 5.85.* O———O *4 μg antimycin A. About 30 % of cytochrome b remains reduced in aerated water or malonate, together with a few percent reduced cytochrome c. A slight curvature at 554 mμ in antimycin A marks the partial reduction of cytochrome* c_1.

chrome appearing after treatment of yeast with antimycin A. It was shown that the shape of the γ- and α-bands of reduced cytochrome b within *ca.* 5 % coincide with the shape of the corresponding bands of cytochrome c, but that oxidized cytochrome b, contrary to cytochrome c, shows low β- and α-bands, too, which are displaced a few mμ towards blue in comparison to the reduced bands (*cf.* Ref.[4]). This fact is able to complicate the *direct spectrum* (recorded with filter paper as reference substance; see Refs.[1,3]) the twobanded weak spectrum of which (in the region 520—570 mμ) is a combination between about 70 % oxidized and 30 % reduced cytochrome b, together with a few percent of reduced cytochrome c (see Fig. 3). A similar weak two-banded spectrum also appears in roots of higher plants as will be shown in a separate publication.

Cytochromes c_1 *and* b_2. These more recently studied enzymes are present in baker's yeast [4]. Cytochrome c_1 has its α-band at 554 and its γ-band at 422 mμ. Its concentration is about 50 % of that of cytochrome c. This cytochrome takes part in the normal aerobic respiration. Cytochrome b_2 has its α-band at 556 mμ and it is closely connected to an approximately equimolar quantity of FP [5,6]. This cytochrome does not participate in the aerobic respiration. Its reduced bands appear after treatment with lactate, primarily in the presence of nitrogen [4,6].

The procedure of corrections. Following the recording of the purified enzymes or coenzymes in intervals of 2 mμ the extinction values are conveniently

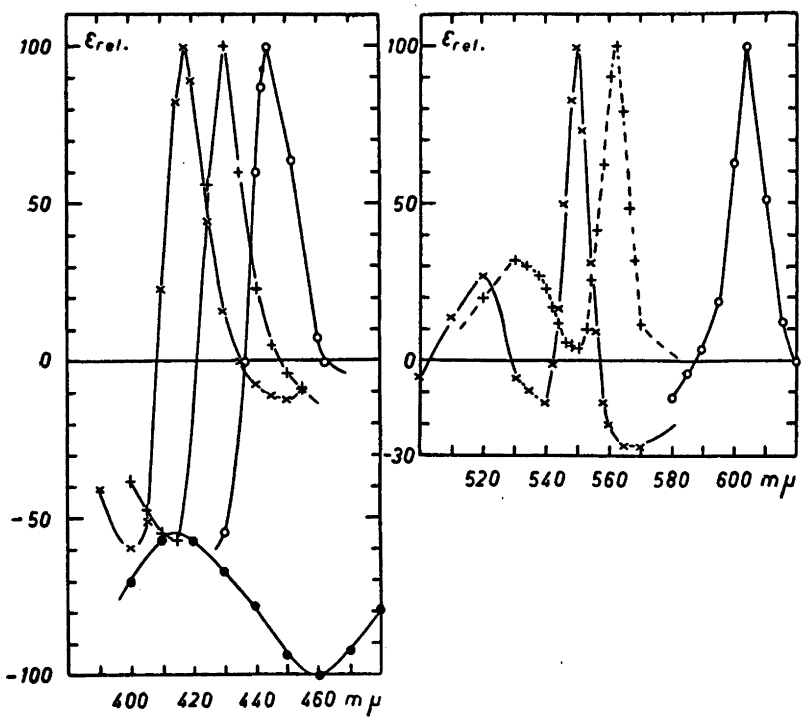


Fig. 4. Difference *curves of preparations of the cytochromes c, b and a* (a_3 + *a*), *and flavoprotein (riboflavin). The reference contains the oxidized and the sample the reduced enzyme. The extinction values are calculated for the purpose of optical analysis,* viz. *the top of the bands set at 100. See the text.*

calculated in percent of the main bands (see Fig. 4). Calculations on spectrograms of living objects ought to be made both from the *direct spectrum* (with strips of filter paper as reference substance [1,3,4]) and from the *difference spectrum* (*e. g.*, oxidized yeast as standard and O_2-free yeast as sample). The difference spectrum is extended on both sides of the zero abscissa which is traversed at the isosbestic points (Fig. 4). The difference spectrum is more convenient to handle and it ought to be mentioned that corrections of records of single band tops (see above) have to be made according to the figures of the difference spectrum (Figs. 5, 6).

Corrections for turbidity. This question has been treated in some detail in a previous communication [4]. The turbidity, *e. g.* of a suspension of yeast, generally lowers the apparent molar extinction of bands in blue and ultraviolet, whereas bands in green and red are far less influenced. The scattering of the light may be to some extent calculated [7], but the only accurate method is here direct determination of the depression of the bands of added pigments. Different objects may behave rather differently. In a suspension of 15 % yeast

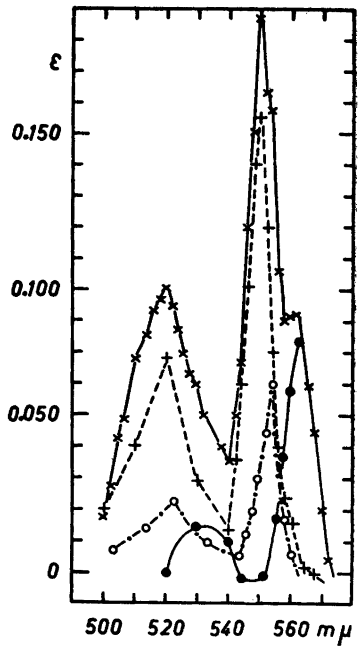


Fig. 5. Example of optical analysis of a spectrogram, according to the procedure mentioned in the text. ×———× *record of a 15 % yeast suspension aerated with nitrogen.* ●———● *spectrum of cytochrome b calculated from the difference 562—570 mμ.* +– – – – + *spectrum of cytochrome c calculated from the difference 550—546 mμ minus the value of* $\frac{1}{3}$ *b at these wave-lengths.* O·····O *spectrum of cytochrome* c_1 *calculated as the observed curve minus c minus b.*

the Soret bands are depressed about 33 % (factor 1.33). The same is true with regard to the band of FP at 450—460 mμ, whereas the values of the DPNH band at 340 mμ have to be corrected with the factor 2.3. Dilution to 5 % here lowers the correction to only 1.25.

Technique for studying rapid changes in the steady states. As shown in Fig. 3 a suspension of washed yeast in aqua dest. or 0.02 M phosphate (pH 6—7) is predominantly oxidized if aerated for some 30 minutes. According to frequent variations in the concentration of DPN the balance may be attained in less than one minute but may occasionally take several minutes. Because there is always a residual reduction of several enzymes, *e. g.* cytochrome b (Fig. 3), in aerated yeast, a fact reflecting the intensive aerobic respiration, observations of the kinetics of reduction have to start from this state as the bottom level. Addition of glucose or still more of ethanol of course moves the steady state far more to the reduced side [4].

Continuous recording of the involved enzymes now shows that reduction does not start immediately after the shifting over from air to nitrogen. As shown in Table 1 the time lag is directly influenced by the intensity of the previous aeration, *viz.* obviously by the quantity dissolved oxygen in the

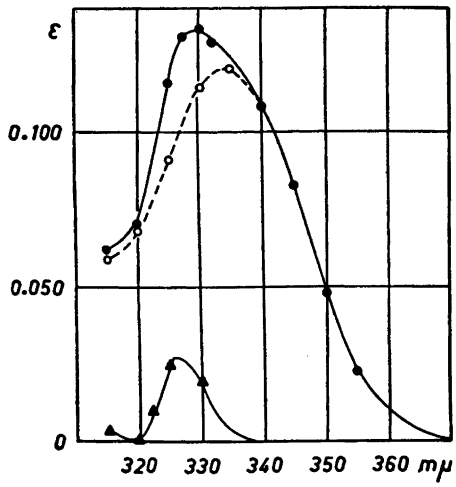


Fig. 6. Optical analysis of the spectrum of DPNH. 3 ml of the sample contained 0.1 mg DPN, 3 mg ADH (from a commercial preparation) and 0.05 ml alcohol. Depth of the cuvette 1 cm. ●——● recorded spectrogram. O- - -O calculated spectrum of DPNH. ▲——▲ the difference between both, corresponding to the spectrum of ADH · DPNH.

medium surrounding the cells. All experiments were performed in "circulation vessels", made of molten quartz and holding 18 ml (Fig. 7). According to the shape of the vessel the suspension is vigorously moved by the stream of air or nitrogen blown from the narrow tube near the bottom. No yeast is accordingly sedimented, a matter of importance for the maintaining of constant light absorption, and the gas exchange is exuberant.

As may be seen from the direct records in Fig. 2 the reduction of the enzymes, primarily those of highest oxidation potential, a + a_3 and c, starts abruptly and proceeds practically linearly, at least up to more than 50 % reduction. This sudden reduction after a comparatively long lag period supports the idea that oxygen forms an adsorption layer in close contact with

Table 1. Relation between the duration of the aeration and the start lag of reduction in N_2. Single values. Times in seconds.

Enzyme	DPN	FP	cytochrome b	cytochrome c	cytochrome a
Band mμ	340	460	562	550	604
5 min. aeration	82	81	70	52	76
2 » »	76	77	69	46	70
1 » »	54	60	60	39	59
30 sec. »	—	43	40	24	—
15 » »	25	25	29	14	20
5 » »	5	5	5	—	5

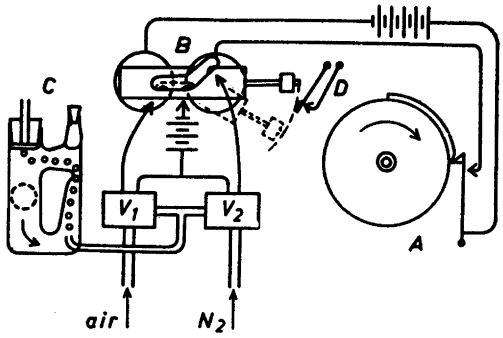


Fig. 7. Scheme of a device for automatic alternating of streams of air and N_2 through the yeast suspension. A *Cam wheel rotating with a speed of one revolution in 110 seconds. The cam closes an electrical contact which changes the position of the relay* B. *A V-shaped mercury contact tube alternately closes the current through the electrical valves V_1 and V_2, one for air the other for nitrogen. On its passage from one position to the other the anchor of the relay touches the contact* D *which by means of a special device draws a short line on the record (see Fig. 2).* C *is the "circulation vessel" made by molten quartz, containing 18 ml yeast suspension, and with a diameter of the main tube of 17 mm. The hatched circle marks the centre of the optical field. The suspension is held in continuous movement by the gas current which escapes through a tube on the top of the vessel. The addition of inhibitors etc. may be made through the smaller tube to the right.*

cytochrome oxidase, a layer operating as a buffer between the dissolved oxygen and the process of electron transfer. It may be tentatively assumed that the absorbed gas layer is carried by a hemoglobin-like pigment (*cf.* Ref.[8]), but it may otherwise be supposed that the apoenzyme of the oxidase adsorbs oxygen.

Preliminary experiments now showed that the lag phase of reduction remains constant within one second or less, if the two gases, air and nitrogen, are alternating in fixed intervals, provided that the gas stream is maintained at a constant value, and that the system has came to a balance. This observation together with the fact that the length of the lag phase is not identically the same for all enzymes served as the basis of a method for determination of the apparent kinetics of a complex system. The experimental outfit is shown in Fig. 7. Air and nitrogen (99.9 %) are fed to the circulation vessel *via* two electrical valves which are operated by means of a relay and a clockwork. Both gas streams are adjusted to the same speed, amounting to about 250 ml in one minute, which gives an intense bubbling in the right side of the vessel. The gas escapes through a tube leading to a flask with a layer of water above the gas outflow. The clockwork was mostly set for periods amounting to 35 seconds for the air and 75 seconds for the nitrogen. In order to obtain a precise record of the start moments the relay is provided with a guide-contact marking a line on the record each time the lever of the relay shifts position.

Apparent velocity constants. Thermodynamical velocity constants cannot be calculated for living enzyme systems, mainly for two reasons: 1) the enzymes are not in true solution but with few exceptions (DPN and possibly cytochrome c) attached to structural moieties ("mitochondria"); each enzyme

is structurally linked to at least one, frequently two or more other enzymes, a situation creating difficulties in clearly distinguishing between individual kinetics and group kinetics. An approximate estimation of the reaction velocity may be calculated from the half-time *ht* (*cf.* Ref.[9]), *viz.* the time elapsing from the start to the point of 50 % increase or decrease of the reduction. The value *ht* is inversely related to the reaction velocity. The apparent velocity constant is calculated as $K_{app} = c/ht$, where c = the apparent molar concentration, *viz.* that fraction of the actually present enzyme which partakes in the reaction.

EXPERIMENTAL RESULTS

Start lag and reaction velocity of the respiratorical enzymes.

The experiments were conducted at 20° C with 15 % baker's yeast (from Svenska Jästfabriksaktiebolaget), washed twice and resuspended in double distilled water. Aeration during 1—2 hours before start.

Table 2. Start lags and apparent reaction velocity at alternating reduction and reoxidation (35 sec. air, 75 sec. N_2). c = μmole × lit.$^{-1}$ moist yeast. Time unit seconds.

Enzyme or coenzyme	a_3	a	c	c_1	b	FP	DPN
Measured band mμ	444	604	550	554	562	460	340
Start lag of reduction	32.1	31.4	32.9	34.5	39.6	38.8	56.2
» » » oxidation	—	2.7	—	—	1.6	2.6	2.5
ht_{red}	1.26	5.42	1.75	—	3.10	4.51	10.0
ht_{ox}	4.36	3.78	5.60	6.7	2.54	4.87	1.3
$K_{app\ red}$	7.1	1.6	11.6	—	5.8	8.6	45.0
$K_{app\ ox}$	2.1	2.3	3.7	—	7.4	8.2	347.0

The start lags of reduction of the group a_3 + a and c show that these enzymes are the first to be "saturated by electrons" when the supply of oxygen is cut off. The slightly schematical picture of the start field in Fig. 8 clearly shows the close connection between a_3 and c, whereas a while starting as rapidly as a_3 takes a quite deviating course of reduction. In its time course it is very similar to c_1. These two enzymes are leading over to group b — FP which enzymes are starting about synchronously with the final stage of reduction of the group a_3 and c. The probably close linkage between cytochrome b and flavoprotein has been emphasized in a recent communication [4]. The existence of a lag of six to seven seconds between the first response of the groups a — c and b — FP points to the presence of a "buffer system" between these two. A member of this intermediate system is probably cytochrome c_1 and possibly also cytochrome a. The situation is complicated by side-lines which are certainly branching off from some of the enzymes, if not all of them, side-lines which imply a display of energy. Studies in the cytochrome

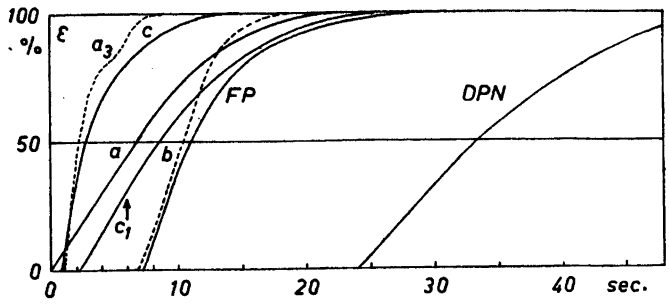


Fig. 8. Slightly schematical reproduction of the course of reduction of the respiratorical enzymes of yeast (cf. Table 6). The start lags are calculated from the moment when the reduction of cytochrome a begins. The first half-part of the reduction approximately follows a straight line, the course of the reduction above the 50 % line is somewhat more varying, but generally slightly curved. The exact position of 100 % reduction is difficult to ascertain.

system of wheat roots strongly support the assumption that the oxidation — reduction of cytochrome b is conducting synthesis of high energy phosphate. Such a coupling between processes giving off and taking up energy will, if they are reversible, act as a buffer system, too [12]. The scheme in Fig. 8, however, may possibly be significant of the pulsations of the stream of electrons, because it shows that the group b — FP does not start reduction until the group a_3 — c is nearly completely reduced, and DPN does not start reduction until the group b — FP is completely reduced. This "pulsation" of the total process cannot be taken as an argument for disruptures in the structural integrity of the total system. It is more likely to assume that it reflects a grouping of oxidation potential states. From this point of view the deviating course of the cytochromes a and c_1 is most interesting. — Certain minimum quantities of DPNH are of course present from the beginning, even in well aerated yeast, and act as a continuously working source of electrons feeding the group b — FP and so on. Electrons are fed to DPN by, among others, the alcohol and glyceraldehyde phosphate dehydrogenases. The proceeding of the reduction of ADH can be measured on the ADH · DPNH band at 323—325 mμ (Ref.[4], Fig. 6). Observations of the time course of the development of this band show that it starts considerably slower than the DPNH band, an observation alluding to the fact that a certain level of DPNH is needed before measurable quantities of the enzyme combination are formed.

Cytochromes a_3 and a. In their important work on the spectral characteristics of the cytochrome system Keilin and Hartree [13] concluded that in respect of cytochrome a "we are dealing here with two distinct but closely allied and intimately connected compounds a and a_3". There has been much discussion in the literature as to this point. One of the main difficulties is the fact that the quantitative relation $\lambda_{444}/\lambda_{604}$ remains constant irrespective of the path of reduction [10]. A fixed combination of two pigments in equimolar concentrations would, however, render a similar result. The present observation of a deviating time course of reduction and reoxidation of the two bands 444 and 604 undoubtedly corroborates the original conception of Keilin and Hartree.

The results clearly show that a_3 is the oxidase, because it reacts about four times as rapidly as a at reduction. Some peculiarities of a were emphasized above. Others are appearing under the influence of antimycin A, as will be shown below.

The actually reacting quantities. As already mentioned these are not necessarily identical with the total quantities. Previous measurements [4] pointed to equimolar total quantities of a, c and b. In the present experiments calculations of the activity of a only give *ca.* 50 % of the total quantity (see Table 3). Calculations from 444 mμ give higher values (see Table 4). Because no really pure preparation of $a + a_3$ is at hand all figures of molar concentrations are somewhat uncertain. The results, however, support the conclusion that under the conditions of the experiments the actually reacting quantities of a_3 and a are not always the same, even if the total amounts may be alike. Regarding the group b and FP the results corroborate the authors previous calculations. Experiments with N_2, lactate, and antimycin A showed [4] that cytochrome b is most probably connected to an equimolar quantity of flavoprotein. A similar close connection has actually been shown to exist [5,6] regarding cytochrome b_2. The fact that the actually reacting quantity of flavoprotein is twice as large as that of b, even if b_2 does not partake in the balance (see above), points to the existence of still another fraction of FP, which participates in the respiratorical chain but is not intimately linked to b. The following experiments with antimycin A will further elucidate this question. The high concentration of DPN in yeast is a well known fact. The experiments show that the total reacting quantity is 50—100 times as large as that of the single cytochromes and that nearly 50 % of DPNH is within 1—2 minutes bound to the alcohol dehydrogenase.

The response to antimycin A. Antimycin is claimed [11] to inhibit the transfer of electrons from cytochrome b to cytochrome c. If this antibioticum is added in increasing quantities to 18 ml of an 15 % yeast suspension (containing 2.7 g yeast) a visible reduction of cytochrome b starts at *ca.* 1 μg and an optimum

Table 3. Reacting quantities of the enzymes. Values in μmole × lit.$^{-1}$ moist yeast.

Enzyme or coenzyme	a_{604}	c_{550}	b_{563}	FP_{460}	$DPNH_{340}$	ADH_{325}
Absolute quantities	9.0	20.3	18.0	39.0	450.0	330.0
Relative, approxim.	1	2	2	4	50	40

Table 4. The effect of antimycin A on the cytochromes c, c_1, and b in 15 % yeast (aerated) in vessels of 17 mm diameter.

Cytochromes	c	c_1	b
Observed extinction in:			
0.0 μg antimycin A	0.000	0.000	0.059
1.2 » » »	0.076	0.038	0.133
2.4 » » »	0.000	0.022	0.144

is attained at *ca.* 2.4 μg antimycin A. Larger quantities do not change the spectroscopic picture. It could, however, be shown that the initial effect of antimycin A is not exclusively confined to cytochrome b. Also cytochrome c is affected in the start period, and cytochrome c_1, too (Table 4). This intermediate reduction of cytochrome c reflects the comparatively slowly proceeding combination of antimycin A with cytochrome b, as can be observed by continued recording of the band 563 mμ. The proportions between quantities of antimycin A needed for optimal effect on b, and the enzyme itself, are about equimolar. The reaction takes at least a couple of minutes. It could furthermore be shown that the reaction stops at *ca.* 80 %, the rest may then be reduced in nitrogen. The residual quantity of noninhibited cytochrome b is possibly responsible for the residual aerobic respiration of about 5—10 %, frequently observed after treatment with antimycin A, but this observation may be explained otherwise, too (see below). The effect of antimycin is reversible. It may be abolished by treatment with some dithionite followed by aeration.

Change of activities after treatment with antimycin A. The deepgoing effects af antimycin A are illustrated in Tables 5 and 6, computed from experiments with alternating reduction and reoxidation. If attention is first paid to the

Table 5. Reacting quantities of cytochromes, FP, and DPN in one experiment with added antimycin A (ca. 4 μg per 2.7 g yeast). Values in μmole × lit.$^{-1}$.

Enzymes and coenzymes	a_{444}	a_{604}	c_{550}	$c_{1\ 554}$	FP	DPN
Control	5.5	8.5	20.3	—	39.0	450.0
Antimycin added	7.5	8.1	18.5	—	23.0	225.0
Relative values, control	100	100	100	100	100	100
» » + antimycin	135	95	91	52	59	50

actually reacting quantities (Table 5) these are remaining practically constant as far as a and c are concerned whereas the activity of b is practically completely abolished (not shown in the table) and that of cytochrome c_1, FP and DPN reduced to 50 %. The apparent rise of the activity of a_3 may be caused either by a more far going activation of the oxidized state under the influence of the lessened effect of the dehydrogenases, or simply by some interfering effect which is still obscure. The first explanation is, however, good enough. The observed 50 % reduction of the reacting quantities of FP strongly support the idea of a close molar linkage between cytochrome b and this pigment. The other half quantity of flavoprotein is obviously cooperating with the rest of the cytochrome system probably *via* the remaining quantities of cytochrome c_1. The fact that the reacting quantity of DPN is reduced to about the same percentage as FP is difficult to understand unless we assume the existence of two different enzymes performing the transference of electrons from DPNH to FP. One of these enzymes will only react with that fraction of total flavo-

Table 6. Effects of antimycin A on the kinetics of the respiratorical enzymes. Values in seconds. — control. + with antimycin A.

Enzymes or coenzymes		a_3	a	c	c_1	b	FP	DPN	ADH
Measured band		444	604	550	554	562	460	340	325
Start lag of reduction	—	40.3	38.5	39.8	—	41.6	47.8	91.0	97.7
	+	149.5	143.0	134.0	152.0	—	155.0	182.0	215.0
Start lag of oxidation	—	values varying between 1.2 and 2.5							
	+	» » » 1.9 » 2.5							
ht_{red}	—	1.1	8.2	1.8	—	4.2	5.4	8.7	10.0
	+	5.0	4.4	4.0	4.3	—	4.2	12.5	15.0
ht_{ox}	—	2.9	1.7	2.5	—	1.7	3.8	1.4	—
	+	1.3	1.8	0.7	1.3	—	1.2	3.3	2.5
$K_{app\ red}$	—	5.0	1.0	11.3	—	—	7.2	52.0	—
	+	1.5	1.8	4.6	—	—	5.5	18.0	—
$K_{app\ ox}$	—	1.9	5.0	8.1	—	—	10.3	32.0	—
	+	5.8	4.5	26.4	—	—	19.1	68.0	

protein which is directly linked to cytochrome b. After blocking the b — FP moiety a corresponding quantity of DPN is put out of circulation.

The strongly reduced oxygen consumption (about 5—10 % of the normal) in yeast which has been treated with antimycin A is illustrated by the increase in the start lag of reduction from about 40 to about 150 seconds (Table 6). The retardation of the velocity of reduction ($K_{app\ red}$) of the cytochromes a_3 and c amounts to about 1/3 and is a consequence of the drop in DPN activity, *viz.* in the intensity of the stream of electrons, at preserved activity of the oxidase. Inversely a slower working mechanism of reduction raises the speed of reoxidation (from 1 to 3). It is significant that these reciprocal relations between K_{app} before and after the addition of antimycin A are less exaggerated with regard to flavoprotein, because the velocities are here calculated on the basis of 50 % lower activity. The residual quantity of FP must then, of course, speed up its $K_{app\ ox}$ in relation to the oxidase. We are in Table 6 again meeting the deviating response of cytochrome a, as compared with a_3 and c. Its activity is seemingly only little affected by the sharp drop in the activity of reduction of DPN. Because it is not hampered with regard to active concentration one must conclude that it is involved in some oxidation-reduction balance outside of the scope of DPN and FP, perhaps in relation to high energy phosphate. This point needs further experimental elucidation.

Alternate pathways of electron transfer. Even if antimycin A is not inactivating cytochrome b to fully 100 % it could be calculated that under the conditions quoted in Table 6 the state of oxidation and reduction of this enzyme is not visibly altered. Reduction only causes a negative response at 562 mμ

(*cf.* Fig. 2) the magnitude of which is quite in accord with the calculated depression of the extinction curves of c and c_1 at this wave-length (see Fig. 4). It must consequently be concluded that the electrons largely bypass the inhibited cytochrome b and from the residual FP go to cytochrome c, probably *via* c_1, the behaviour of which in some way resembles that of b. This would be an alternate pathway of electron transference from DPN to a_3 and oxygen. But this way offers a poor substitute for the main line through cytochrome b which normally transmits 80—95 % of the electrons conducting aerobic respiration. The sharp drop in effectivity is nevertheless surprising, because a reduction of DPN and FP to half activity would only cause a retardation of $\frac{1}{2}$. The real depression, however, approximates $(\frac{1}{2})^3$ or even $(\frac{1}{2})^4$. For explanation two possibilities present themselves. It may either be assumed that the cytochrome b, in spite of the spell under which it is held by antimycin A, still maintains a strongly reduced activity, or it may be assumed that the alternate pathway from FP to c_1 and c is far less convenient (perhaps for structural reasons) as a track for electrons. In view of what was said above of the obvious outruling of cytochrome b and of the fact that its partner, *viz.* the halfpart of the total flavoprotein, is inactivated too, the odds are obviously more in favour of the second scheme of explanation.

The investigation has been aided by a grant from *Statens Naturvetenskapliga Forskningsråd.*

REFERENCES

1. Lundegårdh, H. *Arkiv Kemi* **3** (1951) 69.
2. Chance, B. *Science* **120** (1954) 767.
3. Lundegårdh, H. *Arkiv Kemi* **7** (1954) 451.
4. Lundegårdh, H. *Biochim. et Biophys. Acta* **20** (1956) 469.
5. Appleby, C. A. and Morton, R. K. *Nature* **173** (1954) 749.
6. Boeri, E. and Tosi, L. *Arch. Biochem. and Biophys.* **60** (1956) 463.
7. Rabinowitch, E. *Photosynthesis*, Vol. II, p. 1, New York 1951.
8. Keilin, D. *Nature* **172** (1953) 390.
9. Lundegårdh, H. *Nature* **171** (1953) 521.
10. Lundegårdh, H. *Arkiv Kemi* **5** (1952) 97.
11. Potter, V. and Reif, A. E. *J. Biol. Chem.* **194** (1952) 287.
12. Lundegårdh, H. *Physiologia Plantarum* **8** (1955) 142.
13. Keilin, D. and Hartree, E. F. *Proc. Roy, Soc. London B* **127** (1939) 167.

Received April 26, 1956.

ACTA CHEMICA SCANDINAVICA 10 (1956) 1097—1099

Isolation of N-[D-2,3-Dihydroxy-*n*-propyl]-taurine from *Gigartina leptorhynchos*

BÖRJE WICKBERG

Organisk-kemiska Institutionen, Kungl. Tekniska Högskolan, Stockholm, Sweden

In an investigation of the red alga *Gigartina leptorhynchos* a new internal salt was isolated. This was shown to be N-[D-2,3-dihydroxy-*n*-propyl]-taurine, for which the shorter name D-glyceryltaurine is suggested. Taurine, floridoside, glycerol and small amounts of *meso*-inositol, mytilitol and laminitol were also found.

In previous communications from this institute investigations on the occurrence of internal salts [1] and of low-molecular weight carbohydrates [2] in various algae have been reported. The present paper records the investigation of the red alga *Gigartina leptorhynchos*, *Florideae*, order *Gigartinales*, from which a new internal salt, shown to be N-[D-2,3-dihydroxy-*n*-propyl]-taurine or shortly, D-glyceryltaurine, was isolated. In addition taurine, floridoside, glycerol and small amounts of the cyclitols *meso*-inositol, laminitol and mytilitol were found.

Floridoside is a common constituent of algae belonging to *Florideae* while taurine and its N-methyl derivatives [1] are frequently met with throughout the red algae. The amounts of cyclitols found, being of the order 0.001 %, are so small that these substances could possibly derive from impurities in the material investigated.

The new internal salt was optically active $[\alpha]_D^{23}$ −21° (water) and had a much lower melting point (163.5—164.5°) than taurine and its N-methyl derivatives which all melt in the range 240—340°. On a carbon column the new compound travels at about the rate of a hexitol which is much slower than the rate observed for the other taurines. When paper chromatograms were run in ethyl acetate-acetic acid-water (3:1:1) the R_F-value of the substance was some 10 % higher than for taurine. On the chromatogram the substance could be detected with the silver nitrate-sodium ethoxide reagent and with ninhydrin. With the latter reagent rather strong heating was required and the colour produced was fainter than that observed with taurine, a behaviour which is similar to that of N-methyl taurine. The crude compound could be freed from

carbohydrates by adsorption on Amberlite resin IR 400 in the OH-state and subsequent elution with dilute acetic acid.

Analysis was in fair agreement with the composition $C_5H_{13}O_5NS$, and no solvent of crystallisation was detected. The substance was unaffected by hydrolysis in 2 N HCl for 15 h at 120°. Periodate oxidations indicated a consumption of 2 moles of oxidant with the formation of 2 moles of formaldehyde. From the oxidized material pure taurine was isolated. According to these facts the compound should have structure I. This conclusion was confirmed by the synthesis of D-glyceryl-taurine by reductive coupling of *iso*-propylidene-D-glyceric aldehyde with taurine and subsequent hydrolysis of the *iso*propylidene derivative obtained. The optical rotation, melting point and chromatographic behaviour were the same for the synthetic product as for the substance obtained from the alga, and the mixed melting point for the two preparations showed no depression. The internal salt from the alga thus possesses the D-form of structure I.

$H_3\overset{+}{N}CH_2CH_2SO_3^-$
CH_2
$CH(OH)$
CH_2OH

I. Glyceryltaurine

EXPERIMENTAL

The alga (320 g) was extracted with ether for 2 days and with methanol for 14 days. The methanol extract was concentrated to a syrup which was stirred with water, the mixture was filtered and the filtrate de-ionised with Amberlite IR 120 and IR 4B and concentrated to dryness. The residue (5.5 g) was dissolved in water (100 ml) and the solution added to the top of a carbon-Celite column (35 × 4.5 cm). The column was eluted with water (2 000 ml) and then with aqueous ethanol (4 000 ml) the concentration of which was linearly raised from 0 to 30 %. The eluate was fractionated and investigated by paper chromatography using as solvent ethyl acetate-acetic acid-water. The main fractions were de-ionised as before and concentrated to dryness.

Fraction No. 1 (200 mg) contained only one component and this was ninhydrin-positive. After recrystallisation from aqueous ethanol taurine (150 mg) was obtained, m. p. 320—8° * alone or admixed with an authentic sample.

Fraction No. 2 (112 mg) contained two components with the same R_F-values as *meso*-inositol and glycerol. Separation on Whatman filter paper No. 3 MM yielded *meso*-inositol (15 mg) which after recrystallisation had m. p. 222—225°, alone or admixed with authentic material. The glycerol fraction (90 mg) was benzoylated by the Schotten-Bauman procedure, yielding a benzoate (110 mg) which melted at 74—75° and gave no melting point depression with authentic glycerol tribenzoate.

Fraction No. 3 (30 mg) gave one reducing spot. Recrystallisation and acetylation yielded an acetate which crystallised in needles melting at 170—172° with simultaneous transformation into rhombic crystals melting at 184—186°. The melting points were undepressed on admixture with mytilitol hexa-acetate.

Fraction No. 4 gave a spot indistinguishable from that of laminitol. Recrystallisation yielded a substance (15 mg) a sample of which was acetylated yielding an acetate, m. p. 155—157° alone or admixed with an authentic sample of laminitol hexa-acetate.

Fraction No. 5 (580 mg) contained a substance which gave one strong spot with the silver nitrate and the ninhydrin reagents. It was adsorbed on the Amberlite resin IR 400 in OH-form and subsequently eluted with 5 % aqueous acetic acid. The crude crystalline material so obtained (420 mg) melted when heated under aqueous ethanol and was recrystallised by the careful addition of ethanol to its slightly warmed aqueous solution. M. p. 163.5—164.5°, $[\alpha]_D^{23}$ −21° (water, c = 2.0). (Found: C 30.4; H 6.68; N 6.64; S 14.7. Calc. for $C_5H_{13}O_5NS$: C 30.1; H 6.58; N 7.03; S 16.1.)

* All melting points are corrected.

Fraction No. 6 (2.3 g) contained a substance which was recrystallised from aqueous ethanol. M. p. 125—128°, $[\alpha]_D^{23}$ +152° (water, c = 2). These data and its chromatographic behaviour showed it to be floridoside.

Periodate oxidations of the internal salt from fraction 5. Periodate oxidations were carried out on a micro scale with an aqueous solution containing *ca.* 2 mg/ml of the internal salt from fraction 5.

a) *Periodate consumption.* To each sample (0.5 ml) 0.03 molar sodium metaperiodate solution (1 ml) was added. After varying times saturated sodium bicarbonate solution (1 ml), 0.1 N sodium arsenite (1 ml) and 20 % aqueous potassium iodide (0.2 ml) were added and after standing for 15 minutes the mixture was titrated with 0.02 N standard iodine solution. Within a few minutes the periodate consumed was 2.1 moles/mole substance and this value rose to 2.2 moles overnight.

b) *Formation of formaldehyde and taurine.* The sample (2 ml) was oxidized with sodium periodate and the formaldehyde formed was determined as its dimedone compound as described by Reeves [3]. The dimedone compound had m. p. 193—194°, alone or admixed with an authentic sample and the yield corresponded to the formation of 1.9 moles of formaldehyde per mole of internal salt.

The mother liquors from the dimedone precipitation were freed from excess dimedone by extraction with ether and from inorganic salts by passing the solution through Amberlite resins IR 120 and IR 4B. By evaporation of the de-ionised solution and subsequent recrystallisations from dilute methanol, pure taurine was obtained, m. p. 325—329°, alone or mixed with authentic material.

D-*Glyceryltaurine. Iso*propylidene-D-glyceric aldehyde was prepared from D-mannitol as described by Baer [4,5].

To a solution of freshly distilled *iso*propylidene-D-glyceric aldehyde (6.4 mmole, 0.83 g) and taurine (8 mmole, 1.0 g) in water (10 ml) colloidal platinum solution [6] (4 ml, 8 mg Pt) was added and the mixture shaken with hydrogen for 100 hours at room temperature and atmospheric pressure. The hydrogen uptake was 7.9 mmole. This high value may have been due to the reduction of liberated acetone, as the hydrogenated mixture was found to be slightly acid afterwards.

After hydrogenation the mixture was heated for a short while with a minute amount of hydrochloric acid to remove *iso*propylidene groups, filtered through a small amount of carbon-Celite and the filtrate concentrated and added to the top of a carbon-Celite column (170 ml carbon-Celite 1:1). The column was subjected to gradient elution (2 000 ml, 0—30 % ethanol); the appropriate fractions of the eluate were concentrated to dryness and the residue (0.9 g) was after treatment with Amberlite resins IR 120 and IR 4B recrystallised from dilute ethanol yielding a product (0.67 g, 53 % calc. on *iso*propylidene-D-glyceric aldehyde) which proved to be identical with the internal salt isolated from the alga. M. p. 163—164.5° alone or mixed with the natural product, $[\alpha]_D^{23}$ −19° (water, c = 2), CH_2O formed upon periodate oxidation: 2 moles/mole comp.

Acknowledgements. The author is indebted to *Statens Naturvetenskapliga Forskningsråd* for financial support and to Ing. L. Mikiver for his skilful assistance. The alga was kindly supplied by Dr. Colm O'h Eocha, University of California.

REFERENCES

1. Lindberg, B. *Acta Chem. Scand.* **9** (1955) 1323.
2. Lindberg, B. *Acta Chem. Scand.* **9** (1955) 1097.
3. Reeves, R. E. *J. Am. Chem. Soc.* **63** (1941) 1476.
4. Baer, E. *J. Am. Chem. Soc.* **67** (1945) 338.
5. Baer, E. and Fischer, H. O. L. *J. Biol. Chem.* **128** (1939) 463.
6. Skita, A. and Meyer, W. A. *Ber.* **45** (1912) 3580.

Received May 5, 1956.

ACTA CHEMICA SCANDINAVICA 10 (1956) 1100—1110

*iso*Thiocyanates XIX.* L(-)-5-Methylsulphinylpentyl *iso*Thiocyanate, the Aglucone of a New Naturally Occurring Glucoside (Glucoalyssin)

ANDERS KJÆR and ROLF GMELIN

The Chemical Laboratory of the University of Copenhagen, Denmark

The isolation of L(−)-5-methylsulphinylpentyl *iso*thiocyanate (VII) from seeds of the crucifer *Alyssum argenteum* Vitm. is described. The mustard oil is liberated from its glucosidic precursor, *glucoalyssin*, on enzymic hydrolysis and characterized as its thiourea derivatives, formed upon reaction with ammonia, aniline and benzylamine. The derivative with the last amine, (I), serves to prove the structure of (VII) by transformation into compounds of established structure. The aniline derivative (IX) is compared with a synthetic sample prepared elsewhere.

The mustard oil of glucoiberin is unambiguously proved to be L(−)-3-methylsulphinylpropyl *iso*thiocyanate (XIII). The configurational relationship of the latter, as well as (VII), with (−)-sulphorophene is pointed out. The natural occurrence of sulphoxides is reviewed.

A paperchromatographic survey of the *iso*thiocyanate glucosides in 12 species of *Alyssum* is presented. They appear to contain glucoalyssin, gluconapin, the glucoside of 4-pentenyl *iso*thiocyanate (glucobrassicanapin) and glucoberteroin in various combinations, together with one or two glucosides containing yet undetermined *iso*thiocyanates.

In a previous paper of this series[1] 5-methylthiopentyl *iso*thiocyanate (V) was proved to be the aglucone of a glucoside (glucoberteroin) *ex* the crucifer *Berteroa incana* (L.) DC. Strong, though admittedly inconclusive evidence further suggested that a second glucoside in the same species was derivable from one of the corresponding stereoisomeric sulphoxides. This surmise has now been put beyond dispute, through the isolation and characterization of L(−)-5-methylsulphinylpentyl *iso*thiocyanate (VII), present in various

* Part XVIII of this series: *Acta Chem. Scand.* **10** (1956) 335.

species of the genus *Alyssum* as a glucoside for which the name *glucoalyssin* is proposed *.

Due to insufficient supplies of *Berteroa*, the species *Alyssum argenteum* Vitm.** was selected as a starting material for the isolation of the new *iso*thiocyanate (VII). Paperchromatographic evidence indicated that glucoalyssin is present in *B. incana* as well, the two genera being closely allied with regard to taxonomy ***. *Alyssum* species have been only incidentally quoted as sources of *iso*thiocyanates. Thus, Schultz and Gmelin [2] from paperchromatographic survey work considered sinigrin, glucocochlearin and sinalbin to be present in various species of this genus, in addition to two or three other, less certainly identified or unknown glucosides. In this laboratory, various *Alyssum* species have been subjected to glucoside chromatography by essentially the same method, yet with different conclusions as discussed below.

Glucoalyssin occurs in most *Alyssum* species investigated here (Table 2). In *A. argenteum* Vitm. the glucoside is accompanied by only a trace of glucoberteroin, a fact facilitating the purification considerably; no attempts were made, however, to isolate the glucoside in pure condition. A methanolic extract, partly purified by precipitation of impurities with lead acetate, was subjected to enzymic hydrolysis and the sulphide-*iso*thiocyanate selectively removed by ether extraction. The sulphoxide-mustard oil (alyssin) was then extracted with chloroform and obtained as a colourless, vesicant, *levo*rotatory oil which was used directly for the preparation of solid derivatives. Its rotation value was comparable to those determined by Karrer *et al.* for other sulphoxide-*iso*thiocyanates (Table 1). On reaction with ammonia, benzylamine and aniline, alyssin afforded the corresponding thioureas in good yields. The analytical data left no doubt as to the composition, $C_7H_{13}NOS_2$, for the parent mustard oil. Infra-red spectra strongly indicated the presence of a sulphoxide-grouping in the *iso*thiocyanate, the structure of which was definitely proved through the following series of reactions, starting with the *levo*rotatory benzylthiourea-derivative **** (I).

This compound was transformed into the corresponding benzylurea (II) by a modification of the method of Dixon [5], the reaction probably pro-

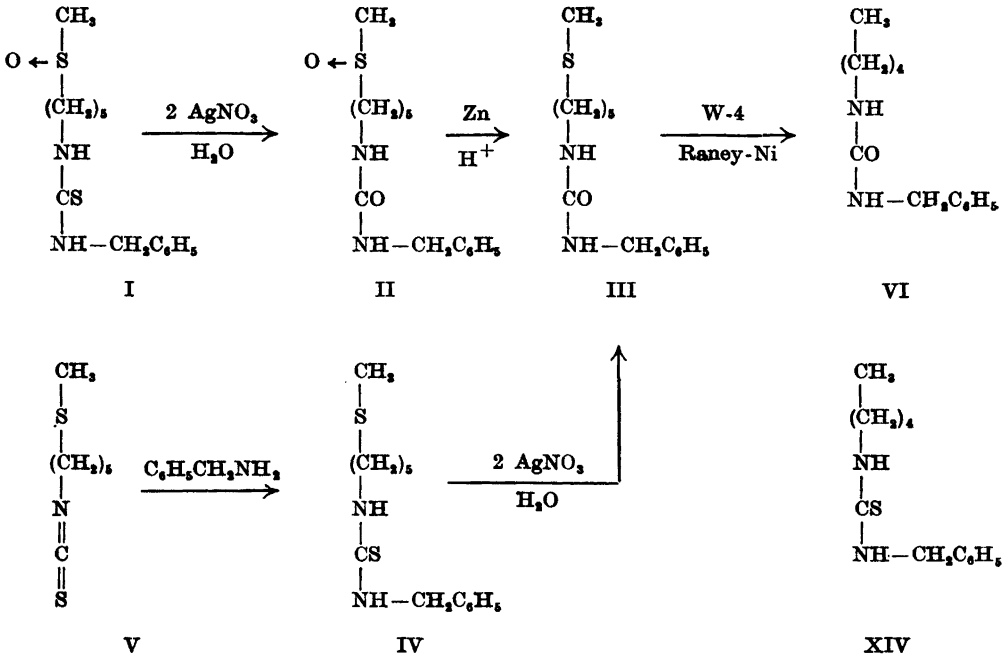
---

* *Note added in proof:* In a recent paper, submitted to publication a few weeks later than the present communication, Schultz and Wagner [27] describe the isolation from seeds of a species named *Alyssum argenteum* Allioni (*cf.* Table 2) of a crystalline tetraacetate of a glucoside, almost certainly identical with and fortuitously named as our glucoalyssin [28]. The formulation of the corresponding mustard oil as 5-methylsulphinylpentyl *iso*thiocyanate, a structure foreshadowed in a previous paper from this laboratory [1], rests solely on analysis of the acetylated glucoside, infra-red data and analogy to previously recognized *iso*thiocyanates of this type. A non-analyzed preparation of the corresponding thiourea, m. p. 112°, is further reported, yet without optical rotation data.

** The generous gift of a substantial seed sample from E. Benary, Hann.-Münden, Germany, is gratefully acknowledged.

*** *Berteroa incana* DC. was originally described by Linné (1753) as *Alyssum incanum*.

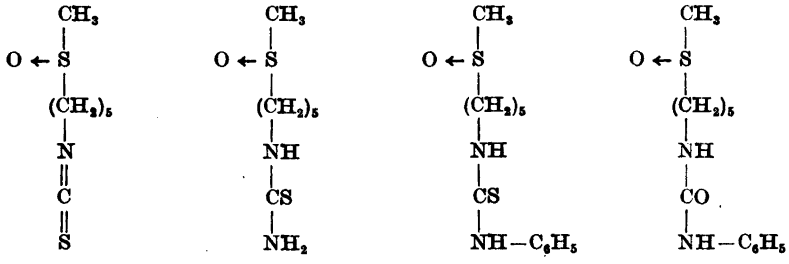
**** For reasons to be discussed in the sequel, (I) is considered to be configurationally related to *levo*-rotatory sulphoraphene, previously proposed by Schmid and Karrer [3] as a configurational reference standard for sulphoxides and arbitrarily allotted the designation L. In this paper, the substances are depicted in conformity with the convention of Karrer *et al.*[4] according to which the oxygen atom is written to the left in the projection formulae of members of the L-series, arranged with the methyl groups at the top.



I II III VI

V IV XIV

ceeding *via* a carbodiimide. Reduction of (II) with zinc dust in acid solution resulted in loss of optical activity, a fact pointing to the sulphoxide-grouping as the sole centre of asymmetry. The identity of the reduced product as 1-benzyl-3-(5′-methylthiopentyl)-urea (III) was established on comparison with an authentic specimen, prepared from the corresponding thiourea (IV) which was, in turn, produced from synthetic 5-methylthiopentyl *iso*thiocyanate [1] (V) and benzylamine. Ultra-violet and infra-red spectra, as well as mixed melting point determination, served as criteria of identity of the two preparations. A specimen of the heretofore unknown 1-benzyl-3-pentylurea (VI), needed in another connection, was produced by hydrogenolysis of (III) with W-4 Raney nickel and also by sulphur exchange of the corresponding thiourea (XIV).



VII VIII IX X

Table 1. Optical rotation data for compounds described in the present paper, (A), together with some previously reported substances of related structures.

Formula	m.p.°	$[\alpha]_D$	$t°$	Solvent	Conc. g/100 ml	Ref.
$CH_3SOCH{=}CHCH_2CH_2NCS$		—108°	18	$CHCl_3$	1.40	7
$CH_3SOCH{=}CHCH_2CH_2NHCSNH_2$	219—220	— 72°	15	H_2O	1.13	7[d]
$CH_3SOCH{=}CHCH_2CH_2NHCSNHC_6H_5$	121	—105°	18	$CHCl_3$	1.03	7
$CH_3SOCH_2CH_2CH_2CH_2NCS$		— 79°	22	$CHCl_3$	1.22	3
$CH_3SOCH_2CH_2CH_2NCS$		— 74°	18.5	C_2H_5OH		6
$CH_3SOCH_2CH_2CH_2NHCSNHC_6H_5$	133—134	— 44°[a]	18	C_2H_5OH		6
$CH_3SOCH_2CH_2CH_2NHCSNHC_6H_5$	137.0—137.5	— 54°	24.5	C_2H_5OH	1.90	A
$CH_3SO(CH_2)_3NHCSNHCH_2C_6H_5$	107.5—108.5	— 51°	24	C_2H_5OH	2.00	A
$CH_3SO(CH_2)_5NCS$		— 9°		C_2H_5OH		6
$CH_3SO(CH_2)_5NCS$[c]		— 69°	24	$CHCl_3$	4.06	A
$CH_3SO(CH_2)_5NHCSNH_2$	106.0—106.5[e]	— 79.5°	24	H_2O	2.00	A
$CH_3SO(CH_2)_5NHCSNHC_6H_5$	123	—19(?)[b]		C_2H_5OH		6
$CH_3SO(CH_2)_5NHCSNHC_6H_5$	126.0—126.5	— 62°	25	C_2H_5OH	2.14	A
$CH_3SO(CH_2)_5NHCSNHCH_2C_6H_5$	103.5—104.0	— 59°	25	C_2H_5OH	1.20	A
$CH_3SO(CH_2)_5NHCONHC_6H_5$	101.5—102.0	— 55°	24	C_2H_5OH	0.76	A
$CH_3SO(CH_2)_5NHCONHCH_2C_6H_5$	105.5—106.5	— 65°	24	C_2H_5OH	0.87	A

[a] *cf.* Foot-note p. 1104. [b] *cf.* Foot-note. [c] Non-analyzed specimen. [d] It has been established in this laboratory that the compound possessing the reported data does not represent authentic sulphoraphene-thiourea. [e] *cf.* Foot-note p. 1101.

The crystalline thiourea-derivatives, (VIII) and (IX), prepared by reaction of alyssin with ammonia and aniline, respectively, possessed properties comparable to those of the above benzyl-derivative. (—)-1-Phenyl-3-(5′-methylsulphinylpentyl)-thiourea (IX), with a specific rotation of —11°, was previously reported by Karrer *et al.*[6] as a reaction product of synthetic (+)-5-methylsulphinylpentyl *iso*thiocyanate (spec. rotat. +4°) and aniline. The corresponding antipodes were reported with the specific rotation values +19°* and —9° for the phenylthiourea and *iso*thiocyanate, respectively.

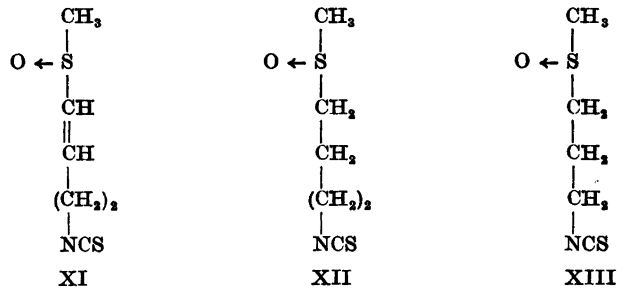
These values differ considerably from those determined in this laboratory for the natural mustard oil (VII) and its derivative (IX) (*cf.* Table 1) and raised doubt as to the stereochemical homogeneity of the formerly described preparations. We are indebted to Professor Karrer for a specimen of the original preparation of the (—)-phenylthiourea which, despite its deviating rotation value, showed hardly any depression of the melting point on admixture with our natural derivative. Moreover, the infra-red spectra of the two specimens were identical save for a few minor details. We are inclined to believe that in-

* A recent redetermination of the specific rotation gave a small negative value (<9°) suggesting that the antipodes had originally been interchanged. In addition, however, a partial racemization must have taken place on storing as estimated from the small numerical value (private communication from Professor Karrer).

completely resolved products account for the numerically low values reported, a suggestion supported by the fact that the rotation data for the natural *iso*thiocyanate and its derivatives are of the same order of magnitude as those found in analogous series (Table 1). In order to extend the number of compounds for comparison purposes, the sulphoxide-phenylthiourea (IX) was also transformed into the corresponding phenylurea-derivative (X).

The first sulphoxide-mustard oil recognized in nature was the *levo*rotatory sulphoraphene (XI), isolated by Schmid and Karrer [7] from seeds of *Raphanus sativus* L. var. *alba* and representing the first natural product in which optical activity was attributable solely to a sulphoxide-grouping. Therefore, (—)-sulphoraphene was proposed [3] as a configurational L-standard for sulphoxides *. The synthetic (—)-dihydroderivative (XII) has been directly related with (—)-sulphoraphene [3] and is consequently to be designated L-sulphoraphane. Comparable rotation values for (—)-3-methylsulphinylpropyl *iso*thiocyanate (XIII), as well as its derivatives afford strong evidence of the relationship also of the latter to the L-series [6]. Schultz and Gmelin [8] suggested the *iso*thiocyanate (XIII) (iberin) as the aglucone of the crystalline glucoside glucoiberin which they isolated from seeds of *Iberis amara* L. They did not succeed in isolating pure iberin and no crystalline derivatives were obtained. The proposed structure (XIII) was based mainly on the composition of the glucoside, infra-red spectra and structural analogy to the long known cheirolin (3-methylsulphonylpropyl *iso*thiocyanate) and sulphoraphene. In order to prove the structure and configurational relationship of iberin we have prepared its crystalline phenylthiourea- and benzylthiourea-derivatives. The former was compared with an authentic, synthetic specimen, generously supplied by Professor Karrer. The natural derivative had the specific rotation —54°, comparable to the reported value [6] (—43.6°) of the synthetic specimen **. Except for this minor deviation in optical rotation, the two products proved to be identical with regard to mixed melting point and infra-red spectra. It is thus established that iberin possesses the structure (XIII) and belongs, as well as alyssin (VII), to the same configurational series as (—)-sulphoraphene. Both are consequently to be designated as L-compounds.

Alyssin (VII) represents a novel addition to the steadily increasing group of naturally occurring sulphoxides. At present it comprises, besides sulpho-



* *Cf.* note added in proof p. 1109.

** A recent redetermination in Professor Karrer's laboratory gave $[\alpha]_D^{22.5}$ —45.4° (*c* 1.76, ethanol) (private communication).

raphene, iberin and alyssin, the active principle of garlic, alliin, which was shown by Stoll and Seebeck [9] to be (+)-S-allyl-L-cysteine sulphoxide; further, the corresponding (+)-S-methyl-L-cysteine sulphoxide, recently recognized as a constituent of cabbage juice [10] and turnip roots [11] by two groups of workers. (+)-Biotin sulphoxide has been isolated from milk residues [12] and the diastereoisomeric (−)-sulphoxide from cultures of *Aspergillus niger* [13]. Again, the so-called β-lipoic acid, isolated from liver residues, has been demonstrated to be a sulphoxide [14].

The recent recognition of so many sulphoxides in nature raises the question as to what extent these compounds shall be regarded as artefacts, formed as a result of secondary oxidation *in vitro*, or rather as species of individual metabolic significance. Although convincing evidence is lacking, various observations point to an independent biochemical role of the sulphoxides.

In Table 2 are summarized the results of paperchromatographic studies of the *iso*thiocyanate glucosides in seeds of several species of the genus *Alyssum*, collected from various botanical gardens *. In every case, paper chromatography of the glucosides in two solvent systems [2], combined with paper chromatography of the thioureas of the corresponding *iso*thiocyanates in several systems (see Experimental), served to make the assignments as correct as possible by this type of approach. Except for two, all species investigated so far contain glucoalyssin ** (A), often in combination with glucoberteroin (D) from which it is probably biogenetically derived by enzymic oxidation. In several species gluconapin (B), a name introduced by Ter Meulen [15], is proved to be present. The *iso*thiocyanate of gluconapin was previously identified as 3-butenyl *iso*thiocyanate in this laboratory [16] and, independently, by Ettlinger and Hodgkins [17], both groups using seed of rape (*Brassica napus* L.) as a starting material. From unpublished survey work, it appears that this mustard oil is one of rather wide distribution. On the paper chromatograms a glucoside (C) was often detectable possessing an R_F-value slightly lower than that of glucoberteroin. The corresponding *iso*thiocyanate is volatile and the glucoside only difficultly distinguishable from glucoerucin, the glucoside containing

* The seed samples have been sowed in the Botanical Garden of the University of Copenhagen with the purpose of controlling their identities. Possible corrections will appear at a later date.

** *Note added in proof:* The formation of glucose and sulphate subsequent to enzymic hydrolysis of glucoalyssin has been established in the present work. This fact, supplemented with the remarkable demonstration by Ettlinger and Lundeen [30] of a revised structural expression for the mustard oil glucosides, lends support to the following formula for glucoalyssin:

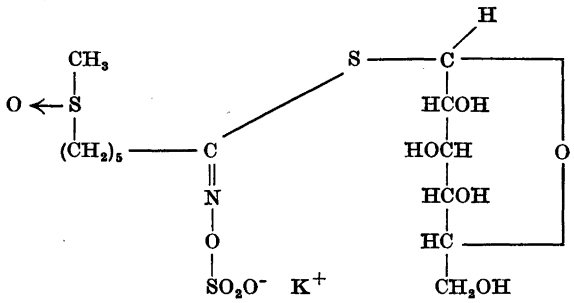


Table 2. iso*Thiocyanate glucoside pattern of seeds of various species of the genus* Alyssum *as determined by paper chromatography.*

Species	A	B	C	D
A. argenteum (All.) Vitm.[b]	+			(+)
A. Bornmuelleri Hausskn.		+		
A. Borzaeanum Nyár.	+			+
A. saxatile L. var. *citrinum*	+	+		+
A. corymbosum Boiss.[a]	+(?)	+		+
A. maritimum Lam.[a,c]	+			
A. montanum L.	+	+		+
A. orientale Ard.	+	+	+	
A. ovirense A. Kern.[a]	+			+
A. saxatile L.	+	+	+	+
A. sinuatum L.	+		+	+
A. alyssoides (L.) L.[a,d]				

A: Glucoalyssin. B: Gluconapin. C: Glucobrassicanapin. D: Glucoberteroin. (+): Traces only. [a] Contains an additional, not yet identified glucoside. [b] Probably identical with the species, less correctly designated as "*A. arg. Allioni*"[20] (=*Lunaria argentea* All.). [c] identical with *Lobularia maritima* Desv. (and *A. Benthamii*[20]). [d] identical with *A. calycinum* L.[20].

4-methylthiobutyl *iso*thiocyanate which we have previously identified in other species [18]. Paper chromatograms of the thiourea corresponding to (C) in special solvent systems, with synthetic 4-pentenylthiourea as a reference substance, leave little doubt, however, that (C) represents a new glucoside containing 4-pentenyl *iso*thiocyanate as the aglucone (glucobrassicanapin). Further evidence of its identity is available in this laboratory and will be presented in a forthcoming communication. It is interesting to note that 4-pentenyl *iso*thiocyanate fits well into the series of allyl and 3-butenyl mustard oil and the formally similar 3-methylthiopropyl [19], 4-methylthiobutyl [18] and 5-methylthiopentyl [1] *iso*thiocyanates. Two additional glucosides are recognized in the *Alyssum* series, the *iso*thiocyanates of which are being further studied.

After this work had been concluded, a paper by Schultz and Wagner [20] appeared, presenting paperchromatographic data for the glucosides of a long series of various plants, including 6 *Alyssum* species, 5 of which are identical with species investigated here. No allocations to specified glucosides are given, but it seems likely that the R_B-values 0.45 and 0.41 in *n*-butanol: acetic acid:water (4:1:3) and *n*-butanol:pyridine:water (6:4:3), respectively, represent glucoalyssin, the values 0.79—0.80 and 0.87—0.95, respectively, gluconapin, 1.06—1.07 (BuOH:HAc:H_2O) the 4-pentenyl *iso*thiocyanate glucoside and 1.16—1.17 (same system) glucoberteroin. Two additional glucosides are listed, one of which, at least, may be identical with one of the still unidentified types observed here (*cf.* Table 2).

The possible significance of the *iso*thiocyanate pattern of the genus *Alyssum* for taxonomical and genetic problems will be discussed in a forthcoming paper.

EXPERIMENTAL

The melting points are uncorrected and determined in capillary tubes in a slowly heated bath. All samples were dried over calcium chloride at room temperature before analysis.

Isolation of (−)-5-methylsulphinylpentyl isothiocyanate (VII). Finely ground seed (200 g) of *Alyssum argenteum* Vitm. was exhaustively extracted with hot 70 % methanol. The filtered extract was freed of methanol by evaporation *in vacuo* to a volume of about 500 ml. Impurities were precipitated by adding excess lead acetate as a 10 % solution. After filtration and removal of excess lead ions as PbS, the filtered solution was again concentrated to *ca.* 500 ml. Solid phosphates were added, in order to buffer the solution at pH 6.6, together with a myrosinase preparation (5 ml), and the mixture was set aside at room temperature for 18 hours. It was then extracted with two 50 ml portions of ether and the extract was discarded. Three extractions with 100 ml portions of chloroform removed all alyssin from the aqueous phase. The organic layer was washed twice with a sodium carbonate solution and finally with water. After drying, the solvent was removed in a vacuum, leaving (VII) as a colourless, vesicant oil (1.01 g) which was used directly for the preparation of the following derivatives. $[\alpha]_D^{24}$ −69° (*c* 4.06, $CHCl_3$).

L(−)-*5-Methylsulphinylpentylthiourea (VIII).* The mustard oil (500 mg) was dissolved in methanol, previously saturated with ammonia at 0°, and the solution kept at room temperature for 24 h in a stoppered flask. After removal of the solvent, a crystalline residue remained which was recrystallized from ethyl acetate, a slight, sticky residue being discarded. After two additional recrystallizations from the same solvent, the thiourea (281 mg) was obtained as colourless compact needles with m.p. 106.0−106.5° (*cf.* foot-note on p. 1101). $[\alpha]_D^{24}$ − 79.5° ± 1.5° (*c* 2.00, H_2O). The ultra-violet spectrum in ethanol was normal, displaying a maximum at 242 mμ (ε 14 200) and a minimum at 222 mμ (ε 3 870). (Found: C 40.28; H 7.60; N 13.29. Calc. for $C_7H_{16}N_2OS_2$: C 40.36; H 7.74; N 13.45).

The thiourea was chromatographed descendingly on Whatman paper No. 1 with the upper layer of the system *n*-butanol:ethanol:water (4:1:4) as the mobile phase, conditions which we previously found useful for certain thioureas [21]. Comparative runs with selected thioureas (Th.) gave the following R_F-values: iberin-Th. 0.44, cheirolin-Th. [22] 0.50, erysolin-Th.[23] 0.53, (VIII) 0.55 and N-methyl-Th. 0.60.

L(−)-*1-Benzyl-3-(5′-methylsulphinylpentyl)-thiourea* (I). From a solution of the mustard oil (VII) (500 mg) in chloroform, containing excess benzylamine, the benzylthiourea (I) crystallized spontaneously after about 5 minutes (616 mg). An analytical specimen was obtained as colourless rhombs after two recrystallizations from aqueous ethanol, m.p. 103.5−104.0°. $[\alpha]_D^{25}$ −58.6° ± 1.0° (*c* 1.20, 96 % ethanol). (Found: C 56.55; H 7.45; N 9.36. Calc. for $C_{14}H_{22}N_2OS_2$: C 56.34; H 7.43; N 9.39). The UV-spectrum in ethanol exhibited a maximum at 242 mμ (ε 14 050) and a minimum at 233 mμ (ε 12 120).

L(−)-*1-Benzyl-3-(5′-methylsulphinylpentyl)-urea (II).* The benzylthiourea (I) (200 mg) was dissolved in a mixture of ethanol (4 ml) and water (5 ml). A solution of silver nitrate (228 mg) in 50 % ethanol (6 ml) was added, resulting in the development of a yellow colour gradually changing to brown. The reaction mixture was heated on the steam bath for 0.5 h and kept neutral by gradual addition of a total of 2.6 ml of 0.5 N NaOH. After filtering through Celite, the solution was taken to dryness *in vacuo* and the benzylurea extracted with hot anhydrous ethanol which was again removed. The crystalline residue was recrystallized from ethyl acetate yielding clusters of small needles (120 mg). An analytical specimen was obtained after a new recrystallization from the same solvent, m.p. 105.5−106.5°. $[\alpha]_D^{24}$ −64.5° ± 1.0° (*c* 0.87, 96 % ethanol). (Found: C 59.30; H 7.51; N 9.63. Calc. for $C_{14}H_{22}N_2O_2S$: C 59.55; H 7.86; N 9.92). The UV-spectrum in EtOH displayed strong end-absorption and low benzyl-group absorption at *ca.* 250 mμ (ε *ca.* 200).

Reduction of (II) to 1-benzyl-3-(5′-methylthiopentyl)-urea (III). The sulphoxide-urea (II) (80 mg) was dissolved in glacial acetic acid (5 ml); this solution had the initial rotation −0.87°. Acid-activated zinc dust (50 mg) and two drops of conc. hydrochloric acid were added and the solution heated on the steam cone. After 4 h, the rotation had

decreased to $-0.07°$, and after standing at room temperature overnight, no optical activity was observable. On evaporation of the solvent and addition of water the reduced benzylurea crystallized (23 mg). Recrystallization from 50 % ethanol afforded the pure compound as rhombic plates, m.p. 86.5—87.5°, alone or in admixture with the synthetic preparation described below. The IR-spectra further served to establish the identity of the two specimens.

1-Benzyl-3-(5'-methylthiopentyl)-thiourea (*IV*). Previously prepared 5-methylthiopentyl *iso*thiocyanate [1] (V) (1.52 g) was gradually added to a solution of benzylamine (1.29 g) in ether (10 ml). Next day, the solvent was removed and the residue recrystallized from aqueous ethanol (1.98 g). An analytical specimen separated as colourless, rhombic plates from the same solvent, m.p. 56.0—57.0°. (Found: C 59.45; H 8.06; N 9.97. Calc. for $C_{14}H_{22}N_2S_2$: C 59.53; H 7.85; N 9.92).

1-Benzyl-3-(5'-methylthiopentyl)-urea (*III*). The benzylthiourea (IV) was transformed into the corresponding benzylurea (III), essentially as described above for the corresponding sulphoxide-derivative (yield 65 %). The reaction product separated from 50 % ethanol as colourless flat needles, m.p. 86.5—87.0°, undepressed on admixture with the specimen prepared above from the natural derivative. (Found: C 62.95; H 8.08; N 10.51. Calc. for $C_{14}H_{22}N_2OS$: C 63.11; H 8.33; N 10.52). The infra-red spectra of the two preparations were identical.

1-Benzyl-3-pentylurea (*VI*). Hydrogenolysis of the methylthio-urea (III) (266 mg) was performed by heating a stirred solution in anhydrous ethanol (30 ml) with a level teaspoon full of freshly prepared W-4 Raney nickel [24] for 2 h at 40°, followed by 2 h at 70°. After filtering, and removal of the solvent, the sulphur-free urea remained (181 mg). It separated from 50 % ethanol as thin platelets, m.p. 93.5—94.5°. (Found: C 70.80; H 9.37; N 12.65. Calc. for $C_{13}H_{20}N_2O$: C 70.88; H 9.15; N 12.72.) No depression was observed on admixture with a specimen produced by treatment of 1-benzyl-3-pentylthiourea with silver nitrate in the usual way.

1-Benzyl-3-pentylthiourea (XIV). A quantitative yield of this thiourea was obtained by reaction of benzyl *iso*thiocyanate with *n*-pentylamine. It separated as colourless, nacreous plates from aqueous ethanol, m. p. 53°. (Found: C 65.95; H 8.51; N 11.80. Calc. for $C_{13}H_{20}N_2S$: C 66.03; H 8.53; N 11.85).

Weller *et al.*[25] report the m. p. 62° for this compound, whereas the value 54° is listed for 1-benzyl-3-*iso*pentylthiourea. A specimen of the latter, prepared in this laboratory, melted at 62°, suggesting an accidental interchange of the two isomerides in the American laboratory. (Found: C 66.15; H 8.58; N 11.79. Calc.: *vide supra*).

L(−)-*1-Phenyl-3-(5'-methylsulphinylpentyl)-thiourea* (*IX*). A solution of the *iso*thiocyanate (VII) (1.00 g) and aniline (2 ml) in chloroform was kept at room temperature for 5 h. On addition of ether an oil separated which rapidly crystallized on scratching. The product separated from chloroform and petroleum ether as small needles (848 mg). An analytical sample was obtained as prisms from aqueous ethanol, m.p. 126.0—126.5° (previously recorded [6] 123°; a mixture melted at 125.0—125.5°). $[\alpha]_D^{25}$ $-61.6° \pm 2.5°$ (*c* 2.14, 96 % ethanol) (*cf.* Table 1). The UV-spectrum in ethanol exhibited a maximum at 247 mμ (ε 14 550), a minimum at 225 mμ (ε 9 000) and a plateau at 260—265 mμ (ε *ca.* 13 100). (Found: C 54.95; H 7.10; N 9.78. Calc. for $C_{13}H_{20}N_2OS_2$: C 54.89; H 7.09; N 9.85). The infra-red spectra of the natural and the synthetic derivative coincided except for a few, very small details.

L(−)-*1-Phenyl-3-(5'-methylsulphinylpentyl)-urea* (*X*). When the above phenylthiourea (IX) (285 mg) was treated with silver nitrate (340 mg) in the usual fashion, the corresponding phenylurea (X) was obtained (138 mg). The pure compound crystallized as thin, rhombic plates from ethyl acetate, m.p. 101.5—102.0°. $[\alpha]_D^{24}$ $-55° \pm 1°$ (*c* 0.76, 96 % ethanol). (Found: C 58.20; H 7.48; N 10.34. Calc. for $C_{13}H_{20}N_2O_2S$: C 58.17; H 7.51; N 10.44). (X) exhibited very intense absorption in the UV-region with maxima at 241 mμ (ε 24 100) and *ca.* 270 mμ (ε 1 700) and a minimum at 265 mμ (ε 1 360). These data are comparable to those reported for similar substances, *e.g.* 1-ethyl-3-phenylurea [25].

L(−)-*1-Benzyl-3-(3'-methylsulphinylpropyl)-thiourea.* A solution of glucoiberin [8] (1.00 g) was dissolved in water (200 ml), 1/15 M phosphate buffer solution of pH 6.6 (50 ml) and a myrosinase preparation (5 ml) were added, and the mixture set aside for 18 h at room temperature. The *iso*thiocyanate (iberin) was extracted with chloroform and the extract divided into two halves, one of which was treated with benzylamine in

the usual way to give a crystalline thiourea (151 mg). An analytical sample separated from ethyl acetate as stout, colourless prisms, m. p. 107.5—108.5. $[\alpha]_D^{24}$ −51° ± 1° (*c* 2.00, 96 % ethanol). (Found: C 53.75; H 6.40; N 10.27. Calc. for $C_{12}H_{16}N_2OS_2$: C 53.30; H 6.71; N 10.36).

L(−)-*1-Phenyl-3-(3'-methylsulphinylpropyl)-thiourea.* The other half of the above chloroform solution of iberin was allowed to react with aniline. The crystalline phenylthiourea (67 mg) separated from water in beautiful, colourless prisms, m.p. 137.0—137.5°. (A synthetic specimen prepared elsewhere [6] had m.p. 134.5—135.0° in the same bath, and a mixture of the two samples melted undepressed at 136.0—136.5°). $[\alpha]_D^{24.5}$ −54° ± 2° (*c* 1.90, 96% ethanol). (Found: C 51.40; H 6.42; N 10.99. Calc. for $C_{11}H_{16}N_2OS_2$: C 51.52; H 6.29; N 10.93). The infra-red spectra of the natural and the synthetic derivative were found to be identical.

Paper chromatography of Alyssum *species.* The seed samples were crushed in a mortar and extracted with hot methanol. Without further purification, these extracts were used for descending paper chromatography in the two solvent systems: (a) *n*-butanol: ethanol: water (4:1:4) and (b) pyridine:amyl alcohol:water (35:30:30), essentially by the method of Schultz and Gmelin [2].

Separate extracts were taken to dryness, dissolved in dilute phosphate buffer (pH 6.6) and hydrolyzed enzymically with myrosinase. The solutions were then extracted with chloroform and transformed into thioureas on treatment with ammonia at room temperature. The concentrated solutions were used for paper chromatography in water-saturated chloroform by our usual method [26], yet modified to the descending technique. Chromatograms in this system, run with suitable authentic reference samples, permitted the unambiguous identification of the thioureas of 3-butenyl and 5-methylthiopentyl *iso*thiocyanates. Also alyssin-thiourea could be clearly distinguished by comparison with an authentic specimen.

In some seed species (*cf.* Table 2) an additional glucoside spot, (C), with an R_F-value slightly lower than that of glucoberteroin, was observed. A corresponding spot appeared in the thiourea-chromatograms with an R_{Ph}-value [26] of *ca.* 0.95, intermediate between those given by benzylthiourea (0.92) and 4-methylthiobutylthiourea (0.99). It was indistinguishable, however, from a reference sample of 4-pentenylthiourea, the synthesis of which will be described in a forthcoming paper. This finding was confirmed in chromatograms, run with the upper layer of the system *n*-heptane:benzene-water (2:9:9) as the mobile phase. In this solvent, the R_F-values of benzyl- and 4-methylthiobutyl-thiourea are depressed to such an extent that they can be clearly differentiated from 4-pentenylthiourea. On the other hand, it is still possible to recognize the latter in the presence of 5-methylthiopentylthiourea. Other evidence (unpublished) is available for the natural occurrence of a glucoside of 4-pentenyl *iso*thiocyanate in nature.

Note added in proof: From a paper by Synge and Wood [10] it appears that an X-ray structural analysis of (+)-S-methyl-L-cysteine sulphoxide has been embarked upon elsewhere with the purpose of relating the sulphoxide configuration directly to that of the *a*-carbon atom, which is known, thus abolishing the need for an arbitrary sulphoxide reference compound.

Microanalyses were performed in this laboratory by Mr. P. Hansen. The technical assistance of Mrs. Dorthe Hansen (B.Sc.) is gratefully acknowledged. We are thankful to Dr. B. Hansen, the *Botanical Museum of the University of Copenhagen*, for botanical advice, and to the *Botanical Garden of the University of Copenhagen* for numerous seed samples.

The work is part of investigations supported by *Statens Almindelige Videnskabsfond (The Danish State Research Foundation)* and *Carlsbergfondet (The Carlsberg Foundation).*

REFERENCES

1. Kjær, A., Larsen, I. and Gmelin, R. *Acta Chem. Scand.* **9** (1955) 1311.
2. Schultz, O.-E. and Gmelin, R. *Z. Naturforsch.* **8b** (1953) 151.
3. Schmid, H. and Karrer, P. *Helv. Chim. Acta* **31** (1948) 1497.
4. Karrer, P., Antia, N. J. and Schwyzer, R. *Helv. Chim. Acta* **34** (1951) 1392.

5. Dixon, A. E. *J. Chem. Soc.* **67** (1895) 556.
6. Karrer, P., Scheitlin, E. and Siegrist, H. *Helv. Chim. Acta* **33** (1950) 1237.
7. Schmid, H. and Karrer, P. *Helv. Chim. Acta* **31** (1948) 1017.
8. Schultz, O.-E. and Gmelin, R. *Arch. Pharm.* **287/59** (1954) 404.
9. Stoll, A. and Seebeck, E. *Advances in Enzymol.* **11** (1954) 377.
10. Synge, R. L. M. and Wood, J. C. *Biochem. J. London* **64** (1956) 252.
11. Morris, C. J. and Thompson, J. F. *J. Am. Chem. Soc.* **78** (1956) 1605.
12. Melville, D. B. *J. Biol. Chem.* **208** (1954) 495.
13. Wright, L. D., Cresson, E. L., Valiant, J., Wolf, D. E. and Folkers, K. *J. Am. Chem. Soc.* **76** (1954) 4163.
14. Reed, L. J., DeBusk, B. G., Hornberger, C. S. Jr. and Gunsalus, I. C. *J. Am. Chem. Soc.* **75** (1953) 1271.
15. Ter Meulen, H. *Rec. trav. chim.* **24** (1905) 475.
16. Kjær, A., Conti, J. and Jensen, K. A. *Acta Chem. Scand.* **7** (1953) 1271.
17. Ettlinger, M. G. and Hodgkins, J. E. *J. Am. Chem. Soc.* **77** (1955) 1831.
18. Kjær, A. and Gmelin, R. *Acta Chem. Scand.* **9** (1955) 542.
19. Kjær, A., Gmelin, R. and Larsen, I. *Acta Chem. Scand.* **9** (1955) 1143.
20. Schultz, O.-E. and Wagner, W. *Z. Naturforsch.* **11b** (1956) 73.
21. Kjær, A. and Gmelin, R. *Acta Chem. Scand.* **10** (1956) 335.
22. Kjær, A., Marcus, F. and Conti, J. *Acta Chem. Scand.* **7** (1953) 1370.
23. Kjær, A. and Conti, J. *Acta Chem. Scand.* **8** (1954) 295.
24. Pavlic, A. A. and Adkins, H. *J. Am. Chem. Soc.* **68** (1946) 1471.
25. Schroeder, W. A., Wilcox, P. E., Trueblood, K. N. and Dehler, A. O. *Anal. Chem.* **23** (1951) 1740.
26. Kjær, A. and Rubinstein, K. *Acta Chem. Scand.* **7** (1953) 528.
27. Schultz, O.-E. and Wagner, W. *Z. Naturforsch.* **11b** (1956) 417.
28. Kjær, A. *Dansk Tidsskr. Farm.* **30** (1956) 117, p. 132.
29. Weller, L. E., Ball, C. D. and Sell, H. M. *J. Am. Chem. Soc.* **74** (1952) 1104.
30. Ettlinger, M. G. and Lundeen, A. J. *J. Am. Chem. Soc.* **78** (1956) 4172.

Received May 8, 1956.

ACTA CHEMICA SCANDINAVICA 10 (1956) 1111—1115

Fungus Pigments

IV. * Aurantiacin, the Pigment of *Hydnum aurantiacum* Batsch

JARL GRIPENBERG

Department of Chemistry, Institute of Technology, Helsingfors, Finland

The fungus, *Hydnum aurantiacum* Batsch has yielded a red pigment, termed aurantiacin. It has been shown that aurantiacin is 2,5-bis(benzoyloxy)-3,6-bis(*p*-hydroxyphenyl)-1,4-benzoquinone, that is, a dibenzoate of the previously known fungus pigment atromentin.

Hydnum aurantiacum Batsch is a fungus growing on the ground, particularily in shady places in spruce forests. The foot of the sporophore is dark red-brown, whereas the cap is lighter in colour with darker streaks. The pigment can very readily be extracted with ether from the fresh material, and somewhat more slowly from the dried fungus. When the extraction is carried out in a Soxhlet apparatus, a red crystalline precipitate is formed in the extraction flask. This precipitate gives after purification, as described in the experimental part, aurantiacin as dark red, small needles, m.p. 285—295°. Aurantiacin gives a yellow acetate, m.p. 235—238° and a colourless leuco-acetate, m.p. 246—253°.

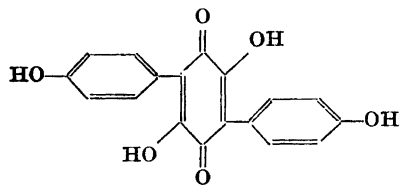
Analytical data indicated a composition $C_{32}H_{20}O_8$ for aurantiacin, $C_{36}H_{24}O_{10}$ for the acetate and $C_{40}H_{30}O_{12}$ for the leuco-acetate. The two derivatives are thus a diacetate and a dihydrotetra-acetate, respectively. Molecular weight determination gave somewhat high values, but this is not considered too important, because the low solubility of the substances necessitated working with relatively low concentrations, making the values obtained rather uncertain.

A clue to the structure of aurantiacin was obtained in an attempt to recover more of the pigment from the highly coloured ether extract. This was shaken first with sodium hydrogen carbonate and then with sodium carbonate solutions, which, however, extracted only minute amounts of material. With 2 N sodium hydroxide, on the other hand, all of the pigment could be removed from the ether solution giving a dark red-brown alkaline solution. When this was acidified and the colouring matter taken up in ether most of it could now

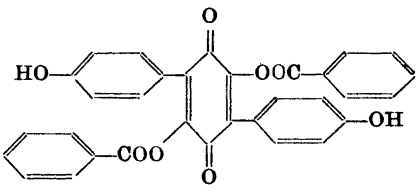
* Part III. *Acta Chem. Scand.* **6** (1952) 587.

be extracted with sodium hydrogen carbonate. Reprecipitation with acid gave a mixture which upon treatment with benzene was separated into two components. The benzene soluble component was identified as benzoic acid. The insoluble component formed upon recrystallisation dark brown leaflets, decomposing without melting at about 300°. This substance corresponds to the formula $C_{18}H_{12}O_6$ and gave a yellow tetra-acetate, $C_{26}H_{20}O_{10}$. This melts at 242—245°, but resolidifies and then melts at 290—294°. A colourless leuco-acetate, $C_{30}H_{26}O_{12}$, m.p. 235—240° was obtained upon reductive acetylation. The formation of these derivatives shows the presence of four hydroxyl groups and a quinone group in the compound $C_{18}H_{12}O_6$. The parent hydrocarbon is thus $C_{18}H_{14}$, which is the composition of terphenyl. Because several diphenylbenzoquinones have been found in fungi [1,2] the formulation of the compound $C_{18}H_{12}O_6$ as a tetrahydroxydiphenylbenzoquinone suggested itself. In fact the properties of this compound and its derivatives are in close agreement with those given by Kögl and Postowsky [3] for atromentin isolated from *Paxillus atrotomentosus* Batsch. The only serious difference is that Kögl and Postowsky report only a single m.p. 240—241° for atromentin tetra-acetate. Through the kindness of Professor Kögl, who sent a very generous sample of authentic atromentin, it could be shown that the compound obtained in the present work was identical with atromentin. When the m.p. of atromentin tetra-acetate was determined in the Kofler hot-stage microscope it showed the same characteristic double m.p. as observed with the acetate of our compound.

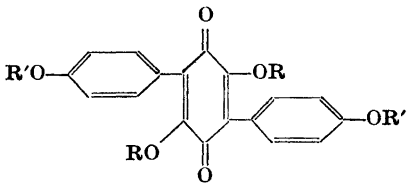
It is obvious that both the benzoic acid and the atromentin have been formed upon treatment of the extract with alkali. This suggests that they might be combined with another in aurantiacin. This was borne out by a separate experiment, where aurantiacin was dissolved in sodium hydroxide, giving atromentin and benzoic acid.



I



II



III ; R = OC—⟨benzene⟩ ; R′ = CH_3

IV ; R = CH_3 ; R′ = OC—⟨benzene⟩

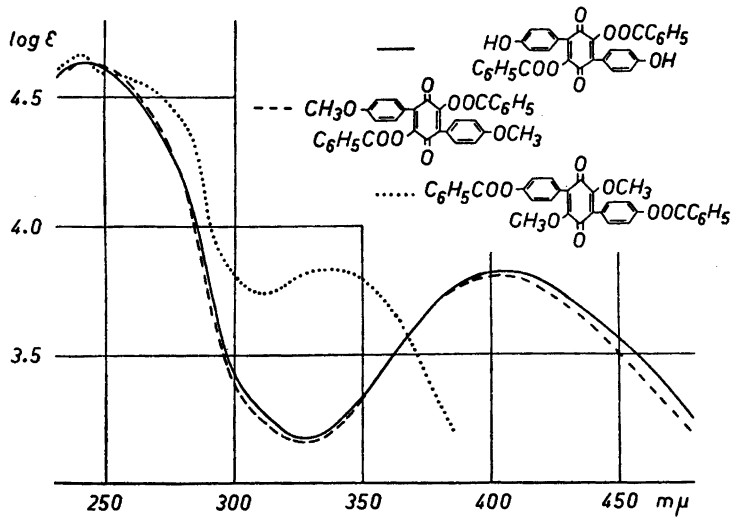


Fig. 1.

Aurantiacin is thus most probably a benzoate of atromentin, and the analyses reported above show that it is a dibenzoate. This view is further supported by benzoylation of aurantiacin to a dibenzoate. which is identical with the tetrabenzoate obtained by benzoylation of atromentin.

The structure of atromentin (I) has been established by Kögl and coworkers, both by degradation [4] and by synthesis [5]. It remains to show which of the four hydroxyl groups are benzoylated in aurantiacin. Three dibenzoates of atromentin are possible and, as will be shown below, aurantiacin must be (II)

This conclusion rests on the following observations. Aurantiacin is only a very weak acid, being insoluble in 2 N sodium carbonate, whereas atromentin is soluble even in sodium hydrogen carbonate. This shows that aurantiacin cannot have any free hydroxyl groups in the quinone ring. The almost instantaneous hydrolysis of aurantiacin, when treated with alkali also indicates that it is the hydroxyl groups in the quinone ring that are benzoylated, giving what can be considered as a vinylogous acid anhydride. Thirdly a comparison of the UV-absorption curve of aurantiacin with the absorption curves of the compounds (III) and (IV) prepared by unambiguous routes from atromentin, shows, as can be seen from Fig. 1, that the spectrum of aurantiacin is very close to that of (III), but quite different from that of (IV). (All spectra in dioxan).

Final proof of the structure (II) for aurantiacin was obtained by methylating it to its dimethyl ether, which was identical with the synthetically prepared (III). This methylation was unexpectedly difficult to achieve. Only a rather low yield (20 %) of the desired compound could be obtained. At least three other compounds were formed in the methylation but they have not been studied further.

EXPERIMENTAL

(All m.p:s have been determined on a Kofler hot-stage microscope, unless otherwise stated. The analyses have been carried out by Dr. A. Bernhardt, Mülheim.)

Isolation of aurantiacin. The finely ground sporophores of the fungus were extracted with ether in a Soxhlet apparatus and the red crystalline precipitate was filtered off. The yield was varying, one batch of 140 g giving 2.7 g, another of 170 g giving 1.7 g of crude pigment. This (100 mg) was dissolved in acetone and chromatographed on acid washed alumina (10 g). In the upper part of the column a narrow green band was formed and immediately below this a broad dark brown zone. Development with acetone caused a slow broadening of the brown zone but no clear separation from the green band could be achieved. The green band was removed from the column and the brown zone was eluated with acetone containing a few drops of acetic acid (3 drops per 40 ml). A dark red eluate was obtained. The pigment could be recovered either by evaporation of the solvent in vacuum, or by addition of water. In either case dark red crystals (85 mg) were obtained. Rechromatography of this gave only the brown zone. The pigment was recrystallised from dioxan giving small orange red needles. Upon standing they slowly turned dark red. They evidently contain dioxan of crystallisation. M.p. 285–295°. (Found: C 72.25; H 3.72; O 23.89; Mol.wt. (Rast) 610; $C_{32}H_{30}O_8$ requires C 72.18; H 3.79; O 24.04; Mol.wt. 532.5).

Aurantiacin diacetate. Aurantiacin (200 mg) was suspended in acetic anhydride (10 ml) containing two drops of pyridine. After standing overnight all the red crystals of aurantiacin had disappeared and the solution contained the yellow crystals of aurantiacin diacetate. These were filtered off (180 mg) and recrystallised from dioxan. M.p. 235–238°. (Found: C 69.61; H 3.88; O 26.85; Mol.wt. 745, 760; $C_{36}H_{24}O_{10}$ requires C 70.13; H 3.92; O 25.95; Mol.wt. 616.5).

Aurantiacin leuco-acetate. Aurantiacin diacetate (100 mg) was suspended in acetic anhydride (2 ml) to which had been added a few drops of pyridine. Zinc powder was then added and the mixture was allowed to stand. The yellow acetate disappeared rapidly and the almost colourless solution was filtered from the zinc, and poured into cold water. A white crystalline precipitate was formed (100 mg) This was recrystallised from acetic acid. M.p. 246–253°. (Found: C 68.35; H 4.50; O 27.30; $C_{40}H_{30}O_{12}$ requires C 68.46; H 4.29; O 27.25).

Aurantiacin dibenzoate. Aurantiacin (100 mg) was dissolved in pyridine (5 ml) and benzoyl chloride (0.25 ml) was added. The mixture turned warm and after some time a mixture of colourless and yellow crystals was formed. The crystals were filtered off and washed with water to remove the colourless pyridine hydrochloride. The remaining yellow aurantiacin dibenzoate was recrystallised from dioxan. M.p. 310–315°. (Found: C 74.22; H 3.93; O 22.02; $C_{46}H_{28}O_{10}$ requires C 74.59; H 3.81; O 21.60).

Treatment of the ether extract. The ether extract obtained in the extraction of one batch of fungus (170 g) was shaken successively with portions of saturated sodium hydrogen carbonate, 2 N sodium carbonate and 2 N sodium hydroxide, each time until the aqueous phase was almost colourless. The two first extracts gave upon acidification only minute amounts of precipitate, which were not further investigated, while the sodium hydroxide extract gave a large precipitate. This was taken up in ether and the extraction repeated as above. The precipitate obtained by acidification of the sodium hydrogen carbonate extract was filtered off and washed with benzene, whereby a part of it dissolved. The mother liquor from the filtration was extracted with ether, the ether was removed and the residue was divided into a benzene soluble and benzene insoluble part, which were combined with the corresponding fractions from the precipitate. 3.3 g of a brown benzene insoluble powder was thus obtained. This was extracted with hot methanol. Upon cooling 1.9 g of dark brown crystals of atromentin separated. By adding dioxan to the mother liquor a further amount (0.35 g) was obtained. Recrystallisation from methanol-dioxan mixture gave orange red crystals which rapidly darken in the air. It decomposes without melting at about 300°. (Found: C 66.68; H 3.96; O 29.54; $C_{18}H_{12}O_6$ requires C 66.67; H 3.73; O 29.60).

The benzene solution obtained above was evaporated leaving a slightly red crystalline mass. Sublimation gave colourless needles, m.p. 120–121°, identified as benzoic acid by mixed m.p.

When pure aurantiacin was dissolved in 2 N sodium hydroxide and the solution acidified a precipitate was obtained that in the same way could be separated into atromentin and benzoic acid.

Atromentin tetra-acetate was prepared from atromentin and acetic anhydride in the presence of pyridine in the same way as aurantiacin diacetate. Recrystallisation from acetic acid and then from dioxan gave yellow needles. When the m.p. was determined in a conventional m.p. apparatus a m.p. of 242—245°, not depressed by admixture of authentic atromentin tetra-acetate was observed. In a m.p. microscope the same initial m.p. was observed, but the melt recrystallised to very characteristic clusters of needles which then melted at 290—294°. The same behaviour was observed also with authentic atromentin tetra-acetate. (Found: C 63.09; H 4.06; O 32.53; $C_{26}H_{20}O_{10}$ requires C 63.41; H 4.09, O 32.49).

Atromentin leuco-acetate. Reductive acetylation in the same manner as described above for aurantiacin gave the colourless leuco-acetate, m.p. 235—240°. Kögl and Postowsky [3] report 235—236°. (Found: C 61.83; H 4.82; O 33.13; $C_{30}H_{26}O_{12}$ requires C 62.28; H 4.53; O 33.19).

Atromentin tetrabenzoate. Atromentin (100 mg) was suspended in pyridine (3 ml) and benzoyl chloride (0.5 ml) was added. The atromentin dissolved and after a short time precipitation began. After standing overnight the crystals were filtered off and washed thoroughly with water. The yellow crystals (140 mg) were recrystallised from anisole, m.p. 308—315°. Gives no depression of m.p. when mixed with aurantiacin dibenzoate. (Found: O 22.19; $C_{46}H_{28}O_{10}$ requires O 21.60).

Aurantiacin dimethylether (III). *a*) From atromentin. Atromentin was converted to its *p,p'*-dimethylether according to Kögl and Becker [4]. This (50 mg) was suspended in pyridine (2 ml) and benzoyl chloride (0.1 ml) was added. After a few hours the same amount of benzoyl chloride was added. After 24 hours the crystalline material was filtered off and washed with water. The residue, after recrystallisation from dioxan-water was obtained as orange red plates, m.p. 243—247°. (Found: C 73.09; H 4.45; $C_{34}H_{28}O_8$ requires C 72.85; H 4.32).

b) From aurantiacin. Aurantiacin (300 mg) was dissolved in dry acetone (50 ml) and dimethyl sulphate (2 ml) and potassium carbonate (3 g) were added. The mixture was boiled one day on a water bath, filtered and the acetone evaporated in vacuum. The residue was dissolved in benzene and the solution chromatographed on alumina. It formed a broad yellow, rapidly moving band and above that several narrow red to brown coloured bands. The eluate of the yellow band was evaporated under vacuum, whereby a partly crystalline residue was obtained. The crystals were filtered off (50 mg) and recrystallised from dioxan-water, giving orange red plates, m.p. 243—246°, no depression when mixed with a specimen prepared according to *a*).

Atromentin-2,5-dimethylether-p,p'-*dibenzoate* (IV). Atromentin-2,5-dimethylether was prepared from atromentin with diazomethane [3]. This (120 mg) was dissolved in pyridine (5 ml) and benzoyl chloride (0.3 ml) was added. After some time crystallisation set in and the mixture was allowed to stand for 2 days. The crystals were removed by filtration and were washed with water and benzene. The residue was recrystallised from pyridine, giving light brown needles, m.p. 278—290°. (Found: C 72.45; H 4.79; $C_{34}H_{24}O_8$ requires C 72.85; H 4.32).

The author wishes to express his indebtedness to Prof. F. Kögl, Utrecht, for a sample of atromentin. A grant from *Statens Naturvetenskapliga Kommission* is gratefully acknowledged.

REFERENCES

1. Mayer, F. and Cook, A. H *The Chemistry of Natural Coloring Matters*, Reinhold Publishing Co., New York 1943, p. 97 ff.
2. Akagi, M. *J. Pharm. Soc. Japan* **62** (1942) 129; *Chem. Abstracts* **45** (1951) 2898.
3. Kögl, F. and Postowsky, J. J. *Ann.* **440** (1924) 19.
4. Kögl, F. and Becker, H. *Ann.* **465** (1928) 211.
5. Kögl, F. *Ann.* **465** (1928) 243.

Received May 8, 1956.

ACTA CHEMICA SCANDINAVICA 10 (1956) 1116—1123

Dyeing of Wool with Lichens and Lichen Substances

YNGVE JOHANNES SOLBERG

Universitetets Kjemiske Institutt, Blindern-Oslo, Norway

Experiments have been carried out in dyeing wool with lichens, lichen substances or their decomposition products and with simple aromatic aldehydes. It is suggested that the formation of azomethine linkages is responsible for the yellow colour obtained under mild dyeing conditions with aldehydic substances. By the usual, more drastic dyeing conditions, where darker colours are developed, the chemical process during dyeing may be more complex.

Some new azomethine compounds with fumarprotocetraric and salazinic acids are described.

I. INTRODUCTION AND GENERAL SURVEY

Dyeing of wool and silk on an industrial scale with lichens has been known in Europe as long as we have records about this craftsmanship, at least as early as the fourteenth century. As a part of domestic industry records may be traced at least 2 000 years further back. The only lichens still used on an industrial scale are giving the well known Orseille dyestuffs. Although the constitution of the pigment is still unknown similar shades may be obtained with other lichens known to contain orcein.

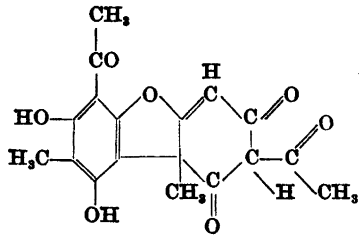
A great number of lichen species which have found use in domestic industry especially for the dyeing of wool does, however, not contain any orcein. By the dyeing procedure mostly used in domestic industry — long boiling of the whole lichens in water followed by introduction of the textiles mostly followed by further boiling — these other lichens give colours ranging from ochre through tawny to a very dull brown.

A broad review of the literature [1-17] revealed that at least 50 different lichen species have been used for dyeing purposes. When the lichens giving Orseille dyes are omitted the 35 species collected in Table 1 remain. In the same table references are given to those of the lichen constituents ("lichen acids") which most reasonably might have some connections with their dyeing properties. Usnic acid (I) one of the most common lichen acids and present in 14 of these lichens is no dyestuff for wool or silk. Most of the aromatic lichen substances are depsides (II) or depsidones (III), compare Table 2.

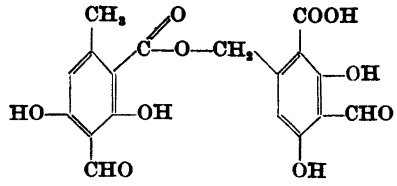
Table 1.

I	II	III	IV
Lichen species	Usnic acid	Depsides or depsidones of aldehydic structure	Other lichen acids
Parmelia centrifuga	1	2	16
» *saxatilis*		2 8	
» *conspersa*	1	2 7	
» *olivacea*		5 6	
» *sulcata*		2 8	
» *physodes*		2 6b	17
» *omphalodes*		2 8	18
» *pertusa*		2 7	
» *encausta*		2 5 6	
» *furfuracea*		2	17
» *stenophylla*	1	2 8	
» *acetabulum*		7b	
» *stygia*		2 5 6	
Cetraria islandica		5	19, 20
» *glauca*		2	21
Ramalina siliquosa	1	7	
» *farinacea*	1	6	12
» *subfarinacea*	1	8	
» *calicaris*	1		10, 14
» *cuspidata*			11
Usnea barbata	1	3	
» *florida*	1	4	
» *hirta*	1	4	
» *plicata*	1	8	
Baeomyces placophyllus		7	
Stereocaulon coralloides		2 7	
Cladonia rangiferina		2 5	
» *pyxidata*		5	
Lobaria pulmonaria		7	
Evernia prunastri	1	2	13, 14
» *vulpina*		2	23
Alectoria cana		2 8 9	16
Haematomma ventosum	1		15
» *coccineum*	1	2	22, one fatty acid
» *leiphaemum*		2	one fatty acid

1) Usnic acid, 2) Atranorin, 3) Barbatolic acid, 4) Thamnolic acid, 5) Fumarprotocetraric acid, 6) Protocetraric acid, 6b) Mono-acetylprotocetraric acid, 7) Stictic acid, 7b) Norstictic acid, 8) Salazinic acid, 9) Psoromic acid, 10) Obtusatic acid, 11) Cuspidatic acid, 12) Sekikaic acid, 13) Barbatic acid, 14) Evernic acid, 15) Divaricatic acid, 16) Alectoronic acid, 17) Physodic acid, 18) Lobaric acid, 19) Protolichesterinic acid, 20) Lichesterinic acid, 21) Caperatic acid, 22) Hymenorhodin, 23) Vulpinic acid.

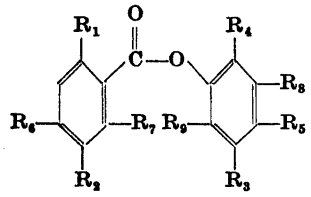


I Usnic acid

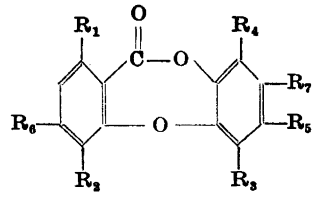


VI Barbatolic acid

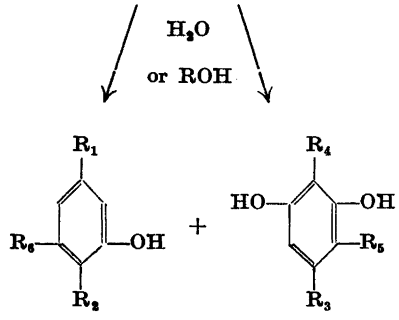
Inspection of Tables 1 and 2 reveals that most of the non-Orseille lichens used for the dyeing of wool contain aromatic compounds with at least one aldehyde function. Of the 12 lichen acids with an aldehyde function in Table 2, four have been tested as pure substances for their dyestuff properties. It turned out that if these aldehydic depsides or depsidones were applied in aqueous acetone or 90 % alcohol at room temperature, the wool took on a bright yellow to yellowish brown colour, whereas boiling under reflux for 2 hours produced the much stronger reddish to brown colours which are usually obtained when dyeing with lichens. In the 2nd chapter is demonstrated that aldehydic depsides or depsidones with different amines give azomethine compounds of yellow to orange colours. Thus it seems probable that the bright colours developed on wool from solutions in organic solvents may be azo-



II Depsides



III Depsidones



IV V

Table 2.

Reference number, Table 1	Depside lichen acids	R_1	R_2	R_3	R_4	R_5	R_6	R_7	R_8	R_9
2	Atranorin	CH_3	*CHO*	CH_3	CH_3	$COOCH_3$	OCH_3	OH	OH	H
4	Thamnolic acid	CH_3	COOH	*CHO*	CH_3	OH	OCH_3	OH	COOH	OH
10	Obtusatic acid	CH_3	CH_3	CH_3	H	COOH	OCH_3	OH	OH	H
12	Sekikaic acid	C_3H_7	H	H	OH	C_3H_7	OCH_3	OH	COOH	OCH_3
13	Barbatic acid	CH_3	CH_3	CH_3	CH_3	COOH	OCH_3	OH	OH	H
14	Evernic acid	CH_3	H	CH_3	H	COOH	OCH_3	OH	OH	H
15	Divaricatic acid	C_3H_7	H	C_3H_7	H	COOH	OCH_3	OH	OH	H
	Depsidone lichen acids									
5	Fumarprotocetraric acid	CH_3	*CHO*	CH_3	CH_2O-CO-CH ‖ CH-COOH	COOH	OH	OH		
6	Protocetraric acid	CH_3	*CHO*	CH_3	CH_2OH	COOH	OH	OH		
6b	Mono-acetylprotocetraric acid	CH_3	*CHO*	CH_3	CH_2O-CO-CH_3	COOH	OH	OH		
7	Stictic acid	CH_3	*CHO*	*CHO*	CH_3	COOH	OCH_3	OH		
7b	Norstictic acid	CH_3	*CHO*	*CHO*	CH_3	COOH	OH	OH		
8	Salazinic acid	CH_3	*CHO*	*CHO*	CH_2OH	COOH	OH	OH		
9	Psoromic acid	CH_3	*CHO*	COOH	CH_3	H	OH	OCH_3		
16	Alectoronic acid	CH_2-CO-$H_{11}C_5$	H	CH_2-CO-$H_{11}C_5$	H	COOH	OH	OH		
17	Physodic acid	CH_2-CO-$H_{11}C_5$	H	C_5H_{11}	H	COOH	OH	OH		
18	Lobaric acid	CO-C_4H_9	H	C_5H_{11}	H	COOH	OCH_3	OH		

methine compounds formed from the aldehydic function of the lichen acids and free amino residues in the wool.

A confirmation of this hypothesis follows from the fact that evernic acid (14, see Table 2) and lobaric acid (18, see Table 2) which do not contain any aldehydic group give no colour on wool. We suppose that the closely related depsides obtusatic acid (10), barbatic acid (13), divaricatic acid (15) and the depsidones alectoronic acid (16) and physodic acid (17) will prove to be wihtout dyeing properties.

That hydroxyaldehydes take part in the dyestuff formation was demonstrated with simple aromatic compounds. Methanolic solutions of salicylic aldehyde, 2,4-dihydroxy-benzaldehyde, 4,6-dimethyl-2-hydroxybenzaldehyde and vanillin all gave strong colours on wool. Piperonal and cinnamic aldehyde, however, also developed yellow colours on wool demonstrating that free hydroxygroups may be absent.

It is well known that lichen depsides are hydrolysed by boiling water II → IV + V (Refs.[18,19]). From atranorin (2) atranol (IV: $R_1 = CH_3$, $R_2 = CHO$, $R_6 = OH$) and β-orcinol carboxylic acid methyl ester (V: $R_3 = R_4 = CH_3$, $R_5 = COOCH_3$) were prepared. The orcinol carboxylic acid methyl ester did not dye wool; atranol refluxed with water and wool gave the same colour as did atranorin (2). The strong tawny colours produced during the process used in domestic industry, could then be due not to the aldehydic lichen acids themselves, but to their decomposition products generated by hydrolysis.

The chemistry of the dyeing process is obviously more complicated in the case of a native lichen than when using the corresponding lichen substances. Experience has really shown that the colour obtained with native lichen is deeper and richer than the colour which results from treatment with the isolated lichen substances. We know to-day that the aldehydic lichen substances are present in a very great number of lichen species (atranorin or chloroatranorin has been demonstrated in more than eighty different species), and that lichens which contain one or more of them always give colour with wool.

In Table 1 *Ramalina calicaris* figures as a dye lichen. This lichen is known to contain usnic (1), evernic (14) and obtusatic acid (10), none of which contains an aldehyde group. As mentioned above usnic acid does not act as a dyestuff. Pure evernic acid (from *Evernia prunastri*) was tested and as expected was found to be negative. Since obtusatic acid is the methyl homologue of evernic acid also this lichen acid most likely is not colour-forming. Since literature gives no informations about the colour obtained with *Ramalina calicaris* dyeing experiments were carried out with the whole lichen. The wool took on a green colour. The dyeing properties of *Ramalina calicaris* thus is due to quite another type of dyestuff formation.

The dye lichens *Ramalina cuspidata* and *Haematomma ventosum* are also said to be free from aldehydic substances. Lack of material has prevented examination of these lichens.

II. NEW AZOMETHINE COMPOUNDS WITH FUMARPROTOCETRARIC ACID AND SALAZINIC ACID

It appears that comparatively few azomethine compounds of depsidone aldehydes and derivatives have been studied [20-26]. Aniline, bromoaniline, phenylhydrazine and *p*-nitrophenylhydrazine have been used as amino components. These azomethine compounds are yellow substances, easily decomposed into their components by treatment with diluted hydrochloric or sulphuric acid. Most frequently they are slightly soluble in the common organic solvents.

The synthesis of five new azomethine compounds is reported in this paper: *p*-aminobenzoic acid-N-fumarprotocetraric acid, glycine methyl ester-N-fumarprotocetraric acid, methyl anthranilate-N-fumarprotocetraric acid, methyl *m*-aminobenzoate-N-fumarprotocetraric acid and di(methyl *m*-aminobenzoate-N-)salazinic acid.

The yellow colour of these azomethine compounds resembles closely the colour obtained when wool is dyed under certain conditions with fumarprotocetraric acid, atranorin, chloroatranol and simpler aromatic aldehydes. This seems to support the suggestion put forward above that azomethine linkages are formed when fibres of wool and silk react with aromatic aldehydes. The fact, however, that the dyeing under other conditions will give darker colours (tawny, brown, redbrown) would indicate that the chemical process in such cases is more complex.

The azomethine compounds described in the experimental part are hygroscopic substances, amorphous or crystalline. They have no definite melting point, but decompose above two hundred degrees.

EXPERIMENTAL

Isolation of lichen substances

The following aldehyde depsidones have been isolated: Fumarprotocetraric acid from *Cetraria islandica* and salazinic acid from *Parmelia saxatilis*. The isolation of the depsidones was carried out mainly according to the methods described by Simon, Hesse, Zopf, Koller, Klein, Pöpl and Asahina [2, 15, 20-23, 27-34].

Preparation of azomethine compounds

I. p-*Aminobenzoic acid-N-fumarprotocetraric acid.* To 2 g of fumarprotocetraric acid, dissolved in the minimum amount of pyridine, was added an ethanolic solution of 0.6 g of *p*-aminobenzoic acid. The mixture immediately turned dark yellow. On dilution with 80 ml hot ethanol and standing, microscopic, yellow needles were precipitated. The condensation product was purified by recrystallization from acetone-petroleum ether (1:2).; Yield: 1.3 g. (Found: C 58.6; H 4.3; N 2.2; equiv.wt. 145.4. Calc. for $C_{29}H_{21}O_{13}N$: C 58.9 H 3.6; N 2.4; equiv.wt. 147.9.)

The substance was easily soluble in cold pyridine and dioxan, soluble in hot acetone and ethanol, insoluble in ether, ethyl acetate, xylene, chloroform and benzene. An ethanolic solution of the compound gave an intensely red colour with *p*-phenylenediamine. The yellow colour of the condensation product disappeared on treatment with diluted hydrochloric acid, indicating that the compound was decomposed. In diluted alkali the compound was stable for some time (5—7 min.).

II. *Glycine methyl ester-N-fumarprotocetraric acid.* Fumarprotocetraric acid (1 g), glycine methyl ester (0.5 g), dry methanol (50 ml) and dry acetone (50 ml) were shaken in a bottle at room temperature for 15 h. By evaporation of the solvents a yellow, amorphous product was precipitated. The condensation product was purified by washing with much petroleum ether and then dried at 80° for 15 h. (Found: C 55.7; H 4.4; N 2.5; CH_3O 5.8. Calc. for $C_{25}H_{21}O_{13}N$: C 55.3; H 3.9; N 2.6; CH_3O 5.7.) The condensation product was found to be easily soluble in ethanol and acetone, slightly soluble in ether, petroleum ether and benzene.

III. *Methyl anthranilate-N-fumarprotocetraric acid.* Fumarprotocetraric acid (1 g), methyl anthranilate (0.5 g), acetone (75 ml) and 96 % ethanol (75 ml) were shaken at room temperature for 15 hours. After filtration the solution was evaporated to dryness. The yellow residue was purified by treatment with petroleum ether. Before analysis the azomethine compound was dried at 60° for 15 h. (Found: C 59.4; H 4.2; N 2.4. Calc. for $C_{30}H_{23}O_{13}N$: C 59.5; H 3.8; N 2.3). The substance was soluble in acetone and ethanol, insoluble in petroleum ether and benzene.

IV. *Methyl* m-*aminobenzoate-N-fumarprotocetraric acid.* This azomethine compound was prepared in two different ways.

a) Fumarprotocetraric acid (1 g) and methyl *m*-aminobenzoate (0.7 g) were shaken with a mixture of 100 ml dry acetone and 100 ml absolute ethanol at room temperature. Yellow, transparent needles precipitated gradually. After 24 h the condensation product was filtered and treated with 75 ml ether for 20 h. Next dried at 100°. (Found: C 59.9; H 4.2; N 2.3; CH_3O 5.1. Calc. for $C_{30}H_{23}O_{13}N$: C 59.5; H 3.8; N 2.3; CH_3O 5.1.) The azomethine compound was insoluble in ether, benzene and petroleum ether, slightly soluble in acetone and ethanol, easily soluble in warm glycol monoethyl ether.

b) Fumarprotocetraric acid (1.5 g) was dissolved in 700 ml hot 80 % acetone. To this solution methyl *m*-aminobenzoate (1 g), dissolved in 150 ml 96 % ethanol, was added. The mixture immediately turned dark yellow. By evaporation of the solvents a yellow, amorphous product was precipitated. The condensation product was purified by shaking it with 50 ml ethanol for 20 h. (Found: C 60.1; H 4.2; N 2.2; CH_3O 5.6. Calc. for $C_{30}H_{23}O_{13}N$: C 59.5; H 3.8; N 2.3; CH_3O 5.1.)

V. *Di(methyl* m-*aminobenzoate-N-)salazinic acid.* Salazinic acid (2.5 g) was dissolved in 600 ml boiling 80 % acetone. Methyl *m*-aminobenzoate (4 g) dissolved in 50 ml acetone was added. The deep yellow solution was filtered and diluted with 1.2 liter cold water. Hereby the condensation product was precipitated. It was purified by recrystallization from acetone-water (1:2). Yield 2.5 g. (Found: C 62.0; H 4.3; N 4.1; CH_3O 9.5. Calc. for $C_{34}H_{28}O_{13}N_2$: C 62.4; H 4.0; N 4.3; CH_3O 9.5). This azomethine compound was easily soluble in hot acetone, slightly soluble in ethanol and insoluble in ether and benzene. An ethanolic solution gave a brown-violet colour with ferric chloride. In conc. sulphuric acid the azomethine compound dissolved with a red colour.

REFERENCES

1. Karr, A. E. *Textile Colorist* **64** (1942) 431.
2. Zopf, W. *Die Flechtenstoffe in Chemischer, botanischer, pharmakologischer und technischer Beziehung*, Jena 1907.
3. Zulkowski, X. and Peters, K. *Monatsh.* **11** (1890) 227.
4. Horwood, A. R. *Science Progress* **23** (1928) 279.
5. Mell, C. D. *Textile Colorist* **57** (1935) 409.
6. Karr, A. E. *Textile Colorist* **65** (1943) 74.
7. Patterson, T. S. *J. Chem. Soc. Ind.* **1924** 189 T.
8. Westring, J. P. *Svenska lafvarnas färghistoria, eller sättet att använda dem till färgning och annan hushållsnytta*, Stockholm 1805.
9. Christensen, H. *Lærebok i farvning med planter*, Kristiania 1908.
10. Bråten, K. and Westby, I. *Håndarbeidsbok for husmorsskoler*, Oslo 1944.
11. Nannfeldt, J. A. and Du Rietz, G. E. *Vilda Växter i Norden (Mossor, Lavar, Svampar, Alger)*. Stockholm 1945.
12. Nolan, T. J. *Thorpe's Dictionary of applied Chemistry* **7** (1946) 284.
13. Krog, H. *Nytt Mag. for Naturv.* **88** 57.

14. Dahl, E. *Extrait de la Revue Bryologique et Lichénoloque*, T. *XXI* (1952) 1.
15. Hesse, O. *J. prakt. Chem.* **57** (1898) 295.
16. Asahina, Y. Mitt. pharm. Inst. kaiserl. Universität zu Tokyo *Acta Phytochim.* **3** (1934) 46.
17. Asahina, Y. Tanase, Y. and Yosioka, I. *Ber.* **69** (1936) 125.
18. Pfau, A. St. *Helv. Chim. Acta* **9** (1926) 650.
19. Pfau, A. St. *Helv. Chim. Acta* **17** (1934) 1319.
20. Asahina, Y. and Tanase, Y. *Ber.* **67** (1934) 411.
21. Asahina, Y. and Asano, J. *Ber.* **66** (1933) 689, 893.
22. Koller, G., Klein, A. and Pöpl, K. *Monatsh.* **63** (1933) 301.
23. Asahina, Y. and Tukamoto, T. *Ber.* **67** (1934) 963.
24. Asahina, Y., Yanagita, M. and Omaki, T. *Ber.* **66** (1933) 943.
25. Asahina, Y. and Yanagita, M. *Ber.* **67** (1934) 1965.
26. Asahina, Y., Yanagita, M. and Yosioka, I. *Ber.* **69** (1936) 1370.
27. Hesse, O. *J. prakt. Chem.* **70** (1904) 455.
28. Simon, O. *Arch. Pharm.* **240** (1902) 521.
29. Asahina, Y. and Tanase, Y. *Ber.* **66** (1933) 700.
30. Asahina, Y. and Yanagita, M. *Ber.* **69** (1936) 120.
31. Asahina, Y. and Yasue, M. *Ber.* **70** (1937) 1053.
32. Asano, M. and Kanematsu, T. *Chem. Abstracts* **25** (1931) 4266.
33. Hesse, O. *J. prakt. Chem.* **68** (1903) 41.
34. Asahina, Y. and Asano, M. *Ber.* **66** (1933) 1215.

Received January 15, 1956.

ACTA CHEMICA SCANDINAVICA 10 (1956) 1124—1131

The First Step in the Swelling of Gelatin with Water. II

CHR. WINTHER

Photochemical Laboratory, Technical University of Denmark, Copenhagen, Denmark

On the basis of a very simple model of the structure of gelatin and of the individual layers of the Christensen-interference plate it is possible to explain the two steps of absorption of water into the interference plate and to show that the final amount of water here is the same as in the corresponding chromated gelatin plate. Moreover it is shown that the diffusion of water throught gelatin is independent of the degree of hardening.

In the first paper in this series [1] I have examined the speed of swelling of the Christensen-interference plate with water. I was thereby forced to assume that about half of the water was taken up practically momentarily, whereas the remaining water was absorbed in the course of some days.

Continued examination of this peculiar phenomenon on various other examples of the said plates has shown its general character. At the same time it has been possible to measure the first "momentary" time and to give a plausible explanation of the two different modes of swelling on the same plate.

1. THE FORMULA

In the said paper was used the formula

$$v_v - \Delta = (v_\infty - \Delta)(1 - 10^{-k \cdot t^{0.5}}) \quad (1)$$

where v_v is the momentary volume of water, Δ the "instantaneous" absorption of water, v_∞ the final absorption of water, all of them per 100 volumes of gelatin, k is a constant and t the time (in minutes) of the slow absorption.

The examination of five other plates has shown that good agreement with this formula can only be obtained if the time t is replaced by $t - t_0$, the formula therefore being

$$v_v - \Delta = (v_\infty - \Delta)(1 - 10^{-k_2(t-t_0)^{0.5}}) \quad (2)$$

and, as the time t_0 is of the order of 0.1—2.0 minutes, it must be understood as the time for the first, "momentary" swelling.

Table 1 contains the results. The 1st column shows the number of the plate. Fig. 1 refers to the upper side of the "broad band"[2], Fig. 2 to the lower side. The 2nd column shows the percentage by volume of unhardened gelatin G′, the 3rd the percentage by volume of silver bromide v_A. Next comes Δ, the first rapid absorption of water, $v_\infty - \Delta$, the second slow absorption, then the observed and calculated values of t_0, the observed and calculated values of k_2, the velocity constant of the slow absorption, and finally k_3 (see below).

Table 1.

Plate No.	G′	v_A	Δ	$v_\infty - \Delta$	t_0		$k_2 \times 10^2$		k_3
					obs.	calc.	obs.	calc.	
20_2	22.2	8.3	94.2	40.2	1.7	1.8	2.88	2.50	23.0
20_1	31.1	15.3	93.3	38.7	2.0	1.7	2.57	2.70	20.6
$14a_2$	22.2	15.0	90.2	38.5	1.5	1.3	3.54	3.36	21.2
$14a_1$	30.2	26.4	87.1	41.9	0.9	1.0	3.47	3.60	24.1
9_2	22.2	14.9	85.7	43.9	1.2	0.9	3.41	3.35	20.0
9_1	30.9	22.9	81.9	46.5	0.5	0.6	3.34	3.32	25.0
28_2	21.9	14.2	82.6	59.4	0.5	0.7	3.11	3.30	24.9
28_1	34.2	23.3	76.7	58.5	0.4	0.3	2.85	3.14	19.8
2_2	22.2	17.3	71.7	76.4	0.1	0.1	3.77	3.60	23.7
2_1	30.6	27.0	69.9	76.5	0.1	0.1	3.23	3.63	18.7
									22.1

The quoted values are means of three independent experiments.

The plates were selected to give the greatest possible variations in properties and composition. No. 20 was watered before treatment with silver nitrate, No. 28 has a special thick coating, No. 2 a special high content of silver bromide, and the remaining two plates are more normal, but still with a marked difference in the extinctions of the original chromated gelatin plates.

2. THE STRUCTURE OF THE GELATIN LAYER

In order to penetrate into this certainly very complex subject it is necessary to use a very simplified working model. Like Sheppard, Lambert and Swinehart [3] I assume that the gelatin molecule has a length of about 100 mμ and a diameter of 0.8—0.9 mμ, and that all the polar groups are found on one side of the molecule, which is therefore hydrophilic, whereas the non-polar groups are found on the other side, which is therefore hydrophobic.

The most simplified model of this structure is shown in Fig. 1, where two hydrophilic surfaces are connected, perhaps with a thin layer of water between them, as air dryed gelatin always contains some water, about 15—20 %. The mutual attraction between these hydrophilic surfaces, with or without the layer of water, will presumably be greater than the attraction between the two adjacent, hydrophobic surfaces.

3. THE CHROMATED GELATIN

If a gelatin layer of the suggested structure is treated with a solution of a chromate, the chromate ions must necessarily be adsorbed on the hydrophilic surfaces, and by the following hardening by light the chromate-bonds must therefore be situated between these surfaces. As to the hydrophobic surfaces, there is accordingly no difference between hardened and unhardened gelatin.

4. THE DIFFUSION OF WATER

In general it is assumed that the rate of diffusion of water in gelatin is independent of the degree of hardening of the gelatin, but it has not been possible to find any literature about this problem. Therefore, I have measured the rate of diffusion directly.

For this purpose four thick layers of photographic gelatin (Stoess, middle hard) were prepared on plate glass which was covered with Zaponlack so that afterwards the layers could be removed and the Zaponlack be dissolved in amyl acetate. One of the layers was hardened with formaldehyde, another, after treatment with a chromate solution, was hardened by prolonged exposure with a mercury lamp, while the two others were not treated in any way.

The thicknesses of the layers were measured directly with a micrometer. Then they were, one at a time, pressed against a Christensen-interference plate, a little water was poured out on the gelatin and the time was measured until the first sign of colour variation on the interference plate was observed. The results are shown in Table 2.

Table 2.

Treatment	Thickness in μ	t sec	sec/μ
Unhardened	65	41	0.63
Unhardened	60	45	0.75
Hardened with formaldehyde	73	60	0.82
Hardened with chromate and light	80	45	0.56
			0.69

Table 2 shows that the rate of diffusion is independent of the degree of hardening. This result must be expected from the suggested model of the structure. The diffusing water must find its way through the lowest possible resistance, *i.e.* between the hydrophobic surfaces. As conditions here are independent of the degree of hardening, the rate of diffusion must be the same for hardened and unhardened gelatin, as was actually found.

5. THE TREATMENT WITH SILVER NITRATE

When the exposed chromated gelatin plate is treated with a solution of silver nitrate the silver ions must be adsorbed on the hydrophilic surfaces, and

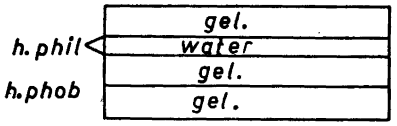


Fig. 1.

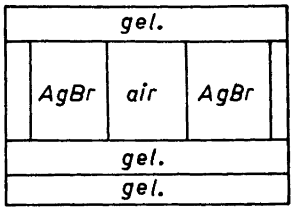


Fig. 2.

by the subsequent treatment with potassium bromide the silver bromide particles must become situated on the same places, probably linking the two adjacent surfaces together. The situation in the plate is now as shown in Fig. 2.

6. THE FIRST "INSTANTANEOUS" SWELLING

The experiments show that the amount of water hereby absorbed agrees with the formula

$$\Delta = 64 + k_3 t_0^{0.5} \tag{3}$$

The values of k_3 and the calculated values of t_0 are shown in Table 1.

The number 64, which means volume of water per 100 volumes of total gelatin, is the same for all the examined plates. As it is independent of time it must refer to the almost instantaneous diffusion of water between the hydrophobic surfaces. It must therefore be independent of the degree of hardening.

In Fig. 3 are shown my earlier measurements [4] of the amounts of water absorbed in differently exposed chromated gelatin. The four curves correspond to plates which are treated with water 2, 4, 7 and 11 days after producing the

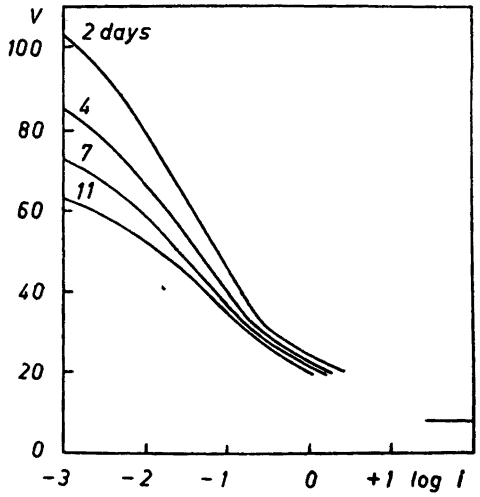


Fig. 3.

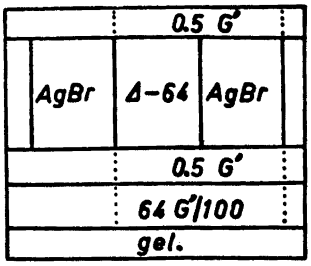


Fig. 4.

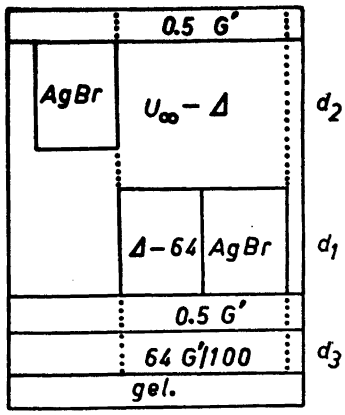


Fig. 5.

plates. The abscissae are the logarithms of the quantities of light, the ordinates the amounts of water per 20 mg of coating. Obviously the curves are not going to zero but are approaching a certain positive value. To the right is marked out the amount of water which corresponds to 64 %. These measurments therefore confirm the conclusion that the very rapid diffusion is independent of the degree of hardening.

When this rapid diffusion has finished the water proceeds to fill the interstices between the gelatin and the silver bromide particles. It is quite natural that the time for this absorption increases with the amount of absorbed water, as shown in formula (3). The measured values, 0.1—2.0 minutes, are in agreement with my earlier measurements, which have shown that the swelling of chromated gelatin is completed in less than 2.5 minutes. Further treatment with water up to 15 minutes shows no difference.

The situation is now as shown in Fig. 4.

7. THE SECOND SWELLING

In my earlier experiments with swelling of exposed layers of chromated gelatin [5] I have found that the adsorption of silver nitrate is somewhat greater than could be expected from the concentration of the solution, so that a selective adsorption of silver nitrate must take place. In other words, the forces between silver ions and gelatin are somewhat stronger than those between water and gelatin. Through the competition between the bonds water-gelatin and AgBr-gelatin, which consequently are not very much different, there will in every moment occur a number of ruptures between gelatin and silver bromide, so that there will always be a very small, but constant, number of free gelatin surfaces. This situation can be written as an equilbirium

$$\text{gel.AgBr.gel.} \rightleftharpoons \text{gel. AgBr} + \text{gel.}$$

The two "concentrations" on the right side are equal, therefore

$$\text{gel.} = K\ (\text{gel.AgBr.gel.})^{0.5}$$

Now, after the first rapid absorption water continues to enter. Thereby the process must be furthered, and the speed must be proportional to the existing free gelatin surface. In accordance herewith the experiments show that

$$k_2 = k_4 \left(\frac{v_A}{G' - \frac{64}{9.3}} \right)^{0.5}$$

The number 9.3 is the swelling factor for this particular type of gelatin [4]. For the results see Table 3 (for k_4) and Table 1 where the observed and calculated values of k_2 are compared.

Now the situation is as shown in Fig. 5. In this figure are indicated the thicknesses of

the gelatin molecule (assumed to be 0.8 mμ),
the silver bromide particle, d_1,
the layer v_∞—Δ, d_2, and
the layer "64", d_3.

These three numbers are given in absolute measure, if the thickness of the gelatin molecule is taken as 0.8 mμ. The following two lengths are only relative.

Table 3.

Plate No.	$k_4 \times 10^2$	d_1	d_2	m	n	v_1	v_2	D	k_5
20_2	3.92	2.78	2.90	13.4	3.0	4.37	5.68	11.9	2.73
20_1	3.23	2.28	1.98	12.8	6.8	5.75	4.26	11.9	2.55
$14a_2$	3.57	2.96	2.78	8.8	5.0	5.18	5.74	15.0	2.35
$14a_1$	3.27	2.62	2.24	8.8	10.1	5.75	4.86	15.0	2.36
9_2	3.45	2.64	3.16	8.2	5.6	5.18	5.80	14.8	2.45
9_1	3.40	2.28	2.60	7.8	10.0	6.27	4.88	14.8	2.52
28_2	3.08	2.36	4.28	7.8	6.0	5.07	6.64	19.3	2.10
28_1	3.08	1.68	2.74	7.4	13.9	5.96	4.42	19.3	2.28
2_2	3.55	1.80	5.52	4.2	9.6	5.18	7.32	15.8	2.06
2_1	3.51	1.80	3.90	4.2	15.0	5.76	5.70	15.8	2.12
	3.40					5.45	5.53		2.38

The length of the silver bromide particle, n, and
the length of the water filled interstice $\Delta - 64$, m.

As $$0.5\ G' = 0.8\ (m + n) \qquad (5)$$

and $$\Delta - 64 + v_A = d_1\ (m + n)$$

then $$d_1 = 1.6\ \frac{\Delta - 65 + v_A}{G'} \qquad m = \frac{\Delta - 64}{d_1} \qquad n = \frac{v_A}{d_1}$$

Further

$$d_2 = d_1 \frac{v_\infty - \Delta}{\Delta - 64 + v_A} \qquad d_3 = 1.6 \frac{64}{100} = 1.0 \text{ m}\mu$$

The last number d_3 must have a constant value as the amount 64 comprises both hardened and unhardened gelatin.

The values of the other quantities are given in Table 3.

For pure chromated gelatin with the swelling factor 9.3 the amount of water in the second slow swelling is 9.3 G′ — 64. The length $m + n$ is calculated for 0.5 G′ (see formula (5)). The amount of water per (relative) unity of length therefore is

$$v_1 = \frac{0.5(9.3\ G' - 64)}{m + n}$$

For the interference plate the corresponding quantity (see Fig. 5) must be

$$v_2 = \frac{(v_\infty - \Delta)\frac{m}{m+n} + \Delta - 64}{m} = d_1 + d_2$$

The values of v_1 and v_2 are shown in Table 3. The values of v_2 must be less exact than those of v_1 because so many different observations take part in the calculations of them, each with its own uncertainty. As a whole there can still be no doubt about the identity of the two series of numbers. The slow absorption of water, therefore, proceeds to the same end in pure chromated gelatin and in the interference plate, indicating that the elastic forces between the gelatin molecules which terminate the absorption are of the same magnitude in the two different cases.

8. THE SPONTANEOUS DRYING OF THE WET PLATE

After the measurement of the final amount of water by the swelling process the plate was with the utmost speed wiped with filter paper and then spectrographed 0.5, 1, 2 . . . minutes after wiping.

During the drying process the water does not need to overcome any elastic or other forces, but the process is a simple diffusion and evaporation. Accordingly the speed of drying must be inversely proportional to the thickness of the coating and directly proportional to the remaining amount of water. Therefore

$$-\frac{dv}{dt} = k_5 \frac{v_V}{D}$$

where D denotes the thickness of the coating in μ. Through integration it follows that

$$v_V = v_\infty\, 10^{-k_5 t/D}$$

Table 3 contains the results. It seems that the constant k_5 decreases a little with increasing thickness of the coating. It must, however be taken into account that the half period for $D = 11.9\ \mu$ is only 1.3 minutes. As the first

spectrograms were taken after 0.5 and 1 minute and the time of exposure must be at least 5 seconds, there must be a systematical error which tends to an apparent increase of the speed of drying, *i.e.* the value of k_5 in this case tends to be too great. For the greater values of D the half period increases up to 2.8 minutes and the measurements are therefore apt to be less erroneous.

After completion of this work I have learned that Bagley and Long [6] have examined a quite analogous case by the sorption of acetone vapour in cellulose acetate. Thereby they have found, first a rapid and thereafter a slow stage of sorption, and they have explained the former as due to diffusion and the latter to breaking of the interchain bonds in the polymer network, just as I have proposed.

REFERENCES

1. Winther, Chr. *Acta Chem. Scand.* **8** (1954) 1053.
2. Winther, Chr. *Trans. Danish Acad. Techn. Sci.* **1953**, No. 5, 27.
3. Sheppard, S. E., Lambert, R. H. and Swinehart, D. *J. Chem. Phys.* **13** (1945) 372.
4. Winther, Chr. *Trans. Danish Acad. Techn. Sci.* **1953**, No. 5, 21.
5. Winther, Chr. *Ibid.* **1953**, No. 5, 19.
6. Bagley, E. and Long, F. A., *J. Am. Chem. Soc.* **77** (1955) 2172.

Received May 12, 1956.

ACTA CHEMICA SCANDINAVICA 10 (1956) 1132—1142

The Diffusion of an Electrolyte Solution in a Superimposed Electric Field

OLE LAMM

Department of Physical Chemistry, Royal Institute of Technology, Stockholm, Sweden

A diffusion effect in electrolyte solutions, arising from an outer field being superimposed in the diffusion direction, is discussed and, in a special case, related to the field characteristics and to the kinetics of the ionization equilibrium.

As is well known, the diffusion of salts in solution is accompanied by a macroscopic electric field, which changes with the nature of the concentration gradient and during the diffusion process. This field, and the ionic migration in it, is characteristic of the gradient diffusion of electrolytes. Phenomena within the gradient, obtained by superimposing an outer electrical field, are naturally considered in connection with the theory of electrophoresis [1], owing to the importance of knowing what happens to the gradient itself (such as sharpening or broadening effects) and of knowing how to define the migration of a boundary. It is in this case the question of a constant outer field. The literature concerning this case is rather large.

In the present article we will investigate the possible ability of the superimposed field to increase the diffusion coefficient of one component of the solution. Such an effect can be foreseen for both alternating current and direct current. In section 3 we will briefly systematize some different reasons for the occurrence of such an electrodiffusion phenomenon, irrespective of whether the order of magnitude is sufficient for an experimental demonstration or not. In sections 1 and 2 we will enter into the quantitative aspect, although only in a special case. We will assume the system to be free of thermal convections, the appearance of which sets a serious limit for the measurements and must be decisive for the choice of experimental conditions.

1. GENERAL PRINCIPLES

Owing to the fact that gegenions, which play no direct role in the above-mentioned electrodiffusion phenomenon possess the disadvantage of increasing the Joule heat, the theory is exemplified by a case with only one single electro-

lyte component *. In the simplest case, this is a weak electrolyte AB. In the ionization equilibrium the constituents A and B are present either as ions or as uncharged AB. This forms a statistical basis for a diffusion effect since the ions are not simply moving up and down as in a completely ionized, simple electrolyte. (This latter is theoretically true only if the statistical changes in the mobility of the ions are neglected. These changes appear to be too rapid for a measurable effect in ordinary cases.)

In the kinetical equilibrium $AB = A^+ + B^-$, an ion has a certain average life-time T. This may not always be the same for the two kinds of ions, $T^+ \neq T^-$. For the present we will assume that the undissociated state AB has a sufficiently long average life-time, with a statistical dispersion large enough, to make the duration of the ionic state of each single A (and B), even for short time intervals, randomly distributed on the time axis of the alternating field.

In the experiments it is not necessary to use a concentration gradient — we can instead measure the self-diffusion using isotopic labelling. Some of the possible systems (see section 3) will give an effect *only* in self-diffusion. In self-diffusion we have, with some exceptions, the disadvantage of a very small density gradient, which may cause difficulties owing to the Joule heat and convection risk **. We will, therefore, assume a real concentration gradient. This complicates the theory because of the Nernst diffusion potential.

Assuming a concentration gradient of the salt as in a differential measurement of the diffusion coefficient, we arrange electrodes at the top and bottom of the diffusion cell or use a technique as in electrophoresis work. Applying an alternating electrical field upon the gradient column, an ion A^+ will move a distance l_+ in one direction, the length of which may depend on the life-time of the ion, on the phase condition at the moment of appearance of the ionic state and on the frequency of the electric field. In addition, l_+ of course depends on the mobility of the ion and on the field strength. After an average time T^+, the ion disappears. In the next ionic state of the same A, the field direction may be the same or opposite, the correlation of phase of the electrical field at the moments of disappearance and reappearance of the ion being supposed to be low according to our suppositions. Under these circumstances, the action of the field will result in a macroscopical net displacement of the ion and the ion constituent A, and therefore also of the substance AB as a component. Thus we have an electrical diffusion effect in addition to the ordinary diffusion.

Assuming ideal statistical conditions, the electrical diffusion effect upon the cations may be expressed by a one-dimensional diffusion coefficient according to *** (see for instance the recent article [2])

$$D^+ = \nu \, l_+^2/2 \qquad (1)$$

* Two solute components is in itself a wider field for practical application. Using a real concentration gradient (mutual diffusion as distinct form self-diffusion), this case will not give an ideal gaussian gradient curve, which means a complication in the evaluation of the experiments.

** The porous disc method is often used, *e. g.* to avoid convections, but would eventually involve troubles from the Joule heat in the membrane and an electroosmotic diffusion effect which is of interest in itself but undesired as a source of error.

*** The number factor 2 is deduced assuming steps of equal length.

where ν is the number of steps per unit time. From eqn. (1) it is seen that the length of the steps (and therefore also the duration of the steps) is more important than the number of steps/sec., since the former appears as a square. As a matter of fact, the kinetical process, and the current frequency as well, has to be comparatively slow if the electro-diffusion shall compete measurably with the ordinary diffusion.

The choice of characteristics of the superimposed field is optional from both theoretical and practical viewpoints. A certain generality and simplicity is achieved by choosing a square field as in Fig. 1.

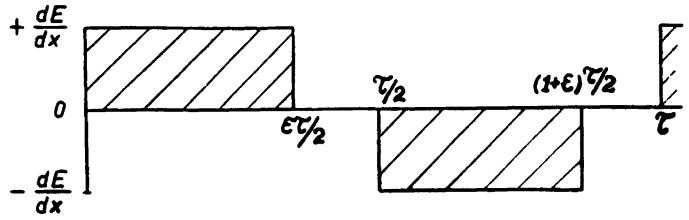


Figure 1.

The period length is τ sec and ε is the fraction of the half-period during which current is conveyed. The reason for choosing $\varepsilon \neq 1$ is that ε is an interesting variable for the magnitude of the diffusion effect. The possibility is also foreseen of using the current-free interval to measure the conductance of the diffusion column, in order to get an exact measure of the average temperature in the column.

It seems that, under certain conditions of current and kinetical characteristics, the regularity of the current variations gives rise to a lower diffusion effect than that which would be obtained if the superimposed field is given a random nature. There is no doubt that such can be experimentally arranged.

We will here treat two extreme cases, the theory for which is elementary. In both cases we assume as above that the uncharged state for A and B is of a comparatively long duration $T°$ and that the statistical dispersion of $T°$ is broad enough to eliminate any correlation between the consecutive phases (on the time axis of the field) with which an ion appears. In this way we also practically exclude the possibility that the ion can appear twice or more during the same period of the current.

The life-time of the ion being T, the two cases we are going to treat are a) $T < \varepsilon\tau/2$ and b) $\varepsilon\tau/2 < T$, $\varepsilon \ll 1$. The latter case corresponds to sudden current shocks, as experimentally used when studying the Wien-effect of electrolytes. In both cases τ is intermediate between T and $T + T°$, which means a kind of broad resonance between the field and the pulsation of the electrolyte.

a) $T < \varepsilon\tau/2$.

The length of each step is $l = \pm Tu$, $\pm u$ being the velocity of the ion in the field $\mathrm{d}E/\mathrm{d}x$. The number of ionic states/sec. is $1/(T+T°)$. Of these states

a fraction ε leads to a step, so that the number of steps/sec. is $\nu = \varepsilon/(T+T^\circ)$. Thus eqn. (1) gives for the electrodiffusion of the cations

$$D^+ = \frac{(T^+u^+)^2\varepsilon}{2(T^+ + T^\circ)} \tag{2}$$

The frequency $1/\tau$ is not directly contained in this formula, compare however the discussion of eqn. (5).

b) $\varepsilon\tau/2 < T$, $\varepsilon << 1$.

The step length is $l = \pm\, \varepsilon\tau u/2$, *i. e.* the duration $\varepsilon\tau/2$ of the step multiplied by the velocity $\pm u$. The number of steps/sec. is the product of the number of + or — shocks $2/\tau$/sec. and the probability $T/(T+T^\circ)$ that a step shall be taken at a certain current shock. Thus $\nu = 2T/\tau(T+T^\circ)$ and, for cations

$$D^+ = \left(\frac{u^+\varepsilon}{2}\right)^2 \frac{T^+\tau}{T^+ + T^\circ} \tag{3}$$

In order to compare cases a) and b), the D^+-values are divided by the Joule effect w watt/cm^3 in each case, which ratio ought to be decisive for the possibility of measuring the effect. This effect is $w = \varepsilon\varkappa(\mathrm{d}E/\mathrm{d}x)^2$, the conductance being denoted by $\varkappa$. The measurements are supposed to be made upon exactly similar diffusion columns, one according to eqn. (2) and the other according to eqn. (3). The allowed potential gradients are different in these cases, and therefore also the velocities u^+. Considering also that $u^+ = U^+\mathrm{d}E/\mathrm{d}x$, where U^+ denotes the ionic mobility, we obtain

$$(D^+/w)_{\text{eqn. (2)}} \,/\, (D^+/w)_{\text{eqn. (3)}} = T^+ \,/\, \tfrac{1}{2}\,\varepsilon\tau \tag{4}$$

Here $\varepsilon\,\tau$ belongs to the conditions of eqn. (3), for which we have assumed $\varepsilon\tau/2 < T^+$. Thus this case is comparatively unfavourable according to eqn. (4).

From eqn. (2) we obtain

$$D^+ \,/\, w = (T^+U^+)^2 \,/\, 2\,\varkappa\,(T^+ + T^\circ) \tag{5}$$

showing that the result is independent of the field characteristic ε. (τ does not enter this formula. However, the greater τ is, the greater must $T^+ + T^\circ$ be according to our suppositions.)

2. DIFFUSION THEORY

The diffusion effect on the two kinds of ions has to be combined with the ordinary diffusion of the ions and undissociated part, due regard being paid to the diffusion potential. For this purpose we first need an expression for the

diffusion of a weak electrolyte A_pB_q, with mole concentration C and degree of dissociation α according to

$$A_pB_q \underset{k'}{\overset{k}{\rightleftharpoons}} pA^{z+} + qB^{z-};\ pz^+ = qz^- \tag{6}$$

$$\begin{array}{lll} C\ (1-\alpha) & pC\alpha & qC\alpha \end{array}$$

$$(pC\alpha)^p\ (qC\alpha)^q = KC(1-\alpha) \tag{7}$$

neglecting for the present the activity coefficients. We will calculate the diffusion coefficient D_{12} using the general expression [3] for the components 1 and 2

$$D_{12} = RTN_1B_{12} / \Phi_2;\ B_{12} = \partial \ln a_2 / \partial \ln N_2 \tag{8}$$

The mole fraction N_1 of the solvent is sufficiently near 1 in the dilute solutions considered here. Φ_2 is the molar friction of the solute, a_2 its activity.

It has been previously shown [3,4] that if a component in solution exists in different forms or molecular sizes, the molar friction Φ of the component depends upon the molar frictions Φ_i of the different species according to

$$\frac{1}{\Phi} = \sum \frac{n\nu_i}{\Phi_i} \tag{9}$$

where ν_i is the fraction of the component which is present in the form i and n is the degree of association ($n = 2$ for double molecules etc.). The molecular weight of the component (necessary for defining Φ) shall correspond to $n = 1$.

Since in our present, simple case with only two kinds of ions, the ions must follow one another in the stoichiometric proportion, eqn. (6) corresponds to a simple conversion, the forms of the electrolyte being A_pB_q with the friction Φ° and ($pA^{z+} + qB^{z-}$) with the friction $\Phi^\pm$. For the friction of the solute Φ_2 we obtain from eqn. (9) simply

$$\frac{1}{\Phi_2} = \frac{1-\alpha}{\Phi^\circ} + \frac{\alpha}{\Phi^\pm} \tag{10}$$

This determines Φ_2 of eqn. (8). We will now proceed to determine B_{12} and may use the concentration of the undissociated part as a measure of the activity of the solute; $a_2 = C(1-\alpha)$. Eqns. (7) and (8) give

$$B_{12} = \frac{p+q}{p+q-\alpha(p+q-1)} \tag{11}$$

This is quite plausible, $\alpha = 0$ giving $B_{12} = 1$ (ideal solute) and $\alpha = 1$ giving $B_{12} = p + q$ (ideal solute of $p + q$ ions per mole salt). The desired expression is then for the very dilute solution ($D_{12} \rightarrow D_2$)

$$D_2 = \frac{RT\ (p+q)}{p+q-\alpha(p+q-1)} \left(\frac{1-\alpha}{\Phi^\circ} + \frac{\alpha}{\Phi^\pm} \right) \tag{12}$$

This expression will now be extended to include the specific electrodiffusion effect. For this purpose it is preferable to use the complete expressions for the stationary motion as functions of forces and frictions. The contribution k^+ of the electrodiffusion to the diffusion force must first be calculated. In the diffusion theory, this force per mole solute, is the gradient in the chemical potential, $k_2 = -RT\partial \ln a_2/\partial x$. Confining our calculation to a dilute component of concentration c_2, eqn. (8) may be written $D_2 = (-RT\partial \ln a_2 \,/\, \partial x) \,/\, (-\Phi_2 \partial \ln c_2/\partial x)$ and from this

$$k_2 = -D_2\, \Phi_2 \partial \ln c_2/\partial x \tag{13}$$

For the cations, eqn. (2) is now assumed (the sign Δ distinguishes electrodiffusion from ordinary diffusion)

$$\Delta\, D^+ = \tfrac{1}{2}\, \frac{(T^+u^+)^2\varepsilon}{T^+ + T^\circ} \tag{14}$$

The concentration is, according to eqn. (6), $pC\alpha$. Further, the velocity $u^+ = U^+ dE \,/\, dx$, U expressing mobility. The electrical force per gram-ion is $-z^+F\ 10^7 dE \,/\, dx$ (F = 1 faraday). From this, since the ratio of force to velocity equals the friction,

$$\Phi^+ = z^+F\ 10^7 \,/\, U^+ \tag{15}$$

Denoting by L the magnitude

$$L^+ = \tfrac{1}{2}\, \frac{\left(T^+ \dfrac{dE}{dx}\right)^2}{T^+ + T^\circ}\ F\ 10^7 \tag{16}$$

we finally get the diffusion force per gram-ion k^+ from equation (13) (D_2 in this case being ΔD^+, $c_2 = pC\alpha$ and $\Phi_2 = \Phi^+$) and by analogy also k^-

$$\begin{aligned} k^+ &= -L^+U^+z^+\partial \ln C\alpha \,/\, \partial x \\ k^- &= -L^-U^-z^-\partial \ln C\alpha \,/\, \partial x \end{aligned} \tag{17}$$

Let v°, v^+, and v^- be the linear velocities of AB, A^+, and B^-, respectively. Considering also the forces originating from the l o c a l potential gradient dE'/dx in the diffusion column, and denoting, as in eqn. (12), the molar friction of AB by Φ°, we obtain by equalizing the forces,

$$v^\circ\ \Phi^\circ = -RT\frac{\partial \ln C(1-\alpha)}{\partial x} \tag{18}$$

$$v^+\ \Phi^+ = -RT\frac{\partial \ln C\alpha}{\partial x} - L^+U^+z^+\ \frac{\partial \ln C\alpha}{\partial x} - z^+F10^7\ \frac{dE'}{dx}$$

$$v^-\ \Phi^- = -RT\frac{\partial \ln C\alpha}{\partial x} - L^-U^-z^-\ \frac{\partial \ln C\alpha}{\partial x} + z^-F10^7\ \frac{dE'}{dx} \tag{19}$$

We have $pz^+ = qz^-$ and, the resulting electricity transport being zero, $pz^+C\alpha v^+ = qz^-C\alpha v^-$. From this, $v^+ = v^-$, and this velocity is denoted v. Expressing the ionic friction in terms of the electrochemical mobilities (eqn. (15), the following is obtained by elimination of dE'/dx from the eqns. (19)

$$F\ 10^7 \left(\frac{1}{U^+} + \frac{1}{U^-}\right) v = -\left[RT\left(\frac{1}{z^+} + \frac{1}{z^-}\right) + (L^+U^+ + L^-U^-)\right]\frac{\partial \ln C\alpha}{\partial x} \quad (20)$$

Calculating the total flow of A_pB_q as a component, according to $J_2 = v^\circ C(1-\alpha) + vC\alpha$, we get from eqns. (18) and (20)

$$J_2 = -\left\{\frac{RT}{\Phi^\circ}\frac{\partial C(1-\alpha)}{\partial C} + \frac{RT\left(\frac{1}{z^+} + \frac{1}{z^-}\right) + (L^+U^+ + L^-U^-)}{F\ 10^7\left(\frac{1}{U^+} + \frac{1}{U^-}\right)}\frac{\partial C\alpha}{\partial C}\right\}\frac{\partial C}{\partial x} \quad (21)$$

Since eqn. (21) is Fick's first law, the expression within the brackets is the total diffusion coefficient D_2. The equilibrium expression (7) provides

$$\frac{\partial C(1-\alpha)}{\partial C} = \frac{(p+q)\ (1-\alpha)}{p+q-\alpha\ (p+q-1)} \quad (22)$$

and similary for $\partial C\alpha/\partial C$. Inserting in eqn. (21) we arrive at

$$D_2 = \frac{RT(p+q)}{p+q-\alpha\ (p+q-1)}\left[\frac{1-\alpha}{\Phi^\circ} + \frac{\alpha\left(\frac{1}{z^+} + \frac{1}{z^-}\right)}{(p+q)F10^7\left(\frac{1}{U^+} + \frac{1}{U^-}\right)}\right] + \\ + \frac{\alpha}{p+q-\alpha\ (p+q-1)}\frac{L^+U^+ + L^-U^-}{F\ 10^7\left(\frac{1}{U^+} + \frac{1}{U^-}\right)} \quad (23)$$

The analogy with eqn. (12) is evident. The last term of eqn. (23) is the contribution ΔD of the superimposed field to the diffusion coefficient of the electrolyte. Thus by eqn. (16)

$$\Delta D = \frac{\frac{1}{2}\alpha\varepsilon\left(\frac{dE}{dx}\right)^2}{p+q-\alpha\ (p+q-1)}\frac{\frac{(T^+)^2U^+}{T^+ + T^\circ} + \frac{(T^-)^2U^-}{T^- + T^\circ}}{\frac{1}{U^+} + \frac{1}{U^-}} \quad (24)$$

We have assumed a real (but small) concentration gradient and thus dE/dx is not exactly constant over the diffusion column. Measuring instead, with isotopic labelling, say AB against A*B, the theory (for the diffusion of the A constituent) is simpler but shall not be given here.

In order to complete our intention of indicating a theory for a simple case, consider the equilibrium scheme of eqn. (6). It is the question of determining average life-times (T°, T^+ and T^-) of the uncharged and the ionic states from the kinetics of the dynamical equilibrium. In a monomolecular reaction, the lifetime of a particle is the inverse of the specific reaction constant k. Assuming an uncomplicated monomolecular reaction, we simply obtain $T^\circ = 1/k$. For the reverse reaction we observe that the process of disappearance of an A^{z+} ion is not limited to a reaction with the ions existing at a certain (zero) time point. Since any A^+ and B^- ion (of equilibrium concentration) can take part, the disappearance of A^{z+} also occurs according to a monomolecular scheme

$$\frac{1}{p}\frac{dA^{z+}}{dt} = k' \, (pC\alpha)^{p-1}(qC\alpha)^q(pC\alpha - A^{z+}) \qquad (25)$$

This equation describes the disappearance of the cations which exist at a certain zero time while the equilibrium is maintained. Since p of A^{z+} must disappear simultaneously for the formation of A_pB_q, each elementary reaction includes the disappearance of a number of the original A^{z+} ions which, on an average, is proportional to the relative content of these amongst the total amount. It seems however that this is accounted for in eqn. (25). It may in this connection be pointed out that the problem is not identical with the rate of disappearance of labelled ions from an original mixture of them with unlabelled salt. In the latter problem, labelled ions successively reappear by dissociation of the molecules formed, a process which is irrelevant to the question of the life-time of an ion, with which we are here concerned.

A complete theory has to consider an eventual exchange reaction, say according to the scheme

$$A_pB_q + (A^{z+})^* \rightarrow A_{p-1}(A^*)B_q + A^{z+} \qquad (26)$$

by which the life-time of the ion, and of the undissociated state of A, are diminished.

Special reaction mechanisms might modify the statistical nature of the kinetics. The same is true in the case of an equilibrium between different states of the salt or a formation of double molecules etc.* — From eqn. (25) we obtain

$$T^+ = T^- = 1/(k'p^pq^q(C\alpha)^{p+q-1}) \qquad (27)$$

The common life-time being denoted by $T^\pm$, this leads to

$$\frac{(T^\pm)^2}{T^\circ + T^\pm} = \frac{\alpha^2}{k(1-\alpha)}; \left(\frac{T^\pm}{T^\circ + T^\pm} = \alpha\right)^{**} \qquad (28)$$

* This may modify the statistical distribution, for short time-intervals, of the life-times. This distribution may be quite abnormal and it may not be self-evident that the calculated kinetical average life-time is identical with the average life-times which are contained in the electrodiffusion eqns. (2) and (24), as is assumed here.

** This expression is directly obtained from $T^\pm/T^\circ$ = the ratio of the ion concentration (divided by the stoichiometric factor) and the concentration of the undissociated state.

Applying this result, eqn. (24) reads

$$\Delta D = \frac{\frac{1}{2}\,\alpha^3\,U^+U^-\varepsilon\left(\frac{dE}{dx}\right)^2}{k\,(1-\alpha)\,[pq\alpha]} \tag{29}$$

$$[pq\alpha] \equiv p + q - \alpha\,(p + q - 1)$$

From the experimental point of view, the current heat is a critical magnitude. Introducing the electrical effect $w = \varepsilon\varkappa\left(\frac{dE}{dx}\right)^2$ watt/cm^3 and the ionic conductances $\Lambda_0^+ \simeq FU^+$, eqn. (29) transforms to

$$\Delta D = \frac{\frac{1}{2}\,\alpha^3\,w}{(1-\alpha)\,[pq\alpha]k}\,\frac{\Lambda_0^+\Lambda_0^-}{F^2\,\varkappa} \tag{30}$$

We will from now on assume $p = q = 1$ and $z = 1$. A modification may be attained by considering $\Lambda \simeq \alpha(\Lambda_0^+ + \Lambda_0^-) = 1\,000\ \varkappa/C$. Eliminating $\varkappa$ and introducing the equilibrium constant K gives

$$\Delta D = \frac{500\,K\,(w/C)}{k(2-\alpha)CF^2}\,\frac{\Lambda_0^+\Lambda_0^-}{\Lambda_0^+ + \Lambda_0^-} \tag{31}$$

The reason for using w/C is that the permitted Joule heat w increases with the density gradient of the column, which latter may be chosen greater with increasing concentration of the salt. Thus, according to eqn. (31), the order of magnitude of a measurable diffusion effect for a given electrolyte in our case varies inversely to the molarity of the salt. Another expression for a numerical estimation is

$$\Delta D = \frac{500\alpha^2\,(w/C)}{(1-\alpha)\,(2-\alpha)kF^2}\,\frac{\Lambda_0^+\,\Lambda_0^-}{\Lambda_0^+ + \Lambda_0^-} \tag{32}$$

obtained from eqn. (31) by eliminating K.

For the present we will prefer the formula

$$\Delta D = \frac{500\alpha^4 w}{(1-\alpha)^2\,(2-\alpha)KkF^2}\,\frac{\Lambda_0^+\Lambda_0^-}{\Lambda^+ + \Lambda_0^-} \tag{33}$$

for an estimation of the electrodiffusion effect, in order to use the value $w = 0.2$ watt/cm^3 which is sometimes given as a maximum value in electrophoresis work at the temperature (approx. 4° C) of the maximum density of water. Our requirements for undisturbed diffusion ought to be greater than those in general electrophoretic work, but on the other hand the cooling of the cell has been considerably improved in our work, so we may use this value as an upper limit. Assuming $\alpha = 1/3$, $K = 10^{-3}$, and the Λ-factor = 40 (international units), we get $\Delta D = 2/3 \cdot 10^{-5}/k$ cm^2/sec. Since $2 \cdot 10^{-5}$ is the

order of magnitude of the diffusion coefficients of common electrolytes in water, the calculation shows that $k = 1/3$ / sec., *i. e.* $T^\circ = 3$ sec., would give a diffusion effect of about 100 %. The molarity is, in this example $C = 0.006$.

With regard to the current to be used (see eqn. (28) the period length is in this example between $T^\circ = 3$ sec. and $T^\circ + T^\pm = 4.5$ sec. The conditions $T^\pm < \varepsilon\tau / 2$ and $T^\pm + T^\circ > \tau$ lead to $\varepsilon > 2\alpha$, independent of k.

These calculations refer to eqn. (2), case a) above, as it was introduced in eqn. (14). The case b), eqn. (3), leads to the expressions

$$\Delta D = \frac{250\alpha\varepsilon\tau(w/C)}{(2-\alpha)\ F^2} \frac{\Lambda_0^+ \Lambda_0^-}{\Lambda_0^+ + \Lambda_0^-} \tag{34}$$

and

$$\Delta D = \frac{250\alpha^3\ \varepsilon\tau w}{(2-\alpha)\ (1-\alpha)\ KF^2} \frac{\Lambda_0^+ \Lambda_0^-}{\Lambda_0^+ + \Lambda_0^-} \tag{35}$$

From these equations it is seen that the use of current shocks leads to an electrodiffusion effect, which is i n d e p e n d e n t of the kinetics of the dynamical equilibrium. This result of the calculation can be seen directly, since sudden shocks do not give an indication of life-times which are comparatively long. The reaction rate is, however, contained in the assumptions regarding order of magnitudes, which were made in case b). A numerical estimate shows clearly that a measurable effect may be obtained also under these conditions.

3. RANGE OF SYSTEMS

If the magnitude or sign of the electric charge of at least one of the constituents changes, then an electrodiffusion effect is possible. The same is true if the mobility of an ionic constituent varies with time, *e. g.* in the case of linear macromolecular ions or longchain polyelectrolytes. The mobility is in this case a function of the actual form of the ion. Other causes are: random changes in solvation, in the instantaneous properties of the medium or in the interionic forces. The reversible formation of micelles and other colloids, the formation of complexes, electron transfers, ampholytes and protolytic systems in general, and exchange reactions within the electrolyte or with an additional component, also belong to this field. An effect upon an added nonelectrolyte or upon the solvent is possible, if this component is bound to ions or reversibly dissolved (solubilized) in micelles. An interesting case may prove to be that of carbon dioxide, say according to the scheme $CO_2 + OH^- = HCO_3^-$. The diffusion of acids, with an equilibrium between *pseudo-* and *aci-*form, belongs to the category theoretically discussed above, since we may here find the delayed kinetics which are necessary in order to provide the region of measurable conditions.

A special field is represented by the presence of a solid structure, such as diffusion in an ion exchange column, in a gel or in an adsorbent.

4. COMPLETIVE REMARKS

Experiments in a special cell, cooled by water to approximately 4° C, have shown that reproducible measurements may be made at somewhat higher electric effects than the figure 0.2 watt/cm^3 given above. We have delayed publication, awaiting experimental evidence of the special effect in question. The publication of Mysels [5,1], in which the principles are the same, although in part rather differently outlined, has now caused the publication of this article.

The connection with the kinetics of the dynamical equilibrium is of interest and may, in special cases, lead to determinations which are difficult to obtain with simpler or more direct methods. It is of special value to obtain an insight into statistical details of the kinetics, which are not revealed by other methods, if this proves to be possible.

This work has been supported by the *Swedish National Research Council.* It has been performed parallel with other investigations and with forced interruptions. The official application to the Council, dated May 1953, contains a description of the electrodiffusion principles and the connection to kinetics.

REFERENCES

1. Ogston, A. G. *Nature* **157** (1946) 193.
2. Lauwerier, H. A. *Appl. Sci. Research* **B 2** (1951) 294.
3. Lamm, O. *J. Phys. Chem.* **51** (1947) 1063.
4. Lamm, O. *Arkiv Kemi Mineral. Geol.* **18A** (1944) No. 10.
5. Mysels, K. J. *J. Chem. Phys.* **24** (1956) 371.

Received May 9, 1956.

ACTA CHEMICA SCANDINAVICA 10 (1956) 1143—1145

The Synthesis of Some Organosilicon Alcohols. I

SUNE BRYNOLF

Department of Organic Chemistry, Chemical Institute of the University, Lund, Sweden

In order to prepare some organosilicon compounds containing hydroxyl groups attached to carbon atoms the reaction between propylene oxide and trimethylsilylmethylmagnesium bromide was investigated. The only silicon-containing alcohol that could be isolated was 4-trimethylsilyl-butanol-2. The constitution of this compound was proved by comparing it with authentic samples of the two alcohols that theoretically could be obtained.

A widely applied method of synthesizing alcohols is to let ethylene oxides react with Grignard compounds. A review is published by Gaylord and Becker [1]. Sommer, Van Strien and Whitmore [2] applied these reactions to silicon-containing materials. The Grignard reagents from chloromethyltrimethylsilane and 3-trimethylsilyl-1-bromopropane yielded on interaction with ethylene oxide 3-trimethylsilyl-propanol-1 and 5-trimethylsilyl-pentanol-1, respectively.

During attempts to repeat the former synthesis with trimethylsilylmethylmagnesium bromide instead of chloride, as in the paper [2], a low yield of the desired alcohol and a large amount of higher boiling materials were obtained. However, when the synthesis was made with the chloride, the stated yield was obtained.

In this work the reaction between propylene oxide and trimethylsilylmethylmagnesium bromide has been studied. Theoretically one or both of the two alcohols (I) and (II) may be formed, depending upon which way the oxide ring is opened.

$(CH_3)_3SiCH_2\text{-}CH_2\text{-}CHOH\text{-}CH_3$ (I)

$(CH_3)_3SiCH_2\text{-}CH(CH_3)\text{-}CH_2OH$ (II)

The only silicon-containing alcohol (A) that could be isolated from the reaction mixture must have had the constitution (I). This was evident partly from the fact that it was non-identical with the alcohol (II) that was obtained from α-methyl-β-trimethylsilyl-propionic acid, prepared by Sommer *et al.* [3] by reduction with lithium aluminium hydride; partly from the fact that those

of its properties that were studied were identical with the corresponding properties of the alcohol (I), obtained from 4-trimethylsilyl-butanone-2 by reduction with lithium aluminium hydride according to Perklev [4]. The data of the alcohols (I), (II) and (A) and their 3,5-dinitrobenzoates are collected in Table 1.

Table 1.

Alcohol	Bp °C	n_D^{20}	d_4^{20}	Mp °C of 3,5-dinitrobenzoate
(A)	81—82°	1.4301	0.8279	65—66° *
(I)	82° **	1.4301 **	—	65.5—66°
(II)	88—89°	1.4357	0.8375	44.5—45.5°

* Mixed m. p. with (I) 65.5—66° C.
** Data recorded by Perklev [4].

EXPERIMENTAL

4-Trimethylsilyl-butanol-2 from propylene oxide (A = I)

58.0 g (1.0 mole) of propylene oxide were dropped with stirring to the Grignard reagent prepared from 83.5 g (0.5 mole) of bromomethyltrimethylsilane, 12.0 g magnesium and 100 ml of absolute ether in a 1-litre flask equipped with a stirrer, a reflux condenser and a dropping funnel, and immersed in an ice-bath. When all the oxide had been added the ice-bath was removed, whereupon the temperature of the mixture generally rose enough to cause boiling. When this ceased the mixture was warmed on a water bath (45°—46°C) for 5—6 hours. The reaction mixture was decomposed with ice-water. Simultaneously the ether, tetramethylsilane and unreacted propylene oxide were distilled over. *Ca.* 8 g (0.1 mole) of tetramethylsilane could be recovered from the distillate by dropping it into concentrated sulphuric acid, cooled in an ice-and-salt bath.

The magnesium hydroxide precipitated by hydrolysis was dissolved by adding a sufficient quantity of dilute hydrochloric acid. The organic layer was separated and the water layer extracted with ether. The combined ether solutions were washed with a small quantity of water.

In an earlier experiment the resulting silicon-containing product was found to contain some bromine, probably due to the presence of propylene bromohydrin, formed upon hydrolysis of the reaction mixture. It was difficult to separate the bromohydrin from the formed silicon-containing alcohol through distillation and, therefore, the ether solution was shaken with small portions of dilute sodium hydroxide solution until a lasting red colour with phenolphthalein was obtained.

The ether layer was separated and the water layer extracted with ether. The combined ether layers were washed with water and dried with anhydrous sodium sulphate. The ether was removed and the mixture distilled in a Claisen flask at 25 mm Hg. A viscous residue was obtained. The distillate was fractionated in an efficient column and the fraction boiling at 81—82° at 25 mm Hg, 29.0 g (0.20 mole), was collected as pure 4-trimethylsilyl-butanol-2. $n_D^{20} = 1.4301$, $d_4^{20} = 0.8279$. (Found: C 57.0; H 12.5; Si 19.2, MR_D 45.6. Calculated for $C_7H_{18}OSi$: C 57.5; H 12.4; Si 19.2, MR_D 45.8).

3,5-Dinitrobenzoate was prepared according to a method described by Vogel [5]. 2.0 g of the 4-trimethylsilyl-butanol-2 were heated with 4.0 g 3,5-dinitrobenzoyl chloride in an oil bath at 110°C until the evolution of hydrogen chloride ceased. The mixture was cooled, and 40 ml of saturated sodium bicarbonate solution was added. The resulting ester was stirred until crystallization occurred. The precipitate was filtered at the pump and washed with a little sodium bicarbonate solution followed by water. The crystals were recrystallized twice from ethanol and water. The yield of crystals melting at 65.0—66.0°C was 2.8 g (*ca.* 60 %). (Found: C 49.1; H 5.8; Si 8.1. Calculated for $C_{14}H_{21}N_2O_6Si$: C 49.4; H 5.9; Si 8.2).

4-Trimethylsilyl-butanol-2 (I) from 4-trimethylsilyl-butanone-2

A few drops of the alcohol (I) were kindly placed at my disposal by Perklev, who synthesized it from 4-trimethylsilyl-butanone-2 by reduction with lithium aluminium hydride [4].

The 3,5-dinitrobenzoate was synthesized in the same way as above for the alcohol (A). M.p. 65.5—66°.

2-Methyl-3-trimethylsilyl-propanol-1 from α-methyl-β-trimethylsilylpropionic acid

22.8 g (0.143 mole) of *a*-methyl-*b*-trimethylsilyl-propionic acid dissolved in 215 ml of absolute ether were dropped into 7.6 g (0.20 mole) of lithium aluminium hydride in 260 ml of absolute ether. When all had been added the mixture was refluxed for 3 hours. Hydrolysis with water and diluted hydrochloric acid and extraction and drying were carried out in the usual way. Fractionation of the ether solution yielded 14.2 g (0.097 mole) of the desired alcohol, b.p. 88—89°C at 25 mm Hg. (Found: C 57.2; H 12.6; Si 19.4, MR_D 45.6. Calculated for $C_7H_{18}OSi$: C 57.5; H 12.4; Si 19.2, MR_D 45.8).

3,5-Dinitrobenzoate. From 2.0 g of 2-methyl-3-trimethylsilylpropanol-1 2.3 g of the 3,5-dinitrobenzoate of m.p. 44.5—45.5° were obtained. (Yield 50 %.)

The author wishes to express his gratitude to Professor Erik Larsson for his kind interest in this work.

REFERENCES

1. Gaylord, N. G. and Becker, E. I. *Chem. Revs.* **49** (1951) 413.
2. Sommer, L. H., Van Strien, R. E. and Whitmore, F. C. *J. Am. Chem. Soc.* **71** (1949) 3056.
3. Sommer, L. H., Goldberg, G. M., Barnes, G. H. and Stone, L. S. *J. Am. Chem. Soc.* **76** (1954) 1609.
4. Perklev, T. *Svensk Kem. Tidskr.* **65** (1953) 253.
5. Vogel, A. I. *Text-Book of Practical Organic Chemistry*, 2:d ed. Longmans, Green and Co, London 1951.

Received May 9, 1956.

ACTA CHEMICA SCANDINAVICA 10 (1956) 1146—1159

Studies on the Interaction of Paraffin-Chain Alcohols and Association Colloids

VII. Microscopic Investigation of the Interaction between some Liquid Alcohols and Sodium Laurate Solutions

PER EKWALL, MILAN SALONEN, INGMAR KROKFORS and INGVAR DANIELSSON

Institute of Physical Chemistry, Åbo Akademi, Åbo, Finland

The formation of a mesomorphic phase as a result of the interaction between aqueous sodium laurate solutions and liquid paraffin-chain alcohols has been studied with the microscope. The first signs of this interaction occur at the L.A.C. The interaction product is predominantly hydrophilic and analyses show that it contains both alcohol and soap. The water content of this product seems to vary; the birefringence diminishes with increasing water content. When decanol interacts with laurate solutions, the molar ratio of alcohol to soap in the separated phase varies from about 1:2 to about 4-5:1, the alcohol content rising as more alcohol is added to the system. The interaction proceeds in several steps. The first amounts of alcohol added form soluble aggregates with the soap, mixed micelles or smaller aggregates. Then alcohol, soap and water separate as a mesomorphic phase. With further alcohol additions, more and more soap is transferred from the aqueous solution to the separated phase until the soap concentration of the solution decreases to a minimum value. Also after this point is reached, the separated phase takes up added alcohol. Finally this uptake reaches a limit and the alcohol appears in the free form. Soap solutions in equilibrium with the mesomorphic phase are not saturated with alcohol. Saturation is reached only when drops of free alcohol appear in the system.

As one of us has shown previously, microscopic observations can be used with advantage to study the interaction between an aqueous soap solution and fatty acid [1–4]. A method based on such observations was developed for the determination of the limiting concentration (L.A.C.) in soap solutions [3]. Subsequently the same method was found to be suitable for the study of the interaction between long-chain alcohols and association colloid solutions [5,6]. In the following we shall describe the results of further investigations in which

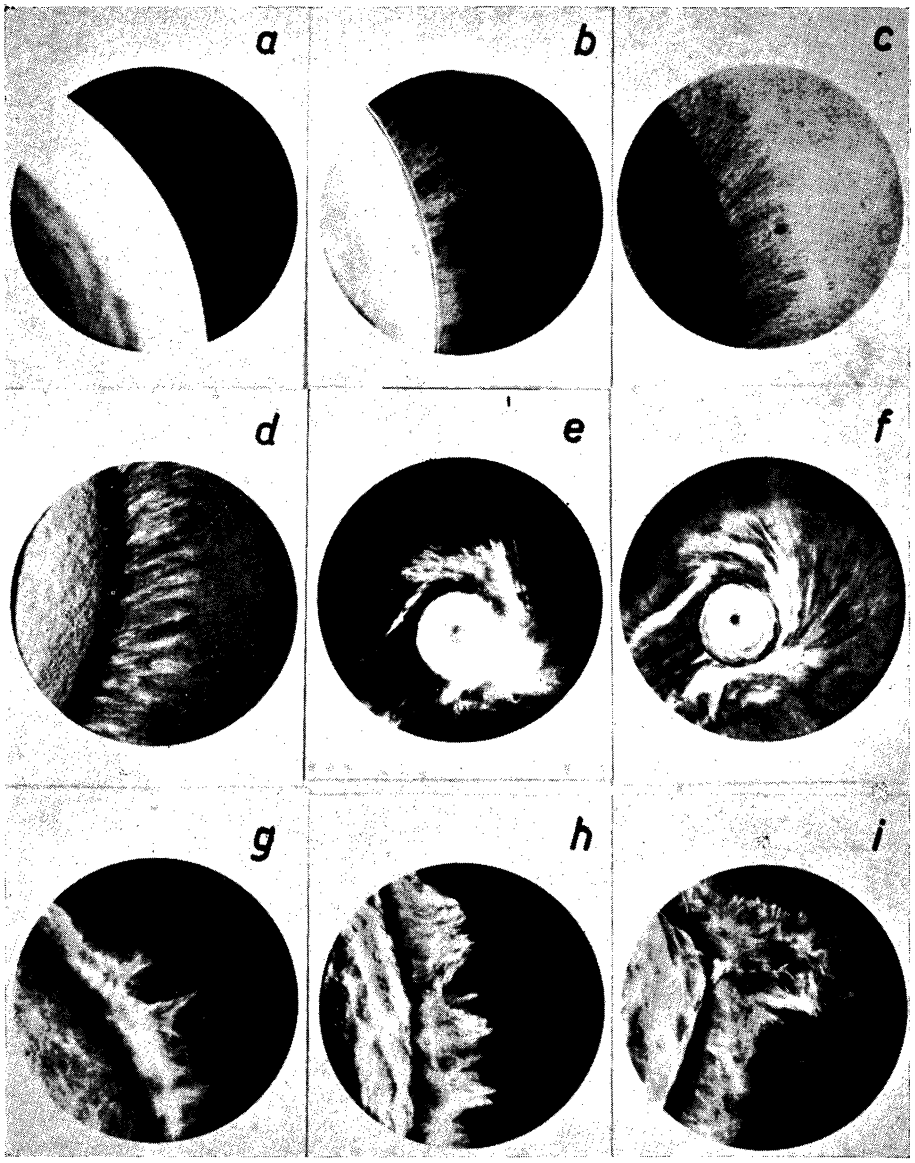


Fig. 1. Microphotographs of the first stages of the interaction between drops of decanol-1 and sodium laurate solutions at room temperature. In the photographs a—d and g—i the decanol drops are seen on the left and the laurate solutions on the right; in photographs e and f, the decanol drops are located near the centres of the photographs. 150 ×.

a) 0.001 M laurate; dark-field condenser
b) 0.006 M laurate; dark-field condenser
c) 0.006 M laurate; transmitted light
d) 0.006 M laurate; phase-contrast condenser
e) 0.006 M laurate; dark-field condenser
f) 0.006 M laurate; phase-contrast condenser
g) 0.014 M laurate; semidark-field condenser
h) 0.030 M laurate; dark-field condenser
i) 0.023 M laurate; dark-field condenser

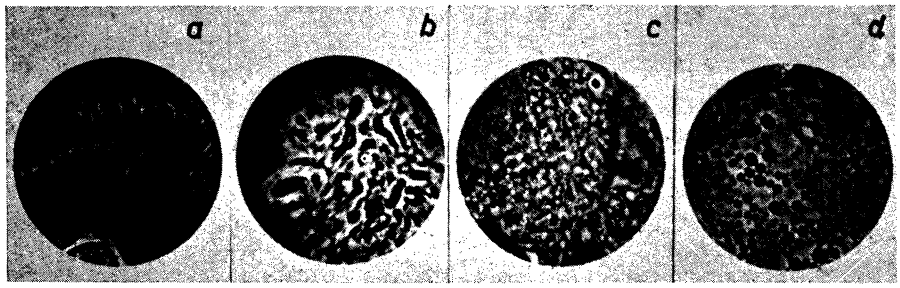


Fig. 2. Later stages of the interaction between decanol and a 0.04 M sodium laurate solution at room temperature.

a) Phase-contrast condenser. 300 ×. Decanol drop in the lower part. Upwards, there is first a layer of interaction product with filamentous structure, then a layer of sausage-shaped and spherical particles of interaction product. Laurate solution in the upper part.
b) Phase-contrast condenser. 600 ×. Myelinic interaction product. A small decanol drop near the centre.
c) Phase-contrast condenser. 150 ×. Sausage-shaped and spherical particles of interaction product streaming out into the solution.
d) Phase-contrast condenser. 300 ×. The interaction product is evenly dispersed in drops throughout the solution.

the same method has been used. In these investigations special attention was directed to the first stages of the interaction, but the appearance of the interaction product at later stages and its composition were also studied.

EXPERIMENTAL

Sodium laurate was prepared in the usual manner from pure lauric acid and sodium ethylate. Conductivity water with a specific conductance less than 1×10^{-6} $ohm^{-1}cm^{-1}$ was employed in the preparation of the soap solutions.

The paraffin-chain alcohols were the same as those used in the previous investigations of this series.

The concentrations of the soap solutions are given in moles per litre of solution, M.

The microscopic observations were made with a Leitz Dialux microscope equipped with phase-contrast and dark-field condensers. Some observations were made also in polarized light (between polaroid plates). While the observations were being made, care was taken to avoid evaporation from the aqueous solutions.

A. INTERACTION BETWEEN DECANOL AND SODIUM LAURATE

The first signs of interaction. The experiments were performed in such a manner that the interface between a decanol drop and the surrounding sodium laurate solution could be examined in the microscope from the moment when they came into contact with each other.

In extremely dilute solutions, when the laurate concentration is below 0.004—0.005 M, the interface between the drop and the solution remains sharply outlined and undergoes no change with time (Fig. 1 a). When the concentration exceeds 0.005—0.006 M, a pronounced change indicating inter-

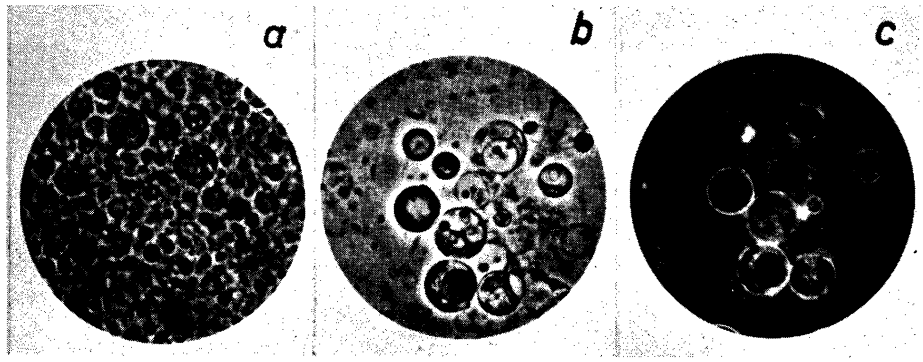


Fig. 3. Final stage of the interaction between decanol and laurate.

a) Laurate concentration 0.05 M + 1 mole of decanol per mole of laurate. Phase-contrast condenser. 600 ×.

b) Laurate concentration 0.014 M + 0.6 mole of decanol per mole of laurate. Phase-contract condenser. 600 ×.

c) The same sample as in b. Dark field condenser. 600 ×.

action between decanol and soap is observed. This change is noted immediately after decanol comes into contact with the laurate solution. The interface becomes uneven, cavities form on the surface of the decanol drop and small particles are dislodged. With the dark-field condenser numerous bright points are seen in vigorous motion in the vicinity of the drop surface. Very soon, however, a corona of hairlike filaments grows from the drop surface (Figs. 1 b, c, d,). Later this corona becomes uneven (Figs. 1 e, f), especially in solutions of high laurate concentration (Figs. 1 g, h, i). (The initial stages of the interaction, before the corona is formed, are difficult to observe, and we have not succeeded in photographing them.)

After the layer of interaction product is formed about the decanol drop, the interaction proceeds much more slowly, particularly in dilute laurate solutions. The outer ends of the filaments in the corona swell and form sausage-shaped figures (myelinic figures) which continue to expand (Figs. 2 a, b). Ultimately the expanded outer ends are disengaged and form clusters of spherical particles which stream out (Fig. 2 c) and are gradually dispersed uniformly in the solution (Fig. 2 d). In the concentration range, 0.02—0.03 M, on both sides of the C.M.C., it is observed that the solubility of the interaction product in the soap solution increases. This has been confirmed by quantitative measurements [6-7].

The final product of interaction. A laurate solution above the C.M.C. is able to solubilize a certain amount of decanol. When an excess of decanol is added, there results a turbidity caused by the separated interaction product. Below the turbidity point, no ultramicroscopic particles are seen on dark-field illumination in decanol-containing laurate solutions, but above this point there occur particles of ultramicroscopic and larger dimensions. The degree of dispersion depends on the mode of preparation and on the decanol and laurate contents of the system. When the decanol content is low, *e.g.* when a new phase

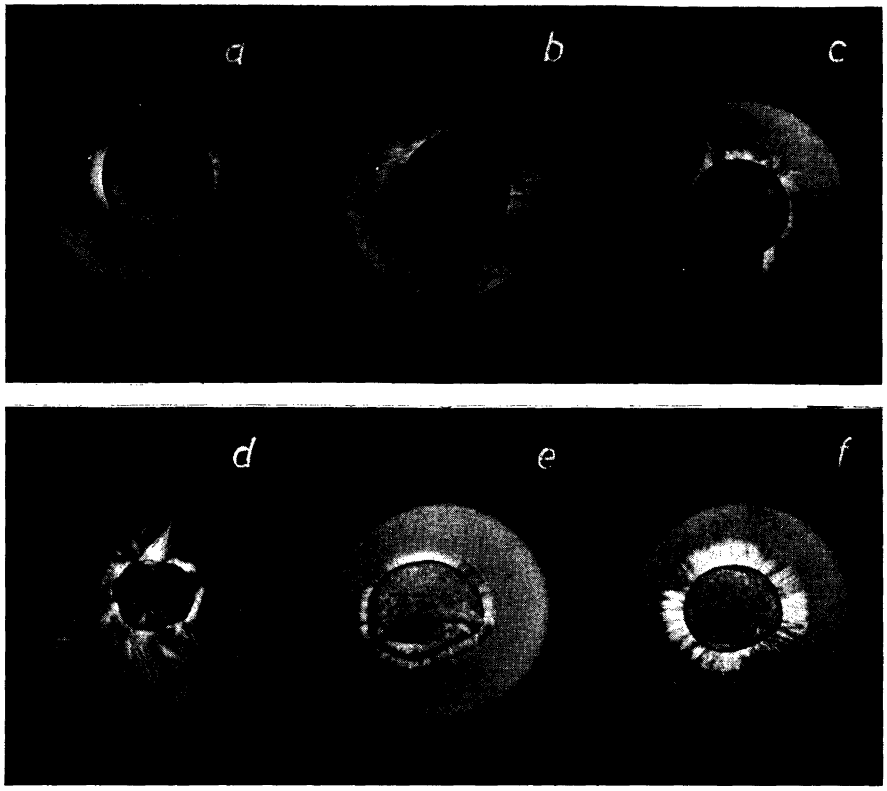


Fig. 4. Microscope observations between crossed polaroid plates of the interaction between decanol and laurate solutions at room temperature. 250×. An isomorphic decanol drop (innermost) surrounded by isomorphic laurate solution (outermost); a layer of birefringent interaction product at the interface.

a) *Laurate concentration 0.005 M · 2 min. from the start of the interaction.*
b) » » *0.005 M · 5* » » » » » » »
c) » » *0.01 M · 5* » » » » » » »
d) » » *0.02 M · 2* » » » » » » »
e) » » *0.04 M · 1* » » » » » » »
f) » » *0.04 M · 5* » » » » » » »

separates on cooling from solutions that are clear at higher temperatures, all the particles are very finely dispersed, ultramicroscopic. When larger amounts of decanol are added to the laurate solutions, the new phase separates in the form of particles of different sizes. The system resembles a semi-transparent emulsion.

In order to be able to examine the final products of the interaction, the following procedure was followed.

A 0.05 M sodium laurate solution containing one mole of decanol per mole of laurate was heated in a sealed ampoule in a water-bath to 75—80°C and shaken thoroughly to

promote the interaction of decanol and the soap. While the shaking was continued, the ampoule was allowed to cool to 40°C, and shaken for two days at this temperature. It was expected that in this way the interaction would be brought to completion.

As seen in Fig. 3 a, the solution now contained an agglomerate of spherical particles of different sizes, from 5—10 μ in diameter downwards. With oil immersion and 900-fold magnification, it was established that there was no lower limit to the sizes of the particles; the number of very small particles was exceedingly large. With the dark-field condenser it could be established that the solution contained numerous ultramicroscopic particles in vigorous Brownian motion.

In some cases another procedure was followed in preparing the solutions.

For example, a 0.014 M sodium laurate solution containing 0.6 moles of decanol per mole of laurate (and 0.05 moles of sodium hydroxide per mole of laurate to suppress the hydrolysis) was thoroughly shaken in a sealed ampoule at room temperature until the decanol was dispersed into small droplets barely visible to the naked eye. The solution was then allowed to stand for two months at room temperature to permit the interaction to continue to completion.

Also in this case the product of interaction was found to consist of spherical particles, but so that smaller particles often were embedded in the larger ones; sometimes one large particle contained many small spheres (Fig. 3 b, c). The refractive index of the substance appeared to differ from sphere to sphere; it seemed as if the decanol content was not the same in all spheres. Also some small drops of unreacted decanol could be seen alongside the interaction products.

It is thus evident that this latter mode of preparation cannot guarantee a complete interaction between the decanol and soap and therefore does not yield an uniform interaction product. The local decrease in the soap concentration of the solution and the accumulation of the separated interaction product, which hinders the contact between solution and decanol, must be prevented by shaking.

0.01—0.05 M sodium laurate solutions with different decanol additions prepared in the first-mentioned manner were investigated systematically. The appearance of the interaction product varied greatly. The sizes of the particles varied from very small particles in vigorous Brownian motion and observable only in dark-field illumination to large spheres about 10^{-2} mm in diameter; the refractive power of the separated phase varied from values near to values greatly deviating from that of the surrounding aqueous solution. At lower laurate concentrations, but above the L.A.C. (*e.g.* in the 0.01—0.014 M sodium laurate solutions) the separated phase appeared as a finely dispersed substance which was indistinct with both phase contrast and dark-field illumination and as fairly large spheres or drops of different sizes which were empty in dark-field and only weakly visible in phase contrast illumination. At higher laurate concentrations, above the C.M.C., (*e.g.* in the 0.04 M sodium laurate solution) and when the decanol additions were relatively small (up to 0.48 mole of decanol per mole of laurate), the separated phase appeared partly as a very finely dispersed substance, partly as small more or less compact spheres clearly outlined in phase contrast and dark-field illumina-

tion. With somewhat higher decanol additions, also in these cases the previously mentioned large, almost invisible spheres appeared. With increasing decanol content, the number of the large spheres increased, but the smaller distinctly outlined spheres did not disappear. There is thus a clear difference in the appearance of the particles of the separated phase above the L.A.C. (up to about 0.02 M sodium laurate) and above the C.M.C. The difference diminishes to some extent when larger amounts of decanol are added.

Observations on the properties of the interaction product. The interaction product is a viscous liquid. Decanol drops covered with a filamentous layer of interaction product approach each other until the ends of the filaments touch. When the drops are pressed together the filaments give way, but when the external force is removed they straighten out again and the drops separate from each other. The filaments are thus elastic. The same applies to the coarser myelinic figures and spherical particles. Examination in polarized light between polaroid plates showed that the interaction product is birefringent (Fig. 4). We have thus a liquid in the mesomorphic state [8,5,6].

In order to determine whether the interaction product is predominantly lipophilic or hydrophilic, the decanol was coloured with a typical fat-soluble dye, Sudan Red.

When the deep-red-coloured decanol interacted in the laurate solution, the dye remained in the decanol drops and the colour of the latter intensified until finally the dye separated as small granules. After all the decanol had been used up in the interaction, small dark red granules of Sudan Red remained among the interaction products at the points where the decanol drops had been earlier.

The dye facilitated the study of the various stages of the interaction. It was now found that sometimes a thin stream of dyed decanol flowed from the decanol drops into the layer of interaction product or into the solution where it more or less rapidly reacted with the soap. Sometimes the connection between the main drop was broken and the decanol formed a new drop that reacted further.

The interaction product was undyed. (A weak rose colour sometimes noted in the layer of the filamentous product was due to minute Sudan Red particles embedded here and there which had separated when the decanol had reacted.) No signs indicating that Sudan Red dissolves in the interaction product were seen. The conclusion was drawn that the interaction product was predominantly hydrophilic.

This was confirmed by experiments in which laurate solutions were coloured with the water-soluble dyes, Azo-blue and Wollecht-violet, which are insoluble in decanol. So far as we could determine, the interaction product was coloured in this case.

The phase formed at the interface between the decanol drop and the soap solution is thus a hydrophilic liquid in the mesomorphic state, probably of the smectic type. This phase seems to swell by taking up more water or soap solution, during which the birefringence diminishes and may disappear completely. The refractive index of the new phase approaches that of the surrounding solution. As mentioned above, this is especially the case in the concentration range above the L.A.C. up to a sodium laurate concentration of about 0.02 M.

Table 1. The decanol and sodium laurate contents of the interaction products formed in 0.014 M sodium laurate solutions to which various amounts of decanol had been added.

Decanol added, moles per mole of sodium laurate	Dried separated product mg	Decanol content of the dry product mg	Sodium laurate content (corrected *) of the dry product mg	Molar ratio of decanol and sodium laurate in the water-free reaction product
0.3	9.9	2.3	7.1	(0.5 :1)
0.3	145.0	29.2	106.4	0.44:1
0.3	89.6	21.3	61.9	0.48:1
0.6	46.9	13.3	29.0	0.64:1
0.6	105.5	31.0	66.9	0.65:1
0.6	416.6	139.0	256.3	0.76:1
1.0	68.4	28.6	35.1	1.2 :1
1.5	46.0	19.7	16.9	1.6 :1
1.5	102.0	42.1	35.8	1.6 :1
2.0	382.0	234.5	125.8	2.6 :1
3.0	425.0	310.5	93.4	4.7 :1

* The correction is based on the assumption that all the water of the isolated product is present as occluded sodium laurate solution. A part of the water belongs, however, to the separated phase itself. The correction is therefore somewhat too large and the decanol-soap ratios in the last column are thus maximum values.

The decanol content of the interaction product. An attempt was made to isolate for analysis the interaction product that appeared as a separate phase, but a complete separation from the solution was not achieved.

A series of 0.014 M sodium laurate solutions containing different additions of decanol were prepared as described above. The solutions were left to stand one month at 40°C, during which time the lighter interaction product gradually rose to the surface from which it was collected. This concentrate was passed through a membrane filter, first under slight pressure and finally by applying suction. The remaining highly viscous product still contained some of the laurate solution that could not be removed.

This product was dried and the water content calculated. Decanol was then removed from the dry residue by distillation and its amount determined. The distillation residue was acidified and the liberated lauric acid extracted with ether. Part of the fatty acid came from the soap dissolved in the occluded laurate solution. The amount of this lauric acid was subtracted and after this correction, the composition of the interaction product was calculated; the water content of the product could not be established. The calculated values are only approximate, but do, however, give an idea of the composition of the separated interaction product.

The data in Table 1 show that the interaction product contains both decanol and sodium laurate. They suggest that in the case of small decanol additions to the solution, the molar ratio of decanol to sodium laurate is near 0.4—0.5. With higher decanol additions, the decanol content of the separating phase increases, the ratio rising to about 1.6 when the amount of added decanol increases to 1.5 moles per mole of laurate. When further amounts of decanol are added, the decanol content of the separated phase increases more rapidly.

As will be shown below, free decanol occurs in the 0.014 M sodium laurate solution only after about 2.5 moles of decanol per mole of laurate have been added.

It is thus evident that the composition of the phase containing decanol and soap is a function of the total decanol content of the system. The interaction between the soap in solution and the decanol does not end when the new phase appears at the turbidity point. The interaction progresses further, but now the decanol is not incorporated in the micelles of the solution but in the separated phase and at the same time more and more soap is removed from the solution. Only after the soap concentration of the solution is decreased to a rather low value, does the interaction with the soap in the aqueous phase end.

Previously we have come to the same conclusion on the basis of conductance measurements.[9] These measurements showed that the decanol content of the separated phase increases with the amount of added decanol at the same time as the concentration of soap in the water phase decreases. The composition of the product which separates from 0.010—0.014 M sodium laurate solutions was calculated (from conductance values) to be 0.6—0.8 mole of decanol per mole of sodium laurate at the turbidity point, but was found to increase to about 4:1 after 1.5 moles of decanol had been added per mole of laurate. (These calculations, which were made on the assumption that the separated phase does not play any part in the transport of current, thus give higher decanol contents than the analyses.)

The calculations made on the basis of conductance measurements also showed that the composition of the separated phase varies with the concentration of the soap solution in which it is formed; in 0.1—0.5 M sodium oleate solutions the composition at the turbidity point was found to be 0.5 moles of decanol per mole of oleate, but at lower oleate concentrations the decanol content increased to 1 mole or more per mole of oleate.

In this connection it may be noted that it was previously found that the mesomorphic acid soap that separates from caprate solutions when capric acid is added has the composition 1 mole of capric acid to 2 moles of sodium caprate and 13—20 moles of water [4]. These acid soaps and the decanol-soap interaction products studied here resemble each other in many of their properties.

The maximum amount of decanol that dissolves in the system. We have previously found that the conductance of the system decreases to a constant value when sufficient decanol has been added. The composition of the separated phase at this point was calculated to be 3.0—3.5 moles of decanol per mole of soap in the 0.010—0.022 M sodium laurate solutions. We have also pointed out that drops of free decanol were observed in the range where the conductance was no longer altered by added decanol.

In a series of 0.010, 0.014, 0.023, 0.030 and 0.040 M sodium laurate solutions containing 0.1—10 moles of decanol per mole of laurate, a study was made of the amount of decanol that a known volume of the soap solution can transfer to the separated mixed phase. Microscopic examinations showed that drops of free decanol occurred in these solutions when the molar ratio of decanol to soap had risen in the respective cases to 2, 2.5, 3.5, 4.0 and 4.5. Considering that only a part (C_{tot}—$C_{L.A.C.}$) of the soap takes part in the formation of the

mesomorphic phase, the ratio in the new phase increases in all cases to 4—5 moles of decanol per mole of laurate. This shows that free decanol occurs in the investigated systems soon after the conductance has decreased to a constant value; small amounts of decanol seem to dissolve in the separated phase even after the interaction with soap in the aqueous phase has gone to completion. (At higher soap concentrations, *e.g.* in the 0.1—0.3 M sodium oleate solutions, the separated phase dissolves appreciable amounts of decanol between the point where the conductance becomes constant and the point where free decanol separates).

B. INTERACTION BETWEEN SODIUM LAURATE AND LIQUID ALCOHOLS OF VARYING CHAIN LENGTH

We have employed the above-described microscopic technique in a study of the interaction of sodium laurate solutions with octanol-1, heptanol-1 and hexanol-1. Similar effects were observed with all alcohols. The solubilities of the alcohols increase, however, with decreasing chain length of the alcohols, and likewise the solubilities of the products of the interaction with soap increase. As a result of this, the interaction proceeds more rapidly and some of the phenomena observed with decanol are weaker or are not observed at all.

On the surfaces of the octanol drops the characteristic layer of filamentous structure composed of birefringent liquid phase was formed. A similar layer developed also on the surfaces of the heptanol drops but did not retard the interaction to the extent noted in the case of decanol and octanol. No continuous layers were produced round the hexanol drops; the dissolution proceeded rapidly and led to complete disappearance of the drops. The end products of the interaction assumed in all cases similar filamentous, myelinic and spherical forms as in the case of decanol.

Separate experiments were made to determine the lowest laurate concentration at which the first signs of interaction with the different alcohols could be detected at 20°C. The laurate solutions employed contained 0.1 mole of sodium hydroxide per mole of laurate to suppress hydrolysis. For decanol, the laurate concentration was found to be 0.0045—0.0055 M; for octanol 0.0055—0.0061 M; for heptanol 0.0061—0.0068 M; and for hexanol 0.0061—0.0068 M. For all alcohols the reaction thus begins in the same relatively narrow laurate concentration range extending from 0.0045 to 0.0068 M. Within this range, the concentration where the first signs of interaction are noted with the microscope varies slightly with the chain length of the alcohol; this may be primarily due to the greater solubility of the reaction product with decreasing chain length of the alcohol.

The observed lowest laurate concentration range, 0.0045—0.0068 M, where interaction with alcohols occurs is in good agreement with the results of our previously published turbidity measurements.

C. INTERACTION WITH CRYSTALLINE ALCOHOLS

Some observations were also made on the interaction between sodium laurate solutions and crystalline dodecanol-1, tetradecanol-1, hexadecanol-1 and octadecanol-1. This interaction differs in principle from that observed with

the lower liquid homologues. The alcohol crystals swell rapidly when they come in contact with the soap solution; they seem to split into thin parallel layers which appear to be held together by a semisolid substance. The alcohol layers also expand in length and breadth; small reacting crystals often move forward quite rapidly, leaving behind a wide tail of interaction product with the layers parallel to the crystal surface. One gets the impression that the soap solution penetrates into the crystal between its double layers of parallel alcohol molecules and that soap concentrates there and also penetrates into the layers of alcohol molecules. The interaction product is birefringent and the interaction with alcohol crystals occurs at rather low laurate concentrations.

The study of this interaction is being continued.

DISCUSSION

In the previously described nephelometric measurements, the first sign of interaction between soap and alcohol at the L.A.C. was the disappearance of the excess of alcohol [10,11]. In the above-described microscopic method, on the other hand, one observes the formation of the mesomorphic phase. Neither of these methods gives information of the changes occurring in the solution, but with the aid of a third method (solubility measurements) we obtain an idea of what happens in the solution; we find that the solubility of the alcohol (decanol-1) increases somewhat above the L.A.C.[6,7]. These three methods give the same value for the concentration (L.A.C.) where the interaction begins; the small differences between the values depend on the fact that the three methods register different phenomena associated with the same process.

In the microscopic observations, the interaction between alcohol and soap solution appears as a reaction taking place at the interface. No changes or processes that take place within the alcohol phase are observed, whereas one gets an idea of the solution of the alcohol in the aqueous phase and of the conditions favouring the formation of the mesomorphic phase when the alcohol concentration increases locally to a certain value. In the interface (also on the alcohol side) there must occur an adsorption of soap and a formation of palisade layers composed of parallel alcohol molecules and soap ions. The interfacial tension must be very low. An extensive dispersion into very fine particles follows ("spontaneous emulsification") and the rapid solution of the alcohol in the water phase in the vicinity of the phase boundary is facilitated. These processes make it possible for the corona to grow out from the interface. The palisade layers of alcohol and soap formed in an environnement rich in alcohol but poor in water take up more water and perhaps more soap with swelling. We refer again to the swelling of the filaments; their strong birefringence decreases and spherical drops are produced. We wish to emphasize that the formation of the mesomorphic alcohol-soap-water phase does not presuppose the presence of soap solution-alcohol interfaces in the system, even if the formation of the corona-like structures does so. This phase can be formed directly from the components in the solution, *e.g.* on cooling the homogeneous solution. Soap solutions in equilibrium with the mesomorphic phase are not saturated with respect to alcohol and the concentration of free alcohol in them is much lower than in a saturated aqueous solution of the alcohol; conditions favouring the

formation of the phase mentioned are produced when the concentrations of soap and free alcohol increase over certain limits.

In the cases we have investigated the interaction between decanol and soap solution passes through several steps. The first amounts of added alcohol (in excess of that which dissolves in the water) form soluble aggregates with the soap; the alcohol solubilizes in micelles or forms smaller soap-alcohol aggregates. When more alcohol is added, a separate phase consisting of alcohol, soap and water is formed; with increasing alcohol additions, more and more soap is removed from the water solution to form more of the separated phase until the soap concentration of the solution is decreased to a minimum value. Also after this minimum value is reached and the interaction with soap in the solution ends, the separated alcohol-soap-water phase takes up added alcohol. Finally also this uptake attains a limit, and the alcohol appears in the free form. Only at this point does the system become saturated with alcohol. In sodium laurate and sodium oleate solutions at 20°C, the system at this point consists of three phases, the aqueous solution, the alcohol-soap-water phase and free decanol.

Both the alcohol-soap ratio and the water content of the alcohol-soap-water phase seem to vary between rather wide limits. If there is a continuous transition between the different compositions and forms of this interaction product or if the product possibly forms more than one phase is not clear. See, for example, the previously described rather sharp turbidity maxima which result when decanol is added to soap solutions in increasing amounts [9].

The character and composition of the substance that separates from association colloid solutions above the L.A.C. when alcohol is added in sufficient amount seems to have been unknown to most of the investigators in this field. This had led to a misinterpretation of the results of the solubility determinations in connection with studies of the solubilization of alcohols. Already in 1947 one of the present writers [8] postulated the difference in the solubilization mechanism of nonpolar and polar compounds and called attention to the fact that a liquid-crystalline product separates from sodium oleate solutions when octanol or hexadecanol is added and that this is accompanied by a fall in the conductance. In the same paper the solubilization of terpineol was also reported and it was shown that terpineol first dissolves readily in a 0.3 M oleate solution, but then causes the system to become heterogeneous when more than 4.5 % is added. The system becomes homogeneous again when still more terpineol is added. The solution was found to be definitely saturated with terpineol only after more than 26 % had been added. At the first turbidity point the viscosity passed through a very pronounced maximum, and after adding 13—16 % terpineol a second, rather low viscosity maximum was noted; the conductance was observed to decrease rapidly above the first turbidity point, but then passed through a minimum. In the saturated systems, both the viscosity and conductance remained constant. It was reported that many other substances effect similar phenomena. Menthol and decamethylene glycol were, however, found to solubilize normally in rather high oleate concentrations, *i.e.* the excess of these substances separated in pure form [8]. These investigations showed the necessity of making observations of the nature of the separated phase in solubilization studies.

Later [5,12] it was shown that a liquid-crystalline product is generally formed when paraffin-chain alcohols interact with aqueous association colloid solutions of the paraffin-chain type (fatty acid soaps, alkyl sulphates, alkyl trimethyl ammonium salts) and that the product contains both alcohol and colloid. It was emphasized that a large part of the colloid can be precipitated in this way from the solution, by adding sufficient amounts of the alcohol. It was also shown that the mesomorphic phase forms only above the L.A.C. and that the maximum solubility of the alcohol increases slightly somewhat above this point (before the system becomes heterogeneous). The great similarities between the interaction between alcohols and association colloid solutions and the formation of acid soaps in the interaction of soap and fatty acid were stressed. Ekwall, Passinen and Danielsson [6] reported on the formation of the mesomorphic alcohol-soap-water phase in a brief survey of their experimental work conducted during 1950—53 on the solubilization of alcohols, and pointed out the differences between the solubilization of alcohols and hydrocarbons. In the present series the results of this work is thoroughly discussed. In Part I [13] it was for instance emphasized that the solubility curves for paraffin-chain alcohols are not comparable with those obtained in studies of hydrocarbon solubilization.

In 1948 Winsor also reported on the separation of birefringent "gels" in systems which, however, contained besides a hydrotropic substance, alcohol, and water, also a hydrocarbon or a mixture of hydrocarbons and thus were rather complex; only in one case did Winsor give experimental data on the formation of a "gel" in a system containing no hydrocarbon (sodium-*n*-butyrate-octanol-water) [14]. Klevens, referring to his own observations and to Winsor's work, mentioned that added polar long-chain compounds and soaps readily form viscous birefringent "gels" [15]. However, in the same paper the solubility curves for alcohols were directly compared with those obtained for hydrocarbons. Lumb investigated the phase equilibria in mixtures of alcohols and aqueous potassium butyrate and octanoate solutions and showed clearly that in some cases a mesomorphic phase composed of soap alcohol and water separates over a wide concentration range [16]. Recently. Hyde, Langbridge and Lawrence, on the basis of extensive experimental observations, primarily on aqueous Teepol-alcohol systems, discussed "soap + water + amphiphile systems" [17]. In their work the study of the formation of a liquid-crystalline phase consisting of alcohol, association colloid and water holds a central place; also the disappearance of this phase on adding greater amounts of alcohol was studied. They showed that there occur two ranges of homogeneous systems (compare Ekwall's [8] observations on the sodium oleate-terpineol systems and Lumb's [16] on the above-mentioned soap-alcohol systems). The viscosities and conductances of the Teepol-systems pass through maxima and minima (somewhat similar to those previously observed in other association colloid-alcohol systems [8,6,9,18]). Lawrence and coworkers state that a similar phase equilibrium pattern has been found to apply to all soaps and all amphiphilic additives of the long-chain type. They emphasize the serious error incurred in many earlier studies when "the initial separation of the liquid-crystalline phase was taken to be emulsion and excess of the amphiphile above saturation . . ."

Summarizing it can be said that Ekwall and coworkers have studied the changes in the aqueous association colloid solutions when alcohol is added both before and after the mesomorphic phase has formed and have attempted an exact determination of the conditions favouring the formation of this phase. They have also studied the properties and composition of this phase, but their investigations were in only a few cases extended to the addition of more than 5 moles of the alcohol per mole of the colloid. The English investigators have studied the systems from the viewpoint of the phase equilibria and have been interested also in those systems where the polar substance predominates; they have attempted to draw equilibrium diagrams for the ternary systems. Only in a few cases have the same systems been studied in these different investigations. They complement each other and give a fairly good idea of the interaction between polar substances and aqueous association colloids, even if there still are many unsolved problems in this field.

REFERENCES

1. Ekwall, P. *Kolloid-Z.* **80** (1937) 77.
2. Ekwall, P. *Kolloid-Z.* **85** (1938) 16.
3. Ekwall, P. *Tek. Fören. i Finland Förhandl.* **1940** 178.
4. Ekwall, P. *Kolloid-Z.* **97** (1941) 71.
5. Ekwall, P. and Danielsson, I. *Acta Chem. Scand.* **5** (1951) 973.
6. Ekwall, P., Passinen, K. and Danielsson, I. *Finska Kemistsamf. Medd.* **1954** 1.
7. Ekwall, P. and coworkers. *To be published later in this series.*
8. Ekwall, P. *VI Nordiska Kemistmötet*, Lund 1947, p. 179.
9. Passinen, K. and Ekwall, P. *Acta Chem. Scand.* **9** (1955) 1438, 1450 (Part II and III of this series).
10. Ekwall, P., Söderberg, O. and Danielsson, I. *Acta Chem. Scand.* **10** (1950) 237 (Part V of this series).
11. Ekwall, P. and Aminoff, Cl. F. *Acta Chem. Scand.* **10** (1955) 227 (Part VI of this series).
12. Ekwall, P. *Svensk Kem. Tidskr.* **63** (1951) 277.
13. Ekwall, P. and Passinen, K. *Acta Chem. Scand.* **7** (1953) 1098 (Part I of this series).
14. Winsor, P. A. *Trans. Faraday Soc.* **44** (1948) 376, 451.
15. Klevens, H. B. *Chem. Revs.* **47** (1950) 1.
16. Lumb, E. C. *Trans. Faraday Soc.* **48** (1951) 1059.
17. Hyde, A. J., Langbridge, D. M. and Lawrence, A. S. C. *Discussions Faraday Soc.* **18** (1954) 239.
18. Passinen, K. and Ekwall, P. *Acta Chem. Scand.* **10** (1956) 215. Part IV of this series).

Received May 12, 1956.

ACTA CHEMICA SCANDINAVICA 10 (1956) 1160—1164

Dimethylsulphoxide, a Solvent for Hemicelluloses

ERIK HÄGGLUND, BENGT LINDBERG
and JOHN McPHERSON

Träkemiska avdelningen, Svenska Träforskningsinstitutet, Stockholm, Sweden and Institutionen för Träkemi, Kungl. Tekniska Högskolan, Stockholm, Sweden

Part of the holocellulose of birch or spruce can be extracted with dimethylsulphoxide and further quantities are extracted from the swollen material by a subsequent treatment with water. The extraction is quite mild, and the fractions still contain a high percentage of the acyl groups (acetyl and formyl) originally present in the wood. Partial fractionation of the hemicellulose components is achieved by the extractions. Dimethylsulphoxide can also be used as a rather selective precipitating agent for hemicelluloses.

In a recent investigation at this Institute [1], it was found that dimethylsulphoxide (D.M.S.) was an excellent solvent for cellulosexanthates of a low D.S., in which the xanthate groups had previously been reacted with chloro-di-N-ethyl-acetamide. It was superior to other solvents, *e. g.* dimethylformamide. We therefore considered it worth while to investigate the possibilities of D.M.S. as a solvent for hemicelluloses, and in the present paper a preliminary study on this subject is reported.

A birch holocellulose, a spruce holocellulose and a spruce sulphite pulp have been investigated. They were all extracted with D.M.S. at room temperature, with cold and with hot water and finally with 18 % sodium hydroxide solution. The fractions were collected and analysed, the results being summarized in Tables 1, 2 and 3. The recovery of extracted material is not quantitative, partly because further fractionations were performed before the fractions were dried and weighed, which involved losses, and partly because the polysaccharides in some extracts were not completely precipitated. In separate experiments, however, it was shown that a good recovery could be obtained.

From the Tables 1, 2 and 3 it is evident that a considerable part of the hemicellulose is extracted with D.M.S. The cellulosic material exhibits considerable inter-micellar swelling during the extraction and this is probably the reason why so much material is extracted during the subsequent treatment with water. In the D.M.S. extract from the birch holocellulose, a high percentage of acyl groups was found, recorded as acetyl, although it is known that

Table 1. Birch holocellulose (Betula verrucosa + B. pubescens).

Fraction	Extraction residue, % of original holocell.	Yield, g	Acetyl, %	Uronic acids % a)	Methoxyl %	Galactose : Glucose : Mannose : Arabinose : Xylose
Holocellulose	100	14.6	5.80	9.5	1.82	b) 1.5 : 58.5 : 0.5 : 0.5 : 39.0
D. M. S. extract	—	4.4	11.2	11.1	2.76	4.7 : 8.1 : (30.4) : 56.8
Water extract	87	4.8	11.4	29.4	4.70	(+) : 2.7 : (3.0) : 94.3
18 % NaOH extract	48	45.8	—	13.0	—	(7.4) : 5.6 : 0 87.0
Residue	—	70.8	—	1.2	—	(+) : 94.7 : 3.0 : (+): 2.3

a) Given as free uronic acids. b) Values taken from Gustafsson *et al.*[2] for *B. verrucosa.*

Table 2. Spruce holocellulose (Picea excelsa).

Fraction	Extraction residue, % of original holocell	Yield, g	Acetyl, %	Uronic Uronic acids, %	(Galactose + Glucose):Mannose: Arabinose : Xylose
Holocellulose	100	77	—	—	74.6 : 15.4 : 0.9 : 9.1
D. M. S. extract	94	—	5.0	18.0	9.7 : 23.4 : 8.3 : 58.6
Water extract	88	—	10.1	12.6	17.7 : 66.4 : 1.5 : 14.4
18 %, NaOH extract	76	—	—	10.9	13.5 : 48.0 : 2.3 : 36.7
Residue	—	58	—	—	85.8 : 13.5 : 0 : 0.7

Table 3. Spruce sulphite pulp (Picea excelsa)

Fraction	Extraction residue, % of original pulp	Uronic acids, %	Methoxyl, %	Glucose : Mannose : Xylose
Pulp	100	—	—	84.5 : 9.5 : 6.6
D. M. S. extract	98.3	12.8	3.85	3.4 : (+) : 96.6
18 %, NaOH extract	89.8	—	—	— — —
Residue	—	—	—	94.8 : 4.4 : 0.8

formyl group are also present. One of the chief advantages of the extraction method is that hemicellulose fractions, with the original acyl groups still present, have been made available for investigation. The xylose still dominates in the D.M.S. fraction but the non-xylan polysaccharides have been considerably enriched, and the fraction is a good starting material for an investigation of these completely unknown polysaccharides. The water extract is essentially a pure xylan with high percentages of acetyl and of uronic acids. As it is possible that the acetic and formic acids in the wood are chiefly combined

with the xylans, this is an especially interesting starting material for further investigations.

The polysaccharides in conifers constitute a complicated mixture, and it is obvious that a considerable partial fractionation has been obtained by the extraction of the spruce holocellulose. There are great differences in composition between the D.M.S. extract and the water extract, xylose dominating in the first and mannose in the second. Also here the acyl groups have survived the extractions. Mannose seems to occur in two different types of polysaccharides, one easily extracted and one very insoluble, which, of course, is known also from previous investigations. It is unknown whether there are structural differences between the two types or if the different solubilities are due to morphological reasons. The two types are enriched in the D.M.S. fraction and in the extraction residue, respectively. The high percentage of arabinose in the D.M.S. fraction probably comes from an arabogalactan, which seems to be present in most conifers, and in this case most of the combined glucose-galactose of this fraction, recorded in Table 2, should be galactose.

From the spruce sulphite pulp, an almost pure xylan, with a high percentage of uronic acids, was obtained from the D.M.S. extract.

It is evident from the experiments described above that some types of polysaccharides are quite soluble in D.M.S. and others are not. One would deduce that the more highly branched or substituted polysaccharides should show the greatest solubility. It was therefore natural to investigate whether D.M.S. could be used, too, as a selective precipitating agent. The 18 % sodium hydroxide fraction from spruce holocellulose in aqueous, neutral solution was added to six times its volume of D.M.S. and after 16 hours, the precipitate was collected. The residual solution was then added to ethanol four times the volume of the original aqueous solution, when further amounts of material precipitated. The analyses of the fractions (Table 4) show that a considerable fractionation has been achieved and that chiefly the mannose-containing polysaccharides were precipitated by D.M.S.

When some of the material precipitated by D.M.S. was treated with 7 % sodium hydroxide solution at room temperature, only part of it went into solution. The insoluble material contained glucose and mannose as the only sugars, with the latter dominating. The recent work of Anthis [3] strongly indicates that at least part of the mannose in conifers is present as a glucomannan, and this fraction thus might be a homogeneous polysaccharide. The material

Table 4. Fractionation with D.M.S. as precipitating agent.

Fraction	Uronic acids, %	(Galactose + Glucose) : Mannose : Arabinose : Xylose
18 % NaOH extract, precipitated with ethanol	11.0	13.5 : 48.0 : 2.3 : 36.2
18 % NaOH extract, precipitated with D.M.S.	8.56	13.7 : 66.5 : 0.7 : 19.1
Residual solution, precipitated with ethanol	16.1	5.3 : 16.0 : 4.2 : 74.5

obtained by precipitation of the residual solution with ethanol was rich in xylose and uronic acids, contained only traces of mannose but other sugars were not detected in the hydrolysate.

When extracted but undelignified wood powder under the same conditions was treated with D.M.S. no significant amounts of carbohydrate material went into solution.

In this preliminary work, no attempts have been made to study the optimum conditions of extraction and precipitation with regard to the concentration and pH of the D.M.S. and of the temperature and duration of the treatment. The D.M.S. is a very slightly alkaline solvent obtained as a white crystalline material (M. p. 18.5° C) and shows partly an "aldehydic" and partly an unsaturated character. It is easily recoverable by distillation under reduced pressure and is miscible with many organic solvents, except the aliphatic hydrocarbons, and with water. As with dimethylformamide it is strongly hygroscopic and at 20° C has an equilibrium moisture content of 10 %. Because of these properties it should have great potentialities in the isolation of undenatured polysaccharides. Whether it effects any marked degradation in the cellulose and hemicellulose components and its exact mode of operation is not yet known. It does appear that the swelling of the pulps and holocelluloses is mainly inter-micellar from experiments on the moisture regain of the samples.

EXPERIMENTAL

The D.M.S. used in this investigation was as obtained from the manufacturer and was not further purified.

All concentrations were carried out at reduced pressure and at about 40° C. All precipitates were investigated by qualitative chromatography after total hydrolysis, using the solvent systems; ethyl acetate-acetic acid-water (3:1:1), butanol-pyridine-water (6:2:3) and butanol-formic acid-water (100:23:77). Most fractions were also investigated by quantitative paper chromatography, using the method of Saeman *et al.*[4]. As aldobiuronic acids are essentially not hydrolysed under the conditions used, the values for xylose are consistently too low.

Birch holocellulose. The birch wood used was a technical mixture of *Betula verrucosa* and *B. pubescens*. The chips were handsorted, ground in a Wiley mill and the fraction of particle size less than 0.5 mm removed by sieving. The remaining wood powder was extracted with acetone in a continous extractor for 24 h, air-dried and delignified, using the sodium chlorite method as modified by Saarnio, Wathén and Gustafsson [5]. The yield of air-dried holocellulose, based on the extracted wood, was 82.7 %, a rather high value, indicating that the delignification was not complete.

The holocellulose (146 g, calc. as oven-dried weight) was extracted with D.M.S. (1 000 ml) at room temperature for 20 h. The extraction was performed in a desiccator and by applying and releasing a vacuum a number of times a good penetration of the solvent was effected. The mixture was filtered and the residue given a further treatment with D.M.S. (760 ml) for 2 h. After this extraction the holocellulose was washed with water (1 000 ml) for five min and filtered. The residue was extracted with water (1 000 ml) at room temperature for 20 h and then with hot water (1 000 ml, 90—95°) for 4 h. To each of the extracts was added four times its volume of ethanol and a few drops of conc. hydrochloric acid and the mixtures were allowed to stand for 24 h. The cold water extract yielded no precipitate but from all the others precipitates were recovered by decantation and centrifugation. The precipitates were washed with ethanol and with benzene and dried under a vacuum, and were thus obtained as white or almost white powders.

Concentration of the residual solutions from the aqueous extracts to small volumes (~ 150 ml) and addition of large excesses of ethanol yielded further precipitates, rather

similar in composition to the first precipitate from the hot water extract. Further concentration of the mother liquors from the aqueous extracts produced no additional amounts of polysaccharide material but deep orange or brown syrups which probably contained modified lignin products. The residues from the D.M.S. extracts were not further investigated but probably contained more soluble polysaccharides.

Part of the holocellulose residue (60 g) after the extractions with D.M.S. and water was given an extraction with 18.1 % sodium hydroxide solution (1 000 ml) for 25 min at room temperature, the mixture was then diluted with water (3 000 ml), stirred for 5 min and filtered. The residue was washed with water, 10 % acetic acid and water again and air-dried in order to determine the yield. The extract was adjusted to pH 6, then to pH 2, and kept at this pH-values for several days at 4°, according to the procedure of McPherson and Rånby [6], but no substancial amounts of material were precipitated. The polysaracchides were then precipitated by addition of ethanol (9 000 ml) and the precipitate washed and dried as described above.

The analyses given in Table 1 for the D.M.S. and the water extracts refer to the first D.M.S. extract and the first precipitate from the hot water extract, but qualitative analyses indicate that they are typical for all the precipitates from the D.M.S. and water extracts, respectively.

Spruce holocellulose. Spruce wood chips were handsorted, extracted with benzene-ethanol and the air-dried extracted wood was converted to holocellulose using sodium chlorite according to the method of Wise *et al.*[7] Yield, 66.1 %. The holocellulose was then extracted and worked up analogously to the birch holocellulose. The various precipitates were divided into a number of subfractions by fractionated precipitation with ethanol. No significant fractionation into different types of polysaccharides was, however, obtained. Quite different and more efficient separations were achieved by using D.M.S. as a precipitating agent for the hemicelluloses extracted by 18 % sodium hydroxide solution, as described in the general part, where also the separation of a subfraction from this fractionation into a "glucomannan" and a xylan by partial dissolution with 7 % sodium hydroxide solution is described.

The second and third analysis given in Table 2 refer to the precipitates from the combined D.M.S. extracts and from the hot water extract, but, as mentioned above, are typical for all the precipitates from the D.M.S. and water fractions, respectively.

Spruce sulphite pulp. The preparation of the chemical grade sulphite pulp is described by McPherson and Rånby [6]. It was extracted and worked up analogously to the birch holocellulose.

REFERENCES

1. Treiber, E., Gierer, J., Rehnström, J. and Schurz, J. *Holzforschung. In press.*
2. Gustafsson, C., Sundman, J., Pettersson, S. and Lindh, T. *Paper and Timber* **B 33** (1951) 300.
3. Anthis, A. F. *Abstracts*, **4 E.** *Am. Chem. Soc. 128th Meeting*, Minneapolis 1955.
4. Saeman, J. F., Moore, W. E., Mitchell, R. L. and Millett, M. A. *Tappi* **38** (1954) 336.
5. Saarnio, J., Wathén, K. and Gustafsson, C. *Acta Chem. Scand.* **8** (1954) 826.
6. McPherson, J. A. and Rånby, B. *In preparation.*
7. Wise, L. E., Murphy, M. and D'Addieco, A. A. *Tech. Assoc. Papers* **29** (1946) 210.

Received May 17, 1956.

ACTA CHEMICA SCANDINAVICA **10** (1956) 1165—1171

Studies on Monoalkyl Carbonates

XIV. The Monoalkyl Carbonates of Sorbitol, Mannitol and Glucose

JØRN THAMSEN

The Royal Danish School of Pharmacy, Copenhagen, Denmark

By addition of carbon dioxide to an aqueous solution of an alcohol and sodium hydroxide, monoalkyl carbonate and carbonate are formed as the carbon dioxide reacts with the alcoholate ion and the hydroxide ion. Sorbitol, mannitol and glucose also form monoalkyl carbonate with carbon dioxide and the velocity constant and the equilibrium constant for the formation of monoalkyl carbonate have been determined. The velocity of the decomposition of monoalkyl carbonate in strongly basic medium has also been investigated and may be explained by assuming that the decomposition is a two-stage reaction *viz.* (1) $RCO_3^- = RO^- + CO_2$; (2) $CO_2 + OH^- = HCO_3^-$

1. The present investigation deals with the equilibrium conditions and the reaction mechanism for the formation and decomposition of the monoalkyl carbonates of sorbitol, mannitol, and glucose.

2. The sorbitol was either D-sorbitol obtained from the Atlas Powder Co., stated to be of great purity, or crystalline D-sorbitol Merck. The melting point, given as 97.7° C for the stable form, was found to be 96—97° C. The mannitol was D-mannitol from the Pfanstiehl Chemical Co., stated to be pure, and had a melting point of 166—167° C. The melting point of mannitol is given as 166° C. The glucose used was 'Dextropur' from the Corn Products Co. Ltd., Copenhagen. Upon analysis it was found to contain 91.2 % glucose and 8.8 % water, thus corresponding very closely to the formula $C_6H_{12}O_6$, H_2O.

3. As it was difficult to isolate the monoalkyl carbonates themselves the solutions were prepared in the following manner: About 0.03 moles carbon dioxide were dissolved in one litre of a solution, which was 0.10—0.50 molar with regard to alcohol and 0.1 molar with regard to NaOH, thus converting about 20—60 % of the carbon dioxide to monoalkyl carbonate and the rest to ordinary carbonate.

4. The method of analysis was the same as in previous investigations, *viz.* separation of the monoalkyl carbonate from the ordinary carbonate by precipitating the carbonate with barium chloride [1]. The data presented are cor-

Table 1 a. 500 ml carbon dioxide solution in 500 ml ROH + NaOH. 0°C.

	Expt. No.	Initial concn. NaOH	Initial concn. ROH	Compositions of the solutions * c_{OH^-} c_{ROH} c_{RO^-}	Absorbed CO_2 mole/litre	% RCO_3^-	% RCO_3^- (corr.)	log $k_{CO_2 \cdot RO^-}$
Sorbitol	1	0.20	0.20	0.1164 0.1164 0.0836 0.0351 0.0757 0.0166	0.028	23.70	27.52	4.15
	2			0.1164 0.1164 0.0836 0.0352 0.0756 0.0166	0.028	24.15	27.86	4.16
Mannitol	3	0.20	0.20	0.1125 0.1125 0.0875 0.0355 0.0735 0.0185	0.027	25.70	29.51	4.15
	4			0.1125 0.1125 0.0875 0.0360 0.0728 0.0186	0.027	28.07	31.83	4.21
	5	0.20	0.50	0.0575 0.3575 0.1425 0.0242 0.2005 0.0345	0.028	48.30	52.35	4.10
	6			0.0575 0.3575 0.1425 0.0216 0.2052 0.0318	0.025	49.91	53.55	4.11
Glucose	7	0.20	0.20	0.0396 0.0396 0.1604 0.0099 0.0479 0.0481	0.023	12.41	17.59	3.10
	8			0.0396 0.0396 0.1604 0.0076 0.0436 0.0414	0.028	12.59	17.81	3.09
	9	0.20	0.50	0.0067 0.3067 0.1933 0.0041 0.1721 0.0729	0.014	28.82	37.13	2.77
	10			0.0067 0.3067 0.1933 0.0047 0.1667 0.0793	0.010	30.78	40.46	2.84
	11	0.20	1.00	0.0034 0.8034 0.1966 0.0016 0.4176 0.0704	0.020	51.74	60.73	2.85
	12			0.0034 0.8034 0.1966 0.0014 0.4214 0.0606	0.028	53.77	62.95	2.89

* *Cf.* footnote to Table 1.

rected for the blank values and for decomposition as mentioned in the next section. The experiments were carried out at 0° C. The velocity constants were calculated by means of Briggs' logarithms and with the time measured in minutes.

I. ON THE FORMATION OF MONOALKYL CARBONATE FROM CARBON DIOXIDE AND ALCOHOL IN BASIC SOLUTIONS, AND ON THE REACTION $RO^- + CO_2 = RCO_3^-$

The first series of experiments was carried out by introducing 500 ml carbon dioxide gas into a 2.5 litre flask containing 1 litre of a basic solution of the alcohol and shaking vigorously for 2 minutes. As the manner in which the

Table 1. Carbon dioxide gas in ROH + NaOH. 0°C.

	Expt. No.	Initial concn. NaOH	Initial concn. ROH	Composition of the solutions * c_{OH^-} c_{ROH} c_{RO^-}	Absorbed CO_2 mole/litre	% RCO_3^-	% RCO_3^- (corr.)	log $k_{CO_2 \cdot RO^-}$
Sorbitol	1	0.1	0.1	0.0700 0.0700 0.0300 0.0435 0.0713 0.0196	0.023	33.62	39.50	4.57
	2			0.0700 0.0700 0.0300 0.0402 0.0716 0.0181	0.026	33.72	39.62	4.57
	3			0.0700 0.0700 0.0300 0.0431 0.0719 0.0195	0.023	30.69	37.32	4.55
Mannitol	4	0.1	0.1	0.0670 0.0670 0.0330 0.0340 0.0710 0.0165	0.031	32.80	39.00	4.50
	5	0.1	0.25	0.0420 0.1920 0.0580 0.0280 0.1960 0.0378	0.025	59.00	64.50	4.51
	6			0.0420 0.1920 0.0580 0.0380 0.1940 0.0508	0.008	56.80	66.00	4.54
	7			0.0420 0.1920 0.0580 0.0300 0.1960 0.0403	0.022	59.30	64.00	4.50
	8	0.2	0.25	0.099 0.1490 0.1010 0.083 0.1550 0.0868	0.021	54.20	59.20	4.54
Glucose	9	0.1	0.1	0.0270 0.0270 0.0730 0.0037 0.0685 0.0229	0.041	12.86	21.09	3.32
	10			0.0270 0.0270 0.0730 0.0065 0.0547 0.0384	0.031	14.59	22.34	3.33
	11			0.0270 0.0270 0.0730 0.0151 0.0371 0.0599	0.014	15.70	21.42	3.33
	12	0.1	0.25	0.0060 0.1560 0.0940 0.0021 0.1957 0.0411	0.035	27.09	37.83	2.96
	13			0.0060 0.1560 0.0940 0.0023 0.1915 0.0441	0.034	30.58	42.22	3.03
	14			0.0060 0.1560 0.0940 0.0039 0.1731 0.0695	0.017	32.33	43.61	3.06
	15	0.2	0.25	0.0240 0.0740 0.1760 0.0129 0.0989 0.1308	0.036	32.00	43.67	3.36
	16			0.0240 0.0740 0.1760 0.0130 0.0989 0.1309	0.035	29.44	39.72	3.39
	17	0.1	0.50	0.0020 0.4020 0.0980 0.0010 0.4390 0.0462	0.038	50.13	60.97	2.90
	18			0.0020 0.4020 0.0980 0.0008 0.4438 0.0381	0.043	47.15	58.01	2.85
	19			0.0020 0.4020 0.0980 0.0012 0.4322 0.0554	0.031	49.84	59.91	2.88
	20	0.2	0.50	0.0060 0.3060 0.1940 0.0035 0.3525 0.1283	0.049	48.91	60.87	3.06

* In the column 'composition of the solutions' are two sets of values. The upper one states the concentrations of hydroxyl ion OH^-, undissociated alcohol ROH, and alcoholate ion RO^- before the addition of carbon dioxide gas, and the lower set states these concentrations immediately after the addition. The lower set of values are corrected for the change in the concentration of alcohol and sodium hydroxide due to the reaction with the carbon dioxide. In further calculations the mean values of the upper and lower figures are used.

carbon dioxide was added to the solution could possibly influence the ratio between monoalkyl carbonate and carbonate (*cf.* the analogous experiments with carbamate and carbonate [2]) a second series of experiments was carried out. In these experiments 500 ml of a 0.06 M solution of carbon dioxide in water was added to 500 ml of the basic solution of alcohol with vigorous stirring. The two series of experiments disagree especially for sorbitol and mannitol. The difference could possibly be ascribed to the different concentrations of the reactants during the addition of the carbon dioxide.

Immediately after the addition of carbon dioxide the reaction solution was analysed for monoalkyl carbonate. The results are listed in the Tables 1 and 1a.

Because of the very rapid decomposition of the monoalkyl carbonate the results are corrected not only with respect to the blanks but also with respect to the decomposition taking place during the time which elapses between the start of the experiment and the separation of the precipitate and the supernatant by centrifugation. The blank values amounted to about 2—5 % of the total concentration of carbon dioxide. The other corrections appear from the tables.

The values in column 5 are computed by means of the following expression

$$\frac{c_{ROH}c_{OH^-}}{c_{RO^-}} = \frac{(a - c_{RO^-})(b - c_{RO^-})}{c_{RO^-}} = \frac{K_{H_2O}}{K_A}$$

where a and b are the total concentrations of alcohol and sodium hydroxide, respectively, thus

$$c_{ROH} + c_{RO^-} = a$$

$$c_{OH^-} + c_{RO^-} = b$$

The acid dissociation constants for sorbitol, mannitol and glucose are: $10^{-14.14}$, $10^{-14.09}$ and $10^{-12.92}$, respectively [3], and $K_{H_2O} = 10^{-14.93}$ at 0° C.

For most of the previously investigated alcohols the dissociation constants were either not known or not known with sufficient accuracy, and it was therefore convenient to compute the velocity constant k' of the gross reaction

$$ROH + OH^- + CO_2 = RCO_3^- + HOH$$

but in this case it is possible to compute the velocity constant $k_{CO_2 \cdot RO^-}$ of the reaction

$$RO^- + CO_2 = RCO_3^-$$

by means of the expression

$$\frac{\% \text{ monoalkyl carbonate}}{\% \text{ carbonate}} = \frac{k_{CO_2 \cdot RO^-} \cdot c_{RO^-}}{k_{CO_2 \cdot OH^-} \cdot c_{OH^-}}$$

where $k_{CO_2 \cdot OH^-} = 10^{+4.39}$

The mean values of $k_{CO_2 \cdot RO^-}$ corresponding to Table 1 are $10^{4.56}$, $10^{4.52}$ and $10^{3.12}$ for sorbitol, mannitol and glucose, respectively. The mean values of $k_{CO_2 \cdot RO^-}$ corresponding to Table 1a are $10^{4.16}$, $10^{4.14}$ and $10^{2.92}$ for sorbitol, mannitol and glucose, respectively.

For comparison it is convenient to state the values of the velocity constant k' computed from the expression $k' = k_{CO_2 \cdot RO^-} K_A / K_{H_2O}$, *viz.* $10^{5.35}$, $10^{5.36}$ and $10^{5.13}$, corresponding to Table 1, and $10^{4.95}$, $10^{4.98}$ and $10^{4.93}$ corresponding to Table 1a for sorbitol, mannitol and glucose, respectively.

II. THE EQUILIBRIUM OF THE REACTION $RCO_3^- + HOH = HCO_3^- + ROH$

The above equilibrium was established in aqueous solutions of alcohol, potassium hydrogen carbonate and sodium carbonate. With the alcohols studied in the present investigation the equilibrium is shifted strongly to the right, and thus the determinations of per cent monoalkyl carbonate may be attended with rather large errors as the blank values are almost of the same order of magnitude as the experimental values, and the computed K_{Eq}-values give only the order of magnitude.

a) Sorbitol. The equilibrium was established at 0° C in a solution 0.25 M with regard to sorbitol, 0.1 M with regard to $KHCO_3$ and 0.1 M with regard to Na_2CO_3.

The monoalkyl carbonate was determined in 100 ml samples and found to be equivalent to 2.35, 2.60, 2.46, 2.50 and 2.44 ml 0.1 N HCl, respectively, with a mean value of 2.47 ml. The blank values corresponded to 1.41, 1.33, 1.38, 1.30 and 1.41 ml 0.1 N HCl, with a mean value of 1.37 ml. The true quantity of monoalkyl carbonate thus corresponds to 1.10 ml 0.1 N HCl, *i. e.* $\frac{1.10 \times 100}{200} = 0.55$ % of the $KHCO_3$ is transformed to monoalkyl carbonate.

b) Mannitol. The equilibrium was established at 0° C in a solution 0.25 M with regard to mannitol, 0.1 M with regard to $KHCO_3$ and 0.1 M with regard to Na_2CO_3. In the equilibrium 0.98 % of the $KHCO_3$ is converted to monoalkyl carbonate.

The monoalkyl carbonate in the samples corresponded to 3.09, 3.30, 3.36, 3.19, 3.41, 3.19, 3.12 and 3.29 ml 0.1 N HCl, with a mean value of 3.24 ml. The blank values corresponded to 1.49, 1.40, 1.58, 1.41, 1.40, 0.98, 1.02 and 0.92 ml 0.1 N HCl, with a mean value of 1.28 ml.

c) Glucose. Equilibrium was established at 0° C in a solution 0.5 M with regard to glucose, 0.1 M with regard to $KHCO_3$ and 0.1 M with regard to Na_2CO_3. In different determinations the monoalkyl carbonate was equivalent to 1.84, 1.94, 2.31, 3.07, 1.56 and 1.52 ml 0.1 N HCl, respectively, with a mean value of 1.87 ml. The blank values were equivalent to 1.03, 0.81, 0.95, 1.05, 1.24, 1.27 and 1.32 ml 0.1 N HCl, respectively, with a mean value of 1.10 ml. In the equilibrium 0.38 % of the $KHCO_3$ is transformed to monoalkyl carbonate.

d) From the above values and

$$K_{Eq} = \frac{c_{ROH} c_{HCO_3^-} f}{c_{RCO_3^-} f}$$

K_{Eq} has the values 45, 25, and 128 for sorbitol, mannitol and glucose, respectively, but as suggested above these values only state the order of magnitude of K_{Eq}.

III. ON THE VELOCITY OF THE REACTIONS $RCO_3^- + HOH = HCO_3^- + ROH$

The solutions mentioned in the Tables 1 and 1a were all directly used for the kinetic determinations. The results corresponding to the experiments represented in the Tables 1 and 1a coincide, and therefore to save space only a limited number of the experiments corresponding to Table 1a are represented in Table 2.

Table 2. Monoalkyl carbonate in NaOH + alcohol. 0°C.

	1	2	3	4	5	6
	Expt. No.	Initial concn. RCO_3^-	Composition of the solutions c_{OH^-} c_{ROH} c_{RO^-}	t min	% RCO_3^- left	k_{mono}
Sorbitol	1	0.0077	0.0351 0.0757 0.0166 0.0287 0.0847 0.0153	10 20 30 40 50 60 Mean	73 53 41 31 24 18	0.014 0.014 0.013 0.013 0.013 0.012 0.013
Mannitol	3	0.0080	0.0355 0.0735 0.0185 0.0287 0.0827 0.0173	10 20 30 40 50 60 Mean	76 56 43 32 25 21	0.012 0.013 0.012 0.012 0.012 0.011 0.012
	5	0.0147	0.0242 0.2005 0.0345 0.0170 0.2230 0.0270	10 25 42 55 70 85 Mean	85 66 50 41 33 27	0.0069 0.0072 0.0071 0.0070 0.0069 0.0068 0.0070
Glucose	7	0.0040	0.0099 0.0479 0.0481 0.0082 0.0542 0.0458	6 12 18 24 Mean	62 43 30 23	0.035 0.031 0.029 0.027 0.030
	10	0.0040	0.0047 0.1667 0.0793 0.0039 0.1739 0.0761	6 12 18 24 30 Mean	71 59 44 36 32	0.025 0.019 0.020 0.018 0.017 0.020
	11	0.0121	0.0016 0.4176 0.0704 0.0010 0.4410 0.0590	6 16 26 36 Mean	81 60 44 34	0.015 0.014 0.014 0.013 0.014

k_{mono} is the value of $\frac{1}{t} \log \frac{a}{a-x}$

In Table 2, column 2, the initial concentration of monoalkyl carbonate are computed from % RCO_3^-(corr.) in Table 1a. The initial compositions of the solutions and the compositions after the reaction is completed are given in column 3. In the kinetic experiments represented in columns 4—6, $t = 0$ corresponds to the fifth minute after the addition of the carbon dioxide.

The mechanism of these reactions is assumed to be similar to that of previously investigated decompositions of monoalkyl carbonates, *i. e.*

(1) $RCO_3^- = RO^- + CO_2$; (2) $CO_2 + OH^- = HCO_3^-$.

k_{mono} may be calculated at pH > 10 by means of the expression

$$k_{mono} = \frac{k_{CO_2 \cdot RO^-} \cdot \frac{K_{Eq} \cdot K_A}{K_{CO_2}}}{1 + \frac{k_{CO_2 \cdot RO^-}}{k_{CO_2 \cdot OH^-}} \cdot \frac{K_A}{K_{H_2O}} \cdot c_{ROH}}$$

the values of K_{CO_2} being $10^{-6.65}$, but in this case the experimental values of K_{Eq} are very uncertain, so it may be better to calculate K_{Eq} from the experimental values of k_{mono}.

By calculation of K_{Eq} by means of the mean values of $k_{CO_2 \cdot RO^-}$ from Table 1a, which may be considered as the most correct values [2], and the mean values of c_{ROH} during the experiments, the following values are obtained (Table 3).

Table 3.

	Expt. No.	K_{Eq}	
		calc.	found
Sorbitol	1	35	45
Mannitol	3	31	25
	5	29	
Glucose	7	79	128
	10	71	
	11	78	

In view of the uncertainty (*cf.* section II) in the experimental values of K_{Eq} they agree quite well with the above calculated values.

The present work has been performed in the Department of Inorganic Chemistry of the Royal Danish School of Pharmacy. The author wishes to thank the head of the department Professor Carl Faurholt for his interest in the work and his valuable advice.

REFERENCES

1. Nøring, I., Jensen, A. and Faurholt, C. *Acta Chem. Scand.* **6** (1952) 404.
2. Jensen, A., Jensen, M. Ballund and Faurholt, C. *Acta Chem. Scand.* **8** (1954) 1129.
3. Thamsen, J. *Acta Chem. Scand.* **6** (1952) 270.

Received May 17, 1956.

ACTA CHEMICA SCANDINAVICA **10** (1956) 1172—1176

Studies on Monoalkyl Carbonates

XV. The Monoalkyl Carbonates of Sucrose and Lactose

BERTEL SMIDT and JØRN THAMSEN

The Royal Danish School of Pharmacy, Copenhagen, Denmark

By addition of carbon dioxide to an aqueous solution of an alcohol and sodium hydroxide, monoalkyl carbonate and carbonate are formed as the carbon dioxide reacts with the alcoholate ion and the hydroxide ion. Sucrose and lactose also form monoalkyl carbonate with carbon dioxide and the velocity constant and the equilibrium constant for the formation of monoalkyl carbonate have been determined. The velocity of the decomposition of monoalkyl carbonate in strongly basic medium has also been investigated and may be explained by assuming that the decomposition is a two-stage reaction, *viz.* (1) $RCO_3^- = RO^- + CO_2$; (2) $CO_2 + OH^- = HCO_3^-$.

1. The present investigation deals with the equilibrium conditions and the reaction mechanism for the formation and decomposition of the monoalkyl carbonates of sucrose and lactose.

2. The sucrose used was nitrogen-free sucrose from 'De danske Sukkerfabriker'. An aqueous solution of 9.995 g sucrose per 100 ml showed an optical rotation of 13.3° at 20° C in a 20 cm tube giving a value for $[\alpha]_D^{20°}$ of 66.53 which agrees with the value given in the literature. The sucrose was thus regarded as fit for use. The lactose was 'Baker's Analyzed' lactose stated to be pure. An aqueous solution of 9.994 g lactose per 100 ml showed an optical rotation of 10.5° at 20° C in a 20 cm tube. Thus $[\alpha]_D^{20°} = 52.53$ which agrees with the value given in the literature. The lactose was thus considered to be usable and corresponded very closely to the formula $C_{12}H_{22}O_{11} \cdot H_2O$.

3. The present investigation is analogous to the investigation concerning sorbitol, mannitol and glucose [1] and the experimental method being similar, it is on the whole sufficient here to state the experimental data and the calculated constants, referring for further information to the investigation of sorbitol, mannitol and glucose.

Table 1. Carbon dioxide gas in ROH + NaOH 0°C.

	Expt. No.	Initial concn. NaOH	Initial concn. ROH	Compositions of the solutions * c_{OH^-} c_{ROH} c_{RO^-}	Absorbed CO_2 mole/litre	% RCO_3^-	% RCO_3^- (corr.)	log $k_{CO_2 \cdot RO^-}$
Sucrose	1	0.1	0.2	0.0185 0.1185 0.0815 0.0127 0.1255 0.0589	0.022	64.70	70.78	4.11
	2			0.0185 0.1185 0.0815 0.0133 0.1235 0.0605	0.021	69.50	76.03	4.24
	3	0.2	0.2	0.0612 0.0612 0.1388 0.0507 0.0633 0.1190	0.024	67.30	73.62	4.47
	4			0.0612 0.0612 0.1388 0.0515 0.0637 0.1214	0.021	64.70	70.80	4.41
	5	0.2	0.1	0.1185 0.0185 0.0815 0.1023 0.0169 0.0639	0.022	41.30	46.13	4.50
	6			0.1185 0.0185 0.0815 0.0960 0.0200 0.0710	0.021	38.40	42.88	4.41
Lactose	1	0.1	0.2	0.0059 0.1059 0.0941 0.0039 0.1165 0.0688	0.021	61.80	69.98	3.49
	2			0.0059 0.1059 0.0941 0.0049 0.1169 0.0681	0.021	62.90	71.23	3.61
	3	0.2	0.2	0.0332 0.0332 0.1668 0.0251 0.0385 0.1472	0.021	62.10	67.93	3.98
	4			0.0332 0.0332 0.1668 0.0251 0.0387 0.1471	0.021	61.60	67.39	3.97
	5	0.2	0.1	0.1059 0.0059 0.0941 0.0723 0.0179 0.0935	0.022	37.60	44.69	4.28
	6			0.1059 0.0059 0.0941 0.0840 0.0066 0.0837	0.021	39.00	46.36	4.35

* Preceding paper [1]: Footnote, Table 1.

ON THE FORMATION OF MONOALKYL CARBONATE FROM CARBON DIOXIDE AND ALCOHOL IN BASIC SOLUTION, AND ON THE REACTION $RO^- + CO_2 = RCO_3^-$

The experimental results concerning the addition of carbon dioxide to sucrose and lactose are in the Tables 1 and 1a.

The acidic dissociation constants of sucrose and lactose are [2]: $10^{-13.36}$ and $10^{-12.75}$, respectively, at 0° C.

The mean values of $k_{CO_2 \cdot RO^-}$ corresponding to Table 1 are $10^{4.36}$ and $10^{3.95}$ for sucrose and lactose, respectively. The mean values of $k_{CO_2 \cdot RO^-}$ corresponding with Table 1a are $10^{3.74}$ and $10^{3.46}$ for sucrose and lactose, respectively. The mean values of k' are $10^{5.93}$ and $10^{6.13}$ corresponding with Table 1, and $10^{5.31}$ and $10^{5.64}$ corresponding with Table 1a for sucrose and lactose, respectively.

Table 1a. 500 ml carbon dioxide solution in 500 ml ROH + NaOH. 0°C.

	Expt. No.	Initial concn. NaOH	Initial concn. ROH	Compositions of the solutions * c_{OH^-} c_{ROH} c_{RO^-}	Absorbed CO_2 mole/litre	% RCO_3^-	% RCO_3^- (corr.)	log $k_{CO_2 \cdot RO^-}$
Sucrose	1	0.2	0.4	0.0217 0.2217 0.1783 0.0099 0.1359 0.0501	0.027	44.79	52.03	3.55
	2			0.0217 0.2217 0.1783 0.0100 0.1352 0.0504	0.027	46.09	53.53	3.60
	3	0.2	0.2	0.0612 0.0612 0.1388 0.0171 0.0551 0.0349	0.029	27.49	34.61	3.77
	4			0.0612 0.0612 0.1388 0.0176 0.0556 0.0364	0.027	23.96	29.48	3.66
	5	0.4	0.2	0.2217 0.0217 0.1783 0.0814 0.0234 0.0706	0.027	18.50	22.25	3.93
	6			0.2217 0.0217 0.1783 0.0790 0.0238 0.0696	0.029	18.92	22.74	3.94
Lactose	1	0.2	0.4	0.0062 0.2062 0.1938 0.0026 0.1304 0.0515	0.032	47.54	56.51	3.06
	2			0.0062 0.2062 0.1938 0.0026 0.1306 0.0504	0.033	48.36	57.48	3.08
	3	0.2	0.2	0.0332 0.0332 0.1668 0.0069 0.0445 0.0463	0.028	25.48	32.83	3.35
	4			0.0332 0.0332 0.1668 0.0068 0.0438 0.0457	0.029	27.76	36.18	3.42
	5	0.4	0.2	0.2062 0.0062 0.1938 0.0660 0.0084 0.0838	0.029	21.07	26.83	3.95
	6			0.2062 0.0062 0.1938 0.0645 0.0089 0.0833	0.030	20.30	25.85	3.92

* Preceding paper [1]. Footnote, Table 1.

THE EQUILIBRIUM OF THE REACTION $RCO_3^- + HOH = HCO_3^- + ROH$

The equilibrium was established in aqueous solutions of the alcohol, potassium hydrogen carbonate and sodium carbonate.

a) Sucrose. Equilibrium was established at 0° C in a solution 0.25 M with regard to sucrose, 0.1 M with regard to $KHCO_3$ and 0.1 M with regard to Na_2CO_3. The monoalkyl carbonate was determined in 100 ml samples. In different determinations the monoalkyl carbonate was equivalent to 3.29, 3.16, 3.09, 3.06, 3.30, 3.34, 3.44 and 3.54 ml 0.1 N HCl, respectively, with a mean value of 3.28 ml. The blank values were equivalent to 1.50, 1.35, 1.37, 1.45, 1.51, 1.35, 1.50, 1.50 and 1.45 ml 0.1 N HCl, respectively, with a mean value of 1.44 ml. The true quantity of alkyl carbonate thus corresponds to 1.84 ml 0.1 N HCl, *i. e.* 0.92 % of the $KHCO_3$ is transformed to monoalkyl carbonate.

Table 2. Monoalkyl carbonate in NaOH + alcohol. 0°C.

	1	2	3	4	5	6
	Expt. No.	Initial concn. RCO_3^-	Composition of the solutions c_{OH^-} c_{ROH} c_{RO^-}	t min	% RCO_3^- left	k_{mono}
Sucrose	4	0.0080	0.0176 0.0556 0.0364 0.0132 0.0672 0.0328	6	76	0.020
				12.5	57	0.020
				18	47	0.018
				24	37	0.018
				30	30	0.017
				36	26	0.016
				Mean:		0.018
	2	0.0144	0.0100 0.1352 0.0504 0.0066 0.1606 0.0394	10	69	0.016
				20	53	0.014
				30	41	0.013
				40	33	0.012
				50	27	0.012
				60	22	0.011
				Mean:		0.013
	6	0.0066	0.0790 0.0238 0.0696 0.0699 0.0279 0.0721	10	65	0.019
				20	44	0.018
				30	36	0.015
				40	26	0.015
				50	20	0.014
				60	15	0.014
				Mean:		0.016
Lactose	3	0.0092	0.0069 0.0445 0.0463 0.0043 0.0603 0.0397	6	76	0.020
				12	50	0.025
				18	37	0.024
				24	30	0.022
				30	25	0.020
				36	19	0.020
				Mean:		0.022
	1	0.0181	0.0026 0.1304 0.0515 0.0014 0.1654 0.0346	10	68	0.017
				20	50	0.015
				30	37	0.015
				40	28	0.014
				50	21	0.014
				60	16	0.013
				Mean:		0.015
	6	0.0078	0.0645 0.0089 0.0833 0.0513 0.0113 0.0887	6	71	0.025
				12	54	0.023
				18	40	0.022
				24	34	0.020
				30	27	0.019
				36	24	0.017
				Mean:		0.021

b) Lactose. The equilibrium was established at 0° C in a solution 0.25 M with regard to lactose, 0.1 M with regard to $KHCO_3$ and 0.1 M with regard to Na_2CO_3. In the equilibrium 0.39 % of the $KHCO_3$ is transformed to mono-

Table 3.

	Expt. No.	K_{Eq}	
		calc.	found
Sucrose	4	26	27
	2	27	
	6	18	
Lactose	3	19	64
	1	24	
	6	11	

alkyl carbonate. The monoalkyl carbonate in the samples was equivalent to 2.24, 2.39, 2.29, 2.25, 2.34, 1.98, 3.00, 3.19 and 2.71 ml 0.1 N HCl with a mean value of 2.49 ml. The blank values correspond to 1.67, 1.72, 2.20, 1.66, 1.80, 1.38 and 1.62 ml 0.1 N HCl with a mean value of 1.72 ml.

Thus K_{Eq} has the values 27 and 64 for sucrose and lactose, respectively, but these values only state the order of magnitude of K_{Eq}.

ON THE VELOCITY OF THE REACTIONS $RCO_3^- + HOH = HCO_3^- + ROH$

The solutions mentioned in the Tables 1 and 1a were all directly used for the kinetic determinations. The results are given in Table 2. To save space only a limited number of the experiments corresponding to Table 1a are represented.

The initial concentration of monoalkyl carbonate computed from $\%\,RCO_3^-$ (corr.) in Table 1a are given in Table 2, column 2.

The initial compositions of the solutions and the compositions after the reaction is completed are given in column 3.

The mean values of c_{ROH} during the experiment and the mean values of $k_{CO_2 \cdot RO^-}$ from Table 1a [1] are used to calculate K_{Eq} from the experimental values of k_{mono} and the following values are obtained (Table 3).

The agreement between the calculated and the experimental values is quite good for sucrose whereas for lactose the experimental value is 3—6 times the calculated and thus not in as good agreement as to be wished.

The present work has been performed in the Department of Inorganic Chemistry of the Royal Danish School of Pharmacy. The authors wishes to thank the head of the department Professor Carl Faurholt for his interest in the work and his valuable advice.

REFERENCES

1. Thamsen, J. *Acta Chem. Scand.* **10** (1956) 1165.
2. Smidt, B. *To be published.*

Received May 17, 1956.

ACTA CHEMICA SCANDINAVICA 10 (1956) 1177—1191

Studies on the Interaction of Paraffin Chain Alcohols and Association Colloids

VIII. The Solubility of Decanol-1 in Soap Solutions below the C.M.C.

PER EKWALL and TUURE VITTASMÄKI

Institute of Physical Chemistry, Åbo Akademi, Åbo, Finland

The solubility of decanol in dilute sodium caprate, laurate and myristate solutions at 40°C up to somewhat above the C.M.C.'s of the pure soaps has been determined with the greatest possible accuracy (maximum error ± 0.005 ml per litre). In all three cases a definite and rapid increase of the solubility begins at a concentration about 30 % lower than the C.M.C. of the pure soap. At this point a rapidly increasing formation of alcohol-soap-micelles begins; the C.M.C. of the decanol-containing soap solution is located at this concentration. The shift of the C.M.C. is caused by the facilitated association of the soap ions due to a decrease in the repulsion of their ionic groups owing to the incorporation of decanol. Below the C.M.C. the decanol solubility changes in a characteristic manner; already immediately above the L.A.C. the solubility increases slightly, passes a maximum and decreases again to a minimum value immediately below the C.M.C. These changes in solubility depend on the formation of small soap ion-decanol aggregates of relatively low solubility. The decanol-soap-water phase separating from all solutions above the L.A.C. has other properties and obviously another composition in the concentration range between the L.A.C. and C.M.C. than above the latter concentration limit. The investigation thus shows that below the C.M.C. there is in the solutions of all soaps a fairly wide concentration range where a limited association of alcohol and soap ions occurs. The degree of this association develops slowly until the critical concentration is reached.

A study has been made of the solubility of decanol in dilute sodium caprate, laurate and myristate solutions in the concentration range below the C.M.C. The solubility determinations made use of the fact that the system becomes turbid when a new phase appears. Since the solubility of decanol is very low below the C.M.C. and the turbidities in some cases were rather weak, the greatest care had to be exercised in the performance of the measurements.

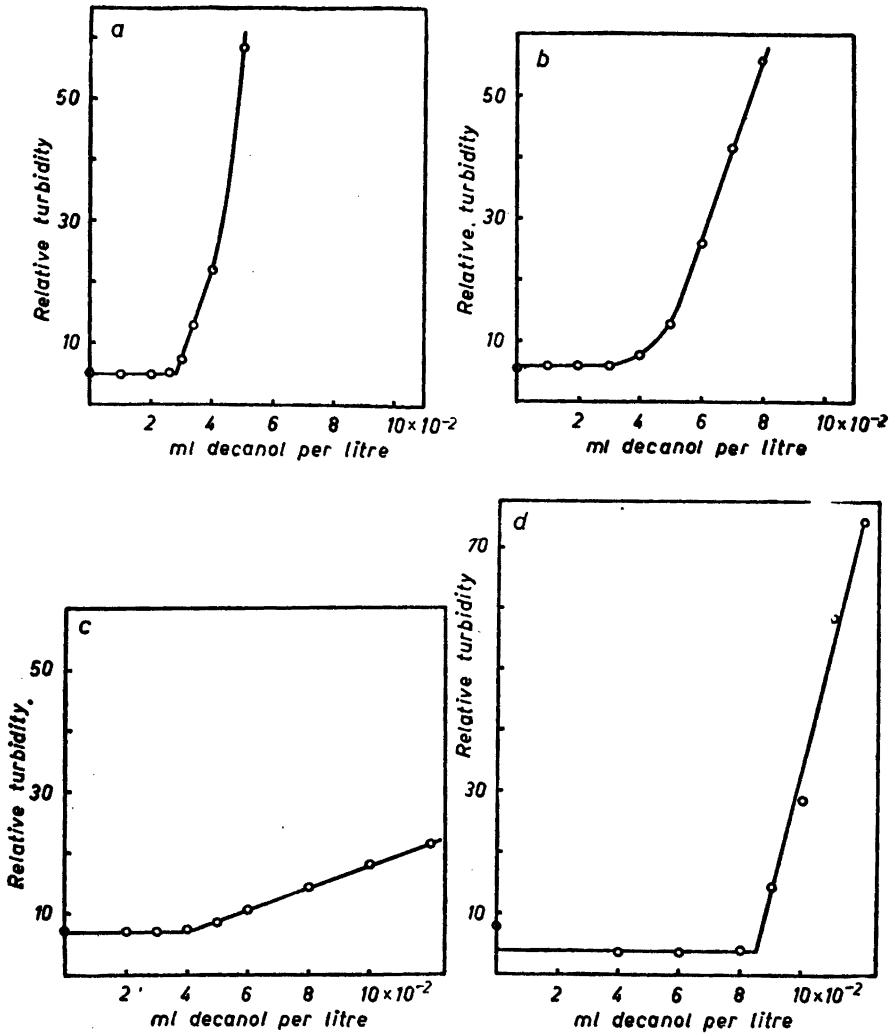


Fig. 1. Typical turbidity curves for soap solutions containing various amounts of decanol.

a. 0.0020 M sodium caprate solution
b. 0.028 M » » »
c. 0.052 M » » »
d. 0.090 M » » »

MATERIALS AND METHODS

The fatty acids were purified by repeated crystallization from ethanol. The melting points of the acids were: capric acid 31—31.5°C, lauric acid 42—43°C, myristic acid 56—57°C. Soaps were prepared from the acids in the usual manner by neutralization in abs. ethanol with sodium ethylate. The decanol was purified by repeated freezing;

the melting point of the final product was −6°C. The specific conductance of the twice distilled water used in the preparation of the solutions was less than 1×10^{-6} ohm^{-1} cm^{-1}.

In most of the experiments, 100-ml cylindrical glass-stoppered Pyrex flasks (30 mm in diameter) were used both as storage vessels and as cuvettes in the turbidity measurements. Several series of solutions were prepared in each of which the soap concentration was constant but the amount of added decanol varied. The flasks were shaken 24 hours in a thermostat at 40° until all decanol had dissolved or the solutions had become saturated and the excess of decanol or separated interaction product was dispersed throughout the solutions. It was found advisable to allow the solutions to stand four hours before measuring the turbidities. The turbidities were measured at 40°C with a Zeiss nephelometer combined with a Pulfrich photometer.

All the flasks were thoroughly cleaned and then rinsed several times with distilled water, after which they were dried and stored so that they did not collect dust.

In order to avoid turbidities caused by separated hydrolytic products, 0.1 mole of sodium hydroxide was added per mole of soap to the solutions.

The decanol was added to the solutions with an Agla micrometer syringe in which the scale is divided into 0.0002 -ml divisions.

EXPERIMENTAL RESULTS

a) The variation of the turbidity with the excess of decanol

Decanol added to a soap solution in excess of the amount dissolved causes the appearance of a turbidity. The turbidity increases with the amount of decanol added but our experiments showed that the increase in turbidity effected per unit volume of decanol added varied greatly with the soap concentration. This is illustrated by the nephelometer curves relating to sodium caprate solutions reproduced in Figs. 1 a, 1 b, 1 c, 1 d.

As seen from the curves, the nephelometric value remains constant when small amounts of decanol are added, but rises when larger amounts are added. The slope of the rising part of the curve is very different in the four cases. The turbidity curve for the 0.002 M caprate solution rises rapidly as soon as decanol is added in excess (Fig. 1a). For the 0.028 M solution the increase is slow at first, but later the curve rises steeply (Fig. 1b). The turbidity curve for the 0.052 M solution rises very slowly above the breakpoint with a constant slope (Fig. 1 c). A linear increase is also seen in the curve for the 0.090 M solution, but the slope is large (Fig. 1d).

It is of interest to note that this variation of the slope of the rising part of the curve is common to all the soaps studied. This is seen in Figs. 2, 3 and 4. The abscissae of these figures give the soap concentrations and the ordinates the slopes of the turbidity curves (above the breakpoint), *i. e.* the increase in turbidity due to a unit volume of decanol in excess per litre of solution. In those cases where the slope is different for small (a) and large (b) excesses of decanol (as in Fig. 1 b), both curves are given. Figs. 2, 3 and 4 are based on all the experimental data obtained in this study. In all cases the slope of the turbidity curve is large in dilute soap solutions, but decreases to a low value as the soap concentration increases; it then remains constant over a certain concentration range and begins to increase again at higher soap concentrations. This shows that the degree of dispersion of the separating substance and/or the refractive index and the nature of the substance causing the turbidity varies in the different concentration ranges.

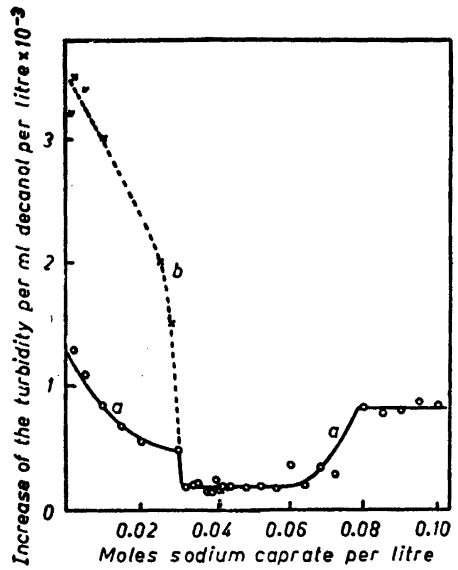


Fig. 2. The dependence of the soap concentration on the increase in turbidity due to a unit volume of decanol per litre of sodium caprate solution. a. Small excesses of decanol above the turbidity point. b. Large excesses of decanol above the turbidity point.

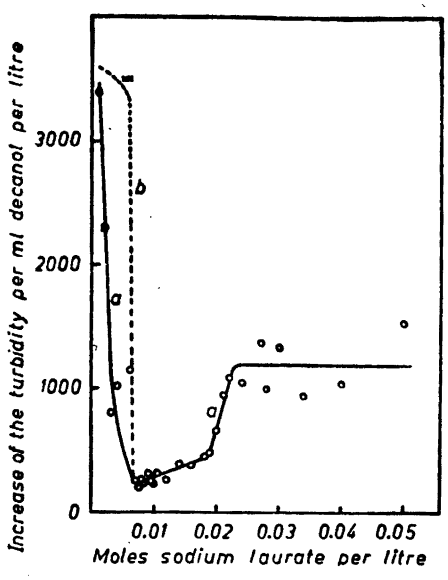
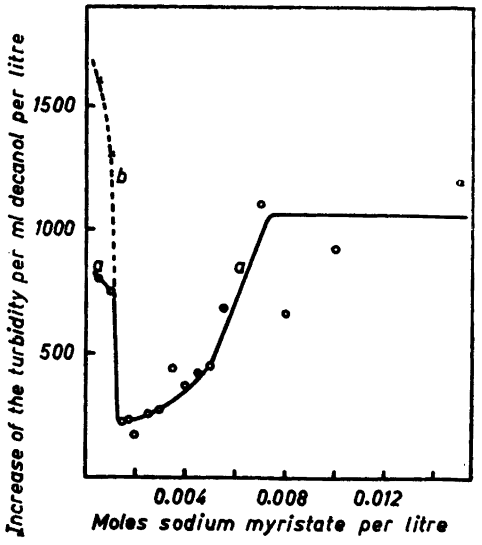


Fig. 3. The dependence of the soap concentration on the increase in turbidity due to a unit volume of decanol per litre of sodium laurate solution. a. Small excesses of decanol above the turbidity point. b. Large excesses of decanol above the turbidity point.

Fig. 4. The dependence of the soap concentration on the increase in turbidity due to a unit volume of decanol per litre of sodium myristate solution. a. Small excesses of decanol above the turbidity point. b. Large excesses of decanol above the turbidity point.



The intermediate concentration ranges, where the turbidity curves rise slowly, *i. e.* the separating substance causes only a slight turbidity, are for the various soaps: sodium caprate, from 0.030 M to 0.064 M; sodium laurate, from 0.007 to 0.019 M; sodium myristate, from 0.0015 to 0.005 M. The lower limits are very close to the limiting concentrations L.A.C., of the soaps, (0.02—0.03 M for sodium caprate, 0.005—0.006 M for sodium laurate and 0.0013—0.0015 M for sodium myristate), where, according to our previous studies, the interaction between decanol and soap begins [1-8]. Whereas the excess of decanol separates below the L.A.C. as emulsified free decanol, the separating substance above this limit is a fine-disperse semitransparent mesomorphic phase composed of decanol, soap and water. Already the turbidity-soap concentration curves reproduced in our earlier papers showed that this latter substance (separating above the L.A.C.) produces a relatively weak turbidity [1,2,5-7]. In those cases where we now found the turbidity-decanol content curves to rise slowly immediately above the turbidity point (as in Fig. 1 b) but later to exhibit a large slope, a mesomorphic phase separates at first, but when decanol is added in greater excess, free alcohol separates and is emulsified. Conductance measurements support this interpretation.

b) The solubility of decanol in the soap solutions

The solubility of decanol is given by the point where the horizontal and rising parts of the nephelometric curves intersect. We have attempted to determine in various ways the accuracy with which this point of intersection can be determined. Only in a few unfavourable cases, in which the slope of the curve was low and the nephelometric values scattered more than normally, the method of least squares gave standard deviations up to $\pm$ 0.005 ml of decanol per litre of solution. In most cases the standard deviation was less than this value.

The solubility values are shown in Tables 1, 2 and 3.

Table 1. The solubility of decanol in sodium caprate solutions at 40°C.

Sodium caprate mole/litre	Decanol ml/litre	Sodium caprate mole/litre	Decanol ml/litre
Aqua	0.028		
0.001	0.028	0.042	0.046
0.002	0.028	0.044	0.049
0.005	0.028	0.048	0.040
0.010	0.028	0.052	0.040
0.015	0.028	0.056	0.038
0.200	0.027	0.060	0.037
0.025	0.029	0.064	0.042
0.030	0.033	0.068	0.100
0.032	0.030	0.072	0.104
0.034	0.030	0.080	0.260
0.035	0.032	0.085	0.535
0.039	0.036	0.090	0.855
0.040	0.037	0.095	1.285
0.041	0.037	0.100	1.700

Table 2. The solubility of decanol in sodium laurate solutions at 40°C.

Sodium laurate mole/litre	Decanol ml/litre	Sodium laurate mole/litre	Decanol ml/litre
Aqua	0.028		
0.0020	0.028	0.0160	0.022
0.0030	0.028	0.0180	0.024
0.0040	0.028	0.0190	0.031
0.0050	0.031	0.0200	0.064
0.0060	0.032	0.0210	0.114
0.0070	0.028	0.0220	0.162
0.0076	0.039	0.0240	0.250
0.0080	0.043	0.0270	0.480
0.0084	0.045	0.0280	0.510
0.0090	0.045	0.0300	0.720
0.0095	0.038	0.0340	1.000
0.0105	0.039	0.0400	1.450
0.0120	0.035	0.0500	2.235
0.0140	0.028		

Table 3. The solubility of decanol in sodium myristate solutions at 40°C.

Sodium myristate mole/litre	Decanol ml/litre	Sodium myristate mole/litre	Decanol ml/litre
Aqua	0.028		
0.00050	0.027	0.00400	0.012
0.00100	0.032	0.00450	0.009
0.00150	0.042	0.00500	0.018
0.00175	0.032	0.00550	0.038
0.00200	0.038	0.00600	0.064
0.00250	0.030	0.00700	0.133
0.00300	0.025	0.00800	0.198
0.00350	0.016	0.0100	0.316
		0.0150	0.630

Fig. 5a shows the variation of the solubility of decanol with the soap concentration in sodium caprate solutions. From 0.065 M caprate upwards, the solubility increases rapidly and especially above the 0.08 M concentration, the solubility curve rises steeply. In pure caprate solutions the critical concentration is 0.097 M at 20° C. The solubility of decanol thus begins to increase rapidly already at a lower concentration, 0.065—0.080 M, of sodium caprate.

A very slight increase in solubility can, however, be detected at even lower concentrations; this is shown by the enlarged lower part of the curve in Fig. 5b. We observed the first signs of an increased solubility already at caprate concentrations between 0.025 M and 0.030 M. The solubility of decanol rises from 0.028 ml of decanol per litre, the solubility in pure water and in very dilute caprate solutions, to a value of 0.049 ml per litre in the 0.044 M caprate

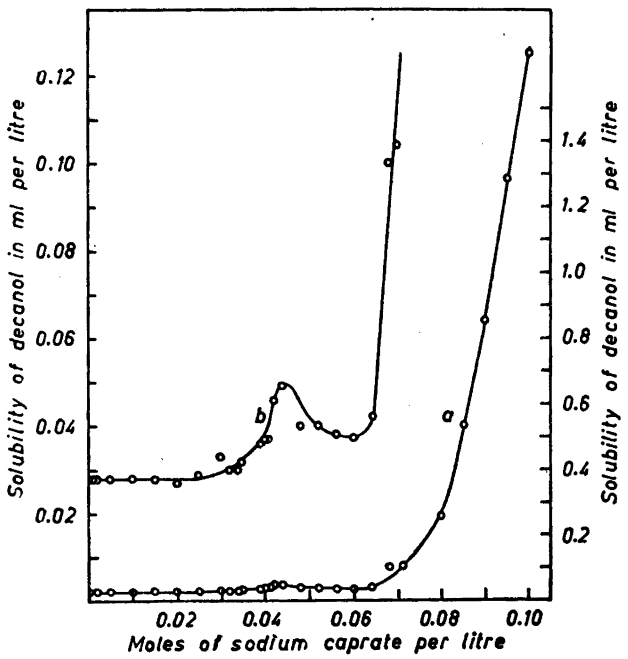


Fig. 5. The solubility of decanol in sodium caprate solutions at 40°C. a. The increase of the solubility around the C.M.C. (scale on the right). b. The solubility between the L.A.C. and the C.M.C. on an enlarged scale (scale on the left).

solutions, an increase of 75 %. At higher caprate concentrations, the solubility decreases again to a minimum in the 0.060 M caprate solution, after which the above-mentioned rapid increase begins.

The first increase in decanol solubility coincides with the limiting concentration, 0.025—0.030 M, of sodium caprate. The range in which the increase and decrease occur, 0.025—0.065 M sodium caprate, is practically the same as the range (0.03—0.064 M caprate) where the effect of the separated substance on the turbidity is especially weak. These two phenomena are thus seen to be closely connected.

Fig. 6a illustrates the variation of the solubility of decanol with the sodium laurate concentration. The solubility begins to increase when the laurate concentration exceeds 0.019—0.020 M. The critical concentration of sodium laurate is 0.028 M (20° C). Decanol thus begins to dissolve in laurate solutions at a laurate concentration somewhat below the C.M.C. of pure sodium laurate.

Also in the laurate solutions a slight increase in solubility is noted even at lower concentrations (Fig. 6b). The first signs of an increase are noted at the laurate concentrations of 0.005—0.007 M. The solubility increases to a value in the 0.008—0.009 M solution which is about 64 % higher than in water. It then undergoes a decrease to a minimum at the 0.016—0.018 M concentration, after which the rapid increase begins.

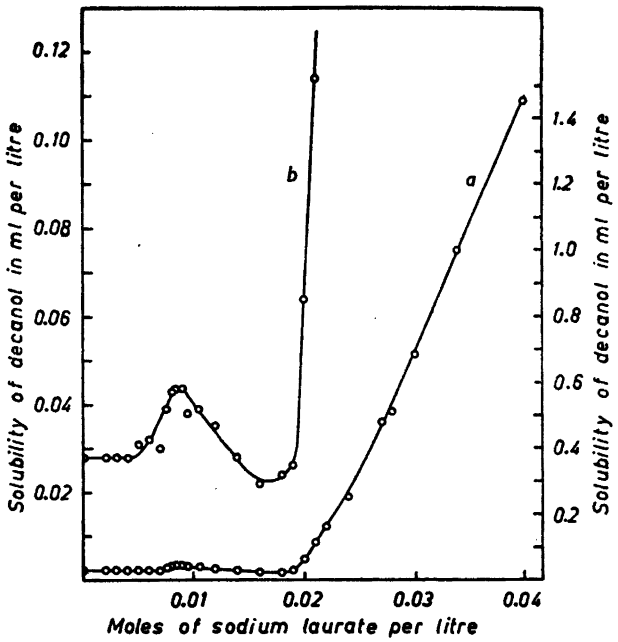


Fig. 6. The solubility of decanol in sodium laurate solutions at 40°C. a. The increase of the solubility around the C.M.C. (scale on the right). b. The solubility between the L.A.C. and the C.M.C. on an enlarged scale (scale on the left).

The first solubility increase begins at the limiting concentration of sodium laurate, 0.005—0.006 M. The solubility variations occur in the same concentration range (0.006—0.019 M laurate) where the separating substance effects only a weak turbidity.

The variation of the decanol solubility in sodium myristate solutions is shown in Fig. 7. The solubility begins to increase when the sodium myristate concentration exceeds 0.0045—0.0050 M and more rapidly when the soap concentration increases above 0.006 M. The critical concentration of sodium myristate is 0.007 M at 40° C. Thus decanol begins to dissolve at a myristate concentration definitely below the C.M.C. of pure sodium myristate. Also in the myristate solutions we have noted solubility changes at still lower concentrations (Fig. 7b). The solubility begins to increase already at the 0.001 M myristate concentration; it is about 50 % higher than the solubility in water in the 0.0015 M myristate solution, but then decreases until it is only one-third of the solubility in water in the 0.0045 M sodium myristate solution. Above this point a rapid increase in the solubility begins.

Also in sodium myristate solutions, the first increase in solubility occurs in the vicinity of the limiting concentration, which is 0.0013 M. The variations in the solubility are observed in the same concentration range (0.0015 M—0.0050 M myristate) where the separating substance effects only a weak turbidity.

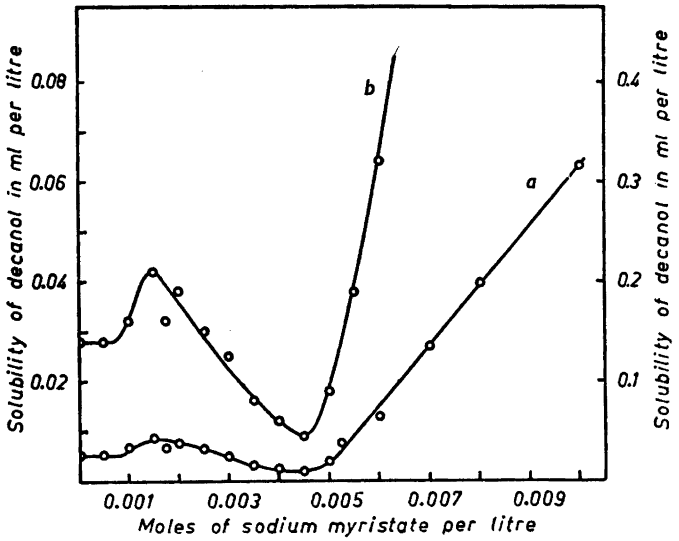


Fig. 7. The solubility of decanol in sodium myristate solutions at 40°C. a. The increase of the solubility around the C.M.C. (scale on the right). b. The solubility between the L.A.C. and the C.M.C. on an enlarged scale (scale on the left).

c) The effect of added sodium hydroxide on the solubility of decanol

In all the above experiments, the solutions contained 0.1 mole of sodium hydroxide per mole of soap to suppress hydrolysis. We have not undertaken any systematical study of the effect of sodium hydroxide or that of the products of hydrolysis on the solubility of decanol, but certain observations throw some light on this question.

The solubility of decanol was measured in 0.008 M sodium myristate solutions containing various amounts of sodium hydroxide up to 0.14 mole per mole of soap. From Fig. 8 it is seen that the solubility is very low in the absence of alkali hydroxide, increases at first rapidly with the amount of sodium hydroxide added but attains a constant limiting value when the concentration of sodium hydroxide increases to about 0.1 mole per mole of soap. A similar increase in the decanol solubility in a 0.006 M myristate solution was also observed when 0.05 and 0.1 mole of sodium hydroxide was added per mole of soap.

The addition of 0.1 mole of sodium hydroxide per mole of soap to a 0.04 M sodium laurate solution increased the solubility of decanol only from 1.30 to 1.44 ml per litre. No increase was noted in the case of a 0.014 M laurate solution when the sodium hydroxide content was increased from 0.05 to 0.15 mole per mole of soap.

The solubility of decanol in a 0.064 M sodium caprate solution did not increase when the sodium hydroxide concentration was increased from 0.1 to 0.15 mole per mole of soap.

In the concentration range immediately above and below the C.M.C. of pure soaps, where we have observed the solubility of decanol to increase rapidly, the sodium hydroxide increases the decanol solubility; 0.1 mole of sodium hydroxide per mole of soap seems, however, to be sufficient to effect maximum solubility of decanol in most cases (in myristate solutions a slightly larger amount may be necessary). In the region above the L.A.C. where the first increase in decanol solubility occurs, sodium hydroxide does not seem to influence the solubility, but the small number of observations does not permit any definite conclusions.

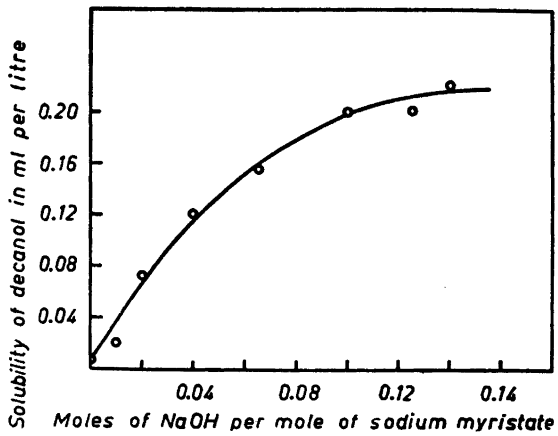


Fig. 8. The influence of added sodium hydroxide on the solubility of decanol in a 0.008 M sodium myristate solution at 40°C.

The addition of sodium hydroxide to a colloid solution generally influences the micelle formation in such a way that the C.M.C. shifts to a somewhat lower value. The effect of sodium hydroxide on the decanol solubility may be partly due to this shift. We think, however, that the results may be considered to indicate that the hydrolysis products (fatty acid, acid soap) present in solutions containing no added alkali decrease the capacity of the soap to dissolve decanol, at least in solutions in which micelle formation has not progressed very far.

d) Solubility of *p*-xylene in soap solutions containing decanol

It is known that soap solutions begin to solubilize hydrocarbons when the critical concentration is exceeded and that the solubilization of hydrocarbons is increased in the presence of long-chain alcohols. We have conducted a few experiments to determine the effect of decanol on the solubilization of *p*-xylene in sodium laurate solutions below the C.M.C. The results are given in Table 4.

The solubility of *p*-xylene in pure water is 0.20 ml per litre at 40°C. The solubility is the same also in dilute soap solutions below the C.M.C. The data in Table 4 show that the solubility is no larger in 0.003 and 0.009 M laurate solutions when these contain

Table 4. The solubilization of p*-xylene in sodium laurate solutions containing different amounts of decanol. The solutions contained 1 mole of sodium hydroxide to 10 moles of soap. 40°C.*

Sodium laurate mole/litre	Decanol ml/litre	*p*-xylene ml/litre
0.003	0.028	0.21
0.009	0.046	0.20
0.018	0.026	0.33
0.023	0.19	0.56

decanol, but a slightly higher solubility is noted in the 0.018 M solution and a definitely higher solubility in the 0.023 M solution.

These results show that solubilization of the hydrocarbon begins at about the same concentration where the solubility of decanol begins to increase rapidly. This seems to indicate that the decanol-laurate mixed micelles are of the usual spheroidal (or double-layer) type. Micelles of this type do not seem to be formed at lower soap concentrations although decanol is present.

DISCUSSION

In the case of all three soaps studied, the first signs of an increase in the decanol solubility appear in the region of the limiting concentration of the soap [1–5]. As the soap concentration is increased, the increase in solubility slows down and the solubility begins to decrease until slightly before the C.M.C. of the pure soap is reached, the solubility again begins to increase [5]. The changes in solubility below the abrupt rise are admittedly rather small, but yet considerably greater than the error of the experimental method. The changes must hence be considered significant.

The regions where these changes in solubility are observed are given in Table 5.

The second increase in the decanol solubility begins at soap concentrations that are about 30 % lower than the C. M. C.'s in pure soap solutions. Above this point the increase in solubility is very rapid. It is obvious that this increase is due to the formation of mixed micelles containing soap and decanol and that their formation progresses rapidly from the solubility minimum upwards. The minimum points thus give the C. M. C. values for soap solutions containing decanol. This is supported by the observation that the 0.018 and 0.023 M laurate solutions begin to solubilize *p*-xylene only after decanol has been added to them. These mixed micelle C. M. C. values lie only a little below the approximate values we have previously obtained for decanol-containing soap solutions by the turbidity method [6]. Our data thus give the lowest soap concentrations to which the C. M. C. can be decreased by decanol at 40° C. These values are appreciably lower than the values recently obtained by Shinoda for decanol-containing soap solutions at 10° and 18° C with the pinacyanol method [9].

Table 5. Variation of the solubility of decanol in soap solutions containing 0.1 mole of NaOH per mole of soap. 40°C.

Soap	L.A.C. M	Soap concentration (mole/l) at which		C.M.C. in pure soap solution M
		the first increase in decanol solubility begins	the second increase in decanol solubility begins	
Sodium caprate	0.022–0.028	0.025–0.030	0.065–0.070	0.097
Sodium laurate	0.004–0.007	0.005–0.007	0.019–0.020	0.027
Sodium myristate	0.011–0.0014	0.001–	0.0045–0.0050	0.0065

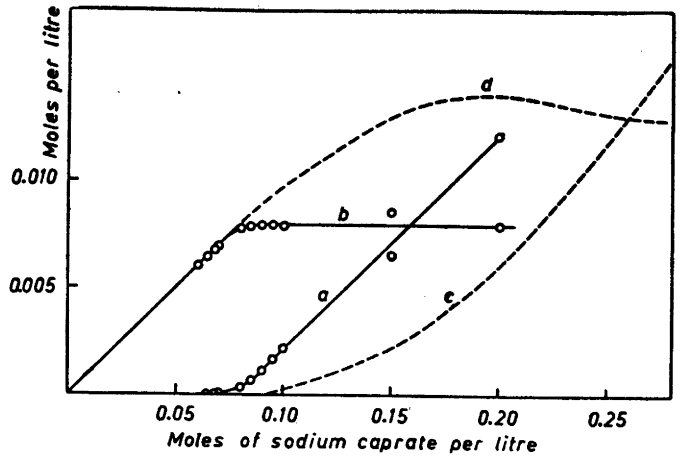


Fig. 9. Micelle formation in sodium caprate solutions. The concentrations of micellar soap (a) and molecular soap (b) in caprate solutions containing decanol, calculated from the solubility of decanol. The concentrations of micellar soap (c) and molecular soap (d) in caprate solutions containing p-*xylene, calculated from the solubility of* p-*xylene.*

On the basis of the solubility values it is possible to estimate the amount of soap bound in the mixed micelles above the critical concentration. Already from concentrations only slightly higher than the C. M. C., the solubility curves begin to rise linearly; this means that the maximum ratio of decanol to soap in the mixed micelles remains constant above this point. The ratio is found to

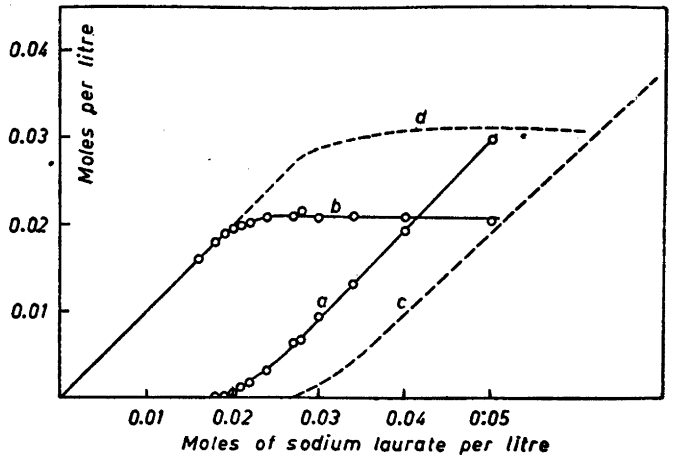


Fig. 10. Micelle formation in sodium laurate solutions. The concentrations of micellar soap (a) and molecular soap (b) in laurate solutions containing decanol calculated from the solubility of decanol. The concentrations of micellar soap (c) and molecular soap (d) in laurate solutions containing p-*xylene, calculated from the solubility of* p-*xylene.*

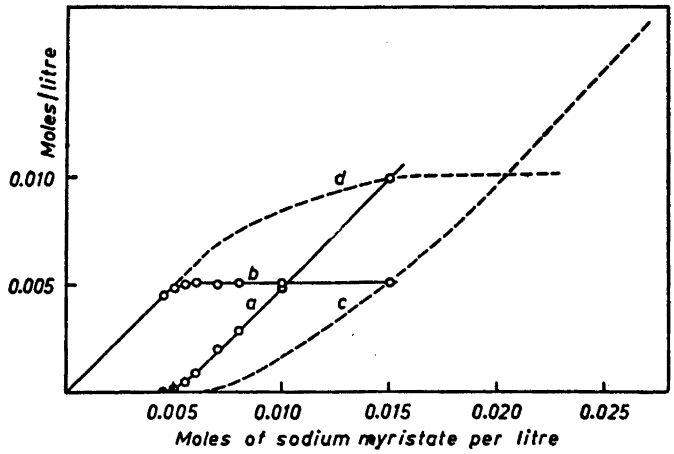


Fig. 11. Micelle formation in sodium myristate solutions. The concentrations of micellar soap (a) and molecular soap (b) in myristate solutions containing decanol calculated from the solubility of decanol. The concentrations of micellar soap (c) and molecular soap (d) in myristate solutions containing p-*xylene calculated from the solubility of* p-*xylene.*

be 0.41 mole of decanol per mole of sodium caprate, 0.39 mole of decanol per mole of sodium laurate, and 0.33 mole of decanol per mole of sodium myristate, at 40° C. If it is assumed that the mixed micelles have the same composition down to the point of minimum decanol solubility, the values given in Figs. 9, 10 and 11 (curves a) can be calculated for the amounts of soap bound in the mixed micelles. Also the amounts of molecular soap calculated from the difference between total and micellar soap are given in the figures (curves b). The curves show that after a relatively narrow transition region, in which the proportion of micellar soap increases rapidly, there is a concentration range where all the added soap is bound in the mixed micelles and hence the concentration of free soap remains constant. This range begins already before the C. M. C. of the pure soap is reached.

For comparison also the amounts of soap present in the micellar state and in the molecular state in decanol-free soap-solutions, calculated in a corresponding manner from the data for the *p*-xylene solubilization, are given in Figs. 9, 10 and 11 (the dotted curves c and d) [11]. In these latter cases the formation of micelles begins at the C. M. C.'s of the pure soaps and proceeds at first much more slowly than in the presence of the alcohol. Though all these values are only approximate, they show clearly the effect of the polar-nonpolar substance on the micelle formation. As we have seen above, the concentration of decanol at the solubility minimum (C. M. C.) is in all cases very low compared with that of the soap (only about 0.5—1.5 % of the latter). Our calculation thus indicates that the effect of decanol is not caused by an increase in the amount of micelle-forming hydrocarbon chains in solutions, but by an increased association of the soap ions due to a decrease in the repulsion

of their ionic groups [7]. In other cases, however, when the solubility of the polar substance is greater, the former factor may play a part in lowering the C. M. C.

The first slight increase in the decanol solubility above the L. A. C. must also be caused by the formation of soluble decanol-soap aggregates. These aggregates are formed only sparingly, however. Therefore the previously (Parts V and VI) described rapid fall at the L. A. C. in the turbidity-soap concentration curves of solutions containing alcohol in excess [6,7] is due only to a minor extent to the increase in the solubility of the alcohol but for the most part to a weak turbidity of the alcohol-soap-water phase formed above the mentioned concentration limit.

It is very interesting to note that the decanol-soap-water phase separating immediately above the L.A.C. effects a much weaker turbidity per unit volume of decanol added than the corresponding phase separating above the C.M.C. This fact conforms with our microscopic observations of the different appearance of the separated phase below and above the latter concentration in sodium laurate solutions (Part VII); these observations suggested that the water content of the former product is greater than that of the latter [8]. On the other hand, we have found (Parts II and III) that the decanol content per mole of soap in the separated phase increases with decreasing concentration of the soap solution in which it is formed [10]. From all these results we conclude that both the properties and the composition of the decanol-soap-water phase formed between L.A.C. and C.M.C. differs from that formed above the latter concentration limit; in the former case the molar ratio of decanol to soap and the water content is larger and the refractive index is nearer that of the aqueous soap solution.

Our investigations thus show that in the concentration range between L.A.C. and C.M.C. the solubility of decanol is different from that in other ranges and the separating phase deviates in properties and composition from those separating in other ranges. As to the composition and properties of the soluble soap ion-alcohol aggregates existing in this range, calculations show that these aggregates are small and composed of only very few soap ions and alcohol molecules. The hydrophilic properties and thus the solubility of such small aggregates must decrease rapidly with increasing molar ratio of decanol to soap. The range of composition of these aggregates is therefore rather limited. If one assumes that two kinds of small aggregates with different decanol-soap ratios, and thus different solubilities, are formed, the course of the observed solubility curve between L.A.C. and C.M.C. with its solubility maximum and decrease to and below the value for pure water can be readily understood. We will return to this question in a later paper of this series.

Now we only wish to emphasize that the solubility measurements presented in this paper show clearly that the limiting concentration should not be confused with the critical concentration [6,7]. Below the latter there is a fairly wide concentration range in solutions of all soaps where a limited association of alcohol and soap ions occurs. The degree of this association increases slowly until the critical concentration is reached.

REFERENCES

1. Ekwall, P. and Danielsson, I. *Acta Chem. Scand.* **5** (1951) 973.
2. Ekwall, P. *Svensk Kem. Tidskr.* **63** (1951) 277.
3. Ekwall, P. *J. Colloid Sci. Suppl.* **1** (1954) 66.
4. Ekwall, P. *Kolloid-Z.* **136** (1954) 37.
5. Ekwall, P., Passinen, K. and Danielsson, I. *Finska Kemistsamfundets Medd.* **63** (1954) 1.
6. Ekwall, P., Danielsson, I. and Söderberg, O. *Acta Chem. Scand.* **10** (1956) 227 (Part V of this series).
7. Ekwall, P. and Aminoff, C. F. *Acta Chem. Scand.* **10** (1956) 237 (Part VI of this series).
8. Ekwall, P., Salonen, M., Krokfors, I. and Danielsson, I. *Acta Chem. Scand.* **10** (1956) 1146 (Part VII of this series).
9. Shinoda, K. *J. Phys. Chem.* **58** (1954) 1136.
10. Passinen, K. and Ekwall, P. *Acta Chem. Scand.* **9** (1955) 1438, 1450 (Parts II and III of this series).
11. Ekwall, P. *6. Nordiska Kemistmötet, Lund* 1947, p. 179.

Received May 19, 1956.

ACTA CHEMICA SCANDINAVICA 10 (1956) 1192—1198

Short Communications

Steric Relations between α-(1-Naphthyl)-propionic Acid and α-(3-Thianaphthenyl)-propionic Acid

BERNDT SJÖBERG

Institute of Chemistry, University of Uppsala, Uppsala, Sweden

In connection with stereochemical studies on aralkyl carboxylic acids, α-(3-thianaphthenyl)-propionic acid has been prepared and resolved into its optical antipodes ($[\alpha]_D^{25} = 80.2°$ in abs. alcohol).

Several methods could be used to determine the configuration of α-(3-thianaphthenyl)-propionic acid and sterically relate it to D-glyceraldehyde. At the present time the simplest and most reliable method is perhaps that of quasi-racemates [1], provided it is possible to find some suitable structurally similar compound.

It may be assumed that the angle γ (Fig. 1) in the thianaphthene molecule ought to be between 113° and 120°, since the corresponding angle in the thiophene molecule is 113° [2] and in the naphthalene molecule

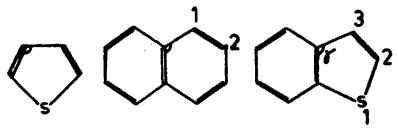


Fig. 1.

120°. The structural dissimilarity between α-(1-naphthyl)-propionic acid and α-(3-thianaphthenyl)-propionic acid should in that case perhaps be small enough to enable a quasi-racemic compound to be formed between the opposite antipodes of these two acids.

The configuration of α-(1-naphthyl)-propionic acid has already been determined by Fredga [3] and the pure antipodes of this acid have been put at my disposal.

By thermal analysis according to Kofler [4] it was shown with the aid of the contact method that a molecular compound was formed between (−)-α-(3-thianaphthenyl)-propionic acid and (+)-α-(1-naphthyl)-propionic acid. After the preliminary experiments the whole curve was determined for this two-component system. As is seen in Fig. 2, a very pronounced quasi-racemic compound is formed from the components in the ratio 1:1.

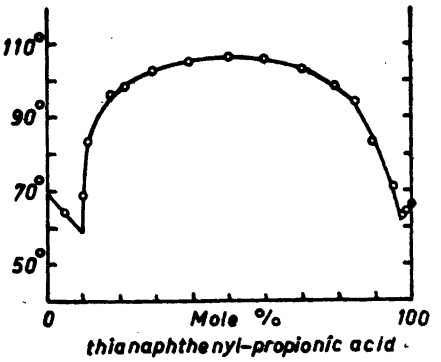
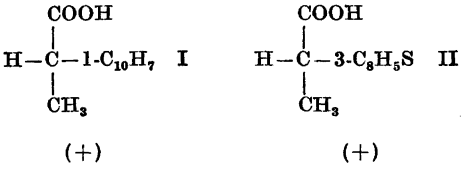


Fig. 2. (−)-α-(3-thianaphthenyl)-propionic acid and (+)-α-(1-naphthyl)-propionic acid.

The melting point curve for the system containing acids with the same direction of rotation was not investigated in detail, but preliminary experiments indicated that no molecular compound was formed.

From the results obtained the conclusion can be drawn that α-(1-naphthyl)-propionic acid and α-(3-thianaphthenyl)propionic acid with the same direction of rotation (measured in alcohol at the wave-length of the D-line) also have the same configuration.

The dextro-rotatory α-(1-naphthyl)-propionic acid has the configuration I. Consequently (+)-α-(3-thianaphthenyl)-propionic acid has a stereo formula corresponding to II.



If the 3-thianaphthenyl group is considered as a substituent on the aliphatic carbon chain, this acid must be assigned to the D-series.

The work described here is part of a stereochemical study of aralkyl carboxylic acids. Full details will be given elsewhere.

A grant from the *Swedish Natural Science Research Council* is gratefully acknowledged.

1. Fredga, A. *"The Svedberg 1884 30/8 1944"*, Uppsala 1944, p. 261.
2. Schomaker, V. and Pauling, L. *J. Am. Chem. Soc.* **61** (1939) 1769.
3. Fredga, A. *Arkiv Kemi* **8** (1955) 463.
4. Kofler, A. and L. *Mikro-Methoden*, Innsbruck 1948.

Received September 4, 1956.

*iso*Thiocyanates XXII *. 3-Benzoyloxypropyl *iso*Thiocyanate, Present as a Glucoside (Glucomalcolmiin) in Seeds of *Malcolmia maritima* (L.) R.Br.

ANDERS KJÆR and ROLF GMELIN

Chemical Laboratory of the University of Copenhagen, Denmark

Paperchromatographic analysis of the *iso*thiocyanate glucosides in a seed extract of the crucifer *Malcolmia maritima* (L.) R. Br. revealed the presence of two glucosides, (a) and (b), possessing R_B-values [1] of 0.34 and 1.36, respectively, in the solvent system: *n*-butanol:ethanol:water (4:1:4). In addition, traces of a third glucoside (R_B 1.03) and substantial amounts of sinapine were recognized in the seed extract, a pattern similar to that obtained elsewhere [1].

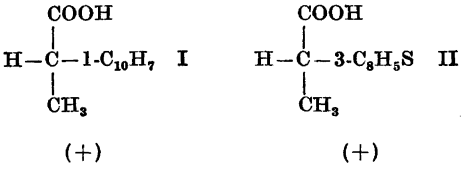
In the present work, the glucoside (a) has been unequivocally identified as glucocheirolin, furnishing cheirolin (3-methylsulphonylpropyl *iso*thiocyanate) on enzymic hydrolysis, a mustard oil formerly recognized as a constituent of *Cheiranthus cheiri* L.** and other species [2]. Crystalline thiourea derivatives have been obtained from enzymically hydrolyzed seed macerates of *M. maritima* after treatment with aniline and benzylamine, identical with reference specimens prepared from synthetic cheirolin [3]. The phenylthiourea has been described previously [2,3] whereas the benzyl derivative is a new compound, m. p. 116° (uncorr.). (Found: C 50.35; H 6.26; N 9.70. Calc. for $C_{12}H_{16}O_2N_2S_2$: C 50.31; H 6.33; N 9.78).

The component (b), for which we propose the name *glucomalcolmiin*, is obviously different from all glucosides heretofore encountered in nature. The corresponding optically inactive, non-volatile *iso*thiocyanate, liberated from a paperchromatographically purified specimen of glucomalcolmiin, displays an ultraviolet absorption spectrum indicative of the presence of a strongly chromophoric system (λ_{max} 230 mμ, λ_{min} 213 mμ in water). The new mustard oil has been characterized as a crystalline thiourea, $C_{11}H_{14}O_2N_2S$, after treatment with ammonia, m. p. 162° (uncorr.). (Found: C 55.40; H 5.91; N 11.75; S 13.59. Calc. for $C_{11}H_{14}O_2N_2S$: C 55.41; H 5.92; N 11.75; S 13.45); UV-spectrum in ethanol: λ_{max} 237 mμ (ε 19 400), λ_{min} 214 mμ (ε 11 180) and low-extinction inflections at 270—272 mμ and 278—280 mμ. The IR-spectrum of the solid thiourea in a KBr disc displayed conspicuous bands at: 3.00 (vs), 5.83 (s, ester-CO), 6.05 (s), 6.41 (vs), 6.76 (s), 7.21 (s), 7.49 (s), 7.75 (vs), 8.44 (m), 8.79 (vs), 8.90 (vs), 9.28 (m), 9.48 (m), 9.70 (m), 9.84 (m), 10.64 (w), 11.00 (m), 12.47 (vs), 13.35 (w, broad), 14.03 (vs) and 14.53 μ (m). This pattern, in conjunction with the composition $C_{11}H_{11}O_2NS$ for the parent mustard oil, points to the new species being a benzoate of a hydroxysubstituted 3-carbon-alkyl *iso*thiocyanate. In accord herewith, alkaline hydrolysis of the thiourea at room temperature afforded benzoic acid in high yield, isolated and identified on comparison with an

* Part XXI of this series: *Acta Chem. Scand.* **10** (1956), *in press*.

** *Malcolmia maritima* R. Br. is *nomen conservandum* over *Cheiranthus maritimus* L.

The dextro-rotatory α-(1-naphthyl)-propionic acid has the configuration I. Consequently (+)-α-(3-thianaphthenyl)-propionic acid has a stereo formula corresponding to II.



If the 3-thianaphthenyl group is considered as a substituent on the aliphatic carbon chain, this acid must be assigned to the D-series.

The work described here is part of a stereochemical study of aralkyl carboxylic acids. Full details will be given elsewhere.

A grant from the *Swedish Natural Science Research Council* is gratefully acknowledged.

1. Fredga, A. *"The Svedberg 1884 30/8 1944"*, Uppsala 1944, p. 261.
2. Schomaker, V. and Pauling, L. *J. Am. Chem. Soc.* **61** (1939) 1769.
3. Fredga, A. *Arkiv Kemi* **8** (1955) 463.
4. Kofler, A. and L. *Mikro-Methoden*, Innsbruck 1948.

Received September 4, 1956.

*iso*Thiocyanates XXII *. 3-Benzoyloxypropyl *iso*Thiocyanate, Present as a Glucoside (Glucomalcolmiin) in Seeds of *Malcolmia maritima* (L.) R.Br.

ANDERS KJÆR and ROLF GMELIN

Chemical Laboratory of the University of Copenhagen, Denmark

Paperchromatographic analysis of the *iso*thiocyanate glucosides in a seed extract of the crucifer *Malcolmia maritima* (L.) R. Br. revealed the presence of two glucosides, (a) and (b), possessing R_B-values [1] of 0.34 and 1.36, respectively, in the solvent system: *n*-butanol:ethanol:water (4:1:4). In addition, traces of a third glucoside (R_B 1.03) and substantial amounts of sinapine were recognized in the seed extract, a pattern similar to that obtained elsewhere [1].

In the present work, the glucoside (a) has been unequivocally identified as glucocheirolin, furnishing cheirolin (3-methylsulphonylpropyl *iso*thiocyanate) on enzymic hydrolysis, a mustard oil formerly recognized as a constituent of *Cheiranthus cheiri* L.** and other species [2]. Crystalline thiourea derivatives have been obtained from enzymically hydrolyzed seed macerates of *M. maritima* after treatment with aniline and benzylamine, identical with reference specimens prepared from synthetic cheirolin [3]. The phenylthiourea has been described previously [2,3] whereas the benzyl derivative is a new compound, m. p. 116° (uncorr.). (Found: C 50.35; H 6.26; N 9.70. Calc. for $C_{12}H_{16}O_2N_2S_2$: C 50.31; H 6.33; N 9.78).

The component (b), for which we propose the name *glucomalcolmiin*, is obviously different from all glucosides heretofore encountered in nature. The corresponding optically inactive, non-volatile *iso*thiocyanate, liberated from a paperchromatographically purified specimen of glucomalcolmiin, displays an ultraviolet absorption spectrum indicative of the presence of a strongly chromophoric system (λ_{max} 230 mμ, λ_{min} 213 mμ in water). The new mustard oil has been characterized as a crystalline thiourea, $C_{11}H_{14}O_2N_2S$, after treatment with ammonia, m. p. 162° (uncorr.). (Found: C 55.40; H 5.91; N 11.75; S 13.59. Calc. for $C_{11}H_{14}O_2N_2S$: C 55.41; H 5.92; N 11.75; S 13.45); UV-spectrum in ethanol: λ_{max} 237 mμ (ε 19 400), λ_{min} 214 mμ (ε 11 180) and low-extinction inflections at 270—272 mμ and 278—280 mμ. The IR-spectrum of the solid thiourea in a KBr disc displayed conspicuous bands at: 3.00 (vs), 5.83 (s, ester-CO), 6.05 (s), 6.41 (vs), 6.76 (s), 7.21 (s), 7.49 (s), 7.75 (vs), 8.44 (m), 8.79 (vs), 8.90 (vs), 9.28 (m), 9.48 (m), 9.70 (m), 9.84 (m), 10.64 (w), 11.00 (m), 12.47 (vs), 13.35 (w, broad), 14.03 (vs) and 14.53 μ (m). This pattern, in conjunction with the composition $C_{11}H_{11}O_2NS$ for the parent mustard oil, points to the new species being a benzoate of a hydroxysubstituted 3-carbon-alkyl *iso*thiocyanate. In accord herewith, alkaline hydrolysis of the thiourea at room temperature afforded benzoic acid in high yield, isolated and identified on comparison with an

* Part XXI of this series: *Acta Chem. Scand.* **10** (1956), *in press*.

** *Malcolmia maritima* R. Br. is *nomen conservandum* over *Cheiranthus maritimus* L.

authentic specimen. On paper chromatography in water-saturated chloroform, the thiourea migrates at a rate corresponding to an R_{Ph}-value [4] of 1.07.

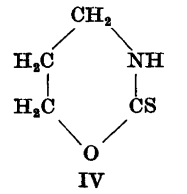
Disregarding the unlikely structures containing a hydroxyl grouping at the α-carbon atom, the alcoholic fragment of the new *iso*thiocyanatoalkyl benzoate may be represented by (I), (II) or (III), the last two structures possessing a centre of asymmetry and thence considered less likely in view of the optically inactive nature of the *iso*thiocyanate.

$HOCH_2CH_2CH_2NCS$ I

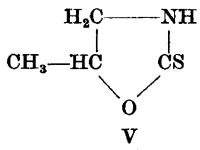
$H_3CCHOHCH_2NCS$ II

$H_3CCH(CH_2OH)NCS$ III

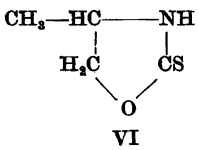
There are good reasons to expect (I), (II) and (III) to undergo spontaneous cyclization to (IV), (V) and (VI), respectively, the last two formulae representing a ring system formerly recognized in various substances derivable from naturally occurring β-hydroxysubstituted *iso*thiocyanates (*cf.* Ref.[5]).



IV



V



VI

$C_6H_5CO-O-(CH_2)_3NCS$ VII

When the thiourea-mixture, obtained by enzymic hydrolysis, solvent extraction and ammonia treatment of a purified seed extract of *M. maritima*, was chromatographed on paper, the pattern shown in Fig. 1 was observed. The results can be interpreted according to the following scheme, and strongly suggest that the new mustard oil is 3-benzoyloxypropyl *iso*thiocyanate (VII).

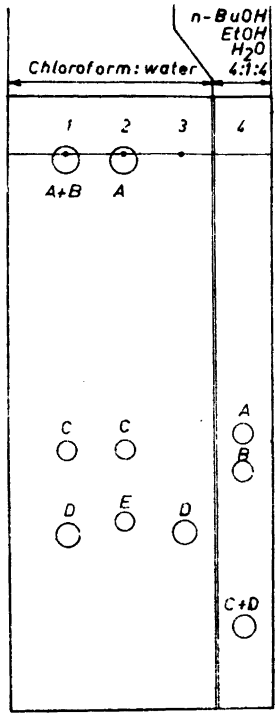


Fig. 1. Schematic, descending paper chromatograms. 1 and 4: thiourea mixture obtained from seeds of Malcolmia maritima; *2 and 3: synthetic reference samples. A: cheirolinthiourea; B: 3-hydroxypropylthiourea; C: tetrahydro-1,3-oxazine-2-thione (IV); D: 3-benzoyloxypropylthiourea; E: (±)-5-methyl-2-oxazolidinethione (V).*

The normal thiourea formation is partly accompanied by ammonolysis of the ester linkage, resulting in the formation of (B) as well as the previously unknown tetrahydro-1,3-oxazine-2-thione (IV). An authentic specimen of the latter, prepared from 3-amino-1-propanol by the method of Hodgkins and Ettlinger [6] for the synthesis of *iso*thiocyanates, was obtained as colourless plates, m. p. 129° (uncorr.). (Found: C 41.05; H 6.21; N 11.86. Calc.

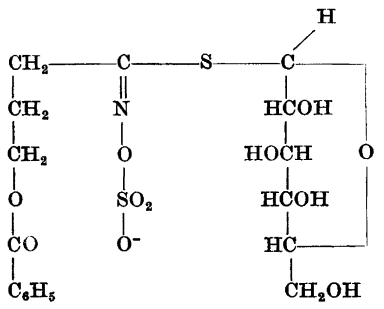
$$CH_3SO_2CH_2CH_2CH_2NCS \xrightarrow{NH_3} CH_3SO_2CH_2CH_2CH_2NHCSNH_2 \quad (A)$$

$$C_6H_5CO-O-CH_2CH_2CH_2NCS \xrightarrow{NH_3} \begin{cases} C_6H_5CO-O-CH_2CH_2CH_2NHCSNH_2 & (D) \\ HOCH_2CH_2CH_2NHCSNH_2 & (B) \\ IV & (C) \end{cases}$$

for C_4H_7ONS: C 40.98; H 6.02; N 11.95). The compound migrated on paper chromatograms at a rate definitely lower than that of a reference sample of (±)-5-methyl-2-oxazolidinethione (V) [7,8] (Fig. 1); it appears likely that the isomeride (VI) [9] will not differ markedly from (V) in its chromatographic behaviour. Synthetic experiments are now in progress to verify the structure (VII).

The possible existence in *Malcolmia* seeds of an additional glucoside, containing (B) as the aglucone and located at the site of glucocheirolin in the paper chromatogram, has been ruled out by chromatography on paper of the free *iso*thiocyanates in chloroform (spray reagent: ammoniacal silver nitrate). Only cheirolin and (VII) were detectable, both travelling near the solvent front, whereas no trace of the expected ring compound (IV) was observed. The present results explain the appearance of two spots in the low R_F-region of the paper chromatogram of *Malcolmia*-thioureas, reported by Schultz and Wagner [1]. One is attributable to cheirolinthiourea (A) whereas the other spot probably represents the artefact (B). In the present work it has been further established that our previously recorded occurrence of methyl *iso*thiocyanate in *Malcolmia* seeds [10] is incorrect.

The presence of glucose and sulphate in glucomalcolmiin has been verified by paper-chromatographic methods. The glucoside thence appears to be of the usual type. Unpublished results from this laboratory, supplemented by the conclusive work of Ettlinger and Lundeen [11] on the revised mustard oil glucoside structure, favour the following expression for the glucomalcolmiinate ion:



A detailed account of the present work will appear in this journal.

Microanalyses by Mr. P. Hansen of this laboratory. The work is part of investigations supported by *Statens Almindelige Videnskabsfond (The Danish State Research Foundation)* and *Carlsbergfondet (The Carlsberg Foundation)*.

1. Schultz, O.-E. and Wagner, W. *Z. Naturforsch.* **11b** (1956) 73.
2. Schneider, W. *Ann.* **375** (1910) 207.
3. Kjær, A., Marcus, F. and Conti, J. *Acta Chem. Scand.* **7** (1953) 1370.
4. Kjær, A. and Rubinstein, K. *Acta Chem. Scand.* **7** (1953) 528.
5. Kjær, A., Gmelin, R. and Boe Jensen, R. *Acta Chem. Scand.* **10** (1956) 432.
6. Hodgkins, J. E. and Ettlinger, M. G. *J. Org. Chem.* **21** (1956) 404.
7. Hopkins, C. Y. *Can. J. Research* **20B** (1942) 268.
8. Rosen, A. A. *J. Am. Chem. Soc.* **74** (1952) 2994.
9. Viscontini, M. and Adank, K. *Helv. Chim. Acta* **33** (1950) 225.
10. Kjær, A., Conti, J. and Larsen, I. *Acta Chem. Scand.* **7** (1953) 1276.
11. Ettlinger, M. G. and Lundeen, A. J. *J. Am. Chem. Soc.* **78** (1956) 4172.

Received September 2, 1956.

A New Modification of Titanium Monoxide

ULF KUYLENSTIERNA and ARNE MAGNÉLI

Institute of Inorganic and Physical Chemistry, University of Stockholm, Stockholm, Sweden

According to Ehrlich [1], titanium monoxide has a structure of sodium chloride type with randomly distributed vacancies in both the titanium and oxygen frameworks and a very broad range of homogeneity. Samples of this phase were prepared by melting mixtures of titanium metal and titanium dioxide (both of high purity) under argon atmosphere in an electric arc furnace. The following data, which are in fair agreement with Ehrlich's results, were obtained for a few of the compositions studied.

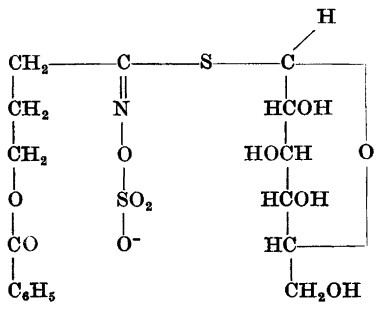
The unit cell dimensions were obtained from powder photographs taken in a Guinier focusing camera with strictly monochromatized Cu$K\alpha_1$ radiation using potassium chloride as an internal standard.

The arc-melted samples were sealed in evacuated silica tubes, heated at 800° C for several days and quenched in water. The Guinier photographs of the preparations TiO_x ($x < 1$) then showed the pattern

for C_4H_7ONS: C 40.98; H 6.02; N 11.95). The compound migrated on paper chromatograms at a rate definitely lower than that of a reference sample of (±)-5-methyl-2-oxazolidinethione (V) [7,8] (Fig. 1); it appears likely that the isomeride (VI) [9] will not differ markedly from (V) in its chromatographic behaviour. Synthetic experiments are now in progress to verify the structure (VII).

The possible existence in *Malcolmia* seeds of an additional glucoside, containing (B) as the aglucone and located at the site of glucocheirolin in the paper chromatogram, has been ruled out by chromatography on paper of the free *iso*thiocyanates in chloroform (spray reagent: ammoniacal silver nitrate). Only cheirolin and (VII) were detectable, both travelling near the solvent front, whereas no trace of the expected ring compound (IV) was observed. The present results explain the appearance of two spots in the low R_F-region of the paper chromatogram of *Malcolmia*-thioureas, reported by Schultz and Wagner [1]. One is attributable to cheirolinthiourea (A) whereas the other spot probably represents the artefact (B). In the present work it has been further established that our previously recorded occurrence of methyl *iso*thiocyanate in *Malcolmia* seeds [10] is incorrect.

The presence of glucose and sulphate in glucomalcolmiin has been verified by paper-chromatographic methods. The glucoside thence appears to be of the usual type. Unpublished results from this laboratory, supplemented by the conclusive work of Ettlinger and Lundeen [11] on the revised mustard oil glucoside structure, favour the following expression for the glucomalcolmiinate ion:



A detailed account of the present work will appear in this journal.

Microanalyses by Mr. P. Hansen of this laboratory. The work is part of investigations supported by *Statens Almindelige Videnskabsfond (The Danish State Research Foundation)* and *Carlsbergfondet (The Carlsberg Foundation)*.

1. Schultz, O.-E. and Wagner, W. *Z. Naturforsch.* **11b** (1956) 73.
2. Schneider, W. *Ann.* **375** (1910) 207.
3. Kjær, A., Marcus, F. and Conti, J. *Acta Chem. Scand.* **7** (1953) 1370.
4. Kjær, A. and Rubinstein, K. *Acta Chem. Scand.* **7** (1953) 528.
5. Kjær, A., Gmelin, R. and Boe Jensen, R. *Acta Chem. Scand.* **10** (1956) 432.
6. Hodgkins, J. E. and Ettlinger, M. G. *J. Org. Chem.* **21** (1956) 404.
7. Hopkins, C. Y. *Can. J. Research* **20B** (1942) 268.
8. Rosen, A. A. *J. Am. Chem. Soc.* **74** (1952) 2994.
9. Viscontini, M. and Adank, K. *Helv. Chim. Acta* **33** (1950) 225.
10. Kjær, A., Conti, J. and Larsen, I. *Acta Chem. Scand.* **7** (1953) 1276.
11. Ettlinger, M. G. and Lundeen, A. J. *J. Am. Chem. Soc.* **78** (1956) 4172.

Received September 2, 1956.

A New Modification of Titanium Monoxide

ULF KUYLENSTIERNA and ARNE MAGNÉLI

Institute of Inorganic and Physical Chemistry, University of Stockholm, Stockholm, Sweden

According to Ehrlich [1], titanium monoxide has a structure of sodium chloride type with randomly distributed vacancies in both the titanium and oxygen frameworks and a very broad range of homogeneity. Samples of this phase were prepared by melting mixtures of titanium metal and titanium dioxide (both of high purity) under argon atmosphere in an electric arc furnace. The following data, which are in fair agreement with Ehrlich's results, were obtained for a few of the compositions studied.

The unit cell dimensions were obtained from powder photographs taken in a Guinier focusing camera with strictly monochromatized Cu$K\alpha_1$ radiation using potassium chloride as an internal standard.

The arc-melted samples were sealed in evacuated silica tubes, heated at 800° C for several days and quenched in water. The Guinier photographs of the preparations TiO_x ($x < 1$) then showed the pattern

Composition	Axial length	Density	Per cent of available atomic sites occupied by titanium atoms	Per cent of available atomic sites occupied by oxygen atoms
$TiO_{0.64}$ (phase limit)	4.202 Å	5.00	96	61
$TiO_{1.00}$	4.182 Å	4.95	85	85
$TiO_{1.26}$ (phase limit)	4.169 Å	4.78	77	97

of the hexagonal α-titanium phase and a great number of extra lines. The latter also appeared in the photographs of samples TiO_x ($1 < x < 1.12$) in addition to a pattern corresponding to titanium monoxide of sodium chloride type of the approximate composition $TiO_{1.15}$. The new phase, the lines of which showed no detectable displacements in samples of different compositions, was pure in the sample $TiO_{1.00}$ and is obviously a new modification of titanium monoxide possessing a very narrow range of homogeneity. The density was found to be 4.91.

Table 1. Part of Guinier powder photograph of $TiO_{1.00}$, prepared at 800° C. CuKa_1 radiation.

I	$\sin^2\Theta_{obs}$
w	0.0191
w	0.0300
w	0.0347
m	0.0421
st	0.0539
m	0.0683
m	0.0761
m	0.0772
w	0.0995
st	0.1018
st	0.1038
st	0.1348
v st	0.1386
v w	0.1574
v w	0.1681
v w	0.1916
w	0.2047
v w	0.2084
w	0.2154
w	0.2212
w	0.2259
v w	0.2346
v v w	0.2447
w	0.2578
m	0.2689
st	0.2729
v st	0.2767
v v w	0.3184
v v w	0.3302

The powder pattern of the new phase, listed in Table 1, is of a rather complicated appearance and probably of low symmetry. So far it has not been possible to index it. However, it shows a noticeable similarity to that of the monoxide of sodium chloride type. Thus the strong reflexions of the former appear as doublets close to those of the latter, *i. e. st* ($\sin^2\Theta = 0.1017$), *v st* (0.1358), and *v st* (0.2714). The similarity seems to indicate the existence of a structural relationship between the two phases. It might be that the structural transformation is associated with an ordering of the atomic vacancies present in the cubic phase.

These studies form part of a research program on metal oxides and related compounds financially supported by the *Swedish Natural Science Research Council*. Further studies on the titanium-oxygen system are in progress. A detailed report of the investigation will be published elsewhere.

1. Ehrlich, P. *Z. Elektrochem.* **45** (1939) 362.

Received September 22, 1956.

The Synthesis of 6-Methoxy-2(3)-benzoxazolinone

PENTTI K. HIETALA and ÖRN WAHLROOS

Laboratory of the Foundation for Chemical Research, Biochemical Institute, Helsinki, Finland

In this laboratory an anti-fungal substance was recently isolated from maize and wheat plants [1]. The structure 6-methoxy-2(3)-benzoxazolinone (IV) was proposed for this substance. This has now been confirmed by the following synthesis:

Composition	Axial length	Density	Per cent of available atomic sites occupied by titanium atoms	Per cent of available atomic sites occupied by oxygen atoms
$TiO_{0.64}$ (phase limit)	4.202 Å	5.00	96	61
$TiO_{1.00}$	4.182 Å	4.95	85	85
$TiO_{1.26}$ (phase limit)	4.169 Å	4.78	77	97

of the hexagonal α-titanium phase and a great number of extra lines. The latter also appeared in the photographs of samples TiO_x ($1 < x < 1.12$) in addition to a pattern corresponding to titanium monoxide of sodium chloride type of the approximate composition $TiO_{1.15}$. The new phase, the lines of which showed no detectable displacements in samples of different compositions, was pure in the sample $TiO_{1.00}$ and is obviously a new modification of titanium monoxide possessing a very narrow range of homogeneity. The density was found to be 4.91.

Table 1. Part of Guinier powder photograph of $TiO_{1.00}$, prepared at 800° C. CuKa_1 radiation.

I	$\sin^2\Theta_{obs}$
w	0.0191
w	0.0300
w	0.0347
m	0.0421
st	0.0539
m	0.0683
m	0.0761
m	0.0772
w	0.0995
st	0.1018
st	0.1038
st	0.1348
v st	0.1386
v w	0.1574
v w	0.1681
v w	0.1916
w	0.2047
v w	0.2084
w	0.2154
w	0.2212
w	0.2259
v w	0.2346
v v w	0.2447
w	0.2578
m	0.2689
st	0.2729
v st	0.2767
v v w	0.3184
v v w	0.3302

The powder pattern of the new phase, listed in Table 1, is of a rather complicated appearance and probably of low symmetry. So far it has not been possible to index it. However, it shows a noticeable similarity to that of the monoxide of sodium chloride type. Thus the strong reflexions of the former appear as doublets close to those of the latter, *i. e. st* ($\sin^2\Theta = 0.1017$), *v st* (0.1358), and *v st* (0.2714). The similarity seems to indicate the existence of a structural relationship between the two phases. It might be that the structural transformation is associated with an ordering of the atomic vacancies present in the cubic phase.

These studies form part of a research program on metal oxides and related compounds financially supported by the *Swedish Natural Science Research Council*. Further studies on the titanium-oxygen system are in progress. A detailed report of the investigation will be published elsewhere.

1. Ehrlich, P. *Z. Elektrochem.* **45** (1939) 362.

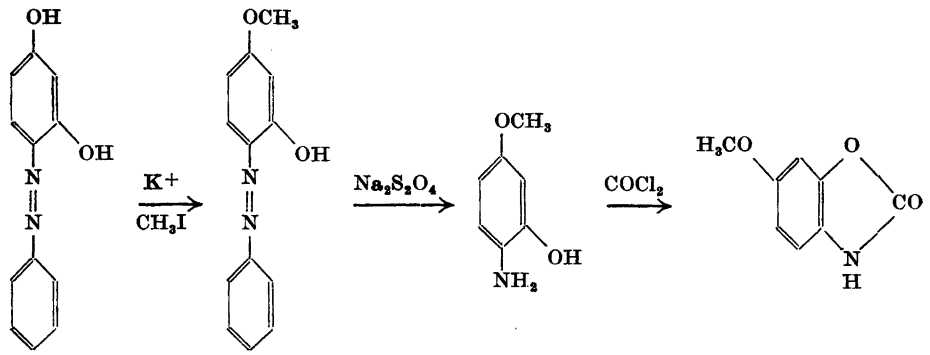
Received September 22, 1956.

The Synthesis of 6-Methoxy-2(3)-benzoxazolinone

PENTTI K. HIETALA and ÖRN WAHLROOS

Laboratory of the Foundation for Chemical Research, Biochemical Institute, Helsinki, Finland

In this laboratory an anti-fungal substance was recently isolated from maize and wheat plants [1]. The structure 6-methoxy-2(3)-benzoxazolinone (IV) was proposed for this substance. This has now been confirmed by the following synthesis:



I II III IV

Pure *p*-benzene-azo-resorcine (I) was obtained by the method of Will and Pukall [2].

The methylation was done by the method of Bechold [3], with the following modifications: a) methyl iodide was used in the proportion 2 moles to 1 mole of the dry potassium salt of I; b) the reaction time was reduced from 6 h to 3 h (yield: 6 h, 1.5 %; 3 h, 14 % theor.).

2-Hydroxy-4-methoxy-aniline (III) is very easily oxidized wherefore the following stages were carried out in a carbon dioxide atmosphere: a) II was reduced in a boiling alcohol solution with a slight excess of a saturated solution of sodium hyposulphite in water [4], the mixture was neutralized with barium carbonate and evaporated almost to dryness (the aniline is removed with the vapour); b) III was extracted from the remaining mixture by peroxide-free ether and after evaporation of the ether it was mixed with glacial acetic acid, about ten times its weight, when the acetate of III precipitated. Phosgene was bubbled through the mixture [5] until the precipitate had dissolved.

After evaporation of the acetic acid *in vacuo*, dissolving the residue in hot water, treating with active carbon to decolourize the solution, and filtrating, IV crystallizes on cooling. Yield 15 % of the theoretical. Through recrystallization from alcohol colourless needles, m. p. 156°, were obtained.

The mixed melting point of this substance and the anti-fungal substance of wheat and maize plants showed no depression. Acetyl derivative m. p. 150° C (no depression).

UV spectra (in water): Synthetic product: Max. 229–230 mμ and 285–286 mμ; Min. 255 mμ; Log ε 286 mμ = 3.74.

Isolated anti-fungal substance: Max. 285–286 mμ; Min. 255 mμ.

Acknowledgement. We are indebted to Professor A. I. Virtanen for his great interest in this work and to the *Rockefeller Foundation* for a grant awarded to the Foundation for Chemical Research.

1. Virtanen, A. I., Hietala, P. K. and Wahlroos, Ö. *Suomen Kemistilehti* **B 29** (1956) 143.
2. Will, W. and Pukall, W. *Ber.* **20** (1887) 1119.
3. Bechold, J. *Ber.* **22** (1889) 2374.
4. Grandmougin, E. *Ber.* **39** (1906) 2494.
5. Zinner, H. and Herbig, H. *Ber.* **88** (1955) 1241.

Received September 18, 1956.

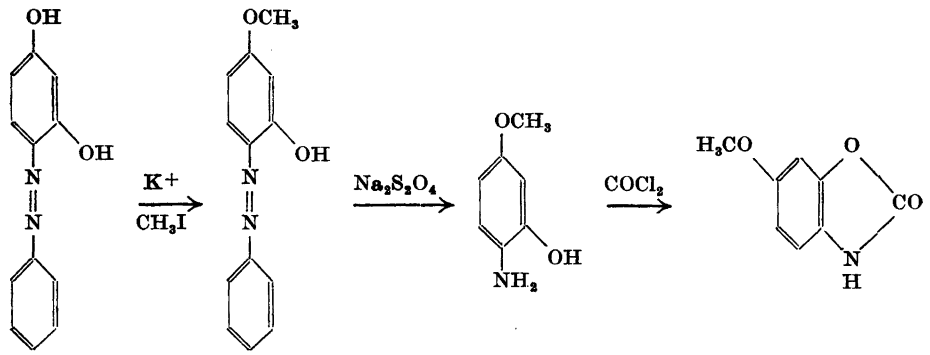
On the Preparation of Alkyl Cyanides

ÅRNE BRÄNDSTRÖM

Research Laboratory, Pharmacia Ltd., Uppsala, Sweden

In an interesting paper Lewis and Susi [1] report that the preparation of alkyl cyanides from the corresponding primary bromides gives very good yields when ethylene glycol is used as solvent.

Glycols seem to be excellent for this reaction, being good solvents of alkali cya-



I II III IV

Pure *p*-benzene-azo-resorcine (I) was obtained by the method of Will and Pukall [2].

The methylation was done by the method of Bechold [3], with the following modifications: a) methyl iodide was used in the proportion 2 moles to 1 mole of the dry potassium salt of I; b) the reaction time was reduced from 6 h to 3 h (yield: 6 h, 1.5 %; 3 h, 14 % theor.).

2-Hydroxy-4-methoxy-aniline (III) is very easily oxidized wherefore the following stages were carried out in a carbon dioxide atmosphere: a) II was reduced in a boiling alcohol solution with a slight excess of a saturated solution of sodium hyposulphite in water [4], the mixture was neutralized with barium carbonate and evaporated almost to dryness (the aniline is removed with the vapour); b) III was extracted from the remaining mixture by peroxide-free ether and after evaporation of the ether it was mixed with glacial acetic acid, about ten times its weight, when the acetate of III precipitated. Phosgene was bubbled through the mixture [5] until the precipitate had dissolved.

After evaporation of the acetic acid *in vacuo*, dissolving the residue in hot water, treating with active carbon to decolourize the solution, and filtrating, IV crystallizes on cooling. Yield 15 % of the theoretical. Through recrystallization from alcohol colourless needles, m. p. 156°, were obtained.

The mixed melting point of this substance and the anti-fungal substance of wheat and maize plants showed no depression. Acetyl derivative m. p. 150° C (no depression).

UV spectra (in water): Synthetic product: Max. 229–230 mμ and 285–286 mμ; Min. 255 mμ; Log ε 286 mμ = 3.74.

Isolated anti-fungal substance: Max. 285–286 mμ; Min. 255 mμ.

Acknowledgement. We are indebted to Professor A. I. Virtanen for his great interest in this work and to the *Rockefeller Foundation* for a grant awarded to the Foundation for Chemical Research.

1. Virtanen, A. I., Hietala, P. K. and Wahlroos, Ö. *Suomen Kemistilehti* **B 29** (1956) 143.
2. Will, W. and Pukall, W. *Ber.* **20** (1887) 1119.
3. Bechold, J. *Ber.* **22** (1889) 2374.
4. Grandmougin, E. *Ber.* **39** (1906) 2494.
5. Zinner, H. and Herbig, H. *Ber.* **88** (1955) 1241.

Received September 18, 1956.

On the Preparation of Alkyl Cyanides

ÅRNE BRÄNDSTRÖM

Research Laboratory, Pharmacia Ltd., Uppsala, Sweden

In an interesting paper Lewis and Susi [1] report that the preparation of alkyl cyanides from the corresponding primary bromides gives very good yields when ethylene glycol is used as solvent.

Glycols seem to be excellent for this reaction, being good solvents of alkali cya-

nides and easily obtainable in a sufficiently anhydrous state to prevent hydrolysis of the alkyl cyanide under the condition of the reaction. The boiling-point of ethylene glycol is, however, somewhat too low to permit easy separation of the alkyl cyanide by means of distillation. In order to eliminate this disadvantage some polymers of ethylene glycol, such as diethylene glycol and polyethylene-glycol-300, have been tried. In these experiments it was surprisingly found that, although the yields were moderate and the reaction slow when bromides were employed, the yields were excellent and the reaction rapid and sometimes vigorous when the corresponding chlorides were used. The reason for this is probably that the reaction is heterogeneous, making solubility a very important factor.

The fact that excellent yields of alkyl cyanides can be obtained from the corresponding alkyl chloride is of great value, since alkyl chlorides are readily available by the chlorination of hydrocarbons and by other methods.

When an alkyl chloride is refluxed with sodium cyanide in polyethylene glycol the temperature in the reaction-flask is at first equal to the boiling-point of the chloride. Since the alkyl cyanide has a much higher boiling-point than the corresponding alkyl chloride, the reaction-temperature will rapidly rise as long as the alkyl cyanide is being formed from the alkyl chloride. This permits an exact determination of the end-point of the reaction as the point where the temperature in the flask no longer rises. The alkyl cyanide is then easily removed from the reaction-mixture by distillation. The crude product obtained in this way contains very little by-products, and is pure enough for most purposes.

If necessary it can easily be purified by means of distillation.

Experimental. In a 5-l round-bottomed flask fitted with an efficient stirrer, a reflux condenser, and a thermometer, were placed 1.5 l of polyethylene-glycol-300, 300 g of sodium cyanide, and 5 moles of the alkyl chloride. The flask was heated by means of an electric heating-mantle so arranged that it could easily be removed if the reaction showed any tendency to become violent. The flask was heated until the temperature was practically constant. The refluxing time varied from about 15 min for *n*-octyl chloride to about 4 h for *n*-butyl chloride. The nitrile was then removed by distillation under reduced pressure as long as any product came over. A temperature of 200° at a pressure of 10 mm was often required to ensure complete removal of the nitrile from the reaction-product. Practically no polyethylene glycol distilled under these conditions. The yield of the crude product varied between 90—95 %, and the yields of the redistilled alkyl cyanides were all in the region of 85—95 % when the chlorides from *n*-butyl to *n*-octyl were employed. When the reaction tended to become violent, which was the case when chlorides higher than *n*-hexyl were used, the reaction was easily controlled by stopping the stirrer and removing the heating-mantle.

1. Lewis, R. N. and Susi, P. V. *J. Am. Chem. Soc.* **74** (1952) 840.

Received September 24, 1956.

ACTA CHEMICA SCANDINAVICA 10 (1956) 1199—1207

La Structure d'un Isomère du Raffinose Isolé des Racines de l'*Angélica archangélica* L. subsp. *norvégica* (Rupr.) Nordh

ALF WICKSTRØM et ANDERS BÆRHEIM SVENDSEN

Universitetets farmasøytiske institutt, Blindern-Oslo, Norvège

A non-reducing trisaccharide occurring in the roots of some *Umbelliferæ* has been isolated on a preparative scale from *Angelica archangelica* L. subsp. *norvegica* (Rupr.) Nordh. The trisaccharide ($[\alpha]_D^{20} = +125°$; water; on anhydrous basis) contains D-fructose, D-glucose and D-galactose, linked together in the same order as in raffinose, and, like raffinose, it yields sucrose on hydrolysis with α-galactosidase. One molecule of the trisaccharide reduces under standard experimental conditions four molecules of periodate, and one molecule of formic acid is simultaneously formed. The fully methylated trisaccharide gives by acid hydrolysis equimolecular amounts of tetramethyl-D-fructofuranose, tetramethyl-D-galactopyranose and 3,4,6-trimethyl-D-glucose. All experimental results obtained agree with the structure of a *2'-α-D-galactopyranosyl-2-α-D-glucopyranosyl-β-D-fructofuranoside*. According to this structure the trisaccharide studied is an *iso*raffinose, in the present paper, however, denoted as *umbelliferose*.

Au cours de ses recherches phytochimiques sur des ombellifères de Norvège l'un de nous [1] a trouvé dans les racines de certaines espèces de cette famille un trisaccharide qui, par quelques unes de ses propriétés, se distingue nettement des trisaccharides naturels décrits dans la littérature antérieure.

Ce sucre a été trouvé dans les racines de *Pimpinella saxifraga* L. et d'*Angélica archangélica* L. subsp. *norvégica* (Rupr.) Nordh., et il est probablement présent dans les racines de quelques autres ombellifères [1].

Le trisaccharide a été isolé en petites quantités à l'aide de chromatographie sur papier épaix. Il est composé de fructose, de glucose et de galactose, arrangés dans le même ordre que dans le raffinose: fructose-glucose-galactose.

Cependant, l'auteur cité [1] a trouvé à ce trisaccharide certaines propriétés permettant de conclure qu'il n'est pas identique au trisaccharide le plus répandu dans les plantes, le raffinose: 1) Après hydrolyse partielle on a isolé du fructose ainsi qu'un disaccharide qui, aux chromatogrammes, se sépare nettement du mélibiose, disaccharide isolé du raffinose par le même procédé. 2) Le trisaccharide nouveau est beaucoup plus résistant vis-à-vis de l'invertase que n'est le raffinose dans les mêmes conditions.

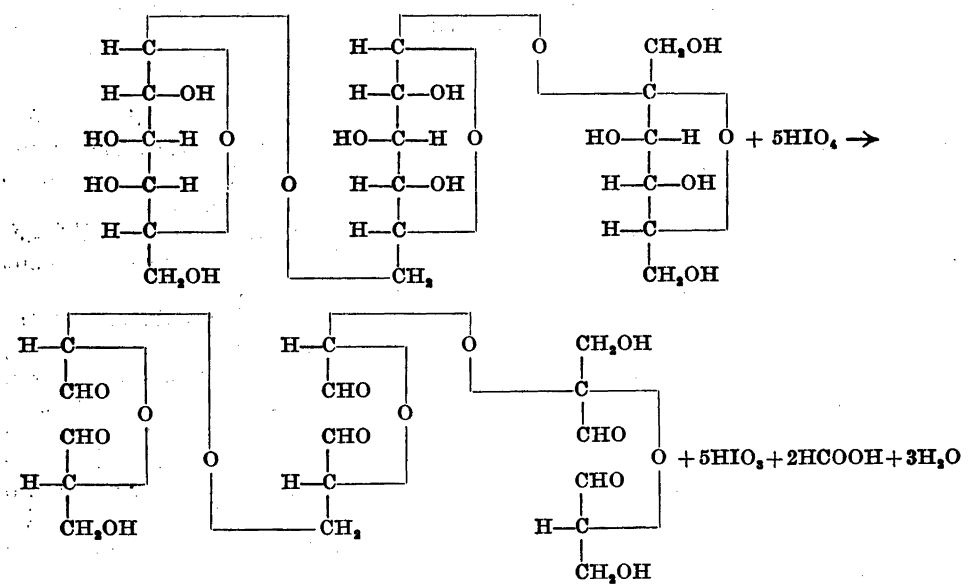
Dans le mémoire présent nous décrivons une téchnique améliorée pour l'isolement du trisaccharide des racines d'*Angélica archangélica* L. subsp. *norvégica* (Rupr.) Nordh. et nous présentons les résultats d'une étude de la structure moléculaire du sucre ainsi isolé. Nous adopterons, pour ce trisaccharide, la dénomination d'umbelliférose.

L'extraction et la purification de l'umbelliférose se trouvent décrites dans la partie expérimentale. 1 000 g de racines desséchées donnent 10 g environ de trisaccharide. Celui-ci se présente sous forme de poudre blanche, amorphe, non réductrice vis-à-vis le réactif cupro-alcalin. Son pouvoir rotatoire spécifique, déterminé sur des échantillons anhydres est de $+125°$ ($c = 2$; eau). Ce chiffre est très voisin de celui indiqué dans la littérature [2] pour le raffinose anhydre, $+123°$.

La vitesse d'hydrolyse de l'umbelliférose par l'α-galactosidase des graines de café est à peu près pareille à celle du raffinose (voir Tableau 1). Une molécule d'umbelliférose, par cette hydrolyse, donne naissance à une molécule de galactose et une molécule d'un disaccharide se composant de fructose et de glucose. Ce disaccharide a été isolé en état cristallin. Toutes ses propriétés chimiques et physiques, y compris le diagramme de diffraction aux rayons X, sont identiques à celles du saccharose (recristallisé de la même manière que le disaccharide inconnu). On en peut conclure que l'umbelliférose est un α-galactoside du saccharose. La présence dans l'umbelliférose de D-galactose sous forme pyranique étant prouvée par des études de méthylation auxquelles nous reviendrons plus bas, nous sommes en droit de conclure que l'umbelli-

SCHÉMA I.

Oxydation du raffinose par l'acide periodique.



férose est un α-D-galactopyranoside du saccharose avec son galactose lié au glucose. Toutefois, cette description ne le distingue en rien du raffinose.

Cependant, l'étude quantitative de l'oxydation de l'umbelliférose par le periodate de sodium a révélé une différence de structure nette entre ce sucre et le raffinose. Le raffinose, étudié par Courtois et Wickström [3], réduit cinq molécules d'acide periodique en donnant naissance à deux molécules d'acide formique au cours de la réaction présentée ci-dessous dans le schéma I. L'umbelliférose, par contre, réduit dans des conditions expérimentales semblables quatre molécules d'acide periodique, ne produisant qu'une seule molécule d'acide formique. Ces résultats, qui se trouvent exposés dans le Tableau 2, sont interprétés de la façon suivante.

L'acide formique est libéré par l'attaque de l'acide periodique sur les trois hydroxyles libres se trouvant dans l'anneau D-galactopyranosique, qui, par conséquent, pour son ouverture, exige la réduction de deux molécules d'acide periodique. Une troisième molécule d'acide periodique est réduite par le D-fructofuranose appartenant à la partie du trisaccharide possédant la configuration du saccharose. Il s'en suit que la quatrième molécule d'acide periodique est réduite, sans libération simultanée d'acide formique, par l'unité centrale du trisaccharide: le D-glucopyranose. Celui-ci, par conséquent, doit posséder deux fonctions alcooliques libres attachées à deux atomes de carbone contigus. La réaction entre l'umbelliférose et l'acide periodique permet d'envisager, pour l'umbelliférose, deux structures différences: 1) celle d'un α-D-galactopyranoside du saccharose avec le pont galactosidique lié au carbone 4 du glucose ou 2) celle d'un α-D-galactopyranoside du saccharose avec le pont galactosidique attaché au carbone 2 du glucose.

Pour nous permettre de choisir entre ces deux possibilités, l'umbelliférose, après méthylation complète, a été soumis à l'hydrolyse et les oses méthoxylés ainsi formés ont été identifiés. Par ce procédé ont été obtenus, en quantités pratiquement égales, le tétraméthyl-D-fructofuranose, le tétraméthyl-D-galactopyranose et le triméthyl-3,4,6-D-glucose. Ce dernier a été identifié par sa réaction caractéristique, décrite par Greville et Northcote [4], avec le periodate de sodium, réaction qui permet de distinguer ce dérivé de tous les triméthyl-D glucoses ne possédant pas, comme le triméthyl-3,4,6-D-glucose, un groupement hydroxyle libre en position 2.

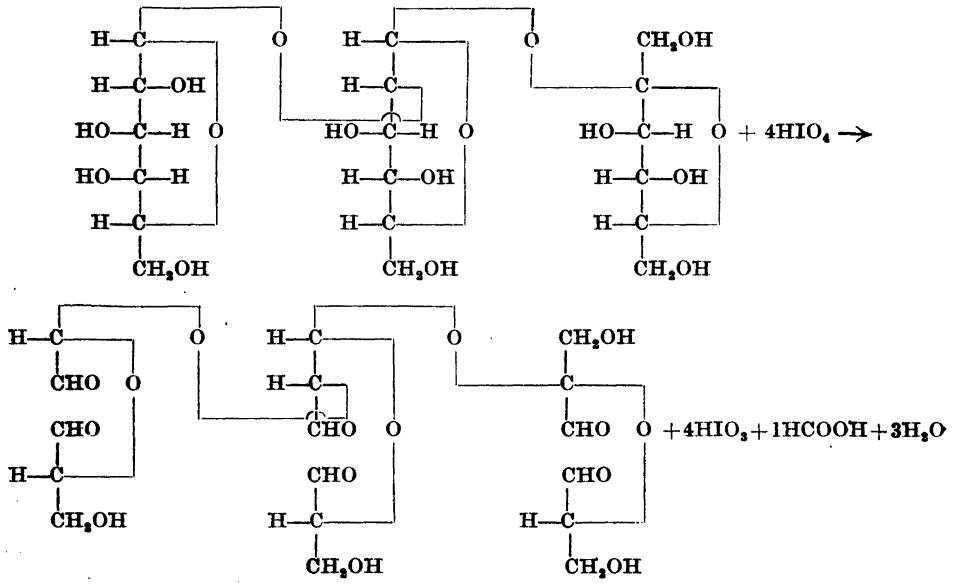
La réaction entre l'umbelliférose et l'acide periodique est représentée par le schema II.

Il convient de noter que l'observation du changement du pouvoir rotatoire pendant l'oxydation de l'umbelliférose par l'acide periodique nous a fourni d'un argument supplémentaire en faveur de la configuration α du carbone 1 du groupement galactopyranosique. Ce changement du pouvoir rotatoire est dû à l'élimination partielle des centres optiquement actifs, principe déjà devenue classique dans les recherches sur les hétérosides simples [5].

Herrisey, Wickstrøm et Courtois [6], étudiant l'oxydation periodique du raffinose, du gentianose et du stachyose, on démontré que la déviation au polarimètre pendant l'oxydation du raffinose et du stachyose, oligosaccharides possédant des liaisons osidiques sous forme α, est toujours positive. Le gentianose, au contraire, qui possède une liaison osidique sous forme β, est transformé par oxydation en substance lévogyre. Or, nous avons trouvé à l'umbelli-

SCHÉMA II.

Oxydation de l'umbelliférose par l'acide periodique.



férose pendant son oxydation une déviation au polarimètre positive et du même ordre de grandeur que celle du raffinose dans les mêmes conditions.

L'ensemble de nos résultats expérimentaux sont en accord avec la structure présentée ci-dessous pour l'umbelliférose:

α-D galactopyranosyl-2′-α-D glucopyranosyl-2 β-D-fructofuranoside.

D'après cette structure la seule différence entre l'umbelliférose et le raffinose se trouve dans la position du pont oxydique reliant le D-galactose au carbone 2 du D-glucose dans l'umbelliférose tandis que dans le raffinose il est lié au carbone 6; voir schéma I et II. L'umbelliférose se classe donc comme un *isoraffinose.*

PARTIE EXPÉRIMENTALE

1. Isolement et purification de l'umbelliférose

Des racines d'*Angélica archangélica* L. subsp. *norvégica* (Rupr.) Nordh. furent cultivées par Vinmonopolet A/S, Oslo, et récoltées en Septembre—Octobre de la première année de végétation.

Les racines, soigneusement lavées, puis grossièrement découpées, ont été stabilisées par l'alcohol à 96 % bouillant additionné de carbonate de calcium. Après ce traitement les racines séchées à la température ordinaire sont découpées et pulvérisées. Un kg de racines pulvérisées est extrait par dix litres d'eau distillée, saturée de toluène, pendant 24 heures à environ 20°. L'extrait aqueux est filtré; ensuite on le fait passer par des colonnes d'échangeurs d'ions, d'abord l'Amberlite IR 120 (H) et ensuite l'Amberlite IRA 400 (OH).

Il est avantageux de soumettre la solution ainsi obtenue à une purification ultérieure par la méthode classique de précipitation des acides par l'acétate de plomb.

On obtient finalement une solution jaune renfermant de l'umbelliférose, du saccharose, des traces d'hexoses et des impuretés colorées. Cette solution est concentrée sous pression réduite. Le résidu est un sirop de couleur jaune très foncé, presque solide. Rendement: 100 g.

Pour le fractionnement du sirop nous avons eu recours à la téchnique chromatographique de Whistler et Durso [7]; emploi d'une colonne de charbon actif et de celite, élution par l'éthanol à titre croissant. Avec le "Carbo activatus siccus Merck, p.a. No. 2186" nous avons obtenu une séparation des sucres aussi satisfaisante qu'avec le charbon "Darco-G-60", utilisé par Whistler et Durso.

L'adsorbant est introduit sur une hauteur d'environ 18 cm dans une colonne de 3,5 cm de diamètre, puis on ajoute 30 ml d'une solution aqueuse à 10 % du mélange saccharique. Ensuite la colonne est lavée, d'abord avec de l'eau distillée (environ 1 litre), puis avec de l'eau renferment 5 % d'éthanol (1,5 à 2 litres) pour éliminer le saccharose. Vers la fin de l'élution la solution sortant de la colonne contient des traces d'umbelliférose. Il est naturellement indispensable de contrôler, par chromatographie sur papier, que toute trace de saccharose est éliminée avant de commencer l'élution de l'umbelliférose avec de l'éthanol à 15 % (0,75 litre).

L'éluate contenant l'umbelliférose est concentré sous pression réduite. Le résidu est repris dans 5—10 ml d'eau distillée, traité par du charbon actif, filtré et concentré de nouveau sous pression réduite. On obtient finalement environ 300 mg d'umbelliférose chromatographiquement homogène, se présentant sous forme de poudre blanche, floconneuse et amorphe. Nous n'avons pas réussi à faire cristalliser l'umbelliférose.

Le pouvoir rotatoire du trisaccharide a été déterminé avec des échantillons séchés jusqu'au poids constant dans le vide en présence d'anhydride phosphorique à 60°. Le pouvoir rotatoire spécifique en solution aqueuse, observé sur plusieurs échantillons provenant de préparations différentes, a toujours été trouve entre $+121°$ et $+125°$ ($c = 2$). Il nous paraît probable que le pouvoir rotatoire le plus élévé, $[\alpha]_D^{20} = +125{,}3°$, corresponde au produit le plus pur.

Il convient à noter que l'umbelliférose est facilement séparé du raffinose par chromatographie sur papier, avec le même système solvant que nous avons utilisé pour contrôler, par chromatographie sur papier, le fractionnement sur colonne du saccharose et le l'umbelliférose. Aux chromatogrammes, réalisés par la technique descendante à 20°—22° avec le système monophasique: *iso*pentanol: 7 vol./pyridine: 7 vol./eau: 6 vol., le cheminement du saccharose au cours de 24 heures est de 24 à 28 cm. Les distance parcourues (R_S) par les trisaccharides par rapport à la migration du saccharose ($R_S = 1{,}00$) sont pour le raffinose 0,62 et pour l'umbelliférose 0,70.

2. Dosage quantitatif des hexoses libérés par hydrolyse acide de l'umbelliférose

a) *Hydrolyse complète:* Environ 50 mg de l'umbelliférose anhydre, exactement pesés, ont été dissous dans 1 ml d'acide sulfurique N/1 et chauffés en ampoule scellée à 100° pendant une heure. Neutraliser avec le carbonate de baryum, centrifuger et séparer les hexoses par chromatographie sur papier avec la phase organique du système solvant: acétate d'éthyle: 2 vol./pyridine: 1 vol./eau: 2 vol. Les hexoses séparés ont été élués à froid [8] et dosés par titration, d'après le protocôle de Hirst et Jones [9], de l'acide formique libéré par oxydation avec le metaperiodate de sodium. Les chiffres suivants, représentant des moyennes de plusieurs chromatogrammes, expriment les proportions moléculaires des hexoses dans l'hydrolysat: glucose: 1,00; galactose: 0,96; fructose: 0,89.

b) *Hydrolyse partielle:* Une solution à 1,874 % d'umbelliférose anhydre dans de l'acide sulfurique 0,01 N (3 ml) est introduite dans une ampoule scellée et chauffée à 100° pendant 40 minutes. Par ce traitement le fructose est selectivement et complètement détaché de la molécule d'umbelliférose. Pendant l'hydrolyse le pouvoir rotatoire change: $\Delta(\alpha)_D^{20}$: $-58{,}3°$, ce qui correspond à un changement du pouvoir rotatoire moléculaire ($\Delta(\alpha)_D^{20}$ x P.M. du trisaccharide) de $-$ 29 410. Ce dernier chiffre est très voisin à ceux

indiqués dans la littérature pour le changement du pouvoir rotatoire moléculaire de certains oligosaccharides, changement provoqué par la rupture d'une liaison β-D-fructofuranosidique [10].

L'hydrolysat a été neutralisé par le carbonate de baryum, puis centrifugé. Le fructose libre a été dosé, sur volumes exactement mesurés avec une micropipette, après séparation chromatographique suivant la méthode décrite ci-dessus. Analyse: Anhydrofructose, $C_6H_{10}O_5$, calc. pour $C_{18}H_{32}O_{16}$: 32,15 %, tr: 31,0 % (moyenne de plusieurs analyses).

3. Hydrolyse de l'umbelliférose par l'α-galactosidase des graines de café

a) *Vitesse d'hydrolyse comparée avec celle du raffinose dans les mêmes conditions:* Mélanger 2 ml d'une solution M/20 du sucre à analyser, avec 0,5 ml d'un tampon contenant de l'acide acétique M/1 neutralisé avec de la soude jusqu'à pH 4,8 et 0,1 ml d'une suspension à 2 % de l'α-galactosidase. Laisser en contact à 37°. Les sucres réducteurs libérés par l'hydrolyse enzymatique sont dosés par leur action réductrice sur le réactif cupro-alcalin d'après la méthode de Lehmann, mise au point par Fleury et Boutot [11]. Nos résultats sont exposés dans le Tableau 1.

b) *Isolement et identification du saccharose après l'hydrolyse enzymatique de l'umbelliférose:* 2,3 g du trisaccharide, dissous dans 10 ml du tampon acétique de pH 4,8, furent additionnés de 5 ml d'une suspension à 1 % de l'α-galactosidase dans l'eau. L'hydrolyse à 37°, en présence d'un peu de toluène, est contrôlée tous les 4 jours au moyen de chromatographie sur papier. Après 16 jours le mélange est filtré et transfert à une colonne de charbon actif-cellite (diamétre: 3,5 cm, hauteur de l'adsorbant: 20 cm). Le galactose et les sels minéraux sont élués par de l'eau distillée (3 litres). Ensuite le disaccharide est récupéré par élution avec de l'éthanol à 5 %. La solution alcoolique fut concentrée sous pression réduite en un sirop visceux et incolore (1 g). Cette substance, après avoir été séchée dans le vide en présence d'anhydride phosphorique, fut obtenu en état cristallin en suivant le procedé décrit par Courtois, Anagnostopoulos et Petek [12]. Rendement 0,47 g.

Un échantillon témoin de saccharose a été recristallisé dans un mélange d'éthanol et d'éther suivant le même protocôle. Le disaccharide formé par détachement de galactose de l'umbelliférose fournit le même diagramme de diffraction aux rayons X que l'échantillon témoin de saccharose. Il est dédoublé par l'invertase d'une vitesse voisine de celle du dédoublement du saccharose. Son point de fusion: 185—188° (déterminé au microscope avec l'appareil de Kofler) n'est pas modifié par mélange avec l'échantillon témoin du saccharose. Son pouvoir rotatoire, $(\alpha)_D^{20} = +66{,}8°$ (c = 2; eau), donc, pareil à celui du saccharose.

4. Oxydation de l'umbelliférose par l'acide periodique; comparaison avec le raffinose

50 ml d'une solution à M/500 du trisaccharide à analyser sont mélangés avec 200 ml d'une solution à M/100 de metaperiodate de sodium ($NaIO_4$). Laisser reposer à 18—20° à l'abri de lumière. Avec des prélèvements de 25 ml on fait a) un dosage de la quantité

Tableau 1. Action de l'α-galactosidase sur l'umbelliférose. Comparaison avec le raffinose.

Durée de contact à 37° (jours)	1	2	4	7
Molécules de galactose libérées par molécule de raffinose	<0,2	0,25	0,36	0,64
Molécules de galactose libérées par molécule d'umbelliférose	0,26	0,46	0,53	0,66

d'acide periodique réduite, dosage effectué d'après la méthode classique à l'anhydride arsénieux-iodure, et b) un dosage de l'acide formique libéré. Ce dosage a été fait par titration avec de la soude M/100 (rouge de méthyle-bleu de méthylène) après addition d'éthylèneglycol neutre (0,5 ml).

Les chiffres trouvé sont présenté dans le Tableau 2. Les résultats obtenus avec le raffinose en suivant la technique décrite ci-dessus sont conformes aux observations antérieures, voir Courtois et Wickstrøm [3].

Dans des essais supplémentaires l'oxydation de l'umbelliférose par l'acide periodique libre est suivie au polarimètre. A titre d'exemple nous citerons une des expériences. 116,80 mg d'umbelliférose anhydre, dissous dans 4 ml d'eau distillée, sont mélangés avec 3,6 ml d'une solution d'acide periodique libre M/2. Compléter à 10 ml et suivre l'oxydation au polarimètre à la température de 20—22°. Lectures (l = 1 dm): Après 15 min: +0,61°; après 2 h: + 0,55°; après 22 h: +0,48°. Après 22 h le pouvoir rotatoire reste constant. Le chiffre de +0,48° correspond à $[M]_D$ = 20 700. calculé en employant le poids moléculaire du polyaldéhyde résultant en théorie de l'oxydation de l'umbelliférose (schéma II). Le chiffre correspondant pour le raffinose est $[M]_D$ = 23 500[6].

Tableau 2. Oxydation de l'umbelliférose et du raffinose par le periodate de sodium.

Sucre	Durée de contact à 18°—20°	24 h	48 h	4 jours	6 jours	8 jours
Umbelliférose	Molécules [a] d'acide periodique réduites	3,57	3,90 3,97	4,06 4,02	4,13 4,17	4,16 4,17
	Molécules [a] d'acide monovalent libéreés	0,68	0,91 0,88	0,95 0,94	0,97 0,88	1,01
Raffinose	Molécules [a] d'acide periodique réduites	4,87	4,98	5,03		
	Molécules [a] d'acide monovalent libérées	1,58	1,82	1,94		

[a] par molécule de trisaccharide.

5. Hydrolyse d'un umbelliférose complètement méthylé et séparation des oses méthylés libérés par l'hydrolyse

3,8 g d'umbelliférose anhydre sont traités trois fois par le diméthylsulfate en présence de soude. Ensuite le produit est traité plusieurs fois par l'iodure de méthyle en présence d'oxyde d'argent. Nous avons suivi sans modifications essentielles le procédé décrit d'une façon détaillée par Laidlaw et Wylam [13] pour la méthylation complète du stachyose.

L'umbelliférose complètement méthylé se présente sous forme de sirop. Il est légèrement jaune. Rendement: 2,35 g. Analyse: CH_3O calc. pour $C_{20}H_{34}O_{10}$: 51,8 %; tr.: 49,5 %. $[\alpha]_D^{20}$: +110° (c = 0,8; eau); $[\alpha]_D^{20}$: +133° (c = 1,2; chloroforme).

2 g du produit méthylé sont dissous dans 100 ml d'acide sulfurique N/1 et chauffés à reflux dans un bain marie bouillant. Lectures du $[\alpha]_D^{20}$: Après 2 h: +52°; après 4 h: +49°. Après chauffage ultérieur le pouvoir rotatoire spécifique reste constant. Après 5 h de chauffage l'hydrolysat est neutralisé par le carbonate de baryum (10 g). La solution est filtrée et ensuite concentrée sous pression réduite. Le résidu est un sirop légèrement jaune. Rendement: 1,5 g.

1,2 g de ce sirop qui, aux chromatogrammes, se comporte comme un mélange de trois hexoses méthylés, est fractionné par chromatographie de partage sur une colonne de poudre de cellulose d'après Hough, Jones et Wadman [14]. Le diamètre intérieur de la

colonne est de 3 cm et la poudre de cellulose (Whatman Ashless Cellulose powder, Standard grade) est introduite sur une hauteur d'environ 65 cm. La phase mobile utilisée pour l'élution des oses méthylés est un mélange de *n*-butanol et d'éther de pétrole, saturé avec de l'eau: *n*-butanol: 3 vol/light petroleum, Eb: 100—120°, B.D.H. Londres: 7 vol. Nous avons récupéré de la colonne trois fractions distinctes, chromatographiquement homogènes, obtenues, après évaporation complète du solvant sous pression reduite, sous forme de sirops incolores ou légèrement jaunes. Rendements: Fraction I: 0,30 g; Fraction II: 0,30 g; Fraction III: 0,25 g.

6. Identification des trois fractions d'hexoses méthylés

Chaque fraction est d'abord purifiée par dissolution dans l'eau, traitement à environ 60° avec un peu de charbon actif, filtration à chaud et ensuite élimination de l'eau sous pression réduite.

Les valeurs de R_G données ci-dessous pour les différentes fractions sont déterminées par chromatographie sur papier avec la phase organique du système solvant: *n*-butanol: 50 vol/éthanol: 10 vol/eau: 40 vol. R_G exprime [15] la distance parcourue par un ose par rapport à la distance parcourue par le tétraméthyl-D-glucopyranose (pour lequel R_G = 1,00), observé sur le même chromatogramme.

Fraction I (0,25 g): Analyse: CH_3O calc. pour $C_{10}H_{20}O_6$: 52,5 %; tr.: 52,0 %. $[\alpha]_D^{20}$: +30,5° (c = 1; eau) R_G: 1,00. Au chromatogrammes la fraction I ne peut être distinguée du tetraméthyl-1,3,4,6-D-fructose, ajouté comme témoin. Les taches sont développées par l'oxalate d'urée et chauffage à 130°. Elles sont de couleur noire ou grise, différente de la couleur brune des taches produites par les méthylfructoses fixés sous forme pyranique [16,17]. Les propriétés trouvées à la fraction I sont identiques à celles signalées pour le tétraméthyl-1,3,4,6-D-fructose [18].

Fraction II (0,25 g): Analyse: CH_3O calc. pour $C_{10}H_{20}O_6$: 52,5 %, tr.: 51,8%. Lectures du $[\alpha]_D^{20}$: (c = 0,8; eau) Après 30 min: +122°, après 2 h: +111°, après 3 h: + 106°. Ensuite, il reste constant. R_G = 0,90. Déméthylation [19] par chauffage avec l'acide bromhydrique à 48 % donne du galactose, caractérisé par chromatographie sur papier. La fraction II, traitée par l'aniline, fournit un anilide qui fond à 196—198° (au microscope avec l'appareil de Kofler). Ce point de fusion n'est pas modifié par mélange avec un échantillon témoin de tétraméthyl-2,3,4,6 N-phényl-D-galactopyranosylamine. Le pouvoir rotatoire spécifique de l'anilide est initialement —70° (c = 1; acétone) avec une mutarotation très lente vers le droite. L'ensemble des résultats permet de conclure que la fraction II est identique au tétraméthyl-2,3,4,6-D-galactose [20].

Fraction III (0,20 g): Analyse: CH_3O calc. pour $C_9H_{18}O_6$: 41,9 %; tr.: 41.1 %. R_G = 0,85. La déméthylation [19] par chauffage avec l'acide bromhydrique à 48 % fournit du glucose. $[\alpha]_D^{18}$: 1) +67°, 2) +73° (c = 1; méthanol anhydre avec 2 % d'acide chlorhydrique). Aucune mutarotation ne peut être décelée. Ce résultat élimine la possibilité de la fraction

Tableau 3. Oxydation de la fraction III (triméthyl-3,4,6-D-glucose) par le periodate de sodium.

Triméthyl-D-glucose ..... 0,002 M, 5 ml
Metaperiodate de sodium ..... 0,01 M, 1,5 ml

Durée de contact à 20°—22° à l'abri de lumière	30 min	60 min.	20 h	48 h
Molécules [a] de periodate réduit	0,62 [b]	0,82	0,95	0,97
Molécules [a] d'acide volatil monovalent formées			0,80	0,89

(a) par molécule de triméthyl-D-glucose.
(b) Les chiffres représentent des moyennes de plusieurs expériences.

III étant identique au triméthyl-2,3,6-D-glucose, qui est le plus souvant caractérisé par l'inversion [21] de son pouvoir rotatoire dans le méthanol en présence d'acide chlorhydrique. On peut déjà constater celle-ci après 24 h dans les conditions expérimentales précisées ci-dessus [22]. Le $[\alpha]_D^{20}$ du triméthyl-3,4,6-D-glucose, au contraire, reste constant à environ +70° (méthanol + HCl) [22].

L'oxydation de la fraction III par le periodate de sodium fut étudiée suivant le procédé de Greville et Northcote [4], qui permet de distinguer d'une façon irréfutable le triméthyl-3,4,6-D-glucose des autres triméthyl-D-glucopyranoses. Nos résultats se trouvent exposés dans le Tableau 3. D'après Greville et Northcote [4] c'est uniquement le triméthyl-3,4,6-D-glucose qui, par oxydation periodique, donne naissance à une molécule d'acide volatil (formique) et qui d'ailleurs est capable de réduire rapidement le periodate. Le triméthyl-2,3,6,-D-glucose ne le réduit point [4]. L'ensemble de nos résultats permet de conclure que la fraction III est identique au triméthyl-3,4,6-D-glucose.

Nous adressons nos plus vifs remercîments à Monsieur le professeur J.-E. Courtois, Paris, qui a bien voulu mettre à notre disposition un échantillon purifié d'α-galactosidase des graines de café.

BIBLIOGRAPHIE

1. Bærheim Svendsen, A. *Zur Chemie norwegischer Umbelliferen* (Thèse) Université, Oslo 1954.
2. Haworth, W. N., Hirst, E. L. et Ruell, D. A. *J. Chem. Soc.* **123** (1923) 3125.
3. Courtois, J. et Wickstrøm, A. *Bull. soc. chim. biol.* **32** (1950) 759.
4. Greville, G. D. et Northcote, D. H. *J. Chem. Soc.* **1952** 1945.
5. Pigman, W. W. et Goepp, R. M. jr. *Chemistry of the Carbohydrates*, New York 1948.
6. Herrisey, H., Wickstrøm, A. et Courtois, J. *Bull. soc. chim. biol.* **34** (1952) 856.
7. Whistler, R. L. et Durso, D. F. *J. Am. Chem. Soc.* **72** (1950) 677.
8. Laidlaw, R. A. et Reid, S. G. *Nature* **166** (1950) 476.
9. Hirst, E. L. et Jones, J. K. N. *J. Chem. Soc.* **1949** 1659.
10. French, D. *Advances in Carbohydrate Chem.* **9** (1954) 149.
11. Fleury, P. et Boutot, L. *J. pharm. chim.* **26** (1922) 209.
12. Courtois, J.-E., Anagnostopoulos, C. et Petek, F. *Enzymologia* **17** (1954) 69.
13. Laidlaw, R. A. et Wylam, Clare B. *J. Chem. Soc.* **1953** 567.
14. Hough, L., Jones, J. K. N. et Wadman, W. H. *J. Chem. Soc.* **1949** 2511.
15. Hirst, E. L. et Jones, J. K. N. *Discussions Faraday Soc.* **1949** 268.
16. Bell, D. J. et Northcote, D. H. *Chemistry & Industry* **1954** 1328.
17. Mitchell, W. E. A. *Thèse Doct. Phil.*, Université, Edimbourg 1953.
18. Barry, C. P. et Honeyman, J. *Advances in Carbohydrate Chem.* **7** (1952) 53.
19. Hough, L., Jones, J. K. N. et Wadman, W. H. *J. Chem. Soc.* **1950** 1702.
20. Bell, D. J. *Advances in Carbohydrate Chem.* **6** (1951) 11.
21. Irvine, J. C. et Hirst, E. L. *J. Chem. Soc.* **121** (1922) 1213.
22. Gränichstädten, H. et Percival, E. G. V. *J. Chem. Soc.* **1943** 54.

Manuscrit reçu le 11 Mai 1956.

ACTA CHEMICA SCANDINAVICA 10 (1956) 1208—1214

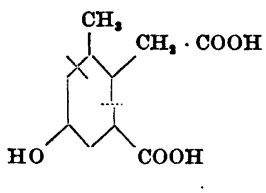
Cyclic Compounds from Acetylpyruvic Esters. Part III
Structure of the Acid $C_{10}H_{10}O_5$

ENDRE BERNER

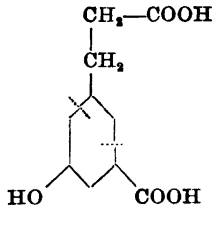
Universitetets Kjemiske Institutt, Blindern-Oslo, Norway

The following three aromatic hydroxy acids have been synthesized, a) 3-hydroxy-5-carboxyhydrocinnamic acid, b) 2-ethyl-5-hydroxybenzoic acid, and c) 2-ethyl-5-hydroxy*iso*phthalic acid. The acid c was found to be identical with the acid $C_{10}H_{10}O_5$ obtained by treatment of the hydrogenated condensation product of methyl acetylpyruvate with barium hydroxide.

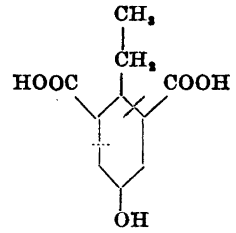
In part I of this series [1] it was shown that the condensation product of methyl acetylpyruvate (in short called methyl product), first described by Claisen [2] as being an open-chained compound, actually must have a cyclic structure. Already Claisen found that the methyl product on heating with barium hydroxide split off oxalic acid and gave 3-methyl-5-hydroxybenzoic acid. Besides verifying this we found that the hydrogenated methyl product, having taken up two moles of hydrogen, on heating with barium hydroxide gave the three compounds: oxalic acid, 3-methyl*cyclo*hexanone-5-carboxylic acid, and an aromatic hydroxy-dicarboxylic acid $C_{10}H_{10}O_5$ with m.p. 267°. For the latter we found that the structural formula I would be in agreement with most of the findings, although we were unable to prove the structure by degradation, either by decarboxylation or by oxidation. Later it was found that an acid with the structure I, 5-hydroxy-3-carboxy-*o*-tolueneacetic acid, had been synthesized by Meldrum and Vaidyanathan [3]. The synthetic acid, having the m.p. 210°, was quite different from our acid, a fact which was verified by repeating the synthesis, and formula I therefore had to be abandoned.



I

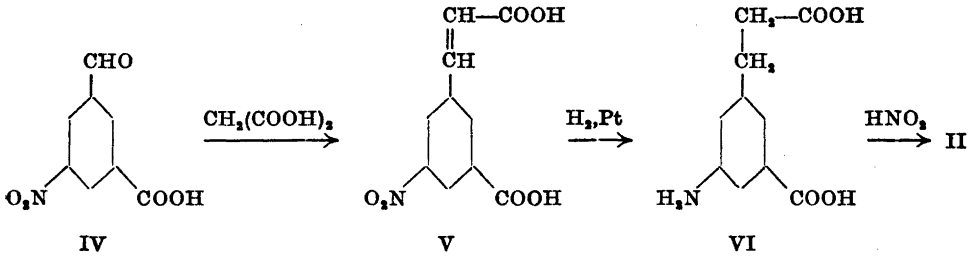


II



III

By further work on the structure of $C_{10}H_{10}O_5$ it was found that the main product obtained on decarboxylating the sodium salt by heating with calcium hydroxide was *p*-ethylphenol, a chromatographic investigation at the same time revealing that small amounts of *m*-ethylphenol and phenol were also formed during the decarboxylation. In order to explain the occurrence of the ethylphenols a structural formula II, 3-hydroxy-5-carboxyhydrocinnamic acid, for the substance $C_{10}H_{10}O_5$ was considered. A corresponding formula for the methyl product would contain the side-chain $-CH_2-CO-COOH$ and thus be able to explain that oxalic acid and 3-methyl-5-hydroxybenzoic acid are formed by treatment with barium hydroxide. The simultaneous occurrence of *p*- and *m*-ethylphenol would at any rate imply that either the ethyl or the hydroxyl group migrates during the decarboxylation. As indicated by dotted lines a skeleton as in formula II would be compatible with the formation of the methyl product from two molecules of acetylpyruvic ester. A synthesis of 3-hydroxy-5-carboxyhydrocinnamic acid (II) also showed, however, that this acid was different from our acid $C_{10}H_{10}O_5$.

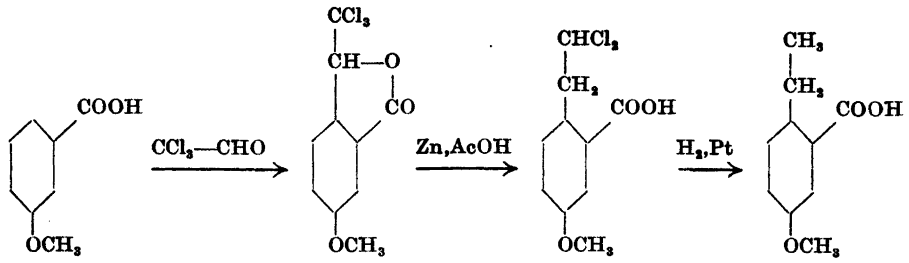


The synthesis was carried out in the following way: *Iso*phthalaldehydic acid on nitration gave 5-nitro*iso*phthalaldehydic acid (IV) in which the 5-position of the nitro group was proved by oxidation of IV to the known 5-nitro*iso*phthalic acid. Condensation of IV with malonic acid gave 3-carboxy-5-nitrocinnamic acid (V). On catalytic hydrogenation the latter was transformed into 3-carboxy-5-aminohydrocinnamic acid (VI) which was diazotized to 3-carboxy-5-hydroxyhydrocinnamic acid (II), having m.p. 200—202°.

The third possibility for the structure of $C_{10}H_{10}O_5$ which suggested itself was formula III, representing the 2-ethyl-5-hydroxy*iso*phthalic acid. It is *a priori* difficult to perceive how a skeleton as in formula III could be compatible with the simultaneous occurrence of the 3-methyl*cyclo*hexanone-5-carboxylic acid when the hydrogenated methyl product was treated with barium hydroxide, and with the formation of 3-methyl-5-hydroxybenzoic acid by treament of the methyl product itself with barium hydroxide. A satisfying explanation of this difficulty has, however, been found and will be dealt with in a later communication. Our present aim is to prove the correctness of formula III for the acid $C_{10}H_{10}O_5$.

As described in part I of this series a methyl ether of the acid $C_{10}H_{10}O_5$ could easily be prepared. A partial decarboxylation of this methyl ether was achieved by heating it with copper chromite, the main product being a crystalline methyl ether of a monobasic hydroxy acid. The corresponding hydr-

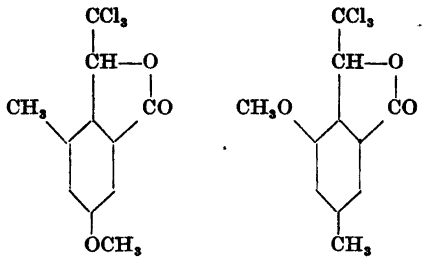
oxy acid, $C_9H_{10}O_3$, m.p. 155°, gave no colour with ferric chloride and on further decarboxylation in the usual way gave *p*-ethylphenol only. The product from the partial decarboxylation must therefore be the methyl ether of 2-ethyl-5-hydroxybenzoic acid (X) which was confirmed by the following synthesis.



VII VIII IX X

According to Fritsch [4] the main product of the reaction between *m*-methoxybenzoic acid (VII) and chloral hydrate in the presence of conc. sulphuric acid is 5-methoxy-2-trichloromethylphthalide (VIII). On heating with zinc powder and glacial acetic acid VIII was reduced to 2-β,β-dichloroethyl-5-methoxybenzoic acid (IX). The substance IX on catalytic dehalogenation gave 2-ethyl-5-methoxybenzoic acid (X) which was found to be identical with the product obtained by partial decarboxylation of the methyl ether of $C_{10}H_{10}O_5$.

Finally an acid with the structural formula III was synthesized along a similar line as that followed by the synthesis of the acid m.p. 155°. Meldrum [5] and later Meldrum and Vaidyanathan [3] showed that 5-methoxy-3-methylbenzoic acid (or its ester) reacted with chloral hydrate to give a mixture of 5-methoxy-3-methyl-2-trichloromethylphthalide (XI) and 3-methoxy-5-methyl-2-trichloromethylphthalide (XII), having m.p. 118° and 143°, respectively.

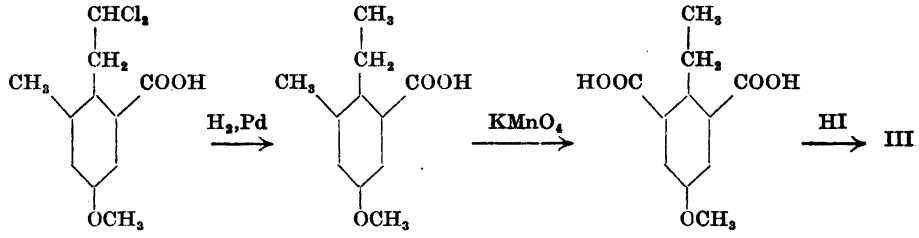


XI XII

A complete separation of the two isomers by crystallization is very difficult to achieve. On repeated crystallizations the lowest melting isomer (XI) was, however, accumulated in the mother liquors and could thus be obtained in a sufficient purity so as to ensure that it was really this isomer which formed the basis for the present synthesis. Having established this fact it was in later

experiments found to be practical to separate the isomeric trichloro-compounds only partially and to use the lower melting, more soluble fraction for the synthesis. A final separation of isomeric reaction products was then undertaken at a later stage as described in the experimental part. The structures of the two isomers XI and XII have been ascertained by Meldrum and Vaidyanathan [3] by transforming them into 5-hydroxy-3-methylphthalic acid (β-coccinic acid) and 3-hydroxy-5-methylphthalic acid (γ-coccinic acid), respectively.

The isomer XI on treatment with zinc powder in glacial acetic acid gave 2-β,β-dichloroethyl-5-methoxybenzoic acid (XIII) which was dehalogenated catalytically to 2-ethyl-3-methyl-5-methoxybenzoic acid (XIV).



XIII XIV XV

The oxidation of XIV to 2-ethyl-5-methoxy*iso*phthalic acid (XV) was effected by potassium permanganate in alkaline solution. The fact that the methyl group alone and not the ethyl group was oxidized must be due to steric hindrance. In the oxidation product itself (XV) in which both *ortho* positions to the ethyl group are occupied by carboxyl groups the steric hindrance is so pronounced that the substance cannot be oxidized at all without breaking up the molecule. The methyl ether XV on treatment with hydroiodic acid gave the corresponding hydroxy acid (III) which had the m.p. 267° and was found to be identical with the acid $C_{10}H_{10}O_5$ obtained from the hydrogenated methyl product.

As mentioned above the decarboxylation of $C_{10}H_{10}O_5$ by the classical method led mainly to *p*-ethylphenol with *m*-ethylphenol and phenol as minor products. In view of formula III the explanation of this result must be that the ethyl group migrates. In some cases it will thereby occupy the position of a carboxyl group when this is expelled, in other cases the ethyl group will not re-enter the molecule at all and phenol will be the final product.

EXPERIMENTAL

(Melting points not corrected)

3-Hydroxy-5-carboxyhydrocinnamic acid

(In part with Stud. real. Asbjørn Baklien)

m-Carboxycinnamic acid, prepared by conventional methods from *m*-nitrocinnamic acid, had m.p. 268–270°. (Found: C 62.27; H 4.21; M by titration 194; Calc. for $C_{10}H_8O_4$ (192.2): C 62.50; H 4.20.). Oxidation to *iso*phthalaldehydic acid: To a solution of *m*-carboxycinnamic acid in 50 ml N sodium carbonate and 400 ml water were added slowly

at 4—5° 80 ml 5 % potassium permanganate, stirring vigorously. The filtrate from manganese dioxide was concentrated to about 150 ml and acidified with 5 N hydrochloric acid, when a mixture of *iso*phthalaldehydic acid, isophthalic acid and unoxidized *m*-carboxycinnamic acid separated. In order to isolate the aldehydic acid, the solid mixture as well as the filtrate from it were extracted with ether in which the two last-mentioned acids are sparingly soluble. The crude *iso*phthalaldehydic acid (3.6 g) was recrystallized from water and had then m.p. 173°.

Nitration: A solution of *iso*phthalaldehydic acid (1.6 g) in conc. sulphuric acid (13 ml) was cooled to +5° and 1.23 g finely powdered potassium nitrate added in small portions. The solution was stirred until all nitrate had dissolved, keeping the temperature below 10°. During half an hour the temperature was raised to 35° and finally to 105—110° where it was kept for 15 min. Pouring the cooled solution on ice some un-nitrated substance (0.7 g) separated. The filtrate from this on extraction with ether gave the nitro*iso*phthalaldehydic acid as a yellow oil (1.0 g) which crystallized slowly when kept in a desiccator. The m.p. was not sharp, clear at 150°, but no attempt was made to recrystallize the acid. In order to prove the position 5 for the nitro group a small quantity of the substance (0.2 g) was oxidized with potassium permanganate to the corresponding nitro*iso*phthalic acid. The methyl ester of the oxidation product (prepared by means of diazomethane) had m.p. 123° and was identical with the methyl ester of the nitrated *iso*phthalic acid.

The 5-nitro*iso*phthalaldehydic acid was condensed with malonic acid, using a method given by Brand and Horn [6]: A mixture of the nitro acid (1 g), malonic acid (0.7 g), pyridine (3 ml), and piperidine (0.3 ml) was heated for half an hour to 70—80°. On raising the temperature to 100° carbon dioxide began to evolve. The temperature was finally raised to 140° and the heating discontinued after 2 ¼ hours. By addition of hydrochloric acid the 5-nitro-3-carboxycinnamic acid separated crystalline (1.2 g). It was recrystallized twice from water, using some Carbex E, and had m.p. 207—211°.

The simultaneous saturation of the double bond and the reduction of the nitro group were effected by catalytic hydrogenation. A solution of 5-nitro-3-carboxycinnamic acid (0.46 g) in methanol (25 ml) to which PtO_2 (0.1 g) had been added did not at first take up any hydrogen. Only after adding more PtO_2 (0.1 g) did the solution in the course of two hours consume 154 ml hydrogen (1 ½ atm.), calculated 160 ml. The filtered solution on evaporation left the amino acid as an oil (0.42 g) which was diazotized directly according to the following method given by Fieser and Lothrop [7]. A solution of the amino acid in 4 ml N sodium carbonate was diluted with water to 6 ml and 0.14 g sodium nitrite in 1 ml water added. The solution was cooled with ice and added slowly under stirring to a mixture of 0.8 ml conc. hydrochloric acid, 4—5 g ice and 0.25 g boric acid. On heating, first on a water-bath, later to boiling, gas evolved. By extraction of the solution with ether the 5-hydroxy-3-carboxyhydrocinnamic acid was obtained as a crystalline, slightly red-coloured mass with m.p. 200°. After recrystallizing twice from water, adding some Carbex E, the acid became practically colourless, m.p. 200—202°. It gave no colour with ferric chloride. (Found: C 57.48; H 4.82. Calc. for $C_{10}H_{10}O_5$ (210.2): C 57.14; H 4.76.)

2-Ethyl-5-hydroxybenzoic acid

3-Methoxybenzoic acid (5.0 g) and chloral hydrate (5.4 g) were dissolved in conc. sulphuric acid (25 ml) and left at room temperature for 24 hours. On dilution with ice and water an oil separated which immediately crystallized. The crystalline mass was crushed in a mortar and recrystallized from ethanol. The first fraction (5.5 g) had m.p. 139° (Fritsch [4] gave m.p. 135°) and the second fraction (1.6 g) m.p. 135—138°. A solution of the first fraction in glacial acetic acid (50 ml) was refluxed for 1 ½ hours with zinc powder (20 g). After adding water (30 ml) the refluxing was continued for half an hour. The clear solution decanted from excess of zinc powder on cooling separated needles (4.0 g) with a somewhat unsharp m.p., clear at 187°. This substance was dissolved in pure methanol (40 ml) and the solution after adding platinum oxide (0.25 g) shaken in an atmosphere of hydrogen. In the course of 1 ½ hours 1 110 ml hydrogen were absorbed. The filtrate from the platinum on evaporation in a vacuum gave a crystalline, halogen-free product (2.9 g) with m.p. about 65°, being the methyl ether of 2-ethyl-5-hydroxybenzoic acid. It was demethylated by refluxing for 3/4 hour with hydroiodic acid (10 ml,

d 1.7). The free hydroxy acid after crystallizing from water had m.p. 155° and showed no depression on mixing with the acid from the partial decarboxylation of $C_{10}H_{10}O_5$. (Found: C 64.97; H 6.05; M by titration 164. Calc. for $C_9H_{10}O_3$ (166,2): C 65.05; H 6.07.)

2-Ethyl-5-hydroxy*iso*phthalic acid

3-Methyl-5-methoxybenzoic acid (22.5 g) and chloral hydrate (22.5 g) were dissolved in conc. sulphuric acid (110 ml). The temperature rose slowly to 29° and then fell again. After standing for 24 hours at room temperature the solution was poured in ice-water. The viscous mass which separated crystallized overnight. It was crushed, filtered, washed and dried (38.7 g) and then crystallized from methanol.

Fraction	I, filtered after short time	21.6 g	m.p.	clear at	115°
»	II, filtered next day	7.8 »	»	» »	112°
»	III, after dilution with water	4.2 »	»	» »	114°

The fractions were treated separately with zinc powder in glacial acetic acid. Fraction I and zinc powder (8 g) in glacial acetic acid (45 ml) reacted on shaking and the solution became warm. In order to finish the reaction the shaking was continued for 3 hours. Afterwards some crystalline material which had separated was redissolved by heating and the solution filtered from excess of zinc. On subsequent addition of water the reduction product (IA, 15.2 g) separated crystalline. Fraction II on treatment in the same way with 3 g zinc powder gave 5.3 g crystalline product (IIA). Equivalent weight by titration 261, calc. for $C_{11}H_{12}O_3Cl_2$ 263. Fraction III on treatment with zinc gave only a partly crystalline reduction product which was discarded.

The fractions IA and IIA were combined and recrystallized from glacial acetic acid and two fractions were collected. Fraction IVA (5.5 g) which separated directly on cooling was not used for further treatment. Fraction IVB (12.8 g) obtained after dilution with water had equiv. wt. 260; it was dehalogenated in the following way. A solution of fraction IVB in 180 ml pure methanol to which had been added 105 ml 25 % methanolic KOH and 6.5 g catalyst (aluminum oxide with 5 % Pd) was shaken in an atmosphere of hydrogen for two hours when about 3 l hydrogen had been adsorbed. On diluting the filtered solution with water the dehalogenated product separated crystalline (7.5 g). It consisted of the methyl ethers of the two isomeric ethylmethylhydroxy-benzoic acids which could be separated by crystallization from petrol ether (45—68°). A solution obtained by refluxing the mixture with 200 ml petrol ether was allowed to evaporate slowly at room temperature in a beaker. The one component crystallizing in thin needles crept up the wall of the beaker. After recrystallization from dilute ethanol it had m.p. 137° and analyzed correctly for a methyl ether of ethylmethylhydroxy-benzoic acid. The other component separated mostly at the bottom of the beaker as clear prisms which could easily be collected (1.7 g). Recrystallized from dilute ethanol, m.p. 90°. (Found: C 68.11; H 7.45; OCH_3 15.98; M by titration 193. Calc. for $C_{11}H_{14}O_3$ (194.2): C 68.02; H 7.27; OCH_3 15.98.) Preliminary experiments had shown that the methyl ether m.p. 90° was derived from the lowest melting of the isomeric trichloro-compounds XI and XII. It must therefore be the 2-ethyl-3-methyl-5-methoxybenzoic acid. Oxidation: The methyl ether (1.6 g) dissolved in 12 ml N sodium hydroxide and 250 ml water was heated on the steam-bath and a solution of 3.1 *g* potassium permanganate (20 % excess) in water (60 ml) added in small portions. After 6 hours the filtrate from manganese dioxide was concentrated to 100 ml and 5 N hydrochloric acid added. The crystalline precipitate (1.2 g) was recrystallized from glacial acetic acid; m.p. 186°, no depression on admixture. It was demethylated by refluxing 1/4 hour with hydroiodic acid. The crude hydroxy acid had m.p. 267° and the m.p. was not altered either on recrystallization from water or on mixing with $C_{10}H_{10}O_5$ prepared from acetylpyruvic ester. (Found: C 57.03; H 4.82. Calc. for $C_{10}H_{10}O_5$ (210.2): C 57.14; H 4.76.)

Decarboxylation of $C_{10}H_{10}O_5$

(With Magister Odd Leander Johansen and Cand. real. Agnes Thoresen)

The sodium salt of the methyl ether of $C_{10}H_{10}O_5$ (3 g) was mixed with twice its weight of calcium hydroxide and heated in a glass tube through which nitrogen passed slowly. The distillate (0.6 ml) was demethylated by refluxing for half an hour with 3 ml hydro-

iodic acid (1.7). The free phenol was taken up in ether, the solution shaken with sodium carbonate and thiosulphate. On distillation the phenol went over at 200—220°. The following derivatives were prepared. 1) Phenylurethane, after recrystallization from petrol ether, m.p. 117—119°. (Found: C 74.98; H 6.29; N 6.20. Calc. for $C_{15}H_{15}O_2N$ (241.3): C 74.66; H 6.27; N 5.81.) The phenylurethane prepared from authentic *p*-ethylphenol had m.p. 120°, mixed m.p. 118—119°. 2) *p*-Ethylphenoxyacetic acid prepared by reaction with monochloroacetic acid and sodium hydroxide; recrystallized from benzene plus petrol ether, m.p. 94°. Prepared from authentic *p*-ethylphenol, m.p. 96—97°, mixed m.p. 96°. 3) Benzoyl derivative crystallized from dilute ethanol, m.p. 55—57°. Corresponding derivative from *p*-ethylphenol, m.p. 60°.

A chromatographic analysis of the product from the decarboxylation was later carried out according to the method of Hossfeld [8]. The product was coupled with diazotized sulphanilic acid and the dyestuffs extracted with ether. Drops of the concentrated ethereal solution were placed on a filter paper (Whatman no 1) which beforehand had been treated with sodium carbonate. For comparison coupling-products of *p*- and *m*-ethylphenol, *p*- and *m*-cresol and phenol were placed on the same paper. The mobile phase was methyl ethyl ketone saturated with water. The chromatogram showed in all five spots of which two were very weak. One yellow spot corresponded to *m*-ethylphenol, one reddish spot to *p*-ethylphenol and another yellow spot to phenol. The two spots of the ethylphenols were of about the same intensity and control experiments showed that mixtures of *m*- and *p*-ethylphenol containing only a minor quantity of the *meta* isomer (5—10 %) would give spots of about equal intensity. The two very weak spots had the same position as those of *m*- and *p*-cresol.

Partial decarboxylation of the methyl ether of $C_{10}H_{10}O_5$: The methyl ether (1.16 g) was mixed with copper chromite (0.3 g) and heated in a test tube through which a slow current of nitrogen passed. At about 290° decarboxylation set in and the temperature was finally raised to 330°. The liquid distillate (0.83 g) crystallized overnight. A sample pressed on porous tile had m.p. 65°. The rest was demethylated in the usual way. The free hydroxy acid after recrystallization from water had m.p. 154°. (Found: C 64.50; H 5.98; M by titration 165.8. Calc. for $C_9H_{10}O_3$ (166.2): C 65.05: H 6.07.)

Most of the synthetic work described in this paper was carried out during a stay in London. The author wants to express his sincere thanks to Dr. R. P. Linstead F.R.S., Rector, of the Imperial College of Science and Technology, at that time Director of the Chemistry Department, for his great kindness in receiving me as a guest in his department. Grants from *Norges Almenvitenskapelige Forskningsråd* and *Fridtjof Nansens Fond* are acknowledged. Magister Odd Leander Johansen wants to thank *A/S Lilleborg Fabrikers Jubilæumsgave* for a scholarship.

REFERENCES

1. Berner, E. and Laland, S. *Acta Chem. Scand.* **3** (1949) 335.
2. Claisen, L. *Ber.* **22** (1889) 3271.
3. Meldrum, A. N. and Vaidyanathan, K. S. *Proc. Indian Acad. Sci.* **1 A** (1935) 510.
4. Fritsch, P. *Ann.* **296** (1897) 344.
5. Meldrum, A. N. *J. Chem. Soc.* **99** (1911) 1712.
6. Brand, K. and Horn, O. *J. prakt. Chem.* [2] **115** (1927) 374.
7. Fieser, L. F. and Lothrop, W. C. *J. Am. Chem. Soc.* **58** (1936) 2050.
8. Hossfeld, R. L. *J. Am. Chem. Soc.* **73** (1951) 852.

Received May 14, 1956.

ACTA CHEMICA SCANDINAVICA 10 (1956) 1215—1227

Studies on the Interaction of Paraffin Chain Alcohols and Association Colloids

IX. The Solubility of Decanol-1 in Solutions of Sodium Caprate, Laurate and Myristate above the C.M.C.

KAAPO PASSINEN and PER EKWALL

Institute of Physical Chemistry, Åbo Akademi, Åbo, Finland

The maximum amounts of decanol that are solubilized by sodium caprate, laurate and myristate solutions before they become turbid have been determined at concentrations above the C.M.C. The solubility curves are linear over a wide concentration range above the C.M.C., slope upwards in a narrow range (A) and continue again as straight lines. Two concentration ranges can hence be distinguished above the C.M.C. with respect to the solubility of decanol, one from the C.M.C. to the break point A and another above this latter point. The break point A in the solubility curve shifts to lower soap concentrations as the number of carbon atoms in the soap increases in the homologous series, but also other factors operate here. The ratios of decanol to soap in the mixed micelles at the turbidity points in the different soap concentration ranges have been calculated from the slopes of the solubility curves. The maximum decanol content of the mixed micelle decreases with increasing number of carbon atoms in the hydrocarbon chain of the soap both in the range between the C.M.C. and the break point A and in the range above the latter point. The maximum decanol content of the mixed micelles depends also on the nature of the ionic group in the association colloid and on the gegenions. It is shown that in the concentration ranges where the break points A are located in the solubility curves also other changes typical of the *2nd* C.M.C. occur in the properties of the solutions. The meaning of the *2nd* C.M.C. and the factors responsible for the separation of the mesomorphic phase that causes the turbidity are discussed.

In Part VIII [1] of this series it was shown how the solubility of decanol varies with the soap concentration in dilute sodium caprate, laurate and myristate solutions. It was found that the first slight increase in solubility occurs already above the limiting association concentration, L.A.C., but that the solubility then passes through a maximum. After a minimum at a concentration about one-third of the critical micelle concentration (C.M.C.) of the pure soap, the

solubility of decanol begins to increase again, the increase being now appreciable. The C.M.C.'s of the decanol-containing soap solutions, *i.e.*, the concentrations where mixed micelles begin to form to a greater extent, are located at these points.

In the present paper data are reported on the solubility of decanol in solutions of the soaps mentioned in the concentration range above the C.M.C. The solubility discussed here is, as in Parts I [2] and VIII [1] of this series, the maximum solubility in the aqueous solution before it becomes turbid owing to the separation of a mesomorphic phase composed of decanol, soap and water. The heterogeneous system as a whole can, as we have shown previously [3-6], bring further, large amounts of decanol into solution, but the decanol is incorporated within the new phase. The solubility relationships when decanol is added in excess of the amount required to produce the turbidity are not considered in this paper.

Previous studies have shown that the micellar substance in solutions of association colloids has constant properties in a relatively wide concentration range above the C.M.C. (in the so-called small micelle range) [7,8]. The saturation capacity of the micellar substance (the solubilizing power expressed as the amount of solubilized substance per mole of micellar soap) has been found to be constant for *p*-xylene, benzene and other hydrocarbons [7,9]. In Part I [2] of this series it was shown that also the maximum amount of decanol that is incorporated in sodium oleate and sodium myristyl sulphate micelles at the turbidity point remains constant over practically the whole small micelle range. We have pointed out earlier that this is the case also for sodium caprate, laurate and myristate solutions [2,3]. The experimental evidence is presented here.

Our earlier studies [2] showed, however, that the linear course of the solubility curve of decanol in solutions of sodium oleate and sodium myristyl sulphate ends at a higher concentration; the curve bends upwards at first and then downwards. The break point is situated in approximately the same concentration range in which the solubilizing power for *p*-xylene and benzene begins to increase more rapidly than at lower concentrations [7,8] and where also many other properties of the solutions undergo a change (see Part IV [6]). Similar results have later been obtained by Markina, Posspelova and Rebinder [10] who studied the solubility of the hydrocarbons benzene, cyclohexane, octane and dodecane and of the polar-nonpolar compounds octanol and acrylonitrile in solutions of sodium oleate. These observations support the view that important changes occur in the properties of oleate (and myristyl sulphate) solutions in the concentration range in question so that one has to assume that changes also occur in the micellar structure. We have investigated whether a corresponding change can also be established in the power of concentrated caprate, laurate and myristate solutions to solubilize decanol.

MATERIALS AND METHODS

The fatty acids were products of Eastman Kodak Co., Rochester. They were recrystallized twice from absolute ethanol. The melting points of the fatty acids were 31.0–31.5°C for capric acid, 42–43°C for lauric acid and 56–57°C for myristic acid. The soaps were prepared in the usual manner by neutralizing the fatty acid with sodium

ethylate in absolute ethanol. The decanol-1 was that used in previous investigations of this series [2].

The solutions were prepared and the solubility was measured as described in Part I [2]. The temperature was 40°C. The solubility values are estimated to be accurate to about ±0.1 ml of decanol per litre of solution in most cases but are perhaps slightly less accurate for the most concentrated myristate solutions owing to the fact that these solutions are gel-like at 40°C and hence very difficult to work with.

The concentrations of the soap solutions are given in moles of soap per 1 000 g of soap solution and denoted by *M*.

EXPERIMENTAL RESULTS

The solubility of decanol has been studied in the following concentration ranges: sodium caprate 0.08—0.5 *M*, sodium laurate 0.02—0.6 *M*, sodium myristate 0.006—0.2 *M* and potassium myristate 0.01—0.06 *M*.

Figs. 1, 2 and 3 show how the solubility of decanol varies with the soap concentration. The solubility values reported in Part VIII have been marked with crosses in these figures; the curves joining the new solubility values (marked with circles) are seen to be continuations of the previously drawn curves. In the case of all soaps the solubility begins to increase definitely a little below the C.M.C. of the pure soap. The solubility curves rise steeply and exhibit a constant slope. The linear course is maintained over a comparatively wide concentration range. In the case of all three soaps there then follows a narrow range (A) where the curves bend upwards and continue as straight lines. (In the solubility curve of myristate (Fig. 3) a weak suggestion of a downward trend can be noted at still higher concentrations. The determination of the course of the curve in this region was a little uncertain owing to the

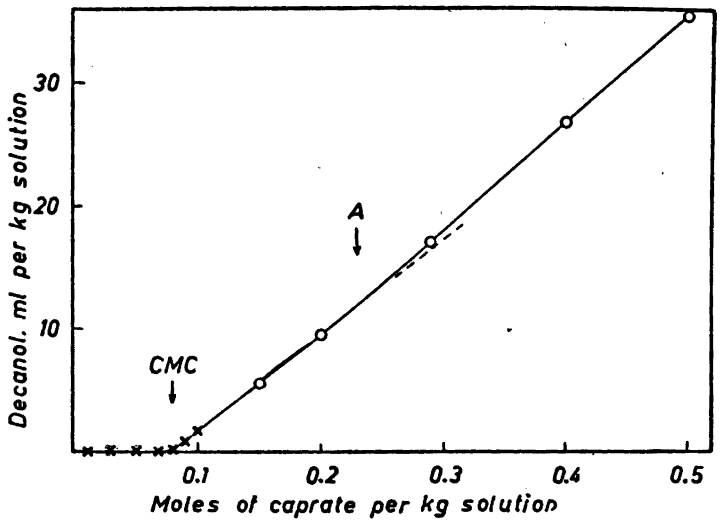


Fig. 1. The maximum amounts of decanol dissolved at the turbidity point in solutions of sodium caprate. 40°C.

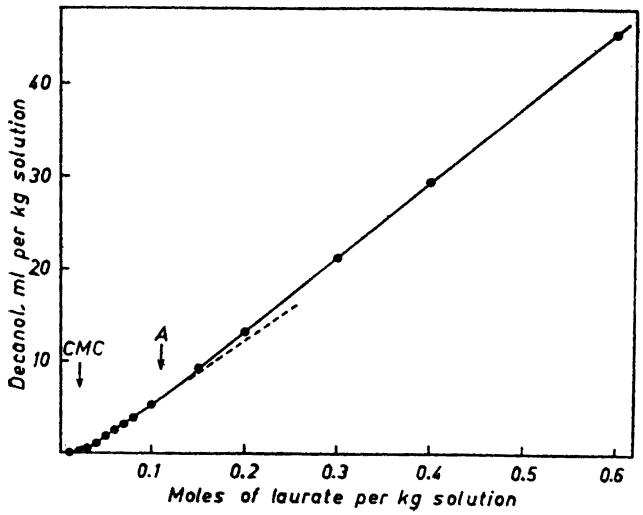


Fig. 2. The maximum amounts of decanol dissolved at the turbidity point in solutions of sodium laurate. 40°C.

difficulty of determining the solubility of decanol in sodium myristate solutions of higher concentrations than about 0.2 *M*; both the pure and the decanol-containing solutions are very viscous in this concentration range.) Above the C.M.C. two concentration ranges can hence be distinguished with respect to the solubility of decanol: one from the C.M.C. to the break point A and another above this latter point.

It should be emphasized that the solubility of sodium myristate in water is so low at 40°C that separated sodium myristate appears in pure myristate

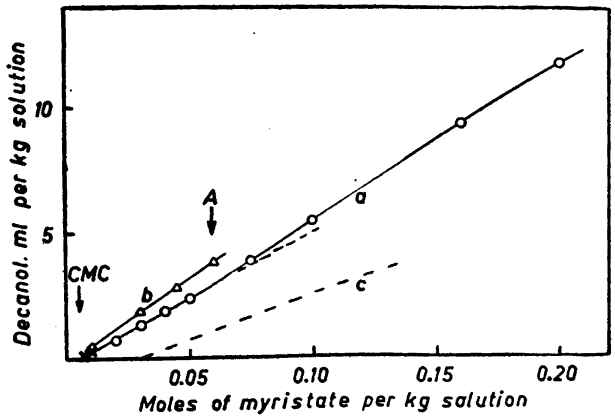


Fig. 3. The maximum amounts of decanol dissolved at the turbidity point. 40°C. a) Sodium myristate solutions, b) Potassium myristate solutions, c) Boundary line separating clear and turbid (lower right) solutions, the turbidity being caused by separated myristate.

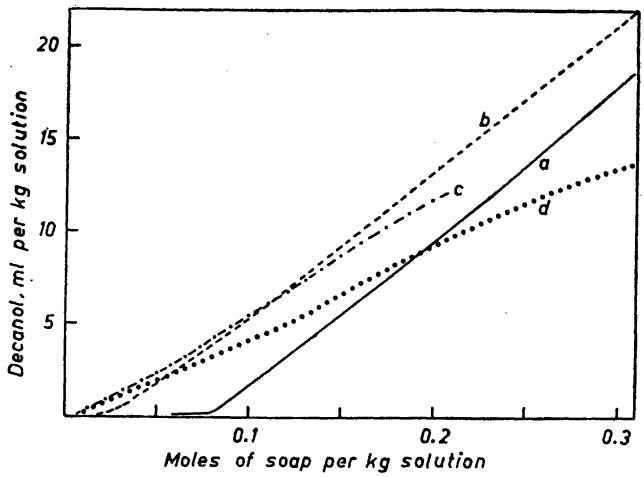


Fig. 4. The maximum amounts of decanol dissolved at the turbidity point. 40°C. a) Sodium caprate solutions, b) Sodium laurate solutions, c) Sodium myristate solutions, d) Sodium oleate solutions.

solutions above about 0.03 *M* in concentration [11]. The solubility of the soap increases, however, when decanol is added to the system. The dotted curve in Fig. 3 has been drawn on the basis of some scattered observations; it gives the approximate amounts of decanol needed to prevent the separation of myristate. Below the dotted curve, the system is heterogenous owing to separated myristate. Between the dotted and the continuous curves, the system is homogeneous but becomes heterogeneous again above the latter curve owing to the separation (above the L.A.C.) of the decanol-myristate-water phase.

The solubility of decanol in potassium myristate solutions was determined at only four soap concentrations (Fig. 3, curve b).

With the purpose of making possible a direct comparison of the solubility curves, the curves for the three soaps and the corresponding curve for sodium oleate have been plotted in the same diagram, Fig. 4. It can be seen that the slopes of the first linear parts of the curves for laurate, myristate and oleate between the C.M.C. and the break point A decrease with increasing number of carbon atoms in the soap; the result is that the curves intersect.

DISCUSSION

The solubility of decanol and its relationship to the molecular structure of the soap and the concentration of the soap solution. It is believed that the molecules of solubilized higher alcohols enter into the palisade layers of the micelles, whereupon mixed micelles are formed. The solubility which results from the solubilization in the micelles is, however, limited by the separation of a new phase composed of decanol, soap and water. As we have already pointed out, the appearance of the new phase does not mean that the system as a whole is

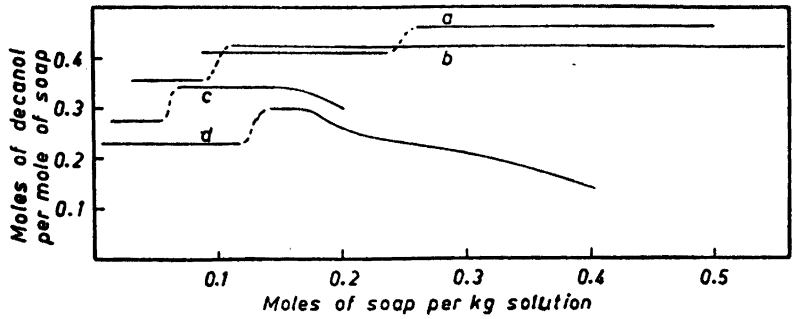


Fig. 5. The decanol content per mole of soap in the mixed micelles. 40°C. a) Sodium caprate solutions, b) Sodium laurate solutions, c) Sodium myristate solutions, d) Sodium oleate solutions.

saturated with decanol. The solubility curves drawn in the figures give only the maximum amounts of decanol which the micelles are able to dissolve before the new phase separates. Hence the solubility values measured at the turbidity point when a polar substance such as a long chain alcohol or fatty acid is solubilized are not comparable with the solubility values obtained in the solubilization of nonpolar compounds since the latter values give the real saturation points above which the pure solubilizate separates [2,7,8]. This difference has been recently stressed also by Hyde, Langbridge and Lawrence [12].

It has previously been customary to compare the solubilities of alcohols (and also hydrocarbons) at the same and often only one concentration of different soaps [13]. Since, as shown by the curves in Fig. 4, the solubility curves have different slopes for different soaps, the results of the comparison depend on the soap concentration chosen. A better survey is obtained when, as has been done in the present study, the slopes of the solubility curves are compared.

The slope of the solubility curve at a certain soap concentration, ∂(solubility)/∂(soap concentration), gives the ratio of decanol and soap in the mixed

Table 1. The compositions of the mixed micelles at the turbidity point expressed as moles of decanol per mole of micellar soap.

Association colloid	Concentration range	Composition, moles of decanol per mole of soap	Break point A	Concentration range	Composition, moles of decanol per mole of soap	Increase of the decanol content of mixed micelles above the break point A (%)
Na-caprate	0.08—0.22 *M*	0.41	0.23 *M*	0.24—0.5 *M*	0.46	12
Na-laurate	0.03—0.10 *M*	0.36	0.11 *M*	0.12—0.6 *M*	0.42	19
Na-myristate	0.01—0.05 *M*	0.28	0.06 *M*	0.07—0.16 *M*	0.34	24
				0.2 *M*	0.30	
K-myristate	0.01—0.05 *M*	0.36				

micelles formed at the soap concentration in question when the turbidity appears. The composition of the mixed micelles is different in different soap concentration ranges, as shown in Fig. 5 and Table 1. The decanol content of the mixed micelles is seen to decrease with the number of carbon atoms in the hydrocarbon chain of the soap both in the range between the C.M.C. and the break point A and in the range above the latter point. The relative increase in the decanol content of the mixed micelles varies in a similar manner in both ranges (Table 1, last column). From Fig. 5 it is also seen that the compositions of the decanol-caprate and decanol-laurate mixed micelles remain constant above the break point over the range studied, whereas the decanol content of the decanol-myristate micelles remains constant at first, but decreases at the higher myristate concentrations. In the case of sodium oleate and sodium myristyl sulphate [2], there is practically no concentration range above the break point where the composition of the mixed micelles remains constant; the decrease in the decanol content of the mixed micelles begins after a very short linear range of fairly high solubility values.

That the decanol content of the mixed micelles at the turbidity point is not dependent solely upon the length of the hydrocarbon chain of the soap is shown by the collected experimental data and has also been emphasized earlier [2]. The nature of the ionic group of the colloid and the presence of a double bond influence the mixed micelle composition. For instance, the decanol content of the mixed decanol-myristyl sulphate micelles in moles per mole of colloid is about 47 % higher than that of the decanol-myristate mixed micelles in both ranges above and below the break point. If the decanol content decreases in the same proportion with increasing chain length as in the series caprate, laurate and myristate, the decanol-stearate mixed micelles should contain 0.12 and 0.18 mole of decanol per mole of soap in the ranges below and above the break point, respectively. For oleate with 18 carbon atoms, considerably higher values, 0.23 and 0.30 mole of decanol per mole of oleate, are obtained [2]; this is evidently to be ascribed to the presence of the double bond in the oleate molecule. Also the gegenion appears to exert some influence since the decanol content on the mixed micelles is higher in potassium myristate solutions than in sodium myristate solutions.

It can be further seen from Fig. 5 that the break point A in the solubility curve shifts to lower soap concentrations as the number of carbon atoms in the soap increases in the homologous series. Also other factors seem to operate here, since the break points lie higher in the curves for oleate and myristyl sulphate than in the myristate curve.

The "Second Critical Concentration". As mentioned in the introduction, we have previously observed that the break point in the solubility curve for decanol lies in oleate and myristyl sulphate solutions in the same narrow concentration range in which also other properties of these solutions undergo marked alterations. We have therefore considered it appropriate (for the lack of a better name) to call this narrow concentration range the "second critical concentration" (*2nd* C.M.C.). Since a similar variation has now been observed in the alcohol solubility in solutions of the saturated fatty acid soaps, it is of interest to examine on the basis of previously reported experimental data whether also other properties of the solutions of these soaps undergo a change

in the concentration range where the break point occurs. It should be noted in this connection that the break points in the decanol solubility curves occur at soap concentrations that are a little lower than those in which changes can be expected to occur in pure soap solutions. This was found to be the case for the oleate and the myristyl sulphate solutions; similarly as decanol lowers the C.M.C. slightly, the "second critical concentration" is evidently also shifted to a lower concentration in the presence of decanol.

One of us has previously shown that the amount of *p*-xylene solubilized at 40°C by sodium myristate solutions increases linearly with the colloid concentration (*i.e.*, the saturation capacity of the micellar substance remains constant) in the concentration range between 0.03 *M* and 0.06 *M*, but increases more rapidly (the saturation capacity has a greater value) above the latter concentration [7]. It has also been found that the equivalent conductance of sodium myristate passes through a shallow minimum at the approximately 0.14 *M* soap concentration (35—80°C) (the change in equivalent conductance is very slight above the 0.08 *M* concentration) [14]. An inspection of the $\partial\varkappa/\partial c$-concentration curve shows that after a rapid fall above the C.M.C. the curve continues horizontally up to the approximately 0.1 *M* concentration and then bends upwards. The break point in the decanol solubility curve is situated in the range from 0.055 *M* to 0.065 *M*.

McBain, Laing and Titley [15] found that a conductance minimum occurs in potassium laurate solutions at the approximately 0.13—0.15 *M* concentration; the horizontal part of the $\partial\varkappa/\partial c$-curve terminates already when the soap concentration is about 0.10 *M*. The break point in the decanol solubility curve occurs approximately in the 0.10—0.12 *M* range.

It is thus seen that also other changes typical of the *2nd* C.M.C. occur in the properties of solutions of at least two of the three soaps in the concentration range where the break point A in the decanol solubility curve is located.

According to Mysels and Dulin [16], the minimum in the equivalent conductance curve (Λ *vs.* $\sqrt{c}$) cannot be taken as an indication that the nature of the solution changes in this region. They emphasize that the specific conductance-concentration curves for soap solutions above the C.M.C. show a continuous upward curvature and that this curvature is almost constant but increases slightly and regularly. We have inspected from this viewpoint numerous conductance measurements of different association colloids by different investigators [4,5,11,14,15,17-22] and found that in nearly all cases the $\varkappa$-*c*-curve is linear and the $\partial\varkappa/\partial c$-curve consequently horizontal over a fairly wide concentration range above the C.M.C. The $\varkappa$-*c*-curve bends upwards at a concentration only slightly below that at which the minimum occurs in the Λ-$\sqrt{c}$-curve; consequently also the $\partial\varkappa/\partial c$-curve deviates from the horizontal at this point. (This applies also to sodium myristate, potassium laurate, sodium oleate and sodium myristyl sulphate.) The conclusion of Mysels and Dulin thus appears to be based on an erroneous interpretation of the experimental data. For the present it seems to us that the course of the conductance curve in the neighbourhood of the minimum of the equivalent conductance (Λ) must be considered a sign that a new factor begins to operate and effects a change in the process of micellization. This is supported by the changes observed in the decanol solubility. New conductance measurements are required before any further conclusions can be drawn.

As the number of micelles increases, a point is sooner or later reached where the electrical double layers of the micelles approach each other so closely that their charged surface layers begin to interfere with each other. This type of interaction may be considered the primary cause of the changes observed in the

properties of colloid solutions at the *2nd* C.M.C. Even if this explanation is sufficient for some of the changes, it can hardly apply to others, *e.g.*, to the variation of the solubilizing power. It is difficult to understand how the interaction between the charged micelle surfaces can alone effect a greater solubilization of hydrocarbons or an increase of the alcohol content of the mixed micelles without the occurrence of a parallel change in the micellar structure. On the basis of various observations many investigators have concluded that only one type of micelle exists, namely, that which is produced in the concentration range immediately above the C.M.C.[23-25] The available experimental evidence relating to this hypothesis is still somewhat uncertain. It seems that the changes in the properties of the micellar substances which have become clearly evident in solubilization studies have not received adequate attention. It must therefore be permissible, until further evidence for the electrical interference theory has been collected, to assume that the changes in the properties of the solutions at the *2nd* C.M.C. are primarily due to changes in the structures and/or sizes of the micelles. Starting from the assumption that the interaction between the micelles leads to further aggregation and rearrangement of the ions and molecules of the micelles (whereupon energetically more stable micelles are formed), one may offer a plausible explanation for the changes noted in the solubilizing power. If the charge density in the outermost palisade layer of the large micelles against the surrounding solution remains sufficiently high when decanol is incorporated in the inner parts of the micelle, the stability of the large micelle in the solution will remain practically unaltered. In this way larger amounts of alcohol per mole of soap can be brought into the solution by the large micelles than by the small micelles. Similarly the micelle aggregation would be expected to increase the solubilization of hydrocarbons.

Irrespective of whether it will be established that either micelle aggregation (or some other change in the micelle) occurs, or if only one type of micelle exists and the changes in the properties of the solutions are due to other yet unknown factors, it is necessary to conclude that a concentration limit is reached in the highly concentrated solutions above which the properties of the association colloid differ from the properties below this limit.

Factors determining the formation of the mesomorphic phase. In all the cases we have studied, the alcohol-soap-water phase separates from solutions that contain higher or lower concentrations of soluble aggregates consisting of soap ions and alcohol molecules; between the L.A.C. and the C.M.C. the aggregates are very small, but above the C.M.C. we have to do with the much larger mixed micelles. There must thus be some relationship connecting the occurrence of the soluble aggregates and the formation of the mesomorphic phase. The question arises whether the association of soap ions and alcohol molecules to soluble aggregates, on one hand, and the association of the components to form the mesomorphic phase, on the other, are two parallel phenomena in which similar factors play a part or whether the presence of soluble soap ion-alcohol aggregates of some kind is a necessary condition for the formation of the phase mentioned. In the latter case it seems probable that the aggregates directly take part in the formation of the new phase and that the shift in the hydrophilic-lipophilic balance of the aggregates caused by the incorporation of alcohol is of importance.

It has previously been established that there is evidently some relationship connecting the balance between the hydrophilic and lipophilic properties of the molecules and ions taking part in mixed micelle formation and the maximum amount of alcohol that the micelles can incorporate before the system becomes turbid due to the separation of the mesomorphic phase [2]. The balance shifts in favour of the hydrophilic properties as the chain length decreases in a homologous series. A similar shift occurs when a double bond is introduced into the hydrocarbon chain of the soap or when the carboxyl group in a fatty acid soap is replaced by a sulphate group. In such cases we have established that the decanol content of the mixed micelles at the turbidity point increases; this result is in agreement with observations of other investigators [26,27]. A similar shift occurs also when the solubilizate is changed: the alcohol content of the micelles at the turbidity point decreases with the chain length of the alcohol (for the heptanol-caprate system the content of heptanol is 1.0 mole of heptanol per mole of soap [28] and for decanol-caprate, 0.43 mole of decanol per mole of soap).

As the hydro-lipophilic balance of the mixed micelle is shifted sufficiently in the direction of the hydrophilic properties, we finally come to a system in which the solubilization of the polar compound is not limited by the separation of a mesomorphic phase but increases to its highest possible value, after which the excess of the polar compound separates in pure form. This has been found to occur, for example, when caproic acid is solubilized in sodium caproate solutions [28], when caprylic acid is solubilized in sodium caprylate solutions [28], when decanediol-1,10 is solubilized in solutions of various soaps [7,28,29], and when decanol-1 is solubilized in solutions of the potassium salts of the α,ω-alkanedioic acids (in some cases a mesomorphic phase appears at higher colloid concentrations; the concentration at which this occurs decreases as the temperature is lowered)[30]. When pure polar substance separates, the solubility values obtained are comparable with those for hydrocarbons, contrary to the solubility values obtained when the phase composed of polar substance, soap and water separates.

We have previously pointed out that the penetration of alcohol molecules between the soap ions in the palisade layers of the micelle leads to changes in the surface of the micelle [2,5]. Weakly hydrophilic groups become located between the strongly hydrophilic ionized carboxylic or sulphate groups. This leads to a decreased charge density on the micelle surface. The decrease should at first be compensated to some degree by a decrease in the number of gegenions bound to the micelle. As more alcohol is solubilized, the hydrophilic properties of the micelle surface will weaken while the number of lipophilic groups in the inner region of the micelle (per unit surface area) will remain practically unaltered (depending on the relative chain lengths of the alcohol and soap). The balance between the lipophilic and hydrophilic properties of the micelle will thus be shifted in favour of the lipophilic properties. As the hydrophilic properties of the micelle surface weaken in this manner, the stability of the micellar solution will decrease and the tendency of the micelles to adhere to each other will increase although the micelles are still charged (this must be true both below and above the *2nd* C.M.C.). The decrease in the hydrophilic properties of the micelle surface must therefore sooner or later lead to the sepa-

ration of a new phase. The process is the same for the small soap ion-alcohol aggregates at concentrations below the C.M.C. when the alcohol-soap ratio increases. As we have pointed out previously (Part VIII), the limits in which this ratio can vary are very narrow, and the hydrophobic properties increase rapidly as the ratio increases.

With the purpose of elucidating the formation of the mesomorphic phase, we have applied the law of mass action to the system containing alcohol, soap and water, irrespective of the fact that considerable errors must be introduced through the neglect of the activity coefficients. As was pointed out above, the formation of the mesomorphic phase can be assumed to occur by either of two ways: A) soap ions and alcohol molecules associate to soluble aggregates which form the mesomorphic phase by aggregation when their alcohol content attains a certain value, or B) soap ions and alcohol and water molecules form the mesomorphic phase directly when the decanol content of the mixed micelles attains a certain value. The calculations must, of course, lead to the same result irrespective of the mechanism chosen.

A. The formation of mixed micelles may be considered a process in which alcohol molecules are incorporated in the ordinary soap micelles or one in which new alcohol-containing micelles are produced. Under certain conditions (concentration, temperature and salt concentration) the molar ratio of alcohol and soap ions in the mixed micelles does not exceed a certain value (y/x). When this value is reached, further addition of alcohol leads to the formation of the mesomorphic phase. At the turbidity point where the soap solution is in equilibrium with the mesomorphic phase, the formation of the mixed micelles in the aqueous phase may be expressed by an equation of the following general type:

$$x\,R'COO^- + yR''OH + z\,Me^+ \rightleftharpoons ((Me^+)_z(R'COO^-)_x(R''OH)_y)^{-(x-z)} \quad (1)$$

$$\frac{[((Me^+)_z(R'COO^-)_x(R''OH)_y)^{-(x-z)}]}{[R'COO^-]^x\,[R''OH]^y\,[Me^+]^z} = K \quad (2)$$

$R'COO^-$ denotes a soap anion, $R''OH$ an alcohol molecule and Me^+ a metal ion. The values of x, y and z need not be the same as for the pure soap micelles. (The formation of the small soap ion—alcohol aggregates occurring in the concentration range between L.A.C. and C.M.C. can be treated in the same way in principle.)

Eqn. (2) may be rewritten as follows:

$$[R'COO^-][R''OH]^{y/x} = \frac{[((Me^+)_z(R'COO^-)_x(R''OH)_y)^{-(x-z)}]^{1/x}}{K'\,[Me^+]^{z/x}} \quad (3)$$

The soap anion concentration may be taken to be approximately equal to the soap concentration at the C.M.C. of the alcohol-containing solution. The alcohol concentration is less than its solubility in water. The decanol content y/x of the mixed micelles at the turbidity point has been determined experimentally and found to be constant below the break point A. When the ratio y/x exceeds a certain value, the mesomorphic phase appears.

If we assume that about 50 % of the gegenions are bound by the micelles, *i.e.* $z/x = 0.50$, it will be seen that the right member of eqn. (3) decreases with increasing soap concentration. Consequently also the concentration of free alcohol, [R″OH], at which the mixed micelles characterized by the ratio y/x are formed, will decrease with increasing soap concentration, at least in the concentration range below the break point A. This may be the explanation for the observation that the alcohol content of the mesomorphic phase decreases with increasing soap concentration below the break point A (see Part II [4]).

B. The conditions resulting in the formation of the mesomorphic phase can also be defined by means of an equation of the solubility product type:

$$[R'COO^-][R''OH]^{y/x}[Me^+]^{z/x} = P \qquad (4)$$

where y/x and z/x denote the molar ratios of alcohol to soap and of gegenions to soap in the mesomorphic phase. The ratios do not have the same values as in eqns. (1)—(3). It has been found that the ratio y/x has a smaller value for the mixed micelles in solution than for the separated phase. Furthermore, the ratio y/x does not remain constant in the separated phase but decreases with increasing soap concentration, at least up to the break point A. According to eqn. (4), the concentration of free alcohol should also decrease with increasing soap concentration.

The ratio z/x has been assumed to have values different from unity and it may hence seem at first sight that the particles of the mesomorphic phase should therefore have an enormously high electrical charge. This is of course not true. The gegenions in the water layers in the mesomorphic phase must be assumed to be partly bound to the soap ions, partly free (analogously as in the micellar solution) so that their activity is the same as in the micellar solution. In the expression for the law of mass action there remains only the activity of the bound gegenion, the activities of the free ions in solution and in the mesomorphic phase cancelling each other. Considerable errors are involved through the neglect of the activity coefficients, which must differ much from unity, especially in the mesomorphic phase.

It should finally be emphasized that the conditions for both equilibria mentioned above, *i.e.* the equilibrium between soap ions, alcohol and mixed micelles and the equilibrium between soap ions, alcohol and mesomorphic phase, must be fulfilled simultaneously.

In the qualitative respect the equations written above seem to be in accord with the observed phenomena. The available experimental data are yet so limited that a quantitative confirmation of the theory is not possible. It seems probable, however, that the soluble small soap ion-alcohol aggregates occurring between the L.A.C. and the C.M.C. and the mixed micelles occurring at concentrations above the C.M.C. partake in the formation of the separating alcohol-soap-water phase and that the increase in hydrophobic properties of these soluble aggregates caused by the incorporation of alcohol is an important factor in this process.

REFERENCES

1. Ekwall, P. and Vittasmäki, T. *Acta Chem. Scand.* **10** (1956) 1177.
2. Ekwall, P. and Passinen, K. *Acta Chem. Scand.* **7** (1953) 1098.
3. Ekwall, P., Passinen, K. and Danielsson, I. *Finska Kemistsamfundets Medd.* **63** (1954) 1.
4. Passinen, K. and Ekwall, P. *Acta Chem. Scand.* **9** (1955) 1438.
5. Passinen, K. and Ekwall, P. *Acta Chem. Scand.* **9** (1955) 1450.
6. Passinen, K. and Ekwall, P. *Acta Chem. Scand.* **10** (1956) 215.
7. Ekwall, P. *6. Nordiska Kemistmötet, Lund* 1947, p. 179.
8. Ekwall, P. *J. Colloid Sci.*, Suppl. **1** (1954) p. 66.
9. Ekwall, P., Hasan, A. and Danielsson, I. *Acta Chem. Scand.* **6** (1952) 440.
10. Markina, S. N., Posspelova, K. A. and Rebinder, P. A. *Chem. Zentr.* **126** (1955) 7852.
11. Ekwall, P. *Z. physik. Chem.* **A 161** (1932) 195.
12. Hyde, A. J., Langbridge, D. M. and Lawrence, A. S. C. *Discussions Faraday Soc.* **18** (1954) 239.
13. Harkins, W. D. and Oppenheimer, H. *J. Am. Chem. Soc.* **71** (1949) 808.
14. Ekwall, P. *Kolloid-Z.* **101** (1942) 135.
15. McBain, J. W., Laing, M. E. and Titley, A. F. *J. Chem. Soc.* **1919**, 1279.
16. Mysels, K. J. and Dulin, C. I. *J. Colloid. Sci.* **10** (1955) 461.
17. Lottermoser, A. and Püschel, F. *Kolloid-Z.* **63** (1933) 175.
18. Ward, A. F. H. *Proc. Roy. Soc. London* **A 176** (1940) 412.
19. Ralston, A. W. and Hoerr, C. W. *J. Am. Chem. Soc.* **64** (1942) 772.
20. Haffner, F. D., Piccione, G. A. and Rosenblum, C. *J. Phys. Chem.* **46** (1942) 662.
21. Gregory, E. T. and Tartar, H. V. *J. Am. Chem. Soc.* **70** (1948) 1992.
22. Voeks, J. F. and Tartar, H. V. *J. Phys. Chem.* **59** (1955) 1190.
23. Hartley, G. S. *Ann. Repts. on Progr. Chem. (Chem. Soc., London)* **45** (1948) 33.
24. Harkins, W. D. and Mittelmann, R. *J. Colloid Sci.* **4** (1949) 367.
25. Debye, P. *J. Phys. Chem.* **53** (1949) 1.
26. Klevens, H. B. *Chem. Revs.* **47** (1950) 1.
27. McBain, M. E. L. and Hutchinson, E. *Solubilization and Related Phenomena*, Academic Press Inc., New York 1955.
28. Ekwall, P. and coworkers, *Unpublished results.*
29. Ekwall, P., Danielsson, I. and Henrikson, S. *Acta Chem. Scand.* **6** (1952) 1297.
30. Danielsson, I. *The Association of Long Chain Dipotassium α,ω-Alkanedioates in Aqueous Solution* (Diss.) Åbo Akademi, Åbo, 1956.

Received May 29, 1956.

ACTA CHEMICA SCANDINAVICA 10 (1956) 1228—1233

Studies on the Interaction of Paraffin Chain Alcohols and Association Colloids

X. The Solubility of Decanol-1 in Sodium Oleate Solutions Containing Sodium Chloride

KAAPO PASSINEN and PER EKWALL

Institute of Physical Chemistry, Åbo Akademi, Åbo, Finland

The maximum amounts of decanol solubilized until sodium oleate solutions containing sodium chloride become turbid have been determined. The solubility of decanol decreases rapidly with increasing sodium chloride concentration. The general shape of the solubility curve is not altered by the addition of 0.05 *M* NaCl. The break point in the solubility curve occurs at a lower oleate concentration in salt-containing than in salt-free solutions. The break point is known to occur at the so-called "*2nd* critical concentration"; this limit is hence not only a function of the concentration of the micelle-forming hydrocarbon-chain ions in the solution, but also a function of the concentration of the gegenions. This indicates that the changes in the micellar structure that take place here do not depend solely on the fact that the micelles come so near each other that disturbances occur in their electrical double layers. The factors responsible for the decrease in the solubility of decanol are discussed.

Investigations of the effects of inorganic salts on the solubilization of simple nonpolar and polar-nonpolar substances have shown that the addition of salt increases the solubilization of nonpolar compounds [1–3], but decreases the solubility of polar-nonpolar substances, *e.g.*, long-chain alcohols [2–5]. This difference has been explained by assuming that nonpolar and polar-nonpolar molecules are incorporated in different regions of the micelles.

In studies of the effect of inorganic salts on the solubilization of very complicated organic molecules, such as dyes, it has been established that in most cases the added salt causes an increase in the solubilizing power of the colloid [6].

In Part I [7] of this series, data were given on the solubility of decanol in oleate solutions at the turbidity point where the separation of a mesomorphic phase begins. It was found that the solubility curve increases linearly up to a colloid concentration of about 0.12 *M*, then curves upwards and finally

downwards as the oleate concentration is increased further. The purpose of the present investigation was to study the effect of sodium chloride on the solubility of decanol in oleate solutions and to determine whether the shape of the solubility curve remains the same as for oleate solutions containing no added salt. It was also of interest to determine whether the breakpoint in the solubility curve at the so-called "2*nd* critical concentration" is displaced when salt is added.

MATERIALS AND METHODS

The same substances and methods have been used as in Part I [7] of this series. The sodium chloride employed was a product from E. Merck.

The experimental error of the solubility values has been estimated to be about ± 0.2 ml of decanol per litre.

The concentrations of sodium oleate and sodium chloride are given in moles per 1 000 g of oleate solution (salt-free) and are denoted by M.

EXPERIMENTAL RESULTS

The solubility of decanol at the turbidity point in 0.100 M sodium oleate solutions containing different amounts of sodium chloride is shown in Fig. 1. The solubility decreases very rapidly with increasing sodium chloride concentration. The solubility of decanol could not be measured when the sodium chloride concentration exceeded about 0.15 M, because the solutions became very viscous, nearly gel-like. The curve has the same form as Klevens has found for the system octanol-potassium myristate-potassium chloride [3].

The solubility of decanol in sodium oleate solutions containing 0.05 mole of sodium chloride per litre is shown by curve *a* in Fig. 2. Curve *b* gives the solubility of decanol at the turbidity point in salt-free oleate solutions (Part I [7]). The form of the solubility curve is similar for salt-containing as for salt-free oleate solutions. At lower oleate concentrations, the solubility increases linearly with the oleate concentration, then begins to increase a little faster, but finally the curve becomes concave against the concentration axis. In the presence of sodium chloride, the departure from linearity occurs at a lower concentration (at about 0.08 M oleate) than in salt-free solutions (at about 0.12 M oleate);

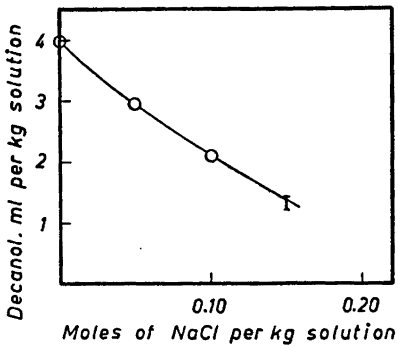


Fig. 1. The effect of sodium chloride on the solubility of decanol in a 0.100 M *sodium oleate solution. 40°C.*

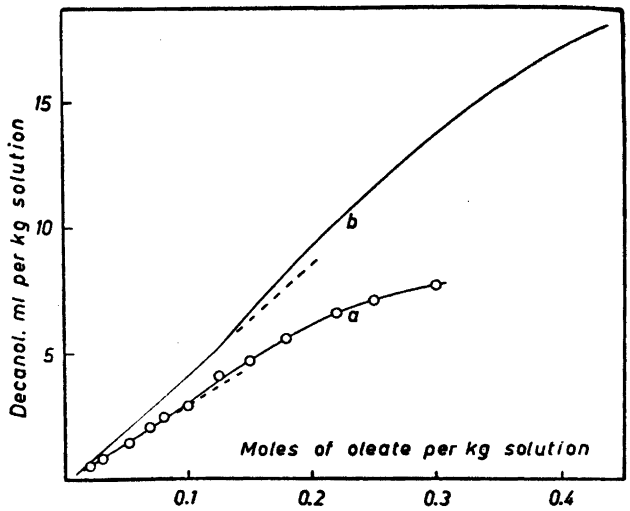


Fig. 2. The solubility of decanol at the turbidity point. 40°C. a) Sodium oleate solutions 0.05 M *in sodium chloride. b) Salt-free oleate solutions.*

the departure is less marked than in salt-free oleate solutions, but exceeds the experimental variation in the solubility determinations. The effect of the salt varies in different concentration ranges; in the linear range below 0.08 *M* oleate, the solubility is decreased by about 26 %, at higher oleate concentrations, the decrease is larger and amounts to about 33 % in the 0.2 *M* and about 44 % in the 0.3 *M* oleate solution.

DISCUSSION

As pointed out earlier [7,8], the solubility curve gives the maximum amount of decanol dissolved by the micelles before the system becomes heterogeneous. The slope of the solubility curve at each point gives the proportion of decanol and soap in the mixed micelles formed at the soap concentration in question. The curve *a* in Fig. 3 and the values in Table 1 show how the decanol content of the mixed micelles (in moles of decanol per mole of oleate) varies with the

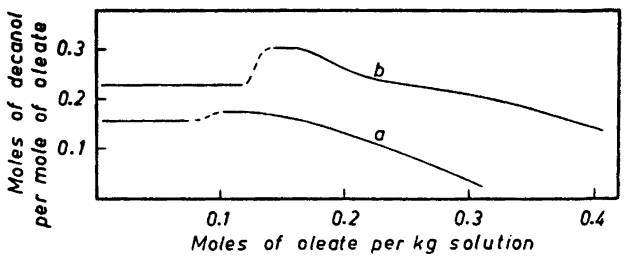


Fig. 3. The decanol content per mole of association colloid in the mixed micelles. 40°C. a) Sodium oleate solutions 0.05 M *in NaCl. b) Salt-free oleate solutions.*

Table 1. Composition of the mixed micelles at the turbidity point in sodium oleate solutions containing sodium chloride.

Concentration of sodium oleate	Maximum proportion of decanol in moles of decanol per mole of oleate		
	Concentration of sodium chloride		
	0.05 *M*	0.10 *M*	0.15 *M*
0.005–0.08 *M*	0.16	(0.11)	(0.07)
0.12 *M*	0.18		
0.20 *M*	0.13		
0.30 *M*	0.04		

oleate concentration in solutions 0.05 *M* in sodium chloride. (The values given in parentheses in Table 1 have been calculated on the basis of only one experimental solubility value and are therefore only approximate.) Curve *b* in Fig. 3 shows the corresponding curve for salt-free oleate solutions. It is seen that in the former case the decanol content of the mixed micelles remains constant at approximately 0.16 mole of decanol per mole of oleate up to an oleate concentration of about 0.08 *M*. The relative decanol content then increases to a low maximum which is about 0.18 mole of decanol per mole of oleate, and finally decreases to a very low value. The addition of sodium chloride seems to smooth out the course of the solubility curve.

We wish to stress the following factors which we hold responsible for the fact that the system becomes heterogeneous at a lower decanol content when salt is present than when the solutions are salt-free. As we pointed out in Part IX [8] of this series, the process that precedes the formation of the new phase can be represented by an equation of the type:

$$x\ \mathrm{R'COO^-} + y\mathrm{R''OH} + z\ \mathrm{Na^+} \rightleftharpoons ((\mathrm{Na^+})_z(\mathrm{R'COO^-})_x(\mathrm{R''OH})_y)^{-(x-z)} \quad (1)$$

$$\frac{[((\mathrm{Na^+})_z(\mathrm{R'COO^-})_x(\mathrm{R''OH})_y)^{-(x-z)}]}{[\mathrm{R'COO^-}]^x\,[\mathrm{R''OH}]^y\,[\mathrm{Na^+}]^z} = K \quad (2)$$

When the ratio of alcohol to soap, y/x, exceeds a certain value, a new phase is formed. This ratio is, as we have shown above, lower in the salt-containing than in salt-free solutions. We have previously assumed that a smaller number of sodium ions are bound per fatty acid ion in the mixed micelles containing alcohol than in the pure soap micelles, *i.e.* the ratio of gegenions to fatty acid anions, z/x, is assumed to be lower in the former case than in the latter. The presence of sodium chloride must lead to an increase in the number of bound gegenions, *i.e.* to a higher z/x-value. The conditions for the formation of the new phase are fulfilled in the salt-containing solutions when mixed micelles with a higher gegenion content (z/x) but smaller alcohol content (y/x) than those present in salt-free oleate solutions are formed. The observed decrease in the solubility of decanol on addition of salt can be explained fairly well on the basis of the law of mass action, eqn. (2), when certain simplifying assumptions are made. Plausible results are also obtained with an equation of the "solubility

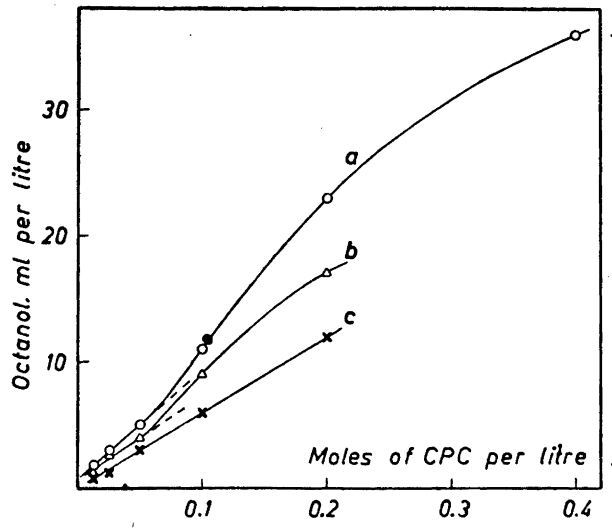


Fig. 4. The solubility of octanol at the turbidity point. 40°C. a) Salt-free cetylpyridinium chloride solutions, b) Cetylpyridinium chloride solutions 0.125 M *in NaCl, c) Cetylpyridinium chloride solutions 0.500* M *in NaCl (Richards and McBain [2])*

product" type (see eqn. (4) in Part IX [8]). It should be noted that in salt-containing soap solutions the C.M.C. is lower and hence the activities of simple ions ($R'COO^-$) are lower than in salt-free solutions.

Also other changes in the structure of the micelles than the above-mentioned, such as changes in their shapes and sizes, may occur when salt is added; this is indicated by light-scattering [9–11] and viscosity [12] measurements.

In Parts I—IV [7,13–15], it was shown that when the oleate concentration of 0.1—0.2 *M* is exceeded, so many important changes occur in the properties of oleate solutions that one has to assume that a change also takes place in the micellar substance and that therefore it is justified to speak of a concentration limit, called the "2*nd* critical concentration". In Part IX [8] it was shown that similar phenomena occur also in solutions of sodium caprate, laurate and myristate and that the concentration limit mentioned is displaced toward lower soap concentrations when the number of carbon atoms in the hydrocarbon chain increases. Our investigations have shown that the solubility of decanol is one of the properties that undergo a characteristic change at this limit. Our present measurements show that the limit is displaced to lower oleate concentrations when sodium chloride is added. The position of this limit is hence not only a function of the amount of the micelle-forming hydrocarbon-chain ions and molecules in the solution, but also a function of the concentration of gegenions (as is the case for the critical concentration). This indicates that the changes in the micellar structure that take place in this concentration range do not depend, solely at least, on the fact that the micelles come so near each other that disturbances occur in their electrical double layers.

We have examined the data on the solubility of alcohols in association colloid solutions published by other workers and have found that in all cases when the measurements have been carried out with sufficient accuracy and when a sufficient number of measurements has been made, the solubility curves (solubility in ml/l, g/l or moles/l plotted against the concentration of association colloid in moles per litre) are linear over a relatively wide concentration range above the C.M.C., then show a breakpoint, slope upwards and finally, in some cases, become concave against the concentration axis [1,2,16]. This is shown especially clearly by the solubility curve for octanol in cetylpyridinium chloride solutions according to measurements of Richards and McBain [2] (Fig. 4, curve a*). Our opinion is therefore that the type of solubility curve that we have found for the solubility of decanol in solutions of fatty acid soaps and of alkyl sulphates is characteristic for at least all the long-chain primary alcohols and all association colloids of the paraffin-chain type.

Richards and McBain reported also some data on the effect of salt on the solubility of alcohol [2]. The effect of 0.125 M sodium chloride on the solubility of octanol in cetylpyridinium chloride solutions (Fig. 4, curve b) is completely analogous to that found by us for sodium oleate solutions 0.05 M in sodium chloride. Our conclusion that a larger addition of salt smooths out the solubility curve is also verified (Fig. 4, curve c). The picture given by Figs. 2 and 4 of the effect of salt on the solubility of long-chain alcohols in solutions of association colloids may therefore be regarded as typical.

REFERENCES

1. Stearns, R. S., Oppenheimer, H., Simon, E. and Harkins, W. D. *J. Chem. Phys.* **15** (1947) 496.
2. Richards, P. H. and McBain, J. W. *J. Am. Chem. Soc.* **70** (1948) 1338.
3. Klevens, H. B. *J. Am. Chem. Soc.* **72** (1950) 3780.
4. Dean, R. B., see McBain, J. W. and Johnson, K. E. *J. Am. Chem. Soc.* **66** (1944) 9.
5. McBain, J. W. and McHan, H. *J. Am. Chem. Soc.* **70** (1948) 3838.
6. McBain, M. E. L. and Hutchinson, E. *Solubilization and Related Phenomena*, Academic Press Inc., New York 1955.
7. Ekwall, P. and Passinen, K. *Acta Chem. Scand.* **7** (1953) 1098.
8. Passinen, K. and Ekwall, P. *Acta Chem. Scand.* **10** (1956) 1215.
9. Debye, P. and Anacker, E. W. *J. Phys. Chem.* **55** (1951) 644.
10. Phillips, J. N. and Mysels, K. J. *J. Phys. Chem.* **59** (1955) 325.
11. Scheraga, H. A. and Backus, J. K. *J. Am. Chem. Soc.* **73** (1951) 5108.
12. Mc Bain, J. W., Willavoys, H. J. and Heighington, H. *J. Chem. Soc.* **1927** 2689.
13. Passinen, K. and Ekwall, P. *Acta Chem. Scand.* **9** (1955) 1438.
14. Passinen, K. and Ekwall, P. *Acta Chem. Scand.* **9** (1955) 1450.
15. Passinen, K. and Ekwall, P. *Acta Chem. Scand.* **10** (1956) 215.
16. Harkins, W. D. and Oppenheimer, H. *J. Am. Chem. Soc.* **71** (1949) 808.

Received May 29, 1956.

* The variation of the solubility of alcohol in colloid solutions is in Fig. 4 plotted in another coordinate system than in the original paper.

ACTA CHEMICA SCANDINAVICA 10 (1956) 1234—1242

Synthesis and Metabolism of 2,2-Dimethylnonadecanoic Acid *

N. TRYDING and G. WESTÖÖ

Department of Physiological Chemistry, University of Lund, Lund, Sweden

The intestinal absorption and metabolism in the rat of 2,2-dimethylnonadecanoic acid has been studied. The main metabolic end-products were 2,2-dimethylglutaric acid and 2,2-dimethylpimelic acid, which were recovered in the urine. Thus the β-oxidation from the carboxyl end of the 2,2-dimethylnonadecanoic acid had been completely hindered and the last step of the degradation from the ω end — from 2,2-dimethylpimelic to 2,2-dimethylglutaric acid — had been retarded by the steric hindrance of the two methyl groups.

The intestinal absorption and metabolism of 2,2-dimethylstearic acid in the rat has been studied in an earlier investigation by Bergström, Borgström, Tryding and Westöö [1]. The acid was well absorbed. The β-oxidation from the carboxyl end of the 2,2-dimethylstearic acid molecule was completely hindered and the main metabolic end product was shown to be 2,2-dimethyladipic acid which was excreted in the urine.

Continuing the study on the influence of steric hindrance at the carboxyl group, we have now investigated the absorption and metabolism of a 2,2-dimethyl fatty acid with an odd number of carbon atoms in the chain. For this reason we have prepared 2,2-dimethyl[1-^{14}C]nonadecanoic acid by a Kolbe electrolysis of heptadecanoic acid and 3-methoxy[^{14}C]carbonyl-3-methylbutyric acid, purification of the methyl ester obtained by chromatography on acid alumina and hydrolysis of the ester.

When administered in olive oil solution *per os* to rats, the acid was well absorbed. The absorbed activity ** was recovered in the urine to 78% (mean for 6 rats), indicating that the carbon skeleton of the ^{14}C-carboxyl end was intact. Rats with a thoracic duct fistula excreted about 21—36 % of the

* Presented in part at the meeting of the Swedish Biochemical Society in Gothenburg, June 4, 1955 and at the IInd International Conference on Biochemical Problems of Lipids, Ghent, Belgium, July 29, 1955.

** Approximately calculated as the difference between the fed activity and the activity excreted in the feces.

absorbed activity in the urine, while 39—64 % was found in the lymph lipids. Thus the acid was absorbed to a considerable extent *via* the portal vessels. 11—20 % of the lymph activity was present as free acid, 77—86 % as neutral fat, while only 2—5 % was incorporated into the phospholipids. A similar distribution in the lymph has been found for 2,2-dimethylstearic acid [2] and for 2,2,17,17-tetramethylstearic acid [3].

The active substances in the urine have been identified by reversed-phase partition chromatography and repeated recrystallizations with synthetic, unlabelled compounds. Two of the urinary metabolic products of 2,2-dimethylnonadecanoic acid were shown to be 2,2-dimethylglutaric (about 55 %) and 2,2-dimethylpimelic acid (about 25 %). Approximately 5 % of these acids were found in conjugated form. There was at least one other minor component, the composition of which has not yet been established. The metabolic products identified indicate that the two methyl groups completely block the degradation from the carboxyl end of the 2,2-dimethylnonadecanoic acid. As the degradation from 2,2-dimethylpimelic acid to 2,2-dimethylglutaric acid was not complete, the last step of the oxidation from the ω end was also influenced by the methyl groups. The steric hindrance thus extends its effect as far as the ∂ carbon atom. There was relatively more 2,2-dimethylpimelic acid in the urine on the first day after the administration than on the following days (Table 5).

Using fatty acids with a phenyl group at the β-carbon atom for blocking the β-oxidation Stevens [4] found that β-phenyldecanoic acid and β-phenyldodecanoic acid were excreted in the urine as β-phenyladipic acid. After feeding acids with an odd number of carbon atoms in the chain no homogeneous product could be isolated from the urine. However, it was clear that dibasic acids were excreted. It is to be noted that substituted acids with less than nine carbon atoms in the chain were excreted mainly unaltered in the urine. Yamakawa [5] administered 2-propyltridecanoic acid to a rabbit. As judged from the mixed melting points of bis-*p*-phenylphenacyl esters the urinary excretion products were suggested to consist of 2-propylglutaric acid (7 parts), and 2-propylpimelic acid (3 parts). Our results confirm these findings.

SYNTHESES

2,2-Dimethyl[1-^{14}C]nonadecanoic acid. A methanol solution (130 ml) of heptadecanoic acid (5.7 g), 3-methoxy[^{14}C]carbonyl-3-methylbutyric acid (0.5 g) and sodium (0.06 g) was electrolysed between Pt-electrodes with a current density of 0.3 A/cm^2 until the pH was 7 (*cf.* Ställberg-Stenhagen [6]). The solution was cooled to room temperature, and the *n*-dotriacontane formed was filtered off. It was extracted twice with boiling methanol and each time filtered off after cooling to room temperature. The combined methanol solutions were evaporated to dryness. The residue was extracted with ether repeatedly. The mixture obtained from the ether extract after evaporation of the solvent was chromatographed on acid alumina (activated at 180° overnight). The hydrocarbons formed were eluted with light petroleum, the methyl 2,2-dimethyl[1-^{14}C]nonadecanoate with benzene, whereas the acids, which had not reacted, and the alcohols formed as byproducts were left on the column.

The colourless crystals of methyl 2,2-dimethyl[1-^{14}C]nonadecanoate (0.5 g) were hydrolysed with a solution of potassium hydroxide (3 g) in water (2 ml) and ethanol (23 ml) for 5 hours in an autoclave at 120°. Water was added to the hydrolysate, which was acidified and extracted twice with ether. The ether solution was washed with water and dried with sodium sulphate, and the ether was evaporated. After recrystallization

from methanol and light petroleum the 2,2-dimethyl[1-^{14}C]nonadecanoic acid melted at 67.2–67.7°. The yield was 0.35 g. (Found: C 77.3; H 13.0; equiv. wt. 326. Calc. for $C_{21}H_{42}O_2$: C 77.2; H 13.0; equiv. wt. 326.5).

2,2-Dimethylglutaric acid. The synthesis of 2,2-dimethylglutaric acid has previously been reported by several investigators. One of the better methods was that described by Franke and Bueren [7], who obtained the acid in a 75 % yield from 4-cyano-2,2-dimethyl-1-butyraldehyde (starting material: 2-methylpropionaldehyde and vinylcyanide).

In the present investigation it was synthesized by a Kolbe electrolysis from methyl hydrogen malonate (4.8 g), 3-methoxycarbonyl-3-methyl-butyric acid (1.6 g) and sodium (0.1 g) in methanol solution (30 ml). The electrolysis was continued until the pH was 7. The methanol was evaporated and the ether-soluble fraction was isolated. The excess methyl hydrogen malonate was removed from the ether solution by the ion exchanger Amberlite IRA-400. The esters (2.7 g of crude product) were partially hydrolysed with potassium hydroxide (3 g), water (2 ml) and ethanol (30 ml) at room temperature, when the hindered ester groups were almost unattacked. After the addition of water (50 ml) the solution was extracted twice with ether to remove methyl tetramethyladipate. The water-ethanol layer was acidified and extracted three times with ether. The ether solution was dried with sodium sulphate, and the solvents were evaporated. Extraction of the residue with ether left most of the succinic acid undissolved. After removal of the ether, the esters were hydrolysed with potassium hydroxide (3 g), water (2 ml) and ethanol (23 ml) in an autoclave at 120° for 5 hours. Water (18 ml) was added to the solution, which was then acidified, saturated with ammonium sulphate and extracted with ether 5 times. The ether solution was dried with sodium sulphate and evaporated to dryness. The mixture of acids obtained was chromatographed twice on hydrophobic Hyflo supercel with 2-ethylhexanol-chloroform (6:5, v/v) as the stationary phase and methanol-water (2:3, v/v) as the moving phase. They were eluted in the order: succinic, dimethylglutaric, tetramethyladipic acid.

The 2,2-dimethylglutaric acid (0.5 g) was recrystallized from concentrated hydrochloric acid and from benzene-light petroleum; m. p. 82°.

2,2-Dimethylpimelic acid. Methyl hydrogen glutarate (7.3 g), 3-methoxycarbonyl-3-methylbutyric acid (1.7 g) and sodium (0.1 g) were electrolysed in methanol (75 ml) as described above. A great excess of glutarate was used in order to suppress the formation of 2,2,5,5-tetramethyladipic acid.

The solution was hydrolysed with potassium hydroxide (8 g) and water (5 ml) in an autoclave at 120° for 3 hours. After acidification the hydrolysate was extracted with ether. From the dry substance of the ether extract, chloroform dissolved the dimethylpimelic and tetramethyladipic acids but left a considerable amount of the glutaric and suberic acid undissolved. The chloroform extract was evaporated to dryness and the solid residue was chromatographed twice on hydrophobic Hyflo supercel with 2-ethylhexanol-chloroform (1:1, v/v) as the stationary phase and methanol-water (2:3, v/v) as the moving phase. The acids appeared in the following order: glutaric, suberic, dimethylpimelic and tetramethyladipic acid.

The 2,2-dimethylpimelic acid (0.66 g) was recrystallized from water and from benzene-light petroleum. M. p. 75.4°. (Found: C 57.6; H 8.4. Calc. for $C_9H_{16}O_4$: C 57.4; H 8.6.)

METABOLIC EXPERIMENTS

A stock solution of 2,2-dimethyl[1-^{14}C]nonadecanoic acid (241.2 mg) with a specific activity of 125 000 counts/min/mg in olive oil (12.3 g) was prepared, and 0.75 — 1 ml of this was given orally in a single dose to adult male rats weighing about 250 g. The radioactivity was determined with a windowless GM-tube (with a background effect of 40 c.p.m.) after direct plating on aluminium planchets. For further experimental details see Bergström, Borgström, Tryding and Westöö [1].

Isotope recovery in excreta after the administration of 2,2-dimethyl[1-^{14}C]nonadecanoic acid

A rat was fed 0.75 ml of the above-mentioned stock solution (1 600 000 counts/min). Feces from the first 24 hours after the administration were shown to contain 17 % of the fed activity. From Table 1 it is seen that the total activity recovered in the feces in one week was 22 % of the amount administered. The total activity found in the urine during one week after the administration, 70 %, corresponds to a recovery of 90 % of the absorbed activity.

The feces from five other rats were collected for 4 days after the administration of the active acid. They contained 9—34 % of the fed activity. In the same experiment 70—91 % of the absorbed activity could be recovered from the urine during the same time.

When part of an ether extract from hydrolysed feces containing 34 % of the fed activity was chromatographed according to Howard and Martin [8] (75 % aqueous acetone as the moving phase and paraffin oil as the stationary phase supported on hydrophobic kieselguhr), 92 % of the activity was found as unaltered 2,2-dimethylnonadecanoic acid. Another part of the same extract was chromatographed on hydrophobic kieselguhr (40 % methanol as the moving phase and 2-ethylhexanol-chloroform (1:1) as the stationary phase) [1]. In this way 3 % of the active substances could be identified as 2,2-dimethylpimelic acid and 2.5 % as 2,2-dimethylglutaric acid. 2.5 %, which was eluted with the front in this system, has not yet been identified. These dicarboxylic acids are real fecal metabolites. They cannot originate from the urine, which for this special animal has been collected separately *via* a plastic funnel, sewn on to the cutis around the penis of the rat. The reason for the presence of dicarboxylic acids in the feces is being investigated.

Table 1. Activity recovered in rat urine and feces after oral administration of 2,2-dimethyl-[1-^{14}C]nonadecanoic acid.

Day No.	Per cent of administered activity found in	
	feces	urine
1	17.4	60.3
2	3.9	6.1
3—4	0.6	3.1
5—7	0.1	0.3

Administration of 2,2-dimethyl[1-^{14}C]nonadecanoic acid to rat with a lymph fistula

Rats with a thoracic duct cannula (Bergström, Blomstrand and Borgström [9]) were fed the stock solution. The lymph was collected at 0° (Table 2, rats 1—3) or in ethanol (Table 2, rats 4—6). During the first 12 hours 52 %

Table 2. Recovery of isotope in lymph and urine after feeding 2,2-dimethylnonadecanoic acid.

Rat No.	Per cent of fed activity absorbed	Per cent of absorbed activity recovered in lymph lipids	Per cent of lymph activity recovered as			Per cent of absorbed activity recovered in urine
			glycerides	free acids	phospholipids	
1	88.2	63.6	86.3	11.1	2.6	29.0
2	66.8	54.0	78.1	19.8	2.1	35.1
3	80.2	55.3	77.2	17.8	5.0	28.7
4	92.5	47.4	82.3	15.9	1.8	35.6
5	74.1	39.5				36.3
6	76.5	52.3				20.6

of the fed activity was recovered in the lymph from rat No. 1 (Table 2). Another 4 % was found during the next 24 hours. Accordingly 24-hour-specimens were collected from the other fistula rats (Table 2). The total fat from the lymph samples was separated into a neutral fat-fatty acid fraction and a phospholipid fraction on a column of silicic acid (Borgström [10]). The phospholipids contained 2—5 % of the activity of the lymph lipids. The neutral fat was separated from free acids on the ion exchanger Amberlite IRA-400 (Borgström [11]). The free fatty acid fraction was shown to contain 11—20 % of the lymph activity.

In addition the excreta from these rats were collected. In four days 8—33 % of the administered activity was found in the feces. During the same period 21—36 % of the absorbed activity was recovered from the urine, while 39—64 % of the absorbed isotope was in the lymph.

Identification of isotopic compounds in the urine after the administration of 2,2-dimethyl[1-^{14}C]nonadecanoic acid

The urine from a noncannulated rat was acidified with hydrochloric acid. When the urine from the first day was extracted three times with two volumes of ether, 77 % of the activity was found in the ether phase. In the same way 60 % of the activity in the urine from the second day and 40 % of the activity from the third day could be extracted with ether. Portions of the urine fractions with a weight of substance less than 50 mg were examined by reversed-phase partition chromatography. The phases and procedures were the same as described earlier [1]. The chromatogram of the ether extract from the first-day urine showed three distinct active bands (*cf.* Fig. 1).

Approximately 15 % (30 mg) of the residue of the ether extract was mixed with inactive 2,2-dimethylglutaric acid (8.4 mg) and subjected to partition chromatography. It is shown in Fig. 1 that this acid corresponds to the second active band. (The front titration peak represents ordinary urine excretion products.) The third active band was rechromatographed together with 7.6 mg

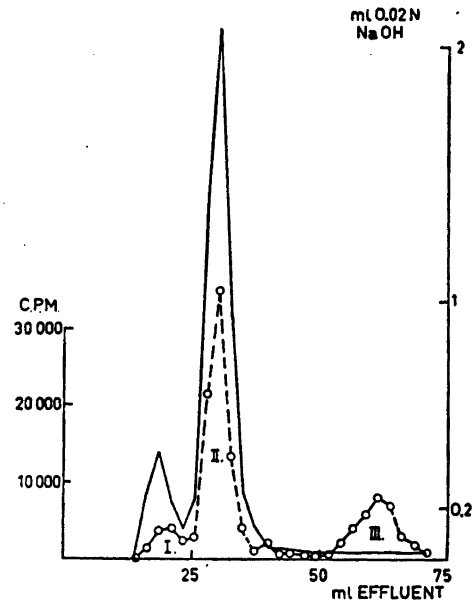


Fig. 1. Partition chromatography of 15 % of the ether extract from the first-day urine together with unlabelled 2,2-dimethylglutaric acid (8.4 mg). Stationary phase: 4 ml of i-octanol (2-ethylhexanol)-chloroform (1:1, v/v) supported on 4.5 g of hydrophobic Supercel. Moving phase: 40 % (v/v) aqueous methanol.

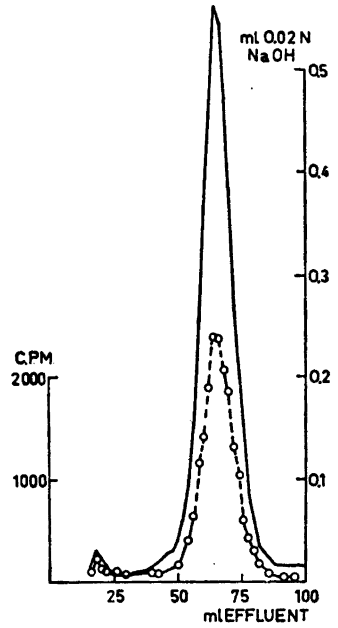


Fig. 2. Chromatography of the third active band from Fig. 1 with unlabelled 2,2-dimethylpimelic acid (7.6 mg). Phases: see Fig. 1.

Table 3. Specific activity of the most active fraction (1.2 mg) from the active band (II) of a chromatogram of urinary extract after recrystallization with inactive 2,2-dimethylglutaric acid (49.7 mg).

Recrystallization from	Crystal weight, mg	Counts / min / mg
benzene-light petroleum	41.5	2 225
water	26.0	2 313
water	14.3	2 280
benzene-light petroleum	9.9	2 307

Table 4. Specific activity of the two most active fractions (1.9 mg) from the active band III of a chromatogram of urinary extract after recrystallization with inactive 2,2-dimethylpimelic acid (79.0 mg).

Recrystallization from	Crystal weight, mg	Counts / min / mg
benzene-light petroleum	59.0	446
water	42.5	470
water	30.1	478
benzene-light petroleum	20.0	485
water	12.8	482

of 2,2-dimethylpimelic acid and the activity and titration peaks were found at the same position (Fig. 2).

The ether extract of the urine from a rat with a lymph fistula was subjected to reversed-phase partition chromatography. The isotope content of each fraction (2 ml) was determined after plating of 0.1 ml samples. The active bands appeared as in Fig. 1.

Table 5. The ratio between the three active bands in chromatograms of urine extracts.

Urine from day No.	Per cent of activity extracted with				Per cent of activity of band No.		
	ether		ethyl acetate from urine saturated with ammonium sulphate		I Conjugates with II and III. A small amount of an unidentified product	II	III
		after hydrolysis		after hydrolysis			
1			90		16	56	28
1				>90	13	58	29
1	80				9	61	30
1		80			8	61	31
2	60				34	55	11
3	40				40	51	9

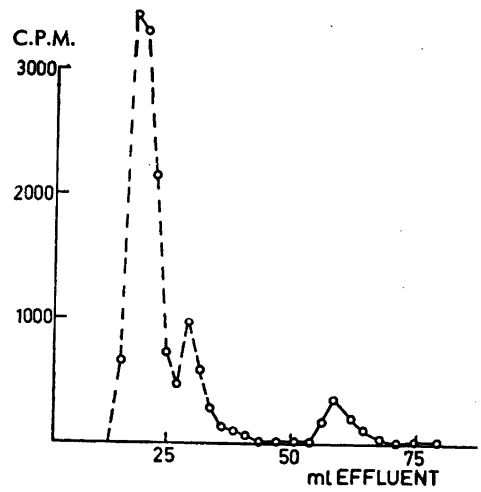


Fig. 3. Chromatogram of metabolites excreted in the urine, extracted with ethyl acetate after extraction with ether and saturation with ammonium sulphate. Phases: see Fig. 1.

The most active fraction from the second band with a weight of substance of 1.2 mg was mixed with 49.7 mg of inactive 2,2-dimethylglutaric acid and crystallized from benzene-light petroleum (b. p. 40—60°) and from water. As shown in Table 3 the activity remained constant indicating that 2,2-dimethylglutaric acid was excreted in the urine. In the same way recrystallization was performed with the two most active fractions from the third active band (with a dry weight of 1.9 mg) and inactive 2,2-dimethylpimelic acid

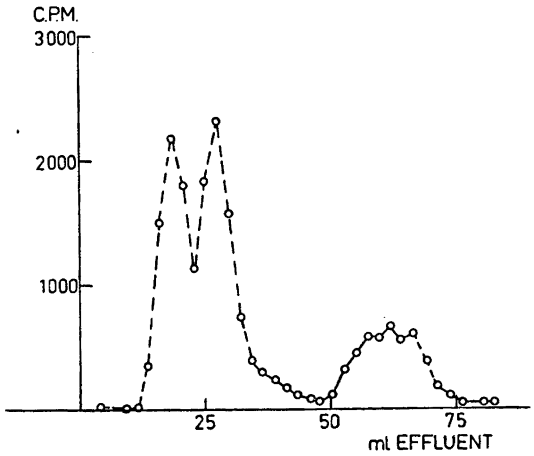


Fig. 4. Chromatogram of metabolites, after hydrolysis extracted as in Fig. 3. Phases: see Fig. 1.

(79.0 mg). From Table 4 it is seen that the activity remained constant. Consequently, 2,2-dimethylpimelic acid was another urinary metabolic product of 2,2-dimethylnonadecanoic acid.

As shown in Table 5 most of the activity of the ether extract was found in the second band (2,2-dimethylglutaric acid). In the chromatograms of the ether extracts of the urine from the second and the third day there was relatively more activity in the first band (unidentified product). The reverse was true for the third band (2,2-dimethylpimelic acid) which was distinctly lowered by the time. The ratio between the three active bands was almost unaltered after hydrolysis of the ether phase from the first-day urine. This indicates that no conjugates were present in the ether extract.

After the extraction with ether, half the water phase was saturated with ammonium sulphate and extracted three times with two volumes of ethyl acetate. In this way 47 % of the remaining activity could be extracted. When subjected to partition chromatography the main part of the activity was in the front band (Fig. 3). The other half of the water phase was hydrolysed for 6 hours at 120° with potassium hydroxide (4 g), water (2 ml) and ethanol (25 ml). After evaporation to dryness, the substance was dissolved in water, acidified, saturated with ammonium sulphate and extracted with ethyl acetate as described above. The activity could be extracted to 70 %.

A comparison between the chromatograms of ethyl acetate extracts of unhydrolysed and hydrolysed water phase of the ether-extracted urine from the first day (Figs. 3 and 4) shows that the front active band contains conjugates with the components in the second and third band. However, all the active substances in the first band could not be hydrolysed, which indicates the existence of a third metabolic product. This product is still being investigated.

We are indebted to Miss K. Sjöström for valuable technical assistance. This investigation has been supported by *Statens naturvetenskapliga forskningsråd*, by *Knut and Alice Wallenbergs Stiftelse*, and by the *Medical Faculty of the University of Lund*, which is gratefully acknowledged.

REFERENCES

1. Bergström, S., Borgström, B., Tryding, N. and Westöö, G. *Biochem. J. London* **58** (1954) 604.
2. Blomstrand, R., Tryding, N. and Westöö, G. *Acta Physiol. Scand.* **37** (1956) 91.
3. Tryding, N. and Westöö, G. *To be published.*
4. Stevens, C. M. *Thesis*, University of Illinois (1941).
5. Yamakawa, T. *J. Biochem. Japan* **37** (1950) 343.
6. Ställberg-Stenhagen, S. *Arkiv Kemi* **2** (1950) 95.
7. Franke, W. and Bueren, J. *Z. Naturforsch.* **5 b** (1950) 122.
8. Howard, G. A. and Martin, A. J. P. *Biochem. J. London* **46** (1950) 532.
9. Bergström, S., Blomstrand, R. and Borgström, B. *Biochem. J. London* **58** (1954) 600.
10. Borgström, B. *Acta Physiol. Scand.* **25** (1952) 101.
11. Borgström, B. *Acta Physiol. Scand.* **25** (1952) 111.

Received June 4, 1956.

ACTA CHEMICA SCANDINAVICA 10 (1956) 1243—1250

Increase of Cholinesterase Content in Mouse Liver Homogenates after Incubation

KARL HÅKON SKRAMSTAD

The Norwegian Defence Research Establishment, Toxicological group, Kjeller, Norway

The rate of hydrolysis of acetyl choline by mouse liver homogenates increases by about 100 % when the homogenates are left either overnight at room temperature or two to three hours at 37° C. Of the organs investigated, only the liver homogenates presented a real "autoactivation". This "activation" takes place in liver homogenates from mice of different ages and both sexes, but is more progressive in the female. The "activation" does not disappear with dialysis and seems to be localized to the particle-fraction of the liver cell upon centrifuging. The "activation" is independent of the isotonic milieu. Kinetic experiments with a selective cholinesterase inhibitor (Nu 683) suggest that one and the same enzyme, *viz.* a pseudo-cholinesterase is responsible for the major part of the activity with acetylcholine as substrate, both prior to and after the "activation" process.

The "activation" takes place with acetylcholine and buturylcholine as substrates, while inactivation results when tributyrine, benzoylcholine and acetyl-β-methylcholine are employed.

This indicates that we are dealing with a butyro-cholinesterase. Besides, it appears as if a benzoyl-cholinesterase is present in mouse liver, an esterase differing from the butyro-cholinesterase.

Wright and Mendel [1] have described an increasing activity towards acetylcholine in rat heart muscle after incubation at 37° C for 4—5 hours. A similar phenomenon in mouse liver homogenates was observed in our laboratory. The present work was an effort to elucidate this matter further.

METHODS

Enzymes. Activity was determined by the standard manometric technique; the temperature was 37° C and pH 7.3. Krebs Ringer's isotonic bicarbonate buffer solution was used as medium (102 parts 0.154 M NaCl, 4 parts 0.154 M KCl, 3 parts 0.11 M $CaCl_2$ and 21 parts 0.154 M $NaHCO_3$).

Readings were taken every fifth minute for half an hour, activity plotted against time and expressed finally as V_{30} values, *i. e.* microlitres carbon dioxide evolved per 30 minutes, as calculated from the linear part of the curve extrapolated to 30 minutes.

Substrates. The substrates were 0.007 M acetylcholine (ACh, La Roche), 0.01 M tributyrin (TB, British Drug Houses), 0.05 M acetyl-β-methylcholine (MeCh, Merck), 0.02 M benzoylcholine (BzCh, Hopkin and Williams) and 0.01 M butyrylcholine (BuCh, synthesized by the author).

The inhibitor was Nu 683 (Ro 2—0683, La Roche) which is dimethyl carbamate of (2-hydroxy-5-phenylbenzyl)-trimethyl ammonium bromide.

Source of enzyme. Ten per cent homogenates of liver, kidney and brain from mice were prepared at 0—5° C in Ringer's buffer solution. Heparinized blood was centrifuged, plasma used without further treatment and the erythrocytes were washed twice with three times their volume of saline. The final concentration of liver homogenates in the Warburg vessels to be analysed was 1 %. The time from the removal of the liver to the first readings of the manometers was usually 30 minutes ("un-activated" liver).

Dialysis. Ten ml 10 % liver homogenate was dialyzed in a refrigerator at 0—1° C against 10 l water, which was renewed twice over a period of two days.

RESULTS

Preliminary experiments

A typical "activation" curve is present in Fig. 2, where activity is plotted against incubation time at 37° C before manometric analysis.

A fresh liver homogenate was centrifuged at high speed (20 000 g) and the precipitate washed and recentrifuged. Activity was estimated in the supernatant and the precipitate, both immediately and after incubation at 20° C for 24 hours. In the "particle fraction" 100 % activation" was found, while the" activity in the supernatant decreased by about 5 %. The "activation" process seems therefore to be associated with the solid particles in the liver cells.

It might be suspected that a concentration gradient between the medium and the particles (nuclei and mitochondria) would cause the membranes to burst with subsequent release of enzymes that were not available for the non-lipoid soluble ACh at the beginning. This would cause a false "enzymatic" activation. However, experiments in strict isotonic milieu, even during the manometric analysis, made clear that the same degree of activation occurred as in the samples under nonphysiological conditions.

As calcium is known to be an activator of cholin-esterase (ChE) [2-5] this ion had to be omitted from the Ringer's solution in order to find out whether "activation" still occurred. Experiments showed that the activity was the same whether calcium was present during incubation or not.

Even when the liver had been homogenized in distilled water and standing overnight at room temperature, its power of splitting ACh increased.

Occurrence of the "activation"

The activities with ACh as substrate, previous to and after two hour's incubation at 37° C are presented in Table 1. Plasma, erythrocytes and brain do not present any "activation". Possibly kidney and certainly liver are "activated".

Fig. 1 shows the "activation" of enzyme with ACh as a substrate after 24 hours at 20° C. The "activation" takes place in liver homogenates from mice of different ages and both sexes, although there are large fluctuations. There

Table 1. Hydrolysis of ACh by some organs of mouse prior to and after incubation at 37° C.

	V_{30}				
	kidney-homogenate	brain-homogenate	liver-homogenate	plasma	erythro-cytes
Prior to incubation	9.5	169	115	196	100
After incubation	14	172	260	200	99.5

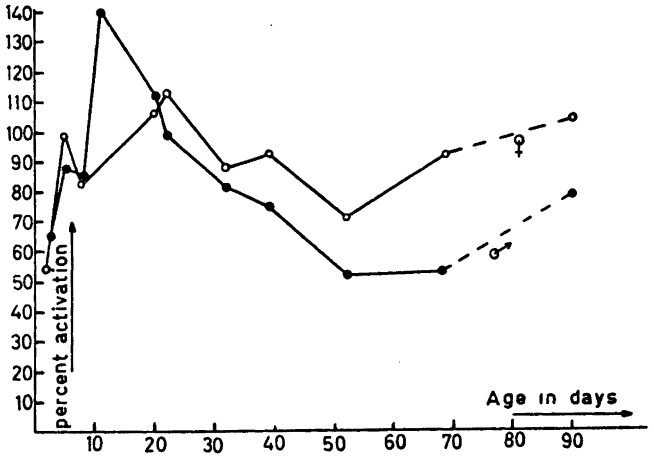


Fig. 1. Increase of cholinesterase content in mouse liver homogenates from animals of different ages and both sexes. "Activation" period lasted for 24 hours at room temperature (20° C).

seems to be a greater "activation" in livers from infantile mice than mature ones. The difference in ChE content in relation to sex is obvious [6].

After one month in the refrigerator the homogenates had lost from 5 to 10 % of their ChE activity, calculated from the 24-hours values.

Dialysis

Table 2 presents the ACh-hydrolysing values after dialysis, as compared to the same preparation not exposed to dialysis. As seen, the degree of "activation" is the same in both cases. Although the "activation" proceeds quite slowly, it might be supposed that the "activation" process is independent of any factor of low molecular weight.

Table 2. "Activation" in liver homogenates after dialysis.

Material	V_{30}
Not dialysed, measured at once	110
Not dialysed, one day at 20° C	150
Dialysed two days, measured immediately after dialysis	150
Dialysed two days, one day at 20° C	140

Different substrates

Acetylcholine. It is seen from Fig. 2 that activity increases within two to three hours at 37° C, whereupon the curve is levelling off. Hydrolysis then decreases slowly, probabely due to thermo-inactivation of the enzyme in question.

"Activation" seems to be more progressive in mature females than in males.

About the same degree of activation takes place in liver homogenates, when left overnight at room temperature (20° C).

Benzoylcholine. With this substrate the course of hydrolysis is the reverse of that with ACh. As seen from Fig. 2, the hydrolysis follows a normal course, with decreasing activity after incubation of the homogenates at 37° C.

Tributyrine. TB presents a course similar to that with BzCh. The curves for BzCh and TB differ to some extent, probably depending on factors such as concentration, pH optima and thermo-stability of the enzymes present. However, thermo-inactivation seems to increase with time of incubation in both cases.

Acetyl-β-methylcholine. True ChE, which is present in very small quantities in the liver [7], was essayed with a concentration of 2 % liver homogenate. The slight tendency of the activity to increase with time, as seen from Fig. 2, is too small to be of any experimental significance. If the "activation" had been caused by true ChE, at least a two-fold increase of the initial activity would be expected.

Buturylcholine. As seen from Fig. 2, the curve apparently is similar to that obtained with ACh as substrate. BuCh is hydrolyzed by pseudo-ChE from human plasma [8,9] and the term butyro-cholinesterase is commonly used for this type of ChE.

In accordance with these experiments one should expect that a butyro-cholinesterase is responsible for the "activation".

Nu 683 as inhibitor

This compound is considered to be a selective inhibitor of plasma-ChE [10]. It was decided to find out whether the I_{50} values prior to and after the "activation" process differed.

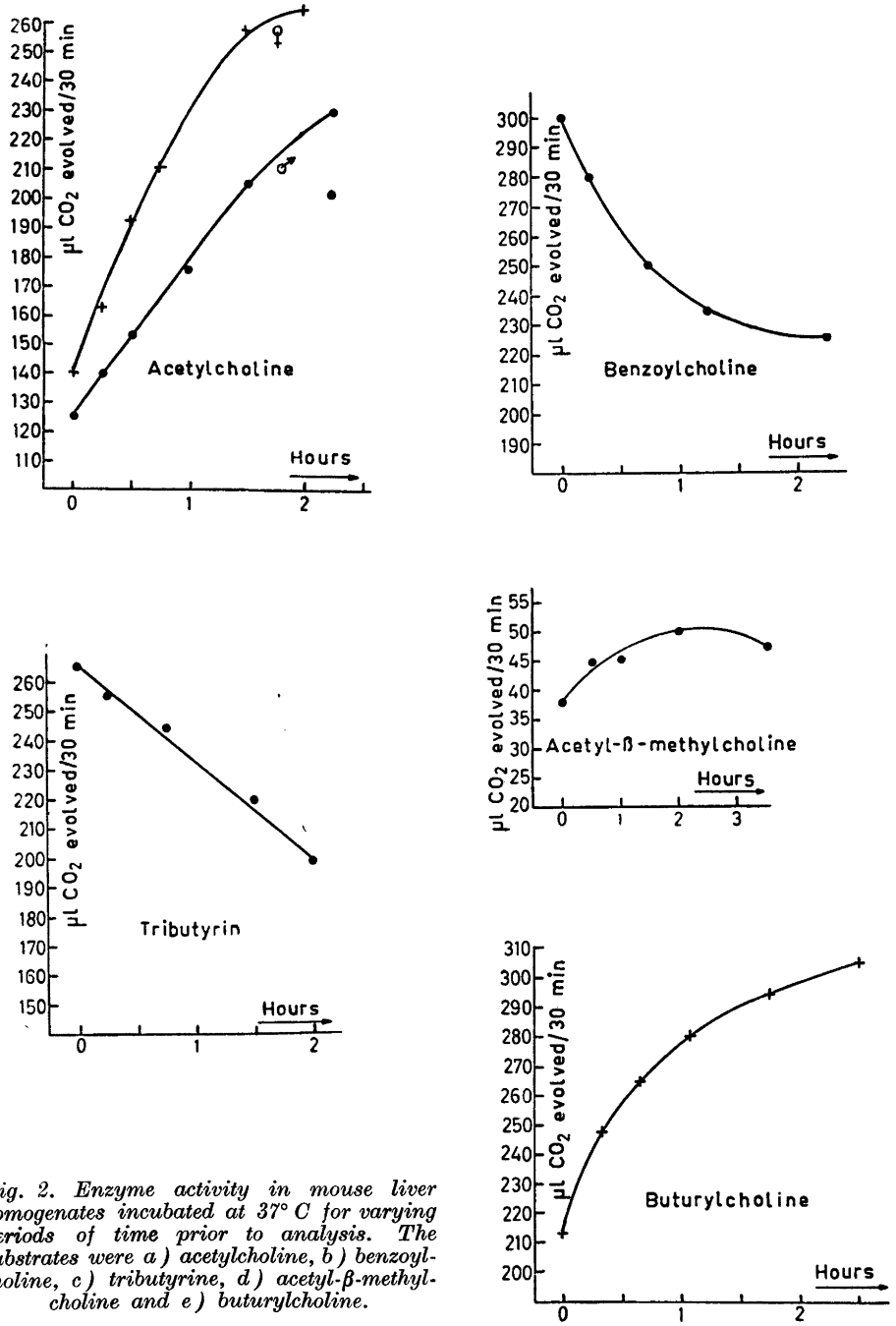


Fig. 2. Enzyme activity in mouse liver homogenates incubated at 37° C for varying periods of time prior to analysis. The substrates were a) acetylcholine, b) benzoylcholine, c) tributyrine, d) acetyl-β-methylcholine and e) buturylcholine.

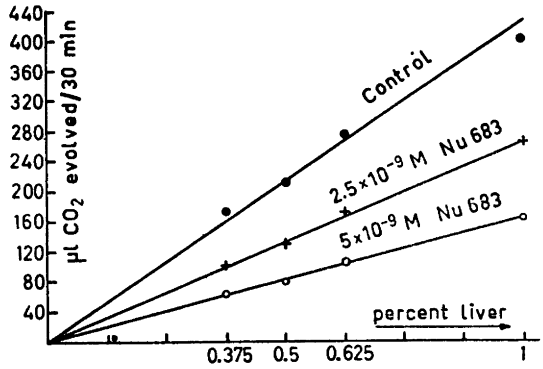


Fig. 3. Acetylcholine hydrolysis in "activated" mouse liver homogenates in presence of inhibitor (Nu 683). Activity is plotted against homogenate concentration.

In preliminary experiments the substrate and enzyme concentrations were held constant, while the inhibitor concentration was varied. A 50 % inhibition was obtained with a concentration between 2.5×10^{-9} M and 5×10^{-9} M. The inhibition was deduced by plotting V/V_i against I, to give a straight line in accordance with the equation for competitive inhibition [11]:

$$\frac{V}{V_i} = 1 + \frac{K_s}{K_i} \cdot \frac{I}{K_s + S}$$

(V and V_i are the velocities of the reaction with or without inhibitor, respectively, S is substrate concentration, I is inhibitor concentration, K_s and K_i are the dissociation constants of the enzyme-substrate and enzyme-inhibitor complexes, respectively.)

The ACh hydrolysis was measured in liver homogenates before incubation. Three samples were used: A) control, B) with 2.5×10^{-9} M Nu 683 and C) with 5×10^{-9} M Nu 683.

Table 3. ACh hydrolysis by "non-activated" and "activated" liver homogenates in the presence of Nu 683.

	control	2.5×10^{-9} M Nu 683		5×10^{-9} M Nu 683		I_{50}
	V_{30}	V_{30}	V/V_i	V_{30}	V/V_i	
"Non-activated" liver	104	73.5	1.42	46	2.26	$4.1.10^{-9}$
"Activated" liver *			1.61		2.62	$3.6.10^{-9}$

* The V/V_i values are deduced from Fig. 3.

After two hour's "activation" at 37° C the three samples were analysed in the presence of four different enzyme concentrations. Fig. 7 shows the result; activity is plotted as a function of the enzyme concentration, giving three straight lines. The ratio between the slopes of the control and the two other curves may be deduced, and from this the two V/V_i values may be found. Hence the I_{50} value, which was found to be 3.6×10^{-9} M for the "activated" liver homogenate. The I_{50} value prior to "activation" is 4.1×10^{-9} M (Table 3).

DISCUSSION

Among the organs investigated (Table 1) "autoactivation" of ACh-hydrolysis prior to incubation exists particularly in liver homogenates. This might be an indication of an increased biosynthesis of plasma-ChE in the liver, as this organ is considered to be the site of production of this esterase [12–14]. Perhaps there is an autocatalytic release of the active enzyme from some precursor, as for instance in the case of pepsinogen-pepsin. The process may be induced after the animal is dead. The transfer of "precursor" to an active enzyme seems to be independent of any dialysable factor and to take place in the solid particles of the liver cells.

It seems rather plain to decide which type of esterase is responsible for the "activation". Among the substrates investigated, only ACh and BuCh present the same "activation" features, and this suggest that a butyro-cholinesterase is the cause of the increase in activity. BzCh, often used as a specific substrate for pseudo-ChE[15], is not hydrolysed at an increased rate after incubation. On the contrary the hydrolysis of this substrate decreases with time. Thus there might perhaps be two pseudo-ChE'es in the mouse liver: one butyro-cholinesterase and one benzoyl-cholinesterase. As known, benzoyl-cholinesterases are occasionally found in the plasma of rabbits [16–18] and in the liver of guinea pigs [7,16,19].

If the "activated" hydrolysis is due to an enzyme which is not inhibited by Nu 683, the I_{50} value might be expected to increase considerably after the "activation". However, the opposite is true. The I_{50} value decreases from 4.1×10^{-9} M to 3.6×10^{-9} M after "activation". If this slight fall should be an experimental error, it might be expected that one and the same enzyme, *viz.* a pseudo-ChE, is responsible for the "autoactivation". If, on the other hand, this fall is experimentally significant, an explanation is simple when it is borne in mind that various enzymes hydrolyse ACh in the mouse liver. In addition to pseudo-ChE, the aliesterase(s) and to a lesser degree, true ChE are present. As true ChE very likely is not inhibited by Nu 683 (at the concentrations here employed) [10], the rate of hydrolysis with inhibitor present prior to "activation", is partly due to enzymes slightly or not inhibitable by Nu 683. Hence the I_{50} value becomes high. After "activation" the relative part of these enzymes (aliesterase, true ChE, benzoylChE) has decreased and thereby caused a reduced I_{50} value. This means that one and the same enzyme, a pseudo-ChE, causes the hydrolysis both prior to and after the "activation". And this pseudo-ChE, in accordance with the aforementioned circumstances, is a butyro-cholinesterase.

Acknowledgement. The author wishes to thank Dr. J. A. B. Barstad for his advice and interest in this work and Mrs. Aa. Lund-Riise for technical aid.

REFERENCES

1. Wright, M. and Mendel, B. *J. Biol. Chem.* **165** (1946) 389.
2. Mendel, B., Mundell, D. B. and Strelitz, F. *Nature* **144** (1939) 479.
3. Massart, L. and Dufait, R. *Nature* **145** (1940) 822.
4. Nachmansohn, D. *Nature* **145** (1940) 513.
5. van der Meer, C. *Chem. Weekblad* **48** (1952) 118.
6. Skramstad, K. H. *Acta Physiol. Scand.* **36** (1956). 383
7. Augustinsson, K. B. *Acta Physiol. Scand.* **15** *Suppl.* **52** (1948).
8. Adams, D. H. and Whittaker, V. P. *Biochem. J. London* **43** (1948) xiv.
9. Whittaker, V. P. *Physiol. Rev.* **31** (1951) 312.
10. Hawkins, R. D. and Gunter, J. M. *Biochem. J. London* **40** (1946) 192.
11. Lineweaver, H. and Burk, D. *J. Am. Chem. Soc.* **56** (1934) 658.
12. Antopol, W., Schifrin, A. and Tuchman, L. *Proc. Soc. exptl. Biol. Med.* **38** (1938) 363.
13. Faber, M. *Acta Med. Scand.* **114** (1943) 59, 72.
14. Sawyer, H. and Everett, J. W. *Am. J. Physiol.* **148** (1947) 675.
15. Mendel, B., Mundell, D. B. and Rudney, H. *Biochem. J. London* **37** (1943) 473.
16. Sawyer, H. *Science* **101** (1945) 385.
17. Levine, M. G., Hoyt, R. E. and Suran, A. A. *Proc. Soc. exptl. Biol. Med.* **73** (1950) 100.
18. Koelle, G. B. *Biochem. J. London* **53** (1953) 217.
19. Blaschko, H., Chou, T. C. and Wajda, I. *Brit. J. Pharmacol.* **2** (1947) 108, 116.

Received May 18, 1956.

ACTA CHEMICA SCANDINAVICA 10 (1956) 1251—1257

Action of Neutral Sulphite Solution on Carbohydrates at High Temperatures. Part I. A Sulphocarboxylic Acid Derived from Xylose

SVEN YLLNER

Department of Wood Chemistry, Swedish Forest Products Research Laboratory, Stockholm, Sweden

When heated in neutral sulphite solution at 135°C xylose is rapidly degraded. From the reaction products an acid was isolated, which was shown to have the structure of α,δ-dihydroxy-γ-sulphovaleric acid. It was degraded to the lactone of β-sulpho-γ-hydroxybutyric acid, which was synthesised by the addition of sulphite to the lactone of γ-hydroxy*iso*crotonic acid.

In account of its technical importance, considerable interest has been devoted to the decomposition of carbohydrates in sulphite solutions at high temperatures. Thus Hägglund and Johnson [1] found that aldoses in acid sulphite solutions are oxidised to the corresponding aldonic acids, and in similar experiments on holocellulose Heiwinkel [2] and Adler [3] showed that a considerable part of the decomposition of carbohydrates must be attributed to the formation of sulphonic acids, which, on account of their stability to alkali, can be distinguished from the well-known aldehyde-bisulphite addition compounds. In continuing the early work of Marusawa *et al.*[4] concerning the action of bisulphite on glucose, Matsui [5] obtained a sulphonic acid, which he suggested was "levoglucosan-6-sulphonic acid".

A sulphonic acid of quite different type was isolated by Hägglund, Johnson and Urban [6] after heating glucose in sodium sulphite-bisulphite solution of pH 6. This acid contained one carboxyl, one carbonyl and one sulphonic acid group. From the reaction product Adler [3] isolated another sulphocarboxylic acid, which lacked the carbonyl function. Moreover, both acids, with the compositions $C_6H_9O_5(SO_3H)$ and $C_6H_{11}O_5(SO_3H)$, respectively, were proved to contain a terminal glycol grouping. The complete structure of these two acids remained unknown.

Recently, the production of wood pulp using the neutral sulphite process has steadily increased. Thus the decomposition of carbohydrates in neutral

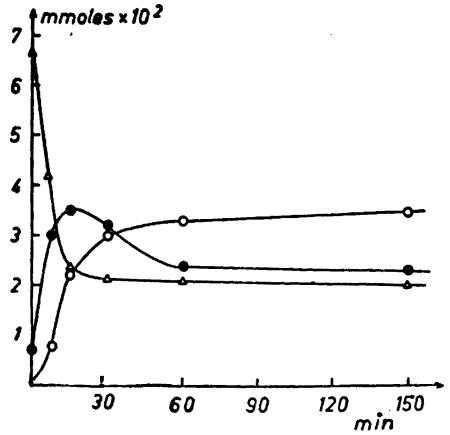


Fig. 1. The reaction of xylose in neutral sulphite solution at 135° C (using for titration 4 ml of the diluted reaction solution).

○ *"Total SO_2" consumed.*
● *"Loosely bound SO_2".*
△ *Reduction capacity calc. for xylose.*

sulphite solution is of current interest, and some additional facts pertaining to this subject have now been uncovered. As even glucose gives rise to rather complicated products, the problem has been somewhat simplified by using xylose as starting material. The present communication deals with the isolation and structural elucidation of α,δ-dihydroxy-γ-sulphovaleric acid, which is formed by heating xylose in neutral sulphite solution. Further work is in progress with the purpose of elucidating the mechanism of the formation of this acid.

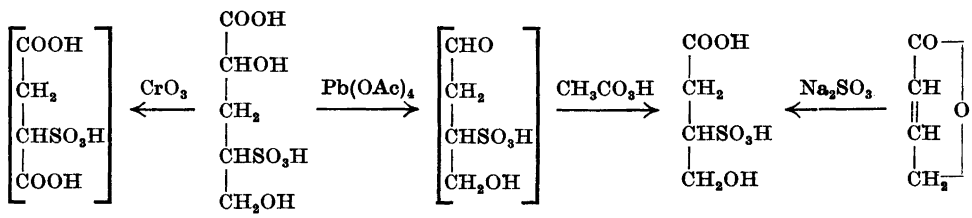
The course of the reaction at 135° C of xylose, dissolved in a solution of sodium sulphite and bisulphite in equimolecular amounts, was followed titrimetrically. The titrimetric method was essentially the same as used by Hägglund, Johnson and Urban [6] in the case of glucose, and the results are shown in Fig. 1.

The reduction capacity, calculated for xylose, decreased rapidly to an almost constant value corresponding to the decomposition of about 70 % of the initial quantity of xylose. Simultaneously "total SO_2" was consumed equivalent to the formation of sulphonic acid in a maximum yield of about 50 % calculated on xylose. The percentage of "loosely bound SO_2" was low at the start of the reaction, but rapidly increased to a maximum after 15 minutes. After one hour further heating produced only insignificant changes in the reduction capacity, "total SO_2" and "loosely bound SO_2". As was also reported by Hägglund, Johnson and Urban [6] in the case of glucose, no appreciable formation of sulphate (in the present investigation determined according to Samuelson and Ögren [7]) was found. The specific rotation calculated on the xylose content in the starting solution was +7.4°, but after 15 minutes at 135° C the reaction mixture no longer showed any optical activity. The pH (determined at room temperature) remained almost constant (6.5) during the cook.

From the reaction solution, after one hour at 135°, were isolated crude, optically inactive barium salts of organic acids containing sulphur and with a Ba to S ratio of 0.93—0.97. For a pure sulphocarboxylic acid this ratio is 1.

Calculated as such the yield of crude barium salt was almost 50 %. Coloured impurities were removed by passing an aqueous solution of the crude product through a carbon column. Although the barium salts thus purified, were almost homogeneous chromatographically (and gave the same analysis as the barium salt described below) they showed no tendency to crystallise. They were therefore converted into the brucine salts, which by crystallisation gave two compounds, one of which was obtained in about 50 % yield. This brucine salt, which could also be obtained directly from the crude barium salts in about 25 % yield, calculated on xylose, was converted back into the barium salt, which now crystallised readily. The pure barium salt was optically inactive.

According to the Ba to S ratio the molecule obviously contained one carboxyl and one sulphonic acid group. The free acid showed no tendency to lactonise in aqueous solution and the titration curve showed that the carboxyl group is strongly acidic. On the assumption of a C_5 unit, and since the substance showed no reducing properties, the remainder of the oxygen could probably be assigned to two hydroxyl groups. The substance thus seemed to be a dihydroxysulphovaleric acid, and closely related to the non-reducing "glucosesulphonic acid" isolated by Adler [3]. Unlike the latter acid it was not oxidised by periodic acid, and thus contains no glycol grouping. On the other hand it consumed one mole of lead tetraacetate with the libration of one mole of carbon dioxide indicating an α-hydroxycarboxylic acid grouping. Strong evidence for the second hydroxyl group being situated in terminal position



Scheme 1.

was obtained by oxidising the acid with dichromate. The consumption of dichromate was practically equal to that calculated (2.67 moles of CrO_3 per mole of sulphonic acid) for the formation of a sulphosuccinic acid (Scheme 1, Table 1).

The formulation of the acid as α,δ-dihydroxy-γ-sulphovaleric acid was supported by the following evidence: The product from the oxidation with lead tetraacetate (a sulphoaldehyde, not isolated) was oxidised with peracetic

Table 1. Oxidation of the sulphocarboxylic acid with dichromate.

Minutes	15	60	120	180	330	1 320
Moles of CrO_3 per mole of acid	1.19	1.81	2.16	2.36	2.60	2.76

acid to β-sulpho-γ-hydroxybutyric acid, which was isolated as the pyridinium salt of the corresponding lactone, the identity of which was shown by analysis and mixed melting point with an authentic sample of β-sulpho-γ-butyrolactone.

This was synthesised by the addition of sulphite to the lactone of γ-hydroxy*iso*crotonic acid, since, according to Schenck and Danishefsky [8], the addition of bisulphite to α,β-unsaturated carboxylic acids directs the sulphonic acid group to the β-position. The free β-sulpho-γ-hydroxybutyric acid lactonised spontaneously and the pyridinium salt of the lactone melted without decomposition and was suitable for the identification mentioned above. The sodium salt melted (with decomposition) about 30° lower than reported for the sodium salt of α-sulpho-γ-butyrolactone [9].

α,δ-Dihydroxy-γ-sulphovaleric acid contains two asymmetric carbon atoms. It therefore seems probable, that the crystalline brucine salt examined (rods), since it gave rise to an optically inactive barium salt, represents one of the two possible DL-forms of the acid. Further work will be done to elucidate the structure of the second brucine salt (needles), which may be derived from the other DL-form of this acid.

EXPERIMENTAL

Course of the reaction of xylose in sodium sulphite-bisulphite solution. Xylose (2.50 g), sodium pyrosulphite (3.7 g) and sodium sulphite hepta hydrate (9.8 g) were dissolved in water, and the solution made up to 100 ml. Samples (10 ml) of this solution were heated in sealed glass tubes in an oil bath at 135° C. When cooled each sample was diluted to 100 ml.

"Free SO_2" was determined by iodine titration of an acidified (pH 2) sample of this solution, and "total SO_2" by iodine titration of a sample buffered with calcium carbonate. "Loosely bound SO_2" was calculated as the difference between "total SO_2" and "free SO_2". The reduction capacity was determined according to Bertrand. The results are shown in Fig. 1.

Fractionation of the reaction products as barium salts. Xylose (5 g), sodium pyrosulphite (7.4 g), and sodium sulphite hepta hydrate (19.6 g) were dissolved in water (100 ml total volume) and the solution was heated in sealed glass tubes for one hour. The faintly yellow reaction mixture was passed through a column of Amberlite IR-120 (300 ml) in the H^+-state. Nitrogen was bubbled through the sodium free solution to remove most of the sulphur dioxide. Saturated barium hydroxide solution was then added until pH 7.5 was reached. Barium sulphate and sulphite were removed by filtration, and the solution, which had turned red, was evaporated *in vacuo* to 30 ml.

To the vigorously stirred solution ethanol (10 ml) was added dropwise, a syrupy precipitate being formed (fraction 1). The clear solution was decanted, another portion of ethanol (4 ml) was added giving a further, somewhat larger syrupy precipitate (fraction 2). Additional ethanol (20 ml) gave rise to only a small precipitate (fraction 3). The solution, containing more than 50 % ethanol, was evaporated *in vacuo* to 10 ml and further precipitation was effected by addition of this solution to ethanol (60 ml). The precipitate was washed with abs. ethanol and ether and dried (fraction 4). The syrupy fractions 1—3 were each dissolved in water (10 ml), precipitated in ethanol (60 ml), washed with ethanol-ether and dried. Amounts and compositions of the fractions 1—4 are shown in Table 2.

Chromatographic examination of the fractions. Samples (200 mg) of the fractions 1—4 were dissolved in water, and the solutions passed through columns of IR-120 in the NH_4^+-state. The ammonium salts were chromatographed on Whatman No. 1 filter paper with a solvent system of ethanol:water (4:1) using the descending technique. The chromatograms were sprayed, according to van Duuren [10], with 4 % formaldehyde and dried at 60° C in order to convert the ammonia to urotropine. The free acids were then detected by spraying with a solution containing starch, potassium iodide and iodate [10]. Fractions 1—3 were found to be very similar giving a few weak spots and one strong spot ($R_F = 0.20$),

Table 2. The crude barium salt fractions.

Fraction. No	g	% Ba	% S	Ba/S molar ratio
1	1.80	37.7	9.09	0.97
2	2.80	36.6	9.04	0.95
3	0.88	36.8	9.23	0.93
4	2.86	32.3	9.52	0.79

which obviously contained the main part of the acids. Fraction 4 on the other hand gave four almost equally strong spots with R_F-values of 0.20, 0.26, 0.30, and 0.36, and a somewhat weaker spot with R_F = 0.40. The identity of the latter four of these, which also appeared as very weak spots in the fractions 1—3 has yet not been established.

By using silver nitrate and sodium hydroxide as spray reagent according to Trevelyan *et al.*[11] no spots were obtained with R_F = 0.20, and only some of the substances in fraction 4 showed reducing properties.

Purification of the crude barium salt. Fractions 1—3 were strongly discoloured, but the impurities could be removed by filtering a water solution of the crude product through a carbon column (Carbo animalis:Celite, 1:1). The barium salt solution thus purified, was evaporated to a small volume and precipitated by pouring into ethanol. (Found: Ba 38.5; S 9.23; C 17.3; H 2.45. Calc. for $C_5H_8O_7SBa$: Ba 39.3; S 9.17; C 17.2; H 2.31.).

The purified amorphous barium salts (490 mg) were dissolved in water and the solution passed through a column (5 ml) of Amberlite IR-120 in the H^+-state. The acids were neutralised by brucine and the solution then evaporated to a small volume. By addition of acetone a rapid crystallisation was achieved. The crystals were quite uniform in the shape of rods, more or less collected in bundles. Yield 0.46 g.

The mother liquor gave a new fraction containing chiefly crystals of the same shape but also a few bundles of long needles. Yield 0.35 g. The two fractions were combined and recrystallised from water-acetone, the product being rods only. (Found: S 3.33; OCH_3 12.1. Calc. for $(C_{23}H_{26}O_4N_2)_2C_5H_{10}O_7S$: S 3.20; OCH_3 12.4).

Additional brucine salt (0.34 g), mainly the needle-like modification, was obtained from the mother liquor.

The brucine salt with rod-like crystals was converted into the barium salt which crystallised readily from a concentrated water solution in the form of short rods and was recrystallised from water-ethanol. (Found: Ba 37.2; S 8.58; C 16.4; H 2.33; H_2O 5.15. Calc. for $C_5H_8O_7SBa$, H_2O: Ba 37.4; S 8.73; C 16.4; H 2.74; H_2O 4.91.)

Oxidation of the sulphonic acid with dichromate. Crystalline barium salt (310 mg) was dissolved in water (25 ml) and a solution (50 ml) of sulphuric acid (5 ml) and potassium dichromate (0.88 g) was added. The reaction mixture was made up to 100 ml, and two samples (5 ml) were immediately taken at room temperature, when the oxidation was slow, and added to a mixture of potassium iodide and sulphuric acid. The liberated iodine was titrated with 0.05 N thiosulphate. After the starting concentration had been determined, the sealed reaction flask was placed in a boiling water bath. The reaction mixture was cooled to room temperature each time samples were taken, and these were titrated as mentioned. Results in Table 1.

Oxidation of the sulphonic acid with lead tetraacetate. a) *Course of the reaction.* The following solutions were made:

A. Crystalline barium salt (70.8 mg) was dissolved in water and the solution made up to 50 ml.

B. A saturated solution (15 ml) of lead tetraacetate in acetic acid was diluted with acetic acid to 100 ml.

C. Potassium iodide (10 g) and sodium acetate (50 g) were dissolved in water. and the solution made up to 100 ml.

Five ml of A were rapidly mixed with 5 ml of B. At the end of the reaction time 5 ml of C were added and the liberated iodine titrated with 0.01 N thiosulphate. In the blank, 5 ml of water were used instead of A. When the reaction time exceeded 20 minutes lead dioxide was precipitated, and correct titration figures could then not be obtained. Results in Fig. 2.

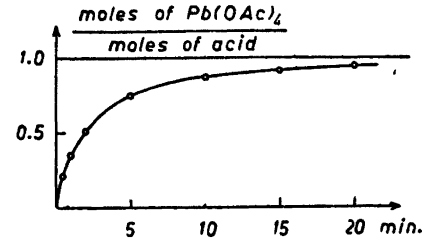


Fig. 2. Oxidation of the sulphocarboxylic acid with lead tetraacetate.

b) *Formation of carbon dioxide.* A test-tube (50 ml) fitted with a side tube and containing a saturated solution of lead tetraacetate in acetic acid (20 ml) was sealed with a rubber stopper fitted with a small separatory funnel and a capillary inlet tube reaching almost to the bottom of the test-tube. For 30 minutes a gentle stream of CO_2-free nitrogen was bubbled through the solution and was afterwards passed firstly through a tube containing $Mg(ClO_4)_2$ and kept at $-20°$ C and secondly through an absorption tube containing NaOH-asbestos. During this time the weight of the absorption tube was constant. The stream of nitrogen was cut off, a solution of the barium salt (209.6 mg) in water (5 ml) was added through the separatory funnel, which was washed out with a few millilitres of water and immediately closed. The stream of nitrogen was again passed through the apparatus, and the reaction tube warmed to 50° C. The absorption tube reached constant weight after about one hour. (Found: 25.0 mg of CO_2. Calc. for $C_5H_8O_7SBa$, H_2O: 25.1 mg of CO_2.)

c) *Degradation to β-sulpho-γ-hydroxybutyric acid.* The barium salt of the sulphonic acid (0.55 g) was dissolved in water and passed through a column (8 ml) of Amberlite IR-120 in the H^+-state. The solution of the free acid was diluted to 50 ml, and added to a saturated solution of lead tetraacetate in glacial acetic acid (50 ml). After 1 hour the reaction mixture was diluted with water (100 ml) in order to destroy excess lead tetraacetate. After filtration, a solution (2.0 ml) of peracetic acid [12] (equal volumes of H_2O_2 (30 %) and acetic anhydride, three days at room temperature) was added, and the reaction mixture kept at 75° C for 90 minutes. After cooling, excess H_2O_2 and CH_3CO_3H was destroyed by shaking the reaction mixture together with 1 g of Pd-asbestos (25 % Pd) overnight. The mixture was filtered, treated with H_2S and filtered again. The solution was evaporated *in vacuo* to 2.5 ml, kept at room temperature for three days for completion of lactonisation, neutralised with pyridine and evaporated to a syrup. This was dissolved in ethanol, some insoluble material was filtered off, and the solution again concentrated to a syrup. This was repeated once. The residual syrup was dissolved in 3 ml of ethanol, and a few drops of ether were added. A rapid crystallisation of the pyridinium salt of β-sulpho-γ-butyrolactone occurred. Recrystallisation from ethanol-ether yielded 0.21 g of optically inactive material. M. p. 160—161 °C. (Found: N 5.49; S 12.8; Calc. for $C_9H_{11}O_5NS$: N 5.72; S 13.1). No m. p. depression with an authentic sample of the pyridinium salt of β-sulpho-γ-butyrolactone was observed.

Synthesis of β-sulpho-γ-butyrolactone. γ-Hydroxy*iso*crotonic acid lactone (0.5 g), prepared according to Glattfeld *et al.*[13], was dissolved in a solution of sodium sulphite hepta hydrate (1.5 g) in water (3 ml). Sulphite was rapidly consumed, and the temperature rose to about 50° C. Next day the solution was passed through a column of Amberlite IR-120 in the H^+-state. The eluate was evaporated to 2 ml and kept at room temperature for three days. The acid was neutralised with pyridine (0.5 ml) and the solution evaporated to a syrup. When this was diluted with ethanol a rapid crystallisation of the pyridinium salt of β-sulpho-γ-butyrolactone occurred. Recrystallisation from ethanol-ether yielded prismatic plates, 1.05 g. M. p. 160—161 °C. (Found: N 5.55; S 13.2. Calc. for $C_9H_{11}O_5NS$: N 5.72; S 13.1.)

The sodium salt melted at 210-215° C (decomp.).

When chromatographed on Whatman No. 1 filter paper using the solvent system ethanol:conc. NH_3:water (20:1:4) and developing according to van Duuren [10] the acid gave two spots with R_F-values 0.28 and 0.41, respectively, the latter probably corresponding to the lactone and the former to the free sulphocarboxylic acid.

REFERENCES

1. Hägglund, E. and Johnson, T. *Svensk Kem. Tidskr.* **41** (1929) 8, 55; Hägglund, E. *Ber.* **62** (1929) 437.
2. Heiwinkel, H. *Svensk Papperstidn.* **47** (1944) 265.
3. Adler, E. *Svensk Papperstidn.* **49** (1946) 339.
4. Marusawa, T., Naito, D. and Uchida, J. *Mem. Ryojun Coll. Eng.* **1** (1929) 351.
5. Matsui, T. *J. Chem. Soc. Japan. Ind. Chem. Sect.* **53** (1950) 411, 427; **54** (1951) 72.
6. Hägglund, E., Johnson, T. and Urban, H. *Ber.* **63** (1930) 1387.
7. Samuelson, O. and Ögren, T. *Svensk Papperstidn.* **49** (1946) 499.
8. Schenck, R. T. E. and Danishefsky, I. *J. Org. Chem.* **16** (1951) 1683.
9. Krzikalla, H. and Tartter, A. *Ger. pat. 800 410* (1950).
10. van Duuren, A. J. *Rec. trav. chim.* **72** (1953) 889.
11. Trevelyan, W. E., Procter, D. P. and Harrison, J. S. *Nature* **166** (1950) 444.
12. Haas, H., Schoch, W. and Ströle, U. *Das Papier* **9** (1955) 469.
13. Glattfeld, J. W. E., Leavell, G., Spieth, G. E. and Hutton, D. *J. Am. Chem. Soc.* **53** (1931) 3164.

Received June 7, 1956.

ACTA CHEMICA SCANDINAVICA 10 (1956) 1258—1266

Kinetics of the Hydrolysis of Methyl-valerate Catalyzed by Horse Liver ali-Esterase

J. A. CHRISTIANSEN and JOHN GRAAE

Universitetets Fysisk-Kemiske Institut, Copenhagen, Denmark

The hydrolysis of methyl-valerate catalyzed by horse liver ali-esterase was investigated by continuous automatic titration of the liberated acid. The reaction was studied with different initial concentrations of enzyme and substrate and followed to a degree of reaction of 99 %. The following chronometric integral can describe the reaction

$$t = A \cdot \frac{a}{E} \cdot a + B \cdot \sqrt{\frac{a}{E}} \left[\ln \frac{1 + \sqrt{a}}{1 - \sqrt{a}} - 2\sqrt{a} \right]$$

where t is time, a initial substrate concentration, E enzyme concentration, a degree of reaction and A and B are constants. It is pointed out that the appearance of square roots in the chronometric integral indicates a reaction between two enzyme-containing molecules. A mechanism of this type is suggested.

Several attempts have been made to elucidate the kinetics of the ali-esterases. It is very often described as a zero order reaction [1–3]. Schønheyder [6] has described it in a particular case as a combination of a zero and a first order reaction, while others [4–5] have described similar cases by a Michaelis-expression, which actually amounts to the same. Many of the investigators have only studied the beginning of the reaction (*i. e.* less than 50 % degree of reaction) and it should be well known that this often leads to misinterpretations of the experimental data. It is the purpose of this investigation to study the kinetics of the enzymic ester hydrolysis including also high degrees of reaction. The substrate was methyl-valerate. This ester was chosen because of its rapid reaction in the presence of esterases [7–10].

The enzyme was obtained from horse liver which has a high content of esterase [11] and is easy to obtain in large quantities.

EXPERIMENTAL

Enzyme. Fresh horse liver was obtained directly from the slaughter house. It was disintegrated in a Waring blendor and washed four times with acetone in order to remove water and fat. After each washing the powder was drained on a Büchner funnel with moderate suction and after the last one it was dried overnight at room temperature. The dry powder was stored in the refrigerator until use. Solutions for the experiments were made by stirring the powder with ten times its weight distilled water for a few hours at room temperature. After centrifugation the clear dark red-brown supernatant was used for the experiments.

Substrate. Methyl-valerate was prepared from butanol (1) which was converted into valeronitril as described by Adams and Marvel [12]. From this nitrile the ester was prepared by interaction with methanol and sulfuric acid. The product was distilled in a Stedman column [13,14], b. p. 127.8/128.3 (uncorr.) at 767.4/768.6 mm Hg.

Apparatus. The hydrolysis of the ester was followed by continuous automatic titration in a pH-stat [14a]. All experiments were made at pH = 8.0, which is the optimum pH [2] and 20.0° C. The reaction chamber was a 100 ml beaker. The experiments were performed in 50 ml 0.1 M KCl, carefully adjusted to pH = 8 with KOH. A suitable amount of ester was added and the experiment was started by adding the desired amount of enzyme solution. Corresponding values of time and amount of KOH added from a syringe necessary to keep pH constant were read. The concentration of ester was found as the titration value when the reaction had finished.

The stability of the enzyme was checked in the following way: An enzyme solution was kept in a thermostat at 20° C. A sample of 3 ml was removed and an experiment performed in the manner described above and continued for about 10 min. This was repeated at suitable intervals for the next 20 hours. As will be seen from Fig. 1 there was no measurable alteration of enzyme activity during this time. The last enzyme sample was heated to about 95° C for 30 min. As also shown by Fig. 1 there was no measurable activity left after this treatment.

The positive interception on the ordinate axis is due to the fact that the enzyme solution has a pH lower than the experimental pH and the final adjustment of this pH is made by the pH-stat. It is seen from the figure that the amount of KOH necessary to make this adjustment is well-defined and it is of course subtracted from all measurements used for the kinetical determinations.

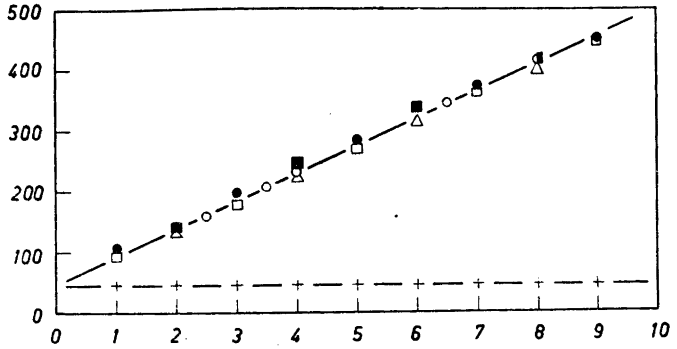


Fig. 1. Experiment with enzyme at different ages. Abscissa: Time in minutes; ordinate: Scale readings on the syringe. One scale reading equals 4.98 10^{-7} eqv. Age of enzyme: O — O — O*: 0 min.* □ — □ — □*: 70 min.* △ — △ — △ *158 min.* ● — ● — ●*: 1 210 min.* ■ — ■ — ■*: 1 283 min.* + — + — +*: Boiled enzyme.*

Tables 1—4. The tables indicate the measured values of time (t_{exp}) and degree of reaction (a), together with times calculated (t_{calc}) from the suggested chronometric integral. If the enzyme concentration used in these experiments equals 1 M the constants A and B are 3 310 and 17.42 minutes, respectively.

Table 1. $a = 13.15 \times 10^{-3}$ M.

t_{exp} min	a	t_{calc} min
0	0	0
3	0.0707	3.10
6	0.1400	6.17
9	0.2028	8.96
12	0.2764	12.26
16.5	0.3742	16.68
20.5	0.4578	20.50
29	0.6357	28.83
33	0.7170	32.78
37	0.7920	36.58
41	0.8710	40.89
46	0.9550	46.56
48	0.9700	48.02
50	0.9870	50.42

Table 2. $a = 6.70 \times 10^{-3}$ M.

t_{exp} min	a	t_{calc} min
0	0	0
2	0.0983	2.21
4	0.1840	4.17
6	0.2612	5.95
8	0.3511	8.05
10	0.4410	10.18
12	0.5183	12.04
14	0.5965	13.97
16	0.6713	15.86
18	0.7584	18.17
20	0.8272	20.12
22	0.8919	22.18
24	0.9480	24.44
28	0.9902	27.73

Table 3. $a = 3.04 \times 10^{-3}$ M.

t_{exp} min	a	t_{calc} min
0	0	0
2	0.2167	2.26
4	0.4056	4.30
6	0.5387	5.81
8	0.7090	7.87
10	0.8483	9.83
12	0.9412	11.63
14	0.9845	13.32

Table 4. $a = 1.08 \times 10^{-3}$ M.

t_{exp} min	a	t_{calc} min
0	0	0
1	0.2435	0.93
2	0.4435	1.75
3	0.6609	2.75
4	0.8000	3.50
5	0.9565	4.89

RESULTS

Experiments were performed at four different substrate concentrations, with the same enzyme concentration. It was found that under these circumstances the reaction could be described by the expression:

$$t = A \cdot a\alpha + B \cdot \sqrt{a}\left[\ln \frac{1+\sqrt{\alpha}}{1-\sqrt{\alpha}} - 2\sqrt{\alpha}\right]$$

where t is time, α degree of reaction, a initial substrate concentration and A and B are constants. The results of these experiments are given in Tables 1—4.

Tables 5—8. The tables indicate the measured values of time (t_{exp}) and degree of reaction (α), together with time calculated (t_{calc}) from the suggested chronometric integral. With the arbitrary values for enzyme concentration used here the constants A and B are 5 699 and 17.39 minutes respectively.

Table 5. $a = 1.314 \times 10^{-2}$ M. $E = 2.005$.

t_{exp} min	α	t_{calc} min
0	0	0
3	0.0865	3.26
6	0.1673	6.32
9	0.2489	9.43
11	0.3018	11.46
15	0.4105	15.67
18	0.4856	18.60
21	0.5608	21.57
24	0.6351	24.55
27	0.7131	27.74
30	0.7818	30.64
33	0.8519	33.75
36	0.9142	36.80
39	0.9614	39.66
42	0.9871	42.14

Table 6. $a = 1.259 \times 10^{-2}$ M. $E = 2.978$.

t_{exp} min	α	t_{calc} min
0	0	0
2	0.0776	1.89
4	0.1626	3.97
6	0.2425	5.95
8	0.3246	8.00
10	0.4022	9.95
12	0.4791	11.90
14	0.5589	13.96
16	0.6305	15.84
18	0.7067	17.89
20	0.7791	19.91
22	0.8455	21.88
24	0.9067	23.88
26	0.9552	25.88
28	0.9873	28.03
30	0.9963	29.61

Table 7. $a = 1.274 \times 10^{-2}$ M. $E = 3.990$.

t_{exp} min	a	t_{calc} min
0	0	0
2	0.1128	2.08
4	0.2197	4.08
6	0.3230	6.03
8	0.4262	8.01
10	0.5265	9.96
12	0.6209	11.85
14	0.7168	13.83
16	0.8097	15.86
18	0.8894	17.80
20	0.9521	19.73
22	0.9830	21.30
24	0.9919	22.17

Table 8. $a = 1.330 \times 10^{-2}$ M. $E = 4.970$.

t_{exp} min	a	t_{calc} min
0	0	0
2	0.1392	2.15
3	0.2042	3.18
4	0.2699	4.22
5	0.3300	5.18
6	0.3943	6.21
7	0.4537	7.18
9	0.5717	9.13
10	0.6339	10.19
12	0.7491	12.23
14	0.8516	14.21
16	0.9420	16.40
18	0.9880	18.50

Four experiments with different enzyme concentrations, but with almost the same substrate concentration were performed. Tables 5—8 show the measured and the calculated times. The following expression was used for the calculations:

$$t = \mathrm{A} \cdot \frac{a}{E} a + \mathrm{B} \cdot \sqrt{\frac{a}{E}} \left[\ln \frac{1 + \sqrt{a}}{1 - \sqrt{a}} - 2 \sqrt{a} \right]$$

The constants A and B used for the calculations were found in the following manner: The chronometric integral was written as:

$$t = \mathrm{A}' \cdot a + \mathrm{B}' \cdot \left[\ln \frac{1 + \sqrt{a}}{1 - \sqrt{a}} - 2\sqrt{a} \right]$$

and the constants A′ and B′ were determined for every experiment. It turned out that empirically A′ could be represented by Aa/E and B′ by $B\sqrt{a/E}$ where A and B are common to all experiments in which the relative values of E are known. The deviation between measured and calculated times seen in some of the experiments are supposed to be due to difficulties in obtaining exactly the

desired enzyme concentration. It may be, however, that the deviations are due to the approximation introduced between formula (12) and (12 a) in the following discussion of the reaction mechanism.

REACTION MECHANISM

To explain the occurrence of the square root of the initial substrate concentration we have assumed that two molecules of enzyme in the same or in different forms combine with one molecule of one of the reactants. As the situation is similar to the state of affairs at certain photochemical reactions, *cf. e. g.* the classical work of Bodenstein *et al.*[15] and Jost [16], some such assumption seems very natural or even necessary.

As it is known that enzymic ester hydrolyses are often inhibited by the acid and not by the alcohol [6] we assume that in our case it is the valerate ion which combines with the enzyme, and suggest the following reaction scheme:

$$X_1 \rightleftharpoons X_2 \qquad (\pm 1)$$
$$X_2 + OH^- \rightleftharpoons X_3 \qquad (\pm 2)$$
$$X_3 + MV \rightarrow X_1 + MOH + V^- \qquad (+3)$$

with the additional equilibrium:

$$2X_3 + V^- \rightleftharpoons X_4 \qquad (\pm 3a)$$

where X_{1-4} are different enzyme forms, MV methyl-valerate, MOH methyl alcohol and V^- valerate ion. From this scheme we can theoretically deduce a chronometric integral identical with the empirical one: Using the steady state method as described by Christiansen [17,18] and with the symbols used by Christiansen we have:

$$s = x_1 w_1 - x_2 w_{-1} \qquad (4)$$
$$s = x_2 w_2 - x_3 w_{-2} \qquad (5)$$
$$s = x_3 w_3 \qquad (6)$$

where s is the steady state rate and the w_i's are reaction probabilities for the steps indicated. The other small letters indicate the concentration of the substance symbolized by the same capital letter.

Solutions of the equations yield:

$$x_1 = s\ (1 + w_{-1}/w_2 + w_{-1}w_{-2}/w_2 w_3)/w_1 \qquad (7)$$
$$x_2 = s\ (1 + w_{-2}/w_3)/w_2 \qquad (8)$$
$$x_3 = s/w_3 \qquad (9)$$

As it is known that the reaction has an energy of activation [19] we assume that X_2 must be on a higher energy level than X_1.

Fig. 2 will account for the energy levels of the enzyme during the reaction. From this it is seen that $w_{-2}/w_3 \ll 1$ and eqns. 7, 8 and 9 can be rewritten as follows:

$$x_1 = s\ (1 + w_{-1}/w_2)/w_1 = q_1 s \qquad (7a)$$
$$x_2 = s/w_2 = q_2 s \qquad (8a)$$
$$x_3 = s/w_3 = q_3 s \qquad (9a)$$

From (3a) we get

$$x_4/x_3^2 v = K \qquad (10)$$

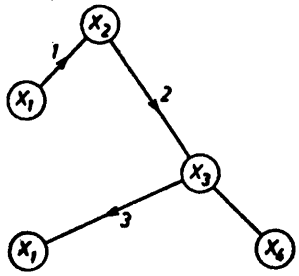


Fig. 2.

where K is an equilibrium constant and v means the concentration of valerate ions. For the total enzyme concentration we have

$$E = x_1 + x_2 + x_3 + x_4$$

Regarding the energy levels it is obvious that x_2 can be neglected and we then have

$$x_4 = E - (x_1 + x_3) \tag{11}$$

Introducing (7a), (9a) and (11) in (10) and solving the equation we find

$$\frac{2}{s} = \frac{q_1 + q_3}{E} + \sqrt{\left(\frac{q_1 + q_3}{E}\right)^2 + \frac{4K \cdot v}{E} \cdot q_3^2} \tag{12}$$

If we require this expression to conform with that derived from the chronometric integral by differentiation we must assume that:

$$\left(\frac{q_1 + q_3}{E}\right)^2 \ll \frac{4K \cdot v}{E} \cdot q_3^2$$

Regarding the energy levels we get:

$$q_3 \ll q_1$$

and eqn. 12 is then reduced to

$$2/s = q_1/E + 2q_3\sqrt{K \cdot v/E} \tag{12a}$$

From the reaction scheme it is seen that

$$\begin{aligned} w_1 &= k_1 \\ w_{-1} &= k_{-1} \\ w_2 &= k_2' \cdot c_{OH^-} \quad \text{or, at constant pH,} \\ w_2 &= k_2 \\ w_3 &= k_3\ (a - v) \end{aligned}$$

where the k's are constants and a is the initial substrate concentration. Introducing this in (12a) we find

$$2/s = 2\mathrm{d}t/\mathrm{d}v = 1/E\ (1/k_1 + k_{-1}/k_1k_2) + 2\sqrt{1/E} \cdot \sqrt{K} \cdot \sqrt{v}/k_3\ (a - v)$$

or

$$\mathrm{d}t/\mathrm{d}v = \mathrm{A}/E + \mathrm{B} \cdot \sqrt{1/E} \cdot \sqrt{v}\,/(a - v) \tag{12b}$$

where A and B are new constants. Integrating this equation and introducing the degree of reaction $\alpha = v/a$ we get

$$t = \mathrm{A} \cdot \frac{a}{E} \cdot \alpha + \mathrm{B} \cdot \sqrt{\frac{a}{E}} \cdot \left[\ln \frac{1+\sqrt{\alpha}}{1-\sqrt{\alpha}} - 2\sqrt{\alpha} \right]$$

which is identical with the empirically found chronometric integral.

It should be noted that (12b) only differs from an ordinary combination of a zero and a first order expression by the factor $\sqrt{E \cdot v}$ in the last term.

DISCUSSION

The reaction scheme suggested here is different from any one earlier found in the literature. It should be noticed that we have followed the reaction nearly to completion, while many of the earlier investigators only studied the first 50 % or less of the range. An exception is Schønheyder [6] who has published an experiment in which he follows the hydrolysis of 1-caprylyl-glycerol by rabbit liver esterase until 98.5 % degree of reaction. However, even his experiments are often followed only to 45—90 % degree of reaction.

It should be mentioned that investigations carried out in order to study the ali-esterase have been performed with enzymes isolated from many different sources and with the most different substrates. We have no reason to be sure that different enzymes will act on different substrates in the same way.

It should be mentioned too, that the chronometric integral found empirically by us could possibly be explained by other reaction schemes. The scheme mentioned must be considered as a suggestion which explains our experimental results, but we cannot postulate that it is the only possible explanation, observe, however, the remark p. 1263 and in the synopsis.

Acknowledgements. Part of this work was carried out with financial support from the *Carlsberg foundation* which is gratefully acknowledged.

We are indebted to Dr. E. Güntelberg for drawing our attention to this subject.

REFERENCES

1. Kastle, I. H. and Loevenhart, A. S. *Am. Chem. J.* **24** (1900) 491.
2. Purr, A. *Biochem. Z.* **322** (1951) 205.
3. Singer, T. P. and Hofstee, B. H. J. *Arch. Biochem.* **18** (1948) 245.
4. Hofstee, B. H. J. *Science* **116** (1952) 329.
5. Lineweaver, H. and Burk, D. *J. Am. Chem. Soc.* **56** (1934) 658.
6. Schönheyder, F. *Biochim. et Biophys. Acta* **6** (1951) 461.
7. Graae, J. *Acta Chem. Scand.* **8** (1954) 356.
8. Matlack, M. B. and Tucker, I. W. *J. Biol. Chem.* **132** (1940) 663.
9. Sobotka, H. and Glick, D. *J. Biol. Chem.* **105** (1934) 199.
10. Weinstein, S. and Wynne, A. *J. Biol. Chem.* **112** (1936) 641.
11. Bamann, E. *Ber.* **62 B** (1929) 1538.
12. Adams, R. and Marvel, C. S. *J. Am. Chem. Soc.* **42** (1920) 313.
13. Stedman, D. F. *Can. J. Research.* **15** B (1937) 383.
14. Klit, A. *Studier over fraktioneret Destillation.* Diss. Copenhagen 1943.

14a. Christiansen, J. A., Drost-Hansen, W. and Nielsen, A. E. *Acta Chem. Scand.* **6** (1952) 333.
15. Bodenstein, M., Jost, W. and Jung, G. *J. Chem. Soc.* **1929** 1153.
16. Jost, W. *Z. physik. Chem.* **134** (1928) 92.
17. Christiansen, J. A. *Acta Chem. Scand.* **3** (1949) 493.
18. Christiansen, J. A. *Advances in Catalysis.* **6** (1953) 311.
19. Connors, W. M., Pihl, A., Dounce, A. L. and Stotz, E. *J. Biol. Chem.* **184** (1950) 29.

Received June 4, 1956.

ACTA CHEMICA SCANDINAVICA 10 (1956) 1267—1275

Kinetics of the Base-catalysed Reaction between Acetamide and Formaldehyde and the Ionization Constants of Formaldehyde and Hydroxymethylacetamide

J. KOSKIKALLIO

Institute of Chemistry, University of Helsinki, Helsinki, Finland

The rate of formation of hydroxymethylacetamide from acetamide and formaldehyde has been measured in aqueous solution at different sodium hydroxide concentrations. The second-order rate constant approaches a limiting value as the concentration of sodium hydroxide is increased. At a constant alkali concentration, the second-order rate constant decreases as the formaldehyde concentration is increased, but a change in the acetamide concentration does not alter the rate constant. The same applies to the reverse reaction. From these results it has been deduced that only the hydroxymethylacetamide and formaldehyde hydrate anions formed in the alkaline solution react. The ionization constants of hydroxymethylacetamide ($K_a = 6.0 \times 10^{-14}$) formaldehyde ($K_a = 8.5 \times 10^{-14}$), both at 20°, have been calculated from the kinetic data. The second-order rate constant of the reaction between acetamide and formaldehyde anion, $k_2 = 0.085$ l mole^{-1}sec^{-1}, and the first-order rate constant of the opposing reaction of hydroxymethylacetamide anion, $k_1 = 3.72 \times 10^{-3}$ sec^{-1} were obtained by an extrapolation method. From measurements made at different temperatures, the heat of the reaction

$$CH_3CONHCH_2OH + HO^- \rightarrow CH_3CONHCH_2O^- + H_2O$$

has been found to be about 1.1 kcal. The parameters of the Arrhenius equation for the formation of acetamide and formaldehyde from the hydroxymethylacetamide anion are $E = 21.8$ kcal. and $\log A = 13.8$.

Two different hydroxymethylamides are formed in the reaction between formaldehyde and an acid amide:

$$R—CO—NH_2 + CH_2O \rightleftharpoons R—CO—NH—CH_2OH \quad (1)$$

$$R—CO—NH—CH_2OH + CH_2O \rightleftharpoons R—CO—N(CH_2OH)_2 \quad (2)$$

Both reactions proceed until an equilibrium state is reached and are catalysed by various acids and bases [1-3]. The reaction between acetamide and formaldehyde was studied kinetically by Grove and Lynch [4]. From polarographic

studies they deduced that formaldehyde, which in neutral and dilute aqueous solution is known to be almost completely in the form of a hydrate (99.99 %) [5], is dehydrated in the presence of alkali, and concluded that formaldehyde reacts with acetamide only in the dehydrated form. Their value for the heat of dehydration (4 kcal.) differs considerably from the value (14.6 kcal.) obtained by Bieber [5].

The similar reaction between urea and formaldehyde has been studied by several authors. de Jong and de Jonge [3] found that the reaction rate is proportional to the hydroxyl and hydrogen ion concentrations of the medium. They believed that in alkaline solution urea forms an anion $NH_2—CO—NH^-$ which reacts with formaldehyde to form the hydroxymethylurea anion. A similar mechanism has been proposed by Okano and Ogata [6] who studied the reaction between melamine and formaldehyde, whereas Grove and Lynch [4] concluded that the amide anion is unable to react with formaldehyde. Iliceto [2] determined the equilibrium constants of the reactions 1 and 2 for various acid amides. At 20° the values for acetamide were found to be 28.2 and 0.117, respectively, and the equilibrium constant remained unchanged over a wide range of pH (7—13.5) and concentration (0.05—6 M). In dilute solutions of formaldehyde and acetamide, the formation of bishydroxymethylacetamide can be neglected. In order to study the role of alkali as catalyst in the reaction between acetamide and formaldehyde, the present author has carried out further kinetic measurements of the reaction.

EXPERIMENTAL

Materials. Acetamide (Merck, purum grade) was purified by crystallization from hot ethanol. Aqueous solutions of formaldehyde were prepared by dissolving paraformaldehyde (Merck, purum grade) in boiling water and filtering after cooling the solution. Hydroxymethylacetamide was prepared according to Einhorn [1] from acetamide and formaldehyde. The product (m. p. 51°) contained 0.98 mole of methylol and 0.01 mole of free formaldehyde per 89 g (the molecular weight) of hydroxymethylacetamide when analysed by the hypoiodite and sulphite methods. The sodium hydroxide solutions were prepared by dilution from a carbonate-free 1:1 mixture with water.

Analytical. Free formaldehyde was determined using the sulphite method [3] and the amount of free and bound (as methylol) formaldehyde with the hypoiodite method [3].

A volume of aqueous sodium sulphite solution which contained about twice the amount of sulphite corresponding to the amount of formaldehyde in the sample was added to the latter. The solution of sulphite also contained the calculated amount of sulphuric acid required to reduce the pH of the final mixture to about 6. After standing for about 30 minutes, the solution was acidified to pH 4 by introducing 3 ml of 1 M acetic acid, and the excess of sulphite titrated with 0.1 N iodine solution. Ten ml of 1 M sodium carbonate were then added and the liberated sulphite was titrated with the same iodine solution using starch as indicator. This latter titration gives the amount of free formaldehyde present in the sample. The method was checked with the aid of hydroxymethylacetamide which was not found to decompose to any appreciable extent in the sulphite solution during periods varying from 30 to 120 minutes. Determinations made on formaldehyde solutions in the concentration range involved in the experiments showed that a standing period of about 30 minutes is sufficient for the formaldehyde-sulphite reaction to go to completion.

In the hypoiodite method 4 ml of 2.5 N sodium hydroxide and 15 ml of 0.1 N iodine solution were added to a sample of 10 ml. After a period of about 15 minutes, the mixture was acidified by adding 10 ml of 1.1 N sulphuric acid, and the excess of iodine was titrated with 0.025 N thiosulphate. The consumption of iodine corresponds to the free

formaldehyde and the methylol groups present. From the data obtained with both methods, the concentration of hydroxymethylacetamide can be calculated. When the hypoiodite method was checked with hydroxymethylacetamide, uniform results were obtained with different standing periods varying from 10 to 60 minutes. Methylenebisacetamide underwent no detectable decomposition in the hypoiodite solution during periods up to 30 minutes, and only some 0.5 % formaldehyde was formed after 60 minutes. Thus if condensation of methylol and acetamide to methylenebisacetamide occurs, it would be detected as a decrease in the hypoiodite titration value. No such decrease was observed when samples were titrated after a reaction period about 20—40 times the half-life.

When a solution of formaldehyde was analysed using both methods, the hypoiodite method gave somewhat higher results (about 1.5 %) than the sulphite method. As no reason could be found for the different results, the same solution was also analysed using the cyanide method of Pfeil and Schroth [7]. The results obtained were similar to those obtained by the sulphite method (about 0.5 % lower), which is therefore believed to give the best values. The effect of the error in the analytical method is negligible when calculating rate constants but the values obtained for equilibrium constants are probably some 5 % too high.

As the hypoiodite titration value is not altered during the experiment, the slow Cannizzaro reaction of formaldehyde in alkaline solution can be neglected [8]. Other reactions such as the hydrolysis of acetamide and hydroxymethylacetamide probably occur to some extent during the experiment. The amount of ammonia and acetic acid liberated in a reaction mixture containing initially 0.01 mole of hydroxymethylacetamide and 0.01 mole of sodium hydroxide per litre was about 4 % during 1 000 minutes (20 times the half-life of the reaction studied) at 20° as determined by potentiometric titration. During the main part of the reaction, the hydrolysis could thus be neglected, but in the determination of the equilibrium constant, a small error results.

Calculations. The kinetic experiments were performed in reaction vessels described by Tommila and Lindholm [9]. The temperatures of the thermostats were electrically controlled to about 0.02°. The reaction was arrested by introducing rapidly a calculated amount of sulphuric acid in order to reduce the pH to about 6 and sulphite to react with the formaldehyde in the mixture. As the reaction did not go to completion in any of the experiments, the equilibrium mixture was analysed after a reaction time of about 20 times the half-life.

$$\mathrm{M} \underset{k_2}{\overset{k_1}{\rightleftharpoons}} \mathrm{F} + \mathrm{A} \tag{3}$$

$$-\frac{\mathrm{dM}}{\mathrm{d}t} = k_1\mathrm{M} - k_2\mathrm{FA} \tag{4}$$

$$k_1 = \frac{2.303}{t} \cdot \frac{\mathrm{M_0} - \mathrm{M_{eq}}}{\mathrm{M_0} + \mathrm{M_{eq}}} \log \frac{\mathrm{M_0^2} - \mathrm{MM_{eq}}}{(\mathrm{M} - \mathrm{M_{eq}})\mathrm{M_0}} \tag{5}$$

Starting from hydroxymethylacetamide (M), the first-order rate constant k_1 can be calculated [10] using eqn. 5. $\mathrm{M_0}$ denotes the initial methylol (hydroxymethylacetamide) concentration, $\mathrm{M_{eq}}$ the methylol concentration at equilibrium and M its concentration at time t; F and A denote formaldehyde and acetamide, respectively.

The second-order rate constant k_2 for the reaction between acetamide and formaldehyde can be calculated using eqn. 6

$$k_2 = \frac{2.303}{t} \cdot \frac{\mathrm{M_{eq}}}{\mathrm{F_0A_0} - \mathrm{M_{eq}^2}} \log \frac{\mathrm{F_0A_0M_{eq}} - \mathrm{M_0M_{eq}^2}}{\mathrm{F_0A_0M_{eq}} - \mathrm{F_0A_0M}} \tag{6}$$

At equilibrium

$$K = \frac{k_2}{k_1} = \frac{M_{eq}}{F_{eq}A_{eq}} \qquad (7)$$

and thus k_1 or k_2 can be calculated easily from the latter equation if one of them is known. Tables 1 and 2 contain two examples of the measurements. Usually a good constancy of the specific rate was obtained over a wide range of the reaction (10—90 %). The rate and equilibrium constants obtained are collected in Tables 3—5.

DISCUSSION

From Tables 3 and 4 it will be seen that the first- and second-order rate constants increase with increasing sodium hydroxide concentration, but no direct proportionality is observed. At high alkali concentrations, the constants

Table 1. The conversion of hydroxymethylacetamide (0.00976 M) into acetamide and formaldehyde in the presence of sodium hydroxide (0.0198 M) at 20°. 10-ml samples.

Time min	0.0125 M I_2 ml	%	10^4 k_1 sec.$^{-1}$
5	0.87	13.9	4.04
8	1.35	21.6	3.79
12	1.90	30.4	3.97
15	2.29	36.7	3.94
19.5	2.94	47.0	4.17
25	3.37	53.5	3.94
35	4.10	65.5	3.84
42.5	4.62	74.0	3.99
48	4.88	78.1	3.92
65	5.44	87.0	3.81
360	6.25	100	mean 3.95

Table 2. The reaction between acetamide (0.500 M) and formaldehyde (0.0507 M) in the presence of sodium hydroxide (0.0503 M) at 20°. 10-ml samples.

Time min	0.0500 M I_2 ml	%	10^4 k_2 l mole^{-1} sec.$^{-1}$
0	10.07	0	
0.25	8.57	16.2	217
0.50	7.18	32.2	219
0.75	6.16	42.1	215
1.00	5.24	52.1	219
1.25	4.63	58.5	212
1.50	4.04	65.0	211
2.0	3.04	75.8	215
3.0	1.94	87.7	215
30	0.80	100	mean 216

Table 3. The equilibrium constants K = *M*/*FA*, *first-order rate constants and activation energies for the reaction: hydroxymethylacetamide → acetamide + formaldehyde. The second-order rate constants for the reverse reaction have been calculated from* $k_2 = k_1 K$.

	Concentrations mole/litre								
	initial		at equilibrium		*K* l/mole	$10^4\ k_1$ sec.$^{-1}$		$10^3 k_2$ litres mole^{-1} sec^{-1}.	*E* kcal
t°	NaOH	Methylol	Methylol	CH_2O and Acetamide		found	calc.		
20°	0.00487	0.00501	0.00057	0.00444	29.0	0.952	1.07	0.635	
	0.0101	0.00986	0.00191	0.00795	30.2	2.10	2.09	0.635	
	0.0101	0.0486	0.0214	0.0272	28.9	1.71	1.73	0.493	
	0.0198	0.00976	0.00190	0.00787	30.6	3.95	3.90		
	0.0499	0.00980	0.00185	0.00795	29.2	8.55	8.50	2.49	
	0.0497	0.0491	0.0220	0.0271	29.9	7.87	7.40		
	0.197	0.00970	0.00168	0.00802	26.1	20.3	20.2	5.30	
	0.197	0.0479	0.00203	0.00276	26.6	19.5	19.3	5.19	
	0.579	0.00981	0.00154	0.00827	22.5	27.9	29.2		
	1.075	0.00983	0.00150	0.00833	21.6	31.5	32.2		
	∞						37.2		
0°	0.0100	0.00500	0.00110	0.00390	72.4	0.175	0.166		
	0.0099	0.00985	0.00293	0.00692	61.2	0.162	0.160		
	0.0099	0.0485	0.0263	0.0222	53.4	0.140	0.132		
	0.0501	0.0100	0.00275	0.00725	52.4	0.669	0.686		
	0.0503	0.0483	0.0265	0.0217	56.2	0.554	0.569		
	0.202	0.00961	0.00232	0.00729	43.7	1.54	1.53		
	∞						2.64		
40°	0.0099	0.00985	0.00160	0.00825	23.5	20.0	20.2		20.5
	0.0502	0.0100	0.00155	0.00845	21.7	88.2	87.9		20.9
	0.202	0.00961	0.00126	0.00835	18.1	223	222		21.2
	∞						441		21.8

Table 4. The equilibrium constants K *and second-order rate constants* k_2 *for the reaction: acetamide + formaldehyde → hydroxymethylacetamide at 20°.*

Concentrations mole/litre						*K* l/mole	$10^3 k_2$ litres mole^{-1} sec^{-1}.	
initial			at equilibrium					
NaOH	CH_2O	Acetamide	Acetamide	CH_2O	Methylol		found	calc.
0.00985	0.00902	0.0500	0.0444	0.00443	0.00556	28.3	0.601	0.616
0.0502	0.0102	0.200	0.191	0.00166	0.00855	26.9	2.46	2.53
0.0501	0.0516	0.0500	0.0273	0.0289	0.0277	28.8	2.17	2.06
0.0503	0.0511	0.200	0.159	0.0100	0.0411	25.9	2.13	2.06
0.0502	0.0505	0.500	0.455	0.00407	0.0454	25.1	2.16	2.06
0.201	0.00947	0.200	0.192	0.00166	0.00834	26.2	5.44	5.31
0.201	0.0505	0.0500	0.0283	0.0287	0.0217	26.7	5.04	5.04
1.46	0.0505	0.0500	0.0294	0.0299	0.0206	23.4		
2.91	0.0505	0.0500	0.0307	0.0312	0.0193	20.1		
∞								8.50

Table 5. The mean values of the equilibrium constants K *given in Tables 3 and 4, and the values of* K′ *calculated from eqn. 21.*

c_{NaOH} mole/l	K obtained in experiments starting from				K' calculated	ΔH kcal
	methylol			formaldehyde-acetamide		
	0°	20°	40°	20°	20°	
0.01	57.3	29.6	20.8	28.3	21.0	4.24
0.05	54.7	29.6	19.2	26.6	20.5	4.47
0.1		28.3			23.2	
0.2	43.7	26.3	18.1	26.7	23.0	3.72
0.58		22.5			21.0	
1.08		21.6		23.4	21.6	
2.9				20.1	19.8	
					mean 21.4	mean 4.14

seem to approach a limiting value. At constant alkali concentration, an increase in the methylol or formaldehyde concentration decreases the rate constant k_1 or k_2, respectively, but when the acetamide concentration is changed, the second-order rate constant remains unaffected. In order to explain these results, the following equilibria may be considered:

$$CH_2O + H_2O \rightleftharpoons HOCH_2OH \tag{8}$$

$$HOCH_2OH + HO^- \rightleftharpoons HOCH_2O^- + H_2O \tag{9}$$

$$CH_3CONHCH_2OH + HO^- \rightleftharpoons CH_3CONHCH_2O^- + H_2O \tag{10}$$

$$HOCH_2O^- + CH_3CONH_2 \underset{k_2}{\overset{k_1}{\rightleftharpoons}} CH_3CONHCH_2O^- + H_2O \tag{11}$$

As already mentioned, in dilute aqueous solutions formaldehyde is almost completely in the hydrated form [5]. In strongly alkaline solutions a considerable proportion of the formaldehyde is present in the anion form [11]. If only the anion form of formaldehyde or methylol reacts, a limiting rate constant should be obtained in concentrated alkali solutions. At different alkali concentrations, the rate should be proportional to the concentration of the anion in the solution.

$$K_1 = \frac{[CH_3CONHCH_2OH] \cdot [HO^-]}{[CH_3CONHCH_2O^-]} = \frac{(M - x)(B - x)}{x} \tag{12}$$

If $B \ll x$, then $B - x \simeq B$ and $x = \frac{M \cdot B}{K_1 + B}$ (13)

$$-\frac{dM}{dt} = k_1 x = k_1 \cdot \frac{B}{K_1 + B} \cdot M = k_{exp} \cdot M \tag{14}$$

$$\frac{1}{k_{exp}} = \frac{K_1}{k_1 B} + \frac{1}{k_1} \tag{15}$$

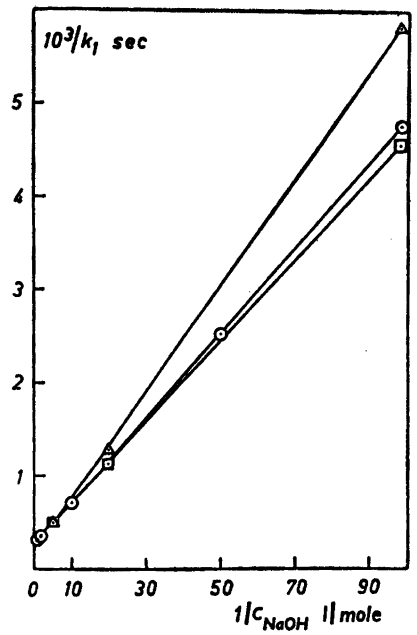


Fig. 1. Plot of the reciprocal of the first-order rate constant k_{exp} *for the reaction: hydroxymethylacetamide → acetamide + formaldehyde at 20° versus the reciprocal of the sodium hydroxide concentration (Equation 15).* △ $c_{methylol} = 0.05$ *mole/l,* ○ $c_{methylol} = 0.01$ *mole/l, and* □ *rate constant values* (k_{exp}) *relating to zero methylol concentration.*

where B and M denote the total concentrations of base and methylol and x the concentration of methylol anion, k_{exp} is the experimentally measured first-order rate constant and k_1 the first-order rate constant for the reaction 11. As the sodium hydroxide was used in excess, B > M and K_1 is large, and hence the assumption made in calculating the amount of unionized methylol (eqn. 13) is justified. In Fig. 1, $1/k_{exp}$ is plotted against 1/B. It will be seen that the curve approaches a straight line at high sodium hydroxide concentrations (Fig. 1, ○△). If the rate constants obtained at constant alkali concentrations are extrapolated to zero methylol concentration, all the points obtained lie on a straight line (Fig. 1, □). This is what is expected because the assumption $B - x \simeq B$ is valid for the extrapolated values.

The first-order rate constant of the methylol anion k_1 and the equilibrium constant K_1 (of reaction 10) can be computed from the intercept and the slope of the line (Table 6). The ionization constant is easily obtained since $K_a = K_1 / K_w$. With aid of the value obtained for the equilibrium constant

Table 6. The equilibrium constants K_1 *and* K_2 *of reactions 9 and 10 and the rate constants* k_1 *and* k_2 *of the reaction 11 calculated using eqn. 15.*

10^4 k_1 sec.$^{-1}$			E	log A	k_2 l mole^{-1} sec.$^{-1}$	K_1 l/mole			ΔH	K_2
0°	20°	40°	kcal		20°	0°	20°	40°	kcal	l/mole 20°
2.64	37.2	441	21.8	13.8	0.085	0.142	0.165	0.194	1.3	0.117

K_1, the amount of methylol anion in any mixture of methylol and sodium hydroxide can be calculated. The corresponding rate constant is $k_1 x/\mathrm{M} = k_{exp}$ (eqn. 14). These calculated rate constants are given in Tables 3 and 4 and are found to be fairly close to the experimental values over more than a 200-fold range of sodium hydroxide concentration. A similar treatment of the second-order rate constant of the reverse reaction gives a limiting rate k_2 and equilibrium constant $K_2 = 0.117$ at 20° (Table 6). From a graph given by Martin [11] which contains values of K_2 obtained by different authors, a mean value $K_2 = 0.111$ is obtained which is fairly close to the above value.

No value was found in the literature for the acid ionization constant of acetamide. When the alkali concentration is held constant, the second-order rate constant remains unaffected when the concentration of acetamide is changed. Thus it is improbable that any detectable amounts of acetamide anion are formed in the reaction mixtures used and that this ion is involved in the reaction mechanism as stated by some authors [3,6].

$$K = \frac{[\mathrm{CH_3CONHCH_2OH} + \mathrm{CH_3CONHCH_2O^-}]}{[\mathrm{CH_3CONH_2}]\,[\mathrm{HOCH_2OH} + \mathrm{HOCH_2O^-}]} \tag{16}$$

$$K' = \frac{[\mathrm{CH_3CONHCH_2O^-}]}{[\mathrm{CH_3CONH_2}] \cdot [\mathrm{HOCH_2O^-}]} \tag{17}$$

The equilibrium constant K calculated using the total methylol and formaldehyde concentrations without taking into account the ionization of these compounds decreases as the alkali concentration is increased (Tables 3—5).

Considering the two equilibria (eqns. 9 and 10)

$$K_1 = \frac{[\mathrm{CH_3CONHCH_2OH}]\,[\mathrm{HO^-}]}{[\mathrm{CH_3CONHCH_2O^-}]} = \frac{(\mathrm{M}-x)(\mathrm{B}-x-y)}{x} \tag{18}$$

$$K_2 = \frac{[\mathrm{HOCH_2OH}][\mathrm{HO^-}]}{[\mathrm{HOCHO^-}]} = \frac{(\mathrm{F}-y)(\mathrm{B}-x-y)}{y} \tag{19}$$

it can again be assumed that $\mathrm{B}-x-y \simeq \mathrm{B}$. Then

$$x = \frac{\mathrm{MB}}{K_1 + \mathrm{B}} \quad \text{and} \quad y = \frac{\mathrm{FB}}{K_2 + \mathrm{B}} \tag{20}$$

$$K' = \frac{x}{\mathrm{A}y} = \frac{\mathrm{M}}{\mathrm{F} \cdot \mathrm{A}} \cdot \frac{K_2 + \mathrm{B}}{K_1 + \mathrm{B}} = K\,\frac{K_2 + \mathrm{B}}{K_1 + \mathrm{B}} \tag{21}$$

where M, F, A and B denote the total concentrations of methylol, formaldehyde, acetamide and sodium hydroxide. According to eqn. 21, K' can be calculated for different sodium hydroxide concentrations from the experimental values of K obtained using total formaldehyde and methylol concentrations by substituting for K_1 and K_2 the values 0.165 and 0.117 obtained from the kinetic measurements at 20° (Table 6). These calculated K' values which are given in Table 5 are fairly constant (mean value $K' = 21.4$) although the K values change considerably when the alkali concentration is altered. The value $K = 22.8$ is obtained from the extrapolated rate constants: $k_2/k_1 =$

$8.5 \times 10^{-2}/3.72 \times 10^{-3}$ (Table 6). This is a further proof that the values of the ionization constants obtained for formaldehyde and methylenebisacetamide from kinetic experiments are of correct order of magnitude. At low alkali concentrations (below 0.05 mole/l) K would be expected to remain fairly constant, as has been found to be the case by several authors *e. g.* Ref.[2]

From the values for different temperatures it will be seen that the unionized form of hydroxymethylacetamide is favoured at higher temperatures, a value of about 1.3 kcal being obtained for the heat of the ionization reaction. Because of this pre-equilibrium (eqn. 10), the activation energy calculated for the reaction 11 does not remain constant when the concentration of alkali is changed (Table 3). The difference between the apparent activation energy obtained for the reaction at low alkali concentrations and the value obtained using the k_1 values for the reaction of the methylol ion (about 1.3 kcal) should be close to the heat of reaction 10 (1.3 kcal).

The energy of activation for the reaction, calculated using the k_1 values given in Table 6, is 21.80 kcal and the frequency factor $A = 7 \times 10^{13}$ which is close to the predicted value for unimolecular reactions [10]. In order to estimate the value of activation energy for the reverse reaction of methylol formation from acetamide and formaldehyde, the heats of the reactions should be of the same order of magnitude. From the value $K_2 = 0.134$ at 40° given by Martin [11] and the above value $K_2 = 0.117$ at 20°, the value $\Delta H_2 = 1.2$ kcal is obtained which is close to value $\Delta H_1 = 1.3$ kcal (Table 6). Thus using the mean value obtained for the heat of reaction 11, $\Delta H = 4.14$ (Table 5), it is found that $E_2 = E_1 - \Delta H = 17.7$ kcal and $A = 1.6 \times 10^{12}$.

All the results obtained show clearly that the reaction between formaldehyde and acetamide occurs in alkaline solution between the anion of formaldehyde hydrate and acetamide (eqn. 11). Similarly, in the reverse reaction, it is the methylol anion that undergoes change. In order to determine whether any reaction occurs between the uncharged molecules, an aqueous solution of hydroxymethylacetamide was kept for several weeks at 20°, but no formaldehyde was found to be liberated. The reaction of the methylol anion is thus at least 10^6 times faster than the reaction of unionized methylol.

Acknowledgement. The author wishes to record his indebtedness to the *Finnish Academy* for a Government research grant for young scientists.

REFERENCES

1. Einhorn, A. *Ann.* **343** (1905) 265.
2. Iliceto, A. *Ann. chim. Roma* **43** (1953) 516; *Chem. Abstracts* **48** (1954) 6208e.
3. de Jong, J. I. and de Jonge, I. *Rec. trav. Chim.* **69** (1950) 1566; **71** (1952) 643, 661, 893; **72** (1953) 88, 139, 169, 202, 207, 213, 356, 1027.
4. Grove, G. A. and Lynch, C. C. *J. Am. Chem. Soc.* **70** (1948) 3795; **71** (1949) 3731; **72** (1950) 3622.
5. Bieber, H. *Helv. Chim. Acta* **30** (1947) 1860.
6. Okano, M. and Ogata, Y. *J. Am. Chem. Soc.* **74** (1952) 5782.
7. Pfeil, E. and Schroth, G. *Ber.* **85** (1952) 293.
8. Pajunen, V. *Ann. Acad. Sci. Fennicae, Ser.* **A.II** (1950) No. 37.
9. Tommila, E. and Lindholm, M. *Acta Chem. Scand.* **5** (1951) 647.
10. Frost, A. A. and Pearson, R. G. *Kinetics and Mechanism*, New York 1953, p. 173.
11. Martin, J. L. *Australian J. Chem.* **7** (1954) 400.

Received June 2, 1956.

ACTA CHEMICA SCANDINAVICA 10 (1956) 1276—1278

Syntheses of *p*-Dimethylaminobenzyl Alcohol and Esters of its Methiodide

LARS-ERIK TAMMELIN

Research Institute of National Defence, Dept. 1, Sundbyberg 4, Sweden

p-Dimethylaminobenzyl alcohol has been synthesized by catalytic hydrogenation of the corresponding aldehyde. Methiodides of the *p*-dimethylaminobenzyl alcohol and esters from acetic-, malonic-, succinic-, glutaric- and adipic acids have been prepared. The conditions for methylation of *p*-dimethylaminobenzyl alcohol are discussed. The esters of *p*-trimethylammoniumbenzyl alcohol have been shown to have neuromuscular blocking effects.

p-Dimethylaminobenzyl alcohol has been synthesized by Smith and Welch [1] who also review earlier literature in this field. The same authors [2] point out that *p*-dimethylaminobenzyl alcohol easily reacts, through loss of water, with phenols and aromatic amines. Reactions of this type occurring as side reactions presumably explains the difficulties of earlier authors to obtain good yields of a pure product. Smith and Welch used the action of formaldehyde on dimethylaniline. Reduction of *p*-dimethylaminobenzaldehyde has also been accomplished by electrolysis [3], sodium amalgame [3], litium aluminium hydride [4] and sodium borofluoride [5]. The latter method provides the best yield (96 %). Since no report has been found on direct catalytic hydrogenation of *p*-dimethylaminobenzaldehyde it seemed reasonable to test that method of synthesis. *p*-Trimethylammoniumbenzyl alcohol and corresponding esters can be expected to have interesting pharmacological actions because of a structural resemblance to choline and the choline esters.

SYNTHESES

p-*Dimethylaminobenzyl alcohol.* One mole of *p*-dimethylaminobenzaldehyde was dissolved in 160 ml of hot abs. ethanol. 1 g of PtO_2 and 2 ml of 0.1 M $FeCl_3$ solution were added to the alcoholic solution and the mixture treated with hydrogen at 10 kg/cm^2 and 50° C. The hydrogenation was considered to be complete when 1.2 moles of hydrogen were consumed. The reaction mixture was filtered and the *p*-dimethylaminobenzyl alcohol purified by fractional distillation *in vacuo*, b. p. 115—120°/1 mm Hg, n_D^{25} 1.5780. Yield 50 %. For analyses see the methiodide.

p-*Trimethylammoniumbenzyl alcohol.* One mole of *p*-dimethylaminobenzyl alcohol and 1.1 moles of methyl iodide were mixed in 8 volume parts of ether in a glass stoppered round

bottomed flask and kept at 25° C. The precipitate formed was filtered off after 4 days and recrystallized twice from methanol, m. p. 261° and yield 60 %. (Found: C 41.3; H 5.4; I 43.4. Calc. for $C_{10}H_{16}ONI$ (293.2): C 41.1; H 5.5; I 43.4).

p-*Trimethylammoniumbenzyl ester of acetic acid.* One mole of acetylchloride and 1 mole of *p*-dimethylaminobenzyl alcohol were boiled in ether for one hour. The reaction mixture was washed with 5 % aqueous sodium bicarbonate solution and dried with sodium sulfate. 1.5 moles of methyl iodide were added to the water free ether solution. After two weeks at 25° C the precipitate formed was filtered off and purified by dissolution in alcohol and reprecipitation with ether. The purified product had a m.p. 186° (decomp.) and was obtained in 33 % yield. (Found: C 43.8; H 5.5; I 38.1. Calc. on $C_{12}H_{18}O_2NI$ (335.2): C 43.0; H 5.4; I 37.8).

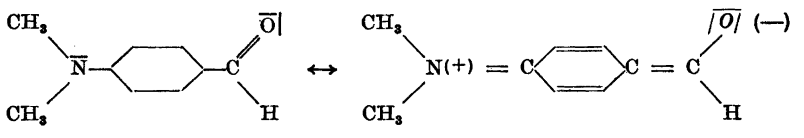
p-*Trimethylammoniumbenzyl esters of aliphatic dicarboxylic acids.* One mole of acid dichloride (malonyl-adipyl) and 2 moles of *p*-dimethylaminobenzyl alcohol were boiled in ether for one hour. The reaction mixture was washed by 5 % aqueous sodium bicarbonate solution and dried with water free sodium sulfate. 2.5 moles of methyl iodide were added and the precipitate formed was filtered off after two weeks at 25° C, and purified by solution in alcohol and reprecipitation with ether. Yield about 30 %. For data see Table 1.

Table 1.

Ester	Formula	Molecular weight	m. p.	C		H		I	
				calc.	found	calc.	found	calc.	found
malonic	$C_{23}H_{32}O_4N_2I_2$	654.3	182	42.3	42.7	4.9	5.1	38.8	38.6
succinic	$C_{24}H_{34}O_4N_2I_2$	668.4	128	43.2	43.4	5.1	5.3	37.9	37.7
glutaric	$C_{25}H_{36}O_4N_2I_2$	682.4	144	44.0	42.9	5.3	5.5	37.2	36.8
adipic	$C_{26}H_{38}O_4N_2I_2$	696.4	147	44.9	44.3	5.5	5.5	36.4	36.1

Good yields from the catalytic hydrogenation of the *p*-dimethylaminobenzaldehyde are obtained only if the aldehyde is completely consumed. The aldehyde seems to provoke side reactions during the distillation, with diminished yield of the alcohol as a consequence. Another complication which has happened a few times is that the catalyst is poisoned during the process of hydrogenation. It is therefore recommended that the completeness of the hydrogenation is tested by the addition of new catalyst, if hydrogen consumption ceases before the calculated amount is consumed. If these possible troubles are overcome the product obtained is well in accordance with the *p*-dimethylaminobenzyl alcohol from the condensation of formaldehyde and dimethylaniline according to Smith and Welch [1] with respect to refractive index and boiling point.

The relative rapidity of the methylation of *p*-dimethylaminobenzyl alcohol gave the impulse to determine whether the *p*-trimethylammoniumbenzaldehyde could be synthesized in a similar way. However, in this case methyl iodide did not react at 25° C in ether. The phenomenon might be described in formulae as follows.



This and other resonance possibilities engage the electron pair at the nitrogen atom. In the case of the alcohol and its esters the corresponding electron pair seems to be more free and thus enables the methylation to proceed.

The present author has not isolated the *p*-dimethylaminobenzyl esters either by crystallization or by distillation *in vacuo*. The quaternary derivatives are easier to isolate but even in this case purification has its obstacles. Dissolution in alcohol and precipitation with ether, which is recommended, is not an ideal method. It does not always lead to the correct composition of the compound especially when the impurities are quaternary products. However, following the given prescriptions for the syntheses, impurities of the type mentioned above seem to have been avoided as follows from the analytical data of the final products.

The iodides of the bis-(*p*-trimethylammoniumbenzyl) esters are water soluble, crystalline, pale yellow substances. Preliminary experiments have shown that they are potent neuromuscular blocking agents and choline esterase inhibitors (although not very potent), effects which could be expected from the structural similarity to the choline esters. The pharmacological data will be published elsewhere [6].

My sincere thanks are due to the Director of this Institute, Professor G. Ljunggren, for his kind interest in this work.

REFERENCES

1. Smith, L. H. and Welch, K. N. *J. Chem. Soc.* **1934** 730.
2. Smith, L. H. and Welch, K. N. *J. Chem. Soc.* **1934** 1136.
3. Clemo, G. R. and Smith, J. M. *J. Chem. Soc.* **1928** 2423.
4. Hass, H. B. and Bender, M. L. *J. Am. Chem. Soc.* **71** (1949) 1767.
5. Chaikin, S. W. and Brown, W. G. *J. Am. Chem. Soc.* **71** (1949) 122.
6. Fredriksson, T. *Acta Pharmacol. Toxicol.* (1957), *in press.*

Received June 9, 1956.

ACTA CHEMICA SCANDINAVICA 10 (1956) 1279—1282

On the "Entropy Effect" in Chelating Processes

SVEND ERIK RASMUSSEN

Chemistry Department A, Technical University of Denmark, Copenhagen, Denmark

The available data on entropies of chelate compounds indicate that an important factor in the so-called "chelate effect" is the difference in number between monodentate and chelate molecules in a chelating reaction. The entropy differences between complex ammonia metal ions and chelate metal ions are found to be relatively small.

Let a reaction between a metal ion and a monodentate ligand be represented by the equation

$$Me(H_2O)_n + nA = MeA_n + nH_2O \quad (1)$$

and that of a metal ion and a chelating agent by

$$Me(H_2O)_n + mCh = MeCh_m + nH_2O \quad (2)$$

where n is the characteristic coordination number.

The equilibrium constant of (2) is generally much higher than that of (1) and there has been much discussion in the literature on the nature of this "chelate effect".

Let us consider a reaction:

$$MeA_n + mCh = MeCh_m + nA \quad (3)$$

which is formally independent of the solvent.

The entropy change is given by

$$\Delta S = n\ S^{\ominus}(A) - m\ S^{\ominus}(Ch) + S^{\ominus}(MeCh_m) - S^{\ominus}(MeA_n)$$

The $S^{\ominus}$s are the partial molar entropies of the species in an arbitrarily chosen standard state at the temperature in question.

In most experiments in complex chemistry the standard state is the hypothetical one molar solution in a neutral salt medium. It is sometimes stated (*e. g.* Young [1]) that equilibrium data obtained in a constant salt medium do not

give "*true thermodynamic*" values. Of course the laws of thermodynamics are applicable also to reactions occurring in a constant salt medium and the thermodynamic data obtained are true enough although more or less different from those determined at extreme dilution.

The partial molar entropies of each of the reactants may in principle be measured using the third law of thermodynamics.

Unfortunately no data exist which permit a complete calculation of the entropies of complex reactions. Not even the entropies of most of the ligands are known. An exception is ammonia. According to *Selected Values of Chemical Thermodynamic Properties* [2] the partial molal entropy of ammonia in water at 25° C is 26.3 cal/degree mole. The atmospheric molar entropy of ammonia gas is 46.01 cal/degree mole at 25° C. Using the vapour pressure measurements of J. Bjerrum [3] and the heat of solution determined by Becker and Roth [4] the partial molar entropy of ammonia in a 2 M NH_4NO_3 solution is calculated to be 25.9 cal/degree mole.

In principle the entropy of a gaseous species may be calculated from statistical mechanics provided that the appropriate spectroscopic data are known. For most of the ligands of complex chemistry no such data are available. Empirical equations have been found, however, which permit a calculation of entropies of many gaseous substances with fair accuracy. Powell and Latimer [5] have proposed an equation which bases the aqueous entropy of neutral species upon the molar volume of the pure liquid state of the solute.

Cobble [6] has combined the different empirical equations and has obtained the following expression for the partial molal entropy in aqueous solution

$$S^{\bullet} = 10 + \frac{3}{2}R\log M + 9.2N - S^{\circ}_{(s)} - 0.22V_m.$$

M is the molecular weight, N represents the number of "skeletal" bonded atoms in the compound (number of bonded atoms — number of hydrogens), $S^{\circ}_{(s)}$ is the entropy loss caused by double bonds, rings and branched chains, and V_m is the molar volume of the pure liquid compound.

For details and for references the reader is referred to the original paper.

For lack of experimental data we shall use this equation for the calculation of the partial molar entropies of ethylenediamine (en) and 1,3-diaminopropane (tn). We get the following values

$$S^{\bullet}(\text{en}) = 45 \text{ cal/degree mole at 1 M and } 25^{\circ}\text{ C}$$

$$S^{\bullet}(\text{tn}) = 50 \text{ cal/degree mole at 1 M and } 25^{\circ}\text{ C}$$

The equation yields for ammonia: $S^{\bullet}(NH_3) = 24$ cal/degree mole while the experimental value is 26. The entropy of gaseous en must be almost equal to that of *n*-butane, which is according to Pitzer [7] 74.17 cal/degree mole (25° C, 1 atm.). In Ref.[2] the entropy of vapourization of en is given as 23.8 cal/degree mole at 117° C and 760 mm Hg. Therefore the entropy of liquid en at 25° C must be about 50 cal/degree mole. It has been found by Copp and Everett [8] and others [9] that the excess entropy of mixing of amines and water is negative. Hence the value calculated for $S^{\bullet}$(en) seems reasonable.

We are now able to obtain approximate values of $nS^{\ominus}(NH_3)$—$mS^{\ominus}(en)$ and $nS^{\ominus}(NH_3)$—$mS^{\ominus}(tn)$ in chelating processes of the type (3).

If the ΔS of the reaction is known we can make rough estimates of the differences $S^{\ominus}(MeCh_m)$—$S^{\ominus}(Me(NH_3)_n)$. Surprisingly few accurate determinations of entropies of reactions of complex compounds exist.

From the recent paper by Poulsen and Bjerrum [10] and from measurements by Bjerrum [11], Fyfe [12] and Davies, Singer and Staveley [13] one obtains the following entropy changes (Standard state 1 M, 25° C)

$Ni(NH_3)_6^{++} + 3\ en = Nien_3^{++} + 6\ NH_3$	$\Delta S = 21$	cal/degree	mole
$Ni(NH_3)_6^{++} + 3\ tn = Nitn_3^{++} + 6\ NH_3$	$\Delta S = 14$	»	»
$Cu(NH_3)_4^{++} + 2\ en = Cuen_2^{++} + 4\ NH_3$	$\Delta S = 15$	»	»
$Cu(NH_3)_4^{++} + 2\ tn = Cutn_2^{++} + 4\ NH_3$	$\Delta S = 11$	»	»
$Zn(NH_3)_4^{++} + 2\ en = Znen_2^{++} + 4\ NH_3$	$\Delta S = 21$	»	»
$Cd(NH_3)_4^{++} + 2\ en = Cden_2^{++} + 4\ NH_3$	$\Delta S = 14$	»	»

From the partial molar entropies of the three ligands we calculate the following differences:

$6\ S^{\ominus}(NH_3)$—$3\ S^{\ominus}(en)$	$= 21$	cal/degree	mole
$6\ S^{\ominus}(NH_3)$—$3\ S^{\ominus}(tn)$	$= 6$	»	»
$4\ S^{\ominus}(NH_3)$—$2\ S^{\ominus}(en)$	$= 14$	»	»
$4\ S^{\ominus}(NH_3)$—$2\ S^{\ominus}(tn)$	$= 4$	»	»

These data yield the following entropy differences:

$S^{\ominus}(Nien_3^{++}) - S^{\ominus}(Ni(NH_3)_6^{++})$	$= 0$	cal/degree	mole
$S^{\ominus}(Nitn_3^{++}) - S^{\ominus}(Ni(NH_3)_6^{++})$	$= 8$	»	»
$S^{\ominus}(Cuen_2^{++}) - S^{\ominus}(Cu(NH_3)_4^{++})$	$= 1$	»	»
$S^{\ominus}(Cutn_2^{++}) - S^{\ominus}(Cu(NH_3)_4^{++})$	$= 7$	»	»
$S^{\ominus}(Znen_2^{++}) - S^{\ominus}(Zn(NH_3)_4^{++})$	$= 7$	»	»
$S^{\ominus}(Cden_2^{++}) - S^{\ominus}(Cd(NH_3)_4^{++})$	$= 0$	»	»

The experimental ΔS values are probably uncertain at about $\pm$ (10—15) %. The estimated entropy values are probably uncertain at about 3—4 cal/degree mole.

An optimistic estimation of the uncertainties involved would yield an indeterminacy of about $\pm$ 10 cal/degree mole for the values of the entropy differences between chelate and non chelate complex ions. This means that their partial molar entropies are almost equal within the experimental uncertainty. An interpretation of the figures obtained seems rather futile.

In the chelating reactions considered the entropy change is largely due to the entropy difference between the monodentate ligands and the chelating ligands. As suggested by Calvin and Bailes [14] this entropy difference is partly caused by the different numbers of monodentate and chelate molecules taking part in the reaction. The numerical value is dependent upon the arbitrary choice of standard state. The entropy differences between the complex ions are of course independent of the standard state.

REFERENCES

1. Young, T. F. *Ann. Rev. Phys. Chem.* **3** (1952) 285.
2. *Selected Values of Chemical Thermodynamic Properties*, Circular of The National Bureau of Standards 500, Washington 1952.
3. Bjerrum, J. *Kgl. Danske Videnskab. Selskab Mat. Fys. Medd.* **11** (1931) No. 5, p. 14.
4. Becker, G. and Roth, W. A. *Z. Elektrochem.* **40** (1934) 841.
5. Powell, R. E. and Latimer, W. M. *J. Chem. Phys.* **19** (1951) 1139.
6. Cobble, J. W. *J. Chem. Phys.* **21** (1953) 1451.
7. Pitzer, K. S. *Chem. Revs.* **27** (1940) 39.
8. Copp, J. L. and Everett, D. H. *Discussions Faraday Soc.* **15** (1953) 174.
9. Hildebrand, J. L. and Scott, R. L. *Solubility of Nonelectrolytes.* 3rd ed. New York 1950.
10. Poulsen, I. and Bjerrum, J. *Acta Chem. Scand.* **9** (1955) 1407.
11. Bjerrum, J. *Metal Ammine Formation in Aqueous Solution.* Copenhagen (1941).
12. Fyfe, W. S. *J. Chem. Soc.* **1952** 2023.
13. Davies, T., Singer, S. S. and Staveley, L. A. K. *J. Chem. Soc.* **1954** 2304.
14. Calvin, M. and Bailes, R. H. *J. Am. Chem. Soc.* **68** (1946) 949.

Received June 1, 1956.

ACTA CHEMICA SCANDINAVICA **10** (1956) 1283—1286

Synthesis and Paper Electrophoresis of the Galactose Monomethyl Ethers

HANS BOUVENG and BENGT LINDBERG

Organisk-kemiska Institutionen and Träkemiska Institutionen, Kungliga Tekniska Högskolan, Stockholm, Sweden

The mono-*O*-methyl ethers of D-galactose have been synthesised by partial methylation of suitable galactose derivatives and the separation of the mixtures of methyl ethers obtained has been performed on carbon columns. — The M_G-values of the monomethyl ethers and of some other galactose derivatives have been determined.

In his studies on paper electrophoresis of glucose derivatives, Foster [1] found that the M_G-values were chiefly dependent on the position of a substituent and only to a lesser extent upon the nature of this substituent. In connection with an investigation of the arabogalactosan in larch wood [2], it was therefore of interest to study the migration of the monomethyl ethers of galactose in electrophoresis and to compare them with those of some oligosaccharides, obtained by partial hydrolysis of the polysaccharide.

Each of the four monomethyl ethers of D-galactose, which can exist in pyranosidic form, is known and has been synthesised by unambiguous methods [3]. The 6-*O*-methyl ether is easily available but the routes leading to the others are more tedious. We therefore prepared them by partial methylation of 4,6-benzylidene-β-methylgalactoside [4] and 6-trityl-β-methylgalactoside, respectively, and separated the mixtures of galactose methyl ethers obtained on carbon columns, using the technique described by Lindberg and Wickberg [5]. The 3- and 4-*O*-methyl ethers, however, could not be separated by this method, but were easily separated when borate was added to the eluting solvent as described by Barker, Bourne and Theander [6].

The partial methylations were performed with the modified Purdie methylation method using N,N-dimethylformamide as solvent, as devised by Kuhn *et al.* [7] for the complete one step methylation of non-reducing sugars. The yield of methoxyl groups, calculated from the added amount of methyl iodide, was 50 % in one experiment and 90 % in another. There is of course a competition for the methyl iodide between the hydroxyl groups of the sugar and the water, present as an impurity in the starting materials and formed during the reaction, and this might explain the difference between these figures.

The monomethyl ethers thus obtained were electrophoretically and chromatographically pure and the melting points and rotations were in good agreement with previously published data. The method of partial methylation and separation on carbon columns of the mixture obtained seems to be of general value for the preparation of less available ethers.

The paper electrophoresis apparatus was similar to that used by Foster [8]. The M_G-values did not differ more than ± 0.02 units from the mean value and no significant influence from differences in the applied voltages or from the use of different papers could be detected. The measurements were performed in a borate buffer of pH 10.

Table 1. M_G*-values of some galactose and glucose derivatives.*

Substance	Complexes formed	M_G	Substance	Complexes formed	M_G
Galactose	X Y β'	0.93	Glucose	X β' C	1.00
β-Methylgalactoside	Y	0.38	β-Methylglucoside		0.19
2-*O*-Methylgalactose	Y β'	0.43	2-*O*-Methylglucose	β'	0.23
3-*O*-Methylgalactose	X β'	0.63	3-*O*-Methylglucose	X β' C	0.82
4-*O*-Methylgalactose	X	0.30	4-*O*-Methylglucose	X	0.24
6-*O*-Methylgalactose	X Y	0.86	6-*O*-Methylglucose	X β' C	0.82
Disaccharide I	—	0.69			
Disaccharide II	—	0.83			

In Table 1 the M_G-values of the galactose monomethyl ethers and some other galactose derivatives are given and compared with the values of the corresponding glucose derivatives, these being taken from Foster's investigation [1]. Foster found that the rate of migration of the glucose derivatives in electrophoresis could be explained by the assumption that essentially three types of borate complexes are formed. The first, X, is due to complex formation between the borate and the hydroxyls at $C_{(1)} : C_{(2)}$ in the α-pyranosidic or α-furanosidic form of the derivative. The two other types are due to complex formation between the borate and two hydroxyls in the β-position in the aldehyde form of the derivative. These hydroxyl groups should be in *cis*-relationship in the Fisher projection formulae (β'C) or one of them should be a primary hydroxyl group (β'). These two possibilities are realised by the hydroxyl groups at $C_{(2)} : C_{(4)}$ and $C_{(4)} : C_{(6)}$, respectively, in the glucose molecule, and Foster found that when both alternatives are possible, β'C takes preference over β'. In galactose, there is no possibility of forming a β'C complex, but there is a contribution from a complex between borate and the two hydroxyls at $C_{(3)} : C_{(4)}$ in the ring forms, here denoted as Y. It is evident from Table 1 that the M_G-values of the galactose derivatives can also be correlated with the structure by application of Foster's theory. The contribution from the Y complexes seems to be of the same order of magnitude as those of X and β'C, and the relatively small contribution from the β' complex is also indicated.

The unexpectedly low migration of 4-*O*-methylgalactose and 4-*O*-methylglucose may be explained by the fact that these substances cannot assume a

furanosidic but only a pyranosidic structure, hence the contribution from X complexes might be reduced.

Two disaccharides (I and II) obtained from the arabogalactosan by partial hydrolysis, and which on further hydrolysis yielded galactose only, were also investigated. From previous investigations of this polysaccharide [9], the disaccharides could be supposed to be 3- and 6-β-galactopyranosyl galactopyranose, respectively, and the observed M_G-values are in good agreement with this assumption.

EXPERIMENTAL

Chromatography. Paper: Whatman No. 1.
Solvent: Butanol:ethanol:water 10:3:5.
Developer: Anisidine hydrochloride.

Electrophoresis. Papers: Whatman No. 1 and Whatman 3 MM.
Borate buffer: 7.45 g boric acid and 4.0 g sodium hydroxide in 1 000 ml of aqueous solution (pH = 10.0).
Developer: Silver nitrate/sodium ethoxide and, in the case of β-methylgalactoside, periodate/benzidine [10], the paper at first being neutralised with acetic acid.
Voltages: 600–800 volts.

All melting points corrected. All evaporations were performed under reduced pressure.

Fractions obtained in the separations were investigated by paper chromatography, paper electrophoresis and determination of the optical rotation.

Partial methylation of 4,6-benzylidene-β-methylgalactoside. To a rapidly stirred solution of 4,6-benzylidene-β-methylgalactoside (6.2 g, 1 mole) and methyl iodide (2.6 ml, 1.95 mole) in 25 ml of dimethylformamide, silver oxide (10 g, 4 mole) was added in portions during 1 hour, the apparatus and the chemicals being previously carefully dried. The temperature was kept below 20° by external cooling and the stirring was continued for another 11 hours. The reaction mixture was worked up according to Kuhn *et al.* [3]. The product obtained was then boiled for 4½ hours in 150 ml of acetone and 75 ml of 0.5 N HCl. The benzaldehyde formed was removed by steam distillation under reduced pressure. The acid was removed by filtering through a column of IR 4B and the solution concentrated to a sirup, which was treated for 14 hours in 28 ml of 0.5 N HCl at 100°, in order to remove the glycosidic group. Neutralisation (IR 4B) and concentration yielded a lightcoloured sirup (4.8 g).

Separation of products from partial methylation of 4,6-benzylidene-β-methylgalactoside. Column: 4.5 × 33 cm. Eluent: 8 l 0–10 % ethanol. Fractions: 26 ml. Amount added: 4.8 g.

Fract. 47– 49. Galactose (traces).
» 81– 98. 0.57 g of 3-methylgalactose (crystallised when seeded).
» 99–131. 1.51 g of a mixture of 2- and 3-methylgalactose of which 0.79 g of 2-methylgalactose crystallised after seeding; the rest gave after some time fairly pure 3-methylgalactose.
» 132–153. 0.30 g cryst. 2-methylgalactose.
» 218–290. 0.87 g 2,3-dimethylgalactose.

Approximate yields: 35 % 2-methyl-, 40 % 3-methyl- and 25 % 2,3-dimethylgalactose.

Partial methylation of 6-trityl-β-methylgalactoside. 6-Trityl-β-methylgalactoside (28.7 g, 1 mole) was treated in the same manner as described above with methyl iodide (6.2 ml, 1.5 mole) and silver oxide (22 g, 3.7 mole) in dimethylformamide (50 ml). The product obtained was detritylated in 100 ml 0.5 N alcoholic hydrochloric acid for 2 hours at room temperature, concentrated and diluted with water and then filtered and neutralised (IR 4B). The solution was concentrated to a sirup and treated for 12 hours in 50 ml of 0.5 N HCl at 100°. Neutralisation (IR 4B) was followed by decolorisation with carbon in 50 % alcohol. Concentration yielded 14.1 g of a light coloured sirup.

Preliminary separation of products from partial methylation of 6-trityl-β-methylgalactoside.

Column: 6.5 × 46 cm. Eluent: 8 l 0–15 % ethanol. Fractions 150–100 ml. Amount added: 14.1 g.

Fract. 22—27. 1.05 g of galactose.
» 28—31. 1.06 g of 3-methyl- and 4-methylgalactose.
» 32—33. 1.06 g of 2-methyl-, 3-methyl- and 4-methylgalactose.
» 34—41. 1.01 g of 2-methylgalactose (cryst.) and 0.71 g of 2-methyl- and 3-methylgalactose (sirup).
» 42—64. 3.71 g of dimethylgalactoses.

50 % ethanol-eluate. 2.77 g of 2,3,4-trimethylgalactose with small amounts of dimethylgalactoses.

Approximate yields: 10 % galactose, 34 % monomethyl ethers, 32 % dimethyl ethers and 24 % of the trimethyl ether.

Separation of 3-O-methyl- and 4-O-methylgalactose (fract. 28—31 above).

Column: 4.5 × 33 cm. Eluent: 1.5 l water + 4 l 0—4 % ethanol, containing 7.45 g boric acid and 4.0 g sodium hydroxide in 1000 ml. Fractions: 26 ml. Added amount: 1.06 g.

Fract. 124—151. 0.69 g of 3-methylgalactose (cryst.)
» 177—188. 0.07 g of 4-methylgalactose (cryst.)

The fractions were neutralized by adding 2 ml of strong cation exchanger (IR 120) to the fractionating tubes. After filtration and concentration the boric acid was evaporated with methanol.

Fractions 32—33 were resolved in exactly the same manner, yielding in the following order: 0.33 g 3-methyl-, 0.37 g 2-methyl- and 0.36 g 4-methylgalactose (cryst.). The separation of 3-methyl- and 2-methylgalactose was not quite complete, but both fractions crystallised on seeding.

The sirupy part of fractions 34—41 (0.71 g) was separated in the usual manner yielding 0.35 g 3-methyl- and 0.33 g 2-methylgalactose.

The approximate ratio of the monomethyl ethers thus obtained is 2-*O*-methyl-: 3-*O*-methyl-: 4-*O*-methylgalactose = 5:4:1.

The 6-*O*-methylgalactose, prepared according to Freudenberg and Hixon [11], failed to crystallise, even when purified by means of carbon column chromatography. It was therefore characterised as its osazone, prepared in the presence of bisulphite, according to Hamilton [12].

Table 2. Properties of Galactose Derivatives.

Compound	M.p.	$[\alpha]_D^{20}(H_2O)$	$R_{Galactose}$	Colour with anisidine-HCl
2-*O*-methylgalactose	149—151°	+ 50 → + 84°(c = 2)	1.50	orange-red
3-*O*-methylgalactose	145—146.5°	+147 → +106°(c = 2)	1.37	light yellow
4-*O*-methylgalactose	206—208°	+ 54 → + 81°(c = 1)	1.37	yellow
6-*O*-methylgalactose			1.39	brown
—, phenylosazone	200—201°			
Disaccharide I				light yellow
Disaccharide II				brownish yellow

The authors are indebted to *Fonden för Skoglig Forskning* for financial support.

REFERENCES

1. Foster, A. B. *J. Chem. Soc.* **1953** 982.
2. Bouveng, H. and Lindberg, B. *Unpublished.*
3. Maher, G. G. *Advances in Carbohydrate Chem.* **10** (1955) 273.
4. Bacon, J. S. D. and Bell, D. J. *J. Chem. Soc.* **1939** 1248.
5. Lindberg, B. and Wickberg, B. *Acta Chem. Scand.* **8** (1954) 569.
6. Barker, S. A., Bourne, E. J. and Theander, O. *J. Chem. Soc.* **1955** 4276.
7. Kuhn, R., Trischmann, H. and Löw, I. *Angew. Chem.* **67** (1955) 32.
8. Foster, A. B. *Chemistry & Industry* **1952** 828.
9. White, E. V. *J. Am. Chem. Soc.* **63** (1941) 2871.
10. Cifonelli, J. D. and Smith, F. *Anal. Chem.* **26** (1954) 1132.
11. Freudenberg, K. and Hixon, R. *Ber.* **56** (1923) 2122.
12. Hamilton, R. H. Jr., *J. Am. Chem. Soc.* **56** (1934) 487.

Received June 19, 1956.

ACTA CHEMICA SCANDINAVICA 10 (1956) 1287—1297

The Crystal Structure of Indium Oxide Chloride and Indium Oxide Bromide

HANS-ERIK FORSBERG

Department of Inorganic and Physical Chemistry, University, and Department of Inorganic Chemistry, Royal Institute of Technology, Stockholm, Sweden

InOCl, and InOBr, have been investigated by X-ray methods. They have an orthorhombic unit cell. Their unit cell dimensions are

InOCl		*InOBr*	
a	= (4.065 ± 0.005) Å	a	= (4.049 ± 0.005) Å
b	= (3.523 ± 0.005) Å	b	= (3.611 ± 0.005) Å
c	= (8.080 ± 0.005) Å	c	= (8.649 ± 0.005) Å
Z	= 2	Z	= 2

A structure is proposed with atomic positions for the indium, halogen, and oxygen atoms in space group No. 59, *Pmmn*. The parameters of the atoms were determined mainly from Patterson and Fourier projections.

The structures are built up of infinite In-O sheets separated by double halogen sheets. They may be described as being of a deformed BiOCl type and are isomorphous with the iron(III)oxide chloride, FeOCl.

Previously, in the Department of Inorganic Chemistry of the Royal Institute of Technology, Stockholm, the hydrolysis of In^{3+} has been studied and polynuclear complexes like In_2O^{3+} have been proved to occur.[1] In connection with this solution work, it was of interest to investigate the coordination between indium and oxygen in solid indium oxide salts. This paper presents a structure determination of indium oxide chloride and indium oxide bromide.

PREPARATION OF THE CRYSTALS

White microcrystalline powders were obtained using the methods described in Gmelin-Kraut's Handbuch (1936)[2] for preparing InOCl and InOBr. By hydrothermal hydrolysis of solutions of indium(III)chloride, only indium hydroxide could be prepared. However, by heating a mixture of indium(III)halide, indium hydroxide and some water at 300°C, crystals of indium oxide chloride and indium oxide bromide were obtained.

Indium(III)chloride and *indium(III)bromide* were prepared by dissolving indium metal (99.96 % pure from the *Consolidated Mining and Smelting Company of Canada*)

in hot conc. hydrochloric or hydrobromic acid, as described by Enslin and Dreyer [3,4]. To oxidize lower oxidation states of indium to In^{3+}, some hydrogen peroxide was added towards the end of the reaction and the solution was then evaporated to dryness, giving $InCl_3(H_2O)_4$ or $InBr_3$.

Indium(III)hydroxide was prepared by precipitation from a solution of indium(III)-nitrate using aqueous ammonia. The precipitate was filtered off, washed with water several times and dried in air at room-temperature. It contained 64.3 % In, corresponding to a hydrated $In(OH)_3$.

Indium oxide chloride was then prepared as follows. A mixture of 280 mg $In(OH)_3$, 2 g $InCl_3(H_2O)_4$ and 0.1 ml H_2O was sealed in a thick-walled glass tube and kept at 300°C in an oven. After 24 h, the tube was cooled and the melt leached with ethanol, thus dissolving the excess of $InCl_3$. The residue was then filtered off and washed with ether. It consisted of clear crystals (plane needles) of InOCl and some indium hydroxide.

Indium oxide bromide was prepared in an analogous manner. The initial mixture consisted of 280 mg $In(OH)_3$, 2.4 g $InBr_3$ and 0.2 ml H_2O. The crystals were of the same shape as those of InOCl.

The crystals of InOCl and InOBr are very slightly soluble in water but dissolve completely in dilute acids.

Analysis

A sample, dried in air, was decomposed by fusion with sodium carbonate. After cooling, the melt was leached with water and the residue filtered off. In the filtrate, the amount of *halide* was determined gravimetrically as silver halide[5].

For the determination of *indium* a sample was dissolved in nitric acid, evaporated, and then ignited and weighed as In_2O_3.

The *density* of the crystals was determined from the loss of weight in benzene.

InOCl	Found		Calculated for InOCl
% Cl	19.8	20.0	21.33
% In	68.1	67.8	69.04
Density	4.6_4	4.6_4	4.77

InOBr	Found		Calculated for InOBr
% Br	35.0	35.0	37.93
% In	55.2	55.2	54.47
Density	5.3_3	5.4_0	5.53

The differences between the experimentally determined percentages of indium and halogen and those calculated from the formula InOX are probably due to slight contaminations of the samples, *e. g.* indium hydroxide.

UNIT CELL AND SPACE GROUP

A crystal was set with (010), the needle axis, as rotation axis and rotation and Weissenberg photographs (*h0l* and *h1l*) were taken with Cu*K* radiation. From these photographs it was concluded that the crystals are orthorhombic with the following cell dimensions.

InOCl	$a \approx 4.1$ Å		*InOBr*	$a \approx 4.2$ Å	
	$b \approx 3.5$ Å			$b \approx 3.6$ Å	
	$c \approx 8.1$ Å			$c \approx 8.6$ Å	

Table 1. Powder photograph of InOCl. Cu Ka_1 *radiation. Photographs were taken with and without KCl as an internal standard.* $a = 6.2930$ Å

hkl	$10^4\sin^2\Theta$ calc	$10^4\sin^2\Theta$ obs	pF^2 calc	*I* obs	*hkl*	$10^4\sin^2\Theta$ calc	$10^4\sin^2\Theta$ obs	pF^2 calc	*I* obs
001	91	90	29	w+	123	3089	3090	40	vw
002	364	359	1	vvw	115	3109		48	
101	450	449	77	st	006	3272	—	1	—
011	569	568	16	w	301	3322	3324	34	w—
102	723	722	37	w	220	3348	3349	80	m—
003	818	—	3	—	024	3366		55	
110	837	836	22	m+	214	3368		1	
012	842	841	135	m+	221	3439	3439	36	w
111	928	928	90	w—	302	3595	3605	18	w
103	1177	1177	34	vvw	106	3631		39	
112	1201	—	0	—	205	3708	3708	24	w—
013	1296	1294	39	vw	310	3709		15	
200	1436	1437	70	m	222	3712		0	
004	1454		42		124	3725		3	
201	1527	1528	29	w	016	3750	—	39	—
113	1655	1656	137	w	311	3800	3800	48	w
202	1800	—	0	—	303	4049	4049	20	vvw
104	1813	—	2	—	312	4073	—	0	—
020	1912	1914	58	m+	116	4109	—	10	—
014	1932	—	0	—	223	4166	—	8	—
021	2003	2004	27	m	025	4184	—	20	—
211	2005		23		215	4186	—	6	—
203	2254	—	10	—	031	4393	4393	9	vvw
005	2272	2276	15	m	007	4453	—	3	—
022	2276		0		313	4527	4520	78	w—
212	2278		176		125	4543		78	
114	2291		73		130	4661	4659	14	w
121	2362	2363	84	m	032	4666		62	
105	2631	2638	55	w—	304	4685	—	1	—
122	2635		48		206	4708	—	0	—
023	2730	2735	12	w—	131	4752	4749	29	vw
213	2732		53		224	4802	4797	84	w
015	2750		4		107	4812		16	
204	2890	2890	62	w					

Reflections systematically absent according to space group No. 59, *Pmmn* have been omitted.

The intensities were calculated from the expression $0.1 \cdot \frac{p}{8} \cdot F^2$, where p is the number of equivalent reflections.

More accurate values were calculated from powder photographs in focusing cameras of Guinier type. (Tables 1 and 2) (Cu*K* radiation, internal standard KCl. $a = 6.2930$ Å [6]).

InOCl
$a = (4.065 \pm 0.005)$ Å
$b = (3.523 \pm 0.005)$ Å
$c = (8.080 \pm 0.005)$ Å
$V = 115.7$ Å^3

InOBr
$a = (4.049 \pm 0.005)$ Å
$b = (3.611 \pm 0.005)$ Å
$c = (8.649 \pm 0.005)$ Å
$V = 126.5$ Å^3

Table 2. Powder photographs of InOBr. CuKa$_1$ radiation. Photographs were taken with and without KCl as an internal standard. a = 6.2920 Å

hkl	$10^4\sin^2\Theta$ calc	$10^4\sin^2\Theta$ obs	pF^2 calc	*I* obs	*hkl*	$10^4\sin^2\Theta$ calc	$10^4\sin^2\Theta$ obs	pF^2 calc	*I* obs
001	79	79	20	w	115	2800	—	48	—
002	317	—	0	—	006	2856	—	3	—
101	441	441	135	st	123	2896	2895	68	vw—
011	534	534	1	vvw	024	3089	3088	69	vvw
102	679	680	8	vw	214	3172	—	4	—
003	714	—	4	—	106	3217	—	39	—
012	772	772	218	m+	220	3268	3267	135	m—
110	817	818	2	vw—	016	3311	—	34	—
111	896	896	137	st	301	3336	3336	62	w
103	1076	1076	48	vw	221	3347		23	
112	1134	1136	14	vvw	205	3431	3443	55	vvw
013	1169	1168	32	vw—	124	3451		53	
004	1269	1268	51	vw	302	3574	—	5	—
200	1448	1447	106	m	222	3585	—	1	—
201	1527	1530	18	m	116	3672	3664	102	vvw
113	1531		203		310	3712	—	2	—
104	1631	1631	37	vvw	311	3791	3791	78	w
014	1724	—	4	—	025	3803		51	
202	1765	—	0	—	215	3886	—	5	—
020	1820	1820	141	m	007	3887	—	0	—
021	1899	—	16	—	303	3971	3970	27	vvw
211	1982	1980	1	vvw	223	3981		4	
005	1983		34		312	4029	—	10	—
114	2086	2088	29	vvw	125	4165	4162	90	vvw
022	2137	—	0	—	031	4174	—	0	—
203	2161	—	3	—	107	4249	—	9	—
212	2220	2220	270	m	206	4303	—	4	—
121	2261	2261	160	m—	017	4342	4340	76	vvw
105	2345	2347	62	vvw	032	4412	4407	97	w—
015	2438	—	3	—	313	4426	4426	123	w—
122	2498	—	12	—	130	4457	—	2	—
023	2534	—	3	—	304	4526	4531	22	w
213	2616	2616	68	vw	131	4536		73	
204	2717	2715	72	vw—	224	4537		137	

Reflections systematically absent according to space group No. 59 *Pmmn* have been omitted.

The intensities were calculated from the expression $0{,}1 \cdot \frac{p}{8} \cdot F^2$, where p is the number of equivalent reflections.

From the observed densities given above, one could calculate that there must be $1.9_5 \approx 2$ formula units InOX in the unit cell.

The same reflections are systematically absent in both compounds and they are thus isomorphous: *hk*0 absent with $h+k$ odd, which is characteristic of the space group No. 59, *Pmmn* [7].

PATTERSON SYNTHESES

In order to find out the indium and halogen positions in the unit cell the Patterson projections, *P*(*upw*), were calculated for both compounds (Fig. 1). Relative intensities of the reflections were estimated visually and the F^2-

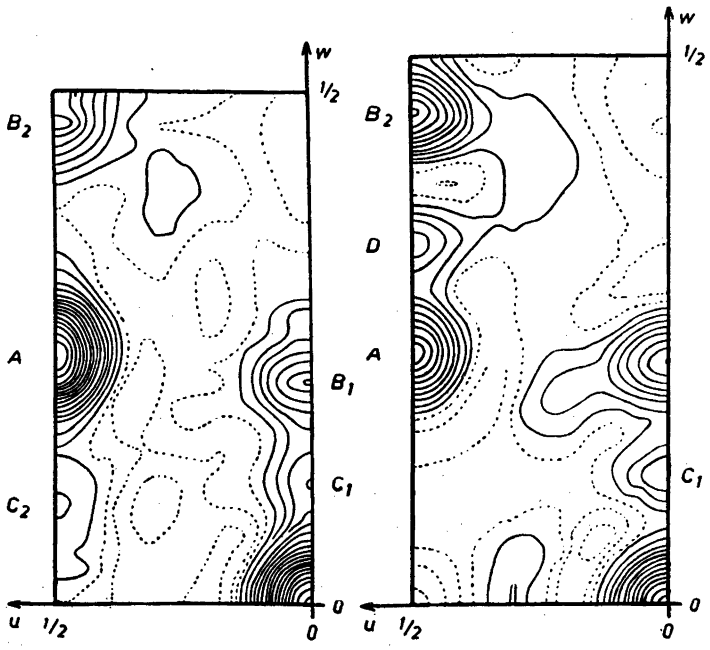


Fig. 1. The Patterson projection P(upw) *for InOCl (left) and InOBr (right). In the peak at the origin only every second contour has been shown. Dashed lines indicate negative values.*

values calculated using the curves given by Lu [8]. In all syntheses the value of $F^2(000)$ has been omitted. Corrections for absorption have not been applied. The maxima have been located by an interpolation table given by Booth [9].

Considering the space group, the indium atoms can only be situated in 2(*a*): 1/4, 1/4, *z*; 3/4, 3/4, $\bar{z}$; or 2 (*b*): 1/4, 3/4, *z*; 3/4, 1/4, $\bar{z}$. The In-In vectors would then be $\pm(\frac{1}{2}, 2z)$ in the *upw* projection.

This must correspond to the pronounced maxima A in the projections at $u = \frac{1}{2}$ and $w = 0.244$ (for InOCl) and $w = 0.229$ (for InOBr). If we assume the indium atoms to be situated in the point position 2(*a*), we thus get the following parameters for the indium atoms (we need only consider the range $0 \leq z_{In} \leq 1/4$)

$$InOCl: z \approx 0.122 \qquad InOBr: z \approx 0.115$$

In addition to the In-In peaks, the Patterson projections show other distinct maxima and we can see that two of them (B_1 and B_2) increase in relative height from the InOCl to the InOBr projection, so they should correspond to distances between indium and halogen atoms. The halogen atoms should then be situated in 2(*a*) or 2(*b*) and the In-X vectors in the *uw* plane would be:

$$\text{I} \pm (0, z_{In} - z_{Br})$$
$$\text{II} \pm (\tfrac{1}{2}, z_{In} + z_{Br})$$

If we now identify I and II with the peaks B_1 and B_2 in Fig. 1, we get the following values for the parameters of the X atoms (we need only consider the range, $0 \leq x \leq 1/4$, $0 \leq z \leq \frac{1}{2}$, if the range for the corresponding y parameter is $0 \leq y \leq 1$):

InOCl

2 Cl in 2(*a*) or 2(*b*) with $z_{Cl} \approx 0.344$

InOBr

2 Br in 2(*a*) or 2(*b*) with $z_{Br} \approx 0.335$

With this value for the Br parameter we could explain the D maximum as a Br-Br vector. The corresponding maximum for Cl-Cl is concealed by the In-In peak in the InOCl projection.

THE ELECTRON DENSITY FUNCTION

The electron density function was studied in order to locate the oxygen atoms and to get more accurate values for the parameters of the heavy atoms.

Since all the atoms of the structure must occupy twofold point positions (2(*a*) or 2(*b*)), the z parameter values may be determined from the line $x = 1/4$ of the projection $\varrho(xpz)$ of the electron density function. This function was thus calculated using the signs of F_{obs} given by the indium and halogen contributions. Fig. 2 shows (1/4, p,z) of InOBr. (The InOCl projection is of the

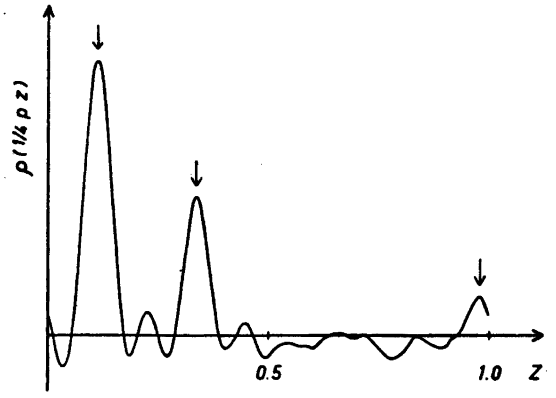


Fig. 2. Electron density of InOBr projected on the xz *plane with* x = 1/4.

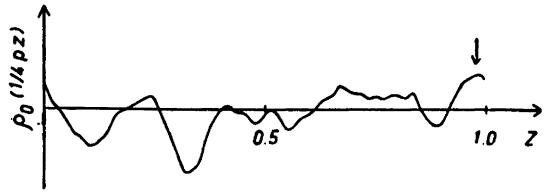


Fig. 3. Electron density of InOBr projected on the xz *plane and with* x = 1/4 *and the indium and bromine atoms substracted.*

same appearance.) It has two very pronounced maxima giving the positions of the indium atom (the highest maximum) and of the bromine atom (the lower maximum). The small peak at $z \approx 0.98$ might give the position of the oxygen atom. However, the peak may be a little displaced from the correct oxygen position by diffraction effects caused by the heavy atoms. To verify the oxygen position, a new electron density projection was calculated with the heavy atoms subtracted (Fig. 3).

Thus, from the electron density projections, the following parameters could be obtained:

InOCl	2 In	in	No. 59,	*Pmmn*	2(*a*)	with	z	=	0.121
	2 Cl	»	»	»	2(*a*) or 2(*b*)	»	z	=	0.345
	2 O	»	»	»	2(*a*) or 2(*b*)	»	z	=	0.97
InOBr	2 In	in	No. 59,	*Pmmn*	2(*a*)	with	z	=	0.113
	2 Br	»	»	»	2(*a*) or 2(*b*)	»	z	=	0.336
	2 O	»	»	»	2(*a*) or 2(*b*)	»	z	=	0.98

With these values for the oxygen parameters, we could explain the small maxima C_1 and C_2 in the Patterson projections in Fig. 1 as In-O distances.

GEOMETRICAL CONSIDERATIONS

From the electron density projections, we have only got values for the x and z coordinates. Now there are two possible values of the y coordinates for the halogen and oxygen atoms, *viz.* $y = 1/4$ or $3/4$, corresponding to the point position 2(*a*) or 2(*b*), and the correct ones can be found by considerations of space.

As 2(*a*) was arbitrarily chosen as the position of the indium atoms, the only possible sites for the halogen atoms will be in 2(*b*), since in 2(*a*) the distances In-X would be too short. (1.8 Å InOCl and 1.9 Å InOBr. In $(NH_4)_2InCl_5\,H_2O$, the In-Cl distance is 2.52 Å. Klug, Kummer and Leroy [10]).

The distance In-O is 2.16 Å in In_2O_3 (Pauling and Shappel [11]) and we should expect about the same in InOX. If the oxygen atoms were situated in 2(*a*) we get too short distances (1.1 Å in InOCl and 1.2 Å in InOBr) and the oxygen atoms must thus be situated in 2(*b*).

FINAL PARAMETERS

The following structure is proposed for InOCl and InOBr. Space group No. 59, *Pmmn*. Two formula units per unit cell.

InOCl	2 In	in	2(*a*)	with	z	=	0.121+0.002
	2 Cl	in	2(*b*)	»	z	=	0.345+0.004
	2 O	in	2(*b*)	»	z	=	0.97 +0.01
InOBr	2 In	in	2(*a*)	»	z	=	0.113+0.002
	2 Br	in	2(*b*)	»	z	=	0.336+0.004
	2 O	in	2(*b*)	»	z	=	0.98 +0.01

Table 3. Comparison between calculated and observed structure factors h0l *from a Weissenberg photograph of InOCl. Cu*K *radiation*

h ↓ \ l →	0	1	2	3	4	5	6	7	8	9	10
0	—	+42 31	+4 —	−12 18	+51 59	−30 36	+9 —	+14 16	+31 31	+29 27	−5 1
1	—	−47 59	−34 47	−32 32	−7 —	+41 38	+35 37	+22 22	+14 13	−20 27	−27 21
2	−66 76	−30 35	−1 —	+12 16	+44 39	+25 17	−2 —	−12 12	−30 27	−26 25	
3	—	+32 36	+24 37	+25 31	+5 —	−32 19	−29 29	−20 22	−12 9		
4	+42 38	+20 27	+1 —	−10 15	−35 26	−21 21					
5	—	−25 23	−19 18								

Table 4. Comparison between calculated and observed structure factors h1l *from a Weissenberg photograph of InOCl. Cu*K *radiation*

h ↓ \ l →	0	1	2	3	4	5	6	7	8	9
0	—	−30 20	−86 59	−46 43	+3 —	+15 16	+46 57	+36 42	−12 —	−12 17
1	−35 34	−50 52	0 —	+61 48	+45 33	+22 38	+16 16	−36 42	−40 45	−23 23
2	—	+25 36	+69 72	+38 41	−5 —	−13 11	−45 42	+35 38	+12 —	+20 20
3	+28 46	+36 47	−3 —	−46 48	−38 42	−31 15	−15 10	+26 33		
4	—	−16 28	−53 56	−28 33	+5 —	+12 11				

Table 5. Comparison between calculated and observed structure factors h0l *from a Weissenberg photograph of InOBr. Cu*K *radiation*

h ↓ \ l →	0	1	2	3	4	5	6	7	8	9	10
0	—	+27 13	+1 —	+12 10	−45 42	−37 42	+11 13	0 —	+16 14	+41 42	+5 —
1	—	+52 67	−13 19	−31 34	−27 18	+35 31	+28 34	+13 22	+31 35	−3 —	−31 29
2	−65 58	+19 30	+2 —	−7 —	+38 42	+33 29	−9 —	0 —	−15 21	−39 37	
3	—	+35 45	+10 21	+23 30	+21 17	−27 27	−23 21	−11 20	−27 28		
4	+44 48	+12 19	−3 —	+5 —	−30 25	−26 20					
5	—	−26 15	−10 9								

Table 6. Comparison between calculated and observed structure factors h1l *from a Weissenberg photograph of InOBr. CuK radiation*

h ↓ / l →	0	1	2	3	4	5	6	7	8	9	10
0	—	−3	−66	−25	+9	−7	+26	+39	−4	−3	−7
		4	45	31	6	10	31	35	6	4	5
1	−6	−37	−12	+45	+17	+22	+32	−15	−27	−6	−23
	11	54	12	47	16	18	30	19	27	9	25
2	—	+3	−52	+26	−6	+7	−23	−36	+3	+5	
		9	55	31	4	—	21	30	4	—	
3	+6	+28	+10	−35	−17	−17	−27	+14	+24		
	13	36	9	33	19	15	18	16	21		
4	—	−2	−39	−21	+6	−4	+20				
		9	35	23	3	—	19				

In Tables 3—6 the calculated structure factors are compared with the observed ones in the Weissenberg photographs *h*0*l* and *h*1*l* of InOCl and InOBr. In all photographs, there is an absorption effect (*cf.* Wells [12]) due to the shape of the crystals (plane needles) which is very pronounced for rays passing along the plane of the crystals. The line with this high absorption has been marked and the structure factors on either side of this line must not be compared with each other. Taking this absorption into account the agreement between calculated and observed structure factors is rather good, the reliability index $R = \frac{||F_{obs}| - |F_{calc}||}{|F_{obs}|}$ being for InOCl *h*0*l* and *h*1*l*, 0.17 and 0.18 and for InOBr 0.21 and 0.19 [8]. (With absent reflections included, InOCl 0.20 and 0.21, InOBr 0.23 and 0.22.) However, for crystals like these containing both heavy and light atoms, the reliability index should not be taken as a definite proof that the structure as a whole is true, but only that the arrangement proposed for the heavy atoms is essentially correct.

DESCRIPTION OF THE STRUCTURE

Fig. 4 shows the structure of InOX. The indium and the oxygen ions form In-O-In layers which are separated by double halogen sheets. The arrangement of the metal and oxygen ions in the In-O sheets has been drawn separately in Fig. 5. The figure shows that the indium and oxygen ions form rectangular sheets and that each oxygen ion is tetrahedrically surrounded by four indium ions.

The indium oxide halides are evidently isomorphous with the iron(III)-oxide chloride, FeOCl (Goldsztaub [13]).

The arrangement of the metal and oxygen ions in the InOX crystals is approximately the same as that found in the corresponding bismuth compounds (Sillén [14]). In BiOX, the bismuth and oxygen ions form square sheets, but in InOX the indium and oxygen ions form rectangular networks.

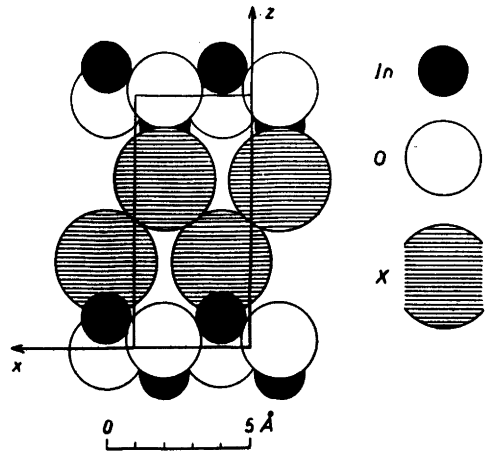


Fig. 4. The structure of InOX, viewed along (010).

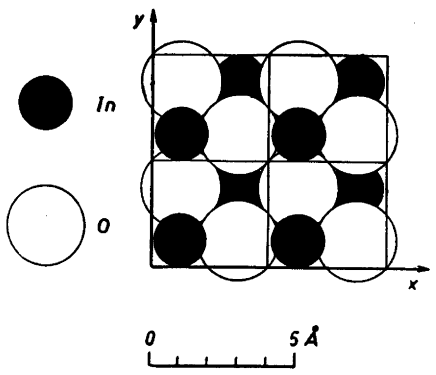


Fig. 5. The In-O sheet. The figure shows the arrangement of the In^{3+} and O^{2-} ions, viewed along (001).

The interatomic distances for the structure proposed will be (in Å):

InOCl	In — In	= 3.35	*InOBr*	In — In	= 3.35
	In — O_1	= 2.1_7		In — O_1	= 2.1_8
	In — O_2	= 2.1_6		In — O_2	= 2.1_5
	In — Cl	= 2.5_1		In — Br	= 2.6_4
	Cl_1 — Cl_1	= 3.52 and 4.07		Br_1 — Br_1	= 3.61 and 4.05
	Cl_1 — Cl_2	= 3.6_9		Br_1 — Br_2	= 3.9_4
	Cl_1 — O_1	= 3.6_8		Br_1 — O_1	= 3.8_4
	Cl_1 — O_2	= 3.0_5		Br_1 — O_2	= 3.0_8
	O_1 — O_2	= 2.7_4		O_1 — O_2	= 2.7_4

The error in the distances is assumed to be = ± 0.1 Å, the only exception being the X_1—O_2 distances with an accuracy of about ± 0.15 Å. The distances from one indium atom to its four indium neighbours are in good agreement with those of 3.38 Å reported for In_2O_3 (Pauling and Shappel [11]). The angles In-O_I-In and In-O_{II}-In are 139° and 109° in InOCl and 136° and 114° in InOBr. The shortest distance between halogen and oxygen is somewhat shorter than that which is expected from the sums of the ionic radii (Cl^- 1.81 Å, Br^- 1.96 Å and O^{2-} 1.40 Å [9]) and which is usually to be found in structures of this type.

Acknowledgements. The author is indebted to Professor Lars-Gunnar Sillén for his helpful criticism and provision of laboratory facilities and, in addition, to Professor Ölander for his kind interest. The author also wishes to thank Dr. Arne Magnéli and Dr. Georg Lundgren for many valuable discussions and Mr. D.G. Gillam for revising the English text.

Thanks are due to the *Consolidated Mining and Smelting Company of Canada, Ltd.* for generously supplying a large amount of indium metal of high purity.

REFERENCES

1. Biedermann, G. *Arkiv Kemi* **5** (1953) 441.
2. *Gmelins Handbuch der anorganischen Chemie*, No. 37, Indium, Verlag Chemie, Berlin 1936.
3. Enslin, F. and Dreyer, H. *Z. anorg. u. allg. Chem.* **249** (1943) 119.
4. Enslin, F. and Dreyer, H. *Z. anorg. Chem.* **254** (1947) 293.
5. Kolthoff, I. M. and Sandell, E. B. *Textbook of Quantitative Inorganic Analysis*, Mac Millan Company, New York 1943, p. 307.
6. Hambling, P. G. *Acta Cryst.* **6** (1953) 98.
7. *International Tables for X-ray Crystallography*, Kynoch Press, Birmingham 1952, Vol. I.
8. Lu, C.-S. *Rev. Sci. Instr.* **14** (1943) 331.
9. Booth, A. D. *Fourier Technique in X-ray Organic Structure Analysis*, University Press, Cambridge 1948, p. 64 and 101.
10. *Internationale Tabellen zur Bestimmung von Kristallstrukturen*, Gebrüder Borntraeger, Berlin 1935, Band 2.
11. Klug, H. P., Kummer, E. and Leroy, A. *J. Am. Chem. Soc.* **70** (1948) 3064.
12. Pauling, L. and Shappel, M. *Z. Krist.* **75** (1930) 128.
13. Wells, A. F. *Z. Krist.* **96** (1937) 451.
14. Goldzstaub, M. S. *Compt. rend.* **198** (1934) 667.
15. Sillén, L. G. *Svensk Kem. Tidskr.* **58** (1941) 39.

Received June 19, 1956.

ACTA CHEMICA SCANDINAVICA 10 (1956) 1298—1302

The Separate Determination of Peroxide-containing Phospholipids and Other Lipoperoxides

J. GLAVIND and S. HARTMANN

Department of Biochemistry and Nutrition, Polytechnic Institute, Copenhagen, Denmark

Methods for the separate determination of peroxide-containing triglycerides (TGPO) and phospholipids (PLPO) have been studied. Tentative methods based on the following principles are described: 1) Precipitation with acetone, 2) determination of TGPO in the filtrate from adsorption on alumina; calculation of PLPO as the difference between total lipoperoxide and TGPO, 3a) determination of TGPO in the filtrate from adsorption on alumina; determination of PLPO by carrying out the colorimetric thiocyanate reaction while the phospholipids are adsorbed on the column, 3b) as in 3a) but with the *indophenol* method. The separate determination of TGPO and PLPO is possible by any of the methods, but the best results are generally obtained by method 2).

In a previous paper[1] we described methods for the determination of peroxide groups in phospholipids and phospholipid-containing fats. In nature, phospholipids are generally found together with triglycerides and other lipids, and the processes whereby peroxide groups are formed most often take place in mixtures of different kinds of lipids. At the same time the phospholipids often have a fatty acid composition different from that of the triglycerides from the same source. The phospholipids are, as a rule, more unsaturated und must be assumed to have a larger tendency towards the formation of peroxide groups. Under such circumstances the problem arises of methods for the determination of how large a fraction of the peroxide groups is situated on the individual kinds of lipids, *e.g.*, methods for the separation of phospholipid peroxides (PLPO) from other lipoperoxides, mainly triglyceride peroxides (TGPO).

In order to carry out such a fractionation it was attempted to use methods similar to those used for the separation of non-peroxidized phospholipids from other lipids, *i.e.*, especially precipitation with acetone, and adsorption. As a result of our studies tentative methods based on different principles of separation were elaborated. They are described in the following together with the results of a comparison of the methods.

METHODS

Method 1. Precipitation with acetone

The presence of peroxide groups does not greatly alter the solubility properties of the lipids, *i.e.*, when acetone is added to a solution of lipids in petro-

leum ether, PLPO are precipitated together with other phospholipids while TGPO and other triglycerides etc. remain in solution.

The lipid is dissolved in 5 ml petroleum ether, and 20 ml acetone is added. After separation by centrifuging and evaporation of the solvents, the two fractions are dissolved in a small amount of chloroform. The peroxide contents are determined in each fraction, with the exclusion of atmospheric oxygen, by the thiocyanate or the indophenol method as described in our first paper.

Method 2. Adsorption on alumina. Determination of TGPO in the filtrate, and of PLPO by substraction from total lipoperoxide

The presence of peroxide groups increases the adsorption affinity of the lipids, but, in general, phosphoric acid groups make the lipids still more strongly adsorbed. By means of a suitable adsorbent, *e.g.* alumina, TGPO and PLPO can be separated. With petroleum ether as a solvent TGPO (and other peroxides) are adsorbed on the column while non-oxidized triglycerides and other substances like carotene are washed through. Petroleum ether is, however, a less suitable solvent for the separation of TGPO and PLPO. Better results are obtained with chloroform as a solvent.

When, accordingly, a solution of lipoperoxides in chloroform is sent through a column of alumina, a fractioning is obtained in such a way that TGPO can be determined in the filtrate by one of the known methods. The PLPO are very strongly adsorbed and difficult to elute. However, when the total amount of peroxide is also determined, the PLPO can be calculated by substracting the TGPO.

The chromatographic adsorption device consists of a 100 × 13 mm glass tube provided with a constriction below which the tube is drawn out. A cotton plug is placed above the constriction, and 5 g alumina (a good commercial preparation for chromatographic use or, preferably, the purified product used in method 3) is put into the tube and packed by gently tapping the tube on the bench. The tube is placed on a suction flask by means of a rubber stopper. The flask is connected to the pump, and by means of an interposed T-tube the pressure can be regulated. The suction flask is filled to about half its volume with glass beads for the convenient placement of a centrifuge tube to collect the filtrate.

Twenty ml chloroform is sucked through the column, and the filtrate is discarded. The lipid dissolved in 5 ml chloroform is filtered through the column and washed with 25 ml chloroform (the pharmacopoea grade which contains a small amount of ethanol). The filtrate is collected in centrifuge tubes, an incidentally occurring precipitate removed by centrifuging, and the solvent evaporated to a small volume. The peroxide content is determined by the thiocyanate or the indophenol method; the result corresponds to the content of TGPO. An identical sample of lipid dissolved in 5 ml chloroform is used for the determination of total lipoperoxide. The content of PLPO is calculated as the difference between the two peroxide determinations.

Method 3. Adsorption on alumina. Determination of TGPO in filtrate, and of PLPO by color development on column

It is possible after chromatographic separation of TGPO and PLPO to carry out the determination of PLPO *in situ*, *i.e.*, by passing a color reagent through the column and measuring the color in the filtrate. Alumina is still a suitable adsorbent, but since commercial preparations are highly impure and would produce very strong colors with the color reagents, it is necessary to carefully purify the alumina in order to remove, as far as possible, all iron and other disturbing substances.

Preparation of purified alumina. Commercial alumina (*e.g.*, Aluminiumoxyd, reinst, Merck; Aluminiumoxyd, standardisiert nach Brockmann, Merck; or Aluminium Oxide for Chromatography, May & Baker) is repeatedly boiled with 5 % hydrochloric acid. The acid is removed by decantation and washing with redistilled water followed by ethanol, and the product is dried at 100 C *in vacuo*.

Method 3a. Thiocyanate procedure

Preparation of the thiocyanate reagent. In a graduated cylinder 50 ml 6 % ammonium thiocyanate in absolute ethanol (or methanol) is mixed with 50 ml chloroform. Oxygen-free nitrogen is bubbled through. After 15 minutes 1 ml ferrous chloride reagent prepared by the method of Loftus Hills and Thiel [2] is added. The reagent is protected from atmospheric oxygen by continuing the passing of nitrogen.

By means of the purified alumina a chromatographic column is prepared as described in method 2. Five ml thiocyanate reagent is filtered slowly through the column followed by absolute ethanol until a volume of about 10 ml is collected in the centrifuge tube. An incidentally occurring precipitate is removed by centrifuging, the volume adjusted to 10 ml, and light absorption at 500 mμ is measured. If the latter is high compared with the absorption of 5 ml thiocyanate reagent +5 ml ethanol, this indicates that the column does still contain traces of iron or other substances that will interfere with the PLPO determination. If that is the case, more portions of thiocyanate reagent followed by ethanol are filtered through until a constant low value is obtained.

With a well-purified alumina a low extinction is obtained in the first filtrate. In that case, the treatment of the column with thiocyanate reagent can be dispensed with, and reagent + ethanol can be used as a blank.

In the case the column has been treated with thiocyanate reagent, thiocyanate is removed by washing with about 20 ml ethanol, and the ethanol washed out with chloroform (about 20 ml). The lipoperoxide mixture containing both TGPO and PLPO dissolved in chloroform is filtered slowly through the column and eluted with about 25 ml chloroform. The filtrates, after incidental precipitates are removed by centrifuging, are evaporated, dissolved in ethanol-chloroform, and the amount of peroxide determined as usual, the result indicating the amount of TGPO present.

Suction is continued until no more chloroform drops from the tube. Then a new centrifuge tube is placed beneath the column and 5 ml thiocyanate reagent is filtered slowly through. When no more reagent is present on the

top of the adsorbent, ethanol is added, and filtration is continued until a total volume of little less than 10 ml is collected. After centrifuging and adjustment of the volume to 10 ml the intensity of the red color is measured, a reagent blank is substracted, and the peroxide content, corresponding to the PLPO content, is calculated.

Method 3b. Indophenol procedure

The method is carried out exactly as in 3a, but TGPO is determined by the indophenol method, and instead of the thiocyanate reagent the following reagent is used for preparation of the column and determination of PLPO.

Preparation of the indophenol reagent. In a graduated cylinder 50 ml 20 % $MgCl_2$,6 H_2O in absolute ethanol is mixed with 50 ml chloroform and oxygen-free nitrogen bubbled through. After 15 minutes 1 ml 2 % leuco-dichlorophenolindophenol and 1 ml 0.1 % ferric chloride, both in absolute ethanol, are added with continued bubbling.

RESULTS AND DISCUSSION

Table 1 illustrates results obtained by the methods described above. Mixtures of a triglyceride (lard) and a phospholipid (egg phosphatides repeatedly precipitated with acetone), both having a peroxide content of about 3 mequiv. per kg, were prepared and the recovery of TGPO and PLPO was determined by the different methods.

The results show that the separate determination of TGPO and PLPO may be carried out by using any of the principles mentioned in the introduction of this paper.

Precipitation with acetone has given the least satisfactory separation. Especially, too little PLPO is found in the precipitate when only a small amount of phospholipid is present. This is in accordance with the well-known fact that acetone does not give a complete precipitation of phospholipids; phospholipids, and probably also PLPO, are somewhat soluble in acetone. In other circumstances, by the examination of phospholipids of other origin than eggs, precipitation with acetone may be more advantageous in comparison with adsorption.

From the TGPO-values found by the different adsorption methods it is seen that the phospholipid preparation used has probably contained a small amount of TGPO. Taking this into consideration, it is seen that the recovery of TGPO has been almost quantitative in methods 1, 2, and 3 a. Pre-treatment of the column with indophenol reagent has resulted in loss of TGPO (method 3b).

PLPO values calculated as the difference between total lipoperoxide and TGPO are in quite good agreement with the "calculated values". In the two adsorption methods where PLPO is determined by carrying out the colorimetric reactions on the columns although oxygen could not be completely excluded, too low PLPO values are regularly found. Generally, a recovery of about 60 % PLPO is found. In most cases, therefore, a determination of PLPO as the difference between total lipoperoxide and TGPO will be the best method. In certain circumstances, the determination of PLPO by the colori-

Table 1. Comparison of different methods for the separate determination of peroxide-containing triglycerides (TGPO) and phospholipids (PLPO).

Mixture	Separation method	Thiocyanate method				Indophenol method	
		"Calculated value"	Method 1	Method 2	Method 3a	"Calculated value"	Method 3b
A	TGPO	0.60	0.61	0.65	0.58	0.36	0.165
	PLPO	0	0.00	(0)	0.00	0	0.02
	Total	0.60	(0.61)	0.60	(0.58)	0.36	(0.185)
B	TGPO	0.54	0.61	0.58	0.56	0.32	0.19
	PLPO	0.06	0.04	(0.02)	0.08	0.04	0.065
	Total	0.60	(0.65)	0.60	(0.64)	0.36	(0.255)
C	TGPO	0.30	0.47	0.36	0.36	0.18	0.06
	PLPO	0.31	0.22	(0.24)	0.24	0.19	0.16
	Total	0.61	(0.69)	0.60	(0.60)	0.37	(0.22)
D	TGPO	0.06	0.33	0.10	0.10	0.04	0.025
	PLPO	0.56	0.33	(0.53)	0.40	0.34	0.16
	Total	0.62	(0.66)	0.63	(0.50)	0.38	(0.185)
E	TGPO	0	0.38	0.05	0.05	0	0.015
	PLPO	0.62	0.28	(0.57)	0.44	0.38	0.265
	Total	0.62	(0.66)	0.62	(0.49)	0.38	0.28

Method 1: Precipitation of PLPO with acetone, TGPO remaining in solution.
„ 2: Adsorption of PLPO on alumina, determination of TGPO in filtrate, calculation of PLPO as difference between total lipoperoxide and TGPO.
„ 3a: Adsorption of PLPO on alumina, determination of TGPO in filtrate, determination of PLPO by carrying out the colorimetric reaction while the phospholipids are adsorbed on the column.
„ 3b: As method 3a, but with the indophenol method instead of the thiocyanate method.

The figures give the extinctions read in the photometer after blanks have been subtracted. The mixtures B, C and D were prepared from the TGPO-solution A, and the PLPO-solution E in the proportions 9:1, 1:1, and 1:9, respectively. "Calculated values" are values calculated from A and E. Values between parentheses (total lipoperoxide in methods 1, 3a, and 3b, and PLPO in method 2) are calculated from the other, directly observed, values presented in the table.

metric reaction on the adsorption column may be preferable, *e.g.*, when the amount of PLPO is very small compared with TGPO. Certain products may contain phospholipids that are not completely adsorbed on alumina. In such cases other adsorbents or the precipitation with acetone may be an advantage.

Acknowledgement. This work was supported by grants from *P. Carl Petersens Fond* and *Laurits Andersen's Fond.*

REFERENCES

1. Glavind, J. and Hartmann, S. *Acta Chem. Scand.* **9** (1955) 497.
2. Loftus Hills, G. and Thiel, C. C. *J. Dairy Res.* **14** (1946) 340.

Received June 23, 1956.

ACTA CHEMICA SCANDINAVICA 10 (1956) 1303—1316

The Acid-soluble Nucleotides of Wheat Plants

ROLF BERGKVIST

Institute of Biochemistry, University of Lund, Sweden

A method is presented for the analysis and isolation of the acid-soluble nucleotides from plant tissue.

The application of this method to wheat plants resulted in the identification of the 5'-triphosphates of adenosine, guanosine, uridine and cytidine beside mono- and diphosphates. The identifications are based on ultraviolet absorption spectra and chromatographic evidence before and after hydrolysis, together with chemical and enzymic analysis.

The demonstration in recent years of the fundamental role of nucleoside polyphosphates in mechanisms of energy transfer and biosynthesis made it desirable to develop methods for their analysis and isolation from plant materials.

The first direct demonstration of the presence of nucleoside polyphosphates in plants originates from Albaum and Umbreit [1], who isolated from germinated oat seedlings an adenine-pentose-pyrophosphate in low yield and of low purity. This compound appeared to be related to, but not identical with 5'-ADP *.

Later, an ATP-like compound was isolated from mung bean sprouts [2], a material chosen because of its low content of polysaccharides, phytic acid and non-specific ultraviolet absorbing substances, which interfered with the isolation from other plant sources. The product obtained originally appeared to be similar to ATP from animal tissue but not identical with it, and was considered [3] to represent a polymerized form of ATP, which with appropriate treatment could be depolymerized to give a compound identical with the ATP found in other tissues.

Among the radioactive compounds observed when algae or green leaves are allowed to photosynthesize in $^{14}CO_2$ Buchanan [4] *et al.* detected a nucleotide fraction, and presented paper chromatographic evidence for the presence of 5'-AMP, 5'-UMP, UDPG, UDPgalactose, an adenosine-containing nucleotide other than ATP, ADP or AMP, and a mannose-containing compound chromatographically similar to a nucleotide.

* Abbreviations used: A, adenosine; G, guanosine; U, uridine; C, cytidine; MP, monophosphate; DP, diphosphate; TP, triphosphate; UDPG, uridine diphosphate glucose; DPN, diphosphopyridine nucleotide; TPN, triphosphopyridine nucleotide.

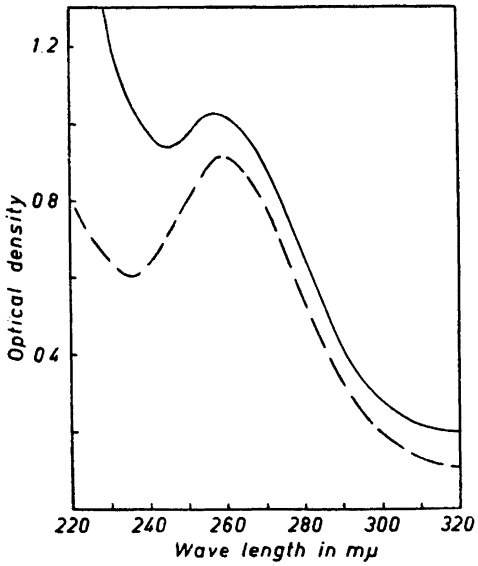


Fig. 1. Norite eluate before ———— *and after* — — — — *ether extraction.*

An ATP-like compound in chlorophyll-containing plants has been detected chromatographically by Simonis and Schwinck [5], and Sebesta and Sorm [6] have determined the ATP content of *Phaseolus vulgaris*.

The determination of the total acid-soluble nucleotide content in plants and isolation of the nucleoside polyphosphates in pure form has generally met with difficulties mainly because the procedures, which were found satisfactory for animal tissue, yielded unsatisfactory results when applied to plant materials [1-3].

The experience of previous authors in this direction was confirmed in the present investigation. Extracts prepared by homogenizing plant material from various sources in cold trichloroacetic or perchloric acids exhibited very complex ultraviolet absorption spectra, and no separation of the nucleotide fraction from other phosphorus-containing or ultraviolet-absorbing substances could be achieved by precipitation of the barium or mercury salts or by any other procedures of purification. Chromatography at this stage proved also impracticable. A crude separation of the nucleotide fraction from non-nucleotide phosphorus compounds could, however, be attained by adsorption on norite, a current method in the nucleotide field. The nucleoside derivatives from the acid extracts were quantitatively retained by norite, and could be recovered by repeated elution with 25 % aqueous ethanol containing 0.5 % ammonia.

Spectrophotometric analysis of the combined eluates showed that the nucleotides were mixed with a large quantity of non-nucleotide material. Precipitation with zinc or barium salts at this point yielded products containing less than 10 % nucleotides. Ion exchange chromatography was also unsuccessful, because of the multitude of ultraviolet absorbing, non-nucleotide fractions. Hence, further purification prior to chromatography was necessary. By the

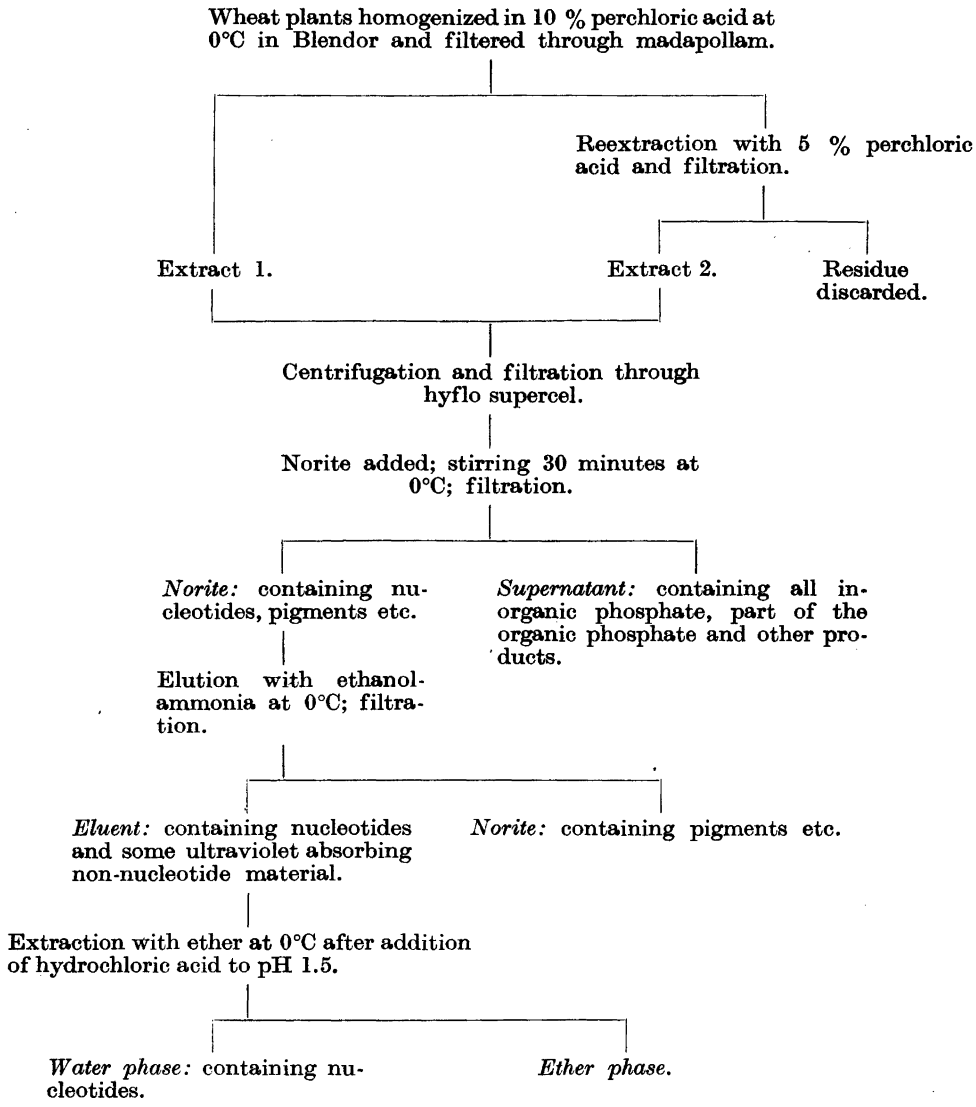


Fig. 2. Isolation of the acid-soluble nucleotide fraction from wheat plants.

addition of hydrochloric acid to pH 1.5 and extraction with ether for several hours the disturbing substances were removed from the norite-eluates. The absorption curves before and after extraction, shown in Fig. 1, indicate the effectiveness of this step in removing ultraviolet absorbing, non-nucleotide material.

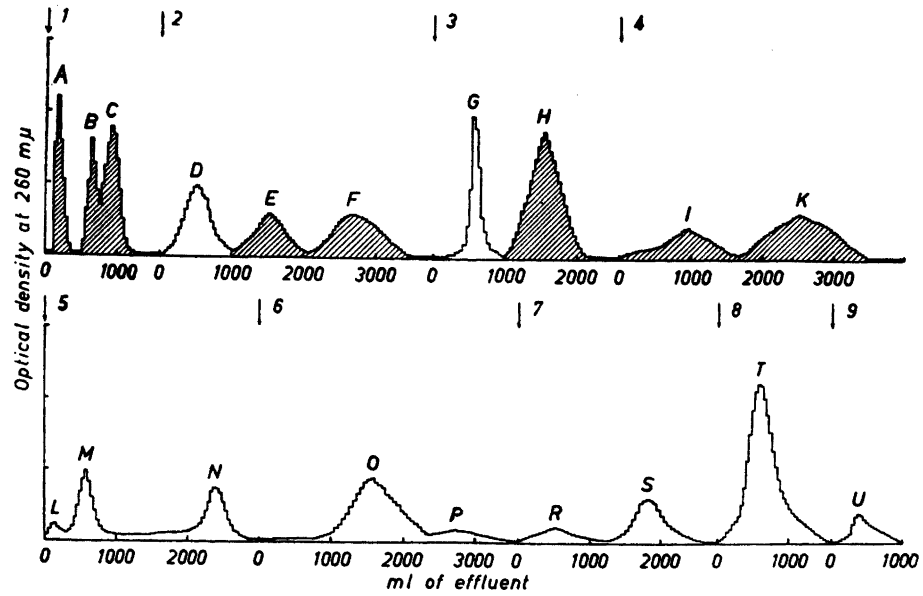


Fig. 3. Ion exchange chromatogram of acid-soluble nucleotides from 500 g of wheat plants. The crossed fractions varied in amounts in different preparations. Exchanger: Dowex 1, X-10, 200 to 400 mesh, 1.6 × 40 cm., formate form; flow rate 1.5 ml/min.

Eluting agents:

1) *0.02 M formic acid*
2) *0.1 M* » »
3) *0.1 M* » » + *0.05 M sodium formate*
4) *0.1 M* » » + *0.1 M* » »
5) *0.1 M* » » + *0.3 M* » »
6) *0.1 M* » » + *0.4 M* » »
7) *0.1 M* » » + *0.6 M* » »
8) *0.2 M* » » + *0.8 M* » »
9) *0.5 M* » » + *1.0 M* » »

By this method, the acid-soluble nucleotide fraction from various plant tissues could be prepared in sufficient purity for further fractionation by chromatography. In the present paper the application of this procedure to wheat plants is reported.

From wheat plants, which had grown out of doors under normal conditions and begun to form grains, only the aerial part was investigated. The acid-soluble nucleotide fraction was isolated as outlined in Fig. 2.

The individual nucleotide compounds were separated by ion exchange chromatography, and the method reported by Bergkvist and Deutsch [7] was used with slight modifications. Because of employing a longer column some changes in the eluting system were necessary.

Fig. 3 shows an ion exchange chromatogram of the acid-soluble nucleotides of wheat plants, as obtained from a formate column.

Table 1. R_F values of effluent fractions.

Solvent systems: (I) *n*-propanol-ammonia-water (60:30:10);
(II) ethanol-1 M ammonium acetate, pH 7.5 (75:30);
(III) ethanol-1 M ammonium acetate buffer, pH 3.8 (75:30);
(IV) *iso*propanol-saturated ammonium sulphate solution-water (2:79:19);
(V) *iso*butyric acid-ammonia-water (66:1:33).
Descending chromatography was used in all systems.
Temperature 20 to 22°C.

Compound	R_F/R_F-5'-AMP	R_F			
	I	II	III	IV	V
B and *C*	1.14	0.17	0.38	0.70	0.39
2'- and 3'-CMP	1.14	0.17	0.38	0.70	0.39
D	1.00	0.14	0.32	0.32	0.44
5'-AMP	1.00	0.14	0.32	0.32	0.44
E	1.18	0.16	0.33	0.28	0.51
2'-AMP	1.18	0.16	0.33	0.28	0.51
F	1.18	0.16	0.33	0.17	0.51
3'-AMP	1.18	0.16	0.33	0.17	0.51
G	0.71	0.18	0.41	0.72	0.23
5'-UMP	0.71	0.18	0.41	0.72	0.23
H	1.00	0.23	0.47	0.70	0.28
2'- and 3'-UMP	1.00	0.23	0.47	0.70	0.28
I	0.69	0.12	0.28	0.54	0.26
2'-GMP	0.69	0.12	0.28	0.54	0.26
K	0.69	0.12	0.28	0.42	0.26
3'-GMP	0.69	0.12	0.28	0.42	0.26
M	0.71	0.23	0.26	0.75	0.24
UDPG	0.71	0.23	0.26	0.75	0.24
N	0.53	0.09	0.20	0.79	0.13
UDP	0.53	0.09	0.20	0.79	0.13
O	0.74	0.07	0.14	0.38	0.32
ADP	0.74	0.07	0.14	0.38	0.32
P	0.52	0.04	0.04	0.82	0.07
CTP	0.52	0.04	0.04	0.82	0.07
R	0.39	0.05	0.10	0.61	0.10
GDP	0.39	0.05	0.10	0.61	0.10
S	0.40	0.04	0.09	0.82	0.08
UTP	0.40	0.04	0.09	0.82	0.08
T	0.56	0.04	0.06	0.47	0.21
ATP	0.56	0.04	0.06	0.47	0.21
U	0.30	0.03	0.04	0.64	0.06
GTP	0.30	0.03	0.04	0.64	0.06

The elution positions and the absorbance ratios E_{250}/E_{260} and E_{270}/E_{260} gave a preliminary identification of the individual fractions.

Peak *A* contained a mixture of purine and pyrimidine bases, which were separated by cation exchange in an acid system according to Cohn [8]. The

Table 2. Analysis of effluent fractions.

Data on absorption spectra, phosphate and ribose content, and base. The chemical data are expressed in terms of moles per mole of base, as determined spectrophotometrically. The absorption spectra were determined in acid and alkaline solutions. The ribose content of the cytosine nucleotides could not be determined by the method of Albaum and Umbreit [15]. The bases were identified by paper chromatography.

Compound	Spectrum type	Phosphate per mole of base		Ribose per mole of base	Base
		Total	Labile		
B	Cytidine	1.00	0	—	Cytosine
C	Cytidine	1.01	0.	—	Cytosine
D	Adenosine	0.96	0	1.00	Adenine
E	Adenosine	1.00	0	1.00	Adenine
F	Adenosine	0.98	0	1.03	Adenine
G	Uridine	1.00	0	0.80	Uracil
H	Uridine	1.01	0	0.86	Uracil
I	Guanosine	0.97	0	1.00	Guanine
K	Guanosine	0.95	0	1.00	Guanine
L	Uridine	—	—	—	Uracil
M	Uridine	2.10	1.00	—	Uracil
N	Uridine	2.01	0.98	0.87	Uracil
O	Adenosine	2.00	1.00	0.97	Adenine
P	Cytidine	3.00	1.98	—	Cytosine
R	Guanosine	2.00	0.97	0.96	Guanine
S	Uridine	2.87	1.90	0.90	Uracil
T	Adenosine	3.00	2.00	0.92	Adenine
U	Guanosine	3.09	2.06	0.94	Guanine

bases adenine, guanine, uracil and cytosine were unequivocally identified by paper chromatography in different solvent systems.

The fractions corresponding to the following peaks were adsorbed on norite with subsequent elution by ethanol-ammonia. The concentrated solutions thus obtained were subjected to paper chromatography in comparison with the authentic products. The results are summarized in Table 1.

Beside elution position, absorbance ratios and paper chromatography, the ultraviolet absorption spectra at different pH values established further the identity of the different fractions.

Total and acid-labile phosphate as well as the pentose content were determined. After hydrolysis and paper chromatography in the *n*-butanol-acetic acid-water (4:1:5) system, the presence of ribose was revealed on development with aniline hydrogen phthalate.

In order to confirm the identity of the bases of the different purine and pyrimidine nucleotide fractions, the free bases were prepared by hydrolysis for one hour at 100°C, in 1 N hydrochloric acid and 70 % perchloric acid, respectively. R_F values identical with those of the corresponding authentic

products were obtained by paper chromatography in three different solvent systems. The ultraviolet absorption curves of the products of hydrolysis were likewise found to be identical with those of the corresponding bases. The results are summarized in Table 2.

Beside uridine and two phosphate groups peak *M* was found to contain glucose. Boiling in 0.01 N acid for 5 minutes liberated practically all the glucose and only a very small portion of the phosphate. After such a treatment uridine diphosphate and glucose could be identified as the breakdown products by paper chromatography and ionophoresis.

Uridine diphosphate glucose was closely associated with another UDP derivative (peak *L*), which on mild acid hydrolysis liberated UDP. This fraction was too small for more complete analysis.

The di- and triphosphates of adenosine were degraded to the monophosphate on heating the free acids for two hours to 100 °C. The uridine polyphosphates were hydrolysed for one hour at 100°C in 1 N hydrochloric acid, which resulted in the formation of the corresponding monophosphate together with orthophosphate, in agreement with the expected behavior of a pyrimidine nucleoside-5'-polyphosphate. Paper chromatography of the products of hydrolysis gave ultraviolet absorbing spots with the same R_F values as 5'-AMP and 5'-UMP, respectively, as seen from Table 3.

The location of the phosphate groups in the different nucleotides was established both by oxidation with periodate [9] and by the action of rattlesnake venom (*Crotalus adamanteus*). Treatment with the venom splits the pyrophosphate linkage between the phosphate group attached to ribose and the next phosphate [10]. The specific 5'-nucleotidase of the venom then splits off the phosphate from any 5'-monophosphate formed, yielding the nucleoside

Table 3. R_F values of the monophosphates obtained by hydrolysis of the different polyphosphates, in comparison with authentic samples.

Solvent systems: (I) ethanol-1 M ammonium acetate, pH 7.5 (75:30); (II) etanol-1 M ammonium acetate buffer, pH 3.8 (75:30); (III) *iso*propanol-saturated ammonium sulphate solution-water (2:79:19). Descending chromatography was used in all systems. Temperature 20 to 22°C.

Compound	R_F		
	I	II	III
AMP from peak *O*	0.14	0.32	0.32
AMP from peak *T*	0.14	0.32	0.32
5'-AMP	0.14	0.32	0.32
2'- and 3'-AMP	0.16	0.33	0.17; 0.28
UMP from peak *M*	0.18	0.41	0.72
UMP from peak *N*	0.18	0.41	0.72
UMP from peak *S*	0.18	0.41	0.72
5'-UMP	0.18	0.41	0.72
2'- and 3'-UMP	0.23	0.47	0.70

Table 4. Periodate oxidation and action of snake venom on effluent fractions.

Periodate oxidation. 0.50 μmole of potassium metaperiodate was added to approx. 0.30 μmole of the sodium salt of the nucleotide in a total volume of 3.0 ml. The amount of periodate consumed was measured at 227 mμ against a blank containing periodate of the same concentration. Reaction time was 60 minutes at 20°C.

Incubation with snake venom. 1 μmole of nucleotide in 1.0 ml of glycine buffer (pH 8.5) and 0.05 ml of 1 M magnesium chloride were treated with 2 mg of lyophilized *Crotalus adamanteus* venom in 0.2 ml of 0.2 % sodium chloride. The mixture was incubated for 60 min. at 38°C. Phosphate was estimated after addition of 0.1 ml of 70 % perchloric acid and centrifugation. The reaction product was isolated from the remaining solution by adsorption on norite and elution with ethanol-ammonia. The products were identified by paper chromatography.

Compound	μmoles of periodate consumed per μmole of nucleotide	μmoles of orthophosphate formed per μmole of nucleotide	Reaction product
B	0.14	0	2'-CMP
C	0.11	0	3'-CMP
D	0.99	0.91	Adenosine
E	0.12	0	2'-AMP
F	0.12	0	3'-AMP
G	1.00	0.90	Uridine
H	0.04	0	2'- and 3'-UMP
I	0.03	0	2'-GMP
K	0.08	0	3'-GMP
M	1.14	0.29	Uridine
N	0.92	0.77	Uridine
O	0.98	0.84	Adenosine
P	0.96	0.30	Cytidine
R	1.04	0.71	Guanosine
S	1.02	0.32	Uridine
T	1.00	0.34	Adenosine
U	0.97	0.20	Guanosine

and orthophosphate. The 2'- and 3'-monophosphates are resistent towards the enzyme and should be unaffected. The reaction products were examined by phosphate analysis and paper chromatography. The results appear in Table 4.

5'-ADP, 5'-ATP, 5-'UTP and 5'-GTP have been isolated as the barium salts; the analyses are shown in Table 5. The results correspond to preparations of about 90 % purity with the exception of GTP, the amount of which was too small for further purification.

As already briefly mentioned, some doubts have arisen in the literature concerning the structural identity of adenosine triphosphate encountered in plants with that from animal tissue. The evidence outlined above leaves little or no doubt about their identity, but as a further test, the reaction with glucose in the presence of hexokinase was studied. ATP from fraction *T* transferred

Table 5. Analysis of the isolated barium salts of nucleotides.

The barium salts were washed with ethanol and ether and dried *in vacuo* over phosphorus pentoxide to constant weight. The base concentrations were calculated from optical densities and ribose concentrations from the values of periodate oxidation. Theoretical values were calculated for barium salts of triphosphates and diphosphate containing 2 and 1.5 barium atoms per mole of nucleotide, respectively, and 4 moles of water per mole of nucleotide.

Compound	Component	Found μmoles/mg	Calculated μmoles/mg	Ratio component/base
ADP from peak *O*	Adenosine	1.18	1.30	
	Total P	2.36	2.60	2.00
	Labile P	1.18	1.30	1.00
	Ribose	1.16	1.30	0.98
ATP from peak *T*	Adenosine	1.05	1.17	
	Total P	3.15	3.51	3.00
	Labile P	2.10	2.34	2.00
	Ribose	1.05	1.17	1.00
UTP from peak *S*	Uridine	1.05	1.21	
	Total P	2.95	3.63	2.81
	Labile P	1.95	2.42	1.86
	Ribose	1.07	1.21	1.02
GTP from peak *U*	Guanosine	0.51	1.15	
	Total P	1.58	3.45	3.10
	Labile P	1.05	2.30	2.06
	Ribose	0.50	1.15	0.98

half of its labile-bound phosphate to glucose, exactly as animal ATP. Furthermore, the effect on the viscosity of actomyosin solutions [11] was identical for ATP from fraction *T* and ATP isolated from muscle.

The qualitative and quantitative analysis of the fractions corresponding to each peak of the chromatogram are summarized in Table 6.

The present work establishes the occurrence in wheat plants of all the four ribonucleosides in the form of acid-soluble 5'-mononucleotides at different levels of phosphorylation, in addition to their occurrence in nucleic acids and in analogy to previous findings on animal tissue.

Nearly 90 % of the acid-soluble nucleotide material in wheat plants consists of adenosine and uridine derivatives, present in practically equimolar amounts. The predominance of uridine, beside adenosine derivatives is of considerable interest and in contrast to the dominating role of adenosine derivatives in animal tissue. But whereas about half of the acid-soluble adenosine and guanosine nucleotides were isolated as the triphosphates, only little over 20 % of the uridine derivatives were found in the form of triphosphate. In the case of cytidine, the triphosphate was the only derivative obtained; neither 5'-CMP and CDP nor 5'-GMP could be detected in any of the experiments. It is probable, that during further isolation work additional nucleotides will be found to occur in small amounts.

Table 6. Amounts and identity of effluent fractions obtained on ion exchange chromatography of the acid-soluble nucleotides from wheat plants. The second column give sthe maximum amounts of 2'- and 3'-phosphates.

Compound	Identity	μmoles/1000 g of wheat plants	μmoles/1000 g of wheat plants
B	2'-CMP		80
C	3'-CMP		80
D	5'-AMP	35	
E	2'-AMP		35
F	3'-AMP		55
G	5'-UMP	44	
H	2'- and 3'-UMP		135
I	2'-GMP		44
K	3'-GMP		89
L	UDPX	4	
M	UDPG	27	
N	UDP	52	
O	ADP	49	
P	CTP	14	
R	GDP	14	
S	UTP	35	
T	ATP	72	
U	GTP	15	
Uridine derivatives		162	135
Adenosine derivatives		156	90
Guanosine derivatives		29	133
Cytidine derivatives		14	160

In addition to nucleoside-5'-polyphosphates, varying amounts of the 2'- and 3'-monophosphates were obtained in some experiments. The fact, that nucleoside 2'- and 3'-derivatives were only encountered in some and not detectable in other experiments, together with the absence of 2'- and 3'-di- and triphosphates in all experiments, makes it possible that the 2'- and 3'-nucleotides originated from the degradation of ribonucleic acid during preparation.

The absence of diphosphopyridine and triphosphopyridine nucleotides in the nucleotide fraction, prepared from wheat plants by the present method, is due to the fact that these compounds, although present in the original acid extract and adsorbed on norite, are not eluted appreciably with ethanol-ammonia. For the isolation of DPN and TPN elution of the norite with pyridine-water is more effective, although this eluent proved unsatisfactory for the isolation of the main bulk of the acid-soluble nucleotides. DPN and TPN have been previously isolated from wheat germ [12] and from other plant materials [13].

EXPERIMENTAL

Isolation of the nucleotide fraction

1 000 g of fresh wheat plants were homogenized in 3 000 ml of ice cold 10 % perchloric acid in a Waring Blendor. The precipitated proteins and fiber masses were separated from the extract by squeezing through madapollam. The residue was re-extracted in the Waring Blendor with 1 000 ml of 5 % perchloric acid and again pressed through madapollam. The combined extracts were further freed from suspended particles by centrifugation and then filtered through hyflo supercel on a Büchner funnel.

The clear, slightly yellow solution was treated with 30 g of norite. The suspension was shaken or stirred vigorously for 30 minutes and then filtered with suction. Experiments with various amounts of norite demonstrated, that under these circumstances all nucleotides were adsorbed on the norite. The norite was washed with water and then dried by suction.

The elution of the nucleotides from the norite was investigated with a number of solvent systems. An aqueous solution containing 25 % ethanol and 0.5 % concentrated ammonia proved to be the most satisfactory for the quantitative elution of the nucleotides with a minimum of disturbing substances. Therefore the norite was suspended in 150 ml of this mixture. The suspension was stirred vigorously in the cold for 30 min. Then the norite was filtered off and the elution repeated. Each fraction was collected in the cold and immediately adjusted to pH 7 with hydrochloric acid. After 5 to 6 extractions no more ultraviolet-absorbing material could be eluted.

The combined fractions were acidified with hydrochloric acid to pH 1.5, and the remaining disturbing substances were removed by continuous liquid-liquid extraction with ether for five hours. The extraction apparatus of Kutscher and Steudel was used, and the solution was cooled with ice during extraction. Thereafter the aqueous phase was freed from the last traces of ether by aeration. Phosphorus analysis before and after extraction showed that no decomposition had occurred. The aqueous phase could now be subjected to ion exchange chromatography.

Ion exchange chromatography

The strong base anion exchange resin Dowex 1, X-10, 200 to 400 mesh, was used. After freeing from fine and coarse particles by sedimentation the resin was converted to the formate form with a mixture of 2 M formic acid and 2 M sodium formate.

A column of 1.6 × 40 cm was supported in a glass tube by a constriction covered with glass wool. The resin was poured as an aqueous slurry and allowed to settle. The column was washed with a large quantity of water until the pH of the effluent was about 7. The column was fed with eluting agent through glass tubing from a container about 1.5 meters above the column.

The nucleotide fraction was put on the column from dilute ammoniacal solution at about pH 10 at the rate of 1.5 ml per min. After washing with water the eluting agents shown in Fig. 3 were used. Fractions of 35 ml were taken with an automatic fraction collector adjustable to different time intervals. Appropriate fractions were pooled and adsorbed on norite (10 mg of norite / μmole of nucleotide), and after washing with water the norite was eluted with small amounts of 50 % aqueous ethanol containing 0.5 % ammonia.

The column could be used several times except for a small layer at the top, which darkened during the run and was replaced each time by fresh resin.

Analytical methods

Ultraviolet absorption. Optical densities were measured in a 1.00 cm quartz cuvette in a Beckman Universal Spectrophotometer, Model DU, with photomultiplier. The course of the elution was followed by measurement of the optical densities of the fractions of chromatogram at 250, 260 and 270 mμ with the suitable eluting agents as the blank. The densities at 250 and 270 mμ assisted in interpretation of the chromatogram since the ratios of the readings E_{250}/E_{260} and E_{270}/E_{260} are characteristic of the various nucleotides.

Table 7. Molar absorbancy and absorbance ratios at pH 1 of the different nucleotides. The values for the polyphosphates followed those obtained for the corresponding monophosphates very closely.

Compound	$a_M \times 10^{-3}$	Absorbance ratios	
		250/260	270/260
Adenosine phosphates	14.5	0.84	0.71
Guanosine phosphates	10.8	0.93	0.73
Cytidine phosphates	6.3	0.47	1.71
Uridine phosphates	10.0	0.76	0.87

The optical densities at 260 mμ of the effluent fractions were plotted against effluent volume to obtain the chromatograph shown in Fig. 3.

The molar absorbancy a_M at 260 mμ and the absorbance ratios in acid solution are shown in Table 7. Each peak was also identified by determining its optical density over the range 220 to 320 mμ in both acid and alkaline solution, compared with authentic samples.

Phosphate. Inorganic phosphate was determined by the method of Allen[14] adapted to a total volume of 5.0 ml (4.0 ml of aqueous sample, 0.40 ml of 70 % perchloric acid, 0.40 ml of amidol-reducer and 0.20 ml of 8.5 % ammonium molybdate). The color was read 15 minutes after mixing, in a Klett-Summerson photoelectric colorimeter with a red filter.

The acid-labile phosphate was determined from the increase in inorganic phosphate after 10 minutes in 1 N hydrochloric acid at 100°C.

For total phosphate, the sample was digested with 0.40 ml of 70 % perchloric acid at 250°C and after cooling the inorganic phosphate was determined without further addition of acid.

Pentose. All fractions were analyzed for pentose with the orcinol reagent according to Albaum and Umbreit[15]. To the sample in 3.0 ml of water, 3.0 ml of 0.1 % ferric-chloride in concentrated hydrochloric acid and 0.3 ml of a reagent, containing 0.4 % orcinol in 95 % ethanol, were added. The reaction tubes were heated for 45 min. in a boiling water bath, cooled, diluted to a total volume of 10.0 ml and read in a colorimeter with a red filter. The results obtained were calculated by use of authentic samples as standards. The values for the uridine nucleotides were very small and therefore uncertain, and the cytidine nucleotides did not give any color.

Paper chromatography

The filter paper used was Whatman No. 1. The papers were in equilibrium with the solvent mixture before the runs were started. The temperature was 20 to 22°C. Standard substances were run in every chromatogram.

The nucleoside derivatives were located by making a contact print in monochromatic ultraviolet light of 254 mμ. For quantitative estimations, spots were cut out and eluted with 0.1 N hydrochloric acid. Standing for a few hours with occasional shaking effected quantitative elution. To allow for ultraviolet absorbing substances in the paper, blanks were cut, equal in area and at equal distances from the starting line, and were eluted and read at the same wave-lengths as the corresponding spots. Aniline hydrogen phthalate was used to demonstrate the position of the sugar spots on the paper chromatograms.

The nucleotides were hydrolysed to the free bases by heating at 100°C for one hour in 1 N hydrochloric acid for the purines, and in 70 % perchloric acid for the pyrimidines. Paper chromatography of the bases was carried out with the following systems: a) *iso*-propanol-hydrochloric acid (*d* 1.180)-water (65:17:18); b) *n*-butanol-acetic acid-water (4:1:5); c) *iso*propanol-saturated ammonium sulphate solution-water (2:79:19).

For paper chromatography of the sugars, the butanol-acetic acid-water system, already described, was used, in addition to ethyl acetate-pyridine-water (2:2:1).

Paper ionophoresis

Ionophoresis on paper was performed with a technique described by Markham and Smith [16] where the paper is kept cold by immersion in carbon tetrachloride. The substances were applied near one end of a long strip of Whatman No. 1 paper (6×50 cm). It was found convenient to wash the paper with 1 N hydrochloric acid and water before use. The carbon electrodes were connected to a d.c. power supply of 900 V thus giving a voltage gradient of about 20 V/cm. Under these conditions a run of 3 h gave good separations with the different buffers used. In ionophoretic as well as in chromatographic experiments, the position on the paper was compared with the position of the authentic substances.

The 5'-phosphate esters of any ribose nucleoside possess one characteristic by means of which they may be separated from the 2'- and 3'-esters of the same nucleoside: the presence of two adjacent hydroxyl groups in the ribose moiety, which can give complexes with boric acid. In 0.1 M sodium tetraborate buffer at pH 9.2 the mobility of the 5'-nucleotide is faster than that of the corresponding 2'- and 3'-nucleotides. The sugars could also be separated with the same buffer.

Separation of mono-, di- and triphosphates was obtained using an acetate buffer of ionic strength 0.1 at pH 5.

Action of snake venom

The estimation was performed as shown in Table 4. Phosphate was determined as described above, but the blue color was read in the colorimeter first after extraction with amyl alcohol, because of interference by magnesium otherwise.

The reaction products were adsorbed on norite and then eluted with small volumes of ethanol-ammonia. The concentrated solutions thus obtained were analyzed by paper chromatography. The solvent systems used were: *iso*propanol-saturated ammonium sulphate solution-water (2:79:19) and 95 % ethanol-1 M ammonium acetate buffer; pH 3.8 (75:30).

Periodate oxidation

Oxidation with periodate was performed according to Dixon and Lipkin [9].

Hexokinase reaction

This reaction was performed according to Colowick and Kalckar [17], and the reaction was followed by the disappearance of the acid-labile phosphate.

0.1 ml of the ATP-solution (10 μmole/ml), 0.1 ml of 0.5 M magnesium sulphate solution, 0.5 ml of 0.04 M sodium bicarbonate solution (pH 7.5), and 0.1 ml of 0.3 M glucose were combined and warmed to 30°C. 0.1 ml of dilute enzyme (10 mg/ml) was added and the mixture was incubated at 30°C for 30 minutes.

The reaction was stopped by the addition of 0.4 ml of 70 % perchloric acid. After centrifugation the acid-labile and total phosphates were determined. The values were compared with similar analyses of a mixture at zero time. Identical results were obtained with ATP from wheat plants and animal tissue.

Effect on actomyosin

The reaction was followed by viscosity measurement in Ostwald viscosimeters at 21°C (time of flow for water, about 40 sec.). The viscosimeters contained 3.5 ml of actomyosin solution in 0.5 M potassium chloride with a protein concentration of approximately 3 mg/ml. 0.4, 0.8 and 1.6 μmoles of triphosphate were added in volumes of 25, 50 and 100 μl.

Materials

The mono-, di- and triphosphates used as standard substances were isolated from muscle as previously described [18,19]. GTP and hexokinase were obtained by courtesy of Sigma Chemical Company.

Acknowledgement. The author wishes to express his gratitude to Dr. A. Deutsch for his encouragement and continued interest in this work, and to *Sigma Chemical Company* for supplies of GTP and hexokinase. Financial support has been obtained from *Kungliga Fysiografiska Sällskapet, Lund* and the *Lilly Foundation.*

REFERENCES

1. Albaum, H. G. and Ogur, M. *Arch Biochem.* **15** (1947) 158.
2. Albaum, H. G. ,Ogur, M. and Hirshfeld, A. *Arch. Biochem.* **27** (1950) 130.
3. Albaum, H. G., *The Biology of Phosphorus*, Michigan State College Press 1952, p. 37.
4. Buchanan, J. G., Lynch, V. H., Benson, A. A., Bradley, D. F. and Calvin, M. *J. Biol. Chem.* **203** (1953) 935.
5. Simonis, W. and Schwinck, L. *Naturwiss.* **40** (1953) 245.
6. Sebesta, K. and Sorm, F. *Chem. Listy* **48** (1954) 1585.
7. Bergkvist, R. and Deutsch, A. *Acta Chem. Scand.* **8** (1954) 1877.
8. Cohn, W. E. *Science* **109** (1949) 377.
9. Dixon, J. S. and Lipkin, D. *Anal. Chem.* **26** (1954) 1092.
10. Fellig, J. *J. Am. Chem. Soc.* **77** (1955) 4419.
11. Bergkvist, R. and Deutsch, A. In print.
12. Pfleiderer, G. and Schulz, W. *Ann.* **580** (1953) 237.
13. Anderson, D. G. and Vennesland, B. *J. Biol. Chem.* **207** (1954) 613.
14. Allen, R. J. L., *Biochem. J. London* **34** (1940) 858.
15. Albaum, H. G. and Umbreit, W. W. *J. Biol. Chem.* **167** (1947) 369.
16. Markham, R. and Smith, J. D. *Biochem. J. London* **52** (1952) 552.
17. Colowick, S. P. and Kalckar, H. M. *J. Biol. Chem.* **148** (1943) 117.
18. Bergkvist, R. and Deutsch, A. *Acta Chem. Scand.* **8** (1954) 1880.
19. Bergkvist, R. and Deutsch, A. *Acta Chem. Scand.* **8** (1954) 1889.

Received June 26, 1956.

ACTA CHEMICA SCANDINAVICA 10 (1956) 1317—1326

Fast-writing Precision Apparatus for Continuous Recording of Electrolytic Resistance

CARL-OVE ANDERSSON and EINAR STENHAGEN

Department of Medical Biochemistry, Institute of Medical Chemistry, University of Uppsala, Sweden

OLOF MELLANDER

Department of Medical Biochemistry, University of Gothenburg, Sweden

A high precision apparatus is described for the continuous recording of resistance. Full-scale response in less than 5 seconds is obtained for resistance-changes within a range variable at will from 2 to 1 900 ohms. The noise-level of the apparatus in its present form is equivalent to resistance-changes of about $1:10^6$ at a cell-resistance of 500 ohms. In practice, sensitivities up to $1:10^5$ may be employed without noise or zero drift in the recordings, provided that resistance-changes due to temperature-drift are eliminated.

During the course of a chemical reaction involving ions and taking place in aqueous solution, some of the ions originally present disappear and new ones are formed, causing change in the electrolytic conductivity of the solution. Analytical procedures involving conductrometric titrations are based upon the fact that the slope of the curve conductivity- added reagent shows an abrupt change in direction at the equivalence point. Similar changes are noted when the state of aggregation of the solute is changed. Measurements of conductivity are therefore useful in following micelle formation in solutions of paraffin-chain salts and bile salts.

Reactions in biological systems such as enzymatic hydrolysis may also be traced by measurement of the conductivity of the solutions. With the methods ordinarily used for following enzymatic hydrolysis it is impossible to cover the initial part of the reaction. In most methods samples are taken after different time-intervals, and the information obtained is thus limited to a series of

* A preliminary report of this work was made at the meeting of the Swedish Biochemical Society at Gothenburg, June 3—4, 1955 [1].

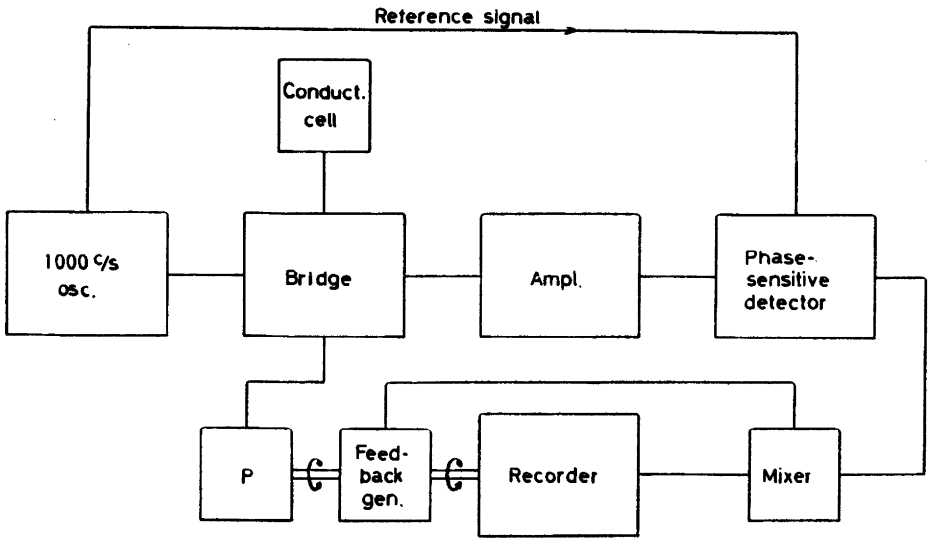


Fig. 1. Block diagram of resistance-recorder

discrete points on the reaction-time curve. The means of stopping the enzymatic reaction in the samples after they have been removed from the system are frequently such that they might influence the analytical results through secondary reactions. In contrast to this, measurement of the conductivity often enables reactions to be followed without interference but, as the ionic strength of the system is usually high and the often rapid reaction produces only small changes in the conductivity of the solution, a fast, sensitive recording system is necessary.

In recent years a number of devices have been described for recording the electrolytic conductivity of the effluent from chromatographic columns [1–6]. In this particular connexion a high recording-speed is not necessary, and none of the devices described appears to possess the combination of speed, accuracy, and stability needed for following chemical reactions of various types.

The conversion of a Shedlovsky precision bridge [7] into a fast-writing resistance recorder is described below. A block diagram of the apparatus is shown in Fig. 1.

The bridge is fed from a 1 000 c/s oscillator. The detector signal is amplified by a three-stage amplifier with automatic gain control, which prevents overloading of the recording system in case of considerable unbalance. The amplified signal and a reference signal from the oscillator are applied to a phase-sensitive detector. After filtering, the output of the phase-sensitive detector is fed *via* a cathode-follower stage to the input of the amplifier of a Speedomax-G recorder. To the potentiometer shaft of this recorder a linear high-precision potentiometer is mechanically coupled (P in Fig. 1), which forms parts of two arms of the bridge (*cf.* Fig. 2), the moving contact being connected to one side of the input of the detector amplifier. A signal from the bridge

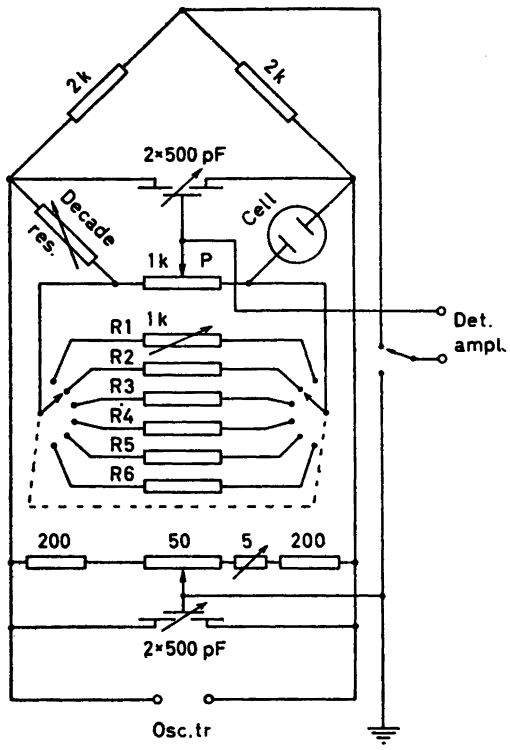


Fig. 2. Bridge circuit (shielding not shown). For details see text.

makes the recorder pen move until balance has been restored through the potentiometer attached to the recorder shaft. In order to prevent hunting of the servo system an adjustable amount of velocity feed-back to the recorder amplifier is introduced *via* a mixer from a tachometer generator geared to the balance motor of the recorder.

The use of a detector amplifier with automatic gain control ('compression amplifier'), variable phase-control in the phase-sensitive detector, velocity feed-back in the servo system, and an electro-mechanical filter in the form of a motor-generator between the A.C. mains and the power supply units of the apparatus, has resulted in very satisfactory sensitivity, stability, and speed of response.

The theory of the alternating-current Wheatstone bridge is found in standard texts [8]. The theoretical aspects of bridges for measuring electrolytic conductivity, and the sources of error involved in such measurements, have been discussed by Jones and Josephs [9] and by Shedlovsky [7]. A precision conductivity-bridge assembly has also been described by Luder [10]. A new type of alternating-current bridge suitable for measuring electrolytic resistance has recently been described by Easton and Lamson [11].

DESCRIPTION OF APPARATUS

Wheatstone bridge. The Shedlovsky type bridge [7] is similar to that used by Mellander and Stenhagen [12]. A shunted 1 000-ohm precision potentiometer P (Fernsteuergeräte PW 70 *), mechanically coupled to the potentiometer shaft of the recorder, is electrically connected between the decade and the conductometric cell as shown in Fig. 2. The movable contact is connected to one side of the primary of the detector input transformer. By means of the variable shunt, R1, the resistance range covered by full-scale travel of the recorder pen can be continuously adjusted from about 2 ohms to 1 900 ohms. Alternatively, a series of fixed shunts is provided for selecting standard resistance ranges of 20, 50, 100, 200, 500, and 1 000 ohms.

In order to determine the initial resistance of the cell, the shunt R1 is shorted, and a pair of headphones connected through a jack to the output side of the detector amplifier. The headphones are also necessary during the initial adjustment of the phase-sensitive detector.

The potentiometer, P, (Fig. 2) has 1 200 turns for 1 000 ohms. The resultant limit of precision is thus, for a recorder scale- range of 1 000 ohms, of the order of 1 ohm (0.1 %), *i.e.* the same as the pen-setting precision of the recorder. On lower scale-ranges the limitation of the precision due to the limited number of turns of the potentiometer is therefore negligible. Early in the development of the apparatus a 100-ohm potentiometer was used, when the recorder could be made to count the number of turns of the winding. The figure obtained in this way agreed with that given by the manufacturer.

All fixed resistors are of manganin wire ** (Ayrton-Perry winding or, for resistances above 200 ohms, single layer on mica card). The values of the fixed resistors R2—R6 must be determined experimentally. The bridge is fed from an oscillator *via* a shielded transformer (Svenska Radiobolaget XLT 504), the voltage across the secondary of which is usually adjusted to one volt. The requirements for low content of harmonics in the output of the oscillator do not seem critical. Both a simple, home-made RC oscillator and a commercial instrument (Philips GM 2307) have been used.

Detector amplifier. The circuit diagram of the detector amplifier is shown in Fig. 3a. Three resistance-capacity coupled stages using two 6SK7 and one 6V6 tubes give a maximum voltage amplification of 70 000 for an input voltage of 10 microvolts. The noise-level of the amplifier at the maximum gain was found to be equivalent to 10 microvolts at the primary of the input transformer. As the input voltage increases in amplitude the gain is reduced by the automatic volume control through the 6H6 diode. At 0.1 mV input at 1 000 cycles/sec the gain is 50 000; at 100 mV input it has been reduced to 600 times. The time constant of the automatic gain-control is about 2 seconds, and the amplifier can handle input signals of up to 0.3 volts without appreciable distorsion. The low gain at low frequencies reduces noise due to 50-cycle pick-up. The shielded input transformer Tr has a turns-ratio of 1:6 (Svenska Radio-

* Obtainable from AB Impuls, Stockholm.
** Made by Svenska Mätapparater Fabriks AB, Enskede.

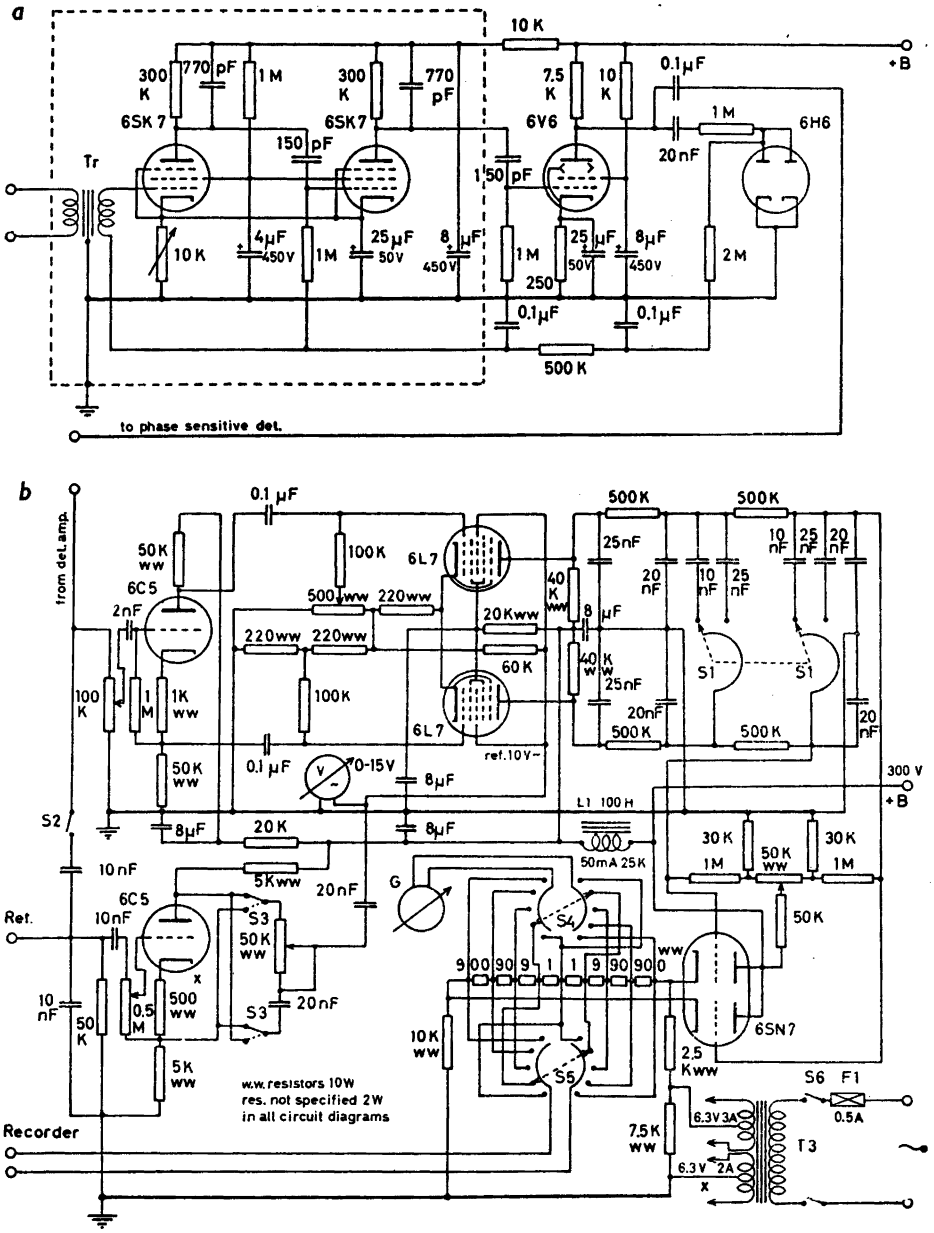


Fig. 3. a) Detector amplifier and b) phase-sensitive detector circuits.

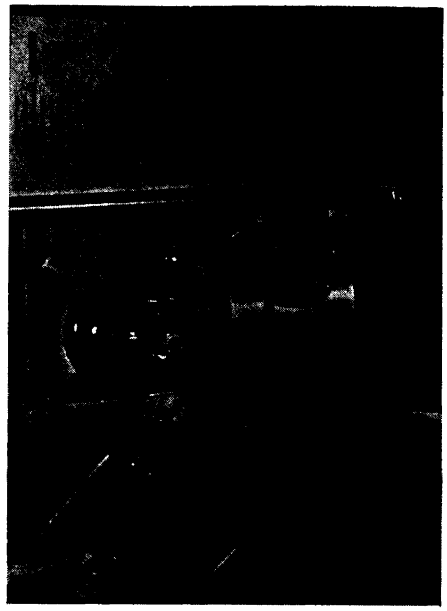


Fig. 4. Mechanical arrangement of feed-back generator in recorder.

bolaget type XLT 505). The position and orientation of this transformer have not proved critical.

Phase-sensitive detector. The circuit (Fig. 3) is almost identical with that used by Kinell [13], who also discusses the theory. (For a general discussion of phase-sensitive detectors see Ahrendt [14]). A small galvanometer with a sensitivity of 2 micro-amperes per scale division (Siemens, 450 ohms internal resistance) indicates the sign and magnitude of the direct-current output of the cathode follower which is fed to the input terminals of the recorder amplifier.

RECORDER AND ARRANGEMENT OF VELOCITY FEED BACK

A Leeds and Northrup Speedomax-G recorder with a pentravel time of 4.5 seconds across the chart is used. As shown in Fig. 4, a small direct-current generator (Pullin 5V/4798 *) is geared directly to the pen-driving motor of the recorder *via* a pair of 1:1 helical gears for crossed axles (Kremp und Söhne, Wetzlar, Germany). There must be no backlash in these gears. To prevent hunting of the servo system, part of the output of the generator is fed back to the input of the recorder amplifier *via* a mixer (Fig. 1) consisting of a 200-ohm potentiometer connected in series with one of the recorder-amplifier input leads. One of the generator terminals is connected to the movable contact,

* Obtained through Ingeniörsfirma Hugo Tillquist, Stockholm.

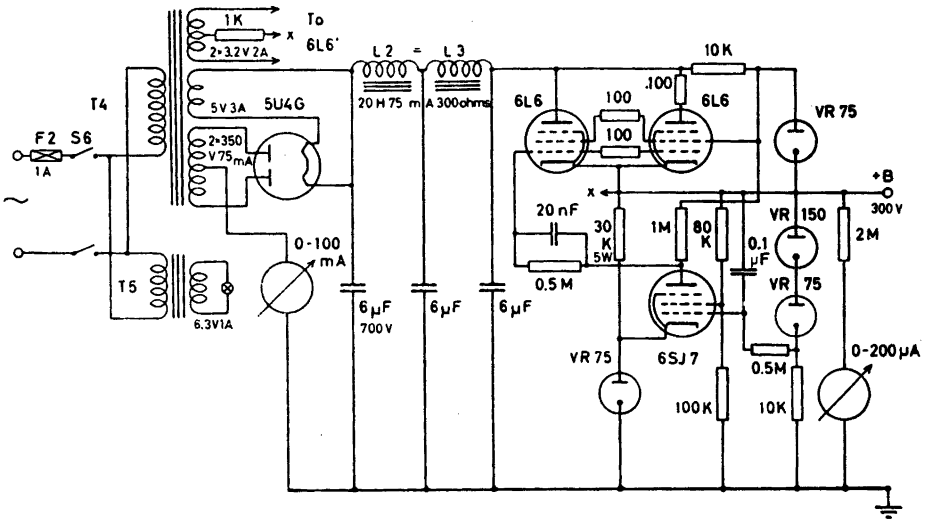


Fig. 5. Anode-voltage power supply.

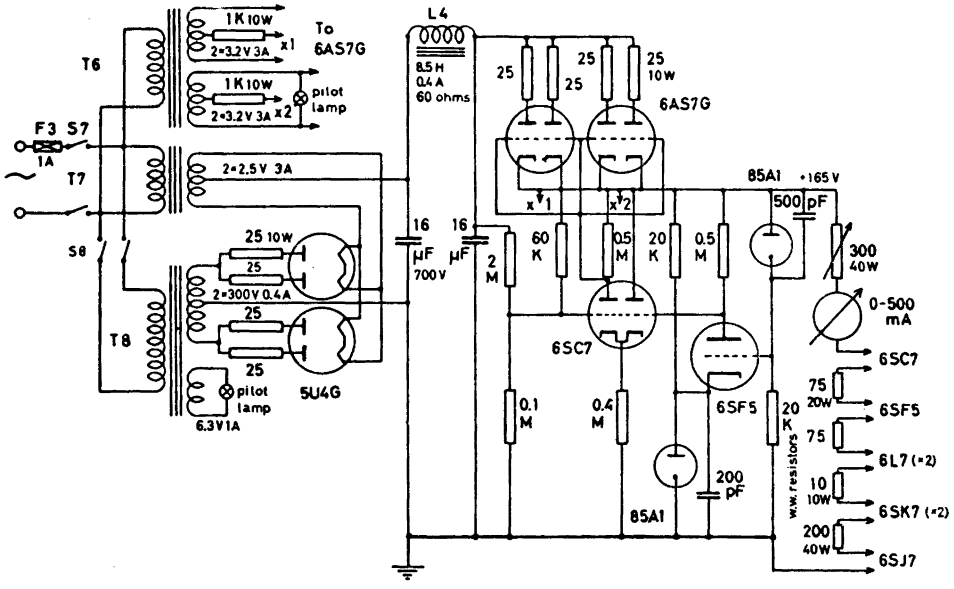


Fig. 6. Filament power supply.

and the other to one end of the potentiometer-winding. By adjusting the potentiometer the desired amount of feed-back can be introduced.

Power-supply. The stabilized anode current supply and the stabilized direct-current filament supply used are identical with those described by Kinell [13]. For convenience the circuit diagrams are reproduced in Figs. 5 and 6.

When first testing the completed apparatus in the laboratory the recordings were very disturbed by irregular 'spikes'. These were evidently caused by disturbances and transients in the 220-volt A.C. mains, as they disappeared completely when the apparatus was connected to a separate 220-volts alternating-current generator driven by a motor connected to the A.C. mains.

PERFORMANCE OF THE APPARATUS

Fig. 7 shows the response of the recorder for step-wise resistance-changes of 10 ohms each on the 100 ohm recorder range for cell-resistance of the order of 1 000 ohms. The pen-positions are reproduced within one pen-line width, *i.e.* the pen-setting precision of the recorder. The feed-back was adjusted to give a slight overshoot for the step-wise resistance change. Between the steps the paper chart was moved forwards by hand. There is complete freedom from noise.

Fig. 8 shows the response to step-wise resistance changes of 100 ohms with the paper travelling at a speed of 14" per hour (5.9 mm per minute).

The performance of the apparatus at high sensitivity is illustrated in Fig. 9, which shows the response of the recorder to resistance changes in steps of 1, 0.1, and 0.05 ohms, respectively, at a total resistance (decade box) of 5 000 ohms and a recorder-range of 6 ohms. The steps of 0.05 ohms correspond to a sensitivity of 1 part per 100 000. Taking into account variable contact resistance in the decade switches it appears that the reproducibility of the apparatus is of the order of 1:200 000, or 0.0005 per cent.

At these high sensitivities the galvanometer across the output of the phase-sensitive detector showed rapid fluctuations equivalent to resistance-changes of 0.005 ohms ($1{:}10^6$), which may be taken as representing the noise-level of the system. Superimposed upon these small rapid fluctuations were slower

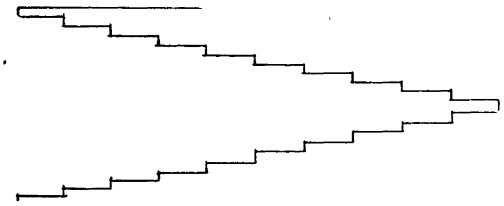


Fig. 7. Recording of step-wise resistance changes of 10 ohms at a recorder range of 100 ohms. Paper moved forward by hand between steps.

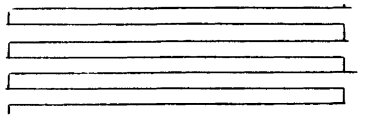


Fig. 8. Recording of step-wise resistance changes of 100 ohms at a recorder range of 200 ohms. Paper speed 5.9 mm per minute.

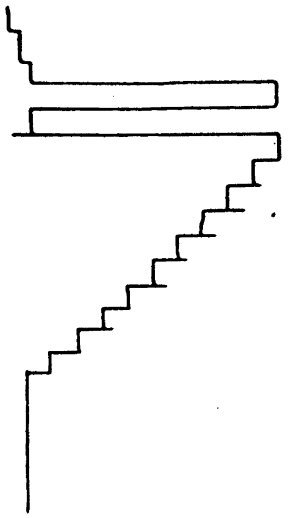


Fig. 9. Recordings of small changes in resistance at a total 'cell' resistance of 5 000 ohms and a recorder-range of 6 ohms. From above downwards: 2 steps of 0.05 ohm; 3 steps of 1 ohm; and 10 steps of 0.1 ohm. Paper speed 5.9 mm per minute.

oscillations equivalent to resistance-changes of about 0.01 ohms. These were found to be caused by small variations in the voltage of the motor generator. It seems likely that a fly-wheel on the shaft of the motor generator or the use of a larger machine * would eliminate this type of noise.

Effect of capacitative unbalance. For a cell-resistance of 500 ohms a capacitative unbalance of 400 pF introduced a zero drift of less than 0.25 ohm, or 0.05 %. The effect on the accuracy and speed of response was negligible. For a cell-resistance of 5 000 ohms the zero drift was more pronounced, and the effect on the accuracy and speed of response became marked at unbalances of about 100 pF. Under the conditions of measurement the zero drift was more marked when the capacitance was decreased, the drift for —350 pF amounting to 21.5 ohms, or about 0.4 %.

It is obvious that the ideal instrument for recording changes in electrolytic resistance should also be capable of continuously correcting errors in the capacitative balance of the bridge, as a change in resistance is usually accompanied by a change in capacitance. Drake [5] has performed some measurements on a conductivity cell using the same voltage across the cell at different conductivities of the solution (electrolyte not specified). He found that the change in capacitance was a linear function of 1/R. From this he inferred that the capacitance of the electrolytic cell is proportional to the current density. If this were true, capacitative unbalance could be corrected by altering the voltage across the bridge. It is found experimentally, however, that an increase in the current density due to an increase in the voltage across the cell has practically no effect on the effective capacitance of the cell. Both the capacitance of the cell and the current density at constant voltage are approximately proportional to the concentration of the electrolyte, but there is no direct connexion between the two.

* The machine used had a capacity of 1.8 kW.

During a run any capacitative unbalance developing may be traced on an oscilloscope connected across the output of the bridge amplifier. If the error becomes too large it may be corrected by manual adjustment. The simplest way to perform this correction automatically seems to be to arrange a separate servo system or recorder to make the adjustment at predetermined intervals as a standardizing operation. By reversal of these functions the instrument can of course be made to record capacitance changes in conducting systems. Such an instrument is being constructed.

Acknowledgements. The phase-sensitive detector and its associated equipment were built by Seve Radio, Mölnlycke, and we are indebted to Mr. S. Severinsson for his cooperation. We wish to thank Mr. P. Olsson (Uppsala) and Mr. G. Rundberg (Gothenburg) for the construction of various mechanical parts. This work has been aided in part by a grant from *The Swedish Medical Research Council.*

REFERENCES

1. Andersson, C.-O., Mellander, O. and Stenhagen, E. *Acta Chem. Scand.* **9** (1955) 1044.
2. Wickbold, R. *Z. anal. Chem.* **132** (1951) 401.
3. James, A. T., Martin, A. J. P. and Randall, S. S. *Biochem. J. London* **49** (1951) 293.
4. Drake, B. *Arkiv Kemi* **4** (1952) 401.
5. de Verdier, C.-H. and Sjöberg, C. I. *Acta Chem. Scand.* **8** (1954) 1161.
6. Drake, B. *Arkiv Kemi* **8** (1955) 159.
7. Shedlovsky, T. *J. Am. Chem. Soc.* **52** (1930) 1793.
8. Hague, B. *Alternating-current Bridge Methods*, 4th Ed. London 1938.
9. Jones, G. and Josephs, R. C. *J. Amer. Chem. Soc.* **50** (1928) 1049.
10. Luder, W. F. *J. Am. Chem. Soc.* **62** (1940) 89.
11. Easton, I. G. and Lamson, H. W. *General Radio Experimenter* **30** (1955) No. 2.
12. Mellander, O. and Stenhagen, E. *Acta Physiol. Scand.* **4** (1942) 349.
13. Kinell, P. O. *A Spectrophotometric Study of Polymethyl Methacrylate*, Ph. D. Thesis, Uppsala 1953, p. 67.
14. Ahrendt, W. R. *Servomechanism Practice*, New York 1954, p. 68.

Received June 28, 1956.

ACTA CHEMICA SCANDINAVICA 10 (1956) 1327—1339

Studies on the Hydrolysis of Metal Ions

18. The Scandium Ion, Sc^{3+}

GEORGE BIEDERMANN, MARTIN KILPATRICK, LEWIS POKRAS and LARS GUNNAR SILLÉN

Department of Chemistry, Illinois Institute of Technology, Chicago, Ill; Department of Inorganic Chemistry, Royal Institute of Technology, Stockholm 70, Sweden

The data of Kilpatrick and Pokras concerning the hydrolysis of Sc^{3+} have been recalculated by using general methods for polynuclear complexes [3-5]. At all temperatures and ionic media studied, the data could be explained assuming the formation of "core + links" complexes of the general formula $Sc((OH)_2Sc)_n^{(3+n)+}$.

From a "direct analysis" of the data it was found that at least the complexes with $n = 1$ and $n = 2$, $Sc_2(OH)_2^{4+}$ and $Sc_3(OH)_4^{5+}$ must exist; there were also indications of the formation of higher complexes. By comparison with the calculated curves from AB II[4], a good approximation was obtained with "hypothesis IIIa". The equilibrium constants obtained with this hypothesis are listed in Table 2. Here k_0k is the equilibrium constant of the reaction $Sc^{3+} + 2\ H_2O + Sc^{3+} \rightleftharpoons Sc(OH)_2Sc^{4+} + 2\ H^+$; k is the equilibrium constant for all following steps $Sc((OH)_2Sc)_n^{(3+n)+} + 2\ H_2O + Sc^{3+} \rightleftharpoons Sc((OH)_2Sc)_{n+1}^{(4+n)+} + 2\ H^+$.

At the lowest total scandium concentration used, a small correction was necessary for the formation of the mononuclear complexes $ScOH^{2+}$ and $Sc(OH)_2^+$. For 25°C and $I = 1.0$ M, the following values of the equilibrium constants were calculated: for $Sc^{3+} + H_2O \rightleftharpoons ScOH^{2+} + H^+$ $\log \beta_1 = -5.1 \pm 0.2$, and for $Sc^{3+} + 2\ H_2O \rightleftharpoons Sc(OH)_2^+ + 2\ H^+$ $\log \beta_2 = -10.2 \pm 0.5$.

Some time ago, Kilpatrick and Pokras published the results of a very careful investigation on the hydrolysis of the Sc^{3+} ion. The most extensive measurements [1] were made at 25°C with an ionic strength 1.0 M (with $NaClO_4$). In a following paper [2], data were also given at other ionic strengths (0.01 M, 0.1 M, and 0.5 M at 25°C) and for 10°C and 40°C at ionic strength 1.0 M.

The hydrogen ion concentration at equilibrium was determined with a quinhydrone electrode since spectrophotometric studies had indicated no complex formation between Sc^{3+} and quinhydrone. The equilibria were found to be established rapidly.

Kilpatrick and Pokras concluded from their data that the chief products of the hydrolysis are $ScOH^{2+}$ and $Sc_2(OH)_2^{4+}$, and that higher polynuclear complexes are probably formed.

In the meantime, general methods for treating polynuclear complex equilibria have been given (AB I[3], AB II[4], AB IV[5]), and applied to the hydrolysis of a number of ions (parts VIII—XIV of this series [7–11]). In the present paper, the same methods have been applied to Kilpatrick and Pokras' data for scandium [1,2], the treatment on the whole confirming the conclusions of these authors and providing, in addition, some information on the higher complexes.

Notation

We shall use the following notation: h is the equilibrium concentration of H^+, b the concentration of free Sc^{3+}, B the total scandium concentration (denoted by C in [1,2]) and Z the average number of hydrogen ions set free per Sc. The ionic strength (as defined in [1,2]) is denoted by I. Instead of Z, the original papers [1,2] give the "hydroxyl number" n. The connection between Z and n is easily shown. Since the solutions are always acidic, the total number of bound OH groups per litre, $BZ = nB + h$, or $Z = n + hB^{-1}$. All concentrations are in M (mole/l) if not otherwise stated.

THE DATA FOR 25°C and I = 1.0 M

Formula of the complexes

The mathematical analysis of the data will be based chiefly on the data for 25°C and $I = 1.0$ since they are much more extensive than those for other temperatures and ionic strengths.

First of all, the original data n $(\log h)_B$ were recalculated and plotted in the form $Z(\log h)_B$. In the resulting diagram, Fig. 1, the points for each of the values of B used (1.25, 2.5, 5, 10, and 20 mM) are given with different symbols. Since the curves for different values of B do not coincide, the process cannot be explained assuming only mononuclear complexes; polynuclear species must also be formed. Moreover, the points are seen to lie on practically parallel curves. From the spacing of the curves, the derivative

$$\left(\frac{\partial \log B}{\partial \log h}\right)_Z \tag{1}$$

is found to be roughly 2.2. The value 2.0 was tested by plotting $y = \frac{1}{2} Z$ as a function of

$$x = \log B - 2 \log h \tag{2}$$

(*cf.* part VIII[7], 14—15 a). The ordinate was taken as

$$y = \frac{Z}{2} \tag{3}$$

to facilitate a comparison with the calculated curves from AB II[4].

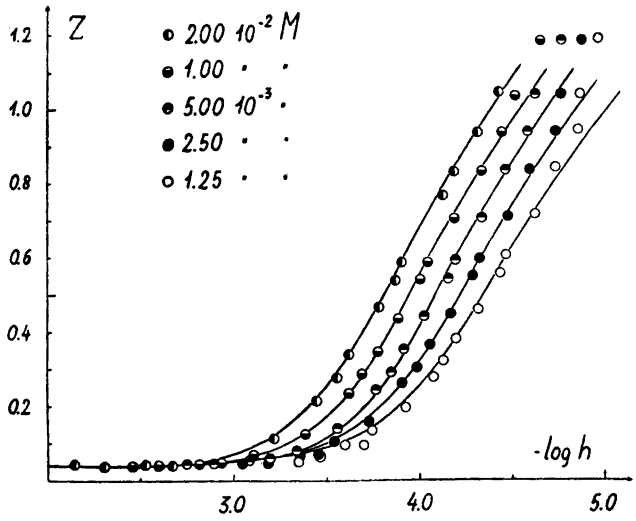


Fig. 1. Hydrolysis of Sc^{3+}. Z *(average number of OH bound per Sc) as a function of log* h, *for five different total concentrations* B. *Experimental data*[1]*: symbols, see figure. Curves calculated assuming a polynuclear unlimited mechanism (14) (IIIa, with* $k_0 = 5$, *log* $k = -6.8$), *together with a mononuclear reaction with log* $\beta_1 = -4.9$; *a correction of +0.04 has been added to the calculated* Z *values.*

From the diagram $y(x)$, Fig. 2, it is seen that the points fall on practically the same curve; only for the very lowest B value (1.25 mM) is a slight positive deviation noted while, for $x > 7$, all the data are seen to diverge.

Disregarding for a moment these small deviations, we would find that Z is a function of log B — 2 log h which, according to AB I[3] and VIII[7], implies

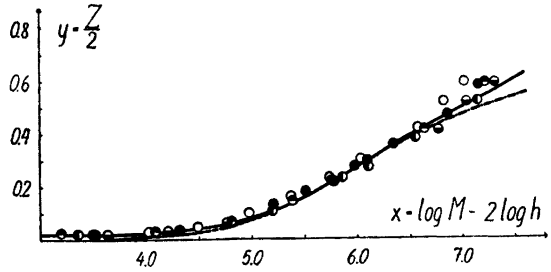


Fig. 2. Hydrolysis of Sc^{3+}. $y = \frac{1}{2}Z$ *as a function of* $x = \log B - 2 \log h$. *Points: experimental data*[1], *symbols as in Fig. 1. Full drawn curve calculated with mechanism IIIa,* $k_0 = 5$, *log* $k = -6.8$, *adding +0.02 to the calculated* y *values. Dotted curve: only two complexes, log* $k_1 = -6.1$, *log* $k_2 = -12.9$; y *corrected; for* $x < 6.4$ *it practically coincides with the full-drawn curve. Broken curve: IIIa,* $k_0 = 5$, *log* $k = -6.7$, *no correction to* y. *For* $x > 5.2$, *it practically coincides with the full-drawn curve.*

that all the predominating complex species can be written in the general "core + links" form

$$Sc((OH)_2Sc)_n^{(3+n)+} \tag{4}$$

The deviations at the lowest B values can be ascribed to the formation of mononuclear complexes, especially $ScOH^{2+}$ (see below), whereas the irregular behavior around $x = 7.0$ may be caused by some slow process, *e.g.* irreversible precipitation.

To the left in Fig. 2 it is seen that, with decreasing x, y approaches a value of 0.02 rather than 0. Similarly Z in Fig. 1 approaches 0.04 instead of 0. This behavior indicates a small systematic error, perhaps in the analysis of the perchlorate concentration in the scandium stock solution.

We shall first treat the main reaction, which leads to the formation of polynuclear complexes $Sc((OH)_2Sc)_n^{(3+n)+}$, and then consider the correction for the mononuclear reaction.

Direct analysis of $y(x)$

We could now draw a smooth curve through the data $y(x)$ and apply equations (AB II, 14 and 15) which yield the function $g(u)$ where

$$u = bh^{-2} = [Sc^{3+}]h^{-2} \tag{5}$$

$$g = \sum k_n u^n = k_1 u + k_2 u^2 + \ldots \tag{6}$$

and k_n is the equilibrium constant of the reaction:

$$(n+1)Sc^{3+} + 2\,n\,H_2O \rightleftharpoons Sc((OH)_2Sc)_n^{(3+n)+} + 2\,n\,H^+;$$
$$k_n = c_n h^{2n} b^{-(n+1)} = c_n b^{-1} u^{-n} \tag{7}$$

(c_n = concentration of n:th complex).

This procedure involves no additional assumptions besides the one, corroborated by the fitting of the data with a single $y(x)$ curve, that all complexes present in appreciable amounts can be written in the "core + links" form (4).

Fig. 3 gives the results, recalculated to

$$gu^{-1} = k_1 + k_2 u + k_3 u^2 + \ldots \tag{8}$$

as a function of u. The points marked ◐ were calculated from a smooth curve, rather similar to the dashed curve in Fig. 2; corrections applied to the integration constant could not eliminate the irregular behavior for low x.

For the dots ○, the experimental y values were corrected by subtracting 0.02 (assuming a systematic error). Disregarding deviations at the lowest values of u, which are very sensitive to small errors in y, the points are seen to lie approximately on a straight line, from the intercept and slope of which we estimate

$$k_1 = 10^{-6.1 \pm 0.1}\ M; \qquad k_2 = 10^{-12.9 \pm 0.4}\ M^2 \tag{9}$$

At the highest u values the points are seen to deviate upwards, indicating the formation of higher complexes; it did not seem possible to estimate k_3 accurately.

The $y(x)$ curve, calculated for the values (9) of k_1 and k_2, is given as a dotted line in Fig. 2.

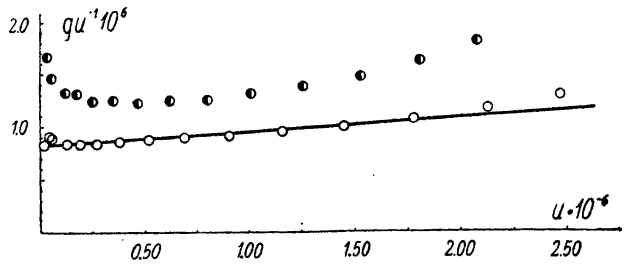


Fig. 3. gu^{-1} *as a function of* u *calculated by "direct analysis" of* y(x). *Circles* ◐ *calculated without correction to* y, *circles* O *by correcting the experimental* y *with* -0.02. *Line:* $gu^{-1} = 0.8 \cdot 10^{-6} + 1.25 \cdot 10^{-13}\,u = 10^{-6.1} + u \cdot 10^{-12.9}$.

From the $g(u)$ data we can calculate also the average number of links per complex

$$\bar{n} = \frac{\mathrm{d} \log g}{\mathrm{d} \log u} \tag{10}$$

To compute $\bar{n}$ it is convenient to apply the equation

$$\bar{n} = y(1 - y - F^{-1})^{-1} \tag{11}$$

where

$$\log F = y \log e + \int_{-\infty}^{x} y\, dx \tag{12}$$

Eqn. (11) can be obtained by combining (10) with eqns. (14) and (15) of AB II[4].

In Fig. 4 $\bar{n}$ is plotted as a function of log u. $\bar{n}$ is seen to start at about 0.90 instead of unity; this is explained by the inaccuracy of the numerical integration for low u values. As u increases, $\bar{n}$ rises monotonically, attaining the maximum value 1.84. Thus the conclusion can be drawn, in agreement with the preceding calculation, that complexes with $n = 1$ and 2 predominate in the u range studied.

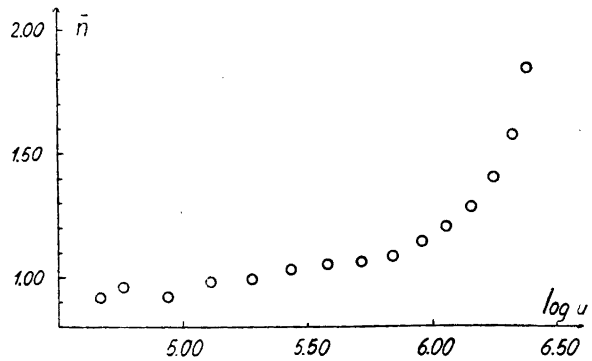


Fig. 4. $\bar{n}$ (*equation 10*) *as a function of log* u. *A correction of* -0.02 *has been added to the experimental* y *values.*

Comparison with $y(x)$ curves for simple mechanisms

Another way of treating the data is to compare the experimental $y(x)$ data with the $y(X)$ curves calculated for various simple mechanisms in AB II[4]. With mechanism I (precipitate formed, in this case *e.g.* $Sc(OH)_2ClO_4$), no good fit could be found. With hypothesis II (only one complex $Sc((OH)_2Sc)_N^{3+N}$ formed), an approximate agreement was found with $N = 1$ for low values of x. With increasing x, y became systematically higher than the calculated curve, showing that complexes higher than $Sc_2(OH)_2^{4+}$ are also formed.

Good agreement could, however, be obtained with the hypotheses IIIa—c assuming a repeated reaction, with the formation of complexes with all n values $n = 1, 2 \ldots$ Since the accuracy did not permit a distinction between IIIa, IIIb, and IIIc, only the simplest hypothesis IIIa was considered in detail:

$$\text{IIIa: } k_n = k_0 k^n \tag{13}$$

This hypothesis has been found satisfactory with Th^{4+}, UO_2^{2+}, and In^{3+} (parts IX[8], X[9], XIV[11]). Except for the lowest y, a good agreement was obtained with hypothesis IIIa, assuming $k_0 = 5$ and $\log k = -6.7 \pm 0.1$; this is the broken curve in Fig. 2.

A still better agreement in the whole range was obtained after correcting the calculated y with $+0.02$, assuming $k_0 = 5$ and $\log k = -6.8 \pm 0.1$ (full-drawn curve in Fig. 2). In the range $x > 5.2$ the curves practically coincide.

We would thus have the reactions and equilibrium constants

$$2\ Sc^{3+} + 2\ H_2O \rightleftharpoons Sc(OH)_2Sc^{4+} + 2\ H^+;\ k_1 = k_0 k = 10^{-6.1 \pm 0.1} \tag{14a}$$

and for all consecutive steps

$$Sc((OH)_2Sc)_n^{(3+n)+} + 2\ H_2O + Sc^{3+} \rightleftharpoons Sc((OH)_2Sc)_{n+1}^{(4+n)+} + 2\ H^+;\quad k_{n+1}/k_n = k = 10^{-6.8 \pm 0.1} \tag{14b}$$

This result, as far as the first two constants are concerned ($k_1 = 10^{-6.1}$, $k_2 = 10^{-12.9}$) is identical with that obtained by the direct analysis (9), and the first one agrees well with the value $k_1 = 10^{-6.0}$ given by Kilpatrick and Pokras [2] (Table IV, where the present k_1 is denoted by "K_0").

In fact, Kilpatrick and Pokras' mechanism, the one (9) obtained by direct analysis, and IIIa (13, 14) may be regarded as three successive approximations to the real mechanism. Kilpatrick and Pokras considered only the first complex, $Sc_2(OH)_2^{4+}$, whereas the data force us to assume also a second complex $Sc_3(OH)_4^{5+}$. Moreover the data indicate that higher complexes are formed, as implied by IIIa. Assuming IIIa and the constants (14) one may calculate the fraction of all Sc present in the form of the various complexes

$$\alpha_0 = [Sc^{3+}]/B;\ \alpha_1 = 2\ c_1/B;\ \ldots\ \alpha_n = (n+1)\ c_n/B \tag{15}$$

where c_n is the concentration of the n:th complex. One finds

$$\text{for } u = 1.5 \cdot 10^6 (Z = 0.9),\ \alpha_0 = 0.20,\ \alpha_1 = 0.51,\ \alpha_2 = 0.19,\ \alpha_3 = 0.06 \tag{16a}$$

$$\text{for } u = 2.4 \cdot 10^6 (Z = 1.2),\ \alpha_0 = 0.11,\ \alpha_1 = 0.41,\ \alpha_2 = 0.24,\ \alpha_3 = 0.13 \tag{16b}$$

Thus the complexes with n higher than 2 would be appreciable only in the region where the data begin to diverge.

Mononuclear complexes

In order to explain the deviations of the experimental data for the lowest B, 1.25 mM, in the $y(x)$ diagram (Fig. 2), it will be assumed that, besides the main hydrolysis products, $Sc((OH)_2Sc)_n$, *mononuclear* species are also present in appreciable concentrations.

It may be inferred from the $y(x)$ diagram that, even for the lowest B, the concentration of the mononuclear ions may amount only to a few percent of the total concentration of the hydrolysis products. Therefore it would not be practical to compute the formation constants of the mononuclear species by using some type of deviation function; this would be inevitably too strongly influenced by the uncertainty in k.

To find simultaneously the equilibrium constants of the polynuclear and mononuclear mechanisms, we shall use an approach [5] which has been worked out especially for such an unfavorable case.

This method is based on the consideration of the function $\log B(x)_Z$, where $x = \log B - t \log h$, as in (2). When only polynuclear complexes of the "core + links" type are formed, the family of functions $\log B(x)_Z$ is represented by lines parallel with the $\log B$ axis, since $x = \text{const.}$ for $Z = \text{const.}$ When mononuclear ions are present exclusively, $\log B(x)_Z$ consists of lines with a slope of unity, since $h = \text{const.}$ for $Z = \text{const.}$ In the intermediate range where both mononuclear and polynuclear species exist in comparable amounts, $\log B(x)_Z$ forms curves with continuously increasing slope.

Thus if the plot $\log B(x)_Z$ is made from the experimental data, a deviation of the points from a vertical line at low B values indicates that mononuclear ions begin to be formed in appreciable amounts. Such a deviation is more conspicuous than deviations of the data for low B from the $y(x)$ curve valid for high B.

The $\log B(x)_Z$ diagram calculated from Kilpatrick and Pokras' data is shown in Fig. 5; points for low B clearly indicate the presence of mononuclear ions.

In order to calculate the formation constants of the mononuclear complexes and a more accurate value for $\log k$, the $\log B(x)_Z$ data will be compared with the calculated curves

$$\log B(X)_Z$$

where $X = x + \log k$, $\log \boldsymbol{B} = \log B + \log k - t \log \beta_1$ (*cf.* eqns. (13) and (14) of [5]). β_1 is the equilibrium constant of the reaction

$$Sc^{3+} + H_2O \rightleftharpoons ScOH^{2+} + H^+ \qquad \beta_1 = [ScOH^{2+}]h[Sc^{3+}]^{-1}$$

If the data are superimposed on the calculated curves $\log B(X)_Z$, the differences $X - x$ and $\log \boldsymbol{B} - \log B$ give in the position of best agreement the most probable values of $\log k$ and $\log \beta_1$.

In the first instance, $\log B(X)_Z$ was calculated by assuming that only one mononuclear species is formed, namely $ScOH^{2+}$. The fit obtained is shown in Fig. 5a. Up to $Z = 0.6$, the agreement is satisfactory but, for higher values of Z, the deviations increase gradually.

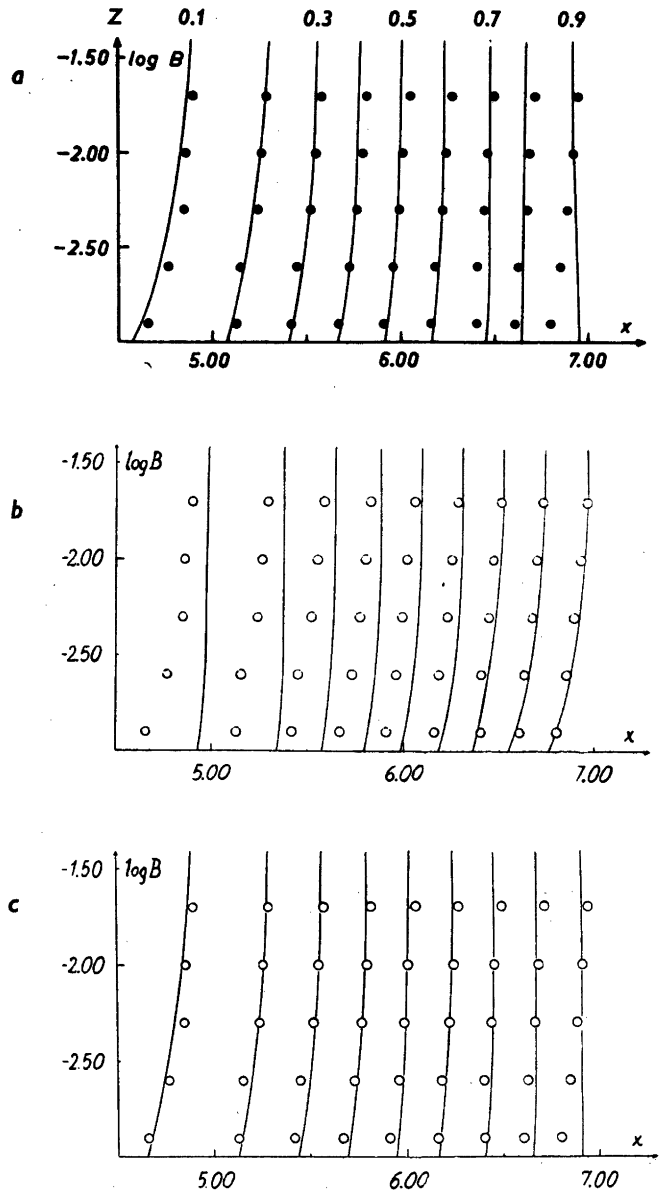


Fig. 5 a, b, c. log B *as a function of* x *for* Z *values of 0.1—0.9. Circles: experimental points. The curves have been calculated assuming the equilibrium constants given in Table 1.*

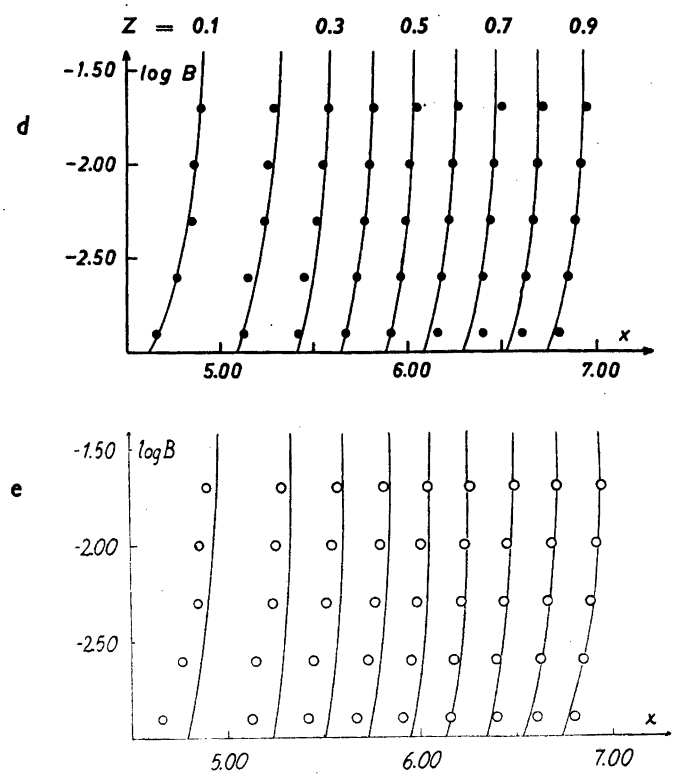


Fig. 5 d, e. log B *as a function of* x *for* Z *values of 0.1—0.9. Circles: experimental points. The curves have been calculated assuming the equilibrium constants given in Table 1.*

Next, log $B(X)_Z$ was computed assuming the equilibrium

$$Sc^{3+} + 2\ H_2O \rightleftharpoons Sc(OH)_2^+ + 2\ H^+ \qquad \beta_2 = [Sc(OH)_2^+]h^2[Sc^{3+}]^{-1}$$

In this case we have *

$$\log B = \log B + \log k - \frac{t}{2} \log \beta_2$$

$$X = x + \log k$$

As Fig. 5b shows, the agreement is acceptable for $Z > 0.6$ but, as Z is decreased, the deviations rapidly increase.

To obtain an agreement for the whole range of Z investigated, we must thus assume that $ScOH^{2+}$ and $Sc(OH)_2^+$ are both present in appreciable amounts.

* Introducing the auxiliary normalized variable $\alpha = \beta_2 h^{-2}$ we get by eqn. (8) of [5] $\log B = \log v - \log k - \frac{t}{2}$ (log α—log β_2) + log(1 + α + g + vg') where $v = k\ u$ and $g = \sum k_n u^n$. Thus for a constant value of Z $\log B = \log B + \log k - \frac{t}{2} \log \beta_2$ is a function of v only.

In this case where three constants, β_1, β_2 and k, should be determined, some assumption must be made on the ratio

$$\beta_2\beta_1^{-2} = l$$

in order to calculate $\log B(X)_Z$. With $l = 1$, the agreement is very satisfactory (Fig. 5d). With $l = 0.1$ (Fig. 5c), the deviations at the highest Z values indicate that l was chosen somewhat too low, on the other hand, with $l = 10$ (Fig. 5e) a reasonable fit is obtained only for $Z > 0.6$, indicating that a too high value of l was taken.

The constants obtained using different assumptions are summarized in Table 1.

Table 1.

l	0	0.1	1	10	infinite
$\log k$	−6.85	−6.84	−6.87	−6.88	−6.90
$\log \beta_1$	−5.0	−5.1	−5.1	(−5.6)	−
$\log \beta_2$	−	(−11.2)	−10.2	−10.2	−10.2
	Fig. 5a	Fig. 5c	Fig. 5d	Fig. 5e	Fig. 5b

We can estimate as the most probable values

$$\log k = -6.87 \pm 0.10$$
$$\log \beta_1 = -5.1 \pm 0.2$$
$$\log \beta_2 = -10.2 \pm 0.5$$

This $\log \beta_1$ value is in good agreement with that given by Kilpatrick and Pokras [1]: -4.9 ± 0.1.

We have found previously, assuming a pure polynuclear mechanism, that $\log k = -6.8 \pm 0.1$; thus no serious error was introduced by neglecting the mononuclear mechanism at $B \geq 2.5$ mM.

DATA AT OTHER TEMPERATURES AND IONIC STRENGTHS

For the other temperatures and ionic strengths, the data for only two values of $\log B$ were generally available. The data were plotted as before, giving $y = Z/2$ as a function of $x = \log B - 2 \log h$ (Fig. 6a, b; Fig. 7a, b). The points for $B = 1.25$ mM were in general found to be somewhat higher (especially for 40° C) than those for the higher concentration (usually 10 mM). Since the effect is rather small, no attempt was made to use these data for calculating accurately the variation of β_1 or β_2 with ionic strength and temperature.

The shape of the curves could be well explained with mechanism IIIa in all cases, assuming $k_0 = 5$ (10 for the lower values of I). The correction +0.02 was made to the calculated y, to account for a possible small analytical error (see above). The results are summarized in Table 2.

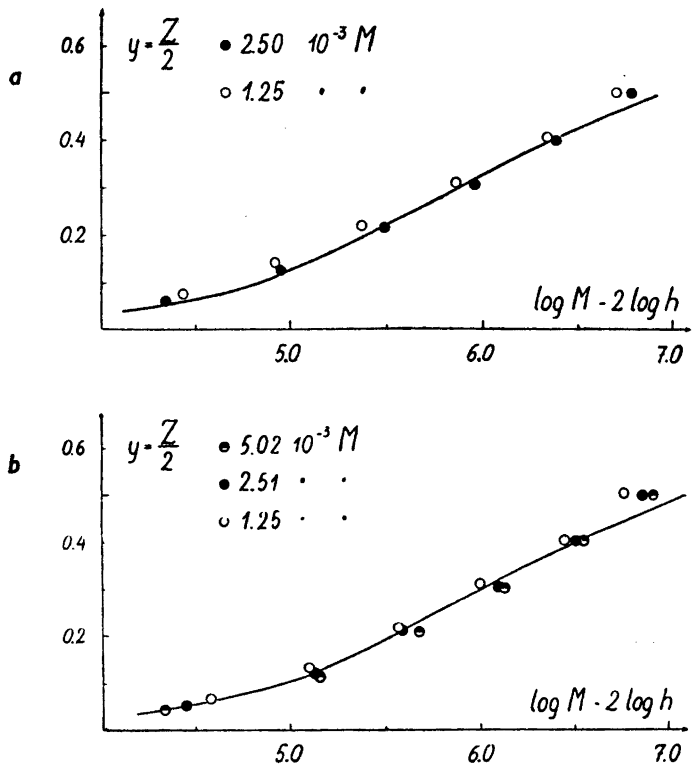


Fig. 6. Hydrolysis of Sc^{3+}. Data[2] for 25°C and ionic strengths 0.5 and 0.1 M plotted in the form y(x), *assuming* t = 2. *Fig. 6a:* I = *0.1 M; curve: IIIa,* $k_0 = 10$, *log* k = −6.8. *Fig. 6b:* I = *0.5 M; curve:IIIa,* $k_0 = 10$, *log* k = −6.9.

Table 2

Temperature °C	*I* M	k_0	log *k*	log k_0k = log k_1	log k_1[2]
25	1.00	5	−6.87 ± 0.1	−6.17 ± 0.1	−6.00
25	0.50	10	−6.9 ± 0.2	−5.9 ± 0.2	−5.90
25	0.10	10	−6.8 ± 0.2	−5.8 ± 0.2	−5.67
10	1.00	5	−7.3 ± 0.2	−6.6 ± 0.2	−6.66
40	1.00	5	−6.2 ± 0.2	−5.5 ± 0.2	−5.50

The last column gives the log k_1 ("log K_0") values given by Kilpatrick and Pokras [2] who, however, considered only the first polynuclear complex. The agreement is very satisfactory.

The formation of the polynuclear complexes is favored by increasing the temperature. From the temperature variation of the constants we may calculate, both for the first step (14a) and for the following (14b), values for ΔH of about 15 kcal, and values for ΔS of about 20 cal degree^{-1}, in good agreement with Kilpatrick and Pokras [2].

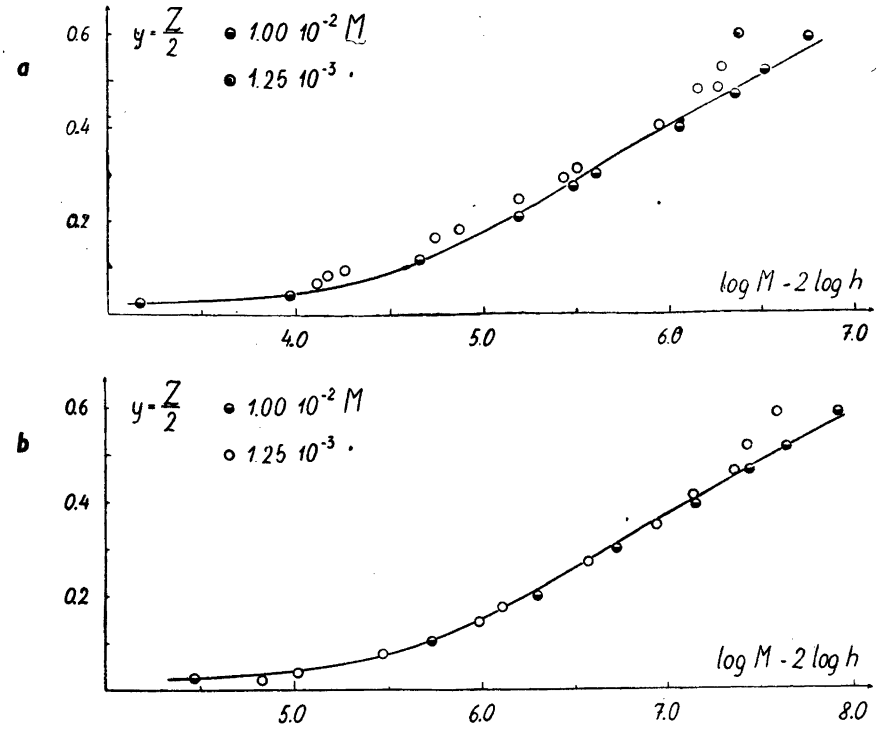


Fig. 7. Hydrolysis of Sc^{3+}. Data[3] for 10°C and 40°C plotted in the form y(x), *assuming* t = 2. *Fig. 7a: 40°C,* I = *1.00 M; curve: IIIa,* k_0 = *5, log* k = −*6.2. Fig .7b: 10°C,* I = *1.00 M; curve: IIIa,* k_0 = *5, log* k = −*7.3.*

From Table 2 it seems that log k is not much affected by changes in I. The increase in log k_0k would imply an increasing predominance of the first complex, $Sc_2(OH)_2^{4+}$, with decreasing I.

DISCUSSION

We may thus conclude that, for all temperatures and ionic media studied by Kilpatrick and Pokras, the data can be explained by the same mechanism, namely the formation of a series of "core+links" complexes, $Sc((OH)_2Sc)_n^{(3+n)+}$, with a small correction for the mononuclear complexes $ScOH^{2+}$ and $Sc(OH)_2^+$.

Complexes of the same general formula have been found for Fe^{3+} (part VII[6]), UO_2^{2+} (part X[9]), and In^{3+} (part XIV[11]). Scandium is seen to take an intermediate place in the range in the following respect. For Fe^{3+}, the data could be explained assuming only one polynuclear complex, with $n = 1$. For Sc^{3+}, we have found that at least two complexes, with $n = 1$ and 2, must be considered. For UO_2^{2+} and In^{3+} at least $n = 3$ must also be considered. However, it seems that the differences are only gradual. One may imagine

that in all cases an unlimited series of complexes may be formed but that the higher complexes do not reach appreciable concentrations within the experimental range which is limited by the precipitation of the hydroxide or some other solid phase at a sufficiently high value of Z.

Another type of reaction seems to be found for Al^{3+}, where the rather scarce data are best explained assuming only one complex, of some complicated composition like $Al_6(OH)_{15}^{3+}$ (part XI[10]). Recent crystal structure data suggest the existence of complexes $Al_{13}(OH)_{32}^{7+}$ [12].

This work is part of a program supported by *Statens Naturvetenskapliga Forskningsråd* (*Swedish Natural Science Research Council*) and *Atomkommittén* (*Swedish Atomic Committee*). One of us (M. K.) would like to express his appreciation to the United States State Department for a Fulbright Research Grant.

REFERENCES

1. Kilpatrick, M. and Pokras, L. *J. Electrochem. Soc.* **100** (1953) 85.
2. Kilpatrick, M. and Pokras, L. *J. Electrochem. Soc.* **101** (1954) 39.
3. Sillén, L. G. *Acta Chem. Scand.* **8** (1954) 299 (AB I).
4. Sillén, L. G. *Acta Chem. Scand.* **8** (1954) 318 (AB II).
5. Biedermann, G. and Sillén, L. G. *Acta Chem. Scand.* **10** (1956) 1011 (AB IV).
6. Hedström, B. O. A. *Arkiv Kemi* **6** (1953) 1 (part VII).
7. Hietanen, S. and Sillén, L. G. *Acta Chem. Scand.* **8** (1954) 1607 (part VIII).
8. Hietanen, S. *Acta Chem. Scand.* **8** (1954) 1626 (part IX).
9. Ahrland, S., Hietanen, S. and Sillén, L. G. *Acta Chem. Scand.* **8** (1954) 1907 (part X).
10. Brosset, C., Biedermann, G. and Sillén, L. G. *Acta Chem. Scand.* **8** (1954) 1917 (part XI).
11. Biedermann, G. *Arkiv Kemi* **9** (1956) 277 (part XIV).
12. Söderquist, R., Johansson, G., Lundgren, G. and Sillén, L. G. *Acta Chem. Scand. To be published.*

Received June 26, 1956.

ACTA CHEMICA SCANDINAVICA 10 (1956) 1340—1344

The Basicity Constant of *p*-Benzoquinone

Comparison of the Quinhydrone Half-cell with the Hydrogen Half-cell in $HClO_4$-$NaClO_4$ Ionic Medium

GEORGE BIEDERMANN

Department of Inorganic Chemistry, Royal Institute of Technology, Stockholm 70, Sweden

Deviations between the quinhydrone and hydrogen half-cells at high acidities in the ionic medium $HClO_4$-$NaClO_4$ at 25°C can be interpreted by assuming the equilibrium

$$OC_6H_4OH^+ \rightleftharpoons OC_6H_4O + H^+, \text{ with } \log K_a = 1.0 \pm 0.2.$$

Investigations on cells containing quinhydrone and hydrogen electrodes [1] have established that in acid solutions of low ionic strength the quinhydrone half-cell can be considered to be equivalent to the hydrogen half-cell. This implies that under the conditions stated the electrode process

$$\text{quinone} + 2\ H^+ + 2\ e^- \rightleftharpoons \text{hydroquinone}$$

is reversible and the ratio of the activities of quinone and hydroquinone, $a_Q a_{QH_2}^{-1}$, is constant. As the ionic strength is increased, $\log (a_Q a_{QH_2}^{-1})$ is found to vary approximately linearly [1] with the concentration of the dissolved electrolytes. The dependence of the activity ratio on the composition of the solution is usually referred to as the "salt error" of the quinhydrone electrode and is explained by assuming that the dissolved substances influence differently the activity factors of quinone and hydroquinone.

Though the salt error introduces a complication, the quinhydrone electrode offers a number of advantages. It comes rapidly to equilibrium and dissolved air is without effect; in addition, the standard potential of $H^+/QH_2Q(s),Pt$ is +699.3 mV at 25°C [1] which makes it applicable to a number of systems which would react with H_2. On account of these features the quinhydrone half-cell has been extensively used to investigate protolytic reactions. So it was often employed to study the hydrolysis equilibria of metal ions [2–7]. These studies on hydrolysis were all carried out in a constant ionic medium [8]. The solutions were made to contain 1 M or 3 M ClO_4^- by the addition of $NaClO_4$, the concentration of the metal ion to be studied was kept low and the hydrogen ion concentration was varied by adding $HClO_4$ or $NaHCO_3$.

In connection with these hydrolysis studies, it was therefore of interest to compare the quinhydrone half-cell with the hydrogen half-cell and thus to ascertain whether $a_Q a_{QH_2}^{-1}$ varies as Na^+ is replaced by H^+ in the ionic media $[ClO_4^-] = 3$ M and 1 M.

EXPERIMENTAL RESULTS

For experimental details reference is made to previous work [8]. The emfs of the following cells were studied at 25°C

— CE/solution S, quinhydrone(s)/Pt + (A)

— Pt, H_2/solution S/CE+ (B)

Here CE denotes the half-cell

Hg, Hg_2Cl_2/4 M NaCl/3 M $NaClO_4$/,

and solution S had the general composition

h M H^+, (3.000 — h) M Na^+, 3.000 M ClO_4^-.

h ranged from 0.0100 to 0.600 M.

The emf of cell (A) can be written at 25°C

$$E_A = E_{0A} + 59.16 \log h + 29.58 \log \left(\frac{a_Q}{a_{QH_2}}\right) + E_j \quad (1)$$

that of cell (B) at $p_{H_2} = 1$ atm

$$E_B = E_{0B} - 59.16 \log h - E_j \quad (2)$$

where E_{0A} and E_{0B} are constants and E_j denotes the liquid junction potential between solution S and 3 M $NaClO_4$. The standard state is defined so that the activity factors of the solutes approximate to unity if the solutes are present in negligible concentrations in the solvent 3 M $NaClO_4$. In previous work [8], evidence was given that f_{H^+} remains practically constant as Na^+ is replaced by H^+ up to $h = 0.6$ M; therefore the concentration of hydrogen ions can be used in (1) and (2) instead of the activity.

If $a_Q a_{QH_2}^{-1}$ remained unchanged as h is varied, $E_A(h) + E_B(h)$ would be a constant. From the plots $E_A(h)$ and $E_B(h)$, it became apparent however that $E_A(h) + E_B(h)$, and thus $a_Q a_{QH_2}^{-1}$, decreases monotonically with h.

In order to analyze these data in more detail the function

$$\delta = \delta(h) = 29.58 \log \left(\frac{a_{QH_2}}{a_Q}\right) \quad (3)$$

is needed. To obtain δ the values of E_{0A} and E_{0B} are required. These can be found by extrapolation. When h approaches zero, E_j and δ become negligible, consequently $E_A - 59.16 \log h = E'_A$ and $E_B + 59.16 \log h = E'_B$ approach E_{0A} and E_{0B}. On plotting E'_A and E'_B against h, both functions proved to be linear up to $h = 0.250$ M. Therefore the error involved in the extrapolations did not exceed ± 0.05 mV, which is the average uncertainty of the emf measurements.

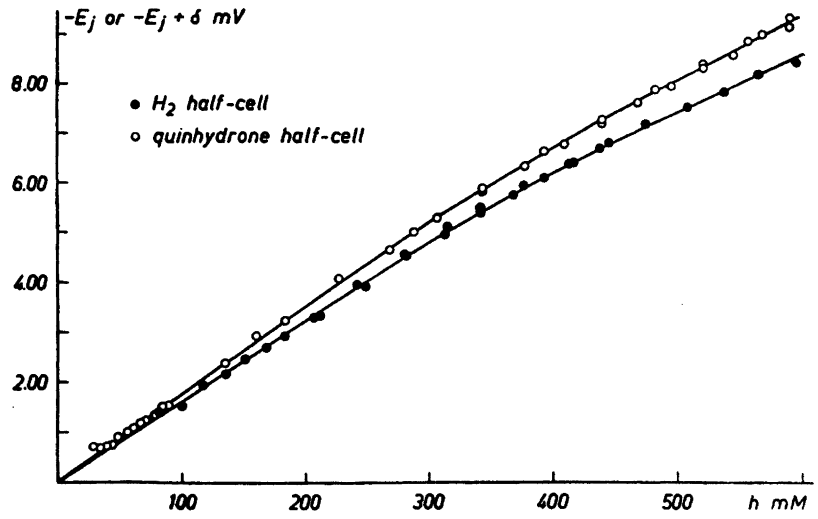


Fig. 1. $E_j - \delta$ *(equation 4) and* E_j *(equation 5) as functions of* h. *The upper curve represents the equation* $E_j - \delta = -59.16 \log\left(1 + \frac{2.00}{3.000}\,h\right) - 29.58 \log(1 + 0.1\,h)$ *mV. The lower curve:* $E_j = -59.16 \log\left(1 + \frac{2.00}{3.000}\,h\right)$ *mV.*

Using these extrapolated E_{0A} and E_{0B} values

$$E_A - E_{0A} - 59.16 \log h = 29.58 \log \left(\frac{a_Q}{a_{QH_2}}\right) + E_j = E_j - \delta \qquad (4)$$

and

$$E_{0B} - E_B - 59.16 \log h = E_j \qquad (5)$$

have been computed as functions of h, these data being plotted in Fig. 1. A smooth curve has been drawn through each set of experimental points. It was found that the curve describing the measurements with the hydrogen electrode coincides within 0.10 mV with the equation

$$E_j = -59.16 \log \left(1 + \frac{2.00\,h}{3.000}\right) \text{mV} \qquad (6)$$

which was found previously [8] to give a good fit in the whole range of h studied.

With the help of these curves, δ, which is equal to (5)—(4), was read off at a number of h values. These δ values are plotted *versus* log h in Fig. 2, where the length of the vertical lines indicates the probable error.

Solutions of $[ClO_4^-] = 1$ M have also been studied. Measurements with silver and hydrogen half-cells have indicated that, in this ionic medium, the activity factors remain constant up to $h \sim 0.100$ M. Therefore the measurements were not extended over $h = 0.200$ M. A comparison of the quinhydrone half-cell with the hydrogen half-cell has shown in this case too that δ increases gradually with h; at $h = 0.200$ M, δ attains a value of 0.20 mV.

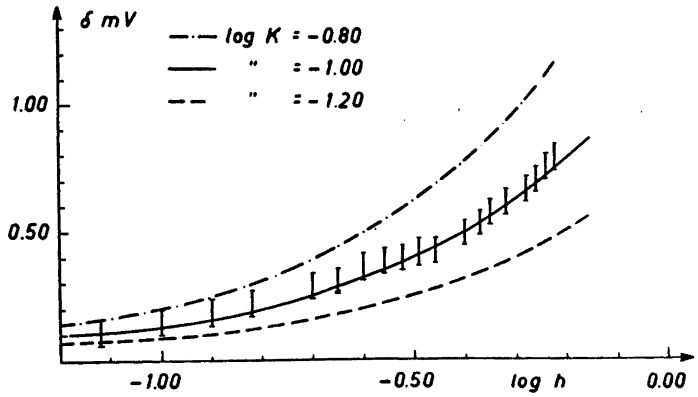


Fig. 2. δ (equation 3) as a function of log h. *Curves calculated with log* K = *−0.80, −1.00 and −1.20.*

DISCUSSION

Previous measurements on the variation of $a_Q a_{QH_2}^{-1}$ have been made [1] in solutions of varying ionic strength and the results have been explained by assuming that the ratio of the activity factors of Q and QH_2 changes with the composition of the solution. This assumption does not seem to be probable in the present case, where only solutions of constant ionic strength were investigated.

It has been shown [8] that, in the ionic medium $[ClO_4^-] = 3$ M, the activity factors of a number of positive ions of different charge, present in concentrations which are small compared with the $[ClO_4^-]$, remain practically constant as Na^+ is replaced by H^+ up to $h = 0.600$ M. It seems reasonable to expect that the ratio of the activity factors of the two *uncharged* species, quinone and hydroquinone, which are present in small concentrations, will not change in the h range where the activity factors of positive ions remain constant.

Assuming the constancy of $f_{QH_2} f_Q^{-1}$, the experimental $\delta(h)$ data are to be explained by the variation of the *concentration* ratio $[QH_2][Q]^{-1}$. Since this ratio increases with h (see Fig. 2), the simplest assumption seems to be that quinone, as a base, reacts with H^+ forming the corresponding acid $OC_6H_4OH^+$. Thus the equilibrium is established:

$$OC_6H_4O + H^+ \rightleftharpoons OC_6H_4OH^+ \qquad K = \frac{[QH^+]}{[Q]h} = K_a^{-1} \tag{7}$$

The acidity constant of hydroquinone is so small, $pK_a \sim 10$ ([9, 10]), that its ionization is negligible in the h range studied.

In order to compute the equilibrium constant K, the solubility and dissociation equilibria of quinhydrone must first be considered:

$$QH_2Q(s) \rightleftharpoons QH_2Q(\text{dissolved}) \rightleftharpoons Q + QH_2 \tag{8}$$

According to (7) and (8)

$$[QH_2] = [Q] + [QH^+] = [Q](1 + Kh) \tag{9}$$

Thus δ, the difference between (5) and (4), will be

$$\delta = 29.58 \log (1 + Kh) \tag{10}$$

K may be conveniently calculated by comparing the experimental $\delta = \delta(\log h)$ values with the function $\delta = 29.58 \log (1 + X)$. Superimposing the experimental data on the curve $\delta(\log X)$, the difference $\log X - \log h$ gives in the position of best agreement the most probable value of $\log K$. The advantages of this graphical method for finding constants from experimental data have been outlined by Sillén [11]. In this way it was calculated that

$$\log K = -1.0 \pm 0.2$$

As Fig. 2 shows, the agreement between the experimental data and the curve calculated with this constant may be considered satisfactory.

A great number of organic compounds containing oxygen have been found to be bases of appreciable strength, see *e.g.* Hammett [12], but of the quinones only anthraquinone has hitherto been investigated. Flexser, Hammett and Dingwall [13] estimated, by spectrophotometric measurements, pK_a of anthraquinone to be -8.2 ± 0.2 in concentrated sulfuric acid solutions. This substance is therefore a much weaker base than *p*-benzoquinone.

This work was financially supported by *Statens Naturvetenskapliga Forskningsråd* (*Swedish Natural Science Research Council*). I am greatly indebted to Professor Lars Gunnar Sillén for valuable criticism. I also want to thank my wife Dr. Clara Bereckí-Biedermann for helpful discussions.

REFERENCES

1. Hovorka, F. J. and Dearing, W. C. *J. Am. Chem. Soc.* **57** (1935) 446. This work contains a complete review of earlier investigations.
2. Granér, F. and Sillén, L. G. *Acta Chem. Scand.* **1** (1947) 631.
3. Ahrland, S. *Acta Chem. Scand.* **3** (1949) 374.
4. Hietanen, S. *Acta Chem. Scand.* **8** (1954) 1626.
5. Kilpatrick, M. and Pokras, L. *J. Electrochem. Soc.* **100** (1953) 85.
6. Biedermann, G. *Arkiv Kemi* **9** (1956) 277.
7. Kakihana, H. and Sillén, L. G. *Acta Chem. Scand.* **10** (1956) 985.
8. Biedermann, G. and Sillén, L. G. *Arkiv Kemi* **5** (1953) 425.
9. Sheppard, S. E. *Trans. Amer. Electrochem. Soc.* **39** (1921) 429.
10. Abichandani, C. T. and Jatkar, S. K. K. *J. Indian Inst. Sci.* **21A** (1938) 417.
11. Sillén, L. G. *Acta Chem. Scand.* **10** (1956) 186.
12. Hammett, L. P. *Physical Organic Chemistry*, McGraw-Hill Book Company Inc. New York 1940.
13. Flexser, L. A., Hammett, L. P. and Dingwall, A. *J. Am. Chem. Soc.* **57** (1935) 2103.

Received June 26, 1956.

ACTA CHEMICA SCANDINAVICA 10 (1956) 1345—1354

Electrode Impedance Measurements on the Cerium(IV)-Cerium(III) Couple in Perchloric Acid Solutions

STURE FRONÆUS

Department of Physical Chemistry, Chemical Institute, University of Lund, Lund, Sweden

A small platinum electrode, immersed in a solution of cerium(III) and cerium(IV) perchlorates in 3 M perchloric acid, is polarized by a sinusoidal alternating voltage of small amplitude, and the impedance of the metal-solution interface is determined. Owing to the high redox potential of the cerium couple the total impedance includes two parallel faradaic impedances, one of them due to the oxygen-water couple. From the measurements the rate of the electron transfer step of the cerium couple is calculated, and the result is shown to be in accord with a previous isotopic exchange investigation.

The rate of the charge transfer of the oxygen evolution on platinum is also obtained from the impedance measurements combined with separate determinations of the over-all rate of reaction. It is found that the rate-determining step is not the charge transfer but a subsequent reaction.

Furthermore, it is demonstrated that the steady-state potential of the platinum electrode is very nearly equal to the redox potential of the cerium couple.

The heterogeneous exchange reaction between cerium(III) and cerium(IV) at platinum surfaces was investigated in a previous work (Fronæus and Östman [1]) by means of a radioactive cerium isotope. At 0°C and in approximately 3 M perchloric acid as an ionic medium the following relationship was obtained for the rate r of the over-all exchange reaction

$$\frac{1}{r} = \frac{1.25 \times 10^{10}}{c^{1.5} q^{0.5}} + \frac{2.0 \times 10^{9}}{c} \qquad (1)$$

when r is expressed in mole $\cdot$ cm^{-2} $\cdot$ sec^{-1} and the concentrations c and q of cerium(IV) and cerium(III) are expressed in mM. The relationship was established for small values (< 10 mM) of c and q.

By comparing this expression with the one theoretically derived [1], it is found that the first term on the right-hand side of (1) is equal to the reciprocal of the rate r_0 of the electron transfer, and the second term is equal to the reci-

procal of the rate r_d of the diffusion of cerium(IV) to and from the electrode. Thus it was concluded that these two steps are the rate-determining ones. Furthermore, the exponent 1.5 of c in the expression for r_0 indicates [1] that the oxidizing species predominating in the electron transfer step is a dinuclear hydrolysis product of cerium(IV).

The purpose of the present investigation was to check these results and, for this reason, electrode impedance measurements were chosen, since by this method [2] it is generally possible to determine the rate of the electron transfer, even if this step is rather rapid in comparison with the diffusion processes. However, the present case is complicated by the fact that water is slowly oxidized at the electrode owing to the high redox potential of the cerium(IV)—cerium(III) couple, and the oxygen-water couple will interfere with the measurements. This complication is common to the electrical methods available.

THEORETICAL

At the platinum electrode we have simultaneously the following two overall electrode reactions

$$\mathrm{Ce(III)} \rightleftharpoons \mathrm{Ce(IV)} + \mathrm{e^-} \tag{2}$$

$$2\mathrm{H_2O} \rightleftharpoons \mathrm{O_2} + 4\mathrm{H^+} + 4\mathrm{e^-} \tag{3}$$

The electron transfer steps of these reactions are denoted

$$\mathrm{A}_n \rightleftharpoons \mathrm{B}_n + \mathrm{e^-} \tag{4}$$

where $n = 1$ refers to the cerium couple and $n = 2$ to the oxygen-water couple. For the current densities $\vec{i}_n$ and $\overleftarrow{i}_n$ of the forward and reverse reactions of (4) we have the expressions [1]

$$\vec{i}_n = k_n' \, [\mathrm{A}_n] \exp\left\{\frac{\alpha_n e F}{RT}\right\} \tag{5}$$

$$\overleftarrow{i}_n = k_n'' \, [\mathrm{B}_n] \exp\left\{-\frac{(1-\alpha_n) e F}{RT}\right\} \tag{6}$$

Here k_n', k_n'', and α_n should be constants, the transfer coefficients α_n fulfilling the condition $0 < \alpha_n < 1$. If the electrode potential e is adjusted at the redox potential e_n of the couple B_n—A_n we get $\vec{i}_n = \overleftarrow{i}_n = i_{0,n}$, where $i_{0,n}$ is the exchange current density of the couple. Then the concentrations of A_n and B_n close to the electrode become equal to the equilibrium values $[\mathrm{A}_n]_0$ and $[\mathrm{B}_n]_0$, and thus for an arbitrary value of e we get

$$\vec{i}_n = i_{0,n} \frac{[\mathrm{A}_n]}{[\mathrm{A}_n]_0} \exp\left\{\frac{\alpha_n (e-e_n) F}{RT}\right\} \tag{7}$$

$$\overleftarrow{i}_n = i_{0,n} \frac{[\mathrm{B}_n]}{[\mathrm{B}_n]_0} \exp\left\{-\frac{(1-\alpha_n)(e-e_n) F}{RT}\right\} \tag{8}$$

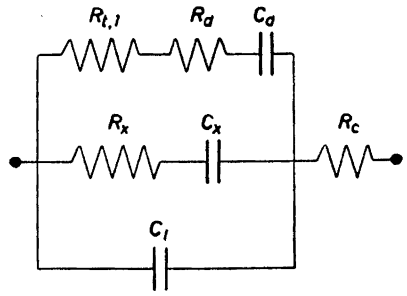


Fig. 1. Equivalent circuit of the electrochemical cell. $R_{t,1}$, R_d, *and* C_d = *transfer resistance, diffusion resistance, and diffusion capacity of the cerium couple;* R_x *and* C_x = *equivalent series resistance and capacity of the oxygen-water couple;* C_l = *double layer capacity;* R_c = *cell resistance.*

Furthermore, for the contribution i_n of the couple B_n—A_n to the total anodic current density we have the relationship

$$i_n = \vec{i}_n - \overleftarrow{i}_n \tag{9}$$

If the measurement cell consists of two platinum electrodes immersed in the solution and a sinusoidal alternating voltage is applied to the cell, the equivalent circuit can be represented as in Fig. 1. There are two so-called faradaic impedances, corresponding to the electrode reactions (2) and (3), and further the ordinary double layer capacity C_l. These parallel impedances are in series with the resistance R_c of the cell solution.

For small amplitudes (< 10 mV) of the applied alternating voltage the faradaic impedance connected with the cerium couple can be divided into the resistance $R_{t,1}$, due to the electron transfer step, and a diffusion impedance, composed of the resistance R_d and the capacity C_d. Under the condition stated $R_{t,1}$ is evidently equal to $(\partial e/\partial i_1)_{[A_1],[B_1]}$ for $e = e_0$, where e_0 is the steady-state potential of the electrode. Now, from an investigation by Sherill, King and Spooner [3] it is found that at a constant concentration (0.5 M) of perchloric acid and at cerium(IV) concentrations <10 mM the dependence of e_0 upon c and q is approximately in accordance with Nernst's formula. Thus it is very probable that e_0 is very nearly equal to the redox potential e_1 of the cerium couple. Then, remembering that $[A_1] = [A_1]_0$ and $[B_1] = [B_1]_0$ for $e = e_1$, we obtain from eqns. (7)—(9)

$$R_{t,1} = \frac{RT}{F} \cdot \frac{1}{i_{0,1}} \tag{10}$$

For diffusion impedances it has been shown before, *e.g.*, by Randles [2], Ershler [4], and Gerischer [5], that $\omega C_d R_d = 1$ and, furthermore, that R_d is proportional to $\omega^{-\frac{1}{2}}$, where $\omega = 2\pi\nu$ and ν is the frequency of the alternating current. Thus, if other experimental conditions are fixed we can put

$$R_d = \frac{K}{\sqrt{\omega}}; \qquad C_d = \frac{1}{K\sqrt{\omega}} \tag{11}$$

where K is a constant.

The expressions for R_x *and* C_x. On the basis of investigations of the oxygen evolution at electrodes (*cf.* Hickling [6] and Bockris [7]) we may presume for the oxygen-water couple that A_2 is equal to OH^- or in acid solutions H_2O, and that B_2 is the radical OH adsorbed on the platinum surface. In this case there is no diffusion impedance, but if the reaction between the adsorbed radicals is a slow process another impedance will result, and we will establish the dependence of the resistance R_x and the capacity C_x (see Fig. 1) upon ω.

For the variation in the electrode potential e with time t the differential equation

$$\frac{de}{dt} = R_x \frac{di}{dt} + \frac{i}{C_x} \tag{12}$$

is valid if i is the alternating current through this impedance. We can put $i = I \sin \omega t$, where I is the amplitude. Hence, we get

$$\frac{de}{dt} = \omega I R_x \cos \omega t + \frac{I}{C_x} \sin \omega t \tag{13}$$

Combining eqns. (7)—(9) we obtain i_2 expressed as a function of e and $[B_2]$, since $[A_2] = [A_2]_0$ according to the presumption above. A differentiation of this function gives

$$\frac{de}{dt} = R_{t,2} \frac{di_2}{dt} + R_{t,2} \frac{\overleftarrow{i_2}}{[B_2]} \frac{d[B_2]}{dt} \tag{14}$$

where $R_{t,2}$ is the electron transfer resistance of the oxygen-water couple at the electrode potential e_0 and is given by the expression

$$\frac{1}{R_{t,2}} = \frac{F}{RT} \left\{ \overrightarrow{i_2} \alpha_2 + \overleftarrow{i_2} (1 - \alpha_2) \right\} \tag{15}$$

For i_2 we have $i_2 = (i_2)_{e=e_0} + I \sin \omega t$ and hence $di_2/dt = \omega I \cos \omega t$.

Now we represent by $f([B_2])$ the rate of the reaction between the radicals adsorbed on the electrode surface. Then, if $[B_2]$ is expressed in moles per unit area, $i_2 F^{-1}$ will be the net rate at which the radicals are supplied by the electron transfer step. Hence, we obtain the differential equation

$$\frac{d[B_2]}{dt} + f([B_2]) = \frac{(i_2)_{e=e_0}}{F} + \frac{I}{F} \sin \omega t \tag{16}$$

where the first term in the right member is a constant.

For *very small amplitudes* the solution of eqn. (16) is of the form

$$[B_2] = a + \frac{I(b \sin \omega t - \omega \cos \omega t)}{(b^2 + \omega^2)F} + \varphi(t) \tag{17}$$

where the constants a and b fulfil the conditions

$$f(a) = \frac{(i_2)_{e=e_0}}{F}; \qquad b = \left(\frac{df}{d[B_2]} \right)_{[B_2]=a} \tag{18}$$

In (17) the non-sinusoidal term $\varphi(t)$ is negligible for t-values which are not very small. Then, differentiating this equation with respect to t and combining the expression obtained with (14) we get

$$\frac{de}{dt} = \omega I R_{t,2} \left\{ \cos\ \omega t + \frac{\overleftarrow{i_2}(b \cos \omega t + \omega \sin \omega t)}{[B_2](b^2 + \omega^2)F} \right\} \tag{19}$$

An equating of the coefficients of cos ωt and sin ωt in (13) and (19) gives the final expressions for R_x and C_x

$$R_x = R_{t,2} \left\{ 1 + \frac{\overleftarrow{i_2}\ b}{[B_2](b^2 + \omega^2)F} \right\} \tag{20}$$

$$\frac{1}{C_x} = \frac{\overleftarrow{i_2}\ R_{t,2}\ \omega^2}{[B_2](b^2 + \omega^2)F} \tag{21}$$

From (21) it is seen that the capacity C_x increases with the concentration of the adsorbed radicals, and if the reaction rate $f([B_2])$ is very low, which means a small value of b, the capacity is but slightly dependent on the frequency. It is also evident from (15) and (21) that if $\overrightarrow{i_2} >> \overleftarrow{i_2}$ for $e = e_0$, then the oxygen-water couple will give rise to the transfer resistance $R_{t,2}$ only.

The determination of the exchange current density $i_{0,1}$. The three parallel impedances in Fig. 1 can be replaced by an equivalent circuit, consisting of a resistance R_p and a capacity C_p connected in parallel. Then, by means of well-known transformation formulas for impedances we get

$$\frac{1}{R_p} = \frac{\omega^2 C_d^2 (R_{t,1} + R_d)}{1 + \omega^2 C_d^2 (R_{t,1} + R_d)^2} + \frac{\omega^2 C_x^2 R_x}{1 + \omega^2 C_x^2 R_x^2} \tag{22}$$

$$C_p = C_l + \frac{C_d}{1 + \omega^2 C_d^2 (R_{t,1} + R_d)^2} + \frac{C_x}{1 + \omega^2 C_x^2 R_x^2} \tag{23}$$

If the expressions for R_d, C_d, R_x, and C_x in eqns. (11), (20), and (21) are taken into consideration the following relationships are approximately valid at high frequencies

$$\frac{1}{R_p} = \frac{1}{R_{t,1}} + \frac{1}{R_{t,2}} - \frac{K'}{\sqrt{\omega}} \tag{24}$$

$$C_p = C_l + \frac{K'}{\omega\sqrt{\omega}} \tag{25}$$

where the coefficient K' is >0 and independent of the frequency.

Accordingly, R_p^{-1} and C_p experimentally determined should be plotted against $\nu^{-\frac{1}{2}}$ and $\nu^{-\frac{3}{2}}$, respectively, and extrapolated to $\nu = \infty$ giving $R_{t,1}^{-1} + R_{t,2}^{-1}$ and C_l. Then, denoting the intercept on the R_p^{-1}-axis by R_t^{-1} and observing that $i_{0,1} = r_0 F$, where the rate of the electron transfer of the cerium couple is expressed in moles per unit area and unit time, we obtain from (10) and (15)

$$\frac{RT}{F^2 R_t} = r_0 + \frac{\overrightarrow{i_2}\alpha_2 + \overleftarrow{i_2}(1-\alpha_2)}{F} \tag{26}$$

If we choose $c = q$ and keep $[H^+]$ at a fixed value the overvoltage $e_0 - e_2$ ($\approx e_1 - e_2$) of the oxygen-water couple will be constant and consequently also the current densities $\vec{i}_2$ and $\overleftarrow{i}_2$. On the other hand, for $c = q$ it is found from (1) that r_0 is proportional to c^2, if the results obtained in the isotopic exchange investigation are reliable. Then, by determining R_t for various values of c we can arrive at the corresponding rates r_0.

A test on the existence of an impedance due to the oxygen-water couple. The two faradaic impedances in Fig. 1 can be replaced by a single impedance, consisting of a resistance R_s and a capacity C_s in series. The expressions for R_s and C_s are rather complicated, but at high frequencies we get the following approximate formulas

$$R_s = \beta\left(R_{t,1} + \frac{K}{\sqrt{\omega}}\right) \tag{27}$$

$$\frac{1}{\omega C_s} = \frac{\beta^2 K}{\sqrt{\omega}} + \frac{(1-\beta)^2}{\omega C_x} \tag{28}$$

where $\beta = R_x(R_{t,1} + R_x + R_d)^{-1}$. Thus, if $R_x = \infty$ we have $\beta = 1$, whereas $\beta < 1$ for finite values of R_x. In the first-mentioned case two parallel straight lines should be obtained, when R_s and $(\omega C_s)^{-1}$ are plotted against $\nu^{-\frac{1}{2}}$. On the other hand, if $\beta < 1$ the quantity $(\omega C_s)^{-1}$ may increase more rapidly than R_s for increasing values of $\nu^{-\frac{1}{2}}$, since according to (21) C_x should be fairly independent of the frequency.

It can be mentioned that ordinarily [8-10] an extrapolation of R_s is used for the determination of R_t. However, in those cases where $C_p - C_l \ll C_p$ but $\omega R_p(C_p - C_l)$ is not $\ll 1$ the resistance R_s cannot be calculated with sufficient accuracy for such a determination.

MEASUREMENTS AND CALCULATIONS

Experimental details. The cell used in the impedance measurements was similar to that of Vetter [8]. The small, polarizable electrode was a platinum wire with a diameter of 0.32 mm and a length of 30 mm. It was placed as the axis of a cylindrical platinum electrode with a diameter of 10 mm and a length of 30 mm. The solution contained cerium(III) and cerium(IV) perchlorates in equal concentrations, and as supporting electrolyte 3.00 M perchloric acid was used [1].

The impedance of the cell was measured with an a.c. Wheatstone bridge circuit, properly shielded. Two of the arms consisted of two equal standard resistors, and in the fourth arm, adjacent to the cell, there were a decade resistor and a decade condenser, connected in parallel for technical reasons. The bridge was fed with an oscillator whose output was adjusted so that the amplitude of the voltage applied to the cell was about 7 mV. A cathode-ray oscillograph combined with a preamplifier served as a balance indicator of high sensitivity.

Calculations. From the readings on the decade resistor and the condenser, when the bridge was balanced, the corresponding values for an equivalent series arrangement of the resistance and the capacity were computed. Since the apparatus did not permit measurements at very high frequencies the eletrolyte resistance R_e could not be determined directly but was calculated from

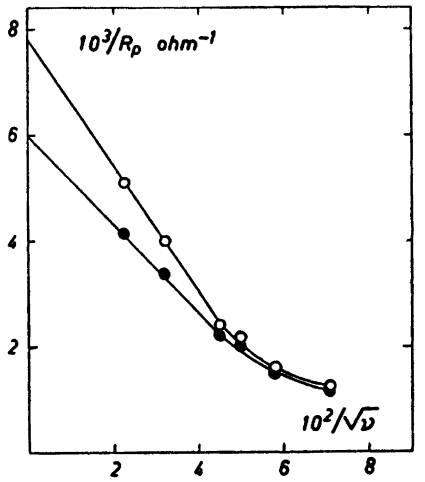


Fig. 2. The conductance R_p^{-1} *as a function of* $\nu^{-\frac{1}{2}}$ *(*ν *= frequency) at the cerium concentrations* c = q = 3.00 *mM* (●) *and* c = q = 6.00 *mM* (○).

the specific conductivity of 3 M perchloric acid and the electrode dimensions (R_c = 0.30 ohm at 20°C). After subtraction of R_c from the series resistance a re-calculation of the equivalent parallel arrangement was performed, giving the values of R_p and C_p.

For the cerium concentrations $c = q$ = 3.00 mM and 6.00 mM, which are within the ranges used in the isotopic exchange investigation [1], the measurements were at first carried out at 20°C. In Fig. 2 R_p^{-1} has been plotted against $\nu^{-\frac{1}{2}}$. Owing to the rather great values of both C_p and R_p the resistance could not be determined with sufficient accuracy at high frequencies, and accordingly R_p has been given only for $\nu \leqq 2\,000$ cycles · sec^{-1}. As predicted by the theory the curves are approximately straight-lined at the lower values of $\nu^{-\frac{1}{2}}$ and can be used for extrapolations to $\nu = \infty$. In Fig. 3 the capacity C_p has been plotted against $\nu^{-\frac{3}{2}}$. Since the variation in C_p is small we should get fairly accurate determinations of the double layer capacity C_l by the extrapolations to $\nu = \infty$.

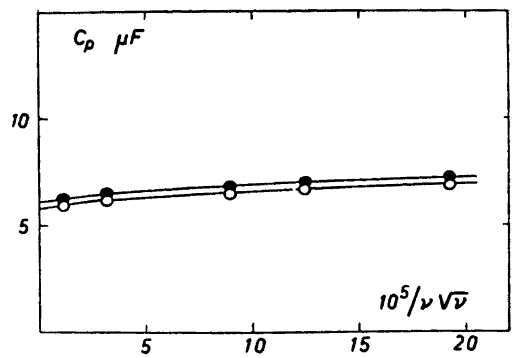


Fig. 3. The capacity C_p *as a function of* $\nu^{-\frac{3}{2}}$ *at the cerium concentrations* c = q = 3.00 *mM* (●) *and* c = q = 6.00 *mM* (○).

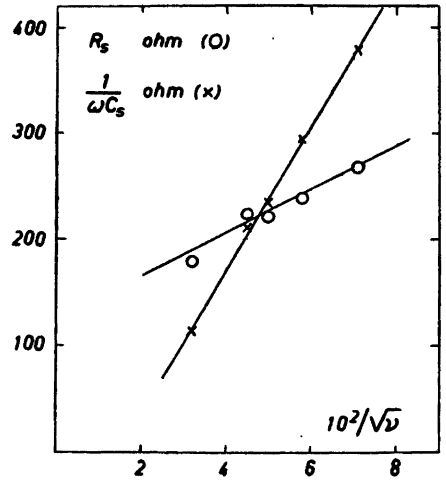


Fig. 4. The quantities R_s (O) *and* $1/\omega C_s$ (×) *as functions of* $\nu^{-\frac{1}{2}}$ *at the cerium concentrations* c = q = 6.00 *mM.*

From R_p and the difference $C_p - C_l$ the equivalent circuit consisting of the resistance R_s and the capacity C_s in series was calculated. In Fig. 4 R_s and $(\omega C_s)^{-1}$ have been plotted against $\nu^{-\frac{1}{2}}$. It is seen that $(\omega C_s)^{-1}$ increases more rapidly than R_s with $\nu^{-\frac{1}{2}}$, and according to the theory above this means that the faradaic impedance due to the oxygen-water couple influences the measurements.

The values of R_t^{-1} and C_l arrived at refer to the two electrodes of the cell. Thus we have to divide by the factor $s_1 s_2 (s_1 + s_2)^{-1} = 0.30$ cm^2, where s_1 and s_2 are the surface areas of the electrodes, in order to obtain the corresponding quantities per unit area of the interface. Since in the present case $s_1 = 0.03\ s_2$ the impedance of the great electrode is only a correction term. For C_l a value of about 20 μF · cm^{-2} is obtained at the cerium concentrations used.

In Table 1 the values of $RTF^{-2}R_t^{-1}$ are given. The corresponding rates r_0 in the next column have been calculated from eqn. (26) as described in the theoretical section. Some impedance measurements were also performed at 0°C, since the isotopic exchange measurements were carried out at this temperature. However, at 0°C it was possible to determine R_p with sufficient accuracy only at low frequencies. Then it was found that the R_p-values were about half as

Table 1. The rate of the electron transfer step of the cerium (IV)-cerium (III) couple on platinum in the presence of 3 M perchloric acid. The quantities in the columns 2—7 are expressed in mole · cm^{-2} · sec^{-1}.

c = q mM	$\frac{RT}{F^2 R_t} \times 10^9$		$r_0 \times 10^9$		$r_0 \times 10^9$	$r_d \times 10^9$
	20°C	0°C	20°C	0°C	Tracer method;0°C	
3.00	5.2	2.5	0.5	0.25	0.72	1.5
6.00	6.8	3.5	2.0	1.0	2.9	3.0

great as the corresponding values obtained at 20°C. Accordingly we may conclude that the same thing is valid for the rate r_0, as is indicated in Table 1.

From the measurements at 20°C the calculations give $\vec{i}_2\alpha_2 + \overleftarrow{i}_2(1 - \alpha_2) = 0.45$ mA · cm^{-2}. Now according to Hickling and Hill [11] the transfer coefficient α_2 is about 0.5 for platinum in acid solution, and using this value we get $\vec{i}_2 + \overleftarrow{i}_2 = 0.90$ mA · cm^{-2}. The current density $i_2 = \vec{i}_2 - \overleftarrow{i}_2$ of the oxygen evolution at the steady-state potential e_0 is equal to the current density of the simultaneous heterogeneous reduction of cerium(IV) and can be measured separately. To this end 15 ml of a solution with $c = q = 20.0$ mM and the perchloric acid concentration 3 M was shaken at 20°C for 45 hours with a platinum foil, the surface area of which was 8 cm^2. Then it was found that as a mean value 5.3×10^{-2} mmoles of cerium(IV) had been reduced. During the same time about 10^{-3} mmoles had been reduced in the homogeneous reaction. Hence we get $i_2 = 4 \times 10^{-3}$ mA · cm^{-2} at the potential[3] $e_0 = 1.67$ V. For the oxygen-water couple we compute $e_2 = 1.25$ V at $[H^+] = 3$ M, giving us the overvoltage $e_0 - e_2 = 0.43$ V. The current density obtained is consistent with the measurements by Hickling and Hill [11]. Combining the values of $\vec{i}_2 + \overleftarrow{i}_2$ and $\vec{i}_2 - \overleftarrow{i}_2$ we obtain $\vec{i}_2 = 0.45$ mA · cm^{-2}. Thus the resultant rate of the oxygen evolution at platinum is much less than the rate of discharge of OH^- or H_2O.

Furthermore, since $i_1 + i_2 = 0$ at the steady-state potential e_0, we get from eqns. (7)—(9) the approximate relationship

$$e_1 - e_0 = \frac{RT\, i_2}{F^2\, r_0} \tag{29}$$

if the value of $e_1 - e_0$ is so small that we can put $[A_1] \approx [A_1]_0$ and $[B_1] \approx [B_1]_0$ and apply the approximation $\exp(y) \approx 1 + y$ to the exponential functions containing $e_1 - e_0$. Combining the i_2-value with the rate r_0 at 20°C we find $e_1 - e_0 = 2$ mV for $c = q = 3.00$ mM, which confirms the validity of the approximation. Consequently, the steady-state mixed potential is very nearly equal to the redox potential of the cerium(IV)-cerium(III) couple.

DISCUSSION

In the last two columns of Table 1 the rate r_0 and the rate r_d of the diffusion of cerium(IV) have been calculated from the two terms in the right member of eqn. (1). It is seen that the impedance measurements and the radioactive tracer method give the same order of magnitude for r_0. The agreement is satisfactory if we take into consideration that possibly the surface states of the electrodes used in the two investigations were not the same, though the platinum wires were treated in the same way [1] prior to use. Thus a very good support is obtained for the result arrived at in the previous investigation [1] that $r_0 \leqq r_d$ for the concentrations used, so that r_0 has a considerable influence upon the over-all rate of the heterogeneous exchange reaction.

From a comparison between the values of $i_2F^{-1} = 4 \times 10^{-11}$ mole · cm^{-2} · sec^{-1} and r_d it is found that the rate of reduction of cerium(IV) at the steady-state potential is only 1 to 2 % of the rate of diffusion of cerium(IV) to and from the electrode. Consequently we have also confirmed the assumption in the previous investigation that the cerium concentrations at the interface are not affected appreciably by this reduction.

On the other hand, at the low cerium(IV) concentrations used, necessitated by the intricate hydrolysis of the cerium(IV) ion in perchloric acid solutions, the term r_0 in the right member of (26) is rather small in comparison with the constant term. Thus, even if several concentrations within the narrow range given are used it is impossible to carry out impedance measurements with such an accuracy that we can get an independent check on the relation $r_0 =$ constant · c^2 (for $c = q$), presupposed in the calculations above. It is evident that in the present case the radioactive tracer method is superior to the impedance measurements.

Interesting information about the heterogeneous oxygen evolution has been obtained in this investigation. From the calculations we arrive at the conclusion that under the conditions given the oxygen evolution is controlled not by the discharge step but by the subsequent reaction between the radicals OH, adsorbed on the platinum. This result is in agreement with recent investigations. Thus according to Bockris [7] the rate-determining step of the oxygen evolution is the following one: 2 OH → H_2O_2, where OH and H_2O_2 are adsorbed on the platinum electrode.

This investigation has been supported by a grant from the *Swedish Natural Science Research Council* which is gratefully acknowledged.

The author wishes to thank Fil.mag. C. O. Östman and Miss K. Anderson for valuable assistance in the measurements.

REFERENCES

1. Fronæus, S. and Östman, C. O. *Acta Chem. Scand.* **10** (1956) 769.
2. Randles, J. E. B. *Discussions Faraday Soc.* **1** (1947) 11.
3. Sherril, M. S., King, C. B. and Spooner, R. C. *J. Am. Chem. Soc.* **65** (1943) 170.
4. Ershler, B. V. *Discussions Faraday Soc.* **1** (1947) 269.
5. Gerischer, H. *Z. physik. Chem.* **198** (1951) 286.
6. Hickling, A. *Quart. Revs.* **3** (1949) 95.
7. Bockris, J. O'M. *Ann. Rev. Phys. Chem.* **5** (1954) 477.
8. Vetter, K. J. *Z. physik. Chem.* **199** (1952) 285.
9. Randles, J. E. B. and Somerton, K. W. *Trans. Faraday Soc.* **48** (1952) 937 and 951.
10. Gerischer, H. *Z. Elektrochem.* **57** (1953) 604.
11. Hickling, A. and Hill, S. *Trans. Faraday Soc.* **46** (1950) 550.

Received June 29, 1956.

ACTA CHEMICA SCANDINAVICA 10 (1956) 1355—1364

Short Communications

Acid Hydrolysis of Some α,β-Unsaturated Aliphatic Esters

EERO A. HALONEN

Institute of Chemistry, University of Helsinki, Finland

The ethyl esters of propiolic, tetrolic and *tert.* butylpropiolic acid and the diethyl ester of acetylenedicarboxylic acid were prepared previously [1]. In the present study, the hydrolyses were carried out in ampoules of Pyrex glass and of about 10.5 ml capacity. The sample volume was 10 ml and the concentrations of sulphuric acid and ester were both 0.02 N in the initial mixture. The reaction was arrested in ice and the acid was titrated with barium hydroxide using phenolphthalein as indicator.

Addition of water to the triple bond of the esters was not observed. If it occurred, ethyl propiolate would have given, *via* acetoacetic acid, acetaldehyde, and, correspondingly, ethyl tetrolate and ethyl *tert.*butylpropiolate would have given ketones. The acid hydrolysis of diethyl acetylenedicarboxylate cannot be studied by using the above mentioned method as the acidic ester resulting from the hydrolysis is decarboxylated at a faster rate than the diethyl ester is hydrolyzed. Also the propiolic acid formed in the hydrolysis of ethyl propiolate is decarboxylated under these conditions [2] and, as a result, a decrease in the rate constant of hydrolysis occurs when the reaction proceeds. Especially at high temperatures, this becomes evident, as the activation energy of decarboxylation is 13 600 cal greater than the activation energy of hydrolysis. Mathematically, the decrease has been shown to agree, quantitatively, with the decarboxylation. The rate constants and the calculated activation energies and frequency factors are given in Table 1.

The ratios of the rates of hydrolysis correspond approximately to those previously obtained in alkaline hydrolysis of these esters [1].

The difference in the rates for ethyl propiolate and ethyl tetrolate is greater than the difference in the rates for ethyl tetrolate and ethyl *tert.*butylpropiolate. When compounds with triple bonds are compared to the corresponding saturated ones [3] and to those with double bonds [4], it will be noted, that the acetylenic compounds will hydrolyze about 40 times slower than the saturated ones but only slightly slower than the ethylenic compounds. The activation energies of the acetylenic and saturated compounds are of the same magnitude and approximately 3 000 cal smaller than the activation energies of the ethylenic compounds. This indicates that the conjugation between the unsaturated bond and the carboxyl carbonyl group has more effect

Table 1. Acid hydrolysis of esters in water and in acetone-water mixtures.

Ester	Solvent composition wt % H_2O	10^5k l mole^{-1} sec.$^{-1}$			E cal	log A
		40.0°	60.0°	80.0°		
$HC{\equiv}C{\cdot}CO_2Et$	100	1.16	5.60	22.4	16 221	4.39
—»—	50	0.437	2.03	7.74	15 680	3.59
$H_3C{\cdot}C{\equiv}C{\cdot}CO_2Et$	100	0.713	3.83	16.4	17 220	4.88
—»—	50	0.300	1.31	5.62	16 113	3.73
$(CH_3)_3C{\cdot}C{\equiv}C{\cdot}CO_2Et$	50	0.276	1.14	4.53	15 860	3.46

on the rate of the hydrolysis than has the inductive effect and, on the basis of the reaction mechanism, this can also be expected. As compared with the ethylenic esters the decrease in the rate is due to the inductive effect of the triple bond. As a result of this either the pre-equilibrium moves from the side of the ionic conjugate acid of ester to the side of the ester or the alkoxyl linkage, after the addition of water, is less readily breakable.

The rates of hydrolysis in 60 % aqueous ethanol at 60° C for the ethyl ester of acetic, monochloroacetic, dichloroacetic and trichloroacetic acids are 1, 0.91, 0.40 and 0.11, respectively, if the rate for ethyl acetate is taken as a unity [5]. The fact that the rates of hydrolysis for the ethyl ester of propiolic and acrylic acids differ only slightly from each other gives support to the assumption that, in the case of chloroacetic acids, steric factors are of importance.

1. Halonen, E. A. *Acta Chem. Scand.* **9** (1955) 1492.
2. Halonen, E. A. *Ann. Acad. Sci. Fennicae* **A. II.** 55 (1954).
3. Tommila, E. and Hella, A. *Ann. Acad. Sci. Fennicae* **A. II.** 53 (1954).
4. Pekkarinen, L. *Ann. Acad. Sci. Fennicae* **A. II.** 55 (1955).
5. Timm, E. W. and Hinshelwood, C. N. *J. Chem. Soc.* **1938** 862; Tommila, E., Hietala, S. and Nyrkiö, J. *Suomen Kemistilehti* **B. 28** (1955) 143; Ingold, C. K. *Structure and Mechanism in Organic Chemistry*, Cornell University Press, New York 1953, p. 777.

Received September 20, 1956.

Paper Chromatographic Separation of Thiamine Phosphates

KARL-HEINZ KIESSLING

Institute of Zoophysiology, Uppsala, Sweden

Several papers have been published about paper chromatographic separation of thiamine phosphates [1-5]. In all solvents described thiamine triphosphate hardly moves at all, and its R_F value coincides in most cases with that of nucleotide di- and triphosphates.

In this paper a paper chromatographic solvent is described in which thiamine triphosphate moves easily, and in which it separates well from other thiamine compounds and from nucleotide phosphates. Also thiamine phosphates with more than three phosphate groups are separated. From a mixture of thiamine phosphates prepared according to Viscontini, Bonetti, and Karrer [6], nine thiamine compounds can be isolated.

The solvent consists of 100 ml *iso*butyric acid, 60 ml N ammonia, and 1.6 ml 0.1 M ethylene diamine tetraacetic acid. It has been used by Krebs and Hems for separating nucleotides [7] and is a modification of a solvent described by Zetterström and Ljunggren [8]. Filter papers Whatman No. 1 are used after washing in aqueous ethylene diamine tetraacetic acid according to the method described by Eggleston and Hems [9].

The di- and triphosphates of inosine, guanosine, uridine, and cytidine all have lower R_F values than adenosine diphosphate [10]. In this investigation thiamine triphosphate was shown to move faster than adenosine diphosphate. It can thus be easily separated from the nucleotides mentioned.

Fig. 1 and 2 show the separation of different amounts of thiamine phosphates prepared according to Viscontini *et al.*[6] One mg of the mixture dissolved in water is linearly spread on the filter paper in Fig. 1. The separation is very distinct. Ten lines can be seen with the naked eye, but only nine are registered on the photographic plate. When the amount of the thiamine phosphate mixture is increased to 3 mg (Fig. 2) the separation is still distinct except between thiamine mono- and diphosphate (lines 3 and 4). Nine lines can be detected.

The lines are cut out, the compounds run off with water, then added as spots on a new filter paper, and developed in the same solvent. The compounds appear as distinct spots with about the same R_F values as the lines on the original paper chromatogram (Fig. 3).

Total and hydrolyzable phosphorus per molecule of thiamine for the compounds 1–7 are seen in Table 1. Thus compound 1 and 2 were identified as different forms of thiamine *. The ratio between total and hydrolyzable phosphorus and thiamine suggests that the compounds 3–7 are thiamine mono-, di-, tri-, tetra- and pentaphosphate, respectively. Compounds

* These two forms have been separated earlier by Gaudiano, Spadoni and Tecce [11].

on the rate of the hydrolysis than has the inductive effect and, on the basis of the reaction mechanism, this can also be expected. As compared with the ethylenic esters the decrease in the rate is due to the inductive effect of the triple bond. As a result of this either the pre-equilibrium moves from the side of the ionic conjugate acid of ester to the side of the ester or the alkoxyl linkage, after the addition of water, is less readily breakable.

The rates of hydrolysis in 60 % aqueous ethanol at 60° C for the ethyl ester of acetic, monochloroacetic, dichloroacetic and trichloroacetic acids are 1, 0.91, 0.40 and 0.11, respectively, if the rate for ethyl acetate is taken as a unity [5]. The fact that the rates of hydrolysis for the ethyl ester of propiolic and acrylic acids differ only slightly from each other gives support to the assumption that, in the case of chloroacetic acids, steric factors are of importance.

1. Halonen, E. A. *Acta Chem. Scand.* **9** (1955) 1492.
2. Halonen, E. A. *Ann. Acad. Sci. Fennicae* **A. II.** 55 (1954).
3. Tommila, E. and Hella, A. *Ann. Acad. Sci. Fennicae* **A. II.** 53 (1954).
4. Pekkarinen, L. *Ann. Acad. Sci. Fennicae* **A. II.** 55 (1955).
5. Timm, E. W. and Hinshelwood, C. N. *J. Chem. Soc.* **1938** 862; Tommila, E., Hietala, S. and Nyrkiö, J. *Suomen Kemistilehti* **B. 28** (1955) 143; Ingold, C. K. *Structure and Mechanism in Organic Chemistry*, Cornell University Press, New York 1953, p. 777.

Received September 20, 1956.

Paper Chromatographic Separation of Thiamine Phosphates

KARL-HEINZ KIESSLING

Institute of Zoophysiology, Uppsala, Sweden

Several papers have been published about paper chromatographic separation of thiamine phosphates [1-5]. In all solvents described thiamine triphosphate hardly moves at all, and its R_F value coincides in most cases with that of nucleotide di- and triphosphates.

In this paper a paper chromatographic solvent is described in which thiamine triphosphate moves easily, and in which it separates well from other thiamine compounds and from nucleotide phosphates. Also thiamine phosphates with more than three phosphate groups are separated. From a mixture of thiamine phosphates prepared according to Viscontini, Bonetti, and Karrer [6], nine thiamine compounds can be isolated.

The solvent consists of 100 ml *iso*butyric acid, 60 ml N ammonia, and 1.6 ml 0.1 M ethylene diamine tetraacetic acid. It has been used by Krebs and Hems for separating nucleotides [7] and is a modification of a solvent described by Zetterström and Ljunggren [8]. Filter papers Whatman No. 1 are used after washing in aqueous ethylene diamine tetraacetic acid according to the method described by Eggleston and Hems [9].

The di- and triphosphates of inosine, guanosine, uridine, and cytidine all have lower R_F values than adenosine diphosphate [10]. In this investigation thiamine triphosphate was shown to move faster than adenosine diphosphate. It can thus be easily separated from the nucleotides mentioned.

Fig. 1 and 2 show the separation of different amounts of thiamine phosphates prepared according to Viscontini *et al.*[6] One mg of the mixture dissolved in water is linearly spread on the filter paper in Fig. 1. The separation is very distinct. Ten lines can be seen with the naked eye, but only nine are registered on the photographic plate. When the amount of the thiamine phosphate mixture is increased to 3 mg (Fig. 2) the separation is still distinct except between thiamine mono- and diphosphate (lines 3 and 4). Nine lines can be detected.

The lines are cut out, the compounds run off with water, then added as spots on a new filter paper, and developed in the same solvent. The compounds appear as distinct spots with about the same R_F values as the lines on the original paper chromatogram (Fig. 3).

Total and hydrolyzable phosphorus per molecule of thiamine for the compounds 1–7 are seen in Table 1. Thus compound 1 and 2 were identified as different forms of thiamine *. The ratio between total and hydrolyzable phosphorus and thiamine suggests that the compounds 3–7 are thiamine mono-, di-, tri-, tetra- and pentaphosphate, respectively. Compounds

* These two forms have been separated earlier by Gaudiano, Spadoni and Tecce [11].

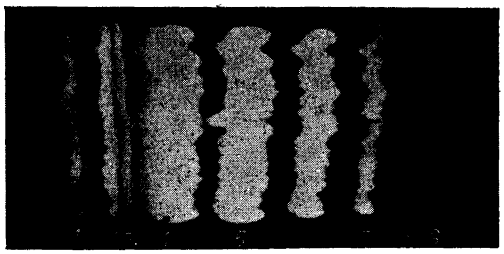


Fig. 1. Paper chromatographic separation of a mixture of thiamine phosphates.

1 mg of the mixture prepared according toViscontini *et al.* and dissolved in water is spread as a line on the filter paper. For solvent see text. Time 19 h. The thiamine compounds on the chromatogram are made visible by spraying the paper with an alkaline ferricyanide solution. In UV of 340 mμ they are seen as blue lines.



Fig. 2. Paper chromatographic separation of a mixture of thiamine phosphates.

3 mg of the mixture is dissolved in water, and placed on the filter paper. Other conditions as in Fig. 1.

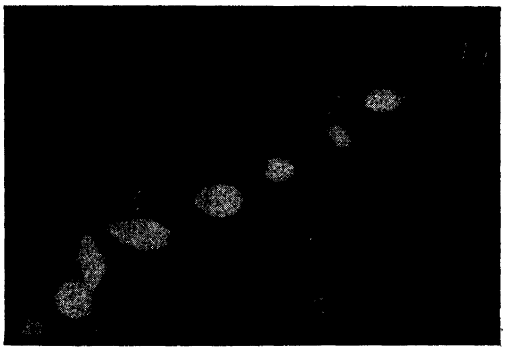


Fig. 3. Subsequent test chromatography of the compounds separated in Fig. 1.

The lines from the chromatogram in Fig. 1 are added as separate spots on a new filter paper, and run with the same solvent. The figures correspond to those in Fig. 1 and in Table 1.

Table 1. Total and hydrolyzable phosphorus of the thiamine compounds separated as in Fig. 1.

Hydrolyzable phosphorus is determined after heating the compounds in 2 N HCl at 100° for 10 min., after which all thiamine polyphosphates appear as thiamine monophosphate. Total phosphorus is determined after wet ashing. Thiamine is oxidized with alkaline ferricyanide to thiochrome, and the fluorescence estimated in a Beckman spectrophotometer with fluorescence attachment.

Compound	hydrolyzable P / total P	P / thiamine	R_F value
1	—	—	0.87
2	—	—	0.79
3	—	1	0.77
4	1/2	2	0.68
5	2/3	3	0.55
6	3/4	4	0.46
7	4/5	5	0.36
8—10		>5	0.24, 0.21 0.16

8—10 have more than five phosphate groups per molecule of thiamine.

The described method has been used for isolating biological thiamine triphosphate from yeast [12], and was found satisfactory for this purpose. The R_F value, however, is somewhat lower than for the synthetic compound depending on the contamination with impurities from the yeast.

1. Viscontini, M., Bonetti, G., Ebnöther, C. and Karrer, P. *Helv. Chim. Acta* **34** (1951) 1384.
2. Rossi-Fanelli, A., Siliprandi, N. and Fasella, P. *Science* **116** (1952) 711.
3. Kiessling, K.-H. and Lindahl, G. *Arkiv Kemi* **6** (1953) 271.
4. Bartley, W. *Biochem. J. London* **56** (1954) 379.
5. Siliprandi, D. and Siliprandi, N. *Biochim. et Biophys. Acta* **14** (1954) 52.
6. Viscontini, M., Bonetti, G. and Karrer, P. *Helv. Chim. Acta* **33** (1949) 1478.
7. Krebs, H. A. and Hems, R. *Biochim. et Biophys. Acta* **12** (1953) 172.
8. Zetterström, R. and Ljunggren, M. *Acta Chem. Scand.* **5** (1951) 291.
9. Eggleston, L. V. and Hems, R. *Biochem. J. London* **52** (1952) 156.
10. Hems, R. *Personal communication.*
11. Gaudiano, A., Spadoni, M. A. and Tecce, G. *Boll. Soc. it. Biol. Sper.* **28** (1952) 701.
12. Kiessling, K.-H. *Biochim. et Biophys. Acta* **20** (1956) 293.

Received August 8, 1956.

*iso*Thiocyanates XXIII*. L (—)-9-Methylsulphinylnonyl *iso*Thiocyanate, a New Mustard Oil Present as a Glucoside (Glucoarabin) in *Arabis* Species

ANDERS KJÆR and ROLF GMELIN

Chemical Laboratory of the University of Copenhagen, Denmark

In the course of a systematic investigation of glucosidically bound *iso*thiocyanates in seeds of various species of the cruciferous genus *Arabis*, it was observed that a glucoside, obviously different from all compounds heretofore recognized in Nature, was present in, *e. g.*, *Arabis alpina* L., a popular flower-garden subject. Paper chromatograms of seed extracts [1] indicated the presence of two glucosides both possessing R_F-values well above that of glucotropaeolin (*cf.* Ref.[2]).

When a purified, methanolic extract of a larger seed sample was subjected to enzymic hydrolysis in a buffered solution (pH 6.5), an ether-soluble *iso*thiocyanate fraction was formed. Homogeneous, optically active, crystalline thioureas were obtained upon reaction of the *iso*thiocyanate solution with various amines. The analytical data clearly indicated the composition $C_{11}H_{21}ONS_2$ for the parent mustard oil. The *thiourea*, recrystallized from ethyl acetate, had the m. p. 103.5—104.5° (uncorr.) (Found: C 50.00; H 9.13; N 10.45; S 24.40. Calc. for $C_{11}H_{24}ON_2S_2$: C 49.96; H 9.15; N 10.60; S 24.25), $[\alpha]_D^{24.5}$ −66° (96 % EtOH, c = 2.1). The infra-red spectrum in a KBr-wafer showed a characteristic strong band at 9.78 μ, attributable to a sulphoxide-grouping. The *phenylthiourea* separated from ethyl acetate in colourless prisms, m. p. 121—122° (uncorr.) (Found:

* Part XXII of this series: *Acta Chem. Scand.* **10** (1956) 1193.

Table 1. Total and hydrolyzable phosphorus of the thiamine compounds separated as in Fig. 1.

Hydrolyzable phosphorus is determined after heating the compounds in 2 N HCl at 100° for 10 min., after which all thiamine polyphosphates appear as thiamine monophosphate. Total phosphorus is determined after wet ashing. Thiamine is oxidized with alkaline ferricyanide to thiochrome, and the fluorescence estimated in a Beckman spectrophotometer with fluorescence attachment.

Compound	hydrolyzable P / total P	P / thiamine	R_F value
1	—	—	0.87
2	—	—	0.79
3	—	1	0.77
4	1/2	2	0.68
5	2/3	3	0.55
6	3/4	4	0.46
7	4/5	5	0.36
8—10		>5	0.24, 0.21 0.16

8—10 have more than five phosphate groups per molecule of thiamine.

The described method has been used for isolating biological thiamine triphosphate from yeast [12], and was found satisfactory for this purpose. The R_F value, however, is somewhat lower than for the synthetic compound depending on the contamination with impurities from the yeast.

1. Viscontini, M., Bonetti, G., Ebnöther, C. and Karrer, P. *Helv. Chim. Acta* **34** (1951) 1384.
2. Rossi-Fanelli, A., Siliprandi, N. and Fasella, P. *Science* **116** (1952) 711.
3. Kiessling, K.-H. and Lindahl, G. *Arkiv Kemi* **6** (1953) 271.
4. Bartley, W. *Biochem. J. London* **56** (1954) 379.
5. Siliprandi, D. and Siliprandi, N. *Biochim. et Biophys. Acta* **14** (1954) 52.
6. Viscontini, M., Bonetti, G. and Karrer, P. *Helv. Chim. Acta* **33** (1949) 1478.
7. Krebs, H. A. and Hems, R. *Biochim. et Biophys. Acta* **12** (1953) 172.
8. Zetterström, R. and Ljunggren, M. *Acta Chem. Scand.* **5** (1951) 291.
9. Eggleston, L. V. and Hems, R. *Biochem. J. London* **52** (1952) 156.
10. Hems, R. *Personal communication.*
11. Gaudiano, A., Spadoni, M. A. and Tecce, G. *Boll. Soc. it. Biol. Sper.* **28** (1952) 701.
12. Kiessling, K.-H. *Biochim. et Biophys. Acta* **20** (1956) 293.

Received August 8, 1956.

*iso*Thiocyanates XXIII*. L (—)-9-Methylsulphinylnonyl *iso*Thiocyanate, a New Mustard Oil Present as a Glucoside (Glucoarabin) in *Arabis* Species

ANDERS KJÆR and ROLF GMELIN

Chemical Laboratory of the University of Copenhagen, Denmark

In the course of a systematic investigation of glucosidically bound *iso*thiocyanates in seeds of various species of the cruciferous genus *Arabis*, it was observed that a glucoside, obviously different from all compounds heretofore recognized in Nature, was present in, *e. g.*, *Arabis alpina* L., a popular flower-garden subject. Paper chromatograms of seed extracts [1] indicated the presence of two glucosides both possessing R_F-values well above that of glucotropaeolin (*cf.* Ref.[2]).

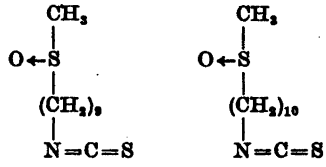
When a purified, methanolic extract of a larger seed sample was subjected to enzymic hydrolysis in a buffered solution (pH 6.5), an ether-soluble *iso*thiocyanate fraction was formed. Homogeneous, optically active, crystalline thioureas were obtained upon reaction of the *iso*thiocyanate solution with various amines. The analytical data clearly indicated the composition $C_{11}H_{21}ONS_2$ for the parent mustard oil. The *thiourea*, recrystallized from ethyl acetate, had the m. p. 103.5—104.5° (uncorr.) (Found: C 50.00; H 9.13; N 10.45; S 24.40. Calc. for $C_{11}H_{24}ON_2S_2$: C 49.96; H 9.15; N 10.60; S 24.25), $[\alpha]_D^{24.5}$ −66° (96 % EtOH, c = 2.1). The infra-red spectrum in a KBr-wafer showed a characteristic strong band at 9.78 μ, attributable to a sulphoxide-grouping. The *phenylthiourea* separated from ethyl acetate in colourless prisms, m. p. 121—122° (uncorr.) (Found:

* Part XXII of this series: *Acta Chem. Scand.* **10** (1956) 1193.

C 60.00; H 8.24; N 8.21. Calc. for $C_{17}H_{33}ON_2S_2$: C 59.97; H 8.29; N 8.23), $[\alpha]_D^{24}$ −54° (96 % EtOH, c = 0.84), whereas the *benzylthiourea* crystallized from acetone as thin, colourless needles, m. p. 119° (uncorr.) (Found: C 60.90; H 8.61; N 7.60; S 18.00. Calc. for $C_{18}H_{30}ON_2S_2$: C 60.97; H 8.53; N 7.90; S 18.09), $[\alpha]_D^{25}$ −64° (MeOH, c = 0.44). Treatment of the latter derivative with silver nitrate furnished in high yield (79 %) the corresponding urea-derivative, separating from ethyl acetate in colourless needles, m. p. 120.5° (uncorr.) (Found: C 63.75; H 8.96; N 8.32; S 9.37. Calc. for $C_{18}H_{30}O_2N_2S$: C 63.87; H 8.93; N 8.28; S 9.47), $[\alpha]_D^{24}$ −56° (96 % EtOH, c = 0.95). Reduction of the latter with zinc dust in HCl-containing ethanol proceeded in quantitative yield, and was accompanied by disappearance of the optical rotation and the characteristic sulphoxide-band in the infra-red spectrum. The reduced benzyl-urea separated from ethyl acetate as tiny, colourless needles, m. p. 99.5° (uncorr.) (Found: C 66.85; H 9.31; N 8.58. Calc. for $C_{18}H_{30}ON_2S$: C 67.01; H 9.38; N 8.69). Hydrogenolysis of this compound with W4-Raney nickel afforded a sulphur-free urea-derivative, which was proved to be identical with an authentic specimen of the previously unknown 1-benzyl-3-nonylurea, m. p. 99.0−99.5° (uncorr.) (Found: C 73.75; H 10.23; N 10.05. Calc. for $C_{17}H_{28}ON_2$: C 73.88; H 10.21; N 10.14), synthesized by oxygen-sulphur exchange with silver nitrate from 1-benzyl-3-nonylthiourea, m. p. 75.5° (uncorr.). (Found: C 69.90; H 9.65; N 9.71. Calc. for $C_{17}H_{28}N_2S$: C 69.81; H 9.65; N 9.58), which was, in turn, produced from benzyl *iso*thiocyanate and *n*-nonylamine.

The above sequence of reactions establishes the structure of the new *Arabis* mustard oil as a methylsulphinylnonyl *iso*thiocyanate, the optical activity of which resides solely in the sulphoxide grouping. This fact, in conjunction with the close analogy to previously recorded natural representatives of the ω-methylthioalkyl *iso*thiocyanates [3-5], strongly suggest that the *Arabis* mustard oil has its methylsulphinyl-grouping located at the terminal carbon-atom *. The physical data, notably the rotation values, are closely comparable to those of the homologous L(−)-10-methylsulphinyldecyl *iso*thiocyanate (II) which we recently established [5] as a naturally occurring species.

Therefore, we conclude that seeds of *Arabis alpina* L. contain L(−)-9-methylsulphinylnonyl *iso*thiocyanate (I) in the traditional glucosidic combination, for which we wish to introduce the name *glucoarabin*. On paper chromatography in various solvent systems, the presence of glucose and sulphate in glucoarabin has been established. A detailed account of this work, supplemented by confirmatory synthetic evidence for the structure (I), will form the subject of a forthcoming communication in this journal.



I II

Microanalyses were performed in this laboratory by Mr. P. Hansen. The experimental assistance of Mr. R. Boe Jensen in part of the work is acknowledged.

The work is part of investigations supported by *Statens Almindelige Videnskabsfond (The Danish State Research Foundation)* and *Carlsbergfondet (The Carlsberg Foundation)*. A special grant from *Kai Hansens Fond* is gratefully acknowledged.

1. Schultz, O.-E. and Gmelin, R. *Z. Naturforsch.* **8b** (1953) 151.
2. Schultz, O.-E. and Wagner, W. *Z. Naturforsch.* **11b** (1956) 73.
3. Kjær, A. and Gmelin, R. *Acta Chem. Scand.* **10** (1956) 1100.
4. Kjær, A. *Dansk Tidsskr. Farm.* **30** (1956) 117, p. 132; *cf.* also: Schultz, O.-E. and Wagner, W. *Z. Naturforsch.* **11b** (1956) 417.
5. Kjær, A., Gmelin, R. and Boe Jensen, R. *Acta Chem. Scand., in press.*

Received September 25, 1956.

* *Note added in proof:* This supposition has now been verified by synthesis.

A Method of Preparing Half-esters of Alkylsuccinic Acids with Free Primary Carboxyl Group. Synthesis and Optical Configuration of Optically Active Methyl 2-Methyl-3-carboxypropanoate

GUNNEL STÄLLBERG

Chemical Institute, and Institute of Medical Chemistry, University of Uppsala, Uppsala, Sweden

The preparation of the half-ester (I) of methylsuccinic acid has proved difficult because the methods usually employed for the synthesis of monoesters of dibasic acids give mixtures of

$$HOOC—CH_2—CH(CH_3)—COOCH_3$$

I

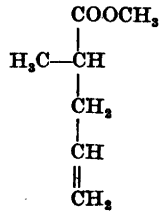
$$HOOC—CH(CH_3)—CH_2—COOCH_3$$

II

the two isomeric half-esters (I) and (II) [1,2]. Hancock and Linstead [2] obtained (I) in crystalline form in very poor yield by fractional crystallization of the ester mixture. The half-ester (I) has recently been prepared from citraconic anhydride by Veibel and Pedersen [3]. None of the methods appears suitable for preparation of (I) in quantity.

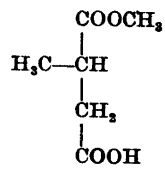
Armstrong and Hilditch [4] obtained methyl hydrogen azelate in very good yield by oxidation of methyl oleate in acetone solution with potassium permanganate. It thus appeared possible to prepare half-esters of the type (I) by oxidation of the corresponding esters of alkylallylacetic acids. It was found that simple distillation of the oxidation products of methyl methylallylacetate gives crude (I) in yields of 60—68 % of the theoretical. The half-ester may be purified by crystallization from low boiling light petroleum. The melting point of pure (I) was found to be 42.2—42.8° C. (Hancock and Linstead give 42.5—43.5° C and Veibel and Pedersen 42—44° C). The melting point was unchanged after distillation at 0.1 mm pressure.

Methyl ester of optically active methylallylacetic acid can be oxidized without racemization to give the enantiomorphs of (I). (+)-Methyl 2L-methyl-$\Delta^{4:5}$-pentenoate (III),



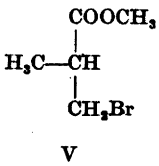
III

$[\alpha]_D^{23}$ +17.0° (homogeneous)



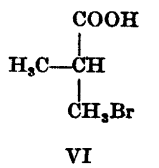
IV

$[\alpha]_D^{25}$ −9.3° (chloroform c = 17.5)



V

$[\alpha]_D^{24}$ +13.6 (homogeneous)



VI

$[\alpha]_D^{27}$ +10.1° (chloroform c = 14.4)

from acid of $[\alpha]_D^{23}$ + 8.2° [5,6,7] on oxidation gave (−)-methyl 2L-methyl-3-carboxypropanoate (IV). The active half-ester isolated by means of simple distillation had $[\alpha]_D^{25}$ −9.3° (chloroform, c = 17.5). A part of the specimen was converted into (−)-methyl methylsuccinate of α_D^{20} −3.45°, l = 0.5. For the antipode Berner and Leonardsen [8] give α_D^{20} + 6.91°, l = 1. This result shows that the oxidation of (III) by means of potassium permanganate proceeds without partial racemization in contrast to the oxidation of optically active methylallylacetic acid with chromic acid [9]. Levorotatory half-ester (IV) can also readily be obtained by resolution of the inactive ester (I) *via* the quinine salt. A specimen of (IV) obtained in this manner had after distillation $[\alpha]_D^{25}$ −9.3° (chloroform, c = 17.4).

The enantiomorphs of methyl 2-methyl-3-carboxypropanoic acid (I) are key compounds for the synthesis of a number of optically active compounds having a methyl group in α-position to a carboxyl group. Work is in progress on the prepara-

tion of the dextrorotatory antipode of (IV) and on the use of the enantiomorphs as intermediates in the synthesis of optically active compounds. For example, (IV) has *via* Hunsdieckers' procedure [10] been converted into (+)-methyl 2L-methyl-3-bromo-propanoate (V), $[\alpha]_D^{24}$ + 13.8° (homogeneous). (Found: Br 44.3. Calc. Br 44.14). Hydrolysis of the ester (V) with hydrogen bromide in glacial acetic acid gave (+)-2L-methyl-3-bromopropanoic acid ((+)-β-bromo*iso*butyric acid), $[\alpha]_D^{27}$ +10.1° (chloroform, c = 14.4). (Found Br 48.2. Calc. Br 47.85).

Experimental. For the oxidation of methyl methylallylacetate the following procedure appears to give the best results. Methyl methylallylacetate, b.p. 134.5—135.0°, 760 mm, $n_D^{22.6}$ 1.4158, (52 g) was dissolved in 450 ml of dry acetone (distilled from potassium permanganate) in a 2 l three-necked round-bottomed flask equipped with a reflux condenser and a Hershberg stirrer. Powdered potassium permanganate (400 g) was added in portions as fast as the vigorous reaction allowed. The addition of permanganate lasted 2 h after which time refluxing and stirring was continued for 4 h. The reaction mixture was filtered on a sintered glass funnel. The filtrate contained practically nothing of the desired oxidation product and was discarded. The mass on the filter was washed with about 1 l of a solution of sulfurous acid. The filtrate was acidified with hydrochloric acid and the mixture was extracted several times with ether (it is preferable to use an apparatus for continuous extraction). The ether solution was washed with a small quantity of water and dried with sodium sulphate. The solvent was distilled off and the residue distilled *in vacuo*. The main fraction (37.8 g, 64 % of the theoretical) distilled at 101—103°, 0.1 mm. On cooling to room temperature most of the material solidified to a mass of large crystals, only a very small part remaining liquid. After treatment with charcoal the half-ester was crystallized from light petroleum at —15°. M. p. 42.2—42.8°.

Preparation of the optically active half-ester (IV). a) by oxidation. The oxidation was performed as described above starting from optically active methylallylacetic acid. Once-distilled half-ester (IV) (n_D^{26} 1.4309; $[\alpha]_D^{25}$ —9.3° (chloroform, c = 17.5)) crystallized on seeding. Crystallization from light petroleum (b. p. 20—40°) after treatment with charcoal gave (IV) with m. p. 31.4—32.3° and $[\alpha]_D^{24}$ —9.3° (chloroform, c = 17.8).

b) by resolution of inactive half-ester (I). Inactive half-ester (I) (16.7 g) was dissolved in a mixture of acetone and water (1:1 by volume, 450 ml) and quinine (43.4 g) was dissolved in the warm solution. The solution was filtered and crystallization allowed to take place at room temperature. After standing overnight the crystals were collected and recrystallized thrice from progressively smaller amounts of the same solvent. The quinine salt was decomposed by means of hydrochloric acid and the half-ester extracted with ether in an apparatus for continuous extraction. After distillation the optically active half-ester (IV) (n_D^{26} 1.4309, super-cooled liquid) showed an optical rotation of $\alpha_D^{24.5}$ —0.81° (chloroform, c = 17.4, l = 0.5) $[\alpha]_D^{24.5}$ —9.3°.

The writer is indebted to Professors A. Fredga and E. Stenhagen for advice and interest.

1. Bone, W. A., Sudborough, J. J. and Sprankling, C. H. G. *J. Chem. Soc.* **85** (1904) 534.
2. Hancock, J. E. H. and Linstead, R. P. *J. Chem. Soc.* **1953** 3490.
3. Veibel, S. and Pedersen, C. *Acta Chem. Scand.* **9** (1955) 1674.
4. Armstrong, E. F. and Hilditch, T. P. *J. Soc. Chem. Ind.* **44** (1925) 43 T.
5. Ställberg-Stenhagen, S. *Arkiv Kemi, Mineral. Geol.* **23 A** (1946) No. 15.
6. Ställberg-Stenhagen, S. *Arkiv Kemi* **1** (1949) 153.
7. Fray, G. I. and Polgar, N. *J. Chem. Soc.* **1956** 2036.
8. Berner, E. and Leonardsen, R. *Ann.* **538** (1939) 1.
9. Ställberg-Stenhagen, S. and Stenhagen, E. *Arkiv Kemi, Mineral. Geol.* **24 B** (1947) No. 9.
10. Hunsdiecker, H. and Hunsdiecker, C. *Ber.* **75** (1942) 291.

Received October 8, 1956.

A Correction of the Crystal Structure of $MoO_3 \cdot 2H_2O$

INGVAR LINDQVIST

Institute of Chemistry, University of Uppsala, Uppsala, Sweden

In order to refine the crystal structure of $MoO_3 \cdot 2H_2O$ [1] a reinvestigation was started in this Institute. Prolonged exposures then showed that the crystal has a considerable superstructure. The new axes a, b, c are related to the earlier a', b', c' in the following way: $a = 4a'$, $b = 2b'$, $c = 2c'$. The cell dimensions are thus $a = 15.08$ Å, $b = 13.82$ Å, $c = 14.68$ Å and $\beta = 90° 40'$. The loss of orthorhombic symmetry which could not be detected in the intensities earlier is now obvious for the superstructure reflexions. It has been checked that the main principles of the suggested structure cannot be influenced by the superstructure but there are of course, small changes in the oxygen positions. The calculated bond distances (except for Mo-Mo) are thus of little value and therefore the basis is removed for the suggestion about the existence of an ion H_4O^{2+}.

Because of change of axes during the work an obvious error has been made in the description of the structure in Ref.[1]: x and z parameters and h and l indices should be interchanged all through the paper to fit the choice of axes.

A complete reinvestigation will be very time-consuming and is not planned at present.

1. Lindqvist, I. *Acta Chem. Scand.* **4** (1950) 650.

Received October 17, 1956.

A Nuclear Magnetic Resonance Study of the Dihydrate of Molybdenum Trioxide

S. MARIČIĆ and J. A. S. SMITH

Department of Inorganic and Structural Chemistry, The University of Leeds, England

A combined proton magnetic resonance and infra-red investigation of the dihydrate of molybdenum trioxide has shown that the formula $(H_4O^{++})MoO_4^{--}$ is very improbable [1].

The second moment of the proton absorption line at 77° K is 27.6 gauss [2]. If a symmetrical H_4O^{++} ion existed in the crystal, this value would predict [2] an O—H distance of 1.16 Å in H_4O^{++}, compared with 0.96 Å in water vapour, and this seems an improbably large increase. In addition, the infra-red spectrum shows frequencies at 3 100 and 1 592 cm^{-1}; if these are interpreted as stretching and bending frequencies associated with O—H groups, they suggest an expansion of the order of 0.04 Å only. It would be difficult to reconcile both of these results with the existence of an H_4O^{++} ion.

We hope to publish these results in detail elsewhere.

1. Lindqvist, I. *Acta Chem. Scand.* **4** (1950) 650.
2. Van Vleck, *Phys. Rev.* **74** (1948) 1168.

Received October 17, 1956.

Metalation of Pyrene

ARNE BERG

Chemical Institute, University of Aarhus, Aarhus, Denmark

Only few strictly aromatic hydrocarbons have been metalated by organolithium compounds [1] and the yields of carboxylic acids obtained upon carbonation have been poor.

Pyrene, in view of its readiness to partake in substitution reactions, and especially of the general rule of substitution in 3-position [2] governing these reactions, seemed an interesting object for metalation.

It has now been found that pyrene, by the action at room temperature of a rather large excess of *n*-butyllithium in diethyl ether not only is metalated as evidenced by the isolation of pyrene carboxylic acids upon carbonation of the reaction mixture, but also is attacked by the organometallic reagent in positions 1 and 4 in addition to the usual 3-position, that is in all isomeric positions in the pyrene molecule. This was shown by the isolation from the acid mixture of three acids two of which were

identical with the known pyrene-3- and pyrene-4-carboxylic acids. The third acid, also being, as shown by analysis, a pyrene-monocarboxylic acid, consequently must be the hitherto unknown pyrene-1-carboxylic acid [5]. Its constitution has been further established by converting it to the known 1-methyl-pyrene *via* 1-pyrenyl carbinol by reduction with lithium aluminium hydride. Also the carbinol is new. The 3-acid itself appeared difficult to isolate in a pure state, but it could be identified as the methyl ester.

The isomer ratio, as roughly estimated from the yields of the three acids in an experiment as described below, was 2:1:0.2, the positions taken in the order 1, 3 and 4. In a typical experiment a conversion of 85 % of pyrene was found, the remainder being recovered. Of converted pyrene 70 % were isolated as acidic products, 70 % of which consisted of the three pyrene-monocarboxylic acids.

More details will appear in a following paper and the present work is continued in different directions.

Experimental. Pyrene (20 g; 0.1 mole) in absolute ether (300 ml) was treated with a filtered solution of *n*-butyllithium, prepared, according to Gilman *et al.* [3], from lithium (8.5 g; 1.22 g. atoms) and *n*-butyl bromide (68.5 g; 0.5 mole) in abs. ether (200 ml). The colour of the solution rapidly turned deep red. After 14 days the solution was pressed into a mixture of dry ice and ether and worked up. From the ether layer pyrene (3.1 g) was recovered. The acidic products were separated by fractionated salting out of the sodium salts. In this way and by recrystallization from acetic acid and chlorobenzene more or less pure fractions of the three pyrene-monocarboxylic acids resulted, amounting to 10.2 g. By repeated recrystallizations pure fractions of the 1- and 4-acids were obtained. The last named acid (m.p. 327—328°) as well as the methyl ester (m.p. 139°; esterification was accomplished with methanolic hydrogen chloride) did not show any depression in mixed m.p. with authentic samples. Not quite pure 3-acid (m.p. about 260°; the pure acid has m.p. 273°) was esterified with methanol and hydrogen chloride and the crude methyl ester chromatographed (in benzene-hexane, 1:1) on alumina. The bulk of the ester was obtained with m.p. 82° and did not show any depression in mixed m.p. with authentic 3-ester (m.p. 83—84°).

Pyrene-1-carboxylic acid. Light yellow fractions with sharp m.p. 275—276° were obtained from chlorobenzene (Found: Equiv. wt. by titration 246.6; C 83.16; H 4.27. Calc. for $C_{17}H_{10}O_2$: Equiv.wt. 246.3; C 82.90; H 4.09). The 1-acid dissolves in conc. sulphuric acid with a yellow colour but without fluorescence (the 3-acid shows a strong yellow-green fluorescence). Esterification in methanolic hydrogen chloride yielded the methyl ester of the 1-acid, m.p. 107—108° (from methanol) (Found: C 83.14; H 4.79. Calc. for $C_{18}H_{12}O_2$ (260.3): C 83.05; H 4.65). Ultraviolet absorption maxima of the ester (in ethanol) were found at: 218.5, 240.4, 253, 280, 310.5, 341.5 and 380.5 mμ.

1-Pyrenyl carbinol. Pyrene-1-carboxylic acid (0.93 g) was extracted down into a stirred suspension of lithium aluminium hydride (0.5 g) in ether in the course of 4 h and the mixture refluxed for an additional hour before it was hydrolyzed and worked up. The organic layer by evaporation of the ether left the carbinol as thin, white needles. Recrystallization from benzene yielded 0.82 g with m.p. 155—155.5° (Found: C 87.50; H 5.18. Calc. for $C_{17}H_{12}O$ (232.3): C 87.88; H 5.21). Ultraviolet absorption maxima were found at 233, 242, 253.5, 264, 274.5, 307.5, 321, 336.7, 351, 363.5 and 373.5 mμ (in ethanol).

The 1-carbinol (0.5 g) was converted to the corresponding chloride as described by Bachmann and Carmack [4] for the 3-carbinol and the chloride then reduced with lithium aluminium hydride in boiling ether. After hydrolysis only a minor part could be identified as definite compounds. The crude product was fractionated from ethanol, and fractions showing a green fluorescence with conc. sulphuric acid (the carbinol does not show this) were chromatographed on alumina (from benzene-hexane, 1:1), when small amounts of 1-pyrenyl carbinol (25 mg) and of not quite pure 1-methyl-pyrene (50 mg) could be isolated. After recrystallization from ethanol the 1-methyl-pyrene fraction (30 mg) showed m.p. 144.5—145°. Repetition of the whole purification procedure brought the m.p. to 147.5—148°. There was no m.p. depression with an authentic specimen of 1-methyl-pyrene whereas a specimen of 4-methyl-pyrene (m.p. 145—146°) depressed the m.p. drastically. The two authentic methyl pyrenes were very kindly supplied by Dr. H. Dannenberg, Max-Planck Institute in Munich and by Dr. O. Kruber, the Gesellschaft für Teerverwertung, Duisberg-Meiderich, to whom I am very much indebted. Also the m.p. of the picrate (228—229°, from

benzene) as well as the ultraviolet absorption spectrum of the hydrocarbon itself agreed with 1-methylpyrene.

1. Gilman, H. *Org. Reactions* **8** (1954) 265. E. A. Braude, *Progr. Org. Chem.* **4** (1955) 201.
2. Vollmann, H., Becker, H., Corell, M. and Streeck, H. *Ann.* **531** (1937) 73.
3. Gilman, H., Beel, J. A., Brannen, C. G., Bulluck, M. V., Dunn, G. E. and Miller, L. S. *J. Am. Chem. Soc.* **71** (1949) 1499.
4. Bachmann, W. E. and Carmack, M. *J. Am. Chem. Soc.* **63** (1941) 2494.
5. Added in proof: Recently a paper by O. Neunhoeffer and H. Woggon [*Ann.* **600** (1956) 34] appeared reporting the formation of pyrene-1-carboxylic acid (m. p. 258° is reported) by the action of metallic sodium on pyrene followed by carbonation. The metalorganic intermediate is shown to be an addition product of 1 sodium atom with 1 molecule of pyrene.

Received October 17, 1956.

A Correction of the Crystal Structure of $MoO_3 \cdot 2H_2O$

INGVAR LINDQVIST

Institute of Chemistry, University of Uppsala, Uppsala, Sweden

In order to refine the crystal structure of $MoO_3 \cdot 2H_2O$ [1] a reinvestigation was started in this Institute. Prolonged exposures then showed that the crystal has a considerable superstructure. The new axes a, b, c are related to the earlier a', b', c' in the following way: $a = 4a'$, $b = 2b'$, $c = 2c'$. The cell dimensions are thus $a = 15.08$ Å, $b = 13.82$ Å, $c = 14.68$ Å and $\beta = 90° 40'$. The loss of orthorhombic symmetry which could not be detected in the intensities earlier is now obvious for the superstructure reflexions. It has been checked that the main principles of the suggested structure cannot be influenced by the superstructure but there are of course, small changes in the oxygen positions. The calculated bond distances (except for Mo-Mo) are thus of little value and therefore the basis is removed for the suggestion about the existence of an ion H_4O^{2+}.

Because of change of axes during the work an obvious error has been made in the description of the structure in Ref.[1]: x and z parameters and h and l indices should be interchanged all through the paper to fit the choice of axes.

A complete reinvestigation will be very time-consuming and is not planned at present.

1. Lindqvist, I. *Acta Chem. Scand.* **4** (1950) 650.

Received October 17, 1956.

A Nuclear Magnetic Resonance Study of the Dihydrate of Molybdenum Trioxide

S. MARIČIĆ and J. A. S. SMITH

Department of Inorganic and Structural Chemistry, The University of Leeds, England

A combined proton magnetic resonance and infra-red investigation of the dihydrate of molybdenum trioxide has shown that the formula $(H_4O^{++})MoO_4^{--}$ is very improbable [1].

The second moment of the proton absorption line at 77° K is 27.6 gauss [2]. If a symmetrical H_4O^{++} ion existed in the crystal, this value would predict [2] an O—H distance of 1.16 Å in H_4O^{++}, compared with 0.96 Å in water vapour, and this seems an improbably large increase. In addition, the infra-red spectrum shows frequencies at 3 100 and 1 592 cm^{-1}; if these are interpreted as stretching and bending frequencies associated with O—H groups, they suggest an expansion of the order of 0.04 Å only. It would be difficult to reconcile both of these results with the existence of an H_4O^{++} ion.

We hope to publish these results in detail elsewhere.

1. Lindqvist, I. *Acta Chem. Scand.* **4** (1950) 650.
2. Van Vleck, *Phys. Rev.* **74** (1948) 1168.

Received October 17, 1956.

Metalation of Pyrene

ARNE BERG

Chemical Institute, University of Aarhus, Aarhus, Denmark

Only few strictly aromatic hydrocarbons have been metalated by organolithium compounds [1] and the yields of carboxylic acids obtained upon carbonation have been poor.

Pyrene, in view of its readiness to partake in substitution reactions, and especially of the general rule of substitution in 3-position [2] governing these reactions, seemed an interesting object for metalation.

It has now been found that pyrene, by the action at room temperature of a rather large excess of *n*-butyllithium in diethyl ether not only is metalated as evidenced by the isolation of pyrene carboxylic acids upon carbonation of the reaction mixture, but also is attacked by the organometallic reagent in positions 1 and 4 in addition to the usual 3-position, that is in all isomeric positions in the pyrene molecule. This was shown by the isolation from the acid mixture of three acids two of which were

ACTA CHEMICA SCANDINAVICA **10** (1956) 1365—1371

*iso*Thiocyanates XX *. 4-Pentenyl *iso*Thiocyanate, a New Mustard Oil Occurring as a Glucoside (Glucobrassicanapin) in Nature

ANDERS KJÆR and ROALD BOE JENSEN

Chemical Laboratory of the University of Copenhagen, Denmark

A new volatile mustard oil has been isolated from seed cake of rape (*Brassica napus* L.) and identified as 4-pentenyl *iso*thiocyanate (III), the higher homologue of 3-butenyl mustard oil, (II), previously recognized in the same material. The structure proof of (III) rests on infra-red data for the corresponding thiourea, and degradation of its derivative with 1-naphthylamine, (V), to compounds of established structure.

A synthesis of pure 4-pentenyl *iso*thiocyanate has been accomplished, and synthetic 1-(1-naphthyl)-3-(4-pentenyl)-thiourea (V) shown to be identical with the product derivable from the natural mustard oil.

The latter occurs in the seed as a glucoside for which the name *glucobrassicanapin* is proposed. The identification of the new *iso*thiocyanate makes possible the establishment of a complete picture of the mustard oils of rape seed. Six individual glucosides are genuinely present, three of which in very small amounts only. They are: glucoiberin (or a closely allied compound, traces only), progoitrin (glucorapiferin), sinalbin (traces), gluconapin, glucobrassicanapin and gluconasturtiin (traces), yielding (−)-3-methylsulphinylpropyl mustard oil (or a related species), (−)-5-vinyl-2-oxazolidinethione, *p*-hydroxybenzyl, 3-butenyl, 4-pentenyl and 2-phenylethyl *iso*thiocyanate, respectively, on enzymic hydrolysis.

In a previous paper of this series [1] it was demonstrated that seed of rape (*Brassica napus* L.) on enzymic hydrolysis furnished three volatile *iso*thiocyanates. Of these, the chief constituent was proved to be 3-butenyl mustard oil (II), a conclusion independently attained at also by Ettlinger and Hodgkins [2]. One of the minor components has now been identified as the homologous and heretofore unknown 4-pentenyl *iso*thiocyanate (III).

$CH_2=CHCH_2NCS$ I $CH_2=CHCH_2CH_2NCS$ II $CH_2=CHCH_2CH_2CH_2NCS$ III

* Part XIX of this series: *Acta Chem. Scand.* 10 (1956) 1100.

The occurrence of more than one species in the volatile mustard oil fraction of rape seed has been suspected for many years. In 1899 Jørgensen [3] considered the possible existence of an "angelyl mustard oil" in admixture with the preponderant C_5-species ("crotyl mustard oil"), mainly on basis of nitrogen analyses of the corresponding crude thiourea-mixtures. Schmalfuss [4] subjected the volatile mustard oil mixture from a total of 50 kg of rape seed to fractional distillation and obtained, in addition to 4-pentenonitrile and what is known today as 3-butenyl *iso*thiocyanate, a higher boiling *iso*thiocyanate furnishing a thiourea with an unsharp m. p. of *ca.* 50°. No analytical data or suggestions as to composition and structure were presented. More recently, André and Delaveau [5] succeeded in obtaining an *iso*thiocyanate with comparable physical properties, again by fractionation of the volatile rape seed (colza) mustard oils. The product was devoid of optical activity, and analytical data of the corresponding crystalline thiourea indicated the composition C_5H_9NCS of the mustard oil. The French authors realized the theoretical existence of 13 isomerides satisfying these conditions but did not attempt any determination of the actual structure. They did present, however, good evidence for the second minor component, which is present in trifling amounts only, being 2-phenylethyl *iso*thiocyanate, a species occasionally encountered also in other crucifer seeds.

The starting material in the present experiments was commercially produced rape seed cake which was subjected to enzymic hydrolysis by the addition of white mustard seed, functioning as a source of myrosinase. It was formerly shown [6] that the latter seed gives rise to traces only of volatile mustard oils, insignificant for the present purpose. Steam distillation furnished a yield of less than 0.1 % of volatile *iso*thiocyanates which were fractionated *in vacuo*. Subsequent to the bulk of 3-butenyl mustard oil, the new *iso*thiocyanate distilled as a colourless product, containing traces only of the 3-butenyl species as estimated by paper chromatography of the corresponding thiourea. For the purpose of structure determination and characterization, the *iso*thiocyanate was transformed into crystalline thiourea-derivatives upon reaction with ammonia and 1-naphthylamine. Analyses of both derivatives indicated the composition C_5H_9NCS of the parent *iso*thiocyanate. The infra-red spectrum of the simple thiourea (IV) suggested the presence of a vinyl-grouping. The unbranched character of the five-carbon chain was demonstrated in the following way. The naphthylthiourea (V) was transformed into the corresponding naphthylurea (VI) which, on catalytic hydrogenation, afforded 1-(1-naphthyl)-3-pentylurea (VII), identified by comparison with an authentic specimen produced from *n*-pentylamine and naphthyl *iso*cyanate.

$$CH_2=CHCH_2CH_2CH_2NHCSNHR \xrightarrow{AgNO_3} CH_2=CHCH_2CH_2CH_2NHCONHR$$

IV: R = H
V: R = 1-naphthyl

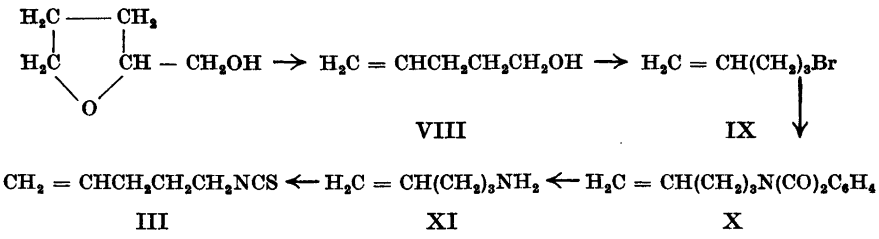
VI

H_2 | Pt

$$CH_3CH_2CH_2CH_2CH_2NH_2 + RNCO \longrightarrow CH_3CH_2CH_2CH_2CH_2NHCONHR$$

VII

As further corroboration the new natural *iso*thiocyanate (III) has been synthesized along conventional lines as shown in the following scheme.



4-Penten-1-ol (VIII), prepared from tetrahydrofurfuryl alcohol [7], was transformed into 5-bromo-1-pentene (IX) as described by La Forge *et al.*[8] N-(4-Pentenyl)-phthalimide (X), obtained according to the described direction [9] as a solid, m. p. 34°, with correct analysis (Ref.[9] m. p. 40°), afforded the requisite 4-pentenylamine (XI), b. p. 98°, on hydrazinolysis. The amine was characterized as an acid oxalate hemihydrate, m. p. 139°. These data deviate somewhat from those previously recorded. v. Braun [10] prepared the amine, b. p. 91—94°, by thermal decomposition of 5-aminopentyltrimethylammonium hydroxide, whereas Paul and Cottin [11] reported the b. p. 105—106° for the anhydrous amine which was also characterized as an acid oxalate, m. p. 129—130°. They apparently ignored the water of crystallization in this salt. Pure 4-pentenyl *iso*thiocyanate (III) was prepared from (XI) by a modification [12] of Dyson's thiophosgene method [13] and converted into 1-(1-naphthyl)-3-(4-pentenyl)-thiourea (V) in the usual way. Analyses, mixed melting point determination and infra-red spectra served to establish the identity of the naphthylthioureas derived from the natural and the synthetic mustard oil.

Three homologous, straight-chain *iso*thiocyanates possessing a terminal double bond, (I), (II) and (III), have thus been recognized in Nature, the first as the aglucone of the classical and widely distributed glucoside sinigrin. It is interesting that the analogous ω-methylthio compounds, *viz.* 3-methylthiopropyl [14], 4-methylthiobutyl [15] and 5-methylthiopentyl [16] *iso*thiocyanate as well as various higher oxidation states of these, have been encountered also as naturally occurring aglucones. This fact suggests a common biogenetic origin, a possibility which is being further considered in this laboratory. As pointed out in a previous paper [21], 4-pentenyl *iso*thiocyanate seems to occur also in various species of the genus *Alyssum*.

Paper chromatography of the *iso*thiocyanate glucosides in rape seed extracts, essentially following the directions given by Schultz and Gmelin [17], indicates the presence of six individual components, three of which appear in very small amounts only (Fig. 1) *. The same pattern has been obtained for several seed samples of different provenance and is therefore regarded as

* In paperchromatographic survey work Gmelin [18] noticed the occurrence of five glucoside spots in a seed extract of *B. napus*. More recent data from the same laboratory [19], however, indicate the presence of only two glucosides in the same material. According to the paperchromatographic values, these may be interpreted as the chief constituents, *viz.* progoitrin [22] (glukorapiferin [23]) and gluconapin [1, 2, 26], respectively.

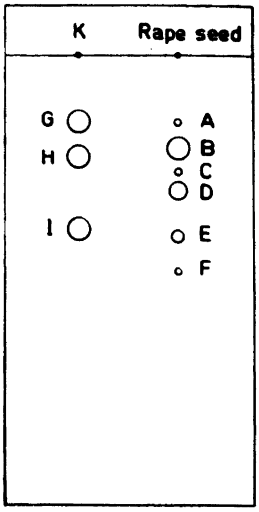


Fig. 1. Schematic, descending paper chromatogram of rape seed iso*thiocyanate glucosides in* n*-butanol : ethanol : water (4 : 1 : 4) (upper phase). A—F: see text. K: reference solution, containing G : glucoiberin [20], H : sinigrin and I : glucotropaeolin (from seeds of* Tropaeolum majus).

characteristic for the species *Brassica napus* L., including several varieties. The component of lowest R_F-value, (A), appears in traces only and may be identical with, or closely related to, glucoiberin, the glucoside previously isolated from *Iberis amara* L.[20] and containing (—)-3-methylsulphinylpropyl *iso*thiocyanate as the aglucone (*cf.* also Ref.[21]). Then follows a spot, (B), attributable to the 2-hydroxy-3-butenyl *iso*thiocyanate glucoside, recently isolated by Greer [22] in crystalline form under the name progoitrin, and almost certainly identical with the glukorapiferin of Schultz and Wagner [23], isolated from seed of a *B. napus* variety and characterized by analysis and melting point of a crystalline pentaacetate.* Enzymic hydrolysis of this glucoside is responsible [22,24,30] for the production of the goitrogenic (—)-5-vinyl-2-oxazolidinethione [25], previously isolated from seeds or fresh parts of various *Brassica* species including rape. A very weak glucoside-spot, (C), can safely be attributed to sinalbin, a long known glucoside containing *p*-hydroxybenzyl *iso*thiocyanate, on account of the correct R_F-value in conjunction with a positive reaction on spraying with diazotized sulphanilic acid [18]. This glucoside has been observed in all *B. napus* species investigated but is consistently present in traces only. Then follow the glucosides giving rise to the volatile mustard oils. First, the progenitor, (D), of the predominant 3-butenyl *iso*thiocyanate [1, 2] for which we have adopted the name gluconapin, introduced in 1905 by Ter Meulen [26] for the glucosidic precursor of the supposedly homogeneous though unidentified volatile mustard oil of rape. With a considerably higher R_F-value follows the 4-pentenyl *iso*thiocyanate glucoside (E) for which we propose the name *glucobrassicanapin*. Lastly, a very faint spot, (F), is consistently apparent, attributable to gluconasturtiin, the 2-phenylethyl *iso*thiocyanate glucoside, an assumption supported by the results of André and Delaveau [5].

* *Added in proof*: Recently, the same authors [30] have indeed presented chemical evidence for the identity of the anions of glukorapiferin and progoitrin.

This picture is regarded as an essentially complete and correct account of the *iso*thiocyanates in rape seeds, a subject of much discussion in the literature through more than five decades. Other species of the genus *Brassica* have been similarly studied in this laboratory. The results will be presented in a forthcoming communication, together with some attempts to correlate the cytological and chemical classification within this important genus.

EXPERIMENTAL

All melting points are uncorrected and determined in capillary tubes in a slowly heated bath.

Isolation. Finely divided rape seed cake (30 kg) was suspended in water (60 l), buffered to pH 6.6 with KH_2PO_4(850 g) and Na_2HPO_4, $2H_2O$ (320 g). Milled seed of white mustard *(Sinapis alba* L.) (5 kg) was added, the suspension was kept at room temperature for 18 hours and steam distilled until about 50 l were collected. The distillate was saturated with salt and extracted three times with a total of 6 l of ether. The extract was dried and the solvent removed over a Vigreux column. The residue was subjected to fractional distillation at 12 mm, using an all-glass column packed with glass-helices and equipped with a total reflux variable take-off head. A forerun, *ca.* 1 g, b. p. 43—60°, was followed by a mustard oil fraction, b. p. 61—70°, redistilled to give 14 g of pure 3-butenyl *iso*thiocyanate (b.p. 64° at 12 mm). Then came a small interfraction (0.6 g), b. p. 71—75°, followed by essentially pure 4-pentenyl *iso*thiocyanate (1.07 g), b. p. 75°. All samples were checked by transformation into thioureas followed by paper chromatography of these in water-saturated chloroform according to our usual method [27]. The last fraction showed a very faint spot only of the 3-butenylthiourea in addition to that of 4-pentenylthiourea and was used directly for preparing the following derivatives.

1-(4-Pentenyl)-thiourea (IV). Treatment of a small sample of the preceding mustard oil with ethanolic ammonia at room temperature furnished a brownish oil which was taken up in benzene. Pentane was added to turbidity, and after one week in the ice-box colourless plates separated, embedded in oily material which was removed by pressing between filter paper. Pure N-(4-pentenyl)-thiourea crystallized from water in thin, nacreous plates, m. p. 43.5—44.0° (Ref.[5] 42.5—43.5°). (Found: C 49.75; H 8.31; N 19.46. Calc. for $C_6H_{12}N_2S$: C 49.97; H 8.39; N 19.43). On descending paper chromatography in water-saturated chloroform an R_{Ph}-value [27] of 0.96 was determined.

The infra-red spectrum, determined in a potassium bromide disc, showed prominent bands at 2.90 (v.s.), 3.27 (m.), 6.08 (v.s.), 6.35 (v.s.), 6.79 (s.), 6.98 (s.), 7.29 (v.s.), 7.60 (m.), 8.27 (m.), 8.54 (m.), 8.79 (w.), 10.01 (s.), 10.92 (v.s.), 11.78 (w.), 13.46 (w.) and 14.06 μ (m.). The bands at 10.01 and 10.92 μ are particularly important in this connexion because they strongly indicate the presence of a vinyl grouping [29]. The ultra-violet absorption spectrum in ethanol was of the usual type, λ_{max} 242 mμ (ε_{max} 14 150), λ_{min} 225 mμ (ε_{min} 5 100).

1-(1-Naphthyl)-3-(4-pentenyl)-thiourea (V). A solution of the natural mustard oil (50 mg) and freshly recrystallized 1-naphthylamine (65 mg) in ethanol (3 ml) was heated to reflux for 2 hours. Removal of the solvent left an oil which crystallized on being rubbed with a few drops of ethanol. Two recrystallizations from aqueous ethanol afforded the pure thiourea (73 mg) as needles, m. p. 102°. (Found: C 70.95; H 6.60; N 10.25. Calc. for $C_{16}H_{18}N_2S$: C 71.06; H 6.71; N 10.36). A week later, the m. p. was found to be 126°, obviously a case of dimorphism. A sample prepared from synthetic 4-pentenyl *iso*thiocyanate and 1-naphthylamine (see below) still appeared as the low-melting form after two recrystallizations from aqueous ethanol, but changed to the high-melting modification on a third recrystallization from the same solvent. Once the high-melting form had appeared, it was no longer possible to realize the low-melting modification. Polymorphism has frequently been observed within the class of thioureas, the present case closely resembling that of *e. g.* 1-(*m*-methoxybenzyl)-3-phenyl-thiourea, recently discussed by Ettlinger and Lundeen [28].

Synthesis of 4-pentenyl isothiocyanate (III). The reaction of 4-penten-1-ol [7] (VIII) and phosphorus tribromide in pyridine, following described directions [8], furnished in somewhat lower yield (70 %) 5-bromo-1-pentene (IX), b. p. 58° at 70 mm. The latter was converted into N-(4-pentenyl)-phthalimide (X) in 75 % yield according to Kharasch and Fuchs [9], b. p. 163° at 2 mm (lit.[9] 155—157° at 2 mm). A sample of the phthalimide, recrystallized twice from aqueous ethanol, melted at 34° (lit.[9] 40°). (Found: C 72.45; H 6.15; N 6.49. Calc. for $C_{13}H_{13}NO_2$: C 72.56; H 6.09; N 6.51).

Hydrazinolysis was performed by refluxing the phthalimide (26 g) and hydrazine hydrate (6.7 ml) in ethanol (150 ml) for one hour. The suspension was digested for another hour at 100° with 500 ml of 6 N HCl, whereupon the ethanol was removed by distillation. The phthalylhydrazide was filtered off, the filtrate concentrated to about 200 ml and made strongly alkaline. Salt was added to saturation, the amine extracted with ether, the extract dried over KOH pellets, and the ether removed over a column. The crude 4-pentenylamine (8.5 g) was further dried over fresh KOH for two days and distilled in a system protected from the atmosphere, b. p. 98°. Analysis indicated that water was still present in the product, though less than corresponding to a monohydrate. (Found: N 15.0. Calc. for $C_5H_{11}N$: N 16.5; for $C_5H_{13}NO$: N 13.6). The amine acid oxalate hemihydrate formed colourless needles from ethanol, m. p. 139.0—139.5° (lit.[11] 129—130°). (Found: C 45.70; H 7.47; N 7.61. Calc. for $C_5H_{11}N$, $C_2H_2O_4$, 0.5 H_2O: C 45.63; H 7.66; N 7.61). Drying of the salt at 100° over P_2O_5 resulted in weight loss, but the extremely hygroscopic nature of the anhydrous product made a quantitative determination of the water of crystallization impossible.

To a solution of thiophosgene (2.08 g) in chloroform (25 ml) was added another solution of 4-pentenylamine (1.7 g) in water (7 ml). 1 N NaOH (39.5 ml) was slowly added to the stirred solution, and the yellow colour gradually disappeared. The chloroform layer was dried, the solvent removed and the residue distilled *in vacuo*. Pure 4-pentenyl *iso*thiocyanate III) (0.9 g) was obtained as a colourless oil possessing a characteristic mustard oil smell, though less penetrant than that of 3-butenyl *iso*thiocyanate, b. p. 75° at 12 mm, n_D^{25} 1.5118 (lit. 73.7°/11.5 mm[4], 76—77°/10 mm[5]; n_D^{18} 1.5187 [4], n_D^{20} 1.5172 [5]). (Found: C 56.30; H 7.28; N 10.97. Calc. for C_6H_9NS: C 56.65; H 7.13; N 11.01).

The synthetic *iso*thiocyanate was transformed into its thiourea derivative with 1-naphthylamine as described above for the natural mustard oil. The stable modification was obtained as colourless needles, m. p. 125°, alone or in admixture with the natural derivative. (Found: C 71.15; H 6.67; N 10.40. Calc. for $C_{16}H_{18}N_2S$: C 71.06; H 6.71; N 10.36). The infra-red spectra were determined for both specimens and found to be identical.

1-(1-Naphthyl)-3-(4-pentenyl)-urea (VI). The thiourea (714 mg), dissolved in ethanol (40 ml), was treated with a solution of silver nitrate (896 mg) in 75 % ethanol (15 ml), resulting in instantaneous separation of silver sulphide. Sodium hydroxide (1 N) was added dropwise to neutral reaction, and the mixture was heated to reflux for two hours. The suspension was filtered through Celite, the precipitate thoroughly washed with ethanol, and the joint filtrate and washing liquor diluted with half the volume of water, resulting in precipitation of the crystalline urea. The product was recrystallized twice from 90 % ethanol and pure 1-(1-naphthyl)-3-(4-pentenyl)-urea (VI) separated as tiny, colourless needles (470 mg), m. p. 152°. (Found: C 75.30; H 7.13; N 11.10. Calc. for $C_{16}H_{18}N_2O$: C 75.58; H 7.13; N 11.02).

1-(1-Naphthyl)-3-pentyl-urea (VII). On mixing equimolecular amounts of naphthyl *iso*cyanate and *n*-pentylamine in ether solution, 1-(1-naphthyl)-3-pentylurea crystallized spontaneously. It separated from aqueous ethanol in colourless needles, m. p. 146.5—147.0°. (Found: C 74.45; H 7.96; N 11.15. Calc. for $C_{16}H_{20}N_2O$: C 74.74; H 7.87; N 10.93).

No depression of the m. p. was observed when this product was mixed with a specimen prepared by catalytic hydrogenation of the corresponding unsaturated urea described above. The reduction was performed in ethanolic solution at ordinary pressure with Adam's platinum catalyst. The infra-red spectra of the two specimens were determined and found to be identical.

Paper chromatography. In the present work, all paper chromatograms were run by the descending technique on Whatman paper No. I in a constant temperature room. Methanolic extracts of the various seed samples were employed without further puri-

fication in the paperchromatographic analyses of the glucoside contents, the spraying and development being performed essentially as described elsewhere[17]. The identity of (B) (Fig. 1) as progoitrin (glukorapiferin) was proved in the following way. A rape seed extract was applied to an 18 cm broad paper strip as a band and chromatographed in the usual way. A small strip, cut from each edge, was developed in order to locate the component (B). The corresponding section of the main strip was cut out, eluted with water and the eluate subjected to enzymic hydrolysis by adding a droplet of a myrosinase solution. After 4 hours, the solution was extracted with ether, the solvent removed and the ultra-violet absorption spectrum determined for an ethanolic solution of the residue. An absorption pattern was obtained, identical with that previously reported for 5-vinyl-2-oxazolidinethione [25]. The other glucoside spots on the paper chromatogram were found devoid of characteristic absorption when tested in a similar way.

Microanalyses were performed in this laboratory by Mr. P. Hansen. Valuable assistance of Mr. I. Larsen in the preliminary experiments is acknowledged. We wish to thank *Dansk Sojakagefabrik* Inc. for the gift of rape seed cake, and *Pharmacia Inc.* for placing at our disposal the necessary technical equipment.

The work is part of investigations supported by *Statens Almindelige Videnskabsfond (The Danish State Research Foundation)* and *Carlsbergfondet (The Carlsberg Foundation)*.

REFERENCES

1. Kjær, A., Conti, J. and Jensen, K. A. *Acta Chem. Scand.* **7** (1953) 1271.
2. Ettlinger, M. G. and Hodgkins, J. E. *J. Am. Chem. Soc.* **77** (1955) 1831.
3. Jørgensen, G. *Landwirtsch. Vers. Sta.* **51** (1899) 311, **52** (1899) 269.
4. Schmalfuss, H. *Forschungsdienst, Sonderheft* **1** (1936) 37.
5. André, E. and Delaveau, P. *Oléagineux* **9** (1954) 591; *cf.* also: Delaveau, P. *Contribution a l'étude biochimique de quelques graines de Crucifères* (Brassica *divers*) *et de leur germination* (Thesis), University, Paris 1954.
6. Kjær, A., Conti, J. and Larsen, I. *Acta Chem. Scand.* **7** (1953) 1276.
7. Brooks, L. A. and Snyder, H. R. *Org. Syntheses Coll. Vol.* **3** (1955) 698.
8. LaForge, F. B., Green, N. and Gersdorff, W. A. *J. Am. Chem. Soc.* **70** (1948) 3707.
9. Kharasch, M. S. and Fuchs, C. F. *J. Org. Chem.* **9** (1944) 359.
10. v. Braun, J. *Ann.* **382** (1911) 1.
11. Paul, R. and Cottin, H. *Bull. soc. chim. France* [5] **4** (1937) 933.
12. Kjær, A., Marcus, F. and Conti, J. *Acta Chem. Scand.* **7** (1953) 1370.
13. Dyson, G. M. and George, H. J. *J. Chem. Soc.* **125** (1924) 1702.
14. Kjær, A., Gmelin, R. and Larsen, I. *Acta Chem. Scand.* **9** (1955) 1143.
15. Kjær, A. and Gmelin, R. *Acta Chem. Scand.* **9** (1955) 542.
16. Kjær, A., Larsen, I. and Gmelin, R. *Acta Chem. Scand.* **9** (1955) 1311.
17. Schultz, O.-E. and Gmelin, R. *Z. Naturforsch.* **8b** (1953) 151.
18. Gmelin, R. *Präparative und analytische Versuche über Senfölglucoside* (Diss.) University, Tübingen 1954.
19. Schultz, O.-E. and Wagner, W. *Z. Naturforsch.* **11b** (1956) 73.
20. Schultz, O.-E. and Gmelin, R. *Arch. Pharm.* **287/59** (1954) 404.
21. Kjær, A. and Gmelin, R. *Acta Chem. Scand.* **10** (1956) 1100.
22. Greer, M. A. *J. Am. Chem. Soc.* **78** (1956) 1260.
23. Schultz, O.-E. and Wagner, W. *Arch. Pharm.* **288/60** (1955) 525.
24. Kjær, A., Gmelin, R. and Boe Jensen, R. *Acta Chem. Scand.* **10** (1956) 432.
25. Astwood, E. B., Greer, M. A. and Ettlinger, M. G. *J. Biol. Chem.* **181** (1949) 121.
26. Ter Meulen, H. *Rec. trav. chim.* **24** (1905) 475.
27. Kjær, A. and Rubinstein, K. *Acta Chem. Scand.* **7** (1953) 528.
28. Ettlinger, M. G. and Lundeen, A. J. *J. Am. Chem. Soc.* **78** (1956) 1952.
29. Bellamy, L. J. *The Infra-red Spectra of Complex Molecules*, Methuen & Co. Ltd., London, 1954.
30. Schultz, O.-E. and Wagner, W. *Arch. Pharm.* **289/61** (1956) 597.

Received July 2, 1956.

ACTA CHEMICA SCANDINAVICA 10 (1956) 1372—1376

Die Capillaritätscorrection von Routine-Viscosimetern

CARL DRUCKER

Physikalisch-chemisches Institut der Universität, Uppsala, Schweden

Durch Beobachtung im rein cylindrischen Teile eines Normalviscosimeters mit gleich weiten Gefässen können die für Capillareffecte corrigierten relativen Auslaufzeiten auf vorläufig 0,05 % genau bestimmt werden. Aus solchen Messungen ergeben sich die Factoren, mittels deren die bei beliebig geformten Routineinstrumenten gefundenen relativen Totalauslaufzeiten zu corrigieren sind. Diese Correctionen können recht wohl 0,5 bis 1 % betragen und dürfen deshalb nicht vernachlässigt werden. Da sie bei beiderseits cylindrischen, gleichweiten Gefässen — mit kurzen conischen Endteilen — wesentlich geringer sind als bei allen anderen Formen, so sollen ungleich weite cylindrische sowie kugelähnliche und doppeltconische Gefässe auch bei gewöhnlichen Routineinstrumenten nach Möglichkeit vermieden werden.

Wenn die Auslaufzeit t einer Flüssigkeit in einem Ostwaldschen Capillarviscosimeter mit der einer Standardsubstanz verglichen wird, so ist die relative Auslaufzeit ($t/t_0 = z$) mit einem Fehler behaftet, der von den Gefässdimensionen und den beiden Capillaritätsconstanten a^2 und a_0^2 abhängt. Um diesen sowohl klein zu halten wie experimentell bestimmen zu können, verfährt man am besten so, dass man beiden Gefässen des Instrumentes cylindrische Form mit gleich grossen Radien gibt.

NORMALVISCOSIMETER

Die Radien der beiden cylindrischen Rohre, deren conische Übergangsteile möglichst niedrig gehalten sind (s. Fig. 1) seien $r_0 = r_u$; ausser den üblichen Marken a und b seien auf dem oberen Gefässe noch zwei feine Ringmarken A und B so angebracht, dass der Meniscus bei A resp. bei B sich völlig im cylindrischen Teile befindet.

Beträgt die mittlere Meniscushöhe einer Standardflüssigkeit — bei den folgenden Versuchen stets Wasser — m_0, so gilt für den Auslauf von A bis B eine mittlere Druckhöhe

$$H_0=\frac{1}{2}\Big\{[(A+m_0)-(A'+m_0)]+[(B+m_0)-(B'+m_0)]\Big\}=\frac{1}{2}[(A-A')+(B-B')]$$

also derselbe Wert, wie wenn gar kein Meniscus vorhanden wäre. Bei Füllung des Instrumentes mit genau demselben Volumen einer anderen Flüssigkeit gilt eine Meniscushöhe m, und stellt man auch hier den oberen Meniscus auf A ein, so steht der untere bei A' + $2(m_0 - m)$ und H_0 geht über in

$$H = \frac{1}{2}\left\{(A + m) - [(A' + m) + 2(m_0 + m)] + (B + m) - [(B' + m) + 2(m_0 - m)]\right\}$$

$$= H_0[1 - \frac{2(m_0 - m)}{H_0} = H_0\,(1 - \lambda_2).$$

Ist $m_0 - m$, so zeigt diese Flüssigkeit eine Auslaufzeit T, welche im Vergleich zu der der Standardsubstanz, T_0, zu gross ist, und ihre wahre relative Auslaufzeit beträgt nicht $Z_m = T/T_0$ sondern $Z'_m = Z_m\,(1 - \lambda_2)$. (Dieser Effect wurde früher [3] als Verdrängungscorrection bezeichnet.) Bestimmt man auch die relative Zeit Z_t des Totalauslaufes zwischen a und b, so ist diese mit dem Factor $F' = Z'_m/Z_t$ zu corrigieren.

Diese vom Einflusse der Capillaritätseffecte befreiten wahren relativen Auslaufzeiten Z'_m müssen mit jedem Normalinstrumente gleich gross gefunden werden, falls die Versuchsbedingungen dieselben sind. Ungleiche Verticalorientierung der Instrumente oder ungenaue Füllung kann Abweichungen verursachen.

Versuche. In einem so gebauten Rohr (Nr 18) mit den Radien $r_0 = r_u = 4{,}20$ mm und der Druckhöhe $H_0 = 158$ mm wurde, mit Wasser als Bezugssubstanz, Folgendes gefunden (Tabelle 1).

Tabelle 1.

	a_2	m	T	t	λ_2	Z_m	Z'_m	Z_t	F'
Wasser	14,68	0,91	1670,8	2171,0	—	—	—	—	—
Dichloressigsäure .. 6,7 %	11,72	0,86	1870,2	2466,7	0,0006	1,1193	1,1186	1,1179	1,0006
o-Xylol	6,80	0,71	1622,9	2101,4	0,0025	0,9713	0,9689	0,9678	1,0013
Aethylenbromid ..	3,61	0,53	1396,5	1801,7	0,0048	0,8358	0,8318	0,8299	1,0023

Die Meniscushöhen m sind in bekannter Weise berechnet [1,2]; aus ihnen ergaben sich die jeweiligen Werte von λ_2.

Ein anderes Normalinstrument (Nr X) von etwas abweichenden Dimensionen ($r_0 = r_u = 5{,}06$ mm, $H_0 = 168$ mm) ergab für F' die Zahlen 1,0002, 1,0012, 1,0020, also fast identisch mit Nr. 18. Die Unsicherheit dieses Factors dürfte 0,0005 nicht erreichen.

F' weicht hier nur wenig von 1 ab, steigt jedoch bei beiden Rohren ein wenig an, antibat zur Capillaritätsconstanten. Dieser Gang braucht nicht in allen Fällen vorzuliegen, da er von Form und Grösse der beiden conischen Endteile mitbestimmt wird. Dies ging bereits aus den früher mitgeteilten

Untersuchungen hervor und kann auch aus der Tabelle 2 entnommen werden. Diese gilt, bei denselben Flüssigkeiten wie oben, für den Totalauslauf in einem Rohr (Nr VI) mit ebenfalls beiderseits gleichen Radien $r_0 = r_u = 7{,}50$ mm.

Tabelle 2.

	t	Z_t	$F = Z'_m / Z_t$
Wasser	1015,4	—	—
Dichloressigsäure 6,7 % ..	1132,8	1,1167	1,0026
o-Xylol	981,6	0,9668	1,0024
Aethylenbromid	843,8	0,8311	1,0010

Die wahren relativen Zeiten Z'_m sind aus Tabelle 1 entnommen, und die in diesem Falle merklich verschiedene Grösse der beiden conischen Teile macht sich in dem umgekehrten Gange von F bemerklich.

Trotzdem kann auch dieses Instrument als »secundäres» Normalinstrument verwendet werden, nachdem seine eigenen Correctionsfactoren ermittelt sind. Es bietet den Vorteil, dass seine Totalauslaufzeit viel kürzer ist als die des primären Instrumentes Nr 18.

ROUTINEVISCOSIMETER

Bei laufenden Messungen verwendet man fast immer anders gebaute Instrumente. Ihre Gefässe sind ungleich weit (Fig. 2, 3) und, wenigstens die oberen, kugelähnlich (Fig. 3) oder doppeltconisch. Infolge dessen ist die Differenz der Meniscushöhen, $m_0 - m$, nicht constant, sondern ändert sich während des Auslaufes beständig und zwar in unberechenbarer Weise.

Die Correctionsfactoren müssen also in diesen Fällen mit Hilfe der in den Normalinstrumenten gewonnenen Resultate ermittelt werden. Über die Grösse, welche sie annehmen können, mögen einige Beispiele Auskunft geben.

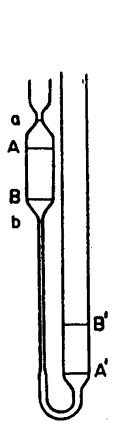
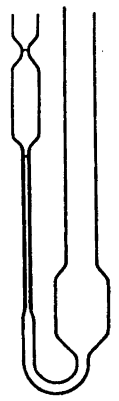
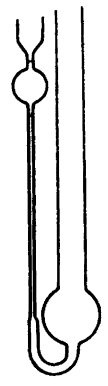


Fig. 1


Fig. 2


Fig. 3

Ein Viscosimeter (Nr XIV) mit beiderseits cylindrischen Rohren, aber verschieden grossen Radien $r_0 = 4{,}01$ und $r_u = 11{,}4$ mm (vgl. Fig. 2), zeigte folgende Totalauslaufzeiten z_t resp. z (s. Tab. 3), aus welchen sich mittels der am Normalinstrumente Nr 18 gewonnenen Zahlen (vgl. Tab. 1) die Correctionsfactoren $F = Z'_m/z_t$ ergeben. Wie man sieht, sind diese weit grösser als F' bei Nr 18.

Tabelle 3.

	t	z_t	Z'_m	$F' = Z'_m/z_t$
Wasser	1061,0	—	—	—
Dichloressigsäure 6,7 %	1180,9	1,1130	1,1186	1,0051
o-Xylol	1020,0	0,9613	0,9689	1,0079
Aethylenbromid	874,7	0,8244	0,8318	1,0091

Ein anderes Instrument (Nr II) mit nahezu kugelförmigen Gefässen, deren unteres etwa doppelt so viel Flüssigkeit fasste wie das obere (vgl. Fig. 3), wurde mit zwei verschiedenen Füllungen v_1 und $v_2 = 2\ v_1$ untersucht. Aus Tab. 4 geht hervor, dass das Verhältnis t_1/t_2 deutlich von der Füllhöhe abhängt, weil die Druckhöhen sich mit den Gefässradien ändern, und zwar, wegen der Verschiedenheit der Capillaritätsconstanten, in ungleicher Weise. Die ebenfalls auf Nr 18 bezogenen Correctionsfactoren F_1 und F_2 weichen wiederum stark von 1 ab und sind sogar unter einander verschieden.

Tabelle 4.

	t_1	t_2	t_2/t_1	Z'_m	z_1	z_2	$F_1 = \frac{Z'_m}{z_1}$	$F_2 = \frac{Z'_m}{z_2}$
Wasser	672,2	708,7	1,0536	—	—	—	—	—
Dichloressigsäure 6,7 %	747,9	789,7	1,0558	1,1186	1,1125	1,1142	1,0055	1,0040
o-Xylol	648,7	685,3	1,0563	0,9689	0,9650	0,9670	1,0050	1,0020
Aethylenbromid	556,0	587,8	1,0571	0,8318	0,8270	0,8293	1,0059	1,0031

In dieser Weise lassen sich also die durch die Capillaritätseffecte bedingten Correctionsfactoren des Totalauslaufes von Routineviscosimetern ermitteln. Sollten etwa bei solchen Aichungen andere Vergleichsflüssigkeiten als hier verwendet werden, so braucht man nur die erforderlichen Werte von F' durch Interpolation nach Massgabe der Capillaritätsconstanten zu bestimmen *.

Da übrigens diese Factoren nur wenig temperaturempfindlich sind, wird man die etwa wie hier bei 25° gefundenen Werte auch bei 20° oder 30° anwenden dürfen.

* Wäre etwa bei Tabelle 1 eine Substanz mit $a^2 = 9{,}00$ mit Wasser verglichen worden, so hätte sich für diese $F' = 1{,}0010$ ergeben.

Routineviscosimeter mit ungleich weiten, nicht cylindrischen Rohren können also Correctionen der relativen Auslaufzeiten um ½ % oder mehr verlangen. Diese dürfen vielleicht bisweilen vernachlässigt werden, doch nicht immer, z.B. nicht, wenn es sich um die Eigenviscosität einer stark capillaractiven Substanz in verdünnter Lösung handelt. Ein solcher Fall sei hier angeführt.

Es wurde in den Viscosimetern (II) und (18) die stark capillaractive Hendekafluorhexylsäure, $C_5F_{11}COOH$, in verdünnter wässriger Lösung gemessen (0,266 %, $a^2 = 11{,}7$.) In Nr II betrug die Auslaufzeit für Wasser 672,0 sec., für die Lösung 673,3 sec., somit $z_t = 1{,}0019$. Im cylindrischen Teile von Nr 18 wurde gefunden 1670,0 resp. 1683,4, also $Z_m = 1{,}0074$. Da λ_2 sich hier zu 0,0006 berechnet, wird $Z'_m = 1{,}0068$. Die Eigenviscosität, wie sie aus Z'_m folgt, ist demnach im Verhältnis 0,0068/0,0019 = 3,5 grösser als nach dem uncorrigierten Werte z_t, dessen Fehlerhaftigkeit hier besonders deutlich zu Tage tritt.

Je näher also die relative Viscosität η/η_0 einer Lösung an 1 liegt, d.h. je verdünnter diese ist, um so falscher ergibt sich die Eigenviscosität, wenn man sie aus dem uncorrigierten Resultate des Routineinstrumentes berechnet, statt dem richtigen Werte des Normalviscosimeters.

LITTERATUR

1. Drucker, C. *Svedberg-Festschrift* **1944**, S. 94.
2. Drucker, C. *Acta Chem. Scand.* **2** (1948) 890.
3. Drucker, C. *Acta Chem. Scand.* **2** (1948) 883.

Eingegangen am 3. Juli 1956.

ACTA CHEMICA SCANDINAVICA 10 (1956) 1377—1380

Synthesis of Compounds Related to Muscarufin

II. 3,6-Dihydroxy-2,5-bis-(2-carboxyphenyl)-benzoquinone

MARTIN NILSSON

Organisk-kemiska Institutionen, Kungl. Tekniska Högskolan, Stockholm, Sweden

3,6-Di-iodo-2,5-dimethoxybenzoquinone has been converted into 3,6-di-iodo-1,2,4,5-tetramethoxybenzene, which on Ullmann coupling with methyl 2-bromobenzoate afforded 2,3,5,6-tetramethoxy-1,4-bis-(2-carbomethoxyphenyl)-benzene (I). This was transformed further into 3,6-dimethoxy-2,5-bis-(2-carbomethoxyphenyl)-benzoquinone (II) and 3,6-dihydroxy-2,5-bis-(2-carboxyphenyl)-benzoquinone (III). The last mentioned compound is related to the fungal pigments muscarufin and polyporic acid.

In the previous communication [1] the synthesis of 2,5-bis-(2-carbomethoxyphenyl)-benzoquinone was reported. The present paper deals with the synthesis of 3,6-dihydroxy-2,5-bis-(2-carboxyphenyl)-benzoquinone (III), which is interesting as an analogue of both muscarufin and polyporic acid although it has not been found in Nature.

Earlier it had been found difficult to introduce further substituents on the central nuclei of 2,5-dimethoxy-1,4-bis-(2-carbomethoxyphenyl)-benzene and 2,5-bis-(2-carbomethoxyphenyl)-benzoquinone. The most suitable approach to the synthesis of the dihydroxyquinone III was therefore considered to be an Ullmann coupling of methyl 2-bromobenzoate with a *p*-di-iodo compound already possessing the essential features of the central nucleus.

Preliminary experiments aiming at the direct iodination of 1,2,4,5-tetramethoxybenzene to 3,6-di-iodo-1,2,4,5-tetramethoxybenzene were unsuccessful and interest was therefore turned to the use of 3,6-di-iodo-2,5-dimethoxybenzoquinone as a starting material. This compound was prepared in poor yield from iodo-anil *via* di-iodo-dimethoxybenzoquinone di-methyl hemiacetal according to Jackson and Bolton [2]. Reduction with phenyl hydrazine and methylation of the hydroquinone thus obtained gave 3,6-di-iodo-1,2,4,5-tetramethoxybenzene.

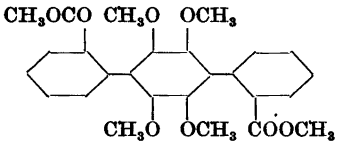
Ullman coupling with methyl 2-bromobenzoate then afforded 2,3,5,6-tetramethoxy-1,4-bis-(2-carbomethoxyphenyl)-benzene (I) in good yield. The product, however, was found to be a mixture of two different types of

crystals, which could not be completely separated. They were readily interconvertible and it may be presumed that they are the *cis*- and *trans*-isomers arising from hindered rotation, the energy barrier between them being low enough to permit rapid equilibration. Similar although stable isomers have been described for 3,6-dibromo-2,5-dihydroxy-1,4-bis-(2,4-dimethylphenyl)-benzene and its derivatives [3].

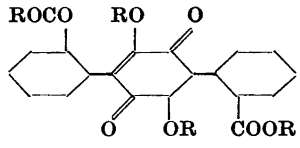
2,3,5,6-Tetramethoxy-1,4-bis-(2-carbomethoxyphenyl)-benzene on cautious treatment with nitric acid yielded 3,6-dimethoxy-2,5-bis-(2-carbomethoxyphenyl)-benzoquinone (II), which on alkaline hydrolysis gave the desired 3,6-dihydroxy-2,5-bis-(2-carboxyphenyl)-benzoquinone (III). This compound is a high melting solid, which can be recrystallised from dioxan giving crystals containing five moles of solvent of crystallisation. It is somewhat soluble in hot water giving a bluish solution and it dissolves readily in aqueous alkali to give an intense violet colour.

The dihydroxyquinone III on reductive acetylation afforded a dilactone diacetate (IV). This behaviour is analogous to that of 2,5-bis-(2-carbomethoxyphenyl)-benzoquinone but is in contrast to that of muscarufin, which on similiar treatment is reported to give a triacetate (*cf.* Ref. [1]).

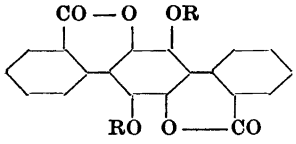
The controlled action of hydrobromic acid on 2,3,5,6-tetramethoxy-1,4-bis-(2-carbomethoxyphenyl)-benzene afforded a dimethoxy dilactone (V) and even when the dihydroxyquinone III itself was heated lactonisation occurred to give a quinonoid dilactone (VI), which was however far less resistant to hydrolysis than the above mentioned dilactones; it dissolved fairly rapidly in cold, dilute aqueous alkali.



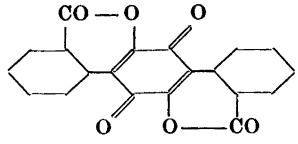
I



II R = CH_3-
III R = H-



IV R = CH_3CO-
V R = CH_3-



VI

EXPERIMENTAL

All melting points are uncorrected.

3,6-Di-iodo-2,5-dimethoxy-1,4-dihydroxybenzene. Bromo-anil was treated with an excess of sodium or potassium iodide (in successive portions) in boiling acetone or ethanol [4,5]. A crude iodo-anil was obtained, which was extracted with hot acetic acid to remove part of the bromo-iodoquinones present, and then recrystallised from large

volumes of ethyl acetate or benzene. The yield of purified iodo-anil was 20—40 %, large scale preparations giving the smaller yields. Treatment with sodium methoxide in methanol [5] (equivalent amount or a moderate excess) afforded the amorphous di-iodo-dimethoxybenzoquinone dimethyl hemiacetal, which on heating with acetic anhydride [2] gave 3,6-di-iodo-2,5-dimethoxybenzoquinone (overall yield from iodo-anil 10—35 %). It was found to be most important to use a thoroughly purified iodo-anil; with less pure material large amounts of ill-defined by-products were obtained and the yield of di-iodo-dimethoxyquinone was considerably diminished.

3,6-Di-iodo-2,5-dimethoxybenzoquinone (7.2 g) was suspended in hot (90°) acetic acid and phenyl hydrazine (2.5 ml) added dropwise with shaking until the nitrogen evolution ceased. After cooling to room temperature the product (5.2 g) was collected and recrystallised from acetic acid to give needles, which slowly darkened in the air, m.p. 240° (decomp.). (Found: C 22.9; H 1.9; I 60.1. Calc. for $C_8H_8O_4I_2$: C 22.8; H 1.9; I. 60.2.)

3,6-Di-iodo-1,2,4,5-tetramethoxybenzene. 3,6-Di-iodo-2,5-dimethoxy-1,4-dihydroxybenzene was dissolved in a mixture of ethanol and excess dimethyl sulphate. The solution was stirred under an atmosphere of coal gas and a 50 % solution of sodium hydroxide in water added. On addition of water the methylated product separated in almost quantitative yield. Recrystallisation from methanol (charcoal) gave long needles, m.p. 136—137°. (Found: C 27.2; H 2.8; I 55.6. Calc. for $C_{10}H_{12}O_4I_2$: C. 26.7; H 2.7; I 54.4.)

2,3,5,6-Tetramethoxy-1,4-bis-(2-carbomethoxyphenyl)-benzene, (I). 3,6-Di-iodo-1,2,4,5-tetramethoxybenzene (11 g), methyl 2-bromobenzoate (21 g) and copper bronze (60 g) were mixed intimately and heated to 200°; a reaction then brought the temperature up to *ca.* 270°. The reaction mixture was allowed to cool and was then exhaustively extracted with chloroform in a Soxhlet apparatus. The solvent was removed and the residue distilled *in vacuo* yielding besides dimethyl diphenate and a small amount of methyl benzoate a fraction b.p. 200—300°, 1 mm (6.6 g), which solidified to a mixture of needles and prisms on trituration with methanol. On recrystallisation from the same solvent it became evident that the two forms were crystalline modifications of the same compound. The prisms (m.p. around 130°) were apparently more stable above 30°, but below this temperature needles (m.p. about 120°) dominated in the mixture. It was not, however, possible to obtain a perfectly homegeneous sample; even after seeding and rapid separation of the various crops contaminated crystals were obtained. The interconvertibility of the forms is shown by the fact that a sample mainly consisting of one form could give a product in which the other form predominated. The product obtained after six recrystallisations from various solvents was sublimed *in vacuo* and analysed (m.p. 122—129°). (Found: C 66.5; H 5.7. Calc. for $C_{26}H_{26}O_8$; C 66.9; H 5.6.)

3,6-Dimethoxy-2,5-bis-(2-carbomethoxyphenyl)-benzoquinone, (II). Nitric acid (15 ml, *d* 1.42) was slowly added to a suspension of finely powdered 2,3,5,6-tetramethoxy-1,4-bis-(2-carbomethoxyphenyl)-benzene (0.50 g) in water (5 ml) and methanol (5 ml). The colour of the mixture turned yellowish red and the crystals dissolved. After some minutes water (50 ml) was added and after 1 h the crystalline precipitate was collected (0.43 g), and recrystallised from *n*-butyl ether and from methanol to give coarse yellow needles m.p. 178—180°. (Found: C 65.9; H 4.9. Calc. for $C_{24}H_{20}O_8$: C 66.0; H 4.6.)

3,6-Dihydroxy-2,5-bis-(2-carboxyphenyl)-benzoquinone, (III). 3,6-Dimethoxy-2,5-bis-(2-carbomethoxyphenyl)-benzoquinone (0.24 g) was added to a solution of sodium hydroxide (2 g) in water (5 ml) and ethanol (15 ml). It slowly dissolved giving a violet solution which was heated on the water bath (20 min.), cooled and acidified. The reddish precipitate was collected (0.17 g) and recrystallised from dioxan giving orange prisms, which slowly crumbled in the air giving off dioxan. They were found to contain *ca.* five moles of dioxan of crystallisation. (Found: 47.4 % loss of weight on drying *in vacuo* at 130°. Calc. for 5 moles of dioxan: 48.7 %.) When heated the dried material sublimed slowly above 280°, began to decompose at *ca.* 350° and melted with decomposition at about 370—375°. The dried material was analysed. (Found: C 63.4; H 3.3. Calc. for $C_{20}H_{12}O_8$: C 63.2; H 3.2.)

3,6-Dihydroxy-2,5-bis-(2-carboxyphenyl)-benzoquinone dilactone, (VI). On sublimation or prolonged heating *in vacuo* at 200° 3,6-dihydroxy-2,5-bis-(2-carboxyphenyl)-benzoquinone turned yellow; apparently water was given off and a dilactone formed. This compound decomposed above 350° and dissolved, although not as rapidly as the parent dihydroxyquinone, in aqueous alkali giving a violet solution. The sublimed product was analysed. (Found: C 69.6; H 2.6. Calc. for $C_{20}H_8O_6$: C 69.8; 2.3.)

3,6-Diacetoxy-2,5-dihydroxy-1,4-bis-(2-carboxyphenyl)-benzene dilactone, (V), (or possibly the isomeric 5,6-diacetoxy-2,3-dihydroxy compound). A small amount of the dihydroxyquinone III was heated under reflux for 0.5 h with acetic anhydride, fused sodium acetate and zinc dust. The white precipitate was collected and recrystallised from large volumes of acetic anhydride giving small needles, m.p. *ca.* 340° (decomp.) (Found: C 66.3; H 3.3. Calc. for $C_{24}H_{14}O_8$: C 67.0; H 3.3.)

3,6-Dimethoxy-2,5-dihydroxy-1,4-bis-(2-carboxyphenyl)-benzene dilactone, (V), (or the isomer, as pointed out for the previous substance). 2,3,5,6-Tetramethoxy-1,4-bis-(2-carbomethoxyphenyl)-benzene (0.25 g) was heated to boiling with hydrobromic acid (2 ml, *d* 1.48) and acetic acid (7 ml). The crystals dissolved immediately but after a few minutes a white precipitate appeared. Heating was continued for a total of 7 min. and the mixture allowed to cool. The precipitate (0.20 g) was recrystallised from acetic acid giving small needles, m.p. *ca.* 316°. (Found: C 70.4; H 4.2. Calc. for $C_{22}H_{14}O_6$: C 70.6; H 3.8.)

If the demethylation procedure was extended over several hours complete demethylation apparently occurred. The product obtained was rather sensitive to air and was partially oxidised on attempts to recrystallise it from acetic acid; it was not further investigated.

The author is indebted to *Statens Tekniska Forskningsråd* for a fellowship.

REFERENCES

1. Erdtman, H. and Nilsson, M. *Acta Chem. Scand.* **10** (1956) 735.
2. Jackson, C. L. and Bolton, E. K. *J. Am. Chem. Soc.* **36** (1914) 1473.
3. Browning, E. and Adams, R. *Ibid.* **52** (1930) 4098.
4. Jackson, C. L. and Bolton, E. K. *Ibid.* **36** (1914) 301.
5. Torrey, H. A. and Hunter, W. H. *Ibid.* **34** (1912) 702.

Received July 3, 1956.

ACTA CHEMICA SCANDINAVICA 10 (1956) 1381—1392

The Chemistry of the Natural Order Cupressales

XVI.* Heartwood Constituents of *Chamaecyparis nootkatensis* (Lamb.) Spach. The Structure of Chamic and Chaminic Acids

H. ERDTMAN, W. E. HARVEY and J. G. TOPLISS

Organisk-Kemiska Institutionen, Kungl. Tekniska Högskolan, Stockholm, Sweden

Chamic acid, $C_{10}H_{14}O_2$, has been shown to be a monoterpene acid of structure (I). The presence of the dimethyl*cyclo*propyl grouping (IX) was demonstrated by the formation of *trans*-caronic acid (VIII) on permanganate oxidation and the relative positions of the carboxyl group and the *cyclo*propane ring were deduced from the transformation of chamic acid into *m*- and *p-iso*propylbenzoic acids (IV, VI) and further into *iso*- and *tere*phthalic acids (V, VII). The position of the double bond followed from a study of the ultra-violet and infra-red absorption spectra of chamic acid and its alkali isomerisation product, *iso*chamic acid (III).

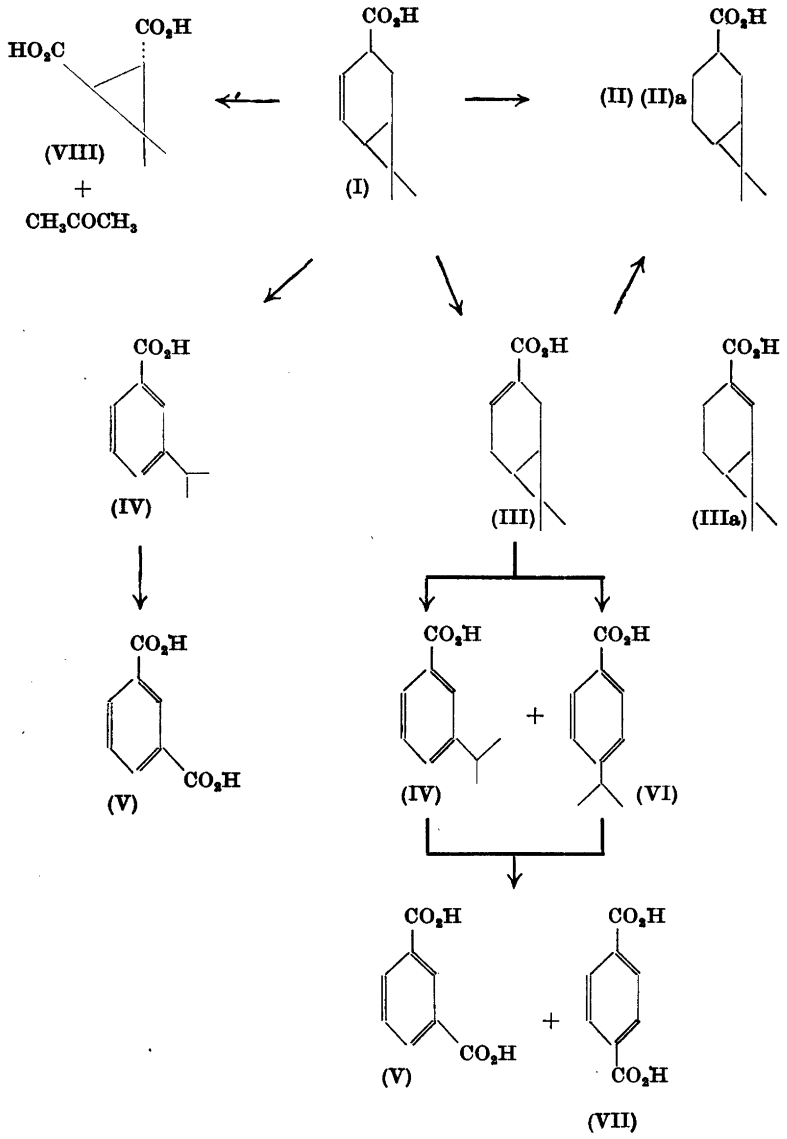
Another acid, chaminic acid, has also been isolated in very small quantities from the heartwood and has been shown to be the optical antipode of *iso*chamic acid.

The isolation of chamic acid from the heartwood of *Chamaecyparis nootkatensis* and its characterisation as the *p*-bromophenacyl ester and the *cyclo*hexylamine and *S*-benzylthiuronium salts has been described in a previous communication [1]. The present communication describes the degradative experiments which have led to the elucidation of the structure of chamic acid and the probable structure of chaminic acid.

Permanganate oxidation of chamic acid under alkaline conditions resulted in extensive decomposition but from the mixture of oxidation products a small quantity of *dl-trans*-caronic acid (VIII) and acetone (as the 2,4-dinitrophenylhydrazone) were isolated and evidence for the presence of dimethylmalonic acid was also obtained. This establishes the presence of the grouping (IX) in chamic acid **. Moreover these results are reminiscent of the results obtained

* Part XV *Acta Chem. Scand.* **9** (1955) 1728.

** The weak infra-red bands at 1 007 cm^{-1}, 998 cm^{-1} and 1 011 cm^{-1} for chamic, *iso*chamic and dihydrochamic acids, respectively, provide additional evidence for the presence of the *cyclo*-propane ring system in these compounds.



on oxidation of Δ^3-carene under similar conditions [2] and suggest that chamic acid may possess a close structural resemblance to the carenes.

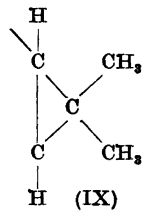
The catalytic reduction of chamic acid in alcoholic solution in the presence of Adams' catalyst resulted in the rapid uptake of one mole of hydrogen affording dihydrochamic acid (II), obtained as an oil but readily characterised by its *p*-bromophenacyl ester m. p. 79—80°. Hence chamic acid has one double bond and therefore could possess a fused *cyclo*propane-*cyclo*hexene ring system.

On hydrogenation of dihydrochamic acid in acetic acid solution with Adams' catalyst one mole of hydrogen was very slowly absorbed and this clearly corresponds to fission of the *cyclo*propane ring.

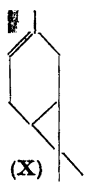
The ultra-violet absorption spectrum of chamic acid contains no strong bands thus indicating that the double bond is not conjugated with the carboxyl group. This deduction is supported by infra-red measurements, the medium intensity band at 1 644 cm^{-1} present in the spectrum of chamic acid but absent in the case of the dihydro-compound corresponding to the isolated double bond in the former substance.

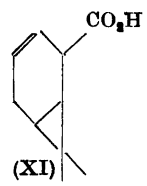
When chamic acid is treated with hot aqueous alkali, crystalline *iso*chamic acid is obtained. The ultra-violet absorption spectrum of *iso*chamic acid has a maximum at *ca.* 218 mμ (ε 7 250), and the infra-red spectrum shows strong bands at 1 684 cm^{-1} and 1 647 cm^{-1} clearly demonstrating that the double bond has moved into conjugation with the carboxyl group.

*Iso*chamic acid when reduced catalytically gave a dihydro-compound (IIa) as an oil which afforded a single *p*-bromophenacyl ester not identical with that prepared from dihydrochamic acid (II) obtained by catalytic reduction of chamic acid. The two dihydro-compounds (II) and (IIa) are presumably diastereoisomers differing according to the *cis* or *trans* relationship of the carboxyl group to the *cyclo*propane ring.

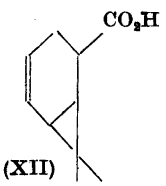


(IX)


(X)



(XI)



(XII)

At this stage structures (I), (XI) and (XII) were probable for chamic acid and clearly the next step was to determine the relative positions of the carboxyl group and the *cyclo*propane ring in the molecule.

Treatment of chamic acid in chloroform solution with an equimolar quantity of bromine in the same solvent resulted in a rapid reaction with no significant formation of hydrogen bromide. Further bromine could be absorbed but at a greatly reduced rate. The crude dibromo-compound was dehydrobrominated directly by heating with dimethylaniline to give a liquid acid mixture in which the presence of a considerable quantity of aromatic material was indicated by ultra-violet and infra-red spectra measurements. In fact the ultra-violet absorption spectrum of the mixture resembled rather closely that of *m-iso*propylbenzoic acid which was therefore probably the main component of the mixture, a deduction subsequently verified. Separation of the acids by partition chromatography or by fractional crystallisation of the *p*-bromophenacyl esters was not successful, but after catalytic hydrogenation of the mixture (palladium, room temperature and pressure) and conversion of the product to the amide *via* the acid chloride, pure *m-iso*propylbenzamide could be isolated by careful chromatography of the amide mixture on alumina. In

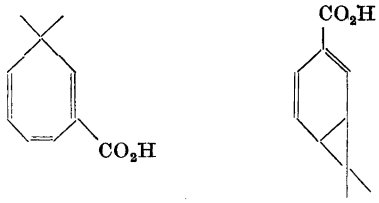
addition, oxidation of the crude acid mixture with dilute nitric acid afforded *iso*phthalic acid, identified as its dimethyl ester.

The addition of a unimolecular quantity of bromine to *iso*chamic acid proceeded at a much slower rate than in the case of chamic acid owing to the conjugation of the double bond with the carboxyl group. Dehydrobromination of the resulting dibromo-compound was accomplished by heating with pyridine to yield a liquid acid mixture which, from its ultra-violet absorption spectrum appeared to consist largely of non-aromatic material. Hydrogenation of the acid mixture, conversion to the amides and chromatography of the latter on alumina gave a small quantity of *m-iso*propylbenzamide as the only recognisable product. The addition of *cyclo*hexylamine to a petroleum ether solution of the acid mixture gave a considerable quantity of insoluble *cyclo*hexylamine salts which after crystallisation from acetone furnished what had every appearance of being a pure salt, not identical with, but according to analysis isomeric with, *iso*chamic acid *cyclo*hexylamine salt. Decomposition of the salt afforded the free acid as a crystalline solid of rather indefinite melting point. The acid (A), which was not optically active, had an ultra-violet absorption spectrum with a maximum at 260 mμ (ε 8 750), and it thus appeared that the acid possessed a conjugated system of two double bonds and a carboxyl group and had arisen by ring opening of the *cyclo*propane ring of *iso*chamic acid probably as a result of the presence of hydrogen bromide in the bromine. However, if the unpurified mixture of *cyclo*hexylamine salts obtained from the acid degradation products was refluxed with an acetic acid-hydrochloric acid mixture, distillation of the acid products gave a small quantity of material boiling at the same temperature as the original acid degradation product and a main fraction which boiled considerably higher. The lower boiling product, which partially crystallised, had an ultra-violet absorption spectrum distinctly resembling that of *p-iso*propylbenzoic acid. The higher boiling main fraction also deposited a crystalline solid, insoluble in petroleum ether, of m. p. 156—160°. The ultra-violet absorption spectrum of this compound showed a maximum at 280 mμ (ε *ca.* 30 000), and it seems very likely that it is a dicarboxylic acid formed by dimerisation of the acid (A) isolated by purification of the *cyclo*hexylamine salt as previously described, or a similar compound. The lower boiling distillate was converted to the amide and by fractional evaporative distillation followed by crystallisation a very small quantity of pure *p-iso*propylbenzamide was isolated. Also oxidation with dilute nitric acid of the acid mixture as obtained directly from the dehydrobromination gave a mixture of *iso-* and *tere*phthalic acids which were separated by fractional crystallisation of their dimethyl esters. Thus these degradations establish conclusively the relative positions of the carboxyl group and the *cyclo*propane ring in chamic acid which must therefore possess structure (I). *Iso*chamic acid consequently must be formulated as (III) or (IIIa), (III) being the most probable since the addition of bromine to, followed by the dehydrobromination of (IIIa), would be expected to give a considerable quantity of *p-iso*propylbenzoic acid (by analogy with the similar degradation of chamic acid in which a bromine atom is situated in an adjacent position to the *cyclo*propane ring) whereas in actual fact, as already described, a complex mixture of acids is formed containing very little aromatic material. However, a con-

clusive distinction between the possible structures (III) and (IIIa) for *iso*-chamic acid cannot be made on the present evidence. Further investigations on this point have been hampered by lack of material.

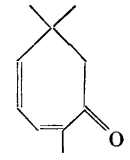
In an earlier paper [1] describing the isolation of chamic acid the presence of small quantities of other acids in the mother liquors from the precipitation of the *cyclo*hexylamine salt of chamic acid was reported. One of these acids, chaminic acid, m. p. 104—105°, $[\alpha]_D$ 6 (± 1)° has now been obtained in the pure state. The infra-red spectrum of chaminic acid is identical with that of *iso*chamic acid, m. p. 105—106°, $[\alpha]_D$ —6 (± 1)°, and chaminic acid is therefore the optical antipode of *iso*chamic acid. The fact that chaminic acid is the *d*-form whereas *iso*-chamic acid formed by isomerisation of chamic acid is the *l*-form eliminates the possibility that chaminic acid is an artefact formed from chamic acid during the isolation process which necessarily involves alkaline treatments.

Although it is clear that *m-iso*propylbenzoic acid is formed directly by the addition of bromine to, followed by dehydrobromination of, *iso*chamic acid, this cannot be stated with certainty in the case of *p-iso*propylbenzoic owing to its method of isolation. *p-Iso*propylbenzoic acid *cyclo*hexylamine salt is insoluble in petroleum ether whereas the *cyclo*hexylamine salt of *m-iso*propylbenzoic acid is soluble. Hence if *p-iso*propylbenzoic acid is a direct product of the degradation then it is possible that its separation from *m-iso*propylbenzoic acid occurred at this stage and that the treatment with acetic acid-hydrochloric acid served only to dimerise acid (A) and thus make possible a separation of *p-iso*propylbenzoic acid on account of its widely different volatility from the dimer of (A). On the other hand if either thujic acid (XIII) or "dehydrochamic acid" (XIV) are the direct products of the degradation then these, after separation as their petroleum ether insoluble salts, would be rearranged by the acetic acid-hydrochloric acid reagent to *p-iso*propylbenzoic acid [3].

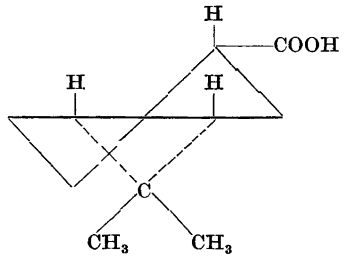


(XIII)

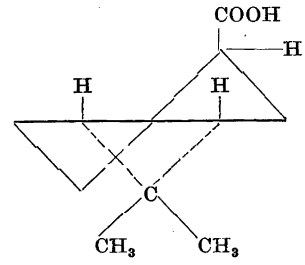
(XIV)



(XV)



(XVI)



(XVII)

The relationship between chamic acid (I), chaminic acid (III), dehydrochamic acid (XIV) and thujic acid (XIII) is of interest particularly in view of their possible common biogenetic origin from carene-like precursors [4]. In this connection it would be desirable to effect the interconversion of chamic acid or chaminic acid and dehydrochamic acid or thujic acid. At this juncture it should be pointed out that dehydrochamic acid and thujic acid may be regarded as valence tautomers and in fact Gripenberg [5] considered the possibility that thujic acid might possess structure (XIV). Similar problems arose in the study of the structures of certain compounds prepared from eucarvone [6] (XV) and were resolved with certainty by the use of nuclear magnetic resonance measurements [7]. This method has been used very recently to distinguish between structures (XIII) and (XIV) for thujic acid [8], the results clearly pointing to structure (XIII). Moreover although one can consider an equilibrium between the *cyclo*heptatriene and *bicyclo*heptadiene structures for these compounds it seems that in all cases so far known one form is so much more stable that it is formed to the exclusion of the other form. Hence the possibility that dehydrochamic acid (XIV) exists as such is remote. The possible formation of thujic acid (in small quantity) as an intermediate product in the degradation of *iso*chamic acid to *p-iso*propylbenzoic acid has already been discussed but no direct evidence for its presence could be obtained. An alternative degradation of *iso*chamic acid involving bromination using N-bromosuccinimide followed by dehydrobromination by heating with base was briefly examined but also gave a complex mixture of acids, none of which predominated.

The formation of *dl-trans*-caronic acid rather than the *cis*-isomer on permanganate oxidation of chamic acid is presumably the result of a *cis-trans* rearrangement and racemisation at some stage in the oxidation as a *trans* ring junction in (I) is unlikely. *l-* and *dl-trans* and *cis*-Caronic acids have all been obtained from the oxidation of Δ^3-carene under different conditions [2,9,10].

The fact that stereoisomeric dihydrochamic acids (II) (IIa) are obtained depending on whether chamic acid or *iso*chamic acid is reduced enables certain deductions to be made concerning the probable stereochemistry of chamic acid. The catalytic reduction of *iso*chamic acid would be expected to give the dihydrochamic acid with an equatorially placed carboxyl group and a *cis* relationship between the carboxyl group and the *cyclo*propane ring (XVI) (*cis*-dihydrochamic acid) (*cf.* Ref.[11]). Thus the dihydrochamic acid obtained from chamic acid should have an axial carboxyl group (XVII; *trans*-dihydrochamic acid) and hence in chamic acid itself the carboxyl group and the *cyclo*propane ring can be assigned a *trans* relationship.

Since oxidation of the methyl group in Δ^3-carene would lead to *iso*chamic acid the selenium dioxide oxidation of Δ^3-carene was investigated with a view to effecting this change *via* the corresponding aldehyde. A similar oxidation of α-pinene is known to give myrtenal [12] but in the case of Δ^3-carene the oxidation apparently took place at the methylene groups adjacent to the double bond and not at the methyl group.

It is hoped to confirm the structure of chamic acid and establish with certainty the structure of chaminic acid by synthetic studies.

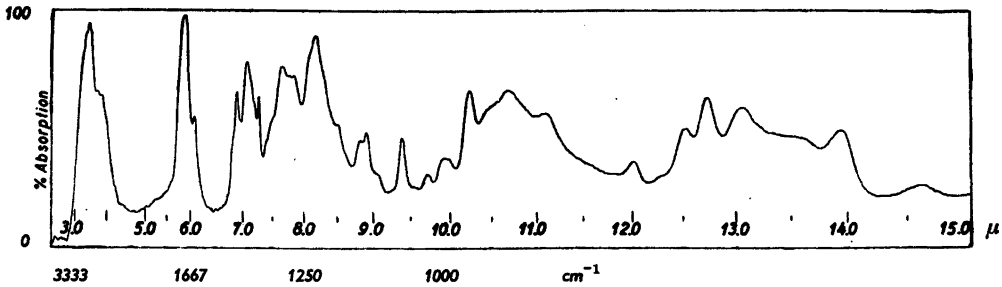


Fig. 1. Infra-red absorption spectrum of chamic acid.

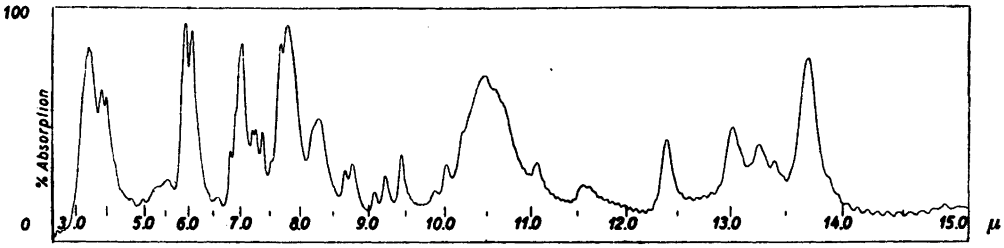


Fig. 2. Infra-red absorption spectrum of isochamic acid.

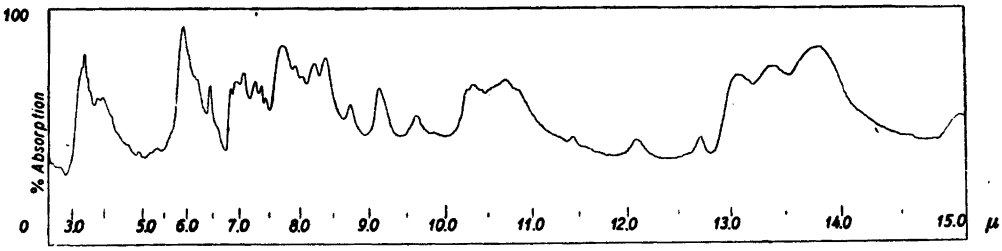


Fig. 3. Infra-red absorption spectrum of thujic acid.

EXPERIMENTAL

Isolation of chamic acid. Wood samples employed included some from large trees grown near Vancouver, Canada, which constituted the major source and some from a small Scandinavian grown tree. The latter sample gave much greater yields of chamic acid. The acetone extraction procedure described previously [1] (with omission of the preliminary ether extraction) was found to be the most convenient method for the extraction of chamic acid. The yields of crude steam volatile acid varied between 3 g and 6 g per 10 kg batch of heartwood. The crude acid normally afforded 60—80 % yields of the crude acetone insoluble *cyclo*hexylamine salt of chamic acid which after recrystallisation gave 40—50 % yields (based on the crude salt) of pure chamic acid *cyclo*hexylamine salt. Hence 0.75—2.0 g of pure chamic acid could usually be obtained from 10 kg of heartwood. In some extractions, however, the yield was much below these average values.

The ultra-violet absorption spectrum of chamic acid showed no strong bands. Infra-red spectrum: (Fig. 1.) Medium intensity band at 1 644 cm^{-1} (isolated double bond), weak band at 1 007 cm^{-1} (*cyclo*propane ring).

Isolation of chaminic acid. The mother liquors from which the *cyclo*hexylamine salt of chamic acid had been precipitated were concentrated to small volume, filtered, and the remaining solvent evaporated under reduced pressure. The free acids were recovered by acidification and ether extraction and were obtained as a faintly coloured viscous oil which slowly deposited a crystalline solid on storage in the refrigerator. The solid material was collected by filtration and recrystallised from petroleum ether yielding pure *chaminic acid*, m. p. 104—105°, $[\alpha]_D$ 6 (± 1)° (*c* 3.9 in methanol). (Found: C 72.6; H 8.56. $C_{10}H_{14}O_2$ requires C 72.3; H 8.49). The infra-red spectrum was identical with that of *iso*chamic acid, m. p. 105—106°, $[\alpha]_D$ −6 (± 1)°. A mixture of approximately equal parts of the *d*- and *l*-isomers melted at the same temperature as either of them, but if the two were mixed in non-equivalent amounts depressions in the melting point of up to 10—12° were obtained. The p-*bromophenacyl ester* was prepared in the usual manner and after recrystallisation from aqueous ethanol formed flat plates, m. p. 72.5—73,° $[\alpha]_D$ −2.6° (methanol).

Oxidation of chamic acid. Chamic acid (1.09 g) was dissolved in a solution of sodium carbonate (0.5 g anhydrous) in water (100 ml) and finely powdered potassium permanganate was added with cooling and shaking until no further reaction occurred. Further potassium permanganate (1 g) was added and the solution was warmed on the water bath, decolourisation rapidly taking place. This process was repeated until no further reaction took place at 100° by which time a total of 10 g of permanganate had been added. The solution was finally heated on the boiling water bath for 1 ½ hours. The resulting solution was cooled to room temperature, acidified with dilute sulphuric acid, treated with sulphur dioxide and steam distilled. The distillate was made alkaline by the addition of sodium hydroxide and steam distilled once more. The second distillate was treated with an aqueous solution of 2:4-dinitrophenylhydrazine hydrochloride and the yellow precipitate which formed in the cold was collected and recrystallised from ethanol giving yellow needles of acetone 2:4-dinitrophenylhydrazone, m. p. 123—124°, undepressed on admixture with an authentic specimen. The residual liquid from the first distillation was diluted with water to dissolve the salts which had separated and extracted with ether (4 × ½ volume). The ether extracts were combined, washed with a little water, dried (Na_2SO_4) and evaporated giving a semi-solid residue. This material gave a strong fluorescein reaction and paper chromatography showed that at least four substances were present although two of these apparently occurred only in small amount. The mixture was triturated with a little chloroform and the insoluble matter was collected and washed with a few drops of chloroform. It melted over a very wide range, gave a strong fluorescein reaction and on paper chromatography gave two well defined spots. The faster moving substance moved at about the same speed as pimelic acid and is in fact caronic acid whilst the slower moving substance travelled at about the same speed as succinic acid or a little faster and is probably dimethylmalonic acid. The mixture of acids was recrystallised repeatedly from water finally yielding a small amount of *dl-trans*-caronic acid, m. p. 212—213°, undepressed on admixture with an authentic specimen of *dl-trans*-caronic acid and behaving identically on paper chromatography.

Hydrogenation of chamic acid. Chamic acid, in ethanol, was shaken in an atmosphere of hydrogen at room temperature and pressure, in the presence of Adams' catalyst until one mole of hydrogen had been absorbed, at which stage the rate of uptake of hydrogen decreased sharply. The catalyst was removed by filtration and the ethanol evaporated under reduced pressure giving an almost colourless oil which was distilled in high vacuum affording *dihydrochamic acid* as a colourless viscous oil, d_{20}^{20} 1.0445, n_D^{20} 1.4835, $[\alpha]_D$ −47° (methanol). (Found: C 71.6; H 9.66. $C_{10}H_{16}O_2$ requires C 71.4; H 9.59.) Infra-red spectrum: No band corresponding to the band at 1 644 cm^{-1} (isolated double bond) found in the spectrum of chamic acid. Weak band at 1 011 cm^{-1} (*cyclo*propane ring). The same product was obtained if the hydrogenation was carried out in ethanol solution using a palladised charcoal catalyst.

Dihydrochamic acid p-*bromophenacyl ester* was prepared in the usual manner and crystallised from aqueous ethanol as long thin plates, m. p. 79—80°. (Found: C 59.45; H 5.74. $C_{18}H_{21}O_3Br$ requires C 59.2; H 5.80.)

In the presence of Adams' catalyst either in alcoholic or, preferably in acetic acid solution, a second mole of hydrogen was very slowly absorbed. The product obtained on removing the catalyst and evaporating the solvent partially solidified but has not been investigated in detail.

Iso*chamic acid*. Chamic acid (1.30 g), in aqueous sodium hydroxide (25 ml 25 %), was heated gently under reflux for 2 h. The solution was cooled and acidified with hydrochloric acid and the precipitate which formed collected by filtration and dried affording almost pure *iso*chamic acid in practically quantitative yield. Recrystallisation was effected from petroleum ether giving *iso*chamic acid as colourless prisms, m. p. 105—106°, $[\alpha]_D$ −6 (± 1)°. (Found: C 72.7; H 8.59. $C_{10}H_{14}O_2$ requires C 72.3; H 8.49). Ultra-violet absorption spectrum: max. *ca.* 218 mμ (ε 7 250). Infra-red spectrum: (Fig. 2.) Strong bands at 1 684 cm^{-1} (conjugated C=O) and 1 647 cm^{-1} (conjugated double bond). Weak band at 998 cm^{-1} (*cyclo*propane ring).

Iso*chamic acid* cyclo*hexylamine salt* was prepared by the addition of *cyclo*hexylamine to an acetone solution of *iso*chamic acid and recrystallised from acetone-ethanol forming fine needles, m. p. 166—167°, subliming readily *in vacuo* below 100°. (Found: C 72.5; H 10.28. $C_{16}H_{27}O_2N$ requires C 72.4; H 10.25).

Iso*chamic acid* p-*bromophenacyl ester* was prepared from the acid and *p*-bromophenacyl bromide by the standard procedure and recrystallised from aqueous ethanol giving colourless plates, m. p. 73.5—74°, $[\alpha]_D$ + 2.3° (methanol). (Found: C 59.6; H 5.36. $C_{18}H_{19}O_3Br$ requires C 59.5; H 5.27).

Hydrogenation of iso*chamic acid*. *Iso*chamic acid, in ethanol, was hydrogenated in the presence of Adams' catalyst until one mole of hydrogen had been absorbed, at which stage the rate of uptake of hydrogen ceased or became very slow. The catalyst was removed by filtration and the solvent evaporated under reduced pressure yielding an oil which was converted directly into the p-*bromophenacyl ester*. The crude ester melted at 53—54° and repeated recrystallisation raised the melting point only to 55.5—56.5° and no evidence was obtained for the presence of more than one component. (Found: C 59.0; H 5.70. $C_{18}H_{21}O_3Br$ requires C 59.2; H 5.80).

Dehydrobromination of dibromochamic acid. To a solution of chamic acid (1.35 g), in chloroform (25 ml) was added dropwise, with shaking, a solution of bromine (1.30 g, 1 mole) in chloroform (10 ml). Immediate decolourisation of the bromine solution took place and no evolution of hydrogen bromide was detected. The chloroform was evaporated and the residue refluxed with freshly distilled dimethylaniline for 1 h. Most of the dimethylaniline was removed by heating on a water bath under reduced pressure. The residue was shaken with ether and dilute hydrochloric acid and the ether layer removed. The acid layer was extracted with fresh ether and the combined ethereal solutions washed with dilute hydrochloric acid followed by water and dried (Na_2SO_4). The ether was removed and the residue distilled *in vacuo* to give 0.66 g of nearly colourless product (A), b. p. *ca* 120—170° (bath temperature) / 0.15 mm. Ultra-violet absorption: max. 230 mμ (ε 7 500); 277 mμ (ε 1 000); *m-iso*propylbenzoic acid: max. 230 mμ (ε 7 500); 277 mμ (ε 1 050). The infra-red spectrum showed bands at 1 652, 1 606 and 1 582 cm^{-1}, indicative of an aromatic carboxylic acid. On paper chromatography using propanol-ammonia-water (80 : 4 : 16) or *t*-butanol-ammonia-water (80 : 4 : 16) as solvents a single spot was obtained. No *cyclo*hexylamine salt was precipitated in acetone or petroleum ether solution. Conversion to the *p*-bromophenacyl esters gave a product m. p. 83—87° (corr.), clearly a mixture, which could not be purified by fractional crystallisation or by chromatography on alumina. The distilled product (A) (0.65 g), in ethanol (15 ml), was hydrogenated in the presence of 10 % palladium charcoal (0.1 g) as catalyst at room temperature and atmospheric pressure. The uptake of hydrogen after 2 h was 45 ml when the hydrogenation had practically ceased. The catalyst was removed by filtration, the alcohol evaporated and the residual acid refluxed for 15—20 min with freshly distilled thionyl chloride. The excess of thionyl chloride was removed by distillation and the residual acid chloride dissolved in dry ether (25 ml). Ammonia gas was passed into the ether solution for 15—20 min. and water was then added. The ether layer was separated and the aqueous layer extracted with fresh ether. The combined ether solutions were washed with a little 2 N sodium hydroxide solution followed by water, dried (Na_2SO_4) and the ether removed to give 0.40 g of brown semi-solid amide. Sublimation of a small portion of this material followed by crystallisation of the solid part of the sublimate from petroleum ether gave needles, m. p. 81—82.5°. This material was undoubtedly impure *m-iso*propylbenzamide (m. p. of the pure compound 93—94° (corr.) since its melting point was not depressed on admixture with the authentic compound and the ultra-violet absorption spectra of the two samples were amost identical. However, the impure sample could not be purified by repeated recrystallisations. The remainder of the semi-

solid amide preparation (0.380 g) was chromatographed on alumina (40 g), (column 22.5 cm × 1.7 cm), in benzene solution and eluted successively with ether-benzene mixtures and finally ether. The ether-benzene eluates yielded small quantities of oily material (total 0.035 g). A total of 18 fractions were obtained from the elution with ether and of these, 12 (total 0.250 g) consisted of substantially pure *m-iso*propylbenzamide judged by mixed melting point and ultra-violet absorption spectra determinations. Recrystallisation of the combined fractions from petroleum ether gave pure *m-iso*propylbenzamide as fine needles, m. p. 93—94° (corr.), (Found: C 73.2; H 8.0; N 8.5. $C_{10}H_{13}ON$ requires C 73.6; H 8.0; N 8.6) undepressed on admixture with authentic *m-iso*propylbenzamide. When this work was carried out *m-iso*propylbenzamide had not been reported in the literature. *m-Iso*propylbenzoic acid[13] was converted into its acid chloride by the action of thionyl chloride and an ethereal solution of the acid chloride treated with ammonia gas. The resulting amide crystallised from petroleum ether in fine needles, m. p. 93—94° (corr.), (Found: C 73.5; H 7.8; N 8.5. $C_{10}H_{13}ON$ requires C 73.6; H 8.0; N 8.6).

Distilled product (A) (0.150 g) from the dehydrobromination was heated overnight at 170—180° in a sealed tube with a mixture of concentrated nitric acid (4 ml) and water (8 ml). The crystalline precipitate which formed was collected and washed with water. It melted above 300°, gave no fluorescein reaction and was readily and completely soluble in barium hydroxide solution (distinction from *tere*phthalic acid). The methyl ester, prepared in ethereal solution with diazomethane, was recrystallised from aqueous methanol giving dimethyl *iso*phthalate as fine needles, m. p. 63—64°, undepressed on admixture with an authentic specimen.

*The dehydrobromination of dibromo*isochamic acid. To *iso*chamic acid (3.45 g, 1 mole) in chloroform (75 ml) was added portionwise over 2 ½ hours, a solution of bromine (3.33 g, 1 mole) in chloroform (50 ml). The reaction was complete 1—2 h after the addition of the last portion of bromine. No detectable amount of hydrogen bromide was evolved. The chloroform was removed and the gummy, pale yellow residue was refluxed in pyridine for 30 min. The reaction mixture was poured into 15 % hydrochloric acid (300 ml), the product extracted with ether (2 × 100 ml) and the ether solution washed with 15 % hydrochloric acid followed by water and then extracted with 2 N sodium hydroxide solution (2 × 50 ml). The alkaline extracts were acidified (hydrochloric acid), the liberated acids, isolated with ether, amounting to 1.70 g. Distillation of the product *in vacuo* gave a practically colourless distillate (B) (1.16 g), b. p. 120—140° / 0.02 mm (bath temp.). The ultra-violet absorption spectrum of this material showed no maxima above 220 mμ. A small higher boiling fraction was also obtained from the distillation. On keeping it partially solidified and was crystallised from aqueous acetic acid (small prisms) m. p. 95—100° (corr.). Recrystallisation from the same solvent increased the melting point to 115—116° (corr.), which was strongly depressed on admixture with *p-iso*propylbenzoic acid, m. p. 117—118° (corr.). The ultra-violet absorption spectrum showed no maxima above 220 mμ and the substance was not further investigated.

Distillate (B) (0.36 g) was hydrogenated in ethanol solution (20 ml) with a 10 % palladium charcoal catalyst (0.50 g), 35 ml of hydrogen (N.T.P.) being absorbed. The hydrogenation product was converted to the acid chloride by refluxing with thionyl chloride (3 ml) for 30 min. and after removal of excess of thionyl chloride ammonia gas was bubbled through a solution of the acid chloride in dry ether (25 ml) for 15 min. The ether solution was washed with water, dilute sodium hydroxide solution and water again, dried (Na_2SO_4) and the ether removed yielding the crude amide as a brown gum (0.235 g). The amide, in benzene solution, was placed on a column of alumina (40 g) and eluted with ether, 30 fractions being taken. The ultra-violet absorption spectra of fractions 11—13 indicated the presence of *m-iso*propylbenzamide. These fractions were combined and recrystallised from petroleum ether affording a small quantity of pure *m-iso*propylbenzamide, m. p. and mixed m. p. 93—94°. Examination of the other fractions yielded only small quantities of impure crystalline material which did not give any characteristic absorption in the ultra-violet and was not further investigated.

To distillate (B) (0.58 g), in petroleum ether (5 ml) was added a solution of *cyclo*hexylamine (0.39 g), in petroleum ether (5 ml). There was a considerable heat of reaction and the *cyclo*hexylamine salt began to separate almost immediately. After 30 min. in the refrigerator the *cyclo*hexylamine salt (C) was filtered off (0.54 g, m. p. 135—140°). The crude salt (0.250 g) was refluxed for 5 h with concentrated hydrochloric acid (5 ml) containing enough glacial acetic acid to produce a homogeneous solution at the boiling

point. The reaction mixture was diluted with water and extracted with ether (2 × 75 ml). The ethereal solution was washed with water, dried (Na_2SO_4) and the ether evaporated. The residue was evaporatively distilled and separated into two fractions. The more volatile fraction (0.035 g) was refluxed with thionyl chloride (2 ml) for 30 min. and the excess of thionyl chloride then removed by distillation. The resulting acid chloride was dissolved in dry ether (25 ml) and ammonia gas bubbled through the solution for 30 min. The ether solution was washed with 2 N sodium hydroxide solution followed by water, dried (Na_2SO_4) and the ether evaporated. Evaporative distillation of the residue gave a small crystalline fraction which, after two recrystallisations from petroleum ether (fine needles), had m. p. 148.5—149.5° (corr.), undepressed on admixture with an authentic specimen of *p-iso*propylbenzamide.

Crude *cyclo*hexylamine salt (C) (0.360 g), repeatedly recrystallised from acetone gave what was apparently a single, pure *cyclo*hexylamine salt (0.07 g), m. p. 170—171° (depresses the melting point of the *cyclo*hexylamine salt of *iso*chamic acid). (Found: C 72.3; H 10.1. $C_{16}H_{27}O_2N$ requires C 72.4; H 10.25). Treatment of this salt with dilute hydrochloric acid followed by ether extraction afforded the free acid which crystallised from aqueous methanol as thin plates of rather indefinite melting point (115—130°). The melting point behaviour was unchanged after further recrystallisation. $[\alpha]_D$ 0° (chloroform). Ultra-violet absorption: max. 260 mμ (ε 8 750).

Distillate (B) (0.200 g) was oxidised with nitric acid (4 ml) and water (8 ml) in a sealed tube at 170—180° overnight and the crystalline product formed was collected and washed with water. This material was not completely soluble in barium hydroxide solution. It was converted to the methyl ester by treatment with phosphorus pentachloride followed by methanol and the crystalline product obtained was recrystallised from methanol forming long flat needles of dimethyl *tere*phthalate, m. p. 139—140°, undepressed on admixture with an authentic specimen. The methanol mother liquors were diluted with water and the crystalline material which precipitated was recrystallised from aqueous methanol yielding fine needles of dimethyl *iso*phthalate, m. p. 63.5—64°, undepressed on admixture with an authentic specimen.

The oxidation of Δ^3-Carene with selenium dioxide. To a stirred refluxing solution of Δ^3-carene (20 g, 1 mole), in ethanol (40 ml), was added over 30 min. a solution of selenium dioxide (18 g, 1. 1 mole) in ethanol (40 ml). The formation of red selenium metal was soon noticed. The reaction mixture was refluxed for 5 h, filtered to remove selenium, and the filtrate concentrated and steam distilled. The steam volatile product was extracted with ether and the ether extract washed with 2 N sodium hydroxide solution. Acidification of the alkali washings revealed the absence of steam volatile acidic material. The ether solution was washed with water, dried (Na_2SO_4) and the ether removed giving 6.67 g of crude product. Distillation *in vacuo* afforded the following fractions as pale yellow oils: (1) b. p. 65—73°/7 mm, 1.07 g (2) b. p. 80—97° (mainly 92—97°)/10 mm, 3.1 g (3) b. p. 115—120°/10 mm, 1.0 g. Ultra-violet absorption: fraction (1) max. 245 mμ; fraction (2) max. 242 mμ.

Fraction (2) (1.0 g), in ethanol (100 ml), containing a trace of sodium hydroxide, was refluxed with freshly precipitated silver oxide (2.32 g, 1.5 mole) for 4 h. The silver and unchanged silver oxide were removed by filtration and most of the solvent was evaporated from the filtrate (A). The inorganic material was treated with dilute nitric acid and the ether washings were added to the concentrated filtrate (A). The ether solution was washed with water and dried (Na_2SO_4). Removal of the ether yielded only a trace of acidic material. A similar treatment of fraction (1) gave the same result.

The authors are indebted to *Statens Naturvetenskapliga Forskningsråd* for financial support, Crown Zellerbach Co., Camas, Washington, for generous gifts of wood, and to Dr. I. Fischmeister, *Medicinsk-Kemiska Institutionen, Uppsala Universitet*, for the infrared spectra determinations.

REFERENCES

1. Carlsson, B., Erdtman, H., Frank, A. and Harvey, W. E. *Acta Chem. Scand.* **6** (1952) 690.
2. Simonsen, J. L. *J. Chem. Soc.* **1920** 570.
3. Gripenberg, J. *Acta Chem. Scand.* **3** (1949) 1137.
4. Erdtman, H. *Experientia*, Supplementum (11), Zürich, 21—27 VII, 1955.

5. Gripenberg, J. *Acta Chem. Scand.* **5** (1951) 995.
6. Corey, E. J. and Burke, H. J. *J. Am. Chem. Soc.* **76** (1954) 5257.
7. Corey, E. J., Burke, H. J. and Remers, W. A. *J. Am. Chem. Soc.* **77** (1955) 4941.
8. Gripenberg, J. *Acta Chem. Scand.* **10** (1956) 487.
9. Semmler, F. W. and von Schiller, H. *Ber.* **60** (1927) 1591.
10. Gibson, C. S. and Simonsen, J. L. *J. Chem. Soc.* **1929** 305.
11. Peppiat, E. G. and Wicker, R. J. *Chemistry & Industry* **1955** 747.
12. Dupont, G. and Zacharewicz, W. *Compt. rend.* **198** (1934) 1699; **200** (1935) 759; *Chem. Zentr.* 1936 (11) 2384.
13. Harvey, W. E. *Acta Chem. Scand.* **8** (1954) 692.

Received July 4, 1956.

ACTA CHEMICA SCANDINAVICA 10 (1956) 1393—1403

Countercurrent Fractionation of Cellulose Derivatives with Porous Charcoal II

HAROLD A. SWENSON* and AGNETA ROSENBERG

Paper Technology Department, Swedish Forest Products Research Laboratory, Stockholm, Sweden

The effect on the resulting cumulative integral and differential DP weight distribution curves, of altering the uptake to the charcoal stages is investigated. This is accomplished through variation of the concentration of the polymer charge and the number of charcoal stages.

In an earlier paper by Swenson [1] it was shown that secondary cellulose acetates could be fractionated with a countercurrent procedure of the Craig type [2] in which porous charcoal was used as the stationary phase.

The separations were shown to occur by the preferential diffusion and adsorption of the lower, in preference to the higher weight molecules, by the charcoal stages, the unadsorbed polymer of higher DP advancing to later stages. The fractionation method and the fifty stage countercurrent apparatus designed for the experiment were also described.

In the present paper, the effect on the resulting integral and differential DP weight distribution curves, of altering the uptake to the charcoal stages is investigated. This is accomplished through variation of the concentration of the polymer charge and the number of charcoal stages.

The fractionation of a high DP secondary cellulose acetate and a cellulose nitrate are also reported and the osmotically determined molecular weights of the original samples and of a limited number of the fractions are given.

The low concentration, fifty stage fractionation of cellulose acetate 1.62

Two grams of the sample — the samples are identified in the text by their intrinsic viscosity values — in 30 ml acetone, were introduced to the first of the 50 stages, each containing 8 g of charcoal saturated with solvent. 5 min. shaking periods were used.

The concentration of the polymer charge was chosen so that the removal of a high percentage of the sample to the charcoal would be obtained while also

* Present address: The Institute of Paper Chemistry, Appleton, Wisc., USA.

taking advantage of all the charcoal stages. It was known that 49 additions of following solvent to the first stage would have resulted in the fractionation effect of no more than 42 of the stages, because of the detaining, countercurrent effect of the charcoal on the polymer [1]. Consequently, 59 additions of 25 ml acetone were made, between the successive shaking and transfer operations which served to spread the polymer to further stages. The 10 extra additions of the solvent, free of polymer, were decanted from the last charcoal stage of the apparatus.

At the conclusion of the run, after the routine removal of the solvent from the transfer reservoirs and the charcoal tubes with a syringe, elution was done by shaking the charcoal stages twice with 25 ml dioxan. The run was then duplicated and the respective fractions combined to afford more material for analyses. The accuracy of the duplication was checked by separate determinations of the amounts and intrinsic viscosities of the unadsorbed polymer found at the later stages in the two runs.

Of the sample 74 % was recovered, 9 % was not taken up by the charcoal. The average intrinsic viscosity of the recovered fractions was 1.47. Correction for irreversible precipitation effects (see Experimental) increased this figure to 1.53.

This run is compared to an earlier fractionation of the same sample [1] in which the amount of polymer charge appreciably exceeded the uptake capacity of the charcoal stages. 5 g of sample 1.62 was introduced in this run in 70 ml acetone to the first two stages followed by 50 additions of 25 ml acetone to the first stage. To elute the adsorbed polymer, two shakings with 25 ml dioxan were used. Of the sample 25 % was in the decanted acetone which, when added to the eluted material accounted for a total recovery of 60 %. The average intrinsic viscosity of the recovered fractions, uncorrected, was 1.53.

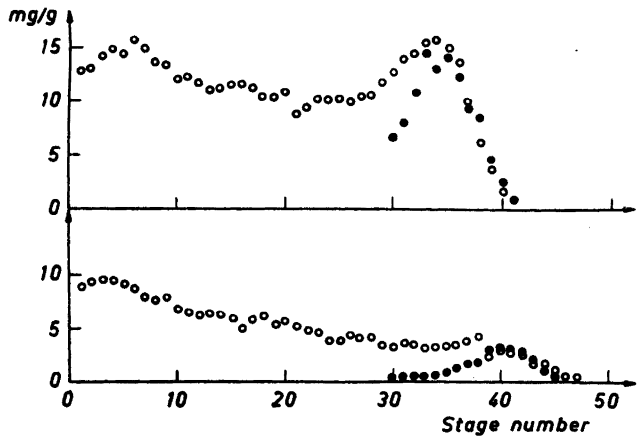


Fig. 1. Eluted and free material expressed as mg/g charcoal found at each stage in fifty stage fractionations of cellulose acetate sample 1.62. Upper figure: Five grams of sample followed by 50 solvent additions. Lower figure: Two grams of sample followed by 60 solvent additions. Open symbols: the eluted fractions. Solid symbols: the material not taken up by the charcoal.

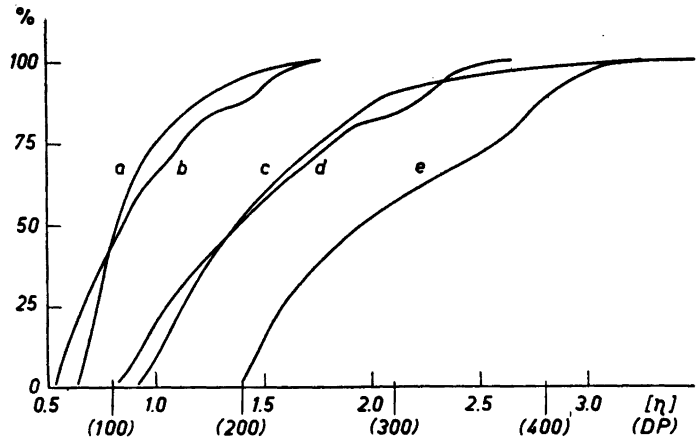


Fig. 2. The cumulative integral fractionation curves from the cellulose acetate fractionations. a. 0.5 g of sample 0.95; 20 stages and 19 additions of solvent. b. 5 g of sample 0.95; 50 stages and 50 solvent additions. c. 2 g of sample 1.62; 50 stages and 60 solvent additions. d. 5 g of sample 1.62; 50 stages and 50 solvent additions. e. 3.6 g of sample 2.24; 50 stages and 60 solvent additions.

In this and subsequent fractionations reported, the amounts eluted from the charcoal are corrected to 100 % recovery assuming, following an earlier finding [1], in which the amounts and intrinsic viscosities from successive elutions were determined, that representative elution of like proportions of the polymer regardless of DP were recovered.

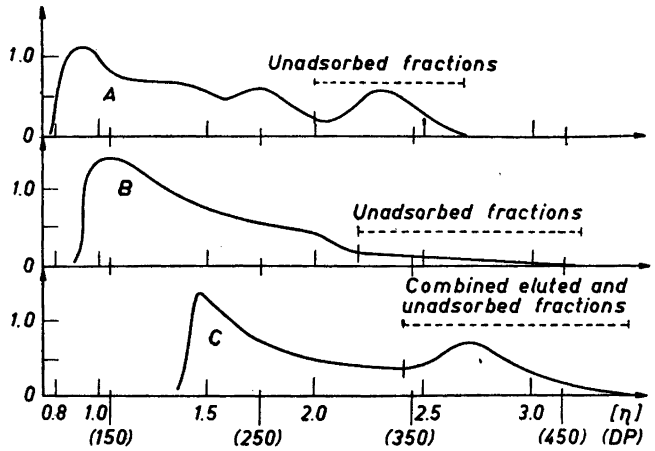


Fig. 3. The differential weight distribution curves of cellulose acetate samples 1.62 and 2.24. A. 5 g, 50 stage fractionation of sample 1.62. B. 2 g, 50 stage fractionation of sample 1.62. C. 3.6 g, 50 stage fractionation of sample 2.24.

The quantities of adsorbed and unadsorbed polymer found at each apparatus stage in the two fractionations are shown in Fig. 1. It can be seen in the lower part of the figure how the polymer has been spread to further charcoal stages in the lower concentration run as a result of the extra additions of solvent.

The integral fractionation curves from the two runs are shown in Fig. 2, curves *c* and *d*. The DP weight distribution curves, obtained by graphical differentiation of the integral curves, are given in Fig. 3, the latter closely reflecting the amounts found at each apparatus stage as shown in Fig. 1.

In the DP weight distribution curve resulting from the high concentration fractionation, Fig. 3 A, the first peak from the right derives from the decanted, unadsorbed material of highest DP and the peak next to the left, the material eluted from the corresponding underlying charcoal stages.

In the lower concentration run, Fig. 3 B, the material in these peaks of less fractionated higher DP polymer have largely been taken up by the charcoal stages resulting in a single maximum distribution curve, an extension of the DP range of the fractions and higher apparent homogeneity of the fractions.

Twenty stage fractionation of cellulose acetate 0.95

To determine how the fractionation is influenced by using fewer stages in combination with high uptake of sample to the charcoal, the low DP sample was run at low concentration. 0.5 g of the sample in 25 ml acetone was introduced to the first of 20 stages, each containing 9 g of charcoal, the effective charcoal capacity of the apparatus.

Nineteen 25 ml additions of acetone were made between successive 5 min. shaking periods. Elution was done by shaking twice for two or more hours with dioxan. Total recovery was 59 %. Less than 4 % of the sample was not taken up by the charcoal. The average intrinsic viscosity of the recovered fractions, which required no correction for irreversible precipitation effects, was 0.94.

This run is compared to an earlier[1] 50 stage fractionation of the same sample in which the amount of sample again exceeded the uptake capacity of the charcoal. 5 g was introduced in 70 ml acetone, in two 35 ml portions to the first two stages of the apparatus followed by fifty additions of acetone. 9 g of charcoal per stage and 5 min. shaking periods were used. Recovery after three elutions with 25 ml dioxan was 92 %, 15 % of the sample was unadsorbed. The average intrinsic viscosity of the recovered fractions, uncorrected, was 0.95.

The experimental integral curves which resulted from the two runs are shown in Fig. 2, curves a and b, and the differential weight distribution curves in Fig. 4. In the latter figure, curve A, from the high concentration 50 stage fractionation, the two peaks from right to left, the unadsorbed material and the material later eluted from the corresponding underlying charcoal stages, respectively, have again resulted from exceeding the uptake capacity of the 50 charcoal stages. More stages or more charcoal per stage were needed to adsorb and further fractionate the free material.

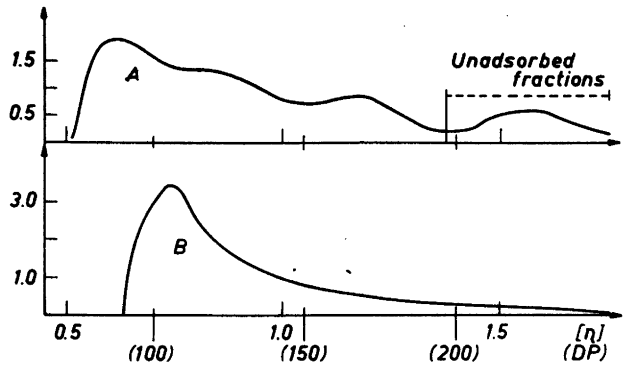


Fig. 4. The differential weight distribution curves of cellulose acetate 0.95. Upper figure: 5 g, 50 stage fractionation. Lower figure: 0.5 g, twenty stage fractionation.

Little polymer material was found in the transfer reservoirs following the 20 stage run and no polymer was found in the first 25 reservoirs after the 50 stage run. This shows, since little or no transfer of polymer was occurring between stages, that the lower DP peaks in the two distribution curves have largely been stabilized by irreversible adsorption. As a result, extending the runs to further stages could not be expected to effect appreciable further fractionation of this lower DP material.

Fractionation of cellulose acetate 2.24

The fractionation of a high DP secondary cellulose acetate was of particular interest since it appeared from earlier fractionations of the lower DP acetate 1.62 that a limit was being approached in the DP of the polymer sample which could be effectively fractionated. In the fractionation run, 3.6 g of acetate 2.24 was introduced in 60 ml acetone in two 30 ml portions to the first stage followed by sixty 25 ml additions of acetone between the successive shaking and transfer operations. 9 g of charcoal were used in each of the 50 apparatus stages and 5 min. shaking periods.

Total recovery, after two 25 ml dioxan elutions was 73 %, 21 % of the sample remaining free of the charcoal. The average intrinsic viscosity of the fractions was 2.00, before correction, and 2.20, after correction for the irreversible precipitation effect.

The experimental integral fractionation curve is given in Fig. 2, curve e, and its graphical differentiation in Fig. 3, curve c. The peak to the right is again the apparent result of too high sample concentration for the uptake capacity of the charcoal stages. The peak contains, however, in contrast to earlier runs with lower DP acetates, both unadsorbed decanted polymer and a smaller amount of adsorbed polymer which was eluted with dioxan. The latter adsorbed material was found in the charcoal stages over the entire DP range of the fractions to DP *ca.* 450 in comparison to the runs with acetate sample 1.62 (*cf.* Fig. 3, A, B), in which the highest DP fractions removed from the charcoal had a DP of *ca.* 300.

A further indication that the experiment shows no apparent limit in the DP of the polymer which can be fractionated, is indicated by the percentage of the sample not taken up by the charcoal, 21 % from 3.6 g of sample 2.24 compared to 25 % not taken up by the charcoal in a similar 50 stage fractionation of 5 g of sample 1.62.

Osmotic pressure determinations

Measurements were made on the original cellulose acetate samples and on the lower DP fractions, Nos. 4, 6 and 8, from the 2 g, 50 stage fractionation of sample 1.62, Fig. 3 B. The small amounts in the fractions were insufficient to allow determinations on more of the fractions from the run.

The measurements were made in Schulz type osmometers at 25° C ± 0.02. The osmotic pressure molecular weight of the original acetate 2.24 and of additional samples not included in the paper were determined at the Institute of Physical Chemistry, Uppsala University, Uppsala, Sweden. Zimm-Myerson osmometers [3] were used in the latter measurements. "Ultracellafilter, allerfeinst" membranes from Membran-Gesellschaft, Göttingen, were used in the determinations with both types of osmometers.

The osmotically determined M_n values and K_m values calculated from the intrinsic viscosities by means of the Staudinger relation $[\eta] = K_m \cdot (DP)$, are listed in Table 1. $K_m = 7 \times 10^{-3}$ was chosen in the present paper to convert the intrinsic viscosity values to DP.

Table 1.

Sample	(η) exp	M_n	$K_m \times 10^3$	M_w (K_m 7.0 × 10^{-3})	DP
0.95	0.95	30 000	8.3	35 300	136
1.63	1.62	62 000	6.8	60 000	230
2.24	2.24	78 000	7.3	83 000	320
Fractions					
4	1.04	38 000	7.1	38 700	149
6	1.09	43 800	6.5	40 500	156
8	1.14	48 000	6.2	42 300	163

It is seen from the table that the M_n of the three fractions rises with the corresponding increase in intrinsic viscosity and fraction number. Because so few analyses on limited amounts from a narrow band of the total distribution could be made, the drop in the K_m value from fraction 4 to fraction 8 cannot safely be interpreted to be due to a corresponding decrease in polydispersity.

The substitution degree of secondary cellulose acetate fractions

Duplicate acetyl analyses were obtained on the eluted fractions 1, 3, 5, 7 and 9 and on combined contiguous eluted fractions Nos. 10 to 44 from the 1.62 fractionation (*cf.* Fig. 3 B) and single analyses on both combined contiguous,

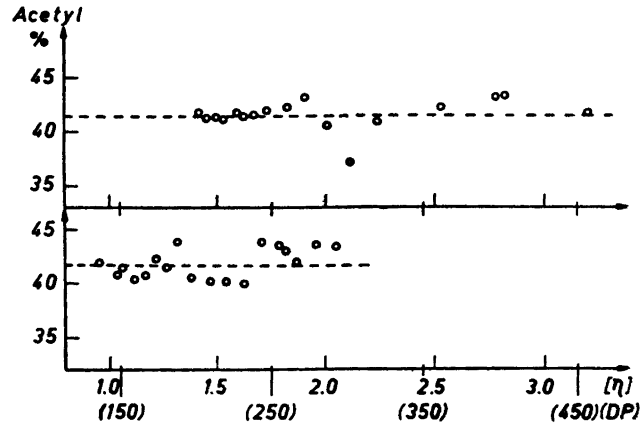


Fig. 5. The acetyl substitution of the fractions versus *their DP. Upper: Fractions from 3.6 g fifty stage fractionation of sample 2.24. Lower: fractions from 2 g fifty stage fractionation of sample 1.62.*

eluted and unadsorbed fractions from the fractionation of sample 2.24 (*cf.* Fig. 3 C).

A plot of the percent acetyl of the fractions *versus* their respective DP values is given in Fig. 5. The original samples 1.62 and 2.24 had 39.1 and 40.1 % acetyl while the average of the analyses on the fractions were 41.0 % and 41.5 %, respectively. The higher average acetyl content of the fractions appears to have been due either to the presence of non-acetyl contaminants or to analytical reasons since the fractions analyzed were largely representative of the entire sample.

No significant variation of acetyl content with DP is apparent from Fig. 5. The variation in acetyl content between fractions, however, is roughly ten times as great as that reported by Staudinger and Eicher [4] following the fractional precipitation of a commercial secondary cellulose acetate of similar DP and substitution degree from acetone with water. The higher apparent non-uniformity shows that the countercurrent fractionation is relatively free of substitution effects. This would be expected since the counter-current separations depend primarily on variations in diffusion rates. Rosenthal and White [5] found variations in substitution of a similar order to those in Fig. 5 by the fractional cross precipitation of secondary cellulose acetates from acetone with water. The variations they reported were also apparently independent of DP.

The five stage fractionation of cellulose nitrate

1.5 g of a cellulose nitrate with intrinsic viscosity 1.95 (see Experimental) was introduced in 25 ml acetone to the first of 5 charcoal stages followed by four 25 ml additions of acetone between 5 min. shaking periods. 9 g of charcoal were used per tube. To elute, the charcoal was shaken twice with 25 ml dioxan.

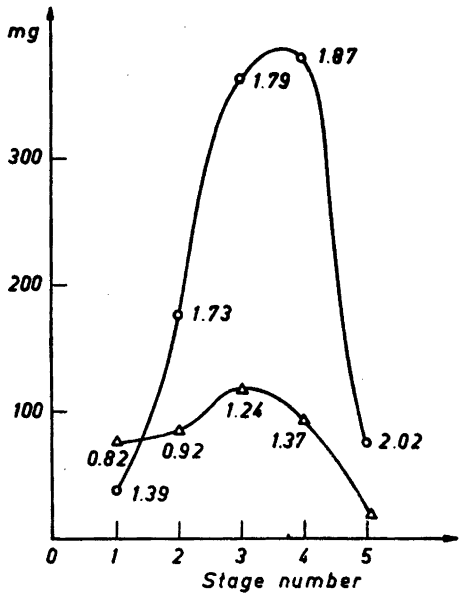


Fig. 6. The amounts of eluted and free material in the fractions from the five stage fractionation of cellulose nitrate 1.95. Circles: the eluted fractions. Triangles: the unadsorbed fractions. The intrinsic viscosities are inscribed for each fraction.

The fractions, in both acetone and dioxan, were precipitated in water, evaporated and further dried under vacuum at room temperature before redispersing in acetone for the viscosity measurements. The total recovery was 95 %, 69 % of which was unadsorbed, decanted, material.

The average intrinsic viscosity of the recovered fractions was 1.62. This low value evidently resulted from degradation of the fractions since the high recovery apparently precluded unrepresentative elution as the cause for the low average intrinsic viscosity of the recovered fractions.

Fig. 6 shows the amounts taken up by each charcoal stage, the amounts decanted at each stage and the intrinsic viscosity of the fractions. The figure, which shows how rapidly and effectively the fractionation begins, also illustrates how the peak of free material appears at an early stage when the uptake capacity of the five charcoal stages is far exceeded. If the run were extended to more charcoal stages the peak of free material would gradually lessen as more material is removed to the charcoal stages. The higher polydispersity of the large fractions in the peak of free material is indicated by their viscosity values which, although the degradation effect must be taken into consideration, are close to that of the original sample.

The result of a 50 stage fractionation of the cellulose nitrate sample is not reported due to the degradation of the fractions which apparently occurred primarily during the precipitation and drying of the fractions. Erratic drops in viscosity were found when some of the fractions in acetone, which had not

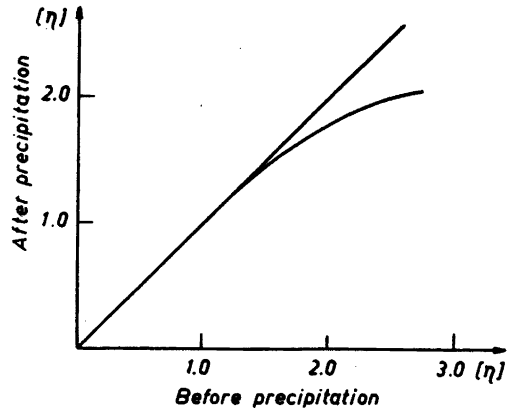


Fig. 7. The intrinsic viscosity of the original cellulose acetate samples after precipitation from dioxan versus *the intrinsic viscosity of the samples dispersed directly in acetone. The figure was used to correct the intrinsic viscosity of some of the eluted fractions.*

altered in viscosity after standing for a week, were reprecipitated in water, dried below 55° C and redispersed in acetone. The viscosity efflux time of the original cellulose nitrate sample in acetone dropped only very slightly after six weeks at room temperature. In dioxan the sample did not change in efflux time after six weeks following an initial drop due to the formation of a slight haze of precipitate which formed after a few days.

EXPERIMENTAL

Materials. The cellulose acetates are Hercules Powder Company products. The samples with intrinsic viscosities of 0.95, 1.62 and 2.24 are substituted to the extent of 2.45, 2.39 and 2.48 respectively. The cellulose nitrate sample from Nitroglycerin AB, Gyttorp, Sweden, had a nitrogen content of 12.02 %, an intrinsic vicosity of 1.95.

The acetone had analytical purity and the dioxan, of *ca.* 99 % purity was used without further treatment. The charcoal, a Norit Company product, is a rather soft, extruded carbon with particle diameter 0.7 mm and with *ca.* 10 % ash content, half of which could be removed with concentrated hydrochloric acid. The untreated charcoal, except for drying, was used in the experiments.

The characteristics sought for in choosing the charcoal were maximum uptake capacity, adequate adsorptive capacity and a particle size from which the polymer solution could be readily decanted. Hard charcoals would be desirable to minimize the charcoal fines that develop from abrasion of soft charcoals during the shaking. Since the uptake capacity was found to increase with increasing softness and porosity, however, the rather soft charcoal was chosen for the experiments. Prior screening and washing of the charcoal was done to minimize the fines. Centrifuging the fraction solutions was necessary [1].

Irreversible precipitation. Evidently due to variations in the purity of the dioxan, it was found that when the cellulose acetates in dioxan were precipitated in water on a steam bath and dried in vacuum at 105° C, theoretical recoveries, on which the concentration values were based were difficult to obtain. Further, the very dry precipitates would not disperse completely in acetone and low viscosity values resulted.

The dioxan fractions were, thereafter, precipitated in water, dried and evaporated at room temperature. The precipitates, containing some moisture, were then dispersed in acetone. The concentration of the latter solutions, used for the viscosity measurements,

was determined on a part of this solution by precipitating in water on the steam bath and drying at 105° C, under vacuum. Theoretical recoveries were obtained in this way but the viscosity values were still low.

To determine the degree of the insolubility effect on the viscosity, varying concentrations of the 0.95, 1.62 and 2.24 cellulose acetates in dioxan were precipitated without heat and the viscosity of the precipitates, redispersed in acetone, determined. The insolubility was found to be independent of the concentration of the solutions precipitated.

In Fig. 7 is shown a plot of the viscosity values on the redispersed precipitates *versus* the viscosity of the original samples dispersed directly in acetone. The graph which was used to correct the viscosity values illustrates that the insolubility increases with increasing DP.

Viscosity measurements. A single measurement method described in the earlier paper [1] was used for the cellulose acetates. The intrinsic viscosity of the cellulose nitrate samples were made by extrapolation of plots of the reduced viscosity *versus* concentration at three or more concentrations below 0.5 g/dl. Ostwald pipettes requiring 2 ml of solution recommended [6] for a range between 0.3 and 5.0 centipoises were used at 25° C ± 0.02.

DISCUSSION

When complete uptake to the charcoal stages was approached in the fractionations of secondary cellulose acetate, single maximum positively skewed, DP weight distribution curves were obtained of the theoretical type to be expected from the random degradation of an original high DP polymer.

While a peak of lower DP material may be expected on theoretical grounds, it is also in the first stages of the apparatus that the highest concentration gradient as well as diffusion rate can be expected to combine in greatest uptake to the charcoal, both effects diminishing as the polymer solution advances to later stages.

Since the fractions in the charcoal stages are held by irreversible adsorption as the runs proceed, the adsorbed material is not further fractionated and the percentage of the sample held by the charcoal stages will determine in part their relative polydispersity. It is important, in consequence, to choose the amount of sample to be fractionated in relation to the uptake capacity, as well as the number, of charcoal stages.

In the countercurrent fractionations, too small a sample in relation to the adsorptive capacity resulted in detention of a higher proportion of lower DP material (*cf.* Fig. 4 B). Too large a sample, on the other hand (*cf.* Fig. 3 A) resulted in the apparent finer fractionation of the lower DP material in the distributions, while higher DP material of consequently higher polydispersity was left unadsorbed since more stages were needed to fractionate the latter material.

The uptake to the charcoal which has been varied in the present experiments by altering the polymer concentration and number of stages while keeping the charcoal capacity and shaking times constant, could also be varied by altering the shaking times, by using a diffusion medium of different porosity and adsorptive capacity or by altering the polarity of the solvent.

Comparison of the first fractions in the two runs in which 0.5 and 5.0 g of acetate 0.95 were introduced to the stages with 9 g charcoal, illustrates the effect of variation in the percentage of sample in the fraction on the selectivity of the separation. The percentages recovered, for example, in the first fraction stage, in the two fractionations, were 10.3 % and 2.6 %, respectively. The

higher apparent polydispersity to be expected of the higher percentage fraction is shown by the intrinsic viscosity, 0.63, compared to that of the low percentage fraction 0.53. The larger percentage fractions from the low concentration 20 stage run also appear to be less sharp when comparison is made of the intrinsic viscosity 0.63 of the single fraction containing 10.3 % of the sample, with the average intrinsic viscosity 0.57 of the first four fraction stages from the high concentration 50 stage run which contained 11.4 % of the sample.

It should be stressed that the solid phase counter-current fractionations are rigorously reproducible, this has been confirmed repeatedly in the course of the experiments. The method, in consequence, is useful for comparative determinations of polymolecularity pending the time when the comparative accuracy of the DP weight distribution curves can be established by determination of the M_w/M_n ratios of the fractions or by other means.

The upper and lower limits in DP which can be fractionated with the method also remain to be established since with the samples investigated, no apparent limit was found. Fractions varying in DP from *ca.* 70 to 500 were obtained in the experiments.

Acknowledgements. The authors wish to express their appreciation to Docent Bengt Rånby, Institute of Physical Chemistry, Uppsala University, Uppsala, Sweden, for the osmotic pressure analyses and also thank Dr. Bertil Enoksson of Nitroglycerin AB, Gyttorp, Sweden, for kindly providing cellulose nitrate samples with accompanying analyses.

The authors are also indebted to Dr. Per Olof Betghe and Miss Rose Marie Persson of the analytical department of this laboratory for the acetyl analyses and to Miss Maj-Britt Eriksson for her assistance in the experiments.

REFERENCES

1. Swenson, H. A. *Acta Chem. Scand.* **9** (1955) 572.
2. Craig, L. C., Hausmann, W., Ahrens, E. H. Jr. and Harfenist, E. J. *Anal. Chem.* **23** (1951) 1236.
3. Zimm, B. H. and Myerson, I. *J. Am. Chem. Soc.* **68** (1946) 911.
4. Staudinger, H. and Eicher, T. *Makromol. Chem.* **10** No. 1 (1953) 235.
5. Rosenthal, A. J. and White, B. B. *Ind. Eng. Chem.* **44** (1952) 2693.
6. Cannon, M. R. and Fenske, M. R. *Ind. Eng. Chem. Anal. Ed.* **10** (1938) 297.

Received July 6, 1956.

ACTA CHEMICA SCANDINAVICA 10 (1956) 1404—1413

Studies on the Chemistry of Lichens

X.* The Structure of Porphyrilic Acid **

CARL AXEL WACHTMEISTER

Kungl. Tekniska Högskolan, Institutionen för Organisk kemi, Stockholm, Sweden

Porphyrilic acid from *Haematomma coccineum* (Dicks.) has been ascribed the structure (III) consistent with the results of oxidative degradations described earlier [1,2] and in harmony with the negative Gibbs' reaction of methyl porphyrilate as well as the negative ferric reaction of O-monomethylporphyrilic acid (IV). The position of the nuclear methyl group has been confirmed by oxidation of O,O-dimethylporphyrilic acid to a tricarboxylic acid (XIII), further degraded to 1,7-dihydroxy-3-methyldibenzofuran (X), obtained synthetically. The acidity of the phenolic groups of porphyrilic acid and its derivatives before and after hydrolysis is discussed.

As described in part VII of this series [2], porphyrilic acid, a lichen acid of the composition $C_{16}H_{10}O_7$ from *Haematomma coccineum* (Dicks.), has been subjected to oxidative degradation, the result of which established the acid as a derivative of 1,7-dihydroxydibenzofuran. A consideration of the properties and colour reactions of the acid together with derivatives and degradation products led to three alternative formulae, (I)—(III), as the most probable structures for the acid itself. Of these, alternative (III) with the carboxyl group in the *para*-position to a phenolic hydroxyl group was rejected since chromatography of porphyrilic acid on buffered paper gave evidence for the formation of a borate complex, characteristic for aromatic *ortho*-hydroxy carboxylic acids [3]. However, porphyrilin [2], the decarboxylation product of porphyrilic acid, has now been found to be retarded on a borate paper as compared with a phosphate paper, provided the pH-values of the buffer solutions are chosen above 9, and hence the borate method is of little value in the present case. Furthermore, methyl porphyrilate, prepared by methanolysis of methyl O,O-diacetylporphyrilate, gave no colour with 2,6-dichloroquinone monochloroimide (Gibbs' reagent) [4] whereas the acid itself gave a clear blue colour with this reagent, as characteristic for phenolic compounds devoid

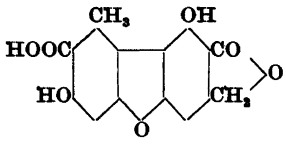
* Part IX: *Acta Chem. Scand.* **9** (1955) 1395.
** Preliminary note: *Chemistry and Industry* **1956** 960.

of ordinary carbonyl functions and containing a free position or an easily removable grouping, *e. g.* a carboxyl group, in the *para*-position to a free hydroxyl group [5,6]. It was therefore necessary to reconsider structure (III), the only formula which accounts for a negative Gibbs' reaction after esterification of the carboxyl group.

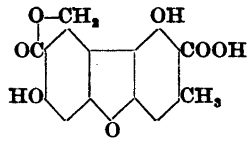
Further evidence in favour of structure (III) has now been obtained by partial methylation of porphyrilic acid. As stated in the experimental part of part VII [2], the acid titrates in the cold approximately as a dibasic acid with thymolphthalein as indicator. The titration is conveniently carried out in aqueous acetone with thymol blue as indicator. Hence, one of the two phenolic hydroxyl groups should be fairly acidic and the acid when treated for a short time with an excess of diazomethane in aqueous acetone at —10° gave a good yield of a methyl O-monomethylporphyrilate, hydrolysed by alkali to O-monomethylporphyrilic acid. These derivatives were only very sparingly soluble in the common solvents, the methyl ether being conveniently purified *via* its acetate, crystallising as a mixed anhydride from acetic anhydride. The methyl ether as well as its methyl ester gave no or at most a faintly yellowish colour with ferric chloride in ethanol, whereas an ethanolic solution of porphyrilic acid of a similar, very low concentration (0.01 %) gave a quite distinct, reddish-blue colour. Since, of the six possible monomethyl ethers derivable from the structures (I)—(III), only the methyl ether (IV) should give a negative ferric reaction, these results point definitely to this structure for the methyl ether and structure (V) for the corresponding methyl ester. The methyl ether (IV), in contrast to its ester (V), gave a clear blue colour with Gibbs' reagent, which constitutes a further confirmation of the proposed structures.

Porphyrilin, according to the above results formulated as (VI), also possesses a phenolic hydroxyl group of a high acidity, as revealed in aqueous acetone or aqueous pyridine when the lactone titrates in the cold approximately as a monobasic acid with thymol blue as indicator. Furthermore, treatment of porphyrilin in aqueous acetone containing a trace of methanol with an excess of ethereal diazomethane for 5—10 minutes at —10° afforded a quantitative yield of a monomethyl ether which gave no ferric reaction but a strong blue colour with Gibbs' reagent and hence must be ascribed the structure (VII). It melted with decomposition at 315—320° which is higher than the melting point of porphyrilin and was conveniently characterized by paper chromatography and by its acetate (VIII), m.p. 254—257°. The same monomethyl ether (VII) of porphyrilin was obtained from O-monomethylporphyrilic acid (III) by sublimation *in vacuo* or more conveniently by prolonged boiling with formic acid.

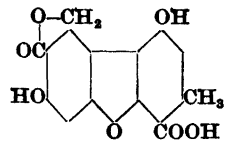
A derivative of porphyrilin containing a free acidic hydroxyl group could be prepared by treatment of its diacetate [2] with aniline at room temperature. The resulting monoacetate, which crystallised directly from the reaction mixture, gave an intense blue ferric reaction but no blue colour with Gibbs' reagent and hence must be ascribed the structure (IX). It titrated in the cold as a monobasic acid with thymol blue as indicator and on methylation with diazomethane yielded the O-monomethylporphyrilin monoacetate (VIII), m. p. 254—257°, mentioned above.



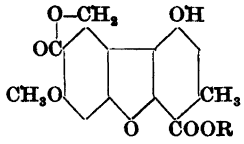
I



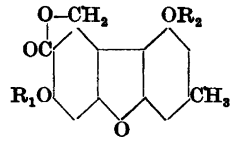
II



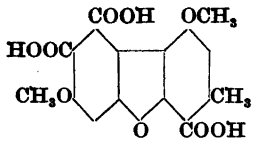
III



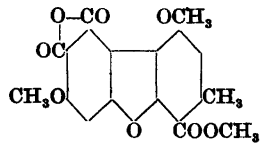
IV : R = H
V : R = CH_3



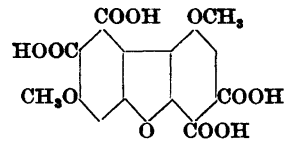
VI : $R_1 = R_2 = H$
VII : $R_1 = CH_3$ $R_2 = H$
VIII : $R_1 = CH_3$ $R_2 = CH_3CO$
IX : $R_1 = H$ $R_2 = CH_3CO$



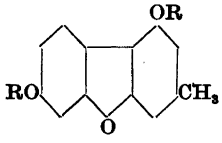
XIII



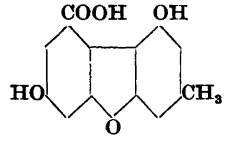
XIV



XV



X : R = H
XI : R = CH_3CO



XII

The colour reactions given by these monosubstituted derivatives of porphyrilin provide strong evidence for formulating this compound as (VI) and hence establish porphyrilic acid as derived from 1,7-dihydroxy-3-methyldibenzofuran (alternatives (II) or (III)), and not from 1,7-dihydroxy-9-methyldibenzofuran (alternative (I)).

The position of the nuclear methyl group has been confirmed by partial oxidation of O,O-dimethylporphyrilic acid [2], carried out in a dilute alkaline solution at 80—90° with an excess of permanganate. The desired tricarboxylic acid (A) could be isolated in a pure state as the monomethyl ester of its anhydride (B) which on prolonged boiling with hydrobromic acid lost two molecules of carbon dioxide with simultaneous demethylation to a dihydroxy-monocarboxylic acid (C), characterised by paper chromatography and by its methyl ester. The methyl ester, like the free acid, gave no distinct ferric reaction.

On decarboxylation with quinoline and a copper chromite catalyst, the acid (C) yielded a phenol $C_{13}H_{10}O_3$, (D), m. p. 165—166°, shown to be identical with 1,7-dihydroxy-3-methyldibenzofuran (X), synthesised by a method analogous to that used for 1,7-dihydroxydibenzofuran [2].

The mixed Ullmann-coupling, carried out with 4-iodo-3,5-dimethoxytoluene and an excess of 4-iodoresorcinol dimethyl ether, yielded a mixture of diphenyls which could not be easily separated into its components. The crude mixture on treatment with boiling hydrobromic acid furnished a mixture of dihydroxydibenzofurans partly freed from 3,7-dihydroxydibenzofuran [7] by crystallisation from benzene. The desired phenol (X) was isolated from the mother liquor by chromatography on thick filter paper or on aluminium oxide. Its identity with the phenol (D), indicated by paper chromatography, was definitely established by mixed melting points of the phenols as well as of their acetates.

Hence the acid (C) must have structure (XII), the carboxyl group of which is not in the *ortho*- or *para*-position to any hydroxyl group. The structure of the tricarboxylic acid (A) and the corresponding ester-anhydride (B) however can be established as (XIII) and (XIV), respectively, only with due regard to the results obtained concerning the position of the carboxyl group of porphyrilic acid. Taking into account these results, the tetracarboxylic acid $C_{18}H_{12}O_{11}$ (tetramethyl ester, m. p. 221.5—223°) obtained earlier [2] must be ascribed the structure (XV), previously considered improbable.

The proposed structure (III) for porphyrilic acid can be substantiated by a more detailed examination of the acidic functions of the acid and its derivatives. It is a well known fact that intramolecular hydrogen bonds in aromatic *ortho*-hydroxy carboxylic acids strikingly affect the dissociation constants of the acidic groups in these acids as compared with their *meta*- or *para*-isomers. Thus salicylic acid and *p*-hydroxybenzoic acid show $pK_1 = 3.0$ and 4.5, respectively [8,9]. The former acid can be titrated with some accuracy even with an indicator such as bromocresol green (pH-range 3.8—5.4) whereas the latter requires at least bromothymol blue (pH-range 6.0—7.6). Porphyrilic acid, when titrated in aqueous acetone, behaves like *p*-hydroxybenzoic acid.

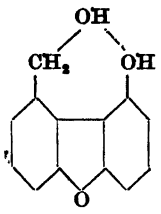
Similarly, the phenolic hydroxyl group in salicylic acid or its esters is of extremely low acidity [9,10], also revealed by the slow reaction of methyl salicylate with diazomethane (compare, *e. g.*, Schönberg and Mustafa [11]). On the other hand, the hydroxyl group of *p*-hydroxybenzoic acid ($pK_2 = 9.3$) [9] is acidic enough to interfere in the titration of this acid using thymol blue and its acidity is still further enhanced in methyl *p*-hydroxybenzoate [10], which can be titrated in aqueous acetone or pyridine with thymolphthalein as indicator. It is therefore in harmony with structure (III) that methyl porphyrilate in cold aqueous pyridine can be titrated fairly sharply as a dibasic acid using the indicator mentioned. Furthermore, porphyrilic acid contains no hydroxyl group showing great resistance towards methylation with diazomethane.

The high acidity of that phenolic hydroxyl group which accounts for the blue ferric reaction of porphyrilic acid and porphyrilin, also found in, *e. g.*, mycophenolic acid [12] or in 7-hydroxy-3-methylphthalide ($pK = 8.5$) [13], is evidently characteristic for *ortho*-hydroxyphthalides containing the hydroxy-group in the *ortho*-position to the lactonised carboxyl group and points to a

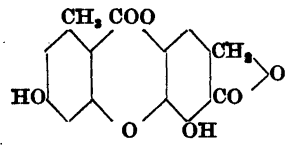
reduced chelation in these compounds as compared with, *e. g.*, methyl salicylate. The rapid methylation with diazomethane in aqueous acetone of the hydroxyl group in question is then explained as is also the very low solubility of porphyrilin even in boiling chloroform. It is of interest that recent infra-red measurements by Duncanson, Grove and Zealley [14] on simple compounds of the types discussed show strongly reduced though still distinct chelation in the 7-hydroxyphthalides.

While the above considerations account for the results obtained by titration in the cold of porphyrilic acid and its derivatives, the hydrolytic titrations require further discussion. Unexpectedly, O-monomethylporphyrilin (VII) titrated fairly sharply as a dibasic acid after hydrolysis with excess of alkali in aqueous ethanol and back titration with thymolphthalein as indicator. The titration could not be performed in an aqueous solution since the lactone, being of the phthalide type, precipitated at high pH-values. Porphyrilin (VI) was still more easily precipitated even from alkaline solutions containing ethanol, but on hydrolytic titration in aqueous pyridine this compound also titrated approximately as a dibasic acid. The result previously reported of the hydrolytic titration of porphyrilin in an aqueous solution with thymol blue as indicator could not be reproduced. Furthermore, porphyrilic acid (III) as well as its monomethyl ether (IV) proved approximately tribasic on hydrolytic titrations using the indicator mentioned.

A possible explanation of the observed low equivalent weights involves the assumption of an intramolecular hydrogen bond between the methylol group and the phenolic hydroxyl group of the partial structure (XVI), resulting in an increased acidity of the phenolic hydroxyl group. It seems quite possible that the postulated hydrogen bond, perhaps weak in an unionized phenol of the type (XVI), becomes fairly strong only after ionization of the phenolic group, but this question clearly requires further investigations on simple model compounds. A somewhat analogous case is given by 1,8-dihydroxynaphthalene [15]. Also 1,9-dihydroxydibenzofuran which titrates sharply as a monobasic acid with thymol blue as indicator offers an interesting example of a similar intramolecular hydrogen bond, which in this case seems to be of a considerable strength in the unionized phenol also [16]. The hydroxyl group in the *ortho*-position to the lactonised carboxyl group is not titrated after hydrolysis of the lactone ring, when the hydroxyphthalide structure changes to a salicylic acid structure (*cf.* [12]).



XVI



XVII

The indigo-blue colour reaction with ferric chloride given by porphyrilic acid and some of its derivatives seems to be of diagnostic value as it is reported also for 7-hydroxyphthalide [14] itself as well as for related compounds such as strepsilin [17] or mycophenolic acid [12]. Salicylic acid and related compounds generally give a violet ferric reaction.

The possibilities for formation of borate complexes of porphyrilic acid and its derivatives seem to be greater than previously supposed. As not only porphyrilin and methyl porphyrilate but also O-monomethylporphyrilic acid is slowed down on a borate paper, no conclusions concerning their structures can be drawn from these results without further studies on model compounds.

The unsymmetrical dihydroxydibenzofuran structure of porphyrilic acid (III) is unique among the lichen acids although there is paper chromatographic evidence for the occurrence of another closely related acid in very small amounts in *H. coccineum*. The crustose lichen *Ochrolechia parella* (L.) Mass. contains an isomeric compound of the depsidone type, variolaric acid, ascribed the structure (XVII) by Murphy, Keane and Nolan [18]. Both porphyrilic acid and variolaric acid are composed of orsellic acid units and contain the hydroxyphthalide structure and they may both be considered as having been formed from the same two phenolic acids by different mechanisms of dehydrogenative coupling. It is possible that in *O. parella* a preformed depside is dehydrogenated with formation of the depsidone, whereas in *H. coccineum* the dehydrogenase system attacks the simple phenolic compounds resulting in the formation of a diphenyl derivative further stabilised by ring closure to the dibenzofuran derivative, porphyrilic acid. The positions involved in the presumed dehydrogenative couplings to variolaric acid and porphyrilic acid are unusual, being *ortho* to both hydroxyl groups of the orcinol skeleton of one of the components, whilst as a rule in the lichen series the coupling involves the *o*-, *p*-positions. The chemical relations discussed may be of special interest in view of the presumed close relations between the genera *Haematomma* and *Ochrolechia*. Thus, in both lichens identical dehydrogenase systems may operate, *H. coccineum*, however, largely lacking the enzymatic requirements for the formation of depsides of the orcinol type.

EXPERIMENTAL *

Unless otherwise stated the paper chromatography was carried out at 25° using the solvent system *n*-butanol-water. Whatman No. 1 paper was used after impregnation with buffer solutions as previously described [2,3,19].

Methyl porphyrilate. Methyl O,O-diacetyl porphyrilate [2] (1 g) was boiled for 30 min. with 1.5 N methanolic hydrogen chloride (50 ml), yielding methyl porphyrilate (0.8 g) which crystallised from the boiling solution. The analytical sample crystallised as needles from a mixture of pyridine and glacial acetic acid (1:1) and was dried *in vacuo* at 150° C. It showed no melting point but decomposed gradually above 320°. The ester gave no colour with Gibbs' reagent [4] when tested in a borate buffer of pH 9 but a light brown colour with *bis*-diazotised benzidine [20] (on buffered filter paper) and a distinct blue colour with ferric chloride in ethanol. R_F-values on phosphate-impregnated papers: 0.65 (0.1 M Na_2HPO_4, pH 8.9); 0.10 (0.1 M Na_3PO_4, pH 12.1) and on borate-impregnated paper: 0.35 (0.1 M borate buffer of pH 9.1).

The equivalent weight was determined by titration of the ester in a cold pyridine solution with 0.05 N aqueous sodium hydroxide using thymolphthalein as indicator. (Found: C 61.9; H 3.60; OCH_3 9.6; equiv. weight, 165. $C_{17}H_{12}O_7$ requires C 62.2; H 3.68; OCH_3 9.5; equiv.weight (as a dibasic acid) 164.1.)

Methyl O-monomethylporphyrilate (V). To a solution of porphyrilic acid (1 g, *ca.* 3 mmole) in acetone (800 ml) and water (75 ml), cooled to −10 – −15°, diazomethane

* All melting points uncorrected.

(20 mmole) in ether (60 ml) was added in a few portions with stirring during 5 min. After another 5 min., the excess of diazomethane was destroyed by the addition of acetic acid. The reaction product, which rapidly crystallised from the cold solution, was collected after a few hours and proved to be fairly pure methyl O-monomethylporphyrilate (0.65 g). It gave no colour with Gibbs' reagent and no or only a faintly yellowish colour with ferric chloride in ethanol. On buffered paper (0.1 M Na_3PO_4) a spot, $R_F = 0.45$, of greenish-white colour in ultra-violet light was obtained, which gave a faint yellowish-brown colour with *bis*-diazotised benzidine. In addition a faint spot of methyl porphyrilate ($R_F = 0.10$) was observed on the chromatogram. The mother liquor on evaporation yielded a second fraction (0.35 g), only partly soluble in cold alkali and evidently containing methyl O,O-dimethylporphyrilate [2]. This compound was obtained as the main reaction product when the methylation was performed at higher temperature or when too large an excess of diazomethane was used.

The analytical sample was crystallised from pyridine and from pyridine-ethanol. Needles, dried *in vacuo* at 150°. M. p. 340–345° (decomp.) after darkening from 300°. (Found: C 63.6; H 4.51; OCH_3 17.7. $C_{18}H_{14}O_7$ requires C 63.2; H 4.12; OCH_3 18.1.)

O-Monomethylporphyrilic acid (IV). Crude methyl O-monomethylporphyrilate (V) (0.3 g) in 0.2 N sodium hydroxide solution (200 ml) was warmed to 50° overnight and the solution then diluted with acetone (200 ml) and acidified with hydrochloric acid, whereupon the monomethyl-derivative (IV) crystallised as microscopic needles containing solvent of crystallisation. It was almost insoluble in dry acetone but could be crystallised from 80 % aqueous acetone (150 ml to 100 mg of the acid). The analytical sample was obtained by hydrolysis of the mixed anhydride of its monoacetate (see below) with equal volumes of 0.1 N sodium hydroxide solution and acetone. It was dried *in vacuo* at 150°. M. p. 305–310° (decomp.). The equivalent weight was determined before hydrolysis by back titration of a solution of the acid in an excess of 0.05 N sodium hydroxide using phenol red as well as after hydrolysis by treatment of the acid with excess alkali for 1 h at 90° and back titration with thymolphthalein as indicator. (Found: C 62.0; H 3.51; OCH_3 8.8; equiv. weight 335 (before hydrolysis) and 114 (after hydrolysis). $C_{17}H_{12}O_7$ requires C 62.2; H 3.68; OCH_3 9.5; equiv. weight 328.3 (as a monobasic acid) and 109.4 (as a tribasic acid).)

O-Monomethylporphyrilic acid (0.01 % in ethanol) gave only a faintly yellowish colour with ferric chloride but a strong blue colour with Gibbs' reagent and a dark wine-red colour when treated with the benzidine reagent on buffered paper. The R_F-values of the acid on buffered paper were 0.20 (Na_2HPO_4), 0.05 (Na_3PO_4) and 0.10 (borate buffer, pH 9.1), respectively. The spots showed a greenish-white fluorescence in ultra-violet light.

Acetylation of O-monomethylporphyrilic acid. Crude monomethyl ether (IV) (0.5 g) was warmed with acetic anhydride (15 ml) and a few drops of pyridine until complete solution had been effected. The acetate crystallised on cooling and was obtained chromatographically pure as needles, m. p. 212–215°, from acetic anhydride. For chromatography, the acetate was dissolved in pyridine and the chromatogram run on buffered paper (Na_3PO_4) when a single spot of the monomethyl ether (IV) was obtained due to hydrolysis of the acetoxyl groups. The acetate which in the crystalline state exhibited an extraordinarily intense white fluorescence in ultra-violet light proved insoluble in cold aqueous sodium hydroxide and was established as a mixed anhydride by the hydroxamate test as well as by analysis. (Found: OCH_3 7.5; CH_3CO 20.7. $C_{21}H_{16}O_9$ requires OCH_3 7.5; CH_3CO 20.9.)

When warmed with glacial acetic acid the above acetate dissolved but acetolysis of the mixed anhydride occurred and the sparingly soluble monoacetate of O-monomethylporphyrilic acid soon crystallised from the hot solution.

The same monoacetate was obtained by acetylation of the monomethyl ether (50 mg) with acetic anhydride (0.5 ml) and pyridine (1 ml). Needles, m. p. 260–270° (decomp.), dried *in vacuo* at 150°. The equivalent weight was determined by hydrolytic titration (thymolphthalein). (Found: CH_3CO 11.0; equiv. weight 95. $C_{19}H_{14}O_8$ requires CH_3CO 11.6; equiv. weight 93.3 (after complete hydrolysis).)

O-Monomethylporphyrilin (VII). a) *Partial methylation of porphyrilin* (VI). Porphyrilin (360 mg, 1.2 mmole) in acetone containing a trace of methanol (200 ml) and water (20 ml) was methylated at −10° with diazomethane (5 mmole) in ether (25 ml), added in portions during 10 min. Acetic acid was then added and evaporation of the solution yielded a crystallisate practically free from porphyrilin as found by paper chromato-

graphy. The substance gave no ferric reaction but an immediate blue colour with Gibbs' reagent. R_F-value on buffered paper (Na_3PO_4): 0.85. It crystallised as colourless needles from acetone and was finally sublimed *in vacuo*, m. p. 315—320° (decomp., darkening from 300°). The equivalent weight was determined by hydrolysis of 50 mg with 0.1 N aqueous sodium hydroxide (6 ml) and ethanol (10 ml) for 1 hour at 90°, followed by back titration of the cooled solution with 0.1 N hydrochloric acid, using thymolphthalein as indicator. (Found: C 67.5; H 4.54; OCH_3 10.8; equiv. weight 140. $C_{16}H_{12}O_5$ requires C 67.6; H 4.25; OCH_3 10.9; equiv. weight (as a dibasic acid) 142.1.)

Acetylation with acetic anhydride and a trace of pyridine yielded O-monomethylporphyrilin monoacetate (VIII), needles from acetone, m. p. 254—257° after sintering from 245°. (Found: CH_3CO 13.1. $C_{18}H_{14}O_6$ requires CH_3CO 13.2.)

b) *Decarboxylation of O-monomethylporphyrilic acid (IV).* The methyl ether (IV) (50 mg) in formic acid (5 ml; $d = 1.22$) was boiled for two days and the solution was then filtered hot and evaporated to dryness. The product obtained, m.p. 305—310° after sublimation *in vacuo*, proved to be identical with the monomethyl ether (VII), obtained from porphyrilin, by its colour reactions, by paper chromatography and finally by conversion to its acetate, m.p. 250—255° (after sintering), undepressed on admixture with the acetate (VIII) described above. The decarboxylation could also be effected by sublimation of the acid (IV) *in vacuo*, although some decomposition then occurred.

Partial deacetylation of porphyrilin diacetate [2]. The diacetate (350 mg) in aniline (10 ml) was kept at room temperature with occasional stirring. The acetate soon dissolved and the crude monoacetate (IX) (120 mg) which gradually crystallised from the reaction mixture was filtered off after 24 h. It crystallised from acetone as needles, m.p. 227—229°, dried *in vacuo* at 150°. The monoacetate gave an intense blue reaction with ferric chloride in ethanol but no blue colour when tested with Gibbs' reagent in a borate buffer of pH 9. The equivalent weight was determined by titration in cold acetone with thymol blue as indicator. (Found: equiv. weight 310. $C_{17}H_{12}O_6$ requires equiv. weight 312.3.)

A small sample of the monoacetate was methylated with ethereal diazomethane yielding a product of m.p. 255—258° which by mixed melting point determination proved identical with the derivative (VIII) described above.

Partial oxidation of O,O-dimethylporphyrilic acid [2]. The dimethyl ether (1.5 g, 4.5 mmole) in 0.2 N potassium hydroxide solution (100 ml) was boiled for 10 min. to hydrolyse the lactone ring. After dilution with water (700 ml) the solution was warmed on the boiling water bath and 0.06 M potassium permanganate solution (130 ml, a 30 % excess of the amount calculated for oxidation of the carbinol group) added dropwise with rapid stirring during 10 h. After filtration, the solution was acidified with conc. hydrochloric acid (10 ml) and heated to boiling, when a yellow crystalline material separated. It was filtered off (1.0 g) and dried *in vacuo* at 180° to complete the formation of the anhydride. The desired anhydride of the tricarboxylic acid (A) proved difficult to isolate in a pure state but after short treatment of the reaction product in acetone suspension with an excess of ethereal diazomethane, the monomethyl ester of the anhydride (B) could be isolated from the reaction product by extraction with hot methyl ethyl ketone. It was obtained in a pure state as yellow needles, (0.3 g), m. p. 286—292°, by recrystallisation from the same solvent. The equivalent weight was determined by titration in aqueous pyridine with thymol blue as indicator. (Found: C 61.3; H 3.80; OCH_3 24.5 equiv. weight 187. $C_{19}H_{14}O_8$ requires C 61.6; H 3.81; OCH_3 25.1; equiv. weight (as a dibasic acid) 185.1.)

Demethylation and decarboxylation of acid (A). The methyl ester monoanhydride (B) of acid (A) (0.24 g) was boiled in a nitrogen atmosphere with hydrobromic acid (25 ml, $d = 1.5$) for two days. After cooling, the crude monocarboxylic acid (C) (0.16 g) was collected by filtration and purified by precipitation with hydrochloric acid from a bicarbonate solution. The acid did not crystallise well but was obtained as a microcrystalline brownish powder, reasonably pure as shown by chromatography on buffered paper (Na_3PO_4; $R_F = 0.45$). The spot which showed a greenish white fluorescence in ultraviolet light gave a red colour with *bis*-diazotised benzidine and an intense blue colour with Gibbs' reagent. A small sample of the acid was purified *via* the methyl ester (see below) and obtained as yellowish needles, m. p. 265—270°, by sublimation *in vacuo* (1 mm, bath-temperature 250—260°). It gave no distinct colour with ferric chloride. (Found: equiv. weight 263. $C_{14}H_{10}O_5$ requires equiv. weight 258.2.)

The methyl ester, obtained by short treatment of the crude acid in ice-cold acetone solution with ethereal diazomethane, crystallised as yellowish prisms from ethanol and

was finally sublimed *in vacuo*. It gave no colour with ferric chloride and showed m. p. 232–235°. (Found: OCH_3 12.1. $C_{15}H_{12}O_5$ requires OCH_3 11.4.)

Decarboxylation of the acid (C). The crude acid (C) (0.13 g) in quinoline (2.5 ml) was boiled for 2 h with a copper chromite catalyst (25 mg). The reaction mixture was diluted with ether, filtered and the insoluble material washed with ether. The combined ether solutions were washed with 4 N sulphuric acid, bicarbonate solution and water, dried with sodium sulphate and evaporated to dryness, yielding the crude phenol (D) as an oil (0.11 g) which crystallised after distillation *in vacuo*. It was crystallised from methanol-water and finally from benzene, yielding prisms, m. p. 165–166°, undepressed on admixture with synthetic 1,7-dihydroxy-3-methyldibenzofuran (X), described below. The two phenols also showed the same R_F-values (0.20; solvent system benzene-water) and gave identical colour reactions: *bis*-diazotised benzidine, red, Gibbs' reagent, blue, and ferric chloride, no colour. (Found: C 72.3; H 4.45. $C_{13}H_{10}O_3$ requires C 72.9; H 4.70.)

The phenol was further characterised by its diacetate which crystallised from methanol in needles, m. p. 129–130°, undepressed on admixture with synthetic 1,7-diacetoxy-3-methyldibenzofuran (XI), m. p. 129–130°. (Found: C 68.6; H 4.70. $C_{17}H_{14}O_5$ requires C 68.5; H 4.73.)

1,7-Dihydroxy-3-methyldibenzofuran. 4-Iodo-3,5-dimethoxytoluene [21] was prepared *via* 4-nitro-orcinol obtained in 5–6 % yield by nitration of orcinol in ether solution and subsequent steam distillation as described by Henrich and Meyer [22]. Methylation of the crude nitro-orcinol with dimethyl sulphate and alkali yielded 4-nitro-3,5-dimethoxytoluene, m. p. 147–148° after crystallisation from ethanol (Posternak *et al.*[21] report m. p. 147–147.5°). It was hydrogenated in ethanol with Adams platinum oxide catalyst to 4-amino-3,5-dimethoxytoluene and the crude product (m. p. 60–62°; Posternak *et al.*[21] give m. p. 64–65°) was diazotised and transformed into 4-iodo-3,5-dimethoxytoluene as described by Posternak *et al.*[21]. After crystallisation from ethanol it showed m. p. 96–97°, in agreement with the value given by Posternak *et al.*[21].

4-Iodo-3,5-dimethoxytoluene (1 g), 4-iodoresorcinol dimethyl ether [23] (9 g) and copper bronze (30 g) were thoroughly mixed and the reaction carried out in an analogous manner to that described in an earlier paper [2]. It proved convenient to extract the reaction product in a Soxhlet apparatus with light petroleum (b. p. 40–60°) for 12 h. In contrast to acetone, this solvent did not extract much resinous by-product, nor the symmetrical 4,4′-dimethyl-2,6,2′,6′-tetramethoxydiphenyl[21] (m. p. 145–146°) which should be formed in minute amounts. The petroleum extract deposited an oil which soon crystallised (3.4 g; m. p. 80–105°). All attempts to isolate the desired unsymmetrical diphenyl derivative in the pure state were unsuccessful.

The mixture of diphenyls (3.0 g) was boiled for 7 h under reflux with hydrobromic acid (60 ml; $d = 1.5$) in a carbon dioxide atmosphere. After cooling overnight in the refrigerator, the deposited crystalline material was collected, washed with water and dried *in vacuo* (yield, 1.9 g). Paper chromatography of the crude product (solvent system: benzene-water) showed one spot (grey colour with Gibbs' reagent) of 3,7-dihydroxydibenzofuran [7], $R_F = 0.07$, and a second spot, $R_F = 0.20$, which gave a blue colour with Gibbs' reagent, as expected for 1,7-dihydroxy-3-methyldibenzofuran. This second spot was in all respects identical with the spot from the phenol (D) described above. On extraction of the crude product with benzene in a Soxhlet apparatus a considerable enrichment of 3,7-dihydroxydibenzofuran in the crystallisate obtained was achieved. The unsymmetrical compound could be isolated from the mother liquor by chromatography on thick filter paper or more conveniently on alumina. The column was constructed in benzene using aluminium oxide (10 g) deactivated with nitric acid [24]. The phenol mixture (200 mg) in benzene (150 ml) was adsorbed on the column and eluted with benzene (750 ml). The fractions (25 ml) were tested with Gibbs' reagent and if necessary analysed by paper chromatography. Ca. 50 mg of chromatographically pure 1,7-dihydroxy-3-methyldibenzofuran (X) was obtained from the fractions Nos. 10–25. It was crystallised from methanol-water, and finally obtained from benzene as prisms, m. p. 166–167°. (Found: C 73.0; H 4.74. $C_{13}H_{10}O_3$ requires C 72.9; H 4.70.)

1,7-Diacetoxy-3-methyldibenzofuran (XI) was obtained from the above phenol by the action of acetic anhydride and pyridine and crystallised from methanol in needles, m. p. 129–130°. (Found: C 68.5; H 4.67. $C_{17}H_{14}O_5$ requires C 68.5; H 4.78.)

Paper chromatography of porphyrilin. The R_F-values of porphyrilin obtained on buffered papers were as follows: With 0.1 M phosphate buffer, pH 8.9: 0.78; pH 10.0: 0.70; pH 10.6: 0.60, and with 0.1 M borate buffer, pH 9.1: 0.55; pH 9.8: 0.40.

Titration of porphyrilin (VI). a) *Before hydrolysis:* The lactone, dissolved in 90 % aqueous acetone or in 90 % aqueous pyridine, was titrated in the cold with 0.05 N aqueous sodium hydroxide, using thymol blue as indicator. (Found: equiv. weight 275 ± 10. $C_{15}H_{10}O_5$ requires equiv. weight 270.2.)

b) *After hydrolysis:* Porphyrilin (40 mg) in 0.1 N sodium hydroxide solution (6 ml) and pyridine (10 ml) was hydrolysed on the boiling water bath for 1 h and back titrated with 0.1 N hydrochloric acid (thymolphthalein). The sample of porphyrilin used gave a yellow solution with alkali (*cf.* [2]) and the end point was somewhat indefinite. (Found: equiv. weight 150 ± 20. $C_{15}H_{10}O_5$ requires equiv. weight 135.1 (as a dibasic acid).)

Titration of porphyrilic acid (III) after hydrolysis. The acid was hydrolysed for 1 h at 90° with an excess of 0.05 N sodium hydroxide solution and back titrated with 0.02 N acid (thymolphthalein). (Found: equiv. weight 109. $C_{16}H_{10}O_7$ requires equiv. weight 104.7 (as a tribasic acid).)

A grant from *Hierta-Retzius' fond för vetenskaplig forskning* is gratefully acknowledged.

REFERENCES

1. Erdtman, H. and Wachtmeister, C. A. *Nature* **172** (1953) 724.
2. Wachtmeister, C. A. *Acta Chem. Scand.* **8** (1954) 1433.
3. Wachtmeister, C. A. *Acta Chem. Scand.* **5** (1951) 976.
4. Gibbs, H. D. *J. Biol. Chem.* **72** (1927) 649.
5. Davidson, V. E., Keane, J. and Nolan, T. J. *Sci. Proc. Roy. Dublin Soc.* **23** (N. S.) (1943) 148.
6. Gierer, I. *Acta Chem. Scand.* **8** (1954) 1319.
7. Hata, K. and Simada, T. *Sci. Papers Inst. Phys. Chem. Research, Tokyo* **6** (1927) 305.
8. Branch, G. E. K. and Yabroff, D. L. *J. Am. Chem. Soc.* **56** (1934) 2568.
9. Kuhn, R. and Wassermann, A. *Helv. Chim. Acta* **11** (1928) 20.
10. Larsson, E. *Z. anorg. Chem.* **183** (1929) 34.
11. Schönberg, A. and Mustafa, A. *J. Chem. Soc.* **1946** 746.
12. Birkinshaw, J. H., Bracken, A., Morgan, E. N. and Raistrick, H. *Biochem. J. London* **43** (1948) 216.
13. Hochstein, F. A. and Pasternack, R. *J. Am. Chem. Soc.* **74** (1952) 3905.
14. Duncanson, L. A., Grove, J. F. and Zealley, J. *J. Chem. Soc.* **1953** 1331.
15. Hoyer, H. *Ber.* **86** (1953) 507.
16. Wachtmeister, C. A. *To be published.*
17. Shibata, S. *Acta Phytochim. Japan* **14** (1944) 177.
18. Murphy, D., Nolan, T. J. and Keane, J. *Sci. Proc. Roy. Dublin Soc.* **23** (N. S.) (1943) 71.
19. Wachtmeister, C. A. *Acta Chem. Scand.* **6** (1952) 818.
20. Koch, J. E. and Krieg, W. *Chem. Ztg* **62** (1938) 140.
21. Posternak, T., Ruelius, H. W. and Tcherniak, J. *Helv. Chim. Acta* **26** (1943) 2036.
22. Henrich, F. and Meyer, W. *Ber.* **36** (1903) 885.
23. Kaufmann, H. and Kieser, F. *Ber.* **45** (1912) 2334.
24. Boissonnas, R. A. *Helv. Chim. Acta* **30** (1947) 1696.

Received July 7, 1956.

ACTA CHEMICA SCANDINAVICA **10** (1956) 1414—1421

Dehydrogenation of Alkaloids of the Yohimbine Type with *tert.*-Butyl Hypochlorite. Conversion of Yohimbine to Pseudoyohimbine

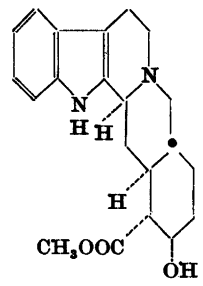
W. O. GODTFREDSEN and S. VANGEDAL

Leo Pharmaceutical Products, Copenhagen, Denmark

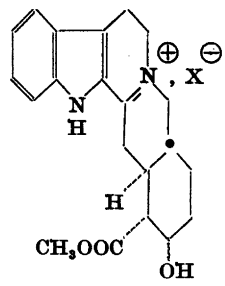
The dehydrogenation of alkaloids of the yohimbine type with *tert.*-butyl hypochlorite is described and the structure of the dehydrogenation products discussed.

It is shown that catalytical hydrogenation of dehydroyohimbine under alkaline conditions leads to the formation of a mixture of yohimbine and pseudoyohimbine.

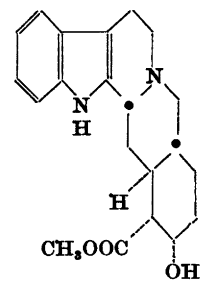
In a recent communication Weisenborn and Diassi [1] describe the oxidation of yohimbine (I) with mercuric acetate to salts of Δ^3-dehydroyohimbine (II).



I



II



III

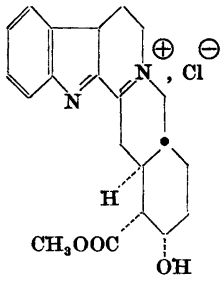
Other alkaloids of the yohimbine type containing an axial hydrogen at C_3 were oxidized in the same manner, while compounds containing an equatorially oriented hydrogen failed to react.

Catalytical reduction of II with platinum in methanol gave only yohimbine, while reduction with zinc and hydrochloric acid yielded a mixture of yohimbine (I) and pseudoyohimbine (III).

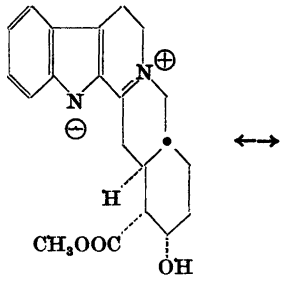
In this paper, it is shown that the same dehydrogenation can be accomplished in good yield with *tert.*-butyl hypochlorite in methylene chloride. By this method, the following compounds have been oxidized: Yohimbine, pseudoyohimbine, corynanthine, α-yohimbine, apoyohimbine, and deserpidine.

It will be seen that compounds containing an axial hydrogen at C_3 (yohimbine, corynanthine, α-yohimbine, and apoyohimbine) as well as compounds with an equatorially oriented hydrogen atom (pseudoyohimbine and deserpidine) can be dehydrogenated in this way.

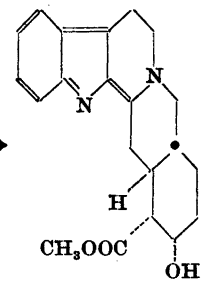
The fact that in the infrared spectrum of Δ^3-dehydroyohimbine chloride no band appears in the NH-region while, on the other hand, all N-unsubstituted indole derivatives are characterized by an intense sharp band at 2.9 μ, suggests that the structure of this compound is better represented by formula IV than by formula II.



IV



V

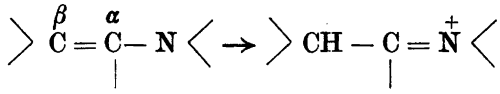


Va

The dehydroyohimbine base is proposed to be a resonance hybrid of the limiting structures V and Va.

The difference between the chromophoric systems in IV and V ⟷ Va is clearly demonstrated by the ultraviolet spectra (curves 1 and 2, Fig. 1).

In this connection it is worth mentioning Leonards [2] observation, that the transformation



takes place when an α,β-unsaturated amine is converted to its salt.

The formulae IV and V ⟷ Va involve a difference between the ultraviolet spectra of the methiodide and the salts of dehydroyohimbine. It is seen from Fig. 1 (curves 1 and 3) that, actually, such a difference is present.

The choice between the structures VI and VII for dehydroyohimbine methiodide was made by catalytical reduction of this compound. The result that the hydrogenation product turned out to be a mixture of yohimbine methiodide and pseudoyohimbine methiodide indicates that VII is the correct structure.

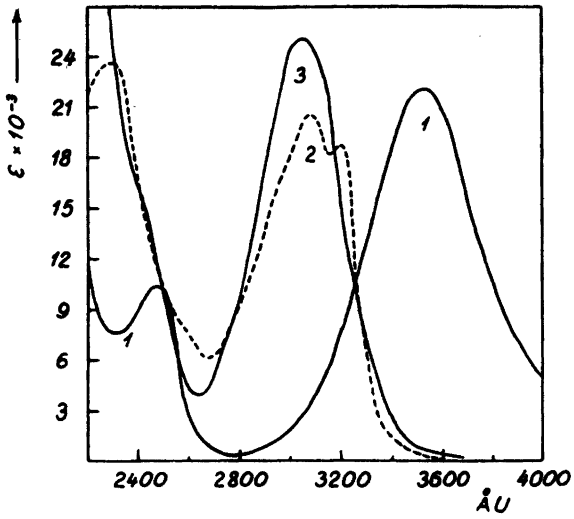
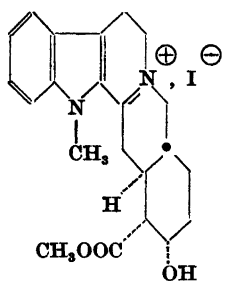
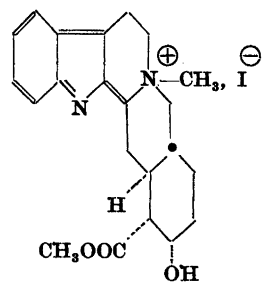


Fig. 1. Ultraviolet absorption spectra.
Curve 1. Dehydroyohimbine chloride.
» *2. The dehydroyohimbine base.*
» *3. Dehydroyohimbine methiodide.*



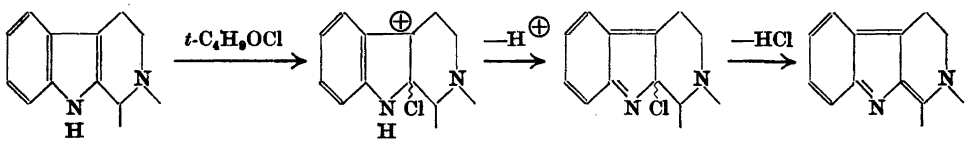
VI



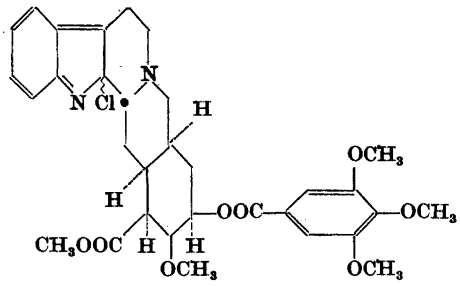
VII

By dehydrogenation of deserpidine a chlorodeserpidine was isolated as an intermediate. This compound was smoothly transformed to dehydrodeserpidine chloride by short treatment with methanolic hydrogen chloride.

The intermediary formation of chloro compounds by dehydrogenation with *tert.*-butyl hypochlorite may be explained by assuming the following reaction sequence:



The assignment of formula VIII to chlorodeserpidine is supported by the experimental findings mentioned below.



VIII

1) The infrared spectrum contains no band in the NH-region (2.9 μ).
2) The substance does not show the oxidizing properties which would be expected for N-chlorodeserpidine.
3) Catalytical reduction with platinum in ethylene glycol monomethyl ether yields only deserpidine.
4) Hydrogen chloride is readily eliminated with the formation of dehydrodeserpidine chloride.

Catalytical reduction of Δ^3-dehydrodeserpidine chloride with platinum in methanol afforded the hitherto unknown compound 3-isodeserpidine, isolated as the nitrate.

We are able to confirm Weisenborn and Diassi's [1] observation that reduction of salts of dehydroyohimbine with hydrogen and platinum in methanol gives only yohimbine. The same result is obtained with sodium borohydride in methanol.

If, however, the catalytical reduction is carried out in basic solution a mixture of yohimbine and pseudoyohimbine is obtained. With Raney nickel in ethylene glycol monomethyl ether the yield of pseudoyohimbine was approximately 50 %.

The influence of the solvent and the catalyst appears from Table 1. It will be seen that the formation of pseudoyohimbine is favoured by a low dielectric constant of the solvent.

EXPERIMENTAL

All melting points are corrected.

Dehydroyohimbine

A stirred solution of 17.7 g (0.05 mole) of yohimbine and 7 ml of triethylamine in 350 ml of dry methylene chloride was cooled to $-10°$ C and, during 45 min, a solution of 7 ml of *tert.*-butyl hypochlorite in 50 ml of dry carbon tetrachloride was added. The cooling bath was removed and, after standing for about 15 min, the resulting solution was washed with two 50 ml portions of water, and dried. The solvent was evaporated *in vacuo* and the oily residue dissolved in 75 ml of absolute ethanol. After acidification with ethanolic hydrogen chloride, the dehydroyohimbine chloride was crystallized by addition of ether.

Yield of crude product: 17.4 g. Recrystallization from methanol-ether gave 17.0 g of yellow needles, m. p. 268–270° C (decomp.). $[\alpha]_D^{20}$ + 213° (1 % in water). Ultraviolet absorption spectrum: λ_{max}^{EtOH} 246 mμ, log ε 4.03; 355 mμ, log ε 4.35. (Found: C 64.68; H 6.40; Cl 9.27; N 7.40. Calc. for $C_{21}H_{25}Cl\,N_2O_3$: C 64.86; H 6.48; Cl 9.12; N 7.21).

The iodide was obtained by addition of aqueous potassium iodide to a methanolic solution of the chloride. Recrystallization from methanol gave yellow needles; m. p. 276–277° C (decomp.). (Found: C 52.36; H 5.22; I 26.17; N 5.83. Calc. for $C_{21}H_{25}I\,N_2O_3$: C 52.50; H 5.25; I 26.42; N 5.83).

The dehydroyohimbine base was precipitated from a solution of 5.0 g of dehydroyohimbine chloride in 50 ml of methanol by addition of concentrated aqueous sodium hydroxide followed by water. Yield of crude product: 3.7 g, m. p. 174–176° C (decomp.). Recrystallization from methanol-water yielded pale yellow crystals, m. p. 176–178° C (decomp.). (Found: C 71.46; H 7.06; N 7.74. Calc. for $C_{21}H_{24}N_2O_3$: C 71.57; H 6.86; N 7.95).

The following alkaloids were dehydrogenated in the same way as yohimbine:

Pseudoyohimbine [3]. Yield of dehydroyohimbine chloride: 65 %. The I. R.-spectrum was identical with the I.R.-spectrum of dehydroyohimbine chloride prepared from yohimbine.

Apoyohimbine [4]. Yield of dehydroapoyohimbine chloride: 73 %. Recrystallization from alcohol-ether gave yellow needles, m. p. 284–285° C (decomp.). (Found: C 67.81; H 6.44; Cl 9.74; N 7.76. Calc. for $C_{21}H_{23}Cl\,N_2O_3$: C 68.01; H 6.25; Cl 9.56; N 7.55). Ultraviolet absorption spectrum: λ_{max}^{EtOH} 246 mμ, log ε 3.95; 355 mμ, log ε 4.31.

Corynanthine *. Yield of dehydrocorynanthine chloride after recrystallization from methanol-ether: 66 %. M. p. 227–229° C (decomp.). Ultraviolet absorption spectrum: λ_{max}^{EtOH} 247 mμ, log ε 4.03; 353 mμ, log ε 4.35. (Found: C 63.62; H 6.63; Cl 8.98; N 7.25. Calc. for $C_{21}H_{25}Cl\,N_2O_3$, ½ CH_3OH: C 63.78; H 6.72; Cl 8.76; N 6.92).

α-Yohimbine *. Dehydro-α-yohimbine chloride was isolated in 77 % yield as a yellow amorphous powder. A crystalline perchlorate was obtained by addition of aqueous sodium perchlorate to a methanolic solution of the chloride. Recrystallization from water gave m. p. 206–208° C. (Weisenborn and Diassi [1] report m. p. 211–212° C). Ultraviolet absorption spectrum: λ_{max}^{EtOH} 246 mμ, log ε 4.01; 355 mμ, log ε 4.33.

Chlorodeserpidine (VIII)

To a stirred solution of 1 734 mg (0.003 mole) of deserpidine ** and 0.45 ml of triethylamine in 30 ml of dry methylene chloride a solution of 0.45 ml of *tert.*-butyl hypochlorite in 5 ml of carbon tetrachloride was added at −10° C during a period of 15 min. After standing for another 15 min. at 0° C, the resulting solution was washed with two 10 ml portions of water, and dried. The solvent was removed *in vacuo* and the solid residue recrystallized from ethanol to give 1 400 mg (76 %) of white crystalline material. M. p. 189–193° C (decomp.). Recrystallization from *iso*propanol raised the melting point to 191–196° C (decomp.). $[\alpha]_D^{20}$ −184.5° in chloroform (c = 1). Ultraviolet absorption spectrum: λ_{max}^{EtOH} 266 mμ, log ε 4.14. (Found: C 62.69; H 6.27; Cl 5.67; N 4.65. Calc. for $C_{33}H_{37}ClN_2O_8$: C 62.69; H 6.08; Cl 5.78; N 4.57).

Dehydrodeserpidine chloride

A suspension of 400 mg of chlorodeserpidine in 6 ml of methanol was acidified with strong methanolic hydrogen chloride and the resulting clear solution was refluxed for five minutes. After cooling dehydrodeserpidine chloride was precipitated as an amorphous powder. Yield: 380 mg. Crystallization from water afforded yellow crystals, m. p. 185–187° C (decomp.).

---

* Kindly supplied by E. Merck AG., Darmstadt.

** Supplied by S. B. Penick & Co., New York.

Ultraviolet absorption spectrum: λ_{max}^{MeOH} 252 mμ, log ε 4.19; 260—265 mμ (shoulder), log ε 4.07; 355 mμ, log ε 4.36. (Found: C 60.13; H 6.60; Cl 5.68; N 4.61. Calc. for $C_{32}H_{37}ClN_2O_3$, 1½ H_2O: C 60.05; H 6.30; Cl 5.54; N 4.38).

Dehydroyohimbine methiodide (VII)

2.5 g of dehydroyohimbine base were dissolved in a mixture of 20 ml of absolute ethanol and 10 ml of methyl iodide. After standing overnight in the dark, 1.87 g of a crystalline methiodide were obtained, which were recrystallized from ethanol. M. p. 213—215° C (decomp.). Ultraviolet absorption spectrum: λ_{max}^{MeOH} 305 mμ, log ε 4.35. (Found: C 52.66; H 5.81; I 24.80; N 5.82. Calc. for $C_{22}H_{27}I N_2O_3$, ½ H_2O: C 52.48; H 5.61; I 25.21; N 5.57).

Hydrogenation of dehydroyohimbine methiodide

A solution of 988 mg of dehydroyohimbine methiodide in 30 ml of ethylene glycol monomethyl ether was hydrogenated at *ca.* 60° C under one atm. of hydrogen in the presence of 200 mg of a platinum oxide catalyst.

When the theoretical amount of hydrogen had been absorbed, the catalyst was removed by filtration and the filtrate evaporated to dryness. The light yellow sirupy residue crystallized on scratching in the presence of a few ml of acetone. The solid was filtered and washed with acetone to give 890 mg of a mixture of yohimbine methiodide and pseudoyohimbine methiodide, which was dissolved in 20 ml of boiling methanol. After cooling yohimbine methiodide crystallized upon seeding while pseudoyohimbine methiodide remained in solution. Filtration and washing with methanol yielded 150 mg of pure yohimbine methiodide which softened at 240—242° C and thereafter was gradually decomposed. The infrared spectrum was indistinguishable from the spectrum of authentic yohimbine methiodide.

Addition of ether to the filtrate afforded 580 mg of pseudoyohimbine methiodide, m. p. 271—272° C (decomp.). The melting point of a mixture with an authentic sample was undepressed and their infrared spectra were identical.

Hydrogenation of chlorodeserpidine (VIII) to deserpidine

A solution of 307 mg (0.0005 mole) of chlorodeserpidine (VIII) in 10 ml of dioxan was shaken at room temperature in the presence of 30 mg of platinum oxide under one atm. of hydrogen. When the theoretical amount of hydrogen had been absorbed (30 min.), the catalyst was removed by filtration and the solution evaporated to dryness under reduced pressure. The residue was dissolved in 10 ml of methanol and the resulting solution basified with aqueous ammonia. Addition of water yielded 220 mg of white crystalline material. M. p. 224—226° C (decomp.). After recrystallization from methanol the melting point was 225—227° C (decomp.) alone and by admixture with deserpidine. $[\alpha]_D^{20}$ —135° in chloroform (c = 1). Schlittler *et al.*[5] report for deserpidine: $[\alpha]_D^{24,5}$ —137° ± 1 in chloroform.

3-Isodeserpidine

235 mg of dehydrodeserpidine chloride were dissolved in 10 ml of methanol and hydrogenated at room temperature under one atmosphere of hydrogen in the presence of 20 mg of a platinum oxide catalyst.

When the theoretical amount of hydrogen had been absorbed (15 min.), the catalyst was removed by filtration. The solution was basified with aqueous ammonia and the hydrogenation product precipitated as a white amorphous powder by addition of water.

The amorphous base was converted to a crystalline nitrate by careful acidification of an ethanolic solution with nitric acid. Filtration and washing with ethanol and ether yielded 170 mg which melted at 189—194° C (decomp.). Recrystallization from ethanol raised the melting point to 194—198° C (decomp.). Ultraviolet absorption spectrum: λ_{max}^{EtOH} 271 mμ, log ε 4.26. (Found: C 58.34; H 6.55; N 6.47. Calc. for $C_{32}H_{39}N_3O_{11}$, H_2O: C 58.25; H 6.28; N 6.37).

The substance was readily distinguishable from deserpidine nitrate [6] by its low melting point, its optical rotation ($[\alpha]_D^{20}$ −153° in pyridine (c = 1)), and its high R_F value in the paper chromatographic system described below.

For deserpidine nitrate Mac Phillamy *et al.*[6] report m. p. 254—260° C (decomp.). The optical rotation was found to be $[\alpha]_D^{20}$ −138° in pyridine (c = 1).

Reduction of dehydroyohimbine

a) With sodium borohydride. To a stirred solution of 777 mg of dehydroyohimbine chloride in 20 ml of methanol was added drop by drop 1 ml of a 10 % methanolic solution of sodium borohydride. From the resulting colourless solution the reduction product was precipitated by addition of 50 ml of water. The precipitate was filtered off, washed with water and dried. Yield: 525 mg of white crystals, m. p. 234—235.5° identified as yohimbine by mixed melting point and by optical rotation $[\alpha]_D^{20}$ +102° in pyridine (c = 1).

b) Catalytically. A series of catalytical hydrogenations were carried out with the aim to study the influence of the solvent, the catalyst, and the addition of base on the content of pseudoyohimbine in the hydrogenation product. The general procedure is described below and the results are summarized in Table 1.

Table 1. Catalytical hydrogenation of dehydroyohimbine chloride.

Solvent	Dielectric constant of the solvent	Catalyst	Mole equivalent triethylamine added	Yield of pseudoyohimbine %
Methanol	32.6	PtO_2 (100 mg)	0	0
—	—	—	1	26
—	—	—	2	27
Ethylene glycol monomethyl ether	16.0	—	2	34
Dioxan *	2.2	—	2	47
Methanol	32.6	5 % Pd on $CaCO_3$ (1.0 g)	2	20
—	—	Raney nickel (*ca.* 0.5 g)	2	30
Ethylene glycol monomethyl ether	16.0	Raney nickel (*ca.* 0.5 g)	2	48

*) In this experiment dehydroyohimbine acetate was dehydrogenated since the chloride was insoluble in dioxan.

General procedure. 1.554 g (0.004 mole) of dehydroyohimbine chloride were dissolved in 40 ml of the appropriate solvent. The catalyst and the base were added and the resulting mixture was shaken at room temperature under one atmosphere of hydrogen. When the theoretical amount of hydrogen had been absorbed (5—60 min.) the catalyst was removed by filtration and the filtrate concentrated *in vacuo* to a volume of 10 ml. The solution was made alkaline with aqueous ammonia and the hydrogenation product precipitated by addition of water. The crystalline precipitate was filtered, washed with water and, after drying, treated with 10 ml of boiling methanol. By this treatment, the yohimbine went into solution, while the highly insoluble pseudoyohimbine, after cooling, was collected on a filter and washed with methanol. From the filtrate the yohimbine was precipitated by addition of water.

The pseudoyohimbine was identified by its melting point (266—268° C (decomp.). and its optical rotation $[\alpha]_D^{20}$ +28° in pyridine (c = 1).

Paper chromatography

It was found that two of the paper chromatographic systems described by Bush [7] for the separation of steroids were well suited for the separation and identification of alkaloids of the yohimbine type.

The relatively polar alkaloids such as yohimbine, corynanthine, and α-yohimbine were best separated in the B5 system, while the B3 system was more convenient for the relatively non-polar alkaloids such as reserpine, deserpidine, and isodeserpidine.

Whatman No. 1 paper was used and the chromatograms were run at 32° C for three hours after equilibration overnight.

The alkaloids were located on the dried papers by their ultraviolet fluorescence after irradiation with ultraviolet light for about ten min. Quantities ranging from 0.5 to about 5 μg could be detected by this method.

It was necessary to use known alkaloids as controls, since the R_F values varied with the amount of material applied.

Acknowledgment. The authors wish to express their gratitude to Dr. E. Frederiksen and Dr. E. Juhl Nielsen for their kind encouragement and advice. We are also indebted to Dr. P. Mørch for the ultraviolet and infrared spectra and to Mr. G. Cornali for the microanalyses.

REFERENCES

1. Weisenborn, F. L. and Diassi, P. A. *J. Am. Chem. Soc.* **78** (1956) 2022.
2. Leonard, N. J. and Gash, V. W. *J. Am. Chem. Soc.* **76** (1954) 2781.
3. Janot, M. M., Goutarel, R., Le Hir, A., Amin, M. and Prelog, V. *Bull. soc. chim.* **19** (1952) 1085.
4. Barger, G. and Field, E. *J. Chem. Soc.* **123** (1923) 1038.
5. Schlittler, E., Ulshafer, P. R., Pandow, M. L., Hunt, R. and Dorfman, L. *Experientia* **11** (1955) 64.
6. MacPhillamy, H. B., Huebner, C. F., Schlittler, E., St. André, A. F. and Ulshafer, P. R. *J. Am. Chem. Soc.* **77** (1955) 4335.
7. Bush, I. E. *Biochem. J. London* **50** (1952) 370.

Received July 11, 1956.

ACTA CHEMICA SCANDINAVICA 10 (1956) 1422—1426

Studies on Lignin

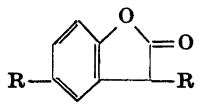
XVII.* Properties of Some 2'-Hydroxydesoxybenzoins

ÅKE SPETZ

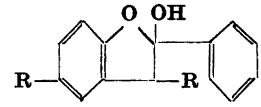
Organisk-kemiska Institutionen, Kungl. Tekniska Högskolan, Stockholm, Sweden

As potential lignin models compounds of *semi*-acetal 2-phenylcoumaranol-(2) type (II) were desired. The reaction between coumaranone-(2) (Ia) and phenylmagnesium bromide yielded 3-(*o*-hydroxyphenylacetyl)-coumaranone-(2) (IV) — also obtained from coumaranone-(2) on treatment with potassium — and a small amount of 2'-hydroxydesoxybenzoin (IIIa) also obtained in good yield by reduction of *o*-hydroxybenzil. 3,5-Dimethylcoumaranone-(2) (Ib) and phenylmagnesium bromide gave exclusively *α*,5'-dimethyl-2'-hydroxydesoxybenzoin (IIIb). The 2'-hydroxydesoxybenzoins were readily dehydrated to the corresponding coumarones when treated with strong acids or subjected to a sulphite cook. Because of their instability it is unlikely that 2-phenylcoumaranol-(2) systems occur in lignin.

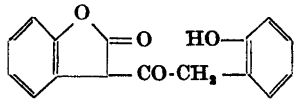
In connection with certain lignin chemical problems we were interested in the stability of compounds of the 2-phenylcoumaranol-(2) type (II)[1]. A convenient method for the preparation of such compounds appeared to be the condensation of coumaranones with suitable phenylmagnesium halides.



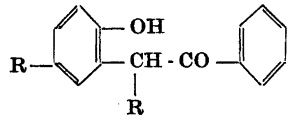
Ia R = H
Ib R = CH_3



IIa R = H
IIb R = CH_3



IV



IIIa R = H
IIIb R = CH_3

* Part XVI. *Svensk Papperstidn.* **55** (1952) 816.

When an ethereal solution of phenylmagnesium bromide was added to coumaranone, $C_8H_6O_2$ (Ia), reaction took place but from the reaction product only a small amount of a substance, $C_{14}H_{12}O_2$ (A), could be isolated. The main product was a pale yellow compound, $C_{16}H_{12}O_4$.

It was suspected that the latter compound might be 3-(*o*-hydroxyphenylacetyl)-coumaranone-(2) (IV) formed by an acetoacetic ester type of condensation from two molecules of coumaranone, the Grignard reagent simply functioning as the base catalyst. The correctness of this assumption was shown by the formation of the same compound when a solution of coumaranone in dry ether was treated with potassium.

Compound A could be more conveniently obtained by reduction of *o*-hydroxybenzil with zinc in the presence of ammonium chloride (compare Pearl [2] for the similar reduction of vanillil to desoxyvanilloin).

3,5-Dimethylcoumaranone-(2) (Ib) was prepared by transforming 2-methoxy-5-methylacetophenone into its cyanohydrin which was hydrolysed to 2-methoxy-5-methylhydratropic acid. The acid was demethylated with pyridinium chloride and distilled to give the desired product. This compound when treated with phenylmagnesium bromide furnished a compound, $C_{16}H_{16}O_2$ (B), in moderate yield. No condensation products of the acetoacetic ester type could be isolated in this case.

Compound A is not the semiacetal 2-phenylcoumaranol-(2) (IIa) but the corresponding 2′-hydroxydesoxybenzoin (IIIa) and compound B is α,5′-dimethyl-2′-hydroxydesoxybenzoin (IIIb). This follows from the close similarity of the U.V. absorptions of compound A, its methyl ether, compound B and desoxybenzoin [3].

Maxima:	mμ	log ε	mμ	log ε
Desoxybenzoin	240	4.10	278*	2.90
2′-Methoxydesoxybenzoin	243	4.03	275*	3.42
2′-Hydroxydesoxybenzoin (comp. A)	242	4.13	275*	3.54
α,5′-Dimethyl-2′-hydroxydesoxybenzoin (comp. B)	245	4.11	283	3.50

* inflexion

In 0.25 N sodium hydroxide solution the phenol-phenolate shift was observed with compound A (max.: 240 mμ, log ε 4.29; infl.: 288 mμ, log ε 3.70). However, above 350 mμ a new maximum was gradually developed (log ε increasing from 2.7 to 3.3 at 400 mμ in 90 minutes). This indicates that some secondary changes take place. Moreover the original absorption was not immediately restored on acidification.

When compound A was treated with acids, water was easily eliminated and 2-phenylcoumarone was formed and similarly when heated with bisulphite cooking acid 2-phenylcoumarone was obtained but no sulphonic acid.

Compound B behaved in exactly the same manner yielding 3,5-dimethyl-2-phenylcoumarone in good yield.

These results indicate that it is unlikely that 2-hydroxy-2-phenylcoumarone systems occur in lignin.

EXPERIMENTAL *

2'-Hydroxydesoxybenzoin (IIIa). Method a. Phenylmagnesium bromide (from 7.8 g bromobenzene) in dry ether (100 ml) was slowly added with mechanical stirring to coumaranone-(2) (10 g) in dry ether (50 ml). The reaction product was decomposed with ammonium chloride in ice-water and the aqueous phase carefully acidified with dilute hydrochloric acid (to pH 2—3) and extracted with ether. The combined ether solutions were washed with cold dilute hydrochloric acid and then extracted with dilute sodium hydroxide. Carbon dioxide was bubbled into the alkaline solution and at pH 9 a pale yellow precipitate formed which was dissolved in ether. The ether solution was dried over magnesium sulphate and evaporated to dryness. The residue (compound A, 1.5 g) was crystallised from ethanol-water. Pale yellow crystals starting to sinter at 110° and, melting at about 120°. The unsharp melting point is probably due to loss of water and partial formation of 2-phenylcoumarone. (Found: C 80.5; H 5.6. Calc. for $C_{14}H_{12}O_2$: C 79.2; H 5.7).

Method b. *o*-Hydroxybenzil (1.6 g) in ethanol (100 ml) and zinc dust (5 g) were heated to boiling and a warm solution of ammonium chloride (5 g) in water (20 ml) added and the mixture boiled under reflux for one hour. The zinc was removed and acetic acid (10 ml) carefully added to the cooled solution which was then concentrated at reduced pressure to a small volume whereupon water (100 ml) was added. The remaining ethanol was now removed by further distillation. On cooling a pale yellow precipitate was obtained. The product (0.9 g) was dissolved in dilute aqueous alkali, filtered and precipitated with carbon dioxide. Crystallisation from ethanol-water gave crystals m.p. 110—120° (decomp.).

2'-Methoxydesoxybenzoin, which is a stable compound with a sharp melting point, was prepared in order to identify the reaction products from *methods a* and *b* by dissolving 2'-hydroxydesoxybenzoin (0.5 g), prepared according to either of the methods, in 2 N aqueous sodium hydroxide (5 ml) and shaking with dimethyl sulphate (0.5 ml). The crystalline reaction product was dissolved in ether and the solution filtered through a short column of aluminium oxide. On evaporation almost pure methyl ether m.p. 59—60° was obtained. Recrystallisation from a small volume of methanol raised the m.p. to 61.5—62°. The products obtained from both preparations were identical (mixed m.p.). (Found: C 79.7; H 6.4; OCH_3 13.6. Calc. for $C_{15}H_{14}O_2$: C 79.6; H 6.2; OCH_3 13.7).

3-(o-Hydroxyphenylacetyl)-coumaranone-(2) (IV). Method 1. On further acidification of the alkaline phase from the preparation of 2'-hydroxydesoxybenzoin according to *method a* (to pH 6—7) a precipitate (3.5 g) was obtained. Crystallisation from ethanol-water yielded pale yellow needles m.p. 150—155° (decomp.) (Found: C 71.5; H 4.7. Calc. for $C_{16}H_{12}O_4$: C 71.6; H 4.5).

Method 2. In a flask fitted with a condenser, potassium (1.2 g) was powdered under dry toluene (100 ml) which was then replaced by dry ether (25 ml). Coumaranone-(2) (4.6 g) in dry ether (50 ml) was added through the condenser with shaking at room temperature. The mixture was then boiled for six hours and left overnight. Acetic acid (2.5 ml) in water (25 ml) was added with vigorous shaking. The ethereal layer was separated, washed with water, dried over magnesium sulphate and evaporated to dryness. Crystallisation of the residue (2 g) from ethanol-water yielded a pale yellow substance m.p. 151—154° not depressed on admixture with 3-(*o*-hydroxyphenylacetyl)-coumaranone-(2) from the previous experiment (*method 1*).

2-Phenylcoumarone. 2'-Hydroxydesoxybenzoin (0.5 g) was dissolved in acetic acid (2 ml) and conc. hydrochloric acid (2 drops) added. On heating the solution to boiling it gave almost instantly a white precipitate. It was collected, dissolved in ether, shaken with dilute aqueous alkali, dried over calcium chloride and the solution evaporated to dryness. Crystallisation of the residue (0.4 g) from ethanol gave white plates exhibiting a blue fluorescence, m.p. 120.5—121°. (Found: C 86.4; H 5.2. Required for $C_{14}H_{10}O$: C 86.6; H 5.2).

2-Methoxy-5-methylhydratropic acid. Concentrated hydrochloric acid (70 ml, *d* 1.18) was added from a dropping funnel in five to ten drop portions to a mixture of 2-methoxy-5-methylacetophenone (82 g) and potassium cyanide (55 g) and ether (100 ml) cooled in

* All melting points uncorrected.

ice-water and vigorously stirred. The pale yellow colour appearing at each addition of the acid was allowed to disappear before the next addition. Towards the end of the reaction the mixture remained yellow. The ethereal layer was separated, washed several times with water, concentrated at reduced pressure and the crude 2-methoxy-5-methylacetophenone cyanohydrin (100 g) used for the next step without further purification.

Crystalline stannous chloride (100 g), acetic acid (100 ml), conc. hydrochloric acid (100 ml) and hydriodic acid (10 ml, *d* 1.7) were added to the crude 2-methoxy-5-methylacetophenone cyanohydrin (100 g). The mixture was heated on a steam bath for five hours. After cooling the mixture was filtered and the filtrate diluted with water and extracted with ether. The ethereal solution was extracted with sodium bicarbonate solution from which on acidification with hydrochloric acid a colourless crystalline product (18 g) was precipitated. The substance crystallised from ethanol-water in plates, m.p. 125—126°. (Found: C 68.5; H 7.3; Equiv. wt. 192. Calc. for $C_{11}H_{14}O_3$: C 68.0; H 7.3; Equiv. wt. 194).

The ethereal solution was then extracted with 2 N sodium hydroxide from which on acidification a crystalline, phenolic substance (about 5 g) was obtained by extraction with ether. The substance crystallised from ligroin in needles m.p. 47—48° undepressed on admixture with 2-hydroxy-5-methylacetophenone. It is evidently formed by demethylation of unchanged 2-methoxy-5-methylacetophenone.

The *amide* of 2-methoxy-5-methylhydratropic acid separated from the aqueous phase on standing and was crystallised from benzene. Plates, m.p. 144—145°. (Found: N 7.25. Calc. for $C_{11}H_{15}O_2N$: N 7.25). It was converted to 2-methoxy-5-methylhydratropic acid, m.p. 125—126° undepressed on admixture with an authentic specimen, by refluxing with 50 % ethanolic potassium hydroxide for five hours.

Concentration of the extracted solution yielded a residue (about 40 g) consisting chiefly of unchanged 2-methoxy-5-methyl-acetophenone.

3,5-Dimethylcoumaranone-(2) (Ib). A mixture of 2-methoxy-5-methylhydratropic acid (17 g) and pyridinium chloride (50 g) was heated to 180° for two hours. The reaction mixture was poured into 2 N hydrochloric acid (500 ml) and extracted with ether. The ethereal solution was washed with dilute hydrochloric acid and with water. After removal of the ether and distillation of the residual oil at reduced pressure a colourless product (12 g) was obtained which readily crystallised. Plates, m.p. 36—37°. Crystallisation from methanol-water and repeated distillation raised the melting point to 39—39.5°. (Found: C 74.3; H 6.5. Calc. for $C_{10}H_{10}O_2$: C 74.1; H 6.2).

a,5'-Dimethyl-2'-hydroxydesoxybenzoin (IIIb). Phenylmagnesium bromide (from 3.1 g bromobenzene) in dry ether (10 ml) was slowly added to a solution of 3,5-dimethylcoumaranone-(2) (4 g) in dry ether (150 ml) with mechanical stirring. The reaction product was worked up exactly in the same way as for 2'-hydroxydesoxybenzoin and yielded a crystalline substance (1.5 g) melting at 125—127°. Recrystallisation from ligroin gave needles m.p. 129.5—130°. (Found: C 80.1; H 6.8. Calc. for $C_{16}H_{16}O_2$: C 80.0; H 6.7).

Sulphite cooking of the desoxybenzoins. The cooking acid was obtained by bubbling sulphur dioxide into 10 % aqueous sodium hydroxide until the desired pH was reached. The heating was carried out in a sealed glass tube. Time 12 hours. Temperature 135°C.

2'-Hydroxydesoxybenzoin. a: pH 1.5. The compound (0.5 g) was heated with cooking acid (10 ml). The reaction mixture was extracted with ether which was then washed with dilute alkali, dried over calcium chloride and concentrated. A crystalline substance (0.5 g) m.p. 118—120° with a blue fluorescence was obtained. Recrystallisation from ethanol yielded plates, m.p. 120—121° showing no depression when mixed with 2-phenylcoumarone. *b*: pH 5.5. The experiment was carried out in a similar way and the alkali-washed ethereal solution on concentration yielded 2-phenylcoumarone (0.4 g). When carbon dioxide was bubbled through the alkaline washings unchanged 2'-hydroxydesoxybenzoin (0.1 g) was recovered.

a,5'-Dimethyl-2'-hydroxydesoxybenzoin. The experiments were carried out as above. At pH 1.4 3,5-dimethyl-2-phenylcoumarone was obtained in a quantitative yield. Crystallisation from methanol gave needles exhibiting a strong blue fluorescence m.p. 69.5—70° (Found: C 86.7; H 6.2. Calc. for $C_{16}H_{14}O$: C 86.5; H 6.3).

No sulphonic acids were found in any of these experiments.

REFERENCES

1. Aulin-Erdtman, G., Björkman, A., Erdtman, H. and Hägglund, S. E. *Svensk Papperstidn.* **50** (B) (1947) 81; Erdtman, H. *Research* **3** (1950) 63.
2. Pearl, L. A. *J. Am. Chem. Soc.* **74** (1952) 4593.
3. Alpen, E. L., Kumler, W. D., Strait, L. A. *J. Am. Chem. Soc.* **72** (1950) 4558.

Received July 20, 1956.

ACTA CHEMICA SCANDINAVICA 10 (1956) 1427—1431

Studies on Lignin

XVIII.* Sulphite Cooking of Salicil

HOLGER ERDTMAN and ÅKE SPETZ

Organisk-kemiska Institutionen, Kungl. Tekniska Högskolan, Stockholm, Sweden

Salicil (II) when subjected to a sulphite cook in neutral or slightly alkaline medium gave phenol, salicoylformic acid and xanthene-9-sulphonic acid (VIII). Similarly 4,5-dihydro-2,3;6,7-dibenzoxepin-dione-(4,5) (IX) and salicilic acid (V), the former in excellent yield, both furnished VIII. Salicil was oxidised to disalicylide (IV) with lead *tetra*-acetate indicating that salicil can react in the cyclised form IIIa.

At one stage in our researches on the sulphonation of lignin it was suggested that "group B" which is sulphonated only at a low pH but not with neutral sulphites might possess a *cyclo*-acetal structure of the type I [1]. However, our further studies especially on the sulphonation of various benzylalcoholic model substances and their ethers soon made this hypothesis superfluous [2] and in a recent publication [3] we have shown that *cyclo-hemi*-acetals of this type (I, R = H) are unstable.

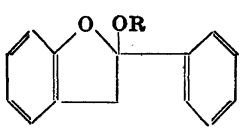
Not entirely unexpectedly salicil (II) shows a greater tendency to react in the *bis-cyclo*-acetal form (IIIa) and for example we have found that it readily forms a dimethyl acetal (IIIb) which will be described in a forthcoming publication. Further it gives disalicylide (IV) in good yield when treated with lead *tetra*-acetate in acetic acid.

Hence it was of interest to investigate whether salicil reacts, when subjected to sulphite cooking, with formation of a sulphonic acid.

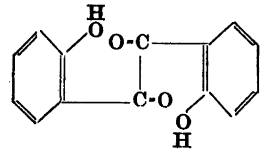
However, salicil did not react with a normal "acid sulphite cooking acid" and was recovered unchanged, but at pH 7—10 a series of interesting reactions occurred resulting in the formation of phenol, salicoylformic acid, and a sulphonic acid, (Scheme 1, VI, VII and VIII, respectively) the sparingly soluble sodium salt of which separated from the reaction mixture on cooling.

The free sulphonic acid was very unstable but the sodium salt when oxidised with permanganate furnished xanthone in good yield. This lead to the assumption that the sulphonic acid was xanthene-9-sulphonic acid and this

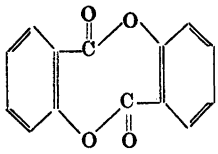
* Part XVII. *Acta Chem. Scand.* **10** (1956) 1422.



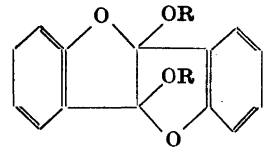
I



II



IV

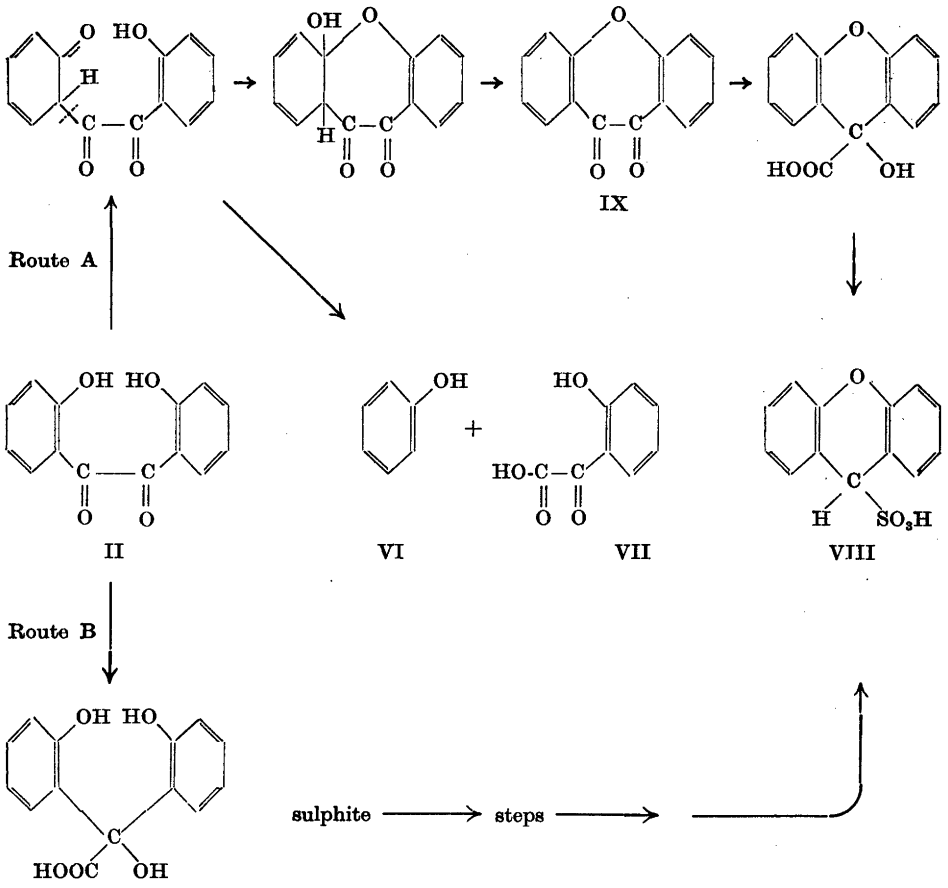


III a R = H
III b R = CH_3

was confirmed by direct sulphonation of xanthydrol and identification of the sodium salts of the sulphonic acids by means of their X-ray powder photographs.

The formation of phenol and salicoylformic acid is easy to understand. It simply represents a hydrolytic fission as indicated in scheme 1 (Route A) and phenol was, moreover, obtained when salicil was heated with a saturated sodium bicarbonate solution in the same way as in the case of the sulphite cook. A similar case has recently been recorded [4].

There are several ways in which the formation of xanthene-9-sulphonic acid can be explained. One is illustrated in scheme 1 (Route B) and involves the intermediate formation of salicilic acid (V) which suffers dehydration, decarboxylation and sulphonation to xanthene-9-sulphonic acid as indicated in the scheme. Salicilic acid was obtained by a rather drastic treatment of salicil with strong alkali although it was impossible to isolate the compound in a completely pure state. It was characterised by conversion into the dimethyl ether and into the diacetate of salicilic acid lactone both of which are readily obtainable in good yield from the crude salicilic acid preparation. This crude preparation, when subjected to a sulphite cook under the conditions employed for salicil furnished xanthene-9-sulphonic acid in moderate yield. In view of this and because it seems improbable that salicil would readily undergo a benzilic acid rearrangement under the conditions employed it appears doubtful that the formation of xanthene-9-sulphonic acid from salicil proceeds *via* salicilic acid. An alternative reaction mechanism was therefore considered involving the intermediate formation of 4,5-dihydro-2,3;6,7-dibenzoxepindione-(4,5) (IX, Scheme 1: route A) which would bear some analogy with tropolones and therefore might readily rearrange to 9-hydroxyxanthene-9-carboxylic acid. A synthesis of this compound was contemplated when recently Mathys, Prelog and Woodward [5] reported its synthesis and also commented upon its facile rearrangement to 9-hydroxyxanthene-9-carboxylic acid with even weak alkali. Through the courtesy of Professor V. Prelog to whom we extend our



Scheme 1.

gratitude, we have been able to investigate the action of sulphite on this compound. It was found to give an excellent yield of xanthene-9-sulphonic acid and it therefore appears probable that the formation of xanthene-9-sulphonic acid from salicil largely follows route A in scheme 1.

EXPERIMENTAL *

Lead tetra-acetate oxidation of salicil. To salicil (0.5 g) in acetic acid (15 ml) was added a solution of lead *tetra*-acetate (1 g) in acetic acid (10 ml). The mixture was heated to 70° and then left for one hour at room temperature. On cooling disalicylide precipitated in rhombic crystals. The crude reaction product (0.4 g, yield 80 %) had a m. p. 165—195° which was raised to 225—230° by repeated crystallisation from chloroform. The compound gave an I. R. spectrum identical with that of authentic disalicylide prepared according to Baker *et al.*[6].

* All melting points uncorrected.

Sulphite cooking of salicil. Here and in the following experiments the "cooking acid" was prepared by bubbling sulphur dioxide into 10 % aqueous sodium hydroxide until the desired pH was reached. The cookings were all carried out in sealed tubes at 135° C.

pH 1.5. Salicil (1.1 g) was heated with "cooking acid" (50 ml) for 20 hours. After cooling the solid (1.07 g) was collected and recrystallised from ethanol to give yellow needles, m. p. 153—154°, undepressed on admixture with salicil.

pH 7.1. Salicil (5 g) was heated with "cooking acid" (70 ml) for 8 hours. After cooling, the sodium salt of the sulphonic acid VIII (1.5 g, yield 25 %) was collected by filtering. The filtrate (pH 6.9) was extracted with ether and the ether solution evaporated to give phenol (1 g, yield 51 %). The aqueous phase was run through a cation exchanger, immediately neutralised with barium carbonate and filtered and evaporated to give the barium salt of salicoylformic acid (3.5 g, yield 72 %).

Identification of phenol (VI). The phenol was transformed into phenoxyacetic acid and into *tri*-bromophenol, both derivatives showing no melting point depression when mixed with authentic specimens.

Identification of salicoylformic acid (VII). The barium salt (1.5 g) was dissolved in water, excess of 2 N sodium hydroxide (5 ml) was added and carbon dioxide bubbled into the solution which was then filtered and weakly acidified with dilute hydrochloric acid. Phenylhydrazine (0.5 ml) was added and the solution heated to boiling. After cooling the reaction product (1 g), m. p. *ca.* 148°, was collected and dissolved in acetic acid (20 ml). Conc. hydrochloric acid (1 drop) was added and the solution heated to boiling. A crude reaction product (about 1 g, yield 67 %) was obtained which was recrystallised from acetic acid to yield yellow prisms, m. p. 184—185°, undepressed on admixture with coumarandion-3-phenylhydrazone prepared according to Fries *et al.*[7].

Identification of the sulphonic acid (VIII). The sodium salt was recrystallised from ethanol to yield white needles. A sample of the salt (0.93 g) was dissolved in water (5 ml) and heated for one hour on a steam bath, finely powdered potassium permanganate (0.59 g) g) being added from time to time. After cooling the reaction mixture was saturated with sulphur dioxide and filtered. A crystalline product (0.4 g, yield 67 %) was obtained which was recrystallised from ethanol to give colourless needles m. p. 172—173°. The reaction product was soluble in conc. sulphuric acid with a yellow colour exhibiting a strong blueish fluorescence. Admixture with xanthone did not depress the melting point.

After drying in a high vacuum a sample of the sodium salt (43.8 mg) was dissolved in water and after cation exchange titrated with 0.0417 N sodium hydroxide (3.68 ml). (Found: Equiv. weight 285. Calc. for $C_{13}H_9O_4S$ Na: Equiv. weight 284). The *cyclohexylammonium salt* of the sulphonic acid was prepared by running an ethanolic solution of the sodium salt through a cation exchanger into an ethereal solution of *cyclo*hexylamine. The crystalline precipitate was collected and recrystallised several times from ethanol yielding white needles without distinct melting point which started to decompose with a red colour at about 230°. (Found: C 62.9; H 6.5; N 4.0; S 8.9. Calc. for $C_{19}H_{23}NO_4S$: C 63.1; H 6.4; N 3.9; S 8.9).

Sulphite cooking of xanthydrol. Xanthydrol (5 g) was heated with "cooking acid" (70 ml, pH 7) for 8 hours. The crystalline reaction product (6.5 g, yield 91 %) was recrystallised from ethanol and the product shown to have an X-ray powder photograph identical with that of the sulphonic acid sodium salt obtained by sulphite cooking of salicil.

Salicilic acid (V). With vigorous mechanical stirring salicil (5 g) in 2 N sodium hydroxide (50 ml) was heated on a steam bath and solid sodium hydroxide (100 g) was added in portions. A yellowish brown semi-solid product was precipitated which crystallised on continued stirring forming an almost colourless suspension. The reaction mixture was poured into finely crushed ice (1 l) and carefully acidified with conc. hydrochloric acid (250 ml) and extracted with ether. The ether solution was washed with water and then extracted with saturated aqueous sodium bicarbonate (2 × 25 ml). The bicarbonate solution was acidified with 2 N hydrochloric acid (40 ml) to yield the reaction product as an oil which crystallised on standing. The crude salicilic acid (5 g) was collected by filtration, washed with cold water and dried. M. p. 100—110°. Repeated attempts to recrystallise the acid from water and from benzene yielded a red-coloured product without distinct melting point.

Salicilic acid dimethyl ether. The crude salicilic acid (2.6 g) was dissolved in 2 N sodium hydroxide (20 ml) and shaken with dimethyl sulphate (3 ml). The reaction mixture was boiled for five minutes, then cooled and acidified with dilute sulphuric acid. The crystalline reaction product (2 g, yield 71 %) was recrystallised several times from ethanol to yield the pure dimethyl ether, m. p. 160.5—161°, undepressed on admixture with *o,o'*-dimethoxybenzilic acid prepared according to Ford-Moore [8].

Salicilic acid lactone diacetate. The crude salicilic acid was dissolved in pyridine and acetic anhydride added. The solution was heated for some minutes and then poured into ice. The crystalline reaction product was collected and recrystallised from ethanol (charcoal) to yield colourless plates, m. p. 167—169.5°. Distillation at 1 mm Hg raised the m. p. to 169—169.5°. (Found: C 66.2; H 4.5. Calc. for $C_{18}H_{14}O_6$: C 66.3; H 4.3).

Sulphite coking of salicilic acid. Crude salicilic acid (0.5 g) was heated with "cooking acid" (10 ml, pH 7) for 8 hours. The reaction mixture was cooled and filtered to yield xanthene-9-sulphonic acid sodium salt (0.1 g, yield 18 %).

Sulphite cooking of 4,5-dihydro-2,3:6,7-dibenzoxepindione-(4,5). The dihydrodibenzoxepindione (90 mg) was heated with "cooking acid" (1 ml, pH 7) for 8 hours. On cooling, the sodium salt of xanthene-9-sulphonic acid (100 mg, yield 87 %) precipitated.

We are indebted to Dr. G. E. H. Lundgren, Inst. för Oorg. Kemi, KTH, Stockholm, for the X-ray determinations.

REFERENCES

1. Aulin-Erdtman, G., Björkman, A., Erdtman, H. and Hägglund, S. E. *Svensk Papperstidn.* **50** (B) (1947) 82; Erdtman, H. *TAPPI* **32** (1949) 76; Erdtman, H. *Research* **3** (1950) 66.
2. Erdtman, H., Lindgren, B. and Pettersson, T. *Acta Chem. Scand.* **4** (1950) 228; Lindgren, B. *Acta Chem. Scand.* **1** (1947) 779, **3** (1949) 1011; Erdtman, H. and Leopold, B. *Acta Chem. Scand.* **2** (1948) 535, **3** (1949) 1358; Leopold, B. *Acta Chem. Scand.* **4** (1950) 971.
3. Spetz, Å. *Acta Chem. Scand.* **10** (1956) 1422.
4. Pfeil, E., Geissler, G., Jacquemin, W. and Lömker, F. *Ber.* **89** (1956) 1210.
5. Mathys, F., Prelog, V. and Woodward, R. B. *Helv. Chim. Acta* **39** (1956) 1095.
6. Baker, W., Ollis, W. D. and Zealley, T. S. *J. Chem. Soc.* **1951** 201.
7. Fries, K. and Pfaffendorf, W. *Ber.* **45** (1912) 157.
8. Ford-Moore, A. H. *J. Chem. Soc.* **1947** 952.

Received August 6, 1956.

ACTA CHEMICA SCANDINAVICA 10 (1956) 1432—1439

A Procedure for the Determination of Proteins and Similar Compounds in Large Numbers of Fractions

BENGT v. HOFSTEN

Institute of Biochemistry, University of Uppsala, Uppsala, Sweden

Fraction collector work gives rise to large numbers of samples, and the chemical analysis of these necessitates methods which are sensitive but as simple as possible. Some of the current methods used when nitrogenous biological material is fractionated have been experimentally evaluated, and their relative merits are discussed.

A relatively simple procedure using a ninhydrin reaction is proposed. In this method a small sample from every fraction is first hydrolyzed with HCl at 120°, after which the acid is removed *in vacuo*. The ninhydrin reaction is then performed on a suitable aliquot of the residue. Useful technical arrangements and precautions are described, and the advantages and limitations of the method are discussed.

Fractionation work using chromatography, electrophoresis or counter current distribution gives rise to a great number of fractions, the analysis of which requires considerable time. The determination of biological or chemical activity in these fractions is often the main problem, but the activity is usually wanted as specific activity. In the case of fractionation of nitrogenous compounds, the specific activity is often expressed as activity per mg dry weight or nitrogen. Dry weight determinations of proteins is no easy matter and requires a comparatively large amount of material. In certain cases the simple method of Johnson [1] can be used to obtain an estimate of total organic matter. In this method, conc. H_2SO_4 and sodium dichromate of known strength reacts with the organic compounds in the sample. The sensitivity of the method is high but the accuracy is rather low, especially when interfering metals are present.

The determination of nitrogen according to Kjeldahl and conversion to protein by multiplication with a certain factor has long been the standard method for protein determinations. Besides the variable nitrogen content of different proteins, all other nitrogen containing substances interfere. Many different methods of precipitating the protein before the determination have been proposed, but it is often difficult to get a quantitative precipitate without co-precipitation [2]. Dialysis or ultrafiltration has been used extensively, but

some proteins tend to become adsorbed to the membranes, and neither precipitation nor dialysis is suitable for compounds of intermediate size such as peptides and certain enzymes.

Ordinary digestion of the sample and distillation of ammonia according to Kjeldahl is not practical with large numbers of fractions and, in addition, samples containing less than 0.1 mg N are difficult to analyse. A hypobromite titration is useful and easy to perform even on a few micrograms of nitrogen, provided small but usually constant errors can be tolerated. As modified by Harvey [3], the titration can be carried out directly in the digestion flasks or tubes without distillation, which is a definite advantage. It is thus possible to perform a large number of determinations in a comparatively short time, provided the approximate nitrogen content is known so that a suitable amount of hypobromite can be added. The method needs to be standardized on samples of known nitrogen content, and its pH-sensitivity is sometimes irritating. Boissonas and Haselbach [4] have used a sulfuric acid digestion followed by neutralization and a ninhydrin reaction to determine the nitrogen content in series of fractions. This elegant method is claimed to give good values in the 1—20 μg range, and it is certainly valuable when the total nitrogen content of fractions is wanted. For accurate determination of small quantities of nitrogen, the diffusion method of Conway [5] combined with the sealed-tube digestion of Greenbaum *et al.*[6] is certainly more exact.

When the available amount of protein is comparatively large, turbidimetric determinations may be useful. A procedure using trichloroacetic acid is very rapid and has been much used by Smith in his work on proteolytic enzymes [7] and by Stadtman *et al.*[8]. More than 20 μg protein per ml is needed for a determination and the precision of the method is rather low because of the inherent difficulties of all turbidimetric determinations.

The method of Greif [9] modified by Nayyar and Glick [10] using bromosulfalein has been developed particularly for use in histochemistry. The acid bromosulfalein reagent is used to precipitate the protein, and the residual concentration of the dye is measured at an alkaline pH. The method is useful down to very small amounts of protein and the specificity is high. In fractionation work, it should be useful in distinguishing between proteins and low molecular weight material, but as it involves a precipitation followed by a centrifugation on a micro-scale, it is of limited use in the analysis of large numbers of fractions.

The much used method of Lowry *et al.*[11], in which a combination of the biuret and Folin reactions is used, has the advantage of being rather specific for proteins. It is definitely the easiest method in many cases, and has a quite high accuracy if it is calibrated with the protein determined. The Lowry method is rather sensitive to the pH of the analyzed solution, and in many cases the only possibility of overcoming this is a preliminary precipitation. The tyrosine content of the sample influences the colour yield, but this disadvantage is balanced by the sensitivity of the method compared to a simple biuret reaction.

For a preliminary localization of protein material in fractions, the absorption of proteins at 280 mμ is often made use of routinely because of the simplicity and relative sensitivity of the method. The reviews by Dannenberg [12] and Beaven and Holiday [13] are useful when ultraviolet absorption data of proteins

are compared. Because of the abundance of ultraviolet absorbing substances in biological materials, it is often difficult to use the absorbance at 280 mμ for strictly quantitative purposes, and some buffers containing aromatic substances nessesitate other methods.

Ninhydrin reacts directly with proteins and peptides, and this has been utilized by Kunkel and Ward [14] for the quantitative determination of serological precipitates. As it is the free amino groups that are responsible for the reaction, different proteins give variable amounts of colour, and a slight contamination of ammonium salts will produce relatively large errors. Moreover, certain peptide linkages seem to be broken up by the comparatively violent reaction involved in the ninhydrin procedure. These factors make the use of a direct ninhydrin reaction of proteins uncertain and unsuitable for material of unknown behaviour.

The purpose of this study is to investigate the possibility of using the ninhydrin reaction of Moore and Stein [15] on aliquots from large numbers of fractions after hydrolysis and subsequent evaporation to dryness over sodium hydroxide. Upon acid hydrolysis, proteins and peptides are broken down chiefly into amino acids and ammonium salts. As the reaction of ninhydrin with these substances, with the exception of proline and hydroxyproline, is practically quantitative, the colour yield is an estimate of the nitrogen content of the samples. It is true that some nucleic acid components may be converted to ninhydrin-reacting compounds during the hydrolysis but ringbound nitrogen does not interfere. The main disadvantage of the method is the high sensitivity for ammonia, but this can be corrected for. The procedure of Boissonas [16] employing a solution of 1 % KOH in methanol to volatilize ammonia without decomposition of the amino acids is relatively simple, and the difference in ninhydrin colour obtained before and after such a treatment is an estimate of ammonium salts, provided the small amounts formed during hydrolysis can be neglected.

DESCRIPTION OF PROCEDURE USING HYDROLYSIS AND NINHYDRIN REACTION

The following procedure is suitable for fractions containing more than about 3 μg of nitrogen (in the form of proteins, peptides, amino acids etc.) per ml, but smaller amounts can also be determined by slight modifications, as will be outlined later.

One-tenth ml from every fraction is pipettes into small ampoules or tubes preferably with the aid of constriction pipets of the Lang-Levy type. Simple, inexpensive 2 or 3 ml ampoules of the sort * shown in Fig. 1 have been found suitable and easy to open and seal. With the aid of a semiautomatic syringe ** shown in the same figure, 0.5 ml of distilled constant-boiling hydrochloric acid is added, after which the ampoules are sealed over a narrow flame. Hydrolysis is carried out in a thermostated oven at 120°C for 10—24 h. The ampoules are then cooled below room temperature and opened with a sharp file. They are put in a desiccator with sodium hydroxide and dried *in vacuo* overnight. 2 ml

* Manufactured by Johnsen & Jorgensen Flint Glass LTD, London.
** Available through KELAB, Stockholm, Sweden.

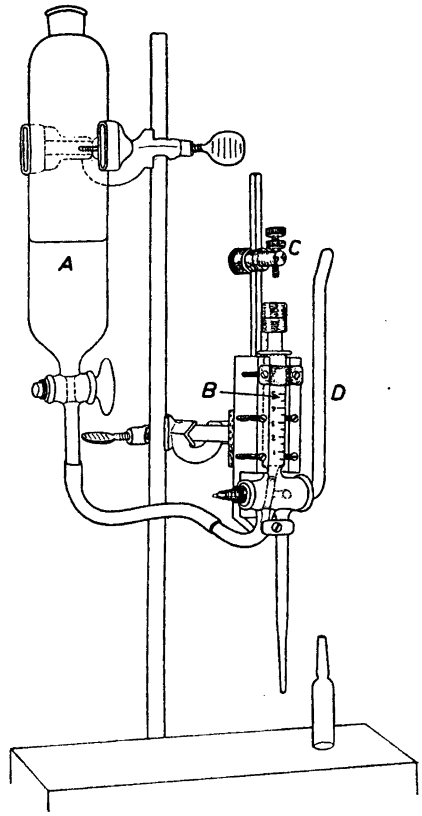


Fig. 1. Semiautomatic syringe used to deliver reagents into ampoules. The solution in A is forced into the all-glass syringe B by means of a slight air pressure. The volume to be delivered is set by the screw C and the plunger, which is filled with mercury, empties the syringe when the handle D of the stopcock is turned.

of water is added to each ampoule with a semi-automatic syringe, and 1 ml of the resulting solution is taken for ninhydrin analysis. This is performed according to Moore and Stein [15] using 1 ml ninhydrin solution prepared by dissolving 2.0 g ninhydrin and 0.3 g hydrindantin in 75 ml methyl cellusolve, adding 25 ml 4 N sodium acetate buffer pH 5.5 immediately before use. The reaction is carried out in test tubes immersed for 15 minutes in a boiling water bath, after which the tubes are immediately cooled and diluted with 3 ml 50:50 ethanol-water. When the tubes have been thoroughly shaken to oxidize any residual hydrindantin, they are read at 570 mμ against blanks from ampoules containing buffer, that have been subjected to the same procedure as the samples to be analysed. It is of special importance to use well cleaned tubes for the reaction, and the use of semi-automatic syringes for the addition of ninhydrin solution and dilution is of great convenience.

When extinction values that are too high are obtained with a final volume of 5 ml, the contents of the tubes can be further diluted with 5 or 10 ml ethanol:water without deviation from the linear relationship between the amount of nitrogen and colour. If the hydrolyzed residue in the ampoules is dissolved in 2 ml of water, of which 1 ml is taken for the ninhydrin reaction, the upper limit of such a determination is about 10 μg N taken from the fractions. However, as the hydrolysis of much larger amounts of protein is complete under the conditions described, as much as 1 mg N can be determined simply by diluting a portion of the 1 ml remaining in the ampoules. Table 1 shows that it is possible to determine very wide range of protein concentrations in this way without significant loss in precision. As test sample, a commercial protein standard, Pro-Sol,

Table 1. Quantitative ninhydrin determination of different amounts of hydrolyzed protein. The extinction values are given for equal amounts of hydrolyzed protein.

μg of protein taken	% of hydrolyzed residue taken for the ninhydrin analysis	extinction at 570 mμ
5 550	0.5	0.38
1 110	0.5	0.39
504	2.5	0.38
111	10	0.41
55.5	50	0.39
11.1	50	0.37
5.55	50	0.39
2.78	50	0.39

distributed by the Standard Scientific Supply Corp., New York, has been used. This standard is a partly purified preparation of bovine serum albumin and has been used throughout this investigation.

It has been found that the concentration of hydrochloric acid during hydrolysis is not critical, as long as it is at least 3 M. When comparatively large and unequal volumes are to be hydrolyzed, samples can be reduced in volume before the addition of HCl, but this is seldom necessary.

If very small amounts of material are available, the following modifications can be made. The hydrolyzed residue in the ampoules is dissolved in only a few tenths of a ml, an aliquot of which is taken for analysis with ninhydrin with a final volume of 1 ml. In this way as little as 0.1 μg of protein N can be determined with comparatively high precision. It is possible to perform the ninhydrin reaction directly in the ampoules, but it is then more difficult to oxidize the residual hydrindantin. For approximate determinations, the ninhydrin colour can then be read in the ampoules, as these vary comparatively little in width.

No detailed investigation of the time necessary for the complete hydrolysis of different proteins has been made; however, it seems advisable to try different times before using the method on samples of unknown behaviour. Since a few hours is sufficient in most cases, and prolonged hydrolysis does not seem to change the colour yield with ninhydrin very much, 24 hours has been used routinely at this laboratory. Fig. 2 shows the influence of different times of hydrolysis of Pro-Sol. As the ninhydrin reaction gives slightly different amounts of colour depending on the reagents and the exact procedure em-

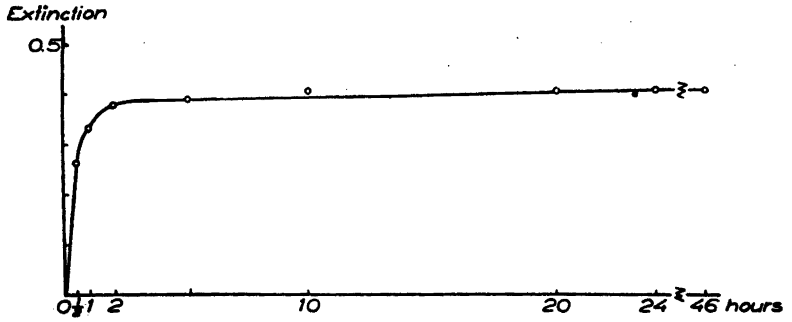


Fig. 2. The relationship between colour yield and time of hydrolysis at 120°.

Table 2. Precision of method. 3.53 µg of Pro-Sol nitrogen pipetted into each of eight ampoules. After hydrolysis at 120° and solution of the dry residue in 2 ml of water, 1 ml was taken for a ninhydrin reaction with a final volume of 5 ml.

	Extinction at 570 mµ minus blank reading			
Samples	0.409	0.410	0.420	0.419
	0.410	0.411	0.420	0.423
Mean value		0.415		
Standard deviation of mean		0.006		

ployed at a laboratory, it is necessary to calibrate the method with proteins of known nitrogen content if accurate quantitative data are wanted. It is then possible to convert the colour to protein nitrogen, but in fractionation work it is often sufficient to compare the colour yields of the different fractions directly. Table 2 illustrates the precision of the method when the same amount of protein is hydrolyzed in a series of ampoules. When other proteins have been tested, they have given similar values, but no detailed comparison between different proteins has been made as yet.

To keep blank readings as low as possible, it is necessary to use ammonia-free reagents and to clean all glassware well. The hydrochloric acid used for hydrolysis is best distilled in Pyrex and kept in a bottle provided with an arrangement to protect it from ammonia in the atmosphere. Water is obtained

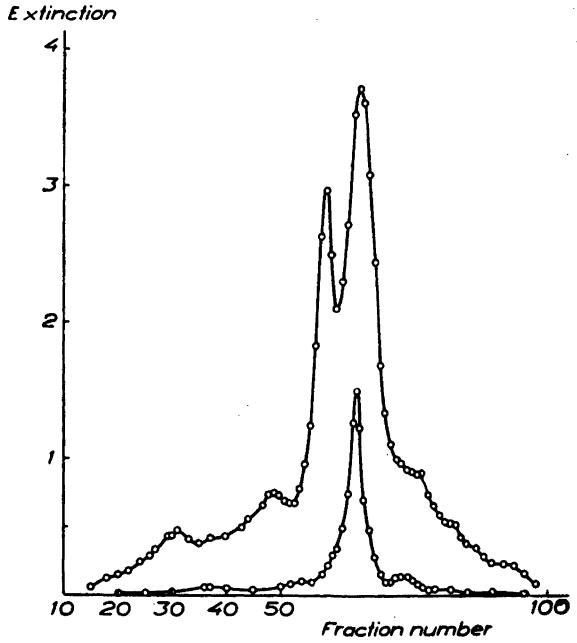


Fig. 3. Electropherogram of an extract from hog neurohypophysis. Lower curve: ninhydrin colour without hydrolysis. Upper curve: ninhydrin colour after hydrolysis with HCl at 120°. The extinction values are given for equal sample size in estimating the two curves.

Table 3. Comparison of some methods of protein determination. The approximate extinction values are given for a concentration of 1 μg of Pro-Sol protein nitrogen per ml measured in a 1 cm cell.

Method	Wavelength used mμ	Extinction
Ultraviolet absorption	280	0.0046
Turbidity with trichloroacetic acid at a final concentration of 3 %	420	0.0082
Direct ninhydrin reaction	570	0.092
Method according to Lowry *et al.*[11]	750	0.124
Hydrolysis and ninhydrin reaction	570	1.17

by distillation from an acid medium in a Pyrex still. The ampoules are sealed when delivered from the manufacturer and therefore do not contribute to high blanks, but the tubes used for the ninhydrin reactions must be kept free from contamination. If fractions can not be analysed soon after collection, they should be stored in a box provided with an acid adsorbent. If blank readings higher than 0.1 on the optical density scale are obtained, the reagents should be tested for impurities.

As an example of the usefulness of the method, Fig. 3 shows an electropherogram of an extract from hog neurohypophysis *. Electrophoresis was carried out in an apparatus described by Porath [17] with a buffer composed of 0.1 M pyridine adjusted to pH 5.0 with acetic acid. The fractions eluted from the column had a volume of approximately 10 ml each, of which 0.25 ml was taken for the ninhydrin reaction without hydrolysis. 0.2 ml was pipetted into ampoules and hydrolyzed for 24 hours with 0.5 ml 6.4 N HCl at 120°C. After removal of HCl, 2 ml of water was added, and 1 ml of the resulting solution taken for the ninhydrin reaction. The extract is a very complicated mixture of amino acids and peptides, and no attempt is made in this connection to discuss its different components. From the shapes of the two curves, it is possible to draw certain conclusions about the contents of the different fractions, because a high ratio between the colour yield of hydrolyzed and unhydrolyzed material indicates the presence of peptide-bound nitrogen. In this special case, it would have been impossible to use either optical density readings at 280 mμ or nitrogen determinations because of the pyridine content of the buffer. Pyridine does not react with ninhydrin and has the advantage of being volatile, so that the fractions can be lyophilized.

Table 3 has been arranged to allow a comparison of some of the colorimetric methods discussed. The values have been obtained from determinations made on the previously mentioned protein standard, Pro-Sol. In order to facilitate a comparison of the sensitivity of the methods, the extinction has been given for 1 μg of protein nitrogen per ml solution measured at the specified wave length.

The author wishes to thank Professor A. Tiselius and colleagues at the Institute for helpful discussions. The technical assistance of Mrs. B. Malmström and Mrs. I. Stark is gratefully acknowledged. This investigation was supported by grants from the *Swedish Natural Science Research Council.*

* Data from experiments by H. Kiessling.

REFERENCES

1. Johnson, M. J. *J. Biol. Chem.* **181** (1949) 707.
2. Gorbach, G., Dedic, G. and Philippi, E. H. *Hoppe-Seylers' Z. physiol. Chem.* **301** (1955) 185.
3. Harvey, H. W. *Analyst* **76** (1951) 657.
4. Boissonas, R. A. and Haselbach, C. H. *Helv. Chim. Acta* **36** (1953) 576.
5. Conway, E. J. *Microdiffusion analysis and volumetric error*, Crosby Lockhood & Son Ltd., 3. Ed. 1950.
6. Grunbaum, B. W., Kirk, P. L., Green, L. G. and Koch, C. W. *Anal. Chem.* **27** (1955) 384.
7. Smith, E. L. *Private communication.*
8. Stadtman, E. R., Novelli, G. D. and Lipman, F. *J. Biol. Chem.* **191** (1951) 365.
9. Greif, R. L. *Proc. Soc. Exptl. Biol. Med.* **75** (1950) 813.
10. Nayyar, S. N. and Glick, D. *J. Histo. Cyto. Chem.* **2** (1954) 282.
11. Lowry, O. H., Rosebrough, N. J., Farr, A. L. and Randall, R. J. *J. Biol. Chem.* **193** (1951) 265.
12. Dannenberg, H. *Angew. Chem.* **63** (1951) 208.
13. Beaven, G. H. and Holiday, E. R. *Advances in Protein Chem.* **7** (1952) 320.
14. Kunkel, H. G. and Ward, S. M. *J. Biol. Chem.* **182** (1950) 597.
15. Moore, S. and Stein, W. H. *J. Biol. Chem.* **211** (1954) 907.
16. Boissonas, R. A. *Helv. Chim. Acta* **33** (1950) 1975.
17. Porath, J. *Acta Chem. Scand.* **8** (1954) 1813.

Received July 3, 1956.

ACTA CHEMICA SCANDINAVICA 10 (1956) 1440—1454

X-Ray and Magnetic Study of Nickel Selenides in the Range NiSe to $NiSe_2$

FREDRIK GRØNVOLD and EINAR JACOBSEN

Kjemisk Institutt A, Universitetet i Oslo, Blindern, Norway

Two nickel selenide phases are identified in the range NiSe to $NiSe_2$ by means of X-rays.

1. *The NiSe phase* has a broad range of homogeneity extending from $NiSe_{1.02}$ to $NiSe_{1.30}$. Its structure is of a NiAs-like type up to the composition $NiSe_{1.20}$. At higher selenium content the structure becomes monoclinic (pseudo-hexagonal) with doubled *c*-axis. The lattice constants vary between these limits:

$NiSe_{1.00}$: $a = 3.6613$ Å, $c = 5.3562$ Å.
$NiSe_{1.30}$: $a = 6.196$ Å, $c = 2 \times 5.232$ Å,
$b = 3.634$ Å, $\beta = 90.78°$.

Weak reflections observed on single crystal photographs of $NiSe_{1.15}$ are due to an orthorhombic superstructure with

$a' = b\sqrt{3} = 6.2932$ Å, $b' = 3b = 10.901$ Å, $c' = 3c = 15.957$ Å.

Density determinations show that the solid solution of selenium in the NiSe phase takes place by subtraction of nickel atoms with increasing selenium content. The observed density decreases from 7.269 g cm^{-3} for $NiSe_{1.00}$ to 6.918 g cm^{-3} for $NiSe_{1.30}$.

2. *The $NiSe_2$ phase* has a structure of the pyrite ($C2$) type and a narrow range of homogeneity on the nickel-rich side of $NiSe_2$, with lattice constant decreasing from $a = 5.9626$ Å for $NiSe_{1.975}$ to $a = 5.9604$ Å for $NiSe_{2.00}$. The shortest selenium selenium distance is determined as 2.40 Å.

Magnetic measurements were carried out by the Gouy method. All samples are weakly paramagnetic and for those richer in selenium than $NiSe_{1.07}$ the susceptibility increases slightly with increasing temperature. The effective magnetic moment at 450° C is 1.08 Bohr magnetons for $NiSe_{1.00}$ and 1.34 Bohr magnetons for $NiSe_{2.00}$.

A nickel selenide was described for the first time by Little [1] in 1859. He obtained a silver white, crystalline, non-magnetic product with composition close to NiSe (found 43.23 % Ni, calc. 42.64 % Ni) by heating a mixture of the elements. Fabre [2] made NiSe in the same way and used the product to determine the enthalpy of formation of NiSe by solution calorimetry in bromine water. His result has been re-evaluated by Rossini *et al.*[3] who give $\Delta Hf° = -10$ kcal/mole at 25° C.

In 1900, Fonzes-Diacon [4] prepared gray, crystalline NiSe by leading selenium vapor diluted with nitrogen over red hot nickel. In another experiment, a gray black mass of $NiSe_2$ was prepared by the action of hydrogen selenide on nickel(II) chloride at about 300° C. If the chloride was kept at red heat, the compounds Ni_2Se_3 or Ni_3Se_4 were formed instead. By heating any of these compounds in hydrogen at bright red heat, Fonzes-Diacon obtained a gold-colored compound which he assumed had the composition Ni_2Se.

The existence of a fifth nickel selenide was claimed by Meyer and Bratke [5] who heated mixtures of nickel powder and selenium with potassium carbonate at 1 250° C. Analysis of the crystalline reaction products gave the result: 37.8 % Ni, 61.6 % Se and on this basis they deduced the formula Ni_5Se_6 or $3NiSe \cdot Ni_2Se_3$, which corresponds to 38.25 % Ni and 61.75 % Se.

Nickel selenides have also been prepared by precipitation. Reeb [6] obtained a black precipitate by the action of hydrogen selenide or potassium selenide on a nickel salt solution containing acetic acid and sodium acetate. His experiments were repeated by Moser and Atynski [7], who found that the products contained 1.4 to 2.8 % more selenium than NiSe. They succeeded, however, in preparing almost stoichiometric NiSe by precipitating it from alcoholic solutions (found Ni:Se = 1:1.035).

Alsén [8] studied NiSe by means of X-rays and found that it had a hexagonal structure of the NiAs ($B8$) type. This was later confirmed by Levi and Baroni [9]. As a result of electron diffraction studies these authors claimed the existence of two more NiSe phases, α-NiSe, which was amorphous, and γ-NiSe, which was found to be isomorphous with millerite (NiS).

The structure of $NiSe_2$ was established by de Jong and Willems [10] by X-ray diffraction studies on a sample prepared by heating a mixture of NiSe and selenium (in slight excess of $NiSe_2$) at 230° C for 48 hours. Although the product contained some elemental selenium, a phase with structure of the pyrite ($C2$) type was recognized. Its lattice constant and atomic parameter were determined. The lattice constant of $NiSe_2$ was later redetermined by Tengnér [11].

The only known nickel selenide mineral is penroseite from Colquechaca, Bolivia. It was first studied by Gordon [12] who proposed the formula $2PbSe_2 \cdot 3CuSe \cdot 5(Ni, Co)Se_2$ or $PbSe \cdot Cu_2Se \cdot 3(Ni, Co)Se_3$. Ten years later, Herzenberg and Ahlfeld [13] also described a nickel selenide mineral from the same locality. They concluded that it had the formula $(Ni, Cu)Se_2$ and gave the name blockite to it. The structural identity of penroseite, blockite and artificial $NiSe_2$ was established by Bannister and Hey [14] by X-ray diffraction and chemical analysis.

In view of the many nickel selenides that have been described and as a continuation of the work going on in this institute on the chalcogenides of the transition elements, a systematic study of the nickel selenium system seemed highly desirable. An X-ray study of this system was therefore started in 1950 by Olaf Holwech [15] on the suggestion of professor Haakon Haraldsen.

The work has been continued by Osvald Knop, now at Nova Scotia Technical College, and by the present authors. While Mr. Knop has mainly been concerned with the nickel-rich region of the system, we have especially studied the selenium-rich region, and an account of our work in the NiSe-$NiSe_2$ region will be given here.

EXPERIMENTAL

The *nickel* used for preparing the alloys was made from "Nickel oxide, low in cobalt and iron" from the British Drug Houses Ltd. by reduction with hydrogen at 600° C until constant weight was obtained. A spectrographic analysis showed only the presence of traces of copper and magnesium as impurities in the metal.

Highly purified *selenium* was placed at our disposal by Bolidens Gruvaktiebolag, Sweden. It contained the following impurities: copper 0.0002 %, iron 0.0007 %, tellurium 0.003 %, sulfur 0.01 %, non volatile matter 0.003 %.

The nickel selenides rich in nickel were synthesized by heating appropriate amounts of the elements in evacuated and sealed silica tubes. Samples in the composition range $NiSe_{0.90}$ to $NiSe_{1.333}$ (50.00 to 57.14 atomic % Se) were kept at 800° C for one day and furnace-cooled. The grayish, sintered products were then ground, homogenized by heating at 550° C for five days in pyrex tubes and afterwards air-cooled. One part of each sample was annealed at 300° C for six weeks and cooled down to room temperature during two weeks. X-ray photographs of these samples were not different from those of the 550° C annealing. The 300° C samples were therefore subjected to another annealing, this time at 400° C. After six weeks, they were slowly cooled. Changes were now noticed in some of the samples.

Samples with composition $NiSe_{1.95}$, $NiSe_{1.975}$, $NiSe_{2.00}$, $NiSe_{2.025}$ and $NiSe_{2.05}$ were prepared by mixing NiSe and selenium. They were heated for four weeks at 300° C but X-ray photographs proved this to be insufficient for complete reaction. After being transferred to new tubes they were heated at 400° C for another week and slowly cooled. Prepared in this way, the samples $NiSe_{1.95}$, $NiSe_{1.975}$ and $NiSe_{2.00}$ looked homogeneous, while small amounts of elemental selenium were observed in the samples $NiSe_{2.025}$ and $NiSe_{2.05}$.

X-Ray powder photographs of the samples were taken at 20 ± 2° C in 11.48 cm diameter cameras with asymmetric film mounting. In most cases filtered copper radiation was used, while iron radiation was used to obtain greater dispersion in the range from $NiSe_{1.80}$ to $NiSe_{1.40}$. The lattice constants are expressed in Å units, taking $\lambda CuK\alpha_1$ = 1.54051 Å and $\lambda FeK\alpha_1$ = 1.93597 Å. The probable error in the lattice constants is estimated as 0.01 % for the cubic structure, 0.02 % for the hexagonal structure and 0.03 % for the monoclinic structure. Lattice constants from earlier investigations have been transformed from kX to Å units by multiplication by the factor 1.00202.

Density determinations were carried out at 25° C by the vacuum pycnometric method. Approximately 2 g of substance were used in each experiment, and the displacement liquid was redistilled kerosene (200°—240° C fraction). The standard error in the density measurements is of the order 0.3 % but the values found for powdered samples of this type are usually about 1 % lower than those calculated on the basis of the unit cell dimensions.

Magnetic measurements were carried out by the Gouy method at different field strengths and temperatures. The samples were filled in thin-walled quartz tubes of about 1 mm internal diameter and to a height of about 80 mm. The field was calibrated at 20° C by means of $Mn_2P_2O_7$, which has a susceptibility of 102 × 10^{-6} per g at 20° C according to Foëx and Brunet [16] and by means of an aqueous $NiCl_2$ solution, for which Nettleton and Sugden [17] have given a formula for the susceptibility in terms of concentration and temperature.

To reduce the corrections for the empty tubes, a piece of quartz tubing was fused on to the bottom end of the specimen tube. In this way a correction for the empty tubes was avoided at room temperature and above, but a slight correction had to be taken into account below room temperature, with a maximum value of 0.043 mg.

RESULTS

A. X-Ray study and density measurements

In the range NiSe to $NiSe_2$ two phases were found, one with a broad range of homogeneity in the region $NiSe_{1.02}$ to $NiSe_{1.30}$, the other with a narrow range

of homogeneity close to $NiSe_{2.00}$. They will here be designated as the NiSe phase and the $NiSe_2$ phase, and the NiSe phase will be considered first.

The NiSe phase. Irrespective of whether samples with the composition $NiSe_{1.00}$ were heat-treated at 550°, 400° or 300° C they consisted of more than one phase. The major phase present was found to have a structure of the NiAs ($B8$) type. In addition, weak lines from phases richer in nickel were observed *.

The results of the lattice constant determinations of the NiSe phase for samples in the range $NiSe_{0.90}$ to $NiSe_{1.40}$ are listed in Table 1. Only the values found for samples heated at 550° C are given in the table, since the differences in cell dimensions due to the heat treatment are very small.

Table 1. Lattice constants of the NiSe phase.

Sample	a, ($b\sqrt{3}$) in Å	b in Å	c in Å	β
$NiSe_{0.90}$	(6.3410)	3.6610	5.3566	(90°)
$NiSe_{1.00}$	(6.3416)	3.6613	5.3562	(90°)
$NiSe_{1.04}$	(6.3330)	3.6564	5.3484	(90°)
$NiSe_{1.07}$	(6.3208)	3.6493	5.3407	(90°)
$NiSe_{1.10}$	(6.3092)	3.6426	5.3331	(90°)
$NiSe_{1.15}$	6.2932	3 × 3.6336	3 × 5.3190	(90°)
$NiSe_{1.175}$	(6.2824)	3.6279	5.3038	(90°)
$NiSe_{1.20}$	(6.2771)	3.6241	5.2951	(90°)
$NiSe_{1.225}$	6.235	3.631	2 × 5.277	90.2°
$NiSe_{1.25}$	6.224	3.635	2 × 5.260	90.52°
$NiSe_{1.275}$	6.206	3.635	2 × 5.250	90.63°
$NiSe_{1.30}$	6.196	3.634	2 × 5.232	90.78°
$NiSe_{1.40}$	6.199	3.635	2 × 5.230	90.77°

Within their limited accuracy the lattice constants found by Alsén [8] for NiSe ($a = 3.67$ Å, $c = 5.34$ Å) agree reasonably well with ours. Alsén studied only a sample with composition ratio 1 : 1 and noted, in agreement with our findings, that NiSe was not a pure product.

At the composition $NiSe_{1.04}$ the interferences belonging to the NiAs type structure are shifted slightly compared to $NiSe_{1.00}$ and the extraneous lines have disappeared. The X-ray photographs show the simple $B8$-pattern in the range from $NiSe_{1.04}$ to $NiSe_{1.20}$. Only the photographs of $NiSe_{1.04}$ and $NiSe_{1.07}$ are, however, free from weak additional lines. From the composition $NiSe_{1.10}$ on, many weak lines are observed in the low angle region, indicating that the true unit cell is larger than the $B8$-cell. In Table 2 are listed the more characteristic lines occurring in the low angle region on a powder photograph of $NiSe_{1.15}$.

After several attempts, some single crystals were obtained of $NiSe_{1.15}$ and by means of Weissenberg photographs the superstructure was found to be orthorhombic with

$$a' = b\sqrt{3} = 6.2932 \text{ Å}, \quad b' = 3b = 10.901 \text{ Å}, \quad c' = 3c = 15.957 \text{ Å}.$$

* The phase relationships in the Ni-rich region are rather complicated. The three intermediate phases that have been identified in this concentration range will be considered in another communication.

Table 2. Superstructure lines observed in the low angle region on a powder photograph of $NiSe_{1.15}$ taken with Cu radiation.

I_{obs}	$\sin^2\Theta \times 10^4$		*hkl*	I_{obs}	$\sin^2\Theta \times 10^4$		*hkl*
	obs	calc			obs	calc	
w	76	73	011	m	606	600	200
m	144	143	012	vw	665	659	033
		150	100			673	211
m	212	210	003	vw	714	723	124
		223	021, 111	vw	769	783	025, 115
w	267	260	013			810	133, 203
w	347	329	120	vst	812	822	034
		360	103			823	041, 221
w	476	472	031	m	848	839	006
w	498		?				

At the composition $NiSe_{1.20}$ the hexagonal structure still exists, but at $NiSe_{1.225}$ many of the reflections are split into several components, indicating a change to lower symmetry. This deformation is even more pronounced at the compositions $NiSe_{1.25}$, $NiSe_{1.275}$ and $NiSe_{1.30}$.

Small crystals were obtained of $NiSe_{1.25}$ in a preparation that had been heated in a sealed quartz tube at 750° C for six weeks and then slowly cooled. By means of Weissenberg photographs the structure * was found to be pseudo-hexagonal, monoclinic, with identity periods: $a = 6.22$ Å, $b = 3.63$ Å, $c = 10.53$ Å.

By means of powder photographs the unit cell dimensions were determined more accurately (see Table 1). The assignment of indices to the powder photograph of $NiSe_{1.25}$ is seen from Table 3. The lattice dimensions of the remaining monoclinic samples, $NiSe_{1.225}$, $NiSe_{1.275}$ and $NiSe_{1.30}$, were then easily found and the results are listed in Table 1.

The unit cell dimensions of the NiSe phase are plotted against composition in Fig. 1. The orthohexagonal cell description is used and the corresponding lattice sub-periods are given in the figure to facilitate the comparison. It is seen that the lattice constants decrease almost linearly with increasing selenium content in the hexagonal range $NiSe_{1.02}$ to $NiSe_{1.20}$. Further addition of selenium causes a slight increase in the length of the b-axes. This is compensated by an abrupt contraction of the a-axis as soon as the monoclinic deformation starts.

From Fig. 1 the selenium-rich limit for the homogeneity range of the NiSe phase appears to be $NiSe_{1.30}$. This is in accordance with the fact that faint lines from the $NiSe_2$ phase are visible on the powder photographs of $NiSe_{1.333}$.

Density determinations were carried out on the NiSe phase in order to ascertain that the solid solution of selenium in NiSe takes place by subtraction of nickel atoms from the NiSe structure. The densities calculated under that assumption are listed in Table 4 together with the observed densities. The

* The atomic arrangement in $NiSe_{1.35}$ and $NiSe_{1.15}$ will be discussed in a forthcoming paper.

Table 3. Powder photograph data of $NiSe_{1.25}$ taken with Fe radiation, a_2 and β lines omitted.

I_{obs}	$\sin^2\Theta \times 10^4$ obs	$\sin^2\Theta \times 10^4$ calc	*hkl*	I_{obs}	$\sin^2\Theta \times 10^4$ obs	$\sin^2\Theta \times 10^4$ calc	*hkl*
vw	325	324	$\bar{1}01$	m	5 262	5 264	404
		329	101	st	5 423	5 418	008
w	340	339	002	vw	5 774	5 785	$\bar{2}17$
w	795	794	011	vw	5 887	5 861	217
vw	950	951	110			5 884	026
vw	965	966	200	w	6 832	6 818	$\bar{2}26$
vw	996	996	$\bar{1}03$			6 849	$\bar{4}06$
vw	1 010	1 012	103	w	6 894	6 882	226
vst	1 284	1 285	$\bar{1}12$	m	6 973	6 956	$\bar{1}32$
st	1 302	1 294	$\bar{2}02$			6 967	132
		1 295	112			6 979	406
m	1 324	1 316	202	w	7 034	7 019	$\bar{4}22$
w	1 355	1 355	004	w+	7 074	7 061	$\bar{5}12$
w+	1 474	1 471	013			7 063	422
w−	1 770	1 765	211	w	7 126	7 115	512
vst	2 295	2 295	$\bar{1}14$	vw	7 216	7 226	$\bar{1}27$
		2 299	$\bar{2}04$	w+	7 974	7 967	$\bar{1}34$
st	2 321	2 317	114	w+	7 999	7 989	134
m	2 350	2 343	204	m	8 023	8 014	$\bar{4}24$
w+	2 425	2 421	$\bar{2}13$	w	8 099	8 100	424
st	2 840	2 836	020	vw	8 164	8 158	514
vst	2 892	2 883	310	st	8 241	8 236	$\bar{3}18$
vw	3 172	3 159	$\bar{1}21$			8 254	028
		3 165	121	m	8 370	8 366	318
		3 175	022	st	8 557	8 555	330
m	3 974	3 982	$\bar{2}06$	w	8 649	8 647	$\bar{4}17$
		3 983	$\bar{1}16$	m	8 698	8 698	600
m	4 021	4 015	116	w	9 386	9 378	$\bar{2}.0.10$
w	4 137	4 130	$\bar{2}22$			9 391	$\bar{1}.1.10$
m	4 158	4 152	222	w	9 439	9 445	1.1.10
w	4 197	4 191	024	w	9 486	9 486	2.0.10
		4 206	$\bar{3}14$	w	9 655	9 655	$\bar{1}36$
vw	4 284	4 270	314	st	9 689	9 685	$\bar{4}26$
vw	4 382	4 371	$\bar{1}07$			9 687	136
m	5 131	5 135	$\bar{2}24$	st	9 728	9 716	$\bar{5}16$
st	5 174	5 178	$\bar{4}04$	w	9 823	9 815	426
		5 179	224	w	9 883	9 878	516

good agreement between the two sets of values confirms the correctness of the above assumption. As to the question why the observed densities are consistently lower than the calculated ones, this seems primarily to be related to the large surface area of the powdered samples, and only to a smaller extent to missing metalloid atoms.

In the case of $NiSe_{1.00}$ there is a significant difference in density due to the heat treatment. This may be understood by comparison with the X-ray results, as the $NiSe_{1.00}$ sample heat-treated at 300° C contained much stronger lines from phases richer in nickel than the sample heated at 550° C. Furthermore, the density of $NiSe_{0.95}$ heated at 300° C was only 7.142 g cm^{-3}.

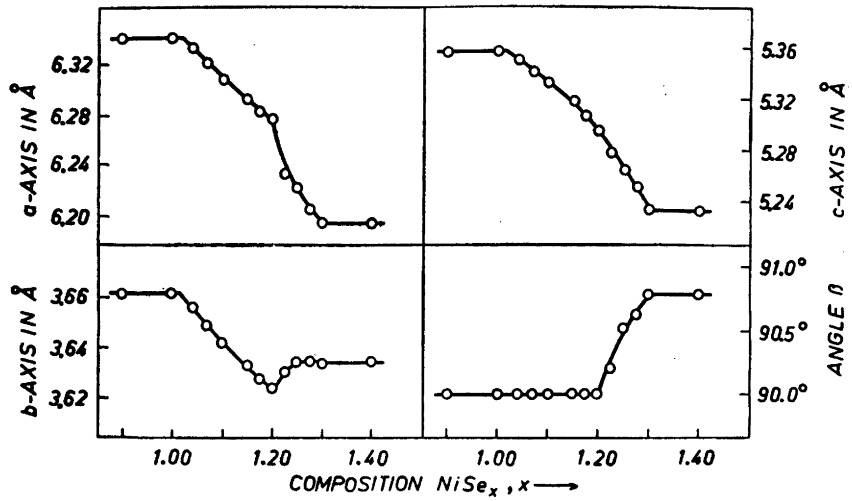


Fig. 1. Lattice constants of the NiSe phase as functions of composition.

In the NiSe structure each nickel atom is surrounded by six selenium atoms at the corners of a deformed octahedron (trigonal antiprism). The distances are 2.50 Å for $NiSe_{1.00}$, and 2.48 Å for $NiSe_{1.20}$. Each nickel atom is further surrounded by two nickel atoms at the distance $c/2 = 2.68$ Å ($NiSe_{1.00}$) and 2.65 Å ($NiSe_{1.20}$). The selenium atoms are arranged in a hexagonal close packing which is compressed in the c-direction so that the shortest distance between selenium atoms in adjacent planes is 3.41 Å against 3.66 Å for nearest neighbors in the hexagonal plane for $NiSe_{1.00}$ and 3.38 Å against 3.62 Å for $NiSe_{1.20}$.

The $NiSe_2$ phase. X-Ray photographs of samples in the $NiSe_2$ region showed the existence of a phase with pyrite ($C2$) structure. While several lines from the NiSe phase were present in $NiSe_{1.95}$, only one line was present in $NiSe_{1.975}$

Table 4. Observed and calculated densities in g cm^{-3} for the NiSe phase. The atomic weight unit is taken as 1.660 × 10^{-23} g.

Sample		D_{obs}	D_{calc}	Sample		D_{obs}	D_{calc}
$NiSe_{1.00}$	550° C	7.269	—	$NiSe_{1.20}$	550° C	6.974	7.051
$NiSe_{1.00}$	300° C	7.217	—	$NiSe_{1.20}$	300° C	6.980	7.051
$NiSe_{1.04}$	300° C	7.219	7.260	$NiSe_{1.225}$	550° C	6.915	7.052
$NiSe_{1.07}$	550° C	7.169	7.214	$NiSe_{1.25}$	550° C	6.890	7.027
$NiSe_{1.10}$	550° C	7.132	7.170	$NiSe_{1.25}$	300° C	6.927	7.027
$NiSe_{1.10}$	300° C	7.127	7.170	$NiSe_{1.275}$	550° C	6.894	7.009
$NiSe_{1.15}$	300° C	7.052	7.098	$NiSe_{1.30}$	300° C	6.918	6.997
$NiSe_{1.175}$	550° C	6.993	7.080	$NiSe_{1.333}$	300° C	6.914	—

that could possibly be attributed to the NiSe phase. No foreign lines were found in $NiSe_{2.00}$, $NiSe_{2.025}$ or $NiSe_{2.05}$.

The lattice constant was determined for these five samples and the results are listed in Table 5. A slight contraction of the unit cell takes place from $NiSe_{1.975}$ to $NiSe_{2.00}$, which denotes that the $NiSe_2$ phase has a narrow range of homogeneity on the nickel-rich side of $NiSe_2$. The lattice constant value found by Tengnér [11] for $NiSe_2$, $a = 5.960$ Å, is in perfect agreement with the present results, while the value $a = 6.034 \pm 0.003$ Å found by de Jong and Willems [10] is considerably higher.

Table 5. Lattice constants and densities of samples in the $NiSe_2$ region.

Composition	a in Å	D_{obs} in g cm^{-3}
$NiSe_{1.95}$	5.9628	6.730
$NiSe_{1.975}$	5.9626	6.724
$NiSe_{2.00}$	5.9604	6.720
$NiSe_{2.025}$	5.9605	6.703
$NiSe_{2.05}$	5.9603	6.693

Results of the density determinations carried out in the $NiSe_2$ region are also listed in Table 5. The observed density of $NiSe_{2.00}$ (6.720 g cm^{-3}) is as usual a little lower than the X-ray density (6.792 g cm^{-3}). The density calculated for $NiSe_{1.975}$ assuming different types of solid solution is given in Table 6. Since a decrease in density from $NiSe_{2.00}$ to $NiSe_{1.975}$ is not compatible with the observations, it is concluded that nickel atoms are taken up interstitially in this range.

Table 6. Calculated densities for $NiSe_{1.975}$. The atomic weight unit is taken as 1.660×10^{-23} g.

Type of solid solution	Formula	D_{calc} in g cm^{-3}
Interstitial	$Ni_{1.012}Se_2$	6.808
Substitutional	$Ni_{1.008}Se_{1.992}$	6.780
Subtractive	$NiSe_{1.975}$	6.723

In structures of the pyrite ($C2$) type, each metal atom is surrounded octahedrally by six metalloid atoms, and each metalloid atom is surrounded tetrahedrally by one metalloid atom and three metal atoms. The metalloid metalloid distance is equal to $a(1-2x)\sqrt{3}$, where x is a parameter to be determined. De Jong and Willems found $x = 0.375$ for $NiSe_2$, which led to a selenium selenium distance of 2.61 Å. This value is rather large, and a redetermination of the parameter was therefore undertaken.

The relative intensities of the $NiSe_2$ reflections were determined photometrically from powder photographs taken with Cu radiation. The best agreement between observed and calculated intensities was obtained with $x = 0.384$. The results are listed in Table 7. In the left column are found the $\sin^2\Theta$ values for the α_1 reflections.

Table 7. Observed and calculated intensities for $NiSe_2$ with $x = 0.384$, Cu radiation.

$\sin^2\Theta \times 10^4$	*hkl*	I_{obs}	I_{calc}	$\sin^2\Theta \times 10^4$	*hkl*	I_{obs}	I_{calc}
499	111	0.2	1.4	6 019	{600 442}	4.6	{0.0 3.4}
674	200	14	31				
837	210	*100*	*100*	6 184	610	5.4	4.3
1 007	211	85	83	6 350	{611 532}	18	{4.8 13}
1 339	220	12	11				
1 502	221	1.5	1.0	6 691	620	1.7	{1.3 1.2 0.1}
1 843	311	50	55				
2 008	222	6.1	3.9	6 854	{621 540 443}	3.8	
2 177	320	25	32				0.7
2 343	321	31	44	7 018	541	0.8	0.5
2 679	400	8.3	7.3	7 184	533	9.0	7.3
2 835	{410 322}	2.0	{0.7 0.5}	7 355	622	2.7	1.8
				7 520	{630 542}	13	{7.1 5.1}
3 001	411	1.3	0.7				
3 159	331	0.7	0.2	7 684	631	13	11
3 351	420	2.7	1.9	8 020	444	3.8	3.6
3 508	421	20	17	8 187	632	2.1	2.2
3 680	332	11	8.4	8 353	543	0.9	0.8
4 015	422	4.5	2.9	8 520	{711 551}	2.7	{0.0 2.9}
4 174	430	1.2	0.6				
4 337	431	2.3	0.8	8 686	640	9.5	11
4 512	{511 333}	23	{18 2.1}	8 853	{720 641}	21	{14 13}
4 834	{520 432}	22	{3.0 16}	9 019	{721 633 552}	23	{20 7.2 7.1}
5 000	521	15	12				
5 349	440	18	18	9 354	642	5.4	8.3
5 511	{522 441}	0.8	{0.1 0.4}	9 523	{722 544}	1.4	{0.6 0.6}
5 681	433	0.5	0.2	9 853	{731 553}	27	{33 47}
5 851	531	0.8	0.4				

According to the present results, the selenium selenium distance is 2.40 Å. The nickel selenium distance is, however, only slightly altered by the new constants, 2.49 Å now against 2.50 Å from the data by de Jong and Willems *.

B. Magnetic properties

All samples studied were found to be weakly paramagnetic and to have susceptibilities that were only slightly dependent on the temperature. In the range NiSe to $NiSe_{1.07}$, the susceptibility decreases with increasing tempera-

* The distance nickel selenium given by de Jong and Willems [10] as 2.47 Å is not consistent with their data. The correct value should be $a\sqrt{3x^2-2x+\frac{1}{2}} = 2.50$ Å.

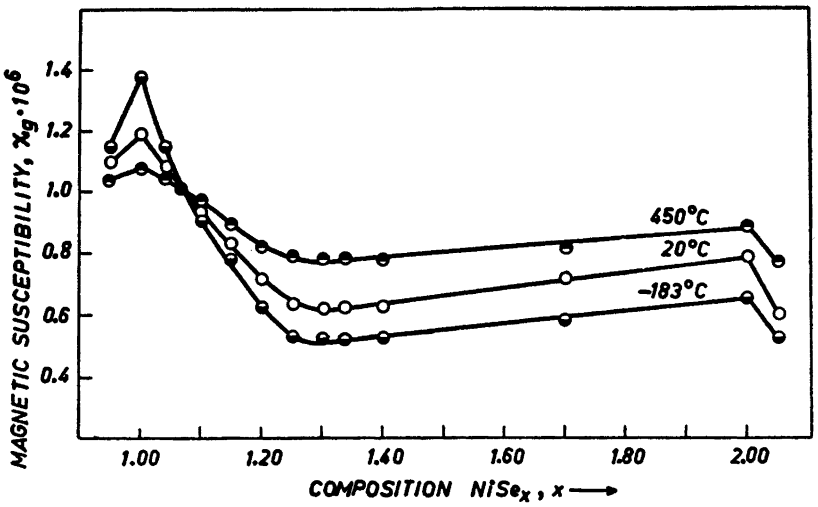


Fig. 2. Magnetic susceptibilities of the nickel selenides at −183°, 20° and 450° C.

ture while the opposite is true for all samples with higher selenium content than $NiSe_{1.07}$ in the temperature range studied. The results of the measurements are listed in Table 8. No specimen was found to have field strength dependent susceptibility and only the mean values of the results at H_{max} = 4 015, 4 700 and 5 110 Ørsteds are recorded in the table.

Table 8. Magnetic susceptibility of the nickel selenides, $\chi_g \times 10^6$.

Sample	Temperature °C					
	−183	−78	20	150	300	450
$NiSe_{0.95}$	1.15	1.12	1.10	1.07	1.05	1.04
$NiSe_{1.00}$	1.38	1.24	1.19	1.13	1.08	1.08
$NiSe_{1.04}$	1.15	1.10	1.08	1.07	1.06	1.05
$NiSe_{1.07}$	1.01	1.00	1.00	0.99	1.00	1.00
$NiSe_{1.10}$	.92	.92	.94	.95	.97	.98
$NiSe_{1.15}$	.79	.82	.84	.85	.87	.90
$NiSe_{1.20}$	.63	.68	.72	.75	.79	.83
$NiSe_{1.25}$	.53	.57	.64	.66	.75	.80
$NiSe_{1.30}$	.53	.57	.62	.67	.74	.79
$NiSe_{1.33}$	.52	.57	.63	.67	.74	.79
$NiSe_{1.40}$	.53	.58	.63	.68	.73	.78
$NiSe_{1.70}$	.58	.65	.72	.75	.80	.82
$NiSe_{2.00}$	.66	.73	.79	.82	.85	.90
$NiSe_{2.05}$	.53	.56	.60	.75	.76	.77

The susceptibility isotherms at —183°, 20° and 450° C are drawn in Fig. 2 and they show the phase relationships very clearly. A pronounced maximum close to $NiSe_{1.00}$ defines the nickel-rich limit of the homogeneity range of the NiSe phase. With increasing selenium content especially the —183° C isotherm has a non-linear character which is indicative of a single phase domain. At about the composition $NiSe_{1.30}$ minima occur in the isotherms and they define the selenium-rich limit of the NiSe phase. From the composition $NiSe_{1.30}$ on, the susceptibilities increase linearly and reach another maximum at $NiSe_{2.00}$. The decrease which is observed from $NiSe_{2.00}$ to $NiSe_{2.05}$ is probably due to the selenium phase.

In cases where the magnetic susceptibility of a substance is inversely proportional to the absolute temperature (*i. e.* the Curie law is fulfilled) a definite electronic state might be ascribed to the magnetic atom. This condition is far from fulfilled for the nickel selenides, and one can therefore only hope to obtain information about the magnetic state of the nickel atom at high temperatures, where the disturbing interactions are smaller. Since the magnetic susceptibility of the nickel selenides does not even obey the Curie-Weiss law, this information is best obtained by calculating the effective magnetic moment of the nickel atom.

This has been done * for NiSe and $NiSe_2$ and the results are shown in Fig. 3. The effective magnetic moment rises to 1.08 B. M. (Bohr magnetons) at 450° C

* The susceptibilities are corrected for induced diamagnetism with the value —17.7 $\times 10^{-6}$ mole^{-1} for Ni^{+2} according to Asmussen [18] and the value —47.58 $\times 10^{-6}$ mole^{-1} for Se^{-2} according to Angus [19].

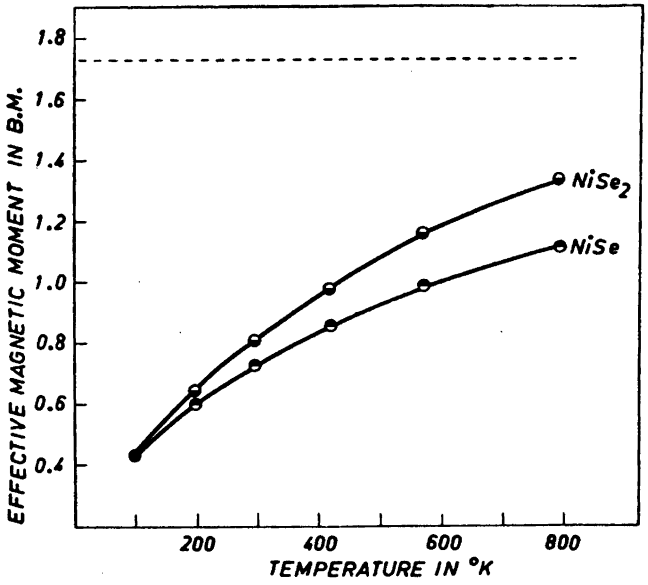


Fig. 3. Effective magnetic moments of NiSe and $NiSe_2$ as functions of temperature.

for NiSe and to 1.34 B. M. for $NiSe_2$. The slope of the curves is rather flat and the effective magnetic moments are of a much smaller magnitude than expected for Ni^{+2} ions.

According to Van Vleck [20], the magnetic moment of the free, gaseous Ni^{+2} ion is 5.56 B. M. at room temperature when the effect of the multiplet width is taken into account. When the crystalline field is so strong as to destroy the coupling of the spin angular momentum S and the orbital angular momentum L to a quantized resultant J, a "spin only" value of 2.83 B. M. is expected for Ni^{+2}. Also in case of nickel(II) forming covalent d^2sp^3 bonds the same value might be expected. The magnetism of the nickel selenides is, however, so weak that it cannot be explained satisfactorily in any of these ways.

The departure of the magnetism from Curie's law shows that strong interactions are present between the paramagnetic ion and its neighbors. It is not yet known to what extent this is due to interactions between paramagnetic ions, leading to antiferromagnetism, and to interactions with neighboring diamagnetic ions.

DISCUSSION

Of all the nickel selenides described by earlier investigators in the composition range NiSe to $NiSe_2$ only the NiSe phase and the $NiSe_2$ phase exist. The variable composition of the NiSe phase might, however, account for the conclusions by some of the earlier investigators about the existence of other intermediate phases. Thus, the compound $3NiSe \cdot Ni_2Se_3$ postulated by Meyer and Bratke [5], falls well within the homogeneity range of the NiSe phase.

The nickel selenide with approximate composition Ni_3Se_4, consisted according to Fonzes-Diacon [4] of a mixture of cubic crystals and a product containing slightly less selenium. It seems probable that the latter product, which he was not able to avoid, was the NiSe phase and that the cubic crystals were of the $NiSe_2$ phase. The polymorphism of NiSe which was found by Levi and Baroni [9] has not been observed in the present study. Their γ-NiSe is presumably identical with one of the phases we have observed on the nickel-rich side of NiSe. The same is probably also the case with the cubic NiSe crystals found by Little [1] and Fonzes-Diacon [4].

The atomic configuration in the NiSe and $NiSe_2$ phases is rather alike in that each nickel atom is surrounded octahedrally by six selenium atoms at practically the same distances, 2.50 Å in NiSe and 2.49 Å in $NiSe_2$. The values for the NiSe phase agree very well with the sum of the metallic radii given by Pauling [21]. In $NiSe_{1.00}$ the coordination number of the nickel atom is 8 and that of the selenium atom is 6 and the radius sum is 1.19 Å + 1.31 Å = 2.50 Å. For $NiSe_{1.20}$ the coordination numbers are 7.3 and 5 and the radius sum is 1.19 Å + 1.29 Å = 2.48 Å, in perfect agreement with the observed value (2.48 Å). In $NiSe_2$, nickel has coordination number 6 and selenium 4 which makes the radius sum 1.15 Å + 1.26 Å = 2.41 Å.

In structures of the pyrite ($C2$) type, the conditions are favorable for deriving characteristic radii since the metalloid atoms are bonded to each other. For $NiSe_2$ the empirical radius of the selenium atom is 1.20 Å (see

p. 1448) and the radius of the nickel atom is thus 2.49 Å — 1.20 Å = 1.29 Å. The nickel radius found here is considerably smaller than the octahedral covalent d^2sp^3 radius 1.39 Å for Ni(II) given by Pauling and Huggins [22]. This is not very surprising, however, as Lewis and Elliott [23] found that $NiSe_2$ is a conductor of electricity. The nickel atom might perhaps more aptly be designated as Ni(III), with electrons transferred to the conduction band. The transition of Ni(II) to Ni(III) causes a decrease in radius of 0.09 Å according to Pauling and Huggins.

A compilation of the interatomic distances in the diselenides of manganese, iron, cobalt and nickel is found in Table 9. $FeSe_2$ has a structure of the marcasite ($C18$) type and it is interesting to note that it has the largest selenium selenium distance among the four compounds. This case is analogous to the sulfide case where Buerger [26] showed that the sulfur sulfur bond distance for marcasite was appreciably larger than for pyrite and for MnS_2, CoS_2 and NiS_2 as well — see Haraldsen [27]. It thus seems that the conditions for the metalloid atoms to form sp^3 bonds are not so favorable in the marcasite structure as in the pyrite structure, which is in keeping with the larger deformation of the tetrahedral configuration. The sp^3 orbitals might therefore to some extent be taken up by unshared pairs, thus increasing the distance between the metalloid atoms and leaving fewer electrons for the conduction band.

Table 9. Shortest interatomic distances in Å for some diselenides.

Substance	Me-Se	Se-Se	Me-Me	Authors
$MnSe_2$	2.70	2.38	4.55	Elliott [24]
$FeSe_2$	2.37	2.50	3.58	Tengnér [11]
$CoSe_2$	2.42	2.43	4.14	Bøhm *et al.*[25]
$NiSe_2$	2.49	2.40	4.22	Present

The selenium selenium distances in $MnSe_2$, $CoSe_2$ and $NiSe_2$ are almost equal with 1.20 Å as mean value for the radius of the selenium atom. A rather abrupt decrease in the distance metal selenium and therefore also in the metal radius is observed as one goes from manganese (r = 1.50 Å) to iron (r = 1.17 Å). From then on the radius rises again to cobalt (r = 1.22 Å) and nickel (r = 1.29 Å). The anomalously large manganese radius was explained by Pauling [21] as a result of $4s4p^3$ resonating bonds for manganese compared to $3d^24s4p^3$ bonds for iron. The magnetic measurements of Haraldsen and Klemm [28] on natural MnS_2 (hauerite-)indicated the presence of five unpaired 3d electrons in manganese at high temperatures, which leaves no 3d orbitals available for bond formation. FeS_2 shows, as recently confirmed by Serres [29], almost zero magnetism so that in this compound all 3d electrons are paired. The six 3d electrons of Fe^{+2} presumably make use of three 3d orbitals, and the remaining two 3d orbitals are utilized in the d^2sp^3 bond formation.

Huggins [30] has suggested that d orbitals with principal quantum number one higher than normal might be used for bond formation in compounds of the

pyrite ($C2$) type and that intermediate bond types comprising both kinds of orbitals were possible. These outer orbitals are not so useless for bond formation as the separation of the energy levels of the free ion indicates, since they have their maximum probability density further out in space and can thus overlap appreciably with orbitals of the surrounding atoms. Actual overlap calculations carried out by Craig *et al.*[31] have confirmed Huggins' predictions and provided support for the view that 4d orbitals may be used for σ-bond formation in "ionic" complexes involving the first transition group metals.

The magnetic behavior of $NiSe_2$ seems to support this view. At low temperatures the octahedral bonds might be of a $3d4s4p^34d$ type with zero magnetism, and as the temperature is raised, the 4d character of the bonds increases. Simultaneously, unpaired electrons populate the available 3d orbitals and the effective magnetic moment of $NiSe_2$ increases. Evidently, the bonds do not relinquish much of their 3d character, since the effective magnetic moment does not even reach the "spin only" value for one unpaired electron per nickel atom at 450° C, *i.e.* 1.73 B.M.

The magnitude and temperature dependence of the effective magnetic moment for the NiSe and $NiSe_2$ phases are rather similar to what was found for the corresponding cobalt selenides by Bøhm, Grønvold, Haraldsen and Prydz [25] and the cobalt tellurides by Haraldsen, Grønvold and Hurlen [32]. Discussion of these relationships will be postponed to a later paper.

The authors wish to express their appreciation to professor Haakon Haraldsen for his encouragement and interest, and for extending to them the facilities of the laboratory. They should like to thank Bolidens Gruvaktiebolag for a generous supply of selenium and to thank siv.ing. Sigurd Rutlin, Sentralinstitutt for Industriell Forskning, for a spectrographic analysis of the nickel used.

REFERENCES

1. Little, G. *Ann. Chem. u. Pharm.* **112** (1859) 211.
2. Fabre, C. *Ann. chim. et phys.* [6] **10** (1887) 472.
3. Rossini, F., Wagman, D. D., Evans, W. H., Levine, S. and Jaffe, I. *Selected Values of Chemical Thermodynamic Properties*, NBS Circular 500, Washington 1952.
4. Fonzes-Diacon, H. *Compt. rend.* **131** (1900) 556.
5. Meyer, J. and Bratke, H. *Z. anorg. u. allgem. Chem.* **135** (1924) 289.
6. Reeb, . *J. pharm. chim.* [4] **9** (1869) 173.
7. Moser, L. and Atynski, K. *Monatsh.* **45** (1924) 235.
8. Alsén, N. *Geol. Fören. i Stockholm Förh.* **47** (1925) 19.
9. Levi, G. R. and Baroni, A. *Z. Krist.* **92** (1935) 210.
10. de Jong, W. F. and Willems, H. W. V. *Z. anorg. u. allgem. Chem.* **170** (1928) 241.
11. Tengnér, S. *Z. anorg. u. allgem. Chem.* **239** (1938) 126.
12. Gordon, S. G. *Proc. Acad. Nat. Sci. Phila.* **77** (1925) 317.
13. Herzenberg, R. and Ahlfeld, F. *Zentr. Mineral. Geol.* **1935**, 277.
14. Bannister, F. A. and Hey, M. H. *Am. Mineralogist* **22** (1937) 319.
15. Holwech, O. *Thesis*, Norges Tekniske Høgskole, Trondheim 1950.
16. Foëx, G. and Brunet, A. *Compt. rend.* **184** (1927) 443.
17. Nettleton, H. R. and Sugden, S. *Proc. Roy. Soc. London A* **173** (1939) 313.
18. Asmussen, R. W. *Magnetokemiske Undersøgelser over uorganiske Kompleksforbindelser*, København 1944.
19. Angus, W. R. *Proc. Roy. Soc. London A* **136** (1932) 573.
20. Van Vleck, J. H. *The Theory of Electric and Magnetic Susceptibilities*, Oxford 1932.

21. Pauling, L. *J. Am. Chem. Soc.* **69** (1947) 542.
22. Pauling, L. and Huggins, M. L. *Z. Krist.* **87** (1934) 205.
23. Lewis, B. and Elliott, N. *J. Am. Chem. Soc.* **62** (1940) 3180.
24. Elliott, N. *J. Am. Chem. Soc.* **59** (1937) 1958.
25. Bøhm, F., Grønvold, F., Haraldsen, H. and Prydz, H. *Acta Chem. Scand.* **9** (1955) 1510.
26. Buerger, M. J. *Z. Krist.* **97** (1937) 504.
27. Haraldsen, H. *Avhandl. Norske Videnskaps-Akad. Oslo I, Mat. Naturv. Kl.* **1947** No. 4.
28. Haraldsen, H. and Klemm, W. *Z. anorg. u. allgem. Chem.* **223** (1935) 409.
29. Serres, A. *J. phys. radium* **14** (1953) 689.
30. Huggins, M. L. *J. Chem. Phys.* **5** (1937) 527.
31. Craig, D. P., Maccoll, A., Nyholm, R. S., Orgel, L. E. and Sutton, L. E. *J. Chem. Soc.* **1954** 332.
32. Haraldsen, H., Grønvold, F. and Hurlen, T. *Z. anorg. u. allgem. Chem.* **283** (1956) 143.

Received June 2, 1956.

ACTA CHEMICA SCANDINAVICA 10 (1956) 1455—1458

Insulin Crystals

I. The Minimum Mole-Fraction of Metal in Insulin Crystals Prepared With Zn^{++}, Cd^{++}, Co^{++}, Ni^{++}, Cu^{++}, Mn^{++}, or Fe^{++}

J. SCHLICHTKRULL

Novo Terapeutisk Laboratorium, Copenhagen, Denmark

Recrystallized insulin is made zinc-free by a simple salting-out process.

The metal-free insulin is crystallized with Zn^{++}, Cd^{++}, Co^{++}, Ni^{++}, Cu^{++}, Mn^{++} and Fe^{++}. Of these metals, Cu^{++}, Mn^{++} and Fe^{++} have not hitherto been known to form crystals with insulin.

After recrystallization without any further addition of metal ions, the recrystallized insulin contained 2 atoms of metal per crystal unit of insulin. This amount of metal is considered a fundamental part of the crystal structure.

Abel [1] crystallized insulin as the first protein hormone in 1926. The rhombohedral crystals were precipitated in the isoelectric region at pH 5.5—5.6 from an insulin solution buffered with brucine, pyridine and ammonium acetate. The rather poor and uncertain yields were increased in 1929 by Harrington and Scott [2] who replaced brucine with saponin. The reason for this improvement was discovered in 1934 by Scott [3] who found that both the insulin crystals obtained with either method as well as the saponin contained zinc. Scott and Fisher [3-5] showed that the presence of either Zn, Cd, Co or Ni ions is an essential condition for the formation of crystals. Other metals were tried, *e. g.* Mg and Fe, but without success.

It was furthermore demonstrated by Scott and Fisher [4,5] that the metal content of the insulin crystals is directly proportional to the atomic weight of the metal (0.52 % Zn, 0.77 % Cd, 0.44 % Co and 0.41 % Ni). Cohn *et al.*[6] observed in 1941 that the zinc content of insulin crystals increases from 0.33 % to 0.65 % when the pH of crystallization is changed from 5.1 to 6.5. Two extremes were reported in the same year by Sahyun [7] (0.15 %) and Eisenbrand and Wegel [8] (0.8 %). In 1951 it was shown by the present author and his associates [9,10] that insulin crystals may combine with zinc to the extent of at least 2.3 % Zn.

Rhombohedral insulin crystals have apparently never been prepared without these metals. In 1949, however, Ellenbogen [11] obtained insulin crystals with various other compounds instead of metals, *e. g.* from a solution of insulin and sodium sulphate made slightly acid with sulphuric acid. These crystals were found to be orthorhombic and their unit weight was only one third of that of the rhombohedral crystal.

The presence of anions is also essential for the crystallization of insulin as shown by Hallas-Møller [12]. Rhombohedral insulin crystals were not formed with zinc and chloride ions alone; an addition of other anions (*e. g.* citrate, phosphate or carbonate) was found necessary.

From the experimental evidence listed above it can be concluded that the zinc content of insulin crystals is not merely defined by the molecular weight of insulin and the crystal structure; the metal content of the insulin crystals is rather dependent on the chemical composition of the suspension medium. It must nevertheless be assumed that at least a part of the metal found in the crystals is somewhat related to the structure, as the metal ions are necessary for the formation of crystals. The amount of metal which is an essential part of the crystal structure is considered identical with the metal content of crystals prepared with the minimum amount of metal necessary for the crystal formation. This minimum metal content was determined experimentally. The investigation was carried out with Zn^{++}, Cd^{++}, Co^{++}, Ni^{++}, Cu^{++}, Mn^{++} and Fe^{++}.

EXPERIMENTAL

Preparation of zinc-free insulin. Three-times-recrystallized insulin from beef pancreas was salted out 5 times (15 % NaCl, 0.5 % insulin, pH = 2—3) and isolated after precipitation at pH = 5. It contained less than 0.01 % zinc calculated on the dry weight of insulin.

First crystallization. The metal-free insulin was first crystallized from a medium containing a surplus of one of the metal ions. The composition of the mixture was as follows: 0.5 % insulin, 0.05 M sodium citrate, 15 % (v/v) acetone, and a salt of one of the metals, pH = 6.0 (glass electrode). It is preferable to use citrate buffer rather than the phosphate buffer, as the phosphate may precipitate the metal ions so that the crystals will be defiled by metal phosphate [13]. The ammonium acetate buffer which is frequently employed for the crystallization of insulin has the disadvantage that it contaminates the insulin crystals with non-protein nitrogen thus invalidating the subsequent Kjeldahl analyses. The acetone prevents the insulin from precipitating as amorphous particles from the supersaturated solution.

The zinc-free insulin was dissolved in water made slightly acid (pH = 2) with hydrochloric acid. The solution was distributed in glass beakers, acetone and metal salt solutions were added and the pH adjusted to 6.0 by adding a solution of sodium citrate. The mixture was stirred mechanically overnight with a glass propeller at room temperature. The precipitate was collected on a sintered glass filter without washing and dried to a water content of 4—7 %. The yield of a crystallization was expressed in % and calculated on the basis of Kjeldahl analysis.

Recrystallizations. The insulin crystals were recrystallized from a medium of the same composition as used for the first crystallization except that no metal salts were added. The crystals thus obtained contained less metal than the original crystals. This procedure was repeated until the crystal shape deteriorated severely (spherical shape) and amorphous particles appeared. The yield of a recrystallization was expressed in % and calculated on the basis of Kjeldahl analysis.

RESULTS

The precipitates are characterized by their microscopical appearance. Normal twinned rhombohedrons are indicated as NC (normal crystals) in Table 1. A tendency towards spherical shape is denoted by DC (defective crystals). Furthermore, if amorphous insulin particles are present in considerable amounts, an A is added.

From the paper by Sanger and co-workers [14] it is known that the smallest molecule of insulin contains 65 atoms of nitrogen. As it is assumed that one crystal unit contains 6 of the small molecular units, it contains 390 atoms of nitrogen. Thus the metal content per crystal unit is calculated as atoms of metal per 390 atoms of nitrogen.

Table 1. Crystallization of insulin with Zn++, Cd++, Co++, Ni++, Cu++, Mn++, and Fe++.

(1)	Zn++ $ZnCl_2$	Cd++ $3CdSO_4$, $8H_2O$	Co++ $CoCl_2$, $6H_2O$	Ni++ $NiCl_2$, $6H_2O$	Cu++ $CuCl_2$, $2H_2O$	Mn++ $MnCl_2$, $4H_2O$	Fe++ $FeCl_2$, $4H_2O$
(2)	94	95	94	96	95	89	93
(3)	94	96	87	95	93	68	61
(4)	85	91	88	93	94	—	—
(5)	46	45	48	48	30	274	135
(6)	2.12	3.28	2.23	2.16	2.07	3.43	2.38
(7)	1.92	1.99	1.90	1.96	1.92	—	—
(8)	1.92	1.91	1.81	1.96	1.90	—	—
(9)	NC	NC	NC	NC	NC	NCA	NC
(10)	NC	NC	DCA	DCA	NC	(DC)A	A
(11)	DC	NC	DCA	DCA	DC	—	—

(1) Metal salt employed.
(2), (3) and (4) Yields from 1st, 2nd and 3rd crystallization, respectively, expressed in per cent nitrogen recovered.
(5) Total amount of metal present during the first crystallization, expressed as atoms of metal per 390 atoms of nitrogen.
(6), (7) and (8) Metal content of crystals from 1st, 2nd and 3rd crystallization, respectively, expressed as atoms of metal per 390 atoms of nitrogen.
(9), (10) and (11) Character of precipitate from 1st, 2nd and 3rd crystallization, respectively. NC = normal appearance of crystals; DC = defective crystals, *i. e.* tendency towards spherical shape; A = amorphous insulin particles present in considerable amounts.

DISCUSSION

It has been a common practice to remove the zinc from insulin by electrodialysis. Preference was, however, given to a more easy method with no detrimental effect on the insulin. As already shown by Netter [15] in 1939, hydrogen ions may displace metal ions bound to insulin. The ordinary salting-out procedure for insulin, using an acid insulin solution and salt, is a similar process, and the zinc actually remains in the solution while the insulin is precipitated. The zinc content of insulin crystals can also be simply extracted by acid saline which does not dissolve the crystals.

It may be inferred from Scott and Fisher's [16] findings that the metal ions are chemically bound to the protein in a stoechiometric relation. The unit weight of the rhombohedral insulin crystal has been found to be 37 000 by Crowfoot [17] in 1935. Thus, the zinc content determined by Scott and Fisher (0.52 %) corresponds to 3 atoms of zinc per unit weight of insulin. The interpretation of the metal content is nevertheless complicated by the later findings of diverging zinc contents. In view of the present investigation it seems that 2 rather than 3 atoms of metal per crystal unit form the structural basis of the insulin crystal.

The metal content of crystals prepared in the presence of a surplus of metal ions (first crystallization) varies considerably, 2.1—3.4 atoms per crystal unit. This variation is explainable, as the metal content of the crystals is known to depend on the concentration of metal ions in the medium.

In the recrystallization process Mn^{++} and Fe^{++} crystals failed to reappear. The Mn^{++} and Fe^{++} ions must be present in a relatively high concentration to bring about crystallization.

The change in metal ion concentration in the medium from the first to the second crystallization did not greatly influence the Zn, Co, Ni and Cu contents of the crystals. This invariability is quite compatible with the concept of a fundamental metal insulin compound.

The minimum metal content of insulin crystals prepared with Zn^{++}, Cd^{++}, Co^{++}, Ni^{++} or Cu^{++} was found to be 2—5% less than 2 atoms per crystal unit. A closer proximity to the integer cannot be claimed when it is considered that the crystal structure becomes visibly imperfect through repeated recrystallization. The structure may already be somewhat defective after the second crystallization.

REFERENCES

1. Abel, J. J. *Proc. Natl. Acad. Sci. U.S.* **12** (1926) 132.
2. Harrington, C. R. and Scott, D. A. *Biochem. J. London* **23** (1929) 384.
3. Scott, D. A. *Biochem. J. London* **28** (1934) 1592.
4. Scott, D. A. and Fisher, A. M. *Biochem. J. London* **29** (1935) 1048.
5. Scott, D. A. and Fisher, A. M. *Trans. Roy. Soc. Can. V* **32** (1938) 55.
6. Cohn, J., Livinggood, J. J. and Blanchard, M. H. *J. Am. Chem. Soc.* **63** (1941) 17.
7. Sahyun, M. *J. Biol. Chem.* **138** (1941) 487.
8. Eisenbrand, J. and Wegel, F. *Hoppe-Seyler's Z. physiol. Chem.* **268** (1941) 26.
9. Hallas-Møller, K., Petersen, K. and Schlichtkrull, J. *Ugeskrift Laeger* **113** (1951) 1761.
10. Hallas-Møller, K., Petersen, K. and Schlichtkrull, J. *Science* **116** (1952) 394.
11. Ellenbogen, E. *The Determination of the Physical-Chemical Properties of Insulin and Their Application to the Equilibrium Between Insulin of Molecular Weights 12 000 and 36 000.* (Diss.) University, Harvard 1949.
12. Hallas-Møller, K. *Chemical and Biological Insulin Studies, I and II.* (Diss.) University, Copenhagen 1945.
13. Petersen, K. *USA Patent 2.626.228*
14. Brown, H., Sanger, F. and Kitai, R. *Biochem. J. London* **60** (1955) 556.
15. Netter, R. *Bull. soc. chim. France* **6** (1939) D 1042.
16. Scott, D. A. *Endocrinology* **25** (1939) 437.
17. Crowfoot, D. *Nature* **135**)1935) 591.

Received July 21, 1956.

ACTA CHEMICA SCANDINAVICA 10 (1956) 1459—1464

Insulin Crystals

II. Shape of Rhombohedral Zinc-Insulin Crystals in Relation to Species and Crystallization Media

J. SCHLICHTKRULL

Novo Terapeutisk Laboratorium, Copenhagen, Denmark

The shape of insulin crystals depends on the species of insulin. When crystallized by ordinary methods (citrate, phosphate, ammonium acetate buffer), recrystallized pig insulin precipitates as single, sharp and perfect rhombohedral bodies. The shape of cattle and sheep insulin crystals often shows a twinned appearance (*e.g.* star shape). The faces are curved.

Pig and cattle insulins are found to have identical biological insulin activities (units per molecule). The confidence limits for the ratio between pig and cattle insulin activity were 0.99 and 1.07 (P = 0.95).

Recrystallized insulin from all tree species yields perfectly shaped rhombohedral single crystals when urea or a halogenide are present in the mother liquid during crystallization.

The angle of a large rhombohedron is measured with an eye-piece goniometer. The estimate, 114°22′, is in agreement with the X-ray analysis, 114°16′.

In 1929 Abel [1] crystallized insulin and observed that the crystals were rhombohedral, and in 1935 this structure was proved by X-ray diffraction analysis by Crowfoot [2]. In the papers by Abel [1], Harrington and Scott [3], Scott [4], Netter [5] (Ni-insulin crystals), Romans *et al.*[6] and Sahyun [7] the rhombohedral shape is apparent from the photomicrographs. Scott [4] showed by means of a movie strip, however, that the crystals were actually twins, and he writes in this connection: "This twinned appearance of insulin crystals is the rule rather than the exception, but of course, is not observed unless the crystal is moved to expose various faces to view". When crystallizing at pH 5.2 instead of at the usual pH 6, Scott [4,8] obtained dumb-bell shaped crystals (wedge-shaped, no plane faces). Crowfoot [9] reviewed the literature dealing with insulin crystals of various shapes and studied some of these crystals by X-ray.

The primary purpose of the present paper is to define, within limits of particular interest, the dependence of the crystal shape on insulin and the conditions of crystallization. A new crystallization medium is introduced contain-

ing saline and sodium acetate. This medium causes the development of rhombohedral shape regardless of insulin species.

The second part of the present paper comprises a goniometric confirmation of the X-ray estimate of the obtuse angle of the rhombohedron, for which purpose large, perfectly shaped rhombohedral single crystals were prepared.

EXPERIMENTS WITH CRYSTAL SHAPES

In order to establish the sources of shape variation, the conditions of crystallization are initially fixed and the quality of insulin varied, with respect to species (pig, cattle and sheep). The dependence of shape on purity within the species cannot be properly studied as the impurities are not well defined.

1. Crystallization from a buffered solution

The crystallization mixture contains 0.5% insulin; 0.04% Zn^{++} (as chloride); 0.05 M sodium citrate; 15 % (v/v) acetone; and the pH = 6.0—6.3. The insulin is dissolved in water containing HCl (pH = approximately 2.5), whereupon acetone and buffer solution are added. The crystallization is carried out at room temperature without stirring.

Only a few observations were made with sodium phosphate or ammonium acetate buffers. The results were identical with those obtained with the citrate buffer.

A. Insulin from pig pancreas. Fig. 1 shows pig insulin crystals obtained by recrystallization. The crystals are beautiful single rhombohedrons. All attempts, without any exception, to obtain this shape by recrystallizing various lots of pig insulin proved successful. The pig insulin crystals (citrate buffer, recrystallized insulin) are thus defined as perfectly shaped, rhombohedral singlecrystals.

B. Insulin from cattle pancreas. Cattle insulin crystals from several times recrystallized insulin are shown in Fig. 2. They have the star-shaped appearance described by Crowfoot [9]. When agitation is avoided the crystals may grow even larger and develop the needle shape [9]. The gradual perfection of shape seen when recrystallizing pig insulin has not been observed in this laboratory in the case of cattle insulin even after as many as ten recrystallizations.

The shape of cattle insulin crystals is correlated with the size of crystals. When agitating, a great number of smaller crystals (5—10 μ) are obtained. These crystals, apparently twins, resemble those shown in the publications listed above. They have rounded edges and faces and their vertices are not well defined. The curved surface of cattle insulin crystals may be explained by the presence of impurities which are not removed by recrystallization. To test this question, cattle insulin was fractionated by salting out with NaCl at pH 3 or by extracting the crystals with neutral citrate or phosphate buffers. No perfect rhombohedral shape could be observed in crystals obtained by crystallization of these fractions.



Fig. 1. Rhombohedral zinc-insulin crystals from pig pancreas. × 250.



Fig. 2. Twinned zinc-insulin crystals from beef pancreas. × 250.

C. Insulin from sheep pancreas. Only one lot of sheep insulin crystals has been examined. After recrystallization the crystals developed a shape similar to that of cattle insulin crystals.

2. Crystallization from a buffered solution of urea or a halogenide

If it is assumed that the impurities of both pig and cattle insulin are removed by the recrystallizations from citrate buffer it follows that the peculiar shape of cattle insulin crystals is not due to impurities. In order to investigate the question of equal purity, the biological activities of recrystallized pig and cattle insulin were estimated by biological assays on rabbits. The activity is expressed in units per molecule of insulin. The ratio between the activities of insulin from the two species was estimated as:

$$\frac{\text{activity of pig insulin}}{\text{activity of cattle insulin}} = 1.03 \pm 0.04 \text{ (confidence limits: } P = 0.95).$$

The activities are found identical. This finding also supports the hypothesis of equal purity.

The crystallization of pig insulin was then compared with the crystallization of cattle insulin in order to find an explanation of the shape difference. Under apparently identical conditions (citrate, pH, acetone, *etc.*) cattle insulin crystals are formed more rapidly than pig insulin crystals, and this is more pronounced when the pH is increased above 6. The solubility of the two species of insulin crystals also presents a difference. By increasing the pH from 6 to a value below 7, the solubility of pig insulin is increased more than

that of cattle insulin. This difference in solubility and rate of crystallization may or may not have any relation to the shape of the crystals. In order to investigate this question, these differences were tentatively eliminated by using solubilizing agents for the crystallization of cattle insulin. Urea, which is known to have solubilizing properties, was added to the citrate medium for the crystallization of cattle insulin. The solubility of the cattle insulin was thereby increased and the rate of crystallization decreased. Sodium chloride which also increases the solubility of the crystals in the citrate buffer was likewise tested.

A. Addition of urea, citrate buffer, cattle insulin. Acetone was tentatively substituted by 20 % urea, which caused the insulin tc stay in solution. 10 % urea was tried with the result that perfect rhombohedrons developed which could not be distinguished from pig insulin crystals. After recrystallization without urea, the beautiful sharp rhombohedrons were transformed into the usual shape typical of cattle insulin. Thus the shape seems to be related to solubility and the rate of crystallization rather than to the presence of impurities.

B. Addition of halogenides. The solubilizing effect of sodium chloride is less pronounced, but when acetone is replaced by 7—8 % sodium chloride, rhombohedrons are obtained which are just as perfect as those obtained with 10 % urea. Sodium acetate, nitrate, sulphate, citrate or phosphate were found ineffective, whereas KCl, NH_4Cl, $CaCl_2$ and $(HOCH_2CH_2)_3NHCl$ produced the effect. Thus the effect seems to be due to the chloride ion.

Sodium fluoride was ineffective, but the following halogenides, KCl, KBr, KI, were all effective, especially KI as judged from the dependence of shape upon molar concentration of the halogenide.

In order to demonstrate that the effect of the halogenides is not contingent on the presence of citrate buffer, the following composition may be employed:

0.5—4.0 % insulin
0.8 % Zn^{++} (as chloride) calculated on the weight of insulin
0.1 M sodium acetate
7.0 % sodium chloride
HCl to pH 5.45—5.55.

The insulin is dissolved in water containing HCl and $ZnCl_2$, whereupon a solution of sodium acetate and sodium chloride is added. The crystallization is carried out at room temperature under mechanical stirring. The process is completed within one or two days. The advantages of this method are the following:

1) The shape of crystals is perfectly rhombohedral irrespective of the species of insulin and, to a certain extent, the purity.
2) Non-protein nitrogen is not introduced (as with ammonium acetate).

When the acid insulin solution is mixed with the alkaline buffer solution to produce pH 5.5, the insulin is precipitated as amorphous particles and gradually converted into crystals. When impure insulin is used, an amorphous

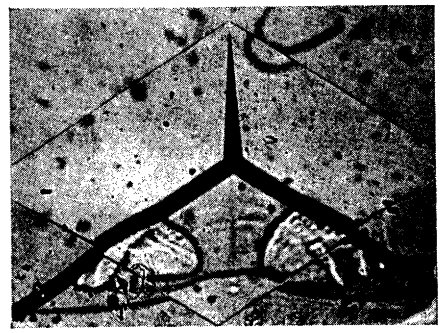


Fig. 3. 1.3 mm large insulin crystal from pig pancreas.

fraction is left which may be removed by acetone (30 % (v/v)). The acetone dissolves the amorphous fraction so that the crystals can be isolated by filtration or centrifugation. When pure, recrystallized insulin is crystallized by this method, only a small fraction, approximately 3 % of the protein, is left as amorphous particles, and the amount of insulin left in solution is of the same magnitude.

The halogenide ions do not alter the shape of pig insulin crystals.

MEASUREMENT OF THE ANGLE BETWEEN THE EDGES OF THE RHOMBOHEDRON

Several times recrystallized insulin from pig pancreas was crystallized from the acetone-citrate buffer at pH 6.2 (1 litre). Agitation was avoided. Within a few days, large (1 mm), beautiful, extremely sharp and colourless rhombohedrons could be observed on the glass walls, at the bottom of the beaker and hanging on the surface. The crystals shrink, harden and become crackled when taken up and left in the air. Therefore, for the microscopical examination, a crystal was placed in its mother liquid on a slide and covered with a cover glass, a ring of vaseline between the glasses providing space for the crystal. The crystal was lying on a face which was therefore in level (see Fig. 3). The horizontal position was checked by adjusting the microscope to the edges of the face. A 10 × objective in connection with a 8 × eye-piece goniometer was used for the measurements. Ten goniometer readings of the obtuse angle between the edges were made with the following result: $\alpha = 114° 22' \pm 4'$ (S.D.). This estimate agrees with the X-ray estimate for wet insulin crystals, *viz.*: $\alpha = 114° 16'$, as determined by Crowfoot and Riley [10].

REFERENCES

1. Abel, J. J. *Proc. Natl. Acad. Sci. U.S.* **12** (1926) 132.
2. Crowfoot, D. *Nature* **135** (1935) 591.
3. Harrington, C. R. and Scott, D. A. *Biochem. J. London* **23** (1929) 384.
4. Scott, D. A. *Endocrinology* **25** (1939) 437.
5. Netter, R. *Bull. soc. chim. France* **6** (1939) D 1042.

6. Romans, R. G., Scott, D. A. and Fisher, A. M. *Ind. Eng. Chem. News Ed.* **32** (1904) 908.
7. Sahyun, M. *J. Biol. Chem.* **138** (1941) 487.
8. Scott, D. A. *Trans. Roy. Soc. Can. V* **26** (1932) 275.
9. Crowfoot, D. *Proc. Roy. Soc. London A* **164** (1938) 580.
10. Crowfoot, D. and Riley, D. *Nature* **144** (1939) 1011.

Received July 21, 1956.

ACTA CHEMICA SCANDINAVICA 10 (1956) 1465—1474

Spectroscopic Conformational Analysis of Some Monohalogenated *Cyclo*hexanes

PETER KLÆBOE, JOHAN J. LOTHE and K. LUNDE

Universitetets Kjemiske Institutt og Sentralinstitutt for Industriell Forskning, Blindern-Oslo, Norway

The vibrational spectra of monohalogenated *cyclo*hexanes in the liquid and solid states have been investigated.

In the liquid state of monochloro- and monobromo-*cyclo*hexane both the *e*- and the *a*-conformation are present, the *e*-conformation preponderating in both compounds. The same dynamic equilibrium between the two conformations of monochloro*cyclo*hexane was observed in the rotating, cubic modification. No cubic modification was found for the monobromo-compound. In the anisotropic modification (at −150° C) only the *e*-conformation of the two compounds could be detected.

Investigation of the spectra of monofluoro*cyclo*hexane in the liquid, cubic (rotating) and anisotropic modification revealed the presence of only one conformation.

The stereochemistry of halogen substituted *cyclo*hexanes has been studied in considerable detail by Hassel and co-workers [1] using X-ray and electron diffraction methods and in some cases dipole moment measurements. As a result of the investigation of *cyclo*hexane Hassel [2] pointed out that for the majority of the substituted *cyclo*hexanes two different conformations are possible through the conversion of the carbon ring. In the vapour the relative amounts of the two conformations present at equilibrium are to a large extent determined by steric factors. In the solid state only one of the two possible conformations has been observed.

The electron diffraction method will in most cases not be sensitive enough to detect a small percentage of one conformation in an equilibrium. The method is furthermore not suited for investigation of the liquid phase.

It was hoped, however, that the infrared spectrophotometric method would be more sensitive to small amounts of a second conformation. The method might also be valuable in elucidating the structure of some of the more complicated halogen substituted *cyclo*hexanes.

A great advantage of the infrared method is that it is equally suited for the solid, liquid and even for the vapour phase of the lower boiling compounds. Since the two conformations of monohalogeno derivatives of *cyclo*-

hexane represent two different molecular species, they will have two different sets of vibrational frequencies. Some of the corresponding infrared bands, at least in the lower frequency region, should be so strongly influenced by the different directions of the halogen substituent that they should be resolved by an infrared spectrophotometer. Provided that only one conformation is present in the solid state it should be possible by noting the disappearance of a set of bands on going from the liquid to the solid state to assign some of the bands to one or another of the two conformations. The more complicated problem to decide which of the two conformations is present in the solid state may be solved either by an X-ray study or in more special cases by direct assignment of some of the bands to each of the two conformations. This assignment is greatly facilitated if polarization data from the Raman spectrum are available, or, as will be discussed in a forthcoming paper [3], if it is possible to displace the conformational equilibrium by changing the solvent.

As an introduction to the spectroscopic study of the stereochemistry of halogen substituted *cyclo*hexanes a discussion of the infrared and Raman spectra of monochloro- and monobromo-*cyclo*hexane and of the infrared spectrum of monofluoro*cyclo*hexane is presented in this paper. In a subsequent paper [3] the spectra of some 1,2-dihalogen substituted *cyclo*hexanes will be dealt with.

An electron diffraction investigation of the vapour of monochloro*cyclo*hexane published in 1943 by Hassel and Viervoll [4] has shown that the *e*-conformation must be present in a concentration considerable greater than the *a*-conformation.

More recently Larnaudie [5] in a study of the infrared spectra of the monohalogenated *cyclo*hexanes concluded from a consideration of the band envelopes of the vapour spectra that both conformations of the iodo-, bromo-, chloro-, and probably also of the fluoro-compound were present in the liquid phase. It is obvious, however, that the band envelopes are not very sensitive to the structure of these molecules of low symmetry (C_s), and the interpretation given by Larnaudie cannot be regarded as conclusive.

It has been known for several years that some simple derivatives of *cyclo*hexane exhibit molecular rotation in the crystals just below the melting point. This phenomenon has been shown both for *cyclo*hexane itself and for monochloro*cyclo*hexane [6]. Usually organic compounds which exhibit rotation below the melting point crystallize in the cubic system. This rotation can, however, not continue down to the absolute zero of temperature. The crystals must consequently undergo a transition into a non-rotating, generally anisotropic modification. This gives us the possibility of learning, by means of polarized light, whether the crystals are in a rotating or a non-rotating state.

The true nature of molecular rotation in the crystal lattice is not very well understood, but it will be shown in this paper that the rotation in the cubic modification permits the free interconversion between the two conformations.

EXPERIMENTAL

The *cyclo*hexane derivatives were synthesized using well known methods and their purity checked by the refractive indices.

Table 1. Raman and infrared spectra of monochlorocyclohexane.

Raman spectrum liquid (20° C)			Infrared spectra liquid (25° C)		rot. cubic modif. (−60° C)	solid modif. (−150° C)
$\Delta\nu$ cm^{-1}	I	ϱ	ν cm^{-1}	I	ν cm^{-1}	ν cm^{-1}
1 461	1		1 462	1	1 462	1 462
1 446	6	0.72	1 450	10	1 449	1 450
1 429	0		1 434	1	1 434	1 438
1 349	2	0.61	1 352	3	1 352	1 352
1 338	2		1 339	4	1 339	1 337
			1 325	1	1 325	1 325
1 302	1	0.80	1 301	0	1 300	1 302
1 270	3	0.69	1 267	10	1 269	1 270
1 261	4		1 262	10	1 261	1 259
1 216	1	0.78	1 217	8	1 218	1 219
1 184	1	0.85	1 186	0	1 186	1 187
1 132	1	0.37	1 132	1	1 134	1 134
			1 098	3	1 098	
			1 088	0	1 088	1 089
1 074	1	0.85				
1 051	1	0.88	1 050	0	1 052	1 056
1 028	4	0.65	1 030	2	1 029	1 031, 1 026
			1 014	4	1 016	
993	3	0.41	993	8	994	994
921	0	p	920	1	920	920
889	0	0.73	888	8	888	888
868	0	p	867	4	869	
			858	5	859	
852	2	0.25	852	2	852	850
818	3	0.19	816	8	817	817
807	3	0.18	806	3	807	
732	8	0.19	728	9 b	726	726
686	2	0.15	683	5	684	
586	0	p				
559	2	0.15	557	7		
512	1	0.18	512	5		
471	0	p	471	3	not recorded	
435	1	0.14	434	2		
382	0	p				
339	10 b	0.19	340	6 b		
			298			
258	1	0.67		2		
199	0	p				

The infrared spectra were recorded with a Perkin-Elmer Model 21 double beam spectrophotometer equipped with sodium chloride and caesium bromide prisms. A cell similar to the one described by Lord *et al.*[7], was used and only minor alterations introduced in order to record the spectra at low temperatures. Teflon spacers were, however, found to be more efficient than the conventional metal spacers to prevent leakage. One welding point of the thermocouple was placed as close as possible to the cell windows and a rough estimate of the temperature gradient between this spot and the sample was made. Before running the spectra the solids were inspected by placing the cell in a light beam between two opposed polaroid films.

The Raman spectra were recorded with a three-prism f : 3, Steinheil spectrograph. The source unit consisted of eight 450 watts mercury lamps surrounded by a cylindrical

Table 2. Raman and infrared spectra of monobromocyclohexane.

Raman spectrum liquid (20° C) $\Delta\nu$ cm^{-1}	I	ϱ	Infrared spectra liquid (25° C) ν cm^{-1}	I	solid modif. (−150° C) ν cm^{-1}
1 446	4	0.84	1 448	10	1 444
1 349	3	0.62	1 346	2	1 346 ?
1 336	1		1 334	6	1 332
1 301	1		1 297	1	1 296
1 273	1				
1 257	5	0.52	1 252	10	1 256
1 195	4	0.53	1 189	10	1 192
			1 139	0	1 138
1 117	2		1 116	6	1 120
1 088	1		1 086	4	1 086 ?
1 061	2				
1 052	2				
1 029	4	0.90	1 026	1	1 026
			1 009	5	
990	5	0.45	987	9	989
			919	1	919
888	1		885	8	886
865	1		862	2	
849	4	0.30	850	6	846
809	6 b	0.54	811 804	8 4	810
688	8	0.40	685	9	684
659	3	0.28	658	6	
503	4 b	0.23	503	5	
460	3	0.35	457	5	
			436	1	
			428	2	
411	2				
371	2				not recorded
298	2		299	1	
262	10	0.30			
243	2				
221	2				

metal jacket the inner surface of which was coated with magnesium oxide [8]. The same source unit, with the addition of a set of parallel baffles inside the circle of mercury lamps, was used in order to obtain polarization data by means of the two-exposure method by Crawford and Horwitz [9].

EXPERIMENTAL RESULTS

The infrared and Raman data for the monochloro- and the monobromo-*cyclo*hexane in the liquid and solid states are reproduced in Tables 1 and 2. The frequencies for the Raman spectra of these compounds are in reasonably good agreement with those reported by Kohlrausch [10]. The most significant difference is found in the Raman spectrum of the chloro compound. We have found two polarized lines of about equal intensity at 807 and 818 cm^{-1}. Kohlrausch observed only one line. The polarization data of Tables 1 and 2 represent the average of four plates and should be more reliable than the results from the rather incomplete investigation by Canals [11].

Table 3. Infrared spectra of monofluorocyclohexane.

liquid (25° C)		rot. cubic modif. (−25° C)	solid modif. (−150° C)
ν cm^{-1}	I	ν cm^{-1}	ν cm^{-1}
			1 495
			1 471
1 456	10	1 454	1 454
			1 394
1 370	10	1 370	1 369
1 350	5	1 350	1 351
1 344	5	1 343	1 343
1 332	5	1 331	1 330
			1 317
			1 297
1 263	4	1 263	1 263
1 247	1	1 249	1 252
1 195	2	1 196	1 194
1 162	6	1 163	1 163
			1 145
1 130	8	1 131	1 129
1 098	4	1 099	1 098
		1 078	1 079
1 050	10	1 050	1 048
1 034	9	1 034	1 034
1 020	10	1 018	1 018
962	10	960	958
942	10	938	939
			926
894	8	896	896
869	3	870	869
847	6	848	844
834	7	834	833
794	6	795	795
		732	733
719	1	719	717
677	0	676	676
662	2	662	660

It is very interesting to note that all of the bands observed in the liquid state of monochloro*cyclo*hexane (Table 1) are also found in the cubic, semi-solid modification. A set of bands has disappeared, however, from the spectrum of the solid, anisotropic modification at —150° C.

For the monobromo-compound only *one* crystalline modification has been found [6]. Inspection in polarized light revealed that the crystals were anisotropic. A comparison of the infrared bands of the two states (Table 2) shows that a set of bands disappeared on going from the liquid to the solid state. Only by very slow cooling and crystallization of the bromo compound could these bands be eliminated.

The infrared data for the monofluoro*cyclo*hexane in the liquid state are in good agreement with a spectrum obtained by Bak [12]. The data for the liquid state and for the two crystalline modifications are given in Table 3. It will be seen that in this case all the bands observed for the liquid state are present in the semi-solid, cubic as well as in the solid, anisotropic modification. The

infrared spectrum of the anisotropic modification was repeatedly investigated with the same result.

The infrared spectra of solutions of the monochloro- and monobromo-compound in different solvents of high and low dielectric constant (nitromethane - *cyclo*hexane) did not reveal any change in the conformational equilibrium, judging from the relative absorbancy values of the bands.

DISCUSSION

The discussion will mainly be concerned with monochloro*cyclo*hexane as this compound exhibits all of the special features of substituted *cyclo*hexanes: Both conformations are present in the liquid state; two solid modifications are found, one cubic, rotating, where both conformations are observed, and one anisotropic, non-rotating, where only one of the two conformations can be present.

The monochloro*cyclo*hexane molecule possesses $3 \times 18 - 6 = 48$ normal modes of vibration which are all active both in the infrared and the Raman spectra. A more detailed consideration indicates that the molecule would be expected to have at most 6 polarized Raman lines below 700 cm^{-1}: 4 ring frequencies, 1 C—Cl stretching and 1 C—Cl bending frequency. The Raman spectrum of liquid monochloro*cyclo*hexane (Table 1) shows, however, a great number of polarized, strong Raman lines in the lower frequency region, 16 below 1 000 cm^{-1} and 9 below 700 cm^{-1}. Already this behaviour indicates strongly that both conformations must be present in appreciable concentrations in the liquid state of monochloro*cyclo*hexane. This assumption is confirmed by the observation that several bands of high intensity in the spectrum of the liquid are lacking from the spectrum of the solid at —150° C. As only one conformation can be present in the true solid state, this behaviour points unequivocally to an equilibrium between the two conformations in the liquid state. Only with molecules of high symmetry, where forbidden bands are observed in the liquid state owing to the breaking-down of the selection rules, may some of these bands disappear on going to the solid state.

The Raman spectrum of liquid monobromo*cyclo*hexane (Table 2) does not as clearly indicate the presence of two conformations as was the case with the chloro compound. Only 5 lines below 700 cm^{-1} can unambigously be identified as polarized. The intensity of the other lines is too low to permit observation of the polarization ratio. A consideration of the total number of frequencies, 15 in all, observed below 700 cm^{-1} in the Raman and infrared spectra indicates, however, that both conformations are probably present in the liquid state as about 9 frequencies only would be expected for monobromo*cyclo*hexane. A comparison of the liquid and solid state infrared spectra of monobromo*cyclo*hexane shows, furthermore, that at least 4 bands of medium intensity are lacking from the solid state spectrum. Unfortunately, the solid state spectrum has only been run in the sodium chloride region, but it is quite probable that a study of the spectrum below 650 cm^{-1} would reveal the absence of other bands. At any rate the presence of both conformations in the liquid state is clearly revealed.

For monofluoro*cyclo*hexane all of the infrared bands present in the liquid persisted in both the cubic and in the anisotropic modification. It seems thus as if only *one* conformation can be detected in the liquid state of the monofluoro compound.

ASSIGNMENTS

It would be of great help for the infrared determination of the structure of polyhalogenated *cyclo*hexanes if some bands could be assigned to definite groupings within the molecules. Attention should especially be paid to the effect of *a*- and *e*-substituents on the position and intensity of the bands.

The infrared spectra of the monohalogenated *cyclo*hexanes would be expected to have at least 3 comparatively strong bands in which the polar carbon-halogen linkage participates to a large extent in the vibration *. The stretching of the carbon-halogen bond, a totally symmetrical vibration and consequently polarized in Raman, would be expected to show up strongly in both the infrared and the Raman spectra. Of the two vibrations connected with the bending of the carbon-halogen bond, one should give a polarized, the other an unpolarized Raman line.

Kohlrausch [10] identifies the C—Cl stretching vibration of monochloro*cyclo*hexane with the very strong, polarized Raman line at 732 cm^{-1}. Kohlrausch did not, however, consider the possibility of two conformations. As the C—Cl stretching frequency is usually found around 700 cm^{-1}, it is reasonable to assign the polarized Raman line at 686 cm^{-1} to the C—Cl stretching frequency of the other conformation. This corresponds well with the observation that the 732 cm^{-1} band persists in the infrared spectrum of the solid, whereas the 686 cm^{-1} band is absent.

The polarized and very strong Raman line at 339 cm^{-1} in the spectrum of the chloro compound is obviously the C—Cl bending vibration. It is somewhat surprising that the corresponding band for the other conformation has not been identified. Probably this band is located in the region below 200 cm^{-1} which is obscured by the exciting Raman lines. It is also possible that the line is covered by the broad 339 cm^{-1} line.

The pair of lines at 807 and 818 cm^{-1}, both equally strongly polarized in the Raman spectrum of monochloro*cyclo*hexane, are probably the symmetrical ring stretching frequencies of the two conformations, corresponding to the line at 802 cm^{-1} in *cyclo*hexane [13].

The bands at 1 014 and 1 098 cm^{-1}, lacking in the spectrum of solid monochloro*cyclo*hexane may be ascribed to the methine C—H group, or possibly to a ring stretching frequency. This question will be discussed more completely in the forthcoming paper on dihalogenated *cyclo*hexanes.

The assignment of the bands in the spectra of monobromo*cyclo*hexane will be mentioned in a few words. The polarized Raman lines at 688 and 659 cm^{-1} are obviously the C—Br stretching vibrations of the two conformations. The very strong and polarized Raman line at 262 cm^{-1} is the symmetrical

* It should be pointed out that the term "polar" here has a real physical signification and should not be mistaken for the old designation used in the *cyclo*hexane stereochemistry instead of an axial -*a*-substituent.

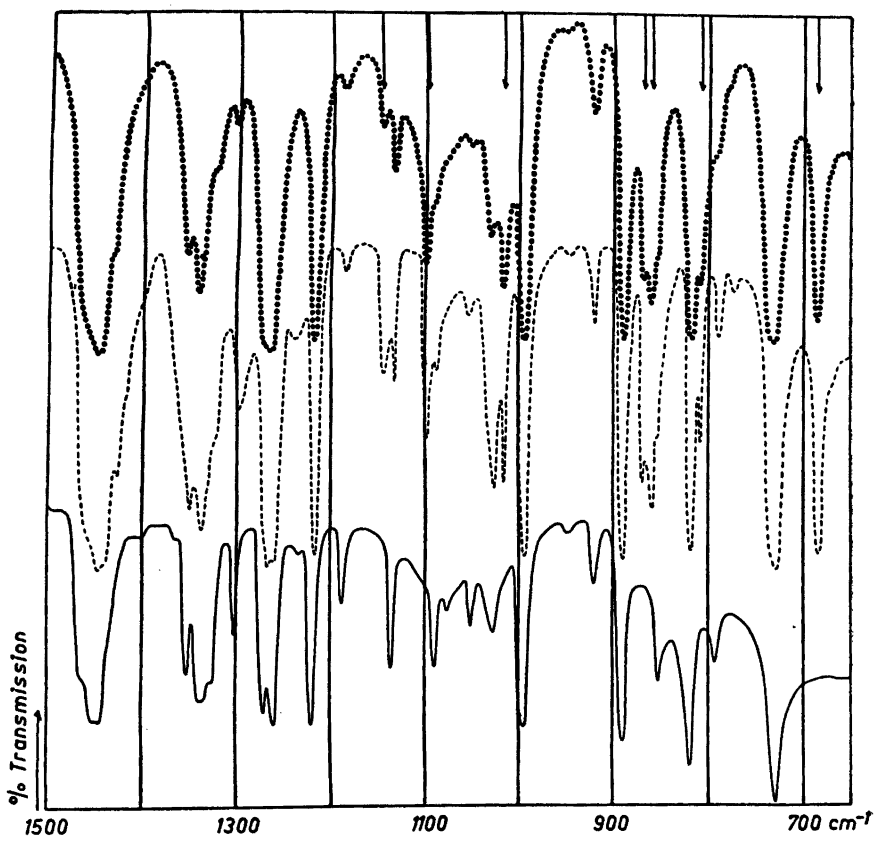


Fig. 1. Infrared spectra of monochlorocyclohexane.
..... *liquid at +20° C*
– – – – – *cubic, rotational modification at −60° C*
——— *solid, anisotropic modification at −150° C*

The bands that are assigned to the a-conformation, are indicated by arrows.

deformation vibration of the C—Br linkage of one of the two conformations. Again it is not quite clear where the C—Br bending frequency of the other conformation is located. The symmetrical ring stretching frequency, at 802 cm^{-1} in *cyclo*hexane, is probably found at 809 cm^{-1} in monobromo*cyclo*hexane. A close inspection of the Raman spectrum reveals that the 809 cm^{-1} band is a doublet. Seemingly the symmetrical ring stretching frequency of the halogeno compounds is not very sensitive to the geometrical direction of the substituent.

The problem of deciding which of the two conformations is present in the solid state of monochloro- and monobromo-*cyclo*hexane is best solved by considering the relative positions of the carbon-halogen stretching frequencies. As will be evident from the forthcoming paper on dihalogenated *cyclo*hexanes,

there are strong indications that the carbon-halogen stretching vibration is of higher frequency in the *e*-conformation than in the *a*-conformation. Consequently, the C—Cl stretching band of monochloro*cyclo*hexane at 728 cm^{-1} should be assigned to the *e*-conformation. The observed ratio of the intensities of the 728 cm^{-1} and the 683 cm^{-1} band is as 2 to 1 in the liquid infrared and somewhat higher in the Raman spectrum; this is in accordance with the general trend of the intensity ratios of other pair of bands in the spectra. Qualitatively, the higher intensity of the *e*-band is in good agreement with the observation by Hassel and Viervoll [2] that only the *e*-conformation could be detected in the vapours by the electron diffraction method.

Correspondingly, of the two C—Br stretching frequencies of monobromo-*cyclo*hexane, the 685 cm^{-1} band should be assigned to the *e*-conformation and the 658 cm^{-1} band to the *a*-conformation.

These assignments make it possible to identify the conformation in the solid. Tables 1 and 2 show that of the carbon-halogen stretching frequencies it is the *a*-bands, 683 cm^{-1} in the monochloro- and 658 cm^{-1} in the monobromo-compound, that disappear in the solid state spectra. Consequently, the *e*-conformations are energetically preferred in the lattice of the anisotropic modifications of both the monochloro- and the monobromo-*cyclo*hexane. A conclusion regarding the conformation present in crystalline monofluoro*cyclo*-hexane cannot be reached at the present time.

ROTATIONAL, SEMISOLID STATE

The observed close similarity of the spectra of monochloro*cyclo*hexane in the liquid state and in the semi-solid, cubic modification is quite interesting but not surprising. The disappearance of a set of bands on going to the solid, anisotropic modification provides a clear evidence for the presence of two conformations both in the liquid and in the cubic modification. As the energy barrier of the conversion of the carbon ring is very low and considering the easy transition of one conformation into the other at the transition-point, a static equilibrium can be excluded. The conclusion must be that the molecular rotation permits an unhindered interconversion of the two conformations in the cubic lattice. Furthermore it must be assumed that the dynamic equilibrium ratio between the two conformations is approximately the same in the liquid and in the rotational, cubic state of monochloro*cyclo*hexane.

Monofluoro*cyclo*hexane also exhibits molecular rotation in the cubic lattice. In this case, however, all spectra of the solid states at any temperature down to —150° C were identical with that of the liquid compound, although a transition from the cubic to an anisotropic modification at a higher temperature was ascertained by inspection in polarized light. This leads to the conclusion that only *one* conformation of the monofluoro*cyclo*hexane can be identified in the solid as well as in the cubic, semi-solid and liquid states of the compound. The physical explanation of this behaviour may possibly involve a stabilizing effect by intramolecular C——H- - -F bonding due to the strong electronegativity of the fluorine atom. The finding that only one conformation prevails, even when steric interactions does not exclude the other conformation, is not unique [14].

The spectrum of the solid monobromo*cyclo*hexane is not changed through the temperature range from just below the melting point to —150° C. This is in full accordance with the lack of a cubic, rotating state for this compound.

One of the authors (K. L.) wishes to thank *Norges almenvitenskaplige forskningsråd* for financial support.

REFERENCES

1. Hassel, O. *Research* **3** (1950) 504.
   Hassel, O. *Quart. Rev.* **VII** (1953) 221.
2. Hassel, O. *Tidskr. Kjemi Bergvesen Met.* **3** (1943) 32.
3. Klæboe, P., Lothe, J. and Lunde, K. *To be published.*
4. Hassel, O. and Viervoll, H. *Tidsskr. Kjemi Bergvesen Met.* **3** (1943) 35.
5. Larnaudie, J. M. Thesis, Paris 1953.
6. Hassel, O. and Sommerfeldt, A. M. *Z. physik. Chem.* **B 40** (1938) 391.
   Finbak, Chr. *Arch. Math. Naturvidenskab* **42** (1938) No. 1.
7. Lord, R. C., Mc Donald, R. S. and Miller, F. A. *J. Opt. Soc. Amer.* **42** (1952) 149.
8. Menzies, A. C. and Skinner, J. *J. Sci. Instr.* **26** (1949) 299.
9. Crawford, B. L. and Horwitz, W. *J. Chem. Phys.* **15** (1947) 268.
10. Kohlrausch, K. W. F. and Stockmair, W. *Z. physik. Chem.* **31** (1936) 382.
11. Canals, E., Mousseron, M., Granger, R. and Gastaud, J. *Bull. soc. chim.* **4** (1937) 2048.
12. Bak, B. *Private communication.*
13. Beckett, C. W., Pitzer, K. S. and Spitzer, R. *J. Am. Chem. Soc.* **69** (1947) 2488.
14. Bastiansen, O. and Hassel, O. *Acta Chem. Scand.* **5** (1951) 1404.
    Lunde, K. *Acta Chem. Scand.* **10** (1956) 690.

Received July 9, 1956.

ACTA CHEMICA SCANDINAVICA 10 (1956) 1475—1487

The Alkaline Hydrolysis of Alkoxymethyl Ureas

J. UGELSTAD* and J. de JONGE

Philips Research Laboratories N. V. Philips Gloeilampenfabriken, Eindhoven, Netherlands

Alkoxy methyl ureas, surprisingly enough, were found to be quite readily hydrolysed in moderately alkaline solution at room temperature, giving urea, formaldehyde and an alcohol as end products. The decomposition of different alkoxymethyl ureas was investigated kinetically. The hydrolysis was found to be proportional to the OH^- ion concentration. Based on kinetic investigations in strongly alkaline solution a choice is made between two possible reaction paths for the reaction. It may be concluded that the reaction involves the breaking of an ether bond, *i.e.* that methylol urea and alcohol are the first decomposition products.

The reaction is specific for ethers of methylol urea, ethers of methylol compounds of carboxylic acid amides being comparatively very stable in alkaline solution.

The reaction mechanism is discussed.

Ethers of methylol urea are usually prepared in acid solution from methylol urea and alcohol.

$$NH_2CONHCH_2OH + ROH \rightleftharpoons NH_2CONHCH_2OR + H_2O$$
$$HOCH_2NHCONHCH_2OH + 2ROH \rightleftharpoons ROCH_2NHCONHCH_2OR$$

As indicated in the above equations these reactions are reversible. The ethers are readily decomposed under the catalytic influence of acids, probably giving the methylol compound and the alcohol as the first decomposition products. The details of this decomposition in acid solution are not yet known.

Contrary to some observations in the literature, it can be shown that such ethers are also hydrolysed in alkaline solutions. The experimental evidence for a hydrolysis of this type of ethers in alkaline aqueous solution is the appearance of free formaldehyde.

This result could be due to the decomposition of the urea part of the ether molecules. The breaking of a C—N bond at one of the places indicated by the dotted lines in equation (a) would result in a total break-down of the ether molecule:

$$NH_2{:}CO{:}NHCH_2OCH_3 + 2H_2O \rightarrow 2NH_3 + CO_2 + CH_2O + CH_3OH \qquad (a)$$

* Present address: Sintef, Norges Tekniske Högskole, Trondheim, Norway.

From what is known of the stability of urea in alkaline solution it is not very probable that such a reaction occurs in the present instance. The conditions under which the alkaline hydrolysis of the ethers appears to occur are so mild that the urea molecule may safely be regarded as stable.

It was possible to confirm this experimentally.

The compound $NH_2CONHCH_2OCH_3$ was hydrolysed practically completely after being dissolved in 0.3 N NaOH for 24 hours at room temperature (95 % free CH_2O). Urea could then be precipitated from the solution as its addition compound with xanthydrol with a yield of 90 % (More details of these experiments are to be found in the experimental part of this chapter).

It is therefore more probable that the ether will break initially at one of the points indicated by a dotted line in $NH_2CONH:CH_2:OR$. In both cases the final products will be urea and formaldehyde, in accord with experimental evidence. Should the C-N bond between the urea fragment and the methylene group be broken initially the decomposition would proceed as follows:

$$\left.\begin{array}{ll} 1. & NH_2CONHCH_2OR \rightarrow NH_2CONH_2 + HOCH_2OR \\ 2. & HOCH_2OR \rightarrow CH_2O + ROH \end{array}\right\} \quad (b)$$

The hemiacetal primarily formed is known to be very unstable in alkaline solution and will quickly decompose into formaldehyde and the alcohol.

If the C-O bond is broken initially the following reaction occurs:

$$\left.\begin{array}{ll} 1. & NH_2CONHCH_2OR \rightarrow NH_2CONHCH_2OH + ROH \\ 2. & NH_2CONHCH_2OH \rightarrow NH_2CONH_2 + CH_2O \end{array}\right\} \quad (c)$$

Under the catalytic influence of hydroxyl ions, the ether is decomposed into the alcohol ROH and methylol urea, this involving the rupture of an ether bridge $—CH_2:OR$. The methylol compound is broken down further in a subsequent reaction into urea and formaldehyde, a reaction which is known to occur in alkaline solution [1].

The two latter reaction paths (b) and (c) are very similar and both involve a series of two subsequent reactions with an unstable intermediate. It is very difficult to show by any chemical method which of these two reactions paths (b) or (c) does in fact predominate since the possible intermediates are both highly unstable compared to the parent compound. Later in this paper arguments will be given that monomethylol urea is the initial product in the ether decomposition (scheme (c)). The evidene for this has been derived from kinetic measurements. The kinectic investigation of the decomposition also gave an insight into the mechanism of the reaction.

KINETIC INVESTIGATIONS

A. General outline of the kinetic measurements

1. The rate of hydrolysis of various alkyl ethers of methylol urea was measured in alkaline solution at 25°C.

$$NH_2CONHCH_2OR \rightarrow NH_2CONH_2 + CH_2O + ROH$$

Formaldehyde was considered to be the component most suitable for determination. It was possible to obtain satisfactory results with "the KCN method"[2]. In alkaline solution formaldehyde reacts very rapidly and completely with KCN by the familiar equation:

$$CH_2O+CN^-+H_2O\rightarrow CH_2(OH)CN+OH^-$$

The excess KCN is titrated with $Hg(NO_3)_2$ after reducing the pH of the sample to about 5.

2. As already indicated the decomposition of the ether may be formulated as a sequence of two reactions:

$$1.\ E\rightarrow I+\ldots \quad 2.\ I\rightarrow F+\ldots,$$

in which E is the ether, I the intermediate (hemiacetal or methylol urea) and F formaldehyde.

If it is required to use rate of formation of free formaldehyde in ascertaining the rate of decomposition, it should be noted that reaction 2 does not go to completion but reaches an equilibrium. This inconvenience can be overcome by arranging for the measured amount of KCN to be present from the very start of a kinetic run. (To keep the pH constant during the run the experiments were carried out in strong phosphate-buffer. More details of the experimental procedure are found in the experimental part).

Under these conditions reaction 2 will be irreversible because in the alkaline solution any free formaldehyde will be completely removed by KCN by an instantaneous reaction. Nothing is known regarding the reversibility of reaction 1. From what is known of similar organic chemical reactions it is to be expected that a possible equilibrium will be far over to the right. In any case under the present experimental conditions, reaction 1 may be considered as going to completion because the concentration of the intermediate will always be very low compared to the concentration of the undecomposed ether.

The system is therefore considered as being a sequence of two irreversible reactions 1 and 2 (scheme b or c). Later in this chapter it will be shown experimentally that the ether decomposition is a first order reaction. The concentration of the compounds in the system can be derived from the following equations:

$$-\frac{d[E]}{dt} = k_1[E] \tag{1}$$

$$\frac{d[I]}{dt} = k_1[E]-k_2[I] \tag{2}$$

in which E is the ether, I is the initially formed intermediate, (hemiacetal or methylol urea) k_1 and k_2 are the rate constants for reaction 1 and 2. This gives:

$$[E] = [E_0]e^{-k_1t} \tag{3}$$

$$[I] = \frac{[E_0]k_1}{k_2-k_1}\left(e^{-k_1t}-e^{-k_2t}\right) \tag{4}$$

Accordingly, for the ratio α of the amount of formaldehyde liberated to the amount of ether decomposed is obtained the expression:

$$\alpha = \frac{[F]}{[E_0]-[E]} = 1 - \frac{k_1}{k_2-k_1} \frac{e^{-k_1 t}-e^{-k_2 t}}{1-e^{-k_1 t}} \quad (5)$$

The required rate constant for the ether decomposition in reaction 1 is given by:

$$k_1 = \frac{1}{t} \ln \frac{[E_0]}{[E_0]-([E_0]-[E])} \quad (6)$$

We define an "experimental rate constant" by:

$$k_1' = \frac{1}{t} \ln \frac{[E_0]}{[E_0]-[F]} \quad (7)$$

which is obtained by substituting for the amount of ether decomposed $[E_0]-[E]$ the measured concentration of formaldehyde liberated [F].

From eqn. (5) it will be seen that the ratio $\alpha = \frac{[F]}{[E_0]-[E]}$ is less than 1 and approaches 1 as the time increases which from eqns. (6) and (7) means that the "experimental rate constant" k_1' will approach the true constant k_1 as the degree of decomposition increases. From eqn. (5) it also follows that the value of α will approach 1 the more rapidly the higher the ratio k_2/k_1 is. The same applies therefore to the way in which k_1' will approach k_1 with increasing reaction time. When k_2 is much larger than k_1 the ratio α will be practically equal to 1 already at low degrees of decomposition and accordingly we shall find that the "experimental rate constant" k_1' is constant and equal to the required rate constant k_1 after a low degree of decomposition. This appeared to be the case for all experiments at moderate pH values. Table 1 shows an example of a run.

Table 1. The decomposition of methoxymethyl urea.
E_0 = 0.02 moles/l. Temp. = 25°C
pH = 11.27–11.30. k_2 = 16.5 10^{-5}
k_2/k_1 = 142.

Time (hours)	$Hg(NO_3)_2$ 0.1073 N	% F	$k_1' \times 10^7$ (sec.$^{-1}$)
0	6.60		
14	6.30	5.4	11.0
24	6.08	9.3	11.1
48	5.64	17.2	10.9
96	4.72	33.6	11.8
168	3.80	50.1	11.5
264	2.84	67.2	11.7

The second column of Table 1 gives the amount of $Hg(NO_3)_2$ required for the titration of excess KCN. The third column gives the % of formaldehyde liberated and in the fourth column are given the values of the rate constant k_1' as calculated from eqn. (7). The value of k_1' is within experimental error constant

already at low degrees of decomposition and may be taken as equal to the required rate constant k_1. With all ethers of methylol urea decomposed at pH 11—12 and 25°C the "experimental rate constant" k_1' was constant at low degrees of decomposition.

As explained above this result means that the second step in the decomposition reaction, the splitting of hemiacetal (scheme b) or the splitting of methylol urea (scheme c), is very fast compared to the ether decomposition. However, the results do not give any indication as to what scheme is the right one, because both possible intermediates decompose very fast compared to the ether decomposition under the given conditions. The hemiacetal may be expected to split practically spontaneously under the conditions cited in Table 1 [3]. The decomposition of methylol urea was measured separately under the same condition. The value for the rate constant is given in the top of Table 1 (k_2) and has indeed also a much higher value than the rate constant of the ether hydrolysis ($k_2/k_1 = 142$). Therefore both schemes b and c are in agreement with the constant value experimentally observed for the "experimental rate constant". The question is further discussed in part D of this chapter.

B. The order of the decomposition reaction

The hydrolysis of methoxymethyl urea is a first order reaction. This follows from the fact that in each separate run we find a constant value for the rate constant as calculated from the equation for a first order reaction (Table 1).

Furthermore the reaction is shown to be first order by decomposition measurements with different initial concentrations of the ether: The degree of decomposition after a certain time is independent of the initial concentration of the ether (Table 2).

Table 2. The decomposition of methoxymethyl urea is a first order reaction. Temp. = 25°C pH = 11.27—11.30.

Time (hours)	24	48	96	168	
% F liberated	9.3	18.3	32.7	49.0	$[E_0]$ = 0.01 mole/l
	9.3	17.2	33.6	50.1	$[E_0]$ = 0.02 mole/l
	9.0	18.0	32.1	49.8	$[E_0]$ = 0.03 mole/l

C. The influence of pH on the rate of decomposition

Table 3 gives the value of the rate constant k_1 for the decomposition of methoxymethyl urea at three different pH values at 25°C. It is evident that the rate is directly proportional to the concentration of hydroxyl ions.

Table 3. The first order rate constant for the decomposition of methoxymethyl urea at different pH values.

pH	11.27—11.30	11.61—11.63	11.97—12.0
$10^7 k_1$(sec^{-1})	11.6	24.8	58.6

D. Evidence that monomethylol urea is initially formed as an intermediate in the decomposition of the ethers

In the introduction it was pointed out that the appearance of free formaldehyde from, *e.g.*, methoxymethyl urea may be described by two different reaction schemes both involving a series of two subsequent reactions. The molecule $NH_2CONH\overset{x}{:}CH_2\overset{y}{:}OCH_3$ may break at x giving the hemiacetal as intermediate product (scheme b) or at y with methylol urea as intermediate (scheme c). As explained above the measurements hitherto described do not give any indication as to which of these two possibilities does in fact occur.

Let us now tentatively assume that methylol urea (UF) is the intermediate, *i.e.* that the reaction course given in scheme c is correct.

$$1. \quad E \xrightarrow{k_1} UF$$

$$2. \quad UF \xrightarrow{k_2} U+F$$

and let us try to find conditions under which the rate of decomposition of methylol urea k_2 (which can be measured separately) is much closer to the value of k_1 than it was under the conditions given in Table 1 ($k_2/k_1 = 142$).

From the discussion of the rate expressions (5) (6) and (7) it will be evident that in this case we shall (if our assumption is right) expect to find that the "experimental rate constant" increases with time and only reaches a constant value after a considerably degree of decomposition.

Ether decomposition experiments at slightly different pH values from 11—12 will not change the ratio of the rates of the two subsequent reactions, because both are proportional to $[OH^-]$. However, the authors have shown in the investigation of the kinetics of formaldehyde — amide reactions [4] that the velocity of the decomposition of monomethylol urea at very high alkalinities (0.1 N NaOH and higher) is not longer proportional to the OH^- concentration but approaches an upper limit where a further increase in $[OH^-]$ no longer affects the rate. Fortunately the hydrolysis of the ether was now found to be still proportional to $[OH^-]$ even in these strongly alkaline solutions. The result is a smaller value of the ratio k_2/k_1 as is required.

The decomposition of methoxymethyl urea was measured in 0.4 and 1 N NaOH at 0°C. The amount of formaldehyde formed was determined with the KCN-method as described. (At such high OH^- concentrations as used here, the increase in $[OH^-]$ due to the reaction of KCN with formaldehyde, is negligible compared to the $[OH^-]$ already present. Therefore no buffers are necessary under these conditions. More details are found in the experimental part.)

The results are shown in Table 4. It can be seen that the rate constant for the hydrolysis of the ether k_1 ($=k_1'$ at high conversions) is indeed still proportional to the OH^- concentration. The independently measured values for the rate constant of the decomposition of monomethylol urea (k_2) are given at the top of the tables. As will be seen the value of k_2 at such high alkalinities is no longer proportional to $[OH^-]$. The result is that the ratio k_2/k_1 is less than its

value at pH 11—12, where k_2/k_1 was about 140. This effect is most obvious at the highest alkalinity.

With this more favourable ratio of k_2/k_1 the predicted increase in the value of k_1' on increasing the reaction time is now clearly observed.

In the tables are also given the values of the ratio $\alpha = [F]/([E_0]—[E])$

Table 4. The decomposition of methoxymethyl urea in 0.4 N and 1 N NaOH at 0°C.

a) $[Na^+] = 0.40$; $k_2 = 2.45 \times 10^{-4}$; $k_2/k_1 = 44.5$

Time in min.	% F	$k_1' \times 10^6$ (sec^{-1})	$\frac{[F]}{[E_0]-[E]}$	k_1 calc. $\times 10^6$
215	4.60	3.66	0.702	5.27
360	9.40	4.57	0.819	5.66
986	26.8	5.28	0.938	5.69
2520	56.0	5.43	0.983	
4200	74.1	5.49		

b) $[Na^+] = 1.00$; $k_2 = 3.44 \times 10^{-4}$; $k_2/k_1 = 24.6$

60	2.18	6.1	0.424	14.4
120	6.10	8.7	0.638	13.9
180	10.5	10.4	0.750	13.9
240	14.6	11.0	0.813	13.8
300	19.5	12.1	0.852	14.4
370	23.9	12.3	0.872	14.3
946	53.7	13.6	0.965	
1251	64.1	13.7		
1675	74.8	13.7		
1749	76.3	13.7		

at the different time intervals, calculated from eqn. (5), using the value of $k_1' = k_1$ for high conversions and the measured value of k_2. With the aid of the values of α and eqn. (6), the rate constant k_1 can now be calculated for low conversions from the [F]-values measured. The values are given in the table as k_1 calc.

It will be seen that these calculated values for k_1 at low conversions are constant, allowance being made for the experimental error, and have practically the same value as $k_1' = k_1$ found at high conversions. This result is a very strong indication that methylol urea is indeed the initial intermediate compound in the splitting of ether since we used the directly measured value of the rate constant for the decomposition of methylol urea (k_2) to obtain this result. It is extremely unlikely that the rate constant for the hydrolysis of the hemi-acetal $HOCH_2OCH_3$ has the same value under these conditions. In fact, the hydrolysis of a hemiacetal should be expected to be spontaneous at such high alkalinities, which means that not even qualitatively an increase in k_1' could have been observed.

E. Influence of the alkyl group on the rate of decomposition

To establish the influence of the alkyl group R on the rate of hydrolysis of the ethers $NH_2CONHCH_2OR$ investigations were made on the methyl, ethyl, propyl and *iso*propyl ethers. These ethers have been prepared by a procedure described by Kadowaki [5]. The propyl and *iso*propyl ethers are new compounds. The results of the decomposition experiments are given in Table 5. As will be seen the rate constant is roughly doubled in going from the *iso*propyl ether to the propyl ether, is nearly unchanged in going from the propyl ether to the ethyl ether and is again doubled in going from the ethyl ether to the methyl ether.

Table 5. The rate of decomposition of various alkyl ethers of methylol urea. Temp. = 25°C; pH = 11.98.

	$k_1 \times 10^6$ (sec^{-1})
$NH_2CONHCH_2OCH_3$	5.87
$NH_2CONHCH_2OC_2H_5$	2.87
$NH_2CONHCH_2OCH_2CH_2CH_3$	2.96
$NH_2CONHCH_2OCH(CH_3)_2$	1.67
$(CH_3)_2NCONHCH_2OCH_3$	27

F. Hydrolysis of di-alkyl ethers of dimethylol urea

A few experiments have been performed with some of the ethers of dimethylol urea $ROCH_2NHCONHCH_2OR$. These compounds were likewise found to hydrolyse readily in alkaline solution, at a higher rate even than the monoethers. It has been observed that practically the theoretical amount of formaldehyde can be obtained from such a di-alkyl ether after a prolonged reaction time which means that both ether bonds can be hydrolysed. The overall reaction is rather complicated. The complexity of the reaction makes it difficult to derive any accurate value for the rate constant in this case.

In the kinetic investigations the hydrolysis of a di-ether was followed up to a degree of conversion, where about 5—10 % of the theoretical amount of formaldehyde had been set free. The hydrolysis of the second ether group then may probably be neglected and the rate of liberation of formaldehyde will be determined by the following two reactions.

1. $ROCH_2NHCONHCH_2OR \xrightarrow{k_1} ROCH_2NHCONHCH_2OH + ROH$

2. $ROCH_2NHCONHCH_2OH \xrightarrow{k_2} ROCH_2NHCONH_2 + CH_2O$

The rate constant k_2 is unknown and cannot be readily determined, because methylol alkoxymethyl ureas are unknown compounds and will be difficult to prepare. However, the experimental rate constant for the appearance of formaldehyde, as calculated from a first order reaction equation, appears to be nearly constant after 10 % conversion, and as explained in connexion with the mono ethers we may therefore assume that in this manner we are measuring the rate of decomposition of the first ether group in the di-ether.

The rate constants at 35°C and pH 11.9 found in this way, for three di-alkyl ethers, are collected in Table 6. As will be seen the rates of decomposition with different alkyl groups vary in the same manner as was observed for the monoethers, *viz.* $CH_3 > C_2H_5 \sim CH_2CH_2CH_3$. The ratios of the rate constants are about the same as those found for the mono ethers.

Table 6. Rate constants for the hydrolysis of some di-alkyl ethers of dimethylol urea. Temp. = = 35°C; pH = 11.90.

	$k_1 \times 10^5$(sec.$^{-1}$)
$CH_3OCH_2NHCONHCH_2OCH_3$	6.4
$CH_3CH_2OCH_2NHCONHCH_2OCH_2CH_3$	3.3
$CH_3CH_2CH_2OCH_2NHCONHCH_2OCH_2CH_2CH_3$	3.6

The fact that a di-ether like $CH_3OCH_2NHCONHCH_2OCH_3$ decomposes in alkaline solution proves that for the decomposition it is not necessary for the molecule to have a free amino group H_2N. An even better proof is provided by the observed decomposition of the methyl ether of N-dimethyl N'-methylol urea $(CH_3)_2NCONHCH_2OCH_3$. The rate constant for the decomposition of this ether is about 5 times higher than for $NH_2CONHCH_2OCH_3$. (The value has been given in Table 5).

G. Hydrolysis of ethers of methylolamides

Urea may be looked upon as a special type of amide, and it might have been expected that ethers of methylol compounds of amides of carboxylic acids would also be hydrolysed in alkaline solution at a rate of the same order of magnitude as the rate of hydrolysis of ethers of methylol urea.

This did not appear to be the case. The methyl ether of methylol benzamide did not liberate any detectable amount of formaldehyde after long intervals under conditions, which had led to a ready break-down of the ethers of methylol urea (pH 11—12, temp. 25°C).

To find any measurable hydrolysis in a reasonable time it was necessary to use a much higher alkalinity. Table 7 gives the result of the hydrolysis of the methyl ether in 1 N NaOH at 25°C.

Table 7. The rate of decomposition for the methyl ether of methylol benzamide. Temp. 25°C; $[OH^-]$ = 1.0 N.

Time (hours)	% F	$k_1 \times 10^7$
24	12.3	15.2
43.5	20.8	14.9
120	50.1	16.0
168	61.3	15.7

However, the experimental conditions in the above hydrolysis are so severe, that the formation of formaldehyde may quite well be due to another reaction, *e.g.* to an amide hydrolysis:

$$C_6H_5CO{:}NHCH_2OCH_3 \rightarrow C_6H_5COOH + NH_3 + CH_2O + CH_3OH$$

Ogato and Okano [6] give $k = 2.14 \times 10^{-4}$ sec^{-1} for the first order rate constant for the hydrolysis of benzamide in 1 N NaOH at 70°C; at 25° the value will be about 5×10^{-6} sec^{-1} at a very rough estimate. The apparent rate constant for the hydrolysis of the ether is calculated from the present measurements to be 1.5×10^{-6} sec^{-1} in 1 N NaOH at 25°C. These values are of the same order of magnitude.

Alkyl ethers of other methylol amides also are known to be fairly stable towards alkali. Haworth, Peacock and Smith [7] observed that ethers of some other methylol amides liberate formaldehyde on treatment with strong alkali. The rate constant for the decomposition, which can be calculated from their experimental data, is of about the same magnitude as the rate constant for the decomposition of N-methoxymethyl benzamide.

REACTION MECHANISM

The decomposition of alkoxymethyl ureas in alkaline solution is shown to be a first order reaction with a rate proportional to the hydroxyl ion concentration. The decomposition probably involves the rupture of an ether bridge:

$$NH_2CONHCH_2OR + H_2O \rightarrow NH_2CONHCH_2OH + HOR$$

While ordinary dialkyl ethers such as CH_3—OR are known to be very stable towards alkali, it is well known that hemiacetals like $HOCH_2$—OR are readily split in alkaline solution. The mutarotation of glucose, which also involves the splitting of an ether bridge in a hemiacetal structure, is known to be catalysed by bases [8].

It is assumed in the literature that the instability of the ether bond in these cases is due to the active hydrogen in the β position to the oxygen atom of the ether group. This is in harmony with the fact that diacetals like RO—CH_2—OR are stable towards alkali. The ethers of methylol urea $NH_2CONHCH_2$—OR also have an active hydrogen in β position, in this case at an N atom. It seems reasonable to assume that with these ethers also the instability is primarily due to this fact. In accordance with the reaction scheme proposed in the literature for the mutarotation of glucose we may assume that the hydrolysis of the ethers of methylol urea in alkaline solution will take place in a sequence of steps as indicated below.

$$a.\quad NH_2CONHCH_2OR + OH^- \rightleftharpoons NH_2C\bar{O}\bar{N}CH_2OR + H_2O$$

$$b.\quad NH_2C\bar{O}\bar{N}CH_2OR \rightleftharpoons NH_2CON{=}CH_2 + OR^-$$

$$c.\quad RO^- + H_2O \rightleftharpoons ROH + OH^-$$

$$d.\quad NH_2CON{=}CH_2 + H_2O \rightleftharpoons NH_2CONHCH_2OH$$

In step *a* a proton is removed from the N atom, and this step is followed by the elimination of the alkoxy group in step *b* with the formation of an unstable Schiff's base. In step *c* the base is formed back by neutralisation of the alkoxy group and in step *d* the Schiff's base reacts with water with formation of the methylol compound. As in the mutarotation of glucose, steps *b* and *c* may be assumed to take place simultaneously in one single step.

Step *c* or *d* cannot be rate determining in this reaction scheme because such an assumption does not lead to the right expression for the rate. Moreover from a chemical point of view these reactions may be expected to be rapid. In principle either reaction *a* or reaction *b* can be the rate-determining step to explain the first order, base-catalysed, decomposition reaction. Most probably

step *b*, the elimination of the alkoxy group, will be rate-determining. With this assumption the rate constant for the decomposition will be given by

$$k = k_b \cdot K_a[OH^-] = k_b \cdot K_N[OH^-]/K_w \qquad (8)$$

where k_b = the rate constant for step *b*.
K_a = the equilibrium constant of step *a*.
K_N = the acid dissociation constant of the ether.
K_w = the ionisation product of water.

The rate of hydrolysis will therefore be determined by two factors: the acidity of the hydrogen at the N atom in β position to the ether group (K_N) and the rate of step *b* (k_b).

It is known that an increased branching of an alkyl group increases the polarisibility of the group while an increase in chain length has hardly any effect in this respect. Thus, when an electron-attracting group *x* is bound to the alkyl group, the electron density at the group *x* will increase in the following order:

$$CH_3x < CH_3CH_2x \sim CH_3CH_2CH_2x < (CH_3)_2CHx$$

The nature of the alkyl group R will hardly influence the value of the acidity constant K_N of the urea methylol ether because the distance between the N atom and the alkyl group is too great. It may, however, be expected to influence the value of k_b appreciably. An increased branching of the alkyl group R in $NH_2CONHCH_2OR$ increases the electron density at the O atom and will counteract the introduction of a negative charge into the O atom as is involved in the transition state of step *b*:

$$NH_2CO\overset{-\delta}{N}{=}CH_2{-}{-}\overset{-\delta}{O}R$$

The value of k_b will therefore be lowered. This explains the experimental observation that the rate of splitting of the urea methylol ethers decreases in the order: methyl>ethyl>*iso*propyl ether.

It is difficult to explain this effect if reaction step *a* is taken as rate determining. Also from a chemical point of view step *a* would be expected to establish equilibrium rapidly since this step involves a proton transfer at an N atom.

On comparing the ether of methylol benzamide and the ether of methylol urea it seems probable that the benzamide compound will have a higher value of K_N which from eqn. (8) should in fact favour the reaction. The surprisingly slow rate of decomposition of the benzamide compound compared with the urea compound as found experimentally must therefore be explained by a low value of k_b. If we formulate the formation of the transition state of step *b* as follows:

$$R'CO\bar{N}CH_2OR \rightleftharpoons R'CO\overset{-\delta}{N}{=}CH_2{-}{-}\overset{-\delta}{O}R$$

it will be seen that the formation of the transition state involves an electron displacement from left to right. This displacement may be expected to be largely influenced by the nature of the group R'; thus it will be hampered by the electron attracting C_6H_5 group and facilitated by the electron releasing

NH_2 group. Therefore we may expect that k_b for the benzamide ether will indeed be lower than for te urea ether and apparently this effect more than outweighs the higher value of K_N for the benzamide ether.

The suggestion that a decreased acidity of the amide favours the rate of decomposition of the ether is further supported by the comparison of the ethers $(CH_3)_2NCONHCH_2OCH_3$ and $NH_2CONHCH_2OCH_3$. The former may be expected to be the less acidic and the rate of decomposition of this ether has been found to be about 5 times higher than that for the ether from urea (Table 5).

EXPERIMENTAL PART

Materials

Monomethylol urea methyl ether (m.p. 91°C), monomethylol urea ethyl ether (m.p 111°C), dimethylol urea dimethyl ether (m.p. 101°C), dimethylol urea diethyl ether (m.p. 124°C) and dimethylol urea di-*n*-propyl ether (m.p. 95°C) were prepared by Kadowaki's method [5] by treating the appropriate methylol compound with the appropriate alcohol in the presence of small amounts of HCl.

Other ethers were prepared for the first time: Methylol urea appeared to be only slightly soluble in propyl or *iso*propyl alcohol. It was therefore found preferable in the preparation of the *n*-propyl and *i*-propyl ether of monomethylol urea to dissolve monomethylol urea in a small amount of water before the addition of the alcohol and the catalysing acid. This appreciably reduces the reaction time and thus reduces the danger of condensation reactions (resinifying) which is otherwise appreciable. The procedure for the preparation of the two new propyl ethers is the same. The preparation of the *n*-propyl ether is given below in detail: 10 g methylol urea were dissolved in 15 ml H_2O at *ca.* 40°C. Thereupon 100 ml propyl alcohol were added, followed by 0.5 ml of 2 N HCl. The temperature was maintained at 40°C for *ca.* 5 minutes. The reaction mixture was then neutralised by shaking with Ag_2O, filtered and evaporated *in vacuo*. The residue was crystallised from propyl alcohol-diethyl ether (1:1) giving *monomethylol urea* n-*propyl ether* in colourless needles, m.p. 86.5—87.5°C.

Monomethylol urea iso*propyl ether* was crystallised from *iso*propyl alcohol-diethyl ether (1:1) giving colourless plates, m.p. 103°C.

	H	N	C
Calculated for $C_5H_{12}O_3N_2$	9.15	21.18	45.43
Found for *n*-propylether	9.08	21.12	45.52
Found for *i*-propylether	9.11	21.33	45.41

N,N-dimethyl-N'-methylol urea methyl ether (m.p. 66°C) was prepared from N,N-dimethyl-N'-methylol urea by a similar procedure as was used for monomethylol urea methylether.

N-methylol benzamide methyl ether has hitherto not been reported in the literature. It was prepared as follows: 5 g N-methylol benzamide were dissolved in 10 ml methyl alcohol at room temperature and 5 drops of conc. HCl were added. After standing for 10 min. at room temperature the solution was neutralised with an excess of Ag_2O, and after filtration the solution was cooled to 0°C. Long, prismatic, colourless crystals separated out and were recrystallised from ether. M.p. 73—74°C. (Found: C 65.47; H 6.68; N 8.57. Calc. for $C_9H_{11}O_2N$: C 65.45; H 6.67; N 8.48).

Isolation of urea after hydrolysis of the ether

208 mg of the methyl ether of monomethylol urea were dissolved in 40 ml of an alkaline KCN solution (0.24 N NaOH, 0.1 N KCN) and the solution was left to stand at room temperature for 24 hours. Then 12 ml of concentrated acetic acid and 12 ml of a 10 % solu-

tion of xanthydrol in ethyl alcohol were added. After 4 h the white finely crystalline precipitate was filtered off, washed 3 times with alcohol and dried at 60°. Yield: 762 mg. Calculated for $C_{27}H_{20}O_3N_2$: 840 mg. In a separate experiment, with the same time of hydrolysis for the ether, a titration was made with $Hg(NO_3)_2$ and 97.1 % of the theoretical amount of formaldehyde was found.

The decomposition of an ether at pH 11-12 and 25°C

The reaction medium was made up of 100 ml Na_2HPO_4 solution (1 M) 50 ml KCN (0.1 N) and a certain volume of NaOH solution (2 N). It was diluted to 200.0 ml with water (the amount of NaOH was variable depending upon the pH value of the solution required). This mixture was transferred into a well stoppered erlenmeyer flask which was placed in a thermostat at 25°C. A weighed amount of the finely powdered ether was added to the solution and dissolved by vigorous shaking. The time when the ether was added was taken as zero time for the kinetic run. A sample of this solution was taken and the pH carefully measured.

In order to follow the decomposition of the ether, samples of 30 ml were drawn out of the solution after suitable time intervals. 5 drops of diphenyl carbazone solution were added and the solution was then acidified with 2 N HNO_3 to the appearance of a faint orange-yellow colour (pH 5—4). The solution was then at once titrated with 0.1 N $Hg(NO_3)_2$ from a micro burette. The time when HNO_3 was added was taken as the time of sampling.

The decomposition of an ether in NaOH solution at 0°C

Solutions were made up consisting of 2 N NaOH, 10 ml 0.1 N KCN and diluted to 50.0 ml with water. The mixture was brought into an erlenmeyer flask which was placed in ice-water. When the temperature of the mixture had reached 0°C, 52 mg of finely powdered methoxymethyl urea were added and dissolved immediately on shaking the mixture.

After a certain time the reaction was stopped by neutralising the mixture with a solution containing as much HNO_3 as is equivalent to the NaOH in the sample and 20 ml of a phosphate buffer (0.5 M KH_2PO_4 + 0.5 M Na_2HPO_4). The excess KCN was determined with $Hg(NO_3)_2$ as described earlier.

REFERENCES

1. de Jong, J. I. and de Jonge, J. *Rec. trav. chim.* **71** (1952) 643.
2. Pfeil, E. and Schroth, G. *Z. anal. Chem.* **34** (1952) 333.
3. Meadows, G. W. and de B. Darwent, B. *Trans. Faraday Soc.* **48** (1952) 1015.
4. Ugelstad, J. and de Jonge, J. *To be published.*
5. Kadowaki, H. *Bull. Chem. Soc. Japan* **11** (1936) 248.
6. Ogata, Y. and Okano, M. *J. Chem. Soc. Japan* **70** (1949) 32.
7. Haworth, R. D., Peakock, D. H., Smith, W. R. and MacGillivray, R. *J. Chem. Soc.* **1952** 2972.
8. Brönsted, J. N. and Guggenheim, E. A. *J. Am. chem. Soc.* **49** (1927) 2554.

Received August 7, 1956.

ACTA CHEMICA SCANDINAVICA 10 (1956) 1488—1490

Identification of Dialkylsulfides as Dialkyl *p*-Bromophenacyl Sulfonium Picrates

STIG VEIBEL and BENT JUHL NIELSEN

Department of organic chemistry, University of Technology, Copenhagen, Denmark

The preparation and the titratability of dialkyl *p*-bromophenacyl sulfonium picrates with perchloric acid in glacial acetic acid has been investigated.

Diarylsulfides and thioanisoles do not react with *p*-bromophenacyl bromide.

Dialkyl sulfides with mobile alkyls (allyl or benzyl), refluxed with *p*-bromophenacyl bromide, form bis-(*p*-bromophenacyl) sulfide instead of dialkyl *p*-bromophenacyl bromide.

Jureček, Večeřa and Gasparič [1], referring to previous work of Bost and Schultze [2], recommended the characterisation of dialkyl sulfides as dialkyl *p*-bromophenacyl sulfonium salts, preferring for the picrates or bromides the perchlorates, as these salts showed the widest range of melting points.

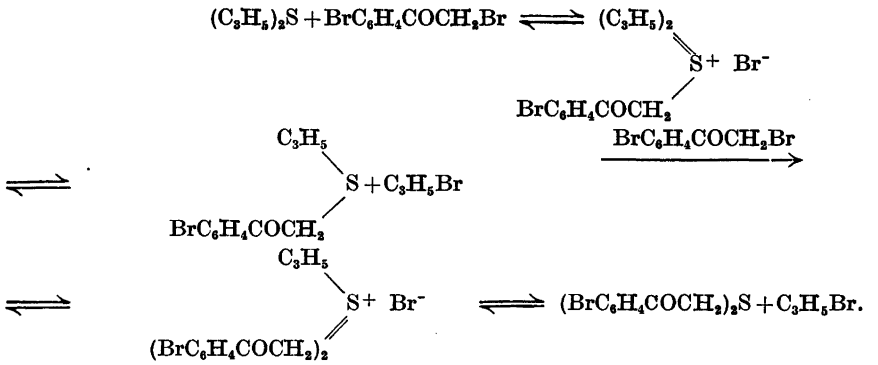
Recalling the very convenient method of estimating alkyl halides by converting them into alkyl thiuronium picrates which are then dissolved in glacial acetic acid and titrated with perchloric acid in the same solvent (Schotte and Veibel [3]), we investigated the preparation of a series of tertiary sulfonium picrates and their titratability with perchloric acid, examining at the same time the possible extension of the method to aromatic sulfides and mixed aromatic-aliphatic sulfides (thioanisoles).

We found that in the case of uncomplicated dialkyl sulfides the preparation of the dialkyl *p*-bromophenacyl sulfonium picrates presented no serious difficulties, although some of the picrates, as stated by Jureček *et al.*[1], may first separate as oils. As expected, the picrates are easily titratable with perchloric acid.

As to the aromatic sulfides, however, no formation of a tertiary sulfonium salt took place, neither from the diaryl sulfides nor from the thioanisoles.

Using aliphatic sulfides where the carbon-sulfur bond may be expected to be weakened, due to the structure of the aliphatic radical (as in diallyl sulfide or dibenzyl sulfide) we were unable to isolate the dialkyl *p*-bromophenacyl sulfonium picrate. Instead of this we isolated a substance which was in both instances bis-(*p*-bromophenacyl) sulfide, formed by exchange of the radicals originally bound to the sulfur atom for *p*-bromophenacyl radicals. Evidently, the sulfide thus formed is unable to combine with *p*-bromophenacyl bromide to form tris-(*p*-bromophenacyl) sulfonium bromide.

In order to explain the formation of bis-(*p*-bromophenacyl) sulfide the mechanism proposed by Ray and Levene [4] is adopted:

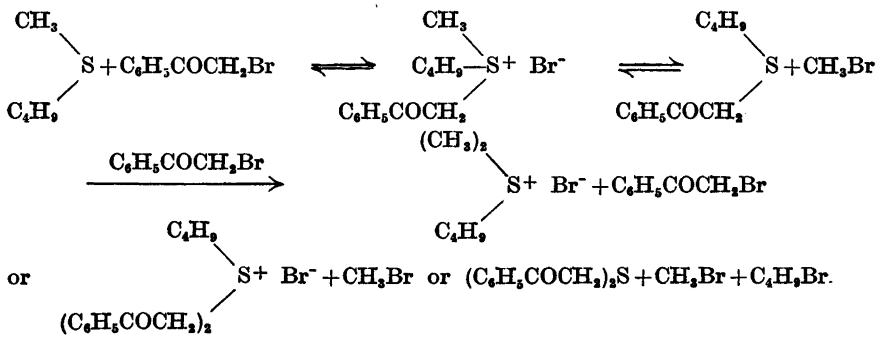


Bost and Schultze [2] indicate that when methyl *n*-butyl sulfide is allowed to react with phenacyl bromide in absolute methanol, the resulting product is dimethyl *n*-butyl sulfonium bromide and not methyl *n*-butyl phenacyl sulfonium bromide, assuming as an explanation the mechanism proposed by Ray and Levene [4]. Jureček *et al.*[1], allowing methyl *n*-butyl sulfide to react with phenacyl bromide or *p*-bromophenacyl bromide in absolute methanol, met no difficulties in obtaining the expected methyl *n*-butyl phenacyl sulfonium perchlorate or methyl *n*-butyl *p*-bromophenacyl sulfonium perchlorate, neither did other unsymmetrical sulfides present such anomalies. They found it difficult, however, to isolate the bromides as these salts separated as oils, but they were converted without difficulty into crystalline picrates or perchlorates.

We, too, repeated the preparation of methyl *n*-butyl phenacyl sulfonium salts and had no trouble in preparing the picrate, which by titration with perchloric acid gave the molecular weight 449.5 (calculated 451.5), whereas M for dimethyl *n*-butyl sulfonium picrate is only 350.4.

Also with *p*-bromophenacyl bromide we found a normal reaction (as did Jureček *et al.*[1]), $M_{Picrate}$ found by titration with perchloric acid 530.1, calculated 530.5.

A possible explanation of the discrepancy may be found in the observation of Jureček *et al.* that the yield of the sulfonium bromides usually decreases when the refluxing time is increased. Accepting the scheme of Ray and Levene [4], prolongation of the refluxing time will favour the precipitation of the slightest soluble of the compounds in an equilibrium mixture as:



just as we obtained the bis-(*p*-bromophenacyl) sulfide by reacting, *e.g.*, diallyl sulfide with *p*-bromophenacyl bromide.

EXPERIMENTAL

The sulfonium bromides were prepared according to Jureček *et al.*[1] by refluxing equivalent amounts of *p*-bromophenacyl bromide and the sulfide under investigation (0.005 mole) in methanol (5 ml) during 10 minutes. After cooling the sulfonium bromide was precipitated by addition of 200 ml of ether, isolated, if possible, by filtration, washed with ether, dissolved in water and precipitated as picrate on addition to a saturated aqueous solution of picric acid. The picrates were recrystallised from ethanol.

0.001 mole was dissolved in 50 ml glacial acetic acid and titrated with 0.1 N perchloric acid in glacial acetic acid (indicator: crystal violet, end point: green). Some results are given in Table 1.

Table 1. Titration of some dialkyl p*-bromophenacyl picrates with perchloric acid in glacial acetic acid.*

Alkyl	M.p. Lit.	M.p. Found	M calc.	M found
Di-*n*-propyl	119°[1]	120°	544.4	545.3 546.6 544.5
Di-*n*-butyl	79°[1]	80—81°	572.5	573.7 573.3 573.8
Methyl hydroxyethyl	—	140—41°	518.3	518.7 517.2 517.5
Methyl *n*-butyl	121—21.5°[1]	119—20°	530.4	530.1
Diallyl		142°		*
Dibenzyl		142°		*

* In these cases a substance (the same for both sulfides) precipitated during the refluxing. The substance was not able to form a picrate with aqueous picric acid, its m. p. (142°) and composition corresponded to that of bis-(*p*-bromophenacyl) sulfide. (Found: C 44.85; H 2.85; Br 37.52; S 7.56. Calc. for $C_{16}H_{12}O_2Br_2S$: C 44.88; H 2.83; Br 37.32; S 7.49.

Reaction between n*-butyl sulfide and phenacyl bromide.* The standard procedure yielded an oily picrate which crystallised after 24 h in the ice box. Purified by recrystallisation from ethanol it showed m.p. 99—100° and M 449.5, calculated for methyl butyl phenacyl sulfonium picrate ($C_{19}H_{21}O_8N_3S$) 451.5.

Financial support from *Rask-Ørsted Fondet* is gratefully acknowledged.

REFERENCES

1. Jureček, M., Večeřa, M. and Gasparič, J. *Chem. Listy* **48** (1954) 542.
2. Bost, R. W. and Schultze, H. C. *J. Am. Chem. Soc.* **64** (1942) 1165.
3. Schotte, L. and Veibel, S. *Acta Chem. Scand.* **7** (1953) 1357.
4. Ray, F. E. and Levene, I. *J. Org. Chem.* **2** (1937) 267.

Received July 28, 1956.

ACTA CHEMICA SCANDINAVICA 10 (1956) 1491—1496

The Flavonoid Glycosides of *Dahlia variabilis*

IV. 3-Glucosido-5-arabinosidocyanidin from the Variety "Dandy"

C. G. NORDSTRÖM

Institute of Chemistry, University of Helsingfors, Finland

A method for the identification of anthocyanins on a micro-scale has been developed and applied to an anthocyanin separated from the petal extracts of the blue dahlia "Dandy". The anthocyanin was identified as 3-glucosido-5-arabinosidocyanidin.

In Part I of this series [1] the presence of a cyanidin glycoside, yielding glucose and arabinose on hydrolysis, was reported in the petal extracts of the variety "Dandy". Further attempts to characterise this compound using methods similar to those developed for the identification of flavone glycosides were then unsuccessful due to the instability of cyanidin in solution. Investigation of the causes of this instability has resulted in the successful development of methods for the determination of the aglycone:sugar ratio and position of carbohydrate attachment in anthocyanins. Application of these methods to investigations of anthocyanins from natural sources gives more precise information regarding their structure than previously used micro-methods [2,3].

As previously described (*cf.* Part I) large scale paper chromatography of the ethanolic hydrochloric acid extracts of the petals of the blue garden dahlia "Dandy" by butanol-acetic acid-water yields, besides a number of flavone glycosides, an anthocyanin which after further purification yielded an aglycone, tentatively identified as cyanidin, arabinose and glucose on hydrolysis. This glycoside was now further tested for homogeneity by running in a number of solvents. Using acetone-0.1 N hydrochloric acid (1:3) an impurity having a weak yellow fluorescence in ultra-violet light was removed and chromatograms of the ethyl acetate extract of the hydrolysed anthocyanin indicated the absence of further impurities. The aglycone which so far had been identified only by its R_F value in one solvent was now conclusively identified as cyanidin by its absorption spectrum in visible light and its R_F values in a number of other solvents [4] (Table 1).

All previous attempts to determine the molar aglycone:sugar ratio of this and other anthocyanins using the methods developed in Part I had so far been

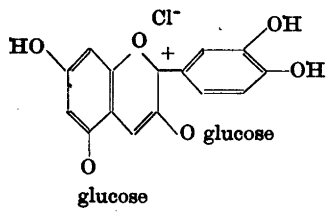
unsuccessful due to the fading of the colour of the anthocyanidins in solution, making spectrophotometric determination of their concentration impossible. Such fading in acid solution in the light has previously been reported by Spaeth and Rosenblatt [5]. It was found that in 0.1 to 2 N hydrochloric acid solutions kept in darkness at room temperature no significant decrease in cyanidin concentration could be detected, whereas when similar solutions were exposed to light the cyanidin concentration decreased fairly rapidly. In six hours the concentration of a solution exposed to diffuse light had decreased by 10 % but in sunlight the decrease of concentration of the solution amounted to about 95 % of the cyanidin initially present. These experiments were repeated in nitrogen atmosphere and although the decrease in cyanidin concentration was slightly less, it was of the same order as in the previous cases. In no case could the cyanidin be restored by increasing the acid concentration. Model experiments on the hydrolysis of cyanin with 2 or 4 N aqueous hydrochloric acid at 100° yielded calculated amounts of cyanidin provided the hydrolysis was carried out in darkness. Thus it was possible to determine spectrophotometrically the cyanidin concentration in hydrolysed extracts of the "Dandy" anthocyanin.

In this connection the effect of the solvent on the main absorption peak of cyanidin and its glycosides should be mentioned. Thus the absorption maximum of cyanidin in 0.1 N 80—100 % ethanolic hydrochloric acid is at 545 mμ moving towards shorter wave-lengths on further decrease of ethanol concentration. In a solution containing 20 % ethanol the maximum lies at 530 mμ. Variations in the acid concentration has no influence provided this concentration is high enough to prevent colour-base formation. Similar solvent effects have been reported by Sondheimer and Kertesz [6] in case of 3-glucosidopelargonidin.

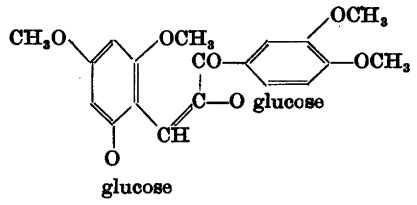
The amount of arabinose in the hydrolysed extracts of the "Dandy" anthocyanin was determined after removal of the aglycone using the orcinol-ferric chloride method described by Fernell and King [7] and the glucose was quantitatively determined directly by the revised anthrone method [1] applying corrections for arabinose and cyanidin. The results of these estimations gave a cyanidin:glucose:arabinose ratio of approximately 1:1:1.

The position of carbohydrate attachment was determined by identification of the compounds obtained on acid and alkaline hydrolysis of the product of methylation of the anthocyanin with dimethyl sulphate in aqueous alkaline solution. In such strongly alkaline solutions the heterocyclic ring of the anthocyanins is broken and chalkones formed but only when the 5-hydroxyl is blocked by a sugar molecule can the anthocyanidin methyl ether be reformed on acid hydrolysis [8]. Thus on methylation of cyanin (I), the chalkone (II) is obtained which yields (III) on hydrolysis.

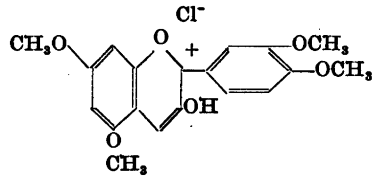
Methylation and subsequent acid hydrolysis of the "Dandy" anthocyanin yielded an anthocyanidin methyl ether indicating that carbohydrate is attached to the 5-hydroxyl. In order to investigate the possibility of further glycosidation in the aromatic nuclei the cyanidin methyl ether was hydrolysed with 10 % aqueous sodium hydroxide solution, a treatment known to degrade 3-hydroxyflavylium compounds and anthocyanins to a phloroglucinol component and an acid component [9], but no compound could be isolated. Experiments with a



I



II



III

3',4',5,7-tetra-*O*-methyl cyanidin showed that relatively large amounts of material had to be used in order to obtain enough degradation products to be detected even by paper chromatography. However, it was found that alkali treatment of methylated cyanin without previous acid hydrolysis gave much better yields of degradation products. When this technique was applied to the "Dandy" anthocyanin, phloroglucinol dimethyl ether and veratric acid were identified (Table 2). Since the cyanidin methyl ether obtained on acid hydrolysis of the methylated "Dandy" anthocyanin, when run alongside 3',4',5,7-tetra-*O*-methyl and 3,3',4',5,7-penta-*O*-methyl cyanidin on paper chromatograms, showed R_F identity with the former compound it must be concluded that the sugars are attached to the 3- and 5-hydroxy-groups.

Partial hydrolysis of the anthocyanin with 1 % aqueous hydrochloric acid yielded a monoside which after separation on streak chromatograms by butanol-acetic acid-water and further purification by running in acetone-0.1 N hydrochloric acid (1:3) on hydrolysis showed the presence of cyanidin and glucose together with traces of arabinose (Table 1). The behaviour of the monoside in a number of specific tests (*i.e.* stability towards ferric chloride, colour in sodium carbonate solution and regeneration on acidification of an alkaline solution) was identical with that of mecocyanin and 3-glucosidocyanidin but different from that reported for 5-glucosidocyanidin [10] and shown by cyanidin and its 3',4',5,7-tetramethyl ether. Since León and Robinson [11] claim that they obtained 5-glucosidocyanidin on partial hydrolysis of cyanin, this latter compound was partially hydrolysed and the resulting monoside purified as described above. The monoside obtained showed all the above mentioned characteristics of a 3-glucoside. Both monosides, on methylation and hydrolysis with alkali, yielded phloroglucinol trimethyl ether and so conclusively proved to be 3-glucosidocyanidin. Consequently the "Dandy" anthocyanin must be 3-glucosido-5-arabinosidocyanidin. This compound has not previously been found to occur in Nature and is a new type of anthocyanin since all previously isolated pentose containing anthocyanins are of the type 3-pentose glucoside.

EXPERIMENTAL

Separation and purification of the "Dandy" anthocyanin. Petals (122 g) of the variety "Dandy" were crushed under 0.1 N ethanolic hydrochloric acid (600 ml), kept at 0° for one week and filtered (total solids 8.2 mg/ml, cyanidin 0.08 mg/ml). The extract was then stored at 0°.

Portions (25 ml) of the extract were applied to Whatman No. 3 MM paper 22 × 22" and the chromatograms developed with butanol-acetic acid-water (6:1:2). The separated anthocyanin band was cut out without previous drying and the glycoside eluted with 0.05 N aqueous hydrochloric acid as described in Part I. The eluate was applied as a streak to No. 3 MM paper and further purified by *iso*propanol-2 N hydrochloric acid. On elution as above the anthocyanin was tested for homogeneity on Whatman No. 1 paper in other solvents. Separation from a yellow fluorescing compound took place in acetone-0.1 N hydrochloric acid (1:3) and the whole eluate was rerun in this solvent. The anthocyanin solution obtained on eluting the final chromatograms was used for further investigation. R_F values and wave -lengths of maximum absorption of the "Dandy" anthocyanin and a few reference compounds are given in Table 1.

Identification of the anthocyanin. (a) *Qualitative hydrolysis.* A portion of the glycoside solution was made 2 N by the addition of concentrated hydrochloric acid and heated in the dark at 100° for 2 h., then cooled and the aglycone extracted with butanol. The extract was washed with water and after removal of the solvent the aglycone was dissolved in 0.1 N ethanolic hydrochloric acid. The aglycone was then identified by compairing its R_F values and main absorption maximum with those of synthetic standards [4] (Table 1).

The identification of the sugar components has been described in Part I of this series [1].

Table 1. R_F values and wave-lengths of the main absorption peaks of the "Dandy" anthocyanin, the products obtained on partial and complete hydrolysis and of reference compounds.

Compound	R_F in					
	BuOH-HOAc-H_2O 6:1:2:	BuOH-2N HCl	$COMe_2$-0.1N HCl 1:3	H_2O-HOAc-conc. HCl 10:30:3	*m*-Cresol-5.5 N-HCl-HOAc 1:1:1	λ_{max} mμ (a)
"Dandy" anthocyanin	0.08	0.03	0.32			533
Aglycone		0.68		0.50	0.69	545
Part. hydrolysed anthocyanin	0.18	0.11	0.19			536
Aglycone		0.68		0.50	0.69	545
Sugar	0.15					
Cyanin	0.07	0.02	0.32			538
Mecocyanin	0.13	0.10	0.55			537
Part.hydrolysed cyanin	0.18	0.11	0.19			536
3-Glucosidocyanidin	0.18	0.11	0.19			536
Cyanidin	0.48(b)	0.68		0.50	0.69	545
»	0.73(c)					
Glucose	0.15					
Arabinose	0.19					

(a) in 0.1 N ethanolic HCl. (b) chloride. (c) colour-base.

Table 2. R_F values of the methylated "Dandy" anthocyanidin, of the products of alkali degradation and of reference compounds.

Compound	R_F in H_2O-HOAc-conc. HCl 10:30:3	R_F in Toluene-HOAc-H_2O 4:1:5	R_F in BuOH-2 N Ammonia
"Dandy" anthocyanin	0.82		
Phenolic component		0.83	
Acid component			0.25
Part. hydrolysed anthocyanin, phenolic component		0.96	
Part. hydrolysed cyanin, phenolic component		0.96	
3,3',4',5,7-Penta-*O*-Me cyanidin	0.97		
3',4',5,7-Tetra-*O*-Me cyanidin	0.82		
Phloroglucinol		0.00	
» Me ether		0.18	
» di-Me ether		0.83	
» tri-Me ether		0.96	
Protocatechuic acid			0.02
Vanillic acid			0.06
*iso*Vanillic acid			0.09
Veratric acid			0.25

(b) *Quantitative hydrolysis.* (i) Determination of aglycone concentration. A portion of the glycoside solution (1 ml) and concentrated hydrochloric acid (0.5 ml) was heated at 100° in total darkness for 30 min. On cooling, the solution was diluted with ethanol to 10 ml. The concentration of the aglycone was determined spectrophotometrically, standards being determined in the same medium. (Cyanidin: λ_{max} 545 mμ, ε 29 270).

(ii) Determination of sugar concentration. Arabinose. A portion of the glycoside solution was made 2 N by the addition of concentrated hydrochloric acid and heated at 100° for 2 h. On cooling the aglycone was extracted with butanol, the extract washed with water and the combined mother liquor and washings made up to 25 ml. The arabinose concentration of this solution was determined by the orcinol-ferric chloride method [7] using a Fisher photoelectric colourimeter. No correction for glucose was necessary.

Glucose. Portions (5 ml) of the glycoside solution were taken to dryness in 3/4" test tubes. The glucose concentration was then measured directly using the revised anthrone method [1]. Glucose and arabinose standards were measured simultaneously and a blank containing the corresponding amount of cyanidin was similarly measured. Corrections for arabinose and cyanidin were then applied. Results: Cyanidin:glucose:arabinose = = 1:0.98:0.95; 1:0.96:0.87.

(c) *Determination of the position of sugar substituents.* A portion of the glycoside solution was carefully taken to dryness under reduced pressure at room temperature, and the glycoside was dissolved in 2—3 drops of 1 N aqueous sodium hydroxide solution. With extremely vigorous stirring freshly distilled dimethyl sulphate (0.5 ml) and 30 % aqueous sodium hydroxide (2 ml) were added dropwise during 1.5—2 h. in nitrogen atmosphere and the stirring was continued for another hour. A part of the mixture was neutralised with 2 N hydrochloric acid and made about 4 N with concentrated hydrochloric acid.

On heating at 100° for 30 min. the cyanidin methyl ether was extracted with chloroform, the extract washed with water and taken to dryness. The residue was dissolved in a small amount of acid ethanol and run on paper chromatograms alongside synthetic standards. Results are given in Table 2. To the remainder of the methylation mixture one half of its volume of 30 % aqueous sodium hydroxide was added and while nitrogen was passed through the solution, it was boiled for 4 h., acidified and boiled for 30 min. longer to hydrolyse any remaining glycosides. On cooling, the products of degradation were extracted with ether. The extract was washed free of acid and separated into a phenolic and an acid fraction. Both fractions were run on paper chromatograms alongside synthetic standards, the phenolic fraction in toluene-acetic acid-water (4:1:5)[13], the spots being made visible with Millons reagent or diazotised *p*-nitroaniline, the acid fraction in butanol saturated with 2 N ammonia, the spots in this case being rendered visible by spraying with dilute aqueous silver nitrate followed by phenol saturated with aqueous sodium hydroxide [13]. Results are given in Table 2.

Identification of the monoside. A final portion of the glycoside solution was carefully taken to dryness and heated with 1 % aqueous hydrochloric acid at 100° for 30 min. The mixture was cooled, applied as a streak to No. 3 MM paper and separated with butanol-acetic acid-water. The monoside was eluted with 0.05 N 70 % ethanolic hydrochloric acid and separated from free sugars on paper chromatograms run in acetone-0.1 N hydrochloric acid. On final elution the monoside was identified in the usual way. Results of this identification are given in the tables.

Cyanin was similarly partially hydrolysed and the 3-monoside identified as described above.

Mecocyanin was partially hydrolysed and the 3-monoside separated in the same way.

The reference compounds needed for this investigation were prepared by recorded methods.

The author gratefully acknowledges a grant from the *Finnish Academy*. Thanks are also due to Dr. T. Swain for the gift of cyanin and mecocyanin specimens.

REFERENCES

1. Nordström, C. G. and Swain, T. *J. Chem. Soc.* **1953** 2764.
2. Robinson, G. M. and Robinson, R. *Biochem. J. London* **25** (1931) 1687.
3. Hayashi, K. and Abe, Y. *Misc. Repts. Research Inst. Nat. Resources (Japan)* **28** (1952) 1.
4. Bate-Smith, E. C. *Biochem. J. London* **58** (1954) 122.
5. Spaeth, E. C. and Rosenblatt, D. H. *Anal. Chem.* **22** (1950) 1321.
6. Sondheimer, E. and Kertesz, Z. I. *J. Am. Chem. Soc.* **70** (1948) 3476.
7. Fernell, W. R. and King, H. K. *Analyst* **78** (1953) 80.
8. León, A., Robertson, A., Robinson, R. and Seshadri, T. R. *J. Chem. Soc.* **1931** 2672.
9. Karrer, P. and Widmer, R. *Helv. Chim. Acta* **10** (1927) 5.
10. León, A. and Robinson, R. *J. Chem. Soc.* **1932** 2221.
11. León, A. and Robinson, R. *J. Chem. Soc.* **1931** 2732.
12. Bate-Smith, E. C. *Chemistry & Industry* **1954** 1457.
13. Löffler, J. E. and Reichl, E. R. *Mikrochim. Acta* **1953** 79.

Received August 3, 1956.

ACTA CHEMICA SCANDINAVICA 10 (1956) 1497—1510

Short Communications

A Diagram for the Determination of the Surface Tension of Mineral Oil Fractions (Hydrogenated and Non-hydrogenated) from their Kinematic Viscosity and Density

J. CORNELISSEN, O. HARVA and H. I. WATERMAN

Institute of Chemical Engineering, The University, Delft, Holland

In a recent publication [1] the present authors presented a method to determine the surface tension at 20°C in dynes/cm, σ_{20}, of *saturated* mineral oil fractions from their kinematic viscosity at 20°C in centistokes, ν_{20}, and refractive index, n_D^{20}. The values obtained by this method are generally as accurate as the experimental values.

In a second publication [2] a method was described to determine σ_{20} of *non hydrogenated* (original) mineral oil fractions from ν_{20}, n_D^{20} and the density at 20°C, d_4^{20}. Use was made of 5 cross-sections for constant ν_{20}-values of the ν-n-d space model [3-5]. Again good results were obtained.

It appears that the lines of constant σ_{20} values are straight and are running parallel to the n_D^{20} axis of the n, d-cross-sections. This means that for a constant

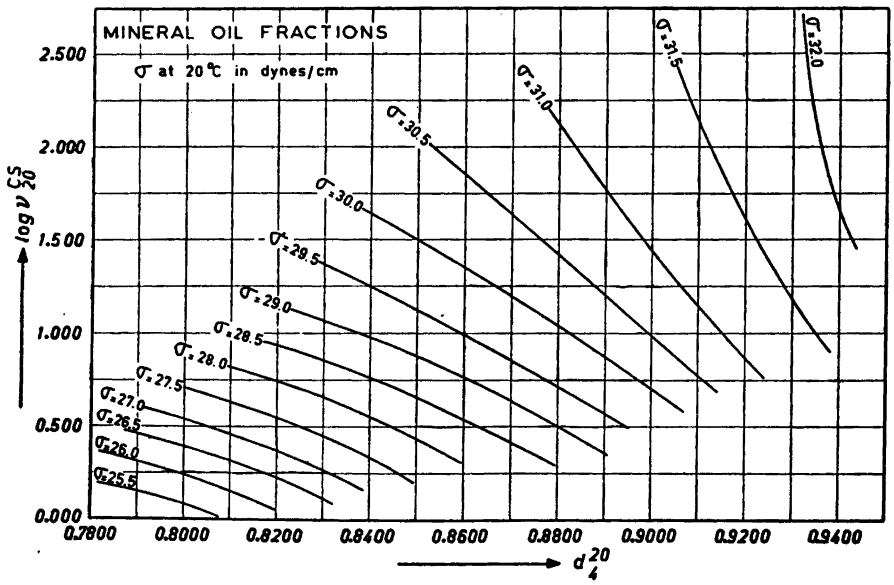


Fig. 1. log ν_{20}, d_4^{20} diagram for the determination of the surface tension at 20°C of non-hydrogenated as well as hydrogenated mineral oil fractions.

Table 1

Fraction	d_4^{20}	log ν_{20}	(σ_{20})pred.	(σ_{20})exp.	$\Delta\sigma =$ (σpred. − σexp.)
Venezuela Tin 1 fr.					
1	0.8158	0.319	26.7	26.6	+0.1
1H	0.7990	0.342	26.3	26.4	−0.1
2	0.8235	0.455	27.3	27.0	+0.3
2H	0.8080	0.458	27.0	27.0	0
3	0.8397	0.602	27.8	27.2	+0.6
3H	0.8154	0.605	27.5	27.7	−0.2
4	0.8363	0.752	28.3	27.8	+0.5
4H	0.8197	0.741	28.0	28.1	−0.1
5	0.8429	0.953	29.0	28.7	+0.3
5H	0.8260	0.926	28.5	28.8	−0.3
6	0.8510	1.129	29.5	29.4	+0.1
6H	0.8320	1.082	29.1	29.4	−0.3
7	0.8594	1.334	30.0	29.8	+0.2
7H	0.8390	1.282	29.5	29.8	−0.3
8	—	—	—	—	—
8H	0.8453	1.472	29.9	30.2	−0.3
Borneo Tin 2 fr.					
1	0.8414	0.324	27.5	27.3	+0.2
1H	0.8325	0.352	27.3	26.7	+0.6
2	0.8530	0.390	28.0	27.9	+0.1
2H	0.8406	0.424	27.7	27.3	+0.4
3	0.8657	0.473	28.5	28.4	+0.1
3H	0.8482	0.488	28.1	27.9	+0.2
4	0.8762	0.543	29.0	29.0	0
4H	0.8554	0.562	28.4	28.3	+0.1
5	0.8868	0.622	29.5	29.5	0
5H	0.8605	0.627	28.7	28.8	−0.1
6	0.8978	0.709	29.9	29.9	0
6H	0.8673	0.708	29.0	29.3	−0.3
7	0.9100	0.816	30.6	30.6	0
7H	—	—	—	—	—
8	0.9186	0.911	31.0	31.0	0
8H	0.8756	0.856	29.6	29.8	−0.2
9	0.9323	1.100	31.5	31.4	+0.1
9H	0.8872	1.025	30.2	30.3	−0.1
10	0.9448	1.360	32.0	32.1	−0.1
10H	0.8945	1.217	30.6	30.8	−0.2
11	0.9612	1.854	32.5	32.6	−0.1
11H	0.9070	1.570	31.2	31.5	−0.3
12H	0.9199	2.181	31.7	32.1	−0.4
Mexico Tin 3 fr.					
1	0.8058	0.311	26.4	25.9	+0.5
1H	0.7944	0.327	26.2	26.0	+0.2
2	0.8187	0.435	26.8	26.8	0
2H	0.8049	0.443	26.8	26.7	+0.1
3	0.8363	0.624	28.0	27.7	+0.3
3H	0.8198	0.631	27.7	27.5	+0.2
4	0.8551	0.871	29.2	28.7	+0.5
4H	0.8337	0.848	28.5	28.4	+0.1
5	0.8723	1.158	30.0	29.5	+0.5
5H	0.8471	1.107	29.4	29.2	+0.2
6	0.8906	1.546	30.8	30.6	+0.2
6H	0.8593	1.442	30.1	29.9	+0.2
7	0.9055	1.977	31.3	31.2	+0.1
7H	0.8717	1.805	30.7	30.7	0
8H	0.8801	2.151	31.0	31.2	−0.2
Borneo Tin 4 fr.					
1	0.8363	0.242	27.1	27.4	−0.3
1H	0.8067	0.288	26.3	26.2	+0.1
2	0.8446	0.299	27.5	27.7	−0.2
2H	0.8140	0.345	26.7	27.0	−0.3
3	0.8537	0.358	28.0	28.0	0
3H	0.8210	0.396	27.1	27.3	−0.2
4	0.8634	0.428	28.4	28.3	+0.1
4H	0.8282	0.464	27.5	27.6	−0.1
5	0.8709	0.489	28.7	28.3	+0.4
5H	0.8331	0.505	27.7	27.9	−0.2
6	0.8766	0.556	29.0	29.0	0
7	0.8804	0.634	29.1	28.9	+0.2
7H	0.8404	0.631	28.2	28.5	−0.3
9	0.8808	0.846	29.7	29.5	+0.2
9H	0.8429	0.798	28.7	28.7	0
Rumania Tin 5 fr.					
1	0.8029	0.254	26.1	25.9	+0.2
1H	0.7857	0.276	25.8	25.9	−0.1
2	0.8123	0.365	26.8	26.6	+0.2
2H	0.7963	0.387	26.3	26.7	−0.4
3H	0.8064	0.507	27.0	27.1	−0.1
4	0.8328	0.649	28.0	27.9	+0.1
4H	0.8153	0.647	27.7	27.7	0
5	0.8390	0.828	28.6	28.4	+0.2
5H	0.8220	0.811	28.2	28.4	−0.2
6	0.8469	1.033	29.2	29.0	+0.2
6H	0.8299	0.993	28.8	29.1	−0.3
7H	0.8389	1.184	29.4	29.9	−0.5
Sumatra Tin 6 fr.					
1	0.8090	0.160	26.0	26.0	0
1H	0.7918	0.202	25.7	25.3	+0.4
2	0.8125	0.196	26.2	26.3	−0.1
2H	0.7944	0.230	25.8	25.4	+0.4
3	0.8178	0.252	26.5	—	—
3H	0.8010	0.277	26.1	25.9	+0.2
4	0.8238	0.312	26.9	26.9	0
4H	0.8077	0.336	26.5	26.4	+0.1
5	0.8302	0.378	27.3	27.2	+0.1
5H	0.8137	0.398	26.9	26.8	+0.1

Fraction	d_4^{20}	log ν_{20}	(σ_{20})pred.	(σ_{20})exp.	$\Delta\sigma =$ $(\sigma$pred.$-\sigma$exp.$)$
6	0.8372	0.447	27.7	27.5	+0.2
6H	0.8195	0.462	27.3	27.2	+0.1
7	0.8444	0.529	28.1	28.0	+0.1
7H	0.8260	0.539	27.6	27.5	+0.1
8	0.8519	0.613	28.5	28.5	0
8H	0.8318	0.638	28.0	28.0	0
9	0.8586	0.713	28.8	28.7	+0.1
9H	0.8375	0.705	28.3	28.3	0
10	0.8651	0.840	29.3	29.2	+0.1
10H	0.8439	0.830	28.7	29.8	—0.1
11	0.8726	1.010	29.8	29.7	+0.1
11H	0.8507	0.979	29.2	29.2	0
12	0.8857	1.244	30.4	30.2	+0.2
12H	0.8605	1.178	29.8	29.8	0
13	0.9065	1.644	31.2	31.0	+0.2
13H	0.8753	1.492	30.5	30.7	—0.2
Sumatra Tin 7 fr.					
1	0.8081	0.228	26.2	26.0	+0.2
2	0.8136	0.283	26.5	26.7	—0.2
2H	0.7953	0.327	26.2	26.4	—0.2
3	0.8213	0.356	27.0	26.9	+0.1
3H	0.8021	0.382	26.5	26.6	—0.1
4	0.8284	0.419	27.3	27.1	+0.2
4H	0.8068	0.445	26.9	27.0	—0.1
5	0.8351	0.493	27.7	27.6	+0.1
5H	0.8121	0.499	27.2	27.2	0
6	0.8401	0.575	28.0	28.3	—0.3
6H	0.8179	0.580	27.5	27.6	—0.1
7	0.8409	0.663	28.3	28.2	+0.1
7H	0.8200	0.663	27.8	27.9	—0.1
8	0.8392	0.765	28.5	28.5	0
8H	0.8208	0.758	28.0	28.2	—0.2
9	0.8380	0.853	28.6	28.2	+0.4
9H	0.8215	0.869	28.3	28.6	—0.3
10	0.8396	1.009	29.0	28.9	+0.1
10H	0.8251	0.993	28.7	29.0	—0.3
Venezuela Tin 8 fr.					
1	0.8400	0.423	27.7	27.5	+0.2
1H	0.8204	0.454	27.3	27.4	—0.1
2	0.8755	0.806	29.5	28.9	+0.6
2H	0.8440	0.750	28.6	28.7	—0.1
3	0.9036	1.309	31.0	30.3	+0.7
3H	0.8635	1.163	29.8	29.8	0
4	0.9255	1.974	31.8	31.5	+0.3
4H	0.8750	1.485	30.5	30.6	—0.1
5	0.9396	2.687	32.1	31.9	+0.2
5H	0.8880	2.155	31.1	31.5	—0.4
Persia (Iran) Tin 9 fr.					
1	0.7982	0.260	26.0	26.0	0
1H	0.7873	0.292	25.9	25.7	+0.2
2	0.8077	0.363	26.6	26.5	+0.1
2H	0.7940	0.368	26.2	26.2	0
3	0.8188	0.474	27.3	27.2	+0.1
3H	0.8027	0.388	26.5	26.7	—0.2
4	0.8305	0.604	27.9	28.0	—0.1
4H	0.8123	0.608	27.5	27.3	+0.2
5	0.8419	0.772	28.5	28.2	+0.3
5H	0.8213	0.754	28.0	27.9	+0.1
6	0.8538	0.960	29.3	29.2	+0.1
7	0.8679	1.183	29.9	29.5	+0.4
7H	0.8390	1.116	29.2	29.1	+0.1
8	0.8814	1.450	30.6	30.5	+0.1
8H	0.8481	1.333	29.7	29.6	+0.1
Texas Tin 11 fr.					
1	0.8082	0.274	26.3	26.5	—0.2
1H	0.7963	0.316	26.1	26.1	0
2	0.8174	0.367	26.9	26.7	+0.2
2H	0.8041	0.389	26.6	26.3	+0.3
3	0.8283	0.488	27.5	27.6	—0.1
3H	0.8125	0.500	27.2	26.9	+0.3
4	0.8379	0.643	28.2	28.3	—0.1
4H	0.8217	0.642	27.7	27.6	+0.1
5	0.8465	0.818	28.8	28.8	0
5H	0.8297	0.812	28.4	28.6	—0.2
6	0.8552	1.032	29.5	29.2	+0.3
6H	0.8362	0.993	29.0	29.0	0
7	0.8665	1.274	30.0	29.9	+0.1
7H	0.8462	1.211	29.5	29.7	—0.2

value of ν_{20} and d_4^{20} the value of σ_{20} is independent of the refractive index. Therefore it is possible to construct a diagram with the coordinates log ν_{20} and d_4^{20}, (Fig. 1). In the diagram lines of equal values of σ_{20} have been given.

This diagram has primarily been constructed for the determination of the surface tension of non-hydrogenated mineral oil fractions.

It appears however to be possible after the necessary extension of the diagram to use it also for the determination of σ_{20} of saturated oil fractions. The diagram (Fig. 1) has been tested on several (164) mineral oil fractions, with the results shown in Table 1. In this table the graphically determined σ_{20} values have been indicated by $(\sigma_{20})_{\text{pred.}}$, and the experimental values of σ_{20} by $(\sigma_{20})_{\text{exp.}} \cdot \Delta\sigma = (\sigma_{20})_{\text{pred.}} - (\sigma_{20})_{\text{exp.}}$ The hydrogenated mineral oil fractions are indicated by H.

As can be seen from the table the results obtained in the determination of the

surface tension at 20°C by means of the new method are as good as those obtained by means of the previous methods [1,2]. The advantages of the new method are that the surface tension at 20°C can be determined for hydrogenated as well as for non-hydrogenated mineral oil fractions by means of only one graph, using two, properly chosen, physical constants.

1. Cornelissen, J., Harva, O., and Waterman, H. I. *Chimie & Industrie. To be published.*
2. Cornelissen, J., Harva, O., and Waterman, H. I. *Erdöl & Kohle. To be published.*
3. Cornelissen, J. and Waterman, H. I. *Constitution of mineral oil fractions. Development of a method to determine the carbon-type composition in a clear and simple way from the viscosity, the refractive index and the density*, University Print, Delft, 1956.
4. Cornelissen, J. and Waterman, H. I. *Chimie & Industrie. To be published.*
5. Cornelissen, J. and Waterman, H. I. *Brennstoffchemie. To be published.*

Received September 10, 1956.

Die Verbreitung der Umbelliferose in der Pflanzenfamilie der Umbelliferen

ANDERS BÆRHEIM SVENDSEN

Pharmazeutisches Institut der Universität Oslo, Oslo-Blindern, Norwegen

Nach der Ermittelung der Konstitution der Umbelliferose [1] (2'-α-D-galactopyranosyl-2-α-D-glucopyranosyl-β-D-fructofuranose) haben wir es von Interesse gefunden, zu untersuchen, ob das neue Trisaccharid, das wir früher in 3—4 verschiedenen Doldenpflanzen nachgewiesen haben [2], ein allgemein vorkommender Bestandteil bei den Umbelliferen sei. Um diese Untersuchung durchführen zu können, haben wir Papierchromatographie benutzt. In einem Flüssigkeitsgemisch von Amylalkohol, Pyridin und Wasser ist es möglich, Trisaccharide — u.a. Raffinose und Umbelliferose — zu trennen. Die erwähnten Zucker passieren bei einer 20—24-stündigen Durchlaufschromatographie (Whatman Filtrierpapier No. 1) etwa 8 cm, beziehungsweise 10 cm.

In einigen der unten beschriebenen Fälle wurde nur der oberirdische Teil der Pflanze, in den meisten Fällen aber wurden sowohl der unterirdische als der oberirdische Teil untersucht; in einigen Fällen wurden sogar Wurzel, Stengel, Blatt, Blumendolde und Dolde mit unreifen, grünen Früchten je für sich untersucht. In sämtlichen Fällen konnte die Umbelliferose in allen Teilen der Pflanze nachgewiesen werden. Die Menge schien von Art zu Art und von Pflanzenteil zu Pflanzenteil etwas zu variieren, ohne dass diese quantitative Frage vorläufig näher behandelt wurde. Neben der Umbelliferose haben wir in allen untersuchten Arten bedeutende Mengen von Saccharose und kleine Mengen von Monosacchariden gefunden. Bei den Untersuchungen wurde wegen der Gefahr eines enzymatischen Abbaus der Umbelliferose immer frisches Pflanzenmaterial nach Stabilisierung in kochendem Alkohol verwendet.

Nachstehend sind die untersuchten Arten tabellarisch zusammengestellt. Sämtliche enthalten Umbelliferose.

Aegopodium podagraria L.
Aethusa cynapium L.
Angelica archangelica L.
subsp. *norvegica* (Rupr.) Nordh.
subsp. *litoralis* (Fr.) Thell.
Angelica silvestris L.
Anthriscus silvestris (L.) Hoffm.
Carum carvi L.
Chaerophyllum aromaticum L.
Conium maculatum L.
Heracleum sphondylium L.
Imperatoria ostruthium L.
Levisticum officinale Koch.
Ligusticum scoticum L.
Meum athamanticum Jacq.
Myrrhis odorata (L.) Scop.
Pimpinella major (L.) Huds.
Pimpinella saxifraga L.
Sium sisarum L.

Aufarbeitung des Pflanzenmaterials: 10—50 g frisches Pflanzenmaterial wurde mit 150—250 ml Äthanol und 1—2 g Kalciumkarbonat in einem "Waring Blendor" 3 Minuten fein zerrieben, worauf das Gemisch sofort zum Sieden gebracht wurde. Das Pflanzenmaterial wurde nach Abkühlen abfiltriert und mit 20—30 ml Wasser ausgewachsen. Die gesammelten Filtrate wurden dann während ein paar Minuten mit etwa 5 ml gequollenem saurem Ionenaustauscher (Amberlite IR 120) und nach Filtrieren in der nämlichen Weise mit Amberlite IRA 400 geschüttelt. Das Filtrat wurde in

surface tension at 20°C by means of the new method are as good as those obtained by means of the previous methods [1,2]. The advantages of the new method are that the surface tension at 20°C can be determined for hydrogenated as well as for non-hydrogenated mineral oil fractions by means of only one graph, using two, properly chosen, physical constants.

1. Cornelissen, J., Harva, O., and Waterman, H. I. *Chimie & Industrie. To be published.*
2. Cornelissen, J., Harva, O., and Waterman, H. I. *Erdöl & Kohle. To be published.*
3. Cornelissen, J. and Waterman, H. I. *Constitution of mineral oil fractions. Development of a method to determine the carbon-type composition in a clear and simple way from the viscosity, the refractive index and the density*, University Print, Delft, 1956.
4. Cornelissen, J. and Waterman, H. I. *Chimie & Industrie. To be published.*
5. Cornelissen, J. and Waterman, H. I. *Brennstoffchemie. To be published.*

Received September 10, 1956.

Die Verbreitung der Umbelliferose in der Pflanzenfamilie der Umbelliferen

ANDERS BÆRHEIM SVENDSEN

Pharmazeutisches Institut der Universität Oslo, Oslo-Blindern, Norwegen

Nach der Ermittelung der Konstitution der Umbelliferose [1] (2'-α-D-galactopyranosyl-2-α-D-glucopyranosyl-β-D-fructofuranose) haben wir es von Interesse gefunden, zu untersuchen, ob das neue Trisaccharid, das wir früher in 3—4 verschiedenen Doldenpflanzen nachgewiesen haben [2], ein allgemein vorkommender Bestandteil bei den Umbelliferen sei. Um diese Untersuchung durchführen zu können, haben wir Papierchromatographie benutzt. In einem Flüssigkeitsgemisch von Amylalkohol, Pyridin und Wasser ist es möglich, Trisaccharide — u.a. Raffinose und Umbelliferose — zu trennen. Die erwähnten Zucker passieren bei einer 20—24-stündigen Durchlaufschromatographie (Whatman Filtrierpapier No. 1) etwa 8 cm, beziehungsweise 10 cm.

In einigen der unten beschriebenen Fälle wurde nur der oberirdische Teil der Pflanze, in den meisten Fällen aber wurden sowohl der unterirdische als der oberirdische Teil untersucht; in einigen Fällen wurden sogar Wurzel, Stengel, Blatt, Blumendolde und Dolde mit unreifen, grünen Früchten je für sich untersucht. In sämtlichen Fällen konnte die Umbelliferose in allen Teilen der Pflanze nachgewiesen werden. Die Menge schien von Art zu Art und von Pflanzenteil zu Pflanzenteil etwas zu variieren, ohne dass diese quantitative Frage vorläufig näher behandelt wurde. Neben der Umbelliferose haben wir in allen untersuchten Arten bedeutende Mengen von Saccharose und kleine Mengen von Monosacchariden gefunden. Bei den Untersuchungen wurde wegen der Gefahr eines enzymatischen Abbaus der Umbelliferose immer frisches Pflanzenmaterial nach Stabilisierung in kochendem Alkohol verwendet.

Nachstehend sind die untersuchten Arten tabellarisch zusammengestellt. Sämtliche enthalten Umbelliferose.

Aegopodium podagraria L.
Aethusa cynapium L.
Angelica archangelica L.
subsp. *norvegica* (Rupr.) Nordh.
subsp. *litoralis* (Fr.) Thell.
Angelica silvestris L.
Anthriscus silvestris (L.) Hoffm.
Carum carvi L.
Chaerophyllum aromaticum L.
Conium maculatum L.
Heracleum sphondylium L.
Imperatoria ostruthium L.
Levisticum officinale Koch.
Ligusticum scoticum L.
Meum athamanticum Jacq.
Myrrhis odorata (L.) Scop.
Pimpinella major (L.) Huds.
Pimpinella saxifraga L.
Sium sisarum L.

Aufarbeitung des Pflanzenmaterials: 10—50 g frisches Pflanzenmaterial wurde mit 150—250 ml Äthanol und 1—2 g Kalciumkarbonat in einem "Waring Blendor" 3 Minuten fein zerrieben, worauf das Gemisch sofort zum Sieden gebracht wurde. Das Pflanzenmaterial wurde nach Abkühlen abfiltriert und mit 20—30 ml Wasser ausgewachsen. Die gesammelten Filtrate wurden dann während ein paar Minuten mit etwa 5 ml gequollenem saurem Ionenaustauscher (Amberlite IR 120) und nach Filtrieren in der nämlichen Weise mit Amberlite IRA 400 geschüttelt. Das Filtrat wurde in

einem heissen Luftstrom bis zu etwa 5 ml eingeengt, durch eine Aluminiumoxydsäule (Aluminiumoxyd alkalifrei "Woelm"), 3 cm × × 1,5 cm, filtriert, die Säule mit 5 ml Wasser ausgewaschen und das fast farblose Filtrat weiter, wie oben beschrieben, eingeengt.

Papierchromatographie: Aus dem isolierten Zuckergemisch wurden variierende Mengen für die papierchromatographischen Untersuchungen entnommen. Die Chromatogramme (Whatman Filtrierpapier No. 1 in Bogen 45 × 18 cm) wurden mit absteigender mobiler Flüssigkeitsphase als 20—24-stündige Durchlaufschromatogramme entwickelt. Flüssigkeitsgemisch: Amylalkohol puriss. "Merck", Pyridin puriss. "Merck", Wasser, 7+7+6 Raumteile (einphasiges Gemisch). Als Vergleichssubstanzen wurden auf jedes Chromatogramm Umbelliferose, Raffinose und Saccharose appliziert.

Sprühreagens: Eine gesättigte, wässerige Lösung von Harnstoff-Oxalat. Nach dem Besprühen des Chromatogramms wurde dies 5 Minuten auf 130—140° im Trockenschrank erwärmt. Ketosehaltige Zucker ergeben grünschwarze Flecke.

Für ökonomische Unterstützung dieser Arbeit bin ich *A/S Norsk Varekrigsforsikrings Fond* zu besonderem Dank verpflichtet.

1. Wickström, A. und Bærheim Svendsen, A. *Acta Chem. Scand.* **10** (1956) 1199.
2. Bærheim Svendsen, A. *Zur Chemie norwegischer Umbelliferen* (Diss.) Universität Oslo, Oslo 1954.

Eingegangen am 18. Oktober 1956.

The Electrostatic Model for Calculation of the Ligand Field Parameter of Octahedral Complexes

OLE BOSTRUP and
CHR. KLIXBÜLL JØRGENSEN

Chemistry Departments B and A, Technical University of Denmark, Copenhagen, Denmark

Since 1951, several authors [1,2] have applied the ligand field theory to the absorption spectra of octahedral complexes with partly filled d-shells and found very good agreement with the observed energy levels, provided that reasonable values are chosen for the ligand field parameter Δ (also denoted by $(E_1 - E_2)$ or $10\,Dq$ or $\frac{10}{21}\,K$), the energy difference between the high γ_3-orbital and the low γ_5-orbital (containing at most four and six electrons, respectively). All the wavenumbers of the Laporte-forbidden bands can be expressed as multiples of Δ plus linear combinations of term distances, which seem [3] to have somewhat smaller values for complexes than the corresponding gaseous ions.

When the observed values of Δ are compared, many regularities are conspicuous, which support the value of the treatment: For a given ligand, Δ increases with the oxidation state of the central ion and with the principal quantum number 3d, 4d, and 5d. For a given central ion, Tsuchida's spectrochemical series can be expressed as increasing values of Δ, depending mainly on the atom in the first coordination sphere:

$$\mathrm{Br} < \mathrm{Cl} < \mathrm{F} < \mathrm{O} < \mathrm{N} < \mathrm{C} \quad (1)$$

Ilse and Hartmann [4] applied an electrostatic model to explain the absolute value of Δ. Six point charges q, representing the ligands, perturb a hydrogen-like 3d-wavefunction yielding an energy difference in atomic units between the two possible energy levels γ_3 and γ_5:

$$\Delta \cong \frac{8}{27} q \cdot \frac{Z_*}{3} \cdot G_4\left(\frac{Z_*}{3} \cdot R\right)$$
$$\text{where } G_4(x) \cong \frac{14\,175}{8x^5} \quad (2)$$

where Z_* is the effective charge acting on the hydrogen-like 3d-wavefunction and R the distance between the centre of the metal ion and the point charge. However, the actual 3d-radial function cannot be hydrogen-like; *e. g.* in a nickel(II) ion, the potential near the nucleus must necessarily correspond to $Z = 28$ and for large distances r to $Z = 3$, while Z_* is some average value between these two limits. Recently, Hartree [5] calculated self-consistent field functions (with exchange) for gaseous ions which support this qualitative argument: When compared to a hydrogen-like function with the same average distance r of the electron from the nucleus, Hartree's function is larger both for small values of r (giving a smaller r_{max}) and for large values of r (vanishing more slowly, corresponding to the external charge plus one), while it is smaller for intermediate r. Thus, it will be more generally valid to write eqn. 2 in the more old-fashioned way, discussed by Belford [6]:

einem heissen Luftstrom bis zu etwa 5 ml eingeengt, durch eine Aluminiumoxydsäule (Aluminiumoxyd alkalifrei "Woelm"), 3 cm × × 1,5 cm, filtriert, die Säule mit 5 ml Wasser ausgewaschen und das fast farblose Filtrat weiter, wie oben beschrieben, eingeengt.

Papierchromatographie: Aus dem isolierten Zuckergemisch wurden variierende Mengen für die papierchromatographischen Untersuchungen entnommen. Die Chromatogramme (Whatman Filtrierpapier No. 1 in Bogen 45 × 18 cm) wurden mit absteigender mobiler Flüssigkeitsphase als 20—24-stündige Durchlaufschromatogramme entwickelt. Flüssigkeitsgemisch: Amylalkohol puriss. "Merck", Pyridin puriss. "Merck", Wasser, 7+7+6 Raumteile (einphasiges Gemisch). Als Vergleichssubstanzen wurden auf jedes Chromatogramm Umbelliferose, Raffinose und Saccharose appliziert.

Sprühreagens: Eine gesättigte, wässerige Lösung von Harnstoff-Oxalat. Nach dem Besprühen des Chromatogramms wurde dies 5 Minuten auf 130—140° im Trockenschrank erwärmt. Ketosehaltige Zucker ergeben grünschwarze Flecke.

Für ökonomische Unterstützung dieser Arbeit bin ich *A/S Norsk Varekrigsforsikrings Fond* zu besonderem Dank verpflichtet.

1. Wickström, A. und Bærheim Svendsen, A. *Acta Chem. Scand.* **10** (1956) 1199.
2. Bærheim Svendsen, A. *Zur Chemie norwegischer Umbelliferen* (Diss.) Universität Oslo, Oslo 1954.

Eingegangen am 18. Oktober 1956.

The Electrostatic Model for Calculation of the Ligand Field Parameter of Octahedral Complexes

OLE BOSTRUP and
CHR. KLIXBÜLL JØRGENSEN

Chemistry Departments B and A, Technical University of Denmark, Copenhagen, Denmark

Since 1951, several authors [1,2] have applied the ligand field theory to the absorption spectra of octahedral complexes with partly filled d-shells and found very good agreement with the observed energy levels, provided that reasonable values are chosen for the ligand field parameter Δ (also denoted by $(E_1 - E_2)$ or $10\,Dq$ or $\frac{10}{21}\,K$), the energy difference between the high γ_3-orbital and the low γ_5-orbital (containing at most four and six electrons, respectively). All the wavenumbers of the Laporte-forbidden bands can be expressed as multiples of Δ plus linear combinations of term distances, which seem [3] to have somewhat smaller values for complexes than the corresponding gaseous ions.

When the observed values of Δ are compared, many regularities are conspicuous, which support the value of the treatment: For a given ligand, Δ increases with the oxidation state of the central ion and with the principal quantum number 3d, 4d, and 5d. For a given central ion, Tsuchida's spectrochemical series can be expressed as increasing values of Δ, depending mainly on the atom in the first coordination sphere:

$$\mathrm{Br} < \mathrm{Cl} < \mathrm{F} < \mathrm{O} < \mathrm{N} < \mathrm{C} \quad (1)$$

Ilse and Hartmann [4] applied an electrostatic model to explain the absolute value of Δ. Six point charges q, representing the ligands, perturb a hydrogen-like 3d-wavefunction yielding an energy difference in atomic units between the two possible energy levels γ_3 and γ_5:

$$\Delta \cong \frac{8}{27} q \cdot \frac{Z_*}{3} \cdot G_4\left(\frac{Z_*}{3} \cdot R\right)$$
$$\text{where } G_4(x) \cong \frac{14\,175}{8x^5} \quad (2)$$

where Z_* is the effective charge acting on the hydrogen-like 3d-wavefunction and R the distance between the centre of the metal ion and the point charge. However, the actual 3d-radial function cannot be hydrogen-like; *e. g.* in a nickel(II) ion, the potential near the nucleus must necessarily correspond to $Z = 28$ and for large distances r to $Z = 3$, while Z_* is some average value between these two limits. Recently, Hartree [5] calculated self-consistent field functions (with exchange) for gaseous ions which support this qualitative argument: When compared to a hydrogen-like function with the same average distance r of the electron from the nucleus, Hartree's function is larger both for small values of r (giving a smaller r_{max}) and for large values of r (vanishing more slowly, corresponding to the external charge plus one), while it is smaller for intermediate r. Thus, it will be more generally valid to write eqn. 2 in the more old-fashioned way, discussed by Belford [6]:

$$\Delta \cong \frac{5}{3} q \cdot \frac{\overline{r^4}}{R^5} \qquad (3)$$

As emphasized by Williams [7], it is a very peculiar feature of the series (1) that neutral ligands such as H_2O and NH_3 produce similar or larger values of Δ than OH^-, Cl^- and other anions. The effect has been explained [4,8] as a perturbation from six dipoles with the point dipole moment μ. It must be pointed out that the parameter μ has no connection at all with the dipole moment of the ligand; only the negative end of a polarized molecule will have any appreciable effect (eqn. 3) independent of the distance to the positive end. Generally, the spatial distribution of charge will have larger effects, according to eqn. 3, than identical charges concentrated on a point. Thus, Δ would be calculated as 3 000 K for $q = 1$, $Z_* = 7.2$ and $R = 2.51$ Å from eqn. 2, while the $CsNiCl_3$ studied by Asmussen and Bostrup[9] actually has $\Delta = 6\,900$ K, even though it contains octahedral environments, $NiCl_6$, of the dimensions given above. However, this can easily be explained by the assumption of spherically symmetrical charge distributions (yielding, of course, no proof for the validity of the electrostatic model), since the most important contribution to Δ is produced by the charge density just outside the nickel(II) ion with radius r_M.

If eqn. 3 is integrated for a sphere with radius r_L and charge q equally distributed in each volume element, one finds by neglecting the angular dependence of the perturbations from charge elements not on the axis containing the ligand's centre, that this expression can be derived:

$$\Delta \cong \frac{5}{12} q \cdot \frac{\overline{r^4}}{r_L^3 r_M^2} \qquad (4)$$

The double segment common to the ligand and the sphere with $r < r_0$ has the volume $\frac{1}{3}\pi h_1^2 (3r_0 - h_1) + \frac{1}{3}\pi h_2^2 (3r_L - h_2)$, which for r_0 not much larger than r_M and $r_L >> r_M$ ($\equiv h_1 >> h_2$) can be written $\pi h_1^2 r_0$, and thus, the volume element is $2\pi r(r - r_M)dr$ and the charge element is $\frac{3r(r-r_M)}{2r_L^3} dr$, which then can be integrated from r_M outwards.

The expression (3) might of course be evaluated for different charge distributions, taking also the angular dependence of the perturbations into account; but these results would not have sufficiently quantitative significance, relative to the necessary effort. The important feature of eqn. 4 is that Δ is much increased, since $r_L^{-3} r_M^{-2}$ generally is larger than $4(r_L + r_M)^{-5}$; i. e. for $r_L = 1.8$ Å and $r_M = 0.7$ Å it is increased by a factor 9. The proportionality to r_L^{-3} seems confirmed to a certain degree by the series (1), even though the low values of Δ for halide complexes (see the Table) may also be connected with π-bonding in the direction from the ligand to the central ion[3].

Ligands:	6 Br^-	6 Cl^-	6 H_2O	6 NH_3
Nickel(II)[9]	6 500	6 900	8 500	10 800
Rhodium(III)[2]	18 900	20 300	27 000	33 900

The latter trend of thought was initiated by Van Vleck [10], who demonstrated that the molecular orbital theory, assuming partly covalent bonding, implies nearly the same results as the electrostatic model. While much evidence for partly covalent bonding can be derived from the decrease of the F^k-integrals, relative to the gaseous ions [11], the most conspicuous difficulty for the electrostatic theory, assuming pure d-orbitals, is the extension of the d-electrons. There is no doubt that a considerable amount of the partly filled shell in the gaseous ion is present [5] outside the crystallographic radius of the metal ion $\sim 0.5 - 0.8$ Å, and this effect is further accentuated in the complexes [3,11]. However, the values of Δ do not seem very much changed from those predicted by the electrostatic model. It is a rather general feature of the theoretical chemistry that the covalent and ionic structures have nearly the same energy, and the intermixing of them therefore does not produce large relative energy differences between the possible excited levels. Actually, the electrostatic model can be considered as yielding the perturbations, which are the further cause of introducing overlap with certain of the ligands' orbitals, as described by the group theory, of which the results are common to both theories.

Recently, several authors have attempted the difficult task of determining the absolute value of Δ from combined electrostatic and molecular orbital theory. Kleiner [12] considered it impossible to apply the electrostatic theory to $Cr(H_2O)_6^{+++}$, since Δ turned out to be slightly negative. However, it can easily be seen that this is caused by the neglect of orthogonality of

the d-wavefunction with the neighbourhood of the oxygen nuclei, since Hartree's function still has a large value there. From a magnetochemical study of FeF_2 and CoF_2, rather small electrostatic field splittings have been obtained [13], which nearly disappear or are reversed by introduction of the overlap. The level scheme does not agree well with the optical spectra of similar compounds, while Tanabe and Sugano [14] have taken up again the chromium(III) problem. Even though Δ turns out to be of the right order of magnitude, it is a small effect as a difference between large quantities. So far, the electrostatic model seems still useful as a first order approximation, and there is much evidence that the partly covalent bonding * has not yet reached the Pauling limiting value [11], even for cobalt(III) and rhodium(III) complexes, while manganese(II) and nickel(II) complexes of the first transition group are nearer to the electrostatic case.

1. Tanabe, Y. and Sugano, S. *J. Phys. Soc. Japan* **9** (1954) 753, 766.
2. Jørgensen, C. Klixbüll *Acta Chem. Scand.* **8** (1954) 1502; **9** (1955) 116, 1362; **10** (1956) 500, 518, 887.
3. Owen, J. *Proc. Roy. Soc. London* **A 227** (1955) 183.
4. Ilse, F. E. and Hartmann, H. *Z. physik. Chem.* **197** (1951) 239.
5. Hartree, R. D. *J. Opt. Soc. Amer.* **46** (1956) 350.
6. Belford, R. L. *Bonding and Spectra of Metal Chelates.* Thesis, Univ. of California 1955. UCRL-3051.
7. Williams, R. J. P. *J. Chem. Soc.* **1956** 8.
8. Ballhausen, C. J. *Kgl. Danske Videnskab. Selskab, Mat.-fys. Medd.* **29** (1955) No. 8.
9. Asmussen, R. W. and Bostrup, O. *Acta Chem. Scand. To be published.*
10. Van Vleck, J. H. *J. Chem. Phys.* **3** (1935) 803, 807.
11. Jørgensen, C. Klixbüll, *Kgl. Danske Videnskab.Selskab., Mat.-fys. Medd.* **30** (1956) No. 22.
12. Kleiner, W. H. *J. Chem. Phys.* **20** (1952) 1784.
13. Moriya, T., Motizuki, K., Kanamori, J. and Nagamiya, T. *J. Phys. Soc. Japan* **11** (1956) 211.
14. Tanabe, Y. and Sugano, S. *J. Phys. Soc. Japan* **11** (1956) 864.
15. Tinkham, M. *Proc. Roy. Soc. London* **A 236** (1956) 535, 549.

Received October 29, 1956.

* Recently, Tinkham [15] investigated the binding of fluoride to Mn(II), Fe(II), Co(II), and Cr(III) by hyperfine-structure of paramagnetic resonance. It was concluded that both 2s, 2p, 3s, and 3p orbitals of fluorine are included, implying very complicated and uncertain expressions for the absolute magnitude of Δ.

Absorption Spectra of Red Uranium(III)Chloro Complexes in Strong Hydrochloric Acid

CHR. KLIXBÜLL JØRGENSEN

Chemistry Department A, Technical University of Denmark, Copenhagen, Denmark

Someya [1] reported that solutions of uranium(III) are red in concentrated hydrochloric acid, while they are greyish green in less acidic solutions. Fig. 1 gives the absorption spectra of grey uranium (III) solutions, which are identical in 2 M and 6 M HCl (and practically coincident with the spectrum, reported by Stewart [2] of the U(III) aquo ion in 1 M $HClO_4$), and of a dark red solution in 11 M HCl. Since the normal redox potential [3] of U(III):U(IV) is -0.64 V, a hydrogen activity, corresponding to 10^{21} atm would be necessary to render the U(III) solutions thermodynamically stable; however, amalgamated zinc can in most cases produce a stationary state after one day, containing $\sim$ 80 % U(III). It cannot be argued that the colour of the grey solution in 6 M HCl is caused by admixed pale green [4] U(IV), since it turns red by addition of a large excess of 12 M HCl after removal of the zinc.

The present author [5] identifies the narrow bands of grey U(III) in the visible as Laporte-forbidden transitions from the groundstate 5 $f^3\ {}^4I_{9/2}$ to the other $5f^3$-levels, while the high and broad bands in the ultraviolet have $5f^26d$-levels as excited levels, to which the transitions are allowed by Laporte's rule. Similar $f^n \rightarrow f^{n-1}d$ transitions have been observed [5] of Ce(III), Sm(II), Eu(II), Pa(IV), Np(III), and Pu (III). The individual $5f^26d$-levels are not easily identified; in U(III) both the ligand

the d-wavefunction with the neighbourhood of the oxygen nuclei, since Hartree's function still has a large value there. From a magnetochemical study of FeF_2 and CoF_2, rather small electrostatic field splittings have been obtained [13], which nearly disappear or are reversed by introduction of the overlap. The level scheme does not agree well with the optical spectra of similar compounds, while Tanabe and Sugano [14] have taken up again the chromium(III) problem. Even though Δ turns out to be of the right order of magnitude, it is a small effect as a difference between large quantities. So far, the electrostatic model seems still useful as a first order approximation, and there is much evidence that the partly covalent bonding * has not yet reached the Pauling limiting value [11], even for cobalt(III) and rhodium(III) complexes, while manganese(II) and nickel(II) complexes of the first transition group are nearer to the electrostatic case.

1. Tanabe, Y. and Sugano, S. *J. Phys. Soc. Japan* **9** (1954) 753, 766.
2. Jørgensen, C. Klixbüll *Acta Chem. Scand.* **8** (1954) 1502; **9** (1955) 116, 1362; **10** (1956) 500, 518, 887.
3. Owen, J. *Proc. Roy. Soc. London* **A 227** (1955) 183.
4. Ilse, F. E. and Hartmann, H. *Z. physik. Chem.* **197** (1951) 239.
5. Hartree, R. D. *J. Opt. Soc. Amer.* **46** (1956) 350.
6. Belford, R. L. *Bonding and Spectra of Metal Chelates.* Thesis, Univ. of California 1955. UCRL-3051.
7. Williams, R. J. P. *J. Chem. Soc.* **1956** 8.
8. Ballhausen, C. J. *Kgl. Danske Videnskab. Selskab, Mat.-fys. Medd.* **29** (1955) No. 8.
9. Asmussen, R. W. and Bostrup, O. *Acta Chem. Scand. To be published.*
10. Van Vleck, J. H. *J. Chem. Phys.* **3** (1935) 803, 807.
11. Jørgensen, C. Klixbüll, *Kgl. Danske Videnskab.Selskab., Mat.-fys. Medd.* **30** (1956) No. 22.
12. Kleiner, W. H. *J. Chem. Phys.* **20** (1952) 1784.
13. Moriya, T., Motizuki, K., Kanamori, J. and Nagamiya, T. *J. Phys. Soc. Japan* **11** (1956) 211.
14. Tanabe, Y. and Sugano, S. *J. Phys. Soc. Japan* **11** (1956) 864.
15. Tinkham, M. *Proc. Roy. Soc. London* **A 236** (1956) 535, 549.

Received October 29, 1956.

* Recently, Tinkham [15] investigated the binding of fluoride to Mn(II), Fe(II), Co(II), and Cr(III) by hyperfine-structure of paramagnetic resonance. It was concluded that both 2s, 2p, 3s, and 3p orbitals of fluorine are included, implying very complicated and uncertain expressions for the absolute magnitude of Δ.

Absorption Spectra of Red Uranium(III)Chloro Complexes in Strong Hydrochloric Acid

CHR. KLIXBÜLL JØRGENSEN

Chemistry Department A, Technical University of Denmark, Copenhagen, Denmark

Someya [1] reported that solutions of uranium(III) are red in concentrated hydrochloric acid, while they are greyish green in less acidic solutions. Fig. 1 gives the absorption spectra of grey uranium (III) solutions, which are identical in 2 M and 6 M HCl (and practically coincident with the spectrum, reported by Stewart [2] of the U(III) aquo ion in 1 M $HClO_4$), and of a dark red solution in 11 M HCl. Since the normal redox potential [3] of U(III):U(IV) is -0.64 V, a hydrogen activity, corresponding to 10^{21} atm would be necessary to render the U(III) solutions thermodynamically stable; however, amalgamated zinc can in most cases produce a stationary state after one day, containing $\sim$ 80 % U(III). It cannot be argued that the colour of the grey solution in 6 M HCl is caused by admixed pale green [4] U(IV), since it turns red by addition of a large excess of 12 M HCl after removal of the zinc.

The present author [5] identifies the narrow bands of grey U(III) in the visible as Laporte-forbidden transitions from the groundstate 5 $f^3\ {}^4I_{9/2}$ to the other $5f^3$-levels, while the high and broad bands in the ultraviolet have $5f^26d$-levels as excited levels, to which the transitions are allowed by Laporte's rule. Similar $f^n \rightarrow f^{n-1}d$ transitions have been observed [5] of Ce(III), Sm(II), Eu(II), Pa(IV), Np(III), and Pu (III). The individual $5f^26d$-levels are not easily identified; in U(III) both the ligand

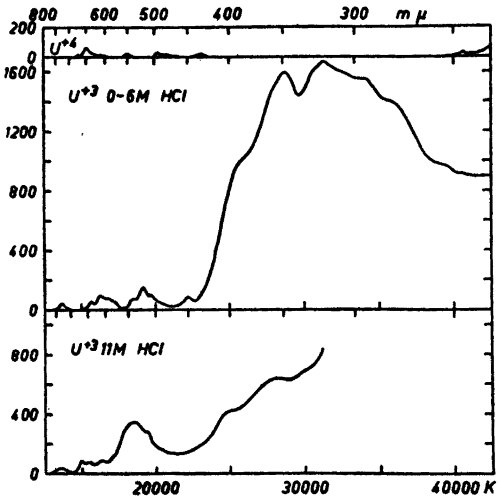


Fig. 1. The absorption spectra of uranium (IV) aquo ions [4] in $HClO_4$ and of 0.001 M to 0.008 M uranium(III) in 2 M—6 M HCl (several solutions of the grey form) and in 11 M HCl (the dark red chloro complexes). Measured on a Cary spectrophotometer at 25°C. The content of U(IV) is corrected [2] for from the absorption ~ 650 mμ. The half-life time for spontaneous evolution of hydrogen is ~ 10 minutes in 11 M HCl and longer in more dilute acids.

field parameters and the intermediate coupling (*i. e.* ζ_{5f} and ζ_{6d}) are not small compared to the energy differences between the multiplet terms with given values of L and S, while usually only one of these conditions prevails (in the d^n-complexes and in the lanthanides, respectively). Thus most of the $\frac{14 \cdot 13}{2} \cdot \frac{10}{2} = 455$ possible $5f^2 6d$-levels may have different energy. In addition to the two principal peaks [2] at 350 and 319 mμ, the shoulders at 390, 327, 294, 280, and ~ 250 mμ are probably caused by such levels or by superposed f^n-transitions. It is remarkable that the broad bands seem only to occur [2] in a range between 400 and 250 mμ.

The narrow f^2-peak at 521 mμ is shifted to a comparatively broad and high band at 540 mμ, having an area and thus an oscillator strength ~ 5 times larger for the red solution in 11 M HCl than for the grey aquo ion. (The reflection spectrum [6,7] of anhydrous UCl_3 exhibits a similar shift to ~ 545 mμ, compared to [7] ~ 510 mμ for UF_3). In the ultraviolet, the $5f^2 6d$-bands are lower and shifted towards higher wavelengths; only the shoulders at 401, 361, and 330 mμ can be observed, because U(IV) in 12 M HCl (as UCl_6^{--}?) has an electron transfer band at 286.5 mμ (ε = 2 300, δ (−) = 1 400 K), which is shifted towards shorter wavelengths by dilution and has disappeared in 4 M HCl. The U(IV) aquo ion is remarkably non-absorbing in the ultraviolet [4] (see the Figure). U(III) in 9 M HBr has a spectrum similar to that of the grey solutions in < 6 M HCl.

It cannot be completely excluded that the red colour in 11 M HCl is caused by a mixed oxidation state U(III, IV) analogous to Ti(III, IV)[8]. However, it is much more probable that a chloro comples of U(III) is formed. Actually, the actinides exhibit other exchange ion properties in strong HCl than do the lanthanides [9], and recently, Ward and Welch [10] reported equilibria between chloride ions and Pu (III), Am(III), and Cm(III): The decreased affinities to cation exchange resins imply formation constants of the monochloro complexes of all three metals equal to 15, when extrapolated to infinite dilution, and 1 to 2.5 in the actual solutions. Further, Pu(III)is strongly bound to anion exchangers in 12.6 M HCl (implying the partial presence of $PuCl_4^-$ or higher complexes). This is not the case for Am(III) or Cm (III) in 12.6 M HCl, nor for Pu(III) in 10 M HCl. Kraus, Moore and Nelson [11] have made a comparative study of quadrivalent metals in HCl and found strong adsorption on anion exchangers of U(IV) above 5.5 M and of Zr(IV) above 7 M HCl, while Th(IV) was not extracted at all.

It is surprising that the trivalent actinides (and also Ce(III)[10]) should occur mainly as monochloro complexes in 1 M HCl, since no change of absorption spectrum can be observed below 6 M HCl. Thus, Hindman [3] investigated Pu(III), and the spectrum of Nd(III)[12] changes only above 6 M HCl. Of course, the f^n-transitions might be less perturbed than the $f^n \rightarrow f^{n-1}d$ transitions. However, the three high bands of Ce(III) at 253, 240, and 222 mμ are identical within the experimental uncertainty of 0.002 M $CeCl_3$ in H_2O, 1 M, 3 M, and 5 M HCl. Only in stronger HCl, a new spectrum appears [12]. The evidence for U(III) in this note is analogous.

It may be questioned whether the chloro complex formation, implied by physicochemical methods, apply to association in the second co-ordination sphere (analogous to $Co(NH_3)_6^{+++}$, I^-) or to substitions of water in the first co-ordination sphere. The old statement that changes of the absorption spectra occur only in the latter case [13] has been highly justified for d^n-transitions in the recent years. The present author believes that the first co-ordination sphere of the aquo ions of trivalent lanthanides and actinides is not changed to a large extent in solutions, containing less than 4 M HCl, while in concentrated HCl actual complexes are formed with one or more chloride ions bound directly to the central ion. J. Bjerrum [14] investigated the case of Cu(II) and the strongly increasing chloride activity of strong HCl. The mass-action law on concentration units is very far from being valid; this is probably caused by the strong tendency towards dehydration of the aquo ions in strong HCl of low H_2O-activity [15]. It is interesting that Katzin effect [16], *i. e.* that complexes with anions are much more readily formed in anhydrous alcohols than in aqueous solutions or in alcohols with 10 % water content, can be described a similar dehydration effect: the spectral changes of Ce(III) in above 10 M aqueous HCl are reproduced by 0.002 M $CeCl_3$ alone in absolute ethanol[12], but not of $Ce(ClO_4)_3$. Thus, water (and amines) have an extraordinarily large tendency to occupy the whole of the first co-ordination sphere (rather independently of the dielectric constant of the solvent), thus displacing anions to form second-sphere associates or leading to complete ionic dissociation.

1. Someya, K. *Z. anorg. Chem.* **161** (1927) 46.
2. Stewart, D. C. *Absorption Spectra II.* ANL-4812 (AECD-3351), Argonne 1952.
3. Seaborg, G. T. and Katz, J. J. *The Actinide Elements. National Nuclear Energy Series* Div. IV, Volume 14B, 1954.
4. Jørgensen, C. Klixbüll *Kgl. Danske Videnskab.Selskab, Mat.-fys. Medd.* **29** (1955) No. 7.
5. Jørgensen, C. Klixbüll *Kgl. Danske Videnskab.Selskab, Mat.-fys. Medd.* **29** (1955) No. 11.
6. Sancier, K. M. and Freed, S. *J. Chem. Phys.* **22** (1954) 928.
7. Staritzky, E. and Douglas, R. M. *Anal. Chem.* **28** (1956) 1055, 1056.
8. Jørgensen, C. Klixbüll *Acta Chem. Scand.* **11** (1957) *in press.*
9. Diamond, R. M., Street, K. and Seaborg, G. T. *J. Am. Chem. Soc.* **76** (1954) 1461.
10. Ward, M. and Welch, G. A. *J. Inorg. Nucl. Chem.* **2** (1956) 395.
11. Kraus, K. A., Moore, G. E. and Nelson, F. *J. Am. Chem. Soc.* **78** (1956) 2692.
12. Jørgensen, C. Klixbüll *Kgl. Danske Videnskab.Selskab. Mat.-fys. Medd.* **30** (1956) No. 22.
13. Bjerrum, N. *Z. anorg. Chem.* **63** (1909) 140.
14. Bjerrum, J. *Kgl. Danske Videnskab.-Selskab, Mat.-fys. Medd.* **22** (1946) No. 18.
15. Bjerrum, N. *Z. anorg. Chem.* **109** (1920) 275.
16. Katzin, L., Jørgensen, C. Klixbüll and Bjerrum, J. *Nature* **175** (1955) 425, 426.

Received October 29, 1956.

The Hump of Ionization Potentials at Half-Filled Shells and the Influence of Spin-Pairing Energy on Standard Oxidation Potentials

CHR. KLIXBÜLL JØRGENSEN

Chemistry Department A, Technical University of Denmark, Copenhagen, Denmark

Recently, many properties of chemical complexes have been related to atomic spectroscopy [1]. Especially, the ligand field stabilization of partly filled d-shells has been evaluated [2] in terms of the parameter Δ (also called $(E_1\text{-}E_2)$ or 10 Dq), determined from the absorption spectra.

The standard oxidation potentials [3] (with the opposite sign of that used by Latimer) express the ionization potentials in aqueous solutions when corrected for the energy necessary for the reaction $\frac{1}{2}H_2 \rightarrow H_{aq}^+ + e^-$. Since the latter energy probably is between 4.5 and 5 eV, the ionization potentials in solution are much lower, 4—7 eV, than for the gaseous ions known from atomic spectroscopy [4]. The divalent and trivalent hexaaquo ions of the first transition group represent the only case where the redox potentials are known for systems having several different numbers of d-electrons. In Table 1, these potentials [3] are corrected for the influence of ligand field stabilization [2] (1 eV = 8 067

It may be questioned whether the chloro complex formation, implied by physicochemical methods, apply to association in the second co-ordination sphere (analogous to $Co(NH_3)_6^{+++}$, I^-) or to substitions of water in the first co-ordination sphere. The old statement that changes of the absorption spectra occur only in the latter case [13] has been highly justified for d^n-transitions in the recent years. The present author believes that the first co-ordination sphere of the aquo ions of trivalent lanthanides and actinides is not changed to a large extent in solutions, containing less than 4 M HCl, while in concentrated HCl actual complexes are formed with one or more chloride ions bound directly to the central ion. J. Bjerrum [14] investigated the case of Cu(II) and the strongly increasing chloride activity of strong HCl. The mass-action law on concentration units is very far from being valid; this is probably caused by the strong tendency towards dehydration of the aquo ions in strong HCl of low H_2O-activity [15]. It is interesting that Katzin effect [16], *i. e.* that complexes with anions are much more readily formed in anhydrous alcohols than in aqueous solutions or in alcohols with 10 % water content, can be described a similar dehydration effect: the spectral changes of Ce(III) in above 10 M aqueous HCl are reproduced by 0.002 M $CeCl_3$ alone in absolute ethanol[12], but not of $Ce(ClO_4)_3$. Thus, water (and amines) have an extraordinarily large tendency to occupy the whole of the first co-ordination sphere (rather independently of the dielectric constant of the solvent), thus displacing anions to form second-sphere associates or leading to complete ionic dissociation.

1. Someya, K. *Z. anorg. Chem.* **161** (1927) 46.
2. Stewart, D. C. *Absorption Spectra II.* ANL-4812 (AECD-3351), Argonne 1952.
3. Seaborg, G. T. and Katz, J. J. *The Actinide Elements. National Nuclear Energy Series* Div. IV, Volume 14B, 1954.
4. Jørgensen, C. Klixbüll *Kgl. Danske Videnskab.Selskab, Mat.-fys. Medd.* **29** (1955) No. 7.
5. Jørgensen, C. Klixbüll *Kgl. Danske Videnskab.Selskab, Mat.-fys. Medd.* **29** (1955) No. 11.
6. Sancier, K. M. and Freed, S. *J. Chem. Phys.* **22** (1954) 928.
7. Staritzky, E. and Douglas, R. M. *Anal. Chem.* **28** (1956) 1055, 1056.
8. Jørgensen, C. Klixbüll *Acta Chem. Scand.* **11** (1957) *in press.*
9. Diamond, R. M., Street, K. and Seaborg, G. T. *J. Am. Chem. Soc.* **76** (1954) 1461.
10. Ward, M. and Welch, G. A. *J. Inorg. Nucl. Chem.* **2** (1956) 395.
11. Kraus, K. A., Moore, G. E. and Nelson, F. *J. Am. Chem. Soc.* **78** (1956) 2692.
12. Jørgensen, C. Klixbüll *Kgl. Danske Videnskab.Selskab. Mat.-fys. Medd.* **30** (1956) No. 22.
13. Bjerrum, N. *Z. anorg. Chem.* **63** (1909) 140.
14. Bjerrum, J. *Kgl. Danske Videnskab.-Selskab, Mat.-fys. Medd.* **22** (1946) No. 18.
15. Bjerrum, N. *Z. anorg. Chem.* **109** (1920) 275.
16. Katzin, L., Jørgensen, C. Klixbüll and Bjerrum, J. *Nature* **175** (1955) 425, 426.

Received October 29, 1956.

The Hump of Ionization Potentials at Half-Filled Shells and the Influence of Spin-Pairing Energy on Standard Oxidation Potentials

CHR. KLIXBÜLL JØRGENSEN

Chemistry Department A, Technical University of Denmark, Copenhagen, Denmark

Recently, many properties of chemical complexes have been related to atomic spectroscopy [1]. Especially, the ligand field stabilization of partly filled d-shells has been evaluated [2] in terms of the parameter Δ (also called $(E_1\text{-}E_2)$ or 10 Dq), determined from the absorption spectra.

The standard oxidation potentials [3] (with the opposite sign of that used by Latimer) express the ionization potentials in aqueous solutions when corrected for the energy necessary for the reaction $\frac{1}{2}H_2 \rightarrow H_{aq}^+ + e^-$. Since the latter energy probably is between 4.5 and 5 eV, the ionization potentials in solution are much lower, 4—7 eV, than for the gaseous ions known from atomic spectroscopy [4]. The divalent and trivalent hexaaquo ions of the first transition group represent the only case where the redox potentials are known for systems having several different numbers of d-electrons. In Table 1, these potentials [3] are corrected for the influence of ligand field stabilization [2] (1 eV = 8 067

Table 1.

Ionization Process	V(II)→(III)	Cr(II)→(III)	Mn(II)→(III)	Fe(II)→(III)	Co(II)→(III)
Standard oxidation potential	—0.25 V	—0.41 V	+1.5 V	+0.77 V	+1.84 V
$\triangle$ of divalent ion	12 600 K	13 900 K	7 800 K	10 400 K	9 700 K
Stabilization of divalent ion	15 100 K	8 300 K	0 K	4 200 K	7 800 K
$\triangle$ of trivalent ion	18 600 K	17 400 K	21 000 K	13 700 K	18 600 K
Stabilization of trivalent ion	14 900 K	20 900 K	12 600 K	0 K	44 600 K —37 000 K
Ligand field correction	—200 K	+12 600 K	+12600 K	—4 200 K	—200 K
Corrected potential	—0.27 V	+1.10 V	+3.0 V	+0.25 V	+1.82 V

K (= cm^{-1})). In the case of tetragonally distorted d^4-systems [2], *viz.* Cr(II) and Mn (III), the stabilization is assumed to be expressed by the increased value of $\triangle$. In the case of the diamagnetic d^6-system Co(III), it is necessary to correct for the large energy $5\ B + 8\ C$ in atomic term differences [5], necessary to obtain the large stabilization $-\ 2.4\ \triangle$ of the magnetically anomalous groundstate.

The last row in the table demonstrates that the oxidation potentials, when corrected for the ligand field stabilization, regularly increase 1.5 V per unit of atomic number, Z, except between manganese and iron, where a hump $\sim$ 4 V occurs. This hump can be ascribed to the special stability of half-filled shells with the maximum value of the total spin S. Actually, the ionization potentials of neutral Al, Si, P, S, Cl, A demonstrates a similar hump $\sim$ 3.4 eV at p^3 besides the regular increase $\sim$ 2.6 eV per unit of Z (*cf.* Koefoed [6]). Orgel [7] and Griffith [8] have recently discussed the spin-pairing energy necessary for formation of magnetically anomalous complexes (*cf.* Co(III) in the table). For a given d^n-electron configuration, the energy necessary in average [9] (of all the terms with the same S) to decrease S by one unit is $S\left(\frac{35}{6}B + \frac{7}{3}C\right) \sim S \times 14\,000$ K. The theoretical comparison of spin-pairing energies in different electron configurations is not as easy; the hump seen from the Table suggests that the ionization process necessitates 32 000 K less energy, when it increases S by a half unit rather than to decrease it. Actually, this value is comparable to the 37 000 K spin-pairing energy of Co(III) from $S = 2$ to $S = 0$.

The ionization potentials [4] of the gaseous divalent d^n-ions are in eV for Sc 24.75, Ti 28.14, V 29.7, Cr 30.95, Mn 33.69, Fe 30.64, Co 33.49, Ni 36.16, Cu 36.83 and for Zn 39.70, corresponding to an increase of 2.2 eV for each unit of Z, and a d^5- hump = 4.8 eV. The small irregularities can be explained, if it is assumed that ions with F-groundstates are stabilized $\frac{3}{10} \cdot 15\ B \sim 4\,000$ K, relative to ions with D- or S-groundstates. Thus, the corrected Cr(II): Cr(III) oxidation potential is also somewhat too low, because the transition is from ^5D to ^4F. Since the similar increase is 1.5 eV per unit of Z for the hexaaquo ions, it can be concluded that the aquation stabilization increases 0.7 eV more for the trivalent than for the divalent ions per unit of Z, corresponding to smaller ionic radii and larger electric potentials near the trivalent ions.

By extrapolation from the table it can be shown that the standard redox potentials would be:

Sc(II) → Sc(III)	— 2.7 V
Ti(II) → Ti(III)	— 1.6
Ni(II) → Ni(III)	+ 3.1
Cu(II) → Cu(III)	+ 2.6
Zn(II) → Zn(III)	+ 4.8

assuming $\triangle$ = 12 000 K for the divalent and 20 000 K for the trivalent ions, and no formation of magnetically anomalous complexes. Thus, Ti(II) is probably a stronger reducing agent than reported [3] (— 0.37 V), and Sc(II) should disproportionate to the metal and Sc(III) in aqueous solution.

Since the d^5-hump has no direct influence on the relative stability of different complexes of the same central ion (as has the competition between $\triangle$ and the spin-pairing energy in Co(III) complexes), it is not surprising that the ^6S-states of d^5 (or ^8S of f^7) exhibit smaller complex formation constants than their neighbours, due to the absence of ligand field stabilization. However, if the integrals of electrostatic interaction between the d-electrons,

forming a part of the d^5-hump energy differences, actually decrease in anion complexes, compared to complexes of neutral ligands [10], it cannot be excluded that this effect will produce a slight decrease of ligand field stabilization in the complexes with stronger partial covalent bonding.

1. Jørgensen, C. Klixbüll *J. Inorg. Nucl. Chem.* **1** (1955) 301.
2. Bjerrum, J. and Jørgensen, C. Klixbüll *Rec. trav. chim.* **75** (1956) 658.
3. Latimer, W. M. *The Oxidation States of the Elements and their Potentials in Aqueous Solutions*, 2 ed. New York 1952.
4. Moore, C. E. *Atomic Energy Levels, Nat. Bur. Stand. Circular* No. 467, Vol. II.
5. Tanabe, Y. and Sugano, S. *J. Phys. Soc. Japan* **9** (1954) 753, 766.
6. Koefoed, J. *Valenskræfterne og de kemiske reaktioner*, Copenhagen 1951.
7. Orgel, L. E. *J. Chem. Phys.* **23** (1955) 1819.
8. Griffith, J. S. *J. Inorg. Nucl. Chem.* **2** (1956) 1, 229.
9. Jørgensen, C. Klixbüll *Acta Chem. Scand.* **11** (1957) *in press.*
10. Jørgensen, C. Klixbüll *Reports to the Xth Solvay Conference*, Bruxelles, May 1956.

Received October 29, 1956.

Table 1.

PTH-amino acid	R_F-value in solvent		
	D	*E*	*F*
Glycine	0.09	0.63	0.62
Alanine	0.18	0.77	0.78
Valine	0.53	0.87	0.89
Isoleucine	0.65	0.92	0.91
Leucine	0.67	0.92	0.92
Serine	0	0.47	0.14
Threonine	0	0.55	0.34
Proline	0.83	0.90	0.89
Hydroxyproline	—	—	0.54
Methionine	0.45	0.89	0.88
Cysteic acid *	0	0	0
Phenylalanine	0.57	0.90	0.91
Tyrosine	0	0.75	0.41
Tryptophan	0.12	0.86	0.82
Aspartic acid	0	0.38	0.16
Glutamic acid	0	0.56	0.27
Asparagine	0	0.31	0.08
Glutamine	0	0.41	0.15
Histidine	0	0.22	0
Arginine	0	0.11	0
ε-PTC-lysine	0.05	0.85	0.81

* PTH-cysteic acid may be identified by paper electrophoresis.

Identification and Semiquantitative Determination of Phenyl Thiohydantoins

PEHR EDMAN and JOHN SJÖQUIST

Department of Physiological Chemistry, University of Lund, Lund, Sweden

In an earlier paper [1], one of us described a paper chromatographic procedure for identification of the phenyl thiohydantoin (PTH) derivatives of natural amino acids. The procedure has now been improved in a way, that permits a semiquantitative determination based on the strong ultraviolet absorption of the PTH. This called for a method of locating the PTH's on the paper without destroying them and also for a low background absorption. For the first purpose a low pressure mercury lamp and a fluorescent screen with excitation in the appropriate ultraviolet region and emission in the visible were used *. In order to cut out the visible light from the mercury lamp a dye emitting in the visible red was used and observations were made through red glasses. The PTH's then appear on the paper as black spots on a red background. The lower limit of sensitivity is approx. 1 μg of PTH in a spot**. For a semiquantitative determination at least 5 μg in each spot is required. After location of the spot the area is cut out, the material extracted from the paper and its absorption measured. The yield varies between 75 and 105 %, the lower figure usually being obtained for the PTH's with highest R_F-values.

The solvents were chosen so that after drying the paper they did not leave material absorbing in the critical UV region around 270 mμ.

* Related procedures have been described for the location of steroids [2] and nucleic acid material [3] on paper chromatograms.

** For identification purposes the iodine-azide reaction [1] should afterwards be applied.

forming a part of the d^5-hump energy differences, actually decrease in anion complexes, compared to complexes of neutral ligands [10], it cannot be excluded that this effect will produce a slight decrease of ligand field stabilization in the complexes with stronger partial covalent bonding.

1. Jørgensen, C. Klixbüll *J. Inorg. Nucl. Chem.* **1** (1955) 301.
2. Bjerrum, J. and Jørgensen, C. Klixbüll *Rec. trav. chim.* **75** (1956) 658.
3. Latimer, W. M. *The Oxidation States of the Elements and their Potentials in Aqueous Solutions*, 2 ed. New York 1952.
4. Moore, C. E. *Atomic Energy Levels, Nat. Bur. Stand. Circular* No. 467, Vol. II.
5. Tanabe, Y. and Sugano, S. *J. Phys. Soc. Japan* **9** (1954) 753, 766.
6. Koefoed, J. *Valenskræfterne og de kemiske reaktioner*, Copenhagen 1951.
7. Orgel, L. E. *J. Chem. Phys.* **23** (1955) 1819.
8. Griffith, J. S. *J. Inorg. Nucl. Chem.* **2** (1956) 1, 229.
9. Jørgensen, C. Klixbüll *Acta Chem. Scand.* **11** (1957) *in press.*
10. Jørgensen, C. Klixbüll *Reports to the Xth Solvay Conference*, Bruxelles, May 1956.

Received October 29, 1956.

Table 1.

PTH-amino acid	R_F-value in solvent		
	D	*E*	*F*
Glycine	0.09	0.63	0.62
Alanine	0.18	0.77	0.78
Valine	0.53	0.87	0.89
Isoleucine	0.65	0.92	0.91
Leucine	0.67	0.92	0.92
Serine	0	0.47	0.14
Threonine	0	0.55	0.34
Proline	0.83	0.90	0.89
Hydroxyproline	—	—	0.54
Methionine	0.45	0.89	0.88
Cysteic acid *	0	0	0
Phenylalanine	0.57	0.90	0.91
Tyrosine	0	0.75	0.41
Tryptophan	0.12	0.86	0.82
Aspartic acid	0	0.38	0.16
Glutamic acid	0	0.56	0.27
Asparagine	0	0.31	0.08
Glutamine	0	0.41	0.15
Histidine	0	0.22	0
Arginine	0	0.11	0
ε-PTC-lysine	0.05	0.85	0.81

* PTH-cysteic acid may be identified by paper electrophoresis.

Identification and Semiquantitative Determination of Phenyl Thiohydantoins

PEHR EDMAN and JOHN SJÖQUIST

Department of Physiological Chemistry, University of Lund, Lund, Sweden

In an earlier paper [1], one of us described a paper chromatographic procedure for identification of the phenyl thiohydantoin (PTH) derivatives of natural amino acids. The procedure has now been improved in a way, that permits a semiquantitative determination based on the strong ultraviolet absorption of the PTH. This called for a method of locating the PTH's on the paper without destroying them and also for a low background absorption. For the first purpose a low pressure mercury lamp and a fluorescent screen with excitation in the appropriate ultraviolet region and emission in the visible were used *. In order to cut out the visible light from the mercury lamp a dye emitting in the visible red was used and observations were made through red glasses. The PTH's then appear on the paper as black spots on a red background. The lower limit of sensitivity is approx. 1 μg of PTH in a spot**. For a semiquantitative determination at least 5 μg in each spot is required. After location of the spot the area is cut out, the material extracted from the paper and its absorption measured. The yield varies between 75 and 105 %, the lower figure usually being obtained for the PTH's with highest R_F-values.

The solvents were chosen so that after drying the paper they did not leave material absorbing in the critical UV region around 270 mμ.

* Related procedures have been described for the location of steroids [2] and nucleic acid material [3] on paper chromatograms.

** For identification purposes the iodine-azide reaction [1] should afterwards be applied.

Another possible use of this procedure, in addition to the determination of the N-terminal amino acids, may be briefly referred to here. In conjuction with a micro procedure for the synthesis of PTH's from amino acids at present being developed in our laboratory [4] it can be used for amino acid analysis. It offers the advantages of rapidity, small material requirements (0.1 —0.2 mg of protein hydrolyzate) and noninterference of salts.

Experimental. *o*-Xylene is shaken three times with 1/10 vol. of conc. H_2SO_4 for 1/2 h with cooling to below 30° C. The organic phase is then washed with water, dried over KOH pellets overnight and distilled.

n-*Butyl acetate* is distilled and the fraction boiling at 126—127° C used.

Propionic acid is refluxed for 4 h with chromic acid (10 g/750 ml), distilled on a Widmer column and the fraction boiling at 140—141° C collected.

n-*Heptane* is shaken three times with 1/10 vol. of conc. H_2SO_4 and then washed successively with water, 10 % aqueous NaOH and water. It is finally dried over Na_2SO_4 and distilled.

Ethylene chloride, puriss (Fluka).

Formic acid, analytical reagent (Merck).

Formamide, analytical reagent (Fluka).

Filter paper. Whatman No. 1. Impregnation with starch prior to use [1] does not interfere with the quantitative determinations.

Fluorescent screen. A fine suspension of fluorescent cadmium borate * in acetone-amyl acetate (2:1) is sprayed evenly on to a 500 × 500 × 2 mm celluloid sheet, dried, and the operation repeated a number of times. When a good and even coverage has been obtained a hot solution of polyethylene in heptane is sprayed on to form a protective coating. The screen is more convenient to use if put in a frame in a slightly curved position.

Mercury lamp. Original Hanau NK 20/40 with main UV emission at 254 mμ.

PTH-references. The synthesis of the PTH-amino acids has been described earlier [5-7]. A molar extinction coefficient in ethanol at 269 mμ of 14 000—16 000 applies to most PTH-amino acids with the exception of PTH-ε-phenyl thiocarbamyl lysine (ε_{269} = 29 000) and PTH-tryptophane (ε_{269} = 19 700). The reference solutions are made up in ethylene chloride (0.5—1.5 mg/ml) except PTH-arginine and PTH-histidine which owing to their low solubility in ethylene chloride are dissolved in hexanol. In solution the PTH-amino acids decompose slowly and should therefore be stored in the cold.

Solvent systems:

D. *o-Xylene/formamide.* The paper is dipped into a solution of formamide in acetone (2:7) and immediately placed horizontally on a filter paper to remove excess solution. The strip is then suspended for a few minutes in the air for the acetone to evaporate. Reference compounds and unknowns in appropriate solvents (*cf.* above) are applied to the paper, and descending elution of the chromatogram immediately started using *o*-xylene.

E. n-*Butyl acetate/propionic acid/formamide.* The paper strip is impregnated with formamide as described for solvent system *D*. The butyl acetate is saturated with water, 3 % (v/v) propionic acid added and this mixture subsequently saturated with formamide. The filter paper lining of the chromatography tank is moistened with the solvent mixture. The paper strip is allowed to equilibrate in the chamber for 1/2 h before starting development.

F. n-*Heptane/ethylene chloride/formic acid.* The upper phase obtained after mixing 1 vol. of *n*-heptane, 2 vols. of 75 % aqueous formic acid and 2 vols. of ethylene chloride is used for developing the chromatogram and the lower phase is poured on the filter paper lining of the chromatography tank. An equilibration time of 1/2 h is required.

For the semiquantitative determination a sample of the unknown (5—20 μg) is applied together with varying, known amounts of the corresponding PTH-reference compound. An empty lane serves as a blank. After development the paper is dried at 90° C for 10 min, the spots marked out on the paper with the aid of the fluorescent screen, and cut out with a margin of *ca.* 3 mm. An area corresponding in size and level is cut out from the blank lane. The spots are eluted with 1.5 ml of ethanol for 2 h at room temperature and the extinctions of the ethanolic extracts read at 269 mμ in a Beckman spectrophotometer model DU provided with micro cuvettes. The accuracy of a single determination is ± 10 % although the yield in absolute terms may be reduced to 75 % for the faster moving spots.

This work has been aided by a grant from Eli Lilly and Company to one of us (P. E.) which is gratefully acknowledged.

* Obtainable from AB Lumalampan, Stockholm 20.

1. Sjöquist, J. *Acta Chem. Scand.* **7** (1953) 447.
2. Haines, W. and Drake, N. *Federation Proc.* **9** (1950) 180.
3. Wallenfels, K. and Christian, W. *Angew. Chem.* **65** (1953) 459.
4. Sjöquist, J. *Biochim. et Biophys. Acta* **16** (1955) 283, and unpublished.
5. Edman, P. *Acta Chem. Scand.* **4** (1950) 277.
6. Ingram, V. M. *J. Chem. Soc.* **1953** 3717.
7. Edman, P. and Lauber, K. *Acta Chem. Scand.* **10** (1956) 466.

Received October 26, 1956.

Isotope Effect in the Hydrolysis of Grignard Compounds. II *

LARS OLOF ASSARSSON

Nobel Institute of Chemistry, Stockholm 50, Sweden

Measurements of the hydrogen isotope effect in the hydrolysis of methylmagnesium iodide and phenylmagnesium iodide in a solution of anisole and pyridine were reported in a previous preliminary paper [1]. Pyridine, with its fairly basic character, and its ability to form addition products, may influence the reaction mechanism. The reactions have now been carried out in a more inert solvent, *i.e.* a mixture of anisole and tetrahydrofuran. The hydrolytic agent was in some of these experiments tritiated water and in others a tritiated mixture of water and hydrochloric acid.

The water was present in at least tenfold excess in all experiments and in the acid experiments the hydrogen chloride was present in twice the amount stoichiometrically needed. (The acid concentration in the acid-water mixture was about 18 % HCl by weight.) The technique was analogous to the one used earlier, *i.e.* the Grignard compound, dissolved in anisole-tetrahydrofuran, was added by means of an injection syringe or a dropping funnel to the water or the dilute hydrochloric acid, both dissolved in tetrahydrofuran. The anisole had been dried according to current methods, while the drying of the tetrahydrofuran was carried out by shaking it with anhydrous $CaCl_2$, thereafter with metallic sodium and finally by distilling it from methylmagnesium iodide. After the preparation of the phenylmagnesium halide, a fraction of the solvent was distilled off at reduced pressure in order to eliminate benzene formed by moisture or other side reactions. The mixture of anisole and tetrahydrofuran in the proportion used

* Ref. [1] is considered as part I.

Table 1. Results in the decomposition of Grignard compounds with water or hydrochloric acid at 20°C.

Grignard compound	Hydrolysis by	k_T/k_H	Number of parallel determinations of tritium in combustion water	Mean value (including error in determination of tritium in initial water)
CH_3MgI	water	0.700	2	0.71 ± 0.02
		0.713	2	
	hydrochloric acid	0.710	1	0.71 ± 0.04
		0.694	1	
		0.738	1	
C_6H_5MgI	water	0.644	1	(0.64 ± 0.04)*
C_6H_5MgBr	water	0.561	2	0.57 ± 0.02
		0.570	1	
	hydrochloric acid	0.579	2	0.57 ± 0.02
		0.567	1	

* Only one experiment.

1. Sjöquist, J. *Acta Chem. Scand.* **7** (1953) 447.
2. Haines, W. and Drake, N. *Federation Proc.* **9** (1950) 180.
3. Wallenfels, K. and Christian, W. *Angew. Chem.* **65** (1953) 459.
4. Sjöquist, J. *Biochim. et Biophys. Acta* **16** (1955) 283, and unpublished.
5. Edman, P. *Acta Chem. Scand.* **4** (1950) 277.
6. Ingram, V. M. *J. Chem. Soc.* **1953** 3717.
7. Edman, P. and Lauber, K. *Acta Chem. Scand.* **10** (1956) 466.

Received October 26, 1956.

Isotope Effect in the Hydrolysis of Grignard Compounds. II *

LARS OLOF ASSARSSON

Nobel Institute of Chemistry, Stockholm 50, Sweden

Measurements of the hydrogen isotope effect in the hydrolysis of methylmagnesium iodide and phenylmagnesium iodide in a solution of anisole and pyridine were reported in a previous preliminary paper [1]. Pyridine, with its fairly basic character, and its ability to form addition products, may influence the reaction mechanism. The reactions have now been carried out in a more inert solvent, *i.e.* a mixture of anisole and tetrahydrofuran. The hydrolytic agent was in some of these experiments tritiated water and in others a tritiated mixture of water and hydrochloric acid.

The water was present in at least tenfold excess in all experiments and in the acid experiments the hydrogen chloride was present in twice the amount stoichiometrically needed. (The acid concentration in the acid-water mixture was about 18 % HCl by weight.) The technique was analogous to the one used earlier, *i.e.* the Grignard compound, dissolved in anisole-tetrahydrofuran, was added by means of an injection syringe or a dropping funnel to the water or the dilute hydrochloric acid, both dissolved in tetrahydrofuran. The anisole had been dried according to current methods, while the drying of the tetrahydrofuran was carried out by shaking it with anhydrous $CaCl_2$, thereafter with metallic sodium and finally by distilling it from methylmagnesium iodide. After the preparation of the phenylmagnesium halide, a fraction of the solvent was distilled off at reduced pressure in order to eliminate benzene formed by moisture or other side reactions. The mixture of anisole and tetrahydrofuran in the proportion used

* Ref. [1] is considered as part I.

Table 1. Results in the decomposition of Grignard compounds with water or hydrochloric acid at 20°C.

Grignard compound	Hydrolysis by	k_T/k_H	Number of parallel determinations of tritium in combustion water	Mean value (including error in determination of tritium in initial water)
CH_3MgI	water	0.700	2	0.71 ± 0.02
		0.713	2	
	hydrochloric acid	0.710	1	0.71 ± 0.04
		0.694	1	
		0.738	1	
C_6H_5MgI	water	0.644	1	(0.64 ± 0.04)*
C_6H_5MgBr	water	0.561	2	0.57 ± 0.02
		0.570	1	
	hydrochloric acid	0.579	2	0.57 ± 0.02
		0.567	1	

* Only one experiment.

dissolved the water or the hydrochloric acid, as well as the magnesium salts formed. The hydrocarbons produced were burnt over cupric oxide, and the radioactivity of the water formed, as well as that of the initial water used for the hydrolysis, was determined by means of a Geiger-Müller counter.

It should be noted that the yields of benzene from phenylmagnesium iodide were not very high. An experiment, done to find the approximate yield in the neutral hydrolysis, gave the result of about 20 %, determined by the method of isotope dilution. However, phenylmagnesium bromide seems to give better yields. In four of the five decompositions reported here the bromide was used.

The results, all obtained at 20°C, are given in Table 1. The reported values have not been corrected for the small change in the activity of the water or the dilute hydrochloric acid occurring during the reaction.

Experiments were also done with *tert.*-butylmagnesium bromide. However, in this case, it was found to be impossible to use tetrahydrofuran as solvent, because it reacts instantly with the Grignard compound with evolution of heat and formation of a white precipitate, after which it will give no gas on admixture with water. Probably other branched chain alkylmagnesium halides will react in the same manner. It has been known for a long time that Grignard compounds react with ethylene oxide [2] and trimethylene oxide [3].

1. Assarsson, L. O. *Acta Chem. Scand.* **9** (1955) 1399.
2. Blaise, E. E. *Compt. rend.* **134** (1902) 551.
3. Derick, C. G. and Bissell, D. W. *J. Am. Chem. Soc.* **38** (1916) 2484.

Received October 22, 1956.

ACTA CHEMICA SCANDINAVICA 10 (1956) 1511—1514

Constituents of the Wood of *Juniperus communis* L.

JOHAN B-SON BREDENBERG and JARL GRIPENBERG

Department of Chemistry, Institute of Technology, Helsingfors, Finland

The neutral part of the extract of the wood of *Juniperus communis* L. contains, in addition to the previously reported sugiol, a substance which most probably is a mixture of ferruginol and some closely related compound, and also a yellow compound termed xanthoperol. Xanthoperol appears to be an artefact and a partial structure is suggested.

We have previously [1] reported the presence of sugiol in the wood of the common juniper (*Juniperus communis* L.). Although this work dealt primarily with the phenolic part of the extract, it could be demonstrated that sugiol occurred also in the neutral part.

A more thorough investigation of this neutral part has now been made. It was divided by steam distillation into a volatile and non-volatile fraction, and it is the investigation of the latter, which forms the subject of the present paper.

This fraction, which amounted to 1.8 % of the air-dried wood, was hydrolysed with alcoholic potassium hydroxide after preliminary experiments had shown that direct chromatography gave no useful results. The acids obtained in the hydrolysis were mainly fatty acids and no separation of them was attempted. The high equivalent weight of a crude preparation indicated, however, the presence of considerable amounts of acids higher than stearic acid.

The unsaponifiable part was chromatographed giving as a first fraction a thick oil, this being followed by two colourless crystalline compounds and finally a yellow compound.

The oil showed absorption at 280 mμ, indicating the presence of a phenol. Further attempted purification by chromatography followed by acetylation failed to give any crystalline material. However, vacuum distillation of the oil gave fractions from which a crystalline acetate could be obtained. This analysed for $C_{22}H_{32}O_2$, corresponding to the composition $C_{20}H_{30}O$ for the parent phenol. Hydrolysis of the acetate gave the phenol as an only partially crystalline material, which indicates that it is a mixture. As there is no reason to believe that the hydrolysis has caused any change in the phenol it can be assumed that even the acetate is a mixture, in spite of the fact that it behaves as a pure compound. The properties of both the acetate and the free phenol

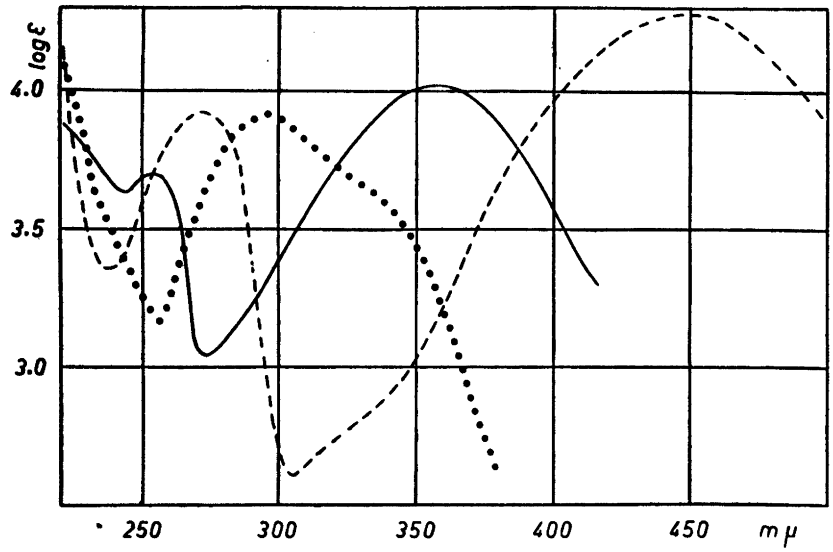


Fig. 1. Ultraviolet absorption curves of (————) *xanthoperol in ethanol,* (— — — —) *xanthoperol in 0.05 N sodium carbonate and* (. . . . . .) *xanthoperol acetate.*

are rather close to those of ferruginol (I), previously isolated from the wood of some conifers [2], suggesting that the present material is a mixture of ferruginol with some other closely related compound, most probably the corresponding dehydroderivative.

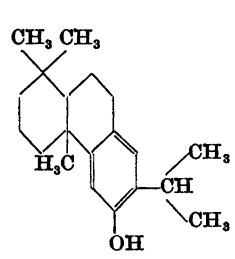
The two colourless compounds that are eluted from the chromatogram in the following fractions have been identified as sugiol and β-sitosterol.

The compound, which was most strongly absorbed on the column was obtained as yellow needles and melts between 255 and 270° with decomposition. It is optically active, with $[\alpha]_D^{20}$ +132,5° (ethanol) and has the composition $C_{20}H_{28}O_3$. The name xanthoperol is proposed for this apparently new compound. The nature of the three oxygen atoms can be deduced from the infra-red spectrum. This shows peaks at 3 436, 1 717 and 1 658 cm^{-1}, which can be attributed to a hydroxyl not involved in a chelate ring formation, an unconjugated ketone in an open chain or a six membered ring and a conjugated ketone, respectively. Further bands at 1 595, 1 567 and 1 502 cm^{-1} are attributed to an aromatic ring. A band at 883 cm^{-1} indicates the presence of isolated hydrogen atoms in the aromatic ring.

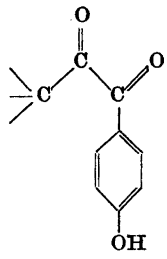
The presence of a hydroxyl group is further demonstrated by the formation of an acetate. That the hydroxyl is phenolic is shown by the large hypsochromic effect of acetylation and bathochromic effect of alkalinisation on its U.V.spectrum (see Fig. 1). This last mentioned shift (~ 90 mμ), taken together with the infra-red evidence presented above, points to the presence of a carbonyl group in the *p*-position to the phenolic hydroxyl, although the shift is even larger than those usually given by this grouping [3,4]. The p*K*-value, which is lower than 8.5 is also in agreement with the presence of such a grouping. The

yellow colour indicates either a 1,2-diketone or a quinone. The latter is, however, incompatible with the infra-red absorption in the carbonyl region.

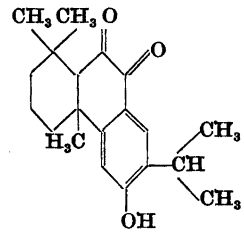
The facts mentioned above lead to the proposal of the partial structure (II), where the aromatic ring must carry at least two substituents in such positions that there are no adjacent hydrogen atoms.



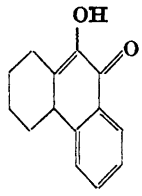
I



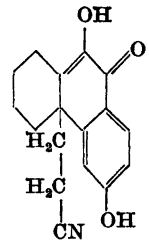
II



III



IV



V

The obvious extension of this to the complete formula (III) must be regarded with some doubt, because such a structure ought to exist mainly in the enolic form. Parham *et al.*[5] have synthesised the compound IV and Gates [6] the compound V. In neither case is there any evidence for the presence of the diketo form.

That xanthoperol does not exist as such in the wood can be seen from the fact that no yellow zone corresponding to that of xanthoperol is observed when chromatographing the material before hydrolysis. This has also been confirmed by a spectrophotometric investigation of fractions obtained in this way. There was in no fraction any selective absorption at 350 mμ in neutral or at 450 mμ in alkaline medium, characteristic of xanthoperol. After hydrolysis certain fractions showed these maxima, indicating that xanthoperol had been formed.

Experiments are in progress aimed at establishing the structure of xanthoperol and its precursor, as well as the nature of the ferruginol-like mixture.

EXPERIMENTAL

(All m.p.s are determined on a Kofler microscope. The microanalyses have been performed by Dr. A. Bernhardt, Mülheim.)

Separation of the compounds. The non-steam volatile portion of the neutral extract [1] was dissolved in ethanol and heated on a water bath with 2 N potassium hydroxide for 2 h. The ethanol was evaporated in a stream of carbon dioxide and water and ether were added. A gelatinous precipitate was thereby formed. The aqueous phase gave, after acidification and recrystallisation from methanol, a mixture of acids, m.p. 61 – 64°, equiv. wt. 308.

The precipitate and the ether soluble part were chromatographed separately but found to yield essentially the same results. Chromatography was carried out on standardised alumina using light petroleum as solvent and light petroleum-ether mixtures followed by ether as eluent, the appropriate fractions being combined.

Light petroleum eluted a comparatively large amount of a non-crystalline material. Ether-containing light petroleum eluted first sugiol, followed by a sterol, and finally the yellow xanthoperol. The last mentioned came out just before changing to ether as eluent. Further elution with ethanol-containing ether or pure ethanol failed to give any recognisable substances.

The non-crystalline light petroleum eluate (36.2 g) was distilled under vacuum. After a forerun boiling at 94—185°/0.2 mm, two main fractions b.p. 175—185°/0.15 mm (7.6 g) and b.p. 185—205°/0.1 mm (7.4 g) were obtained. The residue (18.3 g) was a dark brown resin. The first fraction was acetylated and the acetate subjected to chromatography. Elution with light petroleum gave a crude crystalline acetate, m.p. 50—60° (5.2 g). Acetylation of the second fraction and seeding with crystals from the first one gave a further amount (2.8 g) of the acetate. Recrystallisation from methanol furnished the acetate as colourless rods, m.p. 92—93°, $[\alpha]_D^{20}$ −9±1° (c = 1.5; ethanol). (Found: C 80.6; H 9.7; O 9.9; mol.wt. (Rast) 329. $C_{22}H_{32}O_2$ requires C 80.4; H 9.8; O 9.7; mol.wt. 328.5). λ_{max} (in ethanol) 268 mμ (log ε 3.71).

Hydrolysis with N potassium hydroxide and chromatography in light petroleum-ether mixture gave the free phenol as a semisolid mass, $[\alpha]_D^{15}$ +43 ± 1° (c = 1.5; ethanol), λ_{max} (in ethanol) 282 mμ (log ε 3.70). From this a small amount of crystals with m.p. 56—57° could be obtained.

The benzoate was obtained from the acetate (100 mg) by hydrolysis followed by benzoylation with benzoyl chloride in pyridine. After chromatography, crystallisation from methanol and sublimation it had m.p. 154.5—156° (yield 20 mg).

β-Sitosterol. Recrystallisation of the sterol from alcohol gave leaflets of m.p. 139—139.5,° $[\alpha]_D^{20}$ −35.5±1° (c = 1.0; chloroform). The acetate had m.p. 126—127°, $[\alpha]_D^{20}$ −41.3±1° (c = 1.0; chloroform), the benzoate m.p. 148—149°, $[\alpha]_D^{20}$ −13.0±1° (c = 1.0; chloroform) and the 3,5-dinitrobenzoate m.p. 203.5—205°, $[\alpha]_D^{20}$ −12.5±0.5° (c = 1.0; chloroform). All these values correspond well with those given for β-sitosterol [7].

Xanthoperol. Recrystallisation from benzene gave xanthoperol as yellow needles. It decomposes between 255 and 270°, $[\alpha]_D^{20}$ +132.5±2.5° (c = 1.2; ethanol). (Found: C 76.1; H 8.4; O 15.5; mol.wt. (Rast) 303. $C_{20}H_{26}O_3$ requires C 76.4; H 8.3; O 15.3; mol.wt. 314). IR-maxima: (KBr) 3 380 (s), 2 960 (m), 2 910 (m), 2 870 (m), 1 717 (m), 1 658 (s), 1 595 (s), 1 567 (s), 1 508 (m), 1 470 (m), 1 365 (w), 1 327 (s), 1 290 (s), 1 261 (s), 1 180 (m), 1 163 (m), 1 149 (m) 1 108 (w), 1 047 (w), 917 (w), 883 (w) cm^{-1}.

Xanthoperol is soluble in alkali and conc. sulphuric acid with a strong yellow colour. It gives no colouration either with ferric chloride, or with diazotised benzidine.

Xanthoperol acetate. Xanthoperol (20 mg) mixed with acetic anhydride (1 ml), and pyridine (3 drops) was allowed to stand for 3 days at room temperature. The mixture was poured into water and the precipitate recrystallised from dilute ethanol giving yellow rods (13.5 mg), m.p. 157.5—158.5°. (Found: C 74.0; H 7.95. $C_{22}H_{28}O_4$ requires C 74.1; H 7.9).

This work has been financially supported by a grant from *Statens Naturvetenskapliga Kommission*, which is gratefully acknowledged.

REFERENCES

1. Bredenberg, J. B. and Gripenberg, J. *Acta Chem. Scand.* **8** (1954) 1728.
2. Erdtman, H. in Cook, J. W. (editor) *Progress in Organic Chemistry* **1** (1952) 22.
3. Morton, R. A. and Stubbs, A. L. *J. Chem. Soc.* **1940** 1347.
4. Lemon, H. W. *J. Am. Chem. Soc.* **69** (1947) 2998.
5. Parham, W. E., Wheeler, E. L. and Dodson, R. M. *J. Am. Chem. Soc.* **77** (1955) 1166.
6. Gates, M. *Private communication.*
7. *Elsevier's Encyclopedia of Organic Compounds* **Ser III Vol 14** (1940) 90.

Received August 13, 1956.

ACTA CHEMICA SCANDINAVICA 10 (1956) 1515—1519

Studies on Arabogalactans

I. Products from the Mild Hydrolysis of the Arabogalactan from *Larix occidentalis*

HANS BOUVENG and BENGT LINDBERG

Organisk-kemiska Institutionen och Träkemiska Institutionen, Kungl. Tekniska Högskolan, Stockholm, Sweden

The arabogalactan from *Larix occidentalis* yielded a mixture of arabinose, galactose, two disaccharides and a small trisaccharide fraction when hydrolysed under conditions mild enough to cleave furanosidic linkages almost exclusively. One of the disaccharides was shown to be 3-β-L-arabopyranosyl-L-arabinose which had previously been obtained from a similar polysaccharide by Jones [1]. The other disaccharide was demonstrated to be 6-β-D-galactopyranosyl-D-galactose. The trisaccharide mixture was not further fractionated but on partial hydrolysis the arabopyranosyl-arabinose referred to above was obtained, together with arabinose and galactose.

The water-soluble polysaccharides from species of the *Larix* genus have been subject of several investigations. The literature up to 1952 has been summarised by Whistler and Smart [2]. The polysaccharide is branched and built up from 1,3′- and 1,6′-β-linked D-galactopyranosidic units and terminal L-arabofuranosidic units. Jones [1] isolated a disaccharide, 3-β-L-arabopyranosyl-L-arabinose, after mild hydrolysis of the arabogalactan from *L. decidua*. Considering the mild conditions during the hydrolysis, Jones assumed, that this disaccharide, as well as the free arabinose formed at the same time, is linked through a furanosidic linkage to the rest of the polysaccharide. He indicated the possibility that the free galactose, which is formed in small amounts under these mild conditions, should possess a furanosidic linkage also.

Sedimentation analyses showed that the polysaccharide from *L. occidentalis* consisted of two fractions with molecular weights of 16 000 and 100 000, respectively. Lystad Borgin [3] however, demonstrated that the heartwood contained only the fraction of the highest molecular weight, while both fractions were present in the sapwood.

Polysaccharides of this type are probably present in all Conifers, as indicated by their high percentage of galactose, and an arabogalactan has recently been isolated from *Pinus Jeffreyi* by Wadman, Anderson and Hassid [4].

The present paper is the first in a series with the aim of studying the arabogalactans in coniferous woods. The water-soluble polysaccharide from *L. occidentalis* was subjected to mild hydrolyses, first with 0.01 N hydrochloric acid at 100°C for two hours and then, after separation of the sugars and oligosaccharides, with 0.02 N hydrochloric acid at 100°C for two hours. Even after the last treatment the polysaccharide contained small amounts of arabinose. Chromatograms of the hydrolysates showed the presence of arabinose and galactose in dominating quantities, two disaccharides and traces of substances in the trisaccharide region. As the products from the two hydrolyses gave essentially the same chromatographic picture, they were combined and separated on a carbon column. L-Arabinose (5.9 %), D-galactose (2.2 %), two disaccharides, I (2.0 %) and II (0.8 %), and a mixture of trisaccharides (0.8 %) were isolated. The yield of higher oligosaccharides, eluted from the column with 50 % ethanol, was 2.5 %. The nature of these oligosaccharides is now under investigation.

Considering the high proportions of low-molecular weight saccharides formed under conditions when the velocity constants for hydrolysis of glycosidic linkages (expressed in minutes and Briggs logarithms) are about 10^{-4} for pyranosides and 10^{-1} — 10^{-2} for furanosides [5], it is strongly indicated, that these saccharides are linked to the rest of the molecule through furanosidic linkages, and that only a minute amount of pyranosidic linkages are cleaved during these mild conditions.

On hydrolysis, disaccharide I yielded arabinose only and disaccharide II galactose only. After methylation and hydrolysis, disaccharide I yielded a mixture of two substances, which were separated on a carbon column. One of these was identified as 2,3,4-tri-*O*-methyl-L-arabinose by transferring it into the amide of the corresponding arabonic acid, identical with an authentic specimen. The other substance was identified as 2,4-di-*O*-methyl-L-arabinose. This substance has not yet been synthesised, but its identity has been unambiguously proved [1,6], and it was now characterised as the N-phenylamine derivative and as the amide of the corresponding arabonic acid. The disaccharide therefore is a 3-L-arabopyranosyl-L-arabinose, and from its specific rotation +200°, the β-configuration of the pyranosidic linkage is highly probable. Thus it is identical with the disaccharide isolated by Jones [1] from the arabogalactan obtained from *L. decidua*.

On methylation and hydrolysis of the other disaccharide (II), a mixture of 2,3,4,6-tetra-*O*-methyl-D-galactose and 2,3,4-tri-*O*-methyl-D-galactose was obtained. They were separated by chromatography on thick filter paper and characterised as their N-phenylamine derivatives, identical with authentic specimens. The disaccharide therefore is a 6-D-galactopyranosyl-D-galactose The specific rotation, +30°, indicates a β-pyranosidic structure.

The trisaccharide fraction on total hydrolysis yielded a mixture of arabinose and galactose. On partial hydrolysis with 0.01 N hydrochloric acid for one hour at 100° a substance, chromatographically indistinguishable from disaccharide I above, was also obtained. This indicates that, in at least one of the trisaccharide components, the 3-L-arabopyranosyl-L-arabinose is a structural unit with a furanosidic linkage to either arabinose or galactose.

The rather simple picture of the arabogalactan given by previous investigators was complicated by Jones [1], who demonstrated the presence of

arabopyranosidic units in the molecule. The results of the present investigation introduce further complications. It is not yet settled, whether the polysaccharide is homogeneous or consists of a mixture of a galactan and an arabogalactan; the results of previous sedimentation studies [3] indicate, however, that the material here investigated should be homogeneous. In the highly branched framework of 1,3′- and 1,6′-linked β-galactopyranosidic units, the arrangement of which is not known, arabinose, galactose and di- and higher saccharides of these sugars are linked to the rest of the molecule through furanosidic linkages. In these saccharides some of the linkages between the monomers are pyranosidic, 1,3′-bonds for arabinose to arabinose and 1,6′-bonds for galactose to galactose being demonstrated. Other bonds, however, must be furanosidic, as indicated by the results from the partial hydrolysis of the trisaccharide fraction. The amount of easily hydrolysed parts of the molecule may be estimated at about 25 % of the polysaccharide.

EXPERIMENTAL

All melting points corrected. All evaporations performed under reduced pressure.

Chromatography. Papers: Whatman No. 1 and 3MM. Solvent: Butanol, ethanol, water, 10:3:5. Developers: Silver nitrate/sodium ethoxide and anisidine hydrochloride.

Preparation of arabogalactan. Ground heartwood of *Larix occidentalis* (580 g) was continuously extracted with ether (30 h) and subsequently with methanol (90 h). The wood (540 g) was then extracted with cold water (4 + 2 + 2 l) for 12 – 18 h with continuous stirring. The extracts were separated from the wood by filtering through a cotton cloth and then through paper, using a filter aid (Celite). The extracts were concentrated until they became viscous and then precipitated in anhydrous ethanol. The sticky precipitate was washed with anhydrous ethanol and ether and dried in a desiccator, yielding a light-coloured powder (46.5 g, 8.6 %). $[\alpha]_D^{20}$ + 7.5° (*c*, 2.0 in water).

Partial hydrolysis of arabogalactan. The polysaccharide (25 g) was treated with 0.010 N hydrochloric acid (650 ml) at 100°C for 2 h. After being cooled, the solution was neutralised by filtering through a column of IR 4B and then concentrated to a viscous liquid, which was poured into ethanol to a concentration of 90 % ethanol. The precipitate formed was filtered off and the filtrate treated with active carbon in 50 % ethanol to free it from dextrins and then filtered and concentrated to a colourless syrup (1.42 g).

The precipitate mentioned above was treated with 0.020 N hydrochloric acid (600 ml) at 100°C for 2 h. After neutralisation (IR 4B) and concentration the product was precipitated in ethanol at 90 % concentration and filtered. The precipitate was dissolved in water and the procedure repeated. The filtrates (2.15 and 0.89 g, resp. when concentrated) were combined and yielded, after being treated with carbon in the same manner as described above, a colourless syrup (3.08 g) upon concentration. The amount of high molecular weight material, recovered after the last hydrolysis, was 20.0 g.

Separation of the products from the partial hydrolyses of arabogalactan. Column: 4.5 × × 33 cm. Eluent: 8 l 0 – 20 % ethanol. Fractions: *ca.* 150 – 100 ml. Added amount: 4.50 g.

Fract. 10 – 15. Arabinose (1.47 g). M.p. 157 – 158°. $[\alpha]_D^{20}$ +104° (*c*, 2.0 in water)

» 16 – 21. Galactose (0.54 g). M.p. 164 – 165° $[\alpha]_D^{20}$ + 82° (*c*, 2.0 in water)

» 32 – 37. 0.51 g of an amorphous disaccharide (I), giving a carmine colour with anisidine hydrochloride and on total hydrolysis arabinose only. $[\alpha]_D^{20}$ + 212° (*c*, 2.0 in water).

» 38 – 46. 0.20 g of an amorphous disaccharide (II) (traces of (I) in fract. 38), giving a brown-yellow colour with anisidine hydrochloride and on total hydrolysis galactose only. $[\alpha]_D^{20}$ + 30° (*c*, 2.0 in water).

» 54 – 70. 0.19 g of at least two trisaccharides.

Elution with 50 % ethanol yielded on concentration 0.63 g of higher saccharides. The recovery of 3.48 g of an in all added 4.50 g shows that the added material was not dry.

Methylation of (I) and hydrolysis of the methylated products. 0.51 g of (I) was dissolved in water (5 ml) and methyl sulphate (1 ml) added, the solution being vigorously stirred and the temperature kept at 0°C. During 7 h 30 % sodium hydroxide (2 ml) was added dropwise, and stirring continued for 4 h more, when all methyl sulphate had dissolved. The reaction mixture was then deionised (IR 120 followed by IR 4B).

The product was concentrated and water removed by repeated distillation, first with anhydrous chloroform and then with dimethyl formamide. Complete methylation was performed by adding methyl iodide (2.5 ml) and silver oxide (2.5 g) to a rapidly stirred solution of the premethylated disaccharide in dimethyl formamide (10 ml), the apparatus and reagents being previously carefully dried and the reaction mixture kept below 20°C by external cooling. The silver oxide was added during one hour and the stirring continued for another 11 h. The reaction product was worked up according to Kuhn *et al.*[7]. Yield: 0.56 g (87 %).

The methylated disaccharide was hydrolysed in 0.5 N hydrochloric acid at 100° for 12 h. After neutralisation (IR 4B) the solution was concentrated, yielding a light brown syrup (0.50 g).

Separation on a carbon column of the products from the methylated and hydrolysed disaccharide (I). Column: 3 × 20 cm. Eluent: 4 l. 10 — 40 % ethanol. Fractions: 26 ml. Added amount: 0.50 g.

Fract. 8 — 14. 0.18 g of a substance with a rather high R_F-value (Ia).
» 17 — 32. 0.21 g of a substance with a somewhat higher R_F-value (Ib).

*Identification of (Ia) as 2,4-di-*O*-methyl-*L*-arabinose.* 0.06 g of (Ia) in water (0.7 ml) was oxidised with bromine (0.11 ml) for two days at room temperature. The reaction mixture was neutralised with silver carbonate and the acid liberated with hydrogen sulphide. After filtering and concentration, the product was distilled *in vacuo* in order to obtain the lactone, and then treated with methanolic ammonia over night at 0°C. On concentration the amide crystallised and was recrystallised from ethanol. M.p. 160—161°.

0.06 g of (Ia) was boiled with aniline (0.1 ml) in anhydrous ethanol (3 ml) for 4 h. The reaction mixture was concentrated and dried in a desiccator over phosphorus pentoxide. The 2,4-di-*O*-methyl-N-phenylarabinosylamine was recrystallised from butanol, m.p. 142—144°.

These melting points are in good agreement with those of 2,4-di-*O*-methyl-L-arabonamide and 2,4-di-*O*-methyl-N-phenyl-L-arabinosylamine reported by Smith [6] and Jones [1].

*Identification of (Ib) as 2,3,4-tri-*O*-methyl-*L*-arabinose.* 0.11 g of (Ib) was oxidised with bromine and worked up in the same manner as described above. The amide was crystallised from benzene-acetone-ethanol. M.p. 104—105°, undepressed on admixture with an authentic specimen of 2,3,4-tri-*O*-methyl-L-arabonamide.

Methylation of (II) and hydrolysis of the methylated product. The fraction containing (II) was purified on thick filter paper, yielding 0.11 g of a chromatographically pure (II). This was dissolved in water (5 ml) and methylated with methyl sulphate (1 ml) and 30 % sodium hydroxide (2 ml) in the same manner as described above.

The premethylated disaccharide was carefully dried and methylated with silver oxide (2 g) and methyl iodide (2 ml) in dimethyl formamide and worked up as above. The product formed a soft crystalline mass but no attempt of recrystallisation was made.

Hydrolysis of the completely methylated disaccharide was performed in 0.5 N hydrochloric acid (4 ml) at 100°C for 14 h. Neutralisation (IR 4B) and concentration yielded a light coloured syrup (0.11 g).

The methyl ethers from the hydrolysed disaccharide were separated on thick filter paper yielding 0.05 g of a compound with a relatively high R_F-value (IIa) and 0.04 g of a somewhat slower one (IIb).

*Identification of (IIa) as 2,3,4,6-tetra-*O*-methyl-*D*-galactose.* (IIa) was boiled with aniline (0.1 ml) in anhydrous ethanol (3 ml) for 4 h. After concentration and drying over phosphorus pentoxide, the N-phenylgalactosylamine was recrystallised from ethanol. M.p. 199—200°, undepressed on admixture with authentic 2,3,4,6-tetra-*O*-methyl-N-phenyl-D-galactosylamine.

*Identification of (IIb) as 2,3,4-tri-*O*-methyl-*D*-galactose.* The N-phenylgalactosylamine of (IIb) was prepared in the same manner as above. M.p. 167—169°, undepressed on admixture with authentic 2,3,4-tri-*O*-methyl-N-phenyl-D-galactosylamine.

The authors are indebted to Dr. W. M. Hearon, Crown Zellerbach Corp., Camas, Wash., USA for a generous gift of Western larch wood and to *Fonden för Skoglig Forskning* for financial support.

REFERENCES

1. Jones, J. K. N. *J. Chem. Soc.* **1953** 1672.
2. Whistler, R. W. and Smart, C. L. *Polysaccharide Chemistry*, New York 1953, p. 203.
3. Lystad Borgin, G. *J. Am. Chem. Soc.* **71** (1949) 2247.
4. Wadman, W. H., Anderson, A. B. and Hassid, W. Z. *J. Am. Chem. Soc.* **76** (1954) 4097.
5. Pigman, W. W. and Goepp, R. M. Jr. *Chemistry of Carbohydrates*, New York 1948, p. 206.
6. Smith, F. *J. Chem. Soc.* **1939** 744.
7. Kuhn, R., Trischmann, H. and Löw, I. *Angew. Chem.* **67** (1955) 32.

Received August 17, 1956.

ACTA CHEMICA SCANDINAVICA 10 (1956) 1520—1526

Bond Energies in Transition Metal Complexes

F. ALBERT COTTON

Department of Chemistry, Massachusetts Institute of Technology, Cambridge 39, Mass, U.S.A.

The feasibility of calculating the heat of formation of a gaseous complex ion, $MX_{p(g)}^{+m-px}$, from $M_{(g)}^{+m}$ and $pX_{(g)}^{-x}$ and hence the total bond energy by a procedure similar to the Born-Haber cycle is examined critically. It is concluded that at least in some cases the procedure has merit and application is made to some hexammines of divalent first transition series ions. Some implications of the results with regard to theories of the bonding in such complex ions are noted.

There have been three general theoretical approaches to the problem of bonding in transition metal complexes, *viz.*, the valence bond theory, the crystal field (ligand field) theory, and the molecular orbital theory. The valence bond approach as formulated by Pauling [1] makes the approximation that the energy of the process

$$M^{+m} + pX^{-x} = MX_p^{+m-px} \qquad (1)$$

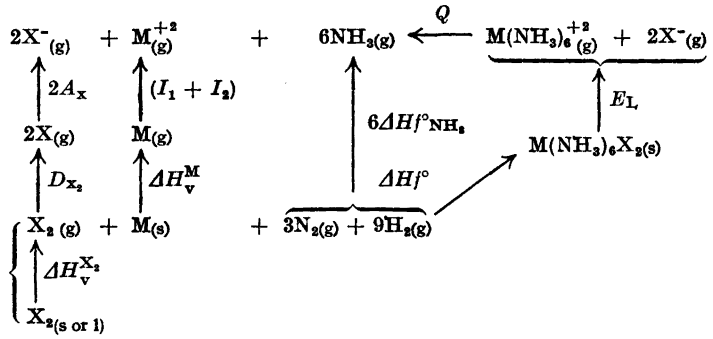
as well as other properties of the resulting complex can be accounted for by the formation of x directed bonds, more or less covalent. While this theory has had considerable qualitative success in accounting for stereochemistry and bulk magnetic properties it is not completely satisfactory even in these respects and fails seriously in dealing with detailed magnetic properties and spectra. The ligand field theory (a term proposed [2] to replace the term "crystal field theory" when the concepts of the latter are applied to complex ions) while saying nothing explicitly about the overall process (and energy) of complex ion formation focuses attention on the effects of an electrostatic field of given symmetry upon the partially filled *d*-shell of the metal ion. It is thus able to account for the spectral and magnetic properties in some cases quantitatively, in general semiquantitatively. It is also successful in explaining the stereochemistry of the complexes, sometimes more reliably than valence bond theory. These successes of ligand field theory for a time led to the suggestion that perhaps, where transition metal complexes were concerned, the valence bond theory was wholly inappropriate, or at least that the formation of directed covalent bonds was a negligible part of the problem. However, there are a

number of points on which a *purely electrostatic* ligand field model is not satisfactory, and it now seems that a molecular orbital theory in which both directed covalent bonding and ligand field effects upon the metal *d*-shell may be simultaneously recognized and their interrelations formulated is the best conceptual approach to the problem *.

With these considerations in mind the various energy terms involved in the overall process (1) are of considerable interest and we may enquire whether the total energy or any of the contributing energies may be calculated from experimental data. It is well known [2] that the energy contribution resulting from ligand field stabilization of the partially filled *d*-shell of the metal ion can be computed from spectroscopic data. It is the purpose of this note to suggest and utilize a simple method for estimating the total energy of the process.

METHOD OF CALCULATION

In principle the total energy, Q, of process (1) for the hexammine of a divalent metal ion may be calculated from the following thermodynamic cycle analogous to the Born-Haber cycle for simple ionic crystals.



(2a)

$$Q = -\Delta Hf^\circ + 6\Delta Hf^\circ_{NH_3} + D_{X_2} + 2A_X + \Delta H_v^{X_2} + (I_1 + I_2) + \Delta H_v^M - E_L \qquad (2b)$$

The symbols have their customary meanings **. It is clear that the energies of all of the steps in this cycle can be evaluated with considerable accuracy from known experimental data with the exception of E_L. The validity of the computed value of Q will thus depend upon the reliability of the method used to evaluate the pseudo-lattice energy, E_L. We have adopted the approximation that the hexammine ion, $M(NH_3)_6^{++}$, can be regarded as a large, spherical, monatomic cation whose interactions with other ions in the lattice is essentially coulombic as is that of Na^+ in the NaCl lattice for example.

If this assumption were strictly correct then we might anticipate calculating E_L with the usual accuracy of the Born approximation, ± 3 %. The two effects which will most appreciably detract from the validity of this approximation

* A good general discussion of these points will be found in Ref. [2], parts b and c.

** For information concerning this general type of calculation see Ref. [4].

are the high polarizability of the large complex ion and the possible existence of other non-central coulombic interactions, especially hydrogen bonding to the halide ions. That these two effects are probably not large in the compounds to be treated below may be inferred from the following facts. (a) Each ion is centrosymmetrically coordinated by a large number of other ions thus tending to balance out polarization effects by symmetry; (b) the lattice does not provide geometry especially suitable for the formation of N—H $\cdots$ X bonds *; and (c) it has been observed that in crystals similar to those treated here various types of free or nearly free rotation occur at room temperature which requires that hindering energies are so small as to be negligible compared to the total lattice energy. Murray and Waugh [3] have found rotation ($\sim$ 5 000 cps) of the ammonia ligands about the metal-ligand axis in several salts of $Co(NH_3)_6^{+3}$ and also rotation *even of the* BF_4^- *ion* in $Co(NH_3)_6(BF_4)_3$. Finally it may be noted that application of the Born equation to lattices containing polyatomic ions has been made before. Sherman [4] used this method to compute the lattice energies of the ammonium halides from which he derived the energy of protonation of ammonia. It is interesting to note that Stephenson [5] has recently concluded that rotation of the NH_4^+ ion may occur in crystalline NH_4I thus lending further confidence to Sherman's calculation. The possible sources of uncertainty in calculating E_L which have been discussed are such as to make the estimate too low, and hence, in view of eqn. (2b), to make the estimated value of Q too high.

One further point requires consideration, namely, the form to be assumed for the repulsive potential. The Born-Mayer equation using an exponential repulsive potential, while fundamentally the most correct, will not be used because of the difficulty of evaluating the constant ϱ [4] in the present case. Instead we shall use the original Born equation

$$E_L = \frac{Az^2e^2}{R}\left(1-\frac{1}{n}\right) \tag{3}$$

in which the repulsive potential is of the form $1/R^n$. Rather than merely assuming n to be equal to 9, an attempt has been made to adjust it to the nature of the ions concerned in this case, and using the usual empirical relation of n to ion size [6] the following values were chosen:

$M(NH_3)_6Cl_2$	8.70
$M(NH_3)_6Br_2$	8.73
$M(NH_3)_6I_2$	8.80

While the number of hexammino, hexaquo (or even hexahalo) salts for which the calculation might be made is large, there are actually very few indeed for which all necessary data are available. It is necessary to know, *inter alia*, the appropriate ionization potential of the metal ion, the heat of formation of the solid salt, the crystal structure of the solid and the Madelung constant for that structure. (Approximations might be made for some of these but it seems undesirable to add unnecessary approximations to an already

* It may also be remarked that hydrogen bonds to Cl are generally only very weak, while hydrogen bonding to Br and I is considered to be negligible.

Table 1.

Values of Q calculated for $M(NH_3)_6^{++}$ ions

Compound M	X	Lattice Constant [a] a_0 in Å	E_L kcal	$-\Delta Hf$ [b] kcal	ΔH_V^M [c] kcal	I_1+I_2 [d] kcal	Q kcal	Average Q for metal M	
Ca	Br	10.71	315.2	310.5	46.0	414.3	414.3	281.1	
	I	11.24	302.5	289.0	46.0	414.3	414.3	283.0	282
Mn	Cl	10.20	329.6	268.9	68.3	533.3	533.3	356.9	
	Br	10.52	326.4	256.1	68.3	533.3	533.3	356.6	
	I	11.04	308.2	232.7	68.3	533.3	533.3	362.2	357
Fe	Cl	10.15	331.2	246.6	96.7	554.7	554.7	382.8	
	Br	10.47	322.2	219.8	96.7	554.7	554.7	370.3	
	I	10.97	310.2	288.9	96.7	554.7	554.7	375.3	376
Co	Cl	10.10	332.8	239.0	105.0	580.0	580.0	407.2	
	Br	10.39	324.6	230.	105.0	580.0	580.0	411.7	
	I	10.91	311.8	188.6	105.0	580.0	580.0	398.0	406
Ni	Cl	10.06	334.3	239.1	101.6	595.6	595.6	418.0	
	Br	10.34	326.2	221.7	101.6	595.6	595.6	414.0	
	I	10.88	312.8	191.2	101.6	595.6	595.6	411.9	415
Zn	Br	10.46	322.6	246.7	31.2	629.1	629.1	405.7	
	I	10.96	310.3	209.8	31.2	629.1	629.1	396.0	401

(a) The lattices are of the fluorite type for which the Madelung constant to be used in conjunction with a_0, the length of the unit cube edge, is 11.637. The a_0 values are from Bödtker-Naess, G. and Hassel, O. *Z. physik. Chem.* **B22** (1933) 471.

(b) All taken from Bichowsky, F. R. and Rossini, F. D. *The Thermochemistry of the Chemical Substances*, Reinhold Publishing Corp., New York 1936. The value they list for $Mn(NH_3)_6I_2$ (201.8) is in error and the above value was recalculated from the supplementary data also listed.

(c) All taken from *Handbook of Chemistry and Physics*, 32nd Ed., Chemical Rubber Publishing Co., Cleveland, Ohio 1954.

(d) All taken from Moore, C. E. *Atomic Energy Levels*, Natl. Bur. Standards, Circular 467, Vols. I, II, 1952.

The quantities $D_{x_2} + 2A_x + 6\,\Delta Hf_{NH_3} + \Delta H_V^{X_2}$ computed from data in *Handbook of Chemistry and Physics*, 32nd Ed., Chemical Rubber Publishing Co., Cleveland, Ohio 1954 and using "best values" of A_x given by Pritchard, H. O. *Chem. Rev.* **52** (1953) 554 for X = Cl, Br, I, respectively, are −184.0, −182.0 and −178.8 kcal.

long list of unavoidable ones.) For the series of salts $M(NH_3)_6X_2$ where M = Ca, Mn, Fe, Co,Ni and Zn and X = Cl, Br and I sufficient data are at hand. The various parameters used and the results of the calculation for this group of compounds are summarized in Table 1.

DISCUSSION

The calculated values of the Q's, the total heats of dissociation of the complex ions, require comment in three respects. It is first to be clearly realized that these are and ought to be lower than the heats of solution of the gaseous

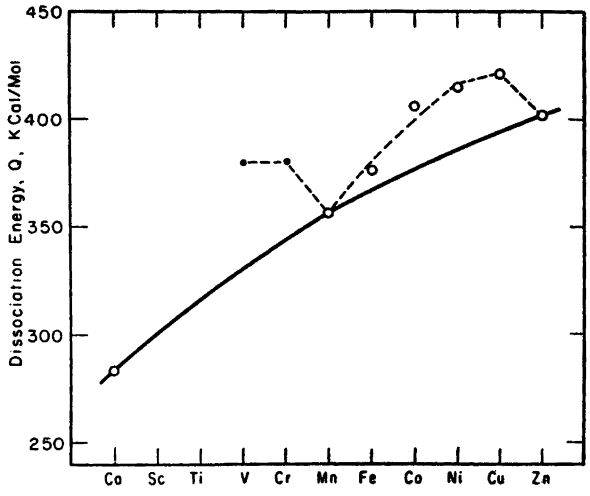


Fig. 1. Energy in kcal/mole of the gas phase dissociation of $M(NH_3)_6^{++}$ ions. Calculated points, O; - - - values predicted by adding ligand field stabilization energies to points on solid curve.

divalent metal ions of the first transition series as quoted by Orgel [7]. The latter values are the sum of an association energy analogous to that calculated here with water instead of ammonia as ligand (and probably not too different in magnitude) plus the heat of solution of the resulting complex ion. The $-Q$'s are about 100 kcal. less than the total heats of solution which is a reasonable magnitude for the heat of solution on an ion of the size and charge of these hexammine cations. Secondly, the mean deviation of the Q values averaged for the several halides of a given hexammine run from 1 to 8 kcal., or 1 to 3 %. While in terms of kilocalories these deviations are rather large, the percentages are less than the expected absolute errors of perhaps 3 to 5 %. It will be observed that the calculated Q's for a given metal ammine vary randomly with the halide ion. This indicates the absence of any important special energy contributions such as hydrogen bonding in the case of the chlorides. Finally, it has been noted by Orgel [7] that when the hydration energies of the divalent cations from Ca^{++} to Zn^{++} are plotted *versus* atomic number and a smooth curve drawn through the points for Ca^{++}, Mn^{++} and Zn^{++}, the ions for which no ligand field stabilization occurs, then the (positive) deviations of the other ions follow very closely the ligand field stabilization energies calculated from spectroscopic data. If the calculated Q's are at least not erratic (which of course indicates little about their *absolute* accuracy) they should show similar behavior. In Fig. 1 the Q's are plotted *versus* atomic number. The dotted line represents the calculated curve through Ca^{++}, Mn^{++} and Zn^{++}. The agreement is seen to be satisfactory. The ligand field stabilization energies were computed from the data summarized by Klixbüll-Jørgensen [2a].

It may also be noted that although the ligand field stabilization energies play a critical role in determining the detailed chemistry of the transition metal

ions, they actually constitute a rather small fraction of the total bond energy. Also the mean ligand-metal bond energies are 60 to 70 kcal. This might be taken to mean that the reactions of the more labile complex ions which have activation energies of 20 to 30 kcal. do not proceed by a simple S_N-1 mechanism in which the activation energy is simply that required to break one metal-ligand bond without some other compensatory action.

Acknowledgement. Thanks are due to Prof. Sv. Å. Schou of Danmarks Farmaceutiske Højskole for the hospitality of his laboratories and to the *John Simon Guggenheim Memorial Foundation* for a Fellowship during the course of this work. Additional support by the *United States Atomic Energy Commission* is acknowledged.

REFERENCES

1. Pauling, L. *The nature of the Chemical Bond*, Cornell University Press, Ithaca, New York, 1939.
2. *Proceedings of the Tenth Solvay Conference*, Brussells, May 1956: Articles by (a) Chr. Klixbüll Jørgensen, (b) L. E. Orgel, (c) R. S. Nyholm.
3. Murray, G. and Waugh, J. S. *Private communication.*
4. Sherman, J. *Chem. Rev.* **11** (1932) 93.
5. Stephenson, C. C., Landers, L. A. and Cole, A. G. *J. Chem. Phys.* **20** (1952) 1044.
6. Ref.[1], page 319.
7. Orgel, L. E. *J. Chem. Soc.* **1952** 4756.

ADDENDUM ADDED IN PROOF

F. A. Cotton and Marilyn C. Verdier

It was felt that the results of a calculation of the type described above applied to $Co(NH_3)_6^{+3}$ might be of interest. This was not done previously because there were no salts of this ion with crystal structures for which the Madelung constant was known. It was found however that $[Co(NH_3)_6]\,I_3$ and the isomorphous $[Co(NH_3)_5H_2O]\,I_3$ crystallize in a cubic structure[1] in which the units to be considered ($[Co(NH_3)_6]^{+3}$, $[Co(NH_3)_5H_2O]^{+3}$, I^-) occur at lattice positions having coordinates which are integral multiples of 1/12 of the unit cell edge. (This structure is the *anti* form of that found by Pauling[2] for $(NH_4)_3AlF_6$ and $(NH_4)_3FeF_6$). The Madelung constant for such a structure may be computed relatively simply from the table compiled by Emersleben[3]. For this structure we have calculated A_{a_0} (*i.e.*, Madelung constant to be used with lattice parameter a_0, the length of the unit cell edge) to be 22.12196. The third ionization potential of Co was taken from C. E. Moore's table. The heats of formation of the above salts were taken as -201.6 and -240.9 kcal/mole respectively[4]. Using these and other data from sources cited above we have obtained for $[Co(NH_3)_6]I_3$, $E_L = 593.8$ kcal/mole and $Q = 854.7$ kcal/mole and for $[Co(NH_3)_5H_2O]I_3$, $E_L = 597.6$ kcal/mole and $Q = 843.3$ kcal/mole. Thus the mean ligand metal bond energies in these complexes of Co^{+3} are about 140 kcal. The ~10 kcal difference accords with the expectation that water would be less strongly bound than ammonia, but is of no quantitative significance in view of the possible errors (perhaps as much as 5—10 kcal/mole).

It has also been found that although no data on $Cu(NH_3)_6X_2$ compounds are given in the general reference for lattice parameters consulted previously, such data are available for $Cu(NH_3)_6Br_2$[5]. The compound has the fluorite structure with $a_0 = 10.30$ Å and the heat of formation (Bichowsky and Rossini) is -193.2 kcal/mole. From these data $E_L =$ $= 327.3$ kcal/mole and $Q = 420.6$ kcal/mole were computed. The use of this crystallographic data requires comment since they were previously criticized on the logical ground that while the structure is given as cubic, the crystals are also said to be *slightly* dichroic. This is not necessarily inconsistent because Jahn-Teller distortion, which would of course occur in $Cu(NH_3)_6^{+2}$, could conceivably give rise to a noticeable spectral effect without causing sufficient steric distortion to be observed in X-ray studies of moderate accuracy.

Thanks are due to Professor R. G. Pearson who read the manuscript and caught a potentially disasterous numerical error.

1. Wyckoff, R. W. G. and McCutcheon, T. P. *Am. J. Sci.* [5], **13** (1927) 223.
2. Pauling, L. *J. Am. Chem. Soc.* **46** (1924) 2738.
3. Emersleben, E. *Phys. Zeits.* **24** (1923) 99.
4. Yatsimirskii, K. B. and Panhova, L. C. *Zhur. Obshchei Khim.* **19** (1949) 617; (*CA* **43** (1949) 7805). This reference first came to our attention in looking for the above heats of formation. The abstract indicates that some calculations of the general type reported here were made, but apparently a number of unnecessary approximations were made.
5. Peyronel, G. *Gazz. Chim. Ital.* **71** (1941) 363.

Received August 9, 1956.

ACTA CHEMICA SCANDINAVICA **10** (1956) 1527—1530

Synthesis of the Racemic and Optically Active Forms of 10-Methylnonadecanoic Acid

ROBERTO CAVANNA

Department of Medical Biochemistry, Institute of Medical Chemistry, University of Uppsala, Uppsala, Sweden

The synthesis of the racemic and optically active forms of 10-methylnonadecanoic acid is described and several physical constants for the acids, methyl esters and amides are given.

The synthesis of the racemic and the optically active forms of 11-methylnonadecanoic acid was described in a previous communication [1]. It was pointed out that none of the acids synthesized could be identical with phytomonic acid from *Agrobacterium tumefaciens* and that data already at hand also showed the non-identity of the racemic or one of the optically active forms of 10-methylnonadecanoic acid with phytomonic acid. The suggestion was made that phytomonic acid was a *cyclo*propane derivative similar to the lactobacillic acid isolated by Hofmann and Lucas [2] from *Lactobacillus arabinosus*. A large-scale growth of *Agrobacterium tumefaciens* was then undertaken at the Istituto Superiore di Sanitá in Rome, with the object of preparing phytomonic acid and investigating its structure. For reasons outside our control the analytical work had to be postponed, and in the meantime Hofmann and collaborators [3] showed that phytomonic acid is indeed a *cyclo*propane derivative as suggested by Ställberg-Stenhagen and the writer [1]. According to Hofmann *et al.* the acid is identical with lactobacillic acid with the proposed structure of *cis*-11,12-methyleneoctadecanoic acid [4,5].

The details of the preparation of the 10-methylsubstituted acids are now given. The synthetic routes used were the same as those for the 11-methyl-substituted isomers. 10DL-Methylnonadecanoic acid of m.p. 26.8—27.2° was prepared by Clemmensen reduction of 8-oxo-10DL-methylnonadecanoic acid. The oxo-acid of m.p. 47.0—47.2° was prepared by the β-oxo-ester synthesis [6] from methyl 3-oxo-5DL-methyltetradecanoate and methyl 6-iodohexanoate. 10DL-Methylnonadecanoic acid prepared from the enantiomorphs melted at 26.8—27.1°.

The optically active forms were synthesized by the Kolbe reaction (*cf.* Ref. 1) from the enantiomorphs of 3-methyldodecanoic acid and methyl hydro-

gen azelate. The active 3-methyldodecanoic acids were also prepared by the Kolbe reaction using the enantiomorphs of methyl hydrogen β-methylglutarate[7] and *n*-nonanoic acid as initial material.

After solidification from the melt optically active 10-methyl-nonadecanoic acids remelt at 12.5°. After crystallization from solvents slightly higher melting points have been recorded. Similar behaviour was encountered by Hallgren [8] in the case of (+)-9D-methyloctadecanoic acid, when it was possible to obtain a higher-melting form by slow crystallization from methanol at a low temperature. It seems likely that the behaviour of the 10-methylnonadecanoic acids also indicates the existence of a higher-melting modification although the conditions for obtaining the acids in this form alone have not been established.

The D-acid, the derived amide, and the methyl ester are all dextrorotatory, although the specific rotations are very small. 9D-Methyloctadecanoic acid and 11D-methylnonadecanoic acid [1] are both dextrorotatory [8], whereas 10D-methyloctadecanoic acid (tuberculostearic acid) is laevorotatory [9,10].

EXPERIMENTAL [1]

3DL-Methyl-5-oxododecanoic acid. Methyl 3DL-methyl-5-ketopimelate (40 g) was alkylated with *n*-hexyl iodide (45 g of b.p. 46°, 4 mm) using dry potassium carbonate (60 g) and methyl-*n*-propyl ketone (300 ml). For details of alkylations of this type see Ref.[6]. After refluxing for 24 h, hydrolysis and ketonic cleavage were performed in the standard manner, using potassium hydroxide (85 g) in water (80 ml) and methanol (1000 ml). The reaction mixture was kept overnight at a temperature of 50°. The product was isolated from the reaction mixture in the usual way. Distillation gave 3DL-methyl-5-oxododecanoic acid as a colourless oil of b.p. 140°, 1 mm. Yield 26 g or 49 % of the theoretical. (Found: C 68.68; H 10.42. Calc. for $C_{13}H_{24}O_3$ (228.3): C 68.50; H 10.51.)

Ethyl 3DL-methyldodecanoate was obtained by Clemmensen reduction of the oxo-acid (15 g) with 250 g of amalgamated zinc in 250 ml of absolute ethanol. A moderate stream of dry hydrogen chloride was led into the reaction mixture for 15 min. every 7th hour. After 70 h the reduced ester was isolated and distilled through a 1 m Podbielniak column. Yield 8 g of b.p. 104°, 0.3 mm (50 % of the theoretical). (Found: C 74.04; H 12.46. Calc. for $C_{15}H_{30}O_2$ (242.4): C 74.32; H 12.48).

3DL-Methyldodecanoic acid was obtained in 75 % yield after hydrolysis of the ester and distillation of the acid. B.p. 137°, 0.5 mm. (Found: C 73.20; H 12.20. Calc. for $C_{13}H_{26}O_2$ (214.3): C 72.84; H 12.23).

Methyl 3-oxo-5DL-methyltetradecanoate was prepared by the general procedure of Ställberg-Stenhagen [11]. 3-DL-Methyldodecanoyl chloride (prepared from 8 g of the acid by means of 5 ml of oxalyl chloride in 25 ml of dry benzene) was condensed with ethyl sodioacetoacetate (from 15 ml of the ethyl acetoacetate and 1.5 g of sodium). Hydrolysis and ketonic cleavage was performed with 1.5 g of sodium in 45 ml of methanol. The oxo-ester distilled at 134°, 0.5 mm. Yield, 6 g (59 % of the theoretical). (Found: C 71.00; H 11.04. Calc. for $C_{16}H_{30}O_3$ (270.4): C 71.06; H 11.18).

3-Oxo-10DL-methylnonadecanoic acid was synthesized from the above oxo-ester (6 g) and methyl 6-iodohexanoate (5.7 g prepared from the silver salt of methyl hydrogen pimelate by bromine degradation according to Hunsdiecker and Hunsdiecker [13]). After hydrolysis and ketonic cleavage in the usual way (*cf.* Ref. [1]) using 15 g of potassium hydroxide in 15 ml of water and 200 ml of methanol, the oxo-acid was crystallized from light petroleum (b.p. below 40°) at a temperature of −18°. Two recrystallizations from the same solvent gave the oxo-acid in the form of fine needles melting at 47.0−47.2°. The X-ray diffraction pattern of the oxo-acid did not show any characteristic series of 00*l* reflexions. (Found: C 73.68; H 11.75. Calc. for $C_{20}H_{38}O_3$ (326.5): C 73.57; H 11.73).

Amide of 10DL-methylnonadecanoic acid. 0.6 g of the oxo-acid was reduced by Clemmensen's method in the manner described for the C_{13} oxo-acid. After saponification, the crude acid was converted into the amide *via* the acid chloride prepared by means of

oxalyl chloride in benzene solution. The amide was crystallized from methanol-water (85:15 by volume). Yield 0.32 g (56 % of the theoretical), m.p. 78.8—79.2°. Long X-ray spacing 41.0 Å. No polymorphism has been observed. (Found: N 4.61. Calc. for $C_{20}H_{41}ON$ (311.5): N 4.50).

*10*DL-*Methylnonadecanoic acid* was obtained by saponification of the amide. Crystallization from light petroleum (b.p. below 40°) gave acid in the form of white crystals melting at 26.8—27.2°. The X-ray diffraction pattern was similar to that of 9DL-methyloctadecanoic acid in that it showed no distinct series of 00*l* reflexions. (Found: C 77.15; H 12.92. Calc. for $C_{20}H_{40}O_2$ (312.5): C 76.86; H 12.90).

*10*DL-*Methylnonadecanoic acid* from the enantiomorphs. Equal amounts of the enantiomorphs described below were mixed, a little ether being added for mixing, and the solvent evaporated at room temperature. After removing the last traces of solvent *in vacuo* the liquid solidified to a mass of fine, hard crystals. The DL-acid prepared in this manner melted without recrystallization at 26.8—27.1°.

(+)-*3*D-*Methyldodecanoic acid* was prepared in a similar way to that described for the next lower homologue in Part I. The initial materials were (+)-methyl hydrogen β-methylglutarate (20.8 g, 0.13 mole) and *n*-nonanoic acid (27 g, 0.171 mole, 25 % excess; the acid had been purified *via* the methyl ester). The anodic synthesis was performed as described in the previous paper [1]. Saponification of the methyl ester and distillation gave 10.2 g of (+)-3D-methyldodecanoic acid, b.p. 121°, 0.2 mm. The optical rotation was $[\alpha]_D^{22}$ +4.16° (homogeneous, *l*,1). n_D^{25} 1.4408.) Found: C 72.71, H 12.20. Calc. for $C_{13}H_{26}O_2$ (214.3): C 72.84; H 12.23). Hallgren [8] gives $[\alpha]_D^{24.5}$ +4.23° (homogeneous), $d_4^{24.5}$ 0.8848 and n_D^{25} 1.4405.

(−)-*3*L-*Methyldodecanoic acid* was obtained in the same way, starting from (−)-methyl hydrogen β-methylglutarate (27 g) and *n*-nonanoic acid (34 g). Yield, 13.5 g of acid distilling at 107°, 0.1 mm. n_D^{25} 1.4408. Optical rotation $[\alpha]_D^{24}$ −2.06° (homogeneous; *l*, 0.5). (Found: C 72.84; H 12.16. Calc. for $C_{13}H_{26}O_2$ (214.3): C 72.84; H 12.23).

Methyl hydrogen azelate was prepared by partial esterification of azelaic acid. The mono-ester used distilled at 137°, 0.5 mm.

(+)-*10*D-*Methylnonadecanoic acid.* 10.2 g (0.05 mole) of methyl hydrogen azelate was electrolyzed together with 8.6 g (0.04 mole) of (+)-3D-methyldodecanoic acid in 250 ml of methanol containing 0.28 g of sodium. The reaction was started with half the above amounts of reagents, the second half being added when the pH of the electrolysis mixture had risen to 7. A current of 5 A were passed through the cell for a total time of 1 h. Near the end of the reaction more methyl hydrogen azelate (2 g) was added in order to use up as much of the optically active acid as possible. The reaction mixture was extracted and saponified in the usual way (*cf.* Ref. [1]). Distillation gave 3.0 g (24 % of the theoretical) of (+)-10D-methylnonadecanoic acid as a thick colourless oil, b.p. 173—174°, 0.1 mm. The properties of the optically active hydrocarbon ((−)-10L,13D-dimethyldocosane) found in the unsaponifiable material have been described by Hallgren [8].

The amount of D-acid of m.p. 12.5° purified *via* the amide was too small to allow the determination of the optical rotation in the 0.5 dm polarimeter tube available. n_D^{25} 1.4521. d_4^{24} 0.880. (Found: C 76.8; H 13.1. Calc for $C_{20}H_{40}O_2$ (312.5): C 76.86; H 12.90). The D-amide melted after crystallization from acetone at 75.0—75.5°. Long X-ray spacing at room temperature 40.0 Å. Optical rotation α_D^{25} +0.05° (chloroform; *l*,1; *c*, 21.5). (Found: N 4.6. Calc. for $C_{20}H_{41}ON$ (311.5): N 4.50).

*Methyl 10*D-*methylnonadecanoate* was prepared by means of diazomethane from a specimen of acid that had been chromatographed on de-activated aluminium oxide. The ester distilled at 142°, 0.2 mm, and had an optical rotation α_D^{25} +0.03° (homogeneous, *l*, 0.5). d_4^{24} 0.861 (Found C 77.0; H 12.6. Calc. for $C_{21}H_{42}O_2$ (326.5): C 77.72; H 12.42).

(−)-*10*L-*Methylnonadecanoic* acid was prepared in an analogous manner starting from (−)-3L-methyldodecanoic acid. The acid distilled at 176—177°, 0.15 mm. The distilled material (5 g) had m.p. 12.5°. After two crystallizations from acetone at −25° the m.p. was 13.0—13.3°. Yield 4.17 g. n_D^{25} 1.4524; d_4^{24} 0.879. Optical rotation α_D^{25} −0.03° ± 0.01° (homogeneous, *l*,1); α_{4358}^{25} −0.07° (homogeneous, *l*,1). Hydrolysis of 0.5 g of the amide described below was carried out with a solution of 5 g of potassium hydroxide in

water (5 ml) and ethanol (30 ml). The solution was refluxed for two days. After acidification the acid was extracted in the usual way and distilled, giving 0.12 g of distilled material of m.p. 12.0—12.6°. Solidification took place at 9.5—9.0°. (Found: C 76.7; H 12.8. Calc. for $C_{30}H_{40}O_2$ (312.5): C 76.86; H 12.90).

(—)-*10*L-*Methylnonadecanamide* was prepared in the same way as the DL-amide, and crystallized from acetone. M.p. 75.0—75.5°. The melting point was the same after the amide had been chromatographed on aluminium oxide. Long X-ray spacing 40.0 Å. Optical rotation α_D^{25} —0.08° (chloroform; *l*,1; *c*,21.25). (Found: N 4.6. Calc. for $C_{30}H_{41}ON$ (311.5): N 4.50).

The writer is indebted to Professor D. Marotta, Director of the Istituto Superiore di Sanità, Rome, for financial support. This work was aided by a grant to S. and E. Stenhagen from the *Swedish National Association for Cancer Research*. The analyses were performed in the microanalytical laboratory of this institute.

REFERENCES

1. Cavanna, R. and Ställberg-Stenhagen, S. *Atti accad. nazl. Lincei* (8) **3** (1950) 31.
2. Hofmann, K. and Lucas, R. A. *J. Am. Chem. Soc.* **72** (1950) 4328.
3. Hofmann, K., Panos, C. and Tausig, F. *Federation Proc.* **13** (1954) 231.
4. Hofmann, K., Jucker, O., Miller, W. R., Young, A. C. Jr. and Tausig, F. *J. Am. Chem. Soc.* **76** (1954) 1799.
5. Hofmann, K. and Panos, C. *J. Biol. Chem.* **210** (1954) 687.
6. Ställberg-Stenhagen, S. and Stenhagen, E. *Arkiv Kemi, Mineral. Geol.* **19A** (1944) No. 1.
7. Ställberg-Stenhagen, S. *Arkiv Kemi, Mineral. Geol.* **25A** (1947) No. 10.
8. Hallgren, B. *Arkiv Kemi* **9** (1956) 389.
9. Ställberg-Stenhagen, S. *Arkiv Kemi, Mineral. Geol.* **26A** (1948) No. 12.
10. Linstead, R. P., Lunt, J. C. and Weedon, B. C. L. *J. Chem. Soc.* **1951** 1130.
11. Ställberg-Stenhagen, S. *Arkiv Kemi, Mineral. Geol.* **20A** (1945) No. 19.
12. Hunsdiecker, H. and Hunsdiecker, C. *Ber.* **75** (1942) 291.

Received July 31, 1956.

ACTA CHEMICA SCANDINAVICA **10** (1956) 1531—1546

Studies on the Hydrolysis of Metal Ions

17. The Hydrolysis of the Uranium(IV) ion, U^{4+}

SIRKKA HIETANEN

Department of Inorganic Chemistry, Royal Institute of Technology, Stockholm 70, Sweden

The hydrolysis of U^{4+} has been studied in a 3 M (sodium) perchlorate medium at 25°C by two series of electrometric titrations; in one, $[H^+] = h$ was measured with glass or hydrogen electrodes, in the other, $b = [U^{4+}]$ was measured with a Pt—Pd redox electrode, after the addition of UO_2^{2+}.

The data could be explained, assuming the mononuclear reaction $U^{4+} + H_2O \rightleftharpoons UOH^{3+} + H^+$, equilibrium constant β_1, and a polynuclear "core+links" reaction, according to hypothesis IIIa: $(n+1)U^{4+} + 3\ n\ H_2O \rightleftharpoons U((OH)_3U)_n^{4+n} + 3\ n\ H^+$, equilibrium constant $k_n = k_0 k^n$. The best agreement was found with $\log \beta_1 = -2.00 \pm 0.1$, $\log k_0 = -1.2 \pm 0.3$, $\log k = -3.4 \pm 0.1$.

By analogy with Th^{4+} and considering the crystal structure of $U(OH)_2SO_4$ it seems plausible that the complexes are chain-like, of formula $U(^{O}_{OH}U)_n^{4+n}$.

Lawrence [1] found that the magnetic susceptibility of uranium(IV) solutions decreases with decreasing $[H^+]$ and ascribed this effect to the hydrolysis of U^{4+} to form UO^{2+}. From his magnetic data he estimated the equilibrium constant $K = [UO^{2+}][H^+]^2[U^{4+}]^{-1} = 5 \times 10^{-3} \sim 10^{-2.3}$ M² in perchlorate solutions. The effect of ionic strength on the activity factors was not considered. (From Lawrence's data one may calculate values of K varying from $10^{-3.41}$ to $10^{-1.41}$. In the range studied by Lawrence, U^{4+} forms predominantly mononuclear complexes according to the present investigation.)

Kraus and Nelson [2] have studied the hydrolytic behavior of U^{4+} by spectrophotometric measurements on chloride and perchlorate solutions. They described the first stages of hydrolysis in terms of the formation of the mononuclear complex UOH^{3+} and calculated the acidity constant $K_a = [H^+][UOH^{3+}][U^{4+}]^{-1}$ for various ionic strengths. For instance, for 2.004 M perchlorate they found $K_a = 2.36 \times 10^{-2}$ M. By extrapolation to zero ionic strength they estimated the true (activity) constant $K_a^\circ = 0.21 \pm 0.02$. According to Kraus, Nelson and Johnson [3], further hydrolysis occurs above pH = 2, to give a polymer of approximate composition $U(OH)_4$; no intermediate product be-

tween UOH^{3+} and the polymer was found. The same authors have found that plutonium(IV) gives a similar polymer, approximately $Pu(OH)_4$ at 0.2 mM Pu(IV) and a pH as low as 1.5.

Kraus and Nelson [4] found the acidity constant 0.0125 at 10°C and 0.100 at 43°C with U(IV) perchlorate solutions on further spectrophotometric investigations for 0.5 ionic strength.

The aim of the present work was to investigate the hydrolysis of uranium(IV) by the methods developed in this laboratory [7,9,12,13]. Among other things, it seemed interesting to compare its behavior with the mechanism previously found for thorium.

METHOD

The hydrolysis of uranium(IV) was studied by two series of potentiometric titrations at 25°C, referred to below as Z and η titrations. We shall denote the concentrations of free H^+ and U^{4+} by

$$[H^+] = h; \; [U^{4+}] = b \tag{1}$$

B is the total concentration of uranium(IV), whether hydrolyzed or not, and H is the analytical excess concentration of H^+, assuming all uranium(IV) to be present as U^{4+}; thus H may be negative. The quantities B and H for each solution are known from the analytical data.

In each Z titration, B was kept constant, and h was measured for varying H. Then one could calculate Z, the average number of OH bound per U(IV) (= the number of H^+ split off per U(IV)):

$$Z = (h—H)/B \tag{2}$$

Curves $Z(\log h)_B$ could thus be calculated from this type of titration.

In the η titrations, both b and h were measured, the former using redox emf:s in the presence of a comparable amount of UO_2^{2+}. From these titrations, each of which was also carried out at constant B, one obtained

$$\eta = \log\frac{B}{b} \tag{3}$$

as a function of h, thus $\eta(\log h)_B$.

By addition of $NaClO_4$, all solutions were made to contain 3 M ClO_4^-, and no other anions. Since h and B were always small compared with $[Na^+]$ and $[ClO_4^-]$, the activity factors of all species were assumed to be constant so that true stoichiometric equilibrium constants could be obtained.

The acidity of the solutions was increased by adding $H^+ClO_4^-$, and decreased by adding $Na^+HCO_3^-$. NaOH was avoided, since local high pH might cause a precipitate which would be hard to redissolve.

Types of cells

In all cells used, the reference electrode was

$$SE\| = Ag|\ 0.01\ M\ AgClO_4,\ 2.99\ M\ NaClO_4|\ 3\ M\ NaClO_4| \tag{4}$$

The three types of cell used, and expressions for their emf:s, were

—Pd, $H_2(g)|H^+||SE+$; $E_h = E_{0h} + jh - 59.16 \log h$ (5)

— glass electrode$|H^+||SE+$; $E_g = E_{0g} + jh - 59.16 \log h$ (6)

— $Pd|U^{4+}, UO_2^{2+}||SE+$; $E_r = E_{0r} + jh - 29.58 \log [UO_2^{2+}] + 29.58 \log b -$
$-118.32 \log h$ (7)

In eqns. (5) to (7), E is the measured emf, E_{0g}, E_{0h} and E_{0r} are constants in each titration (although E_{0r} was found to vary between different titrations). In the liquid junction potential $E_j = jh$, the constant j was 15 mV M^{-1} for E_h, 22 mV M^{-1} for E_g.

In the pH and concentration range studied, the hydrolysis of UO_2^{2+} is negligible according to the data of Ahrland [5].

For the Z titrations, E_g or sometimes E_h was measured; the η titrations required measurements of E_r and E_g, usually in a range of higher acidity. If j is known, the E_0 can be calculated from data at higher acidities (negligible hydrolysis); then one may readily obtain h from E_h or E_g, and b from E_r.

Reagents

The starting material for the *uranyl perchlorate* and *uranium(IV) perchlorate* solutions was an ammonium uranyl hydroxide, which had been precipitated from uranyl nitrate, purified by ether extraction. The hydroxide was heated to form U_3O_8, which was dissolved in HNO_3, and the uranyl nitrate so obtained was repeatedly evaporated with 70—72 % $HClO_4$ under an infrared lamp until no trace of HNO_3 could be detected. This product was used for preparing uranyl perchlorate solutions.

Uranyl perchlorate solution was adjusted to contain about 0.5 M UO_2^{2+} and 2.5 M $HClO_4$; it was then reduced to uranium(IV) by electrolysis, using a mercury cathode and a platinum anode, separated by a diaphragm of sintered glass [6]. Air was kept away with a stream of CO_2. The potential difference between the electrodes was 4—5 V, and the current 0.15—0.25 A. With 6 V and about 1.0 A, chloride ions could be detected after 10 min. The acidity of the $UO_2(ClO_4)_2$ solution to be reduced is important. If it is too low, a black solid (probably UO_2) will precipitate during the electrolysis; if it is too high, H will be unnecessarily high in the uranium(IV) solution, and it is then hard to determine Z accurately.

The uranium(IV) perchlorate solution finally obtained was stored under purified CO_2 in an automatic buret.

Perchloric acid solutions were prepared from 70—72 % $HClO_4$ (Kebo p.a.) and analyzed using HgO + KI, or recrystallized hydrazine sulfate.

Sodium hydrogen carbonate solutions were prepared from $NaHCO_3$ (Riedel-de-Haen p.a.) and titrated with $HClO_4$.

Silver perchlorate solutions were prepared as described in previous papers from this laboratory [7].

Sodium perchlorate solutions were prepared by mixing $HClO_4$ and Na_2CO_3. No Cl^- could be detected. The stock solutions were analyzed as described before [7].

Carbon dioxide, nitrogen, and *hydrogen* were purified as described previously [7].

Analysis

The *total uranium* in the uranium(IV) or uranyl stock solutions was determined by precipitating with oxine, igniting, and weighing as U_3O_8. The concentration of *uranium(IV)* had to be checked repeatedly, since it may easily decrease by oxidation. After each titration, the following convenient method was used: Equal volumes of uranium(IV) solution and conc. HCl were mixed in a measuring cylinder fitted with a glass stopper; then ICl solution and 10 % $FeCl_3$ solution were added, and the free I_2 titrated with KIO_3,

using $CHCl_3$ as indicator. — Another method was to add excess of $FeCl_3$ solution, which oxidizes U^{4+} to UO_2^{2+}, and to determine the Fe^{2+} formed by potentiometric titration with $K_2Cr_2O_7$ solution.

The *perchlorate* ion concentration was determined by ion exchange. First U^{4+} was oxidized to UO_2^{2+} with a stream of air or oxygen, and then the solution was passed through a column of the H^+ form of Amberlite IR 120. The total amount of ClO_4^- was found by titrating the eluate ($H^+ClO_4^-$) with NaOH solution. — When uranium(IV) solution was passed through the same type of ion exchange column without previous oxidation, nevertheless the same total amount of ClO_4^- was found. This shows that uranium(IV) on the ion exchange resin is not associated with any ClO_4^-.

Apparatus

The cell was of the type described by Forsling, Hietanen and Sillén [9]. It was kept in a paraffin oil thermostat at 25.0±0.1°C, and the titrations were carried out in a room thermostated at approximately 25°C.

The hydrogen electrodes were lightly palladinised Pt foils [8]. Two glass electrodes were used, a commercial Radiometer electrode, and one prepared by Mr Erik Blomgren in Uppsala. The redox electrodes were palladinised Pt foils. In measurements of E_T and E_g, air was kept out of the titration vessel by bubbling purified N_2 through the solution.

The emfs of the cells were measured with a Vernier compensator (Cambridge Instrument Co.) and a Multiflex galvanometer type MG 2, or with a valve potentiometer (Radiometer PHM 3i).

PROCEDURE AND DATA

Z Titrations

The data from Z titrations with a glass electrode are given in Fig. 1, those with a hydrogen electrode in Fig. 3, both in the form of plots of $Z(\log h)_B$. As an example, the primary data for a titration with a hydrogen electrode for $B = 10.00$ mM are given in Table 1.

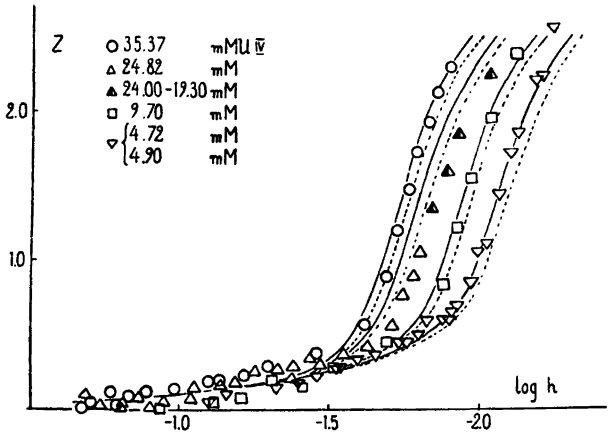


Fig. 1. Data for glass electrode measurements. Vertical axis: Z = *average number of* OH^- *bound per U(IV) atom. Horizontal axis: log* h (*M scale*). *Full drawn curve: calculated for the various values of* B *with "hypothesis IIIa"* $k_0 = 0.06$, *log* $k = -3.37$, *assuming one mononuclear step with* $\log \beta_1 = -1.98$. *Broken curve: calculated for* $k_0 = 0.06$, *log* $k = -3.45$, $\log \beta_1 = -1.95$.

Table 1.

Uranium solution: 20.00 mM U^{4+}, 0.55 mM UO_2^{2+}, 182.00 mM H^+ } v ml; $HClO_4$ 97.80 mM v_1 ml; $NaHCO_3$ 273.6 mM v_2 ml

Acid-base titration. In titration vessel 35.00 ml $HClO_4$

v_1	H	E_0'	E_h
0.00	97.80	837.17	719.42
1.00	87.48	836.76	721.88
2.00	77.72	836.54	724.70
3.00	68.48	836.54	727.95
4.00	59.70	836.07	731.00
6.00	43.44	835.32	738.42
10.00	25.26	834.51	764.50
12.00	2.97	835.00	807.05

Uranium addition 47.00 ml

v	v_2	H	h	E_h	E_0'	Z
0.00	0.00	46.98	47.93	735.30	835.1	0.10
2.00	2.00	41.34	43.24	738.10	834.9	0.19
4.00	4.00	36.14	38.50	740.89	834.7	0.24
10.00	10.00	22.72	25.97	750.60	834.3	0.32
15.00	15.00	13.53	18.03	759.78	834.1	0.45
20.00	20.00	5.70	13.77	766.50	833.9	0.81
24.00	24.00	0.24	12.22	769.67	833.9	1.20
26.00	26.00	−2.27	11.51	771.11	833.9	1.38
28.00	28.00	−4.64	10.81	772.62	833.8	1.54
30.00	30.00	−6.90	10.21	774.08	833.8	1.71
32.00	32.00	−9.03	9.62	775.62	833.8	1.87
34.00	34.00	−11.06	9.01	777.20	833.7	2.01
36.00	36.00	−13.00	8.39	779.03	833.7	2.14

The correction for uranyl is made by reducing E_0' with 0.50 mV.

The titration procedure was practically the same as that used for thorium [7]. Usually, as in Table 1, $E_0' = E_0 + jh$ was obtained from an immediately preceding acid-base titration with no uranium present; sometimes E_0' was calculated from E values measured in the most acidic solutions containing U, where the hydrolysis of U^{4+} could be neglected.

The accuracy of the Z values is lower than for many other ions studied in this series, especially at the highest acidities. At 100 mM H^+, where Z is already about 0.1, an error of 0.2 or 0.3 mV in E will make an error of 0.8 to 1.2 mM in h, which makes the Z value for the lowest values of B (2 or 5 mM) very uncertain. For higher B, and lower h, the accuracy increases.

Influence of uranyl ions. It was practically unavoidable that the uranium(IV) solutions contained 1—2 % of the total uranium in the form of uranyl ions UO_2^{2+}. Fig. 2 shows measurements with glass and hydrogen electrodes on a solution, where the analytical H^+ and uranium(IV) concentrations, H and B, were kept constant, while the concentration of UO_2^{2+} was increased by adding from a buret a uranyl solution, of the same H and B as the original solution. The presence of uranyl ions does not seem to affect the glass electrode,

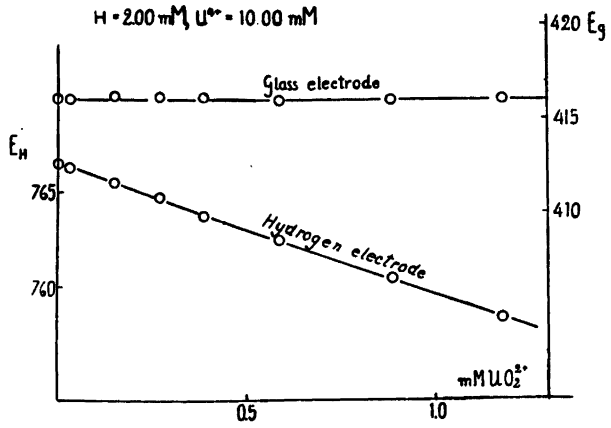


Fig. 2. Influence of uranyl ion on glass and hydrogen electrodes.

whereas E_h (and thus E_{0h}) are seen to decrease. The difference amounted to about 7 mV for 1 mM UO_2^{2+}; in experiments with other values for B and H, approximately the same slope was obtained.

The glass electrode data would thus seem more reliable. To evaluate the hydrogen electrode data, E_{0h} was taken from points of high acidity ($Z = 0$) and assumed to be constant.

η Titrations

In preliminary experiments, various redox electrodes were tried: Pt, Pt—Ir, platinised Pt, palladinised Pt, gilded Pt, Au, and Hg. The emf obtained using Hg electrodes was usually about 6—7 mV lower than with the others. Equilibrium was reached most quickly with the palladinised and platinised Pt electrodes. If a few drops of indigo tetrasulfonate solution was added [11], the gilded Pt electrodes also came to equilibrium rather rapidly.

Palladinised Pt electrodes were used, since they were most easily prepared. New electrodes were palladinised for each titration.

The data, calculated in the form $\eta(\log h)_B$ are given in Fig. 4. Full data for two titrations are given in Table 2, one in which h was increased and one in which h was decreased.

The procedure for η titrations was similar to that of the Z titrations. The hydrogen ion concentration was sometimes measured directly with the glass electrode; in such cases, an acid-base titration preceded the uranium titrations. In other cases, h was calculated as $h = H + BZ$. The correction term BZ for the H^+ split off from U^{4+} was assumed to be a function of h and B and was interpolated from previous Z titrations.

Variation of E_{0r}. When the values of E_{0r} for different titrations were compared, they were found to differ, usually by about 1 mV although sometimes deviations up to 6—8 mV were observed. However, in each titration E_{0r} seemed to be constant, since the difference in E_r values found in parallel

Table 2.

Uranium solution: 20.00 mM U^{4+}, 20.42 mM UO^{2+}, 102.1 mM H^+ } v ml; $HClO_4$ 504.4 mM v_1 ml; $NaHCO_3$ 273.6 mM v_2 ml

In titration vessel 20.00 ml uranium solution + 20.00 ml 3 M $NaClO_4$

v	v_1	v_2	$-E_r$	E_j	H	h	η
3.00		3.00	488.6	0.6	33.20	35.48	0.111
1.00	1.00		476.5	0.8	44.46	46.24	0.067
2.00	2.00		467.4	0.9	54.81	56.24	0.041
3.00	3.00		460.0	1.1	64.36	65.32	0.035
4.00	4.00		454.2	1.2	73.21	73.96	0.019
6.00	6.00		445.1	1.5	89.07	89.64	0.004
8.00	8.00		438.0	1.7	102.9	102.9	0.010
10.00	10.00		432.6	1.9	115.0	115.3	0.001
12.00	12.00		428.4	2.1	125.8	125.9	0.000
15.00	15.00		423.2	2.3	139.8	139.8	0.000
20.00	20.00		416.9	2.6	158.8	158.8	0.000

In titration vessel 20.00 ml uranium solution + 20.00 ml 3 M $NaClO_4$

v	v_2	$-E_r$	E_j	H	h	η
2.00	2.00	482.0	0.7	38.61	40.74	0.099
3.00	3.45	492.0	0.5	30.23	32.59	0.143
4.00	4.00	494.8	0.5	28.25	30.72	0.149
5.00	5.00	500.6	0.4	23.69	26.45	0.210
6.00	6.00	507.7	0.4	19.48	22.39	0.258
7.00	7.00	514.1	0.3	15.58	19.16	0.310
8.00	8.05	521.3	0.3	11.95	16.64	0.311
9.00	8.95	526.7	0.2	8.83	14.62	0.353
10.00	10.07	530.7	0.2	5.12	13.26	0.388
11.00	11.00	532.2	0.2	2.50	12.28	0.468
12.00	12.05	534.1	0.2	−0.47	11.35	0.541
13.00	13.00	534.7	0.2	−2.84	10.69	0.623
14.00	14.04	535.0	0.2	−5.44	10.03	0.725

titrations was always constant. Since in (7) only the difference E_{0r}—E_r is important, and not the absolute value of E_{0r}, η could still be calculated. It is hard to understand the reason for this deviation. The equilibria between U(IV), U(V), and U(VI) should be reached within the times used. There may be differences in the surface of the electrode, but when two electrodes were immersed in the same solution, they gave the same emf within ± 0.2 mV at low values of Z (or η) and within 0.5 mV close to the point of precipitation.

The equilibrium E_r or E_h was obtained within 20-30 min. and E_g much more quickly; it was sometimes checked that E did not change after two hours.

A number of back-titrations were made, adding H^+: Z titrations for $B =$ $= 9.81$ mM (from $Z = 0.50$) and 9.74 mM (from $Z = 0.40$) with the hydrogen electrode, and for $B = 4.90$ (from $Z = 0.85$) with the glass electrode; and η titrations for $B = 10.00$ (from $\eta = 0.11$) $B = 9.32$ mM (from $\eta = 0.260$), $B = 5.00$ (from $\eta = 0.163$ and for $B = 4.78$ (from $\eta = 0.167$). They seem to agree well with titrations in the other direction.

Influence of carbonate. To make sure that no error was caused by carbonate complexes formed on the addition of $NaHCO_3$, the following experiment was carried out. A solution was prepared with $H = 22$ mM, $B = 35$ mM and $[UO_2^{2+}] = 7$ mM. In this solution, $Z \approx 0.35$, and $\eta \approx 0.17$. The redox emf E_r was measured in the cell (7), and then a stream of CO_2 was bubbled through the solution. E_r increased by 1 mV, which may indicate a weak complex formation with uranium(IV). However, when N_2 was again bubbled through the solution, after 10 min. E_r had attained the same value as before the treatment with CO_2. The experiment was repeated and found to be fully reproducible. Thus there is no indication of strong or irreversible complex formation with carbonate.

Precipitation. In order to study the tendency to slow precipitation, four series of solutions were prepared; in each series, the total concentrations of uranium(IV) and uranyl ions were kept constant, whereas the excess of H^+, H, was varied. The solutions which were initially clear were stored in flasks under paraffin oil to avoid oxidation, and the E_r with each solution was measured daily. The flasks were also scrutinized for a possible precipitate.

The maximum change in E was 2 mV, and the variations were usually less than 1 mV. In the most acidic solutions, E often varied by 1 mV during the first day.

The results may be summarized as follows:

B, mM	$[UO_2^{2+}]$, mM	Precipitate at H, mM	no ppt at H, mM
5.05	4.61	0, 2, 5	10, 30, 50...200
10.00	8.65	−10, 0, 5	10, 30...200
25.00	25.00	−10, 0, 5	10, 30...200
50.00	50.00	−20, −15	− 10...

In the most concentrated solution, the black precipitate appeared after three days and in the other solutions after one day. In these experiments, the uranium(IV) perchlorate contained some Cl^-, which had formed on electrolytic reduction of UO_2^{2+}.

In other experiments it was noticed that the presence of UO_2^{2+} ions favored precipitation, which was observed at higher acidities than in the absence of UO_2^{2+}.

The polynuclear mechanism: first approximation

From the plots of $Z(\log h)_B$ in Figs. 1 and 3 or of $\eta(\log h)_B$ in Fig. 4 it is seen that for different values of B the steep part of the curves do not coincide but are parallel. This shows that polynuclear complexes are formed and indicates, as a first approximation, that they can be written in a "core + links" form [12]. The spacing between the curves indicates $t = 3$, whence the formula of the complexes would be $U((OH)_3U)_n^{4+n}$. As a test, the data of the Z and η titrations were recalculated and plotted as functions of the variable

$$x = \log B - 3 \log h \tag{8}$$

For convenience, Z was replaced by the variable

$$y = Z/t = Z/3 \tag{9}$$

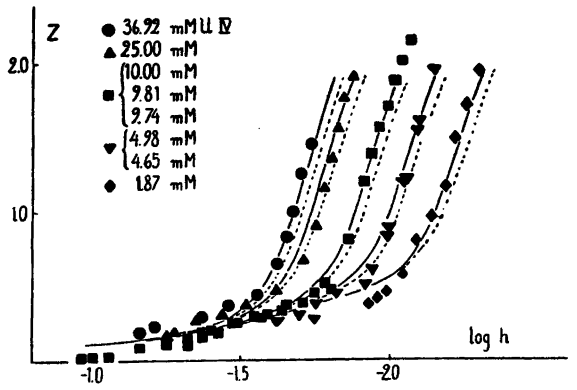


Fig. 3. Data for hydrogen electrode measurements. Vertical axis: Z = *average number of* OH^- *bound per U(IV) atom. Horizontal axis: log* h (*M scale*). *Full-drawn curve: calculated for the various values of* B *with "hypothesis III a"* $k_0 = 0.06$, log k = −3.37, *assuming one mononuclear step with log* $\beta_1 = -1.98$.

The data $y(x)$ are seen to fall on single curves, independent of B, at least in the steep parts of the curves. In the flat part, for higher h(lower x), the agreement is less good; on the other hand, the experimental inaccuracy is also much greater.

It would thus seem that a "core + links" mechanism would give a good approximation.

For two of the titrations in Fig. 5, the values of E'_0 taken differed from those used for calculating Z for Figs. 1 and 3. In one of them, with $B = 4.72$ mM, $E'_{0g} = 202.7$ mV (giving $Z = 0.11$ at $H = 45.88$ mM) was used in Fig. 1, and $E'_{0g} = 202.8$ mV (giving $Z =$ = 0,15) in Fig. 5. In the other, with $B = 36.92$ mM, we used $E'_{0h} = 834.62$ (giving $Z =$ = 0.195 at $H = 62.26$) in Fig. 3, and $E'_{0h} = 832.25$ (giving $Z = 0.030$) in Fig. 5. These

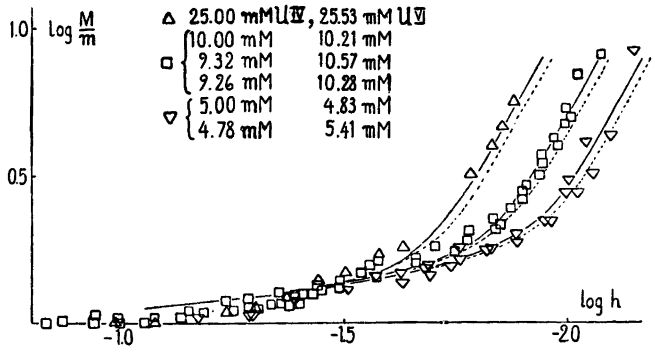


Fig. 4. Data for redox titrations. Vertical axis: $\eta = log$ (B/b); *horizontal axis: log* h (*M scale.*) *Full-drawn curve: calculated for the various values of* B *with "hypothesis III a"* $k_0 = 0.06$, *log* k = −3.37, *assuming one mononuclear step log* $\beta_1 = -1.98$. *Broken curve: calculated for* $k_0 = 0.06$, *log* k = −3.45, *log* $\beta_1 = -1.95$.

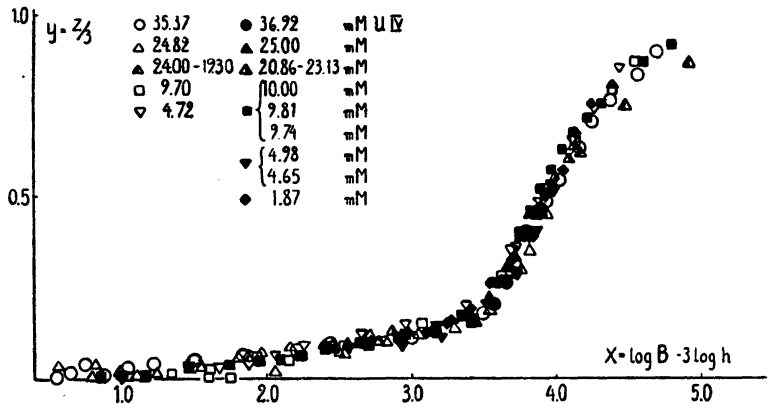


Fig. 5. Data for glass electrode measurements (circles) and hydrogen electrode measurements (dots) recalculated to the form y(x) *assuming* t = 3, x = *log* B − 3 *log* h (*M scale*), y = Z/3.

adjustments were attempted to make the $Z(x)$ curves coincide more closely; large as they may seem, they will influence the Z very little in the steep part of the curve: by about 0.01 in the former case and 0.04 in the latter.

Comparison with simple mechanisms. The $y(x)$ curve was now compared with those calculated for a number of simple mechanisms discussed in AB II[12] and in part 8[13]. The steep part gave no fit with hypothesis I (no soluble complex, precipitate formed) or II (single complex formed, with $n = N$). An acceptable fit was found with hypothesis IIIa, for values of k_0 between 0.1 and 0.01. In mechanism IIIa it is assumed that complexes with all values of n are formed, and that the equilibrium constant k_n for the formation of the n:th "core + links" complex (concentration = c_n) in this case

$$(n+1)U^{4+} + 3\,n\,H_2O \rightleftharpoons U((OH)_3U)_n^{(4+n)+} + 3\,n\,H^+;\ k_n = c_n h^{3n} b^{-(n+1)} \quad (10)$$

is given by

$$k_n = k_0 k^n \quad (11)$$

where k and k_0 are constants.

A better value of k_0 was found using the equation (AB II, 37)

$$k_0 = y[1 - 10^X(1-y)]^2(1-2\,y)^{-2} \cdot 10^{-X} \quad (12)$$

The abscissa x was measured for $y = 0.7$, $0.5(x_{\frac{1}{2}})$, 0.3, 0.2 and, for each value, $10^X = 2 \cdot 10^{(x-x_{\frac{1}{2}})}$ was calculated. This gave $k_0 = 0.042$, $\log k_0 = -1.38$ when $y = 0.7$, $k_0 = 0.06$, $\log k_0 = -1.22$ when $y = 0.3$ and $k_0 = 0.134$, $\log k_0 = -0.87$, $y = 0.2$.

To estimate the uncertainty in k_0 the difference $x(y = 0.633, Z = 1.9) - x(y = 0.267, Z = 0.8)$ was plotted against k_0. The experimental value of this difference varied between 0.45 and 0.55, which would correspond to $\log k_0 = -1.2 \pm 0.3$.

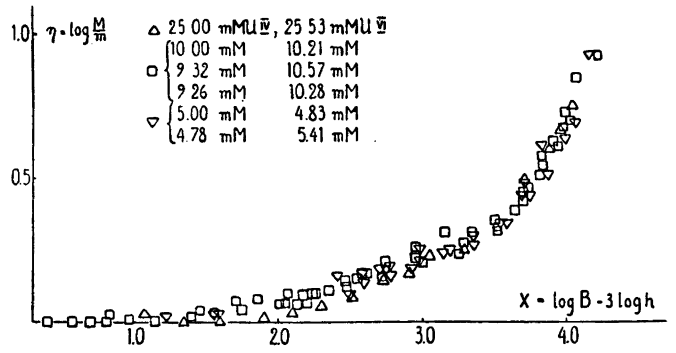


Fig. 6. Data for redox titrations recalculated to the form η (X) *assuming* $t = 3, \eta = log(B/b)$, $x = log\ B - 3\ log\ h$ (*M scale*).

From $x_{\frac{1}{2}}$ one also finds $\log k = \log 2 - x_{\frac{1}{2}} = 3.6 \pm 0.1$.

Direct analysis of the curve $y(x)$. A smooth curve $y(x)$ was drawn through the points of Fig. 5. This curve was used to calculate

$$\log F = y \log e + \int_{-\infty}^{x} y\, dx = \eta \tag{13}$$

$$g = (1-y)F-1; \quad u = 10^x F^{-1} \tag{14}$$

In this case

$$u = bh^{-t} = bh^{-3}; \quad g = \sum k_n u^n \tag{15}$$

The average number of $U(OH)_3$ links per complex is defined by

$$\bar{n} = \sum n c_n / \sum c_n \tag{16}$$

One may calculate $\bar{n}$ either by differentiating $\log g(\log u)$, or directly from y and F. (The second formula may be derived from eqns. 5, 6 and 7 in part 10[5] and eqns. 13 and 14 in this paper)

$$\bar{n} = \frac{\mathrm{d}\ \log\ g}{\mathrm{d}\ \log\ u} = \frac{y}{1-y-F^{-1}} \tag{17}$$

The squares (□) in Fig. 7 were obtained in this way. Whatever the details of the "core + links" reaction, one would expect $\bar{n}$ to start at 1.0 for low x and then to increase with increasing x. The absurd behavior of the function $\bar{n}(x)$ in Fig. 7, with a minimum less than 1, was at first ascribed to analytical errors. So, new $\bar{n}(x)$ curves were calculated, subtracting 0.04 (○) or 0.08 (×) units from each value of y. The $\bar{n}$ curves are still senseless for low x; moreover, these corrections would correspond to a very improbable error in the value of H for the original uranium(IV) solution.

So it was concluded that in the first stages of the hydrolysis, some species other than the "core + links" complexes must be formed. The values of $\bar{n}$

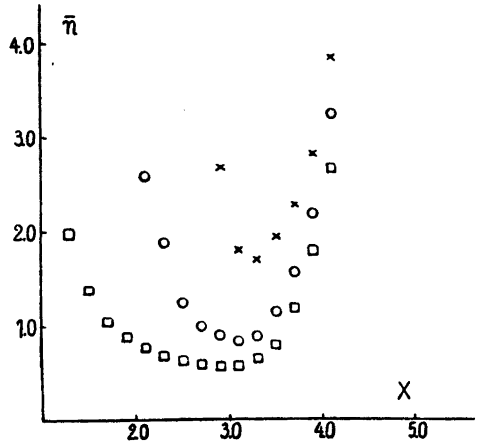


Fig. 7. Direct analysis of y(x) *curve:* $\bar{n}$ *as a function of* x. y = *0* (□) y = *0.04* (○), *y* = = *0.08* (×).

for high values of x, where the "core + links" mechanism seems to predominate, indicate that complexes with $\bar{n}$ greater than 3, *i.e.* with more than 4 U, are present.

Correction for mononuclear reaction

It was found that the Z curves could be explained on the reasonable and simple assumption that, in addition to the "core + links" complexes, the mononuclear complex UOH^{3+} is formed

$$U^{4+} + H_2O \rightleftharpoons UOH^{3+} + H^+;\ \beta_1 = [UOH^{3+}]hb^{-1} \qquad (18)$$

To determine the best values for the constants β_1 for the mononuclear reaction and k for the "core + links" mechanism, a normalized projection map was used as indicated by Biedermann and Sillén [14]. If the "core + links" complexes with $t = 3$, and in addition only the first mononuclear complex are formed, then the total concentration of uranium(IV) is

$$B = b(1+\beta_1 h^{-1}+\sum(n+1)k_n u^n) \qquad (19)$$

and the concentration of OH bound by uranium(IV) is

$$BZ = \beta_1(h^{-1}+3\sum nk_n u^n) \qquad (20)$$

We shall introduce the auxiliary normalized variables

$$\alpha = \beta_1 h^{-1};\ \mathbf{B} = k\beta_1^{-3}B;\ v = ku \qquad (21)$$

and the function $g(v) = \sum k_n u^n;\ vg'(v) = \sum nk_n u^n$ (22)

For the special case of hypothesis IIIa (with an integer value of t) we have

$$g(v) = k_0 v(1-v)^{-1};\ vg'(v) = k_0 v(1-v)^{-2} \qquad (22a)$$

Introducing (21) and (22) we find from (19) and (20)

$$B = b(1+\alpha+g+vg');\ BZ = b(\alpha+3\ vg') \qquad (19a,\ 20a)$$

$$\mathbf{B} = v\alpha^{-3}(1+\alpha+g+vg');\ \mathbf{B}Z = v\alpha^{-3}(\alpha+3\ vg') \qquad (19b,\ 20b)$$

The method consists in preparing a projection map of the experimental data in the form of curves $y(x)_Z$, with the experimental variables

$$x = \log B - 3 \log h;\ y = \log B \qquad (23)$$

This plot is moved parallel to the axes across a projection map of calculated curves $Y(X)_Z$ where the normalized variables are

$$X = \log \mathbf{B}\alpha^3 = x+\log k; \qquad Y = \log \mathbf{B} = y+\log k - 3 \log \beta_1 \qquad (24)$$

In the position which gives the best fit one can at once read the best values of $X-x = \log k$ and $Y-y = \log k - 3 \log \beta_1$

For calculating the normalized projection map one may eliminate α from (19a) and (20a), to find

$$\alpha = (Z(1+g+vg')-3\ vg')(1-Z)^{-1} \qquad (25)$$

$$X = \log v+\log\ (1+g-2\ vg')-\log(1-Z) \qquad (26)$$

$$Y = X-3 \log \alpha = \log v+2 \log(1-Z)+\log(1+g-2\ vg')-$$

$$-3 \log(Z(1+g+vg')-3\ vg') \qquad (27)$$

Thus for a constant value of Z, corresponding values of X and Y can be calculated for various values of the auxiliary variable v. On applying this method (always using $k_0 = 0.01$) and (21a) we found

$$\log k = X-x = -3.40 \pm 0.10 \qquad (28)$$

$$\log k - 3 \log \beta_1 = Y-y = 2.5 \pm 0.3$$

$$\log \beta_1 = -1.95 \pm 0.10$$

The constants k and β_1 can be determined independently from the η titrations, also using normalized projection maps [14]. In this case, an experimental plot $\log B(\log h)_\eta$ and calculated curves $\log \mathbf{B}(\log \alpha)_\eta$ were used. From (19a) and (19)

$$\eta = \log(1+\alpha+g+gv');\ \alpha = 10^\eta - (1+g+vg') \qquad (29)$$

and from (19b)

$$\log \mathbf{B} = \log v+\eta-3 \log \alpha \qquad (30)$$

From the positions of best agreement, we found

$$\log k = \log \mathbf{B} - \log B = -3.30 \pm 0.05$$

$$\log \beta_1 = \log \alpha - \log h = -2.00 \pm 0.10$$

In order to test whether some other value of k_0 could be used successfully, the family of curves $y(x)_Z$ was constructed from the experimental data, when $x = \log B - 3 \log h$ and $y = \log B$. This diagram was compared with projection maps of calculated curves when k_0 was 0.00 and 0.20. These two values could be eliminated in the region of vertical lines, their spacing in the calculated projection map was much too narrow with $k_0 = 0$, and too broad with $k_0 = 0.20$.

A diagram $\log k(\log \beta_1)$ was made in which for each value of $\log k$, the range of $\log \beta_1$ which gave the best fit with the Z and η data, was marked out. From the common area, a middle set and two extreme sets were selected:

$\log k = -3.30$,	$\log \beta_1 = -2.00$
-3.37	-1.98
-3.45	-1.95

With these three sets, theoretical curves $Z(\log h)_B$ were calculated for the different B values used in the Z titrations with hydrogen and glass electrodes. The second (full-drawn) and the third (broken) sets gave the best agreement (Figs. 1 and 3).

The same three sets of constants were also used to calculate curves $\eta(\log h)_B$ (Fig. 4) for the B values used in the titrations. Here also, the second and third set gave the best agreement. It may thus be assumed that

$$\log k = -3.4 \pm 0.1;\ \log \beta_1 = -2.0 \pm 0{,}1;\ \log k_0 = -1.2 \pm 0.3$$

The constant of the mononuclear reaction, β_1, agrees reasonably well with Kraus's constant [2] $\log \beta_1 = -1.63$ in 2 M perchlorate solution. The constant $\log \beta_1 = -1.63$ in 2 M perchlorate is somewhat higher than $\log \beta_1 = -2.0 \pm 0.1$ in 3 M perchlorate as one would expect, especially when one compares it with the constants of Kraus [2] at other ionic strengths:
$\log \beta_1 = -1.56$ for 1 M, $= -1.45$ for 0.55 M, and $= -1.23$ for 0.1 M ClO_4^-
It was tested whether the experimental data could be explained by assuming only the second mononuclear complex $U(OH)_2^{2+}$. The projection map $\log \mathbf{B}(X)_Z$ was calculated when

$$\mathbf{B} = v\alpha^{-3}(1+\alpha^2+g+vg') \quad (31)$$

$$\mathbf{B}Z = v\alpha^{-3}(2\alpha+3\ vg') \quad (32)$$

The experimental data $\log B(x)_Z$ were compared with these curves. The fit was somewhat satisfactory with the high Z values but not with the low Z values.

Then it was assumed that both the mononuclear complexes UOH^{3+} and $U(OH)_2^{2+}$ are formed. The projection map (14) $\log \mathbf{B}\ (X)_Z$ was constructed for

$$\log\ \mathbf{B} = \log v + \log (1+\alpha+l\alpha^2+g+vg') - B \log \alpha \quad (33)$$

$$X = \log v + \log (1+\alpha+l\alpha^2+g+vg') \quad (34)$$

Here $l = \beta_2\beta_1^{-2}$ (35)

where β_1 is the equilibrium constant for the reaction

$$U^{4+} + H_2O \rightleftharpoons U(OH)_2^{2+} + 2H^+ \quad (36)$$

The statistical value $l = 1/4$ was assumed, which means that both protons are split off equally easily. As before, g was taken from (22 a).

The agreement of experimental data with these theoretical curves was somewhat less satisfactory than with the curves when only the first complex UOH^{3+} was assumed. The following constants were calculated from glass electrode and hydrogen electrode measurements.

$$\log \beta_1 = -1.7 \pm 0.2$$
$$\log \beta_2 = -4.0 \pm 0.2$$

The data of the redox electrode measurements were treated in the same way. Only the second complex was at first assumed and the projection map was calculated when

$$\log \alpha = \tfrac{1}{2} \log (10^{\eta} - (1 + g + vg')) \quad (37)$$

and

$$\log \mathbf{B} = \log v + \eta - 3 \log \alpha \quad (38)$$

The experimental data did not fit in this case either and therefore the both complexes with $l = 1/4$ were assumed. The projection map was constructed with

$$\log \mathbf{B} = \log v + \log (1 + \alpha + l\alpha^2 + f + vg') - 3 \log \alpha \quad (39)$$

$$\log \alpha = \log (2\sqrt{1 - (1 + g + vg' - 10^{\eta})} - 2); \quad \eta = \log \frac{B}{b} \quad (40)$$

Also here the fit was not so good as with the assumption that only one mononuclear complex UOH^{3+} is formed. The constants obtained on testing were:

$$\log \beta_1 = -1.7 \pm 0.1$$
$$\log \beta_2 = -4.0 \pm 0.1$$

Influence of uranium (V). In the previous calculations on the η titration data, the presence of uranium(V), UO_2^+, was neglected. According to Kraus [15], $K = 9.6 \times 10^7$ for the reaction $2\,UO_2^+ + 4\,H_3O^+ \rightleftharpoons UO_2^{2+} + U^{4+} + 6\,H_2O$ in 1.96 M perchlorate medium; a specific solution contained 0.361 mM U(IV), 0.536 mM U(V), 2.41 mM U(VI), and 4.95 mM H^+. A rough calculation, using $K = 10^9$, indicates that appreciable amounts of U(V) are present in solutions which contain both U(IV) and U(VI) and $[H^+]$ approximately equal to or less than 10 mM. Then the correct $\eta(x)_B$ curves would be slightly to the left of these now used. The correction would in our experiments be at most of an order of magnitude corresponding to about 1 mV in E_r, which is still within the limits of the experimental error.

STRUCTURE OF THE COMPLEXES

The equilibrium data give no information about the shape of the complexes $U((OH)_3U)_n^{(4+n)+}$. Lundgren [16,17] has studied the crystal structures of two uranium(IV) hydroxide sulfates. In $U_6O_4(OH)_4(SO_4)_6$ he found separate groups, $.U_6O_4(OH)_4^{12+}$; on the other hand, in $U(OH)_2SO_4$ he found infinite chains $(U(OH)_2^{2+})_n$, which are analogous to the chains in the isomorphous compound $Th(OH)_2SO_4$.

It therefore seems reasonable to assume that the uranium(IV) complexes are thread-like, $U(^{O}_{OH}U)_n^{4+n}$, by analogy with the thorium structure.

Acknowledgements. The author is greatly indebted to Professor Lars Gunnar Sillén for many valuable discussions in connection with this work. The author also wishes to thank fil.lic. George Biedermann and fil.lic. Georg Lundgren for helpful suggestions. Mr Frans Ericson is thanked for his help in connection with the equipment.

Thanks are due to Dr Hazel Rossotti, Dr Francis Rossotti and Mr D. G. Gillam for helpful comments during the correction of the English text.

This work has been financially supported by *Atomkommittén (Swedish Atomic Energy Committee)*.

REFERENCES

1. Lawrence, R. W. *J. Am. Chem. Soc.* **56** (1934) 776.
2. Kraus, K. A. and Nelson, F. *J. Am. Chem. Soc.* **72** (1950) 3901.
3. Kraus, K. A., Nelson, F. and Johnson, G. L. *J. Am. Chem. Soc.* **71** (1949) 2510.
4. Kraus, K. A. and Nelson, F. *J. Am. Chem. Soc.* **77** (1955) 3721.
5. Ahrland, S., Hietanen, S. and Sillén, L. G. *Acta Chem. Scand.* **8** (1954) 1907 (Part X).
6. Rosenheim, A. and Loebel, H. *Z. anorg. Chem.* **57** (1908) 234.
7. Hietanen, S. *Acta Chem. Scand.* **8** (1954) 1626 (Part IX).
8. Hamer, W. J. and Acree, S. F. *J. Research Natl. Bur. Standards* **33** (1944) 87.
9. Forsling, W., Hietanen, S. and Sillén, L. G. *Acta Chem. Scand.* **6** (1952) 901 (Part III).
10. Rodden, C. J. and Warf, J. C. *Natl. Nuclear Energy Ser.* **VIII—I** (1950) 68.
11. Ahrland, S. and Larsson, R. *Acta Chem. Scand.* **8** (1954) 137.
12. Sillén, L. G. *Acta Chem. Scand.* **8** (1954) 318 (AB II).
13. Hietanen, S. and Sillén, L. G. *Acta Chem. Scand.* **8** (1954) 1607 (Part VIII).
14. Biedermann, G. and Sillén, L. G. *Acta Chem. Scand.* **10** (1956) 1011.
15. Nelson, F. and Kraus, K. A. *J. Am. Chem. Soc.* **73** (1951) 2157.
16. Lundgren, G. *Arkiv Kemi* **5** (1953) 349.
17. Lundgren, G. *Arkiv Kemi* **4** (1952) 421.

Received August 13, 1956.

ACTA CHEMICA SCANDINAVICA 10 (1956) 1547—1552

Incorporation of ^{59}Fe into Different Iron Compounds of Liver Tissue

ROBERT B. LOFTFIELD* and ROGER BONNICHSEN

Biochemical Department, Medical Nobel Institute and Wallenberg Laboratory of Physiological Chemistry, Stockholm, Sweden

Techniques are described for isolating and radioassaying the iron of individual iron proteins from rat liver. These compounds include two ferritins, catalase, cytochrome b and cytochrome c.

After intraperitoneal injection of ^{59}Fe, radioactivity appears most rapidly in supernatant ferritin, followed by microsome ferritin, cytochrome b and catalase. After four hours, cytochrome b is the most radioactive.

It is suggested that the injected iron reaches the liver over a period of several hours. Because only a part of the iron of ferritin is labile, the average specific activity of ferritin iron does not rise as high as that of intracellular free iron. Cytochrome b which appears to have a turnover time of only a few hours more nearly reflects the free iron specific activity. It is possible that cytochrome b is a precursor of catalase.

There have been several reports of the use of radio-iron to study iron metabolism *in vivo*[1-4]. The techniques used for isolation of individual iron compounds and the rather low specific activity of the iron employed have limited the conclusions to be drawn. By restricting our investigation to a single rather homogeneous organ, rat or guinea pig liver; by utilizing the Hogeboom-Schneider [5] cell fractionation; by using high specific activity iron; and by developing new isolation methods for the iron containing proteins, we hoped to get a closer view of iron metabolism than has heretofore been possible. Following a single injection of radio-iron, ferritin has been isolated from the microsomes and from the 105 000×g supernatant fraction, cytochrome b from the microsomes, cytochrome c from the mitochondria, and catalase from the supernatant fraction and mitochondria. The radio-iron content of these substances has been followed from one hour to fourteen hours.

EXPERIMENTAL

Iron determination. Each substance to be examined was digested with sulfuric acid and hydrogen peroxide and the total iron was determined using the sulfosalicylic acid method [6,1]. In each case additional ferric sulfate was added to bring the total amount to

* Damon Runyon fellow.

500 μg and all the iron was then precipitated as iron sulfide by saturating the solution with hydrogen sulfide. The iron sulfide was filtered on hard paper and assayed with a shielded end-window counter. Under these conditions the counting efficiency for ^{59}Fe was about 3 %.

Table 1. Iron distribution in liver tissue.

	3 rat livers 16 g	3 rat livers 17 g	4 guinea pig livers 191 g	4 guinea pig livers 208 g
Nw. fraction	0.74 mg iron	0.92	2.4	2.4
Mtw. fraction	0.47	0.50	0.81	0.8
Microsomes	1.14	1.30	1.9	1.9
Microsome ferritin	1.10	1.17	0.9	0.8
Supernatant ferritin	2.05	2.80	1.6	1.0
Cytochrome b (hemin iron)	0.029	0.037	0.218	0.22

Fractionation. The rats used were between four and six months old and weighed between 150 and 200 g. They had been on a high iron diet for at least three months. 20 000—100 000 counts per min. of ^{59}Fe (1—5 μg of Fe as ferric ammonium citrate) was administered intraperitoneally to each animal. After the chosen time three to five animals were sacrificed, the livers excised and homogenized in 0.25 M sucrose solution. Fractionation according to the method of Hogeboom and Schneider [5] yielded a nuclear fraction (10 min. 700 × g sediment), mitochondrial fraction (10 min. 5 000 × g sediment), microsomal fraction (40 min. 100 000 × g sediment), and a soluble fraction (100 000 × g supernatant). Table 1 shows average values for the iron content of these fractions and for several iron-proteins.

Supernatant ferritin. To the 100 000 × g supernatant was added one half its volume of saturated ammonium sulfate. The supernatant was saved for isolation of catalase. The precipitate was dissolved in water, repeatedly fractionated with ammonium sulfate (25 to 35 %), and eventually dissolved in water. The solution was heated 5 min. at 70°, and centrifuged to yield a clear solution of ferritin containing between 17 and 20 % iron. When 2 % of cadmium sulfate was added to a very concentrated solution of this ferritin, part crystallized as shown in Fig. 1.

Microsome ferritin. The microsomes were suspended by homogenization in ten volumes of water and the pH was adjusted to 5 by addition of acetic acid. After 30 min., the

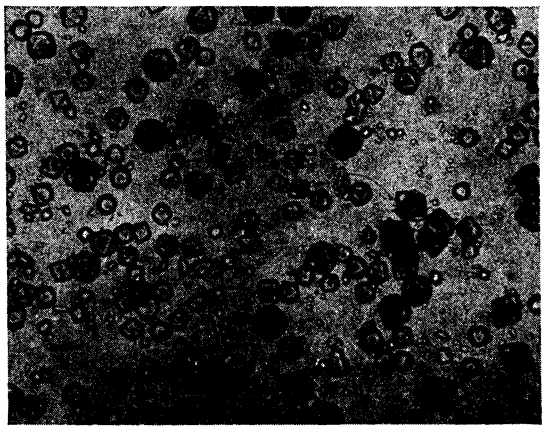


Fig. 1. Rat ferritin crystallized from cadmium sulfate (350 ×).

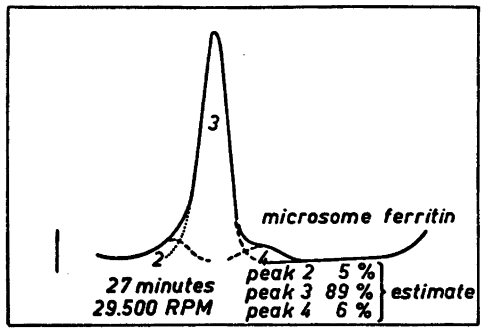


Fig. 2. Ultracentrifugation of microsome ferritin.

suspension was centrifuged and the supernatant was decanted. The sediment was extracted once more with water. The combined supernatants were treated as the supernatant above to isolate the microsome ferritin. This contained 18 to 22 % iron.

Cytochrome b. The sediment remaining after extraction of the ferritin from the microsomes could be solubilized with desoxycholic acid. In agreement with Strittmatter and Ball [7] the only photometrically detectable cytochrome was cytochrome b. Pyridine hemochromogen determinations confirmed this observation. Routinely the extracted microsomes were treated with 1:1 000 HCl-acetone which releases the hemin. The acetone solution was filtered, concentrated and partitioned between water and *peroxide-free* ether. The ether phase was evaporated and ^{59}Fe was determined.

Catalase. To the 100 000 × g supernatant from which ferritin had been isolated more ammonium sulfate was added to 60 % saturation. The precipitate was dissolved in 0.1 M phosphate buffer, pH 7.0, and dialyzed against the same buffer. Four volumes of the dialyzed solution were shaken with one volume of chloroform ethanol (1:3). This denatures all of the hemoglobin present. After centrifugation, the supernatant solution was heated to precipitate the catalase. The precipitate was treated with HCl-acetone and worked up like the cytochrome b. Catalase could also be isolated in the same fashion from the mitochondria.

Cytochrome c. A suspension of mitochondria was adjusted to pH 4.2 with 1.0 N H_2SO_4 and allowed to stand at 4° for one hour. After centrifugation the solution was adjusted to pH 7.0 with 1.0 N NH_4OH and again centrifuged. The clear solution was passed through

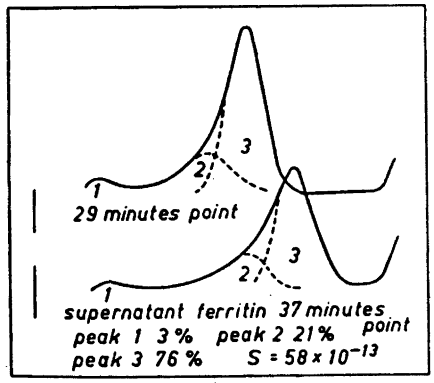


Fig. 3. Ultracentrifugation of supernatant ferritin.

a 4 × 1 cm column of Amberlite XE-69 in the ammonium form. (We are indebted to Rohm and Haas, Inc., and to their associates Chas. Lemming and Co., Ltd., for gifts of this material). All of the cytochrome c is retained by the upper part of the column while hemoglobin and other pigments pass through. After washing with about 20 ml of water, the cytochrome c is eluted with about 4 ml of 1 N sodium sulfate. After reduction with dithionite, cytochrome c was determined by its absorption at 550 mμ. Radio-iron was determined as described above.

RESULTS AND DISCUSSION

Although the isolation of ferritin from rat liver has not been described previously, it was not surprising that ferritin could be obtained. Interestingly, ferritin prepared in this manner from both the microsomes and from the supernatant fraction, gives very sharp peaks in the ultracentrifuge in contrast to previous observations on other ferritins [8] (Figs. 2 and 3). Nonetheless, both of our ferritins give sedimentation constants of 58 and 60×10^{-13} in essential agreement with other workers. Occasionally, we observe in the "supernatant ferritin" a small amount of a colorless protein with a sedimentation constant about 7.5 or 10×10^{-13}. This may be due to apoferritin. The electrophoretic mobilities of our two ferritins are within about 10 % of each other at pH 6.0 namely $-2.2\ u \times 10^{-5}$ for microsome and $-1.95\ u \times 10^{-6}$ for supernatant ferritin. (Figs. 4 and 5).

The radioactivity data is summarized in Table 2 and Fig. 6. The ratios of specific activities at each time interval are quite significant. It appears that ^{59}Fe reaches the liver rather slowly over a period of as much as ten hours. The activity reaching the liver is first incorporated into the "supernatant ferritin" more than twice as rapidly as into the microsome ferritin. This may be compared with earlier observation [9] that ^{14}C-leucine is incorporated into supernatant ferritin ten times as rapidly as into microsome ferritin in a 20 min. period and supports our belief that these two ferritins are biochemically distinct. With the passage of time, iron atoms or perhaps entire ferritin molecules move from the supernatant ferritin pool to the microsome ferritin pool and from ten hours onward the specific activities in each fraction are essentially the same.

It is extremely interesting that the specific activity of the cytochrome b is lower than either ferritin at first and then higher than either. Obviously, the

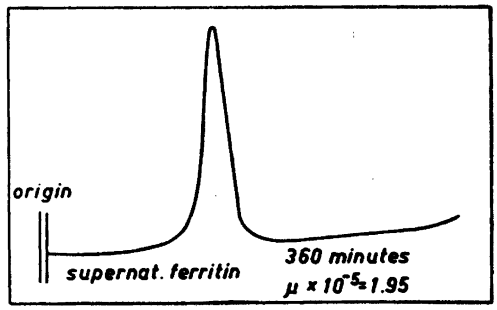


Fig. 4. Electrophoresis of supernatant ferritin.

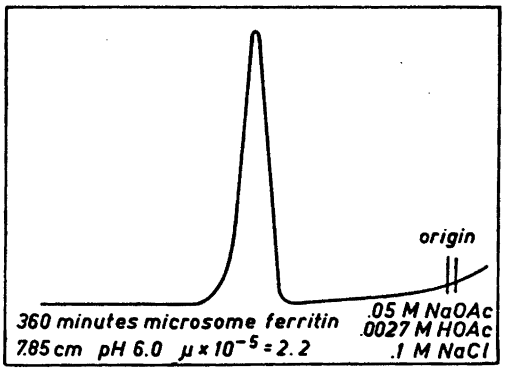


Fig. 5. Electrophoresis of microsome ferritin.

specific activities of all iron precursor substances must have been as high or higher than that of cytochrome b at its highest point. Ultimately, this requirement includes free iron. It would appear that free iron entering the liver is very rapidly picked up or equilibrated with a small amount of the ferritin iron. Accordingly, in the early phase there is a nearly linear rise in the average specific activity of the ferritins and in the total activity of the ferritins, which include about half of the iron of the liver. Because the superficial or most labile ferritin iron (which is in equilibrium with the free iron) is not rapidly equilibrated with the more deeply "buried" iron of the ferritin, the specific activity of the free iron is at all early times higher than the average activity of ferritin iron atoms. Substances synthesized more or less directly from free iron might be expected to reflect the rapid rise in free iron activity to levels much higher than the ferritin average. Cytochrome b appears to be such a substance.

The very high incorporation rate of cytochrome b is made doubly interesting because this substance is found in the microsomes where the bulk of the cell's protein synthetic activity is located. Cytochrome b has as yet no well defined cell function. Perhaps it is a precursor of one or several hemoproteins. If cytochrome b were the precursor of catalase, one might expect the peak of the catalase curve to come at the point that the two curves intersect. This is obviously not the case, but possibilities such as the presence of comparatively

Table 2. Specific activity of the isolated iron compounds in counts per min. per μg Fe from guinea pig livers.

	Minutes						
	80	195	240	320	675	1 170	1 440
Microsome ferritin	0.115	0.251	0.364	0.497	0.335	0.237	0.271
Supernatant ferritin	0.255	0.386	0.350	0.554	0.440	0.374	0.338
Cytochrome b hemin iron	0.055	0.305	0.396	0.983	0.700	0.621	0.528
Catalase	0.029	0.061	0.089	—	0.297	0.268	0.281

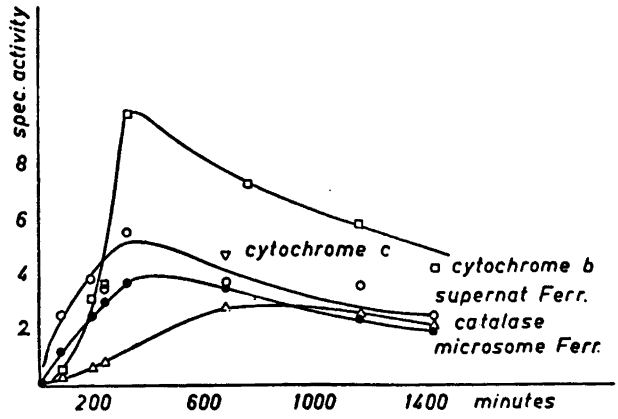


Fig. 6. Specific activity (counts per minutes per μg Fe) of the different iron compounds of liver. The animals were sacrificed 30—1 400 minutes after the injection.

radioactivity inert blood catalase [1] or inert catalase-like substances in the cell extract tend to reduce the observed specific activity of liver catalase by dilution. Hence it is still presumptuous to exclude cytochrome b as a precursor of catalase.

A final noteworthy observation concerns the rather short time required to reach maximum specific activity in each substance in comparison to previous observations [1]. This may very well be due to the much smaller doses of iron and hence the much shorter time required to bring free iron in the liver to its maximum specific activity. From our data we believe that the turnover time of cytochrome b is sufficiently short to permit its being an important precursor of hemoproteins. In turn it is possible that the turnover time of catalase may be short enough to account for the rapid disappearance of catalase on tumor implantation [10]. Liver catalase may also be released to provide part of the blood catalase. The single cytochrome c point serves only to show that liver cytochrome c must also have a rather high turnover rate.

Acknowledgenemt. This work was supported by *Statens Naturvetenskapliga Forskningsråd.*

REFERENCES

1. Theorell, H., Béznak, M., Bonnichsen, R., Paul, K.-G. and Åkeson, Å. *Acta Chem. Scand.* **5** (1951) 445.
2. Granick, S. and Hahn, P. F. *J. Biol. Chem.* **155** (1944) 661.
3. Stevens, A. R., Jr., White, P. L., Hegsted, D. M. and Finch, C. A. *J. Biol. Chem.* **203** (1953) 161.
4. Granick, S. *Physiol. Rev.* **31** (1951) 489.
5. Schneider, W. C. *J. Biol. Chem.* **176** (1948) 259.
6. Lorber, F. *Biochem. Z.* **181** (1927) 391.
7. Strittmatter, C. F. and Ball, E. G. *Proc. Natl. Acad. Sci. U.S.* **38** (1952) 55.
8. Rothen, A. *J. Biol. Chem.* **152** (679) 1944.
9. Loftfield, R. B. *Federation Proc.* **13** (1954) 1525.
10. Greenstein, J. P. and Andervont, H. B. *J. Natl. Cancer Inst.* **4** (1943) 283.

Received August 17, 1956.

ACTA CHEMICA SCANDINAVICA 10 (1956) 1553—1556

Changes in Glycogen and Nitrogen-containing Compounds in *Escherichia coli B* during Growth in Deficient Media

II. Phosphorus and Sulphur Starvation

T. HOLME and H. PALMSTIERNA

Bacteriological Department and Chemical Department I, Karolinska Institutet, Stockholm, Sweden

The glycogen per dry weight and litre of culture did not increase during the starvation phase in phosphorus-starved cultures to the same extent as in nitrogen-starved ones. An addition of phosphate to the phosphorus-starved cultures caused an immediate increase in the rate of glycogen synthesis, followed by a decrease when the rate of synthesis of nitrogen-containing compounds increased.

Some basic mechanism involving the syntheses of both nitrogen-containing compounds and glycogen seemed to be affected during the starvation phase in sulphur-deficient cultures.

In a preceding article [1] experiments have been described which deal with the chemical composition of *Escherichia coli B* starved of the nitrogen or carbon sources. In this paper the observations have been extended to cells starved of the phosphorus or sulphur sources. As in the experiments previously described, the changes in the chemical composition of the cells after addition of the limiting factor was also investigated.

METHODS

The media used in these experiments were modified from Friedlein's salt-sodium lactate medium [2]. In the experiments with the phosphorus source as the limiting factor, the initial concentration of phosphate (KH_2PO_4) was 7.4×10^{-2} M. Instead of the phosphate buffer, 2×10^{-2} M tris(hydroxymethyl)-aminomethane was used. Growth curves of cultures in non-limited media were not affected by this concentration of "tris" buffer. The medium was made 1.3×10^{-2} M with regard to the potassium concentration by adding KCl. After sterilisation, the pH of the medium was 7.0. In the experiments in which the sulphur source was the limiting factor, the initial concentration of the sodium sulphate was 7.0×10^{-5} M. Instead of magnesium sulphate, magnesium chloride was added.

After a certain period of starvation, an amount of the limiting factor was added to the cultures in order to give them the same concentration as in the complete medium. In the event of phosphorus starvation, the phosphate buffer of the Friedlein medium was added. To the sulphur-starved culture, sodium sulphate was added.

The cultivation techniques and chemical methods were the same as those previously described [1].

RESULTS

Phosphorus starvation. (Expts. E and F, Table 1). The duration of the lag phase was about the same as in the complete medium. A starvation phase, characterized by an almost constant cell concentration, followed after an initial multiplication period. The dry weight of cells during the starvation phase was in expt. E 165 mg, and in expt. F 185 mg per litre of culture. After the addition of the limiting factor, a difference occurred in the behaviour of the two cultures. In expt. E there followed a phase of rapid cell division during the first 30 min. after the addition, whereupon a cell division lag of about one hour's duration was noted, followed by a further cell division period. The dry weight of the cells per litre of culture increased independantly.

In expt. F the cell division rate was low during the first hour after the addition of the limiting factor. Then there was a period of more rapid cell division lasting for about two hours before the culture reached the stationary phase.

The glycogen in per cent of the dry weight did not reach the same high values as in nitrogen-starved cultures [1]. These values varied between 1 and

Table 1. Phosphorus starvation.

Expt.	Time after inoculation, min.	Cells per ml × 10^{-6}	Dry weight of cells per litre of culture (mg)	Glycogen-glucose per litre of culture (mg)	Protein-N per litre of culture (mg)	Cold TCA-N per litre of culture (mg)	Hot TCA-N per litre of culture (mg)
E	0	1.0					
	90	1.2					
	120	2.5					
	160	3.6					
	185	3.7	137.4	1.4	13.7	0.8	4.5
	250	4.3	165.4	2.4	16.7	1.3	4.7
	250	addition of phosphate					
	255	5.9	172.2	5.0	16.0	1.2	4.9
	265	7.8	190.4	4.7	18.6	1.2	5.6
	280	9.6	201.3	5.2	19.1	1.2	6.3
	300	10.3	225.8	4.3	21.7	1.5	7.4
	325	10.6	287.2	3.7	28.4	2.3	9.8
	370	12	379.7	4.1	37.4	3.2	12.3
	430	18	490.3	4.5	49.7	2.8	15.1
	540	21	625.6	5.5	59.9	4.4	19.0
F	0	0.9					
	90	1.0					
	150	2.2					
	240	5.0	132.0	5.0	12.4	0.9	4.0
	270	7.4					
	300	7.4					
	345	7.4	184.8	11.6	16.4	1.4	4.1
	345	addition of phosphate					
	350	7.4	184.2	12.9	16.0	1.3	4.2
	360	7.8	183.4	13.9	15.6	1.3	4.3
	375	7.8	202.2	15.6	16.7	1.5	5.8
	395	8.7	232.3	15.3	19.2	1.8	6.5
	420	9.8	265.0	11.4	22.6	2.1	7.8
	525	22.5	413.8	10.3	37.4	3.4	12.5

Table 2. Sulphur starvation.

Expt.	Time after inoculation, min.	Cells per ml $\times 10^{-8}$	Dry weight of cells per litre of culture (mg)	Glycogen-glucose per litre of culture (mg)	Protein-N per litre of culture (mg)	Cold TCA-N per litre of culture (mg)	Hot TCA-N per litre of culture (mg)
G	0	0.9					
	90	1.1					
	150	2.9					
	210	5.7					
	240	6.0	203.6	1.8	18.9	1.4	6.8
	270	6.7					
	300	7.8	272.7	2.6	25.8	2.1	8.5
	300	addition of sodium sulphate					
	305	9.5	279.9	4.0	26.1	1.5	8.6
	315	10	291.6	3.1	26.9	2.0	9.3
	330	11	309.3	3.0	29.4	2.3	9.6
	350	13	347.0	3.2	32.3	2.5	10.7
	375	15	412.9	3.5	38.5	3.1	13.0
	480	27	652.7	5.1	57.8	4.7	18.7
	660	43					
H	0	1.0					
	135	1.8	66.8	2.3			
	180	3.6	111.9	3.0			
	225	5.0	175.9	3.2			
	225	addition of sodium sulphate					
	230	8.0	187.9	3.9			
	240	8.3	204.0	4.5			
	265	10	259.8	4.4			
	315	19	441.8	6.6			
	375	37	860.0	16.3			

4 % of the dry weight at the beginning of the starvation phase, and increased approximately 1.5 times during the first hour of this phase (four experiments). The addition of phosphate was followed within five minutes by a very rapid increase in the rate of glycogen synthesis. Total glycogen (glycogen per dry weight and litre of culture) reached a maximum in about 30 min. from the addition of the limiting factor. The maximum rate in the glycogen increase observed immediately after the addition coincided with a lag in the synthesis of nitrogen-containing compounds. When the synthesis of these compounds was resumed, the total glycogen decreased.

Sulphur starvation. (Expts. G and H, Table 2). During the starvation phase in the sulphur-starved cultures, the dry weight of cells per litre of culture continued to increase, but at a low rate in comparison with the rate in non-limited cultures. In expt. G the cell concentration increased from 5.7 to 7.8×10^8 cells per ml during the starvation phase, which was interrupted after about one hour by the addition of sodium sulphate. After this addition there was a small increase in glycogen in per cent of the dry weight during the first five minutes, but it is doubtful whether it is significant. In fact, the glycogen in per cent of the dry weight remained in the neighbourhood of the lowest values observed in cultures grown in lactate media. When the limiting factor was added after at least one hour's starvation, the rate of increase in the dry

weight remained at the same low level as during the starvation phase (expt. G). If, however, the addition was made at the moment when the starvation phase was expected to begin (expt. H), the increase in dry weight per litre of culture proceeded at about the same rate as during the logarithmic phase in non-limited cultures, grown in lactate medium.

No significant increase in the absorption between 220 and 310 mμ of the cell-free culture medium was observed during phosphorus or sulphur starvation.

DISCUSSION

In previous experiments it was shown [1] that glycogen accumulated rapidly in cultures of *Escherichia coli B* when the synthesis of nitrogen-containing compounds was prevented by nitrogen starvation.

During the starvation phase in phosphorus-starved cultures, there was a considerable difference in glycogen in per cent of the dry weight between different cultures, but the glycogen values never reached the high values observed in nitrogen-starved cultures. There was, however, a slow increase in total glycogen during the starvation phase. During the lag in the synthesis of nitrogen-containing compounds following the addition of phosphate, there was an immediate increase in the rate of glycogen synthesis, showing that it was a lack of phosphate that caused the comparatively low increase in glycogen during the starvation phase. As in all other cases tested, the decrease in total glycogen that followed coincided with an increased rate of synthesis of nitrogen-containing compounds.

As shown in expt. E (Table 1), a synchronous cell division occurred immediately after the addition of phosphate, *i.e.* the cell count was doubled in about 20 min. This was followed by a cell division lag of about one hour's duration, which was followed in turn by a new cell division period. This result indicates that it may be possible to obtain simultaneous cell divisions by using the phosphate starvation technique.

Sulphur starvation caused a slowing down of the synthesis of nitrogen-containing compounds as well as of the glycogen synthesis (expt. G). The fact that these syntheses proceeded at a relatively slow rate even after the limiting factor had been added, indicates that some basic mechanism was affected. It seems probable that this change in the cells occurred during the starvation phase, since the addition of sulphate at the beginning of this phase rendered possible a synthesis of these substances at the same rate as in non-limited cultures.

REFERENCES

1. Holme, T. and Palmstierna, H. *Acta Chem. Scand.* **10** (1956) 578.
2. Friedlein, F. *Biochem. Z.* **164** (1928) 273.

Received August 27, 1956.

ACTA CHEMICA SCANDINAVICA 10 (1956) 1557—1562

On the Glycogen in *Escherichia coli B*; its Synthesis and Breakdown and its Specific Labeling with ^{14}C

T. HOLME and H. PALMSTIERNA

Bacteriological Department and Chemical Department I, Karolinska Institutet, Stockholm, Sweden

A technique has been devised by which it is possible to label the glycogen in *E. coli B* cells with ^{14}C without labeling the protein to any appreciable extent.

It has been shown that those glucose residues that were the last to be incorporated during a net synthesis of glycogen in *E. coli B*, were the first to be split off by the cells when the conditions were changed in order to cause a breakdown of the glycogen.

If there is a pool of substances on the pathway from medium glucose towards glycogen, this pool will not be large enough to cause any measurable dilution of the medium glucose, when it is incorporated in the glycogen.

It appears that cells in the starvation phase in a nitrogen-starved culture do not break down glycogen simultaneously as they synthesize it.

After the injection of ^{14}C-labeled glucose into rats, Stetten and Stetten [1] found that after a short interval the rat liver glycogen was predominantly labeled in those glucose residues that were the first to be split off by enzymic degradation of the glycogen.

The methods employed by us [2,3] have made possible investigations of the synthesis and breakdown of glycogen in metabolizing bacterial cells. *Escherichia coli B* cells accumulate glycogen during nitrogen starvation. During the last part of this accumulation phase the carbon source was labeled with ^{14}C. The conditions were thereupon changed, so as to make the cells break down part of the glycogen that had accumulated. The results indicate that also in this case those glucose residues that were last incorporated in the glycogen were the first to be split off when the glycogen was degraded, in our case, by the cells.

METHODS AND RESULTS

Nitrogen-starved cultures of *E. coli B* were prepared as previously described [2]. Instead of Friedlein's sodium lactate-salt medium, the glucose-salt medium devised by Hook and coworkers was used [4]. The glucose concentration was 1 g/l instead of 4 g as in the original medium. This reduction had no influence on the length of the lag phase nor on the mean generation time in the log phase. It was possible to starve the cells of the nitrogen source by reducing the concentration of ammonium chloride to 50 mg/l of medium. As in nitrogen-starved cultures grown in lactate medium, the dry weight of cells per litre of culture remained constant during the starvation phase.

During the starvation phase, totally labeled ^{14}C-glucose was added to the culture, and the phase was allowed to proceed for another 45 min. in the labeled medium. The cultivation was then interrupted by cooling the culture rapidly to 4°C. The cell suspension was divided into two equal parts which were centrifuged separately. The wet weight of the cells obtained from these centrifugations [5] was the same for both portions. One portion was taken for analysis, and the cells of the other were incubated for a further 90 min. in a medium from which the glucose had been totally omitted. It contained the same amount of ammonium chloride as the complete medium. The sample taken at the end of this incubation period is called +90 (Table 1). Prior to inoculation the cells were washed once with the medium in which they were to be inoculated. During the nitrogen starvation an increase in ultra violet absorption of the cell-free culture medium was observed, just as in lactate-grown, nitrogen-starved cultures [3]. No such absorption was observed in the glucose-free medium. The results are summarized in Table 1 (expt. A).

Cells that had not been subjected to nitrogen starvation were also used (expt. B, Table 2). Cells from an 18 hours' praeculture in the complete medium were harvested and washed, and then inoculated into an ammonium chloride-free medium (volume: 6 l). The incubation was interrupted by cooling after 10 min. The cells were centrifuged and reincubated in a fresh medium (volume: 4 l) of the same composition, but in this case the glucose was totally labeled with ^{14}C. After an incubation period of 30 min. the culture was cooled and the cells centrifuged and washed. Then they were inoculated into a medium (volume: 2 l) containing ammonium chloride in excess (1 g/l) but no glucose, the incubation lasting in this case 60 min. The results are shown in Table 2.

Prior to inoculation into a new medium, the cells were washed once in the medium in which they were to be incubated. In both experiments the initial culture volume was 6 l. Each analysis is based on cells taken from about one third of the culture. When reinoculating cells into a new medium, the volume of this new medium was always the same as that from which they were harvested. In all particulars other than those described in the present paper, the methods employed were the same as those previously reported [2,3,5].

The results obtained from a nitrogen-starved culture with lactate as the carbon source are reproduced in Fig. 1. Isotopic lactate was added in the same way as described in expt. A. The cells treated in this way were incubated in a medium free of lactate, but containing the nitrogen source in excess. The methods and results have already been described in a preliminary paper [2] (expt. C).

Table 1. Experiment A.

Time after inoculation in min.	Glycogen-glucose per litre of culture (mg)	Counts per min. per μg	
		glycogen carbon	protein carbon
0	1.0	—	—
130	11.0	0	0
175	13.4	113	6
+90	10.2	23	24

The isotope was added at 130 min. after inoculation which in this case was the beginning of the starvation phase. At 175 min. after inoculation the cells were harvested and reincubated for 90 min. in the carbon-less, ammonium chloride-containing medium. During the starvation phase there was no increase in protein nitrogen per litre of culture (8.36 mg/l at 130 min. and 8.32 mg at 175 min.). The number of cells, however, increased during this time from 3.4 to 5.3×10^8 cells per ml. The specific activity of the glucose carbon in the medium was 593 c.p.m. per μg.

An experiment was performed in order to follow the breakdown of glycogen and the protein synthesis in a medium free of carbon but containing the nitrogen source in excess. The methods were the same as those described in expt. C, except that no isotope was added, *i.e.* the cells were praecultured for 270 min. in a nitrogen-deficient medium with lactate as the carbon source, and then incubated in a medium of the same basic composition, but containing 1 g/l of ammonium chloride and no lactate. The dry weight of cells per litre of culture and the cell concentration during the nitrogen starvation was the same as during the starvation phase in expt. C. The results are shown in Fig. 2 (expt. D).

In all cases the specific activity of the protein carbon has been estimated in the following way. Nitrogen determinations were performed on the protein (hydrolyzed for 2 h in 6 N HCl), and the specific activity was calculated per μg of protein nitrogen. These values were converted to specific activity per μg of protein carbon by using a N:C ratio of 0.23. The N:C ratio was determined in four samples and found to be 0.23 ± 0.02.

DISCUSSION

The results given in Table 1 and Fig. 1 (expts. A and C) show that if labeled carbon was added during the starvation phase in a nitrogen-starved culture, it was possible to label the glycogen in *E. coli B* without labeling the protein to any appreciable extent.

When cells labeled in this way were incubated in a medium containing ammonium chloride but no carbon source, glycogen was broken down and some protein synthesized, as shown in Fig. 2.

A lowering of the glycogen to about 75 % of the original value caused most of the label in the glycogen to disappear. This means that those glucose residues

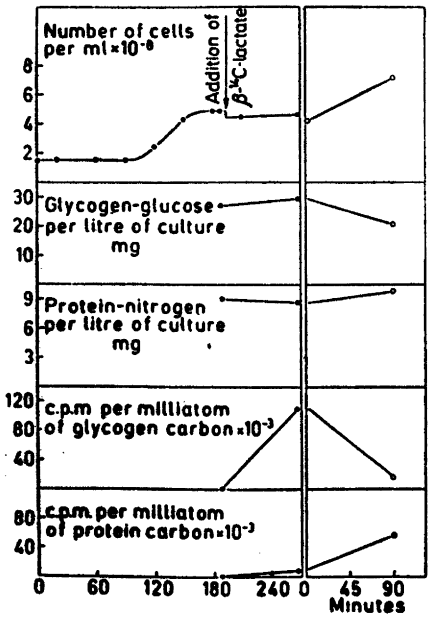


Fig. 1. Experiment C. The curves on the left-hand side of the double line show the course of events during nitrogen starvation. Part of the cells were reincubated in a medium containing the nitrogen source in excess but from which the carbon source was omitted (the curves on the right-hand side of the double line).

that were the last to be incorporated in the glycogen were the first to be split off by the cells, when incubated in a medium containing nitrogen. Under the circumstances the flow of carbon in the cell was directed away from glycogen towards the protein carbon, as shown by the increasing specific activity of the protein carbon.

The results were less marked when cells grown for 18 h in Hook's medium were allowed to accumulate a certain amount of glycogen and were thereupon incubated in a labeled medium (Table 2, expt. B). In these cells the label did not disappear from the glycogen to the same extent when incubated in the carbon-free medium with the nitrogen source in excess. The results show, however, that the specific activity of the glycogen decreased to about 40 % of the original value when the glycogen per litre of culture decreased from 8.9 to 5.1 mg. This shows that the glycogen was not evenly labeled, and that, as in the other experiments, those glucose residues that were the last to be incorpo-

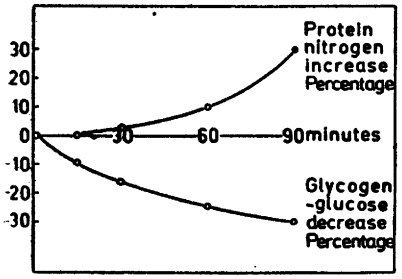


Fig. 2. Experiment D, illustrating the increase in protein nitrogen and decrease in glycogen during the second incubation period in an experiment performed in the same way as expt. C (Fig. 1, the curves on the right-hand side of the double line). The values are represented as increase or decrease in per cent of the values at the moment of inoculation.

Table 2. Experiment B.

Time after inoculation in minutes	Glycogen-glucose per litre of culture (mg)	Counts per min. per μg	
		glycogen carbon	protein carbon
0	1.1	—	—
10	5.8	0	0
40	8.9	348	117
110	5.1	140	320

Media: 0—10 min.: N-free Hook medium, glucose unlabeled.
10—40 min.: N-free Hook medium, glucose labeled.
40—110 min.: N-containing (NH_4Cl), glucose-free Hook medium.
The specific activity of the medium glucose carbon was 590 c.p.m. per μg.

From zero time to the end of the second incubation period (40 min.) the protein nitrogen per dry weight and litre of culture increased from 7.7 mg to 9.1 mg, showing that the cells contained reserves of nitrogen that were incorporated in the protein. At 110 min. the protein nitrogen per litre of culture was 11.5 mg.

rated in the glycogen were the first to be split off. In this case, too, there was an increase in the specific activity of the protein carbon during the last incubation period.

During the time the cells were cultivated in isotope medium in expt. A (130 to 175 min. after inoculation) the glycogen increased from 11.0 to 13.4 mg/l of culture. If this increase had been due solely to glucose of the same specific activity as that of the medium glucose, the specific activity of the glycogen carbon would have been 106 c.p.m. per μg at 175 min. The specific activity noted was 113 c.p.m. per μg of glycogen carbon. This means that during nitrogen starvation there was no large pool of substances on the pathway from glucose to glycogen, at any rate not during the starvation phase. Furthermore, the results may be taken as an indication that in nitrogen-starved cultures there was no appreciable breakdown of glycogen during the starvation phase.*

In expt. B the specific activity of the glycogen should have been 205 c.p.m. per μg when calculated in the same way. The specific activity observed was 348 c.p.m. This means that under the circumstances some of the non-labeled glycogen carbon present at the moment when the cells were inoculated into the labeled medium was broken down during the following incubation period. A net synthesis and a breakdown of glycogen seem to have occurred simul-

* Another possible, but rather unlikely explanation shou'd perhaps be pointed out. If some of the nonlabeled glycogen was broken down, *and* there was a pool of substances on the pathway from medium glucose towards glycogen, the non-labeled substances in this hypothetic pool may have compensated for a loss of non-labeled glycogen, present at the moment when the isotope was introduced. Since the specific activity of the hypothetic pool must have increased during the time in the labeled medium, the culture must have been harvested in this experiment exactly at the time when as much non-labeled carbon had disappeared from the glycogen as had been incorporated in the glycogen from the pool.

taneously in this experiment. This may possibly be attributed to the fact, that there was a considerable protein synthesis during this period in spite of the absence of any nitrogen source in the medium (*cf.* the text under Table 2). As shown by previously reported experiments [3,5] glycogen is utilized by the cells when protein is synthesized.

REFERENCES

1. Stetten, M. R. and Stetten, D. Jr. *J. Biol. Chem.* **213** (1955) 723.
2. Holme, T. and Palmstierna, H. *Acta Chem. Scand.* **10** (1956) 155.
3. Holme, T. and Palmstierna, H. *Acta Chem. Scand.* **10** (1956) 578.
4. Hook, A. E., Beard, D., Taylor, A. R., Sharp, D. G., and Beard, J. W. *J. Biol. Chem.* **165** (1946) 241.
5. Palmstierna, H. *Acta Chem. Scand.* **10** (1956) 567.

Received August 27, 1956.

ACTA CHEMICA SCANDINAVICA 10 (1956) 1563—1567

The Chemistry of the Natural Order Cupressales

XVII.* Heartwood Constituents of *Pilgerodendron uviferum* (D.Don) Florin (=*Libocedrus tetragona* Ends.)

H. ERDTMAN, Z. PELCHOWICZ** and J. G. TOPLISS

Organisk-kemiska Institutionen, Kungl. Tekniska Högskolan, Stockholm, Sweden

The heartwood constituents of *Pilgerodendron uviferum* (D. Don) Florin have been investigated. From the alkali soluble fraction a very small quantity of a highly dextrorotatory crystalline phenol, probably of the flavanone type has been isolated. The large neutral fraction has been shown to contain a mixture of cadinenes and also a new crystalline cadinol for which the name *pilgerol* is proposed.

As already mentioned in a previous communication [1] the genus *Libocedrus sensu lato* does not constitute a natural group and has been subdivided into several small or monotypic genera. It appears that the still very incomplete chemical investigation of the genus is in harmony with the views of modern botanical taxonomists as regards its heterogeneity. The monotypic genus *Pilgerodendron* differs botanically very distinctly from the other species of *Libocedrus s.l.* and as Florin has remarked it seems strange that this genus was ever included in *Libocedrus*. *Pilgerodendron uviferum* grows along the extremely humid western slopes of the Andes in southern Chile (down to Tierra del Fuego) at altitudes of 600—1 000 metres. The wood is renowned as the most durable wood in the country.

Through the good offices of Jägmästare J. Lagerborg, Talca, Chile, to whom our gratitude is expressed, we have been able to subject a sample of this wood to a preliminary chemical investigation. The wood came from a mature tree about one foot in diameter.

From the alkali soluble fraction of the ether soluble part of the acetone extract of the wood, a minute amount of a highly dextrorotatory crystalline compound was isolated which, judging from its ultra-violet absorption and composition, is probably a flavanone derivative but it is doubtful whether the substance was obtained in a completely pure state.

---

* Part XVI *Acta Chem Scand.* **10** (1956) 1381.

** On leave of absence from the Scientific Department, Israeli Ministry of Defence.

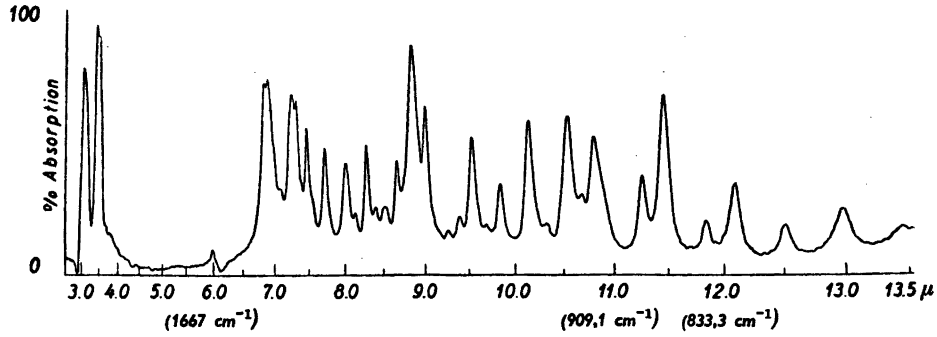
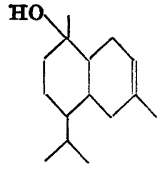
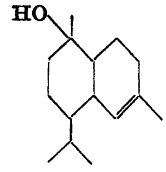


Fig. 1. Infra-red spectrum of pilgerol (KBr disc).

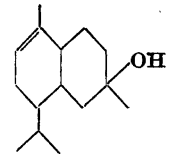
The bulk of the extract was neutral and the steam distillable portion of this was fractionally distilled *in vacuo*. The main hydrocarbon fractions yielded cadalene on dehydrogenation and cadinene dihydrochloride with hydrogen chloride and thus can be considered to be mixtures of cadinenes. From the high boiling fractions a crystalline sesquiterpene alcohol, $C_{15}H_{26}O$, was isolated for which the name *pilgerol* is suggested. It yielded cadalene on dehydrogenation and cadinene dihydrochloride on treatment with hydrogen chloride and is thus a cadinol. Attempts to prepare a crystalline phenylurethane were unsuccessful. Catalytic reduction of pilgerol in ethanol using Adams' catalyst afforded a mixture of diastereoisomeric dihydropilgerols which could be partially separated by fractional sublimation. The infra-red spectrum (Fig. 1) of pilgerol indicated the presence of a trisubstituted double bond (medium-strong band at 873 cm^{-1} and weak band at 1 668 cm^{-1}, both absent in the spectrum of the dihydrocompound). Pilgerol must therefore possess one of the structures (I), (II) or (III). It is hoped to proceed with chemical studies which will distinguish between these three alternatives when more material becomes available.



(I)



(II)



(III)

The remainder of the high boiling fraction from which pilgerol had been separated was chromatographed on alumina and yielded, as the only solid product, a further small quantity of pilgerol. The chromatographic separation was not sharp but of the liquid fractions obtained one, $[\alpha]_D$ —90° ($CHCl_3$), n_D 1.5104 and analysing for $C_{15}H_{26}O$ which corresponded to a peak on the weight per ml of eluate/volume of eluate graph of the chromatogram, was further investigated. On selenium dehydrogenation a good yield of cadalene was obtained but no crystalline hydrochloride was formed by reaction with hydro-

gen chloride. This fraction, therefore, does not appear to consist, in the main, of alcohols of the cadinol type.

Only one crystalline cadinol (m.p. 72.5°, $[\alpha]_D$ —39.4) has previously been reported (from Java-citronella oil [2] and *Chamaecyparis lawsoniana* [3]). Cadinols have been reported to occur in several other species belonging to the natural order Cupressales, *e.g. Cryptomeria*, *Taiwania* [4], *Fokenia* [5], and *Chamaecyparis pisifera* [6]. No tropolones were found in *Pilgerodendron* in contrast to *Heyderia decurrens* (β- and γ-thujaplicin) and *Austrocedrus* (β-thujaplicin) and in no other respect does *Pilgerodendron* appear to exhibit chemical similarities to the other species of *Libocedrus s.l.*

EXPERIMENTAL

All melting points are corrected.

Extraction of the heartwood. The powdered heartwood (9 kg) was extracted continuously with acetone for 32 h and the acetone removed by distillation yielding 550 g of extract. This was vigorously shaken with ether (2.5 l) when it partly passed into solution leaving some of the material (*ca.* 200 g) undissolved. The latter was of the usual "membrane substance" type and was discarded. The ether solution (A) was shaken with a saturated solution of sodium bicarbonate (1.5 l). Ether phase = A′, aqueous phase = B′. Acidification of B′ with dilute sulphuric acid and extraction with ether *etc.* yielded only 3 g of an acidic material (B^{1a}). The ether solution A′ was shaken with a 10 % solution of sodium carbonate (1.5 l). Ether phase = A^2, aqueous phase = B^2. Acidification of B^2 with dilute sulphuric acid and extraction with ether *etc.* yielded another acid fraction (B^{2a}, 14 g). The ether solution A^2 was shaken with a 5 % solution of potassium hydroxide (1.5 l). Ether phase = A^3, aqueous phase = B^3. Acidification of B^3 and extraction with ether etc. yielded still another acidic material (B^{3a}, 25 g). A^3 on evaporation of the ether yielded a neutral fraction (310 g).

Examination of the sodium carbonate extract. The material extractable with 10 % sodium bicarbonate solution (fraction B^{2a}) was dissolved in ether (35 ml) and the solution filtered through a column of aluminium oxide (1.5 × 3.5 cm) which was then washed with ether (100 ml). The solvent was evaporated, the residue treated with methanol and the crystals which separated were recrystallised from a little methanol. After several recrystallisations needles, m.p. 217—219°, were obtained (0.107 g), $[\alpha]_D$ 324° (c = 1.2, acetone). (Found: C 64.6; H 4.9. $C_{16}H_{14}O_6$ requires C 63.6; H 4.7), Ultra-violet absorption: min 248 mμ (ε 725), max 290 mμ (ε 9 000), shoulder 225 mμ (ε 1 800). The acetate was

Fraction	Boiling point	Volume in ml	Refractive index	Rotation (chloroform)
A^{3a1}	95—99	4	1.4903	
A^{3a2}	99.5—100	3	1.4909—1.4914 *	
A^{3a3}	101—105.5	10	1.4918—1.4971	
A^{3a4}	106—111.8	10	1.4981—1.5038	
A^{3a5}	114—115	15	1.5060—1.5092	—19°
A^{3a6}	115	10	1.5092—1.5105	—18°
A^{3a7}	115—116	15	1.5117—1.5130	—16°
A^{3a8}	116.5	25	1.5133—1.5136	—15°
A^{3a9}	116.5	22	1.5140—1.5149	—13°
A^{3a10}	116.5	12	1.5150—1.5158	—12°
A^{3a11}	119—125.7	10	1.5158—1.5070	
A^{3a12}	127—130	41	1.5040—1.5020 —1.5035 **	—59° to —69°
A^{3a13}	130—132°	35	1.5050—1.5111	—73°

* refractive indices from first and last portions
** refractive indices from first, middle and last portions

prepared by dissolving the compound (0.030 g) in a mixture of acetic anhydride (2 ml) and pyridine (3 drops). After 24 h at room temperature water was added and the solid collected. This was recrystallised from ethanol, m.p. 187.5—189°. (Found: C 62.5; H 4.9; OCH_3 8.8. $C_{15}H_8O_2$ $(OCOCH_3)_3OCH_3$ requires C 61.7; H 4.7; OCH_3 7.25.). Ultraviolet absorption max 220 mμ (ε 7 400), min 250 mμ (ε 980), max 278 mμ (ε 4 500).

Examination of the neutral fraction. The neutral fraction A^3 was steam distilled and the steam volatile part, (A^{3a}, 213 g) collected and subjected to fractional distillation at 6.5 mm with the results shown on p. 1565.

Dehydrogenation. Of the distillation fractions, numbers A^{3a5}—A^{3a10} were subjected to dehydrogenation with selenium (14 h, 300°) and all yielded cadalene, identified as the picrate m.p. 114.5—115°, not depressed on admixture with an authentic sample.

Hydrochloride. A sample (0.40 g) corresponding to a mixture of fractions A^{3a5}—A^{3a10} was dissolved in ether (40 ml), and the solution cooled to 0° and saturated with dry hydrogen chloride. After 15 min. the ether and excess of hydrogen chloride were removed and the remaining oil dissolved in ethanol (3 ml). After 24 h in the refrigerator 0.40 g of a crystalline hydrochloride had separated, m.p. 117—118°, $[\alpha]_D$ —36° (c = 1.4 in $CHCl_3$). The melting point was not depressed on admixture with an authentic sample of cadinene dihydrochloride (kindly supplied by Professor F. Šorm, Prague).

Pilgerol. From the highest boiling fraction A^{3a13} crystalline material (2 g) slowly separated and was collected by filtration. After several recrystallisations from ethanol--water followed by sublimation *in vacuo*, pure *pilgerol*, m.p. 138.5—139°, $[\alpha]_D$ —107° (c = 1.1 in $CHCl_3$) was obtained. (Found: C 80.63; H 11.60. $C_{16}H_{26}O$ requires C 81.00, H 11.78.) Infra-red spectrum (Fig. 1): bands at 873 cm^{-1} and 1 668 cm^{-1}, (trisubstituted double band).

Dehydrogenation. Pilgerol was dehydrogenated with selenium (24 h, 300°) giving cadalene (65 % yield), identified as the picrate.

Hydrochloride. Pilgerol (0.100 g) was dissolved in dry ether and dry hydrogen chloride passed into the solution at 0°. After removal of the ether and excess of hydrogen chloride the crystalline residue was recrystallised from ethanol (2 ml) affording cadinene dihydrochloride, m.p. 117—118°, $[\alpha]_D$ —35° ($CHCl_3$), in 80 % yield. The melting point was undepressed on admixture with an authentic sample of cadinene dihydrochloride.

Attempted preparation of the phenylurethane. Pilgerol, when heated with excess of phenyl*iso*cyanate at 90° for 1 h or treated with excess of phenyl*iso*cyanate at room temperature for several days or refluxed with phenyl*iso*cyanate (1.1 mole) in petroleum ether (60—80°) solution for 30 min. did not yield any crystalline phenylurethane.

Hydrogenation. Pilgerol (0.076 g) was hydrogenated in ethanol (15 ml) in the presence of Adams' catalyst (0.044 g), at room temperature and atmospheric pressure for 100 h. The catalyst was then removed by filtration, the alcohol evaporated and the residue sublimed *in vacuo* to give *dihydropilgerol* (*ca.* 0.06 g) as feathery needles, m.p. 79—80°, $[\alpha]_D$ +17° (c = 1.4 in $CHCl_3$), (Found: C 80.39; H 12.60. $C_{15}H_{28}O$ requires C 80.29; H 12.57). The product showed no unsaturation by the tetranitromethane test (in contrast to pilgerol itself) and the infrared spectrum exhibited no bands corresponding to ε double bond. Fractional sublimation, however, gave a small fore-fraction m.p. 74—75° and a main fraction m.p. 80—81°. Resublimation of the latter fraction gave more of the previously obtained fore-fraction m.p. 74—75° and a less volatile fraction m.p. 90—94°. The hydrogenation product thus appears to consist of a mixture of diastereoisomers. Substantially the same result was obtained when the hydrogenation was carried out in glacial acetic acid as solvent.

Chromatography of the sesquiterpene alcohol fraction The distillation fraction A^{3a13} (from which the separated pilgerol had been removed by filtration) (7.5 g) in petroleum ether (25 ml), was placed on a column of alumina (250 g) and eluted successively with petroleum ether, petroleum ether-benzene mixtures, benzene, benzene-ether mixtures, ether and finally methanol. In all 49 fractions were taken. The fractions (total weight 1.74 g) corresponding to a peak in the weight per unit volume of eluate/volume of eluate graph all completely or partially solidified. By addition of a little petroleum ether and filtration the solid material was isolated and recrystallised from petroleum ether (40—60°) (needles) giving pure pilgerol (0.150 g) m.p. 140—141°, undepressed on admixture with pilgerol previously isolated. Other fractions (total weight 1.37 g) corresponded to another main peak in the weight per volume of eluate/volume of eluate graph. A middle fraction of these, $[\alpha]_D$ —90° (c = 2.14 in $CHCl_3$), n_D^{23} 1.5104, was analysed, (Found: C

80.45; H 11.44. $C_{15}H_{26}O$ requires C 81.00; H 11.78.). Further samples were (a) dehydrogenated by heating with selenium powder to give a good yield of cadalene (identified as the picrate, m.p. and mixed m.p. 116—116.5°) and (b) treated with dry hydrogen chloride in dry ether at −10° to 0° when no crystalline hydrochloride could be obtained.

We wish to thank *Statens Naturvetenskapliga Forskningsråd* for financial support and Dr. I. Fischmeister, *Medicinsk-Kemiska Institutionen*, Uppsala Universitet, for the infrared spectra determinations.

REFERENCES

1. Erdtman, H. and Pelchowicz, Z. *Acta Chem. Scand.* **9** (1955) 1728.
2. Plattner, P. A. and Markus, R. *Helv. Chim. Acta.* **25** (1942) 1674.
3. Kritchevsky, G. and Anderson, A. B. *J. Am. Pharm. Assoc.* **44** (1955) 535.
4. Kafuku, K. and Kato, R. *Bull. Chem. Soc .Japan* **6** (1931) 65.
5. Glichitch, L. S. *Parfums France* **8** (1930) 157.
6. Nakatsuka, T. and Hirose, Y. *J. Japan Forestry Soc.* **37** (1955) 452.

Received August 29, 1956.

ACTA CHEMICA SCANDINAVICA 10 (1956) 1568—1575

The Turnover of Polynucleotides and Proteins in Regenerating Rat Liver, Studied with Glycine-^{15}N *

E. HAMMARSTEN, S. ÅQVIST, E. P. ANDERSON** and N. A. ELIASSON

Department of Biochemistry, Karolinska Institutet, Stockholm, Sweden and

B. THORELL

Department of Pathology, Karolinska Institutet, Stockholm, Sweden

An investigation of polynucleotide and protein turnover in regenerating rat liver has been made using ^{15}N-labeled glycine. Ten time stages, between 10 and 80 h after operation, have been studied, and particular attention has been paid to the incorporation pattern during the early period after hepatectomy.

1. The maximum of total cell PNA purine incorporation occurred at 14 h, considerably ahead of any other maximum. There was a smaller, broader peak of uptake into PNA around 26 to 56 h.

2. Incorporation into DNA purines was less than into those of PNA but of the same order of magnitude; the exact ratio between the two nucleic acids varied at different times. The peaks of incorporation into the DNA purines occurred at 26—32 and at 56 h.

3. In both PNA and DNA the two purine bases were not identical either in absolute uptake of ^{15}N or in time changes of incorporation. Guanine consistently showed a greater uptake of isotope than did adenine, but the ratio between the bases varied with time.

4. Total protein and its glycine constituent both showed two peaks of incorporation, at 20—26 and at 44 h, respectively, considerably later than the initial PNA maximum.

5. Cytological studies located the peak of mitosis frequency around 32 h; this coincided rather well with the major peak of isotope incorporation into DNA. Estimations of the relative size of the various cell parts revealed that the nucleolus showed maximum size earlier than did the nucleus and cytoplasm.

* Part of this work was presented at the Ciba Foundation conference on Isotopes in Biochemistry, London, 1951. The work was aided by grants from *Statens Medicinska Forskningsråd.*

** Research fellow of the American Association of University Women and the American Scandinavian Foundation; present address, National Institutes of Health, Bethesda, Maryland.

Previous work from this laboratory [1] undertook an investigation of polynucleotide and protein turnover in regenerating rat liver, as revealed by the incorporation of ^{15}N-glycine. Protein turnover was judged by the uptake of isotope into the glycine constituent of the total protein, and nucleic acid turnover by the incorporation of tracer into the purine bases, which have been shown to be specifically labeled by this precursor [2-7]. This work showed that the maxima of turnover of these substances, particularly the polynucleotides, occurred soon after hepatectomy, rather than in the later stages of regeneration which have been studied in certain other investigations [8-10]. Further work was therefore undertaken to examine the time curve more closely during this early period, under more carefully controlled experimental conditions but similar conditions of isotope administration.

EXPERIMENTAL

The animals used were adult albino rats weighing 180—200 g. The investigation included eleven groups of animals, each comprising five to ten rats; one group of non-hepatectomized rats represented the normal base line of no regeneration, while the other groups represented various time points of regeneration — 10, 12, 14, 17, 20, 26, 32, 44, 56 and 80 h, respectively (time from hepatectomy to death).

Partial hepatectomy was performed as described in previous work [3]. The wet weight of the extirpated portion of liver was recorded in each case and the weight of the remaining portion calculated, as in earlier work [1]. The weight of the total original liver was thus recorded.

Since the voluntary consumption of food by the hepatectomized animals is considerably below normal, especially at early stages after operation, all rats were fed a definite amount of food by means of stomach tube. The diet [11] * was made up as a water suspension containing 10 g per 24 ml, and each rat was given 4 ml of this suspension per 200 g (weight at the beginning of the experiment) every 4 h. Feedings of the hepatectomized rats were begun 4 h after operation. The non-hepatectomized animals were fed in this manner for 32 h, with the last feeding being given 4 h before death.

Labeled glycine (32.9 atom per cent excess ^{15}N) was injected subcutaneously in aqueous solution. The total dosage was 200 mg per 200 g (weight at the time of first injection) divided in half and given in two injections, 5 and 4 h, respectively, before death.

The livers from all animals were removed and weighed. From these figures and the calculated weights of the total original liver, the extent of regeneration was determined (weight of regenerated liver as per cent of weight of total original liver).

Samples of each liver were taken for determination of water content and for cytological examination. In the cytological studies the relative size of the nucleus, nucleolus, and cytoplasm areas (optical cross-section areas), were determined as described previously[1]; the mitosis frequency was also measured [1].

The livers from each group of animals were pooled in alcohol, homogenized, and dried. The material was then disintegrated by vibration with glass beads [12] and extracted with boiling alcohol-ether to remove lipids. Mixed polynucleotides were extracted by the method of Hammarsten [12], hydrolyzed in alkali, and separated into pentose nucleic acid (PNA) and desoxypentose nucleic acid (DNA) with lanthanum nitrate.

The PNA mononucleotides were purified by precipitation with mercuric nitrate and decomposition with hydrogen sulfide, and the purine bases were split off by hydrolysis in

* This synthetic amino acid diet was originally set up as a basis for further investigation on the effect of single amino acid deficiencies on liver regeneration. However, preliminary experiments indicated that a deficiency of one of the essential amino acids produced no decrease in this liver growth or in the incorporation of glycine, and in later work this diet was replaced by a less elaborate one containing 18 % casein instead of the synthetic amino acids. The authors are grateful to Dr. Arvid Wretlind for advice on the composition of the diet and for assistance with the animal experiments.

acid and precipitated with silver, according to established methods [13,14]. The silver purines were decomposed with hydrochloric acid [13], excess hydrochloric acid removed *in vacuo*, and the free bases isolated and purified by starch chromatography, using a solvent system of butanol-water [15]. The pyrimidine bases were not analyzed.

The lanthanum precipitate of DNA was decomposed with potassium carbonate and the DNA precipitated with acid alcohol and dried [16]. The DNA was then hydrolyzed with dry hydrochloric acid in methanol [17]. The purine hydrochlorides were dissolved in water, the excess hydrochloric acid removed, and the pure bases again separated on starch.

All purine bases from both PNA and DNA were analyzed for ^{15}N content in the mass spectrometer, nitrogen being determined by a semi-micro Kjeldahl procedure. Purity was checked in each case by determination of the ultraviolet light absorption and the ratio $E_{max}/\mu g$ N per ml.

The protein residue from the polynucleotide extraction was treated twice with hot 5 % trichloroacetic acid, according to Schneider [18], to remove any remaining traces of polynucleotides. It was then dried, hydrolyzed with 6 N hydrochloric acid, and separated into the constituent amino acids by starch chromatography, according to Åqvist [19]. Both the total unhydrolyzed protein and the isolated glycine constituent were analyzed for excess ^{15}N.

RESULTS

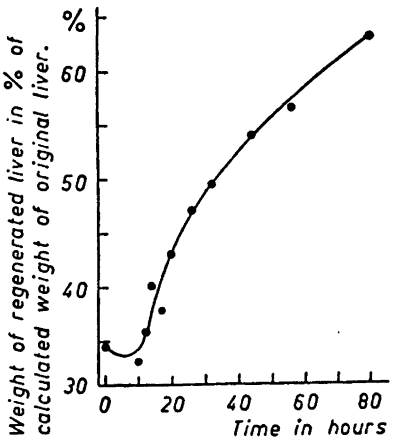
The average extents of regeneration found for these various time stages are shown in Fig. 1. It can be seen that after a slight initial drop the liver weight increased to 63 % of the original weight by 80 h. The differences in extent of regeneration at the earlier time stages are within the limits of biological variation and probably do not indicate significant deviation from the curve of steady increase.

Table 1 shows the figures for the atom per cent excess ^{15}N found in the PNA and DNA purines as well as in the total protein and its glycine constituent. The figures are calculated on the basis of 100 % ^{15}N in the administered glycine.

From these figures it can be seen that when the turnover picture is examined with time intervals so close together in the period soon after hepatectomy, the trends appear to be more complicated than could be seen from previous work with regeneration stages farther apart. The highest peak of PNA incorporation occurred as early as 14 h after operation, considerably ahead of any other maximum. In agreement with earlier work in this laboratory on glycine-^{15}N incorporation *in vivo* [1,3,20], the uptake into guanine was considerably greater than that into adenine, but the ratio between the two bases varied at different regeneration times. The time changes for the PNA purines showed that after 14 h guanine incorporation fell off rapidly to increase again around 26 h, while adenine incorporation decreased somewhat more slowly and then rose to a broader maximum between 26 and 56 h.

The incorporation into DNA was lower than that into PNA, although the figures for both nucleic acids had the same order of magnitude. The exact ratio between PNA and DNA varied with time, as did that between the two purine bases. As in the case of PNA, the DNA guanine showed a greater uptake of tracer than did adenine, but again the two purines did not show the same changes with time, both exhibiting considerable variation with both increases and decreases during the total time range. The highest incorporation was found at 26—32 and at 56 h.

From Table 1 it can also be seen that the total protein and the protein glycine both showed two peaks of isotope incorporation, also in the later stages,



at 20—26 and 44 h, respectively. This is in agreement with previous work [1]. It should be emphasized that this maximum is considerably later than the initial high peak of PNA incorporation.

The results of the cytological studies also showed considerably more variation than previously observed for regeneration stages farther apart in time [1,21]. The nucleolus was the first cell part to increase in size (optical cross-section area), reaching a maximum as early as 10—20 h. Both nucleus and cytoplasm approached maximum size around 26 h. The peak of mitotic activity came rather late in this series, based on the average of results for all livers within each group; the mitosis frequency remained at the normal low level through 20 h of regeneration and then increased to a maximum of about 10 % (per cent of cells counted which were undergoing mitosis) by 32 h. With such close time

Table 1.

Hours of regeneration	^{15}N excess * PNA ** Adenine	PNA ** Guanine	DNA Adenine	DNA Guanine	Protein ** Total	Protein ** Glycine
0	0.122	0.191	0.067	0.134	0.503	3.88
10	0.661	0.762	0.092	0.184	0.731	3.99
12	0.572	0.796	0.116	0.375	0.721	4.06
14	0.754	1.54	0.102	0.415	0.791	4.53
17	0.410	1.10	—	—	0.796	—
20	0.298	1.28	0.113	0.222	0.960	5.43
26	0.517	1.35	0.182	0.771	0.943	6.11
32	0.441	1.15	0.276	0.569	0.926	5.63
44	0.498	0.858	0.110	0.264	1.03	6.14
56	0.491	0.517	0.309	0.519	0.870	5.52
80	0.173	0.434	0.060	0.093	0.819	4.93

* The values are calculated on the basis of 100 % ^{15}N in the administered glycine.

** The curves for the time changes of ^{15}N content in the PNA purines and in the protein have been previously published [23].

intervals it was observed that mitotic activity increased very sharply at a particular time point for each liver, but examination of the individual livers indicated considerable variation among animals in the time point at which this began. Thus, around 26 to 44 h, each liver showed either great mitotic activity or very little mitosis, and the composite figure for each time interval could only be obtained by averaging the extremes for each group.

If the cytological findings are compared with the findings on isotope incorporation, it can be seen that the maximum of mitosis frequency correlated rather well with the major peak of isotope incorporation into DNA. Such correlation has also been emphasized in earlier work [1,22]. By and large, however, the appearance of the cell parts, as expressed in the other cytological magnitudes, does not seem to have a direct relationship to the chemical events reflected in the pattern of isotope incorporation.

DISCUSSION

As pointed out in previous work [1,23], an ideal precursor for isotope experiments would be incorporated directly, or by identical pathways, into all of the materials being analyzed. This situation can almost never be realized for a variety of substances, but a direct incorporation is approached in the uptake of glycine by protein[23]. In this case, therefore, the turnover indicated by glycine incorporation might be assumed to approximate that of the protein itself, with time changes being indicative of actual changes in the protein turnover rather than simply variations in biosynthetic patterns associated with this particular precursor. Explanation of the double maximum in the protein uptake of isotope could, then, be sought in the protein itself. Such a double maximum has been observed previously in this laboratory in a study similar to this [1] as well as in an investigation of the incorporation of ^{15}N-glycine into all the constituents of protein [24]. The double peak has been discussed in this earlier work in connection with heterogeneity of the protein fraction; since the fraction is a composite of cell proteins, the figures for isotope incorporation would be affected by variations in the composition of the total fraction.

Although the incorporation of glycine into polynucleotide purines has also been shown to be specific [2,4–7], the pathway is a complex one [25-29] and the uptake of this amino acid into the purine molecule might be expected to be somewhat more complicated than that into protein; the results in the present study would support this idea. The differences between the two purine bases, not only in extent of incorporation but also in pattern of time changes, indicate non-identical patterns of incorporation in the two cases *cf.* [30-33]. Studies on differences in the pattern of nucleic acid turnover revealed by the incorporation of various precursors [34-39] have served to emphasize the complexity of this problem. Thus, it is known that parts of the pattern found in these results, such as the high guanine to adenine ratios and the comparatively low PNA to DNA ratios, are typical of glycine incorporation and are not as evident with certain other nucleic acid precursors [3,4,6,16,20,23,34,36-44]. It is also apparent that these ratios reflect incorporation by purine bases themselves and are not due only to differences in uptake by the pyrimidine or carbohydrate portions

of the nucleic acid molecule [cf. 36]. Possible factors contributing to differences between dissimilar precursors include the availability of any particular one for biosynthesis in a specific tissue, dilution by unlabeled pools of intermediates, and the metabolic effects of enzyme distribution and activity. Moreover, the incorporation pattern for any one precursor could be affected by independent turnover of specific parts of the molecule being synthesized, so that the problem is the extent to which the incorporation is representative of overall nucleic acid turnover. In the light of the known differences in turnover results, it would seem highly probable that there are different paths of biosynthesis of nucleic acid components and that these paths may coexist in one tissue. Since we know very little about how such paths may vary in importance during function, data with various precursors must be correlated before the incorporation of any particular one can be fully evaluated as an accurate reflection of total nucleic acid turnover during liver regeneration. In addition to reflecting any such effects of a particular precursor, the nucleic acid turnover pattern, like that of the protein, could be affected by any heterogeneity of the material.

All such variations could affect the time changes for both PNA and DNA. The DNA figures here showed particularly irregular changes, but since glycine incorporation into DNA is high even in non-dividing tissue [cf. 41,45], the isotope uptake here might be expected to show variations due to DNA synthesis not associated with cell division, or even to some dynamic turnover having no relation to actual synthesis. The factors mentioned above could enter into such turnover; heterogeneity of DNA has been specifically pointed out [46-48]. DNA is considered to be metabolically a rather stable cell component. However, it may also be that at least the smaller variations in DNA incorporation here represent merely biological variation during regeneration (*cf.* the results on mitosis frequency). This question of the reproducibility of the biological phenomenon being studied must be kept in mind in evaluating all of these time curves, since it is virtually impossible to know to what extent the groups representing the various time points actually correspond to each other in regeneration.

The time changes in PNA incorporation of isotope seemed considerably more distinct, and the double maximum in this incorporation, revealed by this examination of such close time intervals, was of considerable interest. It appeared to be of value to try to investigate further the significance of this curve for PNA in terms of some of the variables discussed above. One possible explanation of the double peak in incorporation was cellular heterogeneity of the PNA; the PNAs from nucleus and cytoplasm are known to show great differences in the absolute uptake of various precursors [1,3,36-38, 49-53] and might well vary also in their changes of incorporation with time. Another possibility was a difference among the various nitrogen atoms of the purines in rate of incorporation. Further work was therefore undertaken to explore these particular possibilities.

The distinction between turnover and synthesis is a difficulty always encountered in the evaluation of isotope incorporation pattern. It is evident that the pattern will be influenced by changes in the equilibrium between synthesis and degradation. In the case of both protein and nucleic acid it appeared desirable, therefore, to determine to what extent the turnover figures

here represented actual net synthesis of new molecules. Towards this end a comparable study was undertaken to determine the quantitative changes in the content of these materials in liver during regeneration.

REFERENCES

1. Eliasson, N. A., Hammarsten, E., Reichard, P., Åqvist, S., Thorell, B. and Ehrensvärd, G. *Acta Chem. Scand.* **5** (1951) 431.
2. Abrams, R., Hammarsten, E. and Shemin, D. *J. Biol. Chem.* **173** (1948) 429.
3. Bergstrand, A., Eliasson, N. A., Hammarsten, E., Norberg, B., Reichard, P. and Ubisch, v. H. *Cold Spring Harbor Symposia Quant. Biol.* **13** (1948) 22.
4. Heinrich, M. R. and Wilson, D. W. *J. Biol. Chem.* **186** (1950) 447.
5. Sutton, W. B., Schlenk, F. and Werkman, C. H. *Arch. Biochem. and Biophys.* **32** (1951) 85.
6. Heidelberger, C. and LePage, G. A. *Proc. Soc. Exptl. Biol. Med.* **76** (1951) 464.
7. Edmonds, M., Delluva, A. M. and Wilson, D. W. *J. Biol. Chem.* **197** (1952) 251.
8. Drabkin, D. L. *J. Biol. Chem.* **171** (1947) 395.
9. Novikoff, A. B. and Potter, V. R. *J. Biol. Chem.* **173** (1948) 223.
10. Lombardo, M. E., Cerecedo, L. R. and Reddy, D. V. N. *J. Biol. Chem.* **202** (1953) 97.
11. Wretlind, K. A. J. and Rose, W. C. *J. Biol. Chem.* **187** (1950) 697.
12. Hammarsten, E. *Acta Med. Scand. Suppl.* **196** (1947) 634.
13. Kerr, S. E. and Seraidarian, K. *J. Biol. Chem.* **159** (1945) 211.
14. Reichard, P. *J. Biol. Chem.* **179** (1949) 763.
15. Edman, P., Hammarsten, E., Löw, B. and Reichard, P. *J. Biol. Chem.* **178** (1949) 395.
16. Reichard, P. *Acta Chem. Scand.* **3** (1949) 422.
17. Vischer, E. and Chargaff, E. *J. Biol. Chem.* **176** (1948) 715.
18. Schneider, W. C. *J. Biol. Chem.* **161** (1945) 293.
19. Åqvist, S. E. G. *Acta Chem. Scand.* **5** (1951) 1031.
20. Reichard, P. *J. Biol. Chem.* **179** (1949) 773.
21. Stowell, R. E. *Arch. Pathol.* **46** (1948) 164.
22. Hammarsten, E., Thorell, B., Åqvist, S., Eliasson, N. A. and Åkerman, L. *Exptl. Cell Research* **5** (1953) 404.
23. Hammarsten, E. *CIBA Foundation Conference, Isotopes in Biochemistrty*, London 1951, p. 203.
24. Åqvist, S. E. G. *Acta Chem. Scand.* **5** (1951) 1065.
25. Greenberg, G. R. *Federation Proc.* **12** (1953) 651.
26. Goldthwait, D. A., Peabody, R. A. and Greenberg, G. R. *J. Am. Chem. Soc.* **76** (1954) 5258.
27. Hartman, S. C., Levenberg, B. and Buchanan, J. M. *J. Am. Chem. Soc.* **77** (1955) 501.
28. Goldthwait, D. A., Greenberg, G. R., and Peabody, R. A. *Biochim. et Biophys. Acta* **18** (1955) 148.
29. Levenberg, B. and Buchanan, J. M. *J. Am. Chem. Soc.* **78** (1956) 504.
30. Carter, C. E. and Cohen, L. H. *J. Am. Chem. Soc.* **77** (1955) 499.
31. Abrams, R. and Bentley, M. *J. Am. Chem. Soc.* **77** (1955) 4179.
32. Lagerkvist, U. *Acta Chem. Scand.* **9** (1955) 1028.
33. Lieberman, I. *J. Am. Chem. Soc.* **78** (1956) 251.
34. Furst, S. S. and Brown, G. B. *J. Biol. Chem.* **191** (1951) 239.
35. Goldthwait, D. A. and Bendich, A. *J. Biol. Chem.* **196** (1952) 841.
36. Payne, A. H., Kelly, L. S. and Jones, H. B. *Cancer Research* **12** (1952) 666.
37. Anderson, E. P. and Åqvist, S. E. G. *J. Biol. Chem.* **202** (1953) 513.
38. Tyner, E. P., Heidelberger, C. and LePage, G. A. *Cancer Research* **13** (1953) 186.
39. Moldave, K. and Heidelberger, C. *J. Am. Chem. Soc.* **76** (1954) 679.
40. Brown, G. B., Roll, P. M., Plentl, A. A. and Cavalieri, L. F. *J. Biol. Chem.* **172** (1948) 469.
41. Brown, G. B. *CIBA Foundation Conference, Isotopes in Biochemistry*, London 1951, pp. 149—150, 164.
42. LePage, G. A. and Heidelberger, C. *J. Biol. Chem.* **188** (1951) 593.

43. Abrams, R. *Arch. Biochem. and Biophys.* **33** (1951) 436.
44. LePage, G. A. *Cancer Research* **12** (1952) 277.
45. Malkin, H. M. *Biochim. et Biophys. Acta* **12** (1953) 585.
46. Chargaff, E., Crampton, C. F. and Lipschitz, R. *Nature* **172** (1953) 289.
47. Brown, G. L. and Watson, M. *Nature* **172** (1953) 339.
48 Bendich, A., Russell, P. J., Jr. and Brown, G. B. *J. Biol. Chem.* **203** (1953) 305
49. Jeener, R. and Szafarz, D. *Arch. Biochem.* **26** (1950) 54.
50. Barnum, C. P. and Huseby, R. A. *Arch. Biochem.* **29** (1950) 7.
51. Smellie, R. M. S., McIndoe, W. M., Logan, R., Davidson, J. N. and Dawson, I. M. *Biochem. J. London* **54** (1953) 280.
52. Smellie, R. M. S., McIndoe, W. M. and Davidson, J. N. *Biochim. et Biophys. Acta* **11** (1953) 559.
53. Smellie, R. M. S. in Chargaff, E. and Davidson, J. N., Eds., *The Nucleic Acids II*, New York 1955, p. 408.

Received September 7, 1956.

ACTA CHEMICA SCANDINAVICA 10 (1956) 1576—1582

Further Studies on the Turnover of Polynucleotides in Regenerating Rat Liver

E. P. ANDERSON* and S. AQVIST

Department of Biochemistry, Karolinska Institutet, Stockholm, Sweden

A further study has been made on polynucleotide and protein turnover in regenerating rat liver, using ^{15}N-labeled glycine. Liver tissue at 14, 18, 26, 37 and 126 h after hepatectomy was fractionated into nuclei and cytoplasm and the incorporation of glycine nitrogen into PNA and DNA purines and into total protein was determined. The purine bases from cytoplasm PNA were further degraded in order to analyze separately ^{15}N incorporation into the amino group, into N_7 of the ring, and into the pool of ring nitrogen atoms 1, 3 and 9.

The time curves of incorporation into both polynucleotides and protein were, for the most part, in agreement with those found in earlier work. Incorporation into cytoplasm PNA purines showed an early peak at 18 h after hepatectomy and a second one at 37 h. Nuclear PNA tended to reach maximum uptake around 26 h, somewhat later than the major peak for cytoplasmic PNA. The peak of incorporation into DNA was at 26—37 h. The curve for incorporation into protein showed two maxima, at 26 and 37 h, respectively.

The animals in this series showed appreciably greater liver regeneration than did those in the earlier study, in which the diet contained synthetic amino acids instead of casein. The absolute levels of incorporation were also higher than those in the previous study.

This study aimed at exploring possible explanations for the double peak found previously in the time curve of PNA incorporation. The two possibilities specifically investigated, cellular heterogeneity of the PNA and differences among the constituent nitrogen atoms of the purines, could not explain this double peak. Although the uptake into nuclear PNA was much greater than into cytoplasm PNA, both showed essentially the same time changes in incorporation. Likewise, the various nitrogen atoms of the purines followed time curves similar to those seen for the parent compounds. The high ratio of incorporation into guanine to that into adenine also carried over into all the constituent nitrogen atoms.

This study was undertaken in conjunction with another more intensive examination of the time curves of polynucleotide and protein turnover in regenerating liver, as indicated by the incorporation of ^{15}N-glycine [1]. This

* Research fellow of the American Association of University Women and the American Scandinavian Foundation; present address, National Institutes of Health, Bethesda, Maryland.

previous study included time intervals very close together in the early period after hepatectomy, and the results revealed a somewhat surprising complexity in the time curves of incorporation for the purine bases of the nucleic acids. Of particular interest was a double maximum in the incorporation into the pentose nucleic acid (PNA) purines, the higher of the two peaks occurring at 14 h, and the second, lower one somewhat later. It was thought possible that this double maximum might be explained by cellular heterogeneity of the PNA, since the previous study had been made on total cell PNA, or by differences among the various nitrogen atoms of the purines, which had not been examined separately. The present study was undertaken to investigate these specific possibilities.

EXPERIMENTAL

The study was again made on groups of animals at various stages of liver regeneration. The present study included fewer time points than did the previous study, and larger groups of animals were used. Five groups of adult albino rats weighing 180—200 g were subjected to partial hepatectomy [2] and the livers allowed to regenerate for 14, 18, 26, 37 and 126 h, respectively (time from operation to death). The groups were made up of 17 to 29 animals, depending upon the amount of liver tissue which could be expected for that particular regeneration stage.

During all but the longest regeneration period the animals were fed every four hours by stomach tube to insure adequate food intake. The diet was somewhat different from that used in the earlier study [1]. The one used previously was made up from synthetic amino acids and was to serve as a basis for further studies of amino acid deficient diets. Since preliminary work indicated no effect on liver growth or isotope uptake from such deficient diets, this rather elaborate diet was abandoned and replaced in the present study by one containing 18 % casein instead. This diet was given as a water suspension containing 10 g per 24 ml, and each rat received 4 ml of this suspension per 200 g (weight at time of hepatectomy) at each feeding. The animals undergoing 126 h of liver regeneration received the same diet in dry form rather than by stomach tube; they obtained and consumed 12 g per day.

An aqueous solution of labeled glycine (32.9 atom per cent excess ^{15}N) was injected subcutaneously at a total dosage of 200 mg per 200 g (weight at time of injection). This was divided into two equal doses given 5 and 4 h, respectively, before death.

The regenerated livers from all animals were removed and weighed, and the average extent of regeneration calculated for each group, as described in previous work [1].

The livers for each group of animals were pooled, homogenized, and fractionated into nuclei and cytoplasm in citric acid, as in earlier work [2,3]. The nuclei were washed, disintegrated by vibration with glass beads in alcohol [4], and extracted with alcohol-ether to remove lipids [1]. The cytoplasm material was precipitated with alkali [3] and similarly extracted with alcohol-ether. From the dried tissue preparations mixed polynucleotides were then extracted by the method of Hammarsten [4], hydrolysed in alkali, and separated into PNA and desoxypentose nucleic acid (DNA) with lanthanum acetate [4].

The solutions of PNA nucleotides were hydrolyzed in 1 N hydrochloric acid at 100°C for 1 h, and the resulting mixture of purine bases and pyrimidine nucleotides was fractionated on Dowex 50, the pyrimidine components being eluted with 0.1 N acetic acid and the purine bases with 2 N hydrochloric acid [5]. Aliquots of each of the purines were purified by starch chromatography and the purity was checked and the ^{15}N content determined in the usual way [1]. This determination constituted the entire examination of the nuclear PNA purines. In the case of cytoplasm PNA, however, only small portions of the purines were used for this estimation of the isotope content in the total compound. The rest of each purine fraction was deaminated with sodium nitrite and hydrochloric acid, according to a modification of the methods of Strecker [6] and Kossel [7], under conditions found from preliminary experiments to give the best recovery of oxypurine in each case. Aliquots of the resulting hypoxanthine and xanthine were further purified by Dowex 50 and starch [8] chromatography in the same way as the amino purines and used for deter-

mination of ^{15}N. Other aliquots of the oxypurines were evaporated to dryness at an alkaline pH to remove contaminating ammonia and further degraded by combustion in 6 N hydrochloric acid at 175°C for 24 h [9] to break the purine ring. This splits off the N_7 atom in the form of glycine, leaving a pool of ammonia from the nitrogen atoms 1, 3, and 9 [10,11,12]. The resulting glycine and ammonia were isolated on Dowex 50 [13,14] and ^{15}N content determined on each.

The lanthanum-DNA was decomposed with potassium carbonate and the DNA precipitated with acid alcohol [1,15], dried, and hydrolyzed with dry hydrochloric acid in methanol [16]. The purines were dissolved, freed of excess hydrochloric acid, and purified on starch for determination of ^{15}N content. The quantities of DNA purines were too low to allow sufficient material for any further degradation.

The protein residues remaining after the extraction of polynucleotides were treated as described in earlier work [1] to determine the content of ^{15}N in the total protein and, when possible, in the glycine constituent as well.

RESULTS

In comparison with the previous series [1], these groups attained appreciably greater liver regeneration. The two earliest stages showed around 40—45 % (weight of regenerated liver as per cent of weight of original liver), in agreement with results found previously for these time intervals, but the regeneration increased to 66 % by 37 h (compared to around 51 % for this time interval in the previous study). This amount of regeneration is equivalent to that found in earlier series at 80 h. In the present series the regeneration then increased to 73 % by 126 h, giving a much less steep curve for the later time period.

Table 1 gives the figures for the ^{15}N content in the various purines and the constituent nitrogen atoms analyzed, as well as in the nuclear and cytoplasmic protein and the glycine constituent of the latter. In general the absolute figures for isotope incorporation were higher than in earlier series.

In the case of protein the levels of incorporation of isotope were approximately the same in both nuclei and cytoplasm. If one compares the time curve of protein or glycine uptake of tracer with that of the previous series, the peaks of incorporation can be seen to occur at about the same time in both cases. The highest figures for the time points included here are at 26 h for the nuclear protein and at 37 h for the total cytoplasmic protein as well as for its glycine constituent. The stages of 44—56 h are not represented in this series.

It is difficult to compare the absolute figures for the purines with those of the earlier series, since those for the nuclear PNA purines here are so much higher than those for the cytoplasm PNA compounds. However, in view of the complexities of nucleic acid turnover [1], such a comparison may be invalid for two series as different as these. If the present series is considered alone, it can be seen that cytoplasm PNA adenine showed two peaks of incorporation, one at 18 h, and a lower one at 37 h. This is in agreement with the earlier series, except that there the initial peak occurred at 14 rather than at 18 h. These time changes could be seen not only in the figures for the purine base itself but also in those for the hypoxanthine obtained by deamination, those for the ammonia nitrogen derived from nitrogen atoms 1, 3, and 9, and those for the N_7 atom isolated as glycine. The latter showed the highest content of ^{15}N, representing the most direct incorporation of the precursor. It can be seen, then, that the various nitrogen atoms did not materially differ except

Table 1.

Hours of regeneration	^{15}N excess * 14	18	26	37	126
Cytoplasmic PNA					
Adenine	0.486	0.592	0.451	0.473	0.095
Hypoxanthine	0.614	0.678	0.504	0.546	0.097
Amino-N	0.000	0.250	0.239	0.183	0.088
N_7-glycine	1.65	1.80	1.32	1.43	0.198
$N_{1,3,9}$-ammonia	0.268	0.303	0.232	0.279	0.029
Guanine	1.51	1.73	1.66	1.30	0.233
Xanthine	1.64	1.88	1.74	1.40	0.227
Amino-N	0.990	1.11	1.33	0.896	0.260
N_7-glycine	4.26	5.00	4.50	3.55	0.573
$N_{1,3,9}$-ammonia	0.916	1.25	1.03	0.928	0.108
Nuclear PNA					
Adenine	1.89	2.33	2.26	2.15	0.568
Guanine	4.32	6.34	7.14	5.52	1.48
DNA					
Adenine	0.040	0.043	0.286	0.288	0.041
Guanine	0.209	0.297	1.09	0.787	0.135
Cytoplasmic protein					
Total	0.734	0.835	1.10	1.15	0.754
Glycine	5.05	5.54	7.03	7.16	4.50
Nuclear protein					
Total	0.798	0.679	1.17	1.14	0.726

* The values are calculated on the basis of 100 % ^{15}N in the administered glycine.

in the level of incorporation; their changes of incorporation with time were essentially the same. The time curve for nuclear PNA adenine also showed an early maximum at 18 h, with the level falling off slowly after that time. This is then not greatly different from the pattern for cytoplasmic PNA adenine.

A comparison of these figures with those for the uptake into guanine shows that, as previously observed [1,17], the incorporation of glycine-^{15}N into guanine was considerably greater than into adenine. From the figures for the degraded purines of cytoplasmic PNA, it can be seen that this difference between guanine and adenine uptake carried over into all the constituent nitrogen atoms and was not due to only one particular part of the respective molecules. The figures for the various time stages showed that, as in the previous series, the two purines did not follow identical time curves of incorporation, although the similarities between the two bases were somewhat greater in the present series. Cytoplasmic PNA guanine again showed an early peak at 18 h, with the level of incorporation falling off rather slowly after that time. Here, too, the same changes with time could be seen in the figures for the oxypurine, the $N_{1,3,9}$ ammonia, and the N_7 glycine, so that there were no real differences among the various nitrogen atoms in the time curve of incorporation. The nuclear PNA guanine also showed only one peak, which occurred, however, at 26 h rather than at 18 h.

The incorporation into the DNA purines was, as in other studies with glycine, less than into those of PNA, although of the same order of magnitude. The time curves of incorporation showed single peaks. There was a high maxi-

mum for guanine at 26 h, with the level decreasing somewhat slowly with time, while adenine showed a broad maximum between 26 and 37 h. Thus, the maximum incorporation into DNA occurred considerably later than did that for PNA; the figures here serve to emphasize the peak found for DNA at 26—32 h in the previous series.

DISCUSSION

The difference between this series and the earlier one in amount of liver regeneration shown by the animals was somewhat unexpected. This difference may have been a result of the change from the synthetic amino acid diet to the casein diet. Other results in this laboratory [18] confirm more extensive liver regeneration on the casein diet than on the other one, and a casein diet has been found by others to be conducive to liver growth [19,20].

It is hard to know what effect more rapid regeneration may have had on the turnover picture, but the higher incorporation figures, compared with the earlier series, may well have been due to this greater extent of regeneration for all time points. Certainly, in view of this difference, it would seem to be somewhat hazardous to compare any absolute turnover figures for the two series.

With regard to the time curves, the two points of maximum protein turnover (26 h for nuclear protein and 37 h for cytoplasmic protein) confirm earlier findings [1,21] within the limitations of the time points included in the present series. In contrast, the time curves of nucleic acid incorporation for this series are somewhat different from those for the previous one. One major difference is the location of the inital PNA peak at 18 instead of at 14 h. It is possible that this delay in PNA uptake could have been due to the difference in diet; the casein diet could conceivably have been more slowly metabolized, which might have affected the incorporation during early stages of regeneration. However, the turnover picture for both PNA and DNA showed essentially the same changes with time as that found previously. Thus, the initial high peak of incorporation into PNA occurred considerably ahead of any other maximum, and there was a second increase in PNA uptake somewhat later; the peak of DNA incorporation of isotope also occurred at a later time. It can be seen, then, from these results that the specific possible explanations for heterogeneity of PNA turnover investigated in these experiments could not explain the time changes. Thus, when the cytoplasmic PNA purines were degraded and individual nitrogen atoms analyzed, the changes of isotope incorporation with time were found to be very nearly the same for all the various atoms. It is apparent, therefore, that the two peaks in the PNA uptake of isotope are not due to differences among these atoms. Especially in the case of adenine, the double peak could again be seen in this series, and the figures for the degradation products showed that the same time curve carried over into all the constituent nitrogen atoms.

It has been noted in previous work that glycine-^{15}N incorporation is greater into nucleic acid guanine than into adenine *cf.*[1] and this was confirmed by the present results. The figures here for the purine degradation products showed that the incorporation into xanthine was similarly high compared with that for hypoxanthine; the high ratio found in these experiments is, therefore, not

due to a difference in the metabolic activity of the amino group, which appears to be approximately the same for both purine bases. In fact, this high ratio also carried over into all the nitrogen atoms of the oxypurines, although it varied somewhat with time in each case. From these data adenine is not an intermediate in the synthesis of guanine from glycine, a finding supported by recent results of *in vitro* experiments [22-25]. Data on adenine incorporation, indicating an adenine to guanine conversion, merely reflect the probability that in this case the biosynthesis follows different pathways.

The double peak in PNA incorporation of isotope was also considered to be, possibly, an effect of the known cellular heterogeneity of PNA [2,3,17,26-34]. However, from these data, differences between cytoplasmic and nuclear PNA would seem to be unable to account for this double peak, since both showed essentially the same time changes in incorporation. In the case of adenine, a double maximum was apparent in the figures for cytoplasmic PNA alone, and the peak for nuclear PNA coincided with the main peak for cytoplasmic PNA. In the case of guanine, the peak for nuclear PNA occurred somewhat later than that for cytoplasmic PNA, and this difference may have, to some extent, contributed to the double maximum observed for guanine in the previous series. However, this contribution must have been small because of the great difference in the amounts of the two fractions, and in view of the slow decrease in cytoplasmic PNA incorporation here, the cytoplasmic PNA would appear to have been the major contributor to the later peak as well as to the first one. These conclusions do not, of course, eliminate the possibility of PNA heterogeneity of some other kind as an explanation of the turnover curve.

The absolute figures for incorporation into nuclear material, compared with cytoplasm, were very high for the PNA purines, in contrast with those for protein, which were approximately, the same in both cases. This has been found in work with various precursors [2,3,26-31], and the possible significance of the finding for the theory of a function of PNA in protein synthesis has been discussed [27]. However, although this nuclear PNA/cytoplasmic PNA ratio remained high throughout the regeneration time curve, the maximum incorporation by nuclear PNA occurred at a later period of regeneration than that by cytoplasm PNA. As pointed out above, this was especially obvious in the guanine figures. This finding may be of relevance in elaborating the relationship between nuclear and cytoplasmic PNA.

This later maximum of nuclear PNA bears upon the cytological findings in the previous paper [1]. In that study, the maximum of nucleolar size was observed around 10—15 h, which coincided rather well with the initial peak in PNA incorporation at 14 h. A correlation of the two is attractive but, on the basis of the present data, would appear to be erroneous, since the PNA of the nuclei is apparently much less important than the cytoplasmic PNA in this first PNA peak. This makes it impossible for the part of the nuclear PNA located in the nucleolus to account for the peak, and the coincidence of the two is, therefore, probably a chance one.

The authors are glad to express their thanks to Professor Einar Hammarsten for his active interest and helpful advice throughout this investigation. The work was aided by grants from *Statens Medicinska Forskningsråd.*

REFERENCES

1. Hammarsten, E., Åqvist, S., Anderson, E. P., Eliasson, N. A. and Thorell, B. *Acta Chem. Scand.* **10** (1956) 1568.
2. Bergstrand, A., Eliasson, N. A., Hammarsten, E., Norberg, B., Reichard, P. and Ubisch, v. H. *Cold Spring Harbor Symposia Quant. Biol.* **13** (1948) 22.
3. Andersson, E. P. and Åqvist, S. E. G. *J. Biol. Chem.* **202** (1953) 513.
4. Hammarsten, E. *Acta Med. Scand., Suppl.* **196** (1947) 634.
5. Cohn, W. E. *Science* **109** (1949) 377.
6. Strecker, A. *Ann.* **118** (1861) 151.
7. Kossel, A. *Hoppe-Seylors Z. physiol. Chem.* **10** (1886) 248.
8. Reichard, P. *J. Biol. Chem.* **179** (1949) 773.
9. Strecker, A. *Z. Chem.* **4** (1868) 215.
10. Fischer, E. *Ber.* **32** (1899) 435.
11. Shemin, D. and Rittenberg, D. *J. Biol. Chem.* **167** (1947) 875.
12. Cavalieri, L. F., Tinker, J. F. and Brown, G. B. *J. Am. Chem. Soc.* **71** (1949) 3973.
13. Stein, W. H. and Moore, S. *Cold Spring Harbor Symposia Quant. Biol.* **14** (1949) 179.
14. Åqvist, S. E. G. *Acta Chem. Scand.* **5** (1951) 1031.
15. Reichard, P. *Acta Chem. Scand.* **3** (1949) 422.
16. Vischer, E. and Chargaff, E. *J. Biol. Chem.* **176** (1948) 715.
17. Eliasson, N. A., Hammarsten, E., Reichard, P., Åqvist, S., Thorell, B. and Ehrensvärd, G. *Acta Chem. Scand.* **5** (1951) 431.
18. Åqvist, S. and Anderson, E. P. *Acta Chem. Scand.* **10** (1956) 1583.
19. Guggenheim, K. and Buechler-Czaczkes, E. *Brit. J. Nutrition* **4** (1950) 161.
20. Arnrich, L., Hunt, C. N., Axelrod, H. E., and Morgan, A. F. *J. Nutrition* **43** (1951) 101.
21. Åqvist, S. E. G. *Acta Chem. Scand.* **5** (1951) 1065.
22. Buchanan, J. M. and Schulman, M. P. *J. Biol. Chem.* **202** (1953) 241.
23. Abrams, R. and Bentley, M. *J. Am. Chem. Soc.* **77** (1955) 4179.
24. Lagerkvist, U. *Acta Chem Scand.* **9** (1955) 1028.
25. Lieberman, I. *J. Am. Chem. Soc.* **78** (1956) 251.
26. Payne, A. H., Kelly, L. S. and Jones, H. B. *Cancer Research* **12** (1952) 666.
27. Tyner, E. P., Heidelberger, C., and LePage, G. A. *Cancer Research* **13** (1953) 186.
28. Jeener, R. and Szafarz, D. *Arch. Biochem.* **26** (1950) 54.
29. Barnum, C. P. and Huseby, R. A. *Arch. Biochem.* **29** (1950) 7.
30. Smellie, R. M. S., McIndoe, W. M., Logan, R., Davidson, J. N. and Dawson, I. M. *Biochem. J. London* **54** (1953) 280.
31. Smellie, R. M. S., McIndoe, W. M. and Davidson, J. N. *Biochem. et Biophys. Acta* **11** (1953) 559.
32. de Lamirande, G., Allard, C. and Cantero, A. *J. Biol. Chem.* **241** (1955) 519.
33. Elson, D., Trent, L. W. and Chargaff, E. *Biochim. et Biophys. Acta* **17** (1955) 362.
34. Smellie, R. M. S. in Chargaff, E. and Davidson, J. N., Eds., *The Nucleic Acids II*, New York 1955, p. 408.

Received September 7, 1956.

ACTA CHEMICA SCANDINAVICA 10 (1956) 1583—1588

The Synthesis of Polynucleotides and Protein in Regenerating Rat Liver

S. ÅQVIST and E. P. ANDERSON*

Department of Biochemistry, Karolinska Institutet, Stockholm, Sweden

A study has been made of the changes in quantitative content of PNA and DNA phosphorus and protein nitrogen in regenerating liver 8 to 80 h after hepatectomy. This study has been correlated with a comparable one made previously on incorporation of ^{15}N-labeled glycine into these same substances, in an attempt to compare the time curves of turnover and synthesis.

During the first 80 h of regeneration the protein, lipid, and DNA content of liver remained relatively constant, *i.e.* these substances increased proportionately with liver weight. In contrast, the content of PNA per mg protein nitrogen increased from the original level to a maximum at 40 h.

The relative increases in these materials, over the normal values, were plotted and compared with that of the liver itself. From these, rates of synthesis could be estimated. PNA showed the first and most rapid increase and attained maximum rate of synthesis between 20 and 25 h. Protein synthesis reached a peak at about 40 h, and the maximum for DNA occurred between these two points. The maximum for protein synthesis corresponded with the peak of PNA content.

Correlation of the time curves for synthesis and turnover showed that the peaks of incorporation and synthesis agreed for protein, and, to a large extent, for DNA. In the case of PNA, the second peak in incorporation correlated with the maximum of synthesis, but the initial high peak apparently represented some turnover process distinct from net synthesis of new molecules.

Other work in this laboratory had undertaken a study of polynucleotide and protein turnover in regenerating liver, using ^{15}N-labeled glycine [1]. From this, time curves of turnover during regeneration were determined for these substances. In an attempt to define to what extent these turnover figures could be due to actual net synthesis of new molecules during this process, another study was made of the changes in the quantitative content of these materials in liver during identical periods of regeneration. This study was made as nearly comparable as possible to the earlier one on isotope incorporation [1].

* Research fellow of the American Association of University Women and the American Scandinavian Foundation; present address, National Institutes of Health, Bethesda, Maryland.

EXPERIMENTAL

The experiments employed adult albino rats weighing 180—200 g. Eight groups of eight to twelve rats were subjected to partial hepatectomy, according to a previously described method [2], and the livers allowed to regenerate for a different period of time in each case — 8, 12, 16, 20, 30, 40, 60 and 80 h, respectively, from operation to death.

The hepatectomized animals were fed by stomach tube every four hours during the period of regeneration in order to insure an equal and adequate consumption of food. The diet administered was the same as that used in the comparable isotope experiments [1], except for the two longest periods of regeneration. The animals in these two groups were fed by stomach tube for only the first 24 h after operation, being given a diet containing 18 % casein instead of synthetic amino acids [3]; after this time they were fed 10 g per day of the same diet in dry form.

The regenerated livers from all animals were removed and weighed, and the extent of regeneration calculated as in the previous work [1]. The livers for each group were pooled, homogenized in alcohol, disintegrated by vibration [4], and extracted with alcohol-ether to remove lipids, in a manner corresponding to that described for other work [1], except that recoveries of all fractions were made quantitatively. The liver removed from one of the groups at the time of hepatectomy was taken as a sample of normal, non-regenerating liver and was treated in the same way.

The lipid extracts were evaporated to dryness, and the dry weight of the extracted material determined.

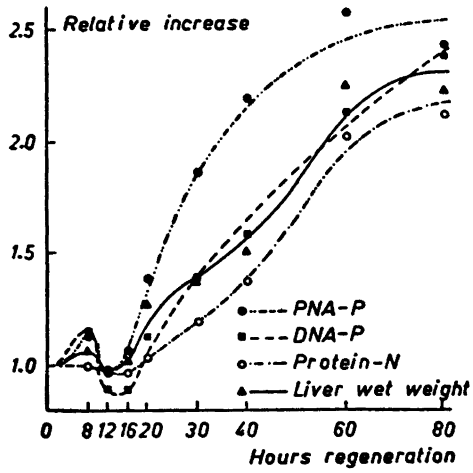
The tissue samples remaining after lipid extraction were treated according to Hammarsten [4] to extract mixed polynucleotides. The method was the same as that usually employed in this laboratory, involving extraction with saturated urea and saturated salt (sodium chloride and ammonium sulfate) solution, precipitation of the extracted polynucleotides with copper, decomposition of the copper salt with potassium acetate and solution of the residue with urea, and final precipitation of the free polynucleotides with alcohol. For this work, however, the exact procedure was somewhat modified in order to insure complete extraction. The extraction was performed on four to twelve weighed aliquots (around 100 mg each) of the original dry, lipid-free tissue, each aliquot being ground by hand during extraction in a small, conical centrifuge tube with a closely fitting ground glass piston. This centrifuge tube constituted a modified McShan-Erway grinder [5]; each tube and its piston were specially ground to fit very closely. The grinder was operated by hand to insure more complete disintegration, since the tissue became rather gummy during the first extraction.

The extracted mixed polynucleotides were hydrolyzed in alkali and separated into pentose nucleic acid (PNA) and desoxypentose nucleic acid (DNA) with lanthanum acetate at pH 2 [4,6]. Both the PNA supernatant and the lanthanum precipitate of DNA were combusted directly for quantitative phosphorus determinations, which were made on aliquots of each digest by the colorimetric method of Fiske and Subbarow [7].

Comparable weighed aliquots of the original dry, lipid-free tissue were also extracted twice with hot trichloroacetic acid (TCA), according to Schneider [8], to obtain a TCA-insoluble protein residue free of salt and other extraneous material. The dry weight of this protein residue was determined for each aliquot, and its nitrogen content estimated by a semi-micro Kjeldahl method.

RESULTS

The time curve of regeneration for these animals is given in Fig. 1, shown as the relative increase in the wet weight of the liver after hepatectomy. In absolute per cent regeneration (weight of regenerated liver as per cent of weight of original liver) the first seven of these groups corresponded very closely to the comparable groups from the previous isotope series [1]. Only the groups representing the two longest time periods showed regeneration much greater in extent. These two groups were fed the casein diet, which has been found in another series [3] to be associated with more extensive liver regeneration. The



amount of regeneration shown by the last two groups in the present series was even more than that previously observed on the casein diet, the figures here being greater than that found previously for 126 h of regeneration. These last two groups seem to have attained almost a plateau of growth, the extent of regeneration being no greater at 80 h than at 60 h.

The figures for the quantitative determinations on liver from these groups are shown in Table 1. This table shows for each group the extent of growth (per cent regeneration), the protein nitrogen content (nitrogen found in the TCA-insoluble protein residue) and the lipid content (dry weight of the residue from lipid extracts) of the dry whole liver tissue, and the content of PNA and DNA phosphorus, expressed per mg protein nitrogen. Because of irregular variations found, from preliminary estimations, in the glycogen content of the liver samples (reflected in the third column of Table 1, giving the protein nitrogen content), the protein nitrogen was considered to be the most constant as well as the most significant basis on which to express the quantitative figures for polynucleotide content.

Table 1.

Hours of regeneration	Per cent regeneration	mg protein N per 100 mg dry weight *	mg lipids per 100 mg dry weight *	μg PNA P per mg protein N	μg DNA P per mg protein N
0	34.6	7.52	19.8	24.9	7.21
8	36.8	7.25	25.3	28.2	8.33
12	34.0	8.31	24.7	25.2	6.65
16	35.3	7.81	23.7	27.6	6.67
20	44.1	6.29	26.3	33.5	7.85
30	47.6	6.64	26.0	38.9	8.40
40	52.4	7.19	27.8	39.8	8.31
60	78.1	6.90	31.7	31.8	8.23
80	77.4	7.39	27.0	28.6	8.09

* Dry weight of whole liver.

From Table 1 it can be seen that the protein content of the whole liver varied irregularly around a figure of approximately 7 mg protein nitrogen per 100 mg dry weight of liver. The lipid content, which was about 25 mg per 100 mg liver, was somewhat more constant, and there was no evidence of accumulation of lipid material during regeneration [9,10]. These substances, then, increased approximately proportionately with liver weight.

From the last column it can be seen that, except for slight irregularity in the early stages of regeneration, the content of DNA as expressed here also remained rather constant throughout the various time stages, *i.e.* the level increased proportionately with protein and with liver weight [cf.11]. The actual figure for DNA content was about 8 μg DNA phosphorus per mg protein nitrogen. Column five gives the values for PNA phosphorus and indicates that this constituent showed initial irregularities during the first 16 hours of regeneration and then increased steadily, compared with the level of protein, to a rather high maximum content at 40 h. If these nucleic acid contents are calculated on the basis of dry weight of liver, the initial irregularities in the curves are less, but the shape of both curves is essentially unchanged, with the maximum in PNA content falling at the same time point.

Figure 1 gives the time curves of regeneration for PNA phosphorus, DNA phosphorus, and protein nitrogen, as well as liver wet weight. These curves represent the change with time of the total amount of each of these constituents, expressed as relative increase over the zero point value. The zero point for each curve represents the content of that constituent in a unit of liver before regeneration has begun. For each time stage the total content of each constituent has then been calculated for the amount of liver expected at that stage of regeneration from this unit of liver. The curves serve to indicate when and with what speed each constituent was produced in the liver during the regeneration process. From them it can be seen that all these constituents increased rather steadily with time. The PNA began its increase somewhat earlier than the other substances and showed a somewhat steeper rise. It must be remembered that the increase in these constituents should actually be less than that seen here for the last two time points, especially the increase between 40 and 60 h, since these two groups had a high extent of regeneration which was out of proportion to that of the earlier groups. With this in mind, if the rates of formation of these materials are estimated from the curves, the maximum rate of PNA synthesis can be seen to have occurred between 20 and 25 h. Protein synthesis reached a maximum at about 40 h, and the peak for DNA occurred between these two points. If these results are compared with the figures in Table 1, it can be seen that the period of maximum rate of protein synthesis coincided with the peak of PNA content.

DISCUSSION

If the results of these quantitative determinations are correlated with those of the corresponding study on incorporation of ^{15}N-labeled glycine [1], some indications can be obtained as to the extent to which the time curves of isotope incorporation reflect net synthesis of protein and nucleic acid molecules. It must be remembered that the time periods recorded in the isotope series

were the duration of life after hepatectomy, and that isotope was administered 5 and 4 h prior to death, so, in making the correlation, these time points should be moved ahead to include this total period.

In the case of protein the highest peak of isotope incorporation was found at 39—44 h. This correlates with the time of most rapid synthesis of protein, as determined in the present series. The earlier, smaller peak of protein uptake of isotope, at 20—26 h, could also have included some lesser contribution from the synthesis of new molecules, since this synthesis had begun by that time. A correlation of the pattern for incorporation into protein with that for net synthesis helps to explain the relatively uncomplicated picture obtained for glycine uptake by protein during regeneration, and supports the claim [1] that this incorporation picture reflects changes in the actual protein rather than simply a biosynthetic pattern associated with this particular precursor.

It is of interest to note the correlation in time between the maximum content of PNA and the maximum rate of protein synthesis. A high PNA content during rapid growth and protein synthesis has been reported by many investigators for various systems of cell growth and function, and has been much discussed in relation to a postulated function of PNA in protein synthesis[2,9,12-27]. Without reviewing the evidence as to the pros and cons of this theory, it can be said that the results in the present study are in agreement with these previous studies in regard to high PNA content during the period of most rapid protein synthesis. However, it should be stressed that data such as these indicate only a time sequence and correlation and can throw no light upon the problem of mechanism for any relationship between these substances.

For DNA the maximum in rate of formation is broader than that for protein and thus harder to place exactly in time, but the curve would indicate that net synthesis of DNA could have materially contributed to the main peak of isotope incorporation around 30 h. This period of synthesis and incorporation also correlates rather well with the maximum of mitosis frequency *cf.*[28]. Actually certain cellular studies have indicated that DNA synthesis occurs during interphase, preceding mitosis [29-31], but the significance of this for a time study of total tissue changes is not clear. Price and Laird [32], using chemical methods, have found a doubling of DNA content just before the maximum of mitosis in regenerating rat liver. Such results cannot be seen from these figures. The picture here is more one of steady increase in the DNA content of the liver, paralleling the total regeneration, and it is difficult to perceive any period of much greater synthesis *cf.* [11,33]. Since the incorporation curve, furthermore, showed variations throughout the time range studied, specific time point correlations are of somewhat doubtful value in the case of DNA.

With respect to the rate of PNA synthesis, in relation to the time curve for PNA incorporation of glycine, the data here show that synthesis attained a maximum between 20 and 25 h, which could have contributed to the second peak in PNA incorporation of isotope. However, the initial high peak of isotope uptake, at 9—14 h, occurred ahead of any material increase in PNA content. It would seem that this peak, therefore, must represent some turnover process quite distinct from net increase in number of molecules. Such turnover might be more likely to depend upon and vary with the precursor used, and its inter-

pretation is more difficult. Thus, it is apparent that the double maximum observed in PNA incorporation [1] reflects the biological complexity of the metabolic processes involved in and contributing to the turnover of this material, but at present the data are still too incomplete to allow a more exact definition of the nature of this complexity.

The authors wish to express their appreciation for the kind help and advice of Professor Einar Hammarsten. Acknowledgement for grants-in-aid is made to *Statens Medicinska Forskningsråd.*

REFERENCES

1. Hammarsten, E., Åqvist, S., Anderson, E. P., Eliason, N. A. and Thorell, B. *Acta Chem. Scand.* **10** (1956) 1568.
2. Bergstrand, A., Eliasson, N. A., Hammarsten, E., Norberg, B., Reichard, P. and Ubisch, v. H. *Cold Spring Harbor Symposia Quant. Biol.* **13** (1948) 22.
3. Anderson, E. P. and Åqvist, S. *Acta Chem. Scand.* **10** (1956) 1576.
4. Hammarsten, E. *Acta Med. Scand., Suppl.* **196** (1947) 634.
5. McShan, W. H., Davis, J. S., Soukup, S. W. and Meyer, R. K. *Endocrinology* **47** (1950) 274.
6. Reichard, P. *J. Biol. Chem.* **179** (1949) 763.
7. Fiske, C. H. and Subbarow, Y. *J. Biol. Chem.* **66** (1925) 375.
8. Schneider, W. C. *J. Biol. Chem.* **161** (1945) 293.
9. Stowell, R. E. *Arch. Pathol.* **46** (1948) 164.
10. Yokoyama, H. O., Tsuboi, K. K., Wilson, M. E. and Stowell, R. E. *Cancer Research* **12** (1952) 312.
11. Nygaard, O. and Rusch, H. P. *Cancer Research* **15** (1955) 240.
12. Caspersson, T. *Symposia Soc. Exptl. Biol.* **1** (1947) 127; *Cell Growth and Cell Function*, New York 1950.
13. Brachet, J. *Symposia Soc. Exptl. Biol.* **1** (1947) 207; Chargaff, E. and Davidson, J. N., Eds., *The Nucleic Acids II*, New York 1955, p. 475.
14. Davidson, J. N. *Cold Spring Harbor Symposia Quant. Biol.* **12** (1947) 50.
15. Malmgren, B. and Hedén, C. G. *Acta Pathol. Microbiol. Scand.* **24** (1947) 417, 448. 472.
16. Novikoff, A. B. and Potter, V. R. *J. Biol. Chem.* **173** (1948) 223.
17. DiCarlo, F. J. and Schultz, A. S. *Arch. Biochem.* **17** (1948) 293.
18. Levy, H. B., Skutch, E. T. and Schade, A. L. *Arch. Biochem.* **24** (1949) 199.
19. Caldwell, P. C., Mackor, E. L. and Hinshelwood, C. *J. Chem. Soc.* **1950** 3151.
20. Fish, C. A., Asimov, I. and Walker, B. S. *Proc. Soc. Exptl. Biol. Med.* **75** (1950) 774.
21. Mitchell, P. D. and Moyle, J. *J. Gen. Microbiol.* **5** (1951) 421.
22. Jeener, R. *Arch. Biochem. and Biophys.* **43** (1953) 381.
23. Price, W. H. *J. Gen. Physiol.* **35** (1952) 741.
24. Wade, H. E. *J. Gen. Microbiol.* **7** (1952) 24.
25. Holloway, B. W. and Ripley, S. H. *J. Biol. Chem.* **196** (1952) 695.
26. Beljanski, M. *Biochim. et Biophys. Acta* **15** (1954) 425.
27. Gale, E. F. and Folkes, J. P. *Biochem. J. London* **53** (1953) 483; *Nature* **173** (1954) 1223; *Biochem. J. London* **59** (1955) 661, 675.
28. Eliasson, N. A., Hammarsten, E., Reichard, P., Åqvist, S., Thorell, B. and Ehrensvärd, G. *Acta Chem. Scand.* **5** (1951) 431.
29. Howard, A. and Pelc, S. R. *CIBA Foundation Conference, Isotopes in Biochemistry*, London 1951, p. 138; *Exptl. Cell Research* **2** (1951) 178.
30. Walker, P. M. B. and Yates, H. B. *Proc. Roy. Soc. London* **B140** (1952) 274.
31. Thorell, B. in Chargaff, E. and Davidson, J. N., Eds. *The Nucleic Acids II*, New York 1955, p. 181.
32. Price, J. M. and Laird, A. K. *Cancer Research* **10** (1950) 650.
33. Drabkin, D. L. *J. Biol. Chem.* **171** (1947) 395.

Received September 7, 1956.

ACTA CHEMICA SCANDINAVICA 10 (1956) 1589—1596

Quantitative Bromination of Phenols

BENGT SMITH

Institutionen för Organisk Kemi, Chalmers Tekniska Högskola, Göteborg, Sweden

The quantitative bromination of 47 phenols was carried out using 0.1 N potassium bromide—bromate solution and glacial acetic acid as the solvent. The required conditions were established for the analysis of various types of phenols whose reactivity toward bromine is also discussed.

For a long time bromination has been an important part of methods for the quantitative determination of phenol. It has also been used in the analysis of a limited number of other types of phenols such as alkylphenols, halophenols and nitrophenols. It was the basis of the first method [1] used for this purpose and, in spite of the introduction of conductometric titration [1-4] and more recently titration in nonaqueous solvents [5] as tools for the analysis of phenols, it is in some respects still superior. Thus the bromination method is the only one by which it is possible to analyze mixtures of isomers, such as the *meta*-substituted phenols in the presence of the corresponding *ortho* or *para* isomers.[6] * Furthermore, unlike the two other methods, bromination reveals the number of free *ortho* and *para* positions in the ring, a fact of great value for the identification of phenols.

Hitherto the quantitative bromination method has been applied only to a limited number of phenols. It was felt that the potential value of the method had not been utilized fully, partly because of the somewhat tedious procedure generally used, and partly because of unsuitable conditions which hinder its application to the quantitative analysis of a larger number of phenols. Furthermore no systematic study has been made of the relationship between the structure of a phenol and the conditions necessary for its quantitative bromination. It was proposed therefore to investigate the possibility of altering the procedure in such a way that the bromination method may be of more general use. Some relationships between structure and reactivity would also be studied. To give the background for the present work it is necessary to discuss, in some detail, the development of the quantitative bromination method.

* Added in proof. After the completion of this work Karrman and Johansson[6a] have reported that a mixture of *o*-, *m*- and *p*-cresol can be analyzed using high frequency titration.

In 1876 Koppeschaar [1] introduced his method for the quantitative determination of phenol which with few alterations has been in use up to now (see, *e.g.* Ref. [7]). The principle of the method was to dissolve the phenol in water and add an excess of a solution containing sodium bromide and sodium bromate. On acidification with hydrochloric acid bromine was liberated, part of which reacted with the phenol to form tribromophenol. After 15 min potassium iodide was added and the iodine liberated titrated with thiosulfate. From the volume of bromide-bromate solution taken and the volume of thiosulfate used in the back-titration the amount of bromine consumed by the phenol could be calculated.

It was not until 1928 that this Koppeschaar "excess" method was tested on several other types of phenols. Thus Day and Taggart [8] were able to analyze about 10 phenols using essentially the same procedure as Koppeschaar. They also tried a so-called "direct" method developed by Callan and Henderson.[9] To the alkaline solution of the phenol a potassium bromide solution was added and then, after acidification, the necessary volume of standard potassium bromate. The end point was determined using spot tests on starch-iodide paper. This "direct" method is reported to be tedious and there is some possibility that bromine might be lost. Most analyses were made therefore using the "excess" method.

The work of Day and Taggart seems still to be the most comprehensive in its field although several papers on the same subject have appeared since. Riemschneider,[10] for example, used sodium sulphite for the reduction of the excess of bromine and determined the sum of the hydrogen bromide formed here and in the bromination reaction by a titration according to Volhard. Singh [11] recently used the Day and Taggart method for the analysis of some phenols with the modification that chloramine-B was substituted for the potassium bromate. Bielenberg *et al.*[12] stated that the Koppeschaar method gave inaccurate results, when applied to phenols other than cresolic acid. They proposed a modified procedure which, however, still utilized water as solvent (concerning water as solvent see below). Bielenberg [13] unsuccessfully tried to indicate the end point of the bromination reaction by methyl orange and other bromine-sensitive dyes.

Of special interest are two investigations by Sprung [14] and Ruderman [15], respectively, concerning the application of the Koppeschaar method to the quantitative analysis of alkylphenols. Sprung found that the method failed for most types of alkylphenols except for some with alkyl groups in the *meta* position or tertiary alkyl groups in the *ortho* or *para* position. Ruderman, varying the excess of bromine, concluded that phenols with primary and secondary alkyl groups *ortho* or *para* to the hydroxyl group tend to overbrominate in the presence of excess bromine while phenols with *ortho*, *meta*, or *para* tertiary alkyl groups brominate quantitatively regardless of the bromine excess. Furthermore hydroxymethyl groups were found to be displaced by bromine in certain instances.

Some attempts have also been made to use a potentiometric method for the indication of the end point in the quantitative bromination of phenols [16,17]. This method should be valuable in the analysis of dark coloured substances,

but the number of phenols to which it has been applied is still too small to permit an estimation of its usefulness.

Day and Taggart reached a high precision in their analyses but at the cost of frequent changes of such variables as dilution, bromination time and the time elapsed between the addition of the potassium iodide and the back titration of the iodine. In spite of this such a simple phenol as *p*-cresol could not be analyzed either by the "excess" method or by the "direct" method. Reliable values for thymol and β-naphthol could be obtained only if chloroform was used as solvent instead of alkali. A decarboxylation reaction was also observed for salicylic acid which consumed 6 equiv. of bromine per molecule instead of the expected 4 equiv. * Another irregularity is the need of allowing the reaction mixture to stand in some cases between the addition of the potassium iodide and the back titration of the iodine. Thus in the case of resorcinol the mixture was kept for 5 min, in the case of *m*-cresol for 60 min. Some of these difficulties might be caused by the choice of solvent. Most of the phenols are not soluble enough in water, but have to be dissolved in alkali. On acidification prior to the addition of bromide-bromate there is a risk that the phenol is partly precipitated and that the reaction thus takes place in an inhomogeneous medium. The long reaction time (30 min) necessary in several cases might be due partly to this circumstance. As mentioned above thymol, which has a low solubility in water, could not be analyzed by the general "excess" method.

From the discussion above it follows that a solvent suitable for general use in the bromination method should have a good dissolving power for phenols. Of course it must be reasonably inert to bromine under the conditions used. It is also desirable that it is mixable with the titrant and has some dissolving capacity for the products of bromination. The last condition arises from the fact that the products of bromination when precipitated might enclose incompletely brominated compounds (*cf.* Ref. [8]). Day and Taggart used chloroform in some of their experiments. It is fairly stable toward bromine but is reported to retain the last of the iodine tenaciously. Furthermore it is not mixable with the titrant. Ethyl alcohol was employed as solvent by Francis and Hill.[6] Its stability toward bromine is, however, reported to be poor.[18] Acetic acid has been used in isolated cases with good results [18]. As it fulfills all the conditions above it was decided to investigate its general usefulness.

It was found that a large number of phenols could be directly titrated in acetic acid solution using 0.1 N bromide-bromate (see Table 1). Instead of the tedious spot test method used by Day and Taggart a small excess of bromide-bromate was added and then immediately back-titrated with standard thiosulfate. The average accuracy of this "direct" method was 0.3 %.

Phenols which could not be quantitatively determined by the "direct" method were analyzed using an "excess" method (see Table 2). In most of the cases the reaction was complete in 3 min with 100 % excess of bromide-bromate. The average accuracy of the "excess" method was 0.4 %.

* Francis and Hill [6], using water, dilute sulphuric acid or ethyl alcohol as the solvent, also reported a decarboxylation to take place in the bromination of the hydroxybenzoic acids. Furthermore carbon monoxide was shown to be formed in the bromination of the hydroxybenzaldehydes, originating from the formyl group which was split off.

It was the objective of the present investigation to develop general procedures which were applicable to the largest possible number of phenols. This was attained so far in that 22 (84 %) of the 26 phenols determined by the "direct" method could be analyzed under identical conditions as could 15 (75 %) of the 20 compounds analyzed by the "excess" method. This unification of the bromination method was partly enabled by the fact that the same number of active centres (*ortho* and *para* positions) were present in each case which also permitted a comparison to be made between the reactivities of the various phenols (see below).

EXPERIMENTAL

Materials. Most of the phenols in Tables 1 and 2 were commercial products. Their purity was tested by melting point or boiling point determinations and they were, if necessary, recrystallized or redistilled.

Procedure for the direct method: 1.5 mequiv. * of the phenol were weighed and dissolved in the prescribed volume of glacial acetic acid (see Table 1). Five ml of conc. hydrochloric acid were added and then dropwise 16 ml of 0.1 N potassium bromide-bromate solution. A larger excess of bromide-bromate solution was never allowed to occur. After addition of 5 ml of a 10 % potassium iodide solution the iodine was immediately titrated with 0.1 N thiosulfate using starch solution as indicator.

Procedure for the excess method. The same amount of the phenol as in the previous method was weighed and dissolved in the prescribed volume of glacial acetic acid in a flask fitted with a ground joint (see Table 2). Thirty ml of 0.1 N potassium bromide-bromate solution were added and then 5 ml of conc. hydrochloric acid. The flask was immediately stoppered, shaken and left for generally 3 min (see Table 2). After that period 10 ml of a 10 % potassium iodide solution were added and the iodine at once titrated as above.

DISCUSSION

In the following the conditions necessary for the quantitative bromination of various types of phenols will be discussed in some detail.

The dominating influence in the bromination of phenols is exerted by the hydroxyl group whose well known activation of the aromatic ring towards electrophilic reagents causes bromine to replace hydrogen at the free *ortho* and *para* positions. Other substituents in the phenol molecule as a rule have only a minor influence on its reactivity.

Phenol and alkylphenols. All of the 5 monoalkylphenols tested (Nos. 2—6) could be analyzed under standard conditions (1.5 mequiv. of the phenol in 10 ml of glacial acetic acid) using the "direct" method. They were found to be more reactive than phenol (No. 1) as the bromine consumption of the latter was too low under standard conditions. This difference in reactivity is natural considering the electron releasing effect of alkyl groups toward the ring. In view of this the dialkyl- and polyalkylphenols might be expected to be even more reactive than the monoalkylphenols. However, for many of the compounds investigated the opposite was the case. Thus, while 2,4- and 2,6-xylenol (Nos. 7 and 8) could be analyzed by the "direct" method the "excess" method had to be used in most cases involving *meta*-substituted dialkyl- and polyalkylphenols (Nos. 27—33). The cause of the decrease in reactivity in those

* It is assumed that each vacant *ortho* or *para* position consumes 2 equiv. of bromine.

Table 1. Bromide-bromate titration of phenols using the "direct" method.

No.	Compound	Ml of glacial acetic acid	Equiv. weight			% Error	Number of bromine atoms entering the molecule
			Found	Mean value	Calc.		
1	Phenol *	5	15.62 15.78	15.70	15.68	0.1	3
2	*o*-Cresol	10	26.96 26.93	26.95	27.03	0.3	2
3	*m*-Cresol	10	18.00 18.02	18.01	18.02	0.1	3
4	*p*-Cresol	10	27.02 26.94	26.98	27.03	0.2	2
5	*p-tert.*-Butylphenol	10	37.84 37.74	37.79	37.55	0.6	2
6	*p-tert.*-Amylphenol	10	41.30 41.28	41.29	41.06	0.6	2
7	2,6-Xylenol	10	61.52 60.92	61.22	61.08	0.2	1
8	2,4-Xylenol	40	61.13 60.84	60.99	61.08	0.1	1
9	2,4-Di-*tert.*-butyl-*m*-cresol	40	109.5 109.2	109.35	110.17	0.7	1
10	2,2-Bis-[*p*-hydroxyphenyl]-propane	10	28.75 28.72	28.74	28.53	0.7	4
11	*o*-Hydroxymethylphenol	10	30.91 31.08	30.99	31.03	0.1	2
12	*p*-Hydroxymethylphenol	10	30.93 30.71	30.82	31.03	0.7	2
13	*o*-Hydroxydiphenyl	10	42.50 42.68	42.59	42.55	0.1	2
14	*p*-Hydroxydiphenyl	10	42.34 42.52	42.43	42.55	0.3	2
15	*β*-Naphthol	10	71.69 71.76	71.73	72.08	0.5	1
16	Resorcinol	10	18.27 18.38	18.32	18.35	0.2	3
17	Phloroglucinol, 2 H_2O	10	27.08 27.05	27.07	27.02	0.2	3
18	2,4-Dihydroxyacetophenone	10	37.62 37.78	37.70	38.04	0.9	2
19	2,4-Dichlorophenol	10	81.39 81.52	81.45	81.50	0.1	1
20	2-Chloro-5-methylphenol	10	35.58 35.46	35.52	35.65	0.4	2
21	*p*-Chloro-*m*-cresol	10	35.60 35.65	35.63	35.65	0.1	2
22	Salicylic acid	10	34.48 34.58	34.53	34.53	0	2
23	*p*-Hydroxybenzaldehyde	10	30.52 30.53	30.53	30.53	0	2
24	*p*-Hydroxyacetophenone	10	34.02 34.10	34.06	34.04	0.1	2
25	*p*-Hydroxypropiophenone	10	37.55 37.52	37.54	37.54	0	2
26	*o*-Hydroxydiphenylether	30	46.24 46.30	46.27	46.55	0.6	2

* Alternatively the "excess" method may be used under standard conditions.

Table 2. Bromide-bromate titration of phenols using the "excess" method.

No.	Compound	Ml of glacial acetic acid	Time (min)	Equiv. weight			% Error	Number of bromine atoms entering the molecule
				Found	Mean value	Calc.		
27	2,3-Xylenol	10	3	30.55 30.39	30.47	30.54	0.2	2
28	2,5-Xylenol	10	3	30.56 30.29	30.43	30.54	0.4	2
29	3,5-Xylenol	10	3	20.26 20.13	20.20	20.36	0.8	3
30	3,4-Xylenol	20	3	30.66 30.41	30.54	30.54	0	2
31	2-*iso*-Propyl-5-methyl-phenol (Thymol)	10	3	37.37 37.49	37.43	37.55	0.3	2
32	2-Methyl-5-*iso*-propyl-phenol (Carvacrol)	10	4	37.88 37.80	37.84	37.55	0.8	2
33	2,3,5-Trimethylphenol	30	3	34.19 33.93	34.06	34.05	0	2
34	*m*-Hydroxymethylphenol	10	3	20.58 20.57	20.58	20.69	0.5	3
35	*o,o'*-Dihydroxydiphenyl	10	3	23.09 23.09	23.09	23.28	0.8	4
36	*o*-Chlorophenol	10	3	32.15 32.05	32.10	32.14	0.1	2
37	*m*-Chlorophenol	10	3	21.42 21.38	21.40	21.43	0.1	3
38	*p*-Chlorophenol	10	3	31.93 32.02	31.98	32.14	0.5	2
39	2,4,5-Trichlorophenol	10	3	98.65 98.61	98.63	98.73	0.1	1
40	*m*-Hydroxybenzoic acid	10	3	22.79 22.90	22.85	23.02	0.8	3
41	*o*-Hydroxybenzaldehyde	30	3	30.55 30.58	30.57	30.53	0.1	2
42	*m*-Hydroxybenzaldehyde	10	3	20.17 20.25	20.21	20.35	0.7	3
43	*o*-Hydroxyacetophenone	10	3	33.88 34.04	33.96	34.04	0.2	2
44	*o*-Nitrophenol	10	3	35.06 34.71	34.89	34.78	0.3	2
45	*m*-Nitrophenol	10	3.5	23.01 23.07	23.04	23.19	0.6	3
46	*p*-Nitrophenol	10	3	34.89 34.52	34.70	34.78	0.2	2
47	2,4-Dinitrophenol	10	3	91.80 91.80	91.80	92.05	0.3	1

cases where a free *ortho* position is flanked by an alkyl group might be, at least in part, that this position is less readily substituted by bromine.*

* In fact it is often observed that substitution in an aromatic nucleus is retarded at a position flanked on both sides by substituent groups.

As seen from Tables 1 and 2 a higher dilution than 10 ml had to be used in some cases as the bromine consumption was too high under standard conditions. The reason for this might be an added substitution at vacant *meta* positions or in side chains. Another possible cause is the formation of compounds of the tribromophenol bromide type [19,20].

The phenols containing hydroxymethyl groups (Nos. 11, 12 and 34) may be discussed in connection with the alkylphenols. The difference in reactivity between the three monosubstituted isomers is here enhanced in comparison with the cresols as the *meta* isomer had to be analyzed by the "excess" method.

Chlorophenols. Four of the five chlorophenols which in addition to the hydroxyl group contained only chlorine (Nos. 36—39) had to be analyzed by the "excess" method. This result is to be expected from the standpoint of the deactivating influence of halogen on the aromatic ring. By introducing a methyl group the reactivity is increased as shown by the results of the titration of the two chlorocresols (Nos. 20 and 21).

Phenols with meta directing substituents. These compounds are conveniently discussed together. Phenols with the following *meta* directing groups have been tested: nitro, carboxyl, formyl and alkylketone (Nos. 22—25 and 40—47). Considering the electronwithdrawing influence of these groups a decreased reactivity in comparison with phenol might be expected *. However, with the exception of the nitrophenols, the *para* isomers (Nos. 23—25) and in one case also the *ortho* isomer (No. 22) are more reactive. The *meta* isomers are less readily substituted than the rest as the "excess" method invariably had to be employed. No splitting off of carboxyl or formyl groups has been observed.

Dihydroxy- and polyhydroxyphenols. Only *meta* isomers could be analyzed by the present bromination method (Nos. 16—18). The "direct" method was applicable.

Diphenylols and naphthols. Of the three diphenylols tested (Nos. 13, 14 and 35) *o*-hydroxy- and *β*-hydroxydiphenyl could be titrated directly, while *o,o'*-dihydroxydiphenyl was less reactive. This fact is obviously a result of decreased resonance due to steric hindrance and hydrogen bonding. *β*-Naphthol (No. 15) consumed only two bromine atoms per molecule although four might be expected **. *α*-Naphthol, on the other hand, consumed four equivalents of bromine. The values are not communicated, however, as the results were less accurate because of discolouration of the solution.

Phenol ethers. The bromination method was tried on several alkoxyphenols. However, it was found to be not suitable for the quantitative analysis of this type of phenols. The result of the direct titration of one aryloxyphenol showed, that only the ring containing the hydroxyl group was attacked (No. 26).

* In the discussion above it has been assumed that alkyl groups increase the nucleophility of a phenol and *meta* directing groups and chlorine decrease it. Such an assumption is not necessarily correct. It must be taken into account that when one of these groups or atoms is substituted for a hydrogen atom in a phenol, the resonance between the oxygen atom of the hydroxyl and the ring also changes. The combined nucleophilic effect may well be contrary to that expected when only the influence of the substituent on the ring is considered. This fact in connection with other effects originating from steric hindrance and hydrogen bonding might explain the apparently contradictory results obtained in some cases.

** To obtain accurate results it is necessary to use a volume of bromide-bromate solution corresponding to the substitution of one hydrogen atom.

With the establishment of the suitable conditions for the quantitative analysis of the phenols collected in Tables 1 and 2 the application of the bromination method to other phenols should be considerably facilitated.

REFERENCES

1. Koppeschaar, W. F. *Z. Anal. Chem.* **15** (1876) 233.
2. Kolthoff, I. M. *Z. anorg. u. allgem. Chem.* **112** (1920) 187.
3. Kolthoff, I. M. *Konduktometrische Titrationen*, Verlag Steinkopff, Dresden 1923.
4. Britton, H. T. S. *Conductometric Analysis*, D. Van Nostrand Co., New York 1934.
5. Fritz, J. S. and Keen, R. T. *Anal. Chem.* **25** (1953) 179. See also *Anal. Chem.* **28** (1956) 784–797.
6. Francis, A. W. and Hill, A. J. *J. Am. Chem. Soc.* **46** (1924) 2498.

6a. Karrman, K. J. and Johansson, G. *Mikrochim. Acta* **11** (1956) 1573.

7. Scott, W. *Standard Methods of Chemical Analysis*, 5th Ed, Vol. II, p. 2253, D. Van Nostrand Co., New York 1939.
8. Day, A. R. and Taggart, W. T. *Ind. Eng. Chem.* **20** (1928) 545.
9. Callan, T. and Henderson, J. A. R. *J. Soc. Chem. Ind.* **41** (1922) 161.
10. Riemschneider, R. *Pharmazie* **1** (1946) 161.
11. Singh, A. *J. Indian Chem. Soc.* **31** (1954) 605.
12. Bielenberg, W., Goldhahn, H. and Zoff, A. *Oel u. Kohle* **37** (1941) 496.
13. Bielenberg, W. *Ber.* **75B** (1942) 686.
14. Sprung, M. M. *Ind. Eng. Chem., Anal. Ed.* **13** (1941) 35.
15. Ruderman, I. W. *Ind. Eng. Chem., Anal. Ed.* **18** (1946) 753.
16. Tomicek, O. and Dolezal, J. *Chem. Listy* **43** (1949) 193.
17. Singh, A. *J. Indian Chem. Soc.* **31** (1954) 609.
18. Buxton, J. and Lucas, H. J. *J. Am. Chem. Soc.* **50** (1928) 249.
19. Price, J. *J. Am. Chem. Soc.* **77** (1955) 5436.
20. Almin, K. E. and Lindberg, B. *Acta Chem. Scand.* **6** (1952) 1561.

Received September 8, 1956.

ACTA CHEMICA SCANDINAVICA 10 (1956) 1597—1602

On some Properties of the Aromatic Constituent of Male Sperm Antagglutin and its "Active Group"

P. E. LINDAHL, J.-E. KIHLSTRÖM and S. ROSS

Institute of Zoophysiology, Uppsala, Sweden

Some properties of an aromatic constituent of the male sperm antagglutin have been studied spectrophotometrically. Its absorption properties like those of its *p*-quinone and its hydroquinone are similar to those of the known tocopherols. On account of many dissimilarities between the substance and the latter its identity with any of the known tocopherols is excluded.

The aromatic compound is part of a protein free complex also containing sulphuric acid, and sugar residues. In this complex it may also occur as quinone.

From male sperm antagglutin we obtained in 1954 [1] a substance which appeared to be aromatic by nature, and which by reason of its absorption curve and its behaviour at oxidation was suggested to be related to vitamin E. It was provisionally denominated as a "tocopherol derivative". Its non-identity with α-tocopherol was, however, stressed, and will be further discussed below.

From samples of bull semen obtained during the spring of 1954 we rather frequently isolated antagglutin which on extraction with ethyl ether from water solution gave the above mentioned aromatic compound. More recently, however, this happened very sporadically only. Accordingly we now consider the occurrence of the aromatic constituent in extractable form as an artefact. So far we have not been able to establish the conditions provoking this state. As the possibilities of splitting off the aromatic residue from the rest of the molecule by means of chemical and physical agents is now being investigated in this laboratory it seems appropriate to publish some early observations on this spontaneously liberated material which has been available in such very minute quantities that it could be studied only by spectrophotometric methods.

EXPERIMENTS AND RESULTS

The semen from which the antagglutin used in these experiments was obtained came chiefly from the A.I.-station of Eskilstuna. The antagglutin was isolated according to Lindahl and Kihlström [2], the procedure including twice repeated salting out with ammo-

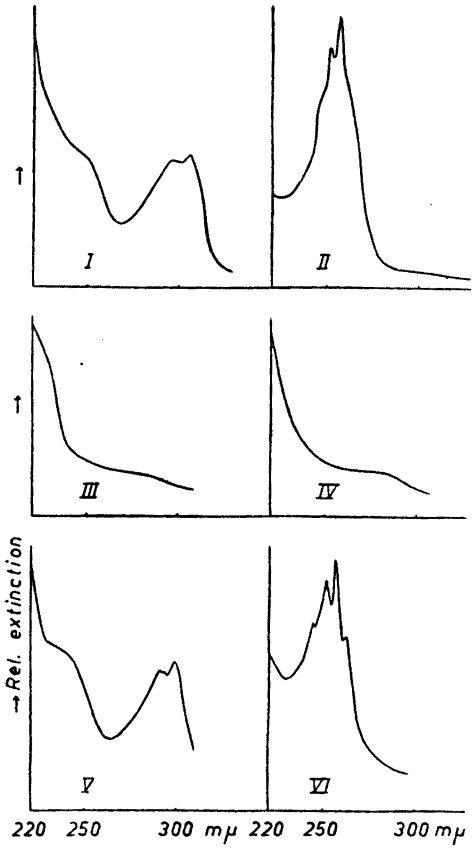


Fig. 1. Absorption curves of the aromatic constituent and the "active group" of male spermantagglutin. I the aromatic constituent in its original form, II after mild oxidation as quinone, III after prolonged oxidation. IV the "active group" split from the protein residue and chromatographed (spectrum of aromatic constituent not visible), V after extraction with ethyl ether showing aromatic constituent in original form, and VI with the aromatic constituent as quinone. I—III in ethanolic, IV—VI in aqueous solution.

nium-sulphate, and subsequent chromatography on calcium carbonate. The antagglutin was always in the reduced form when extracted with ethyl ether, the reduction being generally brought about with hydrogen, and platinum as a catalyst.

The absorption curve (I, Fig. 1) of the extracted compound was measured in absolute ethanol ("Spectroscopically pure", Vin och Spritcentralen, Ltd.) with maxima at 295 and 305 mμ, and a minimum at 268 mμ. Because of the similarity in the general trend of this curve with that of δ-tocopherol in ethanol (*cf.* [3]) a closer comparison is made. The single maximum [4] of δ-tocopherol is at 298 mμ, and its minimum at about 257 mμ. The α-, β-, and γ-tocopherols also have single absorption maxima in ethanol [3]. On the other hand the absorption curve of α-tocopherol in hexane has two maxima [5], and the same was found for δ-tocopherol (from Eastman Kodak Comp.). However, when transferred into hexane ("for spectroscopical use" B.D.H.) our substance yielded a smooth curve without maxima and minima [1] persisting also when the substance was brought back into ethanol again.

In order to provide further comparison our substance was subjected to mild oxidation by being aerated for 16 h at +5°C in ethanolic solution in the presence of $FeCl_3$ and $CuSO_4$ (10^{-4} M). The absorption curve (II, Fig. 1) in ethanol of the product formed has a narrow double peak with maxima at 251 and 256 mμ, with about twice as high extinction coefficient as the substance before oxidation. These absorption data may be compared with those obtained in ethanolic solution for the *o*-quinone of α-tocopherol and the *p*-quinones of the α- and δ-tocopherols (Table 1).

Table 1.

	λ in mμ		max. of ox.prod. / max. of tocoph.	
α-Tocopheryl *p*-quinone	261—263	267—268	6—7	(6)
α-Tocopheryl *o*-quinone	258	(270)	3	(6)
δ-Tocopheryl *p*-quinone	257		2.5	(4)
Ox. antagglutin constituent	251	256	2	

As seen from Table 1 the oxidation product of the antagglutin constituent comes nearest to δ-tocopheryl *p*-quinone which, however, has only one maximum. Further it should be stressed that neither α- nor δ-tocopherol will be oxidized to a quinone under the conditions employed for the antagglutin constituent.

When subjected to catalytic reduction with hydrogen the absorption curve of the oxidized antagglutin constituent changes rapidly. The strong absorption band disappears, and a new weak one around 310 mμ appears, the whole absorption curve now being very similar to the curve of the originally extracted substance. There is, however, a single maximum, and the minimum as well as the maximum absorption occur at longer wavelengths. The existence of a transition stage in the reduction is suggested by the fact that during the first minutes of the reduction, when the high absorption-band of the oxidation product is beginning to decrease, much higher extinction values appear around 310 mμ than those remaining when the reduction is finished.

As the oxidation product appears to be a quinone its reduction should give the corresponding hydroquinone. On account of the different positions of the absorption bands of *ortho*- and *para*-diphenols in general, it may be concluded that we are dealing with a hydroquinone. This hydroquinone is very quickly oxidized to quinone on exposure to air, being in this respect similar to α-tocopheryl hydroquinone [7]. The latter has a single extinction maximum [7] at about 290 mμ, as compared with the maxima of α-tocopherol at 292 and 298 mμ. A corresponding comparison of the extinction maxima of our hydroquinone, about 310 mμ, with those of the originally extracted compound, 292 and 305 mμ, makes probable that besides the quinone-hydroquinone transformation also other changes must have occurred.

Treatment of the tocopherol-like constituent with 4 M hydrochloric acid at 40°C for 11 h in ethanolic solution under H_2-atmosphere did not cause any change in its extinction properties. Thus none of the aromatic hydroxyls may be engaged in an easily hydrolyzed ester bond. In a similar experiment the

H_2-atmosphere was replaced by air. Also here the extinction curve was unchanged, indicating a rather high stability against oxidation by air under these conditions. However, when exposed to air at the same temperature for 48 h with 0.5 M hydrochloric acid the absorption curve was very much changed (Fig. 1, III). It appears from these two experiments that high concentrations of hydrochloric acid protect the substance from being oxidized in air. This is of special interest as acids are known to promote ring closure in α-tocopheryl hydroquinone which is by this process transformed into tocopherol.

Occasionally the *p*-quinone, produced by oxidation of the tocopherol-like substance, may instead of the latter be extracted from antagglutin solutions. In case both are present in a sample the quinone is extracted first, and seems thus to be the more hydrophobic substance of the two. — Also the absorption bands of this quinone are changed in hexane solution under the conditions in question.

The splitting-off of the active group from the protein constituent was performed as a dissociation, promoted by a high pH (9.6) and certain ions. In one type of experiment it was then separated from the protein by adsorption, in the other by ultrafiltration.

In an experiment of the first mentioned type a purified antagglutin sample, dissolved in water, was incubated at 5°C and pH 9.6 with 10^{-4} M $CuSO_4$ and $FeCl_3$ for 44 h. To minimize possibly occurring oxidation the sample was then reduced catalytically with hydrogen at pH 5.5. The solution was afterwards neutralized, brought to pH 8.5 with glycine-sodium hydroxide buffer, and filtered through a column of calcium carbonate, activated by heating for 3 h at 150°C. With CO_2containing water (pH 5.5) an eluate was obtained showing a spectrum without specific absorption (IV). This eluate was evaporated to dryness, and the residue extracted with ethyl ether. The latter was again evaporated, and the remaining substance extracted with water. Part of this residue did not dissolve, and remained as an unwettable coat on the inside of the vessel. This phenomenon was observed regularly when the "active group" had been treated with ether or any other slightly polar solvent. The aqueous extract showed an extinction curve (V) very similar to that (I) of the tocopherol-like substance described above, but with absorption maxima at 290 and 299 mμ. This material contained some impurities, probably salts, which could be further removed by adsorption of the aromatic substance on quartz powder and subsequent washing out which ethyl ether. After this the absorption curve, measured in water, showed a third maximum at 240 mμ (*cf.* Lindahl and Kihlström [1]). This substance which may be dissolved in ether only in a dry state has also appeared spontaneously on some occasions during the isolation of the antagglutin. In such cases it is found in the eluates obtained after the elution of the antagglutin was completed.

In some experiments besides Fe^{3+} and Cu^{2+}, also Mg^{2+}, Mn^{2+}, and Zn^{2+} were present during the incubation in concentrations of 10^{-4} M, and the treatment was shortened to 16 h. In these cases already the eluate showed a characteristic extinction curve (VI), yet with maxima identical with those of the quinone (II). There were, however, two further small peaks at 244 and 263 mμ. Also this substance has occurred spontaneously in some instances (*cf.* above). We are, however, not able to state whether these two small peaks

may be demonstrated also in the extinctior curve of the free quinone or not, as our measurements were not sufficiently extensive at the relevant points.

The ultrafiltration was performed in the following way. The pH of the antagglutin solution was raised to 8.6 with NaOH, and the solution immediately sucked through a washed collodion membrane (Membranfiltergesellschaft, Sartoriuswerke, Göttingen), the pores of which permit the passage of particles corresponding to a max. molecular weight of about 4 000. The filtrate did not give a positive ninhydrin reaction but contained sugar (positive benzidine reaction). The absorption curve was identical with (V). Obtained in this way, the "active group" did not exhibit any antagglutinic activity.

With this method we have also been able to localize the incorporation of radioactive sulphur with the antagglutin molecule (*cf.* [8]) to the "active group". The occurrence of sulphuric acid residues in the "active group" was assumed earlier for different reasons [2,8]. This has now been verified by hydrolyzing the isolated protein-free material obtained from rabbits injected with $Na_2{}^{35}SO_4$ (*cf.* [8]) and following precipitation with Ba^{2+}. The precipitate contained about 95 % of the radioactivity registered in the "active group".

DISCUSSION

The observations on the aromatic constituent of male sperm antagglutin recorded above suggest that we are dealing with a 6-hydroxy-chromane structure, possibly a tocopherol derivative. To decide whether this idea is right or not larger samples of the substance are necessary. The many dissimilarities between this substance and all the known tocopherols, *e.g.* the higher reactivity at oxidation and hydrogenation, the influence of hexane or impurities in the latter on the absorption spectrum, exclude, however, the identity with any known member of the latter group. It was further stated [1] that oxidation of this tocopherol-like substance with nitric acid according to Ungnade and Smith [9] yields a yellow colour instead of the red obtained for the α-, β-, and γ-tocopherols. This is of great interest as it was shown by Smith *et al.*[10] that the presence of an ethylenic bond or a carbonyl group in the side chain of the quinone formed gives rise to a yellow colour instead of a red one. On the other hand also the substituents of the benzene ring in the chromane molecule influence this reaction as δ-tocopherol gives an orange-yellow colour [4].

When the protein constituent has been removed the complex which has been called the "active group" represents the rest of the antagglutin molecule in a more or less denaturated state. Most probably this complex with a molecular weight below 4 000 in its native state has an absorption curve similar to that of the male antagglutin. A moderate change brings about the appearance of the absorption bands of the tocopherol-like constituent — although somewhat displaced towards shorter wavelengths — without impairing the antagglutinic activity. A more far-reaching change abolishes this activity without further altering the absorption spectrum. Oxidation then gives the complex an absorption curve very similar to that of the quinone described above. The occasional spontaneous appearance of the "active group" at the preparation of antagglutin must depend upon some change in the molecule of the latter,

having occurred probably already in the semen. This altered "active group" as well as the tocopherol-like substance extractable with ethyl ether from aqueous solutions must by looked upon as artefacts.

As long as the antagglutin molecule is not in some way denaturated the tocopherol-like constituent seems to be rather resistant against catalytic hydrogenation.

So far the "active group" has been shown to consist of the tocopherol-like substance, sugar, and sulphuric acid residues. The presence of the many hydrophilic groups in the two last mentioned residues causes the water solubility of the complex, and makes it dissolve in ethyl ether only when dry.

We are very much indebted to Drs. B. Ström and T. Svensson for semen material. The financial support of the *Swedish Agricultural, Natural Science* and *Medical Research Councils* is gratefully acknowledged. We thank Prof. E. Stenhagen for reading the manuscript.

REFERENCES

1. Lindahl, P. E. and Kihlström, J.-E. *Nature* **174** (1954) 600.
2. Lindahl, P. E. and Kihlström, J.-E. *Fertility and Sterility* **5** (1954) 241.
3. Baxter, J. G., Robeson, C. D., Tayler, J. D. and Lehman, R. W. *J. Am. Chem. Soc.* **65** (1943) 918.
4. Stern, M. H., Robeson, C. D., Weisler, L. and Baxter, J. G. *J. Am. Chem. Soc.* **69** (1947) 869.
5. Webb, T. J., Smith, L. I., Bostedo, Jr., W. A., Ungnade, H. E., Prichard, W. W., Hoehn, H. H., Wawzonek, S., Opie, J. W. and Austin, F. L. *J. Org. Chem.* **4** (1939) 389.
6. Framton, V. L., Skinner, W. A. and Bailey, P. S. *Science* **116** (1952) 34.
7. John, W., Dietzel, E. and Günther, Ph. *Hoppe-Seylers Z. physiol. Chem.* **252** (1938) 208.
8. Kihlström, J.-E. *Arkiv Kemi* **7** (1954) 399.
9. Ungnade, H. E. and Smith, L. I. *J. Org. Chem.* **4** (1939) 397.
10. Smith, L. I., Iwin, W. B. and Ungnade, H. E. *J. Am. Chem. Soc.* **61** (1939) 2424.

Received September 13, 1956.

ACTA CHEMICA SCANDINAVICA 10 (1956) 1603—1605

Transformation of 2-(Hydroxymethyl)-5-(aminomethyl)-furan into 6-Methyl-3-pyridinol *

NIELS ELMING

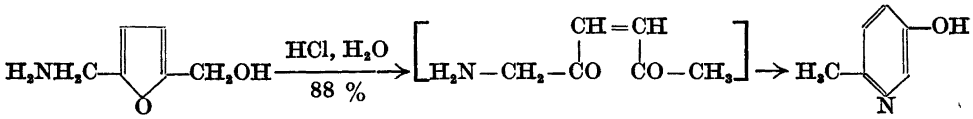
Centrallaboratoriet, Sadolin & Holmblad A/S, Copenhagen, Denmark

NIELS CLAUSON-KAAS

Department of Chemistry, Israel Institute of Technology, Haifa, Israel

6-Methyl-3-pyridinol has been prepared from 2-(hydroxymethyl)-5-(aminomethyl)-furan by the action of hydrochloric acid. Electrolytic methoxylation of 2-(acetoxymethyl)-5-(acetamidomethyl)-furan followed by alkaline hydrolysis and treatment with hydrochloric acid gave 6-(hydroxymethyl)-3-pyridinol.

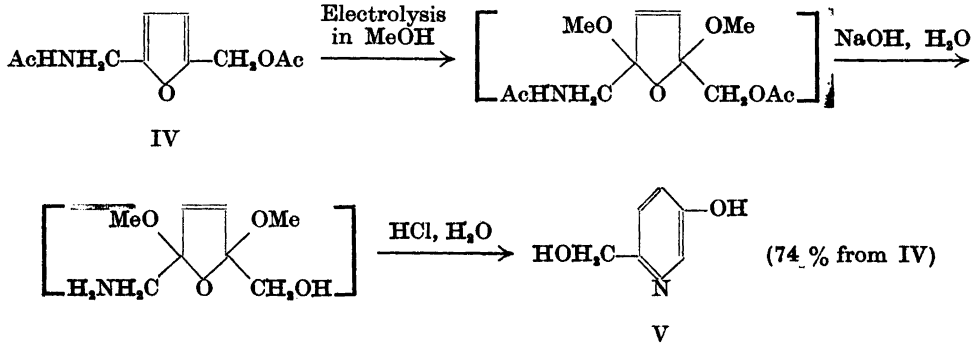
Furfuryl alcohol is transformed by the action of methanolic hydrogen chloride into a mixture of distillable products (yield 42 %) consisting of 2,3 (or 4), 5-trimethoxytetrahydrosilvan, methyl levulinate, methyl levulinate dimethyl ketal and 2 (or 3)-methoxylevulinaldehyde dimethyl acetal [1]. It has been proved [1,2] that this transformation proceeds through *cis*-3-acetylacrolein or its equivalent. We have now found that 2-(hydroxymethyl)-5-(aminomethyl)-furan (I) forms 6-methyl-3-pyridinol (III) by the action of hydrochloric acid. It is reasonable to assume that this transformation also takes place through an unsaturated 1,4-dicarbonyl compound, *viz.* 1-amino-3-hexene-2,5-dione (II) or its equivalent.



I II III

* Presented before the Division of Organic Chemistry at the 9th Scandinavian Chemical Meeting, Århus, Denmark, August 1956.

I is a new compound which was prepared by reductive amination of 5-(hydroxymethyl)-furfural (yield 72 %). It was characterized by the hydrochloride, the diacetate [2-(acetoxymethyl)-5-(acetamidomethyl)-furan (IV)] and by transformation of IV into the known 6-hydroxymethyl-3-pyridinol (V) by the sequence of reactions shown below (*cf.* [3]).



EXPERIMENTAL

Microanalyses by E. Boss and K. Glens

2-(Hydroxymethyl)-5-(aminomethyl)-furan (I). 5-(Hydroxymethyl)-furfural [4] (12.8 g), methanol (30 ml), liquid ammonia (5 ml) and Raney nickel (0.4 g) were mixed and shaken (1 h) under 100 atmospheres of hydrogen at 65—75°. After cooling, the reaction mixture was filtered and the filtrate distilled. The yield was 9.30 g (72 %) of I (pale yellow liquid, b.p. $_{0.1}$ 102—105°, n_D^{25} 1.5278). (Found: C 56.8; H 7.4; N 11.1. Calc. for $C_6H_9O_2N$ (127.1): C 56.7; H 7.1; N 11.0).

2-(Hydroxymethyl)-5-(aminomethyl)-furan hydrochloride. Gaseous hydrogen chloride was passed into a solution of I (130 mg) in ether. The precipitate was removed by filtration, washed with ether and dried. The yield was 120 mg (72 %) of 2-(hydroxymethyl)-5-(aminomethyl)-furan hydrochloride [almost white crystals, m.p. 118—121° (Hershberg apparatus, corr.)]. (Found: C 44.3; H 6.2; N 8.5; Cl 21.2. Calc. for $C_6H_{10}O_2NCl$ (163.6): C 44.1; H 6.2; N 8.6; Cl 21.7).

2-(Acetoxymethyl)-5-(acetamidomethyl)-furan (IV). I (1.27 g) was dissolved in a mixture of acetic anhydride (15 ml) and pyridine (15 ml). The reaction mixture was left standing for 2 days and then evaporated in a vacuum. The residue was crystallized from ether. The yield was 1.93 g (92 %) of IV (white crystals, m.p. 65—67°). (Found: C 56.9; H 6.2; N 6.3; $COCH_3$ 38.5. Calc. for $C_6H_7O_2N(COCH_3)_2$ (211.2): C 56.9; H 6.2; N 6.6; $COCH_3$ 40.8).

6-Methyl-3-pyridinol (III). I (1.27 g) was dissolved in a mixture of N hydrochloric acid (60 ml) and water (40 ml). The reaction mixture was heated under reflux (15 h) and then evaporated in a vacuum. The residue was dissolved in water (15 ml), solid potassium carbonate was added and the mixture continuously extracted with ether overnight. The ether extract was evaporated, the residue washed twice with ether and dried. The yield was 0.96 g (88 %) of III (light-brown crystals, m.p. 168—170°, previously found[5] 167—169°). III gave a red color with aqueous ferric chloride. (Found: C 66.0; H 6.5; N 12.7. Calc. for C_6H_7ON (109.1): C 66.0; H 6.5; N 12.8). Sublimation (150°, 0.05 mm) gave white crystals, m.p. 169—171°.

Picrate. After crystallization from ethanol the m.p. was 205—208° (decomp.), previously found[6] 203°. (Found: C 42.8; H 3.2; N 16.3. Calc. for $C_{12}H_{10}O_8N_4$ (338.2): C 42.6; H 3.0; N 16.6).

6-Methyl-3-pyridinol hydrochloride. In another experiment the reaction mixture was evaporated as described above. The residue was then sublimed (160°, 0.1 mm). The yield

was 75 % of 6-methyl-3-pyridinol hydrochloride (white crystals, m.p. 145—150°). (Found: C 49.6; H 5.7; N 9.9; Cl 24.1. Calc. for C_6H_8ONCl (145.6): C 49.5; H 5.5; N 9.6; Cl 24.4).

6-(Hydroxymethyl)-3-pyridinol (V). IV (1.70 g) and ammonium bromide (200 mg) were dissolved in methanol (15 ml) and the solution electrolyzed with the set-up described previously[7] (temperature of cooling-bath −21°).

Time h	Current Amp.	Potential across the cell during electrolysis Volt	Ampere hours (% of theoretical) amount)	
0.1	0.30	4.6	0.02	(5 %)
0.2	0.29	4.7	0.05	(12 %)
0.5	0.29	4.9	0.14	(33 %)
1.0	0.29	4.9	0.26	(60 %)
2.0	0.22	5.1	0.48	(111 %)

After electrolysis the liquid was poured into a solution of sodium methoxide (from 250 mg of sodium) in methanol (5 ml) and the methanol and the ammonia evaporated in a vacuum. Sodium hydroxide (3 N, 14 ml) was added, the mixture heated under reflux (18 h) and then continuously extracted with ether for 20 h. The ether was evaporated in a vacuum and the mixture heated under reflux (20 min) with hydrochloric acid (N, 15 ml). The mixture was evaporated to dryness in a vacuum and the residue then dissolved in water (15 ml). Solid potassium carbonate was added and the mixture continuously extracted with ether overnight. The ether extract was evaporated, the residue washed twice with ether and dried. The yield was 0.74 g (74 %) of V (light-brown crystals, m.p. 123—125°, previously found[6] 124—125°). V gave a red color with aqueous ferric chloride (Found: C 57.6; H 5.8; N 10.8. Calc. for $C_6H_7O_2N$ (125.1): C 57.6; H 5.6; N 11.2). Sublimation (125°, 0.05 mm) gave white crystals, m.p. 123—125°.

REFERENCES

1. Clauson-Kaas, N. and Nielsen, J. T. *Acta Chem. Scand.* **9** (1955) 475.
2. Dunlop, A. P. and Peters, F. N. *The Furans*, New York 1953, p. 646.
3. Clauson-Kaas, N., Elming, N. and Tyle, Z. *Acta Chem. Scand.* **9** (1955) 1.
4. Haworth, W. N. and Jones, W. G. M. *J. Chem. Soc.* **1944** 667.
5. Marion, L. and Cockburn, W. F. *J. Am. Chem. Soc.* **71** (1949) 3402.
6. Aso, K. *J. Agr. Chem. Soc. Japan* **16** (1940) 249. *Chem. Abstracts* **34** (1940) 6278.
7. Limborg, F. and Clauson-Kaas, N. *Acta Chem. Scand.* **7** (1953) 234.

Received September 13, 1956.

ACTA CHEMICA SCANDINAVICA 10 (1956) 1606—1613

A Kinetic Study by Measurements of Steady-State Potentials of Platinum in Persulphate Solutions Containing Ammonium and Silver Salts

STURE FRONÆUS

Department of Physical Chemistry, Chemical Institute, University of Lund, Lund, Sweden

The oxidation of ammonium ions by silver(II), which is presupposed to be a partial process of the silver(I) catalyzed self-decomposition of ammonium persulphate in acid solution, is investigated by measurements of the steady-state potential of a platinum electrode. From the dependence of the potential upon the concentrations of different ions taking part in the reactions, the kinetic laws of the oxidations of ammonium ions and water are determined. A mechanism of the oxidation of ammonium ions is proposed and is proved to be in accord with the laws obtained.

By measurements of the impedance of the electrode-solution interface it is shown that redox couples formed in the last-mentioned oxidation take part in the electron exchange between the electrode and the solution.

The principal features of the mechanism of the silver(I) catalyzed self-decomposition of ammonium persulphate in aqueous solution were clarified in a previous investigation (Fronæus and Östman [1],) dealing with the silver(I) catalyzed reaction between cerium(III) and ammonium persulphate. A partial process of the mechanism proposed is the reaction between silver(II), formed as an intermediate, and the ammonium ions. Since this reaction is not rate-determining for the over-all reactions studied, the kinetic law for the partial process mentioned could not be obtained from the measurements performed. Actually, no experimental determination of this rate law has been reported but only assumptions (*cf.* Carman [2]), that have not been tested quantitatively.

The purpose of the present investigation is a further elucidation of this problem by determinations of the concentration ratio between silver(II) and silver(I) by emf measurements with a platinum electrode. Since the solutions to be studied contain several redox couples which are not exactly in equilibrium, the steady-state electrode potential is theoretically a so-called mixed potential (for previous literature about this conception, the reader is referred

to papers by Wagner and Traud [3], and Kolthoff and Miller [4]), and this fact should be borne in mind when treating the emf values obtained. In order to determine whether several couples are actually involved in the adjustment of the electrode potential, measurements of the impedance of the electrode-solution interface have been chosen.

THEORETICAL

According to the mechanism for the silver(I) catalyzed decomposition of ammonium persulphate in acid solution, arrived at in the previous paper [1], we have the following set of homogeneous reactions as the predominating ones

$$Ag(I)+S_2O_8^{2-} \rightarrow Ag(II)+SO_4^{-}+SO_4^{2-} \quad (1)$$

$$Ag(I)+SO_4^{-} \rightleftharpoons Ag(II)+SO_4^{2-} \quad (2)$$

$$8\ Ag(II)+NH_4^{+}+3\ H_2O \rightarrow 8\ Ag(I)+10\ H^{+}+NO_3^{-} \quad (3)$$

where (1) is the rate-determining step and reaction (3) certainly involves several steps. The set of reactions has been extended somewhat, in that we take the backward process of (2) into consideration.

Furthermore, we have the oxidation of water, that should be of importance at low ammonium ion concentrations

$$SO_4^{-}+H_2O \rightarrow HSO_4^{-}+OH \quad (4)$$

$$Ag(II)+H_2O \rightarrow Ag(I)+H^{+}+OH \quad (5)$$

$$2\ OH \rightarrow H_2O+\tfrac{1}{2}O_2 \quad (6)$$

Here (5) and (6) are not simple steps [5,6].

In preliminary measurements it was established that the presence of platinum surfaces has no effect on the rate of persulphate decomposition. Evidently the persulphate ions take no appreciable part in the electron exchange with the electrode, and the oxidizing agents formed as intermediates in the reactions above must be responsible for the high steady-state electrode potential obtained. Thus we regard the electrode reactions

$$Ag(I) \rightleftharpoons Ag(II)+e^{-} \quad (7)$$

$$SO_4^{2-} \rightleftharpoons SO_4^{-}+e^{-} \quad (8)$$

and represent by

$$A \rightleftharpoons B+e^{-} \quad (9)$$

the further reactions that may be involved in the adjustment of the potential. The anodic current densities of (7), (8), and (9) are denoted i_1, i_2, and i_3. Thus i_3 is the sum of anodic currents due to the oxygen-water couple and couples formed in the oxidation of the ammonium ion.

When a steady-state electrode potential has been attained the following relationship is valid

$$i_1+i_2+i_3=0 \quad (10)$$

Furthermore, denoting by r_1, $\vec{r}_2$, $\overleftarrow{r}_2$ and $r_3 \cdots r_6$ the rates of the reactions (1)—(6), and applying the steady-state approximation to Ag(II) and SO_4^- in the bulk of the solution by putting $d[Ag(II)]/dt = 0$ and $d[SO_4^-]/dt = 0$ (t = time), we get the equations

$$r_1 + \vec{r}_2 - \overleftarrow{r}_2 - r_3 - r_5 = 0 \tag{11}$$

$$r_1 - \vec{r}_2 + \overleftarrow{r}_2 - r_4 = 0 \tag{12}$$

If r_1 is not equal to r_4 the redox potential e_1 of the silver couple will be different from the redox potential e_2 of the SO_4^-—SO_4^{2-} couple. However, since the reaction (1) is the rate-determining step we can presume that r_1 and r_4 ($<2\,r_1$) are very small in comparison with $\vec{r}_2$ and $\overleftarrow{r}_2$, so that $\vec{r}_2 \approx \overleftarrow{r}_2$ and hence $e_1 \approx e_2$. If we further presume that the absolute value of the difference between $e_1 \approx e_2$ and the steady-state potential e_0 of the electrode is sufficiently small to permit us to put the concentrations of the last-mentioned two couples close to the interface approximately equal to the concentrations in the bulk of the solution, we have the following relationship (*cf.* Fronæus [7]) for i_1 and i_2 at the steady-state potential.

$$i_n = i_{0,n}\left(\exp\left\{\frac{\alpha_n(e_0 - e_1)F}{RT}\right\} - \exp\left\{-\frac{(1-\alpha_n)(e_0-e_1)F}{RT}\right\}\right) \tag{13}$$

($n = 1$ and 2)

Here $i_{0,n}$ is the exchange current density and $0<\alpha_n<1$. But for small absolute values of $(e_0 - e_1)$ this expression can be replaced by

$$i_n = \frac{i_{0,n}(e_0 - e_1)F}{RT} \tag{14}$$

Now $RTF^{-1}i_{0,n}^{-1}$ is equal to the electron transfer resistance [7] $R_{t,n}$ of the electrode reactions (7) and (8), and using eqn. (10) we get

$$e_1 - e_0 = \frac{i_3}{R_{t,1}^{-1} + R_{t,2}^{-1}} \tag{15}$$

In the emf measurements below we will presuppose that the difference $e_1 - e_0$ is negligible and from variations in e_0 calculate the corresponding variations in the concentration ratio between silver(II) and silver(I). It should be emphasized that a very small value of i_3 does not imply that the transfer resistance $R_{t,3}$ of (9) is very high (*cf.* Fronæus [7]).

Adding eqns. (11) and (12) we obtain $r_3 + r_4 + r_5 = 2\,r_1$. According to the results of the previous investigation [1] we have $r_1 = \text{constant} \cdot [Ag(I)][S_2O_8^{2-}]$. If the complex formation between Ag^+ and the anions present is neglected [Ag(I)] can be replaced by $[Ag^+]$. Then we try to use the expression $[Ag^{2+}]^j \cdot \varphi$ for $r_3 + r_4 + r_5$, where φ may be a function of the concentrations of different species except silver(II) and persulphate, and get the relationship

$$\frac{[Ag^{2+}]}{[Ag^+]} = \text{constant}\,\frac{[S_2O_8^{2-}]^{\frac{1}{j}}}{[Ag^+]^{\frac{j-1}{j}}\,\varphi^{\frac{1}{j}}} \tag{16}$$

Thus by determining the dependence of $[Ag^{2+}][Ag^{+}]^{-1}$ upon the different concentrations it should be possible to obtain the value of j and the expression for φ.

MEASUREMENTS AND CALCULATIONS

Chemicals used. Sodium persulphate solutions were prepared by mixing equivalent amounts of solutions containing potassium persulphate and sodium perchlorate, cooling down to about 5°C and filtering off the potassium perchlorate precipitated. The concentration of the sodium persulphate solution was determined as described previously (Fronæus and Östman [8]).

Other chemicals used were prepared as before [1] or were commercial preparations of analytical grade.

Emf measurements. The cells measured were of the following type

−Au	quinh. 10 mM $HClO_4$ 990 mM $NaClO_4$	1000 mM $NaClO_4$	solution	Pt+

The solution of the right half-cell was obtained by mixing different solutions containing ammonium or sodium persulphate, ammonium, silver, and sodium perchlorates, perchloric acid, and ammonium or sodium sulphate. The sodium perchlorate was supplied in order to keep the ionic strength equal to 1 M. The measurements were carried out at a temperature of 25.0°C.

At first when the platinum electrodes were used no steady potentials were obtained. However, when the electrodes had been kept in decomposing persulphate solutions for some days, fairly steady potentials were attained when the electrodes were immersed in new solutions. Probably this fact must be ascribed to the formation of an oxide of platinum on the surface of the electrodes (*cf.* Bowden [9], Ershler [10]). In order to get reliable results every cell solution was freshly prepared many times, and different platinum electrodes were used. Then it was found that within 1 or 2 mV, the same emf mean values were obtained with different electrodes.

For the emf E in mV we have

$$E = E_0 + 59.16 \log \frac{[Ag^{2+}]}{[Ag^{+}]} \qquad (17)$$

where E_0 should be approximately constant. Taking the value 2 000 mV for the standard potential e_1^0 of the silver couple (*cf.* Noyes *et al.* [11]) and 560 mV for the potential of the quinhydrone electrode we get $E_0 \approx 1\,400$ mV. Then we find from the E-values in Tables 1 and 2 that $[Ag^{2+}] < 3 \times 10^{-4}[Ag^{+}]$. Thus, unless the complex formation between Ag^{2+} and the anions of the solutions is very strong, and this is not probable, the concentration of silver(II) is so low that we can put the concentration of silver(I) approximately equal to the total silver concentration. The values of $[H^{+}]$ and $[SO_4^{2-}]$ in the tables were calculated from the concentrations of perchloric acid and sulphate, the secondary dissociation constant $K_s = 8.5 \times 10^{-2}$ M being used for sulphuric acid (Fronæus [12]).

The emf values obtained in the presence of ammonium ions in the cell solutions are collected in Table 1. In order to determine an empirical expression for the right member of (16) we write

$$\frac{[Ag^{2+}]}{[Ag^{+}]} = \text{constant } [Ag^{+}]^a [NH_4^{+}]^b [H^{+}]^c [SO_4^{2-}]^d [S_2O_8^{2-}]^e \qquad (18)$$

Table 1. Emf and electrode impedance measurements on persulphate solutions containing ammonium and silver salts.

$[Ag^+]$ mM	$[NH_4^+]$ mM	$[H^+]$ mM	$[SO_4^{2-}]$ mM	$[S_2O_8^{2-}]$ mM	E mV	R_i^{-1} ohm^{-1}cm^{-2}
3.00	200	380	30	100	1 192	0.40
3.00	500	380	30	100	1 183	0.37
3.00	400	380	0	100	1 188	0.43
3.00	450	145	30	100	1 156	0.40
3.00	500	115	65	100	1 147	0.35
1.50	100	380	30	20	1 134	0.28
3.00	100	380	30	20	1 160	0.32
6.00	100	380	30	20	1 177	0.40
12.00	100	380	30	20	1 192	0.47
6.00	200	380	30	100	1 207	0.67
6.00	500	380	30	100	1 199	0.67

The derivative $\partial E/\partial \log [Ag^+]$ is found to be approximately constant and gives $a = 0.8$, except for the lowest silver(I) concentration, where a higher value is obtained which must be excluded. By combining the other E-values all the exponents in (18) can be determined, and we get $b = -0.4$, $c = 1.1$, $d \approx 0$, and $e = 1.0$. An equating of the right-hand members of (16) and (18) gives $j = e^{-1} = 1.0$ and an expression for φ. Then we have

$$r_3+r_4+r_5 = \text{constant } \frac{[Ag^{2+}][NH_4^+]^{0.4}}{[Ag^+]^{0.8}[H^+]^{1.1}} \qquad (19)$$

In order to obtain an empirical expression for r_4+r_5 emf measurements were also performed in the absence of ammonium ions. The E-values are given in Table 2. Eqn. (18) is applied, and it is found that also in this case $\partial E/\partial \log [Ag^+]$ is constant except for $[Ag^+] = 1.50$ mM. The following exponents are arrived at: $a = 0.8$, $c = 1.0$, $d \approx 0$, and $e = 0.8$. Thus $j = 1.2$ and for r_4+r_5 we get

$$r_4+r_5 = \text{constant } \frac{[Ag^{2+}]^{1.2}}{[Ag^+]^{1.2}[H^+]^{1.2}} \qquad (20)$$

Table 2. Emf and electrode impedance measurements on sodium persulphate solutions containing silver salts.

$[Ag^+]$ mM	$[H^+]$ mM	$[SO_4^{2-}]$ mM	$[S_2O_8^{2-}]$ mM	E mV	R_i^{-1} ohm^{-1}cm^{-2}
3.00	380	30	100	1 215	0.18
3.00	380	0	100	1 223	0.20
3.00	145	30	100	1 190	0.20
3.00	115	65	100	1 185	0.18
1.50	380	30	20	1 162	0.13
3.00	380	30	20	1 182	0.14
6.00	380	30	20	1 197	0.16
12.00	380	30	20	1 213	0.23
6.00	380	30	100	1 230	0.23

It should be emphasized that the real dependence of $r_3+r_4+r_5$ and r_4+r_5 upon $[SO_4^{2-}]$ cannot be ascertained from the measurements without information about the complex formation.

In a previous work [8] we arrived at the conclusion that r_4 is proportional to $[SO_4^-]$. Then, if we have a redox equilibrium between the couple SO_4^-—SO_4^{2-} and the silver couple, r_4 should be proportional to $[Ag^{2+}][Ag^+]^{-1}[SO_4^{2-}]$. For r_5 Noyes *et al.*[13] have found complicated expressions, but at low concentrations of silver(II) r_5 seems to be proportional to $[Ag^{2+}]^2[Ag^+]^{-1}$ and decreases for increasing values of $[H^+]$. Since the two last-mentioned rate laws are of different form, our empirical laws (19) and (20) can be applicable only within limited ranges of concentration.

Electrode impedance measurements. For a description of the apparatus used and the theory on which the calculations are based the reader is referred to a recent work [7]. The impedance of the electrode-solution interface can be represented by an equivalent circuit, consisting of a resistance R_p and a capacity C_p connected in parallel. From the measurements R_p was calculated at different values of the frequency ν of the polarizing alternating current. Then the conductance R_p^{-1} was plotted against $\nu^{-\frac{1}{2}}$ and extrapolated to $\nu = \infty$. For the intercept R_t^{-1} on the R_p^{-1}-axis we have

$$\frac{1}{R_t} = \frac{1}{R_{t,1}} + \frac{1}{R_{t,2}} + \frac{1}{R_{t,3}} \tag{21}$$

Also in these measurements it was found that in the beginning no steady values were obtained. R_t decreased continuously when the small polarizable platinum electrode was immersed in a decomposing persulphate solution, but after a few days the electrode gave reproducible impedances with fresh solutions. It is evident that the exchange current densities increased when a surface oxide was formed on the electrode.

If the over-all electrode reactions (7) and (8) are identical with the corresponding electron transfer steps, then $i_{0,1}$ should be proportional to $[Ag^{2+}]^{\alpha_1}[Ag^+]^{1-\alpha_1}$ and $i_{0,2}$ proportional to $[SO_4^-]^{\alpha_2}[SO_4^{2-}]^{1-\alpha_2}$ (*cf.* Fronæus and Östman [14]). Furthermore, if we have a redox equilibrium between these two couples and assume that the transfer coefficients α_1 and α_2 are approximately equal to 0.5, we should have the relationship

$$\frac{1}{R_{t,1}} + \frac{1}{R_{t,2}} = 10^{0.5E/59}(K_1[Ag^+] + K_2[SO_4^{2-}]) \tag{22}$$

where K_1 and K_2 are constants.

The final values of R_t^{-1} obtained from the measurements are given in the last columns of Tables 1 and 2. It is seen that the differences between the values belonging to one and the same table are rather small, but in Table 2 the variation is on the whole in qualitative agreement with the variation in $R_{t,1}^{-1}$ that can be expected according to eqn. (22). On the other hand, the term $R_{t,2}^{-1}$ seems to be of minor importance.

From (22) it is obvious that for small values of E and $[Ag^+]$ the quantity $R_{t,1}^{-1}$ will be small, and thus the difference e_1—e_0 in eqn. (15) may be appreciable.

Possibly this is the reason of the surprisingly small E-value in Table 1 for $[Ag^+] = 1.50$ mM.

Comparing the values of R_t^{-1} in Table 1 with those in Table 2 we find that, if ammonium ions are supplied but the concentrations of the other ions given in the tables are kept constant, the values of R_t^{-1} *increase* considerably, though the values of E decrease. The only explanation of this fact is that the couples formed in the different stages in the oxidation of ammonium ions take part in the electron exchange between electrode and solution, and thus the term $R_{t,3}^{-1}$ in (21) increases.

DISCUSSION OF THE REACTION MECHANISM

If the concentrations of silver(I) and persulphate are kept constant then we have $r_3+r_4+r_5 =$ constant. From Tables 1 and 2 it is evident that by the supply of ammonium ions the E-values decrease 20—38 mV. This means that $[Ag^{2+}]$ is from 2 to 5 times smaller in the presence of the ammonium ions, and from the empirical law (20) it is seen that approximately the same decrease must be valid for r_4+r_5. Accordingly, for the ammonium ion concentrations used we have $r_4+r_5<r_3<4(r_4+r_5)$.

However, it was found experimentally that the rate of the oxygen evolution was slight in the presence of ammonium ions and not at all as great as could be expected from these calculations. In order to explain this fact it must be presumed that the OH radicals, which are probably formed intermediately in the reactions (4) and (5), are made use of to a certain extent in one (or several) of the steps of the over-all reaction (3). For this reason the following mechanism is proposed for the first steps (*cf.* Fronæus and Östman [1]).

$$Ag^{2+}+NH_4^+ \rightleftharpoons AgNH_3^{2+}+H^+ \qquad (23)$$

$$AgNH_3^{2+}+OH \rightarrow Ag^+ + H^+ + NH_2OH \qquad (24)$$

(23) is presupposed to be a rapid complex equilibrium and (24) a slow step. Then r_3 should be proportional to $[AgNH_3^{2+}][OH]$, and substituting for $[AgNH_3^{2+}]$ the mass law expression we get

$$r_3 = \text{constant}\ \frac{[Ag^{2+}][NH_4^+][OH]}{[H^+]} \qquad (25)$$

Then, since $r_3/8$ is the rate at which ammonium ions are consumed in reaction (3), the steady-state approximation applied to OH in the solution gives

$$r_4+r_5-\frac{r_3}{8}-r_6 = 0 \qquad (26)$$

The mechanism proposed evidently requires that $r_3 \leqq 8(r_4+r_5)$, and this condition is satisfied according to the calculations above. Now we substitute the empirical expression (20) for r_4+r_5 with the exponents rounded off to 1.0.

Furthermore, the rate r_6 of reaction (6) should be proportional to $[OH]^2$, and then we have

$$k_1 \frac{[Ag^{2+}]}{[Ag^+][H^+]} = k_2 \frac{[Ag^{2+}][NH_4^+][OH]}{[H^+]} + k_3[OH]^2 \qquad (27)$$

where k_1, k_2, and k_3 are constants. From (27) it is seen that if the first term in the right member predominates then [OH] is proportional to $[Ag^+]^{-1}[NH_4^+]^{-1}$. On the other hand, if the second term predominates then [OH] is proportional to $[Ag^{2+}]^{0.5}[Ag^+]^{-0.5}[H^+]^{-0.5}$. Thus, within limited ranges of concentration it should be possible to represent [OH] by an expression of the form

$$[OH] = \text{constant } [Ag^{2+}]^{\varepsilon_1}[Ag^+]^{\varepsilon_2}[NH_4^+]^{\varepsilon_3}[H^+]^{\varepsilon_4} \qquad (28)$$

with the following conditions fulfilled

$$\begin{aligned} 0 &< \varepsilon_1 < 0.5 \\ -1 &< \varepsilon_2 < -0.5 \\ -1 &< \varepsilon_3 < 0 \\ -0.5 &< \varepsilon_4 < 0 \end{aligned}$$

For ε-values close to the middles of the intervals we then obtain

$$r_3 = \text{constant } \frac{[Ag^{2+}]^{1.2}[NH_4^+]^{0.5}}{[Ag^+]^{0.7}[H^+]^{1.2}} \qquad (29)$$

Combining this expression with (20) and taking into account that $r_3 > r_4 + r_5$, we can predict that if the resulting expression for $r_3 + r_4 + r_5$ is represented approximately by a law similar to (29) the exponents of $[Ag^{2+}]$ and $[H^+]$ will be unchanged, the exponent of $[Ag^+]$ will be slightly higher and that of $[NH_4^+]$ slightly lower than in (29). This conclusion is verified by the experimentally determined law (19), and it is evident that the mechanism proposed can explain the measurement results in a very satisfactory way.

The author is grateful to Miss K. Anderson for valuable assistance in the experimental work.

REFERENCES

1. Fronæus, S. and Östman, C. O. *Acta Chem. Scand.* **10** (1956) 320.
2. Carman, P. C. *Trans. Faraday Soc.* **30** (1934) 566.
3. Wagner, C. and Traud, W. *Z. Elektrochem.* **44** (1938) 391.
4. Kolthoff, I. M. and Miller, C. S. *J. Am. Chem. Soc.* **62** (1940) 2170.
5. Noyes, A. A., Hoard, J. L. and Pitzer, K. S. *J. Am. Chem. Soc.* **57** (1935) 1221.
6. Weiss, J. *Discussions Faraday Soc.* **12** (1952) 263.
7. Fronæus, S. *Acta Chem. Scand.* **10** (1956) 1345.
8. Fronæus, S. and Östman, C. O. *Acta Chem. Scand.* **9** (1955) 902.
9. Bowden, F. P. *Proc. Roy. Soc. London* **A 125** (1929) 446.
10. Ershler, B. V. *Discussions Faraday Soc.* **1** (1947) 269.
11. Noyes, A. A., De Vault, D., Coryell, C. D. and Deahl, T. J. *J. Am. Chem. Soc.* **59** (1937) 1326.
12. Fronæus, S. *Acta Chem. Scand.* **4** (1950) 72.
13. Noyes, A. A., Coryell, C. D., Stitt, F. and Kossiakoff, A. *J. Am. Chem. Soc.* **59** (1937) 1316.
14. Fronæus, S. and Östman, C. O. *Acta Chem. Scand.* **10** (1956) 769.

Received September 15, 1956.

ACTA CHEMICA SCANDINAVICA 10 (1956) 1614—1619

*iso*Thiocyanates XXI. * (−)-10-Methylsulphinyldecyl *iso*Thiocyanate, a New Mustard Oil Present as a Glucoside (Glucocamelinin) in *Camelina* Species

ANDERS KJÆR, ROLF GMELIN and ROALD BOE JENSEN

Chemical Laboratory of the University of Copenhagen, Denmark

Seeds of the cruciferous species *Camelina sativa* (L.) Crantz, *C. microcarpa* Andrz. and *C. dentata* (Willd.) Pers. contain two *iso*-thiocyanate glucosides according to paperchromatographic analysis. The chief constituent, *glucocamelinin*, has been identified as a glucoside containing (−)-10-methylsulphinyldecyl *iso*thiocyanate (VII) as the aglucone.

The new mustard oil is characterized as crystalline thiourea derivatives, formed by reaction with ammonia, aniline and benzylamine. The derivative with the last amine, (I), is degraded through well-defined steps to the compound (III), identical with a synthetic specimen of the previously unknown 1-benzyl-3-(10-methylthiodecyl)-urea. The mustard oil constitutes an addition to the class of naturally occurring sulphoxide-*iso*thiocyanates discussed in a preceding communication of this series.

In the search for new naturally occurring *iso*thiocyanates it was discovered that seeds of the crucifer *Camelina sativa* (L.) Crantz contained two mustard oils, different from those previously recognized in Nature. Although *C. sativa*, indigenous to the Mediterranean region, has been cultivated as an oil-producing plant since ancient times, its contents of *iso*thiocyanates do not appear to have been recognized previously.

In the present work paper chromatography of a seed extract of *C. sativa*, performed essentially as described by Schultz and Gmelin [1], clearly disclosed the presence of two glucosides (Fig. 1). Schultz and Wagner [2] recently introduced the symbol R_B, *i.e.* the ratio of the movement of the glucoside in question to that of a reference sample of glucotropaeolin, for paperchromatographic characterization of mustard oil glucosides. Adopting this convention we found the R_B-values 1.17 and 1.34 for the glucosides of *C. sativa* by descending chro-

* Part XX of this series: *Acta Chem. Scand.* **10** (1956) 1365.

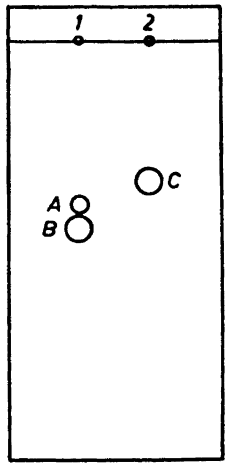


Fig. 1. Descending paper chromatogram of iso*thiocyanate glucosides on Whatman paper No. 1. Solvent system:* n*-butanol:ethanol: water (4:1:4). 1: Extract of seeds of* Camelina sativa *Crantz; 2: extract of seeds of* Tropaeolum majus *L. A: Unidentified glucoside; B: glucocamelinin; C: glucotropaeolin.*

matography on Whatman paper No. 1 with the upper layer of the solvent system *n*-butanol:ethanol:water (4:1:4) as the mobile phase. The glucoside possessing the highest R_B-value appeared to be the predominant constituent. Seed extracts of the closely related species *C. microcarpa* Andrz. and *C. dentata* (Willd.) Pers. showed the same paperchromatographic pattern. The two glucosides were selectively eluted from the proper regions of the paper and subjected to enzymic hydrolysis, followed by spectrophotometric investigation of the individual *iso*thiocyanates. Both exhibited strong end-absorption in the short wave-length region in addition to a low-extinction shoulder at *ca.* 250—260 mμ, attributable to the *iso*thiocyanate grouping. From previous results in this laboratory [3] it appeared that the *iso*thiocyanates were not of the volatile type.

When a larger seed sample was subjected to enzymic hydrolysis in the usual way, a crude *levo*-rotatory *iso*thiocyanate fraction could be isolated by extraction with organic solvents. The product was transformed, without further purification, into crystalline, optically active thiourea derivatives by reaction with ammonia, aniline and benzylamine. After recrystallization, the derivatives were homogeneous as estimated from paper chromatography. Moreover, paperchromatographic comparison of the crude thiourea and an analytical specimen showed that the pure compounds were derivable from the *iso*thiocyanate corresponding to the main glucoside. Analytical data clearly indicated the composition $C_{12}H_{23}ONS_2$ for the parent mustard oil. Infra-red spectra left no doubt as to the presence of the side-chain sulphur atom in a sulphoxide-grouping, narrowing the above formula down to $C_{11}H_{23}(SO)NCS$. In order to elucidate the structure further, the benzylthiourea (I) was transformed into the corresponding benzylurea (II) which, in turn, was reduced to the optically inactive sulphide-urea (III). Consequently, the sulphoxide-grouping represented the sole centre of asymmetry in the parent mustard oil. Raney-nickel hydrogenolysis of (III) furnished a sharp-melting, sulphur-free product which was not homogeneous, however, according to infra-red and analytical data. All

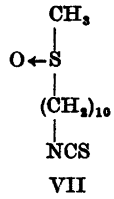
attempts to fractionate the product failed but available data indicated that it consisted of *ca.* 25 % of 1-*cyclo*hexylmethyl-3-decyl-urea and about 75 % of 1-benzyl-3-decyl-urea (IV). An authentic specimen of the latter was prepared from decylamine and benzyl *iso*thiocyanate *via* the thiourea (V), and was found to melt 10° higher than the hydrogenolysis product.

$$\underset{\text{I}}{C_{11}H_{23}(SO)NHCSNHCH_2C_6H_5} \rightarrow \underset{\text{II}}{C_{11}H_{23}(SO)NHCONHCH_2C_6H_5}$$

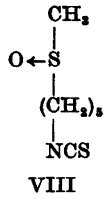
$$\underset{\text{VI}}{CH_3S(CH_2)_{10}NHCSNHCH_2C_6H_5} \rightarrow \underset{\text{III}}{CH_3S(CH_2)_{10}NHCONHCH_2C_6H_5}$$

$$\underset{\text{V}}{CH_3(CH_2)_9NHCSNHCH_2C_6H_5} \rightarrow \underset{\text{IV}}{CH_3(CH_2)_9NHCONHCH_2C_6H_5}$$

In order to establish the structure of (III) in an unambiguous way, a specimen of 1-benzyl-3-(10-methylthiodecyl)-urea was synthetized from the corresponding thiourea (VI) which, in turn, was produced from benzyl *iso*thiocyanate and 10-methylthiodecylamine. Analyses, mixed melting point determination and infra-red spectra served to establish the identity of (III) as 1-benzyl-3-(10-methylthiodecyl)-urea. Consequently, the *Camelina* mustard oil, whence it derives, is 10-methylsulphinyldecyl *iso*thiocyanate (VII).



VII



VIII

The mustard oil (VII) represents a novel addition to the class of naturally occurring, straight-chain ω-methylsulphinylalkyl *iso*thiocyanates. A previous paper of this series [4] described the identification of (—)-5-methylsulphinylpentyl *iso*thiocyanate (VIII), the aglucone of the natural glucoside glucoalyssin, and contained a discussion of various analogous substances and their configurational relationship.* The provenance and sign of rotation of (VII), as well as its thiourea derivatives, indicate that it belongs to the same configurational series as the formerly recognized species. Therefore, the new mustard oil is L(—)-10-methylsulphinyldecyl *iso*thiocyanate (VII), depicted as proposed elsewhere ** (*cf.* Ref. [4]).

* *Added in proof:* After this paper has been submitted for publication we have identified (−)-9-methylsulphinylnonyl *iso*thiocyanate as the mustard oil derivable from the natural glucoside glucoarabin [9].

** *Added in proof:* By means of X-ray structural analysis Hine and Rogers [10] have recently related the configuration at the S atom of (+)-S-methyl-L-cysteine sulphoxide with that at the α-carbon atom, which is known, thus rendering the arbitrary proposal of Schmid and Karrer[11] to use sulphoraphene as a configurational reference compound for sulphoxides superfluous.

The progenitor of this compound is a glucoside for which we wish to propose the name *glucocamelinin*, in accord with general practice in this field. No efforts were made to isolate or characterize the glucoside, but its contents of sulphate and glucose were established by means of paper chromatography *. The nature of the minor glucoside in seeds of the *Camelina* species will be discussed in a forthcoming paper.

10-Methylthiodecylamine, required in the synthetic work, was prepared by Curtius degradation of 11-methylthioundecanohydrazide as described by Walker [5]. The latter compound was obtained by hydrazinolysis of the previously unknown methyl 11-methylthioundecanoate, easily prepared by photo-induced addition of methanethiol to methyl undecenoate in the presence of benzoyl peroxide and mercuric acetate. The addition reaction appears to be a more convenient route to the sulphide-ester than the previously employed four-step reaction from the same starting material [5].

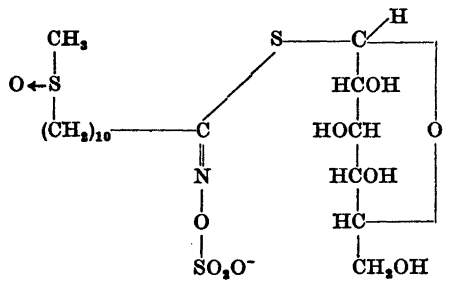
EXPERIMENTAL

All melting points are uncorrected and determined in capillary tubes in a slowly heated bath.

Extraction and purification of glucocamelinin. Finely ground seeds of *Camelina sativa* Crantz (200 g) were defatted and extracted with hot 70 % methanol. The solution was purified by lead salt as previously described for an analogous case [4]. The buffered solution was subjected to enzymic hydrolysis and the liberated *iso*thiocyanates taken up in chloroform. The extract was shaken briefly with a sodium bicarbonate solution in order to remove further impurities. The resulting crude, *levo*-rotatory mustard oil was divided into two halves and treated with ethanolic solutions of excess ammonia and aniline, respectively. Next day, the solvent was removed, and the crystalline derivatives purified by recrystallization from suitable solvents.

(−)-10-Methylsulphinyldecylthiourea. Three recrystallizations from ethyl acetate afforded the pure thiourea (115 mg) as tiny, colourless prisms, m.p. 92−92.5°. (Found: C 51.60; H 9.23; N 9.91; S 22.95. Calc. for $C_{12}H_{26}ON_2S_2$: C 51.75; H 9.41; N 10.06; S 23.03 $[\alpha]_D^{24}$ −65°±1.5° (96 % ethanol, c = 1.03). On paper chromatography in water-saturated chloroform by our usual method [7], the new thiourea possessed the R_{Ph}-value 1.15. The ultra-violet spectrum in ethanol was of the usual type, λ_{max} 242 mμ (ε 13 300) and λ_{min} 224 mμ (ε 3 240). Infra-red analysis of the solid thiourea in a potassium bromide disc

* Glucocamelinin appears to be of the usual glucoside structure type; available evidence in this laboratory, supplemented by the conclusive work by Ettlinger and Lundeen [6] on the revised Gadamer-structure for the mustard oil glucosides, favour the expression:



for the glucocamelinate ion, yet leaving the geometrical isomerism around the C=N linkage undecided.

disclosed conspicuous bands at 2.91 (s)*, 3.30 (s), 6.10 (vs), 6.32 (vs), 6.93 (s), 7.32 (s), 8.59 (w), 9.83 (vs, S→O) and 13.60 μ (m).

(—)-1-(10-Methylsulphinyldecyl)-3-phenylthiourea. The reaction product of the new mustard oil and aniline separated from acetone as flat prisms, m.p. 139°. (Found: C 60.90; H 8.51; N 7.81; S 18.10. Calc. for $C_{18}H_{30}ON_2S_2$: C 60.97; H 8.53; N 7.90; S 18.08). $[\alpha]_D^{24}$ −46°±1.5° (96 % ethanol, c = 0.43). The ultra-violet spectrum in ethanol exerted a maximum at 248 mμ (ε 14 600), a minimum at 228 mμ (ε 9 350) and a plateau at 255—265 mμ (ε 13 950). In the infra-red spectrum a very strong band at 9.99 μ was attributable to the sulphoxide grouping.

(—)-1-Benzyl-3-(10-methylsulphinyldecyl)-urea (II). The thiourea derivative, formed from the new mustard oil and benzylamine, separated from all solvents tested as a gelatinous product which was not brought to analytically pure condition. The benzylthiourea (I) (618 mg) was desulphurized with silver nitrate (573 mg) in dilute ethanol by heating on the steam bath for 10 min. during which period 1 N NaOH (3.4 ml) was gradually added in order to keep the reaction mixture near pH 7. The calculated amount of silver sulphide was filtered off, and the filtrate concentrated to dryness *in vacuo*. The residue was repeatedly triturated with hot ethyl acetate from which the urea (II) separated in tiny, colourless needles on cooling (405 mg), m.p. 113—114° (slight decomp.). (Found: C 64.60; H 9.09; N 7.92; S 9.27. Calc. for $C_{19}H_{32}O_2N_2S$: C 64.74; H 9.15; N 7.95; S 9.10). $[\alpha]_D^{24}$ −53.6°±1.5° (96 % ethanol, c = 1.17).

1-Benzyl-3-(10-methylthiodecyl)-urea (III). The sulphoxide-urea (II) (288 mg) was dissolved in ethanol and treated with acid-activated zinc dust and a few drops of conc. HCl on the steam bath. After the rotation had decreased to practically zero, the solution was filtered hot and the filtrate evaporated to dryness. On digestion with water the solid urea (264 mg) remained. It separated from aqueous ethanol in colourless platelets, m.p. 98.5—99.0°. (Found: C 67.70; H 9.42; N 8.21; Calc. for $C_{19}H_{32}ON_2S$: C 67.83; H 9.59; N 8.33).

1-Benzyl-3-decyl-thiourea (V). This compound was easily obtained from *n*-decylamine and benzyl *iso*thiocyanate as colourless, nacreous plates, m.p. 82.5°. (Found: C 70.50; H 9.87; N 9.06. Calc. for $C_{18}H_{30}N_2S$: C 70.53; H 9.87; N 9.15).

1-Benzyl-3-decyl-urea (IV). The thiourea (V) was desulphurized with silver nitrate, essentially as described above. The urea separated from 80 % ethanol in thin, colourless needles, m.p. 97°. (Found: C 74.60; H 10.47; N 9.69. Calc. for $C_{18}H_{30}ON_2$: C 74.43; H 10.41; N 9.65).

Attempted hydrogenolysis of (III) with W-4 Raney nickel led to a sharply melting mixture (m.p. 87.5°) of (IV) and the corresponding ring-hydrogenated product as estimated from analytical figures and from comparison of the infra-red spectrum of the mixture with that of pure (IV).

Methyl 11-methylthioundecanoate. A mixture of methyl undecenoate (32.6 g), benzoyl peroxide (80 mg) and mercuric acetate (150 mg) was placed together with methanol (50 ml) and methanethiol (7.91 g) in a water-cooled quartz flask, which was exposed to ultraviolet irradiation from a quartz-mercury lamp for 7 hours. Next day, a slight precipitate was filtered off, and methanol was removed from the filtrate by distillation. Pure methyl 11-methylthioundecanoate (31.7 g, 80 %) distilled as a colourless oil, b.p. 119°/0.1 mm; n_D^{25} 1.4651. (Found: C 63.50; H 10.72; S 12.80. Calc. for $C_{13}H_{26}O_2S$: C 63.37; H 10.64; S 13.02).

Hydrolysis of the ester with ethanolic KOH afforded 11-methylthioundecanoic acid, separating from aqueous ethanol in colourless, nacreous plates, m.p. 44° (Ref. [8] m.p. 43—45°).

10-Methylthiodecylamine. The above methyl ester was transformed into the corresponding hydrazide as described elsewhere [5]. The pure hydrazide, separating from aqueous ethanol as flat prisms, was found to melt at 92.0—92.5° (Ref. [5] m.p. 88—89°). (Found: C 58.70; H 10.58; N 11.38. Calc. for $C_{13}H_{26}ON_2S$: C 58.49; H 10.64; N 11.37).

The Curtius degradation of the hydrazide was performed as described by Walker [5], yet in somewhat lower yield. The amine distilled as a viscous, colourless oil at 165°/15 mm. The hydrochloride was prepared, m.p. 161—162° (Ref. [5] m.p. 160—161°).

* vs=very strong; s=strong; m=medium and w=weak.

1-Benzyl-3-(10-methylthiodecyl)-thiourea (VI). The reaction between 10-methylthiodecylamine and benzyl *iso*thiocyanate proceeded smoothly to give a quantitative yield of the thiourea (VI). This separated from 70 % ethanol in colourless, shiny platelets, m.p. 73°. (Found: C 65.10; H 9.06; N 8.00. Calc. for $C_{19}H_{32}N_2S_2$: C 64.73; H 9.15; N 7.95).

Desulphurization of (VI) to (III). When the thiourea was subjected to desulphurization with silver nitrate, essentially as described above, 1-benzyl-3-(10-methylthiodecyl)-urea (III) was obtained in 84 % yield, m.p. 100°, undepressed on admixture with the above specimen, prepared by degradation of the natural derivative. The identity of the two preparations was further substantiated by their coinciding infra-red spectra.

Microanalyses were performed in this laboratory by Mr. P. Hansen. We wish to thank the *Department of Plant Culture of the Royal Danish Veterinary and Agricultural College* for the gift of a substantial sample of *Camelina* seeds.

This work is part of investigations supported by *Statens Almindelige Videnskabsfond (The Danish State Research Foundation)* and *Carlsbergfondet (The Carlsberg Foundation)*.

REFERENCES

1. Schultz, O.-E. and Gmelin, R. *Z. Naturforsch.* **8b** (1953) 151.
2. Schultz, O.-E. and Wagner, W. *Z. Naturforsch.* **11b** (1956) 73.
3. Kjær, A., Conti, J. and Larsen, I. *Acta Chem. Scand.* **7** (1953) 1276.
4. Kjær, A. and Gmelin, R. *Acta Chem. Scand.* **10** (1956) 1100.
5. Walker, J. *J. Chem. Soc.* **1950** 193.
6. Ettlinger, M. G. and Lundeen, A. J. *J. Am. Chem. Soc.* **78** (1956) 4172.
7. Kjær, A. and Rubinstein, K. *Acta Chem. Scand.* **7** (1953) 528.
8. Rapoport, L., Smith, A. and Newman, M. S. *J. Am. Chem. Soc.* **69** (1947) 693.
9. Kjær, A. and Gmelin, R. *Acta Chem. Scand.* **10** (1956) 1358.
10. Hine, R. and Rogers, D. *Chemistry & Industry* **1956** 1428.
11. Schmid, H. and Karrer, P. *Helv. Chim. Acta* **31** (1948) 1497.

Received August 29, 1956.

ACTA CHEMICA SCANDINAVICA 10 (1956) 1620—1634

On the Sulfides, Selenides and Tellurides of Palladium

FREDRIK GRØNVOLD and ERLING RØST

Kjemisk Institutt A, Universitetet i Oslo, Blindern, Norway

The phase relationships in the systems palladium sulfur, palladium selenium and palladium tellurium have been studied by means of X-rays. Density determinations and magnetic susceptibility measurements have also been carried out.

In the Pd-S system five intermediate phases were identified:

1. Pd_4S, with tetragonal structure, $a = 5.1147$ Å, $c = 5.5903$ Å. The observed density is 10.27 g cm^{-3}.
2. $Pd_{2.8}S$, which is only present in quenched preparations. Its structure is unknown.
3. $Pd_{2.8}S$, with cubic structure, $a = 8.9300$ Å and a density of 8.67 g cm^{-3}.
4. PdS, with tetragonal structure. The redetermined lattice constants are $a = 6.4287$ Å, $c = 6.6082$ Å.
5. PdS_2, with orthorhombic structure and unit cell dimensions $a = 5.460$ Å, $b = 5.541$ Å, $c = 7.531$ Å.

In the Pd-Se system four intermediate phases were identified:

1. Pd_4Se, isomorphous with Pd_4S, $a = 5.2324$ Å, $c = 5.6470$ Å. The observed density is 10.74 g cm^{-3}.
2. $Pd_{2.8}^{xx}Se$, with unknown structure.
3. $Pd_{1.1}Se$, with cubic structure and lattice constant $a = 10.604$ Å. It has a density of 8.30 g cm^{-3}.
4. $PdSe_2$, isomorphous with PdS_2 and with lattice constants $a = 5.741$ Å, $b = 5.866$ Å, $c = 7.691$ Å. The observed density is 6.77 g cm^{-3}.

In the Pd-Te system six intermediate phases were identified:

1. Pd_4Te, with cubic structure, $a = 12.674$ Å. The observed density is 11.40 g cm^{-3}. The structure might be looked at as an approximately body-centered arrangement of palladium atoms of which one fifth has been substituted by tellurium atoms.

2, 3 and 4. Three phases have been identified in the range between Pd_4Te and PdTe. Their approximate compositions are Pd_3Te, $Pd_{2.5}Te$ and Pd_2Te.

5. PdTe, with structure of the NiAs-type. The redetermined lattice constants are $a = 4.1521$ Å, $c = 5.6719$ Å.
6. $PdTe_2$, with structure of the $Cd(OH)_2$-type. The redetermined lattice constants are $a = 4.0365$ Å, $c = 5.1262$ Å. No extended mutual solubility of PdTe and $PdTe_2$ was observed.

The magnetic susceptibility of Pd_4S, $Pd_{2.8}S$, Pd_4Se, $Pd_{1.1}Se$, $PdSe_2$ and Pd_4Te has been measured between −183° and 450°C. The compounds Pd_4S, Pd_4Se and Pd_4Te are weakly ferromagnetic with Curie temperatures in the range 20° to 300°C. Above this temperature they have almost zero magnetic susceptibility like the compounds $Pd_{2.8}S$, $Pd_{1.1}Se$ and $PdSe_2$.

Palladium monosulfide was prepared by direct combination of the elements by Berzelius [1] in 1813. It has been studied by many investigators since that time, and the results have been reviewed by Gmelin [2]. Three other palladium sulfides, Pd_2S, Pd_3S_4 and PdS_2, were obtained by Schneider [3]. The existence of the compound Pd_2S has later been confirmed by Petrenko-Kritschenko [4] and Roessler [5]. Furthermore, the compound Pd_4S exists according to Maxted [6], and the compound Pd_3S according to Iwanoff [7].

The region Pd to PdS of the palladium sulfur system was studied by Weibke and Laar [8] by means of thermal, metallographic and X-ray methods. The compounds Pd_4S and PdS were found in slowly cooled samples, and in addition, a phase with composition around 73.5 atomic per cent palladium ($Pd_{2.8}S$) which disproportionated into Pd_4S and PdS at temperatures below 554°C.

A tensimetric analysis of the sulfur-rich part of the system was carried out by Biltz and Laar [9]. No intermediate compounds between PdS and PdS_2 were found.

The crystal structure of PdS was determined by Gaskell [10] by means of single crystals. The structure of the other palladium sulphides are unknown.

Palladium monoselenide was obtained by Rössler [11] as an insoluble product after heating some precipitates containing palladium and selenium and treating them with nitric acid. The existence of PdSe has later been confirmed by Roessler [5] and by Moser and Atynski [12]. Roessler [5] also found a phase with composition Pd_4Se by heating dichlorodiammine palladium with selenium.

Thomassen [13] did not succeed in preparing stoichiometric palladium diselenide from the elements. Laue photographs taken of the crystals showed only twofold symmetry. $PdSe_2$ was later prepared by Wöhler, Ewald and Krall [14] by heating palladium dichloride with excess selenium. As a result of microscopic examination they concluded that the crystals were hexagonal and of the $Cd(OH)_2$-(*C*6)-type.

Palladium monotelluride was prepared by Tibbals, Jr.[15] by precipitation, and later by Thomassen [13] by heating a mixture of the elements. In the same way Thomassen prepared palladium ditelluride. By means of X-ray powder photographs he found that PdTe had a hexagonal structure of the NiAs-(*B*8-) type, and that $PdTe_2$ had a structure of the $Cd(OH)_2$-(*C*6-) type.

EXPERIMENTAL

The *palladium* metal used in this study was kindly placed at our disposal by Falconbridge Nikkelverk A/S, Kristiansand S. To remove adsorbed hydrogen, the metal was heated at 900°C at a pressure of the order 10^{-6} cm Hg. A spectrographic analysis showed that Ag was present in the order of 0.01 % and Cu, Mg, Fe, Si and Na in less than 0.01 % each.

Sulfur from Schering-Kahlbaum A.G. (Sulfur cryst. puriss.) was purified by double distillation in a silica apparatus. Only the middle fractions were used. The highly purified *selenium* was a gift from Bolidens Gruvaktiebolag, Sweden. It carried the analysis: 0.0002 % Cu, 0.0007 % Fe, 0.003 % Te, 0.01 % S and 0.003 % non volatile matter. *Tellurium* from The British Drug Houses Ltd. was subjected to vacuum distillation in silica vessels. According to the spectrographic analysis it contained less than 0.01 % Fe and only traces of Al, Mg and Pb. This analysis and the palladium analysis were kindly carried out by siv.ing. S. Rutlin, Sentralinstitutt for Industriell Forskning, Blindern.

Alloys were prepared by heating mixtures of palladium and sulfur, selenium or tellurium, respectively, in the stoichiometric ratio 1:1 in evacuated and sealed silica tubes.

After being heated for a few days at temperatures ranging between 500° and 800°C the samples were cooled and finely ground. Alloys with other desired compositions were obtained by adding Pd, S, Se or Te in the right proportions to the mono compounds and heating the samples for some days at 600°C. Most of the samples were afterwards annealed at temperatures ranging between 250° and 650°C and cooled slowly to room temperature. In some cases the samples were quenched in ice water. During some of the heat treatments single crystals were formed.

X-Ray single crystal photographs were taken in an oscillation camera with 6.0 cm diameter and a Weissenberg camera with 5.73 cm diameter. The powdered samples were investigated by X-rays in cameras with 11.46 cm effective diameter and asymmetric film mounting. Lattice constants are expressed in Ångström units on basis of the wave lengths $\lambda CuK\alpha_1 = 1.54051$ Å, $\lambda FeK\alpha_1 = 1.93597$ Å and $\lambda CrK\alpha_1 = 2.28962$ Å. Results from earlier investigations, expressed in kX, have been transformed to Å by multiplication by the factor 1.00202.

Lattice constants of the cubic phases were found by extrapolation according to the method given by Nelson and Riley [16]. In this way the lattice constant of palladium was determined as $a = 3.8902$ Å, in perfect agreement with the high precision value $a = 3.89022$ Å given by Owen and Yates [17] for spectrographically pure palladium at 18°C.

The density of the samples was determined by the pycnometric method at 25°C with kerosene as displacement liquid. To remove gases adsorbed by the sample, the pycnometer was filled under vacuum with kerosene. Each sample weighed around 1.5 g.

The magnetic susceptibility of the samples was measured by the Gouy method at three different maximum field strengths at −183°, −78°, 20°, 150°, 300° and 450°C. The samples were filled in thin walled silica tubes of about 0.10 cm internal diameter and to a height of about 8.5 cm.

X-RAY RESULTS

A. Palladium sulfides

In the system palladium sulfur five intermediate phases were identified by means of X-rays: Pd_4S, $Pd_{2.2}S$, PdS, PdS_2 and a high temperature phase with composition around $Pd_{2.8}S$. PdS and samples richer in palladium were brittle and of gray, metallic color. The existence of a compound Pd_3S_4, claimed by Schneider [3], was not confirmed, while all the other palladium sulfides described earlier exist if one associates the compound Pd_3S by Iwanoff [7] with $Pd_{2.8}S$, and Pd_2S by Schneider[3], Petrenko-Kritschenko [4] and Roessler [5] with $Pd_{2.2}S$.

The lattice constant found for palladium in equilibrium with Pd_4S was equal to that of pure palladium within the limits of experimental error. This confirms the observations by Jedele [18] and Weibke and Laar [8] that sulfur is practically insoluble in solid palladium.

The Pd_4S phase. The Pd_4S phase could be indexed on basis of a tetragonal unit cell with dimensions:

$$a = 5.1147 \text{ Å}, \qquad c = 5.5903 \text{ Å}, \qquad c/a = 1.0930.$$

Results of the measurements are listed in Table 1. The systematic missing reflections are of the type $h\,h\,l$ with $l = 2n+1$ and $h\,0\,0$ with $h = 2n+1$. They characterize the space group $P\,\bar{4}\,2_1c$ (D^4_{2d}). The Pd_4S phase is isomorphous with the Pd_4Se phase.

The density of Pd_4S was determined to be 10.27 g cm^{-3} at 25°C, which gives a unit cell content of eight (7.90) palladium and two (1.97) sulfur atoms.

Table 1. Powder photograph data of Pd_4S annealed at 450°C, CuKa radiation. The a_2 reflections have been omitted.

I_{obs}	$\sin^2\Theta \cdot 10^4$	*hkl*	I_{obs}	$\sin^2\Theta \cdot 10^4$	*hkl*	I_{obs}	$\sin^2\Theta \cdot 10^4$	*hkl*
vw	421	101	m	4175	214	vw	7575	424
w	763	002	vw	4541	420	st	7610	513
st	913	200	vw	4622	412	w	7699	325
st	992	102	m	4663	323	w	7743	206
m	1101	201	m	4732	421	w	7903	531
vst	1139	210	w	4847	332	m	7969	216
vst	1219	112	w	5084	304	m	8014	442
st	1330	211	vw	5306	422	vw	8285	523
m	1672	202	w	5571	413	w	8357	601
w	1818	220	vw	5658	205	st	8376	405
st	1899	212	st	5862	501	m	8472	532
w	1940	103			413	m	8580	611
vw	2240	301	m	5890	215	vw	8649	226
vw	2277	310			501	w	8708	504
m	2468	311	m	5994	324			434
vw	2579	222	m	6093	511	vw	8876	306
m	2808	302	vw	6248	423	w	8933	514
vw	2847	213	w	6443	502	w	9102	316
w	2953	320			432	w	9152	612
w	3035	312	vw	6580	520	m	9260	621
m	3143	321	vw	6658	512	st	9281	425
vw	3269	104	m	6773	521	w	9421	533
m	3500	114	w	6841	006	m	9487	541
m	3718	322	w	6902	412	w	9612	520
m	3824	401	vw	7127	334	m	9782	326
w	3866	410	vw	7268	440	m	9830	622
w	3951	204			503			
m	3982	313	w	7385	430			

The $Pd_{2.8}S$ phase. When samples with composition Pd_3S were quenched from 580° and 600°C their X-ray photographs showed the presence of a phase which was not found in the furnace cooled samples. Weak reflections from the Pd_4S phase were found in the quenched Pd_3S sample, while rather strong reflections from the $Pd_{2.2}S$ phase were found in the quenched $Pd_{2.5}S$ sample. The high temperature phase thus seems to have a composition in the vicinity of $Pd_{2.8}S$. This agrees well with the results of Weibke and Laar [8]. We have not yet been able to determine the structure of this phase and only its characteristic reflections are listed in Table 2.

The $Pd_{2.2}S$ phase. In contrast to the results by Weibke and Laar, another intermediate phase between Pd_4S and PdS was found both in slowly cooled samples and in samples quenched from 600°C. The composition of the phase is probably close to $Pd_{2.20}S$ as the powder photograph of this sample contains no lines from other phases, while that of $Pd_{2.25}S$ shows some weak Pd_4S lines and that of Pd_2S shows many lines from the PdS phase.

The powder photograph of $Pd_{2.20}S$ could be indexed as cubic with lattice constant $a = 8.9300$ Å. No significant variation in lattice constant with composition was observed, and in Table 3 is given the indexing for the $Pd_{2.25}S$ sample.

Table 2. Characteristic low angle reflections and interplanar spacings of the $Pd_{2.8}S$ phase as found from a powder photograph of Pd_4S quenched from 600°C, CuKa radiation.

I_{obs}	$\sin^2\Theta \cdot 10^4$	d in Å	I_{obs}	$\sin^2\Theta \cdot 10^4$	d in Å	I_{obs}	$\sin^2\Theta \cdot 10^4$	d in Å
m	314	4.341	vw*	1216	2.209	vw*	2464	1.552
w	474	3.539	m	1250	2.178	w	2617	1.506
m	643	3.037	vst	1332	2.110	w	2687	1.486
vw	764	2.788	st	1413	2.049	vw*	2808	1.454
w*	908	2.556	w	1472	2.008	vw	3041	1.397
st	954	2.494	vw	1724	1.855	vw	3171	1.368
st	985	2.452	vw	1817	1.807	m	3450	1.311
st	1072	2.353	vw*	1898	1.768	w	3529	1.296
w*	1134	2.287	m	1965	1.738	w	3726	1.262
m	1173	2.249	vw	2279	1.614	w	4351	1.168

* Reflections probably from the Pd_4S phase.

Reflections $h\,k\,l$ of the type $h+k+l = 2n+1$ are missing, which is characteristic of a body centered unit cell. The experimentally found density of $Pd_{2.20}S$ is 8.67 g cm^{-3} and the unit cell accordingly contains 30.7 palladium and 13.9 sulfur atoms.

The PdS phase. A redetermination of the lattice constant of the tetragonal PdS phase gave the values:

$$a = 6.4287 \text{ Å}, \qquad c = 6.6082 \text{ Å}, \qquad c/a = 1.0279.$$

Table 3. Powder photograph data of $Pd_{2.25}S$ annealed at 300°C, CuKa radiation.

I_{obs}	$\sin^2\Theta \cdot 10^4$	$h^2+k^2+l^2$	I_{obs}	$\sin^2\Theta \cdot 10^4$	$h^2+k^2+l^2$	I_{obs}	$\sin^2\Theta \cdot 10^4$	$h^2+k^2+l^2$
w	300	4	st	2835	38	m	6409	86
st	449	6	vw	2982	40	vw	6707	90
w	748	10	vw	3135	42	w	7002	94
m	898	12	w	3277	44	w	7152	96
vst	1045	14	m	3430	46	m	7301	98
vw*	1137		w	3580	48	vw	7596	102
m	1193	16	m	3726	50	m	7747	104
vw*	1216		st	4023	54	st	8042	108
st	1347	18	m	4321	58	w	8190	110
w	1493	20	vw	4618	62	w	8489	114
w	1643	22	m	4915	66	vw	8635	116
m	1790	24	vw	5072	68	w	8784	118
vw*	1898		vw	5220	70	vw	8931	120
m	1944	26	w	5368	72	st	9082	122
w	2237	30	m	5514	74	st	9376	126
m	2390	32	m	5667	76	m	9525	128
m	2533	34	st	5817	78	w	9673	130
w	2687	36	vw	6107	82	w	9821	132

* Reflections from the Pd_4S phase.

The determination by Bannister [19] gave $a = 6.44$ Å, $c = 6.60$ Å and the values reported by Gaskell [10], who determined the atomic arrangement in PdS, were $a = 6.44$ Å, $c = 6.64$ Å.

The complete indexing of a powder photograph of PdS taken with chromium radiation is given in Table 4.

Table 4. Powder photograph data of PdS annealed at 300°C, CrKa radiation.

I_{obs}	$\sin^2\Theta \cdot 10^4$	*hkl*	I_{obs}	$\sin^2\Theta \cdot 10^4$	*hkl*	I_{obs}	$\sin^2\Theta \cdot 10^4$	*hkl*
vw	936	111	w	4432	321	vw	8552	511
vw	1273	200	w	4815	004	w	8778	205
st	1521	102	m	5085	400	st	8929	324
st	1573	201	vw	5399	410	m	9050	423
st	1592	210	vw	6297	402	m	9093	215
m	1840	112	vw	6361	420	st	9132	502
vst	1893	211	w	6407	214			432
w	2794	212	w	6611	412	vw	9200	520
m	3745	222	vw	6661	421	m	9449	512
w	3975	203	w	6844	323	m	9497	521
w	4061	302	vw	6921	332	vst	9875	404
w	4130	320	vw	8238	501			
st	4294	213			431			
st	4376	312	vw	8417	333			

The PdS_2 phase. Experiments to get the PdS_2 phase by heating the components were not entirely successful. Even after treating PdS with excess of sulfur for six months at various temperatures between 300° and 500°C, reflections from unreacted PdS could still be seen on the X-ray photographs together with those from another phase, probably PdS_2.

It was then tried to prepare PdS_2 by the method of Wöhler, Ewald and Krall [14] by heating palladium dichloride with excess of sulfur for four days at 450°C in an evacuated silica tube. The product was obtained in form of a black, crystalline powder after washing with carbon disulfide. The X-ray photographs resembled the earlier ones, but all the reflections from PdS had disappeared, and the sample was supposedly pure PdS_2.

The powder photograph could be indexed as orthorhombic with unit cell dimensions:

$$a = 5.460 \text{ Å}, \qquad b = 5.541 \text{ Å}, \qquad c = 7.531 \text{ Å},$$

$$a:b:c = 0.9854:1:1.3591.$$

In Table 5 are found the results of film measurements and indexing.

According to Biltz and Laar [9] the density of PdS_2, synthesized from $PdCl_2$ and sulfur, is 4.833 g cm^{-3}. The unit cell should then contain four (3.883) formula units of PdS_2.

The systematic missing reflections on the powder photograph seem to be the same as those for the $PdSe_2$ phase. Since the number of atoms in the unit cell and the axial ratios are about the same as found for $PdSe_2$, these phases are probably isomorphous.

Table 5. Powder photograph data of PdS_2 annealed at 450°, FeKα radiation.

I_{obs}	$\sin^2\Theta \cdot 10^4$	*hkl*	I_{obs}	$\sin^2\Theta \cdot 10^4$	*hkl*	I_{obs}	$\sin^2\Theta \cdot 10^4$	*hkl*
vst	674	002	w	3885	024	vw	7203	026
vst	798	111	w	3919	204	w	7214	135
vw	987	102	vw	4014	130			206
st	1238	020	w	4228	214	vw	7288	315
st	1273	200			321	w	7543	044
vw	1403	021	m	4566	133	w	7684	404
w	1577	210	m	4646	313	vst	8210	151
w	1720	121	st	4778	115	vst	8340	511
vw	1746	211	m	5145	224	m	8437	226
st	1899	022	vw	5560	323			432
st	1941	202			042	st	8723	117
vst	2128	113			125	m	8791	306
st	2502	220	vw	5699	402			244
w	2665	004			215	m	8898	250
w	2732	023	m	5751	331			424
vw	3073	213	w	6169	240	m	9435	153
st	3159	222	w	6282	420	st	9653	513
vst	3244	131			106	st	9706	335
st	3317	311	m	6824	242	vst	9912	440
vw	3505	302	m	6936	422			
vw	3740	132	m	7087	333			

B. Palladium selenides

Four intermediate phases were identified in the palladium selenium system: Pd_4Se, $Pd_{2.8}Se$, $Pd_{1.1}Se$ and $PdSe_2$. The phases were all obtained both in quenched and slowly cooled preparations. They were of gray, metallic color and also brittle, except $PdSe_2$ which formed soft, platelike crystals.

The $Pd_{2.8}Se$ phase was not found by earlier investigators and the $Pd_{1.1}Se$ phase was given the composition PdSe by Roessler [5], Rössler [11] and Moser and Atynski [12].

The Pd_4Se phase. Powder photographs of Pd_4Se showed great similarities with those of Pd_4S and could be indexed as tetragonal. The unit cell dimensions were found to be:

$$a = 5.2324 \text{ Å}, \qquad c = 5.6470 \text{ Å}, \qquad c/a = 1.0792.$$

A record of the interferences which occur on a powder photograph of Pd_4Se taken with copper radiation is found in Table 6.

After annealing a Pd_4Se sample at 450°C for forty-five days some small crystals had been formed. Weissenberg photographs with the *b*-axis as rotation axis confirmed that the systematic missing reflections were of the type *h h l* absent when $l = 2n+1$ and *h* 0 0 absent when $h = 2n+1$. The characteristic space group is thus $P\,\bar{4}\,2_1c$ (D^4_{2d}) as found for Pd_4S.

The pycnometric density of Pd_4Se is 10.74 g cm^{-3} which means that eight (7.95) palladium and two (1.99) selenium atoms are present in the unit cell. A discussion of the atomic arrangement in the two isomorphous phases Pd_4S and Pd_4Se will be given in a later paper.

Table 6. Powder photograph data of Pd_4Se annealed at 300°C, CuKa radiation.

I_{obs}	$\sin^2\Theta \cdot 10^4$	*hkl*	I_{obs}	$\sin^2\Theta \cdot 10^4$	*hkl*	I_{obs}	$\sin^2\Theta \cdot 10^4$	*hkl*
vw	437	110	w	3569	322	m	7473	325
vw	746	002	m	3661	401	vw	7563	531
m	872	200	st	3850	313	w	7685	442
st	965	102			204	m	7785	216
st	1056	201	w	4066	214	m	7965	523
vst	1092	210	w	4336	420	vst	8121	532
vst	1183	112	m	4498	323			405
vst	1275	211	m	4523	421	st	8208	611
m	1618	202	w	4651	332	w	8614	443
vw	1746	220	vw	4933	304			514
st	1830	212	m	5363	413	vw	8766	612
m	1896	103	vw	5525	205	w	8867	316
w	2148	301	m	5611	431	m	8988	425
w	2177	310	w	5741	215	w	9075	541
m	2362	311	w	5830	511	w	9265	524
vw	2482	222	w	6482	521	w	9414	622
m	2704	302	w	6702	006	m	9516	326
vw	2766	213	w	6876	334	m	9632	542
w	2821	320	vw	7037	522	m	9754	630
m	3011	321	w	7100	503	st	9914	444
vw	3200	104			433			
m	3419	114	st	7314	513			

The $Pd_{2.8}Se$ phase. Powder photographs of samples in the composition range between Pd_4Se and $Pd_{1.1}Se$ contain reflections from a phase with composition around $Pd_{2.8}Se$. The photographs of Pd_3Se show some additional very weak reflections that are probably from the Pd_4Se phase, and the photograph of $Pd_{2.5}Se$ shows rather strong reflections from a phase richer in selenium.

In Table 7 are listed the lines found in the low angle region on a powder photograph of the $Pd_{2.5}Se$ sample. The structure of this phase is unknown. On some photographs a few additional reflections were found that are possibly due to an unidentified phase, perhaps only stable at higher temperatures.

Table 7. Low angle reflections on a powder photograph of $Pd_{2.5}Se$ annealed at 450°C, CuKa radiation.

I_{obs}	$\sin^2\Theta \cdot 10^4$	*d* in Å	I_{obs}	$\sin^2\Theta \cdot 10^4$	*d* in Å	I_{obs}	$\sin^2\Theta \cdot 10^4$	*d* in Å
vw	478	3.523	st*	902	2.564	st	1226	2.199
w*	531	3.341	st	989	2.449	vw	1294	2.142
m*	585	3.184	m	1007	2.428	st	1361	2.088
vw	635	3.056	m	1044	2.384	m*	1426	2.040
vw*	690	2.932	st	1069	2.356			
w*	745	2.820	vst	1190	2.233			

* Reflections probably from the $Pd_{1.1}Se$ phase.

The $Pd_{1.1}Se$ phase (Pd_9Se_8?). Powder photographs of PdSe samples contain some of the strongest reflections from the $PdSe_2$ phase in addition to the characteristic pattern of a cubic phase. These additional reflections are absent on photographs of $Pd_{1.1}Se$ and the cubic phase is therefore assumed to have a composition close to Pd_9Se_8.

A record of the reflections observed for $Pd_{1.1}Se$ is found in Table 8. The unit cell is primitive with lattice constant $a = 10.604$ Å.

A density determination on $Pd_{1.1}Se$ gave 8.30 g cm^{-3} and thus a cell content of 33.7 palladium atoms and 30.0 selenium atoms.

It is interesting to note that Juza, Hülsmann, Meisel and Biltz [20] found a phase at the composition Rh_9S_8 by tensimetric analysis of the rhodium sulfur system. According to X-ray studies by Mr. Ø. Steen in this institute the structure of Rh_9S_8 is also cubic and probably closely related to that of Pd_9Se_8.

Table 8. Powder photograph data of $Pd_{1.1}Se$ annealed at 450°C, CuKα radiation.

I_{obs}	$\sin^2\Theta \cdot 10^4$	$h^2+k^2+l^2$	I_{obs}	$\sin^2\Theta \cdot 10^4$	$h^2+k^2+l^2$	I_{obs}	$\sin^2\Theta \cdot 10^4$	$h^2+k^2+l^2$
vw	215	4	w	2753	52	vw	6764	128
vw	426	8	vw	3009	57	w	6918	131
vw	478	9	vw	3065	58	w	7078	134
st	532	10	st	3122	59	w	7181	136
vst	586	11	vw	3224	61	w	7344	139
vw	632	12	vw	3277	62	w	7602	144
vw	660	?	w	3384	64	vw	7706	146
m	690	13	vw	3433	65	vw	7764	147
st	742	14	w	3488	66	w	8027	152
vw	787	?	w	3538	67	vw	8182	155
vst	903	17	w	3597	68	m	8344	158
m	956	18	vw	3647	69	vw	8446	160
m	1008	19	w	3810	72	w	8497	161
m	1061	20	w	3909	74	w	8553	162
m	1114	21	vw	3962	75	vw	8656	164
vw	1161	22	vw	4226	80	w	8709	165
w	1324	25	vw	4278	81	vw	8925	169
w	1379	26	vw	4330	82	w	8973	170
vst	1430	27	vw	4434	84	st	9025	171
vw	1550	?	w	4541	86	m	9075	$\alpha_1$171
vst	1695	32	vw	4645	88			$\alpha_2$172
vw	1748	33	vw	4706	89	w	9290	176
w	1801	34	vw	4759	90	m	9395	178
m	1906	36	m	5073	96	vst	9446	179
vw	1962	37	m	5232	99	vst	9497	$\alpha_1$179
m	2017	38	vw	5606	106			$\alpha_2$180
w	2115	40	w	5658	107	w	9605	182
m	2170	41	vw	5814	110	m	9762	185
m	2222	42	vw	5968	113	st	9815	$\alpha_1$185
vw	2277	43	m	6130	116			$\alpha_2$186
w	2383	45	vw	6450	122	m	9866	187
vw	2540	48	w	6495	123	w	9916	$\alpha_1$187
w	2648	50	vw	6608	125			

The $PdSe_2$ phase. After annealing $PdSe_2$ for fifty days at 650°C some small, badly developed crystals were obtained. Weissenberg photographs showed that the crystals were orthorhombic and gave the approximate cell dimensions. The powder photograph of $PdSe_2$ could then be indexed as shown in Table 9 and these lattice constants were arrived at:

$$a = 5.741 \text{ Å}, \qquad b = 5.866 \text{ Å}, \qquad c = 7.691 \text{ Å},$$

$$a:b:c = 0.9787:1:1.3111.$$

Missing reflections are of the type 0 $k\,l$ absent when $k = 2n+1$, $h\,0\,l$ absent when $l = 2n+1$ and $h\,k\,0$ absent when $h = 2n+1$. The characteristic space group is thus $P\,b\,c\,a$ (D_{2h}^{15}) and on basis of the observed density 6.77 g cm^{-3} the unit cell contains four (4.00) palladium and eight (8.00) selenium atoms.

Table 9. Powder photograph data of $PdSe_2$ annealed at 450°C, FeKα radiation.

I_{obs}	$\sin^2\Theta \cdot 10^4$	*hkl*	I_{obs}	$\sin^2\Theta \cdot 10^4$	*hkl*	I_{obs}	$\sin^2\Theta \cdot 10^4$	*hkl*
vst	638	002	w	3815	321			341
w	718	111	w	3952	214	w	7076	126
st	922	102	w	4170	133			404
m	1092	020	w	4267	313	w	7113	216
m	1136	200	st	4526	115	m	7254	151
m	1196	112			041			511
m	1253	021	w	4765	224	st	7545	334
m	1415	210	vw	5005	042			235
m	1537	121			233			342
w	1571	211	vw	5087	323	w	7615	325
m	1730	022			304	vw	7935	226
m	1777	202	vw	5174	331	w	8030	512
st	1988	113	w	5279	134			244
vw	2047	212			142	w	8176	424
m	2233	220	w	5340	125	m	8320	045
m	2522	023	vw	5654	332			117
w	2837	104			241	vw	8808	513
		213	vw	5799	043	vw	8853	027
vw	2868	222			421	m	8908	440
st	2903	131	w	6137	234	vw	8974	335
st	2998	311			242	w	9174	217
vw	3100	114	w	6269	116	w	9295	236
w	3200	302			422	w	9375	253
w	3377	132	w	6445	333	w	9453	344
vw	3469	312	vw	6792	026			245
vw	3597	230			315	m	9540	434
vw	3630	024	w	6897	044			442
vw	3677	204						

C. Palladium tellurides

In the palladium tellurium system the following intermediate phases were found: Pd_4Te, Pd_3Te, Pd_2Te, PdTe and $PdTe_2$. In addition, a sixth phase probably exists in the range between Pd_3Te and Pd_2Te. The exact composition limits of the phases have not been determined, and the formulae only indicate

the approximate composition of the phases. All phases have been found both in quenched and in slowly cooled preparations. The samples are gray in color and apart from $PdTe_2$ they are brittle.

The only palladium tellurides described earlier are the monotelluride by Tibbals, Jr.[15] and Thomassen [13] and the ditelluride by Thomassen [13].

The Pd_4Te phase. Single crystals of the Pd_4Te phase were obtained in a sample with gross composition Pd_6Te that had been heated at 550°C for fifty days. Weissenberg photographs showed primitive cubic symmetry, and by means of powder photographs the lattice constant of Pd_4Te was found to be $a = 12.674$ Å.

The single crystal photographs show strong reflections only in the equatorial and fourth layer line while those in the first, second, third, fifth and sixth layer line are weak. This suggests that the true unit cell is a superstructure cell, and as apparent from Table 10 the strong reflections are multiples of $h^2+k^2+l^2 = 32$, indicating that the "subcell" with $a' = 3.168$ Å is approximately body centered.

Table 10. Powder photograph data of Pd_4Te annealed with excess Pd at 500°C, CuKa radiation.

I_{obs}	$\sin^2\Theta \cdot 10^4$	$h^2+k^2+l^2$	I_{obs}	$\sin^2\Theta \cdot 10^4$	$h^2+k^2+l^2$	I_{obs}	$\sin^2\Theta \cdot 10^4$	$h^2+k^2+l^2$
vw	1002	27	vw	4504	122	w	8092	219
vw	1150	?	m	4730	128	vst	8274	224
vst	1193	32	vw	5149	139	w	8681	235
vw	1529	41	m	5922	160	w	8721	236
w	2193	59	w	6330	171	w	9130	?
m	2376	64	vw	6915	187	st	9270	251
vw	3064	83	w	7092	192	vw	9381	254
vw	3141	85	vw	7239	196	m	9453	256
st	3557	96	vw	7460	202	vw	9751	264
w	3962	107	vw	7505	203	w	9861	267
vw	4190	113	vw	7613	206			
vw	4319	117	vw	7831	212			

In agreement with this, the observed density 11.40 g cm^{-3} of Pd_4Te confirms that the number of atoms in the subcell is close to two (1.575 Pd atoms and 0.394 Te atoms). The structure can probably be looked at as a body centered arrangement of palladium atoms of which one fifth has been substituted by tellurium atoms in an ordered way. However, the atoms are slightly displaced from the ideal positions as evidenced especially by the strong $h^2+k^2+l^2 = 251$ reflection.

The phases between Pd_4Te and $PdTe$. Samples in this range give very complicated powder photographs and the phases are not easily identified. The Pd_4Te reflections are found in $Pd_{3.5}Te$ but are absent in Pd_3Te. No lines from a tellurium richer phase are presumably present in Pd_3Te since the powder photographs of Pd_3Te and $Pd_{2.75}Te$ are alike. The low angle reflections found on a powder photograph of Pd_3Te are collected in Table 11.

There also exists a phase with composition around Pd_2Te. Its characteristic low angle reflections are listed in Table 11 too. A sample with composition $Pd_{1.5}Te$ was found to contain both the Pd_2Te and the PdTe phase.

The powder photograph of $Pd_{2.5}Te$ is markedly different from that of Pd_2Te and does not resemble that of $Pd_{2.75}Te$ either, see Table 11. Probably therefore a third phase exists in this range.

Table 11. Characteristic low angle reflections on powder photographs of Pd_3Te, $Pd_{2.5}Te$ and Pd_2Te.

Pd_3Te			$Pd_{2.5}Te$			Pd_2Te		
I_{obs}	$\sin^2\Theta \cdot 10^4$	d in Å	I_{obs}	$\sin^2\Theta \cdot 10^4$	d in Å	I_{obs}	$\sin^2\Theta \cdot 10^4$	d in Å
vw	446	3.65	vw	460	3.59	vw	308	4.39
vw	588	3.18	vw	602	3.14	vw	354	4.09
w	683	2.95	vw	703	2.90	w	525	3.36
w	929	2.53	vw	917	2.54	w	553	3.28
w	958	2.49	w	953	2.50	vw	627	3.08
m	991	2.45	w	986	2.45	vw	732	2.85
w	1101	2.32	vw	1128	2.29	vw	765	2.79
w	1128	2.29	vst	1165	2.26	w	800	2.72
vst	1162	2.26	vw	1192	2.23	m	919	2.54
st	1192	2.23	w	1215	2.21	w	960	2.49
w	1271	2.16	m	1232	2.19	w	1007	2.43
w	1426	2.04	w	1306	2.13	vw	1074	2.35
m	1502	1.99	vw	1343	2.10	m	1117	2.30
vw	1531	1.97	m	1512	1.98	w	1147	2.27
w	1594	1.93	vw	1587	1.93	m	1173	2.25
m	1628	1.91	vw	1654	1.89	st	1198	2.23
vw	1667	1.89	vw	1690	1.87	w	1226	2.20
						vw	1247	2.18
						m	1306	2.13
						w	1349	2.10
						w	1428	2.04
						w	1508	1.98
						m	1539	1.96

The PdTe and $PdTe_2$ phase. A redetermination of the lattice constants of hexagonal PdTe with structure of the NiAs-($B8$-)type gave the result:

$$a = 4.1521 \text{ Å}, \qquad c = 5.6719 \text{ Å}, \qquad c/a = 1.3660.$$

These values are in good agreement with those determined by Thomassen [13] ($a = 4.135 \pm 0.004$ Å, $c = 5.674 \pm 0.005$ Å).

The homogeneity range of the PdTe phase is apparently rather narrow since the lattice constants of the PdTe phase are equal within the limits of experimental error both in $Pd_{1.5}Te$, PdTe and $PdTe_{1.5}$.

The structure of $PdTe_2$ is also hexagonal and for a sample that had been heated with excess tellurium at 300°C for 30 days the following lattice constants were computed:

$$a = 4.0365 \text{ Å}, \qquad c = 5.1262 \text{ Å}, \qquad c/a = 1.2700.$$

According to Thomassen [13] the structure is of the $Cd(OH)_2$-(*C*6-) type and the lattice constants given by him ($a = 4.036 \pm 0.003$ Å, $c = 5.128 \pm 0.004$ Å) are in excellent agreement with ours.

A continuous solid solution between PdTe and $PdTe_2$ is not found, and in general it seems like none of the palladium chalcogenides have extended ranges of homogeneity. Among the chalcogenides of the 3d transition elements solid solutions involving a continuous transition from the *B*8 to *C*6 structure type are quite common. As examples might be mentioned the CoTe - $CoTe_2$ and NiTe - $NiTe_2$ transitions found by Tengnér [21] and the TiTe - $TiTe_2$ transition studied by Ehrlich [22]. Recently, the phases RhTe and $RhTe_2$ have been identified by Geller [23]. RhTe was found to have a structure of the *B*8 type and the high temperature form of $RhTe_2$ a structure of the *C*6 type. No samples with intermediate compositions were studied so it is not known to what extent these phases show mutual solubility.

MAGNETIC PROPERTIES OF THE PALLADIUM CHALCOGENIDES

The magnetic susceptibility of Pd_4S, $Pd_{2.2}S$, Pd_4Se, $Pd_{1.1}Se$, $PdSe_2$ and Pd_4Te was measured at six different temperatures from —183° to 450°C and the results are listed in Tables 12 and 13.

Table 12. Magnetic susceptibility of the palladium chalcogenides, $\chi_g \times 10^6$.

Compound	Temperature °C					
	−183	−78	20	150	300	450
Pd_4S	*	*	*	0.20	0.01	0.06
$Pd_{2.2}S$	0.27	0.25	0.17	0.17	0.14	0.12
Pd_4Se	*	*	*	0.18	0.04	0.00
$Pd_{1.1}Se$	0.07	0.05	0.02	0.00	−0.01	−0.01
$PdSe_2$	−0.26	−0.26	−0.26	−0.26	−0.26	−0.27
Pd_4Te	*	*	*	*	0.51	0.14

* The field strength dependent susceptibilities are listed in Table 13.

Table 13. The field strength dependent susceptibility of the Pd_4X compounds, $\chi_g \times 10^6$.

Compound	*T*°C	H_{max}		
		4 015 Ø	4 700 Ø	5 110 Ø
Pd_4S	−183	19.9	17.5	16.4
	− 78	16.7	14.6	13.5
	20	7.0	6.0	5.4
Pd_4Se	−183	26.2	22.8	21.2
	− 78	11.0	9.5	8.5
	20	1.9	1.7	1.6
Pd_4Te	−183	5.1	4.5	4.3
	− 78	4.7	4.2	3.6
	20	4.3	3.8	3.6
	150	3.6	3.2	3.1

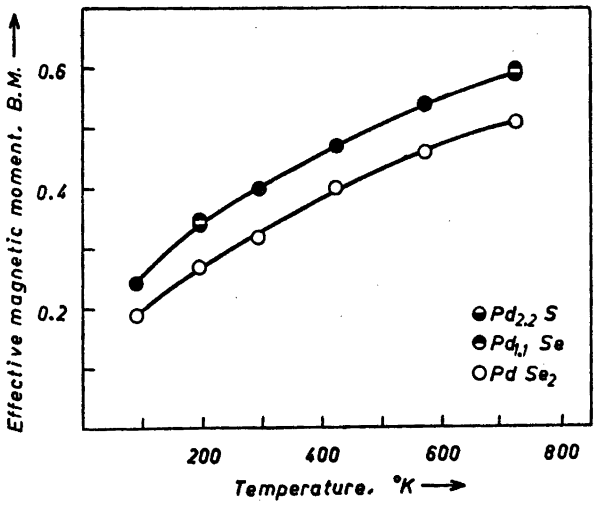


Fig. 1. Effective magnetic moments of the compounds $Pd_{2.2}S$, $Pd_{1.1}Se$ and $PdSe_2$ as functions of temperature.

Disregarding the peculiar behavior of the Pd_4X compounds at low temperatures, the magnetic susceptibilities are exceedingly low. If one subtracts the induced diamagnetism in the palladium (-21.3×10^{-6} per mole Pd^0 according to Hoare and Matthews [24]) and in the chalcogen (-32.6×10^{-6} per mole S^{-2}, -47.6×10^{-6} per mole Se^{-2} and -70.6×10^{-6} per mole Te^{-2} according to Angus [25]) one finds effective magnetic moments in the range 0.19 to 0.60 Bohr magnetons for the compounds $Pd_{2.2}S$, $Pd_{1.1}Se$ and $PdSe_2$, see Fig. 1. Considerable uncertainty is connected with the diamagnetic corrections. They are most probably too high since they refer to completed electron shells, thus resulting in too high effective magnetic moments.

Even so, the magnetic moments are rather small and show that the compounds are of an essentially metallic or covalent type. In case the bonds had been of the ionic type, a magnetic moment of 2.83 B.M. was expected for the Pd^{+2} ion and 4.90 B.M. for the Pd^{+4} ion according to the "spin only" theory. The tendency, present among the nickel chalcogenides, for the magnetism to be weaker than expected, is even more pronounced among the palladium chalcogenides. One possible explanation for this behavior is that interaction between the atoms changes the coupling of the 4d electrons of palladium so that the stable configuration does not have the maximum multiplicity required by the Hund rule.

Below certain temperatures, the magnetic susceptibilities of Pd_4S, Pd_4Se and Pd_4Te are field strength dependent and increase with decreasing temperature. The field strength dependence is observed at room temperature for Pd_4S and Pd_4Se and also at 150°C for Pd_4Te.

The authors should like to express their appreciation to professor Haakon Haraldsen for his interest in this study. They wish to thank Falconbridge Nikkelverk A/S for generously supplying palladium metal and to thank Bolidens Gruvaktiebolag for the selenium. They also wish to thank siv.ing. Sigurd Rutlin, Sentralinstitutt for Industriell Forskning, for carrying out the spectrographic analysis.

REFERENCES

1. Berzelius, J. *Kgl. Svenska Vetenskapsakad. Handl.* **1813** 204.
2. Gmelins *Handbuch der anorganischen Chemie*, System-Nummer 65: Palladium, Berlin 1942.
3. Schneider, R. *Ann. Physik.* **141** (1870) 519; **148** (1873) 625.
4. Petrenko-Kritschenko, P. *Z. anorg. Chem.* **4** (1893) 247.
5. Roessler, F. *Z. anorg. Chem.* **9** (1895) 31.
6. Maxted, E. B. *J. Chem. Soc.* **1919** 1050.
7. Iwanoff, W. N. *Chem.-Ztg*, **47** (1923) 209.
8. Weibke, F. and Laar, J. *Z. anorg. u. allgem. Chem.* **224** (1935) 49.
9. Biltz, W. and Laar, J. *Z. anorg. u. allgem. Chem.* **228** (1936) 257.
10. Gaskell, T. F. *Z. Krist.* **96** (1937) 203.
11. Rössler, H. *Ann.* **180** (1876) 240.
12. Moser, C. and Atynski, K. *Monatsh.* **45** (1924) 235.
13. Thomassen, L. *Z. physik. Chem.* **B2** (1929) 349.
14. Wöhler, L., Ewald, K. and Krall, H. G. *Ber.* **66B** (1933) 1638.
15. Tibbals, C. A. Jr. *J. Am. Chem. Soc.* **31** (1909) 902.
16. Nelson, J. B. and Riley, D. P. *Proc. Phys. Soc. London* **57** (1945) 160.
17. Owen, E. A. and Yates, E. L. *Phil. Mag.* [7] **16** (1933) 606.
18. Jedele, A. *Z. Metallkunde* **27** (1935) 271.
19. Bannister, F. A. *Z. Krist.* **96** (1937) 201.
20. Juza, R., Hülsmann, O., Meisel, K. and Biltz, W. *Z. anorg. u. allgem. Chem.* **225** (1935) 369.
21. Tengnér, S. *Z. anorg. u. allgem. Chem.* **239** (1938) 126.
22. Ehrlich, P. *Z. anorg. Chem.* **260** (1949) 1.
23. Geller, S. *J. Am. Chem. Soc.* **77** (1955) 2641.
24. Hoare, F. E. and Matthews, J. C. *Proc. Roy. Soc. London* **A212** (1952) 137.
25. Angus, W. R. *Proc. Roy. Soc. London* **A136** (1932) 573.

Received July 3, 1956.

ACTA CHEMICA SCANDINAVICA 10 (1956) 1635—1648

Chromatographic Separation of two Vitamin A_2 Isomers

B. BARNHOLDT and WILLY HJARDE

The National Vitamin Laboratory, Copenhagen, Denmark.

The presence of two vitamin A_2 isomers in perch and pike liver extract has been demonstrated, and the spectroscopic properties of the substances have been given.

By the action of iodine on natural vitamin A_2 a vitamin A_2 mixture is obtained which may be separated by chromatography into two substances, *a* and *b*, the ratio of *a* to *b*, expressed by $E_{351m\mu}$, being about 1 to 2. Substance *a* seems to be identical with the neovitamin A_2 occurring in the liver extract. There are some doubts as to whether substance *b* and the vitamin A_2 occurring in Nature are identical. Even though substance *b* and natural vitamin A_2 exhibit a number of similarities both spectroscopically and chromatographically, certain discrepancies as regards spectroscopic properties have made it impossible to ascertain whether *b* is a single substance or a mixture of vitamin A_2 and an irrelevant substance with light absorption in the wavelength range below 310 mμ.

When an isomerized mixture of vitamin A_1 and vitamin A_2 was chromatographed on dicalcium phosphate, the four substances present were eluted in the following order: neovitamin A_1 — substance *a* (neovitamin A_2) — all-*trans* vitamin A_1 — substance *b* (natural vitamin A_2?).

In view of the close relationship between vitamin A_1 and vitamin A_2 (= dehydrovitamin A_1) it is a reasonable assumption that vitamin A_2 may also occur in more than one of the theoretically possible stereoisomeric forms. In their determinations of the content of vitamin A_1 and vitamin A_2 in certain Nile fish Abdullah, Morcos and Salah [1] have assumed the existence of two different geometrical isomers of vitamin A_2 (neovitamin A_2 and vitamin A_2) and have determined the ratio of neovitamin A_2 to vitamin A_2, assuming that under identical experimental conditions the reactions of the two vitamin A_2 isomers with maleic acid anhydride both qualitatively and quantitatively are identical with the corresponding reactions of neovitamin A_1 and all-*trans*-vitamin A_1, respectively.

Since it has been shown to be possible to separate neovitamin A_1 and all-*trans* vitamin A_1 by chromatography (Bro-Rasmussen, Hjarde and Porotnikoff[2]), it would be reasonable to ascertain whether by applying a similar method to a supposed mixture of vitamin A_2 isomers it would be possible to obtain a

separation, or at any rate a partial separation, of the isomers, enabling a further examination of the course of their absorption curves. In the above-mentioned publication from this laboratory it has been suggested that vitamin A_2 may be present in cod liver oil in two stereoisomeric forms, which differ with regard to the readiness with which they are eluted when chromatographed on dicalcium phosphate.

However, preliminary investigations show fresh liver from various freshwater fish to contain almost exclusively one of the vitamin A_2 forms. On chromatography, the greater part of the light-absorbing substances with absorption maximum at about 350 mμ is found to be present in the form of one fraction with an absorption curve which is in good agreement with the one given in the above publication [2]. It was therefore necessary to perform an isomerization of the isolated vitamin A_2 fraction followed by chromatography to separate the isomeric substances.

In the following an account will be given of these experiments and the results obtained.

EXPERIMENTAL

The technique used is, with the exception of the isomerization process, described in the above publication. A few modifications will be referred to in connection with the individual experiments. The isomerization process will be described in section II below. All the chromatographic separations mentioned in the following have been performed at room temperature (22–23°C) and protected against daylight. The spectrophotometric measurements were made with a Beckman spectrophotometer, type D.U., slit-width about 0.15–0.08 mm within the measuring range used in the present investigation.

I,1. ISOLATION OF VITAMIN A_2 FROM PIKE LIVER

A dicalcium phosphate column, 86 cm long, 1.8 cm diam., was used for chromatography of the unsaponifiable fraction from 5.95 g of pike liver, the absorption curve of which when measured in light petroleum displayed three maxima (277 mμ, 287 mμ and 348—352 mμ, $E^{1\%}_{1cm,\ 350\ m\mu} = 0.920$ measured in relation to the liver weight) and $\frac{E_{287\ m\mu}}{E_{350\ m\mu}} = 0.513$. The eluent used was a mixture of light petroleum and diethylether (86:14 v/v). Eluate was collected in 4.7 ml fractions by means of an automatic fraction collector. The fractionation curve is illustrated in Fig. 1. The fractions collected were measured spectrophotometrically (after dilution with light petroleum, if necessary) at the wavelengths 325 mμ and 351 mμ. The value of the ratio $\frac{E_{351\ m\mu}}{E_{325\ m\mu}}$ for each individual fraction is also given in Fig. 1.

The peak fraction (No. 30) and the immediately subsequent fractions all displayed the same value of the ratio $\frac{E_{351\ m\mu}}{E_{325\ m\mu}}$. The vitamin A_2 fraction (No. 31) following the peak fraction with $E^{1cm}_{351\ m\mu} = 6.01$ was evaporated to dryness in a stream of carbon dioxide and redissolved in absolute ethanol. The resulting absorption curve (Fig. 2, curve 1) displayed three maxima (276.5 mμ, 287 mμ

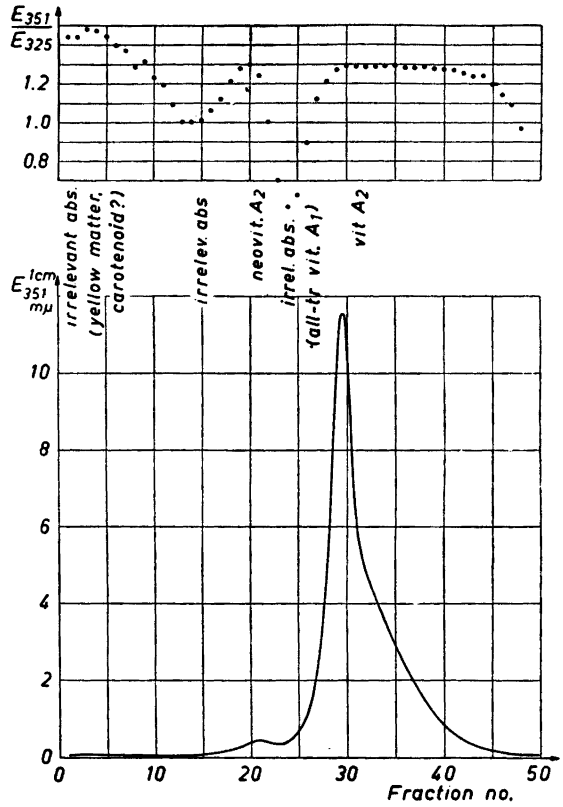


Fig. 1. Fractionation curve for the unsaponifiable fraction from pike liver with a column 86 cm long, diam. 1.8 cm. The upper part of the figure illustrates the ratio $\frac{E_{351\ m\mu}}{E_{325\ m\mu}}$ *for the individual fractions.*

and 351.5 mμ) and two minima (280 mμ and 297 mμ) and the following ratios were found:

$$\frac{E_{276.5}}{E_{351.5}} = 0.388, \quad \frac{E_{280}}{E_{351.5}} = 0.369, \quad \frac{E_{287}}{E_{351.5}} = 0.493, \quad \frac{E_{297}}{E_{351.5}} = 0.298 \quad \frac{E_{325}}{E_{351.5}} = 0.735$$

I,2. ISOLATION OF VITAMIN A_2 FROM PERCH LIVER

A dicalcium phosphate column, 70 cm long, 1.8 cm diam., was used for chromatography of the unsaponifiable fraction from 15.76 g of perch liver ($E^{1\%}_{1cm,\ 350\ m\mu} = 0.085$ measured in light petroleum and calculated in relation to the liver weight). Eluents used: light petroleum-ether mixtures, 300 ml (92:8 v/v), 300 ml (90:10 v/v). Eluate was collected in 3.2 ml fractions. The fractionation curve is illustrated in Fig. 3.

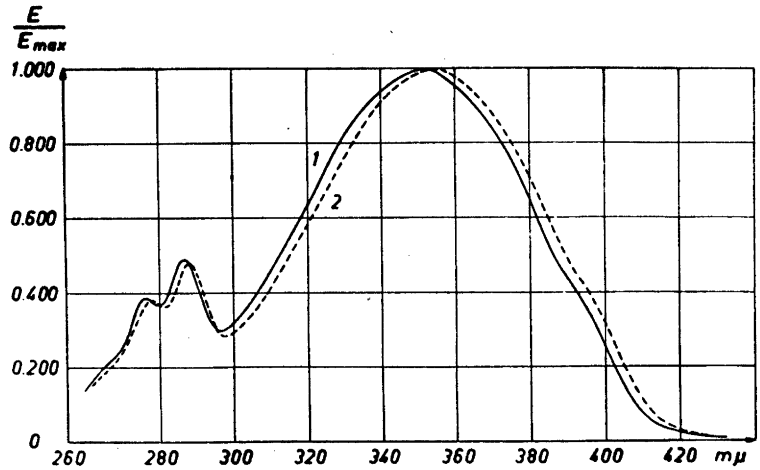


Fig. 2. Light absorption curves for natural vitamin A_2 (curve 1) and the substance a (curve 2). Solvent absolute ethanol.

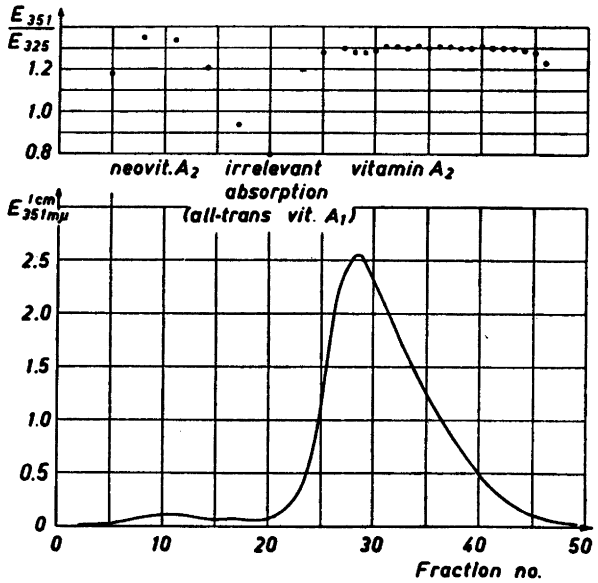


Fig. 3. Fractionation curve for the unsaponifiable fraction from perch liver with a column 70 cm long, diam. 1.8 cm. The upper part of the figure illustrates the ratio $\frac{E_{351\ m\mu}}{E_{325\ m\mu}}$ *for the individual fractions.*

The peak fraction with $E^{1\,cm}_{351.5} = 2.52$ displayed, when dissolved in ethanol, three maxima and two minima at the wavelengths mentioned under I,1. The following ratios were found:

$$\frac{E_{276.5}}{E_{351.5}} = 0.384, \quad \frac{E_{280}}{E_{351.5}} = 0.369, \quad \frac{E_{287}}{E_{351.5}} = 0.490, \quad \frac{E_{297}}{E_{351.5}} = 0.297, \quad \frac{E_{325}}{E_{351.5}} = 0.734.$$

In a subsequent chromatographic isolation on a dicalcium phosphate column, 82 cm long, 1.8 cm diam., of vitamin A_2 from 65 g perch liver (a solution of the unsaponifiable fraction in light petroleum gave $E^{1\,\%}_{1\,cm\ 351\ m\mu} = 0.236$, calculated in relation to the liver weight) all the vitamin A_2-containing fractions for which the ratio $\frac{E_{351.5}}{E_{325}}$ had the same value (1.29—1.31) were combined and again subjected to chromatography on a dicalcium phosphate column, 65 cm long, 1.8 cm diam. Previous to the chromatography, but after activation (*cf.* Brö-Rasmussen, Hjarde and Porotnikoff [2]) this dicalcium phosphate had been washed with ether * on a glass Büchner filter (1.5 l pure, peroxide free ether per 200 g $CaHPO_4$). The washed dicalcium phosphate was transferred into a 500 ml round-bottomed flask and exhausted for half an hour at room temperature. Finally the flask was filled with nitrogen, exhausted and again filled with nitrogen, the process being repeated altogether four times, following which the dicalcium phosphate powder was suspended in light petroleum. According to Schlabach [3], the light petroleum (b.p. 40—60°C) used for the chromatography had been filtered through a column of silica gel (70 cm long, 5.3 cm diam., grain size 100—200 mesh) and subsequently distilled to remove all substances which absorb light within a wavelength range from 240 mμ to 400 mμ when measured against distilled water.

The vitamin A_2 thus isolated by repeated chromatography was dissolved in ethanol and showed an absorption curve with characteristic $\frac{E}{E_{351.5}}$ values in good agreement with those previously given.

The fractionation curves illustrated in Figs. 1 and 3 both display 2 maxima of which the highest correspond to the vitamin A_2 isomer just mentioned. The peak fraction corresponding to the lower maximum of Fig. 1 displayed, when dissolved in absolute ethanol, three maxima, at 277.5 mμ, 287.5 —288 mμ and 353 mμ, and two minima, at 281 mμ and 298 mμ. The following ratios were found:

$$\frac{E_{277.5}}{E_{353}} = 0.46, \quad \frac{E_{281}}{E_{353}} = 0.44, \quad \frac{E_{288}}{E_{353}} = 0.54, \quad \frac{E_{298}}{E_{353}} = 0.36, \quad \frac{E_{325}}{E_{353}} = 0.74$$

The peak fraction corresponding to the lower maximum in the fractionation curve Fig. 3 also displayed three maxima (277 mμ, 287.5 mμ and 353.5 mμ) and two minima (283 mμ and 299.5 mμ), and the following ratios were found (in absolute ethanol):

$$\frac{E_{277}}{E_{353}} = 0.71, \quad \frac{E_{283}}{E_{353}} = 0.63, \quad \frac{E_{287.5}}{E_{353}} = 0.68, \quad \frac{E_{299.5}}{E_{353}} = 0.39, \quad \frac{E_{325}}{E_{353}} = 0.70$$

* The residue obtained by evaporation of the first 400 ml ether filtrate showed after solution in 5 ml absolute ethanol a certain light absorption within the wavelength range 275—325 mμ.

It must be assumed that the substances found in the first fractions by chromatography of pike liver and perch liver are identical, although mixed with different amounts of other light-absorbing substances. The substance which is presumably a vitamin A_2 isomer might be denoted neovitamin A_2 by analogy with neovitamin A_1 which, when chromatographed on a dicalcium phosphate column under corresponding circumstances, leaves the column immediately before all-*trans* vitamin A_1. As the content of this isomer in the liver extracts used is very small (about 1.5 % of the extinction at 351 mμ deriving from the total quantity of eluted neovitamin A_2 + vitamin A_2 is due to neovitamin A_2) and as, moreover, its location in the dicalcium phosphate column is in the transition range between the bands representing the small quantities of the neovitamin A_1 and all-*trans* vitamin A_1 deriving from the liver extract, the fractions containing this neovitamin A_2 cannot, of course, be expected to be pure.

II. ISOMERIZATION

Vitamin A_2 which has been isolated by chromatography according to the method described in section I was dissolved in light petroleum and isomerized by addition of an iodine solution (10 mg iodine per 100 ml light petroleum). To 9 ml of vitamin A_2 solution was added 1 ml iodine solution and after shaking for 30 s the mixture was poured over 0.5 g pulverized sodium thiosulphate ($Na_2S_2O_3$, $5H_2O$) in a 100 ml Erlenmeyer flask, and the flask was shaken until the violet iodine colour disappeared, the sodium thiosulphate precipitate being subsequently removed by filtration through a folded filter. The isomerization process was performed at 23°C, protected against daylight. Three experiments were made, in which the vitamin A_2 solution used had the following values of $E^{1\,cm}_{351\,m\mu}$: 0.980, 7,22 and 34,5 and consequently 0.882, 6.50, and 31.0 at the moment of admixture. After the isomerization $E_{351\,m\mu}$ had dropped by 6—10 % in all three cases. The ratio $\frac{E_{287}}{E_{351}}$ (measured in light petroleum) changed from 0.50 to 0.53—0.55. There was no measurable alteration in the location of the maxima and minima.

Finally an isomerization experiment was made in which 9 ml of a solution of vitamin A_2 in light petroleum, with $E^{1\,cm}_{351\,m\mu} = 0.895$, was mixed with 1 ml of the iodine solution previously mentioned, the iodine being removed after shaking for 100 s as already described. $E^{1\,cm}_{351\,m\mu}$, which at the moment of admixture was 0.805, had after isomerization dropped by about 15 % and $\frac{E_{287}}{E_{351}}$ had altered from 0.495 to 0.629.

III. CHROMATOGRAPHY OF ISOMERIZED VITAMIN A_2

III,1. A sample of 40 ml of a solution of vitamin A_2 in light petroleum which had been isomerized as described in section II (the iodine being allowed to act for a period of 30 s) and with $E^{1\,cm}_{351\,m\mu} = 0.882$ was used for this experiment. For the chromatography a dicalcium phosphate column, length 78 cm, dia-

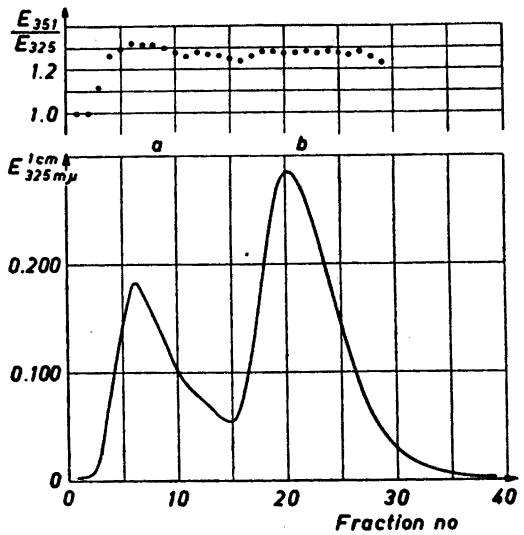


Fig. 4. Fractionation curve for isomerized vitamin A_2 chromatographed on a 78 cm column, diameter 1.8 cm.

meter 1.8 cm, was used. The eluent was a mixture of light petroleum and ether (85:15 v/v). Eluate was collected in 4.7 ml fractions.

The fractionation curve is given in Fig. 4 and shows the presence of two substances with absorption maximum at about 350 mμ. The peak fractions from each of the two curve sections *a* and *b* display the following spectrophotometric properties in absolute ethanol:

Substance a: three maxima: 277.5 mμ, 288—288.5 mμ, and 353.5 mμ
two minima: 281.5 mμ and 298 mμ

$$\frac{E_{277.5}}{E_{353.5}} = 0.432, \quad \frac{E_{281.5}}{E_{353.5}} = 0.415, \quad \frac{E_{288}}{E_{353.5}} = 0.530, \quad \frac{E_{298}}{E_{353.5}} = 0.344, \quad \frac{E_{325}}{E_{353.5}} = 0.724$$

Substance b: three maxima: 276.5 mμ, 287 mμ and 351.5 mμ
two minima: 280 mμ and 297 mμ

$$\frac{E_{276.5}}{E_{351.5}} = 0.472, \quad \frac{E_{280}}{E_{351.5}} = 0.453, \quad \frac{E_{287}}{E_{351.5}} = 0.574, \quad \frac{E_{297}}{E_{351.5}} = 0.339, \quad \frac{E_{325}}{E_{351.5}} = 0.735$$

The ratio of the two substances *a* and *b* may be calculated from the fractionation curve. Ratio *a* to *b* expressed by E_{351} measured directly in the eluate was found to be 34.5/65.5.

III,2. Larger quantities of the two substances *a* and *b* were prepared as follows: The unsaponifiable fraction from 157.6 g of perch liver was subjected to chromatography twice on alumina columns, 18 × 1.8 cm (standardized according to Brockmann). Half of the quantity of purified vitamin A_2 obtained, which in 180 ml light petroleum had an $E^{1\,cm}_{351\,m\mu} = 7.22$ and $\frac{E_{287}}{E_{351}} = 0.50$, was

isomerized as described in section II. After filtration and evaporation, chromatography on a 48×3.0 cm dicalcium phosphate column was applied. The eluents used were various mixtures of diethylether and light petroleum, in the following order:

100	ml	light	petroleum	—	ether	mixture (95: 5 v/v)
100	»	»	»		»	» (92: 8 v/v)
100	»	»	»		»	» (90: 10 v/v)
100	»	»	»		»	» (88: 12 v/v)
300	»	»	»		»	» (86: 14 v/v)
200	»	»	»		»	» (75: 25 v/v)

The eluate was collected in 4.7 ml fractions. The fractionation curve is illustrated in Fig. 5.

It should be mentioned at this point that while it is possible when chromatographing a mixture of neovitamin A_1 and all-*trans* vitamin A_1 on the dicalcium phosphate column to observe a fairly distinct difference in the fluorescence of neovitamin A_1 (yellowish green) and all-*trans* vitamin A_1(more bluish green), the two vitamin A_2 bands displayed only a slight difference in ultraviolet light. Both vitamin A_2 bands displayed a brown fluorescence, that of substance *a* having, however, a slightly reddish tinge while that of substance *b* was of a more violet-brown colour.

The ratio of the quantities in which the two substances *a* and *b* are present is 32: 68, when expressed by E_{351} measured directly on the eluate.

The three peak fractions corresponding to substance *a* which showed the same value of ratios $\frac{E_{288}}{E_{351}}$ and $\frac{E_{351}}{E_{325}}$ were combined, evaporated and rechromatographed on a dicalcium phosphate column, 28×0.8 cm (purified with ether as previously described) ,the eluent used was light petroleum (which had been purified by means of silica gel) mixed with diethylether (86: 14 v/v). Eluate was collected in 2 ml fractions. The fractionation curve showed the presence of one substance only with absorption maximum at about 351 mμ. The values of the ratios $\frac{E_{288}}{E_{351}}$ and $\frac{E_{351}}{E_{325}}$ for the peak fraction and the subsequent fractions were the same. When the peak fraction was dissolved in ethanol, the corresponding curve displayed three maxima and two minima at the wavelengths previously determined (III,1 *a*). The following ratios were found:

$$\frac{E_{277.5}}{E_{353.5}} = 0.383, \quad \frac{E_{281.5}}{E_{353.5}} = 0.364, \quad \frac{E_{288}}{E_{353.5}} = 0.480, \quad \frac{E_{298}}{E_{353.5}} = 0.286, \quad \frac{E_{325}}{E_{353.5}} = 0.674.$$

The absorption curve is illustrated in Fig. 2, (curve 2).

The peak fractions corresponding to substance *b*, for which the value of $\frac{E_{287}}{E_{351}}$ (= 0.55, measured in absolute ethanol) and of $\frac{E_{351}}{E_{325}}$ (= 1.36 = $\frac{1}{0.735}$, measured in absolute ethanol) were found to be the same, were given a corresponding treatment: rechromatography on a 28×0.8 cm column of dicalcium phosphate (purified by means of ether) and elution with a (85: 15 v/v) mixture of light petroleum (purified by means of silica gel) and diethylether.

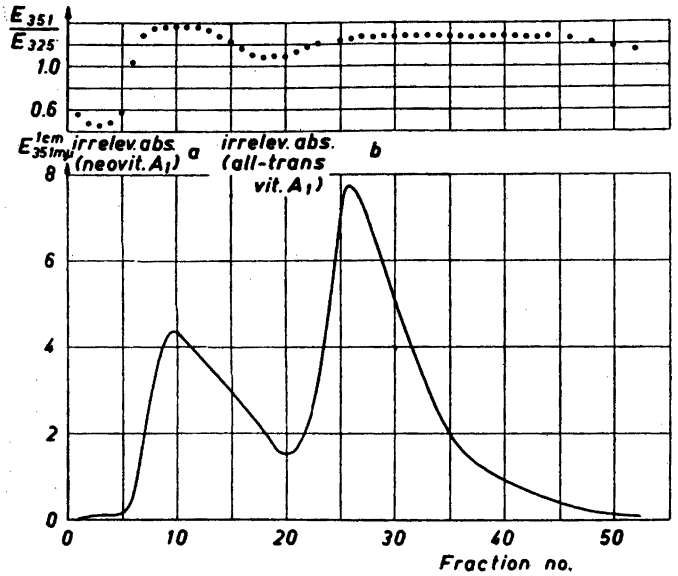


Fig. 5. Fractionation curve for isomerized vitamin A_2 with a column 48 cm long, diameter 3.0 cm.

Eluate was collected in 2 ml fractions. The fractionation curve showed the presence of one substance only with absorption maximum at 351 mμ. When dissolved in ethanol, the peak fraction gave a curve with three maxima and two minima at the wavelengths determined in section III,1 *b*, and the following ratios were found:

$$\frac{R_{276.5}}{R_{351.5}} = 0.445, \quad \frac{E_{280}}{E_{351.5}} = 0.426, \quad \frac{E_{287}}{E_{351.5}} = 0.555, \quad \frac{E_{297}}{E_{351.5}} = 0.321, \quad \frac{E_{325}}{E_{351.5}} = 0.738$$

The peak fractions from the last-mentioned chromatographic separation were combined and rechromatographed on a 58 × 1.0 cm dicalcium phosphate (ether-purified) column, elution with light petroleum (silica gel purified)-diethylether mixtures (90: 10 v/v increasing to 65: 35 v/v). Eluate was collected in 2 ml fractions. The peak fraction dissolved in absolute ethanol gave the same values of the five $\frac{E}{E_{351.5}}$ ratios as the material before it was rechromatographed.

It may be mentioned that after the isomerization experiment described in section II, in which the action of iodine on vitamin A_2 was prolonged for a period of 100 s, the subsequent chromatography resulted in a ratio of *a* to *b* equal to 33.4: 66.6 (expressed by E_{351} measured directly on the collected fractions).

IV. CHROMATOGRAPHY OF A MIXTURE OF VITAMIN A_2 AND SUBSTANCE *b*

A mixture was prepared consisting of 100 ml solution in light petroleum of natural vitamin A_2 purified by chromatography on dicalcium phosphate as described in section I, with $E^{1\,cm}_{351\,m\mu} = 0.466$ and $\frac{E_{287}}{E_{351}} = 0.495$, and 100 ml solution in light petroleum of substance *b*, with $E^{1\,cm}_{351\,m\mu} = 0.428$ an $\frac{E_{287}}{E_{351}} =$ $= 0.555$. The mixture was evaporated and chromatographed on a 78×1.0 cm column of (ether-purified) dicalcium phosphate. Elution by means of mixtures of light petroleum (silical gel purified) and diethylether in the following order:

20	ml	light	petroleum	—	ether	mixture (95: 5 v/v)
20	»	»	»		»	(92: 8 v/v)
40	»	»	»		»	(88: 12 v/v)
40	»	»	»		»	(85: 15 v/v)
20	»	»	»		»	(82: 18 v/v)
100	»	»	»		»	(79: 21 v/v)

Eluate was collected in 2 ml fractions.

The fractionation curve showed the presence of one substance only with absorption maximum at 351 mμ. Direct spectrophotometric measurements on the collected fractions gave $\frac{E_{287}}{E_{351}} = 0.52$—$0.55$. The variation of the ratio throughout the series of fractions did not, however, suggest any pronounced tendency towards separation into two substances. A subsequent, corresponding experiment gave the same result.

V. CHROMATOGRAPHY OF AN ISOMERIZED MIXTURE OF VITAMIN A_1 AND VITAMIN A_2

A mixture was prepared consisting of 15 ml solution of vitamin A_2 in light petroleum ($E^{1\,cm}_{351\,m\mu} = 2.00$) and 15 ml solution in light petroleum of (all-*trans*) vitamin A_1 ($E^{1\,cm}_{325\,m\mu} = 1.920$), and the mixture was isomerized by means of iodine in the manner described in section II. After filtration and evaporation to a volume of about 5 ml, the mixture was chromatographed on a 76×1.0 cm dicalcium phosphate column. Elution with light petroleum-ether mixtures as follows:

100	ml	light	petroleum	—	ether	mixture (90: 10 v/v)
200	»	»	»		»	(86: 14 v/v)

Eluate was collected in 4.7 ml fractions.

The fractionation curve (measurement of $E^{1\,cm}_{335\,m\mu}$ of the eluted fractions) is illustrated in Fig. 6.

Even if a complete separation of the four substances present has not been obtained, it appears clearly from the course of the $\frac{E_{351}}{E_{325}}$ curve that the four substances are eluted in the following order: neovitamin A_1, substance *a* (= neovitamin A_2), all-*trans* vitamin A_1 and finally substance *b* (= all-*trans* vitamin A_2?).

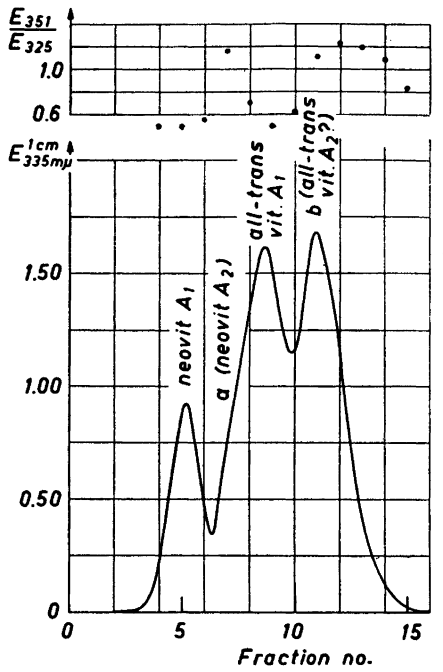


Fig. 6. Fractionation curve for an isomerized mixture of vitamin A_1 and vitamin A_2 with a column 76 cm long, diameter 1.0 cm.

DISCUSSION

Experiments III,1 and III,2 show that it is possible after treatment with iodine of vitamin A_2 prepared by chromatography to isolate from the isomerization product two different substances, *a* and *b*, the absorption curves of which show great similarity, although differing clearly with regard to the location of maxima and minima. In the case of substance *a* the wavelengths of the maxima and minima exceed by about 1—2 mμ those of substance *b* and of natural vitamin A_2, the isolation of which is described in experiments I,1 and I,2.

When bearing in mind that by chromatography on dicalcium phosphate substance *a* is eluted slightly before *b*, it will be seen that there is analogy between substances *a*, *b* and neovitamin A_1, all-*trans* vitamin A_1 — neovitamin A_1 being eluted slightly more readily from dicalcium phosphate than all-*trans* vitamin A_1. It is therefore a reasonable assumption that also as regards geometrical configuration the relationship of the two substances *a* and *b* is as that of neovitamin A_1 and all-*trans* vitamin A_1. In this connection it should also be mentioned that Robeson and Baxter [4] after isomerization for 2 h in daylight of all-*trans* vitamin A_1 anthraquinone-β-carboxylate by the action of iodine dissolved in benzene ascertained that the isomerization product contained 31 % neo-isomer. In the present isomerization experiments on free vitamin A_2 alcohol dissolved in light petroleum, with a reaction period of 30—100 s, the ratio of substances *a* to *b* — expressed by E_{351} — was about 1 to 2.

Keeping in mind the analogy *a*, *b* to neovitamin A_1, all-*trans* vitamin A_1, *a* and *b* might be expected to be identical with neovitamin A_2 and vitamin A_2, respectively, the two vitamin A_2 isomers which occur in the eluate from the liver extracts.

As the amounts of the supposed neovitamin A_2 fractions isolated from the liver extracts were insufficient to allow for further chromatographic purification, additional experiments to confirm the identity of the neovitamin A_2 occurring in the liver extracts and substance *a* have not been made. The location of the maxima and minima for substance *a* and the impure neovitamin A_2 isolated from the liver extracts show fairly good agreement, particularly with regard to the main maximum; at this wavelength (353.5 mμ) less interference from irrelevant substances may also be expected than at lower wavelengths. The difference between $\frac{E}{E_{353.5}}$ for the impure neovitamin A_2 of pike liver extract — which is obviously purer than the neovitamin A_2 isolated from perch liver — and for substance *a*, purified by chromatography, is greatest at the lower wavelengths (270—300 mμ) and small at wavelengths above 350 mμ, which seems to indicate that the difference is due solely to irrelevant light absorbing substances in the neovitamin A_2 isolated directly from liver.

When comparing the spectrophotometric properties of substance *b* and the vitamin A_2 isolated directly from liver, it would be reasonable to establish comparisons with previous investigations on the spectrophotometric properties of vitamin A_2 (Schantz [5], Cama and Morton [6], Farrar, Hamlet, Henbest and Jones [7]).

In Table 1 the experimental results are represented by a series of ratios between the extinctions at the maxima and minima. The table also lists the results of measurements made in this laboratory on chromatographically (dicalcium phosphate) purified synthetic all-*trans* vitamin A_1 and neovitamin A_1 prepared by chromatography after iodine isomerization of synthetic all-*trans* vitamin A_1.

As it will be seen from this table, there is good agreement between the location of the maxima and minima of the natural vitamin A_2 isolated in the present investigation and the synthetic and natural vitamin A_2 preparations described in the literature [5,6,7] although Schantz [5] and Farrar *et al.*[7] do not mention the existence of a maximum at 276.5 mμ, while Cama and Morton [6] mention the presence of an inflexion at 277 mμ. The ratios $\frac{E}{E_{max}}$ and $\frac{E}{E_{min}}$ calculated for the characteristic maxima and minima on the other hand show a certain deviation, since for the range 275—325 mμ the ratio $\frac{E}{E_{351.5}}$ in case of the vitamin A_2 isolated in the present investigation is about 5—20 % below and the ratio $\frac{E_{287}}{E_{297}}$ 9—15 % above the corresponding ratios given in the table for earlier vitamin A_2 preparations [5,6,7]. Maximum difference is observed in the case of the minimum at 297 mμ. The differences seem to suggest a greater purity of the vitamin A_2 prepared in the course of the present investigation.

Table 1. Spectroscopic properties of vitamins A_2 (abs. ethanol solution).

Maxima mμ	Minima mμ	$\frac{E_{276.5}}{E_{280}}$	$\frac{E_{287}}{E_{297}}$	$\frac{E_{297}}{E_{351.5}}$	$\frac{E_{276.5}}{E_{351.5}}$	$\frac{E_{287}}{E_{351.5}}$	$\frac{E_{325}}{E_{351.5}}$		
—, 286, 351	—, 297	(<1)	1.44	0.392*	—	0.561*	0.769	vitamin A_2	(A)
277 (infl), 286, 351	—, 295—97	(ca. 1)	1.38	0.393*	0.435**	0.544	0.810	»	(B)
—, 288, 352	—, 297,5	(<1)	1.45	0.365***	—	0.530†	—	»	(C)
276.5, 287, 351.5	280, 297	1.05	1.66	0.298	0.388	0.493	0.735	»	(D)
276.5, 287, 351.5	280, 297	1.04	1.73	0.321	0.445	0.555	0.738	substance *b*	(D)
277.5, 288, 353.5	281.5, 298	1.01	1.62	0.291	0.373	0.469	0.679	substance *a*	(D)
328	—	0.865	0.625	0.937	0.377	0.585	1.89	neovitamin A_1	(D)
324.5	—	0.860	0.651	1.30	0.524	0.845	2.38	all-*trans* vit. A_1	(D)

1) Schantz [5]
3) Cama and Morton [6]
7) Farrar, Hamlet, Henbest and Jones [7]
D) Barnholdt and Hjarde, work described here.

* $\frac{E}{E_{351}}$ ** $\frac{E_{275}}{E_{351}}$ *** $\frac{E_{297.5}}{E_{352}}$ † $\frac{E_{287}}{E_{352}}$

As already mentioned, substance *b* might be expected to be identical with natural vitamin A_2. With regard to the location of the characteristic maxima and minima the two substances show fairly good agreement, while the ratios $\frac{E}{E_{351.5}}$ at wavelengths below 310 mμ are somewhat higher in the case of substance *b* than in the case of the natural vitamin A_2 isolated according to section I, although at wavelengths above 310 mμ the differences between the ratios are only of a magnitude of 0—0.010. The object of the experiments made with respect to substance *b* has therefore been to find out whether it represented a single substance — a third vitamin A_2 isomer — or a mixture of substances, of which at least one might be expected to be a vitamin A_2 isomer, presumably the vitamin A_2 occurring in nature.

The assumption that substance *b* is identical with natural vitamin A_2, although in a state of incomplete purity, is supported by the agreement existing between the location of the maxima and minima of the absorption curves of the two substances and also by the fact that is has not hitherto been possible

to separate the two substances by chromatography on dicalcium phosphate — as appears from experiment IV.

On the other hand the rechromatographic experiments described in section III suggest that *b* is a single, pure substance; if this is the case, we are thus faced with a vitamin A_2 isomer which cannot, by chromatography on dicalcium phosphate, be separated from the vitamin A_2 occurring in nature, and which has maxima and minima at the same wavelengths as the latter and which only with regard to the ratio $\frac{E}{E_{351.5}}$ at wavelengths below 310 mμ deviates spectrophotometrically from the vitamin A_2 occurring in nature.

Consequently it is not possible on the basis of the results of the present investigation to decide whether substance *b* is a mixture of the vitamin A_2 isolated from pike and perch liver and an impurity deriving from the isomerization process, or a single substance, a third vitamin A_2 isomer, which are not readily separated by chromatography on dicalcium phosphate.

REFERENCES

1. Abdullah, M. M., Morcos, S. R. and Salah, M. K. *Biochem. J. London* **56** (1954) 569.
2. Bro-Rasmussen, F., Hjarde, W. and Porotnikoff, O. *Analyst* **80** (1955) 418.
3. Schlabach, T. D. Jr. *The chromatografic separation and the determination of vitamin D_2 in corn oil*, Thesis, University, Michigan 1952.
4. Robeson, C. D. and Baxter, J. G. *J. Am. Chem. Soc.* **69** (1947) 136.
5. Schantz, E. M. *Science* **108** (1948) 417.
6. Cama, H. R. and Morton, R. A. *Analyst* **78** (1953) 74.
7. Farrar, K. R., Hamlet, J. C., Henbest, H. B. and Jones, E. H. R. *J. Chem. Soc.* **1952** 2657.

Received August 10, 1956.

ACTA CHEMICA SCANDINAVICA 10 (1956) 1649—1662

A Contribution to the Theory of Chromatography

TAGE LANGVAD

Aarhus Universitets kemiske Institut, Aarhus, Denmark

When the adsorption isotherm is linear, the isochrones in elution chromatography are Gauss'ian curves moving along the column at a rate proportional to the flow rate; simultaneously the standard deviation increases proportionally to the square root of the flow rate. Consequently the isoplanes can only in some cases be approximated by Gauss'ian curves, whereas a better approximation is obtained by considering them as Gauss'ian functions of the square root of the eluted volume. As it is very difficult to decide whether or not a series of experimental values fit a certain type of non-linear curve, attention is called to the method of Bliss according to which the problem concerning the normal distribution is converted into an investigation of a linear dependency. The results are tested experimentally in ion-exchange chromatography of chloride ions.

In the theoretical treatment of elution chromatography Vermeulen and Hiester [1] have given a solution of the general case in which the adsorption isotherm is non-linear and the flow rate is too great to obtain equilibrium. Furthermore, several authors have given approximate solutions which in many cases may be satisfactory. All these solutions are, however, rather inconvenient as it is very difficult to make a series of experimental values fit a non-linear curve in such a way that the parameters of the function are determined most accurately. The following elucidation is founded on the plate theory applied by Martin and Synge [2] and Mayer and Thompkins [3].

Consider the column as divided in segments by planes perpendicular to the axis of the column. Each segment contains v ml liquid and they are numbered 0, 1, 2, ... p ... The process is started by pouring v ml solution of the substance in question on the top of the column, and when v ml are drawn off from the bottom, the substance is now in segment No. 0. It is assumed that the adsorption isotherm is linear; then the fraction α of the solute in the liquid phase and the fraction $1-\alpha$ in the solid or stationary phase are independent of the concentration. When adsorption equilibrium has been established, v ml eluant are poured on the top of the column and the whole liquid phase is displaced one segment. The v ml which are hereby drawn off from the bottom of the column are collected as the first fraction, these being numbered 1, 2 ... n ... When equilibrium has again been established the next displace-

ment of one segment takes place. Let the total quantity of solute in the p'th segment after n fractions of v ml have passed the column be $q_{n,p}$ measured in units of the originally introduced quantity. Then the condition of material balance is

$$q_{n,p} = \alpha\ q_{n-1,p-1} + (1-\alpha)\, q_{n-1,p} \tag{1}$$

When n fractions have passed, the total quantity of substance is distributed in the n+1 segments from p = 0 to p = n, while for p > n and p = —1 (pure eluant entering the column) $q_{n,p} = 0$. From these data and $q_{o,o} = 1$, $q_{n,p}$ can be calculated for all values of n and p by successive application of (1). It is however simpler to substitute

$$q_{n,p} = Q_{n,p}\, \alpha^p\, (1-\alpha)^{n-p} \tag{2}$$

by which (1) becomes

$$Q_{n,p} = Q_{n-1,p-1} + Q_{n-1,p} \tag{3}$$

Employing the conditions for $q_{n,p}$ above (2) yields

$$Q_{o,o} = 1,\ Q_{n,-1} = 0 \text{ and } Q_{n,n+1} = 0$$

and as (3) is identical with the recursion formula for the binomial coefficients (2) is converted into

$$q_{n,p} = \binom{n}{p}\, \alpha^p (1-\alpha)^{n-p} \tag{4}$$

In statistics the probability in the binomial distribution, *i.e.* the probability that an event happens p times out of n, the probability of the single event being α, is given by (4). It can be shown [4] that when n increases (4) converges against the normal frequency function

$$q_{n,p} \rightarrow \frac{1}{\sigma}\, \varphi\left(\frac{p-\mu}{\sigma}\right) \tag{5}$$

with the mean value $\mu = n\alpha$ and the standard deviation $\sigma = \sqrt{n\alpha\ (1-\alpha)}$. Here and in the following the Gauss'ian frequency function and distribution function are designated $\varphi\ (x)$ and $\Phi\ (x)$, respectively:

$$\varphi\ (x) = \frac{1}{\sqrt{2\pi}}\, e^{-\frac{x^2}{2}} \text{ and } \Phi\ (x) = \int_{-\infty}^{x} \varphi\ (t)\ dt$$

Measured in units of the initial concentration the concentration in the liquid phase is

$$c = \frac{\alpha \cdot q_{n,p}}{v}$$

Introducing $V = pv$ and $U = nv$ (5) becomes

$$c = \frac{\alpha}{\sqrt{U\alpha\ (1-\alpha)\ v}}\, \varphi\left(\frac{V-\alpha U}{\sqrt{U\alpha\,(1-\alpha)\ v}}\right) \tag{6}$$

which gives the concentration as a function of the two variables V, the distance from the top of the column to the regarded point measured in ml of interstitial volume and U, the eluted volume of liquid.

As the liquid in practice moves continually the above deduction is valid only for infinitely small quantities of substance. Actually the experiment is

started by pouring a finite quantity, say A ml solution on the top of the column. The concentration $c = \mathrm{f}\ (V, U)$ is then the result of a superposition of an infinite number of infinitely small quantities, the first and last of which have moved $V—A$ and V ml along the column, respectively. The total amount of solute that has accumulated in a differential segment with abscissa V when U ml of eluate have passed is given by

$$A \cdot c = \int_{V-A}^{V} \mathrm{f}(V, U)\ \mathrm{d}V = \int_{V-A}^{V} \frac{\alpha}{S}\ \varphi(t)\,\mathrm{d}V,$$

in which

$$S = \sqrt{U\alpha(1—\alpha)\ v} \text{ and } t = \frac{V—\alpha\, U}{S}$$

$$\text{As } \mathrm{d}t = \frac{\mathrm{d}V}{S} \text{ and } t_A = \frac{V—A—\alpha\, U}{S}$$

$$A \cdot c = \alpha \int_{t_A}^{t} \varphi\ (t)\ \mathrm{d}t = \alpha(\Phi(t)—\Phi(t_A))$$

According to the mean value theorem

$$\Phi(t)—\Phi(t_A) = \varphi\left(\frac{V—a—\alpha U}{S}\right)\left(\frac{V—\alpha U}{S} — \frac{V—A—\alpha U}{S}\right)$$

in which $0 < a < A$

Consequently $c = \frac{\alpha}{S}\ \varphi\left(\frac{V—a—\alpha U}{S}\right)$

When $A \ll V$, a may be neglected, and (6) is valid for finite quantities.

The discussion of this formula is divided in two parts: 1°. $U = U_0 = constant\ (isochrones)$. In this case the standard deviation is also a constant and c is a Gauss'ian function of V, the mean value being $\alpha\ U_0$ and the standard deviation $S_0 = \sqrt{U_0\alpha\,(1—\alpha)\,v}$. When U increases this distribution of the solute moves through the column with a rate proportional to that of the eluant, V_{max} being equal to $\alpha\ U$; simultaneously the curve is flattened out, S being proportional to $\sqrt{U}$. 2°. $V = V_0 = constant\ (isoplanes)$. This is the case encountered in practice, the eluate being collected in fractions and the concentrations of solute herein determined in some conventional way. Equation (6) is written

$$c = \mathrm{f}\ (U) = \frac{1}{\sqrt{U\frac{1—\alpha}{\alpha}\,v}}\ \varphi\left(\frac{V_0/\alpha—U}{\sqrt{U\frac{1—\alpha}{\alpha}\,v}}\right) \tag{7}$$

This is not a normal distribution, the "standard deviation" containing the variable U. If, however, U is great compared with $\sqrt{Uv(1—\alpha)/\alpha}$, U_0 may, as a first approximation, be substituted for U in this expression and (7) takes the form of a Gauss'ian equation:

$$c \approx \mathrm{f}_1\ (U) = \frac{1}{s}\ \varphi\left(\frac{U_0—U}{s}\right) \tag{8}$$

in which $U_0 = V_0/a$ and $s = \sqrt{U_0 v(1-a)/a}$
A great ratio between U_0 and s

$$\frac{U_0}{s} = \sqrt{\frac{V_0}{v}\frac{1}{1-a}}$$

means that the longer the column and the greater a the better is the approximation. It should be noticed that in the normal distribution 95 % of the area lies between the values $U_0 \pm 2s$ and 99.7 % lies between $U_0 \pm 3s$.

When necessary, a better approximation may be obtained by the following transcription of (7):

$$c = \frac{1}{\sqrt{U}} \cdot \frac{1}{\sqrt{\frac{1-a}{a} v}} \varphi \left(\frac{(\sqrt{U_0} - \sqrt{U})(\sqrt{U_0} + \sqrt{U})}{\sqrt{U}\sqrt{\frac{1-a}{a} v}} \right)$$

By substituting $\sqrt{U_0}$ for $\sqrt{U}$ in the sum in the numerator and in the denominator in φ we get

$$c \approx f_2(U) = \frac{1}{2\sqrt{U}} \cdot \frac{1}{\frac{1}{2}\sqrt{\frac{1-a}{a} v}} \varphi \left(\frac{\sqrt{U_0} - \sqrt{U}}{\frac{1}{2}\sqrt{\frac{1-a}{a} v}} \right) \qquad (9)$$

If a function $g(U)$ is normally distributed:

$$F(U) = \varphi\left(\frac{g(U) - g(U_0)}{\sigma}\right)$$

the frequency function becomes

$$f(U) = F'(U) = \frac{1}{\sigma} g'(U) \varphi \left(\frac{g(U) - g(U_0)}{\sigma}\right)$$

and as $\frac{d\sqrt{U}}{dU} = \frac{1}{2\sqrt{U}}$ (9) indicates that c is a Gauss'ian function of $\sqrt{U}$, the mean value and standard deviation of which are $\sqrt{U_0}$ and $\frac{1}{2}\sqrt{\frac{1-a}{a} v}$, respectively.

The result of an experiment consists of a table giving the concentration of the solute as a discontinued function of the eluted volume. Even if a continuous curve is drawn by a recording instrument, measuring some physical property of the flowing solution, that varies with concentration, it is necessary to determine from the curve the concentration for some discrete values of the volume. When the fractions or intervals of w ml each are numbered 1, 2 . . . m . . . the problem to solve is whether the stair-shaped curve, which is a result of a plot of c against m, approximates a Gauss'ian curve, and next to determine the mean value and standard deviation thereof. According to statistical methods [6] this is done in the following way: The expressions

$$H(m) = \frac{\sum_{a}^{m} wc}{\sum_{a}^{b} wc} = \frac{\sum_{a}^{m} c}{\sum_{a}^{b} c} \tag{10}$$

are calculated. Here the first and last eluted fraction in which the concentrations are above the analytical error are numbered a and b, respectively. Thus H (m) means the fraction of the total amount of solute contained in the eluted fractions from number a to m inclusive, and it should be valid:

$$H(m) \approx \Phi\left(\frac{m-\mu}{\sigma}\right)$$

in which μ and σ are the mean value and standard deviation, respectively. Consequently the inverse function

$$\Phi^{-1}(H(m)) = \frac{m-\mu}{\sigma}$$

and this equation represents a straight line having the slope $\frac{1}{\sigma}$ and intersecting the abscissa axis in μ. The values of $\Phi^{-1}(x)$, $0<x<1$ are called quantiles; as a rule quantiles + 5 called probits are tabulated [7] in order to avoid negative values.

If the points (m, Φ^{-1} (H(m))) sufficiently well fit a straight line, $c = H(m)$ can be regarded as a Gauss'ian function, the constants of which are determined by the line. As

$$\frac{d\,\Phi^{-1}(x)}{dx} \to \infty \text{ for } x \to 0 \text{ and } x \to 1$$

the points near the ends of the line are rather uncertain and may be neglected. According to (8)

$$w \cdot \mu = U_0 = V_0/\alpha \text{ and } w \cdot \sigma = s = \sqrt{U_0 \frac{1-\alpha}{\alpha} v}$$

and thus α and v can be calculated.

If the line is curved it is tried whether the points ($\sqrt{m}$, Φ^{-1} (H(m))) give a straight line.

In this case the constants are related to the constants of (9) by

$$\sqrt{w} \cdot \mu = \sqrt{U_0} = \sqrt{V_0/\alpha} \text{ and } \sqrt{w} \cdot \sigma = \tfrac{1}{2}\sqrt{\frac{1-\alpha}{\alpha} v} \tag{12}$$

from which α and v may be calculated.

EXPERIMENTAL

The process investigated was the elution of chloride ions through columns containing Amberlite IRA 400 loaded with some other anion, preferably nitrate, the eluant being a solution of a salt containing the same anion:

$$RCl + X^- \rightleftharpoons RX + Cl^-$$

When 1 ml of the column filling contains β ml liquid with a total concentration of l mequiv./ml, and $1-\beta$ ml resin with an exchange capacity of r mequiv. the mass action law for small amounts of chloride gives

$$K_c = \frac{[RX]\,[Cl^-]}{[RCl]\,[X^-]} \approx \frac{[Cl^-]}{[RCl]}\,\frac{r}{l(1-\beta)}$$

The ratio of the total amount of chloride in the liquid phase to that in the resin is

$$\frac{a}{1-a} = \frac{\beta\,[Cl^-]}{(1-\beta)\,[RCl]} = K_c \cdot \frac{\beta\,l}{r}$$

$$K_c = \frac{a}{1-a} \cdot \frac{r}{\beta\,l} \qquad (13)$$

The substitution of [RX] and $[X^-]$ by $r/1-\beta$ and l, respectively, is justified by the fact, that in the experiments performed in this work $[X^-]$ varied between 0.1 and 1, while the maximum chloride concentrations measured in the adsorption bands were between 10^{-3} and 10^{-2}. Three types of column systems were used.

I. The column consisted of a glass tube of 27 mm inner diameter and 100 cm length. The lower end of the tube was narrowed down to the diameter of the outlet tube (inner diameter 1—2 mm, outer 6—7 mm). The filling was Amberlite IRA 400 (NO_3) resting on a glass wool plug. The top of the tube was provided with a three hole rubber stopper, through which were inserted a tube for the eluant, a funnel tube for introducing the chloride solution and a tube for letting out air. The eluant reservoir was a Mariotte bottle, the level of which was adjustable, and a flowmeter was inserted in the line. Immediately after the outlet tube the eluate passed an enlargement of the tube containing a silver-silver chloride electrode and a Radiometer K 9001 reference electrode (saturated K_2SO_4 Hg_2SO_4 / Hg; 650 mV referred to the normal hydrogen electrode). The silver-silver chloride electrode was made by electrolysing with a silver wire 50×0.5 mm as anode a 0.1 M sodium chloride solution with about 5 mA for two minutes. The potential of this cell was measured by a Radiometer PHM 22 and recorded by a Rec. Ia, from the same firm. As it appeared difficult to keep the flow rate constant the eluate after passage of the measuring cell ran to a siphon pipet, the emptying of which operated a relay. This switched the potentiometer to measure the potential of a fixed cell, and as the drainage of the siphon pipette lasted about half a minute, the pen came to rest and put a mark on the record for each fraction eluted.

II. The second type of column was very similar to type I, but it was provided with ten silver—silver chloride electrodes arranged as seen in Fig. 1. In order to prevent the electrolyte solution from creeping along the silver wires, where they pass through the rubber tubings, the central tube was filled with silicone oil. The recording of potentials from all ten electrodes was arranged by means of a selector from an automatic telephone exchange. The selector had eleven positions, and it was operated by minute pulses from the main electric clock of the institute; in this way the ten electrodes were successively connected to one terminal of the potentiometer, while the reference electrode constantly was connected to the other one. In the eleventh position of the selector the terminals of the potentiometer were short-circuited in order to record zero potential. It was thus always easy in the rather confused diagram on the paper strip to identify the marks corresponding to any of the electrodes.

III. The third column system consisted of ten single columns 17 mm inner diameter and 150 cm long. From the outlet tube the eluate passed an electrode system similar to that described in I and next a pump that transported it to the top of the next column. The pumps were magnetically operated pipette rubber bulbs attached to a side tube between two glass valves. The lumina of the measuring cell, valve housings and connecting tubes were chosen as small as practicable in order to avoid mixing. As the time elapsed between the passage of the adsorption band by two consecutive measuring cells was considerably greater in this case, the selector was operated by five minute pulses.

The electromotive force of the measuring cell is related to the chloride concentration by

$$E = 650 - 222 + 58 \log [Cl^-]\ \text{mV},$$

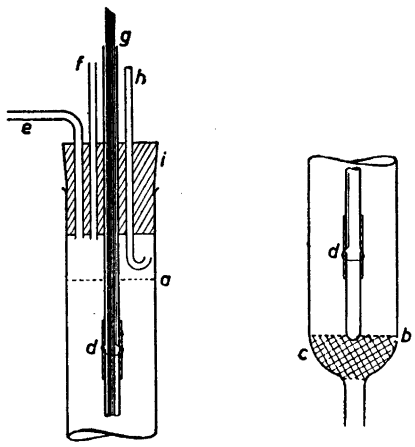


Fig. 1.

a—b ion exchange resin
c glass wool plug
d rubber tubing connecting the parts of the central tube. A silver wire is pricked through the rubber tubing and laid around it. Inside the wire is soldered to a copper wire leading to the selector.
e—f tubes for introducing chloride solution, and eluant
g central tube with ten electrode wires
h electrolytic bridge of the reference electrode
i rubber stopper

the standard potential of the silver—silver chloride electrode being 222 mV at room temperature. Now it proved difficult to keep the standard potential of the cell equal to the theoretical value; it could differ somewhat for different electrodes, and for the same electrode it could alter with time. Another potential also proved to alter with the treatment and age of the electrode, *viz.* the potential in a chloride-free solution. This was as a rule about 200 mV corresponding to a chloride concentration of 10^{-4}.

Because of these facts and as equation (10) contains ratios of concentrations, the potential curves were treated as follows. The horizontal part of the curve immediately before and after the band passage a−1 and b+1, *cf.* eqn. (10) were interconnected by a straight line; as a rule this was parallel to the abscissa axis and only rarely the difference exceeded 10 mV. At appropriate intervals the ordinate differences between this line and the curve were determined, and this potential difference is related to the chloride ion concentration c and the fictive zero concentration c_0 by

$$E = 58 \log (c/c_0)$$

from which

$$c - c_0 = c_0(\text{antilog } (E/58) - 1)$$

The difference $c - c_0$ was taken as a measure of the chloride concentration in the fraction in question; and as the absolute value was irrelevant the expression antilog $(E/58) - 1$ was inserted for c in (10). This procedure was justified by the following experiment: 5 ml 1 M potassium chloride were poured on the top of column I and eluted by 0.5 M potassium nitrate. The fractions were titrated according to Volhard, and the expressions antilog$(E/58) - 1$ with E values referring to the midpoints of the fractions were calculated. The ratios of corresponding values were determined, and the mean error was found to be 3 %.

The interstitial volume of the ion-exchanger was determined by washing down a column with 0.1 M nitric acid until the eluate had the same concentration as the entering

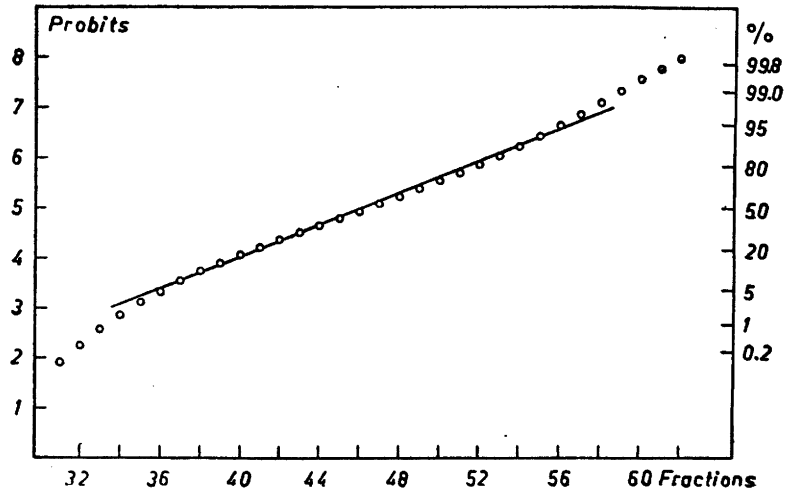


Fig. 2. Column I. 5 ml 1 M potassium chloride eluted with 0.5 M potassium nitrate at 2.3 ml/min. Probits versus *fractions of 20.5 ml each.*

solution. The acid level was adjusted to the surface of the ion-exchanger, and the acid was rinsed out with distilled water and titrated. After removal of the ion-exchanger the volume of the glass wool plug and the buret tip was determined in the same manner. The capacity of the resin was determined in the same column; the nitrate ions were displaced by chloride ions, a 2 M sodium chloride solution being washed through until the eluate gave no reaction for nitrate with sulphuric acid and brucine. After washing out with distilled water the chloride ions were removed by means of 0.5 M potassium nitrate and titrated. The capacity was referred to the nitrate resin. The mean values of duplicate determinations gave the following results: column I and II: $\beta = 0.74$ and $r = 1.55$; column III: $\beta = 0.75$ and $r = 1.45$.

RESULTS

Fig. 2 shows a characteristic diagram of an experiment. As mentioned, the first and last points of the line are rather uncertain; furthermore H(m) is not a stochastic variable, every value containing the errors of the preceding ones. In most cases the lines show a systematic curvature, probably as a result of these facts and also because eqn. (8) is an approximation to eqn. (7), and this, in addition, is derived on assumptions, the validity of which are questionable. The determination of the mean value, the abscissa for probit 5, is only slightly affected hereof, but the estimation of the standard deviation, which is the reciprocal of the slope is made somewhat uncertain. In order to obtain comparable results from the different experiments it was decided to exclude all points, the ordinates of which were less than 3 and greater than 7. This means that the constants of the distribution are determined mainly by the central 95 % of the material as indicated by the Φ values shown at the right hand of the diagram. The straight line has the constants $U_0 = 46.1$ fractions and $s =$ $= 6.29$ fractions. The standard deviation of the observed ordinates from the

corresponding ones of the line between the ordinates 3 and 7 amounts to 0.07. In some other experiments the deviations were calculated and found to be of the same order of magnitude.

A series of five experiments were performed under identical circumstances to try the reproducibility of the procedure. In column I 5 mmoles of potassium chloride were eluted by means of 0.5 M potassium nitrate at a rate of 2.24 ml/min ± 3 %. The mean errors of the 5 sets of values of U_0 and s were found to be 1.5 % and 4 %, respectively.

Tables 1 and 2 show the results of some experiments made to determine the permissible limits to flow rate and initial concentration. It is seen that if the velocity is less than 3.3 ml/min and the quantity of chloride does not exceed 5 mmoles, the constants of the distribution are independent of these two variables. The cross section of column I was 6.0 cm^2 and as the interstitial volume amounted to 74 % of the total volume, the limiting velocity corresponded to 0.8 cm/min. Furthermore the chloride being applied as a 1 M solution occupied 1.2 cm of the column height. These conditions were observed in all the following experiments.

In column II a series of experiments were performed with different concentrations of the eluant, the chloride concentration being recorded at ten places in the column. In two of the experiments some of the electrodes were in disorder, wherefore the corresponding isoplanes could not be calculated. The results are shown in Tables 3—6. In column system III two experiments were carried out to investigate the moving of the adsorption band along a very long column. The travelled distances in the experiments, the results of which

Table 1. 5 ml 1 M potassium chloride eluted with 0.5 M potassium nitrate in column I.

ml/min	U_0 ml	s ml
1.28	964	121
2.32	930	125
3.34	925	123
4.74	934	139
7.15	947	152
12.72	936	161
18.45	947	181

Table 2. Potassium chloride eluted with 0.5 M potassium nitrate in column I. Flow rate: 2.2 ml/min ± 10 %.

1 M KCl ml	U_0 ml	s ml
2	926	133
5	930	125
10	968	126
20	977	130
40	1032	159

Table 3. 0.2 mmoles potassium chloride eluted with 1.0 M potassium nitrate.

V_0 ml	U_0 ml	s ml	a	s^2/V_0
38.4	60.9	6.98	0.631	1.27
64.9	100	9.27	0.648	1.33
91.2	136	11.8	0.669	1.52
118	178	13.1	0.662	1.46
144	218	14.8	0.660	1.52
170	260	18.6	0.656	2.03
197	298	18.4	0.660	1.73
223	339	19.7	0.658	1.74
249	383	20.5	0.651	1.69
276	425	21.8	0.648	1.72
Mean value			0.654	1.60
Mean error			1.5 %	14 %

Table 4. 0.2 mmoles potassium chloride eluted with 0.5 M potassium nitrate.

V_0 ml	U_0 ml	s ml	a	s^2/V_0
38.4	84.2	11.2	0.465	3.23
64.9	135	13.6	0.481	2.85
118	247	21.5	0.478	3.92
144	313	28.4	0.460	5.60
170	362	32.6	0.469	6.25
223	478	28.2	0.467	3.57
249	549	28.6	0.454	3.29
276	606	38.6	0.455	5.40
Mean value			0.466	4.26
Mean error			2 %	30 %

Table 5. 0.2 mmoles potassium chloride eluted with 0.2 M potassium nitrate.

V_0 ml	U_0 ml	s ml	a	s^2/V_0
64.9	262	31.7	0.248	15.7
118	481	58.9	0.246	29.5
144	599	73.6	0.240	38.1
170	731	85.9	0.233	43.4
223	927	82.5	0.240	30.9
249	1050	69.3	0.238	19.1
276	1170	99.5	0.236	36.3
Mean value			0.240	30.4
Mean error			2 %	33 %

Table 6. 0.2 mmoles potassium chloride eluted with 0.1 M potassium nitrate.

V_0 ml	U_0 ml	s ml	α	s^2/V_0
36.5	258	31.8	0.142	27.6
62.8	468	49.0	0.134	38.2
89.0	650	64.5	0.137	46.6
116	840	78.2	0.138	52.6
142	1060	83.0	0.135	48.6
168	1270	100	0.133	59.6
195	1450	106	0.135	57.5
221	1660	118	0.133	63.3
248	1880	121	0.132	59.8
274	2080	129	0.132	60.5
Mean value			0.135	51.4
Mean error			2 %	22 %

Table 7. 2 mmoles potassium chloride eluted with 0.5 M potassium nitrate.

V_0 ml	U_0 ml	s ml	α	s^2/V_0
266	525	34.4	0.507	4.43
529	1062	50.8	0.498	4.88
793	1584	62.2	0.501	4.87
1060	2130	74.7	0.498	5.26
1315	2643	85.8	0.498	5.58
1576	3163	96.4	0.498	5.89
1806	3653	99.3	0.494	5.46
2045	4135	105.0	0.495	5.38
Mean value			0.499	5.22
Mean error			1 %	9 %

Table 8. 2 mmoles potassium chloride eluted with 0.2 M potassium nitrate.

V_0 ml	U_0 ml	s ml	α	s^2/V_0
266	945	54.7	0.282	11.8
529	1782	80.0	0.296	12.1
793	2736	125	0.290	19.7
1060	3720	134	0.285	17.0
1315	4661	167	0.282	21.3
1576	5567	161	0.283	16.4
1806	6394	158	0.284	13.9
2045	7251	163	0.282	13.1
2304	8157	186	0.282	15.5
2570	9117	185	0.282	13.3
Mean value			0.285	15.4
Mean error			2 %	21 %

Table 9. K_c *and* v *are calculated from the results in Tables 3—8 by means of formulas (13) and (11).*

Column	$[KNO_3]$	K_c	v
II	1.0	3.96	1.92
II	0.5	3.66	1.73
II	0.2	3.31	2.30
II	0.1	3.27	1.09
III	0.5	3.85	2.59
III	0.2	3.85	1.75
Mean value		3.65	1.90
Mean error		8 %	27 %

Table 10. Column II with the ion-exchanger in the acetate form. 1 mmole potassium chloride eluted with 1.0 M sodium acetate. $w = 20.18$ *ml per fraction.* a *and* v *are calculated according to (12),* $v = 0.65$ *ml. From (13)* $K_c = 0.100$.

V_0 ml	μ	σ	a
86.2	9.45	0.449	0.0478
113	10.75	0.484	0.0482
139	12.15	0.466	0.0467
165	13.34	0.358	0.0460
192	14.50	0.413	0.0451
218	15.65	0.391	0.0441
244	16.61	0.383	0.0438
271	17.64	0.353	0.0432
Mean value		0.412	0.0456
Mean error		12 %	4 %

Table 11. Column II with ion-exchanger in the acetate form. 1 mmole potassium chloride eluted with 0.5 M sodium acetate. $w = 20.47$ *ml per fraction. Calculated as in the preceding table,* $v = 0.87$ *ml and* $K_c = 0.116$.

V_0 ml	μ	σ	a
26.4	6.59	0.606	0.0297
52.7	9.59	0.606	0.0280
79.1	11.82	0.610	0.0277
105	13.66	0.611	0.0276
132	15.46	0.642	0.0269
158	17.26	0.638	0.0259
185	18.50	0.640	0.0263
211	19.94	0.622	0.0259
237	21.19	0.638	0.0269
264	22.5	0.635	0.0254
Mean value		0.625	0.0270
Mean error		3 %	5 %

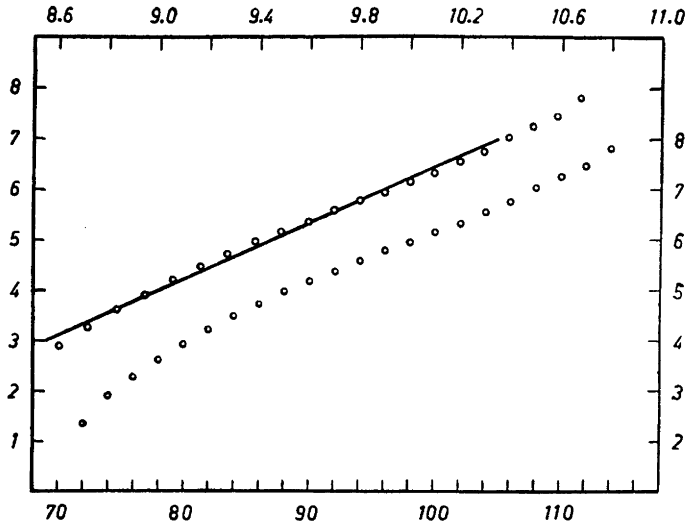


Fig. 3. Column II with the resin in the acetate form. 1 ml 1 M potassium chloride eluted with 1 M sodium acetate at 0.94 ml/min. 20.2 ml per fraction. Lower curve: Probits versus *fractions, coordinates indicated at the right hand and at the bottom. Upper curve: Probits* versus *the square root of fraction numbers, coordinates indicated at the left hand and at the top.*

are shown in Tables 7 and 8, were 12 and 15 m, respectively. A summary of these six experiments are seen in Table 9. The value of the equilibrium constant is in good agreement with the value 3.8 which Wheaton and Bauman [8] found for the chloride-nitrate equilibrium on Dowex 1, which is also a strong base anion exchange resin.

Finally two experiments were made to try if the second approximation (9) was satisfactory when eqn. (8) could not be used, and that is the case if α is small enough. As acetate ions are much weaker adsorbed by the ion-exchanger than chloride ions, the resin in column II was converted into the acetate form and sodium acetate was used as the eluant. In the graphical representations the points (m, Φ^{-1} (H(m))) gave curved lines while the points ($\sqrt{\text{m}}$, Φ^{-1} (H(m))) rather satisfactorily gave straight lines. One example is given in Fig. 3, and the entire results of the two experiments appear in Tables 10 and 11. In this case the agreement of the equilibrium constant with the value 0.17 found by Wheaton and Bauman [8] is not so good, but it should be borne in mind, that although Dowex 1 and Amberlite IRA 400 are of the same type there may be differences in their properties.

The validity of formula (8) requires the constancy of α and s^2/V_0 shown in the two last columns of Tables 3—8. It has been mentioned that the mean error of s is somewhat greater than that of U_0, and consequently the mean error of the last ratio is expected to be considerably greater than that of α. The experimental results indicate, however, these methods of treating elution curves to be a rather good approximation and a valuable tool in designing

columns for chromatographic separations. It should be emphasized that all experimental values constituting the isoplane are used in calculating the parameters. The calculating work is rather easy, but it can be further simplified by plotting H(m) directly against m on "probability paper".

A grant from *Statens almindelige Videnskabsfond (The Danish State Research Foundation)* is gratefully acknowledged.

REFERENCES

1. Vermeulen, Th. and Hiester, N. K. *Ind. Eng. Chem.* **44** (1952) 636.
2. Martin, A. J. P. and Synge, R. L. M. *Biochem. J. London* **35** (1941) 1385.
3. Mayer, S. W. and Tompkins, E. R. *J. Am. Chem. Soc.* **69** (1947) 2866.
4. Hald, A. *Statistiske Metoder*, Det private Ingeniørfond, København 1948, p. 553. Kendall, M. G. *The Advanced Theory of Statistics*, Charles Griffin and Co. London 1947, Vol. I, p. 103.
5. Hald, A. *Statistiske Metoder*, Det private Ingeniørfond, København 1948, p. 154; Kendall, M. G. *The Advanced Theory of Statistics*, Charles Griffin and Co. London 1947, Vol. I, p. 16.
6. Hald, A. *Statistiske Metoder*, Det private Ingeniørfond, København 1948, p. 115; Bliss, C. I. *Ann. Appl. Biol.* **22** (1935) 134.
7. Fischer, R. A. and Yates, F. *Statistical Tables*, Oliver and Boyd, London 1948, p. 50.
8. Wheaton, R. M. and Bauman, W. C. *Ind. Eng. Chem.* **43** (1951) 1088.

Received August 16, 1956.

ACTA CHEMICA SCANDINAVICA 10 (1956) 1663—1676

Short Communications

Crystal Modifications of Bigeranyl Tetrahydrochloride

HARALD SÖRUM, JAN BARSTAD and JOHANNES DALE

Forsvarets Forskningsinstitutt, Kjeller, Norway

Bigeranyl tetrahydrochloride, $C_{20}H_{38}Cl_4$, first described by Sörensen *et al.*[1], is a lower homologue of squalene hexahydrochloride, $C_{30}H_{56}Cl_6$, which has previously been investigated by Sörum and Dale [2], with the result that the two crystalline isomers could be identified as the two *meso*-forms out of the six possible diastereoisomers. From the point of view of a complete structure determination, bigeranyl tetrahydrochloride might be expected to be more favourable than the squalene derivatives, as its carbon chain is only two thirds of that of the latter.

For bigeranyl tetrahydrochloride two diastereoisomers should be possible; one *meso*-form, and one enantiomorphic pair. From the X-ray data given below it was concluded that the crystalline isomer is the *meso*-form. It was not possible to isolate the other isomer, either because it may not be formed at all by the addition of hydrogen chloride to bigeranyl, or, more likely, because it does not readily crystallize. However, it was found that the *meso*-form crystallized in two modifications: thin plates of approximately hexagonal form, melting at 95° C, and long needleshaped crystals, melting at 110° C. The lower melting form can be obtained by crystallization from cold acetone, the higher melting one by evaporation of a carbon disulfide solution at room temperature. The lower melting modification is labile and is spon-

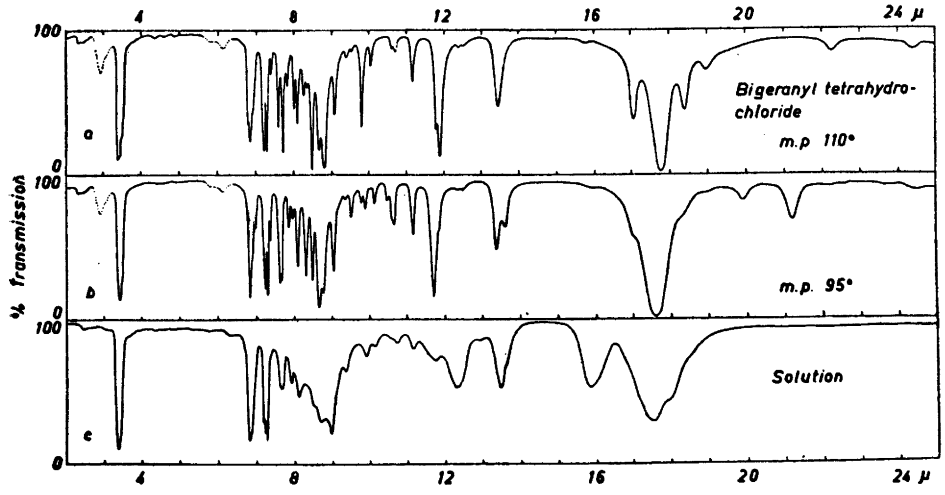


Fig. 1. Infrared absorption spectra from 2—15 μ (NaCl-prism) and from 15—25 μ (KBr-prism) of a) the higher melting and b) the lower melting crystal form of bigeranyl tetrahydrochloride as pressed KBr-disks, and of c) solutions in CCl_4 (2—8 μ, 15—25 μ) and in CS_2 (8—15 μ).

taneously converted in the solid phase to the higher melting and stable modification. This conversion may take several weeks at room temperature, but only minutes or hours at 80° C. After melting at 95° C the substance may solidify on further heating and melt again at 110° C. The degree of conversion may be established by X-ray diffraction, but more conveniently by infrared spectroscopy (Fig. 1).

Some preliminary crystal data for the two modifications of bigeranyl tetrahydrochloride have been collected for further determination of their structures, and shall be reported here. For the *lower melting form* the unit cell dimensions obtained from oscillation and Weissenberg photographs using Cu$K\alpha$ radiation, are: $a = 38.6 \pm 0.1$ Å; $b = 10.20 \pm 0.05$ Å; $c = 5.99 \pm 0.02$ Å, $\gamma = 93.0 \pm 0.3°$, $V = 2\,358$ Å^3, $Z = 4$ mol./u.c., $d_{calc} = 1.181$ g/cm^3, $d_{obs} \approx 1.18$ g/cm^3. Systematic absences are found for $00l$ when l odd; for $hk0$ when k is odd. The same systematic weaknesses of the reflections as for the isomers of squalene hexahydrochloride are also found, *i. e.*, $h00$ when h is odd; $0k0$ when k is odd; and $h0l$ when $h + l$ is odd. Space group $P2_1/b$.

A comparison of these data with those of the squalene hexahydrochloride isomers [2] will show that the a-axis length for bigeranyl tetrahydrochloride is about two thirds of that of squalene hexahydrochloride, the other data being very closely the same for both compounds. A one-dimensional projection of electron density on the a-axis has been calculated, and this synthesis also shows that the low melting modification of bigeranyl tetrahydrochloride closely resembles the squalene hexahydrochloride isomers, especially the higher melting one; hence, it must be the *meso*-form.

A single crystal of the *higher melting form* of approximate size $0.5 \times 1.0 \times 10$ mm has been prepared. This shows good cleavages parallel to (100) and (010), but inferior parallel to (001). The crystal data for this modification are: $a = 20.91 \pm 0.05$ Å; $b = 9.77 \pm 0.02$ Å; $c = 6.04 \pm 0.02$ Å; $\alpha = 87°\ 13' \pm 10'$; $\beta = 92°\ 52' \pm 10'$; $\gamma = 102°\ 55' \pm 10'$; $V = 1\,175$ Å^3; $Z = 2$ mol./u.c.; $d_{calc} = 1.186$ g/cm^3; $d_{obs} \approx 1.19$ g/cm^3.

By comparing the crystal data and the infrared spectra (Fig. 1) of the two crystalline isomers it may be seen that marked differences exist, indicating that we have to do with two different conformational isomers. The spontaneous solid phase conversion of one form into the other can therefore hardly be due to simple translations of the molecules in the crystal lattice, but must rather involve a rotation about some of the bonds in the chain. It is instructive to note the remarkable difference between the spectra of these two conformational isomers even in the C—Cl stretching frequency region, 17—18 μ, where one would expect a fairly constant "group frequency". The solution spectrum represents, of course, the equilibrium mixture of a very large number of conformational isomers and is accordingly more diffuse and less characteristic.

1. Sörensen, N. A., Gillebo, T., Holtermann, H. and Sörensen, J. S. *Acta Chem. Scand.* **5** (1951) 757.
2. Sörum, H. and Dale, J. *Acta Chem. Scand.* **9** (1955) 141.

Received October 23, 1956.

Transformation of 2-(β,β-Dicarbomethoxyethyl)-furan into *m*-Hydroxybenzoic Acid

NIELS ELMING

Centrallaboratoriet, Sadolin & Holmblad A/S, Copenhagen, Denmark

Furans with suitable substituents in the 2-position may be transformed into other systems with aromatic character by methoxylation to cyclic acetals of 1,4-dicarbonyl compounds, followed by intramolecular condensation in acid solution [1-6]. Further application of this principle has led to the transformation of 2-(β,β-dicarbomethoxyethyl)-furan (I) into *m*-hydroxybenzoic acid (III) as shown below.

Trans-2-furanacrylic acid was isolated as a by-product of the reaction (yield 2 %). This indicates that to a small extent an ethylenic linkage has been formed in the side-chain of I by oxidation during electrolysis.

I was prepared from furfuryl chloride as shown below *cf.* [7]. Dimethyl difurfuryl malonate (IV) was isolated as a by-product of this reaction.

taneously converted in the solid phase to the higher melting and stable modification. This conversion may take several weeks at room temperature, but only minutes or hours at 80° C. After melting at 95° C the substance may solidify on further heating and melt again at 110° C. The degree of conversion may be established by X-ray diffraction, but more conveniently by infrared spectroscopy (Fig. 1).

Some preliminary crystal data for the two modifications of bigeranyl tetrahydrochloride have been collected for further determination of their structures, and shall be reported here. For the *lower melting form* the unit cell dimensions obtained from oscillation and Weissenberg photographs using Cu$K\alpha$ radiation, are: $a = 38.6 \pm 0.1$ Å; $b = 10.20 \pm 0.05$ Å; $c = 5.99 \pm 0.02$ Å, $\gamma = 93.0 \pm 0.3°$, $V = 2\,358$ Å^3, $Z = 4$ mol./u.c., $d_{calc} = 1.181$ g/cm^3, $d_{obs} \approx 1.18$ g/cm^3. Systematic absences are found for $00l$ when l odd; for $hk0$ when k is odd. The same systematic weaknesses of the reflections as for the isomers of squalene hexahydrochloride are also found, *i. e.*, $h00$ when h is odd; $0k0$ when k is odd; and $h0l$ when $h + l$ is odd. Space group $P2_1/b$.

A comparison of these data with those of the squalene hexahydrochloride isomers [2] will show that the a-axis length for bigeranyl tetrahydrochloride is about two thirds of that of squalene hexahydrochloride, the other data being very closely the same for both compounds. A one-dimensional projection of electron density on the a-axis has been calculated, and this synthesis also shows that the low melting modification of bigeranyl tetrahydrochloride closely resembles the squalene hexahydrochloride isomers, especially the higher melting one; hence, it must be the *meso*-form.

A single crystal of the *higher melting form* of approximate size $0.5 \times 1.0 \times 10$ mm has been prepared. This shows good cleavages parallel to (100) and (010), but inferior parallel to (001). The crystal data for this modification are: $a = 20.91 \pm 0.05$ Å; $b = 9.77 \pm 0.02$ Å; $c = 6.04 \pm 0.02$ Å; $\alpha = 87°\ 13' \pm 10'$; $\beta = 92°\ 52' \pm 10'$; $\gamma = 102°\ 55' \pm 10'$; $V = 1\,175$ Å^3; $Z = 2$ mol./u.c.; $d_{calc} = 1.186$ g/cm^3; $d_{obs} \approx 1.19$ g/cm^3.

By comparing the crystal data and the infrared spectra (Fig. 1) of the two crystalline isomers it may be seen that marked differences exist, indicating that we have to do with two different conformational isomers. The spontaneous solid phase conversion of one form into the other can therefore hardly be due to simple translations of the molecules in the crystal lattice, but must rather involve a rotation about some of the bonds in the chain. It is instructive to note the remarkable difference between the spectra of these two conformational isomers even in the C—Cl stretching frequency region, 17—18 μ, where one would expect a fairly constant "group frequency". The solution spectrum represents, of course, the equilibrium mixture of a very large number of conformational isomers and is accordingly more diffuse and less characteristic.

1. Sörensen, N. A., Gillebo, T., Holtermann, H. and Sörensen, J. S. *Acta Chem. Scand.* **5** (1951) 757.
2. Sörum, H. and Dale, J. *Acta Chem. Scand.* **9** (1955) 141.

Received October 23, 1956.

Transformation of 2-(β,β-Dicarbomethoxyethyl)-furan into *m*-Hydroxybenzoic Acid

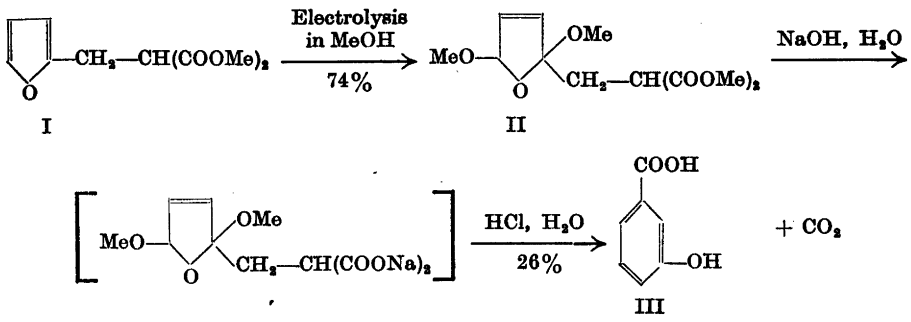
NIELS ELMING

Centrallaboratoriet, Sadolin & Holmblad A/S, Copenhagen, Denmark

Furans with suitable substituents in the 2-position may be transformed into other systems with aromatic character by methoxylation to cyclic acetals of 1,4-dicarbonyl compounds, followed by intramolecular condensation in acid solution [1-6]. Further application of this principle has led to the transformation of 2-(β,β-dicarbomethoxyethyl)-furan (I) into *m*-hydroxybenzoic acid (III) as shown below.

Trans-2-furanacrylic acid was isolated as a by-product of the reaction (yield 2 %). This indicates that to a small extent an ethylenic linkage has been formed in the side-chain of I by oxidation during electrolysis.

I was prepared from furfuryl chloride as shown below *cf.* [7]. Dimethyl difurfuryl malonate (IV) was isolated as a by-product of this reaction.



I II III

The dimethoxydihydrofuran (II) could, as expected, be catalytically hydrogenated to the corresponding tetrahydrofuran, 2,5-dimethoxy-2-(β,β-dicarbomethoxyethyl)-tetrahydrofuran (V).

I, II, IV and V are new compounds, but the free acid and the diethyl ester corresponding to I have been prepared previously [7].

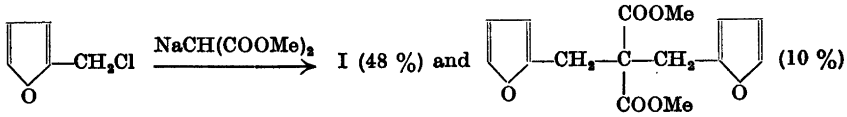
Experimental. 2-(β,β-Dicarbomethoxyethyl)-furan (I). Dimethyl malonate (17.0 g, 0.128 mole) was added to a solution of sodium methoxide in methanol [from sodium (2.80 g, 0.122 mole) and anhydrous methanol (60 ml)]. Furfuryl chloride [8] (14.3 g, 0.123 mole) was added dropwise with stirring during 20 min at 30—40°. The mixture was stirred for a further 10 min at 30° and then heated under reflux with stirring for one hour. The methanol was evaporated in a vacuum and ether added. The mixture was washed twice with cold water and the etheral layer dried with magnesium sulfate. Distillation gave 12.5 g (48 %) of I (colorless liquid, $b.p._{0.1}$ 83—88°, n_D^{25} 1.4667). (Found: C 56.6; H 5.8; OCH_3 29.0. Calc. for $C_8H_6O_3(OCH_3)_2$ (212.2): C 56.6; H 5.7; OCH_3 29.2).

Further distillation gave 1.67 g of pale yellow liquid ($b.p._{0.1}$ 88—130°), which was discarded, and then 2.81 g of pale yellow liquid ($b.p._{0.1}$ 130—136°) which crystallized completely on standing, [m.p. 55—60° (Hershberg apparatus, corr.)]. Crystallization of 500 mg from ether gave 310 mg (10 %) of IV (white crystals, m. p. 67—69°). (Found: C 61.6; H 5.3; OCH_3 21.1. Calc. for $C_{13}H_{10}O_4(OCH_3)_2$ (292.3): C 61.6; H 5.5; OCH_3 21.2).

2-5-Dimethoxy-2-(β,β-dicarbomethoxyethyl)-2,5-dihydrofuran (II). I (4.24 g, 0.020 mole) and concentrated sulfuric acid (412 mg) were dissolved in anhydrous methanol (45 ml) and the solution electrolyzed and worked up as described for the methoxylation of 2-carbomethoxy-5-*iso*propylfuran [9]. The yield was 4.04 g (74 %, current efficiency 59 %) of II (pale yellow liquid, $b.p._{0.2}$ 129—132°, n_D^{25} 1.4560). (Found: C 52.7; H 6.6; OCH_3 44.9. Calc. for $C_8H_6O_3(OCH_3)_4$ (274.3): C 52.6; H 6.6; OCH_3 45.3).

2,5-Dimethoxy-2-(β,β-dicarbomethoxyethyl)-tetrahydrofuran (V). II (2.66 g) and anhydrous methanol (15 ml) were shaken (3 h) with Raney nickel (0.2 g) under hydrogen (100 atm). The product was isolated by distillation. The yield was 2.30 g (83 %) of V (colorless liquid, $b.p._{0.1}$ 129—131°, n_D^{25} 1.4499). (Found: C 52.3; H 7.3; OCH_3 44.8. Calc. for $C_8H_6O_3(OCH_3)_4$ (276.3): C 52.2; H 7.3; OCH_3 44.9).

m-Hydroxybenzoic acid (III) and trans-2-furanacrylic acid. II (4.12 g, 0.015 mole) and N sodium hydroxide (45 ml, 0.045 mole) were mixed and heated under reflux (1 h). After cooling the pH was adjusted to 1—1.5 by addition of concentrated hydrochloric acid. The mixture was heated under reflux for 1 h and the dark brown solution evaporated in a vacuum to about 30 ml. The precipitate formed was removed by filtration, washed once



IV

with water and dried (yield 70 mg). Sublimation (110—120°/0.05 mm) gave 47 mg (2 %) of *trans*-2-furanacrylic acid (white crystals, m. p. 140—142°, mixed m. p. with an authentic specimen of *trans*-2-furanacrylic acid 141—143°). [Found: C 60.9; H 4.6. Neut.equiv. 137.8 (phenolphthalein indicator). Calc. for $C_7H_6O_3$ (138.1): C 60.9; H 4.4].

The filtrate from the crude furanacrylic acid was continuously extracted with ether (2 h), the etheral extract dried with magnesium sulfate and the ether evaporated in a vacuum. 1.45 g of a semisolid residue remained. Crystallization from water followed by sublimation (130—140°/0.05 mm) gave 0.53 g (26 %) of III (white crystals, m. p. 197—200°, mixed m. p. with an authentic specimen of *m*-hydroxybenzoic acid 198—200°). [Found: C 61.0; H 4.5. Neut.equiv. 137.8 (phenolphthalein indicator) Calc. for $C_7H_6O_3$ (138.1); C 60.9; H 4.4].

In another experiment the acid solution was not refluxed. After standing for 6 days at room temperature a 6 % yield of *trans*-2-furanacrylic acid was obtained, but no III could be isolated.

1. Clauson-Kaas, N., Elming, N. and Tyle, Z. *Acta Chem. Scand.* **9** (1955) 1.

2. Elming, N. and Clauson-Kaas, N. *Acta Chem. Scand.* **9** (1955) 23.

3. Nielsen, J. T., Elming, N. and Clauson-Kaas, N. *Acta Chem. Scand.* **9** (1955) 9.

4. Clauson-Kaas, N. and Nedenskov, P. *Acta Chem. Scand.* **9** (1955) 14.

5. Clauson-Kaas, N. and Nedenskov, P. *Acta Chem. Scand.* **9** (1955) 27.

6. Nielsen, J. T., Elming, N. and Clauson-Kaas, N. *Acta Chem. Scand.* **9** (1955) 30.

7. Dunlop, A. P. and Peters, F. N. *The Furans*, New York 1953, p. 611.

8. Kirner, W. R. *J. Am. Chem. Soc.* **50** (1928) 1955.

9. Nedenskov, P., Elming, N., Nielsen, J. T. and Clauson-Kaas, N. *Acta Chem. Scand.* **9** (1955) 17.

Received November 7, 1956.

On the Carbohydrate Components of the α_1-Acid Glycoprotein of Human Plasma

IKUO YAMASHINA

Chemistry Department II, Karolinska Institutet, Stockholm, Sweden

α_1-Acid glycoprotein of human plasma was first isolated in a pure state by Weimer, Mehl and Winzler [1] in 1950. They used ammonium sulphate fractionation under pH control. In 1953, Schmid [2] independently isolated a glycoprotein, called α_1-acid glycoprotein, from the supernatant of fraction V of Cohn's fractionation procedure. Judging from the physicochemical and analytical figures, this substance was considered to be the same one as Weimer *et al.* described.

The α_1-acid glycoprotein is one of the best characterized substances among the numerous plasma proteins. The carbohydrate content is extremely high, amounting to nearly 40 %. Neutral sugars, amino sugars and sialic acids were found by Winzler [1], Schmid [2] and Odin [3].

The present author prepared a certain amount of this glycoprotein for study. After hydrolysis, the substance was analyzed for neutral sugars, amino sugars and sialic acids by means of chromatographic methods. Galactose, mannose, fucose, glucosamine, ovine-type sialic acid and its derivative were determined quantitatively.

In order to investigate the chemical structure proteolytic degradation of the glycoprotein was attempted. At first, the glycoprotein was submitted to a mild hydrolysis in order to remove sialic acids because the intact glycoprotein, was hardly digested by trypsin or papain. The degraded sialic acid free glycoprotein, however, could be digested by trypsin. Actually, a peptide carrying carbohydrate was obtained.

Experimental: Preparation. The electrophoretically pure glycoprotein was prepared principally according to Schmid's method [4]. However, the ethanol concentration was raised to 25 % instead of 20 at the final stage of the fractionation. In this way, the pure substance was regularly obtained, although the yield was somewhat low. Thus, 1 gm of glycoprotein was usually obtained from 50

with water and dried (yield 70 mg). Sublimation (110—120°/0.05 mm) gave 47 mg (2 %) of *trans*-2-furanacrylic acid (white crystals, m. p. 140—142°, mixed m. p. with an authentic specimen of *trans*-2-furanacrylic acid 141—143°). [Found: C 60.9; H 4.6. Neut.equiv. 137.8 (phenolphthalein indicator). Calc. for $C_7H_6O_3$ (138.1): C 60.9; H 4.4].

The filtrate from the crude furanacrylic acid was continuously extracted with ether (2 h), the etheral extract dried with magnesium sulfate and the ether evaporated in a vacuum. 1.45 g of a semisolid residue remained. Crystallization from water followed by sublimation (130—140°/0.05 mm) gave 0.53 g (26 %) of III (white crystals, m. p. 197—200°, mixed m. p. with an authentic specimen of *m*-hydroxybenzoic acid 198—200°). [Found: C 61.0; H 4.5. Neut.equiv. 137.8 (phenolphthalein indicator) Calc. for $C_7H_6O_3$ (138.1); C 60.9; H 4.4].

In another experiment the acid solution was not refluxed. After standing for 6 days at room temperature a 6 % yield of *trans*-2-furanacrylic acid was obtained, but no III could be isolated.

1. Clauson-Kaas, N., Elming, N. and Tyle, Z. *Acta Chem. Scand.* **9** (1955) 1.

2. Elming, N. and Clauson-Kaas, N. *Acta Chem. Scand.* **9** (1955) 23.

3. Nielsen, J. T., Elming, N. and Clauson-Kaas, N. *Acta Chem. Scand.* **9** (1955) 9.

4. Clauson-Kaas, N. and Nedenskov, P. *Acta Chem. Scand.* **9** (1955) 14.

5. Clauson-Kaas, N. and Nedenskov, P. *Acta Chem. Scand.* **9** (1955) 27.

6. Nielsen, J. T., Elming, N. and Clauson-Kaas, N. *Acta Chem. Scand.* **9** (1955) 30.

7. Dunlop, A. P. and Peters, F. N. *The Furans*, New York 1953, p. 611.

8. Kirner, W. R. *J. Am. Chem. Soc.* **50** (1928) 1955.

9. Nedenskov, P., Elming, N., Nielsen, J. T. and Clauson-Kaas, N. *Acta Chem. Scand.* **9** (1955) 17.

Received November 7, 1956.

On the Carbohydrate Components of the α_1-Acid Glycoprotein of Human Plasma

IKUO YAMASHINA

Chemistry Department II, Karolinska Institutet, Stockholm, Sweden

α_1-Acid glycoprotein of human plasma was first isolated in a pure state by Weimer, Mehl and Winzler [1] in 1950. They used ammonium sulphate fractionation under pH control. In 1953, Schmid [2] independently isolated a glycoprotein, called α_1-acid glycoprotein, from the supernatant of fraction V of Cohn's fractionation procedure. Judging from the physicochemical and analytical figures, this substance was considered to be the same one as Weimer *et al.* described.

The α_1-acid glycoprotein is one of the best characterized substances among the numerous plasma proteins. The carbohydrate content is extremely high, amounting to nearly 40 %. Neutral sugars, amino sugars and sialic acids were found by Winzler [1], Schmid [2] and Odin [3].

The present author prepared a certain amount of this glycoprotein for study. After hydrolysis, the substance was analyzed for neutral sugars, amino sugars and sialic acids by means of chromatographic methods. Galactose, mannose, fucose, glucosamine, ovine-type sialic acid and its derivative were determined quantitatively.

In order to investigate the chemical structure proteolytic degradation of the glycoprotein was attempted. At first, the glycoprotein was submitted to a mild hydrolysis in order to remove sialic acids because the intact glycoprotein, was hardly digested by trypsin or papain. The degraded sialic acid free glycoprotein, however, could be digested by trypsin. Actually, a peptide carrying carbohydrate was obtained.

Experimental: Preparation. The electrophoretically pure glycoprotein was prepared principally according to Schmid's method [4]. However, the ethanol concentration was raised to 25 % instead of 20 at the final stage of the fractionation. In this way, the pure substance was regularly obtained, although the yield was somewhat low. Thus, 1 gm of glycoprotein was usually obtained from 50

liters of pooled supernatant of fraction V of Cohn's fractionation procedure (Method 6).

Analytical methods. Total neutral sugars were determined both by the orcinol reaction according to Hewitt [5] and by the cysteine reaction according to Dische [6]. For the chromatographic analysis, Gardell's method [7] was used after hydrolysis with 2 N sulphuric acid for 12 h at 100° C. Amino sugars were determined also according to Gardell's method [8] after hydrolysis with 6 N hydrochloric acid for 8 h at 100° C. For the sialic acid determination, Bial's reagent [9] was used on the intact glycoprotein and Ehrlich's reagent [9] on the fractions of the column chromatography. Paper chromatographic analysis of sialic acid was performed with butanol-acetic acid-water (4:1:5) and butanol-pyridine-water (6:4:3) as solvents according to the directions of Blix, Lindberg, Odin and Werner [10]. The sialic acids were detected by spraying the paper with the orcinol-trichloroacetic acid reagent of Klevstrand and Nordal [11].

Digestion by proteolytic enzymes. For the tryptic digestion, the autoactivation product of trypsinogen was used which was prepared by keeping trypsinogen in borate buffer (0.1 M, pH 8.0) containing 0.1 M $CaCl_2$ for 24 h at 0° C. Trypsinogen was prepared according to Northrop and Kunitz [12] through crystallization and further purification by trichloroacetic acid.

The papain used in this experiment was the product of Worthington (Freehold, New Jersey, U.S.A.).

The digestion was followed by measuring the ninhydrin reaction [13] on the whole reaction mixture.

Results and Discussion. Analytical values on sugar components are given in Table 1 together with the figures given by the earlier workers. As shown in the table, chromatographic values are consistent with the values obtained by direct determination.

From the X-ray diffraction patterns of the isolated and crystallized sialic acid, Odin [3] concluded that the glycoprotein contains sialic acid having N-acetyl group (ovine-type sialic acid). However, two types of sialic acid were found by the present author when the glycoprotein was submitted to a mild hydrolysis (0.01 N H_2SO_4, 100° C, 1 h).

The sialic acids liberated were chromatographed on a Dowex 2 column (formate form) according to the directions of Svennerholm [14]. Thus, the hydrolysate was treated by Dowex 50 (H^+ form) in order to remove the excess amount of $Ba(OH)_2$ used for the neutralization, and the solution was freeze-dried. The residue was dissolved in 0.1 N formic acid and put on a column of Dowex 2 which had been equilibrated by 0.1 N formic acid. A stepwise elution was carried out. A chromatogram on Dowex 2 is shown in Fig. 1.

Table 1. Comparison of analytical values.

	Winzler	Odin	Schmid	Yamashina
Hexose	16.4*%	13.5*%	17.2*%	14.2* %
Galactose	—	—	—	6.5 [7]
Mannose	—	—	—	4.8 [7]
Hexosamine	11.9	12.2	11.5	12.3
Glucosamine	—	12.2 [8]	—	12.3 [8]
Fucose	—	1.4 [6]	—	1.1 [6], 0.9 [7]
Sialic acid	—	10.6 [9]	—	10.8 [9]

* Orcinol reaction.

The sialic acid which was eluted by 0.1 N formic acid was identified as O-sialic acid by means of paper chromatography. The other sialic acid, tentatively named sialic acid II, whose structure is not elucidated yet, migrates faster than the first one on paper chromatography using the aforementioned solvents.

The amount of both types of sialic acid depends on length of hydrolysis time, the total amount being constant and about

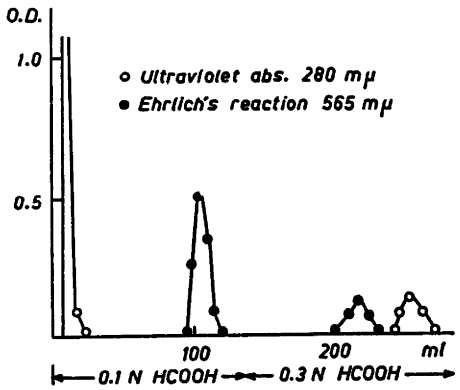


Fig. 1. Chromatogram on Dowex 2 (200—400 mesh), 0.9 × 32 cm. 67 mg of α-acid glycoprotein was hydrolyzed for 40 min. Elution rate: 1 ml per 10 min.

Table 2. Relation between the amount of sialic acids (I and II) and the time of hydrolysis.

Time (Min)	Sialic acid I	Sialic acid II (μg per mg glycoprotein)	Total
30	58	31	89
60	37	43	80
90	27	54	81
120	18	70	88

80—90 % of sialic acid present in the original glycoprotein. The relation between the amount of both sialic acids and the time of hydrolysis is shown in Table 2.

As could be expected, the isolated N-acetyl sialic acid can be converted to sialic acid II by heating in 0.01 N sulphuric acid.

While the structural studies on sialic acid II will be performed in due time, the present findings would provide a definite method for the isolation of sialic acids from glycoproteins. Actually, similar findings, the presence of two transformable sialic acids, were also observed on prothrombin which was prepared according to Seegers [15] and supposed to be a glycoprotein (Magnusson [16]).

After the removal of sialic acid by means of mild hydrolysis as mentioned above, the remaining product was dialyzed against distilled water and freeze-dried. This sialic acid free glycoprotein contained practically the whole amount of sugar present in the original glycoprotein. It behaved as a homogeneous and rather neutral substance, the isoelectric point being higher than 4. Thus, the acidic nature of the original glycoprotein is mainly due to the presence of silaic acid.

While the original glycoprotein is essentially resistant to proteolytic digestion both by trypsin and by papain, the sialic acid free glycoprotein could be digested by trypsin. Thus, to the 0.5 % solution of the sialic acid free glycoprotein in 0.1 M borate buffer (pH 8.0), trypsin was added to a final concentration of 0.25 mg per ml. The digestion was carried out at 25° C for 24 h. The digestion product was separated into two groups, one being dialyzable and the other non-dialyzable. The latter is quite resistant to the further addition of trypsin. The dialyzable part comprises 45 % of the total neutral sugars as determined by the orcinol reaction.

This work was made possible through a research grant to Professor Erik Jorpes from the *Swedish State Medical Research Council*. The author's thanks are also due to Dr. S. Gardell for the analysis of the sugars and to Dr. L. Odin for the gift of sialic acids.

1. Weimer, H. E., Mehl, J. W. and Winzler, R. J. *J. Biol. Chem.* **185** (1950) 561.
2. Schmid, K. *J. Am. Chem. Soc.* **75** (1953) 60.
3. Odin, L. *Acta Chem. Scand.* **9** (1955) 862.
4. Schmid, K. *J. Am. Chem. Soc.* **77** (1955) 742.
5. Hewitt, L. F. *Biochem. J. London* **31** (1937) 360.
6. Dische, Z. and Shettles, L. B. *J. Biol. Chem.* **175** (1948) 595.
7. Gardell, S. *Acta Chem. Scand.* **7** (1953) 201.
8. Gardell, S. *Acta Chem. Scand.* **7** (1953) 207.
9. Werner, I. and Odin, L. *Acta Soc. Med. Upsaliensis* **57** (1952) 230.
10. Blix, G., Lindberg, E., Odin, L. and Werner, I. *Acta Soc. Med. Upsaliensis* **61** (1956) 1.
11. Klevstrand, R. and Nordal, A. *Acta Chem. Scand.* **4** (1950) 1320.
12. Northrop, J. H., Kunitz, M. and Herriott, R. M. *Crystalline Enzymes*, 2nd ed. Columbia Univ. Press, New York 1948, p. 262.
13. Troll, W. and Cannan, R. K. *J. Biol. Chem.* **200** (1953) 803.
14. Svennerholm, L. *Acta Soc. Med. Upsaliensis* **61** (1956) 75.
15. Seegers, W. H. *Record Chem. Progr. Kresge-Hooker Sci. Lib.* 13 (1952) 143.
16. Magnusson, S. *To be published.*

Received November 16, 1956.

The Crystal Structures of Acetyl Choline Bromide and Acetyl Choline Iodide

HARALD SÖRUM

Forsvarets Forskningsinstitutt, Kjeller, Norway

Acetyl choline is known as a very powerful biological reactant showing special effects in the cholinergic nerve system. Chemically, acetyl choline belongs to the choline subgroup of the "onium" compounds or tetrasubstituted ammonium bases. In view of the chemical interest of "onium" compounds in general and the biological importance of this type of compounds in particular it appears worth while to investigate their crystal and molecular structure in detail.

The bromide and the iodide of acetyl choline are easily obtained in crystalline form. The bromide is the more stable compound, the iodide being to some extent decomposed by light. The chloride is more difficult to crystallize, and is furthermore very hygroscopic.

Crystals of acetyl choline bromide were prepared by recrystallization from absolute alcohol. The crystals are colourless, transparent, monoclinic prisms of cell edge ~1 mm or less. The most frequent limiting faces of the crystals are parallel to (010), (110), (1$\bar{1}$0) and (001). Faces parallel to (101), (120), (1$\bar{2}$0) and {111} have been observed, but are less frequent. (100) and (10$\bar{1}$) have not been found as external crystal faces. Cleavage is fairly good parallel to (010), less good along (101).

The crystallographic data for acetyl choline bromide obtained from X-ray diffraction photographs, using Cu$K\alpha$ radiation, are: $a = 10.55 \pm 0.05$ Å, $b = 13.67 \pm 0.05$ Å, $c = 7.18 \pm 0.02$ Å, $\beta = 70.0 \pm 0.03°$, $V = 1\,043$ Å^3, $d_x = 1.43$ g/cm^3 with $Z = 4$ molecules per unit cell. $0k0$ reflexions are absent when k is odd. Possible space groups are $P2_1$ and $P2_1/m$. A Patterson projection on (001) is incompatible with the holohedric space group.

Strictly, however, the unit cell thus described is apparently a pseudo-cell only, as fairly strong superstructure reflexions, indicating very long true repeats, are found in the X-ray photographs. This superstructure seems to be of some peculiar and hitherto unknown type, the superstructure reflexions being defined by:

1. $h0l$ reflexions for h odd integer are absent, but subsidiary reflexions occur slightly displaced from these points.
2. $k = 0$. Subsidiary reflexions occur close to principal reflexions when h even and l even but not for l odd and h even.
3. $k \gtrless 0$. Subsidiary reflexions occur close to principal reflexions for all values of h and l.
4. No subsidiary reflexions accompany the $h00$, $hk0$ reflexions.
5. In terms of the reciprocal lattice the displacement of the subsidiary reflexions from the points corresponding to integral values of hkl is largest near the plane through $0kl$ and decreases towards the plane through $hk0$. In the present case the subsidiary reflexions occur only on one side of the principal reflexions, and not as the more usual pairs of reflexions placed symmetrically to the principal ones.

It cannot be definitely excluded that these extra reflexions in some way may be due to a special sort of twinning. Further investigation on this problem is going on.

The structure of acetyl choline bromide has been solved by Patterson, Fourier and least squares methods, and a detailed report on this work will appear elsewhere.

Acetyl choline iodide crystallizes from alcohol-acetone in very thin, soft, colourless and partly transparent plates. X-Ray oscillation and Weissenberg photographs show that the crystals are pseudo-orthorhombic with axial lengths: $a = 8.32 \pm 0.05$ Å, $b = 16.44 \pm 0.05$ Å, $c = 31.80 \pm 0.1$ Å, $\beta \simeq 90°$, cell volume $V = 2\,172$ Å^3, $Z = 16$ and d_x calculated 1.67 g/cm^3. Reflexions $h00$ are absent when h odd, $0k0$ when k odd and hkl when $h + k$ odd. There is apparently no close similarity between the crystal structure of this compound and that of the bromide. No further structure determination is contemplated for the iodide of acetyl choline.

The crystals used in these investigations were prepared by Mr. G. Aksnes of this Institute.

Received October 29, 1956.

On the Crystal Structures of the Zirconium and Hafnium "Cupferrates"

GEORG NEUMANN, GEORG LUNDGREN and BENGT AURIVILLIUS

Institute of Inorganic and Physical Chemistry, University, Stockholm; Research Institute of National Defence, Dpt 1, Sundbyberg 4; Department of Inorganic Chemistry, Royal Institute of Technology, Stockholm 70, Sweden

Recently Dyrssen investigated the formation of complexes between Th^{4+} ions and the anions of N-nitroso-N-phenylhydroxylamine ($C_6H_5N(NO)OH$) [1]. The question as to how the ligands are arranged in the complexes then arose and, as a hypothesis, Dyrssen suggested a "fourblade propeller" arrangement for $Th(C_6H_5N_2O_2)_4$. The organic ligands could then be arranged either in the *syn* form with both their oxygens in contact with the metal ion or in the *anti* form with one oxygen and one nitrogen per ligand in contact with the metal ion. Dyrssen preferred the first possibility. By investigating the crystal structure of a compound of this formula, it should be possible to reveal the actual structure of the complexes. The heavy thorium atoms, which dominate the X-ray scattering too much, should then preferably be replaced by a lighter tetravalent atom, *i. e.* Zr^{4+}.

From Dr. Dyrssen we obtained crystals of $Me(C_6H_5N_2O_2)_4$, Me being Zr^{4+}, Hf^{4+} and also a mixture of these ions in the

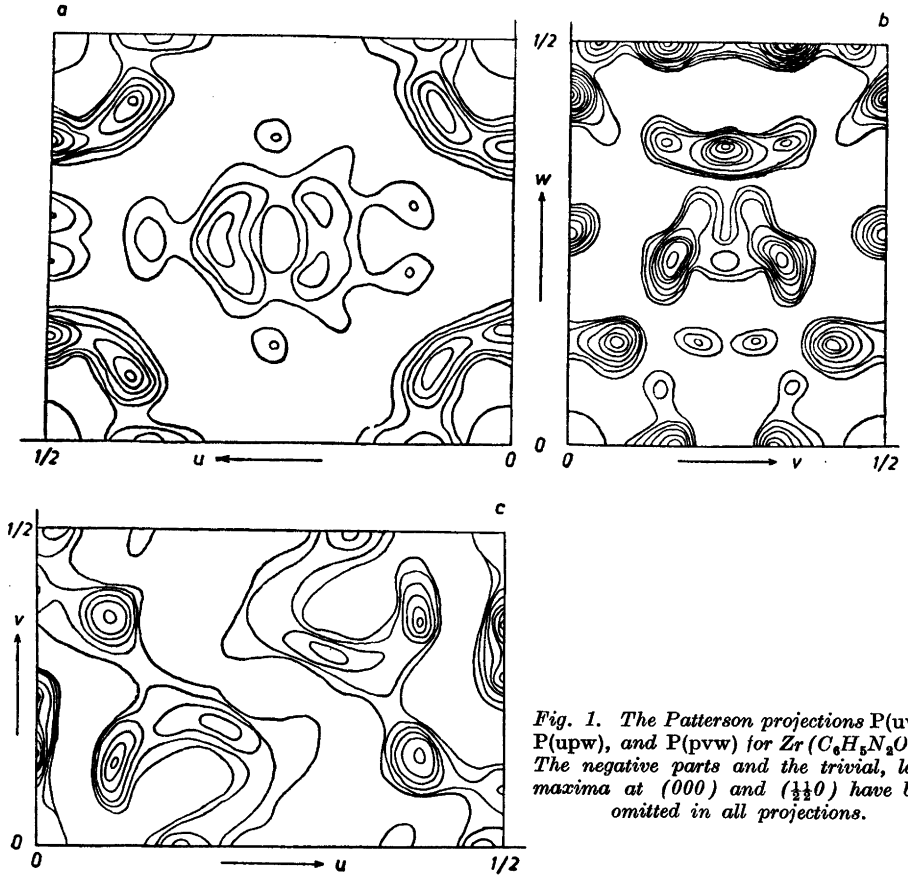


Fig. 1. The Patterson projections P(uvp), P(upw), *and* P(pvw) *for* $Zr(C_6H_5N_2O_2)_4$. *The negative parts and the trivial, large maxima at (000) and* $(\frac{1}{2}\frac{1}{2}0)$ *have been omitted in all projections.*

atomic ratio 1:1. These compounds had been prepared by precipitating water solutions of Me^{4+} perchlorates with the equivalent of "cupferron" (= $NH_4C_6H_5N_2O_2$), dissolving the compounds obtained, preferably in chloroform, and slowly evaporating the solutions. The crystals were light yellow for Me = Zr^{4+}, light yellowish brown for Me = $(Zr, Hf)^{4+}$ and light brown for Me = Hf^{4+}. They were all rather long rods with a rhombic cross-section.

From single crystal photographs of $Zr(C_6H_5N_2O_2)_4$ ($hk0$-$hk7$, $h0l$-$h5l$, $0kl$-$8kl$) taken in Weissenberg cameras with CuK radiation, it was concluded that it is orthorhombic with the following dimensions:

$$a = 16.7 \pm 0.2 \text{ Å}$$
$$b = 11.2 \pm 0.1 \text{ Å}$$
$$c = 14.4 \pm 0.2 \text{ Å}$$
$$V = 2.69 \cdot 10^3 \text{ Å}^3$$

From a few Weissenberg photographs of the (Zr, Hf) and Hf compounds, it was found that the three compounds are isomorphous and that their cell dimensions, within the experimental errors, are identical. For all three compounds, the c axis coincides with the needle axis of the crystals.

From the density of the zirconium compound, 1.573 ± 0.002 g/ml as determined by flotation methods, the cell content was found to be $3.99 \approx 4$ formula units $Me(C_6H_5N_2O_2)_4$.

The following reflections are systematically absent:

$hk0$ with $h + k$ = odd
$h0l$ with l = odd
$0kl$ with k = odd

which is characteristic for the space group No. 60 *Pbcn* [2].

The positions of the metal atoms were determined from the three Patterson projections *P (upw)*, *P (pvw)*, and *P (uvp)* of the zirconium compound (*cf.* Fig. 1). Their parameters were found to be:

4 Zr in *Pbcn* 4(*e*): $\pm(0, y, \frac{1}{4})$;
$\pm(\frac{1}{2}, \frac{1}{2} + y, \frac{1}{4})$ with $y = 0.074$

They are thus situated on the twofold axes in the unit cell and consequently have the special extinction: hkl absent for $h+k$ = odd. The fact that the metal ions are situated in this way is also consistent with a "propeller" arrangement since the organic ligands, lacking twofold symmetry, must be situated outside the twofold axes and, consequently, must be paired within the complexes.

The determination of the O, N, and C parameters has also been begun. It was possible to determine the majority of the signs of F_{hk0} and F_{0kl}, whereas, because of the special extinctions for the Me atoms, only half of the signs of F_{h0l} could be determined. In this way, reliable electron density maps $\varrho(xyp)$ and $\varrho(pyz)$ could be obtained. The work to interpret these projections and to find out the arrangement of the oxygen, nitrogen, and carbon atoms is continuing.

1. Dyrssen, D. *Svensk Kem. Tidskr.* **68** (1956) 212.
2. *International Tables for X-ray Crystallography*, Birmingham 1952, Vol. I, p. 149.

Received November 12, 1956.

Chromatographic Separation of Aliphatic Monocarbonyl Compounds

HENRIK WALLGREN and ERIK NORDLUND

Department of Nutritional Chemistry, University of Helsinki, Viikin Koetila, Malmi, Finland

In work on the chromatographic separation of the 2,4-dinitrophenylhydrazones of aliphatic methylketones and aldehydes, Meigh's two-phase methanol-heptane system [1,2] gave promising results. The separation and identification of components in a mixture was, however, impossible owing to the trailing of the spots. Addition of 10 % glacial acetic acid to the moving phase resulted in well concentrated spots. Ligroin (B.D.H., b.r. 90—110° C) and even a technical petrol fraction (Shell, b.r. 80—110° C) were as effective as pure heptane.

Chromatographic method. The paper (Whatman No. 1) is soaked in methanol, the excess methanol allowed to drip off, and the paper dried for 10—15 minutes at 80° C. It should be used within two hours after this procedure. The hydrazones (0.5—30 μg may be used) are then pipetted on to the paper, which is suspended in a dry trough and left to stand overnight. The chamber should be airtight and the cover provided with holes for filling the troughs. The chamber holds two containers, the one with heptane(ligroin)-in-

atomic ratio 1:1. These compounds had been prepared by precipitating water solutions of Me^{4+} perchlorates with the equivalent of "cupferron" (= $NH_4C_6H_5N_2O_2$), dissolving the compounds obtained, preferably in chloroform, and slowly evaporating the solutions. The crystals were light yellow for Me = Zr^{4+}, light yellowish brown for Me = $(Zr, Hf)^{4+}$ and light brown for Me = Hf^{4+}. They were all rather long rods with a rhombic cross-section.

From single crystal photographs of $Zr(C_6H_5N_2O_2)_4$ ($hk0$-$hk7$, $h0l$-$h5l$, $0kl$-$8kl$) taken in Weissenberg cameras with CuK radiation, it was concluded that it is orthorhombic with the following dimensions:

$$a = 16.7 \pm 0.2 \text{ Å}$$
$$b = 11.2 \pm 0.1 \text{ Å}$$
$$c = 14.4 \pm 0.2 \text{ Å}$$
$$V = 2.69 \cdot 10^3 \text{ Å}^3$$

From a few Weissenberg photographs of the (Zr, Hf) and Hf compounds, it was found that the three compounds are isomorphous and that their cell dimensions, within the experimental errors, are identical. For all three compounds, the c axis coincides with the needle axis of the crystals.

From the density of the zirconium compound, 1.573 ± 0.002 g/ml as determined by flotation methods, the cell content was found to be $3.99 \approx 4$ formula units $Me(C_6H_5N_2O_2)_4$.

The following reflections are systematically absent:

$hk0$ with $h + k$ = odd
$h0l$ with l = odd
$0kl$ with k = odd

which is characteristic for the space group No. 60 *Pbcn* [2].

The positions of the metal atoms were determined from the three Patterson projections *P (upw)*, *P (pvw)*, and *P (uvp)* of the zirconium compound (*cf.* Fig. 1). Their parameters were found to be:

4 Zr in *Pbcn* 4(*e*): $\pm(0, y, \frac{1}{4})$;
$\pm(\frac{1}{2}, \frac{1}{2} + y, \frac{1}{4})$ with $y = 0.074$

They are thus situated on the twofold axes in the unit cell and consequently have the special extinction: hkl absent for $h+k$ = odd. The fact that the metal ions are situated in this way is also consistent with a "propeller" arrangement since the organic ligands, lacking twofold symmetry, must be situated outside the twofold axes and, consequently, must be paired within the complexes.

The determination of the O, N, and C parameters has also been begun. It was possible to determine the majority of the signs of F_{hk0} and F_{0kl}, whereas, because of the special extinctions for the Me atoms, only half of the signs of F_{h0l} could be determined. In this way, reliable electron density maps $\varrho(xyp)$ and $\varrho(pyz)$ could be obtained. The work to interpret these projections and to find out the arrangement of the oxygen, nitrogen, and carbon atoms is continuing.

1. Dyrssen, D. *Svensk Kem. Tidskr.* **68** (1956) 212.
2. *International Tables for X-ray Crystallography*, Birmingham 1952, Vol. I, p. 149.

Received November 12, 1956.

Chromatographic Separation of Aliphatic Monocarbonyl Compounds

HENRIK WALLGREN and ERIK NORDLUND

Department of Nutritional Chemistry, University of Helsinki, Viikin Koetila, Malmi, Finland

In work on the chromatographic separation of the 2,4-dinitrophenylhydrazones of aliphatic methylketones and aldehydes, Meigh's two-phase methanol-heptane system [1,2] gave promising results. The separation and identification of components in a mixture was, however, impossible owing to the trailing of the spots. Addition of 10 % glacial acetic acid to the moving phase resulted in well concentrated spots. Ligroin (B.D.H., b.r. 90—110° C) and even a technical petrol fraction (Shell, b.r. 80—110° C) were as effective as pure heptane.

Chromatographic method. The paper (Whatman No. 1) is soaked in methanol, the excess methanol allowed to drip off, and the paper dried for 10—15 minutes at 80° C. It should be used within two hours after this procedure. The hydrazones (0.5—30 μg may be used) are then pipetted on to the paper, which is suspended in a dry trough and left to stand overnight. The chamber should be airtight and the cover provided with holes for filling the troughs. The chamber holds two containers, the one with heptane(ligroin)-in-

methanol, the other with methanol-in-heptane(ligroin), for saturating the atmosphere. In these are dipped strips of filter paper to increase the evaporating surface. In the morning the moving phase, 10 % acetic acid in heptane(ligroin), is poured into the trough. Freshly prepared solutions should always be used. It is essential that the temperature is kept equal around the whole chamber to prevent condensation. For reasons that will appear below, the chromatogram can be run for *ca.* 1.5 h when the mixture contains hydrazones of the lower aldehydes and ketones. A chromatogram with only higher aldehydes and ketones (5—8 C-atoms) can be run for about 4 h. The spots are clearly brought out in UV-light.

With this method, the following R_F-values were obtained:

Formaldehyde	0.19—0.26	2-Pentanone	0.53—0.59
Acetaldehyde	0.29—0.37	2-Hexanone	0.65
Heptaldehyde	0.65—0.71	2-Heptanone	0.69—0.79
Acetone	0.40—0.52	2-Octanone	0.83
2-Butanone	0.48—0.55		

It is obvious that identification should be based on comparison with runs of known preparations. Complete separation of formaldehyde, acetaldehyde, acetone, 2-butanone, 2-pentanone, and 2-heptanone was achieved. The spots of the higher homologues, especially, are slightly elongated, and therefore 2-hexanone and 2-octanone are partly overlapped by the nearest members of the series. Identification is possible, but not quantitative separation. This is perhaps the chief draw-back of the system, but it can be almost completely overcome with the aid of Matthias' method [8]. Another weakness is that after *ca.* 1.5 h a second solvent front is formed and starts to run up the first one. Apparently this is due to diffusion of the methanol into the acetic acid-heptane mixture and the formation of a new equilibrium. The spots now travel close to the second front and are no longer clearly separated.

Among the methods which the authors have tested [1-9], this has been the most satisfactory for aldehydes and ketones of higher molecular weight, whereas the system of Tarbell *et al.*[3], as modified by Buyske *et al.*[9], is very useful for chromatography of compounds with 5 C-atoms or less. With Matthias' device [8], our method gives equally good separation of these compounds.

Quantitative determination of 2-heptanone and heptaldehyde in fat. The aldehyde or ketone is removed from the fat by steam distillation (20 min) [10-12]. The distillate is collected in a cooled vessel containing 2 ml of a 0.5 % solution of 2,4-dinitrophenylhydrazine in 2 N HCl. The distillate (*ca.* 100 ml) is allowed to stand at least 1 h at room temperature and then extracted with diethyl ether until the ether is colourless. The extract is then washed with 2 N HCl and distilled water, the ether evaporated *in vacuo*, and the residue dissolved in chloroform and chromatographed. The spots are cut out and the pieces of paper crushed in test tubes containing 5 ml of 30 % ethanol made 0.2 N with NaOH. Samples of this solution are sucked out with a pipette provided with a G 2 glass sinter and measured after exactly 20 min in a Beckman spectrophotometer, model DU, at 430 mμ.

The recovery of known amounts of hydrazone run on the paper were: 2-heptanone 76.1 ± 1.17 % (s = 6.5, 31 samples); heptaldehyde 76.2 ± 1.43 % (s = 7.1, 25 samples). When known amounts were mixed in 10 g of lard the recovery was only 35.5 ± 1.43 % in the range 10—200 μg, whereas from 1 000 μg it was 33.1 ± 0.29 %. Thus the variation was considerably smaller when the amounts were greater, but the recovery was not improved. The chief reason for the low percentage recovery was probably incomplete formation of the hydrazones.

The absorption of extracts from pieces of paper treated in the same manner as the chromatograms and of equal size as the spots was 0.031 ± 0.0017 (s = 0.009, 30 samples). Absorption values lower than 0.050 were therefore not concerned, and the lower limit for the determinations is then 1.25 μg of 2-heptanonehydrazone or heptaldehydehydrazone, corresponding to about 0.5 μg of pure ketone or aldehyde. Amounts of about 0.5 μg of hydrazone can, however, be detected in UV-light.

The quantitative method described here cannot be used as such for determination of ketones and aldehydes with lower R_F-values than the two used in this investiga-

tion. Washing of the ether extract with HCl does not remove all the excess dinitrophenylhydrazine, and this forms five spots, of which one travels about as far as 2-hexanone. The method of Pool and Klose[13] could most probably be used, however, for purification of the ether extract.

Acknowledgements. The authors wish to express their gratitude to the Head of the Department of Nutritional Chemistry, Professor Paavo Roine, for his interest and criticism during the work. Financial support was given by *The State Scientific Council*. One of the authors (H.W.) has performed additional experiments especially with the low molecular compounds at the Research Laboratories of the State Alcohol Monopoly, Helsinki. In these experiments, Miss Ingrid Hanika has assisted.

1. Meigh, D. F. *Nature* **169** (1952) 706.
2. Meigh, D. F. *Nature* **170** (1952) 579.
3. Matthias, W. *Naturwiss.* **41** (1954) 17.
4. Huelin, F. E. *Australian J. Sci. Research* **B5** (1952) 328.
5. Kirchner, J. G. and Keller, G. J. *J. Am. Chem. Soc.* **72** (1950) 1867.
6. Rice, R. G., Keller, G. J. and Kirchner, J. G. *Anal. Chem.* **23** (1951) 194.
7. Schmitt, W. J., Moriconi, E. J. and O'Connor, W. F. *Anal. Chem.* **28** (1956) 249.
8. Tarbell, D. S., Brooker, E. G., Vanterpool, A. and Conway, W. *J. Am. Chem. Soc.* **77** (1955) 767.
9. Buyske, D. A., Owen, L. H., Wilder, P. and Hobbs, M. E. *Anal. Chem.* **28** (1956) 910.
10. Isekin, E. *Mitt. Gebiete Lebensm. u. Hyg.* **39** (1948) 310.
11. Patton, S. J. *Dairy Sci.* **33** (1950) 680.
12. Löhr, K. *Biochem. Z.* **320** (1950) 115.
13. Pool, M. F. and Klose, A. A. *J. Am. Oil Chemists' Soc.* **28** (1951) 215.

Received November 7, 1956.

A Low-Resistance Vapour-Phase Chromatograph Column

IB SØRENSEN and P. SØLTOFT

Laboratoriet for almen teknisk Kemi, Danmarks tekniske Højskole, Copenhagen, Denmark

In vapour-phase chromatographic separation of high-boiling compounds, as for instance methyl esters of higher fatty acids, it is convenient to apply low pressures as this enables the use of correspondingly low column temperatures. It is not possible, however, fully to utilize such a pressure reduction in columns of the usual type, as for instance those in which Celite is used as the inert carrier of the static phase, as the pressure drop is very great, about 400 mm mercury pressure in the case of a column length of 1 m. Cropper and Heywood [1] have suggested the substitution of sodium chloride crystals for Celite, enabling a reduction of the pressure drop to 20 mm mercury per metre of column length, and column packing of this type has been used successfully in this laboratory. However, it would be convenient — for several reasons — to be able to reduce the pressure drop further, and since the technique of vapour-phase chromatography offers many points of resemblance to that of fractional distillation, it would be reasonable to assume that packing elements of the types used in lowpressure fractionating columns might also be applied in a vapour-phase chromatograph column. This assumption has been confirmed by experiments with gauze helices of stainless steel, so-called Dixon Gauze Rings, made from fine-mesh steel gauze.

A column packing was prepared with helices of the above-mentioned type, Griffin & George, Ltd., Cat. No. B24—420, dimensions 1/16″ × 1/16″, the helices being carefully mixed with a solution of Dow Corning High Vacuum Silicone Grease in ethyl acetate. After evaporation of the solvent, the grease was left as a film which covered the gauze meshes, but did not fill out the interior of the helix. The helices were packed into a 2 m column of stainless steel tubing with an inside diameter of 8 mm. At 200° C, 20 mm outlet pressure and a rate of flow of carrier gas of 8 ml N_2 per min a pressure drop from one end of the column to the other of 4.5 mm mercury was measured. For purposes of comparison it may be mentioned that the pressure drop measured across the same column when packed with sodium chloride crystals, but otherwise under identical working conditions, was found to be 52 mm.

For our experiments a mixture of methyl esters of C_8—C_{18} fatty acids was used, and it was ascertained that the degree of separation obtained by means of the column was practically the same for both types of packing (see Table 1), but that the elution peaks yielded by the steel gauze packing were of a more perfect shape and more symmetrical. The low pressure drop

tion. Washing of the ether extract with HCl does not remove all the excess dinitrophenylhydrazine, and this forms five spots, of which one travels about as far as 2-hexanone. The method of Pool and Klose[13] could most probably be used, however, for purification of the ether extract.

Acknowledgements. The authors wish to express their gratitude to the Head of the Department of Nutritional Chemistry, Professor Paavo Roine, for his interest and criticism during the work. Financial support was given by *The State Scientific Council*. One of the authors (H.W.) has performed additional experiments especially with the low molecular compounds at the Research Laboratories of the State Alcohol Monopoly, Helsinki. In these experiments, Miss Ingrid Hanika has assisted.

1. Meigh, D. F. *Nature* **169** (1952) 706.
2. Meigh, D. F. *Nature* **170** (1952) 579.
3. Matthias, W. *Naturwiss.* **41** (1954) 17.
4. Huelin, F. E. *Australian J. Sci. Research* **B5** (1952) 328.
5. Kirchner, J. G. and Keller, G. J. *J. Am. Chem. Soc.* **72** (1950) 1867.
6. Rice, R. G., Keller, G. J. and Kirchner, J. G. *Anal. Chem.* **23** (1951) 194.
7. Schmitt, W. J., Moriconi, E. J. and O'Connor, W. F. *Anal. Chem.* **28** (1956) 249.
8. Tarbell, D. S., Brooker, E. G., Vanterpool, A. and Conway, W. *J. Am. Chem. Soc.* **77** (1955) 767.
9. Buyske, D. A., Owen, L. H., Wilder, P. and Hobbs, M. E. *Anal. Chem.* **28** (1956) 910.
10. Isekin, E. *Mitt. Gebiete Lebensm. u. Hyg.* **39** (1948) 310.
11. Patton, S. J. *Dairy Sci.* **33** (1950) 680.
12. Löhr, K. *Biochem. Z.* **320** (1950) 115.
13. Pool, M. F. and Klose, A. A. *J. Am. Oil Chemists' Soc.* **28** (1951) 215.

Received November 7, 1956.

A Low-Resistance Vapour-Phase Chromatograph Column

IB SØRENSEN and P. SØLTOFT

Laboratoriet for almen teknisk Kemi, Danmarks tekniske Højskole, Copenhagen, Denmark

In vapour-phase chromatographic separation of high-boiling compounds, as for instance methyl esters of higher fatty acids, it is convenient to apply low pressures as this enables the use of correspondingly low column temperatures. It is not possible, however, fully to utilize such a pressure reduction in columns of the usual type, as for instance those in which Celite is used as the inert carrier of the static phase, as the pressure drop is very great, about 400 mm mercury pressure in the case of a column length of 1 m. Cropper and Heywood [1] have suggested the substitution of sodium chloride crystals for Celite, enabling a reduction of the pressure drop to 20 mm mercury per metre of column length, and column packing of this type has been used successfully in this laboratory. However, it would be convenient — for several reasons — to be able to reduce the pressure drop further, and since the technique of vapour-phase chromatography offers many points of resemblance to that of fractional distillation, it would be reasonable to assume that packing elements of the types used in lowpressure fractionating columns might also be applied in a vapour-phase chromatograph column. This assumption has been confirmed by experiments with gauze helices of stainless steel, so-called Dixon Gauze Rings, made from fine-mesh steel gauze.

A column packing was prepared with helices of the above-mentioned type, Griffin & George, Ltd., Cat. No. B24—420, dimensions 1/16″ × 1/16″, the helices being carefully mixed with a solution of Dow Corning High Vacuum Silicone Grease in ethyl acetate. After evaporation of the solvent, the grease was left as a film which covered the gauze meshes, but did not fill out the interior of the helix. The helices were packed into a 2 m column of stainless steel tubing with an inside diameter of 8 mm. At 200° C, 20 mm outlet pressure and a rate of flow of carrier gas of 8 ml N_2 per min a pressure drop from one end of the column to the other of 4.5 mm mercury was measured. For purposes of comparison it may be mentioned that the pressure drop measured across the same column when packed with sodium chloride crystals, but otherwise under identical working conditions, was found to be 52 mm.

For our experiments a mixture of methyl esters of C_8—C_{18} fatty acids was used, and it was ascertained that the degree of separation obtained by means of the column was practically the same for both types of packing (see Table 1), but that the elution peaks yielded by the steel gauze packing were of a more perfect shape and more symmetrical. The low pressure drop

Table 1.

200° C, 8 ml N_2/min	Steel gauze		NaCl
Outlet pressure, mm Hg	50	20	20
Pressure drop » »	4	4.5	52
Inlet pressure » »	54	24.5	72
HETP* for C_{12} cm	2.2	4.2	3.6

* HETP has been calculated according to a formula given by van Deemter *et al.* in "Symposium on Vapour Phase Chromatography, London, 30th May—1st June 1956", Butterworth's Scientific Publications, p. A 21.

further enables the use of lower column temperatures or higher outlet pressures, and in both cases the degree of separation obtained from a column is increased considerably. It is also possible to use long columns, the pressure drop in the case of a 4 m column being for instance 8 mm mercury.

It remains to be ascertained whether the type of packing described is also applicable for vapour-phase chromatography at normal pressures, but considering the great similarity between vapour-phase partition chromatography and fractional distillation there is every probability that this is the case.

1. Cropper, F. R. and Heywood, A. *Nature* **174** (1954) 1063.

Received November 15, 1956.

Distribution of Enzymes Involved in the Breakdown of Uracil to β-Alanine in Rat Liver Cells

PER FRITZSON*

Wenner-Gren Institute of Experimental Biology, Department of Physiological Chemistry, University of Stockholm, Stockholm, Sweden, and Norsk Hydro's Institute for Cancer Research, The Norwegian Radium Hospital, Oslo, Norway

Previous studies of the catabolism of ^{14}C-labeled uracil, dihydrouracil (DHU) and β-ureidopropionic acid (BUP) in the rat [1,2] demonstrated the following reactions in rat liver slices *in vitro* and in the intact rat:

Uracil → DHU ⇌ BUP → β-alanine

The results further indicated that the liver is the main site of these reactions. The localization of the enzymes responsible for the different reactions in this process in the liver cells, has now been investigated.

White rats were decapitated, and the livers were homogenized in 0.25 M sucrose as described by Ernster and Löw [3]. Uracil-6-^{14}C *, DHU-6-^{14}C and BUP-3-^{14}C were incubated with the homogenate and with three fractions of the homogenate obtained by successive removal of nuclei, mitochondria and microsomes by fractional centrifugation at 1 600 × g for 10 min, 4 100 × g for 15 min, and 105 000 × g for 45 min, respectively. The reaction mixtures were analyzed for radioactive compounds by paper strip chromatography in *n*-butanol-acetic acid-water (4:1:5) and in collidine saturated with water, and the distribution of radioactivity along the strips was determined, as described previously [1,2]. The total radioactivity of the incubation mixtures before and after incubation was determined by plating aliquots on planchets and subsequent counting, as described by Canellakis [5]. The results showed, within the limits of experimental error, that no volatile, radioactive compounds were formed during incubation, indicating that all the radioactive products can be detected in the chromatograms. The results are recorded in Table 1. The incubations with BUP as substrate show that the yield of β-alanine is the same in the presence of the homogenate and the particle-free supernatant fluid. The removal of nuclei and mitochondria has no effect on the enzymatic activity. These facts clearly demonstrate that the enzyme catalyzing the conversion of BUP to β-alanine is present entirely in the supernatant fraction. The data from the incubations of DHU with homogenate and supernatant fluid are consistent with the finding that the enzyme catalyzing the interconversion of DHU and BUP was present entirely in the supernatant fraction of isotonic KCl homogenates of rat liver [6]. The incubation of uracil with the supernatant fluid demonstrates that β-alanine is the only radioactive product which can be clearly detected in the chromatograms.

* Fellow of the Norwegian Cancer Society, Oslo, Norway.

* The numbering system is that in which uracil is 2,4-dihydroxypyrimidine. The preparation and tests of purity of the labeled compounds are described elsewhere [4,2].

Table 1.

200° C, 8 ml N_2/min	Steel gauze		NaCl
Outlet pressure, mm Hg	50	20	20
Pressure drop » »	4	4.5	52
Inlet pressure » »	54	24.5	72
HETP* for C_{12} cm	2.2	4.2	3.6

* HETP has been calculated according to a formula given by van Deemter *et al.* in "Symposium on Vapour Phase Chromatography, London, 30th May—1st June 1956", Butterworth's Scientific Publications, p. A 21.

further enables the use of lower column temperatures or higher outlet pressures, and in both cases the degree of separation obtained from a column is increased considerably. It is also possible to use long columns, the pressure drop in the case of a 4 m column being for instance 8 mm mercury.

It remains to be ascertained whether the type of packing described is also applicable for vapour-phase chromatography at normal pressures, but considering the great similarity between vapour-phase partition chromatography and fractional distillation there is every probability that this is the case.

1. Cropper, F. R. and Heywood, A. *Nature* **174** (1954) 1063.

Received November 15, 1956.

Distribution of Enzymes Involved in the Breakdown of Uracil to β-Alanine in Rat Liver Cells

PER FRITZSON*

Wenner-Gren Institute of Experimental Biology, Department of Physiological Chemistry, University of Stockholm, Stockholm, Sweden, and Norsk Hydro's Institute for Cancer Research, The Norwegian Radium Hospital, Oslo, Norway

Previous studies of the catabolism of ^{14}C-labeled uracil, dihydrouracil (DHU) and β-ureidopropionic acid (BUP) in the rat [1,2] demonstrated the following reactions in rat liver slices *in vitro* and in the intact rat:

Uracil → DHU ⇌ BUP → β-alanine

The results further indicated that the liver is the main site of these reactions. The localization of the enzymes responsible for the different reactions in this process in the liver cells, has now been investigated.

White rats were decapitated, and the livers were homogenized in 0.25 M sucrose as described by Ernster and Löw [3]. Uracil-6-^{14}C *, DHU-6-^{14}C and BUP-3-^{14}C were incubated with the homogenate and with three fractions of the homogenate obtained by successive removal of nuclei, mitochondria and microsomes by fractional centrifugation at 1 600 × g for 10 min, 4 100 × g for 15 min, and 105 000 × g for 45 min, respectively. The reaction mixtures were analyzed for radioactive compounds by paper strip chromatography in *n*-butanol-acetic acid-water (4:1:5) and in collidine saturated with water, and the distribution of radioactivity along the strips was determined, as described previously [1,2]. The total radioactivity of the incubation mixtures before and after incubation was determined by plating aliquots on planchets and subsequent counting, as described by Canellakis [5]. The results showed, within the limits of experimental error, that no volatile, radioactive compounds were formed during incubation, indicating that all the radioactive products can be detected in the chromatograms. The results are recorded in Table 1. The incubations with BUP as substrate show that the yield of β-alanine is the same in the presence of the homogenate and the particle-free supernatant fluid. The removal of nuclei and mitochondria has no effect on the enzymatic activity. These facts clearly demonstrate that the enzyme catalyzing the conversion of BUP to β-alanine is present entirely in the supernatant fraction. The data from the incubations of DHU with homogenate and supernatant fluid are consistent with the finding that the enzyme catalyzing the interconversion of DHU and BUP was present entirely in the supernatant fraction of isotonic KCl homogenates of rat liver [6]. The incubation of uracil with the supernatant fluid demonstrates that β-alanine is the only radioactive product which can be clearly detected in the chromatograms.

* Fellow of the Norwegian Cancer Society, Oslo, Norway.

* The numbering system is that in which uracil is 2,4-dihydroxypyrimidine. The preparation and tests of purity of the labeled compounds are described elsewhere [4,2].

Table 1. DHU-6-^{14}C and BUP-3-^{14}C incubated for 1 h at 30° C with aliquots of liver preparations representing 0.17—0.19 g of fresh tissue in a final volume of 3 ml of 0.25 M sucrose. Gas phase, air. Uracil-6-^{14}C was incubated at 37° C.

Substrate	Liver preparation	Amounts of radioactive compounds detected after incubation *				Radioactivity recovered after incubation ** (in per cent)
		Uracil	DHU	BUP	β-alanine	
8 μmoles BUP-3-^{14}C	Homogenate	0	0	77	23	
	Mitochondria + microsomes + supernatant	0	0	75	25	
	Microsomes + supernatant	0	0	75	25	
	Supernatant	0	0	77	23	96
8 μmoles DHU-6-^{14}C	Homogenate	0	72	6	22	
	Supernatant	0	73	10	17	102
1 μmole uracil-6-^{14}C	Supernatant	78	0	0	17	96

* Expressed in per cent of the total radioactivity on the paper strip after chromatography.
** Determined by plating TCA-treated aliquots of the incubation mixture.

Additional data from the work of Rutman *et al.*[7] indicate that the ureido carbon of uracil is released as carbon dioxide in the supernatant fluid from rat liver homogenates. The particulate fraction was found to inhibit the enzymatic activity. These results were confirmed by the recent work of Canellakis [5], and it was demonstrated that the enzymatic activity of rat liver slices approximated that of the supernatant fluid. On the basis of these findings it can be concluded that the enzyme catalyzing the reduction of uracil to DHU is present mainly or entirely in the part of the cytoplasm represented by the nonparticulate system.

The author wishes to express his deep appreciation to Dr. Hans Löw, Wenner-Gren Institute, for his valuable advice and assistance in connection with tissue preparations.

1. Fritzson, P. *J. Biol. Chem.* (1957) *In press.*
2. Fritzson, P. and Pihl, A. *J. Biol. Chem.* (1957) *In press.*
3. Ernster, L. and Löw, H. *Exptl. Cell Research*, Suppl. 3 (1955) 133.
4. Fritzson, P. *Acta Chem. Scand.* 9 (1955) 1239.
5. Canellakis, E. S. *J. Biol. Chem.* 221 (1956) 315.
6. Grisolia, S. and Wallach, D. P. *Biochim. et Biophys. Acta* 18 (1955) 449.
7. Rutman, R. J., Cantarow, A. and Paschkis, K. E. *J. Biol. Chem.* 210 (1954) 321.

Received November 24, 1956.

On the Molecular Weights of Human and Ox Pituitary Growth Hormones

A. EHRENBERG and F. HEIJKENSKJÖLD

Biochemical Department, Nobel Medical Institute, and Department of Clinical Biochemistry, Karolinska Sjukhuset, Stockholm, Sweden

A growth-hormone-like principle in human pituitaries has recently been demonstrated by Gemzell and Heijkenskjöld[1]. The human pituitary growth hormone has now been isolated in an electrophoretically pure form [2], and investigations are being carried out concerning its chemical and physical nature. Some preliminary experiments on the sedimentation behaviour and molecular weight of this hormone are re-

Table 1. DHU-6-^{14}C and BUP-3-^{14}C incubated for 1 h at 30° C with aliquots of liver preparations representing 0.17—0.19 g of fresh tissue in a final volume of 3 ml of 0.25 M sucrose. Gas phase, air. Uracil-6-^{14}C was incubated at 37° C.

Substrate	Liver preparation	Amounts of radioactive compounds detected after incubation *				Radioactivity recovered after incubation ** (in per cent)
		Uracil	DHU	BUP	β-alanine	
8 μmoles BUP-3-^{14}C	Homogenate	0	0	77	23	
	Mitochondria + microsomes + supernatant	0	0	75	25	
	Microsomes + supernatant	0	0	75	25	
	Supernatant	0	0	77	23	96
8 μmoles DHU-6-^{14}C	Homogenate	0	72	6	22	
	Supernatant	0	73	10	17	102
1 μmole uracil-6-^{14}C	Supernatant	78	0	0	17	96

* Expressed in per cent of the total radioactivity on the paper strip after chromatography.
** Determined by plating TCA-treated aliquots of the incubation mixture.

Additional data from the work of Rutman *et al.*[7] indicate that the ureido carbon of uracil is released as carbon dioxide in the supernatant fluid from rat liver homogenates. The particulate fraction was found to inhibit the enzymatic activity. These results were confirmed by the recent work of Canellakis [5], and it was demonstrated that the enzymatic activity of rat liver slices approximated that of the supernatant fluid. On the basis of these findings it can be concluded that the enzyme catalyzing the reduction of uracil to DHU is present mainly or entirely in the part of the cytoplasm represented by the nonparticulate system.

The author wishes to express his deep appreciation to Dr. Hans Löw, Wenner-Gren Institute, for his valuable advice and assistance in connection with tissue preparations.

1. Fritzson, P. *J. Biol. Chem.* (1957) *In press.*
2. Fritzson, P. and Pihl, A. *J. Biol. Chem.* (1957) *In press.*
3. Ernster, L. and Löw, H. *Exptl. Cell Research*, Suppl. 3 (1955) 133.
4. Fritzson, P. *Acta Chem. Scand.* 9 (1955) 1239.
5. Canellakis, E. S. *J. Biol. Chem.* 221 (1956) 315.
6. Grisolia, S. and Wallach, D. P. *Biochim. et Biophys. Acta* 18 (1955) 449.
7. Rutman, R. J., Cantarow, A. and Paschkis, K. E. *J. Biol. Chem.* 210 (1954) 321.

Received November 24, 1956.

On the Molecular Weights of Human and Ox Pituitary Growth Hormones

A. EHRENBERG and F. HEIJKENSKJÖLD

Biochemical Department, Nobel Medical Institute, and Department of Clinical Biochemistry, Karolinska Sjukhuset, Stockholm, Sweden

A growth-hormone-like principle in human pituitaries has recently been demonstrated by Gemzell and Heijkenskjöld[1]. The human pituitary growth hormone has now been isolated in an electrophoretically pure form [2], and investigations are being carried out concerning its chemical and physical nature. Some preliminary experiments on the sedimentation behaviour and molecular weight of this hormone are re-

Table 1. Sedimentation constants of human pituitary growth hormones under various conditions.

Buffer	pH	Protein mg/ml	S^0_{20}
Borate	10.0	7	1.99
»	9.9	8	2.12
»	9.9	15	2.30
»	9.9	15	2.20
Acetate	4.1	9	1.6
Phthalate	4.0	5	1.3

ported here and comparison is made with the ox hormone.

Experimental. The sedimentation coefficients were determined in a Spinco ultracentrifuge at 59 780 r.p.m. The molecular weight determinations were carried out in the same centrifuge at lower speeds as will be described elsewhere by Ehrenberg [3].

The human growth hormone was prepared by Heijkenskjöld [2] and the ox hormone was a gift from Dr. C. H. Li [4] to Dr. C. A. Gemzell, who kindly put it at our disposal.

At pH 9.9 a 0.028 M borate buffer was used, and at pH 4 either 0.125 M acetate or 0.045 phthalate. In all cases 1 % sodium chloride was added.

Results and discussion. The sedimentation coefficients from the experiments on the human growth hormone are listed in Table 1. The hormone protein appeared to be homogeneous in the experiments at pH 9.9, whilst the presence of small amounts of both faster and slower components is likely at pH 4. A single experiment on the ox hormone at pH 9.9 gave a sedimentation coefficient of 3.51 S in agreement with previous data [5,6]. As is seen the values for the human hormone are appreciably lower at this pH. The same differences persist in more acid buffers where the ox hormone still shows values above 3 S[6]. At the rather high pH 11.5, however, the sedimentation coefficients of ox hormone [6] are comparable to those of human hormone at pH 4 and 10. These data suggest that the human hormone has a lower molecular weight than the ox hormone at pH 4 and 10.

The molecular weights were determined on both hormones at pH 9.9. Two runs were made on the human hormone (10 and 5 mg/ml), both giving a molecular weight close to 30 000 in the first part of the experiment. In these calculations use was made of the value 0.76 of the partial specific volume of the ox hormone [7]. A decrease in the calculated molecular weight was observed in the later part of the experiment. This behaviour can be explained either by an inhomogeneous sample or by a concentration dependent equilibrium between molecules of different sizes. One experiment with ox hormone, also at pH 9.9 gave in the early part a molecular weight of about 75 000 and in the later part a decrease similar to that just described. Li and Pedersen [6] observed at this H an increase of S^0_{20} with protein concentration, which was explained by the assumption that the ox hormone protein behaves like a mixture of monomeric and dimeric forms. A similar concentration dependence of S^0_{20} of human hormone is indicated by the data of Table 1. There are thus good reasons to assume that this hormone protein also behaves like a mixture of molecules of different sizes at pH around 10.

The molecular weight of the ox hormone at pH 10 calculated by Li and Pedersen [6] from separate sedimentation and diffusion experiments was about 50 000; the sedimentation coefficient was extrapolated to zero protein concentration and the diffusion coefficient was determined at the low concentration of 2.5 mg/ml. This value is likely to correspond to the monomeric ox hormone, and our value of 75 000 to a sample of more or less aggregated molecules. In the later part of the experiment the observed molecular weight decreased towards the value for the monomeric form. By analogy herewith the value of the molecular weight of the human growth hormone of about 30 000 at pH 10 would be a mean for molecules of different sizes. The smallest hormone molecules present at this pH might have molecular weights as low as 15 000 – 20 000.

1. Gemzell, C. A. and Heijkenskjöld, F. *Endocrinology. In press.*
2. Heijkenskjöld, F. *To be published.*
3. Ehrenberg, A. *To be published.*
4. Li, C. H., Evans, H. M. and Simpson, M. E. *J. Biol. Chem.* **159** (1945) 353.
5. Li, C. H. and Moskowitz, M. *J. Biol. Chem.* **178** (1949) 203.
6. Li, C. H. and Pedersen, K. O. *J. Biol. Chem.* **201** (1953) 595.
7. Li, C. H. *J. Phys. & Colloid Chem.* **51** (1947) 218.

Received December 11, 1956.